Right Heart Pathology

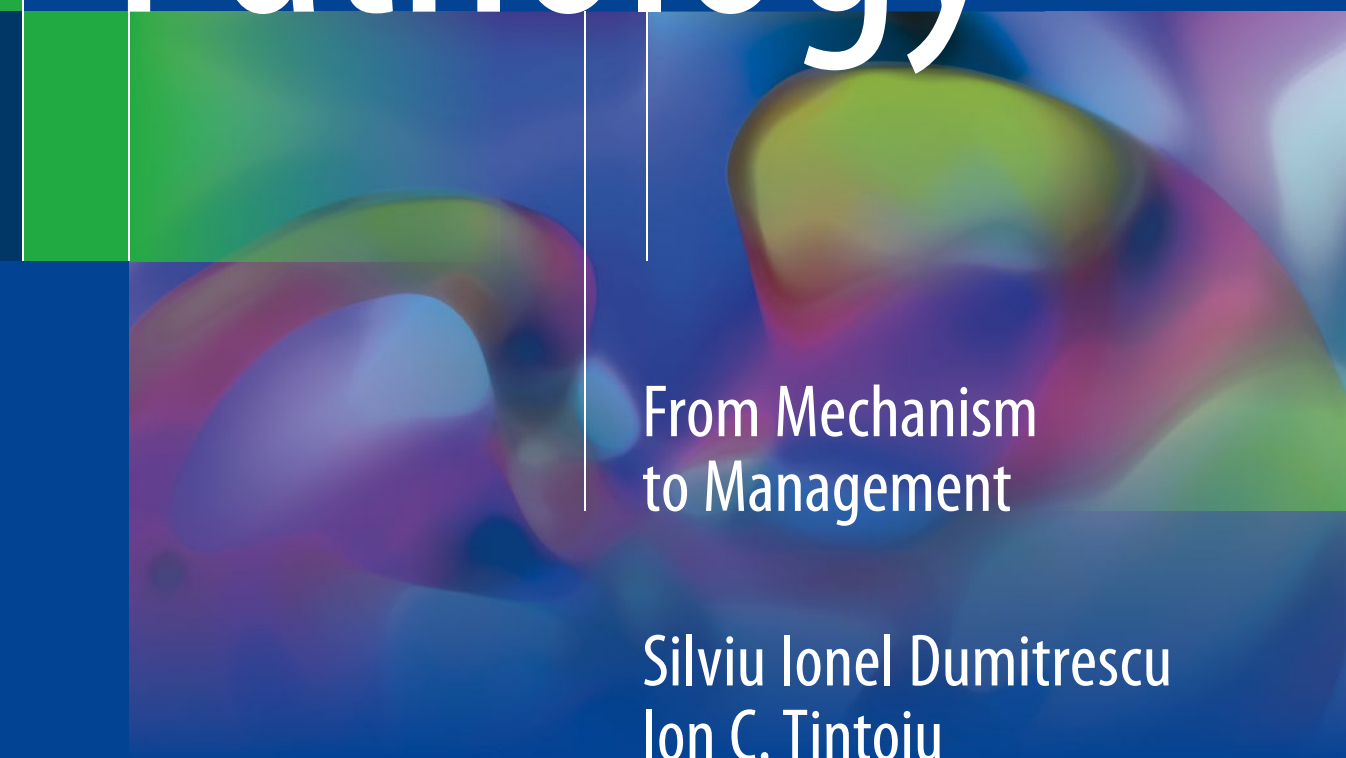

From Mechanism to Management

Silviu Ionel Dumitrescu
Ion C. Țintoiu
Malcolm John Underwood
Editors

Springer

Right Heart Pathology

Silviu Ionel Dumitrescu
Ion C. Ţintoiu
Malcolm John Underwood
Editors

Right Heart Pathology

From Mechanism to Management

Springer

Editors
Silviu Ionel Dumitrescu
Department of Medicine
Titu Maiorescu University
Bucharest
Romania

Malcolm John Underwood
Department of Surgery
Chinese University of Hong Kong
Sha Tin
Hong Kong

Ion C. Ţintoiu
Department of Medicine
Carol Davila University of
Medicine and Pharmacy
Bucharest
Romania

ISBN 978-3-319-73763-8 ISBN 978-3-319-73764-5 (eBook)
https://doi.org/10.1007/978-3-319-73764-5

Library of Congress Control Number: 2018938549

Printed on acid-free paper

This Springer imprint is published by the registered company Springer International Publishing AG part of Springer Nature.
The registered company address is: Gewerbestrasse 11, 6330 Cham, Switzerland

I dedicate this monograph to my professor Vasile Cândea, the mentor of the cardiac surgery school in our hospital.

Thanks to my wife Olga and my daughter Raluca for their patience with which they supported me in the realization of this monograph.

Ion C. Ţintoiu, MD, PhD, FESC

Foreword

Pathology of the right heart has been less studied by medical literature, therefore we have proposed to update the existing data in order to improve the therapeutic solutions.

On the whole, We have reviewed the main elements of embryology, genetics, anatomy, pathophysiology, diagnostic methods, right heart pathology, and up-to-dated therapeutic solutions. We have presented the pathology of the right heart from the point of view of its primary and secondary interests.

The objectives of this monograph were three. The first was to present the general data from anatomy to pathology. The second part of the study was to analyze the main diagnostic methods: exam, classical methods (cardiac catheterization, angiocardiography) as well as modern methods of echocardiography (TEE, 3D, 4D etc), MRI, Angio CT, etc. The third was to individualize the therapeutic solutions for medical and surgical treatments. The authors of this monograph are medical personalities who present their personal experience as well. Each chapter approaches the subject with arguments from literature, graphic examples, and iconography mainly from accumulated knowledge. Arrhythmias, pacing problems, ICD, and CRT are addressed in their complexity from the point of view of procedural techniques as well as complications. The tricuspid valve pathology is treated in its primary and secondary affection and in the context of pulmonary hypertension. The right ventricle dysfunction is presented in its systolic and diastolic components as well as in relation to the left ventricle. Pulmonary thromboembolism is specifically analyzed in a chapter which includes specific surgical and interventional treatment. The repercussions on right ventricle function after liver transplantation and pneumonectomy are tackled as well.

We would like to thank the authors and coauthors of this monograph for their participation in this project.

Bucharest, Romania — Ion C. Ţintoiu

Preface

Pathology of the right heart is less studied in the literature, and that is why we have proposed to update the existing data in order to improve the therapeutic solutions. We have reviewed the main elements of embryology, genetics, anatomy, pathophysiology, diagnostic methods, right heart pathology, and up-to-date therapeutic solutions. We have presented the pathology of the right heart from the point of view of both primary and secondary interests.

The monograph has three objectives. The first is to present the general data from anatomy to pathology. The second is to analyze the main diagnostic methods: exam, classical methods (cardiac catheterization, angiocardiography), and modern methods of echocardiography (TEE, 3D, 4D etc), MRI, Angio CT, etc. The third is to individualize therapeutic solutions for medical and surgical treatment. The authors of this monograph are medical personalities who present their personal experience as well. Each chapter addresses the subject with arguments from literature, graphic, and iconographic examples, generally personal. Arrhythmias, pacing, ICD, and CRT problems are addressed in their complexity from the point of view of procedural techniques and complications. The pathology of the tricuspid valve is treated in its primary and secondary affection and in the context of pulmonary hypertension. Right ventricular dysfunction is presented in its systolic and diastolic components as well as in relation to the left ventricle. Pulmonary thromboembolism is specifically analyzed in a chapter that includes specific surgical and interventional treatment. Repercussions on right ventricular function after liver transplantation and pneumonectomy are also addressed.

We would like to thank the authors and coauthors of this monograph for their participation in this project.

Bucharest, Romania — Silviu Ionel Dumitrescu
Bucharest, Romania — Ion C. Ţintoiu
Sha Tin, Hong Kong — Malcom John Underwood

Contents

Part I

Overview

Heart Embryology: Overview

1

Florentina Radu-Ioniţă, Ecaterina Bontaş, Viorel Goleanu, Bogdan Cîrciumaru, Daniela Bartoş, Irinel Parepa, Ion C. Ţintoiu, and Adrian Popa

Abstract

Human heart has a complex embryological development process driven by genetic mechanisms that have successive and unitary progression in a global context together with other developments of organogenesis. The first elements of cardiogenesis occur prematurely from mesoderm where cellular differentiation at this level acquires cardiogenic specificity by creating the first heart field. From this stage, cellular multiplication is specific for myocardial, endothelial, and smooth muscle cells through the second heart field. Accordingly to up-to-date evidence, the mechanisms of this process are genetically coordinated mainly by NKX2.5, GATA4, Mef2, TBX5 and Hand which establish not only the structure of the embryonic cord but also the sequential evolution of the differentiation and completion of the cardiac structures including the inlet and outlet paths. First field and second field are the initial particular stages of cardiogenesis. In the primary heart tube, the differentiation into adult anatomical cardiac structures (the atrial and ventricular cavities) begins. The heart tube looping initi-

F. Radu-Ioniţă
"Titu Maiorescu" University of Medicine, Bucharest, Romania

"Carol Davila" Central Military Emergency University Hospital, Bucharest, Romania

E. Bontaş (✉) · A. Popa
Department of Cardiology, "Prof. C.C. Iliescu", Emergency Institute for Cardiovascular Diseases, Bucharest, Romania

V. Goleanu
Department of Cardiovascular Surgery, "Dr. Agripa Ionescu" Military Hospital, Bucharest, Romania

B. Cîrciumaru
"Titu Maiorescu" University of Medicine, Bucharest, Romania

Infectious Diseases Department, "Carol Davila" Central Military Emergency University Hospital, Bucharest, Romania

D. Bartoş
Internal Medicine, "Carol Davila" University of Medicine and Pharmacy, Bucharest, Romania

Internal Medicine Department, Emergency Hospital Bucharest, Bucharest, Romania

I. Parepa
Department of Cardiology, "Ovidiu" University Constanta, Emergency County Hospital, Constanta, Romania

I. C. Ţintoiu (✉)
Department of Medicine of Bucharest, "Titu Maiorescu" University, Bucharest, Romania

Center for Cardiovascular Diseases, "Carol Davila" Central Military Emergency University Hospital, Bucharest, Romania

S. I. Dumitrescu et al. (eds.), *Right Heart Pathology*, https://doi.org/10.1007/978-3-319-73764-5_1

ates the separation of the primitive atria, ventricle and outflow tract. The separation between these cavities is made by different but concordant mechanisms. Coronarogenesis is the last stage before embryonic heart becomes functional.

Keywords
Cardiogenesis · Cardiac morphogenesis Normal heart development · First and second heart fields · Linear and looped tube separation Jonctional differentiation · Angiogenesis Conduction system

The norm should be established; embryos should be arranged in stages.

Franklin P. Mall

1.1 Background

Importantly, Kloesel et al. stated that "the embryonic development of the human heart is a complex process" [1]. As well, understanding of cardiac development is based also on "genetics, molecular cell biology, embryology, systems biology and anatomy" [1]. It must also be emphasized that in the heart embryology numerous terms are currently existent for the similar cardiac structures. The extremely difficult molecular biology and genetic taxonomy differentiates a gene from a protein by a general agreement [1]. A human gene is described in italic uppercase letters (e.g., *GATA4*), while the protein obtained from this gene is described in nonitalic uppercase letters (e.g., GATA4) [1].

Recent data regarding cardiogenesis of Kloesel et al. have established nine main successive stages [1]: (1) gastrulation (three germ layers), (2) the first and second heart fields development, (3) heart tube, (4) heart tube looping, convergence, and wedging, (5) septa forming with common atrium and atrioventricular canal, (6) formation of outflow tract, (7) development of cardiac valves, (8) development of vessels (coronary arteries, aortic arches and sinus venous), (9) development of the conduction tissue. The first cardiac structures emerge from the "mesodermal precardiac cells" that shift to the superior part of the primary embryonic framework forming a special cardiac structure called "cardiac crescent" [2]. Equally important, the cardiogenesis process is sustained by transcription factors also known as "primordial genes" implied in cardiac morphogenesis. Therefore, the role of above mentioned genes is to differentiate mesodermal precardiac cells in the myocardial cells, endothelial cells and smooth muscle cells through the process called "the phenomenon of progressive lineage restriction" [3]. Transcription factors responsible for cardiogenesis such as NK2 Homeobox 5 (NKX2.5) [1, 4], GATA-binding protein 4 (GATA4) [1, 5], T-Box protein 5 (TBX5) [1], MADS-box protein (Mef2) [6], and Heart—and neural crest derivatives-expressed protein (Hand) family [6] ensure the control of cardiac differentiation. Specifically, the interrelation between the main three transcription factors (TBX5, GATA4, and NKX2.5) as well the individual action of these elements is fundamental to cardiogenesis.

Embryonic human cardiac development in Carnegie stages 15–23 has important knowledge for clinical and scientific research [7]. Of note, the evolution of the human embryo is based on the *Carnegie Institution of Washington* stages (CS) so that in the first 8 weeks are described 23 stages. Cardiac structures begin differentiation from stage 13 Carnegie and are finalized in stage 23 (see Table 1.1) [7]. Moreover, human embryos cardiac development from Carnegie stages 15–23 offer significant evidence looking embryogenesis, for instance regarding the ventricular trabeculation process [7, 8].

1.2 Heart Fields

At day 16 (CS6-7) of gestation, a part of epiblast cells form by migration the mesoderm with "four cell populations—cardiogenic mesoderm and the paraxial, intermediate, and lateral plate mesoderm" [1, 2]. Further, progenitor cardiogenic mesodermal cells also known as "precardiac cells" generate the first heart field (FHF) [1]. Equally important, the FHF generates further the

Table 1.1 Stages of human development with corresponding events in cardiac development

Carnegie stage (CS)	Human DPC	Characteristics
CS8	17–19	The cardiac crescent forms
CS9	19–21	The embryo folds, the pericardial cavity is placed in its final position, gully of myocardium forms, the endocardial plexus forms, cardiac jelly forms
CS10	22–23	The heart beats, the endocardial tubes fuse, the mesocardium perforates, looping starts, the ventricle starts ballooning
CS11	23–26	The atria balloon, the proepicardium forms
CS12	26–30	The septum primum appears, the right venous valve appears, the muscular part of the ventricular septum forms, cells appear in the cardiac jelly, epicardial growth starts
CS13	28–32	The AV cushions form, the pulmonary vein attaches to the atrium, the left venous valve appears, epicardial mesenchyme appears first in the AV sulcus
CS14	31–35	The AV cushions approach one another, the outflow ridges become apparent, capillaries form in the epicardial mesenchyme
CS15	35–38	The AV cushions oppose one another, the secondary foramen forms, the distal outflow tract septates, the outflow tract ridges reach the primary foramen
CS16	37–42	The primary atrial septum closes, the outflow tract ridges approach the interventricular septum, the entire heart is covered in epicardium
CS17	42–44	Secondary atrial septum appears, the sinus node becomes discernable, the left and right AV connection becomes separate, the proximal outflow tract becomes septated, the semilunar valves develop
CS18	44–48	Papillary muscles appear, the AV valves start to form
CS19	48–51	The left venous valve fuses with the secondary septum, the mural leaflets of the mitral and tricuspid valves are released
CS21	53–54	The main branches of the coronary artery become apparent
CS22	54–56	The chordae tendinae form
CS23	56–60	The septal leaflet of the tricuspid valve delaminates

DPC days postconception
Modified from Kussman and Miller-Hance [7] with permission.
See further reading section for comprehensive data

secondary heart field (SHF) that will create the greater part of the heart [1]. It has to be underlined that the transcription factor islet-1 (Isl1) is exhibited by SHF cells required for the development further in cardiomyocytes, smooth muscle cells and endothelial cells [2, 9]. Both, FHF and SHF form cardiac crescent at day 15 [1].

It is well established that progenitor cardiogenic mesodermal cells (precardiac mesodermal cells) are the first generators in cardiogenesis. Initially, embryonic mesoderm cells convert in "precardiac lineage" that exhibits Mesp-1 with the ability to develop multipotent "cardiac progenitor cells" (CPC, exhibiting NKX2.5). As already mentioned, CPC control by themself the capacity to develop cardiac myocytes, vascular smooth muscle cells, and endothelial cells (Fig. 1.1) [10]. It is postulated that the significant resource for the CPC is SHF that will generate the outflow tract (OFT). However, the increase and generation of both OFT and heart valves is accomplished by "non-mesodermal neural crest cells" (NCC) of the neural fold by migration in the endocardial cushion and the arterial pole through genetic control of Pax3 (see Fig. 1.1) [10].

Between days 15 and 21 (CS7-9) structural evolutionary transformations by cellular multiplication of FHF and SHF lead to linear heart tube development that represents the next step of cardiogenesis. At day 15, first locations of primitive atrial and ventricular cavities appear in FHF sequentially placed in lateral places of cardiac crescent. As well, SHF represents the inside padding of FHF [1].

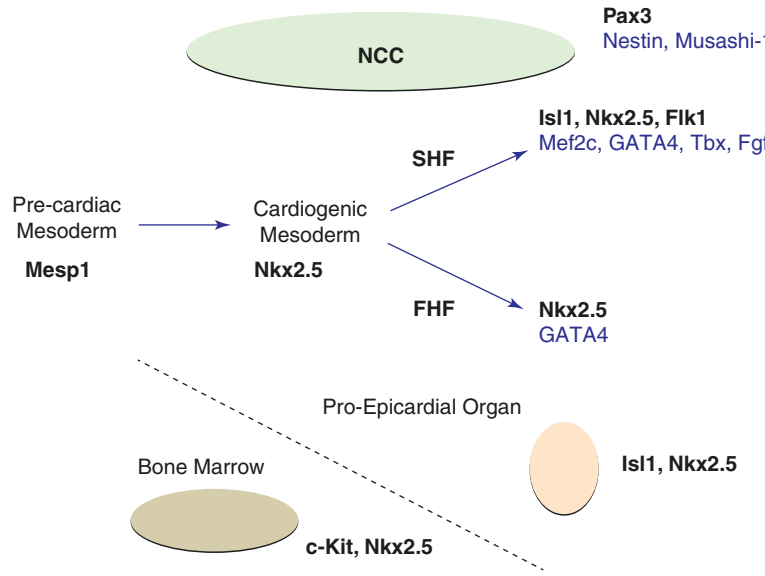

Fig. 1.1 Overview of myocardial CPC Markers in relation to their ontology. Pre-cardiac mesoderm cells express Mesp1 until differentiation to cardiogenic mesoderm, marked by the expression of Nkx2.5. The cardiogenic mesoderm differentiates to form two heart fields. Cells in the first heart field (FHF) express GATA4 in addition to Nkx2.5. Cells of the secondary heart field (SHF) express Isl1 and Nkx2.5. The SHF also becomes populated by neural crest cells (NCC) expressing Pax3. Markers associated with the heart field cells but showing greater variation in their expression are indicated in blue type. In addition to cardiogenic mesoderm, cells from the pro-epicardial organ and also of hematopoietic lineage have been identified in the myocardium. Abbreviations: *NCC* neural crest cells, *SHF* second heart field, *FHF* first heart field. From Chalajour et al. [10]. It is open access chapter.

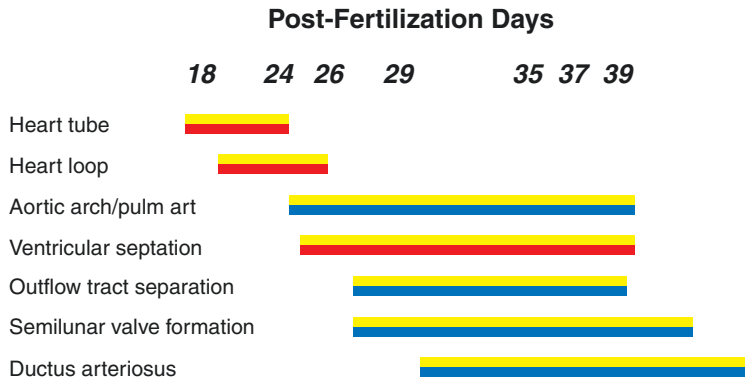

Fig. 1.2 Timeline of outflow tract and semilunar valve development post-fertilization. The colors represent contributions to cardiac development from different cell populations. These contributions are from the first heart field (red), second heart field (yellow) and cardiac neural crest (blue). Modified from Gittenberger-de Groot et al. [11]. From Martin et al. [12]. It is an open access article.

To sum up, FHF along with SHF and the migration of NCC into SHF participate in all stages of cardiogenesis (Fig. 1.2) [1, 10–12].

Consequently, at day 21, the first sites of atrium and ventricle cavities appear in FHF sequentially placed in lateral places of cardiac crescent. As already described above, SHF represents padding through cells placed inside FHF. From day 21 (CS9), cardiac crescent becomes linear heart tube which is a multicellular structure formed from the

upper part to down by truncus arteriosus, bulbus cordis, primitive ventricle and primitive atrium (Fig. 1.3) [1].

The hallmark of this phase is formation of the linear heart tube which initially has an arterial pole in the superior region and a venous one in the inferior region. Additional, Ward et al. showed that the right side of the SHF is partly responsible for the development to the left side of the outflow myocardium [14]. Moreover, the anterior component of the SHF ("anterior heart field") provide the myocardial cells from the right ventricle and the OFT [14].

1.3 Liniar Heart Tube

In the interval of days 19–21 (CS9), the linear heart tube is already built being a multicellular structure formed in the superior area from truncus arteriosus and bulb cordis, and in the lower part from the primitive ventricle and primitive atrium [1]. In fact, Kloesel et al. showed that the linear heart tube is already formed in day 21 (Fig. 1.3) [1]. By the day 28, the linear heart tube changes through the looping process (expansion and elongation of the heart tube) into the right (D-loop) to establish the future arrangement of the cardiac

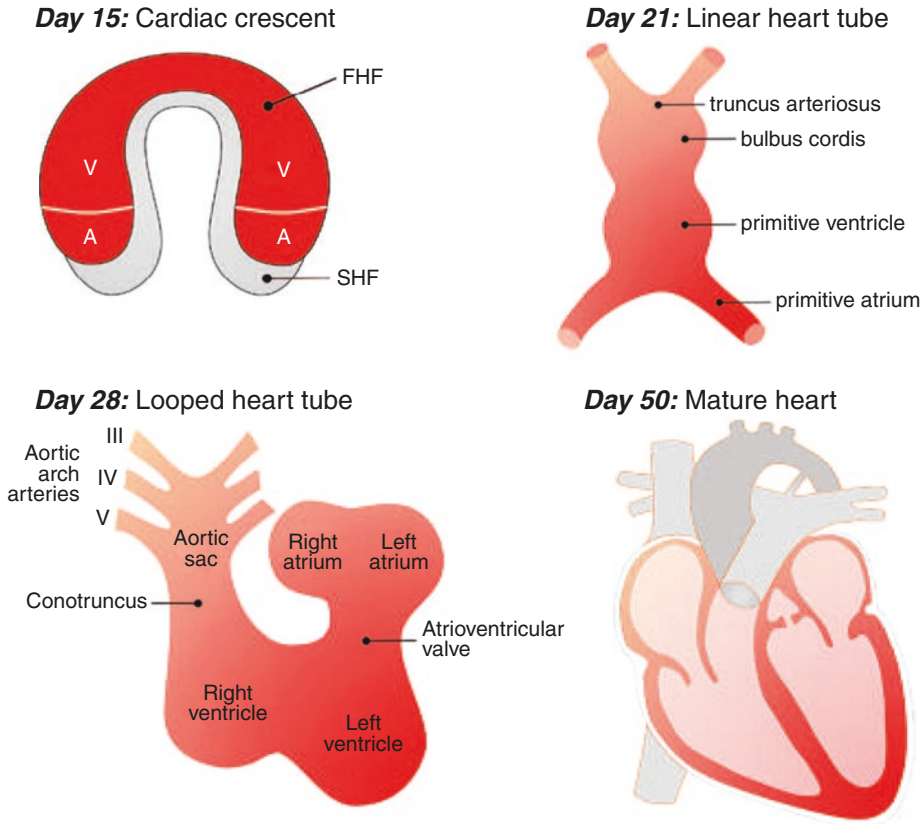

Fig. 1.3 Schematic representation of cardiac embryology. (**a**), Cardiac crescent at day 15. The first heart field is specified to form particular segments of the linear heart tube. The second heart field is located medial and caudal of the first heart field and will later contribute cells to the arterial and venous pole. (**b**) By day 21, cephalocaudal and lateral folding of the embryo establishes the linear heart tube with its arterial (truncus arteriosus) and venous (primitive atrium) poles. (**c**) By day 28, the linear heart tube loops to the right (D-loop) to establish the future position of the cardiac regions (atria [A], ventricles [V], outflow tract). (**d**) By day 50, the mature heart has formed. The chambers and outflow tract of the heart are divided by the atrial septum, the interventricular septum, 2 atrioventricular valves (tricuspid valve, mitral valve) and 2 semilunar valves (aortic valve, pulmonary valve). FHF indicates first heart field; SHF, second heart field. Adapted in modified form from Lindsey et al. [13]. From Kloesel et al. [1] with permission.

areas such as atria, ventricles and OFT (Fig. 1.3) [1, 13]. It has to be underlined that recent evidence shows that the mainly part of heart is created by migration of precursor cells from the SHF with the development of heart tube [1].

Consistently with above data, the comprehensive assessment of Kussman et al. (see Table 1.1) sustains that looping of heart tube has onset during days 22–23 (CS10) [7].

1.4 Looped Heart Tube

Between days 21 and 28 (CS9-13) the linear heart tube rotates and becomes a looped heart tube through the separation of atriums and ventricles; in which atrioventricular valve separates atrium cavities from left ventricle, and conotruncus separates aortic sac from right ventricle (Fig. 1.3) [1].

Of great interest is considerable evidence sustains that the primary linear heart tube under the control of genetic factors transforms through the inner curvature into a new form, process known as looping heart tube. Particularly, it has three fundamental elements in its structure: entry and exit points; and between above mentioned entry and exit points, the primitive atrial and ventricular cardiac cavities structures emerge. As a result, entry tract of the looping heart tube are sinus venosus (SV) and the sinoatrial ring (SAR) that continue with unique atrium. Additionally, an efferent looping pathway comes exclusively from SHT [15].

Gittenberger-de Groot et al. describe looping of the heart tube as the process characterized by "the differentiation of the primary heart tube into cardiac chambers (CC) and transitional zones (TZ)" [16]. Same team points up that many transitional zones are the components of the developing "septa, valves, conduction system, and fibrous heart skeleton" [16]. Moreover, these transitional zones will be in part included in the development of the final right atrium and left atrium, respectively in their right ventricle and left ventricle [16]. In addition, the team of Gittenberger-de Groot et al. showed that "from the venous to the arterial pole there are the sinus venosus and the sinoatrial ring (TZ), the primitive atrium (CC), the atrioventricular canal or ring (TZ), the primitive left ventricle (CC), the primary fold or ring (TZ), the primitive right ventricle (CC), and the ventricular OFT with a proximal and a distal part, also referred to as the ventriculoarterial ring (TZ)" (Fig. 1.4) [16].

The looping process of heart tube joins all above TZ together in the padding of the heart tube, specifically in the inner curvature [16].

Typically, from all TZ, the sinus venosus (SV) and primary fold do not generate endocardial cushions, while the AVC and OFT develop cushions. Importantly, the transition areas (TZ) of looped heart tube are the basic structures in the development of interatrial septum and interventricular septum, of the mitral valve, tricuspid valve, aortic and pulmonary valves, besides conduction tissue (see Fig 1.4) [16].

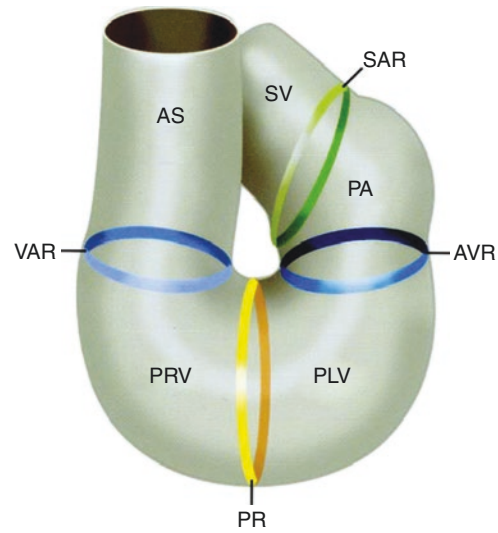

Fig 1.4 Schematic drawing of the looped heart tube with the cardiac chambers and the transitional zones. Following the blood flow from venous to arterial, we can distinguish the sinus venosus (SV), the sinoatrial ring (SAR), the primitive atrium (PA), the atrioventricular ring (AVR) encircling the atrioventricular canal, the primitive left ventricle (PLV), the primary fold or ring (PR), the primitive right ventricle (PRV), the outflow tract ending at the ventriculoarterial ring (VAR), and the aortic sac (AS) From Gittenberger-de Groot et al. [16] with permission.

1.5 Atrial and Ventricular Genesis

The genesis of atriums and ventricles cavities comprises the following stages: left from right ventricle separation, unique atrium, creation of the atrioventricular floor from the common atrioventricular channel, and the entry and exit separation from each ventricle (Fig. 1.5) [17].

Importantly, these processes are developing successively or concomitantly and are developed under genetic control. Precisely, Pitx2 gene determines left-right asymmetry, morphologic or structural differentiation among the right and left heart [18].

1.6 Atrial Septation

Separation of left atrium from right atrium is a progressive process starting with the "septum primum" or primary atrial septum that is covered by a mesenchymal cap and grows from the lowest part toward apex. Meanwhile, another dorsal mesenchymal protrusion advances parallel with septum primum in the common atrium and participate to the downward growing of primary atrial septum (Fig. 1.6) [1]. Before the primary atrial septum is getting to the endocardial cushion, a small hole named ostium primum persists. Moreover, in the cranial part appear fenestrations which become the ostium secundum by cell death mechanism [1].

Kloesel et al. state that around day 33, a second septum forms and further will develop the foramen ovale—a valve that lets the blood of the right atrium to pass on the left atrium during right-to-left shunting, also a feature of placental and systemic venous blood from gestation [1]. On the other hand, Kussman et al. show that during 35–38 days (CS15), the secondary foramen develops. Further, the primary atrial septum closes in CS16 [7]. The ostium primum is closed after joining of the primary atrial septum, mesenchimal cap, dorsal mesechimal protrusion along with the major atrioventricular cushions (Fig. 1.6) [1].

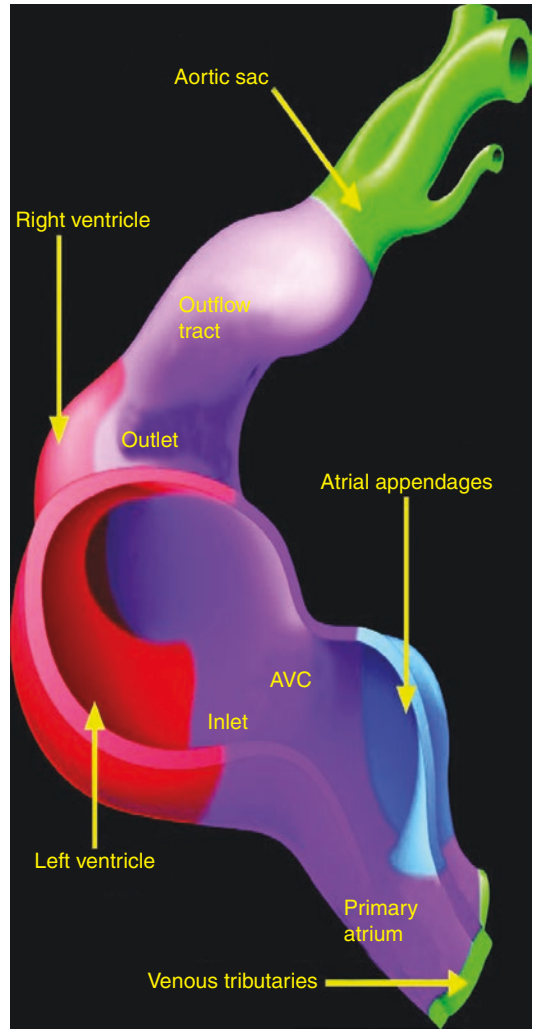

Fig. 1.5 This illustration shows the origin of the components of the developing atriums and ventricles. The myocardium of the primary heart tube is shown in purple, and makes up the primary atrium, the atrioventricular canal (AVC), the inlet and outlet components of the ventricular loop, and the outflow tract. Shown in green are the systemic venous tributaries, which are eventually incorporated within the right atrium, and the aortic sac with its arterial branches. The pulmonary vein is not shown, this being a new development appearing concomitant with the formation of the lungs. The atrial appendages, shown in blue, balloon in parallel from the primary atrial component of the heart tube. The apical parts of the ventricles, in contrast, balloon in series from the primary tube, with the apical part of the left ventricle growing from the inlet component, and the apical part of the right ventricle from the outlet component. From Moorman et al. [17] with permission.

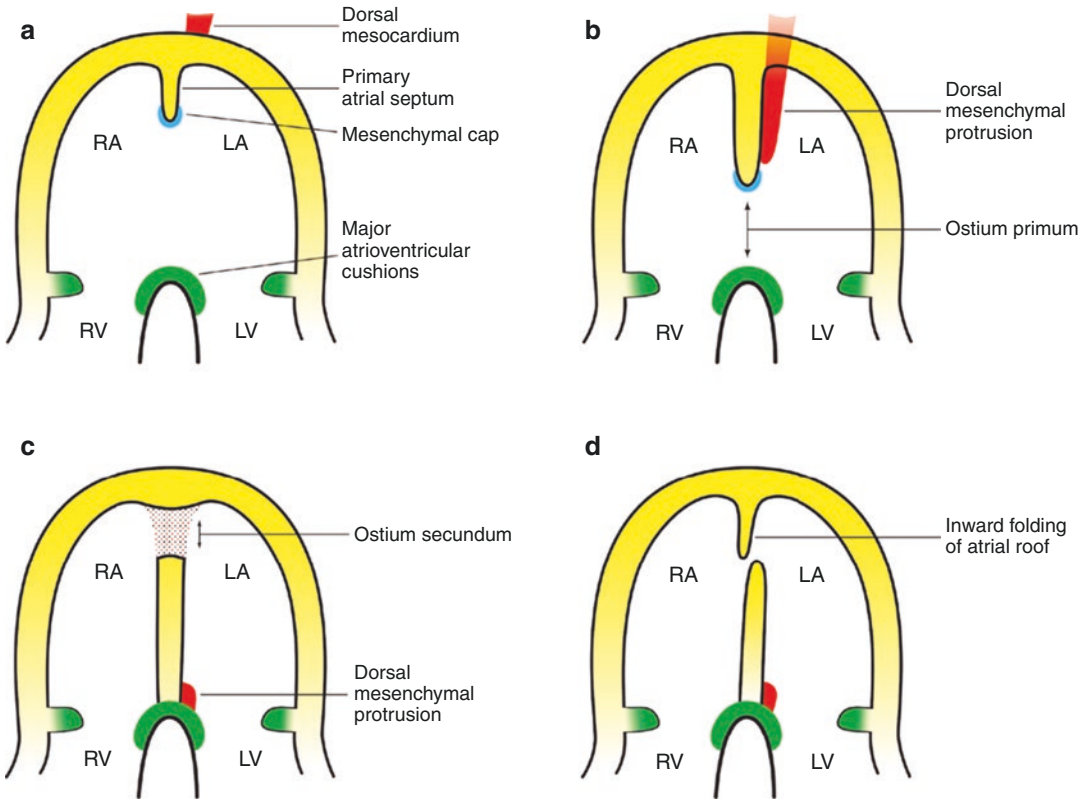

Fig. 1.6 Overview of processes leading to atrial septation. (**a**) Atrial septation begins with formation of the primary atrial septum (septum primum) that extends from the atrial roof downwards towards the major atrioventricular cushions. The leading edge of the primary atrial septum carries a mesenchymal cap. The venous pole of the heart is attached to dorsal mesocardium. (**b**) As the primary atrial septum continues its migration downwards and approaches the major atrioventricular cushions, it closes a gap known as ostium primum. Mesenchmal cells from the dorsal mesocardium have invaded the common atrium and join the downward growing primary atrial septum as the dorsal mesenchymal protrusion. (**c**) After fusion of the primary atrial septum, mesenchymal cap and dorsal mesenchymal protrusion with the major atrioventricular cushions, the ostium primum is closed. At the same time, part of the cranial septum primum breaks down and forms the ostium secundum. (**d**) Inward folding of the myocardium from the atrial roof produces the secondary atrial septum (septum secundum) which grows downwards to occlude the ostium primum by mechanism of a flap-valve (at birth, pulmonary vasculature dilates leading to a drop in right atrial pressure; the higher left atrial pressure pushes the primary atrial septum against the secondary atrial septum). From Kloesel et al. [1] with permission.

Finally, the secondary atrial septum (septum secundum) will occlude the ostium primum at birth (when pulmonary vasculature dilates causing decreasing in right atrial pressures) by mechanism of a flap-valve (Fig. 1.6) [1].

1.7 Ventricles Separation

Separation of the two ventricles starts from the looping heart stage when the univentricular cavity reshapes its primary structure as well as the future entry (inlet) and exit (outlet) paths align in the embryonic structure at the same level [19].

Importantly, the separation of primitive ventricle in the end to the left ventricle and the right ventricle is established by the interventricular septum that has distinctive muscular and mesenchymal constituents. Subsequently, the muscular structure comes up from the interventricular groove by myocardial development of the ventricular wall. Secondly, the mesenchymal constituent comes up above all by combination of the conotruncal endocardial cushions and

atrioventricular endocardial cushion. To same extent, Kloesel et al. concluded that "the complete ventricular septation depends on fusion of the outflow tract (conotruncal) septum, the muscular ventricular septum, and the atrioventricular cushions tissues" [1].

The basic helix-loop-helix (bHLH) transcription factors Hand1 and Hand2 have significant function keys in cardiogenesis [20]. Specifically, Hand1 (eHand, thing1, Hed) and Hand2 (dHand, thing2, Hxt) have important roles in heart development. Also, NKX2.5 and GATA4 genes are expressed in ventricular structures during cardiogenesis. The left ventricle develops under genetic control of Hand1 that is also implied in the formation of the interventricular septum and atrioventricular valve [2, 19]. Hand2 is compulsory for the right ventricle development [2, 19]. Especially, the presence and role of Hand2 in SHF have major contribution to the heart development, as well as the right heart ventricle [20]. Shortly, right ventricle occurs separately from SHF under genetic control of Hand2, and from this genetic control comes the idea that there is no primary direct relationship between the two ventricles during cardiogenesis [2, 19, 20, 54]. To sum up, FHF is exhibiting Hand1, NKX2.5, TBX5 and supports the development of the left ventricle. On the other hand, SHF is exhibiting Hand2, NKX2.5, GATA4, Isl1 and TBX1, and supports right ventricle development.

Franco et al. showed on two different transgenic mouse lines trying to investigate the development of the muscular interventricular septum that the *Mlc1v-nlacZ-24* transgene is exhibited only by the OFT and the right ventricle myocardium [21]. Also, the *Mlc3f-nlacZ-2* transgene is exhibited only by the left ventricle myocardium and the atrial appendages. These results support that the development of the interventricular septum is initiated by a symmetric cooperation of both ventricles constituents [21]. Subsequently, Moorman et al. support that the left–right asymmetry doesn't express the morphological differences between both ventricles [17].

Regarding the initiation and development of the septation process there are two hypotheses, one active from the apex to the atrioventricular layer [22] and a passive one produced by the ballooning of the single ventricular cavity [23]. Moreover, Anderson et al. support the hypothesis of ballooning and proves that between the ascending and descending side of the primary tube, originates the interventricular septum (see Fig. 1.7) [24].

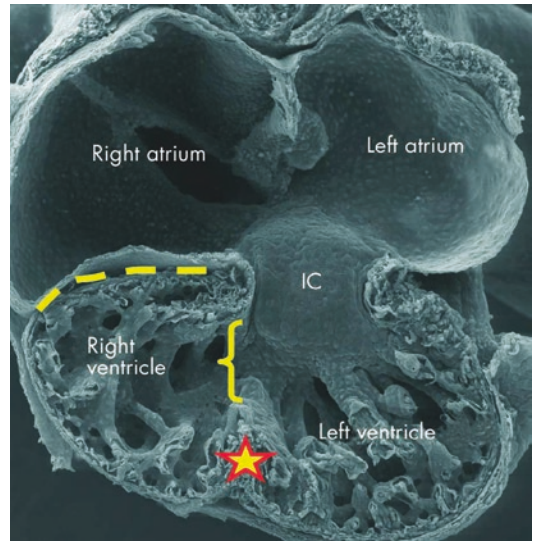

Fig. 1.7 This scanning electron micrograph, from a mouse embryo with 42 somites, shows the formation of the muscular ventricular septum. The specimen was prepared by transecting the heart through the atrioventricular canal, and the photograph is of the posterior segment. Note the inferior cushion (IC) occupying most of the posterior margin of the canal, but note also that the floor of the right atrium is in continuity with the roof of the developing right ventricle at the right margin of the atrioventricular canal, even though the atrioventricular groove interposes between the cavities of right atrium and right ventricle (yellow dashed line). Ballooning of the apical parts of the right and left ventricles from the ascending and descending parts of the ventricular component of the primary heart tube, respectively, has produced the primary muscular ventricular septum between them (star). The primary ventricular foramen (yellow bracket) provides the entrance at this stage to the developing right ventricle. From Anderson et al. [24] with permission.

1.8 Atrioventricular Junction Formation

The atrioventricular junction or atrioventricular canal (AVC) is an embryological structure that consists of the inferior component of the ventricular septum (inlet septum), the lowest area of

interatrial septum ("vestibular septum"), along with the primary structures of the mature atrioventricular valves [2]. To start with, the atrioventricular junction begins from the looping heart tube, particularly from the mesenchyme existent in endocardial cushions of the atrioventricular canal [2]. Initially, during the looping heart phase, the endocardial cushions of AVC join primitive atria with the embryonic left ventricle. Additionally, the embryonic right ventricle and the right part of the primitive atria have no interaction. Only that, during development of the right ventricle due to the migration of myocardial cells from the anterior SHF, the right AVC increases from the dorsal primary fold located among the right part of the AVC and the inner curvature of cardiac crescent [2].

Further, Gittenberger-de Groot et al. come up with their theory about AVC development (Fig. 1.8) [16]. Firstly, they sustain that "the primary heart tube after looping shows an atrioventricular canal, a primitive left ventricle, and a primitive right ventricle that are separated by the primary fold or ring" [16]. The primary interatrial septum (ostium primum) and membranous interventricular septum join in the atrioventricular canal by a progressive differential cellular multiplication process that is the initial stage of the atrioventricular junction. The atrioventricular endocardial cushion channel divides the upstream of atrioventricular junction into the right and left sides. The separation is initiated through a band (primary ring) (PR) (Fig. 1.8a) [16] and it is continued by its expansion to the muscular interventricular septum, thus achieving the initial separation of the atrioventricular canal into the two orifices that will be the future mitral and tricuspid valves (Fig. 1.8b) [16]. Concurrently with the valvular atrioventricular delimitation, a separation band is formed by modifying the primary ring, being a splitting band that begins the formation of the right ventricle (Fig. 1.8c) [16]. The ventriculo-arterial ring forms the separation between the unique ventricle, where the interventricular septum is initiated and the common arterial trunk which is separated by a band (ring) structurally similar with the atrioventricular canal to the initial aorta and the trunk of the pulmonary artery. This also delimits the spaces where the atrioventricular valves and semilunar valves will form (Fig. 1.8d) [16].

Wessel et al. studied fifteen human embryos and fetuses (at least two with same stage) starting with Carnegie Stage 14 forward [25]. They didn't solve the problem of atrioventricular junction genesis, but they stated two possible hypotheses as the mechanism of the atrioventricular junction genesis (Fig. 1.9) [25]. The first hypothesis assumes that the atrioventricular sulcus is the only structure responsible for the development of the fibrous annulus and the atrioventricular valves [26]. In addition, the second hypothesis considers that merging of sulcus tissue and cushion tissue of the ventricular side of the atrioventricular junctional myocardium triggers the division of atrial myocardium from ventricular myocardium (Fig. 1.9) [25].

Lockhart et al. studied the participation of epicardially-derived cells (EPDCs) and endocardially-derived mesenchymal cells (ENDCs) to the atrioventricular junction genesis [27]. According to them, the development of the AV sulcus and the annulus fibrosus is followed by the stage when a subtype of AV-EPDCs move in the components of AV cushions. In particular, the EPDCs populate only components of the lateral AV cushions [27]. On the other hand, the movement of AV-EPDCs to the AV junction and the annulus fibrosus development it is followed by subsequent movement of the AV-EPDCs to the parietal leaflets of atrioventricular valves. Therefore, AV-EPDCs have a significant function in the annulus fibrosus development and they combine with the existent AV-ENDCs being an important factor in the growth of the parietal leaflets of atrioventricular valves (Fig. 1.10) [27].

1.9 Atrioventricular Valves

The initiation of the atrioventricular valves genesis originates in endocardial tissue of AV cushions [28]. The cell population at this level is made up of AV-ENDCs with asymmetric and sequential multiplication forming two first subdivisions, the first one located upper and lower, and the

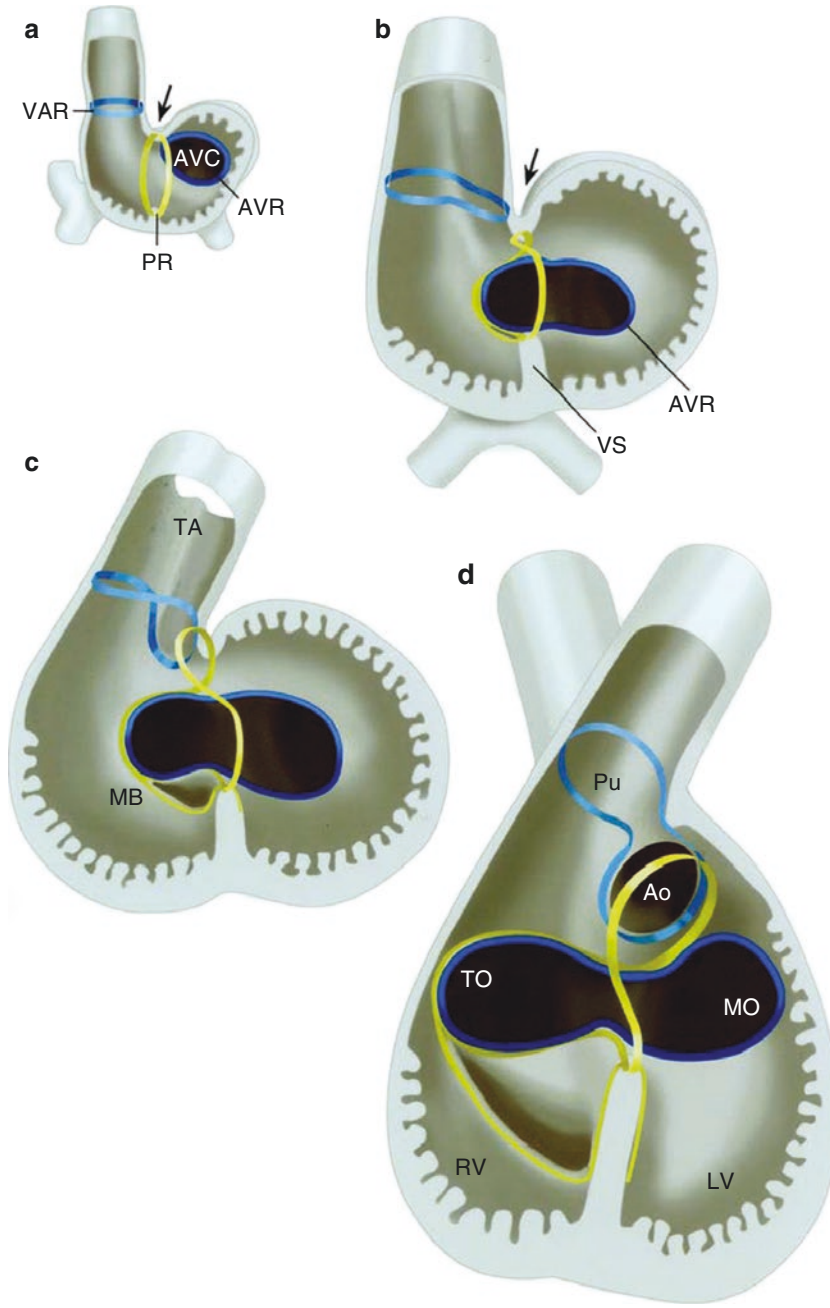

Fig. 1.8 Schematic representation of the remodeling of the cardiac chambers and the transitional zones at the ventricular level. (**a**) internal view of the looped heart tube. The transitional zones are, going from the venous to the arterial pole, the atrioventricular ring (AVR, dark blue), the primary ring (PR, yellow), and, at the distal end of the myocardial outflow tract, the ventriculoarterial ring (VAR, bright blue). (**b**) During looping, with tightening of the inner curvature (arrow), the right part of the AVR moves to the right of the ventricular septum (VS). (**c**) Start of formation of the inflow tract of the right ventricle by excavation of the PR. The lower border is formed by the moderator band (MB). (**d**) Completion of the process with formation of a tricuspid orifice (TO) above the right ventricle (RV) and the aortic orifice (Ao) and the mitral orifice (MO) above the left ventricle (LV). It is easily appreciated that there is aortic-mitral continuity, whereas the distance between the TO and the pulmonary orifice (Pu) is marked. From Gittenberger-de Groot et al. [16] with permission

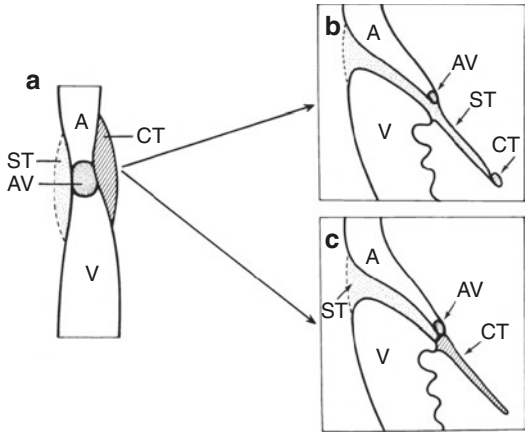

Fig. 1.9 Schematic diagram shows the two current hypotheses for the development of the atrioventricular junction in the human heart. (**a**) The situation at the atrioventricular junction at ~4 to 5 weeks of development. Myocardial continuity between atrium and ventricle is achieved through the myocardium of the atrioventricular canal. The atrioventricular junction is sandwiched between the tissues of the atrioventricular sulcus at the epicardial side and the atrioventricular cushion at the endocardial side. (**b**) The hypothesis in which the atrioventricular sulcus is held responsible for the insulation of atrium and ventricle and is supposed to be the only tissue contributing to the formation of the fibrous annulus and the leaflets of the atrioventricular valves (modified from information presented in Reference [26]). The presumed remnants of the atrioventricular cushions are located on the apical aspects of the leaflets. (**c**) The hypothesis supported by the data presented in this paper. The separation between the atrial and ventricular myocardium in this hypothesis is established by fusion of sulcus tissue and cushion tissue at the ventricular aspect of the atrioventricular junctional myocardium. (Note: The contribution of the myocardium to the formation of the leaflets is not illustrated in this schematic.) *A* indicates atrium, *CT* cushion tissue, *ST* sulcus tissue, *AV* myocardium of the atrioventricular canal, *V* ventricle. From Wessels et al. [25] with permission.

second one on the right and left side wall of AV cushion (Fig. 1.11) [29].

These two components progressively fuse accomplishing AV mesenchymal complex [30]. Process by which they will subsequently cause the primary atrial foramen enclosure (CS16) and accurate atrioventricular separation [7, 30].

Markwald et al. demonstrated how epicardial-derived cells (EPDCs) participate to genesis of the atrioventricular valves by their migration into AV cushion under the control of isoform 4 of morphogenetic bone protein (Bmp4) and TBx2 [28]. The formation of fibrous annulus is initiated by a subset of EPDCs migrated into the atrioventricular valves explaining the presence of these cells in the valvular cusps [29]. Remodeling of the cusps is done by the delamination process. Explicitly, it is separating the muscle tissue from the AV cushion from the mesenchymal tissue of the valvular leaflets that subsequently transform into fibrous tissue and collagen, mediated by fibroblast growth factors (FGF), PTPN11 (PTPN11 encodes the non-membranous protein tyrosine phosphatase), Wnt signaling and periostin [2].

Same mechanism, it is also involved in ENDCs, but the relationship between these cellular groups is not known [27]. Further, Lockhart et al. [29] suggest existence of evidence that derived cells AV-EPDCs may possible transform in various cell types such as interstitial fibroblasts, coronary smooth muscle cells, coronary endothelium, and myocytes [29].

However, there are few AV-EPDCs to the end of the valvulogenesis in the structure of the leaflet fibroblasts, this process being explained by their abundance in the atrioventricular annulus. Decreasing of the AV-EPDCs migration in the valvular tissue is controlled also by the isoform 2 of bone morphogenetic protein (Bmp2). Lockhart et al. showed in one study on mice that blocking the *Bmp receptor Alk3* from epicardial cells and their derivatives, results in reduction of AV sulcus, decrease of EPDCs migration to parietal atrioventricular valve cusps, and the absence of the annulus fibrosus development [29]. Also, this study proves the importance of Bmp signaling in AV valvulogenesis [29].

1.10 Atrioventricular Valvulogenesis

The mesenchyme of the endocardial cushions is common for all four heart valves [2]. Markwald et al. describe four steps in atrioventricular and semilunar valvulogenesis: (1) endocardial-to-mesenchyme conversion in junctional myocardium, (2) development of the mesenchyme as endocardial cushions, (3) remodeling process of

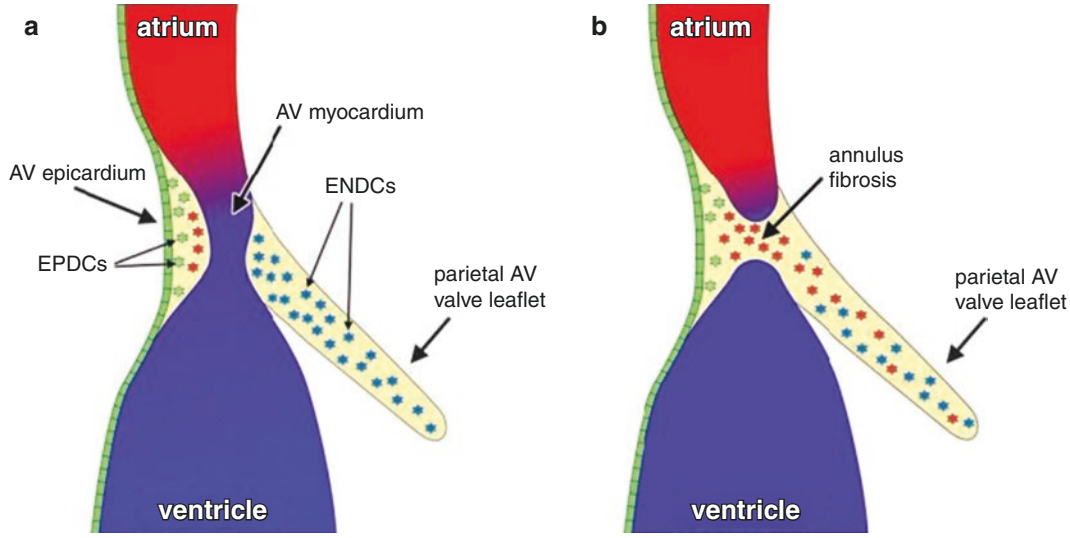

Fig. 1.10 Schematic representation of the contribution of the AV epicardium and the epicardially-derived cells to the development of the AV junction. After formation of the epicardial epithelium (green), epiEMT generates a population of AV-EPDCs (green cells in panel **a**) that, as far as their gene expression profile is concerned, are still very similar to the epicardium itself. However, when the AV-EPDCs migrate further into the AV sulcus and approach the AV myocardium (red cells), the molecular profile of the AV-EPDCs changes drastically as the expression of genes characteristically found in the mesenchyme of the annulus fibrosus (e.g., MMP2) and the AV cushions (e.g., Sox9) is upregulated. These "differentiated" AV-EPDCs (red cells in panel **a**) then penetrate the AV myocardium to form the annulus fibrosus (panel **b**) and migrate into the parietal AV valve leaflets where they intermingle with the endocardially-derived mesenchymal cells (ENDCs; blue cells in panels **a** and **b**). From Lockhart et al. [27]. It is an open access article.

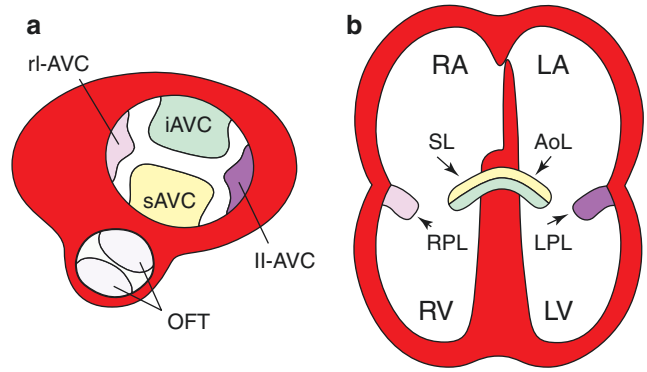

Fig. 1.11 This cartoon shows the fate of the individual AV cushions. The superior and inferior AV cushion (sAVC and iAVC) fuse at the midline and give rise to the septal leaflet of the right AV valve (SL) and the aortic leaflet (AoL) of the left AV valve. The right lateral AV cushion (rlAVC) forms the right parietal leaflet of the right AV valve (RPL), whereas the left lateral AV cushion forms the left parietal leaflet of the left AV valve (LPL). From Lockhart et al. [29] with permission.

mesenchyme into collagen-secreting interstitial valve fibroblasts, and (4) remodeling to the mature valve tissue by "leaflet compaction, attenuation, and formation of fibrous continuities" [31]. Furthermore, both atrioventricular valves have differences looking anatomical configuration and histology. It has to be underlined, that the mitral valve has insertion of the papillary muscles only in the free lateral wall of the left ventricle, and the septal tricuspid valve leaflet attaches directly to interventricular septum.

1.10.1 Mitral Valve

The mitral valve is composed from endocardium and connective tissue. Even if, the anterior and posterior mitral leaflets have same source from

the endocardial cushion of the AVC, their generation and forming are completely other [2].

Both mitral valve leaflets originate in the endocardial cell layer of the AV channel and their subsequent development is linked with septalisation process and aortic valve rotation [2]. Initially, the anterior mitral valve leaflet has only mesenchymal origin with no muscle component, and its papillary muscles are formed just from the free lateral wall of the left ventricle, explaining why the mature mitral valve does not have septal insertion [2, 32]. Also, de Lange et al. state that during formation of the aortic mitral valve leaflet this is connected to myocardium only at its cranial and caudal edges, therefore tendinous cords are forming and attaching to the papillary muscles at these sites [33]. However, there are no tendinous cordal connections of the mitral valve with the interventricular septum.

1.10.2 Tricuspid Valve

Initially, the tricuspid valve is a muscle structure with three developing points from the walls of right ventricle: septal (ventricular septum), anterior (anterior part of the right of the inferior AV cushion) and inferior (inferior right ventricle) [2]. The mesenchymal tissue of the endocardial AV cushions overlay inside all above three myocardial walls [2]. The anterior leaflet of tricuspid valve starts from anterior muscle wall of right ventricle, and this leaflet becomes functional by the process of myocardium apoptosis ("demyocardialization") [2]. Also, septal leaflet and posterior leaflet delaminate from myocardial walls of right ventricle [2]. On the other hand, the anterior leaflet keeps its connection with normal junctional part from the AV junction [2]. The papillary muscles start from the right ventricle walls and by compaction they develop in correlation with the cords of the tricuspid valve leaflets [33]. Finally, tendinous cords have their origin from the mesenchymal tissue of tricuspide valve, and they develop by the process of the remote component fragmentation of the ventricular side of the leaflets being transformed into fibrous structures [2].

1.11 Cardiac Outflow Formation

It also known as "conotruncus", "conus" and "infundibulum" [34]. The primitive OFT of the human heart is an endothelium-lined tube covered by an extracellular matrix layer named "endocardial jelly" that further it is coated by an outer muscular cuff [35].

The cells included within initial structure of OFT originate from anterior heart field (anterior component of the SHF) and cardiac neural crest (CNC) [2]. Therefore, CNC cells may be implied in the development of the smooth muscle cells from the walls of the two great vessels [2]. It seems that the remodelling of OFT into pulmonary and aortic arteries implies the cooperation of different cell types including neural crest cells, myocardium, and endocardium [36]. For instance, the cardiac neural crest signaling to SHF add together cardiomyocytes and smooth muscle cells in development of the OFT [34]. In humans, the OFT rotation has been accepted from Carnegie stage 15 [36]. Also, the myocardial wall rotation of the OFT is part of remodelling process of the OFT, directly correlated with the influx of neural crest [36].

Buckingham et al. believe that conotruncus—forming cells are derived from SHF only by excluding CNC participation in the distal portion of large vessels (truncus), theory unconfirmed by other studies [15]. In the initial stage (day 21), the OFT is found in the linear heart tube in the emerging portion of the single ventricle chamber, followed by the looping stage (day 28) when the differentiation begins in the conotruncus followed by the aortic sac (Fig. 1.12) [12, 37, 38]. As well, CNC cells do signaling process that form the OFT, the aortic arch, ventricular and atrial septae [12]. The ventricular myocardial structure is united with the vascular trunk by a fibrotic cell source called annulus, generated by endothelial derived mesenchyme (Fig. 1.12) [12, 37, 38].

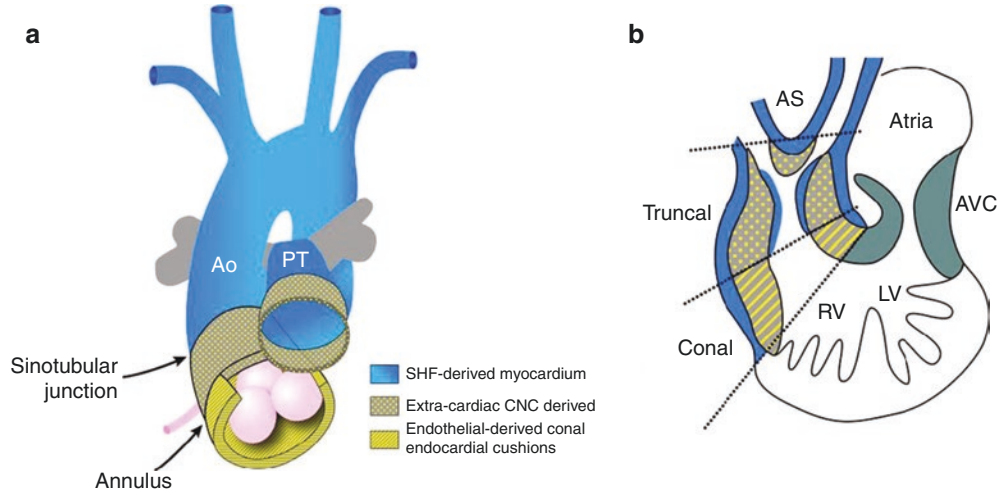

Fig. 1.12 Genesis and cellular contributions to the outflow tract. Schematic shows the locations of outflow tract (OFT) colonization by the extra-cardiac cardiac neural crest (blue), vascular smooth muscle derived from the second heart field (dotted yellow) and the location of myocardium from derived from the second heart field (striped yellow). The aortic annulus or hinge region is formed where myocardial cells meet the vascular smooth muscle cells of the media of the aorta and pulmonary trunk and endothelial derived mesenchyme is the source of the fibroblastic annular tissue. The media of the aorta and pulmonary trunk is derived from secondary heart field proximally (dotted yellow) and the cardiac neural crest distally (blue). The interface between these populations is at the sinotubular junction. Abbreviations: *Ao* aorta, *AS* aortic sac, *AVC* aorto-ventricular cushions, *LV* left ventricle, *PT* pulmonary trunk, *RV* right ventricle. Modified from [37, 38]. From Martin et al. [12]. It is an open access article

1.12 Outflow Separation

OFT septation begins between 23 and 25 days of human embryogenesis. Presently, the separation process mechanisms of OFT are still unclear, therefore there are many hypotheses. As well, there is still confusion looking plentiful terms used to explain "the endocardial ridges" or "cushions", structures implied in the septation of the OFT.

The hypothesis of Van Mierop et al. consider that three components split OFT, that is the aortopulmonary septum with distal and proximal ridges. Firstly, the ridges join and develop a septum that further joins with the aortopulmonary septum. Further, septation joins the proximal ridges developing the proximal conal septum that unifies with the distal septum finishing septation process [39].

The hypothesis of Icardo sustains the spiral septum development. He declares the existence of unconnected proximal and distal ridges. Spiralling is acquired by end-to-end joining of paired proximal ridges with the paired distal ridges, resulting in connected ridges unified lengthways, and intersected at their midpoints [40].

In same time, Bartelings on a human hearts study supposes that the endocardial ridges have no involvement in the OFT septation process [41].

Finally, Webb et al. consider that "it is the distal cushions that divide the distal outflow tract into the intrapericardial parts of the aorta and pulmonary trunk, with the proximal cushions separating both the arterial roots and their ventricular outflow tracts" [42].

Importantly, there is a counterclockwise direction in the rotation process of the junction of the OFT and great arteries align the aorta to the left ventricle and pulmonary artery to the right ventricle [38].

1.13 Aortic and Pulmonary Valves Formation

With development of OFT, its cushion tissue extend in the jelly and generates a spiral pattern around the lumen [35]. Further, the cushions of OFT join in the midline and separate the OFT into its aortic and pulmonary channels [35]. Shortly, the aorta and the pulmonary artery are developing from aortic sac [2]. Semilunar valves genesis begins on days 31–35 starting with the pre-existing endocardial cushions of the OFT and the atrioventricular junction of the primitive heart tube [43].

During the OFT septation process, in the proximal region an invasion of endothelial cells is produced in the contruncal region and fuse with endocardial cushions. This configuration is divided in two sides that contain inferior and posterior septal cushion and two sides of insertion of anterior pulmonary valve and aortic posterior valve. Therefore, from the right posterior side of interposed cushion forms the noncoronary aortic cusp and from the anterior left side forms the anterior pulmonary cusp. From the superior and inferior septal cushion form left and right cusps of the aortic and pulmonary valves (Fig. 1.13) [12].

Recently, based on serial and three-dimensional reconstructions of human embryos in the Shaner Collection at different stages, Milos et al. observed that "the pulmonary semilunar valve regions are more normal and uniform in structure supporting the concept that there is some independence of the development of the aortic and pulmonary semilunar valves from each other" [35].

1.14 Ventriculoarterial Junctions

Anatomic ventriculoarterial junctions represents the connection between a muscular component (infundibular) formed by the interventricular septum separation mechanisms, and the pulmonary

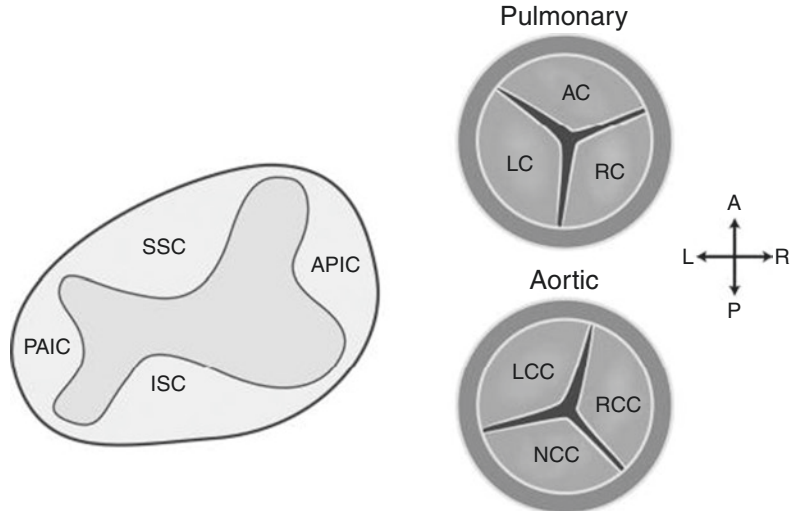

Fig. 1.13 Development of the leaflets of the aortic and pulmonary valves. The semilunar valves arise from the conotruncal and intercalated cushions of the outflow tract. The conotruncal (superior and inferior septal) cushions give rise to the right and left leaflets of each of the semilunar valves. In the aorta, these are the right and left coronary leaflets, while in the pulmonary valve, these are the right and left cusps. The right-posterior and the left-anterior intercalated cushions develop respectively into the posterior aortic (non-coronary cusp of the aortic valve) and the anterior pulmonic (anterior cusp of the pulmonic valve) leaflets. Abbreviations: *AL* anterior leaflet, *APIC* anterior pulmonary intercalated cushion, *CA* coronary artery, *ISC* inferior septal cushion, *LL* left leaflet, *LCL* left coronary leaflet, *NCL* non-coronary leaflet, *PAIC* posterior aortic intercalated cushion, *RCL* right coronary leaflet, *RL* right leaflet. From Martin et al. [12]. It is an open access article.

and aortic valves generated in proximal portion of the arterial trunk. When OFT septation process undergoes, the aortic orifice attaches to the left ventricular outflow tract, meanwhile the pulmonary orifice lies over the right ventricle [16]. Moreover, the team of Gittenberger-de Groot et al. showed by reconstruction the OFT of two human embryos that the condensed mesenchyme is located corresponding to the mesenchymal vessel wall, the arterial orifice level, the cushion tissue and the myocardium (Fig. 1.14) [16].

1.15 The Cardiac Vascular Genesis

1.15.1 Coronary Arteries

There is still a lot of uncertainty about the genesis of the coronary arteries. However, it is clear that the coronary artery connection is the last stage of cardiogenesis being done after the separation of the cardiac cavities, and the inlet and outlet pathways from atria and ventricles. Ventricular endocardial cells represent the main origin of the coronary arter-

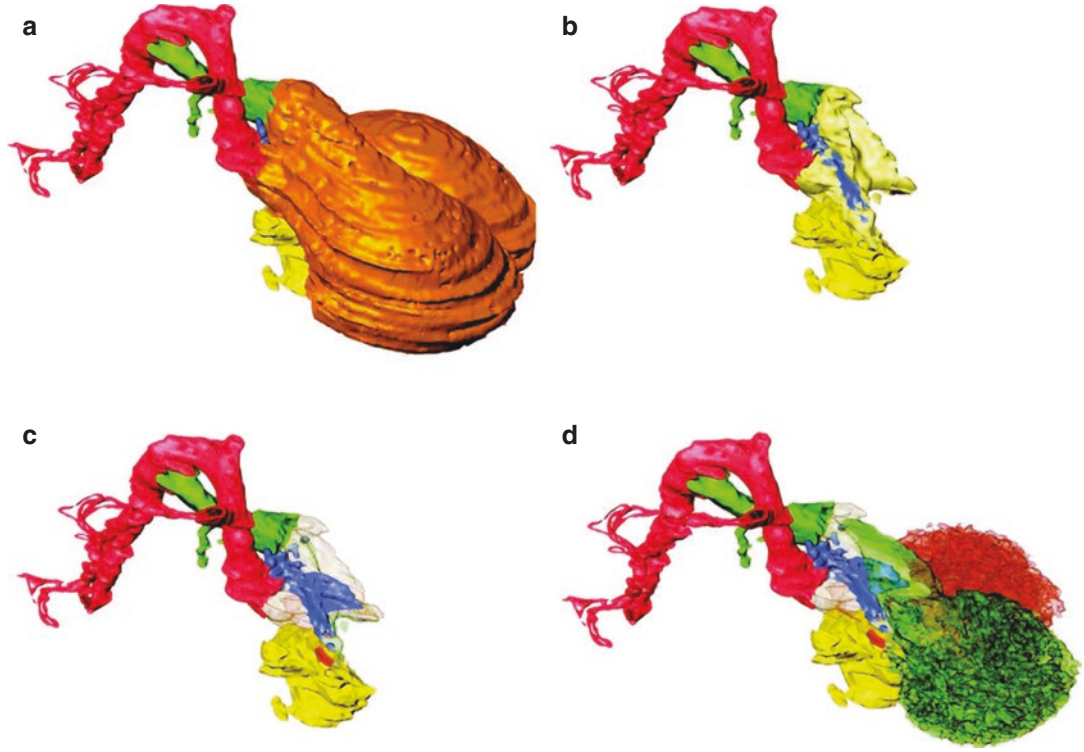

Fig. 1.14 Reconstruction of the heart of a *human embryo* of 5 week development. (**a**) The myocardium (brown) of the ventricles reaches up to the arterial orifice level. The pulmonary trunk (green) arises anteriorly from the right ventricle and the aorta (red) originates at a more caudal and posterior level. (**b**) The myocardium has been removed and the endocardial outflow tract cushions (light yellow) and the atrioventricular cushions (dark yellow) become visible. The condensed mesenchyme (blue), consisting mainly of neural crest cells, is incorporated within the outflow tract cushion mass. It is visible, however, at the entrance site between the arterial orifices (see also a) and as a lateral streak (right side visible, left side not) where the condensed mesenchyme connects to the outflow tract myocardium (removed, see a) At these sites, the myocardialization of the outflow tract septum will take place. The right lateral outflow tract cushion is connected to the atrioventricular cushion mass, whereas the left lateral cushion is not connected to this mass. (**c**) By making the outflow tract cushions translucent, the complete condensed mesenchyme becomes visible extending way out into the cardiac outflow tract. (**d**) Insertion of the right (green) and left (red) ventricular lumen shows how the condensed mesenchyme and thus the outflow tract septum mainly borders the right ventricular pulmonary infundibulum. From Gittenberger-de Groot et al. [16] with permission.

ies and by angiogenesis produce coronary arteries [44]. It seems that myocardial Vegf-a to endocardial Vegfr-2 signaling controls coronary angiogenesis. On contrary, the coronary arteries and veins come up mostly by various origins and mechanisms [44].

Some studies prove that the origin of coronary arteries is in epicardial cells [45]. In fact, Reese et al. state further that "cell lineage commitment and diversification, directed cell migration, control of epithelial/mesenchymal transition, and cell differentiation are some of the hallmarks in the development of coronary arteries" [45].

Also, Red Horse et al. studied based on anatomical and histological analysis the coronary vessel development during mouse embryogenesis using endothelial markers [46]. They concluded that developed and differentiated venous endothelial cells from sinus venosus emerge into myocardium where transform into arteries and capillaries [46]. Therefore, these differentiated venous endothelial cells from sinus venosus extend to develop the coronary plexus, and coronary arteries, capillaries, and veins. Only minor number of the endocardium cells detach to develop blood islands and then join to the coronary plexus nearby the interventricular septum [44, 46].

As a result coronary vessels are generated by complex processes such as: vasculogenesis, angiogenesis, arteriogenesis and remodelling specific to each arterial, venous or capillary vessel [47]. The origin of angiogenesis can be initiated including by proepicardium, sinus venous or endocardium [48]. Of note, Tian et al. consider that complete heart vasculogenesis include all cardiac structures from the epicardium to endocardium, which begins by migration of the subepicardial ECs into myocardial cells of the embryonic ventricle free walls, and finalized with coronary veins and intramyocardial coronary arteries/capillaries (Fig. 1.15) [48].

To sum up, Kloesel et al. synthesize coronarogenesis in the most simplified way [1]. Newly, his team sustains that "the coronary vasculature is derived from proepicardial progenitor cells and venous endothelial angioblasts originating from the sinus venosus". The epithelial progenitors undergo epithelial-to-mesenchymal transformation. After formation of the main coronary vessels, the coronary system connects to aorta by invasion of arterial endothelial cells into the aorta. By day 50, the heart has developed to its mature form [1].

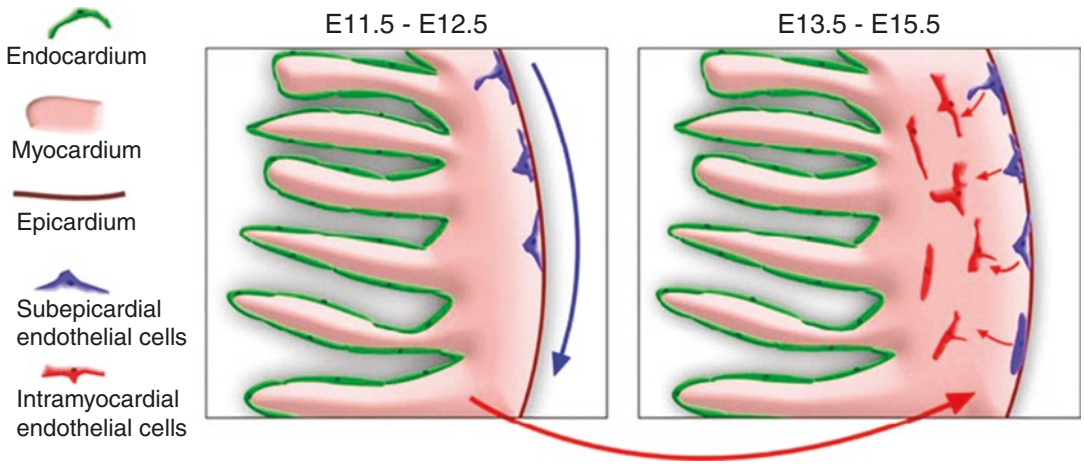

Fig. 1.15 Schematic showing subepicardial ECs as a major source for intramyocardial coronary vessels. During embryogenesis, subepicardial endothelial cells ECs (blue) located beneath the epicardium (brown) migrate along the surface of the heart between E11.5-E12.5 (blue arrow). Subepicardial ECs then migrate into the compact myocardium to become intramyocardial coronary arteries and capillaries at E13.0-E15.5 (red arrows). From Tian et al. [48] with permission.

1.15.2 Aortic Arches

The origin of the aortic arches is the mesoderm of the pharyngeal arches [2]. Further, they join with distal part of aortic sac. Firstly, a part of aortic branches, especially the third, fourth and sixth remodels in the presence of CNC cells to asymmetric great arteries. The third aortic arch developes into the common carotid arteries and the proximal segment of the internal carotid arteries. Further, the fourth aortic arch develops the horizontal aorta. Usually, the fifth aortic arch is not constant. However, the sixth arch develops the arterial duct and first component of the central pulmonary arteries [2].

1.15.3 Sinus Venous

The dorsal mesocardium joins the primitive atria to the dorsal body wall, where the sinus venosus and its contributory veins are blocked [16]. When heart tube is looping, the main veins supplying the sinus venosus (the right anterior and posterior cardinal veins as well as the left anterior cardinal vein) will incorporate into the posterior wall of the right atrium [16]. Also, during this process, a right and a left sinus venosus valve develop, in which blood access into the atrium through a type of channel [16]. Moreover, the left and right venous valves join and develop the septum spurium that is connected with anterior part of the AVC [16].

1.16 Cardiac Conduction System

As cardiogenesis advances with heart remodelling into a four-chambered structure, the myocardium undergo a transformation as "working myocardium" and "conduction system myocardium" [16]. Gittenberger-de Groot et al. [16] stated that the integration of the sinus venosus into the atrium demonstrates existence of the embryonic structures represented by three internodal pathways among the sinoatrial node, the atrioventricular node and the relationship of the pulmonary venous system from the dorsal left atrial wall with the primitive conduction system [16].

In fact, the heart is working with the onset of its development [1]. The primitive heart tube starts to beat about day 21 with pumping blood by day 24 or 25 [1], and the sinoatrial node (the pacemaker of the heart) develops and becomes noticeable in CS17 [7]. In mammalian embryonic ventricles, the contraction signal begins in the inflow part of the heart tube and spread to the ventricles and then to the OFT from base-to-apex [1]. It seems that advanced vertebrates form a "compact myocardium" need to respond to higher heart rhythm and pressure. Of note, this compact myocardium favours developing of the conduction system, with a specific activation from base-to-apex in the trabecular part of the ventricles, and with a specific activation in the subepicardial compact myocardium from apex-to-base, correlated to the His-Purkinje system formation [49].

Wenink et al. studied eight human embryos and the heart of a 90 mm human fetus selected from the collection of the Leiden University and released the "four ring theory" in which tries to explain the developing of cardiac conduction system [50]:

- The conducting rings are inserted between sinus venosus, atrium, ventricle, bulbus and truncus;
- The sinoatrial node develop only from the sinoatrial ring;
- The sinoatrial ring participates to the atrioventricular (AV) node formation;
- Atrioventricular ring develops AV node;
- Ventriculoventricular (primary ring) will be in time bundle His and bundle branches [50]. Although initially controversial, this hypothesis is partially confirmed by studies with immunohistochemical markers [51].

Importantly, the mammalian ventricular conduction system is characterized by biphasic growth and development, but lineage restriction is followed by restricted outgrowth [52].

The spongy myocardium of embryonic mammals allows high ejection fractions and also assists to conduct the ventricular depolarization [53]. Nonetheless, increase of pressure and heart rate cause an evolution to compact myocardium, that further, turn into the early trabecules secondary to force generation, but available to differentiate into fibres of poor contractility and high propagation speeds. In addition, mammals increase compact myocardium ventricular septum while the early trabecules form the septal surfaces with the findings of bundle branches of the His bundle (Fig. 1.16) [53].

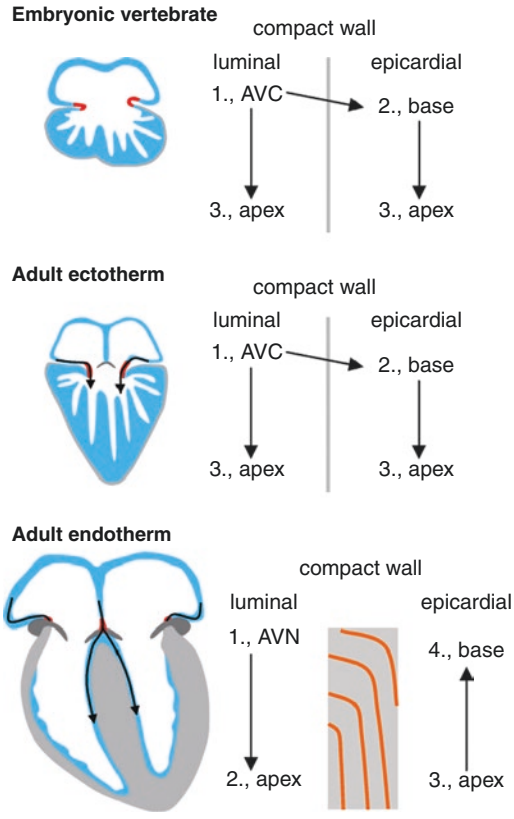

Fig. 1.16 The trabecular myocardium is activated from base to apex in all vertebrates. (**a**–**c**) The trabecular myocardium gives rise to the His-Purkinje system in mammals and birds and remains activated from base to apex. (**c**) On the epicardial surface of septated and thick-walled ventricles, as in the formed hearts of mammals and birds, activation is seen to occur from apex to base and the luminal base-to-apex activation is obscured [53]. It is an open access article.

Conclusions

It is considered that intrauterine life begins with cardiac contraction and heart development is a complex process. Mechanisms of cardiogenesis are sequential, starting from the primary cell differentiation stages to the final processes of cardiogenesis.

Increase in knowledge of genetics, embryology, and molecular medicine offer understanding into the mechanisms of congenital heart disease [1]. For physicians, clear knowledge of cardiac development, including, embryology, genetics, molecular cell biology, and anatomy, provide a better diagnosis of congenital heart diseases [1]. In last years, recent results in cardiac development have proven to improve our knowledge in prenatal diagnosis. Nonetheless, more data are compulsory looking the cardiogenesis in human embryo for an early and accurate diagnosis of congenital heart diseases.

References

1. Kloesel B, DiNardo JA, Body SC. Cardiac embryology and molecular mechanisms of congenital heart disease: a primer for anesthesiologists. Anesth Analg. 2016;123:551–69. https://doi.org/10.1213/ANE.0000000000000014.
2. Schleich JM, Abdulla T, Summers R, Houyel L. An overview of cardiac morphogenesis. Arch Cardiovasc Dis. 2013;106:612–23. https://doi.org/10.1016/j.acvd.2013.07.001.
3. Epstein JA, Franklin H. Epstein lecture. Cardiac development and implications for heart disease. N Engl J Med. 2010;363:1638–47. https://doi.org/10.1056/NEJMra1003941.
4. Olson EN, Srivastava D. Molecular pathways controlling heart development. Science. 1996;272:671–6.
5. Laverriere AC, MacNeill C, Mueller C, Poelmann RE, Burch JB, Evans T. GATA-4/5/6, a subfamily of three transcription factors transcribed in developing heart and gut. J Biol Chem. 1994;269:23177–84.
6. Olson EN. Gene regulatory networks in the evolution and development of the heart. Science. 2006;313:1922–7. https://doi.org/10.1126/science.1132292.
7. Kussman BD, Miller-Hance WC. Chapter 4. Development of the cardiovascular system and nomenclature for congenital heart disease. In: Andropoulos DB, Stayer SA, Mossad EB, Miller-Hance WC, editors. Anesthesia for congenital heart disease. 3rd ed. Massachusetts: Wiley-Blackwell; 2015. p. 43.

8. Hutchins GM, Kessler-Hanna A, Moore GW. Development of the coronary arteries in the embryonic human heart. Circulation. 1988;77:1250–7.
9. Cai CL, Liang X, Shi Y, Chu PH, Pfaff SL, Chen J, Evans S. Isl1 identifies a cardiac progenitor population that proliferates prior to differentiation and contributes a majority of cells to the heart. Dev Cell. 2003;5:877–89.
10. Chalajour F, Ma X, Kirk Riemer R. Myocardial self-repair and congenital heart disease, congenital heart disease - selected aspects. In: Syamasundar Rao P, editor. InTech; 2012. doi:https://doi.org/10.5772/26368. https://www.intechopen.com/books/congenital-heart-disease-selected-aspects/myocardial-self-repair-and-congenital-heart-disease.
11. Gittenberger-de Groot AC, Bartelings MM, Poelmann RE, Haak MC, Jongbloed MR. Embryology of the heart and its impact on understanding fetal and neonatal heart disease. Semin Fetal Neonatal Med. 2013;18:237–44. https://doi.org/10.1016/j.siny.2013.04.008.
12. Martin PS, Kloesel B, Norris RA, Lindsay M, Milan D, Body SC. Embryonic development of the bicuspid aortic valve. J Cardiovasc Dev Dis. 2015;2:248–72.
13. Lindsey SE, Butcher JT, Yalcin HC. Mechanical regulation of cardiac development. Front Physiol. 2014;5:318. https://doi.org/10.3389/fphys.2014.00318.
14. Ward C, Stadt H, Hutson M, Kirby ML. Ablation of the secondary heart field leads to tetralogy of Fallot and pulmonary atresia. Dev Biol. 2005;284:72–83. https://doi.org/10.1016/j.ydbio.2005.05.003.
15. Buckingham M, Meilhac S, Zaffran S. Building the mammalian heart from two sources of myocardial cells. Nat Rev Genet. 2005;6:826–35. https://doi.org/10.1038/nrg1710.
16. Gittenberger-de Groot AC, Bartelings MM, Deruiter MC, Poelmann RE. Basics of cardiac development for the understanding of congenital heart malformations. Pediatr Res. 2005;57:169–76. https://doi.org/10.1203/01.PDR.0000148710.69159.61.
17. Moorman A, Webb S, Brown NA, Lamers W, Anderson RH. Development of the heart: (1) formation of the cardiac chambers and arterial trunks. Heart. 2003;89:806–14.
18. Harvey RP. Patterning the vertebrate heart. Nat Rev Genet. 2002;3:544–56. https://doi.org/10.1038/nrg843.
19. Srivastava D. Making or breaking the heart: from lineage determination to morphogenesis. Cell. 2006;126:1037–48. https://doi.org/10.1016/j.cell.2006.09.003.
20. Vincentz JW, Barnes RM, Firulli AB. Hand factors as regulators of cardiac morphogenesis and implications for congenital heart defects. Birth Defects Res A Clin Mol Teratol. 2011;91:485–94. https://doi.org/10.1002/bdra.20796.
21. Franco D, Meilhac SM, Christoffels VM, Kispert A, Buckingham M, Kelly RG. Left and right ventricular contributions to the formation of the interventricular septum in the mouse heart. Dev Biol. 2006;294:366–75. https://doi.org/10.1016/j.ydbio.2006.02.045.
22. Van Mierop LH, Kutsche LM. Development of the ventricular septum of the heart. Heart Vessel. 1985;1:114–9.
23. Patten BM. The heart. Patten's foundations of embryology. New York: McGraw-Hill; 1954. p. 545–69.
24. Anderson RH, Webb S, Brown NA, Lamers W, Moorman A. Development of the heart: (2) septation of the atriums and ventricles. Heart. 2003;89:949–58.
25. Wessels A, Markman MW, Vermeulen JL, Anderson RH, Moorman AF, Lamers WH. The development of the atrioventricular junction in the human heart. Circ Res. 1996;78:110–7.
26. Van Gils FAW. The development of the human atrioventricular heart valves. J Anat. 1979;128:427.
27. Lockhart MM, Phelps AL, van den Hoff MJ, Wessels A. The epicardium and the development of the atrioventricular junction in the murine heart. J Dev Biol. 2014;2:1–17. https://doi.org/10.3390/jdb2010001.
28. Markwald RR, Fitzharris TP, Manasek FJ. Structural development of endocardial cushions. Am J Anat. 1977;148:85–119. https://doi.org/10.1002/aja.1001480108.
29. Lockhart MM, van den Hoff M, Wessels A. The role of the epicardium in the formation of the cardiac valves in the mouse. In: Nakanishi T, Markwald RR, Baldwin HS, Keller BB, Srivastava D, Yamagishi H, editors. Etiology and morphogenesis of congenital heart disease from gene function and cellular interaction to morphology. Tokyo: Springer; 2016. p. 161–7. https://doi.org/10.1007/978-4-431-54628-3.
30. Snarr BS, Wirrig EE, Phelps AL, Trusk TC, Wessels A. A spatiotemporal evaluation of the contribution of the dorsal mesenchymal protrusion to cardiac development. Dev Dyn. 2007;236:1287–94. https://doi.org/10.1002/dvdy.21074.
31. Markwald RR, Norris RA, Moreno-Rodriguez R, Levine RA. Developmental basis of adult cardiovascular diseases: valvular heart diseases. Ann N Y Acad Sci. 2010;1188:177–83. https://doi.org/10.1111/j.1749-6632.2009.05098.x.
32. Lamers WH, Virágh S, Wessels A, Moorman AF, Anderson RH. Formation of the tricuspid valve in the human heart. Circulation. 1995;91:111–21.
33. de Lange FJ, Moorman AF, Anderson RH, Männer J, Soufan AT, de Gier-de Vries C, Schneider MD, Webb S, van den Hoff MJ, Christoffels VM. Lineage and morphogenetic analysis of the cardiac valves. Circ Res. 2004;95:645–54. https://doi.org/10.1161/01.RES.0000141429.13560.cb.
34. Restivo A, Piacentini G, Placidi S, Saffirio C, Marino B. Cardiac outflow tract: a review of some embryogenetic aspects of the conotruncal region of the heart. Anat Rec A Discov Mol Cell Evol Biol. 2006;288:936–43. https://doi.org/10.1002/ar.a.20367.
35. Milos NC, Nordstrom DB, Ongaro I, Chow AK. Variations in structure of the outflow tract of the human embryonic heart: a new hypothesis for generating bicuspid aortic semilunar valves. Ann Anat. 2017;211:88–103. https://doi.org/10.1016/j.aanat.2016.12.004.
36. Bajolle F, Zaffran S, Kelly RG, Hadchouel J, Bonnet D, Brown NA, Buckingham ME. Rotation of the myocardial wall of the outflow tract is implicated

in the normal positioning of the great arteries. Circ Res. 2006;98(3):421–8. https://doi.org/10.1161/01.RES.0000202800.85341.6e.
37. Neeb Z, Lajiness JD, Bolanis E, Conway SJ. Cardiac outflow tract anomalies. Wiley Interdiscip Dev Biol. 2013;2:499–530. https://doi.org/10.1002/wdev.98.
38. Waldo KL, Hutson MR, Ward CC, Zdanowicz M, Stadt HA, Kumiski D, Abu-Issa R, Kirby ML. Secondary heart field contributes myocardium and smooth muscle to the arterial pole of the developing heart. Dev Biol. 2005;281:78 90. https://doi.org/10.1016/j.ydbio.2005.02.012.
39. Van Mierop LH, Alley RD, Kausel HW, Stranahan A. Pathogenesis of transposition complexes. I. Embryology of the ventricles and great arteries. Am J Cardiol. 1963;12:216–25.
40. Icardo JM. Development of the outflow tract. A study in hearts with situs solitus and situs inversus. Ann N Y Acad Sci. 1990;588:26–40.
41. Bartelings MM. The outflow tract of the heart embryologic and morphologic correlations. Ph.D. thesis. The Netherlands: University of Leiden; 1990. doi:10.1046/j.1469-7580.2003.00168.x.
42. Webb S, Qayyum SR, Anderson RH, Lamers WH, Richardson MK. Septation and separation within the outflow tract of the developing heart. J Anat. 2003;202:327–42.
43. Wirrig EE, Yutzey KE. Conserved transcriptional regulatory mechanisms in aortic valve development and disease. Arterioscler Thromb Vasc Biol. 2014;34:737–41. https://doi.org/10.1161/ATVBAHA.113.302071.
44. Wu B, Zhang Z, Lui W, Chen X, Wang Y, Chamberlain AA, Moreno-Rodriguez RA, Markwald RR, O'Rourke BP, Sharp DJ, Zheng D, Lenz J, Baldwin HS, Chang CP, Zhou B. Endocardial cells form the coronary arteries by angiogenesis through myocardial-endocardial VEGF signaling. Cell. 2012;151:1083–96. https://doi.org/10.1016/j.cell.2012.10.023.
45. Reese DE, Mikawa T, Bader DM. Development of the coronary vessel system. Circ Res. 2002;91:761–8.
46. Red-Horse K, Ueno H, Weissman IL, Krasnow MA. Coronary arteries form by developmental reprogramming of venous cells. Nature. 2010;464:549–53. https://doi.org/10.1038/nature08873.
47. Tomanek RJ. Formation of the coronary vasculature during development. Angiogenesis. 2005;8:273–84. https://doi.org/10.1007/s10456-005-9014-9.
48. Tian X, Hu T, Zhang H, He L, Huang X, Liu Q, Yu W, He L, Yang Z, Zhang Z, Zhong TP, Yang X, Yang Z, Yan Y, Baldini A, Sun Y, Lu J, Schwartz RJ, Evans SM, Gittenberger-de Groot AC, Red-Horse K, Zhou B. Subepicardial endothelial cells invade the embryonic ventricle wall to form coronary arteries. Cell Res. 2013;23:1075–90. https://doi.org/10.1038/cr.2013.83.
49. Gourdie RG, Mima T, Thompson RP, Mikawa T. Terminal diversification of the myocyte lineage generates Purkinje fibers of the cardiac conduction system. Development. 1995;121:1423–31.
50. Wenink AC. Development of the human cardiac conducting system. J Anat. 1976;121(Pt 3):617–31.
51. Jongbloed MR, Mahtab EA, Blom NA, Schalij MJ, Gittenberger-de Groot AC. Development of the cardiac conduction system and the possible relation to predilection sites of arrhythmogenesis. Sci World J. 2008;8:239–69. https://doi.org/10.1100/tsw.2008.40.
52. Miquerol L, Moreno-Rascon N, Beyer S, Dupays L, Meilhac SM, Buckingham ME, Franco D, Kelly RG. Biphasic development of the mammalian ventricular conduction system. Circ Res. 2010;107:153–61. https://doi.org/10.1161/CIRCRESAHA.110.218156.
53. Jensen B, Boukens BJ, Postma AV, Gunst QD, van den Hoff MJ, Moorman AF, Wang T, Christoffels VM. Identifying the evolutionary building blocks of the cardiac conduction system. PLoS One. 2012;7:e44231. https://doi.org/10.1371/journal.pone.0044231.
54. Moorman AF, Christoffels VM. Cardiac chamber formation: development, genes, and evolution. Physiol Rev. 2003;83:1223–67. https://doi.org/10.1152/physrev.00006.2003.

Further Reading

O-Rahilly R, Muller F. Developmental stages in human embryos. Washington: Carnegie Institute; 1987.
Hutchins GM, Kessler-Hanna A, Moore GW. Development of the coronary arteries in the embryonic human heart. Circulation. 1988;77:1250–7.
Oostra RJ, Steding G, Lamers WH, Moorman AFM, Steding S, Viragh S. Scanning electron microscopy atlas of the developing human heart. New York: Springer; 2007.
Arráez-Aybar LA, Turrero-Nogués A, Marantos-Gamarra DG. Embryonic cardiac morphometry in Carnegie stages 15-23, from the Complutense University of Madrid Institute of Embryology Human Embryo Collection. Cells Tissues Organs. 2008;187:211–20. DOI: https://doi.org/10.1159/000112212.

Right Heart Anatomy: A Short Uptodate

2

Mircea Ifrim, Ecaterina Bontaş, Daniel Cochior, and Ion C. Ţintoiu

Abstract

Despite of the first description of Sir William Harvey in 1616 looking the significance of right ventricle function for human heart and lungs, its importance was disregarded in clinical practice. Starting with 1950s until the 1970s, cardiovascular surgeons assessed techniques to treat right-heart hypoplasia and as a result they accepted the significance of right heart function. During last decade, the impact of right heart evaluation has been established for the treatment of cardiopulmonary disorders. Knowledge of the right heart anatomy, imaging pathology and related clinical manifestations is essential to prevent neglected features of cardiovascular diseases and false-positive diagnoses. Understanding image features of the human heart acquired by histological studies, echocardiography, computed tomography (CT), micro-CT studies, or diffusion tensor magnetic resonance imaging (DT-MRI) has a very important role in the correctness of anatomically outlining of the cardiac features, especially those associated to the conduction system. Studying classic anatomy of the heart on cadaveric samplings is a requirement to know what imaging investigations brings for the study of RV anatomy and physiology. Considering that, it has to be underlined important anatomical features of the human right heart.

Keywords

Right heart anatomy · Right atrium · Right ventricle · Interatrial septum · Interventricular septum · Conduction system · Right heart vessels · Myoarchitecture of right heart Computational cardiac modelling and anatomy

M. Ifrim
Academy of Medical Sciences, Bucureşti, Romania

E. Bontaş (✉)
Department of Cardiology, "Prof. C.C. Iliescu" Emergency Institute for Cardiovascular Diseases, Bucharest, Romania

D. Cochior
Department of Medicine, Titu Maiorescu University, Bucharest, Romania

Academic Integration, Department of Surgery and Research, Hospital Monza, Bucharest, Romania

I. C. Ţintoiu
Department of Cardiology, "Titu Maiorescu" University- Department of Medicine of Bucharest, Bucharest, Romania

Center for Cardiovascular Diseases, "Carol Davila" Central Military Emergency University Hospital, Bucharest, Romania

2.1 Background

It has to be underlined that Sir William Harvey was the first who depicted in 1616 the significance of right ventricular (RV) function in his seminal treatise, De Motu Cordis: "Thus the right ventri-

S. I. Dumitrescu et al. (eds.), *Right Heart Pathology*, https://doi.org/10.1007/978-3-319-73764-5_2

cle may be said to be made for the sake of transmitting blood through the lungs, not for nourishing them" [1, 2, 3]. Starting with 1950s until the 1970s, cardiovascular surgeons assessed techniques to treat right-heart hypoplasia, as a result they accepted the significance of right heart function [1]. Cleary during last decade, the significance of right heart evaluation has been established for the treatment of cardiopulmonary disorders [4]. Considering that, it has to be underlined the important anatomical features of the human right heart.

The anterior component or "right atrium proper" derives from the primitive atrium [5, 7]. As widely validated, both ventricles have unrelated embryologic origins. Precisely, the RV arises from progenitory cells of the secondary heart field [8, 9]. On the other hand, the interventricular septum (IVS) has same embryologic origin with the RV [5]. Also, RV and LV wall thickness have identical raise during gestation and both ventricles have almost similar thickness at birth [5, 10]. As well as, both ventricles work similar during fetal life, to maintain the pulmonary and the systemic circulations. After birth, the normal RV is unloaded [11]. Conversely, the pulmonary vascular resistance or the afterload of the RV diminishes gradually [11].

To sum up, these anatomical and physiological differences between right heart and left heart explain the various reactions to pathological disorders.

2.2 Right Atrium

William Harvey was the first to explain the atrium as a 'receptable and store-house' and 'the first chamber to live and the last to die'. Right atrium (RA) is the anatomic chamber that contains the significant components of the conduction system of the heart being the access for difficult electrophysiological procedures that implicate bypass via RA and interatrial septum [12].

Shortly, RA collects deoxygenated blood from the superior vena cavae (SVC), inferior vena cavae (IVC) and from the coronary veins. Further, it propels this blood through the tricuspid valve into RV [5, 13, 14]. Also, from the anatomical location, the RA represents the right border of the human heart. After Cabrera et al. 2014 [15], the RA comprises the right and anterior parts of the heart. This partly covers the right part of the left atrium (LA). The left part of the RA is distinct by the interatrial groove located posteriorly between the SVC and the right pulmonary veins. Further, the interatrial septum (IAS) plane is oblique about 65° from the sagittal plane. Therefore, the LA is located posterior and superior to the RA [15].

It has to be underlined, that from the anteromedial part, the RA continues with the right auricle or right atrial appendage (RAA) that is a large triangular muscular sac (pouch or pouchlike cavity) that enlarges the size of the RA (Fig. 2.1) [12].

A simplified description of the inside of the RA comprises three components: the anterior component, terminalis crest and the posterior component.

The *anterior component* or "atrium proper" is located anterior to terminalis crest and along with

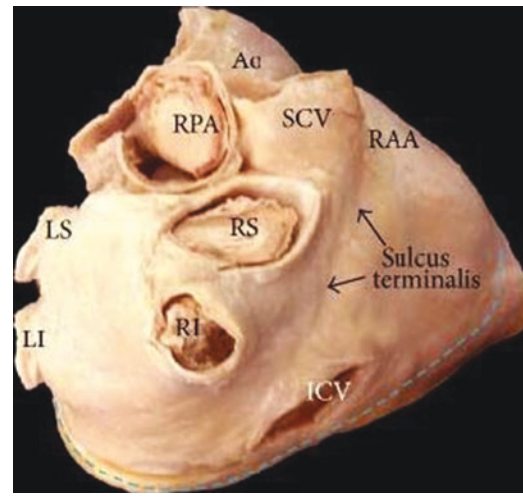

Fig. 2.1 The heart is viewed in attitudinally appropriate position. As can be seen, the right atrium lies anterior to its alleged left-sided counterpart. Note the arrangement of the sulcus terminalis and the atrioventricular or coronary groove (blue broken line). *Ao* aorta, *CSO* coronary sinus orifice, *ICV* inferior cava vein, *LA* left atrium, *LAA* left atrial appendage, *LI* left inferior pulmonary vein, *LS* left superior pulmonary vein, *OF* oval fossa, *PM* pectinate muscles, *PT* pulmonary trunk, *RAA* right atrial appendage, *RCA* right coronary artery, *RI* right inferior pulmonary vein, *RPA* right pulmonary artery, *RS* right superior pulmonary vein, *RVOT* right ventricle outflow tract, *SCV* superior cava vein, *TC* terminal crest, and *TV* tricuspid valve. Modified from [12]. It is an open access article

its length run pectinate muscles [7]. The pectinate muscles extend within the RAA that is a muscular triangular-shaped area located on the superior part of the RA [7]. In fact, the RAA is a triangular superior extension of the RA that wraps around the aortic root [16]. It extends from the SVC almost to the IVC [17]. For patients with a pacemaker and/or an internal cardiac defibrillator, the right atrial lead tip is typically placed at the RAA.

The anterior and posterior components are divided by the *terminal crest (TC)* or *crista terminalis* that is a ridge/fold of muscle [7].

The *posterior component* of the RA is a smooth wall located posterior to the TC. It is known as the *sinus venarum* that is the embryologic "right horn of the sinus venosus" [17]. Specifically, the valve of the sinus venosus degenerates during weeks 9–15 of gestation, with the cranial component developing the TC and the caudal component developing the valves of the IVC (eustachian valve) and coronary sinus (thebesian valve) [5, 14, 16]. To sum up, the posterior component of RA collects in the posteriorlaterally part the SVC, IVC and the CS [17].

Evidence looking the RA size and volume are incomplete [16]. Malik et al. [16] showed that the limits of the RA long- and short-axis dimensions are 3.4–5.3 cm (combined 95% confidence interval [CI]: 3.2, 5.5 cm) and 2.6–4.4 cm (combined 95% CI: 2.4, 4.6 cm), respectively [16].

Viewing from outside, TC corresponds to the sulcus terminalis or terminal groove that is filled

Terminal Crest (TC, Crista Terminalis)

Generally, the TC is a muscular ridge that divides the smooth and muscular components of the RA [16]. The TC has a C-form or ear-shape and is composed by the joint of the sinus venosus and the primitive RA (Fig. 2.2a, b) [12, 18].

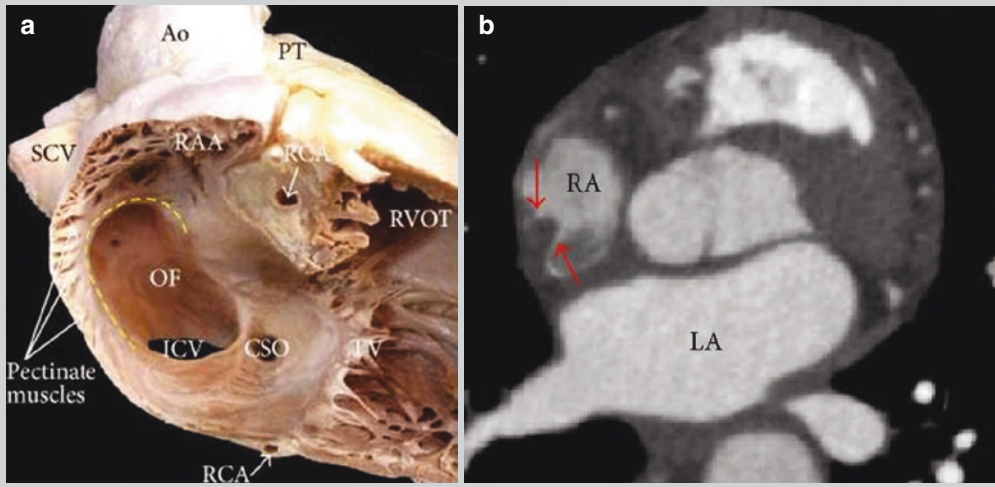

Fig. 2.2 (a) The right atrium is shown in right anterior oblique projection. The terminal crest (yellow broken line) arches anterior to the orifice of the superior caval vein and extends toward the inferior caval vein. *Ao* aorta, *CSO* coronary sinus orifice, *ICV* inferior cava vein, *LA* left atrium, *LAA* left atrial appendage, *LI* left inferior pulmonary vein, *LS* left superior pulmonary vein, *OF* oval fossa, *PM* pectinate muscles, *PT* pulmonary trunk, *RAA* right atrial appendage, *RCA* right coronary artery, *RI* right inferior pulmonary vein, *RPA* right pulmonary artery, *RS* right superior pulmonary vein, *RVOT* right ventricle outflow tract, *SCV* superior cava vein, *TC* terminal crest, and *TV* tricuspid valve. Modified after Sánchez-Quintana et al. [12]. It is an open access article. (**b**) Axial CT angiogram shows a prominent terminal crest (red arrows) in the right atrium. ICV inferior cava vein, *LA* left atrium, *LV* left ventricle, *PM* pectinate muscles, *RA* right atrium, and *TC* terminal crest. Modified after Sánchez-Quintana et al. [12]. It is an open access article

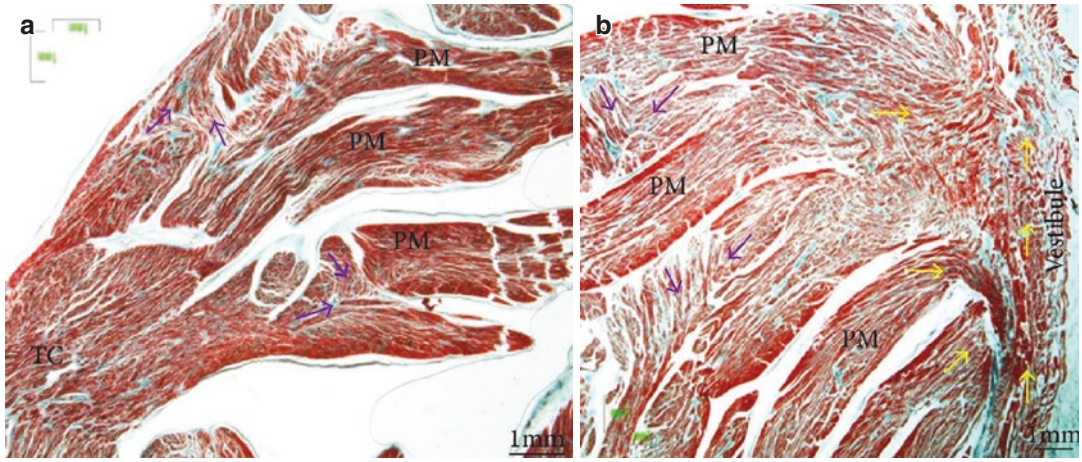

Fig. 2.3 (**a**, **b**) Frontal sections through the *terminal crest* at the origin and ending of the pectinate muscles. Note the irregular alignment (purple arrows) of the muscular myofibrils within the pectinate muscles and between them and the circumferentially arranged myocytes in the vestibule (yellow arrows). *ICV* inferior cava vein, *LA* left atrium, *LV* left ventricle, *PM* pectinate muscles, *RA* right atrium, and *TC* terminal crest. Modified after Sánchez-Quintana et al. [12]. It is an open access article

with fat [7, 12, 14]. Specifically, TC is noticeably on the part of the SVC and then gradually disappears toward the IVC [7].

Accordingly, the mainly myocytes from the TC are parallel with the long axis of the muscle bundle. Myocytes from the outside of TC, specifically from the intercaval area are lined up obliquely. This nonuniform array of the myocytes is a possible explanation for their arrhythmogenicity (see Fig. 2.3a, b) [12, 19, 20].

2.2.1 Pectinate Muscles

Previous anatomical studies depicted the pectinate muscles to originate or "terminate" on the TC in the posterolateral RA [21]. However, the pectinates frequently spread out from the TC onto the sub-Eustachian isthmus and sometimes they are getting within the coronary sinus (Fig. 2.4) [21].

Sánchez-Quintana et al. [12] describe the pectinate muscles as emerging from the TC toward *the vestibular portion* of RA (Fig. 2.5a) [12]. Briefly, the "RA vestibule" is the smooth muscular wall close to the tricuspid orifice and sustains the tricuspid valve leaflets. Also, the RA vestibule is encircled by the pectinate muscles of the

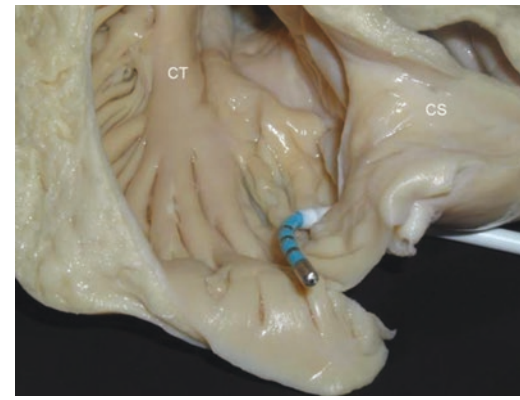

Fig. 2.4 Dissection of an autopsied heart showing left anterior oblique-like view looking through the tricuspid valve into the right atrium with an ablation catheter and guiding sheath placed across the cavotricuspid isthmus. Note the large pectinate muscles emanating from the crista terminalis (CT). Many pectinates are seen encroaching onto the cavotricuspid isthmus and traversing the isthmus into the coronary sinus (CS). Reprinted from [21]. It is an open access article

RA [12]. On particular relevance, the pectinates muscle may not end up in the TC, but more or less traverse the structure of TC and then they end in a secondary ridge or fold that it is more medial and posterior [22]. Also, the team of Sanchez-Quintana et al [12] sustain that the pecti-

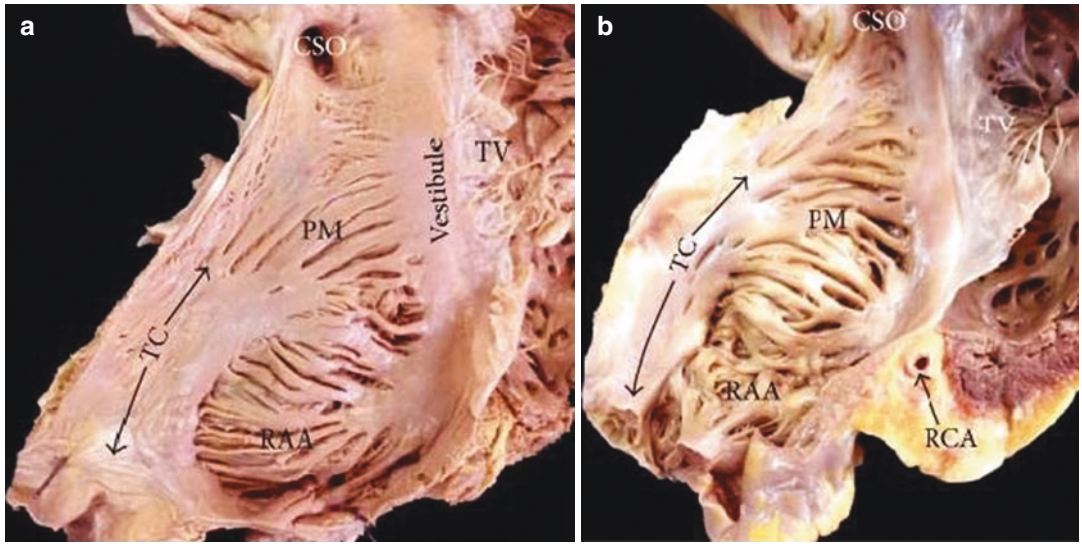

Fig. 2.5 (**a**, **b**) Endocardial aspects of the lateral wall of the right atrium opened. Note in (**a**) that the *pectinate muscles* have a uniform parallel alignment almost without crossovers between them. In contrast, the pectinate muscles in (**b**) have a nonuniform arrangement with abundant interlacing trabeculations between them. *CSO* coronary sinus orifice, *PM* pectinate muscles, *RAA* right atrial appendage, *RCA* right coronary artery, *TC* terminal crest, and *TV* tricuspid valve. Modified after [12]. It is an open access article

nate muscles have a very trabeculated muscle fiber bundles that support the nonuniform conduction of the excitatory impulse (Fig. 2.5a, b) [12].

2.2.2 Cavotricuspid Isthmus or Inferior Isthmus (CTI/CVTI)

Generally, the atrial myocardium from lower part of RA between the tricuspid valve and IVC is named *the cavotricuspid isthmus (CVTI)* (Fig. 2.6a, b) [21, 23]. The *CVTI* is a muscle bundle that begins from the RA anteromedial wall, gets in front of the SVC, and goes down to the IVC to prolong with a disposition of thinner bundles that enter the region of the atrial wall recognized as the *inferior isthmus* or *cavotricuspid isthmus* [23]. It is significant for developing a conduction delay or a reentrant circuit [23] being the anatomic target when ablating typical atrial flutter [21].

Of interest, the CVTI differs regarding length, width and myocardial thickness within the same patient and from patient to patient, and between the septal and free wall locations [24–27].

In fact, [25, 28] in studies of cadaveric hearts they separated the CVTI into three parallel position or levels [25, 28]. Briefly, they recognized and determined the lengths of all three levels of the isthmus: paraseptal (24 ± 4 mm), inferior (19 ± 4 mm), and inferolateral (30 ± 3 mm) [25, 28]. The paraseptal isthmus or septal isthmus represents the base of *Koch's triangle* (see The Conduction system of Right Heart below) [12]. From all three isthmuses, the septal isthmus is the smallest and the widest having the wall varying from 2 to 7 mm on heart specimens. Also, the septal isthmus is nearest to the atrioventricular node, mostly to the inferior nodal elongations [12]. Further, the inferior isthmus or central isthmus with location 6 o'clock on LAO projection is the best possible location for ablation being the thinnest area between the tricuspid valve annulus and the IVC ostium [12]. The morphology and width of the CVTI between the anterior and posterior zones are very different. About 20% of patients may present a pouch-like recess known has the sub-Eustachian (sub-Thebesian) sinus or a recess in the inferior isthmus (Fig. 2.7a, b) [12].

Furthermore, there is a 40% deviation in CVTI length during a single cardiac cycle. Recently,

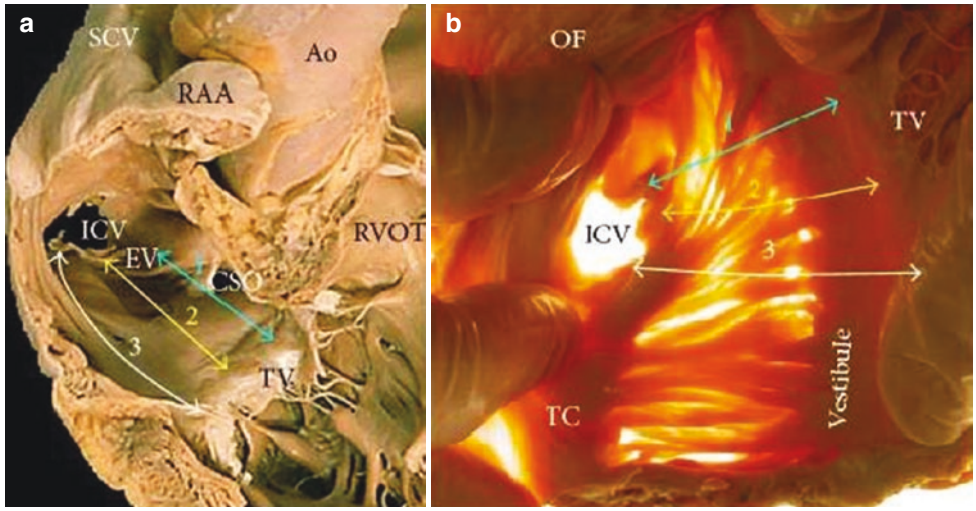

Fig. 2.6 (**a**) The region of the *cavotricuspid isthmus* in simulated right anterior oblique (RAO) view and the paraseptal, inferior, and inferolateral isthmuses are marked 1, 2, and 3, respectively. (**b**) This atrial view shows the cavotricuspid isthmus with transillumination. The lines mark (1) the paraseptal isthmus, (2) the inferior isthmus, and (3) the inferolateral isthmus. Note the smooth vestibule immediately proximal to the tricuspid valve and the pectinate muscles in the posterior regions. *Ao* aorta, *CSO* coronary sinus orifice, *EV* Eustachian valve, *ICV* inferior cava vein, *OF* oval fossa, *RAA* right atrial appendage, *RVOT* right ventricle outflow tract, *SCV* superior cava vein, *TC* terminal crest, and *TV* tricuspid valve. Modified after [12]. It is an open access article

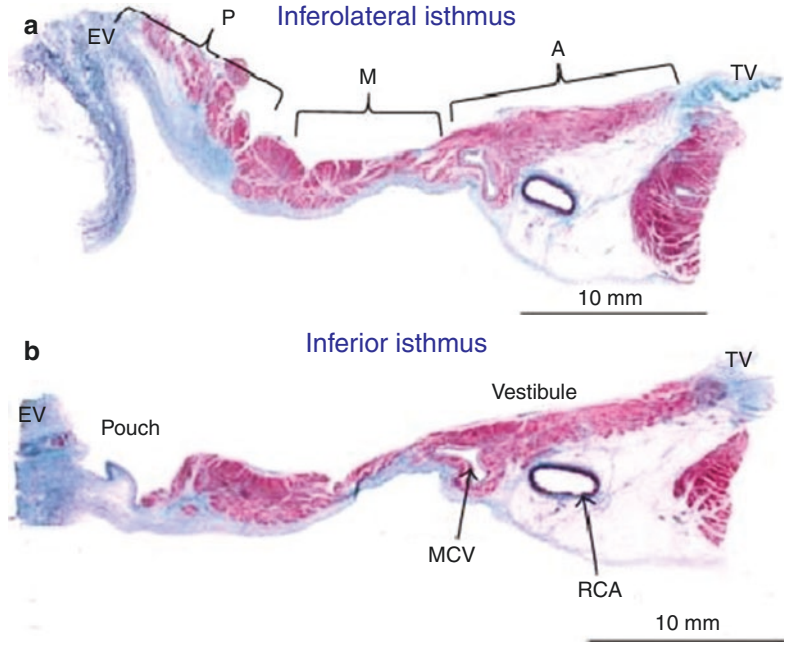

Fig. 2.7 (**a**, **b**) This series of histological sections through inferolateral (A) and inferior (B) isthmuses from a heart with dominance of right coronary artery. Note in (A) the prominent and fibromuscular Eustachian valve in the posterior sector or P, thin myocardium in middle sector or M, and thicker myocardium in the anterior sector (vestibule) or A. In (B), histologic section shows a pouch of the sub-Eustachian recess. Note the lesser transmural thickness in this area. The right coronary artery is in the epicardial fat related to the smooth vestibule. *Ao* aorta, *CSO* coronary sinus orifice, *EV* Eustachian valve, *ER* Eustachian ridge, *ICV* inferior cava vein, *MCV* minor coronary vein, *OF* oval fossa, *PT* pulmonary trunk, *RAA* right atrial appendage, *RCA* right coronary artery, *RVOT* right ventricle outflow tract, *SCV* superior cava vein, *TC* terminal crest, and *TV* tricuspid valve. Modified from [12]. It is an open access article

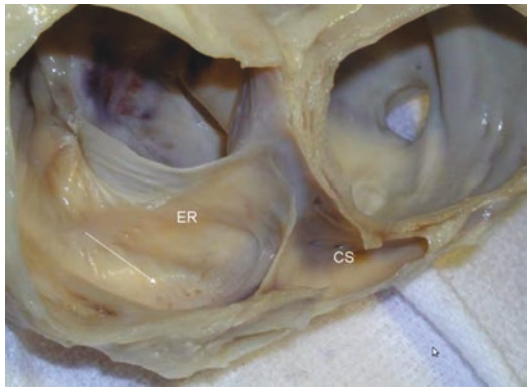

Fig. 2.8 A more realistic view from an actual autopsied heart. The complex regional anatomy of *the cavotricuspid isthmus*. The arrow points to the sub-Eustachian pouch. Note the prominent Thebesian valve guarding the opening of the coronary sinus (CS). A prominent Eustachian ridge (ER) and valve associated with the Eustachian ridge are also visualized. From [21]. It is an open access article

Sanchez-Quintana et al [12] confirmed in 32% of patients using anatomical images studies with CT scan acquired for the period of cardiac cycle that CVTI has the highest length elongation during midventricular systole at all three equivalent levels [12, 29] while the inferior/central isthmus length is over 30 mm [12].

To sum up, the complex anatomical structure of the CVTI from various patients generates substantial problems in case of complete and permanent ablation. The Eustachian ridge (ER), sub-Eustachian pouches, proeminent pectinate muscles, and arrangement of these anatomic deviations, on the whole produce complications (Fig. 2.8) [21].

2.2.3 The Eustachian Valve or Ridge

The Eustachian valve (EV) or the Eustachain ridge (ER) protects the ostium of the IVC [12]. The EV primarily serves to direct blood toward the fossa ovalis in fetal life [5, 6]. Usually, EV is described as a crescentic, thin and unimportant flap [12]. The free edge of the EV carries on as the tendon of Todaro that continues in the muscles of the EV [12]. About 2% of the population presents a "fishnet" EV with different sizes acknowledged as Chiari network [14, 30].

Infrequently, the flap of EV is bulky blocking the entrance to the most posterior component of the isthmus. Therefore, only the whole ablation of oversized EV or ER makes possible the paraseptal isthmus block [31]. Previously, the study of Cabrera et al [28] on cadaveric hearts showed that 26% from hearts had an increased ER with a mean thickness of 3.2 ± 0.8 mm [28]. Also, Heidbuchel H et al [32] showed by an angiographic study increased EV in 24% of patients Heidbuchel H et al [32]. A thicker ER over 4 mm is seen in 24% of the normal population studied with CT scans [29].

Sub-Eustachian Ridge

On the other hand, Sehar N et al [21] consider that EV and ER are two anatomical different structures. His team uses next statement that "the ER along with the Eustachian valve helps in fetal life to direct oxygenated blood from the IVC through the foramen ovale to the left atrium". Furthermore, the ER divides the CVTI into an anterior sub-Eustachian isthmus and a posterior post-Eustachian isthmus [21]. Usually, the sub-Eustachian isthmus is composed from circumferentially atrial myocardial fibers from the base of the ER to the tricuspid valve [21]. Also, the ER differs regarding its protrusion and it is very well expanded as it has been observed in several adult hearts. In ER, the ratio of myocardium to fibrous tissue differs too, as a result the conduction properties of this ridge are also irregular [21]. Also, it should be emphasized, that the most part of hearts have myocardium in the ER, and thus, the ablation technique applied between the tricuspid valve and the ER is not generally effective [21, 33–35].

Sub-Eustachian Pouches

In all patients, the sub-Eustachian component or region of the CVTI is located quite inferior to the ER [21]. However, several patients may present an "excavation of myocardium" causing "an aneurysmal—type dilation" in the sub-Eustachian region named sub-Eustachain pouch (see Fig. 2.8) [21, 27, 31, 33, 36–38]. If these sub-Eustachain pouches develop, they are located closer to the CS ostium than the free wall of the RA, and they differ considerably in the depth as well as the anteroposterior dimension [22, 25, 33]. Of note, it could be an developmental correlation between the protrusion of Eustachian pouches and the prominent of Thebesian valve that protects the ostium of the coronary sinus. Thus, it is unusual to find a large sub-Eustachian pouch without significant evidence of the *Thebesian valve* (Figs. 2.9a–c and 2.10) [12].

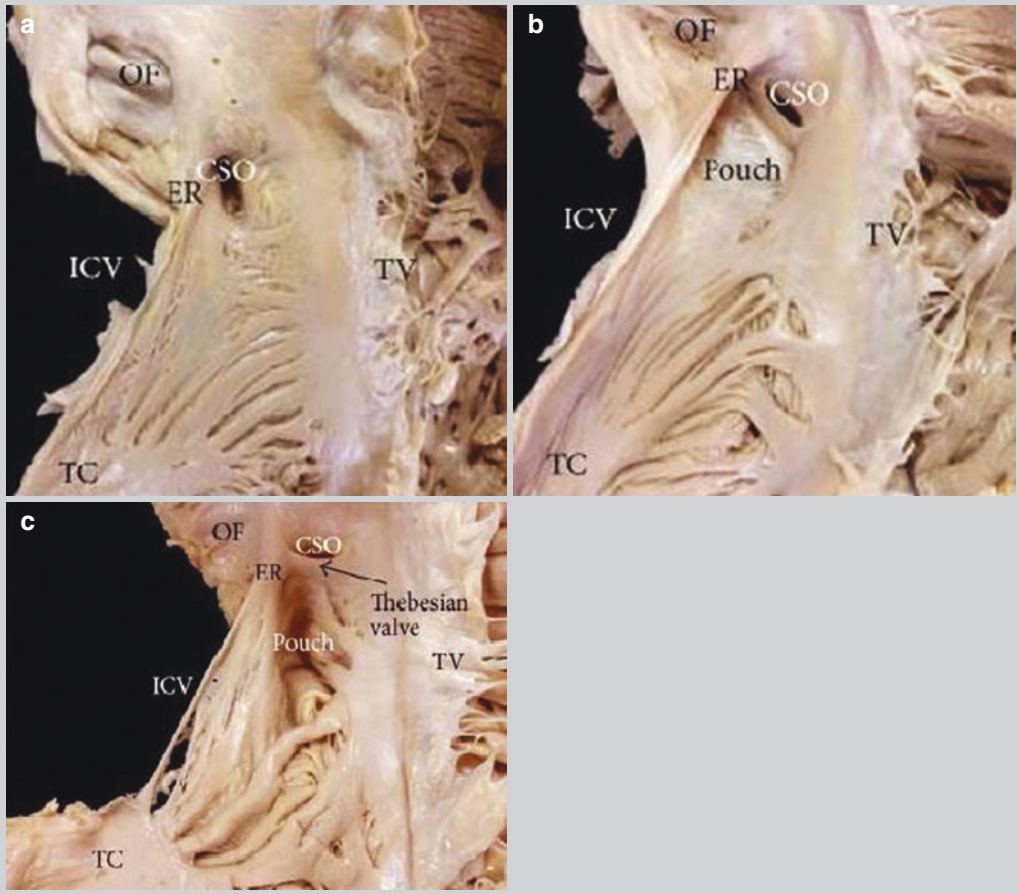

Fig. 2.9 (**a–c**) These hearts show variations in morphology of *the Thebesian valve* guarding the coronary sinus orifice, the sub-Eustachian pouch, and Eustachian ridge. *Ao* aorta, *CSO* coronary sinus orifice, *EV* Eustachian valve, *ER* Eustachian ridge, *ICV* inferior cava vein, *MCV* minor coronary vein, *OF* oval fossa, *PT* pulmonary trunk, *RAA* right atrial appendage, *RCA* right coronary artery, *RVOT* right ventricle outflow tract, *SCV* superior cava vein, *TC* terminal crest, and *TV* tricuspid valve. Modified from [12]. It is an open access article

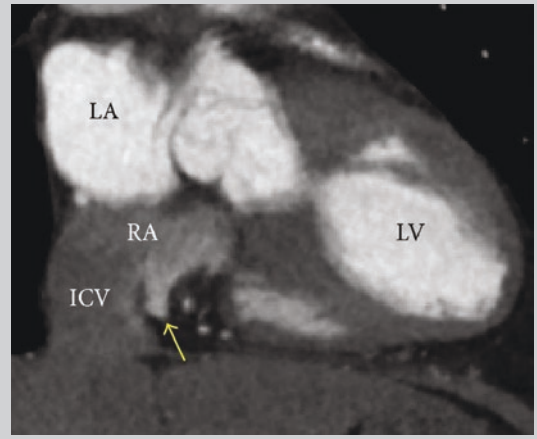

Fig. 2.10 Coronal CT shows a sub-Eustachian pouch (yellow arrow) in the median aspect of the right inferior cavoatrial junction. *ICV* inferior cava vein, *LA* left atrium, *LV* left ventricle, *PM* pectinate muscles, *RA* right atrium, and *TC* terminal crest. Modified from [12]. It is an open access article

The Sub-Eustachian Sinus (Sinus of Keith, Sub-Thebesian Recess)
Attitudinally appropriate nomenclature for this anatomic variant is sub-Thebesian recess [39, 40]. The sub-Eustachian recess is an expansion of a pouch-like isthmus below the ostium of the coronary sinus [12].

The occurrence of a wide sub-Thebesian recess or deep pouches is correlated mainly with RF applications in comparison with undeviating right level of isthmus [27]. This undeviating isthmus can alter local radiofrequency delivery because a limited area from blood flow results in delayed catheter tip cooling. Heidbuchel et al [32] showed in one angiographic study of the CVTI, that pouch was present in 47% of patients with a mean depth of 4.3 ± 2.1 mm (1.5–9.4) [32]. Later, another study of [29] using CT scans in normal population have identified both thick recess associated with a pouch-like over 5 mm in 45% of patients on central isthmus in 45% of mid-diastolic phase images [29]. To sum up, this observation can be valuable in preprocedural techniques when the existence of a wide pouch would determine a "central approach to the ablation" [12].

2.3 The Interatrial Septum

The interatrial septum (atrial septum) splits the atrial chambers from one another [12] representing the posteromedial wall of the RA. The anatomy of the atrial septum is not simple one [41]. Shortly, the interatrial septum is a solid muscular wall with a small central oval-shaped depression called the fossa ovalis (FO) (Fig. 2.11a, b) [41].

Spatial orientation of the anatomic components of the interatrial septum is best shown by CT angiography [29, 42, 43]. The interatrial septum has an interatrial component and an atrioventricular component. In fact, the interatrial septum originates from the embryologic septum primum and septum secundum [13]. Anderson et al [44] define the true interatrial septum as the region confined to the area that is marked by the valve of the FO or "the embryonic septum primum" and the anterior structure of the atrial septum that is the true "secondary septum" [44].

The fossa ovalis (FO) is the rest of the foramen ovale in the foetal heart that let right to left shunting of blood to bypass the lungs. After birth, this embryonic shunt is removed when the valve of the fossa closes against the muscular rim—an infolding of the atrial wall. The superior and posterior parts of the rim are the infolding between the SVC and the right pulmonary veins (Fig. 2.12a, b) [12].

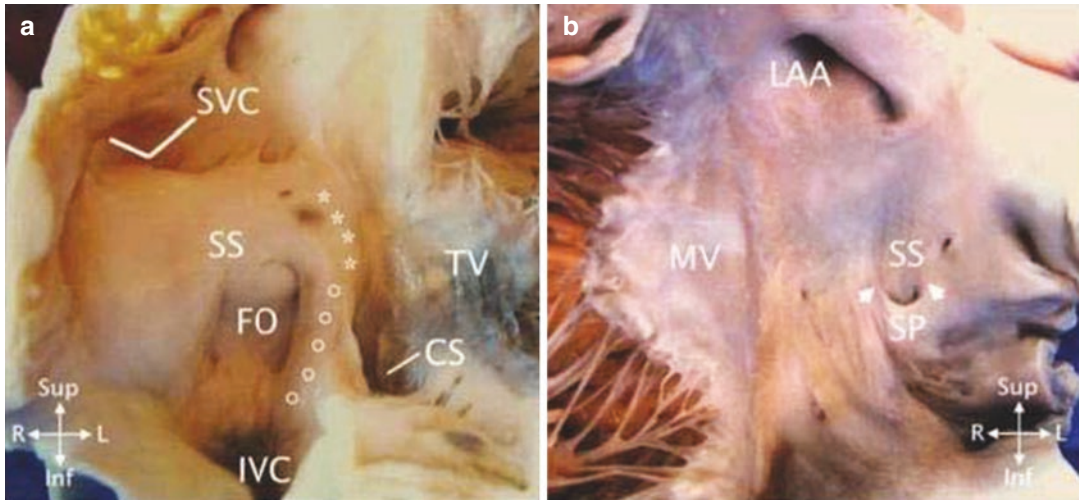

Fig. 2.11 (**a**, **b**) Anatomy of the normal atrial septum. (**a**) Opened right atrium showing the entrance of the superior vena cava (SVC), inferior vena cava (IVC), and coronary sinus (CS). The fossa ovalis (FO) forms the central part of the atrial septum and is bounded superiorly and rightward by septum secundum (SS). Septum primum is the thin floor of the fossa. The muscular base of the atrial septum (o) is between the fossa and the coronary sinus. The AV canal septum ("asterisk") is adjacent to the tricuspid valve (TV). (**b**) On the left atrial side, septum primum (SP) forms a hammock—shaped structure and has insertions (white arrows) on septum secundum (SS). *LAA* left atrial appendage, *MV* mitral valve. From [41]. This is an open-access article distributed under the terms of the Creative Commons Attribution License, which permits unrestricted use, distribution, and reproduction in any medium, provided the original author and source are credited. https://www.omicsonline.org/congenital-heart-defects-in-adults-a-field-guide-for-cardiologists-2155-9880.S8-007.php?aid=6799

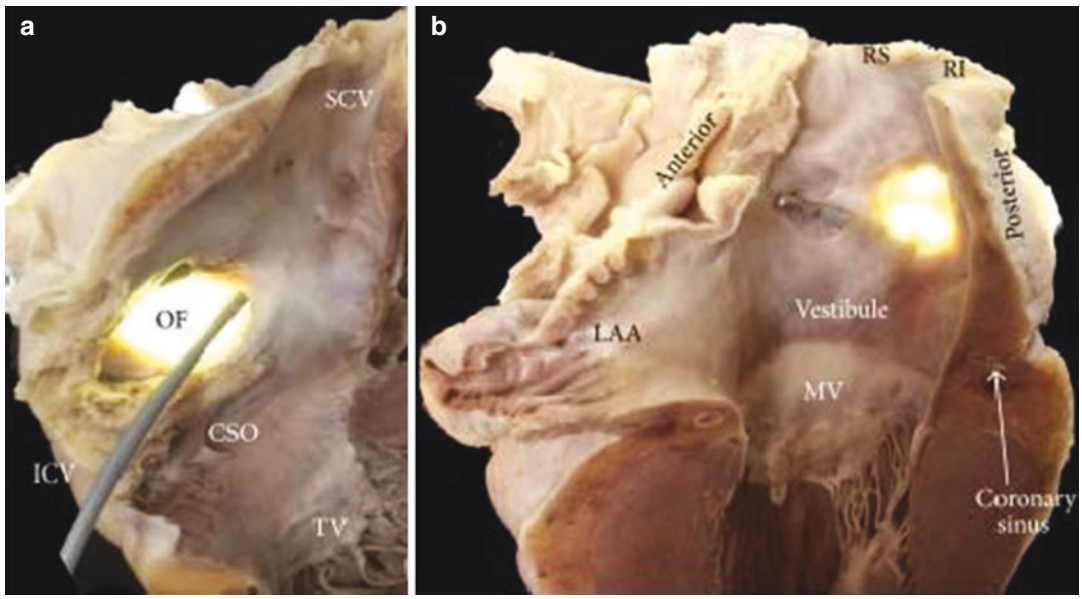

Fig. 2.12 (**a**, **b**) Longitudinal sections through the venous component of the right atrium showing by transillumination in (A) the flap valve of the oval fossa and the muscular rim that surrounds it on the right atrial aspect. In this heart there is probe patency of the oval fossa, leaving a gap in its anterosuperior aspect. The gap can allow a catheter to be slipped between the rim and the valve (A) to enter the left atrium (B). Note in (B) by transillumination the location of the oval fossa in the left side of the septum. *CSO* coronary sinus orifice, *ICV* inferior cava vein, *LAA* left atrial appendage, *OF* oval fossa, *RI* right inferior pulmonary vein, *RS* right superior pulmonary vein, *SCV* superior cava vein, *TC* terminal crest, and *TV* tricuspid valve. Modified from [12]. It is an open access article

The depression of FO is encircled by a muscular ridge known as the limbus fossae ovalis [13]. Also, the FO is located anterior and superior to the both orifices of the IVC and the CS [13]. Further, [5, 41] showed that the FO is bordered superiorly and rightward by septum secundum or superior limbic band [5, 41].

Between the FO and the coronary sinus there is *the inferior muscular bottom* of the atrial septum that has the tendon of Todaro and carry on with the EV. The tendono of Todaro has an obliquely course inside the ER and splits the FO from the coronary sinus to inferior part. It is important to underline the role of the tendon of Todaro that unifies the valve of the IVC to the middle fibrous component of the cardiac skeleton [13]. Furthermore, it looks like a fibrous expansion from the membranous part of the interventricular septum [13]. Importantly, it has a structural role to sustain the IVC and is of use to locate the AV node [13].

This FO is enclosed by a fine septum primum that is more obvious from the left atrial part where the fixation to septum secundum and overlap of both structures are evidently observed [5, 41]. Therefore, the left atrial appearance of the atrial septum has no "crater-like" aspect of the right side because here the fossa valve covers the fossa rim [12, 14]. The component between the FO and the atrioventricular valves has a muscular structure named atrioventricular canal septum [5, 45].

Initially, [46] described patent foramen ovale (patent fossa ovalis) in 10–15% of patients [46]. The team of [12] showed that about one-third of the normal population has patent foramen ovale [12]. Same team of [12] explains that this incomplete adhesion of the valve to the rim, it may be useful. It appears a space frequently in the anterosuperior margin and having a C-shaped mark in the left atrial side. This space can permit the access of a catheter to the LA [12]. Patent foramen ovales has been associated with a right-to-left shunt, paradoxical emboli, cryptogenic stroke, hypoxemia in patients with obstructive sleep apnea, increased risk for decompression sickness among scuba divers, and increased risk for atrial fibrillation after cardiac surgery [46].

There are two major anatomic aspects of the interatrial septum: the lipomatous hypertrophy of the interatrial septum and the large interatrial septal aneurysm [12]. Lipomatous hypertrophy of the interatrial septum is collection of fat in the interatrial groove [42]. The large interatrial septal aneurysm is characterized by a FO with slimmer and elongated valve [12]. Both anatomical variants can be shown precisely by three-dimensional transesophageal echocardiography and CT-derived imaging [29, 42, 43].

Moreover, enlargement of the atrial chambers with raised age or body mass, severe kyphoscoliosis, severe left ventricular hypertrophy or a distended aorta influence the septal plane direction with dislocation of the FO [12, 47].

2.4 Right Ventricle

The right ventricle (RV) collects deoxygenated blood from the RA, and propels it through the pulmonary orifice into the pulmonary artery [14]. On the general whole, the RV is formed by free (anterior and posterior) walls and IVS [48]. In the chest, the RV has an anterior position and is situated just behind the sternum. Also, RV delimitate the inferior margin of the cardiac profile [14, 49].

Anatomically the RV has a complex shape (see Fig. 2.13) [50]. With a quite thin free wall, it has triangular profile observed from a side and crescentic (pyramidal) profile when regarded in cross-section [49]. If heart is observed from the apex, the right edge of the RV is sharp [49]. When heart is observed from the diaphragmatic part, the right ventricle (RV) and left ventricle (LV) lie side by side [14].

Shortly, RV has an odd geometry with a crescent-shaped RV that wraps around conical LV (Fig. 2.14) [14, 48, 51].

RV has three distinct regions with different embryological origins and electrophysiological properties that comprise (Figs. 2.15 and 2.16) [12, 48, 49, 52]:

(1) the inlet/inflow component,
(2) the apical trabecular component,
(3) the outlet/outflow tract component.

The inlet and trabecular components have a common embryological origin. The inflow component is heavily trabeculated by coarse

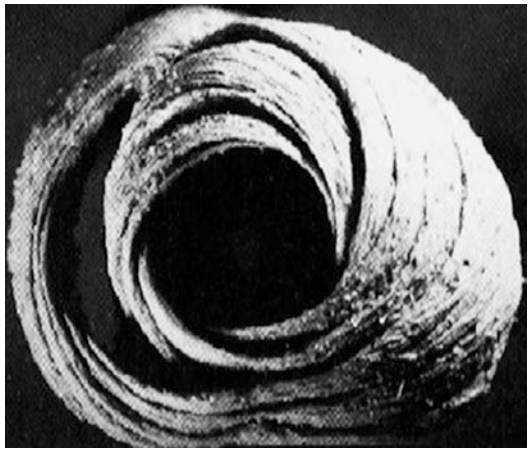

Fig. 2.13 Cross-sectional view of both ventricles demonstrating the crescent shape of the right ventricle and conical form of the left ventricle. The obliquity of the septal muscle structure and its spiral arrangement is clear. Note the thickened septum, and the wrap around basal loop. From [50] with permission

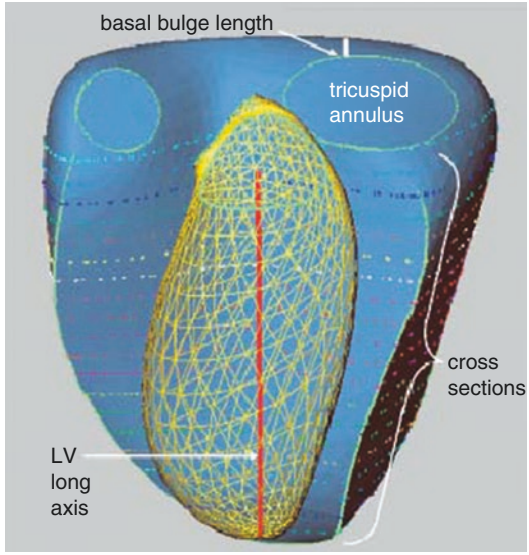

Fig. 2.14 RV shape analysis. Both the total length of the right ventricle (not illustrated) and the basal bulge length were computed parallel to the left ventricular (LV) long axis. Modified from [51] with permission

trabeculae carneae, the outflow component is named infundibulum and contains only a few trabeculae, and the subpulmonic area has a smooth surface [7, 48].

It has to be mentioned that the "tripartite concept in the evaluation of congenitally malformed

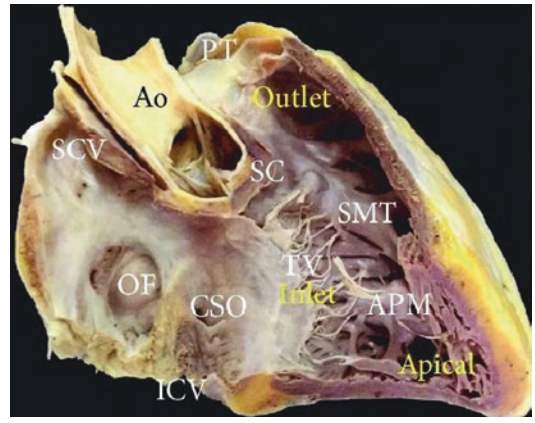

Fig. 2.15 This is a right lateral view showing the three components of the right ventricle and the characteristic muscle bundles as septomarginal trabeculation and supraventricular crest or ventriculoinfundibular fold. Ao aorta, APM anterior papillary muscle, *AV* aortic valve, *CSO* coronary sinus ostium, *ICV* inferior cava vein, *LAA* left atrial appendage, *LV* left ventricle, *LVOT* Left ventricle outflow tract, *OF* oval fossa, *PT* pulmonary trunk, *RAA* right atrial appendage, *RV* right ventricle, *RVOT* right ventricle outflow tract, *SC* supraventricular crest, *SCV* superior cava vein, *SMT* septomarginal trabeculation, and *TV* tricuspid valve. Modified from [12]. It is an open access article

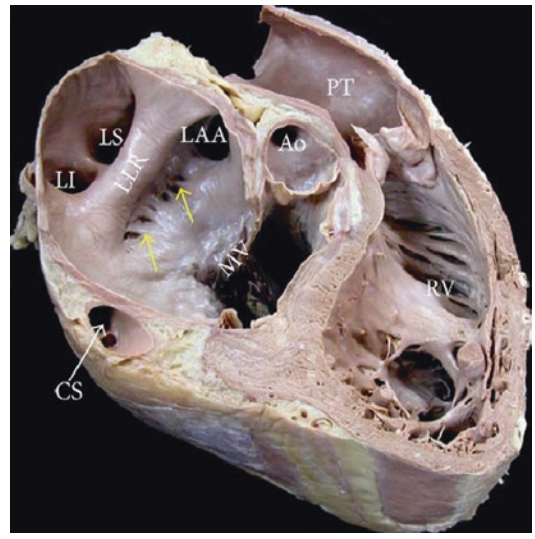

Fig. 2.16 Longitudinal section through the roof of the left atrium showing the endocardial view of the left atrium and *right ventricle*. *LAA* left atrial appendage, *PT* pulmonary trunk, *Ao* aorta, *MV* mitral valve, *RV* right ventricle, *CS* coronary sinus, *LI* left inferior pulmonary vein, *LS* left superior pulmonary vein, *LLR* left lateral ridge, *RI* right inferior pulmonary vein, *RS* right superior pulmonary vein, *OVM* oblique vein of Marshall, and *LCPV* left common pulmonary vein. Modified from [12]. It is an open access article

hearts is more constructive than the traditional division of the RV into sinus and conus components"[49]. It seems that the heart with malformations, one or more of the three components can be absent in one ventricle [5, 49].

The Muscular Inlet/Inflow Component

The posteroinferior component of RV extends from the atrioventricular junction represented by the TV annulus into the insertions of the papillary muscles to the ventricular walls. In other words, it is the area comprising the tricuspid valve (TV) (see Fig. 2.17) [12, 49].

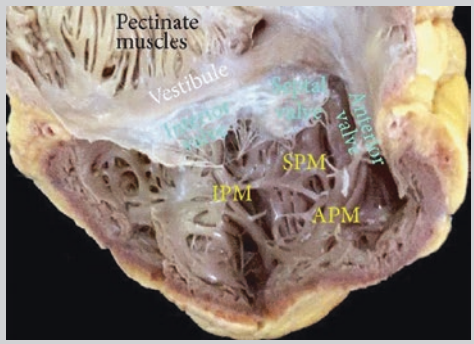

Fig. 2.17 The right side of the heart is opened to show the hinge of the tricuspid valve and the location of the right papillary muscles and leaflets of the tricuspid valve. *Ao* aorta, *APM* anterior papillary muscle, *CSO* coronary sinus ostium, *IPM* inferior papillary muscle, *OF* oval fossa, *RVOT* right ventricle outflow tract, *SC* supraventricular crest, *SCV* superior cava vein, *SMT* septomarginal trabeculation, and *SPM* septal papillary muscle. Modified from [12]. It is an open access article

Tricuspid Valve (TV)

Same to the atrioventricular valve, the tricuspid valve system comprises an annulus, leaflets, papillary muscles, and the chordae tendinae [13, 14]. The TV oriffice is toughened by its annulus fibrosus of the cardiac skeleton. TV annulus is located on the base of RA connected to the membranous region of the septum [13]. TV has the largest annulus in the heart [49, 53], feature that predisposes TV to be fragile to structural changes caused by a persistent increase of pressure or volume load [49]. The anterosuperior component of the TV annulus divides the membranous septum into atrioventricular and interventricular components. Commonly, there is a breach within the leaflet located at the site of the membranous septum.

The *three leaflets* of TV are the anterior (superior, infundibular, anterosuperior), posterior (inferior, mural, marginal), and medial (septal) (see Fig. 2.17) [12, 14]. All leaflets are triangular form with different sizes. *The septal leaflet* is the smallest leaflet with the numerous tendinous cords that have the role to connect septal leaflet right away to the ventricular septum. It begins from the TV annulus and gets on medial part of the IVS. The commisure between the septal and anterior leaflets is sustained by a medial small papillary muscle. Importantly, the septal leaflet is more apical than the anterior mitral leaflet. Further, *the anterior leaflet* is the largest and spreads from the medial part of the IVS to the anterior free wall. In fact, it attaches to the right atrioventricular junction. The anterior leaflet is sustained in its central area by a bulky papillary muscle that as a rule comes up from the moderator band with insertion to the parietal wall. *The inferior leaflet* is sustained by a number of small papillary muscles that come up from the diaphragmatic wall of the RV. It spreads from the lateral free wall to the posterior part of the IVS. It has a mural attachment. The findings of TV such as varying number and disposition of papillary muscles also make a distinction between the TV from the mitral valve that has two groups of papillary muscles with organized grouping [49]. The TV leaflets have a smooth atrial side while the irregular ventricular side offers insertion for the

chordae. Mainly in children, the atrial side of leaflets can have small nodules on the edges, known as the noduli albini [17].

TV has three types of *chordae tendinae* or tendinous cords with the role to insert TV and to prevent its prolapse during systole into the RA [17]. Netter [17] classifies these tendinous cords in primary, secondary and tertiary types. The primary type of chordae attaches the free edge of the leaflets to the papillary muscle by some fine strands. The secondary type of chordae attaches the ventricular component of each leaflet to the papillary muscle. These tendinous cords have reduced number but strongest attachment. In same way, the third type of cords attaches each leaflet to the ventricular myocardium. Typically, septal leaflet has multiple cords insertions to the IVS [17]. In fact, the septal leaflet with its cords or medial papillary muscle attaching directly to the IVS is a feature of the RV [12].

The *commissures* of TV attach the leaflets being classified as anteroseptal, anteroposterior and posteroseptal. These commisures assure only incomplete separation of the leaflets, therefore they don't stretch the annulus of TV [17].

The number of *papillary muscles* that link the leaflets to the walls via the cords are variable. Each papillary muscle gives cords for two adjacent leaflets. The anterior papillary muscle is the largest, while septal papillary muscle is the smallest. Also, the septal papillary muscle is located where the crista supraventricularis meets the septal band, supplying attachment to the cords to the posterior and septal leaflet of the TV [54].

The Trabecular Component

It extends from the papillary muscles of TV to the heart apex [14]. According to [55], the trabecular component of RV contains the static apex (with heavy and coarse trabeculations), two thick intracavitary muscle bands, the crista supraventricularis, and the moderator band [55, 56]. Moderator band is connected to the right ventricular outflow tract (RVOT) and it is extending from the IVS to the anterior RV wall (Fig. 2.18) [12, 55].

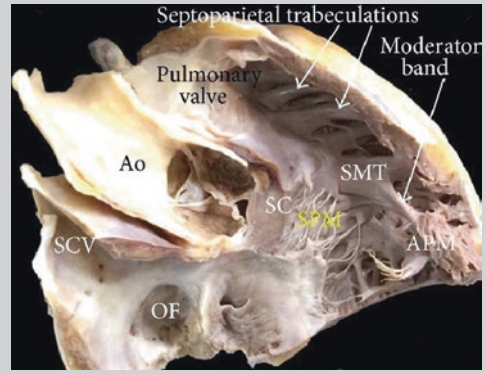

Fig. 2.18 The right ventricle is opened from the front to show the septal papillary muscle, moderator band, and septoparietal trabeculations. *Ao* aorta, *APM* anterior papillary muscle, *CSO* coronary sinus ostium, *IPM* inferior papillary muscle, *OF* oval fossa, *RVOT* right ventricle outflow tract, *SC* supraventricular crest, *SCV* superior cava vein, *SMT* septomarginal trabeculation, and *SPM* septal papillary muscle. Modified from [12]. It is an open access article

In fact, the moderator band is a link between the septomarginal trabeculation (SMT) or septal band to the anterior papillary muscle (see Fig. 2.18). Further, the SMT is a Y-shaped muscular band that attaches to the septal side. Between the extremities of SMT the heart wall infolds and forms the supraventricular crest that divides the inflow and outflow components of the RV and supports the pulmonary valve (PV) [57]. From the anterior edge of the SMT start the septoparietal trabeculations (between five and 22 trabeculations) that go round the free wall parts of the subpulmonary infundibulum [58, 59].

The outlet component (the infundibulum, conus, the RVOT) is a smooth funnel-shaped myocardial outflow tract called infundibulum [49]. Briefly, the RVOT is located leftward and anterior to the left ventricular outflow tract (LVOT) (Fig. 2.19) [60] and the left main coronary artery is closer to the posterior RVOT [12]. This region is particularly important in patients with congenital heart disease [61] and arrhythmias.

The RVOT contains subpulmonary infundibulum and the pulmonary valve [62, 63]. Esentially, the myocardium of the posterior RVOT has

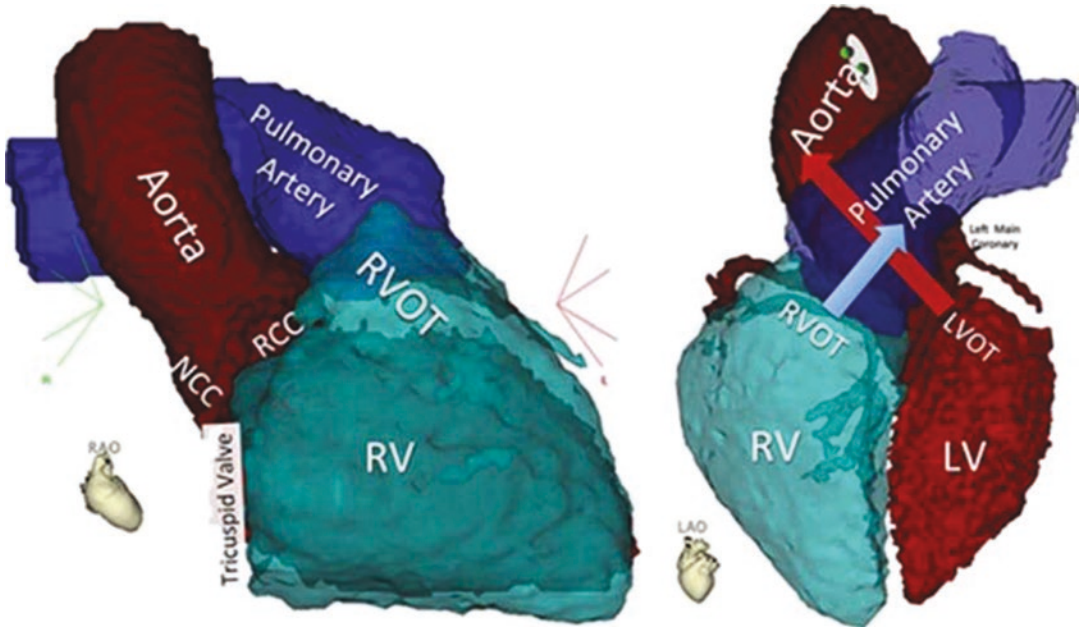

Fig. 2.19 Anatomy of the outflow tract. CT scan 3D reconstruction showing the ventricles, outflow tract and the aorta and pulmonary artery. On the left panel, RAO view, and on the right panel, LAO. The pulmonary artery and the RVOT lie anterior to the LVOT and the aorta. The RV is located to the right, but when it advances into the RVOT and pulmonary artery, they are located on the leftward to the LV, LVOT and aorta. In the opposite, the LVOT and aorta are located rightward to the middle axis of the heart. There is an intimate relationship between the right coronary cusp and the septal aspect of the RVOT. The left main and coronary sinus (not shown in this model) locate to the left of the RVOT and LVOT and anterior to the LV. *CT* computerized tomography; *RAO* right anterior oblique, *LAO* left anterior oblique, *RVOT* right ventricular outflow tract, *LVOT* left ventricular outflow tract, *RV* right ventricle, *LV* left ventricle, *NCC* right coronary cusp, *NCC* non-coronary cusp. From [60]. It is an open access article

continuity with the LVOT and with the closest anterior IVS [12]. The most inferior part of posterior RVOT myocardium is closest to the aortic leaflets (right coronary leaflet and part of the left coronary leaflet). Further, the myocardium is rather thin in the anterior, rightward and subpulmonary valve components of the RVOT, while the posterior infundibular component is adherent to the anterior LVOT as a result the cranial IVS is the thickest. RVOT has a leftward route from proximal-to-distal, as a result the most rightward component of the RVOT is the bundle of His region, and the most leftward component of RVOT is the supravalvar myocardium above the anterior leaflet of the PV [12].

The subpulmonary infundibulum extends from the crista supraventricularis to the pulmonary valve (PV) and is typically without muscular trabeculations. Conversely, bordering subpulmonary infundibulum can exhibit trabeculations from the IVS to the parietal wall. These septoparietal trabeculations can have flat surface, enfolding the parietal wall. Also, they can be hypertrophied with muscular subpulmonary stenosis as in tetralogy of Fallot [49].

The *PV* is a semilunar valve separated from the TV by the ventriculo-infundibular fold that develops the supraventricular crest described above. The PV has no identified annulus to sustain the valve (Figs. 2.20 and 2.21) [12]. The PV looks like the configuration of the aortic valve with the three symmetric, semilunar leaflets or cusps. The cusps are connected to the right ventricular infundibulum and the pulmonary trunk [17]. The leaflets of PV are smooth and thin with a small fibrous nodule (nodulus Arantii) at the center of the free edge [17].

Assessing the both semilunar valves, the level of the PV is superior and almost horizontal, while the level of the aortic valve is inferior with an angle of at least 45° from the median plane. Sánchez-Quintana [12] suggests that the differentiation in levels of arte-

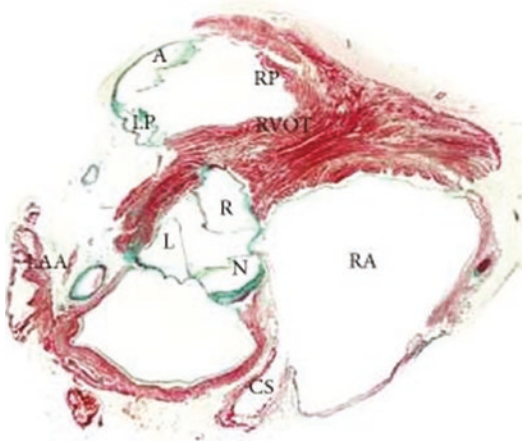

Fig. 2.20 Cross-histological section stained with Masson's trichrome through the left and the right atria. Note the anatomic relation of the *right ventricular outflow tract* with the subaortic outflow. Note that while all of the leaflets of the pulmonary valve are supported by infundibular musculature, only two of the leaflets of the aortic valve have muscular support. Pulmonary sinuses are named according to their relationship to the heart (nonattitudinal), including anterior (A), left posterior (LP), and right posterior (RP) pulmonary sinus. *CS* coronary sinus, *PT* pulmonary trunk, *RVOT* right ventricle outflow tract, and *TV* tricuspid valve. Modified from [12]. It is an open access article

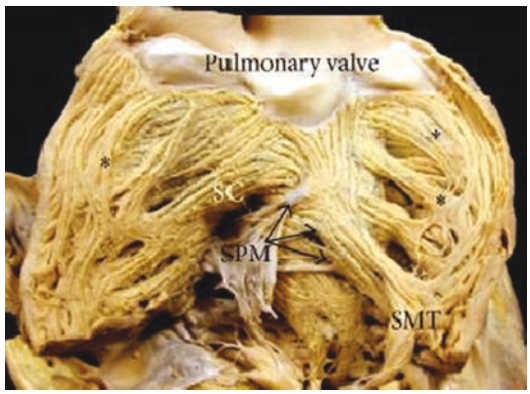

Fig. 2.21 Endocardial view of right ventricular outflow tract (RVOT) is shown (d). Note that endocardial infundibular sleeve consists of septoparietal trabeculations ("asterisk") arising from septomarginal trabeculation (SMT). Note crossing architecture pattern of myocardial strands between septomarginal trabeculation with septoparietal trabeculations and supraventricular crest below pulmonary valve. *L* the left aortic sinus, *LCA* left coronary artery, *M* myocyte, *MV* mitral valve, *N* noncoronary aortic sinus, *LP* left posterior pulmonary sinus, *PF* Purkinje fiber, *PT* pulmonary trunk, *R* right aortic sinus, *RA* right atrium, *RCA* right coronary artery, *RP* right posterior pulmonary sinus, *RVOT* right ventricle outflow tract, *SC* supraventricular crest, *SCV* superior cava vein, *SMT* septomarginal trabeculation, and *SPM* septal papillary muscle. Modified from [12]. It is an open access article

rial semilunar valves can be amplified by the length of infundibulum.

Finally, the *pulmonary trunk* divides into right and left pulmonary arteries. The ligamentum arteriosus that is a residue of the fetal ductus arteriosus joins this division of the pulmonary artery to the inferior plane of the aortic arch [14].

2.5 Interventricular Septal Morphology

The IVS is muscular excluding a very small fibrous part that is the membranous septum. In the normal heart, the curve of the IVS describes the RV as wrapping the LV [14]. The partly covering between left ventricular inlets and outlet locates the LVOT directly at the back of the IVS. As a result, IVS splits LVOT from the RV inlet causing the "wedged" location of the aortic root [14, 49].

The septal side of the RV is a typical muscle band named the septomarginal trabeculation (SMT) as already described above. Ho and Nyhoyannopoulus [49] describe it as a band with Y-shape that holds the ventriculo-infundibular fold between its arms [49]. In the posterior-inferiorly arm inserts the medial papillary muscle. The antero-cranial arm merges into the subpulmonary infundibulum. Frequently, the body of SMT is adherent to the septum. If it is hypertrophied, the SMT can separate the RV cavity into two chambers. Another morphologically feature of the RV is the moderator band that comes up from the body of the Y (SMT) to get to the parietal wall together with a fascicle of the right bundle branch (RBB) of the atrioventricular conduction system [49]. Importantly, the insertion of the medial papillary muscle is the landmark for the most superior part of the right bundle branch (RBB). From there, it descends like a cord in the subendocardium of the SMT [49].

2.6 The Conduction System of Right Heart

The conduction system is also closely associated with the RA. Close to the entry of the SVC is the *sinoatrial (SA) node*, the cardiac pacemaker that produces 60–100 beats per minute (bpm).

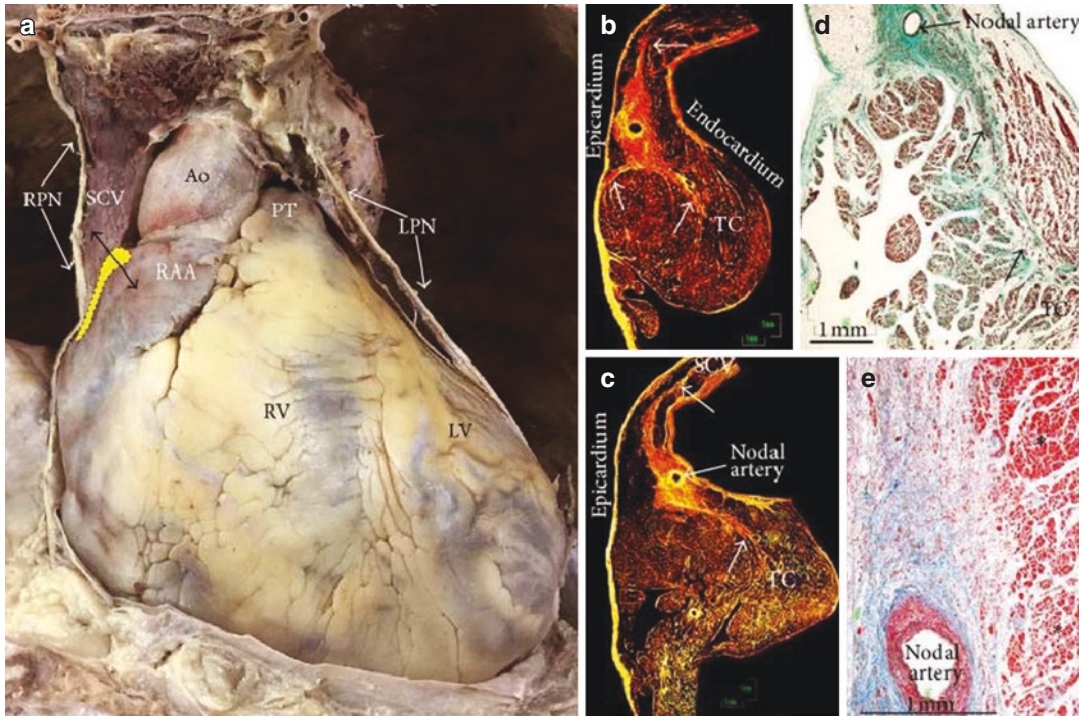

Fig. 2.22 (**a**) Frontal view of the heart in a cadaver that has been dissected to show the course of the phrenic nerves relative to the atria and left ventricle. The anticipated location of *the sinus node* outlined with dots on yellow background. The double-headed arrow represents the sectioning plane used for making the sections through the sinus node and the terminal crest shown in the histological sections. (**b**, **c**) Histological sections with picrosirius red stain and polarized light showing variations in locations of *the sinus node* relative to the epicardial and endocardial surfaces and sizes of the terminal crest. Note nodal extensions (arrows) to superior caval vein, terminal crest, and epicardium. (**d**) With Masson's trichrome stain is recognizable a nodal extension to terminal crest by its fibrous matrix (green). (**e**) Histological section of the nodal body (Masson's trichrome stain). Note the contour of the node towards the neighboring myocardium ("asterisks"). *Ao* aorta, *LPN* left phrenic nerve, and *LV* left ventricle, *PT* pulmonary trunk, *RAA* right atrial appendage, *RPN* right phrenic nerve, *RV* right ventricle, *SCV* superior cava vein, *TC* terminal crest, and *TV* tricuspid valve. Modified from [12]. It is an open access article

Further, the impulse distributes by the interatrial and internodal conduction pathways to get to the *atrioventricular (AV) node*, the *bundle of His* that divides into *left* and *right branches*. Each bundle branch ends in a network of fibers named the *Purkinje fibers* with ventricular contraction. In normal human heart, the dominant pacemaker is the SA node. The AV node and the Purkinje cells have a normal physiologic rate from 25 to 55 bpm [64]. The parasympathetic system dominates at rest and slows the sinoatrial rate.

The SA node is located on the roof of the RA at the junction of the RAA, the SVC, and the sulcus terminalis (Fig. 2.22) [12, 65]. It has been previously described as being located 1 mm under the epicardium, with the length of 10–20 mm and large of 5 mm. It contains the P cells capable of spontaneous depolarization with the formation of the normal cardiac rhythm [65]. Essentially, the SA node is mainly adjusted by sympathetic and parasympathetic efferent innervation.

Interatrial Conduction

From SA node, depolarization spread over both atria. There are disagreements looking the mechanism of impulse conduction through the both atria [65, 66]. Conversely, there are three anatomic conduction pathways from the SA node or from its proximity.

The internodal bundles comprise the anterior internodal bundle that originates from the anterior SA node, coursing the roof of the right IAS and divides into the Bachman's bundle connected to the

LA and a second bundle going downward to the AV node, with the length of the anterior region of the IAS. The middle internodal bundle or Wenckebach's bundle routes anteriorly to the FO within the IAS to get to the AV node. Usually, it is infrequent and undeveloped. The third internodal bundle is named posterior internodal bundle (Thorel's bundle), that routes along the length of the TC via the EV, posteriorly to the coronary sinus [65].

The AV node (node of Tawara) and His bundle. The AV node is situated on the floor of the RA inside the triangle of Koch [12, 49]. To approximate the location of the AV node (see Figs. 2.23 and 2.24) [12], it is necessary to identify the triangle of Koch with its base via the coronary sinus; and the sides are the septal leaflets of the TV and the tendon of Todaro [13].

Therefore, from the components of AV node (transitional zone and compact node) emerges AV bundle and prolongs with the penetrating distal AV bundle (His bundle) [66]. The *bundle of His* is located within the membranous atrioventricular septum and it can be recognized in the central fibrous body. In fact, it represents an anatomically and histologically switch between the AV node and the bundle branches (see above Figs. 2.24c–e and 2.25) [39, 40, 68–70].

The right bundle branch (RBB) of His emerges from the membranous septum to descend subendocardially on the SMT and the moderator band, which carries within it a major fascicle of the RBB [71]. The RBB continues inferiorly as a continuation of the bundle of His in the subendocardic portion of the IVS (Fig. 2.26) [7, 12, 65].

The Purkinje fibers represent the system of conduction fibers emerging from both left and the right bundle branches. It has a rapid conduction. These conduction fibers of Purkinje fibers spread inside the myocardium and the trabeculation of the RV and LV. Specifically, moderator band is the most frequent conduction pathway that comprises Purkinje fibers from the RBB [7].

Future Directions

Recently, [72] using micro-computed tomography (micro-CT) described the first 3D representation of the cardiac conduction system on ex-vivo intact human hearts.

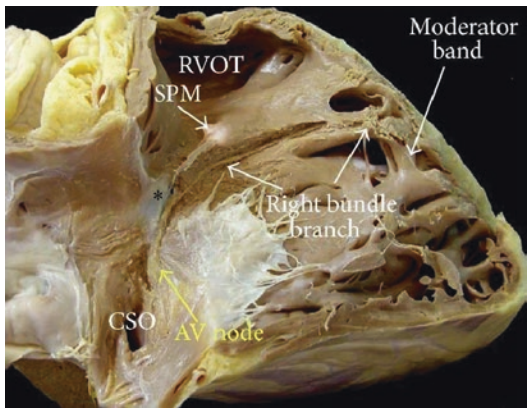

Fig. 2.23 Window dissection of the right heart to show the AV node and right bundle branch crossing the central fibrous body ("asterisk"). *Ao* aorta, *APM* anterior papillary muscle, *CSO* coronary sinus ostium, *IPM* inferior papillary muscle, *OF* oval fossa, *RVOT* right ventricle outflow tract, *SC* supraventricular crest, *SCV* superior cava vein, *SMT* septomarginal trabeculation, and *SPM* septal papillary muscle. Modified from [12]. It is an open access article

It seems that the SA node has a complex 3D shape with multiple emerging extensions (Fig. 2.27) [72]. The SA node gets thinner at the superior cavoatrial junction, and narrows caudally as it continues to the IVC (Fig. 2.27) [72].

Using automatic segmentation, the team of Stephenson [72] had rebuilt the finest elements of SA node (Fig. 2.28). The major body of the SA node has a length = 14.8 mm and width = 4.3 mm. It is located within the intercaval area, however isles and extensions from SA nodal tissue were also observed within the terminal crest, continuing on the way to the epicardial terminal groove, the pectinate muscles, and to the IAS [72].

Accordingly, the study of Stephenson et al [72] confirmed the atrioventricular conduction axis histological data published initially by [73]. Their 3D study validated that the conduction axis stems from the triangle of Koch. Also, the longitudinal micro-CT tomograms confirm histological studies of [73–75] (Fig. 2.29).

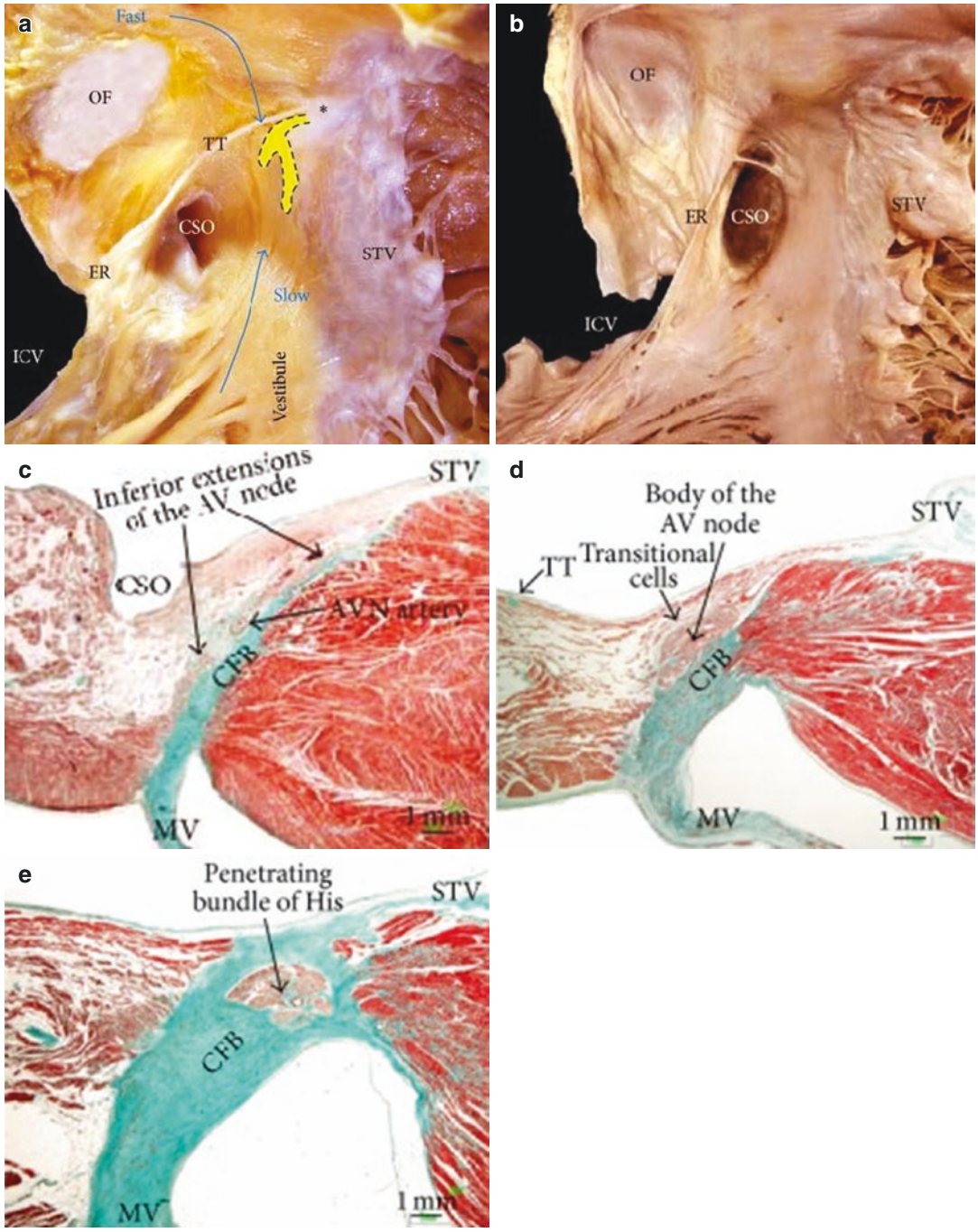

Fig. 2.24 (**a**) Dissection in right anterior oblique view of the right atrium shows the borders of the triangle of Koch. In this view we have depicted the putative fast and slow pathways toward the AV node (dotted shape in yellow). (**b**) Example of small triangle of Koch with a bigger coronary sinus ostium size. (**c**–**e**) A series of histological sections in comparable orientation to the picture (**a**) are taken through the coronary sinus ostium and inferior extensions of the AV node, the body of the AV node, and the penetrating bundle of His. *Asterisk* (∗) central fibrous body, *AVN* artery atrioventricular nodal artery, *CSO* coronary sinus ostium, *CFB* central fibrous body, *ER* Eustachian ridge, *ICV* inferior cava vein, *MV* mitral valve, *OF* oval fossa, *PFO* patent foramen ovale, *STV* septal leaflet of the tricuspid valve, and *TT* tendon of Todaro. Modified from [12]. It is an open access article

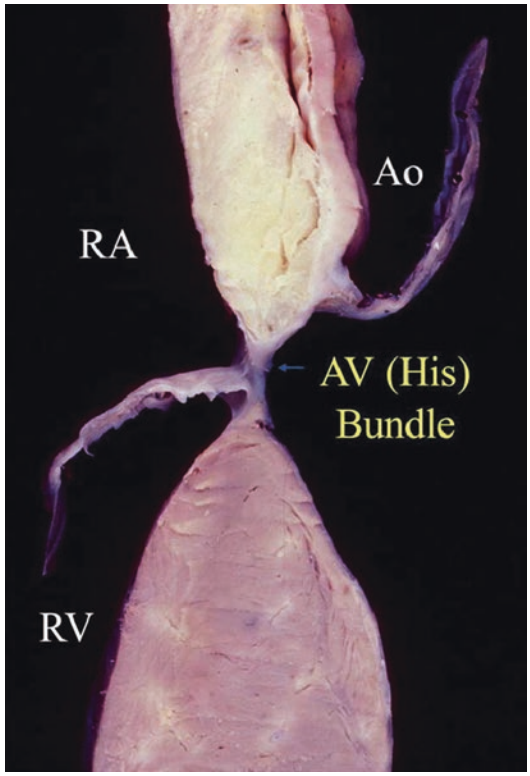

Fig. 2.25 Gross specimen illustrating the location of the penetrating His bundle at the atrioventricular portion of the membranous septum. *RA* right atrium, *RV* right ventricle, *Ao* Aorta, *AV* atrioventricular, *LV* left ventricle. From [67], with permission

Same study of Stephenson et al [72] showed that the bundle branches "as fine low attenuating ribbon-like structures" going down on the endocardial surface of the IVS. The RBB mainly was predominantly outlined in the long-axis micro-CT sections (Fig. 2.30). Distally, RBB continues with the Purkinje network. On the other hand,

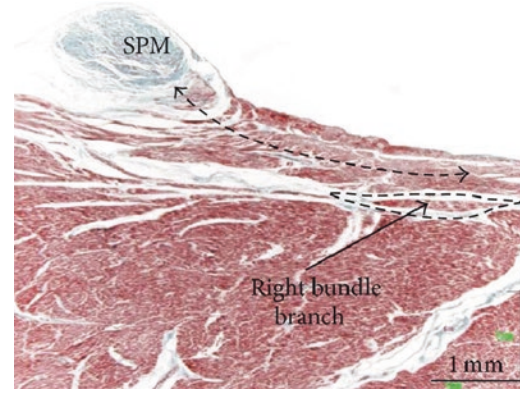

Fig. 2.26 Histological section of the septal papillary muscle (double-headed black broken line). Note the close relationship with *right bundle branch of His*. *Ao* aorta, *APM* anterior papillary muscle, *CSO* coronary sinus ostium, *IPM* inferior papillary muscle, *OF* oval fossa, *RVOT* right ventricle outflow tract, *SC* supraventricular crest, *SCV* superior cava vein, *SMT* septomarginal trabeculation, and *SPM* septal papillary muscle. Modified from [12]. It is an open access article

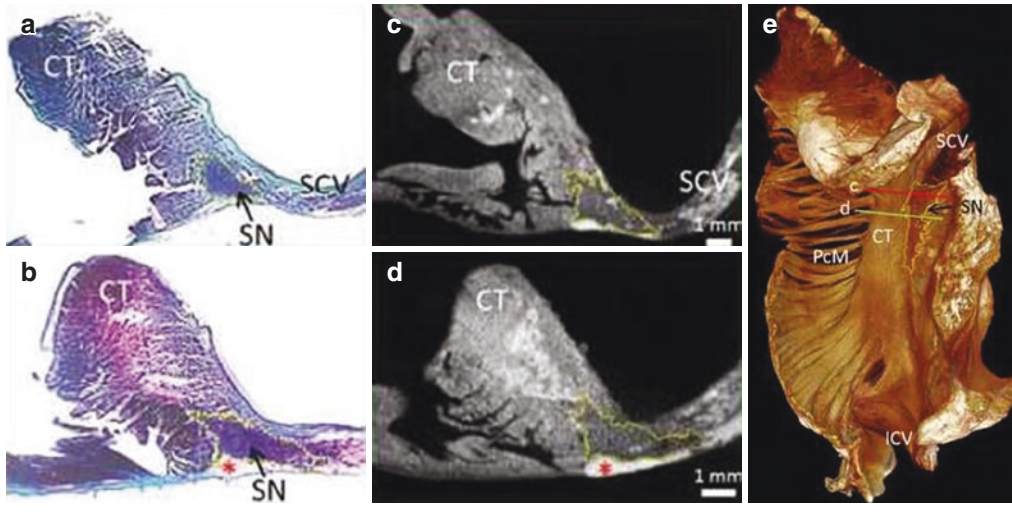

Fig. 2.27 Micro-CT allows objective discrimination of the *human sinus node*. This figure demonstrates high resolution ($28 \times 28 \times 28$ µm^3) micro-CT data from part of the right atrium containing the sinus node. For this figure, the sinus node is outlined in yellow in short-axis micro-CT sections (**c**, **d**) and in matching histological sections taken from the same sample (**a**, **b**). The plane of section in **c** and **d** is shown on the 3D volume rendering (endocardial view) (**e**). *CT* terminal crest, *ICV* inferior caval vein, *PcM* pectinate muscles, *SCV* superior caval vein, *SN* sinus node, "Asterisk" indicates epicardial fat. From [72]. It is an open access article

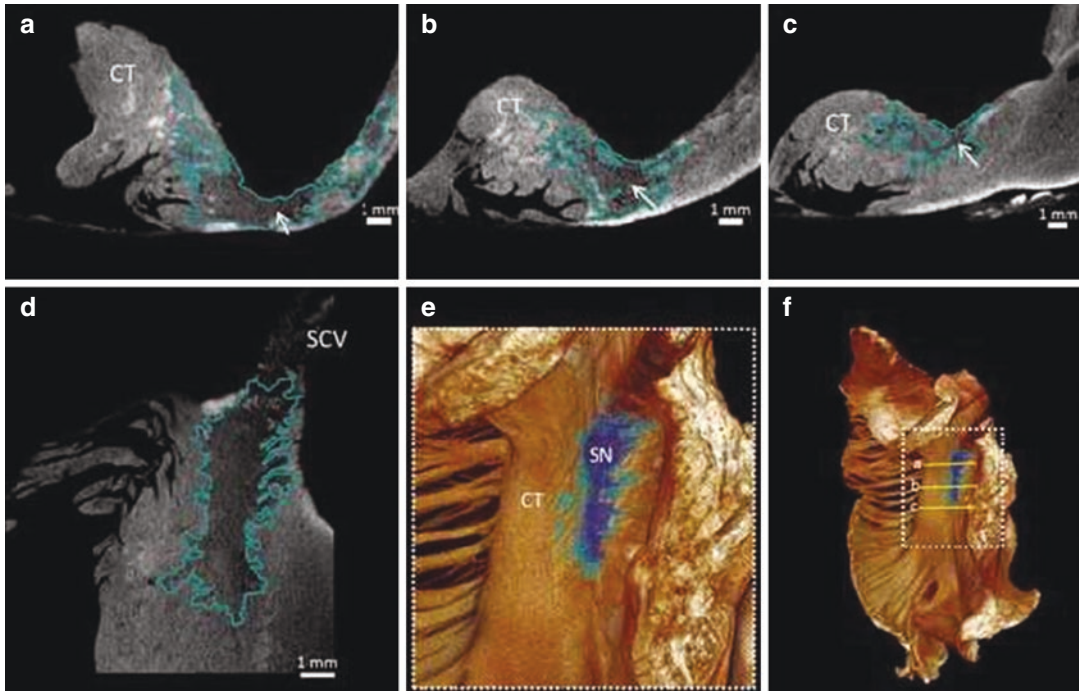

Fig. 2.28 Objective segmentation of the *human sinus node* and its paranodal area. This figure demonstrates high resolution (28 × 28 × 28 μm^3) micro-CT data from part of the right atrium containing the sinus node. The extent of the sinus node and its paranodal area is outlined in short-axis (**a**–**c**) and long-axis (**d**) micro-CT images. (**e**) Volume rendering (endocardial view) showing objective segmentation of the low pixel values corresponding to the body of the sinus node in dark blue; pixel values corresponding to the paranodal area are shown in turquoise. The plane of section in a-c is shown on the 3D volume rendering (**f**). Arrows indicate the approximate seed point for the objective segmentation of the sinus node. Sinus node body length = 14.8 mm, width = 4.3 mm. The sections are available to view without the outlines in the supplementary Fig. S2. *CT* terminal crest, *SN* sinus node. From [72]. It is an open access article

[72] showed that accordingly with previous immunohistochemical studies of [76], there is no confirmation of intramural Purkinje fibres in the human heart.

2.7 Anatomy of Right Heart Vessels: Short Points

The RV has a blood supply assured by the right coronary artery (RCA) and the left (LCA) [14, 48, 67] (Fig. 2.31). The RCA emerges from the right anterior sinus of Valsalva and along with the right atrioventricular sulcus provides two branches: the conus arteriosus branch and the right atrial branches. The conus artery and the communicating arteries from the IVS are a significant collateral blood supply to the LV, anterior regions and anterior two-thirds of the IVS. The right atrial branch gives the SA nodal artery in 50–73% of population [64, 66] and runs along the anterior RA to the SVC, surrounding the vessels prior to getting the SA node. Before the RCA gets to the AV groove, it gives some branches to the RA and RV, including the right marginal branch, which supplies the right margin of the heart [7, 17].

Further, RCA goes along with the sulcus posteriorly until it arrives at the crux cordis [48]. It branches downward to form the posterior interventricular (descending) artery in the posterior interventricular sulcus. It supplies the posterior free wall of the RV and in 85–90% branches into smaller arteries (posterior septal arteries) to supply the distal one third of the IVS [64]. The AV nodal artery runs anteriorly to the base of the atrial septum and supplies the AV node (50–60% of hearts), the proximal part of the bundles of His, and parts of the posterior IVS [7, 17].

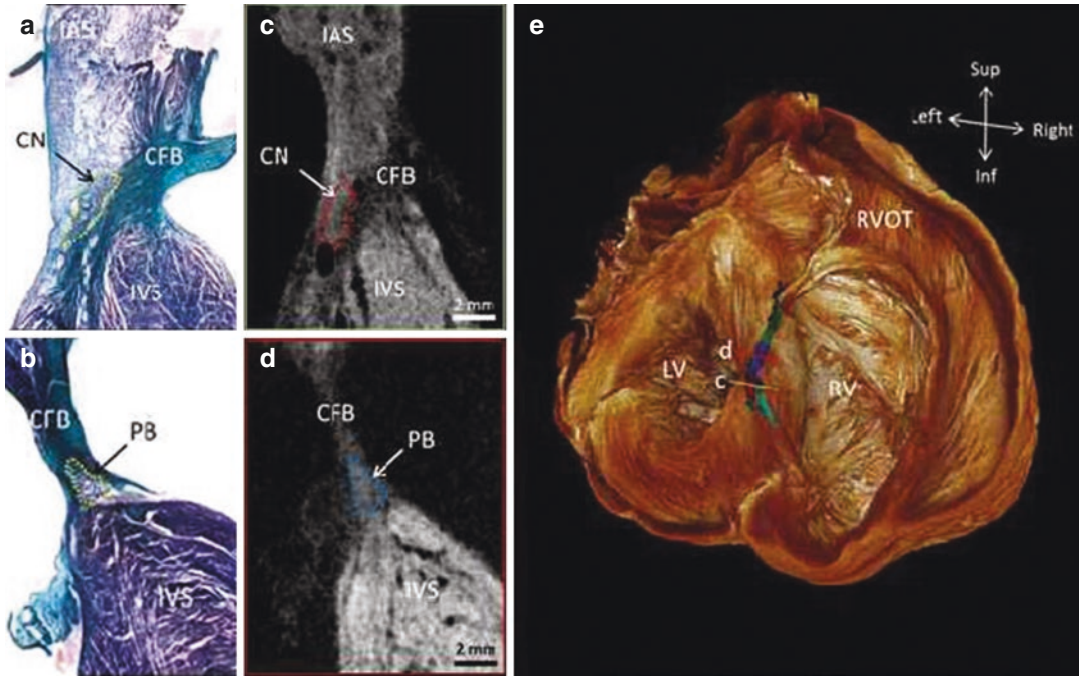

Fig. 2.29 The human atrioventricular conduction axis resolved by micro-CT. This figure demonstrates high resolution (73 × 73 × 73 μm^3) micro-CT data from a whole human heart. It shows the 3D extent and location of the segmented atrioventricular conduction axis across the upper surface of the interventricular septum (**e**). The viewpoint in e is from the atria, looking down into the ventricular chambers. Illustrative long-axis sections from the micro-CT dataset and from corresponding histological sections show the compact node in the right atrium proximally and inferiorly (**a**, **c**), becoming the penetrating bundle (**b**, **d**), and extending anteriorly and slightly rostrally to become the branching bundle (**e**). The plane of section in c and d is shown on the 3D volume rendering (**e**). The sections are available to view without the outlines in the supplementary Fig. S3. Atrioventricular conduction axis colour coding in panel **e**; *turquoise* inferior nodal extension, *red* compact node, *blue* penetrating bundle, *green* branching bundle, *purple* dead-end tract. *CFB* central fibrous body, *CN* compact node, *IAS* interatrial septum, *IVS* interventricular septum, *LV* left ventricle, *PB* penetrating bundle, *RV* right ventricle, *RVOT* right ventricular outflow tract. From [72]. It is an open access article

The venous circulation of heart is separated into three systems: (1) the cardiac venous tributaries forming the coronary sinus, (2) the anterior cardiac veins (anterior right ventricular), and (3) the smallest cardiac (Thebesian) venous system. The satellite venous system, formed by the great, middle and posterior (small) cardiac veins, converge to form the coronary sinus and drain 49% of myocardial blood [7, 64].

2.8 Myoarchitecture of Right Heart

In fact, the helical structure of human heart was described from 500 years by Francisco Torrent-Guasp who described the ventricular wall as a "single myocardial band twisted on itself to form an oblique apical and a transverse basal loop", that is nowadays defined as "double helical myocardial architecture" [77–79].

The microstructure of the atrial tissue is important in the electrical activation [80]. Based on histological studies, micro-CT studies, or diffusion tensor magnetic resonance imaging (DT-MRI), [81] developed a new atrial model that improves their previous 3D model of the human atria (Fig. 2.32) [81]. It seems that their new model RIUNET has amplified anatomical and functional heterogeneity and detailed regional description of fibre direction [81]. Based on the histological analysis, the model was manually separated into 21 regions. Though, some areas were further divided into a total of 53 sub-regions (Fig. 2.32) [81].

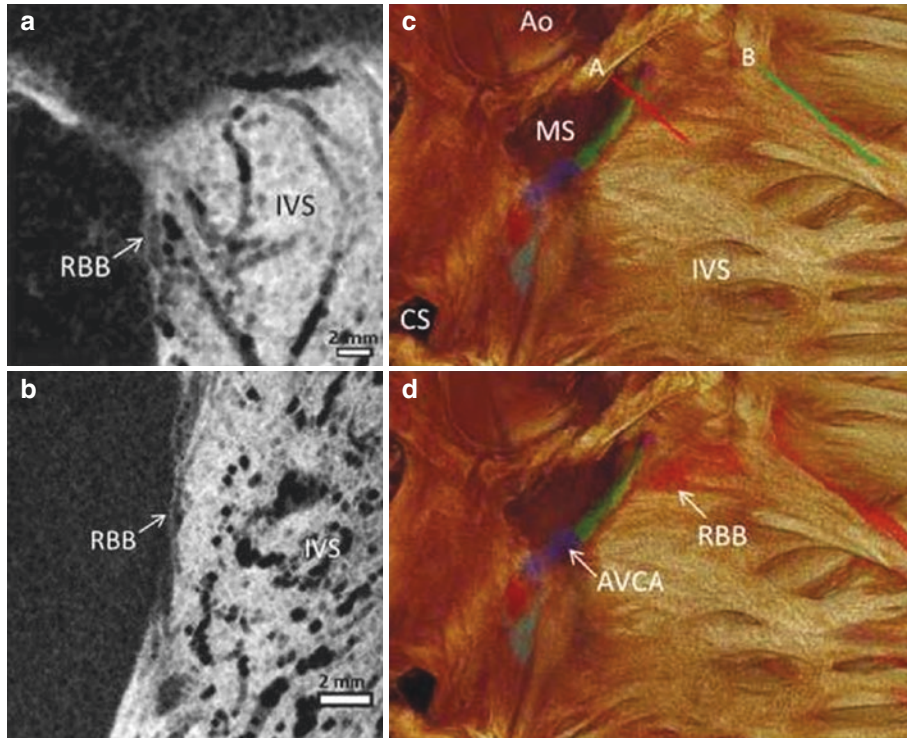

Fig. 2.30 Segmentation of the right bundle branch. The high resolution (73 × 73 × 73 μm^3) micro-CT data from the whole human heart, showing the 3D extent and position of the segmented right bundle branch (red in panel **d**) on the lateral aspect of the interventricular septum (**c**, **d**), as viewed from within the right ventricular cavity. Illustrative long-axis micro-CT sections showing the proximal (**a**) and distal (**b**) aspects of the right bundle branch. From the view in (**d**) a part of the so-called dead-end tract at the anterior/rostral extent of the atrioventricular conduction axis can be identified (purple). The position of the cross-sections (**a**, **b**) are shown in the 3D volume rendering in (**c**). *Ao* aortic root, *AVCA* atrioventricular conduction axis, *CS* coronary sinus, *IVS* interventricular septum, *MS* membranous septum, *RBB* right bundle branch. From [72]. It is an open access article

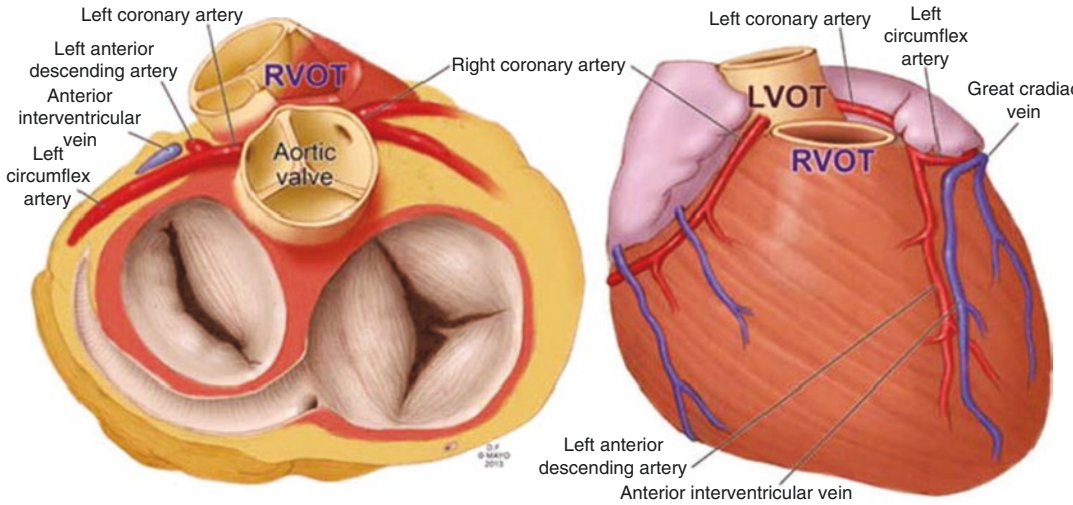

Fig. 2.31 Relationship of the coronary arteries and veins to the ventricular outflow tracts. *RVOT* right ventricular outflow tract, *SVC* superior vena cava. From [67] with permission

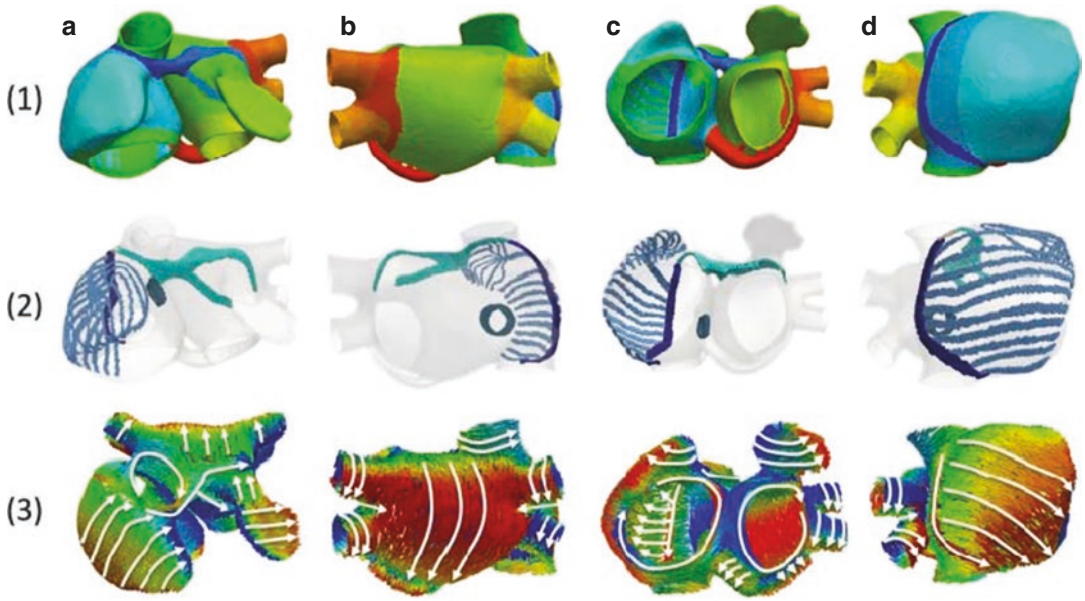

Fig. 2.32 Properties of the 3D atrial model. Row (1) show in colours the division in 21 atrial regions; Row (2) shows preferential conduction bundles; Row (3) shows principal fibre direction; Columns correspond to (**a**) Frontal view; (**b**) rear view; (**c**) inferior view; and (**d**) right lateral view. From [81]. It is an open access article

On the other hand Pashakhanloo et al [82] collected data from 8 human atrial hearts specimen ex-vivo using a 3-dimensional diffusion tensor magnetic resonance imaging sequence on a clinical scanner that makes it possible to image an entire intact human heart specimen ex vivo at submillimeter resolution (Fig. 2.33) [82]. To sum up, the high resolution and reliability of this data could increase our knowledge of structural supports to atrial rhythm and pump disorders and lead to improvements in their targeted treatment [81, 82].

Presently, it is well established that LV contains three layers (superficial/epicardial, middle, and deep/subendocardial), and RV comprises only two layers (superficial/epicardial and deep/subendocardial) [83]. To reiterate, the LV wall comprises superficially/epicardial myofibers with oblique course, middle myofibers with mainly circular course, and deep/subendocardium myofibers with longitudinal course. On the other hand, the LV wall is thicker and myocardial fibers have helical course in a continuous sequence between the subepicardium and subendocardium. Normally, the subepicardial and subendocardial myofibres give the longitudinal contraction of the LV and the middle layer of myofibres gives the circumferential contraction of the LV [83]. For the LV, the middle circumferential constrictor myofibers decrease its diameter during LV ejection. In brief, the subendocardium layer has right handed alignment and the subepicardium layer has a left-handed direction from apex to base [84, 85]. Additionally, the contraction of superficial oblique myofibers shortens LV. Finally, the rotation of LV apex comparative to the base finalizes LV ejection [86]. Because the myocardial geometry has a helical pattern, during systole epicardial myofibres will rotate the base in a clockwise direction and the apex in a counterclockwise direction, whereas the subendocardial myofibers will rotate the LV apex and base in reverse directions ([83]).

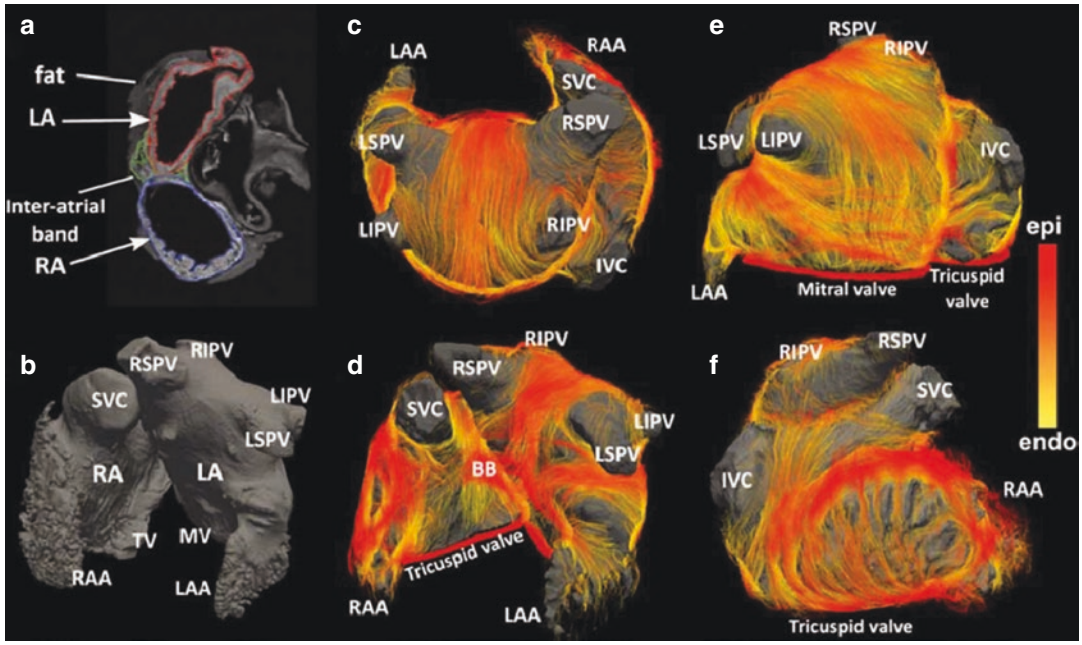

Fig. 2.33 Acquired geometry and fiber visualization results in human atria specimens. Left, Atrial geometry. (**a**) Short-axis view of a nondiffusion-weighted image (b0) with superimposed segmentation of left atrium (*LA* red), right atrium (*RA* blue), and interatrial bundles (green). Fat tissue surrounding the atria is excluded from the segmentation. (**b**) Anterior view of left and right atria created from T1-weighted images; the dark grey volume represents lumen. Right, Fiber visualization using tractography. (**c**) Posterior view of atrial roof. (**d**) Anterior view. (**e**) Inferior and left lateral views. (**f**) View of right atrium. Color encodes the local distance to the endocardial shell: yellow is the endocardial layer, and red is the epicardial layer. *BB* indicates Bachman bundle, *IVC* inferior vena cava, *LAA* left atrial appendage, *LIPV* left inferior pulmonary vein, *LSPV* left superior pulmonary vein, *MV* mitral valve, *RAA* right atrial appendage, *RIPV* right inferior pulmonary vein, *RSPV* right superior pulmonary vein, *SVC* superior vena cava, and *TV* tricuspid valve. From [82] with permission

The myocardium of RV ventricular wall has an intricate three-dimensional network of myocytes in a matrix of fibrous tissue (see Fig. 2.34) [50, 86, 87].

Firstly, the superficial/epicardial myofibers are disposed circumferentially (more than those of the LV) in the subepicardium with a parallel course to the atrioventricular groove surrounding/encircling the subpulmonary infundibulum and deeper subendocardial longitudinal myofibers. Secondly, the subendocardial myofibers contain longitudinal fibres "which pass through the vortices toward papillary muscles to the AV orifices and the arterial orifices, and to the IVS" [83]. Further, the superficial myofibers has a spiral fold inward at the RV apex to shape the deep/subendocardial myofibers that are lined up longitudinally toward the base. On the whole, the thin RV wall has mainly myofibers with circumferential and longitudinal courses. The deep longitudinally layer is disposed from apex to base, allowing only the longitudinal shortening [49]. Longitudinal fibers contract to result in inward/radial thickening. The septal motion is considered to contribute to both LV and RV function [88, 89] and is a major determinant of overall RV performance [88–90]. The IVS is created only by helical fibers that represents ≤40% of the ventricular muscle mass [91].

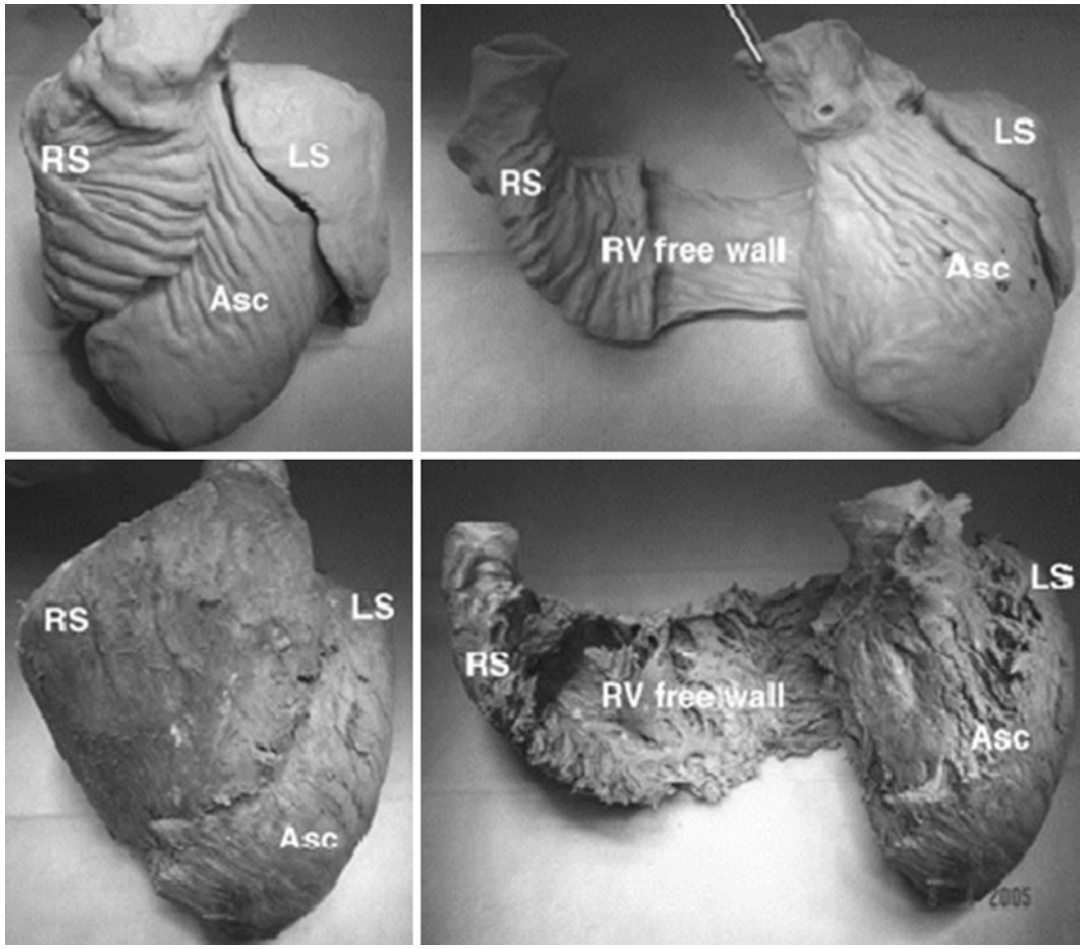

Fig. 2.34 Dissection specimens of the intact heart (left), and the unwrapped free wall that surrounds the underlying septum (right). The upper image shows the helical heart model, and mirrors the dissected ventricle are shown below. The ascending segment fibers (Asc) cover the right side of the septum. The basal loop is shown, and formed by a right segment (RS) and left segment (LS). From [50] with permission

2.9 Computational Cardiac Modelling and Anatomy

The history of modelling for knowing cardiac anatomy, physiology and mechanics has a long history back to Woods [92]. Since work of Woods [92], modelling has developed for understanding the basic anatomical and physiological problems. As in Fig. 2.35, the multiscale anatomy and physiology of the heart play an essential role to cardiac function [95, 96].

Poromechanical Modeling

Recently, the team of Chabiniok et al [95], applied poromechanical modelling to the heart, based on the facts of experimental remarks that disclosed significant additional features [95]. For instance, poromechanical modelling to the heart revealed that cardiac tissue exhibits powerful anisotropic swelling and stiffening effects under perfusion pressure [97], same to skeletal muscle [98].

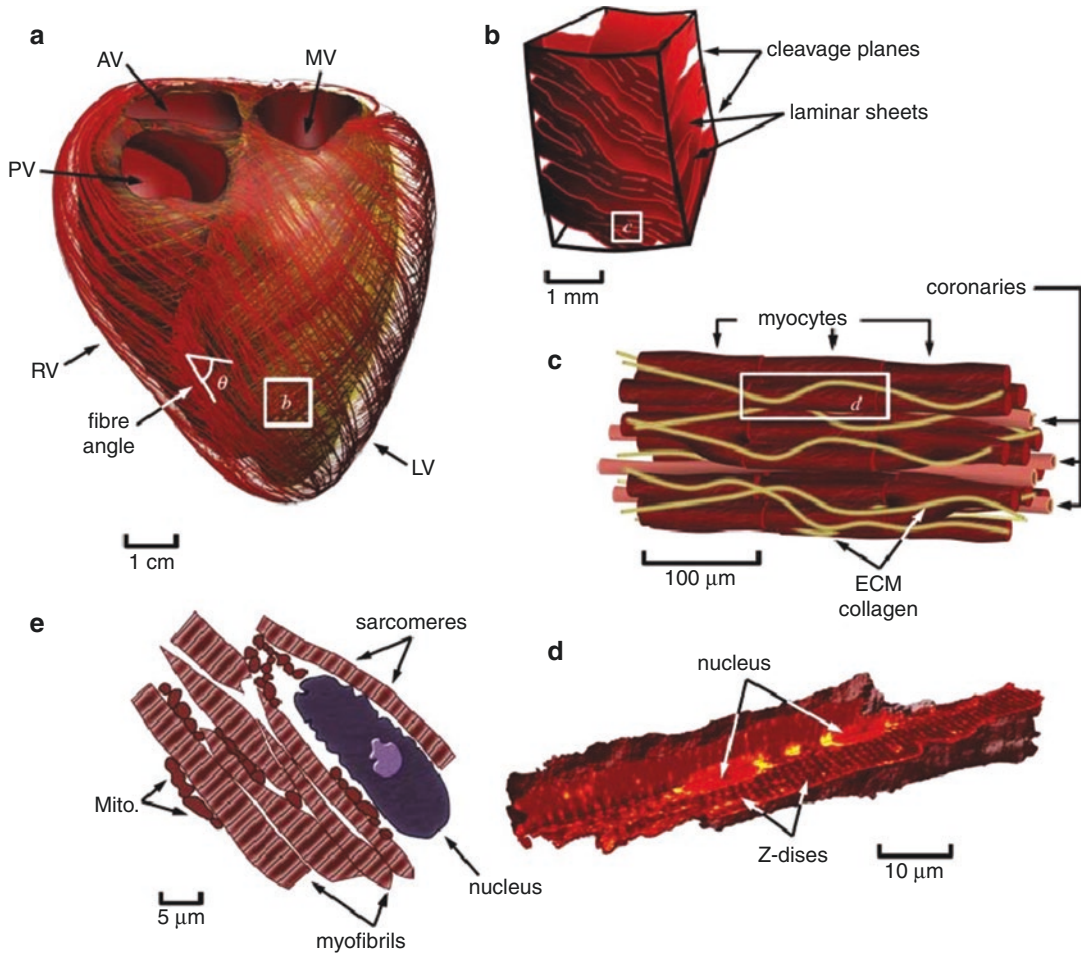

Fig. 2.35 Illustrative representation of multiscale cardiac anatomy. (**a**) Geometric representation of the biventricular anatomy of the heart with streamlines illustrating its fibre architecture, (**b**) tissue block illustrating the laminar structure of the heart comprising fibre bundles arranged into sheets separated by cleavage planes, (**c**) local structural arrangement of myocytes and coronary capillaries, (**d**) 3D view of the cardiomyocyte cut to view internal structures (data courtesy of Dr Rajagopal and Dr Soeller [93, 94]), (**e**) anatomy of the cell illustrating nucleus, myofibres (comprising crossbridges) and mitochondria. *RV* right ventricle, *LV* left ventricle, *PV* pulmonary valve, *AV* aortic valve, *MV* mitral valve, *ECM* extracellular matrix, *Mito.* mitochondria. From [95]. It is an open access article

Also, a dynamic heart shows important coupling effects like the established obstruction flow phenomenon taking place during cardiac systole [99]. On the other hand, heart perfusion is also highly categorized with a blood flow in areas of tissue supplied by particular bigger arteries [100]. To study this aspect, [95], coupled the flow from larger arteries to a distal poromechanical tissue model producing a multiscale depiction that

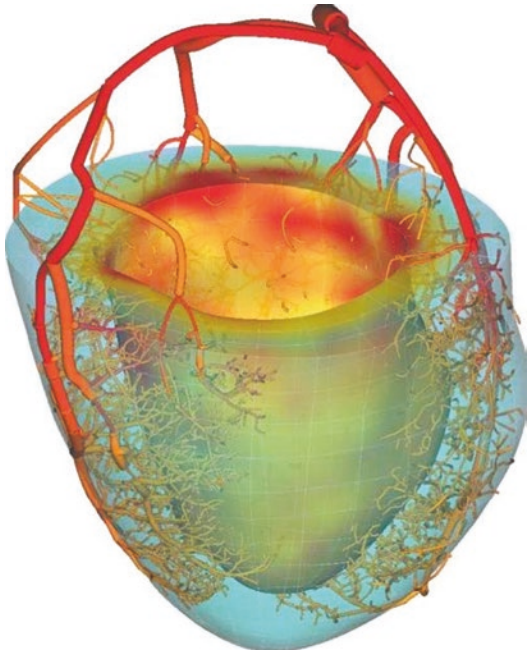

Fig. 2.36 Coupled 1D flow-poroelastic perfusion model shown at early systole. Flow velocities are shown in the vessel segment. The pore pressure in the myocardium shows increased systolic compressive forces preferentially towards the subendocardium [101]. Modified from [95]. It is an open access article

explains the spreading of inflow sites (see Fig. 2.36) [95, 101].

Conclusions

Without a doubt, the RV and the LV are different in their anatomy and physiology. Moreover, morphologically and functionally, both ventricles are comprehensible linked not only in health but also as they react to disease [8].

The better knowledge of the anatomy and physiology of the septum and RV free wall will provide techniques for treating RV dysplasia, RV failure due to pulmonary regurgitation, RV dysfunction after cardiac transplantation, and some right-sided congenital defects that involve LV function. Also, it is compulsory to improve and develop methods that prevent septal injury during cardiac surgery [102].

Understanding the image features of the human heart acquired by histological studies, echocardiography, CT, micro-CT studies, or diffusion tensor magnetic resonance imaging (DT-MRI) has a very important role in the correctness of anatomically outlining of the cardiac features, especially those associated to the conduction system. Studying classic anatomy of the heart on cadaveric samplings is a requirement to know what imaging investigations brings for the study of RV anatomy and physiology [12].

References

1. Haddad F, Hunt SA, Rosenthal DN, Murphy DJ. Right ventricular function in cardiovascular disease, part I: anatomy, physiology, aging, and functional assessment of the right ventricle. Circulation. 2008;117(11):1436–48. https://doi.org/10.1161/CIRCULATIONAHA.107.653576.
2. Harvey W. Exercitatio Anatomica de Motu Cordis et Sanguinis in Animalibus. 1628. Goldstein J. The right ventricle: what's right and what's wrong. Coron Artery Dis. 2005;16:1–3.
3. Goldstein J. The right ventricle: what's right and what's wrong. Coron Artery Dis. 2005;16:1–3.
4. Ghio S, Klersy C, Magrini G, et al. Prognostic relevance of the echocardiographic assessment of right ventricular function in patients with idiopathic pulmonary arterial hypertension. Int J Cardiol. 2010;140:272.
5. Ifrim M, et al. Riscul malformativ in reproducerea umana. (malformation risk in human reproduction). Bucharest: Editura Medicala; 1979.
6. Malouf JF, Edwards WD, Tajik AJ, Seward JB. Functional anatomy of the heart. In: Fuster V, Alexander RW, O'Rourke RA, Roberts R, King SB, Wellens HJJ, eds. Hurt's the Heart. 11th ed. New York, NY: McGraw-Hill, 2005;45–82.
7. Snell RS. The thorax: part II-the thoracic cavity. In: Clinical anatomy by regions. Philadelphia: Lippincott Williams & Wilkins; 2008. p. 77–130.
8. Friedberg MK, Redington AN. Right versus left ventricular failure: differences, similarities, and interactions. Circulation. 2014;129:1033–44.
9. Zaffran S, Kelly RG, Meilhac SM, Buckingham ME, Brown NA. Right ventricular myocardium derives from the anterior heart field. Circ Res. 2004;95:261–8.
10. Firpo C, Hoffman JI, Silverman NH. Evaluation of fetal heart dimensions from 12 weeks to term. Am J Cardiol. 2001;87(5):594–600.
11. Borgdorff MA, Dickinson MG, Berger RM, Bartelds B. Right ventricular failure due to chronic pressure load: what have we learned in animal models since the NIH working group statement? Heart Fail Rev. 2015;20(4):475–91. https://doi.org/10.1007/s10741-015-9479-6.

12. Sánchez-Quintana D, Doblado-Calatrava M, Cabrera JA, Macías Y, Saremi F. Anatomical basis for the cardiac interventional electrophysiologist. Biomed Res Int. 2015;2015:547364. https://doi.org/10.1155/2015/547364.
13. Pelosi A, Rubinstein J. In: Millis R, editor. Cardiac anatomy, advances in electrocardiograms - methods and analysis, PhD: InTech; 2012. doi:10.5772/21737. https://www.intechopen.com/books/advances-in-electrocardiograms-methods-and-analysis/cardiac-anatomy. (Open access article).
14. Ifrim M, et al. Human Atlas of topographical, functional and clinical anatomy viscera. Citrus Heights: ARA Publisher: American Romanian Academy of Arts and Sciences; 2016. ISBN: 978-1-935924-20-3.
15. Cabrera JA, Saremi F, Sánchez-Quintana D. Left atrial appendage: anatomy and imaging landmarks pertinent to percutaneous transcatheter occlusion. Heart. 2014;100(20):1636–50. https://doi.org/10.1136/heartjnl-2013-304464.
16. Malik SB, Kwan D, Shah AB, Hsu JY. The right atrium: gateway to the heart--anatomic and pathologic imaging findings. Radiographics. 2015;35(1):14–31. https://doi.org/10.1148/rg.351130010.
17. Netter FH. In: Netter FH, Dalley AF, editors. Atlas of human anatomy. 5th ed. East Hanover: Navartis; 2010.
18. Matsuyama TA, Inoue S, Kobayashi Y, et al. Anatomical diversity and age-related histological changes in the human right atrial posterolateral wall. Europace. 2004;6(4):307–15. https://doi.org/10.1016/j.eupc.2004.03.011.
19. Akcay M, Bilen ES, Bilge M, Durmaz T, Kurt M. Prominent crista terminalis: as an anatomic structure leading to atrial arrhythmias and mimicking right atrial mass. J Am Soc Echocardiogr. 2007;20(2):e9–e10. https://doi.org/10.1016/j.echo.2006.08.037.
20. Ifrim M, Capusan I. Morfologie normala si patologica a tesutului conjunctiv (normal and pathological morphology of the connective tissue). Bucharest: Editura Medicala; 1983.
21. Sehar N, Mears J, Bisco S, Patel S, Lachman N, Asirvatham SJ. Anatomic guidance for ablation: atrial flutter, fibrillation, and outflow tract ventricular tachycardia. Indian Pacing Electrophysiol J. 2010;10(8):339–56.
22. Asirvatham SJ, et al. Prevalence of a right atrial pouch and extension of pectinate muscles across the tricuspid valve-IVC isthmus. Circulation. 2001;104:409.
23. Sánchez-Quintana D, Anderson RH, Cabrera JA, et al. The terminal crest: morphological features relevant to electrophysiology. Heart. 2002;88(4):406–11. https://doi.org/10.1136/heart.88.4.406.
24. Cabrera JA, et al. Angiographic anatomy of the inferior right atrial isthmus in patients with and without history of common atrial flutter. Circulation. 1999;99:3017.
25. Cabrera JA, Sánchez-Quintana D, Ho SY, Medina A, Anderson RH. The architecture of the atrial musculature between the orifice of the inferior caval vein and the tricuspid valve: the anatomy of the isthmus. J Cardiovasc Electrophysiol. 1998;9(11):1186–95. https://doi.org/10.1111/j.1540-8167.1998.tb00091.x.
26. Cosio FG, et al. Radiofrequency ablation of the inferior vena cava-tricuspid valve isthmus in common atrial flutter. Am J Cardiol. 1993;71:705.
27. Da Costa A, et al. Effect of isthmus anatomy and ablation catheter on radiofrequency catheter ablation of the cavotricuspid isthmus. Circulation. 2004;110:1030.
28. Cabrera JA, Sánchez-Quintana D, Farré J, Rubio JM, Siew YH. The inferior right atrial isthmus: further architectural insights for current and coming ablation technologies. J Cardiovasc Electrophysiol. 2005;16(4):402–8. https://doi.org/10.1046/j.1540-8167.2005.40709.x.
29. Saremi F, Channual S, Raney A, et al. Imaging of patent foramen ovale with 64-section multidetector CT. Radiology. 2008;249(2):483–92. https://doi.org/10.1148/radiol.2492080175.
30. Hightower JS, Taylor AG, Ursell PC, LaBerge JM. The Chiari network: a rare cause of intracardiac guide wire entrapment. J Vasc Interv Radiol. 2015;26(4):604–6. https://doi.org/10.1016/j.jvir.2014.12.004.
31. Chang SL, Tai CT, Lin YJ, et al. The electroanatomic characteristics of the cavotricuspid isthmus: implications for the catheter ablation of atrial flutter. J Cardiovasc Electrophysiol. 2007;18(1):18–22. https://doi.org/10.1111/j.1540-8167.2006.00647.x.
32. Heidbüchel H, Willems R, Van Rensburg H, Adams J, Ector H, Van de Werf F. Right atrial angiographic evaluation of the posterior isthmus: relevance for ablation of typical atrial flutter. Circulation. 2000;101(18):2178–84. https://doi.org/10.1161/01.cir.101.18.2178.
33. El Yaman MM, et al. Methods to access the surgically excluded cavotricuspid isthmus for complete ablation of typical atrial flutter in patients with congenital heart defects. Heart Rhythm. 2009;6:949. https://doi.org/10.1016/j.hrthm.2009.03.017.
34. McKay T. Prominent crista terminalis and Eustachian ridge in the right atrium: two dimensional (2D) and three dimensional (3D) imaging. Eur J Echocardiogr. 2007;8:288. https://doi.org/10.1016/j.euje.2006.03.006.
35. Nakagawa H, et al. Role of the tricuspid annulus and the eustachian valve/ridge on atrial flutter. Relevance to catheter ablation of the septal isthmus and a new technique for rapid identification of ablation success. Circulation. 1996;94:407.
36. Da Costa A, et al. Cavotricuspid isthmus angiography predicts atrial flutter ablation efficacy in 281 patients randomized between 8 mm- and externally irrigated-tip catheter. Eur Heart J. 2006;27(15):1833–40. https://doi.org/10.1093/eurheartj/ehl121.
37. Morton JB, et al. Phased-array intracardiac echocardiography for defining cavotricuspid isthmus anatomy during radiofrequency ablation of typical atrial flutter. J Cardiovasc Electrophysiol. 2003;14(6):591–7.
38. Okishige K, et al. Clinical study regarding the anatomical structures of the right atrial isthmus using intra-cardiac echocardiography:

implication for catheter ablation of common atrial flutter. J Interv Card Electrophysiol. 2005;12(1):9–12. https://doi.org/10.1007/s10840-005-5835-0.
39. Anderson RH, Boyett MR, Dobrzynski H, Moorman AFM. The anatomy of the conduction system: implications for the clinical cardiologist. J Cardiovasc Transl Res. 2013;6:187–96.
40. Anderson RH, Spicer DE, Hlavacek AJ, Hill A, Loukas M. Describing the cardiac components-attitudinally appropriate nomenclature. J Cardiovasc Transl Res. 2013;6(2):118–23. https://doi.org/10.1007/s12265-012-9434-z.
41. Romfh A, Pluchinotta FR, Porayette P, Valente AM, Sanders SP. Congenital heart defects in adults: a field guide for cardiologists. J Clin Exp Cardiol. 2012;2015(Suppl 8):7.
42. Faletra FF, Nucifora G, Ho SY. Imaging the atrial septum using real-time three-dimensional transesophageal echocardiography: technical tips, normal anatomy, and its role in transseptal puncture. J Am Soc Echocardiogr. 2011;24(6):593–9. https://doi.org/10.1016/j.echo.2011.01.022.
43. Mori S, Fukuzawa K, Takaya T, et al. Clinical cardiac structural anatomy reconstructed within the cardiac contour using multidetector-row computed tomography: atrial septum and ventricular septum. Clin Anat. 2015;29(3):342–52. https://doi.org/10.1002/ca.22546.
44. Anderson RH, Spicer DE, Brown NA, Mohun TJ. The development of septation in the four-chambered heart. Anat Rec. 2014;297(8):1414–29. https://doi.org/10.1002/ar.22949.
45. Lai W, Mertens L, Cohen M, Geva T. Echocardiography in pediatric and congenital heart disease: from fetus to adult. Hoboken: Wiley-Blackwell; 2009.
46. Hasan A, Parvez A, Ajmal MR. Patent foramen ovale: clinical significance. J Indian Acad Clin Med. 2004;5(4):339–44.
47. Tzeis S, Andrikopoulos G, Deisenhofer I, Ho SY, Theodorakis G. Transseptal catheterization: considerations and caveats. Pacing Clin Electrophysiol. 2010;33(2):231–42. https://doi.org/10.1111/j.1540-8159.2009.02598.x.
48. Choudhary G, Malik AA, Stapleton D, Reddy PC. In: Lakshmanadoss U, editor. Assessment of right ventricle by echocardiogram, echocardiography in heart failure and cardiac electrophysiology: InTech; 2016. doi: https://doi.org/10.5772/64781. https://www.intechopen.com/books/echocardiography-in-heart-failure-and-cardiac-electrophysiology/assessment-of-right-ventricle-by-echocardiogram. (Open access article).
49. Ho SY, Nihoyannopoulos P. Anatomy, echocardiography, and normal right ventricular dimensions. Heart. 2006;92(Suppl 1):i2–13. https://doi.org/10.1136/hrt.2005.077875.
50. Saleh S, Liakopoulos OJ, Buckberg GD. The septal motor of biventricular function. Eur J Cardiothorac Surg. 2006;29(Suppl 1):S126–38. https://doi.org/10.1016/j.ejcts.2006.02.048.
51. Sheehan FH, Ge S, Vick GW, Urnes K, Kerwin WS, Bolson EL, Chung T, Kovalchin JP, Sahn DJ, Jerosch-Herold M, Stolpen AH. Three-dimensional shape analysis of right ventricular remodeling in repaired tetralogy of Fallot. Am J Cardiol. 2008;101(1):107–13. https://doi.org/10.1016/j.amjcard.2007.07.080.
52. Sánchez-Quintana D, López-Mínguez JR, Macías Y, Cabrera JA, Saremi F. Left atrial anatomy relevant to catheter ablation. Cardiol Res Pract. 2014;2014:289720. https://doi.org/10.1155/2014/289720.
53. Ram F, Dhar M. A modified procedure for calculating person years of life lost. Janasamkhya. 1992;10(1-2):1–12.
54. Rogers JH, Bolling SF. The tricuspid valve: current perspective and evolving management of tricuspid regurgitation. Circulation. 2009;119(20):2718–25.
55. Ostenfeld E, Flachskampf FA. Assessment of right ventricular volumes and ejection fraction by echocardiography: from geometric approximations to realistic shapes. Echo Res Pract. 2015;2(1):R1–R11.
56. Partridge JB, Anderson RH. Left ventricular anatomy: its nomenclature, segmentation, and planes of imaging. Clin Anat. 2009;22(1):77–84. https://doi.org/10.1002/ca.20646.
57. Saremi F, Ho SY, Sánchez-Quintana D. Morphological assessment of RVOT: CT and CMR imaging. J Am Coll Cardiol Img. 2013;6(5):631–5. https://doi.org/10.1016/j.jcmg.2012.06.018.
58. Anderson RH, Razavi R, Taylor AM. Cardiac anatomy revisited. J Anat. 2004;205(3):159–77. https://doi.org/10.1111/j.0021-8782.2004.00330.x.
59. Spicer DE, Anderson RH. Methodological review of ventricular anatomy - the basis for understanding congenital cardiac malformations. J Cardiovasc Transl Res. 2013;6(2):145–54. https://doi.org/10.1007/s12265-012-9432-1.
60. Scanavacca M, Lara S, Hardy C, Pisani CF. How to identify & treat epicardial origin of outflow tract tachycardias. J Atr Fibrillation. 2015;7(6):1195. https://doi.org/10.4022/jafib.1195.
61. Bashore TM. Adult congenital heart disease: right ventricular outflow tract lesions. Circulation. 2007;115(14):1933–47.
62. Foale R, Nihoyannopoulos P, McKenna W, et al. Echocardiographic measurement of the normal adult right ventricle. Br Heart J. 1986;5:633–44.
63. Grant RP, Downey FM, MacMahon H. The architecture of the right ventricular outflow tract in the normal human heart and in the presence of ventricular septal defects. Circulation. 1961;24:223–35.
64. Iaizzo PA, editor. Handbook of cardiac anatomy, physiology, and device. 2nd ed. New York: Springer; 2009. ISBN: 9781603273718.
65. James TN. The internodal pathways of the human heart. Prog Cardiovasc Dis. 2001;43(6):495–535.

66. Anderson RH, Ho SY. The architecture of the sinus node, the atrioventricular conduction axis, and the internodal atrial myocardium. J Cardiovasc Electrophysiol. 1998;9(11):1233–48.
67. Hai JJ, Lachman N, Syed FF, Desimone CV, Asirvatham SJ. The anatomic basis for ventricular arrhythmia in the normal heart: what the student of anatomy needs to know. Clin Anat. 2014;27(6):885–93. https://doi.org/10.1002/ca.22362.
68. Anderson RH, Becker AE, Brechenmacher C, Davies MJ, Rossi L. The human atrioventricular junctional area. A morphological study of the A-V node and bundle. Eur J Cardiol. 1975;3:11–25.
69. Anderson RH, Ho SY. The morphology of the specialized atrioventricular junctional area: the evolution of understanding. PACE. 2002;25:957–66.
70. Anderson RH, Yanni J, Boyett MR, Chandler NJ, Dobrzynski H. The anatomy of the Cardiac Conduction System. Clin Anat. 2009;22:99–113.
71. Loukas M, Klaassen Z, Tubbs RS, et al. Anatomical observations of the moderator band. Clin Anat. 2010;23(4):443–50. https://doi.org/10.1002/ca.20968.
72. Stephenson RS, Atkinson A, Kottas P, Perde F, Jafarzadeh F, Bateman M, Iaizzo PA, Zhao J, Zhang H, Anderson RH, Jarvis JC, Dobrzynski H. High resolution 3-dimensional imaging of the human cardiac conduction system from microanatomy to mathematical modeling. Sci Rep. 2017;7(1):7188. https://doi.org/10.1038/s41598-017-07694-8.
73. Tawara S. The conduction system of the mammalian heart: an anatomico-histological study of the atrioventricular bundle and the purkinje fibers. London: Imperial College Press; 2000.
74. Davies F, Francis ETB. The conducting system of the vertebrate heart. Biol Rev. 1946;21:173–88. https://doi.org/10.1111/j.1469-185X.1946.tb00323.x.
75. Truex RC, Smythe MQ. Reconstruction of the human atrioventricular node. Anat Rec. 1967;158:11–9. https://doi.org/10.1002/ar.1091580103.
76. Oosthoek PW, Virágh S, Lamers WH, Moorman AF. Immunohistochemical delineation of the conduction system. II: the atrioventricular node and Purkinje fibers. Circ Res. 1993;73:482–91. https://doi.org/10.1161/01.RES.73.3.482.
77. Bovendeerd PH, Huyghe JM, Arts T, van Campen DH, Reneman RS. Influence of endocardial-epicardial crossover of muscle fibers on left ventricular wall mechanics. J Biomech. 1994;27(7):941–51.
78. Buckberg GD, Coghlan HC, Torrent-Guasp F. The structure and function of the helical heart and its buttress wrapping. V. Anatomic and physiologic considerations in the healthy and failing heart. Semin Thorac Cardiovasc Surg. 2001;13(4):358–85.
79. Mirsky I, Parmley WW. Assessment of passive elastic stiffness for isolated heart muscle and the intact heart. Circ Res. 1973;33(2):233–43.
80. Ho SY, Sánchez-Quintana D. The importance of atrial structure and fibers. Clin Anat. 2009;22:52–63. https://doi.org/10.1002/ca.20634.
81. Ferrer A, Sebastián R, Sánchez-Quintana D, Rodríguez JF, Godoy EJ, Martínez L, Saiz J. Detailed anatomical and electrophysiological models of human atria and torso for the simulation of atrial activation. PLoS One. 2015;10(11):e0141573. https://doi.org/10.1371/journal.pone.0141573.
82. Pashakhanloo F, Herzka DA, Ashikaga H, Mori S, Gai N, Bluemke DA, Trayanova NA, McVeigh ER. Myofiber architecture of the human atria as revealed by submillimeter diffusion tensor imaging. Circ Arrhythm Electrophysiol. 2016;9(4):e004133. https://doi.org/10.1161/CIRCEP.116.004133.
83. Anderson B. Chapter 2: ventricular systolic function. In: Anderson B, editor. A sonographer's guide to the assessment of heart disease. Sydney: MGA Graphics; 2014. p. 24. www.echotext.info. ISBN:9780992322205.
84. Greenbaum RA, Ho SY, Gibson DG, Becker AE, Anderson RH. Left ventricular fibre architecture in man. Br Heart J. 1981;45(3):248–63.
85. Torrent-Guasp F, Kocica MJ, Corno AF, Komeda M, Carreras-Costa F, Flotats A, Cosin-Aguillar J, Wen H. Towards new understanding of the heart structure and function. Eur J Cardiothorac Surg. 2005;27(2):191–201. https://doi.org/10.1016/j.ejcts.2004.11.026.
86. Sheehan F, Redington A. The right ventricle: anatomy, physiology and clinical imaging. Heart. 2008;94(11):1510–5. https://doi.org/10.1136/hrt.2007.132779.
87. Bleeker GB, Steendijk P, Holman ER, CM Y, Breithardt OA, Kaandorp TA, Schalij MJ, van der Wall EE, Nihoyannopoulos P, Bax JJ. Assessing right ventricular function: the role of echocardiography and complementary technologies. Heart. 2006;92(Suppl 1):i19–26. https://doi.org/10.1136/hrt.2005.082503.
88. Kaul S. The interventricular septum in health and disease. Am Heart J. 1986;112:568–81.
89. Lindqvist P, Morner S, Karp K, Waldenstrom A. New aspects of septal function by using 1-dimensional strain and strain rate imaging. J Am Soc Echocardiogr. 2006;19:1345–9.
90. Klima U, Guerrero JL, Vlahakes GJ. Contribution of the interventricular septum to maximal right ventricular function. Eur J Cardiothorac Surg. 1998;14:250–5.
91. Buckberg G, Athanasuleas C, Saleh S. Septal myocardial protection during cardiac surgery for prevention of right ventricular dysfunction. Anatol J Cardiol. 2008;8(suppl 2):108–16.
92. Woods RH. A few applications of a physical theorem to membranes in the human body in a state of tension. Trans R Acad Med Ireland. 1892;10:417–27. https://doi.org/10.1007/BF03171228.
93. Hou Y, Crossman DJ, Rajagopal V, Baddeley D, Jayasinghe I, Soeller C. Super-resolution fluo-

rescence imaging to study cardiac biophysics: α-actinin distribution and z-disk topologies in optically thick cardiac tissue slices. Prog Biophys Mol Biol. 2014;115:328–39. https://doi.org/10.1016/j.pbiomolbio.2014.07.003.
94. Rajagopal V, et al. Examination of the effects of heterogeneous organization of RyR clusters, myofibrils and mitochondria on Ca2+ release patterns in cardiomyocytes. PLoS Comput Biol. 2015;11:e1004417. https://doi.org/10.1371/journal.pcbi.1004417.
95. Chabiniok R, Wang VY, Hadjicharalambous M, Asner L, Lee J, Sermesant M, Kuhl E, Young AA, Moireau P, Nash MP, Chapelle D, Nordsletten DA. Multiphysics and multiscale modelling, data–model fusion and integration of organ physiology in the clinic: ventricular cardiac mechanics. Interface Focus. 2016;6(2):20150083. https://doi.org/10.1098/rsfs.2015.0083.
96. Opie LH. Heart physiology: from cell to circulation. Philadelphia: Lippincott Williams and Wilkins; 2004.
97. May-Newman K, Omens JH, Pavelec RS, McCulloch AD. Three-dimensional transmural mechanical interaction between the coronary vasculature and passive myocardium in the dog. Circ Res. 1994;74:1166–78. https://doi.org/10.1161/01.RES.74.6.1166.
98. Reeve AM, Nash MP, Taberner AJ, Nielsen PM. Constitutive relations for pressure-driven stiffening in poroelastic tissues. J Biomech Eng. 2014;136:081011. https://doi.org/10.1115/1.4027666.
99. Chapelle D, Gerbeau J-F, Sainte-Marie J, Vignon-Clementel I. A poroelastic model valid in large strains with applications to perfusion in cardiac modeling. Comput Mech. 2010;46:91–101. https://doi.org/10.1007/s00466-009-0452-x.
100. Michler C, et al. A computationally efficient framework for the simulation of cardiac perfusion using a multi-compartment Darcy porous-media flow model. Int J Numer Methods Biomed Eng. 2013;29:217–32. https://doi.org/10.1002/cnm.2520.
101. Lee J, Cookson A, Chabiniok R, Rivolo S, Hyde E, Sinclair M, Michler C, Sochi T, Smith N. Multiscale modelling of cardiac perfusion. In: Quarteroni A, editor. Modeling the heart and the circulatory system. Basel: Springer; 2015. p. 51–96.
102. Buckberg G, Hoffman JI. Right ventricular architecture responsible for mechanical performance: unifying role of ventricular septum. J Thorac Cardiovasc Surg. 2014;148(6):3166–71.e1. https://doi.org/10.1016/j.jtcvs.2014.05.044.
103. Loukas M, Aly I, Tubbs RS, Anderson RH. The naming game: a discrepancy among the medical community. Clin Anat. 2016;29:285–9. https://doi.org/10.1002/ca.22666.
104. Saremi F, Pourzand L, Krishnan S, et al. Right atrial cavotricuspid isthmus: anatomic characterization with multi-detector row CT. Radiology. 2008;247(3):658–68. https://doi.org/10.1148/radiol.2473070819.

3 Molecular and Cellular Biology of the Right Heart

Bogdan Amuzescu and Horia Maniu

Abstract

The present chapter attempts a detailed yet comprehensive account of the exceedingly complex molecular events involved in heart development, including description of the main differentiation signaling pathways, transcription factors, enhancers and gene regulatory networks, with a special emphasis on applying this continuously enlarging body of modern scientific knowledge to the field of stem cell differentiation into cardiomyocytes for diagnostic and therapeutic applications. MicroRNAs are also emerging as an important area of discovery aiming to revolutionize current therapies in cardiology, therefore we describe their involvement in cardiogenesis, proliferation/apoptosis, angiogenesis, fibrosis and hypertrophy. After reviewing the architectural organization, ultrastructure details and functional compartments of cardiomyocytes derived from *in vitro* and *in vivo* studies, we focus on molecular mechanisms involved in cardiac hypertrophy and fibrosis, particularly on calcium signaling events triggering these excessive adaptive responses. Further, we stress the embryogenetic and molecular differences between the right and left ventricle, as well as their pathophysiology specificities and clinical consequences.

Keywords

Heart organizers · Differentiation signaling pathways · Morphogens · Transcription factors · Promoters · Enhancers · Gene regulatory networks · Micro RNAs · Embryonic stem cells · Induced pluripotent stem cells · Cardiomyocyte ultrastructure · Sarcomere · Myofibrils · T tubules · Diads · Sarcoplasmic reticulum · Mitochondria · Extracellular matrix · Proliferation · Apoptosis · Fibrosis · Cardiac hypertrophy · Heart failure

3.1 Introduction

The right myocardium is a territory with distinct embryogenetic origins, appeared relatively recently in phylogenesis, in association with conquest of land by animal species and adaptation from aquatic to atmospheric breathing. Therefore it is subjected to several peculiarities concerning molecular mechanisms involved in its morphogenesis and differentiation, as well

B. Amuzescu (✉)
Department of Biophysics and Physiology, Department of Biology, University of Bucharest, Bucharest, Romania
e-mail: bogdan@biologie.kappa.ro

H. Maniu
Department of Cellular Therapies and Regenerative Medicine, "N. Simionescu" Institute of Cell Biology and Pathology, Bucharest, Romania
e-mail: horia.maniu@icbp.ro

S. I. Dumitrescu et al. (eds.), *Right Heart Pathology*, https://doi.org/10.1007/978-3-319-73764-5_3

as its structural organization and functional features. These differences are particularly significant in pathological states, such as response to pressure or volume overload: the right ventricle is more susceptible to oxidative stress, featuring less developed mechanisms for reactive oxygen species scavenging, has a less robust neoangiogenetic response to hemodynamic stress, and is more prone to cardiomyocyte apoptosis compared to the left ventricle. The coronary blood flow of the right ventricle occurs predominantly during systole, due to a milder pressure regime and lower intraparietal tension, compared to the left ventricle, where it occurs predominantly during diastole. This reduced pressure regime and lower vascular resistance in the pulmonary circulation also explains why the right ventricle average workload is fivefold lower compared to the left ventricle workload, resulting in lower oxygen consumption and metabolic stress. Such peculiarities are extremely important for their clinical and therapeutic consequences, given the specific pathologies leading to right ventricular hypetrophy and right ventricular failure: congenital heart defects with left—right hemodynamic shunt, pulmonary artery stenosis, right heart valvulopathies, other causes of primary pulmonary hypertension, right ventricular myocardial infarction, or rare genetic disorders such as arrhythmogenic right ventricular dysplasia (ARVD).

3.2 Developmental Insights

Cardiomyocyte differentiation is a complex stepwise process controlled via alternating activation and interplay of multiple signaling pathways and gene regulatory networks. We start with a brief presentation of the most important ones.

Wnt1 and β-catenin are the orthologs of *Drosophila melanogaster* genes Wingless and armadillo, required for cardiac specification briefly after gastrulation, via a mechanism independent from Wingless-induced neural segmentation. Wnt ligands are involved in a large variety of embryogenetic processes including anterior-posterior axis formation, primitive streak formation, mesoderm and ectoderm patterning, Hensen node formation (driven mainly by Wnt3 gradients), epithelial-to-mesenchymal transition, and multiple lineage specification. A canonical or β-catenin-related Wnt pathway is activated by ligands Wnt1,2,3A,8A,8B,8C,10A,10B, and can be mimicked by small molecule inhibitors of glycogen synthase kinase 3β (GSK3β) like BIO, LiCl, or the widely used synthetic inhibitor CHIR99021. Another natural inhibitor of the canonical Wnt pathway widely used earlier in cardiomyocyte differentiation protocols is soluble Dickkopf1 (Dkk1), shown to act by isolating LRP6 (low density lipoprotein receptor-related protein 6), a key component of the LRP5/LRP6/Frizzled co-receptor involved in activation of the canonical pathway, in parallel with reduction of β-catenin and an increase in Oct4 expression. The non-canonical Wnt pathways are planar cell polarity and Wnt/Ca^{2+}, activated by non-canonical ligands Wnt4,5A,5B,6,7A,7B,11. Wnt/β-catenin is indispensible for posterior streak mesoderm induction and initial commitment of pluripotent stem cells (PSCs) to cardiomyocytes, but generally it is involved in both mesoderm and endoderm formation. Wnt3A is activated via the PI3K/Akt pathway and promotes cardiopoiesis, while PI3K inhibition triggers GSK3β-induced β-catenin degradation. Another target of Wnt/β--catenin signaling is brachyury (T), an important transcription factor (TF) for mesoderm development and patterning. The T gene promoter features Wnt responsive elements, and is expressed in the mesoderm, primitive (Hensen) node, notochord and notochordal plate during gastrulation. T upregulates in turn Wnt3A, FGF8 (fibroblast growth factor) and AXIN2 in embryonic stem cells (ESC). After mesoderm induction, further cardiomyocytes differentiation requires suppression of canonical Wnt pathway.

Bone morphogenetic (BMP) pathway involves a superfamily of short range morphogens (BMP2,4,5-8) acting as TGF-β (transforming growth factor) ligands, that disrupt ESC self-renewal and induce differentiation. They result in activation of Smad-1, -5, and -8, and all these form complexes with Smad-4 required for transcriptional activation upon nuclear translocation. Competition for Smad-4 generates cross-talk with other signaling pathways, like Nodal/activin. Inhibition of BMP signaling

by Noggin induces neuroectoderm formation. Treatment with BMP-2 and FGF-4 results in cardiogenic induction in non-precardiac mesoderm cells and promotes cell survival and proliferation. Combinatorial co-culture experiments showed that only stage 6 anterior lateral plate endoderm (LPE) induces cardiac differentiation of the anterior lateral plate mesoderm (LPM), uner the action of BMPs, activin A, FGFs and vitamin A, while stage 4–5 anterior LPE and central endoderm induce non-cardiogenic posterior primitive streak cells to cardiomyocytes. The LPM consists of primary and secondary heart field progenitors, with defined spatial boundaries. The primary heart field forms the primary heart tube that generates the right and left atria, the left ventricle, atriovenous inflow tract and atrioventricular canal, while the secondary heart field generates the right ventricle, the ventricular outflow tract, and the smooth muscle cells connecting to the aorta and pulmonary artery trunk. Inhibition of BMP signaling promotes secondary heart field expansion. Asymmetrical BMP activity leads to Smad1 activation only on the right side of developing myocardium. BMP secretion induces cardiac TFs like GATA4, Mef2C, Nkx2.5 via TGF-β-activated kinase 1 (TAK-1), or Tbx2/3 for heart and limb development. BMP-Smad1 promotes the expression of Tbx20, but not of Tbx5 and MHC (myosin heavy chain), via non-canonical Smad-binding elements. In later stages of heart development, Wnt inhibition must be combined with BMP activation.

Nodal/activin is a signaling pathway essential for mesoderm patterning and lineage specification. Smad-2 and -3 deletion leads to suppression of Nodal activity, resulting in impaired specification of axial mesendoderm, while Smad-4 double knockouts lack anterior primitive streak patterning but feature heart formation. Smad-4 induced activation of TGF-β via Smad-2/3 exerts antiproliferative and migratory effects. Beyond induction of anterior mesendoderm that further secretes cardiogenic factors, Nodal is directly involved in cardiac mesoderm formation, in synergy with FGF, reflected in expression of brachyury (T) and Xbra. The Xbra2 promoter features common activin and FGF regulatory sites; thus, low FGF/activin concentrations upregulate Xbra expression, while high concentrations downregulate it via Goosecoid (Gsc), Mix.1 and Xotx2. hESC cardiac differentiation protocols usually include high concentrations (100 ng/ml) of Wnt3A and activin A, and fine modulation of mesoderm cardiogenic differentiation can be achieved by appropriate combinations of BMP4 and activin A.

FGF (fibroblast growth factors) signaling pathway involves the well-known MAPK (mitogen-activated protein kinase) pathway in hESCs, while PI3K preserves pluripotency by nuclear location of β-catenin. Generally, FGFs are involved in a large array of fate decisions in mesendoderm, mesoderm and endoderm. FGF-1, -4, and BMP-2, all required for cardiac differentiation, are secreted by endoderm in the vicinity of anterior LPM, but they can induce cardiogenesis even in remote regions, such as the posterior mesoderm. FGF-8 levels in endoderm beneath cardiogenic mesoderm are regulated by the cardiac region of neural crests, and secreted FGF-8 induces transcription factors Nkx2.5 and Mef2C in BMP-2-exposed cells. Further, FGF-8 and BMP-2 promote cardiogenesis in the secondary heart field. FGFs via FGFR2 induce Sox2, producing Wnt inhibition required for cardiogenesis.

Notch signaling, required for mesoderm differentiation in somites, is upregulated by Wnt signaling along the canonical pathway via induction of Notch ligand Delta-like 1, and further transmits Wnt and BMP-related signals required for cardiac specification, including secreted Frizzled-related proteins.

Sonic hedgehog (Shh) signaling triggers somitic Smad-1 induction and responsiveness to BMP-2/-4 signaling, therefore cardiogenic vs. somitic differentiation requires Shh inhibition. However, Shh contributes transiently to formation of secondary heart field progenitors, therefore it is required for arterial pole development by the right side of the secondary heart field. The Shh agonist puromorphamine has been used for cardiogenic differentiation of the mesoderm in conjunction with inhibition of Wnt/β-catenin and Nodal pathways.

Retinoic acid acts upon binding to two distinct classes of nuclear receptors: retinoic acid

receptors (RARs) and retinoid X receptors (RXRs), both of them with an α, β, and γ isoform. RARs couple only all-trans-RA, while RXRs interact with both the trans and cis isomers. Retinoic acid plays a role in development of the secondary heart field, that produces atrial heart cells, but it also contributes to proliferation of ventricular cells. It has been effectively used as a component of serum-containing supplements required for reprogramming human cardiac mesenchymal stem cells into cardiovascular precursors.

Progress in understanding the signaling pathways involved in cardiomyocytes differentiation led to development of increasingly sophisticated methods and protocols for obtaining *in vitro* cardiomyocyte preparations starting from embryonic stem cells (ESC) and later from induced pluripotent stem cells (iPSC). A first achievement was derivation of human ESC (hESC) from the inner cell mass of human blastocysts by James Thomson et al. in 1998 [1], followed shortly by the proof that embryoid bodies (EB) derived from hESC can generate beating functional cardiomyocytes [2, 3]. Further refinements allowed efficient cardiomyocyte production from several hESC lines [4] and hESC differentiation into cardiomyocytes by co-culture with visceral endoderm-like cells (END2) [5]. Further, cardiomyocyte differentiation from hESC-END2 co-cultures was improved by use of serum-free medium and ascorbic acid [6]. In 2007, Laflamme et al. obtained the first cardiomyocyte differentiation from hESC cultured in monolayers by activin A and BMP4 treatments [7], while Burridge et al. increased cardiomyocytes yields by forced aggregation of hESC into uniform EB [8].

In 2006, Yamanaka and Takahashi reported the first reprogramming of mouse fibroblasts into iPSC that were further differentiated into beating cardiomyocytes [9], a huge achievement that is starting to revolutionize biomedical research and clinical therapies. Their original approach was based on retroviral transfection of 24 candidate pluripotency factors genes, of which only 4 were found to be essential for pluripotent stem cell induction: Oct 3/4 (octamer-binding transcription factor, encoded by Pou5f1), Sox2 (sex-determining region Y-box 2), Klf4 (Kruppel-like factor 4), and the well-known protooncogene c-Myc (similar to myelocytomatosis viral oncogene v-Myc, involved in chromosome 8 translocations in Burkitt lymphoma patients, upregulated in a large variety of human cancers). Although impressive, this procedure resulted in low iPSC yields when applied to adult human fibroblasts (<0.01%), and required several weeks to achieve expandable iPSC colonies [10]. The efficiency of pluripotency induction could be increased via several methods [11], like cell culture medium supplementing with vitamin C, exposure to hypoxia, removal of cell cycle control checkpoints by disrupting signaling pathways involving tumor-suppressor protein p53 and INK4A, or expression of ESC-specific microRNAs. Switching the differentiated human cell source form fibroblasts to juvenile human keratinocytes resulted into an increase of efficiency by two orders of magnitude and halving of the de-differentiation time, with the same set of pluripotency genes inserted by retroviral transfection [12]. Further studies have tested different combinations of pluripotency genes, e.g. by replacement of the highly oncogenic c-Myc and Klf4 with Lin28 and Nanog, and keeping the other two pluripotency factors as in the orginal formulation [13]. It was found that Klf4 transfection was sufficient to trigger endogenous Nanog expression, obviating the need to add this factor to the combination [14]. Other attempts were directed towards replacement of retroviral transfection with less harmful methods, to avoid gene disruption or disregulation upon random insertion of retroviral transcripts into the host cell genome. Thus, Okita et al. were able to generate mouse iPSC using retrovirus/adenovirus vectors or virus-free plasmid transfection under a constitutively active CAG promoter, although with lower efficiency [15]. Chang et al. used a polycistronic excisable self-inactivating lentiviral construct with a loxP site in a truncated 3′LTR (long terminal repeat), that could be almost completely removed from the genome upon exogenous Cre transfection [16]. Other viral vectors that do not result in genome incorporation, such as adenoviruses or modified Sendai viruses, have also been

used for reprogramming with good results, and are nowadays commercially available. Another interesting reprogramming tool is a doxycycline-inducible excisable piggyBac transposon system, requiring only inverted LTRs flanking the construct and transient expression of a transposase to exert insertion or excision events [17, 18]. An alternate reprogramming method relies on overexpression of the miR-302 microRNA up to 1.3-fold the levels in human ESC, resulting in cosuppression of four epigenetic regulators: AOF 1 and 2, MeCP1-p66 and MeCP2 [19]. Yet other attempts succeeded iPSC induction with only two of the four pluripotency factors (Oct4 and Sox2), in combination with valproate acting as deacetylase inhibitor [20], or even with Oct4 alone in combination with small molecules [21].

An even more painstaking process is iPSC differentiation into cardiomyocytes. This requires a multistage protocol recapitulating natural cardiomyocyte differentiation occurring during embyogenesis, composed of the following steps (each featuring several specific cell markers): mesoderm induction (markers: mouse Brachyury homologue or T, FoxC1, DKK1), formation of cardiogenic mesoderm (markers: Mesp1, Isl1, Kdr or VEGFR2), cardiac mesoderm (markers: Nkx2.5, GATA4, Tbx5, Mef2C, Hand1/2), and cardiomyocyte differentiation (markers: ACTN1, MYH6, TNNT2) [22]. *In vitro* approaches attempt to mimick embryonic signaling pathways involved in mesoderm induction: Wnt, BMP, Nodal/activin, FGF, followed by cardiac specification with inhibition of Wnt, BMP and TGF-β pathways [23]. Cell culture methods for ESC or iPSC differentiation into cardiomyocytes have evolved from embryoid body formation-based methods to co-culture based methods, monolayer culture based methods, up to large-scale production methods using suspension cultures and directed differentiation into cardiac subtypes [24]. Burridge et al. described recently an effective method for patient-derived cardiomyocyte generation starting from skin fibroblasts or peripheral blood mononuclear cells using chemically defined media and synthetic matrices [23]. They found that the complex B27 supplement added to RPMI1640 chemically defined cell culture medium, initially used for culture of hippocampal neurons, containing 21 components, many of them of animal origin, can be reliably replaced by a mixture of only three components: RPMI 1640 medium supplemented with L-ascorbic acid 2-phosphate and rice-derived recombinant human albumin. Using such *in vitro* differentiation methods results in heterogeneous and phenotypically diverse cell populations, containing 10–15% cardiomyocytes on the average [25]. These preparations can be further enriched to >95% cardiomyocytes using antibiotic resistance genes coupled to tissue-specific control regions (e.g. a blasticidin-resistance gene controlled by the heavy meromyosin chain MYH6 promoter) [26]. Other cardiomyocyte enrichment methods include glucose-free culture media containing lactate [27], and suspension cultures [28]. A wide variety of commercial human induced pluripotent stem cell-derived cardiomyocyte preparations from documented well-characterized donors are currently available for *in vitro* research purposes, provided by companies such as: Cellular Dynamics International (Madison, WI: iCell® Cardiomyocytes and iCell® Cardiomyocytes^2), Axiogenesis (Cologne, DE: Cor.4U®, VCor.4U™, MaturedCor.4U), Pluriomics (Leiden, NL: Pluricyte® Cardiomyocite Kit) (these two companies merged into Ncardia), and ReproCell (Yokohama, JP: ReproCardio2).

We will further discuss the complex signaling pahways and gene regulatory networks involved in cardiogenesis. A recent study [29] describes identification of the embryonic anterior intestinal portal (AIP—the edge of the endoderm groove that precedes formation of the foregut) as a heart organizer, i.e. a part of the embryo capable to induce and pattern adjacent tissue, even if excised and heterotopically transplanted. To date only a few embryo organizers were known: Hensen's node, inducing and patterning the central nervous system (the amniote equivalent of the amphibian dorsal lip of the blastopore, the first organizer discovered in 1924), the notochord and floor plate (organizing different sets of neurons along the neural tube), the zone of polarizing activity (the caudal edge of limb buds, organizing limb skeletal elements including the fingers),

and the midbrain-hindbrain isthmus (organizing the midbrain-tectum and hindbrain-cerebellum). Experimental approaches started with identification of a gene signature of organizers, via differential microarray profiling of RNA extracts form Hensen's node *vs*. posterior primitive streak, notochord *vs*. dorsal neural tube, and posterior *vs*. anterior upper limb bud edge, resulting in a gene set of 31 enriched transcripts and 17 depleted transcripts. The AIP of chick embryos at different developmental stages showed differential expression of 35 of the 48 genes of the organizer gene set (20 enriched and 15 depleted), including NRP1, FBLN7, KIRREL3, and VTN. Further, the organizing effect of AIP was tested on a paraxial mesoderm region adjacent to Hensen's node (dubbed region #3) that does not contribute to heart when grafted homotopically. In this region AIP was able to induce early cardiac markers like GATA4, Nkx2.5, Tbx5, Isl1, Mef2C, as well as to induce markers of ventricular identity (MYH15, IRX4, NPPB, GJA5) and to suppress markers of atrial identity. AIP from transgenic green fluorescent protein-expressing donors grafted over the cardiogenic mesoderm extended ventricular specification posteriorly into the atrial region, with ventricular marker IRX4 repressing atrial marker AMHC1.

Efforts have been spent to identify the transcription factors involved in heart development, as well as their cofactors and DNA regulatory regions that control cardiac gene expression. Kathiriya et al. describe several strategies used to identify cardiac transcription factors (TF): they can be searched either by evolutionary conservation, or by expression patterns, or by function in cardiovascular development [30]. Many molecular biology and genetics studies have been performed on *Drosophila melanogaster* embryonic development, therefore it makes perfect sense to search for mammalian orthologs of *Drosophila* genes involved in cardiac mesoderm specification and differentiation, as well as for paralogs across the genome once the sequence of a TF has been identified. One good example is identification of mouse Nkx2.5/Csx, a mammalian ortholog of *Drosophila* Tinman (initially named msh-2/NK4, involved in specification of heart and visceral muscles in the fruitfly), by low stringency hybridization [31]. Another example is identification of Hand2 using a phage library of mouse genome with a Hand1 hybridization probe [32]. TF identification by expression patterns is illustrated by discovery of myocardin using an expressed sequence tags library screened for novel sequences specific for cardiac cDNA. Forward genetic screens based on cardiovascular system phenotypes led to identification of Gridlock/Hey2/Hrt2 TF starting from zebrafish mutations induced by *N*-ethyl-*N*-nitrosourea [33]; the same TF was identified via homology screening starting from the bHLH (basic helix-loop-helix) domain [34]. Other important issues in investigating TF roles in cardiac biology are related to the study of TF-TF protein interactions and TF-DNA binding elements. Thus, using candidate gene approaches or yeast 2-hybrid screening revealed TF-TF interactions between Tbx5 and GATA4 [35] or Nkx2.5 [36]. Tbx5 exerts multiple roles in cardiogenesis, being expressed in developing atria, left ventricle, and conduction system. Although Tbx5 double knockout mice show defects in cardiac looping and left ventricle hypoplasia accompanied by early embryonic death (E10.5) [36], ventricle-restricted Tbx5 homozygous deletions result in unique mispatterned ventricle and death at E11.5 in mouse embryos [37]. Targeted Tbx5 deletion by a Cre/loxP system with Cre expression under control of Mef2C anterior heart field enhancer and promoter leads to lack of development of interventricular septum, with normal lateral ventricular walls development and molecular specificity of right and left ventricles [37], while endocardium-specific Tbx5 deletion leads to atrial septal defects without embryonic lethality [38]. TF affinity for DNA binding elements can be assessed via *in vitro* binding and electromobility shift assays; thus, a Tbx5-binding sequence could be identified by similarity to a Brachyury-binding motif [36, 39]. Enhancer elements are DNA regulatory sequences that accelerate assembly of general trascription factors of RNA polymerase II on the promoter sequence, located directly upstream the gene sequence, and help initiation of transcription. For cardiovascular development they

are usually *cis* regulatory sequences, located upstream or downstream of the gene, identified via sequence conservation, chromatin features, or functional assays. Although developmental enhancer elements are active in several related types of tissue, their function is tightly linked with cell-type-specific TFs. Enhancers acting during early cardiac development show the strongest evolutionary conservation [40]. TF binding to enhancer *cis* regulatory elements leads to epigenetic changes that can be subsequently identified, such as histone-3 lysine 27 acetylation induced by p300 (H3K27ac) [40–42], or trimethylation (H3K27me3) of enhancers by polycomb repressive complexes (PRC), or nucleosome depletion leading to DNAse-hypersensitive sites (DHS) preferentially cleaved by *in vitro* DNAse I treatment [43, 44], or preferential access to formaldehyde or transposase, evidenced by FAIRE-seq (formaldehyde-assisted isolation of regulatory elements and sequencing) [45] or ATAC-seq (assay for transposase-accessible chromatin sequencing) [46]. Enhancer identification by regulatory function involves inserting a candidate enhancer sequence akin to a gene promoter coupled to a reporter gene, via a construct inserted in isolated cells or transgene animals as a transient episome or integrated in the genome, e.g. identification of rat NPPA enhancer by transient transfection in cardiomyocytes [47–49]. A high-throughput enhancer detection method is self-transcribing active regulatory region sequencing (STARR-seq) [50]. Once enhancer activity for a reporter gene proved, there is still uncertainty about its role in modulating expression of its target gene in the natural genomic context, that requires *in vivo* functional testing. Another efficient technique, chromosome conformation capture (3C), can directly prove physical contact of proximal or distal enhancers with promoters [51]. An important mechanism for TF activity is epigenetic priming, consisting in chromatin reorganizing leading to changes in physical proximity between distant regulatory regions; these changes are developmentally modulated [52], and result in acquired permissive or occluded states propagated through cellular generations, that allow or forbid transcription activation without persistent expression of TF [53, 54]. Epigenetic priming plays an important role in cardiac development and cardiomyocyte differentiation.

Unfortunately, none of these high-throughput sequencing methods is capable to identify all enhancers active in a tissue. He et al. identified by chromatin immunoprecipitation and high-throughput sequencing (ChIP-seq) 13 genome regions co-occupied by a set of cardiac TF (GATA4, Nkx2.5, Tbx5, SRF, and Mef2A) and p300; of these, 7 regions regulated cardiac gene expression, indicating multiple TF occupancy of a region, a strategy that may lead to identification of developmental enhancers distinct from p300-associated enhancers [55, 196]. Dupays and Mohun discuss the spatiotemporal regulation of enhancers involved in cardiogenesis, emerging from wide-scale ChIP-seq experiments on different preparations, like distinct anatomic regions of embryonic or adult heart and cardiac muscle cell lines, outlining a complex and highly dynamic TF expression in both developing and mature heart [56]. They highlight the role of distant enhancers in congenital heart defects (CHD), by far the most frequent type of birth defects, affecting around 10% of live newborns, that result largely from disregulation of cardiac TF controls. Wamstad et al. present an integrated view of enhancer dynamics during development, whereby lineage-specific TF and chromatin regulators coordinate activation of distal enhancers, providing a tight control of tissue-specific gene expression programs [57]. In their model, pioneer transcription factors (P-TF) bind to enhancers, opening chromatin and priming the region for future activation. Subsequently, master TF responsible for cardiac lineage patterning bind to the same region, *cis*-activating transcription and meanwhile recruiting additional regulators, such as chromatin-modifying enzymes, architectural proteins like Mediator or cohesin and non-coding enhancer RNAs, all of them facilitating bridge formation between the enhancer region and promoters of target tissue-specific genes. Uosaki et al. analyzed several publicly-available gene expression databases containing microarray profiles for different devlopmental stages (from ealry embryonic to adult hearts),

identifying maturation stage-specific gene regulatory networks that include discrete sets of key TF and pathways activated or suppressed during cardiomyocyte maturation [58]. They performed a principal component analysis of 213 microarray datasets, identifying specific regression lines for each maturation stage (early-, mid-, and late-embryonic, neonate, and adult), and studied variances proportions in each principal component. Applying these methods to mouse induced-pluripotent stem cell-derived cardiomyocytes, they proved that their maturation corresponds to a late embryonic stage with inactive peroxisome proliferator-activated receptors and active catenin beta-1. A similar multiple pricipal component analysis and gene regulatory network analysis during mouse cardiogenesis was performed by Parikh et al. as illustrated in Fig. 3.1 [59]. Chen et al. analyzed an equally intriguing developmental phenomenon, the dedifferentiation of adult mammalian cardiomyocytes to cardiac progenitor cells during cardiac tissue repair, combining single-cell transcriptome and whole-genome DNA methylome data to understand the intricacies of epigenomic reprogramming for their *in vitro* model [60].

3.3 miRNAs in Cardiogenesis, Angiogenesis, Fibrosis and Apoptosis

Beyond transcription factors, enhancers and promoters, non-coding RNAs (ncRNA), and particularly microRNAs (miRNA or miR) play important roles in regulation of gene expression that modulates cardiogenesis and other physiological or pathophysiological processes involving the heart. This explains the apparent discrepancy between the small fraction of genome encoding proteins or transcription-regulating sequences (approximately 3%) and the fact that at least 75% of the genome is transcribed [61]. miRNAs represent short stretches of highly conserved non-coding RNA, between 18 and 24 nucleotides in length, that are able to control gene expression primarily at messenger RNA (mRNA) level. They are derived from multi-hairpin primary miRNAs (pri-miRNAs), transcripts of hundreds of KB in length, that are cleaved by nuclear ribonucleases like Drosha (a Class 2 ribonuclease III enzyme) into preliminary miRNAs (pre-miRNAs), hairpins of 70–100 nucleotides in length. Pre-miRNAs leave the nucleus and are further processed by another ribonuclease, Dicer, that cuts the hairpin loop, leaving a double-stranded miRNA approximately 22 nucleotides in length. The strand with less stable 5′-end base pairing is stripped away and transferred to a transport protein named Argonaute 2 (Ago2), part of a RNA-induced silencing complex (RISC). The argonaute protein within the RISC protects the mature miRNA from degradation and transports it to the mRNA target, where it exerts inhibitory effects on translation mainly by mRNA destabilization due to endonuclease function. mRNA targeting can be divergent (same miRNA acting on multiple mRNA targets), convergent (several miRNAs acting on the same mRNA sequence), or combinatorial (several miRNAs binding on different regions of the same mRNA). The total number of miRNA sequences known to date exceeds 2000, and they regulate the expression of approximately 30% of the genes [62]. Although the first miRNAs were discovered in 1993 in *Caenorhabditis elegans* [63, 64], their involvement in pathology was proved in 2002 [65]. Beyond intracellular effects, circulating miRNAs have been detected in association with high-density lipoproteins or Ago2 in extravesicular complexes, or in microparticles, exosomes or apoptotic bodies [66].

miRNAs exert important roles in cardiomyocyte development and control of proliferation/apoptosis. A targeted knock-out of Dicer1 in embryonic cardiomyocytes via Cre expression coupled to Nkx2.5 resulted in double-outlet right-ventricle defect [67], while under cTnT-Cre it led to embryonic lethality at E15.5 due to myocardial wall defects [68], and myocardial inactivation with a MHC-Cre led to dilated cardiomyopathy [69]. Two miRNAs with key functions in cardiogenesis are miR-1 and miR-133, encoded together in a bicistronic unit. In *Drosophila*, miR-1 controls the Notch1 receptor [70]. miR-1 inhibits the translation of TF Hand2, critical for venticular cardiomyocyte development [71], and modulates the insulin-like growth factor 1 pathway either by direct inhibition of

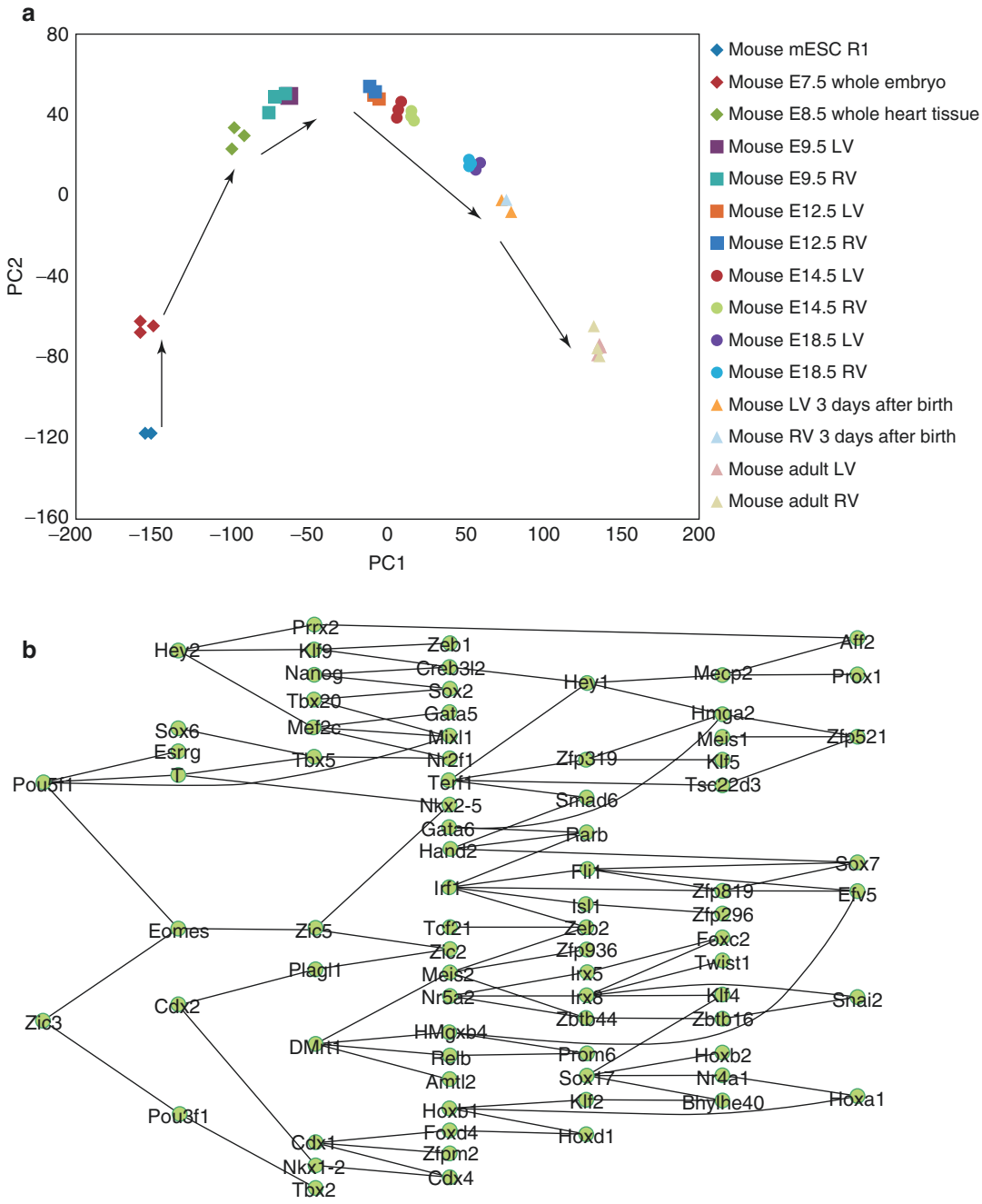

Fig. 3.1 (**a**) Multiple principal component analysis of microarray gene expression data for TF during mouse cardiogenesis showing a spatio-temporal landscape; (**b**) A putative gene regulatory network containing 80 most differentially expressed TF from mouse ESC to embryonic day E8.5 (reproduced with permission from Parikh et al. Signaling Pathways and Gene Regulatory Networks in Cardiomyocyte Differentiation, Tissue Eng. 2015, 21(4):377–92, ©Mary Ann Liebert Inc)

this factor and its receptor [72], or indirectly [73]. miR-133 inhibits cyclin D2 and serum response factor (SRF) [74]. miR-208a, 208b, and 499, encoded in the introns of myosin heavy chains genes, control the expression of myosin via several transcriptional repressors and Thrap1.

miRNAs 17–92 form a cluster that promotes cardiac differentiation in the secondary heart field; their mutation leads to early postnatal death by double-outlet right ventricle and ventricular septal defects. Their transcription is promoted by BMP via SMADs. This miRNA cluster acts by direct repression of cardiac progenitor genes Isl1 and Tbx1. Upregulation of Isl1 and Tbx1 inhibits cardiomyocyte differentiation, as encountered in miRNA 17–92 null embryos or BMP2/4 mutants, while miRNA 17–92 overexpression downregulates Isl1 and Tbx1 [75]. The miRNA-15 family (miR-195, 15a and b, 16 and 497) inhibit cardiomyocyte proliferation and induce apoptosis by targeting Bcl2 [76]. In addition, miR-15 targets the ADP-ribosylation factor-like 2, a protective factor for cardiomyocyte mitochondria. Hence, miR-15 inhibition by locked nucleic acids was shown to rescue myocardium, reducing the size of infarction in a mouse model of ischemia/reperfusion [77]. Similarly, the miRNA 34 family, induced by myocardial infarction, promotes apoptosis. miR-34a derepresses the cardio- and vasculoprotective deacetylase SIRT1 [78], and represses protein phosphatase 1 regulator (PNUTS), involved in DNA damage response and telomere shortening [79]. A miRNA with protective effects at myocardial level that was found to be upregulated after cardiac stress is miR-214 [80]. miR-214 has several targets, including cyclophilin D, Bim, and CaMKIIδ. Cyclophilin D modulates the mitochondrial permeability transition pore (that opens during Ca^{2+} and oxidative damage-induced cell death independent of Bcl2 family pathway). Bim (or Bcl-2-like 11) is also a proapoptotic protein, member of the Bcl2 family, and Ca^{2+}/calmodulin-dependent protein kinase IIδ participates in cardiac hypetrophy. Bim is also targeted by miR-24, therefore miR-24 overexpression was able to reduce myocardial infarct size, decrease cardiomyocyte apoptosis *in vitro* and *in vivo*, and improve cardiac function post-myocardial infarction [81]. Similar antiapoptotic effects at cardiomyocyte level were featured by miR-20a [82]. Many other miRNAs were reported to influence cardiomyocyte proliferation and apoptosis, including miR-17-92, miR-320, miR-199a, miR-590, miR-98, -128, -142 [83, 84]. miR-320 was shown to induce cardiomyocyte apoptosis via inhibition of the cardioprotective factor heat shock protein 20, while miR-98, miR-128, and miR-142 act by TGF-β repression, directly targeting Tgfbr1 mRNA [85]. A complex interplay of miRNAs occurs in post-ischemia-reperfusion remodeling and in ischemic pre- and postconditioning [86–88]. A comprehensive review emphasizes the protective effects of miR-126, miR-210, miR-499, and miR-494, the later targeting both pro-apoptotic genes such as SOCS6 (supressor of cytokine signaling 6), PTEN (phosphatase and tensin homolog), ROCK1 (Rho-associated coiled-coil containing protein kinase 1), CaMKIIδ (Ca^{2+}/calmodulin-dependent protein kinase II), and antiapoptotic genes like FGFR2 (fibroblast growth factor receptor 2), LIF (leukemia inhibitory factor), Api5 (apoptosis inhibitor 5), IGF1R (insulin-like growth factor 1 receptor), FGF7 (fibroblast growth factor 7), several of these genes in both groups acting along the PI3K/Akt pathway (phosphatidylinositol 3′-kinase/Ak [mouse bred] thymoma or protein phosphatase B), promoting cell survival [89]. Akt pathway activation in mesenchymal stem cells (MSC) upon miR-126 overexpression improves their paracrine secretion, resulting in enhanced cell repair after transplantation, but in MSC miR-126 also controlls the Delta-like 4 Notch ligand, promoting ischemic angiogenesis [90].

Other miRNAs were shown to modulate neovascularization after myocardial infarction, particularly miR-92a, which targets integrin α5, preventing endothelial cell apoptosis that is essential for neovessel formation [91], and represses several vasculoprotective genes, such as SIRT1 [92]. Many other miRNAs regulate angiogenesis [93], but their role in neovascularization post-myocardial infarction has been tested for only a few of them [62]. Thus, miR-126 and the miR-17-92 cluster, the expression of which is regulated by VEGF [94], regulate endothelial cell functions, miR-296 and -378 control tumor angiogenesis, miR-143 and -145 control neointima formation and atherosclerosis. Antagonists of miR-24 (antagomirs) targeting GATA2, regulator of endothelin-1 gene expression, and p21-activated kinase 4, improved revascularization post-myocardial

infarction [95], and protected against transition from cardiac hypertrophy to decompensated heart failure [96]. The miR-15 family was also found to inhibit angiogenesis after myocardial or hind limb ischemia [77, 97].

In atherogenic regions, proinflammatory endothelial cells can be controlled by inhibition of proinflammatory molecules like vascular cell adhesion molecule (VCAM-1), E-selectin and NF-κB by miR-10a, or VCAM-1, ICAM-1, and E-selectin by miR-126, miR-181, miR-31, and miR-17-3p [98–100]. Two miRs involved in lipid metabolism (miR-33 and miR-122) can influence cholesterol deposition in the atheromatous plaque [66]. In the arterial intima, LDL uptake by macrophages and their inflammatory modulation is controlled by miR-155 [101] and miR-155a-5p [102], while vascular smooth muscle cell (VSMC) proliferation, marking transition from fatty streak to fibrous atheroma, is regulated by MMP2 and 9 (matrix metalloproteinase) expression under the epigenetic control of miR-29b [103]. miR-145 triggers reversion of transition of VSMC from a contractile to a secretory phenotype, therefore VSMC-specific miR-145 overexpression markedly reduced plaque size in aortic sinuses and increased its collagen contents, representing a potential treatment for plaque stabilizing and avoidance of plaque rupture [104].

Another exciting field of research is related to miR involvement in myocardial fibrosis. miR-21 was shown to exert a pro-fibrotic function [105], being upregulated after acute myocardial infarction [106], therefore its block by antagomirs resulted in enhanced cardiac function [107]. However, miR-21 was also shown to prevent cardiomyocyte cell death induced by exogenous hydrogen peroxide [108], pointing to its antiapoptotic role post-myocardial infarction by targeting the proapoptotic factor ced4 (cell death 4) and the activator protein 1 pathway [109]. The miR-29 family also act as antifibrotic factors, targeting multiple fibrillins, collagens, elastin [106, 110]; miR-29 expression is reduced post-myocardial infarction and repressed by cardiac stressors, e.g. by aortic banding [111]. miR-101 targets the c-fos and TGF-β1 signaling pathways, being downregulated at 4 weeks after acute myocardial infarction; its overexpression resulted in inhibition of cardiac fibroblasts proliferation and collagen secretion [112]. Activation of cardiac regeneration by enhanced cardiomyocyte proliferation and fibroblast reprogramming into functional cardiomyocytes under miR control is an attractive therapeutic approach in cardiology [113, 114]. Combined overexpression of several cardiac transcription factors, including GATA4, Mef2C, Tbx5, Hand2, resulted in direct fibroblast reprogramming into cardiomyocytes [115–117]. These pathways could be activated equally well by a combination of miRs, including miR-1, miR-133, miR-208, and miR-499, resulting in direct cardiomyocyte reprogramming of fibroblasts [118], similar to miR-induced fibroblast reprogramming into stem cells [119].

3.4 Cardiomyocyte Morphology and Ultrastructure

The heart consists of cardiomyocytes (CMC) that represent a dual contractile/conduction cell population system. The myocardium, the muscle of the heart, consists of a three-dimensional arrangement of columnar CMCs, or atrial and ventricular rod-shaped muscle cells (Fig. 3.2a), with one or two large centrally located nuclei surrounded by numerous mitochondria. The cytoplasm contains cross-striated myofibrils, glycogen granules and lipid droplets. CMCs have special intercalated disks—with longitudinal and circular arrangement—that ensure a special networking of interdigitated connection between cardiomyocytes; they branch and their processes interdigitate with neighboring cardiomyocytes. The average dimensions of a mammalian ventricular working cardiomyocyte correspond to a cylindrical shape 100 μm in length and 22 μm in diameter [120]. It is estimated that a mature ventricular CMC is connected to 11 or 12 other CMCs via 11.6 intercalated disks on the average [121]. The intercalated disc area contains (1) gap junctions—allowing cellular communication, (2) desmosomes—ensuring the tight connection between discs (*maculae adherens*), and transverse (3) fasciae, adherent discs. CMCs are surrounded by a basal

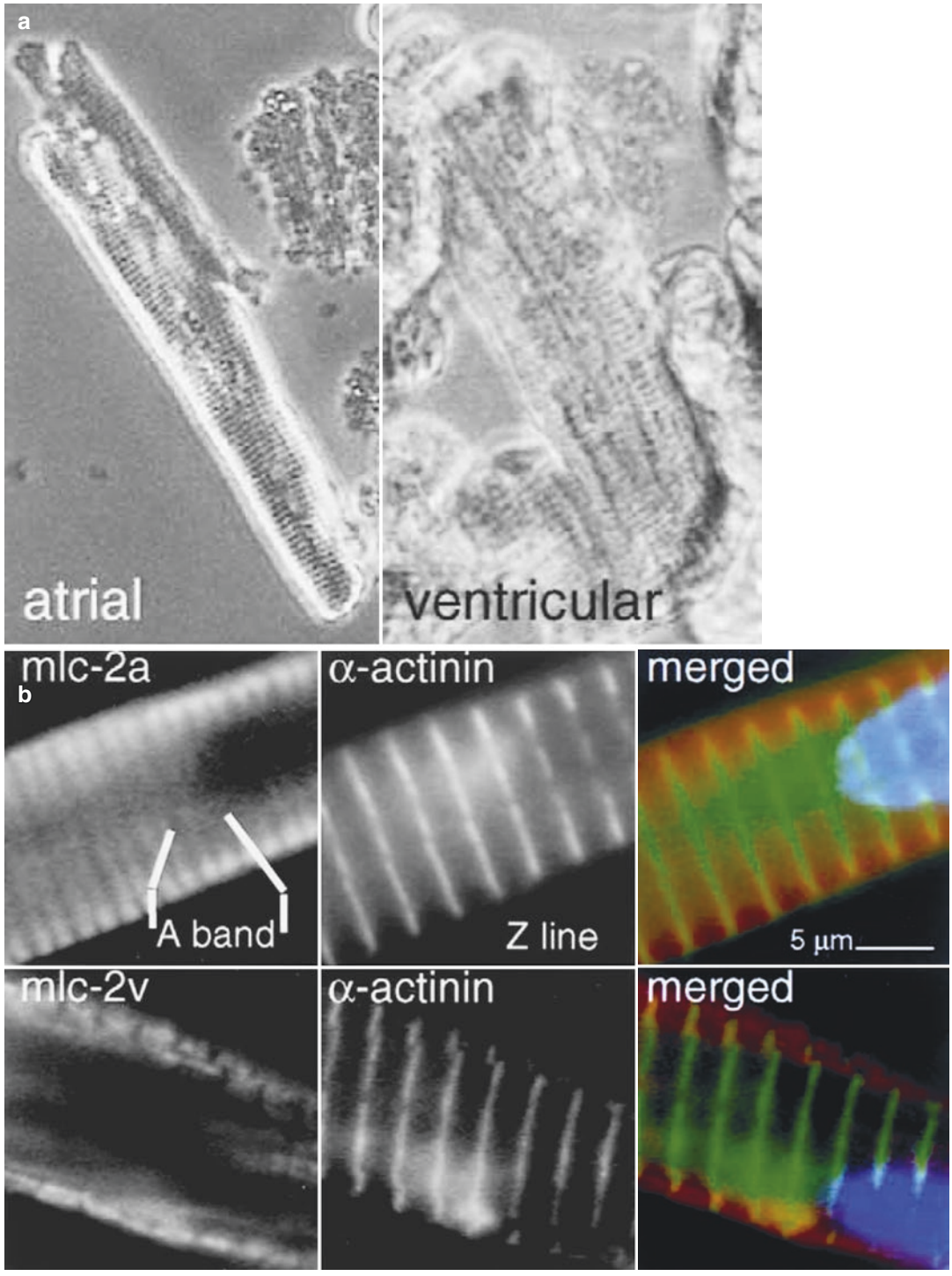

Fig. 3.2 (**a**) Isolation of atrial and ventricular cardiomyocytes from fresh human biopsies (magnification 40×). (**b**) CMC from both atrial and ventricular tissues include rod-shaped atrial and ventricular cells (reproduced from Bird SD et al. The human adult cardiomyocyte phenotype, Cardiovasc Res. 2003, 58(2):423–34, by permission of Oxford University Press)

membrane attached to myocytes and forming the myofibers peripheral to interstitial fibroblasts, blood vessels and the extracellular matrix with a capillary network and intercellular junctions. Each CMC has a bundle of myofibrils divided longitudinally into contractile units or sarcomeres, which consist of myofilaments of contractile proteins including actin and myosin [122]. The ultrastructure of a sarcomere was revealed mainly via transmission electron microscopy studies. The sarcomere is defined as the contractile myofilaments unit between two Z membranes (Z derives from the German term "Zwischenscheibe"), complex cytoskeletal proteins scaffolds that connect the ends of thin (actin) filaments (Fig. 3.2b). The fibrillary actin filaments emerging from the two Z membranes of a sarcomere are intertwinned with thick myosin filaments, the centers of which form the so-called M line (from the German "Mittelscheibe") at the center of the H zone (from the German term "helle"—light), the central light region, containing only myosin, of the anisotropic (A) or dark band of the sarcomere. The A band itself (except for the H zone) is composed of two areas of intertwinning between myosin and actin, while the adjacent isotropic (I) bands, crossed at the center by Z membranes, are formed only of actin filaments. In the dark regions of the A band the S1 heavy meromyosin heads (a meromyosin molecule resembles a golf cross or a musical note, with a heavy meromyosin—HMM—head, and a light meromyosin—LMM—tail; HMM and LMM fragments are the result of trypsin digestion) form crossbridges with actin, and during contraction hydrolysis of ATP bound to a specific site on the HMM head produces a conformational change with bending of the molecule head, that represents the contractile force-generating event. Subsequent to ATP hydrolysis and bending the affinity of the HMM head for actin decreases, the head unbinds from actin, binds a new ATP molecule, and resumes its initial conformation, restarting the cycle. The signal for contraction initiation is represented by an increase in intracellular calcium concentration that results in unmasking of myosin binding sites on actin filaments (double-helical filaments formed by monomeric globular or G-actin) that were previously masked by tropomyosin. Tropomyosin is removed from these myosin-binding sites and unmasks them under the action of trimeric troponin molecules. The 3 troponin subunits are T (required for anchoring on actin), C (containing 4 calcium binding sites represented by EF-hand motifs), and I (required for anchoring on tropomyosin). Apart from actin and myosin filaments, described in the classical microscopy studies of Hugh Huxley [123], the sarcomere contains ultrathin filaments of titin and nebulin. Electron microscopy studies on the conserved relative position of ultrathin N lines within I bands during muscle fiber contraction performed by Eremia in the 1980s [124] led to a proposed complex intertwinned architecture whereby ultrathin nebulin N filaments anchored with one end on a Z membrane connect with actin filaments emerging from the opposite Z membrane of the sarcomere, while ultrathin titin filaments anchor myosin bundles to the Z membranes. This architecture would explain perfect intertwinning between actin and myosin filaments even during muscle fiber recovery from an extreme stretch [125], when the dark bands of intertwinning between actin and myosin disappear completely. In addition to this ordering role, ultrathin filaments may contribute to contractile strength upon ATP hydrolysis in the actin-myosin crossbridge-forming region [126, 127]. The molecular components of the Z membrane are attached to the extracellular matrix via structural proteins forming a costamere (Fig. 3.3d, e). The structure and arrangement of myofibrils and sarcomeres in CMC is similar with those of striated muscle fibers. CMC cultures show a high level of α-sarcomeric actin, and the electron microscopy of CMC illustrates the abundance of mitochondria and well-organized sarcomeric structures [128, 129]. The mitochondrial compartment occupies 26% of the total cell volume for an average ventricular CMC [130]. Atrial CMC are able to reduce water, sodium and adipose loads on the circulatory system, and thereby lower the blood pressure by producing atrial natriuretic peptides with vasodilator role. Another important structure for excitation-contraction coupling in CMC

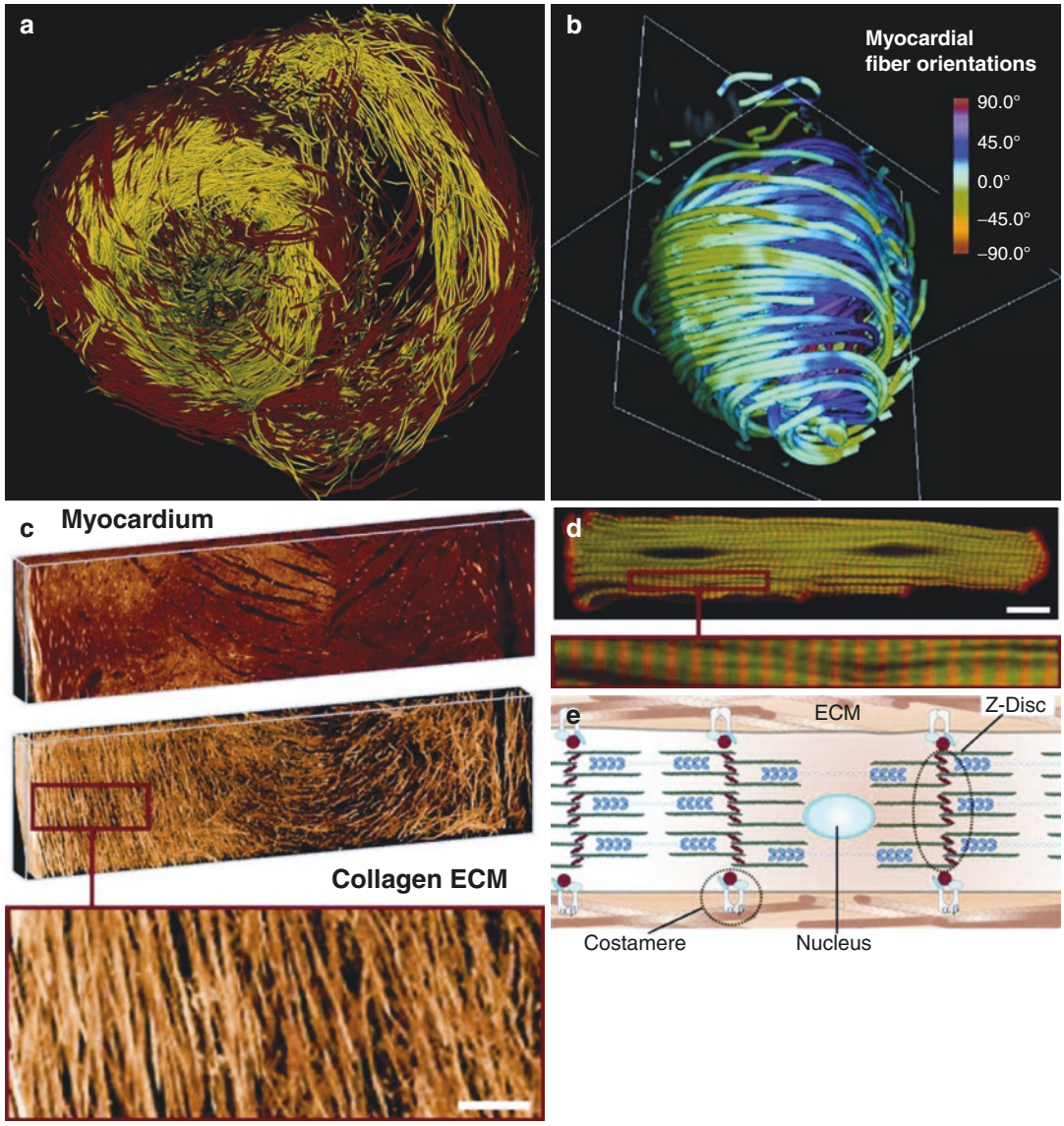

Fig. 3.3 (**a**) Myocardial fiber orientation in right and left ventricle obtained from diffusion tensor MRI of a pig heart; (**b**) Helicoidal arrangement of bundled myofibers around the ventricles—simplified tractography with color scheme representing fiber orientations (reproduced with permission from Poveda F, Gil D, Marti E, Andaluz A, Ballester M, Carreras F. Helical Structure of the Cardiac Ventricular Anatomy Assessed by Diffusion Tensor Magnetic Resonance Imaging With Multiresolution Tractography. Rev Esp Cardiol. 2013;66(10):782–790. Copyright ©2013 Sociedad Española de Cardiologia. Published by Elsevier España, S.L. All rights reserved.) [157] (**c**) The myocardial fibers contribute to the directional contraction; they are arranged parallel with the long axis of the myocardium, and are separated from adjacent laminae by an extracellular collagen network; (**d**) Confocal microscopy image of a cardiomyocyte, with fluorescent markers for F-actin (green) and α-actinin (red); (**e**) Cardiac myofibril ultrastructure, with costamere integrins attaching the Z membranes to the extracellular matrix (reprinted from Adv Drug Deliv Rev. Vol. 96, Capulli et al. Fibrous scaffolds for building hearts and heart parts, 83–102, [158], © 2016, with permission from Elsevier)

is represented by diads, formed by junction between t tubules, protruding from the cell membrane deep inside the myoplasm, and sarcoplasmic reticulum (SR) cisternae, constituting an internal calcium store. In turn, t(transverse) tubules are formed by longitudinal coalescence

of caveolae, the hairpin protein caveolin playing an important role in imposing membrane curvature to these cellular subdomains [131, 132]. Cardiac t tubules, present only in mammalian myocardium and absent in other vertebrates, feature larger diameters (100–300 nm) compared to skeletal muscle t tubules (20–40 nm), and form a complex network with transverse and longitudinal (axial) components, the extension of which is proportional to the heart rate of a particular species [133]. Key signaling processes occur in the narrow diadic subspace between t tubules and SR cisternae during depolarization: the wave of depolarization propagated through the tubules from the cell membrane activates L-type Ca^{2+} channels (better known as dihydropyridine receptors—DHPR), opening them and triggering local increases in calcium concentration that activate much larger Ca^{2+} releases from the SR via ryanodine receptors (mainly RyR2 in myocardium), leading to a phenomenon known as "calcium sparks" [134–137]. In myocardium RyR activation occurs via local calcium concentration increase, while in skeletal muscle via direct mechanical coupling between DHPR and RyR channels (mainly RyR1). This peculiar type of calcium-activated calcium release that occurs in the diadic subspace, featuring a complex modulation, results in systolic transient increases in calcium concentration up to tens of micromol/liter, much larger than in the bulk myoplasm [138–140]. This calcium overload requires large densities of calcium reuptake transporters such as Na^+/Ca^{2+} exchangers (NCX) or sarcoendoplasmic reticulum Ca^{2+} pumps (SERCA) in the junctional SR compared to NCX or plasmalemmal Ca^{2+} pumps (PMCA) densities on the cell membrane [141]. In fact several ion channels and transporters show a preferential location on t tubules (DHPR, cardiac inward-rectifying K^+ channels contributing I_{K1} current) [141, 142] or junctional SR. An interesting phenomenon, from a therapeutic point of view, is the modulation of Ca^{2+} release and reuptake in the diadic subspace by β1-adrenergic receptors and M2 cholinergic receptors on the cell membrane, via adenylate cyclase—protein kinase A (PKA) activation and inhibition, respectively, resulting in phosphorylation changes of DHPR, RyR channels, and phospholamban, which in turn modulates SERCA pumps [141], resulting in direct modulation of the myocardial contractile force. The SR compartment of a cardiomyocyte occupies on average 7% of the cell volume [120, 143, 144]. Another interesting phenomenon with clinical consequences that has revived recently the interest in studying the transverse-axial t tubule system is loss and disorganization of t tubules in heart failure, dilated and hypertrophic cardiomyopathies [133], as well as sheet-like remodeling of transverse t tubule system in heart failure, which hinders functional recovery in response to mechanical unloading by left ventricular assist devices (LVAD) [145].

3.4.1 The Human Adult CMC Phenotype Based on Cell Morphology

CMC morphology was assessed with phase contrast microscopy and indirect immunocytochemistry. Bird et al. described that after isolation procedures, CMC provided a sub-population of rod-shaped atrial and ventricular myocytes that had sharply defined edges and distinctive sarcomeric bands (Fig. 3.2a, b). Rod-shaped cells showed sarcomeric proteins including α-actinin and light chain myosin filaments [146]. CMC shape is an indicator of internal organization and has functional consequences for excitation-contraction coupling, specifically for conduction velocity [147].

Viable adult cardiac myocytes cultured on plastic substrates exhibited after plating a partial or complete loss of sarcomeric structure, although widespread amorphous staining of sarcomeric markers including α -actinin, protein that stained for α-actinin and light chain myosin filaments and tropomyosin, was evident. Cell edges became rounded and remaining sarcomeres appeared disorganized. After 2–3 weeks of cell culture, the same group described that ventricular myocytes adopted two broad but slightly distinct flat cell morphologies. The first CMC-type (Type I) was characterized by flattened spread morphology and extended lamellipodia consisted of beaded stress-like fibers or nascent myofibrils

organized in parallel arrays. The second cell type (Type II) had well-formed sarcomeres radiating in a uniform direction and converging at the cell edges [146]. Hans Michael Piper et al. provided an original method for preserving cylindrical shape and myofibrillary contractile apparatus of dissociated cardiomyocytes during long-term cultures [148].

As *in vitro* models, isolated organs and primary cells from rodents have been the standard in myocardial and CMC research—the animal model most extensively investigated—better models are missing so far. Morphological and functional characterization underlines that these models might become a valuable tool for research on the morphology and ultrastructure mechanisms of normal and pathological CMC for future therapies in human medicine. Thus, CMC transplantation may prove to be an important addition to the armamentarium against myocardial heart diseases. Transplantation of cardiomyocytes stimulated with vascular endothelial growth factor (VEGF) induces angiogenic processes or myogenic properties that improve post-infarction heart function [149].

Cardiomyocytes, the working muscle cells of the heart, are terminally differentiated cells in the adult organism with limited regeneration possibilities. Therefore, ischemia and cardio-toxic compounds can lead to cell death or to an irreversible decline of cardiac function. According to the dogma postulated by Anversa and Kajstura [150], the number of muscle cells in the mammalian heart is defined at birth, and in the absence of cardiac disease, these myocytes persist throughout the life of an individual or animal. The inevitable implication of the dogma is that myocytes are immortal [150]. Actually, myocyte death occurs with aging, but the essential growing and differentiation processes start in the prenatal period: myocyte mitotic division and structural differentiation of the myocyte cytoplasm, involving the synthesis and organization of myofibrils and other cytoplasmic components occurs before birth [151, 152]. The expansion of cardiac mass postnatally is accomplished by increases in myocyte size and number [153, 154].

The recognition that the heart is a self-renewing organ offers novel approaches for the treatment of cardiac diseases. The discovery that CMC can be isolated from small cardiac biopsy specimens and can be expanded *in vitro* for subsequent clinical use or autologous CMC transplants may enable the reconstitution of dead or scarred myocardium. Moreover, the replacement of poorly functional or hypertrophied myocytes of the severely decompensated heart with new, younger, more powerful muscle cells may positively interfere with the onset of terminal heart failure and death [155].

The group of Beltrami et al. [156] challenges the dogma that the heart is a postmitotic organ. Myocyte proliferation may be a component of the growth reserve of the human heart; this mechanism could replace damaged myocardium. The presence of cell division in the nondiseased part of the heart suggests a continuous turnover of cells during the lifespan of the organism. The belief that myocardial infarction constitutes the most obvious demonstration of the incapacity of ventricular myocytes to replicate must be reconsidered [156].

3.4.2 CMC Proliferation Capacity

During development, the proliferative capacity of CMC decreases, so that postnatally they reach a limited capacity to proliferate (~0.5% per year) [159]. A non-proliferative phenotype is considered an indication of terminal differentiation. As CMC transition to a non-proliferative state, many CMC become binucleated, and the proportion of such binucleated cells in the heart is ~25% at birth and remains consistent through to adulthood [159]. Gutstein et al. [160] investigated whether the major cardiac gap junction protein connexin43 may be responsible for regulating adherens junctions, desmosomes and their associated catenins, in terms of abundance and localization at the intercalated discs of cardiomyocytes. The study provides direct evidence that cell adhesion junctions in the heart, comprised of adherens junctions and desmosomes, as well as

their associated catenins and vinculin, are organized independently of the gap junctions. In the absence of connexin43, as detected by immunoblotting and immunofluorescence, and the consequent lack of gap junctions, the localization, abundance and morphology of adherens junctions and desmosomes at the intercalated disc remained unchanged. Furthermore, the localization of catenins associated with the intercalated disc junctions was unchanged, suggesting that decreases in connexin43 expression may not directly influence catenin-dependent signaling. In addition, structural proteins associated with the intercalated disc junctions and vinculin are also unchanged in their distribution despite the loss of connexin43. The results of this study suggest that the gap junction is not necessary for the organization of the cell adhesion junctions and associated proteins in the cardiac intercalated disc. The authors have demonstrated normal cell adhesion junction distribution and morphology in the absence of gap junctions. However, for optimal effect, transplanted cardiomyocytes must be integrated electrically as well as mechanically into the recipient heart [160].

A still widely used method to test the spontaneous, unrestricted differentiation capacity of human pluripotent stem cell lines into CMC was published by Kehat et al. [3], showing the induction of beating cells in embryoid bodies (pluripotent stem cell aggregates primed for differentiation) in 20% fetal-calf-serum-supplemented differentiation medium [3]. However, translation of respective protocols to routine large-scale production of CMC is hampered by high costs of recombinant growth factors supplementation. These high costs, as well as the need for chemically defined and thus GMP-compliant conditions, have spurred the search for alternatives [161]. To more comprehensively quantify CMC content at typical differentiation endpoints between days 7–14 *in vitro*, the flow cytometry analysis of specific sarcomeric markers such as cardiac troponin, sarcomeric actinin and myosin heavy chain is generally accepted as cardiac differentiation standard [162]. Functional characteristics of human pluripotent stem cell-derived CMC include altered Ca^{2+} handling, low Ca^{2+} buffering capacity, low beat rates (~40 BPM), immature sarcoplasmic reticulum and action potential characteristics, abnormal levels of ion currents, negative force-frequency relationships, and abnormal expression of sarcoplasmic reticulum proteins, all indicative of a fetal phenotype, but with physiological contractile function [163]. Kotov et al. [164] demonstrate that in healthy Wistar rats aging is related to changes in myocardial morphology. Age-related remodeling of the cardiac wall is related to cardiomyocyte hypertrophy and interstitial fibrosis. In physiological conditions, the bundles of CMCs are enveloped by thin layers of perimysium and endomysium. In the aging myocardium, transformation of the fibroblasts into myofibroblasts and accumulation of extracellular matrix proteins in the interstitial space are observed. The authors of the study noted that collagen content increases as aging progresses, collagen fibers become thicker and acquire a complex spiral shape; this phenomenon became more pronounced, as aging progressed, in the myocardium of the left ventricle, which was attributed to the higher afterload exerted on the left ventricle and consequently, to the higher degree of injury suffered by the ventricle with progression to senescence. The spatial disposition of cardiac fiber bundles in the two ventricles and texture of collagen extracellular matrix are shown in Fig. 3.3a–c. In conclusion, aging of the myocardium is a dynamic process which involves progressive loss of cardiomyocytes due to necrosis and apoptosis, interstitial fibrosis and reactive hypertrophy of the remaining vital cardiomyocytes [164]. Kuzmicic et al. [167] reported in an electron microscopy study the evidence of a mitochondrial dynamic network, organized and interconnected in package structures arranged along the myofibrils in neonate cardiac myocytes, and extended throughout the cytoplasm, distributed differently than in adults, with a morphology more reminiscent of that observed in other noncardiac cells [165–167].

The group of Burlacu et al. (2008) [128] designed experiments to test the effect of 5-azacytidine on bone marrow stem cells in culture

to commit myogenic differentiation; the significant increase in the number of cells expressing α-sarcomeric actinin suggested enhanced myogenic differentiation. The capability of these cells to express cardiomyogenic markers was indicative of enhanced cell differentiation towards a neonatal cardiac muscle phenotype induced by 5-azacytidine. The appearance of myogenic markers seems to be independent of 5-azacytidine, but is enhanced by this agent, suggesting that 5-azacytidine promotes rather than induces the myogenic differentiation of bone marrow progenitors [128]. Examination of treated and untreated bone marrow stem cells (BMSC) by electron microscopy revealed that 5-azacytidine exposure induced an increase in the cytoskeleton elements and the appearance of parallel intracellular filaments with intercalated mitochondria (Fig. 3.4a, b), somewhat reminiscent of the structure of CMC (Fig. 3.4b, d). Even in the absence of sarcomeric organization, the presence of orderly arranged filaments was observed only in 5-azacytidine-treated BMSC. All these features were not found in untreated cultured BMSC that retained their initial morphology, whereas some cells exhibited numerous vacuoles (Fig. 3.4b, c).

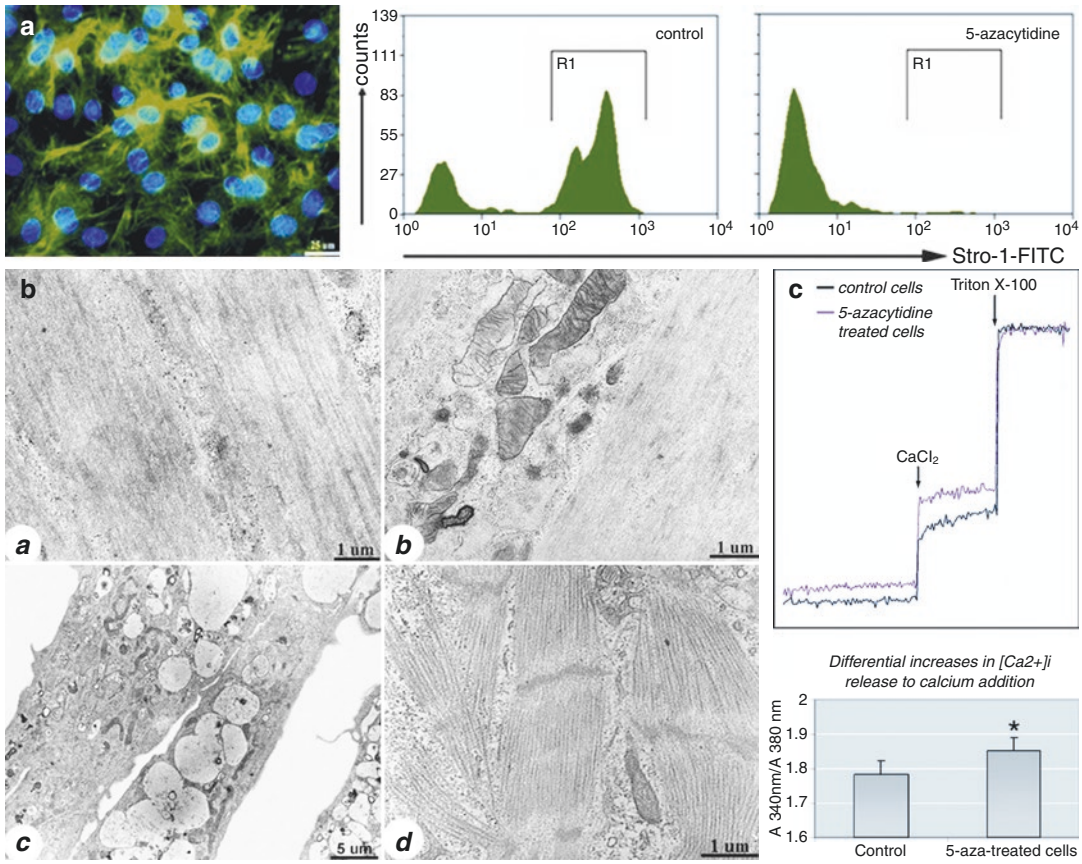

Fig. 3.4 Cardiomyocyte differentiation of BMSC *in vitro* induced by 5-azacytidine. (**a**) Stro-1 expression in BMSC at 21 days *in vitro* (d.i.v.) evidenced by immunofluorescence and flow cytometry in control cultures (70% Stro-1-positive cells, left panel) *vs*. 5-azacytidine-treated culture (no Stro-1-positive cells, right panel). (**b**) Transmission electron microscopy studies of BMSC at 21 d.i.v. **a**, **b**. Sarcomere-like parallel bands with intercalated mitochondria induced by 5-azacytidine treatment. **c**. This pattern was absent in control BMSC, which presented instead cytoplasmic vacuoles. **d**. For comparison, normal sarcomere pattern in neonatal cardiomyocytes. (**c**) Increase in cytosolic free calcium induced by 5-azacytidine treatment, evidenced by Fura-2-AM ratiometric calcium fluorimetry (reprinted from Eur J Cell Biol. Vol. 87(3), Burlacu A, et al. Promoting effect of 5-azacytidine on the myogenic differentiation of bone marrow stromal cells, 173–84, ©2008, with permission from Elsevier)

Freshly isolated adult ventricular CMCs were studied by Liu [168]. However, these CMCs reached a plateau after 4 weeks in culture concomitantly with continuous increase in structural remodeling in long-term cultures. Temporal changes occurred in the morphology of single CMC in gridded long-culture dishes. In a culture with relatively high cell density, attached CMCs were rounded or maintained their original rod shape, and in the first couple of weeks in culture adult ventricular CMCs were able to stretch the cell body with filopodia over 100 μm in length and underwent spontaneous changes in shape, characterized as possible remodeling or transformation processes. CMCs in culture over 17–19 weeks still displayed high capacity of remodeling by stretching filopodia longitudinally concomitant with nuclear relocation ~200 μm from day 149 to day 182 [168].

3.5 Regulatory Molecular Mechanisms and Pathways in Hypertrophy and Fibrosis

Heart failure (HF) represents a complex clinical syndrome that emerges as common complication and endpoint of several cardiovascular diseases, such as ischemic heart disease, particularly myocardial infarction, left ventricular (LV) or right ventricular (RV) pressure overload as a consequence of systemic/pulmonary hypertension, vavulopathies, other cardiovascular malformations (atrial/ventricular septal defects, aortic stenosis, etc.), hypertrophic, restrictive or dilated cardiomyopathies, pericarditis, etc. As a paradoxical consequence of increases in life expectancy resulting from progress in medicine and cure of life-threatening diseases, HF became the most common reason for hospitalization in elderly patients, with mortality and hospitalization rates 90 days after hospitalization for HF reaching 15% and 30%, respectively [169]. The lifetime risk of developing congestive heart failure amounts to 1 in 5 individuals, according to the Framingham Heart Study, while the average rate of 5-year survival is around 50%, even under maximal standard treatment with compounds such as angiotensin converting enzyme (ACE) inhibitors, angiotensin receptor blockers, diuretics, β-adrenergic blockers (in milder cases), cardiotonic glycosides (in fact the first modern treatment, beyond bleeding, introduced by William Withering at the end of the eighteenth century). Therefore there is an imperative demand to discover novel therapies and translate them to clinical application. Neurohumoral imbalances play an important role in the pathophysiology of HF, including increased plasma levels of catecholamines, angiotensin II, aldosterone, endothelin (ET), vasopressin, natriuretic peptides, growth factors and inhibitory cytokines, therefore the potential therapeutic usefulness of endothelin A (ET-A) receptor antagonists (e.g. BQ-123), non-selective ET receptor antagonists (e.g. bosentan), as well as vasopressin receptors non-selective antagonists (e.g. conivaptan) or vasopressin V2 receptor antagonists (e.g. tolvaptan) in congestive HF [170]. A recent study identified 12 elements connected to the nitric oxide (NO)/peroxynitrite ($ONOO^-$) cycle, including oxidative stress, NO, superoxide (O_2^-), NF-κB, inflammatory cytokines, iNOS (inducible nitric oxide synthase), mitochondrial dysfunction, NMDA (*N*-methil D-aspartate glutamate receptors) activity, intracellular Ca^{2+}, TRP (transient receptor potential) channels, and tetrahydrobiopterin depletion, all of them having causal roles in HF, plus two other factors, the small GTPase Rho-actin (RhoA) and ET-1, acting as tissue-limited cycle elements, claiming that the NO/$ONOO^-$ cycle may be the central cause of HF [171]. Another study identifies the myocardial extracellular matrix (ECM) expansion (myocardial fibrosis) as an important component of HF, contributing, beyond impairment of ventricular systolic function, to a relaxation deficit (impaired ventricular diastolic function) [169]. More than two decades ago, Karl Weber coined the concept of "interstitial heart disease", characterized by ECM expansion resulting from excess collagen secretion, recognizing that the myocytes and interstitial compartments of the myocardium are regulated independently, and that activated fibroblasts compartment and subsequent ECM expansion play a central role in the pathophysiology of

HF and ventricular hypertrophy. A large variety of biomarkers have been proposed for this restrictive ventricular dysfunction, including ECM metabolism modulators, matrix metalloproteases (MMPs), cytokines/chemokines/matrikines, and novel therapies addressing this target are under evaluation [172]; a good example is serelaxin, known to reverse myocardial ECM expansion and fibrosis.

TRP channels belonging to the classical or canonical subfamily (TRPC channels) are involved in two types of regulatory responses, playing a role in intracellular Ca^{2+} homeostasis: store-operated Ca^{2+} entry (SOCE) and receptor-operated Ca^{2+} entry (ROCE). In 1986, Putney first postulated the existence of store-operated Ca^{2+} channels (SOCC), starting from the observation that depletion of intracellular Ca^{2+} stores caused subsequent Ca^{2+} influx into the cells [173]. Hoth and Penner described a calcium current in mast cells, activated by depletion of intracellular calcium stores, I_{CRAC} (calcium release-activated calcium current) [174]. The current is carried by very low conductance highly Ca^{2+}-selective channels named ORAI1, the opening of which is regulated by STIM1, a protein located in the endoplasmic reticulum membrane and signaling Ca^{2+} concentration within this intracellular store. Recent studies [175, 176] propose that SOCE channels are heteromeric complexes of TRPC and ORAI subunits associated to lipid rafts, based on experiments showing that expression of ORAI1 in cells stably overexpressing TRPC3 or TRPC6 increased SOCE and that SOCE-enhancing levels of ORAI1 "silence" spontaneous activity of stably overexpressed TRPC3. In contrast to SOCE and I_{CRAC}, Gd^{3+}-sensitive ROCE mediated by TRPC3, TRPC6 or TRPC7 represents Ca^{2+} entry through TRPCs as well as SOCE/I_{CRAC} channels activated secondary to the stimulation of a receptor-$G_{q/11}$-phospholipase C (PLC) signaling pathway, by generated diacylglycerol (DAG), a molecule that activates TRPC3/6/7 but not TRPC1/4/5. Other studies [177, 178] have shown that, in contrast to ORAI, several TRPC channels (1, 2, 4 and 5) are regulated by STIM1 via an electrostatic interaction involving residues 672–685, which explains the role of TRPC1/4 subunits within heteromeric channels in regulating STIM1-independent TRPC3/6 subunits. When expressed at high level, these channels can also function in a STIM1-independent mode.

Several studies have linked increased TRPC channel activity to cardiac hypertrophy and heart failure. Seth et al. have shown that cardiac pressure overload by transverse aortic constriction or chronic angiotensin infusion upregulates a TRPC-like nonselective cation current in cardiomyocytes [179], while protection to hemodynamic stress and neurohormonal excess is conferred in TRPC1-/- mice or upon using the selective TRPC3 inhibitor Pyr3 [180] by altered mechanosensitive signaling through calcineurin/NFAT, mTOR and Akt (calcineurin is also known as protein phosphatase 2b—PP2B). Overexpression of TRPC3 or 6 was shown to induce cardiac hypertrophy through calcineurin/NFAT signaling in transgenic mice [181, 182]. Moreover, Wu et al. used myocytes from hypertrophied hearts of TRPC3/4/6 dominant-negative (dn) mice to show that they lack a unique store-depletion-operated Ca^{2+} influx, which is normally present in cells from wild-type animals. TRPC4 dn inhibited the activity of TRPC3/6/7 in the heart, suggesting that these two types of TRPCs function in coordinated complexes. By double immunofluorescent staining they demonstrated a colocalization of TRPC3 with the Na^{+}/Ca^{2+} exchanger NCX1 in dnTRPC3 cardiomyocytes [183]. Another study performed on cardiomyocytes from insulin-resistant obese *ob/ob* mice [184] showed that insulin fails to potentiate TRPC3 currents in this setting, in contrast to the situation in normal animals. Other anilino-thiazole compounds related to Pyr3 (compounds 14 and 19 in [185]) exert strong potency for TRPC3 and C6 block (in the low nanomolar range), being selective against other TRP channels (TRPA1, V1, V4) as well as against cardiac ion channels (Cav1.2, hERG, Nav1.5).

Calcineurin activation is sufficient to mediate cardiac hypertrophy and progressive heart failure, by dephosphorylation of nuclear factor of the activated T cell (NFAT) family that promotes transcription of multiple hypertrophy genes. This

pathway was first demonstrated in lymphocytes. Interestingly, TRPC1, C3 and C6 genes have conserved NFAT consensus sites in the promoter, resulting in cardiac hypertrophy upon a positive feedback cycle with sustained Ca^{2+} entry. Promoter regions of multiple hypertrophy genes, such as brain natriuretic peptide (BNP), β-MHC (myosin heavy chain), RCAN1 (regulator of calcineurin 1) contain multiple regulatory binding sites (MCAT, GATA, NFAT), resulting in direct activation via NFAT or GATA-binding proteins [186]. Figure 3.5 shows initiation of myocardial hypertrophy by multiple membrane receptors and signaling pathways via the common calcineurin/NFAT pathway [187].

Another study stressed the importance of class I and II histone deacetylases (HDACs), regulated by a transcriptional repressor, neuron-restrictive silencer factor (NRSF, also known as repressor element 1 (RE1) silencig factor—REST), in expression of multiple fetal cardiac genes. TRPC6 plays a key role in this regulation via the calcineurin/NFAT pathway, as well as myocardin-related transcription factor A (MRTF-A), a co-activator of serum response factor (SRF), mediating prohypertrophic signaling by linking RhoA to cardiac gene transcription [188]. Fibroblast proliferation and conversion to myofibroblast are also regulated by the SRF/MRTF and Smad/NFAT pathways, stressing the importance of TRPC channels in myocardial fibrosis, a major risk factor for cardiac arrhythmias and HF [189]; some of these pathways are shown in Fig. 3.6.

Another hallmark feature of HF is altered intracellular Ca^{2+} handling, contributing to impaired contractility. This is a result of SERCA downregulation combined with upregulation of NCX, TRPC4, C5 and C6. In addition, myocardial apoptosis brings an important contribution to HF in both experimental animal models and humans. Apoptosis is triggered by oxidative

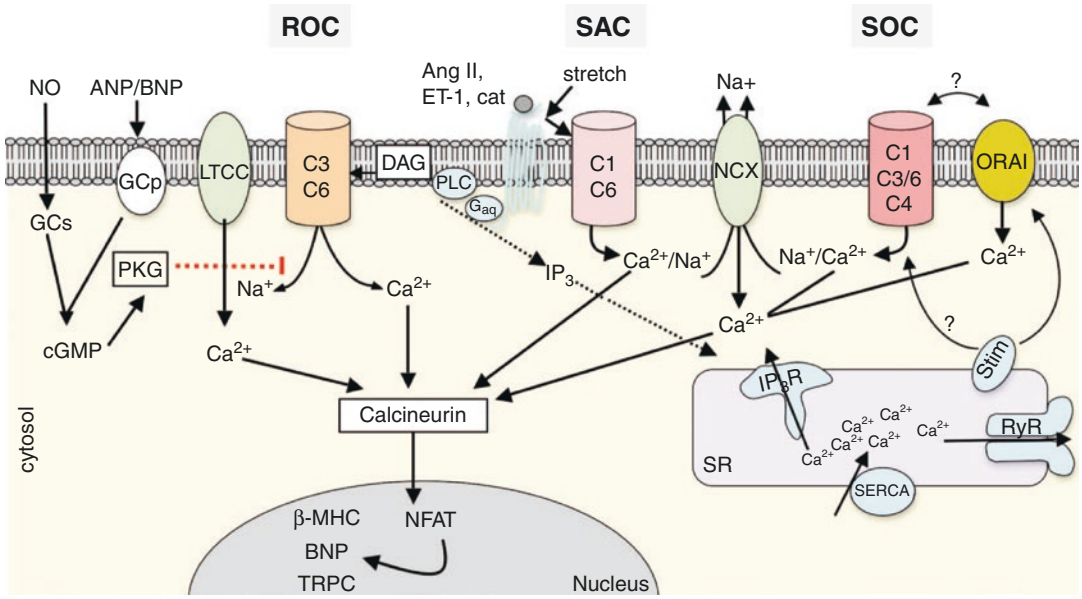

Fig. 3.5 Multiple activation mechanisms of calcineurin/NFAT pathway in cardiac hypertrophy and HF. *ROC* receptor-operated channel, *SAC* stretch-activated channel, *SOC* store-operated channel, *NO* nitric oxide, *ANP/BNP* atrial/brain natriuretic peptide, *AngII* angiotensin II, *ET-1* endothelin 1, *cat* catecholamines, *DAG* diacylglycerol, *PLC* phospholipase C, *LTCC* L-type Ca^{2+} channel, *GCs* soluble guanylate cyclases, *GCp* particulate guanylate cyclases, *PKG* protein kinase G, *SR* sarcoplasmic reticulum, *SERCA* sarcoendoplasmic reticulum calcium pump, *NFAT* nuclear factor of activated T cells, *β-MHC* β-myosin heavy chain (reproduced from Eder P & Molkentin JD: TRPC channels as effectors of cardiac hypertrophy, Circ Res. 2011, 108(2):265–72, with permission of Wolters Kluwer)

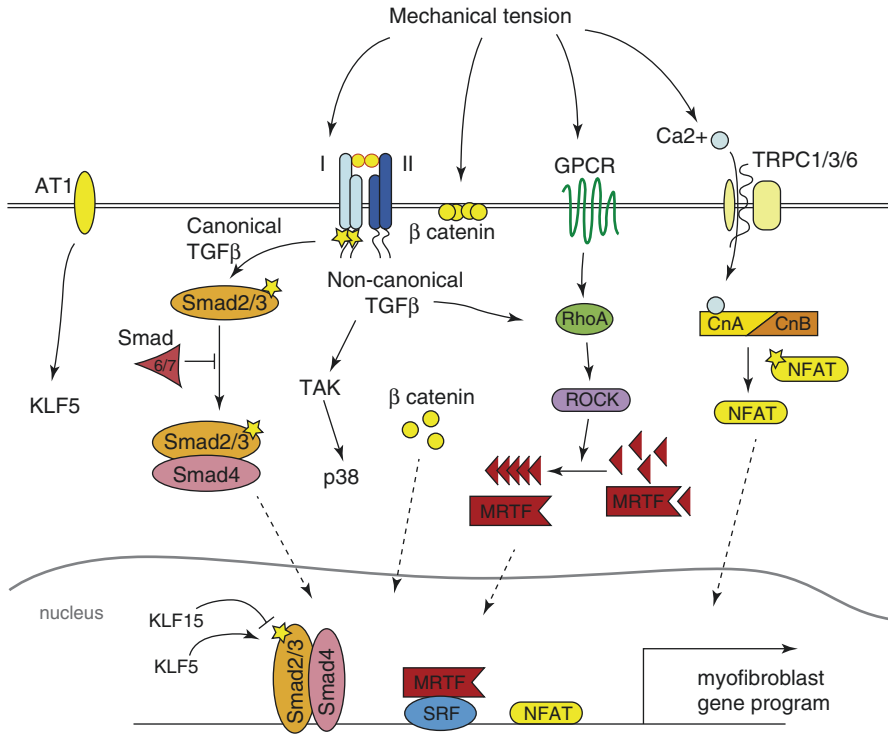

Fig. 3.6 Signaling and transcriptional pathways activated in myocardial fibrosis (reprinted from J Moll Cell Cardiol. Vol. 91, Lighthouse JK and Small EM, Transcriptional control of cardiac fibroblast plasticity, 52–60, ©2016, with permission from Elsevier)

stress, pro-inflammatory cytokines, catecholamines and angiotensin II, intracellular Ca^{2+} elevation playing a central role. Two channels are linked to myocardial apoptosis: the NAD^+/ADP ribose/poly (ADP ribose) polymerase (PARP)-dependent TRPM2 channels that induce Na^+ and Ca^{2+} overload, leading to mitochondrial membrane disruption, cytochrome *c* release, and caspase 3-dependent chromatin fragmentation, as well as TRPC7 channels, related to angiotensin 1 activation [190].

Extensive molecular studies failed to identify a unique pattern of miRNA changes in HF. In acute HF, the only miRNA featuring consistent changes is miR-499, which is significantly (~twofold) elevated [191]. In non-ischemic systolic HF several miRNAs are elevated in correlation with BNP, such as miR-200b, miR-519e, miR-520d, miR-622, miR-1228 and miR-1231 [192]. miR-423-5p and miR-133 are also elevated, but they are not correlated with BNP levels or cardiac remodelling [193]. Of twelve miRNAs with elevated circulating levels in hypertrophic cardiomyopathy, only three showed consistent correlation with cardiac hypetrophy: miR-27a, miR-29a, and miR-199a, and only the second one of these three was also correlated with myocardial fibrosis. A number of miRs regulate cardiomyocyte hypertrophy (miR 21, 133, 150, 195, 214), while the miR-29 family and miR-21 regulate myocardial fibrosis [89] (see Sect. 3.3). miR-208a, regulated during cardiac hypertrophy, is encoded in an α-MHC intron, and can be modulated by a protein interacting with thyroid hormone receptor [194], while miR-1 and miR-133—encoded together in a bicistronic unit - are inversely related to cardiac hypertrophy [195].

A special emphasis has been placed on the roles of miR1/133, deemed to exert protective effects, downregulated by ischemia/reperfusion and upregulated by ischemic postconditioning [55, 196]. However, the two miRs produce

opposite effects *in vitro* on apoptosis induced by H_2O_2: while miR133 downregulates Caspase 9, miR1 downregulates multiple antiapoptosis genes, such as Hsp60, Hsp70, IGF-1 and Bcl2 [89]. Recent studies identified the presence of a cAMP response element (CRE) sequence in the miR1/133a promoter region; in addition, CRE modulator (CREM) is a target of miR1 that acts as a regulator of CRE-binding protein (CREB) signaling, both proteins being activated by β-adrenergic signaling and competing for binding to CRE in gene promoters, which may explain the antiapoptotic effects of β-blockers [197]. The same miRs (miR1 in particular) enhance I_{to} by repressing Iroquois homebox domain 5 (IRX5), a transcriptional inhibitor of Kv4.2. In addition, miR133a enhances expression of KChIP2, the auxiliary subunit of Kv4.x channels contributing to $I_{to\ fast}$ [198]. Other presumed effects of miR133 upregulation include suppression of embryonic cardiomyocytes proliferation, prevention of genetic cardiac hypertrophy, inhibition of apoptosis, repression of HCN2 and hERG expression, and decrease in connective tissue growth factor expression. In HF both miR1 and 133a are dramatically reduced, explaining a main component of electrical remodeling. Therapeutic overexpression of miR133 has been proposed to prevent cardiac remodeling. Since both the calcineurin/NFAT pathway and miR-133 have been shown to play critical roles in cardiac hypertrophy, a relationship between them was postulated by Dong et al. [199]. These authors proved that calcineurin is a target of miR-133 via posttranscriptional repression, and expression of miR-133 is decreased by the calcineurin/NFAT pathway, providing a frame to understanding progressive cardiac hypertrophy [199].

3.6 Molecular Peculiarities of Right Ventricle Cardiomyocytes

Differences between right and left heart appear early during embryonic development. Cardiac progenitor cells appear early during gastrulation in the anterior lateral plate mesoderm: they are organised in a primary heart field (or first heart field), originating in the anterior splanchnic mesoderm, that form the cardiac crescent and then the early heart tube, eventually giving rise to the left ventricle and parts of the atrial chambers, and a secondary heart field, joining the heart tube to its arterial and venous edges from the pharingeal mesoderm and dorsal mesocardium, and giving rise to the main parts of the atrial tissue, right ventricle, and the outflow tract. The primordia of valves and septa derive from endocardial cushions formed by epithelial-to-mesenchymal transition of overlying myocardium, and later differentiate into valvular and septal structures. Neural crest cells migrated through pharyngeal arches from mid-otic placodes and caudal limit of somite 3 join the endocardial cushions to form the aortico-pulmonary (spiral) septum, smooth muscle cells of pharyngeal arteries and interstitial cells of semilunar valves, while epicardial cells derive from the proepicardium organ located near the sinus venosum in embryonic heart.

It is thought that left-right asymmetry of the embryo arises from a leftward extracellular flow of yolk sac fluid produced by rotation of left-right-dynein-containing monocilia on the ventral surface of the embryonic node, and detected by TRPP2 ion channels (belonging to another TRP subfamily, the polycystins) located in flow-sensing nodal cilia at the left margin of the node (as well as primary renal cilia), and their activation leads to asymmetrical Ca^{2+} inflow resulting into oriented differentiation ([200] reviewed by [201, 202]). Thus, TRPP2 knockout mice feature randomization of heart looping and embryonic turning, right pulmonary isomerism and abdominal situs [203], while in other studies TRPP1 or TRPP2 double knockout mice died *in utero* with cardiac septal defects and cyst formation in nephrons and pancreatic ducts [204, 205]. An interesting hypothesis is that, prior to primitive node formation, differential ion channel activity in embryo cells gives rise to unidirectional mRNA flow through gap junctions, resulting in asymmetrical gene expression. An important insight into cardiac asymmetry was obtained recently by Koshiba-Takeuchi and Bruneau by studying differences in transcription factors expres-

sion among different animal species. During phylogenetic evolution of vertebrates, fish have bicameral hearts composed of one atrium and one ventricle, amphibians have tricameral hearts composed of two atria and a common ventricle, lower reptiles have a partially separated ventricle, while crocodiles, birds and mammals have completely separated tetracameral hearts. Via in situ hybridization and qRT-PCR performed in an inferior reptile featuring a single ventricle, the green anole (*Anolis carolinensis*), compared to a superior reptile, the red slider turtle (*Trachemys scripta elegans*) that has a small, incomplete interventricular septum, these authors proved a left-to-right (high-to-low) Tbx5 gradient in the turtle ventricles similar to that in chick or mouse heart, but lacking in anole heart, occurring later during embryonic development [37]. These results provide a molecular mechanism for the evolution of the amniote ventricle, suggesting that restricted Tbx5 expression is required for interventricular septum formation and chamber separation in the vertebrates. Dominant mutations in Tbx5 gene in humans result in Holt-Oram syndrome, with variable congenital heart defects and associated upper limb malformations. The syndrome could be reproduced in Tbx5-mutant mice, with variable degrees of congenital heart defects, milder in animals with a hypomorphic allele ($Tbx5^{lox/+}$) and more pronounced in homozygous hypomorphic ($Tbx5^{lox/lox}$) and haploinsufficient mice ($Tbx5^{del/+}$) or double-knockout mice. Similar congenital heart defects occur in DiGeorge syndrome due to Tbx1 dominant mutations, while non-syndromic congenital heart defects are related to dominant mutations in the homebox transcription factor gene Nkx2.5 and zinc-finger transcription factor gene GATA4 [206]. The conclusion is that Tbx5 exerts a "rheostatic" control of cardiac gene expression, with some genes sensitive to variations as small as 15% in Tbx5 mRNA level, and thus a complex gene network including cardiac transcription factors, intercellular signaling molecules and ion channel proteins is finely tuned during tetracameral heart morphogenesis.

Another interesting hypothesis is that internal right-left asymmetry in vertebrates is controlled by the left-specific Nodal-Pitx2 axis, which is repressed by right-sided epithelial-to-mesenchymal transition (EMT) inducers Snail1 and Prrx1a, the later under control of BMP morphogens; thus, Nodal on the left and BMP on the right form two parallel and mutually repressing pathways along the lateral plate mesoderm, asymmetrically activating transcription factors Pitx2 and Prrx1, driving heart laterality in vertebrates via asymmetrical EMT [207].

Differences between left and right ventricle behavior to pressure or volume overload, particularly in relation to congenital heart diseases, are thoroughly discussed in a recent review [208]. While our current understanding of mechanisms involved in left ventricular hypertrophy and its progression to left ventricular failure is quite accurate, not the same can be said about right ventricular pressure and volume overload and its progression to right ventricular failure, although the topic is obviously of utmost importance for patients with repaired or palliated congenital heart defects or pulmonary hypertension. The authors emphasize a significant number of molecular and functional differences between the two ventricles and their adaptive response to hemodynamic stress. Thus, left and right ventricle feature differences in miR expression levels: in right ventricle miR-28, miR-34a, miR-93, and miR-148a are specifically upregulated during afterload stress, while they remain at steady levels during experimental left ventricular hypertrophy and failure produced by transverse aortic constriction, and miR-34a increases in left ventricle only during ischemia. These differences signal a higher sensitivity of right ventricle, particularly during pressure overload, to ischemia. Indeed, mitochondrial transmembrane potential is lower in right *vs*. left ventricle at rest, but increases during right ventricular hypertrophy via the calcineurin/NFAT pathway. The right ventricle features a deficit of antioxidant enzymes (superoxide dismutase and glutathione peroxidase), particularly during pressure overload, while in the left ventricle these enzymes are activated during such a hemodynamic stress in the compensated stage. Studies also suggest greater mitochondrial reactive oxygen species (ROS) production during right ventricular failure due to hypoxia-inducible factor

(Hif-1α) activation and impaired fatty acid oxydation due to PGC1α (Peroxisome proliferator-activated receptor-gamma coactivator) deficit. In addition, the right ventricle features a lower coronary blood flow and lower oxygen consumption at rest, as well as reduced response to angiogenic factors, rendering it more susceptible to ischemia. While in animal models of pulmonary hypertension induced by injection of monocrotaline (a vascular toxin that selectively affects pulmonary microcirculation) there is an increase in capillary density, in pulmonary artery banding models neoangiogenesis is completely absent, with increased Hif-1α but decreased VEGF. There are also differences between the failing right and left ventricle in relation to neurohormonal activation. In right ventricle failure there is a decreased inotropic response due to down-regulation of several classes of adrenergic receptors (β1, α1, and DA1), decreased cAMP and increased GPCR kinase 2, possibly explaining why beta-blockade does not function in these patients (e.g. in adults with right ventricular failure after repaired tetralogy of Fallot). Data concerning levels of activation of the renin-angiotensin-aldosterone axis in right ventricular failure patients are also controversial, and treatment with angiotensin-converting enzyme inhibitors like enalapril or ramipril or with angoitensin II receptor antagonists like losartan remains elusive.

Another recent study [209] emphasizes the role of Ca^{2+} signaling via TRPC6 channels in relation to TGF-β1 activation (modulated via knockdown of the type I glycoprotein endoglin or CD105, part of the TGF-β1 receptor complex) in right *vs*. left ventricular failure. Studies performed on human right and left ventricular samples from patients with end-stage heart failure *vs*. control subjects showed increased expression of TRPC1, 3, 4, 6, of TRPV2, and decreased expression of TRPM2, 3, and 8, with TRPC1 and 6 levels higher in right *vs*. left ventricular heart failure patients. A study in endoglin single-knockout mice revealed that pumonary artery constriction failed to increase TRP channels expression levels in either ventricle, while in control mice TRP channel expression was differentially increased in the right compared to the left ventricle. The symmetrical model of thoracic aortic constriction resulted in differential increase in TRPC1 and 6 expression in left *vs*. right ventricle irrespective of endoglin gene knockdown.

A study by the group of Antonio Zaza [210] revealed further differences in right *vs*. left ventricular cardiomyocytes in an *in vivo* model of right ventricular hypertrophy induced by monocrotaline injection in rats. Beyond ultrastructural changes, such as increased cardiomyocyte size, increased ECM, disorganized t tubule network, MHC isoform switch, there was an „electrical remodeling" consisting in increased diastolic intracellular calcium levels and Ca^{2+} release from stores, along with down-regulation of K^+ currents and increase in late Na^+ current (I_{NaL}) component, which may explain in part the favorable therapeutic effects of ranolazine in this experimental model of right ventricular pressure overload.

3.7 Concluding Remarks

Within this chapter we have summarized the differentiation signaling pathways, transcription factors, enhancers, and gene regulatory networks involved in cardiogenesis, regulation by microRNAs of cardiomyocyte differentiation, proliferation/apoptosis, angiogenesis, myocardial hypertrophy and fibrosis; we have reviewed the ultrastructural features of cardiomyocytes that transform them into highly efficient contractile elements, ensuring blood pumping in the pulmonary and systemic circulation along the entire lifespan, and we have emphasized molecular mechanisms and adaptive responses involved in myocardial hypertrophy and fibrosis, highlighting the differences between the right and left ventricle concerning response to pressure or volume overload. A number of astounding recent progresses of fundamental biomedical research, such as methods for large-scale differentiation into cardiomyocytes of embryonic or induced pluripotent stem cells, combined with the possibility of genome editing via CRISPR-Cas9 or similar techniques, control of the miRNA regulatory networks with synthetic oligonucleotide inhibitors based on locked nucleic acids, control

of myocardial fibrosis and fibroblast reconversion into functional cardiomyocytes, new drugs and identification of new molecular targets, all these offer promises of new enhanced therapeutic approaches for the benefit of patients with cardiovascular diseases.

Acknowledgements BA expresses his gratitude to Prof. Andrei Dumitru Iacobas for directing his early career in scientific research, and to Prof. Kanigula Mubagwa for introduction in the field of cardiac electrophysiology. This study was funded from Competitiveness Operational Programme 2014–2020 project P_37_675 (contract no. 146/2016), Priority Axis 1, Action 1.1.4, co-financed by the European Funds for Regional Development and Romanian Government funds. The content of this publication does not necessarily reflect the official position of the European Union or Romanian Government.

References

1. Thomson JA, Itskovitz-Eldor J, Shapiro SS, Waknitz MA, Swiergiel JJ, Marshall VS, et al. Embryonic stem cell lines derived from human blastocysts. Science. 1998;282(5391):1145–7.
2. He JQ, Ma Y, Lee Y, Thomson JA, Kamp TJ. Human embryonic stem cells develop into multiple types of cardiac myocytes: action potential characterization. Circ Res. 2003;93(1):32–9.
3. Kehat I, Kenyagin-Karsenti D, Snir M, Segev H, Amit M, Gepstein A, et al. Human embryonic stem cells can differentiate into myocytes with structural and functional properties of cardiomyocytes. J Clin Invest. 2001;108(3):407–14.
4. Xu C, Police S, Rao N, Carpenter MK. Characterization and enrichment of cardiomyocytes derived from human embryonic stem cells. Circ Res. 2002;91(6):501–8.
5. Mummery C, Ward-van Oostwaard D, Doevendans P, Spijker R, van den Brink S, Hassink R, et al. Differentiation of human embryonic stem cells to cardiomyocytes: role of coculture with visceral endoderm-like cells. Circulation. 2003;107(21):2733–40.
6. Passier R, Oostwaard DW, Snapper J, Kloots J, Hassink RJ, Kuijk E, et al. Increased cardiomyocyte differentiation from human embryonic stem cells in serum-free cultures. Stem Cells. 2005;23(6):772–80.
7. Laflamme MA, Chen KY, Naumova AV, Muskheli V, Fugate JA, Dupras SK, et al. Cardiomyocytes derived from human embryonic stem cells in prosurvival factors enhance function of infarcted rat hearts. Nat Biotechnol. 2007;25(9):1015–24.
8. Burridge PW, Anderson D, Priddle H, Barbadillo Munoz MD, Chamberlain S, Allegrucci C, et al. Improved human embryonic stem cell embryoid body homogeneity and cardiomyocyte differentiation from a novel V-96 plate aggregation system highlights interline variability. Stem Cells. 2007;25(4):929–38.
9. Takahashi K, Yamanaka S. Induction of pluripotent stem cells from mouse embryonic and adult fibroblast cultures by defined factors. Cell. 2006;126(4):663–76.
10. Takahashi K, Tanabe K, Ohnuki M, Narita M, Ichisaka T, Tomoda K, et al. Induction of pluripotent stem cells from adult human fibroblasts by defined factors. Cell. 2007;131(5):861–72.
11. Yamanaka S, Blau HM. Nuclear reprogramming to a pluripotent state by three approaches. Nature. 2010;465(7299):704–12.
12. Aasen T, Raya A, Barrero MJ, Garreta E, Consiglio A, Gonzalez F, et al. Efficient and rapid generation of induced pluripotent stem cells from human keratinocytes. Nat Biotechnol. 2008;26(11):1276–84.
13. Yu J, Vodyanik MA, Smuga-Otto K, Antosiewicz-Bourget J, Frane JL, Tian S, et al. Induced pluripotent stem cell lines derived from human somatic cells. Science. 2007;318(5858):1917–20.
14. Chan KK, Zhang J, Chia NY, Chan YS, Sim HS, Tan KS, et al. KLF4 and PBX1 directly regulate NANOG expression in human embryonic stem cells. Stem Cells. 2009;27(9):2114–25.
15. Okita K, Nakagawa M, Hyenjong H, Ichisaka T, Yamanaka S. Generation of mouse induced pluripotent stem cells without viral vectors. Science. 2008;322(5903):949–53.
16. Chang CW, Lai YS, Pawlik KM, Liu K, Sun CW, Li C, et al. Polycistronic lentiviral vector for "hit and run" reprogramming of adult skin fibroblasts to induced pluripotent stem cells. Stem Cells. 2009;27(5):1042–9.
17. Kaji K, Norrby K, Paca A, Mileikovsky M, Mohseni P, Woltjen K. Virus-free induction of pluripotency and subsequent excision of reprogramming factors. Nature. 2009;458(7239):771–5.
18. Woltjen K, Michael IP, Mohseni P, Desai R, Mileikovsky M, Hämäläinen R, et al. piggyBac transposition reprograms fibroblasts to induced pluripotent stem cells. Nature. 2009;458(7239):766–70.
19. Lin SL, Chang DC, Lin CH, Ying SY, Leu D, Wu DT. Regulation of somatic cell reprogramming through inducible mir-302 expression. Nucleic Acids Res. 2011;39(3):1054–65.
20. Huangfu D, Osafune K, Maehr R, Guo W, Eijkelenboom A, Chen S, et al. Induction of pluripotent stem cells from primary human fibroblasts with only Oct4 and Sox2. Nat Biotechnol. 2008;26(11):1269–75.
21. Li Y, Zhang Q, Yin X, Yang W, Du Y, Hou P, et al. Generation of iPSCs from mouse fibroblasts with a single gene, Oct4, and small molecules. Cell Res. 2011;21(1):196–204.
22. Thorrez L, Sampaolesi M. The future of induced pluripotent stem cells for cardiac therapy and drug development. Curr Pharm Des. 2011;17(30):3258–70.

23. Burridge PW, Matsa E, Shukla P, Lin ZC, Churko JM, Ebert AD, et al. Chemically defined generation of human cardiomyocytes. Nat Methods. 2014;11(8):855–60.
24. Talkhabi M, Aghdami N, Baharvand H. Human cardiomyocyte generation from pluripotent stem cells: a state-of-art. Life Sci. 2016;145:98–113.
25. Anson B, Nuwaysir E, Swanson B, Wang WB. Industrialized production of human iPSC-derived cardiomyocytes for use in drug discovery and toxicity testing. BioPharm Int. 2011;2011:58–67.
26. Ma J, Guo L, Fiene SJ, Anson BD, Thomson JA, Kamp TJ, et al. High purity human-induced pluripotent stem cell-derived cardiomyocytes: electrophysiological properties of action potentials and ionic currents. Am J Physiol Heart Circ Physiol. 2011;301(5):2.
27. Tohyama S, Hattori F, Sano M, Hishiki T, Nagahata Y, Matsuura T, et al. Distinct metabolic flow enables large-scale purification of mouse and human pluripotent stem cell-derived cardiomyocytes. Cell Stem Cell. 2013;12(1):127–37.
28. Hemmi N, Tohyama S, Nakajima K, Kanazawa H, Suzuki T, Hattori F, et al. A massive suspension culture system with metabolic purification for human pluripotent stem cell-derived cardiomyocytes. Stem Cells Transl Med. 2014;3(12):1473–83.
29. Anderson C, Khan MA, Wong F, Solovieva T, Oliveira NM, Baldock RA, et al. A strategy to discover new organizers identifies a putative heart organizer. Nat Commun. 2016;7:12656.
30. Kathiriya IS, Nora EP, Bruneau BG. Investigating the transcriptional control of cardiovascular development. Circ Res. 2015;116(4):700–14.
31. Lints TJ, Parsons LM, Hartley L, Lyons I, Harvey RP. Nkx-2.5: a novel murine homeobox gene expressed in early heart progenitor cells and their myogenic descendants. Development. 1993;119(2):419–31.
32. Srivastava D, Cserjesi P, Olson EN. A subclass of bHLH proteins required for cardiac morphogenesis. Science. 1995;270(5244):1995–9.
33. Zhong TP, Rosenberg M, Mohideen MA, Weinstein B, Fishman MC. gridlock, an HLH gene required for assembly of the aorta in zebrafish. Science. 2000;287(5459):1820–4.
34. Iso T, Kedes L, Hamamori Y. HES and HERP families: multiple effectors of the Notch signaling pathway. J Cell Physiol. 2003;194(3):237–55.
35. Garg V, Kathiriya IS, Barnes R, Schluterman MK, King IN, Butler CA, et al. GATA4 mutations cause human congenital heart defects and reveal an interaction with TBX5. Nature. 2003;424(6947):443–7.
36. Bruneau BG, Nemer G, Schmitt JP, Charron F, Robitaille L, Caron S, et al. A murine model of Holt-Oram syndrome defines roles of the T-box transcription factor Tbx5 in cardiogenesis and disease. Cell. 2001;106(6):709–21.
37. Koshiba-Takeuchi K, Mori AD, Kaynak BL, Cebra-Thomas J, Sukonnik T, Georges RO, et al. Reptilian heart development and the molecular basis of cardiac chamber evolution. Nature. 2009;461(7260):95–8.
38. Nadeau M, Georges RO, Laforest B, Yamak A, Lefebvre C, Beauregard J, et al. An endocardial pathway involving Tbx5, Gata4, and Nos3 required for atrial septum formation. Proc Natl Acad Sci U S A. 2010;107(45):19356–61.
39. Hiroi Y, Kudoh S, Monzen K, Ikeda Y, Yazaki Y, Nagai R, et al. Tbx5 associates with Nkx2-5 and synergistically promotes cardiomyocyte differentiation. Nat Genet. 2001;28(3):276–80.
40. Nord AS, Blow MJ, Attanasio C, Akiyama JA, Holt A, Hosseini R, et al. Rapid and pervasive changes in genome-wide enhancer usage during mammalian development. Cell. 2013;155(7):1521–31.
41. Blow MJ, McCulley DJ, Li Z, Zhang T, Akiyama JA, Holt A, et al. ChIP-Seq identification of weakly conserved heart enhancers. Nat Genet. 2010;42(9):806–10.
42. Wamstad JA, Alexander JM, Truty RM, Shrikumar A, Li F, Eilertson KE, et al. Dynamic and coordinated epigenetic regulation of developmental transitions in the cardiac lineage. Cell. 2012;151(1):206–20.
43. Neph S, Stergachis AB, Reynolds A, Sandstrom R, Borenstein E, Stamatoyannopoulos JA. Circuitry and dynamics of human transcription factor regulatory networks. Cell. 2012;150(6):1274–86.
44. Stergachis AB, Neph S, Reynolds A, Humbert R, Miller B, Paige SL, et al. Developmental fate and cellular maturity encoded in human regulatory DNA landscapes. Cell. 2013;154(4):888–903.
45. Gaulton KJ, Nammo T, Pasquali L, Simon JM, Giresi PG, Fogarty MP, et al. A map of open chromatin in human pancreatic islets. Nat Genet. 2010;42(3):255–9.
46. Buenrostro JD, Giresi PG, Zaba LC, Chang HY, Greenleaf WJ. Transposition of native chromatin for fast and sensitive epigenomic profiling of open chromatin, DNA-binding proteins and nucleosome position. Nat Methods. 2013;10(12):1213–8.
47. Knowlton KU, Baracchini E, Ross RS, Harris AN, Henderson SA, Evans SM, et al. Co-regulation of the atrial natriuretic factor and cardiac myosin light chain-2 genes during alpha-adrenergic stimulation of neonatal rat ventricular cells. Identification of cis sequences within an embryonic and a constitutive contractile protein gene which mediate inducible expression. J Biol Chem. 1991;266(12):7759–68.
48. Seidman CE, Wong DW, Jarcho JA, Bloch KD, Seidman JG. Cis-acting sequences that modulate atrial natriuretic factor gene expression. Proc Natl Acad Sci U S A. 1988;85(11):4104–8.
49. Sprenkle AB, Murray SF, Glembotski CC. Involvement of multiple cis elements in basal- and alpha-adrenergic agonist-inducible atrial natriuretic factor transcription. Roles for serum response elements and an SP-1-like element. Circ Res. 1995;77(6):1060–9.
50. Arnold CD, Gerlach D, Stelzer C, Boryń ŁM, Rath M, Stark A. Genome-wide quantitative enhancer

activity maps identified by STARR-seq. Science. 2013;339(6123):1074–7.
51. de Wit E, de Laat W. A decade of 3C technologies: insights into nuclear organization. Genes Dev. 2012;26(1):11–24.
52. Noordermeer D, Duboule D. Chromatin looping and organization at developmentally regulated gene loci. Wiley Interdiscip Rev Dev Biol. 2013;2(5):615–30.
53. Dillon N. Factor mediated gene priming in pluripotent stem cells sets the stage for lineage specification. Bioessays. 2012;34(3):194–204.
54. Lahn BT. The "occlusis" model of cell fate restriction. Bioessays. 2011;33(1):13–20.
55. He A, Kong SW, Ma Q, Pu WT. Co-occupancy by multiple cardiac transcription factors identifies transcriptional enhancers active in heart. Proc Natl Acad Sci U S A. 2011a;108(14):5632–7.
56. Dupays L, Mohun T. Spatiotemporal regulation of enhancers during cardiogenesis. Cell Mol Life Sci. 2016;2016:6.
57. Wamstad JA, Wang X, Demuren OO, Boyer LA. Distal enhancers: new insights into heart development and disease. Trends Cell Biol. 2014;24(5):294–302.
58. Uosaki H, Cahan P, Lee DI, Wang S, Miyamoto M, Fernandez L, et al. Transcriptional landscape of cardiomyocyte maturation. Cell Rep. 2015;13(8):1705–16.
59. Parikh A, Wu J, Blanton RM, Tzanakakis ES. Signaling pathways and gene regulatory networks in cardiomyocyte differentiation. Tissue Eng Part B Rev. 2015;21(4):377–92.
60. Chen X, Chakravarty T, Zhang Y, Li X, Zhong JF, Wang C. Single-cell transcriptome and epigenomic reprogramming of cardiomyocyte-derived cardiac progenitor cells. Sci Data. 2016;3(160079):79.
61. Pennisi E. Genomics. ENCODE project writes eulogy for junk DNA. Science. 2012;337(6099):1159–61.
62. Seeger FH, Zeiher AM, Dimmeler S. MicroRNAs in stem cell function and regenerative therapy of the heart. Arterioscler Thromb Vasc Biol. 2013;33(8):1739–46.
63. Lee RC, Feinbaum RL, Ambros V. The C. elegans heterochronic gene lin-4 encodes small RNAs with antisense complementarity to lin-14. Cell. 1993;75(5):843–54.
64. Wightman B, Ha I, Ruvkun G. Posttranscriptional regulation of the heterochronic gene lin-14 by lin-4 mediates temporal pattern formation in C. elegans. Cell. 1993;75(5):855–62.
65. Calin GA, Dumitru CD, Shimizu M, Bichi R, Zupo S, Noch E, et al. Frequent deletions and down-regulation of micro- RNA genes miR15 and miR16 at 13q14 in chronic lymphocytic leukemia. Proc Natl Acad Sci U S A. 2002;99(24):15524–9.
66. Condorelli G, Latronico MV, Cavarretta E. microRNAs in cardiovascular diseases: current knowledge and the road ahead. J Am Coll Cardiol. 2014;63(21):2177–87.
67. Saxena A, Tabin CJ. miRNA-processing enzyme Dicer is necessary for cardiac outflow tract alignment and chamber septation. Proc Natl Acad Sci U S A. 2010;107(1):87–91.
68. Peng Y, Song L, Zhao M, Harmelink C, Debenedittis P, Cui X, et al. Critical roles of miRNA-mediated regulation of TGFbeta signalling during mouse cardiogenesis. Cardiovasc Res. 2014;103(2):258–67.
69. Chen JF, Murchison EP, Tang R, Callis TE, Tatsuguchi M, Deng Z, et al. Targeted deletion of Dicer in the heart leads to dilated cardiomyopathy and heart failure. Proc Natl Acad Sci U S A. 2008;105(6):2111–6.
70. Kwon C, Han Z, Olson EN, Srivastava D. MicroRNA1 influences cardiac differentiation in Drosophila and regulates Notch signaling. Proc Natl Acad Sci U S A. 2005;102(52):18986–91.
71. Zhao Y, Samal E, Srivastava D. Serum response factor regulates a muscle-specific microRNA that targets Hand2 during cardiogenesis. Nature. 2005;436(7048):214–20.
72. Elia L, Contu R, Quintavalle M, Varrone F, Chimenti C, Russo MA, et al. Reciprocal regulation of microRNA-1 and insulin-like growth factor-1 signal transduction cascade in cardiac and skeletal muscle in physiological and pathological conditions. Circulation. 2009;120(23):2377–85.
73. Varrone F, Gargano B, Carullo P, Di Silvestre D, De Palma A, Grasso L, et al. The circulating level of FABP3 is an indirect biomarker of microRNA-1. J Am Coll Cardiol. 2013;61(1):88–95.
74. Liu N, Bezprozvannaya S, Williams AH, Qi X, Richardson JA, Bassel-Duby R, et al. microRNA-133a regulates cardiomyocyte proliferation and suppresses smooth muscle gene expression in the heart. Genes Dev. 2008;22(23):3242–54.
75. Wang J, Greene SB, Bonilla-Claudio M, Tao Y, Zhang J, Bai Y, et al. Bmp signaling regulates myocardial differentiation from cardiac progenitors through a MicroRNA-mediated mechanism. Dev Cell. 2010;19(6):903–12.
76. Cimmino A, Calin GA, Fabbri M, Iorio MV, Ferracin M, Shimizu M, et al. miR-15 and miR-16 induce apoptosis by targeting BCL2. Proc Natl Acad Sci U S A. 2005;102(39):13944–9.
77. Hullinger TG, Montgomery RL, Seto AG, Dickinson BA, Semus HM, Lynch JM, et al. Inhibition of miR-15 protects against cardiac ischemic injury. Circ Res. 2012;110(1):71–81.
78. Yamakuchi M, Ferlito M, Lowenstein CJ. miR-34a repression of SIRT1 regulates apoptosis. Proc Natl Acad Sci U S A. 2008;105(36):13421–6.
79. Boon RA, Iekushi K, Lechner S, Seeger T, Fischer A, Heydt S, et al. MicroRNA-34a regulates cardiac ageing and function. Nature. 2013;495(7439):107–10.
80. Aurora AB, Mahmoud AI, Luo X, Johnson BA, van Rooij E, Matsuzaki S, et al. MicroRNA-214 protects the mouse heart from ischemic injury by controlling Ca(2)(+) overload and cell death. J Clin Invest. 2012;122(4):1222–32.

81. Qian L, Van Laake LW, Huang Y, Liu S, Wendland MF, Srivastava D. miR-24 inhibits apoptosis and represses Bim in mouse cardiomyocytes. J Exp Med. 2011;208(3):549–60.
82. Frank D, Gantenberg J, Boomgaarden I, Kuhn C, Will R, Jarr KU, et al. MicroRNA-20a inhibits stress-induced cardiomyocyte apoptosis involving its novel target Egln3/PHD3. J Mol Cell Cardiol. 2012;52(3):711–7.
83. Liu N, Olson EN. MicroRNA regulatory networks in cardiovascular development. Dev Cell. 2010;18(4):510–25.
84. Malizia AP, Wang DZ. MicroRNAs in cardiomyocyte development. Wiley Interdiscip Rev Syst Biol Med. 2011;3(2):183–90.
85. Yan S, Jiao K. Functions of miRNAs during mammalian heart development. Int J Mol Sci. 2016;17(5):E789.
86. Fiedler J, Thum T. MicroRNAs in myocardial infarction. Arterioscler Thromb Vasc Biol. 2013;33(2):201–5.
87. Salloum FN, Yin C, Kukreja RC. Role of microRNAs in cardiac preconditioning. J Cardiovasc Pharmacol. 2010;56(6):581–8.
88. Ye Y, Perez-Polo JR, Qian J, Birnbaum Y. The role of microRNA in modulating myocardial ischemia-reperfusion injury. Physiol Genomics. 2011;43(10):534–42.
89. Zhu H, Fan GC. Role of microRNAs in the reperfused myocardium towards post-infarct remodelling. Cardiovasc Res. 2012;94(2):284–92.
90. Huang F, Zhu X, XQ H, Fang ZF, Tang L, XL L, et al. Mesenchymal stem cells modified with miR-126 release angiogenic factors and activate Notch ligand Delta-like-4, enhancing ischemic angiogenesis and cell survival. Int J Mol Med. 2013;31(2):484–92.
91. Bonauer A, Carmona G, Iwasaki M, Mione M, Koyanagi M, Fischer A, et al. MicroRNA-92a controls angiogenesis and functional recovery of ischemic tissues in mice. Science. 2009;324(5935):1710–3.
92. Wu W, Xiao H, Laguna-Fernandez A, Villarreal G Jr, Wang KC, Geary GG, et al. Flow-dependent regulation of kruppel-like factor 2 is mediated by microRNA-92a. Circulation. 2011;124(5):633–41.
93. Bonauer A, Boon RA, Dimmeler S. Vascular microRNAs. Curr Drug Targets. 2010;11(8):943–9.
94. Suárez Y, Fernández-Hernando C, Yu J, Gerber SA, Harrison KD, Pober JS, et al. Dicer-dependent endothelial microRNAs are necessary for postnatal angiogenesis. Proc Natl Acad Sci U S A. 2008;105(37):14082–7.
95. Fiedler J, Jazbutyte V, Kirchmaier BC, Gupta SK, Lorenzen J, Hartmann D, et al. MicroRNA-24 regulates vascularity after myocardial infarction. Circulation. 2011;124(6):720–30.
96. Li RC, Tao J, Guo YB, HD W, Liu RF, Bai Y, et al. In vivo suppression of microRNA-24 prevents the transition toward decompensated hypertrophy in aortic-constricted mice. Circ Res. 2013;112(4):601–5.
97. Yin KJ, Olsen K, Hamblin M, Zhang J, Schwendeman SP, Chen YE. Vascular endothelial cell-specific microRNA-15a inhibits angiogenesis in hindlimb ischemia. J Biol Chem. 2012;287(32):27055–64.
98. Asgeirsdóttir SA, van Solingen C, Kurniati NF, Zwiers PJ, Heeringa P, van Meurs M, et al. MicroRNA-126 contributes to renal microvascular heterogeneity of VCAM-1 protein expression in acute inflammation. Am J Physiol Renal Physiol. 2012;302(12):14.
99. Madrigal-Matute J, Rotllan N, Aranda JF, Fernández-Hernando C. MicroRNAs and atherosclerosis. Curr Atheroscler Rep. 2013;15(5):013–0322.
100. Sun X, Icli B, Wara AK, Belkin N, He S, Kobzik L, et al. MicroRNA-181b regulates NF-kappaB-mediated vascular inflammation. J Clin Invest. 2012;122(6):1973–90.
101. Huang RS, Hu GQ, Lin B, Lin ZY, Sun CC. MicroRNA-155 silencing enhances inflammatory response and lipid uptake in oxidized low-density lipoprotein-stimulated human THP-1 macrophages. J Investig Med. 2010;58(8):961–7.
102. Chen T, Huang Z, Wang L, Wang Y, Wu F, Meng S, et al. MicroRNA-125a-5p partly regulates the inflammatory response, lipid uptake, and ORP9 expression in oxLDL-stimulated monocyte/macrophages. Cardiovasc Res. 2009;83(1):131–9.
103. Chen KC, Wang YS, CY H, Chang WC, Liao YC, Dai CY, et al. OxLDL up-regulates microRNA-29b, leading to epigenetic modifications of MMP-2/MMP-9 genes: a novel mechanism for cardiovascular diseases. FASEB J. 2011;25(5):1718–28.
104. Lovren F, Pan Y, Quan A, Singh KK, Shukla PC, Gupta N, et al. MicroRNA-145 targeted therapy reduces atherosclerosis. Circulation. 2012;126(11 Suppl 1):S81–90.
105. Bauersachs J. miR-21: a central regulator of fibrosis not only in the broken heart. Cardiovasc Res. 2012;96(2):227–9.
106. van Rooij E, Sutherland LB, Thatcher JE, DiMaio JM, Naseem RH, Marshall WS, et al. Dysregulation of microRNAs after myocardial infarction reveals a role of miR-29 in cardiac fibrosis. Proc Natl Acad Sci U S A. 2008;105(35):13027–32.
107. Thum T, Gross C, Fiedler J, Fischer T, Kissler S, Bussen M, et al. MicroRNA-21 contributes to myocardial disease by stimulating MAP kinase signalling in fibroblasts. Nature. 2008;456(7224):980–4.
108. Cheng Y, Liu X, Zhang S, Lin Y, Yang J, Zhang C. MicroRNA-21 protects against the H(2)O(2)-induced injury on cardiac myocytes via its target gene PDCD4. J Mol Cell Cardiol. 2009;47(1):5–14.
109. Cheng Y, Zhu P, Yang J, Liu X, Dong S, Wang X, et al. Ischaemic preconditioning-regulated miR-21 protects heart against ischaemia/reperfusion injury via anti-apoptosis through its target PDCD4. Cardiovasc Res. 2010;87(3):431–9.
110. Boon RA, Seeger T, Heydt S, Fischer A, Hergenreider E, Horrevoets AJ, et al. MicroRNA-29 in aortic dila-

tion: implications for aneurysm formation. Circ Res. 2011;109(10):1115–9.
111. van Rooij E, Sutherland LB, Liu N, Williams AH, McAnally J, Gerard RD, et al. A signature pattern of stress-responsive microRNAs that can evoke cardiac hypertrophy and heart failure. Proc Natl Acad Sci U S A. 2006;103(48):18255–60.
112. Pan Z, Sun X, Shan H, Wang N, Wang J, Ren J, et al. MicroRNA-101 inhibited postinfarct cardiac fibrosis and improved left ventricular compliance via the FBJ osteosarcoma oncogene/transforming growth factor-beta1 pathway. Circulation. 2012;126(7):840–50.
113. Mercola M, Ruiz-Lozano P, Schneider MD. Cardiac muscle regeneration: lessons from development. Genes Dev. 2011;25(4):299–309.
114. Small EM, Olson EN. Pervasive roles of microRNAs in cardiovascular biology. Nature. 2011;469(7330):336–42.
115. Ieda M, JD F, Delgado-Olguin P, Vedantham V, Hayashi Y, Bruneau BG, et al. Direct reprogramming of fibroblasts into functional cardiomyocytes by defined factors. Cell. 2010;142(3):375–86.
116. Qian L, Huang Y, Spencer CI, Foley A, Vedantham V, Liu L, et al. In vivo reprogramming of murine cardiac fibroblasts into induced cardiomyocytes. Nature. 2012;485(7400):593–8.
117. Song K, Nam YJ, Luo X, Qi X, Tan W, Huang GN, et al. Heart repair by reprogramming non-myocytes with cardiac transcription factors. Nature. 2012;485(7400):599–604.
118. Jayawardena TM, Egemnazarov B, Finch EA, Zhang L, Payne JA, Pandya K, et al. MicroRNA-mediated in vitro and in vivo direct reprogramming of cardiac fibroblasts to cardiomyocytes. Circ Res. 2012;110(11):1465–73.
119. Heinrich EM, Dimmeler S. MicroRNAs and stem cells: control of pluripotency, reprogramming, and lineage commitment. Circ Res. 2012;110(7):1014–22.
120. Forbes MS, Sperelakis N. Ultrastructure of mammalian cardiac muscle. In: Sperelakis N, editor. Physiology and pathophysiology of the heart. 2nd ed. Boston: Kluwer Academic Publishers; 1989. p. 3–41.
121. Peters NS, Wit AL. Myocardial architecture and ventricular arrhythmogenesis. Circulation. 1998;97(17):1746–54.
122. Gregorio CC, Antin PB. To the heart of myofibril assembly. Trends Cell Biol. 2000;10(9):355–62.
123. Huxley HE. Memories of early work on muscle contraction and regulation in the 1950's and 1960's. Biochem Biophys Res Commun. 2008;369(1):34–42.
124. Eremia D. Is there a continuity of filaments in the sarcomere? J Theor Biol. 1985;112(1):177–81.
125. Umazume Y, Fujime S. Electro-optical property of extremely stretched skinned muscle fibers. Biophys J. 1975;15(2 Pt 1):163–80.
126. Eremia D. An explanation of shortening heat generation and mechanical performance enhancement during muscle stretch. Sci World J. 2001;1:547–54.
127. Jin JP. Titin-thin filament interaction and potential role in muscle function. Adv Exp Med Biol. 2000;481:319–33. discussion 34–5
128. Burlacu A, Rosca AM, Maniu H, Titorencu I, Dragan E, Jinga V, et al. Promoting effect of 5-azacytidine on the myogenic differentiation of bone marrow stromal cells. Eur J Cell Biol. 2008;87(3):173–84.
129. Rosca AM, Matei C, Dragan E, Burlacu A. Cardiomyocyte apoptosis in ischaemia-reperfusion due to the exogenous oxidants at the time of reperfusion. Cell Biol Int. 2012;36(12):1207–15.
130. Schaper J, Meiser E, Stammler G. Ultrastructural morphometric analysis of myocardium from dogs, rats, hamsters, mice, and from human hearts. Circ Res. 1985;56(3):377–91.
131. Parton RG, Way M, Zorzi N, Stang E. Caveolin-3 associates with developing T-tubules during muscle differentiation. J Cell Biol. 1997;136(1):137–54.
132. Simons K, Toomre D. Lipid rafts and signal transduction. Nat Rev Mol Cell Biol. 2000;1(1):31–9.
133. Ferrantini C, Crocini C, Coppini R, Vanzi F, Tesi C, Cerbai E, et al. The transverse-axial tubular system of cardiomyocytes. Cell Mol Life Sci. 2013;70(24):4695–710.
134. Cannell MB, Cheng H, Lederer WJ. The control of calcium release in heart muscle. Science. 1995;268(5213):1045–9.
135. Cheng H, Lederer WJ, Cannell MB. Calcium sparks: elementary events underlying excitation-contraction coupling in heart muscle. Science. 1993;262(5134):740–4.
136. López-López JR, Shacklock PS, Balke CW, Wier WG. Local calcium transients triggered by single L-type calcium channel currents in cardiac cells. Science. 1995;268(5213):1042–5.
137. Zima AV, Picht E, Bers DM, Blatter LA. Partial inhibition of sarcoplasmic reticulum ca release evokes long-lasting ca release events in ventricular myocytes: role of luminal ca in termination of ca release. Biophys J. 2008;94(5):1867–79.
138. Faber GM, Silva J, Livshitz L, Rudy Y. Kinetic properties of the cardiac L-type Ca2+ channel and its role in myocyte electrophysiology: a theoretical investigation. Biophys J. 2007;92(5):1522–43.
139. Saucerman JJ, Bers DM. Calmodulin mediates differential sensitivity of CaMKII and calcineurin to local Ca2+ in cardiac myocytes. Biophys J. 2008;95(10):4597–612.
140. Shannon TR, Ginsburg KS, Bers DM. Potentiation of fractional sarcoplasmic reticulum calcium release by total and free intra-sarcoplasmic reticulum calcium concentration. Biophys J. 2000;78(1):334–43.
141. Bers DM. Cardiac excitation-contraction coupling. Nature. 2002;415(6868):198–205.
142. Giles WR, Noble D. Rigorous phenotyping of cardiac iPSC preparations requires knowledge of their resting potential(s). Biophys J. 2016;110(1):278–80.
143. Gerdes AM, Kasten FH. Morphometric study of endomyocardium and epimyocardium of the left ventricle in adult dogs. Am J Anat. 1980;159(4):389–94.

144. Severs NJ, Slade AM, Powell T, Twist VW, Jones GE. Morphometric analysis of the isolated calcium-tolerant cardiac myocyte. Organelle volumes, sarcomere length, plasma membrane surface folds, and intramembrane particle density and distribution. Cell Tissue Res. 1985;240(1):159–68.
145. Seidel T, Navankasattusas S, Ahmad A, Diakos NA, WD X, Tristani-Firouzi M, et al. Sheet-like remodeling of the transverse tubular system in human heart failure impairs excitation-contraction coupling and functional recovery by mechanical unloading. Circulation. 2017;135(17):1632–45.
146. Bird SD, Doevendans PA, van Rooijen MA, Brutel de la Riviere A, Hassink RJ, Passier R, et al. The human adult cardiomyocyte phenotype. Cardiovasc Res. 2003;58(2):423–34.
147. Feric NT, Radisic M. Maturing human pluripotent stem cell-derived cardiomyocytes in human engineered cardiac tissues. Adv Drug Deliv Rev. 2016;96:110–34.
148. Piper HM, Jacobson SL, Schwartz P. Determinants of cardiomyocyte development in long-term primary culture. J Mol Cell Cardiol. 1988;20(9):825–35.
149. Yau TM, Fung K, Weisel RD, Fujii T, Mickle DA, Li RK. Enhanced myocardial angiogenesis by gene transfer with transplanted cells. Circulation. 2001;104(12 Suppl 1):I218–22.
150. Anversa P, Kajstura J. Ventricular myocytes are not terminally differentiated in the adult mammalian heart. Circ Res. 1998;83(1):1–14.
151. Anversa P, Olivetti G, Bracchi PG, Loud AV. Postnatal development of the M-band in rat cardiac myofibrils. Circ Res. 1981;48(4):561–8.
152. Anversa P, Vitali-Mazza L, Loud AV. Morphometric and autoradiographic study of developing ventricular and atrial myocardium in fetal rats. Lab Investig. 1975;33(6):696–705.
153. Zak R. Development and proliferative capacity of cardiac muscle cells. Circ Res. 1974;35(suppl II):17–26.
154. Rakusan K. Cardiac growth, maturation, and aging. In: Zak R, editor. Growth of the heart in health and disease. New York: Raven Press; 1984. p. 131–4.
155. Anversa P, Sussman MA, Bolli R. Molecular genetic advances in cardiovascular medicine: focus on the myocyte. Circulation. 2004;109(23):2832–8.
156. Beltrami AP, Urbanek K, Kajstura J, Yan SM, Finato N, Bussani R, et al. Evidence that human cardiac myocytes divide after myocardial infarction. N Engl J Med. 2001;344(23):1750–7.
157. Poveda F, Gil D, Martí E, Andaluz A, Ballester M, Carreras F. Helical structure of the cardiac ventricular anatomy assessed by diffusion tensor magnetic resonance imaging with multiresolution tractography. Rev Esp Cardiol. 2013;66(10):782–90.
158. Capulli AK, MacQueen LA, Sheehy SP, Parker KK. Fibrous scaffolds for building hearts and heart parts. Adv Drug Deliv Rev. 2016;96:83–102.
159. Bergmann O, Bhardwaj RD, Bernard S, Zdunek S, Barnabe-Heider F, Walsh S, et al. Evidence for cardiomyocyte renewal in humans. Science. 2009;324(5923):98–102.
160. Gutstein DE, Liu FY, Meyers MB, Choo A, Fishman GI. The organization of adherens junctions and desmosomes at the cardiac intercalated disc is independent of gap junctions. J Cell Sci. 2003;116(Pt 5):875–85.
161. Ting S, Liew SJ, Japson F, Shang F, Chong WK, Reuveny S, et al. Time-resolved video analysis and management system for monitoring cardiomyocyte differentiation processes and toxicology assays. Biotechnol J. 2014;9(5):675–83.
162. Kempf H, Andrée B, Zweigerdt R. Large-scale production of human pluripotent stem cell derived cardiomyocytes. Adv Drug Deliv Rev. 2016;96:18–30.
163. Batalov I, Feinberg AW. Differentiation of cardiomyocytes from human pluripotent stem cells using monolayer culture. Biomarkers. 2015;10(Suppl 1):71–6.
164. Kotov G, Iliev A, Landzhov B, Jelev L, Dimitrova IN, Hinova-Palova D. Postnatal changes in the morphology of the myocardium in rat ventricles. Arch Anat Physiol. 2017;2(1):11–7.
165. Cereghetti GM, Stangherlin A, Martins de Brito O, Chang CR, Blackstone C, Bernardi P, et al. Dephosphorylation by calcineurin regulates translocation of Drp1 to mitochondria. Proc Natl Acad Sci U S A. 2008;105(41):15803–8.
166. Detmer SA, Chan DC. Functions and dysfunctions of mitochondrial dynamics. Nat Rev Mol Cell Biol. 2007;8(11):870–9.
167. Kuzmicic J, Del Campo A, López-Crisosto C, Morales PE, Pennanen C, Bravo-Sagua R, et al. Mitochondrial dynamics: a potential new therapeutic target for heart failure. Rev Esp Cardiol. 2011;64(10):916–23.
168. Liu SJ. Characterization of functional capacity of adult ventricular myocytes in long-term culture. Int J Cardiol. 2013;168(3):1923–36.
169. Schelbert EB, Fonarow GC, Bonow RO, Butler J, Gheorghiade M. Therapeutic targets in heart failure: refocusing on the myocardial interstitium. J Am Coll Cardiol. 2014;63(21):2188–98.
170. Rehsia NS, Dhalla NS. Potential of endothelin-1 and vasopressin antagonists for the treatment of congestive heart failure. Heart Fail Rev. 2010;15(1):85–101.
171. Pall ML. The NO/ONOO-cycle as the central cause of heart failure. Int J Mol Sci. 2013;14(11):22274–330.
172. Spinale FG, Zile MR. Integrating the myocardial matrix into heart failure recognition and management. Circ Res. 2013;113(6):725–38.
173. Putney JW. Origins of the concept of store-operated calcium entry. Front Biosci. 2011;3:980–4.
174. Hoth M, Penner R. Depletion of intracellular calcium stores activates a calcium current in mast cells. Nature. 1992;355(6358):353–6.
175. Liao Y, Erxleben C, Abramowitz J, Flockerzi V, Zhu MX, Armstrong DL, et al. Functional interactions among Orai1, TRPCs, and STIM1 suggest a STIM-regulated heteromeric Orai/TRPC model for

SOCE/Icrac channels. Proc Natl Acad Sci U S A. 2008;105(8):2895–900.
176. Ong HL, Ambudkar IS. The dynamic complexity of the TRPC1 channelosome. Channels. 2011;5(5):424–31.
177. Cheng KT, Ong HL, Liu X, Ambudkar IS. Contribution and regulation of TRPC channels in store-operated Ca2+ entry. Curr Top Membr. 2013;71:149–79.
178. Yuan JP, Kim MS, Zeng W, Shin DM, Huang G, Worley PF, et al. TRPC channels as STIM1-regulated SOCs. Channels. 2009;3(4):221–5.
179. Seth M, Zhang ZS, Mao L, Graham V, Burch J, Stiber J, et al. TRPC1 channels are critical for hypertrophic signaling in the heart. Circ Res. 2009;105(10):1023–30.
180. Kiyonaka S, Kato K, Nishida M, Mio K, Numaga T, Sawaguchi Y, et al. Selective and direct inhibition of TRPC3 channels underlies biological activities of a pyrazole compound. Proc Natl Acad Sci U S A. 2009;106(13):5400–5.
181. Bush EW, Hood DB, Papst PJ, Chapo JA, Minobe W, Bristow MR, et al. Canonical transient receptor potential channels promote cardiomyocyte hypertrophy through activation of calcineurin signaling. J Biol Chem. 2006;281(44):33487–96.
182. Nakayama H, Wilkin BJ, Bodi I, Molkentin JD. Calcineurin-dependent cardiomyopathy is activated by TRPC in the adult mouse heart. FASEB J. 2006;20(10):1660–70.
183. Wu X, Eder P, Chang B, Molkentin JD. TRPC channels are necessary mediators of pathologic cardiac hypertrophy. Proc Natl Acad Sci U S A. 2010;107(15):7000–5.
184. Fauconnier J, Lanner JT, Sultan A, Zhang SJ, Katz A, Bruton JD, et al. Insulin potentiates TRPC3-mediated cation currents in normal but not in insulin-resistant mouse cardiomyocytes. Cardiovasc Res. 2007;73(2):376–85.
185. Washburn DG, Holt DA, Dodson J, McAtee JJ, Terrell LR, Barton L, et al. The discovery of potent blockers of the canonical transient receptor channels, TRPC3 and TRPC6, based on an anilinothiazole pharmacophore. Bioorg Med Chem Lett. 2013;23(17):4979–84.
186. Kuwahara K, Wang Y, McAnally J, Richardson JA, Bassel-Duby R, Hill JA, et al. TRPC6 fulfills a calcineurin signaling circuit during pathologic cardiac remodeling. J Clin Invest. 2006;116(12):3114–26.
187. Eder P, Molkentin JD. TRPC channels as effectors of cardiac hypertrophy. Circ Res. 2011;108(2):265–72.
188. Kuwahara K, Nakao K. New molecular mechanisms for cardiovascular disease: transcriptional pathways and novel therapeutic targets in heart failure. J Pharmacol Sci. 2011;116(4):337–42.
189. Lighthouse JK, Small EM. Transcriptional control of cardiac fibroblast plasticity. J Mol Cell Cardiol. 2016;91:52–60.
190. Watanabe H, Murakami M, Ohba T, Takahashi Y, Ito H. TRP channel and cardiovascular disease. Pharmacol Ther. 2008;118(3):337–51.
191. Corsten MF, Dennert R, Jochems S, Kuznetsova T, Devaux Y, Hofstra L, et al. Circulating MicroRNA-208b and MicroRNA-499 reflect myocardial damage in cardiovascular disease. Circ Cardiovasc Genet. 2010;3(6):499–506.
192. Vogel B, Keller A, Frese KS, Leidinger P, Sedaghat-Hamedani F, Kayvanpour E, et al. Multivariate miRNA signatures as biomarkers for non-ischaemic systolic heart failure. Eur Heart J. 2013;34(36):2812–22.
193. Bauters C, Kumarswamy R, Holzmann A, Bretthauer J, Anker SD, Pinet F, et al. Circulating miR-133a and miR-423-5p fail as biomarkers for left ventricular remodeling after myocardial infarction. Int J Cardiol. 2013;168(3):1837–40.
194. van Rooij E, Sutherland LB, Qi X, Richardson JA, Hill J, Olson EN. Control of stress-dependent cardiac growth and gene expression by a microRNA. Science. 2007;316(5824):575–9.
195. Carè A, Catalucci D, Felicetti F, Bonci D, Addario A, Gallo P, et al. MicroRNA-133 controls cardiac hypertrophy. Nat Med. 2007;13(5):613–8.
196. He B, Xiao J, Ren AJ, Zhang YF, Zhang H, Chen M, et al. Role of miR-1 and miR-133a in myocardial ischemic postconditioning. J Biomed Sci. 2011b;18(22):1423–0127.
197. Myers R, Timofeyev V, Li N, Kim C, Ledford HA, Sirish P, et al. Feedback mechanisms for cardiac-specific microRNAs and cAMP signaling in electrical remodeling. Circ Arrhythm Electrophysiol. 2015;8(4):942–50.
198. Matkovich SJ, Wang W, Tu Y, Eschenbacher WH, Dorn LE, Condorelli G, et al. MicroRNA-133a protects against myocardial fibrosis and modulates electrical repolarization without affecting hypertrophy in pressure-overloaded adult hearts. Circ Res. 2010;106(1):166–75.
199. Dong DL, Chen C, Huo R, Wang N, Li Z, YJ T, et al. Reciprocal repression between microRNA-133 and calcineurin regulates cardiac hypertrophy: a novel mechanism for progressive cardiac hypertrophy. Hypertension. 2010;55(4):946–52.
200. McGrath J, Somlo S, Makova S, Tian X, Brueckner M. Two populations of node monocilia initiate left-right asymmetry in the mouse. Cell. 2003;114(1):61–73.
201. Clapham DE. TRP channels as cellular sensors. Nature. 2003;426(6966):517–24.
202. Moran MM, Xu H, Clapham DE. TRP ion channels in the nervous system. Curr Opin Neurobiol. 2004;14(3):362–9.
203. Pennekamp P, Karcher C, Fischer A, Schweickert A, Skryabin B, Horst J, et al. The ion channel polycystin-2 is required for left-right axis determination in mice. Curr Biol. 2002;12(11):938–43.

204. Boulter C, Mulroy S, Webb S, Fleming S, Brindle K, Sandford R. Cardiovascular, skeletal, and renal defects in mice with a targeted disruption of the Pkd1 gene. Proc Natl Acad Sci U S A. 2001;98(21):12174–9.
205. Wu G, D'Agati V, Cai Y, Markowitz G, Park JH, Reynolds DM, et al. Somatic inactivation of Pkd2 results in polycystic kidney disease. Cell. 1998;93(2):177–88.
206. Mori AD, Zhu Y, Vahora I, Nieman B, Koshiba-Takeuchi K, Davidson L, et al. Tbx5-dependent rheostatic control of cardiac gene expression and morphogenesis. Dev Biol. 2006;297(2):566–86.
207. Ocaña OH, Coskun H, Minguillón C, Murawala P, Tanaka EM, Galcerán J, et al. A right-handed signalling pathway drives heart looping in vertebrates. Nature. 2017;549(7670):86–90.
208. Reddy S, Bernstein D. Molecular mechanisms of right ventricular failure. Circulation. 2015;132(18):1734–42.
209. Morine KJ, Paruchuri V, Qiao X, Aronovitz M, Huggins GS, DeNofrio D, et al. Endoglin selectively modulates transient receptor potential channel expression in left and right heart failure. Cardiovasc Pathol. 2016;25(6):478–82.
210. Rocchetti M, Sala L, Rizzetto R, Staszewsky LI, Alemanni M, Zambelli V, et al. Ranolazine prevents INaL enhancement and blunts myocardial remodelling in a model of pulmonary hypertension. Cardiovasc Res. 2014;104(1):37–48.

4 Basic Aspects of Cardiac Remodelling

Ecaterina Bontaş, Florentina Radu-Ioniţă, Alice Munteanu, and Iancu Mocanu

Abstract

It has been defined by Conn and colleagues in 2000 that "Cardiac remodelling may be characterized as genome expression, molecular, cellular and interstitial changes that are manifested clinically as changes in size, shape and function of the heart after cardiac injury", associated with ventricular dysfunction, malignant arrhythmias and poor prognosis. Conversely, the various definitions of cardiac remodelling stress on common molecular, biochemical, and mechanical pathways. Although the right ventricle and left ventricle show significant distinctions in embryology, form, and function, they have many similar findings when they adjust to damaging loading or when they fail. Having a number of key differentiations in their molecular response to failure this offer a future platform for right ventricle for a particular therapeutic intervention. It has been suggested by Friedberg and Redington in 2014 that "Focus on the molecular pathways specific to the failing right ventricle, and targeting the interactions between both ventricles may guide to successful treatments for the right ventricle and left ventricle failure". A shortly review is made with updated information for all factors that cause and affect cardiac remodelling process, especially in case of right heart.

Keywords

Right ventricle · Cardiac remodelling · Cardiac remodeling · Heart failure · Reverse remodelling · Right heart

E. Bontaş (✉)
"Prof. C.C.Iliescu" Emergency Institute for Cardiovascular Diseases,, Bucharest, Romania

F. Radu-Ioniţă
"Titu Maiorescu", University of Medicine, Bucharest, Romania

"Carol Davila" Central Military Emergency University Hospital, Bucharest, Romania

A. Munteanu
Department of Interventional Cardiology, "Carol Davila" Central Military Emergency University Hospital, Bucharest, Romania

I. Mocanu
Department of Cardiovascular Surgery, Sanador Hospital, Bucharest, Romania

4.1 Introduction

To date, the term 'cardiac remodelling' (CR) was firstly coined by Hockman and Buckey on myocardial infarction (MI) to study replacement of myocardial injury with scar tissue [1]. Later, Janice Pfeffer applied the name CR to illustrate the progressive dilatation of the left ventricle (LV) on vivo studies [2]. Nonetheless, Pfeffer and

S. I. Dumitrescu et al. (eds.), *Right Heart Pathology*, https://doi.org/10.1007/978-3-319-73764-5_4

Braunwald utilized the term CR for morphological changes caused by MI, especially for LV remodelling [3]. In this regard, an international forum published in 2000 a consensus on CR, that defined "*CR as a group of molecular, cellular and interstitial changes that clinically manifest as changes in size, shape and function of the heart resulting from cardiac injury*" [4]. In biology, the term remodelling characterizes adjustments that cause reorganizing of initial structures [5]. Even if CR was used initially to describe the geometric and structural modifications caused by MI [3, 6], CR is actually applied to a large variety of cardiac conditions. Esentially, Swynghedauw classified etiology of CR as being (1) *acquired diseases* (postmyocardial infarction, hypertensive cardiopathy, valve and congenital disease, myocarditis, and Chagas disease); (2) *genetics* (inherited cardiomyopathies, familial hypertrophic cardiomyopathy, dilated cardiomyopathy, Marfan disease, hemochromatose, transgenic models, transgenic models of cardiac hypertrophy, transgenic models of cardiac failure); and (3) *miscellaneous causes* (aging; heart rate; use of catecholamines, thyroxine, or growth hormone; salt, mineralo- and glucocorticoid; diabetes mellitus; B6 vitamin deficiency; atrophy due to heterotopic transplantation and hypertrophy due to homeotopic transplantation (?)) [5, 7, 8]. Further, CR is separated into *structural* (hypertrophy and fibrosis) and *electrical* remodelling. Shortly, any type of stress induces cardiomyocytes (CMs) to become hypertrophic with altered electrical function, while cardiac fibroblasts (CFs) transform in 'activated' myofibroblasts (MyoFb), which further multiply and boost extracellular matrix (ECM) tissue with fibrosis [9].

During international forum from 2000 [4], two types of CR were established: (1) physiological (adaptive) remodelling and (2) pathological remodelling. Further, Dorn et al. defined CR as being 'adaptive or maladaptive' [10]. It should be noted, that Hill and Olson stated that heart can respond to environmental stimuli by increase of myocardial mass or atrophy starting with a "least 100%" [11]. More important is other mechanisms than remodelling also can alter the evolution of heart disease, even in the absence of remodelling process. To reiterate, CR can be a physiologic or pathologic condition [4]. Physiologic CR is a physiological alteration in size and function of the heart due to physiologic stimuli such as exercise ("athlete's heart") and pregnancy. In addition, pathologic CR occurs with pressure overload conditions (e.g., aortic stenosis, hypertension), with volume overload conditions (e.g., valvular regurgitation), with cardiac injury or coronary artery disease (CAD), and with inflammatory myocardial disease (e.g., myocarditis), or idiopathic dilated cardiomyopathy [4]. Equally, physiologic CR may lead to pathologic remodelling [12].

Constrictive pericardial disease, selected forms of congenital heart diseases (CHD), inflow obstruction, primary myocardial disease, and pressure or volume overload are each well-described causes of *right ventricular (RV) remodelling*, RV systolic dysfunction, and cor pulmonale [13]. Emerging evidence suggests that RV dysfunction is the mainly marker of poor prognosis in pulmonary hypertension (PH) [14, 15].

For simplicity, the first adaptive reaction of the RV to pressure overload is hypertrophy. If untreated, the RV dilates to compensate increased RV preload and to maintain stroke volume according to the Frank-Starling principle. When further increase in RV end-diastolic filling volume do not balance progressive RV contractile dysfunction, clinically evident RV failure ensues. In advanced stages, RV dilation may also impair LV diastolic filling kinetics that contributes further to global pump dysfunction and, consequently, to the congestive heart failure (CHF) syndrome [16].

It should be restated that the RV and the LV don't have same embryologic origins. The RV stems from the secondary/anterior heart tube and the LV from early/primary heart tube [17]. Accordingly, RV formation is specifically controlled by several genes, including Hand2 and

Tbx20 [18]. This different embryologic origin of RV is associated with *cellular divergence* that controls the duration of early development to different LV and RV cardiomyocytes, and go on with distinct cell signalling and Ca^{2+} handling pathways for both chambers, altogether suggestive of certain essential differentiation at the cellular level for both ventricles [19]. For the foetal period, the RV propels blood into the pulmonary circulation, placenta and into the inferior body. Further, during the switch from the foetal circulation to the postnatal circulation with the reduction of pulmonary vascular resistance (PVR), the RV develops into a thin-walled, heavily trabeculated chamber pushing a cardiac output (CO) same to the LV but with lesser energy cost [20]. Normal crescent–shaped RV with thinner walls is a low-pressure chamber that faces the low impedance of pulmonary circulation. Thus, although the RV is a low-resistance and low-capacitance pump, the LV is an high-resistance and high-pressure pump [20]. Additionally, the RV has a different metabolism and morphology in comparison with LV [20]. RV cardiomyoytes are disposed longitudinally and demonstrate faster twitch velocities than the radially oriented LV cardiomyocytes. As a result, because of these anatomical and physiological differences, both ventricles present various reactions to disease forms. According to current evidences, it seems that RV hypertrophy (RVH), RV remodelling and RV failure (RVF) can develop at the same time instead of progression development (Fig. 4.1) [21].

Also, in response to increased afterload, there is an activation of the foetal gene pattern in RV, re-expressing of genes from normal foetal RV. This includes a shift from α- to β-myosin heavy chain expression and an increase in adrenergic receptors, calcineurin activation [22–24], and phosphodiesterase type-5 (PDE5) expression [25]. The foetal gene pattern re-expression, particularly the myosin heavy chain shift from the α to β isoform, an hallmark of foetal gene reactivation, is also triggered in LV failure (LVF) [22].

Further, using microarray gene chip studies of mice, Urashima et al. compared LV hypertrophy (LVH) from aortic banding with RVH from pulmonary banding, and they demonstrated both similar and different LV and RV adaptive mechanisms [26]. One pathway that is more activated in the pressure-loaded RV compared with the pressure-loaded LV is the Wnt signalling pathway (Fig. 4.2) [27–29]. Wnt regulates glycogen synthesis kinase-3b activity, a serine/threonine protein kinase active in multiple intracellular signalling pathways, including cell proliferation, migration, inflammation, glucose regulation, and apoptosis [28, 29]. Also, there are multiple variation concerning the RV and LV in their adaptation to increased loading and likely differences in metabolism, mitochondrial remodelling, and glycolysis-to glucose oxidation coupling. These metabolic changes may subsequently lead to hyperpolarization of the mitochondrial membrane potential in RV hypertrophy, inefficient energy metabolism, and increased lactate production at an earlier stage of maladaptation compared with the LV [30].

In CR process, several *cell markers* may indicate an undergoing CR progression, as well as alterations with an rise in α- and a reduction in β-myosin heavy chain, raised exhibition of Glucose transporter type (GLUT)-1, α-actin, natriuretic peptides, galectin, caveolin, neuronal nitric oxide synthase (NOS), angiotensin-converting enzyme (ACE), reduction of GLUT-4, sarcoplasmic/endoplasmic reticulum Ca(2+)ATPase 2a (SERCA 2a), and a change from free fatty acids oxidation to glucose metabolism [31, 32].

To sum up, cardiac dysfunction is the most important effect of CR. Because of cardiac injury, CR begin with genetic alterations, with reexpression of foetal genes, with cellular and molecular modifications, and gradually damage of ventricular function that develops with signs and symptoms of HF (Fig. 4.3) [4, 31, 33–35].

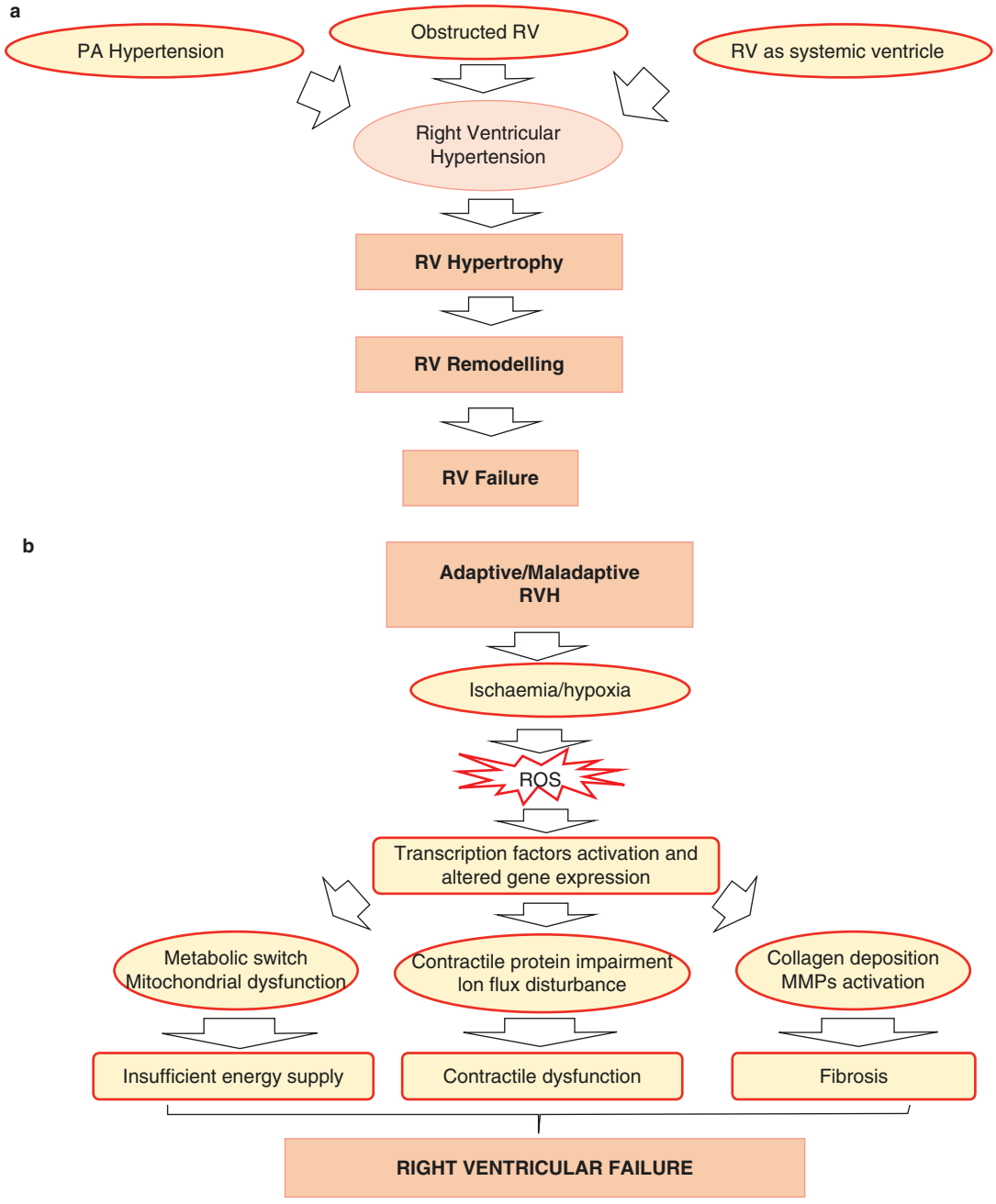

Fig. 4.1 (**a**) An overview of changes associated with RV pressure overload. Key triggers of RV pressure overload include pulmonary hypertension, RV outflow tract obstruction or RV being the systemic ventricle. RV pressure overload induces RVH that, through remodelling, leads to RV failure. It is of note, however, that RV failure is a continuous process and may begin as the time of hypertrophy and remodelling rather than being seen as a sequential process. (**b**) Effect of RVH-induced ischaemia. RVH is characterised by tissue hypoxia arising from ischaemia and microcirculatory insufficiency. Ischaemia-derived ROS, through the activation of transcription factors, drive the metabolic remodelling, contractile dysfunction and fibrosis that occur in RV failure. RVH, RV hypertrophy; PA, pulmonary artery; ROS, reactive oxygen species; MMPs, matrix metalloproteinases. (From Iacobazzi [21]. It is an open access article)

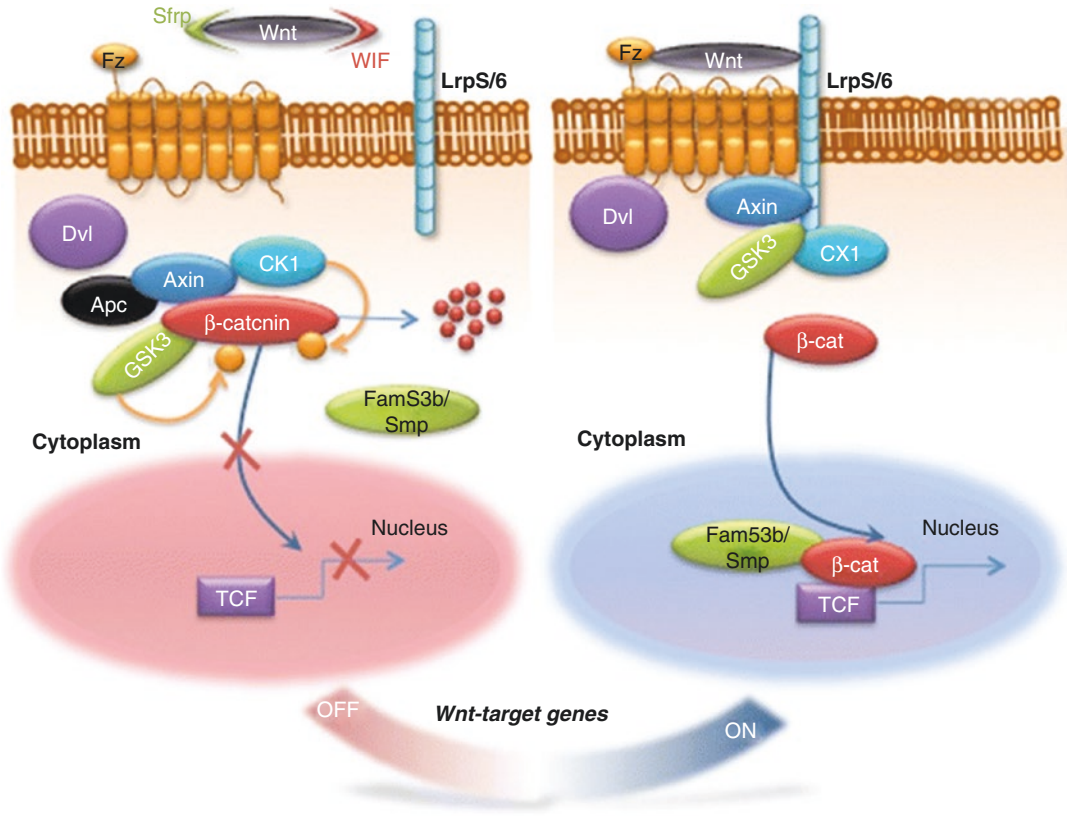

Fig. 4.2 The Wnt/β-catenin signaling pathway. In the Wnt-off state, defined by the absence of an active Wnt ligand, β-catenin is phosphorylated by the destruction complex (formed from the two kinases Gsk3 and Ck1, the scaffolding protein Axin, and the tumor suppressor Apc) and degraded by the ubiquitin-proteasome pathway. In the Wnt-on state, active Wnt ligands interact with the Fz receptors and the Lrp5/6 coreceptor. Phosphorylation of Lrp5/6 by Gsk3 and Ck1 recruits Dvl and Axin to the receptor complex and hence inhibits the destruction complex. This, in turn, inhibits β-catenin phosphorylation and stabilizes β-catenin in the cytoplasm. β-catenin is then translocated into the nucleus, by a complex including Fam53b/Smp, and regulates target gene expression with the Tcf/Lef transcription factors. Many modulators including the inhibitors sFrps and Wif are known to tightly regulate the signaling cascade. (From Ozhan et al. [27]. It is an open access article)

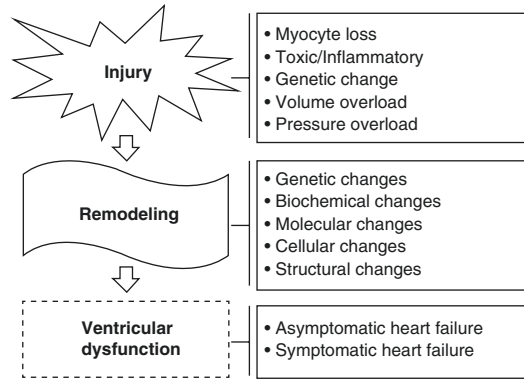

Fig. 4.3 Sequence of events from cardiac injury to cardiac dysfunction. (From Azevedo [33]. It is an open access article)

4.2 Adaptive Versus Maladaptive Cardiac Remodelling

As already stated, CR is an adjusting and a maladaptive process. The adjusting process sustains heart function due to pressure overload or volume overload in case of acute cardiac injury [36]. Even if CAD affects directly RV with regional or global ischemia, RV physiology and RVF are mainly influenced by raised preload or afterload [20]. It has to be underlined that RV is exclusively dependent on afterload. Even small changes in total PVR, as demonstrated by modest increases in mean airway pressure during positive pressure ventilation, can reduce RV contractile performance and lower CO even when RV preload is maintained [37]. In contrast, significant changes in LV afterload may induces only modest changes in LV stroke volume [38]. Although patients with acute changes in systemic vascular resistance can compensate over a wide range, those with acute pulmonary arterial hypertension (PAH) if associate acute lung failure, often develop overt RVF and compromised CO [20]. In the largest part of clinical scenarios, even acute mild/moderate raises in RV afterload produce significant falls in RV output, including PAH and RV outflow obstruction, with the mention that usually changes in afterload are chronic and occur progressively [20]. Undeniably, in the chronic conditions, the relative increase in RV afterload is much greater in PAH than the increase in LV afterload in systemic hypertension [20].

Only that, long-term CR is damaging and correlated with a weak prognosis [39, 40]. Significant CR causes the increase of failing cardiac function [39, 41] that is related with bad prognosis especially for MI [40]. Actually, there is no evidence to suggest the *time of occurrence* from *adaptive* remodelling to *maladaptive* remodelling or if CR can be recognized at right moment. For instance, continuing CR is usual after an initial, moderately large anterior MI, but is uncommon after an initial small inferior MI [41]. CR after acute MI involving the LV may progress with LV dilatation and with later RV dilatation. Biventricular (BiV) remodelling comprises a group of patients with extremely poor outcomes [42]. Importantly, BiV failure is regarded as the terminal phase of CR [43, 44]. On the other hand, there is no clear knowledge regarding the effects of acute MI of LV and RV remodelling. It seems that the most important pathophysiological mechanism is the PH followed by raise of the RV afterload.

It should be mentioned that about 50% of patients with cardiac failing will die in five years. Moreover, about 40% of patients with HF die during first one year of hospitalization [45]. Also, an important number of deaths related with CR and cardiac failing are produced by sudden death [46] suggestive of the fact that an asymptomatic patient doesn't mean a convinced good prognosis. In the face of raised survival with up-to-date current treatments, death rates have inadmissible values [47].

4.3 Basic Concepts of Cardiac Remodelling

As already mentioned that "CR may be characterized as genome expression, molecular, cellular and interstitial changes that are manifested clinically as changes in size, shape and function of the heart after cardiac injury" [4], the myocyte or cardiomyocyte (CM) is the most important cardiac cell implicated in the CR process. Conversely, the various explanations of CR share common *molecular*, *biochemical*, and *mechanical* pathways. Furthermore, the *interstitium*, *fibroblasts*, *collagen*, *coronary vasculature, hemodynamic load*, and *neurohumoral activation* affect the process of CR. A shortly review is made with updated information for all factors that influence CR process especially in case of right heart.

4.3.1 Functional Changes

RV and LV are different in their anatomy and physiology. Moreover, morphologically and functionally, both ventricles are comprehensible linked not only in health but also as they react to disease [20]. In same time, alterations in ventricular mass, and changes in composition

and volume negatively modify the cardiac function [39, 41, 48–50]. As CR continues over time, the heart dilates and becomes spherical instead of elliptical form [51, 52], with thinning of cardiac walls and mitral valve incompetence. Even so, the evolution of CR depends on the primary disease, the severity of the underlying disease, genotype, intermittent ischemia episodes, neuroendocrine activation, and recommended treatment [41, 53, 54].

4.3.2 Cellular and Molecular Changes

It should be emphasized that CR is related with numerous cellular changes as well as myocite hypertrophy, deficit of myocytes due to *apoptosis* [55–57] or *necrosis* [58], *fibroblast proliferation* [59] and *fibrosis* [60, 61]. At molecular level, recent literature has highlighted differences between the RV and LV in the expression of genes involved in the response to pressure loading and failure [62]. Some of these differences are detailed in the following text and are summarized in Table 4.1 [20, 25, 27, 63–69, 71, 72].

4.3.3 The Cardiomyocyte (CM)

Human myocardiums are composed of myocytes tied and hold up by connective tissue mainly created from fibrillar collagen. The adult human heart have about 4–5 billions CMs but the myocardium has insignificant basic regenerative capability, and the damage of an important mass of cardiac muscle causes scar. In fact, the normal myocardium consists of four components that are highly interrelated: CMs, CFs, the microcirculation and the extracellular matrix (ECM) [73]. All four above components have decisive role in the progression of chamber remodelling with hypertrophy [73]. RV myocytes have mainly longitudinal myocyte direction with angulated intrusion of superficial myocytes toward the endocardium creating a peristaltic contraction from the inlet to outlet and a bellows-like motion of the free wall

Table 4.1 Molecular differences between the left and right ventricles in response to adverse loading

Molecular response	Right ventricle	Left ventricle
Wnt pathway activation and glycolysis-to-glucose oxidation metabolism in afterload	Higher activation; potentially inefficient energy metabolism [27]	Lower activation; potentially improved energy metabolism [27]
Fibrotic response to volume loading	Stronger [63]	Weaker [63]
Irx2 transcription factor expression in afterload	Not expressed [64]	Expressed [64]
Atrial natriuretic peptide expression	Not expressed [65]	Expressed [65]
miRNA 133a expression in experimental PAH	Decreased [64]	–
Expression in afterload of clusterin, neuroblastoma suppression of tumorigenicity 1, Dkk3, Sfrp2, formin binding protein, annexin A7, lysyl oxidase	Increased [66]	Not increased [66]
Response to α-1 adrenergic receptor agonists	Decrease contractility [67]	Increase contractility [67]
Response to long-term norepinephrine infusion	No hypertrophy [68]	Hypertrophy [68]
miRNA 28, 148a, and 93 expression in failure	Increased [66]	Decreased [66]
Response to dichloroacetate in hypertrophy	Increased inotropy [27]	Unchanged inotropy [27]
Response to PDE5 inhibitors in hypertrophy	Increased inotropy [25]	Unchanged inotropy [25]
Response to recombinant BNP infusion	Unchanged inotropy [69, 70]	Increased inotropy [64]

BNP indicates brain natriuretic peptide, *Irx2* Iroquois homeobox 2, *miRNA* microRNA, *PAH* pulmonary arterial hypertension, *PDE5* phosphodiesterase type-5
From [20] with permission

toward the septum [74]. In addition, RV myocytes present quicker twitch velocities than LV myocytes [75].

Even if the RV and the LV have related cellular and molecular responses to stress, there are various distinctions at the cellular and molecular levels in their responses to stress such as pressure overload. Furthermore, both ventricles show comparable modifications in genes controlling ECM and cytoskeleton remodelling, but with significant differentiation in genes controlling energy production, mitochondrial function, reactive oxygen species (ROS) production, antioxidant protection, and angiogenesis [26, 70].

Unlike the CMs that comprise almost 1/3 of all heart's cells [76], endothelial cells (ECs) [77], vascular smooth muscle cells (VSMCs) [77], CFs, macrophages and surrounding ECM that exist in the cardiac interstitium are together named as *nonmyocyte cells* [78]. The development of nonmyocyte cells is mentioned as interstitial structural remodelling and is characterized by the increase of collagen [78, 79]. Because the increase of nonmyocytes and myocytes is unrelated of each other, the hypertrophic process may be a similar and proportional or heterogeneous with excessive nonmyocytes raise, correspondingly [80, 81].

Since CMs have low ability for cellular multiplication, it is clear that they can growth by cellular enlargement. Consequently, the cross-sectional area and diameter of CMs are raised. Furthermore, typical characteristics of hypertrophy develop too: (1) sarcomere is intense restructured; (2) raised CMs size and myocardial mass by boost of protein synthesis; and (3) cardiac specific gene expression suffers alterations [11, 82]. A part of these modifications are known as re-activation of foetal gene program that implies only the re-expression of normal genes from embryonic and neonatal heart, together with contractile foetal proteins such as skeletal α-actin, atrial myosin light chain-1 and β-myosin heavy chain, and signal transduction proteins such as atrial natriuretic peptide (ANP) or B-type natriuretic peptide (BNP) [9, 83]. Abnormal existence of these foetal proteins in adult human heart has an effect on cardiac contraction, myocardial metabolism including Ca^{2+} control, resulting in maladaptive CR [84]. Of particular interest, the presence of the foetal gene program does not exist in physiological hypertrophy [85].

Changes of CMs in the size, shape, and function are related with the raise of cell death as well. Deficit of CMs is mainly related to the chronic CR process with progression to HF, increased apoptosis [86], and decreased cardiac function of heart. For that reason, the equilibrium between CMs survival and apoptotic pathways seems the mainly factor of the shift process from hypertrophy to ventricular dilatation [87].

It has previously described that the term *matricellular proteins* don't have any significant role in cardiac tissue structure, but they are stimulated by injury with the alteration of cell to cell and cell to matrix connections [88]. Therefore, the production of matricellular proteins in the cardiac matrix, causes their attachment to growth factors, cytokines, and cardiac cells receptors of transducing signalling cascades. Consequently, matricellular proteins are controlled in CR process and have a significant function in controlling of inflammatory, reparation, fibrotic and angiogenic process [88]. It should be remembered that the term matricellular protein has been created by Bornstein [89] for ECM proteins which have no involvement in the structure of the ECM, except they appear and control cardiac cellular function subsequent to injury. According to current evidence, matricellular proteins implied in CR comprise secreted protein acidic and rich in cysteine (SPARC), osteopontin, thrombospondin (TSP), periostin, and tenascin families [88, 90]. Also, initiation of the matricellular proteins (TSP-1, tenascin-C, SPARC) can produce the process of "de-adhesion" in tissue remodelling. This process may be significant in supporting cell motility during inhibition of cell anoikis [88].

To sum up, the normal adult heart contains CMs, a complicated system of ECM, and nonmyocytes that are more numerous than CMs. Every CM is encircled by collagen (endomysium), and connective tissue (perimysium) demarcates individual fibbers. Also, the normal

mammalian heart has a rich vascular system consisted of capillary, venous and arteriolar endothelial cells, pericytes, smooth muscle cells, numerous CFs, minor numbers of macrophages, mast cells, lymphocytes and dendritic cells [88]. After an injury of sufficient degree, CMs diminish and develop into elongated or hypertrophied cells to sustain stroke volume [49, 50]. As well as, the width of ventricles wall may raise due to myocyte hypertrophy [48–50]. Changing of heart loading conditions like raised preload further causes stretching of cell membranes and increases of wall stress both have the ability to initiate the effect of hypertrophy genes. More precisely, in cardiac myocytes may be triggered new contractile proteins synthesis joining with new sarcomere. The final result is believed to be CMs elongation or the increase of their diameter [91].

It seems that RV dysfunction is described in PAH or RV obstruction [21]. Patients with RV dysfunction are put together even though the CHD can initiate different molecular, cellular and functional remodelling in the RV [21]. In addition, the evaluation of RV function is mainly based on techniques which assess structure and function of RV (e.g. echocardiography, MRI and pulmonary angiography) instead of exploring the cellular and the molecular irregularities of the RV dysfunction from CHD [21]. For instance, some studies demonstrated the alteration of gene expression in signalling pathways that control heart growth in children with Tetralogy of Fallot (TOF). Modifications such as significant suppression of genes in the Notch and Wnt pathways, in VEGF gene expression and numerous ECM proteins are identified as factors that lead to TOF [92, 93]. Another genome-wide array study has demonstrated obvious difference in gene expression between the TOF and other RVH phenotypes, including VSD and ASD. Genes related with cardiac maldevelopment such as SNIP, A2BP1 and KIAA1437 are more active in the TOF group, and genes linked with stress reaction and cell proliferation are more exhibited in the RVH conditions [94].

In addition, a molecular conversion from RV to LV characteristics appears for the period of RV adjustment to pressure overload, with the mention that altered genes from RVH have a normal representation same to the normal LV tissue. Additionally, the association of tissue hypoxia and hypertrophy can boost the protein phosphatase PP1 activity leading to raised phospholamban (PLN-Ser16) dephosphorylation in CMs, followed by cardiac dysfunction [95]. As already described, hypoxia-inducible factor-1 (HIF1α) is a further contributor factor in the RV adjustment to tissue hypoxia and mechanical stress. In acute hypoxia, HIF1α is cardioprotective based on its property to produce angiogenic, metabolic and erythropoietic genes [96]. Conversely, HIF1α sustain transforming growth factor beta TGFβ1-mediated organ fibrosis in chronic hypoxic states [96]. Also, genetic differences of HIF1α change myocardial adjustment to hypoxia during postsurgical period and before RV remodelling process [97]. Therefore, the adjustment of RV to hypoxia prior to TOF surgery is based on the HIF1α pathway and could have an effect on RV phenotype after surgery.

4.3.4 Matricellular Proteins: TSP Family

It should be underlined that one of the *matricellular proteins,* TSP family contains five members divided into two groups. TSP-1 and TSP-2 form homotrimers (Subgroup A), while TSP-3, TSP-4 and TSP-5 (COMP) form homopentamers (Subgroup B) [73, 98–100] (Figs. 4.4 and 4.5).

These matricellular proteins induced by heart injury with CR named TSPs have a significant function during cardiac growth [101]. However, numerous TSP proteins activity increases to stress. They have the capacity to attach with the components of the ECM such as cytokines and growth factors. In addition, it's convenient at this point to discuss that pressure overload quickly raise TSP expression, mainly TSP-1 and TSP-4 [102, 103], and volume overload shows a significant raise in TSP-4 mRNA [104]. In most of the cases, the

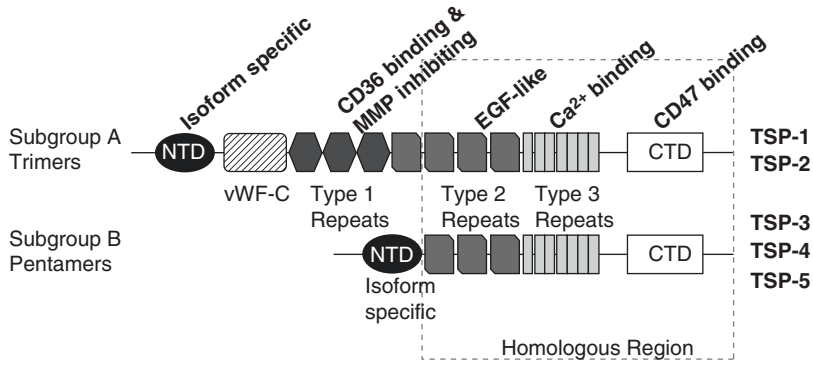

Fig. 4.4 Structure of the two thrombospondin (TSP) subgroups. Subgroup A form homotrimers and consist of TSP-1 and TSP-2, while Subgroup B form homopentamers and consist of TSP-3, TSP-4, and TSP-5 (COMP). Subgroup A has domains that bind to CD36 and inhibit MMPs. The N-terminal domains tend to be family member specific, while the CTD has high homology between the family members. *NTD* N-terminal domain (specific to each family member), *vWF-C* vonWillebrand factor C-type domain, *MMP* matrix metalloproteinase, *EGF* epidermal growth factor, *CTD* C-terminal domain. (From Kirk et al. [73] with permission)

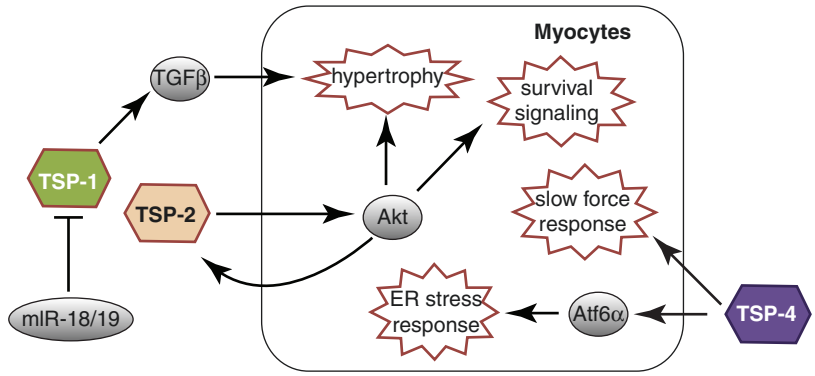

Fig. 4.5 Recent work has identified several roles for TSPs once the heart has transitioned to heart failure. The effects of the TSPs on matrix remodeling and inflammation are still important in HF. However, they also regulate a number of pathophysiologically important elements within the cardiac myocyte, which exhibits hypertrophy, apoptosis, and contractile dysfunction with HF. However, our knowledge of the mechanistic function of each of the TSPs in the HF myocyte is still incomplete. (From Kirk et al. [73] with permission)

mechanisms implied are same to the post-MI, as well as inflammation [105] and fibrosis [106].

4.3.5 Endoplasmic Reticulum Stress

Theoretically, stress factors such as hypoxia, ischemia/reperfusion, hypertrophy, pressure overload, and drug-induced insults can cause activation of *endoplasmic reticulum (ER) stress* in the heart [107]. ER stress being closely implied in the protection of cardiovascular homeostasis, it proves a significant therapeutic aim for cardiovascular diseases treatment. Figure 4.6 shows a schematic illustration of ER stress pathways with particular highlighting on their role in cardiac physiology and pathology [108]. The ER stress response or 'unfolded protein response' (UPR) is essential for normal cellular protection, but in CR like HF can generate apoptosis [107, 108]. A simplistic explanation is TSP-1 and TSP-2 have anti-inflammatory, pro-fibrotic, and antiangiogenic properties, as TSP-4 induces pro-inflammatory and pro-angiogenic consequences [109]. Also, the TSPs are significant aims for stopping the evolution from MI to HF.

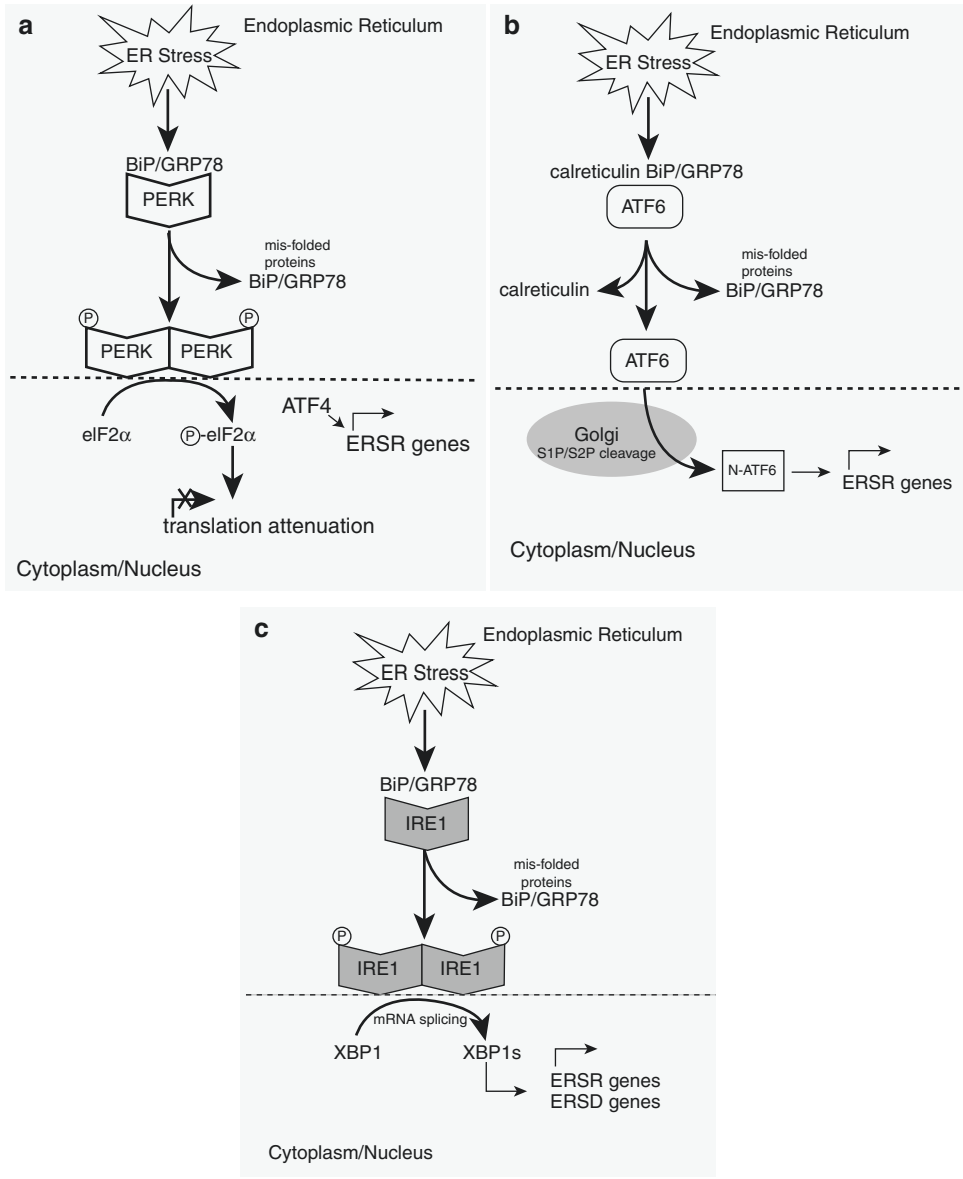

Fig. 4.6 ER stress signaling pathways. (**a**) PERK-dependent pathway activated by ER stress. PERK, a transmembrane kinase and endoribonuclease, interacts with BiP/GRP78 under nonstressed conditions. On activation of ER stress, BiP/GRP78 dissociates from PERK, resulting in dimerization of PERK and activation of its kinase domain, autophosphorylation, and subsequent phosphorylation of eIF2α. Phosphorylation of eIF2α results in attenuation of protein synthesis. However, expression of ATF4 is not inhibited, and the transcription factor induces expression of ERSR-containing genes. (**b**) ATF6 pathway. Under non-stress conditions, ATF6, a transmembrane protein localized to the ER, interacts with BiP/GRP78 and calreticulin. After ER stress, BiP/GRP78 and calreticulin dissociate from ATF6, and the protein translocates to the Golgi, where it undergoes cleavage by S1P and S2P proteases. This cleavage yields a cytoplasmic transcription factor (N-ATF6) that translocates to the nucleus and induces ERSR-containing genes. (**c**) IRE1 pathway. IRE1 is an ER transmembrane protein containing a serine–threonine kinase domain and a carboxyl-terminal endoribonuclease domain in its cytoplasmic region and binds to BiP/GRP78. Under ER stress conditions, BiP/GRP78 is released from IRE1 followed by IRE1 homodimerization and autophosphorylation. Phosphorylation is essential for IRE1 endoribonuclease activity that is responsible for splicing of XBP1 mRNA, yielding spliced XBP1s mRNA encoding a potent transcription factor. The XBP1s splice variant binds to ERSE-containing promoters and activates ERSE genes. XBP1s also binds to a second cis-acting motif, termed the UPRE, resulting in upregulation of genes involved in ERAD. (From Groenendyk et al. [108] with permission)

4.3.6 Pleiotropic Functions of Cardiac Fibroblasts (CFs)

In particular, CFs include over 50% of the cells in the adult heart [110] being implied in the development and deterioration of the cardiac ECM by generating collagens, proteoglycans, MMPs and TIMPs. As well, CFs produce different bioactive mediators such as VEGF-A, fibroblast growth factors (FGFs), transforming growth factor beta (TGF-β), platelet-derived growth factor (PDGF) which affect cardiac angiogenesis and CM proliferation. Furthermore, CFs have an effect on cardiac electrophysiology by protecting CM bundles, spreading of electrical signals, and changing mechanical stimuli in electronic signals [111]. In fact, CFs develop intracellular electrical coupling and interconnect with CMs through gap junctions (Fig. 4.7) [112–114]. Also, CFs being the most abundant cardiac cell type, they monitor CM proliferation during heart development. Therefore, CFs activation is a critical early repair response after cardiac injury.

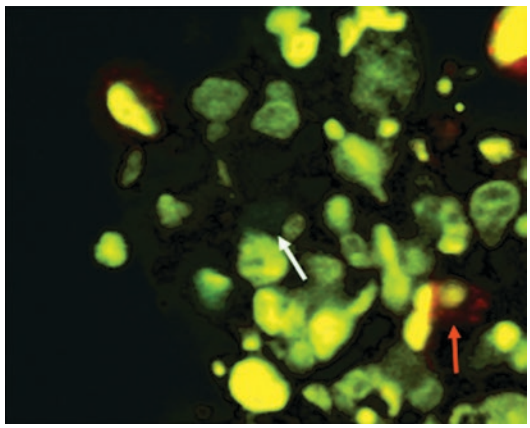

Fig. 4.7 Cell Communication Between Cardiac Fibroblasts and Myocytes. Z-section of a cell aggregate containing cardiac fibroblasts that were dual loaded with Lucifer Yellow and CMRA and myocytes that were unloaded. Cardiac fibroblasts appear as yellow or orange cells. The orange cells are fibroblasts that have transferred their green dye to an adjacent cell (orange arrow). Note the green cells, which are myocytes that have received green dye from an adjacent fibroblast (white arrow). (From Souders et al. [112] with permission)

4.3.7 Collagen Synthesis and Degradation

Collagen is synthesized by interstitial CFs which are degraded by locally formed enzymes named collagenases, such as matrix metalloproteinases (MMPs). The cardiac interstitium consist of 95% of type I and type III collagen fibers. The most important roles of collagen network are to control apoptosis, fix pathological processes, preserve the configuration of structures, control the resistance conduction during fiber shortening, and produce cytokines and growth factors [115]. Each heart has inactive myocardial collagenases in the ventricles but they are activated after a myocardial injury [116]. As already noted above, in any failing heart, CR primarily arises as a preventing reaction to protect the myocardium structure, but with gradually collagen deposit can causes cardiac fibrosis with diastolic and systolic dysfunction [117–120]. Importantly, collagen XIV is necessary to produce and preserve the ECM network in the heart growth [121]. Throughout fibrosis process, CMs undertake hypertrophic modifications, while MyoFb continue with collagen production and scar formation at the site of injury. In addition, collagen XI is necessary for myocardial growth supporting the nucleation of type I and II fibrils [122]. Therefore, the increased activity of collagen type XI alpha 2 chain ($COL_{11}A_2$) gene can be correlated with production of heterotypic fibrils with collagen I that is implicated in CR [123]. Nevertheless, persistence of CFs in injury area leads to chronic scar and remodelling [119].

According to evidence, the atypical deposit of type III collagen and type I collagen was discovered in cardiac injury, produced by several signalling pathways such as TGF-β, endothelin-1 (ET-1), angiotensin II (Ang II), connective tissue growth factor, and PDGF. In this situation, fibrosis is related with raised myocardial stiffness, decreased diastolic function, reduced contraction, failed coronary flow and malignant arrhythmias [124, 125].

As a result, collagen has an important role in the protection of cardiac structure and function.

In CR, the equilibrium between collagen production and degeneration is altered with numerous side effects. To prevent developing of CR to HF is necessary of timely developed stable scar that restores the injured tissue [126]. This equilibrium is preserved to some extent by MMPs that alter the ECM and tissue inhibitors of MMP (TIMPs) [127, 128]. In case of post MI, numerous mechanisms are run by CFs that change into MyoFb [129].

It should be noted, that there is a direct support between TSP-1 and the cardiac collagen. More important, TSP-1 and TSP-2 can preserve ECM normal structure by controlling the MMPs [73, 130, 131] (Table 4.2). TSP-1 and TSP-2 can directly attach to MMP2 and MMP9 through their Type 1 Repeats [132], but this attachment doesn't cause their inhibition directly [133]. When TSPs perform their activation by TGFβ, this diminishes MMP transcription [134]. Also, TSP-1 can attach to collagen V and fibrinogen [135, 136] and hasten fiber growth [137]. On the other hand, TSP-4 increases fibrosis by production of collagens I, II, III, and V [138] that support its direct role on the ECM remodelling process [139]. Essentially, in order to regulate cardiac fibrosis, TSP-4 expression is controlled by the transcription factor Krüppel-like factor 6 (KLF6) [140]. Also, TSP-4 triggers TGF-β [73] necessary for the transdifferentiation of MyoFb from CFs [141]. Further, MyoFb are indispensable to the cardiac fibrosis by production of collagen [142].

Table 4.2 Thrombospondin binding partners. From Kirk et al. [73] with permission

Protein	ECM	Cell surface	Signaling molecules
TSP-1	MMP2, MMP9, collagen V, fibrinogen, fibronectin	CD36, CD47, β1, β3 INTEGRINS	TGF-β, VEGF Ca^{2+}
TSP-2	MMP-2, MMP9	CD36, CD47	Ca^{2+}
TSP-4	Collagens I, II, III, V	B2, β3 integrins	Atf6α

4.3.8 Apoptosis

There are *three main mechanisms* involved in myocyte death: apoptosis or programmed cell death, necrosis and autophagy. According to data, cardiac dysfunction is correlated with modifications produced by autophagy, that can be adaptive or deleterious [143–145]. Initially, Sharov et al. have been suggested that raised cardiac apoptosis with CMs damage increases LV dysfunction with chronic HF [55]. Conversely, Olivetti et al. showed on myocardial samples from patients who underwent heart transplantation that cardiac apoptosis was increased more than 200-fold in the patients with failing heart [57]. In general, apoptosis has an important function in cardiac growth and in various heart diseases with ischemic and non-ischemic origin [146, 147]. However, the major mechanism of CM death from MI is the coagulation necrosis, even if apoptosis is also implied in CMs damage (Fig. 4.8) [148, 149].

It is important to note, that there is a fast triggering of caspase-3 in MI during 1 h after the onset of ischemia [150, 151], and the process of CM apoptosis can be completed within 24 h (Figs. 4.9 and 4.10) [42, 152, 153]. Previous reports have been shown that apoptosis is associated with unfavourable CR and HF post-MI in case of ablated proapoptotic protein Bnip3 [154, 155]. Also, TSP-1 and TSP-2 trigger apoptosis in ECs from microcirculation [156, 157]. Apoptosis inhibits endothelial tubule development and consequently has antiangiogenic effect. Further, vitro studies showed that matricellular proteins relate with the transmembrane glycoprotein CD36 [157–162], being the mainly mechanism that causes the antiangiogenic effect. Also, Primo et al. showed in cultured human ECs the inhibition of angiogenesis by the pathway of the VEGF receptor modulated by TSP-1 [163]. Attachment of TSP-1 to CD36 causes apoptosis of ECs by raise of death receptors and Fas ligand [164].

ADAMTS-7 is a member of the disintegrin and MMPs with TSP motifs (ADAMTS) family [73, 165], being newly recognized to be considerably correlated genome-wide with

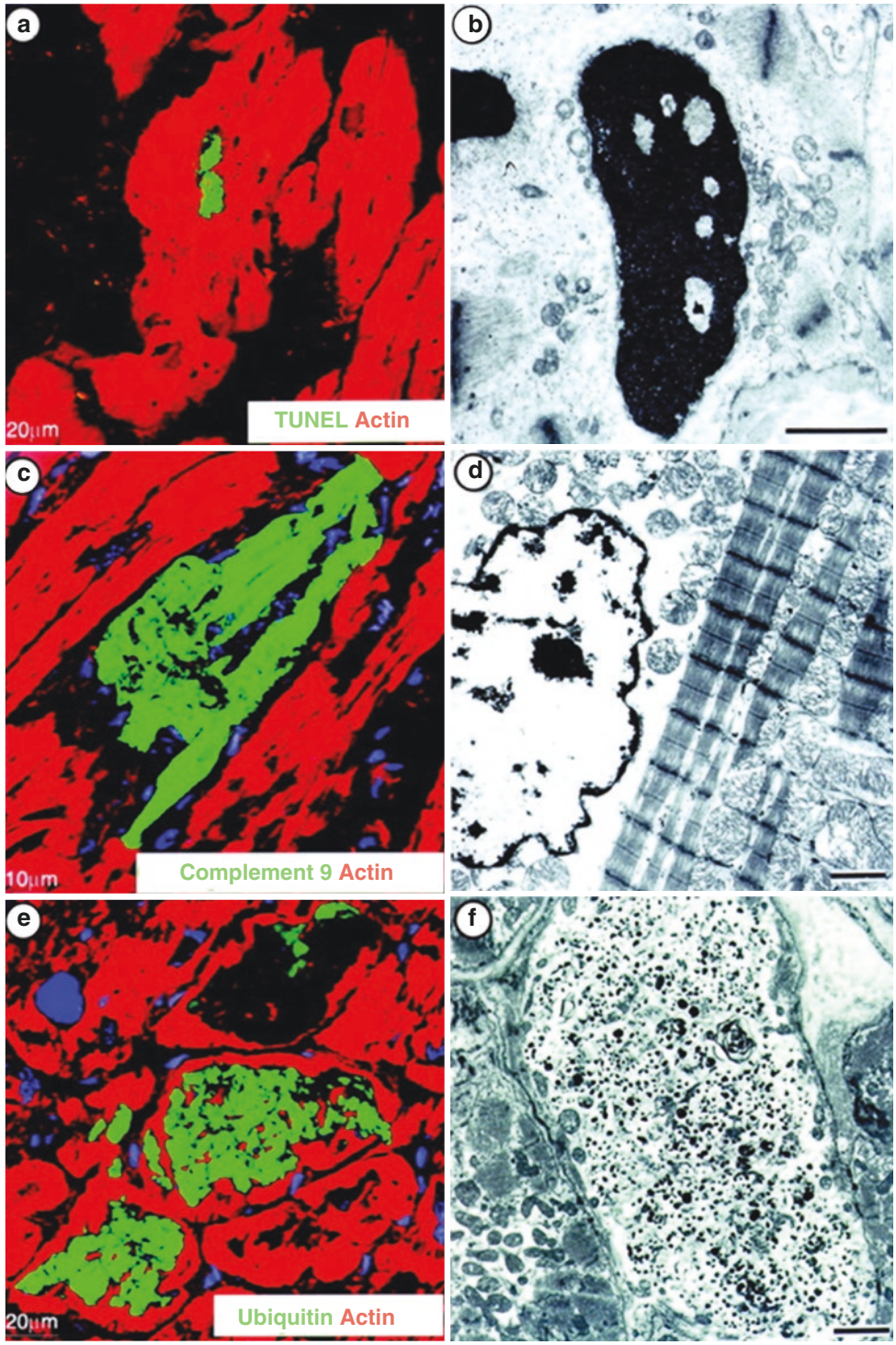

Fig. 4.8 Typical appearance of different types of cell death. (**a**, **c**, **e**) Confocal micrographs: counterstaining for actin, red; nuclei, blue; specific fluorescence, green. (**b**, **d**, **f**) Electron microscopic pictures (all bars = 2 µm). (**a**, **b**) Apoptotic cell death. (**a**) Nuclei with DNA fragmentation are green. (**b**) Nuclei show condensed chromatin. (**c**, **d**) Oncotic cell death. (**c**) Single cell oncosis labeled with C9. (**d**) Nuclei are electron-lucent with clumped chromatin, mitochondria are damaged with flocculent densities. (**e**, **f**) Autophagic cell death. (**e**) Ubiquitin deposition and loss of nuclei. (**f**) Ultrastructural appearance with numerous autophagic vacuoles. (From Kostin et al. [148] with permission)

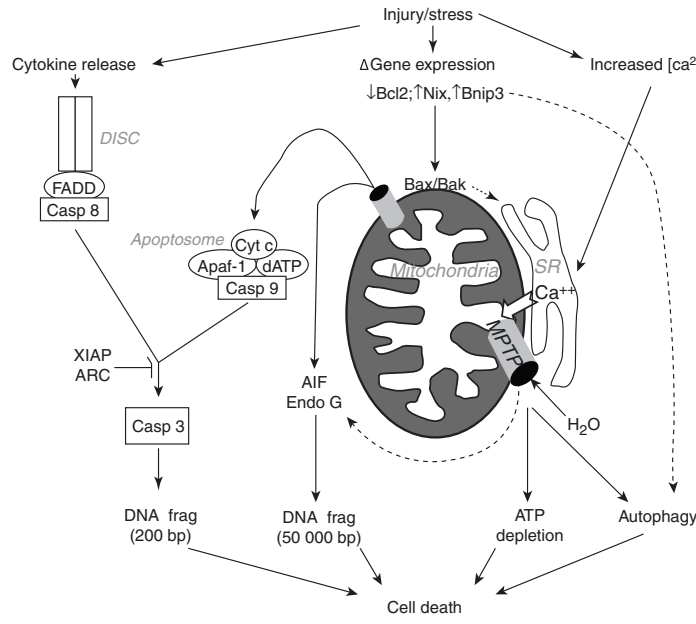

Fig. 4.9 Schematic depiction of pathways leading to programmed cardiomyocyte death, as described in the text. Mechanisms of cell death (bottom) are, from left to right, caspase-dependent apoptosis, caspase-independent apoptosis, programmed necrosis, and authophagy. Solid lines show primary effects; interrupted lines depict cross-talk between pathways. (From Dorn [152] with permission).

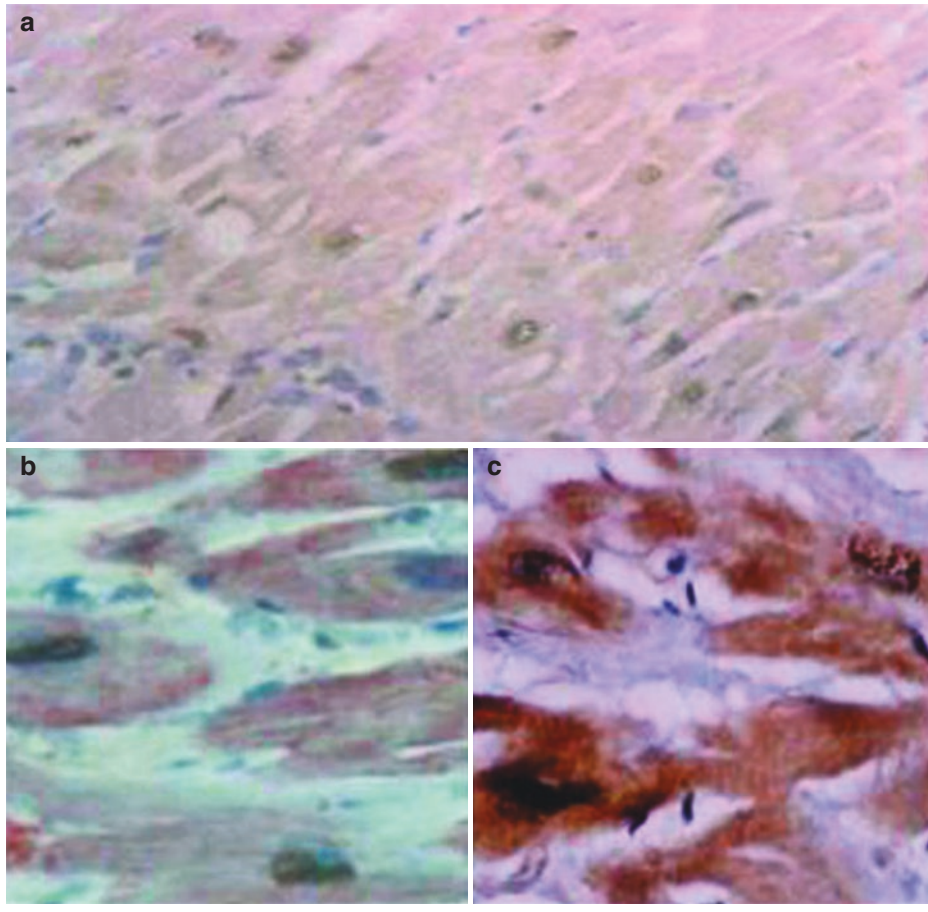

Fig. 4.10 Demonstration of apoptosis. (**a**) Labelling of nuclear DNA fragmentation using terminal deoxynucleotidyl transferase mediated dUTP nick end labelling (TUNEL). Colocalisation of (**b**) TUNEL and actin and of (**c**) TUNEL and activated caspase 3. (From Bussani et al. [42] with permission)

angiographic CAD [73, 166]. It has been previously confirmed that ADAMTS-7 support VSMCs migration and post injury neointima production via degradation of the matrix protein 'Cartilage Oligomeric Matrix Protein' (COMP or TSP-5) [73, 167]. Same researchers demonstrated that ADAMTS-7 breaks down the TSP-1 with re-endothelialization prevention [73, 168]. Also, the extracellular proteases thrombin, cathepsins, leukocyte elastases and plasmin can degenerate the TSPs [169].

Autophagy is defined as the intracellular process that removes needless cytoplasmatic components by lysosomes [144]. To date, the ubiquitin-proteasome system (UPS) and the autophagic-lysosomal pathway (ALP) are two major pathways in charge for most cellular proteins deterioration. Modifications of UPS and ALP pathways are correlated with the increase of proteotoxic defective proteins in the heart, a characteristic of frequent heart disease [144]. Acute ALP inhibition (proteasome inhibition) boost occasionally 'intrinsic proteasome peptidase activities', but chronic ALP inhibition blocks UPS pathway functioning in ubiquitinated protein stage [144]. As a result, autophagy has a significant function in proteotoxicity prevention by the ubiquitin system [144], and chaperones (heat shock protein-HSP) [145]. Particularly, the co-chaperones Bag_3 and HspB8 have significant role in the heart autophagy by chaperone-assisted selective autophagy [170, 171]. Regardless of myocyte death, the gradual decrease of CMs thas a significant function in CR and could be a potential target for therapeutic interventions.

4.4 Fibrosis

Just as RV fibrosis is commonly seen in the setting of both severe RV afterload and chronic pulmonary regurgitation, LV fibrosis is common in both aortic stenosis and regurgitation [172–174]. At the site of MI, acute focal fibrotic scarring provides myocardial healing and prevents rupture [175]. In contrast, chronic diffuse or focal reactive myocardial fibrosis is a result of either pressure overload or volume overload due to persisting hypertension, metabolic disorders, valvular heart diseases, ischemic injury (in areas remote from the infarction), or diffuse myocardial diseases, such as cardiomyopathies [175].

Myocardial fibrosis is defined by dysregulated collagen turnover characterized by increased synthesis that dominates over unaffected or reduced degradation [176, 177] with excessive diffuse collagen accumulation in the interstitial and perivascular spaces [178]. For that reason, the dysregulation of distinct pro- and antifibrotic factors, including cytokines and chemokines, growth factors, proteases, hormones, and ROS, is responsible for the alteration of the collagen matrix (Fig. 4.11) [179, 180].

The degeneration of collagen turnover takes place mainly in phenotypically transformed fibroblasts, termed MyoFb [79, 181]. The shift of CFs in MyoFb implies the expression of α-SMA, a characteristic of SMCs [79, 181–186]. As well as, the development of a wide active ER stimulated by a number of bioactive effectors [79, 181–186]. CFs and particularly MyoFb form collagen type I and III fibrils and develop into cross-linked to form the final fibres [176]. Collagen cross-linking is a significant post-translational stage that raises the resistance of collagen fibres to degradation by MMPs [187, 188]. Only that, myocardial fibrosis disrupts the myocardial architecture, contributes to myocardial disarray, and determines mechanical [189], electrical [190, 191] and vasomotor [192] dysfunction, thus promoting the progression of cardiac diseases to HF [175]. Fibrosis is induced by various genetic disorders, pressure or volume stress, heart injuries, and other diseases. There is evidence that depending on the particular trigger, distinct molecular pathways have varying importance for the individual types of fibrosis. As the development of myocardial fibrosis is characterized by a complex dysregulation of a number of different factors including inflammatory chemokines, angiotensin II (Ang II), and endothelin signalling, *the FIBROTARGETS consortium* that is a multinational consortium with industrial and academic partners, funded by the European Commission is primarily aimed for characterizing novel emerging mechanisms of

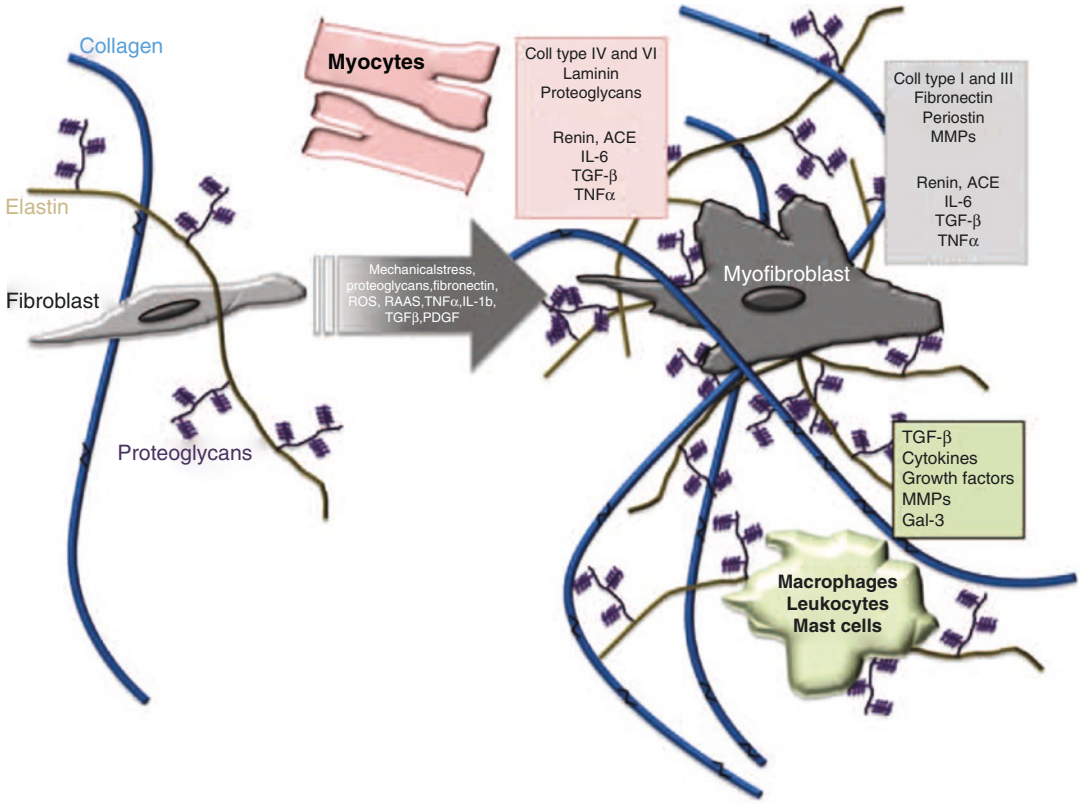

Fig. 4.11 Schematic representation of biochemical and cellular mechanisms of cardiac fibrosis. Under physiological conditions (left), fibroblasts secrete extracellular procollagen chains into the interstitium that assemble into fibrils and are cross-linked by lysyl oxidase. Several cell types are implicated in fibrotic remodelling of the heart either directly by producing matrix proteins (fibroblasts), or indirectly by secreting fibrogenic mediators (macrophages, mast cells, lymphocytes, cardiomyocytes, and vascular cells). Under pathological conditions (right), alterations in the matrix environment, induction and release of growth factors and cytokines, and increase of mechanical stress dynamically modulate fibroblast transdifferentiation into myofibroblasts. Higher collagen cross-linking results in increased myocardial tensile strength. Resistance to degradation by matrix metalloproteinases (MMPs) increases cross-linked collagen, which favours matrisome expansion. Pink, grey, and green boxes list part of the secretome of mycocytes, myofibroblasts, and macrophages/leucocytes/mast cells, respectively, that trigger and maintain fibrosis. *Gal-3* galectin-3, *IL* interleukin, *PDGF* platelet-derived growth factor, *RAAS* renin–angiotensin–aldosterone system, *ROS* reactive oxygen species, *TGF* transforming growth factor, *TNF* tumour necrosis factor. (From Gyöngyösi et al. [179]. It is an open access article)

myocardial fibrosis [180]. Targets and biomarkers under investigation include especially proteins, proteoglycans, and microRNAs (miRNAs) [180].

In increased volume loading, the RV appears more prone than the LV to develop fibrosis [63]. Similarly, patients after surgical repair of TOF who have long-standing RV volume load secondary to pulmonary insufficiency develop RV fibrosis [172]. This is clinically important as risk factor for increased propensity to arrhythmias, exercise intolerance, and RVF [172, 193]. It has been suggested that these differences in response between the RV and LV to volume loading may stem from the different embryological origin of the two ventricles [63].

Several single or multimodal imaging technologies have been used to assess the extent and type of myocardial fibrosis. Besides the direct morphological display of the fibrotic tissue, indirect cardiac functional imaging may evidence fibrosis correlated with decrease of systolic function and increased myocardial stiffness with diastolic

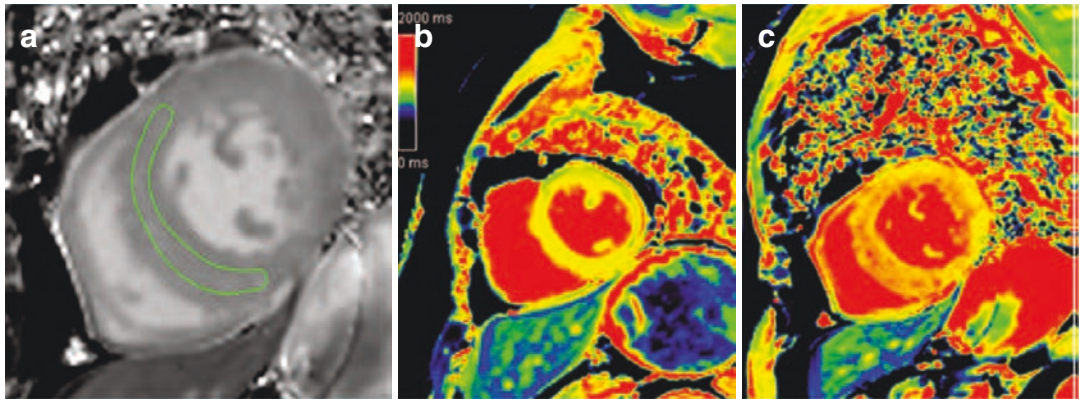

Fig. 4.12 Representative native and T1 cardiac magnetic resonance imaging (cMRI) of diffuse myocardial fibrosis. (**a**) Diffuse myocardial fibrosis on the short-axis view of the cMRI image, with the circumference of the anteroseptal myocardial area (region of interest). (**b**) cMRI T1 map of a patient with moderate aortic stenosis and moderate diffuse myocardial fibrosis. (**c**) cMRI T1 map of another patient with severe aortic stenosis and severe diffuse fibrosis of the left ventricle. (From Gyöngyösi et al. [179]. It is an open access article)

dysfunction [175]. Cardiac magnetic resonance imaging (MRI) provides detailed tissue characterization, identifying focal myocardial fibrotic scars with late gadolinium enhancement (ventricular LGE) and an estimation of diffuse myocardial fibrosis with post-contrast enhanced T1 and T2 mapping (Fig. 4.12) [179, 194].

Positron emission tomography (PET) imaging performed by using ^{15}O-labelled water ($H_2{}^{15}O$) and carbon monoxide ($C^{15}O$) allowed the non-invasive quantification of both myocardial perfusion and fibrosis [195]. Combining PET and MRI has the potential for sensitive and quantitative imaging of cardiovascular anatomy and function with detection of molecular events at the same time [196, 197]. It's worthwhile to specify that PET–MRI (Biograph mMRI, Siemens AG) image allows the simultaneous detection of myocardial global and regional function, ECM volume, and tissue perfusion and metabolism [198].

Histopathological analysis of endomyocardial biopsy specimens is the current gold standard for diagnosis and assessment of cardiac fibrosis. A number of circulating biomarkers, including (pro-) collagen cleavage products, processing enzymes, but also miRNAs (Table 4.3), have been proposed and analysed [179]. Details of these biomarkers and potential targets have been described previously including proteins and proteoglycans that impact fibrosis and miRNAs that act in fibrosis [180]. For their use as cardiac fibrosis biomarkers, it seems reasonable that a combination of several from these increases the predictive power, particularly in the case of miRNAs [199, 200].

As a consequence, the treatment of HF patients improves clinical symptoms, but *does not reverse* fibrosis. Furthermore, the severity of histological proven myocardial fibrosis has been reported to be associated with higher long-term mortality in patients with cardiac diseases, mainly patients with HF [200, 201].

4.4.1 miRNAs

Genetic variations exist among the RV and the LV. Drake et al. [71] note the dissimilarity between gene expression patterns in normal RV and LV in both mRNA and microRNAs (miRNA) types. More precisely, the transcription factor Irx2 is not exhibited in the RV but insulin-like growth factor 1 (IGF-1) is exhibited

Table 4.3 Potential circulating biomarkers for assessment of cardiac fibrosis

Biomarker candidates	Role and correlation to fibrosis	Evidence of associatioan with myocardial fibrosis
ECM formation		
1. Procollagen type I C-terminal propeptide (PICP)	1. Cleaved enzymatically from procollagen I (collagen biosynthesis)	1. Yes
2. Procollagen type I N-terminal propeptide (PINP) Unknown		2. Unknown
3. Procollagen type III N-terminal propeptide (PIIINP)	3. Cleaved enzymatically from procollagen III (collagen biosynthesis)	3. Yes
4. Collagen type I C-terminal telopeptide (CITP)	4. Cleaved by MMP-1 (collagen I degradation), PICP:CITP ratio corresponds to collagen turnover	4. Inconclusive
Fibrolytic enzymes		
1. MMP-1 and other MMPs	1. Degrades collagens I, II, and III	1. Unknown
2. TIMP-1 and other TIMPs	2. Inhibits MMPs	2. No (TIMP-1), unknown (others)
miRNAs		
1. miR-21	1. Correlation with fibrosis in aortic stenosis	1. Inconclusive
2. miR-29a	2. Correlation of plasma levels with hypertrophy and fibrosis in HCM, reduced cardiac expression	2. Unknown
3. miRNA panels	3. Concomitant quantification of several miRNAs increases the diagnostic and prognostic value	3. Unknown
Others		
1. TGF-β1	1. Promotes myofibroblast transactivation and ECM synthesis, deactivates macrophages	1. Inconclusive
2. Osteopontin	2. Matricellular protein involved in macrophage regulation	2. No association
3. Galectin-3	3. Galactosamine binding protein associated with collagen deposition of fibroblasts	3. Inconclusive
4. Cardiotrophin-1	4. Cytokine associated with cardiac fibrosis	4. No association
5. Natriuretic peptides	5. Triggered by myocardial stretch, correlate with HF	5. Unknown

From Gyöngyösi et al. [179]. It is an open access article
ECM extracellular matrix, *HF* heart failure, *HCM* hypertrophic cardiomyopathy, *miRNA* microRNA, *MMP* matrix metalloproteinase, *TIMP* tissue inhibitor of metalloproteinases, *TGF* transforming growth factor

mainly in the LV. Moreover, same team made the assumption that these dissimilarities can be the result of different embryologic origin or the RV is a low-pressure chamber compared to the LV. Also, Reddy et al. [66] demonstrated firstly that changes in miRNAs exist in RV remodeling from RVH to RVF and are mostly comparable to pressure-stressed LV but with separate signalling regulatory pathways.

RV dysfunction is described entirely in RV obstruction or PAH [21]. Only that, all patients with RV dysfunction are put together regardless of the fact that CHD have various functional, molecular and cellular remodelling patterns in the RV [21] (Fig. 4.13). Blood biomarkers, similar to plasma proteins and miRNAs represent an important way to evaluate the function and remodelling of RV [21]. Heart miRNAs are

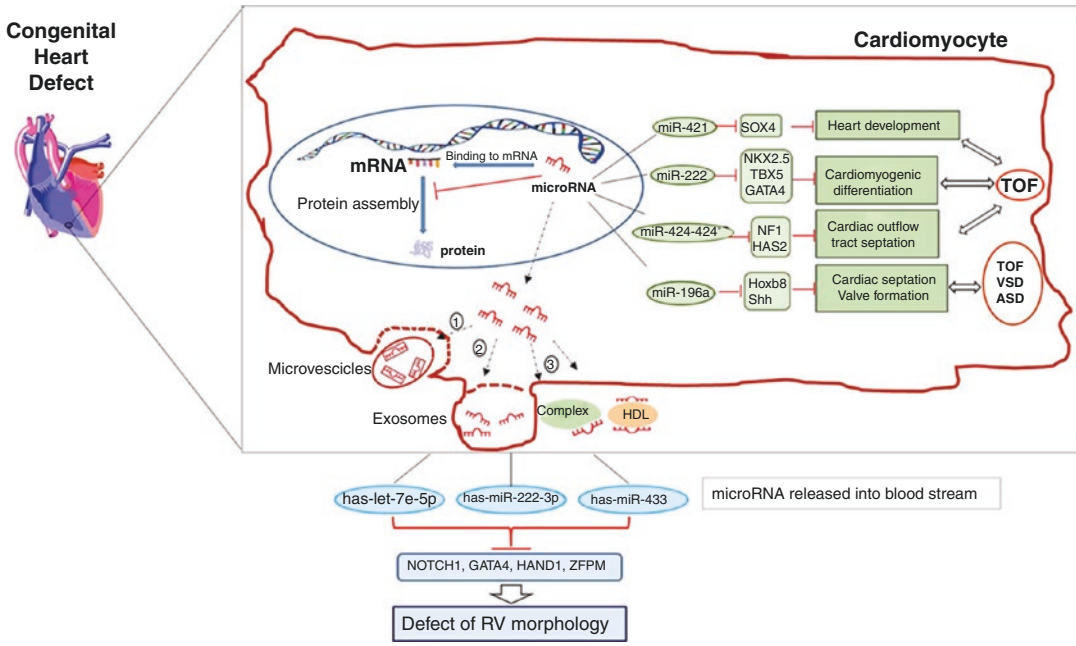

Fig. 4.13 Dysregulated miRNAs in congenital heart diseases (CHDs). A figure showing the link between CHD and miRNAs in cardiomyocytes. Small number of miRNAs are upregulated in cardiomyocyte during CHD. These miRNAs can be released from the cell in microvesicles, by incorporation into exosomes, by linkage to high-density lipoproteins or bound to RNA-binding proteins. Dysregulated levels of miRNAs, crucial in RV development, are found in the bloodstream of children with VSD. The differentially expressed has-miR-222-3p, has-let-7e-5p and has-miR-433 bind with specific transcription factors (NOTCH1, GATA4, HAND1 and ZFPM) associated with RV morphogenesis. (From Iacobazzi et al. [21]. It is an open access article)

constant and quantifiable discharged in the blood flow as exosomes, microvesicles or joining with high-density lipoproteins (HDL) and RNA-binding proteins [21].

There are numerous disrupted miRNAs during CR and RHF [21, 202–205] (Fig. 4.14). miRNAs are non-coding single-stranded RNAs formed from 19–24 nucleotides that adjust in the negative way the exhibition of a particular mRNA via translational degeneration or suppression [206]. According to data, there have been shown in children with VSD in comparison with controls eight various miRNAs. Particularly, NOTCH1 is implied in ventricular growth, and GATA4 has an important function in atrial and ventricular growth, heart partition, and atrioventricular valve development [21, 207].

A low number of studies have studied the blood miRNAs in adult patients diagnosed with systemic RV [21]. Patients with the RV as the SV after transposition of the great arteries (TGA) had altered miRNAs profile. On the whole, from the 24 miRNAs various regulated, miRNA18a and miRNA486-5p related negatively with systemic ventricular contractility [21, 208]. Also, miRNA423_5p defined as a biomarker of LVF, has same expression in healthy adults and in SV after atrial repair of TGA adults [21, 209].

It seems that gene expression in signalling is changed in heart growth of children with TOF [21]. Alteration of VEGF gene expression and of a number of ECM proteins is established as contributors of TOF [92]. Important inhibition of genes in the Notch and Wnt pathways implied in heart growth are also found in children with TOF [21, 93]. Even if RVH is a component of TOF, there is a clear molecular difference between TOF and RVH gene expression, including VSD and ASD [21]. Whereas TOF children have unregulated genes for heart growth such as SNIP, A2BP1 and KIAA1437, RVH has a higher

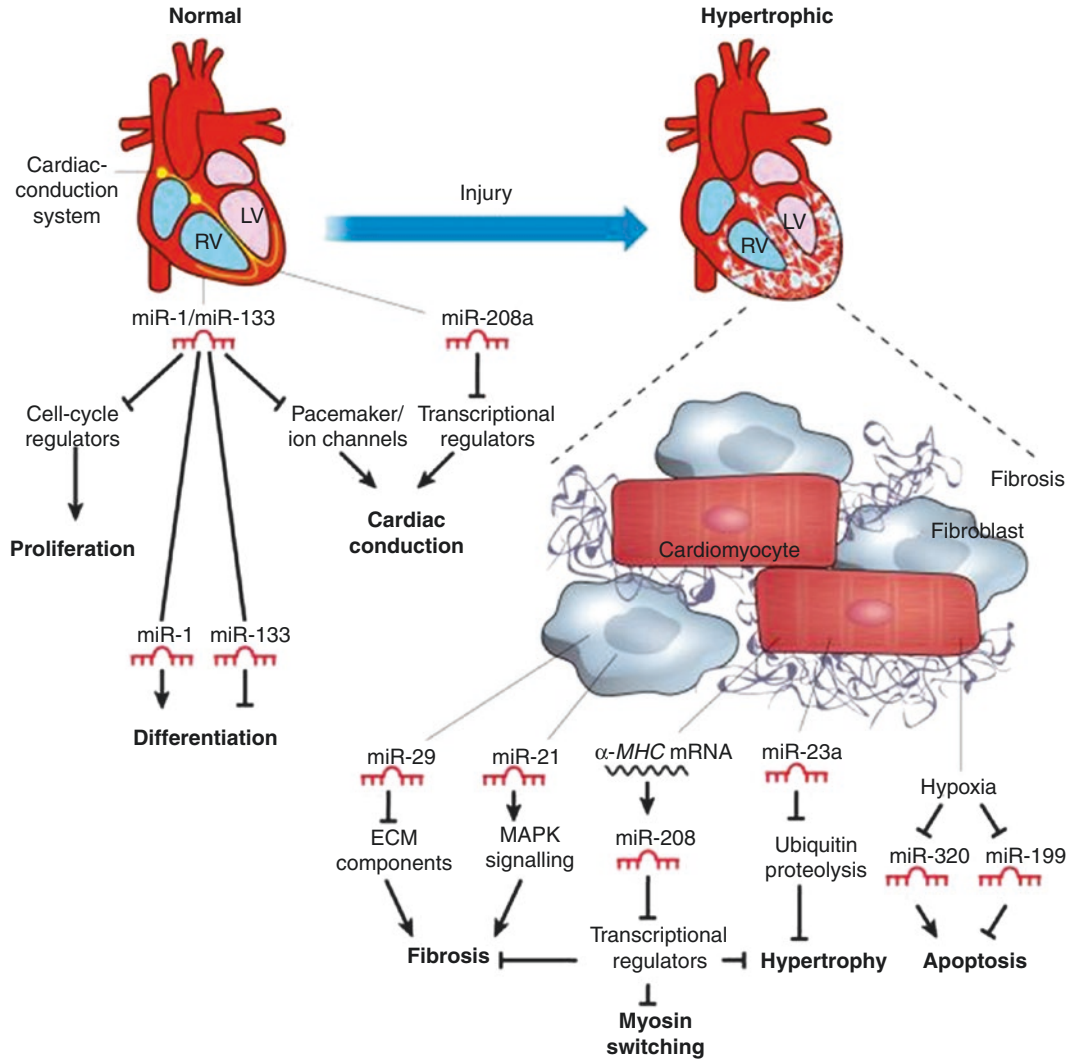

Fig. 4.14 Functional role of miRNAs in the normal and diseased heart. A normal and a hypertrophic heart are shown in schematic form, depicting miRNAs that contribute to normal function or pathological remodelling. The expression of selected miRNAs within the heart is shown, along with their corresponding functions. All arrows denote the normal action of each component or process. miR-1 and miR-133 are involved in the development of a normal heart (left) by regulating proliferation, differentiation and cardiac conduction. For example, proliferation is promoted by cell-cycle regulators, but miR-1 and miR-133 block these regulators, thus blocking proliferation. miR-208a also contributes to the regulation of the conduction system. After cardiac injury (right), various miRNAs contribute to pathological remodelling and the progression to heart failure. miR-29 and miR-21 block and promote cardiac fibrosis, respectively. miR-29 blocks fibrosis by inhibiting the expression of ECM components, whereas miR-21 promotes fibrosis by stimulating mitogen-activated protein kinase (MAPK) signalling. miR-208 controls myosin isoform switching, cardiac hypertrophy and fibrosis. miR-23a promotes cardiac hypertrophy by inhibiting ubiquitin proteolysis, which itself inhibits hypertrophy. Hypoxia results in the repression of miR-320 and miR-199, which promote and block apoptosis, respectively. *ECM* extracellular matrix, *LV* left ventricle, *MHC* myosin heavy chain, *RV* right ventricle. (From Small et al. [205] with permission)

expression of genes implied in stress reaction and cell proliferation [21, 94]. What's more, there is a molecular conversion from RV to LV features that appears during RV adjustment to pressure overload, as a result dysregulated gene phenotype from RVH is same with normal LV [21].

Another study based on cardiac tissues from RV in CHD [95], found dissimilar miRNAs in RV outflow tract obstruction (RVOT) in comparison with RVOT of normal infants [210]. Specifically, miRNA-424 and miRNA-222 had higher expression and they correlated with the decrease of heart growth being correlated with NF1 and HAS2 genes. Correspondingly, the increased expression of miR-421 in RV tissue from children with TOF is correlated with SOX4 gene necessary for cardiac outflow tract formation (Fig. 4.14) [21, 211, 212].

miRNA 133a is thought to suppress cardiac fibrosis and is decreased in LVF secondary to aortic constriction [213, 214]. This aligns with the marked upregulation of connective tissue growth factor/CCN2 and other profibrotic signalling molecules in the course of RV and LV fibrosis in models of RV afterload and RVF [71, 88, 215]. In contrast, miRNA 21 and 34c* may increase during LVF but decrease in RVF [71]. Reddy et al. [66] investigated miRNAs during the transition from RVH to RVF and compared these with miRNA expression in LVH or LVF. During RVH, there was altered expression of miRNAs 199a-3p, which is associated with CM survival and growth. With the progression to RVF and switching on the foetal gene phenotype, there was increased miRNA 208b, miRNA 34, miRNA 21, and miRNA1, which are associated with apoptosis and fibrosis [83]. These patterns of miRNA expression are largely related to LVH and LVF. Conversely, there are important distinction relating RV and LV miRNAs linked to cell survival, proliferation, metabolism, ECM production, and proteasome malfunction (miRNA 28, miRNA 148a, and miRNA 93), which were unregulated in RVH or RVF and downregulated or unchanged in LVH or LVF [66].

Common findings in both RVH and LVH are collagen deposition, fibrosis, and ECM remodelling [216]. The mechanisms inducing fibrosis are multiple, and in the setting of increased ventricular afterload, recognized triggers may include regional ischemia, necrosis, and apoptosis, among others [176]. There is an important match of the miRNA expression phenotype in human HF and foetal hearts in comparison with the adult normal heart tissue [204]. More studies data are necessary for a higher knowledge of these subcellular events that can guide to the development of new ventricle-specific treatments [217].

4.5 Other Factors

Factors that can also contribute to CR comprise *endothelin, cytokines* (tumor necrosis factor-alpha-TNFα and interleukins) [218], *oxidative stress*, *MMPs*, and *peripheral monocytosis* [219].

Endothelins (ET) are powerful vasoconstrictor peptides which increase in HF. The endothelin family of peptides is typically recognized for its vasoconstrictive properties. There are two known receptors for ET-1 in the heart, the ETA and ETB receptors, which have been shown to play differing and sometimes opposing roles. Importantly, ET-1 activation of the ETA receptor is known to increase collagen production in isolated human CFs [220]. Furthermore, MyoFb isolated from scar tissue after experimental MI have elevated levels of ET-1, suggesting an important function for ET within these cells [221].

ET-1 is a 21-amino acid peptide formed and discharged by the ECs and it has a quickest vasoconstrictive effect [222]. Cardiac ET-1 is active in both autocrine and paracrine effects by attaching to ETB receptors from cardiac ECs and ETA receptors from CMs [222]. The attachment of ET-1 to ETB receptors causes the discharge of signalling molecules such as NO and prostaglandin I_2 [222]. If ET-1 attaches to the ETA receptors from CMs, it triggers CM constriction [222, 223]. As a consequence, there may exist a feedback mechanism concerning cardiac ECs and CMs that run CM constriction by the ET-1 system [222]. Also, patients with HF have raised exhibition of cardiac ET receptors and raised plasma ET-1 levels, both linked with disease severity [224]. ET antagonists they will be additionally efficacious in the treatment of pathological fibrosis in the heart [225]. Preliminary trials in humans had demonstrated beneficial hemodynamic and cardiac effects in patients with end-stage HF [226].

Cytokines (tumor necrosis factor-alpha TNFα and interleukins) are small peptides or glycoproteins that are discharged by nucleated cells [227].

Their temporary discharge adjust immune or repair processes by controlling cells growth, process of differentiating, metabolism, and protein synthesis [228]. Fibrinogen is an acute inflammatory regulator discharged by hepatocytes triggered by different cytokines. Also, CRP is an acute-phase reactant synthesized and discharged largely by hepatocytes in response to the cytokine IL-6. The highest levels of CRP are correlated with MI size but are reduced by early reperfusion [229]. It seems that IL-3 is a new biomarker of inflammation and can induce the multiplication of lymphocytes, macrophages, neutrophils, and monocytes with infiltration of heart where trigger the discharge of cytokines from CMs. Moreover, IL-3 can have significant functions in tissue repair. Understanding better inflammatory response could offer measurable ways of immune injury to tissues.

Leukocytosis was studied especially in MI [230, 231]. The ischemic-reperfusion stage produces the discharge of oxygen free radicals, cytokines, and other inflammation markers [231]. The presence of leukocytes in the microcirculation is followed by inflammatory reaction [232]. The transfer of leukocytes from blood flow to the vessel wall with tissue injury and inflammation is regulated by the selectin family of adhesion molecules with attachment of leukocytes to the ECs by involvement of integrins and diapedesis [233, 234]. Recruitment of leukocytes is mediated by complement triggering, TGF-β, IL-8, monocyte chemotactic protein-1 (MCP-1), and platelet activating factor (PAF) [235]. Also, the collection of *neutrophils* in the ischemic-reperfusion tissue could discharge proteolytic enzymes or ROS with further injury of myocytes. ROS directly injure CMs and vascular cells, and by triggering cytokines causes inflammation [236, 237]. Marginated neutrophils exert powerful cytotoxic effects through the adhesion with intercellular adhesion molecule-1 (ICAM-1) expressing CMs [235]. CD11b/ICAM-1 adherence activates the neutrophils respiratory burst resulting in myocyte oxidative injury [235].

Oxidative Stress produces important alteration of sarcolemmal and sarcoplasmic reticulum (SR) membrane, causing raise of intracellular Ca^{2+} levels with severe contraction of CMs, followed by mitochondrial damage and cell death [238, 239]. Specifically, ROS and redox signaling have an important function in apoptosis, including upstream signaling pro-apoptotic pathways and the mitochondria [240, 241]. There are signaling pro-apoptotic pathways that comprise the activation of ASK-1, JNK, p38MAPK, and CaMKII, as well as signaling anti-apoptotic pathways, such as Akt, Bcl2, and HSPs [241].

The cell resources of ROS comprise mitochondrial respiratory chain enzymes, xanthine oxidases (XOs), lipoxygenases, myeloperoxidases, uncoupled nitric oxide synthases (NOSs), and Nox proteins [242, 243]. Moreover, the important sources of ROS in the cardiovascular system comprise mitochondria, NADPH oxidases, NOSs, xanthine oxidases, cytochrome P450-based enzymes, and infiltrating inflammatory cells [243]. ROS are represented by free radicals (species with one or more unpaired electrons) such as superoxide ($O2^{\bullet -}$) and hydroxyl radicals (OH•), and nonradical species such as hydrogen peroxide (H_2O_2) [243]. In healthy adults, production of ROS is inhibited by enzymatic and nonenzymatic antioxidant systems that decrease ROS levels with preserving of a right redox balance in cells and tissues [243].

The first report of the presence of NADPH oxidases in human myocardium is of Heymes et al. [244]. NADPH or NADH-dependent ROS-generating activity are existent in nonphagocytic cell types [243], including VSMC [245, 246], ECs [247, 248], adventitial and CFs [249], and CMs [250]. *Noxs* are multi-subunit transmembrane enzymes that use NADPH as an electron donor to decrease oxygen to superoxide anion (O^{2-}) and hydrogen peroxide (H_2O_2) [243]. Firstly, Noxs were described in phagocytes with the description of the Nox2 isoform that it also named $gp91^{phox}$) [243, 251]. The rest comprise 6 other family members each coded by dissimilar genes, identified as Nox1, Nox3, Nox4, Nox5, dual oxidase 1 (Duox1), and Duox2 [243, 252–254]. All forms of Nox proteins demonstrate 21–59% similarity to Nox2, from which Nox3 is most alike with Nox2 and Nox5 mostly unrelated [243].

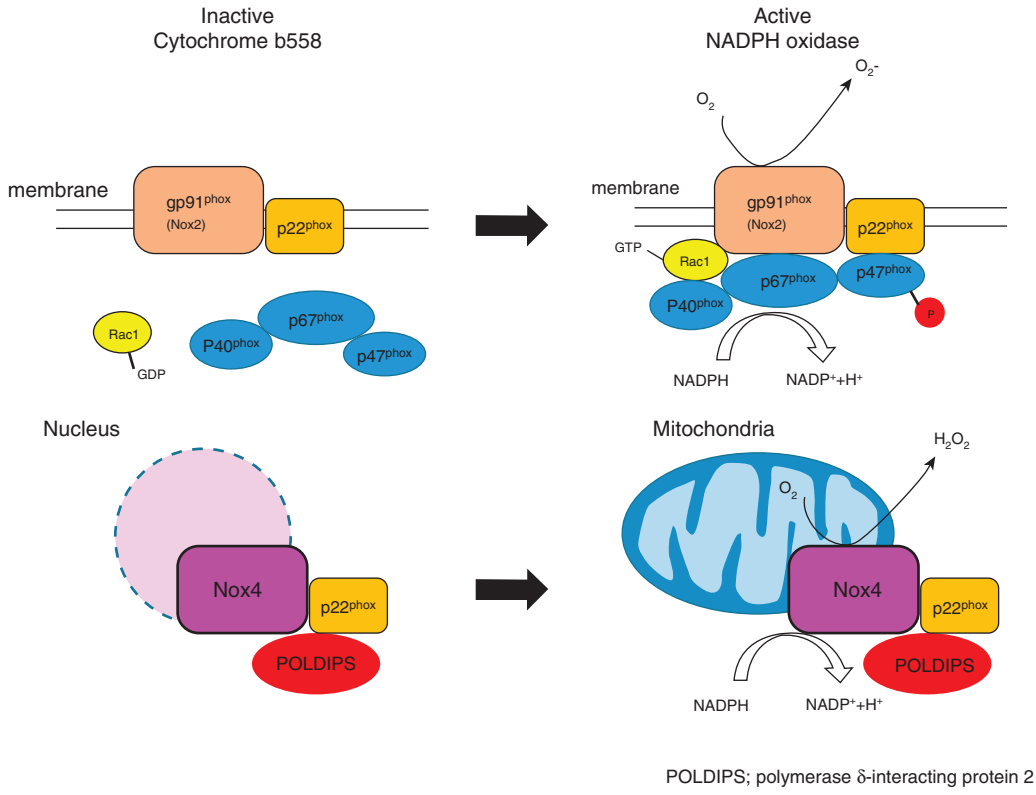

Fig. 4.15 Structure of NADPH oxidase in the heart. NADPH oxidase complex is composed of two major components. Plasma membrane spanning cytochrome b558 composed of $p22^{phox}$ and a Nox subunit ($gp91^{phox}$ (Nox2), Nox4) and cytosolic components composed of four regulatory subunits ($p47^{phox}$, $p67^{phox}$, $p40^{phox}$ and Rac1). The low molecular weight G protein rac1 participates in assembly of the active complex. Upon activation, cytosolic components interact with cytochrome b558 to form an active NADPH oxidase enzyme complex, resulting in release of $\cdot O^{2-}$. The primary Nox subunit isoforms in cardiac cells are Nox2 and Nox4. Nox4 oxidase localizes intracellular organelles around the nucleus. The activity of Nox4 results in the direct release of hydrogen peroxide (H_2O_2) in mitochondria. The mechanisms underlying the generation of hydrogen peroxide by Nox4 oxidase are yet to be fully characterized. (From Kayama et al. [255]. It is an open access article)

Therefore, the NADPH oxidase (Nox) family (Fig. 4.15) is formed from 7 catalytic subunits termed Nox1-5 and Duox1 and Duox2 (for Dual Oxidase), regulatory subunits $p22^{phox}$, $p47^{phox}$ or Noxo1, $p67^{phox}$ or Noxa1, $p40^{phox}$. Further, the Nox1, 2, 4 and 5 enzymes are existent in normal cardiovascular tissues, and trigger the progression of cardiovascular disease. Nox enzymes are located in VSMCs, ECs, adventitial fibroblasts, macrophages, CMs and fibroblasts, plus adipocytes and stem cells. They are associated with hypertension, atherosclerosis, HF, ischemia reperfusion injury and CR, but upregulation can be physiologically beneficial such as in angiogenesis [243, 244, 255, 256]. The acutely upregulation of cardiovascular NADPH oxidase activity by a large various patho-physiological stimuli comprise [243] (a) G-protein coupled receptor agonists such as Ang II and ET-1; (b) growth factors such as VEGF, thrombin, PDGF, and EGF; (c) cytokines such as TNF-β, IL-1 and TGF-β; (d) metabolic factors such as elevated glucose, insulin, free fatty acids, and advanced glycation end products (AGE); (e) oxidized LDL, lysophosphatidylcholine, and hypercholesterolemia; (f) mechanical forces such as oscillatory shear

stress; and (g) ischemia-related stimuli such as nutrient deprivation, membrane depolarization, flow cessation, hypoxia–reoxygenation, and ischemia [243].

Nox2 and Nox4 are the mainly isoform exhibited in CMs. Triggered Nox2 is mainly exhibited at the plasma membrane [244]. According to data, *Nox derived ROS* are implied in CM apoptosis. Pro-apoptotic signaling pathway and generation of CaMKII in pro-apoptotic signaling pathway are triggered both by Ca^{2+}, by Nox2-derived ROS, and downstream of Ang II [257]. Norepinephrine, aldosterone, and doxorubicin are also reported to promote CM apoptosis through the activation of Nox2 [258–260]. Contrary to Nox2 function in Ang II-induced cardiac hypertrophy, Nox2 is not implied in cardiac hypertrophy induced by pressure overload (Fig. 4.16) [261]. The major agonists and stimuli of Nox2 activation in CMs and ECs comprise G-protein coupled receptor agonists (GPCRs) such as Ang II and ET-1, growth factors, cytokines (TNF-α), mechanical forces, metabolic factors (glucose, insulin), glycated proteins [262], and oxidized low-density lipoprotein (ox-LDL) (Fig. 4.17) [261, 263, 264]. To sum up, evidence supports different functions for Nox2 and Nox4 in hypertrophic reaction to pressure overload [243]. Important redox-sensitive downstream signaling pathways in the heart that can be affected by NADPH oxidase activation such as RAS, the MAPKs (p38MAPK, ERK1/2, JNK), c-src, p90RSK, the PI3 kinase (PI3K)/Akt pathway, AP-1, NF-κB, HIF-1, and others [243].

In case of RV, metabolic and ischemic modifications typical to RV remodelling are also correlated with accumulation of ROS [21, 265] (Fig. 4.18). The presence of ROS activates the cellular and molecular modifications with decrease of contractile function, lacking of energy production and fibrosis. Alteration of SM channels by oxidative stress produces damaging of RyR2 activation and decrease of sarco/endoplasmic reticulum Ca2+-ATPase (SERCA) activity, as a result appears temporary malfunction of myocyte Ca^{2+} and contractile dysfunction [21, 92]. Additionally, increased ROS amounts cause conversion of nitrotyrosine rests in TIMPs and discharge active MMPs with CR and fibrosis [21, 266]. To date, vivo studies with histological examination of collagen content in RV samples from pulmonary artery showed a significant raise of ROS, important collagen deposition with high levels of MMP-2, MMP-9 and MMP-13 and diminished TIMP-4 protein amounts. Additionally, ROS are second messengers within CMs for numerous signalling molecules (ATII, TGFβ1, TNFα and ET-1) to generate hypertrophic pathways including MAPKs, PKC and Src [21, 62]. Taken together, raised amounts of ROS can damage cellular, molecular and structural components with CR and failure. It is important to underline that malondialdehyde levels represent an indirect index of oxidative stress and are notably elevated in the RV in comparison with the LV. To sum up, these features support a decreased resistance of RV in oxidative stress being a contributor in the development of HF [267].

Peripheral Monocytosis is a sign of monocyte and macrophage infiltration of the necrotic myocardium which arises two to three days after an acute MI. Likewise, a higher peak monocyte level is related with a larger LV end-diastolic volume and inferior LVEF. It was shown that a peak monocyte count ≥900/μL independently predicts HF, LV aneurysm formation, and cardiac events [219]. It should be stressed that monocytes have the capacity to generate and discharge inhibitory mediators of inflammation such as IL-10 and TGF-β [268]. There are varied monocytes with different functions in inflammatory response showed in humans such as CD16-monocytes that exhibit important amounts of CCR2 with pro-inflammatory properties same to murine Ly6Chi cells [268]. Further, inhibition of inflammatory signal pathways is correlated with Ly6Clo/CX3CR1hi monocytes entrapment that generates angiogenic mediators with infarct healing.

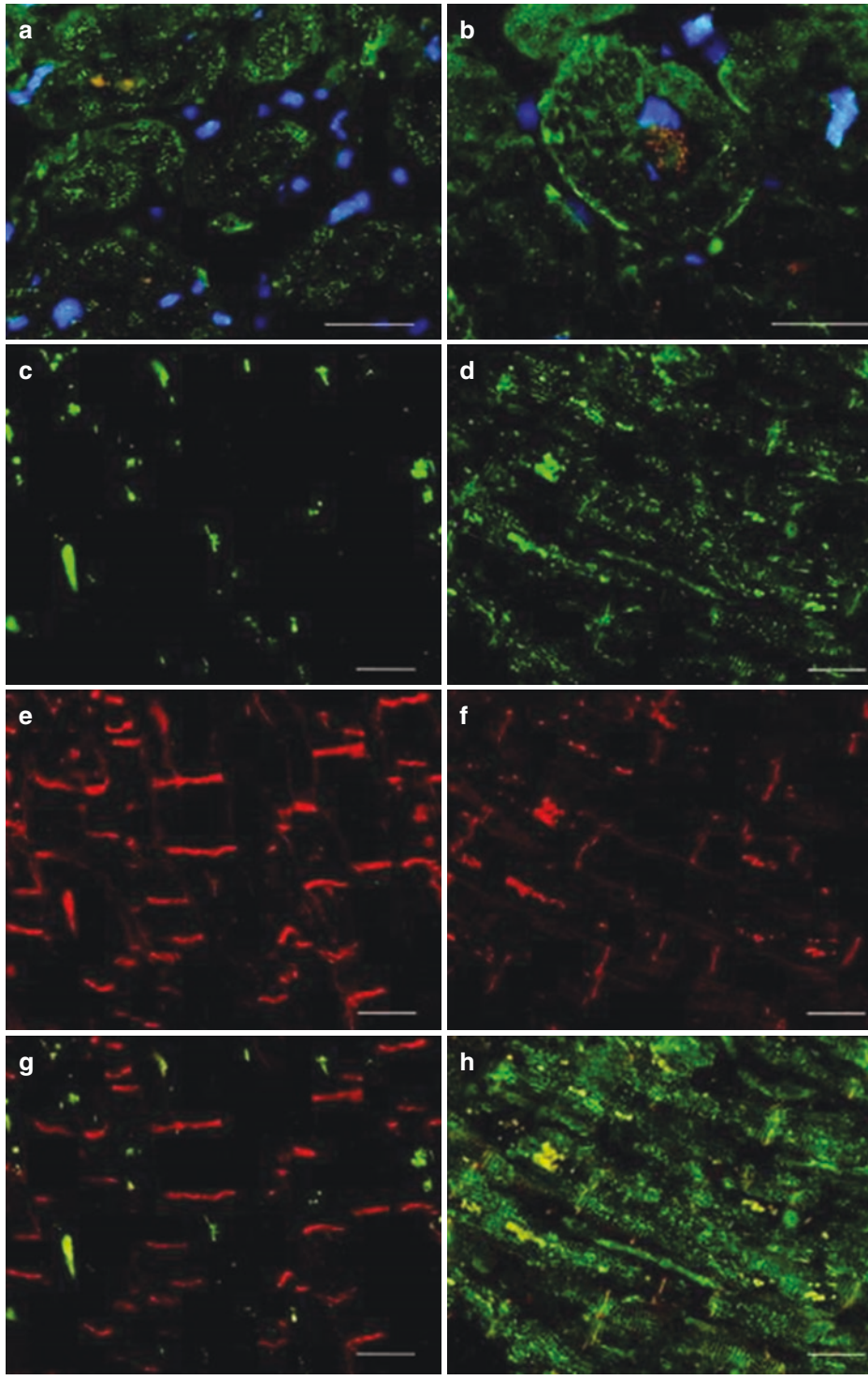

Fig. 4.16 Representative immunofluorescence micrographs of human heart sections labeled for the nicotinamide adenine dinucleotide 3-phosphate (reduced form) oxidase subunit gp91^{phox}. Panels **a**, **c**, **e**, and **g** show nonfailing heart tissue and panels **b**, **d**, **f**, and **h** show end-stage failing tissue. Transverse (**a**, **b**) and longitudinal (**c**, **d**) sections labeled for gp91^{phox} show increased labeling in end-stage heart failure. Labeling for alpha-actinin (**e**, **f**) shows a typical intracellular pattern of myocyte costamer and intercalated disc labeling. Panels **g** and **h** show suprerposition of gp91^{phox} and alpha-actinin labeling. All scale bars = 20 μm. (From Heymes et al. [244] with permission.)

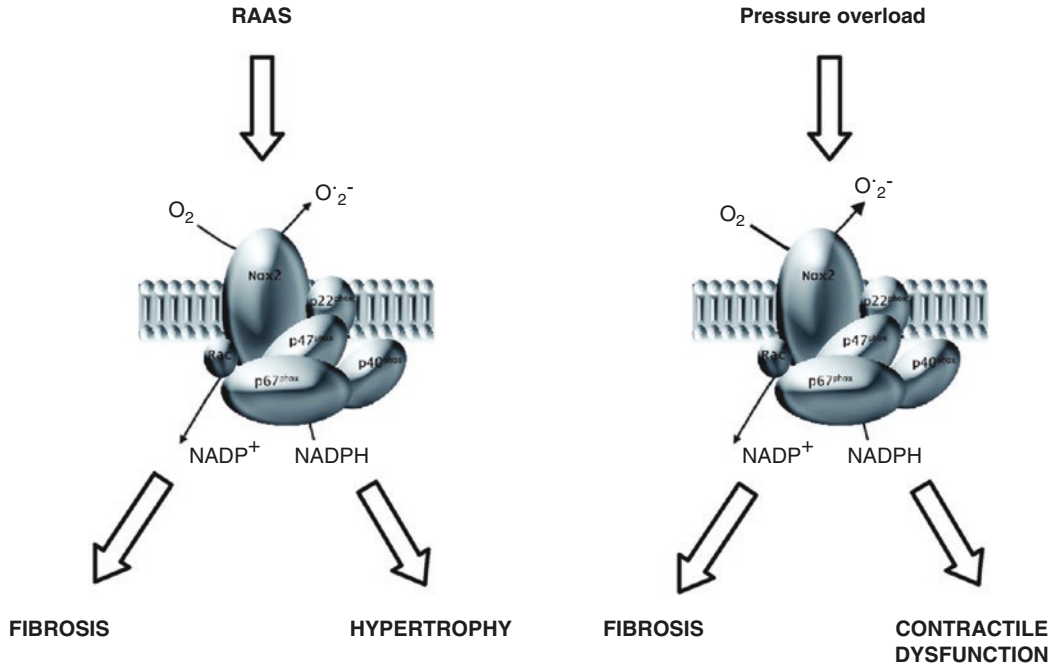

Fig. 4.17 Schematic illustrating involvement of Nox2 NADPH oxidase in the cardiac response to activation of the renin angiotensin aldosterone system (RAAS) or to chronic pressure overload. Hypertrophy in response to short-term RAAS activation is dependent upon Nox2, whereas the hypertrophic response to pressure overload is not. However, Nox2 is essential for the development of interstitial fibrosis in response to either stimulus. (From Murdoch et al. [261] with permission.)

On the other hand, in patients with ST elevation MI, CD14+/CD16-cells have an early peak and are negatively correlated with heart recovery [269].

4.6 Factors Influencing Cardiac Remodelling

4.6.1 Myocardial Infarction

It is the most frequent condition in which CR comes about. Taken together, heart ischemia leads to 'necrotic cell death'. Further, the post-MI evolution implies apoptosis, inflammation, ECM remodelling, fibrotic scar formation, proliferation and differentiation of MyoFb, angiogenesis, and scar maturation [21]. All these reactions are determined to cause healing on short term, but they produce evolution to HF on long time. Therefore, after MI occurrence, the poor evolution continues with additional CR, hypertrophy, dilation, and systolic dysfunction [21, 73].

A number of innate immune pathways are triggered in MI [149]. It appears the production of "damage-associated molecular patterns (DAMP)" by necrotic cells that further trigger membrane-bound "Toll-Like Receptors" (TLRs) [270, 271]. Also, among others innate immune pathways such as the "High mobility group box 1" (HMGB1), the "receptor for advanced glycation end-products" (RAGE) [21, 272] and the complement system are also triggered in the onset of inflammation after MI [21]. As a result, ROS are produced at ischemic injury with further activation of inflammatory signals pathways and myocardial dysfunction [149]. All triggered "innate immune pathways" set off Nuclear Factor NF-κB with further initiation of inflammatory cytokines and chemokines [273]. As already described, pro-inflammatory cytokines significantly modulate the inflammatory reaction to cardiac ischemic injury. IL-1 triggers

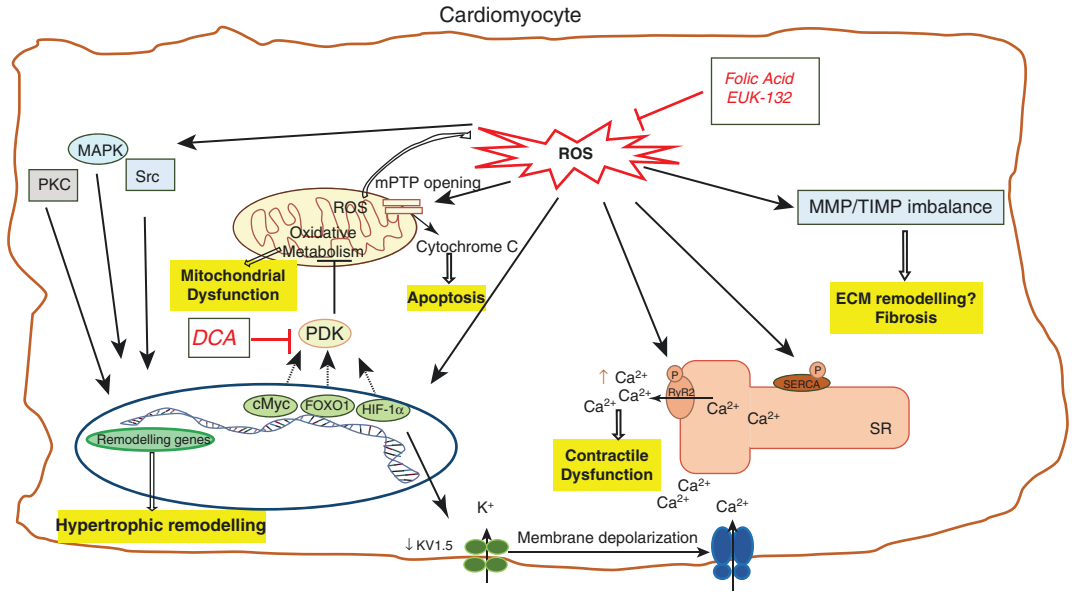

Fig. 4.18 ROS-induced intracellular changes in cardiomyocyte. The increased intracellular ROS levels occurring in RV pressure overload affect several cardiomyocytes functions. ROS can stimulate pro-hypertrophic pathways by targeting key molecules in this process, such as MAPK, PKC and Src proteins. The redox-mediated activation of target transcription factors (HIF-1α, cMyc and FOXO1) might be responsible for the abnormal PKD activation, which inhibits mitochondrial oxidative metabolism, leading to mitochondrial dysfunction. Sustained ROS levels cause mPTP opening and mitochondrial membrane depolarisation. As a consequence, more ROS are produced and cytochrome c is release from mitochondria causing cell apoptosis. HIF-1α activation also decreases the activity of the O2-sensitive Kv channel (Kv1.5), resulting into membrane depolarisation and elevation of cytosolic Ca2+. The surplus of cytosolic Ca2+, in addition to the excessive Ca2+ released from the sarcoplasmic reticulum, as a consequence ROS-mediated RyR2 channel activation and SERCA inhibition, contributes to myocytes contractile dysfunction. ROS are also responsible for the MMPs/TIMPs imbalance that drives ECM remodelling and fibrosis. Antioxidant compounds, like Folic acid or EUK-134, by scavenging the ROS in excess, can help restore the impaired cardiomyocyte function. Furthermore, DCA can restore ROS production and mitochondrial membrane potential by inhibiting PDK and thereby improving glucose oxidation. "Upwards arrow" indicates increase in levels; "Lowerwards arrow" indicates decrease in level. *ROS* reactive oxygen species, *PCK* protein kinase C, *MAPK* mitogen-activated protein kinase, *mPTP* mitochondrial permeability transition pore, *PDK* pyruvate dehydrogenase kinase, *HIF* hypoxia-inducible factor, *FOXO1* Forkhead box protein O1, *cMyc* v-myc avin myelocytomastosis viral oncogene homologue, *RyR2* ryanodine receptor 2, *Kv 1.5* potassium voltage channel, *SR* sarcoplasmic reticulum, *SERCA* sarcoplasmic reticulum Ca2+-ATPase, *MMP* matrix metalloproteinases, *TIMP* tissue inhibitor metalloproteinases, *ECM* extracellular matrix, *DCA* dichloroacetate, *PKD* protein kinase D. (From Iacobazzi et al. [21]. It is an open access article)

chemokines production in MI with entrapment of leukocytes [274]. An inactive precursor named pro-IL-1β generates active IL-1β by the converting enzyme caspase-1. Further, caspase-1 function is strongly controlled in multiprotein complexes named "inflammasomes", which further monitor production of IL-1β [275]. In MI, "inflammasome" initiation is restricted only in leukocytes and CFs with IL-1-mediated inflammatory cell infiltration and cytokine production [276]. ROS production and K^+ efflux have a significant function in inflammasome triggering from CFs. Importantly, chemokines activation is a significant finding of post-MI inflammation [277]. The activation of chemokines receptors from leukocytes in MI exhibit a chemokines profile that controls the composition of the leucocytes infiltrate. Therefore, neutrophils are triggered firstly in MI followed by monocytes and lymphocytes. Apoptotic neutrophils as negative mediators of inflammation are exposed in Fig. 4.19 [149].

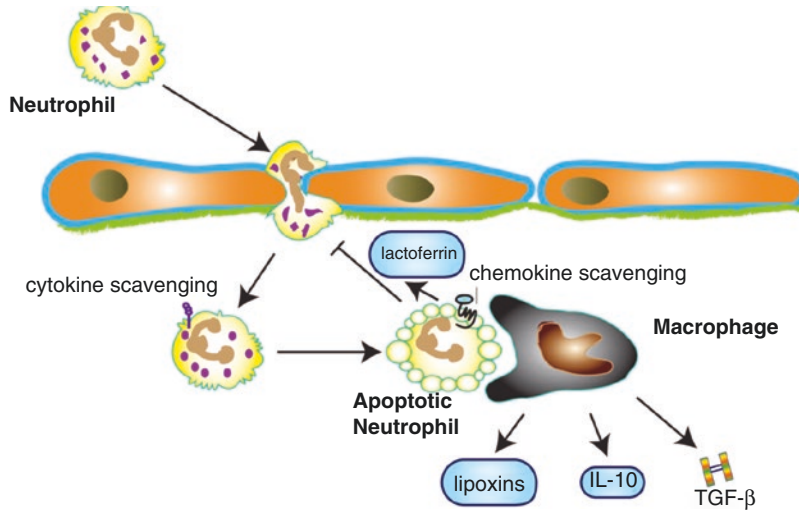

Fig. 4.19 The role of neutrophil clearance in suppression of the inflammatory response. Abundant neutrophils infiltrate the infarcted myocardium. Neutrophils are short-lived cells that undergo apoptosis; dying neutrophils may contribute to repression of the post-infarction inflammatory response through several distinct mechanisms. First apoptotic neutrophils may release lactoferrin, an inhibitor of granulocyte transmigration. Second, during clearance of apoptotic neutrophils, macrophages secrete large amounts of anti-inflammatory and proresolving mediators including IL-10, TGF-β and lipoxins. Third, expression of decoy cytokine receptors by neutrophils may promote cytokine scavenging. Increased expression of chemokine receptors (such as CCR5) in apoptotic neutrophils may serve as a molecular trap for chemokines terminating their action. (From Frangogiannis [149] with permission)

The activation of neutrophils in the MI triggers apoptosis. Shortly, they are eliminated in MI by macrophages which activate powerful inhibitory pathways. Mediators such as TNF-α and IL-1β can maintain activated neutrophils in MI [278]. On the other hand, within 3–7 days after MI, the neutrophils undertake apoptosis [279].

4.6.2 Changes in Hemodynamic Load

In case of patients with anterior MI, the early LV dilation may be increased, as well as ventricular hypertrophy turns up to be a late and restricted modification during the first year [41]. Generally, the outcome of ongoing CR with ventricular dilation and abnormal ventricular hypertrophy causes a significant growing in total LV wall tension [41, 280]. As it will become evident, triggering of wall stress can activate further an amount of mechanisms that in the absence of any efficient therapy may cause further CR with progressive HF [50, 281].

4.6.3 Blood Pressure

Correspondingly, high blood pressure (BP) triggers structural modifications in the LVH with interstitial alterations, which further may produce diastolic dysfunction with HF. Additionally the functional effect of pressure overload hypertrophy may be determined by the features of the CR process. For example, if remodelling is eccentric with LV dilatation with normal relative wall thickness and raised wall stress [282], HF by a functional damage was described. On the other hand, HF does not occur in animals with concentric CR defined as normal chamber volume, raised relative wall thickness and normal wall stress. Previous hypertension may be related with extensive damaging CR and progression of HF after MI. This finding was shown by Richards et al. in 1093 patients, where 68% experienced serial neurohormonal sampling and assessment of LV function one to four days and three to 5 months post-MI [283]. In this study, in comparison with normotensives, hypertensive patients had significantly higher plasma levels of

neurohormones at serial sampling with a significantly enhanced raise in LV volumes by remodelling at five months. Conversely, only normotensive patients had a recovery in LV ejection fraction at five months. Also, previous diagnosis of hypertension was related with a greater risk of HF necessitating hospitalization at a mean follow-up of two years (12.4 versus 5.5% in normotensives) [283]. Moreover, Cingolani et al. discovered that TSP-4 from CMs, adjusts cardiac contraction function to acute stress and it has a major role in chronic CR and HF [21, 284].

4.6.4 Neurohormonal Activation

Progressing HF is connected with an initially compensatory neurohumoral activation that may be a factor to the development of the structural defects. Both the sympathetic system and the renin–angiotensin–aldosterone system (RAAS) are implied in CR. Triggering of both systems turns on intracellular signaling pathways that increase the production of protein in CMs and CFs, with hypertrophy, fibrosis, switching on of growth factors and MMPs [285–287]. Moreover, it appears hemodynamic overload by vasoconstriction and water retention, raise of oxidative stress activity with direct cytotoxic effect, and apoptosis [285–287]. Therefore, the inhibition of these systems can has a major therapeutic role in attenuation or prevention of CR. Unfortunately, elevated plasma norepinephrine, renin activity, and antidiuretic hormone levels [288, 289] are indicators for poor survival in these patients [290]. Even if, neurohumoral activation is firstly adjustable, it is damaging over the long term by pathologic remodelling, especially in case of Ang II and norepinephrine [291]. The studies data are most convincing for the activation of the RAAS. Also, the plasma BNP concentrations are raised in progressive HF and interrelated with prognosis [292]. In spite of this, the release of BNP from myocytes in HF may defend against pathologic remodelling [293].

The RAAS has a significant function in the control of BP and electrolyte equilibrium. Within RAAS, Ang II produces triggering of sympathetic nervous system with vasoconstriction, sodium and water retention, and anorexia [294]. The damaging effects of RAAS in cardiovascular tissues cause CR by local triggering of the RAAS with autocrine and paracrine mechanisms [295–297]. Mainly, the pathophysiological effects of Ang II in the cardiovascular system are controlled by a member of the GPCR family termed the 7 transmembrane (TM7) spanning AT1 receptor [296, 298, 299]. According to recent data, the mechanical stress together with systemically and locally Ang II cause by the triggering of AT1 receptor, cardiac hypertrophy [295–297, 300]. It seems that studies with the AT1 receptor blockers (ARBs) as candesartan showed that switching off of triggered AT1 receptor by mechanical stress, notably reduced hypertrophic reaction in cultured CMs [301–303]. Therefore, mechanical stress causes cardiac hypertrophy in vivo by initiation of the AT1 receptor with no correlation of Ang II [295, 296].

Mechanical stretch and Ang II by attachment to the AT1 receptor causes to its structure to switch on with occurrence of Cys residues inside the ligand-binding pocket. Further, if mechanical stress continues, TM7 undertakes a counter clockwise rotation with a modification in the ligand-binding pocket [304]. It is not determined exactly by current studies the mechanisms by which mechanical stress activates the AT1 receptor perceives its structure change, preparing for dissimilar initiation of particular intracellular signaling mediators [303].

4.6.5 Role of Angiotensin II

Significance of angiotensin II (Ang II) in pathologic CR is demonstrated by data of large trials in humans that have been shown that angiotensin-converting-enzyme inhibitors (ACEI) increase survival in HF by decrease or even reverse of some parameters of CR [305, 306]. Shortly, Ang II is produced and has locally and systemically effects. So that, mechanical stretch directly boost Ang II release from CMs [301]. Also, Ang II seems to sustain directly CR. Previous studies have been showed that human CFs cultured from

cardiomyopathic and ischemic hearts have on CMs the expression of AT1 receptors [307, 308]. In fact, these CFs reply to Ang II with raise of collagen production by activation of AT1 receptor [309–311]. Despite the fact that Ang II is produced locally or systemically, it may directly support CR. In fact, these CFs may reply to Ang II with AT1 receptor-mediated collagen synthesis [309–311]. On the other hand, Ang II acts via the AT1 receptor with boosting of protein synthesis and results in hypertrophy of CMs [309]. Both ACEI and Ang II receptor antagonists can reverse remodelling in HF [212].

Aldosterone secretion is increased by Ang II, and also may be a factor in CR. The heart contains mineralocorticoid receptors and takes out aldosterone after a MI, supporting the post MI remodelling [312]. Moreover, the secondary hyperaldosteronism commonly seen in patients with HF may participate to cardiac hypertrophy and fibrosis [313, 314]. It should be stressed that the benefit effects connected with spironolactone or eplerenone, which both link the mineralocorticoid receptor may result with diminished fibrosis [315].

4.6.6 Energy Metabolism and Cardiac Remodelling

Ischemia, pressure and volume overload are forms of stress that activates human heart to adapt its metabolic function to use glucose instead of the free fatty acids [316]. It seems that free fatty acids provide the highest quantity of ATP to human heart [317]. On the other hand, the glucose metabolism needs a reduced amount of oxygen consuming for same quantity of ATP synthesis, being the most effective alternative in highest metabolic states such as short-term of severe cardiac stress [318]. As a rule, in normal heart, free fatty acids are the main energy substance representing about 60–90% of energy reserves. Both free fatty acids and glucose metabolites undergo β-oxidation and glycolysis in the citric acid cycle, resulting in FADH2 and NADH. Finally, the obtained energy is accumulated and carried as phosphocreatine (Fig. 4.20) [319].

During stress is stopped the normal inhibition of glucose oxidation by free fatty acids [303]. It seems that the nuclear receptor peroxisome proliferator-activated receptor-α (PPARα) is a significant contributory factor that changes from fatty acid metabolism to glucose metabolism [316, 320]. Further, Karbowska et al. showed on ventricular biopsies from 5 patients a 54% fall of PPARα protein levels in end-stage HF in comparison with controls [316, 321]. Therefore, CR implies cardiac dysfunction with energy loss due to the disproportion from the oxygen reserve and use, with a diminished free fatty acids oxidation and raised glucose oxidation [316]. In addition, β-oxidation fall leads to deposit of triglycerides and lipotoxicity, mitochondrial dysfunction [316]. Altogether, these modifications causes for myocardial proteins further low levels of energy reserves with oxidative stress and ROS, with their sides effects (Fig. 4.21) [316, 321–324].

In case of RV, the metabolism data is from the LV studies. As already described, the RV has smaller afterload than the LV due the decreased pulmonary vascular resistance [316]. Even if, RV and LV have similar stroke volumes, the RV has near 25% from the stroke volume of the LV because of the low PVR [316, 325]. Extensive "transcriptional, translational and energetic" disturbances to physiologic and pathophysiologic stress occur in RV. The conversion from pressure overload and volume overload to cardiac hypertrophy and later RVF is correlated with the switch from free fatty acids to glucose metabolism for ATP production. As a result, the RVF is an energy-deprived state with deficient ATP amounts. For this reason, PET using specific radioactive tracers provides a complete description of RV metabolism [316]. These metabolic differences might corelate with the dissimilarities in ventricular wall stress and intraventricular pressure dynamics (Fig. 4.22) [316].

To sum up, metabolic alteration in the hypertrophied RV imitates metabolic alteration of the hypertrophied and failing LV [316]. Nagaya et al. [326] studied 21 patients with RVH due to PH by using magnetic resonance spectroscopic imaging (MRSI) that associates cardiac structure with metabolic function. They found important RV con-

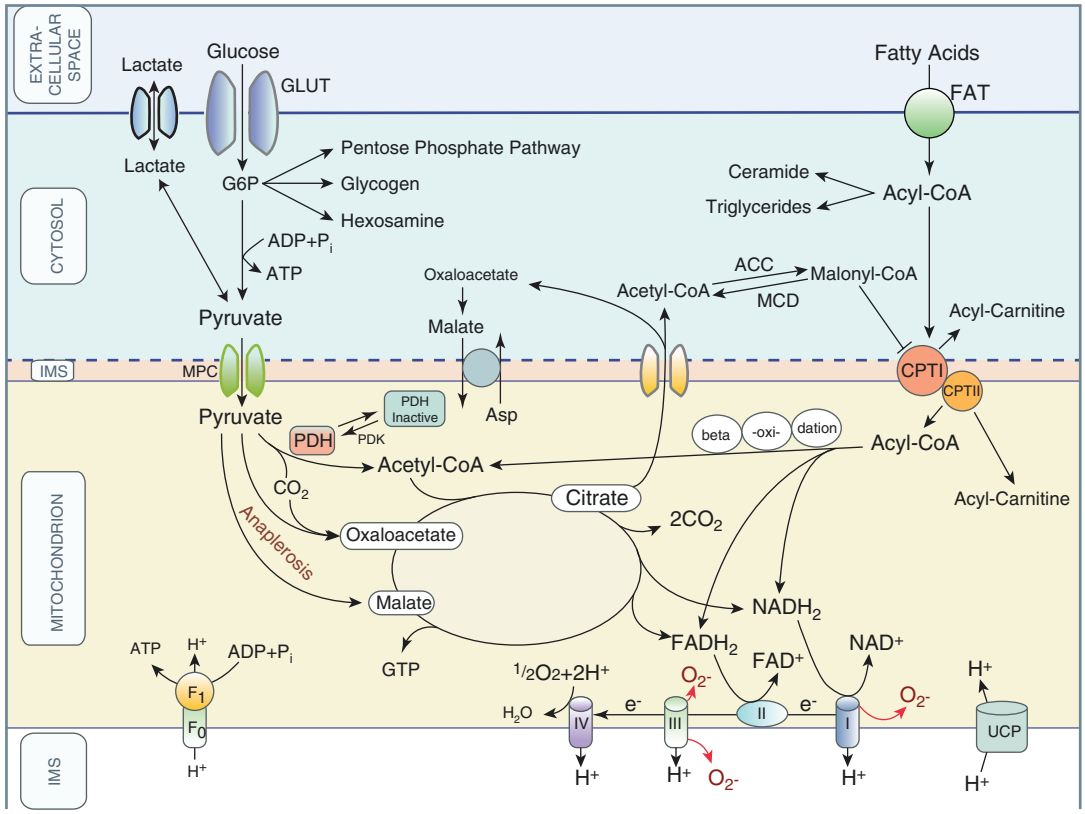

Fig. 4.20 Schematic representation of classic pathways of cardiac metabolism. Substrates are transported across the extracellular membrane into the cytosol and are metabolized in various ways. For oxidation, the respective metabolic intermediates (e.g., pyruvate or acyl-CoA) are transported across the inner mitochondrial membrane by specific transport systems. Once inside the mitochondrion, substrates are oxidized or carboxylated (anaplerosis) and fed into the Krebs cycle for the generation of reducing equivalents (NADH2 and FADH) and GTP. The reducing equivalents are used by the electron transport chain to generate a proton gradient, which in turn is used for the production of ATP. This principal functionality can be affected in various ways during HF thereby limiting ATP production or affecting cellular function in other ways (see text and further Figures for details). *IMS* mitochondrial intermembrane space, *GLUT* glucose transporter, *FAT* fatty acid transporter, *MPC* mitochondrial pyruvate transporter. (Illustration Credit: Ben Smith). (From Doenst et al. [319] with permission)

traction dysfunction in patients with altered myocardial free fatty acid metabolism. Further, in a study of 16 patients with idiopathic PAH, Bokhari et al. proved that PET imaging is for determining myocardial glucose assimilation and use [316, 327]. They demonstrated that RV glucose usage is associated with hemodynamic parameters such as mean PA pressure, doubtlessly implying that RV dysfunction is switched on myocardial glucose metabolism and being a sign of RV dysfunction. Can et al. [328] have been demonstrated same features on 23 patients with PAH and 16 healthy controls evaluated by PET. Their results established that raised fludeoxyglucose (^{18}F) increase in the RV myocardium were connected with raised RV loading conditions and with the existence of elevated pulmonary artery pressures but not with their stage [316, 328].

Also, MRSI for the study of myocardial triglyceride load demonstrated an accurate statistically significance correlation with triglycerides from RV biopsy [316, 329]. Currently, no other study tried to measure in the RV the lipid transitional products.

It is not determined if cardiac metabolic alterations maintain during the development of RVH, that is characterized by important decrease of CO,

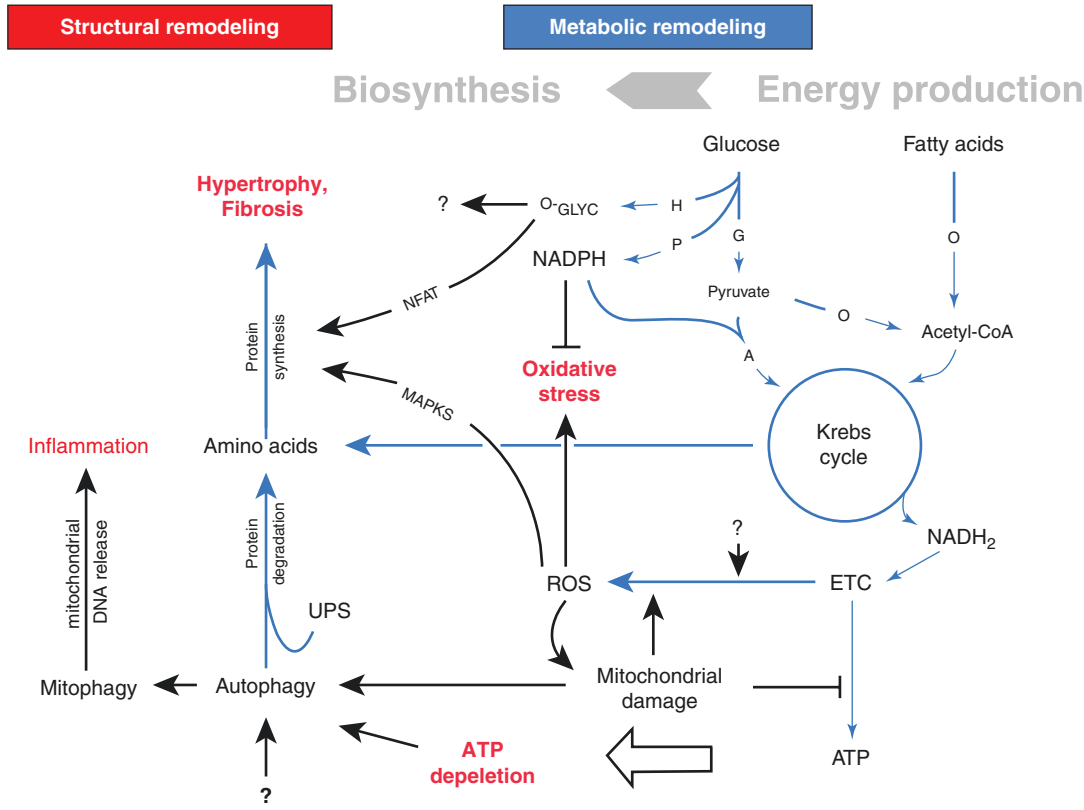

Fig. 4.21 Overview of metabolic remodeling and proposed mechanisms linking it to other processes in the progression to HF. Metabolic pathways are blue. Bold lines indicate pathways/processes that are increased or dominant. Thin lines represent pathways/ processes that are decreased. The question marks imply unknown causes/ effects. In general, metabolic remodeling in cardiac hypertrophy and failure is characterized by a shift away from energy production to activation of biosynthetic pathways required for structural remodeling processes such as ventricular hypertrophy and fibrosis. Particularly, fatty acid oxidation is decreased and may not be sufficiently compensated given the lack of increase in glucose oxidation. These alterations and further mitochondrial defects result in ATP depletion. Instead of being oxidized, pyruvate may be preferentially used for anaplerosis to maintain Krebs cycle moieties, which might be increasingly channeled into protein synthesis. Hypertrophic mediators such as MAPKs and NFAT are activated as a result of increased mitochondrial ROS and flux through the HBP, respectively. Overproduction of mitochondrial ROS causes oxidative damage. Although the flux through the PPP is increased, anti-oxidative defense might be inadequate due to the consumption of NADPH by the anaplerotic malic enzyme. Mitochondrial damage and ATP depletion may stimulate autophagy. Increased activity of autophagy and the UPS may contribute to hypertrophy by providing amino acids and other metabolites. Increase in mitophagy may trigger myocardial inflammation by releasing mitochondrial DNA. *H* hexosamine biosynthetic pathway (HBP), *P* pentose phosphate pathway (PPP), *G* glycolysis, *A* anaplerosis, *O* oxidation, *ETC* electron transport chain, *ROS* reactive oxygen species, *UPS* ubiquitin-proteasome system. (From Doenst et al. [319] with permission)

increase of RV filling pressure and raised fibrosis [21, 330]. Consequently, RVH is correlated with increased mitochondrial ROS, which downregulates HIF1α and triggers p53 pathways, in the end with dysregulated pyruvate dehydrogenase kinase (PDK) and diminished glucose uptake [21, 331]. Raised PDK expression is a frequent feature in RVH during glucose oxidation, as a result there is a decrease in mitochondrial respiration [21, 330]. A number of clinical trials directed on molecular dysfunction in RVH and RV failure are undergoing, even if the precise outcomes for pharmacologic

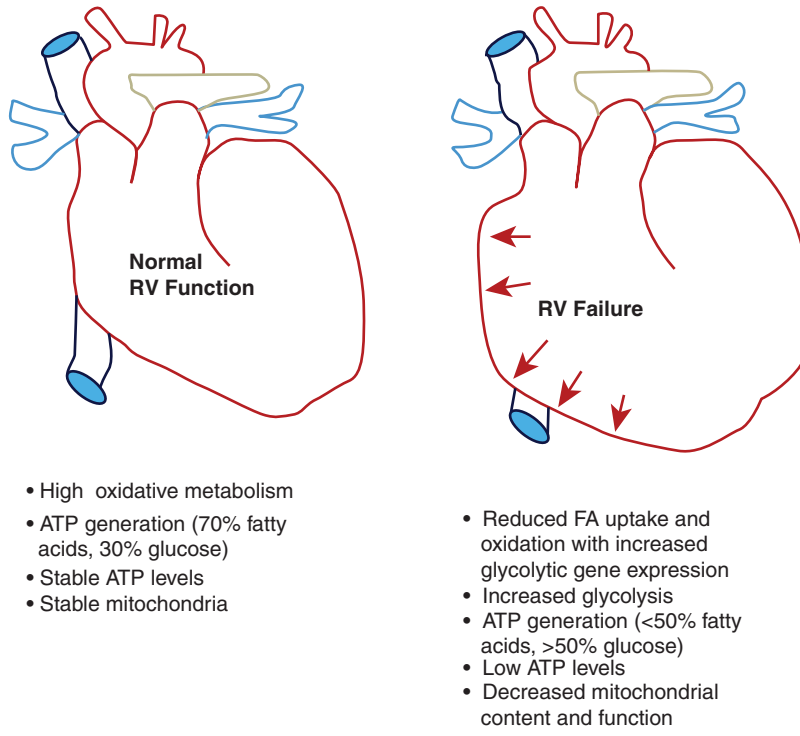

Fig. 4.22 Right ventricular metabolism. (From Altin et al. [316] with permission)

involvements on RV abnormal metabolism are not determined [316].

4.6.7 Electrical Remodelling in Cardiac Remodelling

As already been described, the functional, structural, and electrical modifications of CMs to stress described by hypertrophy, HF, and ischemia define CR, which disposes to raised occurrence of ventricular ectopy and arrhythmias. "Arrhythmia-induced changes in the electrophysiological properties of heart tissue which predisposes to an increased frequency of ventricular ectopy and arrhythmias are referred to as electrical remodelling" [332].

Specifically, Na^+-Ca^{2+} exchanger (NCX) mediates intracellular Ca^{2+} concentration and its activity is controlled by intracellular concentrations of $Ca^{2+,}$ Na^+, ATP, pH, and phosphorylation of NCX, all being modified in HF [332]. Therefore, HF with contractile dysfunction and arrhythmogenesis may be explicated by amplified NCX and diminished SERCa^{2+}a function, consequently with raised Ca^{2+} discharge from CMs and delayed afterdepolarizations [332–334]. Also, during cardiac diastole dysfunction, NCX sustains Ca^{2+} transportation from intracellular space and diminishes SERCa^{2+}a function [332, 333]. It has to be underlined, that NCX activity is mediated in cardiac hypertrophy, function sustained by diminished NCX activity but with raised NCX protein and transcript levels [332]. It seems that calcineurin inhibition weakens the boost of NCX1 transcript and protein levels correlated with pressure overload, advocating that calcineurin is vital in the adjustment of NCX1 transcript synthesis and degeneration [332, 335].

Also, there is a diminished expression and function of Na^+-K^+ATPase in HF [332, 336] that make susceptible cardiac tissue to arrhythmias by raised action potential duration, and increased depolarizing current, and extracellular K^+ [332]. According to experimental cardiomyopathic

studies, ETA receptor blockers demonstrated to stop electrical remodelling and ventricular arrhythmias by diminishing K^+ and Ca^{2+} current expression, rising QT interval and action potential duration [332, 337].

Electrical anisotropy caused by myocardial fibrosis and modifications of intracellular Ca^{2+} could produce the electrophysiological remodelling and arrhythmias from hypertrophy [332]. Further, modification of the collagen amount, type, and cross-linking is correlated with myocardial fibrosis and CR with electrophysiological abnormalities [338].

RVH, dilation, and septal displacement also create RV dyssynchronous motion [339–341] and dyssynchronous RV-LV contraction [341–343]. Delayed RV lateral wall contraction and interventricular dyssynchrony in PAH are not related to QRS duration or abnormal electric activation such as left bundle-branch block but rather to RV wall stress, septal shift, LV end-diastolic volume, and stroke volume [342, 343]. These ventricular-ventricular interactions almost certainly increase the ratio of systolic to diastolic duration because interventricular dyssynchrony is related to lengthening of the RV contraction [343].

To sum up, existing data supports that myocardial hypertrophy form determines the electrical CR and the reverse of it [332, 344]. Nevertheless, in pressure-overload states with reverse of hypertrophy is correlated with the reverse of the electrical remodelling [345–347]. However, the dissimilarity between the reverse of electrical remodelling in pressure-versus volume-overload states is unknowable [332]. Both structure and electrical CR should be regarded as independent clinical disorders [332]. The assessment of risk factors for arrhythmias has a significant function in the regress of hypertrophy and the electrical CR [347].

4.6.8 Coronary Vascular Remodelling in Cardiac Remodelling

Coronary vascular remodelling causes adjustable reactions such as the rapid adaptation of vessel diameter by modifications in smooth muscle tone, changes in vessel diameter structure, adding or elimination of vessels by "angiogenesis (sprouting/splitting)", or "vascular pruning" [348]. It important to underline that physiological vascular adaptation keeps an appropriate perfusion, but vascular maladaptation takes place in disorders such as hypertension [348]. Also, regulatory mechanisms in larger vessels are different from microcirculation that has a vital role in physiological vascular adaptation and pathological states [348]. Generally speaking, growing of size and number of microvessels during exercise or involution with microvascular remodelling because of constant decline of physical activity appear [349]. Reduction of epicardial arteries with hemodynamic- and metabolic modifications causes process of collateralization or arteriogenesis defined by "structural enlargement of arteriolar vessels and arterio-arterial anastomoses" [348, 350].

As a result, constant chronic remodelling of coronary vessels leads to over-prolonged modifications of vessels diameter with or without shifts in wall mass (Fig. 4.23) [348, 352, 353]. Therefore, coronary vessels adjust to mechanical stimuli, such as fluid shear stress acting on ECs, circumferential wall stress and metabolic signals [348, 354, 355].

Essentially, exposure of the LV to afterload stress causes firstly the development of new capillaries or angiogenesis, to sustain the raised blood flow of hypertrophied CMs. In case of angionesis are implied raised production of the proangiogenic factors hypoxia HIF1α and VEGF. If the LV starts to fail, the capillary density starts to decrease. On the other hand, the capillary density of the RV reduces with the beginning of pressure overload upsurge. RVF is a frequent side effect of chronic RV pressure overload with progression to RV ischemia. Specifically, increased pulmonary arterial pressure boosts RV wall tension and oxygen demand in correlation with alteration of coronary blood flow. For instance, Eisenmenger's syndrome produces a level of RV afterload same to idiopathic PAH, only that the survival is longer with latent overt RVF [356]. In addition, PAH during diagnosis protocol have different degrees of RVF even if the RV afterload is highly developed.

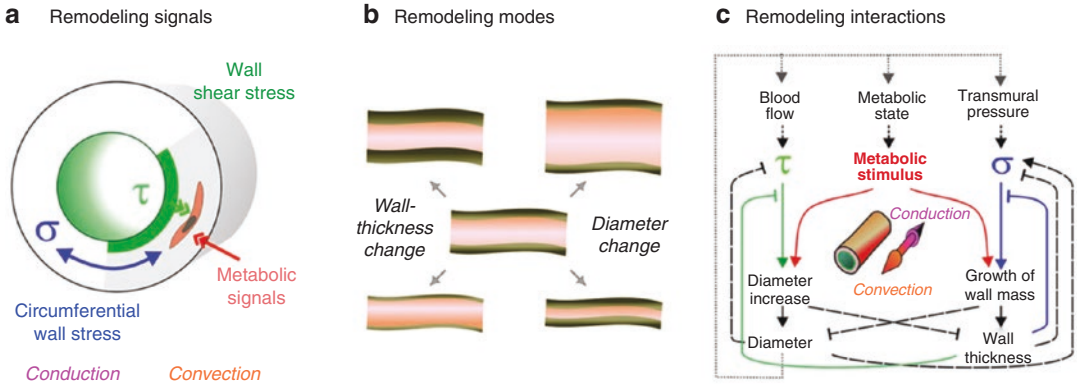

Fig. 4.23 Mechanisms and models of vascular remodelling. Left: Signals for vascular adaptation include wall shear stress at the endothelial surface (*t*), circumferential wall stress (*s*), and metabolic signals. Metabolic signals maybe elicited by low oxygen availability and act as vasodilators and stimulate vascular growth, or they could be vasoconstricting mediators produced at high oxygen partial pressures but in decreasing amounts with decreasing pO2. Metabolic substances are convected downstream, but elicit also a signal that is conducted upstream within the vessel wall. Middle: Vascular responses elicited by these stimuli comprise changes of diameter and wall mass. Right: An integrated model [351] which connects the local conditions (pressure, flow, and metabolic state) with derived stimuli (σ, τ, and metabolic stimuli) and the vascular changes in vessel diameter or wall mass. Lines indicate biological reactions (solid) and physical relations (dashed). (From Pries et al. [348] with permission)

4.7 Reverse Cardiac Remodelling

CR can be reversed with maximized therapy that initiates ongoing recovery of cardiac function and thus enhances prognosis of patients [357]. Even if, reverse CR could arise unexpectedly in heart pathologies, it is more frequently seen as reaction to medical, device-based, or surgical therapies, such as beta-blockers, cardiac resynchronization therapy (CRT), revascularization and valve surgery [358]. The various cardiac pathologies with noticed reverse CR prove that myocardial remodelling is bidirectional and takes place no matter of the myocardial disease aetiology, length, and severity (Fig. 4.24) [358]. Moreover, prognosis is improved in patients with reverted heart dysfunction, for that reason reversal of CR should be the most important treatment aim. Therefore, effective treatment should reverse cardiac remodelling [359].

Both ACEI and Ang II receptor antagonists, also known as angiotensin receptor blockers (ARBs) have been utilized to prevent CR. Preventing raised RAAS stimulation that may limit subsequent maladaptive cardiac remodelling. For instance, RV samples taken from control patients showed higher ventricular weight with raised collagen and foetal contractile protein genes, and diminished SR Ca^{2+}-ATPase. Moreover, ACEI exert antioxidant effects by inhibiting the transcription factor NF-kB that controls the synthesis of various genes associated with inflammatory response, such as cytokines, chemokines, growth factors, and cell adhesion molecules [360–363]. The complexity of the intramyocardial mechanisms involved in CR should also take into account endothelial damage, on which PDE5 inhibition acts positively, as recently demonstrated in a meta-analysis of type 2 diabetic cardiovascular patients [364]. Also, clinically relevant evidence suggests that PDE5 inhibition has favourable direct myocardial effects via cGMP and cAMP activities that may counterbalance hypertrophic and proapoptotic signaling, including adrenergic stimulation [365].

4.7.1 Cardiac Regenerative Medicine

Production of "induced cardiac-like myocytes" (iCLMs) shows all the signs of a new future successful method to regenerate damaged CMs [366]. Replacing lost CMs by injecting cardiac progenitors, cardiospheres, or CMs derived

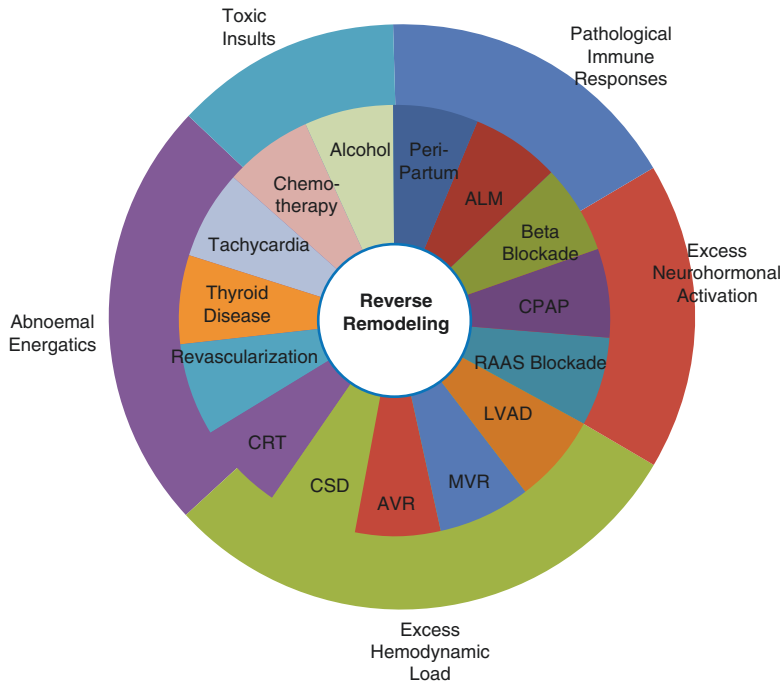

Fig. 4.24 Myocardial recovery in clinical settings. The segments of the outmost ring highlight pathophysiological processes implicated by reverse remodeling in particular clinical settings that comprise the middle ring. Abbreviations: *ALM* acute lymphocytic myocarditis, *CPAP* continuous positive airway pressure, *RAAS* renin–angiotensin–aldosterone system, *LVAD* left ventricular assist device, *MVR* mitral valve repair/replacement, *AVR* aortic valve replacement, *CSD* cardiac support device, *CRT* cardiac resynchronization therapy. (From Hellawell et al. [358] with permission)

from "induced pluripotent stem cells" (iPSCs) and/or "embryonic stem cells" (ESCs) has been researched intensively [367]. Importantly, miRNAs are important for stem cell differentiation, as well as indirect and direct reprogramming to multiple lineages [368–371]. To sum up, miRNA based therapy can be used to promote CMs proliferation, reprogram directly fibroblasts to CMs or indirectly to iPSc as well as driving the differentiation of iPSCs, ESCs or CPCs to CMs (Fig. 4.25) [367]. Another new treatment choice is to release cells in the damaged myocardium. According to evidence, various cell categories have been utilized for heart regeneration, such as ESCs, CMs obtained from iPSCs, mesenchymal stem cells (MSCs), bone marrow MSCs, cardiac stem cells, cardiac progenitor cells, skeletal myoblasts, ECs, adipose tissue-derived stem cells (ATDSCs), and CMs [372]. Nevertheless, studies have still unremarkable outcomes.

4.7.2 Device-Based Therapies

Pharmacological treatments that diminish on either side PVR or systemic vascular resistance can reduce the development of fibrosis in the RV and LV, respectively. Likewise, non-pharmacological mechanical decrease of LV load by LV assist devices (LVADs) can attenuate fibrosis in both ventricles [373].

For instance, cardiac resynchronization therapy (CRT) with biventricular (BiV) pacing is an well-known choice therapy in case of patients with overt HF, diminished LV systolic EF, and delayed ventricular conduction with enlarged QRS complex (e.g. electrical dyssynchrony). In fact, Sachse et al. [374] showed that CRT reduces symptoms and mortality in patients affected by dyssynchronous heart failure (DHF) produced by dyssynchronous electrical and mechanical activation of the left and right ventricle. Also, they concluded that CR of electrophysiological properties, hemodynamic and

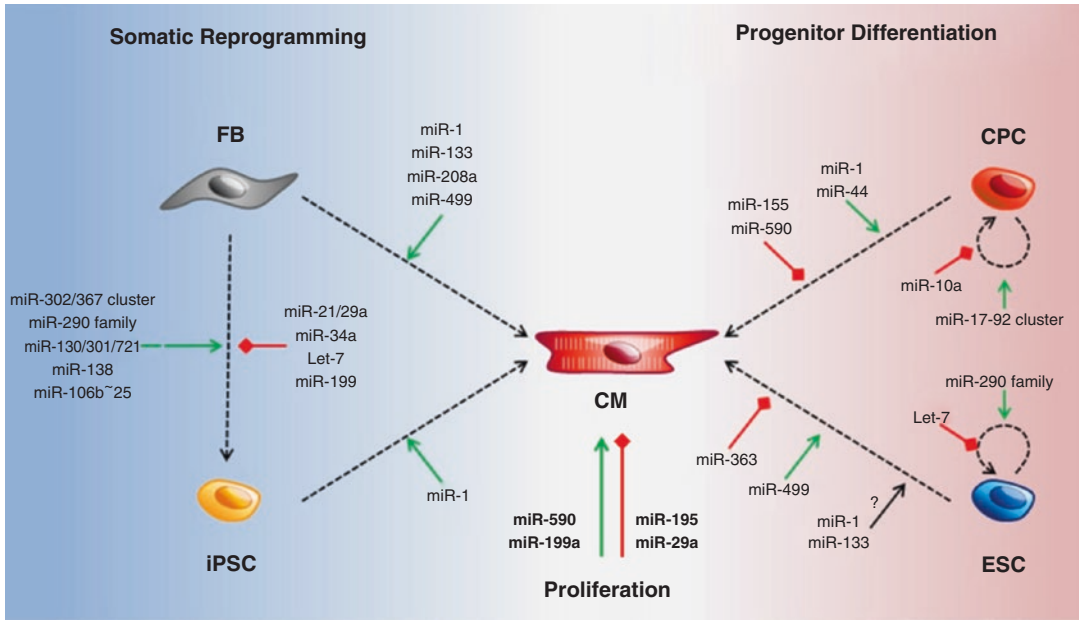

Fig. 4.25 miRNAs and reprogramming. miRNAs promote the generation of cardiomyocytes via a number of mechanisms. Fibroblasts can be reprogrammed into cardiomyocytes by miRNAs directly or through an intermediate iPSC state. miRNAs also promote cardiac progenitor cell (CPC) and embryonic stem cell (ESC) cardiac differentiation. miRNAs can promote or inhibit cardiomycyte proliferation. (From Hodgkinson et al. [367] with permission)

protein expression due to DHF is partially restored by CRT. Specifically, CRT can reverse damages of intracellular structures and function of CMs from HF, with early successful signs of recovery as tubular system structure [374].

Ventricular Assist Devices (VADs) can prevent ongoing CR and produce reverse CR, mainly by decrease of mechanical load of the damaged ventricles [373]. Also, VADs are not same thing with artificial hearts, which are planned for temporary taking up of cardiac function with their latter withdrawal from the patient's heart [373]. VADs are designed to support the LVAD, the right ventricle (RVAD) or both ventricles (BiVAD). LVAD is the most frequent device used in a damaged heart, but in case of increased pulmonary arterial resistance, RVAD will be added to help with cardiac circulation. According to data, the evaluation of LVAD outcomes looking the reverse of RV remodelling, showed there were no change in CMs size among patients with LVADs and control group [373]. Conversely, LVAD therapy produced diminishing of collagen and TNF-α from RV, supporting that LVAD can reduce RVH by inhibiting the paracrine factors [373]. Further, Barbone et al. studied the involvement of these factors in reverse of CR [375]. Shortly, they studied heart samples from patients who required either LVAD or pharmacological treatment for severe HF [375]. Regardless of LVAD type, the RV volume and CM size enlarged, but isolated RV muscle pieces from inserted LVAD showed a diminished force formation at high pacing rates. Finally, they concluded that reverse RV remodelling after LVAD placing is minimum [375]. In conclusion, LVADs implantation is largely helpful for showing biology of reverse CR: changes of mRNA and microRNA profiles, decrease of apoptosis, diminishing of inflammatory cytokines (e.g., TNF-α), ECM remodelling, regression of action potential lengthening, regression of cardiac myocyte hypertrophy, improved contractility, regression of shape

distortions, and improved β-adrenergic responsiveness [358].

Other studies evaluated hearts from end-stage CHF with no VADs, with LVAD or with BiVAD [376]. In comparison with LVAD, BiVAD-supported hearts showed notably diminished right atrium pressures with nearly normal RV end-diastolic pressure-volume interactions. Moreover, the hearts with BiVAD demonstrated normalized RV myocyte diameter and myocardial contraction when isoproterenol perfusion was used. All these modifications were not demonstrated in hearts with LVADs. However, LVADs diminish only RV afterload. To sum up, VADs could induce RV remodelling, but further studies data is necessary [376].

Conclusions

RV remodelling is correlated with functional, cellular and molecular changes [316]. CMs hypertrophy and hyperplasia modify RV geometry, while apoptosis rate and damages of intracellular structures induce further remodelling [316]. RVH and RV dilatation can be correlated with diminished ventricular volume, associated or not with changed hemodynamic status [316]. As a result, physiologic and pathophysiologic stress produces in RV serious transcriptional, translational and energetic modifications [316]. The development of cardiac hypertrophy from pressure and volume overload with failing is correlated with transition from free fatty acids to glucose metabolism for ATP formation [316]. RVF is an energy-depleted condition with lacking ATP levels. Reassuring successful molecular targets are established by ongoing clinical trials studying the molecular alteration from RVH and failure [316]. Ultimately, medical therapy with vasodilators seems to raise both RV stroke volume and CO, while ACEI and ARBs can postpone RVH by diminishing the exhibition of hypertrophy-related genes in the RV. Nonetheless, immunomodulator therapy is correlated with diminishing of RVH and remodelling-related gene expression [316].

References

1. Hochman JS, Bulkley BH. Expansion of acute myocardial infarction: an experimental study. Circulation. 1982;65(7):1446–50.
2. Pfeffer JM, Pfeffer MA, Braunwald E. Influence of chronic captopril therapy on the infarcted left ventricle of the rat. Circ Res. 1985;57(1):84–95.
3. Pfeffer MA, Braunwald E. Ventricular remodeling after myocardial infarction. Experimental observations and clinical implications. Circulation. 1990;81(4):1161–72.
4. Cohn JN, Ferrari R, Sharpe N. Cardiac remodeling--concepts and clinical implications: a consensus paper from an international forum on cardiac remodeling. Behalf of an International Forum on Cardiac Remodeling. J Am Coll Cardiol. 2000;35(3):569–82.
5. Swynghedauw B. Molecular mechanisms of myocardial remodeling. Physiol Rev. 1999;79(1):215–62.
6. Roberts CS, Maclean D, Maroko P, Kloner RA. Early and late remodeling of the left ventricle after acute myocardial infarction. Am J Cardiol. 1984;54(3):407–10.
7. Swynghedauw B. Remodeling of the heart in chronic pressure overload. Basic Res Cardiol. 1991;86(Suppl 1):99–105.
8. Abel ED, Litwin SE, Sweeney G. Cardiac remodeling in obesity. Physiol Rev. 2008;88(2):389–419. https://doi.org/10.1152/physrev.00017.2007.
9. Heineke J, Molkentin JD. Regulation of cardiac hypertrophy by intracellular signalling pathways. Nat Rev Mol Cell Biol. 2006;7(8):589–600. https://doi.org/10.1038/nrm1983.
10. Dorn GW, Robbins J, Sugden PH. Phenotyping hypertrophy: eschew obfuscation. Circ Res. 2003;92(11):1171–5. https://doi.org/10.1161/01.RES.0000077012.11088.BC.
11. Hill JA, Olson EN. Cardiac plasticity. N Engl J Med. 2008;358(13):1370–80. https://doi.org/10.1056/NEJMra072139.
12. Opie LH, Commerford PJ, Gersh BJ, Pfeffer MA. Controversies in ventricular remodelling. Lancet. 2006;367(9507):356–67. https://doi.org/10.1016/S0140-6736(06)68074-4.
13. Haddad F, Doyle R, Murphy DJ, Hunt SA. Right ventricular function in cardiovascular disease, part II: pathophysiology, clinical importance, and management of right ventricular failure. Circulation. 2008;117(13):1717–31. https://doi.org/10.1161/CIRCULATIONAHA.107.653584.
14. D'Alonzo GE, Barst RJ, Ayres SM, Bergofsky EH, Brundage BH, Detre KM, Fishman AP, Goldring RM, Groves BM, Kernis JT, et al. Survival in patients with primary pulmonary hypertension. Results from a national prospective registry. Ann Intern Med. 1991;115(5):343–9.

15. McLaughlin VV, McGoon MD. Pulmonary arterial hypertension. Circulation. 2006;114(13):1417–31. https://doi.org/10.1161/CIRCULATIONAHA.104.503540.
16. Machuca TN, de Perrot M. Mechanical support for the failing right ventricle in patients with precapillary pulmonary hypertension. Circulation. 2015;132(6):526–36. https://doi.org/10.1161/CIRCULATIONAHA.114.012593.
17. Zaffran S, Kelly RG, Meilhac SM, Buckingham ME, Brown NA. Right ventricular myocardium derives from the anterior heart field. Circ Res. 2004;95(3):261–8. https://doi.org/10.1161/01.RES.0000136815.73623.BE.
18. Thomas T, Yamagishi H, Overbeek PA, Olson EN, Srivastava D. The bHLH factors, dHAND and eHAND, specify pulmonary and systemic cardiac ventricles independent of left-right sidedness. Dev Biol. 1998;196(2):228–36.
19. Kondo RP, Dederko DA, Teutsch C, Chrast J, Catalucci D, Chien KR, Giles WR. Comparison of contraction and calcium handling between right and left ventricular myocytes from adult mouse heart: a role for repolarization waveform. J Physiol. 2006;571(Pt 1):131–46.
20. Friedberg MK, Redington AN. Right versus left ventricular failure: differences, similarities, and interactions. Circulation. 2014;129(9):1033–44. https://doi.org/10.1161/CIRCULATIONAHA.113.001375.
21. Iacobazzi D, Suleiman MS, Ghorbel M, George SJ, Caputo M, Tulloh RM. Cellular and molecular basis of RV hypertrophy in congenital heart disease. Heart. 2016;102(1):12–7. https://doi.org/10.1136/heartjnl-2015-308348.
22. Lowes BD, Minobe W, Abraham WT, Rizeq MN, Bohlmeyer TJ, Quaife RA, Roden RL, Dutcher DL, Robertson AD, Voelkel NF, Badesch DB, Groves BM, Gilbert EM, Bristow MR. Changes in gene expression in the intact human heart. Downregulation of alpha-myosin heavy chain in hypertrophied, failing ventricular myocardium. J Clin Invest. 1997;100(9):2315–24.
23. Bakerman PR, Stenmark KR, Fisher JH. Alpha-skeletal actin messenger RNA increases in acute right ventricular hypertrophy. Am J Phys. 1990;258(4 Pt 1):L173–8.
24. Bartelds B, Borgdorff MA, Smit-van Oosten A, Takens J, Boersma B, Nederhoff MG, Elzenga NJ, van Gilst WH, De Windt LJ, Berger RM. Differential responses of the right ventricle to abnormal loading conditions in mice: pressure vs. volume load. Eur J Heart Fail. 2011;13(12):1275–82. https://doi.org/10.1093/eurjhf/hfr134.
25. Nagendran J, Archer SL, Soliman D, Gurtu V, Moudgil R, Haromy A, St Aubin C, Webster L, Rebeyka IM, Ross DB, Light PE, Dyck JR, Michelakis ED. Phosphodiesterase type 5 is highly expressed in the hypertrophied human right ventricle, and acute inhibition of phosphodiesterase type 5 improves contractility. Circulation. 2007;116(3):238–48.
26. Urashima T, Zhao M, Wagner R, Fajardo G, Farahani S, Quertermous T, Bernstein D. Molecular and physiological characterization of RV remodeling in a murine model of pulmonary stenosis. Am J Physiol Heart Circ Physiol. 2008;295(3):H1351–68.
27. Ozhan G, Weidinger G. Wnt/β-catenin signaling in heart regeneration. Cell Regen. 2015;4(1):3.
28. Woodgett JR. Regulation and functions of the glycogen synthase kinase-3 subfamily. Semin Cancer Biol. 1994;5(4):269–75.
29. Embi N, Rylatt DB, Cohen P. Glycogen synthase kinase-3 from rabbit skeletal muscle. Separation from cyclic-AMP-dependent protein kinase and phosphorylase kinase. Eur J Biochem. 1980;107(2):519–27.
30. Nagendran J, Gurtu V, Fu DZ, Dyck JR, Haromy A, Ross DB, Rebeyka IM, Michelakis ED. A dynamic and chamber-specific mitochondrial remodeling in right ventricular hypertrophy can be therapeutically targeted. J Thorac Cardiovasc Surg. 2008;136(1):168–78. 178.e1–3
31. Zornoff LA, Paiva SA, Duarte DR, Spadaro J. Ventricular remodeling after myocardial infarction: concepts and clinical implications. Arq Bras Cardiol. 2009;92(2):150–64.
32. Mesquita ET, Montera MW, de Souza Neto JD, Bernardez-Pereira S, Freitas AF Jr, Volschan A, Biolo A, Nunes Filho AC, Chagas AC, Jorge AJ, Almeida DR, Arteaga E, dos Santos Junior EG, Fernandes F, Ramires FJ, Bacal F, Tarasoutshi F, Feitosa GS, Villacorta H Jr, Ferreira JF, Vieira JM Jr, Moura LA, Pires LJ, Correia LC, Rohde LE, Rivas M, Moreira Mda C, Kaiser SE, Ferreira SM, Martins SM, Martinez TL. Biomarkers in cardiology--part 1--in heart failure and specific cardiomyopathies. Arq Bras Cardiol. 2014;103(6):451–9.
33. Azevedo PS, Polegato BF, Minicucci MF, Paiva SA, Zornoff LA. Cardiac remodeling: concepts, clinical impact, pathophysiological mechanisms and pharmacologic treatment. Arq Bras Cardiol. 2016;106(1):62–9.
34. Anand IS, Florea VG, Solomon SD, Konstam MA, Udelson JE. Noninvasive assessment of left ventricular remodeling: concepts, techniques, and implications for clinical trials. J Card Fail. 2002;8(6 Suppl):S452–64.
35. Heusch G, Libby P, Gersh B, Yellon D, Böhm M, Lopaschuk G, Opie L. Cardiovascular remodelling in coronary artery disease and heart failure. Lancet. 2014;383(9932):1933–43.
36. Sabbah HN, Goldstein S. Ventricular remodelling: consequences and therapy. Eur Heart J. 1993;14(Suppl C):24–9.
37. Henning RJ. Effects of positive end-expiratory pressure on the right ventricle. J Appl Physiol. 1986;61(3):819–26.

38. MacNee W. Pathophysiology of cor pulmonale in chronic obstructive pulmonary disease. Part one. Am J Respir Crit Care Med. 1994;150(3):833–52.
39. Gaudron P, Eilles C, Kugler I, Ertl G. Progressive left ventricular dysfunction and remodeling after myocardial infarction. Potential mechanisms and early predictors. Circulation. 1993;87(3):755–63.
40. White HD, Norris RM, Brown MA, Brandt PW, Whitlock RM, Wild CJ. Left ventricular end-systolic volume as the major determinant of survival after recovery from myocardial infarction. Circulation. 1987;76(1):44–51.
41. Rumberger JA, Behrenbeck T, Breen JR, Reed JE, Gersh BJ. Nonparallel changes in global left ventricular chamber volume and muscle mass during the first year after transmural myocardial infarction in humans. J Am Coll Cardiol. 1993;21(3):673–82.
42. Bussani R, Abbate A, Biondi-Zoccai GG, Dobrina A, Leone AM, Camilot D, Di Marino MP, Baldi F, Silvestri F, Biasucci LM, Baldi A. Right ventricular dilatation after left ventricular acute myocardial infarction is predictive of extremely high peri-infarctual apoptosis at postmortem examination in humans. J Clin Pathol. 2003;56(9):672–6.
43. Oakley C. Importance of right ventricular function in congestive heart failure. Am J Cardiol. 1988;62(2):14A–9A.
44. Di Salvo TG, Mathier M, Semigran MJ, Dec GW. Preserved right ventricular ejection fraction predicts exercise capacity and survival in advanced heart failure. J Am Coll Cardiol. 1995;25(5):1143–53.
45. Liu L, Eisen HJ. Epidemiology of heart failure and scope of the problem. Cardiol Clin. 2014;32(1):1–8. vii
46. Pimentel M, Zimerman LI, Rohde LE. Stratification of the risk of sudden death in nonischemic heart failure. Arq Bras Cardiol. 2014;103(4):348–57.
47. Braunwald E. Heart failure. JACC Heart Fail. 2013;1(1):1–20.
48. McKay RG, Pfeffer MA, Pasternak RC, Markis JE, Come PC, Nakao S, Alderman JD, Ferguson JJ, Safian RD, Grossman W. Left ventricular remodeling after myocardial infarction: a corollary to infarct expansion. Circulation. 1986;74(4):693–702.
49. Anversa P, Olivetti G, Capasso JM. Cellular basis of ventricular remodeling after myocardial infarction. Am J Cardiol. 1991;68(14):7D–16D.
50. Grossman W, Jones D, McLaurin LP. Wall stress and patterns of hypertrophy in the human left ventricle. J Clin Invest. 1975;56(1):56–64.
51. Douglas PS, Morrow R, Ioli A, Reichek N. Left ventricular shape, afterload and survival in idiopathic dilated cardiomyopathy. J Am Coll Cardiol. 1989;13(2):311–5.
52. Mitchell GF, Lamas GA, Vaughan DE, Pfeffer MA. Left ventricular remodeling in the year after first anterior myocardial infarction: a quantitative analysis of contractile segment lengths and ventricular shape. J Am Coll Cardiol. 1992;19(6):1136–44.
53. Weisman HF, Bush DE, Mannisi JA, Bulkley BH. Global cardiac remodeling after acute myocardial infarction: a study in the rat model. J Am Coll Cardiol. 1985;5(6):1355–62.
54. Jugdutt BI. Effect of captopril and enalapril on left ventricular geometry, function and collagen during healing after anterior and inferior myocardial infarction in a dog model. J Am Coll Cardiol. 1995;25(7):1718–25.
55. Sharov VG, Sabbah HN, Shimoyama H, Goussev AV, Lesch M, Goldstein S. Evidence of cardiocyte apoptosis in myocardium of dogs with chronic heart failure. Am J Pathol. 1996;148(1):141–9.
56. Teiger E, Than VD, Richard L, Wisnewsky C, Tea BS, Gaboury L, Tremblay J, Schwartz K, Hamet P. Apoptosis in pressure overload-induced heart hypertrophy in the rat. J Clin Invest. 1996;97(12):2891–7.
57. Olivetti G, Abbi R, Quaini F, Kajstura J, Cheng W, Nitahara JA, Quaini E, Di Loreto C, Beltrami CA, Krajewski S, Reed JC, Anversa P. Apoptosis in the failing human heart. N Engl J Med. 1997;336(16):1131–41.
58. Tan LB, Jalil JE, Pick R, Janicki JS, Weber KT. Cardiac myocyte necrosis induced by angiotensin II. Circ Res. 1991;69(5):1185–95.
59. Villarreal FJ, Kim NN, Ungab GD, Printz MP, Dillmann WH. Identification of functional angiotensin II receptors on rat cardiac fibroblasts. Circulation. 1993;88(6):2849–61.
60. Anderson KR, Sutton MG, Lie JT. Histopathological types of cardiac fibrosis in myocardial disease. J Pathol. 1979;128(2):79–85.
61. Weber KT, Pick R, Silver MA, Moe GW, Janicki JS, Zucker IH, Armstrong PW. Fibrillar collagen and remodeling of dilated canine left ventricle. Circulation. 1990;82(4):1387–401.
62. Bogaard HJ, Abe K, Vonk Noordegraaf A, Voelkel NF. The right ventricle under pressure: cellular and molecular mechanisms of right-heart failure in pulmonary hypertension. Chest. 2009;135(3):794–804.
63. Modesti PA, Vanni S, Bertolozzi I, Cecioni I, Lumachi C, Perna AM, Boddi M, Gensini GF. Different growth factor activation in the right and left ventricles in experimental volume overload. Hypertension. 2004;43:101–8.
64. Colucci WS, Elkayam U, Horton DP, Abraham WT, Bourge RC, Johnson AD, Wagoner LE, Givertz MM, Liang CS, Neibaur M, Haught WH, LeJemtel TH. Intravenous nesiritide, a natriuretic peptide, in the treatment of decompensated congestive heart failure. Nesiritide Study Group. Engl J Med. 2000;343(4):246–53.
65. Raizada V, Thakore K, Luo W, McGuire PG. Cardiac chamber-specific alterations of ANP and BNP expression

with advancing age and with systemic hypertension. Mol Cell Biochem. 2001;216(1-2):137–40.
66. Reddy S, Zhao M, DQ H, Fajardo G, Hu S, Ghosh Z, Rajagopalan V, JC W, Bernstein D. Dynamic microRNA expression during the transition from right ventricular hypertrophy to failure. Physiol Genomics. 2012;44:562–75.
67. Wang GY, McCloskey DT, Turcato S, Swigart PM, Simpson PC, Baker AJ. Contrasting inotropic responses to alpha1-adrenergic receptor stimulation in left versus right ventricular myocardium. Am J Physiol Heart Circ Physiol. 2006;291:H2013–7.
68. Irlbeck M, Muhling O, Iwai T, Zimmer HG. Different response of the rat left and right heart to norepinephrine. Cardiovasc Res. 1996;31:157–62.
69. Michaels AD, Chatterjee K, De Marco T. Effects of intravenous nesiritide on pulmonary vascular hemodynamics in pulmonary hypertension. J Card Fail. 2005;11(6):425–31.
70. Piao L, Marsboom G, Archer SL. Mitochondrial metabolic adaptation in right ventricular hypertrophy and failure. J Mol Med. 2010;88(10):1011–20.
71. Drake JI, Bogaard HJ, Mizuno S, Clifton B, Xie B, Gao Y, Dumur CI, Fawcett P, Voelkel NF, Natarajan R. Molecular signature of a right heart failure program in chronic severe pulmonary hypertension. Am J Respir Cell Mol Biol. 2011;45(6):1239–47.
72. Klinger JR, Thaker S, Houtchens J, Preston IR, Hill NS, Farber HW. Pulmonary hemodynamic responses to brain natriuretic peptide and sildenafil in patients with pulmonary arterial hypertension. Chest. 2006;129(2):417–25.
73. Kirk JA, Cingolani OH. Thrombospondins in the transition from myocardial infarction to heart failure. J Mol Cell Cardiol. 2016;90:102–10.
74. Geva T, Powell AJ, Crawford EC, Chung T, Colan SD. Evaluation of regional differences in right ventricular systolic function by acoustic quantification echocardiography and cine magnetic resonance imaging. Circulation. 1998;98(4):339–45.
75. Rouleau JL, Paradis P, Shenasa H, Juneau C. Faster time to peak tension and velocity of shortening in right versus left ventricular trabeculae and papillary muscles of dogs. Circ Res. 1986;59(5):556–61.
76. Zak R. Cell proliferation during cardiac growth. Am J Cardiol. 1973;31(2):211–9.
77. Vanhoutte PM. Endothelium and control of vascular function. State of the art lecture. Hypertension. 1989;13(6 Pt 2):658–67.
78. Weber KT, Brilla CG. Pathological hypertrophy and cardiac interstitium. Fibrosis and renin-angiotensin-aldosterone system. Circulation. 1991; 83(6):1849–65.
79. Weber KT, Sun Y, Bhattacharya SK, Ahokas RA, Gerling IC. Myofibroblast-mediated mechanisms of pathological remodelling of the heart. Nat Rev Cardiol. 2013;10(1):15–26.
80. Owens GK. Growth response of aortic smooth muscle cells in hypertension. In: Lee RMKW, editor. Blood vessel changes in hypertension: structure and function. Boca Raton: CRC Press; 1989. p. 45–63.42.
81. Weber KT, Clark WA, Janicki JS, Shroff SG. Physiologic versus pathologic hypertrophy and the pressure-overloaded myocardium. J Cardiovasc Pharmacol. 1987; 10(Suppl 6):S37–50.
82. Olson EN. A decade of discoveries in cardiac biology. Nat Med. 2004;10(5):467–74.
83. MacLellan WR, Schneider MD. Genetic dissection of cardiac growth control pathways. Annu Rev Physiol. 2000;62:289–319.
84. Frey N, Katus HA, Olson EN, Hill JA. Hypertrophy of the heart: a new therapeutic target? Circulation. 2004;109(13):1580–9.
85. McMullen JR, Jennings GL. Differences between pathological and physiological cardiac hypertrophy: novel therapeutic strategies to treat heart failure. Clin Exp Pharmacol Physiol. 2007;34(4):255–62.
86. Li Z, Bing OH, Long X, Robinson KG, Lakatta EG. Increased cardiomyocyte apoptosis during the transition to heart failure in the spontaneously hypertensive rat. Am J Phys. 1997;272(5 Pt 2):H2313–9.
87. MacLellan WR, Schneider MD. Death by design. Programmed cell death in cardiovascular biology and disease. Circ Res. 1997;81(2):137–44.
88. Frangogiannis NG. Matricellular proteins in cardiac adaptation and disease. Physiol Rev. 2012;92(2):635–88.
89. Bornstein P. Diversity of function is inherent in matricellular proteins: an appraisal of thrombospondin 1. J Cell Biol. 1995;130(3):503–6.
90. Bradshaw AD. The role of secreted protein acidic and rich in cysteine (SPARC) in cardiac repair and fibrosis: does expression of SPARC by macrophages influence outcomes? J Mol Cell Cardiol. 2016;93:156–61.
91. Francis GS, McDonald KM. Left ventricular hypertrophy: an initial response to myocardial injury. Am J Cardiol. 1992;69(18):3G–7G. discussion 7G–9G
92. Sharma K, Kass DA. Heart failure with preserved ejection fraction: mechanisms, clinical features, and therapies. Circ Res. 2014;115(1):79–96.
93. Bittel DC, Butler MG, Kibiryeva N, Marshall JA, Chen J, Lofland GK, O'Brien JE Jr. Gene expression in cardiac tissues from infants with idiopathic conotruncal defects. BMC Med Genet. 2011;4(1). https://doi.org/10.1186/1755-8794-4-1.
94. Kaynak B, von Heydebreck A, Mebus S, Seelow D, Hennig S, Vogel J, Sperling HP, Pregla R, Alexi-Meskishvili V, Hetzer R, Lange PE, Vingron M, Lehrach H, Sperling S. Genome-wide array analysis of normal and malformed human hearts. Circulation. 2003;107(19):2467–74.
95. Wu Y, Feng W, Zhang H, Li S, Wang D, Pan X, Hu S. Ca^2+-regulatory proteins in cardiomyocytes from the right ventricle in children with congenital heart disease. J Transl Med. 2012;10:67. https://doi.org/10.1186/1479-5876-10-67.

96. Tekin D, Dursun AD, Xi L. Hypoxia inducible factor 1 (HIF-1) and cardioprotection. Acta Pharmacol Sin. 2010;31(9):1085–94. https://doi.org/10.1038/aps.2010.132.
97. Jeewa A, Manickaraj AK, Mertens L, Manlhiot C, Kinnear C, Mondal T, Smythe J, Rosenberg H, Lougheed J, McCrindle BW, van Arsdell G, Redington AN, Mital S. Genetic determinants of right-ventricular remodeling after tetralogy of Fallot repair. Pediatr Res. 2012;72(4):407–13. https://doi.org/10.1038/pr.2012.95.
98. Lawler J, Duquette M, Whittaker CA, Adams JC, McHenry K, DeSimone DW. Identification and characterization of thrombospondin-4, a new member of the thrombospondin gene family. J Cell Biol. 1993;120(4):1059–67.
99. Lawler J, Hynes RO. The structure of human thrombospondin, an adhesive glycoprotein with multiple calcium-binding sites and homologies with several different proteins. J Cell Biol. 1986;103(5):1635–48.
100. Adams JC, Lawler J. The thrombospondins. Cold Spring Harb Perspect Biol. 2011;3(10):a009712.
101. Adams JC. Thrombospondins: multifunctional regulators of cell interactions. Annu Rev Cell Dev Biol. 2001;17:25–51.
102. Xia Y, Dobaczewski M, Gonzalez-Quesada C, Chen W, Biernacka A, Li N, Lee DW, Frangogiannis NG. Endogenous thrombospondin 1 protects the pressure-overloaded myocardium by modulating fibroblast phenotype and matrix metabolism. Hypertension. 2011;58(5):902–11.
103. Mustonen E, Aro J, Puhakka J, Ilves M, Soini Y, Leskinen H, Ruskoaho H, Rysä J. Thrombospondin-4 expression is rapidly upregulated by cardiac overload. Biochem Biophys Res Commun. 2008;373(2):186–91.
104. Melenovsky V, Benes J, Skaroupkova P, Sedmera D, Strnad H, Kolar M, Vlcek C, Petrak J, Benes J Jr, Papousek F, Oliyarnyk O, Kazdova L, Cervenka L. Metabolic characterization of volume overload heart failure due to aorto-caval fistula in rats. Mol Cell Biochem. 2011;354(1-2):83–96.
105. Swinnen M, Vanhoutte D, Van Almen GC, Hamdani N, Schellings MW, D'hooge J, Van der Velden J, Weaver MS, Sage EH, Bornstein P, Verheyen FK, VandenDriessche T, Chuah MK, Westermann D, Paulus WJ, Van de Werf F, Schroen B, Carmeliet P, Pinto YM, Heymans S. Absence of thrombospondin-2 causes age-related dilated cardiomyopathy. Circulation. 2009;120(16):1585–97.
106. Schroen B, Heymans S, Sharma U, Blankesteijn WM, Pokharel S, Cleutjens JP, Porter JG, Evelo CT, Duisters R, van Leeuwen RE, Janssen BJ, Debets JJ, Smits JF, Daemen MJ, Crijns HJ, Bornstein P, Pinto YM. Thrombospondin-2 is essential for myocardial matrix integrity: increased expression identifies failure-prone cardiac hypertrophy. Circ Res. 2004;95(5):515–22.
107. Toth A, Nickson P, Mandl A, Bannister ML, Toth K, Erhardt P. Endoplasmic reticulum stress as a novel therapeutic target in heart diseases. Cardiovasc Hematol Disord Drug Targets. 2007;7:205–18.
108. Groenendyk J, Sreenivasaiah PK, Kim DH, Agellon LB, Michalak M. Biology of endoplasmic reticulum stress in the heart. Circ Res. 2010;107(10):1185–97.
109. Frangogiannis NG, Ren G, Dewald O, Zymek P, Haudek S, Koerting A, Winkelmann K, Michael LH, Lawler J, Entman ML. Critical role of endogenous thrombospondin-1 in preventing expansion of healing myocardial infarcts. Circulation. 2005;111(22):2935–42.
110. Snider P, Standley KN, Wang J, Azhar M, Doetschman T, Conway SJ. Origin of cardiac fibroblasts and the role of periostin. Circ Res. 2009;105(10):934–47.
111. Krenning G, Zeisberg EM, Kalluri R. The origin of fibroblasts and mechanism of cardiac fibrosis. J Cell Physiol. 2010;225(3):631–7.
112. Souders CA, Bowers SL, Baudino TA. Cardiac fibroblast: the renaissance cell. Circ Res. 2009;105(12):1164–76.
113. Chilton L, Giles WR, Smith GL. Evidence of intercellular coupling between co-cultured adult rabbit ventricular myocytes and myofibroblasts. J Physiol. 2007;583(Pt 1):225–36.
114. Baudino TA, McFadden A, Fix C, Hastings J, Price R, Borg TK. Cell patterning: interaction of cardiac myocytes and fibroblasts in three-dimensional culture. Microsc Microanal. 2008;14(2):117–25.
115. Zannad F, Rossignol P, Iraqi W. Extracellular matrix fibrotic markers in heart failure. Heart Fail Rev. 2010;15(4):319–29.
116. Cleutjens JP, Kandala JC, Guarda E, Guntaka RV, Weber KT. Regulation of collagen degradation in the rat myocardium after infarction. J Mol Cell Cardiol. 1995;27(6):1281–92.
117. Segura AM, Frazier OH, Buja LM. Fibrosis and heart failure. Heart Fail Rev. 2014;19(2):173–85.
118. Olivetti G, Capasso JM, Sonnenblick EH, Anversa P. Side-to-side slippage of myocytes participates in ventricular wall remodeling acutely after myocardial infarction in rats. Circ Res. 1990;67(1):23–34.
119. Deb A, Ubil E. Cardiac fibroblast in development and wound healing. J Mol Cell Cardiol. 2014;70:47–55.
120. Spinale FG, Janicki JS, Zile MR. Membrane-associated matrix proteolysis and heart failure. Circ Res. 2013;112(1):195–208.
121. Tao G, Levay AK, Peacock JD, Huk DJ, Both SN, Purcell NH, Pinto JR, Galantowicz ML, Koch M, Lucchesi PA, Birk DE, Lincoln J. Collagen XIV is important for growth and structural integrity of the myocardium. J Mol Cell Cardiol. 2012;53(5):626–38.
122. Ricard-Blum S. The collagen family. Cold Spring Harb Perspect Biol. 2011;3(1):a004978.

123. Gil-Cayuela C, Rivera M, Ortega A, Tarazón E, Triviño JC, Lago F, González-Juanatey JR, Almenar L, Martínez-Dolz L, Portolés M. RNA sequencing analysis identifies new human collagen genes involved in cardiac remodeling. Am Coll Cardiol. 2015;65(12):1265–7.
124. López B, González A, Ravassa S, Beaumont J, Moreno MU, San José G, Querejeta R, Díez J. Circulating biomarkers of myocardial fibrosis: the need for a reappraisal. J Am Coll Cardiol. 2015; 65(22):2449–56.
125. Leask A. Getting to the heart of the matter: new insights into cardiac fibrosis. Circ Res. 2015;116(7): 1269–76.
126. Sun Y, Kiani MF, Postlethwaite AE, Weber KT. Infarct scar as living tissue. Basic Res Cardiol. 2002;97(5): 343–7.
127. Zamilpa R, Lindsey ML. Extracellular matrix turnover and signaling during cardiac remodeling following MI: causes and consequences. J Mol Cell Cardiol. 2010;48(3):558–63.
128. Lindsey ML, Iyer RP, Jung M, DeLeon-Pennell KY, Ma Y. Matrix metalloproteinases as input and output signals for post-myocardial infarction remodeling. J Mol Cell Cardiol. 2016;91:134–40.
129. Booz GW, Baker KM. Molecular signalling mechanisms controlling growth and function of cardiac fibroblasts. Cardiovasc Res. 1995;30(4):537–43.
130. Gonzalez-Quesada C, Cavalera M, Biernacka A, Kong P, Lee DW, Saxena A, Frunza O, Dobaczewski M, Shinde A, Frangogiannis NG. Thrombospondin-1 induction in the diabetic myocardium stabilizes the cardiac matrix in addition to promoting vascular rarefaction through angiopoietin-2 upregulation. Circ Res. 2013;113(12):1331–44.
131. Ma Y, Yabluchanskiy A, Lindsey ML. Thrombospondin-1: the good, the bad, and the complicated. Circ Res. 2013;113(12):1272–4.
132. Bein K, Simons M. Thrombospondin type 1 repeats interact with matrix metalloproteinase 2. Regulation of metalloproteinase activity. J Biol Chem. 2000;275(41):32167–73.
133. Yang Z, Strickland DK, Bornstein P. Extracellular matrix metalloproteinase 2 levels are regulated by the low density lipoprotein-related scavenger receptor and thrombospondin 2. J Biol Chem. 2001; 276(11):8403–8.
134. Hall MC, Young DA, Waters JG, Rowan AD, Chantry A, Edwards DR, Clark IM. The comparative role of activator protein 1 and Smad factors in the regulation of Timp-1 and MMP-1 gene expression by transforming growth factor-beta 1. J Biol Chem. 2003;278(12):10304–13.
135. Leung LL, Nachman RL. Complex formation of platelet thrombospondin with fibrinogen. J Clin Invest. 1982;70(3):542–9.
136. Mumby SM, Raugi GJ, Bornstein P. Interactions of thrombospondin with extracellular matrix proteins: selective binding to type V collagen. J Cell Biol. 1984;98(2):646–52.
137. Bale MD, Mosher DF. Effects of thrombospondin on fibrin polymerization and structure. J Biol Chem. 1986;261(2):862–8.
138. Narouz-Ott L, Maurer P, Nitsche DP, Smyth N, Paulsson M. Thrombospondin-4 binds specifically to both collagenous and non-collagenous extracellular matrix proteins via its C-terminal domains. J Biol Chem. 2000;275(47):37110–7.
139. Mustonen E, Ruskoaho H, Rysä J. Thrombospondin-4, tumour necrosis factor-like weak inducer of apoptosis (TWEAK) and its receptor Fn14: novel extracellular matrix modulating factors in cardiac remodelling. Ann Med. 2012;44(8):793–804.
140. Sawaki D, Hou L, Tomida S, Sun J, Zhan H, Aizawa K, Son BK, Kariya T, Takimoto E, Otsu K, Conway SJ, Manabe I, Komuro I, Friedman SL, Nagai R, Suzuki T. Modulation of cardiac fibrosis by Krüppel-like factor 6 through transcriptional control of thrombospondin 4 in cardiomyocytes. Cardiovasc Res. 2015;107(4):420–30.
141. Desmoulière A, Geinoz A, Gabbiani F, Gabbiani G. Transforming growth factor-beta 1 induces alpha-smooth muscle actin expression in granulation tissue myofibroblasts and in quiescent and growing cultured fibroblasts. J Cell Biol. 1993;122(1):103–11.
142. Ma Y, de Castro Brás LE, Toba H, Iyer RP, Hall ME, Winniford MD, Lange RA, Tyagi SC, Lindsey ML. Myofibroblasts and the extracellular matrix network in post-myocardial infarction cardiac remodeling. Pflugers Arch. 2014;466(6):1113–27.
143. Burchfield JS, Xie M, Hill JA. Pathological ventricular remodeling: mechanisms: part 1 of 2. Circulation. 2013;128(4):388–400.
144. Wang C, Wang X. The interplay between autophagy and the ubiquitin-proteasome system in cardiac proteotoxicity. Biochim Biophys Acta. 2015; 1852(2):188–94.
145. Tarone G, Brancaccio M. Keep your heart in shape: molecular chaperone networks for treating heart disease. Cardiovasc Res. 2014;102(3):346–61.
146. James TN. Normal and abnormal consequences of apoptosis in the human heart. From postnatal morphogenesis to paroxysmal arrhythmias. Circulation. 1994;90(1):556–73.
147. Narula J, Haider N, Virmani R, DiSalvo TG, Kolodgie FD, Hajjar RJ, Schmidt U, Semigran MJ, Dec GW, Khaw BA. Apoptosis in myocytes in end-stage heart failure. N Engl J Med. 1996;335(16):1182–9.
148. Kostin S, Pool L, Elsässer A, Hein S, Drexler HC, Arnon E, Hayakawa Y, Zimmermann R, Bauer E, Klövekorn WP, Schaper J. Myocytes die by multiple mechanisms in failing human hearts. Circ Res. 2003;92(7):715–24.
149. Frangogiannis NG. Regulation of the inflammatory response in cardiac repair. Circ Res. 2012;110(1): 159–73. https://doi.org/10.1161/CIRCRESAHA.111.243162.
150. Freude B, Masters TN, Robicsek F, Fokin A, Kostin S, Zimmermann R, Ullmann C, Lorenz-Meyer S, Schaper J. Apoptosis is initiated by myocardial isch-

emia and executed during reperfusion. J Mol Cell Cardiol. 2000;32(2):197–208.
151. Black SC, Huang JQ, Rezaiefar P, Radinovic S, Eberhart A, Nicholson DW, Rodger IW. Co-localization of the cysteine protease caspase-3 with apoptotic myocytes after in vivo myocardial ischemia and reperfusion in the rat. J Mol Cell Cardiol. 1998;30(4):733–42.
152. Dorn GW. Apoptotic and non-apoptotic programmed cardiomyocyte death in ventricular remodelling. Cardiovasc Res. 2009;81(3):465–73. https://doi.org/10.1093/cvr/cvn243.
153. Maruyama R, Takemura G, Aoyama T, Hayakawa K, Koda M, Kawase Y, Qiu X, Ohno Y, Minatoguchi S, Miyata K, Fujiwara T, Fujiwara H. Dynamic process of apoptosis in adult rat cardiomyocytes analyzed using 48-hour videomicroscopy and electron microscopy: beating and rate are associated with the apoptotic process. Am J Pathol. 2001;159(2):683–91.
154. Diwan A, Krenz M, Syed FM, Wansapura J, Ren X, Koesters AG, Li H, Kirshenbaum LA, Hahn HS, Robbins J, Jones WK, Dorn GW. Inhibition of ischemic cardiomyocyte apoptosis through targeted ablation of Bnip3 restrains postinfarction remodeling in mice. J Clin Invest. 2007;117(10):2825–33.
155. Whelan RS, Mani K, Kitsis RN. Nipping at cardiac remodeling. J Clin Invest. 2007;117(10):2751–3.
156. Dawson DW, Volpert OV, Pearce SF, Schneider AJ, Silverstein RL, Henkin J, Bouck NP. Three distinct D-amino acid substitutions confer potent antiangiogenic activity on an inactive peptide derived from a thrombospondin-1 type 1 repeat. Mol Pharmacol. 1999;55(2):332–8.
157. Dawson DW, Pearce SF, Zhong R, Silverstein RL, Frazier WA, Bouck NP. CD36 mediates the In vitro inhibitory effects of thrombospondin-1 on endothelial cells. J Cell Biol. 1997;138(3):707–17.
158. Asch AS, Silbiger S, Heimer E, Nachman RL. Thrombospondin sequence motif (CSVTCG) is responsible for CD36 binding. Biochem Biophys Res Commun. 1992;182(3):1208–17.
159. Jiménez B, Volpert OV, Reiher F, Chang L, Muñoz A, Karin M, Bouck N. c-Jun N-terminal kinase activation is required for the inhibition of neovascularization by thrombospondin-1. Oncogene. 2001; 20(26):3443–8.
160. Jiménez B, Volpert OV, Crawford SE, Febbraio M, Silverstein RL, Bouck N. Signals leading to apoptosis-dependent inhibition of neovascularization by thrombospondin-1. Nat Med. 2000;6(1):41–8.
161. Simantov R, Febbraio M, Silverstein RL. The antiangiogenic effect of thrombospondin-2 is mediated by CD36 and modulated by histidine-rich glycoprotein. Matrix Biol. 2005;24(1):27–34.
162. Yee KO, Connolly CM, Duquette M, Kazerounian S, Washington R, Lawler J. The effect of thrombospondin-1 on breast cancer metastasis. Breast Cancer Res Treat. 2009;114(1):85–96.
163. Primo L, Ferrandi C, Roca C, Marchiò S, di Blasio L, Alessio M, Bussolino F. Identification of CD36 molecular features required for its in vitro angiostatic activity. FASEB J. 2005;19(12):1713–5.
164. Volpert OV, Zaichuk T, Zhou W, Reiher F, Ferguson TA, Stuart PM, Amin M, Bouck NP. Inducer-stimulated Fas targets activated endothelium for destruction by anti-angiogenic thrombospondin-1 and pigment epithelium-derived factor. Nat Med. 2002;8(4):349–57.
165. Zhang P, Shen M, Fernandez-Patron C, Kassiri Z. ADAMs family and relatives in cardiovascular physiology and pathology. J Mol Cell Cardiol. 2016;93:186–99.
166. Reilly MP, Li M, He J, Ferguson JF, Stylianou IM, Mehta NN, Burnett MS, Devaney JM, Knouff CW, Thompson JR, Horne BD, Stewart AF, Assimes TL, Wild PS, Allayee H, Nitschke PL, Patel RS, Martinelli N, Girelli D, Quyyumi AA, Anderson JL, Erdmann J, Hall AS, Schunkert H, Quertermous T, Blankenberg S, Hazen SL, Roberts R, Kathiresan S, Samani NJ, Epstein SE, Rader DJ, Myocardial Infarction Genetics Consortium; Wellcome Trust Case Control Consortium. Identification of ADAMTS7 as a novel locus for coronary atherosclerosis and association of ABO with myocardial infarction in the presence of coronary atherosclerosis: two genome-wide association studies. Lancet. 2011;377(9763):383–92.
167. Wang L, Zheng J, Bai X, Liu B, Liu CJ, Xu Q, Zhu Y, Wang N, Kong W, Wang X. ADAMTS-7 mediates vascular smooth muscle cell migration and neointima formation in balloon-injured rat arteries. Circ Res. 2009;104(5):688–98.
168. Kessler T, Zhang L, Liu Z, Yin X, Huang Y, Wang Y, Fu Y, Mayr M, Ge Q, Xu Q, Zhu Y, Wang X, Schmidt K, de Wit C, Erdmann J, Schunkert H, Aherrahrou Z, Kong W. ADAMTS-7 inhibits re-endothelialization of injured arteries and promotes vascular remodeling through cleavage of thrombospondin-1. Circulation. 2015;131(13):1191–201.
169. Iruela-Arispe ML. Regulation of thrombospondin1 by extracellular proteases. Curr Drug Targets. 2008;9(10):863–8.
170. Arndt V, Dick N, Tawo R, Dreiseidler M, Wenzel D, Hesse M, Fürst DO, Saftig P, Saint R, Fleischmann BK, Hoch M, Höhfeld J. Chaperone-assisted selective autophagy is essential for muscle maintenance. Curr Biol. 2010;20(2):143–8.
171. Carra S, Seguin SJ, Landry J. HspB8 and Bag3: a new chaperone complex targeting misfolded proteins to macroautophagy. Autophagy. 2008;4(2):237–9.
172. Babu-Narayan SV, Kilner PJ, Li W, Moon JC, Goktekin O, Davlouros PA, Khan M, Ho SY, Pennell DJ, Gatzoulis MA. Ventricular fibrosis suggested by cardiovascular magnetic resonance in adults with repaired tetralogy of fallot and its relationship to adverse markers of clinical outcome. Circulation. 2006;113(3):405–13.

173. Weidemann F, Herrmann S, Störk S, Niemann M, Frantz S, Lange V, Beer M, Gattenlöhner S, Voelker W, Ertl G, Strotmann JM. Impact of myocardial fibrosis in patients with symptomatic severe aortic stenosis. Circulation. 2009;120(7):577–84. https://doi.org/10.1161/CIRCULATIONAHA.108.847772.
174. Hein S, Arnon E, Kostin S, Schönburg M, Elsässer A, Polyakova V, Bauer EP, Klövekorn WP, Schaper J. Progression from compensated hypertrophy to failure in the pressure-overloaded human heart: structural deterioration and compensatory mechanisms. Circulation. 2003;107(7):984–91.
175. Jellis C, Martin J, Narula J, Marwick TH. Assessment of nonischemic myocardial fibrosis. J Am Coll Cardiol. 2010;56(2):89–97. https://doi.org/10.1016/j.jacc.2010.02.047.
176. Kong P, Christia P, Frangogiannis NG. The pathogenesis of cardiac fibrosis. Cell Mol Life Sci. 2014;71(4):549–74. https://doi.org/10.1007/s00018-013-1349-6.
177. Li AH, Liu PP, Villarreal FJ, Garcia RA. Dynamic changes in myocardial matrix and relevance to disease: translational perspectives. Circ Res. 2014;114(5):916–27. https://doi.org/10.1161/CIRCRESAHA.114.302819.
178. Weber KT, Pick R, Jalil JE, Janicki JS, Carroll EP. Patterns of myocardial fibrosis. J Mol Cell Cardiol. 1989;21(Suppl 5):121–31.
179. Gyöngyösi M, Winkler J, Ramos I, Do QT, Firat H, McDonald K, González A, Thum T, Díez J, Jaisser F, Pizard A, Zannad F. Myocardial fibrosis: biomedical research from bench to bedside. Eur J Heart Fail. 2017;19(2):177–91. https://doi.org/10.1002/ejhf.696.
180. Heymans S, González A, Pizard A, Papageorgiou AP, López-Andrés N, Jaisser F, Thum T, Zannad F, Díez J. Searching for new mechanisms of myocardial fibrosis with diagnostic and/or therapeutic potential. Eur J Heart Fail. 2015;17(8):764–71. https://doi.org/10.1002/ejhf.312.
181. Camelliti P, Borg TK, Kohl P. Structural and functional characterisation of cardiac fibroblasts. Cardiovasc Res. 2005;65(1):40–51.
182. Lajiness JD, Conway SJ. Origin, development, and differentiation of cardiac fibroblasts. J Mol Cell Cardiol. 2014;70:2–8. https://doi.org/10.1016/j.yjmcc.2013.11.003.
183. Watson CJ, Phelan D, Collier P, Horgan S, Glezeva N, Cooke G, Xu M, Ledwidge M, McDonald K, Baugh JA. Extracellular matrix sub-types and mechanical stretch impact human cardiac fibroblast responses to transforming growth factor beta. Connect Tissue Res. 2014;55(3):248–56. https://doi.org/10.3109/03008207.2014.904856.
184. Brilla CG, Maisch B, Zhou G, Weber KT. Hormonal regulation of cardiac fibroblast function. Eur Heart J. 1995;16(Suppl C):45–50.
185. Schellings MW, Pinto YM, Heymans S. Matricellular proteins in the heart: possible role during stress and remodeling. Cardiovasc Res. 2004;64(1):24–31.
186. Kumarswamy R, Thum T. Non-coding RNAs in cardiac remodeling and heart failure. Circ Res. 2013;113(6):676–89. https://doi.org/10.1161/CIRCRESAHA.113.300226.
187. Robins SP. Biochemistry and functional significance of collagen cross-linking. Biochem Soc Trans. 2007;35(Pt 5):849–52.
188. Shoulders MD, Raines RT. Collagen structure and stability. Annu Rev Biochem. 2009;78:929–58. https://doi.org/10.1146/annurev.biochem.77.032207.120833.
189. López B, Querejeta R, González A, Larman M, Díez J. Collagen cross-linking but not collagen amount associates with elevated filling pressures in hypertensive patients with stage C heart failure: potential role of lysyl oxidase. Hypertension. 2012;60(3):677–83. https://doi.org/10.1161/HYPERTENSIONAHA.112.196113.
190. Kawara T, Derksen R, de Groot JR, Coronel R, Tasseron S, Linnenbank AC, Hauer RN, Kirkels H, Janse MJ, de Bakker JM. Activation delay after premature stimulation in chronically diseased human myocardium relates to the architecture of interstitial fibrosis. Circulation. 2001;104(25):3069–75.
191. Anderson KP, Walker R, Urie P, Ershler PR, Lux RL, Karwandee SV. Myocardial electrical propagation in patients with idiopathic dilated cardiomyopathy. J Clin Invest. 1993;92(1):122–40.
192. Schwartzkopff B, Brehm M, Mundhenke M, Strauer BE. Repair of coronary arterioles after treatment with perindopril in hypertensive heart disease. Hypertension. 2000;36(2):220–5.
193. Wald RM, Haber I, Wald R, Valente AM, Powell AJ, Geva T. Effects of regional dysfunction and late gadolinium enhancement on global right ventricular function and exercise capacity in patients with repaired tetralogy of Fallot. Circulation. 2009;119(10):1370–7. https://doi.org/10.1161/CIRCULATIONAHA.108.816546.
194. van Oorschot JW, Gho JM, van Hout GP, Froeling M, Hoefer IE, Doevendans PA, Luijten PR, Chamuleau SA, Zwanenburg JJ, Jansen Of Lorkeers SJ. Endogenous contrast MRI of cardiac fibrosis: beyond late gadolinium enhancement. J Magn Reson Imaging. 2015;41(5):1181–9. https://doi.org/10.1002/jmri.24715.
195. Sado DM, Flett AS, Moon JC. Novel imaging techniques for diffuse myocardial fibrosis. Futur Cardiol. 2011;7(5):643–50. https://doi.org/10.2217/fca.11.45.
196. Gyöngyösi M, Blanco J, Marian T, Trón L, Petneházy O, Petrasi Z, Hemetsberger R, Rodriguez J, Font G, Pavo IJ, Kertész I, Balkay L, Pavo N, Posa A, Emri M, Galuska L, Kraitchman DL, Wojta J, Huber K, Glogar D. Serial noninvasive in vivo positron emission tomographic tracking of percutaneously intramyocardially injected autologous porcine mesenchymal stem cells modified for transgene reporter gene expression. Circ Cardiovasc

Imaging. 2008;1(2):94–103. https://doi.org/10.1161/CIRCIMAGING.108.797449.
197. Rischpler C, Nekolla SG, Dregely I, Schwaiger M. Hybrid PET/MR imaging of the heart: potential, initial experiences, and future prospects. J Nucl Med. 2013;54(3):402–15. https://doi.org/10.2967/jnumed.112.105353.
198. Li XG, Roivainen A, Bergman J, Heinonen A, Bengel F, Thum T, Knuuti J. Enabling [(18)F]-bicyclo[6.1.0]nonyne for oligonucleotide conjugation for positron emission tomography applications: [(18)F]-anti-microRNA-21 as an example. Chem Commun. 2015;51(48):9821–4. https://doi.org/10.1039/c5cc02618k.
199. Fang L, Ellims AH, Moore XL, White DA, Taylor AJ, Chin-Dusting J, Dart AM. Circulating microRNAs as biomarkers for diffuse myocardial fibrosis in patients with hypertrophic cardiomyopathy. J Transl Med. 2015;13:314. https://doi.org/10.1186/s12967-015-0672-0.
200. Azevedo CF, Nigri M, Higuchi ML, Pomerantzeff PM, Spina GS, Sampaio RO, Tarasoutchi F, Grinberg M, Rochitte CE. Prognostic significance of myocardial fibrosis quantification by histopathology and magnetic resonance imaging in patients with severe aortic valve disease. J Am Coll Cardiol. 2010;56(4):278–87. https://doi.org/10.1016/j.jacc.2009.12.074.
201. Aoki T, Fukumoto Y, Sugimura K, Oikawa M, Satoh K, Nakano M, Nakayama M, Shimokawa H. Prognostic impact of myocardial interstitial fibrosis in non-ischemic heart failure -comparison between preserved and reduced ejection fraction heart failure. Circ J. 2011;75(11):2605–13.
202. van Rooij E, Sutherland LB, Liu N, Williams AH, McAnally J, Gerard RD, Richardson JA, Olson EN. A signature pattern of stress-responsive microRNAs that can evoke cardiac hypertrophy and heart failure. Proc Natl Acad Sci U S A. 2006;103(48):18255–60.
203. Ikeda S, Kong SW, Lu J, Bisping E, Zhang H, Allen PD, Golub TR, Pieske B, Pu WT. Altered microRNA expression in human heart disease. Physiol Genomics. 2007;31(3):367–73.
204. Thum T, Galuppo P, Wolf C, Fiedler J, Kneitz S, van Laake LW, Doevendans PA, Mummery CL, Borlak J, Haverich A, Gross C, Engelhardt S, Ertl G, Bauersachs J. MicroRNAs in the human heart: a clue to fetal gene reprogramming in heart failure. Circulation. 2007;116(3):258–67.
205. Small EM, Olson EN. Pervasive roles of microRNAs in cardiovascular biology. Nature. 2011;469(7330):336–42. https://doi.org/10.1038/nature09783.
206. Bartel DP. MicroRNAs: genomics, biogenesis, mechanism, and function. Cell. 2004;116(2):281–97.
207. Li D, Ji L, Liu L, Liu Y, Hou H, Yu K, Sun Q, Zhao Z. Characterization of circulating microRNA expression in patients with a ventricular septal defect. PLoS One. 2014;9(8):e106318. https://doi.org/10.1371/journal.pone.0106318.
208. Lai CT, Ng EK, Chow PC, Kwong A, Cheung YF. Circulating microRNA expression profile and systemic right ventricular function in adults after atrial switch operation for complete transposition of the great arteries. BMC Cardiovasc Disord. 2013;13:73. https://doi.org/10.1186/1471-2261-13-73.
209. Tutarel O, Dangwal S, Bretthauer J, Westhoff-Bleck M, Roentgen P, Anker SD, Bauersachs J, Thum T. Circulating miR-423_5p fails as a biomarker for systemic ventricular function in adults after atrial repair for transposition of the great arteries. Int J Cardiol. 2013;167(1):63–6. https://doi.org/10.1016/j.ijcard.2011.11.082.
210. Zhang J, Chang JJ, Xu F, Ma XJ, Wu Y, Li WC, Wang HJ, Huang GY, Ma D. MicroRNA deregulation in right ventricular outflow tract myocardium in nonsyndromic tetralogy of fallot. Can J Cardiol. 2013;29(12):1695–703. https://doi.org/10.1016/j.cjca.2013.07.002.
211. Bittel DC, Kibiryeva N, Marshall JA, O'Brien JE. MicroRNA-421 dysregulation is associated with tetralogy of Fallot. Cells. 2014;3(3):713–23. https://doi.org/10.3390/cells3030713.
212. Tamura T, Said S, Harris J, Lu W, Gerdes AM. Reverse remodeling of cardiac myocyte hypertrophy in hypertension and failure by targeting of the renin-angiotensin system. Circulation. 2000;102(2):253–9.
213. van Rooij E, Sutherland LB, Qi X, Richardson JA, Hill J, Olson EN. Control of stress-dependent cardiac growth and gene expression by a microRNA. Science. 2007;316(5824):575–9.
214. Liu N, Bezprozvannaya S, Williams AH, Qi X, Richardson JA, Bassel-Duby R, Olson EN. microRNA-133a regulates cardiomyocyte proliferation and suppresses smooth muscle gene expression in the heart. Genes Dev. 2008;22(23):3242–54. https://doi.org/10.1101/gad.1738708.
215. Apitz C, Honjo O, Humpl T, Li J, Assad RS, Cho MY, Hong J, Friedberg MK, Redington AN. Biventricular structural and functional responses to aortic constriction in a rabbit model of chronic right ventricular pressure overload. J Thorac Cardiovasc Surg. 2012;144(6):1494–501. https://doi.org/10.1016/j.jtcvs.2012.06.027.
216. Unverferth DV, Fetters JK, Unverferth BJ, Leier CV, Magorien RD, Arn AR, Baker PB. Human myocardial histologic characteristics in congestive heart failure. Circulation. 1983;68(6):1194–200.
217. Montgomery RL, Hullinger TG, Semus HM, Dickinson BA, Seto AG, Lynch JM, Stack C, Latimer PA, Olson EN, van Rooij E. Therapeutic inhibition of miR-208a improves cardiac function and survival during heart failure. Circulation. 2011;124:1537–47.
218. Hwang MW, Matsumori A, Furukawa Y, Ono K, Okada M, Iwasaki A, Hara M, Miyamoto T, Touma M, Sasayama S. Neutralization of interleukin-1beta in the acute phase of myocardial infarction promotes the progression of left ventricular remodeling. J Am Coll Cardiol. 2001;38(5):1546–53.

219. Maekawa Y, Anzai T, Yoshikawa T, Asakura Y, Takahashi T, Ishikawa S, Mitamura H, Ogawa S. Prognostic significance of peripheral monocytosis after reperfused acute myocardial infarction:a possible role for left ventricular remodeling. J Am Coll Cardiol. 2002;39(2):241–6.
220. Hafizi S, Wharton J, Chester AH, Yacoub MH. Profibrotic effects of endothelin-1 via the ETA receptor in cultured human cardiac fibroblasts. Cell Physiol Biochem. 2004;14(4-6):285–92.
221. Katwa LC. Cardiac myofibroblasts isolated from the site of myocardial infarction express endothelin de novo. Am J Physiol Heart Circ Physiol. 2003; 285(3):H1132–9.
222. Hsieh PC, Davis ME, Lisowski LK, Lee RT. Endothelial-cardiomyocyte interactions in cardiac development and repair. Annu Rev Physiol. 2006; 68:51–66.
223. Rich S, McLaughlin VV. Endothelin receptor blockers in cardiovascular disease. Circulation. 2003;108: 2184–90.
224. Zolk O, Quattek J, Sitzler G, Schrader T, Nickenig G, et al. Expression of endothelin-1, endothelin-converting enzyme, and endothelin receptors in chronic heart failure. Circulation. 1999;99:2118–23.
225. Leask A. Potential therapeutic targets for cardiac fibrosis: TGFbeta, angiotensin, endothelin, CCN2, and PDGF, partners in fibroblast activation. Circ Res. 2010;106(11):1675–80. https://doi.org/10.1161/CIRCRESAHA.110.217737.
226. Sütsch G, Kiowski W, Yan XW, Hunziker P, Christen S, Strobel W, Kim JH, Rickenbacher P, Bertel O. Short-term oral endothelin-receptor antagonist therapy in conventionally treated patients with symptomatic severe chronic heart failure. Circulation. 1998;98(21):2262–8.
227. Thomson A. Interleukins. In: Oppenheim JJ, editor. The cytokine handbook. 3rd ed. San Diego: Academic; 1998. p. 146–62.
228. Henry G, Garner WL. Inflammatory mediators in wound healing. Surg Clin North Am. 2003;83(3): 483–507.
229. Pietilä K, Hermens WT, Harmoinen A, Baardman T, Pasternack A, Topol EJ, Simoons ML. Comparison of peak serum C-reactive protein and hydroxybutyrate dehydrogenase levels in patients with acute myocardial infarction treated with alteplase and streptokinase. Am J Cardiol. 1997;80(8):1075–7.
230. Furman MI, Becker RC, Yarzebski J, Savegeau J, Gore JM, Goldberg RJ. Effect of elevated leukocyte count on in-hospital mortality following acute myocardial infarction. Am J Cardiol. 1996;78(8):945–8.
231. Jordan JE, Zhao ZQ, Vinten-Johansen J. The role of neutrophils in myocardial ischemia-reperfusion injury. Cardiovasc Res. 1999;43(4):860–78.
232. Engler RL. Free radical and granulocyte-mediated injury during myocardial ischemia and reperfusion. Am J Cardiol. 1989;63(10):19E–23E.
233. Lasky LA. Selectins: interpreters of cell-specific carbohydrate information during inflammation. Science. 1992;258(5084):964–9.
234. Ebnet K, Vestweber D. Molecular mechanisms that control leukocyte extravasation: the selectins and the chemokines. Histochem Cell Biol. 1999;112(1): 1–23.
235. Frangogiannis NG, Smith CW, Entman ML. The inflammatory response in myocardial infarction. Cardiovasc Res. 2002;53(1):31–47.
236. Lefer DJ, Granger DN. Oxidative stress and cardiac disease. Am J Med. 2000;109(4):315–23.
237. Dhalla NS, Elmoselhi AB, Hata T, Makino N. Status of myocardial antioxidants in ischemia-reperfusion injury. Cardiovasc Res. 2000;47(3):446–56.
238. Hausenloy DJ, Yellon DM. The therapeutic potential of ischemic conditioning: an update. Nat Rev Cardiol. 2011;8(11):619–29.
239. Foo RS, Mani K, Kitsis RN. Death begets failure in the heart. J Clin Invest. 2005;115(3):565–71.
240. Filomeni G, Ciriolo MR. Redox control of apoptosis: an update. Antioxid Redox Signal. 2006;8(11-12): 2187–92.
241. Matsuzawa A, Ichijo H. Stress-responsive protein kinases in redox-regulated apoptosis signaling. Antioxid Redox Signal. 2005;7(3-4):472–81.
242. Giordano FJ. Oxygen, oxidative stress, hypoxia, and heart failure. J Clin Invest. 2005;115(3):500–8.
243. Cave AC, Brewer AC, Narayanapanicker A, Ray R, Grieve DJ, Walker S, Shah AM. NADPH oxidases in cardiovascular health and disease. Antioxid Redox Signal. 2006;8(5-6):691–728.
244. Heymes C, Bendall JK, Ratajczak P, Cave AC, Samuel JL, Hasenfuss G, Shah AM. Increased myocardial NADPH oxidase activity in human heart failure. J Am Coll Cardiol. 2003;41(12):2164–71.
245. Griendling KK, Sorescu D, Lassegue B, Ushio-Fukai M. Modulation of protein kinase activity and gene expression by reactive oxygen species and their role in vascular physiology and pathophysiology. Arterioscler Thromb Vasc Biol. 2000;20(10):2175–83.
246. Ushio-Fukai M, Zafari AM, Fukui T, Ishizaka N, Griendling KK. p22phox is a critical component of the superoxide-generating NADH/NADPH oxidase system and regulates angiotensin II-induced hypertrophy in vascular smooth muscle cells. J Biol Chem. 1996;271(38):23317–21.
247. Görlach A, Brandes RP, Nguyen K, Amidi M, Dehghani F, Busse R. A gp91phox containing NADPH oxidase selectively expressed in endothelial cells is a major source of oxygen radical generation in the arterial wall. Circ Res. 2000;87(1): 26–32.
248. Jones SA, O'Donnell VB, Wood JD, Broughton JP, Hughes EJ, Jones OT. Expression of phagocyte NADPH oxidase components in human endothelial cells. Am J Phys. 1996;271(4 Pt 2):H1626–34.

249. Chamseddine AH, Miller FJ Jr. Gp91phox contributes to NADPH oxidase activity in aortic fibroblasts but not smooth muscle cells. Am J Physiol Heart Circ Physiol. 2003;285(6):H2284–9.
250. Wenzel S, Taimor G, Piper HM, Schlüter KD. Redox-sensitive intermediates mediate angiotensin II-induced p38 MAP kinase activation, AP-1 binding activity, and TGF-beta expression in adult ventricular cardiomyocytes. FASEB J. 2001;15(12):2291–3.
251. Lambeth JD. NOX enzymes and the biology of reactive oxygen. Nat Rev Immunol. 2004;4(3):181–9.
252. Aguirre J, Lambeth JD. Nox enzymes from fungus to fly to fish and what they tell us about Nox function in mammals. Free Radic Biol Med. 2010;49(9):1342–53.
253. Brandes RP, Weissmann N, Schröder K. NADPH oxidases in cardiovascular disease. Free Radic Biol Med. 2010;49(5):687–706.
254. Geiszt M. NADPH oxidases: new kids on the block. Cardiovasc Res. 2006;71(2):289–99.
255. Kayama Y, Raaz U, Jagger A, Adam M, Schellinger IN, Sakamoto M, Suzuki H, Toyama K, Spin JM, Tsao PS. Diabetic cardiovascular disease induced by oxidative stress. Int J Mol Sci. 2015;16(10):25234–63. https://doi.org/10.3390/ijms161025234.
256. Lassègue B, San Martín A, Griendling KK. Biochemistry, physiology, and pathophysiology of NADPH oxidases in the cardiovascular system. Circ Res. 2012;110(10):1364–90. https://doi.org/10.1161/CIRCRESAHA.111.243972.
257. Erickson JR, Joiner ML, Guan X, Kutschke W, Yang J, Oddis CV, Bartlett RK, Lowe JS, O'Donnell SE, Aykin-Burns N, Zimmerman MC, Zimmerman K, Ham AJ, Weiss RM, Spitz DR, Shea MA, Colbran RJ, Mohler PJ, Anderson ME. A dynamic pathway for calcium-independent activation of CaMKII by methionine oxidation. Cell. 2008;133(3):462–74. https://doi.org/10.1016/j.cell.2008.02.048.
258. Gilleron M, Marechal X, Montaigne D, Franczak J, Neviere R, Lancel S. NADPH oxidases participate to doxorubicin-induced cardiac myocyte apoptosis. Biochem Biophys Res Commun. 2009;388(4):727–31. https://doi.org/10.1016/j.bbrc.2009.08.085.
259. Hayashi H, Kobara M, Abe M, Tanaka N, Gouda E, Toba H, Yamada H, Tatsumi T, Nakata T, Matsubara H. Aldosterone nongenomically produces NADPH oxidase-dependent reactive oxygen species and induces myocyte apoptosis. Hypertens Res. 2008;31(2):363–75. https://doi.org/10.1291/hypres.31.363.
260. Li Y, Arnold JM, Pampillo M, Babwah AV, Peng T. Taurine prevents cardiomyocyte death by inhibiting NADPH oxidase-mediated calpain activation. Free Radic Biol Med. 2009;46(1):51–61. https://doi.org/10.1016/j.freeradbiomed.2008.09.025.
261. Murdoch CE, Zhang M, Cave AC, Shah AM. NADPH oxidase-dependent redox signalling in cardiac hypertrophy, remodelling and failure. Cardiovasc Res. 2006;71(2):208–15.
262. Akki A, Zhang M, Murdoch C, Brewer A, Shah AM. NADPH oxidase signaling and cardiac myocyte function. J Mol Cell Cardiol. 2009;47(1):15–22.
263. Lu J, Mitra S, Wang X, Khaidakov M, Mehta JL. Oxidative stress and lectin-like ox-LDL-receptor LOX-1 in atherogenesis and tumorigenesis. Antioxid Redox Signal. 2011;15(8):2301–33. https://doi.org/10.1089/ars.2010.3792.
264. Zhang M, Perino A, Ghigo A, Hirsch E, Shah AM. NADPH oxidases in heart failure: poachers or gamekeepers? Antioxid Redox Signal. 2013;18(9):1024–41. https://doi.org/10.1016/j.yjmcc.2009.04.004.
265. Misra MK, Sarwat M, Bhakuni P, Tuteja R, Tuteja N. Oxidative stress and ischemic myocardial syndromes. Med Sci Monit. 2009;15(10):RA209–19.
266. Qipshidze N, Tyagi N, Metreveli N, Lominadze D, Tyagi SC. Autophagy mechanism of right ventricular remodeling in murine model of pulmonary artery constriction. Am J Physiol Heart Circ Physiol. 2012;302(3):H688–96. https://doi.org/10.1152/ajpheart.00777.2011.
267. Borchi E, Bargelli V, Stillitano F, Giordano C, Sebastiani M, Nassi PA, d'Amati G, Cerbai E, Nediani C. Enhanced ROS production by NADPH oxidase is correlated to changes in antioxidant enzyme activity in human heart failure. Biochim Biophys Acta. 2010;1802(3):331–8.
268. Robbins CS, Swirski FK. The multiple roles of monocyte subsets in steady state and inflammation. Cell Mol Life Sci. 2010;67(16):2685–93. https://doi.org/10.1007/s00018-010-0375-x.
269. Tsujioka H, Imanishi T, Ikejima H, Kuroi A, Takarada S, Tanimoto T, Kitabata H, Okochi K, Arita Y, Ishibashi K, Komukai K, Kataiwa H, Nakamura N, Hirata K, Tanaka A, Akasaka T. Impact of heterogeneity of human peripheral blood monocyte subsets on myocardial salvage in patients with primary acute myocardial infarction. J Am Coll Cardiol. 2009;54(2):130–8. https://doi.org/10.1016/j.jacc.2009.04.021.
270. Arslan F, Smeets MB, O'Neill LA, Keogh B, McGuirk P, Timmers L, Tersteeg C, Hoefer IE, Doevendans PA, Pasterkamp G, de Kleijn DP. Myocardial ischemia/reperfusion injury is mediated by leukocytic toll-like receptor-2 and reduced by systemic administration of a novel anti-toll-like receptor-2 antibody. Circulation. 2010;121(1):80–90. https://doi.org/10.1161/CIRCULATIONAHA.109.880187.
271. Mann DL. The emerging role of innate immunity in the heart and vascular system: for whom the cell tolls. Circ Res. 2011;108(9):1133–45. https://doi.org/10.1161/CIRCRESAHA.110.226936.
272. Andrassy M, Volz HC, Igwe JC, Funke B, Eichberger SN, Kaya Z, Buss S, Autschbach F, Pleger ST, Lukic IK, Bea F, Hardt SE, Humpert PM, Bianchi ME,

Mairbäurl H, Nawroth PP, Remppis A, Katus HA, Bierhaus A. High-mobility group box-1 in ischemia-reperfusion injury of the heart. Circulation. 2008;117(25):3216–26. https://doi.org/10.1161/CIRCULATIONAHA.108.769331.
273. Gordon JW, Shaw JA, Kirshenbaum LA. Multiple facets of NF-κB in the heart: to be or not to NF-κB. Circ Res. 2011;108(9):1122–32. https://doi.org/10.1161/CIRCRESAHA.110.226928.
274. Bujak M, Dobaczewski M, Chatila K, Mendoza LH, Li N, Reddy A, Frangogiannis NG. Interleukin-1 receptor type I signaling critically regulates infarct healing and cardiac remodeling. Am J Pathol. 2008;173(1):57–67. https://doi.org/10.2353/ajpath.2008.070974.
275. Schroder K, Tschopp J. The inflammasomes. Cell. 2010;140(6):821–32. https://doi.org/10.1016/j.cell.2010.01.040.
276. Kawaguchi M, Takahashi M, Hata T, Kashima Y, Usui F, Morimoto H, Izawa A, Takahashi Y, Masumoto J, Koyama J, Hongo M, Noda T, Nakayama J, Sagara J, Taniguchi S, Ikeda U. Inflammasome activation of cardiac fibroblasts is essential for myocardial ischemia/reperfusion injury. Circulation. 2011;123(6):594–604. https://doi.org/10.1161/CIRCULATIONAHA.110.982777.
277. Frangogiannis NG. Chemokines in ischemia and reperfusion. Thromb Haemost. 2007;97(5):738–47.
278. Colotta F, Re F, Polentarutti N, Sozzani S, Mantovani A. Modulation of granulocyte survival and programmed cell death by cytokines and bacterial products. Blood. 1992;80(8):2012–20.
279. Dewald O, Ren G, Duerr GD, Zoerlein M, Klemm C, Gersch C, Tincey S, Michael LH, Entman ML, Frangogiannis NG. Of mice and dogs: species-specific differences in the inflammatory response following myocardial infarction. Am J Pathol. 2004;164(2):665–77.
280. Rumberger JA. Ventricular dilatation and remodeling after myocardial infarction. Mayo Clin Proc. 1994;69(7):664–74.
281. Aikawa Y, Rohde L, Plehn J, Greaves SC, Menapace F, Arnold MO, Rouleau JL, Pfeffer MA, Lee RT, Solomon SD. Regional wall stress predicts ventricular remodeling after anteroseptal myocardial infarction in the Healing and Early Afterload Reducing Trial (HEART): an echocardiography-based structural analysis. Am Heart J. 2001;141(2):234–42.
282. Norton GR, Woodiwiss AJ, Gaasch WH, Mela T, Chung ES, Aurigemma GP, Meyer TE. Heart failure in pressure overload hypertrophy. The relative roles of ventricular remodeling and myocardial dysfunction. J Am Coll Cardiol. 2002;39(4):664–71.
283. Richards AM, Nicholls MG, Troughton RW, Lainchbury JG, Elliott J, Frampton C, Espiner EA, Crozier IG, Yandle TG, Turner J. Antecedent hypertension and heart failure after myocardial infarction. J Am Coll Cardiol. 2002;39(7):1182–8.
284. Cingolani OH, Kirk JA, Seo K, Koitabashi N, Lee DI, Ramirez-Correa G, Bedja D, Barth AS, Moens AL, Kass DA. Thrombospondin-4 is required for stretch-mediated contractility augmentation in cardiac muscle. Circ Res. 2011;109(12):1410–4.
285. Sayer G, Bhat G. The renin-angiotensin-aldosterone system and heart failure. Cardiol Clin. 2014;32(1):21–32. vii
286. Albuquerque FN, Brandão AA, Silva DA, Mourilhe-Rocha R, Duque GS, Gondar AF, Neves LM, Bittencourt MI, Pozzan R, Albuquerque DC. Angiotensin-converting enzyme genetic polymorphism: its impact on cardiac remodeling. Arq Bras Cardiol. 2014;102(1):70–9.
287. Florea VG, Cohn JN. The autonomic nervous system and heart failure. Circ Res. 2014;114(11):1815–26.
288. Cohn JN, Levine TB, Olivari MT, Garberg V, Lura D, Francis GS, Simon AB, Rector T. Plasma norepinephrine as a guide to prognosis in patients with chronic congestive heart failure. N Engl J Med. 1984;311(13):819–23.
289. Vantrimpont P, Rouleau JL, Ciampi A, Harel F, de Champlain J, Bichet D, Moyé LA, Pfeffer M. Two-year time course and significance of neurohumoral activation in the Survival and Ventricular Enlargement (SAVE) study. Eur Heart J. 1998;19(10):1552–63.
290. Lee WH, Packer M. Prognostic importance of serum sodium concentration and its modification by converting-enzyme inhibition in patients with severe chronic heart failure. Circulation. 1986;73(2):257–67.
291. Packer M. The neurohormonal hypothesis: a theory to explain the mechanism of disease progression in heart failure. J Am Coll Cardiol. 1992;20(1):248–54.
292. Maeda K, Tsutamoto T, Wada A, Mabuchi N, Hayashi M, Tsutsui T, Ohnishi M, Sawaki M, Fujii M, Matsumoto T, Kinoshita M. High levels of plasma brain natriuretic peptide and interleukin-6 after optimized treatment for heart failure are independent risk factors for morbidity and mortality in patients with congestive heart failure. J Am Coll Cardiol. 2000;36(5):1587–93.
293. Tamura N, Ogawa Y, Chusho H, Nakamura K, Nakao K, Suda M, Kasahara M, Hashimoto R, Katsuura G, Mukoyama M, Itoh H, Saito Y, Tanaka I, Otani H, Katsuki M. Cardiac fibrosis in mice lacking brain natriuretic peptide. Proc Natl Acad Sci U S A. 2000;97(8):4239–44.
294. Yamamoto R, Akazawa H, Fujihara H, Ozasa Y, Yasuda N, Ito K, Kudo Y, Qin Y, Ueta Y, Komuro I. Angiotensin II type 1 receptor signaling regulates feeding behavior through anorexigenic corticotropin-releasing hormone in hypothalamus. J Biol Chem. 2011;286(24):21458–65.
295. Akazawa H, Yasuda N, Komuro I. Mechanisms and functions of agonist-independent activation in the angiotensin II type 1 receptor. Mol Cell Endocrinol. 2009;302(2):140–7.

296. Kamo T, Akazawa H, Komuro I. Pleiotropic effects of angiotensin II receptor signaling in cardiovascular homeostasis and aging. Int Heart J. 2015;56(3):249–54.
297. Ozasa Y, Akazawa H, Qin Y, Tateno K, Ito K, Kudo-Sakamoto Y, Yano M, Yabumoto C, Naito AT, Oka T, Lee JK, Minamino T, Nagai T, Kobayashi Y, Komuro I. Notch activation mediates angiotensin II-induced vascular remodeling by promoting the proliferation and migration of vascular smooth muscle cells. Hypertens Res. 2013;36(10):859–65.
298. Akazawa H, Yano M, Yabumoto C, Kudo-Sakamoto Y, Komuro I. Angiotensin II type 1 and type 2 receptor-induced cell signaling. Curr Pharm Des. 2013;19(17):2988–95.
299. Sato M. Roles of accessory proteins for heterotrimeric G-protein in the development of cardiovascular diseases. Circ J. 2013;77(10):2455–61.
300. Wu J, You J, Wang S, Zhang L, Gong H, Zou Y. Insights into the activation and inhibition of angiotensin II type 1 receptor in the mechanically loaded heart. Circ J. 2014;78(6):1283–9.
301. Sadoshima J, Xu Y, Slayter HS, Izumo S. Autocrine release of angiotensin II mediates stretch-induced hypertrophy of cardiac myocytes in vitro. Cell. 1993;75(5):977–84.
302. Yamazaki T, Komuro I, Kudoh S, Zou Y, Shiojima I, Mizuno T, Takano H, Hiroi Y, Ueki K, Tobe K, et al. Angiotensin II partly mediates mechanical stress-induced cardiac hypertrophy. Circ Res. 1995;77(2):258–65.
303. Akazawa H. Mechanisms of cardiovascular homeostasis and pathophysiology--from gene expression, signal transduction to cellular communication. Circ J. 2015;79(12):2529–36.
304. Yasuda N, Miura S, Akazawa H, Tanaka T, Qin Y, Kiya Y, Imaizumi S, Fujino M, Ito K, Zou Y, Fukuhara S, Kunimoto S, Fukuzaki K, Sato T, Ge J, Mochizuki N, Nakaya H, Saku K, Komuro I. Conformational switch of angiotensin II type 1 receptor underlying mechanical stress-induced activation. EMBO Rep. 2008;9(2):179–86.
305. Konstam MA, Rousseau MF, Kronenberg MW, Udelson JE, Melin J, Stewart D, Dolan N, Edens TR, Ahn S, Kinan D, et al. Effects of the angiotensin converting enzyme inhibitor enalapril on the long-term progression of left ventricular dysfunction in patients with heart failure. SOLVD Investigators. Circulation. 1992;86(2):431–8.
306. Greenberg B, Quinones MA, Koilpillai C, Limacher M, Shindler D, Benedict C, Shelton B. Effects of long-term enalapril therapy on cardiac structure and function in patients with left ventricular dysfunction. Results of the SOLVD echocardiography substudy. Circulation. 1995;91(10):2573–81.
307. Hafizi S, Wharton J, Morgan K, Allen SP, Chester AH, Catravas JD, Polak JM, Yacoub MH. Expression of functional angiotensin-converting enzyme and AT1 receptors in cultured human cardiac fibroblasts. Circulation. 1998;98(23):2553–9.
308. Matsusaka T, Katori H, Inagami T, Fogo A, Ichikawa I. Communication between myocytes and fibroblasts in cardiac remodeling in angiotensin chimeric mice. J Clin Invest. 1999;103(10):1451–8.
309. Sadoshima J, Izumo S. Molecular characterization of angiotensin II--induced hypertrophy of cardiac myocytes and hyperplasia of cardiac fibroblasts. Critical role of the AT1 receptor subtype. Circ Res. 1993;73(3):413–23.
310. McEwan PE, Gray GA, Sherry L, Webb DJ, Kenyon CJ. Differential effects of angiotensin II on cardiac cell proliferation and intramyocardial perivascular fibrosis in vivo. Circulation. 1998;98(24):2765–73.
311. Kawano H, Do YS, Kawano Y, Starnes V, Barr M, Law RE, Hsueh WA. Angiotensin II has multiple profibrotic effects in human cardiac fibroblasts. Circulation. 2000;101(10):1130–7.
312. Hayashi M, Tsutamoto T, Wada A, Maeda K, Mabuchi N, Tsutsui T, Matsui T, Fujii M, Matsumoto T, Yamamoto T, Horie H, Ohnishi M, Kinoshita M. Relationship between transcardiac extraction of aldosterone and left ventricular remodeling in patients with first acute myocardial infarction: extracting aldosterone through the heart promotes ventricular remodeling after acute myocardial infarction. J Am Coll Cardiol. 2001;38(5):1375–82.
313. Lijnen P, Petrov V. Induction of cardiac fibrosis by aldosterone. J Mol Cell Cardiol. 2000;32(6):865–79.
314. Fullerton MJ, Funder JW. Aldosterone and cardiac fibrosis: in vitro studies. Cardiovasc Res. 1994;28(12):1863–7.
315. Zannad F, Alla F, Dousset B, Perez A, Pitt B. Limitation of excessive extracellular matrix turnover may contribute to survival benefit of spironolactone therapy in patients with congestive heart failure: insights from the randomized aldactone evaluation study (RALES). Rales Investigators. Circulation. 2000;102(22):2700–6.
316. Altin SE, Schulze PC. Metabolism of the right ventricle and the response to hypertrophy and failure. Prog Cardiovasc Dis. 2012;55(2):229–33. https://doi.org/10.1016/j.pcad.2012.07.010.
317. Dias CA, Assad RS, Caneo LF, Abduch MC, Aiello VD, Dias AR, Marcial MB, Oliveira SA. Reversible pulmonary trunk banding. II. An experimental model for rapid pulmonary ventricular hypertrophy. J Thorac Cardiovasc Surg. 2002;124(5):999–1006.
318. Taegtmeyer H, Golfman L, Sharma S, Razeghi P, van Arsdall M. Linking gene expression to function: metabolic flexibility in the normal and diseased heart. Ann N Y Acad Sci. 2004;1015:202–13.
319. Doenst T, Nguyen TD, Abel ED. Cardiac metabolism in heart failure: implications beyond ATP production. Circ Res. 2013;113(6):709–24.

320. Barger PM, Kelly DP. PPAR signaling in the control of cardiac energy metabolism. Trends Cardiovasc Med. 2000;10(6):238–45.
321. Karbowska J, Kochan Z, Smolenski RT. Peroxisome proliferator-activated receptor alpha is downregulated in the failing human heart. Cell Mol Biol Lett. 2003;8(1):49–53.
322. Campos DH, Leopoldo AS, Lima-Leopoldo AP, Nascimento AF, Oliveira SA Jr, Silva DC, Sugizaki MM, Padovani CR, Cicogna AC. Obesity preserves myocardial function during blockade of the glycolytic pathway. Arq Bras Cardiol. 2014;103(4):330–7.
323. Azevedo PS, Minicucci MF, Santos PP, Paiva SA, Zornoff LA. Energy metabolism in cardiac remodeling and heart failure. Cardiol Rev. 2013;21(3):135–40.
324. Santos PP, Oliveira F, Ferreira VC, Polegato BF, Roscani MG, Fernandes AA, Modesto P, Rafacho BP, Zanati SG, Di Lorenzo A, Matsubara LS, Paiva SA, Zornoff LA, Minicucci MF, Azevedo PS. The role of lipotoxicity in smoke cardiomyopathy. PLoS One. 2014;9(12):e113739.
325. Voelkel NF, Quaife RA, Leinwand LA, et al. Right ventricular function and failure: report of a National Heart, Lung and Blood Institute working group on cellular and molecular mechanisms of right heart failure. Circulation. 2006;114(17):1883–91. https://doi.org/10.1161/CIRCULATIONAHA.106.632208.
326. Nagaya N, Goto Y, Satoh T, et al. Impaired regional fatty acid uptake and systolic dysfunction in hypertrophied right ventricle. J Nucl Med. 1998;39:1676–80.
327. Bokhari S, Raina A, Rosenweig EB, et al. PET imaging may provide a novel biomarker and understanding of right ventricular dysfunction in patients with idiopathic pulmonary arterial hypertension. Circ Cardiovasc Imaging. 2011;4:641–7. https://doi.org/10.1161/CIRCIMAGING.110.963207.
328. Can MM, Kaymaz C, Tanboga IH, et al. Increased right ventricular glucose metabolism in patients with pulmonary arterial hypertension. Clin Nucl Med. 2011;36:743–8. https://doi.org/10.1097/RLU.0b013e3182177389.
329. O'Connor RD, Xu J, Ewald GA, et al. Intramyocardial triglyceride quantification by magnetic resonance spectroscopy: in vivo and ex vivo correlation in human subjects. Magn Reson Med. 2011;65:1234–8. https://doi.org/10.1002/mrm.22734.
330. Ryan JJ, Archer SL. The right ventricle in pulmonary arterial hypertension: disorders of metabolism, angiogenesis and adrenergic signaling in right ventricular failure. Circ Res. 2014;115:176–88. https://doi.org/10.1161/CIRCRESAHA.113.301129.
331. Sutendra G, Dromparis P, Paulin R, et al. A metabolic remodeling in right ventricular hypertrophy is associated with decreased angiogenesis and a transition from a compensated to a decompensated state in pulmonary hypertension. J Mol Med. 2013;91(11):1315–27. https://doi.org/10.1007/s00109-013-1059-4.
332. Wasson S, Reddy HK, Dohrmann ML. Current perspectives of electrical remodeling and its therapeutic implications. J Cardiovasc Pharmacol Ther. 2004;9(2):129–44.
333. Hasenfuss G, Schillinger W, Lehnart SE, et al. Relationship between Na+-Ca2+-exchanger protein levels and diastolic function of failing human myocardium. Circulation. 1999;99(5):641–8.
334. Bers DM, Pogwizd SM, Schlotthauer K. Upregulated Na/Ca exchange is involved in both contractile dysfunction and arrhythmogenesis in heart failure. Basic Res Cardiol. 2002;97(Suppl 1):I36–42.
335. Wang Z, Nolan B, Kutschke W, Hill JA. Na+-Ca2+ exchanger remodeling in pressure overload cardiac hypertrophy. J Biol Chem. 2001;276(21):17706–11.
336. Houser SR, Freeman AR, Jaegar JM, et al. Resting potential changes associated with Na+-K+ pump in failing heart muscle. Am J Phys. 1981;240(2):H168–76.
337. Matsumoto Y, Aihara H, Yamauchi-Kohno R, et al. Long-term endothelin a receptor blockade inhibits electrical remodeling in cardiomyopathic hamsters. Circulation. 2002;106(5):613–9.
338. Sipido KR, Volders PG, de Groot SH, et al. Enhanced Ca2+ release and Na+/Ca2+ exchange activity in hypertrophied canine ventricular myocytes: potential link between contractile adaptation and arrhythmogenesis. Circulation. 2000;102(17):2137–44.
339. Kalogeropoulos AP, Georgiopoulou VV, Howell S, Pernetz MA, Fisher MR, Lerakis S, Martin RP. Evaluation of right intraventricular dyssynchrony by two-dimensional strain echocardiography in patients with pulmonary arterial hypertension. J Am Soc Echocardiogr. 2008;21(9):1028–34. https://doi.org/10.1016/j.echo.2008.05.005.
340. López-Candales A, Dohi K, Rajagopalan N, Suffoletto M, Murali S, Gorcsan J, Edelman K. Right ventricular dyssynchrony in patients with pulmonary hypertension is associated with disease severity and functional class. Cardiovasc Ultrasound. 2005;3:23.
341. Vonk-Noordegraaf A, Marcus JT, Gan CT, Boonstra A, Postmus PE. Interventricular mechanical asynchrony due to right ventricular pressure overload in pulmonary hypertension plays an important role in impaired left ventricular filling. Chest. 2005;128(6 Suppl):628S–30S.
342. Feneley MP, Gavaghan TP, Baron DW, Branson JA, Roy PR, Morgan JJ. Contribution of left ventricular contraction to the generation of right ventricular systolic pressure in the human heart. Circulation. 1985;71(3):473–80.
343. Marcus JT, Gan CT, Zwanenburg JJ, Boonstra A, Allaart CP, Götte MJ, Vonk-Noordegraaf A. Interventricular mechanical asynchrony in pulmonary arterial hypertension: left-to-right delay in peak shortening is related to right ventricular overload and left ventricular underfilling. J Am Coll Cardiol. 2008;51(7):750–7. https://doi.org/10.1016/j.jacc.2007.10.041.

344. Peschar M, Vermooy K, Vangat WYR, et al. Absence of reeverse electrical remodeling during regression of volume overload hypertrophy in canine ventricles. Cardiovasc Res. 2003;58(3):510–7.
345. Mayet J, Shahi M, McGrath K, Poulter NR, Sever PS, Foale RA, et al. Left ventricular hypertrophy and QT dispersion in hypertension. Hypertension. 1996;28(5):791–6.
346. Darbar D, Cherry CJ, Kerins DM. QT dispersion is reduced after valve replacement in patients with aortic stenosis. Heart. 1999;82(1):15–8.
347. Reddy HK, Wasson S, Koshy SK, et al. Structural correlates of electrical remodeling in ventricular hypertrophy. Cardiovasc Res. 2003;58(3):495–7.
348. Pries AR, Badimon L, Bugiardini R, Camici PG, Dorobantu M, Duncker DJ, Escaned J, Koller A, Piek JJ, de Wit C. Coronary vascular regulation, remodelling, and collateralization: mechanisms and clinical implications on behalf of the working group on coronary pathophysiology and microcirculation. Eur Heart J. 2015;36(45):3134–46. https://doi.org/10.1093/eurheartj/ehv100.
349. Laughlin MH, Bowles DK, Duncker DJ. The coronary circulation in exercise training. Am J Physiol Heart Circ Physiol. 2012;302(1):H10–23. https://doi.org/10.1152/ajpheart.00574.2011.
350. Schaper W. Collateral circulation: past and present. Basic Res Cardiol. 2009;104(1):5–21. https://doi.org/10.1007/s00395-008-0760-x.
351. Pries AR, Reglin B, Secomb TW. Remodeling of blood vessels: responses of diameter and wall thickness to hemodynamic and metabolic stimuli. Hypertension. 2005;46(4):725–31.
352. Mulvany MJ. Small artery remodelling in hypertension. Basic Clin Pharmacol Toxicol. 2012;110(1):49–55. https://doi.org/10.1111/j.1742-7843.2011.00758.x.
353. Zakrzewicz A, Secomb TW, Pries AR. Angioadaptation: keeping the vascular system in shape. News Physiol Sci. 2002;17:197–201.
354. Koller A. Flow-dependent remodeling of small arteries: the stimuli and the sensors are (still) in question. Circ Res. 2006;99(1):6–9.
355. Pries AR, Reglin B, Secomb TW. Structural adaptation of microvascular networks: functional roles of adaptive responses. Am J Physiol Heart Circ Physiol. 2001;281(3):H1015–25.
356. Hopkins WE, Ochoa LL, Richardson GW, et al. Comparison of the hemodynamics and survival of adults with severe primary pulmonary hypertension or Eisenmenger syndrome. J Heart Lung Transplant. 1996;15(1 Pt 1):100–5.
357. Reis Filho JR, Cardoso JN, Cardoso CM, Pereira-Barretto AC. Reverse cardiac remodeling: a marker of better prognosis in heart failure. Arq Bras Cardiol. 2015;104(6):502–6. https://doi.org/10.5935/abc.20150025.
358. Hellawell JL, Margulies KB. Myocardial reverse remodeling. Cardiovasc Ther. 2012;30(3):172–81. https://doi.org/10.1111/j.1755-5922.2010.00247.x.
359. Kramer DG, Trikalinos TA, Kent DM, Antonopoulos GV, Konstam MA, Udelson JE. Quantitative evaluation of drug or device effects on ventricular remodeling as predictors of therapeutic effects on mortality in patients with heart failure and reduced ejection fraction: a meta-analytic approach. J Am Coll Cardiol. 2010;56(5):392–406. https://doi.org/10.1016/j.jacc.2010.05.011.
360. Ruiz-Ortega M, Lorenzo O, Ruperez M, Konig S, Wittig B, Egido J. Angiotensin II activates nuclear transcription factor kappa B through AT(1) and AT(2) in vascular smooth muscle cells: molecular mechanisms. Circ Res. 2000;86(12):1266–72.
361. Marui N, Offermann MK, Swerlick R, Kunsch C, Rosen CA, Ahmad M, Alexander RW, Medford RM. Vascular cell adhesion molecule-1 (VCAM-1) gene transcription and expression are regulated through an antioxidant-sensitive mechanism in human vascular endothelial cells. J Clin Invest. 1993;92(4):1866–74.
362. Pi XJ, Chen X. Captopril and ramiprilat protect against free radical injury in isolated working rat hearts. J Mol Cell Cardiol. 1989;21(12):1261–71.
363. Chen F, Castranova V, Shi X, Demers LM. New insights into the role of nuclear factor kappa B, a ubiquitous transcription factor in the initiation of diseases. Clin Chem. 1999;45(1):7–17.
364. Santi D, Giannetta E, Isidori AM, Vitale C, Aversa A, Simoni M. Therapy of endocrine disease: effects of chronic use of phosphodiesterase inhibitors on endothelial markers in type 2 diabetes mellitus: a meta-analysis. Eur J Endocrinol. 2015;172(3):R103–14. https://doi.org/10.1530/EJE-14-0700.
365. Pofi R, Gianfrilli D, Badagliacca R, Di Dato C, Venneri MA, Giannetta E. Everything you ever wanted to know about phosphodiesterase 5 inhibitors and the heart (but never dared ask): how do they work? J Endocrinol Investig. 2016;39(2):131–42. https://doi.org/10.1007/s40618-015-0339-y.
366. Nam YJ, Song K, Olson EN. Heart repair by cardiac reprogramming. Nat Med. 2013;19(4):413–5. https://doi.org/10.1038/nm.3147.
367. Hodgkinson CP, Kang MH, Dal-Pra S, Mirotsou M, Dzau VJ. MicroRNAs and cardiac regeneration. Circ Res. 2015;116(10):1700–11. https://doi.org/10.1161/CIRCRESAHA.116.304377.
368. Jayawardena TM, Egemnazarov B, Finch EA, Zhang L, Payne JA, Pandya K, Zhang Z, Rosenberg P, Mirotsou M, Dzau VJ. MicroRNA-mediated in vitro and in vivo direct reprogramming of cardiac fibroblasts to cardiomyocytes. Circ Res. 2012;110(11):1465–73. https://doi.org/10.1161/CIRCRESAHA.112.269035.
369. Rao PK, Kumar RM, Farkhondeh M, Baskerville S, Lodish HF. Myogenic factors that regulate expres-

sion of muscle-specific microRNAs. Proc Natl Acad Sci U S A. 2006;103(23):8721–6.
370. Takaya T, Nishi H, Horie T, Ono K, Hasegawa K. Roles of microRNAs and myocardial cell differentiation. Prog Mol Biol Transl Sci. 2012;111:139–52. https://doi.org/10.1016/B978-0-12-398459-3.00006-X.
371. Joladarashi D, Thandavarayan RA, Babu SS, Krishnamurthy P. Small engine, big power: microRNAs as regulators of cardiac diseases and regeneration. Int J Mol Sci. 2014;15(9):15891–911. https://doi.org/10.3390/ijms150915891.
372. Katz MG, Fargnoli AS, Pritchette LA, Bridges CR. Gene delivery technologies for cardiac applications. Gene Ther. 2012;19(6):659–69. https://doi.org/10.1038/gt.2012.11.
373. Küçüker SA, Stetson SJ, Becker KA, Akgül A, Loebe M, Lafuente JA, Noon GP, Koerner MM, Entman ML, Torre-Amione G. Evidence of improved right ventricular structure after LVAD support in patients with end-stage cardiomyopathy. J Heart Lung Transplant. 2004;23(1):28–35.
374. Sachse FB, Torres NS, Savio-Galimberti E, Aiba T, Kass DA, Tomaselli GF, Bridge JH. Subcellular structures and function of myocytes impaired during heart failure are restored by cardiac resynchronization therapy. Circ Res. 2012;110(4):588-97. Circ Res. 2012;110(4):588–97. https://doi.org/10.1161/CIRCRESAHA.111.257428.
375. Barbone A, Holmes JW, Heerdt PM, et al. Comparison of right and left ventricular responses to left ventricular assist device support in patients with severe heart failure: a primary role of mechanical unloading underlying reverse remodeling. Circulation. 2001;104(6):670–5.
376. Klotz S, Naka Y, Oz MC, Burkhoff D. Biventricular assist device-induced right ventricular reverse structural and functional remodeling. J Heart Lung Transplant. 2005;24(9):1195–201.

Right Ventricular Normal Function

5

Ana Maria Balahura, Daniela Bartoş, and Elisabeta Bădilă

Abstract

The evaluation of right ventricular (RV) morphology and function, although for many centuries forgotten or sidelined, is now recognized to be essential in cardiovascular diseases, as it can be involved in the physiopathology of many disorders. Therefore, appropriate knowledge of RV function in health and disease is mandatory for clinicians. In the present chapter we summarize the current available data on RV function starting with a brief description of anatomy as morphology is closely related to function. We then describe mechanical and haemodynamic aspects of RV contraction. Furtheremore, we discuss methods of assessing RV performance using end-systolic and end-diastolic pressure-volume relationships as well as RV haemodynamic coupling with the pulmonary circulation based on the concept of elastance. Regulatory mechanisms of RV function are also described.

Keywords

Right ventricular function · Physiology · Myocardial contraction · Elastance · Ventriculo-arterial coupling

5.1 Right Ventricle Importance

The right ventricle (RV), although fascinating for the complex anatomy and function, was forgotten or sidelined for centuries, its physiopathological importance in the human body being unrecognized.

The first who noticed RV importance is Sir William Hervey, the father of the modern physiology, who described pulmonary circulation and the importance of the RV in sending the blood to the left ventricle through this circulation, mechanism described in his famous thesis, "De Motu Cordis", in 1616 [1]. The following four centuries were significant in debating the importance of the RV. Publications from the beginning of the twentieth century stated that the RV has only one function, as a conduct, and RV injury would not significantly influence the general circulatory function, statement that was "confirmed" by the successful procedures Glenn and Fontan [2–5]. On the other hand, recognizing the negative effects and even cardiogenic shock as a consequence of RV infarction, overwrite the idea of a passive function of the RV [6, 7]. Moreover, in the second half of the last century,

A. M. Balahura • D. Bartoş • E. Bădilă (✉)
'Carol Davila' University of Medicine and Pharmacy, Bucharest, Romania

Internal Medicine Department, Clinical Emergency Hospital, Bucharest, Romania

S. I. Dumitrescu et al. (eds.), *Right Heart Pathology*, https://doi.org/10.1007/978-3-319-73764-5_5

as the essential role of the RV in many physiologic and pathologic conditions was finally admitted, many researchers have focused on RV function [8].

The evaluation of RV morphology and function is essential in cardiovascular diseases, as it can be involved in the physiopathology or it can be affected by many disorders such as pulmonary hypertension (PH), idiopatic or secondary to the left heart diseases, left ventricle (LV) dysfunction, cardiomyopathies, RV infarction or tricuspid and pulmonary valvulopaties [4, 9].

RV function has an impact on the prognosis of patients with congenital heart diseases (CHD). Conditions as atrial septal defect, tricuspid regurgitation or pulmonary regurgitation, create a volume overload for the RV, whereas pulmonary stenosis or corrected transposition of the great arteries create a pressure overload or even hemodynamic complex modification as in Tetralogy of Fallot (ToF) [10]. Moreover, after surgical intervention in CHD, RV dysfunction secondary to hemodynamic residual overload is a negative long term prognostic factor [11].

The RV is different morphologically and functionally from the LV. It has a complex tridimensional anatomy, hemodynamic pressure load is abolished after birth and it has a different contraction pattern [12]. Consequently, the RV adapts differently than LV at acute and chronic hemodynamic changes. Therefore, the RV is not the LV but is equally important to cardiovascular equilibrium.

5.2 RV Anatomy in Relation to Function

In a normal heart, the RV is the most anteriorly located chamber, in front of the LV and behind the sternum [8].

The RV has a complex tridimensional anatomy, viewed from the front has a triangular shape, but in the cross-section it has a crescent shape. The interventricular septum (IVS) is an important determinant of RV shape. In normal conditions and in the absence of conduction abnormalities, the IVS is concave toward the LV both in systole and in diastole; however in RV overload, the IVS becomes flattened or reversely concave toward the RV, in this condition the RV anatomy being significantly modified [1].

Although in the common echocardiographic windows the RV seems to be smaller than the LV, it has a bigger volume, as it was demonstrated in imaging cardiac studies using cardiac magnetic resonance (CMR): normal end diastolic RV volume is 49–101 ml/m^2 whereas the end diastolic LV volume is 44–89 ml/m^2. On the other hand, the RV mass is only one fifth of the LV mass [13].

The RV chamber has three components: the inlet, the trabecular part situated apically and the outlet/ejection tract/conus. Although it develops embryological from two different components, the sinus (inflow) and the conus (outflow), the definition of the RV in terms of three components described earlier and proposed by Goor and Lillehei in 1975, is the preferred one for practical reasons, as describing congenital abnormalities, when one or more components can be absent [14, 15].

The inlet and trabecular components form the sinus, a functional part with common embryological origin, which contains 80% of the RV volume and it is responsible for 85% of the RV stroke volume, whereas the conus contributes with the rest of 15% [16].

The RV inlet includes the tricuspid valve and it is separated from the trabecular part by the papillary muscle insertion. The trabecular compartment is situated at the apex and it extends to the middle of the free wall. This compartment is characterized by covering with muscular fibers arranged in a grid—muscle trabeculae—whose role appears to be linked in part to intraventricular hemodynamics and on the other hand to the jointing of the papillary muscles with the apex and the walls of the heart [17]. The ejection compartment/tract has different embryological origin and is characterized by the conical shape of the conus and the smooth walls that contribute to the increase in blood flow to the pulmonary artery [1] (Fig. 5.1).

The architecture of the muscle fibres that create the two ventricles is complex and consists of a three-dimensional network of several layers of

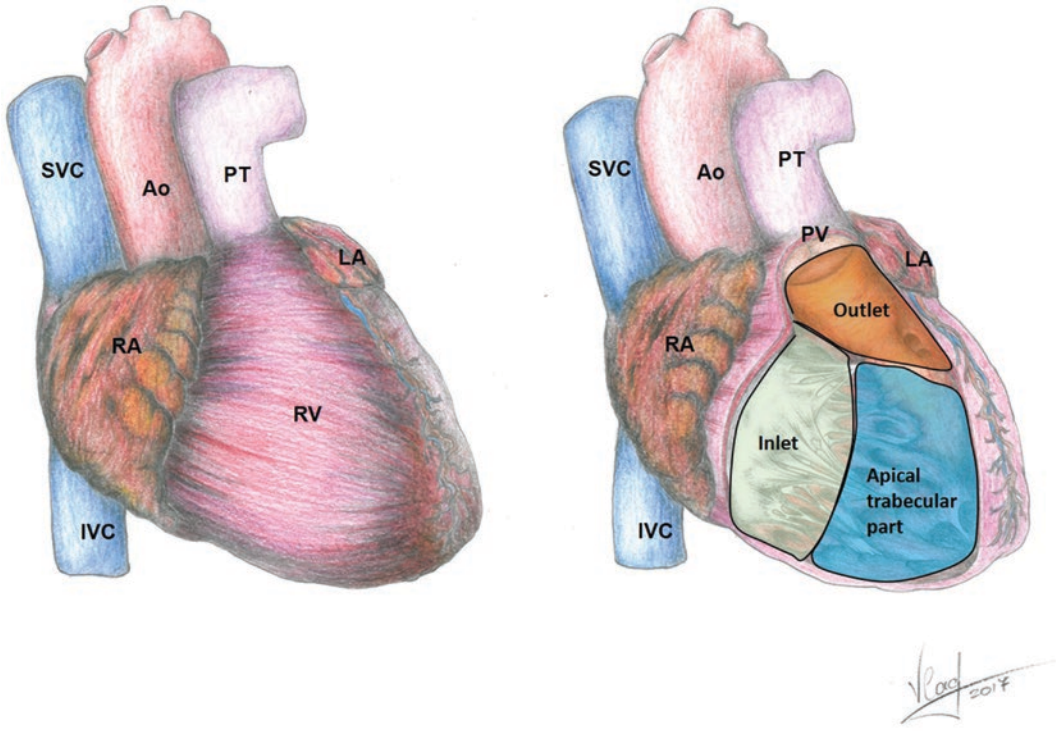

Fig. 5.1 Right ventricle anatomy. *Ao* ascending aorta, *IVC* inferior vena cava, *LA* left atrial appendage, *RA* right atrium, *RV* right ventricle, *PT* pulmonary trunk, *PV* pulmonary valve. With the permission of Dr. Vlad Munteanu

muscle. In contrast to the three-layer muscle architecture of LV, RV consists predominantly of a superficial layer and a deep fibre layer. The thinner subepicardial layer fibres are circumferentially arranged with the fibre direction parallel to the atrioventricular groove. These fibres change the direction on the sternocostal face becoming oblique to the apex and continue into the superficial fibres of the LV. The thicker subendocardic layer has a longitudinal direction from the base to apex [14]. As a result, RV has a predominantly longitudinal contraction and the continuity between the RV and LV muscle fibres functionally connects the two ventricles representing the anatomical base which leads to the RV free wall traction secondary to LV contraction. This continuity also contributes together with the IVS and pericardial contention to the ventricular interdependence [1].

The RV cavity is completed by IVS which belongs to both ventricles, functionally and anatomically [18]. Across the IVS there is an anatomic continuity between the myocardial fibres of the RV and LV contributing to ventricular interdependence.

5.2.1 RV Vascularization

The right ventricle is mostly vascularized by the right coronary artery (RCA). The lateral wall of the RV receives blood from the acute marginal arteries of the RCA, while the posterior wall and the inferior IVS are irrigated by the posterior descending artery (PDA). Thus, RV vascularization also depends on the coronary dominance [19, 20]. In the case of right coronary dominance (85% of cases) and balanced dominance (7.5% of cases) PDA will originate in RCA, whereas in the case of left coronary dominance it will originate in the circumflex artery, which will participate in the RV vascularization [21]. A small part of the anterior wall as well as the anterior IVS are irrigated by the anterior descending artery (ADA) [1]. Vascularization of the infundibulum is performed

by the pulmonary cone artery, which in half of the cases originates in RCA, whilst the other half have a separate origin in the aorta, at the level of the right coronary sinus [21].

Unlike the LV, where myocardial perfusion occurs in diastole, when intra-cardiac pressure drops below the aortic pressure, in the RV, under normal hemodynamic loading conditions, intracardiac pressure remains permanently below the aortic pressure, allowing for myocardial perfusion both in systole and in diastole. Under pathological conditions, however, when RV is subject to significant pressure overload, myocardial perfusion becomes similar to LV [18].

5.3 Right Ventricular Physiology and Adaptation to Hemodynamic Changes

The role of the RV in the body is to take the blood from the venous return and to send it further into the pulmonary circulation. Normally, the RV is connected in series with the LV being thus forced to have substantially the same effective stroke volume (SV) [1]. In spite of a significantly lower ventricular mass, RV is able to achieve the same SV as it is connected to the pulmonary artery characterized by low impedance and high arterial distensibility [22].

5.3.1 Right Ventricle Contraction: Mechanical Aspects

RV contraction occurs sequentially, beginning with the myocardium of the inlet and the trabecular part, then ending with the infundibulum, with a delay of approximately 35 ms between the onset of contraction of the RV apex and that of infundibulum [23]. In addition, the contraction of the infundibular part is longer than that of the inlet [19]. Since anatomically there is an angle of 37.5° between the inlet axis and the ejection tract [24], this peristaltic motion facilitates the transport and ejection of blood from the RV [22]. Under normal hemodynamic conditions, RV contraction is predominantly longitudinal, the contribution of radial myocardial deformation, rotation and twisting being minimal [25, 26].

The RV contraction mechanisms are represented by free wall inward movement, RV shortening in the long axis by contraction of the longitudinal subendocardial fibres which determine the traction of the tricuspid ring to the apex, but also the traction at the attachment points realized by the LV [1].

A significant part, between 20 and 40% of the RV stroke volume is dependent on LV contraction [27, 28]. The interaction between the two ventricles (ventricular interdependence) is determined anatomically by the communication of the RV fibres with the LV ones as mentioned above, by the partially common vascularization, by the pericardium which creates the contention of both ventricles, but especially by the IVS which allows the crossing of the contraction forces between the two ventricles [1, 22, 29]. The fact that the experimental replacement of the RV free wall with a non-contractile patch did not significantly alter pulmonary circulatory hemodynamics comes to reinforce the idea that left ventricular performance directly affects the RV [30].

5.3.2 Right Ventricle Contraction: Hemodynamic Aspects

The right ventricle ejects the blood into a low-impedance arterial system with increased distensibility. In a normal circulatory system, right heart pressures are significantly lower than those of the left heart [18].

The RV pressure curve is characterized by a maximum systolic value of low amplitude (15–30 mmHg), which is reached early, and a subsequent rapid decrease of pressure [1, 17]. Upon initiation of contraction, the RV pressure rapidly exceeds the low pulmonary artery pressure, which makes the duration of the isovolumetric contraction to be low or absent. Another feature of the RV pressure curve is the existence of the so-called 'hangout' interval, which is the continuation of the end systolic flow to the pulmonary artery despite a negative ventriculo-arterial gradient. The explanation for the existence of this interval is related to the complexity of the vetriculo-arterial coupling, given that the total afterload of the RV is determined by the resistive, capacitive, inertial properties and the pulse wave reflection of the pulmonary circulation [20].

5.3.3 Parameters Determining Right Ventricular Function

The RV systolic performance is mainly the reflection of three parameters: contractility, afterload and preload. Additionally, RV performance is also influenced by heart rate, ventricular contraction synchronicity and ventricular interdependence [1].

Contractility is the inherent capacity of the myocardium to contract independently of preload or afterload changes. At the molecular level, the increase in contractility/inotropism is the result of increased interaction between calcium ions and contractile proteins. However, it should be pointed out that any change in contractile status must be independent of the preload and afterload conditions [31].

Preload represents ventricular loading before the start of ventricular contraction, at the end of the diastole. Preload increase leads to end-diastolic ventricular volume augmentation which, through the Frank-Starling mechanism, will cause SV growth without a direct change in contractility [32, 33]. *Afterload* is the systolic pressure imposed on the ventricle after initiation of contraction and is represented by pulmonary vascular resistance (PVR) and dynamic and static pulmonary impedance components [1].

The concepts of preload and afterload are not completely independent since, judging by the Frank-Starling mechanism, an increase in preload will lead to SV growth and an increase in blood pressure which itself represents an increase in afterload. However, ventricular pressure is primarily related to the degree of stretching of myocardial fibres at the end diastole, whereas afterload is related to the parietal stress developed by these fibres during systole [31].

There is a complex interaction between the determinants of RV performance and their understanding usually requires invasive studies of the pressure-volume curves, otherwise it is difficult, in vivo, to differentiate the contribution of one or more factors to the RV performance changes. The pressure-volume curve describes changes in volume and ventricular pressure during a cardiac cycle. The cardiac cycle can be divided into four different phases: (1) the filling phase, (2) the isovolumic contraction phase, (3) the ejection phase, (4) the isovolumic relaxation phase, phases that can be found in the volume-pressure curve [34] (Fig. 5.2).

In order to obtain information on ventricular systolic and diastolic properties, it is necessary to record several such curves preferably by reducing the preload, which can be achieved by vena cava occlusion with a balloon inserted via a catheter. With these curves, the end-systolic pressure-volume relationship (ESPVR) can be defined as the line connecting the end-sistolic points on the curves

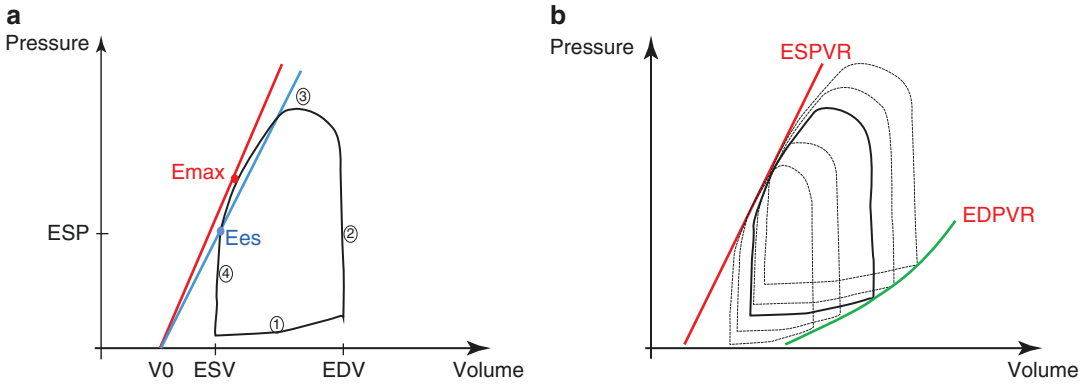

Fig. 5.2 Right ventricular presure-volume curves. (**a**) Represantation of RV pressure-volume loop with the four phases of the cardiac cycle (1—the filling phase, 2—the isovolumic contraction phase, 3—the ejection phase, 4—the isovolumic relaxation phase). The more triangular shape of the RV pressure-volume loop, as opposed to LV, is the reason why maximal elastance (Emax) does not concide with end systolic elastance (Ees). (**b**) Schematic represantation of basic measures of pressure and volume relationships. The end-systolic pressure-volume relationship (ESPVR) and end-diastolic pressure-volume relationships (EDPVR) define the boundaries of the pressure-volume loops for a given contractile state of the ventricle. Changes in preload (as shown with dashed lines) or afterload alter the shape and position of the loops, however, the end-systolic and end-diastolic points will always fall on the ESPVR and EDPVR. Therefore, ESPVR and EDPVR can be used as load independent measures of contractility

previously drawn. By measuring the ESPVR slope, ventricular elasticity (E) is obtained which is considered to be the best parameter for describing myocardial contractility, since it is shown to be independent of preload or afterload [35]. Both E max (maximal elasticity), the maximum value of pressure-to-ventricular volume ratio in one cardiac cycle as well as E es (end-systolic elasticity), being the same ratio at the end of systole, were described [36]. For the LV, the pressure-volume curve is rectangular, therefore, E max and E es overlap. However, the RV works in a low impedance system which causes the blood ejection to continue even after the RV pressure begins to decrease—the so-called 'hangout' period previously described. This phenomenon makes end-systolic identification difficult and contributes to a rather triangular shape of the RV pressure-volume curve. Thus, for RV contractility evaluation, Emax is considered a better parameter than Ees [37] (Fig. 5.2).

Even though very useful in the characterization of RV true function/contractility, the manipulation of venous return through the insertion of a vena cava balloon catheter to generate families of pressure—volume loops make the clinical availability very limited as it increases the invasiveness of the right heart catheterisation (RHC). Several new mehods have been developed in order to increase availability in clinical practice as the use of Valsalva maneouver to generate RV pressure-volume loops at decreased venous return or the use of volume measurements by MRI or three-dimensional echocardiography along with RHC pressure measurements [38, 39]. However, one method has been better validated, initialy for the LV and adapted afterwards for the RV, a method aiming at determining ESPVR from a single pressure-volume loop [40]. This single-beat method relies on the assumption that ESPVR is the same in ejecting and isovolumic beats. In an isovolumic beat, the ESP would reach the highest possible value (Pmax) for a given contractility. Moreover, in the single-beat method, it is assumed that the pressure curve of an isovolumic contraction can be approximated by a sine wave and that the sine wave can be extrapolated from normal ejecting beats [40, 41]. Pmax is estimated as the peak value of the sine wave and the ESPVR is calculated from the slope of a tangent from *P* max to the pressure–volume curve [42] (Fig. 5.3).

Heart rate is an important additional parameter in determining ventricular function in both normal heart and as a mechanism of acute adaptation to

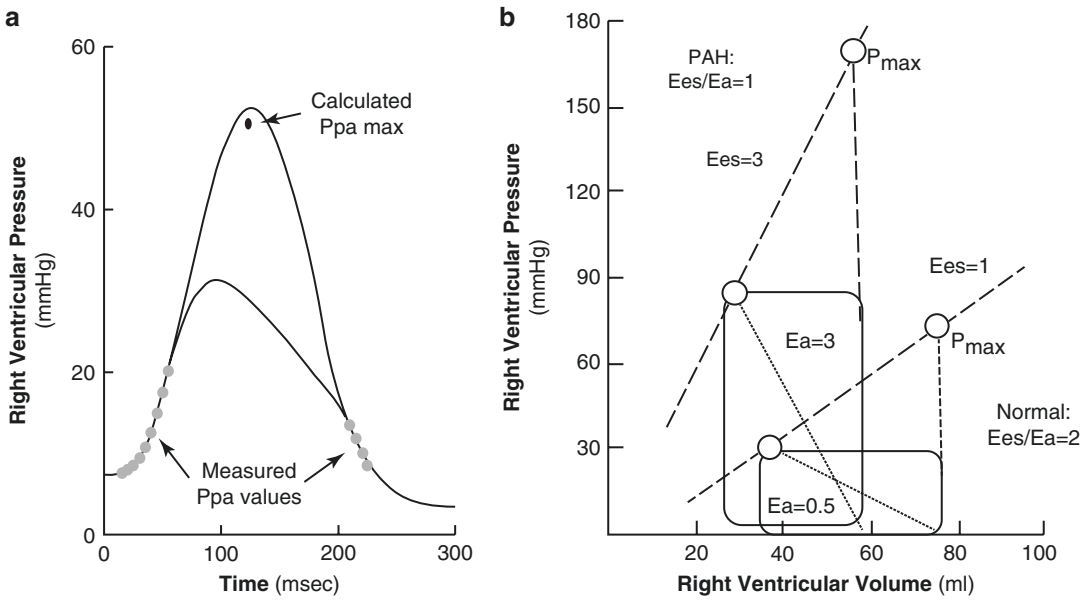

Fig. 5.3 The single-beat method for deriving right ventricular and arterial elastance and right ventricular–arterial coupling (*Ees* and *Ea*). (**a**) Calculation of P max (maximal isovolumic pulmonary arterial pressure) (**b**) Calculation of Ees and Ea for both a normal patient and one with pulmonary hypertension (*PAH*) using the single beat method. Reproduced with permission from [43]

hemodynamic changes. The force-rate relationship or Bowditch effect has been described both in vitro and in vivo and refers to the increase in contractile force as a result of increased heart rate. In vivo, however, at increased heart rate, the effect is counterbalanced by reduced diastole and implicitly by reduced ventricular filling [44].

Cardiac rhythm and contraction synchronicity are mechanisms that can influence ventricular performance, especially in the presence of RV dysfunction. In the case of acute myocardial infarction or chronic right ventricular failure, the onset of atrial fibrillation or atrioventricular block cause worsening of the clinical and hemodynamic picture [1]. Asynchronous contraction of RV may lead to decreased ventricular performance by suboptimal coordination of mechanical function. The importance of this mechanism has been demonstrated especially in pathological situations such as PH or CHD such as Tetralogy of Fallot [45, 46].

5.3.4 Regulatory Mechanisms of Right Ventricular Function

As in the case of the LV, the acute adjustments of RV function in response to haemodynamic changes are done through heart rate, Frank-Starling mechanism and neurovegetative system [1, 18, 19].

The RV displays an increased responsiveness to adrenergic drive than LV, with studies suggesting an intrinsic difference in miocitic intracellular signiling [47]. There is a difference in the response to sympathetic stimulation withing the RV as well, current data supporting an increased inotropic response of the infundibular compartiment in comparison with the inlet [48].

The RV function regulatory mechanisms, when in the physiologic range, are in general the consequences of changes in preload (for instance the increase in venous return with legs lift) and afterload (exercise) and rarely are the result of the direct action of different factors on inotropy [34].

In both the physiological and the pathological range, the RV has several mechanisms to adapt to pressure or volume overload. In acute pressure overload, three mechanisms potentially contribute to increased contractility such as the heterometric adaptation (Frank-Starling effect), homeometric adaptation (Anrep effect) and the neurohormonal induced inotropic changes (especialy the simpatetic nervous system) (Fig. 5.4). The Anrep effect represents the homeometric adaptation (without changes in cavitary dimen-

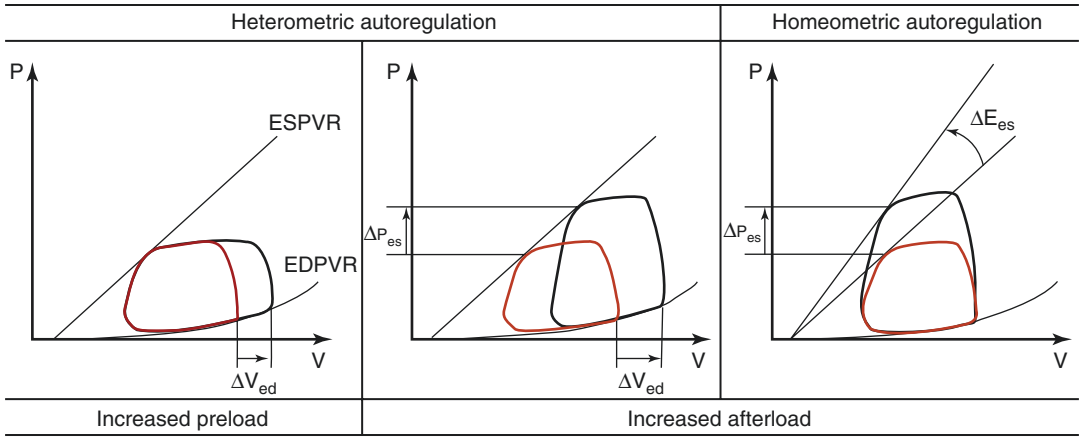

Fig. 5.4 Representation of heterometric and homeometric autoregulation of the right ventricle. *Left panel*—increased preload leads to an increase in SV by the same ΔV_{ed} through heterometric autoregulation. When afterload increases, both heterometric and homeometric responses are activated. In heterometric autoregulation (*center panel*), an increase in EDV (ΔV_{ed}) leads to an increase in pressure (ΔP_{es}) with no change in SV and inotropy. In homeometric autoregulation (*right panel*), a pressure increase (ΔP_{es}) to match increased afterload is achieved by increasing RV contractility (ΔE_{es}) with no change in SV and preload. The end-systolic pressure-volume relationship (ESPVR) line and the end-diastolic pressure-volume relationship (EDPVR) line define the limits of RV working conditions. *EDV* end diastolic volume, *EDPVR* end diastolic pressure volume relationship, *ESPVR* end diastolic pressure volume relationship, *SV* stroke volume. Reproduced with permission from [41]

sions) consisting in contractility increase in the absence of other external regulatory factors such as the intervention of the neurovegetative system. Even though its existence has been debated, there are evidences suggesting the Anrep effect is the first mechanism for initial adaptation to increased afterload [49–51]. The Frank-Starling mechanism or heterometric adaptation allows stroke volume preservation despite increased pressure load due to end-diastolic RV volume increase [34, 36]. Sympathetic tone increase and its inotropic effect can be induced through arterial hypotension and baroreceptor activation due to RV stroke volume reduction secondary to pressure overload or by primary myocardial catecholamine release [52]. Acute increase in volume overload is primarily accompanied by changes in RV end-diastolic volume and inotropic increase through Frank-Starling mechanism [53, 54].

The adaptative particularities of the RV are related to myocardial structure and oxygen demand as well. The RV is characterized by an increased resistence to ischemia resulting from multiple mechanisms: (1) Lower oxygen demand probably related to a lower mithocondrial density at the myofilament level [55], (2) higher oxygen extraction capacity than LV in the setting of haemodynamic stress [56] and (3) coronary circulation properties that allow myocardial perfusion both in systole and diastole along with an increased vasodilatatory response to adrenergic stimulation than LV [1, 57].

5.3.5 Ventriculo-Arterial Coupling

Right ventricular performance depends on the appropriate ventricular myocardial function, on LV function through interventricular interdependence, as well as on the efficient haemodynamic interaction with the pulmonary circulation [1, 41]. If in the past research, for instance in PH, was focused on studying either the RV function or the pulmonary circulation as separate entities, it has now become evident the importance of studying the cardiopulmonary system as a unit [18].

Interaction between RV and the pulmonary circulation has been studied both in physiologic as well as pathologic states through the concept of ventriculo-arterial coupling (VAC) [41]. In this view, the ventricle and the arterial system are seen as elastic chambers and their properties are described in the same measurement unit. The most frequently utilized model is the one where RV and pulmonary circulation characteristics are expressed in elastance [58]. Elastance (E) is defined as the change in pressure per volume unit and it can be evaluated through pressure-volume curves. Arterial elastance (Ea) can be measured on the pressure-volume curve by dividing pressure in the Emax point (maximum ventricular elastance) by SV [41] (Fig. 5.3).

The load independency of indices of ventricular function or contractility referes to the immediate 'beat-by-beat' independency as contractility or Emax adapts to afterload after several beats. This reflects the homeometric adaptation (starting after 30 s) replacing the initial heterometric adaptation. Therefore, the interest of measuring Ea is that it corresponds to the hidraulic load faced by the right ventricle and allows the correction of Emax for afterload. Moreover, they can be measured on the same pressure-volume loop [42].

In an electrical or mechanical system, power transmission is done with maximal efficiency when the impedance emitted by the power producing system is equal to the impedance received by the power receiving system [18, 59]. Therefore, as elastance is closely related to impedance, it is probable that the maximal power transmission from the ventricle to the vascular system is achieved when Emax is equal to Ea. However, in the human pulmonary circulatory system, where the mechanical properties vary with time, current data suggests that maximal efficiency is obtained at a ratio of Emax/Ea of approximately 1.5–2 [60, 61].

In the right heart circulation, in normal haemodynamic conditions, the RV performs at maximal efficiency and submaximal mechanical work. If the RV becomes dysfunctional, E max and Emax/Ea decreases indicated inappropriate coupling and decreased myocardial efficiency. In the case of inappropriate afterload increase such as in PH, VAC is initialy maintained through RV contractility increase whereas in the later disease stages, the association between ventricular dysfunction and arterial pressure increase leads to an important ventriculo-arterial mistmach [38].

Conclusion

The right ventricle, once the forgotten chamber, has now been recognized as an important determinant of cardiovascular function in both health and disease. It has a complex three dimensional shape and contracts in a sequential pattern from the inlet to the outlet part. The RV systolic performance is highly influenced by preload and afterload and adaptation to changes in filling condition are done mainly through heterometric autoregulation. However, RV diastolic and systolic function can be described by a time varying elastance.

Right ventricular performance depends on the appropriate ventricular myocardial function as well as on the efficient haemodynamic interaction with the pulmonary circulation, assessment of ventriculo-arterial coupling being possible through the concept of elastance.

References

1. Haddad F, Hunt SA, Rosenthal DN, Murphy DJ. Right ventricular function in cardiovascular disease, part I anatomy, physiology, aging, and functional assessment of the right ventricle. Circulation. 2008;117(11):1436.
2. Starr I, Jeffers WA, Meade RH. The absence of conspicuous increments of venous pressure after severe damage to the right ventricle of the dog, with a discussion of the relation between clinical congestive failure and heart disease. Am Heart J. 1943;26(3):291.
3. Kagan A. Dynamic responses of the right ventricle following extensive damage by cauterization. Circulation. 1952;5(6):816.
4. Voelkel NF, Quaife RA, Leinwand LA, Barst RJ, McGoon MD, Meldrum DR, et al. Right ventricular function and failure report of a national heart, lung, and blood institute working group on cellular and molecular mechanisms of right heart failure. Circulation. 2006;114(17):1883.
5. Bakos AC. The question of the function of the right ventricular myocardium: an experimental study. Circulation. 1950;1(4):724.
6. Cohn JN, Guiha NH, Broder MI, Limas CJ. Right ventricular infarction: clinical and hemodynamic features. Am J Cardiol. 1974;33(2):209.
7. Kinch JW, Ryan TJ. Right ventricular infarction. N Engl J Med. 1994;330(17):1211.
8. Jurcut R, Giusca S, La Gerche A, Vasile S, Ginghina C, Voigt J-U. The echocardiographic assessment of the right ventricle: what to do in 2010? Eur Heart J Cardiovasc Imaging. 2010;11(2):81.
9. Chin KM, Kim NH, Rubin LJ. The right ventricle in pulmonary hypertension. Coron Artery Dis. 2005; 16(1):13.
10. Davlouros P, Niwa K, Webb G, Gatzoulis M. The right ventricle in congenital heart disease. Heart. 2006; 92(Suppl 1):i27.
11. Norozi K, Wessel A, Alpers V, Arnhold JO, Geyer S, Zoege M, et al. Incidence and risk distribution of heart failure in adolescents and adults with congenital heart disease after cardiac surgery. Am J Cardiol. 2006;97(8):1238.
12. Bartelds B, Borgdorff MA, Berger RM. Right ventricular adaptation in congenital heart diseases. J Cardiovasc Dev Dis. 2014;1(1):83.
13. Haddad F, Couture P, Tousignant C, Denault AY. The right ventricle in cardiac surgery, a perioperative perspective: I. Anatomy, physiology, and assessment. Anesth Analg. 2009;108(2):407.
14. Ho S, Nihoyannopoulos P. Anatomy, echocardiography, and normal right ventricular dimensions. Heart. 2006;92(Suppl 1):i2.
15. Armour J, Pace J, Randall W. Interrelationship of architecture and function of the right ventricle. Am J Physiol. 2017;218:174.
16. Geva T, Powell AJ, Crawford EC, Chung T, Colan SD. Evaluation of regional differences in right ventricular systolic function by acoustic quantification echocardiography and cine magnetic resonance imaging. Circulation. 1998;98(4):339.
17. Ginghina C. Mic tratat de cardiologie. Romania: Editura Academiei Romane; 2010.
18. Greyson CR. The right ventricle and pulmonary circulation: basic concepts. Rev Esp Cardiol. 2010; 63(1):81.
19. Dell'Italia LJ. The right ventricle: anatomy, physiology, and clinical importance. Curr Probl Cardiol. 1991;16(10):653.
20. Dell'Italia LJ. Anatomy and physiology of the right ventricle. Cardiol Clin. 2012;30(2):167.
21. Carmen G, Marinescu M, Dragomir D. Indreptar de diagnostic si tratament in infarctul miocardic acut. In: Ginghina C, editor. Indreptar de diagnostic si tratament in infarctul miocardic acut. Bucureşti: InfoMedica; 2002. p. 15.
22. Giusca S, Jurcut R, Ginghina C, Voigt J-U. The right ventricle: anatomy, physiology and functional assessment. Acta Cardiol. 2010;65(1):67.
23. Meier GD, Bove AA, Santamore WP, Lynch PR. Contractile function in canine right ventricle. Am J Physiol Heart Circ Physiol. 1980;239:H794.
24. Henein M, Lam Y-Y, Waldenström A, Henein MY. Atrial interaction in the form of 'cross talk' in patients with ventricular outflow tract obstruction. Int J Cardiol. 2011; 147(3):388.
25. Kukulski T, Hübbert L, Arnold M, Wranne B, Hatle L, Sutherland GR. Normal regional right ventricular function and its change with age: a Doppler myocardial imaging study. J Am Soc Echocardiogr. 2000; 13(3):194.
26. Leather HA, Missant C, Rex S, Rademakers FE, Wouters PF. Longitudinal but not circumferential deformation reflects global contractile function in the right ventricle with open pericardium. Am J Phys Heart Circ Phys. 2006;290(6):H2369.

27. Santamore WP, Dell'Italia LJ. Ventricular interdependence: significant left ventricular contributions to right ventricular systolic function. Prog Cardiovasc Dis. 1998;40(4):289.
28. Feneley MP, Gavaghan TP, Baron DW, Branson JA, Roy P, Morgan J. Contribution of left ventricular contraction to the generation of right ventricular systolic pressure in the human heart. Circulation. 1985;71(3):473.
29. Buckberg GD. The ventricular septum: the lion of right ventricular function, and its impact on right ventricular restoration. Eur J Cardiothorac Surg. 2006;29(Suppl 1):S272.
30. Hoffman D, Sisto D, Frater RW, Nikolic SD. Left-to-right ventricular interaction with a noncontracting right ventricle. J Thorac Cardiovasc Surg. 1994; 107(6):1496.
31. Mann DL, Zipes DP, Libby P, Bonow RO. Braunwald's heart disease: a textbook of cardiovascular medicine. Philadelphia: Elsevier Health Sciences; 2014.
32. Jacob R, Dierberger B, Kissling G. Functional significance of the Frank-Starling mechanism under physiological and pathophysiological conditions. Eur Heart J. 1992;13:7.
33. Moss RL, Fitzsimons DP. Frank-Starling relationship: long on importance, short on mechanism. Circ Res. 2002;90(1):11.
34. Trip P, Westerhof N, Noordegraaf A. Function of the right ventricle. In: Gaine SP, Naeije R, Peacock AJ, editors. The right heart. London: Springer; 2014. p. 9.
35. Starling MR, Walsh RA, Dell'Italia LJ, Mancini GB, Lasher JC, Lancaster JL. The relationship of various measures of end-systole to left ventricular maximum time-varying elastance in man. Circulation. 1987; 76(1):32.
36. Naeije R, Brimioulle S, Dewachter L. Biomechanics of the right ventricle in health and disease (2013 Grover Conference series). Pulm Circ. 2014;4(3):395.
37. Dell'italia LJ, Walsh RA. Application of a time varying elastance model to right ventricular performance in man. Cardiovasc Res. 1988;22(12):864.
38. Sanz J, Garcia-Alvarez A, Fernandez-Friera L, Nair A, Mirelis JG, Sawit ST, et al. Right ventriculo-arterial coupling in pulmonary hypertension: a magnetic resonance study. Heart. 2012;98(3):238.
39. Herberg U, Linden K, Dewald O, Gatzweiler E, Seehase M, Duerr GD, et al. 3D real-time echocardiography combined with mini pressure wire generate reliable pressure-volume loops in small hearts. PLoS One. 2016;11(10):e0165397.
40. Brimioulle S, Wauthy P, Ewalenko P, Rondelet B, Vermeulen F, Kerbaul F, et al. Single-beat estimation of right ventricular end-systolic pressure-volume relationship. Am J Physiol Heart Circ Physiol. 2003; 284(5):H1625.
41. Bellofiore A, Chesler NC. Methods for measuring right ventricular function and hemodynamic coupling with the pulmonary vasculature. Ann Biomed Eng. 2013;41(7):1384.
42. Naeije R, Manes A. The right ventricle in pulmonary arterial hypertension. Eur Respir Rev. 2014; 23(134):476.
43. Pinsky MR. The right ventricle: interaction with the pulmonary circulation. Crit Care. 2016;20:266.
44. Barry WH. Heart physiology from cell to circulation, 4th ed. Circulation. 2004;110(12):e313.
45. Badagliacca R, Poscia R, Pezzuto B, Papa S, Gambardella C, Francone M, et al. Right ventricular dyssynchrony in idiopathic pulmonary arterial hypertension: determinants and impact on pump function. J Heart Lung Transplant. 2015;34(3):381.
46. Hui W, Slorach C, Dragulescu A, Mertens L, Bijnens B, Friedberg MK. Mechanisms of right ventricular electromechanical dyssynchrony and mechanical inefficiency in children after repair of tetralogy of fallot. Circ Cardiovasc Imaging. 2014;7(4):610.
47. Molina CE, Johnson DM, Mehel H, Spatjens RL, Mika D, Algalarrondo V, et al. Interventricular differences in beta-adrenergic responses in the canine heart: role of phosphodiesterases. J Am Heart Assoc. 2014;3(3):e000858.
48. Heerdt PM, Pleimann BE. The dose-dependent effects of halothane on right ventricular contraction pattern and regional inotropy in swine. Anesth Analg. 1996;82(6):1152.
49. von Anrep G. On the part played by the suprarenals in the normal vascular reactions of the body. J Physiol. 1912;45(5):307.
50. Cingolani HE, Pérez NG, Cingolani OH, Ennis IL. The Anrep effect: 100 years later. Am J Physiol Heart Circ Physiol. 2013;304:H175.
51. Taquini AC, Fermoso JD, Aramendia P. Behavior of the right ventricle following acute constriction of the pulmonary artery. Circ Res. 1960;8:315.
52. Hon JK, Steendijk P, Khan H, Wong K, Yacoub M. Acute effects of pulmonary artery banding in sheep on right ventricle pressure-volume relations: relevance to the arterial switch operation. Acta Physiol Scand. 2001;172(2):97.
53. Hon JK, Steendijk P, Khan H, Wong K, Yacoub M. Acute effects of pulmonary artery banding in sheep on right ventricle pressure-volume relations: relevance to the arterial switch operation. Acta Physiol Scand.
54. Kjaergaard J, Snyder EM, Hassager C, JK O, Johnson BD. Impact of preload and afterload on global and regional right ventricular function and pressure: a quantitative echocardiography study. J Am Soc Echocardiogr. 2006;19(5):515.
55. Singh S, White FC, Bloor CM. Myocardial morphometric characteristics in swine. Circ Res. 1981;49(2):434.
56. Takeda K, Haraoka S, Nagashima H. Myocardial oxygen metabolism of the right ventricle with volume loading and hypoperfusion. Jpn Circ J. 1987;51(5):563.
57. Saito D, Yamada N, Kusachi S, Tani H, Shimizu A, Hina K, et al. Coronary flow reserve and oxygen metabolism of the right ventricle. Jpn Circ J. 1989;| 53(10):1310.
58. Sunagawa K, Maughan WL, Burkhoff D, Sagawa K. Left ventricular interaction with arterial load studied in isolated canine ventricle. Am J Phys Heart Circ Phys. 1983;245(5):H773.

59. Burkhoff D, Sagawa K. Ventricular efficiency predicted by an analytical model. Am J Phys Regul Integr Comp Phys. 1986;250(6):R1021.
60. Champion HC, Michelakis ED, Hassoun PM. Comprehensive invasive and noninvasive approach to the right ventricle–pulmonary circulation unit state of the art and clinical and research implications. Circulation. 2009;120(11):992.
61. Brimioulle S, Wauthy P, Ewalenko P, Bt R, Vermeulen F, Kerbaul F, et al. Single-beat estimation of right ventricular end-systolic pressure-volume relationship. Am J Phys Heart Circ Phys. 2003;284(5):H1625.

Effect of Endurance Sport on the Right Heart

6

Antonis S. Manolis and Antonis A. Manolis

Abstract

The right ventricle (RV) responds differently to prolonged exhaustive and competitive exercise, usually with enlargement, than does the left ventricle. Evidence has accumulated indicating that regular intense endurance exercise and sporting can promote electrical and structural remodeling of the RV, leading to fibrosis. This "exercise-induced cardiomyopathy" mimics features observed in arrhythmogenic right ventricular dysplasia/cardiomyopathy (ARVD/C). In addition, exercise-induced impairment in atrial function (atrial remodeling), mostly in the right atrium related to RV systolic dysfunction, has also been suggested which favors the development of atrial arrhythmias. It should be noted that these adverse effects seem to be limited to extreme intensity levels of exercise and not related to recreational or moderate exercise levels. These deleterious effects of heavy endurance exercise on the right heart can be studied by several methods, including standard and newer echocardiographic techniques, stress testing methods, standard ECG, cardiac magnetic resonance imaging, biomarkers, electroanatomical mapping and/or an electrophysiology study, and in specific cases by genetic testing. All these issues are reviewed in this chapter.

Keywords

Exercise · Endurance sport · Right heart · Right ventricle · Cardiac arrhythmias · Sudden death · Arrhythmogenic right ventricular cardiomyopathy/dysplasia · Echocardiography · Electrocardiography · Cardiac magnetic resonance imaging

Abbreviations

AF	Atrial fibrillation
ARVD/C	Arrhythmogenic right ventricular dysplasia/cardiomyopathy
CMR	Cardiac magnetic resonance imaging
ECG	Electrocardiogram
RBBB	Right bundle branch block
RV	Right ventric-le (-ular)

6.1 Introduction

It has been suggested since over 25 years ago that the right ventricle (RV) responds differently to prolonged competitive exercise, usually with enlargement, than does the left ventricle

A. S. Manolis (✉)
Third Department of Cardiology, Athens University School of Medicine, Athens, Greece
e-mail: asm@otenet.gr

A. A. Manolis
Patras University School of Medicine, Patras, Greece

S. I. Dumitrescu et al. (eds.), *Right Heart Pathology*, https://doi.org/10.1007/978-3-319-73764-5_6

Table 6.1 Endurance sports with high intensity dynamic and/or static exercise component (partial list) [48]

• Distance cycling
• Distance running (marathon)
• Distance track and field
• Distance swimming
• Triathlon
• Cross-country skiing
• Boxing
• Rowing
• Canoeing

[1]. Since then, accumulating evidence suggests that regular intense endurance exercise and sporting can promote structural and electrical changes or remodeling of the RV, culminating in fibrosis, mimicking features which are observed in arrhythmogenic right ventricular dysplasia/cardiomyopathy (ARVD/C) [2, 3]. This "exercise-induced cardiomyopathy" relates to adaptive remodeling of the heart during exercise, with the heaviest toll falling on the RV, which may become pro-arrhythmic [4, 5]. Furthermore, exercise-induced impairment in atrial function, mostly in the right atrium related to RV systolic dysfunction, has also been suggested and this atrial remodeling may favor the development of atrial arrhythmias [6]. However, these adverse effects seem to be limited to extreme intensity levels of exercise (Table 6.1) and not related to recreational or moderate exercise levels. It appears that the RV is most vulnerable during extreme exercise, as the RV wall stress at peak exercise in athletes may increase by 170% compared with only a 23% increase in left ventricular wall stress. [7] Thus, intense endurance exercise causes acute dysfunction of the RV, but not of the left ventricle. Repetitive insults of the RV sustained by endurance sports may lead to chronic RV dysfunction and arrhythmogenesis, particularly in individuals who may unknowingly be carriers of desmosomal or other elusive mutations [8].

The adverse effects of extreme compared to moderate exercise were recently shown in an experimental long-term endurance training rat model, in which the investigators assessed the relationship between RV remodeling and exercise load [9]. They showed a biphasic, unbalanced RV remodeling response with increasing doses of exercise. A physiological adaptation after moderate training turned adverse and maladaptive with intensive training, leading to disproportionate RV dilatation, decreased contractility and impaired diastolic function.

Table 6.2 Assessment of the right heart in intense endurance athletes or athletes presenting with arrhythmias

Echocardiography
Standard techniques
Newer techniques (e.g. speckle tracking and strain imaging/exercise strain imaging/3D echo)
ECG
Holter monitor
CMR with gadolinium enhancement
Stress testing (ETT/Exercise echo/exercise CMR)
Biomarkers (cTn/BNP)
Electroanatomical mapping
Electrophysiology study
Genetic testing

BNP brain natriuretic peptide, *CMR* cardiac magnetic resonance imaging, *cTn* cardiac troponin, *ECG* electrocardiogram, *ETT* exercise tolerance test

There are several tools that may be used for assessing the right heart in intense endurance athletes or athletes presenting with arrhythmias, which will be herein briefly reviewed (Table 6.2).

6.2 Echocardiography

Echocardiography, a widely available imaging technique, can provide useful data in the field of sports cardiology particularly for pre-participation screening and also and importantly for analysis of the cardiac adaptation induced by exercise [10]. RV dimensions, as measured by echocardiography, are larger in endurance athletes than those described by "normal ranges" and frequently meet the major criteria for the diagnosis of ARVD/C [11]. However, functional assessment of RV strain has been proposed to aid in this differential diagnosis [12]. Ambiguous resting measures in endurance athletes could be clarified by exercise strain rate imaging [13]. Examining the influence of high-intensity endurance exercise on global ventricular tissue deformation (strain) may be able to discern whether exercise-induced functional cardiac disturbances are global or segmental.

A recent echocardiographic study showed that changes in ventricular strain following high-intensity exercise were more profound in the RV than in the left ventricle, as expected; however, reductions in left ventricular strain were unique to the septal myocardium and may reflect ventricular interactions secondary to exercise-induced RV dysfunction [14].

The physiological adaptation of the RV in response to endurance training was also investigated in 63 elite athletes, 58 athletes, and 61 healthy controls with conventional echocardiography, tissue Doppler imaging, and 2D strain echo [15]. Left ventricular and RV dimensions were significantly increased in both groups of athletes compared with controls, while RV systolic velocities and displacement were not different between the groups. RV strain and strain rate values were reduced in the RV basal and mid-segment in athletes. Athletes with marked RV dilatation showed lower strain and strain rate values in the basal and mid segment, whereas athletes without RV dilatation showed no significant difference compared with the controls. The authors concluded that reduced regional deformation and deformation rates in the basal RV segment in athletes, most pronounced in athletes with RV dilatation, represent normal adaptation to exercise.

Thus, as regular physical exercise induces mild left ventricular hypertrophy which can be considered an adaptive consequence to exercise, [16] similarly, an *increase of RV dimensions without RV dysfunction* induced by endurance training may be considered a physiologic adaptation and expression of the athlete's heart [17, 18]. However, extreme exercise can confer some deleterious effects, mostly affecting the RV [4]. A meta-analysis of 14 studies, comprising 329 healthy adult participants, and reporting RV function pre-endurance and post-endurance exercise, indicated that intense prolonged exercise is associated with a measurable reduction in RV function while LV function is relatively unaffected [19].

An acute RV impairment has been demonstrated after a trail-running race, related to the amount of exercise, albeit with a high inter-individual variability [20]. More advanced right heart (RV and right atrial) morphological and functional remodeling has been detected by speckle-tracking echocardiography induced by strenuous and chronic exercise training during ultra-trail (mountain) running compared to conventional marathon running [21]. Long-term endurance training may induce bi-ventricular remodeling, which is similar in males and females [22]. However, males may have larger RV size and lower bi-ventricular deformation.

Although different types of extreme sports (Table 6.1) involve different types of stress, and may have distinct influences on left ventricular volume and mass parameters, it appears that they may induce similar degrees of RV dilation [23].

Even in athletes with apparently normal cardiac function at rest, who have ventricular arrhythmias, echocardiographic and cardiac magnetic resonance (CMR) imaging measures of RV function performed during exercise may detect RV dysfunction during exercise separating them from healthy individuals [24].

In addition to RV dysfunction, right atrial function impairment may also be induced by extreme exercise. According to an echocardiography study performed in 55 healthy adults at baseline and after a 3-stage trail race, an acute exercise-dose dependent impairment in atrial function was observed, which was related to RV systolic dysfunction. The authors concluded that the impact on atrial function of long-term endurance training might lead to atrial remodeling, favoring atrial arrhythmia development [6].

6.3 Surface Electrocardiogram (ECG)

As already detailed, prolonged high-intensity exercise has been reported to exert a profound effect on cardiac function, particularly on the right heart which appears to be more susceptible to this deleterious effect [25]. A recent study examined the ECG changes in the right-sided leads in 30 highly trained athletes induced by a 100-mile endurance run [25]. Pre- to post-race, a significant increase in P wave amplitude

(29%) and QTc interval (4%) could be detected on a standard 12-lead ECG. Also, a 23% (P = 0.01) and 38% (P = 0.03) increase in J point amplitude in V1R and V2R and a 22% (P = 0.05) increase in ST segment integral in V2R and V3R were evident. T wave inversion was evident in leads V2R-V6R in 50–90% of athletes. Close examination revealed marked heterogeneity in individual ECGs. The authors concluded that completion of a 100-mile ultramarathon resulted in significant changes in the right-sided ECG alongside more marked responses in specific individuals. P wave, ST segment and T wave changes post-race were considered indicative of acute exercise-induced right heart electrical adaptation.

The ECG plays a significant role in the differentiation between physiological adaptations to endurance exercise and underlying RV pathology such as ARVD/C [26–30]. In Caucasian endurance athletes, T-wave inversion in the right precordial leads is relatively common, however, as this ECG sign also characterizes ARVD/C, it should prompt extensive evaluation for ARVD/C. In black athletes, convex ST-segment elevation with biphasic T-wave inversion in leads V1–V4 is a common benign finding, but if symmetrical anterior T-wave inversion in V1–V3 is preceded by isoelectric or downsloping ST segments, it should lead to further investigation to rule out ARVD/C. Also, symptoms of palpitations or presyncope or syncope in athletes with even minor diagnostic ECG-findings should prompt extensive evaluation including echocardiography, Holter monitoring, maximal exercise-ECG testing and possibly a CMR and an electrophysiology study. Similarly, voltage ECG signs of RV hypertrophy and right axis deviation and/or deep right precordial T wave inversion defines abnormal RV afterload and should trigger further evaluation [27].

Thus, physiological cardiac adaptation to regular exercise may include biventricular dilation and T-wave inversion, which may create diagnostic overlap with ARVD/C. A study compared athletes with T-wave inversion (n = 45), athletes without T-wave inversion (n = 35), and ARVD/C patients (n = 35) [30]. There were no electrical, structural, or functional cardiac differences between athletes with or without T-wave inversion. Compared with ARVD/C patients, markers of physiological remodeling or nonspecific parameters, and indicators of RV pathology could be identified (Table 6.3).

Table 6.3 Classification of ECG and other findings in athletes

Markers of physiological remodeling
• Early repolarization
• Biphasic T-wave inversion
• Voltage criteria for RVH or LVH
• Symmetrical cardiac enlargement
• RBBB (incomplete or complete)
Nonspecific findings
• Prolonged QRS terminal activation
• ≤2 abnormal signal averaged ECG parameters
• RV dilation without wall motion abnormalities
• RV outflow tract ectopy
• Exercise-induced T-wave pseudo-normalization
Indicators of RV pathology
• Symmetrical anterior T-wave inversion in $V_{1–3}$ preceded by isoelectric or down-sloping ST segment
• RVH and right axis deviation and/or deep right precordial T wave inversion
• Q waves or precordial QRS amplitudes <1.8 mV
• 3 abnormal signal averaged ECG parameters
• Delayed gadolinium enhancement
• RV ejection fraction ≤45%, or wall motion abnormalities at CMR
• >1000 PVCs (or >500 non-RV outflow tract PVCs) per 24 h on Holter monitor
• Syncope
• Symptoms, ventricular tachyarrhythmias, or attenuated blood pressure response during exercise

CMR cardiac magnetic resonance (imaging), *LVH* left ventricular hypertrophy, *PVC* premature ventricular contraction, *RBBB* right bundle branch block, *RV* right ventricle, *RVH* right ventricular hypertrophy

Another study analyzed ECGs in competitive rowers (n = 330, 56% male) [31]. The majority (94%) of rowers had one or more training-related ECG patterns including sinus bradycardia (51%), sinus arrhythmia (55%), and incomplete right bundle branch block (RBBB) (42%). Males were more likely than females to have isolated voltage criteria for left ventricular hypertrophy (51% vs 8%, $p < 0.001$) and early repolarization pattern (76% vs 23%, $p < 0.001$). The authors concluded that training-related ECG patterns with several

gender-based differences are common among competitive rowers.

The 12-lead ECG and echocardiographic data from 510 competitive athletes were analyzed and compared to 51 age-, sport type-, and gender-matched athletes with normal QRS duration [32]. The 44 athletes with incomplete RBBB (9%) and 13 with complete RBBB (3%) had larger RV dimensions. Athletes with complete RBBB also had a relative reduction in the RV systolic function at rest. QRS prolongation was associated with parallel increases in interventricular dyssynchrony. Despite these findings, no athlete with RBBB was found to have pathologic structural cardiac disease. The authors concluded that among trained athletes, complete or incomplete RBBB appear to be markers of a structural and physiological cardiac remodeling triad characterized by RV dilation, a relative reduction in the RV systolic function at rest, and interventricular dyssynchrony.

6.4 Cardiac Magnetic Resonance (CMR)

Cardiac magnetic resonance imaging (CMR) performed pre- and post-exercise demonstrated biventricular systolic and diastolic dysfunction occurring after 14 min of high-intensity exercise in endurance trained athletes, a phenomenon not observed in normally active individuals [33].

Myocardial fibrosis detected by CMR has been reported in athletes, predominantly identified in the intraventricular septum and where the RV joins the septum [34]. The underlying mechanisms remain unknown, although some studies have suggested that there may be evidence for genetic predisposition, silent myocarditis, pulmonary artery pressure overload, and prolonged exercise-induced repetitive microinjury as contributors.

Contrariwise, according to a recent study examining the cardiac structure and function in 33 long-term elite master endurance athletes (age range, 30–60 years) with special focus on the RV by contrast-enhanced CMR, RV ejection fraction did not differ between athletes and control subjects (n = 33) [35]. Pathological late gadolinium enhancement on CMR was detected only in one athlete. The authors concluded that based on their results, chronic RV damage in elite endurance master athletes with lifelong high training volumes seems to be unlikely, and suggest that the hypothesis of an exercise-induced ARVD/C has to be questioned.

A study performing CMR imaging in community-based participants without clinical cardiovascular disease, demonstrated that higher levels of physical activity in adults were associated with greater RV mass and volumes (exercise-associated RV remodeling) independent of the associations with LV mass [36].

RV enlargement, detected by echo, almost always occurs in presence of LV enlargement in athletes. When isolated RV enlargement is present, underlying disease should be suspected. CMR may be particularly helpful to image morphologic RV changes and differentiate between athlete's heart and ARVD/C [37]. High-spatial resolution imaging with CMR can provide accurate quantification of RV volumes and function while reliably identifying RV focal wall motion abnormalities, which support a diagnosis of ARVD/C. In addition, CMR can identify fatty infiltration of the RV via tissue characterization, and although imaging of fat is currently not one of the criteria for diagnosis, its presence can be helpful. Finally, late gadolinium enhancement of the RV free wall can be seen in ARVD/C, a finding not encountered in athlete's heart. Thus, CMR should now be regarded as an integral part of the contemporary assessment of athletes in whom a suspicion of structural heart disease is entertained.

6.5 Biomarkers

According to a systematic review and metaanalysis (45 studies) of biomarker and cardiovascular imaging changes after endurance exercise, across all studies, cardiac troponin T (cTnT) exceeded the cutoff value (0.01 ng/mL) in 51% of participants [38]. The measured pooled changes from baseline for high-sensitivity cTnT (hs-cTnT)

were +26 ng/L, for cTnI +40 ng/L, for BNP +10 ng/L, for NT-proBNP +67 ng/L, and for d-dimer +262 ng/mL. Right ventricular end diastolic diameter increased and RV ejection fraction as well as the ratio of the early to late transmitral flow velocities decreased after exercise, while no significant changes were observed in left ventricular ejection fraction. The authors concluded that cardiovascular biomarkers (cTnT, hs-cTnT, BNP, NT-proBNP, and d-dimer) that are used in clinical diagnosis of pulmonary embolism, acute coronary syndrome, and heart failure are prone to alterations due to strenuous exercise, with the major toll falling on the RV. Nevertheless, other investigators have asserted that exercise-induced cardiac troponin release is not a marker of exercise-induced pathology but likely a physiologic response to exercise [39].

A study conducted in 40 well-trained endurance athletes by measuring cytokines, cardiac troponin and BNP and performing echocardiography prior to and immediately following one of four endurance sporting events ranging from 3 to 11 h duration, demonstrated cardiac, mainly RV, dysfunction following intense endurance exercise to be associated with increased expression of pro-inflammatory cytokines [40].

According to a study which screened 60 non-elite participants before and after the 2004 and 2005 Boston Marathons, with echocardiography and serum biomarkers (cardiac troponin T and N-terminal pro-brain natriuretic peptide), completion of the marathon was associated with correlative biochemical and echocardiographic evidence of RV dysfunction and injury, and this risk was increased in those participants with less training [41].

6.6 Electroanatomical Mapping

In competitive athletes presenting with recent-onset ventricular arrhythmias and an apparently normal heart, electroanatomical mapping has been suggested that it may diagnose concealed myocardial diseases, such as ARVD/C [42]. Electroanatomical mapping during catheter ablation of ventricular tachycardia (VT) in athletes has also suggested a new clinical entity of an isolated anterior subepicardial RV outflow tract scar serving as a substrate for fast VT in high-level endurance athletes that can be successfully treated by ablation [43]. This scar pattern may allow distinguishing exercise-induced arrhythmogenic remodeling from ARVD/C and post-inflammatory cardiomyopathy, whereby scars involve the subtricuspid RV area.

6.7 RV Arrhythmogenesis

Whether intense and sustained exercise can induce an RV cardiomyopathy similar to heritable ARVD/C [2] or it facilitates the clinical unveiling of latent ARVD/C in desmosomal carriers [8] has not been definitely demonstrated. In either case, extreme exercise may confer deleterious cardiac effects in certain elite endurance athletes and this needs to be considered when evaluating these individuals, whereby exercise restriction may need to be recommended in order to mitigate the arrhythmogenic risk and protect them from sudden cardiac death; in symptomatic patients, implantation of an implantable cardioverter defibrillator may need to be considered. Such a recommendation can be certainly facilitated by performance of clinical *genetic testing* for ARVD/C in selected athletes, who may be clinically unaffected mutation carriers, particularly when they come from families with a proband diagnosed with ARVD/C [8, 44].

According to a study involving 46 high-level endurance athletes with ventricular arrhythmias, RV arrhythmogenic involvement was manifest in 59% of the athletes, and suggestive in another 30% [2]. The authors concluded that complex ventricular arrhythmias do not necessarily represent a benign finding in endurance athletes. An *electrophysiology study* with programmed electrical stimulation is indicated for risk evaluation, both by defining inducibility and identifying the arrhythmogenic mechanism, and finally guiding therapy.

Other investigators have examined the disproportionate role of exercise in the pathogenesis of ARVD/C in patients without desmosomal

(gene-elusive) mutations [45]. They studied 82 ARVD/C patients (39 desmosomal) by interviewing them about regular physical activity from age 10. All gene-elusive patients were endurance athletes. Family history was less prevalent among gene-elusive patients (9% vs 40% desmosomal, $P < 0.001$), suggesting a greater environmental influence. Gene-elusive patients who had done the most intense exercise prior to presentation had a younger age of presentation ($P = 0.025$), greater likelihood of meeting ARVD/C diagnostic criteria (100% vs 43%, $P = 0.02$), and shorter survival free from a ventricular arrhythmia at follow-up ($P = 0.002$). The authors concluded that gene-elusive, non-familial ARVD/C is associated with very high intensity exercise suggesting exercise has a disproportionate role in the pathogenesis of these cases.

As already alluded to, in athletes with arrhythmias, some investigators [24] have promoted the use of exercise echocardiographic and CMR imaging to measure the RV function during exercise in order to identify athletes with subtle RV dysfunction which only becomes apparent under the hemodynamic stress of exercise, and thus discern from the healthy ones the very small group of athletes who are at greater risk of serious arrhythmias.

In view of ARVD/C being one important cause of sudden cardiac death in ~4–13% among athletes, [46] findings of RV remodeling in an athlete create a diagnostic dilemma. In the endurance athlete, the RV outflow tract may be dilated compared to healthy controls, however, the RV inflow appears to be dilated to a greater degree, albeit without an impairment of RV function [47]. In contrast, it is predominantly the RV outflow that is enlarged in ARVD/C, also combined with RV dysfunction. As already mentioned, strain and/or exercise imaging can aid in the differential diagnosis, as well; the lower RV global strain values found in elite endurance athletes are due to a reduction in basal function, suggesting that global RV strain is likely to be a useful indicator of physiological adaptation, as well as an enhanced contractile reserve of the basal RV segment during exercise [13, 15]. Thus, the presence of RV inflow dilatation, normal RV function during exercise and the lack of RV outflow aneurysm(s) or diverticuli are consistent with physiological adaptation [47].

Conclusion

Regular intense endurance exercise can promote structural and electrical changes or remodeling of the RV, mimicking features which are observed in ARVD/C. Exercise-induced impairment in right atrial function has also been suggested and this atrial remodeling may favor the development of atrial arrhythmias. These deleterious effects of heavy endurance exercise on the right heart can be studied by several methods, including standard and newer echocardiographic techniques, stress testing methods, standard ECG, CMR, biomarkers, electroanatomical mapping and/or an electrophysiology study, and in specific cases by genetic testing. Thus, assessment of the right heart and its arrhythmogenic potential should constitute an integral component of risk assessment in intense and prolonged endurance athletes or in athletes presenting with arrhythmias.

Conflict of Interest None declared.

References

1. Douglas PS, O'Toole ML, Hiller WD, et al. Different effects of prolonged exercise on the right and left ventricles. J Am Coll Cardiol. 1990;15:64–9.
2. Heidbuchel H, Hoogsteen J, Fagard R, et al. High prevalence of right ventricular involvement in endurance athletes with ventricular arrhythmias. Role of an electrophysiologic study in risk stratification. Eur Heart J. 2003;24:1473–80.
3. O'Keefe JH, Patil HR, Lavie CJ, et al. Potential adverse cardiovascular effects from excessive endurance exercise. Mayo Clin Proc. 2012;87:587–95.
4. D'Andrea A, Morello A, Iacono AM, et al. Right ventricular changes in highly trained athletes: between physiology and pathophysiology. J Cardiovasc Echogr. 2015;25:97–102.
5. Manolis AS, Manolis AA. Exercise and arrhythmias: a double-edged sword. Pacing Clin Electrophysiol. 2016;39:748–62.
6. Sanz-de la Garza M, Grazioli G, Bijnens BH, et al. Acute, exercise dose-dependent impairment in atrial performance during an endurance race: 2d ultrasound speckle-tracking strain analysis. JACC Cardiovasc Imaging. 2016;9:1380–8.

7. La Gerche A, Burns AT, Mooney DJ, et al. Exercise-induced right ventricular dysfunction and structural remodelling in endurance athletes. Eur Heart J. 2012; 33:998–1006.
8. James CA, Bhonsale A, Tichnell C, et al. Exercise increases age-related penetrance and arrhythmic risk in arrhythmogenic right ventricular dysplasia/cardiomyopathy-associated desmosomal mutation carriers. J Am Coll Cardiol. 2013;62:1290–7.
9. Sanz-de la Garza M, Rubies C, Batlle M, et al. Severity of structural and functional right ventricular remodeling depends on training load in an experimental model of endurance exercise. Am J Physiol Heart Circ Physiol. 2017;313:H459–68. https://doi.org/10.1152/ajpheart.00763.2016.
10. Grazioli G, Sanz M, Montserrat S, et al. Echocardiography in the evaluation of athletes. F1000Research. 2015; 4:151.
11. D'Ascenzi F, Pisicchio C, Caselli S, et al. RV remodeling in olympic athletes. JACC Cardiovasc Imaging. 2017;10:385–93.
12. Oxborough D, Sharma S, Shave R, et al. The right ventricle of the endurance athlete: the relationship between morphology and deformation. J Am Soc Echocardiogr. 2012;25:263–71.
13. La Gerche A, Burns AT, D'Hooge J, et al. Exercise strain rate imaging demonstrates normal right ventricular contractile reserve and clarifies ambiguous resting measures in endurance athletes. J Am Soc Echocardiogr. 2012;25:253–262.e251.
14. Stewart GM, Chan J, Yamada A, et al. Impact of high-intensity endurance exercise on regional left and right ventricular myocardial mechanics. Eur Heart J Cardiovasc Imaging. 2017;18:688–96.
15. Teske AJ, Prakken NH, De Boeck BW, et al. Echocardiographic tissue deformation imaging of right ventricular systolic function in endurance athletes. Eur Heart J. 2009;30:969–77.
16. Galanti G, Stefani L, Mascherini G, et al. Left ventricular remodeling and the athlete's heart, irrespective of quality load training. Cardiovasc Ultrasound. 2016;14:46.
17. D'Ascenzi F, Pelliccia A, Valentini F, et al. Training-induced right ventricular remodelling in pre-adolescent endurance athletes: the athlete's heart in children. Int J Cardiol. 2017;236:270–5.
18. D'Ascenzi F, Pelliccia A, Corrado D, et al. Right ventricular remodelling induced by exercise training in competitive athletes. Eur Heart J Cardiovasc Imaging. 2016;17:301–7.
19. Elliott AD, La Gerche A. The right ventricle following prolonged endurance exercise: are we overlooking the more important side of the heart? A meta-analysis. Br J Sports Med. 2015;49:724–9.
20. Sanz de la Garza M, Grazioli G, Bijnens BH, et al. Inter-individual variability in right ventricle adaptation after an endurance race. Eur J Prev Cardiol. 2016;23:1114–24.
21. Ujka K, Bruno RM, Catuzzo B, et al. P260Right cardiac chambers remodeling in marathon and ultra-trail athletes detected by speckle-tracking echocardiography. Eur Heart J Cardiovasc Imaging. 2016;17:ii45–8.
22. Sanz-de la Garza M, Giraldeau G, Marin J, et al. Influence of gender on right ventricle adaptation to endurance exercise: an ultrasound two-dimensional speckle-tracking stress study. Eur J Appl Physiol. 2017;117:389–96.
23. Wasfy MM, Weiner RB, Wang F, et al. Endurance exercise-induced cardiac remodeling: not all sports are created equal. J Am Soc Echocardiogr. 2015; 28:1434–40.
24. La Gerche A, Claessen G, Dymarkowski S, et al. Exercise-induced right ventricular dysfunction is associated with ventricular arrhythmias in endurance athletes. Eur Heart J. 2015;36:1998–2010.
25. Lord R, George K, Somauroo J, et al. Exploratory insights from the right-sided electrocardiogram following prolonged endurance exercise. Eur J Sport Sci. 2016;16:1014–22.
26. Claessen G, Brosnan M, La Gerche A, et al. Signs of RV overload on the athlete's ECG. J Electrocardiol. 2015;48:399–406.
27. Brosnan M, La Gerche A, Kalman J, et al. Comparison of frequency of significant electrocardiographic abnormalities in endurance versus nonendurance athletes. Am J Cardiol. 2014;113:1567–73.
28. Corrado D, Pelliccia A, Heidbuchel H, et al. Recommendations for interpretation of 12-lead electrocardiogram in the athlete. Eur Heart J. 2010;31:243–59.
29. Drezner JA, Ackerman MJ, Anderson J, et al. Electrocardiographic interpretation in athletes: the 'Seattle criteria'. Br J Sports Med. 2013;47:122–4.
30. Zaidi A, Sheikh N, Jongman JK, et al. Clinical differentiation between physiological remodeling and arrhythmogenic right ventricular cardiomyopathy in athletes with marked electrocardiographic repolarization anomalies. J Am Coll Cardiol. 2015;65:2702–11.
31. Wasfy MM, DeLuca J, Wang F, et al. ECG findings in competitive rowers: normative data and the prevalence of abnormalities using contemporary screening recommendations. Br J Sports Med. 2015;49:200–6.
32. Kim JH, Noseworthy PA, McCarty D, et al. Significance of electrocardiographic right bundle branch block in trained athletes. Am J Cardiol. 2011;107:1083–9.
33. Scott JM, Esch BT, Haykowsky MJ, et al. Effects of high intensity exercise on biventricular function assessed by cardiac magnetic resonance imaging in endurance trained and normally active individuals. Am J Cardiol. 2010;106:278–83.
34. van de Schoor FR, Aengevaeren VL, Hopman MT, et al. Myocardial fibrosis in athletes. Mayo Clin Proc. 2016;91:1617–31.
35. Bohm P, Schneider G, Linneweber L, et al. Right and left ventricular function and mass in male elite master athletes: a controlled contrast-enhanced cardiovascular magnetic resonance study. Circulation. 2016;133:1927–35.
36. Aaron CP, Tandri H, Barr RG, et al. Physical activity and right ventricular structure and function. The MESA-Right Ventricle Study. Am J Respir Crit Care Med. 2011;183:396–404.

37. Hundley WG, Bluemke DA, Finn JP, et al. ACCF/ACR/AHA/NASCI/SCMR 2010 expert consensus document on cardiovascular magnetic resonance: a report of the American College of Cardiology Foundation Task Force on Expert Consensus Documents. Circulation. 2010;121:2462–508.
38. Sedaghat-Hamedani F, Kayvanpour E, Frankenstein L, et al. Biomarker changes after strenuous exercise can mimic pulmonary embolism and cardiac injury – a meta-analysis of 45 studies. Clin Chem. 2015;61:1246–55.
39. Shave R, Oxborough D. Exercise-induced cardiac injury: evidence from novel imaging techniques and highly sensitive cardiac troponin assays. Prog Cardiovasc Dis. 2012;54:407–15.
40. La Gerche A, Inder WJ, Roberts TJ, et al. Relationship between inflammatory cytokines and indices of cardiac dysfunction following intense endurance exercise. PLoS One. 2015;10:e0130031.
41. Neilan TG, Januzzi JL, Lee-Lewandrowski E, et al. Myocardial injury and ventricular dysfunction related to training levels among nonelite participants in the Boston marathon. Circulation. 2006;114:2325–33.
42. Dello Russo A, Pieroni M, Santangeli P, et al. Concealed cardiomyopathies in competitive athletes with ventricular arrhythmias and an apparently normal heart: role of cardiac electroanatomical mapping and biopsy. Heart Rhythm. 2011;8:1915–22.
43. Venlet J, Piers SR, Jongbloed JD, et al. Isolated subepicardial right ventricular outflow tract scar in athletes with ventricular tachycardia. J Am Coll Cardiol. 2017;69:497–507.
44. Dalal D, James C, Devanagondi R, et al. Penetrance of mutations in plakophilin-2 among families with arrhythmogenic right ventricular dysplasia/cardiomyopathy. J Am Coll Cardiol. 2006;48:1416–24.
45. Sawant AC, Bhonsale A, te Riele AS, et al. Exercise has a disproportionate role in the pathogenesis of arrhythmogenic right ventricular dysplasia/cardiomyopathy in patients without desmosomal mutations. J Am Heart Assoc. 2014;3:e001471.
46. Maron BJ, Haas TS, Ahluwalia A, et al. Demographics and epidemiology of sudden deaths in young competitive athletes: from the United States National Registry. Am J Med. 2016;129:1170–7.
47. George K, Whyte GP, Green DJ, et al. The endurance athletes heart: acute stress and chronic adaptation. Br J Sports Med. 2012;46(Suppl 1):i29–36.
48. Levine BD, Baggish AL, Kovacs RJ, et al. Eligibility and disqualification recommendations for competitive athletes with cardiovascular abnormalities: task force 1: classification of sports: dynamic, static, and impact:A Scientific Statement From the American Heart Association and American College of Cardiology. J Am Coll Cardiol. 2015;66:2350–5.

7 Systolic and Diastolic Right Ventricular Dysfunction

Diana Morvey, Shashank Gupta, Anjali Chandra, and Ernst R. von Schwarz

Abstract

The right ventricle (RV) was often considered clinically insignificant owing to its less muscular structure and its restricted blood flow to a single organ system, the pulmonary system. These misconceptions have resulted in this chamber being understudied; and therefore, limited available research data. The truth is, both ventricles are highly dependent on each other for normal functioning of the cardiovascular system. Therefore, abnormalities in one ventricle adversely impact the function of the other. Recent research on RV implicated that the RV is an important contributor in cardiovascular diseases processes. Thus, this chapter tries to elucidate some of the importance of the RV and its contribution to right ventricular dysfunction.

Keywords

Right ventricle · Systolic right ventricular dysfunction · Diastolic right ventricular dysfunction · Prevalence of right ventricular dysfunction · Autoimmune · Valvular disease

D. Morvey · S. Gupta · A. Chandra
E. R. von Schwarz (✉)
Heart Institute, Southern California Hospital, Culver City, CA, USA
e-mail: dr.ernstschwarz@gmail.com

7.1 Introduction

In the past, the importance of the right ventricle (RV) has been underestimated. The RV was often considered clinically insignificant owing to its less muscular structure and restricted blood flow to a single organ system, the pulmonary system [1]. Due to this misconception, assessment and diagnostic measures for right ventricular dysfunction were understudied. Thus, there is limited information on right ventricular function and its role in various cardiac diseases when compared to the left ventricle (LV) [2]. However, both ventricles are highly dependent on each other for normal functioning of the cardiovascular system; and abnormalities in either ventricle adversely impact the function of the other [1]. Recent research on this chamber implicated the RV as a significant contributor to cardiovascular disease processes [3]. Therefore, the National Heart, Lung, and Blood Institute highlights the importance of better understanding of the RV physiology as its failure continues to burden the medical community [4], necessitating further understanding of ill-defined functional parameters and its role in various cardiovascular diseases [2].

According to a study by Bassem, acute decompensated heart failure due to RV failure accounts for 2.2% of all cases. However, in one fifth (20%) of cases, RV failure presents secondary to acute left ventricular failure [1]. In Egypt, for example, 4.5% of patients with acute heart failure are due

S. I. Dumitrescu et al. (eds.), *Right Heart Pathology*, https://doi.org/10.1007/978-3-319-73764-5_7

to RV failure. This could be due to the higher incidence of rheumatic heart disease which often times affects the mitral valve [1].

7.2 The Normal Right Ventricle

The normal RV is a thin wall structure that is made up RV free wall, interventricular septum and the RV outflow tract [5]. The RV muscle fibers are composed of two layers namely a circumferential superficial layer and a longitudinal deeper layer [6]. The right ventricular wall is thinner; however, it is more compliant than the LV as it works against a significantly lower afterload that is pulmonary vascular resistance [2]. Due to the low pressure in the pulmonary circulation system, the pressure in the right heart are concomitantly lower compared to the left heart; and in conditions with a modest rise in afterload (pulmonary vascular resistance), a reduction in RV stroke volume is observed [6].

The RV wall is supplied predominantly by the right coronary artery (RCA), delivering equal amounts of blood during systole and diastole [2]. The oxygen demand of the right ventricular wall is lower due to the low pressure and RV wall stress during systole. Oxygen uptake by the RV at rest is an estimated 50% as opposed to an estimated 75% by the LV [7]. The blood flow in the RCA supplying the RV is correspondingly lower than the LV allowing for a sizable oxygen and flow reserve in the RV [6].

7.3 Physiology

7.3.1 Systolic Function

In normal cardiac performance, the RV ejects an equivalent amount of blood as the LV; however, uses only 25% effort in comparison to the LV [2, 6]. The ejection fraction (EF) of the RV ranges from 40 to 76% [8]. The RV systolic function is attributed to three mechanisms: (1) shortening of the fibers longitudinally compared to the twisting and rotational contraction of left ventricular fibers, (2) ventricular free wall motion towards the inside assisting in pumping blood out of the ventricle and (3) contraction of the LV due to the shared fibers in the intervetricular septum pulling the right ventricular free wall, creating negative tension in the muscle fibers [5, 9]. Inotropy, afterload and preload are other factors that also contribute to the systolic function of the RV. The interrelations between these factors are better understood with ventricular pressure-volume loops as in the Frank-Starling curve [8].

According to Frank Starling's law of the heart, a physiological rise in the venous return to the heart results in an increased in the myocardial contraction and stroke volume in both ventricles. In order to maintain the same stroke volume (SV) as the LV, the RV, due to its high surface area to volume ratio, needs to generate only a fraction of inward movement in comparison to the LV. The regular series of right ventricular muscle fiber contractions originates in the inlet and trabecular portions of the right heart, with contraction terminating at the smooth outflow tract known as the infundibulum. The period between the start and the end of contraction ranges from 25 to 50 ms. But, the contraction of the right ventricular inflow tract lasts less than that of the outflow tract (RVOT) [8].

The pressure in the left heart is significantly higher compared to the right heart, but high pressure in the RV during systole surpasses the diastolic pressure in the pulmonary artery in a short period resulting in a brief isovolumetric contraction. When compared to the rounded left ventricular pressure tracing, the pressure in the RV exhibits a sharp rise earlier in time followed by sudden decrease in the pressure [8].

The interventricular septum (IVS) between the two ventricles is responsible for maintaining the systolic ventricular interdependence [5]; and is capable of preserving normal function, even in the presence of a right ventricular scar. In contrast to diastolic ventricular interdependence, the pericardium does not play a significant role in systolic ventricular interdependence. Any disturbance in the interdependence results in abnormal functional changes in the RV [5, 8]. Thus, the ventricular interdependence plays a crucial role in the RV dysfunction [8].

7.3.2 Diastolic Function

The diastolic period lasts longer in the RV than the LV. During the cardiac cycle, the volume of blood within the relaxed RV remains constant i.e. isovolumetric relaxation and has decreased early (E) and late (A) filling velocity values, resulting in a lower E/A ratio. A prolonged filling period leads to a rise in right ventricular stroke volume. The RV is better adapted at distending and increasing its volume capacity (compliance) in comparison to the LV [8].

The RV preload is affected by numerous factors such as the relaxation or filling period, compliance, heart rate, pericardium, atria, diastolic filling of LV, and the volume of blood in the circulatory system. The pericardial sac exerts more external pressure on the RV as compared to the LV, due to its thinner and more compliant structure. As evidenced by numerous research studies, ventricular interdependence in diastole is a significant factor in normal functioning of the heart. Unlike systolic ventricular interdependence, the pericardial sac plays an essential role in determining the diastolic ventricular interdependence [8].

7.4 Etiology and Pathophysiology

Abnormalities in RV systole and diastole are identified as RV dysfunction, while the overt failure of the right-sided heart can occur in structural or functional disorders of the cardiovascular system and is manifested clinically with wide range of clinical signs and symptoms such as fluid retention, Congestive hepatomegaly and cardiac cirrhosis [3].

7.4.1 Etiology

The right ventricular function can be compromised due to intrinsic factors (vulvular disorder, congenital anomalies) [10]; extrinsic factors (Left Ventricular failure, pulmonary artery Hypertension, hyperthyroidism) [3]; autoimmune (SLE, sarcoidosis, Behcet's disease, Eosinohils granulomatosis with polyangiitis) [11] and idiopathetic.

The right ventricular function is compromised in underlying conditions such as intrinsic myocardial abnormalities, congenital (Tetralogy of Fallot, Pulmonary artery stenosis, Transposition of Great vessels) [12], atherosclerosis and idiopathic pulmonary arterial hypertension (IPAH) [13]. However, LV failure remains the leading cause of RV failure [5].

Autoimmune diseases such as systemic sclerosis can also lead to pulmonary artery hypertension secondary to inflammation of lung tissue and pulmonary arteries resulting in right ventricular filling dysfunction [6]. Cor pulmonale attributed to structural and functional changes in the RV secondary to pulmonary diseases such as chronic obstructive pulmonary disease (COPD), IPAH, obstructive sleep apnea (OSA), and kyphoscoliosis also lead to a rise in pulmonary arterial pressure [14].

7.4.2 Pathogenesis

7.4.2.1 Systolic and Diastolic Dysfunction

The RV dysfunction can be categorized as systolic or diastolic dysfunction. The genesis of RV dysfunction begins with insults (increase in volume and pressure) to the myocardium. This in turn leads to alterations in gene expressions, activation of cytokines and ventricular remodeling to adapt to the prevailing condition [3]. According Haddad et al., it was noted that the "RV adapts better to volume overload compared pressure overload. The RV can withstand the volume overload over a long period of time without significant decrease in RV systolic function." Pressure overload, on the contrary, may lead to RV dilatation and failure [3].

Microscopically, the histological changes observed in the RV are more noticeable in conditions with high pressure states as compared to the conditions resulting in volume overload. Typically the RV better adapts to high volume states than pressure overload [3]. Right ventricular dysfunction is worsened by a reduction in blood flow and

oxygen supply secondary to pressure overload. According to a study on mice by Reddy et al., "a model of pulmonary insufficiency (PI) and pulmonary stenosis (PS) were used to demonstrate clinical settings in RV dysfunction. In the study, mice were assessed weekly over a 3-month period after the creation of pulmonary insufficiency and pulmonary stenosis. The pulmonary artery band gradient and the RV systolic pressure remained stable over time while the RV internal diameter and RV end-diastolic area progressively increase from 1 month to 3 months. Diastolic dysfunction developed starting at 1 month after generation of PI + PS which was evidence by increase in the on echo Doppler triscupid valve E/a ratio which was consistent with restrictive RV filling and elevated RV end- diastolic pressure on catheterization. At 2 months, there was noted diastolic dysfunction but no signs of RV failure. By the 3 months, systolic dysfunction has developed and this was evidenced by decrease in RV outflow tract shorting and by this time developed overt clinical signs of RV failure such as edema, tachypnea" [15].

Obstruction of the pulmonary vasculature due to thromboembolism causes a sudden rise in the pulmonary artery pressure. The acute rise in afterload leads to dilatation of the ventricle and early dysfunction. In certain long standing abnormalities such as congenital pulmonary stenosis and Eisenmenger Syndrome, the RV is capable of withstanding high pressure states for a longer period of time without causing systolic or diastolic dysfunction [3]. Additionally, the RV tolerates chronic high volume overload in the setting of a septal defect between the atria and regurgitated tricuspid valve with minimal significant functional changes [6]. Extreme volume overload in the RV, due to vulvular heart defect, congenital cardiac anomalies [10], results in compression of the LV and subsequent biventricular dysfunction. The enlarged RV causes a leftward displacement of the ventricular septum with resultant LV dimensional changes and creates tension in the pericardium, limiting the movement of both ventricles. The ability of the LV to distend is markedly reduced as a result of pericardial constraint, ultimately decreasing the cardiac output.

Arrhythmogenic right ventricular cardiomyopathy (ARVC) is a rare hereditary disorder in which cardiac myocytes are replaced by fibrous and fatty connective tissue resulting in distorted right ventricular morphology and function. It has an autosomal dominant pattern of inheritances with variable penetrance and expressivity [16]. Early stages of ARVC are difficult to diagnose because of the overlapping clinical features such as syncope, palpitations and pre-syncope, sustained ventricular tachycardia, with several other cardiac diseases such as myocarditis, outflow ventricular tachycardia of the right ventricle and Brugada Syndrome. However, the principal characteristics of ARVC are arrhythmia and sudden death [17].

Right diastolic dysfunction is defined as inadequate relaxation of cardiac myocytes and/or reduced chamber compliance of the RV during filling or resting phase of the cardiac cycle [18]. Impaired right ventricular relaxation results in pressure buildup in the right atrium which subsequently leads to the distension of the inferior vena cava (IVC) and reversed blood flow to the hepatic veins during atrial contraction [19]. The filling phase of the right ventricle is also impaired in right ventricular dysfunction and leads to decreased cardiac output [3].

Persistent high pulmonary arterial pressure (afterload) leads to hypertrophy of cardiac myocytes resulting in enlargement of the right ventricle and ultimately right ventricular diastolic dysfunction [20]. A number of conditions are associated with the right heart diastolic dysfunction such as cystic fibrosis (CF), long standing narrowed aortic valve, high blood pressure, hypertrophic cardiomyopathy (HCM), obesity with a body mass index (BMI) above 30 kg/m^2, Chagas disease and pulmonary hypertension [18].

7.4.2.2 Combined Dysfunction

Alcohol (i.e. ethanol) is an established risk factor in systolic and diastolic dysfunction of the RV (and the LV). Chronic alcohol abuse has direct toxic effects on cardiac myocytes. This effect result in functional changes and eventually lead to development of dilated cardiomy-

opathy. A positive association exists between the quantity of alcohol intake and the risk of developing dysfunction [21].

Alcohol-induced right ventricular diastolic dysfunction is linked to the dense fibrous connective tissue formed in response to toxicity and stiffening of myocardium resulting in impaired relaxation. The cardiac remodeling process is also impaired in alcoholism [21]. Biologically, heavy alcohol consumption leads to programmed cell death, pathological changes in the filaments of muscle fibrils, impairment of cellular organelles, disturbances in calcium metabolism, and excessive collagen deposition in the cardiac muscle; ultimately, causing a negative inotropic effect on cardiac myocytes [21].

7.5 Clinical Presentation

The principal clinical presentations of right ventricular dysfunction include dyspnea on exertion, fatigue, epigastric fullness, and right upper quadrant discomfort or pain, ankle swelling and generalized and peripheral edema. These clinical symptoms are a result blood pooling in the veins and decreased cardiac output [1]. The signs of RV dysfunction include raised jugular venous pressure (JVD), accentuated secondary pulmonary heart sound, left parasternal shit, pansystolic murmur over the tricuspid area [1].

Initially, the clinical manifestations are silent due to physiologic mechanism of cardiovascular system to maintain homeostasis and circulation. As heart failure progresses, clinical signs become apparent and include tachycardia as the heart attempts to improve cardiac output, bilateral lower extremity edema resulting from venous backflow, increased abdominal girth from fluid accumulation in peritoneal cavity (ascites), right upper quadrant pain due to hepatic congestion and enlargement with hepatojugular reflux [22].

"A rise in the JVP reflects an increase in right atrial pressure. It is a specific sign for right heart failure." [1]. Kussmaul sign, which is a rise in JVP on inspiration also indicates RV dysfunction resulting from myocardial infarction in the RV and other conditions such as constrictive pericarditis. Kussmaul sign is a consequence of abnormal RV diastolic compliance and increased venous return to the right side of the heart [1].

7.6 Diagnostic Workup

RV assessment can be carried out via non-invasive and invasive methods. Echocardiography, Doppler, isotopic technology, cardiac magnetic resonance imaging are non-invasive tests whereas cardiac heart catheterization is undeniably an invasive method [23].

7.6.1 Noninvasive Methods Assessing Systolic Function

7.6.1.1 Echocardiography

Echocardiographic measures include two methods: (1) qualitative and (2) quantitative.

1. Qualitative ("Eyeball") Method
   This is the most frequently used technique to assess the systolic function. It is a subjective estimate of the RV functions and is highly dependent on the judgment of a skilled radiologist. The study is limited by lack of sensitivity and marked variability in the interpretation, as it is unable to differentiate between the degree of severity in the systolic dysfunction and the lack of similarity in the results among the interpreters [19].
2. Quantitative Methods using Two Dimensional Echocardiographic (2DE) Parameters
   (a) Tricuspid Annular Plane Systolic Excursion (TAPSE)
   During the normal cardiac cycle, the atrioventricular tricuspid valve moves outward towards the cardiac apex of the heart during diastole. This movement is calculated as the difference in the distance traveled by the valve at the end of the diastole and end of the systole [19]. TAPSE is dependent on the load, angle and left ventricular function, and can be measured by simple two-dimensional view cardiac echocardiography or apical

four-chamber view [19]. A normal value is identified by movement of more than 16 mm [24]. Clinically, measuring TAPSE has a prognostic value and adequately distinguishes high-risk patients with pulmonary embolism requiring immediate intervention [25].

TAPSE is proven to be very useful in monitoring pulmonary artery hypertension in both adult and pediatric patient populations [19]. Furthermore, TAPSE correlates well with the right ventricular ejection fraction determined by cardiac magnetic resonance imaging (MRI) and radionuclide ventriculography. TAPSE is considered both reliable and reproducible; therefore it is used to make an initial diagnosis and in follow up assessment of RV function [24].

(b) Fractional Area Change (FAC)

This form of measurement can be determined by using the two-dimensional cardiac echocardiography in apical four-chamber view. The value is derived from the difference in area of the RV at the end of diastole and the difference at the end of systole over the area during the end of diastole [19]. In order to accurately visualize the inner right ventricle chamber and the difference in area, the sonographic image is enhanced to highlight the endocardial surface. The FAC is measured as a percentage and a value of more than 35% in adults is accepted as normal [19].

In comparison to TAPSE, the FAC value is more closely related to the right ventricular ejection fraction obtained by a cardiac MRI, especially in adults with surgical repair of pulmonic valve in ToF. FAC measurements are the method of choice in evaluating RV function after pericardiotomy, as it is maintained postoperatively. It is a prognostic indicator in patients affected by pulmonary artery hypertension and myocardial infarction [19]. Furthermore, in adults, the measured FAC values tend to be repeatedly similar as opposed to TAPSE [19].

7.6.1.2 Doppler

Doppler measures include: (1) tissue Doppler-derived right ventricular systolic excursion velocity S′, (2) myocardial acceleration during isovolumic contraction and (3) speckle tracking echocardiography.

1. Right Ventricular Systolic Excursion Velocity S′

   This Doppler derived measurement resembles TAPSE, as it determines the longitudinal systolic performance of right ventricle by measuring the tricuspid annulus velocity in systole [19]. This technique is advantageous especially for pediatric patients with right heart dysfunction, as it has normal reference values for patients in this age group. A right ventricular dysfunction with an ejection fraction less than 45% is correlated to the S′ velocity of less than 11.5 cm/s. Patient with surgically repaired ToF, a reduced velocity that is inversely proportionally to the end-diastolic volume is measured [19].

   In addition to being a reproducible measure, the tricuspid annulus velocity is also easily measured using a pulsed Doppler. This technique is similar to TAPSE, therefore the limitations such as angle and load dependency also applies to S′ velocity measure. Tethering is a unique drawback to this parameter that can give inaccurate velocity values due to the movement of the affected cardiac muscle by the pulling action of surrounding normal tissue [19].

2. Myocardial Acceleration During Isovolumic Contraction (IVA)

   Myocardial acceleration during isovolumic contraction is a measure of RV contractile function derived from Doppler tissue imaging (TDI) and measured as the ratio of myocardial peak velocity in systole (isovolumetric contraction) over the myocardial acceleration time [26]. An acceleration value of more than 1.1 m/s^2 in the free right ventricular wall is normal [19].

   Isovolumic acceleration is an important and unique index for measuring right ventricular function as it is independent of conditions

causing volume and/or pressure overload [9]. IVA is also used to evaluate the contractile reserve of the myocardium during cardiac stress test since it is dependent on the heart rate [19]. It is noted that certain cardiac conditions including congenital heart diseases such as transposition of the great arteries, ToF and thromboembolism cause a reduction in IVA values [19].

3. Speckle Tracking Echocardiography (STE)
   STE uses myocardial deformation imaging to assess various motions of the myocardium including longitudinal, radial, and circumferential [9]. This Doppler or non-Doppler dependent study allows strain and strain rate measurements as the right ventricular longitudinal systolic function [19].
   Strain is the percent of alteration (deformation) in the diseased myocardium. A positive percentage value indicates myocardial tissue lengthening and thickening whereas a negative value indicates the opposite, shortening and thinning. The myocardial deformation rate in s−1 is identified as the strain rate [17].
   STE measures both global and regional function of the myocardium since it is unaffected by angle or load and can be applied to diagnose and manage conditions such as right sided heart failure, pulmonary hypertension, arrhythmogenic right ventricular dysplasia, and congenital heart disease [24]. STE is also used to measure the function of the RV in alcohol-induced diastolic dysfunction during the early stages [21].
   Patients with surgical repair of ToF tend to have reduced global longitudinal strain (GLS) and the strain value is reduced prior to clinically apparent right heart failure. Despite the absence of normal reference values, STE reproduces similar results repeatedly [19].

7.6.1.3 Three Dimensional Echocardiography (3DE)

Three-dimensional echocardiography enables clear visualization of the right ventricular anatomy components and is used to evaluate various congenital heart diseases, including atrial septal defect (ASD), ToF and Ebstein's anomaly, and right ventricular cardiomyopathy [24]. Compared to cardiac MRI, the 3DE is readily available and despite having false low values of the right ventricular volume it is a more cost-effective alternative [19]. 3DE easily assesses the contractile strength of the RV by measuring the ejection fraction. An EF value of more than 45% indicates adequate systolic function of the right heart [24].

7.6.1.4 Right Ventricular DP/DT

RV dp/dt (rate of pressure rise in the RV) is not a commonly used index. It is a measurement obtained as the period required for the tricuspid regurgitation jet to accelerate between 1 and 2 m/s interval. It correlates well with TAPSE despite the lack of data on RV and its dependence on load [24].

7.6.2 Noninvasive Methods Assessing Diastolic Function

Measuring the right ventricular diastolic function requires the use of echocardiography and Doppler measures to determine several distinct values during the various stages of cardiac resting phase [19].

(a) Echocardiography (2DE)
   Routine echocardiography is very useful in diseases like pulmonary hypertension where diastolic dysfunction occurs prior to systolic dysfunction. It is also a valuable tool in follow-up assessment in congenital heart disease patients needing re-intervention procedures due to factors like advancing dilatation of the RV [19].

(b) Doppler Measure
   Diastolic function of the right heart is assessed using Doppler indices such as tricuspid inflow, interrogation of the lateral tricuspid valve annulus, hepatic veins, and IVC size and collapsibility [19]. Doppler hepatic vein flow signal showing either

reduced or inverted systolic waveform indicates abnormality in RV diastolic function [18]. High pressures in the right atrium can occur in right ventricular diastolic dysfunction resulting in decreased or even absence of IVC collapsibility which can easily be seen via two-dimensional view cardiac echocardiography or apical four-chamber view. Reverse flow of blood to the IVC and hepatic veins with every contraction of the right atrium might be present [19].

(c) Myocardial Velocities

The early filling phase of diastole is represented as the E wave whereas the A wave indicates atrial contraction during the late phase of diastole and both are measured by tissue Doppler. The early diastolic velocity (e′) and E deceleration time signify relaxation of the right ventricle [19]. By calculating the tricuspid E/A ratio, the diastolic dysfunction can be classified into (1) mild (impaired relaxation; type 1), (2) moderate (pseudo normal; type 2) and (3) severe (restrictive pattern; type 3). An E/A ratio of less than 0.8 is seen in mild dysfunction, whereas moderate dysfunction is observed when E/A is ranges from 0.8 to 2.1 or in the presence of an E/e′ of more than 6. Severe diastolic function is present with an E/A of more than 2.1 with deceleration time of less than 120 ms [24].

7.6.2.1 Cardiac Magnetic Resonance (CMR)

Right heart function in this non-invasive imaging study is generally evaluated by measuring the ejection fraction of the RV, which is obtained by measuring the blood volume at the end of diastole and at the end of systole in the short-axis plane [27]. This is considered the most accurate radiological procedure for evaluating right ventricular volume. MRI flow studies provide information to accurately calculate the amount of blood pumped out to the system, the percent of blood that flows back to the LV through the aortic valve, and shunt fraction by assessing the normal blood flow through all the heart valves [8].

7.6.3 Invasive Methods for Assessing Systolic and Diastolic Function

7.6.3.1 Right Heart Catheterization

Right cardiac catheterization is the gold standard diagnostic procedure for PAH. Although echocardiography and other noninvasive screening methods help identify PAH, they only provide estimates of right ventricular pressures. Cardiac catheterization provides accurate values and combined with clinical findings, allows for better therapeutic management and monitoring. PAH is defined as a resting mean pulmonary arterial pressure (MPAP) of more than or equal to 25 mmHg. Pulmonary artery/capillary wedge pressure (PAWP) and a pulmonary vascular resistance (PVR) are other indices that can be measured during right cardiac catheterization to determine the presence of PAH; with PAWP ≤15 mmHg and PVR of >3 Wood units being indicative of PAH. Added prognostic value is obtained during the procedure by determining the extent of hemodynamic deterioration, and assessing the positive effect of treatment to better predict the outcome of disease [28] (Table 7.1).

Table 7.1 Values of RV systolic and diastolic parameters [24]

	Unit	Abnormal
Systolic function		
TAPSE	mm	<17
Systolic myocardial velocity (S′)	cm/s	<9.5
Fractional area change	%	<35
Pulsed Doppler RIMP	–	>0.43
RV dp/dt	mmHg/s	<400
RVEF (3DE)	–	<46%
Diastolic function		
E/A ratio	–	<0.8 or >2.1
E′	cm/s	<8
E/E′ ratio	–	>6
E deceleration time	ms	<119 or >242

7.7 Treatment and Management

7.7.1 Chronic Right Heart Failure [29]

The treating modality of RV dysfunction depends on the underlying etiology. The intervention(s) can either be supportive, pharmacological or surgical.

Pulmonary Artery Hypertension (PAH) PAH depending on the etiology can be managed either supportively or pharmacologically. Under supportive treatment, patients must avoid strenuous exercise. If supportive treatment fails, patient is started on pharmacological regimens which include Oxygen, diuretics, digoxin, oral anticoagulants, and inhaled nitric oxide (iNO). PAH due to positive vasoreactivity can be managed on oral calcium channel blockers (CCB) such as amlodipine. In connective tissue diseases, Immunomodulators are adequate. In primary pulmonary hypertension, Lung transplantation is indicated for patients who did not respond to medical treatment. In cases of chronic thromboembolic pulmonary hypertension (CTEPH), medical management include anticoagulant and it is surgically managed my pulmonary thromboendarterectomy (PTE) [29].

The New York Heart Association developed a risk stratefication model to assess the cardiac risk of heart failure. A high risk (NYHA-IV) will present with syncope, walking a distance less than 300 m, increase Brain Natriuretic peptide (BNP), and right atrium pressure greater than 20 mmHg. The management for this class is prostanoids such as IV epoprostenol, SQ treprostinil, Inhaled iloprost, oral beraprost. A low risk patient (NYHA-I/II/III) can walk less than 400 m and normal BNP. Management includes phosphodiesterase-5 inhibitors (Sildenafil Citrate), Endothelin receptor blocker (Bosentan, Tezosentan). A combination therapy is indicated for suboptimal clinical response.

Sildenafil citrate works by inhibiting the PDE-5 enzymes expressed in the right ventricle specifically the hypertrophied myocardium and smooth muscles of coronary arteries, where it helps promotes the systolic function of right ventricle by improving the right ventricle as well as pulmonary arterial remodeling. When administered to patients with PAH, dobutamine tends to lowers the pressure in the pulmonary arteries by relaxing the vascular smooth muscles cells and improves the cardiac contractility [29]. In a failed treatment, Lung or heart transplanted in recommended.

In Congenital heart disease such as Tetralogy of fallot (ToF), the management requires valvular repair and Implantable cardioverter defibrillator (ICD). In atrioventricular valve disease such as tricuspid valve disorder, the management is valve repair or replacement [29].

In RV Myocardial infarction (RVMI), Reperfusion therapy is indicated. Early reperfusion therapy is proven to be very beneficial in improving or maintaining the systolic function of RV and preventing heart block in patients who have endured RV myocardial infarction. The use of pulmonary vascular relaxant like inhaled nitric oxide is limited due to ineffective gaseous intake by patients. Resynchronization therapy has a rate controlling effect suffering from right heart failure whereas atrial septostomy is more of a palliative form of therapy which can be used in severe right heart failure as it known to cause RV decompression by shunting blood from right to left atrium [29].

The management of Systolic right ventricular failure includes angiotensin converting enzyme-inhibitors such as (Benazepril, lisinopril) or angiotensin receptor blocker (losartan). There are new drugs like Myosin activators, Na/K ATPase inhibitor, vasopressin antagonist, micro RNA modulators. The surgical management involves cardiac resynchronization therapy, RV assist device implantation and cardiac transplantation [29].

7.7.2 Heart Transplantation (HTx)

Due to insufficient supply of organs, decision for HTx should be guided by standard protocol as to only include eligible patients. HTx is

recommended in patients with refractory right heart failure unresponsive to medical therapy and congenital heart defects. Patients with intractable pulmonary hypertension have the option to undergo double lung transplantation or heart-lung transplantation. Right ventricle failure is one of many complications of transplant therapy, which is usually an indication for RVAD or mechanical support [29]. Other indications for HTx include severe biventricular dysfunction, and continuous unresponsive ventricular arrhythmias [16].

7.7.3 Prophylactic Treatment

Prophylactic therapy is beneficial in cases with ARVC as it may prevent sudden cardiac death (SCD). As previously mentioned, implantable cardioverter defibrillator (ICD) is the most important method of preventing SCD in such patients. Radiofrequency ablation (RFA) or combination therapy with antiarrhythmic drugs; beta-blockers and amiodarone can be considered in those with irregular cardiac rhythm. Patients with history of sustained ventricular tachycardia, loss of consciousness, widespread disease can be managed with ICD [16].

7.7.4 Emerging Stem Cell Therapy

The arterial changes in pulmonary hypertension can be reversed (partially or completely) using mesenchymal stem cells (MSC) or endothelial progenitor cells (EPC), which restores the integrity of affected blood vessels within the lungs, thereby normalizing the pressure in the pulmonary circulation and decreasing the right ventricular afterload [20], however, more research is needed to establish the role of stem cell therapy for this indication.

Stem cells are primitive cells that have the ability to give rise to all types of bodily cells and form clones. Progenitor cells are undifferentiated early descendants of stem cells that have the ability to develop into cells of single lineage. Endothelial progenitor cells have the intrinsic capacity to undergo maturation and evolve into fully developed endothelial cells. EPCs originate from the marrow of the bones and are found circulating in the blood [20].

Both Mesenchymal stem cells and progenitor cells act specifically in the damaged areas of the lungs and result in neovascularization by producing various vascular growth factors like VEGF, Angiopoietin-1. They also form factors that suppress apoptosis and inflammation in the body. Bcl-2 protein is an inhibitor of apoptosis whereas interferon-γ, interleukin-10, hepatocyte growth factor have anti-inflammatory effect. MSCs are capable of escaping and avoiding recipient's immune system as they're unable to mount an immune response due to their low immunogenicity; therefore treatment with these cells is considered optimal for number disorders involving the lungs [20].

7.8 Prognosis

The ability to perform maximum physical activity is notably associated with the systolic function (ejection fraction) of right ventricle and has been found to be of prognostic value in patients with left-sided heart failure. Due to the investigative difficulties faced by researchers, the mortality rate linked with right ventricular diastolic function has only been acknowledged by limited papers. One such difficulty is measuring the load dependant indices of right ventricular diastolic filling. Deranged diastolic function of right ventricle in those with failure of left heart is interrelated with higher chances of admissions to the hospital for complications associated with heart failure. Quantitative measures like tricuspid annular velocity in both cardiac phases and right ventricular myocardial performance index are also associated with poor prognosis in heart failure patients [21].

7.9 Recommendation

Even with limited data on right ventricular dysfunction, it is quite clear that the right ventricular dysfunction plays a vital role if cardiovascular disease. It is therefore imperative that further research efforts are invested towards better understanding of the right ventricular chamber and its alteration in disease process. Research studies must be carried out on the human myocardium to

better understand and appreciate the right heart function as well as its dysfunction.

In future, more treatment options need to focus primarily on the dysfunctional area rather than the entire heart. Gender specific research must be given more importance in order to accurately understand the biological differences in the function and structure of the right ventricle, thereby accurately treating patients on an individual basis [4].

Conclusion

Like the left ventricle, the contractility of right ventricle is also under the control of autonomic nervous system and multiple other regulatory factors such as the Frank Starling's law and heart rate [6]. Various additional factors such as preload, afterload, pericardial constraint, ventricular contractility and interdependence all play a major role in normal functioning and physiology of the right ventricle [8].

Despite the fact that right heart is often ignored in the cardiovascular research studies, the right ventricle in reality is greatly affected by its counterpart as evident by the ultimate failure of right side of the heart in those with left heart failure [1] and recent studies indicates that it is an independent predicator of morbidity and mortality [5] Number of other conditions such as infarction of right myocardium, congenital cardiac disorders and pulmonary arterial hypertension can affect the right ventricle function [8].

Often used interchangeably, the diastolic dysfunction and diastolic heart failure are separate entities and must be carefully differentiated from each other by extensively researching and studying the already available data [18].

References

1. Bassem SI. Right ventricular failure. EJ Cardiol Pract. 2016;14(32). https://www.escardio.org/Journals/E-Journal-of-Cardiology-Practice/Volume-14/Right-ventricular-failure.
2. Voelkel NF, Quaife RA, Leinwand LA, Barst RJ, McGoon MD, Meldrum DR, et al. Right ventricular function and failure. Circulation. 2006;114:1883–91. https://doi.org/10.1161/CIRCULATIONAHA.106.632208.
3. Haddad F, Doyle R, Murphy DJ, Hunt SA. The right ventricular function in cardiovascular disease, part II. Pathophysiology, clinical importance and mangement of right ventricular failures. Contemporary reviews in cardiovascular medicine. Circulation. 2008;117:1717–31. https://doi.org/10.1161/CIRCULATIONAHA.107.653584.
4. Lahm T, McCaslin CA, Wozniak TC, Ghumman W, Fadl YY, Obeidat OS, et al. Medical and surgical treatment of acute right ventricular failure. J Am Coll Cardiol. 2010;56(18):1435–46. https://doi.org/10.1016/j.jacc.2010.05.046.
5. Ryan JJ, Tedford R. Diagnosing and treating the right ventricular function in cardiovascular disease. Curr Opin Cardiol. 2015;30(3):292–300.
6. Walker LA, Buttrick PM. The right ventricle: biologic insights and response to disease: updated. Curr Cardiol Rev. 2013;9(1):73–81. https://doi.org/10.2174/157340313805076296.
7. Zong PI, Tune JD, Downey HF. Mechanisms of oxygen demand/supply balance in the right ventricle. Exp Biol Med (Maywood). 2005;230(8):507–19. https://www.ncbi.nlm.nih.gov/pubmed/16118400/.
8. Haddad F, Hunt SA, Rosenthal DN, Murphy DJ. Right ventricular function in cardiovascular disease, part I. Anatomy, physiology, aging, and functional assessment of the right ventricle. Circulation. 2008;117:1436–48. Retrieve from https://doi.org/10.1161/CIRCULATIONAHA.107.653576.
9. Toyono M, Harada K, Tamura M, Yamamoto F, Takada G. Myocardial acceleration during isovolumic contraction as a new index of right ventricular contractile function and its relation to pulmonary regurgitation in patients after repair of tetralogy of Fallot. J Am Soc Echocardiogr. 2004;17(4):332–7. https://doi.org/10.1016/j.echo.2003.12.022.
10. Trivedi DV, Adhikari AS, Sarkar SS, Ruppel KM, Spudich JA. Hypertrophic cardiomyopathy and the myosin mesa: viewing an old disease in a new light. Biophys Rev. 2017. https://doi.org/10.1007/s12551-017-0274-6.
11. Comarmond C, Cacoub P. Myocarditis in Autoimmune or auto-inflmmatory disease. Autoimmun Rev. 2017;16(8) 811–6. Retrieve from https://doi.org/10.1016/j.autev.2017.05.021.
12. Reddy S, Bernstein D. Molecular mechanisms of right ventricular failure. Circulation. 2015;132(18):1734–42. https://doi.org/10.1161/CIRCULATIONAHA.114.012975.
13. Ho SY, Nihoyannopoulos P. Anatomy, echocardiography, and normal right ventricular dimensions. Heart. 2006;92(Suppl 1):i2–i13. https://doi.org/10.1136/hrt.2005.077875.
14. Garrison D, Memon J. Cor Pulmonale. In: StatPearls [Internet]. Treasure Island: StatPearls Publishing; 2017. Available from https://www.ncbi.nlm.nih.gov/books/NBK430739.
15. Reddy S, Zhao M, Fajardo G, Katnelson E, Spin JM, Bernstein D. Physiologic and molecular char-

acterization of a murine model of right ventricular volume overload. Am J Physiol Heart Circ Physiol. 2013;304(10):H114–H1327. https://doi.org/10.1152/ajpheart.00776.2012.
16. Pinamonti B, Brun F, Mestroni L, Sinagra G. Arrhythmogenic right ventricular cardiomyopathy: from genetics to diagnostic and therapeutic challenges. World J Cardiol. 2014;6(12):1234–44. https://doi.org/10.4330/wjc.v6.i12.1234.
17. Lemarié J, Huttin O, Girerd N, Mandry D, Juillière Y, Moulin F, Lemoine S, Beaumont M, Marie PY, Selton-Suty C. Usefulness of speckle-tracking imaging for right ventricular assessment after acute myocardial infarction: a magnetic resonance imaging/echocardiographic comparison within the relation between aldosterone and cardiac remodeling after myocardial infarction study. J Am Soc Echocardiogr. 2015;28(7):818–27. https://doi.org/10.1016/j.echo.2015.02.019.
18. Schwarz ER, Dashti R. The clinical quandary of left and right ventricular diastolic dysfunction and diastolic heart failure. Cardiovasc J Afr. 2010;21(4):212–20. https://doi.org/10.5830/CVJA-2010-018.
19. DiLorenzo MP, Bhatt SM, Mercer-Rosa L. How best to assess right ventricular function by echocardiography. Cardiol Young. 2015;25(8):1473–81. Retrieve from https://doi.org/10.1017/S1047951115002255.
20. Van der Laarse A, Cobbaert CM, Umar S. Stem and progenitor cell therapy for pulmonary arterial hypertension: effects on the right ventricle (2013 Grover Conference Series). Pulm Circ. 2015;5(1):73–80. https://doi.org/10.1086/679701.
21. Meng S, Guo L, Li G. Early changes in right ventricular longitudinal function in chronic asymptomatic alcoholics revealed by two-dimensional speckle tracking echocardiography. Cardiovasc Ultrasound. 2015;14:16. https://doi.org/10.1186/s12947-016-0058-3.
22. Inamdar AA, Inamdar AC. Heart failure: diagnosis, management and utilization. J Clin Med. 2016;5(7):62. https://doi.org/10.3390/jcm5070062.
23. Fayssoi A, Abasse S, Nardi O. Right ventricular assessment with echocardiography. Med Sci (Paris). 2009;25(5):513–8. Retrieve from https://doi.org/10.1051/medsci/2009255513.
24. Kossaify A. Echocardiographic assessment of the right ventricle, from the conventional approach to speckle tracking and three-dimensional imaging, and insights into the "right way" to explore the forgotten chamber. Clin Med Insights Cardiol. 2015;9:65–75. https://doi.org/10.4137/CMC.S27462.
25. Schmid E, Hilberath JN, Blumenstock G, Shekar PS, Kling S, Shernan SK, Nowak-Machen M. Tricuspid annular plane systolic excursion (TAPSE) predicts poor outcome in patients undergoing acute pulmonary embolectomy. Heart Lung Vessel. 2015;7(2):151–8.
26. Schattke S, Knebel F, Grohmann A, Dreger H, Kmezik F, Riemekasten G, Baumann G, Borges A. Early right ventricular systolic dysfunction in patients with systemic sclerosis without pulmonary hypertension: a Doppler tissue and speckle tracking echocardiography study. Cardiovasc Ultrasound. 2010;8:3. https://doi.org/10.1186/1476-7120-8-3.
27. Jorstig S, Waldenborg M, Thunberg P. Right ventricular ejection fraction measurements using two-dimensional transthoracic echocardiography by applying an ellipsoid model. Cardiovasc Ultrasound. 2017;15:4. https://doi.org/10.1186/s12947-017-009-5.
28. Rosenkranz S, Preston IR. Right heart catheterisation: best practice and pitfalls in pulmonary hypertension. Eur Respir Rev. 2015;24(138):642–52. https://doi.org/10.1183/16000617.0062-2015.
29. Skhiri M, Hunt SA, Denault AY, Haddad F. Evidence-based management of right heart failure: a systematic review of an empiric field. Rev Esp Cardiol. 2010;63(4):451–71. https://doi.org/10.1016/S1885-5857(10)70094-3.

8 Hypertrophy and Dilatation, Markers of Dysfunction

Ecaterina Bontaş, Florentina Radu-Ioniţă, and Liviu Stan

Abstract

Known as "the forgotten ventricle", right ventricle (RV) is presently not anymore regarded as a needless or inactive component of the normal circulation. In addition, the importance of right ventricular function in cardiovascular disease and cardiac surgery has been recognized from several years. RV dysfunction has been shown to be an independent significant prognostic factor in heart failure, congenital heart disease, valvular disease, and cardiac surgery. Nowadays, significant basic science work proved that the RV has an essential function in the pathogenesis and prognosis of numerous cardiovascular diseases including the numerous acquired and congenital cardiac diseases. As a result, there is an increasing research focused on the significance of the individual RV function, in addition to its effect on global heart function through biventricular relationships. The aim of this chapter is to underline that pathologic hypertrophy and dilatation may represent markers of right ventricle dysfunction.

Keywords

Right heart · Right heart mechanics · Physiopathology · Hypertrophy · Right heart dilatation · Right ventricle failure · Right atrium · Right ventricle · Preload · Overload

The same thing that makes you live can kill you in the end.

Neil Young

8.1 Introduction

Known as "the forgotten ventricle", right ventricle is presently not anymore regarded as a needless or inactive component of the normal circulation. Nowadays, significant basic science work proved without a doubt that the right ventricle has an essential function in the pathogenesis and prognosis of numerous cardiovascular diseases including the numerous acquired and congenital cardiac diseases. As a result, there is an increasing research focused on the significance of the individual right ventricle function, in addition to its effect on global heart function through biventricular relationships.

E. Bontaş (✉)
Department of Cardiology, "Prof. C.C. Iliescu" Emergency Institute University for Cardiovascular Diseases, Bucharest, Romania

F. Radu-Ioniţă
"Titu Maiorescu" University of Medicine, Bucharest, Romania

"Carol Davila" Central Military Emergency University Hospital, Bucharest, Romania

L. Stan
Department of Cardiovascular Surgery, Central Clinic Emergency Military Hospital "Carol Davila", Bucharest, Romania

S. I. Dumitrescu et al. (eds.), *Right Heart Pathology*, https://doi.org/10.1007/978-3-319-73764-5_8

Moreover, the evaluation of RV function is significant in the care of right ventricular cardiomyopathies, pulmonary hypertension, subpulmonary or systemic right ventricle dysfunction in congenital heart disease, left ventricular dysfunction and cardiac transplantation. What is more, Sheehan and Redington [1] consider that it is absurd to regard the RV abnormalities uniqueness and vice versa.

In conclusion, the described modifications in size, shape, and function of the right heart include atrial as well as ventricular hypertrophy and dilatation. The aim of this chapter is to emphasize the role of right ventricle hypertrophy and dilatation as markers of right heart dysfunction.

8.2 Righ Heart Physiopathology

Right Heart Anatomy A comprehensive aknowlegeded of right heart anatomy is Chap. 2. However, we put emphasis on short outlines. Both ventricles have with early progress embryological, genetics, developmental and functional findings. This diferentiation starts with the primary and secondary heart fields (see Chap. 1), causing the separation of right ventricle (RV) and left ventricle (LV) cardiomyocytes during early development, and ends up with chamber-specific variations in cell signaling and Ca^{2+} handling, all suggestive of essential variation between both ventricles at the cellular level as well [2].

Embryological and structural anatomical differentiation between the RV and LV are already described in previous chapters. However, it has to be underlined that same to heart embryology, there are different anatomical descriptions of right heart. Recently, D'Alto et al. [3] and Sánchez-Quintana et al. [4] described right atrium (RA) as having three anatomical components: "the appendage, the venous part, and the vestibule or the active structure with various roles of reservoir, conduit, and booster pump function" [3, 4]. It is well established that RV has also three components: the inlet, the apex and the infundibulum (outlet, conus) (Fig. 8.1b) [5].

Therefore, *morphologically*, RV is differentiated from LV by possessing coarser trabeculae, a moderator band, and no fibrous continuity between its inlet and outflow valves (Table 8.1) [1, 5–7].

Right Heart Mechanics: Short Outlines It is well established that normal RV contractile function is especially dependent on that of the LV. As mentioned above, the RV has a different metabolism and morphology in comparison with LV, including the helical muscle fibre arrangement (Fig. 8.1, Table 8.1) [7, 8].

Therefore, it is not surprising that as a result of these anatomical and physiological differences, the two chambers display different responses to adverse conditions. On the other hand, the complex geometry of RV is also determined by the interventricular septum (IVS) location [5]. In fact, the IVS is the most important determinant of the shape of the RV. The IVS motion is considered to contribute to both LV and RV function [9, 10] and is a major determinant of overall RV performance [9–11].

Cardiac contraction is three dimensional [12] and consistent with published data longitudinal shortening strain, %, circumferential shortening strain, %, and radial thickening strain, % could be determined in three directions which form three perpendicular axes if they are placed as a Cartesian system in heart [13].

It seems that RV myocytes being mainly longitudinal, they produce a "peristaltic contraction from the inlet to outlet and a bellows-like motion of the free wall toward the septum" [1, 14]. Moreover, some RV myocardium is not the same with the LV myocardium because isolated RV muscle bundles have more rapidly twitch velocity than LV [1, 15–17]. Moreover, early studies demonstrated that the force production of RV papillary muscle per unit mass is smaller than that of LV papillary muscle, even though as stated above the shortening velocity of isolated RV muscle bundles is higher in comparison with the LV [18, 19].

The dominant movements of the RV include longitudinal shortening with pressing of the free wall against the septum, contraction of the IVS, and a "wringing" action of the LV (Table 8.2) [20].

RV contraction is *sequentially* [5]. Importantly, the whole RV contraction is mainly longitudinally

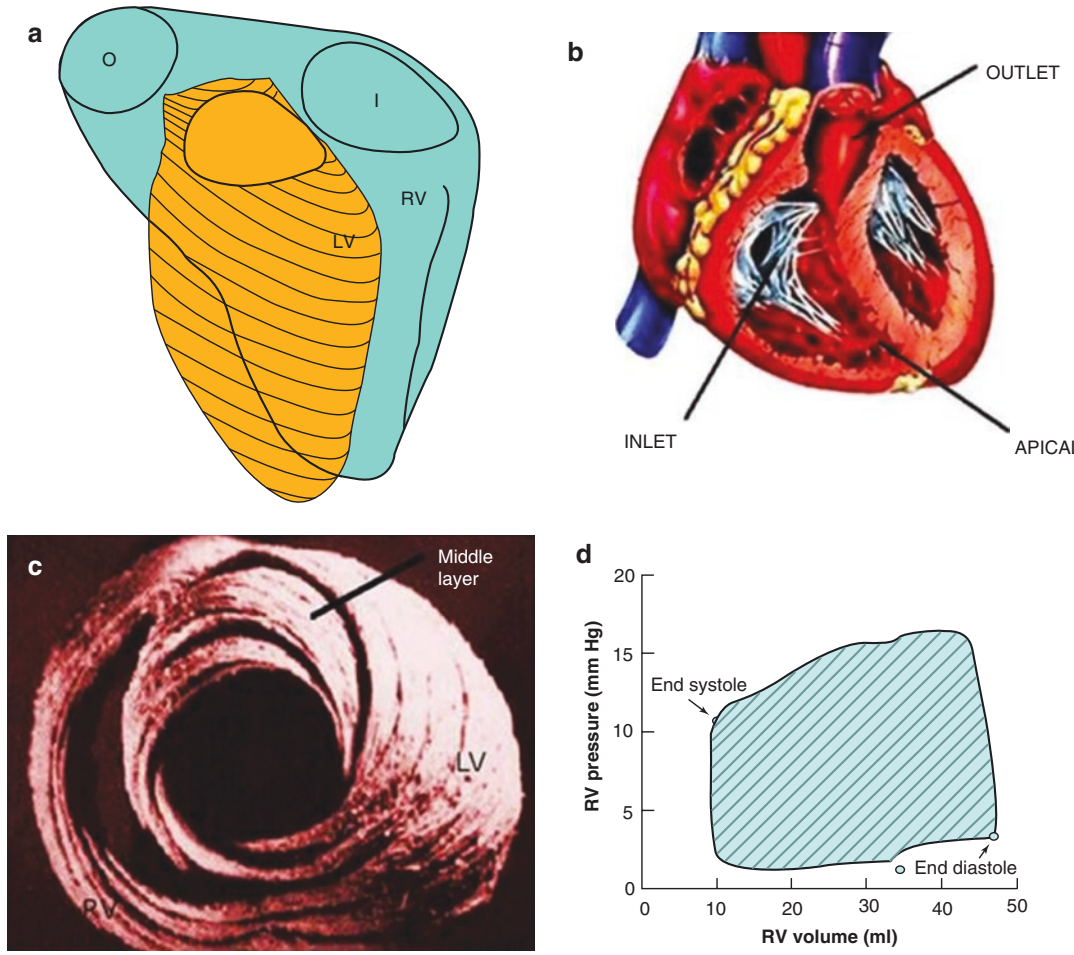

Fig. 8.1 RV anatomy and physiology. (**a**) RV complex shape compared to ellipsoid LV shape. (**b**) Three component parts of RV inside cavity: inlet, apical trabecular, and outlet. (**c**) RV and LV wall fibers layers. The LV middle layer is shown (absent in the RV). (**d**) RV pressure/volume loop. The RV has the same stroke volume compared to the LV but with approximately 25% of stroke work (dashed area under the curve). *I* inlet chamber, *O* outlet chamber. From Vitarelli and Terzano [5] with permission.

Table 8.1 Morphological differences between the RV from the LV

• More apical position of the tricuspid valve as compared to the mitral valve
• Presence of a moderator band
• Presence of more than three papillary muscles
• Three leaflets of the tricuspid valve with septal papillary attachments
• Presence of trabeculations (trabeculations can also be seen in the left ventricle in case of pathological noncompaction of the left ventricle)

From Choudhary et al. [7]. It is an open access chapter.

Table 8.2 Right ventricular contractile functions

1. Longitudinal/twisting motion (septal contraction) – *Interventricular septum shares fibers with both ventricles* – *LV maintains 20–40% RV contractile function*	80%
2. Transverse motion (free wall contraction)	20%
3. Traction of the RV free wall at the points of binding to the LV	

From Kırali et al. [20]. It is an open access chapter.

than radially [5]. Normally, RV afterload is very low, and blood flow gets from the RV into the pulmonary system circulation both during systole and during the early part of diastole, with the lack of isovolumetric relaxation [21]. Step by step, following the description of Vitarelli and Terzano [5] and Leng [22], the period of the isovolumic contraction is caused by subepicardial fibers that shortens RV in a circumferential direction. Subsequently, during the period of the ejection phase caused by subendocardial fibers, the RV shortens longitudinally [5, 22]. On the whole, the RV contraction begins with rapid inlet or the trabeculated myocardium contraction but finishes after 25–50 ms with a longer contraction of the infundibulum with RV ejection [23]. As a result it appears this characteristic "peristaltic" RV contraction. To sum up, Leng [22] and Vitarelli and Terzano [5] described RV contraction having three different mechanisms: (1) "bellows effect"—the inward movement of the free wall, (2) RV shortening in long axis due to contraction of the longitudinal fibers, and (3) "traction on the free wall at the points of attachment secondary to LV contraction" [5, 22].

To date, Damiano et al. [24] studied the significance of systolic ventricular interdependence on RV function, using a single electrically isolated RV free wall preparation. Undeniable, this study showed that the LV contraction is very essential for RV and showed how pressure and volume outflow arised [24]. These results also advocate that the normal geometry of the RV covering LV in its short axis causes RV shortening, along with the end-diastolic transseptal pressure gradient that attributes RV pressure formation. Also, the study of Damiano et al. [24] prove the afterload dependency of RV contractile function [24].

Right Ventricle Physiology Both ventricles pump blood into circulation. In case of RV, its main function is to collect systemic venous return and to pump it into the pulmonary system (Table 8.3) [25–27].

As already described, normal RV is a low-pressure chamber with thinner walls in comparison with the LV (high-pressure chamber) because it faces a low impedance of pulmonary vascular circulation [1, 8]. There is a great difference between systemic and pulmonary circulation. Shortly, the RV pumps against the low-resistance pulmonary circulation, while the LV pumps against the high-resistance systemic circulation [28]. Also, the normal pulmonary vascular resistance is about 10% from the systemic circulation resistance [28]. Moreover, the pulmonary circulation benefits from a decreased pulmonary vascular resistance with higher widening of pulmonary artery [5]. If to take into account only the LV afterload, the LV "workload" is five times higher owing to the higher systemic vascular resistance, than the RV characterized by the low resistance of pulmonary circulation [8, 29].

Interestingly, the cardiac ouput or stroke volume of both ventricles are almost the same because both ventricles are connected in series [26], but the RV pumps blood into pulmonary circulation at 20% of the energy cost [28]. If it is of note, Vitarelli and Terzano [5] affirmed that RV output is realized with about 25% of stroke work, therefore with a reduced amount of energy cost. Also, they stated that this lower energy cost is due to the low pressure of pulmonary circulation and the RV pressure-volume relationship has its distinctive features (Figs. 8.1d and 8.2) [1, 5].

Table 8.3 Comparison of RV and LV Properties [27]. It is an open access article.

Properties	RV	LV
EDV, mL/m^2	75 ± 13 (49–100)	65 ± 12 (44–90)
Mass, g/m^2	26 ± 5 (17–34)	87 ± 12 (64–110)
Wall thickness, mm	2–5	7–11
Ventricular pressure, mmHg	25/4 [(15–30)/ (1–7)]	130/8 [(90–140)/ (5–12)]
Ventricular elastance mmHg/mL	1.30 ± 0.84	5.48 ± 1.23
Afterload (PVR and SVR) (dyne.s.cm^{-5})	70 (20–130)	1100 (700–1600)
Accommodation to imposed load	Better in response to volume overload	Better in response to pressure overload

EDV end-diastolic volume, *PVR* pulmonary vascular resistance, *SVR* systemic vascular resistence

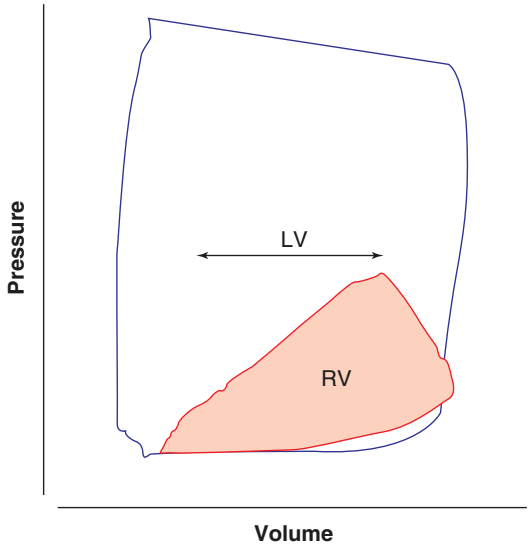

Fig. 8.2 Schematic showing normal human left (LV) and right ventricular (RV) pressure–volume relationships. Unlike the rectangular LV loop, the RV is more trapezoidal, with poorly defined isovolumic periods. Note the continued ejection from the RV during pressure decline (arrow), correlating with the hangout period described by Shaver et al. [37]. See text for details. From Sheehan and Redington [1] with permission

Further, Sheehan and Redington [1] proposed that about 30% of the contractile energy of the RV is created by that of the LV [1]. In same year, Markel et al. [30] proposed that about 40% the RV contractile force comes from LV contraction [30].

There are disagreements looking the RV mass in comparison with LV mass. Firstly, Dell'Italia [25], D'Alto et al. [3], and Kırali et al. [20] sustain that the RV has a mass about one sixth from the LV mass [3, 20, 25]. Conversely, Haddad et al. [26] sustain that mass of the RV is only about one third of the ventricular mass of the LV [26]. Importantly, both hypotheses come up with the idea that RV has lower oxygen consumption in comparison with the LV.

On the echocardiographic examination, RV seems smaller than the LV. However, based on cardiac magnetic resonance imaging (CMRI), the RV volume is larger than the LV volume. Therefore, normal range of RV end-diastolic volume (RVEDV) is 49–101 mL/m^2 whereas the normal range of LV end-diastolic volume (LVEDV) is 44–89 mL/m^2 [23, 31, 32].

LV coronary blood is supplied primarily through diastole. On the other hand, the coronary blood flow of RV is provided during systole and diastole, mainly during cardiac systole [33]. As a result, LV coronary blood flow is not considerably receptive to LV afterload modifications like aortic stenosis. On the other hand, LV has better adaptation to pressure overload states [26]. By definition, *RV afterload* is the load that the RV has to overcome during ejection. Currently, the mainly index used for RV afterload is pulmonary vascular resistance (PVR) [26, 34].

Of note, RV systolic *elastance* is smaller than of the LV. This feature also means that the RV is greatly responsive to raises in *afterload* [35, 36].

The normal human left (LV) and right ventricular (RV) pressure–volume relationships is showed by Fig. 8.2 [1].

As expected, the RV is susceptible to RV afterload modifications such as RV outflow tract obstruction (pulmonary stenosis) and pulmonary hypertension, with raised risk for subendocardial ischemia followed by fibrosis [28, 33]. Also, RV has upper compliance than of LV and enhanced adjustment to *overload states* [26].

It must be emphasized that *the heart–lung relationship* must be taken into consideration in any evaluation of RV function [1]. In particular, the side effect of increased mean airway pressure on the RV function is enhanced even if the RV function is solely altered including pulmonary embolism or after cardiopulmonary bypass [1]. Therefore, the smallest alteration in total pulmonary vascular resistance (PVR) causes diminished contractile function and altered cardiac output of RV [38].

In spite of embryological, anatomical and physiological distinctions, in case of normal states, the RV and LV have almost *same energetic profiles*, including glycolytic, tricarboxylic acid cycle (TCA), oxidative phosphorylation (Ox-Phos) enzyme activities, cellular aerobic capacity and volume fraction of mitochondria, excluding the fact that the RV has with a exception a minor decrease in fatty acid binding protein (FABP) [39].

Consequently, various factors adjust *PVR*, as well as cardiac output, pulmonary volume and

pressure, hypoxia, hypercarbia, and specific molecular pathways—mainly the nitric oxide pathway (vasodilation), the prostaglandin pathway (vasodilation), and the endothelin pathway (vasoconstriction) [25, 26, 40].

To sum up, RV pump function depends on contractility, afterload, preload, heart rate, rhythm, pericardial constraint, interaction with the LV, and valve function [26, 41, 42]. Being a thin-walled chamber, it is not suited to sustain high pressure. The RV can provide great raises in volume better than raises pressure [43].

Right Ventricle Pathophysiology As mentioned above, the RV undergo easier volume overload better than the LV. This can be explained mechanically, because RV has an enhanced muscle compliance that clinically is demonstrated by the finding that RV systolic function greatly conserved even in the case of chronic volume overload, i.e. due to an atrial septal defect (ASD) or tricuspid regurgitation [44].

On the other hand, the adult RV seems to inadequately support the acute raises in the afterload. Among others, MacNee [45] was the first who demonstrated this [45]. They showed by experimentally studies that an acute raise in pulmonary artery pressure (PAP) of 20 mmHg caused a 30% deterioration in RV stroke volume in comparison with increased LV afterload that caused only a 10% decline in stroke volume of LV. Also, they implied mechanisms such as the thin walls with reduced elastance of RV [35]. For instance, moderate to severe pulmonary hypertension typically evoluates in RV dilation and failure. Moreover, even moderate raises in acute pulmonary vascular resistance due to acute pulmonary embolization can alter RV function with inability to produce enough systolic pressure and of a course sudden decrease of the RV stroke volume [46].

Of crucial importance, the RV in comparison with the LV undergo ischaemic injury better because it has a "lesser oxygen demand, higher oxygen extraction reserve capability during stress, dual anatomical supply from the right and left coronary arteries, relatively homogeneous transmural perfusion across the cardiac cycle, and increased propensity to acute collateral development" [47, 48]. Contrary, Ohuchi et al. [49] showed in an experimental study using 3D micro-CT in a porcine model that the RV is more vulnerable to ischemia when stressed [49]. However, these results should be more studied.

On the other hand, various patients with raised RV afterload are able to preserve a near normal cardiac output for long time, whereas others undergo fast decline and death [50, 51]. When faced with a sudden increase in afterload, the normally thin-walled RV is unable of generating a mean pulmonary artery pressure >40 mmHg acutely [52]. Conversely, in case of acute pressure-overload conditions like significant pulmonary embolism, a normal RV has not the ability to produce instantly a mean pulmonary artery pressure >40 mmHg, as a result RV failure arises [46].

The pathophysiology of the pressure-loaded RV is shown in Fig. 8.3 [53].

8.3 Right Heart Hypertrophy

On the whole, cardiac hypertrophy is a powerful clue for the progress of heart failure, arrhythmia, and sudden death [54]. Of note, RV hypertrophy is an independent risk factor for heart failure and cardiovascular mortality [55].

Cardiomyocytes Hypertrophy At cellular level, cardiac injury triggers the adjustement mechanisms like cardiac hypertrophy to preserve cardiac function. Importantly, cardiomyocytes hypertrophy is the main adaptable mechanism for the heart in response to chronic stress. In case of chronic RV increased workload, hypertrophy is related with enhanced interstitial fibrosis, apoptosis, and eventually heart failure [56]. Basically, cardiomyocytes remodelling comprises myocyte hypertrophy [57–59], myocytes number diminishing by apoptosis [57–59] or necrosis [60], fibroblast proliferation [61], and fibrosis [62, 63].

As already described, cardiomyocytes hypertrophy are caused by modifications in the hemodynamic workload [64–66]. Cardiomyocytes reactions during hypertrophy comprise raise in cell size and resetting of the fetal cardiac genes [67].

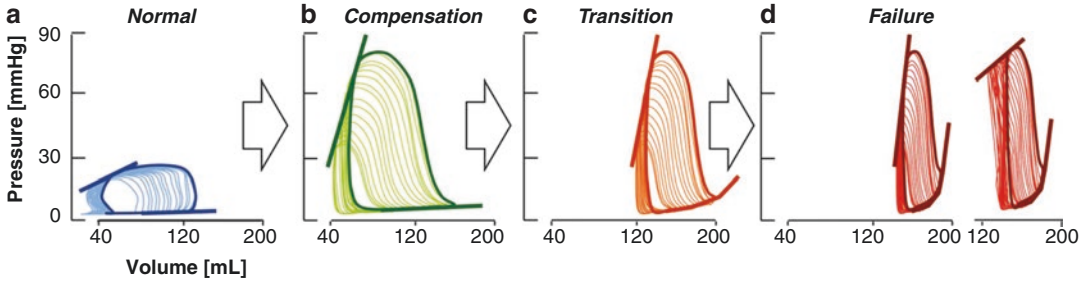

Fig. 8.3 Pathophysiology of the pressure-loaded RV. Conceptual representation of the progression of pathophysiological changes in the pressure-loaded RV. Typical pressure–volume (PV) loops from compensation to failure. Volumetric changes were derived from experimental studies and extrapolated using previously published normal values. Straight lines represent the end- systolic elastance (Ees), dotted lines represent the end-diastolic elastance (Eed). (**a**) PV loop in the unloaded RV, showing normal systolic and diastolic function. (**b**) PV loop in compensated RV, showing increased systolic function (Ees) and RV dilatation (increased end-diastolic volume) but normal diastolic function (Eed). (**c**) PV loop in transition to failure showing increased systolic function (Ees) and impaired diastolic function (Eed). (**d**) PV loop in RV failure showing increased or pseudonormalized systolic function (Ees) and further impaired diastolic function (Eed). From Borgdorff et al. [53]. It is an open access article.

Nonetheless, cardiac hypertrophy needs gene regulation at multiple levels: epigenetic, transcriptional, post-transcriptional, and translational regulation [68]. The mainly trigger for cardiac hypertrophy are mechanical stress and neurohumoral factors [69]. Therefore, without a doubt, hemodynamic overload triggers cardiac hypertrophy partially due to the catecholamines. Further, various cellular reactions modify gene expression, protein synthesis, sarcomere assembly, ion channel function, and energy metabolism (Fig. 8.4) [67, 69].

Inside process, hypertrophy is described by "myocytes enlargement, increase in myocyte size, enhanced protein synthesis, reorganization of sarcomeres, and stereotypical changes in gene expression" [70, 71]. Inside every cardiomyocyte, the response to stress is checked by a system of cyclic nucleotide, mitogen-activated protein kinases (MAPK), Ca^{2+} and phosphoinositide-dependent intracellular signaling pathways (Fig. 8.5) [72, 73].

Right Ventricle Hypertrophy Mechanisms: Outlines Not too much is acknowledged looking the original mechanisms that control the conversion from a pressure-overloaded hypertrophic, normocontractile RV to the dysfunctional and failing RV in various pathological conditions [51]. However, as hypertrophy of the RV rises, the oxygen requirement and distribution by flow upsurge, produce a necessity for a elevated oxygen supply [74, 75].

Same to the LV, the RV has its various adaptable mechanisms that control extremely RV function, including heart rate, the Frank-Starling mechanism, and the autonomic nervous system [25, 26]. Nahrendorf et al. [76] observed that RV has a rather constant hemodynamics even with RV hypertrophy, signifying that pressure/volume overload is not enough to trigger RV hypertrophy, and the involvement of local and systemic renin-angiotensin-aldosterone system activation is possible [76]. The initially increase of neurohormonal activity is to maintain adaptable mechanisms. As described before, same to cardiac remodelling, the pathophysiological Frank-Starling mechanism is also initially triggered to maintain adaptable mechanisms [77–80].

Consequently, the augmentation of RV afterload causes progress of the RV contraction function and its remodelling too [3]. Conversely, if there is no involvement to decrease RV afterload, coronary blood flow to the RV myocardium will decrease with RV ischaemia and cardiomyocytes apoptosis. The hypertrophied RV will gradually dilate, stiffen, and the RV filling and RV stroke volume are equally damaged [81], and RV start to slowly depending on right atrial (RA) function.

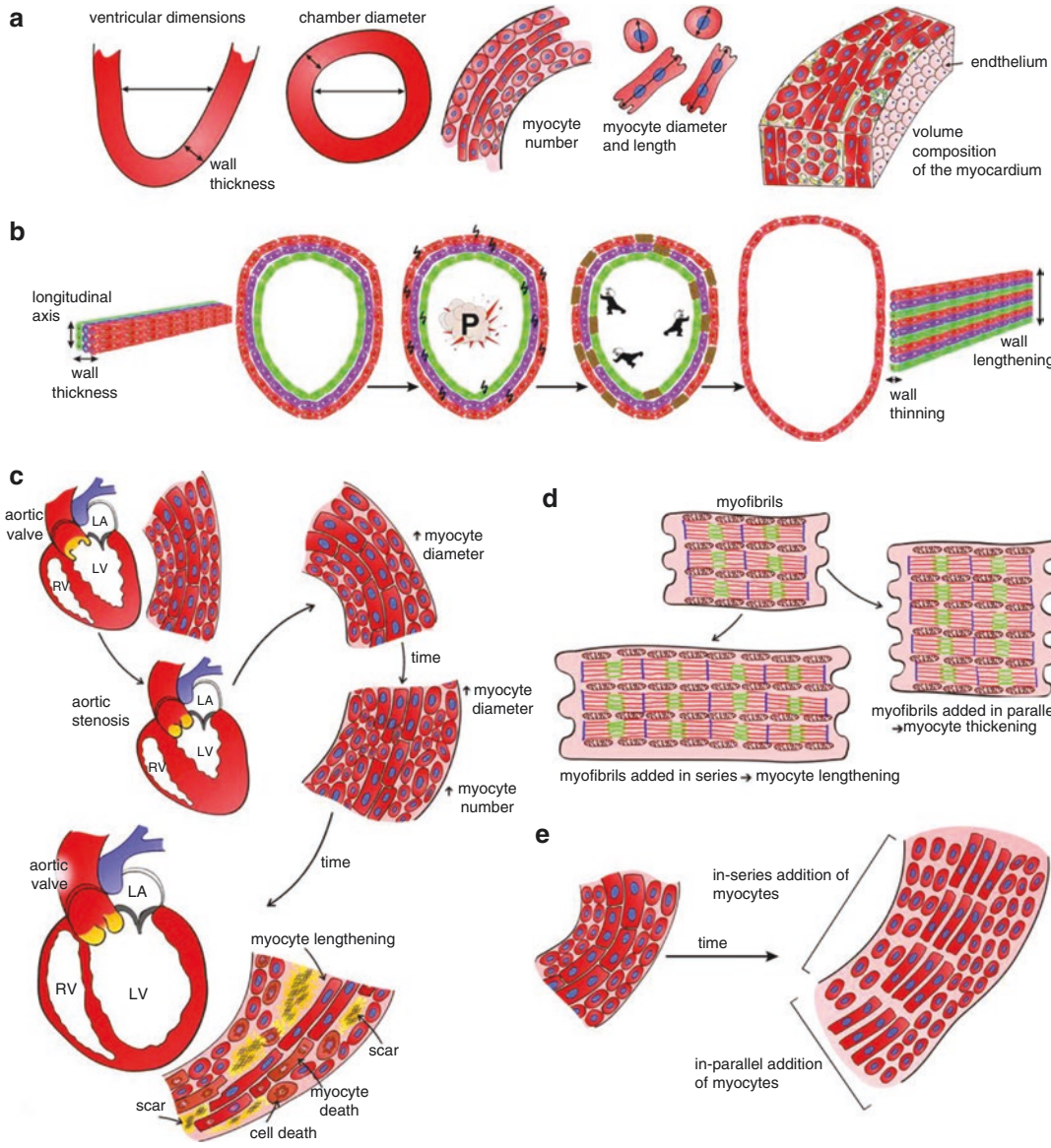

Fig. 8.4 Cellular basis of ventricular remodelling. (**a**) Structural determinants of wall thickness and chamber diameter. (**b**) Sudden increases in diastolic stress (P) affect the architectural integrity of myocyte bundles by triggering apoptotic cell death (thunderbolt; brown cells) which allows the redistribution of myocyte layers within the wall, i.e., side-to-side slippage of cells. This event decreases the number of myocytes across the wall resulting in wall thinning and cavitary dilation as shown in a simplified form in cross and longitudinal orientation of cells. (**c**) Anatomical and cellular changes, together with tissue damage and collagen accumulation, characterize the evolution of pressure overload hypertrophy to cardiac failure. (**d**) The pattern of sarcomere growth conditions increase in myocyte length and diameter. (**e**) New myocytes can be added in series (chamber dilation), or in parallel (wall thickening), or both (chamber dilation and wall thickening). From Leri et al. [67] with permission.

As already is acknowledged for left atrial (LA) function in the pressure-overloaded left heart, a similar adjustement increase in RA contractility and distensibility (reservoir function) happens to preserve filling of the pressure-overloaded stiffened RV [82, 83]. Consequently, increased afterload with increased RV diastolic pressure and distended RA signifies high RA pressure.

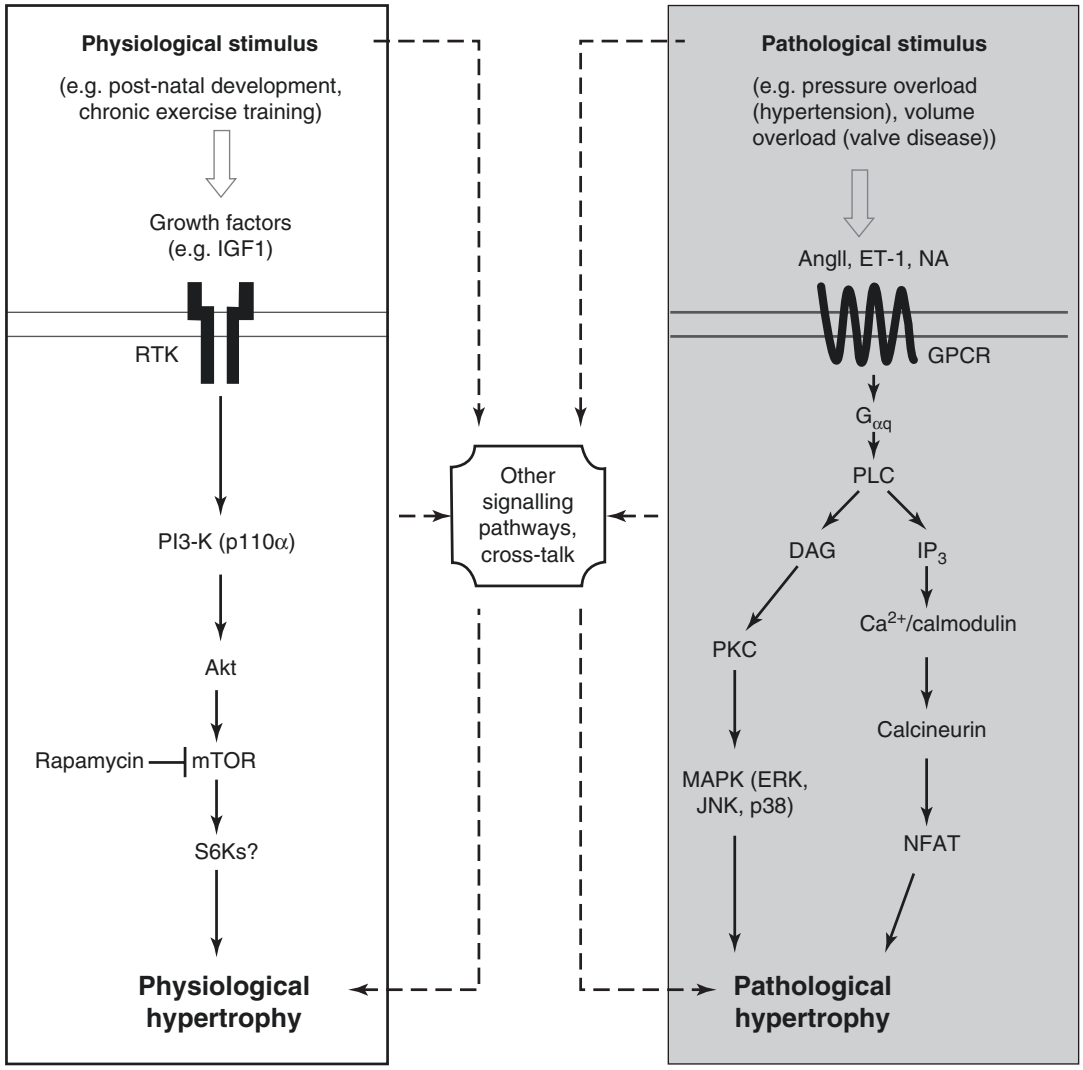

Fig. 8.5 A schematic illustrating the signalling pathways involved in the induction of pathological and physiological cardiac hypertrophy. *RTK* receptor tyrosine kinase, *mTOR* mammalian target of rapamycin, *NA* noradrenaline, *PLC* phospholipase C, *DAG* diacylglycerol, *IP3* inositol 1,4,5-trisphosphate, *MAPK* mitogen-activated protein kinase, *JNK* c-jun amino-terminal kinase, *PKC* protein kinase C, *PI3-K* phosphoinositide-3 kinase, *ERK* extracellular signal-regulated kinase, *AngII* angiotensin II, *ET-1* endothelin 1, *GPCR* G-protein-coupled receptor, *NFAT* nuclear factor of activated T cells, *IGF1* insulin-like growth factor 1, *S6Ks* ribosomal S6 kinases. From McMullen and Jennings [73] with permission.

Nonetheless, RA area is a strong predictor for poor clinical outcome, e.g. in pulmonary arterial hypertension. Similarly, clinical manifestations and prognosis of patients diagnosed with severe pulmonary hypertension, some congenital heart diseases (CHD), and Eisenmenger syndrome, are considerably reliant on the RV function and its adjustment to a chronic raised afterload [3]. It has to be remembered, that the hypertensive heart can present RV hypertrophy with a prevalence of 30% from a meta-analysis of subjects with systemic hypertension [84, 85].

Under these circumstances, a constant pressure overload in RV will end up in diminished cardiac output, heart failure, and deficient end-organ perfusion [86].

Intriguingly, it has been shown that an *acute RV pressure overload* there is no important modification in RV diastolic function, even if the RV elastance increased two- to three- times [87, 88]. Conversely, *chronic RV pressure overload* such as progressive pulmonary artery banding or exposure to chronic normobaric or hypobaric hypoxia, frequently produces RV diastolic dysfunction with increased diastolic relaxation times and raised diastolic stiffness. Together these modifications take place in the hypertrophied RV that is still able to assure its contractile function and cardiac output [51].

As stated above, normal RV muscle mass is decreased in comparison with the LV, the RV being more susceptibile to afterload modifications [89]. For that reason, RV hypertrophy has been correlated with raised RV afterload in numerous human studies [90, 91]. Even if, the RV geometry, hypertrophy, and pressure-volume relationships (Figs. 8.1 and 8.2) are often interconnected, these studies showed a relatively stable RV hemodynamics regardless of RV hypertrophy, signifying that RV hypertrophy is caused mainly by a non significant pressure/volume overload, and a single hypertrophic process may not be a damaging process [76, 90, 92].

As RV hypertrophy evolves and it happens in connection with myocardial fibrosis this modifies "electrical coupling between cells, slows conduction, and dispersion of refractoriness, all of which predispose to arrhythmia's, syncope, and sudden death" [93].

Further, the heart reacts to various cardiopathological disorders with hypertrophic growth by extending each myocyte to diminish ventricular wall tension and to enhance cardiac contractile function. Firstly, this cardiac hypertrophic growth is a frequent adaptable counteract process, but with time it becomes maladaptive. While, RV afterload rises step by step in a constant way in developed disease, it appears an important RV adjustment and patients survive when pulmonary artery pressures are higher than of systemic circulation pressures. At first, the RV end-diastolic volume rises with recovery of cardiac output by the Frank-Starling mechanism. For the moment, this development of adjustment to myocardial hypertrophy is to decrease wall tension/stress and to preserve the normal stroke volume. For instance, RV hypertrophy was observed through 96h of raised afterload in animal studies with the mention when the RV is more concentric and the IVS flattens [94].

There is a switch point between adaptative RV hypertrophy and maladaptative RV hypertrophy [95]. The conversion into maladaptive RV hypertrophy is characterized by diminishing in angiogenesis, inhibition of HIF-1α in the RV, and diminishing in glucose uptake [96]. Further, maladaptive RV hypetrophy causes a "chamber-specific dysregulation of the autonomic nervous system with desensitization and downregulation of α-, β- and dopaminergic receptors in the RV" [97]. Moreover, most of changes from maladaptive RV hypertrophy continue into the LV [97].

Types of Right Ventricle Hypertrophy Cardiac hypertrophy is a complicated remodelling process of the heart due to raised workload triggered by physiological or pathological factors [98, 99]. There are two types of hypertrophy "physiological or adaptive" hypertrophy and "pathological or maladaptive" hypertrophy (Table 8.4) [56, 73].

Even if both pathological and physiological cardiac hypertrophyies are correlated with the development of muscle heart, pathological hypertrophy is related with an intricate display of procedures, mainly "upregulation of fetal genes, histopathology and cardiac dysfunction". The inverse, physiological hypertrophy is correlated with normal cardiac structure and normal or increased cardiac function. In conclusion, it is obviously that pathological and physiological hypertrophyies occur by different signalling molecules [73].

With respect to previous science work, William Osler that wrote the textbook *The Principles and Practice of Medicine* in 1892, was the first who explained that hypertrophy is adaptative and maladaptative [100]. In fact, he related that human heart responds to overload states by three stages that are described with his words:

1. development of hypertrophy depending on the nature of the underlying abnormality.
2. "full compensation," in which hypertrophy allows the heart to meet the increased hemodynamic demand. This concept is now called adaptive hypertrophy.

Table 8.4 Characteristics of pathological and physiological cardiac hypertrophy

	Pathological cardiac hypertrophy	Physiological cardiac hypertrophy
Stimuli	Pressure load in a disease setting (e.g. hypertension, aortic coarction) or volume load (e.g. valvular disease)	Regular physical activity or chronic exercise training
		Volume load (e.g. running, walking, swimming)
	Cardiomyopathy (familial, viral, toxic, metabolic)	Pressure load (e.g. strength training: weight lifting)
Cardiac morphology	Increased myocyte volume	Increased myocyte volume
	Formation of new sarcomeres	Formation of new sarcomeres
	Interstitial fibrosis	
	Myocyte necrosis and apoptosis	
Fetal gene expression	Usually upregulated[a]	Relatively normal[a]
Cardiac function	Depressed over time	Normal or enhanced
Completely reversible	Not usually	Usually
Association with heart failure and increased mortality	Yes	No

From McMullen and Jennings [73] with permission.
[a]Biological significance not clear

3. "broken compensation," which can result in pulmonary edema but more commonly evolves slowly as the result of "degeneration and weakening of the heart muscle." This concept is now called maladaptive hypertrophy.

Physiological hypertrophy characterizes the normal growth of the heart from birth to early adulthood, the growth of maternal heart during pregnancy, and the growth of athletes' heart as a result of physical exercise [101]. It is an adaptive mechanism to normalize ventricular wall stress in response to injury [98]. As expected, physiological hypertrophy is described by the increase of the heart and cardiomyocytes size without cell division, with a better cardiac function with no fibrosis [72]. Notably, during physiological hypertrophy, there is a cardiac structure and function conservation correlated with initiation of myocardial angiogenesis but with no initiation of fibrosis [66].

Pathological hypertrophy signifies cardiac hypertrophy from cardiovascular disorders such as neurohumoral stresses (too much release of hormones and cytokines), various forms of hemodynamic stress (myocardial infarction, hypertension, ischemia) associated with coronary heart disease, valvulopathies, cardiomyopathy or dysfunctions or inherited mutations of genes coding for contractile proteins [54]. By definition, it is characterized by abnormal metabolic, structural and functional findings including fibrosis, cell death and failing function [99]. On long time cardiac hypertrophy can cause diastolic dysfunction, chamber dilatation, and interstitial fibrosis, congestive heart failure, arrhythmia, and sudden death [98, 102].

8.3.1 Concentric and Eccentric Hypertrophy

On the other hand, Göktepe et al. [103] define cardiac hypertrophy or growth as being connected with a broad various pathologies, classified as concentric and eccentric hypertrophy (Fig. 8.6) [54, 103].

Concentric hypertrophy is correlated with wide ventricular walls, impaired filling and diastolic heart failure [104]. Currently, concentric hypertrophy is usually assumed to be determined by pressure overload [105].

Eccentric hypertrophy is connected with dilation of the ventricles, decreased pump function and systolic heart failure [104]. Normally, eccentric hypertrophy is caused by volume overload [105].

Both types of hypertrophy can involve the left and/or right side of the heart [106]. Nonethelesss, in case of RV hypertrophy, it is an adaptable response to reduce wall stress (Laplace's Law) and to enhance contractility [54].

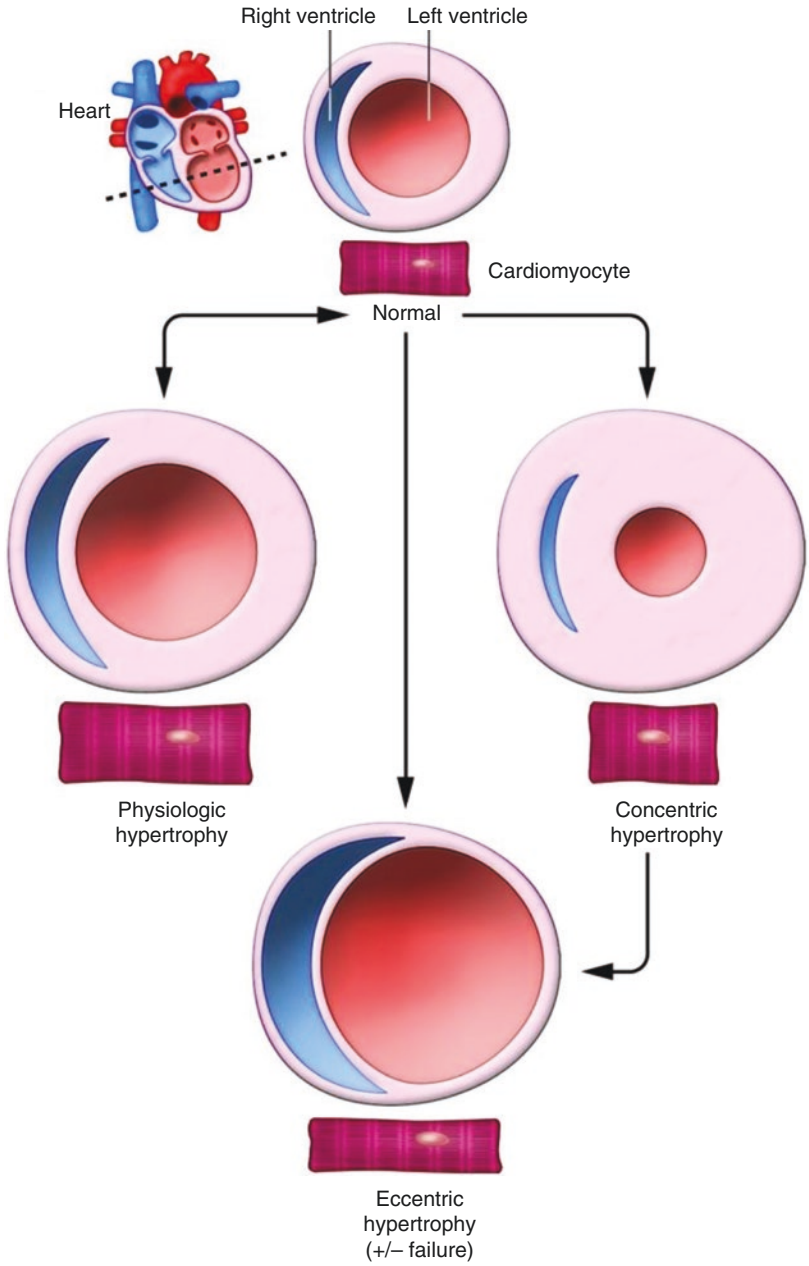

Fig. 8.6 Stimulus-specific hypertrophic responses of the heart and how they affect wall stress (*c*), which, at equal pressures, is proportional to the ratio of internal ventricular radius at end diastole (*r*) and ventricular wall thickness (*h*). From Dorn (2007) with permission (Dorn GW 2nd. The fuzzy logic of physiological cardiac hypertrophy. Hypertension. 2007 May;49(5):962–70. doi: 10.1161/HYPERTENSIONAHA.106.079426)

Figures 8.7 and 8.8 are scanning electron microscopy of human myocardial samples that supports that concentric hypertrophy causes increase in the number of cardiomyocytes branches while eccentric hypertrophy causes their diminishing [107].

8.4 Right Heart Dilatation

The dictum 'left heart failure begets right heart failure' is well known to most clinicians and involves *ventricular interdependence* [108]. Obviously, the failure of one ventricle will cause

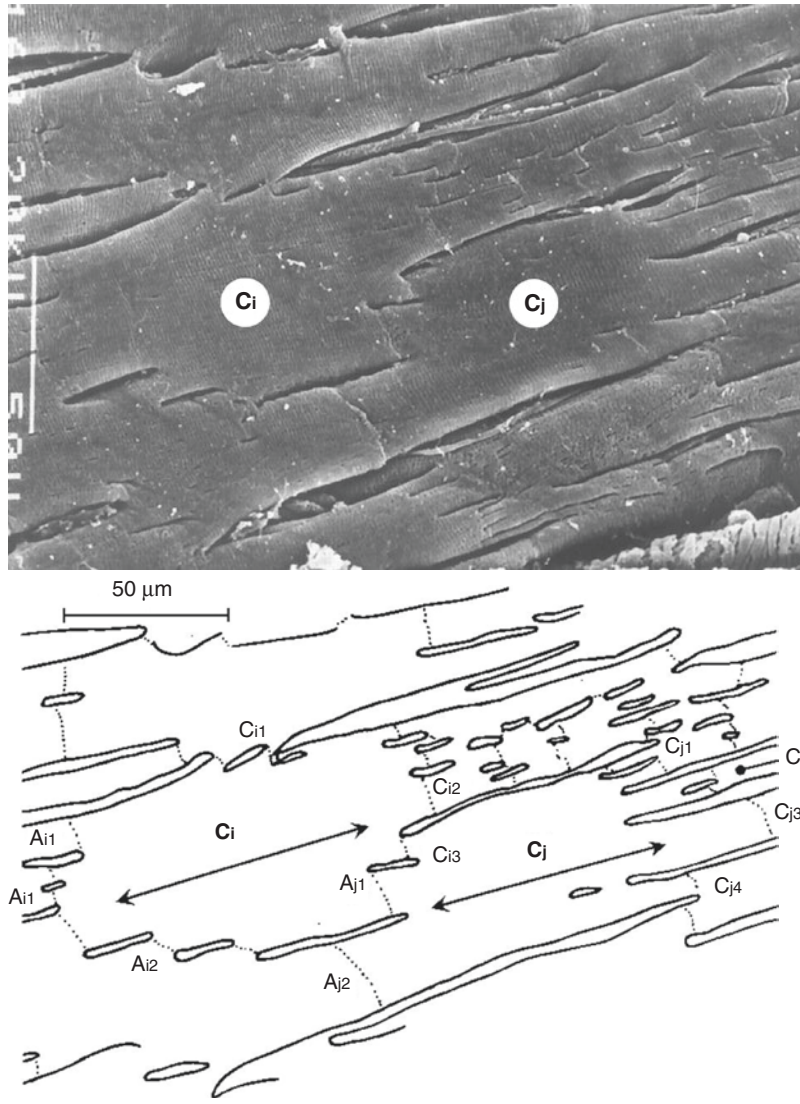

Fig. 8.7 Scanning electron micrograph (top) and a drawing (bottom) of the myocardial fibers of a heart with concentric hypertrophy. The cardiocyte Ci connects with seven cardiocytes in all, and the cardiocyte Cj connects with six in all. From Yamamoto et al. [107] with permission.

in time the failure of the other [108]. A frequent adaptative reaction of the overloaded heart is switching of cardiac hypertrophy to *dilatation* [109, 110]. Further, heart dilatation will try to maintain its normal cardiac output by increasing the number of cardiac muscle bundles with parallel diminishing of wall stress and enhancing of the wall thickness of the myocardium [111]. On the whole, the right-sided overload conditions produces cardiac remodeling with the right ventricular growth and right heart failure characterized by sluggish venous blood flow return, altered pulmonary flow and as a result with insufficient LV preload.

As largely mentioned, the RV has no ability to carry on fast and great raises in PAP pressure. On the other hand, it has same capacity as the LV to preserve *ventriculo-arterial coupling* by adjustement of its systolic function. Therefore, in acute raises of PAP pressure (some minutes), the RV adjust its systolic function by Anrep's law of the heart (homeometric functional modification).

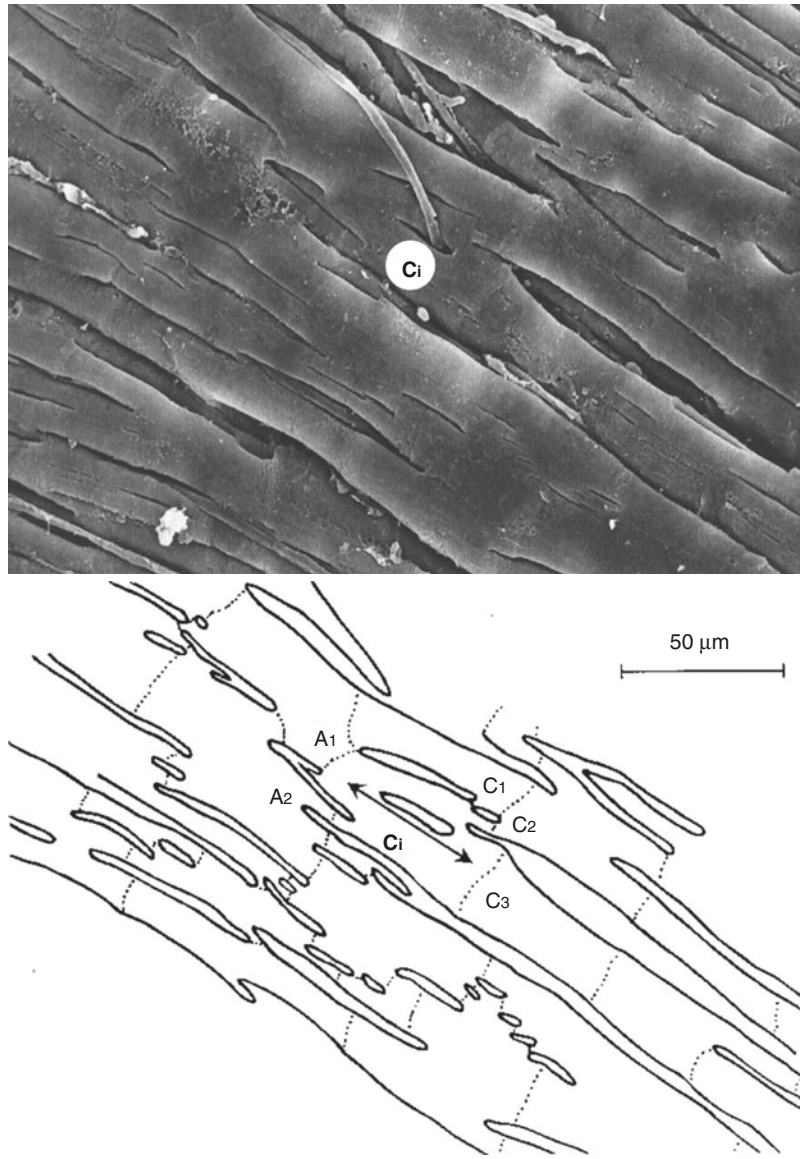

Fig. 8.8 Scanning electron micrograph (top) and a drawing (bottom) of the myocardial fibers of a heart with eccentric hypertrophy. The cardiocyte Ci connects with five cardiocytes in all. From Yamamoto et al. [107] with permission.

Conversely, in chronic raises of PAP pressure, the RV applies Starling's law of the heart (heterometric or dimensional modification) to maintain flow output. Failure of systolic function adjustment in both above situations results in insufficient cardiac output, systemic hypotension and cardiogenic shock. Characteristically, during the initial RV adjustment to raised systolic function appears dyssynchrony (inhomogeneous regional contraction). While, the RV dilates significantly with IVS shift arises asynchrony (late RV systole) when the RV is still pumping and the LV is already filling. At this moment, in fact the systolic ventricular interactions are altered and the LV turns into low supplied chamber with secondary hypotension. Ultimately, the RV dilatation evoluates further in systemic congestion.

Step by step in a RV pressure overloaded often secondary to LV pressure overloaded there is initially myocardial hypertrophy. This process is not enough to normalize wall stress and RV dysfunction as dilatation develops [94]. Further, RV

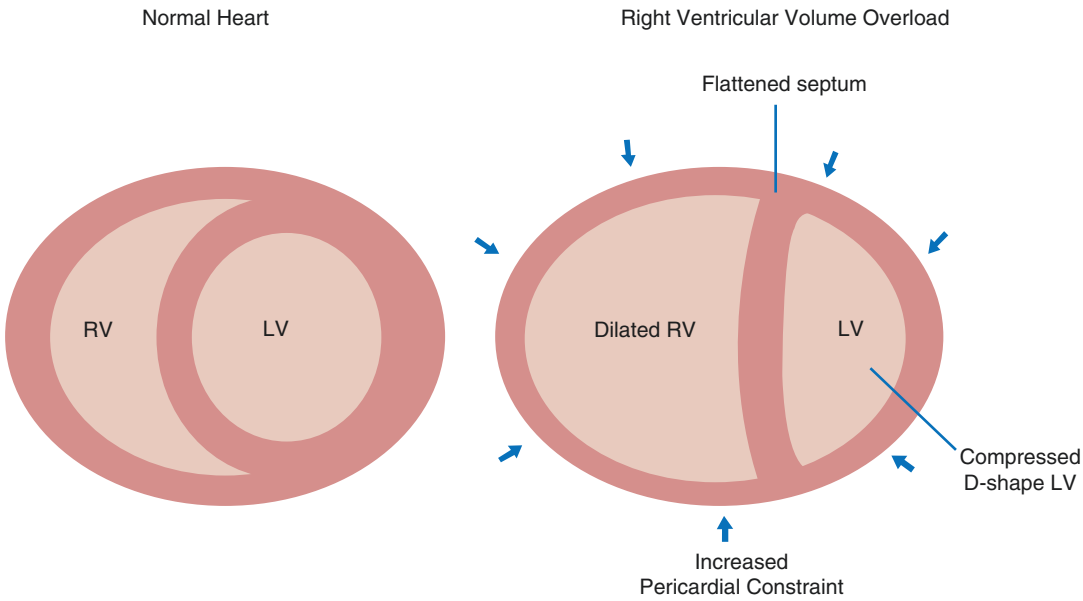

Fig. 8.9 Ventricular interdependence in RV failure. Dilatation of the RV shifts the interventricular septum toward the left, changing LV geometry. Acute RV distension also may lead to an increase in pericardial constraint (arrows). These changes may contribute to low cardiac output state by decreasing LV distensibility, preload, and ventricular elastance. From Haddad et al. [55]. It is an open access article.

develops gradually increasing of filling pressures with diminishing of contraction function, rising RV sphericity, enlargement of tricuspid annulus with functional tricuspid regurgitation [86, 112, 113]. Consequently, there is a progressively volume overload of the RV that is functionally better endured. However, this vicious cycle continues with RV cavity dilation, ventricular wall stress rising, RV contraction function alteration, and diminishing of RV cardiac output.

Conversely, as RV dilates, the ventricular interdependence is gradually evident. As a result, these modifications cause the diminishing of LV distensibility, decreasing of LV end-diastolic volume, decreasing of LV preload with diminishing LV cardiac output [114]. Nonetheless, the LV elastance may be reduced by the mechanisms of ventricular interdependence [115]. As previously mentioned, RV dilatation and/or pressure overload determine a leftward shift of the IVS with modified LV geometry mainly associated with the pericardium constraint (Fig. 8.9) [55].

Another issue is the role of global ischemia even if the RV tolerates better ischemia in comparison with the LV [25]. What's more, in volume overloaded conditions states, there is a dilated and rotated clockwise RV from apex position. The normal crescentic form of RV becomes step by step a cylindrical form, and the IVS is shifted into the LV cavity for the most part of end-diastole [116]. In this case, LV cavity gets a D-shape configuration and the eccentry index is over 1 [117].

The alteration of myocardium in RV causes activation of multiple mechanisms such as adrenergic activation that hyperphosphorylates the sarcoplasmic reticulum and boosts circulating free fatty acids. The presence of circulating free fatty acids inhibit mitochondrial function at the level of acyl carnitine transferase, and further inhibits fatty acid oxidation and synthesis of ATP. Also, circulating free fatty acids inhibit pyruvate dehydrogenase with enhancing of anaerobic glycolysis instead of oxidative metabolism [119, 120].

It is fair to note, that right ventricular function is the most significant independent predictor of survival [121–125]. Moreover, the RV dysfunction does not correlate with the peak of PAP and/or RV pressure does not correlate with the RV dysfunction. In keeping with this finding RV dysfunction is better tolerated in pulmonary stenosis. But RV dysfunction is poor tolerated in

pulmonary vascular hypertension and inflammatory lung disease even if PAPs have same value.

8.4.1 Etiologies of Right Ventricle Dilatation: Short Overview

Without a doubt, RV dilatation is the most frequent cause of tricuspid regurgitation [126]. Causes of primary tricuspid regurgitation include rheumatic heart disease; infective endocarditis; congenital disorders such as Ebstein anomaly; tricuspid valve prolapse; papillary muscle dysfunction caused by ischemia, trauma, connective tissue disorders such as Marfan syndrome; carcinoid heart syndrome; pacemaker leads; radiation therapy; and specific drug-based treatments [126]. Nonetheless, moderate to severe acquired pulmonary hypertension in the adult causes frequently RV dilatation and failure [86]. Most patients with idiopathic pulmonary arterial hypertension develop gradually RV dilatation with RV dysfunction. According to clinical studies, though some patients with pulmonary hypertension acquire RV failure faster in comparison with others even if the pulmonary pressures have same value. Voelkel et al. [127] suggest that modified gene expression and neurohormonal activation are partially responsible for this variation [127].

Intringuily, anterior myocardial infarction (MI) is a common cause of RV dilatation. The study of Hirose and colleagues showed after a 5-year follow-up period of patients with anterior MI that RV volumes upsurge is parallel with LV volumes increase (Figs. 8.10 and 8.11) [128, 129].

In a subsequent study, Beygui et al. [130] showed in patients with inferior wall MI in the absence of RV infarction evaluated by magnetic resonance imaging the existence of RV modifications with biventricular remodeling [130]. Same study also showed that the premature RV dilatation has positive outcomes for LV remodeling, most probably as a result of pericardium constraint determined by RV with stopping of LV dilation after MI [130]. Nonetheless, after an acute myocardial infarction of RV, RV has a significant capacity to recuperate its systolic function at rest and during exercise, showing its resistance to irreversible ischemic injury [115].

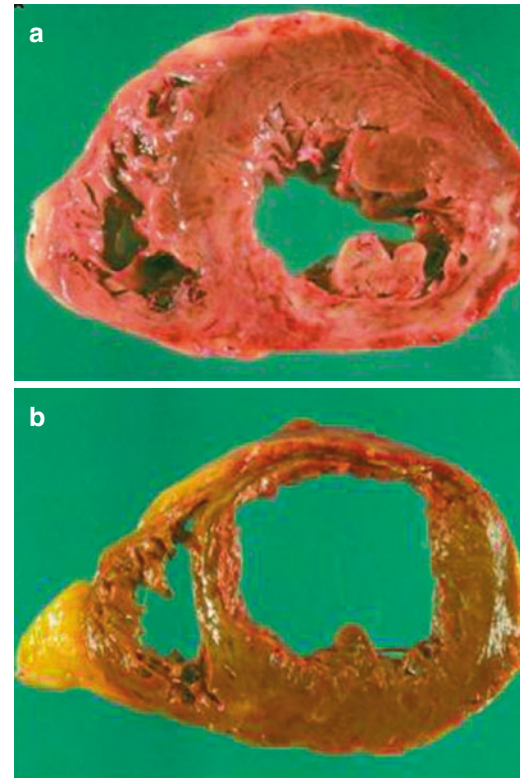

Fig. 8.10 Left ventricular and biventricular enlargement. (**a**) A case of recent posterior wall acute myocardial infarction (day 17) complicated by mild left ventricular dilatation. (**b**) A case of severe biventricular remodelling following anterior wall acute myocardial infarction (day 15). From Bussani et al. [128] with permission.

According to current evidence, RV dilation is a finding after heart transplant. Bhatia and colleagues observed in patients with orthotopic cardiac transplantation a gradually dilation of RV end-diastolic sizes at 1 day and 1 month after surgery compared with control group. In the 1-year after surgery, the RV cavity dimensions diminished in comparison with those from 1 day but still higher compared to control subjects [131]. Same study showed in group with orthotopic cardiac transplantation that increasing of RV dimensions were correlated with tricuspid regurgitation in 67% patients at 1-day, and in 36% at 1-year follow-up [131].

Most common congenital causes of right heart dilatation in adults are pretricuspid left-to-right shunts (secundum ASD—see Fig. 8.12, partially anomalous pulmonary venous connection), post-tricuspid left-to-right shunts, tricuspid valve

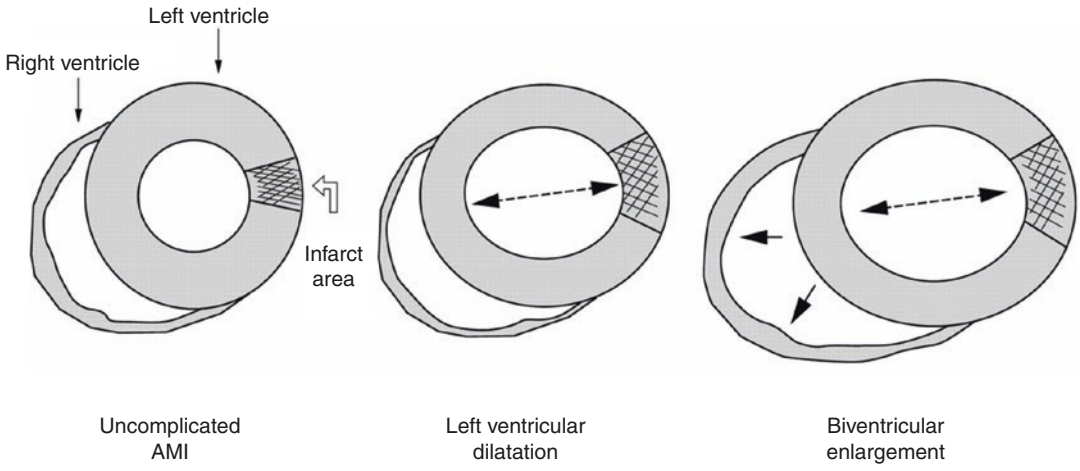

Fig. 8.11 Progressive post-infarction cardiac remodelling. Cardiac remodelling after acute myocardial infarction (AMI) involving the left ventricle may determine progressive left ventricular dilatation and subsequent right ventricular enlargement. Biventricular remodelling identifies a group of patients with an extremely unfavourable prognosis. From Bussani et al. [128] with permission.

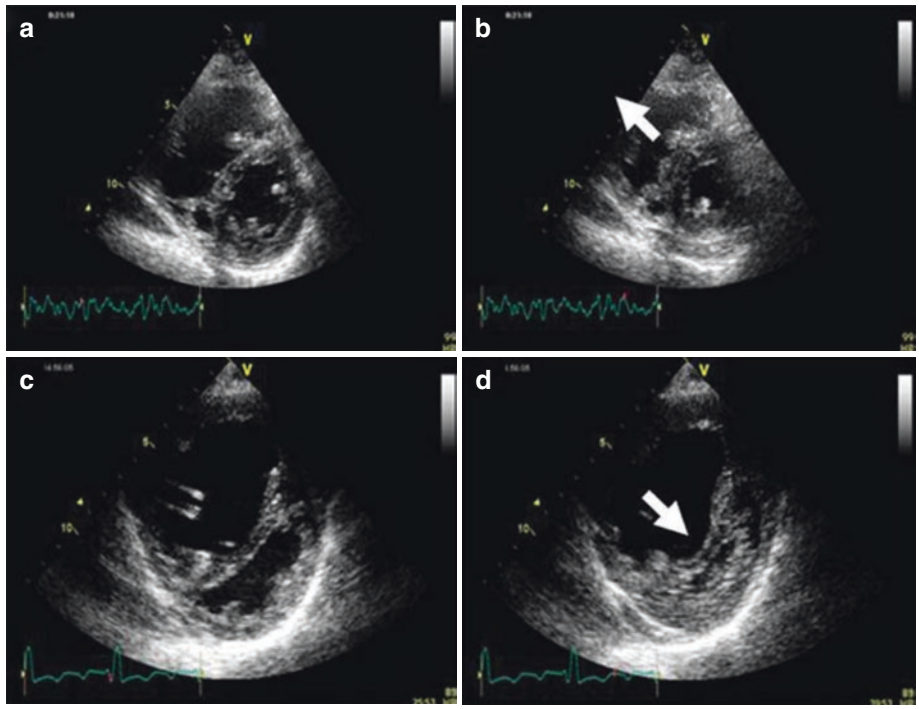

Fig. 8.12 Parasternal short-axis views at the mid-ventricular level. (**a**, **b**) Patient with *atrial septal defect type ostium secundum*, consequent right ventricular volume overload, and mildly elevated pulmonary artery pressures—flattening of the interventricular septum at end diastole (**a**) and recovering of shape at end systole (arrow) (**b**). (**c**, **d**). Patient with severe pulmonary arterial hypertension and consequent severe right ventricular pressure overload—flattening of the interventricular septum both at end diastole (**c**) and end systole (arrow) (**d**). From Jurcut et al. [118] with permission.

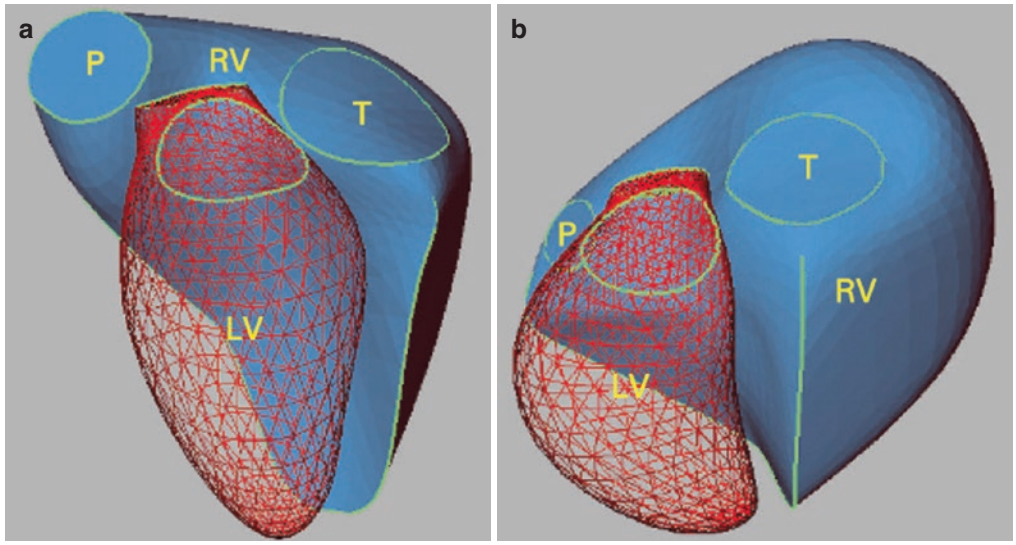

Fig. 8.13 Three dimensional reconstructions of the right ventricle (RV) illustrating its complex shape in a normal subject (**a**). RV remodelling in diseased hearts can result in profound shape change, as in this patient (**b**) with dilated RV due to severe pulmonary regurgitation following repair of tetralogy of Fallot. The mesh surface is the left ventricle. *LV* left ventricle, *P* pulmonary valve, *RV* right ventricle, *T* tricuspid valve. From: Sheehan and Redington [1] with permission.

regurgitation (Ebstein's anomaly), myocardium, and pulmonary valve regurgitation (postsurgical repair of right ventricular outflow tract obstruction as tetralogy of Fallot—see Fig. 8.13) [132]. In fact, Cook et al. [132] split left-to right shunts into pretricuspid and posttricuspid shunts. The pretricuspid shunts dilate the right heart, while the posttricuspid shunts dilate the left heart. Also, the structural abnormalities of the right-sided valves and the myocardium are correlated with right heart chambers dilation [132].

It has to be mentioned that in case of patients with congenital pulmonary stenosis, the RV has initially a higher hypertrophy with earlier elliptic form but dilation arises later in this disease in the absence of a severe stenosis [23].

In addition, patients with successful atrial septal defect repair may frequent present residual RV dilatation and paradoxical ventricular septal motion. According to the study of Pearlman et al. [133] even the mean RV dimensions diminished after surgery and only 23% patients were within normal values of RV dimensions [133].

Conclusions

In 2006, the National Heart, Lung, and Blood Institute recognized RV physiology as a main concern in cardiovascular research [127]. Obviously, the significance of RV function in the biventricular circulation and the pathogenesis and prognosis of numerous cardiovascular diseases it is increasing. However, the last two decades enhanced knowledge about the physiologic importance of the RV triggering opening for better therapeutic interventions [1]. In conclusion, "right and left heart are interdependent and work in synergy, but they are also independent as they are genetically, embriologically, and pathopysiologically different" [5].

References

1. Sheehan F, Redington A. The right ventricle: anatomy, physiology and clinical imaging. Heart. 2008;94(11):1510–5. https://doi.org/10.1136/hrt.2007.132779.
2. Kondo RP, Dederko DA, Teutsch C, Chrast J, Catalucci D, Chien KR, Giles WR. Comparison of contraction and calcium handling between right and left ventricular myocytes from adult mouse heart: a role for repolarization waveform. J Physiol. 2006;571:131–46.
3. D'Alto M, Scognamiglio G, Dimopoulos K, Bossone E, Vizza D, Romeo E, Vonk-Noordergraaf A, Gaine S, Peacock A, Naeije R. Right heart and pulmonary

vessels structure and function. Echocardiography. 2015;32(Suppl 1):S3–10. https://doi.org/10.1111/echo.12227.
4. Sánchez-Quintana D, Doblado-Calatrava M, Cabrera JA, Macías Y, Saremi F. Anatomical basis for the cardiac interventional electrophysiologist. Biomed Res Int. 2015;2015:547364. https://doi.org/10.1155/2015/547364.
5. Vitarelli A, Terzano C. Do we have two hearts? New insights in right ventricular function supported by myocardial imaging echocardiography. Heart Fail Rev. 2010;15(1):39–61. https://doi.org/10.1007/s10741-009-9154-x.
6. Goor DA, Lillehei CW. Congenital malformations of the heart. 1st ed. New York: Grune and Stratton; 1975. p. 1–37.
7. Choudhary G, Malik AA, Stapleton D, Reddy PC. Assessment of right ventricle by echocardiogram, echocardiography in heart failure and cardiac electrophysiology, Lakshmanadoss U, editor. Intech; 2016. https://doi.org/10.5772/64781. Available from https://www.intechopen.com/books/echocardiography-in-heart-failure-and-cardiac-electrophysiology/assessment-of-right-ventricle-by-echocardiogram. Open access chapter.
8. Friedberg MK, Redington AN. Right versus left ventricular failure: differences, similarities, and interactions. Circulation. 2014;129(9):1033–44. https://doi.org/10.1161/CIRCULATIONAHA.113.001375.
9. Kaul S. The interventricular septum in health and disease. Am Heart J. 1986;112:568–81.
10. Lindqvist P, Morner S, Karp K, Waldenstrom A. New aspects of septal function by using 1-dimensional strain and strain rate imaging. J Am Soc Echocardiogr. 2006;19:1345–9.
11. Klima U, Guerrero JL, Vlahakes GJ. Contribution of the interventricular septum to maximal right ventricular function. Eur J Cardiothorac Surg. 1998;14:250–5.
12. Blessberger H, Binder T. Non-invasive imaging: two dimensional speckle tracking echocardiography: basic principles. Heart. 2010;96(9):716–22. https://doi.org/10.1136/hrt.2007.141002.
13. Thomas JD, Popović ZB. Assessment of left ventricular function by cardiac ultrasound. Am Coll Cardiol. 2006;48(10):2012–25. https://doi.org/10.1016/j.jacc.2006.06.071.
14. Geva T, Powell AJ, Crawford EC, Chung T, Colan SD. Evaluation of regional differences in right ventricular systolic function by acoustic quantification echocardiography and cine magnetic resonance imaging. Circulation. 1998;98:339–45.
15. Bleeker GB, Steendijk P, Holman ER, Yu CM, Breithardt OA, Kaandorp TA, Schalij MJ, van der Wall EE, Nihoyannopoulos P, Bax JJ. Assessing right ventricular function: the role of echocardiography and complementary technologies. Heart. 2006;92(Suppl 1):i19–26. https://doi.org/10.1136/hrt.2005.082503.
16. Lindqvist P, Calcutteea A, Henein M. Echocardiography in the assessment of right heart function. Eur J Echocardiogr. 2008;9(2):225–34. https://doi.org/10.1016/j.euje.2007.04.002.
17. Rouleau JL, Paradis P, Shenasa H, et al. Faster time to peak tension and velocity of shortening in right versus left ventricular trabeculae and papillary muscles of dogs. Circ Res. 1986;59:556–61.
18. Brooks WW, Bing OH, Blaustein AS, Allen PD. Comparison of contractile state and myosin isozymes of rat right and left ventricular myocardium. J Mol Cell Cardiol. 1987;19(5):433–40.
19. Harding SE, O'Gara P, Jones SM, Brown LA, Vescovo G, Poole-Wilson PA. Species dependence of contraction velocity in single isolated cardiac myocytes. Cardioscience. 1990;1(1):49–53.
20. Kırali K, Özer T, Özgür MM. Pathophysiology in heart failure, cardiomyopathies – types and treatments, Kırali K, editor. Intech; 2017. https://doi.org/10.5772/66887. Available from https://www.intechopen.com/books/cardiomyopathies-types-and-treatments/pathophysiology-in-heart-failure. Open access chapter.
21. Berlin DA, Bakker J. Understanding venous return. Intensive Care Med. 2014;40:1564–6.
22. Leng J. Right ventricle. In: Weyman AE, editor. Principle and practice of echocardiography. Philadelphia: Lippincott Williams & Wilkins; 1994. p. 901–21.
23. Haddad F, Couture P, Tousignant C, Denault AY. The right ventricle in cardiac surgery, a perioperative perspective: I. Anatomy, physiology, and assessment. Anesth Analg. 2009;108(2):407–21. https://doi.org/10.1213/ane.0b013e31818f8623.
24. Damiano RJ Jr, La Follette P Jr, Cox JL, Lowe JE, Santamore WP. Significant left ventricular contribution to right ventricular systolic function. Am J Phys. 1991;261(5 Pt 2):H1514–24.
25. Dell'Italia LJ. The right ventricle: anatomy, physiology, and clinical importance. Curr Probl Cardiol. 1991;16:653–720.
26. Haddad F, Hunt SA, Rosenthal DN, Murphy DJ. Right ventricular function in cardiovascular disease. I. Anatomy, physiology, aging, and functional assessment of the right ventricle. Circulation. 2008;117(11):1436–48. https://doi.org/10.1161/CIRCULATIONAHA.107.653576.
27. Walker LA, Buttrick PM. The right ventricle: biologic insights and response to disease: updated. Curr Cardiol Rev. 2013;9(1):73–81. Open access article.
28. Gentles TL, Mayer JE Jr, Gauvreau K, Newburger JW, Lock JE, Kupferschmid JP, Burnett J, Jonas RA, Castañeda AR, Wernovsky G. Fontan operation in five hundred consecutive patients: factors influencing early and late outcome. J Thorac Cardiovasc Surg. 1997;114(3):376–91.
29. Tedford RJ. Determinants of right ventricular afterload (2013 grover conference series). Pulm Circ. 2014;4:211–9.
30. Markel TA, Wairiuko GM, Lahm T, Crisostomo PR, Wang M, Herring CM, Meldrum DR. The right heart and its distinct mechanisms of development, function, and failure. J Surg Res. 2008;146:304–13.

31. Lorenz CH, Walker ES, Morgan VL, Klein SS, Graham TP Jr. Normal human right and left ventricular mass, systolic function, and gender differences by cine magnetic resonance imaging. J Cardiovasc Magn Reson. 1999;1:7–21.
32. Mahler DA, Matthay RA, Snyder PE, Pytlik L, Zaret BL, Loke J. Volumetric responses of right and left ventricles during upright exercise in normal subjects. J Appl Physiol. 1985;58:1818–22.
33. Reddy S, Bernstein D. The vulnerable right ventricle. Curr Opin Pediatr. 2015;27(5):563–8. https://doi.org/10.1097/MOP.0000000000000268.
34. Goldstein JA. Pathophysiology and management of right heart ischemia. J Am Coll Cardiol. 2002;40(5):841–53.
35. Dell'Italia LJ, Walsh RA. Application of a time varying elastance model to right ventricular performance in man. Cardiovasc Res. 1988;22(12):864–74.
36. Guyton AC, Lindsey AW, Gilluly JJ. The limits of right ventricular compensation following acute increase in pulmonary circulatory resistance. Circ Res. 1954;2(4):326–32.
37. Shaver JA, Nadolny RA, O'Toole JD, et al. Sound pressure correlates of the second heart sound. An intracardiac sound study. Circulation. 1974;49:316–25.
38. Shekerdemian LS, Bush A, Lincoln C, Shore DF, Petros AJ, Redington AN. Cardiopulmonary interactions in healthy children and children after simple cardiac surgery: the effects of positive and negative pressure ventilation. Heart. 1997;78:587–93.
39. Phillips D, Aponte AM, Covian R, Neufeld E, ZX Y, Balaban RS. Homogenous protein programming in the mammalian left and right ventricle free walls. Physiol Genomics. 2011;43:1198–206.
40. McLaughlin VV, McGoon MD. Pulmonary arterial hypertension. Circulation. 2006;114(13):1417–31. https://doi.org/10.1161/CIRCULATIONAHA.104.503540.
41. Naeije R, Brimioulle S, Dewachter L. Biomechanics of the right ventricle in health and disease (2013 Grover Conference series). Pulm Circ. 2014;4:395–406.
42. Voelkel NF, Gomez-Arroyo J, Abbate A, Bogaard HJ. Mechanisms of right heart failure-a work in progress and a plea for failure prevention. Pulm Circ. 2013;3:137–43.
43. Kosiborod M, Wackers FJ. Assessment of right ventricular morphology and function. Semin Respir Crit Care Med. 2003;24:245–62.
44. Webb G, Gatzoulis MA. Atrial septal defects in the adult: recent progress and overview. Circulation. 2006;114(15):1645–53.
45. MacNee W. Pathophysiology of cor pulmonale in chronic obstructive pulmonary disease. Part One. Am J Respir Crit Care Med. 1994;150(3):833–52.
46. Goldhaber SZ, Visani L, De Rosa M. Acute pulmonary embolism: clinical outcomes in the International Cooperative Pulmonary Embolism Registry (ICOPER). Lancet. 1999;353(9162):1386–9.
47. Laster SB, Ohnishi Y, Saffitz JE, Goldstein JA. Effects of reperfusion on ischemic right ventricular dysfunction. Disparate mechanisms of benefit related to duration of ischemia. Circulation. 1994;90:1398–409.
48. Laster SB, Shelton TJ, Barzilai B, Goldstein JA. Determinants of the recovery of right ventricular performance following experimental chronic right coronary artery occlusion. Circulation. 1993;88:696–708.
49. Ohuchi H, Beighley PE, Dong Y, Zamir M, Ritman EL. Microvascular development in porcine right and left ventricular walls. Pediatr Res. 2007;61:676–80.
50. Bristow MR, Zisman LS, Lowes BD, Abraham WT, Badesch DB, Groves BM, Voelkel NF, Lynch DM, Quaife RA. The pressure-overloaded right ventricle in pulmonary hypertension. Chest. 1998;114(Suppl. 1):101S–6S.
51. Pokreisz P, Marsboom G, Janssens G. Pressure overload-induced right ventricular dysfunction and remodelling in experimental pulmonary hypertension: the right heart revisited. Eur Heart J Suppl. 2007;9(Supplement H):H75–84. https://doi.org/10.1093/eurheartj/sum021.
52. Schulman DS, Matthay RA. The right ventricle in pulmonary disease. Cardiol Clin. 1992;10:111–35.
53. Borgdorff MA, Dickinson MG, Berger RM, Bartelds B. Right ventricular failure due to chronic pressure load: What have we learned in animal models since the NIH working group statement? Heart Fail Rev. 2015;20(4):475–91. Open access article.
54. van Berlo JH, Maillet M, Molkentin JD. Signaling effectors underlying pathologic growth and remodeling of the heart. J Clin Invest. 2013;123(1):37–45. https://doi.org/10.1172/JCI62839.
55. Haddad F, Doyle R, Murphy DJ, Hunt SA. Right ventricular function in cardiovascular disease, part II: pathophysiology, clinical importance, and management of right ventricular failure. Circulation. 2008a;117(13):1717–31. https://doi.org/10.1161/CIRCULATIONAHA.107.653584.
56. Frey N, Olson EN. Cardiac hypertrophy: the good, the bad, and the ugly. Annu Rev Physiol. 2003;65:45–79. https://doi.org/10.1146/annurev.physiol.65.092101.142243.
57. Sharov VG, Sabbah HN, Shimoyama H, Goussev AV, Lesch M, Goldstein S. Evidence of cardiocyte apoptosis in myocardium of dogs with chronic heart failure. Am J Pathol. 1996;148(1):141–9.
58. Teiger E, Than VD, Richard L, Wisnewsky C, Tea BS, Gaboury L, Tremblay J, Schwartz K, Hamet P. Apoptosis in pressure overload-induced heart hypertrophy in the rat. J Clin Invest. 1996;97(12):2891–7.
59. Olivetti G, Abbi R, Quaini F, Kajstura J, Cheng W, Nitahara JA, Quaini E, Di Loreto C, Beltrami CA, Krajewski S, Reed JC, Anversa P. Apoptosis in the failing human heart. N Engl J Med. 1997;336(16):1131–41.
60. Tan LB, Jalil JE, Pick R, Janicki JS, Weber KT. Cardiac myocyte necrosis induced by angiotensin II. Circ Res. 1991;69(5):1185–95.

61. Villarreal FJ, Kim NN, Ungab GD, Printz MP, Dillmann WH. Identification of functional angiotensin II receptors on rat cardiac fibroblasts. Circulation. 1993;88(6):2849–61.
62. Anderson KR, Sutton MG, Lie JT. Histopathological types of cardiac fibrosis in myocardial disease. J Pathol. 1979;128(2):79–85.
63. Weber KT, Pick R, Silver MA, Moe GW, Janicki JS, Zucker IH, Armstrong PW. Fibrillar collagen and remodeling of dilated canine left ventricle. Circulation. 1990;82(4):1387–401.
64. Akazawa H, Komuro I. Roles of cardiac transcription factors in cardiac hypertrophy. Circ Res. 2003;92(10):1079–88.
65. Kamo T, Akazawa H, Komuro I. Cardiac nonmyocytes in the hub of cardiac hypertrophy. Circ Res. 2015;117(1):89–98.
66. Oka T, Akazawa H, Naito AT, Komuro I. Angiogenesis and cardiac hypertrophy: maintenance of cardiac function and causative roles in heart failure. Circ Res. 2014;114(3):565–71.
67. Leri A, Kajstura J, Anversa P. Role of cardiac stem cells in cardiac pathophysiology: a paradigm shift in human myocardial biology. Circ Res. 2011;109(8):941–61. https://doi.org/10.1161/CIRCRESAHA.111.243154.
68. Dassanayaka S, Jones SP. Recent developments in heart failure. Circ Res. 2015;117(7):e58–63.
69. Siri FM, McNamara JJ. Effects of sympathectomy on heart size and function in aortic-constricted rats. Am J Phys. 1987;252(2 Pt 2):H442–7.
70. Finn SG, Dickens M, Fuller SJ. c-Jun N-terminal kinase-interacting protein 1 inhibits gene expression in response to hypertrophic agonists in neonatal rat ventricular myocytes. Biochem J. 2001;358:489–95.
71. Sundaresan NR, Gupta M, Kim G, Rajamohan SB, Isbatan A, Gupta MP. Sirt3 blocks the cardiac hypertrophic response by augmenting Foxo3a-dependent antioxidant defense mechanisms in mice. J Clin Invest. 2009;119:2758–71.
72. Heineke J, Molkentin JD. Regulation of cardiac hypertrophy by intracellular signalling pathways. Nat Rev Mol Cell Biol. 2006;7(8):589–600. https://doi.org/10.1038/nrm1983.
73. McMullen JR, Jennings GL. Differences between pathological and physiological cardiac hypertrophy: novel therapeutic strategies to treat heart failure. Clin Exp Pharmacol Physiol. 2007;34(4):255–62. https://doi.org/10.1111/j.1440-1681.2007.04585.x.
74. Rain S, Handoko ML, Vonk Noordegraaf A, Bogaard HJ, van der Velden J, de Man FS. Pressure-overload-induced right heart failure. Pflugers Arch. 2014;466:1055–63.
75. Ruiter G, Ying Wong Y, de Man FS, Louis Handoko M, Jaspers RT, Postmus PE, Westerhof N, Niessen HW, van der Laarse WJ, Vonk-Noordegraaf A. Right ventricular oxygen supply parameters are decreased in human and experimental pulmonary hypertension. J Heart Lung Transplant. 2013;32:231–40.
76. Nahrendorf M, Hu K, Fraccarollo D, et al. Time course of right ventricular remodeling in rats with experimental myocardial infarction. Am J Physiol Heart Circ Physiol. 2002;284:241–8.
77. Bocchi EA, Marcondes-Braga FG, Bacal F, et al. Updating of the Brazilian guideline for chronic heart failure – 2012. Arq Bras Cardiol. 2012;98(1 Suppl 1):1–33.
78. Jessup M, Brozena S. Heart failure. N Engl J Med. 2003;348(20):2007–18.
79. Colucci WS. Molecular and cellular mechanisms of myocardial failure. Am J Cardiol. 1997;80(11A):15L–25L.
80. Schrier RW, Abraham WT. Hormones and hemodynamics in heart failure. N Engl J Med. 1999;341(8):577–85.
81. Mebazaa A, Karpati P, Renaud E, Algotsson L. Acute right ventricular failure: from pathophysiology to new treatments. Intensive Care Med. 2004;30:185–96.
82. Gaynor SL, Maniar HS, Bloch JB, Steendijk P, Moon MR. Right atrial and ventricular adaptation to chronic right ventricular pressure overload. Circulation. 2005a;112(Suppl. 9):I212–8.
83. Gaynor SL, Maniar HS, Prasad SM, Steendijk P, Moon MR. Reservoir and conduit function of right atrium: impact on right ventricular filling and cardiac output. Am J Physiol Heart Circ Physiol. 2005;288:H2140–5.
84. Cuspidi C, Negri F, Giudici V, Valerio C, Meani S, Sala C, et al. Prevalence and clinical correlates of right ventricular hypertrophy in essential hypertension. J Hypertens. 2009;27:854–60.
85. Cuspidi C, Sala C, Muiesan ML, De Luca N, Schillaci G. Right ventricular hypertrophy in systemic hypertension: an updated review of clinical studies. J Hypertens. 2013;31:858–65.
86. Chin KM, Kim NH, Rubin LJ. The right ventricle in pulmonary hypertension. Coron Artery Dis. 2005;16:13–8.
87. de Vroomen M, Cardozo RH, Steendijk P, van Bel F, Baan J. Improved contractile performance of right ventricle in response to increased RV afterload in newborn lamb. Am J Physiol Heart Circ Physiol. 2000;278:H100–5.
88. Hon JK, Steendijk P, Khan H, Wong K, Yacoub M. Acute effects of pulmonary artery banding in sheep on right ventricle pressure-volume relations: relevance to the arterial switch operation. Acta Physiol Scand. 2001;172:97–106.
89. Kowalewski J, Brocki M, Dryjanski T, Kapron K, Barcikowski S. Right ventricular morphology and function after pulmonary resection. Eur J Cardiothorac Surg. 1999;15:444–8.
90. Eltzschig HK, Mihaljevic T, Byrne JG, Ehlers R, Smith B, Shernan SK. Echocardiographic evidence of right ventricular remodeling after transplantation. Ann Thorac Surg. 2002;74:584–6.
91. Rozenberg VD, Nepomnyashchikh LM. Postinfarction remodeling of the heart: types of pathomorphological

changes in the right ventricle. Bull Exp Biol Med. 2003;136:291–5.
92. Gardner JD, Brower GL, Janicki JS. Gender differences in cardiac remodeling secondary to chronic volume overload. J Card Fail. 2002;8:101–7.
93. Hill JA. Electrical remodeling in cardiac hypertrophy. Trends Cardiovasc Med. 2003;13:316–22.
94. Dias CA, Assad RS, Caneo LF, et al. Reversible pulmonary trunk banding. II. An experimental model for rapid pulmonary ventricular hypertrophy. J Thorac Cardiovasc Surg. 2002;124(5):999–1006.
95. Sutendra G, Dromparis P, Paulin R, Zervopoulos S, Haromy A, Nagendran J, Michelakis ED. A metabolic remodeling in right ventricular hypertrophy is associated with decreased angiogenesis and a transition from a compensated to a decompensated state in pulmonary hypertension. J Mol Med (Berl). 2013;91:1315–27.
96. Sugden MC, Langdown ML, Harris RA, Holness MJ. Expression and regulation of pyruvate dehydrogenase kinase isoforms in the developing rat heart and in adulthood: Role of thyroid hormone status and lipid supply. Biochem J. 2000;352(Pt 3):731–8.
97. Piao L, Fang YH, Parikh KS, Ryan JJ, D'Souza KM, Theccanat T, Toth PT, Pogoriler J, Paul J, Blaxall BC, Akhter SA, Archer SL. Grk2-mediated inhibition of adrenergic and dopaminergic signaling in right ventricular hypertrophy: therapeutic implications in pulmonary hypertension. Circulation. 2012;126:2859–69.
98. Olson EN. A decade of discoveries in cardiac biology. Nat Med. 2004;10(5):467–74. https://doi.org/10.1038/nm0504-467.
99. Hill JA, Olson EN. Cardiac plasticity. N Engl J Med. 2008;358(13):1370–80. https://doi.org/10.1056/NEJMra072139.
100. Osler W. Section V. Diseases of the circulatory system. Hypertrophy and Dilatation by Osler, William, Sir, 1849-1919. In: The principles and practice of medicine, designed for the use of practitioners and students of medicine. 1st edition, 2nd state of British edition; cf. R.L. Golden & C.G. Ronad, Sir William Osler, no. 1440. Publisher Edinburgh; London: Young J. Putland; 1892.
101. Akazawa H. Mechanisms of cardiovascular homeostasis and pathophysiology – from gene expression, signal transduction to cellular communication. Circ J. 2015;79(12):2529–36.
102. Lorell BH, Carabello BA. Left ventricular hypertrophy: pathogenesis, detection, and prognosis. Circulation. 2000;102(4):470–9.
103. Göktepe S, Abilez OJ, Parker KK, Kuhl E. A multiscale model for eccentric and concentric cardiac growth through sarcomerogenesis. J Theor Biol. 2012;265:433–42. https://doi.org/10.1016/j.jtbi.2010.04.023.
104. Genet M, Lee LC, Baillargeon B, Guccione JM, Kuhl E. Modeling pathologies of systolic and diastolic heart failure. Ann Biomed Eng. 2015;44:112–27. https://doi.org/10.1007/s10439-015-1351-2.
105. Kerckhoffs RCP, Omens JH, McCulloch AD. A single strain-based growth law predicts concentric and eccentric cardiac growth during pressure and volume overload. Mech Res Commun. 2012;42:40–50. https://doi.org/10.1016/j.mechrescom.2011.11.004.
106. Rausch MK, Dam A, Göktepe S, Abilez OJ, Kuhl E. Computational modeling of growth: systemic and pulmonary hypertension in the heart. Biomech Model Mechanobiol. 2011;10(6):799–811. https://doi.org/10.1007/s10237-010-0275-x.
107. Yamamoto S, James TN, Sawada K, Okabe M, Kawamura K. Generation of new intercellular junctions between cardiocytes. A possible mechanism compensating for mechanical overload in the hypertrophied human adult myocardium. Circ Res. 1996;78:362–70.
108. Saleh S, Liakopoulos OJ, Buckberg GD. The septal motor of biventricular function. Eur J Cardiothorac Surg. 2006;29(Suppl 1):S126–38.
109. Carabello BA. Concentric versus eccentric remodeling. J Card Fail. 2002;8(6 Suppl):S258–63. https://doi.org/10.1054/jcaf.2002.129250.
110. Swynghedauw B. Molecular mechanisms of myocardial remodeling. Physiol Rev. 1999;79(1):215–62.
111. Fedak PWM, Verma S, Weisel RD, Li R. Cardiac remodeling and failure from molecules to man (Part I). Cardiovasc Physiol. 2005;12:1–11.
112. Boxt LM, Katz J, Kolb T, Czegledy FP, Barst RJ. Direct quantitation of right and left ventricular volumes with nuclear magnetic resonance imaging in patients with primary pulmonary hypertension. J Am Coll Cardiol. 1992;19(7):1508–15.
113. Chen EP, Craig DM, Bittner HB, Davis RD, Van Trigt P. Pharmacological strategies for improving diastolic dysfunction in the setting of chronic pulmonary hypertension. Circulation. 1998;97(16):1606–12.
114. Louie EK, Lin SS, Reynertson SI, Brundage BH, Levitsky S, Rich S. Pressure and volume loading of the right ventricle have opposite effects on left ventricular ejection fraction. Circulation. 1995;92(4):819–24.
115. O'Rourke RA, Dell'Italia LJ. Diagnosis and management of right ventricular myocardial infarction. Curr Probl Cardiol. 2004;29:6–47.
116. Davlouros PA, Niwa K, Webb G, Gatzoulis MA. The right ventricle in congenital heart disease. Heart. 2006;92(Suppl 1):i27–38.
117. Domingo E, Aguilar R, López-Meseguer M, Teixidó G, Vazquez M, Roman A. New concepts in the invasive and non invasive evaluation of remodelling of the right ventricle and pulmonary vasculature in pulmonary arterial hypertension. Open Respir Med J. 2009;3:31–7.
118. Jurcut R, Giusca S, La Gerche A, Vasile S, Ginghina C, Voigt JU. The echocardiographic assessment of the right ventricle: what to do in 2010? Eur J Echocardiogr. 2010;11(2):81–96.
119. Heusch G, Libby P, Gersh B, Yellon D, Böhm M, Lopaschuk G, Opie L. Cardiovascular remodelling

in coronary artery disease and heart failure. Lancet. 2014;383(9932):1933–43.
120. Opie LH. The metabolic vicious cycle in heart failure. Lancet. 2004;364:1733–4.
121. D'Alonzo GE, Barst RJ, Ayres SM, et al. Survival in patients with primary pulmonary hypertension. Results from a national prospective registry. Ann Intern Med. 1991;115(5):343–9.
122. de Groote P, Millaire A, Foucher-Hossein C, et al. Right ventricular ejection fraction is an independent predictor of survival in patients with moderate heart failure. J Am Coll Cardiol. 1998;32(4):948–54.
123. Di Salvo TG, Mathier M, Semigran MJ, Dec GW. Preserved right ventricular ejection fraction predicts exercise capacity and survival in advanced heart failure. J Am Coll Cardiol. 1995;25(5):1143–53.
124. Polak JF, Holman BL, Wynne J, Colucci WS. Right ventricular ejection fraction: an indicator of increased mortality in patients with congestive heart failure associated with coronary artery disease. J Am Coll Cardiol. 1983;2(2):217–24.
125. Sandoval J, Bauerle O, Palomar A, et al. Survival in primary pulmonary hypertension. Validation of a prognostic equation. Circulation. 1994;89(4):1733–44.
126. Malik SB, Kwan D, Shah AB, Hsu JY. The right atrium: gateway to the heart – anatomic and pathologic imaging findings. Radiographics. 2015;35(1):14–31. https://doi.org/10.1148/rg.351130010.
127. Voelkel NF, Quaife RA, Leinwand LA, Barst RJ, McGoon MD, Meldrum DR, Dupuis J, Long CS, Rubin LJ, Smart FW, Suzuki YJ, Gladwin M, Denholm EM, Gail DB. Right ventricular function and failure: report of a National Heart, Lung, and Blood Institute Working Group on Cellular and Molecular Mechanisms of Right Heart Failure. Circulation. 2006;114:1883–91.
128. Bussani R, Abbate A, Biondi-Zoccai GG, Dobrina A, Leone AM, Camilot D, Di Marino MP, Baldi F, Silvestri F, Biasucci LM, Baldi A. Right ventricular dilatation after left ventricular acute myocardial infarction is predictive of extremely high peri-infarctual apoptosis at postmortem examination in humans. J Clin Pathol. 2003;56(9):672–6.
129. Hirose K, Reed JE, Rumberger JA. Serial changes in regional right ventricular free-wall and left ventricular septal wall lengths during the first 4-5 years after index anterior wall myocardial infarction. J Am Coll Cardiol. 1995;26:394–400.
130. Beygui F, Furber A, Delepine S, et al. Assessment of biventricular remodeling by magnetic resonance imaging after successful primary stenting for acute myocardial infarction. Am J Cardiol. 2004;94:354–7.
131. Bhatia SJS, Kirshenbaum JM, Shemin RJ, et al. Time course of resolution of pulmonary hypertension and right ventricular remodeling after orthotopic cardiac transplantation. Circulation. 1987;4:819–26.
132. Cook AL, Hurwitz LM, Valente AM, Herlong JR. Right heart dilatation in adults: congenital causes. AJR Am J Roentgenol. 2007;189(3):592–601. https://doi.org/10.2214/AJR.07.2420.
133. Pearlman AS, Borer JS, Clark CE, et al. Abnormal right ventricular size and ventricular septal motion after atrial septal defect closure. Am J Cardiol. 1972;41:295–301.

Physiopathology of Right Heart Failure

9

Cătălina Arsenescu-Georgescu,
Carmen Elena Pleşoianu, and Delia Şălaru

Abstract

The physiopathology of the right heart failure is tightly linked to the particular features of the right ventricle (RV). Its small dimension along with the specific geometry ensures the compliance of the RV which is able to accommodate extreme variations in venous return. Myocardial dysfunction, pressure overload, volume overload, and preload reduction are the main mechanisms of right heart failure. Due to its particular pattern of contraction, the RV better adapts to volume overload than to pressure overload. There are several aspects underlying the relative resistance of the RV to ischemia: its lower oxygen demand, dual coronary supply, and perfusion during both systole and diastole. Another key role in the pathophysiology of RV dysfunction is the ventricular interdependence. In case of acute pressure or volume overload, the RV dilates shifting the interventricular septum to the left, which along with the increased pericardial constraint determines low cardiac output. As the filling pressures rise, the auto aggravation of the low cardiac output state becomes an irreversible vicious cycle.

Keywords

Ventricular interdependence · Pressure overload · Volume overload

9.1 Introduction

The right heart failure is of extreme importance as it involves a high mortality burden. The involvement of the right ventricle (RV) in inferior myocardial infarction, for example, confers an eightfold increase in mortality [1], while RV dysfunction in acute pulmonary embolism is a predictor of mortality independent of systemic hemodynamics [2]. Moreover, acute RV failure worsens mortality rates more than acutely decompensated left heart failure [3], with an in-hospital mortality rates reaching 5–17% [4].

Right ventricular failure may be defined as the inability of the RV of the heart to provide adequate blood flow through the pulmonary circulation at a normal central venous pressure [5]. Right ventricular failure is a complex clinical syndrome that can result from any structural or functional cardiovascular disorder that impairs the ability of the RV to fill or to eject

C. Arsenescu-Georgescu (✉) · C. E. Pleşoianu · D. Şălaru
Department of Cardiology and Internal Medicine, "Gr. T. Popa" University of Medicine and Pharmacy, Iasi, Romania

Department of Cardiology, "George I.M. Georgescu" Cardiovascular Diseases Institute, Iasi, Romania

S. I. Dumitrescu et al. (eds.), *Right Heart Pathology*, https://doi.org/10.1007/978-3-319-73764-5_9

blood [6]. Clinical right heart failure is identified by signs and symptoms of venous congestion due to elevated central venous pressure along with evidence of right ventricular contractile dysfunction and right ventricular pressure overload [7] while RV dysfunction refers to abnormalities of filling or contraction without reference to signs or symptoms of heart failure [6].

9.2 Causes of Right Ventricular Failure

Right heart failure can be associated with a wide variety of clinical settings ranging from pulmonary pathologies such as respiratory failure [8], primary pulmonary hypertension [9] or chronic obstructive pulmonary disease [10] to acute or chronic cardiac diseases such as pulmonary embolism [11], idiopathic dilated cardiomyopathy [12] or coronary ischemia [13].

Pulmonary embolism determining acute right heart failure or pulmonary hypertension complicating severe long-standing pulmonary obstructive diseases are among the most frequent causes of right ventricular failure. Sepsis can directly induce dysfunction of the right ventricle [14]. Severe tricuspid regurgitation causes or aggravates symptoms and signs of right heart failure. Left-heart failure due to dilated cardiomyopathy leads to right-heart failure that aggravates its prognosis [15]. A variety of congenital heart defects are associated with RV failure, usually from increased afterload, volume overload or both. In the settings of a right ventricle acute myocardial infarction the coronary occlusion produces right ventricular failure through a direct mechanism—ischemia [13], whereas in acute ventricular septal defect or acutely decompensated left heart failure ischemia becomes an indirect mechanism.

In all these pathologies that may be encountered in critical care units right ventricular failure can be a disease by itself with different degrees of severity or a major complicating factor of another underlying disease.

9.3 Particular Features of the Right Ventricle Significant to the Physiopathology of the Right Heart Failure

The physiopathology of the RV is tightly linked to the particular features of this chamber.

The RV performs 1/4 of the stroke work of the left ventricle (LV) as the pulmonary vascular resistance is one-tenth of the systemic vascular resistance [16]. Due to the low pressure the pulmonary valve opens early in systole once RV pressure reaches the (relatively low) pulmonary artery (PA) pressure. Little time is spent in isovolumic contraction, giving a triangular-shaped pressure–volume loop, in contrast to the almost square loop of the LV. Therefore, the RV performs primarily volume rather than pressure work. Because of the low resistance presented by the pulmonary circulation, the RV continues to eject through the early phase of systole. As such, there is no isovolumic relaxation phase on the right side. Impedance of the pulmonary vascular bed represents the afterload of the RV and remains low as long as the vascular bed can be recruited. In the average person, the systolic pressure of the RV reaches 25 mmHg compared to 120 mmHg which is the systolic pressure of the LV [17]. This particularity has a very important physiopathological consequence: the RV is perfused in both systole and diastole as the aortic systolic pressure (and consequently the systolic pressure of the right coronary artery) exceeds the RV tissue pressure.

The mass of the RV is about 1/6 of the LV [16] resulting in a lower oxygen consumption [18]. The right ventricular free wall blood supply is predominantly from the right coronary artery and receives about equal flow during systole and diastole.

The RV has a thin wall which rarely exceeds 2–3 mm at end-diastole compared with 8–11 mm in the case of LV [5]. This small dimension along with the specific geometry ensures the compliance of the RV which is able to accommodate extreme variations in venous return resulting from changes in volume status, position, and respiration

with little change in pressure [5]. The preload of the RV is determined by venous return and the distensibility of the right ventricular wall. As with the LV, the Frank-Starling mechanism is obeyed, however the RV requires lower filling pressures to create the same ventricular output due to pulmonary vascular resistance being considerably lower than systemic vascular resistance. The RV compensates for changes in preload through stretching of the muscle wall (compliance) without loss of contractility (i.e. large increase in end-diastolic volume without increase in end-diastolic pressures). The same hemodynamic mechanisms apply to the RV as for the LV: as the right heart fails, a higher filling pressure is required to maintain right heart output.

The contraction pattern is another important feature that influences RV adaptive capacity. The RV contraction is enabled by three main mechanisms: the bellows-like inward movement of the free wall, the contraction of the longitudinal fibres drawing the tricuspid annulus toward the apex and the traction on the free wall as a result of left ventricular contraction [19]. This pattern of contraction is optimized for moving large and varying volumes of blood but is poorly adapted to generating high pressure [5]. As a result, the RV better adapts to volume overload than to pressure overload.

Another important aspect with a key role in the pathophysiology of RV dysfunction is the ventricular interdependence. It refers to the concept that the size, shape, and compliance of one ventricle may affect the size, shape, and pressure-volume relationship of the other ventricle through direct mechanical interactions [20]. Consequently, LV contraction may contribute to approximately 20–40% of RV systolic pressure and volume outflow [20]. The interdependence of the two ventricles results from their shared interventricular septum and the surrounding pericardium [16]. The septum mainly mediates the systolic ventricular interdependence while the pericardium is involved in the diastolic ventricular interdependence [18]. In case of acute volume or pressure overload, the RV dilatation shifts the interventricular septum toward the left, changing the LV geometry and increasing pericardial constraint that results in low cardiac output state due to decreased LV distensibility, preload and ventricular elastance [18, 21]. The pericardium plays a major role in modulating the interaction between the RV and the LV and in limiting RV dilatation during volume or pressure overload [5].

9.4 Molecular Mechanisms Involved in Right Ventricle Failure

There are several mechanisms involved in the physiopathology of RV failure [6]. Excessive sympathetic adrenergic stimulation may impair ventricular remodelling and decrease survival in patients with RV failure [22]. Moreover, elevated catecholamine levels are associated with higher pulmonary vascular resistance and lower cardiac index in patients with pulmonary hypertension (PHTN) [23] and higher New York Heart Association class in patients with congenital heart disease [22]. The renin-angiotensin-aldosterone system seems to be involved in the fluid retention and ventricular remodelling in patients with cor pulmonale [24]. Endothelin system activation also plays a role in the pathology of pulmonary vascular disease and right heart failure as elevated endothelin-1 levels are associated with decreased exercise capacity and more severe ventricular dysfunction [6]. Modulation of the endothelin system with endothelin receptor antagonists in PHTN may lead to an improvement in exercise capacity, a decrease in pulmonary vascular resistance, and better ventricular remodelling in patients with PHTN [22, 25]. High levels of B-type natriuretic peptide and activation of cytokines are associated with increased risk of mortality in patients with idiopathic PHTN [26] and more symptomatic disease in patients with RV failure [27].

Recent research on RV adaptation and failure secondary to PHTN has provided insight into the cellular and molecular changes in the afterload-stressed RV. It should be mentioned from the beginning that the RV adaptation to pressure and

volume overload due to congenital heart disease (associated with hypoxia and hypoxemia) is different from the response of the RV to PHTN [28], where local and systemic inflammation is involved due to primary pulmonary vascular pathology [29].

Although the two ventricles develop similar alterations in genes regulating extracellular matrix and cytoskeletal remodelling in response to pressure overload stress, there are several discrepancies concerning genes regulating energy production, mitochondrial function, reactive oxygen species production and antioxidant protection, and angiogenesis [30, 31]. In response to increased afterload, the RV reverts to a fetal gene pattern, re-expressing genes normally expressed in the fetal but not postnatal RV. This includes a shift from α- to β-myosin heavy chain expression and an increase in adrenergic receptors, calcineurin activation [32–34], and phosphodiesterase type-5 expression [35].

In right ventricular failure due to PHTN, as the RV hypertrophy develops, a metabolic shift from mitochondrial oxidative phosphorylation to cytoplasmic glycolysis has been described [36]. This increase in glycolysis is accompanied by a decrease in fatty acid oxidation, because there is less oxygen consumed per adenosine-triphosphate (ATP) generated than with fatty acid metabolism. Although this shift is beneficial during acute stress, chronic dependence on glycolysis for energy production cannot meet the needs of the myocardium to maintain a normal function [28]. In PHTN, the accompanying increase in RV afterload induces ischemia, due at least in part to compromised right coronary artery blood flow [37].

In an ischemic myocardium associated with hypertrophy, mitochondria-dependent apoptosis is suppressed and there is a decrease in the production of mitochondria-derived reactive oxygen species (mROS) [38]. While the RV remains in a compensated state, there is an increase in Hypoxia-Inducible Factor 1α (HIF1α), which might promote angiogenesis to satisfy the oxygen demands of the hypertrophied RV. When the RV decompensates, there is an increase in mROS and a decrease in HIF1α, followed by decreased angiogenesis, exacerbation of ischemia, and finally RV failure [39].

9.5 Physiopathology of Right Ventricular Failure

The normal function of RV is dependent on the preload, afterload, contractility, pericardial constraint, interaction with the LV, and cardiac rhythm [4]. In case of alteration of any of these parameters, compensatory mechanisms are triggered.

From a pathophysiologic point of view RV failure may be due to: (1) myocardial dysfunction (RV myocardial infarction, cardiomyopathies, arrythmogenic RV dysplasia, sepsis), (2) pressure overload (in cases of LV failure—the most common entity, pulmonary embolism—acute or chronic, pulmonary hypertension of different etiologies, obstructive congenital heart diseases), (3) volume overload (tricuspid regurgitation, pulmonary regurgitation, atrial/ventricular septal defect), and (4) preload reduction (pericardial diseases) [16].

RV adaptation to disease is complex and depends on many factors such as: the type and severity of myocardial injury or stress, the time course of the disease (acute or chronic), and the time of onset of the disease process (newborn, pediatric, or adult years) [6].

9.5.1 The Consequences of RV Pressure Afterload

In case of RV pressure overload, the opening of the pulmonary valve in systole is delayed. Thus, isovolumic contraction time is prolonged and the pressure–volume curve assumes a shape similar to that of the LV. Isovolumic contraction implies pressure work with greater oxygen consumption than volume work. The next consequence is that the relatively compliant RV dilates to maintain stroke volume (Frank–Starling mechanism). However, this causes an increase in myocardial wall stress because of the thin walls of the RV (law of Laplace). Myocardial wall stress is a major determinant of oxygen demand. An increased right ventricular end-diastolic pressure causes right coronary perfusion to assume a profile similar to that of the left coronary system (flow predominantly or solely in diastole). These

factors result in decreased oxygen supply at a time of greatly increased demand [40].

Dilatation of the RV chamber leads to dilatation of the tricuspid annulus causing tricuspid regurgitation, further exacerbating dilatation. Over time, hypertrophy occurs as a natural response to increased wall stress. As the RV expands, the crescentic shape of the RV cavity is lost. In addition, the interventricular septum bulges into the LV cavity. This occurs because the pericardium necessarily limits the space available for cardiac expansion, and thus an increase in RV volume must be accommodated by a decrease in LV volume (Fig. 9.1). Septal shift impairs filling of the LV and therefore impairs LV function due to ventricular interdependence. As the LV fails, systemic perfusion pressure and right coronary perfusion pressures decrease, further compromising the RV [40]. Once all mechanisms of contractile reserve are exhausted, systemic pressure begins to fall, followed by a potentially irreversible decrease in RV contractile function.

The RV is exposed to pressure overload in pulmonary valve stenosis and pulmonary hypertension of different etiologies. Initially, the myocardium responds by hypertrophy, followed by progressive contractile dysfunction [41]. Dilatation of the RV allows compensatory preload and maintains stroke volume despite reduced fractional shortening during the compensated

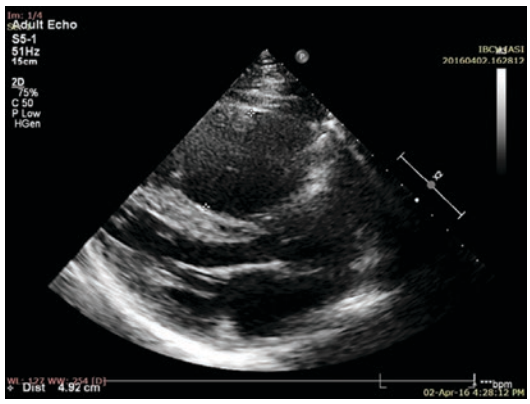

Fig. 9.1 Ecocardiography, parasternal long-axis view, in a patient with severe pulmonary hypertension. Note the important dilation of the right ventricle and the interventricular septum bulging into the LV cavity, impairing its function.

state of the RV failure. As the process continues, the filling pressures rise, diastolic dysfunction becomes evident, and the cardiac output decreases. Functional tricuspid regurgitation due to annular dilatation appears, and the clinical signs of congestion progress.

Even small changes in total pulmonary vascular resistance, as demonstrated by modest increases in mean airway pressure during positive pressure ventilation, reduce RV contractility and diminish cardiac output even with normal RV preload [39]. In animal models, even modest increases in afterload lead to major decreases in RV stroke volume [42].

The idea that the enlargement of the LV influences the function of the RV was first advanced in 1910 [43]. In 2006, Voelkel et al. [41] defined several mechanisms of right ventricular dysfunction associated with left ventricular dysfunction: (1) in case of left ventricular dysfunction the afterload increases by increasing pulmonary venous pressure; (2) several types of cardiomyopathies may affect both ventricles; (3) myocardial ischemia might also involve both ventricles; (4) left ventricular impairment may contribute to decreased pressure of right ventricular coronary perfusion; (5) septal dysfunction may enhance the ventricular interdependence and (6) left ventricular dilatation in a limited pericardial compartment may restrict right ventricular diastolic function.

Santamore et al. [44] studied the importance of LV-to-RV myocardial cross-talk and identified the effects of LV volume loading and dysfunction on RV developed pressure. Reducing LV volume from its normal volume to zero caused a 5.7% decrease in RV developed pressure. Furthermore ligating the coronary supply to the LV free wall resulted in an additional 9.3% decrease in RV developed pressure. Cutting the LV free wall from developing any contractile force determined a 45% decrease in RV developed pressure. All these changes in RV developed pressure correlated with the degree of septal bulging in the RV cavity during systole, suggest that the septum plays an important role in mediating ventricular-ventricular interactions. According to these authors, more than 50% of the normal RV

mechanical work may be generated by LV contraction and that the LV free wall plays a pivotal role in RV function [44].

Because of the variate interconnections between right ventricular dysfunction and left ventricular failure, right ventricular status may constitute a "common final pathway" in the progression of congestive heart failure and therefore may be a sensitive indicator of impending decompensation or poor prognosis [41].

The fundamental differences in the mechanisms of RV versus LV failure are well demonstrated by the divergence in the response of the two ventricles to heart failure therapies. Multiple clinical trials have shown that standard heart failure drugs (β-blockers, angiotensin-converting enzyme inhibitors, angiotensin II receptor blockers) do not improve function or survival in patients with RV failure [45–47].

In acute settings, RV uses a homeometric or systolic functional adaptation (Anrep's law of the heart) within minutes of pressure overload while in chronically situations it implements a heterometric or dimensional adaptation (Frank-Starling's law of the heart) in order to preserve flow output [4].

9.5.1.1 Acute RV Pressure Overload

Conditions of acute RV increased afterload are represented by pulmonary embolism, positive pressure ventilation, acute respiratory distress syndrome, and increased pulmonary vascular resistance.

In the acute settings, RV function is optimized by several adaptive mechanisms including heart rate, the Frank-Starling mechanism, and the autonomic nervous system [48].

In acute pulmonary embolism, the RV is not capable to overcome the high mean pulmonary artery pressure generated by the embolic burden resulting in rapid RV failure [2].

The rapid onset of this compensatory mechanism due to acute pressure overload defines the acute cor pulmonale, a pathological condition which is reversal if the underlying cause is promptly treated [49]. However, if neglected, this can set the premises of a vicious cycle—the autoaggravation cycle of RV failure. Dilatation of the RV can determine tricuspid annular dilatation resulting in tricuspid regurgitation, increase of RV end-diastolic volume and leftward movement of the septum, with impairment of the LV [16]. Tricuspid insufficiency can aggravate splanchnic congestion with decreased RV preload which further worsens the low preload state of the LV. The low cardiac output determines hypotension and impairment in organ perfusion and coronary artery perfusion with consequent ischaemia which further aggravates cardiac performance [17]. The RV poorly tolerates acute pressure overload. Severe right-ventricular pressure overload can cause a progressive and persistent decline in right-ventricular function after only 90 min, due to activation of endogenous proteases or induction of apoptosis [7].

If in acute settings the compensatory mechanisms of the RV are rapidly exhausted, in case of gradual increase in afterload the RV adapts by changes in morphology and function.

9.5.1.2 Chronic RV Pressure Overload

Chronically elevated right-ventricular pressure more typically causes progressive adverse remodelling and right-ventricular contractile dysfunction [50]. In case of chronic RV pressure overload as in patients with chronic pulmonary hypertension of any etiology, the sequence of events is marked by initial RV hypertrophy. From a morphologic point of view, the RV wall becomes thicker through assembly of new sarcomeres and increased protein synthesis, making the RV more concentric with concomitant flattening of the interventricular septum [48]. Secondary to sarcomere synthesis, cardiomyocyte length increases, allowing for a larger stroke volume and the maintenance of cardiac output [6]. This compensatory RV hypertrophy, however, leads to increased oxygen demand and a reduction in the perfusion flow with consequent RV dysfunction. In case of persistent pulmonary hypertension, further modifications occur. The RV enlargement leads to tricuspid annular dilatation and tricuspid regurgitation. The increase of RV end diastolic pressure has two major consequences that aggravate RV dysfunction. On one hand, the elevated intraventricular pressure causes the compression of the coronary flow

to the RV wall leading to RV ischemia. On the other hand, in order to overcome the pressure overload, the contraction of the RV takes longer leading to an abnormal condition where the RV is still contracting while the LV is already relaxing leading to a leftward displacement of the septum. Consequently the diastolic area of the LV diminishes with a subsequent suboptimal filling and altered cardiac performance.

RV function worsens parallel to elevation of the pulmonary artery pressure [16]. However, studies imply that RV failure occurs differently in the settings of the same degree of pulmonary pressure suggesting the implication of other mechanisms such as altered gene expression and neurohormonal activation [41].

Prolonged high pulmonary arterial flow can also cause progressive right-ventricular contractile dysfunction and right heart failure independent of changes in the pulmonary vasculature, possibly due to activation of inflammatory and apoptotic factors in the RV [7, 51].

It must be highlighted that RV remodelling seems to be highly reversible as patients with RV failure showed significant improvement of RV function after lung transplant, even if preoperative RV dysfunction was classified as severe [48].

9.5.2 RV Volume Overload

The RV is a compliant chamber, with high capacity of accommodating large volumes of blood [16]. This is sustained by the favorable evolution of patients with cardiac congenital heart diseases that imply RV volume overload or tricuspid regurgitation that are well tolerated for a long time without a significant RV systolic dysfunction [52].

Patients with atrial septal defect (ASD) maintain the RV ejection fraction at higher end-diastolic and end-systolic volumes [53, 54] and can remain undiagnosed until adulthood [55] demonstrating the ability of the RV to adapt to increased filling volumes [48]. Patients with Eisenmenger's syndrome (ES) have a much higher survival rate than those with idiopathic pulmonary hypertension, which is believed to relate to the fact that in ES the RV has been exposed and primed to high pressures since birth and therefore is better adapted [48]. It is postulated that regression of right ventricular wall thickness never occurs and contractile function is preserved for a longer period in patients with ES compared with idiopathic pulmonary arterial hypertension (PAH), resulting in a fetal RV phenotype [48].

9.6 Physiopathology of RV Failure in Special Settings

9.6.1 Pulmonary Embolism

Pulmonary embolism is one of the most common causes of acute cor pulmonale.

It is a representative condition for acute increase of RV afterload. During the acute phase both the right atria and the RV show signs of hypertrophy and elevated right atrial pressure, with reversal of trans-septal diastolic pressure gradient with reduction in left ventricular diastolic area due to the leftward movement of the septum [56]. RV dilates and reduces the stroke volume. Initially the increase of end diastolic volume provides transient compensation to reduced cardiac output, and then the acute dilatation leads to RV dysfunction with failure to produce adequate flow [16].

9.6.2 Pulmonary Hypertension

The specific mechanisms underlying the development of right ventricular failure secondary to pulmonary hypertension are still under debate as it is uncertain whether some patients develop right ventricular myocardial ischemia, whether there is microvascular endothelial cell dysfunction, and whether or not myocytes undergo apoptosis [41].

In idiopathic pulmonary arterial hypertension the RV suffers alterations in terms of volume, mass and conformation. It presents an increased end-diastolic volume, varying degrees of hypertrophy and a crescentic trapezoid conformation reaching

in severe cases to a spherical shape with a greater cross-sectional area than the LV leading to an abnormal septal function that impairs LV performance [41].

9.6.3 Myocardial Dysfunction: Right Ventricular Infarction

The incidence of RV involvement in patients with inferior myocardial infarction ranges between 30 and 50% [57]. Acute RV failure as the primary cause of cardiogenic shock has been reported in 16% of cases of patients with myocardial infarction (MI) [58].

RV MI often results when there is an occlusion of the proximal right coronary artery (RCA) [16]. However, the occlusion of the RCA is not always followed by significant RV necrosis and dysfunction. RV is particularly resistant to irreversible ischemic injury and myocardial stunning plays an important part in the pathophysiology of RV dysfunction [6]. Several aspects can explain the relative resistance of the RV to irreversible ischemic injury: its lower oxygen consumption, dual anatomical supply from the right and left coronary arteries, relatively homogeneous transmural perfusion across the cardiac cycle, increased propensity to acute collateral development, and its ability to increase oxygen extraction during stress [18, 59, 60]. Moreover, the right ventricle may remain viable for days after an infarct [61], making late reperfusion an important resource in the management of patients with inferior MI complicated by RV dysfunction.

RVMI may be associated with an increased risk of death, cardiogenic shock, ventricular tachycardia or fibrillation, and high-grade atrioventricular block [62].

9.6.4 Surgery

RV failure is a leading cause of morbi/mortality early after cardiac transplant [63] and following several other cardiothoracic procedures [64].

RV failure is usually due to acute increase in afterload in non-cardiac surgery and volume overload, myocardial ischaemia, preexisting RV dysfunction, or arrhythmias in cardiac surgery [19, 65].

The risk factors for postoperative RV failure are previous pulmonary hypertension, RV dysfunction, severe LV dysfunction and long cardiopulmonary bypass periods while the intraoperative mechanisms that may lead to RV failure are represented by suboptimal myocardial protection, myocardial stunning after long durations on cardiopulmonary bypass, air or thromboembolism to the right coronary artery, and mechanical occlusion or kinking of the right coronary button or bypass graft [4].

9.6.5 Valvular Disease

Both left-sided and right-sided valvular heart disease can result in RV failure.

In patients with left-sided valvular diseases, the elevated left atrial filling pressure prevents central venous pressure from maintaining pulmonary arterial flow causing RV dysfunction.

In case of tricuspid regurgitation which is the most frequent right-sided valvular disease, the RV failure is secondary to volume overload and RV enlargement. The same mechanism is responsible for the RV dysfunction in the settings of right heart infective endocarditis (estimated at 5–10% of all cases of infective endocarditis) whether it affects native valves, prosthetic valves, congenital heart defects or implanted devices [4].

9.6.6 Intensive Care Setting

The incidence of acute RV failure caused by acute respiratory distress syndrome (ARDS) ranges from 25% to 50% [66, 67]. The pathological mechanism is dual. It is linked both to the severity of the distal occlusion of the pulmonary arterial bed and the mechanical ventilation settings as the majority of patients require intermittent positive pressure ventilation.

Positive pressure ventilation can contribute to an uncoupling between the pulmonary circulation and the RV, predisposing to an inability to sustain sufficient blood flow, especially if myocardial contraction is also impaired [4] as the preload of RV decreases and the afterload increases [17].

Once right heart failure develops, elevated intrathoracic pressure from ventilator therapy may exacerbate it with important detrimental effect on of high-frequency ventilation with high mean airway pressure [7].

9.6.7 Arrythmias

RV pressure overload causes dyssynchronous contraction of the RV and LV with paradoxical septal motion contributing to diminished cardiac output and increased filling pressures leading to further deterioration of RV function [7]. Maintenance of sinus rhythm and AV synchrony is especially important in the presence of RV dysfunction [18]. Asynchrony of the RV occurs early in the adaptation of the RV and has implications in the physiopathology of RV failure. It appears when the RV dilates and the septum shifts toward the left resulting in a suboptimal filled LV, with resultant systemic hypotension and cardiogenic shock [4].

Bradycardia, high-grade atrioventricular block, ventricular tachycardia, and rupture of the interventricular septum may occur more often in patients with RV infarction [57, 68].

9.6.8 Sepsis

Right ventricular dysfunction reaches 32% in sepsis [69].

9.7 Pericardial Disease

The limitation of the diastolic filling of the heart caused by the rigid pericardium or the pericardial effusion increases the diastolic pressure in all cardiac chambers resulting in diastolic pressure equalization. Deep inspiration, although it does not reduce systemic venous pressure, determines an increased right ventricular filling that shifts the interventricular septum towards the left ventricle with the occurrence of the paradoxical pulse [70].

Conclusions

RV failure is inherently an unstable condition, with a tendency toward abrupt and irreversible decompensation. The physiopathology of RV is linked to its particular size, shape, compliance, contraction pattern, and coronary perfusion. Right heart failure can be caused by myocardial dysfunction, pressure overload, volume overload, and pericardial disease. The complex interaction of the RV and the LV makes clinical assessment and therapeutic management a challenging issue.

References

1. Zehender M, Kasper W, Kauder E, et al. Right ventricular infarction as an independent predictor of prognosis after acute inferior myocardial infarction. N Engl J Med. 1993;328:981–8.
2. Goldhaber SZ, Visani L, De Rosa M. Acute pulmonary embolism: clinical outcomes in the International Cooperative Pulmonary Embolism Registry (ICOPER). Lancet. 1999;353:1386–9.
3. Nieminen MS, Brutsaert D, Dickstein K, et al. EuroHeart failure survey II (EHFS II): a survey on hospitalized acute heart failure patients: description of population. Eur Heart J. 2006;27:2725–36.
4. Harjola VP, Mebazaa A, Čelutkienė J, Bettex D, Bueno H, Chioncel O, Crespo-Leiro MG, Falk V, Filippatos G, Gibbs S, Leite-Moreira A, Lassus J, Masip J, Mueller C, Mullens W, Naeije R, Nordegraaf AV, Parissis J, Riley JP, Ristic A, Rosano G, Rudiger A, Ruschitzka F, Seferovic P, Sztrymf B, Vieillard-Baron A, Yilmaz MB, Konstantinides S. Contemporary management of acute right ventricular failure: a statement from the Heart Failure Association and the Working Group on Pulmonary Circulation and Right Ventricular Function of the European Society of Cardiology. Eur J Heart Fail. 2016;18(3):226–41.
5. Greyson CR. Pathophysiology of right ventricular failure. Crit Care Med. 2008;36(Suppl. 1):857–65.
6. Haddad F, Doyle R, Murphy DJ, Hunt SA. Right ventricular function in cardiovascular disease, part II: pathophysiology, clinical importance, and management of right ventricular failure. Circulation. 2008; 117:1717–31.

7. Greyson CR. Right heart failure in the intensive care unit. Curr Opin Crit Care. 2012;18:424–31.
8. Zapol WM, Snider MT. Pulmonary hypertension in severe acute respiratory failure. N Engl J Med. 1977; 296:476–80.
9. Rubin LJ. Primary pulmonary hypertension. N Engl J Med. 1997;336:111–7.
10. Naeije R. Pulmonary hypertension and right heart failure in chronic obstructive pulmonary disease. Proc Am Thorac Soc. 2005;2:20–2.
11. Hirsh J, Hoak J. Management of deep vein thrombosis and pulmonary embolism: a statement for healthcare professionals: Council on Thrombosis (in consultation with the Council on Cardiovascular Radiology), American Heart Association. Circulation. 1996;93:2212–45.
12. La Vecchia L, Zanolla L, Varotto L, et al. Reduced right ventricular ejection fraction as a marker for idiopathic dilated cardiomyopathy compared with ischemic left ventricular dysfunction. Am Heart J. 2001; 142:181–9.
13. Goldstein JA. Pathophysiology and management of right heart ischemia. J Am Coll Cardiol. 2002;40: 841–53.
14. Lambermont B, Ghuysen A, Kolh P, et al. Effects of endotoxic shock on right ventricular systolic function and mechanical efficiency. Cardiovasc Res. 2003; 59:412–8.
15. Ghio S, Tavazzi L. Right ventricular dysfunction in advanced heart failure. Ital Heart J. 2005;6:852–5.
16. Guarracino F, Cariello C, Danella A, Doroni L, Lapolla F, Vullo C, Pasquini C, Stefani M. Right ventricular failure: physiology and assessment. Minerva Anestesiol. 2005;71(6):307–12.
17. Cecconi M, Johnston E, Rhodes A. What role does the right side of the heart play in circulation? Crit Care. 2006;10(Suppl 3):S5.
18. Haddad F, Hunt SA, Rosenthal DN, Murphy DJ. Right ventricular function in cardiovascular disease, part I: anatomy, physiology, aging, and functional assessment of the right ventricle. Circulation. 2008;117(11): 1436–48.
19. Haddad F, Couture P, Tousignant C, Denault AY. The right ventricle in cardiac surgery, a perioperative perspective: I. Anatomy, physiology, and assessment. Anesth Analg. 2009;108:407–21.
20. Santamore WP, Dell'Italia LJ. Ventricular interdependence: significant left ventricular contributions to right ventricular systolic function. Prog Cardiovasc Dis. 1998;40:289–308.
21. Dell'Italia LJ. The right ventricle: anatomy, physiology, and clinical importance. Curr Probl Cardiol. 1991;16:653–720.
22. Bolger AP, Sharma R, Li W, Leenarts M, Kalra PR, Kemp M, Coats AJ, Anker SD, Gatzoulis MA. Neurohormonal activation and the chronic heart failure syndrome in adults with congenital heart disease. Circulation. 2002;106:92–9.
23. Nootens M, Kaufmann E, Rector T, Toher C, Judd D, Francis GS, Rich S. Neurohormonal activation in patients with right ventricular failure from pulmonary hypertension: relation to hemodynamic variables and endothelin levels. J Am Coll Cardiol. 1995;26:1581–5.
24. Kiely DG, Cargill RI, Lipworth BJ. Angiotensin II receptor blockade and effects on pulmonary hemodynamics and hypoxic pulmonary vasoconstriction in humans. Chest. 1996;110:698–703.
25. Channick RN, Simonneau G, Sitbon O, Robbins IM, Frost A, Tapson VF, Badesch DB, Roux S, Rainisio M, Bodin F, Rubin LJ. Effects of the dual endothelin-receptor antagonist bosentan in patients with pulmonary hypertension: a randomised placebo-controlled study. Lancet. 2001;358:1119–23.
26. Nagaya N, Nishikimi T, Uematsu M, Satoh T, Kyotani S, Sakamaki F, Kakishita M, Fukushima K, Okano Y, Nakanishi N, Miyatake K, Kangawa K. Plasma brain natriuretic peptide as a prognostic indicator in patients with primary pulmonary hypertension. Circulation. 2000;102:865–70.
27. Sharma R, Bolger AP, Li W, Davlouros PA, Volk HD, Poole-Wilson PA, Coats AJ, Gatzoulis MA, Anker SD. Elevated circulating levels of inflammatory cytokines and bacterial endotoxin in adults with congenital heart disease. Am J Cardiol. 2003;92:188–93.
28. Reddy S, Bernstein D. Molecular mechanisms of right ventricular failure. Circulation. 2015;132(18):1734–42.
29. Gomez-Arroyo J, Sakagami M, Syed AA, et al. Iloprost reverses established fibrosis in experimental right ventricular failure. Eur Respir J. 2015;45(2):449–62.
30. Piao L, Marsboom G, Archer SL. Mitochondrial metabolic adaptation in right ventricular hypertrophy and failure. J Mol Med (Berl). 2010;88(10):1011–20.
31. Urashima T, Zhao M, Wagner R, et al. Molecular and physiological characterization of RV remodeling in a murine model of pulmonary stenosis. Am J Physiol Heart Circ Physiol. 2008;295(3):H1351–68.
32. Lowes BD, Minobe W, Abraham WT, et al. Changes in gene expression in the intact human heart. Downregulation of alpha-myosin heavy chain in hypertrophied, failing ventricular myocardium. J Clin Invest. 1997;100(9):2315–24.
33. Bakerman PR, Stenmark KR, Fisher JH. Alpha-skeletal actin messenger RNA increases in acute right ventricular hypertrophy. Am J Phys. 1990;258(4 Pt 1): L173–8.
34. Bartelds B, Borgdorff MA, Smit-van Oosten A, et al. Differential responses of the right ventricle to abnormal loading conditions in mice: pressure vs. volume load. Eur J Heart Fail. 2011;13(12):1275–82.
35. Nagendran J, Archer SL, Soliman D, et al. Phosphodiesterase type 5 is highly expressed in the hypertrophied human right ventricle, and acute inhibition of phosphodiesterase type 5 improves contractility. Circulation. 2007;116(3):238–48.

36. Archer SL, Fang YH, Ryan JJ, Piao L. Metabolism and bioenergetics in the right ventricle and pulmonary vasculature in pulmonary hypertension. Pulm Circ. 2013;3(1):144–52.
37. Bogaard HJ, Natarajan R, Henderson SC, et al. Chronic pulmonary artery pressure elevation is insufficient to explain right heart failure. Circulation. 2009;120(20): 1951–60.
38. Sutendra G, Dromparis P, Paulin R, et al. A metabolic remodeling in right ventricular hypertrophy is associated with decreased angiogenesis and a transition from a compensated to a decompensated state in pulmonary hypertension. J Mol Med (Berl). 2013;91(11):1315–27.
39. Henning RJ. Effects of positive end-expiratory pressure on the right ventricle. J Appl Physiol. 1986;61(3):819–26.
40. Kevin LG, Barnard M. Right ventricular failure. Contin Educ Anaesth Crit Care Pain. 2007;7(3):89–94.
41. Voelkel NF, Quaife RA, Leinwand LA, national heart, lung, and blood institute working group on cellular and molecular mechanisms of right heart failure, et al. Right ventricular function and failure: report of a National Heart, Lung, and Blood Institute working group on cellular and molecular mechanisms of right heart failure. Circulation. 2006;114(17):1883–91.
42. MacNee W. Pathophysiology of cor pulmonale in chronic obstructive pulmonary disease. Part one. Am J Respir Crit Care Med. 1994;150(3):833–52.
43. Bernheim D. De l'asystole veineuse dons l'hypertrophie du coeur gauche par stenose concomitante du ventricule droit. Rev Med (Paris). 1910;30:z785.
44. Santamore WP, Lynch PR, Heckman JL, et al. Left ventricular effects on right ventricular developed pressure. J Appl Physiol. 1976;41(6):925–30.
45. Winter MM, Bouma BJ, Groenink M, et al. Latest insights in therapeutic options for systemic right ventricular failure: a comparison with left ventricular failure. Heart. 2009;95:960–3.
46. Szymañski P, Klisiewicz A, Hoffman P. Therapeutic options for systemic right ventricular failure. Heart. 2009;95:1950–1.
47. Shaddy RE, Boucek MM, Hsu DT, Pediatric Carvedilol Study Group, et al. Carvedilol for children and adolescents with heart failure: a randomized controlled trial. JAMA. 2007;298:1171–9.
48. Poels EM, da Costa Martins PA, van Empel VP. Adaptive capacity of the right ventricle: why does it fail? Am J Physiol Heart Circ Physiol. 2015;308(8): H803–13.
49. Mebazaa A, Karpati P, Renaud E, Algotsson L. Acute right ventricular failure- from pathophysiology to new treatments. Intensive Care Med. 2004;30:185–96.
50. Bogaard HJ, Abe K, Vonk Noordegraaf A, Voelkel NF. The right ventricle under pressure: cellular and molecular mechanisms of right-heart failure in pulmonary hypertension. Chest. 2009;135:794–804.
51. Rondelet B, Dewachter C, Kerbaul F, et al. Prolonged overcirculation-induced pulmonary arterial hypertension as a cause of right ventricular failure. Eur Heart J. 2012;33:1017–26.
52. Davlouros PA, Niwa K, Webb G, Gatzoulis MA. The right ventricle in congenital heart disease. Heart. 2006;92(Suppl 1):i27–38.
53. Fogel MA, Rychik J. Right ventricular function in congenital heart disease: pressure and volume overload lesions. Prog Cardiovasc Dis. 1998;40: 343–56.
54. Popio KA, Gorlin R, Teichholz LE, Cohn PF, Bechtel D, Herman MV. Abnormalities of left ventricular function and geometry in adults with an atrial septal defect. Ventriculographic, hemodynamic and echocardiographic studies. Am J Cardiol. 1975;36:302–8.
55. Lindsey JB, Hillis LD. Clinical update: atrial septal defect in adults. Lancet. 2007;369:1244–6.
56. Jardin F, Dubourg O, Gueret P, Delorme G, Bourdarias JP. Quantitative two dimensional echocardiography in massive pulmonary embolism: emphasis on ventricular interdependence and leftward septal displacement. J Am Coll Cardiol. 1987;10:1201–6.
57. Bueno H, Lopez-Palop R, Perez-David E, Garcia-Garcia J, Lopez-Sendon JL, Delcan JL. Combined effect of age and right ventricular involvement on acute inferior myocardial infarction prognosis. Circulation. 1998;98:1714–20.
58. Brodie BR, Stuckey TD, Hansen C, Bradshaw BH, Downey WE, Pulsipher MW. Comparison of late survival in patients with cardiogenic shock due to right ventricular infarction versus left ventricular pump failure following primary percutaneous coronary intervention for ST-elevation acute myocardial infarction. Am J Cardiol. 2007;99:431–5.
59. Laster SB, Shelton TJ, Barzilai B, Goldstein JA. Determinants of the recovery of right ventricular performance following experimental chronic right coronary artery occlusion. Circulation. 1993;88:696–708.
60. Laster SB, Ohnishi Y, Saffitz JE, Goldstein JA. Effects of reperfusion on ischemic right ventricular dysfunction. Disparate mechanisms of benefit related to duration of ischemia. Circulation. 1994;90:1398–409.
61. Dell'Italia LJ, Lembo NJ, Starling MR, Crawford MH, Simmons RS, Lasher JC, Blumhardt R, Lancaster J, O'Rourke RA. Hemodynamically important right ventricular infarction: follow-up evaluation of right ventricular systolic function at rest and during exercise with radionuclide ventriculography and respiratory gas exchange. Circulation. 1987;75:996–1003.
62. Mehta SR, Eikelboom JW, Natarajan MK, Diaz R, Yi C, Gibbons RJ, Yusuf S. Impact of right ventricular involvement on mortality and morbidity in patients with inferior myocardial infarction. J Am Coll Cardiol. 2001;37:37–43.
63. Stobierska-Dzierzek B, Awad H, Michler RE. The evolving management of acute rightsided heart failure

in cardiac transplant recipients. J Am Coll Cardiol. 2001;38:923–31.
64. Kaul TK, Fields BL. Postoperative acute refractory right ventricular failure: Incidence, pathogenesis, management and prognosis. Cardiovasc Surg. 2000;8: 1–9.
65. Haddad F, Couture P, Tousignant C, Denault AY. The right ventricle in cardiac surgery, a perioperative perspective: II. Pathophysiology, clinical importance, and management. Anesth Analg. 2009;108:422–33.
66. Vieillard-Baron A, Price LC, Matthay MA. Acute cor pulmonale in ARDS. Intensive Care Med. 2013; 39:1836–8.
67. Jardin F, Vieillard-Baron A. Is there a safe plateau pressure in ARDS? The right heart only knows. Intensive Care Med. 2007;33:444–7.
68. Bueno H, Lopez-Palop R, Bermejo J, Lopez-Sendon JL, Delcan JL. In-hospital outcome of elderly patients with acute inferior myocardial infarction and right ventricular involvement. Circulation. 1997;96:436–41.
69. Jardin F, Brun-Ney D, Auvert B, Beauchet A, Bourdarias JP. Sepsis related cardiogenic shock. Crit Care Med. 1990;18:1055–60.
70. Georgescu GIM, Arsenescu C. Bolile pericardului. In: Tratamentul rational al bolilor cardiovasculare majore. Iasi: Polirom; 2001. p. 123–32.

Acute Right Heart Failure

10

Camille Abigael P. Alcantara, Anjali Chandra, Diana Morvey, and Ernst R. von Schwarz

Abstract

Heart failure is defined as a life-threatening complex clinical syndrome with exacerbation of symptoms signifying decompensation and requires emergent treatment. In its acute state it presents within 24 hours with symptoms such as shortness of breath, volume overload including pulmonary edema, sometimes forward failure and even cardiogenic shock. Two forms of acute heart failure exist: newly diagnosed "de novo" or acutely decompensated chronic heart failure. This chapter summarizes the clinical and prognostic classification of acute right heart failure, epidemiology, diagnostic work-up and the principles behind treatment and management options that focus on preload optimization, afterload reduction and improvement of contractility.

Keywords

Right heart failure · Cardiomyopathy · Acute heart failure · Congestive heart failure

C. A. P. Alcantara · A. Chandra · D. Morvey
Heart Institute, Southern California Hospital, Culver City, CA, USA

E. R. von Schwarz (✉)
Heart Institute, Southern California Hospital, Culver City, CA, USA

Cedars Sinai Medical Center, Los Angeles, CA, USA

University of California Los Angeles, Los Angeles, CA, USA

University of California Riverside, Riverside, CA, USA

10.1 Introduction

Research efforts have disproportionately concentrated on the left ventricle in heart failure, however recent efforts recognize the need to achieve a comprehensive understanding of the right ventricle. In the past, the general laws regarding cardiac mechanics and treatment modalities to improve cardiac performance have been similar in both the right ventricle (RV) and left ventricle (LV). However, the RV is distinct from the LV in regards to structure, geometry, and mechanics [1]. During the past two decades, with the help of imaging modalities, RV function has proved to be an important contributor in the prognosis of heart failure regardless of underlying etiology [2].

Heart failure (HF) is generally a chronic medical condition with exacerbation of symptoms signifying decompensation and requires medical attention. It is a complex syndrome that is caused by structural or functional cardiac disorders leading to impairment of either ventricle to fill or eject blood. It can, however, present as an acute condition within 24 h as seen in pulmonary edema or cardiogenic shock [3]. Right HF is now more frequently identified in current clinical practice due to the increase in the prevalence of predisposing conditions in the population such as LV failure and myocardial infarction [2]. The clinical syndrome presents predominantly as systemic congestion leading to jugular venous regurgitation and ankle swelling [3].

S. I. Dumitrescu et al. (eds.), *Right Heart Pathology*, https://doi.org/10.1007/978-3-319-73764-5_10

10.2 Epidemiology

The prevalence of HF is estimated at 1–2% in Western countries and the incidence is about 5–10 per 1000 persons per year [3]. It is estimated that five million Americans are diagnosed with heart failure. The majority of HF patients are hospitalized for acute heart failure. The median length of stay in hospital is 3 days [4]. HF is one of the most common diseases affecting adults in Europe today. In Germany, for example, HF is reported to be the most common diagnosis leading to hospitalization. In persons aged 20–40 years, the prevalence is under 0.5%, however in persons over age 60 years, the prevalence reaches as high as 10% in men and 8% in women [5]. The high prevalence is attributed to the aging population, advances in medicine in primary and secondary prevention of coronary events, as well as in available treatment options. In developed countries, the mean age of patients with HF is 75 years [3].

10.3 Prognosis

Due to recent advancements in medicine such as drug therapy providing beneficial long-term effects, implantable defibrillators and cardiac resynchronization systems, the five-year mortality rate of patients with chronic HF has decreased. A study using enalapril as treatment for HF patients demonstrated significant reduction in cardiac death (hazard ratio was 0.90 for treatment group) and extension of median survival by 9.4 months [6]. Implantable cardioverter-defibrillator (ICD) could reduce mortality rate by 23% among patients with HF [7]. However, minimal improvement in the prognosis among patients with acute HF has been demonstrated. The in-patient mortality rate is reportedly 7% according to the Euro Heart Failure Survey, with a one-year mortality rate at 20–30%. Cardiogenic shock notably has the highest mortality rate, followed by pulmonary edema, and then followed closely by de novo acute HF and right HF [5].

10.4 Etiology and Pathophysiology

Two forms of acute HF exist: (1) newly arisen or "de novo" and (2) acutely decompensated chronic heart failure (ADCHF). Two thirds of all patients with acute HF have a previous history of HF [5].

Common causes of de novo HF include coronary heart disease, mainly acute coronary syndrome and its mechanical complications (e.g. ventricular septal defect, acute mitral insufficiency, right heart infarct), valvular diseases, myocarditis, hypertensive crisis, arrhythmias, circulatory failure (e.g. acute pulmonary embolism, pericardial tamponade, aortic dissection), and surgical intervention and associated perioperative complications [5].

ADCHF is associated with delayed clinical deterioration, such as infections (endocarditis), acute exacerbation of chronic obstructive pulmonary disease and asthma, anemia, worsening renal failure, inadequate fluid and salt intake, non-compliance with medication, adverse drug reaction and interaction (e.g. non-steroidal anti-inflammatory drugs, corticosteroids), uncontrolled arterial hypertension, hypo- or hyperthyroidism, and substance abuse [5].

10.4.1 Acute Right Ventricular Failure

RV dysfunction is a result of pressure overload or volume overload, or a combination of both [2]. Notably, the thin-walled chambers and lesser elasticity of the RV structure accommodate changes in volume overload better than the LV, making the RV more afterload-dependent [1]. Additionally primary loss of myocardium leads to right HF, however it is a rare cause and not confined to the right heart [2].

The RV systolic function remains well-preserved despite long-standing volume-overload secondary to atrial septal defect (ASD) or tricuspid regurgitation (TR). However, due to ventricular interdependence, shift of the interventricular septum, and increased pericardial constraint, these valvular abnormalities lead to

decreased LV cardiac output and LV elasticity. The over circulation of the pulmonary vasculature causes fixed pulmonary hypertension and increased RV afterload [1].

In adults, the RV cannot tolerate acute increases in afterload. An increase in pulmonary artery pressure of 20 mmHg results in a 30% decline in RV stroke volume. Pulmonary hypertension thereby leads to RV dilation and subsequent failure, as seen in acute pulmonary embolism with a sudden drop in RV systolic volume [1].

There are several causes of right HF [2]. The most common cause of RV dysfunction is LV dysfunction and failure resulting in pressure overload and pulmonary venous hypertension [8]. The causes of right heart failure and their corresponding mechanisms are listed in Table 10.1.

Table 10.1 Causes and corresponding mechanisms of right heart failure [2]

Causes of right heart failure	
Left ventricle failure or arrhythmia	
Right ventricle ischemia or injury	RV infarction secondary to pressure overload
Increased afterload	Acute pulmonary embolism
	Pulmonary microthrombi (sepsis)
	Pulmonary arterial hypertension (PAH)
	Hypoxic vasoconstriction
	Mechanical ventilation
	Post CABG
Decreased preload	Hypovolemia
	Capillary leak
	Sepsis
	Superior vena cava (SVC) syndrome
	Right ventricle outflow tract (RVOT) obstruction
	Mechanical ventilation
	Tamponade
Myocardial disease	Left ventricle cardiomyopathies
	Arrhythmogenic right ventricular dysplasia (ARVD)
	Cytokines (sepsis)
Congenital/Valvular	Mitral valve disease
	Ebstein anomaly
	Tetralogy of Fallot
	Transposition of great vessels (TOGV)
	Atrial septal defect (ASD)
	Tricuspid regurgitation (TR)
	Pulmonic regurgitation (PR)
Pericardial	Constrictive pericarditis

10.4.2 Acute Pressure Overload

As a response to increased pressure, the RV compensates via the Frank-Starling mechanism by increasing its contractile state. An increase in ventricular inotropy as a result of a sudden increase in afterload, known as the Anrep effect, is mediated through changes in calcium dynamics and occurs by maintaining the adrenergic state. Catecholamines also contribute to the increase in RV pressure by increasing the inotropy. With a further increase in the afterload, the subsequent dilated RV relies on the Frank-Starling mechanism to function. However, when all of the adaptive mechanisms in response to pressure overload are exhausted, the systemic pressure begins to fall, with a sudden, dramatic, and irreversible decrease in the contractile function of the RV. This concept was first demonstrated in 1954 by Guyton et al. in which it was established that a steady rise in the pressure of the RV secondary to the progressive constriction of the main pulmonary artery to the point where the RV can no longer compensate would lead to a sudden decrease in systemic pressure and cardiac output [9].

Acute pulmonary embolism serves as the prototype of RV failure due to acute pressure overload. Pre-existing cardiac or pulmonary disease and anatomic severity of the obstruction influence the cascading events seen in pulmonary thromboembolism. As vasoconstrictive factors are released from the thrombus and in response to hypoxia, the pulmonary vascular resistance increases, with subsequent increase in pulmonary artery pressure. The result is a dilated and hypokinetic RV. The myocardial oxygen demand increase and eventually leads to myocardial ischemia or infarction [2]. Ischemia or infarc-

tion then causes both a decrease in RV ejection and a septal shift, thereby reducing the LV preload. Ultimately, the heart is unable to maintain cardiac index and arterial pressure, leading to cardiogenic shock [2].

10.4.3 Chronic Pressure Overload

Chronic pressure overload leads to multiple episodes of decompensation, as seen in PAH. The adaptive response of the RV to pressure overload is myocardial hypertrophy and a change in shape from the normal conformation to a spherical geometry. This is a result of increased protein synthesis and increase in cell size. Paracrine, autocrine, and neurohormonal signals such as the renin-angiotensin-aldosterone system (RAAS) and enhanced sympathetic activity, as well as stretch, induce protein synthesis. The long term effect causes the pressure overload to eventually decrease the cardiac contractile force. The accompanying extracellular matrix synthesis impacts the RV function and morphology, thus leading to electrical instability [2]. The adaptive mechanism of the RV in chronic pressure overload due to congenital heart disease, where the RV shape is concentric with preserved function, is attributed to persistent expression of fetal genes [8].

The RV adequately adapts to chronic pressure overload in contrast to acute pressure overload. It is reported that 55% of incident patients with PAH and chronic pressure overload average a survival rate of 3 years. However, some patients with severe PAH remain highly functional (New York Heart Association Functional Class I) for years without developing RV failure [10].

In maladaptive cardiac remodeling, the alpha to beta isotype switching of the myosin heavy chains (MCH) causes a reduction of the alpha-MCH isotype, which represents one third of the total MCH in adults. This type of remodeling is seen in PAH-associated right heart failure. Since beta-MCH has lower adenosine triphosphate (ATP) activity than alpha-MCH, a reduction in systolic function is seen. Additionally, the phosphorylation of troponin T by protein kinase C inhibits the binding of troponin T to tropomyosin, resulting in inhibition of maximal myofibrillar ATP and contraction. Maladaptive remodeling also demonstrates abnormalities in enzymes and ion channels, mitochondrial effects, depletion of myocardial ATP and changes in myocardial substrate use (from fatty acids to glucose) [2].

10.4.4 Right Heart Failure Secondary to Left Heart Failure

Multiple mechanisms contribute to RV failure secondary to LV dysfunction: (1) LV failure increases the afterload by increasing pulmonary arterial pressure, (2) cardiomyopathy in the LV may simultaneously affect the RV, (3) MI that may involve both ventricles, (4) LV dysfunction affecting the systolic driving pressure of the RV coronary perfusion, (5) through ventricular interdependence due to septal dysfunction, and (6) RV diastolic function could be restricted in the setting of LV dilation with a limited pericardial compartment [11].

In the setting of an inferior MI, acute RV failure is a result of LV dysfunction and elevated LV filling pressure. The increase in LV and left atrial pressure leads to a corresponding increase in mean pulmonary artery pressure to maintain the same cardiac output at the same pulmonary resistance. These events lead to a simultaneous decrease in RV contractile function [9].

In left HF, although RV dysfunction appears to be more common in non-ischemic cardiomyopathy, it is also seen in ischemic cardiomyopathy. RV dysfunction in this setting more closely parallels LV dysfunction. RV ejection fraction is a strong and independent predictor for mortality in left HF [12].

The RV may be unable to maintain the flow volume required to keep adequate left ventricular preload in LV failure. The RV status serves as a common final pathway in the progression of congestive HF due to the multiple factors that influence RV function in LV failure. Thus, this is a sensitive indicator of poor prognosis or impending decompensation [11].

10.4.5 Ischemic RV Failure and RV Infarction

Coronary artery disease (CAD) represents the main preceding event (around 70%) in heart failure. The high prevalence of reduced flow reserved

in patients with HF and non-significant stenosis in the main coronary arteries suggests that microvascular impairment contributes to myocardial dysfunction [3].

In acute myocardial infarction (MI), the death of myocytes in one or more ventricular segments results in scarring resulting in inadequate relaxation in diastole and impaired contraction in systole. The lack of synchronicity in the movement connected to the infarcted area reduces the efficiency of pump function [3].

Coronary ischemia leads to a decrease in the contractile function of the RV. It is commonly a consequence of acute coronary syndrome; however, other causes include severe pulmonary hypertension and/or decreased systemic pressure. The blood supply of the RV originates from the right coronary artery, and supplies the inferior wall of the heart in about 90% of the population [9].

The RV is more adept at tolerating ischemia in comparison to the LV due to lower oxygen demand and the presence of coronary collateral flow. RV failure due to RV infarct may improve simultaneously overtime. However, if the RV infarct is hemodynamically significant, mortality is high [9].

RV infarction occurs in the setting of an inferior MI. This is often unrecognized, as an isolated decrease in the RV contractile function with preserved RV outflow pressure is a clinically silent phenomena. In this setting, normal right atrial function is crucial to prevent a loss of atrioventricular synchronicity contributing to cardiogenic shock [9].

Infarction of the RV could cause sufficient myocardial damage resulting in heart failure, shock, arrhythmias, and death in the absence of any superimposed volume or pressure overload, and unrelated to the extent of LV damage. The enlarged hypocontractile right ventricle plays an important role in compromising the overall circulatory status. Patients with right HF and defective RV are found to be more susceptible to deterioration [11].

Tachyarrhythmias, such as nonsustained ventricular tachycardia (NSVT) and atrial fibrillation and flutter (AF), impact right atrial function. In AF, atrial contraction is reduced leading to a decrease in ventricular filling and stroke volume. In NSVT, the systolic volume is diminished due to atrioventricular dissociation and the consequent preload drop. Further decreasing the filling and cardiac output is the shortened diastolic time. Persistent tachyarrhythmias lead to tachycardia-induced myopathy (tachycardiomyopathy) [3].

10.4.6 Congenital Heart Disease and RV failure

RV failure is a common consequence of congenital heart disease (CHD). In patients with large atrial septal defect (ASD), left-to-right shunting and volume overload is seen in the RV. The long-standing volume overload is associated with increased mortality and morbidity, such as HF, decreased exercise tolerance, and arrhythmias. Incomplete RV and right atrial remodeling, and increased risk of arrhythmias are correlated with older patients (>40 years of age) with delayed repair or closure. In comparison to ventricular septal defects, only a small percentage of patients with ASD develop Eisenmenger syndrome presenting later in life. This is attributed to two factors: (1) the timing of the shunting, which is delayed until RV hypertrophy regresses and maturation of pulmonary vasculature occurs, and (2) the absence of high-pressure shear forces as seen in VSD [12].

Ebstein's anomaly is a congenital heart defect in which there is apical displacement of the septal and posterior tricuspid leaflet exceeding 8 or 20 mm/m^2 in the adult. The result is an atrialized portion of the RV and moderate to severe tricuspid regurgitation. Associated congenital defects include ASD with bi-directional shunt, pulmonary stenosis, and accessory pathways. Due to the volume overload of the RV and the inability of the hypoplastic RV chamber to adequately handle systemic venous return, RV failure ensues. Surgical management depends on the valve morphology (attachment, commissures, surface) and the size of the functional RV before repair can be considered [12].

A number of congenital abnormalities such as pulmonary valve stenosis, double-chambered RV, infundibular hypertrophy, or dynamic obstruction of the RV lead to RV outflow tract obstruction. When pulmonary valve stenosis is severe, the RV maintains the ability to adapt. Symptoms rarely manifest during childhood and adolescence; however, long-standing, untreated severe

obstruction lead to RV failure and tricuspid regurgitation. Adults present with symptoms of fatigue and dyspnea which reflect the inability to increase cardiac output during exercise [12].

A common surgical complication of Tetralogy of Fallot is severe pulmonic regurgitation (PR) associated with RV dysfunction, decreased exercise capacity, atrial and ventricular arrhythmias, and sudden death. Timely replacement of the pulmonic valve protects patients from post-surgical complications [13].

In patients with D-transposition of the great arteries who underwent atrial switch surgery and patients with congenitally corrected L-transposition of the great arteries, the anatomic RV supports systemic circulation. These patients present with late-onset RV failure since the RV properties and mechanics are not designed to support the systemic circulation. A progressive decline in RV function due to myocardial perfusion defects, uncoordinated myocardial contraction, and systemic atrioventricular valve (tricuspid valve) regurgitation is seen in patients who have undergone atrial switch surgery. Congenital correction of the L-transposition of the great arteries is associated with moderate to severe systemic atrioventricular (tricuspid valve) regurgitation and increased mortality. Replacement of the tricuspid valve slows the progression of the RV failure [12].

10.5 Clinical Presentation

In the emergency setting, the most common presentation in patients with acute right HF is dyspnea. However, dyspnea is a non-specific symptom that includes pulmonary etiologies, such as asthma and COPD exacerbation, and various cardiac etiologies, such as myocardial infarction [14]. Dyspnea has a high sensitivity of 84–100%, but a poor specificity (17–34%). Paroxysmal nocturnal dyspnea is more specific at 80–84%, but it has low sensitivity at 39–41% [15]. Other clinical presentations include orthopnea, fatigue, weakness and lethargy, as well as peripheral edema and abdominal distention. Orthopnea has a specificity of 77% and a sensitivity of 50% [14]. Right hypochondrial pain is mostly likely due to right sided heart failure, with a specificity of 80% and sensitivity of 23% [15].

Furthermore patients with right HF present with jugular venous distention, lower extremity edema and parasternal holosystolic murmur that is compatible with tricuspid regurgitation [16]. On physical examination, the presence of a third heart sound has the highest specificity of 99%, but has a very low sensitivity of 13%. Jugular venous distention and presence of murmurs have specificities of 90% but they also have low sensitivities of around 30% [14]. In critically ill patients, the most recognizable signs are elevated right-sided filling pressures, such as jugular venous distention and peripheral edema. A parasternal heave may also be felt over the right sternal border [17]. Rales and lower extremity edema both have specificity of 78% but their sensitivity is at 60% and 50%, respectively. Wheezing has low sensitivity and specificity, at 22% and 58%, respectively [14]. Hepatojugular reflux and ascites are not frequently found in HF but they both have a high specificity of more than 96%, but their sensitivity is only at 24% and 1%, respectively [15]. In patients with right to left shunting or severely low cardiac output, cyanosis can also be present [16].

10.6 Diagnostic Work Up

Since most symptoms of acute right HF have either low sensitivity or specificity, it is essential to complete a thorough medical history and physical examination. Recommended investigations for each patient include: (1) 12-lead electrocardiogram, (2) laboratory evaluation, (3) chest radiograph, and (4) echocardiogram [14].

10.6.1 Electrocardiography (EKG)

Obtaining an EKG is routinely done to assess the cardiac rhythm, QRS duration, and presence of atrioventricular conduction block [16]. Although specific, EKG lacks sensitivity [18].

10.6.2 Echocardiography

Echocardiography plays a significant role in the diagnosis of right heart failure. RV enlargement, RV systolic dysfunction, tricuspid regurgitation, pulmonary hypertension, congenital heart defects, valvular heart disease, or left heart disease are consistent in patients with RHF [16].

In the parasternal short-axis view, changes in the RV associated with hemodynamic overload could be seen. The crescent-shaped RV is lost while the septum becomes flat. The LV becomes non-spherical (D shape) resulting in impaired LV filling and decreased cardiac output [2].

Because of the complex structure of the RV, only diameters and areas are used in echocardiographic assessment of RV size. The normal free wall thickness is at 5 mm, and measurements above 5 mm are considered hypertrophy. Using the apical 4-chamber view, the long- and short-axis views can be measured and the end-systolic and end-diastolic area are determined. Normally, the RV area and mid-cavity diameter are smaller than the LV. Visual echocardiographic assessment is inaccurate for identification of functional abnormalities [2].

Three-dimensional echocardiography can be used determine volumes and ejection fraction without geometrical assumptions. This has been proven to be accurate and reproducible compared to cardiac MRI [2].

Measurement of right atrial pressure and cardiac index are the strongest prognosticators in PAH and a more accurate reflection of RV function than PAP. A right atrial pressure of ≥15 mmHg or a cardiac index ≤2 l/min/m^2 is an indication for transplantation referral in PAH [18].

10.6.3 Magnetic Resonance Imaging (MRI) and Computerized Tomography Scan (CT scan)

MRI is the gold standard for quantifying the RV chamber, right heart structure and function [2]. This is especially useful in patients with complex congenital heart defects such as Ebstein's anomaly and hypoplastic RV, precise quantification of valvular regurgitation, and planning of complex surgeries. Recent studies have also shown the prognostic value of RV end-diastolic volumes and pulmonary compliance as assessed by MRI in PAH [16].

Tricuspid annular plane systolic excursion (TAPSE) is most commonly used in clinical practice to evaluate global RV function. It is easily measured by using an M-mode cursor that is passed through the tricuspid lateral annulus in a 4-chamber view. The extent of systolic motion of the lateral portion of the tricuspid ring towards the apex is then measured. This exhibits a good correlation with isotope-derived RV ejection fraction [2]. It has an established prognostic value in patients with PAH and values of <1.8 cm indicates significantly decreased survival [18].

Cardiac CT can provide accurate assessment of structure and function, including the coronary arteries. However, in patients with tachycardia, the cardiac CT and MRI has lower accuracy [15].

10.6.4 Right Heart Catheterization

Cardiac catheterization remains the gold standard for assessing hemodynamics of the pulmonary circulation. It measures the pressures directly and estimates the flow indirectly. Right heart catheterization is useful in confirming the presence of pulmonary hypertension (mean pulmonary arterial pressure at ≥25 mmHg at rest), defining the underlying causes and providing prognostic information [2].

Indications for right heart catheterization include assessment of pulmonary vascular resistance or impedance, pulmonary pressures, cardiac output shunt fraction, and pulmonary vasoreactivity [16].

10.6.5 Exercise Stress Testing

Exercise stress testing is very useful is objective assessment of clinical deterioration in patients with PAH or congenital heart disease. However, this is contraindicated in patients with severe pulmonary vascular disease [16].

10.6.6 Brain Natriuretic Peptide (BNP)

HF-specific tests include brain natriuretic peptide (BNP) and N-terminal proBNP (NT-proBNP). A neuro-hormone, BNP is the activated form of proBNP, and is stored in secretory granules in both ventricles and lesser in the atria. ProBNP is secreted into the ventricles and is broken down into its two cleaved form—the inert N-terminal fragment (NT-proBNP) and its biologically active hormone BNP as a response to volume expansion and pressure overload. If measured in patients with acute dyspnea, BNP levels of less than 100 pg/ml have a negative predictive value (NPV) of 90%, while values of more than 500 pg/ml have a positive predictive value (PPV) of 81%. Its level is a strong predictor of risk of death and cardiovascular events in patients who are previously diagnosed with heart failure or cardiac dysfunction [15]. BNP could predict survival in patients with acute RVH in PAH. Increased levels are associated with increased mortality (1415 pg/ml vs 628 pg/ml) [18].

NT-proBNP has a longer half-life of 72 h compared to 4 h of BNP. They have no clinically significant difference, aside from NT-BNP levels are less affected by obesity. Elevated levels have been associated with renal failure, pulmonary embolism, pulmonary hypertension, and chronic hypoxia. Obese and overweight individuals are found to have relatively low BNP levels [15].

10.6.7 Other Tests

Chest radiography can be used to evaluate cardiac size, pulmonary congestion, and to detect other cardio-pulmonary diseases that are contributory to the patient's symptoms [15]. Once the chest radiograph shows signs of RV dysfunction, RVF is usually advanced and is associated with high mortality [18].

Baseline renal and liver function tests, albumin, uric acid levels and B-type natriuretic peptide could help in determining the prognosis of right heart disease [16]. Sodium levels ≤136 mml/l could predict RVF and increased risk of death in patients with PAH. Creatinine could also predict survival as increased levels suggest increased mortality. Elevated levels of C-reactive protein are associated with increased mortality. Liver transaminases, though its prognostic value has not been established, could reflect hepatic congestion and/or hypoperfusion due to compromised LV function and forward failure [18].

In patients with PAH, the following tests are also obtained: ventilation perfusion scan, pulmonary function tests, overnight oximetry, and serology for human immunodeficiency virus (HIV) and connective tissue diseases. To determine protein-losing enteropathy, stool alpha-1 antitrypsin is also obtained [16].

10.7 Treatment and Management

Treatment of acute right heart failure focuses on three targets: (1) preload optimization, (2) afterload reduction, and (3) improvement of contractility [18]. The primary goal in the setting of acute RHF is to avoid systemic hypotension in order to prevent sequela events such as myocardial ischemia and further hypotension [16].

In etiology-specific management, the treatment options include early revascularization for RV infarction, thrombolysis for pulmonary embolism, antibiotics for endocarditis, and surgical repair. In ST-elevation myocardial infarction (STEMI) involving the right ventricle, early reperfusion has been shown to improve RV ejection fraction and decrease the incidence of complete heart block [16].

In critically ill patients admitted to the intensive care unit (ICU), acute RV failure is mostly a combination of established pulmonary vascular disease complicated by acute derangements in one or all of the following: (1) RV preload, (2) RV afterload, and (3) RV contractility. For example, in an ICU patient who develops cor pulmonale from emphysema and subsequent severe pneumonia, management is directed at optimizing RV function. In patients with acute RV failure secondary to a massive pulmonary embolism, the targeted treatment is to reduce the increased afterload [17].

10.7.1 Optimizing the Preload

Most of the clinical conditions that lead to RHF are associated with increased RV afterload. Diuretics or hemofiltration reduce the excessive RV preload, and thereby reduce RV dilatation and free wall tension. This minimizes ischemia and improves contractility [19]. Progressive diuresis of 500–1000 ml daily is the target goal in patients with volume overload. In patients with hypovolemia, a bolus of 500 ml is given [16].

Generally maintaining moderately high RV diastolic filling pressure of 8–12 mmHg is optimal in RHF [19]. It is then adjusted to optimize RV function and cardiac output. In ICU patients, a central venous catheter is used to monitor superior vena cava oxygen saturation (Sv_{O2}) and central venous pressure, which help in assessing right-sided filling pressures and oxygen delivery. The normal range for Sv_{O2} and lower values suggest reduced cardiac output [17]. In conditions like acute RV infarction (further discussed below) where the RV output is impaired due to contractile dysfunction but the afterload is normal, a higher preload is needed to keep the forward flow [19].

10.7.2 Reducing the Afterload

Pulmonary vasodilators are used in conditions with high pulmonary vascular resistance (PVR). Increased PVR is seen in critically ill patients with acidosis, hypoxia, and hypercapnia. Using lung protective ventilation (using lower effective plateau pressure, tidal volume, and positive end-expiratory pressure) while avoiding hypoxemia and hypercarbia, helps improve RV preload and afterload [19]. The Sa_{O2} is ideally kept above 92% and ventilator settings are adjusted to achieve a lung volume near functional residual capacity and a P_{CO_2} and pH that are near normal as possible [17].

The pulmonary vasodilator agent of choice in critically ill patients is inhaled nitric oxide (iNO), used off-label. Its pharmacologic properties of rapid onset of action and short-half-life have been shown to improve pulmonary hemodynamics in RHF [19]. It improves oxygenation by diverting blood flow away from areas of very low ventilation-perfusion ratio or shunt. In patients with acute respiratory distress syndrome (ARDS), iNO does not improve the outcome but has been shown to improve the RV ejection fraction and end-diastolic volume and improve mixed venous oxygenation saturation in patients with acute RV failure. It must be noted that systemic administration of pulmonary vasodilators can worsen gas exchange and impair ventilation-perfusion matching [17].

Prostanoids are used in patients with PAH and RV infarction [16]. Similar to iNO, three prostacyclin derivatives are currently available in the United States for the treatment of pulmonary arterial hypertension: (1) epoprostenol, (2) treprostinil and (3) iloprost. These agents act as potent pulmonary vasodilators with rapid onset of action and short half-lives. They function to increase the intracellular cAMP level, and provide inotropic effects. These agents are administered via inhalation, thus minimizing the systemic effects [17].

Phosphodiesterase-5 (PDE5) inhibitors are alternate therapeutic agents used to manage patients with acute RHF and underlying chronic pulmonary hypertension. They act by decreasing the pulmonary arterial pressure and increasing the cardiac output in both acute and chronic pulmonary hypertension. However, the potential adverse effect of causing systemic hypotension and blunting hypoxic pulmonary vasoconstriction must be taken into consideration [19].

Other pulmonary vasodilator agents such as the endothelin receptor antagonists and the soluble guanylate cyclase stimulator, riociguat, should also be used with caution in management of acute RV failure. Endothelin receptor antagonists have reportedly been associated with increased mortality in left heart failure. Riociguat has significant systemic vasodilator effects, especially in conditions like sepsis wherein the endogenous nitric oxide production may be increased. Calcium channel blockers should also be avoided because of associated negative inotropic effects and the potential to increase RV stroke work index [17].

10.7.3 Improving Contractility

Supraventricular tachyarrhythmias (SVTs) can further compromise cardiac function. In the setting of chronotropic incompetence, atrial or atrioventricular sequential pacing may improve cardiac output in RHF. Electrical cardioversion is performed on patients with tachyarrhythmias, while pacemaker implantation is performed in patients with high grade AV block [16].

The therapeutic goal in patients who are hypotensive with severely elevated pulmonary artery pressure is to maintain the systemic arterial pressure higher than the pulmonary arterial pressure. Vasopressin, which binds to vasopressin-1 (V1) receptors on vascular smooth muscles, can cause pulmonary vasodilation at low doses (0.01–0.03 U/min). However, at higher doses, it causes coronary vasoconstriction by increasing catecholamine responsiveness [19].

In patients with acute RHF and signs of low cardiac output, inotropic therapy is indicated. Dobutamine acts to increase cardiac index and stroke volume while maintaining preload. At doses of 2–5 mcg/kg/min, dobutamine increases cardiac output while decreasing pulmonary vascular resistance in PAH. Its combination with iNO in pulmonary hypertension has shown to increase cardiac index, decrease pulmonary vascular resistance, and significantly increase PaO2/FiO2 ratio. In hypotensive patients, the preferred agent is dopamine, whereas milrinone is preferred in patients with tachyarrhythimas [16].

If the patient remains hemodynamically unstable after preload optimization, in which dobutamine is primarily used, mechanical support options such as extra corporeal membrane oxygenation (ECMO) and right ventricular assistive device (RVAD) are considered, as well as urgent transplantation and surgery in selected cases [16].

Levosimendan, a calcium sensitizer with inotropic properties, improves RV function or pulmonary hemodynamics in patients with biventricular failure or ARDS [16]. It functions to increase contractility without increasing oxygen consumption. This effect is achieved by sensitizing cardiac troponin C to the effects of intracellular calcium. However, its use is limited by adverse effects, such as hypotension and arrhythmias, especially with bolus dosing [18]. Future studies are needed to determine its role in managing patients with acute RHF [16]. It is currently approved in Europe, but not in the U.S. [18].

10.7.4 Treatment of RV Ischemia and Infarction

RV ischemia presents with both systolic and diastolic dysfunction which causes a serious deficit in LV preload and a resultant drop in cardiac output, leading to systemic hypotension. Adequate filling (preload) of the RV is crucial to maintain sufficient RV output volume and LV function. Initial therapy includes administration of adequate volume and avoidance of therapeutic agents that cause venodilation and decreased RV filling, such as diuretics and nitrates. Initial recommendation is a volume challenge of 300–600 ml of normal saline over 10–15 min via a central line or through a large-bore peripheral intravenous site. Invasive hemodynamic monitoring is preferred since further infusion is damaging when additional increases in the RV volume prevent sufficient LV filling, due to interventricular interactions and intra-pericardial pressure equalization [20].

Although conventional management of RV infarction is initially volume replacement, recent studies have cautioned against excessive volume loading. Traditionally, the initial therapy in hypotensive patients with severe RV infarction without pulmonary congestion is volume expansion when the central venous pressure is <15 mmHg. The accepted regimen is administration of normal saline (40 ml/min, up to 2 L) while maintaining the right atrial pressure at <18 mmHg to prevent volume overload. However, recent clinical studies show that volume loading further elevates the right-sided filling pressure without improving cardiac output. Berisha et al. conducted a study demonstrating that the mean optimal pulmonary wedge pressure (PWP), which reflected maximum LV stroke work index in each patient, was 16 mmHg [21].

Early and complete revascularization of the affected vessels, including the major RV branch, is significant in the recovery of RV

function. Adequate heart rate and maintenance of atrioventricular synchrony by electrical stabilization are key factors in preserving cardiac output in RV infarction. Extracorporeal support devices have been used to support RV failure due to infarction which improve RV shock [21].

References

1. Walker L, Buttrick P. The right ventricle: biologic insights and response to disease: updated. Curr Cardiol Rev. 2013;9(1):73–81. https://doi.org/10.2174/157340313805076296.
2. Apostolakis S, Konstantinides S. The right ventricle in health and disease: insights into physiology, pathophysiology and diagnostic management. Cardiology. 2012;121:263–73. https://doi.org/10.1159/000338705.
3. Pazos-Lopez P, Peteiro-Vazquez J, Carcia-Campos A, Garcia-Bueno L, Abugattas de Torres J, Castro-Beiras A. The causes, consequences, and treatment of left or right heart failure. Vasc Health Risk Manag. 2011;7:237–54. https://doi.org/10.2147/VHRM.S10669.
4. Storrow A, Jenkins C, Self W, Aexander P, Barrett T, Han J, McNaughton C, Heavrin B, Gheorghiade M, Collins S. The burden of acute heart failure on U.S. emergency departments. JACC Heart Fail. 2014;2(3):269–77. https://doi.org/10.1016/j.jchf.2014.01.006.
5. Hummel A, Empen K, Dorr M, Felix S. De novo acute heart failure and acutely decompensated chronic heart failure. Dtsch Arztebl Int. 2015;112(17):298–310. https://doi.org/10.3238/arztebl.2015.0298.
6. Jong P, Yusuf S, Rousseau M, Ahn S, Bangdiwala S. Effect of enalapril on 12-year survival and life expectancy in patients with left ventricular systolic dysfunction: a follow up study. Lancet. 2003;361(9372):1843–8. https://www.ncbi.nlm.nih.gov/pubmed/12788569/.
7. Bardy GH, Lee KL, Mark DB, Poole JE, Packer DL, Boineau R, Domanski M, Troutman C, Anderson J, Johnson G, McNulty SE, Clapp-Channing N, Davidson-Ray LD, Fraulo ES, Fishbein DP, Luceri RM, Ip JH, Sudden Cardiac Death in Heart Failure Trial (SCD-HeFT) Investigators. Amiodarone or an implantable cardioverter-debrillator for congestive heart failure. N Engl J Med. 2005;352(3):225–37. https://www.ncbi.nlm.nih.gov/pubmed/15659722/.
8. Farha S, Lundrgrin E, Erzurum S. Novel therapeutic approaches to preserve the right ventricle. Curr Heart Fail Rep. 2013;10(1):12–7. https://doi.org/10.1007/s11897-012-0119-3.
9. Guyton AC, Lindsey AW, Gilluly JJ. The limits of right ventricular compensation following acute increase in pulmonary circulatory resistance. Circ Res. 1954;4:326–32.
10. Voelkel N, Gomez-Arroyo J, Abbate A, Bogaard H. Mechanisms of right heart failure – a work in progress and a plea for failure prevention. Pulm Circ. 2013;3(1):137–43. https://doi.org/10.4103/2045-8932.109957.
11. Voelkel N, Quaife R, Leinwand L, Barst R, McGoon M, Meldrum D, Dupuis J, Long C, Rubin L, Smart F, Suzuki Y, Gladwin M, Denholm E, Gail D. Right ventricular function and failure: report of a national heart, lung, and blood institute working group on cellular mechanisms of right heart failure. Circulation. 2006;114:1883–91. https://doi.org/10.1161/CIRCULATIONAHA.106.632208.
12. Haddad F, Doyle R, Murphy D, Hunt S. Right ventricular function in cardiovascular disease, part II: pathophysiology, clinical importance, and management of right ventricular failure. Circulation. 2008;117(13):1717–31. https://doi.org/10.1161/CIRCULATIONAHA.107.653584.
13. Davlouros P, Niwa K, Webb G, et al. The right ventricle in congenital heart disease. Heart. 2006;92:i27–38. http://heart.bmj.com/content/92/suppl_1/i27.
14. Teichman S, Maisel A, Alan S. Challenges in acute heart failure critical management: optimizing care despite incomplete evidence and imperfect drugs. Crit Pathw Cardiol. 2015;14(1):12–24. https://doi.org/10.1097/HPC.0000000000000031.
15. Inamdar AA, Inamdar AC. Heart failure: diagnosis, management and utilization. J Clin Med. 2016;5(7):62. https://doi.org/10.3390/jcm5070062.
16. Skhiri M, Hunt S, Denault A, Haddad F. Evidence-based management of right heart failure: a systematic review of an empiric field. Rev Esp Cardiol. 2010;63:451–71. https://doi.org/10.1016/S1885-5857(10)70094-3.
17. Ventetuolo C, Klinger J. Management of acute right ventricular failure in the intensive care unit. Ann Am Thorac Soc. 2014;11(5):811–22. https://doi.org/10.1513/AnnalsATS.201312-446FR.
18. Lahm T, McCaslin C, Wozniak T, Ghumman W, Fadl Y, Obeidat O, Schwab K, Meldrum D. Medical and surgical treatment of acute right ventricular failure. J Am Coll Cardiol. 2010;56(18):1435–46. https://www.clinicalkey.com/#!/content/playContent/1-s2.0-S0735109710034996?returnurl=http:%2F%2Flinkinghub.elsevier.com%2Fretrieve%2Fpii%2FS0735109710034996%3Fshowall%3Dtrue&referrer=https:%2F%2Fwww.ncbi.nlm.nih.gov%2F.
19. Mehmood M, Frank T. Treatment of right heart failure: Is there a solution to the problem? EJ Cardiol Pract. 2016;14(33). https://www.escardio.org/Journals/E-Journal-of-Cardiology-Practice/Volume-14/Treatment-of-right-heart-failure-is-there-a-solution-to-the-problem.
20. Ondrus T, Kanovsky J, Novotny T, Anderson I, Spinar J, Kala P. Right ventricular myocardial infarction: from pathophysiology to prognosis. Exp Clin Cardiol. 2013;18(1):27–30. https://www.ncbi.nlm.nih.gov/pmc/articles/PMC3716484/.
21. Inohara T, Kohsaka S, Fukuda K, Venu M. The challenges in the management of right ventricular infarction. Eur Heart J Acute Cardiovasc Care. 2013;2(3):226–34. https://doi.org/10.1177/2048872613490122.

Chronic Right Heart Failure

11

Kaan Kırali, Özge Altaş Yerlikhan, and Davut Çekmecelioglu

Abstract

Right heart failure (RHF) represents a disturbance or dysfunction in any of the components that constitute the right heart circulatory system. The right ventricle is overshadowed by the left ventricle and the crescent-shaped right ventricle is anatomofunctionally different from the conical-shaped left ventricle due to its myocardial structure. The central component of the anatomofunctional relationship between both ventricles is the interventricular septum. Several pathologies affecting the right ventricle do not usually impair right ventricular functions because the interventricular septum remains intact in most cases, thus enabling the right ventricle to withstand acute or chronic cardiac dysfunctions for long periods and delaying the development of RHF. On the other hand, RHF leads several pathological changes involve not only the cardiovascular system, but also the hepatic, renal, neuroendocrinological, immunological, musculoskeletal, hematologic, gastrointestinal systems, and nutritional status. Congestive multiorgan dysfunctions should be treated initially, and then these patients should be listed for transplantation or mechanical assist device implantation. Understanding of pathophysiology and structural changes of the right ventricle will open new treatment options in near future. Percutaneous right heart bypass systems will also take first place to support the right-sided cardiac output; maybe, for long-term implantation.

Keywords

Right ventricular failure · Right heart failure
Right ventricular dysfunction · Pulmonary hypertension · Pulmonary vascular resistance
Tricuspid regurgitation · Volume overloading
Septal contractility

11.1 Introduction

Right heart failure (RHF) represents a disturbance or dysfunction in any of the components that constitute the right heart circulatory system (i.e., from systemic veins to pulmonary capillaries), which is not restricted to the right ventricle (RV); rather, right ventricular failure (RVF) is one of the most important causes of RHF [1].

Right heart failure is a major determinant of the outcomes in patients with primary pulmonary arterial hypertension (PAH), corrected congenital heart diseases (c-CHDs), and advanced left ventricular failure (LVF). Recent clinical observations, scientific investigations, and experimental studies have cast new light on the importance of

K. Kırali (✉) · Ö. A. Yerlikhan · D. Çekmecelioglu
Department of Cardiovascular Surgery, Division of Heart Transplantation and Mechanical Assist Device, Kartal Koşuyolu Education and Research Hospital, Istanbul, Turkey

S. I. Dumitrescu et al. (eds.), *Right Heart Pathology*, https://doi.org/10.1007/978-3-319-73764-5_11

the RV in normal cardiac physiology and its prominent role in the pathophysiology of RHF. The main difference of the RV is the dependence of right ventricular afterload on fetal and postnatal life, wherein the RV works as a systemic ventricle during fetal life and pulmonic ventricle after birth. During fetal life, the RV and the left ventricle (LV) work in parallel to support the systemic and pulmonary circulation. Elevated pulmonary vascular resistance (PVR), which is associated with higher systemic afterload, maintains the physiologic right ventricular hypertrophy (RVH) because the RV accounts for approximately 60% of the total cardiac output (CO). However, these circulations are serially connected after birth due to a progressive decrease in pulmonary afterload when both lungs begin to function during respiration, thus resulting in the unloading of right ventricular pressure and a subsequent physiologic regression. Pathological increase in pulmonary afterload, after birth, will lead to a chronically compensated state with increased RVH, right ventricular dysfunction (RVD), or clinical symptomatic RVF.

The RV has been overshadowed by the LV, which conforms better to geometric models and is more accessible to noninvasive imaging tests, especially transthoracic echocardiography (TTE), due to its simpler anatomy. The crescent-shaped cavity of the RV is anatomofunctionally different from the conical-shaped cavity in the LV due to its myocardial structure, which includes dense transverse fibers that create the framework of the thin free wall and scanty oblique helical fibers that form the interventricular septum (IVS). Moreover, the LV cavity is only capable of long-axis shorting and mild circumferential narrowing. Early studies on cardiac function have falsely concluded that the RV did not contribute significantly to the generation of CO. However, advanced imaging techniques including cardiac magnetic resonance imaging (cMRI) have provided critical information about the anatomical, physiological, and pharmacological actions and response mechanisms of the RV, allowing for true measurements of the right ventricular ejection fraction (RVEF), right ventricular stroke work index (RVSWI) and right ventricular fractional area change (RVFAC).

Several pathologies affecting the RV do not usually impair right ventricular functions because the IVS remains intact in most cases, thus enabling the RV to withstand acute or chronic cardiac dysfunctions for long periods and delaying the development of RHF. The IVS can be defined as the main power source of the RV and the LV; it compensates for the lack of functional support from the rest of the ventricles and counterpoises the ventricular stroke volume (SV) of both ventricles. This functional interaction between both ventricles is termed as ventricular interdependence, which transmits the contractile force from one ventricle to the other, particularly from the LV to the RV, through the myocardium and pericardium independent of neural, humoral, and circulatory mechanisms [2]. An intact IVS constitutes approximately 35–40% of the ventricular muscle mass and produces approximately 80% of the right ventricular contraction (close to 60% of the RVEF), which prevents right ventricular suppression. Intact septum protects right ventricular function for a long period, despite the destruction of the free wall by infarction or surgical intervention, even in the presence of supranormal PVR; on the contrary, septal damage causes severe RVD within a short time despite the preservation of free wall functions, even in the absence of PHT [3].

Recently, researchers have witnessed several paradigm shifts in studies involving PAH because of its progressive nature, which affects both the pulmonary vasculature and the heart. Knowledge about insufficiency between pulmonary vascular tone and lung vessel constriction helped understand the pathology of severe forms of PHT. Recently, RV is thought to be a specific contributor to the pathobiology of PAH and a part of the axis between the diseased lung circulation and the RV. In spite of the fact that the RV can adapt to increased pulmonary afterload via concentric hypertrophy, this compensatory mechanism can inhibit right ventricular function to a certain extend; however, failure can result in RVD. In PAH, pulmonary vascular damage inevitably affects the entire cardiopulmonary unit.

Yet, RVD is the most important determinant of long-term outcomes, and prolonged survival is related more to the degree of RVF than to pulmonary hemodynamics [4].

The final determinant of chronic RHF is the intrinsic breakdown of degenerating myocytes. Genetic disorders involving the heart, congenital heart defects, acquired myocardial infiltrative diseases, and specific myocardial pathologies affecting the RV worsen systolic and/or diastolic right ventricular functions, resulting in chronic RHF. Contractile dysfunctions can be tolerated by septal systolic contraction, but diastolic dysfunction causes severe symptoms.

Chronic RHF, like LHF, should be defined as a syndrome characterized by specific symptoms (e.g., dyspnea and fatigue) and signs (e.g., edema, ascites, hepatomegaly, and anasarca edema) on physical examination. Furthermore, it should be graded as "physiologic hypertrophy, asymptomatic RVD, symptomatic RVF, and end-stage RHF". While it is not difficult to recognize the signs and symptoms of severe RHF, it is challenging to define and to predict the transition of an individual patient from a compensated to a decompensated state. Possibly, the condition "at risk of developing RVF" best describes asymptomatic patients with varying etiologies (Table 11.1), who demonstrate mild or compensated abnormalities in the TTE or cMRI.

Table 11.1 Etiology of chronic RVF

1.	Increased afterload
	(a) Postcapillary
	• PHT group II (LHF, left-sided CMPs)
	• Increased LVEDP (e.g., AS, LVOT obstructions)
	• Increased LAP (e.g., MS, MR)
	(b) Capillary
	• Pulmonary embolism (thrombotic, septic, amniotic, fat, air, injectate, other)
	• Hypoxic pulmonary vasoconstriction
	• Mechanical ventilation
	• Vaso-occlusive sickle cell crisis
	(c) Precapillary
	• RVOT obstructions (e.g., PS, diffuse hypertrophic CMP, infundibular hypertrophy)
	• CHDs (e.g., ASD, APVR)
	• Valvular insufficiency (e.g., TR, PR)
2.	Right ventricular myocardial abnormality
	(a) Right ventricular infarction
	(b) Infiltrative or restrictive CMPs
	(c) ARVD
	(d) Amyloid, sarcoid
	(e) Right ventricular ischemia
	(f) Microvascular diseases and capillary rarefaction
3.	Decreased preload
	(a) Hypovolemia (e.g., systemic vasodilatory shock, anaphylaxis, extensive burn injury, sepsis)
	(b) Tamponade
	(c) Constrictive pericarditis
	(d) Superior and/or inferior VC syndrome
	(e) TS
4.	Mixt
	(a) Post-LVAD RHF

APVR anomalous pulmonary venous return, *ARVD* arrhythmogenic right ventricular dysplasia, *AS* aortic stenosis, *ASD* atrial septal defect, *CHD* congenital heart disease, *CMP* cardiomyopathy, *LAP* left atrial pressure, *LHF* left heart failure, *LVAD* left ventricular assist device, *LVEDP* left ventricular end-diastolic pressure, *LVOT* left ventricular outflow tract, *PR* pulmonary regurgitation, *PS* pulmonary stenosis, *RHF* right heart failure, *RVOT* right ventricular outflow tract, *TR* tricuspid regurgitation, *TS* tricuspid stenosis, *VC* vena cava

11.2 Contractile Anatomy of the Right Ventricle

To understand the anatomic structure of the RV, it is important to recognize that both ventricles are embryologically, architecturally, structurally, geometrically, physiologically, and adaptationally different from each other. The LV is less complex to analyze and more accessible to imaging than the RV. Both ventricles consist of three parts: the inflow tract in front, a trabecular body in the middle, and an outflow tract at the end, which gives the appearance of a differently shaped ballooned tube in the middle of each ventricle. The central component of the anatomofunctional relationship between both ventricles is the IVS, which separates the LV and RV chambers. The IVS is formerly considered as a part of the LV because it comprises the same oblique fiber elements of the free left ventricular wall.

The helical ventricular myocardial band model details the geometric structure and the spatial myofiber configuration of the heart, comprising two interconnected loops (i.e., the basal and apical components) [5]. The basal loop is an external structure comprised predominantly of transverse fibers that wrap around both ventricles. A central myocardial fold occurs where the right basal segment becomes the left basal segment (i.e., the IVS). The RV free wall mainly containing the transverse basal loop provides an external cover for the IVS, thereby changing the orientation of the fibers in an oblique direction resulting a helical arrangement of the apical loop. Some of these oblique apical loop fibers also contribute to the RV outflow tract (RVOT).

The LV originates from the primary heart field and has a conical architecture as if folded by the two flow paths, like a horseshoe, with both paths adjacent to each other. The LV, along with the IVS, accounts for >70% of the weight of the heart with the IVS constituting approximately 35% of the entire ventricular myocardial mass in the adult [6]. Myocardial structure is thicker (≥10 mm) and consists of three layers at the free wall (i.e., superficial oblique fibers, subendocardial longitudinal fibers, and circumferential fibers in between). The oblique helical fibers crossing each other at 60° angles are generally responsible for systolic ejections against higher systemic afterload via *helical motions* (spiral contraction). This ability of systolic contraction is the main factor that differentiates it from the RV, thus enabling the LV to adapt to the acutely elevated systemic afterload without LVF. Chronic elevation of systemic afterload induces a concentric hypertrophy to counterbalance the increase in resistance and to provide systemic SV for a long time, possibly life long, if myocardial ischemia and/or structural changes (e.g., excessive hypertrophy or valvular pathologies) do not develop.

The RV originates from the secondary heart field and has a triangular or crescent-shaped architecture, wrapping around the LV with both flow paths unbound to each other. The RV, with its thin free wall myocardium (≤5 mm), constitutes <30% of the weight of the heart and comprises only two myofiber layers: the superficial muscle fibers are arranged circumferentially parallel to the atrioventricular groove in continuity with the LV, whereas the trabecular subendocardial longitudinal fibers are aligned along the base to the apex. Because the free-wall of the RV is composed mostly of transverse fibers with scanty longitudinal fibers and no helical fibers, it can normally create a systolic ejection against lower pulmonary afterload using the *bellows-type motion* (peristaltic contraction). This type of contraction has limited ability to cause a marked increase in afterload, thus resulting in symptomatic RVF within a short period. In the same way, chronic elevation of pulmonary afterload can induce a concentric RVH to maintain pulmonary SV up to a certain time, but the RV fails soon with signs of right-sided low cardiac output syndrome (LCOS).

11.3 Physiology of the Right Ventricle

Normal RV function is hugely complex and dependent on multiple factors (Fig. 11.1). The forward RVEF (i.e., forward blood flow) is essential to maintain systolic function. Right ventricular stiffness is dependent on the hydraulic pressure in the right coronary artery (thus on systemic pressure), the end-systolic volume, and the degree of fibrosis in the myocardium [7]. The

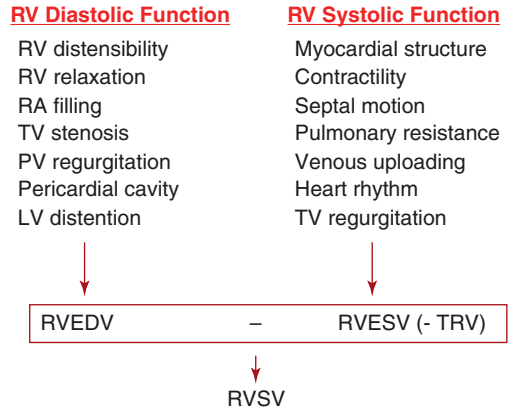

Fig. 11.1 Factors affected right ventricular function. *LV* left ventricle, *PV* pulmonary valve, *RA* right atrium, *RV* right ventricle, *RVEDV* right ventricular enddiastolic volume, *RVESV* right ventricular endsystolic volume, *RVSV* right ventricular stroke volume, *TRV* tricuspid regurgitant volume, *TV* tricuspid valve

generally thin RV is capable of filling and pumping the same amount of blood as the stronger, thick-walled LV. The contractility of the RV is weaker than that of the LV because of lower myocardial mass, a crescent-shaped cavity, and spindly papillary muscles; however, the structure of the trabeculae carneae in the RV gains power for ejection without excessive concentric hypertrophy. Lower pulmonary resistance (i.e., one-sixth the amount of systemic resistance) of highly distensible pulmonary vessels prevents the thin and expandable RV myocardium from increasing in pulmonary afterload, which may prove injurious under circumstances of pressure overload, and maintains significantly lower pressures in the RV. Therefore, the RV is more dependent on the afterload compared with the LV. This is probably due to the characteristics of the pulmonary arterial circulation as opposed to systemic arterial circulation for systolic motions and the characteristics of the systemic venous circulation as opposed to the pulmonary venous circulation for the diastolic behavior.

The trapezoidal right ventricular pressure-volume loop reflects the changes during the cardiac cycle. Right ventricular ejection starts early during pressure generation and maintains a "hang-out period" to continue the antegrade flow into the low resistance pulmonary circuit despite the onset of right ventricular relaxation. The right ventricular end systolic pressure (RVESP) falls before the closure of the pulmonic valve during end-systole, whereas the LV continues to generate systolic pressure until the closure of the aortic valve during whole systole. The RV takes advantage of this physiology by producing CO identical to that of the LV with markedly reduced work (25% of the left ventricular stroke work) and myocardial energy demand (20% of the left ventricular energy cost): *the low cavity pressure determines lower wall stress and lower oxygen demands*.

The unique anatomy, myocardial ultrastructure, and coronary physiology of the RV reflect the characteristics of a "high-volume/low-pressure" pump with a complex contraction mechanism (Table 11.2). Right ventricular ejection (by twisting and thickening) and filling (by untwisting and lengthening) is usually regulated by septal contraction and relaxation. During systole, right ventricular contraction proceeds sequentially, by initiating in the inlet, continuing through the apex, and concluding in the infundibulum. At the inflow tract, a longitudinal shortening from base to apex occurs via tricuspid annular plane systolic excursion (TAPSE) strengthened by the helical contraction of the IVS. This contraction is the dominant systolic motion of the RV to eject blood into the low resistance pulmonary circulation; yield alone an ejection more than 60% (*longitudinal strain*), supported by the bellows effect due to the pressing of the RV free-wall against the septum; yield alone an ejection fraction close to 30–35% (*circumferential strain*). The last effectiveness will be clinically evident for the prevention of postoperative RVF despite the frequent occurrence of early septal dysfunction following many conventional cardiac operations, when PVR continues to remain low postoperatively, and provides enough SV to maintain the right-sided CO. On the contrary, septal dysfunction related to any reason results in significant right-sided LCOS when the pulmonary afterload following surgical procedures is elevated.

Ventricular systolic interdependence plays an important role in the physiology of this contraction of the RV. Physiological dependence of both ventricles works according to the Frank Starling mechanism wherein one is obliged to provide optimal preload to another to maintain circulation. The anatomical interaction between both

Table 11.2 Systolic contraction mechanism of the RV

1. Longitudinal shortening	80%
(a) TAPSE (*contraction of longitudinal fibers that draw the tricuspid annulus toward the RV apex)*	
(b) Ventricular interdependence (*LV assistance to RV contraction by way of the shared interventricular septum and contiguous LV and RV circumferential fibers*)	
(c) Basal loop constriction	
(d) Infundibular contraction toward the end of systole	
2. Bellows motion (inward movement of the free wall)	15-20%
3. Traction of RV free wall at the points of binding to the LV	<5%

LV left ventricle, *RV* right ventricle

ventricles is more complicated. The LV contributes to significant amounts (20–40%) of right ventricular contractility and even higher (approximately 50%) of right ventricular pressure generation. Right ventricular dysfunction causes right ventricular dilatation with or without pressure overload resulting in a leftward shift of the IVS and a change in the left ventricular geometry. Moreover, it increases the constraining effect of the pericardium resulting in right heart diastolic tamponade. These changes contribute to the aggravation of LCOS, which means that the contractile state of one ventricle can influence the entire performance of the heart.

Preload determines the functions of both ventricles as well as the IVS (Fig. 11.2). Diastolic

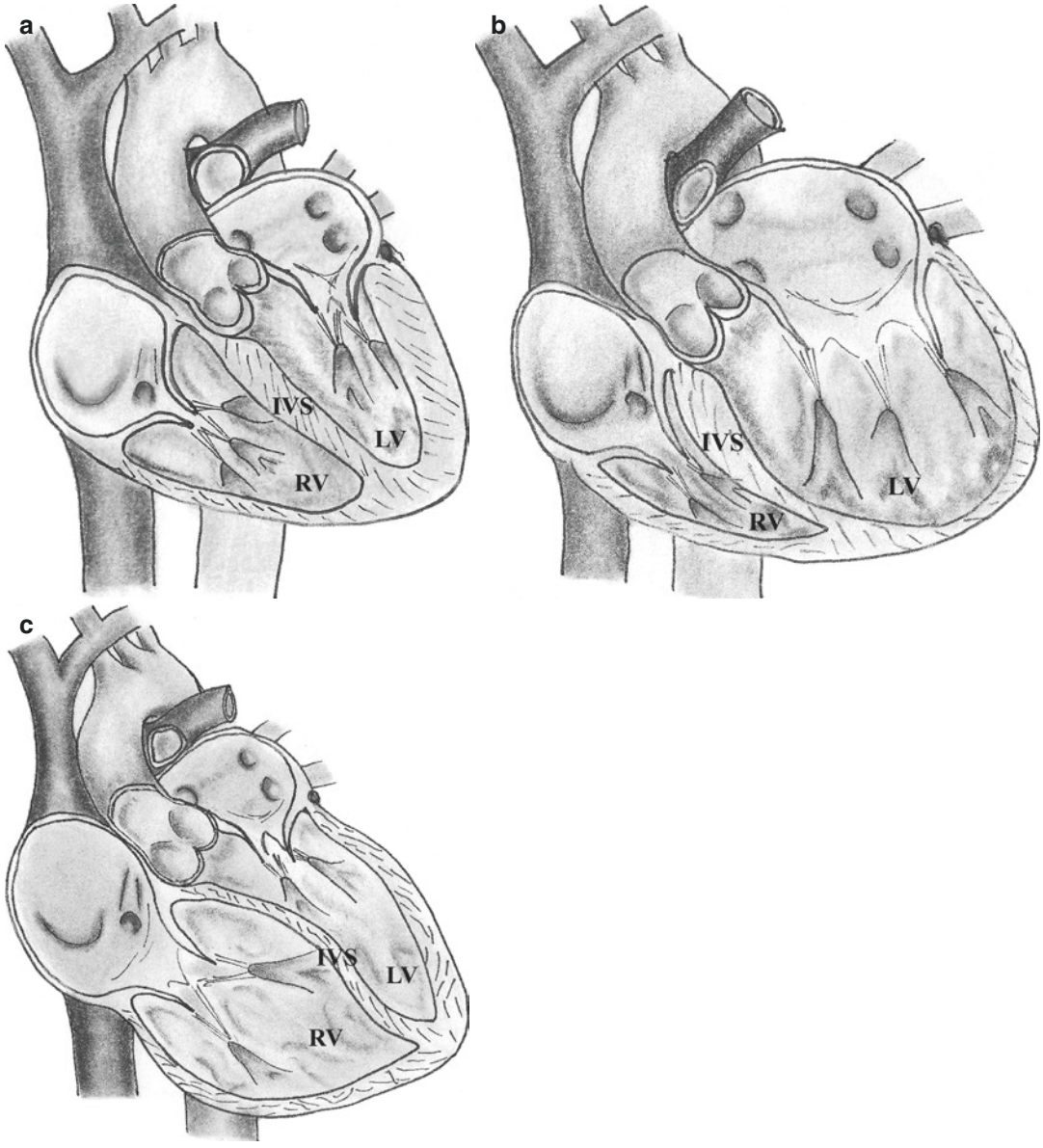

Fig. 11.2 Interventricular volume and/or pressure overload shifts the IVS into the other ventricular cavity. (**a**) Normal-loaded LV and RV. (**b**) Overloaded LV and collapsed RV. (**c**) Overloaded RV and collapsed LV. *IVS* interventricular septum, *LV* left ventricle, *RV* right ventricle

interdependence significantly crystalizes only under pathological conditions, when the volume or pressure overloaded ventricle shifts the IVS into the other chamber, resulting in a decreased preload and an impairment of SV. Volume or pressure overloaded RV shifts the IVS into the LV, decreasing left ventricular diastolic filling and SV [8]. Diastolic mutuality is a result of the common pericardial sac. The pericardium is limited in its ability to accommodate chronic ventricular dilatation. As the RV is the more compliant chamber, this diastolic interaction most commonly occurs during the volume overload state of the RV (e.g., atrial septal defect). Right ventricular diastolic function is not affected during acute elevation of the pulmonary afterload, whereas chronic pressure overloading impacts diastolic dysfunction caused by a prolonged diastolic relaxation time and increased diastolic stiffness [9].

Besides, right ventricular function is determined by the heart rhythm and right heart synchrony because preserved functions of both atria affect the RV more than the LV. Maintenance of sinus rhythm and atrio-ventricular synchrony is crucial for right ventricular function, especially in chronic RVF.

11.4 Assessment of Right Ventricular Functions

The goals of the initial evaluation of patients with chronic RVF are to better characterize the etiology, severity of dysfunction, associated cardiac pathologies, and possible treatments. It is technically more difficult to image the RV than the LV due to its changeable physiological and anatomical structures during the filling and ejecting phases in the presence of normal loading, unloading or uploading of the RV. The RV works and shapes according to the afterload, which is caused by an elevated pulmonary arterial pressure (PAP), a rightward shifted IVS, an increased intrathoracic pressure, or raised pulmonary arterial resistance. Afterload mismatch is the most important prognostic factor for systolic RVD in pressure overload conditions. Imaging studies play a crucial role during the initial assessment and serial monitoring of right ventricular functions.

Noninvasive imaging tools are preferred to evaluate right ventricular functions, primarily TTE or cMRI. Echocardiography plays a key role in the diagnosis of right heart diseases due to its ease of use, low cost, and accessibility. However, cMRI is the gold standard for evaluating right heart structure and function, and it is particularly useful in patients with complex congenital heart defects (e.g., Ebstein's anomaly, hypoplasic RV), requiring a complex surgery. Moreover, cMRI provides information on ventricular hypertrophy, the presence of infiltrative diseases, and the presence of fibrosis. Several parameters can be measured via TTE to present the final, but instant situation of the RV (Table 11.3). Load-dependent measurements such as TAPSE, RVFAC, and RVEF cannot directly evaluate the intrinsic right ventricular contractility and may provide varying information under different hemodynamic conditions, because the right ventricular functions fluctuate while determining the parameters via two-dimensional TTE, which is due to the lack of accurate ventricular volumes and the sensitivity of the RV to loading conditions. The well-known method used to diagnose RVD is TAPSE, the vertical motion of the tricuspid valve annulus from the base of the RV to the apex during the cardiac cycle, because the contraction and release phases of the RV occur via longitudinal shortening. However, it cannot be used as a prognostic after cardiac surgery as it is affected by LV function owing to septal dysfunction or loss of pericardial constraint. Furthermore, it is not used in patients with cCHDs and multivariable evaluation is a more appropriate method for the diagnosis of RVD in this group. Measurement of pulmonary artery systolic pressure (PASP) is the gold standard for PAH diagnosis. The relationship between longitudinal right ventricular fiber shortening (i.e., TAPSE) and developed pressure (i.e., PASP) may be viewed as a useful clinical index of the length/force relationship (TAPSE/PASP $\geq$0.36 mm/mmHg); the ratio of the variables potentially possesses a more discerning ability to detect disease severity compared with either of the two variables, separately [10].

Table 11.3 Echocardiographic measurements for the normal and pathologic RV

Parameter	Mean values (min–max)	RVD	RVF
RV basal diameter (mm)	33 (24–40)	41–45	>45
RV midcavity diameter (mm)	28 (20–35)		>35
RV longitudinal diameter (mm)	71 (56–86)		
RV subcostal wall thickness (mm)	≥5		<5
RVEDA (cm^2)	18 (10–25)		
RVESA (cm^2)	9 (4–14)		
TAPSE (mm)	23 (16–30)	10–15	<10
S′ (cm/s)	≥10	5–10	<5
E/E′	≤6	7–10	>10
FAC (%)	49 (35–63)		<35
RV strain			
Lateral longitudinal strain (%)	−26 (−20 to −32)	−9 to −20	>−9
Free wall strain (%)	−27 (−24 to −29)	−20 to −24	>−20

E/*E′* trans-tricuspid filling velocity/early diastolic velocity ratio, *FAC* fractional area change, *RV* right ventricle, *RVD* right ventricular dysfunction, *RVEDA* right ventricular end-diastolic area, *RVESA* right ventricular end-systolic area, *RVF* right ventricular failure, *S* peak tissue Doppler systolic velocity in the tricuspid annulus, *TAPSE* tricuspid annular plane systolic excursion

Strain imagines are increasingly being utilized to assess right ventricular function. Free-wall right ventricular longitudinal strain best predicts clinical outcomes in patients with RVD referred for heart transplantation and in patients with other types of PAH [11].

Invasive measurements of cardiac parameters by right heart catheterization are often required to diagnose the condition, to determine the appropriate therapeutic approach, and to observe the clinical course in patients with chronic RHF. Additionally indications for cardiac catheterization include assessment of PVR, CO, left-to-right shunt fraction, and pulmonary vasoreactivity. Hemodynamic variables obtained with right heart catheterization will give more details about right heart function because the relation between right ventricular pressure and right ventricular volume is the gold standard for the assessment of right ventricular function and the effect of afterload (Table 11.4). Moreover, measures of pressure-volume coupling are particularly attractive because RV–PA coupling can quantify systolic and diastolic function regardless of loading conditions, and it may help identify subclinical RHF.

11.5 Physiologic Responses of the RV Against Pathologic Overload

Small acute changes in PVR can impair right ventricular contractile performance and decrease SV even when preload is maintained, in contrast to the LV. The RV can adapt to chronic pathological elevation of pulmonary afterload via increased contractility, dilatation and hypertrophy, whereas clinical RVF is associated with progressive diastolic deterioration and disturbed ventricular–arterial coupling, despite an increase in contractility. Right ventricular adaptation to reduce wall stress and improve contractility is a complex response and dependent on many factors. The most important factors appear to be the type and severity of myocardial stress and/or injury, the time course of the underlying pathology, and the time of onset of the pathologic process (pediatric or adult groups). Other factors include neurohormonal activation (e.g., adrenergic and angiotensin pathways), altered gene expression, and ventricular remodeling [12]. The last important determinants are coronary perfusion and myocardial metabolism, which

Table 11.4 Normal invasive parameters for normal and pathologic RV

Parameter	Normal values	RVD	RVF
CVP (mmHg)	2–6	≥16	>18
PCWP (mmHg)	6–12	≤18	≤18
CVP/PCWP	<1/2	>2/3	>1
s/m/dPAP (mmHg)	<30/18/15		≥50/25
PAPP (sPAP − dPAP)	variable		
TPG (mmHg) *(mPAP − PCWP)*	≤12	>12	
DPG (mmHg) *(dPAP − PCWP)*	≤7	>7	
RVEDVI (mL/m^2)	65 (40–90)	>90	>100
RVESVI (mL/m^2)	28 (12–45)	>45	>60
SV (mL/beat) *(RVEDV − RVESV) (CO/HR)*	60–100	<50	<40
SVI (mL/m^2/beat) *(CI/HR)*	35–47	<35	
CO (L/min) *(SV × HR)*	4–8	<4	<3.5
CI (L/min/m^2) *(CO/BSA)*	2.5–4	2–2.2	<2
RVEF (%)	57 (45–69)	30–44	<30
PVR (dynes-s/cm^5) (<3 Woods) *(80 × (TPG/CO))*	<250		
RVSWI (g/m^2/beat) *(SVI × (mPAP − RAP) × 0.0136)*	5–10	<5	<4.4
0.0136 converts mmHg × L/m^2 *to* g × m/m^2	*>0.4*	*0.25–0.40*	*<0.25*
PAPi (PAPP/RAP)	>3.5	2–3.5	<2
PACi (mL/mmHg/m^2) *(SV/PAPP/BSA)*	>1	0.85–1	<0.85

BSA body surface area, *CI* cardiac index, *CO* cardiac output, *CVP* central venous pressure, *HR* heart rate, *s/m/dPAP* systolic/mean/diastolic pulmonary artery pressure, *PACi* pulmonary arterial compliance index, *PAPi* pulmonary artery pulsatility index, *PAPP* pulmonary artery pulse pressure, *PCWP* pulmonary capillary wedge pressure, *PVR* pulmonary vascular resistance, *RAP* right atrial pressure, *RV* right ventricle, *RVEDV* right ventricular end-diastolic volume, *RVEF* right ventricular ejection fraction, *RVESV* right ventricular end-systolic volume, *RVSWI* right ventricular stroke work index, *SV* stroke volume, *SVI* stroke volume index, *TPG* transpulmonary gradient

stimulate or block myocardial apoptotic pathways via mitochondrial activity. Adaptive remodeling is characterized by more concentric remodeling (higher mass-to-volume ratio) and preserved systolic and diastolic function (e.g., ventricular remodeling observed in patients with Eisenmenger syndrome), whereas maladaptive remodeling is associated with increased eccentric hypertrophy and decreased systolic and diastolic functions (e.g., remodeling observed in patients with PAH associated with connective tissue disease or idiopathic PAH) [4].

A simple, but hopefully not too simplistic approach to the pathobiology of chronic RVF is to distinguish between intrinsic mechanisms and extrinsic influences (Fig. 11.3).

Right ventricular afterload is described on a pressure-volume loop as the sum of RV systolic pressure occurring throughout ejection [13]. By LaPlace's law, RV wall stress is dependent on the pressure during ejection and the division of the ventricular radius to the free wall thickness. The ventricular radius during ejection and wall thickness are relatively small and constant; hence, wall stress is generally proportional to the ejection pressure of the RV (i.e., systolic PAP). Pulmonary afterload depends on the amount of blood flow ejected by the RV and the pulmonary arterial resistance against it (Fig. 11.4). The primary response of the RV to counterbalance increased pulmonary afterload is to strengthen contractility, defined as right ventricular end-systolic elastance (RV-Ees), and to maintain SV against the increased pulmonary afterload, which is defined as pulmonary arterial elastance (PA-Ea). When the increase in RV-Ees is less than that of PA-Ea, the Ees/Ea ratio (denoting the approximate SV value) decreases and leads to

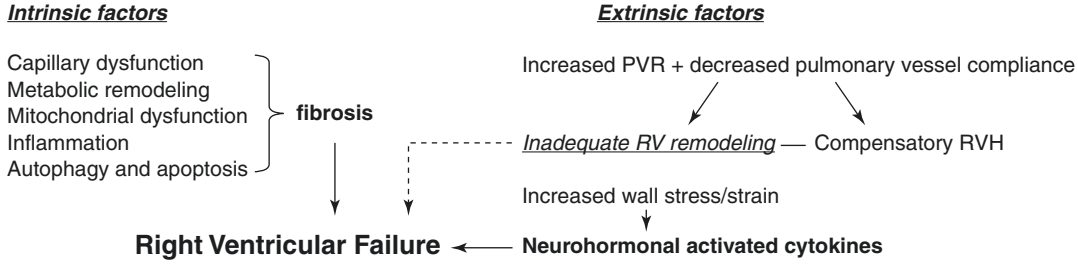

Fig. 11.3 Intrinsic and extrinsic factors leading to RVF. *PVR* pulmonary vascular resistance, *RV* right ventricle, *RVH* right ventricular hypertrophy

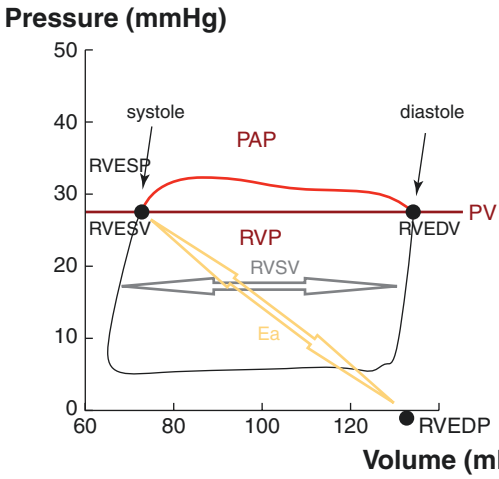

Fig. 11.4 Right ventricular pressure × volume loop. Rigth ventricular afterload can be described as the sum of RVP throughout ejection (light red line), which is affected by RVSV (=RVEDV − RVESV) (light grey bidirectional arrow) and pulmonary artery Ea (=RVESP/RVSV) (light orange bidirectional arrow). *Ea* pulmonary arterial elastance, *PAP* pulmonary artery pressure, *PV* pulmonary valve, *RVEDP* right ventricular end-diastolic pressure, *RVEDV* right ventricular end-diastolic volume, *RVESP* right ventricular end-systolic pressure, *RVESV* right ventricular end-systolic volume, *RVP* right ventricular pressure, *RVSV* right ventricular stroke volume

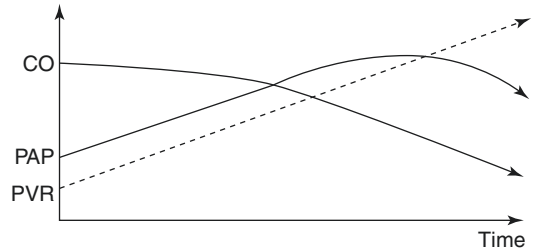

Fig. 11.5 Time-dependent relation between pressure overload and right ventricular ejection. *CO* cardiac output, *PAP* pulmonary arterial pressure, *PVR* pulmonary vascular resistance

ventricular–arterial uncoupling, which is regarded as a pathophysiological sign of RVF [14]. Increased loading in the early phase of an acute pulmonary overload improves right ventricular ejection and avoids right ventricular dilatation; however, the RV will immediately deteriorate if this increase in loading is not treated. In contrast, the Frank–Starling's mechanism processes the compensation of chronic pressure overloading to sustain adequate right-sided CO, whereas ventricular dilatation develops with time and causes a decrease in Ees/Ea ratio, leading to increase in wall stress and a resultant systolic dysfunction. Reversal of this vicious circle improves RV-PA coupling, leading to reduction in right ventricular wall stress and dilatation. Chronic elevation of pulmonary afterload also aggravates progressive deterioration of diastolic dysfunction represented by increase in right atrial pressure. At the beginning, the right atrium attemps to compensate for diastolic RVD by increasing its own contractility and enlarges to serve as a reservoir. Deterioration of right ventricular diastolic function is the main factor responsible for the transition from compensated RVD to RVF (Fig. 11.5).

The second most important factor influencing pulmonary afterload is the relationship between resistance and compliance in the lung vasculature, which is different from that in the systemic vasculature. In spite of compliance in systemic circulation changes independent of resistance,

there is a close inverse hyperbolic relation between them during pulmonary circulation, which is not significantly effected by changes in heart rate. Vascular architecture, which results compliance or resistance, is also inverse in systemic and pulmonary circulations: the proximal aorta accounts for most of the total arterial compliance, while the distal vessels are responsible for most of the resistance. Alternatively, proximal PA may account for only ~20% of the total arterial compliance, and the distal vessels are responsible for most of the resistance and capacitance, because the number of distal arterioles is roughly ten times larger in the pulmonary vasculature compared with the systemic vasculature (i.e., normal PVR is about 10% of systemic vascular resistance). Pulmonary vascular compliance, which can be calculated easily by the division of the right ventricular SV to PA pulse pressure, decreases when PVR elevates because the RV needs stronger systolic pressure to eject blood.

In general, the RV adapts better to volume overload than to pressure overload. The RV may tolerate volume overload such as in atrial septal defect or tricuspid regurgitation (TR) for a long time without a significant decrease in right ventricular systolic function. However, pressure overload may lead to RVD with or without dilatation along with myocardial ischemia, which may further aggravate RVD. Interestingly, the timing of onset of pressure overload is a crucial determinant of the right ventricular response, which explains why the RV in Eisenmenger patients takes much longer to be compensated for when compared with patients with acquired PHT. Intrinsic myocardial diseases affecting only the RV may impair right ventricular contractility without pulmonary arterial uploading and can play a significant role in the development of RHF.

Chronic pressure overload in pulmonary circulation is the end-stage of many cardiovascular and pulmonary diseases, where the RV adapts to this increased afterload through multiple compensatory mechanisms. Myocyte hypertrophy and the expansion of the extracellular matrix result in an increase in chamber thickness. According to Laplace's law, wall stress is directly proportional to the right ventricular pressure during ejection and the chamber radius, and inversely proportional to the chamber thickness. The primary result of these initial adaptations is to reduce wall stress, thus countering the effect of the rise in afterload. The result of chronic pressure overloading is concentric hypertrophy, followed by reduction in contractility and progressive ventricular dilatation. Other causes for myocardial dysfunction during chronic pressure overloading are (1) increase in myocardial energy demand due to progressive increase in right ventricular systolic pressure relative to aortic systolic pressure, resulting in the simultaneous reduction of the right coronary perfusion and oxygen delivery; (2) a shift in myocardial energy production from fatty acid metabolism to glycolysis, causing a reduction in oxidative capacity, whereas both the RV and LV myocardium utilize free fatty acids for biosynthesis and energy production in the normal fasting state; (3) the absence of washout of metabolites or electrical remodeling in the failing RV, leading to arrhythmias; (4) early failure of right ventricular antioxidant defenses due to nonactivation of antioxidant enzymes during the compensation stage of RVD, resulting in early myocardial damage compared with the LV; and (5) a progressive decline in mitochondrial number and mass. This supply-demand mismatch further compromises right ventricular performance and ultimately leads to RVF if the PAH remains untreated. Both CO and PAPs fall when the contractile reserve of the RV is no longer sufficient to maintain an adequate SV (Fig. 11.4).

Chronic volume overload of the RV can be tolerated for several years before RVD develops because of the ability of the thin distensible RV, which can adapt to large volume changes without significant changes in pressure. Acute volume uploading primarily impairs right ventricular diastolic function, whereas the systolic function of the RV is preserved. During the chronic phase of volume overload, diastolic dysfunction worsens with the onset of fibrosis, whereas similar to the clinical situation, systolic function at this stage is still largely preserved. Myocardial dysfunction develops with similar mechanisms during chronic

pressure overload. There is a shift away from fatty acid metabolism to glycogenolysis similar to those developed during left-sided overload. The two effects of constant RV dilatation are deformation of the tricuspid annulus and septal shift. Dilatation of the tricuspid annulus results in TR, which can further worsen the volume overload of the RV, while septal shift can weaken LV filling and adversely affect LV functions. Lastly, prolonged volume overload may induce an increase in PAPs due to the increase in flow through the pulmonary circuit. The development of PAH is often a trigger for the decompensation of the chronic volume overloaded state, as the dilated RV lacks the compensatory mechanisms to augment its contractility in the setting of an increased afterload.

11.6 Pathologic Changes During Chronic RVF

The response of both ventricles to afterload increase is similar in acute situations and includes contraction enhancement, preload elevation (i.e., increase in ventricular filling volume), and stimulation of vascular resistance reducing biomarkers. On the contrary, during chronic afterload increase, both ventricles also exhibit similar alterations in genes regulating the extracellular matrix and cytoskeletal remodeling; however, there are important differences in genes regulating energy production, mitochondrial function, reactive oxygen species production and antioxidant protection, and angiogenesis [15].

11.6.1 Cardiac Hypertrophy

The RV that suffers from a chronically elevated afterload initially undergoes myocardial strengthening via myocardial hypertrophy in order to successfully adapt to the increase in wall stress and strain. This compensation mechanism of the RV against pressure overloading comprises an increase in RV free wall thickness via accumulation of muscle mass and modification to a more rounded shape. There are several differences in metabolism, mitochondrial remodeling, and glycolysis-to-glucose oxidation coupling between both ventricles during the process of adapting to the increase in afterload. The hypertrophic response of cardiomyocytes to pathological conditions leads to changes at the transcriptional level, such as an increase in protein synthesis, the number of sarcomeres, and the size of the myocytes. Particularly, new protein synthesis, turnover, and lysis are very important during this transition phase, which is directly enhanced by autocrine, paracrine, and neurohumoral influences.

The mechanism of transition from compensated hypertrophy to failure appears to be, fundamentally, a matter of balance between cell survival and death. During cardiac hypertrophy, a mismatch between the numbers of capillaries and the size of the cardiomyocytes (chronic oxygen demand-supply mismatch) can result in myocardial hypoxia, contractile dysfunction, and apoptosis. In contrast, the coronary perfusion can primarily occur during diastole in patients with RVF, secondary to pulmonary afterload while coronary perfusion is present throughout the cardiac cycle in the unstressed RV. At present, it is not known as to whether the microvessels in RVH dissapear or whether angiogenesis matches the degree of hypertrophy. If the RVH in PAH is initially compensatory, then factors promoting growth and preserving the integrity of the microvessels try to balance the increased blood flow caused by cardiomyocyte hypertrophy. In contrast, capillary density decreases in the decompensated RVH cases, rendering the stressed RV more susceptible to microischemic injury, even at the onset of pressure overload.

Energy utilization shift from fatty acid oxidation to glucose and lactate, and then from complete glucose oxidation via the Krebs cycle to glycolysis only is observed in pressure-loaded RV, which results in increased expression of glycolysis-related genes, and acts as an adaptive mechanism against decreased blood flow (decreased oxygenation). While this shift is beneficial during acute overloading, chronic dependence on glycolysis for energy production is not sufficient to meet the demands of the myocardium

and to maintain normal function, leading to an energy-starved state and contributing to heart failure [16]. As a power storage of cardiomyocytes, mitochondrial activity increases some processes such as the formation of oxygen radicals, induction of apoptosis, and inflammation to regulate increased oxidative stress, which triggers the production of oxygen radicals. Pressure load stimulates apoptosis due to mechanic damage, oxidative stress, and neurohumoral signaling, which contributes to heart failure even at mildly increased rates. Impaired proteins and organelles, if not removed from the cells by autophagy, accumulate and become toxic or trigger apoptotic death.

In response to increased afterload, the RV reverts to a fetal gene pattern, re-expressing genes normally expressed in the fetal but not postnatal RV, which includes a shift from α- to β-myosin and an increase in adrenergic receptors, calcineurin activation, and phosphodiesterase type-5 expression [17]. This adaptive phenotype provides a lower energetic cost profile to the failing myocardium, as α-myosin heavy chains are usually involved in stronger and faster contractions, whereas ß-myosin heavy chains account for lower contractile potential [18]. Because α-myosin requires larger amounts of adenosine triphosphate, a decrease in α-myosin and an increase in ß-myosin may prevent ischemic cascade due to the energy-sparing profile, as appropriate glycolysis. In the failing RV, the gene expression pattern (RV failure gene expression program) is characterized by a depressed cell growth pattern, along with increased proteolysis and apoptosis, a shift from cell growth to cell death. Cardiac autophagy can be a maladaptive response to chronic hemodynamic stress and a hallmark of myocardial hibernation. Inhibition of autophagy during the development of hypertrophy may be harmful, but may prove useful when the autophagy becomes maladaptive and plays a role in the progression of heart failure.

11.6.2 Cardiac Fibrosis

The next step of transition from compensated RVD to collapse of the RV is adverse remodelling of the extracellular matrix, which is characterized by an increase in myocardial fibrosis. There appears to be a syncytial relationship among cardiomyocytes, fibroblasts, and the cardiac matrix. The normal heart muscle contains about 50% fibroblasts, which are essential for the adaptive response of the heart to pressure overload. Right ventricular fibrosis develops after the increase in right ventricular mass. Cardiac fibrosis is a hallmark of maladaptive hypertrophy and is characterized by increased deposition of the fibrillary collagens type I and III [19]. Collagen synthesis increases when wall stress enhancement begins, and rate of collagen production remains higher than that in the normal RV owing to decrease in the degradation process. Upregulation of the activities of specific genes such as transforming growth factor (TGF)-β1, connective tissue growth factor, and endothelin-1, results in myocardial fibrosis, while the upregulation of matrix metalloproteinases leads to extracellular matrix degeneration; these processes are linked in a complex fashion and will adversely affect the myocardial systolic and diastolic functions [20]. Increased collagen content in the heart (fibrosis) is tightly linked to TGF-β1. Fibrosis may impair the electrical coupling between cardiomyocytes and can reduce capillary density, thereby influencing myocyte metabolism. Endothelial cell–mesenchymal transition (EMT) is another mechanism by which cardiac fibrosis may occur. Although EMT is an embryonic mechanism and is inactive in adults, hypoxia, injury, inflammation, or aging can sitmulate this process, and it has been shown that the fibroblasts formed in fibrotic lesions in the heart may be of endothelial origin [21].

11.6.3 Intrinsic Myocardial Disease

A few cardiomyopathies are characterized by the replacement of the ventricular myocardium with non-contractile tissues, as seen in an arrhythmogenic RV. It may present with focal RVD at the sites of involvement and ultimately progress to dilatation and global RVF. The typical clinical presentation is ventricular arrhythmias, whereas

congestive symptoms develop late during the course of the pathology. Therefore, most patients with RVD can be present without any significant symptoms for decades due to the continuance of a normal PVR. However, when the PVR is raised, it is associated with rapid cardiac decompensation suggesting that the progression of RVD to RVF may require the presence of an additional stressor, such as PAH.

11.7 Chronic Non-Cardiac Organ Dysfunctions

Heart failure leads several pathological changes involve not only the cardiovascular system, but also the hepatic, renal, neuroendocrinological, immunological, musculoskeletal, hematologic, gastrointestinal systems, and nutritional status. Advanced HF is often characterized by an increasing inability to meet the metabolic requirements of end organs or skeletal muscle. Currently, studies are being carried out in order to clarify the pathophysiology of the systemic complications related to heart failure and to propose treatments that improve quality of life and increase survival. All these chronic adverse progresses should be treated medically and/or mechanically (e.g., right ventricular assist devices) before heart, lung or heart-lung transplantation. The worst cituation is anasarca edema, which is characterized with gode dropping tissue edema on the upper legs and whole abdomen, and it is the most sensitive indicator for adverse prognosis and also the most serious risk factor for surgery (e.g., heart transplantation or mechanical assist device implantation). The optimal strategy to solve the anasarca edema should be aggressive medical treatment with or without ultrafiltration (or directly dialysis) and/or right ventricular bypass (see Chap. 53).

11.7.1 Congestive Hepatopathy (Cardiohepatic Syndrome; Cardiac Cirrhosis)

Hepatic pathologies secondary to cardiac decompansations develop step by step due to the following underlying reasons: chronic passive congestion, centrcilobular necrosis, and cardiac cirrhosis. Chronic congestion is usually a consequence of right-sided HF, whereas centrcilobular necrosis is generally caused due to severe hypotension or shock. Cardiac cirrhosis includes a wide spectrum of hepatic disorders developed secondary to passive hepatic congestion due to RHF, without an intrinsic hepatic pathology. Right-sided cardiac pathology can generate right-sided LCOS with elevated CVP, which reflects in the hepatic sinusoid and increases intrahepatic venous pressure. Venous congestion caused by RHF can induce a transient increase in liver stiffness, which is assessed by elastography, and can mislead the diagnosis of liver cirrhosis. Congestive hepatopathy is the chronic course of a chronic RHF and is characterized by sinusoidal dilatation resulting in hypoperfusion, edema, and hypoxia. These adverse alterations impair hepatocytes with accompanied hemorrhagic injury resulting in modification of the hepatocyte architecture, atrophy with associated collagen deposition, and fibrosis in the hepatic veins and sinusoids. Severe extended hepatic congestion can eventually lead to the development of cardiac cirrhosis, which histologically, in the early stages of the disease process, shows a distinguishing reverse lobulation pattern in which fibrous septa form bridges between the central veins. In long-prolonged or severe cases, the cell loss and collapse of normal architecture might diffuse to incorporate some portal tracts. However, the presence of portal inflammatory cells or bile ductular proliferation is rare, which helps distinguish a cardiac etiology from others more commonly encountered in adults.

Advanced RHF may present with liver-related symptoms including abdominal distention, intermittent right upper quadrant discomfort, nausea, early satiety, or anorexia [22]. Symptoms are difficult to distinguish from primary hepatobiliary or gastrointestinal conditions such as cholelithiasis, peptic ulcer disease, or even ischemic colitis. Acute cardiogenic liver injury or ischemic hepatitis is related to elevated right-sided or venous filling pressures, whereas between 40 and 70% of these patients have the underlying diagnosis of

chronic RHF. Because patients remain asymptomatic for a long period, the clinical appearance is evident only after a marked elevation in serum hepatocyte markers such as serum alanine aminotransferase (ALT), aspartate aminotransferase, and lactic dehydrogenase (LDH) levels to 10–20 times normal, and γ-glutamyl-transpeptidase along with the prolongation of coagulation period (thrombin and prothrombin time) [23]. A ratio of serum ALT to LDH <1.5 early in the course of liver injury is characteristic of cardiogenic injury as opposed to other etiologies of hepatitis. Hyperbilirubinemia and hypoalbuminemia are accurate diagnostic biomarkers showing severe hepatic insufficiency, whereas hepatomegaly and ascites confirm the diagnosis of cardiac cirrhosis. The ascites fluid typically reveals a high protein content (>2.5 g/dl), which is associated with rupture of the hepatic lymphatics and leakage of protein-rich fluid. A serum to ascites albumin gradient >1.1 reflects portal hypertension (i.e., irreversible cardiac cirrhosis). Total bilirubin, an independent predictor of adverse prognosis, has potentially become an important risk factor of chronic RHF [24]. A bleeding diathesis from acquired coagulopathy may also develop due to impaired production of coagulation factors. These abnormalities peak at 1–3 days after onset of symptoms and, in patients who survive, return to normal within 5–10 days after onset.

There are some clinical characteristics and laboratory tests that can help in distingushing cardiac-related liver disease from primary diseases of the liver. Measurement of the diameter of the IVC might be the best marker for severe venous congestion due to its low interobserver variation. Therefore, evaluation of the IVC diameter may provide supportive information as with measurements of plasma concentrations of biomarkers in outpatients with chronic HF [25].

11.7.2 Congestive Nephropathy

Chronic kidney disease can be observed in up to 60% of patients with advanced RHF [26]. Cardiorenal syndrome (CRS) is defined as a complex pathophysiological disorder of the heart and kidneys in which acute or chronic dysfunction in one organ may induce acute or chronic dysfunction in the other. CRS type 2 (CRS2) is characterized by chronic abnormalities in cardiac function leading to kidney injury or dysfunction. A low cardiac index (CI) seems to develop in parallel with renal impairment, cirrhosis, and ascites and may play an important role during this stage of the disease. One of the principle roles of a properly functioning cardiorenal axis is the maintenance of extracellular fluid volume homeostasis. A complex system of volume and pressure sensors, afferent and efferent feedback loops, local and distant vasoactive substances and neurohormonal systems with built-in redundancies serves to continuously monitor and adapt to changing extracellular fluid volume and blood pressure. When such systems are intact and working properly, they respond rapidly to the ever-changing hemodynamics and volume status, and ensure adequate tissue perfusion and oxygen delivery.

Impaired renal function is common and is one of the most powerful determinants of outcome in chronic RHF that causes worsening of renal function due to increased CVP and/or intraabdominal pressure (IAP) generated by severe ascites. This increase in venous pressure causes worsening of the kidney function, where tubular damage plays a major role and simultaneously constitutes a stimulus for peripheral synthesis and the release of inflammatory mediators [27]. Normal IAP measurements in healthy adults are between 5 and 7 mmHg, whereas a small increases in IAP, in the range of 8–12 mmHg, is associated with impaired renal function. In critically ill patients, IAP >12 mmHg is a common cause of organ dysfunction [28]. Persistance of significant reduction in glomerular plasma flow together with elevated intra-glomerular filtration pressure (i.e., efferent arteriolar constriction) produces focal and segmental glomerulosclerosis. On the contrary, chronic RHF associated with LCOS results in renal ischemia, which is the dominant factor for decrease in glomerular filtration.

Experimental and clinical data indicate that CRS2 is characterized by mild-to-moderate proteinuria, a progressive decline in glomerular

filtration rate, and an elevated expression of renal injury biomarkers. Important pathophysiological triggers of renal disease progression include chronic increases in renal venous pressure, maladaptive activation of the renin-angiotensin-aldosterone axis and the sympathetic nervous system, as well as a chronic inflammatory state. Intrarenal oxidative stress and proinflammatory signaling precipitate structural injury, including glomerulosclerosis and tubulointerstitial fibrosis. With increase in the level of aldosterone in the kidney due to impairment of the renin-angiotensin-aldosterone axis, pronounced oxidative stress occurs via signaling from the paracrine glycoprotein galectin-3. Pro-fibrotic cytokine TGF-β is upregulated followed by an increase in fibronectin, leading to renal fibrosis and glomerulosclerosis. Furthermore, venous congestion may increase the gut absorption of endotoxin leading to additional inflammatory responses, while venous congestion itself acts as a stimulus for peripheral synthesis and release of inflammatory mediators.

A similar cardio-renal relation is seen in patients with HF, along with the co-existence of cardiac and renal failure that amplify the progression of failure of the individual organs; the key physiological factor in this case is arterial underfilling. It may induce or amplify disturbances in cardio-renal homeostasis and neurohumoral integrity, which is caused due to arterial vasodilation and a decrease in CI (relative or absolute). Albumin expands central blood volume and increases both CI and mean arterial pressure; hence, amelioration of arterial underfilling can prevent the development of hepatorenal syndrome.

11.7.3 Anasarca Edema

Variable spectrum of fluid retention ranging from acute pulmonary oedema to chronic peripheral edema can be encountered in patients with LHF. On the contrary, patients with RHF, acute and/or chronic fluid retention is the main problem causing peripheral or generalized edema. Generalized edema, otherwise known as anasarca, is a common presentation in various conditions including liver, and/or renal disease or malnutritional. Additionally, congestive RHF may lead itself to hepato-renal impairment, resulting in generalized edema. The mechanisms of generalized edema contain decreased plasma oncotic pressure due to reduction of plasma protein, increased hydrostatic pressure leading more water outwards to the interstitium, obstruction of lymphatic flow due to congestion, and increased vessel permeability with mediators causing decrease of plasma proteins in circulation. Fluid is primarily extravasated to peripheral tissues and abdominal viscera; however, anasarca is characterized by a puffiness of the face (most noticeable in the periorbital area) and the persistence of an indentation over the medial aspect of the ankle following the application of pressure. Patients with anasarca present with complaints of feeding difficulties (in pediatric patients), excessive sweating, failure to thrive, respiratory distress, and cyanosis. They may also have a history of orthopnea, dyspnea, and syncopal symptoms. Furthermore, the following signs may also be present: nontender peripheral pitting edema (digital pressure leaves visible and palpable imprints, sometimes quite deep) in the feet and ankles; an enlarged and sometimes pulsatile liver palpable below the right costal margin; abdominal swelling and ascites; and visible elevation of the jugular venous pressure, sometimes with large a or v waves that are visible even when the patient is seated or standing.

11.7.4 Cardiac Cachexia

It needs to be acknowledged that cachexia is representing a major burden for patients and the healthcare system. Heart failure was recorded for 19% of cachexia admissions and was the third most common chronic comorbidity (Table 11.5) [29]. The heart-failure induced cachexia is defined as non-edematous wight loss of 6% of the usual body weight in the last 6 months, in the absence of other diseases such as neoplasias, infection or hypothyroidism. Cachexia is an important predictive factor in the reduction of

Table 11.5 Defination of cachexia

1. Wight loss ≥5% in <4 months
2. BMI <20 kg/m^2
3. Presence of a chronic disease (the first five reasons)
(a) Malignancy
(b) Chronic obstructive pulmonary disease
(c) Chronic heart failure
(d) Infection
(e) Thyroid dysfunctions
4. At least three of the following criteria
(a) Reduced muscle strength
(b) Fatigue
(c) Anorexia
(d) Reduction of the fat free mass index
(e) Inflammation
(f) Anemia
(g) Low serum albumin

BMI body mass index

survival in heart failure, independent from important variables such as age, functional status, ejection fraction and capacity to perform physical activity. However, it is often difficult to diagnose cachexia in heart failure patients, since edema, especially anasarca, impairs body weight evaluation and other anthropometric measures. Cachexia is mainly the result of an imbalance in the homeostasis of muscle protein synthesis and degradation due to a lower activity of protein synthesis pathways and an over-activation of protein degradation, where the overall net catabolic outcome is systemic tissue wasting (e.g., skeletal muscle, bone, and fat compartments) [30]. The pathophysiology of cardiac cachexia is complex and multifactorial including several factors interacting in a complex system with immune, metabolic, and neurohormonal consequences. The key points are global anabolic blunting and insulin resistance and catabolic overactivity. Besides anorexia, other factors may lead to the reduction of food ingestion, such as early fullness due to significant hepatomegaly, reduced energy ingestion due to low lipid ingestion, and dyspnea at rest. On the other hand, reduced food consumption can be secondary to anorexia and various factors, such as tasteless diets, particularly due to the low sodium content, intestinal hypomotality and passive visceral congestion [31].

Conclusion

Chronic RHF is growing and repressing isolated LHF and has become more serious public health problem than it, especially after LVAD. Severe RHF leads life-threatening several pathological changes involve not only the cardiovascular system, but also the hepatic, renal, neuroendocrinological, immunological, musculoskeletal, hematologic, gastrointestinal systems, and nutritional status. Therefore, RHF should always be kept in mind as compared to LHF and it would be more appropriate to delay further treatment protocols unless controlled by severe and aggressive medical therapy. Particularly, since anazarca edema is pointing to severe multiorganic deterioration, heart transplantation should be postponed after it has been treated.

References

1. Mehra MR, Park MH, Landzberg MJ, Lala A, Waxman AB. Right heart failure: toward a common language. J Heart Lung Transplant. 2014;33(2):123–6. https://doi.org/10.1086/674750.
2. Santamore WP, Dell'Italia LJ. Ventricular interdependence: significant left ventricular contributions to right ventricular systolic function. Prog Cardiovasc Dis. 1998;40(4):289–308. https://doi.org/10.1016/S0033-0620(98)80049-2.
3. Buckberg G, Hoffman JI. Right ventricular architecture responsible for mechanical performance: unifying role of ventricular septum. J Thorac Cardiovasc Surg. 2014;148(6):3166–3171.e1-4. https://doi.org/10.1016/j.jtcvs.2014.05.044.
4. Vonk-Noordegraaf A, Haddad F, Chin KM, Forfia PR, Kawut SM, Lumens J, Naeije R, Newman J, Oudiz RJ, Provencher S, Torbicki A, Voelkel NF, Hassoun PM. Right heart adaptation to pulmonary arterial hypertension: physiology and pathobiology. J Am Coll Cardiol. 2013;62(25 Suppl):D22–33. https://doi.org/10.1016/j.jacc.2013.10.027.
5. Torrent-Guasp F, Whimster WF, Redmann K. A silicone rubber mould of the heart. Technol Health Care. 1997;5(1):13–20.
6. Plunkett MD, Buckberg GD. Pathophysiologic implications of the helical ventricular myocardial band: considerations for right ventricular restoration. Semin Thorac Cardiovasc Surg Pediatr Card Surg Ann. 2007;10:68–75. https://doi.org/10.1053/j.pcsu.2007.01.011.
7. Chin KM, Coghlan G. Characterizing the right ventricle: advancing our knowledge. Am J Cardiol.

2012;110(6 Suppl):3S–8S. https://doi.org/10.1016/j.amjcard.2012.06.010.
8. Tadic M. Multimodality evaluation of the right ventricle: an updated review. Clin Cardiol. 2015;38(12):770–6. https://doi.org/10.1002/clc.22443.
9. Gaynor SL, Maniar HS, Bloch JB, Steendijk P, Moon MR. Right atrial and ventricular adaptation to chronic right ventricular pressure overload. Circulation. 2005;112(9 Suppl):I212–8. https://doi.org/10.1161/CIRCULATIONAHA.104.517789.
10. Guazzi M, Bandera F, Pelissero G, Castelvecchio S, Menicanti L, Ghio S, Temporelli PL, Arena R. Tricuspid annular plane systolic excursion and pulmonary arterial systolic pressure relationship in heart failure: an index of right ventricular contractile function and prognosis. Am J Physiol Heart Circ Physiol. 2013;305(9):H1373–81.
11. Ryan JJ, Tedford RJ. Diagnosing and treating the failing right heart. Curr Opin Cardiol. 2015;30(3):292–300. https://doi.org/10.1097/HCO.0000000000000164.
12. Kholdani CA, Fares WH. Management of right heart failure in the intensive care unit. Clin Chest Med. 2015;36(3):511–20. https://doi.org/10.1016/j.ccm.2015.05.015.
13. Tedford RJ. Determinants of right ventricular afterload. Pulm Circ. 2014;4(2):211–9. https://doi.org/10.1086/676020.
14. Borgdorff MA, Dickinson MG, Berger RM, Bartelds B. Right ventricular failure due to chronic pressure load: what have we learned in animal models since the NIH working group statement? Heart Fail Rev. 2015;20(4):475–91. https://doi.org/10.1007/s10741-015-9479-6.
15. Reddy S, Bernstein D. The vulnerable right ventricle. Curr Opin Pediatr. 2015;27(5):563–8. https://doi.org/10.1097/MOP.0000000000000268.
16. Reddy S, Bernstein D. Molecular mechanisms of right ventricular failure. Circulation. 2015;132(18):1734–42. https://doi.org/10.1161/CIRCULATIONAHA.114.012975.
17. Friedberg MK, Redington AN. Right versus left ventricular failure differences, similarities, and interactions. Circulation. 2014;129(9):1033–44. https://doi.org/10.1161/CIRCULATIONAHA.113.001375.
18. Guihaire J, Noly PE, Schrepfer S, Mercier O. Advancing knowledge of right ventricular pathophysiology in chronic pressure overload: insights from experimental studies. Arch Cardiovasc Dis. 2015;108(10):519–29. https://doi.org/10.1016/j.acvd.2015.05.008.
19. Bogaard HJ, Abe K, Vonk Noordegraaf A, Voelkel NF. The right ventricle under pressure: cellular and molecular mechanisms of right-heart failure in pulmonary hypertension. Chest. 2009;135(3):794–804. https://doi.org/10.1378/chest.08-0492.
20. Creemers EE, Pinto YM. Molecular mechanisms that control interstitial fibrosis in the pressure-overloaded heart. Cardiovasc Res. 2011;89(2):265–72. https://doi.org/10.1093/cvr/cvq308.
21. Zeisberg EM, Tarnavski O, Zeisberg M, Dorfman AL, McMullen JR, Gustafsson E, Chandraker A, Yuan X, WT P, Roberts AB, Neilson EG, Sayegh MH, Izumo S, Kalluri R. Endothelial-to-mesenchymal transition contributes to cardiac fibrosis. Nat Med. 2007;13(8):952–61. https://doi.org/10.1038/nm1613.
22. Samsky MD, Patel CB, DeWald TA, Smith AD, Felker GM, Rogers JG, Hernandez AF. Cardiohepatic interactions in heart failure: An overview and clinical implications. J Am Coll Cardiol. 2013;61(24):2397–405. https://doi.org/10.1016/j.jacc.2013.03.042.
23. Çağlı K, Başar FN, Tok D, Turak O, Başar Ö. How to interpret liver function tests in heart failure patients? Turk J Gastroenterol. 2015;26(3):197–203. https://doi.org/10.5152/tjg.2015.0086.
24. Allen LA, Felker GM, Pocock S, McMurray JJ, Pfeffer MA, Swedberg K, Wang D, Yusuf S, Michelson EL, Granger CB, Investigators CHARM. Liver function abnormalities andoutcome in patients with chronic heart failure: data from the Candesartan in Heart Failure: Assessment of Reduction in Mortality and Morbidity (CHARM) program. Eur J Heart Fail. 2009;11(2):170–7. https://doi.org/10.1093/eurjhf/hfn031.
25. Pellicori P, Carubelli V, Zhang J, Castiello T, Sherwi N, Clark AL, Cleland JG. IVC diameter in patients with chronic heart failure: Relationships and prognostic significance. JACC Cardiovasc Imaging. 2013;6(1):16–28. https://doi.org/10.1016/j.jcmg.2012.08.012.
26. Di Lullo L, Bellasi A, Barbera V, Russo D, Russo L, Di Iorio B, Cozzolino M, Ronco C. Pathophysiology of the cardio-renal syndromes types 1-5: an uptodate. Indian Heart J. 2017;69(2):255–65. https://doi.org/10.1016/j.ihj.2017.01.005.
27. Angelini A, Castellani C, Virzì GM, Fedrigo M, Thiene G, Valente M, Ronco C, Vescovo G. The role of congestion in cardiorenal syndrome type 2: new pathophysiological insights into an experimental model of heart failure. Cardiorenal Med. 2015;6(1):61–72. https://doi.org/10.1159/000440775.
28. Verbrugge FH, Dupont M, Steels P, Grieten L, Malbrain M, Tang WH, Mullens W. Abdominal contributions to cardiorenal dysfunction in congestive heart failure. J Am Coll Cardiol. 2013;62(6):485–95. https://doi.org/10.1016/j.jacc.2013.04.070.
29. Loncar G, Springer J, Anker M, Doehner W, Lainscak M. Cardiac cachexia: hic et nunc. J Cachexia Sarcopenia Muscle. 2016;7(3):246–60.
30. Saitoh M, Ishida J, Doehner W, von Haehling S, Anker MS, Coats AJS, Anker SD, Springer J. Sarcopenia, cachexia, and muscle performance in heart failure: review update 2016. Int J Cardiol. 2017;238:5–11. https://doi.org/10.1016/j.ijcard.2017.03.155.
31. Okoshi MP, Romeiro FG, Paiva SA, Okoshi K. Heart failure-induced cachexia. Arq Bras Cardiol. 2013;100(5):476–82. https://doi.org/10.5935/abc.20130060.

Systemic Consequences of Right Ventricular Failure

12

Vlad Damian Vintilă and Ana-Maria Vintilă

Abstract

Right ventricular failure can occur as an acute or chronic dysfunction. It can occur during an acute pathology of the right heart (for example, inferior acute myocardial infarction with right ventricle involvement) or of the lungs (for example massive venous thromboembolism). It can also arise in a chronic situation as a secondary dysfunction of the lungs or of the heart (for example pulmonary hypertension, pulmonary infiltrative diseases or pulmonary stenosis). There are multiple organ dysfunctions involved in heart failure. It is difficult to separate right ventricle for left ventricle dysfunction since there is an interventricular mechanism of loading, pressure and contraction. Quantitation of the degree of heart failure is difficult since the most frequent biomarkers have altered clearance in right heart failure.

Keywords

Systemic disorder · Interventricular coupling
Organ failure · Biomarkers

V. D. Vintilă (✉)
Department of Cardiology, University Emergency Hospital, "Carol Davila" University of Medicine and Pharmacy, Bucharest, Romania

A.-M. Vintilă
Department of Internal Medicine, Colţea Clinical Hospital, "Carol Davila" University of Medicine and Pharmacy, Bucharest, Romania

12.1 Etiology. Acute Versus Chronic Decompensation

The etiology of the right ventricle (RV) failure is variate and apart from the acuteness of the disease it can be split into cardiac causes and extracardiac causes [1, 2]:

Cardiac causes

1. Isolated right ventricle myocardial infarction
2. Right ventricle involvement in left sided myocardial infarction
3. Mitral valve disease with secondary pulmonary hypertension
4. Congenital septal defects and other congenital conditions
5. Isolated infiltrative myocardial disease
6. Hypereosinophilic syndrome

Extracardiac causes

7. Chronic Obstructive Pulmonary Disease (COPD) and Chronic Bronchitis
8. Acute respiratory distress syndrome (ARDS)
9. Acute Pulmonary Hypertension (primary and secondary)
10. Acute overload in perioperative situations
11. Massive Pulmonary Embolus
12. Recurrent Thromboembolism
13. Obstructive Sleep Apnea
14. Morbid Obesity
15. Important resection of lung tissue
16. Primary pulmonary infiltrative disease

S. I. Dumitrescu et al. (eds.), *Right Heart Pathology*, https://doi.org/10.1007/978-3-319-73764-5_12

RV failure can develop as a spontaneous condition or can arise during an invasive or surgical maneuver and in such cases the pathological disturbance can determine or promote acute right heart failure decompensation. These conditions are summarized below [3]:

1. Acute pulmonary embolus/air embolus/fat embolus
2. Hypoxemia
3. Hypercarbia which might increase pulmonary vascular resistance
4. Elevated positive-end-expiratory-pressure (PEEP) which decrease preload and influence cardiac output
5. Volume overload which may generate functional tricuspid regurgitation

The acute decompensation of the right ventricle usually determines various degrees of hypotension, while the chronic decompensation generates a wider systemic response with lung, hepatic, renal involvement as well as inflammatory response [4] with pro-inflammatory response, activation of TNF-ά (tumor necrosis factor ά) and decrease in myocardial contractility.

12.2 Physiology of the Right Heart Function

To consider RV a simple conduit is by far a medical misjudgment. There are two main functions for right ventricle [5]: first it is a reservoir, providing adequate pulmonary pressure and pulmonary blood flow to maintain a continuous gas exchange at the membrane level of the lungs and secondly, it allows a low pressure into the lungs and by thus prevents organ damage (Fig. 12.1).

Being a volume reservoir, right ventricle function is susceptible to variation in both preload and afterload. It is also influenced by the function of left ventricle (LV), being well established an interventricular coupling mechanism [6].

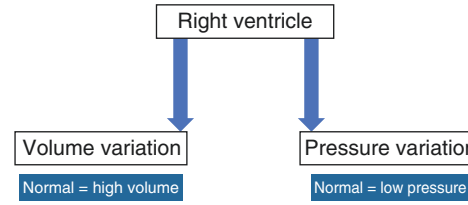

Fig. 12.1 Right ventricle essential functions

The passive filling of the ventricle during atrial systole represents the preload. It can be physiologically enhanced during intense muscle activity or it can reflect a pathological condition such as increased venous return (for example shunts). Decreased filling can occur in physiological conditions such as low gravity or dehydration with volume underload and in various pathological conditions.

There are differences between contraction of LV and RV. In 1975 Curtiss described the difference in shape of the two pressure curves, the right ventricle presenting a pressure curve without a plateau, with a continuous ejection of the blood into the lungs event at the beginning of relaxation (Fig. 12.2).

This type of ejection allows a low-pressure ejection without high oxygen consumption. The downgrade of this model is the rapid influence of the increased lung vascular resistance and of the left ventricle due to the difference in pressure between the two chambers.

Due to the low workload of the right ventricle, the right myocardium is thin. The special curve shape of the right ventricle which wraps around the left ventricle allows the usage of left ventricular contraction for blood expulsion from the right ventricle. It has been continuously studied and a special model of the successive layers of myocardial fibers has been developed [7, 8]. For a complete picture of the normal function of the right heart see also Chap. 3.

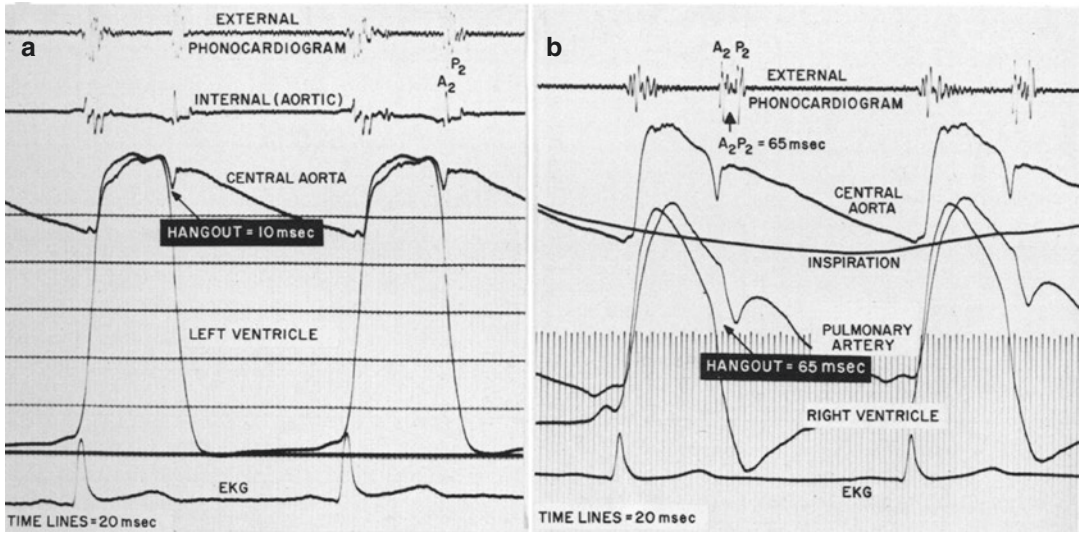

Fig. 12.2 Difference in pressure curves for normal left (LV) and right ventricles (RV). Adapted from Curtiss EI, Matthews RG, Shaver JA. Mechanism of normal splitting of the second heart sound. Circulation. 1975 Jan;51(1):157–64

12.3 Pathophysiology of the Right Heart

Because of the relatively weak myocardial contraction within the right heart any changes in the blood volume or pressure caused by a left heart condition or a lung condition is immediately transferred into the right heart function, first to the right ventricle and immediately after into the right atrium. A change in volume load and/or pressure load into the right heart generates a systemic venous response [9].

In case of acute right heart decompensation due to the lack of compliance of both right ventricle and right atrium, the systemic venous response is immediate. It is the case for acute liver decompensation in acute exacerbation of right heart failure with increased blood levels of hepatic enzymes.

In case of a chronic decompensation, the mechanism is more complex [2]. The initial volume overload generates tricuspid annular distension while right ventricle pressure overload generates right free wall hypertrophy. Over time this generates changes of the form of the RV from the curvilinear shape towards oval shape [10]. As consequence, the tricuspid valve is tethered, and the tricuspid annulus is distorted. All these generate tricuspid regurgitation. Because of the pericardial fix dimensions, the pressure increases in the right heart and the interventricular septum is bounced toward the left side (Fig. 12.3). This movement diminishes the left ventricular load which consequently increases the pulmonary afterload with immediate response onto the right heart volume and pressure load and further decompensation [1, 11]. There is similar cardiac output for RV and LV, but with different pressures (Fig. 12.4). When pressure curves are plotted, there is a shift towards lower left when RV is compared with LV pressure. During RV decompensation, the diastolic pressure rises and this

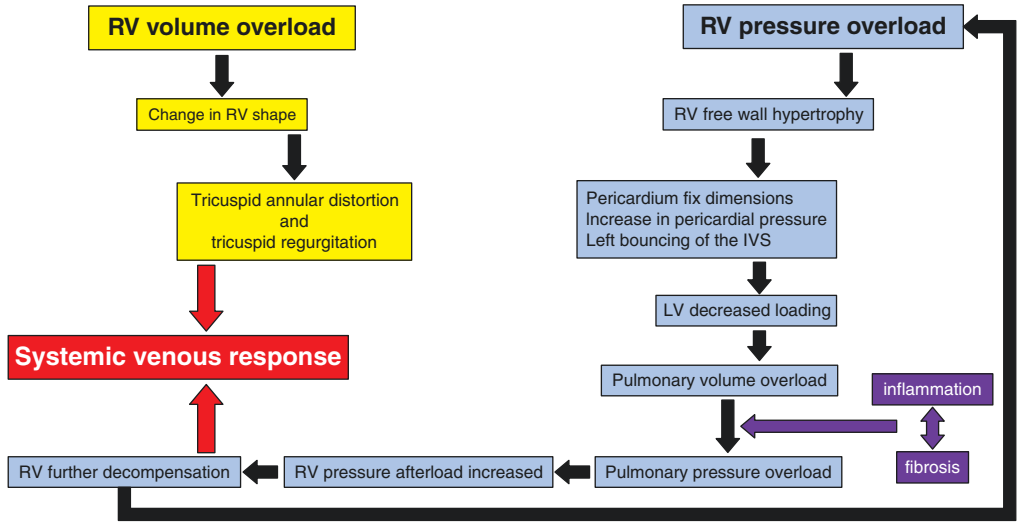

Fig. 12.3 Pathological mechanisms in chronic right ventricle failure. *RV* right ventricle, *LV* left ventricle, *IVS* interventricular septum

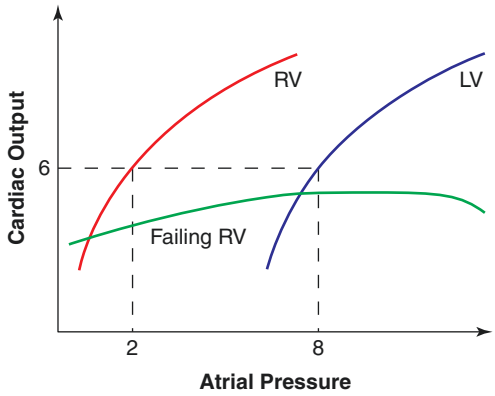

Fig. 12.4 Cardiac output and pressures (reprint with permission from Hrymak C, Strumpher J, Jacobsohn E Acute Right Ventricle Failure in the Intensive Care Unit: Assessment and Management. Can J Cardiol. 2017 Jan;33(1):61–71. doi: 10.1016/j.cjca.2016.10.030)

increases the oxygen consumption of the myocytes [9, 12] (Fig. 12.5).

Congestion plays an important role in decreasing the quality of life, but this is doubled by a prognostic role. There are series of patients in which congestion by itself (univariate analysis) increases the risk of total death by 50% [13]. It is a continuous balance between forward and backward cardiac dysfunction.

In case of intrinsic heart disease, inflammation is less involved. When the RV failure occurs due to a chronic pathology of the lungs, inflammation plays an important role. In obstructive sleep apnea, both intermittent hypoxia and hypercapnia rise the oxidative stress which is part of the onset of a high inflammatory status [4, 14]. There is secondary stimulation of fibrotic process. This applies not only for the lungs, but for other organs as well (Fig. 12.6).

12.4 Systemic Determinations of Right Heart Failure

It is of great importance to evaluate each important organ which might be affected in the decompensating organism. We will discuss the gastrointestinal involvement, the renal decompensation, the brain, and the bone marrow (Fig. 12.7).

Apart from the inflammation mechanism, stasis can play an important role in development of systemic consequences in case of right ventricle failure. There is a higher incidence of strokes in people suffering of chronic obstructive pulmonary disease (COPD) [15].

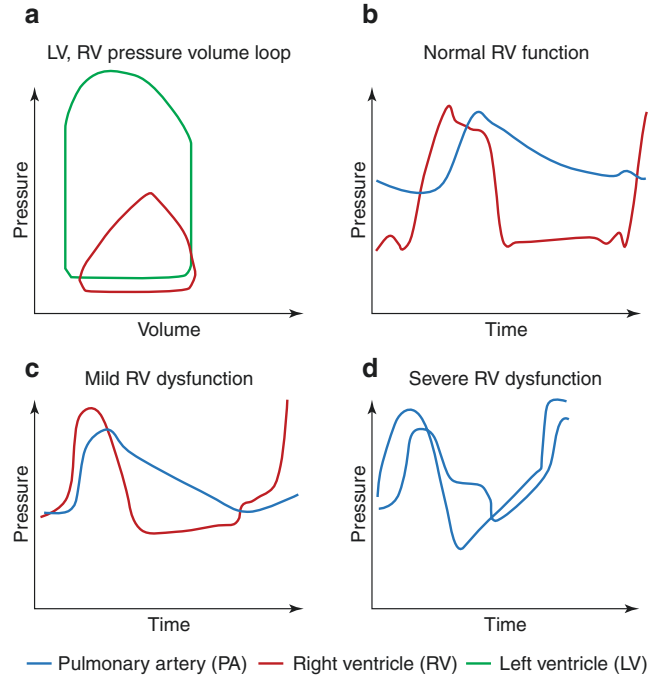

Fig. 12.5 Pressure curves in right (RV) and left ventricles (LV). (**a**, **b**) Normal function, (**c**) mild RV dysfunction, (**d**) Severe RV dysfunction (reprint with permission from Hrymak C, Strumpher J, Jacobsohn E. Acute Right Ventricle Failure in the Intensive Care Unit: Assessment and Management. Can J Cardiol. 2017 Jan;33(1):61–71. doi: 10.1016/j.cjca.2016.10.030)

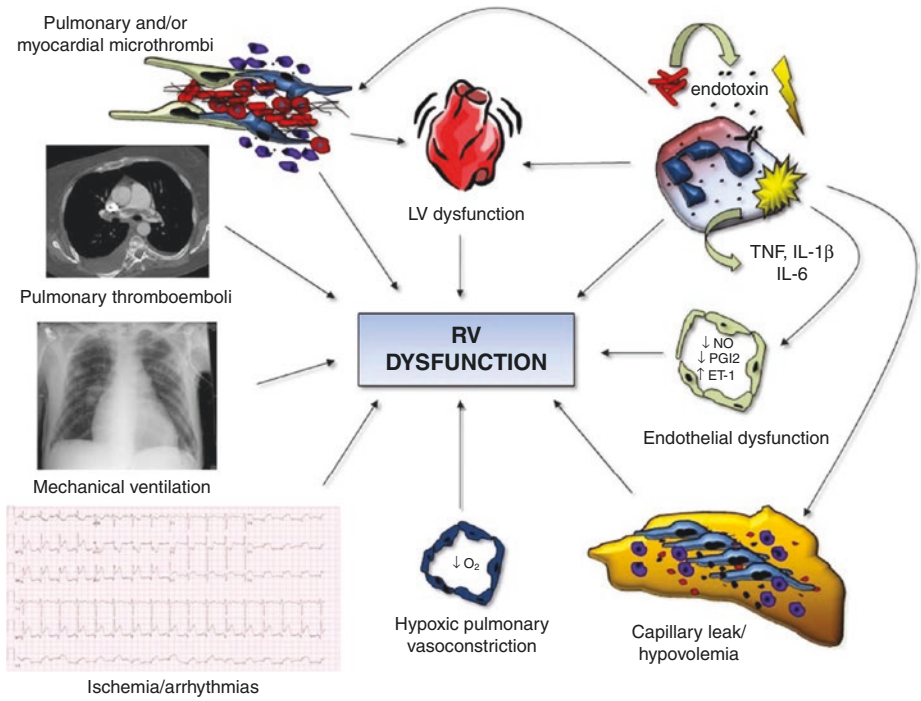

Fig. 12.6 Mechanisms of RV Dysfunction in Critically Ill Patients (reprint with permission from Lahm T, McCaslin CA, Wozniak TC, Ghumman W, Fadl YY, Obeidat OS, Schwab K, Meldrum DR. Medical and surgical treatment of acute right ventricular failure. J Am Coll Cardiol. 2010 Oct 26;56(18):1435–46. doi: 10.1016/j.jacc.2010.05.046

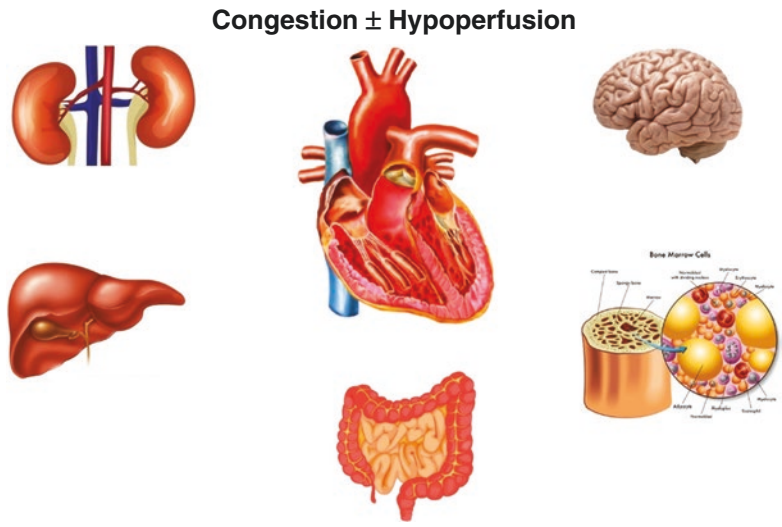

Fig. 12.7 Various organs damaged during right heart decompensation

Hepatic cytolysis in acute heart failure setting is a common finding. Two potential mechanism are involved. The first one is hepatic ischemia due to decrease in blood pressure. The second one is retrograde stasis in the liver and this can explain less acute changes in the hepatic function driven by irritative mechanism and fibrosis. This second mechanism is more often involved in liver decompensation in chronic heart failure [16]. The increase in venous pressure in RV dysfunction leads to the atrophy of hepatocytes and perisinusoidal edema. This impairs the oxygen and nutrients diffusion to the hepatocytes [17]. It also determines enhanced hepatic lymph formation, leading to ascites. Moreover, increased pressure within the hepatic sinusoid favors bile duct damage by disrupting endothelial cells and the interhepatocytic tight junctions which delineates the extravascular space from the bile canaliculus. Finally, stagnant flow causes thrombosis within sinusoids, hepatic venules, and portal ducts. This recurrent process determines liver fibrosis [18–20]. The most frequent changes on microscopy examination in cases of hepatic venous hypertension are the prominence of central veins, central vein hemorrhage, and sinusoidal engorgement [21]. In cases of forward LV heart failure with low blood pressure, ischemic liver injury might be present and the morpho-pathological aspect is fully different. It is characterized by centrolobular necrosis of the hepatocytes in the absence of histological evidence of inflammation characteristic of viral hepatitis [22–24] (Table 12.1).

The cardio-renal syndrome is most often described in heart failure with reduced LV ejection fraction (LVEF) and decreased blood flow in the periphery. It is characterized by profound alteration of both liver and kidney function and implies active cardiac support management. In case of RV failure, the decrease in blood flow in the peripheral organs is less important, the principal patho-physiological feature being a raised central venous pressure. The changes in organ function are thus less impressive, but might be persistent towards multiorgan failure. The presence of cardio-renal syndrome in RV failure is less frequent [25], but in cases with high central venous pressure renal congestion is promoted. A powerful direct correlation between change in renal venous pressure and reduction in urine flow has been demonstrated. The kidney blood flow is predominantly reduced by an increase in venous pressure than by an equivalent decrease in arterial pressure [26]. These changes occur independently of the decrease in cardiac output and/or mean arterial pressure. These pathological changes occur later on the pathway of heart failure [27, 28] (Fig. 12.8).

Table 12.1 Comparison between acute and chronic hepatic changes in heart failure

	Chronic congestive hepatopathy	Acute ischemic hepatitis
Aetiology	Chronic heart failure	Acute heart failure
Pathophysiology	Perisinusoidal edema	Tissue hypoxia
	Increased lymph flow	Zone 3 necrosis
	Zone 3: alternating necrosis and hemorrhage	
	Sinusoidal thrombosis	
Manifestations	Right hypochondrial pain	Asymptomatic or nonspecific
	Edema, ascites, jaundice	nausea, vomiting, jaundice, right hypochondrial pain
Laboratory data		
Bilirubin	Mild increase	Marked elevation
ALT and AST	Normal mild elevation	Marked elevation
LDH	Normal or mild elevation	Marked elevation
ALT/LDH		<1.5
Prothrombin time	Prolonged	Normal/prolonged
ALP	Normal/mild elevation	Increased
Albumin	Hypoalbuminemia	Normal
Treatment	ACE inhibitors	Oxygen therapy
	b-blockers	Avoid precipitating factors
	Diuretic	Inotropic agents with caution
	Amiodarone	Vasopressor with caution
	Statins with caution	Diuretics in hypervolemia
Prognosis	Slowly progressive course	Benign and usually self-limited

Modified from Fouad YM, Yehia R. Hepato-cardiac disorders. World J Hepatol. 2014 Jan 27;6(1):41–54. doi: 10.4254/wjh.v6.i1.41. This is an Open Access article. Copyright ©2014 Baishideng Publishing Group Co., Limited. All rights reserved

ALT alanin-amino-transpherase, *AST* aspartate-amino-transpherase, *LDH* lactat-dehydrogenase, *ALP* alkaline-phosphatase, *ACE* angiotensin-converting-enzime

There are series of patients with renal failure with/without RV failure. In the group of patients in whom the renal function improved under treatment, right ventricular dysfunction was more prominent. In the group that had worse renal function, the least decrease appeared in those patients without RV dysfunction [29]. This might seem an apparent paradox. It can be explained through a decrease of RV filling pressure during treatment of HF which increases the glomerular filtration rate (GFR). Two mechanisms are involved, a decrease of renal venous pressure and a decrease of LV filling through the interdependent ventricular function. This second mechanism leads to secondary decrease of arterial renal pressure, a compensatory useful process in this phase of the disease.

HF generates pathological changes of the bowel. RV failure generates congestion which in turn might lead to increased permeability of intestinal wall for pro-inflammatory endotoxin. This can cause also malabsorption/maldigestion. Another potential mechanism might be venous thrombosis in the splanchnic vessels.

The bone marrow is altered in RV failure [30]. Cultures of isolated CD34(+) haematopoietic progenitor cells were exposed to increasing doses of erythropoietin (EPO) and/or myeloid growth factors. The CD34(+) cells from CHF patients produced a twofold lower number of erythrocytes precursor colonies compared with controls. The resistance to EPO was associated with markedly increased apoptosis during erythroid differentiation in CHF patients. In the myeloid cultures, the

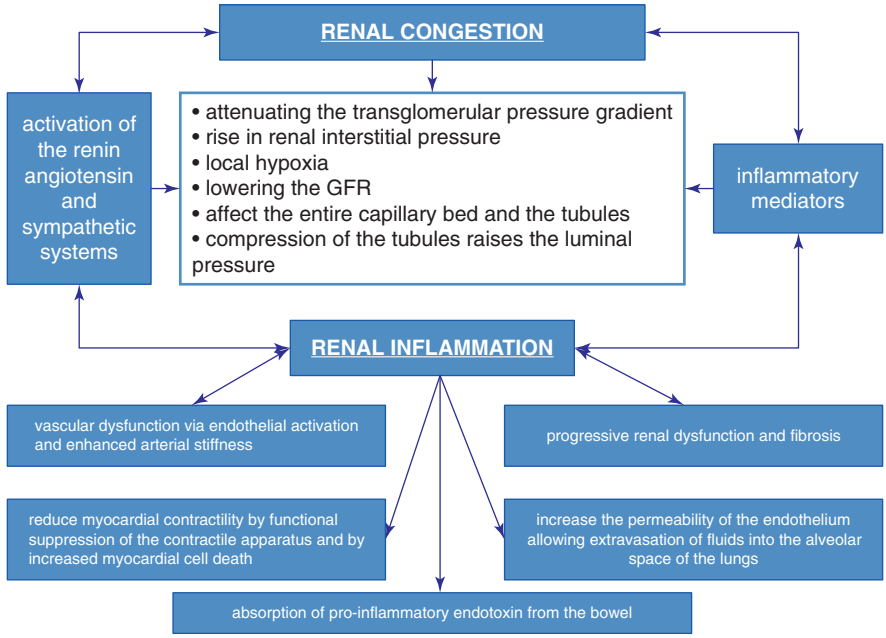

Fig. 12.8 Mechanisms of increased inflammation during venous congestion. (reprint from Afsar B, Ortiz A, Covic A, Solak Y, Goldsmith D, Kanbay M. Clin Kidney J. 2016 Feb; 9(1): 39–47. Published online 2015 Nov 29. doi: 10.1093/ckj/sfv124. Copyright © The Author 2015. Published by Oxford University Press on behalf of ERA-EDTA. This is an Open Access article distributed under the terms of the Creative Commons Attribution Non-Commercial License (http://creativecommons.org/licenses/by-nc/4.0/), which permits non-commercial re-use, distribution, and reproduction in any medium, provided the original work is properly cited

number of promyeloid colonies was also twofold lower in CHF patients. In the mixed-culture assay, myelopoiesis and erythropoiesis were reduced to a similar magnitude in CHF patients. There was an inverse relation between the number of erythrocytes precursor colonies and the severity of heart failure irrespective of the quantification of HF, by symptoms—NYHA class or by biomarkers—NT-proBNP level.

Anemia worsens the prognosis in HF patients. There are multiple mechanisms involved, including haematogenic marrow, liver, kidney and bowel alterations (Fig. 12.9).

There are series of patients with increased incidence of stroke without arterial or atherosclerotic causes who associates lung comorbidities. Their pathology might be explained through increased venous stasis [12]. An extensive search of the literature failed recently to identify a unique patho-physiological pathway between stroke and lung disease as a precursor of RV failure [31], only one of the considered mechanism being stasis.

There is RV involvement in various pulmonary comorbidities. Patients with sarcoidosis may experience various degrees of RV dysfunction before clinical overt manifestations of secondary pulmonary hypertension [32]. There are reports of worse prognosis in patients which associate sarcoidosis and subtle subclinical changes in RV function.

Important hemodynamical changes have been described in heart failure. Most of them refer to left heart decompensation and in a lesser magnitude to primary right heart decompensation. According to Frank Starling law the decrease in cardiac output in heart failure is further influenced by increase of pulmonary stasis. The myocardial contractions of both RV and LV are linked, a interventricular coupling mechanism being described. A decreased LV contraction triggers less RV contraction.

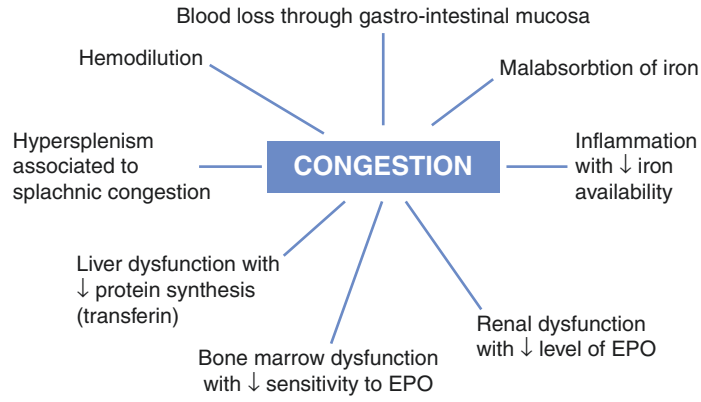

Fig. 12.9 Multiple mechanism of worsening HF through anemia

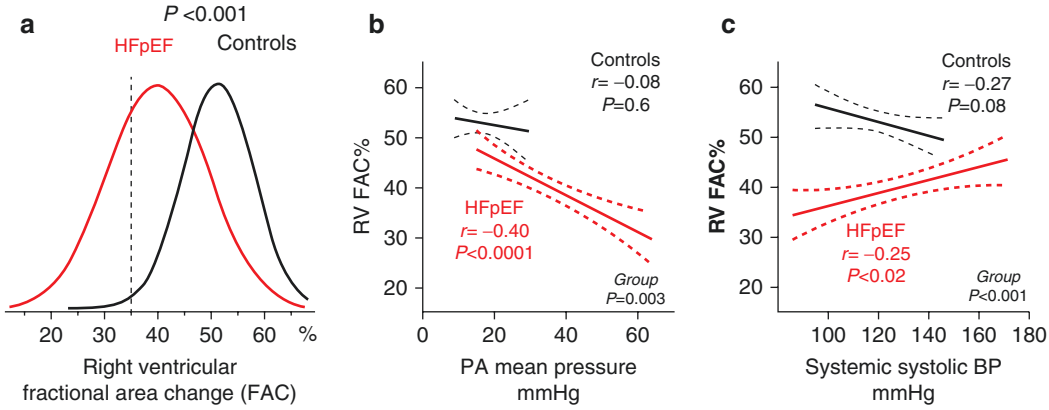

Fig. 12.10 RV and LV interaction. RV dysfunction in patients with HFpEF. (**a**) RV fractional area change (FAC) comparison between normal and HFpEF patients. (**b**) Increase of pulmonary artery (PA) mean pressure for a similar RV FAC in HFpEF patients. (**c**) Decrease of systolic blood pressure (BP) in HFpEF patients (reprint with permission from Vojtech Melenovsky, Seok-Jae Hwang, Grace Lin, Margaret M. Redfield, Barry A. Borlaug. Right heart dysfunction in heart failure with preserved ejection fraction. Eur Heart J. 2014 Dec 21; 35(48): 3452–3462. Published online 2014 Jun 30. doi: 10.1093/eurheartj/ehu193)

In an acute setting, the RV failure generates less contraction without increase in right chambers compliance. The systemic response in this situation will be generated by organ stasis in the two vena cava territories with a more obvious expression in the inferior vena cava drainage system and secondary inflammation cascade.

In patients with LV preserved ejection fraction and mild symptoms of heart failure (HFpEF) [33] there are reports of early involvement of RV [34, 35]. These changes can be explained through increase of pulmonary arterial pressure (PA), but not through variation in blood volume (Fig. 12.10).

12.5 Paraclinical Findings in Right Heart Failure

Having a less impressive clinical picture of the organ damage, one would need an exact paraclinical evaluation to proper assess the prognosis of a patient with chronic RV dysfunction. Brain natriuretic peptide (BNP), one of the most reliable biomarker in heart failure [36] is of lesser importance in case of liver dysfunction due to changes in hepatic metabolization [37]. Troponin suffers the same alteration in absolute value following the same pattern. Also in kidney disease the troponin I and T level are modified and the

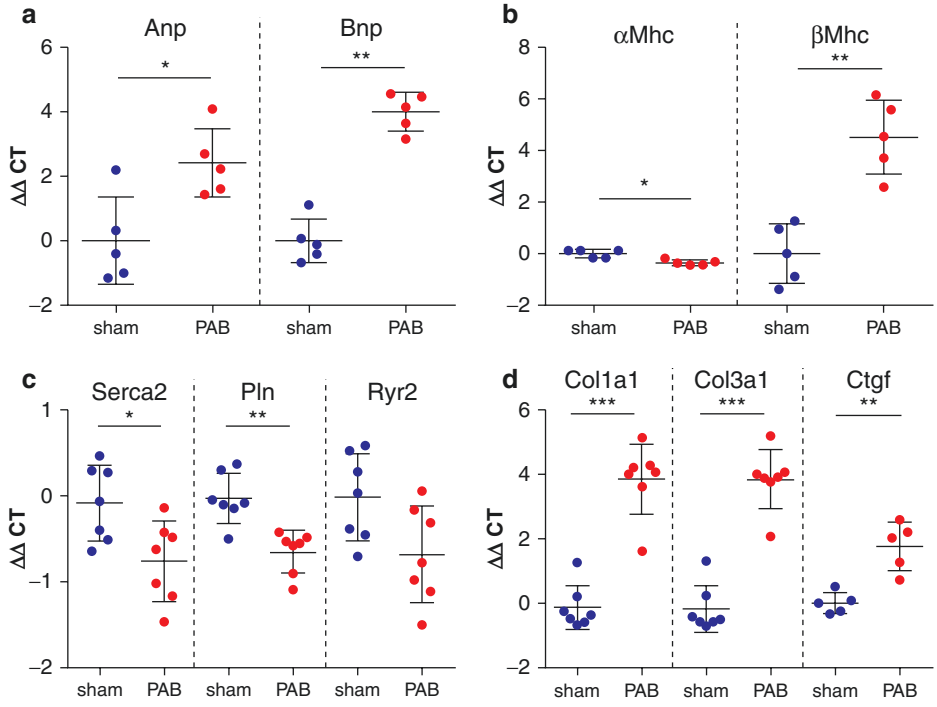

Fig. 12.11 Different markers for fibrosis elevated in RV wall in patients with induced pulmonary induced arterial hypertension through banding (PAB). Comparison with controls without PAB. (**a**) Anp atrial natriuretic peptide, Bnp brain natriuretic peptide, (**b**) fetal gene program activation (αMhc and βMhc), (**c**) Ca^{2+}-handling proteins (Ryr2, Serca2, and Pln), (**d**) collagens (Col1a1 and Col3a1) and profibrotic factor Ctgf was determined by real-time polymerase chain reaction in RV tissue samples (reprint with permission from Bakytbek Egemnazarov, Albrecht Schmidt, Slaven Crnkovic, Akylbek Sydykov, Bence M. Nagy, Gabor Kovacs, Norbert Weissmann, Horst Olschewski, Andrea Olschewski, Grazyna Kwapiszewska, Leigh M. Marsh. Pressure Overload Creates Right Ventricular Diastolic Dysfunction in a Mouse Model: Assessment by Echocardiography. J Am Soc Echocardiogr. 2015 Jul;28(7):828–43. doi: 10.1016/j.echo.2015.02.014

possibility to differentiate true from false positive results may be altered [38]. There are several proteins elevated in right ventricular involvement, but their clearance in a liver or renal comorbidity is not yet clearly defined [39] (Fig. 12.11).

There are studies in which gene expressions and different proteins are analyzed directly from RV wall samples in animal models. When determination in blood or urine of such proteins will be available it might be possible to evaluate better the RV dysfunction and define the prognosis of such patients.

Conclusions

Right heart failure represents a complex pathological condition with multiple faces: different etiologies induce different evolutive patterns (RV volume overload, RV pressure overload, intrinsic RV dysfunction). Venous systemic congestion is the main physio-pathological consequence, but low cardiac output may be associated, independent of LV function. Organ dysfunction or failure driven by venous congestion and secondary hypoperfusion involves different organs with possible pathological influence on one each other.

Organ dysfunction influence the reliability of current biomarkers. There are no current biomarkers of clinical utility to be used irrespective of systemic expansion of cardiac failure. RV and LV failure frequently coexist and there is great difficulty to establish which dys-

function is dominant. More specific biomarkers for RV are needed.

References

1. Haddad F, Doyle R, Murphy DJ, Hunt SA. Right ventricular function in cardiovascular disease, part II: pathophysiology, clinical importance, and management of right ventricular failure. Circulation. 2008;117(13):1717–31.
2. Kevin LG, Barnard M. Right ventricular failure. Contin Educ Anaesth Crit Care Pain. 2007;7(3):89–94.
3. Piazza G, Goldhaber SZ. The acutely decompensated right ventricle: pathways for diagnosis and management. Chest. 2005;128(3):1836–52.
4. Lahm T, McCaslin CA, Wozniak TC, Ghumman W, Meldrum DR. Medical and surgical treatment of acute right ventricular failure. J Am Coll Cardiol. 2010;56(18):1435–46.
5. Bleeker GB, Steendijk P, Holman ER, Yu C-M, Breithardt OA, Kaandorp TAM, Schalij MJ, van der Wall EE, Nihoyannopoulos P, Bax JJ. Assessing right ventricular function: the role of echocardiography and complementary technologies. Heart. 2006;92:i19–26. https://doi.org/10.1136/hrt.2005.082503.
6. Gayat E, Mebazaa A. Normal physiology and pathophysiology of the right ventricle. In: Acute heart failure. London: Springer. p. 63–9. isbn:978-1-84628-781-7.
7. Lunkenheimer PP, Muller RP, Konermann CHR, Lunkenheimer A, Kohler F. Architecture of the myocardium in computed tomography. Investig Radiol. 1984;19:271–8.
8. Torrent-Guasp F, Kocica MJ, Corno AF, Komeda M, Carreras-Costa F, Flotats A, Cosin-Aguillar J, Wen H. Towards new understanding of the heart structure and function. Eur J Cardiothorac Surg. 2005;27:191–201.
9. Hrymak C, Strumpher A, Jacobsohn E. Acute right ventricle failure in the intensive care unit: assessment and management. Can J Cardiol. 2017;33:61–71.
10. Averin K, Michelfelder E, Sticka J, Cash M, Hirsch R. Changes in ventricular geometry predict severity of right ventricular hypertension. Pediatr Cardiol. 2016;37(3):575–81.
11. Harjola VP, Mebazaa A, Čelutkienė J, Bettex D, Bueno H, Chioncel O, Crespo-Leiro MG, Falk V, Filippatos G, Gibbs S, Leite-Moreira A, Lassus J, Masip J, Mueller C, Mullens W, Naeije R, Nordegraaf AV, Parissis J, Riley JP, Ristic A, Rosano G, Rudiger A, Ruschitzka F, Seferovic P, Sztrymf B, Vieillard-Baron A, Yilmaz MB, Konstantinides S. Contemporary management of acute right ventricular failure: a statement from the Heart Failure Association and the Working Group on Pulmonary Circulation and Right Ventricular Function of the European Society of Cardiology. Eur J Heart Fail. 2016;18(3):226–41.
12. Denault AY, Haddad F, Jacobsohn E, Deschamps A. Perioperative right ventricular dysfunction. Curr Opin Anaesthesiol. 2013;26:71–81.
13. Drazner MH, Eduardo Rame J, Stevenson LW, Dries DL. Prognostic importance of elevated jugular venous pressure and a third heart sound in patients with heart failure. N Engl J Med. 2001;345:574–81.
14. Lévy P, Ryan S, Oldenburg O, Parati G. Sleep apnoea and the heart. Eur Respir Rev. 2013;22:333–52.
15. Orea-Tejeda A, Bozada-Gutiérrez K, Pineda-Juárez J, González-Islas D, Santellano-Juárez B, Keirns-Davies C, Peláez-Hernández V, Hernández-Zenteno R, Sánchez-Santillán R, Cintora-Martínez C. Right heart failure as a risk for stroke in patients with chronic obstructive pulmonary disease: a case-control study. J Stroke Cerebrovasc Dis. 2017;26:2988–93. https://doi.org/10.1016/j.jstrokecerebrovasdis.2017.07.027.
16. Fouad YM, Yehia R. Hepato-cardiac disorders. World J Hepatol. 2014;6(1):41–54.
17. Dunn GD, Hayes P, Breen KJ, Schenker S. The liver in congestive heart failure: a review. Am J Med Sci. 1973;265(3):174–89.
18. Wanless IR, Liu JJ, Butany J. Role of thrombosis in the pathogenesis of congestive hepatic fibrosis (cardiac cirrhosis). Hepatology. 1995;21(5):1232–7.
19. Møller S, Bernardi M. Interactions of the heart and the liver. Eur Heart J. 2013;34(36):2804–11.
20. Cogger VC, Fraser R, Le Couteur DG. Liver dysfunction and heart failure. Am J Cardiol. 2003;91(11):1399.
21. Lefkowitch JH, Mendez L. Morphologic features of hepatic injury in cardiac disease and shock. J Hepatol. 1986;2(3):313–27.
22. Caraceni P, Bianchi C, Domenicali M, Maria Pertosa A, Maiolini E, Parenti Castelli G, Nardo B, Trevisani F, Lenaz G, Bernardi M. Impairment of mitochondrial oxidative phosphorylation in rat fatty liver exposed to preservation-reperfusion injury. J Hepatol. 2004;41:82–8.
23. Alvarez AM, Mukherjee D. Liver abnormalities in cardiac diseases and heart failure. Int J Angiol. 2011;20:135–42.
24. Lindenfeld J, Albert NM, Boehmer JP, Collins SP, Ezekowitz JA, Givertz MM, Katz SD, Klapholz M, Moser DK, Rogers JG, et al. HFSA 2010 comprehensive heart failure practice guideline. J Card Fail. 2010;16:e1–194.
25. House AA. Cardio-renal syndrome type 4: epidemiology, pathophysiology and treatment. Semin Nephrol. 2012;32(1):40–8.
26. Ganda A, Onat D, Demmer RT, et al. Venous congestion and endothelial cell activation in acute decompensated heart failure. Curr Heart Fail Rep. 2010;7:66–74.
27. Blake WD, Wegria R, Keating RP, et al. Effect of increased renal venous pressure on renal function. Am J Phys. 1949;157:1–13.
28. Afsar B, Ortiz A, Covic A, Yalcin S, Goldsmith D, Kambay M. Focus on renal congestion in heart failure. Clin Kidney J. 2016;9(1):39–47.

29. Testani JM, Khera AV, St John Sutton MG, Keane MG, Wiegers SE, Shannon RP, Kirkpatrick JN. Effect of right ventricular function and venous congestion on cardiorenal interactions during the treatment of decompensated heart failure. Am J Cardiol. 2010;105(4):511–6.
30. Westenbrink BD, Voors AA, de Boer RA, Schuringa JJ, Klinkenberg T, van der Harst P, Vellenga E, van Veldhuisen DJ, van Gilst WH. Bone marrow dysfunction in chronic heart failure patients. Eur J Heart Fail. 2010;12(7):676–84.
31. Morgan AD, Sharma C, Rothnie KJ, Potts J, Smeeth L, Quint JK. Chronic obstructive pulmonary disease and the risk of stroke. Ann Am Thorac Soc. 2017;14(5):754–65.
32. Joyce E, Kamperidis V, Ninaber MK, Katsanos S, Debonnaire P, Schalij MJ, Taube C, Bax JJ, Delgado V, Ajmone Marsan N. Prevalence and correlates of early right ventricular dysfunction in sarcoidosis and its association with outcome. J Am Soc Echocardiogr. 2016;29(9):871–8.
33. Piepoli MF, Hoes AW, Agewall S, Albus C, Brotons C, on behalf of the Authors/Task Force Members, et al. 2016 European Guidelines on cardiovascular disease prevention in clinical practice: The Sixth Joint Task Force of the European Society of Cardiology and Other Societies on Cardiovascular Disease Prevention in Clinical Practice. Eur Heart J. 2016;37(29):2315–81.
34. Melenovsky V, Hwang SJ, Lin G, Redfield MM, Borlaug BA. Right heart dysfunction in heart failure with preserved ejection fraction. Eur Heart J. 2014;35(48):3452–62.
35. Aschauer S, Kammerlander AA, Zotter-Tufaro C, Ristl R, Pfaffenberger S, Bachmann A, Duca F, Marzluf BA, Bonderman D, Mascherbauer J. The right heart in heart failure with preserved ejection fraction: insights from cardiac magnetic resonance imaging and invasive haemodynamics. Eur J Heart Fail. 2016;18:71–80.
36. Ponikowski P, Voors AA, Anker SD, Cleland JGF, et al. 2016 ESC Guidelines for the diagnosis and treatment of acute and chronic heart failure. Eur Heart J. 2016;37(27):2129–200.
37. Metwaly A, Khalik AA, Nasr FM, Sabry AI, Gouda MF, Hassan M. Brain natriuretic peptide in liver cirrhosis and fatty liver: correlation with cardiac performance. Electron Physician. 2016;8(2):1984–93.
38. Willging S, Keller F, Steinbach G. Specificity of cardiac troponins I and T in renal disease. Clin Chem Lab Med. 1998;36(2):87–92.
39. Egemnazarov B, Schmidt A, Crnkovic S, Sydykov A, Nagy BM, Kovacs G, Weissmann N, Olschewski H, Olschewski A, Kwapiszewska G, Marsh LM. Pressure overload creates right ventricular diastolic dysfunction in a mouse model: assessment by echocardiography. J Am Soc Echocardiogr. 2015;28(7):828–43.

Essential in Genetic Etiology of Congenital Heart Diseases

13

Mariana Jinga, Silviu Dumitrescu, Liviu Stan, Ecaterina Bontaş, Tudor Păduraru, Ion C. Ţintoiu, Vasile Murgu, and Rabia Denis El Zoabi

Abstract

Congenital heart disease (CHD) represent another unsolved problem of the present, although new techniques of exploration like fluorescence in situ hybridization (FISH), high resolution array-comparative genomic hybridization (array-CGH), single nucleotide polymorphisms (SNPs), comparative genomic hybridization (CGH) and spectral karyotyping (SKY) explain some genetic mechanisms implied in the genesis of this pathology. However, there are many unresolved issues. Structural modifications of chromosomes by duplication and also by deletion determine variable phenotypes depending on the altered structural site. Given that, the genetic defect affects only one gene or more but determines repercussions over the cardiac anatomy or/and other non-cardiac systems, as a result the phenotype can be syndromic or nonsyndromic. The raised or low number of chromosomes was the first explanation for CHD. Trisomy 21 (Down's syndrome), 18 (Edward's syndrome), 13 (Patau's syndrome), monosomy X (Turner's syndrome), deletion at chromosome 7q11.23 and 22q11.2, multiple gene mutations, are the most frequent chromosomal or sub-chromosomal destructuring along with syndromic phenotype. Copy number variations (CNVs) is defined as subchromosomal mechanism that by deletion or multiplication produces in general nonsyndromic phenotype. Transcription factors T-Box protein 5 (TBX5), mNK2 Homeobox 5 (NKX2.5), GATA-binding protein 4 (GATA4) are specific proteins that sending information from DNA to RNA messenger can undergo structural denaturations and if this happens these proteins cannot send correct messages resulting in alteration of the

M. Jinga
"Carol Davila" University of Medicine and Pharmacy, Bucharest, Romania

"Carol Davila" Central Military Emergency University Hospital, Bucharest, Romania

S. Dumitrescu · I. C. Ţintoiu (✉)
Department of Interventional Cardiology, "Carol Davila" Central Military Emergency University Hospital, Bucharest, Romania

L. Stan
Department of Cardiovascular Surgery, Central Clinic Emergency Military Hospital "Carol Davila", Bucharest, Romania

E. Bontaş
Department of Cardiology, "Prof. C.C. Iliescu" Emergency Institute for Cardiovascular Diseases, Bucharest, Romania

T. Păduraru
Department of Anesthesiology, "Carol Davila" Central Military Emergency University Hospital, Bucharest, Romania

V. Murgu · R. D. El Zoabi
Department of Medicine, "Titu Maiorescu" University, Bucharest, Romania

S. I. Dumitrescu et al. (eds.), *Right Heart Pathology*, https://doi.org/10.1007/978-3-319-73764-5_13

normal chain of cardiogenesis. Combination between these mechanisms and unitary action produce CHD in different forms, syndromic or nonsyndromic.

Keywords
Chromosome abnormality · Gene defects · Syndromic · Nonsyndromic · Duplication · Deletion · Congenital heart diseases · Developmental delay

13.1 Introduction

CHDs represent the single largest cause of infant morbidity and mortality worldwide [1, 2], and CHD genetics is increasing with a fast rate [3]. However, CHDs continue to have unresolved issues because of multiple aetiologies forms such as chromosome abnormalities caused by environmental factors and genetic disorders; single or multiple gene mutations; de novo mutations; abnormal RNA; single nucleotide polymorphism; copy number variations (CNVs).

Mechanisms of genesis and understanding of congenital cardiac malformations have concerned scientific societies over two decades. Although genetic elucidation of cardiogenesis enlightened some of the issues, there are still many unknown mechanisms that presently are in stage of hypothesis. However the progression of understanding the involvements of molecular and genetic mechanisms which trigger the defects in cardiac structure was progressive mainly with the help of new modern techniques used in studies of this pathology (Table 13.1) [4].

Table 13.1 Conceptual evolution of the genetics of congenital heart diseases

Concepts	Examples
Multifactorial inheritance	All heart diseases
Major role of the environment	Teratogenic: Rubella, thalidomide
Unique mechanism of anatomically different heart disease: One genetic abnormality–several heart diseases	Deletion of chromosome 22q1.1 and conotruncal heart diseases
Monogenic nature of many heart diseases	Interatrial communication, atrioventricular canals, tetralogy of Fallot
Failure of strategies of partial phenocopy: Genetically different syndrome and non-syndrome associated heart diseases	Interatrial communication and Holt-Oram syndrome (*TBX5*), tetralogy of Fallot and deletion of chromosome 22q1.1, atrioventricular canals and critical cardiac region of trisomy 21
Notion of phenotype continuum or gravity spectrum	Bicuspid aortic valve, aortic stenosis and coarctation, shone syndrome, hypoplasia of left heart
Variability of intrafamilial expression for a same molecular abnormality	Familial heart diseases of deletion of chromosome 22q1.1
Genetic heterogeneity of congenital heart diseases: One malformation–several genes	Interatrial communication and mutations in *NKX2.5*, *GATA4*, *MYH7*
Heterogeneity of mechanisms for a same heart disease	Common arterial trunk: Septation disease of the efferent pathway or of myocardium rotation from the base of the efferent pathway
Redefinition of the phenotype in relation to the mechanism	Double outlet right ventricles

From Bajolle et al. [4]

13.2 Causes of Congenital Heart Defects

New concepts regarding the etiology of CHD sustain genetic and nongenetic factors. Among genetic factors the most important are structural alteration of chromosomes responsible for cardiogenesis, genetic mutations (8%), restructuring of RNA, epigenetic factors, single nucleotide polymorphism and multifactorial factors (90%) (Fig. 13.1) [5].

It has to be mentioned that James Nora suggested in 1968 the contribution of combining genetic and environmental factors in the develop-

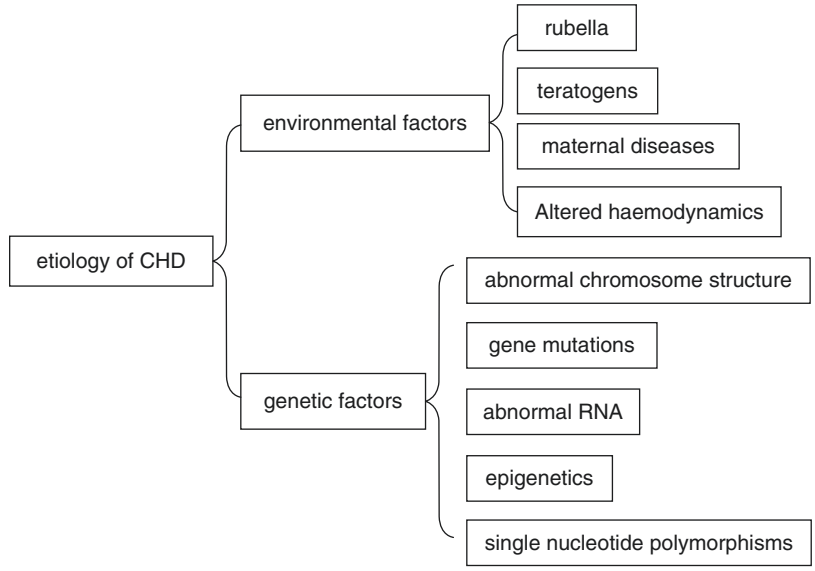

Fig. 13.1 Etiology of congenital heart defects [5]. *It is open access chapter*. Attribution 3.0 Unported (CC BY 3.0)

ment of a human heart defects that can be used in prevention of CHD [6, 7]. Recently, Akhirome et al. [6] showed in a comprehensive review that genetic etiologies of CHD comprise an high number of unknown causes (61.7%), the rest being known (Table 13.2) [6]. Importantly, the known causes of CHD are de novo or inherited genetic abnormalities [6].

Table 13.2 Genetic disorders in congenital heart defects (adapted from Akhirome et al. [6])

Genetic disorder	%	References
Chromosomal syndrome	12	[8, 9]
De novo copy number variations (CNV)	15	[10]
De novo gene mutation	10	[11–13]
Inherited gene mutation	1.3	[13]
Unknown	61.7	[6]

13.3 Chromosomal Abnormalities

Chromosomal aneuploidy is the most frequent cause of chromosome destructuring that modifies the normal genetic information. Due to the new techniques of study like fluorescence in situ hybridization—FISH, spectral karyotyping (SKY) and comparative genomic hybridization (CGH), it appeared new concepts as cells genetics (molecular cytogenetics) in the last decades. These new concepts established that deletion and duplication (microdeletions and microduplications) are new genetic mechanisms of chromosome destructuring in CHD [14].

Genetic modifications that affect only the heart are classified in the nonsyndromic CHD category, however those that involve heart and other organs are named syndromic CHD. Recently, Chung and Rajakumar [15] classified by a study the chromosomal anomalies from CHD into three categories [15]:

1. Modification of chromosomes implied in cardiogenesis such as trisomy 21 (Down's syndrome), 18 (Edward's syndrome), 13 (Patau's syndrome), monosomy X (Turner's syndrome), Tetrasomy 22q [15];
2. Chromosomes deletion: 22q11, 7q11.23, 1p36, and 22q11.2;
3. Gene mutations: multiple (TFAP2B), or single (TFAP2B) (Table 13.3) [15].

Moreover, the most frequent congenital malformations with modification of chromosomes implied in cardiogenesis are: atrial septal defect (ASD) with all its types (ostium primum, ostium secundum, and common atrioven-

Table 13.3 Representative chromosomal disorders associated with congenital heart defects [16]

Chromosomal disorder	Main features	Percent with CHD	Heart anomaly	References
Deletion 4p (Wolf-Hirschhorn syndrome)	Pronounced microcephaly, widely spaced eyes, broad nasal bridge (Greek helmet appearance), downturned mouth, micrognathia, preauricular skin tags, elongated trunk and fingers, severe mental retardation and seizures; 1/3 die in infancy	50–65	ASD, VSD, PDA, LSVC, aortic atresia, dextrocardia, TOF, tricuspid atresia	[17, 18]
Deletion 5p (cri-du-chat)	Catlike cry, prenatal and postnatal growth retardation, round face, widely spaced eyes, epicanthal fold, simian crease, severe mental retardation, long survival	30–60	VSD, ASD, PDA	[17, 19, 20]
Deletion 7q11.23 (Williams-Beuren syndrome)	Infantile hypercalcemia, skeletal and renal anomalies, cognitive deficits, "social" personality, elfin facies	53–85	Supravalvar AS and PS, PPS	[21–23]
Trisomy 8 mosaicism	Skeletal/vertebral anomalies, widely spaced eyes, broad nasal bridge, small jaw, high arched palate, cryptorchidism, renal anomalies (50%), long survival	25	VSD, PDA, CoA, PS, TAPVR, truncus arteriosus	[17, 24–27]
Deletion 8p syndrome	Microcephaly, growth retardation, mental retardation, deep-set eyes, malformed ears, small chin, genital anomalies in males, long survival	50–75	AVSD, PS, VSD, TOF	[28–30]
Trisomy 9	Severe prenatal and postnatal growth retardation, marked microcephaly, deep-set eyes, low-set ears, severe mental retardation; 2/3 die in infancy	65–80	PDA, LSVC, VSD, TOF/PA, DORV	[17, 31]
Deletion 10p	Frontal bossing, short down-slanting palpebral fissures, small low-set ears, micrognathia, cleft palate, short neck, urinary/genital, upper-limb anomalies	50	BAV, ASD, VSD, PDA, PS, CoA, truncus arteriosus	[17, 32, 33]
Deletion 11q (Jacobsen syndrome)	Growth retardation, developmental delay, mental retardation, thrombocytopenia, platelet dysfunction, widely spaced eyes, strabismus, broad nasal bridge, thin upper lip, prominent forehead	56	HLHS, valvar AS, VSD, CoA, Shone's complex	[34]
Trisomy 13 (Patau syndrome)	Polydactyly, cleft lip and palate, scalp defects, hypotelorism, microphthalmia or anophthalmia, colobomata of irides, holoprosencephaly, microcephaly, deafness, profound mental retardation, rib abnormalities, omphalocele, renal abnormalities, hypospadias, cryptorchidism, uterine abnormalities; 80% die in first year	80	ASD, VSD, PDA, HLHS, laterality defects, atrial isomerism	[35, 36]
Trisomy 18 (Edwards syndrome)	IUGR, polyhydramnios, micrognathia, short sternum, hypertonia, rocker-bottom feet, overlapping fingers and toes, TEF, CDH, omphalocele, renal anomalies, biliary atresia, profound mental retardation; 90% die in first year	90–100	ASD, VSD, PDA, TOF, DORV, D-TGA, CoA, BAV, BPV, polyvalvular nodular dysplasia	[17, 37, 38]
Deletion 20p12 (Alagille syndrome)	Bile duct paucity, cholestasis, skeletal or ocular anomalies, broad forehead, widely spaced eyes, underdeveloped mandible	85–94	Peripheral PA, hypoplasia, TOF, PS, (left-sided heart lesions and septal defects less common)	[39, 40]

Table 13.3 (continued)

Chromosomal disorder	Main features	Percent with CHD	Heart anomaly	References
Trisomy 21 (Down syndrome)	Hypotonia, hyperextensibility, epicanthal fold, simian crease, clinodactyly of fifth finger, brachydactyly, variable mental retardation, premature aging	40–50	AVSD, VSD, ASD, (TOF, D-TGA less common)	[17, 41–46]
Deletion 22q11 (DiGeorge, velocardiofacial, and conotruncal anomaly face syndrome)	Hypertelorism, micrognathia, low-set posteriorly rotated ears, "fish mouth," thymic and parathyroid hypoplasia, hypocalcemia, feeding/speech/learning/ behavioral disorders, immunodeficiency, palate/skeletal/renal anomalies	75	IAA-B, truncus arteriosus, isolated aortic arch anomalies, TOF, conoventricular VSD	[47, 48]
Monosomy X (turner syndrome, 45,X)	Lymphedema of hands and feet, widely spaced hypoplastic nipples, webbed neck, primary amenorrhea, short stature, normal intelligence	25–35	CoA, BAV, valvar AS, HLHS, aortic dissection	[17, 49–53]
Klinefelter syndrome (47,XXY)	Usually normal appearing, tall stature, small testes, delayed puberty, emotional and behavioral problems common, variable mental retardation	50	MVP, venous thromboembolic disease, PDA, ASD	[17, 54]

Abbreviations: *CHD* indicates congenital heart defects, *ASD* atrial septal defect, *VSD* ventricular septal defect, *PDA* patent ductus arteriosus, *LSVC* persistent left superior vena cava, *TOF* tetralogy of Fallot, *AS* aortic stenosis, *PS* pulmonic stenosis, *PPS* peripheral pulmonary stenosis, *CoA* coarctation of the aorta, *TAPVR* total anomalous pulmonary venous return, *AVSD* atrioventricular septal defect, *TOF/PA* tetralogy of Fallot with pulmonary atresia, *DORV* double-outlet right ventricle, *BAV* bicuspid aortic valve, *HLHS* hypoplastic left heart syndrome, *IUGR* intrauterine growth retardation, *TEF* tracheoesophageal fistula, *CDH* congenital diaphragmatic hernia, *D-TGA* D-transposition of the great arteries, *BPV* bicuspid pulmonary valve, *PA* pulmonary artery, *IAA-B* interrupted aortic arch type B, and *MVP* mitral valve prolapse

tricular canal), ventricular septal defect, and patent ductus arteriosus (PDA). For instance, trisomy 21 (Down's syndrome) has a frequency of 40–50% from cases [55], and 1 from 2500 female newborns have monosomy X (Turner's Syndrome) [56]. Importantly, heart defects are present in 35% cases of trisomy 13 (Patau's syndrome) and in 45% cases of trisomy 18 (Edward's syndrome) [57].

Also, the known genetic mechanisms that are assigned to chromosome modifications implied in cardiogenesis or chromosome deletion are present in Table 13.3 [16].

13.4 Copy Number Variations (CNVs)

According to current evidence, along with modification of chromosomes, microdeletion and genetic mutations, another mechanism may induce subchromosomal changes in genome structure known as Copy Number Variations (CNVs). These subchromosomal changes or destructuring have outcomes over cardiogenesis and it is accomplished by multiple mechanisms but mainly by deletions and duplications (Fig. 13.2) [60].

In particular, investigations such as fluorescence in situ hybridization (FISH), high-resolution array-comparative genomic hybridization (array-CGH) and single nucleotide polymorphisms (SNPs) are the most frequent methods used for identification of CNVs and their connection to CHD [60].

Richards et al. [61] on a study of 40 childrens with CHD using fluorescence in situ hybridization (FISH) consider that this technique is more precisely in detection of modifications induced by deletions, duplications or translocations, especially in subthelomeric analyzing explaining fundamental chromosomal and subchromosomal mechanisms in genesis of CHD (Fig. 13.3) [61].

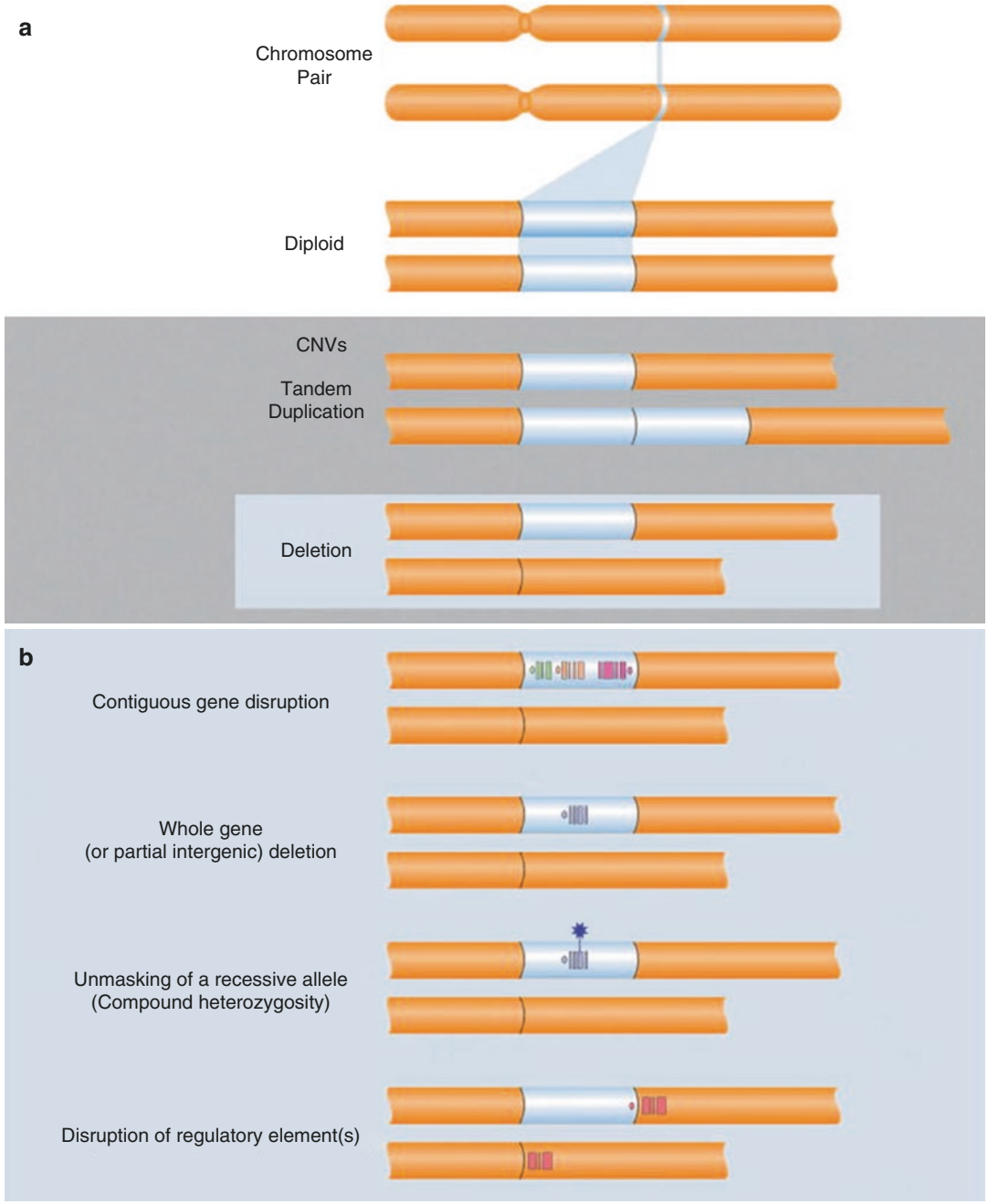

Fig. 13.2 Examples of CNV and associated disease mechanisms. (**a**) Normal diploid status and two examples of CNV (a simple deletion and a tandem duplication). Not pictured are the diverse other forms of CNV, including non-contiguous insertions, higher-order copy number changes (multi-allelic CNV), and more complex rearrangements. CNVs may involve no, one or multiple genomic elements. (**b**) Selected mechanisms underlying disease effects of copy number losses (deletions). A gene is indicated by a contiguous monochromatic set of rectangles, and a regulatory element (e.g., promoter) by an oval. The definition of 'gene' extends beyond protein-coding genes to potentially include noncoding elements like microRNAs and long noncoding RNAs. Of note, duplications can effect change through increased copy number of a dosage sensitive gene (not pictured) or via the mechanisms depicted for deletions (e.g., via disruption at a breakpoint or partial intragenic duplication). Inspired by Fig. 1 in Bassett et al. [58] and Fig. 2 in Lee and Scherer [59]. From Costain et al. [60]. *It is an open access article*. Attribution 4.0 International (CC BY 4.0)

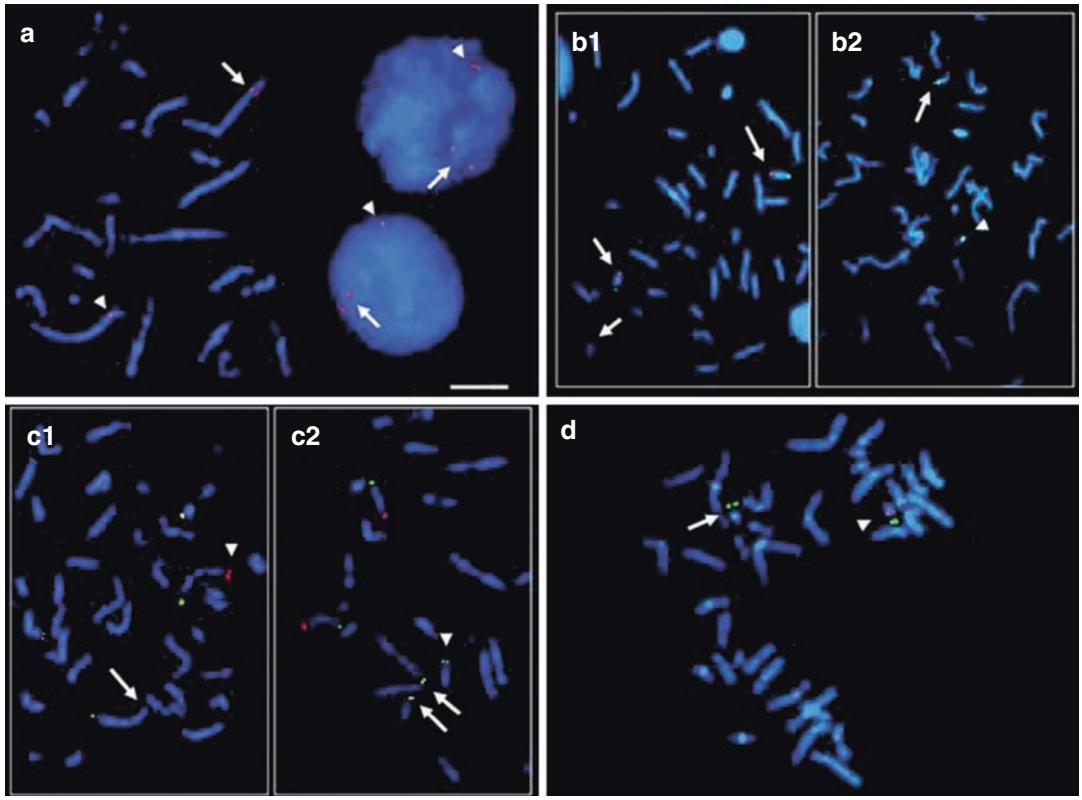

Fig. 13.3 FISH demonstrates chromosomal abnormalities in five subjects with CHD and additional anomalies. (**A**) Interstitial duplication of long arm of chromosome (ch) 2. FISH using custom BAC clones shows normal hybridization signals to the normal homologue of ch2 (*arrowhead*) and duplicated hybridization signals to the abnormal homologue of ch2 (*arrow*). Hybridization signals are also seen in interphase cells (right) with long arrows showing two signals (duplication) and arrowhead showing a single signal (normal). (**B**) Unbalanced translocation involving the long arm of chromosome 16 and short arm of ch19. (**B1**) FISH using subtelomeric probes to the short arm (*green signal*) and long arm of ch16 (*red signal*) indicate trisomy for the terminal region of ch16. (**B2**) FISH using probes for the subtelomeres of the short arm (*green*), long arm (*red*), and centromere (aqua) of ch19. Absence of the green signal (*arrowhead*) indicative of deletion of the distal segment of the short arm of ch19 when compared with normal ch19 (arrow). (**C**) Unbalanced translocation involving the long arm of ch1 and the long arm of ch15. (**C1**) FISH using subtelomeric sequences for the short arm (*green*) and the long arm (red) of chromosome 1. Arrow identifies the distal long arm of the abnormal chromosome 1 (signal missing), arrowhead identifies the distal long arm of the normal chromosome 1. Additional signals (*yellow*) in C1 identify Xp/Yp subtelomeric regions used as reporter sequences. (**C2**) Arrows identify hybridization signals for the subtelomeric sequences of ch15. *Arrowhead* indicates a ch15q hybridization signal on the long arm of ch1. Additional signals in C2 indicate short arm of ch10 (*green*) and long arm of 10 (*red*) as reporter sequences. (**D**) FISH showing normal hybridization to the DiGeorge/velo-cardio-facial syndrome critical region at chromosome 22q11.2 using a TUPLE1 probe. *Arrowhead* identifies normal hybridization pattern (*red*), arrow points to the deleted region. Green signal identifies distal ch22q, a reporter sequence encoding the arylsulfatase A gene. (**E**) Unbalanced translocation involving the long arm of ch7 and the long arm of ch17. (**E1**) FISH showing hybridization of subtelomeric sequences to the short arm (*red*) and the long arm (*green*) of ch7. *Arrows* indicate hybridization to the long arms of both the normal and abnormal homologues of ch7 indicating that the subtelomeric sequences on the abnormal chromosome are intact. The second set of signals is a reporter and identifies ch14. (**E2**) *Arrowhead* identifies hybridization to the telomeres of the long arms of the normal homologues of ch17. *Arrow* identifies a ch17 hybridization signal on the distal long arm of ch7. The scale bar in (**A**) represents 5 μm and the same magnification of 600× is used in all images. From Richards et al. [61]

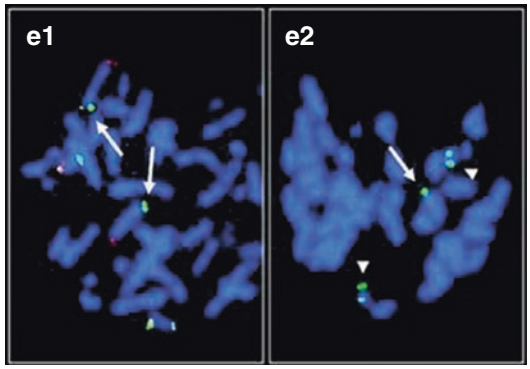

Fig. 13.3 (continued)

Fahed et al. [62] evaluated recently in a metanalysis the variation of CNVs based on the number and type of genes involved in the developmental of a pathological phenotype in patients with non-syndromic CHD. The alteration mechanism of CNVs is either the deletion or duplication. The number of involved genes can be one or multiple and their destructuring generate various types of CHD. For instance the most frequent modified genes in genesis of Fallot tetralogy are only one (*PPM1K, MID1*) or multiple (*RAF J, TMEM40, EDIL3, VCAN, SSBP2, TMEM167A, CNOT6, GFPT2, FLT4, ZNF879, ZNF345C, ADAMTS2, NSD1, GATA4, NEIL2, FDFT1, CSTB, SOX7, NOTCH1, EHMT1, TNFSF11, MIER2, CNN2, FSTL3, PTBP1, WDR18, GNA11, S1PR4*), that further causes de novo CNVs responsible for the genesis of Fallot tetralogy, when while both parents have normal karyotype. Also, this metaanalysis showed that 5–10% of patients are estimated to have non-syndromic CHD while both parents have normal karyotype (see Table 13.4) [62].

13.5 Transcription Factors

Transcription factors (sequence-specific DNA-binding factor) are specific proteins with the role to control the transfer of genetic information from DNA to RNA messenger [71]. This process is accomplished through mechanisms of activation or blockage of RNA polymerase [72–74].

In the differentiation and embryological evolution of cardiac structures with effects on anatomical integrity the main role belongs to the transcription factors which are T-Box protein 5 (*TBX5*, NK2 Homeobox 5 (*NKX2.5*), GATA-binding protein 4 (*GATA4*). They control transcription of the information from DNA to RNA messenger through RNA polymerase [71, 75].

TBX5, *GATA4*, and *NKX2* are the main factors of transcription that control the differentiation and development of cardiac structures and they are responsible for the congenital malformations. These can relate each other or they can act alone in the genesis of CHD. Thus, in case of ASD and VSD, each of them can be implied in the development of congenital malformation. For ASVD, both transcription factors like *TBX5* and *GATA4* can be involved. The specificity of one transcription factor exists in Ebstein disease (*NKX2-5*) and hypoplasic left ventricle; for paroxistic atrial fibrillation and Holt-Oram Syndrome is responsible only *TBX5*. Further, for Fallot tetralogy is implied only *NKX2-5,* and for AV block the same *NKX2-5*. Also one transcription factor is responsible for the pulmonary valve stenosis known as *GATA4*. Combinations between these major transcription factors participate to genesis of cardiac structures, therefore *TBX5* with *NKX2-5* control beginning with the first heart field (FHF) stage cellular differentiation and later the specific genes for cardiac cavities and conduction system of cardiac tissue. Moreover, *GATA4* and *NKX2-5* promote proteins from sarcomeric genes, and *GATA4* + *TBX5* sustain gene expression for protein synthesis from AV node and gap-junction (Fig. 13.4) [76].

To sum up, these hypotheses don't clarify the questions regarding why same gene modifications can develop more types of CHD, thus the mutations of *TBX5* can lead to ASD phenotype and also to VSD, or mutations of *TBX5*, *TBX20*, *GATA4* and *NKX2.5* can produce different phenotype on a patient than to another patient [76]. Furthermore, they don't explain why only one mutation can decide a unique phenotype, for example *NKX2-5* for Fallot Tetralogy and *GATA4* for pulmonary valve stenosis. However, Kloesel et al. [76] consider that the explanation for these situations are realized by transcriptional/translation and by interaction of multiple genes [76].

Table 13.4 Copy number variations (CNVs) associated with recurrent cases of non-syndromic CHD

Locus	Size range (Kbp)	No of cases	Inheritance	CNVs	No of genes	Genes[a]	Phenotype	Reference(s)
1q21.1	418–3981	21	De novo, inherited, n/a	Gain, loss	3–45	*PRKAB2, FM05, CHD1L, BCL9, ACP6, GJA5, CD160, PDZK1, NBPF11, FMO5, GJA8*	TOF, AS, CoA, PA, VSD	[63–67]
3p25.1	175–12,380	3	De novo, inherited	Gain	2	*RAF J, TMEM40*	TOF	[64, 68]
3q22.1–3q26.1	680–32,134	3	Inherited, n/a	Gain, loss	0–300	*FOXL2, NPHP3, FAM62C, CEP70, FAIM, PIK3CB, FOXL2, BPESC1*	DORV, TAPVR, AVSD	[69, 67, 70]
4q22.1	45	2	De novo inherited	Gain	1	*PPM1K*	TOF	[64, 63]
5q14.1-q14.3	4937–5454	2	De novo	Gain	41,103	*EDIL3, VCAN, SSBP2, TMEM167A*	TOF	[63, 65]
5q35.3	264–1777	4	De novo, n/a	Gain	19–38	*CNOT6, GFPT2, FLT4, ZNF879, ZNF345C, ADAMTS2, NSD1*	TOF	[63, 67]
7q11.23	330–348	2	n/a	Gain	5–8	*FKBP6*	HLHS, Ebstein's	[67]
8p23.1	67–12,000	10	n/a	Gain, loss	4	*GATA4, NEIL2, FDFT1, CSTB, SOX7*	AVSD, VSD, TOF,ASD, BAV	[63, 67]
9q34.3	190–263	3	De novo	Loss	2–9	*NOTCH1, EHMT1*	TOF, CoA, HLHS	[63, 67]
11p15.5	256–271	2	n/a	Gain	13	*HRAS*	DILV, AS	[67]
13q14.11	555–1430	3	n/a, de novo	Gain	7	*TNFSF11*	TOF, TAPVR, VSD,BAV	[65, 69]
15q11.2	238–2285	12	n/a	Loss	4	*TUBGCP5, CYFIP1, NIPA2, NIPA1*	CoA, ASD, VSD, TAPVD, complex left-sided	[63]
16p13.11	1414–2903	3	n/a	Gain	11–14	*MYH11*	Malformatio-ns HLHS	[67]
18q11.1–18q11.2	308–6118	2	n/a	Gain	1–28	*GATA6*	VSD	[67]
19p13.3	52–805	3	n/a, de novo	Gain, loss	1–34	*MIER2, CNN2, FSTL3, PTBP1, WDR18, GNA11, S1PR4*	TOF	[65, 63]
Xp22.2	509–615	2	n/a	Gain	2–4	*MID1*	TOF, AVSD	[65]

From Fahed et al. [62]

[a]Genes listed are encompassed by the CNV and were reported by the authors as candidate genes that are responsible for CHD. Only CNVs that have recurred in ≥1 CHD patient are listed. *CNVs* copy number variants, *AVSD* atrioventricular septal defects, *ASD* atrial septal defect, *VSD* ventricular septal defect, *CoA* coarctation of aorta, *PS* pulmonary stenosis, *TOF* tetralogy of Fallot, *BAV* Bicuspid Aortic Valve, *AS* Aortic Stenosis, *PAPVR* Partial Anomalous Pulmonary Venous Return, *TAPVR* Total Anomalous Pulmonary Venous Return, *TAPD* Total Anomalous Pulmonary Venous Drenaige, *HLHS* Hypoplastic left heart syndrome, *DILV* Double Inlet Left Ventricle, *DORV* Double outlet right ventricle

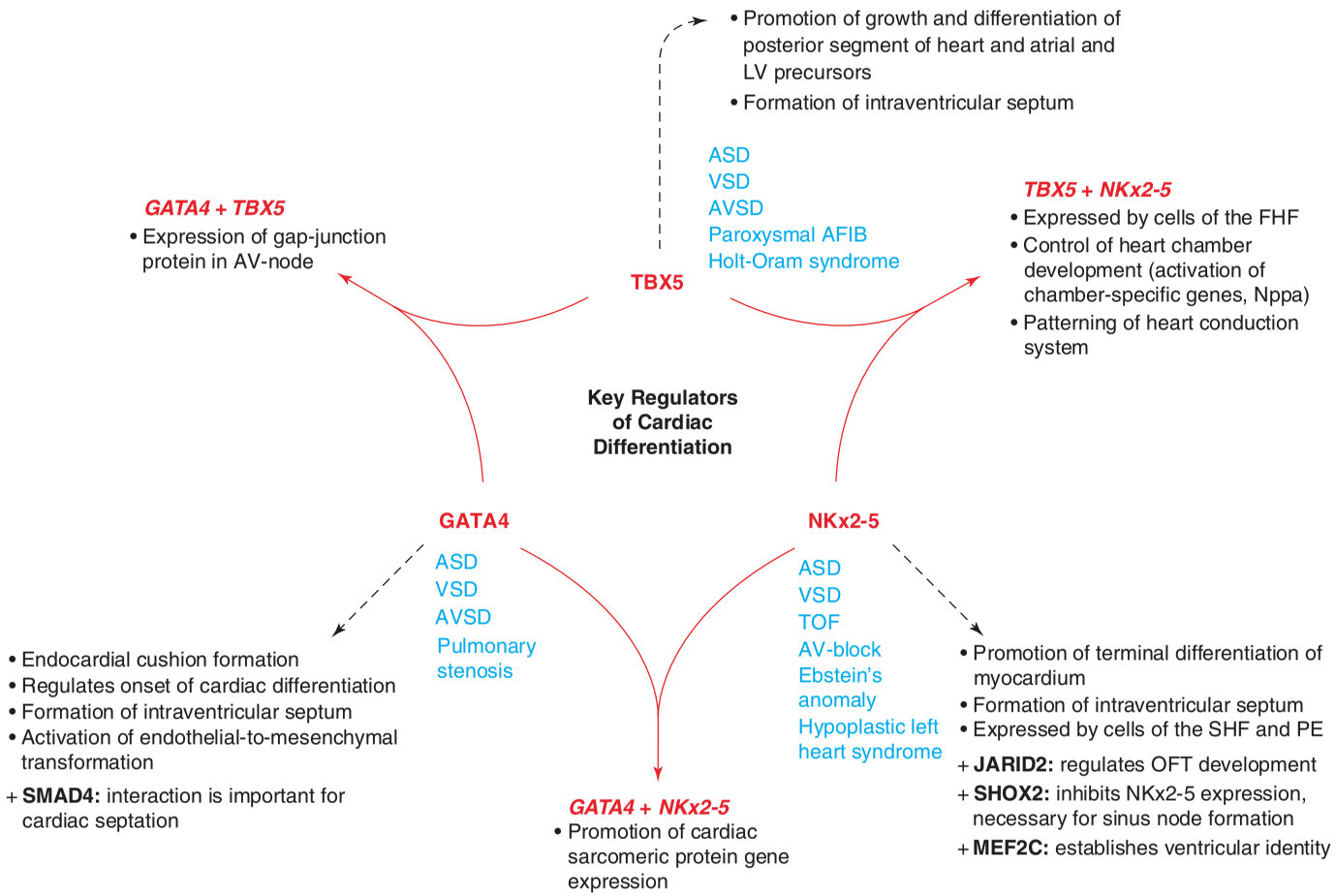

Fig. 13.4 Condensed overview of the function and interaction between three major transcription factors that are viewed as key regulators of cardiac differentiation: T-Box protein 5 (TBX5), GATA-binding protein 4 (GATA4), and NK2 Homeobox 5 (NKX2.5). AFiB indicates atrial fibrillation; ASD, atrial septal defect; AVSD, atrioventricular septal defect; FHF, first heart field; OFT, outflow tract; PE, proepicardium; SHF, second heart field; VSD, ventricular septal defect. From Kloesel et al. [76].

13.6 Syndromic CHD

Precisely, genetic defects responsible for congenital heart diseases are generating damage of the cardiac phenotype (non-syndromic CHD) or they are accompanied by other extracardiac defects (syndromic CHD).

Genetic mechanisms responsible for both conditions are multiple, some of them in hypotheses stage. For syndromic CHD there are genetic mechanisms which include disorders of chromosomes number (chromosomal anueploidy), chromosomal microdeletions, single gene defects, gene mutations. As a result, specific genetic defects are accomplished by mechanisms such as deletion (22q11.2), microdeletion (*ELN*, 20p12, 12q21, 2-q22), mutations [*ELN*, *TBX5*, *JAG1* or *Notch1*, *PTPN11*, *SOS1*, *RAF1*, *KRAS*, *BRAF*, *MEK1*, *MEK2*, and *HRAS*, *CHD7*, *SEMA3E*, *TFAP2B*, *EVC* or *EVC2*, *HRAS*, *Fibrillin-1*), outlining a clinical picture specific for each genetic defect. These mechanisms can act alone or combined, as a consequence we have different clinical pictures depending on the type of the genetic defect (Table 13.5) [77].

Table 13.5 Syndromes manifesting congenital heart disease and their genetic cause

Syndrome with CHD	Genetic cause for CHD
Disorders of chromosome dosage	
Trisomy 21 (Down syndrome)	Unknown
Turner	Unknown
Chromosomal microdeletions	
Di Georges syndrome	22q11.2 deletion resulting in absent *TBX1* gene
Williams-Beuren syndrome	Microdeletion of *ELN* gene; mutations in *ELN* gene
Single gene defects	
Holt-Oram syndrome	*TBX5* mutations
Alagille syndome	*JAG1* or *Notch1* mutations; microdeletion or rearrangement at 20p12 resulting in absent *JAG1*gene
Noonan syndrome	Mutations in *PTPN11, SOS1, RAF1, KRAS, BRAF, MEK1, MEK2*, and *HRAS*
CHARGE association	Mutations in *CHD7* and *SEMA3E*; microdeletion at 22q11.2
Char syndrome	Mutations in *TFAP2B*
Ellis-van Creveld syndrome	Mutations in *EVC* or *EVC2*
Cardiofaciocutaneous syndrome	Mutations in *KRAS, BRAK, MEK1*, or *MEK2*; Microdeletion at 12q21.2-q22
Costello syndrome	Mutations in *HRAS* (overlap with Noonan and Cardiofaciocutaneous syndrome)
Marfan syndrome	Mutations in *Fibrillin-1*

From [77]. *It is open access chapter*. This is an open access chapter distributed under the terms of the Creative Commons Attribution License (http://creativecommons.org/licenses/by/3.0), which permits unrestricted use, distribution, and reproduction in any medium, provided the original work is properly cited. Attribution 3.0 Unported (CC BY 3.0)

13.7 Non-syntromic CHD

Non-syndromic CHDs are the result of only one modified gene that shapes its own structure in an abnormal way, and that doesn't respect the genetic code of cardiogenesis. *NKX2.5*, *GATA4*, *MYH6*, *BMPR2*, *CRELD1*, *ALK2*, *NOTCH1* and *PROSIT-240* are the most frequent involved genes which can produce by themself cardiac congenital malformations (Table 13.6) [78].

13.8 New Approach

There are still many unknowns in understanding the gene dysfunction in congenital heart disease. Presently, there is knowledge about 50 genes that by mutations cause CHD. Recent studies establish a more precise relationship between genetic mutations and CHD genesis [79].

Zaidi et al. [11] analyzed the mutations on 4169 genes and they found an excess of a new protein in the group of heart-specific genes (high heart expression (*HHE*) gene), establishing 8 gene mutations in patients with cardiac malformations. These mutations were produced by the modification of histone via methylation of H3K4me (histone H3, lysine 4). This pathway

Table 13.6 Non-syndromic CHD resulting from single gene defects [78]

Cardiac anomalies	Gene
ASD atrioventricular conduction delay, *TOF* tricuspid valve abnormalities	NKX2.5
ASD, VSD	GATA4
ASD, hypertrophic cardiomyopathy	MYH6
Cardiac septation defects associated with PHTN	BMPR2
Endocardial cushion defects	CREDLD1, ALK2
BAV, early valve calcification	NOTCH1
d-TGA	PROSIT-240

It is an open access article.
Abbreviations: *ASD* atrial septal defect, *TOF* tetralogy of Fallot, *VSD* ventricular septal defect, *TGA* transposition of the great arteries, *BAV* bicuspid aortic valve, *PHTN* pulmonary hypertension

is recognized as responsible for gene mutations *MLL2*, *KDM6A*, and *CHD7* [11].

Later, Homsy et al. [12] studied the genetic differences between patients with syndromic heart disease (S-CHD) and non-syndromic CHD (NS-CHD) and suggested that de novo protein-truncating variants (PTVs) are markedly present in the case of patients with NS-CHD representing one significant landmark that we are trying to elucidate in differentiation between NS-CHD and S-CHD [12].

Most gene mutations responsible for NS-CHD and S-CHD occur in both forms (ABCC9, ACTC1, COL1A1, NOTCH1, and NOTCH2,) and therefore it is considered that the genetic mechanisms of differentiation between these forms are not known [79].

To sum up, these studies suggest that there may be other gene mutations which can do the differentiation between NS-CHD and S-CHD. Recently genes like CDK13, CHD4, and PRKD1 have been isolated, being involved in the generation of S-CHD.

Conclusions

According to current evidence the causes of CHD are exogenous and endogenous factors. The genetic mechanisms of CHD are multiple and include, among others, destructuring and numerical multiplication of chromosomes, sub-chromosomal changes (CNV), abnormal interrelationship between transcription factors, gene destructuring, deletion and duplication, mutations, and so on. There are still many congenital heart diseases with unknown etiology (61.7%). Syndrome CHDs are congenital malformations that include other genetic defects while non-syndromic CHD are clinical forms that manifest only by cardiac involvement. Monogene or polygenes mutations can produce both syndromic and non-syndromic phenotypes and further means that the interrelation between the original genetic factors is not yet elucidated.

The transcription factors responsible for cardiogenesis that regulate the differentiation of cardiac structures are T-Box protein 5 (TBX5), GATA-binding protein 4 (GATA4) and NK2 Homeobox 5 (NKX2.5) and the abnormal interrelation between them generates multiple forms of CHD. In the genetic sequence of CHD the beginning damage that has many starting points, ends with the phenotype specific to each genetic aberration.

Far from being puzzling, knowledge of normal cardiac development and the mechanisms of congenital heart diseases are essential to daily practice, as much for the daily examination of heart diseases as for genetic counselling before birth or in the case of familial forms [4]. For that reason, clinical geneticists and genetic counselors will have important responsibilities in patient care, to make certain correct diagnosis and helpful communication of inheritance and recurrence risks [3].

References

1. Centers for Disease Control and Prevention (CDC). Hospital stays, hospital charges, and in-hospital deaths among infants with selected birth defects–United States, 2003. MMWR Morb Mortal Wkly Rep. 2007;56:25–9.
2. Hoffman JI, Kaplan S. The incidence of congenital heart disease. J Am Coll Cardiol. 2002;39:1890–900.
3. Cowan JR, Ware SM. Genetics and genetic testing in congenital heart disease. Clin Perinatol.

2015;42(2):373–93, ix. https://doi.org/10.1016/j.clp.2015.02.009.
4. Bajolle F, Zaffran S, Bonnet D. Genetics and embryological mechanisms of congenital heart diseases. Arch Cardiovasc Dis. 2009;102(1):59–63. https://doi.org/10.1016/j.acvd.2008.06.020.
5. Huang J, Liang J. Molecular mechanisms of congenital heart disease. In: Syamasundar Rao P, editor. Congenital heart disease - selected aspects. InTech; 2012. https://doi.org/10.5772/27902. Available from https://www.intechopen.com/books/congenital-heart-disease-selected-aspects/molecular-mechanisms-of-congenital-heart-disease. Under CC BY 3.0 license.
6. Akhirome E, Walton NA, Nogee JM, Jay PY. The complex genetic basis of congenital heart defects. Circ J. 2017;81(5):629–34. https://doi.org/10.1253/circj.CJ-16-1343.
7. Nora JJ. Multifactorial inheritance hypothesis for the etiology of congenital heart diseases: the genetic-environmental interaction. Circulation. 1968;38:604–17.
8. Ferencz C, Neill CA, Boughman JA, Rubin JD, Brenner JI, Perry LW. Congenital cardiovascular malformations associated with chromosome abnormalities: an epidemiologic study. J Pediatr. 1989;114:79–86.
9. Hartman RJ, Rasmussen SA, Botto LD, Riehle-Colarusso T, Martin CL, Cragan JD, et al. The contribution of chromosomal abnormalities to congenital heart defects: a population-based study. Pediatr Cardiol. 2011;32:1147–57.
10. Glessner JT, Bick AG, Ito K, Homsy JG, Rodriguez-Murillo L, Fromer M, et al. Increased frequency of de novo copy number variants in congenital heart disease by integrative analysis of single nucleotide polymorphism array and exome sequence data. Circ Res. 2014;115:884–96.
11. Zaidi S, Choi M, Wakimoto H, Ma L, Jiang J, Overton JD, et al. De novo mutations in histone-modifying genes in congenital heart disease. Nature. 2013;498:220–3.
12. Homsy J, Zaidi S, Shen Y, Ware JS, Samocha KE, Karczewski KJ, et al. De novo mutations in congenital heart disease with neurodevelopmental and other congenital anomalies. Science. 2015;350:1262–6.
13. Sifrim A, Hitz MP, Wilsdon A, Breckpot J, Turki SH, Thienpont B, et al. Distinct genetic architectures for syndromic and nonsyndromic congenital heart defects identified by exome sequencing. Nat Genet. 2016;48:1060–5.
14. Bejjani BA, Shaffer LG. Clinical utility of contemporary molecular cytogenetics. Annu Rev Genomics Hum Genet. 2008;9:71–86.
15. Chung IM, Rajakumar G. Genetics of congenital heart defects: the NKX2-5 gene, a key player. Genes (Basel). 2016;7(2):E6. https://doi.org/10.3390/genes7020006.
16. Pierpont ME, Basson CT, Benson DW, Gelb BD, Giglia TM, Goldmuntz E, McGee G, Sable CA, Srivastava D, Webb CL. Genetic basis for congenital heart defects: current knowledge, a scientific statement from the American Heart Association Congenital Cardiac Defects Committee, Council on Cardiovascular Disease in the Young: endorsed by the American Academy of Pediatrics. Circulation. 2007;115:3015–38. https://doi.org/10.1161/CIRCULATIONAHA.106.183056.
17. Pierpont MEM, Moller JH. Chromosomal abnormalities. In: Pierpont MEM, Moller JH, editors. The genetics of cardiovascular disease. Boston: Nijhoff; 1987. p. 13–24.
18. Zollino M, Di Stefano C, Zampino G, Mastroiacovo P, Wright TJ, Sorge G, Selicorni A, Tenconi R, Zappala A, Battaglia A, Di Rocco M, Palka G, Pallotta R, Altherr MR, Neri G. Genotype-phenotype correlations and clinical diagnostic criteria in Wolf-Hirschhorn syndrome. Am J Med Genet. 2000;94:254–61.
19. Wilkins LE, Brown JA, Nance WE, Wolf B. Clinical heterogeneity in 80 home-reared children with cri du chat syndrome. J Pediatr. 1983;102:528–33.
20. Pierpont MEM. Genetic etiology of cardiac syndromes. Prog Pediatr Cardiol. 1996;6:29–41.
21. Eronen M, Peippo M, Hiippala A, Raatikka M, Arvio M, Johansson R, Kahkonen M. Cardiovascular manifestations in 75 patients with Williams syndrome. J Med Genet. 2002;39:554–8.
22. Bruno E, Rossi N, Thuer O, Cordoba R, Alday LE. Cardiovascular findings, and clinical course, in patients with Williams syndrome. Cardiol Young. 2003;13:532–6.
23. Wu YQ, Sutton VR, Nickerson E, Lupski JR, Potocki L, Korenberg JR, Greenberg F, Tassabehji M, Shaffer LG. Delineation of the common critical region in Williams syndrome and clinical correlation of growth, heart defects, ethnicity, and parental origin. Am J Med Genet. 1998;78:82–9.
24. Riccardi VM. Trisomy 8: an international study of 70 patients. Birth Defects Orig Artic Ser. 1977;13:171–84.
25. Fineman RM, Ablow RC, Howard RO, Albright J, Breg WR. Trisomy 8 mosaicism syndrome. Pediatrics. 1975;56:762–7.
26. Berry AC, Mutton DE, Lewis DG. Mosaicism and the trisomy 8 syndrome. Clin Genet. 1978;14:105–14.
27. De Michelena MI, Sanchez R, Munoz P, Cabello E, Rojas P, de Olazaval E. Trisomy 8: an additional case with unique manifestations [published correction appears in Am J Med Genet. 1993;46:605]. Am J Med Genet. 1992;43:697–700.
28. Dobyns WB, Dewald GW, Carlson RO, Mair DD, Michels VV. Deficiency of chromosome 8p21.1–8pter: case report and review of the literature. Am J Med Genet. 1985;22:125–34. https://doi.org/10.1002/ajmg.1320220114.
29. Digilio MC, Marino B, Guccione P, Giannotti A, Mingarelli R, Dallapiccola B. Deletion 8p syndrome. Am J Med Genet. 1998;75:534–6.
30. Marino B, Reale A, Giannotti A, Digilio MC, Dallapiccola B. Nonrandom association of atrioventricular canal and del (8p) syndrome. Am J Med Genet. 1992;42:424–7.

31. Wooldridge J, Zunich J. Trisomy 9 syndrome: report of a case with Crohn disease and review of the literature. Am J Med Genet. 1995;56:258–64.
32. Shapira M, Borochowitz Z, Bar-El H, Dar H, Etzioni A, Lorber A. Deletion of the short arm of chromosome 10 (10p13): report of a patient and review. Am J Med Genet. 1994;52:34–8.
33. Monaco G, Pignata C, Rossi E, Mascellaro O, Cocozza S, Ciccimarra F. DiGeorge anomaly associated with 10p deletion. Am J Med Genet. 1991;39:215–6.
34. Grossfeld PD, Mattina T, Lai Z, Favier R, Jones KL, Cotter F, Jones C. The 11q terminal deletion disorder: a prospective study of 110 cases. Am J Med Genet A. 2004;129:51–61.
35. Wyllie JP, Wright MJ, Burn J, Hunter S. Natural history of trisomy 13. Arch Dis Child. 1994;71:343–5.
36. Benacerraf BR, Miller WA, Frigoletto FD Jr. Sonographic detection of fetuses with trisomies 13 and 18: accuracy and limitations. Am J Obstet Gynecol. 1988;158:404–9.
37. Van Praagh S, Truman T, Firpo A, Bano-Rodrigo A, Fried R, McManus B, Engle MA, Van Praagh R. Cardiac malformations in trisomy-18: a study of 41 postmortem cases. J Am Coll Cardiol. 1989;13:1586–97.
38. Matsuoka R, Misugi K, Goto A, Gilbert EF, Ando M. Congenital heart anomalies in the trisomy 18 syndrome, with reference to congenital polyvalvular disease. Am J Med Genet. 1983;14:657–68.
39. McElhinney DB, Krantz ID, Bason L, Piccoli DA, Emerick KM, Spinner NB, Goldmuntz E. Analysis of cardiovascular phenotype and genotype-phenotype correlation in individuals with a JAG1 mutation and/or Alagille syndrome. Circulation. 2002;106:2567–74.
40. Alagille D, Estrada A, Hadchouel M, Gautier M, Odievre M, Dommergues JP. Syndromic paucity of interlobular bile ducts (Alagille syndrome or arteriohepatic dysplasia): review of 80 cases. J Pediatr. 1987;110:195–200.
41. Pueschel SM. Clinical aspects of Down syndrome from infancy to adulthood. Am J Med Genet Suppl. 1990;7:52–6.
42. Goldhaber SZ, Rubin IL, Brown W, Robertson N, Stubblefield F, Sloss LJ. Valvular heart disease (aortic regurgitation and mitral valve prolapse) among institutionalized adults with Down's syndrome. Am J Cardiol. 1986;57:278–81.
43. Goldhaber SZ, Brown WD, Sutton MG. High frequency of mitral valve prolapse and aortic regurgitation among asymptomatic adults with Down's syndrome. JAMA. 1987;258:1793–5.
44. Freeman SB, Taft LF, Dooley KJ, Allran K, Sherman SL, Hassold TJ, Khoury MJ, Saker DM. Population-based study of congenital heart defects in Down syndrome. Am J Med Genet. 1998;80:213–7.
45. Hijii T, Fukushige J, Igarashi H, Takahashi N, Ueda K. Life expectancy and social adaptation in individuals with Down syndrome with and without surgery for congenital heart disease. Clin Pediatr (Phila). 1997;36:327–32.
46. Kallen B, Mastroiacovo P, Robert E. Major congenital malformations in Down syndrome. Am J Med Genet. 1996;65:160–6.
47. McDonald-McGinn DM, Kirschner R, Goldmuntz E, Sullivan K, Eicher P, Gerdes M, Moss E, Solot C, Wang P, Jacobs I, Handler S, Knightly C, Heher K, Wilson M, Ming JE, Grace K, Driscoll D, Pasquariello P, Randall P, Larossa D, Emanuel BS, Zackai EH. The Philadelphia story: the 22q11.2 deletion: report on 250 patients. Genet Couns. 1999;10:11–24.
48. Ryan AK, Goodship JA, Wilson DI, Philip N, Levy A, Seidel H, Schuffenhauer S, Oechsler H, Belohradsky B, Prieur M, Aurias A, Raymond FL, Clayton-Smith J, Hatchwell E, McKeown C, Beemer FA, Dallapiccola B, Novelli G, Hurst JA, Ignatius J, Green AJ, Winter RM, Brueton L, Brondum-Nielsen K, Stewart F, Van Essen T, Patton M, Paterson J, Scambler PJ. Spectrum of clinical features associated with interstitial chromosome 22q11 deletions: a European collaborative study. J Med Genet. 1997;34:798–804.
49. Lin AE, Lippe BM, Geffner ME, Gomes A, Lois JF, Barton CW, Rosenthal A, Friedman WF. Aortic dilation, dissection, and rupture in patients with turner syndrome. J Pediatr. 1986;109:820–6.
50. Natowicz M, Kelley RI. Association of Turner syndrome with hypoplastic left-heart syndrome. Am J Dis Child. 1987;141:218–20.
51. Mazzanti L, Cacciari E. Congenital heart disease in patients with Turner's syndrome: Italian Study Group for Turner Syndrome (ISGTS). J Pediatr. 1998;133:688–92.
52. Lin AE, Lippe B, Rosenfeld RG. Further delineation of aortic dilation, dissection, and rupture in patients with Turner syndrome. Pediatrics. 1998;102:e12.
53. Prandstraller D, Mazzanti L, Picchio FM, Magnani C, Bergamaschi R, Perri A, Tsingos E, Cacciari E. Turner's syndrome: cardiologic profile according to the different chromosomal patterns and long-term clinical follow-up of 136 nonpreselected patients. Pediatr Cardiol. 1999;20:108–12.
54. Visootsak J, Aylstock M, Graham JM Jr. Klinefelter syndrome and its variants: an update and review for the primary pediatrician. Clin Pediatr. 2001;40:639–51.
55. Antonarakis SE, Lyle R, Dermitzakis ET, Reymond A, Deutsch S. Chromosome 21 and Down syndrome: from genomics to pathophysiology. Nat Rev Genet. 2004;5:725–38.
56. Bondy CA. Turner syndrome 2008. Horm Res. 2009;71(Suppl 1):52–6.
57. Pont SJ, Robbins JM, Bird TM, Gibson JB, Cleves MA, Tilford JM, Aitken ME. Congenital malformations among liveborn infants with trisomies 18 and 13. Am J Med Genet A. 2006;140:1749–56.
58. Bassett AS, Scherer SW, Brzustowicz LM. Copy number variations in schizophrenia: critical review and new perspectives on concepts of genetics and disease. Am J Psychiatry. 2010;167(8):899–914. https://doi.org/10.1176/appi.ajp.2009.09071016.
59. Lee C, Scherer SW. The clinical context of copy number variation in the human genome. Expert

Rev Mol Med. 2010;12:e8. https://doi.org/10.1017/S1462399410001390.
60. Costain G, Silversides CK, Bassett AS. The importance of copy number variation in congenital heart disease. NPJ Genom Med. 2016;1:16031. https://doi.org/10.1038/npjgenmed.2016.31.
61. Richards AA, Santos LJ, Nichols HA, Crider BP, Elder FF, Hauser NS, Zinn AR, Garg V. Cryptic chromosomal abnormalities identified in children with congenital heart disease. Pediatr Res. 2008;64(4):358–63. https://doi.org/10.1203/PDR.0b013e31818095d0.
62. Fahed AC, Gelb BD, Seidman JG, Seidman CE. Genetics of congenital heart disease: the glass half empty. Circ Res. 2013;112:707–20.
63. Soemedi R, Wilson IJ, Bentham J, et al. Contribution of global rare copy-number variants to the risk of sporadic congenital heart disease. Am J Hum Genet. 2012;91:489–501.
64. Greenway SC, Pereira AC, Lin JC, et al. De novo copy number variants identify new genes and loci in isolated sporadic tetralogy of Fallot. Nat Genet. 2009;41:931–5.
65. Silversides CK, Lionel AC, Costain G, Merico D, Migita O, Liu B, Yuen T, Rickaby J, Thiruvahindrapuram B, Marshall CR, Scherer SW, Bassett AS. Rare copy number variations in adults with tetralogy of fallot implicate novel risk gene pathways. PLoS Genet. 2012;8:e1002843.
66. Christiansen J, Dyck JD, Elyas BG, Lilley M, Bamforth JS, Hicks M, Sprysak KA, Tomaszewski R, Haase SM, Vicen-Wyhony LM, Somerville MJ. Chromosome 1q21.1 contiguous gene deletion is associated with congenital heart disease. Circ Res. 2004;94:1429–35.
67. Tomita-Mitchell A, Mahnke DK, Struble CA, Tuffnell ME, Stamm KD, Hidestrand M, Harris KD, Goetsch MA, Simpson PM, Bick DP, Broeckel U, Pelech AN, Tweddell JS, Mitchell ME. Human gene copy number spectra analysis in congenital heart malformations. Physiol Genomics. 2012;44:518–41.
68. Luo C, Yang YF, Yin BL, Chen JL, Huang C, Zhang WZ, Wang J, Zhang H, Yang JF, Tan ZP. Microduplication of 3p25.2 encompassing RAF1 associated with congenital heart disease suggestive of Noonan syndrome. Am J Med Genet A. 2012;158A:1918–23.
69. Erdogan F, Larsen LA, Zhang L, Tumer Z, Tommerup N, Chen W, Jacobsen JR, Schubert M, Jurkatis J, Tzschach A, Ropers HH, Ullmann R. High frequency of submicroscopic genomic aberrations detected by tiling path array comparative genome hybridisation in patients with isolated congenital heart disease. J Med Genet. 2008;45:704–9.
70. Priest JR, Girirajan S, Vu TH, Olson A, Eichler EE, Portman MA. Rare copy number variants in isolated sporadic and syndromic atrioventricular septal defects. Am J Med Genet A. 2012;158A(6):1279–84.
71. Latchman DS. Transcription factors: an overview. Int J Biochem Cell Biol. 1997;29(12):1305–12.
72. Lee TI, Young RA. Transcription of eukaryotic protein-coding genes. Annu Rev Genet. 2000;34:77–137. https://doi.org/10.1146/annurev.genet.34.1.77.
73. Nikolov DB, Burley SK. RNA polymerase II transcription initiation: a structural view. Proc Natl Acad Sci U S A. 1997;94(1):15–22.
74. Roeder RG. The role of general initiation factors in transcription by RNA polymerase II. Trends Biochem Sci. 1996;21(9):327–35.
75. Karin M. Too many transcription factors: positive and negative interactions. New Biol. 1990;2(2):126–31.
76. Kloesel B, DiNardo JA, Body SC. Cardiac embryology and molecular mechanisms of congenital heart disease: a primer for anesthesiologists. Anesth Analg. 2016;123(3):551–69. https://doi.org/10.1213/ANE.0000000000001451.
77. Fahed AC, Nemer GM. Genetic causes of syndromic and non-syndromic congenital heart disease. In: Cooper D, editor. Mutations in human genetic disease. InTech; 2012. https://doi.org/10.5772/48477. Available from https://www.intechopen.com/books/mutations-in-human-genetic-disease/genetic-causes-of-syndromic-and-non-syndromic-congenital-heart-disease.
78. Richards AA, Garg V. Genetics of congenital heart disease. Curr Cardiol Rev. 2010;6(2):91–7. https://doi.org/10.2174/157340310791162703.
79. Wilsdon A, Sifrim A, Hitz MP, Hurles M, Brook JD. Recent advances in congenital heart disease genomics. F1000Res. 2017;6:869. https://doi.org/10.12688/f1000research.10113.1.

Congenital Heart Disease and Right Heart

14

Silvia Iancovici and Maria Dorobanţu

Abstract

In the field of congenital heart disease (CHD) the right heart is frequently affected, therefore understanding its dysfunction and discovering new modalities of evaluation may have clinical implications. In patients with CHD, the right ventricle (RV) is either considered the subpulmonary ventricle as is the case in atrial septal defects, pulmonary stenosis, and Tetralogy of Fallot, either the systemic ventricle, e.g. in transposition of the great arteries (TGA). Without corrective surgery for these lesions, right-sided heart failure may develop and severely complicate the evolution of these patients. Consequently, finding new means to evaluate the right ventricle is highly important and has prognostic relevance. The anatomy and shape of the right ventricle (RV) are complex, making its assessment more difficult. Generally, several imaging modalities can be utilized, mainly echocardiography, but also radionuclide imaging and, more recently, computed tomography (CT) and cardiac magnetic resonance (CMR). As mentioned before, in CHD the RV can functionally serve as the sub-pulmonary ventricle, however, it can also function as the systemic ventricle, in order to support pressure or volume overload or both.

Keywords

Congenital heart disease · Right heart · Right-sided heart failure · Atrial septal defect · Ventricular septal defect · Ebstein anomaly · Fallot tetralogy Pulmonary regurgitation · Tricuspid regurgitation Transposition of the great arteries

14.1 Anatomy and Imaging

It is important to understand the anatomy and characteristics of the RV in order to differentiate between the two ventricles in the different types of congenital heart malformations. In the normal heart, the RV is the most anteriorly located cardiac chamber and lies closely behind the sternum.

The shape of the left ventricle (LV) is conical and easier to evaluate by 2D echocardiography. On the contrary, shape of the RV is complex, semilunar or "croissant"-like, which makes it more difficult to evaluate by 2D echocardiography, as it is impossible to visualize all the RV segments in one plane.

The RV consists of three different parts: inlet, apical trabecular, and outlet. The inlet RV extends from the tricuspid valve (TV) annulus to

S. Iancovici (✉)
Cardiology Department, Emergency Clinical Hospital, Bucharest, Romania

M. Dorobanţu
Cardiology Department, Emergency Clinical Hospital, Bucharest, Romania

Cardiology, "Carol Davila" University of Medicine and Pharmacy, Bucharest, Romania

S. I. Dumitrescu et al. (eds.), *Right Heart Pathology*, https://doi.org/10.1007/978-3-319-73764-5_14

the insertion of the papillary muscles; the trabeculated apical myocardium extends from there, followed by the outlet (infundibulum or conus), which consists of a smooth myocardial outflow section. The TV has 3 leaflets: the septal, anterosuperior, and inferior (or mural).

One of the typical characteristics of the TV is represented by the insertions of the tendinous cords to the interventricular septum. This TV feature, along with the apical displacement of the TV and the presence of the moderator band, are used in echocardiography to distinguish TV from the mitral valve and the morphological LV from the morphological RV.

The RV trabeculations are coarse compared to the smoothly trabeculated left ventricle. Moreover, the RV outflow tract is muscular and elongated, ending in the pulmonary valve, that does not have a real valvular annulus [1].

Angiographic assessment of the RV used to be the "gold standard" for the evaluation of the right heart, however, it has recently been replaced by CMR. Angiography is an irradiating, invasive procedure that also involves the use of contrast agents; the right heart angiographic assessment can reveal information concerning hemodynamic parameters, the pressure within the right chambers, O_2 saturations, and the presence of atrial shunts. It is still used to measure the gradients through the pulmonary valve in cases of stenosis before and after balloon dilatations. However, it is less revealing when it comes to the geometrical characteristics and the function of the right chambers.

Echocardiography is the first-line imaging modality for right heart assessment. Two-dimensional echocardiography offers information about the dimensions of the RV and the right atrium (RA), the systolic and diastolic function of the RV, flow through the tricuspid and the pulmonary valve, and the presence of valvular stenosis or regurgitation.

The CMR is the preferred imaging modality for quantitative assessment of RV volume, mass, and function, regardless of its position in the thorax (subpulmonary *or* systemic RV) [1].

CMR with late gadolinium enhancement can detect myocardial fibrosis. The limitations of CMR are breath-holding, requirement of a regular heart rhythm, the exclusion of patients with implantable metallic devices, and its high cost [1].

Multiscan CT is an alternative, especially for patients with implantable devices, with the limitation of using ionizing radiation [1].

14.2 The Volume-Overloaded RV

There are several CHD where the main consequence is dilatation of the right chambers—atrial septal defects, significant pulmonary regurgitation and tricuspid regurgitation.

14.2.1 Atrial Septal Defect

Is the second most common congenital defect, preceded by bicuspid aortic valve [2]. Three types of ASD are more frequent: ostium secundum ASD, sinus venosus ASD, ostium primum ASD. Ostium secundum defects account for 70% of all ASD. Sinus venosus ASD and ostium primum defect represent 5 and 10% of all ASD, respectively [2].

The ostium secundum ASD represents a defect of the atrial septum at the fossa ovalis (Figs. 14.1 and 14.2).

The ostium primum defect is included in the spectrum of the atrioventricular (AV) septal defects (Fig. 14.3).

The sinus venosus ASD is a defect usually located at the junction of the superior vena cava with the RA and is almost always associated with partial anomalous pulmonary venous return. There are two other uncommon types of ASDs: inferior vena cava type of sinus venosus ASD and "unroofed" coronary sinus.

The isolated ASD leads to a left-to-right shunt and secondary dilatation of the right chambers: RA, RV and the pulmonary artery. Transthoracic echocardiography (TTE) reveals the right chamber dilatation and the diagnosis of ASD is established based on the presence of a defect at different levels of the interatrial septum, as described above. Sometimes, transesophageal echocardiography (TEE) may be necessary to confirm the diagnosis, especially in sinus

venosus ASD and may assist in the evaluation of pulmonary venous drainage.

Sometimes, the RV dilates severely due to the left-to-right shunt, however the systolic and diastolic function are normal [1]. In patients with longstanding volume overload due to ASD, regional RV tissue Doppler imaging may show relaxation abnormalities [3].

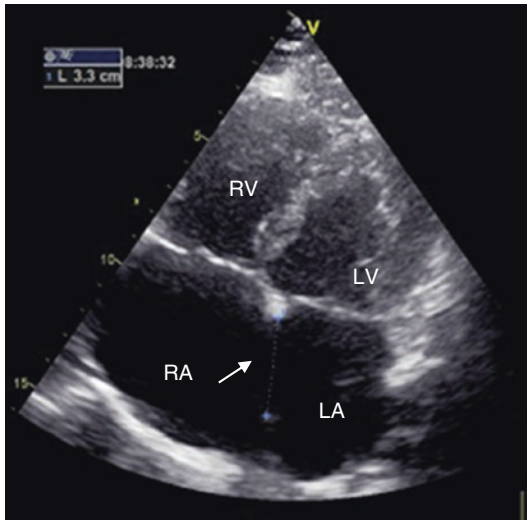

Fig. 14.1 Two-dimensional echocardiogram, apical four-chamber view. There is dilatation and hypertrophy of the right ventricle, that is larger than the left ventricle. A large atrial septal defect (ASD) is present (white arrow). *LA* left atrium, *LV* left ventricle, *RA* right atrium, *RV* right ventricle

It has been proven that longstanding dilatation of the right chambers leads to increased risk of complications, such as heart failure, arrhythmias, embolic events and increased mortality [4]. After closure of the ASD, reverse-remodeling of the right chambers can be noticed. The degree of reverse-remodeling varies with age, generally in older patients the RV/RA remodeling is incomplete [5]. Some trials showed that the process of reverse-remodeling develops over 1–24 months after ASD closure [6].

Closure of the ASD depends on the type. For ostium primum ASD and sinus venosus ASD, the solution is solely surgical; in contrast, for ostium secundum ASD, treatment may be either surgical or interventional, using a special device (Figs. 14.4 and 14.5). Establishing closure indication is based on the enlargement of the right chambers [7]. Another indication of closure is paradoxical embolism, regardless of the size of the ASD [7]. With rigorous patient selection, device closure in adults leads to clinical improvement and increased exercise capacity, and is associated with fewer complications and shorter hospitalization compared to surgery [8].

An untreated large ASD leads to a progressive increase in pulmonary pressures, that may become fixed, thus implying the development of Eisenmenger syndrome. In Eisenmenger syndrome, due to high pressures in the right atrium,

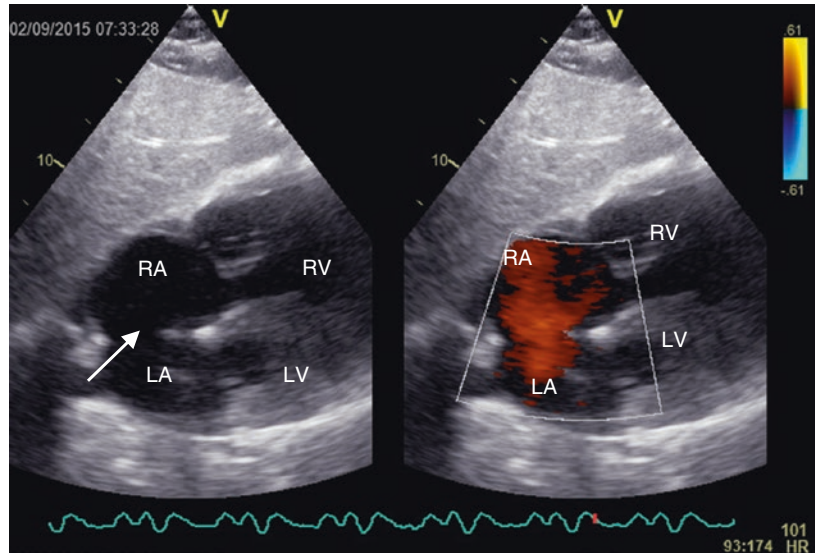

Fig. 14.2 Left: Two-dimensional echocardiogram, apical subcostal four-chamber view. There is a large ostium secundum ASD (Arrow). Right: Color Doppler evaluation: the left-to-right shunt is seen through the ASD (red color). *LA* left atrium, *RA* right atrium, *RV* right ventricle

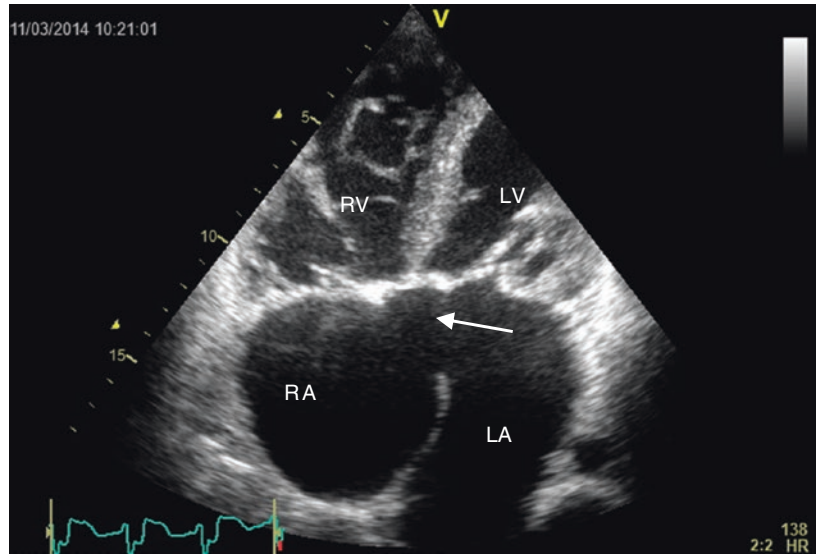

Fig. 14.3 Two-dimensional echocardiogram, apical four-chamber view. There is dilatation and hypertrophy of the right ventricle. A large atrial septal defect ostium primum is present (white arrow). Also noticeable is the insertion of the atrio-ventricular valves at the same level. *LA* left atrium, *LV* left ventricle, *RA* right atrium, *RV* right ventricle

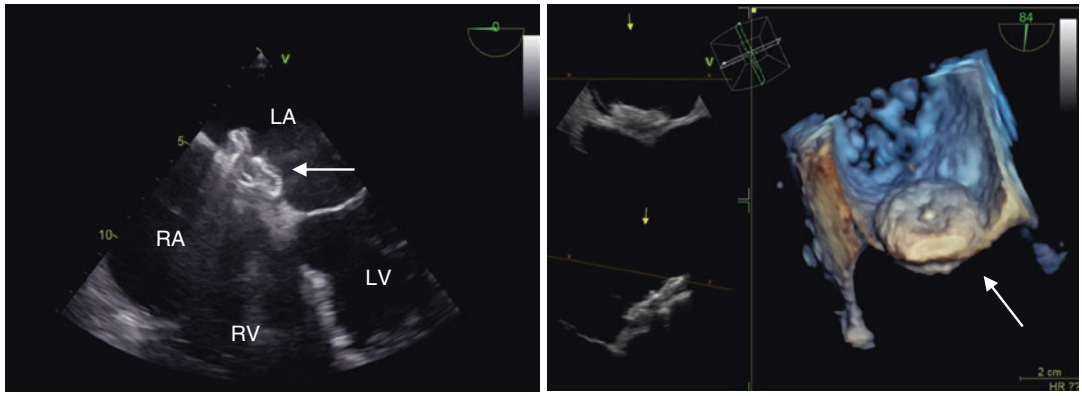

Fig. 14.4 Transesophageal echocardiography. Left: two-dimensional echocardiogram (0°). The ASD closure device can be seen at the level of the atrial septum (arrow). Right: 3D zoom real time echocardiography left atrial view. The ASD device can be seen at the level of inter-atrial atrial septum (arrow)

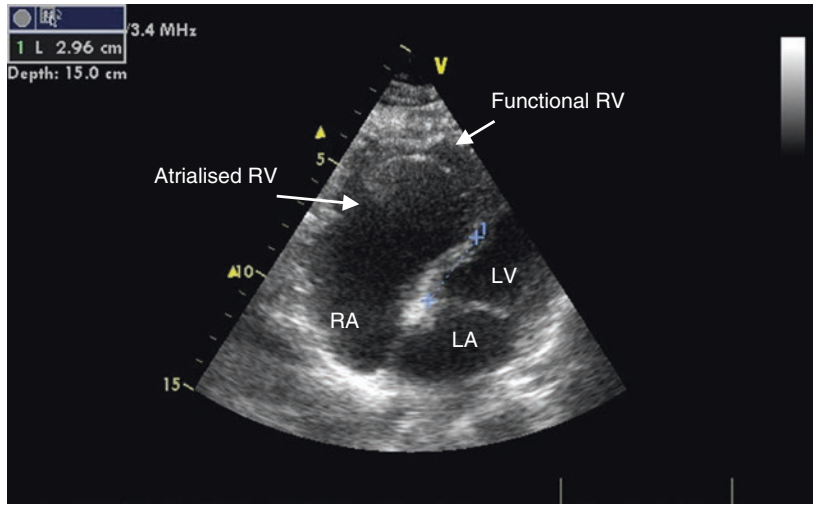

Fig. 14.5 Two dimensional echocardiogram, apical four chamber view. There is dilatation of the right ventricle. The apical insertions of the septal tricuspid leaflet are measured at a distance of 29 mm from the atrioventricular annulus (dotted blue line). *LA* left atrium, *LV* left ventricle, *RA* right atrium, *RV* right ventricle

the shunt becomes initially bidirectional and then switches right-to-left. The presence of Eisenmenger syndrome is a contraindication for ASD closure [7].

Once pulmonary arterial hypertension (PAH) develops, the already dilated RV becomes hypertrophied. Over time, with longstanding PAH, diastolic and systolic dysfunction appear. Furthermore, due to the enlargement of the right ventricle, the tricuspid annulus dilates and functional tricuspid regurgitation develops.

The appearance of PAH can be evaluated by echocardiography by estimating systolic pulmonary arterial pressure (sPAP). Thus, sPAP is obtained by measuring the RV-to-RA gradient and adding the RA pressure. Furthermore, the systolic dysfunction of the RV can be estimated by echocardiography using several parameters, such as: tricuspid annular excursion (TAPSE), fractional area change, S wave measured by Tissue Doppler, RV performance index (Tei index). Patients with RV systolic dysfunction, severe tricuspid regurgitation may develop signs of right-sided heart failure.

14.2.2 Pulmonary Regurgitation (PR)

Mild PR may be noticed while performing an echocardiogram in most examinations. In the congenital heart disease field, more significant forms of PR are commonly seen following repaired tetralogy of Fallot, or following intervention (transcatheter or surgical) for pulmonary stenosis. Severe PR is rarely seen as an isolated lesion [1]. Severe PR after tetralogy of Fallot is associated with RV dilatation and systolic dysfunction, diminished exercise capacity, atrial and ventricular arrhythmias, and sudden death [1]. It is known that following 2 decades of exposure to significant volume-overload, RV systolic dysfunction occurs [9]. Therefore, the echocardiographic follow-up of the RV systolic function and degree of PR is essential. In addition to echocardiography, CMR is considered the gold standard to assess systolic function and degree of PR [1].

In order to evaluate the severity of PR, several echocardiography parameters can be measured. Using Doppler echocardiography, a new Doppler index (the PR index, represented by the ratio of PR duration to diastolic duration) has been shown to correlate well with the MRI-derived pulmonary regurgitant fraction [10]. A PR index of less than 0.77 yields 100% sensitivity and 85% specificity for identifying patients with a PR fraction >24.5%—that is, patients with significant PR [10]. In addition, a PR pressure half-time <100 ms has been found to be a reliable indicator of hemodynamically significant regurgitation [11].

Treatment consists of replacement of the pulmonary valve, keeping in mind that identifying the optimal moment for intervention prevents complications. Patients with repaired tetralogy of Fallot should be followed-up by performing an echocardiogram yearly and a CMR scan every 2 years [12]. It is recommended to refer the patient for pulmonary valve replacement in the presence of symptoms and severe PR, or when the subsequent are noticed at follow-up: progressive dilatation of the RV, decrease in functional capacity, progressive RV systolic dysfunction, progressive TR, sustained atrial/ventricular arrhythmias [7]. After pulmonary valve replacement, the RV volume usually decreases, as evidenced by different imaging techniques: echocardiography [13], radionuclide angiography (RNA) [14] or CMR [15].

In patients with operated tetralogy of Fallot, there is a considerable arrhythmia risk. These patients usually have right bundle branch block, as well as signs of RV hypertrophy on the electrocardiogram.

Prolongation of the QRS duration correlates well with progressive RV dilatation and dysfunction [9]. Therefore, following QRS duration is relevant, with a QRS rate of change >4 ms/year having been associated with an increased risk of sustained ventricular tachycardia and sudden cardiac death [16]. Other predictors of ventricular tachycardia and sudden cardiac death include a QRS duration >180 ms and LV dysfunction [16].

The main concern is deciding implantation of an internal cardiac defibrillator (ICD) in these patients and there is still uncertainty regarding the optimal moment for the intervention. There are several risk factors that should place the

patient in a high risk category for sudden cardiac death: large RVOT aneurysms [17], QRS > 180 ms [18], inducible ventricular tachycardia [19], extensive late gadolinium enhancement evaluated by CMR [20] or associated LV dysfunction [21].

14.2.3 Tricuspid Regurgitation (TR)

Mild, physiologic TR may be noticed on most transthoracic echocardiograms. When significant, TR may be primary, as in Ebstein anomaly, dysplasia of the tricuspid valve, or it may be secondary to the dilatation of the tricuspid annulus, as seen in patients with operated tetralogy of Fallot, or in other conditions with RV enlargement (arrhythmogenic right ventricular dysplasia).

Ebstein anomaly may be associated with other congenital heart defects (ASD, pulmonary stenosis, pulmonary atresia or hypoplastic pulmonary arteries, subaortic stenosis, bicuspid aortic valve, mitral valve prolapse and ventricular septal defect), as well as accessory conduction pathways (Wolff-Parkinson-White syndrome) [9].

Ebstein anomaly consists of a complex congenital disease characterized by the apical displacement of the septal and posterior leaflets exceeding 20 mm or 8 mm/m^2 body surface area in adults [22] (Fig. 14.5). Secondary to the apical displacement of the septal and posterior leaflet, the right ventricle divides in two: the atrialised RV (above the valve) and the functional RV (beneath the valve). The malformation leads to severe TR, affecting the RV function. Diagnosis is usually established by echocardiography, where the apical displacement of the leaflets in the four-chamber view can be observed. Echocardiography can also establish the severity of the disease, which depends on the ratio between the "atrialised RV" and the "functional RV", as well as the mobility of the anterior leaflet.

The dimensions and parameters for assessing the systolic function of the RV can be estimated by echocardiography. CMR remains, however, the gold standard for an accurate assessment of both the volume and systolic function of the RV [23]. Treatment for Ebstein anomaly is surgical, with transverse plication of the atrialised chamber and tricuspid valvuloplasty if feasible, or tricuspid valve replacement [24]. Referral to surgery is recommended if more-than-moderate TR is present and symptoms associated, with a decrease in exercise capacity, progressive dilatation of the RV or reduction of RV systolic function [7]. Of crucial importance, prior to performing the procedure, the patient should undergo a complete assessment of the tricuspid valve anatomy, RV dimensions and function by echocardiography and, if possible, supplemented by CMR. Three-dimensional echocardiography may offer useful information, in addition to the 2D evaluation, in order to understand the valve anatomy.

TR may also be significant in patients with operated tetralogy of Fallot. TR, in this case, is related to RV dilatation due to severe PR and, possibly, valvular trauma during reparative surgery [25]. If severe, the TR contributes to further RV dilatation [25]. As discussed above, in these patients, a significant TR is an indication for pulmonary valve replacement [7]. However, when TR is severe, reoperation is associated with high surgical mortality and poor long term results due to postoperative RV dysfunction [26].

14.3 Pressure-Loaded RV

14.3.1 Right Ventricular Outflow Tract Obstruction: Isolated Pulmonary Stenosis

Valvular pulmonary stenosis (PS) represents 80–90% of the right ventricular obstruction cases [1]. Less frequently, stenosis appears above (supra-) or below (subvalvular) the pulmonary valve. The main consequence of obstruction is the hypertrophy of the RV. The degree of hypertrophy depends on the severity of the obstruction. When prominent, RVOT hypertrophy can lead to secondary dynamic subvalvar stenosis [9]. PS

can also result in post-stenotic dilatation of the pulmonary trunk, which is common in the doming form of PS and often extends to the proximal left pulmonary artery [9].

The assessment of the stenosis is performed by echocardiography with a 2D visualization of the valve. The pulmonary valve can be "dome"-shaped, the most frequent morphological feature in PS cases, but it can also be dysplastic (10–20% of PS cases [9]). The degree of PS is established using continuous Doppler assessment by measuring the peak gradient through the valve. Cardiac catheterization should be used when balloon valvuloplasty is contemplated [12]. Sometimes, catheterization may also be needed for diagnosis, especially in cases of infundibular stenosis. More sophisticated methods, mainly CMR, may be used for detailed imaging of the RVOT and for assessment of RV size and function [1].

A hypertrophied RV can maintain its function for years [9]. If there is no other volume-loading condition associated, the RV is usually able to maintain its function well into the fourth or fifth decade of life [27]. There is little progression in PS severity when the gradient is less than 30 mmHg; these patients should be followed up at least every 5 years with a clinical examination and Doppler echocardiography.

Treatment of RVOT obstruction is recommended if the gradient through the obstruction is above 64 mmHg, when the RV function is normal and there is no need for valve replacement, as stipulated in the European Society of Cardiology guidelines [7]. Balloon valvulotomy is the method of choice in valvular PS. The same guidelines mention that intervention in patients with a gradient <64 mmHg should be considered in the presence of: symptoms related to PS or decreased RV function or double-chambered RV (which is usually progressive) or important arrhythmias or right-to-left shunting via an ASD or VSD [7].

The American College of Cardiology/American Heart Association guidelines recommend balloon valvulotomy for asymptomatic patients with dome-shaped pulmonary valve and a peak instantaneous Doppler gradient >60 mmHg or a mean Doppler gradient >40 mmHg [12]. For symptomatic patients, balloon valvulotomy is indicated when a peak instantaneous Doppler gradient >50 mmHg or a mean Doppler gradient >30 mmHg is present [12].

In the long term, the outcome following balloon valvulotomy is excellent [28], with a low rate of restenosis. The latter was found to be more common when a residual gradient was present immediately after the procedure [29]. Sometimes, significant PR may develop following the intervention and may lead to progressive dilatation of the RV.

14.3.2 The Systemic RV

The morphological systemic RV is seen in two conditions: congenitally corrected transposition (ccTGA) and surgically corected TGA by atrial switch (Mustard or Sennning) [9]. In the systemic position, the RV faces the left arterial pressures, consequently leading to changes in the myocardium, with important hypertrophy.

Congenitally corrected TGA is a rare congenital disease, consisting of a double discordance: atrio-ventricular and ventriculo-arterial. The right atrium is connected to the right-sided morphological LV that, in turn, connects to the pulmonary artery through the pulmonary valve (Fig. 14.6). The left atrium is connected to the left-sided morphological RV that, in turn, connects to the aorta through the aortic valve. ccTGA may be associated with other congenital malformations, adding to the general prognosis.

Echocardiography establishes the diagnosis: in the four-chamber view the inverted ventricles can be noticed. The morphological RV is left-sided and characterized by: apical displacement of the tricuspid valve, the presence of the moderator band, and the tricuspid septal valve has cordal insertion on the inlet septum (Fig. 14.6). Another criteria for the diagnosis ofTGA is the side by side position of the great arteries. Accurate assessment of systemic RV function and the degree of systemic AV valve regurgitation is essential. Just as is important is to identify associated lesions.

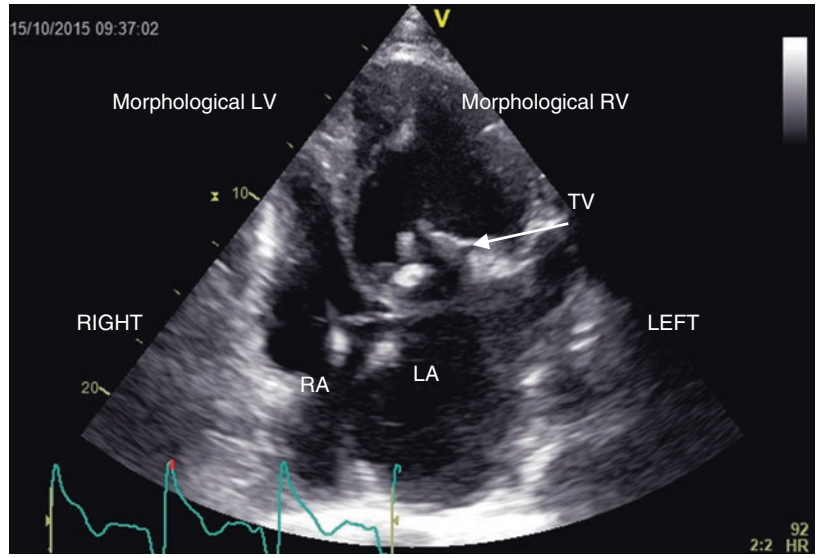

Fig. 14.6 Two-dimensional echocardiogram, apical four-chamber view of a patient with ccTGA. The LA communicates with the left-sided morphological RV. The RA communicates with the right-sided morphological LV. *LA* left atrium, *LV* left ventricle, *RA* right atrium, *RV* right ventricle, *TV* tricuspid valve

CMR provides complementary information on the anatomy and accurate assessment of RV size and function [9].

The prognosis of ccTGA depends on the presence of associated lesions [9]. Without any associated lesions these patients may survive until the seventh to eighth decade of life [9]. However, in the long term, the clinical course deteriorates even in patients without any associated lesions due to the possible appearance of complications such as: tricuspid valve regurgitation [30], RV systolic dysfunction [31] and complete heart block [32]. The presence of more-than-moderate tricuspid regurgitation associated with RV dysfunction is related to increased mortality [31], TR being the most significant independent predictor of outcome [33].

Although it is difficult to assess the RV systolic dysfunction by echocardiography, there are several parameters that offer an estimation of systolic function. In addition, the degree of TR can be appreciated by echocardiography using the standard evaluation: the reverse flow into the pulmonary veins, the vena contracta, estimating the regurgitant volume and area using the PISA method. The severity of TR also influences the RV systolic function; RV dysfunction usually develops within 5 years from TR onset in ccTGA patients (without associated lesions or surgery) [33]. In addition, the severity of TR gradually increases with progression of RV dilatation and dysfunction.

When systemic RV function deteriorates in the presence of systemic AV valve regurgitation, particularly when intrinsic abnormalities of the valve are present, TV replacement should always be considered, before irreversible systemic RV dysfunction ensues [12].

Complete transposition of the great arteries (*TGA*) appears in around 5% of congenital heart malformations [9]. In these patients, the aorta arises from the morphological RV, and the pulmonary artery from the morphological LV; the aorta and the pulmonary artery are parallel, usually with the aorta situated anterior and to the right. Associated lesions may also be present. This anomaly is incompatible with life without a surgical switch of the circulation either at the atrial or great arterial level.

The treatment of choice for patients with TGA is the arterial switch procedure, which has been used for more than two decades. However, most of the adults with TGA have had an atrial switch procedure (Mustard or Senning operation) that results in the RV as the systemic ventricle. These patients may develop systemic ventricular dysfunction, arrhythmias or baffle-related problems, and warrant annual follow-up

in specialized adult congenital heart disease (ACHD) centers [12].

Cumulative survival 25–30 years after the Mustard repair is as high as 80% [1]. RV dysfunction appears as the TR becomes more severe [9]. TV replacement is recommended in patient with severe TR due to primary TV disease (which may be iatrogenic from VSD closure or due to other factors such as endocarditis) [12]. The systolic function of the systemic RV can be estimated by echocardiography, however the primary modality for RV function and size assessment remains CMR. Moreover, the systemic and pulmonary venous pathways can be evaluated more accurately. When CMR is contraindicated, gated CT-angiography may be an alternative [9]. The decline in RV function, cumulated with residual lesions like baffle obstruction or leakage, residual ventricular septal defect, and pulmonary valve stenosis, may lead to late morbidity and mortality manifested as reduced exercise capacity, heart failure, endocarditis, supraventricular arrhythmias, reoperation, and cardiac death [34].

Echocardiographic assessment of RV function is difficult, but echocardiography also provides information on baffle patency, leaks (with contrast studies), valvular regurgitation or stenosis and, in experienced hands, semiquantitative information on RV function [35]. Lissin et al. showed that MRI-derived RV volumes correlate positively with echo-derived RV inlet dimensions and negatively with the dP/dT of the tricuspid regurgitant jet [35]. Furthermore, RV longitudinal function (M mode: wall excursion measured from the apex) correlates with CMR-derived RV ejection fraction [35].

Conclusions

The complete evaluation of the RV remains a challenge, due to its complex shape and function; in the field of CHD, the RV is an essential chamber and its function has prognostic implications. Echocardiography remains the first line of investigation, offering important information on RV size and function, and it is also very useful for follow-up. In addition, CMR is the main imaging technique, offering an accurate and complete exploration of RV. The use of CMR has led to an important progress and a better understanding of the role and the evolution of RV in CHD.

References

1. Davlouros PA, Niwa K, Webb G, Gatzoulis MA. The right ventricle in congenital heart disease. Heart. 2006;92(Suppl 1):i27–38. https://doi.org/10.1136/hrt.2005.077438.
2. Guihaire J, Haddad F, Mercier O, Murphy DJ, Wu JC, Fadel E. The right heart in congenital heart disease, mechanisms and recent advances. J Clin Exp Cardiolog. 2012;8(10):1–11. https://doi.org/10.4172/2155-9880.S8-010.
3. Pascotto M, Caso P, Santoro G, et al. Analysis of right ventricular Doppler tissue imaging and load dependence in patients undergoing percutaneous closure of atrial septal defect. Am J Cardiol. 2004;94(9):1202–5. https://doi.org/10.1016/j.amjcard.2004.07.098.
4. Vasquez AF, Lasala JM. Atrial septal defect closure. Cardiol Clin. 2013;31(3):385–400. https://doi.org/10.1016/j.ccl.2013.05.003.
5. Kort HW, Balzer DT, Johnson MC. Resolution of right heart enlargement after closure of secundum atrial septal defect with transcatheter technique. J Am Coll Cardiol. 2001;38(5):1528–32. https://doi.org/10.1016/S0735-1097(01)01547-9.
6. Schussler JM, Anwar A, Phillips SD, Roberts BJ, Vallabhan RC, Grayburn PA. Effect on right ventricular volume of percutaneous Amplatzer closure of atrial septal defect in adults. Am J Cardiol. 2005;95(8):993–5. https://doi.org/10.1016/j.amjcard.2004.12.046.
7. Baumgartner H, Task Force on the Management of Grown-up Congenital Heart Disease of the European Society of Cardiology (ESC), et al. ESC Guidelines for the management of grown-up congenital heart disease (new version 2010). Eur Heart J. 2010;31:2915–57. https://doi.org/10.1093/eurheartj/ehq249.
8. Du ZD, Hijazi ZM, Kleinman CS, Silverman NH, Larntz K. Comparison between transcatheter and surgical closure of secundum atrial septal defect in children and adults: results of a multicenter nonrandomized trial. J Am Coll Cardiol. 2002;39(11):1836–44. https://doi.org/10.1016/S0735-1097(02)01862-4.
9. Alonso-González R, Dimopoulos K, Ho S, Oliver JM, Gatzoulis MA. The right heart in adults with congenital heart disease. Rev Esp Cardiol. 2010;63(9):1070–86. https://doi.org/10.1016/S1885-5857(10)70211-5.
10. Li W, Davlouros PA, Kilner PJ, et al. Doppler-echocardiographic assessment of pulmonary regurgitation in adults with repaired tetralogy of Fallot: comparison with cardiovascular magnetic resonance imaging. Am Heart J. 2004;147(1):165–72. https://doi.org/10.1016/s0002-8703(03)00527-1.

11. Silversides CK, Veldtman GR, Crossin J, et al. Pressure half-time predicts hemodynamically significant pulmonary regurgitation in adult patients with repaired tetralogy of Fallot. J Am Soc Echocardiogr. 2003;16(10):1057–62. https://doi.org/10.1016/S0894-7317(03)00553-4.
12. Warnes CA, Williams RG, Bashore TM, et al. ACC/AHA 2008 guidelines for the management of adults with congenital heart disease: executive summary: a report of the American College of Cardiology/American Heart Association Task Force on Practice Guidelines (writing committee to develop guidelines for the management of adults with congenital heart disease). Circulation. 2008;118(23):2395–451. https://doi.org/10.1161/CIRCULATIONAHA.108.190811.
13. Discigil B, Dearani JA, Puga FJ, et al. Late pulmonary valve replacement after repair of tetralogy of Fallot. J Thorac Cardiovasc Surg. 2001;121(2):344–51. https://doi.org/10.1067/mtc.2001.111209.
14. d'Udekem Y, Rubay J, Shango-Lody P, et al. Late homograft valve insertion after transannular patch repair of tetralogy of Fallot. J Heart Valve Dis. 1998;7(4):450–4.
15. Vliegen HW, Van Straten A, De Roos A, et al. Magnetic resonance imaging to assess the hemodynamic effects of pulmonary valve replacement in adults late after repair of tetralogy of Fallot. Circulation. 2002;106(13):1703–7. https://doi.org/10.1161/01.CIR.0000030995.59403.F8.
16. Gatzoulis MA, Balaji S, Webber SA, et al. Risk factors for arrhythmia and sudden cardiac death late after repair of tetralogy of Fallot: a multicentre study. Lancet. 2000;356(9234):975–81. https://doi.org/10.1016/S0140-6736(00)02714-8.
17. Nollert GDA, Däbritz SH, Schmoeckel M, Vicol C, Reichart B. Risk factors for sudden death after repair of tetralogy of Fallot. Ann Thorac Surg. 2003;76(6):1901–5. https://doi.org/10.1016/S0003-4975(03)01065-8.
18. Gatzoulis MA, Till JA, Somerville J, Redington AN. Mechanoelectrical interaction in tetralogy of Fallot: QRS prolongation relates to right ventricular size and predicts malignant ventricular arrhythmias and sudden death. Circulation. 1995;92(2):231–7. https://doi.org/10.1161/01.CIR.92.2.231.
19. Khairy P, Landzberg MJ, Gatzoulis MA, et al. Value of programmed ventricular stimulation after tetralogy of Fallot repair: a multicenter study. Circulation. 2004;109(16):1994–2000. https://doi.org/10.1161/01.CIR.0000126495.11040.BD.
20. Babu-Narayan SV, Kilner PJ, Li W, et al. Ventricular fibrosis suggested by cardiovascular magnetic resonance in adults with repaired tetralogy of Fallot and its relationship to adverse markers of clinical outcome. Circulation. 2015;113(3):405–14. https://doi.org/10.1161/CIRCULATIONAHA.105.548727.
21. Ghai A, Silversides C, Harris L, Webb GD, Siu SC, Therrien J. Left ventricular dysfunction is a risk factor for sudden cardiac death in adults late after repair of tetralogy of Fallot. J Am Coll Cardiol. 2002;40(9):1675–80. https://doi.org/10.1016/S0735-1097(02)02344-6.
22. Oechslin E, Buchholz S, Jenni R. Ebstein's anomaly in adults: Doppler-echocardiographic evaluation. Thorac Cardiovasc Surg. 2000;48(4):209–13. https://doi.org/10.1055/s-2000-6900.
23. Nihoyannopoulos P, McKenna WJ, Smith G, Foale R. Echocardiographic assessment of the right ventricle in Ebstein's anomaly: relation to clinical outcome. J Am Coll Cardiol. 1986;8(3):627–35. https://doi.org/10.1016/S0735-1097(86)80193-0.
24. Chauvaud S, Berrebi A, D'Attellis N, Mousseaux E, Hernigou A, Carpentier A. Ebstein's anomaly: repair based on functional analysis. Eur J Cardiothorac Surg. 2003;23:525–31. https://doi.org/10.1016/S1010-7940(02)00836-9.
25. Mahle WT, Parks WJ, Fyfe DA, Sallee D. Tricuspid regurgitation in patients with repaired tetralogy of Fallot and its relation to right ventricular dilatation. Am J Cardiol. 2003;92(5):643–5. https://doi.org/10.1016/S0002-9149(03)00746-X.
26. Conte S, Jashari R, Eyskens B, Gewillig M, Dumoulin M, Daenen W. Homograft valve insertion for pulmonary regurgitation late after valveless repair of right ventricular outflow tract obstruction. Eur J Cardiothorac Surg. 1999;15(2):143–9. https://doi.org/10.1016/S1010-7940(98)00306-6.
27. Warnes CA. Adult congenital heart disease importance of the right ventricle. J Am Coll Cardiol. 2009;54(21):1903–10. https://doi.org/10.1016/j.jacc.2009.06.048.
28. Jarrar M, Betbout F, Farhat MB, et al. Long-term invasive and noninvasive results of percutaneous balloon pulmonary valvuloplasty in children, adolescents, and adults. Am Heart J. 1999;138(5):950–4. https://doi.org/10.1016/S0002-8703(99)70022-0.
29. Sadr-Ameli MA, Sheikholeslami F, Firoozi I, Azarnik H. Late results of balloon pulmonary valvuloplasty in adults. Am J Cardiol. 1998;82(3):398–400. https://doi.org/10.1016/S0002-9149(98)00302-6.
30. Lundstrom U, Bull C, Wyse RK, Somerville J. The natural and "unnatural" history of congenitally corrected transposition. Am J Cardiol. 1990;65(18):1222–9. https://doi.org/10.1016/0002-9149(90)90978-a.
31. Graham TP, Bernard YD, Mellen BG, et al. Long-term outcome in congenitally corrected transposition of the great arteries: a multi-institutional study. J Am Coll Cardiol. 2000;36(1):255–61. https://doi.org/10.1016/S0735-1097(00)00682-3.
32. Daliento L, Corrado D, Buja G, John N, Nava A, Thiene G. Rhythm and conduction disturbances in

isolated, congenitally corrected transposition of the great arteries. Am J Cardiol. 1986;58(3):314–8.
33. Prieto LR, Hordof AJ, Secic M, Rosenbaum MS, Gersony WM. Progressive tricuspid valve disease in patients with congenitally corrected transposition of the great arteries. Circulation. 1998;98(10):997–1005. https://doi.org/10.1161/01.CIR.98.10.997.
34. Roos-Hesselink JW, Meijboom FJ, Spitaels SEC, et al. Excellent survival and low incidence of arrhythmias, stroke and heart failure long-term after surgical ASD closure at young age: a prospective follow-up study of 21-33 years. Eur Heart J. 2003;24(2):190–7. https://doi.org/10.1016/S0195-668X(02)00383-4.
35. Lissin LW, Li W, Murphy DJ, et al. Comparison of transthoracic echocardiography versus cardiovascular magnetic resonance imaging for the assessment of ventricular function in adults after atrial switch procedures for complete transposition of the great arteries. Am J Cardiol. 2004;93(5):654–7. https://doi.org/10.1016/j.amjcard.2003.11.044.

Primary and Secondary Pulmonary Hypertension

15

Carmen Ginghină and Roxana Enache

Abstract

Pulmonary hypertension (PH) is a complex syndrome that may complicate different cardiovascular, respiratory and systemic disorders. Once considered an orphan disease, currently things have changed in recent years due to major progress seen towards the understanding of this multidisciplinary disorder. PH is defined as an increase in mean pulmonary artery pressure (PAP) ≥25 mmHg at rest as measured invasively by right heart catheterization (RHC). According to common pathophysiological and therapeutic characteristics, 5 clinical groups of PH are defined. Pulmonary arterial hypertension (PAH) or group 1 of PH includes idiopathic and heritable PAH, PAH associated with connective tissue disorders, congenital heart diseases, toxins and drugs, HIV infection and portal hypertension. The common feature of these PH forms is involvement of the distal pulmonary arteries. In PH, the right ventricle (RV) adapts to a dual pressure overload composed by the fixed pulmonary vascular resistance and the pulsatile pressure overload due to pulmonary artery stiffness. RV function is the main determinant of the outcome in PH patients. Based on clinical suspicion or screening of high risk populations, transthoracic echocardiography establishes the probability of PH while the RHC is mandatory to confirm the diagnosis, to assess the severity of haemodynamic impairment and to perform pulmonary vasoreactivity testing in selected PAH patients and to assess the response to PAH treatment or confirm disease worsening. Other diagnostic tools are useful to identify the different forms of PAH and PH and to test the exercise capacity of the patients. Treatment of PAH has evolved considerably over the past 30 years, in part due to the advances in knowledge of the disease and the availability of drugs that target known pathways in the disease pathobiology. Despite this real progress, PAH remains a chronic progressive disorder. Current therapeutic approaches are medical therapy, interventional and surgical procedures.

Keywords

Pulmonary hypertension · Right ventricular function · Pulmonary vasodilator therapy

C. Ginghină (✉) · R. Enache
Carol Davila University of Medicine and Pharmacy, Bucharest, Romania

Department of Cardiology, "Prof. C.C. Iliescu" Emergency Institute for Cardiovascular Diseases, Bucharest, Romania

Pulmonary hypertension (PH) is a complex syndrome that may complicate various cardiovascular, respiratory and systemic disorders.

S. I. Dumitrescu et al. (eds.), *Right Heart Pathology*, https://doi.org/10.1007/978-3-319-73764-5_15

Once considered an orphan disease, currently things have changed due to major progress of recent years seen towards the understanding of this complex and multidisciplinary disorder.

15.1 Definition and Classifications

PH is defined as an increase in mean pulmonary artery pressure (PAP) ≥25 mmHg at rest as measured invasively by right heart catheterization [1], since normal values of mean PAP in the general population are 14 ± 3 mmHg, with an upper limit of the normal range of 21 mmHg at rest [2].

The term primary PH was used to define an idiopathic increase in pulmonary vascular pressure while secondary PH was employed for all the forms of PH in which an underlying cause could be identified. Nowadays, according to common pathophysiological and therapeutic characteristics, the current guidelines on the management of PH define 5 clinical groups of PH (Table 15.1).

Pulmonary arterial hypertension (PAH) or group 1 of PH requires an increase in mean PAP ≥25 mmHg, a normal pulmonary arterial wedge pressure (PAWP) ≤15 mmHg and high pulmonary vascular resistance (PVR) ≥3 Wood units [1].

Besides the clinical classification of PH, of great clinical use is the functional classification, an adaptation of the NYHA classification of heart failure, which allows grading the clinical severity of this disorder (Table 15.2).

Table 15.1 Clinical classification of pulmonary hypertension (adapted from [1])

1. Pulmonary arterial hypertension
1.1. Idiopathic
1.2. Heritable
1.2.1. *BMPR2* mutation
1.2.2. Other mutations (*ACVRL-1, ENG, SMAD9, CAV1, KCNK3*)
1.3. Drugs and toxins induced
1.4. Associated with:
1.4.1. Connective tissue disease
1.4.2. Human immunodeficiency virus infection
1.4.3. Portal hypertension
1.4.4. Congenital heart disease
1.4.5. Schistosomiasis
1′. Pulmonary veno-occlusive disease and/or pulmonary capillary haemangiomatosis
1′.1. Idiopathic
1′.2. Heritable
1′.2.1. Mutația *EIF2AK4*
1′.2.2. Alte mutații
1′.3. Drugs, toxins and radiation induced
1′.4. Associated with:
1′.4.1. Connective tissue disease
1′.4.2. Human immunodeficiency virus infection
1″. Persistent pulmonary hypertension of the newborn
2. Pulmonary hypertension due to left heart disease
2.1. Left ventricular systolic dysfunction
2.2. Left ventricular diastolic dysfunction
2.3. Left valvular heart disease
2.4. Congenital/acquired left heart inflow/outflow tract obstruction and congenital cardiomyopathies
2.5. Congenital/acquired pulmonary veins stenosis
3. Pulmonary hypertension due to lung diseases and/or hypoxia
3.1. Chronic obstructive pulmonary disease
3.2. Interstitial lung disease
3.3. Other pulmonary diseases with mixed restrictive and obstructive pattern
3.4. Sleep-disordered breathing
3.5. Alveolar hypoventilation disorders
3.6. Chronic exposure to high altitude
3.7. Developemental lung diseases
4. Chronic thromboembolic pulmonary hypertension and other pulmonary artery obstructions
4.1. Chronic thromboembolic pulmonary hypertension
4.2. Other pulmonary artery obstructions
4.2.1. Angiosarcoma
4.2.2. Other intravascular tumors
4.2.3. Arteritis
4.2.4. Congenital pulmonary arteries stenoses
4.2.5. Parasites (hydatidosis)
5. Pulmonary hypertension with unclear and/or multifactorial mechanisms
5.1. Haematological disorders: chronic haemolytic anaemia, myeloproliferative disorders, splenectomy
5.2. Systemic disorders, sarcoidosis, pulmonary histiocytosis, lymphangioleiomyomatosis
5.3. Metabolic disorders: glycogen storage disease, Gaucher disease, thyroid disorders
5.4. Others: pulmonary tumoral thrombotic microangiopathy, fibrosing mediastinitis, chronic renal failure (with/without dialysis), segmental pulmonary hypertension

Table 15.2 Functional classification of pulmonary hypertension modified after the New York Heart Association (NYHA) functional classification of heart failure according to the World Health Organization (WHO) [3]

WHO class	Definition
I	Patients with pulmonary hypertension but without resulting limitation of physical activity. Ordinary physical activity does not cause undue dyspnoea or fatigue, chest pain or near syncope
II	Patients with pulmonary hypertension resulting in slight limitation of physical activity. They are comfortable at rest. Ordinary physical activity causes undue dyspnoea or fatigue, chest pain or near syncope
III	Patients with pulmonary hypertension resulting in marked limitation of physical activity. They are comfortable at rest. Less than ordinary activity causes undue dyspnoea or fatigue, chest pain or near syncope
IV	Patients with pulmonary hypertension with inability to carry out any physical activity without symptoms. These patients manifest signs of right heart failure. Dyspnoea and/or fatigue may even be present at rest. Discomfort is increased by any physical activity

A third classification of PH reflects the variability of haemodynamic parameters (PVR, PAWP) in PH. According to this haemodynamic classification, PH may be defined as:

- *Pre-capillary PH*: mean PAP ≥25 mmHg and PAWP ≤15 mmHg. This haemodynamic profile is found in clinical groups 1, 3, 4, 5 [1].
- *Post-capillary PH*: mean PAP ≥25 mmHg and PAWP >15 mmHg. This haemodynamic profile is found in clinical groups 2 and 5. According to the diastolic pressure gradient (DPG, the difference between the diastolic PAP and the mean PAWP), post-capillary PH is defined as *isolated post-capillary PH* (DPG <7 mmHg and/or PVR ≤3 Wood units) or *combined post-capillary and pre-capillary PH* (DPG ≥7 mmHg and/or PVR >3 Wood units) [1].

15.2 Epidemiology, Genetics and Risk Factors

The reported incidence of PAH in developed countries is 1.1–7.6 cases per million adults per year, and the prevalence is 6.6–26 cases per million adults [4]. For Europe, the prevalence and incidence of PAH is 15 cases per million adults and 2.4 cases per million adults per year, while the prevalence of idiopathic PAH is 5.9 cases per million adults [1]. The ratio females:males is 1.7–3.5 but the survival rates are greater in female patients [4]. While the first American Registry on PAH reported a mean age of 36 years for the patients with idiopathic PAH, the current registries data report a mean age of 50–65 years at diagnosis [1, 4]. Most American and European registries report idiopathic PAH as the most common type of PAH (50–60% of all cases), followed by PAH associated to connective tissue disease, congenital heart disease and porto-pulmonary PAH [4]. PH due to left heart disease is found in 60% of patients with left ventricular severe systolic dysfunction, in 70% of patients with left ventricular diastolic dysfunction, in all patients with severe symptomatic mitral valve disease and in 65% of patients with severe symptomatic aortic stenosis [1]. The prevalence of PH in advanced stages of chronic obstructive pulmonary disease is increased (18–50%) but the PAP values are not very high, while in interstitial fibrosis is 32–39% [1, 4]. The incidence of chronic thromboembolic pulmonary hypertension (CTEPH) is 3–30 cases per million general population per year [5], and 0.5–2% of patients with an episode of acute pulmonary embolism develop CTEPH [1].

Idiopathic PAH occurs predominantly as sporadic cases, without known history of familial cases of PAH or risk factors. The prevalence of heritable PAH is between 6% and 10%, most cases (75%) occur due to a mutation in *BMPR2 (bone morphogenetic protein receptor 2)* gene that encodes a type 2 receptor (BMPR2) belonging to the TGF-β receptor superfamily. The BMPR2 receptor is involved in the regulation of growth, differentiation, and apoptosis of pulmonary artery endothelial and smooth muscle cells [6, 7]. Over 300 independent *BMPR2* mutations were identified in familial cases of PAH but also in 25% of sporadic cases of PAH [6]. Heritable PAH affects twice as many females as males. Also, *BMPR2* mutation carriers are younger at the time of diagnosis of PAH and have more severe haemodynamic compromise (higher

mean PAP, lower cardiac output, higher PVR, and a lower likelihood of having an acute vasodilator component). Therefore *BMPR2* mutation carriers are more likely to die sooner or to undergo transplantation than patients with idiopathic PAH [6]. A personal or familial history of hereditary hemorrhagic telangiectasia in patients with PAH led to the identification of other genes involved in the development of PAH: activin A receptor type II–like kinase 1 (*ACVRL1* or *ALK1*) and endoglin (*ENG*). Furthermore, mutations in other genes (i.e., *BMPR1B*, *CAV1*, *SMAD9* and *KCNK3*) have been identified but are less common (5% of cases) [1, 6]. Approximately 20% of families with heritable PAH have no detectable known mutation [8].

In patients with pulmonary veno-occlusive disease (PVOD)/pulmonary capillary haemangiomatosis (PCH) other heritable forms of PH have been described. Recessive mutations in *EIF2AK4* gene that encodes a serine-threonine kinase which can induce changes in gene expression in response to amino acid deprivation were detected in all families with PVOD studied in the French National Registry and in 5 of 20 histologically confirmed sporadic cases of PVOD/PCH [9].

A number of drugs and toxins have been identified as risk factors for the development of PAH and they were categorized according to the strength of evidence, as definite, likely, possible, or unlikely [8]. Table 15.3 displays the risk factors currently associated with PAH development.

15.3 Pathology and Pathobiology of Pulmonary Circulation and Adaptive Mechanisms of the Right Ventricle

Due to the heterogeneity of PH forms, different pathologic features characterize the diverse clinical groups. In PAH the disease affects mainly the distal pulmonary arteries (≤500 μm in diameter) and the characteristic lesions are medial hypertrophy, intimal proliferation and fibrosis, adventitial thickening with moderate perivascular inflammatory infiltrates, plexiform and dilation lesions and thrombotic lesions [10]. In PVOD, the septal veins and preseptal venules are involved and exhibit occlusive fibrotic lesions, venous muscularization, patchy capillary proliferation, pulmonary edema, occult alveolar hemorrhage, lymphatic dilation with lymph node enlargement, and inflammatory infiltrates and also the distal pulmonary arteries are affected by medial hypertrophy, intimal fibrosis, and uncommon complex lesions [10].

In PH due to left heart disease, the pathologic features are enlarged and thickened pulmonary veins, dilated capillaries, interstitial edema, alveolar hemorrhage, and enlargement of the lymphatic vessels and lymph nodes. The distal pulmonary arteries may also be involved with medial hypertrophy and intimal fibrosis. In PH due to lung diseases and/or hypoxia, medial hypertrophy and intimal obstructive proliferation of the distal pulmonary arteries are observed. In CTEPH, organized thrombi are attached to the medial layer in the elastic pulmonary arteries and replace the normal intima and may occlude the lumen or form different grades of stenosis, webs, and bands. In non-occluded areas, a pul-

Table 15.3 Risk factors for drugs and toxin-induced pulmonary arterial hypertension (adapted from [3])

1. Definite	2. Likely	3. Possible
Aminorex	Amphetamines	Cocaine
Fenfluramină	Dasatinib	Phenylpropanolamine
Dexfenfluramină	L-tryptophan	St. John's Wort
Toxic rapeseed oil	Methamphetamines	Amphetamine-like drugs
Benfluorex Selective serotonin reuptake inhibitors		Interferon α and β Chemotherapeutic agents (mytomycine C, cyclophosphamide)

monary arteriopathy similar to that of PAH is found. Collateral arteries from the systemic circulation (from bronchial, costal, diaphragmatic, and coronary arteries) can develop and perfuse the areas distal to complete occlusions [10].

In PH there is an imbalance in vasoconstriction and vasodilation, thrombosis, and cell proliferation and remodeling of pulmonary arterial wall that contributes to increased PVR. Pulmonary vascular remodeling involves the three layers of small arteries (intima, media, adventitia) and all cell types (endothelial, smooth muscle, and fibroblast), as well as inflammatory cells and platelets. Excessive pulmonary vasoconstriction is due to an abnormal function or expression of potassium channels and to endothelial dysfunction. Endothelial dysfunction is characterized by impaired production of vasodilators such as nitric oxide (NO) and prostacyclin, along with overexpression of vasoconstrictors such as endothelin-1. Recent research showed the role of other mediators such as angiopoietins, serotonin, bone morphogenetic proteins (BMPs), and growth factors (platelet-derived growth factor [PDGF], fibroblast growth factor [FGF], epidermal growth factor [EGF], and the transforming growth factor-beta [TGF-β] superfamily) in the PH pathobiology. Abnormal proteolysis of the extracellular matrix, autoimmunity, inflammation, altered metabolism and mitochondrial function seem also involved in pulmonary vascular remodeling in PH [11].

In PH, the right ventricle (RV) has to adapt to a dual pressure overload composed by the fixed pulmonary vascular resistance and the pulsatile pressure overload due to the pulmonary artery stiffness. The RV adapts to the pressure overload by an increase in wall thickness. Initially, the RV hypertrophy maintains a normal wall stress due to the Laplace law and also a normal performance of RV with a normal cardiac output at rest. In time, this adaptive mechanism fails and RV dilation and contractile dysfunction occur with a supplemental increase in wall stress and RV hypertrophy. RV myocardial ischemia may develop due to an increase in wall pressure and a decrease in the right coronary artery perfusion. Thus, the RV adaptation and remodeling in PH is a complex process influenced not only by the severity of pulmonary vasculopathy but also by the interaction between the neurohormonal activation, the coronary perfusion and the myocardial metabolism. Also, the time of PH onset, the underlying PH etiology and genetic factors may also impact this process. There are two forms of RV remodeling in PH based on the above-mentioned factors: adaptive RV remodeling with a concentric hypertrophy and preserved systolic and diastolic function (seen in patients with Eisenmenger syndrome) and maladaptive RV remodeling with eccentric hypertrophy and systolic and diastolic dysfunction (seen in patients with idiopathic PAH or PAH associated with connective tissue disease) [12]. The concept of ventriculo-arterial coupling, meaning the enhancing in RV contractility in order to maintain flow in the presence of an increased vascular load, is essential in understanding the RV pathophysiology in PH. Due to ventriculo-arterial coupling the stroke volume changes little while preserving ventricular efficiency. In time, RV dilation occurs in an attempt to limit the reduction in stroke volume and to maintain RV contractility. Consequently, increased wall stress, leftward septal bowing and impaired RV and left ventricular function occur. In the final stages of the disease, ventriculo-arterial uncoupling induces high metabolic demand and reduced cardiac output [13].

15.4 Diagnosis

Clinical Presentation The onset of *symptoms* may be insidious in PH, delaying the moment of diagnosis with more than 2 years [14]. The most common symptom is exertional dyspnoea that is progressive to resting dyspnoea. A reduced exercise capacity, fatigue, weakness, lightheadedness and dry cough occur in the first stages of the disease, while in the advanced stages patients may experience exertional syncope due to the RV inability of increasing the cardiac output during exertion and exertional angina due to functional

ischemia of the RV, dilation of the pulmonary artery during effort or extrinsic compression of the left main coronary artery by the dilated pulmonary trunk [1, 15]. Also, in the advanced stages symptoms of right heart failure occur with abdominal distention and lower extremity edema. Other symptoms are haemoptysis related to rupture of hypertrophied bronchial arteries, hoarseness due to the compression of the left recurrent laryngeal nerve, wheeze caused by large airway compression. Significant dilation of the pulmonary artery may result in its rupture or dissection, leading to signs and symptoms of cardiac tamponade [1].

The *physical examination* can be nonspecific or may reveal typical PH signs: accentuated pulmonary component and/or split S_2, early systolic click and midsystolic ejection murmur in the pulmonary area, left parasternal lift, right ventricular S_4. In more advanced cases, there are signs of severe PH, such as holosystolic murmur of tricuspid regurgitation, diastolic murmur of pulmonary regurgitation, increased jugular v waves, pulsatile liver and hepatojugular reflux and signs of RV failure, such as right ventricular S_3, distension of jugular veins, hepatomegaly, peripheral edema, ascites, low blood pressure, cool extremities. Crackles are usually absent [1].

The clinical examination may suggest a possible underlying cause of PH. Central cyanosis and clubbing indicate a congenital heart disease or hypoxemia, intrapulmonary shunt, POVD. Systolic and diastolic murmurs of the left heart may reveal a left heart disease. Telangiectasia, digital ulceration, sclerodactyly, Raynaud phenomenon are seen in scleroderma. Inspiratory crackles, protracted expiration, accessory musle use, productive cough may point towards interstitial lung disease and spider naevi, testicular atrophy, palmar erythema, icterus, ascites suggest liver disease [1].

Electrocardiogram may be normal but usually suggests right heart involvement with right atrial enlargement, right-axis deviation, and right ventricular hypertrophy (Fig. 15.1), often with a

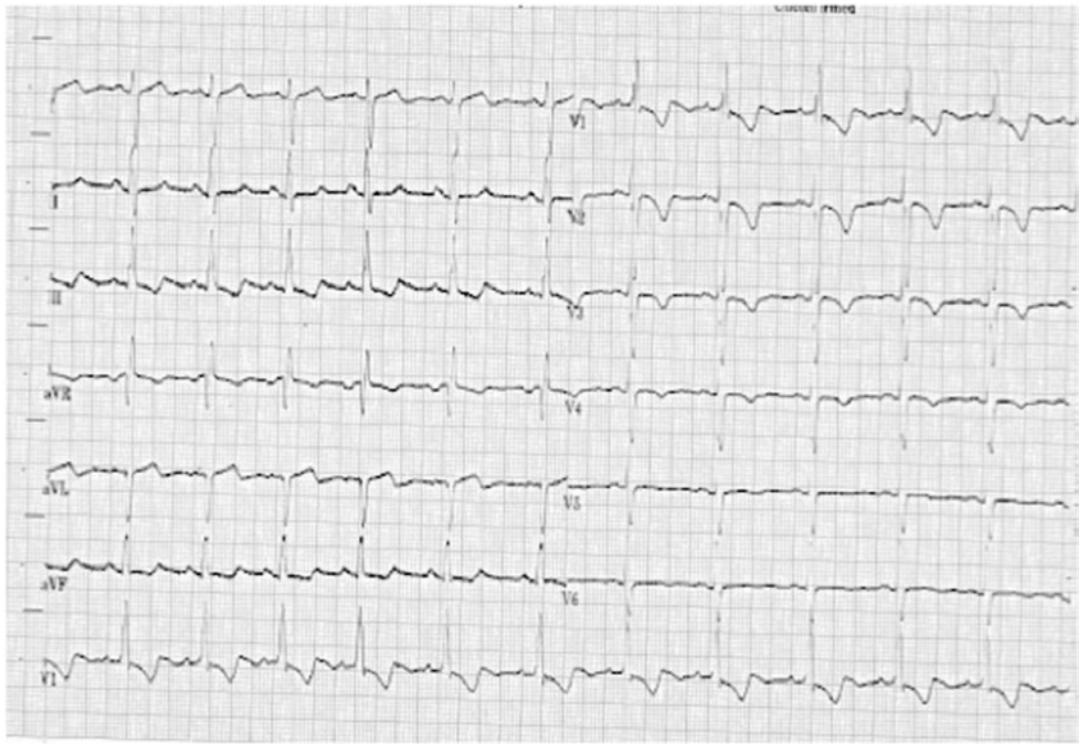

Fig. 15.1 Electrocardiogram of a patient with PAH: sinus rhythm, 73 bpm, QRS axis + 120°, incomplete right bundle branch block, right ventricular hypertrophy with inverted T waves in V1–V4, lead III and aVF

strain pattern, right bundle branch block, and QTc prolongation [1, 16]. Atrial arrhythmias (atrial flutter, atrial fibrillation) may be present in advanced disease.

Chest radiograph is abnormal in 90% of patients at the moment of diagnosis [14]. Chest X-ray reveals central pulmonary arterial dilatation (Fig. 15.2), which contrasts with 'pruning' (loss) of the peripheral blood vessels. Right atrium (RA) and RV enlargement may be seen in advanced cases. It is also useful in the diagnosis of PH due to left heart disease with pulmonary venous congestion and enlargement of the left heart or PH due to lung disease [1].

Transthoracic echocardiography is an essential investigation in patients with PH: it establishes the probability of PH in patients with clinical suspicion, it may reveal the PH etiology (congenital heart disease, left heart disease, CTEPH with thrombi in pulmonary artery trunk or its main branches), it evaluates the PH consequences on right chambers size, RV function and left ventricular function, it allows patients' follow-up with or without specific PH treatment. Also, echocardiography is a useful noninvasive screening tool in populations at risk of developing PH (scleroderma patients, relatives of patients with idiopathic PAH or PH mutation carriers).

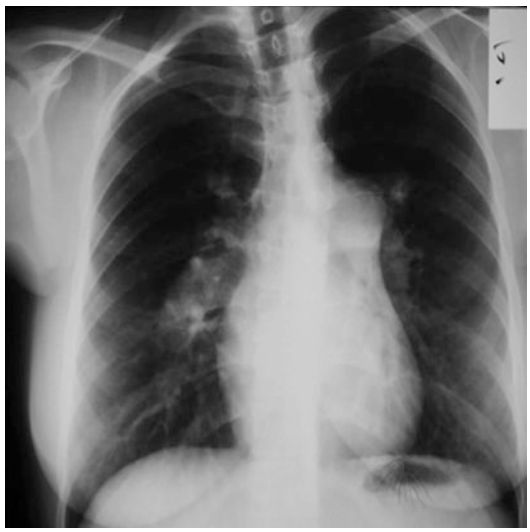

Fig. 15.2 Chest radiograph of a patient with PAH: enlarged main and hilar pulmonary artery shadows with attenuation of the peripheral vasculature and right chambers enlargement

Echocardiography offers an estimation of pulmonary artery pressures: systolic PAP based on the tricuspid regurgitation jet velocity (Fig. 15.3), mean and diastolic PAP based on the pulmonary regurgitation jet (Fig. 15.4), using the Bernoulli equation: RV-RA pressure gradient = 4 × (peak velocity)^2 and the estimation of right atrial pressure based on the dimensions and the respiratory variability of the inferior vena cava [17]. Also, an estimation of PVR using echocardiography is possible but the available formulas are applicable only for PVR less than 8 Wood units [17].

Echocardiography shows also indirect signs of PH presence: flattening of the interventricular septum with a D-shape left ventricle (LV), enlargement of the RV with a RV/LV ratio >1.0 at basal level (Fig. 15.5), enlarged pulmonary artery trunk (>25 mm), pulmonary regurgitation with an early diastolic velocity >2.2 m/s, RV outflow acceleration time > 105 ms and/or midsystolic notching (Fig. 15.6), enlargement of the RA (end-systolic area >18 cm^2), enlarged inferior vena cava (>21 mm) with decreased inspiratory collapse (<50% with a sniff) (Fig. 15.7). Considering the peak tricuspid regurgitation velocity and the presence of indirect signs of PH, the probability of PH can be establish using the echocardiography (Table 15.4) [1].

The presence of pericardial effusion revealed by echocardiography is a parameter of worse prognosis in PH patients. Echocardiography is also required for the assessment of parameters of systolic and diastolic RV function, these parameters and not PAP values being useful as prognostic factors in the follow-up of PH patients. Tricuspid annular plane systolic excursion (TAPSE), TDI-derived RV free-wall systolic velocity (S-wave), Tei index, RV fractional area change, RV isovolumic acceleration, RV free-wall longitudinal strain as parameters of RV systolic function (Figs. 15.8, 15.9, and 15.10) and E/A ratio at tricuspid level, RV free-wall e′ and E/e′ ratio as parameters of RV diastolic function are frequently used to assess RV function in clinical practice.

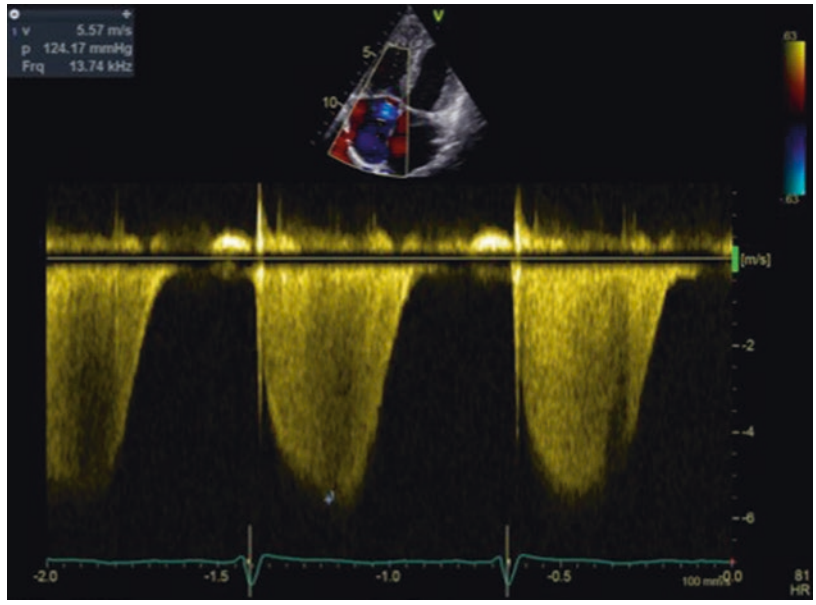

Fig. 15.3 Transthoracic echocardiography, apical 4-chambers view, continuous-wave Doppler examination at the level of tricuspid valve: a peak tricuspid regurgitation velocity of 5.57 m/s is measured, allowing an estimation of systolic PAP of 129 mmHg

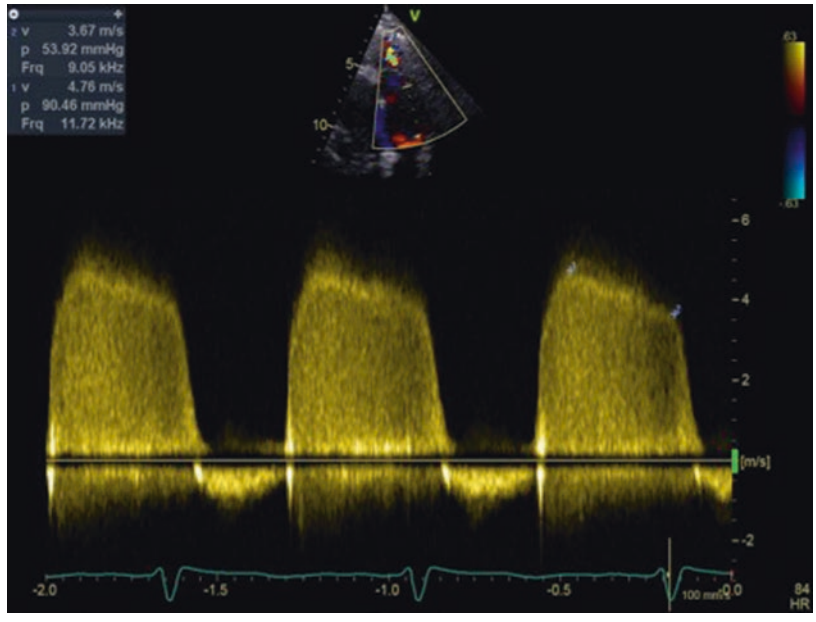

Fig. 15.4 Transthoracic echocardiography, parasternal short axis view, continuous-wave Doppler examination at the level of pulmonary valve: an early diastolic pulmonary regurgitation velocity of 4.76 m/s and an end-diastolic pulmonary regurgitation velocity of 3.67 m/s is measured, allowing an estimation of mean PAP of 96 mmHg and diastolic PAP of 59 mmHg

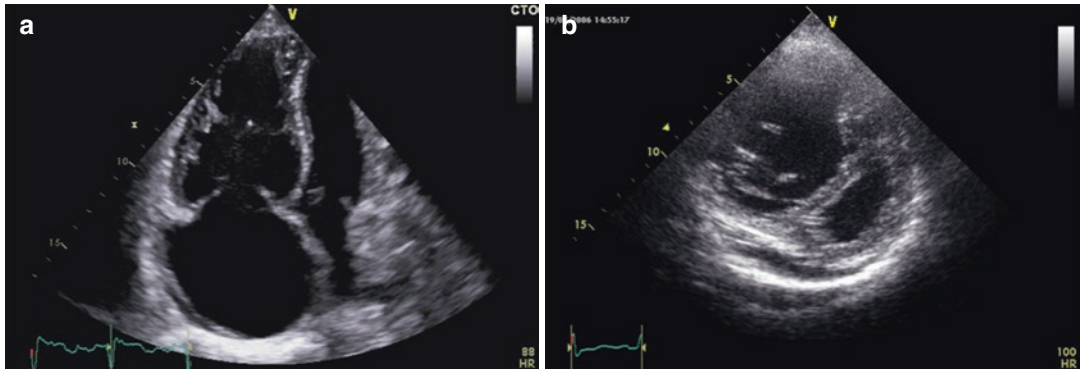

Fig. 15.5 Transthoracic echocardiography, 2D examination: indirect signs of pulmonary hypertension based on the ventricles with RV dilation an RV/LV ratio >1 in apical 4-chambers view (**a**) and flattening of the interventricular septum with left ventricular eccentricity index >1.1 in parasternal short axis view (**b**)

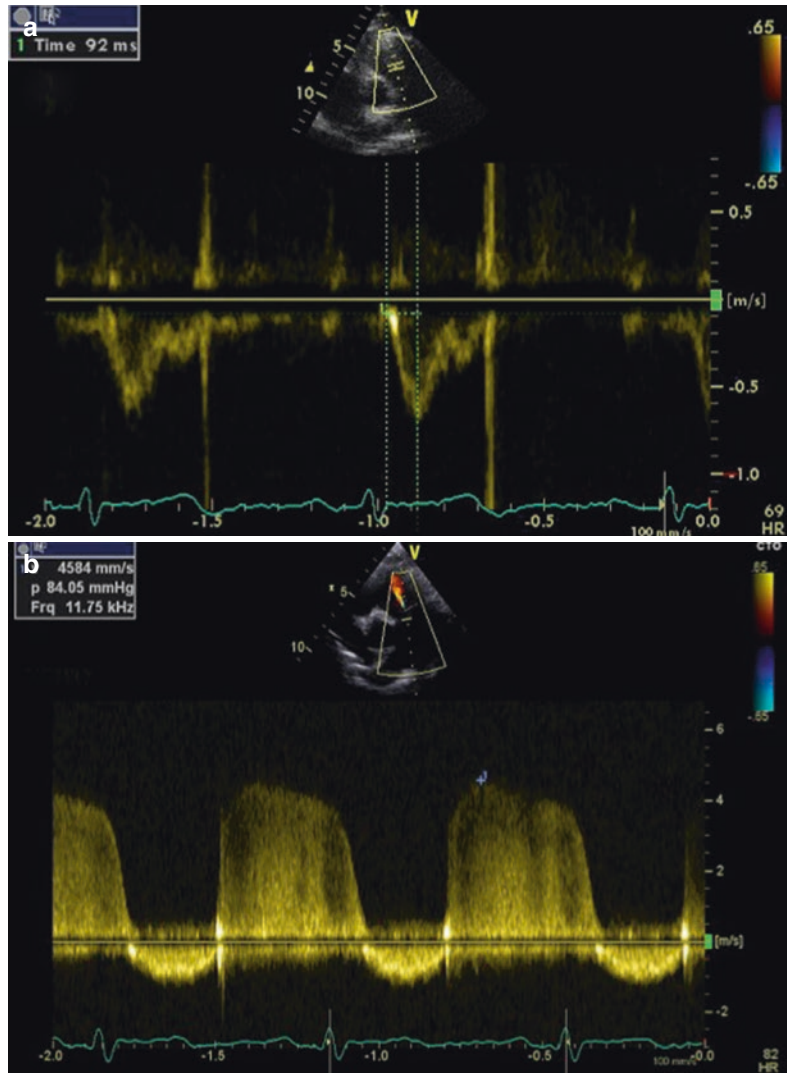

Fig. 15.6 Transthoracic echocardiography: indirect signs of pulmonary hypertension based on the pulmonary artery: short right ventricular outflow acceleration time (92 ms) and midsystolic notching (**a**), pulmonary regurgitation with early diastolic velocity of 4.5 m/s (**b**) and pulmonary trunk dilation of 52 mm (**c**)

Fig. 15.6 (continued)

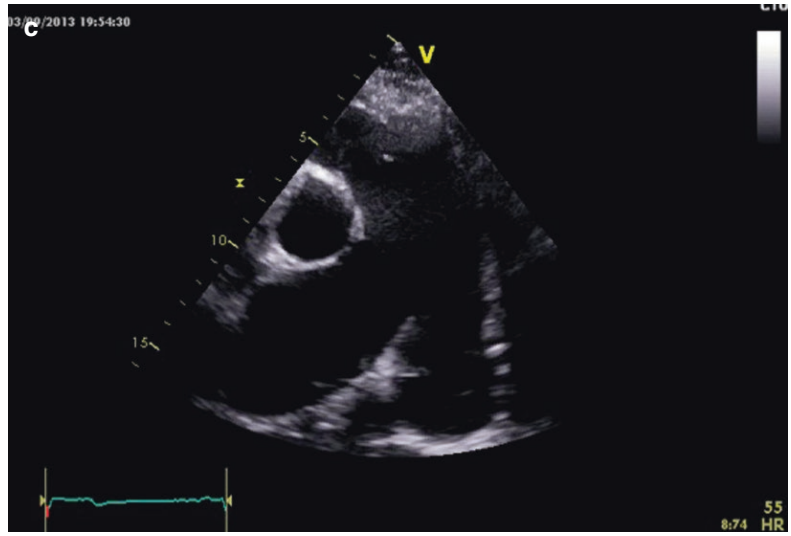

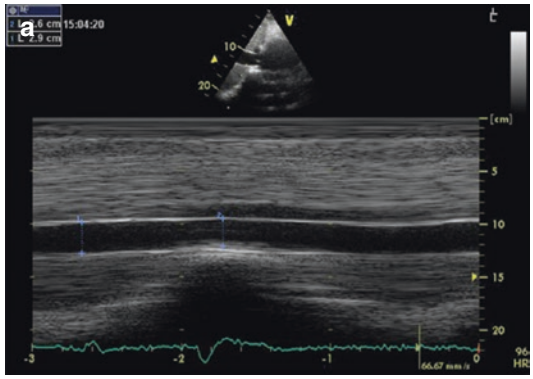

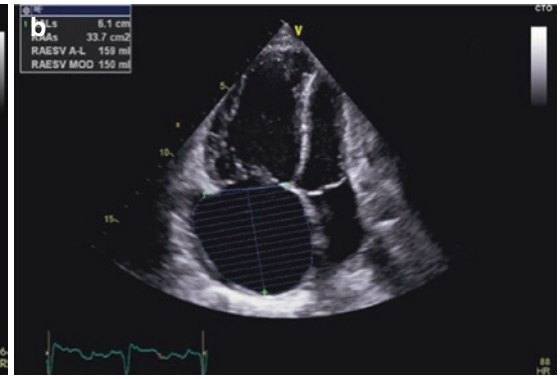

Fig. 15.7 Transthoracic echocardiography: indirect signs of pulmonary hypertension based on the right atrium (RA) and inferior vena cava (IVC): IVC dilation (29 mm) with decreased inspiratory collapse of 10% (**a**) și RA enlargement with end-systolic area of 33.7 cm^2 (**b**)

Table 15.4 Echocardiographic probability of pulmonary hypertension (adapted from [1])

Peak tricuspid regurgitation velocity	Indirect echo signs of PH[a]	Echocardiographic probability of PH
≤2.8 m/s or not measurable	No	Low
≤2.8 m/s or not measurable	Yes	Intermediate
2.9–3.4 m/s	No	
2.9–3.4 m/s	Yes	High
> 3.4 m/s	Not required	

[a]Indirect echo signs of PH are discussed in the text and illustrated in Figs. 15.5, 15.6, and 15.7. *PH* pulmonary hypertension

Ventilation/perfusion lung scan should be performed in all patients with PH as a screening test in order to exclude CTEPH as it is more sensitive than computed tomography pulmonary angiogram [18]. A normal or low-probability ventilation/perfusion scan excludes CTEPH with a sensitivity of 90–100% and a specificity of 94–100%. In PAH and also in PVOD the ventilation/perfusion scan may be normal or it may show small peripheral unmatched and non-segmental perfusion defects. When a ventilation/perfusion scan is not available, a recent chest radiograph or a high-resolution computed tomography of the lungs can be matched with a perfusion lung scan (Fig. 15.11) [1].

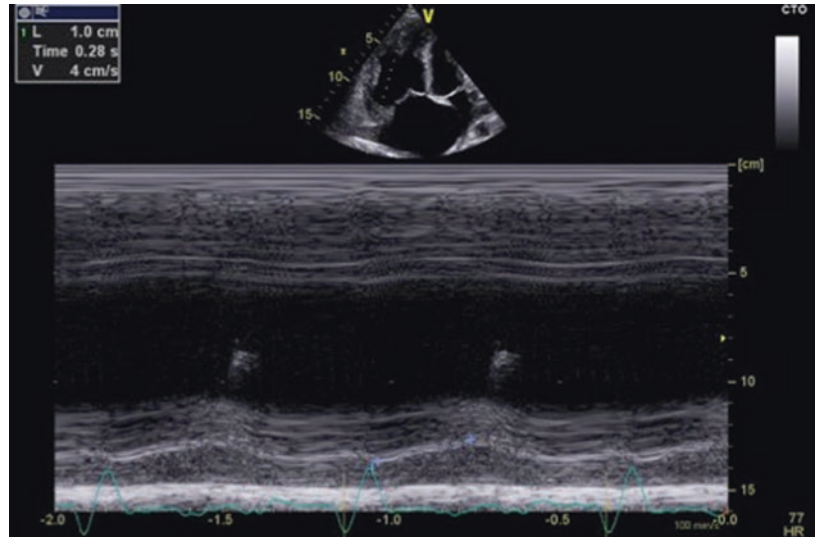

Fig. 15.8 Transthoracic echocardiography, apical 4-chambers view, mode M examination at the lateral tricuspid annulus: a decreased TAPSE (10 mm) is measured in a patient with PAH and severe RV global systolic dysfunction

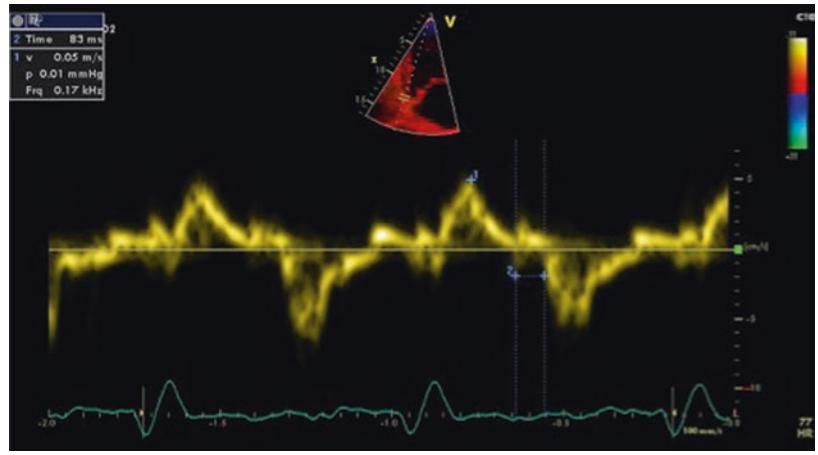

Fig. 15.9 Transthoracic echocardiography, apical 4-chambers view, tissue Doppler imaging at the lateral tricuspid annulus: there is longitudinal RV dysfunction in a patient with PAH and severe RV global systolic dysfunction (S wave 5 cm/s)

High-resolution computed tomography is an important tool in the assessment of patients with PH. It may suggest the presence of PH showing the enlargement of pulmonary artery or the right chambers, it identifies the underlying etiology of PH in lung diseases or CTEPH or it brings important information and supports the diagnosis when there is a clinical suspicion of PVOD (interstitial oedema with diffuse central groud-glass opacification and thickening of interlobular septa) or PCH (diffuse bilateral thickening of the interlobular septa and the presence of small, centrilobular, poorly circumscribed nodular opacities) [1]. However, ground-glass abnormalities are also present in PAH (Fig. 15.12), occurring in more than one-third of patients [19].

Pulmonary angiography is mandatory in CTEPH patients in order to identify those who would benefit from pulmonary endarterectomy or balloon pulmonary angioplasty [1].

Cardiac magnetic resonance imaging provides a very accurate assessment of RV size, morphology and function and allows non-invasive assessment of blood flow, including stroke volume, cardiac output, pulmonary artery distensibility [1]. It helps to define better congenital heart diseases when echocardiography is incomplete and it may diagnose CTEPH in patients with contraindication to CT examination. Also, CMR provides prognostic information in PAH patients: a RV end-diastolic volume index lower than 84 mL/m^2, a LV end-diastolic volume

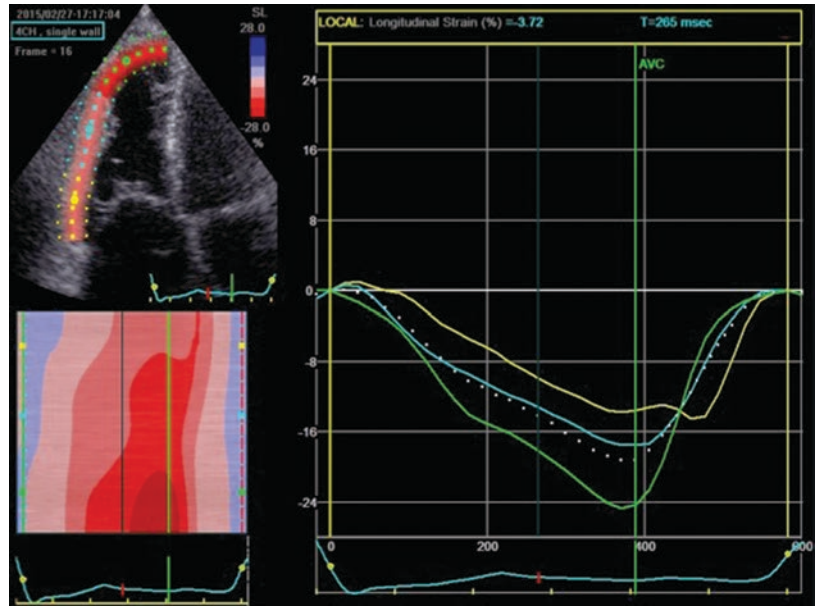

Fig. 15.10 Transthoracic echocardiography, apical 4-chambers view, speckle-tracking examination: a RV free-wall strain of −19% is measured in a patient with PAH and mild RV systolic dysfunction

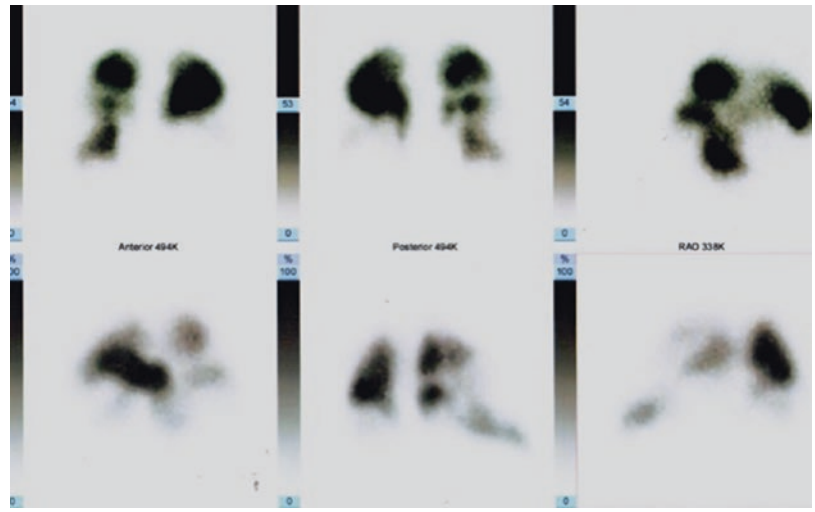

Fig. 15.11 Perfusion lung scan in a patient with proximal CTEPH: perfusion defects are observed in the middle and inferior right lobes and in the entire inferior left lobe

index higher than 40 mL/m^2, and a stroke volume index higher than 25 mL/m^2 are associated with better survival in patients with idiopathic PAH [20]. A RV ejection fraction lower than 35% on CMR is also predictive of mortality [21].

Pulmonary function tests and arterial blood gases are useful to assess for obstructive or restrictive lung disease. Patients with PAH may have mild restriction and mildly reduced diffusion capacity of carbon monoxide (DLCO). A severely decreased DLCO is associated with a poor outcome. A severely decreased DLCO requires the differential diagnosis with scleroderma- associated PAH, PVOD or interstitial lung diseases [1].

Blood tests and immunology studies are required to screen for connective tissue diseases, HIV disease, and liver disease in the diagnostic

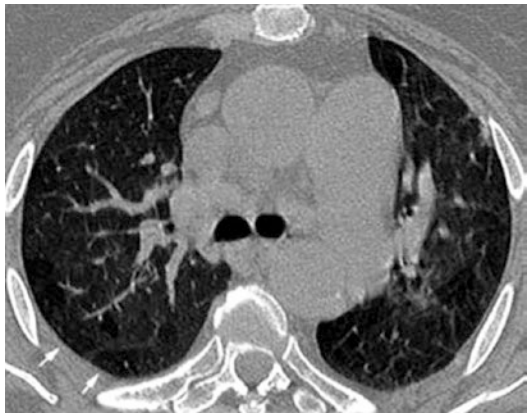

Fig. 15.12 High-resolution computed tomography in a patient with PAH: enlargement of the pulmonary artery and ground-glass abnormalities are observed

evaluation. Patients with CTEPH should undergo thrombophilia screening [1]. Brain natriuretic peptide (BNP) and N-terminal pro-brain natriuretic peptide (NT-proBNP) may be elevated in patients with PH and these biomarkers are independent risk predictors in these patients.

Other investigations such as *abdominal ultrasound* and *overnight oximetry* are useful in establishing the etiology of certain forms of PH.

Functional assessment is useful to establish the exercise capacity in patients with PH. *The 6-minute walk test (6MWT)*, a test easy to perform, inexpensive and familiar to patients, it is a useful prognostic tool and an important parameter in the clinical assessment of disease progression and treatment effect. The 6MW distance has been the primary endpoint of almost every clinical trial involving PAH to date; at present, it remains useful in the longitudinal assessment of the individual patient. *Cardiopulmonary exercise testing (CPET)* provides information on exercise capacity, gas exchange, ventilator efficacy and cardiac function during exercise. Patients with PAH show a typical pattern with a low end-tidal partial pressure of carbon dioxide (pCO_2), high ventilator equivalents for carbon dioxide (VE/VCO_2), low oxygen pulse (VO_2/HR) and low peak oxygen uptake (peak VO_2). Several variables determined by CPET provide prognostic information, although peak VO_2 is most widely used for therapeutic decision [1, 22].

Right heart catheterization (RHC) is mandatory to confirm the diagnosis of PAH and CTEPH, to assess the severity of haemodynamic impairment and to perform pulmonary vasoreactivity testing in selected patients: patients with idiopathic PAH, heritable PAH and drugs and toxin-induced PAH [1]. RHC is also useful to assess the response to PAH treatment or to confirm disease worsening. In patients with PH group 2 or 3, RHC may assist in the differential diagnosis and the decision-making process, including the referral for organ transplantation. Besides confirming the presence of PH by measuring a mean PAP $\geq$25 mmHg, RHC allows various haemodynamic measurements such as PAP pressures, PAWP, RA pressure, RV pressures, cardiac output and cardiac index, PVR, calculated as (meanPAP-PAWP)/cardiac output, and total PVR, calculated as meanPAP/cardiac output, oxygen saturation. Measurement of PAWP is of most importance as it helps discriminate between pre-capillary PH forms that may benefit from specific treatment and post-capillary PH. It should be measured at end-expiration and in several different segments of the pulmonary vasculature. When PAWP measurement is inaccurate, measurement of LV end-diastolic by left heart catheterization is required in order to correctly classify a pre- or post-capillary PH. Sometimes the effect of an acute volume challenge on left heart filling pressures (e.g., a fluid bolus of 500 mL) may distinguish between PAH patients and patients with LV diastolic dysfunction in whom initial PAWP was reduced due to diuretic treatment [23].

Acute pulmonary vasoreactivity testing for identification of patients suitable for high-dose calcium channel blocker treatment is performed at the time of RHC using inhaled nitric oxide (NO) at 10–20 parts per million or, as alternatives, intravenous epoprostenol, intravenous adenosine or inhaled iloprost. A positive acute vasodilator response is defined as a reduction of

the mean PAP ≥10 mmHg to an absolute mean PAP value ≤40 mmHg with an increased or unchanged cardiac output. Only about 10% of patients with idiopathic PAH will meet these criteria and only a small percentage of these acute responders will maintain a long-term vasodilator response to calcium channel blockers. Vasoreactivity testing is not recommended in other types of PAH except for idiopathic PAH, heritable PAH and drugs-induced PAH nor in PH groups 2, 3, 4 and 5 [1].

Genetic testing and counseling should be offered to patients with sporadic PAH or PVOD/PCH, anorexigen-induced PAH and to patients with a family history of PAH or PVOD/PCH [1].

15.5 Prognostic Evaluation and Risk Assessment

During the 1980s, an American registry was established to study the natural history of patients with primary pulmonary hypertension (i.e., idiopathic PAH or heritable PAH) receiving no PAH-specific therapy. From this registry, a median survival of 2.8 years was reported in the overall population, with 1-, 3-, and 5-year survival rates of 68%, 48%, and 34%, respectively [14]. From the National Institutes of Health (NIH) registry dataset, a formula was developed to predict the mortality risk for idiopathic PAH or heritable PAH and anorexigen-associated PAH on the basis of 3 baseline haemodynamic parameters (mean PAP, mean RA pressure, and cardiac index) [24]. Many long-term studies have compared predicted survival on the basis of this formula to observed survival in various PAH populations, and in nearly every report, the comparison has favoured specific PAH therapy. Recent data from several contemporary PAH registries have suggested that survival estimates as predicted by the NIH formula may no longer be accurate in the current era of PAH specific therapy. In 247 patients with idiopathic, familial, and anorexigen-associated PAH from the Pulmonary Hypertension Connection registry (i.e., etiologies similar to those in the NIH model) who received various PAH treatments from 1991 to 2007, observed survival was significantly higher than NIH-predicted survival at 1 year (92% vs. 65%), 3 years (75% vs. 43%), and 5 years (66% vs. 32%), respectively. Another registry of 354 adults in France with idiopathic, familial, or anorexigen- associated PAH who received various PAH treatments also observed similar 1-, 3-, and 5-year survival rates (83%, 67%, and 58%, respectively), which were approximately 10% points higher than those predicted by the NIH formula [25]. Although none of the recent registry studies specifically examined the response to therapy as a predictor of survival, several developed new predictive models that include multiple risk factors known to be influenced by current medical therapy (e.g., 6MWD, B-type natriuretic peptide, hemodynamic parameters, WHO functional class). Therefore, specific PAH therapy should have a positive impact on survival in patients whose response to therapy places them in a better risk category for these models [25].

According to current guidelines, the evaluation of disease severity and the patients' outcomes using the 1-year mortality risk assessment before the initiation and during the PAH treatment is obtained by periodic follow-up of the patients at 3–6 months intervals and at every clinical worsening. In order to assess the risk of clinical worsening and/or mortality, a panel of clinical, functional, biological, echocardiographic and haemodynamic parameters with recognized prognostic value in patients with PAH is recommended (Table 15.5). According to these parameters, 1-year risk of mortality is established: less than 5% (low risk), 5–10% (intermediate risk) and more than 10% (high risk). Also, considering these predictive factors the treatment response is assessed: an adequate treatment response is defined by achievement/maintenance of a low-risk profile [1].

Table 15.5 One-year mortality risk assessment in pulmonary arterial hypertension [1]

Prognostic factors	Low risk <5%	Intermediate risk 5–10%	High risk >10%
Clinical signs of right heart failure	Absent	Absent	Present
Progression of symptoms	No	Slow	Rapid
Syncope	No	Occasional syncope	Repeated syncope
WHO functional class	I, II	III	IV
6-minute walk distance	>440 m	165–440 m	<165 m
Cardiopulmonary exercise testing	Peak VO_2 > 15 mL/min/kg (>65% predicted) VE/VCO_2 slope <36	Peak VO_2 11–15 mL/min/kg (35–65% predicted) VE/VCO_2 slope <36–44.9	Peak VO_2 < 11 mL/min/kg (<35% predicted) VE/VCO_2 slope ≥45
BNP/NT-proBNP plasma levels	BNP <50 ng/L NT-proBNP <300 ng/mL	BNP 50–300 ng/L NT-proBNP 300–1400 ng/mL	BNP >300 ng/L NT-proBNP >1400 ng/mL
Imaging (echocardiography, CMR imaging)	RA area <18 cm^2 No pericardial effusion	RA area 18–26 cm^2 No or minimal pericardial effusion	RA area >26 cm^2 Pericardial effusion
Haemodynamics	RAP <8 mmHg CI ≥2.5 L/min/m^2 S_vO_2 > 65%	RAP 8–14 mmHg CI 2.0–2.4 L/min/m^2 S_vO_2 60–65%	RAP >14 mmHg CI <2.0 L/min/m^2 S_vO_2 < 60%

BNP brain natriuretic peptide, *CI* cardiac index, *CMR* cardiac magnetic resonance, *NT-proBNP* N-terminal pro-brain natriuretic peptide, *RA* right atrium, *RAP* right atrial pressure, *SvO_2* mixed venous oxygen saturation, *VE/VCO_2* ventilatory equivalents for carbon dioxide, *VO_2* oxygen consumption, *WHO* World Health Organization

15.6 Treatment of Pulmonary Arterial Hypertension

Treatment of PAH has evolved considerably over the past three decades, in part due to the advances in knowledge of the disease and the availability of agents that target known pathways in the disease pathobiology. Despite this real progress, PAH remains a chronic progressive disorder. Current therapeutic approaches are medical therapy, interventional and surgical procedures.

General Measures *Education* of the patients and their family on the disease state is an important aspect in the care of patients with PAH. Low-level progressive *aerobic exercise* such as walking, cycling and swimming is recommended. Patients are advised against heavy physical exertion and isometric exercise due to the risk of exertional syncope. The benefits of cardiopulmonary rehabilitation with increased exercise tolerance, distance at 6MWT and quality of life have been demonstrated [26]. A *low sodium diet* is advised especially for the management of volume status in patients with right ventricular failure.

The haemodynamic fluctuations of pregnancy, labor, delivery, and the postpartum period are potentially life-threatening in patients with PAH, with a maternal mortality rate of 30–50% [7]. Accordingly, current guidelines recommendation is to avoid pregnancy in women with PAH [1] and effective birth control methods, especially barrier methods or progesterone-only preparations, should be discussed. A contemporary account of pregnancies in patients with PAH described 26 pregnancies at 13 PAH centers in women with well-controlled PAH, with three deaths, a case of refractory right-sided heart failure in one patient, who underwent heart-lung transplantation postpartum, two spontaneous and six induced abortions and an overall pregnancy success rate of 62% (a healthy baby without maternal complications) [27].

Routine immunizations, such as those against influenza and pneumococcal pneumonia, *supplemental O_2 during prolonged flights* in patients with

PAH in WHO functional class III and IV and those with arterial blood O_2 pressure consistently less than 8 kPa (60 mmHg), and *epidural anaesthesia* in the need of elective surgery are recommended [1].

Supportive Therapy *Oxygen supplementation* to keep saturation higher than 91% and arterial blood O_2 pressure more than 8 kPa (60 mmHg) is advisable [1]. This may not be possible in patients with intracardiac shunts (including a patent foramen ovale).

Diuretics are indicated to manage fluid overload in decompensated right heart failure, with close monitoring of serum electrolytes and renal function to avoid hypokalaemia and the effects of decreased intravascular volume leading to prerenal failure [1]. The risk of hypotension is not significant since the decreased cardiac output is mainly due to the high PVR and not due to the decreased vascular volume.

Digoxin is used to decrease the ventricular rate in patients with PAH who develop atrial tachyarrhythmias.

The rationale of using *oral anticoagulants* in PAH is the presence of vascular thrombotic lesions in the pulmonary vasculature, abnormalities in coagulation and fibrinolytic pathways and the risk factors for venous thromboembolism. Survival benefit of anticoagulants is confined to patients with idiopathic, heritable and anorexigens-induced PAH, but data supporting this evidence is from uncontrolled observational series, generally retrospective and single-centre. Data from registries and randomized controlled trials are inconclusive [28]. That is why current guidelines recommendation regarding oral anticoagulation in the above-mentioned types of PAH has a class IIb, level of evidence C indication. Little evidence is available on anticoagulation in patients with other forms of PAH, although most experts recommend oral anticoagulation in those with more advanced disease, such as patients receiving continuous intravenous therapy, in the absence of contraindications [1].

Iron deficiency has been reported in 43% of patients with idiopathic PAH, 46% of patients with scleroderma-associated PAH and 56% of patients with Eisenmenger syndrome and it should be treated in these patients, as it may be associated with reduced exercise capacity, and with a higher mortality, independent of the presence or severity of anaemia [1].

The use of angiotensin-converting enzyme inhibitors, angiotensin-2 receptor antagonists, beta-blockers and ivabradine is not recommended in patients with PAH unless required by comorbidities (i.e. systemic hypertension, coronary artery disease or left heart failure) [1].

Specific PAH Drug Therapy *Calcium channel blockers* are recommended in patients with idiopathic, heritable and anorexigens-induced PAH who demonstrate a favorable response to acute vasodilator testing. The rationale of using calcium channel blockers in PAH is the mechanism of action of this class of drugs which block the L-type calcium channels reducing the intracellular calcium and thus inducing vasodilation. The daily doses of these drugs that have shown efficacy in idiopathic PAH are relatively high: 120–240 mg for nifedipine, 240–720 mg for diltiazem and up to 20 mg for amlodipine. Because of its potential for negative inotropic effects, verapamil should be avoided. Patients with idiopathic PAH who meet the criteria for a positive acute vasodilator response and are treated with calcium channel blockers should be followed closely for reasons of both safety and efficacy, with a complete reassessment after 3–4 months of therapy including RHC. If the patient does not show an adequate response, defined as WHO functional class I or II with a marked haemodynamic improvement (near normalization), specific PAH therapy should be initiated. In some cases the combination of calcium channel blockers with the PAH drugs is required because of further clinical deterioration in the attempt of withdrawal of the calcium channel blocker [1]. As stated above, very few patients maintain a long-term response to this type of vasodilator therapy (less than 7% of patients with idiopathic PAH) [29].

Prostacyclin Analogues and Prostacyclin Receptor Agonists Administration of prostanoids which act on the prostacyclin I2 pathway in the pathophysiology of PAH has been a mainstay of

PAH therapy for almost two decades, due to the vasodilator and antiprofiferative effects of this class. Currently, multiple prostanoids are available: epoprostenol (continuous intravenous), treprostinil (continuous subcutaneous, continuous intravenous, intermittent inhaled, oral), iloprost (intermittent inhaled, continuous intravenous), beraprost (oral).

Epoprostenol was the first therapy approved for the indication of idiopathic PAH in 1995, randomized controlled clinical trials demonstrating improvements in exercise tolerance, haemodynamics, quality of life, and survival [30]. Observational series have also reported favorable effects of intravenous epoprostenol in patients with other forms of associated PAH. Epoprostenol must be delivered by continuous intravenous infusion and it is commonly started in the hospital at a dose of 2–4 ng/kg/min and titrated upward to 20–40 ng/kg/min, depending on the symptoms of PAH and the adverse effects of the therapy. Common side effects include jaw pain, flushing, nausea, diarrhea, rash, and musculoskeletal pain. Infections and interruptions in infusion with rebound symptoms can be life-threatening [1].

Treprostinil is a tricyclic benzidine analogue of epoprostenol stable at ambient temperature, thus allowing administration by intravenous and subcutaneous routes. The subcutaneous administration of treprostinil is accomplished by a microinfusion pump and a small subcutaneous catheter. The effects of subcutaneous treprostinil in PAH were assessed in a randomized controlled trial and showed improvements in exercise capacity, haemodynamics and symptoms [31]. Treatment with subcutaneous treprostinil is initiated at a dose of 1–2 ng/kg/min, with doses increasing at a rate limited by side effects (local site pain, flushing, headache). The optimal dose varies, ranging in the majority of patients between 20 ng/kg/min and 80 ng/kg/min [1]. Adverse effects have included pain and erythema at the site of the subcutaneous infusion in 85% of patients, leading to discontinuation of the treatment in 8% of cases on active drug and limiting dose. Other common side effects included headache, diarrhea, rash, and nausea. Based on bioequivalence data, treprostinil has also been approved to be delivered on a continuous intravenous basis. Also, a randomized controlled trial with inhaled treprostinil in PAH patients already on background therapy with either bosentan or sildenafil showed improvements in exercise capacity, NT-proBNP and quality of life measures [32].

Iloprost is a chemically stable prostacyclin analogue available for intravenous, oral or aerosol administration. Inhaled iloprost has been evaluated in one randomized controlled trial in which daily repetitive iloprost inhalations (6–9 times, 2.5–5 μg/inhalation, median 30 μg daily) were compared with placebo inhalation in patients with PAH and CTEPH and demonstrated an increase in exercise capacity and improvement in symptoms, PVR and clinical events [33]. Overall, inhaled iloprost was well tolerated, with flushing and jaw pain being the most frequent side effects. Continuous intravenous administration of iloprost appeared to be as effective as epoprostenol in a small series of patients with PAH and CTEPH. The effects of oral iloprost have not been assessed in PAH [1].

Beraprost is the first chemically stable and orally active prostacyclin analogue that have shown an improvement in exercise capacity for 3–6 months in randomized controlled trials but without haemodynamic improvements or long-term outcome benefits [1].

Selexipag is an orally available, selective prostacyclin IP receptor agonist which showed its clinical efficacity in an event-driven phase 3 randomized controlled trial that enrolled 1156 patients. In this trial selexipag in monotherapy or in combination therapy with endothelin receptor antagonists and/or phosphodiesterase type 5 inhibitors reduced by 39% a composite morbidity and mortality endpoint (including death from all causes, hospitalization for worsening of PAH, worsening of PAH) [34].

Endothelin Receptor Antagonists Endothelin-1 is a potent vasoconstrictor and smooth muscle mitogen that contributes to the pathogenesis of PAH. Three endothelin receptor antagonists, bosentan, ambrisentan, and macitentan, that act on the endothelin pathway in the treatment of PAH are currently available.

Bosentan is an oral active dual endothelin receptor type A and B antagonist and the first molecule of its class to be synthesized and it is available since 2001. This compound has been studied in multiple randomized placebo-controlled trials of idiopathic PAH, connective tissue disease-associated PAH and Eisenmenger syndrome which showed improvement in exercise capacity, functional class, haemodynamics, echocardiographic parameters and time to clinical worsening. Bosentan is currently used widely in patients with PAH, with dosing starting at 62.5 mg twice daily and increased to 125 mg twice daily. Increases in hepatic aminotransferases occurr in approximately 10% of the patients and are dose dependent and reversible after dose reduction or discontinuation. For these reasons, liver function testing is recommended monthly in patients receiving bosentan [1]. Other side effects include headache, anemia, and edema.

Ambrisentan is an endothelin receptor antagonist that preferentially binds with endothelin receptor type A that has been studied in two multicenter, randomized, placebo-controlled trials in 394 patients with PAH and demonstrated an improvement on symptoms, exercise capacity, haemodynamics and time to clinical worsening in patients with idiopathic PAH and PAH associated with connective tissue diseases and HIV infection [35]. Approved dose is 5 mg daily that may be increased to 10 mg daily. The incidence of abnormal liver function tests is less than with bosentan (0.8–3%). Other side effects of ambrisentan include headache and lower extremity edema [1].

Macitentan, a dual endothelin receptor antagonist, has been studied in a phase III long-term morbidity and mortality trial in which the primary endpoint was time to first occurrence of a composite endpoint of death, atrial septostomy, lung transplantation, initiation of treatment with parenteral prostanoids, or worsening PAH. 742 patients were randomly assigned to either placebo; macitentan, 3 mg; or macitentan, 10 mg daily. There was a 30% and 45% risk reduction in the primary endpoint with the 3-mg and 10-mg doses, respectively and also an increase in exercise capacity. The most frequent adverse events were headache, nasopharyngitis, and anemia. The incidence of edema and elevated liver function test results was similar in the placebo and macitentan groups [36].

Phosphodiesterase Type-5 (PDE5) Inhibitors The reduction in NO synthase in patients with PAH impacts the cyclic guanosine monophosphate (GMP) pathway. PDE5 inhibition has the potential to inhibit the hydrolysis of cyclic GMP and has proved to be an effective therapy for PAH.

Sildenafil is an orally active, potent and selective inhibitor of PDE5. Four randomized controlled trials in PAH patients treated with sildenafil have confirmed favorable results on exercise capacity, symptoms and/or haemodynamics. Sildenafil is currently approved at a dosage of 20 mg three times daily. More impressive hemodynamic improvements were achieved with higher doses, and some patients were treated with doses of up to 80 mg three times daily [37]. Most side effects of sildenafil are mild to moderate and mainly related to vasodilation (headache, flushing, epistaxis, dyspepsia, myalgia,).

Tadalafil is a once daily dispensed PDE5 inhibitor. It was studied in a multicenter, randomized, placebo-controlled trial in 406 patients treated with 2.5, 10, 20 or 40 mg once daily and demonstrated favorable results on exercise capacity, symptoms, haemodynamics and time to clinical worsening at the highest dose [38]. The side-effect profile was similar to that of sildenafil.

Vardenafil is a twice-daily dispensed PDE5 inhibitor that showed in 66 treatment-naive PAH patients treated with a dose of 5 mg twice daily favorable results on exercise capacity, haemodynamics and time to clinical worsening [39]. The side-effect profile was similar to that of sildenafil.

Soluble Guanylate Cyclase Stimulators Riociguat is a first-in-class agent that directly stimulates soluble guanylate cyclase independent of NO and increases the sensitivity of soluble guanylate cyclase to NO. A randomized controlled trial of 443 patients with PAH (some previously treated

with endothelin receptor antagonists or nonparenteral prostanoids) treated with riociguat up to 2.5 mg three times daily demonstrated an improvement in the primary endpoint of 6 MW distance, as well as multiple secondary endpoints, including PVR, NT-pro-BNP, functional class, and time to clinical worsening with riociguat [40]. The most common adverse events included headache and syncope. The combination of riociguat and PDE-5 inhibitors is contraindicated due to hypotension and other relevant side effects.

Combination Therapy in PAH In recent years clinical trials showed the efficacy of combination therapy in PAH, meaning the simultaneous administration of two or three drugs from different classes either simultaneously or sequentially initiated in order to obtain an adequate response to therapy. *Initial (upfront) combination therapy* was recently studied in a multicentre, blinded, placebo-controlled trial that compared first-line monotherapy with tadalafil or monotherapy with ambrisentan with upfront combination therapy with tadalafil and ambrisentan in de novo PAH patients in functional class II or III and showed a 50% reduction in clinical failure events (death, hospitalization, PAH progression and unsatisfactory clinical status) and improvements in exercise capacity, rate of satisfactory clinical response and NT-proBNP plasma levels in the combination group [41]. Moreover, a pilot study on an initial triple combination therapy (bosentan + sildenafil + intravenous epoprostenol) in 19 patients in WHO functional class III and IV has provided evidence of the long-term benefits of upfront triple combination therapy in patients with severe PAH [42].

Sequential combination therapy is the most widely used strategy both in clinical trials and in clinical practice: from monotherapy there is an addition of a second and then a third drug in cases of inadequate clinical response or in cases of deterioration. The therapy is considered adequate only if the targets are met. The goal-oriented treatment strategy has different targets, including WHO functional class I or II, and the near-normalization of resting cardiac index and/or of NT-proBNP plasma levels. Sequential combinations with strong evidence from clinical trials are macitentan added to sildenafil, riociguat added to bosentan, selexipag added to an entothelin receptor antagonist or/and a PDE5 inhibitor, sildenafil added to epoprostenol (for PAH patients in WHO functional class III) [1].

According to the PAH treatment algorithm proposed by the current version of the European guidelines on the management of PH [1], initial oral combination therapy may be considered in a PAH patient with low or intermediate risk (WHO class II–III) and initial combination therapy including an intravenous prostacyclin analogue is recommended in a PAH patient with high risk (WHO class IV). Double or triple sequential combination therapy is recommended in PAH patients with inadequate clinical response to monotherapy or initial double combination therapy.

Interventional procedures in PAH Atrial septostomy creates a right-to-left interatrial shunt, decreases right-sided heart filling pressure, improves RV function, and improves left-sided heart filling and cardiac output. Published reports suggest a benefit in patients in WHO functional class IV with right heart failure refractory to medical therapy or with severe syncopal symptoms and in patients awaiting lung transplantation with unsatisfactory clinical response on maximal medical therapy or when medical therapy is not available. Balloon atrial septostomy should be avoided in end-stage patients presenting with a baseline mean RA pressure more than 20 mmHg and O_2 saturation at rest less than 85% on room air. Atrial septostomy should be regarded as a palliative or bridging procedure [1].

Lung Transplantation According to current guidelines recommendations, it seems reasonable to consider eligibility for lung transplantation after an inadequate clinical response to the initial monotherapy/combination therapy and to refer the patient for transplantation immediately after an inadequate clinical response is confirmed on maximal combination therapy. The PAH etiology

may also help the decision-making process since the prognosis varies according to the underlying condition: PAH associated with connective tissue diseases has a worse prognosis than idiopathic PAH, while patients with PAH associated with congenital heart disease have a better survival. Patients with PVOD and PCH have the worst prognosis due to the lack of effective medical treatments; these patients should be listed for transplantation at diagnosis. Both heart–lung and double-lung transplantation have been performed in PAH patients, although the threshold for unrecoverable RV systolic dysfunction and/or LV diastolic dysfunction is not clear. Recent data show that survival after double-lung transplantation is 52–75% at 5 years and 45–66% at 10 years [1].

15.7 Pulmonary Arterial Hypertension Subsets

Pulmonary arterial hypertension (PAH) group includes various clinical conditions with very different demographics, clinical manifestations and outcomes united by a common haemodynamic measurable parameter of an underlying pulmonary vasculopathy (increased pulmonary vascular resistence due to the arterial component).

Idiopathic PAH Formerly named primary pulmonary hypertension, idiopathic PAH is a rare disease of unknown cause and is the most common type of PAH in current-day registries. Idiopathic PAH corresponds to a sporadic disease in which there is neither a family history of PAH nor an identified risk factor. Its diagnosis requires exclusion of all other known causes of PH and PAH and confirmation by RHC.

Heritable PAH This PAH type requires identification of a family member with PAH or a known PAH gene mutation. Hereditary transmission of PAH has been reported in approximately 6–10% of patients with PAH.

Drugs and Toxin-Induced PAH An association between anorexigens (appetite-suppressant drugs that increase release and block reuptake of serotonin) and PAH was initially observed in the 1960s. Epidemiologic studies have also linked the development of PAH to rapeseed oil, L-tryptophan, and illicit drugs such as methamphetamines. More recently, the tyrosine kinase inhibitor dasatinib has been associated with the development of PAH. From the approval of dasatinib in November 2006 to September 2010, nine incident cases of PAH in patients treated with dasatinib were identified in the French National Registry [43]. Improvement is usually observed after cessation of the dasatinib therapy.

PAH Associated with Congenital Heart Diseases (CHD) This type of PAH includes a very heterogenous patient population illustrated by the clinical classification included in Table 15.6. An important feature of PAH in patients with CHD is the RV adaptive response to elevated PAH (RV adaptive remodeling). With onset early in life, marked hypertrophy and preservation of a fetal-like phenotype occur. As a result, these patients can sustain increased afterload with better RV function for many years or decades than can those in whom PAH develops later in life. The RV is also relieved by the right-to-left shunt, sustaining cardiac output at the expense of hypoxaemia and cyanosis. Survival of patients with Eisenmenger syndrome is better than those with idiopathic PAH, with a 3-year survival rate of 77% compared with 35% for untreated idiopathic PAH [44]. Moreover, the worst survival was observed in patients with persistent PAH after defect repair or with small/coincidental defects as compared with patients with Eisenmenger syndrome or those with prevalent systemic-to-pulmonary shunts [45].

Operability may be considered in patients with prevalent systemic-to-pulmonary shunting if PVR <2.3 Wood units (<4 Wood units m^2), while this is not recommended if PVR >4.6 Wood units (<8 Wood units m^2). No prospective data are available on the usefulness of vasoreactivity testing, closure test or lung biopsy for operability assessment. Surgical or percutaneous intervention is contraindicated in patients with Eisenmenger syndrome and likely is useless in patients with small/coincidental defects [1].

Table 15.6 Clinical classification of PAH associated with congenital heart disease (adpated from [1])

Clinical condition	Description
1. Eisenmenger's syndrome	Includes all large intra- and extra-cardiac defects that begin as systemic-to-pulmonary shunts and progress with time to severe elevation of PVR and to reversal (pulmonary-to-systemic) or bidirectional shunting; cyanosis, secondary erythrocytosis, and multiple organ involvement are present
2. PAH associated with prevalent systemic-to-pulmonary shunts	• Correctable • Non-correctable Includes moderate to large defects; PVR is mildly to moderately elevated, there is a predominant systemic-to-pulmonary shunting; cyanosis at rest is not a feature
3. PAH with small/coincidental defects	Marked elevation in PVR in the presence of small cardiac defects (usually ventricular septal defects <1 cm and atrial septal defects <2 cm assessed by echo), which themselves do not account for the development of elevated PVR; the clinical picture is very similar to idiopathic PAH. Closing the defects is contra-indicated
4. PAH after defect correction	Congenital heart disease is repaired, but PAH either persists immediately after correction or recurs/develops months or years after correction in the absence of significant postoperative haemodynamic lesions

PAH pulmonary arterial hypertension, *PVR* pulmonary vascular resistance

The use of oral anticoagulants in Eisenmenger syndrome is controversial: a high incidence of PA thrombosis and stroke is reported, but there is also an increased risk of haemorrhage and haemoptysis. Secondary erythrocytosis is beneficial for adequate tissue O_2 delivery and routine phlebotomy should be avoided. If symptoms of hyperviscosity are present when the haematocrit is >65%, phlebotomy with isovolumic replacement should be performed. Iron deficiency should be corrected. The empirical use of calcium channel blockers in Eisenmenger syndrome should be avoided [1]. Currently approved PAH-specific therapies have demonstrated benefit in patients with Eisenmenger syndrome. Bosentan has been shown to improve 6MWT and decrease PVR after 16 weeks of treatment in WHO functional class III patients [46]. Although a beneficial effect of bosentan on exercise capacity and quality of life in this group of patients was demonstrated, an effect on mortality remains uncertain [47]. Experiences with other endothelin receptor antagonists and the PDE-5 inhibitors sildenafil and tadalafil show favorable functional and haemodynamic results in patients with PAH associated with CHD and Eisenmenger syndrome [1].

PAH Associated with Connective Tissues Disease (CTD) The prevalence of PAH is greatest in patients with the scleroderma spectrum of diseases, although PAH can occur in the setting of any of the CTD (systemic lupus erythematosus, mixed CTD and, to a lesser extent, rheumatoid arthritis, dermatomyositis and Sjögren's syndrome) [1]. PAH associated with CTD is the second most prevalent type of PAH after idiopathic PAH in developed countries [4]. Prospective studies using echocardiography as a screening tool and hemodynamic confirmation by RHC found a prevalence of PAH in the scleroderma patients of approximately 5–12% [1]. Currently, echocardiography is the most common screening tool for PH detection in scleroderma patients but, recently, a novel screening approach was developed that involves a two-step algorithm, including clinical, pulmonary function test, and echocardiographic variables (DETECT algorithm) [48].

In patients with scleroderma, PH may occur in association with interstitial lung disease or as a result of an isolated pulmonary vascular disease, which may affect pre-capillary arterioles (PAH) and post-capillary venules (PVOD) or they may experience LV diastolic dysfunction. Compared with idiopathic PAH, patients with CTD and PAH are predominantly women (female:male ratio 4:1), are older (mean age at diagnosis >60 years), may present concomitant disorders (interstitial lung disease, left heart disease) and have shorter survival times [1]. The 3-year survival rate of patients with scleroderma-associated PAH in the French National Registry was 56% [49].

Treatment of patients with CTD-associated PAH is more complex than idiopathic PAH therapy. Immunosuppressive therapy combining glucocorticosteroids and cyclophosphamide shows clinical improvement in patients with PAH associated with systemic lupus erythematosus or mixed CTD. Long-term favorable response to calcium channel blockers is reported in <1% of cases. In scleroderma patients, the long-term risk: benefit ratio of oral anticoagulation is less favorable than in idiopathic PAH due to an increased risk of bleeding [1].

Treatment of PAH in patients with CTD should follow the same treatment algorithm as in idiopathic PAH, as the patients with CTD have been included in most of the major randomized controlled trials for approval of PAH therapy, including those with combination therapy. Indications and contraindications for lung transplantation should be adapted to the specificities of scleroderma patients with a special focus on digestive (gastro-oesophageal reflux disease and intestinal disease), cardiac, renal and cutaneous involvement [1].

PAH Associated with HIV Infection PAH is a rare, but well-established complication of human immunodeficiency virus (HIV) infection. Population studies of HIV-infected patients suggest that the prevalence of PAH is approximately 0.5% and it did not changed with the widespread use of highly active antiretroviral therapy. The pathogenesis is unknown, but the hemodynamics and clinical course are similar to that of idiopathic PAH. The prognosis of HIV-associated PAH has improved in recent years. In a recent single-center observation, the survival rate was 88% at 1 year and 72% at 3 years, with a cardiac index >2.8 L/min/m^2 and a CD4 lymphocyte count >200 cells/μL being independent predictors of survival [50]. Echocardiographic screening for PAH in HIV-infected patients is not recommended due to its relatively low prevalence, although PAH should be considered in HIV-infected patients with symptoms of dyspnoea in whom another cause cannot be found. PAH is an independent risk factor for death in HIV-infected patients. In patients with PAH associated with HIV infection, the same treatment algorithm used for patients with idiopathic PAH should be considered, taking into consideration co-morbidities and drug–drug interactions. Anticoagulation is not recommended because of a lack of data on the efficacy:risk ratio [1].

PAH Associated with Portal Hypertension PAH associated with elevated pressure in the portal circulation is defined as portopulmonary hypertension and it should be differentiated from hepatopulmonary syndrome that is characterized by abnormal pulmonary vasodilation and hypoxemia. Portal hypertension, and not the underlying liver disease, is the risk factor for PAH development. Neither the severity of the liver disease nor the degree of portal hypertension predicts the presence or severity of portopulmonary hypertension. Epidemiologic studies have estimated the prevalence of PAH in patients with portal hypertension of 1–5%, but it may be higher in those referred for liver transplantation. Echocardiographic screening is recommended in symptomatic patients with liver disease or portal hypertension and in all candidates for liver transplantation and PAH confirmation by RHC is required [1]. The distinction between the high-flow state of the underlying disease or the high-output cardiac failure with elevated left-sided cardiac filling pressure and the true portopulmonary hypertension is mandatory.

The presence of PAH increases the risk associated with liver transplantation. Mild PH with normal or near-normal PVR in the presence of high cardiac output is usually well tolerated and tends to be reversible after transplantation. PAH, in contrast, is a major risk factor in the setting of liver transplantation. Based on observational cohorts, the mortality rate was 100% in patients with PAPm ≥50 mmHg and 50% in patients with PAPm between 35 and 50 mmHg and a PVR ≥250 dyn s cm^{-5} [51]. So liver transplantation is contraindicated in patients with severe and uncontrolled PAH.

The treatment of portopulmonary hypertension follows the algorithm for other forms of PAH, but there are some special considerations. These patients often have an elevated bleeding

risk and anticoagulation is usually not recommended. Beta-blockers, which are frequently used to lower the portal pressure, should be avoided in patients with portopulmonary hypertension, as they worsen haemodynamics and exercise capacity in this patient population [52]. Specific PAH therapies may be used in this patient population and liver transplantation may be considered in selected patients responding well to PAH therapy [1].

15.8 Pulmonary Veno-Oclusive Disease and Pulmonary Capillary Hemangiomatosis

PVOD and PCH are two conditions associated with PH with pathological, genetic and clinical similarities and differences with PAH thus being classified together in a distinct subgroup of the clinical classification of PH (Table 15.1). These two condition overlap and have similar pathologic features, clinical characteristics with worse prognosis than PAH and a risk of developing pulmonary oedema with specific PAH therapy. In addition to the histology of PAH, these entities also exhibit the findings of pulmonary venous hypertension, including pulmonary hemosiderosis, interstitial edema, and lymphatic dilation. The true incidence of PVOD/PCH is still unknown because many cases are misclassified as PAH. The proportion of idiopathic cases of PAH that fulfil the criteria for PVOD/PCH is likely to be around 10% (lowest estimates of PVOD/PCH incidence and prevalence are <1 case/million) [53, 54]. In contrast to IPAH, there is a male predominance in PVOD and the prognosis appears to be worse. Familial cases of PVOD/PCH have been described, often in consanguineous families and typically occur in the young siblings of one generation with unaffected parents, indicating that the disease segregates as a recessive trait. Recessive mutations in *EIF2AK4* (also called *GCN2*) cosegregated with PVOD in 100% of familial and 25% of sporadic cases of histologically confirmed PVOD/PCH. These findings suggest that *EIF2AK4* is the major gene linked to the development of PVOD/PCH [9]. Identification of a bi-allelic EIF2AK4 mutation is recommended to confirm a diagnosis of heritable PVOD/PCH without histological confirmation [1]. Like PAH, PVOD/PCH may complicate the course of associated conditions (scleroderma, HIV infection, etc.) and exposure to drugs or toxins (cyclophosphamide, mitomycin, etc.) [53].

The diagnosis of PVOD/PCH can be established with a high probability by the combination of clinical suspicion, physical examination, pulmonary functional tests, bronchoscopy and radiological findings. Physical examination may reveal digital clubbing and crackles on lung auscultation, these being unusual in PAH. Patients with PVOD/PCH are more severely hypoxemic and have much lower DLCO levels (<55%) than in other forms of PAH because of the presence of chronic interstitial pulmonary oedema and pulmonary capillary proliferation typical of PVOD/PCH. Chest radiography may reveal Kerley B lines, mediastinal lymph node enlargement and peripheral interstitial infiltrate, in addition to other signs of PH. High-resolution CT of the chest is an essential investigation that reveals typical findings suggestive of PVOD/PCH: the presence of subpleural thickened septal lines, centrilobular ground-glass opacities (Fig. 15.13) and mediastinal lymphadenopathy. The presence of these findings seems to closely correlate with the risk of pulmonary oedema with PAH drugs. Bronchoscopy with bronchoalveolar lavage may show occult alveolar haemorrhage. The haemo-

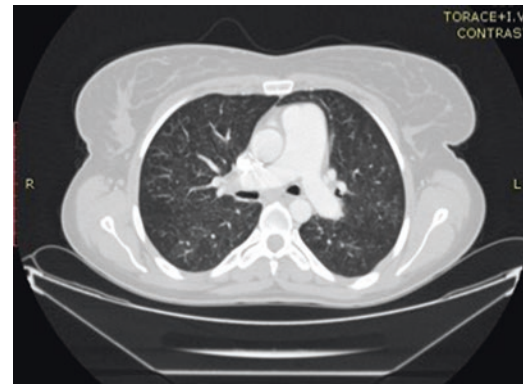

Fig. 15.13 High-resolution computed tomography in a patient with PVOD: centrilobular ground-glass opacities are observed

dynamic presentation of PVOD is similar to idiopathic PAH. Importantly, PAWP is almost invariably normal, because the pathological changes occur in small venulae and capillaries and do not affect the larger pulmonary veins. Vasoreactivity testing may be complicated by acute pulmonary oedema [1, 53, 55]. Histologic proof is required for definitive diagnosis of PVOD/PCH, but surgical lung biopsy is a high-risk procedure in these patients and is therefore contraindicated [1]. The rapid development of pulmonary edema after the administration of PAH-specific therapy is sometimes the first clue to the appropriate diagnosis and can be life-threatening.

Survival of patients with PVOD is poor. There is no established medical therapy for PVOD/PCH. Specific PAH therapy and, in particular, intravenous epoprostenol must be used with great caution because of the high risk of severe drug-induced pulmonary oedema. However, there are reports of sustained clinical improvement in individual patients treated with these medications [55] but these therapies should be undertaken only at centres with extensive experience in the management of PH. High-dose diuretics and O_2 therapy are also recommended [53]. The only curative therapy for PVOD/PCH is lung transplantation, and eligible patients with PVOD/PCH should be referred to a transplant centre for evaluation as soon as the diagnosis is established [1].

15.9 Pulmonary Hypertension Due to Left-Sided Heart Disease

PH due to left heart disease (PH-LHD) can complicate any left heart disorder, such as valvular heart diseases, congenital defects, heart failure and with preserved or reduced ejection fraction. When present, PH-LHD is associated with more severe symptoms and worse exercise tolerance and is a significantly negative prognostic factor. Compared with PAH, patients with PH-LHD (especially in the case of heart failure due to LV diastolic dysfunction) are older (more than 65 years), female, with a higher prevalence of cardiovascular co-morbidities amongst which persistent atrial fibrillation and many of the features of metabolic syndrome [1].

In LHD there is a passive backward transmission of filling pressures, mainly due to LV diastolic function, enhanced by exercise-induced mitral regurgitation and a reduced LA compliance. In some patients, these purely mechanical components of venous congestion may trigger a superimposed component, combining pulmonary vasoconstriction, decreased NO availability, increased endothelin expression and vascular remodelling. This results in a further increase in PAPm in excess of the elevation of PAWP that may lead to pulmonary vascular disease, increased RV afterload and RV failure [56]. Therefore, the haemodynamic classification of post-capillary PH according to the diastolic pressure gradient in isolated post-capillary PH and combined pre- and post-capillary PH is important in order to better define the patients' outcome since a diastolic pressure gradient more than 7 mmHg seems associated with worse prognostic in patients with heart failure [56].

The diagnosis of PH-LHD is suspected when patients with known left heart involvement develop symptoms and signs of right heart failure. The electrocardiogram may reveal left ventricular hypertrophy, left atrial dilation, left bundle branch block, atrial fibrillation or flutter, pathologic Q waves. The chest radiograph shows Kerley B lines, pleural effusion, pulmonary oedema, LA enlargement. The transthoracic echocardiography is the essential diagnostic tool as it distinguishes between a right and left phenotype of PH, i.e. pre-capillary PH and post-capillary PH. In PH-LHD there are structural left heart abnormalities with left heart valves diseases, LA dilation, bowing of the interatrial septum to the right, LV systolic dysfunction, LV hypertrophy, signs of increased LV filling pressures with increased E/e'. Also RV dysfunction and pericardial effusion are rare findings in this

setting [1, 56, 57]. The role of exercise testing to uncover PH-LHD in patients with heart failure with preserved ejection fraction is not yet standardized [1].

The primary goal of therapy in PH-LHD is the best management of the underlying condition prior to considering specific PH therapies. This includes repair of valvular heart disease when indicated and aggressive therapy for heart failure with reduced systolic function. In severe heart failure, optimizing volume status is essential. In addition, the implantation of an LV assist device has been shown to lower pulmonary pressures through LV unloading without increasing the risk of post implantation RV failure. Risk factors for cardiovascular diseases and features of metabolic syndrome should also be controlled. Comorbidities leading to PH should be identified and treated, including chronic obstructive pulmonary disease, sleep apnoea syndrome and pulmonary embolism [1].

The PAH specific therapies were studied in patients with PH-LHD as acute or short-term studies using prostanoids, endothelin receptor antagonists and PDE-5 inhibitors had reported improvements in haemodynamics, exercise capacity and symptoms. But there is no evidence suggesting that acute changes in pulmonary circulation may have a value outside of the setting of major cardiac surgery such as heart transplantation and/or LV assist device implantation [57].

There is a population of patients with risk factors for left heart disease presenting with precapillary PH that is characterized by disease features lying in between typical idiopathic PAH and PH-LHD and there are patients with heart failure and combined pre- and postcapillary PH. These patients may benefit from PH-targeted therapies, especially PDE-5 inhibitors since endothelin receptors agonists or at least those studied so far failed to show clinical benefit and were associated with frequent side effects, predominantly fluid retention. Still, according to the current guidelines on the management of pulmonary hypertension, the use of PAH-approved therapies is not recommended in PH associated with left heart disease [1].

15.10 Pulmonary Hypertension Due to Lung Diseases and/or Hypoxia

The most common lung diseases associated with PH are chronic obstructive pulmonary disease (COPD), interstitial lung disease and combined pulmonary fibrosis and emphysema included in PH group 2 from the clinical classification of PH. Other conditions such as Langerhans cell granulomatosis or sarcoidosis associated with PH are classified as group 5 due to the multifactorial mechanisms involved in PH development (Table 15.1). In any lung disease, the development of PH is accompanied by a decrease in exercise capacity, worsening of hypoxemia and shorter survival [58]. The predictive factors for the presence of PH in these patients are a disproportionally low DLCO and a low pCO_2. Usually the values of pulmonary artery pressures are low in PH associated with chronic lung diseases, a mean PAP more than 35 mmHg in patients with COPD or a mean PAP more than 25 mmHg in the presence of a low cardiac output (less than 2.5 L/min) suggests severe PH and other potential associated causes of PH should be excluded in these cases or the diagnosis of PAH with associated lung disease should be considered [1]. In some situations, such as exercise, sleep, and COPD exacerbations, PH may worsen.

In patients with more severe symptoms than expected for the impairment in their lung function the transthoracic echocardiography is recommended in order to screen for PH or associated left heart disease. Patients with clinical or echocardiographic signs of severe PH and/or severe RV dysfunction should be referred to a PH centre. RHC is required to confirm or exclude PH diagnosis in candidates for surgical treatments (transplantation, lung volume reduction), in cases of suspected associated PAH or CTEPH or in frequent episodes of RV failure in cases with a high level of suspicion of PH and potential therapeutic implications [1].

There is no specific therapy for PH associated with lung diseases. Patients with lung disease

and PH who are hypoxemic should receive long-term O_2 therapy, as long-term O_2 administration has been shown to partially reduce the progression of PH in COPD [59], while the role of long-term O_2 therapy on PH progression in interstitial lung diseases is less clear. Treatment of the underlying lung disease should be optimized. Treatment with conventional vasodilators such as calcium channel blockers is not recommended because they may impair gas exchange due to the inhibition of hypoxic pulmonary vasoconstriction. The use of drugs approved for PAH is not recommended for patients with PH due to lung disease [1].

15.11 Chronic Thromboembolic Pulmonary Hypertension

The definition of chronic thromboembolic pulmonary hypertension (CTEPH) is based on findings described after at least 3 months of effective anticoagulation: presence of precapillary PH and at least one segmental perfusion defect detected by lung scanning, multidetector CT angiography, and/or pulmonary angiography or specific diagnostic signs seen by multidetector CT angiography, MR imaging or pulmonary angiography, such as ring-like stenoses, webs/slits and chronic total occlusions. CTEPH is caused by chronic obstruction of major pulmonary arteries and should be differentiated from other obstructive diseases of the pulmonary vasculature (Table 15.1). CTEPH has a cumulative incidence of 0.1–9.1% within 2 years after a symptomatic event [60], but a significant number of cases develop in the absence of previous acute pulmonary embolism. In the pathogenesis of CTEPH it has been suggested that pulmonary embolism may be followed by a pulmonary vascular remodeling process modified by infection, immune phenomena, inflammation, circulating and vascular-resident progenitor cells, and malignancy. Hypercoagulation, "sticky" red blood cells, high platelet counts, and uncleavable fibrinogens contribute to major vessel obliteration in CTEPH. Other risk factors for CTEPH include splenectomy, ventriculoatrial shunt for hydrocephalus therapy, and inflammatory bowel disease [61].

The symptoms of CTEPH are similar to those of idiopathic PAH but oedema and haemoptysis occur more often in CTEPH, while syncope is more common in idiopathic PAH. The ventilation/perfusion lung scan remains the main imaging modality for CTEPH, with a 96–97% sensitivity and a 90–95% specificity for the diagnosis [18]. A negative scan excludes the diagnosis of CTEPH. Multidetector CT pulmonary angiography has become an established imaging modality for confirming CTEPH, but this investigation alone cannot exclude the disease [18]. Perfusion inequalities manifest as a mosaic parenchymal pattern, with dark areas corresponding to relatively decreased perfusion. CT pulmonary angiography may help to identify complications of the disease such as PA dilatation and hypertrophied bronchial arterial collaterals, which may lead to hemoptysis. MR imaging of the pulmonary vasculature is still considered inferior to CT, but this technique, as well as cone beam CT, angioscopy, intravascular ultrasound or optical coherence tomography, may be complimentary [1]. RHC is a mandatory diagnostic tool. Preoperative and immediate postoperative PVR is a long-term predictor of prognosis [62]. The selective pulmonary angiography (Fig. 15.14) in the anterior–posterior and lateral projections is recommended preoperatively and it illustrates ring-like stenosis, webs ('slits'), pouches, wall irregularities, complete vascular obstructions as well as bronchial collaterals, and supports the assessment of operability.

The pulmonary endarterectomy is the gold standard of treatment in CTEPH with a perioperative mortality of 4.7% across European centres [5]. CTEPH treatment requires a true bilateral endarterectomy through the medial layer of the pulmonary arteries, which is performed under deep hypothermia and circulatory arrest [61]. According to the surgical specimen, there are four anatomic types of CTEPH: type 1 disease (25% of cases) involving the main and lobar pulmonary arteries with fresh red thrombus superimposed on white obstructions; type 2 disease (40% of cases) with intimal thickening and fibro-

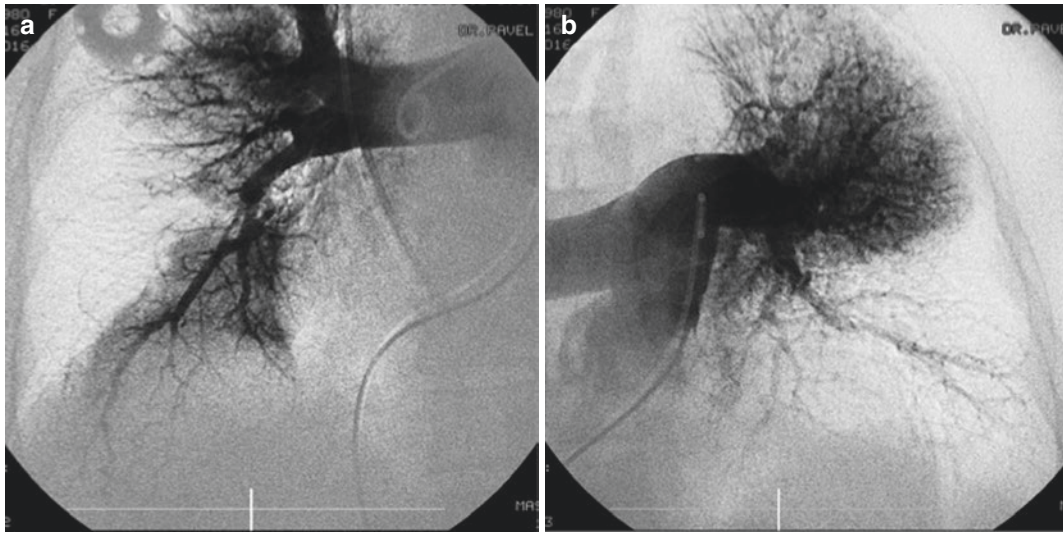

Fig. 15.14 Pulmonary angiography in a patients with CTEPH: segmental obstructions in the upper and middle right lobe, nearly complete occlusion of the right lower lobe (**a**) and complete occlusion of the left lower lobe (**b**)

sis proximal to segmental arteries; type 3 disease (30% of cases) with fibrosis, intimal webbing, and thickening confined to distal segmental and subsegmental arteries; and type 4 disease (≤5% of cases) defined by microscopic distal arteriolar vasculopathy without visible thrombus. Type 4 is not operable. Operability should be assessed by a multidisciplinary team in centres with expertise in pulmonary endarterectomy. General operability criteria include WHO functional class II–IV; preoperative PVR higher than 300 dyn s cm^{-5}; surgical accessibility of thrombi in the main, lobar, or segmental pulmonary arteries; absence of severe comorbid diseases [61]. There are no contraindications to pulmonary endarterectomy related to patient's age, PVR values or RV dysfunction [1]. Early postoperative reperfusion oedema may require veno-arterial ECMO, and severe persistent PH may be bridged to emergency lung transplantation with veno-venous ECMO [1]. International CTEPH registry data indicate 3-year survival rates in operated patients as high as 89.3%, in contrast to 70.5% in non-operated cases [61].

Some centers currently propose balloon pulmonary angioplasty for inoperable CTEPH with an average number of 4.8 sessions is needed per patient to improve parameters of RV function and the procedure has a risk of reperfusion pulmonary oedema [1].

Optimal medical treatment for CTEPH consists of anticoagulants and diuretics, and supplemental O_2 in cases of heart failure or hypoxemia. Lifelong anticoagulation with antivitamin K drugs is recommended, even after PEA; no data exist on the efficacy and safety of new oral anticoagulants [1].

Pulmonary microvascular disease in CTEPH has provided the rationale for off-label use of drugs approved for PAH. PAH-targeted therapy may be recommended in technically non-operable patients, in the presence of an unacceptable surgical risk:benefit ratio or in patients with persistent or recurrent PH after surgery [1]. Riociguat was administered to 261 of 446 screened patients with non-operable CTEPH or persistent/recurrent PH after pulmonary endarterectomy and led to an increase in exercise capacity (6MWD) and a reduction in PVR but the time to clinical worsening remained unchanged [63]. The use of PAH-targeted therapy in operable patients with severe haemodynamic compromise as a bridge to pulmonary endarterectomy is not supported by definite scientific evidence.

15.12 Perspectives

Over recent decades a substantial progress has been made in the understanding of the pathogenesis and treatment of PAH. Patients with PAH currently have a better quality of life and survival than they had previously, but their survival is still suboptimal, and more advances in medical therapies are needed. Data from important registries continue to highlight important prognostic parameters and may help guide the appropriate therapeutic strategies.

Although considerable advances were made in the treatment of PAH, clinical trial data for the more common group 2 and 3 PH are still needed. Off-label use of PAH-specific therapy in these populations is possible in clinical practice, but there is little evidence regarding the efficacy and safety data. Clinical trials in patients with PH associated with left heart disease or lung disease are more and more necessary.

References

1. Galie N, Humbert M, Vachiery JL, et al. 2015 ESC/ERS guidelines for the diagnosis and treatment of pulmonary hypertension. Eur Heart J. 2016;37:67–119.
2. Kovacs G, Berghold A, Scheidl S, Olschewski H. Pulmonary arterial pressure during rest and exercise in healthy subjects: a systematic review. Eur Respir J. 2009;34:888–94.
3. Barst RJ, McGoon M, Torbicki A, et al. Diagnosis and differential assessment of pulmonary arterial hypertension. J Am Coll Cardiol. 2004;43(Suppl 1):S40–7.
4. Hoeper MM, Humbert M, Souza R, et al. A global view on pulmonary hypertension. Lancet Respir Med. 2016;4:306–22.
5. Pepke-Zaba J, Delcroix M, Lang I, et al. Chronic thromboembolic pulmonary hypertension (CTEPH): results from an international prospective registry. Circulation. 2011;124:1973–81.
6. Soubrier F, Chung WK, Machado R, et al. Genetics and genomics of pulmonary arterial hypertension. J Am Coll Cardiol. 2013;62:D13–21.
7. McLaughlin VV, McGoon MD. Pulmonary arterial hypertension. Circulation. 2006;114:1417–31.
8. Simonneau G, Gatzoulis MA, Adatia I, et al. Updated clinical classification of pulmonary hypertension. J Am Coll Cardiol. 2013;62:D34–41.
9. Eyries M, Montani D, Girerd B, et al. EIF2AK4 mutations cause pulmonary veno-occlusive disease, a recessive form of pulmonary hypertension. Nat Genet. 2014;46:65–9.
10. Dorfmuller P. Pathology of pulmonary vascular diseases. In: Peacock AJ, Naeije R, Rubin LJ, editors. Pulmonary circulation. Diseases and their treatment. 4th ed. Boca Raton: CRC Press, Taylor & Francis Group; 2016. p. 61–78.
11. Ormiston ML, Morrell NW. Pathobiology of pulmonary hypertension. In: Peacock AJ, Naeije R, Rubin LJ, editors. Pulmonary circulation. Diseases and their treatment. 4th ed. Boca Raton: CRC Press, Taylor & Francis Group; 2016. p. 79–95.
12. Vonk-Noordegraaf A, Haddad F, Chin KM, et al. Right heart adaptation to pulmonary hypertension: physiology and pathobiology. J Am Coll Cardiol. 2013;62:D22–33.
13. Vonk-Noordegraaf A, Westerhof BE, Westerhof N. The relationship between the right ventricle and its load in pulmonary hypertension. J Am Coll Cardiol. 2017;69:236–43.
14. Rich S, Dantzker DR, Ayres S, et al. Primary pulmonary hypertension. A national prospective study. Ann Intern Med. 1987;107:216–23.
15. Rich S, McLaughlin VV, O'Neill W. Stenting to reverse left ventricular ischemia due to left main coronary artery compression in primary pulmonary hypertension. Chest. 2001;120:1412–5.
16. McGoon M, Gutterman D, Stern V, et al. Screening, early detection and diagnosis of pulmonary arterial hypertension. Chest. 2004;126:14S–34S.
17. Rudski LG, Lai WW, Afilalo J, et al. Guidelines for the echocardiographic assessment of the right heart in adults: a report from the American Society of Echocardiography endorsed by the European Association of Echocardiography, a registered branch of the European Society of Cardiology, and the Canadian Society of Echocardiography. J Am Soc Echocardiogr. 2010;23:685–713.
18. Tunariu N, Gibbs SJR, Win Z, et al. Ventilation-perfusion scintigraphy is more sensitive than multidetector CTPA in detecting chronic thromboembolic pulmonary disease as a treatable cause of pulmonary-hypertension. J Nucl Med. 2007;48:680–4.
19. Rajaram S, Swift AJ, Condliffe R, et al. CT features of pulmonary arterial hypertension and its major subtypes: a systematic CT evaluation of 292 patients from the ASPIRE registry. Thorax. 2015;70:382–7.
20. van Wolferen SA, Marcus JT, Boonstra A, et al. Prognostic value of right ventricular mass, volume, and function in idiopathic pulmonary arterial hypertension. Eur Heart J. 2007;28:1250–7.
21. van de Veerdonk MC, Kind T, Marcus JT, et al. Progressive right ventricular dysfunction in patients with pulmonary arterial hypertension responding to therapy. J Am Coll Cardiol. 2011;58:2511–9.
22. Blumberg FC, Arzt M, Lange T, et al. Impact of right ventricular reserve on exercise capacity and survival in patients with pulmonary hypertension. Eur J Heart Fail. 2013;15:771–5.
23. Fujimoto N, Borlaug BA, Lewis GD, et al. Hemodynamic responses to rapid saline loading: the impact of age, sex, and heart failure. Circulation. 2013;127:55–62.

24. D'Alonzo GE, Barst RJ, Ayres SM, et al. Survival in patients with primary pulmonary hypertension. Results from a national prospective registry. Ann Intern Med. 1991;115:343–9.
25. Gomberg-Maitland M, Dufton C, Oudiz RJ, Benza RL. Compelling evidence of long-term outcomes in pulmonary arterial hypertension? A clinical perspective. J Am Coll Cardiol. 2011;57:1053–61.
26. Chan L, Chin LM, Kennedy M, et al. Benefits of intensive treadmill exercise training on cardiorespiratory function and quality of life in patients with pulmonary hypertension. Chest. 2013;143:333–43.
27. Jaïs X, Olsson KM, Barbera JA, et al. Pregnancy outcomes in pulmonary arterial hypertension in the modern management era. Eur Respir J. 2012;40:881–5.
28. Olsson KM, Delcroix M, Ghofrani HA, et al. Anticoagulation and survival in pulmonary arterial hypertension: results from the Comparative, Prospective Registry of Newly Initiated Therapies for Pulmonary Hypertension (COMPERA). Circulation. 2014;129:57–65.
29. Sitbon O, Humbert M, Jais X, et al. Long-term response to calcium channel blockers in idiopathic pulmonary arterial hypertension. Circulation. 2005;111:3105–11.
30. Barst RJ, Rubin LJ, Long WA, et al. A comparison of continuous intravenous epoprostenol (prostacyclin) with conventional therapy for primary pulmonary hypertension. N Engl J Med. 1996;334:296–302.
31. Simonneau G, Barst RJ, Galie N, et al. Continuous subcutaneous infusion of treprostinil, a prostacyclin analogue, in patients with pulmonary arterial hypertension. A double-blind, randomized, placebo-controlled trial. Am J Respir Crit Care Med. 2002;165:800–4.
32. McLaughlin VV, Benza RL, Rubin LJ, et al. Addition of inhaled treprostinil to oral therapy for pulmonary arterial hypertension. A randomized controlled clinical trial. J Am Coll Cardiol. 2010;55:1915–22.
33. Olschewski H, Simonneau G, Galiè N, AIR Study Group, et al. Inhaled iloprost in severe pulmonary hypertension. N Engl J Med. 2002;347:322–9.
34. Sitbon O, Channick R, Chin KM, GRIPHON Investigators, et al. Selexipag for the treatment of pulmonary arterial hypertension. N Engl J Med. 2015;373:2522–33.
35. Galiè N, Olschewski H, Oudiz RJ, et al. Ambrisentan for the treatment of pulmonary arterial hypertension. Results of the ambrisentan in pulmonary arterial hypertension, randomized, doubleblind, placebo-controlled, multicenter, efficacy (ARIES) study 1 and 2. Circulation. 2008;117:3010–9.
36. Pulido T, Adzerikho I, Channick RN, et al. Macitentan and morbidity and mortality in pulmonary arterial hypertension. N Engl J Med. 2013;369:809–18.
37. Galie N, Ghofrani AH, Torbicki A, Sildenafil Use in Pulmonary Arterial Hypertension (SUPER) Study Group, et al. Sildenafil citrate therapy for pulmonary arterial hypertension. N Engl J Med. 2005;353:2148–57.
38. Galiè N, Brundage BH, Ghofrani HA, et al. Tadalafil therapy for pulmonary arterial hypertension. Circulation. 2009;119:2894–903.
39. Jing Z-C, Yu Z-X, Shen J-Y, et al. Vardenafil in pulmonary arterial hypertension: a randomized, double-blind, placebo-controlled study. Am J Respir Crit Care Med. 2011;183:1723–9.
40. Ghofrani H-A, Galiè N, Grimminger F, et al. Riociguat for the treatment of pulmonary arterial hypertension. N Engl J Med. 2013;369:330–40.
41. Galiè N, Barberà JA, Frost AE, et al. Initial use of ambrisentan plus tadalafil in pulmonary arterial hypertension. N Engl J Med. 2015;373:834–44.
42. Sitbon O, Jaïs X, Savale L, et al. Upfront triple combination therapy in pulmonary arterial hypertension: a pilot study. Eur Respir J. 2014;43:1691–7.
43. Montani D, Bergot E, Günther S, et al. Pulmonary arterial hypertension in patients treated by dasatinib. Circulation. 2012;125:2128–37.
44. Hopkins WE, Ochoa LL, Richardson GW, Trulock EP. Comparison of the hemodynamics and survival of adults with severe primary pulmonary hypertension or Eisenmenger syndrome. J Heart Lung Transplant. 1996;15:100–5.
45. Manes A, Palazzini M, Leci E, et al. Current era survival of patients with pulmonary arterial hypertension associated with congenital heart disease: a comparison between clinical subgroups. Eur Heart J. 2014;35:716–24.
46. Galiè N, Beghetti M, Gatzoulis MA, et al. Bosentan therapy in patients with Eisenmenger syndrome: a multicenter, double-blind, randomized, placebo-controlled study. Circulation. 2006;114:48–54.
47. Gatzoulis MA, Beghetti M, Galiè N, et al. Longer-term bosentan therapy improves functional capacity in Eisenmenger syndrome: results of the BREATHE-5 open-label extension study. Int J Cardiol. 2007;127:27–32.
48. Coghlan JG, Denton CP, Gruenig E, et al. Evidence-based detection of pulmonary arterial hypertension in systemic sclerosis: the DETECT study. Ann Rheum Dis. 2014;73:1340–9.
49. Launay D, Sitbon O, Hachulla E, et al. Survival in systemic sclerosis-associated pulmonary arterial hypertension in the modern management era. Ann Rheum Dis. 2013;72:1940–6.
50. Nunes H, Humbert M, Sitbon O, et al. Prognostic factors for survival in human immunodeficiency virus-associated pulmonary arterial hypertension. Am J Respir Crit Care Med. 2003;167:1433–9.
51. Krowka MJ, Plevak DJ, Findlay JY, et al. Pulmonary hemodynamics and perioperative cardiopulmonary-related mortality in patients with portopulmonary hypertension undergoing liver transplantation. Liver Transpl. 2000;6:443–50.
52. Provencher S, Herve P, Jaïs X, et al. Deleterious effects of beta-blockers on exercise capacity and

hemodynamics in patients with portopulmonary hypertension. Gastroenterology. 2006;130:120–6.
53. Montani D, O'Callaghan DS, Savale L, et al. Pulmonary veno-occlusive disease: recent progress and current challenges. Respir Med. 2010; 104:S23–32.
54. Best DH, Sumner KL, Austin ED, et al. EIF2AK4 mutations in pulmonary capillary hemangiomatosis. Chest. 2014;145:231–6.
55. Montani D, Achouh L, Dorfmuller P, et al. Pulmonary veno-occlusive disease: clinical, functional, radiologic, and hemodynamic characteristics and outcome of 24 cases confirmed by histology. Medicine (Baltimore). 2008;87:220–33.
56. Vachiery JL, Adir Y, Barbera JA, et al. Pulmonary hypertension due to left heart disease. J Am Coll Cardiol. 2013;62:D100–8.
57. D'Alto M, Romeo E, Argiento P, et al. Echocardiographic prediction of pre- versus post-capillary pulmonary hypertension. J Am Soc Echocardiogr. 2015;28:108–15.
58. Kessler R, Faller M, Weitzenblum E, et al. "Natural history" of pulmonary hypertension in a series of 131 patients with chronic obstructive lung disease. Am J Respir Crit Care Med. 2001;164:219–24.
59. Weitzenblum E, Sautegeau A, Ehrhart M, et al. Long-term oxygen therapy can reverse the progression of pulmonary hypertension in patients with chronic obstructive pulmonary disease. Am Rev Respir Dis. 1985;131:493–8.
60. Lang IM, Pesavento R, Bonderman D, Yuan JX. Risk factors and basic mechanisms of chronic thromboembolic pulmonary hypertension: a current understanding. Eur Respir J. 2013;41:462–8.
61. McLaughlin VV, Humbert M. Pulmonary hypertension. In: Braunwald's heart disease: a textbook of cardiovascular medicine. 10th ed. Philadelphia: Elsevier; 2015. p. 1682–702.
62. Skoro-Sajer N, Marta G, Gerges C, et al. Surgical specimens, haemodynamics and long-term outcomes after pulmonary endarterectomy. Thorax. 2014;69:116–22.
63. Ghofrani HA, D'Armini AM, Grimminger F, et al. Riociguat for the treatment of chronic thromboembolic pulmonary hypertension. N Engl J Med. 2013;369:319–29.

Tricuspid Valve Pathology

16

Shahzad G. Raja

Abstract

Tricuspid valve pathology has increasingly become the focus of attention in recent years. Both primary and secondary disease processes involve the tricuspid valve. Depending on the underlying disease process the predominant hemodynamic lesion can be either tricuspid valve stenosis or regurgitation. Whereas tricuspid stenosis is uncommon, tricuspid regurgitation is frequently encountered and is most often secondary in nature. Patients with tricuspid valve disease are usually in an advanced stage of multivalvular heart disease and constitute a high-risk group. Recent improved understanding of the pathophysiology of tricuspid valve disease coupled with substantial advances in assessment and management have improved the outlook for patients with tricuspid valve pathology. This chapter provides an overview of tricuspid valve pathology focusing on pathophysiology, diagnosis, management and emerging transcatheter therapies.

Keyword

Atrioventricular valve · Tricuspid valve
Tricuspid stenosis · Tricuspid regurgitation
Functional regurgitation

Tricuspid valve (TV) often referred to as the forgotten valve has become the focus of attention in recent years. The past decade has particularly seen a massive increase in publications emphasizing the need to aggressively treat TV disease and the long term implications of failure to address it [1–4]. Multiple entities affect the tricuspid leaflets, annulus, chordae and papillary muscles and can cause severe tricuspid regurgitation (TR) or stenosis in the initial absence of either pulmonary hypertension or right ventricular (RV) dysfunction (Table 16.1). Over time, these entities can cause progressive right atrial, RV, and annular dilatation, sometimes with atrial fibrillation leading to poor patient outcomes. A variety of surgical approaches with promising immediate and long

S. G. Raja
Department of Cardiac Surgery, Harefield Hospital, Harefield, Middlesex, UK

S. I. Dumitrescu et al. (eds.), *Right Heart Pathology*, https://doi.org/10.1007/978-3-319-73764-5_16

Table 16.1 Causes of tricuspid valve pathology

Tricuspid stenosis
Rheumatic fever
Carcinoid heart disease
Endocarditis
Endomyocardial fibrosis
Systemic lupus erythematosus
Congenital tricuspid stenosis
Tricuspid regurgitation
Secondary to left-sided valvular heart disease
Rheumatic fever
Myxomatous degeneration
Ebstein anomaly
Endomyocardial fibrosis
Endocarditis
Blunt chest trauma
Pacing wire(s)
Pulmonary thromboembolism
Left ventricular dysfunction
Pulmonary hypertension
Chronic lung disease
Right ventricular ischaemia
Myocardial disease
Left to right shunt
Carcinoid heart disease
Cleft tricuspid valve

term outcomes have been introduced in recent years [5]. This chapter provides an overview of the current understanding of the TV pathology in terms of diagnosis, prognosis and treatment.

16.1 Embryology

The septation of atria and ventricles in the fetal circulation is followed by formation of endocardial cushions at the crux of the heart. The atrioventricular (AV) valves develop subsequently. The architecture of the two AV valves is intimately tied to the corresponding ventricles. This relationship demonstrates that the mitral valve is connected to the anatomic left ventricle and the TV to the anatomic right ventricle. This relationship is emphasized in the congenitally corrected transposition of great arteries with functionally intact circulation, such that the anatomic right ventricle becomes the systemic ventricle and anatomic left ventricle the pulmonary ventricle [6]. The corresponding AV valves are transposed along with the ventricles. Thus, the TV becomes a left sided valve between the left atrium and anatomic right ventricle, which is the systemic ventricle connected to the aorta. Similarly the mitral valve is transposed with anatomic left ventricle, which is the pulmonary ventricle connected to the pulmonary artery and low resistance pulmonary circulation. Congenitally corrected transposition in absence of other malfunctions is compatible with life into the sixth and seventh decades. This speaks to the adaptation of the anatomic right ventricle and TV to high pressure, high resistance systemic circulation [6].

Since the formation of AV cushions at the crux of the heart are central to distinctive anatomy of the two atrioventricular valves, the congenital absence of AV cushions, partial or complete, results in striking abnormalities of the two AV valves [6]. The attachment of the septal leaflet of the TV is normally more apical than the mitral valve, and a small defect is capable of providing shunting of blood from the left ventricle to the right atrium. This defect, when isolated, is anatomically small and is known as Gerbode defect. Another anatomic consideration is that the septal leaflet of the TV is attached to membranous ventricular septum. Thus, perimembranous ventricular septal defects distort this portion of the TV, which can grow over the defect, resulting in spontaneous closure of small membranous ventricular septal defect in childhood [6].

16.2 Valve Anatomy

The TV is most caudally located and has the largest orifice of the 4 intracardiac valves. It functions as a unidirectional valve permitting systemic venous blood flow from right atrium and hence from the 2 vena cava to advance to the right ventricle during diastole and prevents backflow or regurgitation during systole. The TV apparatus is composed of the annulus, the leaflets, the chordae and papillary muscles. Its coordinated function is also influenced by the geometric alterations of the right ventricle and the right atrium [6].

The tricuspid annulus is oval in shape, but assumes a more circular shape on dilatation. It has been shown to have a more complex nonplanar shape with postero-septal commissure the highest point. The shape, besides becoming more circular, flattens out and becomes more planar in presence of severe "functional" regurgitation. The annular diameter, circumference and area are all larger than the mitral valve by about 20%. Although major tricuspid annular diameter values of 30–35 mm are described for normal adults (BSA 1.5–1.7 m^2), the orifice size is influenced by overall body size as reflected in body surface area [6]. Thus, while a measured diameter of 40 mm in an average size normal adult represents dilated annulus, this may be normal for a person with BSA in excess of 2.0 m^2. Thus, size of an individual patient must be considered in assigning the given measure as normal or abnormal. The average normal annular diameter is 21 mm/m^2. A hemodynamic consequence of a larger tricuspid annulus orifice is lower velocities and lower pressure drops during diastolic inflow than in the normal mitral valve. The annulus exhibits a dynamic behavior similar to the mitral annulus, with expansion of the orifice in diastole and reduction in systole [7]. The maximum to minimum area reduction is nearly 30%. This dynamic behavior promotes forward flow while maintaining low right atrial and thus systemic venous pressures.

The TV has 3 leaflets namely anterior, septal and posterior, the anterior being the largest and septal being the smallest. The septal leaflet attachment is from posterior ventricular wall across the interventricular septum, its insertion being more apical relative to the anterior leaflet. The anterior leaflet is attached to the right AV junction. The posterior leaflet has mural attachment [6].

The tendinous chords are attached to the ventricular surface of the leaflets or the free edges of the leaflets to the papillary muscle supporting the leaflet. There may be accessory chords that attach from the septal leaflet to the moderator band or the right ventricular free wall.

There are 3 sets of papillary muscles, each set being composed of up to 3 muscles. The chordae arising from each set are inserted into 2 adjacent leaflets [6]. Thus, the anterior set of chordae insert into half of the anterior and half of the posterior leaflets, the medial set provides chordae to anterior and septal leaflets. The third, posterior, set is more rudimentary and is attached to the diaphragmatic wall of the right ventricle [8].

16.3 Normal Tricuspid Valve Function

The diastolic opening of the valve along with corresponding expansion of the annulus provides a tricuspid orifice area of 7–9 cm^2. This large orifice provides unimpeded flow both at rest and with physical activity without elevations in central venous pressures. The systolic narrowing of the orifice provides an effective seal for valve closure; however, a degree of TR detected by Doppler echocardiography is observed in 80–90% of normal subjects. The majority of patients with physiologic TR are in the mild category, but a small number of otherwise healthy individuals may have moderate regurgitation. A failure to appreciate this may result in identifying as abnormal what is a normal variant [6].

16.4 Tricuspid Valve Dysfunction

The TV disease is generally classified as primary or intrinsic valve pathology or secondary or functional valve dysfunction [9, 10]. The primary valve disease results from structural abnormality of the valve apparatus. The secondary or functional TV disease results from factors that generally lead to tricuspid annular dilatation, commonly from left heart disease and resulting right ventricular hypertension, dilatation and dysfunction [11].

16.4.1 Clinical Presentation

The abnormal valve function may be in form of: (a) pure or predominant tricuspid stenosis; (b) pure or predominant TR; or (c) mixed.

In case of TV regurgitation is more commonly seen than stenosis. Almost 75% of severe TR is

classified as functional and is secondary to left-sided valvular disease leading to pulmonary hypertension, right ventricular dysfunction, or a combination of both. Non-functional TR occurs when there is damage to the tricuspid leaflets, chordae, papillary muscles, or annulus, independent of right ventricular dysfunction or pulmonary hypertension. The entities that cause non-functional TR include rheumatic and myxomatous disease, acquired and genetic connective tissue disorders, endocarditis, sarcoid, pacing, RV biopsy, blunt trauma, radiation, carcinoid, ergot alkaloids, dopamine agonists, fenfluramine, cardiac tumors, atrial fibrillation, and congenital malformations [12].

Generally the symptoms of left heart disease predominate in those with secondary TV disease. The symptoms specific to advanced TV disease are related to: (a) decreased cardiac output, for example, fatigue; (b) right atrial hypertension, for example, liver congestion resulting in right upper quadrant discomfort, or gut congestion with symptoms of dyspepsia, indigestion, or fluid retention with leg edema and ascites. It may be emphasized that significant TV disease may not be associated with any symptoms until a late stage of the disease involving progressive right ventricular dysfunction. Symptoms caused by underlying etiology such as flushing, diarrhea, abdominal pain, etc. associated with carcinoid heart disease point to the etiology.

Physical findings include signs related to TV disease and those secondary to chronic venous congestion, that is, leg edema and ascites. Tricuspid stenosis results in characteristic changes in the jugular venous pulse in form of a slow "V" to "Y" descent and prominent "A" waves. The liver is enlarged with a firm edge, and pulsatile in presystole. Auscultation reveals a low-to-medium-pitched diastolic rumble with inspiratory accentuation. This is usually localized to the lower sternal border [13].

TR results in the jugular venous pulse exhibiting a prominent "C-V" wave or systolic wave. There is often a parasternal lift from right ventricular enlargement. The liver shows systolic pulsations, is enlarged and often tender. The cardiac auscultation reveals a soft early or holosystolic murmur which is augmented with inspiratory effort (Carvallo sign). A systolic honk may be present with TV prolapse [14]. Substantial TR may exist without the classic ausculatory findings. Thus, neither presence nor quantitation of TR can be reliably judged by auscultation. The pulsatile liver is a sign of severe regurgitation.

16.4.2 Investigations

Electrocardiogram There are no specific markers of TV disease, although the following clues may be present: (a) right ventricular hypertrophy and "strain" with right QRS axis; and (b) right atrial enlargement with prominent P waves. Specific ECG signs of primary etiology may be noted, such as left axis deviation and complete right bundle branch block in AV canal defect associated with cleft valve, and Ebstein's anomaly may exhibit wide QRS.

Chest Radiograph Cardiomegaly associated with prominent right-heart borders may be noted. There are no specific findings to suggest a diagnosis of TV disease.

Transthoracic Echocardiography Two dimensional echocardiogram combined with spectral and color flow Doppler evaluation provides the most accurate laboratory test in detection and quantitation of TV disease (Fig. 16.1).

Color flow Doppler and spectral Doppler are sensitive for detection of valve regurgitation and generally accurate for semiquantitative assessment of tricuspid stenosis and regurgitation [15]. Tricuspid stenosis is detected with color flow imaging by demonstrating a central core of high velocity jet. The continuous wave Doppler permits measurements of mean and end-diastolic gradients. The normal mean gradient is less than 3 mmHg and the end diastolic gradient nearly zero. Severe stenosis is associated with mean gradient of 5 mmHg and pressure half time measured in end inspiratory beat is greater than 190 ms. It has been proposed, but not well validated, that TV area may be determined by 190 divided by pressure half time.

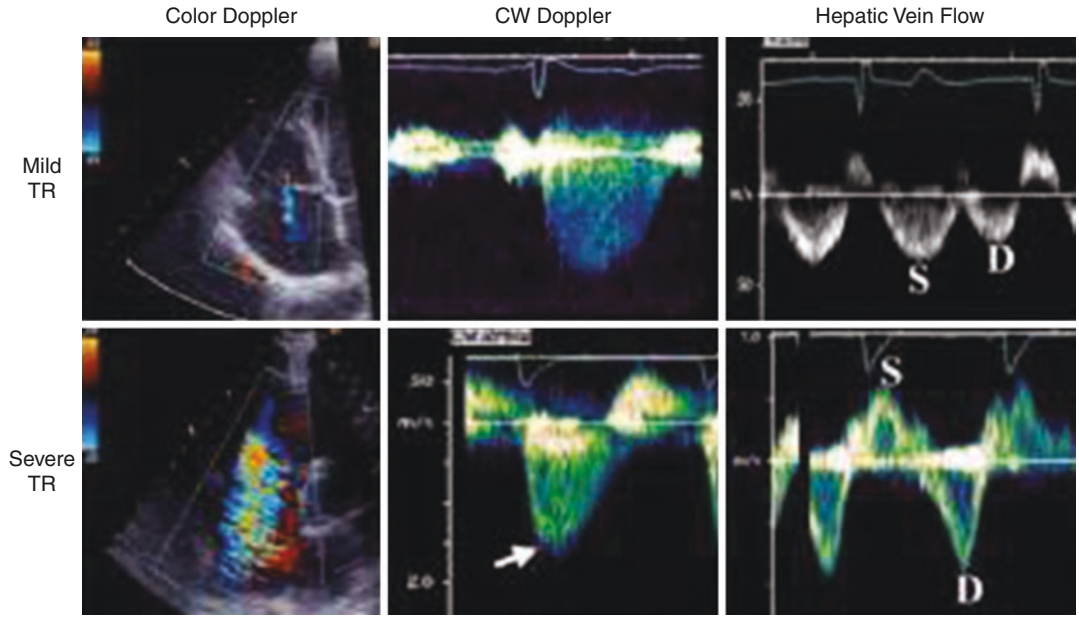

Fig. 16.1 2D echocardiogram demonstrating evaluation of severity of tricuspid regurgitation

TR using color flow imaging is readily recognized from parasternal tricuspid inflow view, short axis view, and apical or subcostal four chamber cross sections. Regurgitant jet area correlates roughly with severity of regurgitation, being less than 5 cm^2 in mild, 6–10 cm^2 in moderate and greater than 10 cm^2 in severe cases. In clinical practice, a visual estimate rather than actual planimetry is utilized. A more accurate estimate may be obtained by utilizing flow acceleration and PISA (Proximal Isovelocity Surface Area) measurements from which regurgitant orifice area may be calculated. The measured PISA radius is by itself a good guide to severity of regurgitation. The technique is important. The color flow baseline should be shifted in direction of regurgitation to get aliased velocity of approximately 30 cm/s. The radius of hemispherical PISA of greater than 9 mm indicates severe, 5–9 mm moderate, and less than 5 mm mild regurgitation. The spectral Doppler image of TR represents pressure gradient between right ventricle and right atrium through systole. The shape of TR velocity profile using continuous wave Doppler provides a clue to this relationship. The regurgitation profile is generally parabolic except in severe cases, where high right atrial "C-V" waves result in rapid equalization with right ventricular pressure giving a profile with rapid deceleration, also described as 'V' wave cut off sign [16].

Additional indirect clues of regurgitation severity are density of continuous wave Doppler profile, size of right ventricle and atrium, paradoxical interventricular septal motion, and systolic bulge of interatrial septum toward left atrium. The hepatic vein flow may exhibit systolic reversal of flow in severe cases.

A calculation of right ventricular systolic pressure (ie, pulmonary artery systolic pressure in absence of outflow obstruction) using peak TR velocity is extremely useful in clinical practice. The formula used is: Right Ventricular Systolic Pressure = 4 × TR velocity + right atrial pressure [16]. The latter may be assumed to be 7–10 mm, or more accurately determined from size of inferior vena cava and its collapse with sniff test. It is important to emphasize that height of TR velocity is not indicative of severity of regurgitation, but rather the degree of right ventricular systolic pressure or pulmonary hypertension.

In addition, the TV morphology provides clues of underlying etiology and pathophysiology of valve dysfunction [17].

Ebstein's anomaly is characterized by apical displacement of the septal tricuspid leaflet into the right ventricle by more than 8 mm/m^2 from the insertion point of the anterior mitral leaflet from the crux. The right atrium is enlarged, composed of anatomic right atrium proper and atrialized proximal inflow right ventricle. The residual right ventricle is reduced in size (Fig. 16.2).

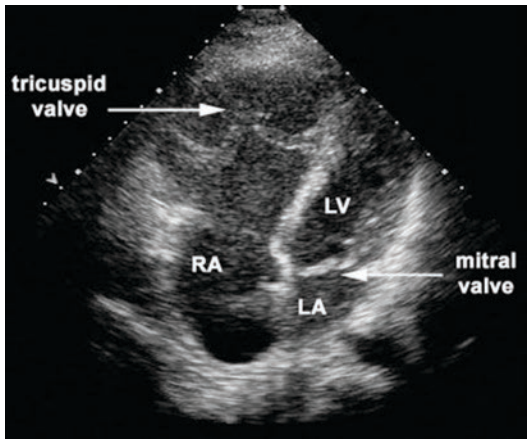

Fig. 16.2 2D echocardiogram demonstrating Ebstein's anomaly

AV cushion defect with associated cleft valve abnormality is best seen in apical 4 chamber view. The mitral and TVs are seen as a common valve straddling the defect. The cleft may be visualized with confirmation by color flow image showing the regurgitation jet going across the valve abnormality.

Carcinoid heart disease is characterized by thickened immobile valve leaflets held in half open position, resulting in appearance of stenosis as well as free flowing regurgitation with color flow Doppler [18] (Fig. 16.3).

Rheumatic TV disease is nearly always associated with rheumatic mitral and/or aortic valve

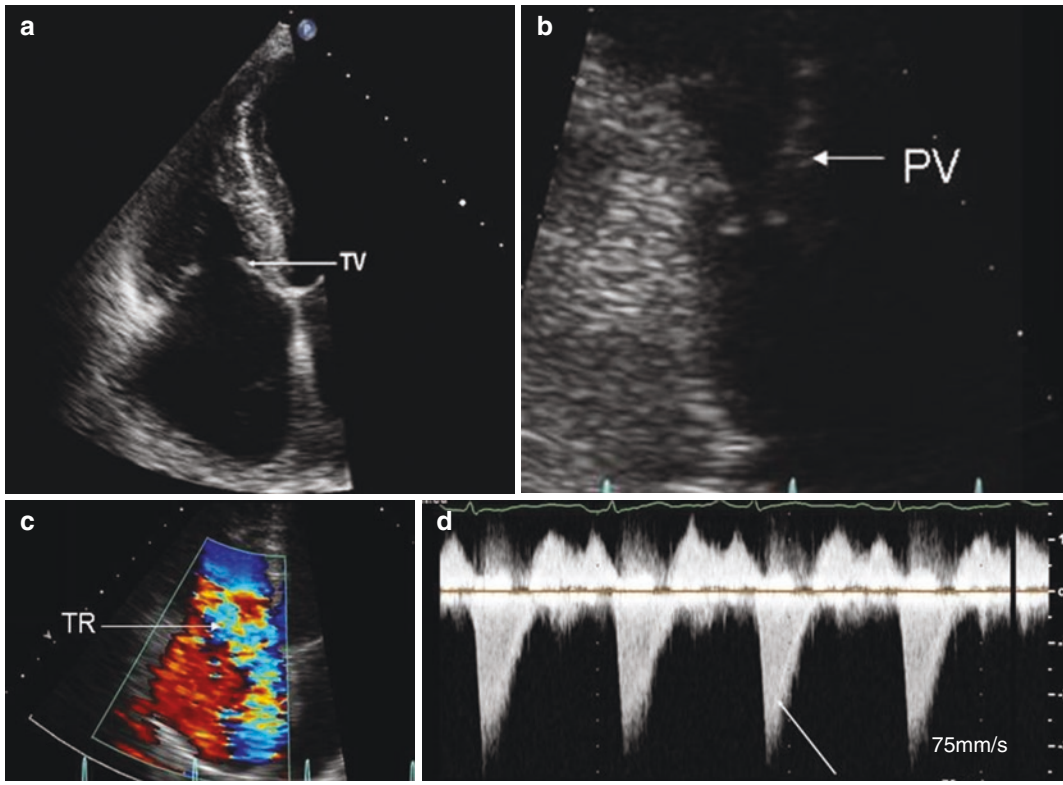

Fig. 16.3 2D echocardiogram in carcinoid heart disease. (**a**) Thickened, retracted, fixed tricuspid valve (TV) leaflets which do not co-apt. (**b**) Thickened, fixed and retracted pulmonary valve (PV) cusps. (**c**) Color Doppler demonstrating severe tricuspid regurgitation (TR). (**d**) Continuous wave Doppler demonstrating "Dagger" shaped profile of severe tricuspid regurgitation

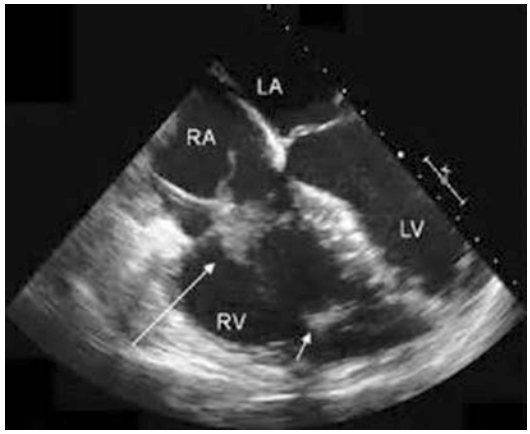

Fig. 16.4 2D echocardiogram demonstrating pacemaker lead and tricuspid valve endocarditis

disease. The valve leaflets are thickened and exhibit some doming in diastole.

TV prolapse is seen in nearly 30% of patients with mitral valve prolapse. The characteristic appearance includes dilated annulus, billowing prolapse, less commonly chordae rupture with flail leaflet [18]. Apart from the general syndrome of degenerative valve disease, TV prolapse has been described in congenital heart disease associated with systemic right ventricles.

Infective endocarditis is generally apparent with demonstration of mobile vegetation with transthoracic echocardiography (Fig. 16.4). In some cases, the transesophageal approach may be used for confirmation. Differentiation of vegetation from a tumor requires clinical correlation [18].

Valvulopathy associated with Phen-Fen and methysergide consists of thickened, fibrotic, less mobile tricuspid leaflets. These appearances are non-specific and require historical confirmation of drug use.

Pacemaker lead related trauma exhibits leaflet entrapment by a pacemaker lead. The color flow jet of TR may be localized at the pacemaker contact site along the tricuspid leaflet. Less commonly, leaflet perforation may be noted.

Secondary or functional TR is characterized by annular dilatation, generally the annular diameter greater than 40 mm, and tethering of leaflets with tenting distance in excess of 8 mm. In extreme cases, the leaflets fail to coapt with wide open regurgitation. Severe right ventricular hypertension is associated with shift of the interventricular septum toward the left ventricle, resulting in asymmetric tethering. In addition, characteristic appearances of RV infarction, arrhythmogenic RV dysplasia, or myocarditis and cardiomyopathy may be observed.

Transesophageal Echocardiography (TEE) Transthoracic echocardiography is often of diagnostic quality because the TV and RV are closer to the anterior chest wall and several parasternal, apical, and subcostal views are used to image these structures. However, TEE is indicated for better anatomic definitions of the valve lesions or precise measurement of the tricuspid annulus. The assessment of severity of tricuspid stenosis or TR is generally more accurate with transthoracic echocardiography. This is especially true in the intraoperative setting, where severity of TR may be underestimated as a result of lowered pulmonary vascular resistance from the anesthetic agents. It is therefore erroneous to use the severity of TR in the operating room to decide if a surgical procedure is to be performed on the TV. In the intraoperative setting, TEE is especially used for measuring the tricuspid annulus diameter. This is done in the midesophageal four-chamber view and a plane perpendicular (90°) to it.

Cardiac Catheterization and Selective Angiography Prior to the advent of diagnostic echocardiography, cardiac catheterization was used to confirm the presence and severity of tricuspid stenosis. It was recognized that simultaneous recordings of right atrial and right ventricular diastolic pressures was needed for accurate assessment because the pressure gradients are small and there is considerable respiratory variation in the pressure wave forms. The diagnosis of TR posed a greater challenge, as selective angiography into the right ventricle would often distort the TV. The pressure wave form in the right atrium shows the characteristic prominent systolic V wave with rapid descent only in the most severe cases. Diagnostic cardiac catheterization should rarely, if ever, be undertaken for the diagnosis or quantitation of TV disease alone.

16.5 Treatment

The treatment of TV disease must entertain two important questions, namely when to treat and how to treat.

16.5.1 Indications and Timing of Intervention

The decision to treat TV disease is based largely on hemodynamic and functional consequences of the diseases as well as coexistence of other associated valvular or congenital lesions. As an isolated lesion, mild or moderate TV disease does not need to be treated. Mild or even moderate TR may be observed using current echo-Doppler techniques in normal subjects. In the absence of structural changes such as annular dilatation or leaflet disruption, such lesions are not known to progress. On the other hand, severe TV disease results in enlargement of right atrium and RV and increase in right atrial and systemic venous pressures. If untreated, RV dysfunction with reduction in cardiac output develops first with exercise and subsequently at rest. This is accentuated by development of atrial fibrillation. In addition, chronic hepatic congestion results in fibrosis and development of cardiac cirrhosis. The liver function tests become increasingly abnormal. Progressive dilatation of right heart chambers brings about progressive annular dilatation, worsening severity of regurgitation. Thus, chronic severe regurgitation often begets more regurgitation. For isolated severe TV disease, intervention should be considered as earliest signs of RV and/or hepatic dysfunction develop.

The rules governing management are different when moderate TV dysfunction is associated with other valvular or myocardial disorders. The timing of intervention is generally dictated by considerations relating to accompanying left heart disease. Approximately 40% of patients exhibit regression of TR following mitral valve surgery, with reduction in pulmonary hypertension. Since it fails to regress in nearly 60% of patients, it is a recommended practice to treat tricuspid lesion more aggressively during the mitral valve surgery [19].

The 2014 AHA/ACC guidelines recommend TV surgery for patients with severe TR undergoing left-sided valve surgery [20]. According to these guidelines TV repair can be beneficial for patients with mild, moderate, or greater functional TR at the time of left-sided valve surgery with either (1) tricuspid annular dilation or (2) prior evidence of right heart failure. TV surgery can also be beneficial for patients with symptoms due to severe primary TR that are unresponsive to medical therapy. TV surgery may be considered for patients with moderate functional TR and pulmonary hypertension at the time of left-sided valve surgery as well as for asymptomatic or minimally symptomatic patients with severe primary TR and progressive degrees of moderate or greater RV dilation and/or systolic dysfunction. In patients who have undergone previous left-sided valve surgery and who do not have severe pulmonary hypertension or significant RV systolic dysfunction, reoperation for isolated tricuspid valve repair or replacement may be considered for persistent symptoms due to severe TR.

Surgery is recommended for patients with severe tricuspid stenosis at the time of surgery for left-sided valve disease as well as for patients with isolated, symptomatic severe tricuspid stenosis. Percutaneous balloon tricuspid commissurotomy may be considered for patients with isolated, symptomatic severe tricuspid stenosis without accompanying TR [20].

16.5.2 Medical Treatment

TR secondary to pulmonary hypertension may be treated by medical management of underlying etiology, when feasible. Thus, appropriate treatment of myocarditis or depressed left ventricular function may result in amelioration of functional TR. Similarly, improvement in lung function in chronic obstructive lung disease or appropriate control of sleep apnea may improve the associated TR. It is worth emphasizing that functional TR may be dynamic, being load dependent. Intensive medical treatment of heart failure may improve dramatically the severity of TR. This is especially relevant when a patient is undergoing surgery of left heart disease (such as mitral or aortic valve disease) following intensive medical treatment of heart failure, such that the most recent echocardiogram may fail to show signifi-

cant TR. In this setting even if the TR is mild to moderate, it will require surgical treatment.

16.5.3 Surgical Treatment

Primary or intrinsic TV disease with severe dysfunction nearly always requires surgery, with the possible exception of rheumatic tricuspid stenosis which may be approached by percutaneous balloon valvuloplasty.

16.6 Surgical Treatment of Rheumatic Tricuspid Stenosis

The most common cause of organic tricuspid disease worldwide is rheumatic fever. It usually affects the mitral valve and frequently affects the aortic valve concomitantly. Despite the dramatic decline of acute rheumatic fever in developed countries, significant morbidity and mortality are still associated with rheumatic heart disease in developing nations [21]. Rheumatic tricuspid stenosis is nearly always associated with rheumatic mitral valve disease. Successful mitral and TV repair may be carried out, although long term results are poor. Mitral valve replacement with TV replacement may be considered in patients unwilling to entertain a risk of reoperation. These patients will require mechanical prosthesis, being in a younger age group [21].

16.7 Surgical Treatment of Functional Tricuspid Regurgitation

Functional TR is the most frequent cause of tricuspid insufficiency and is often secondary to left-sided valve diseases. The correction of left-sided valve diseases without concomitant repair of functional TR is associated with significant late morbidity and mortality. This occurs on account of progressive right ventricular dysfunction and increasing need for reoperation [22]. A variety of techniques for valve repair have been used over the years. These fall broadly into 2 categories; suture techniques and annuloplasty techniques.

16.7.1 Suture Techniques

De Vega Purse String Repair De Vega developed his popular technique of semicircular suture annuloplasty in the early 1970s, which consists of plication of the posterior and anterior portion of the annulus, preserving the septal portion, with a double continuous suture [23] (Fig. 16.5). It is one of the most effective frequently used techniques for surgical correction of FTR. It appears to be safe, easily reproducible, and efficacious in the short-term. It is reliable when used for minor degrees of tricuspid regurgitation in the absence of right heart dilatation. Physiologic annular motions

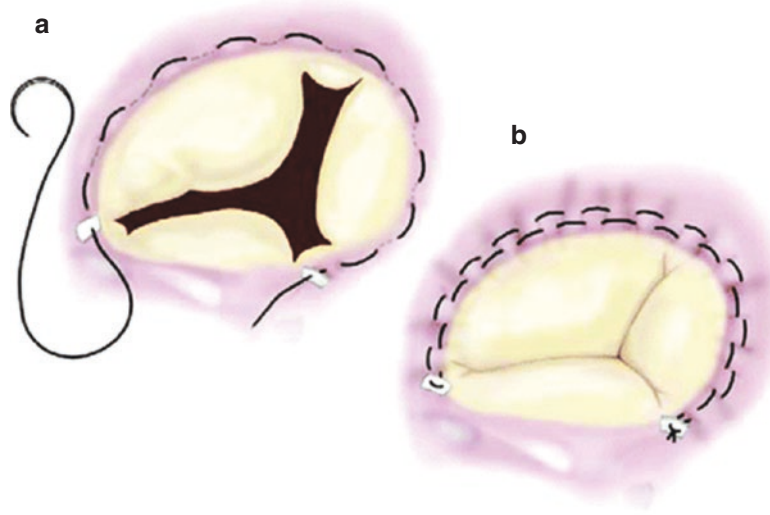

Fig. 16.5 (**a**) Suture annuloplasty commencing at posteroseptal commissure going upto anteroseptal commissure (**b**) Completed suture annuloplasty with a double continuous suture preserving the septal portion

are protected by De Vega annuloplasty. However, recurrent tricuspid regurgitation secondary to Bowstring (Guitar string) phenomenon is seen after De Vega suture annuloplasty as a result of gliding (jiggle) effect especially in the setting of moderate to severe regurgitation [5]. It is a more practical and economical approach in developing countries with high incidence of rheumatic mitral disease being operated on at early age [5].

Several modifications of the De Vega annuloplasty technique have been described in recent years with potential benefits. However, despite the suggested advantages of these modifications none has been followed up for long enough to validate these benefits [22].

Annuloplasty Techniques There is a growing body of evidence to support improved outcome and durability of TV repair using a prosthetic annuloplasty ring. Tang et al. reported that long-term survival, event-free survival and freedom from recurrent TR were significantly better in the ring group, and there was a trend toward fewer TV reoperations compared to a De Vaga procedure without the prosthetic ring. Multivariable analysis demonstrated that the use of an annuloplasty ring was an independent predictor of long-term survival (hazard ratio [HR], 0.7; 95% confidence interval [CI], 0.5–1.0; P = 0.03) and event-free survival (HR, 0.8; CI, 0.6–1.0; P = 0.04) [23]. McCarthy et al. also reported a higher rate of failed TV repair without use of rings. They observed 30% of patients with De Vega procedure had severe regurgitation at 8 years as compared to none with ring annuloplasty [5].

A variety of annuloplasty rings and bands have been used over the years. Peri-Guard annuloplasty consists of customized semicircular annuloplasty using bovine pericardium. A high rate of early and late recurrence of TR has been reported. This approach is not favored at the present time [5].

Carpentier ring devised for the TV introduced more than 30 years ago has been extensively used. This semi-rigid ring has had excellent early and late outcome. Special care has to be taken to avoid injury to the AV node [5].

Fig. 16.6 Clover technique

Duran flexible ring has been proposed in order to preserve the normal annular function of dilatation in diastole and reduction in systole. Good early and late outcome has been reported using the flexible ring [5].

Annuloplasty bands or incomplete rings are used to avoid risk of AV node injury. A partial ring specially devised with knowledge of 3-dimensional geometry of the TV (MC3 ring) has been introduced with promising early and mid-term outcome [24].

Other Techniques To improve the feasibility and efficacy of TV repair in the setting of complex lesions like prolapse or flail of multiple cusps or myxomatous degeneration of TV, Debonis and associates developed a new surgical approach, which consists of stitching together the central part of the free edges of the leaflets producing a 'clover' shaped valve [25, 26] (Fig. 16.6).

Suture bicuspidization originally conceptualized and described by Kay, Maselli-Campagna, and Tsuji in 1965 is a relatively simple technique that involves figure-of-eight suture plication of the posterior leaflet to reduce annulus size [27] (Fig. 16.7).

Autologous pericardial patch extension of anterior tricuspid leaflet combined with pros-

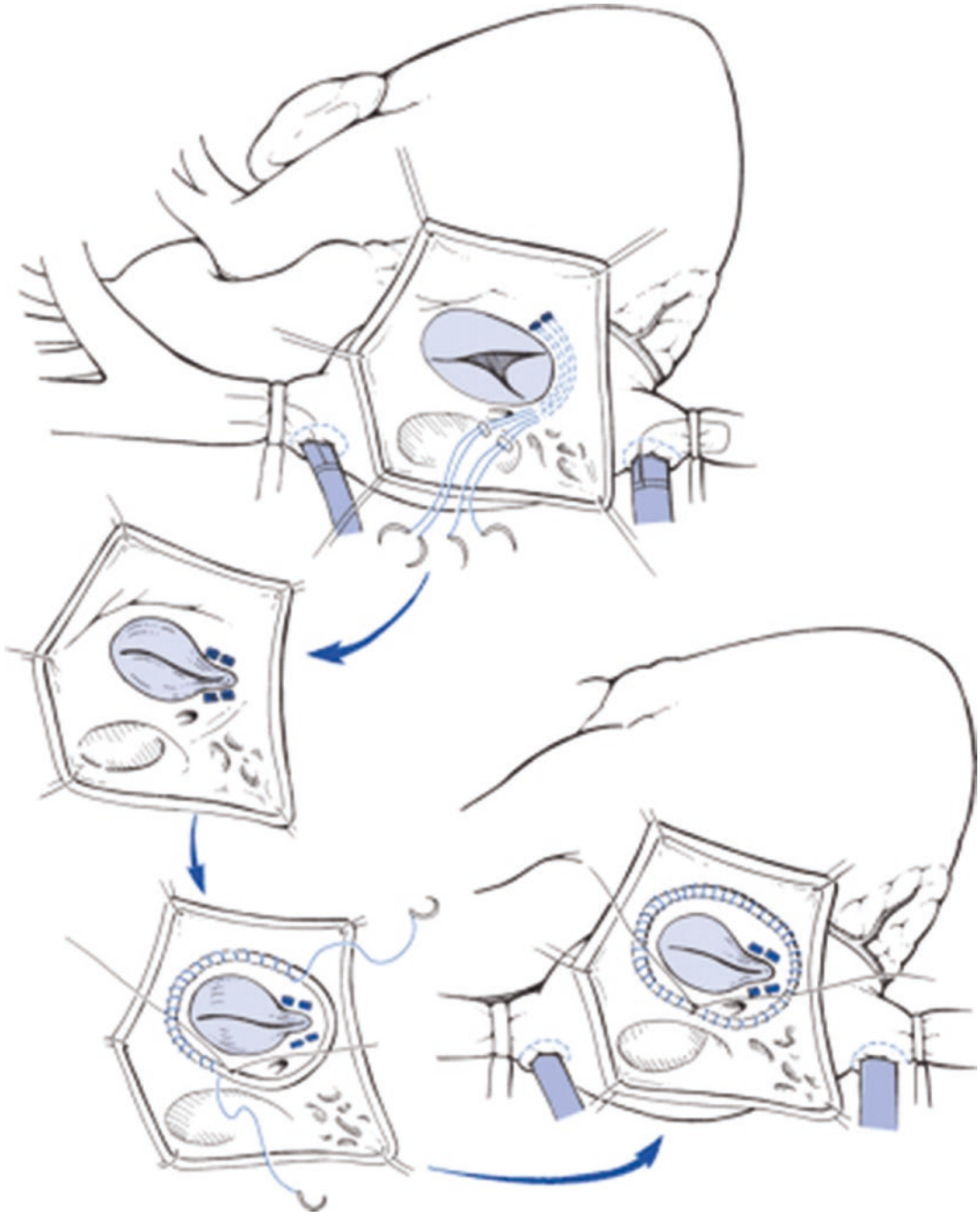

Fig. 16.7 Suture bicuspidization technique

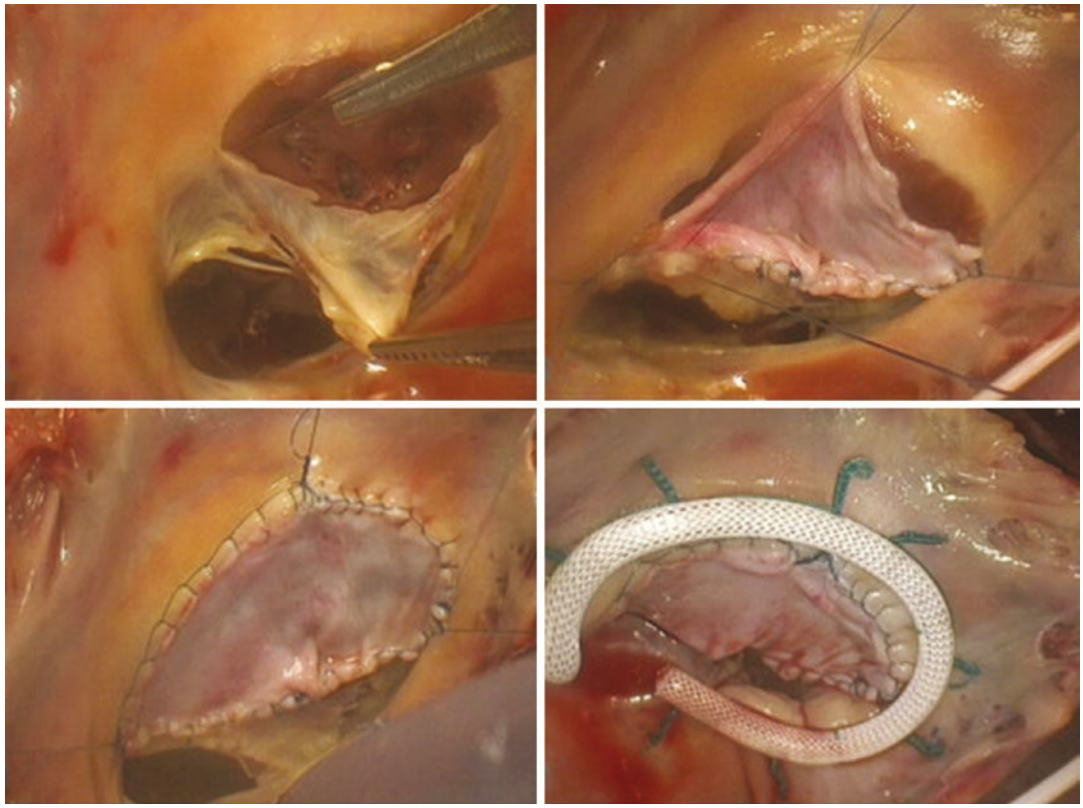

Fig. 16.8 (**a**) Anterior leaflet detached from the annulus (**b**) Pericardial patch being sewn onto the detached edge of the anterior leaflet (**c**) Pericardial patch completely sewn onto the anterior leaflet and annulus (**d**) Completed repair with annuloplasty ring

thetic annuloplasty ring is another innovative and easily reproducible technique that is claimed to virtually eliminate residual/recurrent TR in cases of severe leaflet tethering in the short-term [28] (Fig. 16.8).

Tricuspid Valve Replacement Although most studies have reported a better early and long term outcome with valve repair, there are some cases with marked distortion of the annulus and severe leaflet tethering in which valve replacement may be necessary. Generally bioprosthetic valves are preferred, since valve thrombosis and infection following mechanical valve replacement are recognized risks [4]. Some studies have shown no significant difference in long term outcome between tissue and mechanical valves [29–31]. Residual regurgitation following TV replacement is lower than after valve repair; however, the perioperative midterm survival and event free survival is better with valve repair [4].

16.8 Surgical Treatment of Primary Tricuspid Valve Regurgitation

16.8.1 Rheumatic Valve Disease

The surgical options include valve repair techniques similar to those employed for rheumatic mitral valve disease. In rare cases with extreme fibrotic distortion of the valve, TV replacement may need to be considered. In a study of 328 patients followed over a mean 8.7 years, in-hospital mortality was 7.6% and late mortality was 52.1%. Valve repair had a more favorable outcome [21].

16.8.2 Ebstein's Anomaly

TV repair may be feasible in milder cases, although the majority requires valve replacement. Good long term outcomes and survival are reported. A study examined outcome of 40 consecutive patients at one center. The valve was repaired in 18 patients, in 12 in association with cavo-pulmonary shunt. Twenty-two underwent replacement, 11 with cavo-pulmonary shunt. There were 2 postoperative deaths and 5 late deaths during follow-up of 6.7 (4.8) years. Arrhythmias were the most common late complication [32]. The experience reported from the Mayo Clinic in 539 patients showed survival at 5, 10, 15, and 20 years of 94%, 90%, 86%, and 76% respectively. Thirty-six percent experienced atrial fibrillation or flutter and 27% had endocarditis [33].

16.8.3 Carcinoid Heart Disease

Symptomatic patients with severe TV dysfunction despite treatment with somatostatin analogues generally require valve replacement. Surgical intervention, aside from relief of symptoms, is also credited with improved survival in this lethal disease. Balloon valvuloplasty has been used in rare cases with predominant tricuspid stenosis. This represents a high risk surgical group [34]. The published experience of surgery for carcinoid heart disease is limited and there is no consensus at present about timing, indications of surgery or choice of prosthetic valves [35].

16.8.4 Infective Endocarditis

Infection of the tricuspid is commonly related to intravenous drug abuse and poses a significant challenge in management. Early cases may undergo successful valve repair with resection of vegetation, focal leaflet resection and annuloplasty. However, the large majority have significant valve destruction and are candidates for valve replacement. The chances of reinfection in drug addicts is considerable and medical follow-up is likely to be sporadic. Hence, tricuspid valvectomy has been utilized with good initial results, since the resulting TR in absence of pulmonary hypertension is hemodynamically well tolerated [36]. However, the long-term results are discouraging. Replacement with bioprosthesis may be preferred despite young age of the patient, owing to lack of reliance on oral anticoagulation therapy in this group of patients [37].

16.8.5 Cleft Tricuspid Valve

Most adult patients presenting with cleft TV have milder pathology and are successfully repaired. Younger patients with extremely malformed valves may require valve replacement [38].

16.8.6 Iatrogenic Tricuspid Regurgitation

TR associated with pacemaker trauma is generally amenable to valve repair. Rare cases with secondary fibrotic changes may require valve replacement [39].

16.9 Percutaneous Approaches

In recent years, the TV has been regarded as a potential target for new percutaneous treatments in view of the increasing recognition that long-term surgical results are suboptimal due to residual/recurrent regurgitation and repeat surgery carries a significant risk. Percutaneous valve implantation is feasible in degenerated prosthetic tricuspid valves, and may improve haemodynamic and functional status [40]. The differences in reported approaches show that there is no consensus for the best strategy in these complex procedures. Larger series and long-term follow-up are needed to better assess the role of this technique in the future. Moreover, whereas results for valve-in-valve procedures are good, paravalvular leaks occurring with rigid annuloplasty rings are a source of concern. This issue may improve in the near future with dedicated devices, which should offer longer covered lengths [40].

For the native tricuspid valve, preliminary results with the two bicuspidization techniques validate their feasibility [41, 42]. More experience is needed to assess their clinical benefit and define the best candidates. Finally, a number of other devices are in preclinical development, and there is no doubt that the next decade will see the full recognition of the tricuspid valve in the field of transcatheter treatments [43, 44].

Conclusions

Tricuspid disease is predominantly characterized by TR, which is mainly secondary to left-sided heart valve disease. Tricuspid disease has long been ignored, with the belief that TR would improve after surgical correction of left-sided valve disease. A large body of evidence now supports the negative effect of significant TR, and this recognition has led to more frequent indications for combined as well as occasionally isolated tricuspid surgery, with the inherent risk of subsequent dysfunction of tricuspid repair or replacement. A variety of repair techniques have been developed over the years with repair using a prosthetic annuloplasty ring regarded as superior to suture techniques. Despite the efficacy of repair techniques, residual/recurrent TR is a universally recognized phenomenon. Similarly, replacement with a bioprosthetic valve is fraught with structural valve degeneration. Whatever the clinical context, redo TV surgery is often associated with high morbidity and mortality rates. Following the recent development of transcatheter therapies for aortic and mitral valve diseases, the possibility of lower-risk tricuspid valve intervention is therefore particularly attractive and the emerging literature on the subject makes encouraging reading.

References

1. Shah PM, Raney AA. Tricuspid valve disease. Curr Probl Cardiol. 2008;33:47–84.
2. Bruce CJ, Connolly HM. Right-sided valve disease deserves a little more respect. Circulation. 2009;119:2726–34.
3. Guenther T, Norbauer C, Mazzitelli D, Busch RB, Tassani-Prell P, Lange R. Tricuspid valve surgery: a thirty-year assessment of early and late outcome. J Cardiothorac Surg. 2008;34:402–9.
4. Singh SK, Tang GHL, Maganti MD, Armstrong S, Williams WG, David TE, et al. Midterm outcomes of tricuspid valve repair versus replacement for organic tricuspid disease. Ann Thorac Surg. 2006;82:1735–41.
5. McCarthy PM, Bhudia SK, Rajeswaran J, Hoercher KJ, Lytle BW, Cosgrove DM, et al. Tricuspid valve repair: durability and risk factors for failure. J Thorac Cardiovasc Surg. 2004;127:674–85.
6. Shah PM. Tricuspid and pulmonary valve disease evaluation and management. Rev Esp Cardiol. 2010;63:1349–65.
7. Tei C, Pilgrim JP, Shah PM, Ormiston JA, Wong M. The tricuspid valve annulus: study of size and motion in normal subjects and in patients with tricuspid regurgitation. Circulation. 1982;6:665–71.
8. Joudinaud TM, Flecher EM, Duran CM. Functional terminology for the tricuspid valve. J Heart Valve Dis. 2006;15:382–8.
9. Waller BF, Moriarty AT, Eble JN, Davey DM, Hawley DA, Pless JE. Etiology of pure tricuspid regurgitation based on annular circumference and leaflet area: analysis of 45 necropsy patients with clinical and morphologic evidence of pure tricuspid regurgitation. J Am Coll Cardiol. 1986;7:1063–74.
10. Waller BF, Howard J, Fess S. Pathology of tricuspid valve stenosis and pure tricuspid regurgitation part III. Clin Cardiol. 1995;18:225–30.
11. Shiran A, Sagie A. Tricuspid regurgitation in mitral valve disease. J Am Coll Cardiol. 2009;53:401–8.
12. Adler DS. Non-functional tricuspid valve disease. Ann Cardiothorac Surg. 2017;6:204–13.
13. Wooley CF, Fontana ME, Kilman JW, Ryan JM. Tricuspid stenosis: atrial systolic murmur, tricuspid opening snap, and right atrial pressure pulse. Am J Med. 1985;78:375–84.
14. Tei C, Shah PM, Tanaka H. Phonographic-echographic documentation of systolic honk in tricuspid prolapse. Am Heart J. 1982;103:294–5.
15. Rivera JM, Vandervoort PM, Vazquez de Prada JA, Mele D, Karson TH, Morehead A. Which physical factors determine tricuspid regurgitation jet area in the clinical setting? Am J Cardiol. 1993;72:1305–9.
16. Zoghbi WA, Enriquez-Sarano M, Foster E, Grayburn PA, Kraft CD, Levine RA, et al. Recommendations for evaluation of the severity of native valvular regurgitation with two-dimensional and Doppler echocardiography. A report from the American Society of Echocardiography's nomenclature and standards committee and the task force on valvular regurgitation. J Am Soc Echocardiogr. 2003;16:777–802.
17. Tei C, Shah PM, Cherian G, Trim PA, Wong M, Ormiston JA. Echocardiographic evaluation of normal and prolapsed tricuspid valve leaflets. Am J Cardiol. 1983;52:796–800.

18. Fuster V, O'Rourke RA, Poole-Wilson P. Tricuspid valve, pulmonary valve and multiple valve disease. Hurst's The Heart. 2009;13:1745–56.
19. Dreyfus GD, Corbi PJ, Chan KM, Bahrami T. Secondary tricuspid regurgitation or dilatation: which should be criteria for surgical repair? Ann Thorac Surg. 2005;79: 127–32.
20. Nishimura RA, Otto CM, Bonow RO, Carabello BA, Erwin JP, Guyton RA, O'Gara PT, Ruiz CE, Skubas NJ, Sorajja P, Sundt TM 3rd, Thomas JD, ACC/AHA Task Force Members. 2014 AHA/ACC guideline for the management of patients with valvular heart disease: executive summary: a report of the American College of Cardiology/American Heart Association task force on practice guidelines. Circulation. 2014; 129:2440–92.
21. Bernal JM, Pontón A, Diaz B, Llorca J, García I, Sarralde A, Diago C, Revuelta JM. Surgery for rheumatic tricuspid valve disease: a 30-year experience. J Thorac Cardiovasc Surg. 2008;136:476–81.
22. Raja SG, Dreyfus GD. Surgery for functional tricuspid regurgitation: current techniques, outcomes and emerging concepts. Expert Rev Cardiovasc Ther. 2009; 7:73–84.
23. De Vega NG. Selective, adjustable and permanent annuloplasty. An original technic for the treatment of tricuspid insufficiency. Rev Esp Cardiol. 1972;25:555–6. [Spanish].
24. Hata H, Fujita T, Shimahara Y, Sato S, Kobayashi J. Early and mid-term outcomes of aggressive tricuspid annuloplasty with the MC3 ring. J Heart Valve Dis. 2014;23:601–8.
25. Alfieri O, De Bonis M, Lapenna E, Agricola E, Quarti A, Maisano F. The "clover technique" as a novel approach for correction of post-traumatic tricuspid regurgitation. J Thorac Cardiovasc Surg. 2003;126:75–9.
26. Lai YQ, Meng X, Bai T, Zhang C, Luo Y, Zhang ZG. Edge-to-edge tricuspid valve repair: an adjuvant technique for residual tricuspid regurgitation. Ann Thorac Surg. 2006;81:2179–82.
27. Kay JH, Maselli-Campagna G, Tsuji KK. Surgical treatment of tricuspid insufficiency. Ann Surg. 1965; 162:53–8.
28. Dreyfus GD, Raja SG, John Chan KM. Tricuspid leaflet augmentation to address severe tethering in functional tricuspid regurgitation. Eur J Cardiothorac Surg. 2008;34:908–10.
29. Tanaka M, Ohata T, Fukuda S, Kigawa I, Yamashita Y, Wanibuchi Y. Tricuspid valve supra-annular implantation in adult patients with Ebstein's anomaly. Ann Thorac Surg. 2001;71:582–6.
30. Ratnatunga CP, Edwards MB, Dore CJ, Taylor KM. Tricuspid valve replacement: UK heart valve registry mid-term results comparing mechanical and biological prostheses. Ann Thorac Surg. 1998;66:1940–7.
31. Rizzoli G, Vendramin I, Nesseris G, Bottio T, Guglielmi C, Schiavon L. Biological or mechanical prostheses in tricuspid position? A meta-analysis of intra-institutional results. Ann Thorac Surg. 2004;77:1607–14.
32. Al-Najashi KS, Balint OH, Oechslin E, Williams WG, Silversides CK. Mid-term outcomes in adults with Ebstein anomaly and cavopulmonary shunts. Ann Thorac Surg. 2009;88:131–6.
33. Brown ML, Dearani JA, Danielson GK, Cetta F, Connolly HM, Warnes CA, et al. Functional status after operation for Ebstein anomaly. J Am Coll Cardiol. 2008;52(6):460–6.
34. Moller JE, Pellikka PA, Bernheim AM, Schaff HV, Rubin J, Connolly HM. Prognosis of carcinoid heart disease analysis of 200 cases over two decades. Circulation. 2005;112:3320–7.
35. Raja SG, Bhattacharyya S, Davar J, Dreyfus GD. Surgery for carcinoid heart disease: current outcomes, concerns and controversies. Futur Cardiol. 2010;6:647–55.
36. Yee ES, Khonsari S. Right-sided infective endocarditis: valvuloplasty, valvectomy or replacement. J Cardiovasc Surg. 1989;30:744–8.
37. Konstantinov IE. Total resection and complete reconstruction of the tricuspid valve in acute infective endocarditis. J Thorac Cardiovasc Surg. 2008;136(2):531.
38. Veerbhadran SP, Pillai VV, Sasidharan B, Karunakaran J. Surgery for congenital tricuspid valve cleft: tricuspid valve repair with neochordae and annuloplasty. J Heart Valve Dis. 2015;24:525–7.
39. Uehara K, Minakata K, Watanabe K, Sakaguchi H, Yamazaki K, Ikeda T, et al. Tricuspid valve repair for severe tricuspid regurgitation due to pacemaker leads. Asian Cardiovasc Thorac Ann. 2016;24:541–5.
40. Bouleti C, Juliard JM, Himbert D, Iung B, Brochet E, Urena M, et al. Tricuspid valve and percutaneous approach: no longer the forgotten valve! Arch Cardiovasc Dis. 2016;109:55–66.
41. Schofer J, Bijuklic K, Tiburtius C, Hansen L, Groothuis A, Hahn RT. First-in-human transcatheter tricuspid valve repair in a patient with severely regurgitant tricuspid valve. J Am Coll Cardiol. 2015;65: 1190–5.
42. Latib A, Agricola E, Pozzoli A, Denti P, Taramasso M, Spagnolo P, et al. First-in-man implantation of a tricuspid annular remodeling device for functional tricuspid regurgitation. JACC Cardiovasc Interv. 2015;8: e211–4.
43. Ruiz CE, Kliger C, Perk G, Maisano F, Cabalka AK, Landzberg M, et al. Transcatheter therapies for the treatment of valvular and paravalvular regurgitation in acquired and congenital valvular heart disease. J Am Coll Cardiol. 2015;66:169–83.
44. Rogers T, Ratnayaka K, Sonmez M, Franson DN, Schenke WH, Mazal JR, Kocaturk O, Chen MY, Faranesh AZ, Lederman RJ. Transatrial intrapericardial tricuspid annuloplasty. JACC Cardiovasc Interv. 2015;8:483–91.

Right Heart in Cardiac Pacing

17

Antonis S. Manolis, Antonis A. Manolis, and Theodora A. Manolis

Abstract

Conventional right heart pacing with leads placed at the right atrial appendage (RAA) and right ventricular (RV) apex produces iatrogenic dyssynchrony. Atrial dysssynchrony may favor the development of atrial tachyarrhythmias, but the data have been relatively limited and have not yet had any influence on clinical practice. However, the evidence of deleterious effects of the iatrogenic dyssynchrony in the form of left bundle branch block (LBBB) which is produced by RV apical pacing has been compelling and has led to some degree of a paradigm shift in our approach to conventional RV pacing by adopting selective site pacing and avoiding the RV apex, at least for patients with left ventricular (LV) dysfunction and/or heart failure, who are the ones who seem to be afflicted the most and are apparently better responders to non-RV apical pacing. The type of inter- and intra-ventricular dyssynchrony produced by classical RV apical pacing (iatrogenic LBBB) leads to *pacing-induced cardiomyopathy* similar to the dyssynchrony conferred by spontaneous LBBB, both manageable by biventricular pacing or cardiac resynchronization therapy (CRT). The evidence regarding the adverse effects of conventional right heart pacing is analyzed and reviewed in this chapter together with the data concerning selective or alternate site right heart pacing.

Keywords

Cardiac pacing · Alternate site pacing · Right ventricular apical pacing · Right ventricular septal pacing · Right ventricular outflow tract pacing · His bundle pacing · Cardiac resynchronization therapy · Biventricular pacing

Abbreviations

AF	Atrial fibrillation
AV	Atrioventricular
CRT	Cardiac resynchronization therapy
ICD	Implantable cardioverter defibrillator
LBBB	Left bundle branch block
LV	Left ventric-le(-ular)
LVEF	Left ventricular ejection fraction
RAA	Right atrial appendage
RV	Right ventric-le(-ular)
RVA	Right ventricular apex
RVOT	Right ventricular outflow tract
RVS	Right ventricular septum

A. S. Manolis (✉)
Third Department of Cardiology, Athens University School of Medicine, Athens, Greece
e-mail: asm@otenet.gr

A. A. Manolis
Patras University School of Medicine, Patras, Greece

T. A. Manolis
Zakynthos Hospital, Zakynthos, Greece

S. I. Dumitrescu et al. (eds.), *Right Heart Pathology*, https://doi.org/10.1007/978-3-319-73764-5_17

17.1 Conventional Right Heart Pacing

Dual-chamber atrioventricular (AV) pacing had been heralded and quoted as "physiological" or "universal" cardiac pacing when first made technically feasible and clinically available. [1–4] This conventional dual-chamber pacing system provides AV synchrony by pacing the right atrial appendage (RAA) at the atrial level and the right ventricular (RV) apex at the ventricular level (Fig. 17.1). Furthermore, these traditional pacing sites are easily accessible and provide stable lead positioning and reliable chronic pacing and sensing thresholds, mostly with use of passive fixation leads. However, nobody initially suspected that this type of cardiac stimulation was far from physiological pacing as it produced an iatrogenic left bundle branch block (LBBB) (Fig. 17.1), the consequences of which we came to realize at a much later stage [5–9]. Most likely this must have been the reason that the benefits of dual- over single-chamber pacing could never have been clearly demonstrated in several analyses with regards to hard-end-points, such as survival [1, 10], apparently negated by the deleterious effects of the produced dyssynchrony [11–13].

Indeed, over the last two decades, several studies have demonstrated the harmful consequences of intraventricular conduction delay, particularly those produced by intrinsic left bundle branch block (LBBB), which has been reported to afflict about 20–30% of heart failure patients [14–18]. In the presence of LBBB, ventricular dyssynchrony can confer hemodynamic and clinical deterioration due to a resultant reduction of stroke volume and cardiac output, further leading to clinical worsening in patients with left ventricular (LV) dysfunction and heart failure. In certain patients, long-standing LBBB may even be an identifiable reversible cause of cardiomyopathy [19]. All these ailments produced by this type of dyssynchrony are alleviated by cardiac resynchronization therapy (CRT) effected via biventricular pacing [20, 21]. Several studies have demonstrated over the years that CRT offers substantial clinical improvement and survival benefit in these patients [22].

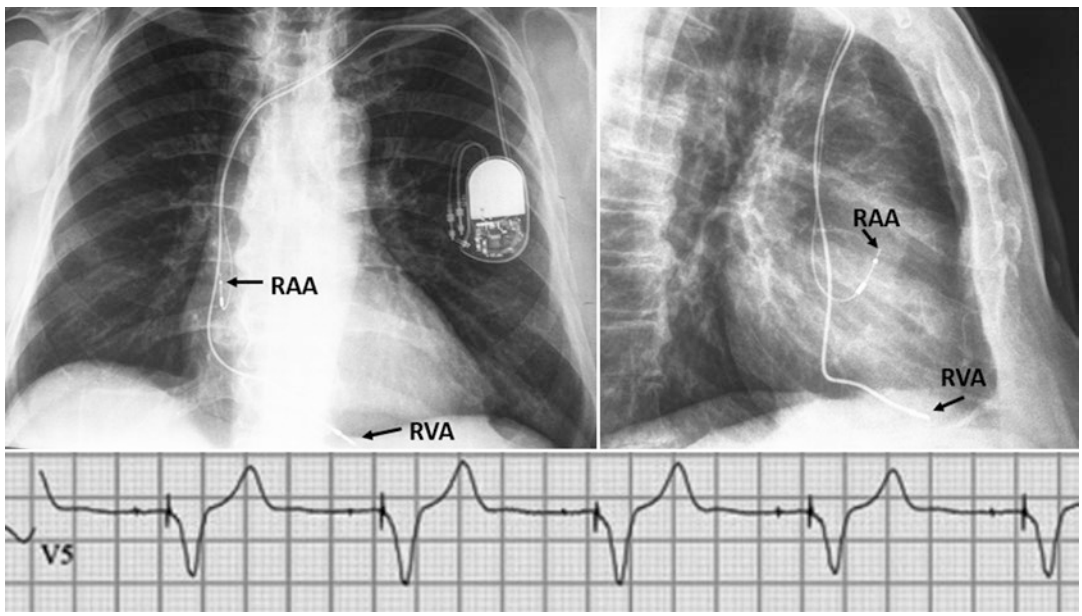

Fig. 17.1 Conventional dual-chamber right heart pacing entails anchoring or screwing an atrial lead into the right atrial appendage (RAA) and a ventricular lead at the RV apex (RVA). An anteroposterior view is viewed on the left panel and a right anterior oblique view on the right displaying the respective leads. The ECG at the lower panel displays an LBBB-like morphology with very wide QRS indicating the degree of ventricular dyssynchrony

Although it has become abundantly clear that LBBB is functionally deleterious, there are still those who continue producing iatrogenic LBBB by applying conventional permanent cardiac pacing in their practices. Indeed, in concert with the above data regarding the adverse hemodynamic and clinical effects of the spontaneous LBBB, data are accumulating, which convincingly indicate that the iatrogenic LBBB, produced by our conventional RV apical pacing technique employed in permanent cardiac pacing, is equally harmful [11, 13, 23]. The evidence of a deleterious effect of RV apical pacing on both otherwise healthy individuals and heart failure patients is such that we cannot afford being complacent with such a routine practice any longer.

Similar to the ventricular dyssynchrony produced by conventional RV pacing, conventional RAA pacing has been implicated in producing atrial dyssynchrony that can lead to atrial tachyarrhythmias (atrial fibrillation) and compromised atrial mechanical function [24, 25].

17.2 Clinical Studies of Harm Conferred by RV Apical Pacing/RV Pacing-Induced Cardiomyopathy

The realization of a serious adverse effect of dual-chamber conventional pacing came abruptly when the results of the DAVID trial were published in 2002, showing that in 506 patients fitted with an implantable cardioverter defibrillator (ICD) device, also having a LV ejection fraction (LVEF) of ≤40%, dual-chamber pacing in 250 patients compared with ventricular backup pacing in 256 patients was actually detrimental by increasing the combined end point of death or hospitalization for heart failure [26]. Over 1 year, the hazard ratios for the DDDR pacing group compared with the VVI group were 1.61 for heart failure hospitalization or death, 1.54 for heart failure hospitalization and 1.61 for death. Similar results were subsequently reported by a MADIT II substudy comprising 567 patients [27]. According to this study, during a 20-month follow-up, 369 patients having high cumulative RV pacing (>50%), had a higher incidence of new or worsened heart failure (50% vs 20%, $p < 0.001$; hazard ratio 2.1) and heart failure or death (hazard ratio 1.9) compared to 198 patients with infrequent RV pacing. In addition, patients in the high pacing group had significantly more episodes of ventricular tachycardia events requiring shock or antitachycardia pacing by the ICD than did patents in the low pacing group ($p < 0.001$).

However, even before the results of the DAVID trial, several studies and case reports had been providing clues indicating a plethora of harmful effects of long-term RV apical pacing (Table 17.1) [5, 6, 8, 28, 29]. Importantly, a longitudinal controlled study reported the long-term effects of RV apical pacing in 24 young patients (mean age of 19.5 years) who received conventional permanent pacemakers [7]. These patients were followed for a mean of 9.5 years. The duration of RV apical pacing ranged from 0.7 to 18.9 years (median 10). Right ventricular apical pacing led to irreversible LV dysfunction. Both LV systolic and diastolic function indexes were impaired in comparison with the indexes of 33 age- and basal surface area-matched healthy control individuals. Paced QRS interval and age were found to significantly influence global LV contraction in these patients. The same group performed myocardial biopsies in 14 patients with congenital complete heart block and

Table 17.1 Adverse effects of right ventricular apical pacing

• LV dyssynchrony (iatrogenic LBBB)
• Pacing-induced cardiomyopathy
• LV remodeling (dilatation, hypertrophy)
• Systolic and diastolic LV dysfunction
• Decreased cardiac output/increased filling pressure
• Heart failure
• Myocardial perfusion defects
• Functional mitral regurgitation
• Altered myocardial histology
• Increased left atrial diameter
• Atrial fibrillation
• Increased sympathetic nerve activity
• Promotion of ventricular arrhythmias
• Increased morbidity and mortality

LBBB left bundle branch block, *LV* left ventricle

otherwise normal cardiac anatomy, demonstrating altered cardiac histology produced by chronic RV apical pacing, potentially explaining the compromised LV function observed clinically [30]. These results clearly point to a newly recognized pathology, that of "pacing-induced cardiomyopathy" [31]. This is defined as a ≥10% decrease in LVEF, with resultant LVEF <50% in patients being chronically paced at the RV apex. An incidence of 9–26% has been reported in various studies when the percentage of constant ventricular pacing exceeds 40% [32, 33]. However, some investigators have suggested that this type of cardiomyopathy (CM) may develop even at lower pacing percentages; in one study, 13% of patients developed this type of cardiomyopathy with pacing percentages between 20 and 40 [31]. Other studies have found a lower percentage of LV function deterioration (6%) with RV pacing percentage not being predictive of outcome [34].

Some investigators have suggested that development of early (at 1 month) pacing induced dyssynchrony could predict reduction of LV systolic function with long-term RV apical pacing, which could be prevented by biventricular pacing [35]. The percentage of early pacing induced dyssynchrony could be as high as 50%; significant LVEF reduction (defined as ≥5%) occurred in ~72% of patients with dyssynchrony vs only in 30% in those without dyssynchrony [35]. Importantly, at long-term follow-up (median 4.8 years), LVEF was reduced with RV apical pacing even in patients (up to 1/3) who did not exhibit early dyssynchrony. In a recent CRT study comprising 914 patients (117 with conventional pacemakers and 797 with intrinsic LBBB), mechanical dyssynchrony was observed in 51% of patients with chronic RV pacing vs 77% in patients with intrinsic LBBB [36]. In both groups, CRT produced a favorable effect on reverse remodeling and long-term (4-year) survival, mainly determined by the presence of mechanical dyssynchrony and not by the nature of LBBB. Thus, mechanical dyssynchrony develops quite commonly in patients with chronic RV apical pacing; importantly, whether iatrogenic or intrinsic the nature of LBBB, when it produces mechanical dyssynchrony, CRT appears to be the appropriate therapeutic modality.

Studies quantifying the QRS duration have suggested that QRS duration is a significant and independent predictor of cardiovascular mortality in a general medical population [37]. Similar results have been obtained in patients with an abnormal electrocardiogram, a bundle branch block, and a paced rhythm. Thus, an inordinately prolonged (>190 ms) paced QRS may confer adverse clinical outcomes [38]. In a study of 247 patients undergoing long-term RV apical pacing (>90% ventricular pacing with AV synchrony for more than 1 year) for acquired AV block and normal LV systolic function (LVEF >50%), over a mean follow-up of 6.9 years, a duration of paced QRS >163 ms and axis > −65° predicted adverse clinical outcomes [39]. Similar findings regarding the detrimental effect of prolonged paced QRS duration (>160 ms) on long-term cardiac function during RV apical pacing have been reported in studies of patients with complete AV block receiving a permanent pacemaker [33, 40]. On the other hand, in another study, a normal paced QRS axis was associated with a preserved LV function [41]. Based on the potential adverse effect of a prolonged paced QRS, some investigators have proposed that patients with frequent RV pacing and paced QRS duration ≥150 ms should be screened by echocardiogram to assess for pacing-induced CM [42].

More data on the adverse effect of RV apical pacing have become available via studies assessing the prevalence of congestive heart failure or LV dysfunction among chronically paced patients, comprising both single- and dual-chamber pacing [43, 44]. Thus, ventricular desynchronization imposed by RV pacing even when AV synchrony is maintained increases the risk of heart failure hospitalization, in addition to the risk of atrial fibrillation (AF), in sinus node dysfunction with normal baseline QRS duration. Other data have suggested that atrial pacing is preferred over RV apical pacing in patients with sick sinus syndrome and normal AV conduction, as it avoids the adverse effects of RV apical pacing, which include both the promotion of AF

probably by causing left atrial dilation and the reduction of LV function [45].

Thus, studies have demonstrated that pacing-induced cardiomyopathy can emerge in a wide range of percentages among patients receiving long-term RV apical pacing, afflicting both patients with LV dysfunction and patients with normal LV function at baseline. This calamity has been amply shown to be prevented or managed with biventricular pacing and CRT [46], however, the role of alternate site pacing of the RV in preventing and/or managing these patients is not clear yet.

17.3 Selective or Alternate Site Right Ventricular Pacing

Considering the harmful effects of RV apical pacing, alternate sites of ventricular stimulation have been sought (Fig. 17.2). Selective or alternate site pacing involves pacing of other RV sites (outflow or septal sites) [11, 47, 48]. However, there has now been abundant experience with biventricular or LV pacing modes, which have immensely benefited patients with spontaneous or pacing-induced LBBB [22, 36]. Thus, the advantages of CRT effected by biventricular pacing are clear for certain groups of patients, particularly for patients with LV dysfunction (LVEF ≤35%) and New York Heart Association (NYHA) class II-ambulatory IV symptoms of heart failure [20–22, 49]. Left univentricular pacing has also been reported to be advantageous [50]. Studies have compared RV apical pacing with CRT in patients with refractory heart failure, confirming the benefits of biventricular pacing over RV pacing [11, 51, 52]. CRT may lead to reversal of some of the chronic deleterious effects of ventricular dyssynchrony. Studies using Doppler echocardiograms and tissue Doppler imaging techniques, have shown that CRT significantly improved LV function and reversed LV remodeling during long-term follow-up [53–56]. Whether this can be achieved with other alternate site RV pacing methods remains to be elucidated in future

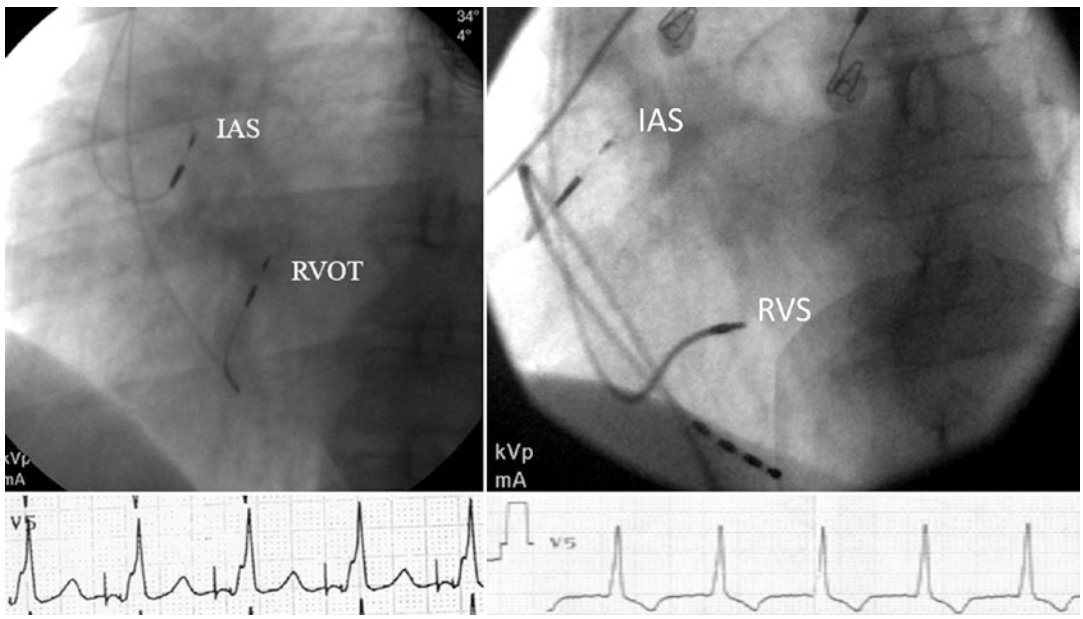

Fig. 17.2 Alternate or selective site pacing was effected in these patients by placing the right atrial (RA) lead at the inter-atrial septum (IAS) in juxtaposition of the Bachman's bundle and the ventricular lead either at the RV outflow tract (RVOT) (left panel) or the RV septum (RVS) at a parahisian position (right panel). Pacing at the RVOT produces a wide QRS (left lower panel), while parahisian (RVS) pacing results in a QRS of much shorter duration (right lower panel), indicating minimized dyssynchrony

studies. Thus, issues dealing with CRT will not be analyzed further in this review, and we will limit the discussion to selective site RV pacing. Whether biventricular pacing provides better CRT when a combination of RV apical and LV pacing or RV septal and LV pacing is used, remains a moot point and probably clinically non-relevant, since the data indicate that either way of CRT remains equally effective [57].

In search of alternate RV pacing sites, the RV outflow tract has been more extensively studied [58–60]. (Fig. 17.2). A pooled analysis of 9 prospective studies, evaluating the hemodynamic effects of RV outflow-tract pacing in 217 patients, indicated a modest but significant hemodynamic benefit compared with RV apical pacing (odds ratio of 0.34) [29]. Apart from the pooled analysis, there are additional studies, which compare RV apical with alternate site pacing and suggest better performance of alternate site pacing [61]. However, it is difficult from these studies to discern which site may be optimal, as there is a lack of a uniform definition and identification of each specific site, but most of them agree that at least the data point to a site away of the RV apex. New pacing lead systems of novel technology have been introduced to assist in this direction, such as very thin active-fixation leads bearing no lumen and thus no guiding stylet, with insertion and endocardial positioning being facilitated by a steerable guiding catheter [47, 62].

RV septal pacing has been proposed as a better choice compared to RV apical pacing, with emerging evidence that pacing from the RV septum is associated with less dyssynchrony, a shorter duration of activation (Fig. 17.2), improved hemodynamics, and less LV remodeling [9, 63–65]. In a small crossover randomized pilot study of 28 patients with permanent AF who received permanent pacing with two leads placed at the RV apex and RV septum, septal pacing was associated with shorter QRS (145 ± 4 ms vs 170 ± 4 ms, $P < 0.01$) and normal axis (40° ± 10° vs −71 ± 4°, $P < 0.01$) [66]. At 3 months, among patients with baseline LVEF ≤45%, LVEF was 42 ± 5% after septal pacing vs 37 ± 4% after apical pacing ($P < 0.001$). The authors concluded that in contrast to RV apical pacing, chronic RV septal pacing preserved LVEF in patients with baseline LVEF ≤45%. In another study comprising 149 patients undergoing implantation of a dual chamber pacemaker for AV block with either RV septal-pacing or RV apical-pacing, the rates of mortality and hospitalization due to heart failure were significantly lower in the RV septal-pacing group (event free RV septum: 1 year, 98% and 2 years, 98%; RV apex: 1 year, 85% and 2 years, 81%; $p < 0.05$) [67]. None of the patients died from heart failure in the RV septal-pacing group, while 4 patients died from heart failure in the RV apical-pacing group within 2 years after pacemaker implantation. The paced QRS interval was significantly shorter with RV septal pacing. The authors concluded that RV septal pacing is feasible and safe with more favorable clinical benefits than RV apical pacing. Similarly, favorable results were obtained with RV septal pacing in another retrospective comparative study of 3 groups of patients; 244 patients with RV high septal parahisian site pacing; 22 patients with low percentage of pacing (<20%); and 33 patients with high percentage, i.e. >80%, RV apical pacing, followed for 21 months [68]. A recent retrospective study of 3450 patients compared at 5 years patients with apical and septal leads (n = 238), apical and non-septal non-apical (n = 733), and apical and septal with >40% ventricular pacing [69]. Septal lead position was associated with a lower mortality compared to apical leads (24% vs 31%, $p = 0.02$). In patients with >40% pacing, septal leads were associated with higher rates of incident AF compared to apical leads (49% vs 34%, $p = 0.04$). Non-septal non-apical lead positions were associated with a significantly higher rate of lead dislodgement (4% vs 2%, $p = 0.005$) and need for revision (8% vs 5%, $p = 0.005$). In a small randomized study, among 71 patients having 98% ventricular pacing, at implant, QRS duration was significantly greater in the apical (158 ms) (n = 34) than the septal group (146 ms; $P = 0.018$), the QRS axis was left in the apical and normal in the septal group ($P < 0.001$) [70]. At 1 year, although the 6-min walk improved similarly, the LVEF increased significantly only in the septal group (from 0.57 to 0.61; $P = 0.008$). Among 273

patients with permanent AF and low (<30%) LVEF needing a pacemaker implantation, those (n = 113) with mid-septal RV pacing were clinically improved and had a significant (5%) increase in LVEF at 18 months compared with patients (n = 120) who had RV apical pacing (P = 0.01) [71].

However, other studies have not shown a distinct clinical benefit of RV septal pacing over RV apical pacing in similar or much larger cohorts of patients with normal baseline LVEF over short- or medium-term (~1 to 2-years) follow-up period [72–78]. However, one relevant problem may relate to inadvertent placement of the lead to anterior or other sites rather than septal positions [77, 79], while data on QRS duration are lacking in these studies, as some studies have proposed that QRS duration can better predict outcome compared to pacing site alone [80, 81]. Thus, the target for pacing site optimization might be a paced QRS as narrow as possible. Such a relatively narrow QRS could be obtained with a para-Hisian pacing site (Fig. 17.2), which appears to preserve LVEF and mechanical synchrony [82].

Permanent His-bundle pacing has also been suggested and animal and patient data indicate that this may be feasible, albeit technically challenging, and it might be a safe and effective option of attaining physiologic pacing [83–85]. Nevertheless, a more practical approach might be para-Hisian pacing (Fig. 17.2) which does not require insertion of an electrode catheter and recording of the His bundle electrogram [82, 86, 87]. Selective conduction system pacing has been suggested as a better terminology to indicate attempts to selectively pace the conduction system to produce a short QRS morphology without practically capturing the ventricular myocardium [88]. Para-Hisian pacing has also been proposed to decrease the incidence of AF compared with RV apical or septal pacing [89].

Finally, in patients with technically difficult or failed coronary sinus lead placement, some investigators have shown satisfactory results with bifocal RV pacing, with one lead placed at the RV apex and a second lead placed high at the RV outflow tract [90, 91]; in non-responders to standard CRT, triple site (LV plus bifocal RV) pacing has been proposed [48]. Alternatively, His bundle pacing might be an option in lieu of a left ventricular lead to attain CRT in patients with LBBB [92, 93], or parahisian pacing may be selected for patients with RBBB, in whom conventional CRT with biventricular pacing may not be expected to be efficacious [94–97].

17.4 Clinical Implications

The adverse hemodynamic effects of *spontaneous LBBB* have well been established [14, 15]. LBBB produces asynchronous myocardial activation (dyssynchrony) which may trigger ventricular remodeling. This ventricular dyssynchrony can lead to both systolic and diastolic LV dysfunction and the development or worsening of heart failure symptoms. In the presence of LBBB, reversible myocardial perfusion defects have been demonstrated on radionuclide scintigraphy in the absence of significant coronary artery disease, while some patients with intermittent LBBB may even develop angina concurrently with the onset of LBBB [98]. In patients with dilated cardiomyopathy, LBBB is accompanied by progressive LV dilation and mitral regurgitation, shortening of LV filling time, lower LVEF, increased symptomatology and poor prognosis with reduced survival [14, 15, 98]. Restoring LV synchrony with CRT has been demonstrated to have a significant impact on both patients' symptomatology, and on their survival [21, 22].

Although the deleterious effects of spontaneous LBBB have been well described, it is only over the last 1–2 decades that we are becoming poignantly aware of the harmful consequences of the *iatrogenic LBBB* (*pacing-induced cardiomyopathy*) produced by RV apical pacing in patients with conventional permanent pacemakers [11, 23, 99, 100]. Taking into account all the evidence accumulated to date on the adverse effects of the iatrogenic LBBB, many arrhythmologists have reconsidered their approach to conventional RV apical pacing [101]. A practical approach is proposed in the algorithm depicted in Fig. 17.3. Firstly, for those patients already having conventional pacing systems, particularly in the presence

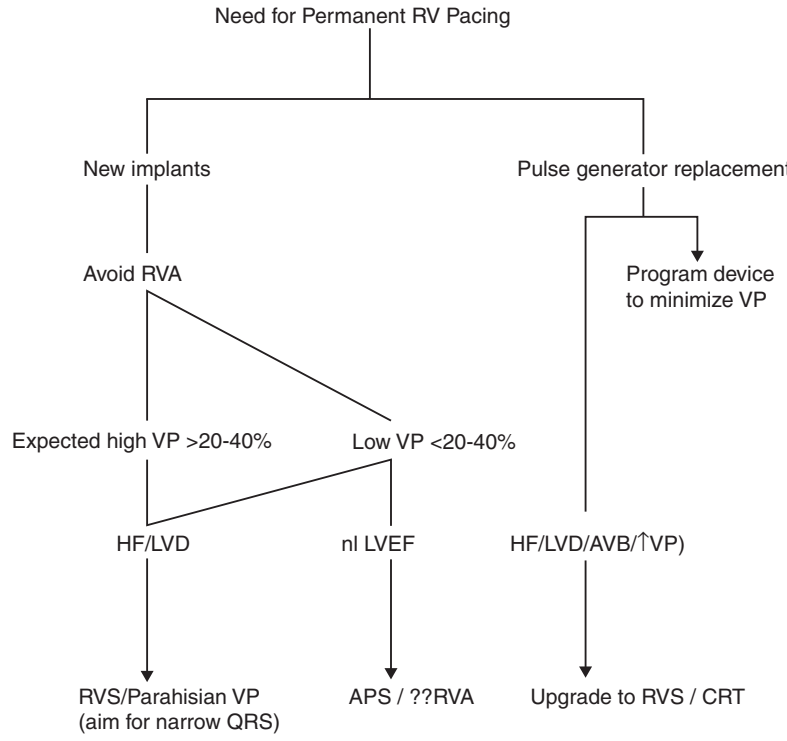

Fig. 17.3 An algorithm is proposed for patients receiving an RV pacing lead (see text for discussion). *APS* alternate pacing site, *AVB* atrioventricular block, *CRT* cardiac resynchronization therapy, *HF* heart failure, *LVD* left ventricular dysfunction, *LVEF* left ventricular ejection fraction, *nl* normal, *RVA* right ventricular apex, *RVS* right ventricular septum, *VP* ventricular pacing

of LV dysfunction or heart failure, pacemaker programming should be employed to minimize RV pacing [102]. Over the recent years, pacemaker devices are equipped with special automated algorithms minimizing ventricular pacing [23, 103]. Thus, in patients with sinus node dysfunction but with normal AV conduction, functional AAIR pacing is established for most of the time either by activating these algorithms, or when unavailable, by programming a long AV delay (≥250 ms) [45]. With regards to patients with AV block, use of alternate site pacing becomes imperative, particularly when dealing with patients with compromised LV function [12, 104]. However, for those patients who already have an implanted conventional pacemaker, either a dual-chamber pacing system in the presence of sinus rhythm or a single-chamber system in cases of permanent AF, one should seriously consider upgrading them to biventricular systems if moderate or severe LV dysfunction is present [53, 105, 106]. In select cases, RV septal pacing alone may be hemodynamically more advantageous than RV apical pacing [101, 107]. Choosing a specific alternate pacing site remains at the operator's discretion, but evidence suggests that RV septal pacing, particularly para-Hisian, or, of course, His-bundle pacing, albeit a more tedious and elaborate procedure for now, appears to be the preferred approach [68, 82, 86]. In general, avoiding the conventional RV apical position seems to be the way to go in every patient in need for cardiac pacing for any bradyarrhythmic cause. A suggested guidance might aim for a septal site producing a relatively narrow paced QRS (≤150 ms) [42]. Some promising data of RV septal pacing producing narrow QRS in patients with RBBB are emerging that might hopefully translate into a form of cardiac resynchronization for such patients, in whom CRT with biventricular pacing has not been shown to have a consistent benefit in this particular group of patients [94, 95]. Even in patients requiring CRT where the LV lead implantation fails, this approach might present as an alternative strategy [97].

A systematic review and meta-analysis of 14 randomized controlled trials involving 754 patients, indicated that compared with subjects

randomized to RV apical pacing, those randomized to RV non-apical pacing had greater LVEF at the end of follow-up [61]. Importantly, LVEF improvement was greater in trials with follow-up ≥12 months, and those conducted in patients with baseline LVEF ≤40–45%; while no significant difference was observed in trials of patients whose baseline LVEF was preserved. The authors concluded that while randomized controlled trials suggest that LVEF is higher with RV non-apical than with RV apical pacing, there remains a need for larger trials to compare the safety and efficacy of RV non-apical and RV apical pacing. Another systematic review and meta-analysis of 24 studies (n = 1628 patients) showed that among studies reporting a difference (in favor of RV non-apical pacing), the weighted mean difference in LVEF between RV non-apical and RV apical pacing at follow-up was 5.40%, related in part to group's RV apical arm demonstrating a significant reduction (mean loss −3.31%) in LVEF between study baseline and end of follow-up [104]. The studies that showed a difference more frequently included patients with poor baseline LVEF (<40%) and had a follow-up >12 months. The authors concluded that in patients requiring chronic RV pacing where there is inclusion of impaired baseline LVEF (<40%), RV apical pacing is associated with deterioration in LV function relative to RV non-apical pacing.

Finally, a recently published randomized study, the Right Ventricular Apical and High Septal Pacing to Preserve Left Ventricular Function (Protect Pace) study, had disappointing results, at least for the mid-term follow-up, showing that in patients with a high-grade AV block and preserved LV function requiring a high percentage of ventricular pacing, high septal pacing did not provide a protective effect on LV function over RV apical pacing in the first 2 years [74]. Thus, other ongoing studies, such as the Right Ventricular Apical versus Septal Pacing (RASP) and RIGHT PACE studies, comparing RV apical and septal pacing, will have to provide more definitive information about the impact of the RV pacing on the LV dyssynchrony, and about acute and chronic responses to selective site pacing, as adopted in current clinical practice [108]. Importantly, attention should be paid in such studies to avoid heterogeneity of pacing sites [79], or in other words, anatomic identification of the true pacing site is a most significant factor of consistency in comparative studies for more precise determination of true efficacy and impact of selective site pacing.

17.5 Conventional Atrial Pacing/ Atrial Dyssynchrony/ Alternate Atrial Site Pacing

Atrial pacing is traditionally effected via pacing the RAA as it contains trabeculations to anchor the pacing lead [109], is easily accessible and provides stable lead position and pacing parameters. A much less commonly discussed or appreciated problem relates to atrial dyssynchrony produced by conventional atrial pacing at the RAA [110]. This is inferred by the results of several studies. According to a randomized, controlled study, RAA pacing (n = 28) produced atrial dyssynchrony with prolongation of the atrial, interatrial and AV conduction times compared with atrial septal pacing (n = 28) [111]. Atrial septal pacing decreased the P wave duration, left atrial electromechanical delay, and interatrial interval ($P < 0.001$). The authors concluded that atrial septal pacing avoids this undesirable prolongation of the atrial, interatrial, and AV conductions observed during RAA pacing. In addition, septal pacing creates a slight reversal of the timing of the atrial systoles and induces a shortening of PR interval, the extent of which could depend on the height of the pacing site on the septum.

According to an echocardiography study, in 30 patients with sinus node dysfunction and paroxysmal AF, right low atrial septal pacing (n = 15) significantly improved global and regional atrial mechanical function and synchronized inter-atrial electromechanical contraction compared with RAA pacing (n = 15) [112].

According to a study applying dual-site right atrial pacing in patients with AF requiring demand pacing, atrial pacing resulted in a marked decline in AF recurrences [113]. Per their

long-term experience with dual-site atrial pacing in 30 patients with paroxysmal and chronic drug-refractory AF, the investigators reported that 78% of patients were free of AF recurrence at 1 year, 63% at 2 years, and 56% at 3 years. Rhythm control was achieved in 86% of patients during a follow-up period of 3 years. Concomitantly, they observed a marked reduction in need for anticoagulation, type I antiarrhythmic drugs, and cardioversion therapies.

In another study, conventional right atrial-paced rhythm (n = 52) conferred a higher incidence of AF (15.4% vs 4%) compared to atrial-sensed rhythm (n = 100) (P = 0.023) among 152 patients (108 men; mean age 73) over a mean follow-up of ~4 years [114]. The authors suggest that VDD pacing may be a better choice than the DDD system for patients with AV block, but without clinical evidence of sinus node dysfunction, and if an atrial lead is required, it should be placed close to the Bachmann's bundle. Other investigators report that a pacemaker program combining atrial antitachycardia pacing with minimized ventricular pacing may confer reverse atrial remodeling resulting in lower incidence of early AF recurrences, [115] and even delay AF disease progression [116].

According to a meta-analysis of 10 controlled, randomized clinical trials on interatrial septum (IAS) vs conventional pacing, comprising 1245 patients, compared to conventional atrial pacing, IAS pacing conferred no additional benefit on the persistent/permanent AF free survival; however, it was associated with reduced device-detected AF burden and AF frequency. Lead-related complications and major adverse events were similar in the two groups [117]. Similarly, the SAFE study which randomized 385 patients with paroxysmal AF and sick sinus syndrome requiring pacemaker implantation to ON/OFF RAA or IAS pacing, did not show a benefit of alternate site pacing in preventing the development of persistent AF [118].

In summary, earlier reviews indicated that atrial tachyarrhythmia prevention by biatrial or dual-site right atrial pacing reported in small studies was not confirmed by randomized trials [117, 119]. Small studies showed a reduced atrial arrhythmia recurrence rate in patients with septal pacing at the triangle of Koch or at Bachmann's bundle [120–122]. Another more recent study, the controlled randomized Electrophysiology-Guided Pacing Site Selection (EPASS) Study, showed similar results [123]. It randomly assigned 97 patients with sinus disease (77 ± 7 years) to interatrial septal pacing vs RAA pacing; 11 (16.6%) patients met the primary end point of time to development of permanent or persistent AF within a 2-year follow-up: 2 septal pacing vs 9 RAA pacing ($P = 0.047$) [123]. The authors concluded that in patients with sinus node dysfunction and intra-atrial conduction delay, low septal pacing was superior to RAA pacing in preventing progression to persistent or permanent AF.

In general, the hypothesis that has been advanced regarding the potential benefits of septal or biatrial pacing suggest that these pacing modes may reduce or slow the progression of pro-arrhythmic substrate by reducing atrial activation time and improving atrial mechanical efficiency during atrial overdrive pacing [124]. Although the mechanism remains unclear, alternate site pacing at the atrial level may improve atrial mechanical efficacy by synchronization of atrial activation via stimulation at the level of Bachman's bundle or via multisite atrial pacing [25].

The deleterious effects of conventional RAA pacing may extend to CRT patients. According to a study of 17 CRT patients studied about 10 months after implantation, conventional right-atrial-paced (DDD) compared to right-atrial-sensed (VDD) biventricular paced rhythm had unfavorable hemodynamic effects on cardiac resynchronization therapy [125]. The authors concluded that avoidance of right atrial pacing results in a higher degree of LV resynchronization, in a substantial prolongation of the LV filling period, and in an improved myocardial performance. Thus, the VDD mode seems to be superior to the DDD mode in CRT patients. Whether alternate atrial site pacing may benefit these patients remains unknown.

Conclusion

Conventional right heart pacing with leads placed at the RAA and RV apex produces

iatrogenic dyssynchrony. At the atrial level, the data for a harmful effect of conventional RAA pacing are meagre and have not yet led to a change in the practice of atrial pacing. However, the data of a plethora of deleterious effects of the iatrogenic LBBB which is produced by RV apical pacing have been compelling and have led to some degree of a paradigm shift in our approach to conventional RV pacing by adopting selective site pacing and avoiding the RV apex. There is still considerable room for improvement so that alternative site pacing may penetrate the pacing community further and thus one can avoid the potentially harmful effects of RV apical pacing at least for patients with LV dysfunction and/or heart failure, who are the ones who seem to be afflicted the most and are apparently better responders to non-RV apical pacing. The iatrogenic LBBB produced by classical RV apical pacing apparently leads to a form of *pacing-induced cardiomyopathy* which creates inter- and intra-ventricular dyssynchrony similar to the dyssynchrony conferred by spontaneous LBBB, both remedied by CRT. In the same direction, there is some, albeit less strong, evidence that conventional RAA pacing may produce dyssynchrony at the atrial level with a pro-arrhyhmic result (AF), which may be obviated by alternate site pacing, particularly at the high inter-atrial septum (Bachman's bundle).

Conflict of Interest None declared.

References

1. Sutton R, Perrins EJ, Morley C, et al. Sustained improvement in exercise tolerance following physiological cardiac pacing. Eur Heart J. 1983;4:781–5.
2. Hayes DL, Holmes DR Jr, Vlietstra RE, et al. Changing experience with dual chamber (DDD) pacemakers. J Am Coll Cardiol. 1984;4:556–9.
3. Rosengarten MD, Chiu RC. Artificial cardiac stimulation: a current view of physiologic pacemakers. Can Med Assoc J. 1983;128:1377–81.
4. Hayes DL, Holmes DR Jr, Vlietstra RE. Early experience with a universal (DDD) pacing device. Mayo Clin Proc. 1983;58:301–6.
5. Tanabe A, Mohri T, Ohga M, et al. The effects of pacing-induced left bundle branch block on left ventricular systolic and diastolic performances. Jpn Heart J. 1990;31:309–17.
6. Modena MG, Mattioli AV, Mattioli G. Right ventricular pacing and left ventricular filling pattern. An echo-Doppler study. Chest. 1991;100:744–7.
7. Tantengco MV, Thomas RL, Karpawich PP. Left ventricular dysfunction after long-term right ventricular apical pacing in the young. J Am Coll Cardiol. 2001;37:2093–100.
8. Tse HF, Yu C, Wong KK, et al. Functional abnormalities in patients with permanent right ventricular pacing: the effect of sites of electrical stimulation. J Am Coll Cardiol. 2002;40:1451–8.
9. Karpawich PP, Mital S. Comparative left ventricular function following atrial, septal, and apical single chamber heart pacing in the young. Pacing Clin Electrophysiol. 1997;20:1983–8.
10. Das A, Kahali D. Physiological cardiac pacing: current status. Indian Heart J. 2016;68:552–8.
11. Manolis AS. The deleterious consequences of right ventricular apical pacing: time to seek alternate site pacing. Pacing Clin Electrophysiol. 2006;29:298–315.
12. Sweeney MO, Prinzen FW. A new paradigm for physiologic ventricular pacing. J Am Coll Cardiol. 2006;47:282–8.
13. Tops LF, Schalij MJ, Bax JJ. The effects of right ventricular apical pacing on ventricular function and dyssynchrony implications for therapy. J Am Coll Cardiol. 2009;54:764–76.
14. Baldasseroni S, Opasich C, Gorini M, et al. Left bundle-branch block is associated with increased 1-year sudden and total mortality rate in 5517 outpatients with congestive heart failure: a report from the Italian network on congestive heart failure. Am Heart J. 2002;143:398–405.
15. Hesse B, Diaz LA, Snader CE, et al. Complete bundle branch block as an independent predictor of all-cause mortality: report of 7,073 patients referred for nuclear exercise testing. Am J Med. 2001;110:253–9.
16. Lee SJ, McCulloch C, Mangat I, et al. Isolated bundle branch block and left ventricular dysfunction. J Card Fail. 2003;9:87–92.
17. Clark AL, Goode K, Cleland JG. The prevalence and incidence of left bundle branch block in ambulant patients with chronic heart failure. Eur J Heart Fail. 2008;10:696–702.
18. Tabrizi F, Englund A, Rosenqvist M, et al. Influence of left bundle branch block on long-term mortality in a population with heart failure. Eur Heart J. 2007;28:2449–55.
19. Blanc JJ, Fatemi M, Bertault V, et al. Evaluation of left bundle branch block as a reversible cause of non-ischaemic dilated cardiomyopathy with severe heart failure. A new concept of left ventricular dyssynchrony-induced cardiomyopathy. Europace. 2005;7:604–10.

20. Abraham WT, Fisher WG, Smith AL, et al. Cardiac resynchronization in chronic heart failure. N Engl J Med. 2002;346:1845–53.
21. Manolis AS. Cardiac resynchronization therapy in congestive heart failure: ready for prime time? Heart Rhythm. 2004;1:355–63.
22. Leyva F, Nisam S, Auricchio A. 20 years of cardiac resynchronization therapy. J Am Coll Cardiol. 2014;64:1047–58.
23. Akerstrom F, Pachon M, Puchol A, et al. Chronic right ventricular apical pacing: adverse effects and current therapeutic strategies to minimize them. Int J Cardiol. 2014;173:351–60.
24. Padeletti L, Michelucci A, Pieragnoli P, et al. Atrial septal pacing: a new approach to prevent atrial fibrillation. Pacing Clin Electrophysiol. 2004;27:850–4.
25. Dabrowska-Kugacka A, Lewicka-Nowak E, Rucinski P, et al. Atrial electromechanical sequence and contraction synchrony during single- and multisite atrial pacing in patients with brady-tachycardia syndrome. Pacing Clin Electrophysiol. 2009;32:591–603.
26. Wilkoff BL, Cook JR, Epstein AE, et al. Dual-chamber pacing or ventricular backup pacing in patients with an implantable defibrillator: the Dual Chamber and VVI Implantable Defibrillator (DAVID) trial. JAMA. 2002;288:3115–23.
27. Steinberg JS, Fischer A, Wang P, et al. The clinical implications of cumulative right ventricular pacing in the multicenter automatic defibrillator trial II. J Cardiovasc Electrophysiol. 2005;16:359–65.
28. Nunez A, Alberca MT, Cosio FG, et al. Severe mitral regurgitation with right ventricular pacing, successfully treated with left ventricular pacing. Pacing Clin Electrophysiol. 2002;25:226–30.
29. de Cock CC, Giudici MC, Twisk JW. Comparison of the haemodynamic effects of right ventricular outflow-tract pacing with right ventricular apex pacing: a quantitative review. Europace. 2003;5:275–8.
30. Karpawich PP, Rabah R, Haas JE. Altered cardiac histology following apical right ventricular pacing in patients with congenital atrioventricular block. Pacing Clin Electrophysiol. 1999;22:1372–7.
31. Khurshid S, Epstein AE, Verdino RJ, et al. Incidence and predictors of right ventricular pacing-induced cardiomyopathy. Heart Rhythm. 2014;11:1619–25.
32. Yu CM, Chan JY, Zhang Q, et al. Biventricular pacing in patients with bradycardia and normal ejection fraction. N Engl J Med. 2009;361:2123–34.
33. Zhang XH, Chen H, Siu CW, et al. New-onset heart failure after permanent right ventricular apical pacing in patients with acquired high-grade atrioventricular block and normal left ventricular function. J Cardiovasc Electrophysiol. 2008;19:136–41.
34. Ebert M, Jander N, Minners J, et al. Long-term impact of right ventricular pacing on left ventricular systolic function in pacemaker recipients with preserved ejection fraction: results from a large single-center registry. J Am Heart Assoc. 2016;5(7):e003485. https://doi.org/10.1161/JAHA.116.003485.
35. Fang F, Luo XX, Zhang Q, et al. Deterioration of left ventricular systolic function in extended Pacing to Avoid Cardiac Enlargement (PACE) trial: the predictive value of early systolic dyssynchrony. Europace. 2015;17(Suppl 2):ii47–53.
36. Stankovic I, Prinz C, Ciarka A, et al. Long-term outcome after CRT in the presence of mechanical dyssynchrony seen with chronic RV pacing or intrinsic LBBB. JACC Cardiovasc Imaging. 2017;10(10 Pt A):1091–9.
37. Desai AD, Yaw TS, Yamazaki T, et al. Prognostic significance of quantitative QRS duration. Am J Med. 2006;119:600–6.
38. Miyoshi F, Kobayashi Y, Itou H, et al. Prolonged paced QRS duration as a predictor for congestive heart failure in patients with right ventricular apical pacing. Pacing Clin Electrophysiol. 2005;28:1182–8.
39. Sohn J, Lee YS, Park HS, et al. Predictors of an adverse clinical outcome in patients with long-term right ventricular apical pacing. J Cardiol. 2017;70:420–4.
40. Chen S, Yin Y, Lan X, et al. Paced QRS duration as a predictor for clinical heart failure events during right ventricular apical pacing in patients with idiopathic complete atrioventricular block: results from an observational cohort study (PREDICT-HF). Eur J Heart Fail. 2013;15:352–9.
41. Kim SH, Oh YS, Nam GB, et al. Paced QRS axis as a predictor of pacing-induced left ventricular dysfunction. J Interv Card Electrophysiol. 2014;41:223–9.
42. Khurshid S, Liang JJ, Owens A, et al. Longer paced QRS duration is associated with increased prevalence of right ventricular pacing-induced cardiomyopathy. J Cardiovasc Electrophysiol. 2016;27:1174–9.
43. Thackray SD, Witte KK, Nikitin NP, et al. The prevalence of heart failure and asymptomatic left ventricular systolic dysfunction in a typical regional pacemaker population. Eur Heart J. 2003;24:1143–52.
44. Sweeney MO, Hellkamp AS, Ellenbogen KA, et al. Adverse effect of ventricular pacing on heart failure and atrial fibrillation among patients with normal baseline QRS duration in a clinical trial of pacemaker therapy for sinus node dysfunction. Circulation. 2003;107:2932–7.
45. Nielsen JC, Kristensen L, Andersen HR, et al. A randomized comparison of atrial and dual-chamber pacing in 177 consecutive patients with sick sinus syndrome: echocardiographic and clinical outcome. J Am Coll Cardiol. 2003;42:614–23.
46. Guglin M, Barold SS. The role of biventricular pacing in the prevention and therapy of pacemaker-induced cardiomyopathy. Ann Noninvasive Electrocardiol. 2015;20:224–39.
47. Manolis AS, Simeonidou E, Sousani E, et al. Alternate sites of permanent cardiac pacing: a randomized study of novel technology. Hellenic J Cardiol. 2004;45:145–9.
48. Manolis AS, Sakellariou D, Andrikopoulos GK. Alternate site pacing in patients at risk for heart failure. Angiology. 2008;59:97S–102S.

49. Brignole M, Auricchio A, Baron-Esquivias G, et al. 2013 ESC guidelines on cardiac pacing and cardiac resynchronization therapy: the task force on cardiac pacing and resynchronization therapy of the European Society of Cardiology (ESC). Developed in collaboration with the European Heart Rhythm Association (EHRA). Eur Heart J. 2013;34:2281–329.
50. Burri H, Prinzen FW, Gasparini M, et al. Left univentricular pacing for cardiac resynchronization therapy. Europace. 2017;19:912–9.
51. Yu CM, Lin H, Fung WH, et al. Comparison of acute changes in left ventricular volume, systolic and diastolic functions, and intraventricular synchronicity after biventricular and right ventricular pacing for heart failure. Am Heart J. 2003;145:E18.
52. Leclercq C, Walker S, Linde C, et al. Comparative effects of permanent biventricular and right-univentricular pacing in heart failure patients with chronic atrial fibrillation. Eur Heart J. 2002;23:1780–7.
53. Erol-Yilmaz A, Tukkie R, Schrama TA, et al. Reversed remodelling of dilated left sided cardiomyopathy after upgrading from VVIR to VVIR biventricular pacing. Europace. 2002;4:445–9.
54. St John Sutton MG, Plappert T, Abraham WT, et al. Effect of cardiac resynchronization therapy on left ventricular size and function in chronic heart failure. Circulation. 2003;107:1985–90.
55. Sogaard P, Egeblad H, Kim WY, et al. Tissue Doppler imaging predicts improved systolic performance and reversed left ventricular remodeling during long-term cardiac resynchronization therapy. J Am Coll Cardiol. 2002;40:723–30.
56. Lau CP, Yu CM, Chau E, et al. Reversal of left ventricular remodeling by synchronous biventricular pacing in heart failure. Pacing Clin Electrophysiol. 2000;23:1722–5.
57. Leclercq C, Sadoul N, Mont L, et al. Comparison of right ventricular septal pacing and right ventricular apical pacing in patients receiving cardiac resynchronization therapy defibrillators: the SEPTAL CRT Study. Eur Heart J. 2016;37:473–83.
58. Giudici MC, Thornburg GA, Buck DL, et al. Comparison of right ventricular outflow tract and apical lead permanent pacing on cardiac output. Am J Cardiol. 1997;79:209–12.
59. Victor F, Leclercq C, Mabo P, et al. Optimal right ventricular pacing site in chronically implanted patients: a prospective randomized crossover comparison of apical and outflow tract pacing. J Am Coll Cardiol. 1999;33:311–6.
60. Bourke JP, Hawkins T, Keavey P, et al. Evolution of ventricular function during permanent pacing from either right ventricular apex or outflow tract following AV-junctional ablation for atrial fibrillation. Europace. 2002;4:219–28.
61. Shimony A, Eisenberg MJ, Filion KB, et al. Beneficial effects of right ventricular non-apical vs. apical pacing: a systematic review and meta-analysis of randomized-controlled trials. Europace. 2012;14:81–91.
62. Gammage MD, Lieberman RA, Yee R, et al. Multicenter global evaluation of electrical efficacy and safety of a catheter-delivered, lumenless permanent pacemaker lead implanted in traditional and specific right-heart sites. Eur Heart J. 2005;26:175.
63. Hillock RJ, Mond HG. Pacing the right ventricular outflow tract septum: time to embrace the future. Europace. 2012;14:28–35.
64. Zou C, Song J, Li H, et al. Right ventricular outflow tract septal pacing is superior to right ventricular apical pacing. J Am Heart Assoc. 2015;4:e001777.
65. Yoshikawa H, Suzuki M, Tezuka N, et al. Differences in left ventricular dyssynchrony between high septal pacing and apical pacing in patients with normal left ventricular systolic function. J Cardiol. 2010;56:44–50.
66. Victor F, Mabo P, Mansour H, et al. A randomized comparison of permanent septal versus apical right ventricular pacing: short-term results. J Cardiovasc Electrophysiol. 2006;17:238–42.
67. Kikuchi M, Tanno K, Miyoshi F, et al. Long-term effectiveness of right septal pacing vs right apical pacing in patients with atrioventricular block. J Arrhythm. 2012;28:214–8.
68. Occhetta E, Quirino G, Baduena L, et al. Right ventricular septal pacing: safety and efficacy in a long term follow up. World J Cardiol. 2015;7:490–8.
69. Witt CM, Lenz CJ, Shih HH, et al. Right ventricular pacemaker lead position is associated with differences in long-term outcomes and complications. J Cardiovasc Electrophysiol. 2017;28:924–30.
70. Molina L, Sutton R, Gandoy W, et al. Medium-term effects of septal and apical pacing in pacemaker-dependent patients: a double-blind prospective randomized study. Pacing Clin Electrophysiol. 2014;37:207–14.
71. Muto C, Ottaviano L, Canciello M, et al. Effect of pacing the right ventricular mid-septum tract in patients with permanent atrial fibrillation and low ejection fraction. J Cardiovasc Electrophysiol. 2007;18:1032–6.
72. Mizukami A, Matsue Y, Naruse Y, et al. Implications of right ventricular septal pacing for medium-term prognosis: propensity-matched analysis. Int J Cardiol. 2016;220:214–8.
73. Zhang HX, Qian J, Hou FQ, et al. Comparison of right ventricular apex and right ventricular outflow tract septum pacing in the elderly with normal left ventricular ejection fraction: long-term follow-up. Kardiol Pol. 2012;70:1130–9.
74. Kaye GC, Linker NJ, Marwick TH, et al. Effect of right ventricular pacing lead site on left ventricular function in patients with high-grade atrioventricular block: results of the Protect-Pace study. Eur Heart J. 2015;36:856–62.
75. Bai M, Li Q, Jiang G, et al. Comparison of effectiveness of right ventricular mid-septal pacing vs. apical pacing: a randomized-controlled trials. Eur Heart J Suppl. 2016;18:F12–F18.

76. Cano O, Osca J, Sancho-Tello MJ, et al. Comparison of effectiveness of right ventricular septal pacing versus right ventricular apical pacing. Am J Cardiol. 2010;105:1426–32.
77. Domenichini G, Sunthorn H, Fleury E, et al. Pacing of the interventricular septum versus the right ventricular apex: a prospective, randomized study. Eur J Intern Med. 2012;23:621–7.
78. Kypta A, Steinwender C, Kammler J, et al. Long-term outcomes in patients with atrioventricular block undergoing septal ventricular lead implantation compared with standard apical pacing. Europace. 2008;10:574–9.
79. Ng AC, Allman C, Vidaic J, et al. Long-term impact of right ventricular septal versus apical pacing on left ventricular synchrony and function in patients with second- or third-degree heart block. Am J Cardiol. 2009;103:1096–101.
80. Chan NY, Yuen HC, Choy CC, et al. Left ventricular volumes and systolic function after long-term right ventricular pacing may be predicted by paced QRS duration, but not pacing site. Heart Lung Circ. 2014;23:43–8.
81. Hayashi K, Kohno R, Fujino Y, et al. Pacing from the right ventricular septum and development of new atrial fibrillation in paced patients with atrioventricular block and preserved left ventricular function. Circ J. 2016;80:2302–9.
82. Kronborg MB, Mortensen PT, Poulsen SH, et al. His or para-His pacing preserves left ventricular function in atrioventricular block: a double-blind, randomized, crossover study. Europace. 2014;16:1189–96.
83. Sharma PS, Subzposh FA, Ellenbogen KA, et al. Permanent His-bundle pacing in patients with prosthetic cardiac valves. Heart Rhythm. 2017;14:59–64.
84. Vijayaraman P, Dandamudi G. How to perform permanent His bundle pacing: tips and tricks. Pacing Clin Electrophysiol. 2016;39:1298–304.
85. Dandamudi G, Vijayaraman P. History of His bundle pacing. J Electrocardiol. 2017;50:156–60.
86. Occhetta E, Bortnik M, Marino P. Permanent parahisian pacing. Indian Pacing Electrophysiol J. 2007;7:110–25.
87. Zanon F, Barold SS. Direct His bundle and paraHisian cardiac pacing. Ann Noninvasive Electrocardiol. 2012;17:70–8.
88. Mulpuru SK, Cha YM, Asirvatham SJ. Synchronous ventricular pacing with direct capture of the atrioventricular conduction system: functional anatomy, terminology, and challenges. Heart Rhythm. 2016;13:2237–46.
89. Pastore G, Zanon F, Baracca E, et al. The risk of atrial fibrillation during right ventricular pacing. Europace. 2016;18:353–8.
90. Res JC, Bokern MJ, de Cock CC, et al. The BRIGHT study: bifocal right ventricular resynchronization therapy: a randomized study. Europace. 2007;9:857–61.
91. Manolis AS, Metaxa S, Sakellaris N. Bifocal right ventricular pacing: alternative to biventricular pacing for cardiac resynchronization therapy? Hosp Chronicles. 2014;9:280–2.
92. Ajijola OA, Upadhyay G, Macias C, et al. Permanent His-bundle pacing for cardiac resynchronization therapy: initial feasibility study in lieu of left ventricular lead. Heart Rhythm. 2017;14:1353–61.
93. Lustgarten DL, Crespo EM, Arkhipova-Jenkins I, et al. His-bundle pacing versus biventricular pacing in cardiac resynchronization therapy patients: a crossover design comparison. Heart Rhythm. 2015;12:1548–57.
94. Giudici MC, Abu-El-Haija B, Schrumpf PE, et al. Right ventricular septal pacing in patients with right bundle branch block. J Electrocardiol. 2015;48:626–9.
95. Manolis AS, Tolis P. Right ventricular septal pacing: in lieu of biventricular pacing for cardiac resynchronization in a patient with right bundle branch block? Rhythmos. 2015;10:62–3.
96. Manolis AS, Voyiantzakis N, Lazaros G. Improved cardiac output with right ventricular septal pacing in a patient with right bundle branch block and left ventricular dysfunction. Rhythmos. 2016;11:12–3.
97. Alhous MH, Small GR, Hannah A, et al. Right ventricular septal pacing as alternative for failed left ventricular lead implantation in cardiac resynchronization therapy candidates. Europace. 2015;17:94–100.
98. Littmann L, Symanski JD. Hemodynamic implications of left bundle branch block. J Electrocardiol. 2000;33:115–21.
99. Padeletti L, Lieberman R, Valsecchi S, et al. Physiologic pacing: new modalities and pacing sites. Pacing Clin Electrophysiol. 2006;29(Suppl 2): S73–7.
100. De Sisti A, Marquez MF, Tonet J, et al. Adverse effects of long-term right ventricular apical pacing and identification of patients at risk of atrial fibrillation and heart failure. Pacing Clin Electrophysiol. 2012;35:1035–43.
101. Mond HG, Vlay SC. Pacing the right ventricular septum: time to abandon apical pacing. Pacing Clin Electrophysiol. 2010;33:1293–7.
102. Gillis AM. Optimal pacing for right ventricular and biventricular devices: minimizing, maximizing, and right ventricular/left ventricular site considerations. Circ Arrhythm Electrophysiol. 2014;7:968–77.
103. Boriani G, Tukkie R, Manolis AS, et al. Atrial antitachycardia pacing and managed ventricular pacing in bradycardia patients with paroxysmal or persistent atrial tachyarrhythmias: the MINERVA randomized multicentre international trial. Eur Heart J. 2014;35:2352–62.
104. Hussain MA, Furuya-Kanamori L, Kaye G, et al. The effect of right ventricular apical and nonapical pacing on the short- and long-term changes in left ventricular ejection fraction: a systematic review and meta-analysis of randomized-controlled trials. Pacing Clin Electrophysiol. 2015;38:1121–36.
105. Leon AR, Greenberg JM, Kanuru N, et al. Cardiac resynchronization in patients with congestive heart failure and chronic atrial fibrillation: effect of upgrad-

ing to biventricular pacing after chronic right ventricular pacing. J Am Coll Cardiol. 2002;39:1258–63.
106. Baker CM, Christopher TJ, Smith PF, et al. Addition of a left ventricular lead to conventional pacing systems in patients with congestive heart failure: feasibility, safety, and early results in 60 consecutive patients. Pacing Clin Electrophysiol. 2002;25:1166–71.
107. Tse HF, Wong KK, Siu CW, et al. Upgrading pacemaker patients with right ventricular apical pacing to right ventricular septal pacing improves left ventricular performance and functional capacity. J Cardiovasc Electrophysiol. 2009;20:901–5.
108. Muto C, Calvi V, Botto GL, et al. Is there a right place to pace the right ventricle? Evaluation of apical and septal positions in a pacemaker population: study protocol for a prospective intervention-control trial. Contemp Clin Trials. 2014;39:320–6.
109. Manolis AS, Varriale P, Baptist SJ. Necropsy study of right atrial appendage: morphology and quantitative measurements. Clin Cardiol. 1988;11:788–92.
110. Xie JM, Fang F, Zhang Q, et al. Atrial dysfunction and interatrial dyssynchrony predict atrial high rate episodes: insight into the distinct effects of right atrial appendage pacing. J Cardiovasc Electrophysiol. 2012;23:384–90.
111. Hermida JS, Carpentier C, Kubala M, et al. Atrial septal versus atrial appendage pacing: feasibility and effects on atrial conduction, interatrial synchronization, and atrioventricular sequence. Pacing Clin Electrophysiol. 2003;26:26–35.
112. Wang M, Siu CW, Lee KL, et al. Effects of right low atrial septal vs. right atrial appendage pacing on atrial mechanical function and dyssynchrony in patients with sinus node dysfunction and paroxysmal atrial fibrillation. Europace. 2011;13:1268–74.
113. Saksena S, Delfaut P, Prakash A, et al. Multisite electrode pacing for prevention of atrial fibrillation. J Cardiovasc Electrophysiol. 1998;9:S155–62.
114. Kong CW, Yu WC, Chen SA, et al. Development of atrial fibrillation in patients with atrioventricular block after atrioventricular synchronized pacing. Pacing Clin Electrophysiol. 2004;27:352–7.
115. Boriani G, Tukkie R, Biffi M, et al. Atrial antitachycardia pacing and atrial remodeling: a substudy of the international, randomized MINERVA trial. Heart Rhythm. 2017;14:1476–84.
116. Padeletti L, Purerfellner H, Mont L, et al. New-generation atrial antitachycardia pacing (Reactive ATP) is associated with reduced risk of persistent or permanent atrial fibrillation in patients with bradycardia: results from the MINERVA randomized multicenter international trial. Heart Rhythm. 2015;12:1717–25.
117. Shali S, Su Y, Ge J. Interatrial septal pacing to suppress atrial fibrillation in patients with dual chamber pacemakers: a meta-analysis of randomized, controlled trials. Int J Cardiol. 2016;219:421–7.
118. Lau CP, Tachapong N, Wang CC, et al. Prospective randomized study to assess the efficacy of site and rate of atrial pacing on long-term progression of atrial fibrillation in sick sinus syndrome: Septal Pacing for Atrial Fibrillation Suppression Evaluation (SAFE) Study. Circulation. 2013;128:687–93.
119. Israel CW, Hohnloser SH. Pacing to prevent atrial fibrillation. J Cardiovasc Electrophysiol. 2003;14:S20–6.
120. Padeletti L, Pieragnoli P, Ciapetti C, et al. Randomized crossover comparison of right atrial appendage pacing versus interatrial septum pacing for prevention of paroxysmal atrial fibrillation in patients with sinus bradycardia. Am Heart J. 2001;142:1047–55.
121. Kale M, Bennett DH. Atrial septal pacing in the prevention of paroxysmal atrial fibrillation refractory to antiarrhythmic drugs. Int J Cardiol. 2002;82:167–75.
122. Bailin SJ, Adler S, Giudici M. Prevention of chronic atrial fibrillation by pacing in the region of Bachmann's bundle: results of a multicenter randomized trial. J Cardiovasc Electrophysiol. 2001;12:912–7.
123. Verlato R, Botto GL, Massa R, et al. Efficacy of low interatrial septum and right atrial appendage pacing for prevention of permanent atrial fibrillation in patients with sinus node disease: results from the electrophysiology-guided pacing site selection (EPASS) study. Circ Arrhythm Electrophysiol. 2011;4:844–50.
124. Tse HF, Hettrick DA, Mehra R, et al. Improved atrial mechanical efficiency during alternate- and multiple-site atrial pacing compared with conventional right atrial appendage pacing: implications for selective site pacing to prevent atrial fibrillation. J Am Coll Cardiol. 2006;47:209–12.
125. Bernheim A, Ammann P, Sticherling C, et al. Right atrial pacing impairs cardiac function during resynchronization therapy: acute effects of DDD pacing compared to VDD pacing. J Am Coll Cardiol. 2005;45:1482–7.

18 Importance of Right Ventricular and Left Ventricular Lead Placement in Cardiac Resynchronisation Therapy

Radu Ciudin and Leonard Alexandru Mandes

Abstract

Cardiac resynchronisation therapy was a major advancement in the treatment of patients with heart failure, improving both the symptoms and left ventricular ejection fraction while reducing left ventricular volumes and increasing survival. Nevertheless, in spite of all the advancements in the technique and the numerous studies aimed at choosing the suitable candidates for device implantation or the optimal site for lead placement, some important questions still remain unanswered since a relatively large number of patients fail to have an adequate response to left ventricular pacing (Zareba and Klein, Circulation 123:1061–72, 2011; Daubert et al., Europace 14(9):1236–86, 2012). Therefore, having a better insight on the means to achieve the optimal technique and the different approaches suitable for selected, difficult cases might help in increasing the number of adequate responders. Beside optimal patient selection, choosing an appropriate site for right and left ventricular lead placement is paramount for a successful resynchronisation. Numerous studies advocate for targeted left ventricular lead placement, by using either radiological markers, electrical parameters or multimodality imaging aimed at finding the latest viable activated left ventricular wall segment (Mortensen et al., Europace 12(12):1750–6, 2010; Zhou et al., JACC Cardiovasc Imaging 7(12):1239–48, 2014). Moreover, when the conventional approach for pacing in the left ventricle fails, other techniques might prove to be the right solution, such as endocardial/epicardial (by surgery) methods or leadless pacing (DeRose et al., J Am Coll Cardiol 41:1414–9, 2003; Garrigue et al., Am J Cardiol 88:858–62, 2001; Auricchio et al., Europace 16(5):681–8, 2014; Neuzil et al., Europace 16(Suppl. 2):35, 2014). Finally, other studies affirm that the right ventricular lead position has an important influence over the success of resynchronisation (Merchant et al., Pacing Clin Electrophysiol 33:575–82, 2010; Heist et al., Am J Cardiol 96:685–90, 2005).

Keywords

Cardiac resynchronisation therapy · Lead placement · Pacing site · LV dysfunction · Electrical dyssynchrony

R. Ciudin (✉)
"Carol Davila" University of Medicine and Pharmacy, Bucharest, Romania

Cardiology Department, "Prof. C.C. Iliescu" Emergency Institute for Cardiovascular Diseases, Bucharest, Romania

L. A. Mandes
Cardiology Department, "Prof. C.C. Iliescu" Emergency Institute for Cardiovascular Diseases, Bucharest, Romania
e-mail: leonardmandes@gmail.com

S. I. Dumitrescu et al. (eds.), *Right Heart Pathology*, https://doi.org/10.1007/978-3-319-73764-5_18

18.1 Introduction

For almost 20 years, cardiac resynchronisation therapy (CRT) has been one of the cornerstones in treating patients with heart failure, reduced ejection fraction and interventricular conduction delay, as several large trials have established its crucial role in improving symptoms and left ventricular (LV) function, while reducing heart failure (HF) hospitalisations and mortality [1, 11–13]. However, despite its large availability and significant technical advancements compared with its early days, one of the major limitation of CRT in current medical practice is the large proportion of patients who fail to show an improvement in functional and structural parameters—with an estimated rate between 20 and 40% [2]. Therefore, efforts have been made not only to predict beforehand who will respond to CRT, but also to optimise the procedure for maximal clinical benefit [14]. Current approach is focused on better patient selection, targeted LV and right ventricular (RV) lead placement to reduce mechanical and electrical dyssynchrony, ideally assisted by multimodality imaging, while using different surgical techniques for accessing the optimal pacing site and better device programming.

18.2 The Influence of Right Ventricular Lead Location Over CRT Success

While the LV pacing site is very important for a successful resynchronization therapy, data regarding an optimal position for the right ventricular (RV) lead is still controversial and its overall impact on CRT outcome remains unclear [15]. Practice usually varies from centre to centre, but conventionally an apical location is preferred, especially for CRT with defibrillation function (CRT-D), as it allows the entire distal coil to lie in the RV, which may lower the defibrillation threshold and decrease the odds of damaging the tricuspid valve [2, 15, 16].

Alternate pacing sites for placing the RV lead have been proposed (high septal/mid-septal—the Hiss-bundle area, or RV outflow tract). The explanation for choosing the septal region for RV lead placement during CRT procedure lies in observations derived from previous studies that showed that single-site RV apical pacing is deleterious for myocardial performance [17–20]. Faster ventricular activation (resulting in a narrower QRS), improvements in myocardial perfusion [20], and hemodynamic parameters [17, 19] and a decrease in wall motion abnormalities and adverse histopathological changes (myofibrilar disarray) have been associated with choosing a septal pacing site. However, other studies didn't show the superiority of this approach in single-site RV pacing [21, 22]. Such discrepancies might be explained by the difficulty of placing the RV lead in the proximity of the Hiss-bundle area and the different follow-up periods, since adverse anatomical and histopathological changes require a certain amount of time to become apparent [20, 23].

Most studies that evaluated the impact of alternative RV pacing sites in CRT-receivers are derived form post hoc analyses of main large trials. For example, in the REVERSE trial there were no significant differences regarding premature death or the time before the first hospitalization for heart failure [24]. In another retrospective study based on the MADIT-CRT trial cohort, Kutyifa et al. found no influence over clinical outcome (heart failure or death) between apical and non-apical RV lead position, while a higher risk for arrhythmic death due to ventricular tachycardia or ventricular fibrillation was noted (mainly in the first year after device implantation) in patients with a nonapical lead location [25]. While some observational, non-randomised studies hinted at a potential benefit from RV septal pacing (further narrowing of the QRS—although a shorter QRS was not related to better clinical outcomes—probably because temporal synchrony is not fully superimposable with spatial synchrony, and better LV reverse remodelling) [23], the results of other small, prospective studies further supported the fact that the RV lead position is not a major determinant for CRT success, with no significant differences regarding LV reverse remodelling after 6 months of follow up [26]. Moreover, the SEPTAL-CRT trial—a multicentre, randomized

trial that assigned 263 patients in a 1:1 ratio either to RV septal pacing or RV apical pacing found no difference between the two groups regarding the clinical outcome, improvement of LV ejection fraction and LV end-systolic volume reduction [27]. As discussed above, the possible confounding factors that might lead to such differences are the short follow up period (6 months for almost all the studies), the lacking of precise localization of the Hiss bundle only by using fluoroscopy and probably the most important factor—the influence of the relative position of the RV lead in relation to the LV lead [28]. Indeed, there are several studies that further advanced the hypothesis that interlead distance (mainly the anterior-posterior or horizontal separation) measured during fluoroscopy in the standard left anterior oblique (LAO) and right anterior oblique (RAO) projections or on postoperative chest X-rays might be correlated with reverse remodelling. Both Merchant et al. and Heist and co-workers found a positive link between a greater separation of the two leads and acute hemodynamic improvement with better electrical separation between the two ventricles and LV lead electrical delay, which translated in more positive outcomes [9, 10]. The same findings were supported by a study led by Miranda et al., which further showed that a mid-septal RV lead position is associated with improved electrical separation [29]. However, another study with similar design failed to show a link between interlead distances and reverse remodelling, although there was no assessment of clinical, functional and quality of life parameters [30]. Possible explanations for these results might lie in the relative small number of patients recruited, the inclusion of patients with ischemic HF (where the presence of scarring tissue is a limitation for CRT success) and the difficulty in assessing the real distance between the two leads only from bidimensional standard projections [30].

To conclude, there are no definite recommendations for RV lead placement for CRT receivers and we are in dire need for long-term multicentre randomized trials to assess the benefit of alternative RV pacing sites and the maximisation of interlead distance in the CRT population, ideally by using complementary imaging techniques to identify the optimal pacing site (contrast angiography for RVOT, echocardiography—speckle tracking/3D echo/intracardiac echography, cardiac magnetic resonance imaging (MRI) or cardiac computed tomography (CT)) [31]. Moreover, in the presence of severe myocardial disease or extensive scar tissue, adequate pacing threshold and sensing may limit the available sites for the RV lead placement [2].

18.3 Left Ventricular Lead Placement: Available Techniques

18.3.1 Conventional Approach

The mainstay of LV lead placement is the transvenous approach by cannulating one of the branches of the coronary sinus (CS). Usually the RV lead is positioned first, since trauma to the right bundle branch during CS cannulation may lead to complete heart block and immediate need for pacing [2]. Strategies for CS cannulation include using a guide sheath with a J-shaped curve (ideally adjusted to right atrium (RA) size) in combination with an ablation catheter (deflectable)/angiography guide catheter/J-guidewire or, for difficult cases (prominent sub-eustachian pouch, prominent thebesian valve, a large left ventricle or right atrium) using a secondary Amplatz-type catheter, hydrophilic guidewires or balloon dilation of the coronary sinus, in addition to small injections of contrast media [2, 31]. The CS cannulation is possible in over 95% of the cases. Usually, after a successful CS cannulation, retrograde angiography is performed, either by direct injection, or by using a balloon occlusion catheter—this allows for a better anatomical assessment and selection of the optimal branch for lead positioning. Obtaining two projections is recommended—LAO projection allows for branch localization, while the anterior-posterior (AP) projection permits the visualisation of branch origin from the CS (Fig. 18.1) [2].

CS cannulation and angiography are followed by advancement of the lead through the selected

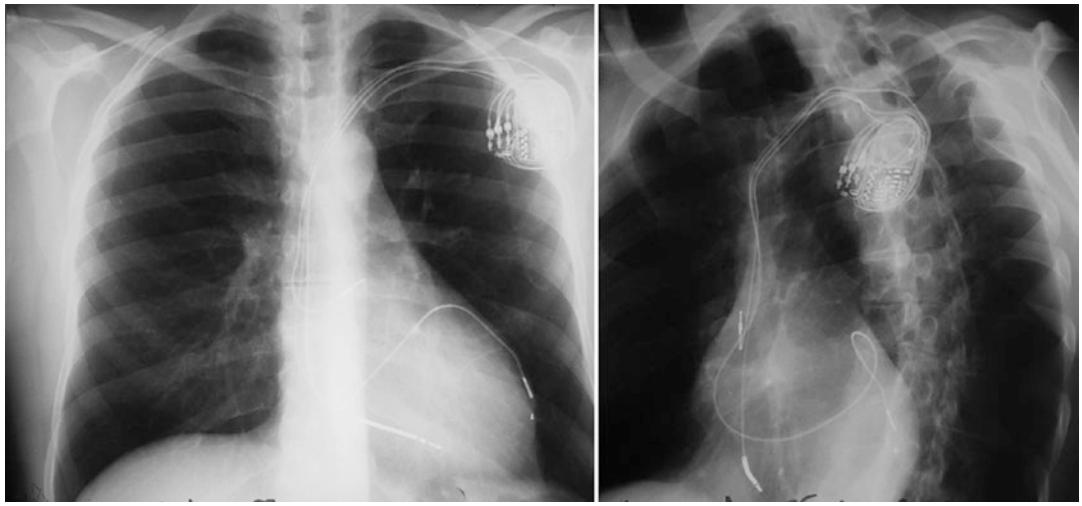

Fig. 18.1 The importance of using multiple radiological views for the correct assessment of the final LV lead position. On the left X-ray (PA), the LV lead has a false anterior position, while on the right (LAO), we can correctly predict that the final LV lead pacing site is on the lateral wall

branch—commonly a lateral branch. Advancing within the coronary sinus might prove difficult in some cases—the presence of CS stenosis/CS spasm/CS dissection may need low-pressure balloon dilation (or even using coronary stents for particular cases) or selection of proximal posterior veins, valves in the coronary sinus require usage of stiffer guidewires or deflectable catheters for valve opening while soft guide-wires with frequent venographies are useful for excessive tortuosity [2, 31, 32]. Placement of the LV pacing lead on the lateral wall can be further impeded by lead instability/dislodgement (Fig. 18.2), small or absent lateral veins (anastomotic branches and collaterals that drain to the lateral wall might prove a solution—snares can be used to capture the distal end of a long hydrophilic wire and retracted, offering support for lead advancement [32]), variceal veins (usage of larger leads with "corkscrew" curvature is advised [31] and selection of normal-sized third or fourth-order branches), extensive myocardial scar leading to increased thresholds and capture latency or phrenic nerve stimulation [31].

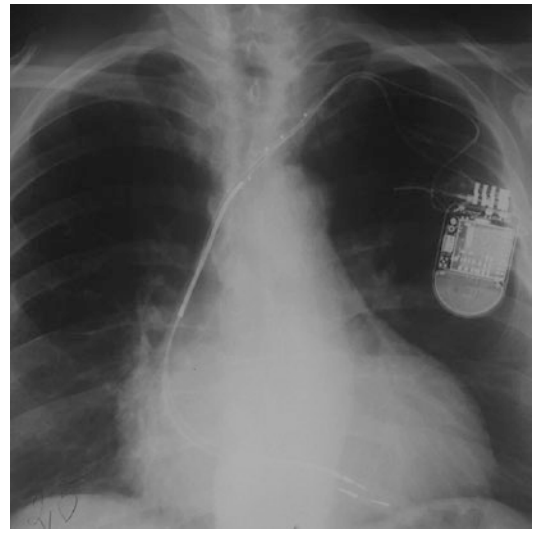

Fig. 18.2 PA Chest X-ray in a CRT-D receiver with no LV pacing on the surface ECG showing quadripolar LV lead dislodgement, with the lead migrated in the superior vena cava

An interventional approach to lead placement using a telescoping system of inner directional catheters and guide sheaths for increased stability and direct lead delivery to the desired CS branch might be better than the classical over-the-wire implant [14, 33, 34]. The selective catheter connected to the contrast injection system and the steerable guide wires for navigating difficult vein branches provide additional support and allow for direct LV lead delivery into the chosen branch [33].

A non-randomized study comparing the two techniques showed fewer LV lead failures (1.9% vs 8.1%), better targeted lead placement and decreased fluoroscopy times [34]. LV lead placement failure in the two most recent CRT randomized trials by using the conventional approach ranges between 7.5% and 10% [35, 36]. The REVERSE trial reported a 12-month rate of dislodgement of 3.4% [37]. Most failures are caused by inability to access the CS or to advance into a suitable and stable position [33]. Obtaining an adequate capture threshold without phrenic nerve capture can be another challenging endeavour. Using multipolar leads should be encouraged, since they allow for a large range of available pacing polarities, both for avoiding phrenic stimulation and for maintaining long term CRT success—especially because over 36% of the patients with CRT experience therapy failure, in part due to loss of LV capture (Fig. 18.3) [2]. Moreover, lower rates of dislodgements were noted for multipolar leads versus conventional bipolar/unipolar leads (1.7% vs 4.6%), probably because multipolar leads are available in a wide range of lead tip shapes [2]. Mapping of the targeted vein to determine the course of the phrenic nerve is recommended [2].

In addition to multipolar leads, preformed curves provide increased stability and proximal fixation (avoiding apical positions), provided that the proximal preformed element resides within the target vessel [38, 39]. When CS cannulation has failed, additional imaging techniques can be useful. CT angiography and late filling of the cardiac veins during left heart catheterization may provide sufficient information regarding distal venous anatomy and CS location [2]. Intraoperative, transoesophageal echocardiography can be helpful [40], but intracardiac echocardiography is usually more tolerable in conscious patients [41]. Nevertheless, the EHRA committee recommends these methods only when CS cannulation has failed or in the case of suspected structural anomalies [2].

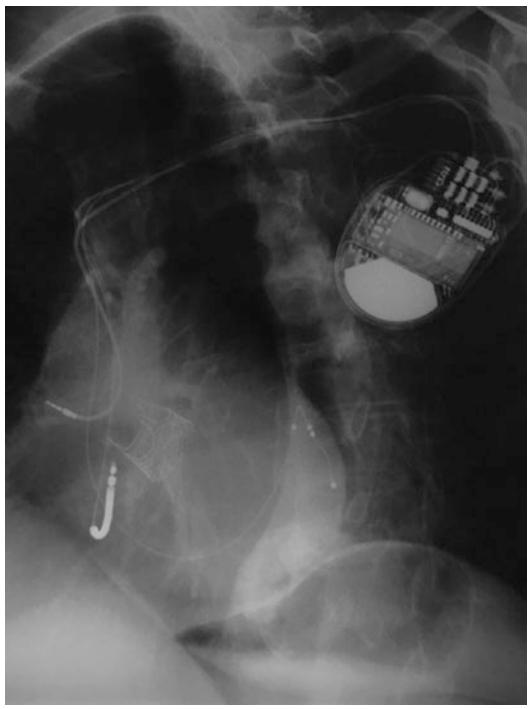

Fig. 18.3 Successful implantation of a CRT-D device in a patient using a quadripolar LV lead. LAO Chest X-ray shows a good positioning of the lead on the lateral LV wall

18.3.2 Endocardial Approach

Endocardial pacing might provide superior results to epicardial pacing, since physiologically electrical depolarization originates in the endocardium and the site for LV pacing is not limited by the CS anatomy. The reversal of normal activation sequence in epicardial pacing may lead to electrical dispersion, with the potential for an arrhythmogenic substrate [42]. Moreover, the faster impulse conduction through the endocardium compared to the epicardium results in a more synchronous activation and contraction of the left ventricle. Some safety issues might be raised because of the increased thromboembolic risk, and, subsequently, an increase in the bleeding risk due to the need for permanent anticoagulation (similar to mechanical valves) and the possibility of lead infection [43].

Several small studies using different approaches and delivery systems showed a potential benefit of endocardial pacing versus epicardial pacing on clinical status and LV performance [6, 44]. Other technical approaches

using the subclavian vein to perform an interventricular septal puncture is under investigation in the LV-CONSEPT trial. Yet another study described a transapical method for accessing the LV endocardium, bypassing the need for transseptal puncture and the risk of damaging the mitral valve, reducing the implant time and allowing for LV lead repositioning, albeit on a very small cohort of 12 patients [44]. Additionally, the ALSYNC trial, a prospective, multicentric clinical investigation sought to evaluate the feasibility and safety of left ventricular endocardial pacing by using an investigational lead delivery system and LV lead, by a pectoral transseptal approach through the mitral valve. 138 patients unsuitable for conventional CRT or that were nonresponsive to conventional CRT were enrolled [45]. The primary endpoint of the study was freedom from complications. The results from the trial were encouraging, with a 89% success rate and freedom of complications for 82.2% of the patients at 6 months, meeting the primary endpoint. Complications ranged form lead dislodgement and pocket haematoma to stroke, intracardiac thrombus, aorta puncture, pericardial effusion and pneumothorax. There were no deaths due to the procedure or mitral valve complications. About 60% of the patients were responders, with an improvement in LV ejection fraction and LV reverse remodelling [45]. The main limitation of the study was the lack of comparison with other techniques in improving clinical outcomes. Therefore, although LV endocardial pacing looks promising, this approach still remains investigational until further comparative studies will prove its clinical effectiveness and safety [42].

18.3.3 Surgical Epicardial Approach

As aforementioned, transvenous lead implantation is plagued by some technical difficulties that may compromise the success of CRT—in up to 8–10% of the patients undergoing the procedure there is a failure to cannulate the CS or to have a proper lead placement in an adequate venous branch [5, 46]. Moreover, lead dislodgement is responsible for another 5–10% late LV pacing failures [5]. A possible solution for these patients is open surgery lead placement (Fig. 18.4), a technique that is able to circumvent some of the disadvantages of the conventional transvenous approach.

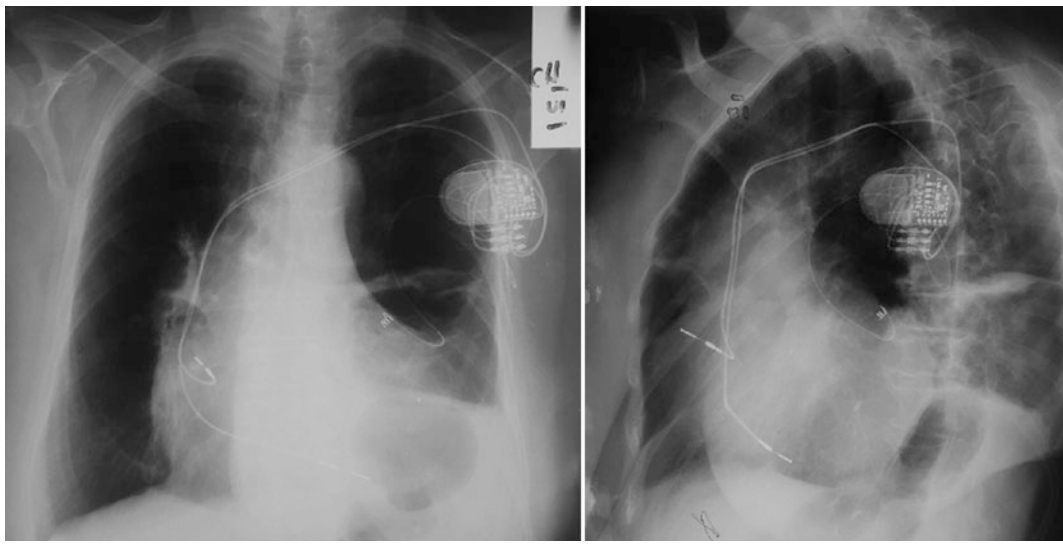

Fig. 18.4 PA and LAO Chest X-rays of a patient with surgically implanted epicardial electrode on the lateral LV wall. The patient didn't have a suitable CS vein anatomy, with no suitable venous branches on the posterolateral or anterolateral LV wall

There are various surgical techniques that are used for implanting the LV lead—either by a left anterior or lateral mini-thoracotomy or by video-assisted thoracoscopy approach [47–49]. The *da Vinci robot system* can also be used, allowing for high-resolution, real time three-dimensional vision of the left ventricle, while using as an access route a small thoracotomy incision [5]. Moreover, the surgical approach enables the operator to choose exactly the site for LV lead implantation, especially when robotic assistance is used, and it might be a first choice when the transvenous approach is unfeasible [5]. After surgery, in the mid-term, the patients had better clinical outcomes and improvements in LV performance with stable pacing parameters [5, 46]. However, in patients with advanced heart disease and significant comorbidities, the surgical risk might be to high, requiring alternative approaches—these patients have increased perioperative morbidity and mortality, while reverse remodelling of the LV may not occur (a possible explanation for less LV reverse remodelling is the operator tendency to place the epicardial LV lead in an anterior position rather than on the LV lateral wall, since it's readily accessible) [5].

For CRT-D receivers that lack an adequate venous access, the placement of epicardial defibrillator leads might be required. A case report by Sugumar et al. describes a successful technique for a total epicardial CRT-D system. After a midline sternotomy multiple single coil active fixation defibrillation leads are placed anteriorly into the RV outflow tract and posteriorly in the AV groove. The leads are then sutured over the visceral epicardium and tunnelled from the pericardium to the lateral abdominal wall. Follow-up at 2 years showed stable electrical parameters [49].

18.3.4 Percutaneous Epicardial Approach

While surgical epicardial lead placement is associated with higher perioperative morbidity, an epicardial lead delivered percutaneously through a subxiphoid approach similar to the technique used for electrophysiology procedures would, in theory, lower the complications, while maintaining the advantage of choosing the exact site for pacing [50]. The only available studies thus far have only assessed the LV lead safety and stability over time in small series of animal models (porcine and canine models), with favourable results [51]. However, the tools and lead fixation strategies are still in development, so this technique although promising, is momentarily still investigational and far from reaching clinical practice.

18.3.5 Leadless Left Ventricular Pacing

The WiCS LV system (manufactured by EBR Systems, Inc) is a device that allows leadless LV endocardial pacing, combining the advantages of the endocardial approach while minimising the risk of mitral valve injury and thromboembolic events—the main disadvantages of using regular electrodes for endocardial pacing. A small electrode is implanted in the LV endocardial wall using femoral access via a retrograde aortic approach, while a pulse generator is inserted subcutaneously in an adjacent intercostal space [52]. The system is dependent on previously implanted conventional devices (implantable cardiac defibrillators (ICD), pacemakers or CRT devices)—RV pacing by these devices is detected by the subcutaneous pulse generator, which in turn uses ultrasound to trigger LV stimulation [52]. The device was tested in two prospective, multicentre, nonrandomized trials. Both had as primary outcome measures the safety and feasibility of the system, while the secondary endpoints were the changes in clinical composite scores and echocardiographic (LVEF, LV end-diastolic volume and end-systolic volume) and bioumoral (NT-pro BNP level) changes [7, 8].

The WiSE-CRT trial, which included 17 patients in three groups—those with failed CS lead implantation, non-responders to traditional CRT and patients with previously implanted devices (ICD's and pacemakers) that required an upgrade to CRT—reported a success rate of 76.5%, with complications ranging from lead

failure (5.8%) to pericardial effusion (17.6%). Up to two thirds of the patients had a significant improvement in both the LVEF and clinical status (at least one NYHA functional class) after 6 months of follow up [7].

The SELECT-LV trial enrolled 35 patients with failed conventional CRT (difficult CS anatomy, non-responders, high LV pacing thresholds or phrenic nerve capture) and achieved a success rate of 97.1%, albeit with serious procedure or device-related events in 22.9% of the patients after 1 month of follow-up. The majority of the patients had a significant improvement in the clinical composite score (84.8%) and echocardiographic parameters (66%) at 6 months [8].

Although both studies supported the clinical feasibility for the WiSE-CRT system, the device is not FDA approved, and some safety and efficacy concerns have been raised regarding the widespread utilisation in clinical practice. However, as with every new technique, with better operator experience come improved outcomes.

18.3.6 Multisite Pacing

While conventional CRT uses a single lead to achieve LV pacing, small trials have raised the hypothesis that CRT nonresponders might benefit from multisite pacing, by placing one, two or even three additional LV leads, allowing for better myocardial recruitment. Patients with very large left ventricles, extremely wide and fragmented QRS (suggestive for extensive fibrosis), myocardial scarring and those with permanent atrial fibrillation (marker of a more severe disease) seem to benefit the most in several small trials, with significant improvements in NYHA class, VO2 max and 6 min walk distance [53]. Another study by Ginks et al. [54] compared LV endocardial multi-site pacing (performed after a complete electrophysiology study with non-contact mapping of LV endocardium for scar detection) with conventional CRT pacing in 10 patients, while measuring hemodynamic parameters. A statistically significant improvement in dP/dt was observed in both groups, with better results for those with endocardial pacing, although the difference was not statistically significant due to the small number of study participants [54]. Similar results were reported by Pappone et al. [55], who also found a further reduction by 22% in QRS duration during multisite pacing. Recent results from the TRUST-CRT trial, a randomized unicentric study that compared triple-site pacing with conventional CRT in 100 patients, supported the abovementioned findings, showing a marked improvement in NYHA functional class after 1 year of follow up in patients with multisite pacing, while the incidence of serious complications was similar in both groups [56].

Another randomized, multicentric trial is underway—the DIVA trial, where dual site pacing is compared with standard CRT by evaluating the clinical composite score for heart failure at follow up. Interestingly, there is no trial that compares multi-site pacing achieved by placing multiple standard bipolar leads with that achieved by using a single quadripolar lead.

18.4 Left Ventricular Lead Placement: Anatomic Versus Targeted Strategy

Choosing an appropriate LV lead position is the cornerstone for CRT success—even if is dependent on the anatomy of the cardiac venous system, an optimal site should have good pacing parameters and lead stability while avoiding phrenic nerve stimulation. Current practice uses an “anatomical approach”, where a lateral wall position is desirable, although this strategy has not been validated by mutlicentric studies [57]. However, the lack of an appropriate clinical and echographic response in about a third of the patients undergoing CRT (Fig. 18.5) suggest that beside unfavourable CS anatomy or suboptimal pacing parameters precluding the lead positioning in the desired site, other factors play a key role, like different electrical and mechanical activation patterns specific for each patient (especially since many patients don’t have a typical left bundle branch block (LBBB) morphology

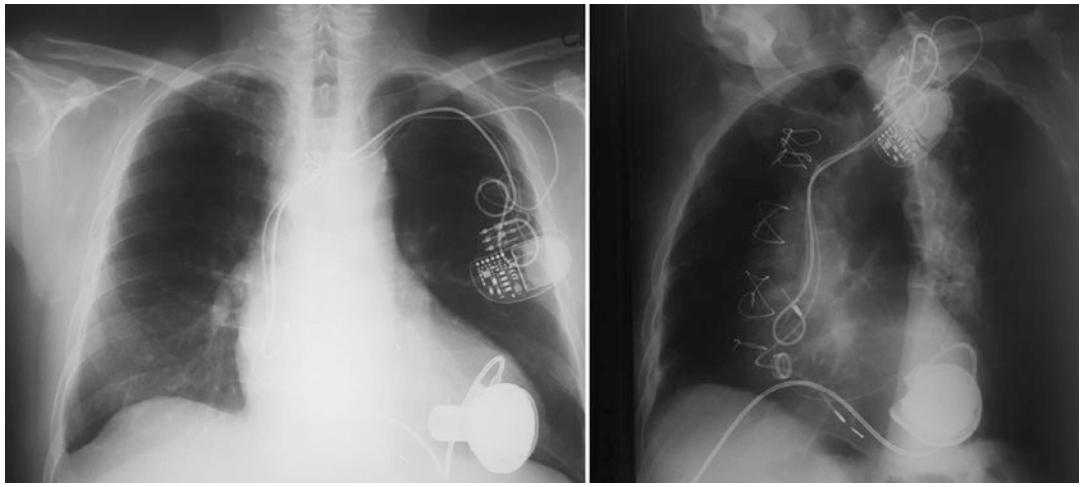

Fig. 18.5 Lack of CRT response in a patient with apparent anatomic optimal LV lead position (PA and LAO chest X-rays). The patient required a left ventricular assist device for refractory HF as a bridge to transplant

that translates into a contraction pattern of opposing wall motion with apical rocking—meaning a different activation sequence that might respond different to the usual pacing site), the presence of myocardial scarring and device optimisation (AV and VV delay) [2].

18.4.1 Anatomical Strategy

LBBB morphology has a detrimental effect on LV remodelling by increasing end-systolic and end diastolic volumes and the myocardial wall stress, leading to a decline in myocardial function [58]. Pacing at the most delayed activated site was beneficial in early clinical trials, reducing LV remodelling and improving the ejection fraction. Mostly for LBBB, it corresponds with posterolateral and LV free wall pacing, as found by some of the studies [57, 59]. Another retrospective study on 457 CRT recipients (either with or without a defibrillator) analysing whether a posterolateral/anterolateral position was better than an anterior position for the LV lead found that clinical improvement (assessed by NYHA class), LV EF increase and survival were more likely for the lateral position [60].

The REVERSE study also favoured lateral LV pacing sites regarding a favourable response by reverse LV remodelling and the composite time to death or first HF hospitalisation [15]. While the above studies clearly are in favour of choosing a lateral position for the LV lead, a post-hoc analysis of the COMPANION trial found no difference between lead position and mortality/heart failure hospitalisation, with clinical improvement in most CRT receivers [61].

In the MADIT-CRT trial where the LV lead location was determined by using venograms from two orthogonal views, during follow-up the primary endpoint (HF hospitalization and death) was similar between anterior, lateral and posterior positions, while only the apical position correlated with adverse outcomes [1].

The PROSPECT trial supported this result, with no relation between optimal and non-optimal position and adverse outcomes, although in group subanalysis a suboptimal LV lead position (mid-apical anterior position) was detrimental for patients with LBBB and non-ischemic cardiomyopathy [3].

18.4.2 Impact of Myocardial Scarring and Targeted LV Lead Placement

Clinical response and myocardial scarring have been inversely correlated in CRT receivers, since an LV lead with the electrodes placed in a scar

area is less likely to effectively pace the LV (both due to high threshold and delayed activation through the fibrotic tissue). Although initial studies didn't report a significant difference between patients with and without ischemic cardiomyopathy, most studies supported the idea that CRT success is dependent on the aetiology of cardiomyopathy [62]. In the MIRACLE study, patients with non-ischemic HF and mild-to moderate mitral regurgitation benefited the most from reverse remodelling and LV EF improval [11]. The current accepted gold standard for assessing the location and extent of myocardial scarring (transmural/endocardial/mid-wall location) is cardiac magnetic resonance imaging (MRI) with delay enhancement. In a study by Bleeker et al. [63] that used contrast MRI for scar detection and quantification, CRT nonresponders were prone to have transmural scarring in the posterolateral LV wall, and mechanical dyssynchrony (assessed by tissue Doppler imaging) didn't have a significant impact on CRT success in these patients. Other trials supported the abovementioned result [64, 65].

Echocardiographic studies using speckle tracking two dimensional (2D) radial strain to determine the latest LV mechanical activation might be useful in guiding a successful CRT, as reported by the TARGET trial, a randomized study that assessed the impact of targeted LV lead placement on the outcomes, and found at 6 months of follow-up that patients with echocardiography-guided implantation fared better, with improved clinical response, LV reverse-remodelling and fewer HF hospitalizations, albeit with no significant changes in mortality. After multivariate analysis, the impact was greater for those without myocardial scarring, whereas those that had a scar in the target area for LV lead placement had a much lower benefit form CRT [66]. Another randomized study, the STARTER trial, that compared standard fluoroscopic anatomical lead placement with echo-guided placement using 2D speckle tracking confirmed the benefits found in the TARGET trial and enforced the superiority of the echographic method – those with concordant LV lead placement assessed by echocardiography had better outcomes, with a significand reduction in end-points (HF hospitalization/death) [67].

Another approach for identifying the area of latest electrical activation is by measuring electrical delay form surface ECG/intracardiac electrogram—derived parameters, usually assessed by the QLV interval, which is the time form QRS onset on the surface ECG to the first identifiable peak of the LV electrogram measured at the time of CRT implant [68]. The QLV interval is a strong predictor of acute hemodynamic improvement, both in biventricular and LV only pacing. A study by Gold et al. found that pacing in an area with the longest QLV (>120 ms) was linked to better clinical outcomes and significant echographic improvement (LV volume reduction and EF increase) [68]. These findings were also supported by the PEGASUS-CRT trial, where another measure of electrical delay (RV-LV interval) was adversely correlated with HF events [69]. Moreover, other recent trials also supported QLV importance (interval greater than the median 95 ms) in influencing CRT response, independent of the HF aetiology, LBBB or non-LBBB morphology and QRS duration (130–150 ms or wider than 150 ms) [70].

Other imaging techniques can be useful both for assessing myocardial viability and mechanical dyssynchrony—Gated single photon emission-computed tomography myocardial perfusion imaging (SPECT MPI) and positron emission tomography (PET) can easily provide such information in a single scan [71–73]. Several studies showed that SPECT MPI is able to identify with accuracy myocardial scarring (less than 50% tracer uptake) and the latest LV activated site (by calculating the mean phase for each segment—the segment with the maximal value being the latest activated segment), having a positive outcome on CRT success—patients with LV lead placement at the latest activated sites with reasonable myocardial viability had improved LV function and clinical response compared with those with discordant lead positions after 6 months of follow-up [72, 74]. Similar results were obtained by using PET-CT as guidance—responders (defined as having clinical improvement with an increase in EF) were more likely to

have LV pacing leads in area with the most dyssynchronous and viable segments [75, 76]. The main limitations of these studies were their retrospective nature and the relatively small numbers of participants enrolled (between 19 and 90 patients).

CMR can provide high quality data regarding the circumferential strain enabling accurate assessment of mechanical dyssynchrony [77]. A retrospective study that enrolled 559 patients that underwent CRT where LV placement was either guided or not by CMR found that after 9 years of follow-up patients with CMR-targeted LV placement had significantly better outcomes (HF hospitalization/CV death) than patients with LV leads placed in scar tissue or without imaging guidance [78]. Other studies validated the placement of LV leads in the latest activated viable segment by using CMR as a superior method, with up of 3 times more reverse remodelling in such patients [79, 80].

18.4.3 LV Lead Placement by Using Image Fusion Techniques

While echocardiography, SPECT/PET–CT and CMR can provide useful data regarding the optimal LV pacing site, such information must also be available in real time during the CRT procedure, since without a clear image of the myocardial wall during conventional fluoroscopy the operator is unable to accurately correlate the venous anatomy with the corresponding myocardial segment, thus resulting in suboptimal LV lead placement [81]. Therefore, hybrid imaging techniques might overcome such a disadvantage. Both the TARGET trial and the STARTER trial integrated the venous anatomy obtained form venograms in the LAO plane with the corresponding short-axis echocardiographic image, while the RAO plane was used for correction and adjustment to assess if the LV lead position was in the basal, middle or apical segments [66, 67]. However, the concordance between the final LV pacing site and the optimal segment identified by echocardiography varied significantly in the two studies—over 64% for the TARGET trial and under 30% for the STARTER trial [66, 67].

Another single centre study evaluated the feasibility of LV lead placement by using a 3D generated model from LGE-CMR data that was projected and matched on 2D intraprocedural fluoroscopy. The final LV lead tip location was assessed by postprocedural ECG-gated cardiac CT. The optimal pacing site was achieved in over 97% of the patients [82]. In yet another CMR study, both the vein anatomy and the anatomical LV 3D model were obtained using magnetic resonance, combined with real-time fluoroscopy, achieving high accuracy in optimal lead positioning [83]. The main disadvantages of such techniques is their costs, limited availability and the fact that they are time-consuming [82, 83].

Other possible methods include using CT venography obtained preoperatively and 2D fluoroscopy-derived venograms combined with LV anatomy/viability models obtained by CMR or SPECT-CT [4]. The CT venography was used to assess if the venograms and the SPECT MPI images were correctly fused. A prospective study validated this approach in the clinical setting, with an accuracy of 87% [4]. However, the extra imaging time and additional radiation exposure are still a concern [4, 82, 83]. These novel imaging techniques are a step forward and they might have a significant positive impact on CRT success.

18.5 Future Perspectives

While the development of new tools and techniques has greatly advanced the field of cardiac resynchronization therapy compared to its early days, further improvements are still needed. Active fixation leads might reduce the risk of depositioning while multipolar leads that allow for a much larger array of pacing configuration may prevent phrenic nerve capture and improve capture thresholds.

Better patient selection and “targeted” implant strategies tailored to the patient, with optimal programming might also prove the solution for a significant decrease in CRT nonresponders. Hybrid techniques using fluoroscopy and echography/MRI or SPECT-CT are promising since

they enable the operator to select the optimal LV lead site in real time, but further studies are warranted (ideally randomized, controlled trials), since most data are derived from small, nonrandomized retrospective studies.

References

1. Zareba W, Klein H, Cygankiewicz I, et al. Effectiveness of cardiac resynchronization therapy by QRS morphology in the Multicenter Automatic Defibrillator Implantation Trial-Cardiac Resynchronization Therapy (MADIT-CRT). Circulation. 2011;123:1061–72.
2. Daubert JC, Saxon L, Adamson PB, Auricchio A, Berger RD, Beshai JF, Breithard O, Brignole M, Cleland J, DeLurgio DB, Dickstein K, Exner DV, Gold M, Grimm RA, Hayes DL, Israel C, Leclercq C, Linde C, Lindenfeld J, Merkely B, Mont L, Murgatroyd F, Prinzen F, Saba SF, Shinbane JS, Singh J, Tang AS, Vardas PE, Wilkoff BL, Zamorano JL, Anand I, Blomström-Lundqvist C, Boehmer JP, Calkins H, Cazeau S, Delgado V, Estes NA, Haines D, Kusumoto F, Leyva P, Ruschitzka F, Stevenson LW, Torp-Pedersen CT. 2012 EHRA/HRS expert consensus statement on cardiac resynchronization therapy in heart failure: implant and follow-up recommendations and management. Europace. 2012;14(9):1236–86.
3. Mortensen PT, Herre JM, Chung ES, Bax JJ, Gerritse B, Kruijshoop M, Murillo J. The effect of left ventricular pacing site on cardiac resynchronization therapy outcome and mortality: the results of a PROSPECT substudy. Europace. 2010;12(12):1750–6.
4. Zhou W, Hou X, Piccinelli M, Tang X, Tang L, Cao K, Garcia EV, Zou J, Chen J. 3D fusion of LV venous anatomy on fluoroscopy venograms with epicardial surface on SPECT myocardial perfusion images for guiding CRT LV lead placement. JACC Cardiovasc Imaging. 2014;7(12):1239–48.
5. DeRose JJ, Ashton RC, Belsley S, Swistel DG, Vloka M, Ehlert F, et al. Robotically assisted left ventricular epicardial lead implantation for biventricular pacing. J Am Coll Cardiol. 2003;41:1414–9.
6. Garrigue S, Jais P, Espil G, Labeque JN, Hocini M, Shah DC, et al. Comparison of chronic biventricular pacing between epicardial and endocardial left ventricular stimulation using Doppler tissue imaging in patients with heart failure. Am J Cardiol. 2001;88:858–62.
7. Auricchio A, et al. Feasibility, safety, and short-term outcome of leadless ultrasound-based endocardial left ventricular resynchronization in heart failure patients: results of the Wireless Stimulation Endocardially for CRT (WiSE-CRT) study. Europace. 2014;16(5):681–8.
8. Neuzil P, et al. Wireless LV endocardial stimulation for CRT: SELECT-LV study. Europace. 2014;16(Suppl. 2):35.
9. Merchant FM, Heist EK, Nandigam KV, Mulligan LJ, Blendea D, et al. Interlead distance and left ventricular lead electrical delay predict reverse remodeling during cardiac resynchronization therapy. Pacing Clin Electrophysiol. 2010;33:575–82.
10. Heist EK, Fan D, Mela T, Arzola-Castaner D, Reddy VY, et al. Radiographic left ventricular-right ventricular interlead distance predicts the acute hemodynamic response to cardiac resynchronization therapy. Am J Cardiol. 2005;96:685–90.
11. Abraham WR, Fisher WG, Smith A, MIRACLE Study Group, et al. Cardiac resynchronization in chronic heart failure. N Engl J Med. 2002;346:1845–53. https://doi.org/10.1056/NEJMoa013168.
12. Birnie DH, Ha A, Higginson L, et al. Impact of QRS morphology and duration on outcomes after cardiac resynchronization therapy: results from the Resynchronization-Defibrillation for Ambulatory Heart Failure Trial (RAFT). Circ Heart Fail. 2013;6:1190–8.
13. Egoavil CA, Ho RT, Greenspon AJ, Pavri BB, et al. Cardiac resynchronization therapy in patients with right bundle branch block: analysis of pooled data from the MIRACLE and Contak CD trials. Heart Rhythm. 2005;2:611–5.
14. Lewis G, Gold M. Developments in cardiac resynchronisation therapy. Arrhythm Electrophysiol Rev. 2015;4(2):122–8.
15. Thébault C, Donal E, Meunier C, Gervais R, Gerritse B, Gold MR, Abraham WT, Linde C, Daubert JC, REVERSE Study Group. Sites of left and right ventricular lead implantation and response to cardiac resynchronization therapy observations from the REVERSE trial. Eur Heart J. 2012;33(21):2662–71.
16. Kindermann M, Frohlig G, Berg M, Lawall P, Schieffer H. Atrial lead implantation during atrial flutter or fibrillation? Pacing Clin Electrophysiol. 1998;21:1531–8.
17. Giudici MC, Thornburg GA, Buck A, et al. Comparison of right ventricular outflow tract and apical lead permanent pacing on cardiac output. Am J Cardiol. 1997;79:209–12.
18. Karpawich PP, Justice CD, Chang CH, et al. Septal ventricular pacing in the immature canine heart: a new prospective study. Am Heart J. 1991;121:827.
19. Schwaab B, Frohlich G, Alexander C, et al. Influence of right ventricular stimulation site on left ventricular function in atrial synchronous ventricular pacing. J Am Coll Cardiol. 1999;33:317–23.
20. Tse H, Yu C, Wong KK, et al. Functional abnormalities in patients with permanent right ventricular pacing. J Am Coll Cardiol. 2002;40(8):1451.
21. Buckingham TA, Candinas R, Attenhofer C, et al. Systolic and diastolic function with alternate and combined site pacing in the right ventricle. Pacing Clin Electrophysiol. 1998;21:1077–84.

22. Victor F, Leclercq C, Mabo P, et al. Optimal right ventricular pacing site in chronically implanted patients. J Am Coll Cardiol. 1999;33:311–6.
23. Riedlbauchova L, Cihak R, Bytesník J, Vancura V, Frídl P, Hoskova L, Kautzner J. Optimization of right ventricular lead position in cardiac resynchronisation therapy. Eur J Heart Fail. 2006;8:609–14.
24. Linde C, William TA, Michael G, Sutton MSJ, Ghio S, Daubert C. Randomized trial of cardiac resynchronization in mildly symptomatic heart failure patients and in asymptomatic patients with left ventricular dysfunction and previous heart failure symptoms. J Am Coll Cardiol. 2008;52(23):1834. https://doi.org/10.1016/j.jacc.2008.08.027.
25. Kutyifa V, Kloppe A, Zareba W, Solomon SD, McNitt S, Polonsky S, Barsheshet A, Merkely B, Lemke B, Nagy VK, Moss AJ, Goldenberg I. The influence of left ventricular ejection fraction on the effectiveness of cardiac resynchronization therapy: MADIT-CRT (Multicenter Automatic Defibrillator Implantation Trial With Cardiac Resynchronization Therapy). J Am Coll Cardiol. 2013;61(9):936–44. https://doi.org/10.1016/j.jacc.2012.11.051.
26. Kristiansen HM, Vollan G, Hovstad T, Keilegavlen H, Faerestrand S. A randomized study of haemodynamic effects and left ventricular dyssynchrony in right ventricular apical vs. high posterior septal pacing in cardiac resynchronization therapy. Eur J Heart Fail. 2012;14(5):506–16.
27. Leclercq C, et al. Comparison of right ventricular septal pacing and right ventricular apical pacing in patients receiving cardiac resynchronization therapy defibrillators: the SEPTAL CRT Study. Eur Heart J. 2016;37(5):473–83.
28. Auricchio A, Leclercq C. Location and characteristics of pacing leads and cardiac resynchronization therapy outcomes - right and left ventricular lead optimization. In: Clinical cardiac pacing, defibrillation and resynchronization therapy. 5th ed. Philadelphia: Elsevier; 2017.
29. Miranda RI, et al. Maximal electrical separation-guided placement of right ventricular lead improves responders in cardiac resynchronization defibrillator therapy. Circ Arrhythm Electrophysiol. 2012;5:927.
30. Zoppo F, et al. Pacing inter-lead fluoroscopic RAO and LAO distance and cardiac resynchronization therapy response. J Clin Exp Cardiolog. 2014;5(9):336.
31. Srivatsa SS. A proposed technique for right ventricular septal pacing. J Invasive Cardiol. 2014;26(3):140–7.
32. Morgan J, Delgado V. Lead positioning for cardiac resynchronization therapy: techniques and priorities. Europace. 2009;11:v22–8.
33. Jackson K. Left ventricular lead placement for cardiac resynchronization therapy. J Innov Card Rhythm Manag. 2013;4:1284–91.
34. Zanon F, Baracca E, Pastore G, et al. Implantation of left ventricular leads using a telescopic catheter system. Pacing Clin Electrophysiol. 2006;29:1266–72.
35. Moss AJ, Hall WJ, Cannom DS, et al. Cardiac-resynchronization therapy for the prevention of heart-failure events. N Engl J Med. 2009;361:1329–38.
36. Tang AS, Wells GA, Talajic M, et al. Cardiac-resynchronization therapy for mild-to-moderate heart failure. N Engl J Med. 2010;363:2385–95.
37. Daubert C, Gold MR, Abraham WT, et al. Prevention of disease progression by cardiac resynchronization therapy in patients with asymptomatic or mildly symptomatic left ventricular dysfunction: insights from the European cohort of the REVERSE (Resynchronization Reverses Remodeling in Systolic Left Ventricular Dysfunction) trial. J Am Coll Cardiol. 2009;54:1837–46.
38. Biffi M, Moschini C, Bertini M, Saporito D, Ziacchi M, Diemberger I, et al. Phrenic stimulation: a challenge for cardiac resynchronization therapy. Circ Arrhythm Electrophysiol. 2009;2:402–10.
39. Hansky B, Vogt J, Gueldner H, Lamp B, Tenderich G, Krater L, et al. Left heart pacing—experience with several types of coronary vein leads. J Interv Card Electrophysiol. 2002;6:71–5.
40. Bashir JG, Frank G, Tyers O, Lampa M, Yamaoka R. Combined use of transesophageal ECHO and fluoroscopy for the placement of left ventricular pacing leads via the coronary sinus. Pacing Clin Electrophysiol. 2003;26:1951–4.
41. Shalaby AA. Utilization of intracardiac echocardiography to access the coronary sinus for left ventricular lead placement. Pacing Clin Electrophysiol. 2005;28:493–7.
42. van Deursen C, van Geldorp IE, Rademakers LM, van Hunnik A, Kuiper M, Klersy C, et al. LV Endocardial pacing improves resynchronization therapy in canine LBBB hearts. Circ Arrhythm Electrophysiol. 2009. https://doi.org/10.1161/CIRCEP.108.846022.
43. van Gelder BM, Scheffer MG, Meijer A, Bracke FA. Transseptal endocardial left ventricular pacing: an alternative technique for coronary sinus lead placement in cardiac resynchronization therapy. Heart Rhythm. 2007;4:454–60.
44. Jais P, Takahashi A, Garrigue S, Yamane T, Hocini M, Shah DC, et al. Mid-term follow-up of endocardial biventricular pacing. Pacing Clin Electrophysiol. 2000;23:1744–7.
45. Morgan J, et al. ALternate Site Cardiac ResYNChronization (ALSYNC): a prospective and multicentre study of left ventricular endocardial pacing for cardiac resynchronization therapy. Eur Heart J. 2016;37(27):2118–27.
46. Fernandez AL, Garcia-Bengochea JB, Ledo R, Vega M, Amaro A, Alvarez J, et al. Minimally invasive surgical implantation of left ventricular epicardial leads for ventricular resynchronization using video-assisted thoracoscopy. Rev Esp Cardiol. 2004;57:313–9.
47. Mair H, Jansens JL, Lattouf OM, Reichart B, Dabritz S. Epicardial lead implantation techniques for biventricular pacing via left lateral mini-thoracotomy, videoassisted thoracoscopy, and robotic approach. Heart Surg Forum. 2003;6:412–7.

48. Rivero-Ayerza M, Jessurun E, Ramcharitar S, van BY, Serruys PW, Jordaens L. Magnetically guided left ventricular lead implantation based on a virtual threedimensional reconstructed image of the coronary sinus. Europace. 2008;10:1042.
49. Sugumar H, et al. Epicardial CRT-D in a pacing dependant patient without transvenous options. Heart Lung Circ. 2017;26:e48–9.
50. Boyle NG, Shivkumar K. Epicardial interventions in electrophysiology. Circulation. 2012;126:1752–69. https://doi.org/10.1161/CIRCULATIONAHA.111.060327.
51. John R, Morgan K, Brennecke L, Benser M, Jais P. Acute and chronic performance evaluation of a novel epicardial pacing lead placed by percutaneous subxiphoid approach in a canine model. Circ Arrhythm Electrophysiol. 2015;8:659–66.
52. Auricchio A, Delnoy PP, Regoli F, Seifert M, Markou T, Butter C, Collaborative Study Group. First-in-man implantation of leadless ultrasound-based cardiac stimulation pacing system: novel endocardial left ventricular resynchronization therapy in heart failure patients. Europace. 2013;15(8):1191–7.
53. Lenarczyk R, Kowalski O, Kukulski T, et al. Mid-term outcomes of triple-site vs. conventional cardiac resynchronization therapy: a preliminary study. Int J Cardiol. 2009;133:87–94.
54. Ginks MR, Shetty AK, Lambiase PD, et al. Benefits of endocardial and multisite pacing are dependent on the type of left ventricular electric activation pattern and presence of ischemic heart disease: insights from electroanatomic mapping. Circ Arrhythm Electrophysiol. 2012;5:889–97.
55. Pappone C, Rosanio S, Oreto G, et al. Cardiac pacing in heart failure patients with left bundle branch block: impact of pacing site for optimizing left ventricular resynchronization. Ital Heart J. 2000;1:464–9.
56. Lenarczyk R, Kowalski O, Sredniawa B, Pruszkowska-Skrzep P, Mazurek M, Jędrzejczyk-Patej E, Woźniak A, Pluta S, Głowacki J, Kalarus Z. Implantation feasibility, procedure-related adverse events and lead performance during 1-year follow-up in patients undergoing triple-site cardiac resynchronization therapy: a substudy of TRUST CRT randomized trial. J Cardiovasc Electrophysiol. 2012;23:1228–36.
57. Butter C, Auricchio A, Stellbrink C, Fleck E, Ding J, Yu Y, et al. Effect of resynchronization therapy stimulation site on the systolic function of heart failure patients. Circulation. 2001;104:3026–9.
58. Xiao HB, Roy C, Gibson DG. Nature of ventricular activation in patients with dilated cardiomyopathy: evidence for bilateral bundle branch block. Br Heart J. 1994;72(2):167–74.
59. van Campen CM, Visser FC, de Cock CC, Vos HS, Kamp O, Visser CA. Comparison of the haemodynamics of different pacing sites in patients undergoing resynchronisation treatment: need for individualisation of lead localisation. Heart. 2006;92(12):1795–800.
60. Dong YX, Powell BD, Asirvatham SJ, Friedman PA, Rea RF, Webster TL, Brooke KL, Hodge DO, Wiste HJ, Yang YZ, Hayes DL, Cha YM. Left ventricular lead position for cardiac resynchronization: a comprehensive cinegraphic, echocardiographic, clinical, and survival analysis. Europace. 2012;14(8):1139–47.
61. Saxon LA, Olshansky B, Volosin K, Steinberg JS, Lee BK, Tomassoni G, Guarnieri T, Rao A, Yong P, Galle E, Leigh J, Ecklund F, Bristow MR. Influence of left ventricular lead location on outcomes in the COMPANION study. J Cardiovasc Electrophysiol. 2009;20(7):764–8.
62. Linde C, Leclercq C, Rex S, Garrigue S, Lavergne T, Cazeau S, McKenna W, Fitzgerald M, Deharo JC, Alonso C, Walker S, Braunschweig F, Bailleul C, Daubert JC. Long-term benefits of biventricular pacing in congestive heart failure: results from the MUltisite STimulation in cardiomyopathy (MUSTIC) study. J Am Coll Cardiol. 2002;40(1):111–8.
63. Bleeker GB, Kaandorp TA, Lamb HJ, Boersma E, Steendijk P, de Roos A, van der Wall EE, Schalij MJ, Bax JJ. Effect of posterolateral scar tissue on clinical and echocardiographic improvement after cardiac resynchronization therapy. Circulation. 2006;113(7):969–76.
64. Adelstein EC, Saba S. Scar burden by myocardial perfusion imaging predicts echocardiographic response to cardiac resynchronization therapy in ischemic cardiomyopathy. Am Heart J. 2007;153(1):105–12.
65. Jaffe LM, Morin DP. Cardiac resynchronization therapy: history, present status, and future directions. Ochsner J. 2014;14(4):596–607.
66. Khan FZ, Virdee MS, Palmer CR, Pugh PJ, O'Halloran D, Elsik M, Read PA, Begley D, Fynn SP, Dutka DP. Targeted left ventricular lead placement to guide cardiac resynchronization therapy: the TARGET study: a randomized, controlled trial. J Am Coll Cardiol. 2012;59(17):1509–18.
67. Saba S, Marek J, Schwartzman D, Jain S, Adelstein E, White P, Oyenuga OA, Onishi T, Soman P, Gorcsan J 3rd. Echocardiography-guided left ventricular lead placement for cardiac resynchronization therapy: results of the speckle tracking assisted resynchronization therapy for electrode region trial. Circ Heart Fail. 2013;6(3):427–34.
68. Gold MR, Birgersdotter-Green U, Singh JP, Ellenbogen KA, Yu Y, Meyer TE, Seth M, Tchou PJ. The relationship between ventricular electrical delay and left ventricular remodelling with cardiac resynchronization therapy. Eur Heart J. 2011;32(20):2516–24.
69. Martin DO, Day JD, Lai PY, et al. Atrial support pacing in heart failure: results from the multicenter PEGASUS CRT trial. J Cardiovasc Electrophysiol. 2012;23:1317–25.
70. Kandala J, Upadhyay GA, Altman RK, Bose A, Heist EK, Mela T, Singh JP. Electrical delay in apically positioned left ventricular leads and clinical outcome after cardiac resynchronization therapy. J Cardiovasc Electrophysiol. 2013;24(2):182–7.
71. AlJaroudi W, Chen J, Jaber WA, Lloyd SG, Cerqueira MD, Marwick T. Nonechocardiographic imaging in

evaluation for cardiac resynchronization therapy. Circ Cardiovasc Imaging. 2011;4(3):334–43.
72. Boogers MJ, Chen J, van Bommel RJ, Borleffs CJ, Dibbets-Schneider P, van der Hiel B, Al Younis I, Schalij MJ, van der Wall EE, Garcia EV, Bax JJ. Optimal left ventricular lead position assessed with phase analysis on gated myocardial perfusion SPECT. Eur J Nucl Med Mol Imaging. 2011;38(2):230–8.
73. Chen J, Boogers MJ, Bax JJ, Soman P, Garcia EV. The use of nuclear imaging for cardiac resynchronization therapy. Curr Cardiol Rep. 2010;12(2):185–91.
74. Friehling M, Chen J, Saba S, Bazaz R, Schwartzman D, Adelstein EC, Garcia E, Follansbee W, Soman P. A prospective pilot study to evaluate the relationship between acute change in left ventricular synchrony after cardiac resynchronization therapy and patient outcome using a single-injection gated SPECT protocol. Circ Cardiovasc Imaging. 2011;4(5):532–9.
75. Lehner S, Uebleis C, Schüßler F, Haug A, Kääb S, Bartenstein P, Van Kriekinge SD, Germano G, Estner H, Hacker M. The amount of viable and dyssynchronous myocardium is associated with response to cardiac resynchronization therapy: initial clinical results using multiparametric ECG-gated [18F]FDG PET. Eur J Nucl Med Mol Imaging. 2013;40(12):1876–83.
76. Uebleis C, Ulbrich M, Tegtmeyer R, Schuessler F, Haserueck N, Siebermair J, Becker C, Nekolla S, Cumming P, Bartenstein P, Kääb S, Hacker M. Electrocardiogram-gated 18F-FDG PET/CT hybrid imaging in patients with unsatisfactory response to cardiac resynchronization therapy: initial clinical results. J Nucl Med. 2011;52(1):67–71.
77. Bilchick KC, Kuruvilla S, Hamirani YS, Ramachandran R, Clarke SA, Parker KM, Stukenborg GJ, Mason P, Ferguson JD, Moorman JR, Malhotra R, Mangrum JM, Darby AE, Dimarco J, Holmes JW, Salerno M, Kramer CM, Epstein FH. Impact of mechanical activation, scar, and electrical timing on cardiac resynchronization therapy response and clinical outcomes. J Am Coll Cardiol. 2014;63(16):1657–66.
78. Leyva F, Foley PW, Chalil S, Ratib K, Smith RE, Prinzen F, Auricchio A. Cardiac resynchronization therapy guided by late gadolinium-enhancement cardiovascular magnetic resonance. J Cardiovasc Magn Reson. 2011;13:29.
79. Sohal M, Shetty A, Duckett S, Chen Z, Sammut E, Amraoui S, Carr-White G, Razavi R, Rinaldi CA. Noninvasive assessment of LV contraction patterns using CMR to identify responders to CRT. JACC Cardiovasc Imaging. 2013;6(8):864–73.
80. Taylor RJ, Umar F, Panting JR, Stegemann B, Leyva F. Left ventricular lead position, mechanical activation, and myocardial scar in relation to left ventricular reverse remodeling and clinical outcomes after cardiac resynchronization therapy: a feature-tracking and contrast-enhanced cardiovascular magnetic resonance study. Heart Rhythm. 2016;13(2):481–9.
81. Sommer A, Kronborg MB, Poulsen SH, Böttcher M, Nørgaard BL, Bouchelouche K, Mortensen PT, Gerdes C, Nielsen JC. Empiric versus imaging guided left ventricular lead placement in cardiac resynchronization therapy (ImagingCRT): study protocol for a randomized controlled trial. Trials. 2013;14:113.
82. Laksman Z, Yee R, Stirrat J, Gula LJ, Skanes AC, Leong-Sit P, Manlucu J, McCarty D, Turkistani Y, Scholl D, Rajchl M, Goela A, Islam A, Thompson RT, Drangova M, White JA. Model-based navigation of left and right ventricular leads to optimal targets for cardiac resynchronization therapy: a single-center feasibility study. Circ Arrhythm Electrophysiol. 2014;7(6):1040–7.
83. Ma YL, Shetty AK, Duckett S, Etyngier P, Gijsbers G, Bullens R, Schaeffter T, Razavi R, Rinaldi CA, Rhode KS. An integrated platform for image-guided cardiac resynchronization therapy. Phys Med Biol. 2012;57(10):2953–68.

Right Heart in Dilated Cardiomyopathy

19

Anjali Chandra, Sami Merie, Diana Morvey, Yasemin Saylan, and Ernst R. von Schwarz

Abstract

Dilated cardiomyopathy (DCM) is a significant burden affecting 5 people in 100,000, it is also the most common cardiomyopathy encountered. The condition can be a result of underlying diseases, which can comprimise the heart's contractility such as any insult to the heart, for example several viral or bacterial infections can lead to myocarditis, whereas other agents such as alcohol or illicit drug use can exert direct cardiotoxic effects destabilizing the normal cardiac function. In many cases, however, no causing effect can be identified and thus, the condition is referred to as, idiopathic non ischemic (dilated) cardiomyopathy. This chapter is dedicated to understand the etiology, pathogenesis, clinical manifestation, diagnosis and treatment of DCM. Although left ventricular dysfunction is seen as the primary outcome of the disease, the right heart function and dysfunction does plays an important role. Physical examination, a complete history and assessment of current symtoms as well as an electrocardiogram, laboratory testing including metabolic panel, brain natriuretic peptide levels and echocardiogram are mainly utilized in the initial diagnostic work-up if cardiomyopathy as a reason for heart failure symptoms is suspected. Due to subtle symptoms of the disease patients oftentimes do not seek medical advice early in the course of the disease but only after severe and debilitating heart failure symptoms occur. Modern therapy is tailored to 1) alleviate symptoms, 2) improve outcomes and reduce mortality and morbidity, and 3) remove or ease the underlying causes in cases of secondary DCM. Whereas vasodilators such as nitrates and diuretics are often the first-line therapy to ease symptoms of shortness of breath and volume overload, early treatment with Angiotensin Converting Enzyme Inhibitors (ACEI) and Angiotensin Receptor Blockers (ARB) is initiated in order to used to prevent cardiac remodeling. Beta blockers have shown promising results to potentially reverse ventricular dilatation and further prevention of structural changes.

Keywords

Cardiomyopathy • Heart failure • Cardiac remodeling

A. Chandra • S. Merie • D. Morvey • Y. Saylan
Heart Institute, Southern California Hospital, Culver City, CA, USA

E. R. von Schwarz (✉)
Heart Institute, Southern California Hospital, Culver City, CA, USA

Cedars-Sinai Medical Center, Los Angeles, CA, USA

University of California Los Angeles, Los Angeles, CA, USA

University of California Riverside, Riverside, CA, USA

S. I. Dumitrescu et al. (eds.), *Right Heart Pathology*, https://doi.org/10.1007/978-3-319-73764-5_19

19.1 Introduction

In cardiomyopathies the heart muscle demonstrates a reduced contractile function secondary to a failure of the cardiomyocytes. Cardiomyopathies of different origins represent a major contributor to overall cardiovascular morbidity and mortality [1]. The underlying etiology may be genetic as in the cases of hypertrophic cardiomyopathy, arrhymogenic right ventricular cardiomyopathy/dysplasia (ARVC/D), mitochondraial cardiomyopathy; or genetic and acquired as in dilated cardiomyopathy and restrictive cardiomyopathy [2].

The advancement in genomic studies has elucidated the pathophysiology of the cardiomyopathies as a result of mutations at the genetic level. According to Dadson et al., "Modern genomics has identified mutations that are common in these populations, while in vitro and in vivo experimentation with these mutations have provided invaluable insight into the molecular mechanisms native to these diseases. For example, increased myosin heavy chain (MHC) binding and ATP utilization lead to the hypercontractile sarcomere in HCM, while abnormal protein–protein interaction and impaired Ca2+ flux underlie the relaxed sarcomere of DCM" [2]. The main focus of this chapter is right ventricular dilated cardiomyopathy.

Dilated cardiomyopathy (DCM) is characterized by dilation and impaired contraction of the ventricles [3]. It is the most common cardiomyopathy accountings for approximately 55% of all cases [1]. It has an incidence rate of 2–8/100,000 in adults and about 0.57/100,000 in children and a prevalence rate is 1/2500 [1]. Unlike most part of the world, DCM is very common in Africa due to the advent of the human immunodeficiency virus (HIV) infection and its association with cardiomyopathies; and it is the major cause of heart failure throughout the continent [3].

19.2 Etiology and Pathogenesis of Dilated Cardiomyopathy

DCM is a progressive disorder of the myocardium characterized by ventricular chamber dilatation and reduced systolic function that eventually leads to the development of heart failure, arrhythmias, thromboembolic complications, heart failure-associated multi-organ failure and sudden or HF-related death [1]. DCM can be classified into primary and secondary cardiomyopathies as a result of the underlying etiology. Primary dilated cardiomyopathy includes acquired and familial or genetic causes, whereas secondary cardiomyopathy are mainly acquired due to myocardial damage from systemic diseases such as myocardial ischemia, inflammation, infection, increased myocardial pressure or volume load and toxic agents [3]. Idiopathic DCM is diagnosed when all possible underlying causes are for the changes in the heart muscle and chambers are excluded.

In primary cardiomyopathy, genetic causes account for 20–30% of all DCM cases and up to 60 genes have been linked to the aetiology of the disease [4]. In most cases, DCM displays an autosomal dominant transmission; however, autosomal recessive, X-linked inheritance and mitochondrial inheritance pattern have been reported in some cases [5]. Firstly, recent genetic analysis has implicated Titin (TTN) as the predominant DCM causing gene in multicohort studies [6]. In order to understand TTN mutations, one must first look at the interactions the gene has with other sarcomere proteins. The TTN gene interacts with four protein bands, Z-disk, I-Band, M-Band and A-band. The Z-disk contains the first 826 amino acids and interacts with N-residues, moreover, the Z-disk TTN structurally and functionally interacts with myofibrillar and sarcolemmal proteins and as a result is important for myofibrillar assembly, stability and signalling [7]. The meta-transcript of I-band TTN is mainly composed of Ig domains, cardiac N2B region, skeletal N2A and Pro-Glu-Val-Lyrs TTN domain, in which they all contribute to TTN related elasticity. Taking everything into account, this makes the I-band TTN a highly interactive structure with potential for alternative splicing [8]. A-band TTN mainly consists of Ig and Fibronectin motifs, in contrast to previously listed bands; it is inextensible as it provides binding sites for myosin [9]. Finally, the M-band contains the putative serine/threonine kinase domain and consequently its function revolves around its kinase domain activity [10]. TTN is a DCM locus

and is located on chromosome 2q31 and is the largest protein known in biology [8]. TTN has a huge potential to be alternatively spliced and increasing complexity of protein isoforms can be introduced due to various mutations such as point mutations, premature termination codes and insertions/deletions [11].

Secondly, the wingless (Wnt) pathway has been strongly associated with the pathogenesis of DCM. Patients with DCM are characterized by deregulated systemic and myocardial Wnt signaling involving Wnt4a and the Wnt antagonist sFRP3, a study on 102 patients diagnosed with idiopathic DCM concluded. High levels of circulating Wnt5a correlated with increased pulmonary artery pressures, decreased right ventricular (RV) function and adverse outcome. A higher Wnt5a/sFRP3 ratio in the right ventricle correlated with NFAT activation and pulmonary artery pressure [12].

Thirdly, arrhythmogenic right ventricular cardiomyopathy (ARVC) is a primary disease of the heart muscle that results from fibrofatty replacement of the right ventricle and the subpericardial region of the left ventricle. Familial studies have implicated that ARVC is caused by genetic alterations in desmosomal proteins, especially plakoglobin and desmoplakin. Thus, ARVC is proposed to be a result of an underlying inflammatory process modulated by the aforementioned genes [13].

Primary acquired DCM can be further divided into four main subtypes namely: Takotsubo cardiomyopathy, peripartum cardiomyopathy, tachycardia-induced cardiomyopathy, and inflammatory cardiomyopathy.

Takotsubo cardiomyopathy (TCM) it was first described in Japan in 1991. It is a transient cardiac syndrome that involves left ventricular apical akinesis and mimics the clinical presentation of acute coronary syndrome (ACS). The disease initially presents with chest pain and/or dyspnea, the electrocardiographic changes and elevated serum cardiac markers observed in TCM patients often result in the misdiagnosis of TCM as ACS [14]. In order to properly diagnose TCM, it is necessary to perform echocardiography to evaluate wall motion abnormality and coronary angiography to confirm the absence of significant stenotic lesions [14].

Peripartum cardiomyopathy (PCM), according to Fett, is defined as a new heart failure in a previously heart-healthy peripartum patient. It is necessary to rule out all other known causes of heart failure before accepting a diagnosis of PCM. An echocardiography with an ejection fraction less than 45% from 1 to 5 month of delivery, it is defined as pregnancy associated cardiomyopathy [15].

Immune system changes during pregnancy play an important part in the pathogenesis of PCM. T-cells and innate immunity activations are increased during pregnancy. For example, T cells ($CD3^+$ $CD4^-$ $CD8^-$ CD38) are increased in PCM patients compared to healthy postpartum patients. Natural killer (NK) cells ($CD3^-$ $CD56^+$ $CD16^+$) are significantly reduced in PCM patients compared to healthy postpartum women [15].

Long standing tachycardia is an identified cause of heart failure and left ventricular dysfunction and has led to the definition of a condition referred to as tachycardia-induced cardiomyopathy (TIC) [16]. Inflammatory cardiomyopathy on the other hand is defined as inflammation of the cardiomyocytes associated with impaired function of the myocardium. This is triggered mostly by viral infections [17].

In secondary DCM, the myocardial damage usually is a result of systemic diseases. Inflammation of the myocardium due to an infectious process is the most common cause. For example, infectious myocarditis can be caused by bacterial, fungal, parasitic, spirochetal, protozoal, rickettsial and most commonly viral infections. Coxsackievirus A and B are frequent causes. Myocarditis related DCM which was previously thought to be idiopathic in nature, is found to be oftentimes associated with Parvovirus B19, HHV-6 and Enterovirus infections [18]. A recent study demonstrated that 23.1% of patients who were previously classified under idiopathic DCM were found to have biomarkers that are indicative of a prior enterovirus infection, whereas 76.9% of patients had a parvovirus viral load but lacked biomarkers indicating the association between viral infection and DCM. The study concluded that more optimal results could be obtained by revising endomyocardial biopsy protocols [19].

Histopathologic criteria can be used to further classify myocarditis. These include lymphocytic

(viral), eosinophilic, polymorphous, giant cell and granulomatous. Other causes of myocarditis include autoimmune conditions, which are further divided into allergic, alloantigens and autoantigens. In autoimmune myocarditis, the body forms circulating antibodies that attack the myocardium. Finally, Toxicity from drugs, heavy metals, hormones and physical agents can cause myocarditis [20].

19.3 Pathological Findings in DCM

Grossly, the hallmark of dilated cardiomyopathy is dilated and enlarged ventricles. The heart is described as large, floppy, and often with thinned ventricular walls [21]. In a study conducted on 64 explanted hearts diagnosed clinically with DCM, 55 patients did have dilated cardiomyopathy on autopsy, whereas in 9 patients pathologic examination revealed other conditions. From the following 55 patients, 38 showed typical 4 chamber dilation, 5 exhibited features of left ventricular noncompaction, 4 showed minimal gross or histologic changes, and 3 had a patterns of healed myocarditis [22]. Therefore, macroscopic findings are ventricular chamber dilation with normal or thickened walls (cardiac remodeling). Valvular dilation of the orficies can be found secondary to ventricular chamber dilation. Coronary artieries usually display normal anatomy. However, the presence of non-occlusive atherosclerotic plaques is often noted. Thrombi are frequently visible in ventricles and atrial appendagees [23]. In a study conducted to examine the relevance of scars in non-ischemic cardiomyopathy, myocardial scars have been detected by delayed enhancement cardiac magnetic resonce imaging studies (MRI-DE-CMR). In addition, over half of the patients displayed macroscopic evidence of cardiac tissue replacement with fibrous tissue [24].

Microscopic findings in biopsies show minimal variation in myofiber size, but display features of myofiber loss, interstial fibrosis, and noticable variation between myofiber sizes. Negative findings are essential in the microscopic examination in order to exclude secondary causes. In 25% of patients, specific diagnoses such as amyloidosis and hemochromatosis had been established [3]. Myocardial necrosis is rare, but predominantly found in the sub-endocardium [24].

19.4 Clinical Presentation of Dilated Cardiomyopathy

In a case study by Fitchett et al. [39] 14 patients with right ventricular dilated cardiomyopathies were studied, most of the patients presented with arrhythmia (70%), right heart failure, ventricular tachycardia which lead to syncope and different forms of arrhythmia [39]. Other common clinical scenarios include signs and symptoms of congestive heart failure, thromboembolism, and sudden death. The age of manifestation is from new-born through late adulthood, but most patients are diagnosed in their second to fifth decades [1]. Arrhythmias can be a part of the initial clinical presentation, or can occur at a later stage of the disease as the heart undergoes structural changes that contribute to arrhythmogenic potential [25]. According to Towbin "DCM can also present with muscular involvement and may be the presenting or primary clinical feature of several multi-system conditions, including Emery-Dreifuss muscular dystrophy (EDMD), Barth syndrome, myofibrillar myopathy, limb-girdle muscular dystrophy (LGMD), and Duchenne or Becker muscular dystrophy (DMD/BMD)" [1].

On physical examination, the patients might present in distress, with peripheral edema or other signs of volume overload, with dyspnea, tachypnea, tachycardia, possibly with a positive jugular venous distension, and patients might demonstrate systolic murmurs as a result of mitral and tricuspid regurgitation during cardiac auscultation. The former presents with pansystolic murmur heard at the apex, whereas the latter presents with holosystolic murmur best heard at the left sternal border. Carvallo's sign, murmur that intensifies on inspiration, is observed in cases with right-sided involvement of the heart. In both cases a third heart sound (S3) can be present as an additional finding [26].

19.5 Diagnostic Approach

Diagnosing DCM is challenging due to the variety of presentations. Therefore, a multi step approach is used. The initial step include a detailed history including the assessment of possible risk factors as well as a family history. Physical examination includes a complete assessment including inspection of the skin, legs, genitals, back, neck, eyes, assessment of peripheral pulses on arms and legs bilaterally, as well as auscultation of the heart and lungs and stomach, including palpitation and percussion.

Echocardiography is usually the initial method to assess cardiac function, according to an article published in 2016 by the American College Of Cardiology, cardiovascular magnetic resonance is the gold standard to assess ventricular function, as well as being an alternative to more invasive procedures used previously for the same purpose such as coronary angiogram. In suspicion of hereditary cases, genetic testing, though it is not recommended as initial approach, can be ordered to detect previously mentioned mutations commonly associated with DCM [27]. This approach may give a clue to the underlying mechanism for the IDCM.

A multiple step approach is recommended by the most recent guidelines of the British Society of Echocardiography. As first line diagnostic tool, a transthoracic echocardiogram (TTE) is recommended, since it determines the severity of impairment caused by wall thickness changes and ventricular dysfunction. Mostly the LV is affected first; although RV involvement may be present, it is not used as a diagnostic criterion [28].

Echocardiography is useful in determining the functionality of the left ventricle and vulvular involvement. Left ventricular dilatation and left ventricular ejection fraction (LVEF) less than 45% is considered diagnostic in IDCM. Mitral regurgitation and tricuspid regurgitation are common findings, indicating LV and RV dilatation [28].

Current guidelines recommend additional testing as initial approach such as metabolic panel, chest X-ray (shows cardiomegaly in advanced cases), an ECG and 24 h Holter monitoring to determine arrhythmias and QRS duration changes associated with DCM. The investigations discussed above are performed on the basis of initial evaluation [29].

19.6 Treatment

Management modalities are important in increasing the quality of life of the patient, relieving the exacerbation of the symptoms and possibly reversing the pathological events that took place in the heart due to DCM.

Reversal of the cardiac structural changes are called reversed remodeling and is established by medications mostly exerting their effect through the sympathetic and renin- angiotensin- aldosterone system [30]. A prognostic factor used to assess the severity of disease is the degree of cardiac dilation. Not all patients benefit from the treatment in the same way, moderate and severely affected venctricles in some cases show better recovery than minimally affected ones [31]. Angiotensin converting enzyme inhibitors (ACEI) and angiotensin receptor blockers (ARBs) are an effective treatment for the improvement of cardiac function by reverse remodeling [32]. Although ACEI play a role in increasing the ejection fraction by small amounts and improvement of the cardiac dilation by preventing further changes to the heart muscle, beta blockers such as carvedilol are more effective in reversing the dilation and improving the EF [33, 34].

Management of the patient is planned depending on the etiology and clinical manifestations of DCM. In cases of secondary causes, like amyloidosis additional therapy aimed at the underlying disease such as anti plasma cell therapy is proven to be beneficial [35]. Furthermore, more invasive measures such as cardiac defibrillator or pacemaker implantation are used in patients presenting with arrhythmias and conduction delays. This approach prevents sudden cardiac arrest and leads to the reduction of hospitalization in patients with systolic dysfunction [36].

For patients with chronic heart failure due to DCM in its advanced stages, cardiac transplantation is the ultima ratio therapeutic option,

however, is limited to a relatively small number of patients, depending on eligibility due to co-morbidities, age and other factors which might influence the outcome of transplantation. DCM was responsible for more than 50% of cardiac transplantations performed between 2006 and 2012 [37]. Survival post-transplant between ischemic and IDCM were found to be similar with cases of pure myocarditis suffering less infections post operatively [37, 38]. Further treatment options include right (and/or left) ventricular assist devices, the implantation of the total artificial heart. The right ventricular assist devices (as well as the total artificial heart) are mainly used temporarily as a bridge to either recovery or to transplantation. Future options might include stem cell and immunologic therapies, and other surgical (myoplastic) procedures.

Conclusion

Cardiomyopathies are disease that adversely affects the cardiomyocytes. There are various types, but dilated cardiomyopathy (DCM) is the most common cardiomyopathy which is characterized by dilated ventricles and low ejection fraction [1, 39]. There are several genetic dispositions and environmental influences. Under the genetic causes of DCM, "there is a disruption in the "final common pathyway" linking the sarcomere and sarcolemma. The mutation in this affected genes codes of cytoskeletal and cardiac muscles that are dysfunctional [1]. The poor functioning of the ventricles lead to dilatation of the ventricles and poor contractility which later might result in the formation on thrombi in the ventricles as a result of stasis.

This type of cardiomyopathy has male preponderance and presents with arrhythmia, ventricular tachycardia leading to syncope, right and left heart failure [39].

The presentation of DCM can be vague. It is therefore important to take a detail history with emphasis on family history and a detailed clinical examinations looking for clues that to will aid in eliminating other differential diagnosis.

References

1. Towbin JA. Inherited cardiomyopathies. Circ J. 2014;78(10):2347–56.
2. Dadson K, Hauck L, Billia F. Molecular mechanisms in cardiomyopathy. Clin Sci. 2017;131(13):1375–92. https://doi.org/10.1042/CS20160170.
3. Mayosi BM, Somers K. Cardiomyopathy in Africa: heredity versus environment. Cardiovasc J Afr. 2007;18(3):175–9.
4. Ackerman MJ, Banner RN, Christodoulou D, Cirino AL, Conner L, Di Lenarda A, et al. Truncations of titin causing dilated cardiomyopathy. N Engl J Med. 2012;366:619–28. https://doi.org/10.1056/NEJMoa1110186.
5. Chauveau C, Rowell J, Ferreiro A. A rising titan: TTN review and mutation update. Hum Mutat. 2014;35:1046–59. https://doi.org/10.1002/humu.22611.
6. Walsh R, Thomson KL, Ware JS, Funke BH, Woodley J, McGuire KJ, et al. Reassessment of Mendelian gene pathogenicity using 7,855 cardiomyopathy cases and 60,706 reference samples. Genet Med. 2017;19(2):192–203. https://doi.org/10.1038/gim.2016.90.
7. Knöll R, Linke WA, Zou P, Miocic S, Kostin S, Buyandelger B, et al. Telethonin deficiency is associated with maladaptation to biomechanical stress in the mammalian heart. Circ Res. 2011;109(7):758–69. https://doi.org/10.1161/CIRCRESAHA.111.245787.
8. Kontrogianni-Konstantopoulos A, Ackermann MA, Bowman AL, Yap SV, Bloch RJ. Muscle giants: molecular scaffolds in sarcomerogenesis. Physiol Rev. 2009;89(4):1217–67. https://doi.org/10.1152/physrev.00017.2009.
9. Muhle-Goll C, Habeck M, Cazorla O, Nilges M, Labeit S, Granzier H. Structural and functional studies of titin's fn3 modules reveal conserved surface patterns and binding to myosin S1—a possible role in the Frank-Starling mechanism of the heart. J Mol Biol. 2001. https://doi.org/10.1006/jmbi.2001.5017.
10. Bogomolovas J, Gasch A, Simkovic F, Rigden DJ, Labeit S, Mayans O. Titin kinase is an inactive pseudokinase scaffold that supports MuRF1 recruitment to the sarcomeric M-line. Open Biol. 2014;4(5):140041. https://doi.org/10.1098/rsob.140041.
11. Roberts AM, Ware JS, Herman DS, Schafer S, Baksi J, Bick AG, et al. Integrated allelic, transcriptional, and phenomic dissection of the cardiac effects of titin truncations in health and disease. Sci Transl Med. 2015;7(270):270ra6. https://doi.org/10.1126/scitranslmed.3010134.
12. Abraityte A, Lunde IG, Askevold ET, Michelsen AE, Christensen G, Aukrust P, et al. Wnt5a is associated with right ventricular dysfunction and adverse outcome in dilated cardiomyopathy. Sci Rep. 2017;7:3490. https://doi.org/10.1038/s41598-017-03625-9.
13. Burke AP. Arrhythmogenic right ventricular cardiomyopathy pathology. Overview, Etiology Epidemiology. News and Perspective. 2016. https://emedicine.medscape.com/article/2017949-overview. 1 July 2017.
14. Sanchez-Jimenez EF. Initial clinical presentation of Takotsubo cardiomyopathy with-a focus on electro-

cardiographic changes: a literature review of cases. World J Cardiol. 2013;5(7):228–41. https://doi.org/10.4330/wjc.v5.i7.228.
15. Fett JD. Peripartum cardiomyopathy: a puzzle closer to solution. World J Cardiol. 2014;6(3):87–99. https://doi.org/10.4330/wjc.v6.i3.87.
16. Ellis ER, Josephson ME. What about tachycardia-induced cardiomyopathy? Arrhythm Electrophysiol Rev. 2013;2(2):82–90. https://doi.org/10.15420/aer.2013.2.2.82.
17. Krejci J, Mlejnek D, Sochorova D, Nemec P. Inflammatory cardiomyopathy: a current view on the pathophysiology, diagnosis, and treatment. Biomed Res Int. 2016. https://doi.org/10.1155/2016/4087632.
18. Kuhl U, Pauschinger M, Noutsias M, Seeberg B, Bock T, Lassner D, Poller W, Kandolf R, Schultheiss HP. High prevalence of viral genomes and multiple viral infections in the myocardium of adults with idiopathic left ventricular dysfunction. Circulation. 2005;111(7):887–93. https://doi.org/10.1161/01.CIR.0000155616.07901.35.
19. N'Guyen Y, Lesaffre F, Metz D, Tassan S, Saade Y, Boulagnon C, Fornes P, Renois F, Andreoletti L. Enterovirus but not Parvovirus B19 is associated with idiopathic dilated cardiomyopathy and endomyocardial CD3, CD68, or HLA-DR expression. J Med Virol. 2017;89:55–63. https://doi.org/10.1002/jmv.24600.
20. Caforio ALP, Bottaro S, Iliceto S. Dilated cardiomyopathy (DCM) and myocarditis: classification, clinical and autoimmune features. Appl Cardiopulm Pathophysiol. 2012;16:82–95. http://www.applied-cardiopulmonary-pathophysiology.com/fileadmin/downloads/acp-2012-1_20120301/06_caforio.pdf.
21. Kransdorf EP, Fishbein MC, Czer LS, Patel JK, Velleca A, et al. Pathology of chronic chagas cardiomyopathy in the United States: a detailed review of 13 Cardiectomy cases. Am J Clin Pathol. 2016;146:191–8. https://doi.org/10.1093/AJCP/AQ098.
22. Zhang M, Tavora F, Huebner T, Heath J, Burke A. Allograft pathology in patients transplanted for idiopathic dilated cardiomyopathy. Am J Surg Pathol. 2012;36(3):389–95. https://doi.org/10.1097/PAS.0b013e31823b02f5.
23. Sisakian H. Cardiomyopathies: evolution of pathogenesis concepts and potential for new therapies. World J Cardiol. 2014;6(6):478–94. https://doi.org/10.4330/wjc.v6.i6.478.
24. Kadish A, Rubenstein JC. Connecting the dots: the relevance of scar in non-ischemic cardiomyopathy. J Am Coll Cardiol. 2009;53(13):1146–7. https://doi.org/10.1016/j.jacc.2008.12.027.
25. Agabegi ED, Agabegi SS. Chap. 1: diseases of the cardiovascular system/section: valvular heart disease. In: Step-up to medicine, Step-up series. Philadelphia: Lippincott Williams & Wilkins; 2008. isbn:0-7817-7153-6.
26. Rivero-Carvallo JM. Signo para el diagnostico de las insuficiencias tricuspideas. Arch Inst Cardiol Mex. 1946;16:531.
27. Japp AG, Gulati A, Cook SA, Cowie MR, Prasad SK. The diagnosis and evaluation of DCM. J Am Coll Cardiol. 2016;67(25):2996–3010. https://doi.org/10.1016/j.jacc.2016.03.590.
28. Mathew T, Williams L, Navaratnam G, Rana B, Wheeler R, Collins K, British Society of Echocardiography Education Committee, et al. Diagnosis and assessment of dilated cardiomyopathy: a guideline protocol from the British Society of Echocardiography. Echo Res Pract. 2017;4(2):G1–G13. https://doi.org/10.1530/ERP-16-0037.
29. Bozkurt B, Colvine M, Cook J, Cooper LT, Deswal A, Fonorow GC, Francis GS, et al. Current diagnostic and treatment strategies for specific dilated cardiomyopathies. Circulation. 2016;2016(134):e579–646. https://doi.org/10.1161/CIR.0000000000000455.
30. Reis Filho JR d AR, Cardoso JN, Cardoso CM d R, Pereira-Barretto AC. Reverse cardiac remodeling: a marker of better prognosis in heart failure. Arq Bras Cardiol. 2015;104(6):502–6. https://doi.org/10.5935/abc.20150025.
31. Wong M, Staszewsky L, Latini R, Barlera S, Glazer R, Aknay N, Hester A, Anand I, Cohn JN. Severity of left ventricular remodeling defines outcomes and response to therapy in heart failure Val-HeFT echocardiographic data. J Am Coll Cardiol. 2004;43(11):2022–7. https://doi.org/10.1016/j.jacc.2003.12.053.
32. Konstam MA, Patten RD, Thomas I, Ramahi T, La Bresh K, Goldman S, Lewis W, et al. Effects of losartan and captopril on left ventricular volumes in elderly patients with heart failure: results of the ELITE ventricular function sub study. Am Heart J. 2000;139(6):1081–7. https://doi.org/10.1067/mhj.2000.105302.
33. Hoshikawa E, Matsumura Y, Kubo T, Okawa M, Yamasaki N, et al. Effect of left ventricular reverse remodeling on long-term prognosis after therapy with angiotensin-converting enzyme inhibitors or angiotensin II receptor blockers and betablockers in patients with idiopathic dilated cardiomyopathy. Am J Cardiol. 2011;107(7):1065–70.
34. Khattar RS. Effects of ACEI and beta blockers on left ventricular remodeling in chronic heart failure. Minerva Cardioangiol. 2003;51(2):143–54. https://doi.org/10.1016/j.amjcard.2010.11.033.
35. Siddiqi OK, Ruberg FL. Cardiac amyloidosis: an update on pathophysiology, diagnosis and treatment. Trends Cardiovasc Med. 2017. https://doi.org/10.1016/j.tcm.2017.07.004.
36. Papadakis MA, Mcphee SJ, Rabow MW. Current medical diagnosis and treatment 2017. 56th ed. New York: McGraw Hill Education; 2017.
37. Lund LH, Edwards LB, Kuvheryevaya AY, et al. The registery of the international society for heart and lung transplantation: 30th official adult heart transplant report 2013. J Heart Lung Transplant. 2013;32(10):951–64.
38. Jawitz OK. Outcomes following heart transplantation in a national cohort: an analysis of the organ procurement and transplantation network's database. Yale University-EliScholar. 2016.
39. Fitchett DH, Sugrue DD, MacArthur CG, Oakley CM. Right ventricular dilated cardiomyopathy. Br Heart J. 1984;51(1):25–9.

Left Heart Pathology and Right Ventricle Function

20

Sebastian Onciul and Maria Dorobanţu

Abstract

Pulmonary hypertension and right ventricular dysfunction are both common in left-sided heart failure. The classical belief that in left-sided heart disease, right ventricular dysfunction develops secondary to pulmonary hypertension is not always true and exceptions to this rule may occur frequently in clinical practice. The shared myofibers between left and right ventricles, the dysfunctional interventricular septum and the shared pericardium are more important mechanisms of right ventricular dysfunction in left heart failure. As pulmonary hypertension and right ventricular dysfunction do not always coexist in the same patient, they have independent prognostic value, and therefore each of them should be regarded as separate entities in the process of risk stratification of patients with left heart failure. In this chapter we discuss the currently accepted mechanisms of right ventricular damage in the context of left heart disease. We also present epidemiological data as well as the predictive value of right ventricular dysfunction in some of the most frequent etiologies of left heart failure such as heart failure with reduced ejection fraction, heart failure with preserved ejection fraction, aortic stenosis and mitral regurgitation.

Keywords

Right ventricle dysfunction · Left-sided heart failure · Pulmonary hypertension · Valvulopathies

20.1 Introduction

20.1.1 How Frequent is Right Ventricular Dysfunction in the Context of Left Heart Disease?

Studies aiming to clarify the prevalence and the prognostic significance of right ventricular dysfunction (RVD) in left heart failure (HF) have returned significantly different numbers depending on the imaging technique employed to diagnose RVD as well as the various cut-off values for different parameters used to define RVD. For example, a cut-off value for tricuspid annular plane systolic excursion (TAPSE) of 15, 16 or 17 mm has been used to define RVD in various two-dimensional echocardiography studies.

The highly variable figures also depend on the etiology and severity of the left HF. The prevalence of RVD is higher in HF with reduced ejection fraction (HFrEF) than in HF

S. Onciul (✉) · M. Dorobanţu
University of Medicine and Pharmacy Carol Davila, Bucharest, Romania

Cardiology Department, Clinical Emergency Hospital of Bucharest, Bucharest, Romania

S. I. Dumitrescu et al. (eds.), *Right Heart Pathology*, https://doi.org/10.1007/978-3-319-73764-5_20

with preserved ejection fraction (HFpEF) or left-sided valvulopathies. As a general rule, RVD becomes more frequent with more severe left heart pathology.

According to a meta-analysis including 11 studies and 4732 patients, almost half of the patients with left ventricular dysfunction may associate RVD [1]. Moreover, only one third of the HFpEF patients associate RVD [2]. Similarly, one third of the patients with left-sided valvular disease have RVD. Using cardiovascular magnetic resonance (CMR), the gold standard for the assessment of RV volumes and function, it was demonstrated that approximately one third of the patients with non-ischemic cardiomyopathy have RV ejection fraction (RVEF) ≤45% [3]. In this population RVD proved to be a powerful, independent predictor of transplant-free survival and adverse HF outcomes [3].

20.2 Prognostic Significance of Right Ventricle Dysfunction in Left Heart Disease

Pulmonary hypertension (PH) has been long time recognized as a risk factor for morbidity and mortality in patients with left sided HF of various etiologies. Historically, it was considered that in left-sided HF, RVD occurs secondary to high systolic pulmonary artery pressure (sPAP). However this is not always true and exceptions to this rule may occur frequently in clinical practice. RVD may be present in left sided HF, without the coexistence of high sPAP (see Mechanisms below). Conversely, RV function may be preserved despite elevated sPAP.

The reasons for which some patients with left-sided HF develop severe PH and RVD whereas others do not, remain largely unknown [4]. This might be explained by a genetic susceptibility of pulmonary vasculature and RV myocardium or might as well be explained by the length of time for which RV had been exposed to an increased afterload. In other words the development of RVD in response to a chronic increase in sPAP is time-dependent [4].

Rosenkranz et al. described a progression from a 'left ventricular phenotype' to a 'right ventricular phenotype' across the natural history of HF (Fig. 20.1) [4]. Mortality increases as the RV phenotype develops. Consequently, the therapeutic strategies also change along the spectrum of RVD, consisting in correction of the underlying cardiac pathology when the patient is still in the 'left ventricular phenotype', changing to

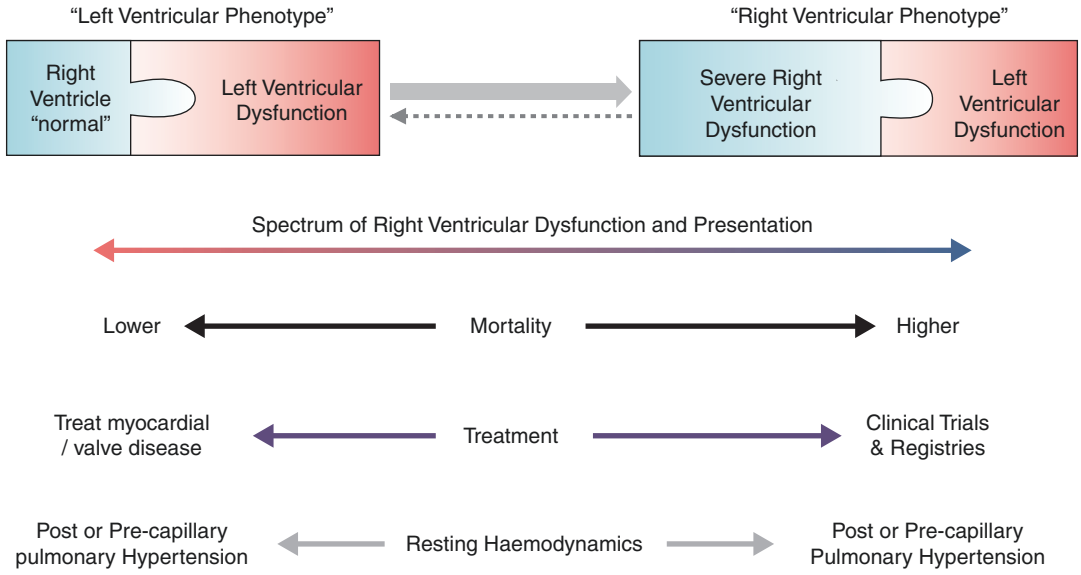

Fig. 20.1 'Left ventricular phenotype' vs. 'right ventricular phenotype' in pulmonary hypertension associated with left heart disease. Shown is the spectrum of right ventricular dysfunction and presentation, the impact on mortality, therapeutic implications, and resting pulmonary haemodynamics. From Rosenkranz et al. [4] with permission

inclusion in clinical trials and registries for patients with 'right ventricular phenotype'.

Taking into account the fact that PH and RVD doesn't always coexist, however each of them have its own prognostic value, it is reasonable to consider that an accurate prognostic stratification of patients with chronic left HF requires the knowledge of both sPAP and RV performance. Future risk scores should combine both sPAP values and parameters of RV function. Right ventricular function as well as PH can be easily assessed with conventional echocardiography. Simple TAPSE assessment may provide an useful objective surrogate of RV function with a strong prognostic value [5].

20.3 Mechanisms of Progression from Left Heart Failure to Right Ventricular Dysfunction

The most common cause of RVD is left-sided HF. The left heart causes of PH are synthesized in Fig. 20.2 [6]. There are multiple mechanisms by which left-sided HF can result in RVD [7]:

- Backwards transmission of the elevated pressures from left heart chambers to the pulmonary circulation with subsequent development of PH and secondary RVD;
- The RV may be involved in a global biventricular cardiomyopathic process such as arrhythmogenic right ventricular cardiomyopathy or dilated cardiomyopathy;
- Myocardial ischemia of both LV and RV;
- Ventricular interdependence due to interventricular septal dysfunction and shared myocardial fibers between RV and LV.

The classical pathophysiological paradigm states that increased LV filling pressures are transmitted backwards to the left atrium and then to pulmonary circulation. The co-existence of mitral regurgitation may augment the backward transmission of high atrial pressures. In this pathophysiological process left atrium plays an important role in modulating the transmission of high ventricular pressures to pulmonary venous circulation. Depending on its distensibility, the left atrium may enlarge in order to accommodate a larger volume of blood or may act as a stiff chamber transmitting the LV high pressures to pulmonary veins.

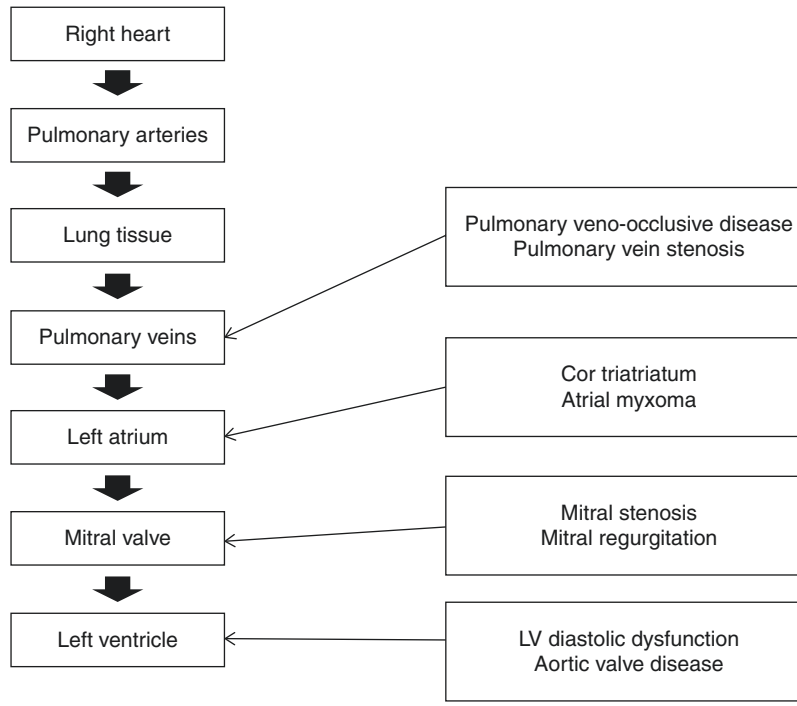

Fig. 20.2 Anatomic organization of left heart causes of pulmonary hypertension from the right ventricle through the lungs to the left ventricular outflow tract. From Kiefer and Bashore [6]. It is an open access article

Chronic elevated left-sided filling pressures may induce changes in the concentration of several mediators involved in pulmonary vasoconstriction [8]. These changes may result in pulmonary arterial vasoconstriction and vascular wall remodeling [4].

However, RVD in left-sided HF cannot be explained only by chronic pulmonary hypertension [7]. In clinical studies, RVD was independently associated with LV systolic dysfunction and atrial fibrillation, but not with sPAP, suggesting that PH is not the single mechanism of RV dysfunction in left HF [9].

20.4 Ventricular Interdependence Theory

The theory of ventricular interdependence states that RV systolic impairment is in part a consequence of interventricular septum dysfunction as well as structural changes of the RV myocardium independent of the severity of PH. Left and right ventricles share both the interventricular septum as well as the pericardial space. They also share common myocardial fibers that originate in the superficial layer of the LV and continue to the RV (Fig. 20.3) [10]. Through these pathways, LV contraction contributes to RV pressure development [7].

Even subtle alterations in LV myocardial fibres can be transmitted to the RV wall—a phenomenon sometimes referred to as *myocardial cross-talk*. This mechanism may explain the development of RVD in left-sided heart pathologies in the absence of elevated sPAP. The concept was proven in left-sided diseases such as aortic stenosis or mitral regurgitation.

The relative contribution of LV performance on RV function was elegantly demonstrated by Santamore et al. in paced rabbit hearts beating isovolumically [11]. Reducing LV volume caused a 5.7% decrease in RV developed pressure (RVDP). Producing ischaemia of the LV free wall resulted in an additional 9.3% decrease in RVDP. Finally, cutting the LV free wall caused a 45% further decrease in RVDP [11].

Conversely, chronic increased RV afterload results in LV adverse remodeling. Friedberg et al. showed using animal model that chronic increase in RV afterload by pulmonary artery banding resulted in biventricular hypertrophy, fibrosis, and apoptosis [12].

20.5 Right Ventricular Dysfunction in Heart Failure with Preserved Ejection Fraction

Right ventricular dysfunction occurs in approximately 1/3 of patients with HFpEF [2]. Generally patients with HFpEF who associate RVD tend to have more severe HF: lower cardiac output, more severe diastolic dysfunction, lower EF albeit in the normal range and a higher prevalence of atrial fibrillation (AF).

The exact mechanisms by which HFpEF can result in RVD are not known. Increased rates of atrial fibrillation (AF) in HFpEF patients with right ventricular systolic dysfunction (RVSD) suggest that AF may be one of the common pathophysiological links between left and right HF. Enlargement and remodeling of both atria predispose to development of AF. In this scenario the harmful tachyarrhytmic effects may be more pronounced on the thinner RV myocardium.

The new paradigm in the pathophysiology of HFpEF states that this syndrome occurs secondary to a cluster of systemic factors such as: diabetes mellitus, obesity, chronic obstructive pulmonary disease and salt-sensitive hypertension [13]. All these comorbidities induce a systemic proinflammatory state which in turn causes coronary microvascular endothelial inflammation [13]. Whether this microvascular dysfunction might induce a decrease in the contractility of the much thinner RV myocardium is not known.

Regardless of the mechanisms of RV impairment in HFpEF, RVD plays an important role in predicting outcomes in this category of patients. Risk stratification is particularly difficult in HFpEF patients in which left ventricular ejection fraction (LVEF) or dimensions cannot be used as prognostic markers. Mohammed et al. showed that the presence of RVD assessed semiquantitatively by 2D-echocardiography was associated with higher all-cause and cardiovascular mortality as well as higher HF hospitalizations rates [2].

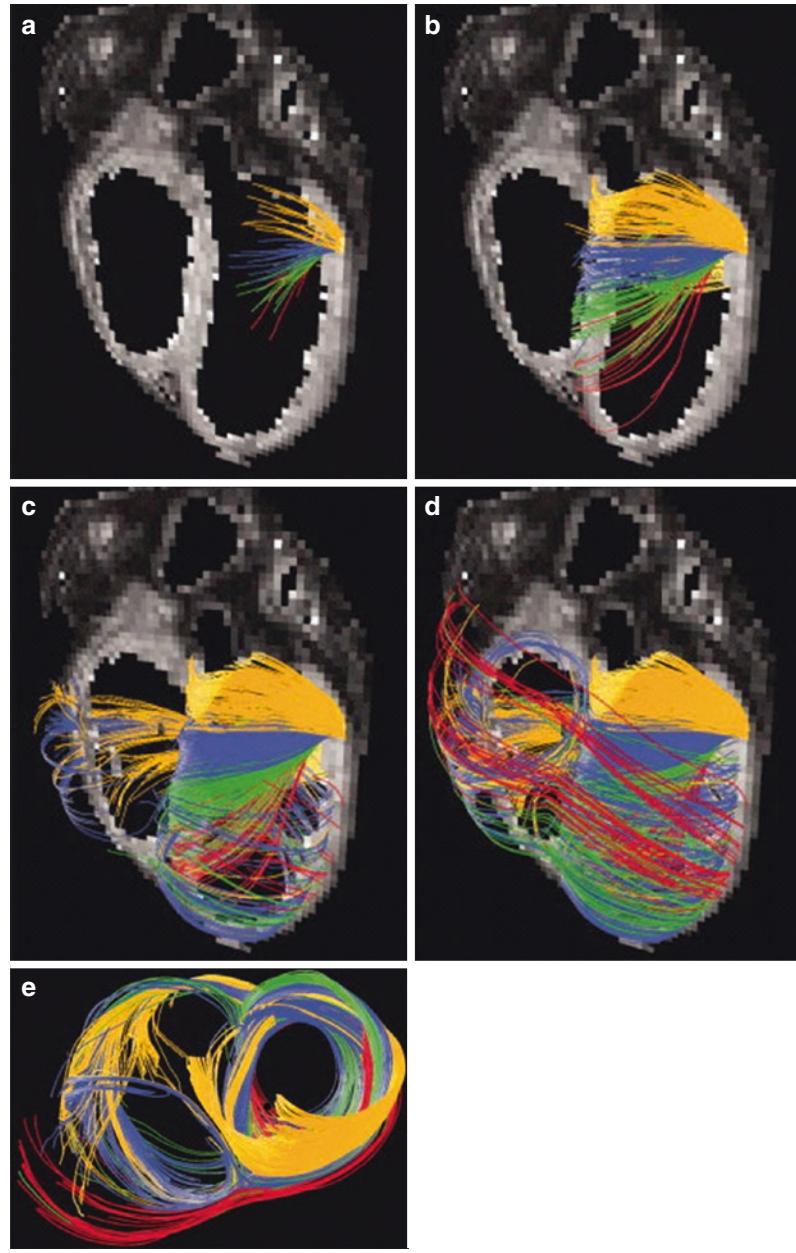

Fig. 20.3 Diffusion tensor magnetic resonance image demonstrating orientation of myocytes. The figure shows clearly the right ventricle is composed by tracks from the parietal walls of the left ventricle (**a**–**d**). Image (**e**) shows the basal circumference of the left ventricle. From Smerup et al. [10] with permission

20.6 Right Ventricle Dysfunction in Left-Sided Valvular Disease

Right ventricular dysfunction is common in left-sided valvular disease. In the context of mitral stenosis, RVD results secondary to high RV afterload due to increased pressures initially in venous and then in the arterial pulmonary circulation.

In what concerns the other left-sided valvular disease it seems that the classical increase in sPAP is not the main mechanism responsible for RVD. Instead, other mechanisms such as LV remodeling, septal dysfunction and 'myocardial cross-talk' phenomenon (see above) are more important in the pathophysiology of RVD.

Regardless of the mechanisms linking left-sided valve disease to RVD, numerous studies have demonstrated that both PH as well as RVD

are important prognostic factors for patients with left-sided valvulopathies. Although severe PH is one of the guidelines indications for valve intervention, RVD has been neglected by the guidelines. Similarly, neither EuroSCORE nor the Society of Thoracic Surgeons' risk models account for preoperative RV function although RVD is one of the strongest predictors of RV failure after cardiac surgery [14]. Furthermore, biventricular dysfunction has been shown to be the strongest predictor of cardiovascular mortality in both severe aortic stenosis (AS) as well as organic mitral regurgitation (MR) (Figs. 20.4 and 20.5) [15, 16].

20.7 Aortic Stenosis

Approximately half of the patients with severe AS have mild to moderate PH, whilst 15–20% of them have a sPAP value >50 mmHg [17, 18]. Interestingly, the severity of PH doesn't correlate with the aortic valve area or LVEF. Instead, the severity of PH correlates with LV end-diastolic pressures and some studies suggest a reactive component of PH in patients with severe AS [17].

Right ventricle dysfunction is also common in patients with severe AS. Using two-dimensional echocardiography, it was shown that approximately one quarter of severe AS patients have RVD defined as a TAPSE ≤17 mm. In this population, biventricular dysfunction (TAPSE ≤17 mm and LVEF ≤50%) proved to have the strongest predictive value for cardiovascular death [15].

In patients with "low-flow, low-gradient severe AS" the prevalence of RVD is even higher and is independently associated with all-cause mortality [19].

The mechanisms by which RV is affected in AS patients are complex. The backward transmission of elevated left atrial pressures to pulmonary circulation increasing RV afterload is only one of them. Galli et al. showed using two-dimensional echocardiography that LVEF and global longitudinal strain (GLS) correlate with TAPSE whereas the association between sPAP and TAPSE is mild or absent [15].

The structural alterations characteristic of LV remodeling in AS might spread to the RV along the anatomical pathways described above. Furthermore, the neuro-hormonal milieu which predispose to remodeling and fibrosis in the LV myocardium acts as well on RV myocardium. In other words, LV pressure/volume overload induces LV as well as RV myocardial fibrosis. It was demonstrated that even

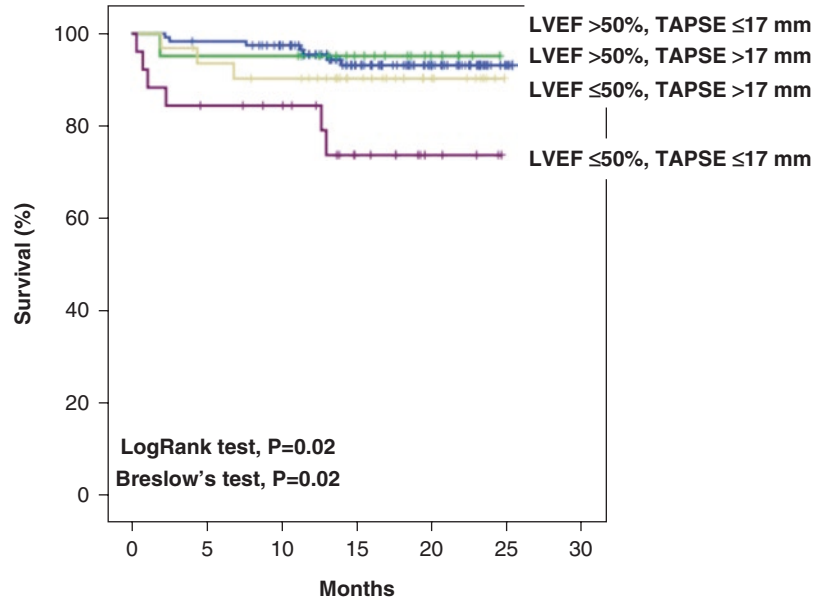

Fig. 20.4 Kaplan–Meier survival plot illustrating cardiovascular survival in severe aortic stenosis according to combined LVEF and TAPSE. *LVEF* left ventricular ejection fraction, *TAPSE* tricuspid annular plane systolic excursion. From Galli et al. [15] with permission

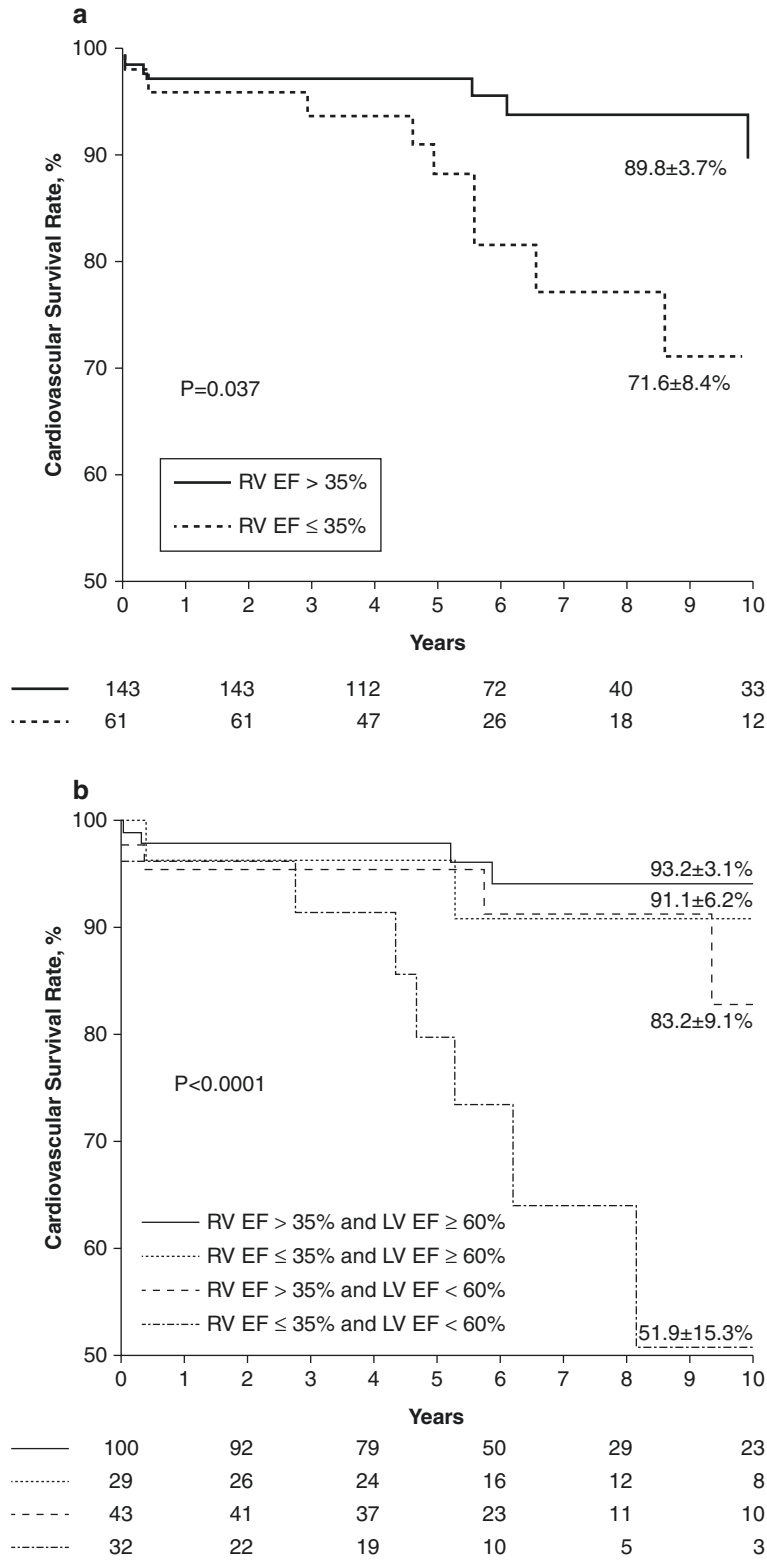

Fig. 20.5 (**a**) Ten-year cardiovascular survival rate after mitral valve surgery in patients with preserved (>35%) versus depressed (≤35%) RV EF (P = 0.037). (**b**) Ten-year cardiovascular survival rate after mitral valve surgery in patients with normal RV and LV systolic function (—), isolated depression of RV EF (•|•|•|•), isolated depression of LV EF (–|–|–) and biventricular impairment (–|•|–|•|–). Note the dramatic decrease in 10-year cardiovascular survival in patients with biventricular impairment in comparison with the remaining patients (P < 0.0001). *EF* indicates ejection fraction, *LV* left ventricle, and *RV* right ventricle. From Le Tourneau et al. [16] with permission

mild to moderate, uncomplicated systemic hypertension is associated with concentric RV remodeling, confirming that the unstressed RV is not immune to the effects of systemic hypertension [20].

Additionally, the fibrotic processes in the two ventricles are interconnected as it was demonstrated by a CMR study analysing severe AS patients 6 months after they had their aortic valve replacement surgery. It was shown that RV systolic performance decreases 6 months after surgical aortic valve replacement in patients with LV myocardial fibrosis, while in patients without any evidence of baseline LV fibrosis, no significant change in RV function was seen following surgical aortic valve replacement [21].

20.8 Right Ventricular Function After Treatment of Aortic Stenosis

Both PH and RVD are associated with poor prognosis in patients with severe AS. The perioperative mortality is high for patients with severe AS and severe PH undergoing aortic valve replacement surgery (SAVR). However, mortality is even higher in those treated conservatively [17]. Interestingly, if the AS patients survive SAVR, the PH regresses and these patients have a similar prognostic to those without preoperative severe PH.

Transcatheter aortic valve replacement (TAVR), may lead to substantial reduction in pulmonary artery pressure. FRANCE 2 Registry which analysed a total of 2435 patients whose pre-TAVR sPAP was known, demonstrated that the procedural success, early complications, and 30-day mortality were statistically similar regardless of the pre-intervention sPAP values [22]. However, moderate and severe PH (sPAP ≥40 mmHg) was associated with increased 1-year mortality [22].

To sum up, there are conflicting results regarding the prevalence of RVD after SAVR comparative to TAVR. One of the explanations for these divergent results may be again the different imaging modalities employed: two-dimensional or three-dimensional echocardiography or CMR.

Nonetheless, some studies suggest that the prevalence of RVD is higher after SAVR compared to TAVR. Two-dimensional echocardiography studies showed a decrease in RV function (TAPSE, RV longitudinal strain and RV fractional area change) in patients with severe AS undergoing SAVR while TAVR did not affect the post-intervention standard parameters of RV systolic function [23]. The pathophysiologic mechanisms of this finding are not entirely understood but they may be explained by the detrimental effects of pericardiotomy and cardiopulmonary bypass on RV function [23].

Contradictory findings are coming from studies employing three-dimensional echocardiography. Keyl et al. showed that there is no difference between three-dimensional derived RV function after SAVR compared to TAVR [24]. Although postoperative TAPSE was markedly reduced in patients undergoing SAVR, but not in patients undergoing TAVR, fractional shortening of the RV mid-cavity transverse diameter actually increased after SAVR in contrast to TAVR. Overall, the three-dimensional right ventricular ejection fraction (RVEF) remained unchanged in both patient groups.

Using CMR, the gold standard technique for assessing RV size and function, it was demonstrated that RV systolic function is impaired 6 months after SAVR [25]. Right ventricle function is not incorporated yet in the currently employed peri-operative risk scores. Real life prospective studies are needed to verify if the presence of RVD in severe AS patients should indicate TAVR over SAVR.

20.9 Mitral Regurgitation

Right ventricular dysfunction is also common in MR patients. In a radionuclide angiography study approximately one third of the patients with severe organic MR had RVEF <35% [16].

Chronic MR can lead to RVD through several mechanisms. The increased sPAP is probably the least important, while LV remodeling and interventricular dependence play a more important role. In the above mentioned study, RVEF correlated weakly with sPAP ($\beta = -0.14$, $P = 0.047$), while the correlation with LV septal function and LV end-diastolic diameter was stronger ($\beta = -0.22$, $P = 0.002$) [16]. Volume overload in chronic MR conducts to LV spherical enlargement. As the two ventricles are enclosed in the same pericardial envelope, the phenomenon of ventricular interdependence and interventricular septal function alteration are important mechanisms for development of RVD [26].

The association of RVD portends a worse prognosis for patients undergoing mitral valve sugery. The significant work by Le Tourneau et al. showed that the biventricular impairment (RVEF ≤35% and LVEF <60%) dramatically reduced 10-year cardiovascular survival and 10-year overall survival even after adjustment for known predictors (Fig. 20.5) [16].

Similar impact of RVD on outcomes was reported in patients with secondary MR. Kaneko et al. showed that RVD (TAPSE <15 mm) was associated with worse survival after MitraClip implantation [27].

Conclusions

The spectrum of RVD extends from minimal subclinical anomalies to overt right HF and modern non-invasive imaging techniques are able to diagnose RVD early, allowing for timely intensive treatment as well as better risk stratification in this patient population.

The mechanisms of RV impairment in the context of left-sided heart disease are complex and the backwards transmission of increased pressures to pulmonary circulation is just one piece of the puzzle. Right ventricular dysfunction is associated with increased mortality in patients with left HF independently of other risk factors such as LV EF. A rigorous risk stratification of patients with left heart pathology should take into consideration RV function.

References

1. Iglesias-Garriz I, Olalla-Gomez C, Garrote C, Lopez-Benito M, Martin J, Alonso D, et al. Contribution of right ventricular dysfunction to heart failure mortality: a meta-analysis. Rev Cardiovasc Med. 2012;13(2–3):e62–9.
2. Mohammed SF, Hussain I, AbouEzzeddine OF, Takahama H, Kwon SH, Forfia P, et al. Right ventricular function in heart failure with preserved ejection fraction: a community-based study. Circulation. 2014;130(25):2310–20.
3. Gulati A, Ismail TF, Jabbour A, Alpendurada F, Guha K, Ismail NA, et al. The prevalence and prognostic significance of right ventricular systolic dysfunction in nonischemic dilated cardiomyopathy. Circulation. 2013;128(15):1623–33.
4. Rosenkranz S, Gibbs JSR, Wachter R, De Marco T, Vonk-Noordegraaf A, Vachiéry J-L. Left ventricular heart failure and pulmonary hypertension. Eur Heart J. 2016;37(12):942–54. Available from http://www.ncbi.nlm.nih.gov/pmc/articles/PMC4800173/.
5. Kjaergaard J, Akkan D, Iversen KK, Kober L, Torp-Pedersen C, Hassager C. Right ventricular dysfunction as an independent predictor of short- and long-term mortality in patients with heart failure. Eur J Heart Fail. 2007;9(6–7):610–6.
6. Kiefer TL, Bashore TM. Pulmonary hypertension related to left-sided cardiac pathology. Pulm Med. 2011;2011:381787.
7. Bogaard HJ, Natarajan R, Henderson SC, Long CS, Kraskauskas D, Smithson L, et al. Chronic pulmonary artery pressure elevation is insufficient to explain right heart failure. Circulation. 2009;120(20):1951–60. Available from http://circ.ahajournals.org/content/120/20/1951.abstract.
8. Vachiery J-L, Adir Y, Barbera JA, Champion H, Coghlan JG, Cottin V, et al. Pulmonary hypertension due to left heart diseases. J Am Coll Cardiol. 2013;62(25 Suppl):D100–8.
9. Bosch L, Lam CSP, Gong L, Chan SP, Sim D, Yeo D, et al. Right ventricular dysfunction in left-sided heart failure with preserved versus reduced ejection fraction. Eur J Heart Fail. 2017. https://doi.org/10.1002/ejhf.873.
10. Smerup M, Nielsen E, Agger P, Frandsen J, Vestergaard-Poulsen P, Andersen J, et al. The three-dimensional arrangement of the myocytes aggregated together within the mammalian ventricular myocardium. Anat Rec. 2009;292(1):1–11.
11. Santamore WP, Lynch PR, Heckman JL, Bove AA, Meier GD. Left ventricular effects on right ventricular developed pressure. J Appl Physiol. 1976;41(6):925–30.
12. Friedberg MK, Cho M-Y, Li J, Assad RS, Sun M, Rohailla S, et al. Adverse biventricular remodeling in isolated right ventricular hypertension is mediated by

increased transforming growth factor-beta1 signaling and is abrogated by angiotensin receptor blockade. Am J Respir Cell Mol Biol. 2013;49(6):1019–28.
13. Paulus WJ, Tschöpe C. A novel paradigm for heart failure with preserved ejection fraction: comorbidities drive myocardial dysfunction and remodeling through coronary microvascular endothelial inflammation. J Am Coll Cardiol. 2013;62(4):263–71. Available from http://www.sciencedirect.com/science/article/pii/S0735109713018901.
14. Shahian DM, O'Brien SM, Filardo G, Ferraris VA, Haan CK, Rich JB, et al. The Society of Thoracic Surgeons 2008 cardiac surgery risk models: part 1—coronary artery bypass grafting surgery. Ann Thorac Surg. 2009;88(1 Suppl):S2–22.
15. Galli E, Guirette Y, Feneon D, Daudin M, Fournet M, Leguerrier A, et al. Prevalence and prognostic value of right ventricular dysfunction in severe aortic stenosis. Eur Heart J Cardiovasc Imaging. 2015;16(5):531–8.
16. Le Tourneau T, Deswarte G, Lamblin N, Foucher-Hossein C, Fayad G, Richardson M, et al. Right ventricular systolic function in organic mitral regurgitation: impact of biventricular impairment. Circulation. 2013;127(15):1597–608.
17. Malouf JF, Enriquez-Sarano M, Pellikka PA, Oh JK, Bailey KR, Chandrasekaran K, et al. Severe pulmonary hypertension in patients with severe aortic valve stenosis: clinical profile and prognostic implications. J Am Coll Cardiol. 2002;40(4):789–95. Available from http://www.sciencedirect.com/science/article/pii/S0735109702020028.
18. Faggiano P, Antonini-Canterin F, Ribichini F, D'Aloia A, Ferrero V, Cervesato E, et al. Pulmonary artery hypertension in adult patients with symptomatic valvular aortic stenosis. Am J Cardiol. 2000;85(2):204–8. Available from http://www.sciencedirect.com/science/article/pii/S0002914999006438.
19. Cavalcante JL, Rijal S, Althouse AD, Delgado-Montero A, Katz WE, Schindler JT, et al. Right ventricular function and prognosis in patients with low-flow, low-gradient severe aortic stenosis. J Am Soc Echocardiogr. 2017;29(4):325–33. https://doi.org/10.1016/j.echo.2015.12.001.
20. Todiere G, Neglia D, Ghione S, Fommei E, Capozza P, Guarini G, et al. Right ventricular remodelling in systemic hypertension: a cardiac MRI study. Heart. 2011;97(15):1257–61.
21. Musa TA, Uddin A, Fairbairn TA, Dobson LE, Kidambi A, Ripley DP, et al. Right ventricular function following Surgical Aortic Valve Replacement (SAVR). J Cardiovasc Magn Reson. 2015;17(1):P177. https://doi.org/10.1186/1532-429X-17-S1-P177.
22. Luçon A, Oger E, Bedossa M, Boulmier D, Verhoye JP, Eltchaninoff H, et al. Prognostic implications of pulmonary hypertension in patients with severe aortic stenosis undergoing transcatheter aortic valve implantation. Circ Cardiovasc Interv. 2014;7(2):240–7. Available from http://circinterventions.ahajournals.org/content/7/2/240.abstract.
23. Kempny A, Diller G-P, Kaleschke G, Orwat S, Funke A, Schmidt R, et al. Impact of transcatheter aortic valve implantation or surgical aortic valve replacement on right ventricular function. Heart. 2012;98(17):1299–304.
24. Keyl C, Schneider J, Beyersdorf F, Ruile P, Siepe M, Pioch K, et al. Right ventricular function after aortic valve replacement: a pilot study comparing surgical and transcatheter procedures using 3D echocardiography. Eur J Cardiothorac Surg. 2016;49(3):966–71.
25. Al Musa T, Uddin A, Fairbairn TA, Dobson LE, Steadman CD, Kidambi A, et al. Right ventricular function following surgical aortic valve replacement and transcatheter aortic valve implantation: a cardiovascular MR study. Int J Cardiol. 2016;223:639–44.
26. le Tourneau T. Right ventricle impairment: are we changing the paradigm in organic mitral regurgitation? Arch Cardiovasc Dis. 2013;106:419–22.
27. Kaneko H, Neuss M, Weissenborn J, Butter C. Prognostic significance of right ventricular dysfunction in patients with functional mitral regurgitation undergoing MitraClip. Am J Cardiol. 2016;118(11):1717–22.

Myocardial Infarction of the Right Ventricle

21

Antonis S. Manolis, Antonis A. Manolis, and Theodora A. Manolis

Abstract

Right ventricular (RV) myocardial infarction (MI) usually occurs in the setting of an inferior MI (IMI) when the acute occlusion of the right coronary artery (RCA) is located proximally to the acute RV marginal branches, which commonly provide blood supply to the RV. RV MI may result in severe right heart failure with hemodynamic compromise and cardiogenic shock which distinctly differs from the cardiogenic shock secondary to left ventricular (LV) dysfunction, presenting with the clinical triad of low-output hypotension, clear lungs, and jugular venous distention despite intact global LV systolic function. The ECG provides further confirmation by examining the right precordial leads, V1 and more specifically V4R displaying ST elevation. Management of this type of cardiogenic shock is also grossly different from the management of LV shock requiring fluid resuscitation and/or vasopressors as the most important initial approach; however more definitive treatment is similar to any type of acute MI with prompt mechanical reperfusion therapy, most effectively achieved via primary percutaneous coronary intervention (PCI) of the culprit coronary artery occlusion.

Keywords

Myocardial infarction · Right ventricle · Coronary angiography · Percutaneous coronary intervention · Hypotension · Cardiogenic shock

Abbreviations

AF	Atrial fibrillation
IMI	Inferior wall myocardial infarction
LV	Left ventric-le(-ular)
MI	Myocardial infarction
PCI	Percutaneous coronary intervention
RA	Right atrium
RCA	Right coronary artery
RV	Right ventric-le(-ular)
STEMI	ST elevation myocardial infarction

21.1 Introduction

For a long time, the right ventricle (RV) had been the neglected chamber as it was felt that RV contraction was not that important in the circula-

A. S. Manolis (✉)
Third Department of Cardiology, Athens University School of Medicine, Athens, Greece
e-mail: asm@otenet.gr

A. A. Manolis
Patras University School of Medicine, Patras, Greece

T. A. Manolis
Zakynthos Hospital, Zakynthos, Greece

S. I. Dumitrescu et al. (eds.), *Right Heart Pathology*, https://doi.org/10.1007/978-3-319-73764-5_21

tion and that, despite loss of RV systolic function, pulmonary flow could be sustained by a passive gradient from an overloaded venous system and active right atrial (RA) contraction [1]. However, it has now been quite a while that the significant hemodynamic effects of RV systolic dysfunction have become evident and universally recognized, particularly with the description of the clinical and hemodynamic consequences of severe RV myocardial infarction (MI), resulting in severe right heart failure, clear lungs, and low-output hypotension despite intact global left ventricular (LV) systolic function [2]. Nearly 50% of patients with acute inferior ST elevation MI (STEMI) exhibit RV involvement by noninvasive studies, albeit with a much lower percentage of evident hemodynamic effects [3, 4].

It appears that a variety of other factors determine the magnitude of hemodymamic consequences of RV MI in addition to the extent of RV free wall contraction abnormalities, as some patients tolerate severe RV systolic dysfunction, whereas others develop severe hemodynamic compromise and shock. It also appears that the term RV "infarction" may not best describe the ischemic stunning of the RV, as, in most cases, the myocardium involved gradually recovers over time, especially after successful reperfusion and even after prolonged periods of infarct-related coronary artery occlusion [5].

21.2 Epidemiology

Nearly half of all cases of inferior wall MI (IMI) are complicated by RV MI. Isolated RV MIs constitute about 3% of all MIs conferring considerable morbidity [3]. RV MI is associated with higher in-hospital morbidity and mortality due to significant hemodynamic and electrophysiological consequences. RV MI has been reported to occur more frequently in women than in men. In a group of 517 patients with STEMI, 32 (23.5%) of 136 women and 42 (11%) of 381 men had RV MI (odds ratio 2.48; $p = 0.001$) [6].

21.3 RV Physiology

The RV has the same cardiac output as the left ventricle, but one sixth the muscle mass; the resistance that it encounters during blood ejection (pulmonary vascular resistance) is considerably less that the systemic vascular resistance that the LV runs into [7].

The RV derives its blood supply predominantly from the acute marginal branch of the right coronary artery (RCA) for its lateral wall, the posterior descending artery for its posterior wall and the septum, and the conus artery for its anterior wall. The conus artery has the lowest incidence of occlusion than any other artery connected to the aorta, hence its importance in providing collaterals to the other vessels and also preserving the systolic function of the RV outflow tract in cases of RV MI.

It appears that the RV is less susceptible to infarction compared to the LV, as the oxygen demand is significantly lower in the RV due to its much smaller muscle mass and lower afterload, while there is more extensive collateral flow from left to right coronary arteries [1, 8].

21.4 Pathogenesis

The majority of RV infarctions occur when the RCA occludes proximally to its acute marginal branches or a minority (~15%) happen when the left circumflex (LCx) coronary artery occludes in cases of a left dominant coronary anatomy [1–4]. Nevertheless, only half of all occlusions proximally to the acute marginals result in RV involvement as the myocardial injury may be prevented or mitigated by better collaterals and/or ability of better oxygen extraction. RV MI is often associated with left ventricular infarction (14–84%). Only rarely has isolated RV MI been reported that mimics left anterior MI [9]. Scarce studies have challenged the notion that RCA is the most common infarct-related artery in RV MI [10, 11]. In one study, the RCA was involved only in approximately a half of the RV MI patients. Anterior wall STEMI and the left ante-

rior descending coronary artery were associated with a good proportion (~24%) of ECG signs of RV MI, however with no apparent clear mechanism explaining such an RV involvement in these cases [10].

21.5 Pathophysiology of RV Infarcts

Consequences of RV MI comprise reduction of RV systolic pressure, LV end-diastolic volume, cardiac output, aortic pressure, and equalization of RV and LV diastolic pressures. The severity of RV MI depends on the extent of infarct and restraining effect of pericardium and/or the RV interaction with the LV. Left ventricular septal contraction that bulges into the RV generates systolic force sufficient for pulmonary perfusion. Augmented atrial contractility overcomes RV stiffness. Diminution of preload with use of diuretics and/or nitrates or loss of atrioventricular (AV) synchrony confers profound hemodynamic effects. Impairment of RA reservoir and conduit functions has also been demonstrated in patients with IMI plus RV MI compared with patients with IMI alone [12].

21.6 Diagnosis

Accurate diagnosis of RV MI is important because management differs from left ventricular MI. RV MI should be always suspected and the diagnosis sought in all cases of inferior MIs (Table 21.1). On physical examination, the characteristic *clinical triad of hypotension, clear lungs, elevated jugular venous pressure* is nearly pathognomonic. On ECG, the right precordial leads should always be obtained in cases of inferior MIs. A 1-mm ST elevation in V4R has 70% sensitivity and is 100% specific [13]. Hemodynamic assessment, if performed, reveals RA pressure >10 mmHg and within 1–5 mmHg of the pulmonary capillary wedge pressure (PCWP). The echo reveals RV dilatation, RV wall asynergy, abnormal interventricular septal motion. The suspicion of RV MI should also be entertained when the patient with acute MI develops hypotension with administration of nitroglycerin and/or morphine.

Table 21.1 Diagnosis of Right Ventricular (RV) Myocardial Infarction (MI)

• Setting: IMI
• Clinical triad: hypotension, elevated jugular venous pressure and clear lungs
• ECG: ≥1-mm ST elevation in right-sided leads (e.g. V4R)
• Hemodynamics: RA pressure >10 mmHg and within 1–5 mmHg of the PCWP
• Echo: RV dilatation, RV wall asynergy, abnormal interventricular septal motion
• CMR with late gadolinium enhancement (LGE): impaired RV function, a regional wall motion abnormality with corresponding edema on T2W images and subendocardial hyperenhancement on LGE
• Isolated RV MI (<3% of STEMI cases): ST elevation in V1–2 (mimics anterior LV infarction)
• Considered when patient with acute MI develops hypotension with administration of nitroglycerin and/or morphine

ECG electrocardiogram, *IMI* inferior wall myocardial infarction, *LV* left ventricle, *PCWP* pulmonary capillary wedge pressure, *RA* right atrium, *RV* right ventricle

However, in rare cases, isolated RV MI may occur that mimics anterior LV infarction in both clinical presentation and ECG recordings, ascribed to the anterior anatomical position of the RV, overlying the left ventricle [9]. Thus, isolated RV MI may present with anterior ST elevation attributed to either isolated occlusion of the RV branch of the RCA, occlusion of a nondominant or a codominant RCA, or occlusion of a nondominant RCA with an anomalous origin [9, 14, 15]. This type of RV MI may account for <3% of STEMI cases [3, 14]. Combined ST elevation in both inferior and anterior leads may also be encountered in cases of proximal occlusion of a large RCA and underlying RV enlargement or hypertrophy which may result in a shift of the electrical forces of injury towards the anterior leads [16].

In a study of 114 patients with IMI undergoing primary PCI of the RCA, cardiac magnetic resonance imaging (CMR) with late gadolinium enhancement (LGE) was performed 3–5 days post-PCI for RV MI assessment [17]. RV MI

Table 21.2 Differential Diagnosis (DDx) of RV MI

• Pericarditis with pericardial tamponade (DDx by echocardiography)
• Anteroseptal MI (ST elevation in leads V1–2, also seen with an RV injury pattern)
• Pulmonary embolism (DDx by ECG, echo, D-dimers, CT scanning or ventilation/perfusion scanning)
• Pre-existent pulmonary hypertension (>45–50 mmHg) (DDx by Swan-Ganz catheter)

CT computed tomography, *MI* myocardial infarction, *RV* right ventricle

was detected in 48 (42%) patients. Multivariate regression analysis identified TIMI flow <2 in at least one RV branch after PCI as an independent angiographic predictor of RV MI (odds ratio -OR 143.00, $p < 0.001$]. ST-segment elevation ≥1 mm in V4R was present in 83 (73%).

Differential diagnosis may include *pericarditis with pericardial tamponade* which may mimic RV MI with the ST elevation present in several leads, including right-sided leads (Table 21.2). In this circumstance, the diagnosis is aided by echocardiography which excludes pericardial effusion and confirms RV chamber dilatation and impaired RV free wall motion in patients with RV MI. *Anteroseptal MI* may also occasionally present some difficulty in differential diagnosis as it presents ST elevation in leads V1 and V2, also seen with an RV injury pattern. However, the most common condition that may be confused with RV MI is *pulmonary embolism* (PE) which may present with chest pain and findings of hypotension (or shock) and clear lungs and can also exhibit ST elevation in the right-sided precordial leads caused by RV "strain". Pleuritic chest pain in PE may help in making the distinction. The ECG is helpful to discern the two; ST elevation in the inferior leads is rarely present in patients with PE. Echocardiography may also assist to distinguish these two conditions. RV systolic dysfunction may be seen in both; however, sparing of the RV apex ("McConnell's sign") has been suggested by some as specific for a large PE. However, additional testing may be needed, such as measuring D-dimers and performing CT scanning or ventilation/perfusion scanning to further establish the diagnosis.

Pre-existent pulmonary hypertension (>45–50 mmHg) produces echocardiographic abnormalities of the RV structure and function, including RV dilatation and tricuspid regurgitation, that mimic some of the findings of RV MI. In difficult cases, placement of a pulmonary artery (Swan-Ganz) catheter may provide additional diagnostic information, albeit with caution to avoid catheter-induced ventricular arrhythmias. Hemodynamically significant RV MIs produce elevations in RA pressure to ≥10 mmHg and a ratio of RA pressure to PCWP increased from a normal of <0.6 to >0.8. The diastolic filling pressures in the RA, RV, PCWP, and the LV, may be elevated and equalized. There may be a Kussmaul's sign (inspiratory augmentation of venous return due to a dilated and non-compliant right heart) evident in the RA pressure trace or the jugular venous pulse.

21.7 Identifying the Culprit Artery of Acute Occlusion by ECG

In cases of ST elevation in the inferior leads, the culprit artery of acute occlusion may be the RCA or the LCX. By analysis of lead I, ST elevation >0.5 mm points to the LCx; ST depression >0.5 mm indicates RCA occlusion [18]. If ST is isoelectric or ST elevation or depression is <0.5 mm, then leads II and III should be analyzed; ST elevation is greater in lead II than III in LCx occlusion. If ST elevation is greater in lead III, then a proportionally greater sum of ST depression in V1–3 than a sum of ST elevation in II, III, aVF points to LCx, while the opposite (greater sum of ST elevation in II, III, aVF than ST depression in V1–3) indicates the RCA. ST elevation in V1 or ST depression <0.5 mm or isoelectric indicates proximal RCA occlusion and therefore possible extension of the ischemia to the RV [19]; greater ST depression in V1 indicates distal RCA occlusion. Of course, ST elevation in lead V4R confirms RV MI [4].

21.8 Complications

Shock is the most serious complication of RV MI (Table 21.3) which differs from LV cardiogenic shock, as it will be described below. Additional

Table 21.3 Complicating and prognostic factors of RV MI

Acute RV failure/shock
Bradyarrhythmias: high-degree or complete AV block
Tachyarrhythmias: AF, VT/VF
Right atrial MI
Mechanical complications: post-MI ventricular septal defect (VSD), tricuspid regurgitation
RV thrombus formation
Acute pericarditis
Concomitant LV dysfunction: a/w greater hemodynamic compromise and higher in-hospital mortality
Pre-discharge RV dysfunction: a/w worse long-term prognosis

AF atrial fibrillation, *AV* atrioventricular, *a/w* associated with, *MI* myocardial infarction, *LV* left ventricle, *RV* right ventricle, *VF* ventricular fibrillation, *VT* ventricular tachycardia

complications may include both *brady- and tachy-arrhythmias* which are more frequently encountered in RV MIs compared with 'simple' inferior or anterior wall left ventricular MIs. High degree or complete AV block may occur in ~50% of patients which portends poor prognosis. Atrial fibrillation is encountered in 1/3 of patients. RV MIs are associated with increased incidence of ventricular tachycardia (VT)/ventricular fibrillation (VF). Other complications may also occur, such as right atrial MI, post-MI ventricular septal defect (VSD), RV thrombus formation, tricuspid regurgitation, and acute pericarditis.

Thus, several important complicating factors may worsen the hemodynamic status of patients with RV MI (Table 21.3). When the RCA occludes proximally to the atrial branches (supplied by the RCA in ~60% and by the LCx in ~40%), concomitant RA ischemia or MI can impair RA function with serious hemodynamic consequences due to compromise or lack of the right atrial kick that may even lead to shock [20]. Other manifestations of right atrial MI may comprise sinoatrial nodal abnormalities such as exit blocks and AF, again depending on the location of the occlusion and the presence or not of collaterals. *Concomitant LV dysfunction* may significantly exacerbate the hemodynamic status, not only due to LV pump failure, but also due to the lack of a strong LV septal contraction on which a severely depressed RV relies on to forward blood into the pulmonary circulation. Furthermore, *tricuspid regurgitation*, caused by ischemia to the papillary muscle or by dilatation of the tricuspid annulus may impose further circulatory burden. Even mechanical complications of RV MI, such as *post-MI ventricular septal defect* from septal rupture can occur with the left-to-right shunting further compromising left ventricular output and worsening the RV dysfunction.

Sinoatrial or atrioventricular nodal dysfunction due to ischemia accounts for the bradyarrhythmias observed in RV MIs, although activation of cardioinhibitory (Bezold-Jarisch) reflexes may also be responsible for both severe bradycardia and hypotension, arising from stimulation of vagal afferents located in the ischemic LV infero-posterior wall but also in the ischemic RV. Finally, ventricular arrhythmias, including VT and VF, may complicate up to one-third of cases of RV MI. Both these types of arrhythmias may also manifest as reperfusion arrhythmias [21].

21.9 Acute RV Failure/Shock

Patients with acute RV MI may present with signs of acute RV failure, usually manifesting with low cardiac output state, hypotension, hypoxemia, cold extremities, central nervous system dysfunction, oliguria, all signs of shock [22]. However, this type of cardiogenic shock is entirely different from the shock state produced by acute LV failure. It is characterized by signs of systemic congestion (jugular venous distention, hepatojugular reflex, peripheral edema, congestive hepato-splenomegaly, ascites, anasarca) but clear lungs (in the absence of concomitant LV dysfunction). An S3 may be heard, as well as a systolic murmur of tricuspid regurgitation. An increase of biochemical markers may be present, such as increased lactate levels, natriuretic peptides (BNP or NT-proBNP, cardiac troponin I or T, abnormal liver biochemistry (e.g. elevated transaminases, bilirubin, prolonged prothrombin time), and abnormal renal function (blood urea nitrogen, creatinine).

In the presence of IMI, development of hypotension or cardiogenic shock without signs of LV

failure and 1 mm ST segment elevation in the V4R lead, a diagnosis of RV MI can be made, if not already confirmed. In this occasion, specific treatment includes prompt administration of fluid loading and vasopressors. In addition, patients with RV MI require continuous careful monitoring because they are at a significantly higher risk for life-threatening ventricular arrhythmias (sustained VT or VF) and high-degree AV block, which may impact overall prognosis [23].

21.10 Cardiac Imaging Findings

In patients with RV MI, *echocardiography* may reveal normal or slightly elevated pulmonary artery pressure, RV dilation, global and regional hypokinesia, abnormal septal motion, reduced tricuspid annular plane systolic excursion (TAPSE), reduced S′ velocity, congested inferior vena cava (IVC) despite normal or low systolic RV pressure, and signs of elevated right atrial and diastolic RV pressure [22]. In other studies, the presence of a severe tricuspid regurgitation and of an abnormal septal motion in patients with acute MI indicates involvement of the RV [24].

Cardiac magnetic resonance (CMR) imaging with late gadolinium enhancement (LGE) is a very useful test for the detection of RV infarction, a diagnosis that may be frequently missed. The typical CMR pattern of acute RV MI is impaired RV function, regional wall motion abnormalities with corresponding edema and hyperenhancement on T2W and LGE images respectively [25]. CMR with LGE has also been utilized for risk stratification by visualization of wall motion, edema, and delayed-enhancement. In a study of 450 STEMI patients undergoing primary PCI, a high RV myocardial mass (odds ratio, 2.06; $P = 0.012$) and a low TIMI flow before PCI (odds ratio, 0.50; $P = 0.011$) were associated with RV MI [26]. Cox regression analysis indicated that RV MI detected by CMR was a strong and independent predictor of clinical outcome after acute reperfused STEMI (hazard-ratio, 3.36 for predicting time to major adverse cardiac events; $P < 0.001$).

21.11 Treatment

Management strategies comprise early maintenance of RV preload, reduction of RV afterload, inotropic support of dysfunctional RV and early reperfusion (Table 21.4). Early reperfusion constitutes the cornerstone of the management. Avoidance of diuretics and nitrates which may produce severe hypotension is also important.

Volume loading with several liters is the initial step, followed by *dobutamine and/or dopamine* if cardiac output fails to improve. *AV synchrony* is essential; one should consider cardioversion of AF early if the patient is hemodynamically compromised. "Unloading" the left ventricle with afterload reduction may be beneficial if there is also LV dysfunction, even with resorting to intra-aortic balloon pump (IABP) when needed. In refractory cases, more aggressive and drastic therapeutic options, such as

Table 21.4 Treatment of RV MI

• Maintenance of RV preload (volume loading)
• Reduction of RV afterload (even by resorting to IABP, Tandem-Heart, etc.)
• Inotropic support of dysfunctional RV (dobutamine and/or dopamine)
• Early reperfusion (cornerstone) (PPCI of RCA/ should include major RV branches)
• Treat reperfusion arrhythmias promptly: e.g. cardiovert VT/VF, atropine for bradycardia and hypotension (Bezold-Jarisch reflex)
• Avoidance of diuretics and nitrates
• AV synchrony: cardiovert AF/avoid temporary RV apical pacing which produces lack of AV synchrony plus iatrogenic dyssynchrony that may lead to hypotension/use either AV pacing or atropine or isoproterenol to accelerate heart rate/more importantly, expedite mechanical reperfusion via PCI that may help restore a physiological rhythm and AV synchrony
• Remember that the optimal LV filling pressure (PCWP) needed to restore hemodynamics and reverse hypotension for a damaged heart is quite different (15–18 mmHg) from that of a normal heart (5–12 mmHg)

AF atrial fibrillation, *AV* atrioventricular, *IABP* intra-aortic balloon pumping, *LV* left ventricle, *MI* myocardial infarction, *PCI* percutaneous coronary intervention, *PCWP* pulmonary capillary wedge pressure, *PPCI* primary PCI, *RV* right ventricle, *VF* ventricular fibrillation, *VT* ventricular tachycardia

Tandem-Heart or percutaneous cardiopulmonary support systems, where and when available, may be lifesaving [27].

Indeed, hypotension and shock may respond to volume repletion and restoration of atrioventricular synchrony (if compromised) and maintenance of a physiologic rhythm. Refractory cases usually respond to parenteral inotropes, though in some cases mechanical support is required. Vasodilators and diuretics should generally be avoided. The RV is relatively resistant to infarction and usually recovers even after prolonged occlusion. Acute percutaneous mechanical reperfusion enhances recovery of RV performance and improves the clinical course and survival of patients with RV MI [1].

Indeed, as myocardial reperfusion greatly benefits patients with LV infarction, similarly reperfusion has been demonstrated to favorably affect the recovery of RV performance in patients with RV MI. In these latter patients, successful mechanical reperfusion via *primary PCI* of the RCA should include the major RV branches in order to confer complete recovery of RV free wall function. Contrariwise, failure to restore flow to the major RV branches may be associated with lack of recovery of RV performance, even if flow is restored in the main RCA. This may further prolong hemodynamic compromise with its attendant increase in in-hospital mortality. Importantly, upon achieving reperfusion, significant bradycardia with hypotension may ensue, as a manifestation of reperfusion arrhythmias, which could respond to administration of atropine [21]. However, marked bradycardia may be followed by ventricular fibrillation necessitating electrical cardioversion.

A concerning and important caveat should be added here for a potential deleterious hemodynamic effect of temporary RV apical pacing in patients with RV MI complicated by bradyarrhythmias [28]; apparent lack of AV synchrony during RV pacing plus the iatrogenic dyssynchrony that this mode of pacing produces may lead to hypotension. Either AV pacing may be attempted to be established or one may rely on the temporary effect of atropine or isoproterenol if it ever succeeds to provide some heart rate acceleration, or more importantly, one should expedite mechanical reperfusion via PCI that may help restore a physiological rhythm and AV synchrony.

Finally, a reminder of cardiac physiology, albeit frequently underestimated during hemodynamic monitoring, relates to the range of LV filling pressures that are optimal for a damaged heart which is quite different from that of a normal heart. Specifically, a normal range of 5–12 mmHg of a PCWP does not suffice to maintain a normal cardiac output and restore blood pressure in a patient who has sustained an MI; according to the Frank-Starling principle, an MI patient with compromised systolic function and hypotension or shock will need a filling pressure of 15–18 mmHg to restore hemodynamics and achieve normal blood pressure; otherwise one may be facing a refractory hypotensive state and may be misled in resorting to more aggressive modes of therapy [29].

21.12 Prognosis

In-hospital mortality up to 31% has been reported for IMI with RV MI vs 6% for IMI without RV infarction. In the vast majority of survivors, treated with primary PCI, hemodynamics and RV dysfunction return to normal [30]. However, even in the era of successful primary PCI, RV MI is still associated with high (18%) in-hospital mortality [31].

According to the SHOCK trial registry, RV shock patients, despite the younger age, lower incidence of anterior MI, and higher prevalence of single-vessel coronary artery disease, compared with left ventricular shock patients, and their similar benefit from revascularization, had unexpectedly an equally high mortality (53% vs 61%; $p = 0.3$) [32].

Other studies have suggested that in patients with acute IMI complicated by RV MI, *depressed LV ejection fraction* is associated with greater hemodynamic compromise and higher in-hospital mortality [33]. Furthermore, *pre-discharge RV systolic dysfunction* appears to correlate independently with worse long-term prognosis in patients after IMI with preserved or slightly impaired LV systolic function [34].

Conclusion

The significant hemodynamic effects of RV systolic dysfunction have been amply recognized, particularly with the description of the clinical and hemodynamic consequences of severe RV myocardial infarction (MI). RV MI usually occurs in the setting of an IMI when the acute occlusion of the RCA is located proximally to the acute RV marginal branches which commonly provide blood supply to the RV. RV MI resulting in severe right heart failure will present with the *clinical triad of low-output hypotension, clear lungs, and jugular venous distention* despite intact global LV systolic function. The ECG provides further confirmation by examining the right precordial leads, V1 and more specifically V4R displaying ST elevation. Fluid resuscitation and/or vasopressors may be the most important initial management; however more definitive treatment is prompt mechanical, if possible, reperfusion therapy with primary PCI.

Conflicts of Interest None declared.

References

1. Goldstein JA. Acute right ventricular infarction: insights for the interventional era. Curr Probl Cardiol. 2012;37:533–57.
2. Cohn JN, Guiha NH, Broder MI, et al. Right ventricular infarction. Clinical and hemodynamic features. Am J Cardiol. 1974;33:209–14.
3. Kinch JW, Ryan TJ. Right ventricular infarction. N Engl J Med. 1994;330:1211–7.
4. Haji SA, Movahed A. Right ventricular infarction–diagnosis and treatment. Clin Cardiol. 2000;23:473–82.
5. Goldstein JA. Pathophysiology and management of right heart ischemia. J Am Coll Cardiol. 2002;40:841–53.
6. Obradovic S, Dzudovic B, Djuric I, et al. Women have right ventricular infarction more frequently than men. Acta Cardiol. 2015;70:343–9.
7. Dell'Italia LJ. Anatomy and physiology of the right ventricle. Cardiol Clin. 2012;30:167–87.
8. Haupt HM, Hutchins GM, Moore GW. Right ventricular infarction: role of the moderator band artery in determining infarct size. Circulation. 1983;67:1268–72.
9. Harnett DT, LaHaye SA, Wilkinson JS. Isolated right ventricular myocardial infarction: a sheep in wolf's clothing. JAMA Intern Med. 2016;176:1207–10.
10. Kanovsky J, Kala P, Novotny T, et al. Association of the right ventricle impairment with electrocardiographic localization and related artery in patients with ST-elevation myocardial infarction. J Electrocardiol. 2016;49:907–10.
11. Pourafkari L, Joudi S, Ghaffari S, et al. ST-segment elevation in the right precordial leads in patients with acute anterior myocardial infarction. Balkan Med J. 2016;33:58–63.
12. Nourian S, Hosseinsabet A, Jalali A, et al. Evaluation of right atrial function by two-dimensional speckle-tracking echocardiography in patients with right ventricular myocardial infarction. Int J Cardiovasc Imaging. 2017;33:47–56.
13. Lopez-Sendon J, Coma-Canella I, Alcasena S, et al. Electrocardiographic findings in acute right ventricular infarction: sensitivity and specificity of electrocardiographic alterations in right precordial leads V4R, V3R, V1, V2, and V3. J Am Coll Cardiol. 1985;6:1273–9.
14. Finn AV, Antman EM. Images in clinical medicine. Isolated right ventricular infarction. N Engl J Med. 2003;349:1636.
15. Franco JJ, Brown M, Bashir R, et al. Acute anterior ST-elevation myocardial infarction and electrical storm secondary to nondominant right coronary artery occlusion. Tex Heart Inst J. 2014;41:335–7.
16. Peters A, Lakhter V, Bashir R. Under-pressure: right ventricular infarction. Am J Med. 2015;128:966–9.
17. Tomala M, Miszalski-Jamka T, Zajdel W, et al. Angiographic result of index PCI determines the presence of right ventricular infarction in patients with acute inferior myocardial infarction. Int J Cardiovasc Imaging. 2015;31:1591–601.
18. Fiol M, Cygankiewicz I, Carrillo A, et al. Value of electrocardiographic algorithm based on "ups and downs" of ST in assessment of a culprit artery in evolving inferior wall acute myocardial infarction. Am J Cardiol. 2004;94:709–14.
19. Garcia-Niebla J, Fiol M, Carrillo-Lopez A, et al. Electrocardiographic diagnosis of right ventricular infarction by proximal occlusion of a very dominant right coronary artery. Am J Med. 2016;129:e41–2.
20. Lu ML, De Venecia T, Patnaik S, et al. Atrial myocardial infarction: a tale of the forgotten chamber. Int J Cardiol. 2016;202:904–9.
21. Chiladakis JA, Patsouras N, Manolis AS. The Bezold-Jarisch reflex in acute inferior myocardial infarction: clinical and sympathovagal spectral correlates. Clin Cardiol. 2003;26:323–8.
22. Harjola VP, Mebazaa A, Celutkiene J, et al. Contemporary management of acute right ventricular failure: a statement from the heart failure association and the working group on pulmonary circulation and right ventricular function of the european society of cardiology. Eur J Heart Fail. 2016;18:226–41.
23. Ondrus T, Kanovsky J, Novotny T, et al. Right ventricular myocardial infarction: from pathophysiology to prognosis. Exp Clin Cardiol. 2013;18:27–30.

24. Mattioli AV, Bastia E, Mattioli G. Doppler echocardiographic findings in patients with right ventricular infarction. J Ultrasound Med. 1998;17:297–301.
25. Fairbairn TA, Motwani M, Greenwood JP, et al. CMR for the diagnosis of right heart disease. JACC Cardiovasc Imaging. 2012;5:227–9.
26. Grothoff M, Elpert C, Hoffmann J, et al. Right ventricular injury in ST-elevation myocardial infarction: risk stratification by visualization of wall motion, edema, and delayed-enhancement cardiac magnetic resonance. Circ Cardiovasc Imaging. 2012;5:60–8.
27. Inohara T, Kohsaka S, Fukuda K, et al. The challenges in the management of right ventricular infarction. Eur Heart J Acute Cardiovasc Care. 2013;2:226–34.
28. Gopalakrishnan A, Sanjay G, Nair KK, et al. Deleterious effects of isolated right ventricular pacing in right ventricular myocardial infarction. Int J Cardiol. 2016;222:995–6.
29. Manolis A, Varriale P, Nobile J. Low filling pressure cardiogenic pulmonary-edema–a complication of venodilatory therapy. N Y State J Med. 1986;86:411–3.
30. Gorter TM, Lexis CP, Hummel YM, et al. Right ventricular function after acute myocardial infarction treated with primary percutaneous coronary intervention (from the glycometabolic intervention as adjunct to primary percutaneous coronary intervention in ST-segment elevation myocardial infarction III trial). Am J Cardiol. 2016;118:338–44.
31. Aissaoui N, Sorbets E, Sleiman C, et al. Characteristics, mortality and prognostic factors of acute right ventricular myocardial infarction: a case-control study. Ann Cardiol Angeiol (Paris). 2017;66:15–20.
32. Jacobs AK, Leopold JA, Bates E, et al. Cardiogenic shock caused by right ventricular infarction: a report from the SHOCK registry. J Am Coll Cardiol. 2003;41:1273–9.
33. Goldstein JA, Kommuri N, Dixon SR. Left ventricular systolic dysfunction is associated with adverse outcomes in acute right ventricular infarction. Coron Artery Dis. 2016;27:277–86.
34. Smarz K, Zaborska B, Jaxa-Chamiec T, et al. Right ventricular systolic function as a marker of prognosis after ST-elevation inferior myocardial infarction 5-year follow-up. Int J Cardiol. 2016;221:549–53.

Pulmonary Disease and Right Ventricular Function

22

Emma Weiss and Elisabeta Bădilă

Abstract

Respiratory diseases have become major players in mortality and morbidity charts and their influence on cardiac function has brought them in research focus, especially when investigating their role on the pathobiology of the less well understood right ventricle. By insulting pulmonary vasculature it leads to micro and macrovessel injury which results in pulmonary hypertension, increased right ventricle afterload along with its consequences—right ventricle hypertrophy and dilation. From the initial physical stimuli of hypoxia, translated by the vessel wall cells into a biological response of vasoconstriction and remodeling, pulmonary hypertension develops in a process modulated by the endothelium and many other epigenetic factors. Pulmonary hypertension is rarely severe when associated purely with chronic lung disease but carries a poor prognosis nevertheless, especially when associating right ventricle dysfunction. The primary diagnostic tools remain the echocardiography parameters generally used in all forms of the disorder and invasive procedures are infrequently necessary for evaluation. Unfortunately, this class of pulmonary hypertension shares much of the prognosis and complications with other groups of the, disorder, but less of the therapeutic arsenal which has become more recently available in the latter.

Keywords

Chronic lung disease · Hypoxia-induced pulmonary vasoconstriction · Right ventricle dysfunction in respiratory disease

22.1 Background

Cardiovascular diseases have become the leading cause of mortality in developed worlds and this led to an era when cardiology has developed to become left ventricle focused. Much less importance has been given to its younger brother, the right ventricle. However, there are four respiratory disease categories in the global top ten causes of mortality (lower respiratory infections, chronic obstructive pulmonary disease, tuberculosis, trachea/bronchus/lung cancer) and together they account for one in six deaths and one in ten disability-adjusted life-years lost [1]. Pulmonary diseases, such as lower respiratory infections and chronic obstructive pulmonary disease, are reported as the third and fourth causes of mortality worldwide [1]. Chronic hypoxemia and disruption of pulmonary vascular beds, as consequences of lung diseases, lead to right

E. Weiss (✉) · E. Bădilă
Internal Medicine, Emergency Clinical Hospital Bucharest, University of Medicine and Pharmacy Carol Davila Bucharest, Bucharest, Romania

S. I. Dumitrescu et al. (eds.), *Right Heart Pathology*, https://doi.org/10.1007/978-3-319-73764-5_22

ventricle dysfunction through a series of pathophysiological cardiopulmonary mechanisms, the understanding of which has become available and increased substantially since its first description by Laennec over 200 years ago. The past decades have brought much insight into a more accurate description of pathophysiological mechanisms underlying the development of right heart disease as a result of chronic pulmonary diseases.

22.1.1 The Importance of the Right Ventricle

The circulatory system is a closed one, with both ventricles acting as interdependent chambers each affecting the other's performance. As the most common cardiac diseases affect primarily the left ventricle (LV), the importance of the other has been neglected initially. It is obviously less frequently involved in diseases of epidemic proportions, and thus little interest has been given to the mechanisms underlying right ventricular (RV) dysfunction, its detection and evaluation, or to the specific molecular and cellular mechanisms contributing to failure of maintenance of normal right ventricular function [2, 3]. This lack of devotion to research was probably a consequence of the study by Starr et al. who concluded that as long as normal lung function is ensured, normal RV function is unnecessary for circulatory stability [4], and the RV ventricle was, at the time, seen as a passive conduit pumping blood to only one organ, the lungs. Over three decades ago, right ventricular dysfunction emerged as a negative prognostic indicator, being associated with increased mortality and reduced exercise capacity in patients with heart failure [5–8]. More recently, right heart dysfunction was shown to be associated with increased mortality in preserved ejection fraction heart failure patients [9]. Currently, it has become broadly known that the right ventricle is deleteriously influenced by, but also contributes to, several disease processes, pulmonary hypertension (PH) being the foremost of all, as it develops in the setting of a variety of lung or pulmonary vascular diseases. Right ventricular dysfunction is a rather heterogeneous syndrome, recognizing varied etiologies, each with different therapeutic options. In the case of chronic lung diseases, chronic hypoxia, in a pathophysiological cascade, leads to the development of PH, eventually altering RV morphology and function. Pulmonary hypertension in the setting of chronic hypoxemia is the third of the main groups, according to the Clinical Classification of Pulmonary Hypertension adopted first in 1998 (the Evian-Venice classification), updated later in 2008 (Dana Point) and 2013 (Nice). This classification brings together different manifestations of the disease, sharing similarities in pathophysiologic mechanisms, clinical presentation, and therapeutic approaches [10].

22.1.2 The Right Ventricle and Pulmonary Hypertension

The RV is the most anterior positioned chamber of the heart, located immediately behind the sternum, anterior to the left ventricle, curving over it and marking the inferior border of the cardiac silhouette in the normal posteroanterior view of a normal chest X-ray examination. It is delimited by the annulus of the tricuspid valve and by the pulmonary valve. Compared to its left counterpart, bearing a concentric ellipsoidal shape, the right ventricle has a rather complex shape, mostly pyramidal, with a triangular shape when viewed from the front, and a crescent-like cavity in cross section view [11]. Its muscular mass is only one sixth of that of the left ventricle, while they are held together by spiraling muscle bundles encircling them to form a single unit [12]. Deeper from these superficial circular fibers, there are longitudinal fibers which run from the apex to the base of the heart and shorten to become the major contributor of RV contraction, along with the inward motion of the RV free wall and the traction exerted by the LV contraction.

The RV has a thinner free wall (3–4 mm in end-diastole), operates at volumes slightly greater than the LV, and has greater chamber distensibility [13]. The interventricular septum is thicker

and accounts for a significant part of RV systolic function [14]. It normally remains concave toward the LV throughout the whole cardiac cycle. The thin-walled ventricle is designed to accommodate the entire systemic venous return and further pump it, for gas exchange, into the pulmonary circulation, a high-flow low-pressure system [15]. It thus ejects the same stroke volume as the LV but against a lower resistance, thus the necessary stroke work is decreased to a 1/6 of that of the LV [14]. With a greater end-diastolic volume than the one of the LV, and with a similar stroke volume, RV ejection fraction is slightly less than that of the LV. In the case of wide flow fluctuations, the lung adapts by recruiting previously nonperfused vessels from its superior portions, and by distention in the rest of its capillary bed, while the highly complaint RV dilates, working together to maintain low-pressures even with large changes in RV output [4]. As RV afterload is low under normal resting conditions, blood flows from the RV into the pulmonary circulation during systole and early diastole, leading to the absence of isovolumetric relaxation [16]. The RV cannot easily handle large or rapid increases in afterload. There are, nevertheless, mechanisms through which it can adapt its systolic function to preserve ventriculo-arterial coupling and preservation of flow output. In the case of an acute rise in pulmonary artery pressure (PAP), the RV increases its systolic force both through a dimensional beat-to-beat adaptation (Starling's law), and over the first 5–10 min through the slow force response (Anrep's Law) which leads to increased myocardial contractility [17]. When adaptation mechanisms are overwhelmed, in case of either volume overload or pressure overload, RV dilates and dysfunction occurs, eventually leading to decreased cardiac output and systemic congestion. In the case of chronically evolving increased afterload conditions, i.e. pulmonary hypertension, the RV adapts by progressive hypertrophy, a response which allows the maintenance of cardiac output over time, up to the point of end-stage disease when dilation occurs along with the same decreased cardiac output and systemic congestion as described above [18].

22.2 Pathophysiology of Pulmonary Hypertension in Chronic Lung Disease

In the setting of diffuse lung diseases or other conditions causing hypoxemia, pre-capillary pulmonary hypertension develops through a series of mechanisms which will further be detailed, and is classified as Group 3 pulmonary hypertension according to the World Health Organization updated classification.

This group comprises several pathologies—chronic obstructive pulmonary disease (COPD), interstitial lung disease (ILD), other pulmonary diseases with mixed restrictive and obstructive pattern (i.e. combined pulmonary fibrosis and emphysema), sleep-disordered breathing, alveolar hypoventilation disorders, chronic exposure to high altitude, developmental lung diseases [10]. However, the mechanisms leading to PH and secondary RV dysfunction have been mostly investigated in COPD patients and individuals subjected to high altitudes. The mechanism of PH in patients with interstitial lung fibrosis (ILF) or sleep disordered breathing (SDB) is presumed to generally share the same major mechanisms, especially considering that in many cases such diseases overlap with COPD. Currently, the strongest evidence points towards hypoxic pulmonary vasoconstriction (HPV) and consequent remodeling of the lung vascular bed as the leading etiologies in Group 3 PH. However, more data has accumulated to sustain that other disease-specific mechanisms may likely be involved in addition to those, but, eventually, all these concert together leading to irreversible arterial narrowing.

The idea that chronic hypoxia is necessary and sufficient alone to induce both rapid and significant changes in human pulmonary arteries is fairly supported by a 30 years old study "Operation Everest II" which simulated a 40 days climb on Mount Everest—a gradual decompression to the Everest summit equivalent. Healthy volunteers showed increased PAPs on right heart catheterization (RHC) at rest and on exercise, compared to those obtained in response to acute hypoxia before "the climb". The lack of

vasodilator response to acute administration of 100% oxygen further pointed to an already occurring structural remodeling in the vascular bed [19].

As described below, mediators derived from the pulmonary vascular endothelium act as either brakes in the setting of PH (i.e. nitric oxide, prostacyclin) or as facilitators (endothelin-1). They have an obviously significant physiological effect on hypoxia-induced vasoconstriction without, however, having an effect on the initiation of the primary response. It has remained somewhat controversial whether the endothelium is necessary for HPV to occur, as there are fairly old studies evaluating HPV after endothelial removal showing both the abolishment [20] and the enhancement of the HPV response [21]. Its role in modulation is nevertheless well established. So far, most of research has been carried out mostly on animals, with much less evidence in humans, which may cast some doubt on the applicability of some of those findings in clinical practice.

22.2.1 Initiation of Hypoxia-Induced Pulmonary Vasoconstriction

It appears that HPV is the primary mechanism to elevate pulmonary vascular resistance (PVR), and thus PAP, in hypoxic conditions. Following this, other pathways—activation of pressure-independent hypoxia-sensitive inflammatory and proliferative pathways, may contribute to sustained PVR elevation and vascular remodeling [2, 3]. The latter has an early onset, a few hours apart from the initiating hypoxic event, with the increased gene transcription of collagen and growth factors [22].

Under normal conditions, HPV occurs as a physiological process, at different degrees and at different sites, in order to optimize ventilation-perfusion matching throughout the entire lung parenchyma and to optimize gas exchange [23]. This vasoconstriction by the pulmonary vasculature is a reflex contraction of vascular smooth muscle as a response to a decreased regional partial pressure of oxygen in a rapid breath-to-breath manner [24]. This hemodynamic feature is a fundamental physiological difference from the systemic circulation, which reacts to hypoxemia through vasodilation. In the isolated, buffer-perfused lung, HPV starts at a partial pressure of oxygen <100 mmHg [24, 25], and its effect is the regional redistribution of blood flow from poorly-ventilated lung regions to well-ventilated ones, thus leading to an increase in overall efficiency of gas exchange. When occurring in response to environmental hypoxia, HPV is global, but, in clinical practice, may be associated more frequently with localized ventilation-perfusion disturbances (atelectasis, pneumonia).

There is a series of factors influencing HPV: age, as HPV is more intensified in fetal and neonatal circulations, serum pH and presence of hypercapnia (possibly augmenting HPV, but effects are variable among species), temperature, and even iron availability as described further on [26].

HPV involves several interacting mechanisms, which differ in the case of an acute immediate reaction versus a more sustained one. The effector cell for this phenomenon is the pulmonary artery smooth muscle cell (PASMC). This is located along the entire pulmonary arterial bed, from the large arteries to the small arterioles [27]. The sensor for hypoxia lies within the PASMC mitochondria [28, 29]. The major oxygen-sensing mechanism is the hypoxia-inducible factor pathway [30]. There has been controversy on whether hypoxia leads to an increase or fall in ROS/hydrogen peroxide levels. Studies have found that hypoxia is associated with high ROS levels [31, 32], but they are in disagreement with findings showing it be a reduced stated with low ROS levels [33, 34]. There is agreement, however, that the mitochondrial redox signal involving a coordinated response from voltage- and redox-sensitive K and Ca channels triggers the initiation of HPV [34].

The HPV response comes in two phases. Acute hypoxia is followed by a rapid (in a few seconds), transient vasoconstriction and secondary increase in pulmonary artery pressure, lasting for up to 10–15 min, followed by a slower developing, but sustained vasoconstriction lasting as

long as hypoxia is present [35, 36]. In case of moderate sustained hypoxia (pO2 30–50 mmHg, 30–60 min), this second phase begins and continues to raise PVR, reaching a peak at 2 h. Furthermore, if this second phase is triggered, the return to baseline vascular tone once normoxia is reached does not occur immediately [36]. In case acute hypoxia occurs on top of several hours of sustained hypoxia, the vascular response is considerably enhanced [37].

The underlying mechanisms of the two phases share a common pathway—contraction occurs when intracellular calcium concentration is increased by the hypoxic induced inhibition of voltage-gated potassium channel α subunits of PASMCs [38], which leads to membrane depolarization and: (1) calcium influx through L-type calcium channels; (2) release of calcium from the sarcoplasmic reticulum with further influx of calcium through store-operated calcium channels, receptor-operated calcium channels and transient receptor potential channel 6; (3) increased sensitivity of actin/myosin to any particular level of calcium, mediated by increased activity of Rho kinase [34]; but they also differ, in that the second (sustained) phase is dependent on RhoA/Rho kinase mediated Ca sensitization [35].

22.2.2 Modulation of Hypoxia-Induced Pulmonary Vasoconstriction

Modulation refers to processes that influence the evolution of the primary mechanism but are not crucial to its initiation or cessation [23]. Both intrinsic and extrinsic mechanisms balance each other in their alteration of the initial process.

22.2.2.1 Epigenetic Modulation of Hypoxia-Induced Pulmonary Vasoconstriction

Oxygen-sensing mechanisms are responsible for maintaining tissue homeostasis. In case of chronic hypoxia such mechanisms respond to alter metabolism in a manner that helps cells adapt to the low oxygen environment [30]. The primary oxygen-sensing mechanism within the cell is the hypoxia-inducible factor (HIF) pathway, and it plays a major role in hypoxia-induced pulmonary hypertension [39]. The cellular response to hypoxia is controlled by HIFs, DNA-binding transcription factors which alter the expression of over 1000 genes in the process of adaptation to hypoxia [40]. There are three members of the HIF family and each consists of an oxygen-sensitive α-subunit and a constitutively expressed β-subunit. In normoxic conditions HIFα is degraded through hydroxylation mediated by prolyl hydroxylases (PHD 1–3) in an oxygen, iron, 2-oxoglutarate, and ascorbate dependent activity. After hydroxylation, HIFα is bound by the von Hippel-Lindau (VHL) protein, which marks it for subsequent degradation. In hypoxic conditions, the prolyl hydroxylases 1–3 are lacking their oxygen substrate, cannot hydroxylate and degrade HIFα, and thus allow them to accumulate in the nucleus and activate their target genes [30]. The following steps in promoting tolerance to hypoxia include the metabolic shift from oxidative phosphorylation to glycolysis, promotion of angiogenesis by stimulating secretion of vascular endothelial growth factor (VEGF), increase in hematocrit by stimulation of erythropoietin production [41].

The role of HIFα subunits in promotion of PH has been suggested by both animal and human studies. First, in mouse models exposed to chronic hypoxia: (1) the heterozygous deficiency of HIF-1α or HIF-2α was associated with development of an attenuated PH with low increase in RV pressure and RV hypertrophy; (2) the presence of hetero- or homozygous mutations in stabilizing HIF-2α was associated with spontaneous development of PH [39]. In a study subjecting two strains of rats (one with known physiological attenuated vasoconstrictive response to acute hypoxia) to identical hypoxic hypobaric conditions, HIF-1 activity and HIF-mediated protein expression were elevated in the "resistant" strain [42].

Secondly, genetic studies carried on specific human populations adapted to high altitudes proved the role of HIF-2α in PH pathophysiology. A study, comparing indigenous highlanders of the Tibetan Plateau with lowland Han, carried

out genome-wide allelic differentiation scanning and found a genome-wide significant divergence across eight SNPs located near the gene encoding HIF-2α, probably a natural selection process in a population living at high altitudes over thousands of years, which leads to reduced erythropoiesis and attenuated PH at high altitudes [43]. Another genetic mechanism for Tibetan high-altitude adaptation was described in the high-frequency missense mutation of the EGLN1 gene encoding PHD2, once again explaining adaptive low hemoglobin levels in this population [44].

Another population in whom genetic studies brought significant insight into the role of HIFs in the physiopathology of PH is the Chuvash population with its endemic Chuvash polycythemia, a disease associating early onset severe PH, dramatically increased erythropoietin levels with secondary polycythemia and high VEGF and ET-1 expression as a result of HIFα metabolism alteration. It is caused by loss of function mutations in the von Hippel-Lindau protein responsible for HIF marking for degradation [45].

In COPD patients HIF-1α levels were found to be elevated in serum and lung tissue, and they were positively correlated with the severity of airflow limitation [46]. Cigarette smoking, the major risk factor for the development of COPD, involved in lung cellular stress and small airway remodeling, was found to induce concentration- and time-dependent accumulation of HIF-1α even under non-hypoxic conditions [47].

22.2.2.2 Endothelium Derived Modulation

Similarly to other locations, the endothelium is responsible for the paracrine modulation of smooth muscle contraction as it generates several vasoactive mediators acting on smooth muscle cells, balancing vasoconstriction with vasodilation to establish the low basal vascular tone of the pulmonary circulation, affecting contraction, migration and cell proliferation. Endothelial dysfunction has been described in all forms of pulmonary hypertension and eventually can alter vascular remodeling in its interaction with fibroblasts, coagulation factors, and the subsequent inflammatory process [48].

In healthy individuals, pulmonary vascular tone is the result of interaction between several vasoconstrictors (thromboxane A2, endothelin-1, serotonin) and vasodilators (nitric oxide, prostacyclin) [49]. The normal lung endothelium is different in ultrastructure and function from systemic endothelium, and has a significant heterogeneity itself [50]. Endothelial cells in pulmonary vessels are the first to sense hypoxic stress and react through the secretion of vasoactive mediators.

Nitric oxide is a locally produced potent vasodilator that inhibits smooth muscle tone, proliferation and migration. It is found in the lungs in all its three isoforms, and its high concentration in the upper and lower airways also affect pulmonary vascular tone [51]. Its role in vascular tone regulation has been evident in several animal studies, but there has been little evidence from human studies to support a significant contribution of hypoxic-inhibition of NO synthesis in PH [52]. Even if it has been considered that NO may contribute only marginally in the PA tone and PVR in conditions of normoxia, the inhibition of endothelial NO synthase (eNOS) potentiates HPV in preparations where flow is present, thus suggesting its relation to shear stress [52]. Furthermore, in patients with COPD, eNOS expression is downregulated and eNOS activation is inhibited, mechanisms which are thought to underlie the reduction in NO in these patients [53].

Prostacyclin (PGI_2) is a naturally occurring prostaglandin synthetized from cyclooxygenase via the arachidonic pathway in the vascular endothelium. Along with NO, PCI2 inhibits platelet proliferation and aggregation [54]. It has a lesser role in vasodilation in normoxia, and rather protects against hypoxia-induced vasoconstriction [48, 54]. Its low levels in patients with PH explain its role in the modulation of HPV. The enzyme responsible for PGI2 production, prostacyclin synthase, is deficient in the pulmonary endothelium of patients with severe PH, and was found to be markedly diminished in patients with COPD [55].

Its role in pathogenesis is most evident from its clinical use in severe and deteriorating PH, however this is mostly limited to Group 1 PH.

Thromboxane A2 shares the same production pathway as PGI_2 and similar vasoconstrictive effects. In primary PH, it has an increased production [56] and an elevated expression of receptors [57], which suggested initially a possibility for the development of a novel therapeutic target. However, studies using thromboxane A2 inhibitor have not been, so far, conclusive [58].

Endothelin-1 (ET-1), is a potent vasoconstrictor peptide widely distributed in the human endothelium. Its expression is elevated in PH both in animal and human studies [59–61]. Its effects are mediated through two types of receptors: ETA and ETB. It leads to vasoconstriction when acting on ETA and ETB receptors on smooth muscle cells, and vasodilation when acting on ETB receptors on endothelial cells to release NO and prostanoids, thus having a significant, but nonspecific, potentiating effect on HPV [52]. It has proven its role by the very effective clinical use in Group 1 PH, beneficial in Group 4 and 5, although rather detrimental in Group 2 and 3 PH.

Serotonin, a neuronal vasoconstriction mediator, promotes smooth muscle cell proliferation, PA vasoconstriction and local formation of microthrombosis [62]. In SMC it generates vasoconstriction by activating mitogen-activated protein kinase and Rho-kinases and enhancing the formation of serotonin dependent reactive oxygen species. It represents the substrate on which anorexigenics act to induce PH [62]. In patients with PH, several mechanisms in the serotonin pathway have been described to explain its role in vasoconstriction: (1) hyperactivity of SERT (serotonin transporter protein); (2) hyperexpression of the tryptophan hydroxylase 1 (TPH1) gene responsible for serotonin synthesis; (3) increased serotonin plasma concentrations; (4) increased production from endothelial cells, or (5) abnormal storage in platelets [49].

The Vascular Endothelial Growth Factor is a protein signaling angio- and vasculogenesis, processes through which it plays an important role in promoting survival in low-oxygen conditions [30]. In PH, both endothelial cells and platelets express high levels of VEGF. Its blockade results in PH, while its overexpression was shown to be protective against the disease [63, 64], an effect which may be mediated through the release of NO and PGI2 in a similar way as in the aortic endothelium.

22.2.2.3 Other Mechanisms of Hypoxia-Induced Pulmonary Vasoconstriction Modulation

There is an increase in pulmonary vascular pressure seen when hematocrit levels rise with altitude as a result mainly of higher blood viscosity. There has been no evidence of significant deformability changes influencing HPV. There are however erythrocyte-mediated PVR changes which balance vascular tone: (1) endothelial cell NO scavenging by oxyhemoglobin and ROS generation by hypoxic erythrocytes, thus enhancing vasoconstriction versus (2) NO generation, either directly by eNOS expressed on erythrocytes, or via hemoglobin desaturation, which favors vasodilation [40].

Neuromodulation of HPV is carried out through both sympathetic and parasympathetic fibers which act together to alter vascular tone. The alpha-1 adrenergic stimulation by norepinephrine is opposed by the release of neuropeptide Y and vasoactive intestinal peptide, and by the NO-dependent parasympathetic innervation. The neuromodulatory effect is influenced by signals from peripheral chemoreceptors (loss of such input leading to increased HPV), and by input via the vagus nerve (vagotomy reduces HPV) [40]. There has been discrepancy on the actual influence of neurohumoral component of HPV, but this mediation has been less studied so far.

There are individuals with an increased susceptibility to pulmonary hypertension or high altitude pulmonary edema in whom the HPV response is more evident [40]. Serum pH and presence of hypo or hypercapnia also modulate HPV, however studies have had conflicting results [65].

22.2.3 Role of Hypoxia-Induced Pulmonary Vasoconstriction in Respiratory Disease and Clinical Significance

The undebated relevance of HPV in clinical practice is in thoracic surgery patients receiving single-lung anesthesia when induction of hypoxia in the target lung (non-ventilated) leads to diminished perfusion, thus minimizing shunt and systemic hypoxemia, and excessive bleeding [66].

The role of HPV in clinical practice is to optimize systemic oxygenation by reducing ventilation-perfusion mismatch and shunting. In the acute setting of atelectasis or pneumonia or other acute lung injury its protective effect is beneficial and HPV remits once the pathogenic state resolves.

In the case of chronic respiratory disease states, the role of HPV is emphasized by the response to oxygen therapy. In stable asthma patients or status asthmaticus requiring mechanical ventilation, and in COPD patients, breathing 100% oxygen worsens matching and increases shunt [26]. In COPD patients the inhibition of HPV by a calcium channel blocker causes oxygenation deterioration [23]. This proves the dependency of COPD patients on HPV to ensure adequate matching. When high levels of inspired oxygen are administered, HPV in poor ventilated regions decreases, shunt is increased, and this may further lead to an increase in arterial partial pressure of CO2, especially if the patient is not awake to compensate by increasing ventilation [26]. Despite all this, long-term (>15 h/day) oxygen therapy improves survival and pulmonary hemodynamics in COPD patients with severe resting chronic hypoxemia, but not in those with stable COPD and resting or exercise-induced moderate arterial oxygen desaturation [67].

Group 3 PH includes however a diversity of diseases and it appears that the case is different for fibrotic lung diseases. Several studies have proven that there is no significant vasodilator response, or difference in matching, with the administration of 100% oxygen, and furthermore, there is no improvement in survival with oxygen therapy, thus showing less support for the contribution of HPV in PH in these pathological states [40].

As described previously, endothelium-derived mediators of HPV response have been investigated in all spectrum of PH, including in that secondary to chronic lung disease. Up to this point, evidence points toward a more significant vasoconstrictive pattern of effect and the use of such findings has been explored, as most mediators have become treatment targets in PH during the past decades. Unfortunately, their use in Group 3 PH has been proven as either lacking benefit, or, in fact, detrimental.

22.2.4 Endothelial Dysfunction: Inflammatory Changes and Vascular Remodeling

In chronic lung diseases, such as COPD or asthma, which are characterized by a significant inflammatory state, the endothelium is the medium through which inflammatory cells migrate to cause cell damage. Endothelial dysfunction appears to develop early in the disease process as it was reported being already present in the pulmonary arteries from patients with mild COPD [68]. Endothelial dysfunction is associated with severity of COPD, is related to forced expiratory volume in one second, and to clinical outcomes and prognosis [69].

The past decades have brought insight into the major role endothelial dysfunction plays in the pulmonary circulation compromise and alteration, mainly by shifting the balance towards more cell growth and proliferation, vasoconstriction and platelet adhesion, with intensive clustering of inflammatory cells in perivascular spaces [70].

Endothelial apoptosis has been proposed as the primary mechanism leading to emphysema. Studies in COPD patients have investigated the underlying processes and it was found that VEGF secretion, Cystic Fibrosis Transmembrane Regulator, and alpha-1 antitrypsin deficiency may lead to endothelial cell death induced emphysema [69].

Transendothelial migration, or diapedesis, refers to the process by which inflammatory cells

pass through the endothelial layer to reach the target tissue at the site of inflammation in an orchestrated dialogue between leukocytes and endothelial cells using signaling molecules [71]. In the case of chronic diseases with an important inflammatory component, such as COPD and asthma, findings have shown that diapedesis is upregulated, along with an increase in levels of many of the endothelium adhesion molecules, which suggests an important role in the development of inflammation, remodeling, and pathogenesis of airway obstruction. As both clinical settings associate endothelial dysfunction, this probably augments the expression of cell adhesion molecules [72].

In a study carried out by Oelsner et al. on seven cohorts, gathering little over 26,000 patients with COPD, serum levels of intercellular adhesion molecule 1 (ICAM-1), ET-1 and P-selectin were inversely related to lung function [73]. Among the 1,865 participants in the Multi-Ethnic Study of Atherosclerosis, higher levels of serum ICAM-1 were independently associated with progression of emphysema [74]. An older comparative study between COPD patients and controls found significantly increased levels of circulating ICAM-1 in the serum and in the bronchial lavage of COPD patients, along with higher levels of serum circulating E-selectin. The latter also correlated significantly with the forced expiratory volume in one second [75].

Levels of circulating adhesion molecules are increased in both allergic and non-allergic asthma patients, proving the activation of endothelial cells [76]. ICAM-1 mediated inflammation is present in asthma patients and its use as a therapeutic target has been proposed for controlling asthma [77]. Leucocyte infiltration to the site of inflammation was shown to be partially regulated by the expression of ICAM-1, vascular cell adhesion molecule 1 (VCAM-1), and E-selectin in a study employing human bronchial tissue from patients undergoing lung cancer surgery which had been previously passively sensitized with serum from atopic asthma patients [78].

Much less investigation has been carried out in patients with other pulmonary diseases to search for endothelial dysfunction. Scarce data shows that early inflammatory markers and signal molecules, and cytokines may be increased and involved in the pathophysiology of other respiratory diseases such as idiopathic pulmonary fibrosis [79], obstructive sleep apnea (OSA) [80], combined pulmonary fibrosis and emphysema (CPFE) [81].

The breakthrough discovery of the HIF (hypoxia-induced factor) family of proteins has closed the gap between the two major mechanisms leading to hypoxia-induced pulmonary hypertension: hypoxia-induced vasoconstriction, as an initial local response of lung vasculature to a physical stimuli, and vascular remodeling, as long term structural and functional vascular changes with variable degrees of reversibility. As hypoxia occurs, HIF proteins target and activate genes involved both in all levels of modulation of vasoconstriction, and in the inflammatory changes leading to vascular remodeling [30].

Under chronic hypoxic conditions, smooth muscle cells go through a process of phenotypic modulation to differentiate from a contractile to a synthetic phenotype [39]. Changes occur at all levels of the vascular bed, but animal models have shown that the degree and modulation of change differs among species. In the large PAs, the media and adventitia become thickened, as matrix proteins (collagen and elastin) markedly accumulate secondary to the activation of intracellular signaling pathways in the now proliferative-prone smooth muscle cell populations [82]. These cells become hypertrophied, the main mechanism involved in medial thickening in humans [70]. The primary site of hypoxic pulmonary vasoconstriction is however at the level of the distal muscular pulmonary arteries. The results again differ according to the studied species, but in human SMC greater proliferative responses to mitogens were reported. In nonmuscular alveolar wall vessels there is a most characteristic "muscularization" of vascular segments which lack, under normal conditions, a muscular component, thus deeming them structurally resistant. Cells become hypertrophied, hyperplasic, and loose contractility and migration, increasing wall thickness [82]. A variable degree of destruction of vascular bed is present in emphysematous

and fibrotic areas [49]. These changes have been described even at the early stage of COPD, and in non-COPD smokers [83]. In end-stage COPD they were shown to correlate with the severity of PH, and in these cases even plexiform lesions were observed—the hallmark of severe PH [84].

In the intricate play of endothelial dysfunction in pulmonary hypertension, endothelial progenitor cells (EPCs) were shown to play a role in vasculogenesis, vascular repair and regeneration by their capacity to infiltrate the vascular wall and to secrete vasoactive factors [85]. EPCs mobilize from the bone marrow, circulate in the blood stream and have the ability to home on sites of vascular injury and restore endothelial integrity. Research on EPCs in PH has so far proved their role in attenuating primary hypertension and has reached as far as investigating tolerability and efficacy of eNOS gene-enhanced progenitor cell therapy in what was a first in man phase 1 clinical trial for PAH patients [86]. In hypoxia-induced PH, EPCs were shown to contribute to pulmonary vessel remodeling, however chronic hypoxia was reported to significantly alter their phenotype, impairing their capacity to migrate, adhere and augment neovascularization in injured sites[87].

22.2.5 The Altered Vascular Structure: From Bad to Worse, or to Adaptation

From studies of pulmonary artery hypertension in congenital heart disease findings have pointed to the role of increased hemodynamic shear stress as a modulator of vascular remodeling and PH. In the development of PH as a consequence of hypoxia and inflammatory vascular remodeling, the already narrowed pulmonary circulation, must accommodate the same blood volume which increases vessel wall shear stress, which will augment resistance and PH [88].

Regardless of the initial stimuli, once the structural changes specific to PH have developed they further progress to remodeling, described above, and rarefaction. The latter refers to the reduction in numbers of blood vessels in a similar way as it occurs in systemic arterial hypertension [89], and it has been long described in both animal and human models of pulmonary hypertension. As opposed to the systemic circulation, initial studies of the pulmonary vascular bed did not find significant evidence of a counteraction to this phenomenon by increased angiogenesis, and thus, it has been hypothesized that rarefaction plays a major role in the structural development of hypoxic PH [88]. More recently though, the employment of new stereological techniques in animal studies successfully identified hypoxia-induced angiogenesis in the adult pulmonary circulation as an important adaptation mechanism [90] and showed that inhibitors of angiogenesis aggravate PH, further supporting the concept of hypoxic induced new vessel formation in the lung [91]. The role of such findings in human models remains less explored.

22.2.6 Other Disease-Specific Mechanisms

22.2.6.1 Obstructive Sleep Apnea

During episodes of hypopnea or apnea, the decrease in systemic oxygenation triggers the adaptive mechanisms of hypoxia-induced vasoconstriction, which makes OSA share the same major mechanisms of PH development with other hypoxemic disorders. However, considering the hypoxic events develop mostly during sleep and their episodic occurrence, a causative link between such events and the persistent diurnal increase of PAP has been questioned [92]. There is proof from animal studies that short, but recurring, hypoxemia over a few weeks is enough to determine muscularization of distal pulmonary arteries, pulmonary arterial remodeling and RV hypertrophy [93]. Obviously, the same cannot be blindly ascertained in humans, and the fact that OSA is frequently associated with obesity and other chronic or heart disorders makes "pure" OSA studies difficult to perform. However, some evidence has built up to show that sleep related hypoxemic events are the most probable drive of PH in this patient category, and that CPAP therapy has a favorable effect on pulmonary hemodynamics [92]. The characteristic mechanisms of

OSA induced diurnal persistent PH described so far are: (1) repeated hypoxia induced vasoconstriction; (2) wild swings in intrathoracic pressure during sleep; (3) sympathetic overstimulation during apnea/hypopnea episodes leading to systemic hypertension, and cardiac arrhythmias which further result in left heart disease and secondary PH (Group 2). Considering systemic arterial hypertension is more prevalent in OSA that pulmonary hypertension, this latter mechanism might be "more" responsible for the PH found in these patients than other mechanisms [74, 93].

All pathways eventually cause vascular remodeling, through classically described mechanisms, and pulmonary hypertension, with usually mild increases in PA pressure in the range of 20–30 mmHg.

22.2.6.2 Interstitial Lung Disease

In addition to the two main processes involved in the development of PH in chronic lung diseases (HPV and vascular remodeling), there are few pathophysiological factors unique to interstitial lung diseases. Fibrosis in the vicinity of pulmonary beds may traction and disrupt vessels, reducing blood distribution volume and increasing pressure. The heterogeneity of macro and microalterations may also affect the vasculature by its proximity and involvement of the bronchoalveolar bundles [94]. In PH associated with diffuse scleroderma or other connective tissue disorders pathophysiological mechanisms include inflammatory vascular remodeling, antiendothelial antibodies and other autoimmune vascular injury and arteritis, thromboembolic disease due to the hypercoagulable state, and associated left heart disease [95]. Furthermore, in such diseases with overactive inflammatory responses, one may hypothesize at the molecular alterations that cytokines have on cardiac function which could precede PH development but nevertheless induce RV dysfunction. In addition, the therapeutics of such disorders (immunosuppressants, corticoids) are known to have cardiotoxic effects [96], and thus ILDs may associate RV dysfunction without there being a causality relation between the two.

22.2.6.3 Combined Pulmonary Fibrosis and Emphysema

Combined pulmonary fibrosis and emphysema was first described by Wiggins et al. as high-resolution computer tomography evidence of co-existence of emphysema in the upper lobes and pulmonary fibrosis in the lower lobes [97]. The syndrome was individualized first by Cottin et al. in 2005 and was characterized in patients with abnormal spirometry, severe impairment of gas exchange, high prevalence of pulmonary hypertension, and poor survival [98]. The co-existence of emphysema and fibrosis dictates the pathophysiological mechanisms of PH in this case—both hypoxia induced vasoconstriction, and subsequent remodeling and fibrosis with destruction of vascular bed.

Eventually, the evolution of these processes and the subsequent development of all the above mentioned lesions lead to the narrowing and obliteration of vessel lumen in a setting of increased vascular tone. The initially low-resistance low-flow system of the pulmonary vasculature now becomes an increased resistance system forcing an elevated afterload on the right ventricle, which now struggles to defeat the high pressures by hypertrophy and eventually dilation and failure.

22.3 Effect of Chronic Lung Disease on Heart Structure and Function

With sustained, hours to days, hypoxic exposure, pulmonary elasticity decreases, pulmonary arterial pressure increases, tachycardia ensues, all leading to an increased workload on the right ventricle.

Hypoxic vasoconstriction leading to alterations in pulmonary micro- and macrovasculature, which are both observed in chronic lung disease patients, leads to an increase in pulmonary vascular resistance, the *sine qua non* of Group 3 PH. Consequently, this increase in right ventricular afterload leads to right ventricular remodeling, namely RV wall hypertrophy and RV dilatation, which eventually end in RV functional

deterioration. The clinical depiction of this syndrome is known as cor pulmonale. As evident from its name, this is a clinical syndrome in which a primarily pulmonary disease leads to alterations of the structure and function of the right heart. This definition excludes the clinical setting in which the RV anomaly is generated by a primarily left-sided heart disease [99]. Therefore all Groups of PH may lead to a form of another of this syndrome, except for Group 2. Cor pulmonale can present either as an acute development, a chronic progression of disease, or an acute decompensation of the chronic syndrome. Currently, however, there is no widely accepted definition of this syndrome (apart from the one settled upon over 50 years ago by the WHO [100]), for which reason its use has been restricted mainly to the latter two clinical presentations. Acute cor pulmonale, preferably known as acute RV failure, is characterized by RV dilation and dysfunction, with a frequently rapid inextricable evolution towards cardiogenic shock, and it can be the consequence of a variety of disorders [18]. Symptoms and clinical signs are similar to an acute decompensation of a previously chronic cor pulmonale, which occurs when the compensatory mechanisms (RV hypertrophy and dilation) either fail, or are overwhelmed by abrupt changes in hemodynamics (i.e. COPD exacerbations, pulmonary embolism, exercise).

In opposition, chronic cor pulmonale or chronic RV failure as seen in Group 3 PH, generally has a more benign evolution as a consequence of slow increases in mean PAP and the mild to moderate PH seen in these patients, in whom it rarely exceeds 35–40 mmHg. Such levels are considered "out of proportion" PH and suggest an additional component for the etiology of PH in a chronic pulmonary disease patient (left heart disease, sleep apnea syndrome) [101]. With 1–3 mmHg/year increments in mean PAP, the RV has time to compensate and hypertrophy, the foremost effect of chronic pulmonary disease, while maintaining myocardial systolic function and possibly associating an impaired diastolic function [102]. In fact, the increase of mean resting PAP over 25mmHg already evokes the destruction of over half the pulmonary vascular bed [103]. Therefore, the clinical syndrome of cor pulmonale speaks of a rather long-lasting and severe alteration of the lung vasculature.

Besides the pressure challenge exerted by hypoxic PH on the RV, the significant changes in intrathoracic pressure in the setting of chronic pulmonary disease may add to the altering of size and function of both ventricles. In COPD and emphysema, hyperinflation increases pressure on the heart, and smaller chamber sizes were reported in COPD patients, in whom the increase in severity was associated with decrease in chamber size (the association was stronger between degree of hyperinflation and size than airway obstruction or diffusion capacity) [104]. Altered lung mechanics leads to impaired LV filling, cardiac output and stroke volume, which may decrease RV perfusion pressure and further worsen RV function [105].

22.3.1 From Pulmonary Hypertension to Right Ventricle Dysfunction

The first response of the RV to chronic steady increases in pressure is hypertrophy, characterized by an increase in ventricular mass and decrease of internal chamber radius, assuming a more rounded shape [106]. This adaptive hypertrophy translates at the cardiomyocyte level into increased protein synthesis, cell size and cytoskeletal remodeling, as these cells are fully differentiated and their only means to adapt is by cell growth and fetal program re-initiation. A crucial role in this process is that of integrins and focal adhesion complexes which couple mechanical stress with biochemical pathways. They function as mechanotransducers; tortional stress induces structural alterations in extracellular matrix proteins which makes them recognizable by integrins, which will now connect to them through their extracellular domain, and to the cytoskeleton through their intracellular domain, this way further inducing intracellular signaling and protein expression to stimulate cell growth and survival [107]. In parallel, both the extracellular matrix and the supporting vessels

have increased synthesis. All these structures, the cardiomyocytes with their cytoskeleton and contractile apparatus, the extracellular matrix and their supportive vasculature, influence each other in the pathobiology of diastolic and systolic function impairment [106].

Further there is significant variability in the development of greater or lesser hypertrophy, evolution towards RV failure, and the timing of such events in the affected population. There are disease specifics, such as the slow progression of increase PA pressures in chronic lung disease, and the rare development of RV failure in such patients [102], which may account for such phenotypical diversity. In other clinical scenarios, polymorphisms in specific enzymes have supported a concept of a genetically controlled RV hypertrophy [108].

The transition from hypertrophy to failure in the case of the RV is far from having a sound and clear description of its underlying pathophysiological mechanisms. So far we know that extrapolating knowledge from the processes described in the left ventricle is not warranted, considering their differences in, amongst others, embryologic origin, morphology and response to stress [109]. The road from hypertrophy to failure is designed by a series of epigenetic, inflammatory and metabolic mechanisms, the details of which have been only more recently investigated by translational studies. While the development of LV hypertrophy to counteract systemic hypertension is an adaptive phenomenon able to prolong time to symptoms with decades, the RV is less optimal in its adaptation, and, without treatment, the survival prognosis is far more severe. The recent review of Samson and Paulin gives an overview of current knowledge on these mechanisms [109]. The dysfunction of contractility has been explained as a result of α- and β-myosin heavy chain ratio alteration in cardiomyocytes as an adaptive mechanism to preserve energy. In addition, the role of thyroid disease has been proposed as a key regulator of contractility in the hypertrophied RV. A series of evidence is also building up to support the role of epigenetic mechanisms such as DNA methylation, modification of histone proteins and microRNAs to explain the suboptimal response to stress-induced hypertrophy in the RV. Inflammation further takes its toll, as the development of RV failure is predominant in those with a higher inflammatory burden (i.e. scleroderma), and cytokines such as tumor necrosis factor-α, interleukin-6 and interleukin-1 were shown to mediate and promote fibrosis, cardiac hypertrophy and failure. The evolution from normal size and function to hypertrophy seems to go through a metabolic switch from lipolysis to predominant glycolysis in the adaptive processes of both ventricles. A recent hypothesis suggests that such an adaptive switch becomes reversed when the progression towards RV failure occurs. Along with this, going from hypertrophy to failure appears to be associated with significant loss of mitochondria, with the remaining displaying abnormal structure and functionality. In addition, the growth in muscular mass seems to be accompanied by either a suppressed or inadequate neovascularization, and becomes therefore more prone to failure. This pathobiology has been described mostly in animal models of induced pulmonary arterial hypertension, and the degree to which all forms of PH in humans adhere to these mechanisms is unknown.

In pulmonary disease, the progression from RV hypertrophy to failure is the primary complication of RV dysfunction, but this is a rather rare occurrence. It is more frequently seen in an acute exacerbation of lung disease, characterized by additional ventilation-perfusion mismatch and further decrease in systemic oxygenation, all these putting additional pressure on an already stressed RV which may now fail, if it had not done so in a clinically obvious manner before. When PH is increased to "out of proportion" levels other etiologies of both PH and RV failure may be considered, most frequently left heart disease [102]. In a cohort of the National Emphysema Treatment Trial only 5% of severe emphysema patients had PAP >35 mmHg [110], while a cohort study on COPD patients showed that only 2.7% had severe PH, and in more than half of cases a different etiology than COPD was demonstrated [111].

Nevertheless, the development of RV failure is associated with a much worse prognosis. And

this is much more relevant if we consider the findings reported by Hilde et al. who showed that alterations in RV structure, size, and function are present in COPD patients even in the absence of resting PH and are actually late markers of pulmonary vasculature disease. The study evaluated 98 patients with COPD stages II to IV, and divided them in two groups—with PH, if mean PA pressure ≥25 mmHg on right heart catheterization, and without PH, otherwise, and performed thorough echocardiographic measurements of RV performance and structure. The results showed that RV systolic function, RV hypertrophy, and RV dilation were present in COPD patients even in the absence of PH [103]. This may support a concept of parallel synchronously mechanisms involving inflammation, endothelial dysfunction and metabolic shifts in both heart and lungs in an overlapping process of developing PH and RV disease. However, one must also consider that the absence of PH at rest does not exclude its presence in usual life conditions when the minimal or moderate exertion of daily living and the secondary desaturations during it or during sleep may be accompanied by temporary, but frequently recurring increases in PA pressure and therefore RV stress.

22.3.2 Prevalence and Characteristics of Pulmonary Hypertension and Right Ventricle Dysfunction Among Lung Disease Patients

Chronic lung diseases (CLD) associating Group 3 PH are COPD, interstitial lung disease, other pulmonary diseases with mixed restrictive and obstructive pattern as the more recently defined combined pulmonary fibrosis and emphysema, sleep-disordered breathing, and alveolar hypoventilation disorders. The prevalence of PH in CLD was reported at 13.8% in a series of ≥65 years old patients [112]. Among these, COPD is the most common cause of PH, probably due to its high prevalence in the general population [101].

22.3.2.1 Chronic Obstructive Pulmonary Disease

The actual prevalence of PH secondary to COPD is unknown; studies have reported extremely variable percentages in the range of 25–90% owing to the different population investigated—from stable less-severe COPD to those with severe emphysema which are candidates for lung resection [113]. Normal mean PAP is considered <20 mmHg at rest, and <30 mmHg during exercise; PH has been defined in different studies as either mean PA pressure >20 mmHg or >25 mmHg. Either way, Group 3 pH is mainly characterized by a mild-moderate increase in mean PA pressure, which rarely exceeds 35–40 mmHg, measurements carried out in stable patients, outside exacerbations when PAP may temporarily increase [101]. Actually, in these latter cases, such increases in PAP parallel worsening hypoxemia and hypercapnia, underlying the role of hypoxia induced vasoconstriction. As described previously, alterations in RV structure and function may precede the actual presence of PH that can be documented at rest, and this may be a consequence of several characteristics of PH in COPD patients which subjects them to frequently recurring episodes of increased pulmonary pressure: (1) exercise increases vascular pressure in CLD patients, but not in normal subjects; (2) COPD patients may overlap other CLD such as SDB or hypoventilation syndromes; (3) hypoventilation and perfusion mismatch during sleep in the absence of such comorbidities, usually during REM when muscle tone is diminished; (4) exacerbations of COPD [101]. RV hypertrophy has been reported in as much as 76% of advanced COPD patients at autopsy and can precede resting hypoxia. Probably as a consequence, it appears that RV myocardial contractility is generally preserved in COPD, thus systolic function is less frequently affected, but RV diastolic function may be more commonly impaired, a feature also present in healthy individuals under acute hypoxia [102].

22.3.2.2 Interstitial Lung Diseases

The prevalence of PH in interstitial ILD varies just as much as in COPD patients, and this

reflects mostly the heterogeneity of the pathologies comprised in this group (idiopathic pulmonary fibrosis, connective tissue diseases, pneumoconiosis). Reports have varied from 30 to 90% of ILD patients [113]. Data on RV disease associated with PH in ILD is scant. The most widely used diagnostic tool to evaluate the RV, transthoracic echocardiography, has significant limitations in such patients. Arcasoy et al. showed that the estimation of systolic PAP by echocardiography was inaccurate in 52% of patients with advanced lung disease, leading to over-diagnosis of PH [114].

22.3.2.3 Sleep-Disordered Breathing

Most research on sleep-disordered breathing and pulmonary hypertension has focused on obstructive sleep apnea, and PH has been described as mild to moderate [115]. Failure of the RV associated to OSA alone is a rare find, and the case is usually of RV dysfunction associating PH in a patient with OSA and other comorbidities, such as COPD, left heart disease or obesity [92]. In subjects of the Framingham Heart Study who were also part of the Sleep Heart Health Study, RV wall thickness was reported increased in those with SDB [116], but these findings have not been consistent across literature. Considering the frequent association of OSA with obesity, other chronic respiratory diseases, systemic hypertension, arrhythmias and left heart disease, it is difficult to pinpoint the exact etiology of right heart disease in these patients. "Pure" OSA has been investigated in small size studies including 12–220 patients, and in these cases the PH prevalence has ranged from 17 to 79% [92]. Nevertheless, the link between OSA, PH and RV failure can be, at least partially, tested through a therapeutic approach—CPAP therapy, and there have been studies showing a significant reduction in PAP after CPAP therapy. Many of them are fraught with limitations—small sample size, confounding factors such as underlying lung disease, obesity and hypoventilation disorders, lack of detailed etiology and right heart catheterization especially as a result of patients' low PAP in the first place. There has been inconsistency in their findings, but generally CPAP therapy has so far been proven to lower PAP and pulmonary circulation reactivity, thus supporting the link between SDB and, usually, mild PH [93, 115].

22.3.2.4 Combined Pulmonary Fibrosis and Emphysema

The prevalence of PH in CPFE patients was reported ranging from 28 to 47%, and it seems to occur more frequently in CPFE than in the case of COPD alone, or ILF alone, but shares the same pathophysiology and characteristics. As in the case of ILD, the accuracy of transthoracic echocardiography studies are limited by the presence of significant emphysema [117]. As a special feature of this disorder, in a recent retrospective analysis of patient characteristics, the prognosis of CPFE was shown to be significantly worse than that of IPF alone [118].

22.4 Diagnostic Evaluation of Pulmonary Hypertension and Right Ventricle Dysfunction in Chronic Lung Disease

Pulmonary hypertension does not equate RV dysfunction, although there is both a correlation and a causation relation between the two, depending on the clinical setting they occur in.

Pulmonary hypertension is defined as present when an increase in mean PAP ≥25 mmHg at rest is documented by right heart catheterization, considering normal mean PAP values are under 20 mmHg and mean PAP ranging from 20 to 25 mmHg has unclear clinical significance [119]. Only a small percentage of CLD patients associate PAP values >35 mmHg, and Seeger et al. have recently suggested defining severe PH in COPD/IPF/CPFE patients as having either mean PAP ≥35 mmHg, or mean PAP ≥25 mmHg with a low cardiac index < 2 l/min/m^2 [120]. In CLD patients the presence of PH is an important indicator of severe prognosis and it will most probably lead to RV dysfunction. One cannot consider and discuss the presence of either PH or RV dysfunction, taken together or alone, in the absence of proper

means to assess their parameters in a reliable and reproducible manner. Which leads to the non-invasive and invasive techniques of measuring PH and RV function in CLD patients, as detailed below.

22.4.1 Physical Examination

The diagnostic algorithm passes through the initial phase of physical examination. The presence of PH alone in a patient can hardly be suggested by clinical signs, in the absence of concomitant RV dysfunction. In an otherwise stable CLD patient, severe aggravating dyspnea during exercise or rapidly decreasing oxygen saturation may point to underlying PH, when such symptoms cannot be explained by the severity of the lung disease. In contrast, the clinical diagnosis of cor pulmonale is rather evident in a patient with systemic venous congestion and low cardiac output. The symptoms and clinical signs will evoke the diagnosis of RV failure without reliably disclosing its etiology, which can be suggested but not fully elucidated by patient medical history. Considering that in CLD patients PH progresses slowly over the years, the symptoms of RV failure will gradually follow. Most frequently, dyspnea occurs in the initial stages and it becomes more severe with the progression of RV failure. Bloating and early satiety follow hepatic venous congestion. Peripheral edema with ankle swelling and ascites may suggest RV failure in the absence of other causes (i.e. hypoalbuminemia, LF failure). It is uncommon in ILD patients and rarely develops in COPD patients without hypercapnia [102]. Fatigue and dizziness may signal low cardiac output. Significant clinical signs are an increased jugular venous pulse, an accentuated second pulmonary sound, and right ventricular gallop, to name a few, all suggestive of RV failure. However, the prominent jugular V wave, indicative of tricuspid regurgitation, can be hard to asses in patients with hyperinflation and widely variable intrathoracic pressures, and heart auscultation becomes more difficult on a hyperinflated chest or in the presence of rhales.

22.4.2 Non-Invasive Evaluation

Pulmonary functional testing such as spirometry, lung volumes and DLCO and assessment of exercise capacity (6 min walk test, cardiopulmonary exercise testing) do not bring information on RV function, but abnormal measurements on these tests have been associated with PH in ILD and COPD patients [102].

Serological testing in CLD is scarce. The most investigated biomarkers with a prognostic benefit are those suggesting RV failure—BNP and NT-proBNP, peptides released from myocytes in response to wall stress. They correlate with myocardial dysfunction in almost any cardiac disease, and are not specific for PH. In COPD patients, both BNP and NT-proBNP were shown to independently strongly predict long term mortality after acute exacerbations [121], increased length of in-hospital stay, and need for intensive care [122], and accurately reflect impact of an acute exacerbation on RV function [123]. Elevated BNP levels were shown to identify patients with clinically significant PH (PAP >35 mmHg) with a sensitivity of 85% and specificity of 88%, and to predict mortality independent from lung functional impairment and hypoxemia in multivariate analysis [124].

Electrocardiographic findings alone do not bring highly sensitive or highly specific information in CLD patients with RV dysfunction, and they are the same as described in other etiologies of both PH and RV dysfunction.

In opposition, the chest radiography, a hardly reliable test for degree of PH and RV dysfunction, in CLD can bring valuable information on the etiology of the disease as it remains an important tool in assessing lung disease (hyperinflation or parenchymal abnormalities) and skeletal disorders. In COPD patients, a high cardiothoracic index and a width of the right descending PA >16 mm were shown to correlate well with the presence of PH [99]. It cannot give any information on degree of severity of either PH or RV dysfunction.

Multidetector computer tomography (MDCT) scanning has been employed to asses RV structure and function and has been validated against

echocardiography and MRI studies [125]. In COPD patients mean RV mass and ejection fraction correlated with COPD severity as assessed by forced expiratory volume in one second [126, 127]. Pulmonary artery cross-section diameter was also shown to correlate well with PAP [102]. However, the use of MDCT to this end is limited due to the exposure to high dose radiation and iodinated contrast agents, but may become more useful in CLD patients who frequently have an indication for such testing as a consequence of their underlying respiratory disorder.

The standard method employed in clinical practice to evaluate RV function in CLD patients remains echocardiography. The CLD patient should undergo echocardiography when PH is suspected (enlarged pulmonary arteries on other imaging techniques—chest X ray, MDCT; clinical signs of RV dysfunction as exemplified above; severely abnormal functional testing as compared to the underlying respiratory disease). The anatomical complexity of the RV makes it difficult to be assessed even in the general population, and on the emphysematous chest of a CLD patient echocardiography loses ever more accuracy. To complement conventional studies, novel approaches such as real-time 3D assessment of RV ejection fraction, tissue Doppler imaging (TDI) velocities, and strain and strain rate have emerged during the past decade [103].

Conventional echocardiography will mostly reveal changes in echo parameters as in other forms of PH: increased RV wall thickness, increased RV diameter and decreased tricuspid annular plane systolic excursion to name some of the more reproducible parameters even in CLD patients. When using TDI and strain rate imaging, the disadvantage of geometric assumptions and endocardial border tracing, as in 2D imaging, can be overcome. These techniques have been more recently evaluated in COPD patients in association with pulmonary functional testing and have proven to correlate with RV dysfunction, and have a high sensitivity and specificity; in COPD patients strain rate imaging had high feasibility as it could be employed even in those with poor 2D imaging [128].

Isovolumetric acceleration and tricuspid annular systolic velocity by TDI have been proven to correlate well with RV failure in COPD patients, having a good interobserver and intraobserver reliability [129]. In a study carried out by Ozben et al. on 30 COPD patients during an acute exacerbation versus 30 controls, both isovolumetric acceleration and tricuspid annular systolic velocity by TDI were reported as reliable indices for the evaluation of RV function in COPD patients, with the more classical PAP actually showing the most accuracy, sensitivity, specificity, positive and negative predictive value compared to other echo parameters in predicting a COPD exacerbation. This underlines the importance of this more commonly measured index and vets its further use in such clinical conditions [130]. Echocardiographic markers of RV function in 87 CLD patients with moderate-severe decreases in predicted forced expiratory volume in one second were evaluated, and RV dimensions, RV area and Doppler indices all strongly associated with survival. The study reported that right ventricular end-diastolic diameter was the most significant variable in the multivariate model and independently predicted survival [131]. In ILD patients too, the echocardiography measured parameters RV systolic pressure, tricuspid annular plane systolic excursion, and RV fractional area change were proven to significantly correlate with outcome [132].

As echocardiography has its limitations, magnetic resonance imaging is the gold standard for the evaluation of right ventricle volumes and function. However, this is not routinely carried out in CLD patients. It also does not give information on lung parenchyma which makes its use in CLD even less frequent. Cardiac magnetic resonance is an accurate reproducible method but it has low availability as compared to even modern echocardiographic methods for estimation of RV function. Parameters derived from this technique, such as RV end-systolic volume and RV ejection fraction were more recently proven to correlate with mortality [132]. Nevertheless, currently, its use is limited to clinical studies and to those cases in which an echocardiographic study is indicated but cannot be performed with proper accuracy.

22.4.3 Invasive Hemodynamic Measurements

Currently, the gold standard evaluation for PH diagnosis is right heart catheterization, but not every CLD patient requires it and such testing cannot be carried out in all CLD patients mainly for ethical reasons [101]. As an invasive procedure it has its risks, and the lack of further diagnostic and therapeutic benefits do not overcome these risks, considering that most CLD patients have mild to moderate PH. Considering the practice from expert centers and in the absence of specific guidelines, in this Group 3 PH population right heart catheterization is generally considered beneficial and indicated if: (1) another etiology of PH is suspected, considering that such finding may improve outcomes and survival by benefiting from specific PH therapies; (2) severe PH is suspected giving prognostic information on transplant candidacy; (3) severe PH is suspected in those with low-quality echocardiography [113]. On right heart catheterization Group 3 PH is characterized by pre-capillary PH with mean PAP ≥25 mmHg and a pulmonary artery wedge pressure ≤15 mmHg [119].

22.5 Therapeutic Options

The mainstay in therapy of COPD is inhaled bronchodilators, anticholinergics and corticoids [67] which reduce inflammation, ameliorate obstruction and prevent exacerbations. In addition to these, there are several adjunct therapies such as phosphodiesterase-4 inhibitors and long-term antibiotics which were shown to reduce exacerbations. The effects of such medications are beneficial on respiratory mechanics which may therefore improve PAP. When reducing exacerbations they have an indirect effect on RV function, as it was shown before that with every exacerbation RV dysfunction progresses. On the contrary, there are no currently available therapies in ILD to significantly improve disease progression, and the data supporting corticoid use in these cases is scarce [102].

Long term oxygen therapy is recommended in COPD patients with severe, not moderate, resting chronic hypoxemia, as it improves survival [67]. Even though it initially aggravates ventilation-perfusion matching, long term use >15 h a day was shown to reduce RV afterload, and stabilize but not improve mean PAP, suggesting that it has no influence on the already fixed vascular remodeling [102].

Although it is widely used in ILD patients with chronic respiratory failure, long term oxygen therapy has not been proven to influence survival; in contrary, it may even have a deleterious effect considering hyperoxia-mediated oxidative injury may play a major role in the development of ILDs [102].

In OSA patients, both PAP and RV function were proven to modestly improve with the correction of hypoxemic events either by weight loss or uvulopalatopharyngoplasty [102]. Most importantly, long term nocturnal continuous positive airway pressure therapy (>3 months) was proven to significantly reduce PAP in several case series and cohorts, and more recently in a randomized sham-controlled study in whom RV systolic pressure decreased after 12 weeks of therapy [93].

Attempting to use the information gathered from pathophysiological studies on PH in CLD, therapeutic research has shifted its aim towards novel molecules in all groups of PH patients.

NO has entered the therapeutic arsenal. The NO effect in the COPD patient is supported by a trial conducted in 40 patients with PH secondary to COPD which showed that the “pulsed” inhalation of NO with oxygen caused a significant decrease in mean pulmonary artery pressure and pulmonary vascular resistance index while maintaining a good safety profile [133]. Currently, FDA approval has been given for its use only for hypoxic respiratory failure in the term and near-term neonates with evidence of PH, but its effectiveness on other clinical scenarios of PH is also being evaluated in several studies. Clinical investigation is ongoing but results have not yet been published in the treatment for bronchopulmonary dysplasia [134]. A Phase 2 trial is carried out in patients with difficult to treat PH associated with

idiopathic pulmonary fibrosis [135]. In the Phase II PHiano study [136] a NO delivery system is used in patients with PAH or PH secondary to idiopathic pulmonary fibrosis.

When approaching the more recent molecules used in PH, research in Groups 2–5 is limited, and that is most probably as a consequence of the initial disappointing results. ET1 receptor antagonists in Group 3 PH have been discouraging, with bosentan failing to improve exercise capacity and worsening hypoxemia and functional status after 12 weeks of therapy in a double blind randomized placebo-controlled trial of 30 patients with severe and very severe COPD [137]. In a subpopulation of the Ambrisentan therapy in a diverse population of patients with pulmonary hypertension (ARIES-3) study, after 24 weeks of therapy those with non-Group 1 PH did not show an improvement of exercise capacity [138]. However, another trial showed conflicting results as 18 months of therapy in 16 patients improved PAP, PVR, and functional capacity [139]. Evidently there are serious limitations in these studies which explain an apparent controversy of conclusions, considering that all of them have included a small number of patients and that the selected cases widely differ in patient characteristics and degree of underlying vascular disease.

Similarly with prostacyclins and phosphodiesterase-5 inhibitors, investigations have led to contrasting results which so far impede their use in clinical practice. Even though in several cases an improvement of either capacity or pulmonary hemodynamics was noted, the long term effects may even have deleterious effects [140]. Therefore, currently, the lack of strong evidence in the field determined the CHEST Guideline and Expert Panel Report to underline that none of the pulmonary arterial hypertension specific therapies is approved in Group 3 PH [141].

Calcium channel blockers have been the first vasodilator option in the treatment of pulmonary arterial hypertension, but with more recent advances it is believed that only a minute fraction of patients may benefit from this therapy and this has severely restricted its use [142]. In COPD they are considered to worsen ventilation-perfusion and hypoxemia, and the recent NICE guideline do not recommend their use to treat cor pulmonale patients [143].

In severe COPD lung volume reduction surgery may become an option to improve functional status, but data supporting its beneficial effect on pulmonary hemodynamics and cardiac function is lacking. A study conducted on a small subpopulation of the National Emphysema Treatment Trial comparing medical therapy versus medical therapy plus lung volume reduction surgery found no significant improvement in PAP and cardiac function in those receiving surgery [144].

22.6 Complications. Clinical Outcomes. Prognosis

Once RV dysfunction has occurred, the main complication will be its progression to RV failure [102] and this may come as a result of: (1) so-called natural disease progression (in the sense that pathogenics are far from being fully elucidated); (2) exacerbations of underlying CLD which may lead to a more or less temporary deterioration of cardiac function; (3) overlapping acute or chronic disorders which further alter RV function (i.e. pulmonary embolism, ischemic heart disease); (4) deleterious effects of CLD therapies on cardiac function.

The presence of RV hypertrophy and remodeling is frequent in COPD patients but it rarely develops into RV failure [102]. The coexistence of left heart disease is fairly frequent in COPD patients, especially smokers, thus accelerating progression of heart failure.

Cor pulmonale, in its acutely decompensated form, is a classical clinical presentation of RV failure, having COPD as its most common etiology in North America [99]. In acute CLD exacerbations, the ventilation-perfusion mismatch is aggravated along with hypoxemia and hypercapnia which deteriorates PH and thus RV dysfunction. In a recent study carried out on 33 patients with an acute COPD exacerbation without clinical signs of RV dysfunction, the authors showed that RV function is altered during the acute event, and only partially recovers after the episode, thus

proving that COPD exacerbations have a deleterious effect on the long-term in terms of RV function [130].

Most COPD and CPFE patients are heavy smokers, share a high inflammatory burden, and this evidently increases their global cardiovascular risk and mortality, which in a significantly high proportion is caused by cardiovascular complications as the Lung Health Study proved [145]. Hypertension, heart failure and arrhythmias are frequent comorbidities in COPD patients, and up to 33.6% of a large 400,000 cohort of COPD US veterans were found to have coronary artery disease. PAP increases, either due to left heart disorders or during CLD exacerbations, can reduce right coronary artery flow, leading to an aggravation of RV dysfunction, which will only be severed in the presence of preexistent atherosclerotic lesions in this territory. RV ischemia can be either a result of increased PAP, especially in those overlapping diverse comorbidities (COPD, OSA, ILD, hypertension, arrhythmias), or an atherosclerotic cause of additional RV dysfunction [146].

The acute exacerbation of a chronic lung disease becomes an interplay between the underlying chronic inflammatory state characteristic of these disorders, and the additional impact of the acute inflammation dynamics of an infection. Knowing their role on coagulation, one may hypothesize on the increased risk of pulmonary embolism (PE) in acute exacerbations of COPD. Furthermore, the Global Initiative for Chronic Obstructive Lung Disease Report from 2014 recommended enhancing thromboprophylactic measures in COPD patients during an acute exacerbation acknowledging their higher risk for deep vein thrombosis and PE [147]. As a recent review by Aleva et al. has discussed, there have been population studies supporting this concept but are balanced by others showing no association at all. In their investigation, the authors went from the idea the PE might be the cause of acute exacerbation of COPD in those 30% of cases when the etiology of the event remains unknown, and concluded that it should be so considered when associated with suggestive clinical signs such as pleuritic chest pain and acute right heart failure in the absence of a clearly associated infection [148].

Right heart failure is said to be "the end point of all forms of PH" [105], and an elevated PAP is definitely an independent predictor of poor outcomes in many forms of CLD, reducing survival in COPD and OSA patients, increasing morbidity and mortality in cystic fibrosis and idiopathic pulmonary fibrosis, and sarcoidosis [102, 149]. In CPFE patients, PH may deteriorate far worse than in IPF patients, and 1 year survival in these patients is reduced to only 60% when PH has developed [98]. For the minority of COPD patients with severe "out of proportion" PH in the ASPIRE registry (Assessing the Spectrum of Pulmonary hypertension Identified at a REferral centre) 1 and 3 years survival was far worse than in those with mild-moderate PH (70 and 33% vs 83 and 55%) [150].

However, neither PAP nor RV dysfunction have been included in severity scores such as the BODE index, St George's Respiratory Questionnaire, or the 36-item Medical Outcomes Study Short Form questionnaire, which are generally used in practice. As mentioned before, early, non clinically evident markers of RV dysfunction can be present in COPD patients even with slight or absent increases in PAP. But as therapeutic options for PH associated to CLD are limited compared to other groups of PH, once it has occurred it speaks of poor prognosis with limited solutions.

References

1. WHO. The top 10 causes of death. 2017. http://www.who.int/mediacentre/factsheets/fs310/en/.
2. Voelkel NF, Gomez-Arroyo J, Abbate A, Bogaard HJ. Mechanisms of right heart failure-A work in progress and a plea for failure prevention. Pulm Circ. 2013;3(1):137–43.
3. Voelkel NF, Mizuno S, Bogaard HJ. The role of hypoxia in pulmonary vascular diseases: a perspective. AJP. 2013;304(7):L457–65.
4. Rigolin VH, Robiolio PA, Wilson JS, Kevin Harrison J, Bashore TM. The forgotten chamber: the importance of the right ventricle. Physiology. 1995;28:18–28.
5. Baker BJ, Wilen MM, Boyd CM, Dinh H, Franciosa JA. Relation of right ventricular ejection fraction to

exercise capacity in chronic left ventricular failure. Am J Cardiol. 1984;54(6):596–9.
6. de Groote P, et al. Right ventricular ejection fraction is an independent predictor of survival in patients with moderate heart failure. J Am Coll Cardiol. 1998;32(4):948–54.
7. Polak JF, Holman BL, Wynne J, Colucci WS. Right ventricular ejection fraction: an indicator of increased mortality in patients with congestive heart failure associated with coronary artery disease. J Am Coll Cardiol. 1983;2(2):217–24.
8. Di Salvo TG, Mathier M, Semigran MJ, Dec GW. Preserved right ventricular ejection fraction predicts exercise capacity and survival in advanced heart failure. J Am Coll Cardiol. 1995;25(5):1143–53.
9. Melenovsky V, Hwang S-J, Lin G, Redfield MM, Borlaug BA. Right heart dysfunction in heart failure with preserved ejection fraction. Eur Heart J. 2014;35(48):3452–62.
10. Simonneau G, et al. Updated clinical classification of pulmonary hypertension. J Am Coll Cardiol. 2013;62(25 Suppl):D34–41.
11. Ho SY. Anatomy, echocardiography, and normal right ventricular dimensions. Heart. 2006;92(suppl_1):i2–13.
12. Dell'Italia LJ. Anatomy and physiology of the right ventricle. Cardiol Clin. 2012;30(2):167–87.
13. Voelkel NF, Dietmar S. The right ventricle in health and disease. New York: Springer; 2014.
14. Haddad F, Hunt SA, Rosenthal DN, Murphy DJ. Right ventricular function in cardiovascular disease, part I: anatomy, physiology, aging, and functional assessment of the right ventricle. Circulation. 2008;117(11):1436–48.
15. West JB. Role of the fragility of the pulmonary blood-gas barrier in the evolution of the pulmonary circulation. AJP. 2013;304(3):R171–6.
16. Berlin DA, Bakker J. Understanding venous return. Intensive Care Med. 2014;40(10):1564–6.
17. Kass DA. Alterations in ventricular function in systolic heart failure - beat-to-beat regulation of systolic function. In: Mann DL, Felker GM, editors. Heart failure: a companion to Braunwald's heart disease. Philadelphia: Elsevier; 2016.
18. Harjola V-P, et al. Contemporary management of acute right ventricular failure: a statement from the Heart Failure Association and the working group on pulmonary circulation and right ventricular function of the European Society of Cardiology. Eur J Heart Fail. 2016;18(3):226–41.
19. Wagner PD. Operation everest II. High Alt Med Biol. 2010;11(2):111–9.
20. Demiryurek AT, Wadsworth RM, Kane KA, Peacock AJ. The role of endothelium in hypoxic constriction of human pulmonary artery rings. Am Rev Respir Dis. 1993;147(2):283–90.
21. Ohe M, Ogata M, Katayose D, Takishima T. Hypoxic contraction of pre-stretched human pulmonary artery. Respir Physiol. 1992;87(1):105–14.
22. Berg JT, Breen EC, Fu Z, Mathieu-Costello O, West JB. Alveolar hypoxia increases gene expression of extracellular matrix proteins and platelet-derived growth factor-B in lung parenchyma. Am J Respir Crit Care Med. 1998;158(6):1920–8.
23. Sylvester JT, Shimoda LA, Aaronson PI, Ward JPT. Hypoxic pulmonary vasoconstriction. Physiol Rev. 2012;92(1):367–520.
24. Weissmann N, Grimminger F, Walmrath D, Seeger W. Hypoxic vasoconstriction in buffer-perfused rabbit lungs. Respir Physiol. 1995;100(2):159–69.
25. Peake MD, Harabin AL, Brennan NJ, Sylvester JT. Steady-state vascular responses to graded hypoxia in isolated lungs of five species. J Appl Physiol Respir Environ Exerc Physiol. 1981;51(5):1214–9.
26. Lumb AB, Slinger P. Hypoxic pulmonary vasoconstriction physiology and anesthetic implications. Anesthesiology. 2015;122(4):932–46.
27. Kay JM. Comparative morphologic features of the pulmonary vasculature in mammals 1, 2. Am Rev Respir Dis. 1983;128(2P2):S53–7.
28. Hong Z, et al. Role of dynamin-related protein 1 (Drp1)-mediated mitochondrial fission in oxygen sensing and constriction of the ductus arteriosus. Circ Res. 2013;112(5):802–15.
29. Longo DL, Archer SL. Mitochondrial dynamics — mitochondrial fission and fusion in human diseases. N Engl J Med. 2013;369(23):2236–51.
30. Palmer BF, Clegg DJ. Oxygen sensing and metabolic homeostasis. Mol Cell Endocrinol. 2014;397(1–2):51–8.
31. Waypa GB, et al. Mitochondrial reactive oxygen species trigger calcium increases during hypoxia in pulmonary arterial myocytes. Circ Res. 2002;91(8):719–26.
32. Waypa GB, Chandel NS, Schumacker PT. Model for hypoxic pulmonary vasoconstriction involving mitochondrial oxygen sensing. Circ Res. 2001;88(12):1259–66.
33. Weir EK, Archer SL. Counterpoint: hypoxic pulmonary vasoconstriction is not mediated by increased production of reactive oxygen species. J Appl Physiol. 2006;101(3):995 LP–998.
34. Weir EK, López-Barneo J, Buckler KJ, Archer SL. Acute oxygen-sensing mechanisms. N Engl J Med. 2005;353:2042–55.
35. Moudgil R, Michelakis ED, Archer SL, Archer SL. Hypoxic pulmonary vasoconstriction. J Appl Physiol. 2005;123:390–403.
36. Talbot NP, Balanos GM, Dorrington KL, Robbins PA. Two temporal components within the human pulmonary vascular response to ~2 H of isocapnic hypoxia. J Appl Physiol. 2005;98(3):1125–39.
37. Smith TG, et al. The increase in pulmonary arterial pressure caused by hypoxia depends on iron status. J Physiol. 2008;586(24):5999–6005.
38. Wang J, Juhaszova M, Rubin LJ, Yuan XJ. Hypoxia inhibits gene expression of voltage-gated K+ channel alpha subunits in pulmonary artery smooth muscle cells. J Clin Investig. 1997;100(9):2347–53.

39. Charolidi N, Carroll VA. Hypoxia and pulmonary hypertension. In: Zheng J, editor. Hypoxia and human diseases. Rijeka: InTech; 2017.
40. Swenson E. Hypoxic pulmonary vasoconstriction and chronic lung disease. Adv Pulm Hypertens. 2013;12(3):135–44.
41. Weidemann A, Johnson RS. Biology of HIF-1alpha. Cell Death Differ. 2008;15(4):621–7.
42. Engebretsen BJ, et al. Acute hypobaric hypoxia (5486 M) induces greater pulmonary HIF-1 activation in hilltop compared to Madison rats. High Alt Med Biol. 2007;8(4):312–21.
43. Beall CM, et al. Natural selection on EPAS1 (HIF2α) associated with low hemoglobin concentration in Tibetan highlanders. Proc Natl Acad Sci U S A. 2010;107(25):11459–64.
44. Lorenzo FR, et al. A genetic mechanism for tibetan high-altitude adaptation. Nat Genet. 2014;46(9):951–6.
45. Sarangi S, et al. The homozygous VHL(D126N) missense mutation is associated with dramatically elevated erythropoietin levels, consequent polycythemia, and early onset severe pulmonary hypertension. Pediatr Blood Cancer. 2014;61(11):2104–6.
46. Tao H, et al. Expression and significance of hypoxia-inducible factor-1alpha in patients with chronic obstructive pulmonary disease and smokers with normal lung function. Chin J Cell Mol Immunol. 2014;30(8):852–5.
47. Daijo H, et al. Cigarette smoke reversibly activates hypoxia-inducible factor 1 in a reactive oxygen species-dependent manner. Sci Rep. 2016;6:34424.
48. Budhiraja R, Tuder RM, Hassoun PM. Endothelial dysfunction in pulmonary hypertension. Circulation. 2004;109(2):159–65.
49. Quy S, Duong. Physiopathology of pulmonary hypertension: from bio-molecular mechanism to target treatment. J Vasc Med Surg. 2016;4(6):294.
50. Aird WC. Endothelial cell heterogeneity. Crit Care Med. 2003;31(Supplement):S221–30.
51. Tonelli AR, Haserodt S, Aytekin M, Dweik RA. Nitric oxide deficiency in pulmonary hypertension: pathobiology and implications for therapy. Pulm. Circ. 2013;3(1):20–30.
52. Aaronson PI, Robertson TP, Ward JPT. Endothelium-derived mediators and hypoxic pulmonary vasoconstriction. Respir Physiol Neurobiol. 2002;132(1):107–20.
53. Yang Q, et al. NO and EDHF pathways in pulmonary arteries and veins are impaired in COPD patients. Vasc Pharmacol. 2012;57(2–4):113–8.
54. Tuder RM, Zaiman AL. Perspective prostacyclin analogs as the brakes for pulmonary artery smooth muscle cell proliferation is it sufficient to treat severe pulmonary hypertension. Am J Respir Cell Mol Biol. 2002;26:171–4.
55. Tuder RM, et al. Prostacyclin synthase expression is decreased in lungs from patients with severe pulmonary hypertension. Am J Respir Crit Care Med. 1999;159(6):1925–32.
56. Christman BW, et al. An imbalance between the excretion of thromboxane and prostacyclin metabolites in pulmonary hypertension. N Engl J Med. 1992;327(2):70–5.
57. Katugampola SD, Davenport AP. Thromboxane receptor density is increased in human cardiovascular disease with evidence for inhibition at therapeutic concentrations by the AT(1) receptor antagonist losartan. Br J Pharmacol. 2001;134(7):1385–92.
58. Langleben D, et al. Effects of the thromboxane synthetase inhibitor and receptor antagonist terbogrel in patients with primary pulmonary hypertension. Am Heart J. 2002;143(5):E4.
59. Frasch HF, Marshall C, Marshall BE. Endothelin-1 is elevated in monocrotaline pulmonary hypertension. Am J Phys. 1999;276(2 Pt 1):L304–10.
60. Giaid A, et al. Expression of endothelin-1 in the lungs of patients with pulmonary hypertension. N Engl J Med. 1993;328(24):1732–9.
61. Li H, et al. Enhanced endothelin-1 and endothelin receptor gene expression in chronic hypoxia. J Appl Physiol. 1994;77(3):1451 LP–459.
62. MacLean MR, Herve P, Eddahibi S, Adnot S. 5-Hydroxytryptamine and the pulmonary circulation: receptors, transporters and relevance to pulmonary arterial hypertension. Br J Pharmacol. 2000;131(2):161–8.
63. Le C, Timothy D, Markham NE, Tuder RM, Voelkel NF, Abman SH. Treatment of newborn rats with a VEGF receptor inhibitor causes pulmonary hypertension and abnormal lung structure. Am J Physiol. 2002;283(3):L555–62.
64. Partovian C, et al. Adenovirus-mediated lung vascular endothelial growth factor overexpression protects against hypoxic pulmonary hypertension in rats. Am J Respir Cell Mol Biol. 2000;23(6):762–71.
65. Ketabchi F, et al. Effects of hypercapnia with and without acidosis on hypoxic pulmonary vasoconstriction. Am J Physiol. 2009;297(5):L977–83.
66. Dunham-Snary KJ, et al. Hypoxic pulmonary vasoconstriction: from molecular mechanisms to medicine. Chest. 2017;151(1):181–92.
67. Vogelmeier CF, et al. Global strategy for the diagnosis, management and prevention of chronic obstructive lung disease 2017 report. Respirology. 2017;22(3):575–601.
68. Peinado VI, et al. Endothelial dysfunction in pulmonary arteries of patients with mild COPD. Am J Phys. 1998;274(6):908–13.
69. Green CE, Turner AM. The role of the endothelium in asthma and chronic obstructive pulmonary disease (COPD). Respir Res. 2017;18:20.
70. Tuder RM, Voelkel NF. Angiogenesis and pulmonary hypertension: a unique process in a unique disease. Antioxid Redox Signal. 2002;4(5):833–43.
71. Muller WA. Transendothelial migration: unifying principles from the endothelial perspective. Immunol Rev. 2016;273(1):61–75.
72. Liao JK. Linking endothelial dysfunction with endothelial cell activation. J Clin Invest. 2013;123(2):540–1.

73. Oelsner EC, et al. Adhesion molecules, endothelin-1 and lung function in seven population-based cohorts. Biomarkers. 2013;18(3):196–203.
74. Aaron CP, et al. Intercellular adhesion molecule 1 and progression of percent emphysema: the MESA lung study. Respir Med. 2015;109(2):255–64.
75. Riise GC, Larsson S, Lofdahl CG, Andersson BA. Circulating cell adhesion molecules in bronchial lavage and serum in COPD patients with chronic bronchitis. Eur Respir J. 1994;7(9):1673–7.
76. Janson C, et al. Circulating adhesion molecules in allergic and non-allergic asthma. Respir Med. 2005;99(1):45–51.
77. Mukhopadhyay S, Malik P, Arora SK, Mukherjee TK. Intercellular adhesion molecule-1 as a drug target in asthma and rhinitis. Respirology. 2014;19(4):508–13.
78. Hirata N, et al. Allergen exposure induces the expression of endothelial adhesion molecules in passively sensitized human bronchus: time course and the role of cytokines. Am J Respir Cell Mol Biol. 1998;18(1):12–20.
79. Malli F, et al. Endothelial progenitor cells in the pathogenesis of idiopathic pulmonary fibrosis: an evolving concept. PLoS ONE. 2013;8(1):e53658.
80. Lu D, Li N, Yao X, Zhou L. Potential inflammatory markers in obstructive sleep apnea-hypopnea syndrome. Bosn J Basic Med Sci. 2017;17(1):47–53.
81. Portillo K, Morera J. Combined pulmonary fibrosis and emphysema syndrome: a new phenotype within the spectrum of smoking-related interstitial lung disease. Pulm Med. 2012;2012:867870.
82. Stenmark KR, Fagan KA, Frid MG. Hypoxia-induced pulmonary vascular remodeling: cellular and molecular mechanisms. Circ Res. 2006;99(7):675–91.
83. Santos S, et al. Characterization of pulmonary vascular remodelling in smokers and patients with mild COPD. Eur Respir J. 2002;19(4):632–8.
84. Carlsen J, et al. Pulmonary arterial lesions in explanted lungs after transplantation correlate with severity of pulmonary hypertension in chronic obstructive pulmonary disease. J Heart Lung Transplant. 2013;32(3):347–54.
85. Chen H, Strappe P, Chen S, Wang L-X. Endothelial progenitor cells and pulmonary arterial hypertension. Heart Lung Circ. 2014;23(7):595–601.
86. Granton J, et al. Endothelial NO-synthase gene-enhanced progenitor cell therapy for pulmonary arterial hypertension: The PHACeT trial. Circ Res. 2015;117(7):645–54.
87. Marsboom G, et al. Sustained endothelial progenitor cell dysfunction after chronic hypoxia-induced pulmonary hypertension. Stem Cells. 2008;26(4):1017–26.
88. Hopkins N, McLoughlin P. The structural basis of pulmonary hypertension in chronic lung disease: remodelling, rarefaction or angiogenesis? J Anat. 2002;201(4):335–48.
89. Feihl F, Liaudet L, Waeber B, Levy BI. Hypertension: a disease of the microcirculation? Hypertension. 2006;48(6):1012–7.
90. Howell K, Preston RJ, McLoughlin P. Chronic hypoxia causes angiogenesis in addition to remodelling in the adult rat pulmonary circulation. J Physiol. 2003;547(Pt 1):133–45.
91. Pascaud M-A, et al. Lung overexpression of angiostatin aggravates pulmonary hypertension in chronically hypoxic mice. Am J Respir Cell Mol Biol. 2003;29(4):449–57.
92. Sajkov D, McEvoy RD. Obstructive sleep apnea and pulmonary hypertension. Prog Cardiovasc Dis. 2009;51(5):363–70.
93. Kholdani C, Fares WH, Mohsenin V. Pulmonary hypertension in obstructive sleep apnea: is it clinically significant? A critical analysis of the association and pathophysiology. Pulmonary Circulation. 2015;5(2):220–7.
94. Shlobin OA, Nathan SD. Pulmonary hypertension secondary to interstitial lung disease. Expert Rev Respir Med. 2011;5(2):179–89.
95. Fagan KA, Badesch DB. Pulmonary hypertension associated with connective tissue disease. Prog Cardiovasc Dis. 2002;45(3):225–34.
96. Authors/Task Force Members, et al. 2016 ESC Position Paper on cancer treatments and cardiovascular toxicity developed under the auspices of the ESC Committee for Practice Guidelines: The Task Force for cancer treatments and cardiovascular toxicity of the European Society of Cardiology (ESC). Eur Heart J. 2016;37(36):2768–801.
97. Wiggins J, Strickland B, Turner-Warwick M. Combined cryptogenic fibrosing alveolitis andemphysema: the value of high resolution computed tomography in assessment. Respir Med. 2017;84(5):365–9.
98. Cottin V, Nunes H, Brillet P. Combined pulmonary fibrosis and emphysema: a distinct underrecognised entity. Eur Respir J. 2005;26(4):586–93.
99. Budev MM, Arroliga AC, Wiedemann HP, Matthay RA. Cor pulmonale: an overview. Semin Respir Crit Care Med. 2003;24(3):233–43.
100. World Health Organization. Chronic cor pulmonale: a report of the expert committee. Circulation. 1963;27:594–8.
101. Weitzenblum E, Chaouat A, Canuet M, Kessler R. Pulmonary hypertension in chronic obstructive pulmonary disease and interstitial lung diseases. Crit Care. 2009;1(212):458–70.
102. Kolb TM, Hassoun PM. Right ventricular dysfunction in chronic lung disease. Cardiol Clin. 2012;30(2):243–56.
103. Hilde JM, et al. Right ventricular dysfunction and remodeling in chronic obstructive pulmonary disease without pulmonary hypertension. J Am Coll Cardiol. 2013;62(12):1103–11.
104. Watz H, et al. Decreasing cardiac chamber sizes and associated heart dysfunction in COPD: role of hyperinflation. Chest. 2010;138(1):32–8.

105. Zangiabadi A, De Pasquale CG, Sajkov D. Pulmonary hypertension and right heart dysfunction in chronic lung disease. Biomed Res Int. 2014;2014:739674.
106. Bogaard HJ, Abe K, Noordegmaf AV, Voelkel NF. The Right ventricle under pressure. Chest. 2009;135(3):794–804.
107. Harston RK, Kuppuswamy D. Integrins are the necessary links to hypertrophic growth in cardiomyocytes. J Signal Transduction. 2011;2011:1–8.
108. Voelkel NF, et al. Right ventricular function and failure: report of a national heart, lung, and blood institute working group on cellular and molecular mechanisms of right heart failure. Circulation. 2006;114(17):1883–91.
109. Samson N, Paulin R. Epigenetics, inflammation and metabolism in right heart failure associated with pulmonary hypertension. Pulm Circ. 2017;7(3):572–87.
110. Scharf SM, et al. Hemodynamic characterization of patients with severe emphysema. Am J Respir Crit Care Med. 2002;166(3):314–22.
111. Chaouat A, et al. Severe pulmonary hypertension and chronic obstructive pulmonary disease. Am J Respir Crit Care Med. 2005;172(2):189–94.
112. Pugh ME, et al. Causes of pulmonary hypertension in the elderly. Chest. 2014;146(1):159–66.
113. Klings ES. Pulmonary hypertension due to lung disease and/or hypoxemia (Group 3 pulmonary hypertension): epidemiology, pathogenesis, and diagnostic evaluation in adults. UpToDate. 2017. https://www.uptodate.com/contents/pulmonary-hypertension-due-to-lung-disease-and-or-hypoxemia-group-3-pulmonary-hypertension-epidemiology-pathogenesis-and-diagnostic-evaluation-in-adults?source=see_link#H1538627010.
114. Arcasoy SM, et al. Echocardiographic assessment of pulmonary hypertension in patients with advanced lung disease. Am J Respir Crit Care Med. 2003;167(5):735–40.
115. Javaheri S, Javaheri S, Javaheri A. Sleep apnea, heart failure, and pulmonary hypertension. Curr Heart Fail Rep. 2013;10(4):315–20.
116. Bradley TD, et al. Role of daytime hypoxemia in the pathogenesis of right heart failure in the obstructive sleep apnea syndrome. Am Rev Respir Dis. 1985;131(0003–0805):835–9.
117. Tzilas V, Bouros D. Combined pulmonary fibrosis and emphysema, a clinical review. COPD Res Pract. 2016;2(1):2.
118. Sugino K, Ishida F, Kikuchi N. Comparison of clinical characteristics and prognostic factors of combined pulmonary fibrosis and emphysema versus idiopathic pulmonary fibrosis alone. Respirology. 2014;19:239–45.
119. Galiè N, Humbert M, Vachiery JL. 2015 ESC/ERS guidelines for the diagnosis and treatment of pulmonary hypertension: The Joint Task Force for the diagnosis and treatment of pulmonary hypertension of the European Society of Cardiology (ESC) and the European Respiratory Society (ERS): endor. Eur Respir J. 2015;46:903–75.
120. Seeger W, et al. Pulmonary hypertension in chronic lung diseases. J Am Coll Cardiol. 2013;62(25 Suppl):D109–16.
121. Høiseth AD, Omland T, Hagve T-A, Brekke PH, Søyseth V. NT-proBNP independently predicts long term mortality after acute exacerbation of COPD – a prospective cohort study. Respir Res. 2012;13(1):97.
122. Adrish M, Nannaka VB, Cano EJ, Bajantri B, Diaz-Fuentes G. Significance of NT-pro-BNP in acute exacerbation of COPD patients without underlying left ventricular dysfunction. Int J Chron Obstruct Pulmon Dis. 2017;12:1183–9.
123. Ouanes-Besbes L, Hamouda Z, Ouanes I, Dachraoui F, Abroug F. NT-proBNP accurately reflects the impact of severe COPD exacerbation on the right ventricle (RV). Eur Respir J. 2014;42(Suppl 57):P2434.
124. Leuchte HH, et al. Brain natriuretic peptide is a prognostic parameter in chronic lung disease. Am J Respir Crit Care Med. 2006;173(7):744–50.
125. Dupont MVM, Drăgean CA, Coche EE. Right ventricle function assessment by MDCT. Am J Roentgenol. 2011;196(1):77–86.
126. Gao Y, et al. Evaluation of right ventricular function by 64-row ct in patients with chronic obstructive pulmonary disease and cor pulmonale. Eur J Radiol. 2012;81(2):345–53.
127. Hur J, Kim TH, Kim SJ, Ryu YH, Kim HJ. Assessment of the right ventricular function and mass using cardiac multi-detector computed tomography in patients with chronic obstructive pulmonary disease. Korean J Radiol. 2007;8(1):15–21.
128. Vitarelli A. Assessment of right ventricular function by strain rate imaging in chronic obstructive pulmonary disease. Eur Respir J. 2006;27(2):268–75.
129. Turhan S, et al. Value of tissue doppler myocardial velocities of tricuspid lateral annulus for the diagnosis of right heart failure in patients with COPD. Echocardiography. 2007;24(2):126–33.
130. Ozben B, et al. Acute exacerbation impairs right ventricular function in COPD patients. Hell J Cardiol. 2015;56(4):324–31.
131. Burgess MI, et al. Comparison of echocardiographic markers of right ventricular function in determining prognosis in chronic pulmonary disease. J Am Soc Echocardiogr. 2002;15(6):633–9.
132. Kato S, et al. Prognostic value of cardiovascular magnetic resonance derived right ventricular function in patients with interstitial lung disease. J Cardiovasc Magn Reson. 2015;17(1):10.
133. Vonbank K, et al. Controlled prospective randomised trial on the effects on pulmonary haemodynamics of the ambulatory long term use of nitric oxide and oxygen in patients with severe COPD. Thorax. 2003;58(4):289–93.
134. ClinicalTrials.gov. Inhaled nitric oxide to prevent and treat bronchopulmonary dysplasia (NO-BPD) NCT01503801. 2017. https://clinicaltrials.gov/ct2/show/NCT01503801.

135. Warren NJ. Bellerophon to Present Positive Clinical Data on INOpulse® at the American Thoracic Society 113th International Conference. 2017. http://investors.bellerophon.com/phoenix.zhtml?c=253899&p=irol-newsArticle_print&ID=2268250"ID=2268250.
136. ClinicalTrials.gov. Study in subjects with PAH and PH secondary to IPF using inhaled GeNOsyl. (PHiano) NCT01503801. 2017. https://clinicaltrials.gov/ct2/show/NCT01265888.
137. Stolz D, et al. A randomised, controlled trial of Bosentan in severe COPD. Eur Respir J. 2008;32(3):619–28.
138. Badesch DB, et al. ARIES-3: ambrisentan therapy in a diverse population of patients with pulmonary hypertension. Cardiovasc Ther. 2012;30(2):93–9.
139. Valerio G, Bracciale P, D'Agostino AG. Effect of Bosentan upon pulmonary hypertension in chronic obstructive pulmonary disease. Ther Adv Respir Dis. 2009;3(1):15–21.
140. Duarte JD, Hanson RL, Machado RF. Pharmacologic treatments for pulmonary hypertension: exploring pharmacogenomics. Futur Cardiol. 2013;9(3):335–49.
141. Taichman DB, et al. Pharmacologic therapy for pulmonary arterial hypertension in adults: CHEST guideline and expert panel report. Chest. 2014;146(2):449–75.
142. Medarov BI, Judson MA. The role of calcium channel blockers for the treatment of pulmonary arterial hypertension: how much do we actually know and how could they be positioned today? Respir Med. 2017;109(5):557–64.
143. Nice Guidelines. Chronic obstructive pulmonary disease in over 16s: diagnosis and management; 2010. pp. 1–31.
144. Criner GJ, et al. Effect of lung volume reduction surgery on resting pulmonary hemodynamics in severe emphysema. Am J Respir Crit Care Med. 2007;176(3):253–60.
145. Wise R, Connett J, Weinmann G, Scanlon P, Skeans M. Effect of inhaled triamcinolone on the decline in pulmonary function in chronic obstructive pulmonary disease. N Engl J Med. 2000;343(26):1902–9.
146. Mapel DW, Dedrick D, Davis K. Trends and cardiovascular co-morbidities of COPD patients in the veterans administration medical system, 1991-1999. COPD. 2005;2(1):35–41.
147. Global Initiative for Chronic Obstructive Lung Disease. Global strategy for diagnosis, management, and prevention of chronic obstructive pulmonary disease (Updated 2014). i-84. 2014.
148. Aleva FE, et al. Prevalence and localization of pulmonary embolism in unexplained acute exacerbations of COPD: a systematic review and meta-analysis. Chest. 2017;151(3):544–54.
149. Rowan SC, Keane MP, Gaine S, McLoughlin P. Hypoxic pulmonary hypertension in chronic lung diseases: novel vasoconstrictor pathways. Lancet Respir Med. 2016;4(3):225–36.
150. Hurdman J, et al. Pulmonary hypertension in COPD: results from the ASPIRE registry. Eur Respir J. 2013;41(6):1292 LP–1301.

Arrhythmias in Right Heart Disease

23

Stefan Bogdan, Radu Vătăşescu, and Maria Dorobanţu

Abstract

Right heart disease can be associated with increased risk for arrhythmias, both ventricular and supraventricular. Right sided arrhythmias may occur in the setting of structural disease predominantly affecting the right heart—such as cardiomyopathies (arrhythmogenic right ventricular dysplasia, cardiac sarcoidosis) and congenital heart disease (corrected tetralogy of Fallot, Ebstein's anomaly, atrial septal defect), as well as in the absence of structural heart disease, with substrate (Mahaim fibers, Coumel type tachycardia) or without substrate (idiopathic right ventricular outflow tract ventricular tachycardia). The most common cause for right heart failure is secondary pulmonary hypertension due to left heart diseases, a setting in which the underlying left heart condition will be the main determiner for prognosis and risk of arrhythmia. Still, right heart failure secondary to pulmonary arterial hypertension is also associated with increased risk for arrhythmic events. Advanced cardiac imaging, especially cardiac MRI, as well as invasive procedures (right/left heart catherization; electrophysiological study; endomyocardial biopsy) play an important role in the differential diagnosis. Modern treatment relies on interventional techniques (implantable cardioverter defibrillator; radiofrequency ablation).

Keywords

Arrhythmogenic right ventricular dysplasia Cardiac sarcoidosis · Tetralogy of Fallot Ebstein's anomaly · Ventricular tachycardia Sudden cardiac death

23.1 Introduction

The following chapter will focus on arrhythmogenic diseases with specific right heart involvement (cardiomyopathies, congenital heart diseases), as well as on arrhythmias originating from the right heart, despite a structurally normal heart or in the setting of pulmonary arterial hypertension.

S. Bogdan · R. Vătăşescu
"Carol Davila" University of Medicine and Pharmacy, Bucharest, Romania

Cardiology Department, Clinical Electrophysiology and Cardiac Pacing Laboratory, Clinical Emergency Hospital, Bucharest, Romania

M. Dorobanţu (✉)
"Carol Davila" University of Medicine and Pharmacy, Bucharest, Romania

Cardiology Department, Clinical Emergency Hospital, Bucharest, Romania

S. I. Dumitrescu et al. (eds.), *Right Heart Pathology*, https://doi.org/10.1007/978-3-319-73764-5_23

23.2 Arrhythmogenic Cardiomyopathies with Specific Right Heart Involvement

Arrhythmogenic cardiomyopathies with specific right heart involvement are rare diseases. Current data regarding their management and treatment comes mainly from registries and scarce registry-based meta-analysis. Modern invasive therapies for ventricular arrhythmia treatment and sudden cardiac death prevention have been applied empirically, in the absence of specific large randomized trials, with overall good clinical results, as confirmed also by registries.

23.2.1 Arrhythmogenic Right Ventricular Cardiomyopathy

Arrhythmogenic right ventricular cardiomyopathy (ARVC) is considered a genetic disorder, with mainly an autosomal dominant pattern of transmittance and a variable penetrance of 20–30% [1]. Most mutations affect proteins composing desmosomes–intracellular adhesion complexes that provide mechanical connections between cardiac myocytes [2]. Disrupted intercellular connections result in myocyte cell death and an inflammatory repair process, leading to the development of fibrolipomatous (fibrofatty) lesions within the myocardium [3]. Fibrofatty tissue progressively replaces the normal myocardium resulting in localized (micro-aneurysm) or generalized dilatation of the right ventricle (RV) and myocardial wall thinning in the dilated regions. The initially described sites of RV involvement included the RV inflow tract, the RV outflow tract, and posterolateral LV—characterizing the so-called "triangle of dysplasia". However, recent data has shown that RV apex is typically affected only during late-stage disease, thus rendering the triangle concept moot [4].

ARVC is a progressive disease during which RV myocardium replacement by fibro-fatty tissue alternating with residual viable myocardial cell leads to inhomogeneous and arrhythmogenic scar formation, as well as right ventricular systolic dysfunction, in late-stage disease. While the disease may remain asymptomatic for a long period of time, the most common symptoms include palpitations (67%) and syncope (32%), related to ventricular arrhythmias [5]. Sudden cardiac death (SCD) can be the first clinical presentation of the disease and ARVC is an important cause of SCD in young adults (11% overall; 22% in athletes in a study from Northern Italy) [6].

Ventricular arrhythmias range from isolated ventricular premature complex (PVC) to sustained ventricular tachycardia (VT). The most common ventricular arrhythmia is VT originating from the RV (inflow/outflow tract or apex) therefore manifesting a left bundle branch block (LBBB) morphology [7] (Fig. 23.1).

Ventricular arrhythmia burden appears to be correlated with disease severity—as studies have reported a prevalence of 100% in patients with severe ARVC as opposed to 82% in those with moderate and 23% in those with mild disease [8]. Malignant ventricular arrhythmia may be exercise-induced in ARVC, therefore ARVC patients should avoid competitive and endurance physical exercise [8]. Severe RV involvement may lead to specific ECG changes—the epsilon wave in V1, negative T waves V1–V3 (Fig. 23.2) [9].

ARVC should be suspected in patients presenting with VT of LBBB morphology in the absence of apparent heart disease, in patients with multiple right sided PVCs and VT inducible during electrophysiology study (EPS), and in patients with exercise induced VT or SCD [10].

Diagnosing ARVC can often be challenging and relies on a 2010 revised task force criteria (minor/major; six categories) [9]. Cardiac MRI has gained significant importance in ARVC evaluation, as it offers information useful to differential diagnosis and may guide endo-myocardial biopsy when necessary.

With the advent of SCD prevention by interventional procedures life expectancy in ARVC has improved significantly. Treatment relies primarily on SCD prevention by implantable cardioverter defibrillator (ICD) implantation. A 2013 meta-analysis has demonstrated that cardiac and non-cardiac annual mortality rates are low in ARVC patients after ICD implantation (0.9%;

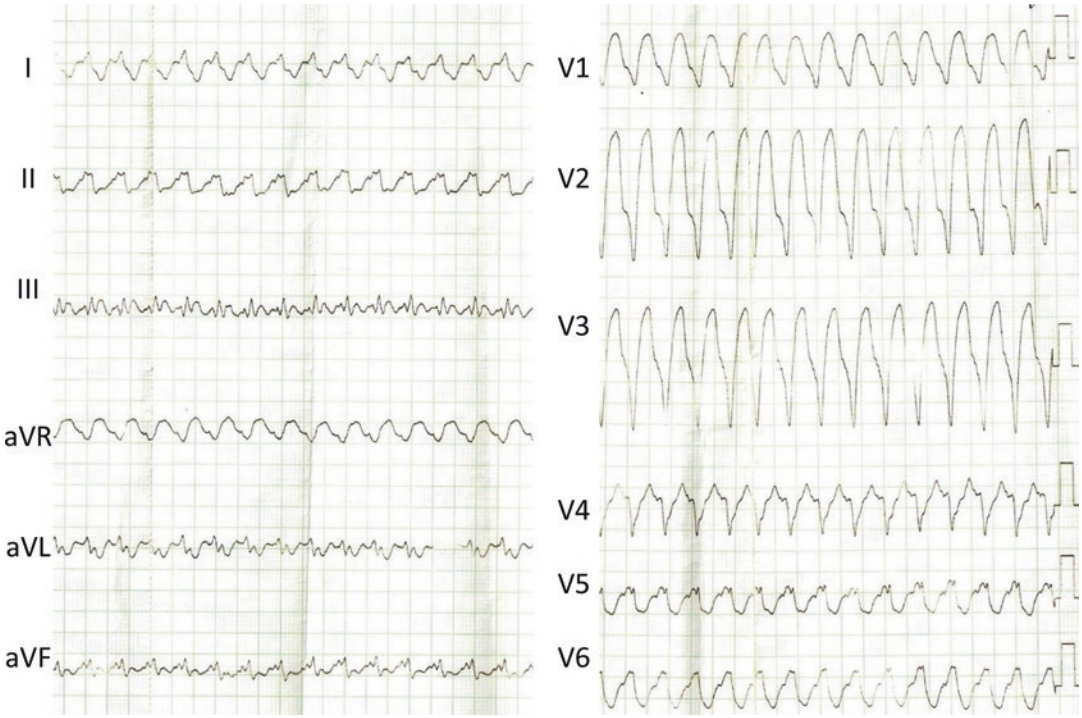

Fig. 23.1 Right ventricle free-wall tachycardia in a patient with ARVC

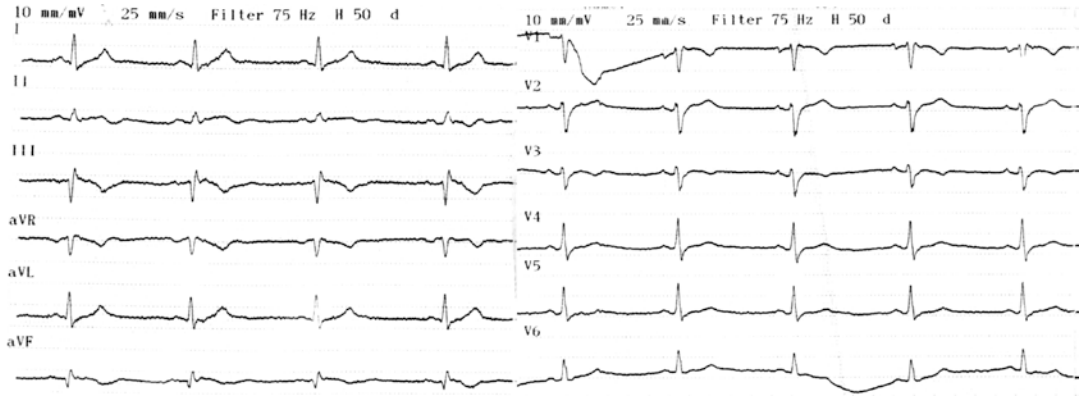

Fig. 23.2 Sinus rhythm with discrete epsilon wave in V1 (same patient as in Fig. 23.1, following cardioversion)

0.8%, respectively). Appropriate ICD therapies occur at a rate of 9.5% per year while inappropriate interventions occur at a rate of 3.7% per year and are associated with considerable ICD-related morbidity [11].

Electrophysiology study with ablation for VT and substrate modification plays an important part in secondary prevention, especially in the setting of recurrent drug-refractory VT or VT storm. Its role in ARVC patients with low arrhythmia burden or in primary prevention remains to be defined, due to the progressive nature of the disease [12]. A recent meta-analysis has shown that VT ablation in ARVC patients is feasible with a high acute and long-term efficacy. Pooled estimate of acute efficacy was 96% (95% confidence

interval: 87–100%) for endocardial ablation strategy and 98% (95% confidence interval: 91–100%) for endo-epicardial ablation strategy. Pooled estimate for long-term efficacy with endo-epicardial ablation strategy (82%, 95% CI: 72–90%) was numerically higher than individual endocardial ablation strategy (63%, 95% CI: 51–74%) [13]. Beta-blockers and sotalol represent the first line of pharmacological treatment, while amiodarone, which has also proven its efficacy, should remain a second line option [14].

Recent data suggested that atrial remodeling and atrial tachy-arrhythmias may be common in ARVC [15]. Atrial fibrillation was shown to be a predictor for lethal arrhythmias at follow-up in ARVC patients [16]. Further studies are required to determine the role of atrial tachyarrhythmias in ARVC. *[For further details, see specific chapter on ARVC].*

23.2.2 Cardiac Sarcoidosis

Sarcoidosis is a systemic disease of unknown etiology, with non-caseating granulomatous lesions formation that can affect any organ within the body, including the heart. Cardiac sarcoidosis can rarely be diagnosed alone, precede, follow or occur simultaneously with another organ involvement (usually the lung) [17]. Initial small registry studies suggested a low prevalence (5–10%) of cardiac involvement during sarcoidosis. Autopsy studies showed subclinical cardiac involvement in up to 25% of sarcoidosis patients [18].

The sarcoid inflammatory process results in scarring most commonly of the interventricular septum, left ventricular posterior and anterior wall, and right ventricle [19]. Isolated cases of RV involvement alone have been reported [20].

Depending upon the location and extent of the granulomatous lesions, clinical manifestations include conduction abnormalities, tachyarrhythmias, cardiomyopathy, congestive heart failure and SCD [21].

Complete heart block is the most common finding in sarcoidosis patients with symptomatic heart involvement. Heart block in sarcoidosis occurs at younger ages by comparison to other etiologies [22]. Other types of conduction disorders (first degree atrio-ventricular block, intraventricular conduction defects) are also common, and may progress towards symptomatic complete heart block.

Ventricular arrhythmias (VT (sustained and non-sustained) as well as VPCs) are the second form of presentation in symptomatic cardiac sarcoidosis. Myocardial sarcoid granulomas may present abnormal automaticity or triggered activity related to inflammation; however, the most likely mechanism is macro-reentry around areas of granulomatous scar. Ventricular arrhythmia was present in up to 22% patients with sarcoidosis [22]. It was suggested that corticoid treatment may convert granulomas to scar tissue, contributing to the formation of ventricular aneurysms, potentially mimicking ARVC [23].

In addition, other types of arrhythmias have been associated with cardiac sarcoidosis including sinus arrest secondary to granulomatous involvement of the sinus node, atrial fibrillation and atrial flutter [24].

Sudden death due to complete heart block or malignant ventricular arrhythmias accounts for 25–65% of death secondary to cardiac sarcoidosis [22, 23].

Diagnosing cardiac sarcoidosis can be very challenging depending upon clinical manifestation and concomitant organ involvement. Advanced cardiac imaging (cardiac MRI or FDG-PET) and biopsy (extracardiac or guided endomyocardial biopsy) are required [25].

Cardiac sarcoidosis may present similar features to ARVC, including the epsilon wave /RV VT, and can fulfil the task force criteria for ARVC [26]. Establishing a differential diagnosis is important because the management differs significantly between the diseases (immunosuppressive therapy versus family screening in ARVC). Besides guided endomyocardial biopsy, cardiac MRI studies have shown that left ventricular septal involvement could only be seen in cardiac sarcoidosis [25].

Device implantation is the mainstay treatment for cardiac sarcoidosis related life-threatening arrhythmias. When considering a patient with cardiac sarcoidosis and acquired heart block for

device implantation, a recent HRS consensus suggests an ICD to be taken into consideration instead of regular permanent pacemaker [25]. While studies have shown that immunosuppression, anti-arrhythmic drugs and ablation therapy may play a role in ventricular arrhythmia management, ICD implantation remains the first line of therapy for secondary prevention as well as primary prevention. When considering patients with cardiac sarcoidosis for an ICD in primary prevention, cardiac MRI (presence/absence of late gadolinium enhancement (LGE)) and electrophysiology study (VT inducibility) have been proven excellent tools for risk stratification [25].

A recent meta-analysis has shown that among patients referred to MRI for known or suspected cardiac sarcoidosis, the presence of LGE was associated with the occurrence of ventricular arrhythmia (5.9% per year in LGE positive versus 0% per year in LGE negative patients; relative risk 19.5, $p = 0.003$) and cardiovascular mortality (1.9% per year in LGE positive versus 0.3% per year in LGE negative; relative risk 10.7, $p = 0.03$) [27]. So cardiac MRI not only holds positive and differential diagnostic value, but also has prognostic value in patients with cardiac sarcoidosis.

23.2.3 Myocarditis

Myocarditis is an inflammatory disease involving the myocardium, that can be produced by a variety of causes (infectious, immune-mediated, toxic). In developed countries, viral infection is presumed to be the most frequent cause. Despite histology remaining the gold standard for diagnosis (the Dallas criteria) [28], low-risk patients are often presumed to have myocarditis based on a clinical scenario suggestive for new onset inflammatory cardiomyopathy and cardiac MRI.

Clinical presentation varies from subclinical to acute coronary syndrome—like, heart failure, cardiogenic shock, arrhythmias and sudden death [29]. It usually involves the left or both ventricles as well as the atria.

Isolated right ventricular myocarditis has been reported [30]. Several case reports have highlighted the importance of early diagnosis in this setting. If not recognized and untreated, it may progress to serious sequel and death—due to arrhythmic complications or heart failure.

23.2.4 Brugada Syndrome

The Brugada syndrome is an autosomal dominant genetic disorder, more commonly affecting men than women, characterized by abnormal findings on the surface electrocardiogram (ECG)—the presence of a pseudo right bundle branch block with persistent ST segment elevation in leads V1–V2. It is associated with an increased risk of ventricular tachyarrhythmias and SCD.

Several factors are considered to contribute to the electrocardiographic and clinical manifestations in the Brugada syndrome: mutations involving the cardiac sodium channel SCN genes, right ventricular abnormalities, autonomic tone, fever and the use of cocaine and other psychotropic drugs.

Sodium gene mutations result in a loss of function which reduces the duration of normal action potentials. Ventricular arrhythmias probably result from the heterogeneity of myocardial refractory periods within the right ventricle. The heterogeneity results from the presence of both normal and abnormal sodium channels within the same tissue (mainly RV) and from the differential impact of sodium current on the three myocardial layers [31].

Despite usually presenting without apparent structural heart disease, the Brugada syndrome has been shown to be associated with microscopic structural abnormalities, including inflammation and fibrosis, commonly affecting the RV outflow tract (RVOT) [32]. Noninvasive ECG mapping has shown delayed activation, slow conduction, and steep repolarization gradients between the RVOT and the rest of the RV, further supporting the role of the RVOT as the primary location of abnormal electrophysiologic substrate in the Brugada syndrome [33]. The main mechanism for ventricular arrhythmias is considered to be phase 2 reentry, which may precipitate sustained, usually polymorphic, VT.

Atrial fibrillation seems to be more common in Brugada patients and appears correlated with

higher risk for future ventricular tachyarrhythmias [34].

The main treatment for SCD prevention in the Brugada syndrome is ICD implantation, for secondary prevention or primary prevention in high risk patients. Defining high-risk patients for primary ICD prevention remains a challenge. The clinical features—presence of symptoms (syncope) and spontaneous type 1 ECG pattern, are important determinants of arrhythmia risk [35]. The use of EPS for SCD risk stratification remains questionable, especially in non-high-risk profile patients. Recent meta-analysis has shown that positive programmed ventricular stimulation is associated with future ventricular arrhythmia risk, and the induction with fewer extra stimuli is associated with higher risk. However, clinical risk factors were also important, and the negative predictive value was poor, particularly in patients with high-risk clinical features [35].

Drug therapy with quinidine or amiodarone can be useful for preventing recurrent VTs resulting in ICD therapies or in patients who refuse the ICD [36].

23.3 Congenital Heart Diseases Affecting the Right Heart, Associated with Increased Risk for Arrhythmia

A significantly increasing number of patients with congenital heart disease are surviving to adulthood. This has led to the appearance of novel complications secondary to the underlying congenital heart disease, related surgical interventions and associated comorbidities. A recent large North-American registry analysis has shown that around 25% of admissions in adults with congenital heart disease are associated with arrhythmia. The most prevalent arrhythmia in grown-ups with congenital heart disease (GUCH) was atrial fibrillation (86%) followed by atrial flutter (20%). The largest arrhythmia burden was observed in those with tricuspid atresia (59% prevalence) followed by Ebstein's anomaly (39% prevalence) [37]. SCD, mainly secondary to malignant ventricular arrhythmias, has been identified as main mode of death in some categories of GUCH after corrective surgery. ICD implantation is the main treatment for GUCH surviving a cardiac arrest, after exclusion of reversible causes (IB). Current guidelines give a class IC recommendation to EPS with catheter ablation in GUCH with spontaneous sustained VT. Surgical resection of arrhythmogenic substrate can also be taken into consideration [38].

23.3.1 Surgically Corrected Tetralogy of Fallot

Surgical correction for the tetralogy of Fallot (TOF) has been successfully performed for over 40 years. Studies have shown that SCD is the most common mode of death in patients with surgically corrected TOF [39]. There is a significant increase in mortality after 25 years following surgical correction for TOF, from 0.24% to 0.94% ($p = 0.003$), mainly related to RV malignant arrhythmias [40]. Still, the absolute rates remain small. While ICD implantation is clearly recommended for secondary SCD prevention (aborted SCD) in the absence of identifiable reversible causes [12], risk stratification for primary prevention remains a challenge.

Factors associated with higher arrhythmic risk after surgically corrected TOF are summarized in Table 23.1 [41].

However, a multivariable analysis showed only NSVT and left ventricular end-diastolic pressure ≥12 mmHg to be independent

Table 23.1 Factors associated with higher arrhythmic risk after surgically corrected tetralogy of Fallot

Age	≥30 years from corrective surgery
Related to surgical technique	Ventriculotomy incision
	Use of transannular patch
	Prior palliative shunt
ECG	QRS duration ≥180 ms
	Documented non-sustained VT
Electrophysiological study	Inducible monomorphic or polymorphic VT
Hemodynamic features	Left ventricular end-diastolic pressure ≥12 mmHg

ECG electrocardiogram, *VT* ventricular tachycardia

predictors for appropriate therapies in corrected TOF patients implanted with ICD [42]. Sustained VT, both monomorphic and polymorphic, inducible by EPS has also been shown to predict future clinical VT and SCD [43].

Based on the aforementioned factors, a multiparameter risk stratification approach has been suggested, classifying surgically corrected TOF patients into low (<1% per year), intermediate (1–11.5% per year) and high (>11.5% per year) risk for SCD. For the intermediate risk category, a negative EPS is considered re-assuring, while a positive EPS mandates ICD implantation. For high risk patients, a negative EPS is not considered re-assuring enough, and ICD implantation should be performed [41]. EPS and VT ablation can be successful in surgically corrected TOF patients, with both acute [44] and long-term benefits [45], especially in cases of monomorphic recurrent sustained VT. In this setting, current guidelines suggest an ICD to be implanted only if radiofrequency ablation fails to eliminate the tachycardia.

Careful evaluation when considering ICD implantation should be performed, as device-related complication rates are extremely high (up to 29%) in corrected TOF patients [42]. The advent of the subcutaneous ICD offers new therapeutical options in GUCH, especially in corrected TOF patients—with possibly lower complication rates and similar efficacy profile by comparison with classic ICD, as demonstrated by recent data [46].

23.3.2 Ebstein's Anomaly

Ebstein's anomaly is a rare congenital heart disease in which the septal and posterior leaflets of the tricuspid valve are displaced towards the apex of the RV. About 50% of patients with Ebstein's anomaly have evidence of Wolff-Parkinson-White syndrome with sometimes multiple right sided accessory pathways, secondary to atrialized right ventricular tissue [47].

Ebstein's anomaly has been associated with increased risk for sudden death during childhood and also in adults [48], not only related to the presence of the accessory pathways and increased risk for atrial fibrillation, but also secondary to malignant ventricular arrhythmia [49]. Surgical repair alone is considered insufficient, and Ebstein patients should undergo thorough electrophysiological evaluation including EPS, especially in the presence of Wolff-Parkinson-White syndrome [50, 51], where successful radiofrequency ablation can significantly reduce even normalize the risk for SCD.

23.3.3 Atrial Septal Defect

Left-to-right shunts, such as in atrial septal defects (ASD), may lead to right-side volume overload, pulmonary hypertension and right heart cavities remodeling and dilatation. Right atrium remodeling may be associated with increased risk for typical atrial flutter.

Typical and atypical right atrial flutters are common following surgical corrections of ASD.

Radiofrequency catheter ablation of the cavotricuspid is associated with high acute success rates and low recurrence rates in the absence of significant structural heart disease (with or without previous cardiac surgery) and therefore should be recommended as first line therapy for typical atrial flutter [52].

Furthermore, long-term follow-up data has demonstrated the efficacy of electroanatomic guided radiofrequency ablation of late onset macro-reentrant atrial arrhythmias in patients with surgically corrected ASD. Therefore radiofrequency ablation should be considered early in this setting [53].

23.4 Right Heart Arrhythmias in the Setting of a Structurally Normal Heart

23.4.1 Rare Types of Right-Sided Accessory Pathways

There are two types of rare accessory pathways with typical right-side insertion: Mahaim fibers and Coumel type.

Mahaim fibers are defined as decrementally conducting connections between the right atrium or the AV node and the right ventricle in or close to the right bundle branch. They are typically responsible for antidromic reentrant tachycardia with LBBB morphology, while sinus rhythm ECG is usually normal. Rarely, typical right-side pre-excitation may be noticed during sinus rhythm [54]. Although generally benign, in rare cases it can be responsible for tachycardia induced cardiomyopathy [55]. Because of atypical RV insertion, radiofrequency ablation may be challenging and require electroanatomic mapping support [56].

Coumel type tachycardia refers to permanent junctional reciprocating tachycardia (PJRT). It is an orthodromic atrio-ventricular reentrant tachycardia through an atypical accessory pathway with retrograde decremental conduction properties usually located in the right postero-septal area [57]. PJRT is most commonly diagnosed in children but can sometimes be discovered in adults as well [58]. Because of the persistent recurrent nature, PJRT is associated with increased risk for tachycardia induced cardiomyopathy [59]. Radiofrequency ablation is usually very efficient and should be taken into consideration early during the disease.

23.4.2 Right Ventricular Outflow Tract Ventricular Tachycardia

Some VT syndromes can occur in normal hearts and have a benign prognosis [60]. The most common origin for idiopathic repetitive monomorphic VT is the RVOT. The main mechanism is triggered activity and can be adenosine sensitive.

The diagnostic work-out in patient with RVOT VT is targeted at eliminating any suspicion of underlying heart condition (structural heart disease or channelopathy)—as idiopathic VT remains an exclusion diagnosis. The main differential diagnosis is with ARVC.

The findings in patients with idiopathic VT are summarized below:

- Normal rest ECG between arrhythmia episodes
- Functional studies for left and right ventricle should be within limits when assessed in sinus rhythm
- Exercise stress test should be normal—negative for myocardial ischemia, with no exercise inducible arrhythmia
- Normal coronary angiogram—if considered necessary to be performed
- Cardiac MRI may be normal or reveal mild structural abnormalities of the RV, primarily affecting the free wall (focal thinning, fatty infiltration, wall motion abnormalities); the significance of these findings remain unclear unless they can be seen in the RVOT as well [61]
- RV radionuclide imaging may help distinguish between idiopathic VT and dilated cardiomyopathy, myocarditis and ARVC [62]
- Endomyocardial biopsy, if performed, should be normal

In rare cases, a high arrhythmia burden (>20,000 PVCs/day) may lead to tachycardia induced cardiomyopathy, in which case differential diagnosis with dilated cardiomyopathy may prove difficult. It is important however to recognize this entity as arrhythmia elimination by radiofrequency ablation may result in heart function normalization [63].

Otherwise the treatment is mainly symptom-driven and depends upon arrhythmia burden. Due to limited efficacy and potential side effects of anti-arrhythmic drugs, the main treatment for patients with symptomatic idiopathic RVOT VT is radiofrequency ablation, with success rates ranging from 80% to 100%, depending upon the site of origin [64]. Recent meta-analysis has shown that radiofrequency catheter ablation significantly reduces the number of PVCs from the RVOT by an average of 30,089/24-hours ($p < 0.00001$) and improves left ventricular ejection fraction by a mean of 10.36 ($p < 0.00001$) [65], underlining its role as first line option for a curative treatment in RVOT VT.

23.5 Arrhythmias Secondary to Pulmonary Arterial Hypertension

Longstanding pressure and volume overload due to pulmonary arterial hypertension (PAH) leads to electro-anatomical remodeling of the right heart cavities and right heart failure. In combination with changes in autonomic tone, repolarization abnormalities and ischemia, it increases arrhythmogenicity in patients with PAH. Supraventricular arrhythmias—usually atrial fibrillation and atrial flutter, as well as atrioventricular nodal reentrant tachycardia (AVNRT), can occur during the course of the disease, and are associated with worsened prognosis [66]. Radiofrequency ablation is highly efficient for treating typical atrial flutter and AVNRT, with high acute success rates (over 80%), resulting in clinical and hemodynamic improvement; recurrence rates may be higher as compared to other heart conditions, because of evolving right atrial substrate [66]. There is no specific data regarding atrial fibrillation management in PAH patients.

SCD and RV failure account for almost 2/3 of deaths in PAH patients [67]. In contrast with patients suffering from left heart disease, malignant ventricular arrhythmias are relatively rare events in PAH patients. The main cause for SCD seems to be bradycardia and electromechanical dissociation. The main prognosis factor in PAH is RV function and SCD is more likely to occur in the setting of severe RV systolic dysfunction and hypoxia [68]. The role of anti-bradycardia pacing or ICD has not been established in PAH patients.

Conclusion

Arrhythmia management in right heart disease is based upon assessing the clinical and hemodynamic impact as well as understanding the underlying heart disease and substrate. As opposed to left heart disease, structural right heart disease may be less obvious to diagnose and require advanced cardiac imaging–mainly cardiac MRI, invasive studies and in some cases—endomyocardial biopsy. Differential diagnosis for VT originating in the RV is crucial, due to the frequent nature of idiopathic RVOT VT and the possible overlap of ARVC with cardiac sarcoidosis. Among grown-ups with congenital heart disease involving RV, those with surgically corrected tetralogy of Fallot and Ebstein's anomaly are at highest risk for arrhythmic events, including VT and sudden death. Arrhythmia treatment and SCD prevention in right heart disease is similar to left heart disease and is based on ICD implantation and electrophysiology study with radiofrequency ablation.

References

1. Dalal D, James C, Devanagondi R, Tichnell C, Tucker A, Prakasa K, Spevak PJ, Bluemke DA, Abraham T, Russell SD, Calkins H, Judge DP. Penetrance of mutations in plakophilin-2 among families with arrhythmogenic right ventricular dysplasia/cardiomyopathy. J Am Coll Cardiol. 2006;48:1416–24.
2. Basso C, Czarnowska E, Della Barbera M, et al. Ultrastructural evidence of intercalated disc remodelling in arrhythmogenic right ventricular cardiomyopathy: an electron microscopy investigation on endomyocardial biopsies. Eur Heart J. 2006;27:1847–54.
3. Basso C, Thiene G, Corrado D, Angelini A, Nava A, Valente M. Arrhythmogenic right ventricular cardiomyopathy. Dysplasia, dystrophy, or myocarditis? Circulation. 1996;94:983–91.
4. Te Riele ASJM, James CA, Philips B, et al. Mutation-positive arrhythmogenic right ventricular dysplasia/cardiomyopathy: the triangle of dysplasia displaced. J Cardiovasc Electrophysiol. 2013;24:1311–20.
5. Hulot J-S, Jouven X, Empana J-P, Frank R, Fontaine G. Natural history and risk stratification of arrhythmogenic right ventricular dysplasia/cardiomyopathy. Circulation. 2004;110:1879–84.
6. Corrado D, Basso C, Schiavon M, Thiene G. Screening for hypertrophic cardiomyopathy in young athletes. N Engl J Med. 1998;339:364–9.
7. Dalal D, Nasir K, Bomma C, et al. Arrhythmogenic right ventricular dysplasia: a United States experience. Circulation. 2005;112:3823–32.
8. Nava A, Bauce B, Basso C, Muriago M, Rampazzo A, Villanova C, Daliento L, Buja G, Corrado D, Danieli GA, Thiene G. Clinical profile and long-term follow-up of 37 families with arrhythmogenic right ventricular cardiomyopathy. J Am Coll Cardiol. 2000;36:2226–33.
9. Marcus FI, McKenna WJ, Sherrill D, et al. Diagnosis of arrhythmogenic right ventricular cardiomyopathy/dysplasia: proposed modification of the task force criteria. Circulation. 2010;121:1533–41.

10. Niroomand F, Carbucicchio C, Tondo C, Riva S, Fassini G, Apostolo A, Trevisi N, Bella PD. Electrophysiological characteristics and outcome in patients with idiopathic right ventricular arrhythmia compared with arrhythmogenic right ventricular dysplasia. Heart. 2002;87:41–7.
11. Schinkel AFL. Implantable cardioverter defibrillators in arrhythmogenic right ventricular dysplasia/cardiomyopathy: patient outcomes, incidence of appropriate and inappropriate interventions, and complications. Circ Arrhythm Electrophysiol. 2013;6:562–8.
12. Priori SG, Blomström-Lundqvist C, Mazzanti A, et al. 2015 ESC guidelines for the management of patients with ventricular arrhythmias and the prevention of sudden cardiac death: the task force for the management of patients with ventricular arrhythmias and the prevention of sudden cardiac death of the European Society of Cardiology (ESC). Endorsed by: Association for European Paediatric and Congenital Cardiology (AEPC). Eur Heart J. 2015;36:2793–867.
13. Jiang H, Zhang X-L, Yang Q-L, Zhu S-H, Yu H-S, Xu B, Huang W. Catheter ablation for ventricular tachycardia in patients with arrhythmogenic right ventricular dysplasia/cardiomyopathy: a systematic review and meta-analysis. Acta Cardiol. 2016;71:639–49.
14. Smith W. Members of CSANZ cardiovascular genetics working group: guidelines for the diagnosis and management of arrhythmogenic right ventricular cardiomyopathy. Heart Lung Circ. 2011;20:757–60.
15. Wu L, Guo J, Zheng L, Chen G, Ding L, Qiao Y, Sun W, Yao Y, Zhang S. Atrial remodeling and atrial tachyarrhythmias in arrhythmogenic right ventricular cardiomyopathy. Am J Cardiol. 2016;118:750–3.
16. Mazzanti A, Ng K, Faragli A, et al. Arrhythmogenic right ventricular cardiomyopathy: clinical course and predictors of arrhythmic risk. J Am Coll Cardiol. 2016;68:2540–50.
17. Statement on sarcoidosis. Joint statement of the American Thoracic Society (ATS), the European Respiratory Society (ERS) and the World Association of Sarcoidosis and Other Granulomatous Disorders (WASOG) adopted by the ATS board of directors and by the ERS executive committee, February 1999. Am J Respir Crit Care Med. 1999;160:736–55.
18. Hulten E, Aslam S, Osborne M, Abbasi S, Bittencourt MS, Blankstein R. Cardiac sarcoidosis-state of the art review. Cardiovasc Diagn Ther. 2016;6:50–63.
19. Jeudy J, Burke AP, White CS, Kramer GBG, Frazier AA. Cardiac sarcoidosis: the challenge of radiologic-pathologic correlation: from the radiologic pathology archives. Radiographics. 2015;35:657–79.
20. Ueberham L, Paetsch I, Jahnke C, Klingel K, Dinov B. Right ventricular thickening and extensive late gadolinium enhancement in a patient with rare case of isolated cardiac sarcoidosis and initially negative biopsy. Eur Heart J Cardiovasc Imaging. 2017;18(12):1427–8.
21. Patel MR, Cawley PJ, Heitner JF, Klem I, Parker MA, Jaroudi WA, Meine TJ, White JB, Elliott MD, Kim HW, Judd RM, Kim RJ. Detection of myocardial damage in patients with sarcoidosis. Circulation. 2009;120:1969–77.
22. Yoshida Y, Morimoto S, Hiramitsu S, Tsuboi N, Hirayama H, Itoh T. Incidence of cardiac sarcoidosis in Japanese patients with high-degree atrioventricular block. Am Heart J. 1997;134:382–6.
23. Yigla M, Badarna-Abu-Ria N, Tov N, Ravell-Weiller D, Rubin A-HE. Sarcoidosis in northern Israel; clinical characteristics of 120 patients. Sarcoidosis Vasc Diffuse Lung Dis Off J WASOG. 2002;19:220–6.
24. Iwai K, Sekiguti M, Hosoda Y, DeRemee RA, Tazelaar HD, Sharma OP, Maheshwari A, Noguchi TI. Racial difference in cardiac sarcoidosis incidence observed at autopsy. Sarcoidosis. 1994;11:26–31.
25. Birnie DH, Sauer WH, Bogun F, et al. HRS expert consensus statement on the diagnosis and management of arrhythmias associated with cardiac sarcoidosis. Heart Rhythm. 2014;11:1305–23.
26. Nery PB, Keren A, Healey J, Leug E, Beanlands RS, Birnie DH. Isolated cardiac sarcoidosis: establishing the diagnosis with electroanatomic mapping-guided endomyocardial biopsy. Can J Cardiol. 2013;29:1015.e1–3.
27. Hulten E, Agarwal V, Cahill M, Cole G, Vita T, Parrish S, Bittencourt MS, Murthy VL, Kwong R, Di Carli MF, Blankstein R. Presence of late gadolinium enhancement by cardiac magnetic resonance among patients with suspected cardiac sarcoidosis is associated with adverse cardiovascular prognosis: a systematic review and meta-analysis. Circ Cardiovasc Imaging. 2016;9:e005001.
28. Caforio ALP, Pankuweit S, Arbustini E, et al. Current state of knowledge on aetiology, diagnosis, management, and therapy of myocarditis: a position statement of the European society of cardiology working group on myocardial and pericardial diseases. Eur Heart J. 2013;34:2636–48. 2648a–2648d
29. Olinde KD, O'Connell JB. Inflammatory heart disease: pathogenesis, clinical manifestations, and treatment of myocarditis. Annu Rev Med. 1994;45:481–90.
30. Virk HUH, Munir MB. Isolated right ventricular myocarditis: rarely reported pathology. Case Rep Cardiol. 2015; [cited Oct 29, 2017]. Available from: https://www.hindawi.com/journals/cric/2015/790246/.
31. Gussak I, Antzelevitch C, Bjerregaard P, Towbin JA, Chaitman BR. The Brugada syndrome: clinical, electrophysiologic and genetic aspects. J Am Coll Cardiol. 1999;33:5–15.
32. Frustaci A, Priori SG, Pieroni M, Chimenti C, Napolitano C, Rivolta I, Sanna T, Bellocci F, Russo MA. Cardiac histological substrate in patients with clinical phenotype of Brugada syndrome. Circulation. 2005;112:3680–7.
33. Zhang J, Sacher F, Hoffmayer K, et al. Cardiac electrophysiological substrate underlying the ECG phenotype and electrogram abnormalities in Brugada syndrome patients. Circulation. 2015;131:1950–9.
34. Kusano KF, Taniyama M, Nakamura K, et al. Atrial fibrillation in patients with Brugada syndrome relationships of gene mutation, electrophysiol-

ogy, and clinical backgrounds. J Am Coll Cardiol. 2008;51:1169–75.
35. Sroubek J, Probst V, Mazzanti A, et al. Programmed ventricular stimulation for risk stratification in the Brugada syndrome: a pooled analysis. Circulation. 2016;133:622–30.
36. Priori SG, Wilde AA, Horie M, et al. HRS/EHRA/APHRS expert consensus statement on the diagnosis and management of patients with inherited primary arrhythmia syndromes: document endorsed by HRS, EHRA, and APHRS in May 2013 and by ACCF, AHA, PACES, and AEPC in June 2013. Heart Rhythm. 2013;10:1932–63.
37. Loomba RS, Buelow MW, Aggarwal S, Arora RR, Kovach J, Ginde S. Arrhythmias in adults with congenital heart disease: what are risk factors for specific arrhythmias? Pacing Clin Electrophysiol PACE. 2017;40:353–61.
38. Baumgartner H, Bonhoeffer P, De Groot NMS, et al. ESC guidelines for the management of grown-up congenital heart disease (new version 2010). Eur Heart J. 2010;31:2915–57.
39. Gatzoulis MA, Balaji S, Webber SA, Siu SC, Hokanson JS, Poile C, Rosenthal M, Nakazawa M, Moller JH, Gillette PC, Webb GD, Redington AN. Risk factors for arrhythmia and sudden cardiac death late after repair of tetralogy of Fallot: a multicentre study. Lancet Lond Engl. 2000;356:975–81.
40. Nollert G, Fischlein T, Bouterwek S, Böhmer C, Klinner W, Reichart B. Long-term survival in patients with repair of tetralogy of Fallot: 36-year follow-up of 490 survivors of the first year after surgical repair. J Am Coll Cardiol. 1997;30:1374–83.
41. Khairy P, Dore A, Poirier N, Marcotte F, Ibrahim R, Mongeon F-P, Mercier L-A. Risk stratification in surgically repaired tetralogy of Fallot. Expert Rev Cardiovasc Ther. 2009;7:755–62.
42. Khairy P, Harris L, Landzberg MJ, et al. Implantable cardioverter-defibrillators in tetralogy of Fallot. Circulation. 2008;117:363–70.
43. Khairy P, Landzberg MJ, Gatzoulis MA, Lucron H, Lambert J, Marçon F, Alexander ME, Walsh EP. Value of programmed ventricular stimulation after tetralogy of fallot repair: a multicenter study. Circulation. 2004;109:1994–2000.
44. Grieco D, Peichl P, Cihák R, Kautzner J. Successful ablation of ventricular tachycardia after correction of tetralogy of Fallot. Herzschrittmachertherapie Elektrophysiologie. 2014;25:116–20.
45. Laredo M, Frank R, Waintraub X, Gandjbakhch E, Iserin L, Hascoët S, Himbert C, Gallais Y, Hidden-Lucet F, Duthoit G. Ten-year outcomes of monomorphic ventricular tachycardia catheter ablation in repaired tetralogy of Fallot. Arch Cardiovasc Dis. 2017;110:292–302.
46. Moore JP, Mondésert B, Lloyd MS, Cook SC, Zaidi AN, Pass RH, John AS, Fish FA, Shannon KM, Aboulhosn JA, Khairy P, Alliance for Adult Research in Congenital Cardiology (AARCC). Clinical experience with the subcutaneous implantable cardioverter-defibrillator in adults with congenital heart disease. Circulation: Arrhythmia and Electrophysiology. 2016;9(9). pii:e004338.
47. Attenhofer Jost CH, Connolly HM, Dearani JA, Edwards WD, Danielson GK. Ebstein's anomaly. Circulation. 2007;115:277–85.
48. Freeman A, Byard RW. Ebstein anomaly and sudden childhood death. J Forensic Sci. 2017 Sep 20. doi: 10.1111/1556–4029.13652.
49. Sherwin ED, Abrams DJ. Ebstein anomaly. Card Electrophysiol Clin. 2017;9:245–54.
50. Huang CJ, Chiu IS, Lin FY, Chen WJ, Lin JL, Lo HM, Wu MH, Chu SH. Role of electrophysiological studies and arrhythmia intervention in repairing Ebstein's anomaly. Thorac Cardiovasc Surg. 2000;48:347–50.
51. Chauvaud SM, Brancaccio G, Carpentier AF. Cardiac arrhythmia in patients undergoing surgical repair of Ebstein's anomaly. Ann Thorac Surg. 2001;71:1547–52.
52. Dallaglio PD, Anguera I, Jiménez-Candil J, et al. Impact of previous cardiac surgery on long-term outcome of cavotricuspid isthmus-dependent atrial flutter ablation. Europace. 2016;18:873–80.
53. Scaglione M, Caponi D, Ebrille E, Di Donna P, Di Clemente F, Battaglia A, Raimondo C, Appendino M, Gaita F. Very long-term results of electroanatomic-guided radiofrequency ablation of atrial arrhythmias in patients with surgically corrected atrial septal defect. Europace. 2014;16:1800–7.
54. Katritsis DG, Wellens HJ, Josephson ME. Mahaim accessory pathways. Arrhythmia Electrophysiol Rev. 2017;6:29–32.
55. Gul I, Roziman Q, Khan AH. Mahaim tachycardia induced cardiomyopathy. J Coll Physicians Surg Pak. 2016;26:S80–2.
56. Asakai H, Fenwick L, Hamilton RM. Electroanatomical voltage mapping of atrial Mahaim potentials to guide catheter ablation. Hear Case Rep. 2016;2:499–501.
57. Tseng ZH, Scheinman M. Persistent long R-P tachycardia. Card Electrophysiol Clin. 2010;2:225–9.
58. Ho RT. Diagnosis and ablation of long RP supraventricular tachycardias. Curr Treat Options Cardiovasc Med. 2015;17:370.
59. Vollmann D, Hansen C. Permanent junctional reciprocating tachycardia causing cardiomyopathy in an adult woman. Herzschrittmachertherapie Elektrophysiologie. 2016;27:404–7.
60. Brooks R, Burgess JH. Idiopathic ventricular tachycardia. A review. Medicine (Baltimore). 1988;67:271–94.
61. Globits S, Kreiner G, Frank H, Heinz G, Klaar U, Frey B, Gössinger H. Significance of morphological abnormalities detected by MRI in patients undergoing successful ablation of right ventricular outflow tract tachycardia. Circulation. 1997;96:2633–40.
62. Eguchi M, Tsuchihashi K, Nakata T, Hashimoto A, Shimamoto K. Right ventricular abnormalities assessed by myocardial single-photon emission computed tomography using technetium-99m

sestamibi/tetrofosmin in right ventricle-originated ventricular tachyarrhythmias. J Am Coll Cardiol. 2000;36:1767–73.
63. Yarlagadda RK, Iwai S, Stein KM, Markowitz SM, Shah BK, Cheung JW, Tan V, Lerman BB, Mittal S. Reversal of cardiomyopathy in patients with repetitive monomorphic ventricular ectopy originating from the right ventricular outflow tract. Circulation. 2005;112:1092–7.
64. Rodriguez LM, Smeets JL, Timmermans C, Wellens HJ. Predictors for successful ablation of right- and left-sided idiopathic ventricular tachycardia. Am J Cardiol. 1997;79:309–14.
65. Lamba J, Redfearn DP, Michael KA, Simpson CS, Abdollah H, Baranchuk A. Radiofrequency catheter ablation for the treatment of idiopathic premature ventricular contractions originating from the right ventricular outflow tract: a systematic review and meta-analysis. Pacing Clin Electrophysiol PACE. 2014;37:73–8.
66. Tongers J, Schwerdtfeger B, Klein G, Kempf T, Schaefer A, Knapp J-M, Niehaus M, Korte T, Hoeper MM. Incidence and clinical relevance of supraventricular tachyarrhythmias in pulmonary hypertension. Am Heart J. 2007;153:127–32.
67. Tateno S, Niwa K, Nakazawa M, Iwamoto M, Yokota M, Nagashima M, Echigo S, Kado H, Shima M, Gatzoulis MA. Risk factors for arrhythmia and late death in patients with right ventricle to pulmonary artery conduit repair–Japanese multicenter study. Int J Cardiol. 2006;106:373–81.
68. McLaughlin VV. Looking to the future: a new decade of pulmonary arterial hypertension therapy. Eur Respir Rev Off J Eur Respir Soc. 2011;20:262–9.

Pulmonary Thromboembolism

24

Letícia Oliveira and Edmo Atique Gabriel

Abstract

Pulmonary Thromboembolism is the clinical entity due to the obstruction of pulmonary vessels by venous thrombi, leading to nonspecific clinical manifestations, making it difficult to early diagnosis. Predisposition results from genetic and acquired factors contributing to the venous thromboembolism. When the diagnosis of Pulmonary Thromboembolism (PT) is confirmed and effective therapy is instituted, the recurrence of embolism is rare and death is usually uncommon, with mortality rate around 20–30%.

Keywords

Pulmonary thromboembolism · Vessels · Diagnosis · Anticoagulation

24.1 Introduction

The pulmonary thromboembolism (PT) is defined by a pulmonary vein obstruction caused by an embolus originating, most commonly, from the deep venous system. By means of the right cardiac chambers the trombus reaches the pulmonary vein and can present a nonspecific clinical picture, which makes its early diagnosis.

USA has an incidence of 1:1000 individuals, and a mortality rate of up to 15% in the first 3 months. In about 10% of cases, sudden death. Its main complication, in long term, is the pulmonary hypertension [1].

Virchow's triad (Fig. 24.1) is the physiopathological basis of the PT, and therefore is any state that expresses venous stasis, endothelial injury or hypercoagulability able to trigger the formation of thrombi. In the PT occurs the release of inflammatory cytokines (especially Thromboxane A2 and Serotonin) which induces vasoconstriction with initial increases of pulmonary vascular resistance after PT, and may be reversed with the use of vasodilators. The abrupt increase in pulmonary vascular resistance generates the dilation of the right ventricle, through the Frank-Starling mechanism. The increased tension on the wall of the right ventricle promotes the stretch myocytes. All these compensatory mechanisms together generate an increase in pulmonary arterial pressure in the attempt to compensate for the pulmonary vascular obstruction. Because the properties of the right ventricle (thin walls and lack of conditioning) is not able to withstand high pressures in the pulmonary artery.

Because of dyssynchrony between the ventricles, it might install a right bundle branch block, with the reduction in preload for left ventricle,

L. Oliveira (✉) · E. A. Gabriel
União das Faculdades dos Grandes Lagos (UNILAGO), São José do Rio Preto, SP, Brazil

S. I. Dumitrescu et al. (eds.), *Right Heart Pathology*, https://doi.org/10.1007/978-3-319-73764-5_24

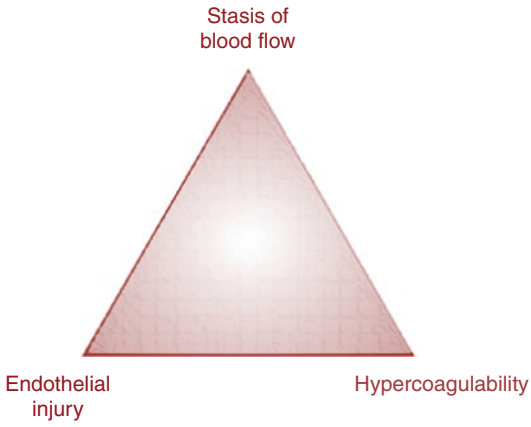

Fig. 24.1 Main risk factors for the development of pulmonary thromboembolism

that won't be able to keep a good cardiac output, culminating with the installation of hypotension and shock causing hemodynamic instability to the individual.

Respiratory failure in pulmonary embolism is predominantly hemodynamics. The low cardiac output results in desaturation of mixed venous blood. In addition, the flow in clogged vessels, combined with overflowing in the capillary zones served by vessels that are not blocked, ventilation-perfusion mismatch contributes to hypoxemia. In about a third of patients, the right-to-left shunt foramen ovale can be detected by echocardiography: this is caused by a pressure gradient reversed between the right atrium and the left atrium that can lead to severe hypoxemia and an increased risk of paradoxical embolization and stroke. Finally, even if it doesn't affect the hemodynamics, small distal emboli may create areas of hemorrhage resulting in hemoptysis, pleuritis and pleural effusion, which usually is mild. This clinical presentation is known as pulmonary infarction. Its effect on gas exchange is usually light [2].

Individuals who are in the fourth decade of life have an increased risk when compared to younger people. Environmental and genetic factors are involved in the genesis of the PT. The most common risk factors include: smoking, male, obesity, cardiac arrhythmias, heart failure, difficult surgery, neurological patients (spinal cord injury, traumatic brain injury, cerebrovascular accident), patients with long immobility, women in oral contraceptive use within the last 6 weeks–3 months, post menopause in use of hormone replacement therapy, some types of cancers, thrombophilia, previous episodes of PT or deep vein thrombo-

Table 24.1 Risk factors for pulmonary thromboembolism

Risk factors (relative risk between 5 and 20)	
Surgical	Abdominal or pelvic surgery, large
	Hip prosthesis or knee
	Need for ICU postoperatively
	Multiple trauma/spinal cord trauma
Obstetric	Pregnancies
	Cesarean delivery
	Puerperium
Problems in lower limbs	Fracture
	AVC with paralysis of limbs
Malignancy	Abdominal or pelvic neoplasm
	Advanced or metastatic disease
	Chemotherapy
> Immobility 3 days	Hospitalization
	Institutionalization
Thrombophilia	Antithrombin deficiency
	Protein C deficiency
	Protein S deficiency
	Antifosfolipideo syndrome
	Homozygous factor V Leiden
	Homozygosity for prothrombin gene mutation
Other	Previous embolic event
Minor risk factors (relative risk between 2 and 4)	
Cardiovascular diseases	Congenital heart diseases
	Congestive heart insufficiency
	Age
	Superficial thrombophlebitis/ varicose veins
	Central venous catheter
Estrogens	Oral contraceptive
	Hormone replacement therapy
Thrombophilia	Heterozygosity for factor V Leiden
	Heterozygosity for prothrombin gene mutation
	Hyperhomocisteinemia
Other	Exacerbation of COPD
	Neurological deficiencies
	Occult malignancy
	Extended trips
	Obesity

Adapted of J Bras Pneumol. v. 36

sis (DVT), among others. In the table below are listed the main risk factors according to the risk presented (Table 24.1).

The clinical picture is variable, and it may present as a finding in asymptomatic patient or in sudden death cases with the presence of massive emboli. The most common symptoms are chest pain, tachycardia and dyspnea. However they have low specificity. Conversely, evidence of massive PT include: syncope, hypotension, shock, cyanosis, metabolic acidosis and engorgement of the neck veins. The main signs and symptoms in PT in order of frequency according to some studies [3] are tachypnea, tachycardia, decreased breath sounds, pulmonary rales, friction, wheezing, hypotension, fever, cyanosis, signs of DVT, Homan's sign.

The diagnosis can be obtained from the clinical history and physical examination wide. According to the degree of suspicion some additional specific examinations are requested. To define the probability of being or not PT some scores are used. The most used in our midst is the Wells score (below) (Table 24.2):

Table 24.2 Two levels DVT Wells score

Clinical feature	Points
Active cancer (treatment ongoing, within 6 months, or palliative)	1
Paralysis, paresis or recent plaster immobilisation of the lower extremities	1
Recently bedridden for 3 days or more or major surgery within 12 weeks requiring general or regional anaesthesia	1
Localised tenderness along the distribution of the deep venous system	1
Entire leg swollen	1
Calf swelling at least 3 cm larger than asymptomatic side	1
Pitting oedema confined to the symptomatic leg	1
Collateral superficial veins (non-varicose)	1
Previously documented DVT	1
An alternative diagnosis is at least as likely as DVT	−2
Clinical probability simplified score	
DVT likely	2 points or more
DVT unlikely	1 point or less

Adapted with permission from Wells PS et al. (2003) Evaluation of D-dimer in the diagnosis of suspected deep-vein thrombosis

Some additional tests may be useful for diagnosing of PT: electrocardiogram (EKG) and chest x-ray may show changes, nonspecific features or normal findings. Pulmonary scintigraphy with hypoperfusion and preserved ventilation areas suggests pulmonary embolism. In contrast, a normal scintigraphy makes the diagnosis [4]. In approximately 50% of cases, a helical computed angiotomography can confirm the diagnosis. The echocardiography is useful for the stratification of PT severity since it is able to detect right ventricular dysfunction-marker of poor prognosis, as we shall see below. Angiography-the 'gold standard'- should be reserved for cases where the aforementioned tests were unable to establish the diagnosis, because of its invasive nature and risks associated with the contrast [5].

The alterations found in pulmonary thromboembolism may be the most diverse. Among them can be mentioned: chest x-ray: normal (12%); atelectasis (69%); unilateral pleural effusion (47%); hypoperfusion area (Westermark sign); Hampton sign.

Rare/specific: Palla sign; Diaphragmatic elevation; EKG: changed in 70% cases with the right bundle branch block; axis deviation to the right; the default S1Q3T3; T wave inversion in the precordial leads (V1–V4); the sinus arrhythmia (sinus catecholamine); arterial blood gases: the hypoxemia with respiratory alkalosis; the hypoxemia with respiratory acidosis (in massive/circulatory collapse); the normal PO^2 in 18% patients.

D-Dimer: its main utility is in association with pretests, to remove suspicion when negative diagnosis persists. Should not be required for patients with high clinical pretest probability.

Duplex scan of legs: it makes the diagnosis of PT, to DVT; Sensitivity and specificity over 90% to the proximal venous thrombosis.

Ventilation/Infusion scintigraphy normal: deletes PT (25% examinations);

The low or medium likelihood: No diagnosis, it pursues research (65% examinations); the high probability: diagnosis of PT (10% examinations); Helical computed tomography: Method

more sensitive for identifying thrombi in the main branches, and segmental lobar bronchi. Echocardiogram: important for function evaluation of RV (only 30–40% have disorders): the increase in the size of right ventricle; the RV function; the Tricuspid Regurgitation; the side wall of RV Hypokinesia (McConnell); Troponins: acute injury to myocytes; Elevation smaller and shorter in the PT; Direct relationship with severity; >0.07 values: sensitivity—70 to 65% for disease specific prognosis [6].

Pulmonary Arteriography: "gold standard" method for the diagnosing PT with visualization of pulmonary circulation, after injection of iodine contrast. The main complications of method are anaphylaxis and nefro-induced contrast toxicity, which can be minimized with proper hydration.

The differential diagnosis of PT includes acute coronary syndrome, thoracic aortic aneurysm, acute pericarditis, cardiac tamponade, tension pneumothorax, pneumomediastium, thoracic tumors, fractures of ribs, intercostal neuralgia, congestive heart failure, decompensated acute asthma, exacerbation of chronic obstructive pulmonary disease, tuberculosis, bronchiectasis and pneumonia.

General measures aimed at clinical and hemodynamic stability should be instituted as soon as possible. Critical patients will need intensive care.

Anticoagulation should be undertaken judiciously in patients with PT.

In the treatment of venous thromboembolism, intravenous unfractionated heparin (UFH) is the most frequent used with proven efficacy of therapeutic approach. The subcutaneous injection can be the alternative to administration of UFH, however with much greater variability than the intravenous, and should be avoided [7]. The average daily dose of UFH in the treatment of venous thromboembolism ranges from 24,000 to 30,000 U in 24 h. Continuous infusion of UFH provides greater stability in serum heparin levels, with less occurrence of bleeding when compared to intermittent administration. The recommended strategy uses 80 U/Kg as bolus loading dose, followed by a maintenance dose of 18 U/Kg/h, which should be adjusted according to changes in the APTT. Intermittent administration, the dose of UFH is 5000 U every 4 hours and the APTT is evaluated before each dose, until they get stability, when, then, may be evaluated at larger intervals. The treatment time with no fractional heparin, usually 5–7 days, coincident with the time required to achieve adequate anticoagulation with the use of oral anticoagulants, being considered effective and safe strategy. The subcutaneous route, when used, requires the same care of laboratory control. The dose of unfractionated heparin subcutaneously is 17,500 U every 12 h. Its use requires laboratory follow-up through evaluations of APTT. The therapeutic goal is to maintain serum levels of APTT between 1.5 and 2.5 times the baseline of patient.

In the treatment of DVT, the use of Low-Molecular-Weight Heparin (LMWH) is established through studies that showed its efficacy and safety when compared to UFH. In PT studies, although outnumbered, all point in the same direction, making the use of LMWH a therapeutic option. Staying in hospitals of patients treated with LMWH has been orientation of some studies, however, in others, outpatient treatment is recommended. The dose of LMWH depends on PT presentation and should be individualized [8].

Fondaparinux, a factor Xa inhibitor, has been shown to be at least as effective and safe as unfractionated heparin for the treatment of pulmonary embolism in hemodynamically stable patients and may be considered a therapeutic option when is commercially available.

Oral anticoagulants: Coumarins are oral anticoagulants that act by inhibiting the synthesis of vitamin K-dependent (II, VII, IX and X) coagulation factors, in addition to the anticoagulant, protein C and protein S. Laboratory control of anticoagulation in patients using oral anticoagulants is classically performed through time measurement and prothrombin activity. The therapeutic objective of the use of oral anticoagulants in the treatment of pulmonary thromboembolism is to maintain INR between 2.0 and 3.0, a range in which good antithrombotic efficacy with a low incidence of bleeding was demonstrated. The initial dose of warfarin is 5 mg/day and may be initiated concomitantly with heparin on the first day

of treatment. Doses greater than 5 mg showed a small reduction in time to obtain the appropriate INR, but, however with significantly increased cases of bleeding. In general, the average time to achieve adequate anticoagulation with warfarin is 5 days, during which time the patient should be in concomitant use of heparin. The duration of treatment with oral anticoagulants will depend on, fundamentally, the risk factors and their possibility of being removed. Patients with only those factors considered to be removable, such as the use of estrogen or with a surgical procedure, may be treated for 3 months, as long as they are suspended on exposure to these situations. Idiopathic thrombosis, in its first episode, requires treatment for at least 6 months. In patients with recurrent idiopathic thrombosis, or in those with non-removable risk factors, treatment may extend for 12 months or longer. The therapeutic strategy for cases of thrombophilia is individualized according to each specific clinical situation [9].

Antithrombinics: ximelagatran is the first antithrombin available for oral use and was evaluated in patients undergoing orthopedic surgery. Ximelagatran showed to be superior to warfarin with an equivalent prevalence of bleeding, being considered a promising alternative to coumarins. Thrombolytics: The use of thrombolytic in the treatment of PT has its rational basis based on the fact that these drugs are more effective than heparin to dissolve the thrombi and, consequently, provide a better clinical result. On the other hand, the use of thrombolytic agents may induce bleeding, and therefore, its indication is limited to subgroups of patients presenting greater clinical severity.

The Food and Drug Administration (FDA) approved streptokinase in 1977 and, in 1990, tissue plasminogen activator (rt-PA) for the treatment of pulmonary thromboembolism. Patients with hemodynamic instability and right ventricular dysfunction, characterizing massive pulmonary embolism, represent the subgroup of worse prognosis, and are indicated for thrombolytic use. Despite being considered the best therapeutic strategy for hemodynamically unstable patients, only one randomized study showed a significant difference in mortality in favor of the group receiving streptokinase (1,500,000 U in 1 h) when compared to the group receiving heparin. The greatest controversy for the use of thrombolytics in PT is in normotensive patients with evidence of RV dysfunction, which can represent 40–50% of cases. In this subgroup, thrombolysis improved perfusion on lung scintigraphy, RV dysfunction on echocardiogram, and resolution of thrombus at arteriography, but did not reduce mortality when compared to heparin.

Surgery: Embolectomy is indicated in massive PE with contraindications for the use of thrombolytic or, more rarely, for those who have not responded to thrombolysis and remain unstable despite intensive treatment. The best surgical result is reserved for cases of subtotal obstruction of the trunk of the pulmonary artery or its main branches. The mortality of patients submitted to embolectomy is high, mainly due to the severity of those who perform such procedure.

Vena cava filter: Vena cava filters are indicated for the prevention of PT in patients with contraindication to anticoagulation and in those who present recurrence of venous thromboembolism despite anticoagulant treatment. In patients with severe cardiac or pulmonary dysfunction–situations of high risk of thromboembolism–the vena cava filter is suggested by some authors, as well as in those submitted to embolectomy [10].

Conclusions

Heparin should be used in patients with intermediate or high clinical probability, even before imaging (C). Low molecular weight heparin should be considered in relation to UFH in the treatment of patients with hemodynamically stable PT, having equal efficacy and safety, with greater ease of administration (A) (Fig. 24.2).

The use of thrombolytic agents is indicated in hemodynamically unstable patients with right ventricular dysfunction (B).

The use of thrombolytic therapy in clinically stable patients with right ventricular dysfunction does not promote a reduction in mortality, but may have greater benefits in relation to heparin use (B).

Invasive approach (thrombus fragmentation and vena cava filter) should be considered where there is experience in performing procedure (C).

Oral anticoagulation should only be initiated in the cases of confirmed PT (C). In the oral anticoagulation phase, the ideal INR should be between 2.0 and 3.0. When this index is reached, heparin can be discontinued (A).

The duration of oral anticoagulation: 4–6 weeks for temporary risk factor (A); 3 months for idiopathic risk factor (A); At least 6 months for the other (C).

Level of evidence A	Data derived from multiple randomized clinical trials or meta-analyses.
Level of evidence B	Data derived from a single randomized clinical trials or large non-randomized studies.
Level of evidence C	Consensus of opinion of the experts and/or small studies, retrospective studies, registries.

Fig. 24.2 Pulmonary embolism probability scoring for diagnosing pulmonary embolism

References

1. Heit JA, Cohen AT, Anderson FA, VTE Impact Assessment Group. Estimated annual number of incident and recurrent, non-fatal and fatal venous thromboembolism (VTE) events in the U. S. Blood. 2005;107:277a.
2. Aujesky D, Jiménez D, Mor MK, Geng M, Fine MJ, Ibrahim SA. Weekend versus weekday admission and mortality after acute pulmonary embolism. Circulation. 2009;119:972–8.
3. Junger M, Diehm C, Storiko H, Hach-Wunderle V, Heidrich H, Karasch T, et al. Mobilization versus immobilization in the treatment of acute proximal deep venous thrombosis: a prospective, randomized, open, multicentre trial. Curr Med Res Opin. 2006;22:593–602.
4. Agnelli G, Prandoni P, Becattini C, Silingardi M, Taliani MR, Miccio M, et al. Extended oral anticoagulant therapy after a first episode of pulmonary embolism. Ann Intern Med. 2003;139:19–25.
5. Endorsed by the European Respiratory Society (ERS). Eur Heart J. 2014;35(43):3033–73. https://doi.org/10.1093/eurheartj/ehu283.
6. Klok FA, van Kralingen KW, van Dijk AP, Heyning FH, Vliegen HW, Kaptein AA, Huisman MV. Quality of life in long-term survivors of acute pulmonary embolism. Chest. 2010;138(6):1432–40.
7. Cohen AT, Agnelli G, Anderson FA, Arcelus JI, Bergqvist D, Brecht JG, Greer IA, Heit JA, Hutchinson JL, Kakkar AK, Mottier D, Oger E, Samama MM, Spannagl M. Venous thromboembolism (VTE) in Europe. The number of VTE events and associated morbidity and mortality. Thromb Haemost. 2007;98(4):756–64.
8. Roy PM, Colombet I, Durieux P, Chatellier G, Sors H, Meyer G. Systematic review and meta-analysis of strategies for the diagnosis of suspected pulmonary embolism. BMJ. 2005;331(7511):259.
9. Caramelli B, et al. Diretriz de Embolia Pulmonar. Arq Bras Cardiol. 2004;83(suppl 1):1–8. https://doi.org/10.1590/S0066-782X2004002000001.
10. Eur Heart J. 2014;35:3033–80. doi:https://doi.org/10.1093/eurheartj/ehu283.

Right Ventricular Dysfunction in Hypertrophic Cardiomyopathy

25

Lucian Florin Dorobanţu

Abstract

Hypertrophic cardiomyopathy (HCM) is one of the primary diseases affecting the cardiac muscle and is characterized by heterogeneous genetic, morphological, functional and clinical features. It is the most common genetic heart disease, with an estimated prevalence at 0.2%. Structural abnormalities in the RV are present in a great proportion of patient with HCM. With advancements of echocardiography, and improved diagnosis the percentage of RV hypertrophy (RVH) in HCM is augmented to 53%. The main common finding in this situation is the mild ventricular obstruction.

There are no specific symptoms related to the RV dysfunction in HCM. There is no demonstrated correlation between the sites and the severity of the LV obstruction and the clinical symptoms. Therefore, the development of the heart failure signs and symptoms, ventricular and/or supraventricular arrhythmias or sudden deaths are most often impossible to predict. There is no specific medical treatment for RV dysfunction in HCM. In absence of the significant gradient in the LV outflow, the patients are treated with "normal" therapy of HCM, consisting in beta-blockers and calcium-channel blockers. In case of significant RV gradient, surgical intervention has been reported. The standard surgical approach consist in myectomy (Morrow procedure) and relief of the RV gradient by resection and patch enlargement. The results are very good, symptoms are improved at intermediate-term follow-up and sudden deaths are rare.

Keywords

Right ventricle · Hypertrophic cardiomyopathy
Right ventricle dysfunction

25.1 Introduction

Hypertrophic cardiomyopathy (HCM) is one of the primary diseases affecting the cardiac muscle and is characterized by heterogeneous genetic, morphological, functional and clinical features. It is the most common genetic heart disease, with an estimated prevalence at 0.2% [1].

HCM is classically considered as a disease of the left ventricle, characterized by impaired myocardial function despite increased left ventricle (LV) thickness [2]. This hypertrophy usually occurs in a nondilated left ventricle in the absence of a secondary cause, like systemic hypertension or aortic stenosis [1, 3, 4]. Right ventricular abnormalities, present in HCM, can be a consequence of a primary cause (sarcomere mutation) or a secondary one (ventricular interdependence,

L. F. Dorobanţu
Cardiomyopathy Center, Monza Hospital, Bucharest, Romania

S. I. Dumitrescu et al. (eds.), *Right Heart Pathology*, https://doi.org/10.1007/978-3-319-73764-5_25

afterload changes), knowing the fact that the main trigger isn't certain.

25.2 Morphologic Aspects

Myocardial hypertrophy, the classical phenotypic presentation of this condition, can be found at any location, including the right ventricle [5]. This situation is not as rare as it seems. In Teare's original report from 1958 of sudden death in young adults with asymmetric hypertrophy, 5 of 8 patients had right as well left ventricular hypertrophy (LVH) [6].

It is clear that nowadays the concept that HCM is a disease limited to the LV is changing, so that the morphological biventricular involvement is an accepted concept. The first information about RV abnormalities are based on autopsy case reports [6].

Unlike the LV involvement in HCM, it is not documented yet if the RV involvement is associated with specific genetic abnormalities or transmission patterns.

25.3 Prevalence

Structural abnormalities in the RV are present in a great proportion of patient with HCM [7]. In an old study published in 1987, Seo et al. [8] suggested that about 67% of patents with HCM presented hypertrophied RV wall (Fig. 25.1).

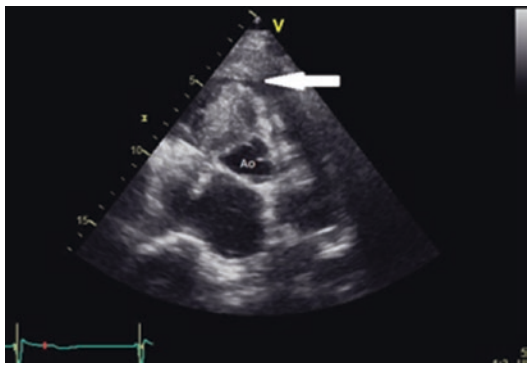

Fig. 25.1 RV hypertrophy with midventricular obstruction

In a larger study of 73 patients, 44% of patients presented moderate to mild RV hypertrophy (max 12 mm) and only one patient had severe RV hypertrophy [7]. This study, one of the first studies using extensive echocardiographic protocol for the assessment of RV morphology, showed also the difficulties of obtaining valuable information about the anatomy of the RV, due to the complex geometry of the RV and the limited resolution of echocardiography at that time.

With advancements of this technique, the results improved and the percentage of RV hypertrophy (RVH) in HCM augmented to 53% [9]. The main common finding in this situation is the mild ventricular obstruction.

While the clinical, anatomic and genetic heterogeneity of the LV abnormalities are well described, the extent and the importance of the RV abnormalities and dysfunction are not very well documented in the literature.

Usually the septum is involved but there is also involvement of the anterior, lateral, inferior or posterior walls [1, 3, 10]; even the crista terminals may be involved [11].

The incidence of significant RV involvement (with an intraventricular gradient greater than 50 mmHG) (Fig. 25.2) is not very well documented; published results are offering poor results on this topic.

25.4 Mechanisms of RV Dysfunction

There is no consensus in the way to identify the RV dysfunction because there are many patterns of involvement of the RV.

Like the LV function in HCM, the RV systolic function seems to be at normal values for long period of time [12] but the diastolic function is abnormal from very early; this findings were demonstrated both by echocardiography [13] and by cardiac magnetic resonance (CMR) [14].

Thus, knowing that longitudinal shortening generates 80% of the stroke volume, the assessment of the RV longitudinal function, the assessment of the longitudinal function is meaningful. There are studies which demonstrate that RV strain parameters

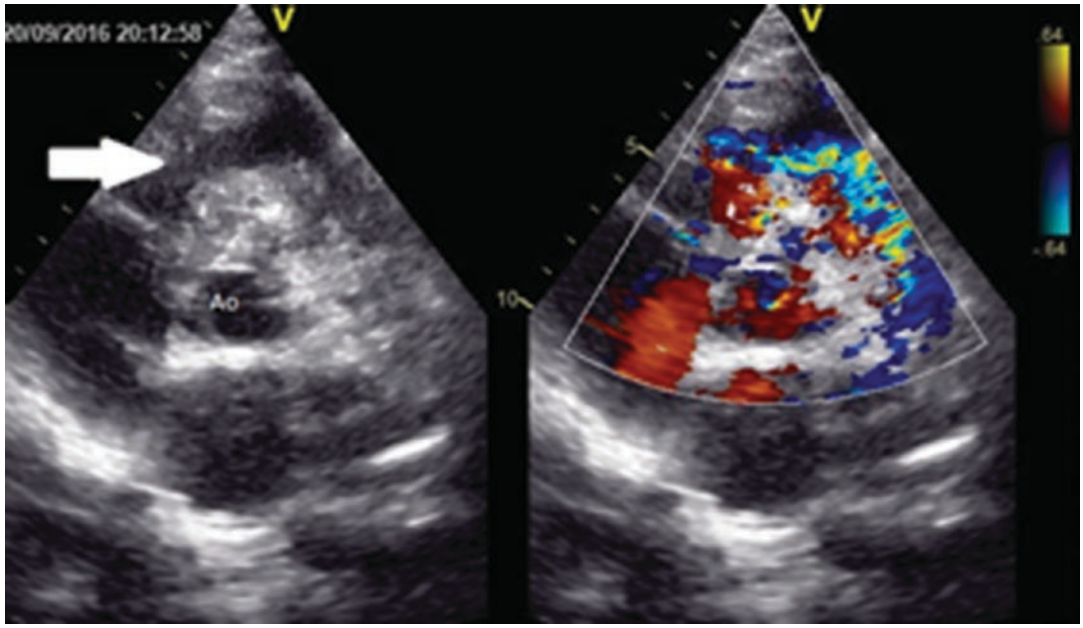

Fig. 25.2 RV hypertrophy and obstruction (arrow) causing RV gradient

were the only RV functional parameters impaired in the HCM patients; the usual ones like TAPSE or RV FAC were unreliable [9].

There is not a strong relation between RV remodeling and the clinical features. Whereas RV remodeling is a common process in HCM, there are no evidence to determine if this is a primary disorder or is secondary to LV dysfunction, the sites and/or severity of the LV hypertrophy and the secondary pulmonary hypertension. There are studies suggesting that RV hypertrophy is independently related to the LVH, but the RV dysfunction is related to the LV longitudinal dysfunction [7, 9, 12]; these data support the interdependence ventricular function determinism, knowing the fact that both ventricles share the hypertrophied ventricular septum.

25.5 Signs and Symptoms

There are no specific symptoms related to the RV dysfunction in HCM. The clinical course of HCM is extremely heterogeneous and unpredictable. There is no demonstrated correlation between the sites and the severity of the LV obstruction and the clinical symptoms, and the development of the heart failure signs and symptoms, ventricular and/or supraventricular arrhythmias or sudden deaths are most often impossible to predict. There are some mechanism like compromised left atrium function [15], LV dyssynchrony, impaired LV diastolic function involved in the development of heart failure symptoms.

Sudden death is the most common modality of death in HCM and occurs more often in young asymptomatic or only mildly symptomatic patients [16–19]. There is a large agreement about the clinical signs indicators regarding sudden death in HCM. They are mainly family history of sudden death, extreme hypertrophy (≥30 mm), unexplained syncope, non-sustained ventricular tachycardia, abnormal blood pressure response to exercise. The low clinical risk profile is attributed to patients with mild left ventricular hypertrophy (wall thickness <20 mm) and without any risk factor [16–19].

There is no correlation described in the literature between the sudden death and the RV dysfunction or hypertrophy. There are reports that confirm the correlations between RV free wall thickness and the severity of heart failure symp-

toms [7, 9], due to the increased RV stiffness and fibrosis. So the RV dysfunction contributes to the severity of symptoms in HCM.

25.6 Diagnosis

Hypertrophic cardiomyopathy is usually suspected because of recent development of dyspnea or palpitations, after identifying a heart murmur during routine clinical evaluation or a routine EKG exam, showing marked electrocardiographic abnormalities [16–18].

Because the definition of HCM is based on cardiac morphologic features, and usually the patients have no or mild symptoms, cardiac imaging often precedes the patient interview.

The diagnosis of HCM is certified by an echocardiographic exam showing a hypertrophied and non-dilated LV in absence of other cardiac causes of hypertrophy [7, 16] (Fig. 25.3).

Identification of elongated and anteriorly displaced mitral leaflets with important SAM and LV outflow obstruction strongly support the diagnosis of HCM.

The RV involvement is impossible to suspect among the clinical settings; both echocardiography and cardiac MRI are useful to show the RV hypertrophy.

When RV dysfunction is suspected, both echocardiography and cardiac catheterization are useful to determine systolic and diastolic function, to evaluate diastolic pressure and outflow gradients. Regarding the echocardiographic assessment of the RV function, the RV strain appears to be a more effective measurement than TAPSE or RV FAC [9].

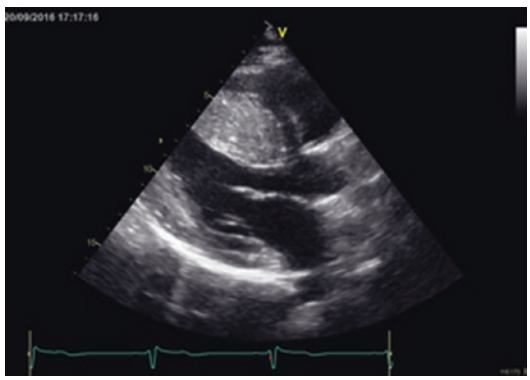

Fig. 25.3 RV hypertrophy in HCM

In recent years, the high resolution of CMR has proved to give very useful information; it is very useful to determine the RV involvement whenever it is suspected.

There are no data regarding the tricuspid valve involvement in RV dysfunction in HCM. To our knowledge, there is no tricuspid incompetence reported due to the morphologic changes of RV in HCM.

25.7 Treatment

There is no specific medical treatment for RV dysfunction in HCM. In absence of the significant gradient in the LV outflow, the patients are treated with "normal" therapy of HCM, consisting in beta-blockers and calcium-channel blockers; there is no great experience on this subject and appears there are even patients who have not responded at this therapy [17].

To our knowledge, there is no septal ablation experience in this subject, because is impossible to reduce the gradient in both ventricles after alcohol injection in septal branches.

Surgical intervention has been reported. In 1993, Maron [11] reported a first series of five patients with HOCM and RV involvement, with a RV outflow gradient >50 mmHg in which they performed myectomy (Morrow procedure) and relief of the RV gradient by resection and patch enlargement. The same technique was used in 11 patients from the same center reported in 2015 by Quintana et al. [20] with good early outcomes. Symptoms in this group were improved at intermediate-term follow-up and sudden death was rare.

In our experience of 31 patients with HOCM we had only 2 patients with RV involvement. We performed myectomy and mitral valve repair with resection of secondary chordae of the mitral valve in all patients; due to the fact that the RV outflow tract gradient was maximum 40 mmHg, we didn't performed surgical relief of the RV gradient.

References

1. Wynne J, Braunwald E. The cardiomyopathies and myocarditides. In: Braunwald E, editor. Heart disease: a textbook of cardiovascular medicine. 5th ed. Philadelphia: WB Saunders Company; 1997. p. 1414.
2. Elliott P, Andersson B, Arbustini E, Bilinska Z, Cecchi F, Charron P, et al. Classification of the cardiomyopathies: a position statement from the European society of cardiology working group on myocardial and pericardial diseases. Eur Heart J. 2008;29: 270–6.
3. Maron BJ, Bonow RO, Cannon RO, Leon MB, Epstein SE. Hypertrophic cardiomyopathy: interrelations of clinical manifestations, pathophysiology, and therapy (first of two parts). N Engl J Med. 1987;316:780–9.
4. Maron BJ, Bonow RO, Cannon RO, Leon MB, Epstein SE. Hypertrophic cardiomyopathy: interrelations of clinical manifestations, pathophysiology, and therapy (second of two parts). N Engl J Med. 1987;316:844852.
5. Elliott PM, Anastasakis A, Borger MA, Borggrefe M, Cecchi F, Charron P, et al. ESC guidelines on diagnosis and management of hypertrophic cardiomyopathy: the task force for the diagnosis and management of hypertrophic cardiomyopathy of the European Society of Cardiology (ESC). Eur Heart J. 2014;35: 2733–79.
6. Teare D. Asymmetrical hypertrophy of the heart in young adults. Br Heart J. 1958;20:1–8.
7. McKenna WJ, Kleinebenne A, Nihoyannopoulos P, Foale R. Echocardiographic measurement of right ventricular wall thickness in hypertrophic cardiomyopathy: relation to clinical and prognostic features. J Am Coll Cardiol. 1988;11:351–8.
8. Seo T, Yokota Y, Kumaki T, Takarada A, Kubo M, Kaku K, Toh S, Fukuzaki H. Regional right ventricular hypertrophy in hypertrophic cardiomyopathy and hypertension. J Cardiogr. 1985;15:339–46.
9. Rosca M, Calin A, Beladan C, et al. Right ventricular remodeling, its correlates and its clinical impact in hypertrophic cardiomyopathy. J Am Soc Echocardiogr. 2015;28(11):1329–38.
10. Klues HG, Schiffers A, Maron BJ. Phenotypic spectrum and patterns of left ventricular hypertrophy in hypertrophic cardiomyopathy: morphologic observations and significance as assessed by two-dimensional echocardiography in 600 patients. J Am Coll Cardiol. 1995;26:1699–708.
11. Maron BJ, McIntosh CL, Klues HG, Cannon RO, Roberts WC. Morphologic basis for obstruction of right ventricular outflow in hypertrophic cardiomyopathy. Am J Cardiol. 1993;71:1089–94.
12. Maron MS, Hauser TH, Dubrow E, Horst TA, Kissinger KV, Udelson JE, Manning WJ. Right ventricular involvement in hypertrophic cardiomyopathy. Am J Cardiol. 2007;100(8):1293.
13. D'Andrea A, Caso P, Bossone E, Scarafile R, Riegler L, Di Salvo G, et al. Right ventricular myocardial involvement in either physiological or pathological left ventricular hypertrophy: an ultrasound speckle-tracking two-dimensional strain analysis. Eur J Echocardiogr. 2010;11:492–500.
14. Amundsen BH, Helle-Valle T, Edvardsen T, Torp H, Crosby J, Lyseggen E, et al. Noninvasive myocardial strain measurement by speckle tracking echocardiography: validation against sonomicrometry and tagged magnetic resonance imaging. J Am Coll Cardiol. 2006; 47:789–93.
15. Rosca M, Popescu BA, Beladan CC, Călin A, Muraru D, Popa EC, et al. Left atrial dysfunction as a correlate of heart failure symptoms in hypertrophic cardiomyopathy. J Am Soc Echocardiogr. 2010;23:1090–8.
16. Spirito P, Seidman CE, McKenna WJ, Maron BJ. The management of hypertrophic cardiomyopathy. N Engl J Med. 1997;336:775–85.
17. Maron BJ. Hypertrophic cardiomyopathy. A systematic review. JAMA. 2002;287:1308–20.
18. Elliott P, McKenna WJ. Hypertrophic cardiomyopathy. Lancet. 2004;363:1881–91.
19. Spirito P, Autore C. Management of hypertrophic cardiomyopathy. BMJ. 2006;332(7552):1251–5.
20. Quintana E, Johnson N, Rotes S, et al. Surgery for biventricular obstruction in hypertrophic cardiomyopathy in children and youn adults: technique and outcomes. Eur J Cardiothorac Surg. 2015;47:1006–12.

Right Ventricular Function in Systemic Autoimmune Diseases

26

Ioan Tiberiu Nanea and Gabriela Silvia Gheorghe

Abstract

Systemic autoimmune diseases (SAD) can be defined as inflammatory diseases with an immune mechanism, of unknown etiology, involving at least 2 organs or systems. This category includes collagen-vascular diseases, vasculitides, granulomatous diseases, while excluding systemic inflammatory diseases with known causes. Cardiovascular changes are among the most frequent causes of morbimortality in patients with SAD by many mechanisms, including sustained systemic inflammation. Chronic right ventricular (RV) involvement in SAD may be due to long-term left ventricular (LV) decompensation, inflammation and myocardial fibrosis generated by the disease itself, pulmonary parenchymal changes and/or pulmonary hypertension (PAH), chronic repetitive pulmonary embolism. These differ in type, prevalence, intensity between the various forms of SAD. Systemic sclerosis (SSc) is the most frequent disease that causes lung and cardiac involvement. SS generates PAH by multiple mechanisms mainly in the cutaneous form, although it induces myocardial perfusion defects especially in the diffuse form. The RV involvement occurs earlier in SSc than in other forms of PAH and the prognosis is more severe. However, the new cardiac imaging techniques prove the occurrence of the systolic and diastolic dysfunction in right and left ventricles in cases without established PAH and clinical heart involvement. Systemic erythematosus lupus (SLE), mixed connective-tissue disease (MCTD), Sjogren syndrome (SjS), rheumatoid arthritis (RA) determine less often PAH and RV involvement. There are also other mechanisms for the cardiac involvement in SAD, like coronaritis, accelerated atherosclerosis or pericarditis.

Keywords

Systemic sclerosis · Systemic erythematosus lupus · Rheumatoid arthritis · Pulmonary hypertension · Right ventricular function · TAPSE · TEI index · Longitudinal strain · Longitudinal strain rate

26.1 Introduction

Definition. Systemic autoimmune diseases (SAD) can be defined as inflammatory diseases with an immune mechanism, of unknown etiology, involving at least 2 organs or systems [1]. This category includes

I. T. Nanea (✉) · G. S. Gheorghe
University of Medicine and Pharmacy "Carol Davila", Bucharest, Romania

"Prof Dr Th Burghele" University Hospital, Bucharest, Romania

S. I. Dumitrescu et al. (eds.), *Right Heart Pathology*, https://doi.org/10.1007/978-3-319-73764-5_26

Table 26.1 Systemic inflammatory diseases [2]

Disease group	Examples
Collagen-vascular diseases	Systemic erythematosus lupus
	Rheumatoid arthritis
	Scleroderma
	Dermatomyositis
	Polymyositis
	Mixed connective-tissue disease
	Sjogren syndrome
Vasculitides	
Large-medium arteries	Giant-cell arteritis/temporal arteritis
	Polymyalgia rheumatica
	Takayasu arteritis
Medium arteries	Polyarteritis nodosa
	Kawasaki disease
Small vessel	
ANCA positive vasculitis	Churg Strauss syndrome
	Microscopic polyangiitis
	Wegener's granulomatosis (Granulomatosis with Polyangiitis)
Non ANCA positive vasculitis	Henoch-Schonlein purpura
Rare vasculitis	Behcet disease
	Buerger disease

collagen-vascular diseases, vasculitides, granulomatous diseases (Table 26.1), excluding systemic inflammatory diseases with known causes: infectious (such as infectious endocarditis), infiltrative (i.e., hemochromatosis, amyloidosis), hereditary (such as Mediterranean fever), toxic (lead, cocaine, amphetamines), iatrogenic (amiodarone, chloroquine) [2].

Cardiovascular changes are among the most frequent causes of morbi-mortality in patients with SAD, and may take the form of myocardial ischemia, arrhythmias, heart failure, accelerated atherosclerosis and pericarditis. Sustained systemic inflammation plays a key role in the occurrence of cardiovascular involvement [3].

26.1.1 Systemic Atherosclerosis and Myocardial Ischemia

Chronic inflammation leads to early onset of atherosclerosis and plaque destabilization. Ischemic heart disease and chronic inflammatory diseases have common inflammation mediators: tumor necrosis factor superfamily (TNF), interleukine-1 family (IL-1) [4, 5]. CD4+28-T lymphocytes are present in unstable angina, as well as in some patients with RA. Expression of the immunoglobuline superfamily of adhesion molecules ICAM and VCAM increases on the vascular endothelium. Anticardiolipin antibodies, anti 2 glycoprotein 1 antibodies (Anti 2-GPI) present in some patients with SLE, contribute to the rapid evolution of atherosclerosis [6]. The nitric oxide (NO) availability is reduced, as ascertained by the increase of serum asymmetric dimethylarginine (ADMA), the main endogenous NO-synthase inhibitor [1]. In these patients, atherosclerotic disease occurs at younger ages.

In addition to vascular changes related to atherosclerosis, SAD may induce changes in all cardiac structures: pericardium, myocardium, endocardium, valves.

26.1.2 Chronic right ventricle involvement in SAD

Chronic right ventricle (RV) involvement in SAD may be due to long-term LV decompensation, inflammation and myocardial fibrosis generated by the SAD itself, pulmonary parenchymal changes and/or PAH, chronic repetitive pulmonary embolism.

The *parenchymal pulmonary changes and the vascular pulmonary changes* are the most important causes of RV involvement in SAD but differ in type, prevalence and intensity between the various forms of SAD.

- *Parenchymal pulmonary changes* consist of various types of interstitial fibrosis and changes in pulmonary circulation.
- Diffuse interstitial lung changes mostly appear in SSc (60% of cases), RA (10–25% of cases), polymyositis/dermatomyositis (PM/DM) (30% of cases) [3], rarely in SLE, SjS, MCDT and very rarely in ankylosing spondylitis (AS) [7].
- In RA, the most common forms of parenchymal pulmonary involvement are nonspecific interstitial pneumonia (NSIP) and cryptogenic organizing pneumonia (COP), while in PM/DM,

COP is the most common. SSc induces NSIP more frequently, as well as usual interstitial pneumonia (UIP). SLE produces especially diffuse alveolar damage (DAD), along with NSIP, UIP. SjS leads to bronchiectasis and lymphoid interstitial pneumonia (LIP), MCTD is associated with NSIP and UIP, PM/DM generate NSIP and organizing pneumonia (OP) [7]. The evolution of interstitial fibrosis in collagen vascular disease is milder than in idiopathic interstitial fibrosis, probably in correlation with the NSIP histological type, more commonly encountered and more benign compared to UIP, more severe and more common in idiopathic fibrosis. However, collagen vascular diseases complicated with interstitial lung fibrosis are associated with increased mortality, 20% on average, within the first 5 years of diagnosis [8].

- Other types of lung involvement are also possible. SLE is commonly associated with pleural effusion, vasculitis and respiratory muscular dysfunction. RA may be responsible for the appearance of pulmonary nodules, pleural effusion, vasculitis. MCTD may be associated with pleural effusion [7].
- *PAH*. Patients with SAD have a higher risk of PAH than those without SAD. PAH appears isolated or associated with interstitial lung involvement [8]. PAH develops in SSc (10–33% of cases), especially the cutaneous form [5] and also in SLE (5–10%), MCTD, RA, PM/DM and SjS. PAH develops almost never in AS [7, 8]. Histopathological changes in pulmonary circulation are similar to those in idiopathic pulmonary hypertension (IPAH) [6] but the clinical evolution of PAH in SAD may be more severe than that of IPAH [8]. In collagen vascular diseases, vasculitis, is defined as an inflammatory process that leads to the destruction of the vascular wall by fibrinoid fibrosis, often located in small muscular arteries and arterioles and capillaries. These lesions appear in SLE, RA, PM/DM, MCTD [7]. In SLE, as in SSc, the histological changes of the pulmonary arteries are similar to those in IPAH: plexogenic arteriopathy, medial and intimal proliferation in the pulmonary arteries and arterioles [7, 9], histologically distinct from changes in hypoxic pulmonary hypertension, in which medial hypertrophy is dominant [7, 9].
- *Mechanisms of PAH in SAD*. PAH develops because of an increase in vascular resistance, as a consequence of pulmonary arteries remodeling, pulmonary capillary rarefaction, volume overload, vasoconstriction induced by inflammation mediators and hypoxia. Pulmonary embolism contributes to PAH especially in SLE and in antiphospholipid syndrome. Pulmonary vascular resistance (PVR) includes arterial, capillary and pulmonary vein resistance [10]. The formula is PVR = (mPAP − PAWP)/CO (with mPAP = mean pulmonary arterial pressure, PAWP = pulmonary arterial wedge pressure and CO = cardiac output) [10]. Characteristics of pulmonary circulation render systolic pulmonary arterial pressure (sPAP) and diastolic pulmonary arterial pressure (dPAP) proportional to mPAP, according to the following formulas: dPAP = 0.36 sPAP; mPAP = 0.6 sPAP [10]. Usually, PVR is small and allows blood circulation through the lungs at low pressure gradients, ranging from 10 to 15 mmHg [11]. Vascular and parenchymal pathological changes lead to an increase in PVR. PVR and total pulmonary arterial compliance (TAC) are inversely proportional, and their product called arterial time constant is constant [10]. The relationship between PVR and TAC can be described as a hyperbola curve, which explains the more significant reduction in TAC when PVR increases from normal values, rather than from higher one [10]. Thus, the reduced pulmonary artery compliance is an early marker of the increase in PVR [10]. PVR increases more than 4 times before PAH develops [12]. PAH induces changes in RV, which depend on the rapidity of the development of PAH and its severity.

26.1.3 Mechanisms of Chronic RV Involvement in SAD

Typically, RV ejection starts after a brief period of isovolumetric contraction and early diastolic filling is not preceded by isovolumetric relax-

ation [13]. These differences from the left ventricle (LV) arise because the pulmonary circulation operates at low pressure.

RV can intensify its contractility by 4–5 times [10].

RV adaptation to the rapid increase of PVR, beat by beat, is performed by the Starling heterometric mechanism, involving dilatation and elongation of the sarcomeres.

RV adaptation to chronic increase of PVR is due to the homeometric mechanism described by Anrep, which involves increasing contractility without augmenting RV size [11].

RV contractility is expressed by the relationship between the RV end-systolic pressure and the end-systolic volume. The gold standard of systolic function is the maximum elastance (Emax), or the maximal value of the ratio of pressure to volume. RV afterload is assessed either by maximum ventricular wall stress, or by arterial hydraulic load [11], which can be evaluated by arterial elastance (Ea): Ea = PVR multiplied by heart rate. According to Arnet's law, contractility increases as the afterload rises up to a certain point. This relationship defines RV-arterial coupling, expressed as the ratio between Emax and Ea. The Emax/Ea ratio is a surrogate evaluation of RV mechanical efficiency. Sunagawa et al. [11] showed that a ratio between 1 and 2 correlates with normal RV effectiveness. The ratio increases as RV boosts its contractility, and the optimal energy transfer from RV to the pulmonary circulation happens when Emax/Ea is 1.5–2 [11]. Reducing the Emax/Ea ratio signifies decoupling the RV and pulmonary circulation.

RV failure in PAH occurs when the RV coupling with its load, represented by pulmonary circulation pressure and/or volume overload, is disrupted. In PAH, RV initially increases its contractility by 4–5 times. This occurs by RV hypertrophy, which leads to an increase in wall thickness, and by changes in muscular properties per se. RV hypertrophy modifies its diastolic function, as RV becomes rigid. In evolution, hypertrophy ceases and stroke volume of the RV (RSV) tends to decrease. Maintaining RSV at this point involves RV dilation. Tachycardia occurs, myocardial O_2 consumption increases, Ea rises and the Emax/Ea ratio decreases. RV decoupling initially occurs upon effort, then also at rest. Unlike LV failure, RV decoupling occurs late in the evolution of pulmonary hypertension. RV dilatation and RSV reduction lead to increasing wall tension and RV pressure, inducing increased O_2 consumption, reduced O_2 efficiency and changes in cardiac myocytes leading to an augmented RV stiffness.

RV O_2 consumption is determined by wall tension and PAP. O_2 consumption increases if RV dilates and pulmonary pressure aggravates. O_2 input is limited in pulmonary hypertension. RV efficiency decreases by 20–25% with PAH progression, due to increased O_2 consumption. Systolic and diastolic relaxation velocities assessed by tissue Doppler imaging (TDI) depend on myocardial structure, interstitial fibrosis and adrenergic receptor density [13].

RV–pulmonary circulation coupling lasts longer in IPAH than in the PAH of SSc in which RV failure occurs earlier, proving an earlier decoupling between RV and pulmonary circulation in PAH of SSc that could be explained by inflammation, loss of capillaries, myocardial interstitial fibrosis, oxidative stress [12].

Evaluation of the RV function is performed by measuring the RV ejection fraction (RVEF), RSV, RV end-diastolic volume (RVEDV) and RV end-systolic volume (RVESV), RSV/RVEF ratio. RSV and RVEF are inversely correlated by the formula RSV/RVEF = RVEF/(1 − RVEF). RSV/RVESV may be a more sensitive indicator for RV function in patients with severe PAH [14, 15].

26.1.4 Ventricular Interaction

Usually, interventricular interaction in normal subjects is negligible. In PAH, ventricular interdependence manifests itself through the paradoxical motion of the interventricular septum (IVS) and reduced LV filling because of reduced RSV. IVS paradoxical motion is due to the lengthening of the RV contraction time versus LV contraction time. This generates a hampered LV

early diastolic filling. RV contraction continues while LV has reached early diastole. The pulmonary valve closes, even if RV has not completed its contraction. Post- systolic isovolumetric contraction of the RV occurs, which contributes to the mechanical inefficiency, as the energy used does not serve the guarantee of an antegrade flow. Post-systolic isovolumetric time increase in PAH correlates with the expansion of wall stress and with disease severity. RV dilation in the fixed pericardial sack also induces a drop in LV size and filling. The decline in LV filling causes a decrease in coronary flow and RV ischemia, which enhances its mechanical failure. Also, the reduced LV filling favors myocyte atrophy, inducing heart failure [10, 11, 15].

Increased RV stiffness can be indirectly assessed by right atrial (RA) pressure and volume, as well as by using the strain and strain rate techniques.

26.2 Systemic Sclerosis

Clinically manifestations of the cardiac involvement occur in 20% of patients with SSc, while necropsy documents pathologic involvement in as many as 80% of patients. SSc can impair all the heart structures. Apparently its impact on RV is not due only to the PAH but also there is an involvement of the RV independent of pulmonary hypertension [13]. Cardiac changes in SSc are classified as primary and secondary [13].

Primary changes are due to the involvement of the myocardium and microcirculation by scleroderma per se, with impaired diastolic function and reduced coronary reserve. Functional and anatomical coronary microcirculation compromise produces recurrent ischemia and, finally, fibrosis, responsible for functional myocardial damage. Diastolic function is impaired earlier, compared to the systolic function. The epicardial coronary arteries are normal.

Secondary damage occurs due to pulmonary vascular and interstitial changes, pulmonary capillary and arteriole obliteration, and interstitial fibrosis [13]. It leads to pulmonary hypertension by increasing PVR due to endothelial dysfunction, vasoconstriction, vascular remodeling, and in situ thrombosis induced by hypoxia, inflammation, acidosis, and high arterial wall tension. Ten percent of patients with scleroderma, especially CREST syndrome, have plexogenic arteriopathy in the pulmonary arteries. Pulmonary hypertension coexists with interstitial lung changes [15].

In both primary and secondary cardiac changes, there is LV and RV myocardial fibrosis occurring as interstitial deposits, without respect to any coronary territory and without a predominantly subendocardial distribution. In SSc there are cardiac alterations in all of the layers and in the conduction system of the heart: myositis, focal myocardial fibrosis that extends to pericardium, pericarditis, arrhythmias, impairment of the conduction system, acceleration of atherosclerosis [15]. These changes can occur independently of the severity of PAH [15].

According to the general classification of PAH, PAH in SSc is classified in the group 1 and has the worst prognosis compared to the other causes of PAH in this group. The survival time from diagnosis is 5 years, compared to 8 years in IPAH [9]. The explanation would consist, on the one hand, of the more important pulmonary arteries stiffness in SSc, and on the other hand, of the myocardial changes per se occurring in SSc (fibrosis, microcirculation damage). Pathological changes of pulmonary circulation are similar in IPAH and PAH from SSc: intimal hyperplasia, medial hypertrophy, adventitial fibrosis, concentric obliteration of small vessels, angioproliferative lesions. Less plexiform lesions but more intimal fibrosis develop. Endothelial apoptosis occurs by activating inflammatory cells, expression of adhesion molecules, procoagulant status. Intrinsic proliferation and adventitial fibrosis are minimal [16]. In PAH from SSc and in IPAH there are anti-fibrillarin and anti-endothelial antibodies, stimulating cellular adhesion and apoptosis; anti-fibroblasts antibodies inducing proinflammatory/fibrotic cytokine-induced response; growth factors that increase collagen synthesis. In SSc, soluble vas-

cular cell adhesion molecules, vascular endothelial growth factor and angiostatic factors suggesting endothelial injury and abnormal angiogenesis have been identified in the blood, with a possible role in the development of PAH. The cardiac index and right atrial pressure correlate with survival in IPAH, but not in SSc-associated PAH. In SSc-associated PAH, RV function is depressed, unlike in IPAH.

Studies have shown poor RV adaptation to hemodynamic pulmonary changes in patients with PAH due to SSc compared to patients with IPAH [15]. SSc patients compared to IPAH patients had lower RV contractility as measured by end-systolic elastance and the coupling of right ventricle contractility with afterload at the same PVR, pulmonary compliance and Ea [15]. A decrease in RV contractility was noted even in patients with SSc without PAH. It was thought that this was due to extended myocardial fibrosis in SSc, but Overbeek et al. [16] showed that SSc patients did not have more extensive myocardial fibrosis, but inflammatory infiltrates compared to patients with IPAH.

Vonk et al. [12] demonstrated than patients with SSc and PAH had a similar prevalence of RV dilatation and higher prevalence of LV diastolic dysfunction, LV dilatation and pericardial effusion comparing to patients with IPAH, whilst the LV systolic function was normal in both groups [17]. In SSc with PAH the isovolumetric contraction time and the isovolumetric relaxation time (IVRT) increase and the ejection time decreases. Tricuspid annular plane systolic excursion (TAPSE) is significantly lower in patients with SSc and PAH versus patients with IPAH at the same afterload level [17].

Using TDI technique, the E′/A′ ratio at the RV lateral wall was reduced, the isovolumetric relaxation time of RV was longer in SSc patients without any other echocardiographic RV and LV changes [17]. Through speckle tracking technique, strain rates were reduced in the RV free wall in the basal, middle, and apical segments, as well as in the LV free wall, in the basal and middle segments. Reduced strain rates were also noted in patients with SSc but without PAH [18].

Pigatto et al. [19] studied RV diastolic function by 3D and speckle tracking techniques in 45 patients with SSc in relation to PAP and PVR, compared with 43 healthy subjects. Patients had no clinical cardiac manifestations. SSc patients had higher RV end-diastolic and end-systolic volumes, low systolic RV function (TAPSE; fractional area changes), higher sPAP and PVR compared to the control group, without reaching the pathological cutoff. The global strain and RV free wall strain did not differ between the two groups. The authors concluded that RV changes in SSc patients occur early, prior to symptomatology and are due to the increase in PAP rather than to an intrinsic change in RV contractility.

Loureiro et al. [20] performed an echocardiographic stress test in 24 patients with collagen vascular disease (SSc, CREST, SLE, MCTD) with no cardiac changes at rest and showed that 33% of them developed PAH upon exertion.

Vonk et al. [17] studied the accuracy of TEI index for RV in PAH prediction in patients with collagen vascular disease. The study group included 98 patients with SSc, SLE, MCTD and 43% of them had a TEI index significantly higher than normal. 19 patients out of the 28 patients (67%) with PAH proven by catheterization and 1 patient out of the 7 (14%) without PAH at catheterization had an elevated TEI, above 0.36. The myocardial performance index for RV (TEI) > 0.36 has a predictive value in these patients.

Giuntta et al. [21] studied RV diastolic function in 77 patients with SSc and showed that 40% of them had abnormalities of RV diastolic filling independently of PAP values and LV diastolic filling. Diastolic dysfunction correlates with scleroderma-induced myocardial fibrosis, which is patchy in both RV and LV, does not affect subendocardial layers, does not respect the distribution of epicardial coronary arteries, is not accompanied by ventricular hypertrophy and is not associated with hemosiderin deposits.

Rosato et al. [22] studied regional LV diastolic dysfunction in 67 patients with SSc by transmitral Doppler, TDI and speckle tracking.

They found abnormalities of the transmitral E/A ratio in 24 patients, whilst in 41 patients, they identified an E′/A′anomaly at TDI and the speckle tracking technique documented systolic abnormalities of the longitudinal but not the radial fibers. The basal segments of LV were more affected than the mid segments of LV. The authors found a correlation between the E′/A′ abnormalities and the contraction abnormalities of the longitudinal fibers. Diastolic abnormalities correlated with disease duration.

D'Andrea et al. [14] studied the diastolic function of LV and RV, as well as LV and RV strain and strain rate parameters in 25 patients with SSc versus normal subjects. LV mass, LV diameters, TAPSE were comparable between the groups of patients. The RV end-diastolic diameter was significantly higher in the group of patients with SSc. The tricuspid E/A ratio was reduced in the group with SSc versus the control group and 43.2% of the SSc patients with reduced tricuspid E/A ration had PAH. TDI of the tricuspid annulus showed a reduction in the early diastolic LV filling velocity and an increase in the regional relaxation time, calculated as the time elapsed between the end of the systolic wave (Sm) and the beginning of the diastolic E'wave (RTm). The TDI technique also showed a prolonged interval between the beginning of Q wave (ECG) and the beginning of Sm wave (TDI) at the RV level, in patients with SSc; Sm velocities were not different between the groups of patients. Peak systolic strain rate and peak systolic strain at the base, middle and apex of the RV lateral wall, as well as at the basal and middle segments of the LV lateral wall were significantly reduced. A decrease of the E′ velocity <0.11 m/s in RV correlated with the severity of skin and lung damage. Early RV diastolic dysfunction was also correlated with the presence of antitropoisomerase antibodies. sPAP and pulmonary fibrosis were the only independent factors correlated with the reduction of RV strain rate [14].

Myocardial scintigraphy showed that SSC patients have ventricular perfusion defects [23]. The gated myocardial perfusion technique SPECT demonstrated diastolic abnormalities in SSc patients with normal cardiac perfusion and systolic function [23].

The RV ejection fraction evaluated by radionuclide imaging with 99mTc ventriculography was reduced in patients with SSC without PAH compared to healthy subjects. Scintigraphy with thallium 201 and single-photon emission tomography showed reversible myocardial perfusion defects induced by a cold stimulus infusions and effort especially in patients with diffuse SSc and anti SCL-70 antibodies [24].

Cardiac MRI is more sensitive than other noninvasive imaging methods in assessing RV changes in patients with asymptomatic SSc. Areas of medium-ventricular localized fibrosis, in the IVS and in the LV free wall, without respecting to any coronary territory, have been noted. Myocardial signal intensity in T2 increases, LV and RV ejection fractions are lower, LV diastolic dysfunction occurs, LV kinetic abnormalities, RV dilatation and pericardial effusion are documented [24].

We report some original illustrative cases of patients with ongoing SSc in which the echocardiography documented altered RV function.

By color kinesis images, we noted a reduced displacement of the tricuspidian annulus which is a sensible criterion for the RV systolic dysfunction (Fig. 26.1).

We analyzed by speckle tracking technique the deformation of the longitudinal muscular fibres of the free wall of the RV (Fig. 26.2).

The apical segment of the RV showed a reduced systolic longitudinal deformation compared with the basal segments (Fig. 26.3). In normal persons there is a more important systolic longitudinal deformation of the RV basal segments than of the apical ones [25].

Using color tissue Doppler technique, we found in another patient a reduced systolic longitudinal shortening of the basal third of the RV free wall (Fig. 26.4). However, the shortening velocities of the different segments of the RV free wall, including the basal ones, are normal as they are evaluated by color tissue Doppler technique (Fig. 26.5).

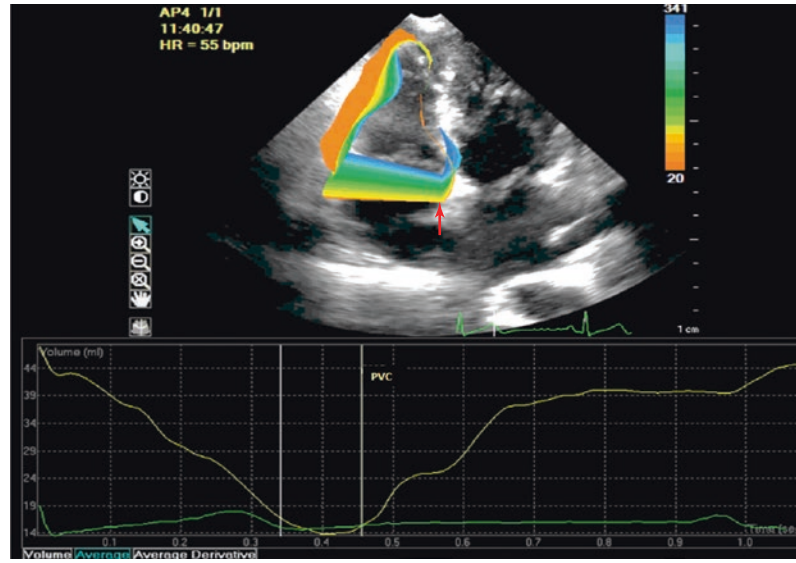

Fig. 26.1 Color kinesis images. There is a reduced displacement of the tricuspidian annulus especially in its septal segment (red arrow) in a patient with SSc. Personal case

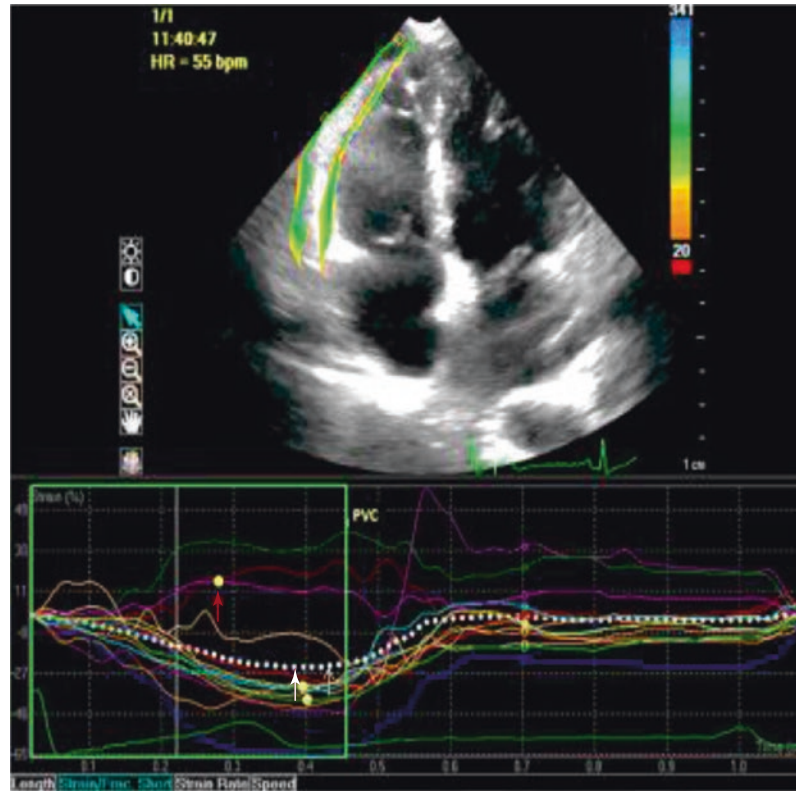

Fig. 26.2 RV free wall deformation evaluated by speckle tracking technique in a patient with SSc. There is a reduced deformation of the free wall (white arrow) and a paradoxical deformation of its apical segment (red arrow). Personal case

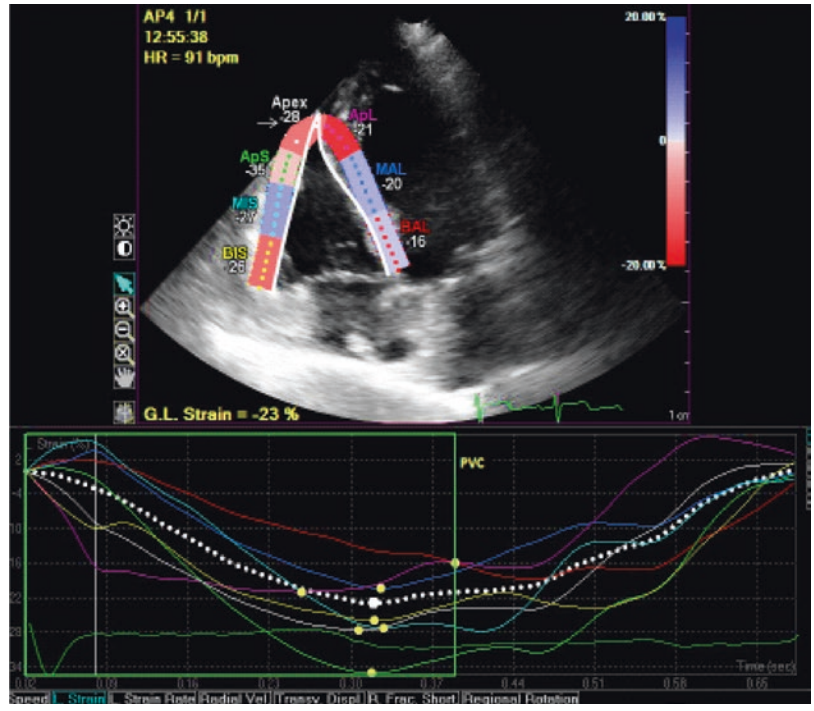

Fig. 26.3 Speckle tracking image technique. Reduced longitudinal systolic deformation of RV (plotted white line), more important at the RV apex (red line) than at the RV basal segments (yellow line). Personal case

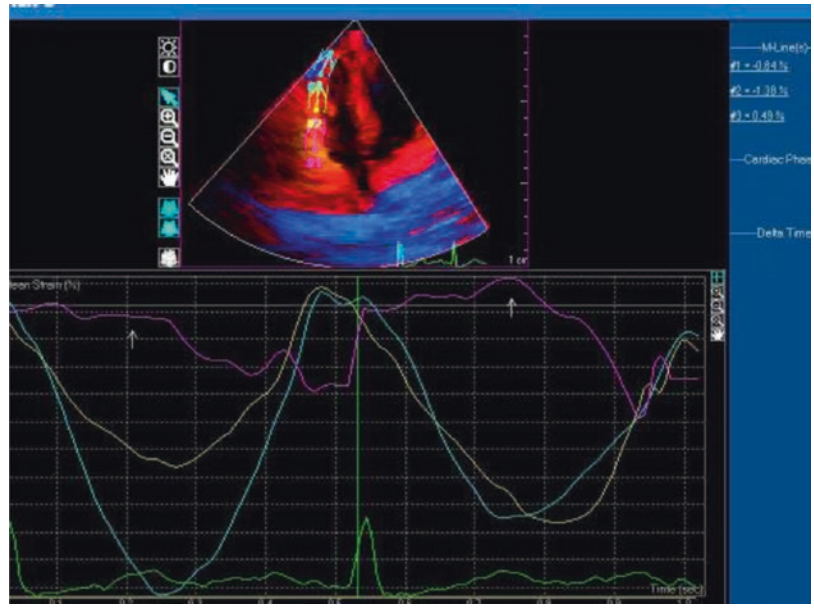

Fig. 26.4 Color tissue Doppler technique. There was a reduced of the longitudinal shortening of the basal third of the RV free wall in a patient with SSc (white arrows). Personal case

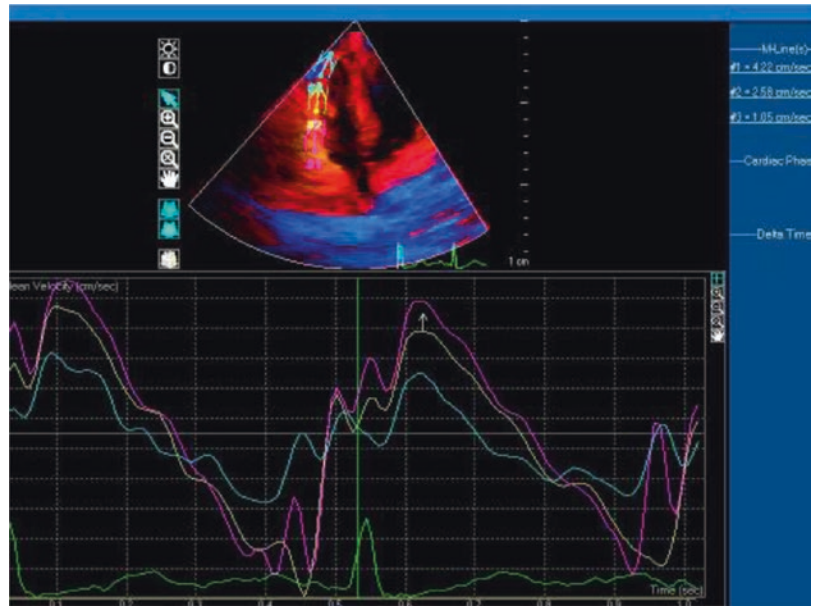

Fig. 26.5 Color tissue Doppler. The systolic longitudinal shortening velocities of the different segments of the RV free wall, including the basal ones, are normal in a patient with SSc (white arrow). Personal case

26.3 Systemic Erythematosus Lupus

SLE affects all the structures of the heart: pericardium, myocardium, endocardium, coronary arteries. The most frequently affected structure is the pericardium, 43–83% of SLE patients having pericarditis, clinically apparent in 25% of patients. 97.8% of patients with SLE have pleural and lung involvement: pleural effusions (77%), bacterial infections (58%), alveolar hemorrhage (26%), pulmonary embolism, in patients with antiphospholipid syndrome, respiratory muscle dysfunction (25%), bronchiolitis (5%). Although interstitial pulmonary damage is rare, 38% of patients with normal pulmonary radiographs have high resolution computed tomography exams showing interstitial disease, especially UIP, lymphocytic interstitial pneumonitis, NSIP, and organizing pneumonia [7, 9]. Atelectasis, reduction in lung volume and pulmonary vascular changes also occur [7, 9], whilst 1–9% of patients with SLE have pulmonary hypertension associated with plexogenic vasculopathy [6], especially in correlation with Raynaud's phenomena, the presence of anti-ribonucleoproteins (anti-RNP) antibodies, antiphospholipid syndrome, rheumatoid factor. Twenty percent of the necropsy cases have small vessel vasculitides [6]. The presence of anti-RNP antibodies is more frequently associated with pulmonary vascular changes and pulmonary shrinking [24].

Poorzand et al. [26] studied 45 patients with SLE without cardiovascular symptoms versus 25 healthy subjects by echocardiography for 5.5 ± 3.4 years. The two groups did not show differences in LV, left atrium size, LV ejection fraction, RV systolic function, RV and LV diastolic function, and pulmonary artery pressure. The LV global longitudinal strain was less in SLE patients ($-18.56 \pm 2.50\%$ vs. $-19.89 \pm 1.94\%$, $P = 0.028$).

Basant et al. [27] studied by transthoracic echocardiography (TTE) and TDI techniques 56 patients with SLE versus 50 normal subjects, revealing diastolic and subclinical biventricular systolic dysfunction. LVEF was similar in both groups, mitral E′ and A′ were lower in the group of SLE patients. TAPSE was lower in the group of SLE patients compared to the control group, RV E′ and A′ were significantly lower, especially

in the interventricular septum. Transmitral and transtricuspid pulsed Doppler flows showed higher A wave velocities in the group of SLE patients compared to the control group.

Tektonidou et al. [28] studied diastolic dysfunction in 164 patients with anticardiolipin antibodies, 56 of whom had SLE, compared to 43 SLE patients without anti-cardiolipin antibodies, 29 patients with anticardiolipin antibodies without SLE and 36 normal volunteers. At the tricuspid annulus, the E wave deceleration time and the isovolumetric relaxatiom time (IVRT) was prolonged in all patient groups. The anticardiolipin antibodies titer was the most important predictor of the aforementioned changes.

Leal et al. [29] studied by speckle-tracking echocardiography RV systolic function in childhood-onset SLE and found reduce RV global systolic longitudinal strain and global systolic longitudinal strain rate comparing with the normal subjects. The values of RV longitudinal strain were positively correlated with TAPSE and negatively correlated with TEI index.

26.4 Rheumatoid Arthritis

PAH is common in RA, but is mild [24]. It is rather the consequence of changes in lung parenchyma (bronchial dilation in 30–40% of cases, ground glass opacities in 15–25% of cases, thickening of the bronchial wall in 12–22% cases, parenchymal micronodules in 15–20% of cases), than pulmonary vascular changes [24]. Pleural effusions also arise. Pulmonary vascular disease is the rarest pulmonary complication in RA. Fibroproliferative proliferative arteriopathy, diffuse alveolar hemorrhage due to pulmonary capillaritis rarely develop [24].

26.5 Polymyositis/ Dermatomyositis

PM/DM. 50–70% of patients with positive anti-Jo-1 antibodies and 10% of anti-Jo-1 negative patients have interstitial lung changes (ILD), especially NSIP and OP [9].

26.6 Sjogren's Syndrom

SjS. SjS causes thickening of the bronchial walls, bronchiectasis, air-trapping, interstitial fibrosis, interstitial lymphoid pneumonia, subpleural nodules, peribronchovascular, centrilobular, pulmonary hypertension [9].

26.7 Mixed Connective Tissue Disease

MCTD affects the lung in 20–80% of cases, the changes being similar to SSc, SLE, PM/DM: NSIP, UIP, centrilobular nodules, honeycombing, aspiration pneumonia, PAH. PAH is the consequence of repetitive pulmonary embolism, plexogenic arteriopathy, hypoxic vasoconstriction secondary to interstitial changes [26]. The prognosis of PAH in MCTD is similar to that of PAH associated with SLE, SSc. The respiratory muscles weakness can induce restrictive ventilatory dysfunction, hypercapnic respiratory failure. The presence of PAH reduces the 5-years survival rate from 96% to 73% [27].

Vég et al. [30] studied 51 patients with MCTD versus 30 healthy subjects by TTE and TDI. Twenty of the MCTD patients had been diagnosed with PAH over the past 2 years. All patients had LV and RV diastolic dysfunction, the impaired relaxation type. The LV TEI index was significantly increased in the PAH group (0.36 ± 0.07) versus non-PAH (0.28 ± 0.04) patients. These patients had the RV TEI index similar to normal subjects.

Conclusion

SSc causes lung and cardiac involvement, generating PAH mainly in the cutaneous form, although it induces myocardial perfusion defects especially in the diffuse form. PAH is produced by multiple mechanisms, and the histological changes in pulmonary circulation are similar to those in IPAH. However, RV failure by ventriculo-arterial decoupling occurs earlier in SSc than in IPAH, and the prognosis is more severe. This is explained by myocardial histological changes (inflamma-

tion, fibrosis) developing in SSc and not in IPAH. SLE affects all the structures of the heart: pericardium, myocardium, endocardium, coronary arteries and 1–9% of patients with SLE have pulmonary hypertension associated with plexogenic vasculopathy. There is not a specific involvement of the RV in SLE patients but some echocardiographic studies performed with the new techniques show impaired biventricular diastolic and systolic function even in patients without clinical cardiac dysfunction. MCTD can be associated with severe PAH by repetitive pulmonary embolism, plexogenic arteriopathy, hypoxic vasoconstriction secondary to interstitial changes. RA is frequently associated with mild PAH, rather by changes in lung parenchyma than by pulmonary vascular changes. PM/DM, SjS determine pulmonary parenchymal changes, PAH, but no specific involvement of the heart.

References

1. Knockaert DC. Cardiac involvement in systemic inflammatory diseases. Eur Heart J. 2007;28(15):1797–804.
2. Luqmani RA, Suppiah R, Grayson PC, Merkel PA, Watts R. Nomenclature and classification of vasculitis—update on the ACR/EULAR Diagnosis and Classification of Vasculitis Study (DCVAS). Clin Exp Immunol. 2011;164(Suppl 1):11–3.
3. Lazzerini PE, Capecchi PL, Laghi-Pasini F. Systemic inflammation and arrhythmic risc: lessons from rheumatoid arthritis. Eur Heart J. 2017;38(22):1717–27.
4. Dinarello CA. Immunological and inflammatory functions of the interleukin-1 family. Annu Rev Immunol. 2009;27:519–50.
5. Watts TH. TNF/TNFR family members in costimulation of T cell responses. Annu Rev Immunol. 2005;23:23–68.
6. Shoenfeld Y, Gerli R, Doria A, Matsuura E, Cerinic MM, Ronda N, Jara LJ, et al. Accelerated atherosclerosis in autoimmune rheumatic diseases. Circulation. 2005;112(22):3337–47.
7. Cosgrove GP, Schwarz MI. Pulmonary manifestations of the collagen vascular diseases. https://thoracickey.com/pulmonarymanifestationsofthecollagenvasculardiseases/.
8. Capobianco J, Grimberg A, Thompson BM, Antunes VB, Jasinowodolinski D, Meirelles GSP. Thoracic manifestations of collagen vascular diseases. Radio Graphics. 2012;32(1):33–50.
9. Cosgrove GP, Schwarz MI. Pulmonary manifestations of the collagen vascular diseases, chapter 60, p 902–918. In: Fishman' s pulmonary diseases and disorders. 15th ed. New York: McGraw-Hill; 2015.
10. Noordegraaf AV, Westerhof BE, Westerhof N. The relationship between the right ventricle and its load in pulmonary hypertension. J Am Coll Cardiol. 2017;69(2):236–43.
11. Naejije R, Brimioulle S, Dewachter L. Biomechanics of the right ventricle in health and disease (2013 Grover conference series). Pulm Circ. 2014;4(3):395–406.
12. Vonk-Noordegraaf A, Haddad F, Chin KM, Forfia PR, Kawut SM, Lumens J, et al. Right heart adaptation to pulmonary arterial hypertension: physiology and pathobiology. J Am Coll Cardiol. 2013;62(suppl 25):D22–33.
13. Condliffe R, Howard LS. Connective tissue disease-associated pulmonary arterial hypertension. F1000Prime Rep. 2015;7:06. https://doi.org/10.12703/P7-06.
14. D'Andrea A, Stisi S, Bellissimo S, Vigorito F, di Uccio FS, Tozzi N, et al. Early impairment of myocardial function in systemic sclerosis: non-invasive assessment by Doppler myocardial and strain rate imaging. Eur J Echocardiography. 2005;6(6):407–18.
15. Hassoun PM. The right ventricle in scleroderma (2013 Grover conference series). Pulm Circ. 2015;5(1):3–14.
16. Overbeek MJ, Mouchaers KTB, Niessen HM, Hadi AM, Kupreishvili K, Boonstra A, et al. Characteristics of interstitial fibrosis and inflammatory cell infiltration in right ventricles of systemic sclerosis-associated pulmonary arterial hypertension. Int J Rheumatol. 2010:604615. https://doi.org/10.1155/2010/604615.
17. Vonk MC, Sande MH, van den Hoogen FHJ, van Riel PLCM, Verheugt FWA, van Dijk APJ. Right ventricle Tei-index: a tool to increase the accuracy of non-invasive detection of pulmonary arterial hypertension in connective tissue diseases. Eur J Echocardiogr. 2007;8(5):317–21.
18. Kepez A, Akdogan A, Sade LE, Deniz A, Kalyoncu U, Karadag O, Hayran M, Aytemir K, Ertenli I, Kiraz S, Calguneri M, Kabakci G, Tokgozoglu L. Detection of subclinical cardiac involvement in systemic sclerosis by echocardiographic strain imaging. Echocardiography. 2008;25(2):191–7.
19. Pigatto E, Peluso D, Zanatta E, Polito P, Miatton P, Bourji K, et al. Evaluation of right ventricular function performed by 3d-echocardiography in scleroderma patients. Reumatismo. 2014;66(4):259–63.
20. Loureiro MJ, Cotrim C, Simoes O, Cordeiro A, Santos MJ, Silva C, et al. Exercise Doppler echocardiography in the detection of pulmonary arterial hypertension in collagen vascular disease, P 1139, European congress of echocardiography. Eur J of Echocardiogr. 2005;6(suppl 1):S184–5.
21. Giunta A, Tirri E, Maione S, Cangianiello S, Mele A, DeLuca A, et al. Right ventricular diastolic abnormal-

ities in systemic sclerosis. Relation to left ventricular involvement and pulmonary hypertension. Ann Rheum Dis. 2000;59(2):94–8.
22. Rosato E, Maione S, Vitarelli A, Giunta A, Fontanella L, de Horatio LT, et al. Regional diastolic function by tissue Doppler echocardiography in systemic sclerosis: correlation with clinical variables. Rheumatol Int. 2009;29(8):913–9.
23. Nakajima K, Taki J, Kawano M, Higuchi T, Sato S, Nishijima C, et al. Diastolic dysfunction in patients with systemic sclerosis detected by gated myocardial perfusion SPECT: an early sign of cardiac involvement. J Nucl Med. 2001;42(2):183–8.
24. Lynch DA. Lung disease related to collagen vascular disease. J Thorac Imaging. 2009;24(4):299–309.
25. Lang R, Goldstein SA, Kronzon I, Khandheria BK, Mor-Avi V. ASE's comprehensive echocardiography. 2nd ed. Amsterdam: Elsevier; 2016.
26. Poorzand H, Mirfeizi SZ, Javanbakht A, Alimi H. Comparison of echocardiographic variables between systemic lupus erythematosus patients and a control group. Arch Cardiovasc Imaging. 2015;3(2):e30009. https://doi.org/10.5812/acvi.30009.
27. Elnady BM, Abdelghafar ASM, Khalik ESA, Algethami MM, Basiony AS, Al-otaibi MDA, et al. The implication of tissue Doppler echocardiography and cardiopulmonary exercise in early detection of cardiac dysfunction in systemic lupus erythematosus patients. Eur J Rheumatol. 2016;3(3):109–17. https://doi.org/10.5152/eurjrheum.2016.16002.
28. Tektonidou MG, Ioannidis JP, Moyssakis I, Boki KA, Vassiliou V, Vlachoyiannopoulos PG, et al. Right ventricular diastolic dysfunction in patients with anticardiolipin antibodies and antiphospholipid syndrome. Ann Rheum Dis. 2001;60(1):43–8.
29. Leal GN, Silva KF, Franca CM, Lianza AC, Andrade JL, Campos LM, et al. Subclinical right ventricle systolic dysfunction in childhood-onset systemic lupus erythematosus: insights from two-dimensional speckle-tracking echocardiography. Lupus. 2015;24(6):613–20.
30. Vég J, Hegedűs I, Szegedi G, Zeher M, Bodolay E. Diastolic function of the heart in mixed connective tissue disease. Clin Rheumatol. 2007;26(2):176–81.

Right Heart Involvement in Haematologic Disorders

27

Ana-Maria Vintilă, Mihaela Horumbă, and Vlad Damian Vintilă

Abstract

Haematologic patients are set apart by specific complications like immunosuppression, thrombocytopenia, sometimes associating coagulopathy and multiple points of entry for infection (central venous catheters and mucositis).

The right-sided heart is of particular importance in this type of patients as it is the preferred location of both primary and secondary cardiac tumours and is more frequently affected by radiation therapy due to its more anterior position in the thorax.

Chemotherapeutics may determine pulmonary hypertension and thus put a strain on the right ventricle.

Moreover, investigation of right-heart parameters like tricuspid annular plane systolic excursion and strain rate may reveal early cardiac dysfunction and establish prognosis in cardiac amyloidosis.

Keywords

Primary cardiac lymphoma · Cardiac metastases · Cardiotoxicity · Radiation therapy Anthracyclines · Tricuspid endocarditis · AL amyloidosis · Right ventricle dysfunction Right heart failure · Haematologic malignancies

27.1 Cardiac Tumors

Heart tumors are very rare disorders due to particularities of anatomy and physiology like rhythmic contraction, metabolism, continous blood flow and lack of lymphatic drainage. However, both primary cardiac tumors, involving only the myocardium and pericardium and metastases of solid tumors and haematologic malignancies may develop. Due to the lower pressure regimen, both primary and secondary tumors affect predominantly the right chambers of the heart. Most remain asymptomatic until post-mortem examination unless they are actively sought for or determine heart failure, arrhythmia, ST-T changes or B symptoms. Prognosis is poor due to late diagnosis, and therapy is limited to palliation.

27.1.1 Cardiac Metastases

Except for central nervous system neoplasms, every other type of malignancy has the ability to

A.-M. Vintilă (✉)
Department of Internal Medicine, Colţea Clinical Hospital, "Carol Davila" University of Medicine and Pharmacy, Bucharest, Romania

M. Horumbă
Department of Internal Medicine, Colţea Clinical Hospital, Bucharest, Romania

V. D. Vintilă
Department of Cardiology, University Emergency Hospital, "Carol Davila" University of Medicine and Pharmacy, Bucharest, Romania

S. I. Dumitrescu et al. (eds.), *Right Heart Pathology*, https://doi.org/10.1007/978-3-319-73764-5_27

metastasize to the heart—most common are lung, breast, oesophagus and pancreatic cancer, malignant melanoma, lymphoma and leukemia [1, 2].

Cardiac metastases are 10–20 times more common than primary cardiac tumors with a reported incidence of 1.5–13.9% [3]. The low overall incidence of cardiac metastases is due to several conditions: (1) the strong kneading action of the myocardium (2) metabolic particularities of striated muscle, (3) the rapid blood flow, (4) the lymph flow normally moving away from the heart [4–6].

There are various pathways of tumor dissemination: direct invasion (in the case of lung, mediastinal or oesophageal neoplasms), lymphatic (retrograde embolisation may occur in mediastinal involvement [2]) or haematogenous metastasis and extension through the vena cava or the pulmonary veins [3]. Uncommonly, metastatic cells may be sequestrated in fibrin networks giving rise to tumor thrombi that occupy heart chambers [7].

Cardiac haematological malignancies include metastases of Hodgkin and non-Hodgkin lymphoma (B or T-cell lymphoma), leukemic infiltration (chloroma) and extramedullary manifestations of multiple myeloma (cardiac plasmacytoma [8]). Onset of cardiac symptoms without an evident cause in a patient with known malignancy must raise clinical suspicion over the possibility of cardiac metastases [2].

Cardiac metastases have a higher incidence in patients over 50 years of age, 60 in the case of plasmacytoma [8]. Infiltration is associated with more advanced disease and, in the case of leukemia, a higher count of blast cells [9].

From a clinical standpoint, heart metastases are usually silent though patients may report palpitations, shortness of breath, cough, chest pain or pedal oedema [2]. Tumors may generate heart murmurs similar to authentic valvular murmurs [10] when they become large enough to obstruct normal blood flow, pericardial rubs due to pericardial thickening or infiltration of the pericardial cavity. Cases presenting with pericardial effusion may have diminished heart sounds and examination reveals serosanguinous fluid [2] (Fig. 27.1).

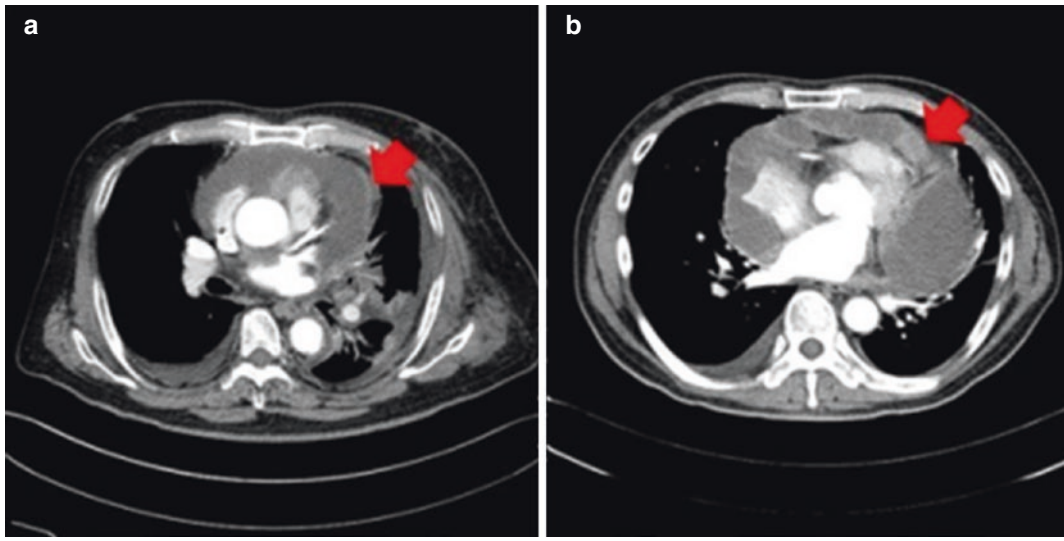

Fig. 27.1 Computed tomography showing cancer-related pericardial thickening and a pericardial nodule. Jeon HW, Cho DG, Park JK, Hyun KY, Choi SY, Suh JH et al. Prognostic factors affecting survival of patients with cancer-related pericardial effusion managed by surgery. World J Surg Oncol 2014; 12(1):249. Copyright © 2014 Jeon et al.; licensee BioMed Central Ltd. This is an Open Access article distributed under the terms of the Creative Commons Attribution License (http://creativecommons.org/licenses/by/2.0), which permits unrestricted use, distribution, and reproduction in any medium, provided the original work is properly credited. The Creative Commons Public Domain Dedication waiver (http://creativecommons.org/publicdomain/zero/1.0/) applies to the data made available in this article, unless otherwise stated

On the ECG, large nodular lesions may mimic myocardial infarction as they displace normal cardiac structures, while small nodular tumors produce T wave changes emulating chronic ischemia [10]. The ECG may also show sinus tachycardia and low voltage—indicative of pericardial involvement, atrial flutter and fibrillation or bundle branch block [2] (Fig. 27.2).

Radiographic examination may reveal cardiomegaly or signs of pericardial effusion [2]. Transthoracic echocardiography shows cardiac metastases as isoechogenic structures, while computed tomography visualizes hypodense structures with moderate enhancement after intravenous (IV) administration of contrast medium. On magnetic resonance imaging (MRI), secondary tumors show up as hyperintense on T2-weighted images, hypointense or isointense on T1-weighted images with enhancement after administration of IV contrast medium [8].

According to size, cardiac metastases have been grouped into large-nodular (over 1 cm in diameter), small-nodular (diameter smaller than 1 cm) and solitary globular metastatic lesions (structures up to 5 cm in diameter clearly delineated from the surrounding tissue) [10].

As opposed to primary cardiac tumors, that are typically left-sided (except for primary cardiac lymphoma), cardiac metastases are most often found in either the right atrium or the right ventricle with sparing of the valves [3] (with the exception of metastatic thrombi that may adhere to pre-existing valvular lesions [7]).

Microscopic infiltration of the pericardium (producing pericardial thickening up to the obliteration of the pericardial space), lymphatic and haematogenous embolisation are commonplace [10]. Malignant cells invading lymphatic channels may give rise to carcinomatous lymphangitis [7].

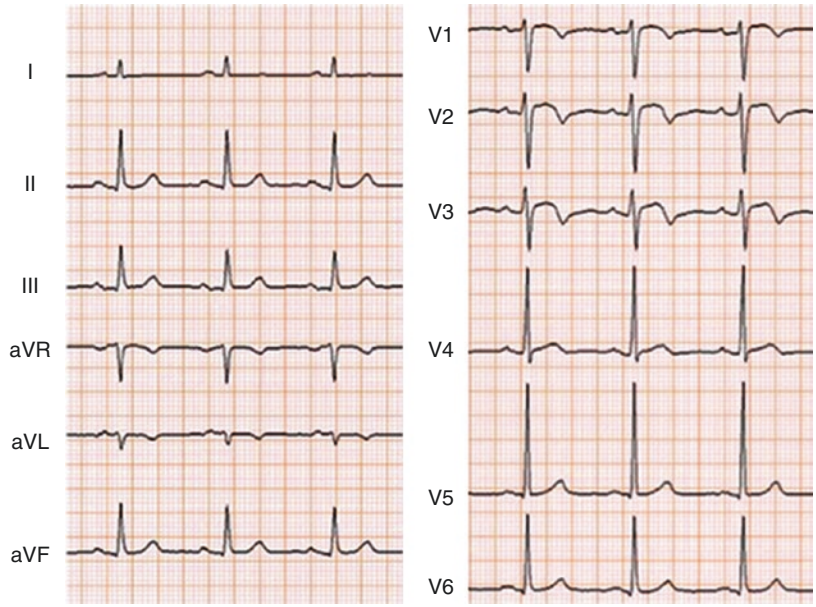

Fig. 27.2 Electrocardiography showing mild ST elevation and T wave inversion in V1–V3 due to cardiac metastases. Nakashima Y, Tanioka K, Kubo T, Yamasaki N, Yamasaki I, Syuin T et al. Metastatic cardiac tumor from urothelial carcinoma detected by transthoracic echocardiography: a case report. J Med Case Rep 2015; 9(1):257. Copyright © Nakashima et al. 2015. This is an Open Access article distributed under the terms of the Creative Commons Attribution 4.0 International License (http://creativecommons.org/licenses/by/4.0/), which permits unrestricted use, distribution, and reproduction in any medium, provided you give appropriate credit to the original author(s) and the source, provide a link to the Creative Commons license, and indicate if changes were made. The Creative Commons Public Domain Dedication waiver (http://creativecommons.org/publicdomain/zero/1.0/) applies to the data made available in this article, unless otherwise stated

Macroscopically, heart metastases are firm, small and nodular, resembling the primary lesions [7]. In lymphoma and leukemic metastases, however, the lesions are white, homogenous, gelatinous masses that adhere to ventricular or atrial walls and only seldom to the valves. Microscopic examination reveals large cells with a high nucleus to cytoplasm ratio, prominent nucleoli and amphophilic cytoplasm [11]. In leukemia in particular, metastatic cancer cells invade the lumen or infiltrate the tissue surrounding blood vessels [7].

Chloroma, also known as granulocytic sarcoma, is leukemic infiltration of soft tissue (commonly the skin), lymph nodes and bone, occurring before, concomitant with or late after a diagnosis of acute myelogenous leukemia (AML) has been established [12]. Cardiac chloroma is particularly rare (affecting less than 1% of patients with AML [13]). Leukemia and lymphoma are the haematological malignancies most likely to metastasize to the heart in pediatric patients [14] and cardiac infiltrates have been detected in up to 30–65% of leukemia patients at autopsy [1, 15].

Chloroma (thus named due to characteristic tan-green skin lesions [15]) is made up of masses of immature granulocytic cells, with or without bone marrow involvement [16]. It may arise from any chamber of the heart, with a predilection for the right-sided heart like all secondary cardiac tumors [17], the pericardium or myocardium. It may cause intractable heart failure [13], superior vena cava syndrome [12] or mimic myocardial infarction [18]. Certain cytogenetic abnormalities like t(8;21)(q22;q22) and inv(16)(p13q22) have been cited in association with cardiac chloroma [17].

Treatment is based on chemotherapy or radiotherapy and may be curative or palliative [13] in the attempt to limit life threatening arrhythmia, pericardial effusion or ischemia. In selected cases, radiation therapy is preferred (especially where localised lesions are involved), due to the fact that chloroma occurrence is most often a sign of drug resistant leukemia [19].

Plasma cell neoplasia may present as plasma cell leukemia, extramedullary plasmacytoma (EMP), multiple myeloma and solitary plasmacytoma of the bone [20]. Extramedullary plasmacytoma generally develop in patients aged 50–70, with a male predominance [20], mainly in the soft tissue of the head and neck, but without bone marrow involvement [21]. Overall survival is estimated at 100 months and progression free survival is longer than in the case of solitary plasmacytoma of the bone—over 71% of patients are progression free at 10 years [22].

Cardiac plasmacytoma is extremely rare. To our knowledge, only nine cases have been reported. Cardiac EMP has been presumed to disseminate haematogenously thus more commonly involves the right atrium; patients present with intractable right-sided heart failure, dyspnea and cyanosis [23].

Diagnosis is made on microscopic examination of biopsy specimens. Further evaluation must rule out multiple myeloma (absence of lytic bone lesions, negative bone marrow biopsy, absence of Bence-Jones proteins in urine [21]).

Treatment involves surgical excision, radiotherapy, chemotherapy for multiple myeloma and autologous stem cell transplantation [20].

In the assessment of intracardiac masses, the differential diagnosis of cardiac metastases includes primary cardiac tumors, intracavitary thrombi (haematologic patients are more prone to develop venous thrombi that may embolize to the heart [24]) and infectious endocarditis (though rare in haematologic patients, it must be actively searched for).

Throughout history, neoplastic spread to the heart has been, in most cases, diagnosed postmortem, but with the advent of cardiac imaging such as echocardiography, CT and MRI, patients are more likely to receive treatment. However, the prognosis remains poor. The therapeutic approach is mostly palliative, with chemotherapy and radiation therapy used to limit further spread and manage life threatening symptoms (for example pericardial window in large pericardial effusions) [6].

27.1.2 Primary Cardiac Lymphoma

Primary cardiac lymphoma (PCL) is an extremely rare entity that, as per the definition provided by the Armed Forces Institute of Pathology, involves only the heart and the pericardium [25]. Only 1.3% of primary cardiac tumors [8] prove to be PCL, though metastatic involvement of the heart by malignant lymphoma, leukemia or multiple myeloma [8] is more common, occurring in up to 20% of autopsy specimens [26].

Usually, primary cardiac lymphoma is located in the right chambers of the heart—chiefly the right atrium, interventricular septum and sometimes the tricuspid valve [27].

In terms of its origin, PCL has been thought to derive from the totipotential mesenchymal cells in the heart after suppression of the immune system, either through viral infection (HIV, EBV) or due to drugs associated with cardiac and renal transplant or Hodgkin disease treatment [25, 27, 28]. Another hypothesis is that PCL is not actually a primary tumor of the heart but an extranodal metastasis of an otherwise occult systemic lymphoma, disseminated through the thoracic duct, superior vena cava and into the right atrium [29].

Histologically, in immunocompetent hosts, most cardiac lymphomas are diffuse large B-cell lymphoma [25, 30], while T-cell [31], Burkitt-like [32], small lymphocytic [29] and plasmablastic lymphoma have been described in immunocompromised patients [33]. In the case of a CD30+ anaplastic and plasmablastic lymphoma, Epstein-Barr virus RNA has been detected in neoplastic cells.

PCL incidence is equal among men and women, though a male predominance has been reported in immunocompromised patients [33]. Patient age ranges from 14 months to 84 years [25], albeit PCL is most commonly diagnosed in the fifth decade of life [33].

PCL used to be a postmortem finding—delay in diagnosis was due to the few and nonspecific clinical signs. The tumor remains mostly asymptomatic until its growth produces a mass effect obstructing the right ventricle (RV) ejection tract, causes local invasion or pulmonary embolization [28]. Depending on tumor location [34], patients may present with signs of intractable *right-sided heart failure* (low cardiac output, hypotension [35], tachypnea, rapid onset dyspnea, ankle oedema, jugular vein distension, with or without hepatomegaly [28]), *arrhythmia* caused by infiltration of the conduction system [26], *pericardial effusion* [25] as severe as cardiac tamponade, and *superior vena cava syndrome* [27]. The most common ECG findings are tachycardia, various degrees of AV block [37], low voltage and nonspecific ST-T changes [31]. Occasionally, patients may present with typical "B symptoms" like weight loss, fever, night sweats and generalised pruritus [33] (Fig. 27.3).

Common laboratory findings are elevated erythrocyte sedimentation rate, C reactive protein [33] and LDH [30]. In cases presenting with pericardial effusion, the analysis of the pericardial fluid may be diagnostic, but most often reveals a transudate with negative histology [37].

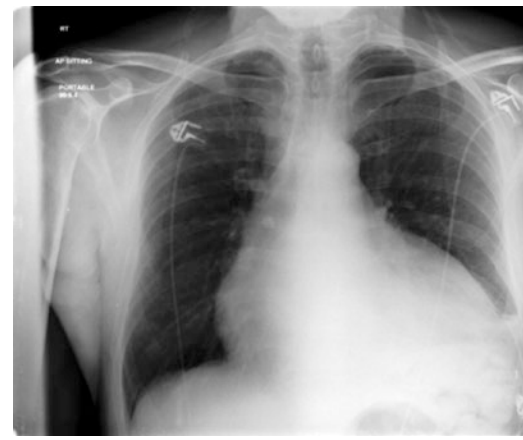

Fig. 27.3 Chest X-ray showing enlargement of cardiac silhouette due to pericardial effusion. Kaul P, Javangula K. Burkitt lymphoma masquerading as cardiac tamponade. J Cardiothorac Surg. 2007; 2(1):30. Copyright © 2007 Kaul and Javangula; licensee BioMed Central Ltd. This is an Open Access article distributed under the terms of the Creative Commons Attribution License (http://creativecommons.org/licenses/by/2.0), which permits unrestricted use, distribution, and reproduction in any medium, provided the original work is properly cited

Another source for cytological examination is biopsy of either the pericardium or the myocardium [34].

Macroscopically, PCL has been described as a mass comprising multiple polypoid, grey-white nodules, some with superficial haemorrhagic discoloration [27]. Microscopic examination reveals large lymphoid cells containing vesicular nuclei with prominent nucleoli [27] and a high mitotic index, positive for B-cell markers such as CD45, CD20, CD5 and bcl2 and negative for CD3, CD68, CD10, CD23 or CD45R0 [28]. There is never involvement of lymph nodes or other organs [25].

Imaging techniques like echocardiography, computed tomography (CT) and magnetic resonance imaging (MRI) may assist in reaching the correct diagnosis. Echocardiographic findings are hypoechoic structures within the myocardium, and pericardial effusion [38]. Transoesophageal echocardiography is superior to transthoracic echocardiography [39] and has been recommended for the evaluation of intracardiac masses [40] (Fig. 27.4).

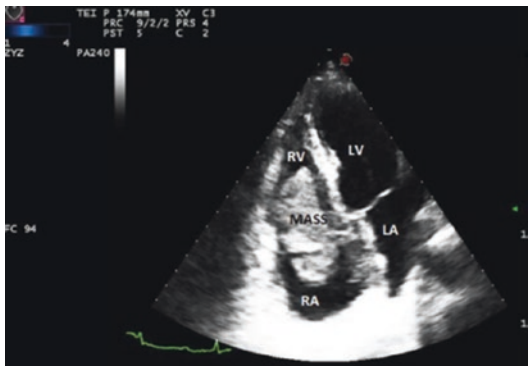

Fig. 27.4 Primary cardiac lymphoma involving the right atrium and ventricle. Montoro J, Mattia L, Bertazzoni P, Liptrott S, Colombo N, Civelli M et al. Primary cardiac lymphoma with isolated parenchymal central nervous system relapse: report of two cases and review of the literature. Ecancermedicalscience 2014; 8. Copyright © the authors; licensee ecancermedicalscience. This is an Open Access article distributed under the terms of the Creative Commons Attribution License (http://creativecommons.org/licenses/by/3.0), which permits unrestricted use, distribution, and reproduction in any medium, provided the original work is properly cited

On CT examination, PCL is isodense to the adjacent myocardium. Contrast-enhanced CT reveals a heterogeneously enhancing, poorly marginated mass, most likely due to clusters of lymphomatous cells infiltrating the normal myocardium. ECG gated MRI[1] reveals a mass isointense to cardiac muscle on both T1 and T2-weighted imaging [38].

Post-gadolinium T1-weighted sequences demonstrate heterogeneous enhancement, which may disappear once specific treatment is started [38, 41].

Coronary angiography may reveal a displacement of a coronary branch, surrounding an akinetic area which corresponds to the tumor itself [38], though as a diagnostic method it has poor sensibility and specificity [42].

PCL usually has a fulminant evolution that is often fatal, though developments in imaging have dramatically improved survival [38]. The treatment of choice is chemotherapy with lymphoma oriented drug regimens like CHOP (cyclophosphamide, doxorubicin, vincristine and prednisone) and COPP [34] (cyclophosphamide, doxorubicin, procarbazine, prednisone). Patients are at increased risk of death days after chemotherapy, possibly due to tissue necrosis (in cases with myocardial infiltration) and anthracycline cardiotoxicity. It appears that avoidance of doxorubicin and use of halved doses of cyclophosphamide and adriamycin have a lower risk of sudden cardiac death [33].

Though radiation therapy has been attempted in association with chemotherapy, no improvement in survival of patients was noted [29]; moreover, radiotherapy is associated with an increase in tumor volume, probably due to local inflammation [33]. Surgery is often difficult and

[1]The isointensity to normal myocardium on T1 and T2-weighted imaging and heterogeneity of enhancement on MRI are unique to PCL. Furthermore, MRI has the advantage of being able to differentiate between primary cardiac tumors: cardiac lipomas have high signal intensity on T1-weighted and intermediate signal on T2-weighted imaging (similar to mediastinal fat on MRI), fibromas have low signal intensity on T1 and T2 -weighted sequences (consistent with fibrous tissue), and pericardial cysts have low T1 signal intensity and high T2 signal intensity (as is the case with simple fluid).

incomplete due to local invasion and should be used only in those cases where intracardiac blood flow is compromised by tumor location [32].

PCL has a poor prognosis, partly because of its nonspecific symptoms that delay the diagnosis and partly due to difficult tumor access [42]. Median survival is 7–12 months after the initial diagnosis [33], though cases with left ventricle involvement have a worse prognosis with overall survival of only 1 month [29]. Lack of left ventricular (LV) involvement and presence of arrhythmia lead to an earlier diagnosis and are associated with better outcomes.

27.2 Cardiotoxicity Associated with Lymphoma Treatment: Radiation Therapy and Chemotherapy

Lymphoma treatment includes radiotherapy and anthracyclines—a class of drugs known for causing cardiotoxicity. Both radiation therapy and chemotherapy regimens induce left and right ventricular remodeling through oxidative stress, endothelial dysfunction and accelerated atherosclerosis and thus lead to ischemia, fibrosis, cavity dilation and pulmonary hypertension. Though fewer traditional cardiovascular risk factors are present in lymphoma survivors, cardiovascular disease has a high prevalence and coronary artery disease, heart failure, constrictive pericarditis and valvular lesions are common.

27.2.1 Radiation Therapy

It is estimated that around 50% of patients with cancer are treated with radiation therapy (RT) [43]. Among patients with a history of Hodgkin lymphoma, cardiovascular disease (CVD) is the main cause of death either through coronary artery disease, valvular heart disease, congestive heart failure or pericardial disease—conditions that may develop up to 19 years after radiation therapy [43, 44].

For a long time, the heart had been considered a radioresistant organ, considering the premise that cardiomyocytes are well differentiated and relatively radioresistant cells [45]. With the advent of newer diagnostic technology, long term consequences are seen in most patients treated for childhood mediastinal Hodgkin lymphoma. After radiation therapy, healthy cardiac tissue is damaged and replaced with fibrosis, which leads to a number of complications like pericardial, myocardial, valve and coronary artery disease [46].

The risk of developing CVD is 3–5 times higher in RT treated patients and the odds of having a fatal myocardial infarction are up to 3 times greater than in radiation naive patients [43, 44].

Cardiovascular side effects depend on cumulative radiation dose, dose per treatment, delivery technique, volume of irradiated myocardium, proximity of tumor to the heart, patient age and comorbidities (including coexisting risk factors [43, 45]). Exposure to over 15 Gray (Gy) increases the risk of heart disease up to six times over individuals not exposed to radiation—the current dose for Hodgkin lymphoma being 35 Gy [45].

The right ventricle is situated more anteriorly in the mediastinum and the right ventricular (RV) free wall receives a higher dose of radiation than the left ventricle (LV). Hence, right ventricular structure, systolic and diastolic function, and strain are significantly impaired after exposure to radiation. The mechanisms behind RV remodeling include micro and macrovascular ischemia, myocardial fibrosis, accelerated atherosclerosis, endothelial dysfunction and oxidative stress [45, 46].

Radiotherapy-induced endothelial injury causes activation of matrix metalloproteinases, leading to destruction of the endothelial basal cell membrane and accumulation of proinflammatory cells at the site of tissue injury, endothelial proliferation and obstruction of the microcirculation [45]. Endothelial lesions produce thrombomodulin, promoting adherence of local macrophages and monocytes that generate cytokines and growth factors (TNF, TGF-β1, IL-1β, IL 6, IL 8, IGF, PDGF [44, 47]). TGF-β1 promotes terminal differentiation of progenitor fibroblasts to post-mitotic

functional fibrocytes by inducing collagen gene expression, thus enhancing collagen production and inhibiting catabolism via decrease of collagenase activity [47].

Endothelial dysfunction caused by radiation therapy is due to reactive oxygen species like superoxide and peroxide and activation of NF-kB (nuclear factor-kappa B) [48].

Moreover, endothelial injury causes activation of the coagulation cascade and formation of fibrin deposits. Obstruction of the microcirculation and thrombus formation lead to apoptosis and replacement of cardiomyocytes with fibrotic tissue, producing a thinning myocardium with impaired function [45, 46].

Another mechanism inducing fibrosis of irradiated tissue is through impaired nitric oxide synthase expression, which leads to impaired endothelial function and vasodilation [44].

As with all cardiovascular diseases, smoking, diabetes, hyperlipidemia act as atherosclerosis promoting factors, though coronary artery disease may also develop in patients without traditional risk factors. Consequently, traditional modifiable risk factors should be treated more aggressively in patients exposed to radiotherapy [44]. Patients at high risk of developing coronary artery disease (CAD) should be monitored through minimally invasive testing such as computed tomography angiography, single-photon emission computed tomography or stress echocardiography [43].

Intimal proliferation of fibrous tissue leads to luminal narrowing, and, as opposed to typical atherosclerotic changes, mainly affects the vascular media; furthermore, the adventitia is thickened and fibrotic and there is a loss of smooth muscle cells in both the media and the adventitia [44] (Fig. 27.5).

Radiation damage affects the vascular endothelium of capillaries (causing telangiectasia) or larger vessels (leading to thrombosis, inflammation and fibrosis) in the irradiated field and may produce histologic alterations of the pericardium, myocardium, valves, peripheral, coronary or carotid arteries [44]. Minimal fibrotic changes may lead to an increase in wall rigidity and decrease in ventricular compliance, whereas advanced fibrosis is more commonly associated with symptomatic heart failure [46]. Radiation therapy induces vascular damage and a decrease in capillary density with the subsequent formation of ischemic myocardium islands [48].

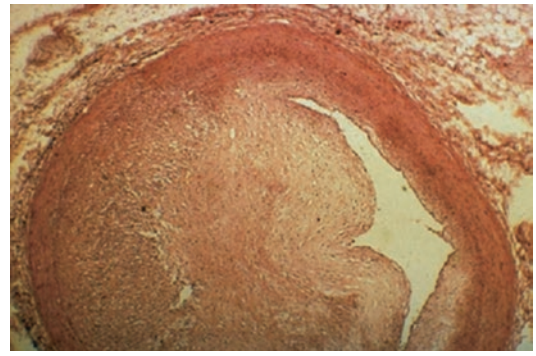

Fig. 27.5 Fibrosis of the left anterior descending artery after radiation therapy. Taunk NK, Haffty BG, Kostis JB, Goyal S. Radiation-induced heart disease: pathologic abnormalities and putative mechanisms. Front Oncol 2015; 5.

Chronic oxidative stress through the production of free radicals increases the risk of atherosclerotic disease development [45]. The time to onset of radiation-induced coronary artery disease (RICAD) is around 82 months. RICAD affects younger patients than typical CAD, specifically survivors of childhood or adolescence cancers [44]. It most often involves proximal arteries and is associated with perfusion defects in non-anatomical territories suggesting small-vessel damage [43].

Treatment of chronic or acute RICAD is similar to typical CAD, though coronary artery bypass graft surgery is associated with a higher incidence of complications as a result of mediastinal fibrosis. Moreover, the internal mammary

artery may be compromised due to its inclusion in the radiation field [44]. Revascularization in cancer patients poses problems due to postprocedural management requiring antiplatelet therapy in patients who often associate bleeding diatheses [49, 50]. Therefore, the use of drug eluting stents in haematologic patients must be done with caution, only after careful consideration of haemorrhagic and thrombotic risks.

CAD is due to vascular endothelial damage associated with extensive fibrosis of the adventitia, destruction of the media and atherosclerotic luminal narrowing [43].

There have been reports of radiation-induced sudden death and its cause may be diffuse fibrointimal hyperplasia in all coronary vessels and ostial lesions [44], particularly of the left anterior descending—as it courses the anterior surface of the heart [48].

Valve disease in patients exposed to radiation therapy occurs predominantly in the mitral and aortic valves, probably due to the higher pressure regimens, though tricuspid and pulmonary valve disease has also been described. The mean time to onset of symptoms is 98 months. Morphologic valve alterations include focal dystrophic calcification and marked thickening [44].

The conduction system is least commonly affected by radiation therapy [51]. Conduction system damage leads to nonspecific ST-T changes that may resolve spontaneously [52], right bundle branch block [44, 46], and infranodal atrioventricular block [53]. The right bundle branch is the most anterior structure of the conduction system and is thus more severely affected by mediastinal irradiation. Right bundle branch damage may result either directly from irradiation or as a consequence of local inflammation and ischemia. Post-mortem studies have shown an increased prevalence of atherosclerosis of the atrioventricular (AV) node and marked fibrosis of the AV node, AV bundle and both bundle branches. One of the most serious manifestations associated with conduction system damage is complete atrioventricular block (AVB) and it may occur any time after completion of radiation therapy [44].

Radiotherapy-induced AV block is suspected based on several criteria: age of onset (AVB in the young usually correlates with RT), delay between RT and onset of symptoms (after an average of 12 years—dose of radiation), AVB confirmation by electrophysiologic study, pericardial involvement and associated lesions demonstrating cardiac effects of radiation therapy [51].

Radiation therapy also leads to alteration in the pericardium, especially that of the right ventricle, either through pericardial effusion (an acute effect) or pericardial thickening (at least after 18 months) [54]. The RV is a thin walled chamber, working under low pressure regimens; thus pericardial disease, particularly pericardial thickening—*constrictive pericarditis*—impairs diastolic function, increases RV filling pressure and ultimately alters RV systolic function [45].

Due to their position in the chest, lungs are also affected by RT. The effects of radiation therapy on the lung can be either acute—*radiation pneumonitis*—or chronic—*pulmonary fibrosis*. Radiation pneumonitis, the earliest effect of radiation, is caused by vasodilation and increase in capillary permeability [48], eventually leading to a decrease in lung volume and impaired diffusion capacity [47]. Pulmonary fibrosis occurs when there is an imbalance between the ratio of progenitor cells and postmitotic fibrocytes responsible for the synthesis of extracellular matrix components like collagen and proteoglycans, with subsequent remodeling and progression of the fibrotic phenotype [47]. As a consequence, there is an increase in pulmonary resistance and pulmonary wedge pressure leading to RV remodeling [45], and ultimately RV dysfunction (Fig. 27.6).

Cardiac biomarkers like BNP, troponin and CK-MB may be used to monitor radiation-induced cardiotoxicity, though there is conflicting evidence on this aspect. An increase in troponin may result from a transient membrane leak from cardiomyocytes damaged by radiation, while BNP is a sign of myocardial cell inflammation and residual diastolic dysfunction [52].

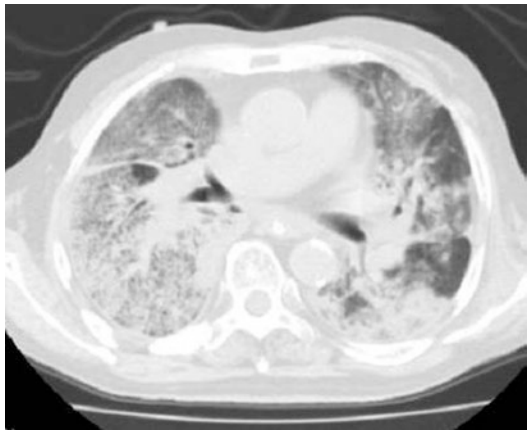

Fig. 27.6 Computed tomography of radiation pneumonitis. Yamashita H, Kobayashi-Shibata S, Terahara A, Okuma K, Haga A, Wakui R et al. Prescreening based on the presence of CT-scan abnormalities and biomarkers (KL-6 and SP-D) may reduce severe radiation pneumonitis after stereotactic radiotherapy. Radiat Oncol 2010; 5(1):32.

27.2.2 Chemotherapy Induced Cardiotoxicity

Chemotherapy induces left and right ventricular remodeling, including RV fibrosis, dilation, decline in systolic and diastolic function and impairment of strain. The pathophysiology of RV involvement may be a consequence of the direct destructive effect of chemotherapy on myocardial fibers, oxidative stress, endothelial dysfunction or pulmonary hypertension [55].

As new therapies have developed in the treatment of haematologic malignancies, so has overall survival increased and with it the incidence of long-term chemotherapy-induced side effects. Type and extent of myocardial alteration are dependent upon various factors like type of chemotherapeutics used, cumulative dose, associated radiation therapy, age and comorbidities.

In terms of chemotherapy-associated toxicity, two types have been described: type 1 is irreversible, dose-dependent and associated with anthracycline therapy and type 2 is associated with the use of trastuzumab (commonly used in the treatment of breast cancer).[2]

The chemotherapeutic agents most commonly associated with a decline in RV function are anthracyclines, trastuzumab, cyclophosphamide and dasatinib [55].

Among antineoplastic drugs, anthracyclines (doxorubicin, daunorubicin, epirubicin) are well known to cause cardiac toxicity [54]. The mechanism behind anthracycline induced cell damage is oxidative stress; thus, reactive oxygen species react with iron and produce mitochondrial damage, vacuolar swelling, myofibrillar disarray and ultimately cell apoptosis [55].

Topoisomerase IIα is an enzyme involved in replication, transcription and chromosomal segregation, thus it is highly active in neoplastic cells. As such, antineoplastic therapies, namely anthracyclines, have been developed to target topoisomerase IIα. However, anthracyclines are not particularly selective in terms of substrate and cross-react with topoisomerase IIβ, a structurally similar isoenzyme with the same catalytic mechanism expressed by cardiac myocytes, thus explaining the cardiotoxic effects of anthracycline therapy [55, 56].

On the short term, cardiac effects may manifest with nonspecific ST-T interval abnormalities. However, on the long run, anthracycline toxicity may lead to heart failure, the cardiotoxic effect depending on cumulative dose (generally considered to be over 550 mg/m^2) [54].

Up to date, dexrazoxane is the single approved agent in providing protection against doxorubicin-induced toxicity during anthracycline infusions and acts by reducing oxidized iron levels [57]. Recently, empagliflozin, a selective inhibitor of sodium-glucose cotransporter 2, has been shown to attenuate doxorubicin induced cardiotoxicity in a mouse model [58]. Moreover, carvedilol, a nonspecific beta blocker with antioxidant and antiapoptotic properties, and ACE inhibitors

[2] As lymphoma and breast and gastric cancer usually respond to similar chemotherapy regimens and/or radiation therapy, the two entities have most commonly been studied together.

(particularly in patients who also associate high blood pressure) have been shown as effective in managing anthracycline cardiac toxicity.

Cyclophosphamide is an alkylating agent that interferes with DNA replication; its cardiotoxic effects are caused by a metabolite that induces damage in cardiomyocytes and endothelial cells. Cyclophosphamide, along with mitomycin C and cisplatin are also associated with veno-occlusive disease [55]. As opposed to anthracyclines, the total dose of an individual course rather than the cumulative dose is what produces cardiac side effects. Association of anthracyclines with RT produces worse outcomes [54]. Fortunately, the side effects of cyclophosphamide therapy, ischemia leading up to acute myocardial infarction, seem to last only up to 6 days after treatment, without long-term toxicity in survivors. Cisplatin, however, does have long term consequences and can cause heart failure or myocardial infarction up to 20 years after treatment [54].

Dasatinib is a tyrosine kinase inhibitor approved for the treatment of chronic myeloid leukemia and acute lymphoblastic leukemia. Dasatinib induces endothelial cell damage, oxidative stress and leads to pulmonary hypertension (tipping the balance in favor of pro-proliferative factors of endothelial and pulmonary arterial smooth muscle cells). Discontinuation of dasatinib has been reported to improve pulmonary hypertension [55, 59, 60].

Used in the treatment of multiple myeloma, thalidomide lowers levels of TNF-β and may be useful in the treatment of heart failure. As such, it is not known to cause cardiac toxicity and its side effects may be managed through dose reduction. However, deep vein thrombosis has been described in relation to thalidomide treatment [54]. Pulmonary embolisation from the affected veins could impact right heart function depending on the severity of the embolism.

Even in patients naive to chemotherapy, RV function deteriorates, possibly due to cancer-related proinflammatory interleukins, reactive oxygen species and neurohormonal changes [55].

The right ventricle (RV) is anatomically and physiologically different from the left ventricle (LV); it consists of two muscle layers (as opposed to three), has a larger volume and works against a lower afterload. Thus, it is expected that the two ventricles behave differently—up to a molecular level [61]—after exposure to cardiotoxic treatment [62].

In terms of imaging techniques, means for echocardiographic evaluation of right ventricular structure and function are less readily available than for the left ventricle and the current gold standard is cardiac magnetic resonance. However, due to its higher cost, it has been less used in the evaluation of haematologic patients [45].

RV dimensions do not change in patients treated with chemotherapy or radiation therapy, but there are slight alterations in function, namely: global function—fractional area change (FAC), longitudinal function—tricuspid annular plane systolic excursion (TAPSE), RV free wall strain and peak systolic velocities of the tricuspid annulus (s') [63]. RV free wall strain seems to be a more sensitive indicator of subtle dysfunction than FAC [64]. RV systolic dysfunction is apparent in patients who have undergone cardiotoxic treatment (either by RT or anthracyclines) [63].

TAPSE is reduced in Hodgkin lymphoma survivors irrespective of the therapy used (radiation therapy or anthracyclines). Furthermore, a reduction in tricuspid s' was detected in patients who had received high-dose radiotherapy (>30 Gy). In patients treated with RT, RV FAC and RV strain are also lower [62].

The cumulative dose of anthracyclines is not associated with RV dysfunction [62] and TAPSE, s' and FAC all remain within the normal range [45]. As expected, RV dysfunction is more prevalent in patients who also associate left ventricular dysfunction [62].

27.3 Central Venous Catheter Associated Endocarditis

Infective endocarditis (IE) usually involves the mitral or aortic valve and in only up to 5–10% of cases has been described in relation to right-sided heart valves—commonly in intravenous drug users, alcoholics, burn victims and the immunocompromised [65, 66]. Out of all right

heart IE cases, only up to 5–10% occur in non-drug users [65].

The lower incidence of tricuspid valve endocarditis correlates with a lower incidence of rheumatic involvement of the right heart, lower pressure regimens and presence of deoxygenated blood [65].

Clinical suspicion is raised when patients develop fever, dyspnea, tricuspid regurgitation murmurs, evidence of pulmonary emboli—atelectasis, pleural effusion, cavitation and alveolar infiltrates [67]—or exhibit vegetations on echocardiography. Moreover, systemic embolisation occurs in patients with patent foramen ovale. Other clinical signs are mucosal and cutaneous lesions (Osler's nodules, Janeway lesions), splenomegaly and splinter haemorrhages [68]. Chest X-rays usually reveal multiple infiltrates in the lower lobes [65]. Blood culture and Gram stain examination are the gold standard for diagnosis, but in the case of unculturable bacteria PCR allows for rapid and reliable detection [66, 68].

The bacterium most commonly associated with central venous catheter (CVC) endocarditis is coagulase-negative *Staphylococcus* [66], though pathogens like *Pseudomonas aeruginosa*, *Klebsiella pneumoniae* and *Candida* spp. have been reported in cases of tricuspid [66, 69] or pulmonary valve endocarditis [70] (Fig. 27.7).

Haematologic patients are particularly prone to develop carbapenem-resistant *K. pneumoniae* infections as a result of the chronic use of broad-spectrum antibiotics, frequent neutropenia, long-term hospitalization and mucositis induced by chemotherapy [71].

Nonbacterial thrombotic endocarditis (NTBE) or marantic endocaditis [72] (thus named due to its primarily affecting patients with chronic wasting diseases [67]) occurs when valvular endothelial lesions are capped by fibrin and platelet deposits stimulated by tissue factor production [66]. The thrombus may remain sterile and eventually lead to pulmonary embolisation [73] or, as with immunocompromised hosts, microorganisms may adhere to the fibrin and platelet mesh and generate micro-colonies producing true infective endocarditis [70].

Blood culture negative IE accounts for up to 2.5–3.1% of cases and is due to prior antibiotic treatment or colonisation with atypical microorganisms – common in immunocompromised hosts like acute leukemia patients and those undergoing myeloablative treatment for stem cell transplantation [66].

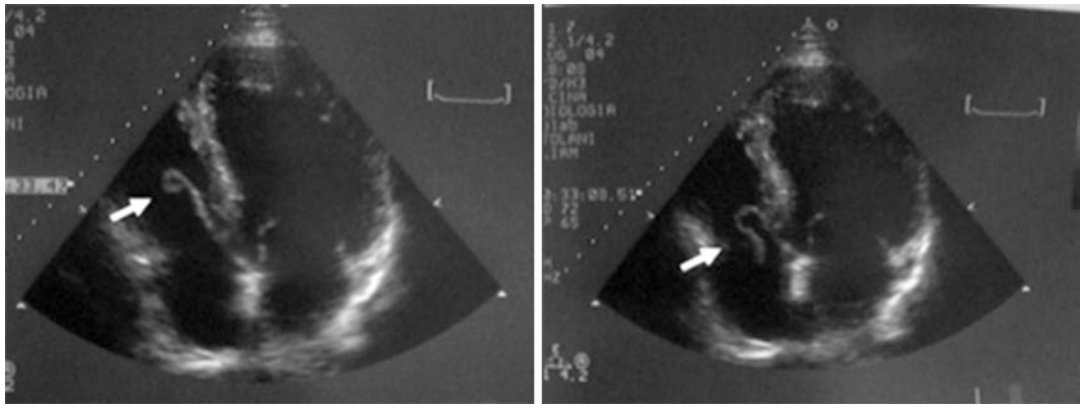

Fig. 27.7 Tricuspid valve vegetation viewed on transthroacic echocardiography. Chesi G, Colli A, Mestres CA, Gambarati G, Boni F, Gherli T. Multiresistant-MRSA tricuspid valve infective endocarditis with ancient osteomyelitis locus. BMC Infect Dis 2006; 6(1):124. Copyright © 2006 Chesi et al.; licensee BioMed Central Ltd. This is an Open Access article distributed under the terms of the Creative Commons Attribution License (http://creativecommons.org/licenses/by/2.0), which permits unrestricted use, distribution, and reproduction in any medium, provided the original work is properly cited

In haematologic patients, infection is one of the most feared complications as it raises mortality either directly or indirectly by delaying chemotherapy and thus decreasing its efficiency [74]. Central venous catheters are a common occurrence in haematologic patients as they are used to deliver blood products, drugs, fluids and parenteral nutrition, sometimes remaining in place for very long periods of time [75]. Active search for right-heart endocarditis is warranted whenever such a patient develops an unexplainable fever.

Central venous catheter placement is a known risk factor for infective endocarditis with a reported incidence of up to 7–29%, depending on catheter type, frequency of manipulation, underlying disease, and setting of insertion (CVCs placed in an urgent setting have a higher risk of colonization due to poor aseptic measures). Tricuspid valve injury associated with CVC placements poses diagnostic difficulties as it occurs in patients without structural heart abnormalities [76].

Endocarditis is a rare occurrence among haematologic patients despite the presence of endothelial injury caused by aggressive chemotherapy regimens and CVC placement, immunosuppression secondary to the haematologic disorder and its therapy and the existence of points of entry for pathogens [70]. However, patients undergoing stem cell transplantation are more prone to develop CVC-related IE—catheters remain in position for longer periods of time, myeloablative therapy leads to long-lasting neutropenia and mucositis and graft-versus-host-disease result in mucosal injury and may favour sepsis [72].

The low incidence of EI In haematologic patients may be due to the low platelet count preventing thrombus formation and bacterial colonization. However, thrombus formation in patients with a low thrombocyte count [77] may be due to endothelial and platelet dysfunction [78] and excess of procoagulant factors [79]. Underdiagnosis is another possible reason behind the low incidence, since fever caused by coexisting factors may hide IE [70].

Long term broad spectrum antibiotic therapy and valve surgery are the mainstay of tricuspid valve IE treatment, along with CVC removal, except for cases where the insertion of a new CVC is particularly problematic and the pathogen is not highly virulent. In such cases, antibiotic therapy is started and the catheter is extracted only if fever persists for up to 48–72 h [36]. Surgery is indicated in patients with intractable right heart failure, persistent sepsis, abscess formation, recurrent septic embolisation [71] and failure to control symptoms despite adequate medical therapy [69]. In the case of recurrent sterile pulmonary emboli—as sterile vegetations may continue to embolise into the pulmonary circulation—respiratory distress and pulmonary hypertension are reversible over time and surgery is not indicated [65].

Vegetation size of over 20 mm, heart failure secondary to severe tricuspid regurgitation without response to diuretics and fungal colonization are negative outcome predictors and weigh in favor of surgery [66]. Timing of the intervention is also important and depends on coexisting left-sided heart failure, cause of endocarditis (the presence of a prosthetic valve or pacemaker warrant urgent intervention), etiology (fungi and *S. aureus* require more aggressive treatment) and toxicity of medical treatment [71]. Valvuloplasty without prosthetic replacement of the tricuspid valve is the current choice of treatment [65], as tricuspid valve replacement requires long term anticoagulation that is often contraindicated in haematologic patients [71].

27.4 Amyloidosis and the Right Heart

Amyloidosis is the condition caused by precipitation of insoluble extracellular proteins into β pleated sheets [80] of amyloid in tissues and organs. Such structures occur in any of the following conditions: immunoglobulin amyloidosis (AL), familial or senile systemic amyloidosis (ATTR—familial transthyretin associated), secondary amyloidosis (AA—due to protein A formation)—secondary to chronic inflammationin tuberculosis, leprosy, inflammatory bowel syndrome—and finally, hemodialysis-associated

amyloidosis (β2-microglobulin deposits [81]). Chemical, mechanical and electrical stimuli cause amino acid substitutions, leading to protein instability and eventually to formation of amyloid [82]. Moreover, amyloid deposits act as scaffolds for further buildup—"amyloid begets amyloid" [83].

In the case of AL amyloidosis, monoclonal immunoglobulin light chain proteins precipitate into amyloid, hence the association with immunoglobulin dyscrasias like multiple myeloma, B-cell lymphoma and Waldenstrom macroglobulinemia [82]. In multiple myeloma, the bone marrow is infiltrated with 5–10% plasma cells (less than 4% in normal individuals [82, 83]). Amyloidosis can exist as a condition in itself or may accompany multiple myeloma. Differentiation among the two is made by bone marrow infiltration, presence of osteolytic lesions and monoclonal proteins in urine and serum; however, prognosis does not vary and the therapeutic strategy is the same [81]. While in healthy individuals there is a κ light chain predominance (3:1), in multiple myeloma the κ to λ ratio is 3:2, and in AL amyloidosis 1:3 [83].

Patients, commonly over 40 years of age, complain of weakness, fatigue (due to heart failure) and weight loss (malabsorption and gastrointestinal disturbances caused by amyloid infiltration of the gut and autonomic nervous system) [83].

The clinical presentation of amyloidosis differs according to the site of predominant involvement, though all organs, with the exception of the central nervous system, seem to be somewhat affected. *Hepatomegaly* is due either to amyloid infiltration or right-sided heart failure; *macroglossia* may associate taste disturbances and sometimes leads to sleep apnea; *dysphonia* is caused by amyloid infiltration of the vocal chords [81]; *proteinuria*, often of nephrotic range, along with hypoalbuminemia and generalised oedema characterize amyloidosis of the kidney; *neuropathy* may be either *autonomic*, presenting with orthostatic hypotension, impotence and diarrhea or *peripheral*, that includes carpal tunnel syndrome [83] and has a distal and symmetric distribution; atraumatic, periorbital *ecchymoses* and facial *purpura* without thrombocytopenia [81], occur due to amyloid infiltration of the vasculature; major haemorrhage is rare and is due to binding of calcium-dependent clotting factors by amyloid [83] (Fig. 27.8).

Laboratory findings include anemia (caused either by multiple myeloma, gastrointestinal bleeding or kidney disease), elevated creatinine and hypoalbuminemia. Serum protein electrophoresis and immunoelectrophoresis are highly suggestive of amyloidosis or multiple myeloma but are not a mandatory finding [81].

The diagnosis of amyloidosis is made through examination of biopsy samples (usually abdominal fat biopsy [81]) with Congo red staining under a light microscope. Amyloid has a typical apple-green birefringence under polarized light [82] (attributed to its β-pleated sheet structure) [83] (Fig. 27.9).

In particular, cardiac involvement is common in AL amyloidosis due to affinity of lambda light chains to cardiac tissue [82]. Clinical signs consist of a restrictive pattern cardiomyopathy (amyloid accumulation in the myocardium), arrhythmia and conduction disturbance (buildup in the conduction system). Moreover, amyloid infiltration may also affect the cardiac vasculature through endothelial dysfunction and smooth muscle proliferation [82, 84, 85], leading to ischemia with subsequent angina or myocardial infarction [84] and pulmonary hypertension. Consequent to the occurence of restrictive cardiomyopathy, elevated jugular venous pressure, pedal oedema and hepatomegaly are present in amyloidosis of the heart [83].

At the onset of cardiac involvement, neither the left nor the right ventricle show alterations in size or function [83]. Echocardiographic findings in AL amyloidosis consist of uniform thickening and hypokinesia of the septum and the posterior wall (with characteristic granular sparkling [81]), a decreased LV end-diastolic volume and systolic function [84]. Furthermore, right ventricle dilation is associated with increased wall thickness due to pulmonary hypertension and increased afterload as a consequence of restrictive patterns of left ventricular filling. Diastolic dysfunction of the RV occurs later than

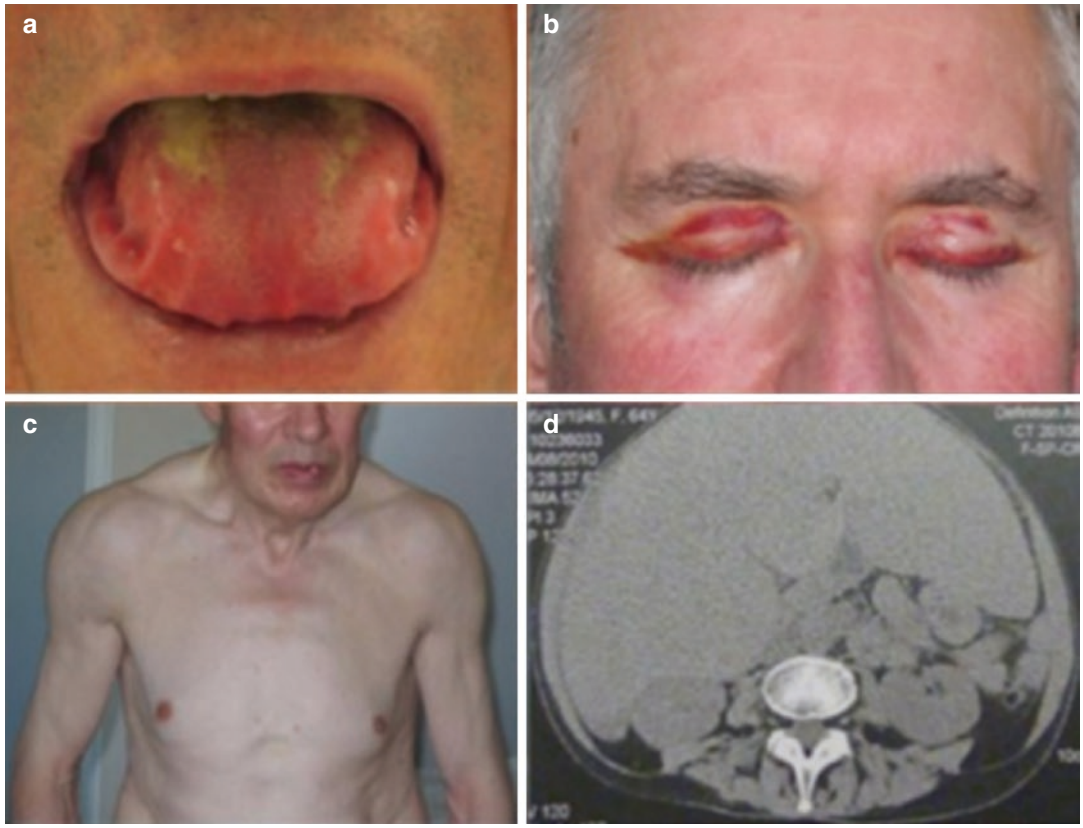

Fig. 27.8 Amyloidosis manifestations: (**a**) Macroglossia. (**b**) Periorbital ecchymoses. (**c**) Pseudo athletic appearance due to muscular infilatration. (**d**) Hepatomegaly. Desport E, Bridoux F, Sirac C, Delbes S, Bender S, Fernandez B et al. AL amyloidosis. Orphanet J Rare Dis 2012; 7(1):54. Copyright ©2012 Desport et al.; licensee BioMed Central Ltd. This is an Open Access article distributed under the terms of the Creative Commons Attribution License (http://creativecommons.org/licenses/by/2.0), which permits unrestricted use, distribution, and reproduction in any medium, provided the original work is properly cited

alterations in left ventricular function [80, 82] (Fig. 27.10).

Doppler myocardial imaging is the most useful tool in estimating systolic dysfunction of the right ventricle (RV) early on during the course of the disease, even while other echocardiographic parameters remain normal. Assessment of tricuspid annular plane systolic excursion (TAPSE), a measure of longitudinal systolic function, and systolic strain of the basal segment of the RV free wall are the most accurate means of diagnosing right ventricular dysfunction. Moreover, RV systolic pressure and systolic strain rate of the middle segment are independent predictors of outcome in amyloidosis patients. Furthermore, TAPSE and RV free wall thickness are accurate in differentiating patients with amyloidosis who have cardiac involvement [86].

While in the case of the left ventricle, a chamber with high afterload and low wall excursion, strain (longitudinal deformation of the myocardial fibers) offers information on function and prognosis, for the right ventricle, a chamber with low afterload and high wall excursion, strain rate (rate of deformation) is more relevant [86].

Amyloid deposits in the right ventricular wall lead to myocardial thickening and diastolic dysfunction. In early stages, increased atrial filling velocity (A) with decreased E/A ratio suggests a higher contribution of atrial systole to ventricular

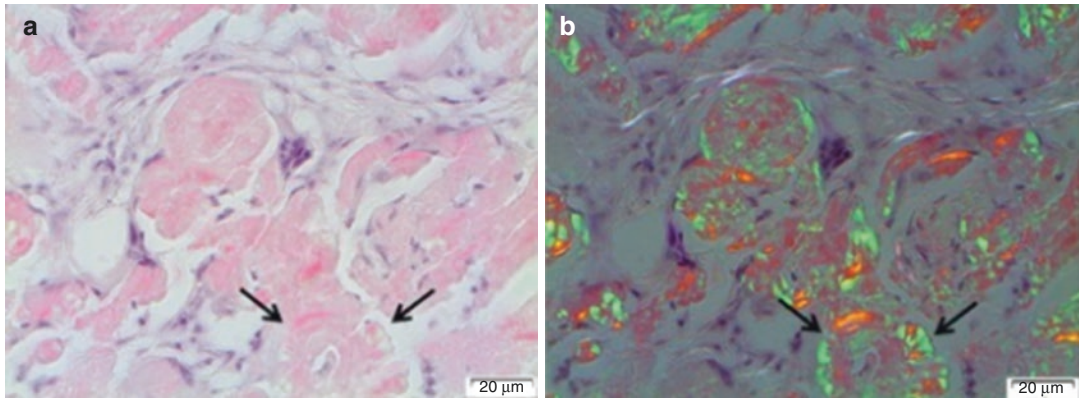

Fig. 27.9 Typical green birefringence in polarized light after Congo red staining of amyloid infiltrated tissue. Westermark P. Localized AL amyloidosis: a suicidal neoplasm? Ups J Med Sci 2012; 117(2):244–250. Copyright © Informa Healthcare. This is an open-access article distributed under the terms of the Creative Commons Attribution Noncommercial License which permits any noncommercial use, distribution, and reproduction in any medium, provided the source is credited

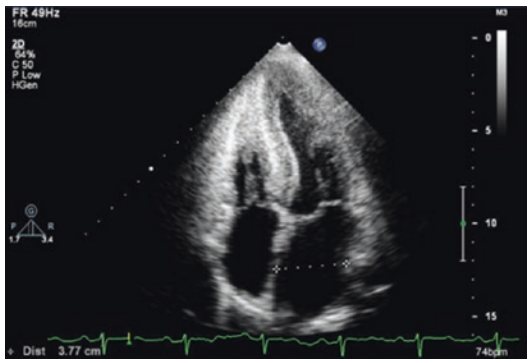

Fig. 27.10 Transthoracic echocardiography: typical aspect of cardiac amyloidosis with septal thickening and "snowstorm" appearance. Wang C, Li Y, Jin Y, Zhou W, Zhu Y, Yao F et al. Chronic diarrhea as the presenting feature of primary systemic AL amyloidosis: serendipity or delayed diagnosis? BMC Gastroenterol 2013; 13(1):71. Copyright © 2013 Wang et al.; licensee BioMed Central Ltd. This is an Open Access article distributed under the terms of the Creative Commons Attribution License (http://creativecommons.org/licenses/by/2.0), which permits unrestricted use, distribution, and reproduction in any medium, provided the original work is properly cited

filling, while in more advanced stages a restrictive pattern of diastolic dysfunction develops, with shortened deceleration time of the rapid filling wave velocity (E) and increased E/A ratio. Impaired function of the left ventricle leads to a more pronounced right ventricular dysfunction and a more severe restrictive filling pattern, suggesting ventricular filling interdependence [87].

The pathophysiology of restrictive cardiomyopathy in amyloidosis has been linked to myocardial amyloid infiltration leading to poor diastolic relaxation due to altered calcium transmembrane shifts; in contrast, in cases with gross ventricular thickening, necrosis of myocardial fibers produces an increase in rapid early filling and poor ventricular compliance in systole [87].

Among the different types of amyloidosis, AL has the worst prognosis with a mean survival in the absence of treatment of approximately 13 months, that may be increased to 17 months with melphalan and prednisone therapy [82]. Depending on the site of major involvement, presence of pulmonary effusion, β2-macroglobulin [81] and troponin T levels [86], the median survival may vary—with worse outcomes in patients with amyloidosis and cardiac involvement [83].

Calcium-channel blockers are ineffective since diastolic dysfunction is due to amyloid deposits rather than cardiomyocyte dysfunction and paradoxically may increase peripheral vascular resistance [88]. Beta blockers worsen hypotension caused by autonomic neuropathy and may aggravate bradycardia and digoxin binds amyloids fibrils with an increase in susceptibility to

digitalis toxicity. Cardiac transplantation has been attempted but shows little promise, as recurrence is inherent and mortality high [82]. As with multiple myeloma, autologous stem cell transplantation seems to induce remission in AL amyloidosis patients. Unfortunately, however, cardiac involvement is a contraindication [86]. Finally, studies have shown in vitro efficacy of treatment with 4′-iodo-4″-deoxydoxorubicin that seems to bind amyloid fibrils and prevents precipitation [83].

References

1. Nikdoust F, Sani ZA, Tabatabaei SA. Right ventricle tumoral mass in acute promyelocytic leukemia (AML M3): cardiac magnetic resonance findings. Iranian Heart J. 2016;17(3):46–50.
2. Young J, Goldman IR. Tumor metastasis to the heart. Circulation. 1954;9(2):220–9.
3. Amano J, Nakayama J, Yoshimura Y, Ikeda U. Clinical classification of cardiovascular tumors and tumor-like lesions, and its incidences. Gen Thorac Cardiovasc Surg. 2013;61(8):435–47.
4. Goudie RB. Secondary tumours of the heart and pericardium. Br Heart J. 1955;17(2):183.
5. Laws JW, Annes GP, Bogren HG. Primary malignant tumors of the heart. Calif Med. 1973;118(4):11.
6. Mukai K, Shinkai T, Tominaga K, Shimosato Y. The incidence of secondary tumors of the heart and pericardium: a 10-year study. Jpn J Clin Oncol. 1988;18(3):195–201.
7. Hanfling SM. Metastatic cancer to the heart. Circulation. 1960;22(3):474–83.
8. Voigt P, Wienbeck S, Weber M-A, Oyama-Manabe N, Beimler M, Schob S, et al. Cardiac hematological malignancies: typical growth patterns, imaging features, and clinical outcome. Angiology. 2017;69(2):170–6. https://doi.org/10.1177/0003319717713581.
9. Barbaric D, Holley D, Lau K-C, McCowage G. It is ALL in the heart: a patient with acute lymphoblastic leukemia and cardiac infiltration at time of diagnosis. Leuk Lymphoma. 2002;43(12):2417–9.
10. Skhvatsabaja L. Secondary malignant lesions of the heart and pericardium in neoplastic disease. Oncology. 1986;43(2):103–6.
11. Perry DJ, McCormick D, Veasey S, Cohen IS. Right heart obstruction due to intracavitary prolymphocytic leukemia. Am J Med. 1986;81(1):131–4.
12. Dingerkus H, Völler H, Albrecht A, Hennig L, Stein H, Schröder R. Mediastinal chloroma affecting the right heart with superior vena cava syndrome. Am Heart J. 1994;127(2):465–8.
13. Makaryus AN, Tung F, Liu W, Mangion J, Kort S. Extensive neoplastic cardiac infiltration in a patient with acute myelogenous leukemia: role of echocardiography. Echocardiography. 2003;20(6):539–44.
14. Hunkeler N, Canter CE. Antemortem diagnosis of gross cardiac metastasis in childhood leukemia: echocardiographic demonstration. Pediatr Cardiol. 1990;11(4):225–6.
15. Foucar K, Foucar E, Willman C, Horvath A, Gerety RL. Nonleukemic granulocytic sarcoma of the heart: a report of a fatal case. Am J Hematol. 1987;25(3):325–32.
16. Marcos-Alberca P, Ibáñez B, Rey M, Román A, Rábago R, Orejas M, et al. Cardiac granulocytic sarcoma (chloroma): in vivo diagnosis with transesophageal echocardiography. J Am Soc Echocardiogr. 2004;17(9):1000–2.
17. Mawad R, Wu D, Abkowitz JL, Walter RB. Myeloid sarcoma of the heart. Leuk Lymphoma. 2012;53(12):2511–4.
18. Attallah A, Cheong BY, Bernicker E, Wilson JM. Cardiac chloroma: novel presentation and subsequent diagnosis with cardiac magnetic resonance imaging. Tex Heart Inst J. 2010;37(2):242.
19. Mignano JE, Chan MD, Rosenwald IB, Kimmelstiel CD, Wolfe LC. Intracardiac chloroma. J Pediatr Hematol Oncol. 2009;31(12):977–9.
20. Fernandez L, Couban S, Sy R, Miller R. An unusual presentation of extramedullary plasmacytoma occurring sequentially in the testis, subcutaneous tissue, and heart. Am J Hematol. 2001;67(3):194–6.
21. Singh B, Lahiri A, Kakar P. Extramedullary plasmacytoma. J Laryngol Otol. 1979;93(12):1239–44.
22. Knowling MA, Harwood AR, Bergsagel DE. Comparison of extramedullary plasmacytomas with solitary and multiple plasma cell tumors of bone. J Clin Oncol. 1983;1(4):255–62.
23. Keung Y, Lau S, Gill P. Extramedullary plasmacytoma of the heart presenting as cardiac emergency: review of literature. Am J Clin Oncol. 1994;17(5):427–9.
24. Nanjappa MC, Shankarappa RK, Kalpana SR, Bhat P, Moorthy N. Intracardiac thrombi in acute myeloid leukemia: an echocardiographic and autopsy correlation. Echocardiography. 2010;27(1):E4–8.
25. McAllister HA, Hall RJ, Cooley DA. Tumors of the heart and pericardium. Curr Probl Cardiol. 1999;24(2):59–116.
26. Roberts WC, Glancy DL, Devita VT. Heart in malignant lymphoma (Hodgkin's disease, lymphosarcoma, reticulum cell sarcoma and mycosis fungoides): a study of 196 autopsy cases*. Am J Cardiol. 1968;22(1):85–107.
27. Curtsinger CR, Wilson MJ, Yoneda K. Primary cardiac lymphoma. Cancer. 1989;64(2):521–5.
28. Chalabreysse L, Berger F, Loire R, Devouassoux G, Cordier J-F, Thivolet-Bejui F. Primary cardiac lymphoma in immunocompetent patients: a report of three cases and review of the literature. Virchows Arch. 2002;441(5):456–61.
29. Petrich A, Cho SI, Billett H. Primary cardiac lymphoma. Cancer. 2011;117(3):581–9.

30. Gowda RM, Khan IA. Clinical perspectives of primary cardiac lymphoma. Angiology. 2003;54(5):599–604.
31. Nakayama Y, Uchimoto S, Tsumura K, Morii H. Primary cardiac lymphoma with infiltration of the atrioventricular node: remission with reversal of the atrioventricular block induced by chemotherapy. Cardiology. 1997;88(6):613–6.
32. Legault S, Couture C, Bourgault C, Bergeron S, Poirier P, Sénéchal M. Primary cardiac Burkitt-like lymphoma of the right atrium. Can J Cardiol. 2009;25(3):163–5.
33. Miguel CE, Bestetti RB. Primary cardiac lymphoma. Int J Cardiol. 2011;149(3):358–63.
34. Chim C, Chan A, Kwong Y, Liang R. Primary cardiac lymphoma. Am J Hematol. 1997;54(1):79–83.
35. Woods J, Monteiro P, Rhodes A. Right ventricular dysfunction. Curr Opin Crit Care. 2007;13(5):532–40.
36. Fortún J. Principales infecciones en el paciente oncológico: manejo práctico. An Sist Sanit Navar. 2004.
37. Chen K-W, Chang J-H, Yeh S-P, Lu C-R. Primary cardiac B-cell lymphoma with atrioventricular block and paroxysmal ventricular tachycardia. J Cardiothorac Surg. 2012;7(1):70.
38. Dorsay TA, Ho VB, Rovira MJ, Armstrong MA, Brissette MD. Primary cardiac lymphoma: CT and MR findings. J Comput Assist Tomogr. 1992;17(6):978–81.
39. Mügge A, Daniel WG, Haverich A, Lichtlen PR. Diagnosis of noninfective cardiac mass lesions by two-dimensional echocardiography. Comparison of the transthoracic and transesophageal approaches. Circulation. 1991;83(1):70–8.
40. Moore JA, DeRan BP, Minor R, Julie A, Fraker TD. Transesophageal echocardiographic evaluation of intracardiac lymphoma. Am Heart J. 1992;124(2):514–6.
41. Cho SW, Kang YJ, Kim TH, Cho SK, Hwang MW, Chang W, et al. Primary cardiac lymphoma presenting with atrioventricular block. Korean Circ J. 2010;40(2):94–8.
42. Ceresoli GL, Ferreri AJ, Bucci E, Ripa C, Ponzoni M, Villa E. Primary cardiac lymphoma in immunocompetent patients. Cancer. 1997;80(8):1497–506.
43. Nielsen KM, Offersen BV, Nielsen HM, Vaage-Nilsen M, Yusuf SW. Short and long term radiation induced cardiovascular disease in patients with cancer. Clin Cardiol. 2017;40(4):255–61.
44. Yusuf SW, Sami S, Daher IN. Radiation-induced heart disease: a clinical update. Cardiol Res Pract. 2011;2011:317659.
45. Tadic M, Cuspidi C, Hering D, Venneri L, Grozdic-Milojevic I. Radiotherapy-induced right ventricular remodelling: the missing piece of the puzzle. Arch Cardiovasc Dis. 2017;110(2):116–23.
46. Brosius FC, Waller BF, Roberts WC. Radiation heart disease: analysis of 16 young (aged 15 to 33 years) necropsy patients who received over 3,500 rads to the heart. Am J Med. 1981;70(3):519–30.
47. Burger A, Loffler H, Bamberg M, Rodemann HP. Molecular and cellular basis of radiation fibrosis. Int J Radiat Biol. 1998;73(4):401–8.
48. Taunk NK, Haffty BG, Kostis JB, Goyal S. Radiation-induced heart disease: pathologic abnormalities and putative mechanisms. Front Oncol. 2015;5:39.
49. Khakoo AY, Yeh ET. Therapy insight: management of cardiovascular disease in patients with cancer and cardiac complications of cancer therapy. Nat Clin Pract Oncol. 2008;5(11):655–68.
50. Torbey E, Yacoub H, McCord D, Lafferty J. Two cases and review of the literature: primary percutaneous angiography and antiplatelet management in patients with immune thrombocytopenic purpura. ISRN Hematol. 2013;2013:174659.
51. Slama MS, Guludec D, Sebag C, Leenhardt AR, Davy J, Pellerin DE, et al. Complete atrioventricular block following mediastinal irradiation: a report of six cases. Pacing Clin Electrophysiol. 1991;14(7):1112–8.
52. Gomez DR, Yusuf SW, Munsell MF, Welsh JW, Liao Z, Lin SH, et al. Prospective exploratory analysis of cardiac biomarkers and electrocardiogram abnormalities in patients receiving thoracic radiation therapy with high-dose heart exposure. J Thorac Oncol. 2014;9(10):1554–60.
53. Orzan F, Brusca A, Gaita F, Giustetto C, Figliomeni M, Libero L. Associated cardiac lesions in patients with radiation-induced complete heart block. Int J Cardiol. 1993;39(2):151–6.
54. Yeh ET, Tong AT, Lenihan DJ, Yusuf SW, Swafford J, Champion C, et al. Cardiovascular complications of cancer therapy. Circulation. 2004;109(25):3122–31.
55. Tadic M, Cuspidi C, Hering D, Venneri L, Danylenko O. The influence of chemotherapy on the right ventricle: did we forget something? Clin Cardiol. 2017;40(7):437–43.
56. Vejpongsa P, Yeh E. Topoisomerase 2β: a promising molecular target for primary prevention of anthracycline-induced cardiotoxicity. Clin Pharmacol Ther. 2014;95(1):45–52.
57. Lemez P. Delayed administration of dexrazoxane provides cardioprotection against anthracyclines in breast cancer or acute myeloid leukemia. J Clin Oncol. 1997;15(10):3293–5.
58. Sabatino J, Yauda M, De Rosa S, Tamme L, Ianconetti C, Albanese M, Mignona C, Aquila I, Donato G, Indolfi C. Empagliflozin reduces the doxorubicine-induced myocardial dysfunction. Eur Heart J. 2017. https://doi.org/10.1093/eurheartj/ehx504.P4230.
59. Kong JH, Jeon Y-W, Lee S-E, Choi SY, Kim S-H, Oh YJ, et al. Long-term assessment of Dasatinib-induced pulmonary arterial hypertension in chronic myeloid leukemia. Blood. 2014;124:5535.
60. Yun S, Anwer F, Vincelette ND. Dasatinib-induced pulmonary hypertension in chronic myelogenous leukaemia. BMJ Case Rep. 2014;2014:bcr2014204477.
61. Lenčová-Popelová O, Jirkovský E, Mazurová Y, Lenčo J, Adamcová M, Šimůnek T, et al. Molecular remodeling of left and right ventricular myocardium

in chronic anthracycline cardiotoxicity and post-treatment follow up. PLoS One. 2014;9(5):e96055.
62. Murbraech K, Holte E, Broch K, Smeland KB, Holte H, Rösner A, et al. Impaired right ventricular function in long-term lymphoma survivors. J Am Soc Echocardiogr. 2016;29(6):528–36.
63. Christiansen JR, Massey R, Dalen H, Kanellopoulos A, Hamre H, Ruud E, et al. Right ventricular function in long-term adult survivors of childhood lymphoma and acute lymphoblastic leukaemia. Eur Heart J Cardiovasc Imaging. 2016;17(7):735–41.
64. Calleja A, Poulin F, Khorolsky C, Shariat M, Bedard PL, Amir E, et al. Right ventricular dysfunction in patients experiencing cardiotoxicity during breast cancer therapy. J Oncol. 2015;2015:609194.
65. Chan P, Ogilby JD, Segal B. Tricuspid valve endocarditis. Am Heart J. 1989;117(5):1140–6.
66. Chaudhary N, Vishwanath M, Pahuja M, Borker A. Candida albicans endocarditis in a child with acute lymphoblastic leukemia: a dreaded complication of intensive chemotherapy. Indian J Med Paediatr Oncol. 2013;34(1):28.
67. Nandakumar R, Raju G. Isolated tricuspid valve endocarditis in nonaddicted patients: a diagnostic challenge. Am J Med Sci. 1997;314(3):207–12.
68. Baddour LM, Wilson WR, Bayer AS, Fowler VG, Tleyjeh IM, Rybak MJ, et al. Infective endocarditis in adults: diagnosis, antimicrobial therapy, and management of complications. Circulation. 2015;132(15):1435–86.
69. Kantarcioglu B, Bekoz HS, Olgun FE, Cakal B, Arkan B, Turkoglu H, et al. Allogeneic stem cell transplantation in a blast-phase chronic myeloid leukemia patient with carbapenem-resistant Klebsiella pneumoniae tricuspid valve endocarditis: a case report. Mol Clin Oncol. 2016;5(4):347–50.
70. Barshay J, Nemets A, Ducach A, Lugassy G. Pseudomonas aeruginosa endocarditis in acute myeloid leukemia: a rare complication. Int J Biomed Sci. 2008;4(4):330.
71. Yong MS, Coffey S, Prendergast BD, Marasco SF, Zimmet AD, McGiffin DC, et al. Surgical management of tricuspid valve endocarditis in the current era: a review. Int J Cardiol. 2016;202:44–8.
72. Kuruvilla J, Forrest D, Lavoie J, Nantel S, Shepherd J, Song K, et al. Characteristics and outcome of patients developing endocarditis following hematopoietic stem cell transplantation. Bone Marrow Transplant. 2004;34(11):969.
73. Chrissoheris MP, Libertin C, Ali RG, Ghantous A, Bekui A, Donohue T. Endocarditis complicating central venous catheter bloodstream infections: a unique form of health care associated endocarditis. Clin Cardiol. 2009;32(12):E48–54.
74. Malagola M, Peli A, Damiani D, Candoni A, Tiribelli M, Martinelli G, et al. Incidence of bacterial and fungal infections in newly diagnosed acute myeloid leukaemia patients younger than 65 yr treated with induction regimens including fludarabine: retrospective analysis of 224 cases. Eur J Haematol. 2008;81(5):354–63.
75. Roguin A, Reisner S. Right atrial mass related to indwelling central venous catheters in patients undergoing dialysis. Eur J Echocardiogr. 2000;1(3):222–3.
76. Kale SB, Raghavan J. Tricuspid valve endocarditis following central venous cannulation: the increasing problem of catheter related infection. Indian J Anaesth. 2013;57(4):390.
77. Liepman MK, Jones PG, Kauffman CA. Endocarditis as a complication of indwelling right atrial catheters in leukemic patients. Cancer. 1984;54(5):804–7.
78. Kravitz MS, Shoenfeld Y. Thrombocytopenic conditions—autoimmunity and hypercoagulability: commonalities and differences in ITP, TTP, HIT, and APS. Am J Hematol. 2005;80(3):232–42.
79. Solomons P. Acute promyelocytic leukaemia associated with acute myocardial infarction-a case report. S Afr Med J. 1986;70(1):117–8.
80. Cappelli F, Porciani MC, Bergesio F, Perlini S, Attanà P, Moggi Pignone A, et al. Right ventricular function in AL amyloidosis: characteristics and prognostic implication. Eur Heart J Cardiovasc Imaging. 2011;13(5):416–22.
81. Kyle RA, Gertz MA. Primary systemic amyloidosis: clinical and laboratory features in 474 cases. Semin Hematol. 1995;32(1):45–59.
82. Hassan W, Al-Sergani H, Mourad W, Tabbaa R. Amyloid heart disease: new frontiers and insights in pathophysiology, diagnosis, and management. Tex Heart Inst J. 2005;32(2):178.
83. Falk RH, Comenzo RL, Skinner M. The systemic amyloidoses. N Engl J Med. 1997;337(13):898–909.
84. Child JS, Levisman JA, Abbasi AS, MacAlpin RN. Echocardiographic manifestations of infiltrative cardiomyopathy: a report of seven cases due to amyloid. Chest. 1976;70(6):726–31.
85. Lehtonen J, Kettunen P. Pulmonary hypertension as a dominant clinical picture in a case of amyloidosis and smoldering multiple myeloma. Int J Cardiol. 2007;115(1):E29–30.
86. Bellavia D, Pellikka PA, Dispenzieri A, Scott CG, Al-Zahrani GB, Grogan M, et al. Comparison of right ventricular longitudinal strain imaging, tricuspid annular plane systolic excursion, and cardiac biomarkers for early diagnosis of cardiac involvement and risk stratification in primary systematic (AL) amyloidosis: a 5-year cohort study. Eur Heart J Cardiovasc Imaging. 2012;13(8):680–9.
87. Klein AL, Hatle LK, Burstow DJ, Taliercio CP, Seward JB, Kyle RA, et al. Comprehensive Doppler assessment of right ventricular diastolic function in cardiac amyloidosis. J Am Coll Cardiol. 1990;15(1):99–108.
88. Griffiths B, Hughes P, Dowdle R, Stephens M. Cardiac amyloidosis with asymmetrical septal hypertrophy and deterioration after nifedipine. Thorax. 1982;37(9):711.

Right Heart Involvement in Hepatic Diseases

28

Ana-Maria Vintilă, Monica Dobrovie, and Vlad Damian Vintilă

Abstract

It is well known there is a relationship between the heart and the liver. A significant proportion of patients with heart failure have suffered at some point from congestive hepatopathy or developed ischemic hepatitis in acute situations. The aim of this chapter is to raise awareness about another situation involving the liver and the heart: patients with primary liver disease that affects the heart. It is a very interesting field, with lots of unknowns, but which deserves our attention as liver disease is prevalent amongst patients worldwide.

In the first part, we will briefly explain the pathophysiology of portal hypertension (PoH), and its systemic consequences that influence heart function. Then, we will focus on three relevant clinical pathologies: cirrhotic cardiomyopathy (CCM), portopulmonary hypertension (PoPH) and hepatopulmonary syndrome (HPS). In the end we will briefly mention other liver disease that may affect the right heart.

Keywords

Portal hypertension · Cirrhotic cardiomyopathy · Portopulmonary hypertension · Hepatopulmonary syndrome

28.1 From Portal Hypertension to Hyperdynamic Circulation

In order to understand the pathophysiology of heart involvement in liver disease, one has to be familiar with haemodynamic changes which take place as a result of liver disease and portal hypertension (PoH).

The most common two causes of portal hypertension are liver cirrhosis and schistosomiasis, depending on geographical area [1]. But these are not the only causes of portal hypertension. Although in Western society sinusoidal PoH as a consequence of liver cirrhosis is the most prevalent situation, PoH may be a consequence of noncirrhotic pathologies, which altogether account for only 10% of PoH cases [1]. Some examples of noncirrhotic PoH are: for presinusoidal PoH: primary biliary cirrhosis, obliteration of inferior vena cava in oncologic disease; for sinusoidal PoH: AL-amyloidosis and fibrosis of the space of

A.-M. Vintilă (✉)
Department of Internal Medicine, Colţea Clinical Hospital, "Carol Davila" University of Medicine and Pharmacy, Bucharest, Romania

M. Dobrovie
Department of Internal Medicine, Colţea Clinical Hospital, Bucharest, Romania

V. D. Vintilă
Department of Cardiology, University Emergency Hospital, "Carol Davila" University of Medicine and Pharmacy, Bucharest, Romania

S. I. Dumitrescu et al. (eds.), *Right Heart Pathology*, https://doi.org/10.1007/978-3-319-73764-5_28

Disse and for postsinusoidal PoH: Budd-Chiari syndrome [2].

Portal hypertension has two major pathophysiologic components, which interact to induce its complications and which should both be taken into account when treating patients:

1. Portal resistance
2. Blood flow (splanhnic and systemic)

The pathophysiology of PoH in liver cirrhosis is briefly illustrated in Fig. 28.1.

28.1.1 Portal Resistance

Liver circulation is impaired because of structural changes in liver architecture, which lead to increased portal resistance. One pathological process is fibrosis and development of regenerative liver nodules, which induces a *fixed impairment of blood flow* [3]. Furthermore, stellate cells, which reside in the space of Disse (between hepatocytes and sinusoids) and are known for their role in vitamin A storage, are transformed to myofibroblasts as a reaction to inflammatory cytokines [4]. The myofibrobalsts contract because of increased vasoconstrictor activity, which is promoted mainly by activation of endothelin 1 (ET-1) production [5]. Reduced NO bioavailability is related to oxidative stress, with production of superoxide radicals that spontaneously bind NO [6] and inhibition of endothelial NO synthase [7]. This results in *dynamic, reversible obstruction of blood flow* through the liver and accounts for as much as 30% of portal resistance [8].

28.1.2 Blood Flow

High portal pressure causes an increase in shear stress in the splanchnic vessels and translocation

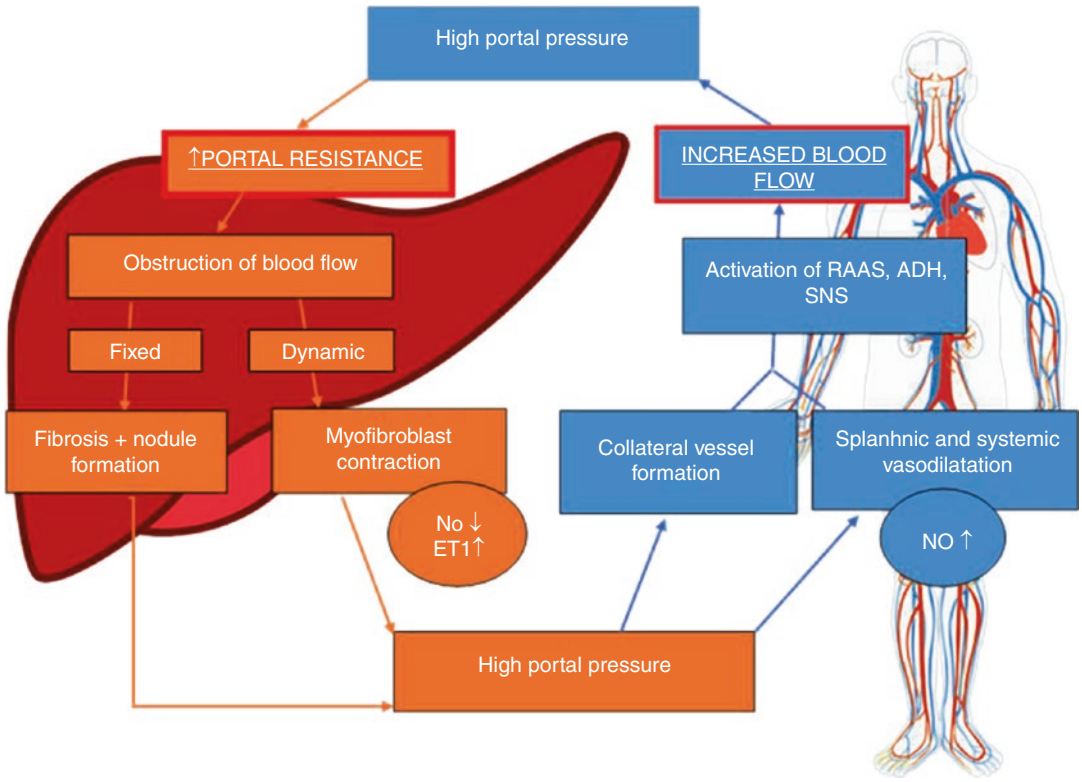

Fig. 28.1 Mechanisms of portal hypertension (see text for explanation). *NO* nitric oxide, *ET1* endothelin 1, *RAAS* renin angiotensin aldosterone system, *ADH* antidiuretic hormone, *SNS* sympathetic nervous system

of bacterial lipopolysaccharides in the systemic circulation. Both processes produce an inflammatory reaction with cytokine formation, which subsequently stimulate endothelial NO synthase [9]. The excessive NO formation results in vasodilatation and consequently decrease in blood pressure. This activates the renin-angiotensin-aldosterone axis, antidiuretic hormone and the sympathetic nervous system, inducing vasoconstriction, sodium and water retention, which further increase circulatory volume and blood flow [4]. Still overall the vasodilator effects dominate both the splanchnic and systemic circulation.

Blood flow is also increased by collateral vessel opening. This is caused by the porto-systemic pressure gradient, which opens pre-existing vessels, but also through angiogenesis [10]. Experimental models show a 18–78% reduction in porto-systemic collaterals as a consequence of anti-angiogenic medication like anti-vascular endothelial growth factor (anti-VEGF) and anti-placental growth factor (anti-PlGF) [11, 12].

Only in later stages of portal hypertension, hyperdynamic circulation develops.

It is characterized by high cardiac output, increased heart rate, increased total blood volume and decreased total systemic vascular resistance, as well as a normal or decreased arterial pressure. Peripheral systemic resistance decreases gradually and animal models point out that sympathetic nerve atrophy in the mesenteric arteries may be incriminated [13, 14].

If splanchnic vasodilation progresses beyond the compensatory capacity of hyperdynamic circulation, central arterial blood volume (heart, lungs, kidneys) decreases, inducing relative hypovolemia and complications like hepatorenal syndrome [15, 16].

28.2 Consequences of Hepatic Diseases on the Heart

As described above, liver pathology starts by affecting splanchnic circulation and ends up triggering a cascade of systemic reactions. The heart can be affected directly and here we will describe a recognized pathologic entity, the cirrhotic cardiomyopathy. Systemic repercussion of liver disease and portal hypertension also causes pulmonary pathology, which may itself affect the heart subsequently, especially the right heart. We will present two pathological entities: portopulmonary hypertension and hepatopulmonary syndrome, as the most important liver-lung-heart syndromes.

28.2.1 Cirrhotic Cardiomyopathy

Patients who suffer from cirrhosis exhibit chronic alterations in cardiac function, including systolic, diastolic and electrical abnormalities, leading to the recognition of a new pathologic entity named Cirrhotic cardiomyopathy (CCM) [17].

CCM was discussed at the 2005 World Congress of Gastroenterology in Montreal and *diagnostic criteria* were established. These include resting or exercise induced systolic dysfunction and diastolic dysfunction, as well as *supportive criteria*, comprising electrical abnormalities (chronotopic incompetence, prolonged QTc interval, dyssynchrony), increased left atrium dimensions, increased ventricular mass and elevated biomarkers. Criteria for the diagnosis of CCM are detailed in Table 28.1.

Prevalence of CCM is estimated between 3 and 23% [18].

CCM remains asymptomatic for a long time because of decreased afterload through systemic vasodilatation. Importantly, CCM becomes clinically apparent especially after interventions on the liver which increase preload, like transjugular intrahepatic porto-systemic shunt (TIPS) or liver transplantation [19]. Heart failure resulting from cirrhotic cardiomyopathy is a common cause of death in liver transplant patients, accounting for 2.6–42% of deaths [20, 21]. This shows the importance of screening patients for CCM before invasive procedures and accurately monitoring them post-intervention.

Cardiac abnormalities of CCM can be grouped into three categories: systolic dysfunction, diastolic dysfunction and electrical abnormalities. Although diagnostic criteria refer to left heart involvement in CCM, the disease is not confined

Table 28.1 Definition of cirrhotic cardiomyopathy

Systolic dysfunction	1. Blunted increase in cardiac output with stress
	2. Resting LVEF <55%
Diastolic dysfunction	1. E/A ratio < 1
	2. Prolonged DT (>200 msec)
	3. Prolonged IVRT (>80 msec)
Supportive criteria	1. Electrophysiological abnormalities
	2. Altered chronotropic response
	3. Electromechanical dyssynchrony
	4. Prolonged QTc
	5. Enlarged LA
	6. Increased cardiac mass
	7. Increased BNP/proBNP
	8. Increased troponin I

(Figueiredo A, Romero-Bermejo F, Perdigoto R, Marcelino P. The end-organ impairment in liver cirrhosis: appointments for critical care. 2012; 2012. Copyright © 2012 Antonio Figueiredo et al. This is an open access article distributed under the Creative Commons Attribution License, which permits unrestricted use, distribution, and reproduction in any medium, provided the original work is properly cited)

to the left-sided heart. Recent studies prove that evaluation of the right heart involvement is strongly advisable since it is correlated with adverse clinical outcomes after liver transplantation [22, 23].

Being widespread, cheap and noninvasive, transthoracic echocardiography is the best imaging method to search for systolic and diastolic dysfunction associated to CCM. It is worth to mention that presence of gross ascites might influence the quality of the exam by not allowing subcostal views and modifying the intrathoracic position of the heart. Modified views may be required in order to obtain the most accurate data. In difficult cases, transesophagial echocardiography and/or cardiac magnetic resonance imaging may be required to complete the evaluation of the heart.

28.2.1.1 Systolic Dysfunction

Up to 25% of patients show impaired systolic function, which manifests as reduced LVEF at rest (<55%) or lack of exercise reserve. Typically, patients are evaluated through dobutamine stress testing or exercise stress testing, where they show no increase in heart rate and ejection fraction [24, 25]. Resting systolic dysfunction can also be identified by means of peak velocity at tissue Doppler imaging [26], as well as by speckle tracking analysis with identification of a decreased left ventricular systolic strain [27]. Right ventricular systolic function is also affected in CCM, although alterations may be more subtle, thus requiring speckle tracking analysis (Fig. 28.2), which identifies a decreased right ventricular systolic strain even in the presence of normal values of conventional parameters (right ventricular fractional area change, TAPSE) [27].

The pathophysiology of systolic dysfunction is incompletely known, but decreased number and sensitivity of beta adrenergic receptors has been shown to be one possible mechanism in animal models [28].

28.2.1.2 Diastolic Dysfunction

Diastolic dysfunction is present in the majority (45–56%) of cirrhotic patients and its mild form has no serious clinical implication [29]. Evidence of pathologic mechanisms points towards myocardial hypertrophy, altered collagen structure and fibrosis [30]. More advanced dysfunction is related to prognosis as it is associated to circulatory dysfunction, ascites and hepatorenal syndrome [29].

28.2.1.3 Electrical Abnormalities

QT Interval Prolongation

The most important electrical abnormality in cirrhotic patients is QT interval prolongation. Delayed repolarization which results from defective K-channels as well as increased sympathetic nervous system expression were incriminated in the pathophysiology of QT interval prolongation in cirrhotic patients [31]. QT interval prolongation always associates portal hypertension and porto-systemic shunts [32, 33]. It relates to liver disease severity, as 60% of patients with advanced stage of cirrhosis present with QT interval prolongation. It is also associated with

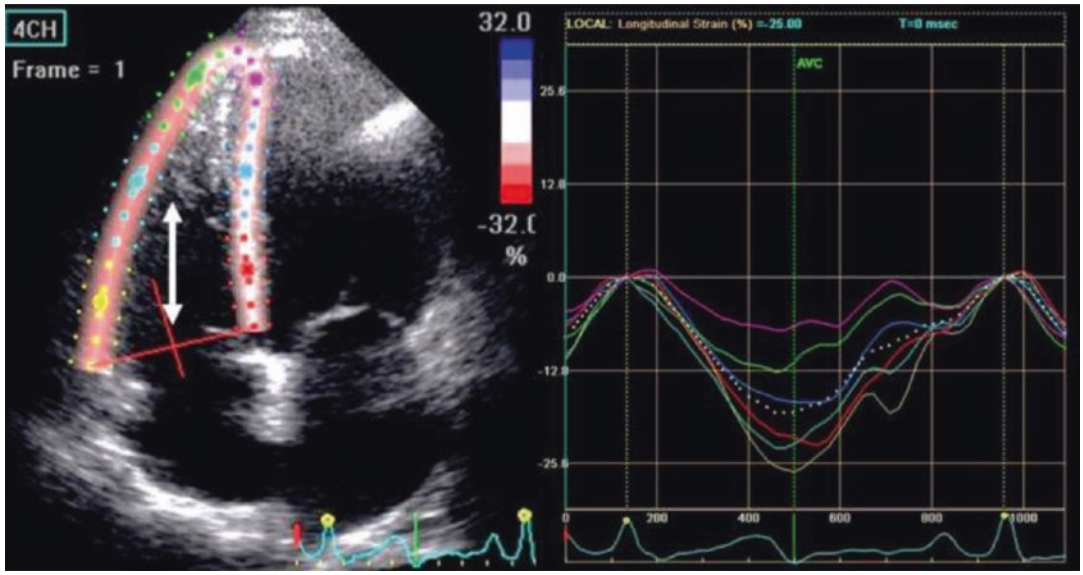

Fig. 28.2 An example of right ventricle (RV) systolic strain at longitudinal direction measured by 2-dimensional speckle tracking analysis from the apical four-chamber view. Each color denotes a regional segmental strain (a total of six segments) and the RV systolic strain is calculated as the average value for peak strain of the six segments. The white arrow denotes the directions of longitudinal strain. Reproduced with permission from Chen et al. [27]

poor survival [31]. Fridericia's and not Bazett formula should be used for QTc calculation in CCM patients [34].

Chronotropic incompetence and disrupted circadian HR variability—probably due to β adrenergic receptor alteration, is also present in CCM patients [35, 36].

Tachcycardia can occur in advanced stages of cirrhosis through excessive sympathetic stimulation as part of the hyperdynamic circulation.

Cardiac biomarkers such as BNP, NT-proBNP and troponin are elevated in CCM patients [37]. NT-proBNP level correlates with the severity of cirrhosis and cardiac involvement [38].

28.2.1.4 Treatment of CCM

Due to systemic vasodilatation angiotensin converting enzyme inhibitors should be avoided [39].

Diuretics should be used only if water retention is present. Aldosterone antagonists improve LV dilatation and LV wall thickness [40]. Nonselective beta-blockers are widely used in the prevention of variceal bleeding, for they decrease portal pressure. They also show benefit in QT interval prolongation [41, 42].

Liver transplantation can reverse abnormalities typical of CCM [43]. Not only left heart, but also right heart structure and function improve after liver transplantation, as shown by reduced biventricular dilatation and improved biventricular systolic strain in one study [27].

28.2.2 Portopulmonary Hypertension (PoPH) Versus Hepatopulmonary Syndrome (HPS)

Interestingly, although the two have opposite pathologic determinants: PoPH being mainly defined by vasoconstriction, while HPS is characterized by vasodilatation, the pathologic mechanisms incriminated in these diseases are the same.

One important factor is the *hyperdynamic circulation,* which produces shear stress and activation of inflammatory pathways. This in turn is

believed to stimulate ET1 production, which seems to play a role in both pathologic entities [44]. Endothelin has two major receptors: ETA - inducing mainly vasoconstriction, and ETB - inducing mainly vasodilatation. Factors which influence the expression of the different receptors, and thus determine the effect of ET1, remain unknown. The role of vasoconstriction induced by ET1 in PoPH is demonstrated by the benefit of endothelin receptor antagonists such as bosentan in the treatment of these patients [45]. On the other hand, patients with HPS have increased expression of ETB receptor in the pulmonary circulation, which stimulates endothelial NO synthase and induces NO mediated vasodilatation.

Other important factors are *bacterial lipopolysaccharides translocation* and *portosysthemic shunts*, which are incriminated in increased phagocytosis in the lung vessels [46]. In both PoPH and HPS, there is evidence of pulmonary macrophage activation, which is hypothesized to induce tissue modification in PoPH, and angiogenesis in HPS [44, 47, 48].

Bacterial endotoxins also induce TNFa activation, which directly stimulates pulmonary NO production in HPS, further contributing to vasodilatation [49]. This theory is also supported by the observation that intestinal flora decontamination with norfloxacin improves HPS in cirrhosis patients [50].

In the end, pathophysiologic changes in PoPH induce vasoconstriction and remodeling of lung circulation, while HPS is characterized by vasodilatation and hypoxia.

We will discuss the most important characteristics of these two pathologic entities using a clinical case for each one. Table 28.2 summarizes the main features to keep in mind for both pathologies.

28.2.2.1 Portopulmonary Hypertension

Case 1

49 years old woman with compensated VHB cirrhosis, Child-Pugh score A (Bilirubin 1,8 mg/dL, Albumin 3,6 g/dl, INR 1.6, mild ascites, no encephalopathy) with progressive exertional dyspnea over the last 3 months. She was diagnosed with portal hypertension 5 years ago, while suffering haemathemesis from oesophageal variceal bleeding. She receives carvedilol 25 mg twice daily since then.

PoPH is a rare disease developing in only 1–5% [56] of portal hypertension cases. Nevertheless, because of its clinical importance, we should keep a low suspicion threshold and screen patients with portal hypertension and dyspnea for signs of pulmonary hypertension and right heart involvement with transthoracic echocardiography. Our patient suffers from liver cirrhosis, the most common cause of PoH in Western society. She is in the typical age of onset of PoH: the fifth decade of life, compared to patients suffering from idiopathic pulmonary hypertension which are diagnosed in their third and fourth decade of life [58]. PoPH is linked to female sex [53] and is most often diagnosed 4–7 years after PoH [56]. This also applies to our case, the patient carrying the diagnosis of PoH 5 years before the described episode. Thus PoPH seems a likely diagnosis in our patient.

Echocardiography is the next step in patient evaluation whenever there is clinical suspicion of PoPH. It may reveal tricuspid regurgitation and may estimate the right ventricular systolic pressure on the basis of the pressure gradient between the right ventricle and the right atrium, calculated from spectral Doppler recording of tricuspid regurgitation flow and status of inferior vena cava (dimension and variation with respiration), which correlates to the right atrial pressure. The pulmonary artery systolic pressure is considered equal to the right ventricular systolic pressure, provided there is no pulmonary stenosis (Fig. 28.3). Other echocardiographic signs of pulmonary hypertension and right heart involvement may also be identified: right chambers dilation, short pulmonary artery acceleration time, paradoxical septal motion with leftward displacement of the interventricular septum, right ventricular wall motion abnormalities.

Right heart catheterization with calculation of pulmonary vascular resistance is recommended by the AASLD and AHA/ACCF in order to

Table 28.2 Portopulmonary hypertension and hepatopulmonary syndrome

	Portopulmonary hypertension	Hepatopulmonary syndrome
Diagnostic criteria	Pulmonary hypertension class 1	Three criteria:
	Two criteria:	1. Liver disease
	1. Portal hypertension	2. Hypoxia: Alveolar-arterial oxygen gradient ≥15 mmHg (or ≥20 mmHg in patients over 64 years)
	+	3. Intrapulmonary vasodilatation ± shunting (positive transthoracic bubble contrast echocardiography or macroaggregated albumin lung perfusion study) [52]
	2. Precapillary PHT [51]	
	• Assessed by right heart catheterization:	
	– PAPm >25 mmHg	
	– PCWP <15 mmHg	
	– PVR >3 wood units	
Clinical features	Diagnosed in the fifth decade of life	Diagnosed in the sixth decade of life
	Linked to female gender and autoimmune liver disease [53]	No gender difference, no predisposing liver disease
	Portal hypertension is a prerequisite	Neither portal hypertension nor liver cirrhosis are a prerequisite
		Can appear in chronic and also acute conditions i.e. fulminant hepatitis A [54] or ischemic hepatitis [55]
Prevalence	1–5% of portal hypertension cases [56]	20% of liver cirrhosis patients [52]
Pathophysiology	Vasoconstriction	Vasodilatation
		Arteriovenous shunting
Symptoms	Progressive dyspnea	Dyspnea (platypnea)—aggravated while sitting upright
		Cyanosis (orthodeoxia)—aggravated while assuming orthostatism
		Finger clubbing
Severity degrees	Classified after *mPAP* value:	Classified after PaO_2 value:
	Mild: >25 to <35 mmHg	**Mild:** ≥80 mmHg
	Moderate: ≥35 to <45 mmHg	**Moderate**: ≥60 to <80 mmHg
	Severe: ≥45 mmHg	**Severe**: ≥50 to <60 mmHg
		Very severe: <50 mmHg
Treatment	Medications used for idiopathic PAH	Liver transplantation
	Oral anticoagulation and BB not recommended	
	Liver transplantation	
	Feasible only if not severe or uncontrolled PAH	
	May be considered in patients responding well on PAH terapy (ESC CLAss IIb) [51]	
	For selected patients liver- lung or liver-heart- lung transplantation [57]	

mPAP mean pulmonary arterial pressure, *PCWP* pulmonary capillary wedge pressure, *PVR* pulmonary vascular resistance, PaO_2 arterial partial pressure of oxygen, *PAH* pulmonary arterial hypertension.

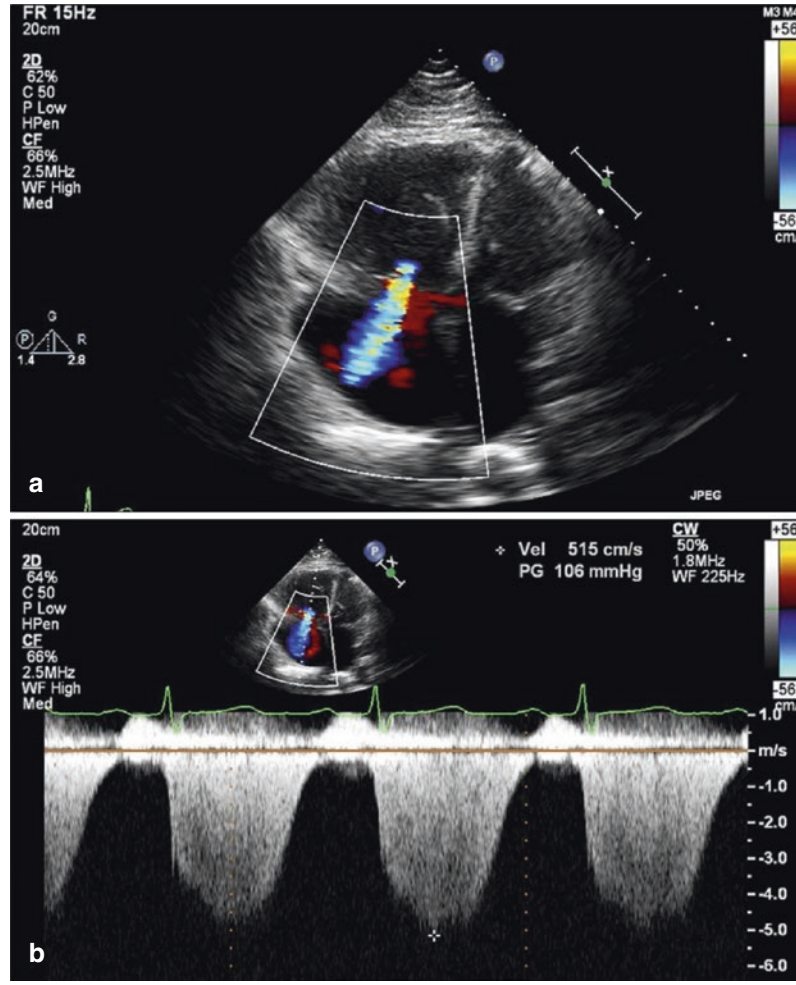

Fig. 28.3 A 57-Year-Old Man With PPH Related to ESLD. (**a**) The apical four-chamber view reveals a markedly dilated right ventricle and right atrium and moderate tricuspid regurgitation. (**b**) Continuous wave Doppler documents a 106-mmHg gradient between the right ventricle and the right atrium consistent with severe pulmonary hypertension. *PPH* portopulmonary hypertension, *ESLD* end-stage liver disease. Reproduced with permission from Garg and Armstrong [59]

confirm the diagnosis of PoPH when echocardiography reveals a right ventricular systolic pressure of 45–60 mmHg [60, 61].

> In our patient, echocardiography showed signs of pulmonary hypertension and the right heart catheterization confirmed the diagnosis of severe precapillary pulmonary hypertension (medium pulmonary artery pressure (PAPm) 50 mmHg, pulmonary vascular resistance (PVR) 5 WU, pulmonary capillary wedge pressure (PCWP) 8 mmHg).

The patient has known PoH and precapillary pulmonary hypertension so we can conclude that she has PoPH. Severity of PoPH is not associated with liver disease severity [54], as is the case of our patient, who suffers from severe PoPH while the liver disease is in a compensated state.

Therapy

Liver transplantation may reverse PoPH, if it did not reach a severe, uncontrolled stage. In patients with PAPm >50 mmHg mortality after liver transplantation can reach 100% and for moderate PoPH 50%, as was shown in a case series of the Mayo Clinic [62].

That is the reason why all patients listed for liver transplantation must undergo echocardiographic screening for PoPH [51]. The degree of secondary right heart dysfunction is an important predictor of mortality in PoPH patients [63].

Therapy with specific PHT drugs, may improve PoPH and render patients suitable for heart transplantation [64–67]. Specific pulmonary hypertension drugs were tested on few

PoPH patients. Only 13 patients with PoPH were included in PATENT study, showing improvement with the soluble guanylate cyclase stimulator, riociguat [68]. Although the endothelin receptor antagonist bosentan demonstrated benefits, it should be used with caution as it is hepatotoxic [69]. Newer drugs of this class, macitentan and ambrisentan, have lower liver toxicity [70, 71].

Decreased pulmonary prostacyclin is also incriminated in the development of PoPH [72] and prostacyclin analogs have shown good results in the treatment of these patients [73].

Supportive medical therapy consists of careful diuretic treatment. Beta-blockers (BB) are contraindicated because they can aggravate heart dysfunction through negative chronotropic and inotropic properties and were shown to decrease exercise capacity in PoPH patients [74].

Our patient was on BB therapy as a prevention for variceal bleeding, which was stopped after the PoPH diagnosis. Actually all patients with PoPH are at increased bleeding risk, so oral anticoagulation is not recommended [51].

28.2.2.2 Hepatopulmonary Syndrome

Case 2

58 years old men suffering from alcohol-induced liver cirrhosis with multiple ascitic decompensations is admitted because of dyspnoea aggravated when standing, accompanied by cyanosis. He has noticeable finger clubbing and moderate ascites, without pulmonary effusion on chest X ray.

Our patient's symptoms point towards HPS. Dyspnea is common in cirrhotic patient and present in 50% of HPS patients, so it is unspecific [75]. Platypnea and orthodeoxia are much more specific for HPS. Finger clubbing is also a very common finding in PHS patients (up to 50%) as compared to chronic liver disease (2%) [76]. Our patient has the typical diagnosis age of HPS: the sixth decade of life.

Although HPS is not linked to liver disease severity [75], there are reports pointing out that especially patients with hypoxemia have more advanced liver disease, as is the case of our patient [77].

Hypoxia and dyspnea are common features of HPS, and are aggravated upon standing (orthodeoxia and plathypnea). These symptoms are caused by vasodilatation and angiogenesis typical of liver disease and portal hypertension, through three main mechanisms:

1. *Oxygen (O_2) diffusion limitation*:
   Dilatation of capillaries increases the distance to be traversed by O_2. Hyperdynamic circulation is limiting the time available for O_2 diffusion [78].
2. *Ventilation-perfusion mismatch:*
   Vasodilatation is more pronounced in the lower lobes, which are not so well ventilated. Experimental work also shows a decreased vasoconstriction response to hypoxia [79].
3. *Intrapulmonary arteriovenous shunts:*
   These shunts are represented especially in the lower lobes. This explains the characteristic symptoms of HPS: plathypnea and orthodeoxia.

The peripheral O_2 saturation was 94% and the calculated alveolar/arterial gradient was 50 mmHg with pO_2 of 52 mmHg while inspiring room air. We performed an echocardiographic bubble contrast test, and there was evidence of bubble appearance in the left atrium five cardiac cycles after passing the right atrium.

Diagnosis of HPS implies evidence of low oxygenation and pulmonary vasodilation in the context of liver disease. Peripheral blood oxygen saturation <96% is a red flag and warrants arterial blood gas analysis. This should be performed in room air, preferably while sitting. Using age, inspired O_2 percent, atmospheric pressure, PaO_2 and $PaCO_2$ we can estimate the alveolo-arterial O_2 gradient (A-a O_2 gradient) with the aid of a calculator. An A-a O_2 gradient of >15 mmHg is a diagnostic criterion for HPS [52].

Indeed the presented case exhibits decreased peripheral O_2 saturation (94%) and an increased A-a O_2 gradient (50 mmHg).

The next step is to demonstrate pulmonary vasodilatation ± shunting. The most sensitive and accessible method is the bubble contrast echocardiography [80, 81]. If agitated saline is injected intravenously, the contrast first appears in the

right atrium. The bubbles have diameters of about 25 μm, so they cannot pass the normal lung vessels, which are only 5–8 μc in diameter. In HPS, the bubbles pass through the dilated pulmonary vessels and reach the left atrium after more than three cardiac cycles (as opposed to intracardiac shunts, were bubbles pass during the first cardiac cycle). One example is given in Fig. 28.4. Again, the presented case shows positive test, results, suggesting pulmonary vasodilation.

We can now conclude that our patient has HPS.

HPS severity is classified on the basis of the arterial oxygen pressure (PaO_2) value. Mild and moderate HPS implies a PaO_2 between 60 and 80 mmHg and should be monitored every 6–12 months. Severe HPS with $PaO_2 < 60$ mmHg warrants liver transplant evaluation and oxygen therapy [52].

The only definitive treatment for HPS remains liver transplantation and with recent advances in post-transplant care mortality is reported to be only 9% in patients with very severe HPS ($PaO_2 < 50$ mmHg) [82].

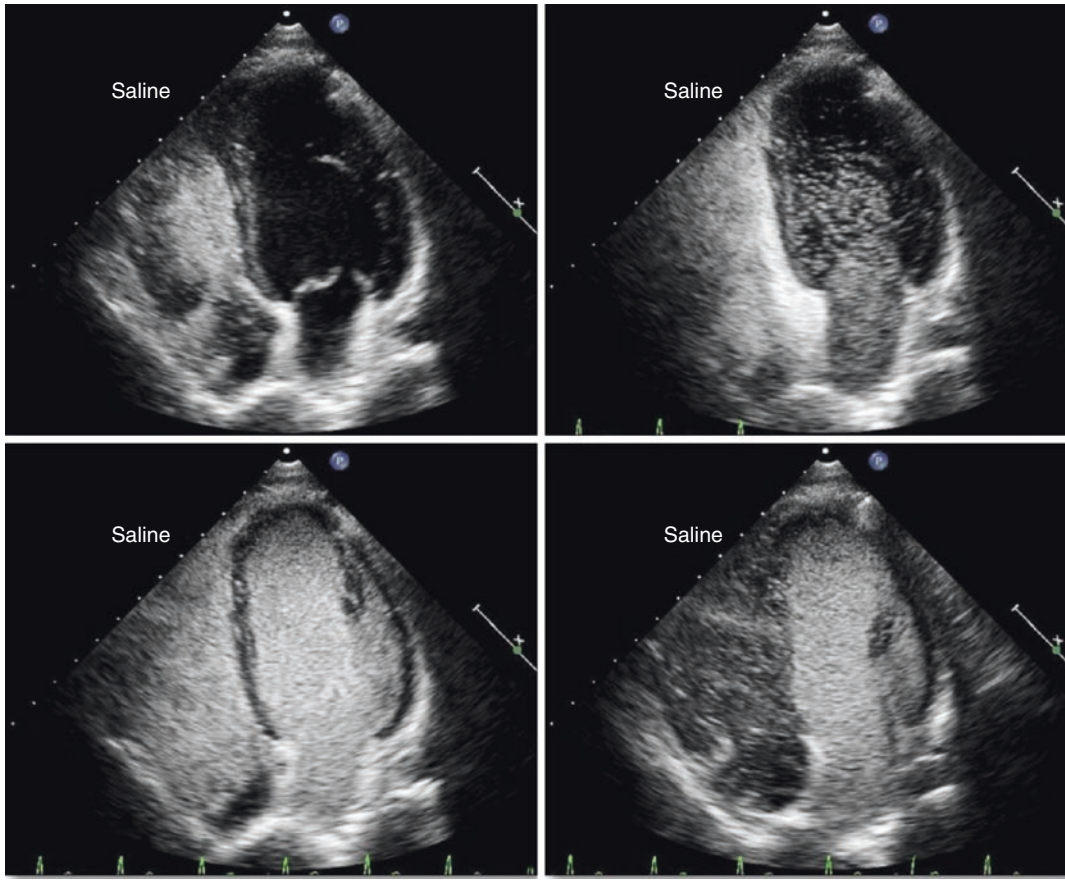

Fig. 28.4 Saline Contrast Echocardiography Performed in a Patient With ESLD Revealing Marked Right-to-Left Shunt Through Pulmonary AVM. The upper left panel is immediately after appearance of contrast in right heart. The upper right panel is five beats following appearance and reveals nearly continuous flow into the LA and LV. The lower left panel is approximately 10 s after injection of contrast and reveals equal contrast in both the right and left ventricles and the lower right panel is recorded 15 s following injection of contrast and reveals continued appearance of contrast into the LV when contrast is diminishing in the right ventricle. *AVM* arteriovenous malformation. Reproduced with permission from Garg and Armstrong [59]

28.2.3 Right Cardiac Involvement in Other Hepatic Diseases

28.2.3.1 Hepatitis C

Patients with hepatitis C virus (HCV) may experience dilated or hypertrophic cardiomyopathy [83]. The pathophysiologic mechanism is not fully understood, but some case reports show reversal of acute heart failure after interferon-free virus-selective antiviral treatment [84]. Cardiac involvement in these patients seems to be linked to higher mortality [85].

28.2.3.2 Primary Biliary Cirrhosis (PBC)

The majority of PBC patients have increased cholesterol levels but this usually does not result in increased cardiovascular risk [86, 87]. While LDL and total cholesterol are elevated, the low incidence of atherosclerosis may be due to increased HDL and adiponectin levels and low levels of lipoprotein(a) in these patients [86–88]. Patients with PBC also have an increased incidence of autonomic dysfunction [89]. Right heart involvement may be a consequence of portopulmonary hypertension, which frequently complicates autoimmune liver diseases, as it was mentioned above.

28.2.3.3 Hepatocellular Carcinoma (HCC)

Although a rare finding, case reports show HCC extension through the inferior vena cava to the right atrium and metastases to the right ventricle with potential risk of outflow obstruction [90–92].

The prognosis of patients is poor due to advanced stage of the oncologic disease, and treatments are palliative [93].

References

1. Berzigotti A, Seijo S, Reverter E, Bosch J. Assessing portal hypertension in liver diseases. Expert Rev Gastroenterol Hepatol. 2013;7(2):141–55.
2. Schouten JN, Garcia-Pagan JC, Valla DC, Janssen HL. Idiopathic noncirrhotic portal hypertension. Hepatology. 2011;54(3):1071–81.
3. Rockey DC. Cell and molecular mechanisms of increased intrahepatic resistance and hemodynamic correlates. In: Portal hypertension. Berlin: Springer; 2005. p. 37–50.
4. Reynaert H, Thompson M, Thomas T, Geerts A. Hepatic stellate cells: role in microcirculation and pathophysiology of portal hypertension. Gut. 2002;50(4):571–81.
5. Pinzani M, Milani S, De Franco R, Grappone C, Caligiuri A, Gentilini A, et al. Endothelin 1 is overexpressed in human cirrhotic liver and exerts multiple effects on activated hepatic stellate cells. Gastroenterology. 1996;110(2):534–48.
6. Gracia-Sancho J, Lavina B, Rodríguez-Vilarrupla A, García-Calderó H, Fernández M, Bosch J, et al. Increased oxidative stress in cirrhotic rat livers: a potential mechanism contributing to reduced nitric oxide bioavailability. Hepatology. 2008;47(4):1248–56.
7. Shah V, Toruner M, Haddad F, Cadelina G, Papapetropoulos A, Choo K, et al. Impaired endothelial nitric oxide synthase activity associated with enhanced caveolin binding in experimental cirrhosis in the rat. Gastroenterology. 1999;117(5):1222–8.
8. Toubia N, Sanyal AJ. Portal hypertension and variceal hemorrhage. Med Clin North Am. 2008;92(3):551–74.
9. Feldman M, Friedman LS, Brandt LJ. Sleisenger and Fordtran's gastrointestinal and liver disease E-book: pathophysiology, diagnosis, management, expert consult premium edition-enhanced online features, vol. 1. Amsterdam: Elsevier; 2010.
10. Sieber CC, Sumanovski LT, Stumm M, van der Kooij M, Battegay E. In vivo angiogenesis in normal and portal hypertensive rats: role of basic fibroblast growth factor and nitric oxide. J Hepatol. 2001;34(5):644–50.
11. Fernandez M, Mejias M, Angermayr B, Garcia-Pagan JC, Rodés J, Bosch J. Inhibition of VEGF receptor-2 decreases the development of hyperdynamic splanchnic circulation and portal-systemic collateral vessels in portal hypertensive rats. J Hepatol. 2005;43(1):98–103.
12. Van Steenkiste C, Geerts A, Vanheule E, Van Vlierberghe H, De Vos F, Olievier K, et al. Role of placental growth factor in mesenteric neoangiogenesis in a mouse model of portal hypertension. Gastroenterology. 2009;137(6):2112–24. e2116.
13. Coll M, Martell M, Raurell I, Ezkurdia N, Cuenca S, Hernández-Losa J, et al. Atrophy of mesenteric sympathetic innervation may contribute to splanchnic vasodilation in rat portal hypertension. Liver Int. 2010;30(4):593–602.
14. Ezkurdia N, Coll M, Raurell I, Rodriguez S, Cuenca S, González A, et al. Blockage of the afferent sensitive pathway prevents sympathetic atrophy and hemodynamic alterations in rat portal hypertension. Liver Int. 2012;32(8):1295–305.
15. Møller S, Bendtsen F, Henriksen JH. Effect of volume expansion on systemic hemodynamics and central and arterial blood volume in cirrhosis. Gastroenterology. 1995;109(6):1917–25.

16. Salerno F, Gerbes A, Ginès P, Wong F, Arroyo V. Diagnosis, prevention and treatment of hepatorenal syndrome in cirrhosis. Postgrad Med J. 2008;84(998):662–70.
17. Mocarzel LOC, Rossi MM, BdM M, Lanzieri PG, Gismondi RA. Cirrhotic cardiomyopathy: a new clinical phenotype. Arq Bras Cardiol. 2017;108(6):564–8.
18. Enache I, Oswald-Mammosser M, Woehl-Jaegle M-L, Habersetzer F, Di Marco P, Charloux A, et al. Cirrhotic cardiomyopathy and hepatopulmonary syndrome: prevalence and prognosis in a series of patients. Respir Med. 2013;107(7):1030–6.
19. Lotterer E, Wengert A, Fleig WE. Transjugular intrahepatic portosystemic shunt: short-term and long-term effects on hepatic and systemic hemodynamics in patients with cirrhosis. Hepatology. 1999;29(3):632–9.
20. Fouad TR, Abdel-Razek WM, Burak KW, Bain VG, Lee SS. Prediction of cardiac complications after liver transplantation. Transplantation. 2009;87(5):763–70.
21. Vogt DP, Henderson JM, Carey WD, Barnes D. The long-term survival and causes of death in patients who survive at least 1 year after liver transplantation. Surgery. 2002;132(4):775–80.
22. Kia L, Shah S, Wang E, Sharma D, Selvaraj S, Medina C, et al. Role of pretransplant echocardiographic evaluation in predicting outcomes following liver transplantation. Am J Transplant. 2013;13(9):2395–401.
23. Le Pavec J, Humbert M, Hervé P, Simonneau G, Sitbon O. Screening for portopulmonary hypertension with transthoracic echocardiography: implications for early mortality associated with liver transplantation. Am J Respir Crit Care Med. 2009;180(4):378–9.
24. Naqvi IH, Mahmood K, Naeem M, Vashwani AS, Ziaullah S. The heart matters when the liver shatters! Cirrhotic cardiomyopathy: frequency, comparison, and correlation with severity of disease. Prz Gastroenterol. 2016;11(4):247.
25. Shaikh S, Abro M, Qazi I, Yousfani A. Frequency of cirrhotic cardiomyopathy in patients with cirrhosis of liver: a tertiary care hospital experience. Pak J Med Sci. 2011;27(4):744–8.
26. Kazankov K, Holland-Fischer P, Andersen NH, Torp P, Sloth E, Aagaard NK, et al. Resting myocardial dysfunction in cirrhosis quantified by tissue Doppler imaging. Liver Int. 2011;31(4):534–40.
27. Chen Y, Chan AC, Chan S-C, Chok S-H, Sharr W, Fung J, et al. A detailed evaluation of cardiac function in cirrhotic patients and its alteration with or without liver transplantation. J Cardiol. 2016;67(2):140–6.
28. Ma Z, Miyamoto A, Lee SS. Role of altered beta-adrenoceptor signal transduction in the pathogenesis of cirrhotic cardiomyopathy in rats. Gastroenterology. 1996;110(4):1191–8.
29. Wong F, Villamil A, Merli M, Romero G, Angeli P, Caraceni P, et al. Prevalence of diastolic dysfunction in cirrhosis, and its clinical significance. Hepatology. 2011;54(4):475A–6A.
30. Heuer A, Gehl A, Püschel K, Sydow K, Lohse A, Lüth S. 160 high rate of cardiac abnormalities in a post-mortem analysis of patients suffering from liver cirrhosis. J Hepatol. 2011;54:S69.
31. Bernardi M, Calandra S, Colantoni A, Trevisani F, Raimondo ML, Sica G, et al. Q-T interval prolongation in cirrhosis: prevalence, relationship with severity, and etiology of the disease and possible pathogenetic factors. Hepatology. 1998;27(1):28–34.
32. Trevisani F, Merli M, Savelli F, Valeriano V, Zambruni A, Riggio O, et al. QT interval in patients with non-cirrhotic portal hypertension and in cirrhotic patients treated with transjugular intrahepatic porto-systemic shunt. J Hepatol. 2003;38(4):461–7.
33. Ytting H, Henriksen JH, Fuglsang S, Bendtsen F, Møller S. Prolonged Q–T c interval in mild portal hypertensive cirrhosis. J Hepatol. 2005;43(4):637–44.
34. Zambruni A, Di Micoli A, Lubisco A, Domenicali M, Trevisani F, Bernardi M. QT interval correction in patients with cirrhosis. J Cardiovasc Electrophysiol. 2007;18(1):77–82.
35. Bernardi M, Trevisani F, De Palma R, Ligabue A, Capani F, Baraldini M, et al. Chronobiological evaluation of sympathoadrenergic function in cirrhosis: relationship with arterial pressure and heart rate. Gastroenterology. 1987;93(6):1178–86.
36. Ramond M, Comoy E, Lebrec D. Alterations in isoprenaline sensitivity in patients with cirrhosis: evidence of abnormality of the sympathetic nervous activity. Br J Clin Pharmacol. 1986;21(2):191–6.
37. Pateron D, Beyne P, Laperche T, Logeard D, Lefilliatre P, Sogni P, et al. Elevated circulating cardiac troponin I in patients with cirrhosis. Hepatology. 1999;29(3):640–3.
38. Licata A, Corrao S, Petta S, Genco C, Cardillo M, Calvaruso V, et al. NT pro BNP plasma level and atrial volume are linked to the severity of liver cirrhosis. PLoS One. 2013;8(8):e68364.
39. Møller S, Henriksen JH. Cardiovascular complications of cirrhosis. Postgrad Med J. 2009;85(999):44–54.
40. Pozzi M, Grassi G, Ratti L, Favini G, Dell'Oro R, Redaelli E, et al. Cardiac, neuroadrenergic, and portal hemodynamic effects of prolonged aldosterone blockade in postviral child a cirrhosis. Am J Gastroenterol. 2005;100(5):1110.
41. Henriksen JH, Bendtsen F, Hansen EF, Møller S. Acute non-selective β-adrenergic blockade reduces prolonged frequency-adjusted Q–T interval (QT c) in patients with cirrhosis. Gan To Kagaku Ryoho. 2004;40(2):239–46.
42. Zambruni A, Trevisani F, Di Micoli A, Savelli F, Berzigotti A, Bracci E, et al. Effect of chronic β-blockade on QT interval in patients with liver cirrhosis. J Hepatol. 2008;48(3):415–21.
43. Torregrosa M, Aguadé S, Dos L, Segura R, Gónzalez A, Evangelista A, et al. Cardiac alterations in cirrhosis: reversibility after liver transplantation. J Hepatol. 2005;42(1):68–74.
44. Benjaminov F, Prentice M, Sniderman K, Siu S, Liu P, Wong F. Portopulmonary hypertension in decompensated cirrhosis with refractory ascites. Gut. 2003;52(9):1355–62.

45. Hoeper M, Halank M, Marx C, Hoeffken G, Seyfarth H, Schauer J, et al. Bosentan therapy for portopulmonary hypertension. Eur Respir J. 2005;25(3):502–8.
46. Nunes H, Lebrec D, Mazmanian M, Capron F, Heller J, Tazi KA, et al. Role of nitric oxide in hepatopulmonary syndrome in cirrhotic rats. Am J Respir Crit Care Med. 2001;164(5):879–85.
47. Thenappan T, Goel A, Marsboom G, Fang Y-H, Toth PT, Zhang HJ, et al. A central role for CD68 (+) macrophages in hepatopulmonary syndrome: reversal by macrophage depletion. Am J Respir Crit Care Med. 2011;183(8):1080–91.
48. Zhang J, Yang W, Luo B, Hu B, Maheshwari A, Fallon MB. The role of CX 3 CL1/CX 3 CR1 in pulmonary angiogenesis and intravascular monocyte accumulation in rat experimental hepatopulmonary syndrome. J Hepatol. 2012;57(4):752–8.
49. Liu L, Liu N, Zhao Z, Liu J, Feng Y, Jiang H, et al. TNF-α neutralization improves experimental hepatopulmonary syndrome in rats. Liver Int. 2012;32(6):1018–26.
50. Rabiller A, Nunes H, Lebrec D, Tazi KA, Wartski M, Dulmet E, et al. Prevention of gram-negative translocation reduces the severity of hepatopulmonary syndrome. Am J Respir Crit Care Med. 2002;166(4):514–7.
51. Galiè N, Humbert M, Vachiery J-L, Gibbs S, Lang I, Torbicki A, et al. 2015 ESC/ERS Guidelines for the diagnosis and treatment of pulmonary hypertension: the Joint Task Force for the Diagnosis and Treatment of Pulmonary Hypertension of the European Society of Cardiology (ESC) and the European Respiratory Society (ERS): endorsed by: Association for European Paediatric and Congenital Cardiology (AEPC), International Society for Heart and Lung Transplantation (ISHLT). Eur Heart J. 2015;37(1):67–119.
52. Rodriguez-Roisin R, Krowka MJ, Herve P, Fallon M. Pulmonary–hepatic vascular disorders (PHD). Eur Respir J. 2004;24(5):861–80.
53. Kawut SM, Krowka MJ, Trotter JF, Roberts KE, Benza RL, Badesch DB, et al. Clinical risk factors for portopulmonary hypertension. Hepatology. 2008;48(1):196–203.
54. Regev A, Yeshurun M, Rodriguez M, Sagie A, Neff G, Molina E, et al. Transient hepatopulmonary syndrome in a patient with acute hepatitis a. J Viral Hepat. 2001;8(1):83–6.
55. Fuhrmann V, Madl C, Mueller C, Holzinger U, Kitzberger R, Funk GC, et al. Hepatopulmonary syndrome in patients with hypoxic hepatitis. Gastroenterology. 2006;131(1):69–75.
56. Krowka MJ, Swanson KL, Frantz RP, McGoon MD, Wiesner RH. Portopulmonary hypertension: results from a 10-year screening algorithm. Hepatology. 2006;44(6):1502–10.
57. Grannas G, Neipp M, Hoeper MM, Gottlieb J, Lück R, Becker T, et al. Indications for and outcomes after combined lung and liver transplantation: a single-center experience on 13 consecutive cases. Transplantation. 2008;85(4):524–31.
58. Porres-Aguilar M. Emphasizing the importance of the clinical classification for pulmonary hypertension. Ann Hepatol. 2009;8(3):267–8.
59. Garg A, Armstrong WF. Echocardiography in liver transplant candidates. JACC Cardiovasc Imaging. 2013;6(1):105–19.
60. Lentine KL, Costa SP, Weir MR, Robb JF, Fleisher LA, Kasiske BL, et al. Cardiac disease evaluation and management among kidney and liver transplantation candidates. Circulation. 2012;126(5):617–63.
61. Murray KF, Carithers RL. AASLD practice guidelines: evaluation of the patient for liver transplantation. Hepatology. 2005;41(6):1407–32.
62. Krowka MJ, Plevak DJ, Findlay JY, Rosen CB, Wiesner RH, Krom RA. Pulmonary hemodynamics and perioperative cardiopulmonary-related mortality in patients with portopulmonary hypertension undergoing liver transplantation. Liver Transpl. 2000;6(4):443–50.
63. Robalino BD, Moodie DS. Association between primary pulmonary hypertension and portal hypertension: analysis of its pathophysiology and clinical, laboratory and hemodynamic manifestations. J Am Coll Cardiol. 1991;17(2):492–8.
64. Ashfaq M, Chinnakotla S, Rogers L, Ausloos K, Saadeh S, Klintmalm G, et al. The impact of treatment of portopulmonary hypertension on survival following liver transplantation. Am J Transplant. 2007;7(5):1258–64.
65. Austin MJ, McDougall NI, Wendon JA, Sizer E, Knisely AS, Rela M, et al. Safety and efficacy of combined use of sildenafil, bosentan, and iloprost before and after liver transplantation in severe portopulmonary hypertension. Liver Transpl. 2008;14(3):287–91.
66. Plotkin JS, Kuo PC, Rubin LJ, Gaine S, Howell CD, Laurin J, et al. Successful use of chronic epoprostenol as a bridge to liver transplantation in severe portopulmonary hypertension1. Transplantation. 1998;65(4):457–9.
67. Raevens S, De Pauw M, Reyntjens K, Geerts A, Verhelst X, Berrevoet F, et al. Oral vasodilator therapy in patients with moderate to severe portopulmonary hypertension as a bridge to liver transplantation. Eur J Gastroenterol Hepatol. 2013;25(4):495–502.
68. Ghofrani H-A, Galiè N, Grimminger F, Grünig E, Humbert M, Jing Z-C, et al. Riociguat for the treatment of pulmonary arterial hypertension. N Engl J Med. 2013;369(4):330–40.
69. Savale L, Magnier R, Le Pavec J, Jaïs X, Montani D, O'Callaghan DS, et al. Efficacy, safety and pharmacokinetics of bosentan in portopulmonary hypertension. Eur Respir J. 2013;41(1):96–103.
70. Galiè N, Olschewski H, Oudiz RJ, Torres F, Frost A, Ghofrani HA, et al. Ambrisentan in Pulmonary Arterial Hypertension, Randomized, Double-Blind, Placebo-Controlled, Multicenter, Efficacy Studies (ARIES) Group. Ambrisentan for the treatment of pulmonary arterial hypertension: results of the

ambrisentan in pulmonary arterial hypertension, randomized, double-blind, placebo-controlled, multicenter, efficacy (ARIES) study 1 and 2. Circulation. 2008;117(23):3010–9.
71. Pulido T, Adzerikho I, Channick RN, Delcroix M, Galiè N, Ghofrani H-A, et al. Macitentan and morbidity and mortality in pulmonary arterial hypertension. N Engl J Med. 2013;369(9):809–18.
72. Tuder RM, Cool CD, Geraci MW, Wang J, Abman SH, Wright L, et al. Prostacyclin synthase expression is decreased in lungs from patients with severe pulmonary hypertension. Am J Respir Crit Care Med. 1999;159(6):1925–32.
73. Sakai T, Planinsic RM, Mathier MA, de Vera ME, Venkataramanan R. Initial experience using continuous intravenous treprostinil to manage pulmonary arterial hypertension in patients with end-stage liver disease. Transpl Int. 2009;22(5):554–61.
74. Provencher S, Herve P, Jais X, Lebrec D, Humbert M, Simonneau G, et al. Deleterious effects of β-blockers on exercise capacity and hemodynamics in patients with portopulmonary hypertension. Gastroenterology. 2006;130(1):120–6.
75. Fallon MB, Krowka MJ, Brown RS, Trotter JF, Zacks S, Roberts KE, et al. Impact of hepatopulmonary syndrome on quality of life and survival in liver transplant candidates. Gastroenterology. 2008;135(4):1168–75.
76. Fallon MB, Abrams GA. Pulmonary dysfunction in chronic liver disease. Hepatology. 2000;32(4):859–65.
77. Schenk P, Schöniger-Hekele M, Fuhrmann V, Madl C, Silberhumer G, Müller C. Prognostic significance of the hepatopulmonary syndrome in patients with cirrhosis. Gastroenterology. 2003;125(4):1042–52.
78. Katsuta Y, Honma H, Zhang X-J, Ohsuga M, Komeichi H, Shimizu S, et al. Pulmonary blood transit time and impaired arterial oxygenation in patients with chronic liver disease. J Gastroenterol. 2005;40(1):57–63.
79. Carter EP, Sato K, Morio Y, McMurtry IF. Inhibition of K Ca channels restores blunted hypoxic pulmonary vasoconstriction in rats with cirrhosis. Am J Physiol Lung Cell Mol Physiol. 2000;279(5):L903–10.
80. Abrams GA, Jaffe CC, Hoffer PB, Binder HJ, Fallon MB. Diagnostic utility of contrast echocardiography and lung perfusion scan in patients with hepatopulmonary syndrome. Gastroenterology. 1995;109(4):1283–8.
81. Lange PA, Stoller JK. The hepatopulmonary syndrome. Ann Intern Med. 1995;122(7):521–9.
82. Gupta S, Castel H, Rao R, Picard M, Lilly L, Faughnan M, et al. Improved survival after liver transplantation in patients with hepatopulmonary syndrome. Am J Transplant. 2010;10(2):354–63.
83. Matsumori A, Ohashi N, Hasegawa K, Sasayama S, Eto T, Imaizumi T, et al. Hepatitis C virus infection and heart diseases. Jpn Circ J. 1998;62(5):389–91.
84. Poller W, Kaya Z, Muche M, Kasner M, Skurk C, Kappert K, et al. High incidence of cardiac dysfunction and response to antiviral treatment in patients with chronic hepatitis C virus infection. Clin Res Cardiol. 2017;106(7):551–6.
85. Terrier B, Karras A, Cluzel P, Collet J-P, Sène D, Saadoun D, et al. Presentation and prognosis of cardiac involvement in hepatitis C virus-related vasculitis. Am J Cardiol. 2013;111(2):265–72.
86. Longo M, Crosignani A, Battezzati P, Giussani CS, Invernizzi P, Zuin M, et al. Hyperlipidaemic state and cardiovascular risk in primary biliary cirrhosis. Gut. 2002;51(2):265–9.
87. Propst A, Propst T, Lechleitner M, Hoppichler F, Kathrein H, Vogel W, et al. Hypercholesterolemia in primary biliary cirrhosis is no risk factor for atherosclerosis. Dig Dis Sci. 1993;38(2):379–80.
88. Floreani A, Variola A, Niro G, Premoli A, Baldo V, Gambino R, et al. Plasma adiponectin levels in primary biliary cirrhosis: a novel perspective for link between hypercholesterolemia and protection against atherosclerosis. Am J Gastroenterol. 2008;103(8):1959.
89. Keresztes K, Istenes I, Folhoffer A, Lakatos PL, Horvath A, Csak T, et al. Autonomic and sensory nerve dysfunction in primary biliary cirrhosis. World J Gastroenterol. 2004;10(20):3039.
90. Agelopoulou P, Kapatais A, Varounis C, Grassos C, Kalkandi E, Kouris N, et al. Hepatocellular carcinoma with invasion into the right atrium. Report of two cases and review of the literature. Hepato-Gastroenterology. 2006;54(79):2106–8.
91. Lin TY, Chiu KM, Chien CY, Wang MJ, Chu SH. Unusual sites of metastatic involvement: case 1. Right ventricular outflow obstruction caused by metastatic hepatocellular carcinoma. J Clin Oncol. 2004;22(6):1152–3.
92. Oncale M, Lewis B. Hepatocellular carcinoma with extension to the heart via the inferior vena cava. Proc (Bayl Univ Med Cent). 2015;28(2):229.
93. Hayashi N, Yasunori H, Soma I, Fukuchi N, Izawa H, Yoshida T, et al. Non-surgical treatment of hepatocellular carcinoma with tumor thrombus in the right atrium. Gan To Kagaku Ryoho. 2004;31(11):1918–20.

Primary Cardiac Tumors

29

Ji-Gang Wang

Abstract

Primary cardiac tumors are rare. The most frequent location is left atrium. Only a small minority of primary tumors occur frequently in the right heart (hemangioma, angiosarcoma, leiomyomatosis, and lymphoma). In this chapter, we discussed several types of primary cardiac tumors in the 2015' edition of WHO classifications of cardiac tumors, including myxoma, rhabdomyoma, hemangioma, fibroma, papillary fibroelastoma, lipoma, schwannoma, paraganglioma, inflammatory myofibroblastic tumor, angiosarcoma, undifferentiated pleomorphic sarcoma, myxofibrosarcoma, leiomyosarcoma, synovial sarcoma, rhabdomyosarcoma, osteosarcoma, and lymphoma.

Keywords

Primary cardiac tumors · Cardiac myxoma · Primary cardiac sarcoma · Primary cardiac lymphoma · Pathology

29.1 Introduction

Primary cardiac tumors are uncommon with an incidence of 0.02% per person-year [1]. About 75–90% of primary cardiac tumors are benign, and only a small minority are malignant [2, 3]. Myxoma represents the majority of benign tumors in adults, while rhabdomyoma is the most common benign tumor in infants and children [4, 5]. Most primary cardiac malignancies are soft tissue sarcomas, of which there are many types, and all have a common mesenchymal origin. According to previous reports, the most frequent cardiac sarcoma in adult is angiosarcoma, while in children is rhabdomyosarcoma [6, 7]. Metastatic tumors, on the other hand, are the most common tumors of the heart with the reported ratio of cardiac metastases to primary cardiac tumors ranging from 100:1 to 1000:1 [8, 9]. However, the precise prevalence of primary cardiac tumors in the general population is still unknown since the data are based on postmortem studies and surgeons' experiences.

In 2015, the World Health Organization (WHO) released a new histologic classification of primary cardiac tumors (Table 29.1). Tumors are separated into benign tumors, tumors of uncertain biologic behavior, germ cell tumors, and malignant tumors. The revised classification has simplified the classification of sarcomas with a predilection for the left atrium. However, the lack of diagnostic agreement among experts in soft-tissue pathology makes classification of similar tumors in the heart difficult.

The prevalence of each histological type is highly age-related. Also, each histological type

J.-G. Wang
Department of Pathology, The Affiliated Hospital of Qingdao University, Qingdao, China

S. I. Dumitrescu et al. (eds.), *Right Heart Pathology*, https://doi.org/10.1007/978-3-319-73764-5_29

Table 29.1 Tumors of the Heart in WHO classifications

Tumors and tumor-like conditions	ICD-O codes
Benign	
Rhabdomyoma	8900/0
Histiocytoid cardiomyopathy	
Hamartoma of mature cardiac myocytes	
Adult cellular rhabdomyoma	8904/0
Cardiac myxoma	8840/0
Papillary fibroelastoma	
Hemangioma, NOS	9120/0
Capillary hemangioma	9131/0
Cavernous hemangioma	9121/0
Arteriovenous malformation	9123/0
Intramuscular hemangioma	9132/0
Cardiac fibroma	8810/0
Lipoma	8850/0
Cystic tumor of the atrioventricular node	8454/0
Granular cell tumor	9580/0
Schwannoma	9560/0
Tumors of uncertain biologic behavior	
Inflammatory myofibroblastic tumor	8825/1
Paraganglioma	8680/1
Germ cell tumors	
Teratoma, mature	9080/0
Teratoma, immature	9080/3
Yolk sac tumor	9071/3
Malignant tumors	
Angiosarcoma	9120/3
Undifferentiated pleomorphic sarcoma	8830/3
Osteosarcoma	9180/3
Myxofibrosarcoma	8811/3
Leiomyosarcoma	8890/3
Rhabdomyosarcoma	8900/3
Synovial sarcoma	9040/3
Miscellaneous sarcomas	
Cardiac lymphomas	
Metastatic tumors	

ICD-O International Classification of Diseases for Oncology, *NOS* not otherwise specified

has preferential anatomical locations. In the reported series, most tumors occur in the left atrium (such as myxoma and most soft tissue sarcomas). Only a small minority of primary cardiac tumors most frequently involve the right heart (for example, hemangioma, angiosarcoma, leiomyomatosis, and lymphoma) [10]. The underlying mechanism on the location predilection is still unclear.

29.2 Benign Tumors

29.2.1 Myxoma

Cardiac myxoma is the only relatively common primary heart tumor and considered as a true neoplasm. It accounts for 75–90% of all primary cardiac tumors [10–14]. The tumor occurs in all age groups with a peak age ranging from 40 to 70 years [10, 11, 14–19]. It occurs more commonly in females than in males with a female/male ratio of 1.5 [11, 14]. The cells giving rise to the tumor are considered to be multipotential mesenchymal cells that persist as embryonal residues during septation of the heart [20, 21].

The clinical presentation of myxomas is diverse and dependent upon tumor location, size and mobility [22–24]. The tumor can cause cardiovascular obstruction related symptoms (dyspnea, palpitation, angina, cough, and edema), cerebral embolism (cerebral infarction, vertigo, and syncope), and constitutional symptoms (weight loss, fever, and fatigue). Dyspnea is the most common symptom, and then followed by palpitation [10, 11]. These presentations are a consequence of atrioventricular valve obstruction. The intracardiac obstruction may also lead to narrowing outflow tract and atrial fibrillation, which could aggravate dyspnea and palpitation. Cough is a result of pulmonary venous hypertension and frank pulmonary edema. Angina may be caused by insufficient blood supply [25]. Embolism is also relatively common which may be caused by the tumor fragments. Since most myxomas are located in the left atrium, systemic embolism is relatively frequent [26]. The cause of some constitutional disturbances is still unclear. Some findings suggest the cytokine interleukin-6 (IL-6) may be responsible for that. The relationship between IL-6 and constitutional syndromes is still controversial [26–32]. In addition, about 20% of cardiac myxomas are asymptomatic; they are usually smaller than 4 cm [11].

Cardiac myxoma is an intracavitary endocardial lesion, most often arising in the left atrium, in the region of the fossa ovalis [33]. Less than 20% of cardiac myxomas occur in the right heart [10, 11, 14, 17, 22]. Most right-sided

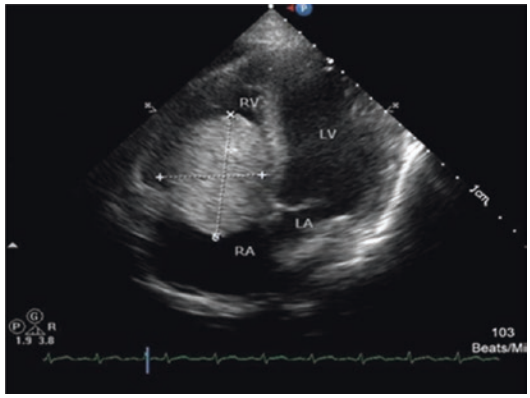

Fig. 29.1 Echocardiographic appearance of a right ventricle myxoma

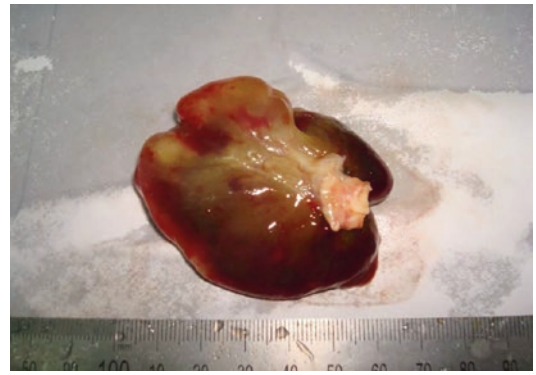

Fig. 29.2 The tumor mass is soft, gelatinous, and very friable. The surface is smooth and glistening

myxomas are located in the right atrium (5.6–15%) which arise from the interatrial septum. The right ventricular myxoma is extremely rare, only accounting for 0.8–7.4% [11, 12, 14, 15, 17, 18, 34, 35] (Fig. 29.1). A few isolated case reports have described right ventricular myxomas in adults and older children [36–44]. The tumor may attach to the outflow tract [37, 39, 40], tricuspid leaflets [42, 43], papillary muscle [45], or interventricular septum [36]. In some cases, cardiac myxoma is multicentric, which is usually the case in the setting of Carney complex [25, 46]. Sporadic myxomas arising in all the four cardiac chambers have been rarely reported [47].

The right atrial myxomas may mimic stenosis of tricuspid valves. Pulmonary embolism and pulmonary hypertension are so-morbidities. Besides the possible disturbance of heart activity due to valve obstruction, bleeding and fragmentation can also occur with subsequent embolism. The ventricular myxomas can directly obstruct the right ventricular outlet tract and pulmonary valves, which may cause complications such as syncope, pulmonary embolism, and sudden death [48–54].

On gross examination, the tumor mass is soft, gelatinous, and very friable. The tumor appearance can be either solid or villous. The solid type is globular or elongated, with a smooth, shiny, and sometimes undulant surface. The villous type has an irregular, often friable, papillary surface. Embolization may occur from the friable fronds themselves or from surface thrombi. Most cardiac myxomas have stalks, and some are broad-based (Fig. 29.2) [33].

Variable amounts of thin walled blood sinus or thick walled blood vessels are often present. Hemorrhagic foci, fibrinoid necrosis, hemasiderin-laden macrophages, and inflammatory cells are also frequent. The tumor cells may be spindle, polygonal, or stellate, and have round to oval nuclei with inconspicuous nucleoli, eosinophilic cytoplasm, and indistinct borders. Mitoses are rare. The cells can be arranged in single, in nests or cords, or in vasoformative ring structures. Small or large mucous halos are frequently observed to surround the myxoid cells, the cords or vasoformative ring structures (Fig. 29.3). In fact, most myxomas are combined with the above two or three structures. The tumor of solid type have a tendency to form vasoforming structures [11]. Occasionally, mucous glandular epithelium may present, which is considered as the rests of entrapped embryonic foregut (Fig. 29.4). However, the morphological features have no correlation with the clinical presentations. Immunohistochemical studies show the tumor cells bear a diffuse, and positive expression for Vimentin, and focal expressions for CD34, CD68, and smooth muscle actin [11]. This finding support the hypothesis that cardiac myxoma is originated from multipotential

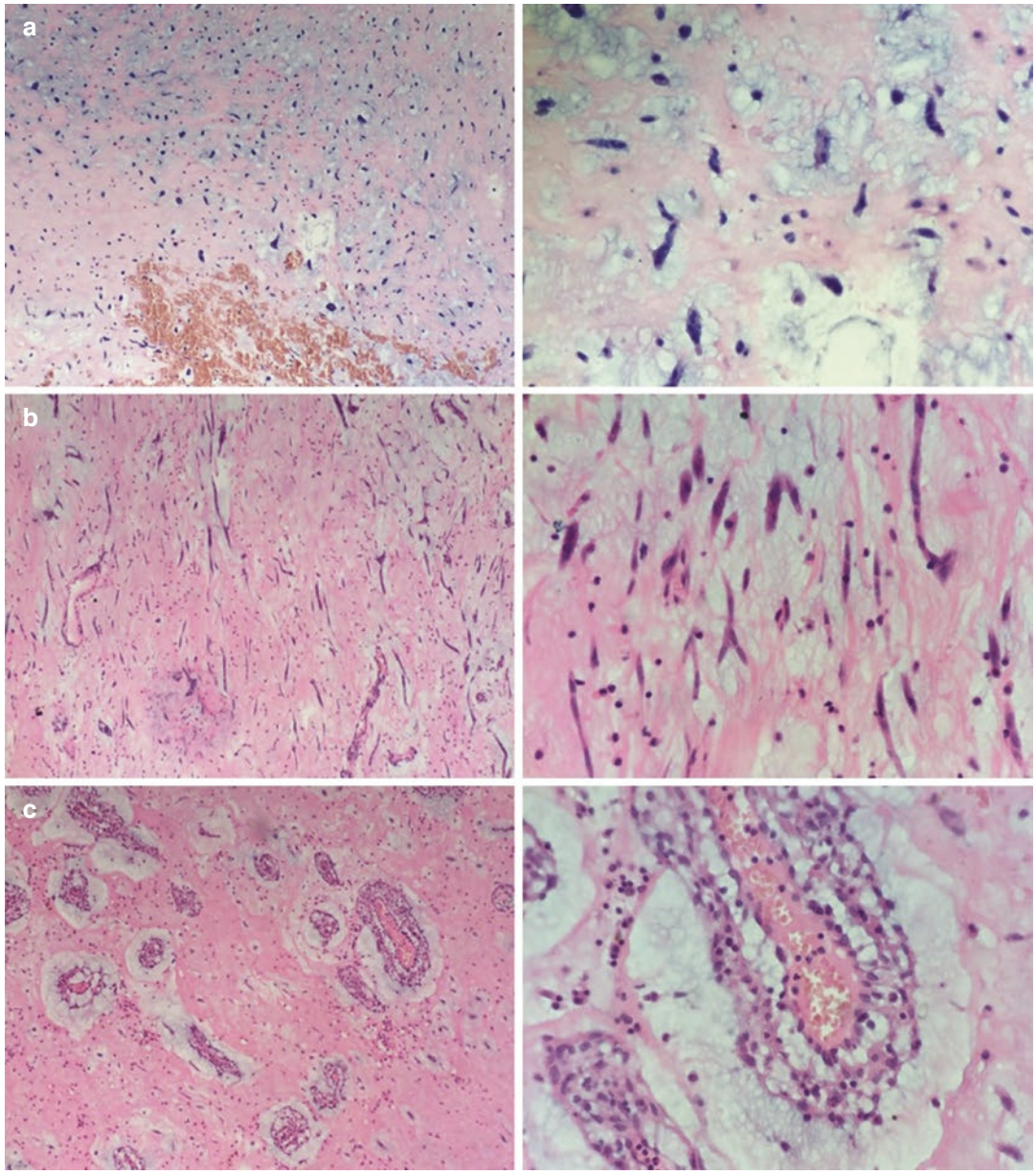

Fig. 29.3 Three cell arrangement subtypes of cardiac myxoma. (**a**) single cell predominant subtype; the single myxoid cells were scattered; (**b**) cell cord predominant subtype; myxomas of this type showed a rudimentary "chicken-wire" vessels like appearance, with few and scattered single myxoid cells in the stroma; (**c**) vasoformative ring predominant subtype; myxomas of this type showed a hemangioma-like appearance, containing distended blood sinus and distinct mucous halo

mesenchymal cells. The typical mucous glands may represent rests of entrapped embryonic foregut. In addition, the tumor cells may be immunoreactive-positive for S100, neuron specific enolase, and Calretinin [55–57].

Bone and brain metastases from glandular cardiac myxomas have been reported in the recent literature [45, 58–63]. The most frequent metastatic site for cardiac myxomas is cerebrum [59]. Several reports have reviewed cerebral

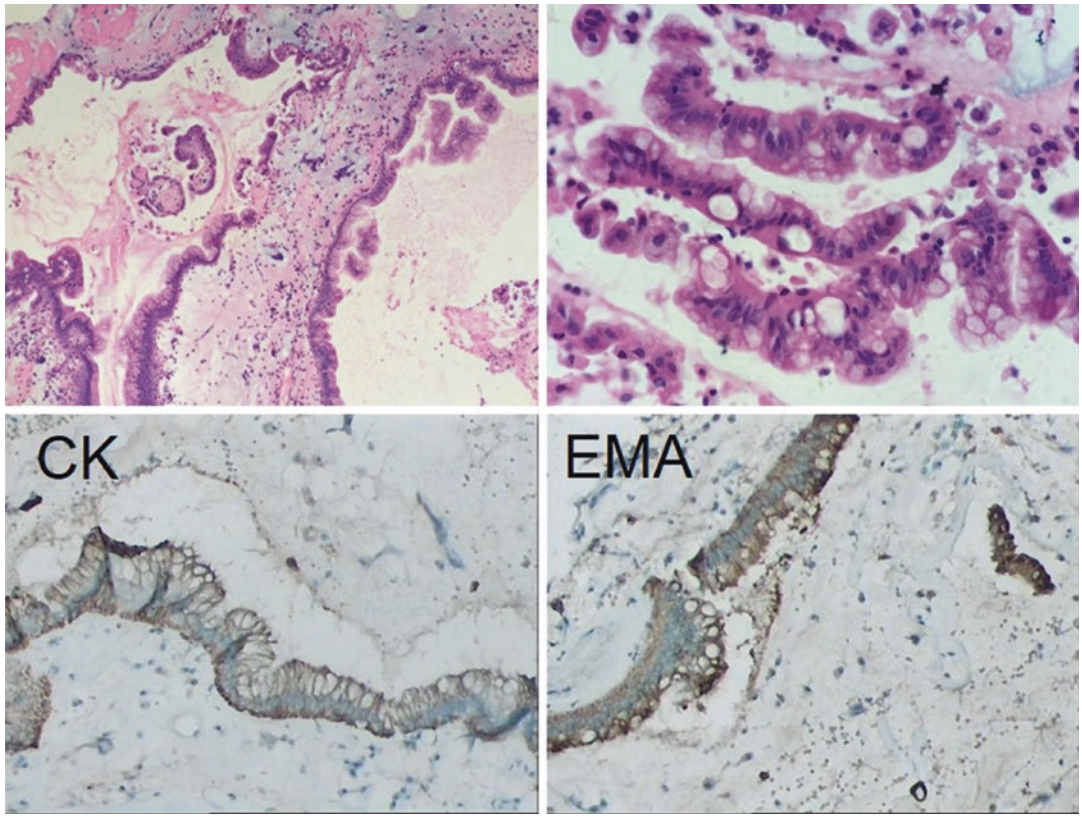

Fig. 29.4 Typical glandular structures in a glandular myxoma. Well-defined mucous glands, containing goblet cells interspersed between cells, formed by columnar epithelium were observed; the glandular structures bear positive expression of CK (cytokeratin) and EMA (epithelial membrane antigen)

metastasis cases [60, 61]. The tumor fragments metastasized to cerebral vessel walls may penetrate through the vessel wall, forming intra-atrial metastases.

The prognosis of cardiac myxomas is good after surgical resection, regardless of the tumor location. There is no evidence to show that right-sided myxomas have poorer prognosis than their counterparts in left atrium. The tumor recurrence is relatively low in non-syndromic patients (less than 5%), but approaches 10–20% in Carney complex patients [10, 33].

29.2.2 Rhabdomyoma

Rhabdomyomas represent the most common primary cardiac neoplasm in pediatric age, with an estimated prevalence of 60–86% of primary fetal cardiac tumors [64]. Rhabdomyomas are present within the myocardium and are often multiple. The tumor is derived from myocytes although there has been debate whether it might arise from purkinje cells, i.e. conduction tissue myocytes. It is regarded as a hamartoma of cardiac myocytes which is associated with the tuberous sclerosis syndrome [65]. If one is found as an incidental finding the family will need investigation. In many patients, however, the tumors regress, and there are often no cardiac symptoms if the patient survives the first month of life. Sporadic rhabdomyomas are more likely solitary endocardial based lesions that may cause ventricular outflow tract obstruction requiring surgical excision, or induce cardiac arrhythmias. However, there is an overlap between the

morphologic findings in patients with and without tuberous sclerosis [66].

Echocardiographically, rhabdomyomas appear as well-circumscribed, homogenous echogenic masses. This is an important feature to distinguish them from thrombi, myxomas, and other tumors. The finding of multiple cardiac masses is highly suggestive of rhabdomyomas, especially in patients with tuberous sclerosis [65].

Grossly, rhabdomyomas are well-demarcated yellow-tan nodules. The tumor size can range from a few millimeters to several centimeters in size. They often occur within the myocardium or on the endocardial surface, but are most commonly found in the ventricles and interventricular septum [65]. Rhabdomyomas are composed of enlarged vacuolated cells with sparse cytoplasm. The characteristic cell is the vacuolated "spider cell," which possesses strands of cytoplasm emanating from the nucleus. The apparent spaces within the cell contain large amounts of glycogen. Ultrastructurally, there are glycogen granules, myofibers, dispersed Z-band material, and intercalated disks along the cell periphery. On immunohistochemistry, the tumor cells are immune-positive for striated muscle markers, i.e. myogenin, Desmin, and Vimentin [65, 67].

Diffuse cardiac rhabdomyomatosis is a rare cause of pediatric cardiomyopathy presenting as sudden cardiac death [67, 68]. Histologically, there is diffuse involvement of the myocardium by rhabdomyoma-like cells with infiltrating borders associated with significant fibrosis. The large clear cells contain glycogen and are periodic acid- Schiff (PAS) positive as reported in the classic rhabdomyoma [56, 57].

Cardiac rhbdomyomas have a tendency for spontaneous regression, especially throughout the first year, and up to 5 years of age [69, 70]. Approximately one-third of patients may be either still-born or die within the first few days of life. Tuberous sclerosis is difficult to diagnose at this stage. Death is caused by the obstruction of cardiac valves when the intracavity tumors are large [68]. In those who survive into children, the tumor may spontaneously regress [71]. About one-third of patients have clinical evidence of tuberous sclerosis. The rhabdomyomas are incidental findings at autopsy, being small and embedded in the myocardium. Other patients have single intracavity tumors with marked obstructions of blood flow in at least one cardiac chamber and clinically there is no evidence of tuberous sclerosis. They often present with cardiac symptoms of congestive cardiac failure and ventricular arrhythmia [72]. Surgery is necessary for these severely symptomatic patients. Generally, clinical follow-up, associated with oral medication, is usually recommended [65].

29.2.3 Hemangioma

Primary cardiac hemangiomas are uncommon, accounting for less than 5% of all benign cardiac tumors [10, 19, 35]. They can occur in patients of all ages with equal frequency in both sexes. The average age at diagnosis is about 44-year-old [73]. The clinical manifestations are varied. Most cardiac hemangiomas are asymptomatic and found incidentally, either radiologically, during cardiac surgery, or at autopsy. The most common presentation in symptomatic cases is decreased exercise tolerance, followed by palpitation, syncope, edema, angina, and stroke [73, 74]. Sudden death have also been reported [75–78]. These symptoms depend primarily on the tumor location, size, and extension.

Cardiac hemangiomas may involve any part of the heart, including the endocardium and heart valves, myocardium, epicardium, and pericardium. The right atrium is the most common site of involvement, accounting for about 26% [73]. The most frequent locations are the anterior wall of the right ventricle, the lateral wall of the left ventricle, and the interventricular septum. Congenital hemangiomas most often involve the right atrium [79].

Most cardiac hemangiomas are small, endocardial nodules, either polypoid or sessile, and without evidence of infiltration. Intramural hemangiomas tend to be poorly circumscribed masses with a hemorrhagic or congested appearance (Fig. 29.5). The basic pathologic types of

cardiac hemangiomas include capillary type, cavernous type (Fig. 29.6), arteriovenous type, and mixed type. The capillary type tends to be circumscribed whereas the cavernous and intramuscular types tend to be infiltrative [79, 80]. The capillary type and cardiac myxomas have overlapping features. If a myxoid background is present, the capillary hemangioma may be misdiagnosed as myxomas [74].

Cardiac hemangiomas have a good prognosis after complete resection. About 90% of patients remained stable without tumor regrowth. Tumor recurrence is rare but may be more likely if resection is incomplete. Cardiac hemangiomas confined to the septum are considered to contribute to a higher risk of preoperative death [73].

29.2.4 Fibroma

Cardiac fibroma is a benign congenital mesenchymal tumor, composed of fibroblasts or myofibroblasts in a variably collagenized stroma [81]. It is the second most common primary cardiac tumor of childhood (following rhabdomyoma). Cardiac fibroma is synonymed as fibrous hamartoma as someone considered the lesion is hamartomatous rather than neoplastic.

Cardiac fibroma is more commonly encountered in patients with Gorlin syndrome. Mutations of the tumor suppressor gene *PTCH1* are the underlying cause of Gorlin syndrome [82, 83]. The clinical manifestations are determined by the tumor size and location. The most common syndrome in symptomatic patients is

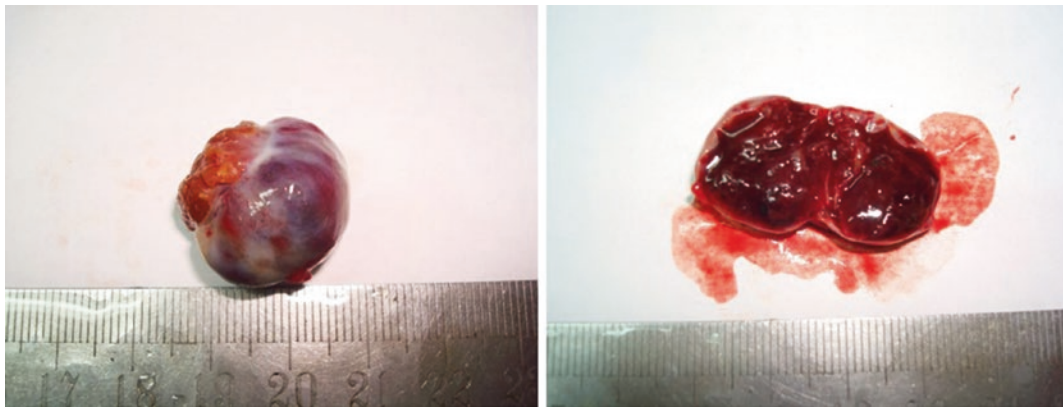

Fig. 29.5 Gross appearance of a right atrial endothelial hemangioma: the tumor surface is smooth and the cut surface is favaginous

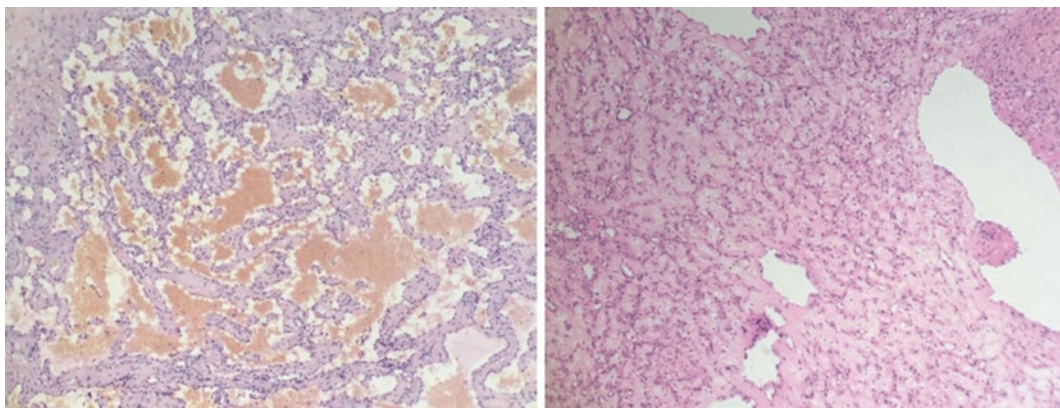

Fig. 29.6 The pathologic appearences of cavernous-type hemangioma (left) and capillary-type hemangioma (right)

ventricular arrhythmias and conduction disturbances [81]. The tumor with a large volume may impede blood flow or displace or directly involve mitral and aortic valves and result in severe mechanical obstruction [84]. In some patients cardiac fibromas may present as sudden unexpected death in adolescence [85, 86]. Interestingly, the tumor rarely causes symptoms in Gorlin syndrome patients, although they can reach significant size [87].

Cardiac fibromas arise predominantly in the interventricular septum or left ventricular free wall and appear to be well circumscribed. The most common location is within the myocardium of the left ventricular free wall or septum [88]. Right ventricular fibromas are uncommon, and the atrial (left and right) tumors are extremely rare. The tumor is usually solid, white, and fibrous. Histologically, the tumor is composed of spindle cells (myofibroblasts) in a collagenous background (Fig. 29.7). Myocardial infiltration at the periphery is often apparent. The cellularity of the lesion varies with age. The proportion of collagen is increasing with the age [79].

Generally, cardiac fibromas have a good prognosis after surgical resection. Sometimes, the tumor in infancy is not resectable because of extensive myocardial infiltration [86].

29.2.5 Papillary Fibroelastoma

Papillary fibroelastoma is a benign endocardial tumor which is characterized by endothelium overlying avascular fibroelastic fronds. In western countries, it is the second most common primary cardiac tumor (after cardiac myxoma) and the most common cardiac valvular tumor, which can occur in any age [89]. The incidence is relatively low in East Asia. The tumor accounts for no more than 1% of

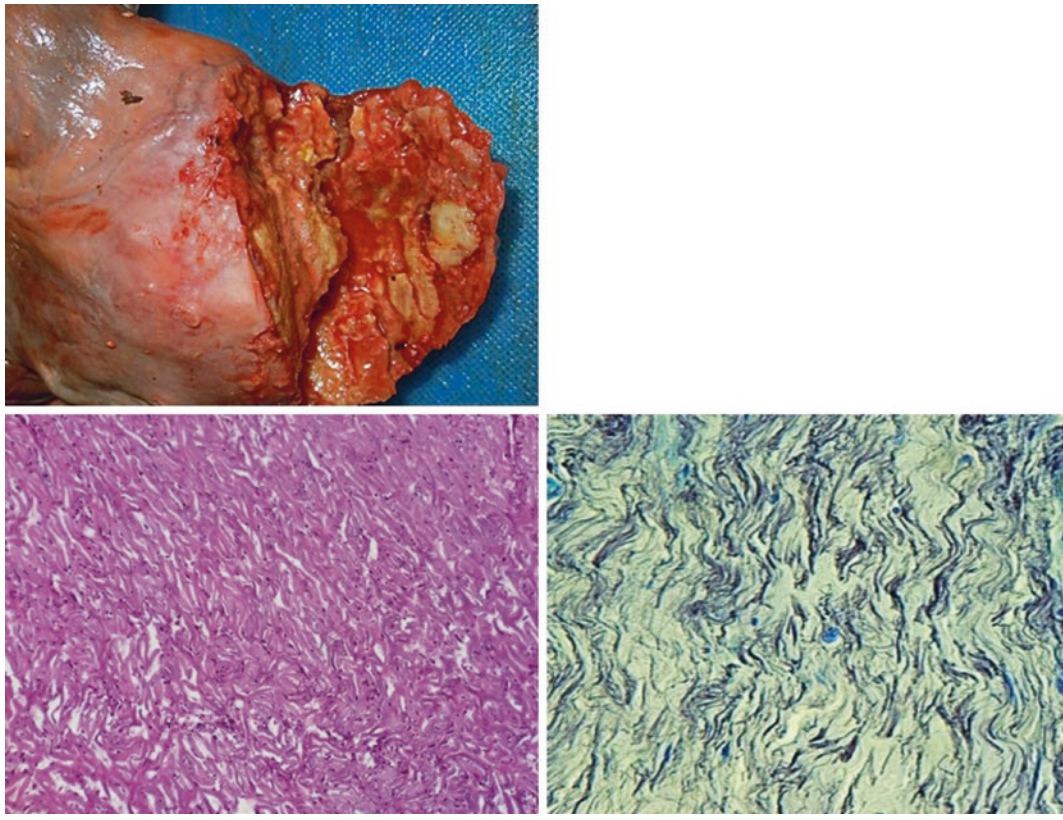

Fig. 29.7 Gross appearance, H&E stain (lower left) and Van-Gieson (lower right) stain of a cardiac fibroma. The patient was a 25-year-old female who suffered sudden death; The autopsy revealed a tumor mass measured 6×5×5 cm in the right ventricular free wall; the tumor was composed of bland cells in a collagenous matrix; the figures was obtained from the internet (www.91360.com)

primary cardiac tumors in large surgical series in China. The discrepancy may be due to the population difference [10]. The pathogenesis of papillary fibroelastoma is still unknown, and it is unclear if it is a reactive or hamartomatous process [90, 91]. Thrombi may occur on the surface of the proliferation, and dislodged clots are responsible for embolic symptoms. Some researchers suggested that it is hamartomas because of its mimicry of tendinous cords, whereas some think that it is organizing thrombi, a theory supported by the presence of fibrin within the cores [92]. Some authors believe that papillary fibroelastoma represents giant form of Lambl's excrescence, evolving from a thrombotic phenomenon due to traumatization of the endothelial cells at the level of the valves which have an increased pressure gradient [93]. Abnormal blood flow might also explain the presence of organized thrombus. Papillary fibroelastoma has been shown to contain fibrin, hyaluronic acid, and elastic fibers, in keeping with organized thrombus [89].

Most patients with papillary fibroelastomas are asymptomatic and these are incidental findings during echocardiography, cardiac surgery, or autopsies. However, left-sided lesions may cause symptoms by embolization of attached fibrin clots or prolapse into the coronary orifices. The most common symptoms are transient neurological defects and myocardial ischemia, although sudden death has also been reported [94].

The left sided valves are most commonly involved, with aortic valves being the usual sites. The right sided valves, heart chambers, and papillary muscles are unusual sites [95]. Grossly, papillary fibroelastomas have a sea anemone appearance with a gelatinous surface and a stalk with multiple papillary projections. They generally are around 1.0 cm in diameter, but range in size from 0.2 to 7 cm. Microscopically, papillary fibroelastomas are avascular and are composed of collagen, elastic, and reticulin (Fig. 29.8). Stains for elastin reveal the presence of elastic fibers, from which

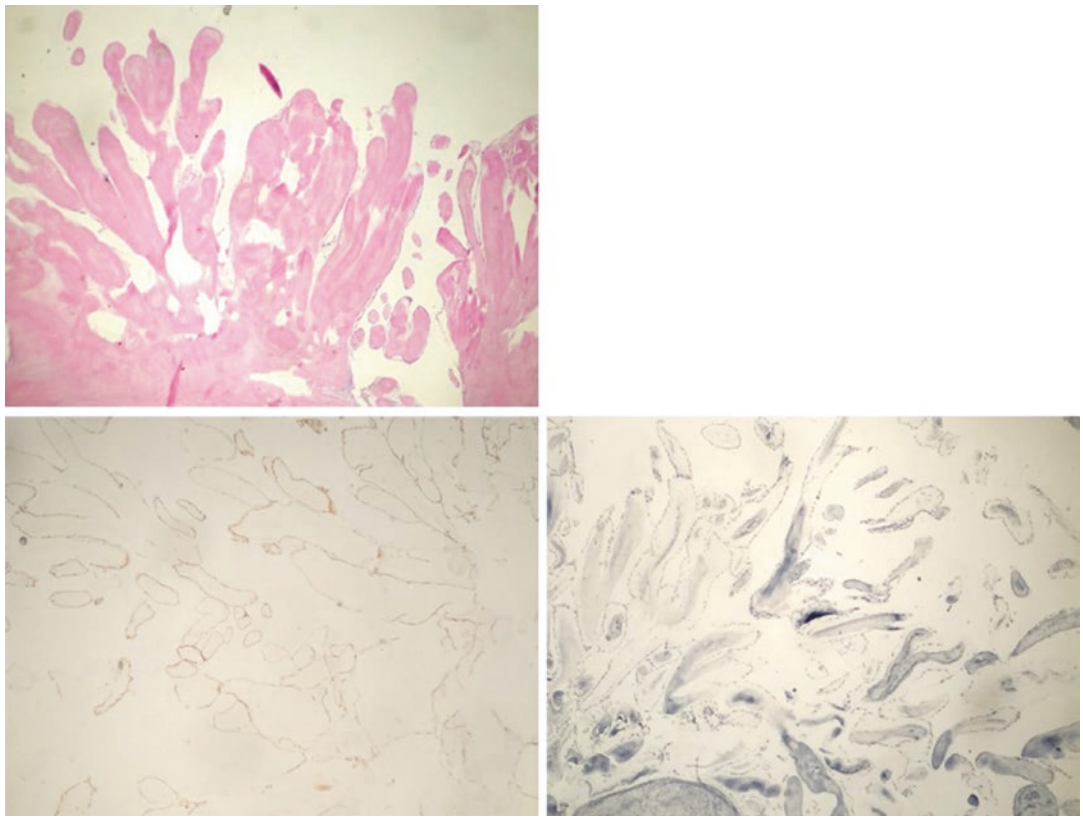

Fig. 29.8 Papillary fibroelastoma is composed of mainly avascular fronds, coated by bland endothelium. The fronds usually arise from a common central stalk; the lining cells are positive for CD34 (lower left), and elastic fibers are positve for elastin stain (lower right)

the lesion derives its name. The cells covering the surface are positive for vimentin, factor VIII-related antigen, and CD34, in keeping with their presumed vascular endothelial origin. Collagen type IV showed multilayered linear staining beneath the surface that is virtually identical to the staining pattern for elastic tissue [90]. Usually, papillary fibroelastoma are single, small, and may be pedunculated. There is no infiltration of the underlying valve leaflet [89]. Previous study has reported an "infiltrative" papillary fibroelastoma on the anterior leaflet of the mitral valve [91, 96].

Owing to the tumor's thromboembolic potential, surgical resection is recommended, although the fibroelastoma is morphologically benign. The long-term outcomes are excellent after resection, without recurrence even when the resection is insufficient. Anticoagulation drugs are also used when thromboembolic signs are present [89].

29.2.6 Lipoma

Cardiac lipoma is a well-defined, benign mass composed of mature, white adipocytes. The tumor is rare and accounts for only 0.5–3% of excised heart tumors. They can occur at any age with equal frequency in both sexes. True cardiac lipomas are encapsulated and much less frequent than lipomatous hypertrophy of the interatrial septum [97, 98].

Most cardiac lipomas are epicardial or endocardial tumors, although any site of the heart may be affected. They may also occupy the pericardial space or be intracavitary. The tumor maybe located more frequently in the left ventricle or right atrium [99]. Rarely, they are intramyocardial. Invasive lipomas are also reported [100]. The tumor can occur in patients with Cowden syndrome [101]. Although typically solitary, multiple cardiac lipomas may be reported [102].

The size of cardiac lipomas varies, and those that are left in situ when they are asymptomatic may grow to large dimensions [103]. The presentation of cardiac lipomas is varied and depends on their location and size. The epicardial lipomas tend to be large [104]. They are mostly asymptomatic and may be discovered incidentally. The tumor can cause arrhythmias, syncope, embolization, and even compression of the coronary arteries or blood flow within the heart. Those adjacent to valves present early with murmurs or valvular obstruction. Tumors of the right atrium, interatrial septum, and right ventricle can predispose to arrhythmias [97]. Histopathologically, the tumor was composed of mature adipose cells (Fig. 29.9).

Excision of cardiac lipomas is indicated if clinical symptoms develop or it is not possible to confidently exclude liposarcoma. Surgical excision generally provides complete cure and a good long-term prognosis [105].

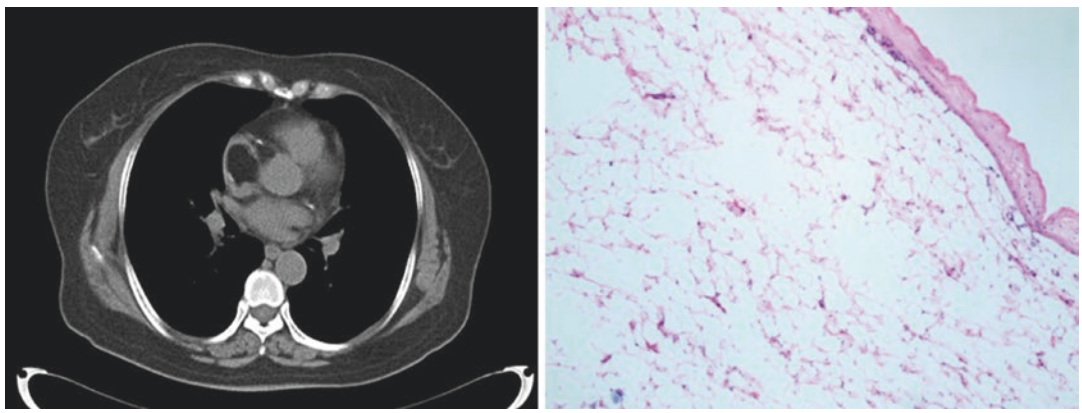

Fig. 29.9 Right atrial lipoma. The patient was a 66-year-old female; the tumor was located under the endocardium with a fibrous capsule

29.2.7 Schwannoma

Primary cardiac schwannoma is an extremely rare disease. No more than 20 cases have been reported in the literature so far. It is considered to originate from the cardiac plexus or the cardiac branch of the vagus nerve [106]. Primary schwannoma of the heart tends to be located in the right heart, frequently close to the cardiac plexus and in the right atrium [107]. However, the tumor can be found in other sites of the heart, including left atrium [106, 108, 109], interatrial septum [10, 110], and left ventricle [111, 112].

Just as other primary cardiac tumors, the symptoms of primary cardiac schwannoma vary depending on the location and size of the tumor, the rate of growth rather than the histopathology. Grossly, the tumor is a well-circumscribed, nodular mass with fibrous capsule. Microscopically, the tumor is composed of variable amounts of hypercellular Antoni A and hypocellular Antoni B areas (Fig. 29.10). It may continue to grow and compress the cardiac chambers. The most common symptoms are chest pain, dyspnea, orthopnea, distal edema, and syncope. After surgical treatment and complete resection, good outcomes have been reported in the reported cases [106–113].

29.3 Intermediate Tumors

29.3.1 Paraganglioma

No more than 300 patients with cardiac paraganliomas are described in the PubMed database. The mean age at diagnosis is about

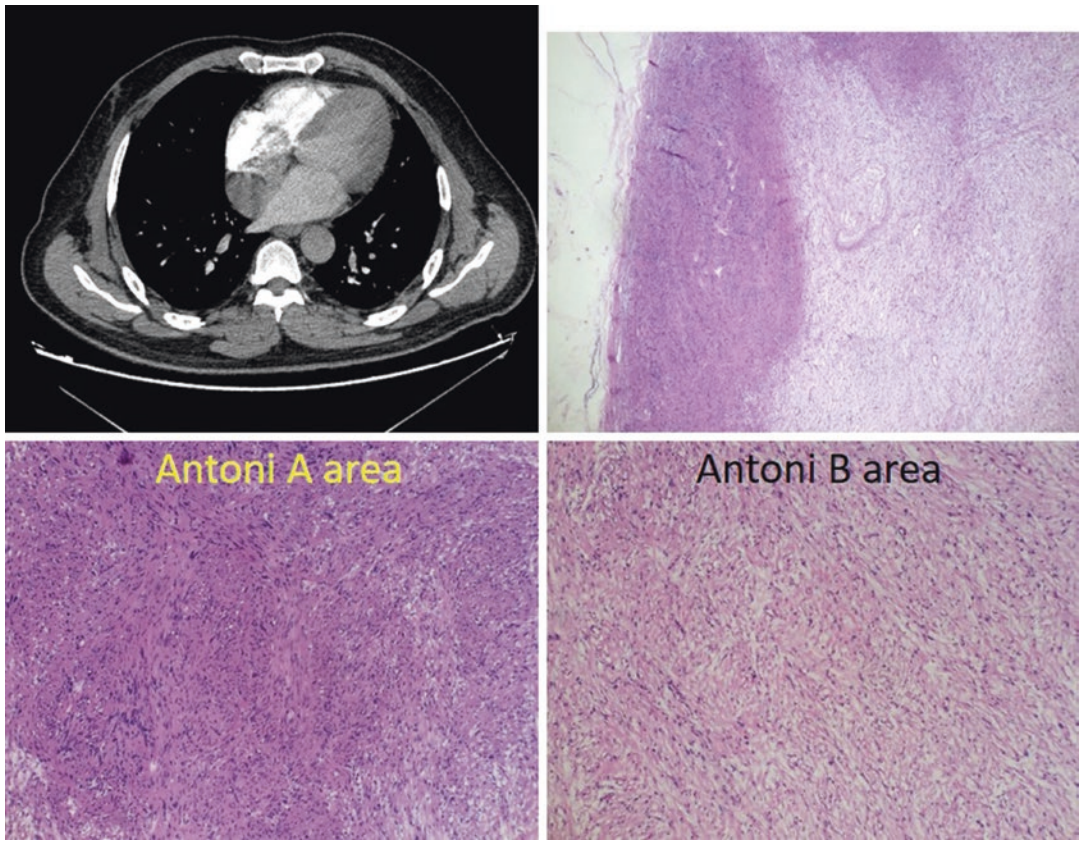

Fig. 29.10 Right atrial (interatrial septum) schwannoma. The patient was a 59-year-old male who appeared asymptomatic; the tumor was embedded in the myocardium of the interatrial septum measuring 4.5×3.5×3 cm in size; typical areas of Antoni A and B were observed

40 years, with a slightly female predominance [114]. Cardiac paragangliomas may originate from the sympathetic nervous system as they usually display catecholamine-related symptoms which affect 77% of all patients (e.g., hypertension, flushing, sweating, diaphoresis, perspiration, palpitation, tachycardia, headache, dizziness, and syncope). Most patients bear serious hypertension (affecting 70%). However, dyspnea is quite uncommon, with an incidence of 20%. Moreover, chest pain (distress, discomfort, tightness, heaviness, or angina) is reported in about 20% patients, and the nonspecific systematic symptoms such as fatigue, fever, and weight loss are documented in about 10% patients [114, 115]. Asymptomatic cases are also reported [116, 117].

Cardiac paragangliomas are often intrapericardiac, and mostly arise from the epicardium (including interatrial groove, and atrioventricular groove) and the root of the great vessels (including aorta, pulmonary artery, pulmonary vein, and vena cava). Published reports suggest that cardiac paragangliomas are closely related to left atrium, and the right-sided tumors are rather uncommon [114]. However, most tumors (about 60%) obtain blood supply from the right coronary artery.

Grossly, cardiac paragangliomas are often well-defined and high vascularized with a hemorrhagic cut surface. The adherence between the tumors and surrounding structures may be caused by compression rather than direct invasion. However, extensive myocardial infiltration could also be observed. The maximal diameter is about 5.3 cm [114]. On microscopy, cardiac paragangliomas composed mainly of so-called chief cells, grouped together in cell clusters or organoid ("Zellbellen") surrounded by a capillary network (Fig. 29.11). Pigmented tumors are reported in three patients [118–120].

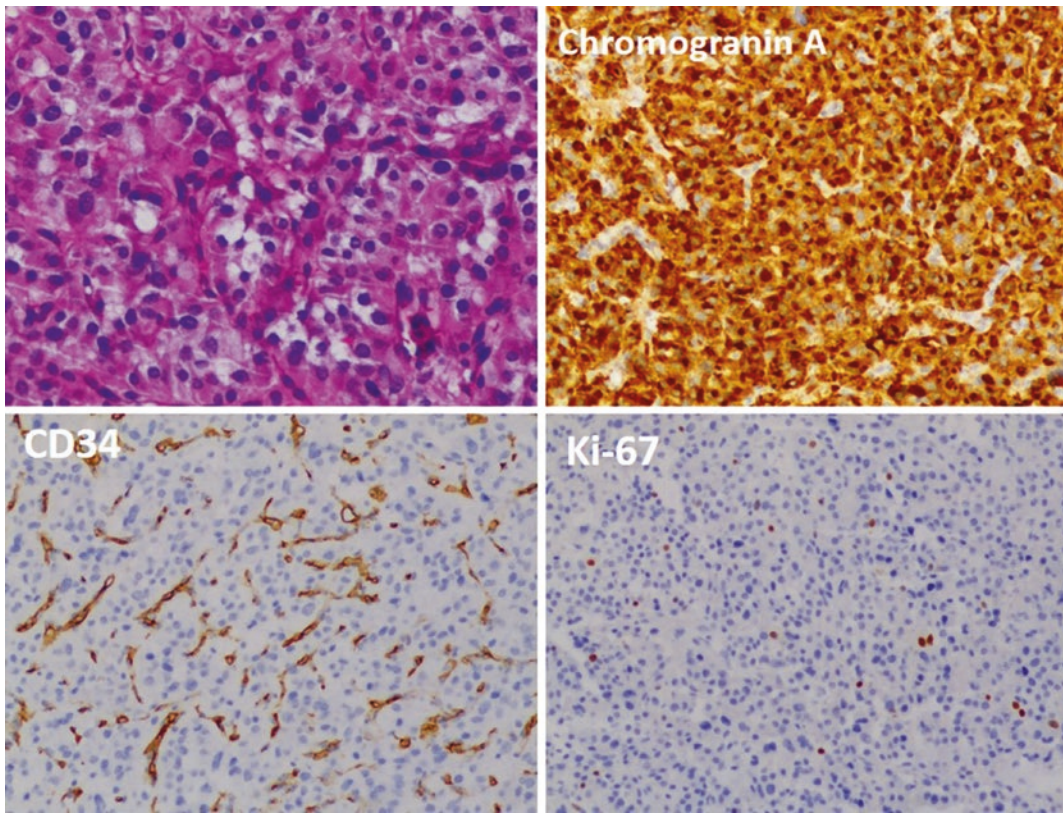

Fig. 29.11 Primary cardiac paraganglioma. The patient was a 42-year-old female who presented with hypertension for one year; the tumor was composed mainly of so-called chief cells, grouped together in cell clusters surrounded by a capillary network; Chromogranin A was diffusely positive; CD34 stain highlighted the capillary network; Ki-67 index was low

Cardiac paraganglioma-related hypertension can be controlled by α-adrenergic blockers (urapidil, doxazosin, phenoxybenzamine), β-adrenergic blockers (esmolol, atenolol, metoprolol), calcium channel antagonists (amlodipine, nifedipine), and angiotensin-converting enzyme inhibitors (ramipril). The most effective therapeutic strategy is surgery. In most cases, the tumor is firmly adherent to the adjacent tissues; therefore, a portion of the affected structures had to be excised (the reported structures including left and right atrial wall, interatrial septum, pulmonary artery/vein, right ventricular wall, aortic sinus, aortic valve leaflets, and superior vena cava), and the defects are repaired by patches of pericardium (autologous or bovine), Dacron or polytetrafluoroethylene. The affected coronary artery can be revascularized using a saphenous vein graft. The prognosis after complete resection is rather good. The one- and 5-year overall survival rates are 98.2 and 78.8%, respectively [114]. For the malignancies, the follow-up information is obtained in five patients, in which four expired with a longest follow-up period of 48 months [121–125]. Adjunctive chemotherapy and radiotherapy are reported, but the effects are still uncertain.

29.3.2 Inflammatory Myofibroblastic Tumor

Cardiac inflammatory myofibroblastic tumor is an extremely uncommon tumor. The exact incidence is unknown due to very different terms used to designate the lesion and the lack of uniform diagnostic criteria. With our best knowledge, less than 100 cases of cardiac inflammatory myofibroblastic tumors have been published in English. The majority of these lesions have been described in children and young adults, although there have been infrequent reports in older adolescents. No gender predominance is found. Owing to its extremely rarity, the etiology of inflammatory myofibroblastic tumors still remains unresolved and the immunologic and infectious postulates are still to be validated.

Cardiac inflammatory myofibroblastic tumor is typically located within the endocardium. The tumor usually forms polypoid masses within the right atrium, less frequently within the ventricles or valves [126]. The left-sided tumor is relatively uncommon.

Patients with cardiac inflammatory myofibroblastic tumor are usually asymptomatic until hemodynamic changes and local invasion leading to cardiac insufficiency. Decreased exercise tolerance may be the most common symptom. The signs of respiratory and cardiovascular failure in our patients resulted from the tumor compressing the right heart, the confluence of great vessels and pericardial fluid, as well as airway compression on the right. The natural history is unpredictable. Patients undergoing surgical resection of the tumor usually have a favorable prognosis, while patients with an unresectable tumor may have a poor one because of the unpredictable progression of the tumor, like sudden death or embolism [127].

Tumor resection is a treatment of choice, and there is consensus about surgical treatment in symptomatic patients [128]. In patients with unresectable tumors, steroid therapy may be considered [129, 130].

29.4 Malignant Tumors

29.4.1 Angiosarcoma

Angiosarcoma is considered as the most common type of right heart sarcoma in most reports. The age range is 9–80 years, with a mean of 40 years [80]. Unlike other cardiac sarcomas, there is a marked right-sided predominance, nearly 90% occurring in the right atrium near the AV groove. Because of the propensity for pericardial involvement, cardiac tamponade occurs more frequently than with other types of cardiac sarcomas [131]. Metastases occur in 66–89% of patients, most often to the lungs [132].

The tumor mass or masses are typically dark red or brown. The size ranges from 2.0 to 17 cm in greatest dimension. Invasion of the vena cava and tricuspid valve is common, but the atrial septum and pulmonary artery are usually spared. The pericardium is frequently involved, and may be the only site of the tumor.

The histological appearance of cardiac angiosarcoma does not differ from that of angiosarcoma

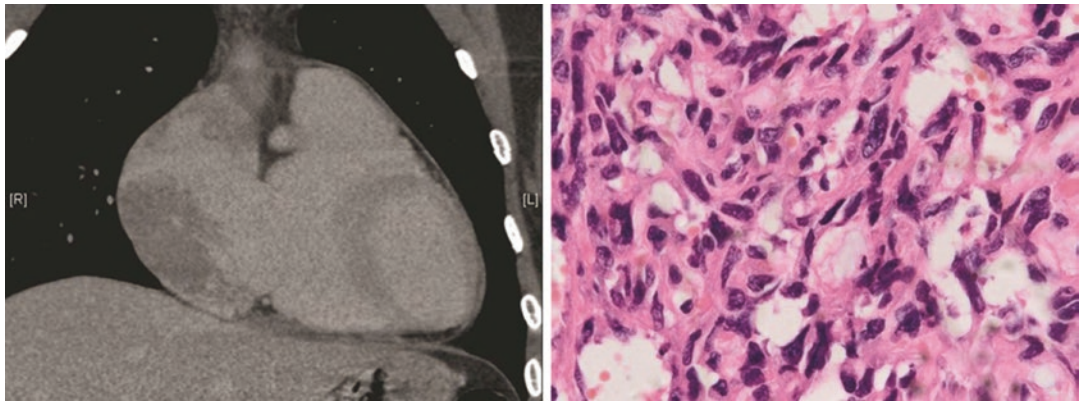

Fig. 29.12 Right atrial angiosarcoma. Angiosarcoma is often highly infiltrative and not well demarcated. The patient was a 31-year-old female who presented with abdominal distension and generalized edema. Radiology image showed a huge tumor mass in the right atrium. She died 6 months after surgery. Histopathologically, tumor cells formed irregular, anastomosing vascular channels in well-differentiated areas, and endothelial cell lining may show multilayering or intraluminal tufting

found elsewhere (Fig. 29.12). Histological grade is not an independent prognostic indicator in cardiac angiosarcomas and is not statistically correlated with survival [133].

Despite earlier presentation than in the past, the prognosis for cardiac angiosarcoma is very poor. Patients die either from localized effects of the tumor, which may include cardiac rupture, or metastatic disease, commonly to the lungs or brain. There is an increased incidence in brain metastases following surgical intervention. This is postulated to be due to dissemination of tumor cells occurring at the time of surgery. Patients who do not undergo surgical resection have a mean survival of 3.8 months, whereas the mean postoperative survival for those who undergo cardiac transplantation or total or partial resection is 10.6 months. Occasional long-term" (up to 53 months) survivors have been documented [131, 133, 134].

29.4.2 Undifferentiated Pleomorphic Sarcoma

Undifferentiated pleomorphic sarcoma, formerly named malignant fibrous histiocytoma, is considered as the second commonest sarcoma arising from the right heart. The tumor manifests a broad range of histological appearances with three-types described: storiform-pleomorphic, giant cell, and inflammatory. The mean age at diagnosis is about 42 years. The tumor is often located in the left atrium, but can involve any site, including all chambers, mitral or tricuspid valve, and pericardium [135]. Just as with cardiac myxomas, cardiac undifferentiated pleomorphic sarcoma often manifests cardiorespiratory symptoms in which dyspnea is most common. Gastrointestinal symptoms, such as abdominal pain, diarrhea, appetite loss, and nausea, which appear more common than that of myxomas [136]. These extra-cardiorespiratory manifestations may be illustrated by hemodynamic changes of gastrointestinal circulation and growth of the malignancy: invasion, necrosis or immune response. In addition, the systemic presentations such as fever and fatigue and central nervous symptoms such as cerebral embolic symptoms are also reported. They are more likely to be attributed to thrombus produced by hemodynamic changes rather than tumor fragments, since the tumor is usually not so friable. The little tumor size (maximal diameter, 3.5 cm) is thought to account for the lack of symptoms [135].

The maximal diameter of the tumor ranged from 2.6 to 10 cm. The laboratory tests appeared to be non-specific. The tumor is composed of storiform, fascicular, or patternless arrangement of highly atypical spindled cells. Marked nuclear pleomorphism is observed in most cases. Abundant mitoses, often abnormal, and necrosis are apparent. The tumor may contain chronic

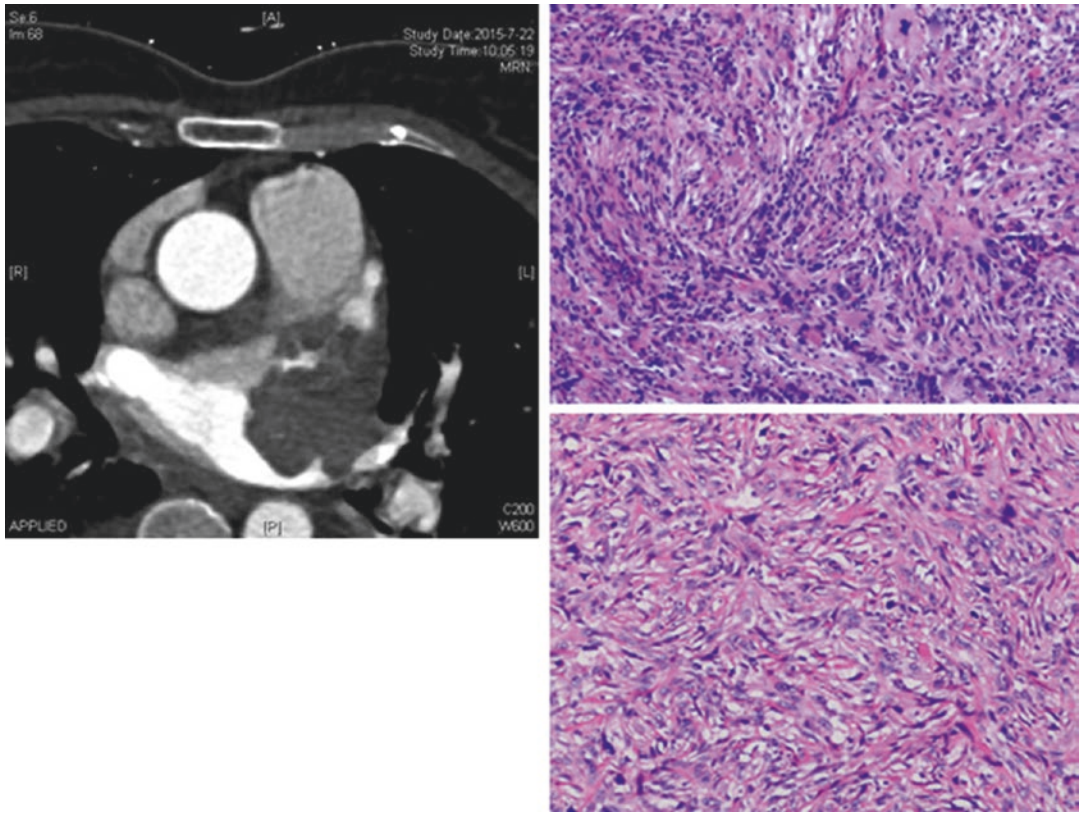

Fig. 29.13 Undifferentiated pleomorphic sarcoma show markedly atypical cytologic features with marked nuclear enlargement, hyperchromasia, and pleomorphism. Mitotic figures are also easily identified

inflammatory infiltrate or osteoclastlike giant cells (Fig. 29.13). On radiography and echocardiography, the tumor is easily taken as myxoma or thrombus. Therefore, it is difficult to make an appropriate preoperative diagnosis, unless a distinct invasive growth pattern or pericardial effusion is noted when the lesion is suggestive of a malignancy [135].

The median overall survival of those diagnosed ante-mortem is approximately 18 months. The survival analysis showed the outcome is not related to variables of tumor location, tumor size, chemotherapy/radiotherapy, and surgery [135].

29.4.3 Myxofibrosarcoma

Primary myxofibrosarcoma rarely arises in the heart. Less than 30 cases can be retrieved from PubMed database by far. According to the previous reports, patients' age ranged from 6 to 81 years with a mean age of 40 years. The most common symptom is dyspnea, which is similar to other benign tumors such as cardiac myxomas [137].

The tumors involved predominantly the left atrium (Fig. 29.14). No more than five right sided cases are reported by far [138, 139]. Histopathologically, the tumor is composed of a myxoid matrix with incomplete fibrous septa. The tumor cells are plump and spindled, with ill defined, slightly eosinophilic cytoplasm and atypical, enlarged, hyperchromatic nuclei (Fig. 29.15). Cardiac myxofibrosarcomas are usually asymptomatic until an advanced stage, which could lead to a narrowed outflow tract contributing to dyspnea and palpitations. Like other sarcomas, myxofibrosarcomas show an infiltrative growth pattern and are usually large at diagnosis, resulting in incomplete

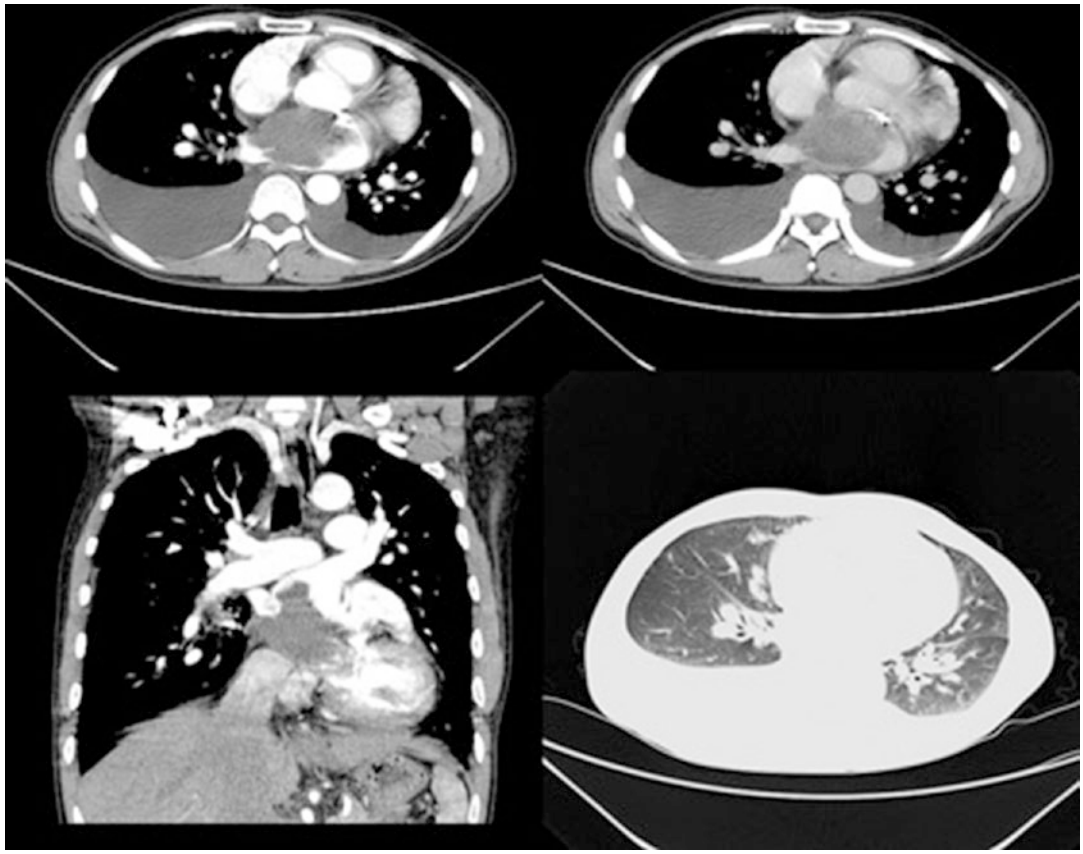

Fig. 29.14 A 42-year-old man who presented with dyspnea and palpitation of 1 month's duration. Contrast-enhanced computed tomography revealed a lobular filling defect in the left atrium

surgical resection and local recurrence (recurrences occur in up to 50–60% of cases, unrelated to histological grade). Sometimes, patients only present with an incidentally observed, slowly enlarging and painless mass. A more embarrassing dilemma is that myxofibrosarcoma is insensitive to chemotherapy and radiotherapy. Thus, even a low-grade myxofibrosarcoma may have a fatal outcome. The outcomes of the patients are disappointing, although some of them received aggressive postoperative radiotherapy and chemotherapy. Of all patients, only two achieved complete recovery [140, 141].

29.4.4 Leiomyosarcoma

It is well known that leiomyosarcoma is a common form of soft tissue sarcoma that is composed of cells showing distinct smooth muscle features. There have been no more than 200 cases of primary cardiac leiomyosarcoma reported in the literature to date [142, 143]. According to previous studies, the age at presentation is about 48 years (range 6 months to 86 years). The congestive heart failure related symptom is the most frequent complaint at diagnosis, affecting 78% [144].

Primary cardiac leiomyosarcoma predominately arises from the left atrium (60%). Other documented locations includ the right ventricle (20%), right atrium (15%), and left ventricle (5%). Sometimes, the tumor may display an infiltrative growth pattern and involve the cardiac valve or occupy two or more heart chambers (22%). Unlike cardiac myxoma, this tumor rarely has a stalk, and rarely originates from the interatrial septum [144].

Grossly, primary cardiac leiomyosarcomas often appear multilobular, nodular, or polypoid. Thus the tumor may often be taken as myxoma on imaging detection, especially when it is located in the left atrium. The median maximal diameter is 6.0 cm (range 1.5–13 cm). The tumor cell may appear spindle, epithelioid, or pleomorphic.

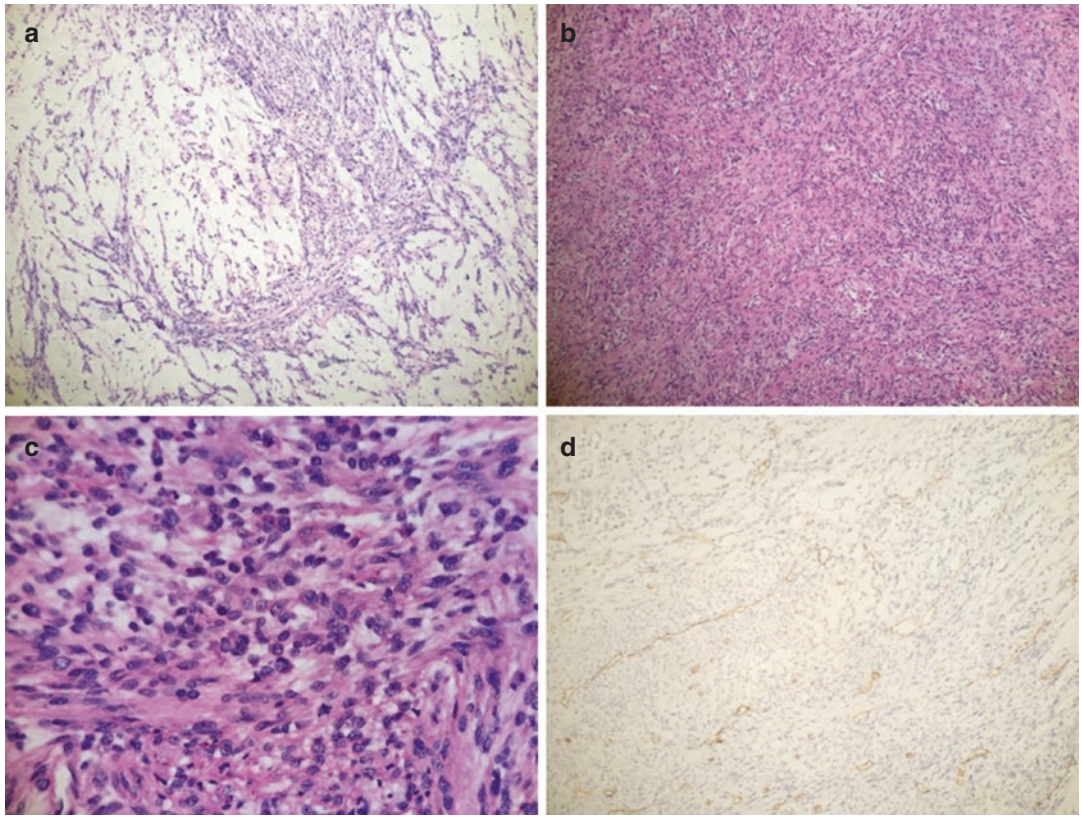

Fig. 29.15 Hematoxylin and eosin and immunohistochemical staining of myxofibrosarcoma. (**a**–**c**) Hematoxylin and eosin staining showed a myxoid matrix containing elongated, curvilinear vessels with a minor solid component. Mitotic figures were infrequent (**d**) CD34 staining defined the characteristic blood vessels

Nearly half of patients undergo postoperative recurrence and metastasis, even complete resection is performed. The 5-year overall survival and local and metastatic recurrence-free survival rates are 25 and 15%, respectively. On univariate analysis, the known prognostic markers of age and operation are significant variables. There is a trend for patients with adjunctive therapy to have better outcomes than those without further therapy. The median recurrence-free survival is about 14 months (range 3 weeks to 5 years) [144].

29.4.5 Synovial Sarcoma

Primary cardiac synovial sarcoma is an extremely rare entity. An analysis of reviews shows that it is calculated to account for approximately 4.2%. The tumor appeared to have a striking male predominance (male/female ratio is approximately 3:1). At presentation, patients are a mean age of 37.1 years (range, 13–70 years). Dyspnea is the most common presenting symptom [145].

The most common location is pericardium (40%), followed by right atrium (24%) and left atrium (8%). On gross appearance, the tumor mass is often polypoid, solid, or lobulated, with a smooth or well-circumscribed external surface. It usually appears as a bulky mass and does not diffusely infiltrate the surrounding structures, so the initiation site can be well distinguished. Most tumors have a broad base, and some have a pedicle or stalk. Sections through the tumor mass show variable patterns: some have firm, glazed, or elastic consistency, or are friable with some necrotic regions; others show cystic changes. It is tan-white or reddish with hemorrhage, and cream-yellow with necrosis. This is related to the histopathologic features: soft and tan when cells are rich, especially with glandular architectures, and elastic and white when abundant with fibrous

stroma. Synovial sarcoma is biphasic or monophasic (the tumor of this case is monophasic and composed of spinal cells) [145]. The t(X;18)(p11; q11), as the cytogenetic hallmark of synovial sarcoma, could be detected using traditional cytogenetics or combined binary fluorescence in situ hybridization [146].

Some tumors with a broad base that showed an infiltrative growth pattern made it impossible to perform a complete resection, and usually, tumor residues or a positive margin are left. Local recurrence and distant metastasis after the initial operation are the two most common adverse events. The median overall survival of the patients diagnosed antemortem is approximately 24 months. Survival rates are approximately 59.9% at 1 year and 29.9% at 5 years. Adjunctive chemotherapy and radiotherapy, as well as age, affected the overall survival pattern [145].

29.4.6 Liposarcoma

Liposarcoma is a malignant tumor of mesenchymal origin that is one of the most common primary neoplasms in the thigh or retroperitoneum. Depending on their size and location within the heart, liposarcomas may present with chest pain, symptoms of right- or left-sided heart failure, pericarditis with or without cardiac tamponade, palpitation, rhythm disturbances, syncope, angina, cough and constitutional symptoms like fever and weight loss. Dyspnea is the most common symptom. In cases where the tumor does not interfere with cardiac function, patients may be entirely asymptomatic [147–149].

Pericardium is the most common location of liposarcomas. All the four histologic subtypes: well-differentiated (or atypical lipoma), dedifferentiated, myxoid/round cell and pleomorphic, are reported in the literature. Well-differentiated liposarcoma accounts for 40–45% of all liposarcomas and the lipoma-like form is by far the most common of its variants. S-100 protein immunoreactivity may help highlight the presence of multivacuolated lipoblasts (Fig. 29.16).

Primary cardiac liposarcomas are often asymptomatic and may reach a considerable size before causing any symptoms related to direct invasion or compression of other thoracic organs [147]. Prognosis of liposarcoma is influenced by some factors: age, site, tumor size, surgicalmargins, surgical procedure, and radiation therapy. Complete tumor resection and adjuvant radiation therapy contribute to reduce the risk of local recurrence and metastasis [150].

29.4.7 Rhabdomyosarcoma

Rhabdomyosarcoma is the most common primary cardiac malignancy in the pediatric age group, but can occasionally occur in adults. It should be noted that the rarity of rhabdomyosarcomas, as a primary cardiac tumor, means that epidemiological and other data are based on relatively few cases. Current

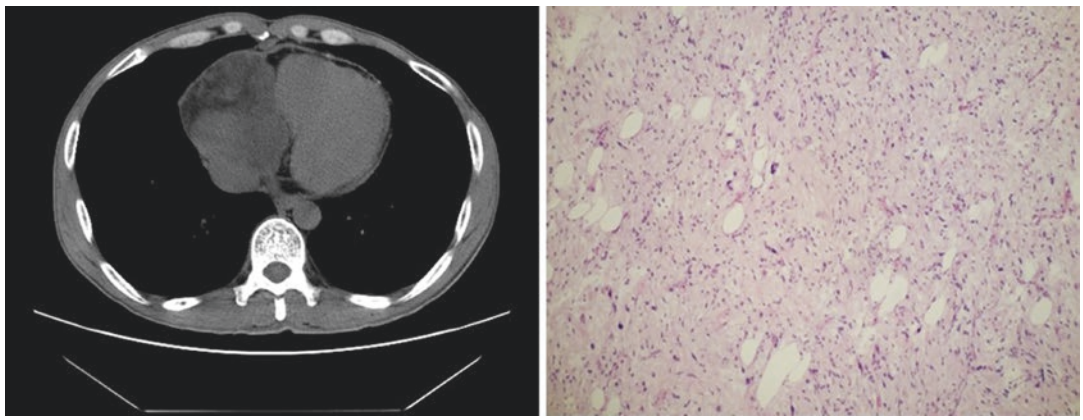

Fig. 29.16 Primary pericardial liposarcoma. The patient was a 42-year-old man who presented with dyspnea. CT-scan demonstrated a non-homogeneous density mass in pericardial sac, and a histopathologic diagnosis of liposarcoma was made

evidence shows that rhabdomyosarcoma occurs equally in both sexes, and 75% occur in children less than 1-year-old [151].

Rhabdomyosarcoma may originate anywhere in the heart, and 60% of cases appear multicentric. They tend to arise within the myocardium, with no chamber bias, rather than as intraluminal masses. Cardiac rhabdomyosarcoma is slightly more common in males than females at a ratio of 1.4:1. Primary cardiac rhabdomyosarcoma always involves the myocardium, and may display intracardiac or extra-cardiac extension. The tumor is bulky, invasive tumors that may exceed 10 cm in the greatest diameter [80]. Rhabdomyosarcoma cannot be distinguished from other cardiac tumors by means of the usual CT imaging; indeed, the radiological appearance is often misinterpreted as cardiac myxoma. In soft tissue tumor pathology, Rhabdomyosarcoma is classically divided into three major subtypes: embryonal (including botroid and spindle cell variants), alveolar (including a solid variant), and pleomorphic. The majority is of the embryonal type and may be well differentiated with numerous tadpole-shaped rhabdomyoblasts [152]. Prognostically spindle cell rhabdomyosarcoma in children have a better outcome when compared with the other classic forms of rhabdomyosarcoma, however, in adults from the available data, the prognosis is worse, but not as bad as that with pleomorphic rhabdomyosarcoma. Recurrences and systemic (lung and bones) metastases, with death intervening within a short period (less than 2–3 years), are well on record [152].

29.4.8 Osteosarcoma

Primary cardiac osteosarcoma is extremely rare. Pathologically, there is a debate as to whether this type of tumor should be classified as extraskeletal osteosarcoma or undifferentiated pleomorphic sarcoma with osteosarcomatous differentiation. Therefore, this tumor is not listed in the previous WHO classifications of cardiac tumors. In the fourth edition of WHO classification released in 2015, it is added as a sole tumor type with an ICD-O code of 9180/3 [153]. Until now, only about a dozen cases of isolated primary cardiac osteosarcoma could be retrieved.

The mean age at presentation is 44 years ranging from 14 to 77 years without sex predominance. The most common presentation is congestive heart failure related symptoms. Central nervous system symptoms, for example, syncope, headache, dizziness, and hemiparesis, are also reported [154].

Primary cardiac osteosarcoma predominantly involves the left atrium (77%). Right heart osteosarcomas are documented in about 20% cases. The tumor often occupies two or more cardiac cavities, diffusely involving the surrounding structures with a broad-base. Sometimes, the tumor is attached the myocardium with a stalk.

Grossly, the tumor mass may appear multidistributed, multilobular, fungating or rounded. The external surface may be either smooth or rough. Gross invasion of the surrounding structures is often evident. The cut section is often yellowish-grey and firm in consistency, and it is fresh and hemorrhagic when tumor necrosis occurred. In some cases, cystic changes and hemorrhage are observed. All of the three common subtypes of conventional osteosarcoma that arise in the bone (osteoblastic, chondroblastic, and fibroblastic type) are reported in the heart (Fig. 29.17) [154].

In most cases, the tumor is usually hardly removed completely due to the extensive infiltration. Despite aggressive surgery and chemotherapy, the prognosis of the tumor is still very poor. Postoperative recurrence and distant metastasis are almost inescapable. Brain and bone are two of the most common metastatic sites. Based on the available data, the 5-year overall survival and disease-free survival is 33.5 and 6.3%, respectively. The median overall survival of the patients diagnosed antemortem is approximately 20 months. On univariate analysis, the clinical parameters of sex, tumor size, and adjunctive chemo/radiotherapy are significant variables [154].

29.4.9 Lymphoma

Primary cardiac lymphoma occurs with far lower frequency than cardiac involvement of disseminated lymphoma. The incidence of primary cardiac lymphoma is about 0.05% [155]. There are more than 300 cases described in PubMed database by far. The male-to-female ratio is 2:1, with

a median age of 63 years. Previous studies demonstrated that the tumor is related to HIV infection. Dyspnea is the most common presenting symptom. Constitutional complaints and chest pain are the next two most common symptoms.

Primary cardiac lymphoma favors the right side of the heart, of which 92% have either the right-side involvement. The reason for this phenomenon remains unclear. A possible explanation might be that the right heart would more readily and frequently be exposed to any preexisting nodal lymphoma [156]. The most common subtype is diffuse large B cell lymphoma, accounting for more than 80% (Fig. 29.18). Other documented subtypes include Burkitte lymphoma, small lymphocytic lymphoma, T-cell lymphoma, and plasmablastic lymphoma.

The median overall survival of those diagnosed antemortem is approximately 12 months. The prognosis of primary cardiac lymphoma is relatively good after chemotherapy. No effect of surgery, radiation, and histology on overall survival is found.

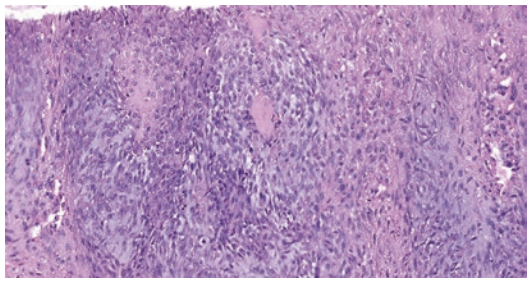

Fig. 29.17 Histopathologic features of primary cardiac osteosarcoma. Atypical spindle cells and osteoid structures were observed

Acknowledgement This work was supported by the grants from the Postdoctoral Applied Research Fundation of Qingdao City and "Clinical Medicine + X" Project of Qingdao University (No. 2017Q12 and 2017238).

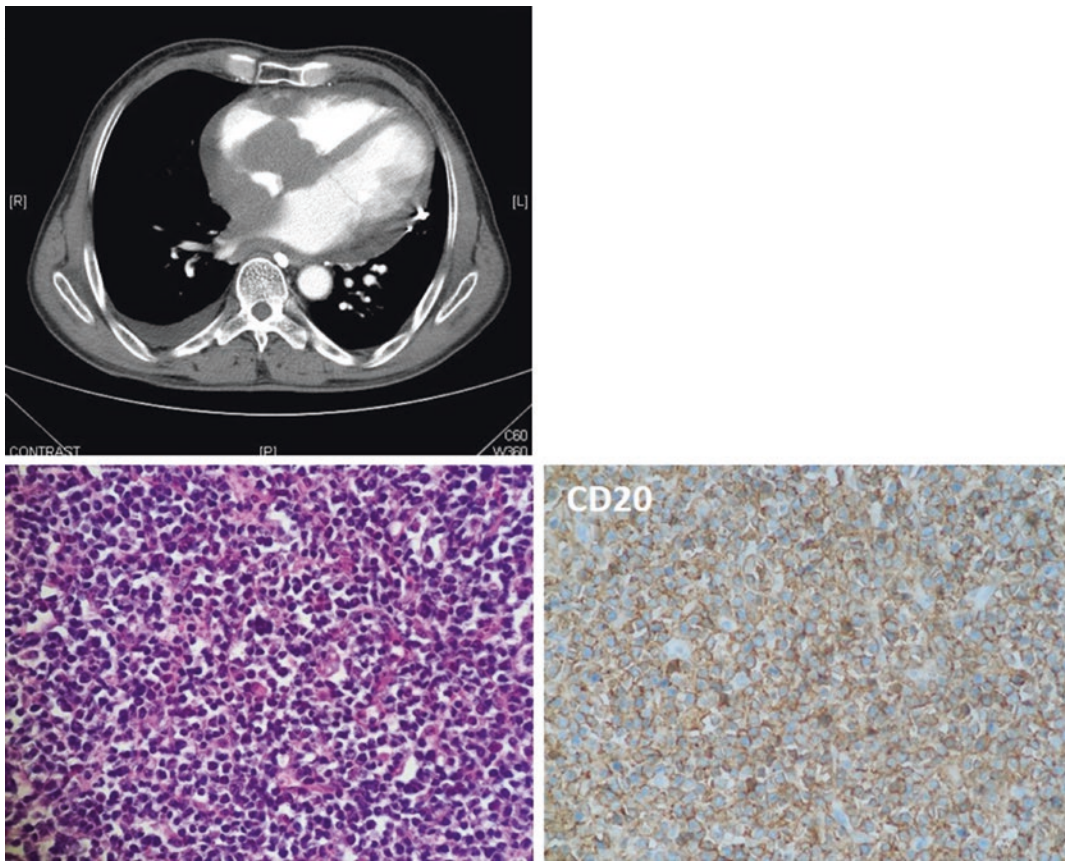

Fig. 29.18 Primary right atrial cardiac lymphoma (diffuse large B cell lymphoma). Primary cardiac lymphomas usually arise from right atrium and diffusedly invade the adjacent myocardium with a smooth surface. The most common pathologic subtype is diffuse large B cell lymphoma. CD20 is diffusely expressed in diffuse large B cell lymphoma

References

1. Reynen K. Frequency of primary tumors of the heart. Am J Cardiol. 1996;77(1):107.
2. Wang JG, Liu H, Yu WJ, Li YJ, Xin FJ. Primary cardiac neoplasms: a clinicopathologic analysis of 81 cases. Zhonghua Bing Li Xue Za Zhi. 2012;41(12):808–12. https://doi.org/10.3760/cma.j.issn.0529-5807.2012.12.004.
3. Strecker T, Rosch J, Weyand M, Agaimy A. Primary and metastatic cardiac tumors: imaging characteristics, surgical treatment, and histopathological spectrum: a 10-year-experience at a German heart center. Cardiovasc Pathol. 2012;21(5):436–43. https://doi.org/10.1016/j.carpath.2011.12.004.
4. Delmo Walter EM, Javier MF, Sander F, Hartmann B, Ekkernkamp A, Hetzer R. Primary cardiac tumors in infants and children: surgical strategy and long-term outcome. Ann Thorac Surg. 2016;102(6):2062–9. https://doi.org/10.1016/j.athoracsur.2016.04.057.
5. Ying L, Lin R, Gao Z, Qi J, Zhang Z, Gu W. Primary cardiac tumors in children: a center's experience. J Cardiothorac Surg. 2016;11(1):52. https://doi.org/10.1186/s13019-016-0448-5.
6. Tazelaar HD, Maleszewski JJ. Tumors of the heart and pericardium. In: Fletcher CDM, editor. Diagnostic histopathology of tumors. 4th ed. Philadelphia: Churchill Livingstone; 2013. p. 6–41.
7. Randhawa JS, Budd GT, Randhawa M, Ahluwalia M, Jia X, Daw H, Spiro T, Haddad A. Primary cardiac sarcoma: 25-year cleveland clinic experience. Am J Clin Oncol. 2016;39(6):593–9. https://doi.org/10.1097/coc.0000000000000106.
8. Hoffmeier A, Schmid C, Deiters S, Drees G, Rothenburger M, Tjan TD, Schmidt C, Loher A, Maintz D, Spieker T, Mesters RM, Scheld HH. Neoplastic heart disease -- the muenster experience with 108 patients. Thorac Cardiovasc Surg. 2005;53(1):1–8. https://doi.org/10.1055/s-2004-830389.
9. Yu K, Liu Y, Wang H, Hu S, Long C. Epidemiological and pathological characteristics of cardiac tumors: a clinical study of 242 cases. Interact Cardiovasc Thorac Surg. 2007;6(5):636–9. https://doi.org/10.1510/icvts.2007.156554.
10. Wang JG, Wang B, Hu Y, Liu JH, Liu B, Liu H, Zhao P, Zhang L, Li YJ. Clinicopathologic features and outcomes of primary cardiac tumors: a 16-year-experience with 212 patients at a Chinese medical center. Cardiovasc Pathol. 2018;33:45–54. https://doi.org/10.1016/j.carpath.2018.01.003
11. Wang JG, Li YJ, Liu H, Li NN, Zhao J, Xing XM. Clinicopathologic analysis of cardiac myxomas: seven years' experience with 61 patients. J Thorac Dis. 2012;4(3):272–83. https://doi.org/10.3978/j.issn.2072-1439.2012.05.07.
12. Barreiro M, Renilla A, Jimenez JM, Martin M, Al Musa T, Garcia L, Barriales V. Primary cardiac tumors: 32 years of experience from a Spanish tertiary surgical center. Cardiovasc Pathol. 2013;22(6):424–7. https://doi.org/10.1016/j.carpath.2013.04.006.
13. Habertheuer A, Laufer G, Wiedemann D, Andreas M, Ehrlich M, Rath C, Kocher A. Primary cardiac tumors on the verge of oblivion: a European experience over 15 years. J Cardiothorac Surg. 2015;10:56. https://doi.org/10.1186/s13019-015-0255-4.
14. Isogai T, Yasunaga H, Matsui H, Tanaka H, Hisagi M, Fushimi K. Factors affecting in-hospital mortality and likelihood of undergoing surgical resection in patients with primary cardiac tumors. J Cardiol. 2017;69(1):287–92. https://doi.org/10.1016/j.jjcc.2016.05.008.
15. Elbardissi AW, Dearani JA, Daly RC, Mullany CJ, Orszulak TA, Puga FJ, Schaff HV. Survival after resection of primary cardiac tumors: a 48-year experience. Circulation. 2008;118(14 Suppl):S7–15. https://doi.org/10.1161/circulationaha.107.783126.
16. Barnes H, Conaglen P, Russell P, Newcomb A. Clinicopathological and surgical experience with primary cardiac tumors. Asian Cardiovasc Thorac Ann. 2014;22(9):1054–8. https://doi.org/10.1177/0218492314528922.
17. Aval ZA, Ghaderi H, Tatari H, Foroughi M, Mirjafari SA, Forozeshfard M, Fani K, Khaheshi I. Surgical treatment of primary intracardiac myxoma: 20-year experience in "Shahid Modarres Hospital"--a tertiary university hospital--Tehran, Iran. TheScientificWorldJOURNAL. 2015;2015:303629. https://doi.org/10.1155/2015/303629.
18. Baikoussis NG, Papakonstantinou NA, Dedeilias P, Argiriou M, Apostolakis E, Koletsis E, Dougenis D, Charitos C. Cardiac tumors: a retrospective multicenter institutional study. J BUON. 2015;20(4):1115–23.
19. Cresti A, Chiavarelli M, Glauber M, Tanganelli P, Scalese M, Cesareo F, Guerrini F, Capati E, Focardi M, Severi S. Incidence rate of primary cardiac tumors: a 14-year population study. J Cardiovasc Med (Hagerstown). 2016;17(1):37–43. https://doi.org/10.2459/jcm.0000000000000059.
20. Lie JT. The identity and histogenesis of cardiac myxomas. A controversy put to rest. Arch Pathol Lab Med. 1989;113(7):724–6.
21. Burke AP, Virmani R. Cardiac myxoma. A clinicopathologic study. Am J Clin Pathol. 1993;100(6):671–80.
22. Bjessmo S, Ivert T. Cardiac myxoma: 40 years' experience in 63 patients. Ann Thorac Surg. 1997;63(3):697–700.
23. Pinede L, Duhaut P, Loire R. Clinical presentation of left atrial cardiac myxoma. A series of 112 consecutive cases. Medicine. 2001;80(3):159–72.
24. Gabe ED, Rodriguez Correa C, Vigliano C, San Martino J, Wisner JN, Gonzalez P, Boughen RP, Torino A, Suarez LD. Cardiac myxoma. Clinical-pathological correlation. Revista espanola de cardiologia. 2002;55(5):505–13.
25. Reynen K. Cardiac myxomas. N Engl J Med. 1995;333(24):1610–7. https://doi.org/10.1056/nejm199512143332407.
26. Acebo E, Val-Bernal JF, Gomez-Roman JJ, Revuelta JM. Clinicopathologic study and DNA analysis of

37 cardiac myxomas: a 28-year experience. Chest. 2003;123(5):1379–85.
27. Kanda T, Umeyama S, Sasaki A, Nakazato Y, Morishita Y, Imai S, Suzuki T, Murata K. Interleukin-6 and cardiac myxoma. Am J Cardiol. 1994;74(9):965–7.
28. Mochizuki Y, Okamura Y, Iida H, Mori H, Shimada K. Interleukin-6 and "complex" cardiac myxoma. Ann Thorac Surg. 1998;66(3):931–3.
29. Shiraishi I, Yamagishi M, Kato R, Okumura Y, Sato H, Tanaka T, Hamaoka K. A case in a child of giant left-atrial myxoma associated with recurrent high fever and myxoma cells expressing interleukin-6. Eur J Pediatr. 2006;165(5):346–7. https://doi.org/10.1007/s00431-005-0061-4.
30. Morishima A, Marui A, Shimamoto T, Saji Y, Nishina T, Komeda M. A case of interleukin-6-producing cardiac myxoma resembling multicentric Castleman's disease. J Thorac Cardiovasc Surg. 2009;138(2):499–501. https://doi.org/10.1016/j.jtcvs.2008.05.048.
31. Soeparwata R, Poeml P, Schmid C, Neuhof H, Scheld HH. Interleukin-6 plasma levels and tumor size in cardiac myxoma. J Thorac Cardiovasc Surg. 1996;112(6):1675–7. https://doi.org/10.1016/s0022-5223(96)70031-4.
32. Mendoza CE, Rosado MF, Bernal L. The role of interleukin-6 in cases of cardiac myxoma. Clinical features, immunologic abnormalities, and a possible role in recurrence. Tex Heart Inst J. 2001;28(1):3–7.
33. Jain D, Maleszewski JJ. Cardiac myxoma. In: Travis WD, Brambilla E, Burke AP, Marx A, Nicholson AG, editors. WHO classification of tumours of the lung, pleura, thymus and heart. 4th ed. Lyon: IARC; 2015. p. 311–4.
34. Tasoglu I, Tutun U, Lafci G, Hijaazi A, Yener U, Yalcinkaya A, Ulus T, Aksoyek A, Saritas A, Birincioglu L, Pac M, Katircioglu F. Primary cardiac myxomas: clinical experience and surgical results in 67 patients. J Card Surg. 2009;24(3):256–9. https://doi.org/10.1111/j.1540-8191.2008.00797.x.
35. Yin L, He D, Shen H, Ling X, Li W, Xue Q, Wang Z. Surgical treatment of cardiac tumors: a 5-year experience from a single cardiac center. J Thorac Dis. 2016;8(5):911–9. https://doi.org/10.21037/jtd.2016.03.87.
36. Gopal AS, Arora NS, Messineo FC. Right ventricular myxoma. N Engl J Med. 2000;342(4):295. https://doi.org/10.1056/nejm200001273420418.
37. Kern JH, Aguilera FA, Carlson DL, Galantowicz M. Right ventricular myxoma obstructing the right ventricular outflow tract. Circulation. 2000;102(2):E14–5.
38. Karagounis A, Sarsam M. Myxoma of the free wall of the right ventricle: a case report. J Card Surg. 2005;20(1):73–6. https://doi.org/10.1111/j.0886-0440.2005.05006.x.
39. Vadivelmurugan S, Senthamarai, Sakthimohan, Janarthanan, Balanayagam, Anand V, Venkateswaran KJ, Ramkumar, Selvaraj. Right ventricular myxoma. J Assoc Physicians India. 2015;63(10):79–80.
40. Gribaa R, Slim M, Kortas C, Kacem S, Ben Salem H, Ouali S, Neffati E, Remadi F, Boughzela E. Right ventricular myxoma obstructing the right ventricular outflow tract: a case report. J Med Case Rep. 2014;8:435. https://doi.org/10.1186/1752-1947-8-435.
41. Sardar MR, Lahoti A, Khaji A, Saeed W, Maqsood K, Zegel HG, Romanelli JE, McGeehin FC. Recurrent right ventricular cardiac myxoma in a patient with carney complex: a case report. J Med Case Rep. 2014;8:134. https://doi.org/10.1186/1752-1947-8-134.
42. Cho SH, Shim MS, Kim WS. The right ventricular myxoma which attached to the tricuspid valve: sliding tricuspid valvuloplasty. Korean J Thorac Cardiovasc Surg. 2015;48(3):228–30. https://doi.org/10.5090/kjtcs.2015.48.3.228.
43. Rao PA, Nagendra Prakash SN, Vasudev S, Girish M, Srinivas A, Guru Prasad HP, Jayakumar P, Anandaswamy VG. A rare case of right ventricular myxoma causing recurrent stroke. Indian Heart J. 2016;68(Suppl 2):S97–s101. https://doi.org/10.1016/j.ihj.2016.05.001.
44. Hajsadeghi S, Pazoki M, Moradians V, Iranpour A, Jebeli M, Babaheidarian P. Right ventricular myxoma originating from a papillary muscle: a case report. Echocardiography. 2016;33(12):1913–5. https://doi.org/10.1111/echo.13373.
45. Moiyadi AV, Moiyadi AA, Sampath S, Kalpana SR, Mahadevan A, Shankar SK, Srikanth SG. Intracranial metastasis from a glandular variant of atrial myxoma. Acta Neurochir. 2007;149(11):1157–62. https://doi.org/10.1007/s00701-007-1291-1.
46. Toufan M, Jodati A, Safaei N, Kazemi B, Pourafkari L. Myxomas in all cardiac chambers. Echocardiography. 2012;29(10):E270–2. https://doi.org/10.1111/j.1540-8175.2012.01803.x.
47. Satish OS, Aditya MS, Rao MA, Mishra RC. Sporadic cardiac myxoma involving all the cardiac chambers. Circulation. 2013;127(4):e360–1. https://doi.org/10.1161/circulationaha.112.105528.
48. Jara-Palomares L, Serrano-Gotarredona MP, Lopez-Haldon J, Rodriguez-Puras MJ, Bibiloni-Lage I, Ruiz-Solano E, Otero-Candelera R. Right atrium mass in a 28-year-old patient with pulmonary embolism taking contraceptives. J Atheroscler Thromb. 2011;18(9):829–32.
49. Cheema U, Thomas J. A giant right atrial myxoma presenting as acute pulmonary emboli. Eur Heart J Cardiovasc Imaging. 2012;13(9):799. https://doi.org/10.1093/ehjci/jes080.
50. Subban V, Lakshmanan A, Sethurathinam R, Ajit MS. Right atrial myxoma--an unusual cause of pulmonary embolism. J Card Surg. 2012;27(5):604. https://doi.org/10.1111/j.1540-8191.2011.01414.x.
51. Jung J, Hong YS, Lee CJ, Lim SH, Choi H, Lee S. Successful surgical treatment of a right atrial myxoma complicated by pulmonary embolism.

Korean J Thorac Cardiovasc Surg. 2013;46(1):63–7. https://doi.org/10.5090/kjtcs.2013.46.1.63.
52. Liu Q, Zuo C, Lv T, Cui B. Pulmonary embolism caused by right atrial myxoma on FDG PET/CT. Clin Nucl Med. 2013;38(11):928–30. https://doi.org/10.1097/rlu.0000000000000226.
53. Gu S, Liu Y, Yan J, Zhang X, Gao J, Xin Y, Su P. Surgical treatment of right atrial myxoma and pulmonary embolism. Chin Med J. 2014;127(1):187–8.
54. Sivakumar K, Singhi A, Mohanraj A, Ezhilan J. Tumor embolism from a right atrial myxoma leads to acute right heart failure after surgery and atrial septal patch dehiscence. J Am Coll Cardiol. 2014;63(23):2579. https://doi.org/10.1016/j.jacc.2014.02.608.
55. Pucci A, Gagliardotto P, Zanini C, Pansini S, di Summa M, Mollo F. Histopathologic and clinical characterization of cardiac myxoma: review of 53 cases from a single institution. Am Heart J. 2000;140(1):134–8. https://doi.org/10.1067/mhj.2000.107176.
56. Terracciano LM, Mhawech P, Suess K, D'Armiento M, Lehmann FS, Jundt G, Moch H, Sauter G, Mihatsch MJ. Calretinin as a marker for cardiac myxoma. Diagnostic and histogenetic considerations. Am J Clin Pathol. 2000;114(5):754–9. https://doi.org/10.1309/nr6g-t872-f090-lbrw.
57. Acebo E, Val-Bernal JF, Gomez-Roman JJ. Thrombomodulin, calretinin and c-kit (CD117) expression in cardiac myxoma. Histol Histopathol. 2001;16(4):1031–6.
58. Uppin SG, Jambhekar N, Puri A, Kumar R, Agarwal M, Sanghvi D. Bone metastasis of glandular cardiac myxoma mimicking a metastatic carcinoma. Skelet Radiol. 2011;40(1):107–11. https://doi.org/10.1007/s00256-010-0966-5.
59. Shimono T, Makino S, Kanamori Y, Kinoshita T, Yada I. Left atrial myxomas. Using gross anatomic tumor types to determine clinical features and coronary angiographic findings. Chest. 1995;107(3):674–9.
60. Altundag MB, Ertas G, Ucer AR, Durmus S, Abanuz H, Calikoglu T, Ozbagi K, Demirkasimoglu A, Kaya B, Bakkal BH, Altundag K. Brain metastasis of cardiac myxoma: case report and review of the literature. J Neuro-Oncol. 2005;75(2):181–4. https://doi.org/10.1007/s11060-005-1859-7.
61. Rodrigues D, Matthews N, Scoones D, Aziz F, Nath F. Recurrent cerebral metastasis from a cardiac myxoma: case report and review of literature. Br J Neurosurg. 2006;20(5):318–20. https://doi.org/10.1080/02688690601000394.
62. Castano-Leon AM, Hernandez-Lain A, Maronas L, Lopez P, Ayuso LL, Ramos A, Perez-Regadera J, Roldan LJ. Pathology-confirmed cerebral arterial invasion and recurrent multiple brain metastasis from cardiac myxoma without evidence of disease after surgery and radiotherapy. Clin Neuropathol. 2016;35(2):84–8. https://doi.org/10.5414/np300900.
63. Badrisyah I, Saiful R, Rahmat H, Naik VR, Tan YC. Brain metastasis of atrial myxoma: case report. Med J Malaysia. 2012;67(6):613–5.
64. Chao AS, Chao A, Wang TH, Chang YC, Chang YL, Hsieh CC, Lien R, Su WJ. Outcome of antenatally diagnosed cardiac rhabdomyoma: case series and a meta-analysis. Ultrasound Obstet Gynecol. 2008;31(3):289–95. https://doi.org/10.1002/uog.5264.
65. Basso C. Rhabdomyoma. In: Travis WD, Brambilla E, Burke AP, Marx A, Nicholson AG, editors. WHO classification of tumours of the lung, pleura, thymus and heart. 4th ed. Lyon: IARC; 2015.
66. Groves AM, Fagg NL, Cook AC, Allan LD. Cardiac tumours in intrauterine life. Arch Dis Child. 1992;67(10 Spec):1189–92.
67. Neri M, Di Donato S, Maglietta R, Pomara C, Riezzo I, Turillazzi E, Fineschi V. Sudden death as presenting symptom caused by cardiac primary multicentric left ventricle rhabdomyoma, in an 11-month-old baby. An immunohistochemical study. Diagn Pathol. 2012;7:169. https://doi.org/10.1186/1746-1596-7-169.
68. De Rosa G, De Carolis MP, Pardeo M, Bersani I, Tempera A, De Nisco A, Caforio L, Romagnoli C, Piastra M. Neonatal emergencies associated with cardiac rhabdomyomas: an 8-year experience. Fetal Diagn Ther. 2011;29(2):169–77. https://doi.org/10.1159/000320483.
69. Hoshal SG, Samuel BP, Schneider JR, Mammen L, Vettukattil JJ. Regression of massive cardiac rhabdomyoma on everolimus therapy. Pediatr Int. 2016;58(5):397–9. https://doi.org/10.1111/ped.12816.
70. Dogan V, Yesil S, Kayali S, Beken S, Ozgur S, Ertugrul I, Bozkurt C, Orun UA, Karademir S. Regression of symptomatic multiple cardiac rhabdomyomas associated with tuberous sclerosis complex in a newborn receiving everolimus. J Trop Pediatr. 2015;61(1):74–7. https://doi.org/10.1093/tropej/fmu056.
71. Wu SS, Collins MH, de Chadarevian JP. Study of the regression process in cardiac rhabdomyomas. Pediatr Dev Pathol. 2002;5(1):29–36.
72. Sheppard M. Cardiac tumours. In: Sheppard M, editor. Practical cardiovascular pathology. 2nd ed. London: CRC Press; 2011.
73. Li W, Teng P, Xu H, Ma L, Ni Y. Cardiac hemangioma: a comprehensive analysis of 200 cases. Ann Thorac Surg. 2015;99(6):2246–52. https://doi.org/10.1016/j.athoracsur.2015.02.064.
74. Montpreville VT, Maleszewski JJ. Haemangioma. In: Travis WD, Brambilla E, Burke AP, Marx A, Nicholson AG, editors. WHO classification of tumours of the lung, pleura, thymus and heart. 4th ed. Lyon: IARC; 2015. p. 318.
75. Patel J, Sheppard MN. Sudden death owing to right atrial hemangioma. J Forensic Sci. 2011;56(2):529–30. https://doi.org/10.1111/j.1556-4029.2010.01667.x.

76. Krous HF, Chapman AJ, Altshuler G. Cardiac hemangioma: a rare (or possible) cause of sudden death in children. J Forensic Sci. 1978;23(2):375–8.
77. Cina SJ, Smialek JE, Burke AP, Virmani R, Hutchins GM. Primary cardiac tumors causing sudden death: a review of the literature. Am J Forensic Med Pathol. 1996;17(4):271–81.
78. Zerbo S, Argo A, Maresi E, Liotta R, Procaccianti P. Sudden death in adolescence caused by cardiac haemangioma. J Forensic Legal Med. 2009;16(3):156–8. https://doi.org/10.1016/j.jflm.2008.08.020.
79. Rassl DM, Davies SJ. Cardiac tumors. In: Suvarna SK, editor. Cardiac pathology: a guide to current practice. London: Springer; 2013. p. 201–21.
80. Ladich E, Virmani R. Tumors of the cardiovascular system: heart and blood vessels. In: Buja LM, Butany J, editors. Cardiovascular pathology. 4th ed. London: Academic Press; 2016. p. 735–72.
81. Shibuya K, Burke AP. Cardiac fibroma. In: Travis WD, Brambilla E, Burke AP, Marx A, Nicholson AG, editors. WHO classification of tumours of the lung, pleura, thymus and heart. 4th ed. Lyon: IARC; 2015. p. 320–1.
82. Scanlan D, Radio SJ, Nelson M, Zhou M, Streblow R, Prasad V, Reyes C, Perry D, Fletcher S, Bridge JA. Loss of the PTCH1 gene locus in cardiac fibroma. Cardiovasc Pathol. 2008;17(2):93–7. https://doi.org/10.1016/j.carpath.2007.08.001.
83. Yan AT, Coffey DM, Li Y, Chan WS, Shayne AJ, Luu TM, Skorstad RB, Khin MM, Brown KA, Lipton MJ, Kwong RY. Images in cardiovascular medicine. Myocardial fibroma in gorlin syndrome by cardiac magnetic resonance imaging. Circulation. 2006;114(10):e376–9. https://doi.org/10.1161/circulationaha.105.605832.
84. Jha NK, Kiraly L, Tamas C, Talo H, Khan MD, El Badaoui H, Jain A, Hammad A. Large cardiac fibroma and teratoma in children- case reports. J Cardiothorac Surg. 2015;10:38. https://doi.org/10.1186/s13019-015-0242-9.
85. Cronin B, Lynch MJ, Parsons S. Cardiac fibroma presenting as sudden unexpected death in an adolescent. Forensic Sci Med Pathol. 2014;10(4):647–50. https://doi.org/10.1007/s12024-014-9582-3.
86. Mecchia D, Lavezzi AM, Matturri L. Primary cardiac fibroma and cardiac conduction system alterations in a case of sudden death of a 4-month-old infant. Open Cardiovasc Med J. 2013;7:47–9. https://doi.org/10.2174/1874192401307010047.
87. Gorlin RJ. Nevoid basal cell carcinoma (Gorlin) syndrome. Genet Med. 2004;6(6):530–9. https://doi.org/10.1097/01.gim.0000144188.15902.c4.
88. Parmley LF, Salley RK, Williams JP, Head GB. The clinical spectrum of cardiac fibroma with diagnostic and surgical considerations: noninvasive imaging enhances management. Ann Thorac Surg. 1988;45(4):455–65.
89. Maloszowski J, Agaimy A. Papillary fibroelastoma. In: Travis WD, Brambilla E, Burke AP, Marx A, Nicholson AG, editors. WHO classification of tumours of the lung, pleura, thymus and heart. 4th ed. Lyon: IARC; 2015. p. 315–7.
90. Rubin MA, Snell JA, Tazelaar HD, Lack EE, Austenfeld JL, Azumi N. Cardiac papillary fibroelastoma: an immunohistochemical investigation and unusual clinical manifestations. Mod Pathol. 1995;8(4):402–7.
91. Ownbey RT. Invading papillary fibroelastoma. J Thorac Cardiovasc Surg. 2006;132(6):1256. https://doi.org/10.1016/j.jtcvs.2006.08.040.
92. Kumar TK, Kuehl K, Reyes C, Talwar S, Moulick A, Jonas RA. Multiple papillary fibroelastomas of the heart. Ann Thorac Surg. 2009;88(6):e66–7. https://doi.org/10.1016/j.athoracsur.2009.08.005.
93. Darvishian F, Farmer P. Papillary fibroelastoma of the heart: report of two cases and review of the literature. Ann Clin Lab Sci. 2001;31(3):291–6.
94. Somers GR, Smith CR, Perrin DG, Wilson GJ, Taylor GP. Sudden unexpected death in infancy and childhood due to undiagnosed neoplasia: an autopsy study. Am J Forensic Med Pathol. 2006;27(1):64–9. https://doi.org/10.1097/01.paf.0000203267.91806.ed.
95. Erdogan M, Guney MC, Ayhan H, Kasapkara HA, Uguz E, Durmaz T, Keles T, Bozkurt E. An unusual presentation of papillary fibroelastoma originating from right ventricular outflow tract. Echocardiography. 2017;34(3):476–7. https://doi.org/10.1111/echo.13465.
96. Fayad G, Modine T, Le Tourneau T, Azzaoui R, Decoene C, Copin MC, Bauters C, Warembourg H. An unusual case of papillary fibroelastoma "invading" the mitral valve. J Thorac Cardiovasc Surg. 2006;132(6):1472–3. https://doi.org/10.1016/j.jtcvs.2006.06.045.
97. Bois MC, Bois JP, Anavekar NS, Oliveira AM, Maleszewski JJ. Benign lipomatous masses of the heart: a comprehensive series of 47 cases with cytogenetic evaluation. Hum Pathol. 2014;45(9):1859–65. https://doi.org/10.1016/j.humpath.2014.05.003.
98. Zhang J, Chong E, Chai P, Poh KK. Contrasting fatty involvement of the right ventricle: lipoma versus lipomatous hypertrophy. Singap Med J. 2009;50(10):e342–5.
99. Ismail I, Al-Khafaji K, Mutyala M, Aggarwal S, Cotter W, Hakim H, Khosla S, Arora R. Cardiac lipoma. J Community Hosp Intern Med Perspect. 2015;5(5):28449. https://doi.org/10.3402/jchimp.v5.28449.
100. D'Souza J, Shah R, Abbass A, Burt JR, Goud A, Dahagam C. Invasive cardiac lipoma: a case report and review of literature. BMC Cardiovasc Disord. 2017;17(1):28. https://doi.org/10.1186/s12872-016-0465-2.
101. Ceresa F, Calarco G, Franzi E, Patane F. Right atrial lipoma in patient with Cowden syndrome. Interact Cardiovasc Thorac Surg. 2010;11(6):803–4. https://doi.org/10.1510/icvts.2010.245001.
102. Smith MA. Multiple synchronous atrial lipomas. Cardiovasc Pathol. 2007;16(3):187–8. https://doi.org/10.1016/j.carpath.2006.10.002.
103. Wu S, Teng P, Zhou Y, Ni Y. A rare case report of giant epicardial lipoma compressing the right atrium with septal enhancement. J Cardiothorac Surg. 2015;10:150. https://doi.org/10.1186/s13019-015-0375-x.

104. Noly PE, Mongeon FP, Rochon A, Romeo P, Lamarche Y. Pericardial constriction caused by a giant lipoma. Circulation. 2016;133(17):1709–12. https://doi.org/10.1161/circulationaha.115.020318.
105. Wang H, Hu J, Sun X, Wang P, Du Z. An asymptomatic right atrial intramyocardial lipoma: a management dilemma. World J Surg Oncol. 2015;13:20. https://doi.org/10.1186/s12957-015-0441-9.
106. Hwang SK, Jung SH. Schwannoma of the heart. Korean J Thorac Cardiovasc Surg. 2014;47(2):141–4. https://doi.org/10.5090/kjtcs.2014.47.2.141.
107. Stolf NA, Santos GG, Sobral ML, Haddad VL. Primary schwannoma of the right atrium: successful surgical resection. Clinics. 2006;61(1):87–8. https://doi.org/10.1590/S1807-59322006000100016.
108. Anderson CD, Hashimi S, Brown T, Moyers J, Farivar RS. Primary benign interatrial schwannoma encountered during aortic valve replacement. J Card Surg. 2011;26(1):63–5. https://doi.org/10.1111/j.1540-8191.2010.01158.x.
109. Sirlak M, Uymaz OK, Tasoz R, Erden E, Ozyurda U, Akalin H. Primary benign schwannoma of the heart. Cardiovasc Pathol. 2003;12(5):290–2.
110. Son KH, Kim KW, Ahn CB, Choi CH, Park KY, Park CH, Lee JI, Jeon YB. Surgical planning by 3D printing for primary cardiac schwannoma resection. Yonsei Med J. 2015;56(6):1735–7. https://doi.org/10.3349/ymj.2015.56.6.1735.
111. Sevimli S, Erkut B, Becit N, Aksakal E, Polat P. Primary benign schwannoma of the left ventricle coursing under the left anterior descending artery. Echocardiography. 2007;24(10):1093–5. https://doi.org/10.1111/j.1540-8175.2007.00529.x.
112. La Francesca S, Gregoric ID, Cohn WE, Frazier OH. Successful resection of a primary left ventricular schwannoma. Ann Thorac Surg. 2007;83(5):1881–2. https://doi.org/10.1016/j.athoracsur.2006.12.012.
113. Miller AD, McDonough S. Interthalamic hematoma secondary to cerebrovascular atherosclerosis in an aged grizzly bear (Ursus Arctos Horribilis) with primary cardiac schwannoma. J Zoo Wildl Med. 2008;39(4):659–62. https://doi.org/10.1638/2007-0128.1.
114. Wang JG, Han J, Jiang T, Li YJ. Cardiac paragangliomas. J Card Surg. 2015;30(1):55–60. https://doi.org/10.1111/jocs.12455.
115. Khan MF, Datta S, Chisti MM, Movahed MR. Cardiac paraganglioma: clinical presentation, diagnostic approach and factors affecting short and long-term outcomes. Int J Cardiol. 2013;166(2):315–20. https://doi.org/10.1016/j.ijcard.2012.04.158.
116. Ramlawi B, David EA, Kim MP, Garcia-Morales LJ, Blackmon SH, Rice DC, Vaporciyan AA, Reardon MJ. Contemporary surgical management of cardiac paragangliomas. Ann Thorac Surg. 2012;93(6):1972–6. https://doi.org/10.1016/j.athoracsur.2012.02.040.
117. Yendamuri S, Elfar M, Walkes JC, Reardon MJ. Aortic paraganglioma requiring resection and replacement of the aortic root. Interact Cardiovasc Thorac Surg. 2007;6(6):830–1. https://doi.org/10.1510/icvts.2007.161737.
118. Miraldi F, Taffon C, Toscano M, Barretta A. Black cardiac paraganglioma in a multiple paraganglioma syndrome. Eur J Cardiothorac Surg. 2007;32(6):940–2. https://doi.org/10.1016/j.ejcts.2007.08.026.
119. Mikolaenko I, Galliani CA, Davis GG. Pigmented cardiac paraganglioma. Arch Pathol Lab Med. 2001;125(5):680–2. https://doi.org/10.1043/0003-9985(2001)125<0680:pcp>2.0.co;2.
120. Gonnella C, Messa FC, Confessore P, Greco C. Angiographic evidence of pigmented cardiac paraganglioma. J Cardiovasc Med. 2008;9(3):319. https://doi.org/10.2459/JCM.0b013e32801411d1.
121. Yamaguchi S, Hida K, Nakamura N, Seki T, Iisaki Y. Multiple vertebral metastases from malignant cardiac pheochromocytoma--case report. Neurol Med Chir. 2003;43(7):352–5.
122. Jirari A, Charpentier A, Popescu S, Boidin P, Eisenmann B. A malignant primary cardiac pheochromocytoma. Ann Thorac Surg. 1999;68(2):565–6.
123. Arai A, Naruse M, Naruse K, Tanabe A, Yoshimoto T, Iwama T, Kusakabe K, Obara T, Demura R, Demura H. Cardiac malignant pheochromocytoma with bone metastases. Intern Med. 1998;37(11):940–4.
124. Cruz PA, Mahidhara S, Ticzon A, Tobon H. Malignant cardiac paraganglioma: follow-up of a case. J Thorac Cardiovasc Surg. 1984;87(6):942–4.
125. Nonaka K, Makuuchi H, Naruse Y, Kobayashi T, Goto M. Surgical excision of malignant pheochromocytoma in the left atrium. Jpn J Thorac Cardiovasc Surg. 2000;48(2):126–8.
126. Mizia-Malarz A, Sobol-Milejska G, Buchwald J, Wos H. Inflammatory myofibroblastic tumor of the heart in the infant: review of the literature. J Pediatr Hematol Oncol. 2016;38(8):e298–302. https://doi.org/10.1097/mph.0000000000000558.
127. Li L, Burke A, He J, Chang L, Zielke HR, Fowler DR. Sudden unexpected death due to inflammatory myofibroblastic tumor of the heart: a case report and review of the literature. Int J Legal Med. 2011;125(1):81–5. https://doi.org/10.1007/s00414-010-0496-7.
128. Kelly SJ, Lambie NK, Singh HP. Inflammatory myofibroblastic tumor of the left ventricle in an older adult. Ann Thorac Surg. 2003;75(6):1971–3.
129. Pearson PJ, Smithson WA, Driscoll DJ, Banks PM, Ehman RL. Inoperable plasma cell granuloma of the heart: spontaneous decrease in size during an 11-month period. Mayo Clin Proc. 1988;63(10):1022–5.
130. Chou P, Gonzalez-Crussi F, Cole R, Reddy VB. Plasma cell granuloma of the heart. Cancer. 1988;62(7):1409–13.
131. Look Hong NJ, Pandalai PK, Hornick JL, Shekar PS, Harmon DC, Chen YL, Butrynski JE, Baldini EH, Raut CP. Cardiac angiosarcoma management and outcomes: 20-year single-institution experience. Ann Surg Oncol. 2012;19(8):2707–15. https://doi.org/10.1245/s10434-012-2334-2.

132. Dong Y, Zhu D, Dong L, Ren L. Primary cardiac angiosarcoma with pulmonary and lumbar metastases presenting as unexplained pericardial effusion in a 41 year-old man. Heart Lung Circ. 2014;23(5):e145–6. https://doi.org/10.1016/j.hlc.2014.01.008.
133. Ge Y, Ro JY, Kim D, Kim CH, Reardon MJ, Blackmon S, Zhai J, Coffey D, Benjamin RS, Ayala AG. Clinicopathologic and immunohistochemical characteristics of adult primary cardiac angiosarcomas: analysis of 10 cases. Ann Diagn Pathol. 2011;15(4):262–7. https://doi.org/10.1016/j.anndiagpath.2011.02.007.
134. Butany J, Yu W. Cardiac angiosarcoma: two cases and a review of the literature. Can J Cardiol. 2000;16(2):197–205.
135. Wang J, Jiang Y, Wang Y, Yu W, Zhao P, Li Y, Lin D, Xin F. Primary pleomorphic malignant fibrous histiocytoma of the heart. Acta Histochem. 2013;115(7):761–6. https://doi.org/10.1016/j.acthis.2013.02.001.
136. Reinecke P, Steckstor M, Schmitz M, Gabbert HE, Gerharz CD. Chemotherapeutic potential of plant alkaloids and multidrug resistance mechanisms in malignant fibrous histiocytoma of the heart. Oncol Rep. 2004;11(3):641–5.
137. Wang JG, Li YJ, Liu H, Zhao P. Primary cardiac myxofibrosarcoma: a case report and review of the literature. Tumori. 2012;98(6):165e–8e. https://doi.org/10.1700/1217.13514.
138. Gupta P, Jain M. Right-sided low grade myxofibrosarcoma of the heart in an adult. Asian Cardiovasc Thorac Ann. 2013;21(2):208–10. https://doi.org/10.1177/0218492312450291.
139. Shiga Y, Miura S, Nishikawa H, Sugihara H, Nakashima Y, Takamatsu Y, Koga K, Koga S, Katayama Y, Yoshida T, Iisaki H, Saku K. Very rare case of large obstructive myxofibrosarcoma of the right ventricle assessed with multi-diagnostic imaging techniques. Intern Med. 2014;53(7):739–42.
140. Pasquale M, Katz NM, Caruso AC, Bearb ME, Bitterman P. Myxoid variant of malignant fibrous histiocytoma of the heart. Am Heart J. 1991;122(1 Pt 1):248–50.
141. Yoo Sang Y, Cheol Joo L, Joon Kyu K, Hyung Tai K, Ho C, Kyi Beom L. Primary left atrial myxofibrosarcoma: a case report. Korean J Thorac Cardiovasc Surg. 2003;36(6):422–6.
142. Behi K, Ayadi M, Mezni E, Meddeb K, Mokrani A, Yahyaoui Y, Ksontini F, Rais H, Chrait N, Mezlini A. Two years survival of primary cardiac leiomyosarcoma managed by surgical and adjuvant therapy. Clin Sarcoma Res. 2017;7:5. https://doi.org/10.1186/s13569-017-0069-3.
143. Muthukumar L, Jan MF, Taylor R, Crouch J, Neitzel G, Tajik AJ. Biatrial high-grade leiomyosarcoma with nine-year post-surgical survival. Ann Thorac Surg. 2017;103(1):e43–5. https://doi.org/10.1016/j.athoracsur.2016.06.063.
144. Wang JG, Cui L, Jiang T, Li YJ, Wei ZM. Primary cardiac leiomyosarcoma: an analysis of clinical characteristics and outcome patterns. Asian Cardiovasc Thorac Ann. 2015;23(5):623–30. https://doi.org/10.1177/0218492315574197.
145. Wang JG, Li NN. Primary cardiac synovial sarcoma. Ann Thorac Surg. 2013;95(6):2202–9. https://doi.org/10.1016/j.athoracsur.2013.01.030.
146. Goldblatt J, Saxena P, McGiffin DC, Zimmet A. Pericardial synovial sarcoma: a rare clinical entity. J Card Surg. 2015;30(11):801–4. https://doi.org/10.1111/jocs.12609.
147. Zanini G, Gorga E, Pasini F, Salemme M, Petrilli G, Bercich L, Lorusso R, Pasini GF. Seaweed floating in the pericardium: a rare case of primary dedifferentiated liposarcoma. Cardiovasc Pathol. 2016;25(4):333–5. https://doi.org/10.1016/j.carpath.2015.10.003.
148. Papavdi A, Agapitos E. Undiagnosed primary cardiac liposarcoma in an adult: a case report and review of the literature. Am J Forensic Med Pathol. 2013;34(4):299–301. https://doi.org/10.1097/PAF.0b013e31828cff50.
149. Sandoval E, Quintana E, Ninot S, Castella M. Myxoid liposarcoma: an unusual primary cardiac tumour. Eur J Cardiothorac Surg. 2012;42(2):379. https://doi.org/10.1093/ejcts/ezs054.
150. Wang JG, Wei ZM, Liu H, Li YJ. Primary pleomorphic liposarcoma of pericardium. Interact Cardiovasc Thorac Surg. 2010;11(3):325–7. https://doi.org/10.1510/icvts.2010.239723.
151. Skopin II, Serov RA, Makushin AA, Sazonenkov MA. Primary rhabdomyosarcoma of the right atrium. Interact Cardiovasc Thorac Surg. 2003;2(3):316–8. https://doi.org/10.1016/s1569-9293(03)00059-8.
152. Fraternali Orcioni G, Ravetti JL, Gaggero G, Bocca B, Bisceglia M. Primary embryonal spindle cell cardiac rhabdomyosarcoma: case report. Pathol Res Pract. 2010;206(5):325–30. https://doi.org/10.1016/j.prp.2009.06.002.
153. Burke A, Tavora F. Osteosarcoma. In: Travis WD, Brambilla E, Burke AP, Marx A, Nicholson AG, editors. WHO classification of tumours of the lung, pleura, thymus and heart. 4th ed. Lyon: IARC; 2015. p. 333.
154. Wang JG, Liu B, Gao H, Li YJ, Zhao P, Liu XP. Primary cardiac osteosarcoma. Heart Lung Circ. 2016;25(7):698–704. https://doi.org/10.1016/j.hlc.2016.01.006
155. Lam KY, Dickens P, Chan AC. Tumors of the heart. A 20-year experience with a review of 12,485 consecutive autopsies. Arch Pathol Lab Med. 1993;117(10):1027–31.
156. Petrich A, Cho SI, Billett H. Primary cardiac lymphoma: an analysis of presentation, treatment, and outcome patterns. Cancer. 2011;117(3):581–9. https://doi.org/10.1002/cncr.25444.

Part II

Diagnostic

Clinical Signs and Electrocardiography

30

Elisabeta Bădilă

Abstract

Right ventricular failure is a complex clinical syndrome that can result from any structural or functional cardiovascular disorder that impairs the ability of the right ventricle to fill or to eject blood. The approach to the patient with known or suspected right heart pathology begins with a directed history and targeted physical examination, the scope of which depends on the clinical context at the time of presentation. These exams are augmented by a series of paraclinic tests that help to accurately establish etiology and classify severity. Symptoms of right heart disease are often due to the underlying disease and depend on the severity of the condition. In acute life threatening situations, i.e. acute pulmonary embolism or right ventricular myocardial infarction, the clinical presentation may be dominated by hemodynamic instability even progressing to cardiogenic shock. The clinical signs encountered in patients with chronic right heart pathology are initially due to the development of pulmonary hypertension; afterwards, they are completed by the development of right ventricular hypertrophy and a typical picture of right ventricular failure, dominated by systemic congestion.

The electrocardiogram is a standard part of the initial assessment of every patient with suspected right heart failure and also in previously diagnosed patients presented for a routine examination or for a new decompensation. Right ventricular hypertrophy, right axis deviation, and right bundle-branch block may suggest chronic right ventricular pressure overload. The sensitivity of the ECG for the diagnosis of pulmonary hypertension is poor, whereas the specificity of signs of right ventricular hypertrophy is high. Electrocardiographic changes do not correlate with disease severity or prognosis.

Keywords

Right ventricular failure · Right ventricular hypertrophy · Pulmonary hypertension Systemic congestion · Electrocardiography in right heart disease

30.1 Overview

Right heart pathology most frequently manifests as right ventricular failure (RVF). The two widely used terms of right versus left ventricle failure refer to the two clinical syndromes where pulmonary versus systemic congestion dominate. The

E. Bădilă
"Carol Davila" University of Medicine and Pharmacy, Bucharest, Romania

Internal Medicine Department, Clinical Emergency Hospital Bucharest, Bucharest, Romania

S. I. Dumitrescu et al. (eds.), *Right Heart Pathology*, https://doi.org/10.1007/978-3-319-73764-5_30

concept of congestive heart failure refers to global heart failure, comprising both systemic and pulmonary venous stasis (congestion). The term "cor pulmonale" is popular, however, currently, it has no consensual definition, and it seems more appropriate to define this condition by the presence of pulmonary hypertension (PH) resulting from diseases affecting the structure and/or the function of the lungs: PH results in right ventricular enlargement and may lead, with time, to right heart failure (RHF) [1].

Right heart failure can occur in the development of left sided heart failure, in this case leading to global heart failure, or can occur separately, as in the case of primary pulmonary hypertension, pericarditis, left to right shunt (atrial septal defect, ventricular septal defect, anomalous pulmonary venous return), Eisenmenger syndrome, pulmonary embolism, mitral stenosis, stenosis of the pulmonic valve or pulmonary artery. Other examples of right ventricular diseases include right ventricular myocardial infarction and various types of cardiomyopathy affecting the right ventricle. Chronic obstructive pulmonary disease (COPD) is the most common cause of cor pulmonale, while idiopathic pulmonary fibrosis and the obesity-hypoventilation syndrome are much less frequent etiologies [1].

Right ventricular (RV) failure is therefore a complex clinical syndrome that can result from any structural or functional cardiovascular disorder that impairs the ability of the RV to fill or to eject blood. The cardinal clinical manifestations of RV failure are: (a) fluid retention, which may lead to peripheral edema, ascites, and anasarca; (b) decreased systolic reserve or low cardiac output, which may lead to exercise intolerance and fatigue; or (c) atrial or ventricular arrhythmias. RV dysfunction, on the other hand, refers to abnormalities of filling or contraction without reference to signs or symptoms of heart failure (HF) [2].

History taking and the clinical examination still remain key diagnostic elements and are augmented by a series of paraclinic tests that help to accurately establish etiology and classify severity. In general, when addressing the clinical manifestations of the right heart pathology, we consider two distinct categories of patients: those with an acute presentation (pulmonary embolism, RV infarction, arrhythmogenic RV dysplasia), and those with chronic pulmonary arterial hypertension (PAH) who develop RV failure [3]. Chronic pulmonary hypertension develops over weeks to months, and leads to RV concentric hypertrophy, without inflammation, that may progress slowly to RV failure. In contrast, pulmonary embolism (PE) results in an abrupt vascular occlusion leading to increased pulmonary artery pressure within minutes to hours, which causes immediate deformation of the RV. Right ventricular injury is secondary to mechanical stretch, shear force, and ischemia that together provoke a cytokine and chemokine-mediated inflammatory phenotype that amplifies injury [4].

The approach to the patient with known or suspected right heart pathology begins with a directed history and targeted physical examination, the scope of which depends on the clinical context at the time of presentation. In those presenting for a routine check-up, a more detailed or thorough examination may be conducted, whilst in the case of patients presented at the emergency room, a more focused approach should be taken. When taking past medical history it is very important to inquire about the presence of coronary artery disease, emphysema/chronic bronchitis, history of deep venous thrombosis, recurrent abortions, autoimmune diseases, and infections.

Right ventricular failure shows signs and symptoms which are distinct from those seen in the case of left ventricular failure. Most patients may display clinical findings which easily clarify the diagnosis; however, the elderly may prove paucisymptomatic, showing only a typical manifestations such as asthenia, abdominal discomfort or obnubilation. Conversely, in those with typical findings, such as dyspnoea and oedema, the underlying etiology may prove to be lung disease, chronic venous insufficiency, or obesity, in the absence of significant cardiac disease.

30.2 Symptoms of Right Heart Disease

Symptoms of right heart disease are often due to the underlying disease and depend on the severity of the condition. Symptoms may be divided into

those that accompany right ventricular heart failure and the additional findings of biventricular failure.

Dyspnea, the subjective complaint of discomfort while breathing, develops later than in the case of left ventricular failure (LVF) and is rarely a dominant complaint. In lone right heart failure, which does not occur as a consequence of LVF, pulmonary congestion is absent and orthopnea is not noted. Dyspnea in right heart failure is the result of the following mechanisms: (a) decreased pulmonary function secondary to decreased compliance and increased airway resistance; (b) increased ventilatory drive secondary to hypoxemia due to increased pulmonary capillary wedge pressure (PCWP), ventilation/perfusion (V/Q) mismatching due to increased PCWP, and low cardiac output; (c) increased carbon dioxide production; (d) respiratory muscle dysfunction, with decreased respiratory muscle strength, decreased endurance, and ischemia [5]. When hydrothorax develops, dyspnea usually intensifies because of further reductions in vital capacity.

Pulmonary hypertension (whether primary or secondary) contributes to increased dyspnea by increasing pulmonary pressure during exercise, even leading to exercise intolerance. When cardiac output becomes markedly reduced in patients with terminal RHF (in the late stages of primary pulmonary hypertension and pulmonary thromboembolic disease), severe dyspnea at rest may occur.

Exertional chest pain or pressure (i.e., angina) may occur as a result of secondary right myocardial ischemia due to subendocardial hypoperfusion from increased filling pressure, poor cardiac output, or hypotension and hypoxemia. Even in the absence of significant obstructive atherosclerotic coronary disease, patients with chronic PAH are at risk for RV myocardial ischemia due to imbalances in myocardial supply and demand, reduced diastolic right coronary perfusion, increased wall stress, that can develop with perturbations in RV preload and afterload, precipitating even acute RV failure [3].

Individuals with chronic PAH poorly tolerate atherosclerotic coronary lesions. Chest pain can be occasionally caused by the dynamic compression of the left main coronary artery by an enlarged pulmonary artery; this risk is greatest for patients with a pulmonary artery trunk at least 40 mm in diameter [6, 7].

Palpitations can be secondary to sinus tachycardia due to hypoxemia, to decompensated heart failure, or more commonly, to tachyarrhythmias. Patients with chronic PAH are at risk for atrial and ventricular tachyarrhythmias, both being poorly tolerated and able to lead to rapid RV failure, clinical decompensation and hemodynamic instability.

There are several conditions which precipitate the occurrence of arrhythmias in patients with RV failure. Chronic PAH is commonly associated with tricuspid regurgitation and annular dilatation. As the right atrium dilates to accommodate the regurgitant volume, fibrosis ensues. Areas of macro or micro re-entry can subsequently develop, and the conditions for atrial flutter and fibrillation are thus created. Periods of increased atrial stretch (occurring with volume overload) and premature atrial contractions are enough to trigger re-entry in those patients who are susceptible [2]. Many studies have demonstrated that atrial flutter or atrial fibrillation is associated with an increased risk of morbidity or mortality in patients with pulmonary hypertension [8].

Metabolic disturbances, including hypoxia and acidosis, become a source for atrial and ventricular arrhythmias that arise from myocardial automaticity [3]. Atrial tachycardia and multifocal atrial tachycardia are two such arrhythmias commonly encountered in patients with chronic PAH and RV failure.

Ventricular tachycardia arising from the RV may occur in RV myocardial infarction, pulmonary arterial hypertension, coronary heart disease, arrhythmogenic RV dysplasia, and idiopathic RV outflow tract tachycardia [9].

Sinus node dysfunction and atrioventricular conduction blocks (in RV myocardial infarction, infiltrative disease, and myocarditis) may also contribute to exercise intolerance and hemodynamic instability in patients with RV dysfunction.

Exertional syncope is due to the inability to increase cardiac output during activity or reflex bradycardia that is secondary to mechanoreceptor activation in the right ventricle.

Sudden death in patients with RV disease often is caused by tachyarrhythmia or bradycardia. Less common non-arrhythmogenic etiologies of sudden death should also be considered, include massive pulmonary embolism, pulmonary haemorrhage, mechanical complications associated with RV myocardial infarction [2] or rare cases of dissection or rupture of the pulmonary artery [10].

In the modern era of PAH management, sudden cardiac death is still responsible for about 28% of deaths [9]. In contrast to patients with advanced left heart disease, malignant ventricular arrhythmias such as ventricular tachycardia and ventricular fibrillation are relatively rare in patients with PAH and RV pathology. In these patients, pulseless electrical activity is often heralded by bradycardia.

Gastrointestinal symptoms of right heart failure are caused by congestion of the hepatic and gastrointestinal venous circulation, and include anorexia, nausea, vomiting, weight loss, bloating, and constipation. Right upper quadrant abdominal pain, epigastric pain, and increased abdominal girth are also due to the systemic congestion. Constipation is a common complaint among patients with heart failure, and it can be a manifestation of decreased intestinal transit secondary to poor perfusion. In pre-terminal heart failure, inadequate bowel perfusion can cause abdominal pain, distention, and bloody stools.

Asthenia and fatigue are the expression of hypoxia and deconditioning of skeletal muscles, and can become severe, worsening with decreased cardiac output. Asthenia is worsening by hypovolaemia and implicitly by diuretic treatment.

Cardiac cachexia is found in longstanding right ventricle heart failure, because of anorexia from hepatic and intestinal congestion. Cachexia may lead to an extensive workup for malignant disease [11].

Neurologic symptoms may appear due to decreased cardiac output and hypoxemia.

Other symptoms are related to the pathology that caused right ventricular failure. Thus, pulmonary hypertension can cause more typical symptoms like exertional chest pain, exertional syncope, anorexia, abdominal pain, but also uncommon symptoms including cough, hemoptysis, and hoarseness may appear. The hoarseness (Ortner's syndrome) is caused by compression of the left recurrent laryngeal nerve by a dilated main pulmonary artery [12].

In the case of pulmonary embolism common findings are dyspnea, anxiety, thoracic pain, palpitations, but also signs of deep vein thrombosis, hemoptysis, or even fulminant RV failure. Patients with acute RV failure in the setting of acute massive pulmonary embolism usually present dramatically with the typical symptoms of PE along with syncope, cardiogenic shock, hypoxia, and/or cardiac arrest [13]. A rapid differentiation between acute and chronic pulmonary embolism is required as management strategies, follow-up, and prognosis differ. Patients with chronic pulmonary hypertension are at risk for pulmonary embolism, both from in situ pulmonary arterial clot formation and central venous catheter and deep venous sources.

In chronic obstructive pulmonary disease, symptoms such as wheezing, chronic productive cough, dyspnea on exertion, and fatigue are generally present in advanced chronic respiratory disease with or without pulmonary hypertension. In COPD, they are essentially the consequence of airflow limitation and hyperinflation rather than PH.

Symptoms associated with biventricular heart failure are as follows: progressive dyspnea, orthopnea, paroxysmal nocturnal dyspnea, wheezing and/or cough (i.e., cardiac asthma), anxiety (multifactorial causes include dyspnea, palpitations, and increased sympathetic tone) [12].

More details regarding pulmonary embolism, pulmonary hypertension (primary or secondary), RV infarction, arrhythmia in RV pathology, pulmonary disease, and RV dysfunction are provided in other dedicated chapters of this book.

30.3 Clinical Signs

The physical examination of the patient depends on the pathology that causes RV failure and its onset. In acute life threatening situations, i.e. acute pulmonary embolism or RV myocardial

infarction, the clinical presentation may be dominated by hemodynamic instability even progressing to cardiogenic shock. The clinical signs encountered in patients with chronic right heart pathology are initially due to the development of pulmonary hypertension; afterwards, they are completed by the development of RV hypertrophy and a typical picture of right ventricular failure, dominated by systemic congestion.

The evaluation for the presence and severity of heart failure should include consideration of the patient's general appearance, measurement of vital signs, examination of the cardiovascular system, and assessment of other organs for evidence of congestion, hypoperfusion, or indications of comorbid conditions.

When performing the physical examination one should follow signs of peripheral retrograde stasis, cardiac signs and general signs.

30.3.1 Signs of Peripheral Retrograde Stasis

These occur due to chronic marked elevation of systemic venous pressure secondary to elevated right sided heart pressures, transmitted backward into the vein circulation.

Jugular venous distention (Fig. 30.1) consists of engorgement of jugular and other neck veins. The assessment should be done with the patient in dorsal decubitus at 45°. Normally, jugular venous pressure (JVP) declines with inspiration. The paradoxical rise of JVP during inspiration in RV failure is a finding sign known as the Kussmaul sign; it is the result of the increase in venous return, in right atrial pressure, and therefore right sided heart failure. This finding, however, may not be very obvious with marked venous distension. Kussmaul sign may indicate not only right ventricular failure, and can also be found in constrictive pericarditis, tricuspid stenosis, or cor pulmonale.

The jugular vein is very pulsatile and may be confused with the carotid arterial pulse. Arterial pulsations in the neck can be differentiated from venous pulsations on the basis of contour; an arterial pulse has its predominant (more rapid) motion directed outward, whereas a venous pulse tends to collapse inward. A systolic thrill may be felt over the jugular vein in patients with severe tricuspid regurgitation.

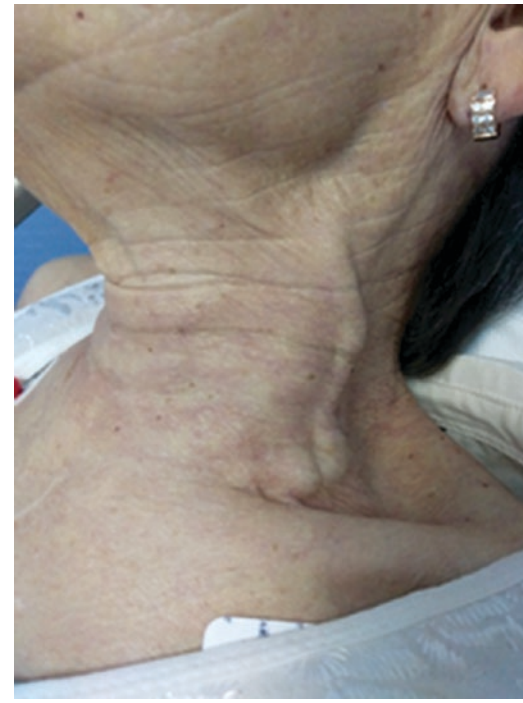

Fig. 30.1 Jugular venous distension in a 78-year-old female patient with tricuspid disease (moderate stenosis, severe regurgitation), with a surgical intervention for mitral stenosis in 1993, with metallic prosthesis, with severe right heart failure symptoms (image from personal collection with patient permission)

The evidence of congestion does not always indicate with certainty that right heart failure is present. A more definitive test for assessment of a patient's volume status is by the measurement of jugular venous pressure. The JVP is usually assessed by observing the right side of the patient's neck; measurement is best performed with the patient comfortably seated on an examining table in a warm, well-lighted room with the neck fully exposed from the clavicle to the ear. Assessment of JVP is usually initiated with the patient's upper torso elevated at a 30- to 45-degree angle, but it can be performed at virtually any angle so long as the true height of the meniscus of the venous pulse can be identified. The vertical distance of the venous pulse above the angle of

Louis at the second intercostal space of the sternum is then determined, and 5 cm (to account for the vertical distance to the mid-portion of the right atrium) is added to determine right atrial pressure [11]. Normally, JVP does not exceed 3–4 cm above the sternal angle; adding the approximately 5 cm since the right atrium below the sternal angle, the JVP corresponds to 9 cm H_2O = 7 mmHg [14]. An elevated JVP means over 4 cm above sternal angle. Both sensitivity and specificity of the JVP in detecting congestion can be improved by exerting pressure on the right upper quadrant of the abdomen while assessing venous pulsations in the neck (i.e., hepatojugular or abdominojugular reflux). An elevated JVP detects both systemic congestion as well as increased right atrial pressures in patients with PAH on the basis of abnormalities in the lung or pulmonary vasculature itself or when injury (such as infarction) to the right ventricle occurs. There is also a good sensitivity (70%) and specificity (79%) between high JVP and elevated left-sided filling pressure [11].

The normal jugular venous pulse has a shape characterized by the presence of several individual components that can be usually identified. It contains three positive waves; by convention these are labeled *a*, *c*, and *v* (Fig. 30.2).

These positive deflections occur, respectively, before the carotid upstroke and just after the P wave of the ECG (*a* wave); simultaneous with the upstroke of the carotid pulse (*c* wave); and during ventricular systole until the tricuspid valve opens (*v* wave). The *a* wave is generated by atrial contraction, which actively fills the right ventricle in end-diastole. The *c* wave is caused either by transmission of the carotid arterial impulse through the external and internal jugular veins or by the bulging of the tricuspid valve into the right atrium in early systole. The *v* wave reflects the passive increase in pressure and volume of the right atrium as it fills in late systole and early diastole. Normally the crests of the *a* and *v* waves are approximately equal in amplitude. The negative waves of the jugular venous pulse occur between the *a* and *c* wave (*x* descent), between the *c* and *v* wave (*x′* descent), and between the *v* and *a* wave (*y* descent). The x and x′ descents reflect movement of the lower portion of the right atrium toward the right ventricle during the final phases of ventricular systole. The y descent represents the abrupt termination of the downstroke of the *v* wave during early diastole after the tricuspid valve opens and the right ventricle begins to fill passively. Normally the *y* descent is neither as brisk nor as deep as the *x* descent [14]. Abnormalities in the jugular venous pulse may be reflected in either the mean pressure, amplitude, or configuration of the positive waves or negative troughs, or in the sequence or absence of the positive waves.

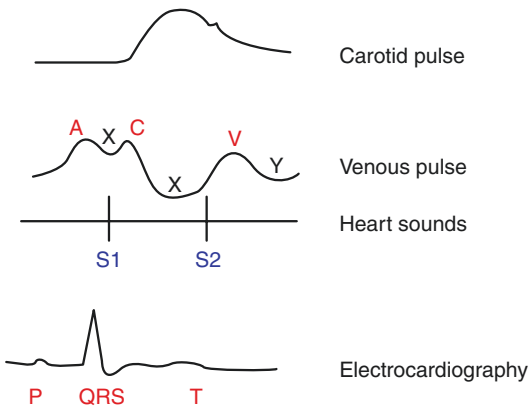

Fig. 30.2 Timing of the jugular venous pulse is displayed in relation to the carotid arterial tracing, first (S_1) and second (S_2) heart sounds, and the electrocardiogram

In right ventricular pathology, the jugular pulse may have a prominent *a* wave, indicating elevated right atrial pressure. Prominent *v* waves with rapid *y* descent indicate tricuspid regurgitation. Progression to a systolic or *c*-*v* wave occurs in severe tricuspid insufficiency and may appear as systolic liver pulsations [15].

The hepatojugular reflux is the distention of the jugular vein induced by applying manual pressure over the liver for as long as 1 min. The evaluation is done with the patient also positioned at a 45° angle. Pressure applied on the abdomen in the right upper quadrant leads to compression on the inferior vena cava, increased venous return, and increased central venous pressure. The hepatojugular reflux is not specific to any one disorder, but is a reflection of a right ventricle that cannot accommodate augmented

venous return. Hepatojugular reflux occurs in patients with elevated left sided filling pressures and reflects elevated capillary wedge pressure (greater than 15 mmHg) and left sided heart failure [11]. Constrictive pericarditis, right ventricular infarction, and restrictive cardiomyopathy are other common causes of a positive finding. The one diagnosis not seen with abdominojugular reflux is cardiac tamponade [16].

Congestive hepatomegaly with painful liver on palpation is common in patients with chronic right sided heart failure, but it may also occur rapidly in acute heart failure. When hepatomegaly occurs acutely, the liver is usually tender. In patients with considerable tricuspid regurgitation, a prominent systolic pulsation of the liver, attributable to an enlarged right atrial *v* wave, is often noted. A presystolic pulsation of the liver, attributable to an enlarged right atrial *a* wave, can occur in tricuspid stenosis, constrictive pericarditis, restrictive cardio-myopathy involving the right ventricle, and primary or secondary pulmonary hypertension.

Cardiac cirrhosis includes by definition a spectrum of hepatic changes occurring in evolution of right sided heart failure [1]. Despite its name, cardiac cirrhosis rarely satisfies strict pathologic criteria for cirrhosis. The terms congestive hepatopathy and chronic passive liver congestion are more accurate, but the name *cardiac cirrhosis* has become conventionally used in these cases. In patients with long-term evolution of right heart failure, liver cirrhosis may occur, which usually implies congestive hepatopathy that results in liver fibrosis. The deleterious effects of HF on the liver are a consequence of chronic congestion in the systemic venous system secondary to volume and pressure overload, compromised liver perfusion by reduced cardiac output causing hypoxic injury and fatty liver changes. Cardiac failure may also be accompanied by changes in liver enzymes. Approximately 25% of patients enrolled in the Romanian Acute Heart Failure Syndromes (RO-AHFS) registry were found to have abnormally high transaminases levels, and these were most prevalent in patients classified as suffering from right HF or cardiogenic shock upon initial presentation. Most importantly, more pronounced elevations in transaminases are suggestive of progressive pump failure, and are independently associated with increased short-term mortality in patients hospitalized for HF [17]. Distinguishing cardiac cirrhosis from *ischemic hepatitis* is important. The latter involves massive hepatocellular necrosis caused by sudden cardiogenic shock or other hemodynamic collapse. Typically, sudden and dramatic serum hepatic transaminase elevations lead to its discovery.

Congestive splenomegaly with pain on palpation in the left hypochondium may be found.

Peripheral edema is frequently perimaleolar or pretibial, but also affects the abdominal wall (the skin appears as of an orange peel, *"peau d'orange"*) or the lower back (sacral edema) especially in immobilized patients. The edema is cold and in time becomes harsh, with cyanosis of the overlying skin, and non-pitting edema. Most often, in heart failure, lower extremities are symmetrical, but sometimes they may evolve asymmetrically [18]. Chronic edema may be associated with lower extremity pigmentation, induration, and cellulitis. Although edema is a cardinal manifestation of heart failure, it does not correlate well with the level of systemic venous pressure. Usually, a substantial gain of extracellular fluid volume (i.e., a minimum of 5 L in adults) must occur before peripheral edema develops [11]. Edema in the absence of dyspnea or other signs of volume overload is nonspecific for heart failure and can be observed in many other conditions. Pedal edema may be the result of chronic venous insufficiency (particularly after saphenous veins have been harvested for coronary artery bypass grafts; there are often additional signs of venous disease, such as extensive varicosities, medial ulcers, or brownish pigmentation from hemosiderin deposition), a side effect of medications (e.g., dihydropyridine calcium channel blockers, thiazolidinediones), a consequence of portal hypertension in a cirrhotic patient or of nephrotic syndrome, or other syndromes of hypoproteinemia. In heart failure, edema may also indicate the presence of secondary hyperaldosteronism induced by functional renal insufficiency [19]. Asymmetrical swelling can reflect local or

unilateral venous thrombosis, lymphatic obstruction, or the sequelae of previous vein graft harvesting. Homans' sign (calf pain on forceful dorsiflexion of the foot) is neither specific nor sensitive for deep venous thrombosis [11]. In conclusion, the presence of peripheral edema is not synonymous with right heart failure.

Transudative serous effusions—pleural, peritoneal, and pericardial, are not uncommon in patients with congestive right heart failure. *Pleural effusion or hydrothorax* results from increased interstitial fluid in the lung due to elevated pulmonary capillary pressure and less often may occur in association with isolated right HF [20]. The presence of a pleural effusion is usually indicative of increased filling pressures on both the right and left sides of the heart. When hydrothorax develops, dyspnea usually intensifies because of further reductions in vital capacity. Dullness to percussion and diminished breath sounds at one or both lung bases suggest the presence of a pleural effusion. Bilateral pleural effusions are most common, but when an effusion is present unilaterally, it is usually right sided; only ~10% occur exclusively on the left side [11]. The fluid typically meets the biochemical characteristics of a transudate, although in 25% of the cases it may fall into the exudative range [20]. Testing for natriuretic peptides, such as NT-proBNP, significantly aids in diagnosing or excluding HF in patients with pleural effusion of unknown origin. The measurement of pleural fluid NT-proBNP is the best means to identify pleural effusions that meet the exudative criteria of Light but are due to HF. At a cut-off point of ≥1714 pg/mL, the test has a sensitivity of 99%, a specificity of 99% for the diagnosis of heart failure [21]. The test may be especially useful in heart failure patients with exudates who have been treated with diuretics. However, if natriuretic peptide assays are not available, calculation of the serum to pleural fluid albumin gradient represents a good substitute for making this distinction [20].

Ascites occurs in patients with increased pressure in the hepatic veins and in the veins draining into the peritoneum, and usually reflects long-standing systemic venous hypertension. History and physical examination provide clues to the possible etiology of ascites formation. Sometimes, abdominal paracentesis with appropriate ascitic fluid biochemical analysis is considered the most cost-effective method for diagnosing the cause of ascites. Due to the low specificity of Light criteria for the differentiation between peritoneal effusions, serum ascites albumin gradient (SAAG) has been proposed more recently as a physiologically based alternative to the traditional classification of ascites into transudates/exudates. SAAG is calculated as the difference between serum and ascites albumin concentration and was demonstrated to correlate directly with measured portal pressure. Consequently, SAAG ≥11 g/L suggests the presence of portal hypertension (as in the case of RHF), while SAAG values <11 g/L are found in patients with normal portal pressure [22].

Transudative *pericardial effusion* may sometimes be seen in the clinical picture of heart failure. Hydropericardium forms only with elevation of the right-sided filling pressure in the heart. In patients with biventricular failure, there is no evidence that elevated left-sided pressure, in the absence of elevated right-sided pressure, can cause a pericardial effusion [23]. Echocardiography is used to diagnose the presence of pericardial effusions, but cannot be used to clearly determine their etiology.

The association of serous effusions with generalized edema, usually evident in congestive heart failure, defines *anasarca* [18]. Anasarca is rare in heart failure unless long-standing, untreated, and accompanied by hypoalbuminemia [11].

30.3.2 Cardiac Findings

Cardiac signs depend on the pathology that caused right heart failure. In the chronic disease associated with pulmonary hypertension, patients develop physical signs as they progress from PH alone to PH associated with right ventricular failure.

Palpable pulmonary artery pulsations, pulmonic valve closure, or an abnormal systolic sternal or left parasternal lift suggests both pulmonary and right ventricular hypertension (particularly if it is accompanied by pulsations in the subxiphoid

region) [11]. When the right ventricle is enlarged, it may become palpable in the epigastric region (Hartzer sign) [18].

Most cardiac signs that are present in right ventricular pathology are found at auscultation.

Tachycardia may be present as a sign of increased adrenergic activity.

Signs of pulmonary hypertension include a closely split S_2 with a *loud pulmonic component* P_2. Accentuation of P_2 heart sound is a cardinal sign of increased pulmonary artery pressure; it disappears or improves after treatment of heart failure. The second heart sound is narrowly split or single in patients with preserved right ventricular function. Right ventricular failure (or a right bundle branch block) widens the splitting of the second heart sound [12].

A *right sided* S_3 *sound* is often associated with an extremely dilated right ventricle. A *right* S_4 *sound* may also be heard if there is significant right ventricular hypertrophy; it results from right atrial contraction into a noncompliant right ventricle. An increase in the intensity of either gallop sound during inspiration indicates that it originated in the right ventricle [11]. Right ventricular third and fourth heart sounds are commonly appreciated at the lower left sternal border of the sternum or over the xiphoid.

In some patients with severe and progressive RV failure, pulmonary arterial pressure may decrease as a consequence of low cardiac output [2]. Therefore, the interpretation of pulmonary pressure in patients with PH should always take into account the degree of RV failure and effective cardiac output.

Auscultation may often reveal a murmur of *tricuspid regurgitation.* Tricuspid regurgitation (TR) is classically associated with a holosystolic murmur that is best heard at the right or lower left sternal border or at the subxiphoid area. When the right ventricle is very enlarged, the murmur may be displaced laterally and may even be appreciated at the apex. There is usually little radiation of the murmur, and a thrill is generally not palpable. However, the murmur of TR may be soft or absent, even when regurgitation is severe [24]. The tricuspid insufficiency murmur may also become softer as volume overload is treated, and a reduction in ventricular size improves valve competency.

Tricuspid regurgitation in adults is most commonly functional, defined as regurgitation with apparently anatomically normal leaflets and chords. The cause of functional TR is most likely the dilatation of the right atrium and right ventricle with dilation of the tricuspid annulus and poor leaflet coaptation [25]. These modifications may result from any condition that directly involves the right ventricle or causes elevation in right ventricular systolic pressure.

The murmur intensifies with inspiration and decreases with expiration (Rivero Carvallo sign). During inspiration, the venous blood flow into the right atrium and ventricle are increased, which increases the stroke volume of the right ventricle during systole. As a result, the leak of blood from the right ventricle into the right atrium is larger during inspiration, causing the murmur to become louder. Respiratory variation in the intensity of the murmur may be observed especially in patients with mild to moderate TR, and may not be appreciated in patients with severe TR or marked RV enlargement and dysfunction [24]. The murmur may also become louder after a premature beat and prolonged diastole.

A significant tricuspid regurgitation may further aggravate RV volume overload and decrease cardiac output. Right ventricular diastolic dysfunction and tricuspid regurgitation may accentuate right-to-left shunting through a patent foramen ovale and lead to hypoxemia [2].

Tricuspid regurgitation can be differentiated from mitral regurgitation by the location of the murmur, an increased intensity during inspiration, and the presence of prominent *v* waves in the jugular venous pulse. The murmur of mitral regurgitation becomes louder during expiration due to the increase in venous return from the pulmonary veins to the left heart.

Diastolic murmurs are usually absent in tricuspid regurgitation, although a diastolic rumble may be heard particularly if there is associated tricuspid stenosis or when there is substantial blood flow across the tricuspid valve during diastole, which may occur with an atrial septal defect [24].

A *diastolic pulmonic regurgitation murmur* can be heard in the setting of a more severe disease. This is known as the *Graham Steell*

murmur and it is a high-pitched, blowing diastolic murmur beginning with a loud P_2 and continuing through most of diastole. Pulmonary regurgitation murmur may be absent in mild to moderate situations, but in severe regurgitations, especially determined by pulmonary hypertension, causes a high-pitched diastolic murmur that might be misinterpreted as aortic regurgitation.

Cardiac findings in acute situations get a more dramatic clinical picture. The physical exam in *acute pulmonary embolism* is similar to that encountered in chronic PAH patients with acute RV failure. The jugular venous pulse is often elevated with a prominent *v* wave. A parasternal RV heave may be palpable. On auscultation, a tricuspid murmur, increased S_2, and in ~25% of patients, a right-sided S_4 may be present [13]. Patients with massive pulmonary embolism are in shock. They have systemic hypotension, poor perfusion of the extremities, tachycardia, and tachypnea. In addition, patients appear weak, pale, sweaty, and oliguric and develop impaired mentation.

In *right ventricular myocardial infarction*, there is a classic clinical triad which includes distended neck veins, clear lung fields, and hypotension [26]. Much less frequently, clinical manifestations include right ventricular S_3 and/or S_4 heart sounds. A tricuspid regurgitation murmur, Kussmaul's sign and pulsus paradoxus are signs of significant hemodynamic effects due to RV ischemia. A disproportionate elevation of right-sided filling pressures compared with left-sided hemodynamics represents the hallmark of right ventricular infarction. Other presentations include high-grade atrioventricular block, tricuspid regurgitation, cardiogenic shock, right ventricular free wall rupture, and cardiac tamponade [27].

30.3.3 General Signs

Jaundice may be evident in patients with severe heart failure. The most common mechanism is passive hepatic venous congestion due to increased central venous pressure which may cause elevations of liver enzymes and both direct and indirect serum bilirubin. Jaundice due to heart failure tends to be mild, and a key feature is the association with dyspnea [28].

Central *cyanosis* is present with significant right-to-left shunting at the level of the heart or lungs, which allows deoxygenated blood to reach the systemic circulation. Peripheral or acrocyanosis of the fingers, toes, nose, and ears reflects reduced blood flow because of small vessel constriction seen in severe heart failure or shock [11].

Rales on lung examination indicate often biventricular congestive HF. In patients with COPD one may find hyper-resonance of the lungs on percussion, wheezes and crackles on auscultation.

Oliguria may be present when there is a decrease in glomerular filtration rate (GFR). *Nocturia* may occur because recumbency reduces the deficit in cardiac output in relation to oxygen demand, renal vasoconstriction diminishes, and urine formation increases.

Protein losing enteropathy may rarely occur, as a consequence of an impaired intestinal absorption of fat. Protein-losing enteropathy is seen occasionally after the Fontan procedure, in constrictive pericarditis, in severe tricuspid regurgitation, and in RV failure [2]. Its origin is multifactorial and cannot be explained simply by elevated right atrial pressure alone. This complex condition may lead to profound hypoproteinemia, malnutrition, and immunological deficiencies [29]. Protein-losing enteropathy with subsequent reduction of plasma oncotic pressure may also exacerbate ascites.

Cardiac cachexia is found in long-standing right ventricular failure, because of anorexia from hepatic and intestinal congestion. Other possible causes are increased total metabolism secondary to augmentation of myocardial oxygen consumption, excessive work of breathing, and elevated levels of circulating tumor necrosis factor (TNF) [11].

Some patients may also have the signs and symptoms of the underlying cause of PH (i.e. connective tissue disease).

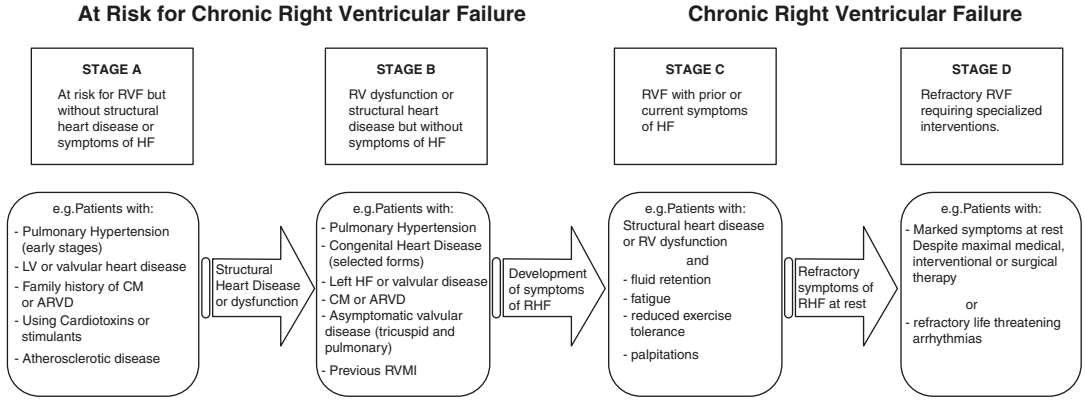

Fig. 30.3 Stages of chronic RV failure. *RVF* right ventricular failure, *HF* heart failure, *LV* left ventricle, *CM* cardiomyopathy, *ARVD* arrhythmogenic RV dysplasia, *RVMI* right ventricle myocardial infarction. Reprint with permission from Haddad et al. [2]

30.4 Stages of RV Failure

The development of RV failure may be described in terms of progressive stages as it has been in the case of left heart failure. RV failure may progress from stage A to stage D (Fig. 30.3).

Stage A is described in a patient at risk for RV failure, but without structural heart disease or symptoms of HF.

Stage B refers to RV dysfunction or structural heart disease in the absence of symptoms of HF.

In *stage C* the patient has symptomatic RV failure with prior or current symptoms of HF.

Stage D corresponds to refractory RV failure requiring specialized interventions [2].

It is important to note the potential of recovery of the failed RV (i.e. after lung transplantation in patients with PAH).

30.5 Electrocardiography in Right Heart Pathology

The electrocardiogram (ECG) is a standard part of the initial assessment of every patient with suspected right heart failure, and also in previously diagnosed patients presented for a routine examination or for a new decompensation. Most ECG signs are specific but not sensitive for the detection of right ventricular disease. ECG changes do not correlate with disease severity or prognosis [30, 31].

In patients with right heart pathology, the ECG may reveals sinus tachycardia due to sympathetic nervous system activation in advanced stage of heart failure or during episodes of decompensation. Evidence of atrial enlargement, ventricular hypertrophy, or prior myocardial infarction is common in chronic disease. The presence of left ventricular hypertrophy can provide clues about the cause (e.g., arterial hypertension or valvular disease). Increased P wave amplitude in lead II suggests right atrial abnormality. Right ventricular hypertrophy, right axis deviation, and right bundle-branch block may suggest chronic right ventricular pressure overload. The sensitivity of ECG for the diagnosis of pulmonary hypertension is poor (20–40%), whereas the specificity of signs of right ventricular hypertrophy is high [32].

As with any ECG interpretations, the sequence of ECG assessment in RV pathology should start from heart rate, rhythm, P-QRS-ST-T morphology, amplitude, duration and axis. It is important to observe ECG patterns in all 12 leads. Patient's age, gender, medication and/or device therapy should be taken into consideration during ECG assessment.

Below is the summary of the main criteria of electrocardiographic diagnosis that one may find as a consequence of changes induced by right heart disease.

30.5.1 Right Atrial Abnormalities

With severe pulmonary hypertension, two ECG patterns are characteristic of right atrial abnormalities: right atrial hypertrophy and P pulmonale. The term right atrial abnormality is preferred now over other terms, such as right atrial enlargement or hypertrophy, which suggest a particular underlying pathophysiology [11].

The underlying mechanism is that greater right atrial mass generates greater electrical force early during atrial activation. Because right atrial forces are responsible for only the early part of the P wave, any increase in the duration of right atrial activation usually does not prolong the total duration of the P wave.

The electrocardiographic features of right atrial abnormality are [11, 12] (Figs. 30.4 and 30.5):

P wave tall in amplitude, narrow in duration, especially prominent in II, III, aVF and right precordial leads (V_1, V_2);

- peaked P waves with amplitudes in lead II > 2.5 mm (0.25 mV) (P pulmonale);
- prominent initial positivity in lead V_1 or V_2 > 1.5 mm (0.15 mV);
- rightward shift of mean P wave axis in frontal plane to more than +75°;
- increased area under initial positive portion of the P wave in lead V_1 to >0.06 mm/s;
- the terminal negative component of the P wave is absent in lead V_1.

An abnormally tall P wave in the right precordial leads is a more specific finding for right atrial abnormality than the diagnostic criteria based on the limbs leads (Fig. 30.5). The P

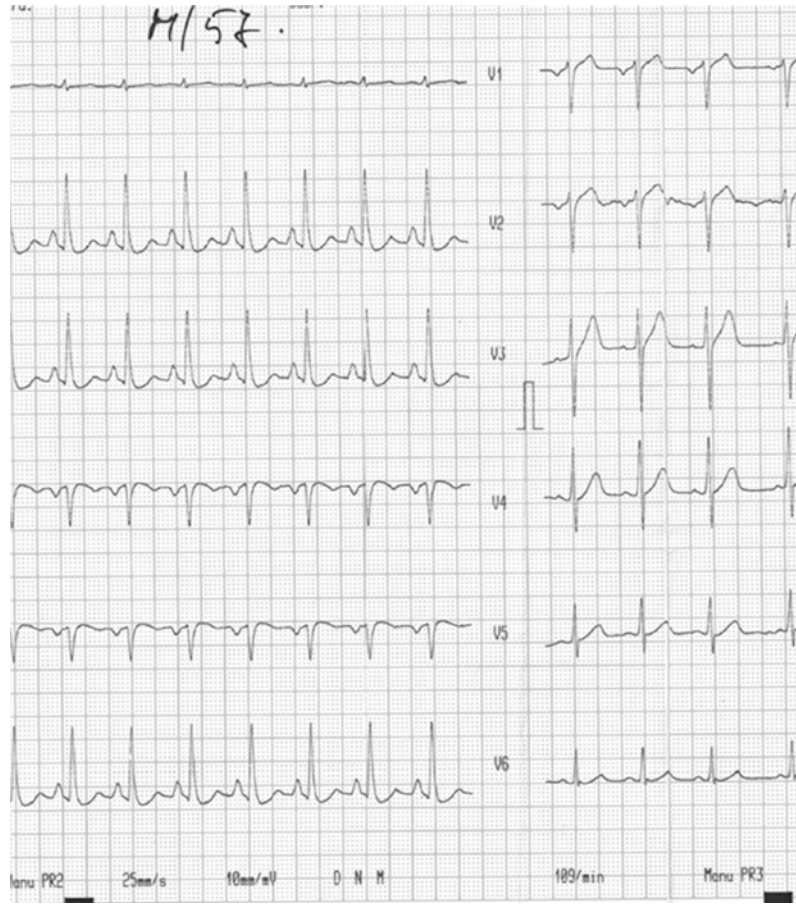

Fig. 30.4 ECG of a 57-year-old man with acute exacerbation of COPD. There are P waves in leads II, III, aVF tall in amplitude (3.5 mm), narrow in duration; the P wave axis is at +80°. We can also see the atrial repolarization (negative deflections in II, III, aVF leads as apparent depression of the ST segment). Image from personal collection

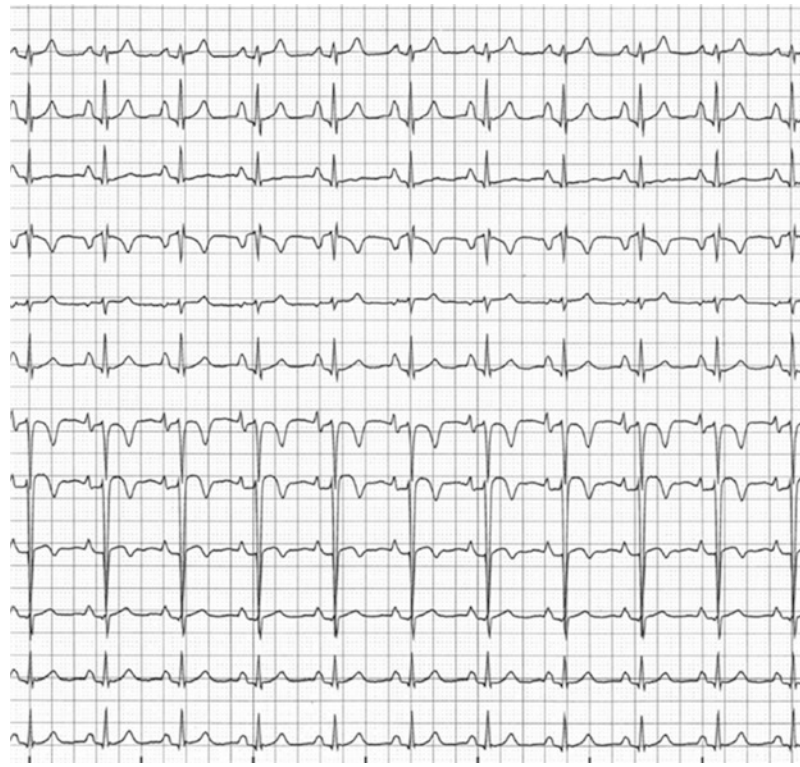

Fig. 30.5 ECG of a 30-year-old woman with severe pulmonary arterial hypertension. There are tall and narrow P waves in leads II, III, aVF (4 mm amplitude in lead II) and in the right precordial leads (prominent initial positivity 2.5 mm in V_1 lead); the QRS axis is at +90°; the ST segment is slightly elevated with negative T waves in V_1–V_3 (like in acute ST elevation myocardial infarction) suggesting RV pressure overload. Image from personal collection

pulmonale pattern is more frequently seen in patients with pressure overload from congenital heart disease, such as pulmonic stenosis, tetralogy of Fallot, Eisenmenger syndrome, and in patients with pulmonary hypertension not caused by COPD. A rightward shift of the P wave more than +90° is uncommon; it is associated especially with COPD. In patients with severe lung disease caused by interstitial pulmonary fibrosis, the P waves are usually normal, suggesting that the axis shift is due to the hyperinflation of the lungs [33].

The atrial repolarization is represented by the Ta wave. The Ta is usually directed opposite to the main P wave axis. The atrial gradient (area under P + Ta) is normally close to zero. In patients with right ventricular pathology, a prominent atrial T wave (Ta) often accompanies a tall P wave. The amplitude of the negative deflection in the inferior leads may exceed 0.1 mV. Because the atrial T wave may last as long as 0.45 s, the negative deflection in these leads may cause apparent depression of the ST segment [33] (Fig. 30.4).

The electrocardiographic findings of right atrial abnormality have limited sensitivity, but high specificity for detecting right atrial enlargement [34]. The P wave pattern does not correlate with right atrial pressure, but patients with COPD and P pulmonale have more severe pulmonary dysfunction and significantly reduced survival than others [11].

The P pulmonale pattern has been described also in patients with coronary artery disease. Ischemia of the left atrium was considered to be the cause of the increased voltage of the P wave and the rightward shift of the P wave axis [35].

On the other hand, P pulmonale may be present in healthy individuals with asthenic body built and is probably related to the vertical position of the heart [33].

If atrial fibrillation is present, the fibrillatory waves may be coarse and of increased amplitude, reflecting right atrial hypertrophy.

Obviously that in RV failure secondary to an associated left-sided heart failure, *left atrial abnormalities* are often present: prolonged P wave duration >120 ms in lead II; prominent notching of P wave, usually most obvious in lead II, with interval between notches of 0.40 ms (P mitrale); increased duration and depth of terminal-negative portion of P wave in lead V_1 (P terminal force) so that area subtended by it >0.04 mm/s; leftward shift of mean P wave axis to between −30° and −45° [11].

Patients with abnormalities in both atria—*biatrial abnormality*—can have electrocardiographic patterns reflecting each defect.

30.5.2 Right Ventricular Hypertrophy

Increasing dominance of the right ventricle changes the ECG in fundamental ways. Generally, RV produces electrical forces much lower than left ventricle; these are normally directed anteriorly and rightward. For right ventricular hypertrophy (RVH) to become manifested on ECG, it must be severe enough to overcome the masking effects of the larger left ventricular forces. In mild cases, no apparent change may be detected on the ECG.

Because the right ventricle is located anteriorly as well as to the right of the left ventricle, the effects produce increased potentials in leads directed in these directions. Thus, on the ECG one may find tall R waves in anteriorly and rightward-directed leads (leads aVR, V_1, and V_2), and deep S waves and abnormally small r waves in leftward-directed leads (I, aVL, and lateral precordial leads V_5–V_6). There will be a reversal of normal R wave progression in the precordial leads, a shift in the frontal plane QRS axis to the right, and the presence of S waves in leads I, II, and III ($S_1S_2S_3$ pattern) [11]. The QRS duration may be slightly increased.

In some cases, the increased rightward forces are directed posteriorly instead of anteriorly; consequently, no apparent abnormality is seen in V_1 lead, but the left precordial leads may reveal deep S waves and the limb leads show right axis deviation [33].

The QRS changes are accompanied by the secondary T wave changes and the deviations of the ST segment. The T waves are directed opposite to the main QRS vector (i.e., inverted in the right precordial leads). Sometimes, the ST and T changes may be seen without apparent QRS abnormalities and are attributed to myocardial ischemia of the right ventricle, or right ventricular strain [33].

The ECG abnormalities of RVH can be divided in three types: (1) typical RVH pattern with anterior and rightward displacement of the main QRS vector; (2) incomplete right bundle branch block (RBBB); and (3) posterior and rightward displacement of the main QRS axis, predominantly in patients with chronic lung disease.

In the diagnostic of right ventricular hypertrophy (RVH) , the ECG may provide the following key findings [11, 12, 33, 36]:

- R wave amplitudes in $V_1 \geq 7$ mm (0.7 mV) (Fig. 30.6);
- presence of a tall R wave in V_1 to V_2 with R > S or R/S > 1 and R ≥ 5 mm;
- dominant S wave in V_5 or $V_6 > 7$ mm (0.7 mV) (or R/S ratio < 1);
- the sum of R in V_1 and S in V_5 or $V_6 > 10.5$ mm (1.05 mV);
- S wave in $V_1 < 2$ mm (0.2 mV);
- R wave in V5 or V6 < 5 mm (0.5 mV);
- R in aVR > 5 mm (0.5 mV);
- presence of qR or QR complex in V_1 (or in V_{3R});
- presence of a rSR′ pattern in V_1 with R′ > 10 mm;
- incomplete (or rarely complete) right bundle branch block (Fig. 30.7);
- right QRS axis deviation greater than +90–100°;
- S_1Q_3 sau $S_1Q_3T_3$ pattern;
- $S_1S_2S_3$ pattern;
- ST-T wave abnormalities secondary to hypertrophy.

These criteria have high specificity but low sensitivity [33]. The changes commonly occur in advanced RV diseases such as severe pulmonary

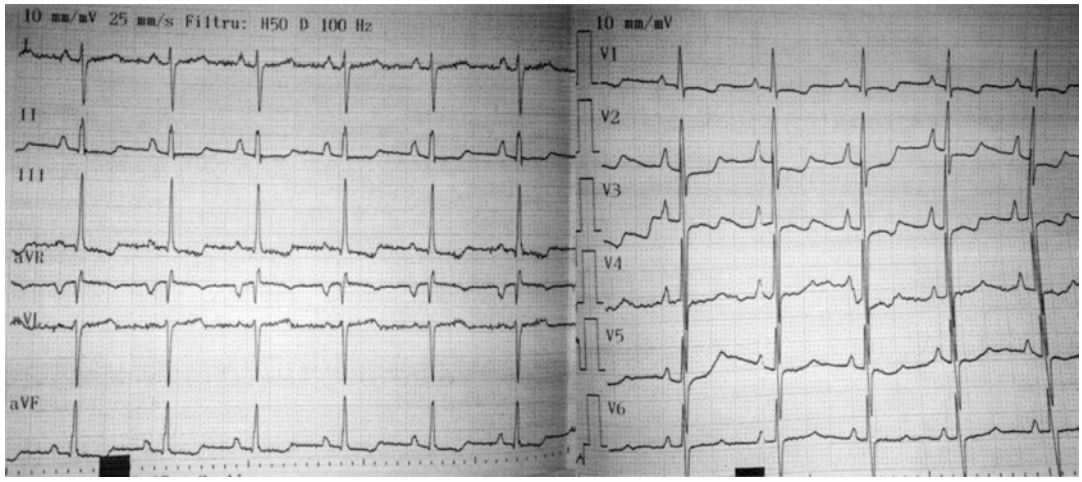

Fig. 30.6 The ECG of a woman, 27 year-old, with primary pulmonary hypertension, which reveals normal sinus rhythm, right atrial abnormality; R wave amplitudes in V1 8 mm, presence of a tall R wave in V1 and V2 with R/S > 1; dominant S wave in V5 and V6; right QRS axis deviation +120°; negative T waves in V1–V3 suggesting RV pressure overload. Image from personal collection

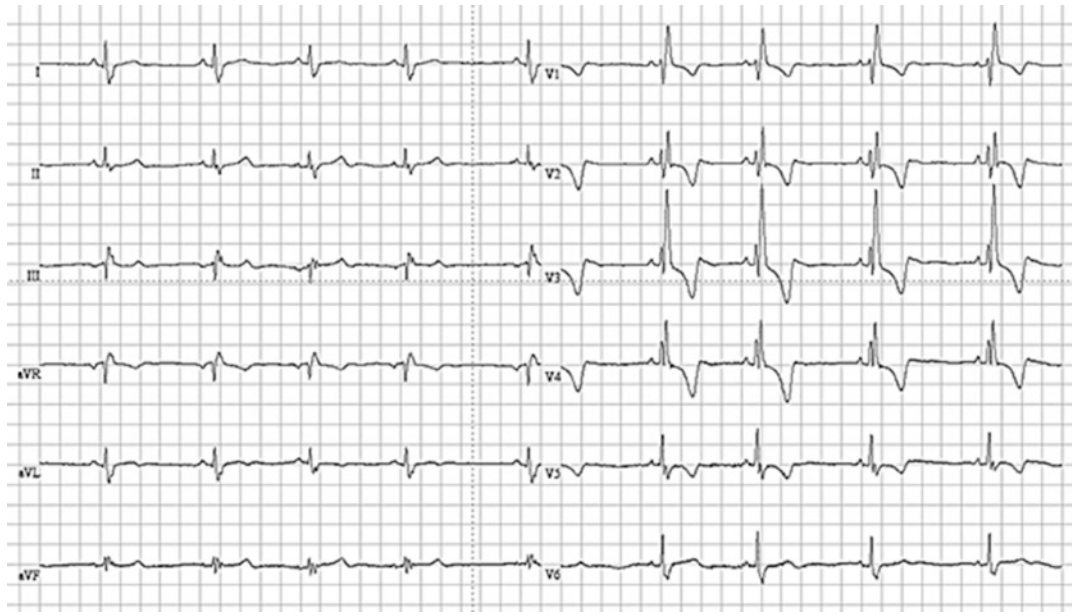

Fig. 30.7 Incomplete right bundle branch block with increased R wave amplitude in right precordial leads in a 16 year-old boy who had undergone surgical correction of tetralogy of Fallot during childhood, with pulmonary regurgitation in present. Courtesy of Ana Maria Balahura, MD

hypertension and pulmonary stenosis. The greater the number of features, the higher the sensitivity for RVH. The typical RVH pattern with tall R waves in the right ventricular leads and right axis deviation in the frontal plane is characteristic for patients with congenital disease or with primary pulmonary hypertension, conditions in which the right ventricular mass tends to approach or even exceed the left ventricular mass. The qR pattern in V_1 lead is one of the most specific signs of severe RVH (Fig. 30.8).

In patients with COPD, the axis can be shifted to +90° in the absence of pulmonary hypertension. In this case, the diagnosis of RVH is difficult, but in patients without hypertrophy, the amplitude of the entire QRS complex in V_1 lead tends to be small. Pathognomonic of emphysema in the absence of myocardial infarction is low voltage with a posteriorly and superiorly oriented QRS vector and an axis of the P waves >60° in the limb leads. Patients with cor pulmonale secondary to chronic pulmonary thromboembolism, idiopathic pulmonary hypertension, or obesity hypoventilation syndrome are more likely to have a tall R wave in V1 than are those with pulmonary emphysema [33].

In right ventricular volume overload (e.g., atrial septal defect), ECG abnormalities may be limited to an rSr′ pattern in V_1 and persistence of S waves in the left precordial leads [11].

An ECG with a tall R wave, a small S and an increased R/S ratio in V_1 lead may be also seen in normal young adults or in patients with true posterior infarction, left septal fascicular block, displacement of the heart due to pulmonary disease (massive pulmonary effusion or pneumothorax), and Wolff-Parkinson-White pattern (in posterior and leftward insertion of the atrioventricular bypass tract) [33].

In the case of a $S_1S_2S_3$ pattern, the S wave amplitude is greater in lead II than in lead III, with the QRS axis in the frontal plane directed rightward and superiorly. Incomplete RBBB can signify hypertrophy, dilation, or overload of the right ventricle (Fig. 30.9). This pattern may also be seen in normal individuals, in acute right ventricular dilatation, in true posterior myocardial infarction, and in extracardiac abnormalities as pectus excavatum [33].

The ST-T abnormalities are seen most commonly in the right precordial leads. In other cases, one can see peaked T waves in inferior leads (II, III, aVF leads) and ST depression and T wave inversion in leads V_2 through V_6 [12]. If the T waves are biphasic in the right precordial leads, it is useful to observe the following configuration: an abnormal negative-positive biphasic T wave (often seen in patients with RVH); a possibly normal positive-negative T wave.

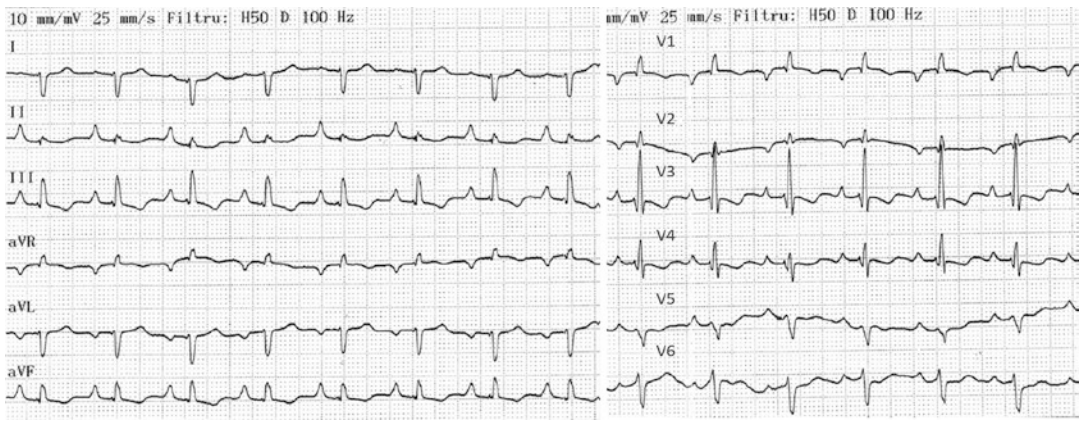

Fig. 30.8 ECG of a 62 year-old man, obese, with severe COPD and chronic respiratory failure, showing sinus rhythm, right QRS axis deviation, qR pattern in V_1 (as specific sign of RVH), and S waves in the left precordial leads. We also note right and left atrial abnormalities. Image from personal collection

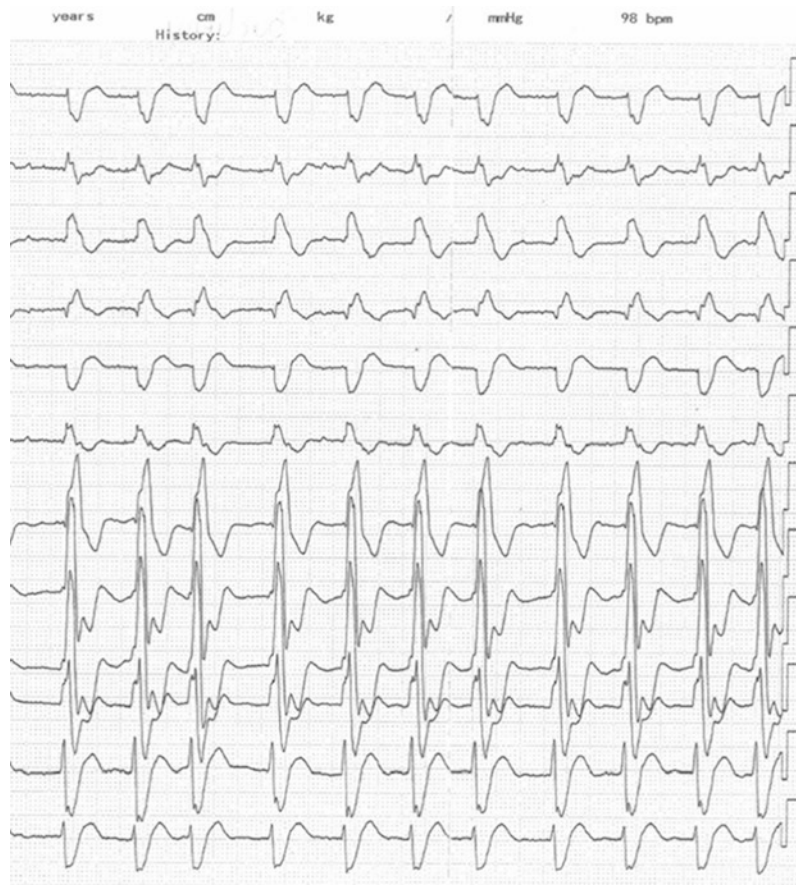

Fig. 30.9 ECG of a 78 year-old man, with chronic post-embolic pulmonary hypertension, showing atrial fibrillation, right QRS axis deviation (+135°), RBBB (with tall R waves in V_1) with secondary ST-T abnormalities, S waves in the left precordial leads. Image from personal collection

30.5.3 Right Ventricular Strain

RV strain consists in a repolarization abnormality due to right ventricular hypertrophy or dilatation, leading to an ECG pattern similar with that from Fig. 30.10. The ECG features are ST depression and T wave inversion in the right precordial leads (V_1–V_3, often extending to V_4) and in the inferior leads (II, III, aVF) often most pronounced in lead III (the most rightward-facing lead).

30.5.4 Biventricular Hypertrophy

The results of biventricular hypertrophy is more complex than in the case of biatrial enlargement, and is not the sum of the two categories of abnormalities. The anterior forces generated by right ventricular hypertrophy (RVH) may be canceled by the posterior forces generated by left ventricular hypertrophy (LVH). Therefore, the specific ECG pattern for RVH or LVH is modified, to the following [11]:

- tall R waves in the right and left precordial leads;
- vertical heart position or right axis deviation in the presence of criteria for LVH;
- deep S waves in the left precordial leads in the presence of electrocardiographic criteria for LVH;
- a shift in the precordial transition zone to the left in the presence of LVH.
- The specificity of the ECG diagnosis of combined ventricular hypertrophy is limited.

30.5.5 ECG Abnormalities in Pulmonary Embolism

There are several EKG abnormalities associated with pulmonary embolism (PE), but none of them

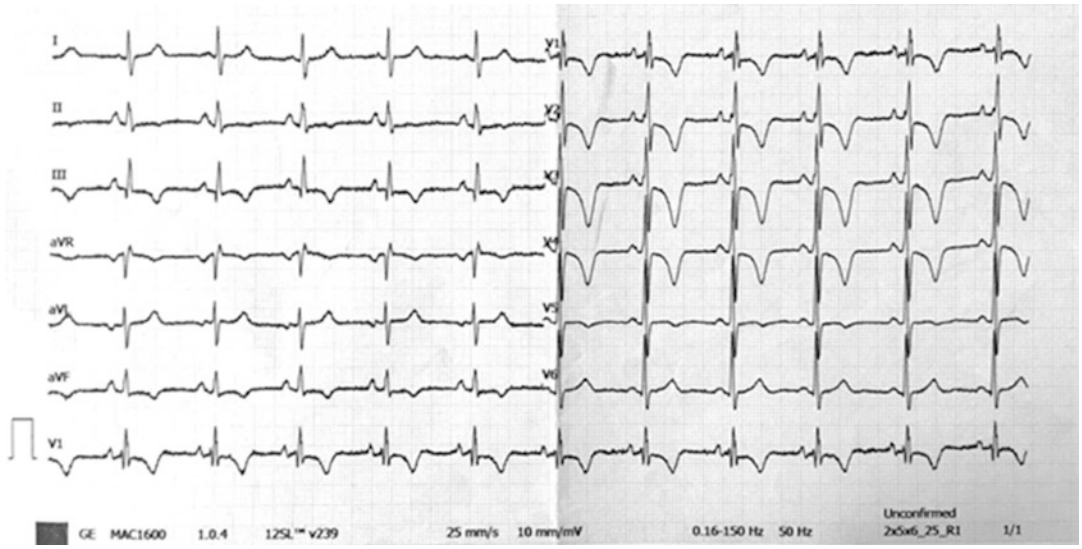

Fig. 30.10 Typical right ventricular strain pattern with ST depression and T-wave inversion in V1–4, plus lead III. We also note right atrial abnormality. In this case, abnormalities are due to right ventricular hypertrophy in a 39 year-old male with diagnosis of Langerhans cell histiocytosis. Courtesy of Claudia Toma, MD

is highly specific or sensitive. In patients with acute RV failure by pressure overloading, the ECG may show [3, 11, 33]:

- sinus tachycardia;
- $S_1Q_3T_3$ pattern with a S wave in lead I and new or increased Q waves in lead III and with T wave inversion in this lead (Fig. 30.11);
- a qR or QR pattern in lead V_1;
- ST-segment elevation in V_1 (Fig. 30.11);
- T wave inversions in leads V_1–V_3 (Fig. 30.11);
- signs of RV strain;
- a complete or incomplete right bundle branch block (RBBB);
- poor R wave progression in the right precordial leads (clockwise rotation);
- a right axis deviation >+90°;
- atrial arrhythmias.

The transient appearance of the P pulmonale has also been observed in patients with acute pulmonary embolism. Acute cor pulmonale secondary to pulmonary embolism sometimes simulates an inferior and anterior infarction (Fig. 30.12). The S_1Q_3 pattern is usually associated with a QR or QS complex, but not an rS in aVR. Furthermore, acute cor pulmonale per se does not cause prominent Q waves in II (only in III and aVF) [37] and the ST segment may be slightly elevated in these leads; the degree of elevation is usually less than in the presence of an acute inferior myocardial infarction. Sometimes, ST segment may be also elevated in leads V_{4R}–V_{6R} [38].

Approximately two-thirds of patients with massive or sub-massive PE exhibit no such changes on EKG [13]. The ECG may show little more than minor or nonspecific waveform changes, or it may be normal even with major pulmonary artery obstruction [11].

The T wave inversion in the anterior precordial leads is correlated with the severity of PE and the presence of RV dysfunction; normalization of these abnormalities implies a favorable outcome [39].

30.5.6 ECG Abnormalities in Right Ventricular Infarction

Right ventricular myocardial infarction (RV MI) often accompanies an inferior or infero-posterior infarction (MI). Thus, the ECG will most

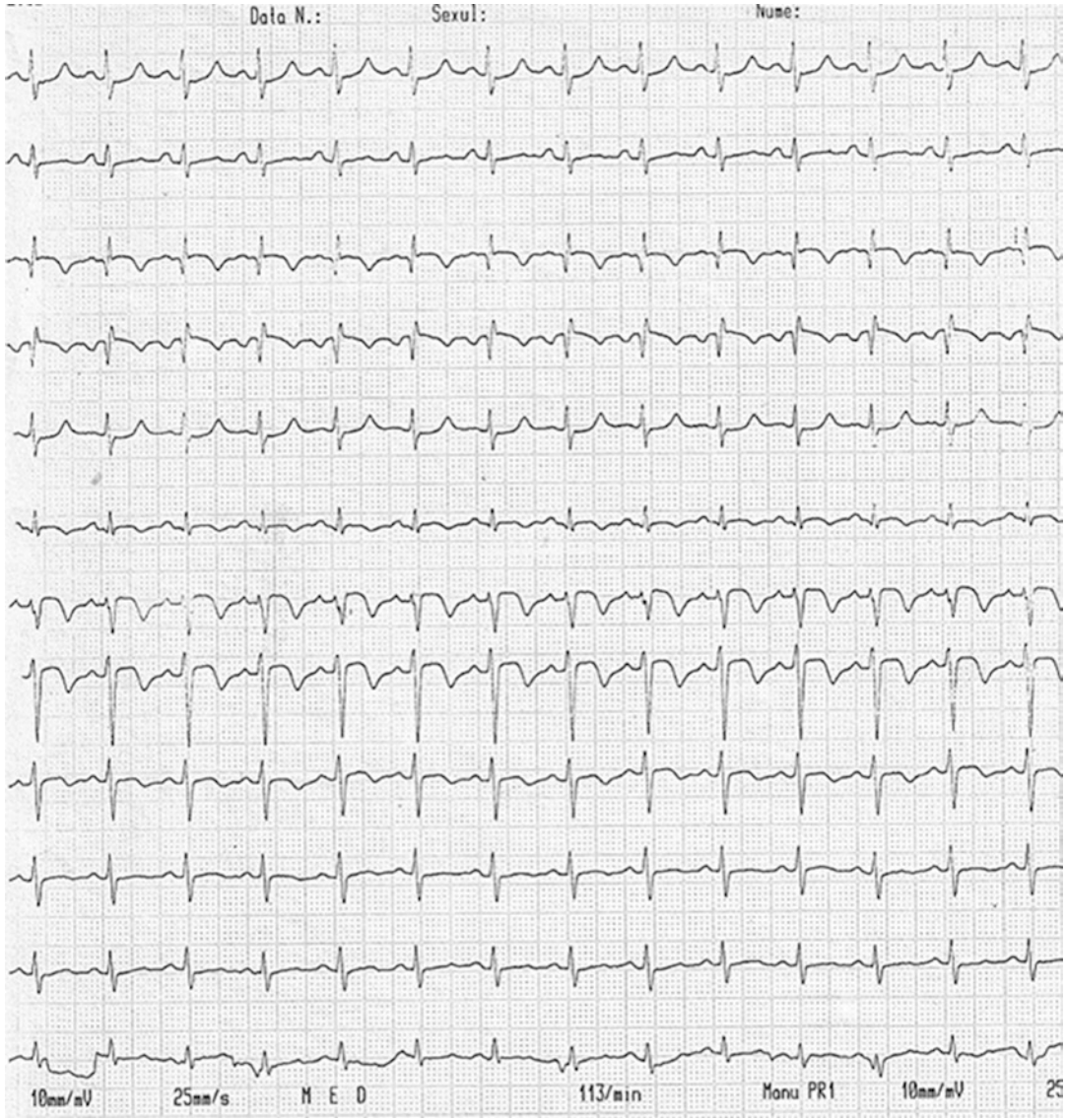

Fig. 30.11 Pulmonary embolism that mimics myocardial infarction. Note the presence of sinus tachycardia, S1Q3T3 pattern, slight ST elevation in III, V_1, V_2 leads, qr in aVR, T wave inversions in leads V_1–V_3. Image from personal collection

commonly show these signs, with >1 mm ST elevation in leads II, III, and aVF, with or without concomitant ST changes in lead V_1, V_2 (Fig. 30.13).

For the diagnosis of RV myocardial infarction, it is mandatory to perform a right-sided ECG with V_{4R} precordial lead (Fig. 30.14). An ST elevation in this lead (V_{4R}) has a sensitivity of 88% and specificity of 78% for diagnosing RV infarction [40]. The right-sided precordial leads may also demonstrate Q waves, particularly in V_{3R} to V_{5R} leads [37].

RV infarction occurs in most cases secondary to coronary stenosis, typically with a proximal occlusion of the right coronary artery; it can also be seen with left anterior descending (moderator branch artery) and circumflex artery occlusions [3].

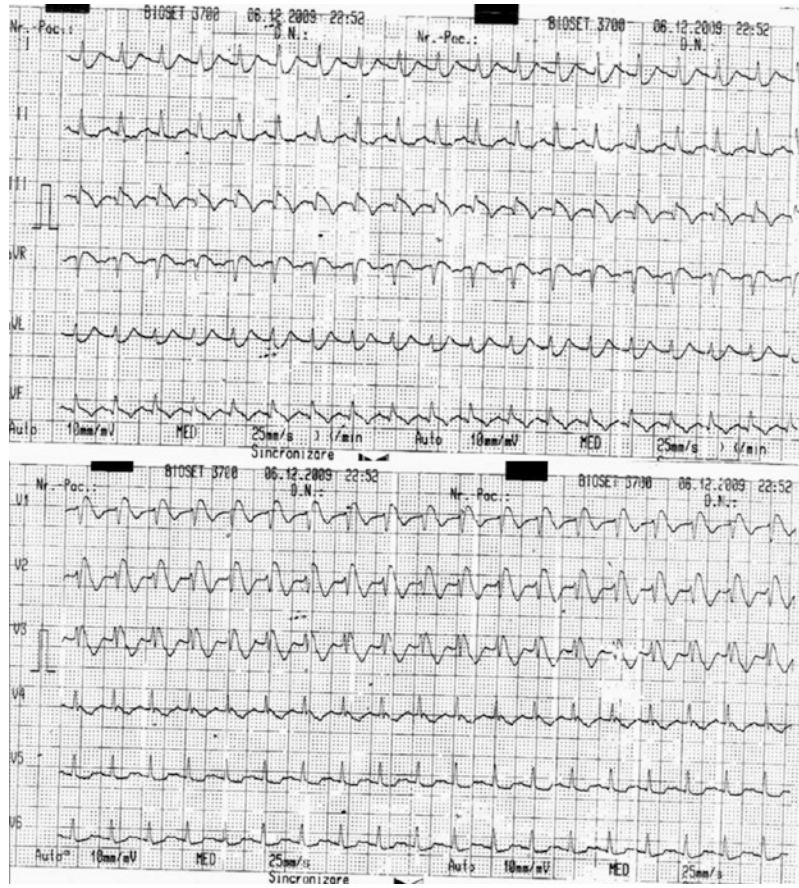

Fig. 30.12 ECG of a 23 year-old man with acute cor pulmonale secondary to life-threatening massive pulmonary embolism showing sinus tachycardia, S_1Q_3 pattern, ST elevation in III, aVF, V1–V3 leads and T wave inversions in these leads. Image from personal collection

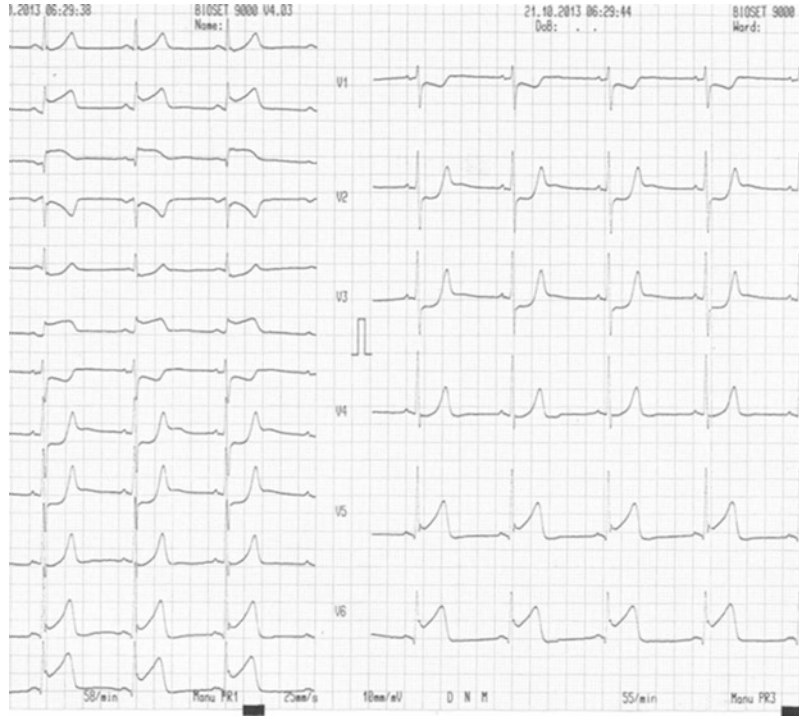

Fig. 30.13 Acute infero-posterior myocardial infarction (ST elevation in II, III, aVF, V_5, V_6 leads and ST depression in V_1, V_2 leads). Image from personal collection

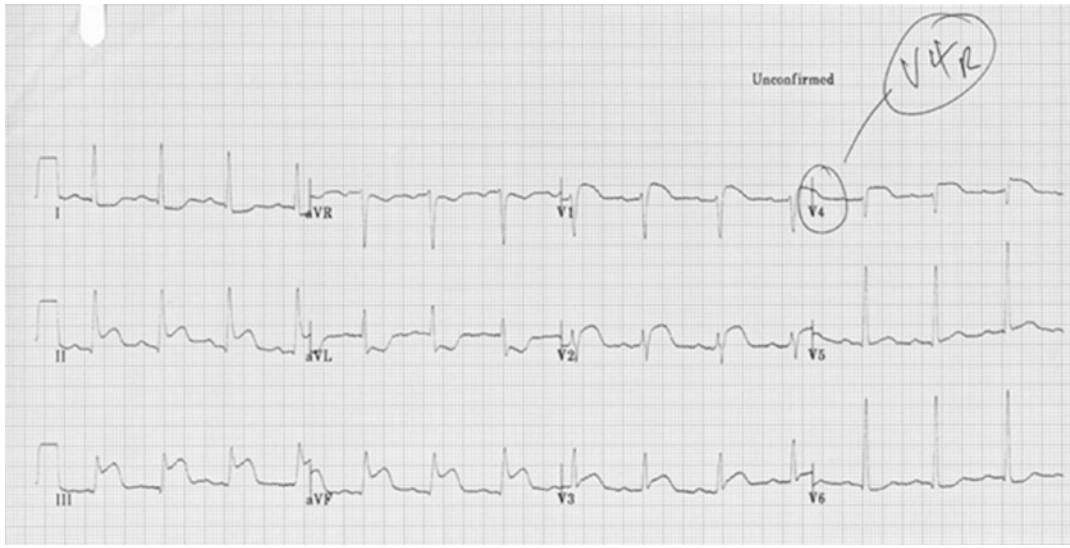

Fig. 30.14 ECG in a patient with acute inferior myocardial infarction (ST elevation in II, III, aVF); the V_{4R} precordial lead also shows us ST elevation suggesting right ventricular myocardial infarction. The correct precordial V_1–V_6 leads are not displayed on the ECG. Image from personal collection

30.5.7 ECG Abnormalities in Arrhythmogenic Right Ventricular Dysplasia

The ECG is abnormal in most patients with arrhythmogenic right ventricular dysplasia (ARVD). There are several ECG features in the criteria diagnosis of ARVD: T wave inversion in V_1 trough V_3 (minor diagnostic criterion, but one of most common ECG abnormality present in 85% of patients); QRS duration 110 ms in V_1 through V_3; epsilon wave (electric potentials after the end of the QRS complex; it is a major diagnostic criterion found in up to 30% of cases of ARVD) [41, 42]. Other ECG markers of ARVD have been reported: QRS and QT dispersion; right ventricular parietal block (defined as a QRS duration in leads V_1–V_3 that exceeds the QRS duration in lead V_6 by >25 ms); a prolonged S-wave upstroke in V_1–V_3 = 55 ms (it was seen as the most prevalent ECG feature in 95% of ARVD); ventricular tachycardia in the morphology of left bundle branch block [41, 43].

Atrial premature contractions, flutter and atrial fibrillation are not uncommon in ARVD especially in those with moderate/severe tricuspid regurgitation and markedly enlarged right ventricles; they can occur prior to or during manifest ventricular arrhythmia [44].

The increased susceptibility to ventricular tachyarrhythmia and sudden cardiac death is a main feature of ARVD. More details are offered in a specific chapter dedicated to ARVD.

30.5.8 ECG Abnormalities in Chronic Obstructive Pulmonary Disease

In chronic obstructive pulmonary disease (COPD), the heart changes its position within the chest, the lungs are hyperinflated and the diaphragm are flattened. Typical ECG changes include [11, 33]:

- peaked P waves >0.25 mV in leads II, III, aVF;
- P wave axis to the right of 80° in the frontal plane;
- reduced QRS amplitude in all limb leads <0.5 mV;
- QRS axis deviated to the right more than 90° in the frontal plane;
- delayed transition in the frontal plane (clockwise rotation);

- QRS amplitude <0.5 mV in lead V_5 or V_6 or R wave <0.7 mV in lead V_5 or R wave <0.5 mV in lead V_6;
- R/S ratio < 1 in lead V_5 or V_6;
- $S_1S_2S_3$ pattern with R/S ratio < 1 in leads I, II, and III

Chou suggests that COPD is likely to be present if one or more of these P wave changes and one or more of these QRS changes are identified [33].

Deep S waves in the lateral precordial leads, an $S_1Q_3T_3$ pattern, a QR pattern in lead V_1, are suggestive for RV hypertrophy. The electrocardiographic presence of RVH signs is not equivalent to severe lung disease or severe pulmonary hypertension. QRS changes do not generally appear until ventilatory function is significantly depressed, with the earliest change commonly being a rightward shift in the mean QRS axis, and the correlation with ventilatory function or hemodynamics is poor. The presence of right atrial abnormality, an $S_1S_2S_3$ pattern, or both is associated with reduced survival [11].

Sometimes, in patients with cor pulmonale, one can find transient changes during exacerbations of pulmonary insufficiency: T waves inversions in right precordial leads; ST segment depressions in leads II, III, and aVF; transient RBBB [45]. The arrhythmias in COPD are mostly supraventricular in origin and they tend to be transient. Multiform atrial tachycardia is almost pathognomonic for the presence of pulmonary insufficiency [38].

Taking into account all these electrocardiographic aspects, one can state that this part of examination is mandatory in every patient with confirmed or suspected right ventricular heart disease. More details about specific ECG aspects are offer in the dedicated chapters.

References

1. Weitzenblum E, Chaouat A. Cor pulmonale. Chron Respir Dis. 2009;6(3):177–85.
2. Haddad F, Doyle R, Murphy DJ, Hunt SA. Right ventricular function in cardiovascular disease, part II: pathophysiology, clinical importance, and management of right ventricular failure. Circulation. 2008;117(13):1717–31.
3. Matthews JC, McLaughlin V. Acute right ventricular failure in the setting of acute pulmonary embolism or chronic pulmonary hypertension: a detailed review of the pathophysiology, diagnosis, and management. Curr Cardiol Rev. 2008;4(1):49–59. http://www.pubmedcentral.nih.gov/articlerender.fcgi?artid=2774585&tool=pmcentrez&rendertype=abstract.
4. Watts JA, Marchick MR, Kline JA. Right ventricular heart failure from pulmonary embolism: key distinctions from chronic pulmonary hypertension. J Card Fail. 2010;16(3):250–9. https://doi.org/10.1016/j.cardfail.2009.11.008.
5. Dumitru I, Baker MM, Ooi HH. Heart failure clinical presentation. eMedicine; 2014 from: http://emedicine.medscape.com/article/163062-clinical.
6. Mesquita SM, Castro CR, Ikari NM, Oliveira SA, Lopes AA. Likelihood of left main coronary artery compression based on pulmonary trunk diameter in patients with pulmonary hypertension. Am J Med. 2004;116:369.
7. Safi M, Eslami V, Shabestari AA, Saadat H, Namazi MH, Vakili H, et al. Extrinsic compression of left main coronary artery by the pulmonary trunk secondary to pulmonary hypertension documented using 64-slice multidetector computed tomography coronary angiography. Clin Cardiol. 2009;32(8):426.
8. Tongers J, et al. Incidence and clinical relevance of supraventricular tachyarrhythmias in pulmonary hypertension. Am Heart J. 2017;153(1):127–32. https://doi.org/10.1016/j.ahj.2006.09.008.
9. Rajdev A, Garan H, Biviano A. Arrhythmias in pulmonary arterial hypertension. Prog Cardiovasc Dis. 2012;55(2):180–6. https://doi.org/10.1016/j.pcad.2012.06.002. http://www.ncbi.nlm.nih.gov/pmc/articles/PMC3832144/.
10. Arena V, De Giorgio F, Abbate A, Capelli A, De Mercurio D, Carbone A. Fatal pulmonary arterial dissection and sudden death as initial manifestation of primary pulmonary hypertension: a case report. Cardiovasc Pathol. 2004;13:230.
11. Mann DL, Zipes DP, Libby P, Bonow RO. Braunwald's heart disease: a textbook of cardiovascular medicine. 10th ed. Philadelphia: Saunders; 2014.
12. Rubin LJ, Hopkins W. Clinical features and diagnosis of pulmonary hypertension in adults. Uptodate Topic 8249 Version 22.0; 2017.
13. Tapson VF. Acute pulmonary embolism. Cardiol Clin. 2004;22:353.
14. Applefeld MM. The jugular venous pressure and pulse contour. In: Hurst JW, Walker HK, Hall WD, editors. Clinical methods: the history, physical, and laboratory examinations. Boston: Butterworths; 1990.
15. Shapira Y, Porter A, Wurzel M. Evaluation of tricuspid regurgitation severity: echocardiographic and clinical correlation. J Am Soc Echocardiogr. 1998;11(6):652.

16. Wiese J. The abdominojugular reflux sign. Am J Med. 2000;109(1):59.
17. Ambrosy AP, et al. The predictive value of transaminases at admission in patients hospitalized for heart failure: findings from the RO-AHFS registry. Eur Heart J Acute Cardiovasc Care. 2013;2(2):99–108. http://journals.sagepub.com/doi/10.1177/2048872612474906.
18. Dorobantu M, Badila E. Insuficienta Cardiaca Cronica. In: Dorobantu M, editor. Compendiu de Boli Cardiovasculare. Bucharest: Editura Universitara Carol Davila; 2010.
19. Farber MO, et al. Hormonal abnormalities affecting sodium and water balance in acute respiratory failure due to chronic obstructive lung disease. Chest. 1984;85(1):49–54. https://doi.org/10.1378/chest.85.1.49.
20. Porcel JM. Pleural effusions from congestive heart failure. Semin Respir Crit Care Med. 2010;31(6):689.
21. Han CH, Choi JE, Chung JH. Clinical utility of pleural fluid NT-pro brain natriuretic peptide (NT-proBNP) in patients with pleural effusions. Intern Med. 2008;47(19):1669–74. https://www.jstage.jst.go.jp/article/internalmedicine/47/19/47_19_1669/_pdf.
22. Kopcinovic LM, Culej J. Pleural, peritoneal and pericardial effusions – a biochemical approach. Biochem Med. 2014;24(1):123–37. http://www.ncbi.nlm.nih.gov/pmc/articles/PMC3936968/.
23. Natanzon A, Kronzon I. Pericardial and pleural effusions in congestive heart failure. Anatomical, pathophysiologic, and clinical considerations. Am J Med Sci. 2009;338(3):211–6. https://doi.org/10.1097/MAJ.0b013 e3181a3936f.
24. Otto CM. Etiology, clinical features, and evaluation of tricuspid regurgitation. UpToDate Topic 8119 Version 10.0; 2017.
25. Fukuda S, Gillinov AM, Song JM, Daimon M, Kongsaerepong V, Thomas JD, Shiota T. Echocardiographic insights into atrial and ventricular mechanisms of functional tricuspid regurgitation. Am Heart J. 2006;152:1208.
26. Chockalingam A, et al. Right ventricular myocardial infarction: presentation and acute outcomes. Angiology. 2005;56(4):371–6. https://doi.org/10.1177/000331970505600 402.
27. Silverman BD, Carabajal NR, Chorches MA, Taranto AI. Tricuspid regurgitation and acute myocardial infarction. Arch Intern Med. 1982;142(7):1394–5. https://doi.org/10.1001/archinte.1982.00340200164031.
28. van Lingen R, Warshow U, Dalton HR, Hussaini SH. Jaundice as a presentation of heart failure. J R Soc Med. 2005;98(8):357–9. http://www.ncbi.nlm.nih.gov/pmc/articles/PMC1181835/.
29. Feldt RH, et al. Protein-losing enteropathy after the Fontan operation. J Thorac Cardiovasc Surg. 1996;112(3):672–80. https://doi.org/10.1016/S0022-5223(96)70051-X.
30. Ahearn GS, Tapson VF, Rebeiz A, Greenfield JC Jr. Electrocardiography to define clinical status in primary pulmonary hypertension and pulmonary arterial hypertension secondary to collagen vascular disease. Chest. 2002;122:524.
31. Bossone E, Paciocco G, Iarussi D, Agretto A, Iacono A, Gillespie BW, et al. The prognostic role of the ECG in primary pulmonary hypertension. Chest. 2002;121:513.
32. Oswald-Mammosser M, Oswald T, Nyankiye E, Dickele MC, Grange D, Weitzenblum E. Noninvasive diagnosis of pulmonary hypertension in chronic obstructive pulmonary disease. Comparison of ECG, radiological measurements, echocardiography and myocardial scintigraphy. Eur J Respir Dis. 1987;71:419.
33. Surawicz B, Knilans T. Chou's electrocardiography in clinical practice. 6th ed. Philadelphia: Saunders; 2008.
34. Hancock EW, et al. AHA/ACCF/HRS recommendations for the standardization and interpretation of the electrocardiogram. Part V: electrocardiogram changes associated with cardiac chamber hypertrophy a scientific statement from the american heart association electrocardiography. J Am Coll Cardiol. 2009;53(11):992–1002. https://doi.org/10.1016/j.jacc.2008.12.015.
35. Gross D. Contributions to the functional morphology of the P wave. Am Heart J. 1961;61:436.
36. Murphy ML, et al. Reevaluation of electrocardiographic criteria for left, right and combined cardiac ventricular hypertrophy. Am J Cardiol. 1984;53(8):1140–7. https://doi.org/10.1016/0002-9149(84)90651-9.
37. Goldberger AL. Myocardial infarction: electrocardiographic differential diagnosis. 4th ed. St. Louis: Mosby-Year Book; 1991.
38. Chia BL, Tan HC, Lim YT. Right sided chest lead electrocardiographic abnormalities in acute pulmonary embolism. Int J Cardiol. 1997;61:43.
39. Ferrari E, et al. The ECG in pulmonary embolism: predictive value of negative t waves in precordial leads - 80 case reports. Chest. 1997;111(3):537–43. https://doi.org/10.1378/chest.111.3.537.
40. Zehender M, et al. Right ventricular infarction as an independent predictor of prognosis after acute inferior myocardial infarction. N Engl J Med. 1993;328(14):981–8. https://doi.org/10.1056/NEJM199304083281401.
41. Nasir K, et al. Electrocardiographic features of arrhythmogenic right ventricular dysplasia/cardiomyopathy according to disease severity. Circulation. 2004;110(12):1527 LP–1534. http://circ.ahajournals.org/content/110/12/1527.abstract.
42. Perez Diez D, Brugada J. Diagnosis and management of arrhythmogenic right ventricular dysplasia. Eur J Cardiol Pract. 2008;7(6)
43. Zhang L, Liu L, Kowey PR, Fontaine GH. The electrocardiographic manifestations of arrhythmo-

genic right ventricular dysplasia. Curr Cardiol Rev. 2014;10(3):237–45.http://www.ncbi.nlm.nih.gov/pmc/articles/PMC4040875/.

44. Chu AF, Zado E, Marchlinski FE. Atrial arrhythmias in patients with arrhythmogenic right ventricular cardiomyopathy/dysplasia and ventricular tachycardia. Am J Cardiol. 2010;106(5):720–2. https://doi.org/10.1016/j.amjcard.2010.04.031.

45. Incalzi RA, Fuso L, De Rosa M, Di Napoli A, Basso S, Pagliari G, Pistelli BT. Electrocardiographic signs of chronic cor pulmonale: a negative prognostic finding in chronic obstructive pulmonary disease. Circulation. 1999;99:1600–5. https://doi.org/10.1161/01.CIR.99.12.1600.

Chest X-ray in Right Heart Disease

31

Zhonghua Sun, Dongting Liu, and Zhanming Fan

Abstract

Right heart pathology receives less attention from clinicians than left-sided heart disease, and knowledge of the importance of right heart, in particular right ventricle in disease development lags behind that of the left ventricle. In recent years, increasing evidence shows that right heart disease has significant impact on morbidity and mortality, thus highlighting the importance of recognizing right heart disease in clinical practice. Although ultrasound and computed tomography are the most commonly used diagnostic image techniques in the diagnosis of right heart disease, chest radiography still remains the first line technique in many applications. Despite non-specific findings in most of the situations, chest X-ray provides useful information for further diagnostic imaging tests of assessing right heart disease. This chapter provides an overview of applications of chest X-ray in the diagnosis of various right heart diseases.

Z. Sun (✉)
Department of Medical Radiation Sciences, Curtin University, Perth, WA, Australia
e-mail: z.sun@curtin.edu.au

D. Liu · Z. Fan
Department of Radiology, Beijing Anzhen Hospital, Capital Medical University, Beijing, China

Keywords

Chest radiography · Diagnosis · Imaging techniques · Right heart disease

31.1 Introduction

Little attention has been paid to the investigation of right heart disease, mainly because of less muscular role to pumping blood through the right ventricle when compared to the left side. This is mainly due to the fact that the left ventricle is more frequently involved in diseases of epidemic proportions such as myocardial ischemia or infarction, cardiomyopathy, or valvular disease [1, 2]. Although limited information is associated with right heart function, the impact of right heart pathology on patient's outcome should draw clinicians' attention about understanding of pathophysiology of right heart disease, choosing appropriate diagnostic imaging tests and referring patients for timely intervention and treatment to prevent adverse complications.

Chest X-ray (CXR) is a useful imaging technique in diagnosing cardiac disease although its role has been ignored to a greater extent because of increasing use of echocardiography, computed tomography (CT) and magnetic resonance imaging (MRI) imaging

S. I. Dumitrescu et al. (eds.), *Right Heart Pathology*, https://doi.org/10.1007/978-3-319-73764-5_31

modalities for more accurate assessment of cardiac anatomy and physiology. As a simple, quick and cheap test, the CXR offers diagnostic information about heart size and lung pathology (Fig. 31.1). Further, the CXR provides useful information for serial comparison of the pathology with low radiation dose [3, 4]. This chapter provides an overview of the diagnostic applications of CXR in various right heart diseases.

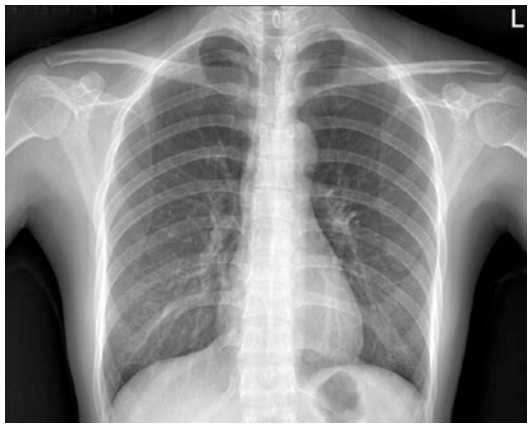

Fig. 31.1 Normal chest radiograph. Bony thorax is symmetrical, with lung field clear. Bilateral hilar appearances are normal, and mediastinum is not widened. The heart shape is normal and its size is within normal limit. Costophrenic angles are sharp

31.2 Normal Right Heart

The right ventricle has complex geometry which makes it different from the left ventricle in several areas: the tricuspid valve configuration of having trileaflet, presence of coarse trabeculation, presence of three or more papillary muscles, and only one-fifth mass of that of the left ventricle [5]. Thus, the right ventricular wall is much thinner than that of the left ventricle as shown in Fig. 31.2. The right ventricle is connected to the left side through the following structures: by an interventricular septum (a shared wall), by sharing the pericardial space and epicardial fibers.

The unique morphological features of right ventricle allow it to serve as a volume-loaded pump with stroke volume identical to that of the left ventricle. However, due to a much smaller mass, the right ventricle is more sensitive to pressure-loaded situations, thus is at risk for developing acute and chronic right heart failure [6]. The blood supply to the right ventricle is mainly provided by the right coronary artery, while anterior two-thirds and inferoposterior one third of the ventricular septum are provided by the left anterior descending coronary artery and the posterior descending artery, respectively. Figure 31.3 shows normal right and left coronary arteries by coronary CT angiographic images.

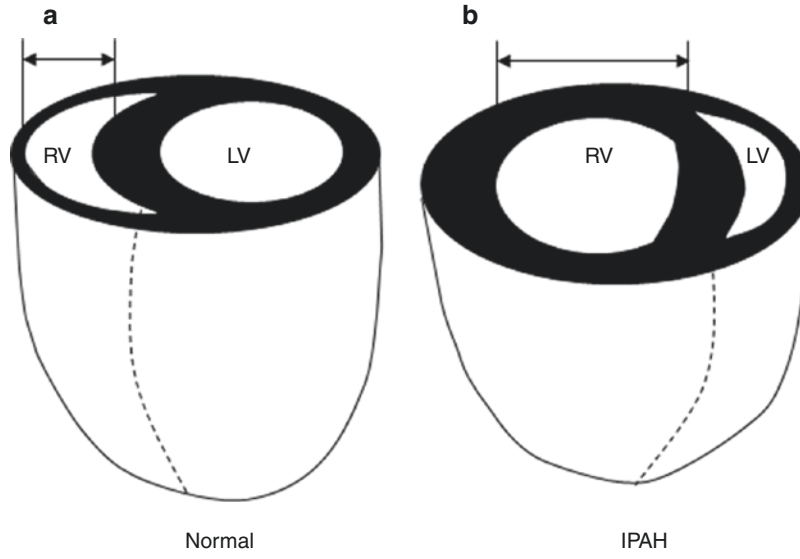

Fig. 31.2 Normal and enlarged right ventricle. (**a**) Diagram shows thinned-wall right ventricle (RV) when compared to the left ventricle (LV). (**b**) In idiopathic pulmonary arterial hypertension (IPAH), the RV is characterized by increased end-diastolic volume, leading to varying degrees of right ventricular hypertrophy. Modified from Voelkel et al. [2]

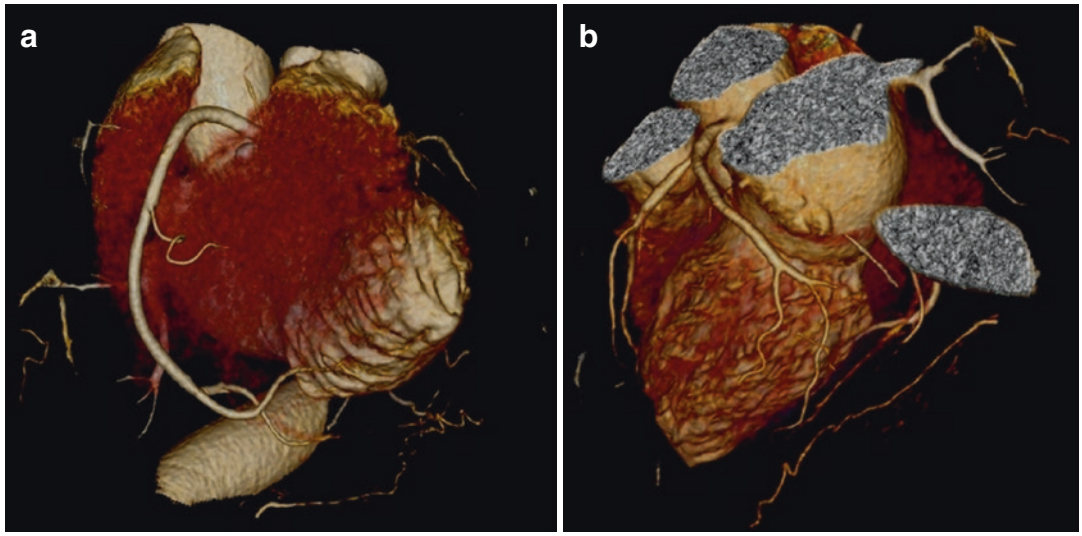

Fig. 31.3 Normal coronary arteries on coronary CT angiography. 3D volume rendering CT angiographic images demonstrate the normal right coronary artery (**a**) and left coronary artery (**b**)

31.3 Right Heart Failure

The right ventricle plays an important role in the management and prognosis of many cardiovascular diseases. The underlying mechanisms of causing right heart dysfunction or failure are not fully understood as opposed to the left ventricular failure. Although multiple factors affect right heart failure due to its association with the left heart failure, and variations exist in the methodologies of assessment of right ventricular function, it is generally agreed that the right ventricular dysfunction or failure predicts an inferior outcome [2]. Studies showed that patients with impaired left ventricular function developed worse right ventricular function [7], or presence of both right and left ventricular dysfunction resulted in higher mortality when compared to the left ventricular failure alone [8]. This highlights the predictive role of a negative outcome by right ventricular dysfunction or failure [9]. Decreased right ventricular function has been reported as a critical prognostic factor [10, 11].

The role of CXR for diagnostic assessment of right heart failure is limited as it is predominantly assessed by echocardiography. Assessment of right ventricular morphology and function can be adequately achieved by transthoracic echocardiography in most patients, with additional imaging modalities (such as cardiac magnetic resonance imaging or cardiac computed tomography) required in the presence of poor quality or for further functional assessment [12–15]. Figure 31.4 is an example of CXR showing the right heart failure.

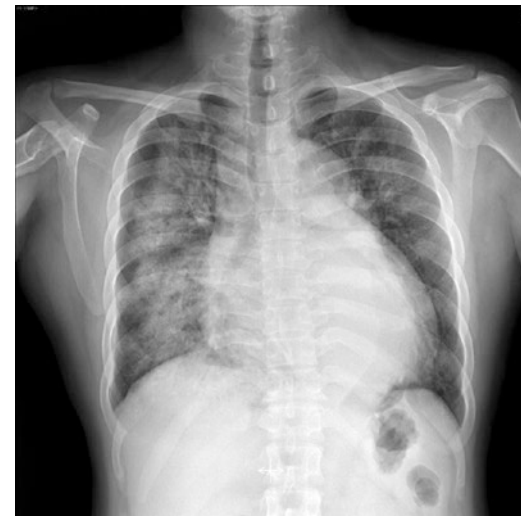

Fig. 31.4 Right heart failure in a 34-year male with chest discomfort after exercise. The patient presented with symptoms of edema at the upper and lower extremities. Chest radiograph shows that lung markings increased, especially apparent on the right side, with patchy shadows on the right lung. The heart size is enlarged

31.4 Pulmonary Hypertension

Pulmonary hypertension is a life-threatening condition with progressive pulmonary vascular abnormalities. It occurs when resting mean pulmonary arterial pressure is increased to more than 25 mmHg measured by right heart catheterization [16, 17]. Although the exact etiology of pulmonary hypertension is unclear, patients with pulmonary hypertension are associated with high mortality in spite of therapy [18].

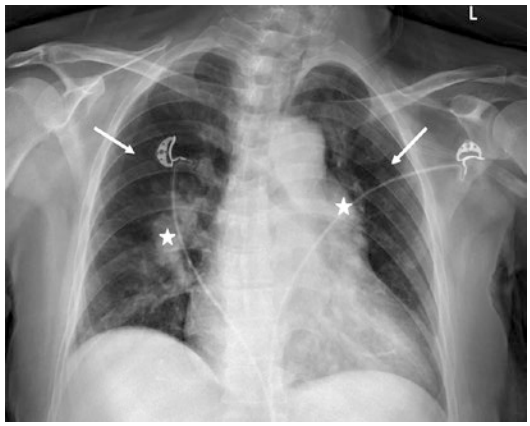

Fig. 31.5 Pulmonary hypertension in a 64-year-old woman with history of chest discomfort after exertion for 4 years, and hypertension for 5 years. Chest radiograph shows prominent dilated pulmonary arteries (stars) with rapid pruning of peripheral pulmonary vessels (arrows), and cardiomegaly

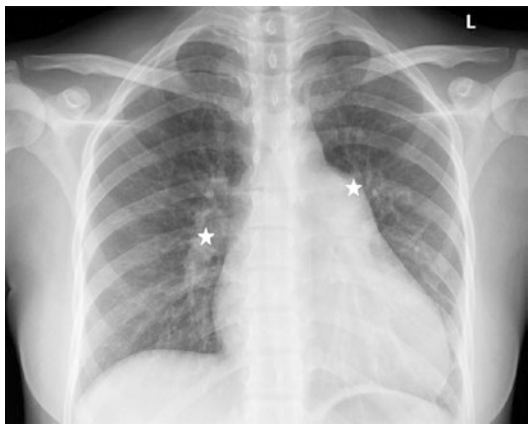

Fig. 31.6 Pulmonary hypertension in a 29-year-old woman with 27 weeks of pregnancy. Chest radiograph reveals dilated pulmonary arteries (stars), and right atrium and right ventricle enlargement

CXR is usually performed as the baseline imaging technique in patients with suspected pulmonary hypertension. Although a normal CXR does not exclude pulmonary hypertension, an abnormal CXR is commonly seen in confirmed diseases [19]. CXR findings include cardiomegaly due to enlarged right atrium and right ventricle; reduced or loss of peripheral pulmonary vessels (Fig. 31.5), and dilation of main pulmonary arteries [20].

The characteristic feature of pulmonary hypertension is manifested as the increased diameter of central pulmonary arteries, with diminished peripheral pulmonary vessels frequently observed in patients with pulmonary hypertension [21, 22] (Fig. 31.6). CXR also plays a role in the differential diagnosis by diagnosing left-sided heart disease and providing information about lung parenchymal abnormalities such as interstitial lung disease and pulmonary embolism [20]. Despite its widespread use in clinical practice, CXR is limited by its nonspecific findings and low diagnostic value to assess disease extent. CT has become the preferred imaging modality for the diagnostic evaluation of pulmonary hypertension because of the superior spatial and temporal resolution, with capability of providing comprehensive assessment of the cardiopulmonary structures and lung parenchyma [20, 23–25].

31.5 Right Ventricular Hypertrophy

Assessment of right ventricular size and function comprises an essential part of routine echocardiographic examination in patients with chronic conditions, such as pulmonary hypertension and cardiomyopathy. While two-dimensional (2D) measurements of right ventricular wall thickness are commonly performed, three-dimensional (3D) echocardiography is increasingly used for assessment of right ventricular volumes because it has been found to be reliable and accurate in different diseases such as pulmonary hypertension and congenital heart

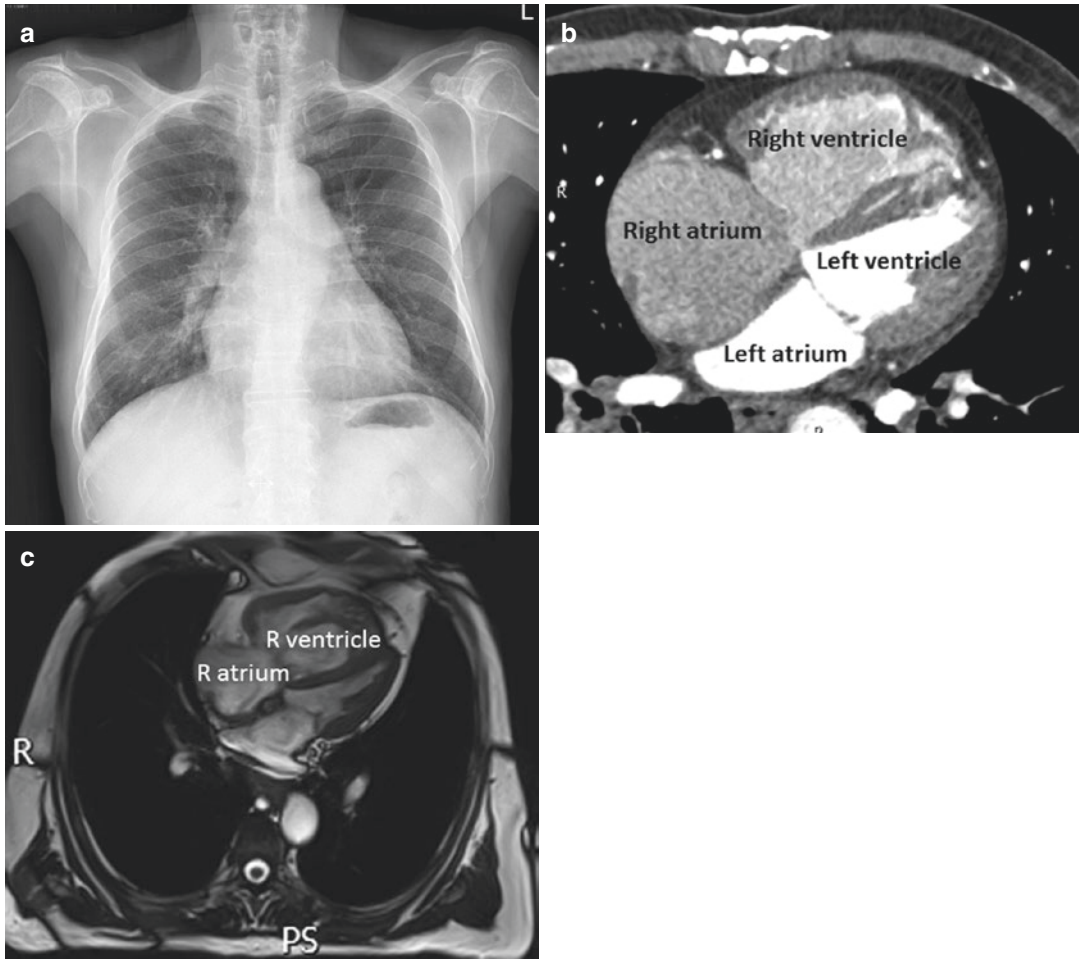

Fig. 31.7 Right ventricular hypertrophy in a 72-year-old male with cough and breathing difficulty after exertion for 4 years, with chest discomfort worsening over the last 2 days. (**a**) Chest radiograph demonstrates cardiomegaly, in particular, enlarged cardiac silhouette. Cardiac CT and cardiac magnetic resonance (**b** and **c**) show enlarged right atrium and right ventricle when compared to the left side

disease [26–28]. Studies have reported good agreement between 3D echocardiography and cardiac magnetic resonance (CMR) imaging measurements of right ventricular volumes and functions [28–30]. Guidelines are available for echocardiographic assessment of the right ventricle for the adult and pediatric patients [31, 32].

CXR is limited in the assessment of right ventricular hypertrophy as it can only detect the cardiac enlargement, while cardiac CT and CMR are more accurate in visualizing heart chamber changes (Fig. 31.7). CMR is still the gold standard for right ventricular assessment [13].

31.6 Right Pulmonary Embolism

Pulmonary embolism is one of the most common causes of cardiovascular death. Untreated pulmonary embolism is associated with an increase in morbidity and mortality [33]. CT pulmonary angiography (CTPA) is currently the method of choice for diagnosis of suspected pulmonary embolism due to its high sensitivity and specificity that is available with modern CT scanners. The widespread availability and high diagnostic value have led to the increasing use of CTPA as a reliable diagnostic imaging modality to detect or

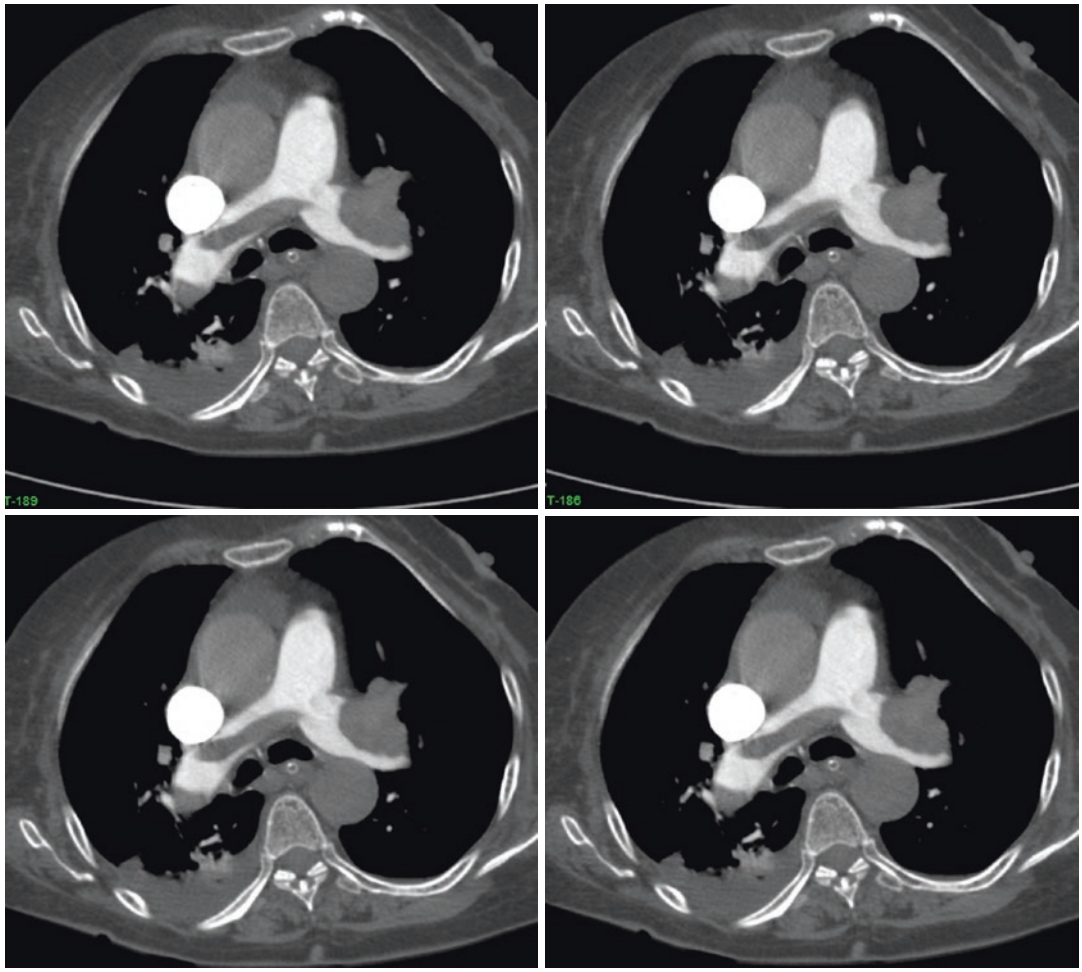

Fig. 31.8 CT pulmonary angiography of pulmonary embolism in an 85-year-old man. 2D axial image show large filling defects in the left and right main pulmonary arteries consistent with pulmonary embolism. Right pleural effusion is also noticed

exclude pulmonary embolism both in the emergency department and in-patient setting [34–39]. With improved spatial resolution, CTPA allows for detection of segmental and subsegmental pulmonary embolism with high accuracy as shown in Fig. 31.8. Although CT is considered a high radiation dose modality, recent studies have shown the feasibility of double low-dose CTPA protocol in the diagnosis of pulmonary embolism [40–44].

Despite its limited diagnostic value, CXR is commonly performed in patients with suspected pulmonary embolism to rule out other pulmonary diseases such as acute or chronic airway disease because the co-existing cardiopulmonary disease contributes to indeterminate results for isotope lung scanning [45]. In addition, it has been reported that nearly 50% of patients with an abnormal CXR require further testing [46, 47] (Fig. 31.9). The sensitivity, specificity, positive predictive value and negative predictive value of CXR in the detection of pulmonary embolism are found to be 36%, 92%, 38% and 76%, respectively, while the corresponding values for CTPA are more than 90% [48].

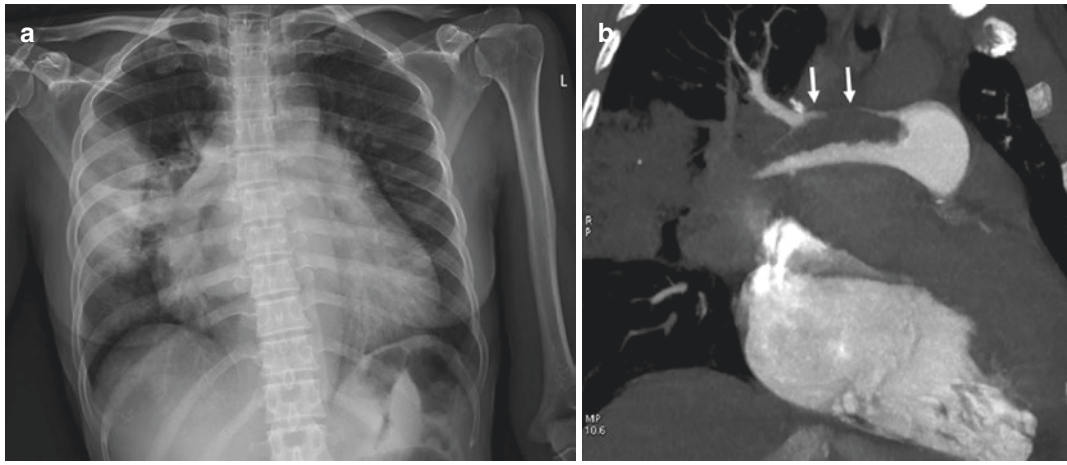

Fig. 31.9 Right pulmonary embolism in a 48-year-old woman with developing sudden cough and bloody sputum. (**a**) Chest X-ray shows large, patchy high-density shadow in the right lung field. (**b**) Coronal CT reformation demonstrates low-density large filling defect (arrows) in the right pulmonary artery, with abruption of distal pulmonary artery. Right lung consolidation is visualized

31.7 Right Cardiac Tumours

Primary cardiac tumours are very rare with reported incidence of between 0.0017% and 0.028% [49], while metastatic tumours are more common. Most of the primary cardiac tumours (up to 90%) are benign, whereas metastatic tumours are malignant [50, 51]. The benign tumours consist of fibromas, hemangiomas, lipomas, pericardial cysts and teratomas, while malignant tumours include various types of sarcomas such as fibrosarcoma, liposarcoma, myxosarcoma and leiomyosarcoma, etc.

Of various imaging modalities for assessment of cardiac tumours, 2D echocardiography is usually the first line test for examining patients presenting with cardiac symptoms. Combining transthoracic echocardiography with transesophageal echocardiography together allows more accurate assessment of the tumour size, shape, morphology and hemodynamic changes [50, 52]. CXR may detect cardiomegaly caused by cardiac tumours, although its imaging appearances are non-specific. Cardiac CT and CMR are also useful for diagnosis of cardiac tumours, including further characterization and differential diagnosis. Cardiac CT is able to help identification of fat with high specificity [53, 54].

Figure 31.10 is an example of cardiac tumour in the right atrium with fat attenuation on cardiac CT images, while Fig. 31.11 is another example of cardiac tumour in the right ventricle with fat attenuation.

31.8 Congenital Heart Disease

Congenital heart disease (CHD) is the most common congenital anomalies [55]. The prevalence of CHD is reported to be 9.1 per 1000 live births, but geographic variations are reported, with the highest prevalence at 9.3 per 1000 live births in Asia, and the lowest prevalence at 8.2 per 1000 live births in Europe [56–58]. The difference in these reported figures is mainly due to the discrepancies in disease definition and identification, use of advanced diagnostic modalities and other factors such as hereditary and environmental factors [56, 58].

A number of imaging techniques are used in the diagnosis of CHD including chest radiography, echocardiography, cardiac CT and CMR with each of them having advantages and limitations. Electrocardiogram and CXR serve as the preliminary diagnostic tools of CHD. Electrocardiogram can help detection of cardiac defects or rhythm abnormalities through

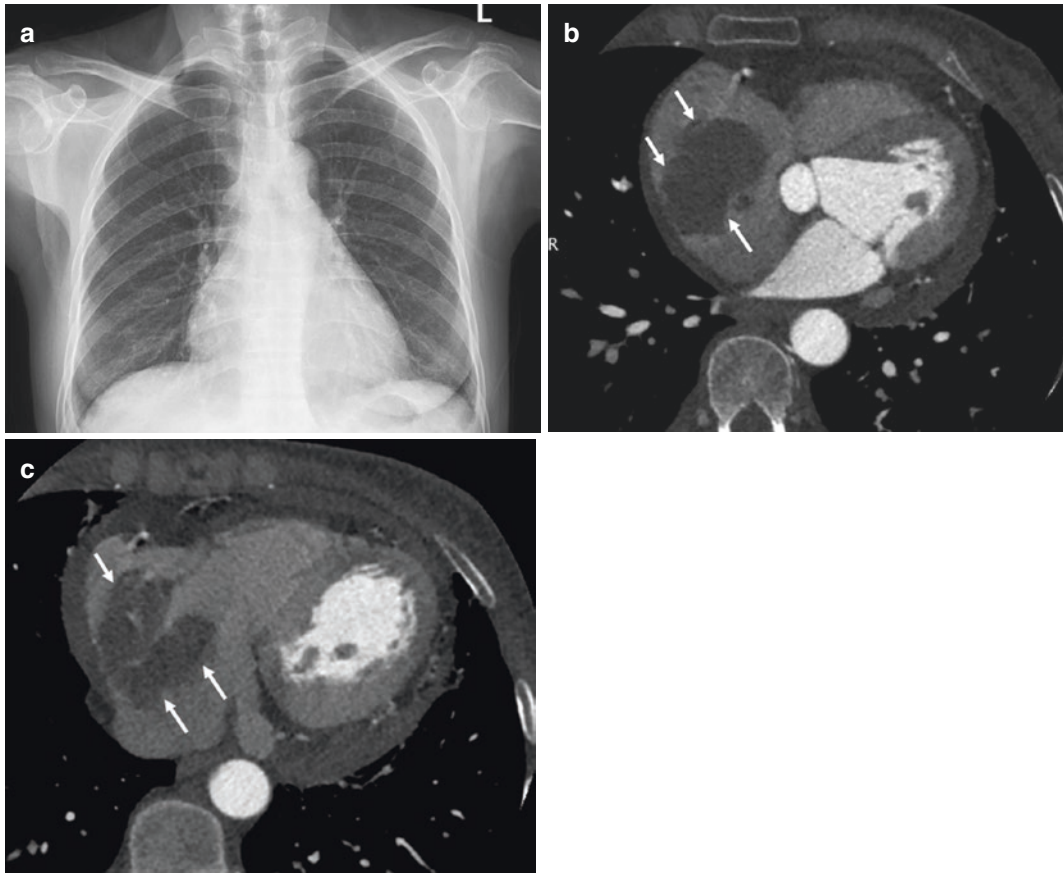

Fig. 31.10 Right atrial tumour in a 53-year-old woman with persistent fever for 3 months. Echocardiography shows a space-occupying lesion in the right atrium. (**a**) Chest radiograph shows right atrium enlargement. (**b** and **c**) Contrast-enhanced CT images show a low-attenuating mass (arrows) with no enhancement. The tumour is measured 5.2 × 3.9 cm in the right atrium with CT attenuation consistent with fat

recording the electrical activity, while CXR plays an important role in determining if the heart is enlarged or lungs are abnormal due to extra blood or fluid which could result in heart failure [59].

31.8.1 Atrial Septal Defect

CXR may demonstrate changes of cardiomegaly due to increased blood volume to the right atrium and right ventricle caused by atrial septal defect (ASD), as well as increased pulmonary markings and dilatation of the pulmonary artery and its branches [60]. However, in children with ASD, CXR was found to be limited value in the diagnosis of defect-specific lesions [61]. In adults with ASD, right ventricular hypertrophy can be visualized on chest radiograph due to long-standing right ventricular volume overload. Figure 31.12 shows a pediatric ASD with right atrium and right ventricle enlargement.

31.8.2 Ventricular Septal Defect

CXR provides diagnostic value in the detection of ventricular septal defect (VSD), depending on the disease extent. Small VSD is generally not associated

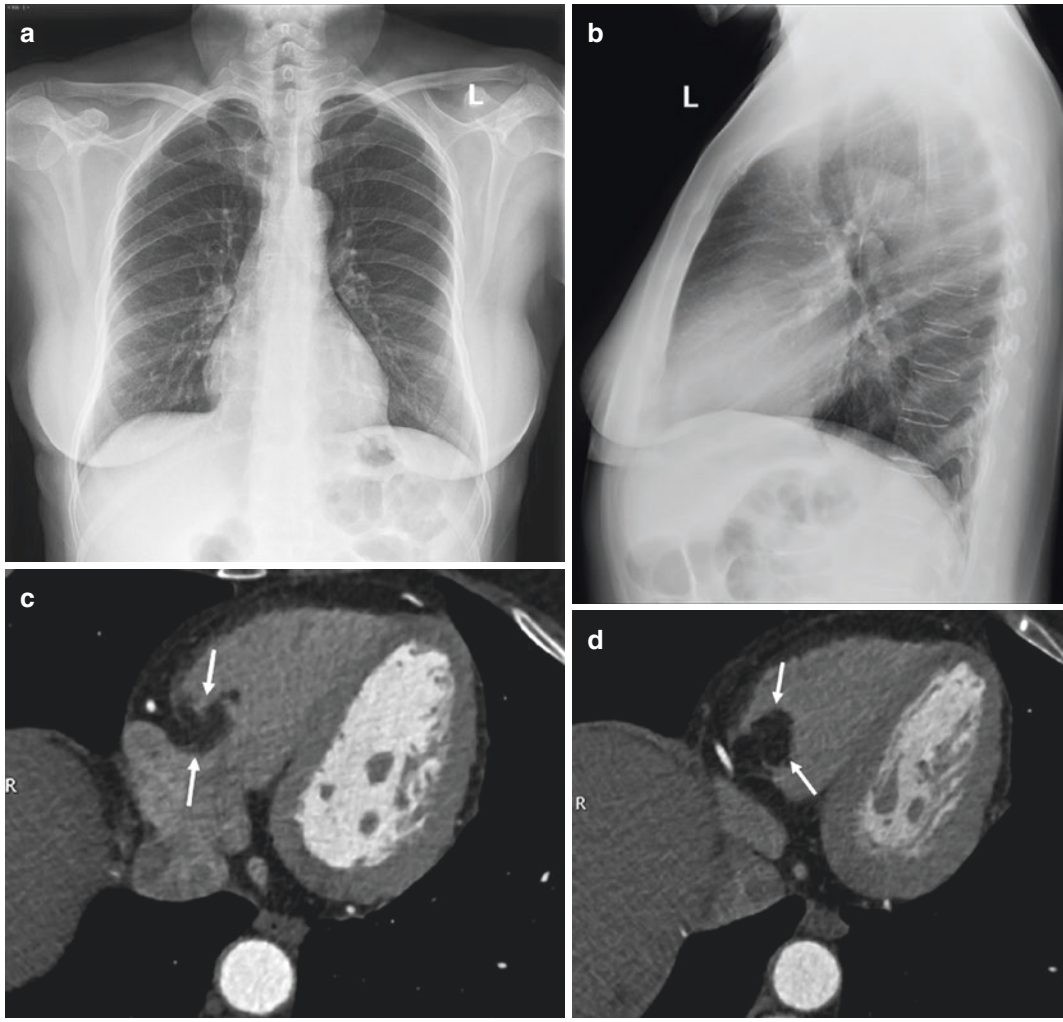

Fig. 31.11 Right ventricular tumour in a 63-year-old female. (**a** and **c**) PA and lateral chest radiographs show that lung fields are clear with hilar normal. The cardiac silhouette is slightly enlarged. (**c** and **d**) Contrast-enhanced CT images reveal a 2.9 × 3.0 cm low-attenuation tumour (arrows) in the right ventricle. The tumour is well defined showing no enhancement

with abnormal X-ray findings, thus showing no relationship between use of X-ray and diagnostic accuracy [61]. For intermediate to large VSD, CXR is able to demonstrate radiographic changes by assisting clinician's diagnosis of VSD. Abnormal chest radiographic findings include cardiomegaly and increased pulmonary arterial markings. An independent association was reported between use of CXR and higher level of suspicion for intermediate to large VSD, indicating the enhancing role of CXR for detection of VSD [61]. Figure 31.13 is an example of VSD in a pediatric patient with enlargement of both ventricles.

31.9 Tricuspid Valve Disease

Tricuspid valve is considered by most surgeons as a second-class structure or the "forgotten valve", leading to the fact that tricuspid valve

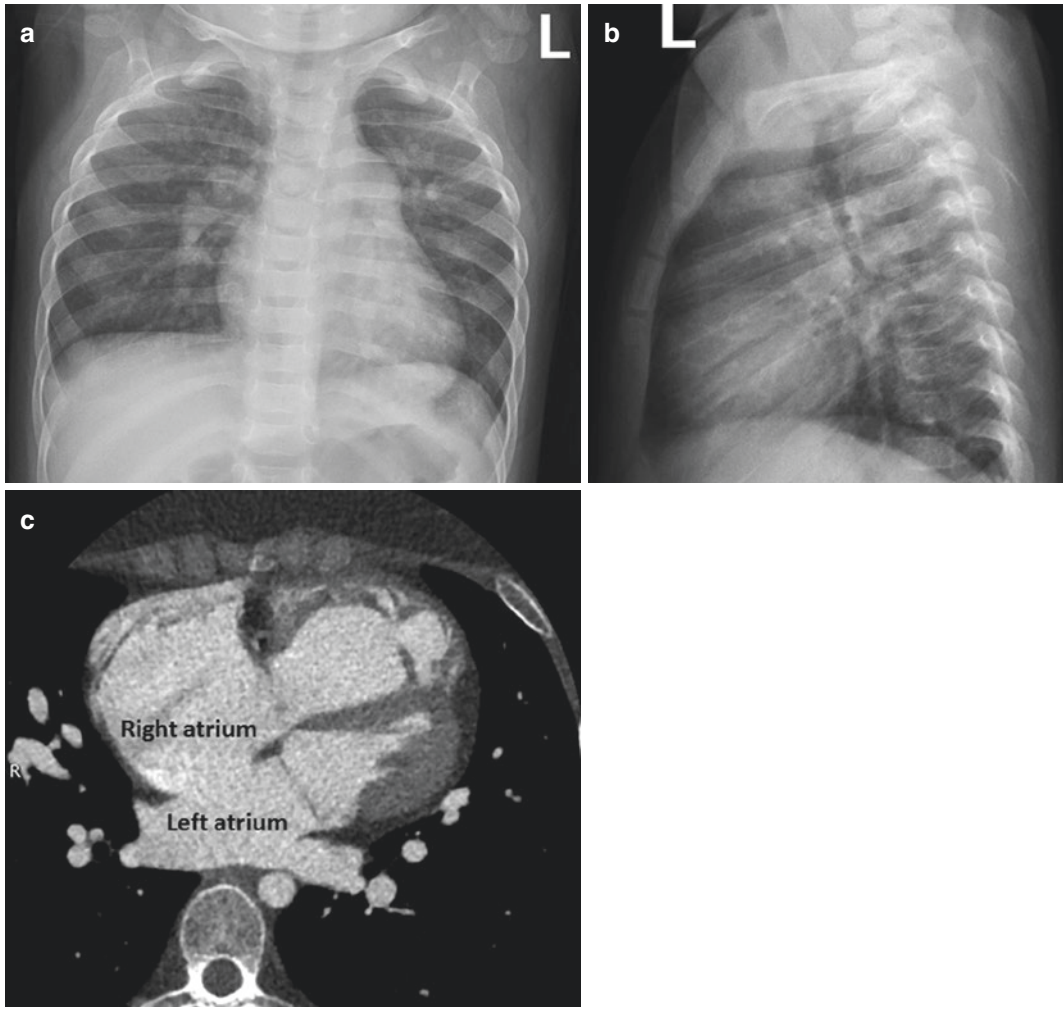

Fig. 31.12 Atrial septal defect (ASD) in a 1-year-old girl with cardiac murmur for 1 month. Echocardiographic examination reveals ASD. (**a** and **b**) PA and lateral chest radiographs show increased lung markings, prominent pulmonary arteries, enlargement of right atrium and right ventricle. (**c**) Contrast-enhanced CT shows right atrium and right ventricle enlargement, with interatrial septum disrupted, with defect size measured 3.4 × 3.0 cm

disease has been often neglected, receiving lesser importance than that of left-sided valvular heart disease [62, 63]. Recent advances in surgical and percutaneous transcatheter techniques have improved understanding of the long-term consequences of tricuspid valve disease, in particular, the effective management of severe tricuspid regurgitation [64–66].

Tricuspid value is more complex than left-sided valves, thus, it is necessary to have a better understanding of its anatomy to assist differentiating normal appearances from pathological changes [67, 68]. Figure 31.14 shows normal tricuspid valve anatomy and adjacent structures. Echocardiography is the preferred diagnostic technique for determining the etiology and severity of tricuspid valve disease, in addition to its value for assessment of right ventricular size and function. Figure 31.15 is an example of multiple transthoracic windows from echocardiographic examination allowing for comprehensive assessment of the tricuspid valve.

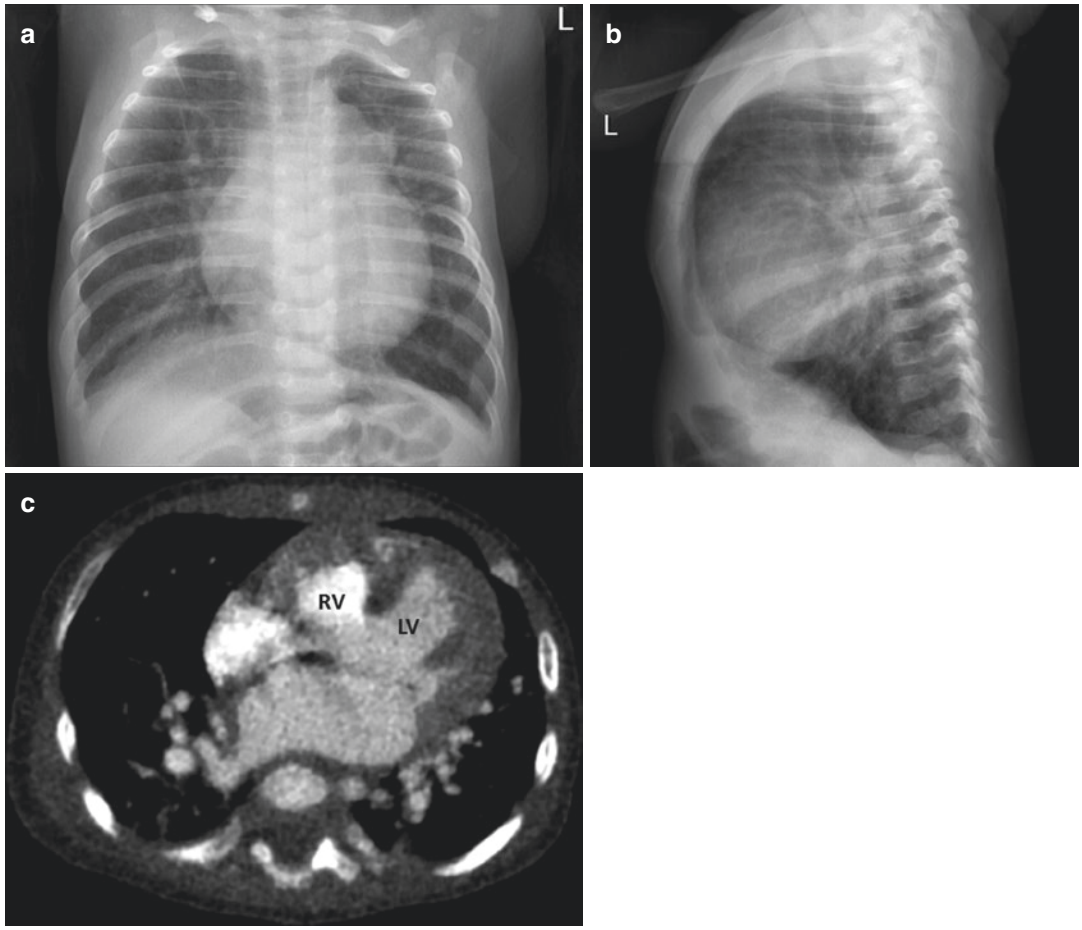

Fig. 31.13 Ventricular septal defect (VSD) in a 4-month-old baby with cardiac murmur for 1 month. (**a** and **b**) PA and lateral chest radiographs show increased lung markings, prominent pulmonary arteries and cardiomegaly. (**c**) Contrast-enhanced CT confirms left atrium and left ventricle enlargement. The interatrial septum is intact, but interventricular septum is disrupted with the defect size measured 5.9 × 11.2 cm, consistent with VSD. *LV* left ventricle, *RV* right ventricle

31.9.1 Tricuspid Stenosis

Tricuspid stenosis is a very rare and uncommon condition when compared to tricuspid regurgitation. The development of tricuspid stenosis is mainly due to congenital defects, rheumatic heart disease, and right atrial tumours [62]. Of these causes, rheumatic heart disease accounts for nearly 90% of cases. Further, rheumatic tricuspid stenosis often coexists with mitral valve disease and tricuspid regurgitation. While echocardiography is commonly used for diagnostic assessment of tricuspid stenosis including calculation of tricuspid gradient by Doppler echocardiography [69–71], CXR may show cardiopulmonary changes as shown in Fig. 31.16, although these findings are non-specific for clinical diagnosis.

31.9.2 Tricuspid Regurgitation

Tricuspid regurgitation is a common valvular disease with more than 80% belonging to secondary in nature caused by tricuspid annular dilatation, pulmonary hypertension and right ventricular infarction, while primary origin results from congenital or acquired disease processes [62]. Volume overload of the right ventricle due to

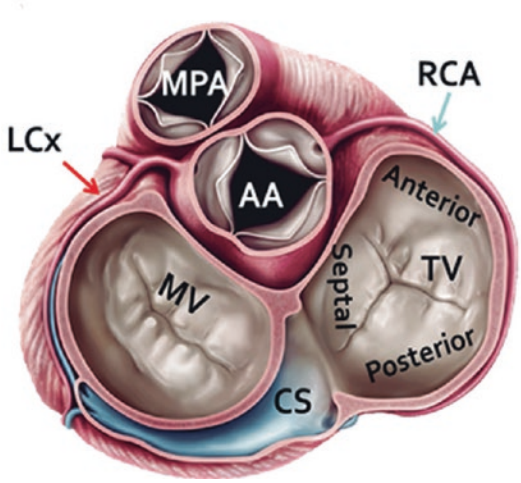

Fig. 31.14 Tricuspid value (TV) anatomy. Tricuspid valve (TV) anatomy and adjacent structures. *AA* ascending aorta, *CS* coronary sinus, *LCx* left circumflex artery, *MV* mitral valve, *MPA* main pulmonary artery, *RCA* right coronary artery. Reprinted with permission from Rodes-Cabau et al. [64]

tricuspid regurgitation results in right ventricular size and functional changes. With chronic volume overload, the right ventricular hypertrophy develops. Patients with long-standing severe tricuspid regurgitation lead to right heart failure.

Transthoracic echocardiography combined with Doppler imaging provides qualitative and quantitative assessment of tricuspid regurgitation, such as identifying the cause and severity of disease, measuring the dimensions of the tricuspid annulus, right ventricular function and right atrial and pulmonary arterial pressures [62]. Recently, 3D echocardiography has been shown to be more accurate than standard 2D techniques in the detection of tricuspid anatomy and annular dimensional changes [72–75]. CMR is not widely available and has some limitations, while cardiac CT allows precise measurements of the tricuspid value and annular structures [76, 77]. CXR has limited diagnostic value as the findings of cardiomegaly are non-specific (Fig. 31.17).

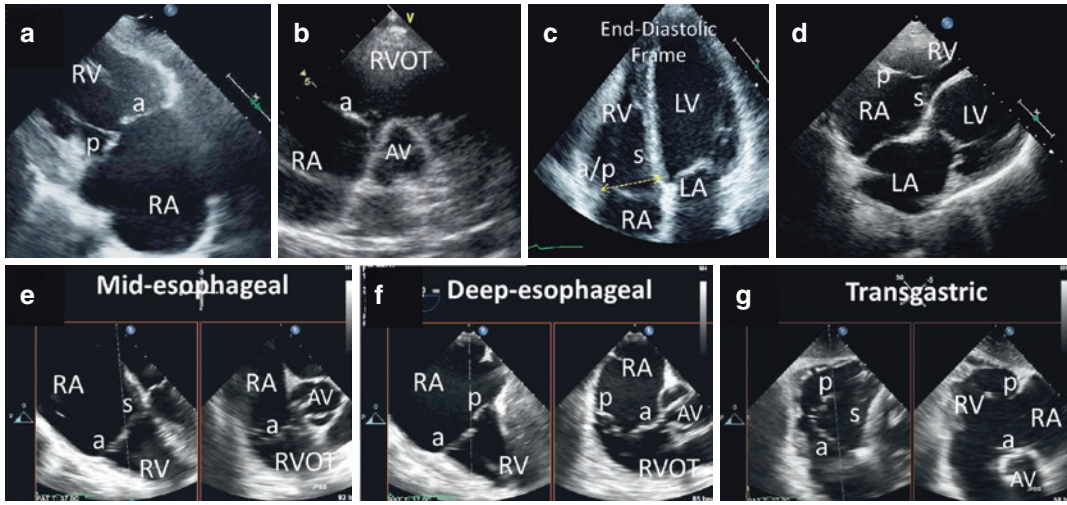

Fig. 31.15 Transthoracic and transesophageal imaging planes for the tricuspid valve. Multiple transthoracic imaging planes (**a** to **d**) should be performed for comprehensive imaging of the tricuspid valve (TV). The parasternal inflow view (**a**) images the anterior (a) and posterior (p) leaflets when no ventricular septum is in the imaging plane. (**b**) Parasternal short-axis view at the level of the aortic valve; when the transducer is angled anteriorly, only the anterior (a) leaflet is seen (with no other leaflet coaptation). (**c**) On-axis 4-chamber view with the left ventricle (LV) in the apex of the sector. The end-diastolic frame shown should be used to measure the annular diameter (dashed yellow double arrow). A subcostal view is shown in (**d**). Transesophageal imaging planes (**e** to **g**) should be performed from multiple levels. These examples from the mid-esophageal view (**e**), the deep-esophageal view (**f**), and the transgastric view (**g**) are simultaneous multiplane images showing the primary imaging plane on the left of each panel, and the orthogonal (rotated 90°) image on the right side of each panel. *AV* aortic valve, *LA* left atrium, *RA* right atrium, *RV* right ventricle, *RVOT* right ventricular outflow tract, *s* septal leaflet. Reprinted with permission from Rodes-Cabau et al. [64]

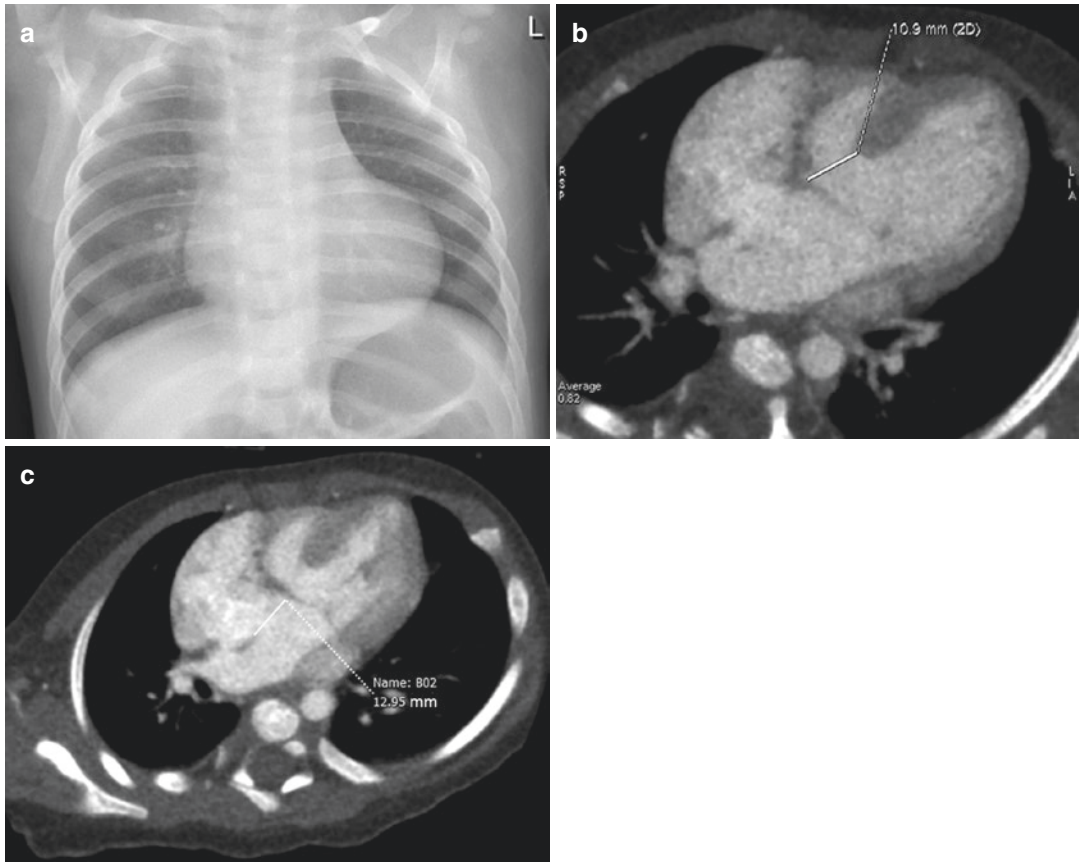

Fig. 31.16 Tricuspid stenosis in an 8-month-old boy with cyanosis after birth, and cardiac murmur for 1 month. (**a**) Chest radiograph shows decreased blood supply to the lung fields, with pruning of hilar vessels. The cardiac silhouette is enlarged. (**b** and **c**) Contrast-enhanced CT images confirm enlarged right atrium and right ventricle, with discontinued interatrial and interventricular septa with defects measured 13.5 × 12.9 and 13.0 × 10.9 mm, respectively

31.10 Pulmonary Valve Stenosis

Most of the pulmonary valve stenosis is caused by congenital diseases, while rheumatic cause is uncommon. Electrocardiogram in severe pulmonary valve stenosis shows right atrium enlargement, right ventricular hypertrophy and right ventricular strain pattern [1, 78]. The most typical feature of pulmonary valve stenosis is dilatation of the main pulmonary artery. Other findings that can be detected on chest radiograph include right-sided heart enlargement, diminished pulmonary vascular markings (Fig. 31.18) [1, 61, 78]. The heart may be within normal size, but can be enlarged in half of the patients. Transthoracic echocardiography is recommended as the imaging technique for diagnosis and follow-up of pulmonary valve stenosis [79].

31.11 Pulmonary Regurgitation

Pulmonary regurgitation is most commonly caused by congenital heart disease such as Tetralogy of Fallot. Less common causes include rheumatic disease, trauma, endocarditis and pulmonary artery dilation [1].

Patients with long-standing history of pulmonary regurgitation are associated with development of progressive right ventricular enlargement and reduced right ventricular function. Chest radiograph may show cardiomegaly involving

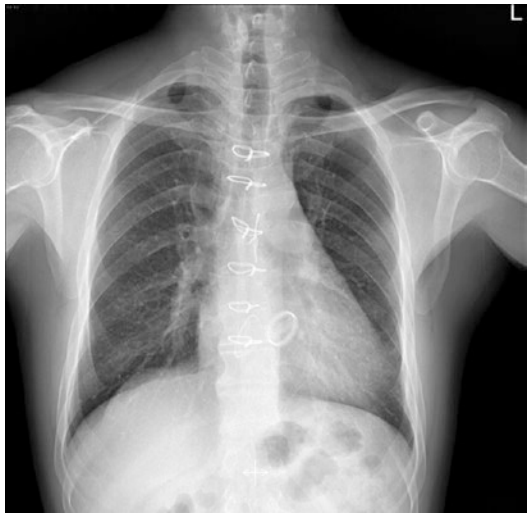

Fig. 31.17 Tricuspid regurgitation in a 50-year-old man with chest discomfort after exertion for 5 years. Echocardiography reveals tricuspid regurgitation with severe reflux, mitral valve slightly stenosed. Mitral valve replacement is noted. Chest radiograph shows that pulmonary arteries are slightly prominent, with left atrium and right ventricle enlargement

the right atrium and right ventricle as well as pulmonary artery enlargement (Fig. 31.19). Echocardiography is usually used for diagnostic assessment of pulmonary regurgitation, when combined with Doppler imaging it enables evaluation of the degree of regurgitation, right ventricular and pulmonary pressure changes [80, 81]. Currently, CMR is the reference standard for evaluation of pulmonary regurgitation and right ventricular performance [82–84].

31.12 Summary

There has been significant progress in the recognition and management of right heart disease owing to the increased impact of right heart disease on morbidity and mortality and rapid developments in imaging techniques. A variety of imaging modalities are available for clinicians to choose for diagnostic purpose, ranging from general chest X-ray to 2D and 3D echocardiography,

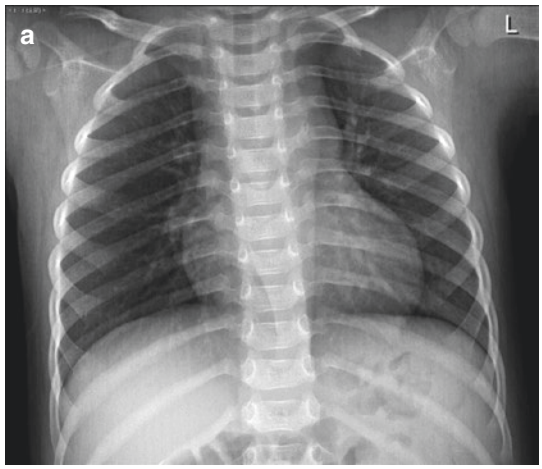

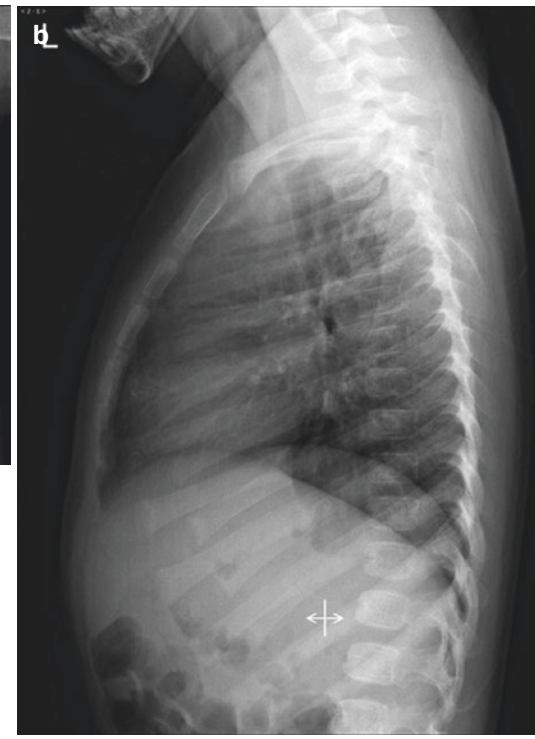

Fig. 31.18 Pulmonary valve stenosis in a 16-month-old boy with heart murmur detected 3 months after birth. Chest radiographs (**a** and **b**: PA and lateral views) show cardiac silhouette is enlarged, mainly involving the right ventricle. Lung blood supply is decreased with prominent pulmonary arteries

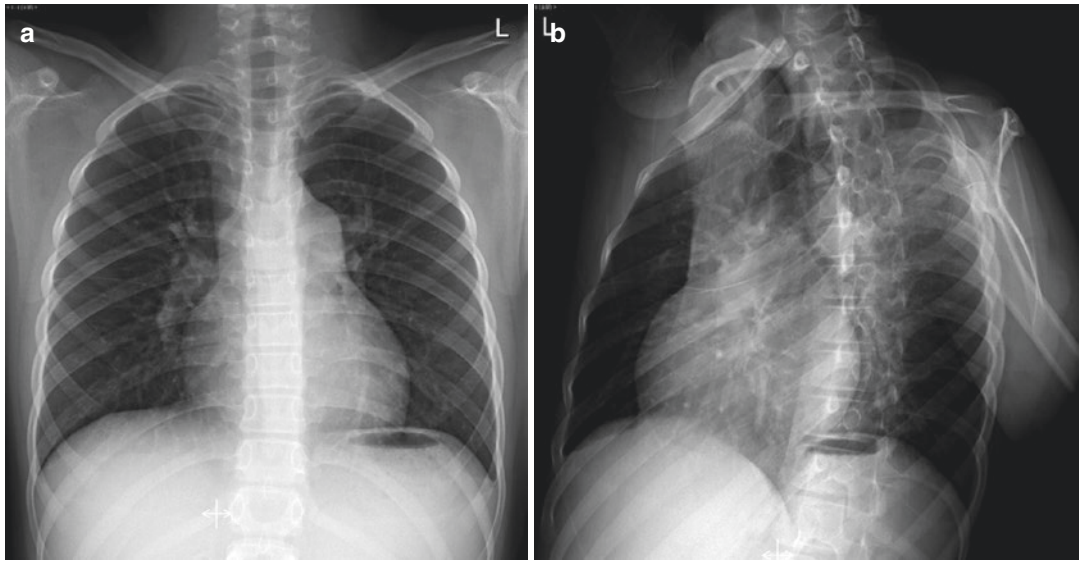

Fig. 31.19 Pulmonary regurgitation in a 12-year-old boy with chest discomfort after exercise. Echocardiography shows pulmonary regurgitation, pulmonary hypertension and tricuspid valve regurgitation. Chest radiographs (**a** and **b**: PA and lateral views) show that lung markings are clear and hilar are normal. Pulmonary arteries are shown to be prominent and right ventricle is slightly enlarged. Cardia apex is elevated

cardiac computed tomography, cardiac magnetic resonance, and cardiac nuclear medicine imaging. Despite limitations, chest X-ray is still commonly used as the first line technique in the diagnostic assessments of right heart disease. Radiographic findings with chest X-ray provide useful information for further imaging examinations.

References

1. Bruce CJ, Connolly HM. Right-sided valve disease deserves a little more respect. Circulation. 2009;119:2726–34. https://doi.org/10.1161/CIRCULATIONAHA.108.776021.
2. Voelkel NF, Quaife RA, Leinwand LA, et al. Right ventricular function and failure: report of a national heart, lung, and blood institute working group on cellular and molecular mechanisms of right heart failure. Circulation. 2006;114:1883–91. https://doi.org/10.1161/CIRCULATIONAHA.106.632208.
3. Somerville J, Grech V. The chest X-ray in congenital heart disease 1. Total anomalous pulmonary venous drainage and coarctation of the aorta. Images Paediatr Cardiol. 2009;11:7–9.
4. Somerville J, Grech V. The chest X-ray in congenital heart disease 2. Images Paediatr Cardiol. 2010;12:1–8.
5. Haddad R, Hunt SA, Rosenthal DN, et al. Right ventricular function in cardiovascular disease, part I: anatomy, physiology, aging, and functional assessment of the right ventricle. Circulation. 2008;117:1436–48. https://doi.org/10.1161/CIRCULATIONAHA.107.653576.
6. Sheehan F, Redington A. The right ventricle: anatomy, physiology and clinical imaging. Heart. 2008;94:1510–5. https://doi.org/10.1136/hrt.2007.132779.
7. Polak JF, Holman L, Wynne J, Colucci WS. Right ventricular ejection fraction: an indicator of increased mortality in patients with congestive heart failure associated with coronary artery disease. J Am Coll Cardiol. 1983;2:217–24. https://doi.org/10.1016/S0735-1097(83)80156-9.
8. Shah PK, Maddahi J, Staniloff HM, et al. Variable spectrum and prognostic implications of left and right ventricular ejection fractions in patients with and without clinical heart failure after acute myocardial infarction. Am J Cardiol. 1986;58:387–93. https://doi.org/10.1016/0002-9149(86)90001-9.
9. Mendes LA, Dec GW, Picard MH, Palacios IF, Newell J, Davidoff R. Right ventricular dysfunction: an independent predictor of adverse outcome in patients with myocarditis. Am Heart J. 1994;128:301–7.
10. Warnes CA. Adult congenital heart disease importance of the right ventricle. J Am Coll Cardiol. 2009;54:1903–10. https://doi.org/10.1016/j.jacc.2009.06.048.
11. de Groote P, Millaire A, Foucher-Hossein C, et al. Right ventricular ejection fraction is an independent predictor of survival in patients with moderate heart failure. J Am Coll Cardiol. 1998;32:948–54. https://doi.org/10.1016/S0735-1097(98)00337-4.
12. Kossaify A. Echocardiographic assessment of the right ventricle, from the conventional approach to

speckle tracking and three-dimensional imaging, and insights into the "right way" to explore the forgotten chamber. Clin Med Insights Cardiol. 2015;9:65–75. https://doi.org/10.4137/CMC.S27462. eCollection 2015.
13. Mertens LL, Friedberg MK. Imaging the right ventricle-current state of the art. Nat Rev Cardiol. 2010;7:551–63. https://doi.org/10.1038/nrcardio.2010.118. Epub 2010 Aug 10.
14. Valsangiacomo Buechel ER, Mertens LL. Imaging the right heart: the use of integrated multimodality imaging. Eur Heart J. 2012;33:949–60. https://doi.org/10.1093/eurheartj/ehr490.
15. Portnoy SG, Rudski LG. Echocardiographic evaluation of the right ventricle: a 2014 perspective. Curr Cardiol Rep. 2015;17:21. https://doi.org/10.1007/s11886-015-0578-8.
16. Galiè N, Humbert M, Vachiery JL, et al. 2015 ESC/ERS Guidelines for the diagnosis and treatment of pulmonary hypertension: The Joint Task Force for the Diagnosis and Treatment of Pulmonary Hypertension of the European Society of Cardiology (ESC) and the European Respiratory Society (ERS): Endorsed by: Association for European Paediatric and Congenital Cardiology (AEPC), International Society for Heart and Lung Transplantation (ISHLT). Eur Heart J. 2016;37:67–119. https://doi.org/10.1093/eurheartj/ehv317.
17. Hoeper MM, Bogaard HJ, Condliffe R, et al. Definitions and diagnosis of pulmonary hypertension. J Am Coll Cardiol. 2013;62(25 Suppl):D42–50. https://doi.org/10.1016/j.jacc.2013.10.032.
18. Farber HW, Miller DP, Poms AD, et al. Five-year outcomes of patients enrolled in the REVEAL Registry. Chest. 2015;148:1043–54. https://doi.org/10.1378/chest.15-0300.
19. Rich S, Dantzker DR, Ayres SM, et al. Primary pulmonary hypertension. A national prospective study. Ann Intern Med. 1987;107:216–23. https://doi.org/10.7326/0003-4819-107-2-216.
20. Ascha M, Renapurkar RD, Tonelli AR. A review of imaging modalities in pulmonary hypertension. Ann Thorac Med. 2017;12:61–73. https://doi.org/10.4103/1817-1737.203742.
21. Helmberger M, Pienn M, Urschler M, et al. Quantification of tortuosity and fractal dimension of the lung vessels in pulmonary hypertension patients. PLoS One. 2014;9:e87515. https://doi.org/10.1371/journal.pone.0087515.
22. Hopkins N, McLoughlin P. The structural basis of pulmonary hypertension in chronic lung disease: remodelling, rarefaction or angiogenesis? J Anat. 2002;201:335–48. https://doi.org/10.1046/j.1469-7580.2002.00096.x.
23. Abel E, Jankowski A, Pison C, Luc Bosson J, Bouvaist H, Ferretti GR. Pulmonary artery and right ventricle assessment in pulmonary hypertension: correlation between functional parameters of ECG-gated CT and right-side heart catheterization. Acta Radiol. 2012;53(7):720. https://doi.org/10.1258/ar.2012.120009.
24. Bolen MA, Renapurkar RD, Popovic ZB, et al. High-pitch ECG-synchronized pulmonary CT angiography versus standard CT pulmonary angiography: a prospective randomized study. AJR Am J Roentgenol. 2013;201:971–6. https://doi.org/10.2214/AJR.13.10597.
25. Kreitner KF. Noninvasive imaging of pulmonary hypertension. Semin Respir Crit Care Med. 2014;35:99–111. https://doi.org/10.1055/s-0033-1363456.
26. Shimada YJ, Shiota M, Siegel RJ, Shiota T. Accuracy of right ventricular volumes and function determined by three-dimensional echocardiography in comparison with magnetic resonance imaging: a meta-analysis study. J Am Soc Echocardiogr. 2010;23:943–53. https://doi.org/10.1016/j.echo.2010.06.029.
27. Grewal J, Majdalany D, Syed I, Pellikka P, Warnes CA. Three-dimensional echocardiographic assessment of right ventricular volume and function in adult patients with congenital heart disease: comparison with magnetic resonance imaging. J Am Soc Echocardiogr. 2010;23:127–33. https://doi.org/10.1016/j.echo.2009.11.002.
28. Niemann PS, Pinho L, Balbach T, et al. Anatomically oriented right ventricular volume measurements with dynamic three-dimensional echocardiography validated by 3-Tesla magnetic resonance imaging. J Am Coll Cardiol. 2007;50:1668–76. https://doi.org/10.1016/j.jacc.2007.07.031.
29. Leibundgut G, Rohner A, Grize A, et al. Dynamic assessment of right ventricular volumes and function by realtime three-dimensional echocardiography: a comparison study with magnetic resonance imaging in 100 adult patients. J Am Soc Echocardiogr. 2010;23:116–26. https://doi.org/10.1016/j.echo.2009.11.016.
30. Grapsa J, O'Regan DP, Pavlopoulos H, et al. Right ventricular remodelling in pulmonary arterial hypertension with threedimensional echocardiography: comparison with cardiac magnetic resonance imaging. Eur J Echocardiogr. 2010;11:64–73. https://doi.org/10.1093/ejechocard/jep169.
31. Rudski LG, Lai WW, Afilalo J, et al. Guidelines for the echocardiographic assessment of the right heart in adults: a report from the American Society of Echocardiography endorsed by the European Association of Echocardiography, a registered branch of the European Society of Cardiology, and the Canadian Society of Echocardiography. J Am Soc Echocardiogr. 2010;23:685–713.; quiz 786–788. https://doi.org/10.1016/j.echo.2010.05.010.
32. Lopez L, Colan SD, Frommelt PC, et al. Recommendations for quantification methods during the performance of a pediatric echocardiogram: a report from the Pediatric Measurements Writing Group of the American Society of Echocardiography Pediatric and Congenital Heart Disease Council. J Am Soc Echocardiogr. 2010;23:465–95; quiz 576–577. https://doi.org/10.1016/j.echo.2010.03.019.
33. Wittram C, Maher MM, Yoo AJ, Kalra MK, Shepard JA, McLoud TC. CT angiography of pulmonary

embolism: diagnostic criteria and causes of misdiagnosis. Radiographics. 2004;24:1219–38. https://doi.org/10.1148/rg.245045008.
34. Righini M, Le GG, Aujesky D, et al. Diagnosis of pulmonary embolism by multidetector CT alone or combined with venous ultrasonography of the leg: a randomised non-inferiority trial. Lancet. 2008;371:1343–52. https://doi.org/10.1016/S0140-6736(08)60594-2.
35. Ghanima W, Almaas V, Aballi S, et al. Management of suspected pulmonary embolism [PE] by D-dimer and multislice computed tomography in outpatients: an outcome study. J Thromb Haemost. 2005;3:1926–32. https://doi.org/10.1111/j.1538-7836.2005.01544.x.
36. Mos IC, Klok FA, Kroft LJ, DE RA, Dekkers OM, Huisman MV. Safety of ruling out acute pulmonary embolism by normal computed tomography pulmonary angiography in patients with an indication for computed tomography: systematic review and meta-analysis. J Thromb Haemost. 2009;7:1491–8. https://doi.org/10.1111/j.1538-7836.2009.03518.x.
37. Carrier M, Righini M, Wells PS, et al. Subsegmental pulmonary embolism diagnosed by computed tomography: incidence and clinical implications. A systematic review and meta-analysis of the management outcome studies. J Thromb Haemost. 2010;8:1716–22. https://doi.org/10.1111/j.1538-7836.2010.03938.x.
38. Kaur M, Vijayananthan A, Kumar G, Jayarani K, Ng KH, Sun Z. Use of 100 kV versus 120 kV in computed tomography pulmonary angiography in the detection of pulmonary embolism: effect on radiation dose and image quality. Quant Imaging Med Surg. 2015;5:524–33. https://doi.org/10.3978/j.issn.2223-4292.2015.04.04.
39. Sun Z, Almoudi M, Cao Y. CT angiography in the diagnosis of cardiovascular disease: a transformation in cardiovascular CT practice. Quant Imaging Med Surg. 2014;4:376–96. https://doi.org/10.3978/j.issn.2223-4292.2014.10.02.
40. Aldosari S, Almoudi M, Sun Z. Double-low dose protocol of CT pulmonary angiography in the diagnosis of pulmonary embolism: a feasible approach for reduction of both contrast medium and radiation dose. Heart Res Open J. 2017;4:33–8. https://doi.org/10.17140/HROJ-4-139.
41. Lu G, Luo S, Meinel FG, et al. High-pitch computed tomography pulmonary angiography with iterative reconstruction at 80 kVp and 20 ml contrast agent volume. Eur Radiol. 2014;24:3260–8. https://doi.org/10.1007/s00330-014-3365-9.
42. Boos J, Kropil P, Lanzman RS, et al. CT pulmonary angiography: simultaneous low-pitch dual-source acquisition mode with 70 kVp and 40 ml of contrast medium and comparison with high-pitch spiral dual-source acquisition with automated tube potential selection. Br J Radiol. 2016;89:20151059. https://doi.org/10.1259/bjr.20151059.
43. Laqmani A, Kurfurst M, Butscheidt S, et al. CT pulmonary angiography at reduced radiation exposure and contrast material volume using iterative model reconstruction and iDose^4 technique in comparison to FBP. PLoS One. 2016;11:e0162429. https://doi.org/10.1371/journal.pone.0162429.
44. Laqmani A, Regier M, Veldhoen S, et al. Improved image quality and low radiation dose with hybrid iterative reconstruction with 80 kV CT pulmonary angiography. Eur J Radiol. 2014;83:1962–9. https://doi.org/10.1016/j.ejrad.2014.06.016.
45. British Thoracic Society Standards of Care Committee Pulmonary Embolism Guideline Development Group. British Thoracic Society guidelines for the management of suspected acute pulmonary embolism. Thorax. 2003;58:470–83. https://doi.org/10.1136/thorax.58.6.470.
46. Hartmann I, Hagen P, Melissant C, et al. Diagnosing acute pulmonary embolism: effect of chronic obstructive pulmonary disease on the performance of D-dimer testing, ventilation/perfusion scintigraphy, spiral computed tomographic angiography, and conventional angiography. Am J Respir Crit Care Med. 2000;162:2232–7.
47. Forbes KP, Reid JH, Murchison JT. Do preliminary chest X-ray findings define the optimum role of pulmonary scintigraphy in suspected pulmonary embolism? Clin Radiol. 2001;56:397–400. https://doi.org/10.1164/ajrccm.162.6.2006030.
48. Sadigh G, Kelly AM, Cronin P. Challenges, controversies, and hot topics in pulmonary embolism imaging. AJR Am J Roentgenol. 2011;196:497–515. https://doi.org/10.2214/AJR.10.5830.
49. Lam KY, Dickens P, Chan ACL. Tumors of the heart – a 20-year experience with a review of 12485 consecutive autopsies. Arch Pathol Lab Med. 1993;117:1027–31.
50. Maleszewski JJ, Anavekar NS, Moynihan TJ, Klarich KW. Pathology, imaging, and treatment of cardiac tumours. Nat Rev Cardiol. 2017;14:536–49. https://doi.org/10.1038/nrcardio.2017.47.
51. Sheppard MN, Mohiaddin R. Tumors of the heart. Futur Cardiol. 2010;6:181–93. https://doi.org/10.2217/fca.09.62.
52. Jain S, Maleszewski JJ, Stephenson CR, Klarich KW. Current diagnosis and management of cardiac myxomas. Expert Rev Cardiovasc Ther. 2015;13:369–75. https://doi.org/10.1586/14779072.2015.1024108.
53. Anavekar NS, Bonnichsen CR, Foley TA, et al. Computed tomography of cardiac pseudotumors and neoplasms. Radiol Clin N Am. 2010;48:799–816. https://doi.org/10.1016/j.rcl.2010.04.002.
54. Araoz PA, Eklund HE, Welch TJ, Breen JF. CT and MR imaging of primary cardiac malignancies. Radiographics. 1999;19:1421–34. https://doi.org/10.1148/radiographics.19.6.g99no031421.
55. Dolk H, Loane M, Garne E, European Surveillance of Congenital Anomalies (EUROCAT) Working Group. Congenital heart defects in Europe: prevalence and perinatal mortality, 2000 to 2005. Circulation. 2011;123:841–9. https://doi.org/10.1161/CIRCULATIONAHA.110.958405.
56. van der Linde D, Konings EE, Slager MA, et al. Birth prevalence of congenital heart disease worldwide: a systematic review and meta-analysis. J Am Coll

Cardiol. 2011;58:2241–7. https://doi.org/10.1016/j.jacc.2011.08.025.
57. Yeh SJ, Chen HC, Lu CW, et al. Prevalence, mortality, and the disease burden of pediatric congenital heart disease in Taiwan. Pediatr Neonatol. 2013;54:113–8. https://doi.org/10.1016/j.pedneo.2012.11.010.
58. Tse KS, Ip JJK, Leong LLY. Imaging of congenital heart disease in Hong Kong: from invasive to non-invasive cardiac imaging. CVIA. 2017;1:124–32. https://doi.org/10.22468/cvia.2016.00122.
59. Sun RR, Liu M, Lu L, Zheng Y, Zhang P. Congenital heart disease: causes, diagnoses, symptoms and treatments. Cell Biochem Biophys. 2015;72:857–60. https://doi.org/10.1007/s12013-015-0551-6.
60. Zaver AG, Nadas AS. Five congenital cardiac defects: study of their profile and natural history. Atrial septal defect—secundum type. Circulation. 1965;31(Suppl III):III-24–32.
61. Danford DA, Gumbiner CH, Martin AB, Fletcher SE. Effects of electrocardiography and chest radiography on the accuracy of preliminary diagnosis of common congenital cardiac defects. Pediatr Cardiol. 2000;21:334–40. https://doi.org/10.1007/s002460010075.
62. Rodes-Cabau J, Taramasso M, O'Gara PT. Diagnosis and treatment of tricuspid valve disease: current and future perspectives. Lancet. 2016;388:2431–42. https://doi.org/10.1016/S0140-6736(16)00740-6.
63. Fawzy H, Fukamachi K, Mazer CD, et al. Complete mapping of the tricuspid valve apparatus using three-dimensional sonomicrometry. J Thorac Cardiovasc Surg. 2011;141:1037–43. https://doi.org/10.1016/j.jtcvs.2010.05.039.
64. Rodes-Cabau J, Hahn RT, Latib A, et al. Transcatheter therapies for treating tricuspid regurgitation. J Am Coll Cardiol. 2016;67:1825–45. https://doi.org/10.1016/j.jacc.2016.01.063.
65. Nath J, Foster E, Heidenreich PA. Impact of tricuspid regurgitation on long-term survival. J Am Coll Cardiol. 2004;43:405–9. https://doi.org/10.1016/j.jacc.2003.09.036.
66. Vahanian A, Alfieri O, Andreotti F, et al. Guidelines on the management of valvular heart disease (version 2012). Eur Heart J. 2012;33:2451–96. https://doi.org/10.1093/eurheartj/ehs109.
67. Tretter JT, Sarwak AE, Anderson PH, Spicer DE. Assessment of the anatomical variation to be found in the normal tricuspid valve. Clin Anat. 2016;29:399–407. https://doi.org/10.1002/ca.22591.
68. Martinez RM, O'Leary PW, Anderson RH. Anatomy and echocardiography of the normal and abnormal tricuspid valve. Cardiol Young. 2006;16(Suppl 3):4–11. https://doi.org/10.1017/S1047951106000709.
69. Fawzy ME, Mercer EN, Dunn B, al-Amri M, Andaya W. Doppler echocardiography in the evaluation of tricuspid stenosis. Eur Heart J. 1989;10:985–90. https://doi.org/10.1093/oxfordjournals.eurheartj.a059423.
70. Perez J, Ludbrook P, Ahumada G. Usefulness of Doppler echocardiography in detecting tricuspid valve stenosis. Am J Cardiol. 1985;55:601–3. https://doi.org/10.1016/0002-9149(85)90266.
71. Xiong TY, Zheng MX, Wei X, et al. Hemodynamic changes after transcatheter aortic valve implantation during sequential follow-ups in patients with bicuspid aortic valve compared with tricuspid aortic valve. Cardiol J. 2017;24:350–7. https://doi.org/10.5603/CJ.a2017.0020.
72. Nesser HJ, Tkalec W, Patel AR, et al. Quantitation of right ventricular volumes and ejection fraction by three-dimensional echocardiography in patients: comparison with magnetic resonance imaging and radionuclide ventriculography. Echocardiography. 2006;23:666–80. https://doi.org/10.1111/j.1540-8175.2006.00286.x.
73. Anwar AM, Soliman OI, Nemes A, van Geuns RJ, Geleijnse ML, Ten Cate FJ. Value of assessment of tricuspid annulus: real-time three-dimensional echocardiography and magnetic resonance imaging. Int J Cardiovasc Imaging. 2007;23:701–5. https://doi.org/10.1007/s10554-006-9206-4.
74. Sugeng L, Mor-Avi V, Weinert L, et al. Multimodality comparison of quantitative volumetric analysis of the right ventricle. JACC Cardiovasc Imaging. 2010;3:10–8.
75. Ling LF, Marwick TH. Echocardiographic assessment of right ventricular function: how to account for tricuspid regurgitation and pulmonary hypertension. JACC Cardiovasc Imaging. 2012;5:747–53. https://doi.org/10.1016/j.jcmg.2011.08.026.
76. van Rosendael PJ, Joyce E, Katsanos S, et al. Tricuspid valve remodelling in functional tricuspid regurgitation: multidetector row computed tomography insights. Eur Heart J Cardiovasc Imaging. 2016;17:96–105. https://doi.org/10.1093/ehjci/jev140.
77. Lee JW, Song JM, Park JP, Lee JW, Kang DH, Song JK. Long-term prognosis of isolated signifi cant tricuspid regurgitation. Circ J. 2010;74:375–80. https://doi.org/10.1253/circj.CJ-09-0679.
78. D'Alfonso A, Scioti G, Milano A. Images in cardiovascular medicine. Combined aortic and pulmonary stenosis in a 79-year-old man. Ital Heart J. 2000;1:848.
79. Bonow R, Carabello B, Kanu C, American College of Cardiology/American Heart Association Task Force on Practice Guidelines, Society of Cardiovascular Anesthesiologists, Society for Cardiovascular Angiography and Interventions, Society of Thoracic Surgeons, et al. ACC/AHA 2006 guidelines for the management of patients with valvular heart disease: a report of the American College of Cardiology/American Heart Association Task Force on Practice Guidelines (writing Committee to Revise the 1998 guidelines for the management of patients with valvular heart disease): developed in collaboration with the Society of Cardiovascular Anesthesiologists: endorsed by the Society for Cardiovascular Angiography and Interventions and the Society of Thoracic Surgeons. Circulation. 2006;114:e84–e231. https://doi.org/10.1161/CIRCULATIONAHA.106.176857.
80. Zoghbi WA, Enriquez-Sarano M, Foster E, et al. Recommendations for evaluation of the severity of

native valvular regurgitation with twodimensional and Doppler echocardiography. J Am Soc Echocardiogr. 2003;16:777–802. https://doi.org/10.1016/S0894-7317(03)00335-3.

81. Groves P, Lewis N, Ikram S, Maire R, Hall R. Reduced exercise capacity in patients with tricuspid regurgitation after successful mitral valve replacement for rheumatic mitral valve disease. Br Heart J. 1991;66:295–301. https://doi.org/10.1136/hrt.66.4.295.
82. Geva T. Repaired tetralogy of Fallot: the roles of cardiovascular magnetic resonance in evaluating pathophysiology and for pulmonary valve replacement decision support. J Cardiovasc Magn Reson. 2011;13:9. https://doi.org/10.1186/1532-429X-13-9.
83. Pennell DJ, Sechtem UP, Higgins CB, European Society of cardiology; Society for Cardiovascular Magnetic Resonance, et al. Clinical indications for cardiovascular magnetic resonance (CMR): Consensus Panel report. J Cardiovasc Magn Reson. 2004;6:727–65.
84. Mercer-Rosa L, Yang W, Kutty S, et al. Quantifying pulmonary regurgitation and right ventricular function in surgically repaired tetralogy of Fallot: a comparative analysis of echocardiography and magnetic resonance imaging. Circ Cardiovasc Imaging. 2012;5:637–43. https://doi.org/10.1161/CIRCIMAGING.112.972588.

Echocardiography of Right Heart

32

Julia Grapsa

Abstract

A significant part of right heart failure management is the accurate imaging of right heart chambers with the means of conventional echocardiography as well as advanced imaging. Because of the orientation of the right ventricular fibers, global assessment of the RV is difficult, with the two main sections contracting perpendicular to each other: the inflow portion longitudinally and the outflow portion circumferentially. The aim of this review manuscript is to highlight important measurements from two dimensional echocardiography as well as explaining how we implement three dimensional echocardiography as well as speckle tracking into right heart imaging.

Keywords

Right heart · Two dimensional echocardiography · Three dimensional echocardiography Speckle tracking

Abbreviations

3D	Three dimensional
MPI	Myocardial performance index
RA	Right atrium
RV	Right ventricle
TAPSE	Tricuspid annular plane systolic excursion
TDI	Tissue Doppler imaging

32.1 Introduction

Pulmonary hypertension is a debilitating disease with limited treatment options and prognosis. A significant part of right heart failure management is the accurate imaging of right heart chambers with the means of conventional echocardiography as well as advanced imaging. The aim of this review manuscript is to highlight important measurements from two dimensional echocardiography as well as explaining how we implement three dimensional echocardiography as well as speckle tracking into right heart imaging.

32.2 Right Ventricular Anatomy

Right ventricle (RV) has a complex anatomy which may jeopardise the conventional 2D imaging, especially due to the irregular shape of the cavity and its heavy trabeculation [1–3]. It is the

J. Grapsa
Department of Imaging, Cardiology, Heart & Vascular Institute, Cleveland Clinic Abu Dhabi, Abu Dhabi, United Arab Emirates

S. I. Dumitrescu et al. (eds.), *Right Heart Pathology*, https://doi.org/10.1007/978-3-319-73764-5_32

most anteriorly situated cardiac chamber, located immediately behind the sternum and it is more triangular in shape when viewed from the front. It also marks the inferior border of the cardiac silhouette. It curves over the left ventricle and this results in the right ventricular outflow tract riding the left ventricular outflow tract. RV is divided into three different parts [4, 5]: the inlet (from the tricuspid valve annulus to the proximal infundibulum), the apical trabecular (the right ventricular body to the apex), and the outlet (also called infundibulum or conus, from the right ventricular outflow tract to the pulmonary valve). As opposed to the normal left ventricle, the RV is highly trabeculated and present several muscle bands including three prominent muscular bands [3]. The musculature of the RV extends from the atrioventricular to the ventriculo-arterial junctions: The inflow portion of the RV is mainly composed of circumferential fibres in the subepicardium and longitudinal fibers in the subendocardium. The outflow portion of the RV is composed of both subendocardial and subepicardial fibres running longitudinally, overlaid by fibres running at right angle to the outlet long axis in a circumferentially, which can be traced to the crista supraventricularis and to the anterior ventricular sulcus, serving to bind the two ventricles together. Because of the orientation of the right ventricular fibers, global assessment of the RV is difficult, with the two main sections contracting perpendicular to each other: the inflow portion longitudinally and the outflow portion circumferentially.

32.3 Right Atrial Anatomy

The right atrium is divided into two distinct parts: the thin-walled sinus venosus posteriorly and the auricle or RA appendage, anteriorly [6–8]. The sinus venosus is attached medially to the left atrium and postero-laterally to the crista terminalis. It includes the venous part (insertion of the inferior and superior vena cava), the vestibulum, and the atrial septum. The pectinated RA appendage merges postero-laterally from the crista terminalis and overlies the aortic root. Just posterior to the tricuspid valve, at its most superior edge is the orifice of the coronary sinus. A membranous structure, the Thebessian valve is often seen at the opening of the coronary sinus. The fossa ovalis, thin membrane between the right and left atria, lies at the middle portion of right atrium posterior wall, at the lower part of the septum, above and to the left of the orifice of the inferior vena cava. The limbus fossa ovalis is a prominent oval margin of the fossa ovalis. The Eustachian valve (inferior vena caval valve) is a stick-like, semilunar, extension of the inferior vena cava, with wide variability in length and shape. In the fetus this valve serves to direct the blood from the inferior vena cava, through the foramen ovale, into the left atrium. The Chiari's network is a congenital remnant of the right valve of the sinus venosus [8].

32.4 Right Ventricular Pathophysiology

The RV is connected to the pulmonary vascular bed, which, in healthy volunteers, is a low-resistance system [9]. It adapts better to volume loading than pressure-loading. Ventricular interdependence is crucial in right heart disease and is ensured by the interventricular septum. In healthy volunteers, the considerably higher pressures in the left ventricular cavity render it circular in cross-section and the septum bows in to the RV. Pressure-loading of the RV resulting from increased pulmonary artery pressure, causes the septum to flatten in systole as the right and left ventricular pressures begin to converge and when the RV becomes severely pressure loaded, the septum may even bulge in to the left ventricular cavity. In a volume-loaded RV with diastolic dysfunction and high end-diastolic pressures, the septum will flatten in diastole. These changes will impact on both left ventricular systolic and diastolic function.

In acute pressure-loading, such as pulmonary embolic disease, the RV will dilate and its free wall will become hypokinetic, but chronic progressive pressure-loading, as in pulmonary hypertension, will lead to right ventricular

remodeling, notably hypertrophy [10–12]. The process is not like the physiological hypertrophy of an athlete's heart, but will also result in myocardial fibrosis, inflammation, myocyte apoptosis and necrosis (forms of cell death) and abnormal contractile function. Right ventricular systolic and diastolic function will therefore deteriorate and it is thought these parameters determine exercise capacity, symptoms and prognosis.

The filling pattern of the RV will alter as diastolic function worsens. As relaxation first becomes impaired, early diastolic filling is reduced and there is an increase in filling due to atrial contraction. This results in the reversal of the transtricupsid E:A ratio in association with prolonged isovolumic relaxation time. With progressive diastolic impairment, right atrial pressure increases, leading to increased early diastolic filling, so that the diastolic filling pattern pseudonormalises. With very severe impairment, isovolumic relaxation time may shorten due to high right atrial pressure and the restrictive characteristics of the RV.

Proximal coronary blood flow to the RV occurs in systole and diastole. More distally, flow is predominantly diastolic. Ventricular hypertrophy, increased wall tension in systole and diastole and impaired cardiac output reduce coronary artery driving pressure and increased oxygen demand, which may result in right ventricular ischemia [10].

32.5 Echocardiography in Pulmonary Hypertension

32.5.1 Two Dimensional Echocardiography

32.5.1.1 Qualitative Assessment

Three components are important for the qualitative right ventricular assessment which will give a preview and maybe indicate towards the etiology of pulmonary hypertension, if that is yet unknown: dilatation, hypertrophy and contractility [7]. Normally the RV is 1/3 of the size of the left ventricle in the parasternal long axis view. One of the first changes in the RV in response to the increased preload and afterload is dilatation, which progresses with worsening pulmonary hypertension. Dilatation of the RV can be assessed in the parasternal long axis, short axis and the apical four-chamber view [11]. With regards to hypertrophy, when right ventricular afterload is chronically elevated, the right ventricular walls become hypertrophied. One of the first anatomical elements to do so is the moderator band, which in normal subjects it is thin and sometimes difficult to see. From the apical four chamber view, right ventricular hypertrophy is defined by a free wall thickness of more than 5 mm. Finally, as far as contractility is concerned, in pulmonary hypertension, right ventricular impairment is global: this is in contrast to other conditions affecting the RV, such as right ventricular infarction or arrhythmogenic right ventricular cardiomyopathy, where there will be regional wall motion abnormalities [11–13].

32.5.2 Right Atrial Pressure

Measurement of the diameter of the inferior vena cava at end-expiration and during an inspiratory manœuvre provides an estimate of right atrial pressure. If the inferior vena cava diameter is normal (1.5–2.5 cm) and the segment adjacent to the right atrium collapses by at least 50% with respiration, then right atrial pressure is normal. Failure to collapse with respiration and/or dilation of the inferior vena cava and hepatic veins is associated with higher right atrial pressures. When there is no response with normal respiration, the patient is asked to "sniff". This generates a sudden decrease in intrathoracic pressure, normally resulting in a decrease in inferior vena cava diameter [14] (Fig. 32.1).

32.5.3 Right Ventricular Systolic Pressure

Right ventricular systolic pressure is calculated through the Bernoulli equation and via the tricuspid regurgitant velocity. The latter is derived

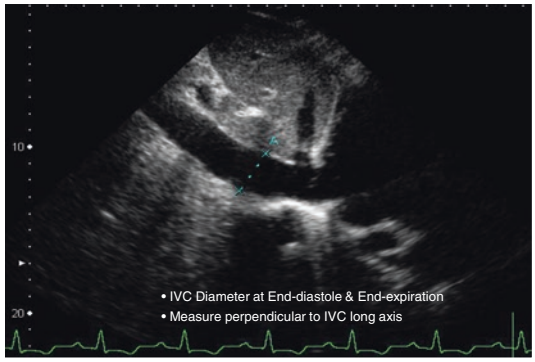

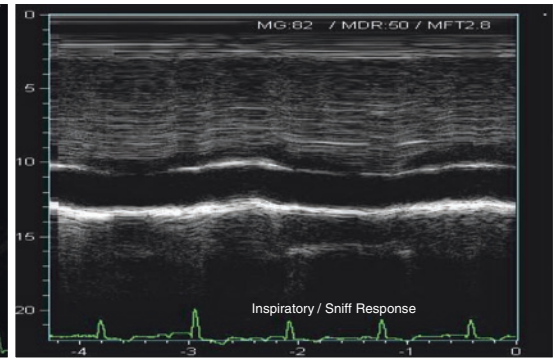

Mean RAP (mmHg)	IVC ∅ (mm)	Inspiratory Collapse
0–5	< 15	Complete
5–10	15–25	> 50%
10–15	15–25	< 50 %
15–20	> 25	< 50 %
> 20	>25	No change

Fig. 32.1 Estimation of right atrial pressure (RAP) through inferior vena cava diameter (IVC) and inspiratory collapse

from the application of continuous wave (CW) Doppler mapping on the tricuspid regurgitant jet, from the apical four chamber view or from the parasternal right ventricular inflow view, if the regurgitant jet is eccentric [6]. The peak velocity is measured in m/s.

The velocity reflects the right ventricular to right atrial pressure difference, ΔP, and when pulmonary stenosis is absent, right ventricular systolic pressure (RVSP) is assumed to equal pulmonary artery systolic pressure (PASP), and is calculated through the Bernoulli Equation:

$$\text{PASP} = \text{RVSP} = 4\left(\text{V}_{\text{TR}}\right)^2 + \text{RAP}$$

[V_{TR}: tricuspid regurgitant velocity; RAP: right atrial pressure]

The normal expected upper limit of PASP depends on age and body mass index (BMI). In the largest study to date, the estimated upper 95% limit for PASP was 37.2 mmHg in low-risk subjects (VTR 2.6 m/s), whereas the estimated upper 95% limit for subjects aged 60 and over was 43.6 mmHg (VTR 2.9 m/s). In those with a BMI > 30 kg/m^2 the limit was 40 mmHg (VTR 2.8 m/s). In all these measurements, right atrial pressure was assumed to be 10 mmHg [15].

Note that in cases of severe free-flow tricuspid regurgitation, the Bernoulli equation is not valid and the tricuspid regurgitant velocity will underestimate the transtricupsid pressure gradient: however, the severity of the tricuspid regurgitation is predictive of survival regardless of the PASP, irrespective of the underlying disease [16–18].

32.5.4 Pulmonary Artery Mean and Diastolic Pressure

As with the tricuspid regurgitant jet, the Bernoulli Equation can be applied to calculate pulmonary arterial end-diastolic pressure (PEDP) [6, 7]:

$$\text{PEDP} = 4\left(\text{V}_{\text{ED}}\right)^2 + \text{RAP}$$

[V_{ED}, end-diastolic pulmonary regurgitant velocity]

Mean pulmonary artery pressure, may also be derived from the pulmonary regurgitant velocity:

$$\text{Mean PAP} = 4\left(\text{PR V}_{\text{BD}}\right)^2$$

[V_{BD}, beginning of diastole pulmonary regurgitant velocity]

Measurement of PEDP and mPAP is not routinely used in the diagnosis or follow-up pulmonary hypertension, but may be useful in its identification when tricuspid regurgitant velocity cannot be used or relied upon.

32.5.5 Right Ventricular Outflow Tract Acceleration Time

Right ventricular outflow tract acceleration time is the time in milliseconds from the beginning of the pulmonary ejection until the maximum of the systolic velocity. It is measured by pulsed-wave Doppler with the sample volume positioned at the centre of the pulmonary artery, ideally at the annulus, in the parasternal short axis view of the right ventricular outflow tract.

In normal people, the acceleration time exceeds 140 ms and it shortens in pulmonary hypertension. There is an inverse relationship between acceleration time and mean PAP and several equations have been described [19, 20].

$$\text{Mean PAP} = 79 - (0.45 \times \text{AT})$$

$$\text{Mean PAP} = 90 - (0.62 \times \text{AT})$$

$$\log 10 \text{mean PAP} = 0.0068.\text{AT} + 2.1$$

but these are not commonly used to derive pressure in clinical practice as they have been superseded by tricuspid regurgitant velocity. Nonetheless, acceleration time may be a useful measure when the tricuspid velocity cannot be measured, particularly at diagnosis. A value below 105 ms is suggestive of pulmonary hypertension [7].

32.5.6 Right Atrial Volume Index

The measurement of RA volume index is usually performed from the apical four chamber view or from the subcostal view. Atrial volume is measured at end-systole, where the maximum atrial volume can be obtained [14].

The single plane area-length method is used and RA volume is measured using the area and the long axis length of the atrium [14]:

$$\text{RA volume index} = (0.85\,\text{A}2 / \text{L}) / \text{BSA}$$

[A, area of atrium in any view (cm^2); L, long axis length of atrium (cm); BSA, body surface area]

An alternative method for measuring right atrial volume index from the apical four-chamber is the method of discs or Simpson's rule. In this plane, the disc diameters at various levels of the atria are used to determine the cross-sectional area. Three-dimensional echocardiography is an alternate imaging modality for the accurate assessment of right atrial volume (Fig. 32.2).

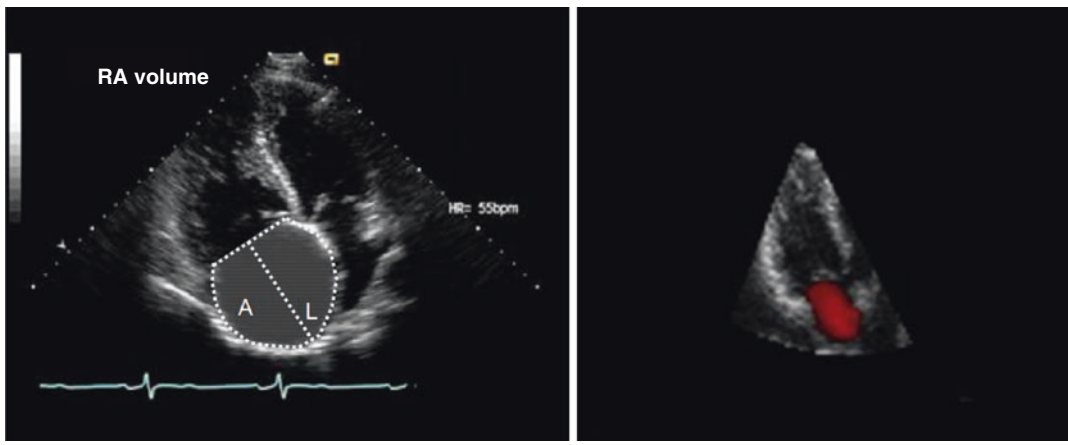

Fig. 32.2 Right atrial volume index assessment: on the left, two dimensional echocardiographic assessment where A is the right atrial area and L is the length of right atrium. On the right, we present the three dimensional echocardiographic approach

The normal ranges for 2D echocardiographic RA volume are 25 + 7 mL/m^2 in men and 21 + 6 mL/m^2 in women [8, 14].

32.5.7 Right Ventricular Fractional Area Change

Right ventricular fractional area change (FAC) is calculated as follows:

$$\text{RV FAC}(\%) = (\text{AED} - \text{AES}) / \text{AED}$$

where AED is end-diastolic area and AES is end systolic area, measured from the apical four chamber view. It is a simple method for assessment of right ventricular systolic function which has been shown to correlate with ejection fraction measured using cardiac MRI and prognosis in pulmonary hypertension. It also correlates with response to treatment [21, 22].

32.5.8 Eccentricity Index of the Left Ventricle

Eccentricity index is measured by the parasternal short-axis at the level of left ventricular papillary muscles. It is measured as the ratio of the minor axis of the left ventricle parallel to the septum (D2), divided by the minor axis perpendicular to the septum (D1).

The index is measured in end-diastole and end-systole. In a purely pressure-loaded RV, there is flattening of the interventricular septum in end-systole, which results in increased end-systolic left ventricular eccentricity index. In pure volume-loading, the eccentricity index will be increased in end-diastole [11, 23].

32.5.9 Myocardial Performance Index

Myocardial Performance Index, also known as Tei Index [7, 24–26], combines a combination of systolic and diastolic measurements. The normal range for RV MPI is 0.28–0.329 [25, 26]. It is relatively unaffected by heart rate, loading conditions or the presence and the severity of tricuspid regurgitation. In patients with idiopathic pulmonary arterial hypertension, the index correlates with symptoms and values above 0.88 predict poor survival [25].

The advantages of its use are good reproducibility, quick calculation, no need for use of geometric models and appliance even in the presence of a difficult acoustic window. There are two different approaches for the measurement of MPI. Colour Doppler (Two views: apical tricuspid inflow and parasternal right ventricular inflow): Two different views are needed for the determination of MPI—the apical four-chamber view for the tricuspid inflow pattern and the parasternal short axis right ventricular outflow tract view for the determination of ejection time.

Tissue Doppler Imaging (One view: Pulsed-wave Doppler of the right ventricular free wall): TDI can also be used to derive the same parameters as colour Doppler, but only one view is required (Fig. 32.3).

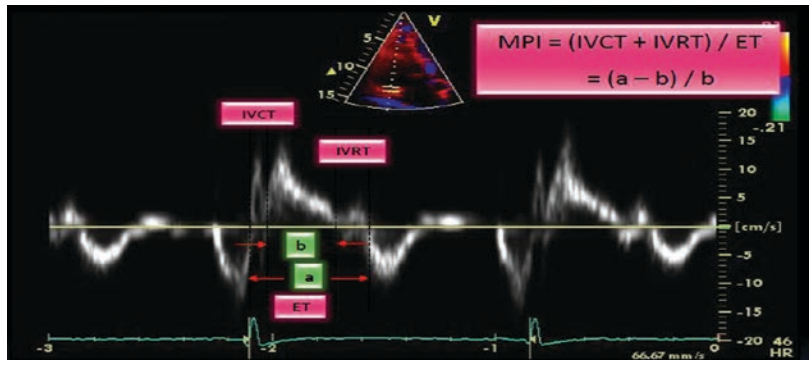

Fig. 32.3 Calculation of myocardial performance index (MPI) of the right ventricle. *IVCT* isovolumic contraction time, *IVRT* isovolumic relaxation time, *ET* ejection time

32.6 Tricuspid Annular Plane Systolic Excursion (TAPSE)

TAPSE is the reflection of the movement the base to apex shortening of the RV in systole (longitudinal function). During ventricular systole, long axis shortening is created by motion of both atrioventricular valve annulae toward the cardiac apex. Because the septal attachment of the tricuspid annulus is relatively fixed, the majority of tricuspid annular motion occurs in its lateral aspect.

The measurement of TAPSE is derived from the apical four chamber view. Special care has to be taken for the whole RV to be included in the view with no dropout in the endocardial outline along the interventricular septum and RV free wall. The width of sector should be limited onto the right ventricular free wall, and the M-mode cursor should be positioned on the lateral portion of the tricuspid annulus, measuring in control sweep mode [7].

Maximal TAPSE is defined by the total excursion of the tricuspid annulus from its highest position after atrial ascent to the peak descent during ventricular systole. Earlier studies using 2D echocardiography showed that in the normal RV this value exceeds 16 mm. Using M-mode the normal range is higher (24.9 ± 3.5 mm; 25.4 ± 4.9 mm) and a value of 20.1 mm has been shown to be a useful cut-off in identifying pulmonary hypertension [27, 28].

In a volume-loaded ventricle with preserved function, such as in the presence of an atrial septal defect, TAPSE may be very high, over 30 mm. In a volume- and pressure-loaded RV, such as a dilated, hypertrophied RV with significant functional tricuspid regurgitation, TAPSE may become pseudonormalised.

32.6.1 Three Dimensional Echocardiography

3D echocardiography has over the last 20 years evolved from a challenging experimental technique requiring outstanding image quality, the use of large 3D transducers, and time-consuming post-processing steps, into a modality on the brink of clinical routine usage, with highly improved spatial and temporal resolution as well as a relatively small transducer footprint.

Current transthoracic 3D transducers, the so-called "fully sampled matrix transducers", while still slightly heavier and larger than 2D transducers, have a similar footprint to standard 2D transducers and are capable of imaging the entire RV with frame rates of 20–30 frames/s Apical acquisition of volumes is recommended in the adult population. An effort should be made to include the tricuspid valve, the apex, and the outflow tract with the pulmonary valve in the full volume. As it is often difficult to include the whole RV volume in the acquisition sector, a modified apical view can be advantageous. The modified view is off-axis compared with the standard 2D apical four-chamber view. One way (the medial approach) is to move the transducer medially to the RV modified apical four-chamber view and then tilt the transducer cranially and anteriorly—and even rotate—to include the pulmonary valve in the guidance images (Fig. 32.4). Another way (the lateral approach) is to displace the transducer laterally with an anterior tilt. To include both the pulmonary and tricuspid valves, it can sometimes be of use to move the transducer further laterally than the RV-focused apical four-chamber view and even to a more cranial intercostal space, as well as rotating the transducer.

32.6.2 Analysis of Data

There are several software packages available for endocardial delineation of cardiac chambers, with some being dedicated to the RV. Pronounced trabeculations, prominent moderator band, or anterior papillary muscle are difficult to differentiate from the anterior RV wall using the semi-automatic delineation software, especially with limited image quality. Owing to the fact that as much as 25% of the RV volumes may originate from the RV outflow tract, semi-automated border tracing can miss out considerable parts of the volume if manual correction is not performed (Fig. 32.5). The underestimation of volumes in comparison to cardiac MRI decreases when manual correction is performed, yet at the cost of

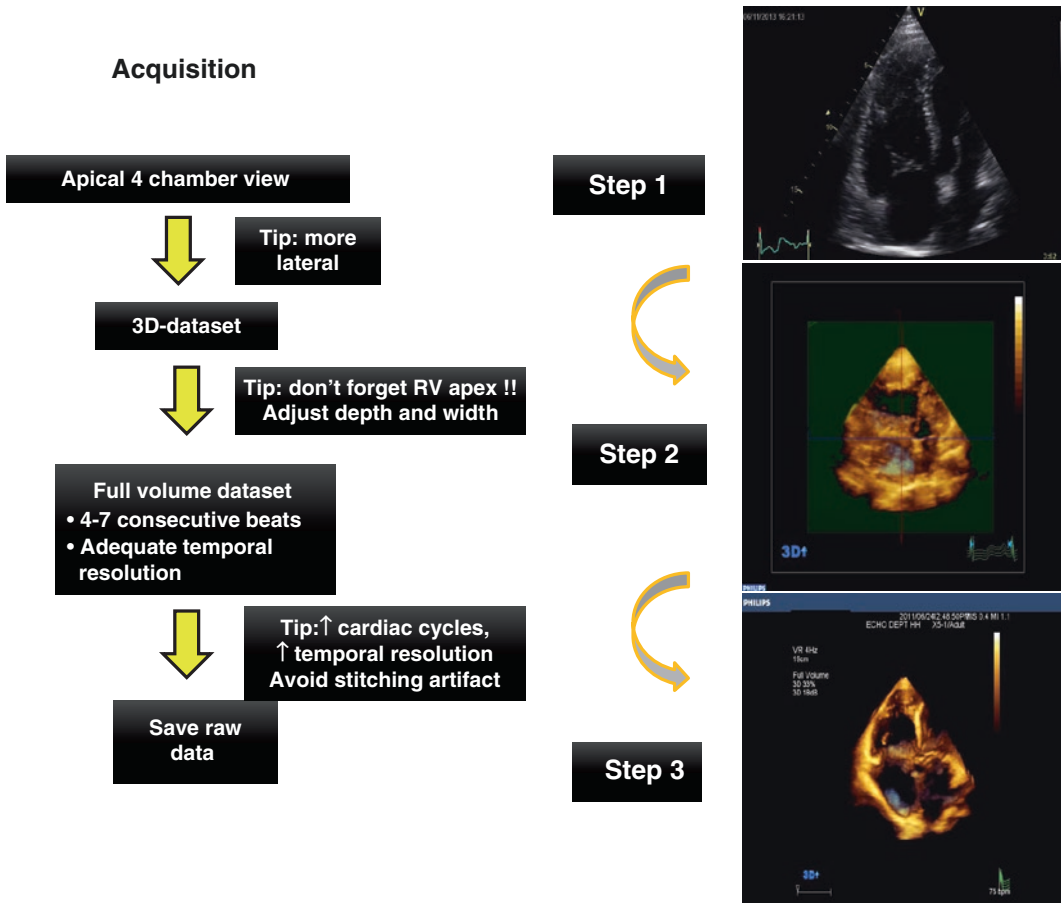

Fig. 32.4 Three dimensional echocardiography: acquisition of sequences

substantially increased time requirements for analysis. Manual correction of semi-automated border delineation can take three to four times longer than the uncorrected delineation, which on average takes 4 min; it is even longer than the time that manual delineation of a transversal stack of magnetic resonance images would take. With the development of new softwares, encouraging test–retest reliability for RV 3D echocardiographic volumes has been reported, with variabilities of 7% for end-diastolic volumes.

32.6.3 Right Ventricular Speckle Tracking

Up to recently, RV strain analysis focused on the longitudinal values only taking into consideration that the RV free wall was best visualized from the apical view, while avoiding transverse strain values because of its thin cross section. Three dimensional strain helped overcoming this obstacle. RV systolic function is predominantly directed by the longitudinal arrangement of myocardial fibers. When compared to the left ventricle, the RV lacks the middle layer of myocardial fibers that is why in healthy volunteers and pulmonary hypertensive patients, circumferential strain has the smallest magnitude of the three vectors [29]. Despite this anatomical documented knowledge, the reduction in strain is proved to be due to circumferential stretch and subsequent reduction in contractility. Failure of the outer layer to contract circumferentially may signify oblique myocardial arrangement in the superficial subepicardium [30].

Radial strain derives from the superficial, obliquely arranged subepicardial fibers with an inwards wave-like contraction, whereas the

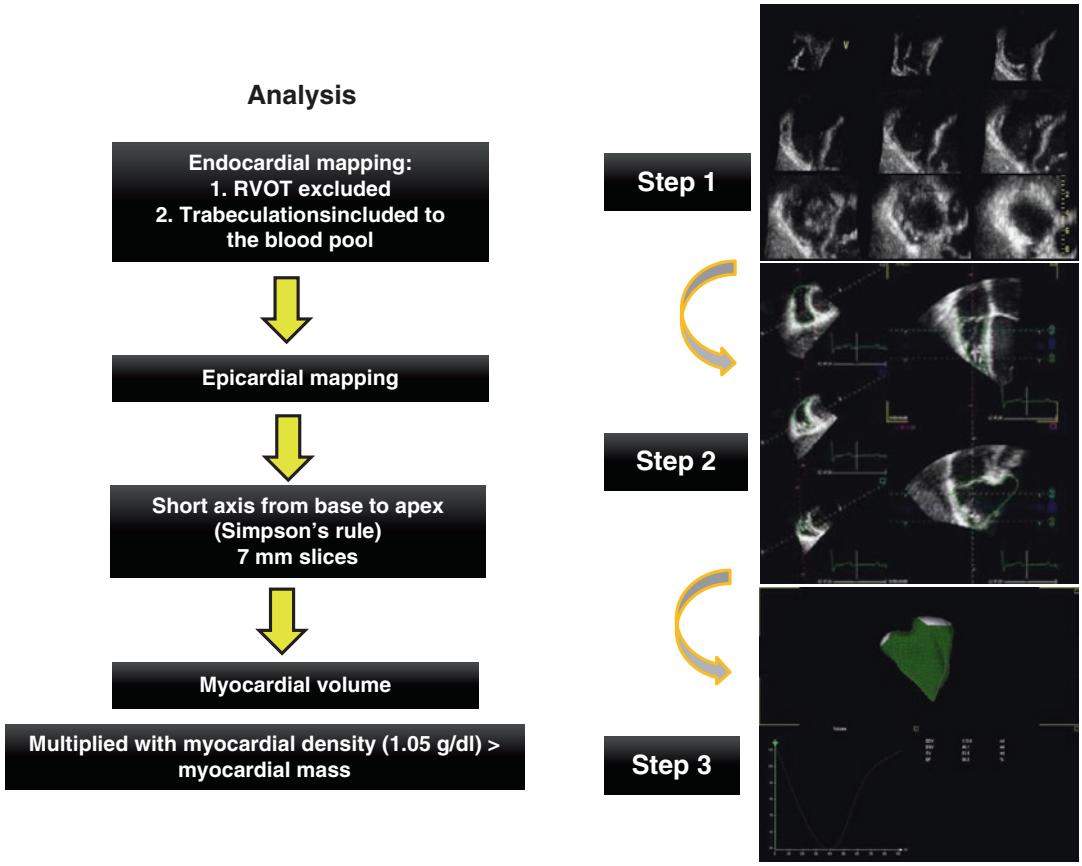

Fig. 32.5 Three dimensional echocardiography: analysis of sequences

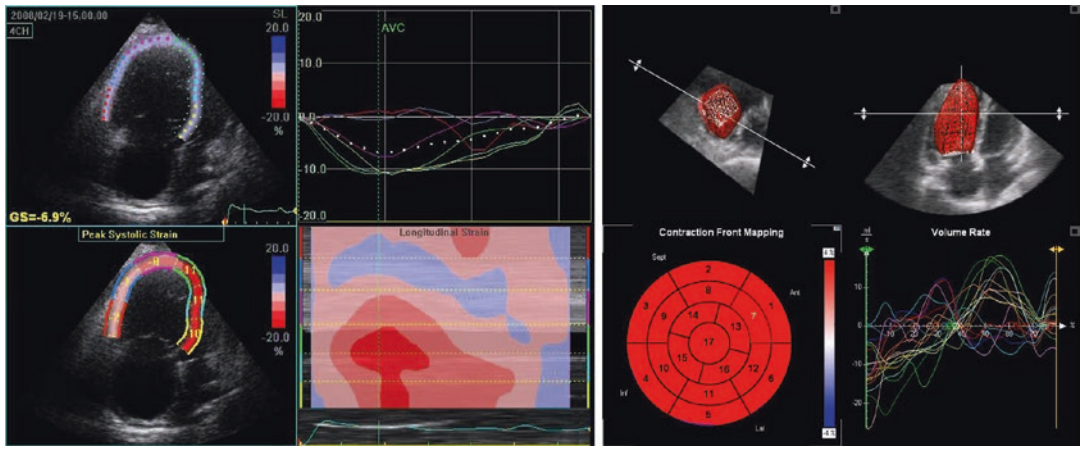

Fig. 32.6 (on the left): Two dimensional speckle tracking of the right ventricle, (on the right): three dimensional speckle tracking of the right ventricle

wave-like base-to-apex contraction is coming from the longitudinal fibers [31].

When pulmonary hypertensive patients are compared to controls, radial strain is the predominant variable in systolic volume variation and has the greatest reduction when compared to healthy volunteers [32, 33] (Fig. 32.6).

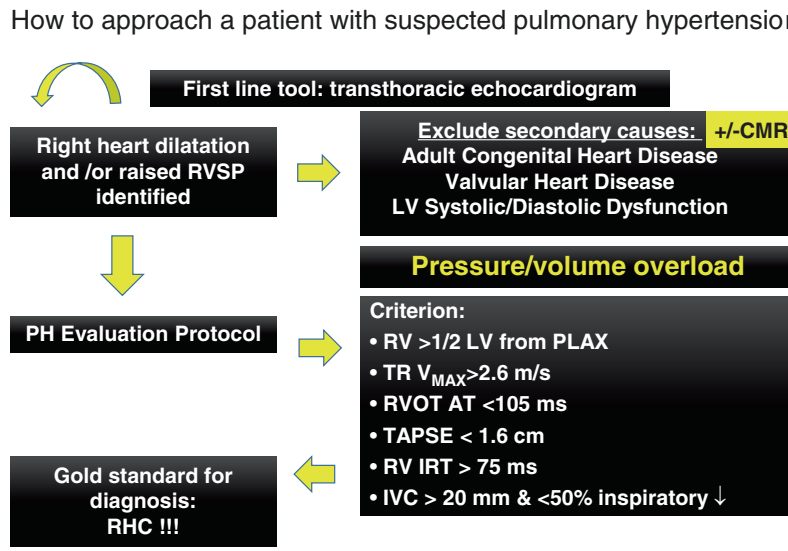

Fig. 32.7 How to approach a patient with suspected pulmonary hypertension. *RVSP* right ventricular systolic pressure, *LV* left ventricle, *CMR* cardiac magnetic resonance, *PH* pulmonary hypertension, *RV* right ventricle, *PLAX* parasternal long axis, *TR* tricuspid regurgitation, *RVOT* RV outflow tract, *AT* acceleration time, *TAPSE* tricuspid annular plane systolic excursion, *IRT* isovolumic relaxation time, *IVC* inferior vena cava, *RHC* right heart catheterization

Conclusion

As a conclusion, transthoracic echocardiography remains the first line imaging tool on a patient with suspected pulmonary hypertension. All imaging indices should be taken into consideration when assessing a patient. Always remember that should we want to exclude other causes, we need to address to multimodality imaging. Finally, right heart catheterization remains the gold standard method for the diagnosis of pulmonary hypertension. Figure 32.7 is a suggested algorithm of how to approach a patient with suspected pulmonary hypertension.

32.7 References

1. Haddad F, Hunt SA, Rosenthal DN, et al. Right ventricular function in cardiovascular disease, part I: anatomy, physiology, aging, and functional assessment of the RV. Circulation. 2008;117:1436–48.
2. Haddad F, Doyle R, Murphy DJ, et al. Right ventricular function in cardiovascular disease, part II: pathophysiology, clinical importance, and management of right ventricular failure. Circulation. 2008;117:1717–31.
3. Ho SY, Nihoyannopoulos P. Anatomy, echocardiography, and normal right ventricular dimensions. Heart. 2006;92(Suppl 1):i2–13.
4. Triulzi M, Gillam LD, Gentile F, et al. Normal adult cross-sectional echocardiographic values: linear dimensions and chamber areas. Echocardiography. 1984;1:403–26.
5. Goor D, Lillehei C. Congenital malformations of the heart: embryology, anatomy, and operative considerations. New York: Grune & Stratton; 1975. p. 1–37.
6. Rudski LG, et al. Guidelines for the echocardiographic assessment of the right heart in adults: a report from the American Society of Echocardiography endorsed by the European Association of Echocardiography, a registered branch of the European Society of Cardiology, and the Canadian Society of Echocardiography. J Am Soc Echocardiogr. 2010;23(7):685–713; quiz 786-8.
7. Howard LS, Grapsa J, Dawson D, Bellamy M, Chambers JB, Masani ND, Nihoyannopoulos P, Simon R, Gibbs J. Echocardiographic assessment of pulmonary hypertension: standard operating procedure. Eur Respir Rev. 2012;21(125):239–48.
8. Rudski LG, Grapsa J. Chapter: Right atrium. ASE Dynamic Echocardiography; 2015.
9. Galiè N, Humbert M, Vachiery JL, Gibbs S, Lang I, Torbicki A, Simonneau G, Peacock A, Vonk Noordegraaf A, Beghetti M, Ghofrani A, Gomez Sanchez MA, Hansmann G, Klepetko W, Lancellotti P, Matucci M, McDonagh T, Pierard LA, Trindade PT, Zompatori M, Hoeper M, Aboyans V, Vaz Carneiro A, Achenbach S, Agewall S, Allanore Y, Asteggiano R, Paolo Badano L, Albert Barberà J, Bouvaist H, Bueno H, Byrne RA, Carerj S, Castro G, Erol Ç, Falk V, Funck-Brentano C, Gorenflo M, Granton J, Iung B, Kiely DG, Kirchhof P, Kjellstrom B, Landmesser U, Lekakis J, Lionis C, Lip GY, Orfanos SE, Park MH, Piepoli MF, Ponikowski P, Revel MP, Rigau D, Rosenkranz S, Völler H, Luis Zamorano J. 2015 ESC/ERS Guidelines for the diagnosis and treatment of pulmonary hypertension: The Joint Task Force for the Diagnosis and Treatment of Pulmonary

Hypertension of the European Society of Cardiology (ESC) and the European Respiratory Society (ERS): Endorsed by: Association for European Paediatric and Congenital Cardiology (AEPC), International Society for Heart and Lung Transplantation (ISHLT). Eur Heart J. 2016;37(1):67–119.
10. Champion HC, Michelakis ED, Hassoun PM. Comprehensive invasive and noninvasive approach to the RV-pulmonary circulation unit: state of the art and clinical and research implications. Circulation. 2009;120(11):992–1007.
11. Feneley M, Gavaghan T. Paradoxical and pseudo-paradoxical interventricular septal motion in patients with right ventricular volume overload. Circulation. 1986;74:230–8.
12. Foale R, Nihoyannopoulos P, McKenna W, et al. Echocardiographic measurement of the normal adult RV. Br Heart J. 1986;56:33–44.
13. Santamore WP, Dell'Italia LJ. Ventricular interdependence: significant left ventricular contributions to right ventricular systolic function. Prog Cardiovasc Dis. 1998;40:289–308.
14. Lang RM, Badano LP, Mor-Avi V, Afilalo J, Armstrong A, Ernande L, Flachskampf FA, Foster E, Goldstein SA, Kuznetsova T, Lancellotti P, Muraru D, Picard MH, Rietzschel ER, Rudski L, Spencer KT, Tsang W, Voigt JU. Recommendations for cardiac chamber quantification by echocardiography in adults: an update from the American Society of Echocardiography and the European Association of Cardiovascular Imaging. Eur Heart J Cardiovasc Imaging. 2015;16(3):233–70.
15. McQuillan BM, Picard MH, Leavitt M, et al. Clinical correlates and reference intervals for pulmonary artery systolic pressure among echocardiographically normal subjects. Circulation. 2001;104:2797–802.
16. Grapsa J, Pereira Nunes MC, Tan TC, Cabrita IZ, Coulter T, Smith BC, Dawson D, Gibbs JS, Nihoyannopoulos P. Echocardiographic and hemodynamic predictors of survival in precapillary pulmonary hypertension: seven-year follow-up. Circ Cardiovasc Imaging. 2015;8(6):e002107.
17. Afilalo J, Grapsa J, Nihoyannopoulos P, Beaudoin J, Gibbs JS, Channick RN, Langleben D, Rudski LG, Hua L, Handschumacher MD, Picard MH, Levine RA. Leaflet area as a determinant of tricuspid regurgitation severity in patients with pulmonary hypertension. Circ Cardiovasc Imaging. 2015;8(5):e002714.
18. Grapsa J, Rudski L. Tricuspid regurgitation: 2015 reflections and re-evaluation. Curr Treat Options Cardiovasc Med. 2015;17(10):405.
19. Kitabatake A, Inoue M, Asao M, et al. Noninvasive evaluation of pulmonary hypertension by a pulsed Doppler technique. Circulation. 1983;68:302–9.
20. Maeba H, Nakatani S, Sugawara M, et al. Different time course of changes in tricuspid regurgitant pressure gradient and pulmonary artery flow acceleration after pulmonary thromboendarterectomy: implications for discordant recovery of pulmonary artery pressure and compliance. Circ J. 2007;71:1771–5.
21. Anavekar NS, Skali H, Bourgoun M, et al. Usefulness of right ventricular fractional area change to predict death, heart failure, and stroke following myocardial infarction (from the VALIANT ECHO Study). Am J Cardiol. 2008;101:607–12.
22. Wang J, Prakasa K, Bomma C, et al. Comparison of novel echocardiographic parameters of right ventricular function with ejection fraction by cardiac magnetic resonance. J Am Soc Echocardiogr. 2007;20:1058–64.
23. Ryan T, Petrovic O, Dillon JC, et al. An echocardiographic index for separation of right ventricular volume and pressure overload. J Am Coll Cardiol. 1985;5:918–27.
24. Tei C, Dujardin KS, Hodge DO, et al. Doppler echocardiographic index for assessment of global right ventricular function. J Am Soc Echocardiogr. 1996; 9:838–47.
25. yeo TC, Dujardin KS, Tei C, et al. Value of a Dopplerderived index combining systolic and diastolic time intervals in predicting outcome in primary pulmonary hypertension. Am J Cardiol. 1998;81:1157–61.
26. Alam M, Wardell J, Andersson E, et al. Characteristics of mitral and tricuspid annular velocities determined by pulsed wave Doppler tissue imaging in healthy subjects. J Am Soc Echocardiogr. 1999;12:618–28.
27. Hammarstrom E, Wranne B, Pinto FJ, et al. Tricuspid annular motion. J Am Soc Echocardiogr. 1991;4:131–9.
28. Lopez-Candales A, Dohi K, Rajagopalan N, et al. Defining normal variables of right ventricular size and function in pulmonary hypertension: an echocardiographic study. Postgrad Med J. 2008;84:40–5.
29. Sheehan F, Redington A. The RV: anatomy, physiology and clinical imaging. Heart. 2008;94:1510–5.
30. Smith BC, et al. Three-dimensional speckle tracking of the RV: toward optimal quantification of right ventricular dysfunction in pulmonary hypertension. J Am Coll Cardiol. 2014;64(1):41–51. https://doi.org/10.1016/j.jacc.2014.01.084.
31. Meier GD, Bove AA, Santamore WP, et al. Contractile function in canine RV. Am J Physiol. 1980;239: H794–804.
32. Carlsson M, Ugander M, Heiberg E, et al. The quantitative relationship between longitudinal and radial function in left, right, and total heart pumping in humans. Am J Physiol Heart Circ Physiol. 2007;293:H636–44.
33. Suever J, et al. Right ventricular strain, torsion, and dyssynchrony in healthy subjects using 3D spiral cine DENSE magnetic resonance imaging. IEEE Trans Med Imaging. 2017;36(5):1076–85. https://doi.org/10.1109/TMI.2016.2646321.

33 Transthoracic Echocardiography: Improved Practice by Real-Time 3D Acquisition and Automation

Kuan-Chih Huang, Jiunn-Lee Lin, and Lung-Chun Lin

Abstract

Right ventricular ejection fraction (RVEF) has been approved of important prognostic in many cardiac diseases. However, RVEF in these studies was mostly evaluated by cardiac magnetic resonance imaging (CMR), radionuclide imaging or even angiography, but not the most accessible echocardiography. Most difficulties of right ventricular assessment by two-dimensional echocardiography come from the unusual crescent shape, the anterior location and the complex contraction mechanism. With recently available dedicated software, three-dimensional echocardiography should bring the innate accessibility in to full play, putting in the last piece, the right ventricle, of puzzle of ventricles.

Keywords

Automatic analysis · Imaging acquisition · Morphological remodeling · Right ventricular ejection fraction · Three-dimensional echocardiography

K.-C. Huang
Division of Cardiology, Heart Center, Cheng Hsin General Hospital, Taipei, Taiwan, Republic of China

J.-L. Lin · L.-C. Lin (✉)
Section of Cardiology, Department of Internal Medicine, National Taiwan University Hospital, Taipei, Taiwan, Republic of China
e-mail: jiunnlee@ntuh.gov.tw; anniejou@ms28.hinet.net

33.1 Introduction

For many years, right ventricle (RV) has continuously been challenging echo-cardiologists with its complex geometry and unique way of contraction. These unresolved obstacles made the RV a forgotten chamber, and indirectly opened the era of "the left cardiology". From left ventricular ejection fraction (LVEF) based systolic function to diastolic function that comprises spectral Doppler envelop of mitral inflow and basal tissue velocity of LV septal and lateral walls to recently widely adapted spectral tracking derived strain analysis, comprehensive LV evaluations gradually become an unaffordable workflow with limited prognostic applications due to complicate inter-vendor variations. Nowadays, the only echo-derived therapeutic indicator remained LVEF alone, and there are lots of controversies in strain analysis. As the LV evaluation cannot catch up the rapidly improving steps of medical and interventional treatments, the focus of cardiologists returned back to the selectively forgotten chamber. Intuitively, right ventricle should have prognostic value in any group of pulmonary hypertension (PH). As a result, more and more reappraisals of the importance of RV were launched in the group 2 PH, such as severe decompensated heart failure, heart failure with preserved ejection fraction, post myocardial infarction status and valvular heart diseases. Radionuclide and cardiac magnetic resonance imaging (CMR) have been already applied for

S. I. Dumitrescu et al. (eds.), *Right Heart Pathology*, https://doi.org/10.1007/978-3-319-73764-5_33

evaluation of RV function [1, 2], but echocardiogram, the imaging modality with the greatest availability, regained its reliable application on RV very recently [3]. In this chapter, we will go through traditional two dimensional echocardiography (2DE) RV evaluation, describe the superiority of three dimensional echocardiography (3DE), introduce basic technique of image acquisition and discuss further application of 4D volumetric analysis.

33.2 Relationship Between Right and Left Ventricles

RV performs the very first of the in-series double pumps, as a result, its functioning reflects a composite result of fluid status, pulmonary vascular resistance and left heart function. Besides, the anatomical connection via septum, pericardium and the anatomical continuous outer layer of myocardium with LV constitute the ventricular interdependence. Experimental animal studies showed that approximately 20% to 40% of RV systolic pressure and volume outflow results from LV contraction [4]. Mitral regurgitation was reported to correlate with RV dilatation and enlargement of right coronary artery [5]. Sabe and colleagues also found that mitral regurgitation (as measured by effective orifice area) appears to be a significantly independent predictor of RVEF in patients with ischemic cardiomyopathy [6]. LA function was recently reported to associate with right sided Ventricular-arterial (VA) uncoupling [7]. Conversely, dilatation of RV could also lead to elevation of left ventricular end-diastolic pressure (LVEDP) and impair LV elastance [4, 8]. With these perceptions, evaluation of right heart should not be an isolated branch or even a competition with the previously well-established LV cardiology. Cardiologist should re-unite these physiologically in-series and anatomically parallel chambers to consider each phenotype of cardiac disease more comprehensively.

33.3 Two-Dimensional Echocardiography (2DE)

A comprehensive 2DE RV analysis includes precise measurements of dimension, estimations of loading status and assessments of contractile function.

33.3.1 Dimension

For the complex geometry of RV, guideline suggested comprehensive 14 acquisition views (including 7 RV specific views) and defined five dimensions (Fig. 33.1) to complete a 2DE RV analysis [9]. The normal RV measurements by 2DE are: basal diameter (RVD1) 24–42 mm, mid cavity diameter (RVD2) 20–35 mm, longitudinal diameter (RVD3) 56–86 mm, proximal RVOT in parasternal long axis 18–33 mm, and distal RVOT in parasternal short axis 17–27 mm. Maximal RV dimension should be acquired under judicious angular change of transducer under RV focused four-chamber view.

33.3.2 Loading Status

IVC diameter and collapsing response toward respiration were adopted for RA pressure estimation [10], but underestimation might occur in the condition of severe tricuspid regurgitation as the highest estimated RA pressure was only 15 mmHg. In the absence of pulmonic stenosis, right ventricular systolic pressure (RVSP) is equal to systolic pulmonary arterial pressure and can be estimated by the equation: $RVSP = 4(V)^2 + RAP$ [11], where V is the peak velocity of tricuspid regurgitation (TR) jet. Pulmonary diastolic pressure (PADP) can be estimated by the equation: $PADP = 4 \times (\text{end-diastoic PR velocity})^2$ and mean PAP by the equation $4 \times (\text{early PR velocity})^2$ [12]. For better temporal resolution of the regurgitant envelope, sweep speeds above 100 mm/s was suggested. Echo contrast enhancement of Doppler

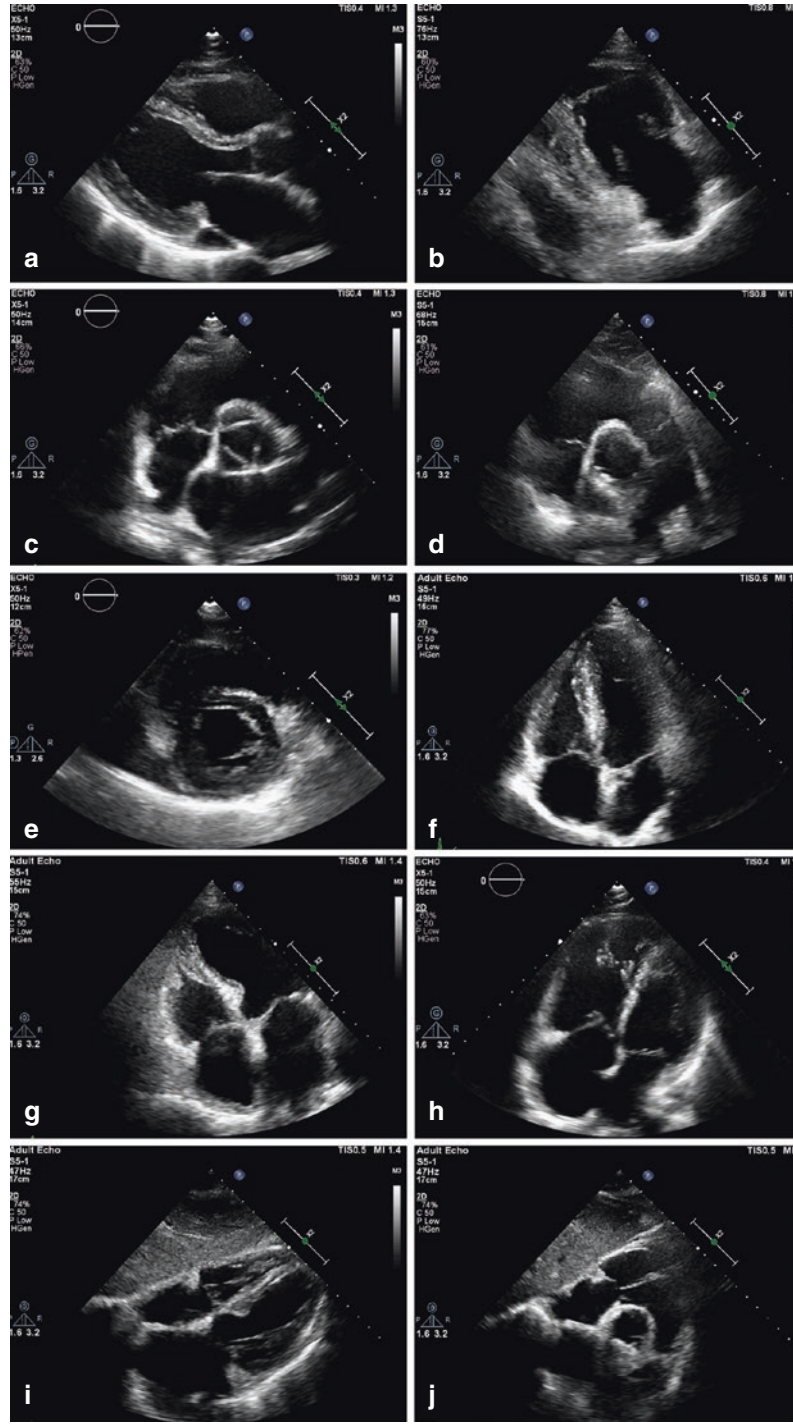

Fig. 33.1 Commonly used views for right ventricular evaluation according to guideline. (**a**) Parasternal long-axis of RV anterior wall*; (**b**) Parasternal long-axis view of RV inflow; (**c**) Parasternal short-axis of basal RV; (**d**) Parasternal short-axis of bifurcation of the pulmonary artery*; (**e**) Parasternal RV short-axis at papillary muscle level; (**f**) Apical 4-chamber*; (**g**) RV focused apical 4-chamber; (**h**) RV modified apical 4-chamber; (**i**) RV subcostal 4-chamber; (**j**) Subcostal short-aixs of basal RV. *Views suggested for chamber quantification

signal might not be necessary for native tricuspid valve with significant heart disease, but could be helpful in the condition of post-tricuspid surgery or PAH with competent tricuspid valve. Normal RVSP is below 40 mmHg and PAH is diagnosed as mPAP beyond 25 mmHg. Pulmonary vascular resistance (PVR) could be estimated by the Abbas equation: PVR (WU) = (TRVmax (m/s) × 10/PV VTI (cm)) + 0.16 [13], underestimation would happen in high resistant status and need correction by Dahiya equation [14].

33.3.3 Contractile Function

Normal RV ejection fraction has a mean value of 52.3 ± 6.2% with 40% being the lower limit [9]. However, due to the complex geometry, no ideal equation of RVEF by 2DE has been developed. Instead, many surrogate parameters have been studied, including fractional area change (FAC), tricuspid annular plane systolic excursion (TAPSE) and RV strain. FAC is a convenient tool for RV function evaluation with lower normal limit of 35%. Because the requirement of clear RV border at the apical four-chamber view with maximal RV dimension and the angular sensitivity of RVD2, the scanning plane should pass both center points of the mitral and tricuspid valves (Fig. 33.2). As a result, the consistency of FAC limits its use. TAPSE has been widely adopted as a surrogate RV index. As Sakuma and colleague demonstrated in an angiographic study [15], the bellow effect (septum—free wall dimension) plays an important role in RV systolic function. But when RVEF is <40%, the contribution of longitudinal shortening increased. This might provide the theoretical support of using TAPSE for risk stratification but we cannot forget the effect of circumferential deformational change, which means not only anatomical continuity with LV but also an early sign on the very beginning of deterioration of RV function. However, due to its relative low absolute value, TAPSE is mostly used as a dichotomic tool with a reference of 16 mm [9]. Recently, a composite parameter TAPSE/PASP has been developed to represent right sided VA coupling [16, 17], broadening the use of TAPSE. Speckle tracking analysis derived RV strain has been widely adapted for risk stratification in various cardiac diseases by software originally designed for left ventricle, as a result, global RV strain, free wall strain and of other different regional of interest were all reported and claimed to have association with prognosis [18–21]. Even though the development of dedicated software for RV is in full wing, the inter-vendor consistency should be an issue to be dealt with as in their left counterpart. It is noteworthy to reclaim the idea of the composite character of these non-invasive indices of RV function. As studied in a porcine model, these parameters are more correlated with Ees/Ea rather than Ees [22], which means that these indices are more like a reflection of VA coupling than of RV contractility.

33.4 Why Is 3DE Important?

Most difficulties of RV assessment by 2DE come from the unusual crescent shape, the anterior location and the complex contraction mechanism. Even though several dimensions have been defined to depict the RV geometry, these are still not satisfactory for clinical pathophysiology. For example, the apical dilatation of RV, a typical type of morphological remodeling, cannot be described by the guideline suggested measurements. As the reflection point of myocardial fibers, the dilatation of RV apex will result in difficult decision of the reference point for further analysis of TAPSE and RV strain. On the other hand, the different RV adaptation toward pulmonary arterial hypertension and pulmonary venous hypertension (Fig. 33.3) could only be represented by RVD2, which is the most angular sensitive dimension of RV. 3D-assisted 2DE could provide a second sector of adjustable rotational angle to make sure the maximal coronal RV area is acquired. When the first sector is adjusted to of maximal RVD2, the second sector could be chosen to of tilting function, avoiding underestimation of RVD3 from taking moderator band as the border of RV apex.

The RV is the most anteriorly situated cardiac chamber and lies immediately behind the sternum. Such geographical condition brings the

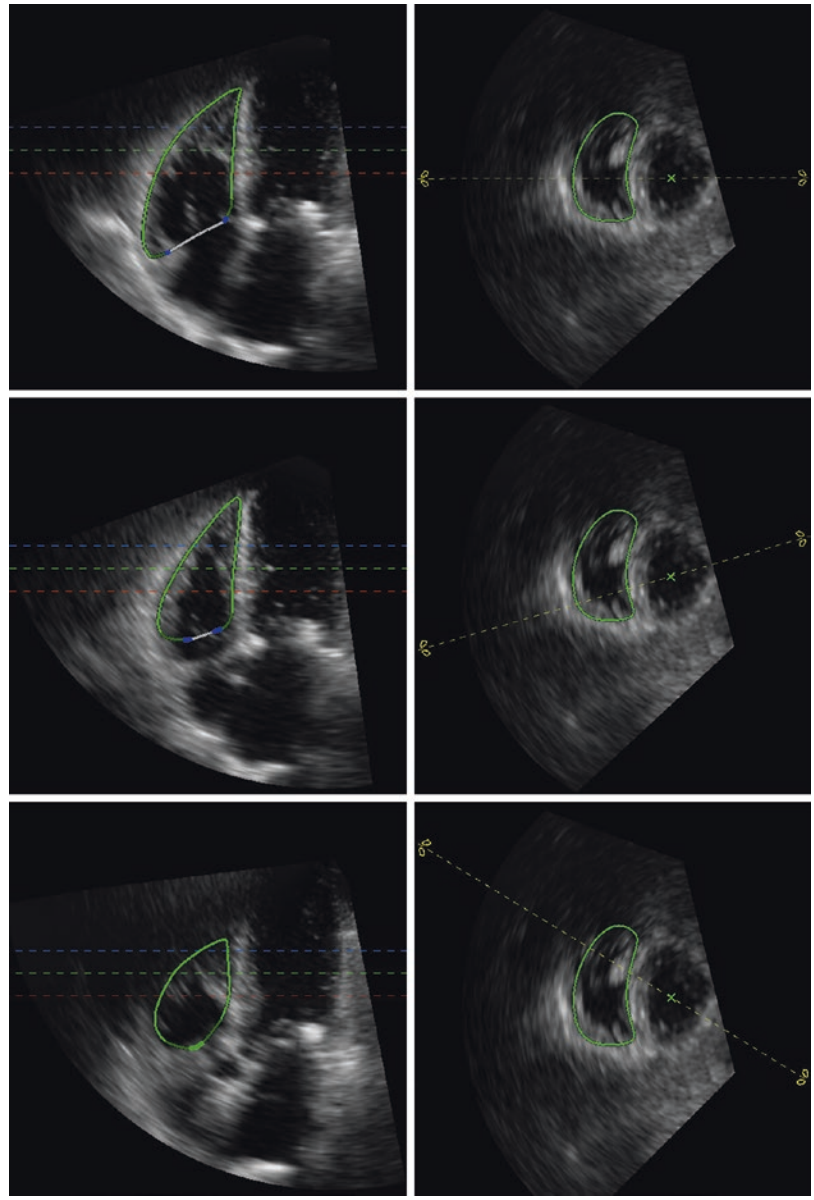

Fig. 33.2 Angular sensitivity of right ventricular dimension. The scanning plane should pass both center points of the mitral and tricuspid valves (upper panel) to acquire suitable four chamber view for RV chamber quantification

need of compromise between prevention of foreshortened imaging and clear RV free wall border in longitudinal RV functional evaluation. Foreshortening would not be an issue in 3DE, as long as the whole volume is included in the dataset, as the axis can be corrected in the post-processing step.

The RV contracts by 3 separate mechanisms: (1) inward movement of the free wall, which produces a bellows effect; (2) contraction of the longitudinal fibers, which shortens the long axis and draws the tricuspid annulus toward the apex; and (3) traction on the free wall at the points of attachment secondary to LV contraction [23]. Besides, RV contraction is sequential, starting with contraction of the inlet and trabeculated myocardium and ending with contraction of the infundibulum. As a result, RV alters its shape continuously throughout its unique peristalsis-like contraction, and the dynamic pumping process has been over-

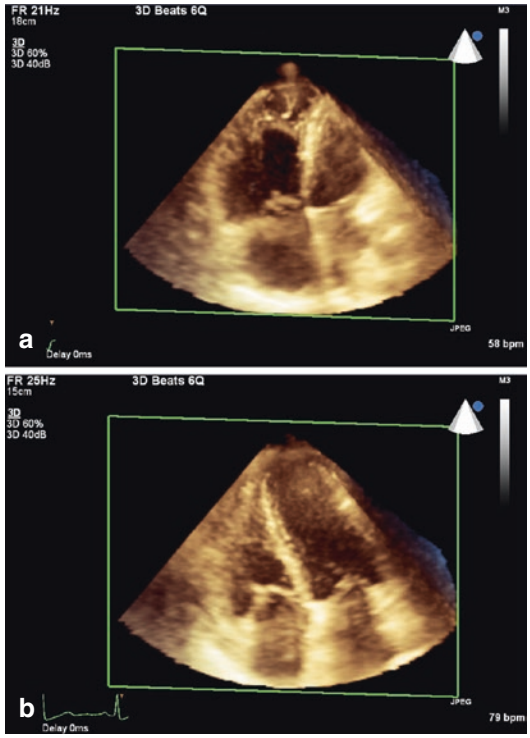

Fig. 33.3 RV adaptation to PAH (**a**) and PVH (**b**)

looked as has the individual contractive contribution made by each of the three parts of the RV. This makes most static 2DE RV parameters only of modest predictive value in the prognosis of heart disease. 3DE with dedicated software could provide volumetric analysis in each part of RV or as a whole, giving cardiologist the opportunity to jump out the left sided boundary to observe RV.

RVEF has been approved of important prognostic in many cardiac diseases (Table 33.1). However, RVEF in these studies was mostly evaluated by CMR, radionuclide imaging or even angiography, but not the most accessible echocardiography. Reliability between RVEF and those surrogate 2DE parameters has only been proved in specific group at well-defined conditions. Previous comparing studies also revealed that the correlation of RVESV with CMR is relatively lower in 2DE [41]. With recently available dedicated software, RV 3DE should bring the innate accessibility in to full play, putting in the last piece of puzzle of ventricles.

33.5 3DE Assessments of RV

With the development and improvement of matrix transducer, 3D echocardiography has evolved from a challenging experimental technique into a possible daily practice. The following will introduce some tips and tricks of RV 3DE acquisition and basic analytic methods.

33.5.1 Acquisition

In traditional apical four-chamber view, the border of RV free wall could be shielded by right lung lobe or might intermittently be out of the scanning sector. Complete inclusion of the chamber of interest is the base of 3DE volumetric analysis. Selection of suitable approach during acquisition could increase the rate of successful inclusion of dilated RV (Fig. 33.4) [42].

33.5.1.1 Lateral Approach (RV Focused Apical Four-Chamber)

This acquisition can be achieved by starting from the ASE guideline described RV focused apical 4-chamber view, displacing the transducer laterally, then adding an anterior tilt. Sometimes a more cranial intercostal space and slight rotation of transducer could help much to include both the pulmonic and tricuspid valves. Like liver enhanced penetration in pediatric echocardiography, such approach used the LV to increase the RV free wall echogenicity, but is challenged by far-field resolution, ribs and artifacts from lungs. The lateral approach is suitable in group 2 PAH, except rheumatic mitral stenosis, as the LV constitutes the greatest part of heart. This is also the official recommended acquisition from one of the dedicated RV 3DE analysis software [3].

33.5.1.2 Medial Approach (RV Modified Apical 4-Chamber)

For typical group 1 PAH and rheumatic mitral stenosis, the right ventricle is usually more enlarged then LV and occupied the apex. In this situation, the lateral approach is not suitable as the relative small LV cannot provide enough

Table 33.1 Prognostic applications of RV systolic function in different cardiac diseases

Study	Population (n)	Modality	RV indices & cut point	Major findings
Zornoff et al. [24] 2002	ICMP, LVEF ≤40% (416)	2DE	RVFAC <32.2%	RV function is an independent predictor of total mortality, cardiovascular mortality and HF
Van der Mass et al. [25] 2012	ICMP (347)	Radionuclide	RVEF <40%	A decreased RVEF was associated with a 2.15 (1.34–3.43)-fold increase in the risk of cardiac hospitalization and a 5.11 (2.32–11.23)-fold risk of cardiac death
Sabe et al. [6] 2016	ICMP (588)	CMR	RVEF <35%	Although decreasing RVEF was associated with a poor prognosis in the nonrepair group (hazard ratio, 1.28; 95% confidence interval, 1.12–1.47; P < 0.001), it was not associated with death in the mitral valve repair or replacement group (P for interaction = 0.046)
La Vecchia et al. [26] 2006	DCM, LVEF <55% (120)	Aniography	RVEF <34%	At multivariate analysis, independent predictors of transplant-free survival were RVEF (P = 0.001), right ventricular stroke work index (P = 0.015), right ventricular end-diastolic volume (P = 0.034) and left ventricular end-diastolic volume (P = 0.048), but not LVEF
Kawata et al. [27] 2017	DCM, LVEF <35% (68)	2DE	RVFAC <26.7%	Receiver-operating characteristic curve analysis showed that the optimal FAC cut-off value to identify patients with an event was <26.7% (area under the curve = 0.74)
Mikami et al. [28] 2017	Systolic HF (314)	CMR	RVEF <45%	RV dysfunction is a strong, independent predictor of arrhythmic events
Tamaki et al. [29] 2015	LVEF <40% (63)	MIBG	RVEF <37%	RVEF and MIBG wash-our rate were independent predictors of unplanned WHF hospitalization
Ghio et al. [16] 2016	CHF (1663)	2DE	TAPSE/PASP <0.36 mm/mmHg	Regardless of the extent of LV dysfunction, the TAPSE/PASP ratio is a powerful independent predictor of prognosis in all heart failure patients
Iacoviello et al. [30] 2017	CHF (315)	2DE	(RVGLS/PASP) <0.36; (RV free wall strain/PASP) <0.66	Both RV-GLS/PASP and RV-fwLS/PASP were significantly associated with an increased risk of death
Antoni et al. [31] 2010	STEMI (621)	2DE	FAC <32%, TAPSE <15 mm, GLS > −22.1%	After multivariable analysis, only RVFAC (hazard ratio, 0.96; 95% CI, 0.92–0.99) and RV strain (hazard ratio, 1.08; 95% CI, 1.03–1.13) independently predicted the composite end point
Larose et al. [32] 2007	30 days after myocardial infarction (147)	CMR	RVEF <40%	By multivariable analysis that adjusted for patient age, left ventricular (LV) infarct size, and LVEF, RVEF <40% remained a significant independent predictor of mortality (adjusted hazard ratio 2.86; P = 0.03)
Murata et al. [33] 2016	PH with mPAP >35 mmHg (86)	3DE	RVEF <28%	K–M analysis showed that patients with 3DRVEF less than 28% had significantly shorter event-free survival in patients with mPAP >35 mmHg

(continued)

Table 33.1 (continued)

Study	Population (n)	Modality	RV indices & cut point	Major findings
Courand et al. [34]	PH (78)	Radionuclide	RVEF <25%	Patients of baseline RVEF >25% or stable RVEF during follow up had better prognosis
Jensen et al. [35] 2015	PH ES (48)	CMR	RVEF <40% (in conjunction with LVEF <50% for given. Failure)	Impaired right, left, or biventricular systolic function derived from baseline CMR are associated with mortality in adult patients with ES
da Costa et al. [18] 2017	Group 1 PH (66)	2DE	RV free wall strain > −14%	Multivariate analysis identified RVFreeWSt ≤ −14% as the only 2DE independent variable associated with combined endpoints (hospitalization for worsening PAH or cardiovascular death) [HR 4.66 (1.25–17.37); P < 0.05]
Haeck et al. [19]	PH (150)	2DE	RV free wall strain > −19%	RV free wall strain is significantly associated with all-cause mortality
Bodez et al. [36] 2016	Caridac amyloidosis (TTR) (82)	2DE	TAPSE <14 mm	Low TAPSE independently predicted major adverse cardiac event (MACE) defined as death, heart transplantation and acute heart failure
Cappelli et al. [20]	AL amyloidosis (52)	2DE	Average of RV strain from 3 free wall segment > −17%	Cox multivariate analysis showed that N-terminal pro-Brain natriuretic peptide and RV longitudinal strain were the strongest death predictor
Bootsma et al. [37] 2017	Cardiovascular surgery (1109)	Thermal filament	RVEF <20%	Right ventricular function is associated independently with 2-year all-cause mortality in a heterogenic cardiac surgery population
Dahou et al. [21] 2016	LFLG AS (211)	DSE	Stress RV free wall strain > −14%	After adjustment for rest RVLS, stress RVLS <|14|% remained independently associated with mortality (HR = 3.29; 95% CI 1.17–9.25; P = 0.024), whereas rest RVLS was not (P > 0.05)
Le Tourneau et al. [38] 2013	Organic MR (208)	Radionuclide	RVEF <35%	RV function impairment depends more on LV remodeling and septal function than on PASP. RV function is a predictor of postoperative cardiovascular survival
Burri et al. [39] 2010	CRT (44)	Radionuclide	RVEF <35%	Patients with a baseline RVEF < or = 0.35 (n = 19) were less likely to improve in NYHA class (P = 0.016), and also tended to improve less in 6MWD and LVEF (P < 0.06)
Alpendurada et al. [40] 2011	CRT (60)	CMR	RVEF <30%; TAPSE <10 mm	Patients with marked RV dysfunction (RVEF <30%) had a particularly low response rate (18.2%) to CRT

echogenicity. A medical approach, derived by moving the transducer medially from the guideline described RV modified apical four-chamber view, could be adopted for these patients. This is because the dilated RV contact the chest wall more closely, providing a possible acoustic window for better resolution of RV anterior and free wall. Apex from this approach is challenged by near-field resolution, ribs, and the sternum.

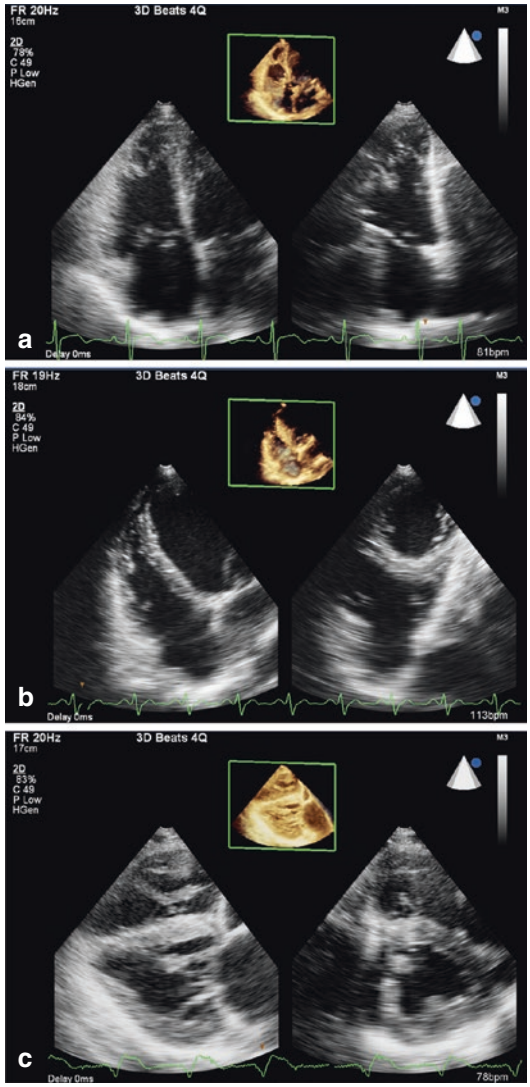

Fig. 33.4 Acquisition windows and corresponding views: (**a**) medial approach, (**b**) lateral approach, (**c**) subcostal approach

33.5.1.3 Subcostal Approach

As a bailout choice, subcostal approach is a theoretical solution, as 3DE analytic software allows inspector to define anatomical reference landmarks. However, the innate limitation that the lateral resolution is always lower than the axial resolution for any ultrasound imaging might compromise the 3D RV strain analysis and the RV volumetric analysis has not yet been validated with CMR. Possible compression from transducer might also lead to misinterpretation of RV function because there is no physical protection from the thoracic cage during subcostal echocardiography. Nevertheless, subcostal approach is a helpful to perform echocardiography on patients of chronic obstructive pulmonary disease (i.e. Group 3 PAH).

33.5.2 Imaging Optimization During Acquisition

Complete inclusion of RV in the 3D pyramidal dataset is not enough, while the adequate frame rate (usually above 20 Hz) is the foundation of volumetric analysis. For the beginners, the adjustment of sector width is a major obstacle to simultaneously consider these mutually exclusive characters of echocardiography. Fortunately, real time multiple planar reconstruction is now available during 3DE acquisition in many echocardiography machines. For example, on the Philips IE33 and Epiq 7 systems (Philips Medical Systems, Andover, MA), four-screen demonstration provides two apical 2D multiplanar reconstruction (MPR) views, one short axis MPR view and the 3D volume view when apical approach (either medial or lateral) is adopted. The apical 2D view could help examiner to adjust sector width for the inlet and sinus part of RV, and the short axis 2D view could help to make sure the inclusion of outlet part. When multiple beats reconstruction is chosen for higher frame rate, real time MPR also provide better check of any stitching artifacts that would be difficult to detect in the 3D volume view without familiar 3D rotation examination. For patients with arrhythmia or those cannot hold breath for multiple beats reconstruction, high volume rate (HRV) mode is another choice at the expanse of resolution as the number of scanning lines was reduced.

33.5.3 Analysis of 3DE Datasets

Three-dimensional echocardiographic data sets should be stored digitally and used for off-line

analysis. Quantitative analysis can be performed using dedicated software (4D RV-Function 2.0, a module of TomTec-Arena; TomTec Imaging Systems, Unterschleissheim, Germany) to measure RV volumes and EF using a semi-automated algorithm. The first step of analysis is to manually define the LV and RV long axes at end-diastole in both apical two- and four-chamber views, left ventricular outflow tract diameter in the apical three-chamber view, the anterior and posterior junction points of the RV free wall on the interventricular septum, and the longest dimension of the RV cavity between the septum and the free wall, both in a single short-axis view (Fig. 33.5a). These anatomic landmarks are then used automatically to extract from the 3DE data set of the right ventricle–focused four-chamber view and a series of short-axis views from base to apex at both end-systole and end-diastole (Fig. 33.5b). The software will then track the RV surface rendering model throughout the cardiac cycle by speckle-tracking technology (Fig. 33.5c). Interactive fine-tuning of the RV border with the assisted of MPR technique is allowed at end-diastole and end-systole. The following analysis will then performed automatically to generate RVEDV, RVESV, RVEF, 3D assisted FAC and TAPSE, and 3D RV strain of free wall and septal wall.

Besides these 3D static data, a 4D RV volume to time curve will also be generated for further volumetric analysis. For example, in our experimental study, a continuous wave Doppler envelope of tricuspid regurgitation was transformed into a pressure gradient recording and conjugated with the RV volume-to-time curve to yield a systolic pressure gradient-volume (PG-V) curve. The area under the curve could then represent RV stroke work.

33.6 Limitations and Future of RV 3DE

There are still some problems of RV 3DE analysis remained to be resolved. Dropout artifacts are an innate weakness of echo imaging, especially for the infundibulum of RV. For example, the rate of exclusion due to sub-optimal imaging was as high as 21% in a 3DE analysis for pulmonary hypertension [43]. Similar issue of the left side counter part is about the near-field resolution of LV apex, and A.I. assisted model selection system seems to provide a possible solution. The right heart version of such software should help much, as the infundibulum assessments might have important role in the field of VA coupling of right heart. On the other hand, the paradoxical septal movement, which is not uncommon in patients that would induce our interests in RV, would lead to inadequate septal tracking during dynamic analysis and limited the value of volumetric analysis. Custom software has been developed for curvature analysis of this special phenomenon during RV remodeling [44–47], the clinical significance and application depends on further works. In summary, the technique-demanding tool, the technique-challenging chamber and time consuming post-processing steps might let the RV 3DE analysis become another frustrating workload before bringing clinical benefits, not to mention the serial examinations that are more necessary in this load-sensitive chamber. To replace the quickly and easily obtained parameters, like TAPSE, FAC and basal RV free wall tissue velocity, the development of user-friendly and accurate on-cart analytic software is imperative and will be indispensable in the future.

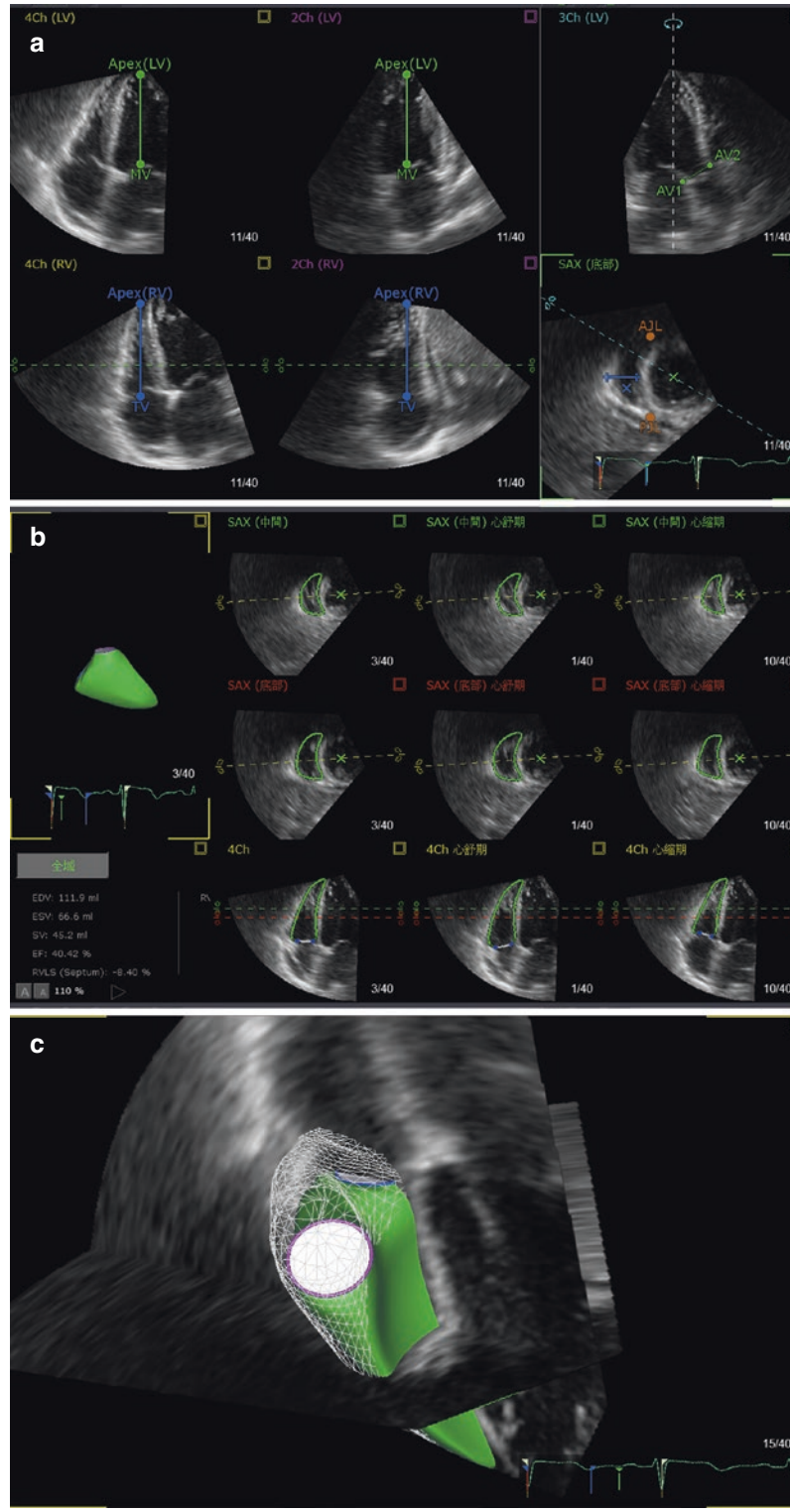

Fig. 33.5 Steps of volumetric right ventricular 4D analysis. (**a**) Decision of anatomical landmarks. (**b**) Automatic tracking of endocardial border with allowed interactive fine-tuning under the assistance of MPR technique at end-diastolic and end-systolic phase. (**c**) Result of 4D dynamic surface rending model (green), end-diastolic endocardial mesh (white), and corresponding MPR 2D echo planes; pink ring = pulmonic valvular plane, blue ring = tricuspid valvular plane

References

1. Kawut SM, Al-Naamani N, Agerstrand C, Berman Rosenzweig E, Rowan C, Barst RJ, et al. Determinants of right ventricular ejection fraction in pulmonary arterial hypertension. Chest. 2009;135:752–9. https://doi.org/10.1378/chest.08-1758.
2. Moledina S, Pandya B, Bartsota M, Mortensen KH, McMillan M, Quyam S, et al. Prognostic significance of cardiac magnetic resonance imaging in children with pulmonary hypertension. Circ Cardiovasc Imaging. 2013;6:407–14. https://doi.org/10.1161/CIRCIMAGING.112.000082.
3. Medvedofsky D, Addetia K, Patel AR, Sedlmeier A, Baumann R, Mor-Avi V, et al. Novel approach to three-dimensional echocardiographic quantification of right ventricular volumes and function from focused views. J Am Soc Echocardiogr. 2015;28:1222–31. https://doi.org/10.1016/j.echo.2015.06.013.
4. Santamore WP, Dell'Italia LJ. Ventricular interdependence: significant left ventricular contributions to right ventricular systolic function. Prog Cardiovasc Dis. 1998;40:289–308.
5. Vassalli G, Hess OM, Krogmann ON, Villari B, Corin WJ, Turina M, et al. Coronary artery size in mitral regurgitation and its regression after mitral valve surgery. Am Heart J. 1993;126:1091–8.
6. Sabe MA, Sabe SA, Kusunose K, Flamm SD, Griffin BP, Kwon DH. Predictors and prognostic significance of right ventricular ejection fraction in patients with ischemic cardiomyopathyclinical perspective. Circulation. 2016;134:656–65. https://doi.org/10.1161/CIRCULATIONAHA.116.022339.
7. Sugimoto T, Bandera F, Generati G, Alfonzetti E, Bussadori C, Guazzi M. Left atrial function dynamics during exercise in heart failure. JACC Cardiovasc Imaging. 2016;10(10 Pt B):1253–64. https://doi.org/10.1016/j.jcmg.2016.09.021.
8. Dell'Italia LJ. The right ventricle: anatomy, physiology, and clinical importance. Curr Probl Cardiol. 1991;16:653–720.
9. Rudski LG, Lai WW, Afilalo J, Hua L, Handschumacher MD, Chandrasekaran K, et al. Guidelines for the echocardiographic assessment of the right heart in adults: a report from the American Society of Echocardiography. J Am Soc Echocardiogr. 2010;23:685–713. https://doi.org/10.1016/j.echo.2010.05.010.
10. Kircher BJ, Himelman RB, Schiller NB. Noninvasive estimation of right atrial pressure from the inspiratory collapse of the inferior vena cava. Am J Cardiol. 1990;66:493–6.
11. Currie PJ, Seward JB, Chan K-L, Fyfe DA, Hagler DJ, Mair DD, et al. Continuous wave Doppler determination of right ventricular pressure: a simultaneous Doppler-catheterization study in 127 patients. J Am Coll Cardiol. 1985;6:750–6.
12. Abbas AE, Fortuin FD, Schiller NB, Appleton CP, Moreno CA, Lester SJ. Echocardiographic determination of mean pulmonary artery pressure. Am J Cardiol. 2003;92:1373–6.
13. Abbas AE, Fortuin FD, Schiller NB, Appleton CP, Moreno CA, Lester SJ. A simple method for noninvasive estimation of pulmonary vascular resistance. J Am Coll Cardiol. 2003;41:1021–7.
14. Dahiya A, Vollbon W, Jellis C, Prior D, Wahi S, Marwick T. Echocardiographic assessment of raised pulmonary vascular resistance: application to diagnosis and follow-up of pulmonary hypertension. Heart. 2010;96:2005–9. https://doi.org/10.1136/hrt.2010.204834.
15. Sakuma M, Ishigaki H, Komaki K, Oikawa Y, Katoh A, Nakagawa M, et al. Right ventricular ejection function assessed by cineangiography. Circ J. 2002;66:605–9.
16. Ghio S, Guazzi M, Scardovi AB, Klersy C, Clemenza F, Carluccio E, et al. Different correlates but similar prognostic implications for right ventricular dysfunction in heart failure patients with reduced or preserved ejection fraction: RV function in heart failure. Eur J Heart Fail. 2017;19:873–9. https://doi.org/10.1002/ejhf.664.
17. Guazzi M, Dixon D, Labate V, Beussink-Nelson L, Bandera F, Cuttica MJ, et al. RV contractile function and its coupling to pulmonary circulation in heart failure with preserved ejection fraction. JACC Cardiovasc Imaging. 2017;10(10 Pt B):1211–21. https://doi.org/10.1016/j.jcmg.2016.12.024.
18. da Costa Junior AA, Ota-Arakaki JS, Ramos RP, Uellendahl M, Mancuso FJ, Gil MA, et al. Diagnostic and prognostic value of right ventricular strain in patients with pulmonary arterial hypertension and relatively preserved functional capacity studied with echocardiography and magnetic resonance. Int J Cardiovasc Imaging. 2017;33:39–46. https://doi.org/10.1007/s10554-016-0966-1.
19. Haeck ML, Scherptong RW, Marsan NA, Holman ER, Schalij MJ, Bax JJ, et al. Prognostic value of right ventricular longitudinal peak systolic strain in patients with pulmonary hypertension. Circ Cardiovasc Imaging. 2012;5:628–36.
20. Cappelli F, Porciani MC, Bergesio F, Perlini S, Attana P, Moggi Pignone A, et al. Right ventricular function in AL amyloidosis: characteristics and prognostic implication. Eur Heart J Cardiovasc Imaging. 2012;13:416–22. https://doi.org/10.1093/ejechocard/jer289.
21. Dahou A, Clavel M-A, Capoulade R, Bartko PE, Magne J, Mundigler G, et al. Right ventricular longitudinal strain for risk stratification in low-flow, low-gradient aortic stenosis with low ejection fraction. Heart. 2016;102:548–54. https://doi.org/10.1136/heartjnl-2015-308309.
22. Guihaire J, Haddad F, Boulate D, Decante B, Denault AY, Wu J, et al. Non-invasive indices of right ventricular function are markers of ventricular-arterial coupling rather than ventricular contractility: insights from a porcine model of chronic pressure overload.

Eur Heart J Cardiovasc Imaging. 2013;14:1140–9. https://doi.org/10.1093/ehjci/jet092.
23. Weyman AE. Principles and practice of echocardiography. 2nd ed. Philadelphia: LWW; 1994. p. 1335.
24. Zornoff LAM, Skali H, Pfeffer MA, St John Sutton M, Rouleau JL, Lamas GA, et al. Right ventricular dysfunction and risk of heart failure and mortality after myocardial infarction. J Am Coll Cardiol. 2002;39:1450–5.
25. van der Maas N, Braam RL, van der Zaag-Loonen HJ, Meerman J, Cozijnsen L, Scholte AJ. Right ventricular ejection fraction measured by multigated planar equilibrium radionuclide ventriculography is an independent prognostic factor in patients with ischemic heart disease. J Nucl Cardiol. 2012;19:1162–9. https://doi.org/10.1007/s12350-012-9613-y.
26. La Vecchia L, Varotto L, Zanolla L, Spadaro GL, Fontanelli A. Right ventricular function predicts transplant-free survival in idiopathic dilated cardiomyopathy. J Cardiovasc Med. 2006;7:706–10.
27. Kawata T, Daimon M, Kimura K, Nakao T, Lee SL, Hirokawa M, et al. Echocardiographic assessment of right ventricular function in routine practice: which parameters are useful to predict one-year outcome in advanced heart failure patients with dilated cardiomyopathy? J Cardiol. 2017;70:316–22. https://doi.org/10.1016/j.jjcc.2017.02.007.
28. Mikami Y, Jolly U, Heydari B, Peng M, Almehmadi F, Zahrani M, et al. Right ventricular ejection fraction is incremental to left ventricular ejection fraction for the prediction of future arrhythmic events in patients with systolic dysfunction. Circ Arrhythm Electrophysiol. 2017;10(1):e004067. https://doi.org/10.1161/CIRCEP.116.004067.
29. Tamaki S, Yamada T, Morita T, Furukawa Y, Iwasaki Y, Kawasaki M, et al. Risk stratification of patients with chronic heart failure using cardiac iodine-123 metaiodobenzylguanidine imaging: incremental prognostic value over right ventricular ejection fraction. ESC Heart Fail. 2015;2:116–21.
30. Iacoviello M, Monitillo F, Citarelli G, Leone M, Grande D, Antoncecchi V, et al. Right ventriculo-arterial coupling assessed by two-dimensional strain: A new parameter of right ventricular function independently associated with prognosis in chronic heart failure patients. Int J Cardiol. 2017;241:318–21. https://doi.org/10.1016/j.ijcard.2017.04.051.
31. Antoni ML, Scherptong RW, Atary JZ, Boersma E, Holman ER, van der Wall EE, et al. Prognostic value of right ventricular function in patients after acute myocardial infarction treated with primary percutaneous coronary intervention. Circ Cardiovasc Imaging. 2010;3:264–71. https://doi.org/10.1161/CIRCIMAGING.109.914366.
32. Larose E, Ganz P, Reynolds HG, Dorbala S, Di Carli MF, Brown KA, et al. Right ventricular dysfunction assessed by cardiovascular magnetic resonance imaging predicts poor prognosis late after myocardial infarction. J Am Coll Cardiol. 2007;49:855–62.
33. Murata M, Tsugu T, Kawakami T, Kataoka M, Minakata Y, Endo J, et al. Prognostic value of three-dimensional echocardiographic right ventricular ejection fraction in patients with pulmonary arterial hypertension. Oncotarget. 2016;7:86781–90. https://doi.org/10.18632/oncotarget.13505.
34. Courand PY, Pina Jomir G, Khouatra C, Scheiber C, Turquier S, Glérant JC, et al. Prognostic value of right ventricular ejection fraction in pulmonary arterial hypertension. Eur Respir J. 2015;45:139–49. https://doi.org/10.1183/09031936.00158014.
35. Jensen AS, Broberg CS, Rydman R, Diller G-P, Li W, Dimopoulos K, et al. Impaired right, left, or biventricular function and resting oxygen saturation are associated with mortality in eisenmenger syndrome: a clinical and cardiovascular magnetic resonance study. Circ Cardiovasc Imaging. 2015;10(1):e003596. https://doi.org/10.1161/CIRCIMAGING.115.003596.
36. Bodez D, Ternacle J, Guellich A, Galat A, Lim P, Radu C, et al. Prognostic value of right ventricular systolic function in cardiac amyloidosis. Amyloid. 2016;23:158–67.
37. Bootsma IT, de Lange F, Koopmans M, Haenen J, Boonstra PW, Symersky T, et al. Right ventricular function after cardiac surgery is a strong independent predictor for long-term mortality. J Cardiothorac Vasc Anesth. 2017;31(5):1656–62. https://doi.org/10.1053/j.jvca.2017.02.008.
38. Le Tourneau T, Deswarte G, Lamblin N, Foucher-Hossein C, Fayad G, Richardson M, et al. Right ventricular systolic function in organic mitral regurgitation: impact of biventricular impairment. Circulation. 2013;127:1597–608. https://doi.org/10.1161/CIRCULATIONAHA.112.000999.
39. Burri H, Domenichini G, Sunthorn H, Fleury E, Stettler C, Foulkes I, et al. Right ventricular systolic function and cardiac resynchronization therapy. Europace. 2010;12:389–94. https://doi.org/10.1093/europace/eup401.
40. Alpendurada F, Guha K, Sharma R, Ismail TF, Clifford A, Banya W, et al. Right ventricular dysfunction is a predictor of non-response and clinical outcome following cardiac resynchronization therapy. J Cardiovasc Magn Reson. 2011;13:68. https://doi.org/10.1186/1532-429X-13-68.
41. Jenkins C, Chan J, Bricknell K, Strudwick M, Marwick TH. Reproducibility of right ventricular volumes and ejection fraction using real-time three-dimensional echocardiography: comparison with cardiac MRI. Chest. 2007;131:1844–51.
42. Ostenfeld E, A Flachskampf F. Assessment of right ventricular volumes and ejection fraction by echocardiography: from geometric approximations to realistic shapes. Echo Res Pract. 2015;2:R1–R11. https://doi.org/10.1530/ERP-14-0077.
43. Smith BC, Dobson G, Dawson D, Charalampopoulos A, Grapsa J, Nihoyannopoulos P. Three-dimensional speckle tracking of the right ventricle toward optimal quantification of right ventricular dysfunction in

pulmonary hypertension. J Am Coll Cardiol. 2014;64:41–51. https://doi.org/10.1016/j.jacc.2014.01.084.

44. Garimella RV, Swartz BK. Curvature estimation for unstructured triangulations of surfaces. Los Alamos Natl Lab. 2003. https://www.researchgate.net/profile/Rao_Garimella/publication/245825677_Curvature_Estimation_for_Unstructured_Triangulations_of_Surfaces.
45. Sciancalepore MA, Maffessanti F, Patel AR, Gomberg-Maitland M, Chandra S, Freed BH, et al. Three-dimensional analysis of interventricular septal curvature from cardiac magnetic resonance images for the evaluation of patients with pulmonary hypertension. Int J Cardiovasc Imaging. 2012;28:1073–85. https://doi.org/10.1007/s10554-011-9913-3.
46. Addetia K, Maffessanti F, Yamat M, Weinert L, Narang A, Freed BH, et al. Three-dimensional echocardiography-based analysis of right ventricular shape in pulmonary arterial hypertension. Eur Heart J Cardiovasc Imaging. 2016;17:564–75. https://doi.org/10.1093/ehjci/jev171.
47. Addetia K, Uriel N, Maffessanti F, Sayer G, Adatya S, Kim GH, et al. 3D morphological changes in LV and RV during LVAD ramp studies. JACC Cardiovasc Imaging. 2017. https://doi.org/10.1016/j.jcmg.2016.12.019.

34 Transoesophageal Echocardiography

Magdalena Gurzun and Silviu I. Dumitrescu

Abstract

The multimodality imaging has improved considerable our understanding and possibility to evaluate the right heart cavities and became mandatory for right ventricle evaluation nowadays. However, echocardiography remains the most accessible, fast and cheap modality in every day clinical practice and transesophageal echocardiography became a very useful tool in some clinical scenarios for diagnosis and monitoring purposes as well (peri-operative or peri-intervention, suboptimal transthoracic echocardiography quality).

Keywords

Transesophageal echocardiography · Right ventricle · Intraoperative echocaradiography

M. Gurzun (✉)
Emergency Central Military Hospital, Bucharest, Romania

Euroecolab, Carol Davila University of Medicine and Pharmacy, Bucharest, Romania

S. I. Dumitrescu
Emergency Central Military Hospital, Bucharest, Romania

Department of Medicine, Titu Maiorescu University, Bucharest, Romania

34.1 Introduction

The multimodality imaging has improved considerable our understanding and possibility to evaluate the right heart cavities and became mandatory for right ventricle evaluation nowadays. However, echocardiography remains the most accessible, fast and cheap modality in every day clinical practice and transesophageal echocardiography (TEE) became a very useful tool in some clinical scenarios (peri-operative or peri-intervention, suboptimal transthoracic echocardiography quality).

34.2 Right Ventricle Anatomy

The right ventricle is the most anteriorly located heart cavity, right behind the sternum. Therefore, the visualization of right ventricle may be more appropriate by transthoracic echocardiography (TTE) than by TEE due the shorter distance between the probe and the mentioned structure.

The right ventricle has a particular shape, being triangular in frontal view and crescent in cross sectional view [1]. The right ventricle extends from the tricuspid valve and atrio-ventricular junction leftward to the apex and after that turns superiorly to the pulmonary valve or ventriculo- arterial junction. The pulmonary valve marks the superior margin and the tricuspid valve the right margin. The complex shape of low pressure right ventricle is partially produced

S. I. Dumitrescu et al. (eds.), *Right Heart Pathology*, https://doi.org/10.1007/978-3-319-73764-5_34

by the indentation of high pressure left ventricle, the right ventricle wrapping around left ventricle.

The cavity of the right ventricle is formed by three parts: the inlet or the inflow tract bordered by the tricuspid valve, the apex and the outlet or the outflow tract bordered by pulmonary valve [2]. The inlet part of right ventricle extends from the tricuspid valve to the insertion of the papillary muscles to the ventricular walls but a clear delimitation between outlet and the apex is absent due to presence of trabeculation. The subpulmonary infundibulum is free of trabeculation and the delimitation between outlet and apex is clear. On the septum of right ventricle there is a characteristic muscle band termed the septomarginal trabeculation. This trabeculation has a Y shape and the moderator bands take off from the Y body, while the two-arms point postero-inferiorly and antero-superiorly. Classically there are described three right ventricle walls: anterior, inferior and lateral wall (also named right ventricular free wall) and each wall can be devided into basal, mid and apical segments [3].

The morphological difference between right and left ventricle are: the presence of moderator band, the presence of more than two papillary muscle and apical trabeculations and the discontinuity between the inflow and outflow valves. The moderator band is a muscular band interposed between the interventricular septum and anterior papillary muscle having inside the fascicle of the right bundle branch of the atrio-ventricular conduction system. The pulmonary valve is separated from the tricuspid valve by crista supraventricularis, a muscular fold extended from septum to subpulmonary infundibulum of right ventricular outlet. Another important element is the atrio-ventricular correspondent valve. For the right ventricle, the tricuspid valve has three leaflets and the distinctive feature is the septal leaflet. The septal leaflet is located closer to the left ventricle apex comparing to mitral valve leaflets and has multiple tendinous cords attaching it directly to the ventricular septum [1].

There are two important components determining the right ventricle contraction: the interventricular septum and the right ventricle free wall [4]. The interventricular septum is a central structure, composed by crisscross oblique fibers and their contraction contribute to right ventricle contraction [5, 6]. The right ventricle wall is thin, 3–5 mm thick not including trabeculations [7] and is formed mainly by two layers of myofibres: the outflow tract has a circumferentially superficial or subepicardial myofibres and a deep layer of longitudinally apex to base aligned myofibres while the outflow tract is formed by longitudinal fibers in both subendocardial and subepicardial layers [8]. The inflow tract produces a systolic longitudinal shortening completed by a radial contraction while the outflow region has a predominant peristaltic motion [9]. Therefore, the contraction of right ventricle starts in the apex and propagates towards outflow tract.

To conclude the anatomical and functional details about right ventricle are very important for appropriate understanding of right ventricle visualization and function assessment by TEE.

34.3 Transesophageal Echocardiography Views for Right Ventricle Imaging

Transesophageal echocardiography became an important tool in every day clinical practice, not only for diagnostic purposes but also for monitoring the patient during interventional procedures, intra and perioperative in the operating theatre or on the intensive care unit [10]. Given mainly the importance of right heart in the perioperative settings, efforts have been made for a better visualization using TEE [11]. The classical transesophageal views allow the imaging of the right ventricle: the inflow tract is visualized in four chamber view, short axis view of the aorta and deep transgastric view while the outflow tract is visualized in long axis view of the aorta and short axis view of the

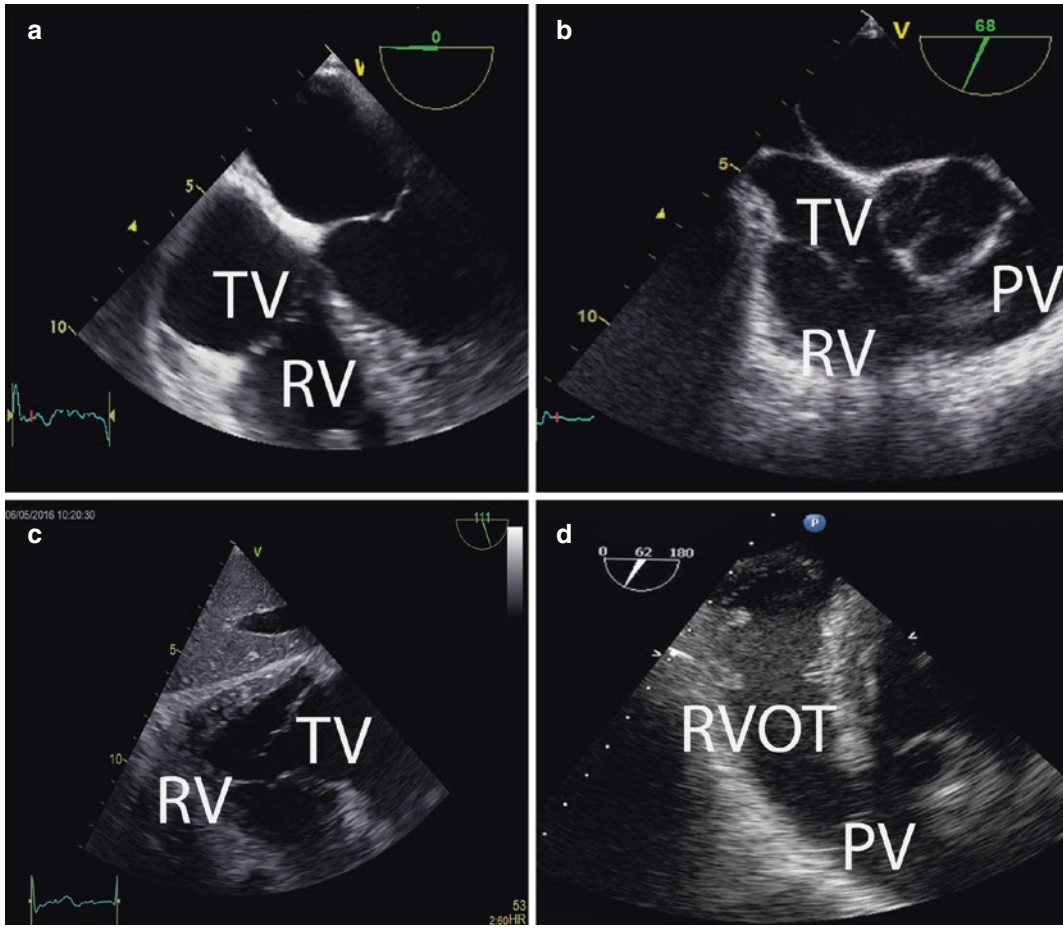

Fig. 34.1 Right ventricle assessment by transesophageal echocardiography: classical and more often used views- four chamber view (**a**) and inflow-outflow (**b**) and recently described transgastric views- inflow view (**c**) and outflow view (**d**) (*TV* tricuspid valve, *RV* right ventricle, *PV* pulmonary valve, *RVOT* right ventricle outflow tract)

aorta (Fig. 34.1). Specific TEE views have been described lately, mainly used for right ventricle imaging. Therefore, beginning from classical four chamber view the lateral wall of right ventricle is better visualized when tricuspid annulus is maximized, cutting at the level where the right ventricle has the greatest dimension or starting from classical short axis view of the aorta the lateral wall is completely visualized when the cutting plane cross it at 60–70°. The transgastric short axis view focus on right ventricle allow the visualization of entire right ventricle (the three walls and interventricular septum in cross section) from apex to base, just changing the cutting plane by flexing or withdrawing slightly the probe. Recently have been described two transgastric views that permit the visualization of inflow and outflow tract of the right ventricle (Fig. 34.1). The inflow transgastric view of right ventricle is useful for visualization of the inferior RV wall while the outflow transgastric view of right ventricle shows the anterior RV wall. The outflow view is also very important for hemodynamic monitorization allowing the estimation of cardiac output [12] (Table 34.1).

Table 34.1 Right ventricle visualization by TEE [13–15]

View	Graphic representation and TEE view[a]	Probe manipulation	Analyzed structures
Modified four chamber view	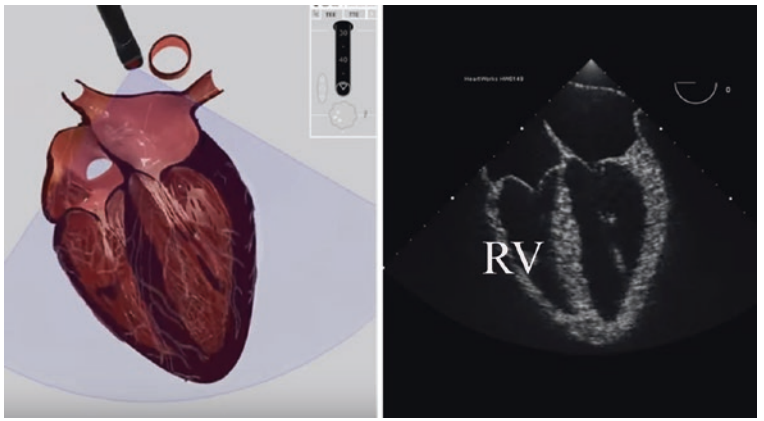	– Insert the probe to the mid-esophagus, behind de left atrium for obtaining four chamber view – Adjust the multiplane to 0–20° for maximizing tricuspid annulus	– Left heart cavities and mitral valve – Right atrium – Right ventricle – Tricuspid valve (septal and anterior/posterior leaflet) – Interventricular and interatrial septum
Inflow-outflow view		– From four chamber view flex or withdraw and adjust the multiplane to 30–60° for obtaining an aortic valve short axis view – Rotate the omniplane to 60–75°	– Aortic valve – Right and left atrium – Pulmonary valve and right ventricle outflow tract- – Pulmonary artery main trunk – Right ventricle free wall – Tricuspid valve (anterior/ septal and posterior leaflet)

Long axis view	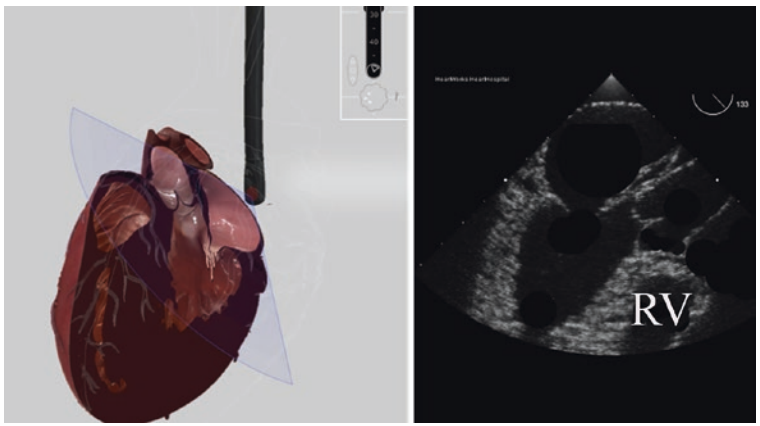	– From four chamber view rotate the omniplane angle to 120°	– Aortic valve – Left ventricle and left ventricle outflow tract – Mitral valve – Left atrium – Right ventricle outflow tract
Transgastric RV short axis view	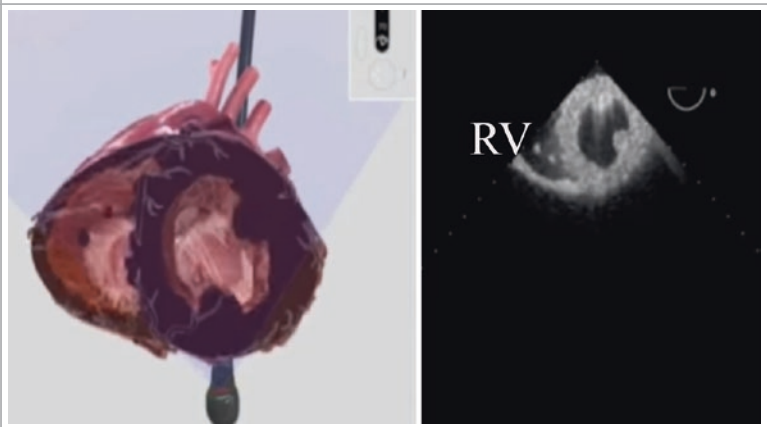	– Insert the probe into the stomach and flex for obtaining the short axis view of left ventricle – Rotate the probe to the right	– Right ventricle cross section with an interventricular septum and right ventricle free wall

(continued)

Table 34.1 (continued)

View	Graphic representation and TEE view[a]	Probe manipulation	Analyzed structures
Trangastric RV inflow view		– From transgastric RV short axis view adjust the omiplane angle to 90°	– Tricuspid valve (posterior and anterior leaflet) – Right ventricle posterior and anterior walls
Transgastric RV outflow view		– From transgastric RV short axis view adjust the omiplane angle to 40°	– Pulmonary valve – right ventricle outflow tract

Deep transgastric view	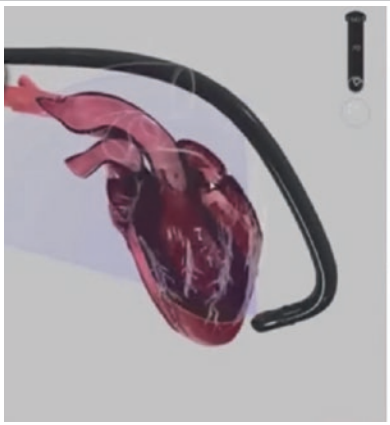	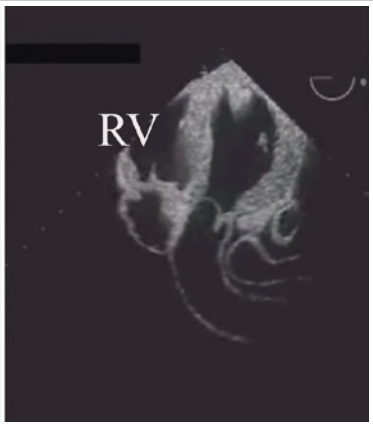	– Advance the probe into stomach at 0° until left ventricle apex is seen – Excessive anteflexion the probe	– Left ventricle – Right ventricle – Aortic valve – Left ventricle outflow tract – Mitral valve

[a]With courtesy of Heartworks (Lifesim, Romania)

34.4 Right Ventricle Size by Transesophageal Echocardiography

Right ventricle size and function is most commonly performed by transthoracic echocardiography but there are some clinical situations when transesophageal echocardiography may be used (poor image quality, limited transductor access to the chest, perioperative settings). However, the right ventricle is situated in the far field and the image resolution may be not appropriate for accurate assessment in some circumstances. The current guideline regarding the performing of transesophageal echocardiographic examination [14] underline the fact that to date there are no specific recommendation for values for right ventricle size and function TEE.

Therefore, transthoracic echocardiography is the standardized method for right ventricle size estimation [16] but it may by assessed off labeled by TEE. The recommended view is a modified mid-esophageal four chamber view. For obtaining the optimal view for right ventricle size estimation it is recommended to pass through the left ventricle apex and to use de multiplane for maximize the tricuspid annulus diameter, generally towards 10–20° [17]. Due to the crescent shape of right ventricle the obtained values are dependent on probe rotation and the inter and interobserver variability is high. Therefore, it is very important to use the multiplane for obtaining the biggest value of the tricuspid annulus and to perform the measurements in this view. The measured diameters are basal and mid right ventricle diameters and base to apex length (Fig. 34.2) and the values may be extrapolated from the current transthoracic recommendations [16]. The normal range for right ventricle basal diameter is considered 25–41 mm, for right ventricle mid-diameter 19–35 mm and for right ventricle longitudinal diameter 59–83 mm.

Although there is no recommendation regarding the estimation of right ventricle outflow tract diameter by transesophageal echocardiography, these diameters may be measured similar to transthoracic echocardiography in aortic valve short axis view and the values may be extrapolated from transthoracic echocardiography. The normal range for proximal right ventricle outflow tract is 21–35 mm and for distal right ventricle outflow tract is 17–27 mm [16].

The right ventricle end-systolic and end-diastolic right ventricle areas may be calculated by manual tracing of endocardial border in modified four chamber view (Fig. 34.2). There are no specific values for measurement of right ventricle areas by transesophageal echocardiography. The normal range by transthoracic echocardiography for diastolic area are 10–24 cm^2 for men and 8–20 cm^2 for women and for systolic area are 3–15 cm^2 for men and 3–11 cm^2 for women.

The right ventricle volume can be estimated by three-dimensional echocardiography, overcoming the limitations of conventional bi-dimensional views. Although technically difficult method, several studies have demonstrated that 3D transesophageal right ventricle volumes (Fig. 34.2) assessment is feasible and valuable [18–20]. The normal values have been reported for transthoracic echocardiography [21].

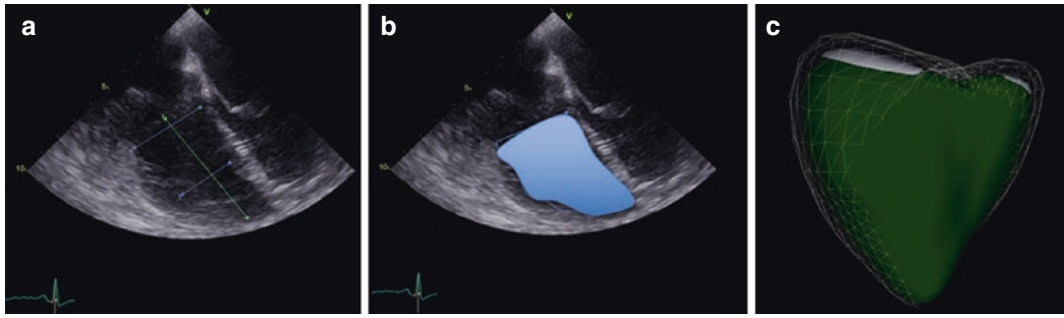

Fig. 34.2 Right ventricle size assessment by TEE: basal and mid diameter measurement in four chamber view, diastolic frame (**a**), end-diastolic right ventricle area (**b**) and right ventricle end-diastolic volume by 3D (**c**)

Often, in every day clinical practice, right ventricle size is visually assessed comparing to left ventricle dimensions (Fig. 34.3) and is considered normal if it is less than two thirds of left ventricle [14].

Although there are no data regarding the measurement of right ventricle free wall by TEE, we can have extended the knowledge from TTE and measure the right ventricle free wall thickness in short axis view, at the level of great vessel. The normal value is considered by TTE less than 5 mm (Fig. 34.3). The measurement can be performed either by M mode or 2D TEE, at end-diastole, below the tricuspid annulus at a distance equal to anterior tricuspid leaflet and zoom imaging is preferred. Papillary muscle and trabeculae should be excluded [16].

34.5 Right Ventricle Function by Transesophageal Echocardiography

The estimation of right ventricle function by TEE generally is done by visual assessment (eye balling). However, the TTE parameters described for right ventricle function estimation may be used with specific conditions for TEE evaluation too (Table 34.2). For example, the right ventricle area change calculated in four chamber view proved to correlate with de right ventricle ejection fraction calculated by 3D echocardiography [22].

With the development of tridimensional echocardiography and specific software for right ventricle assessment, 3D TEE proved to be a feasible and useful tool for estimation of right ventricle

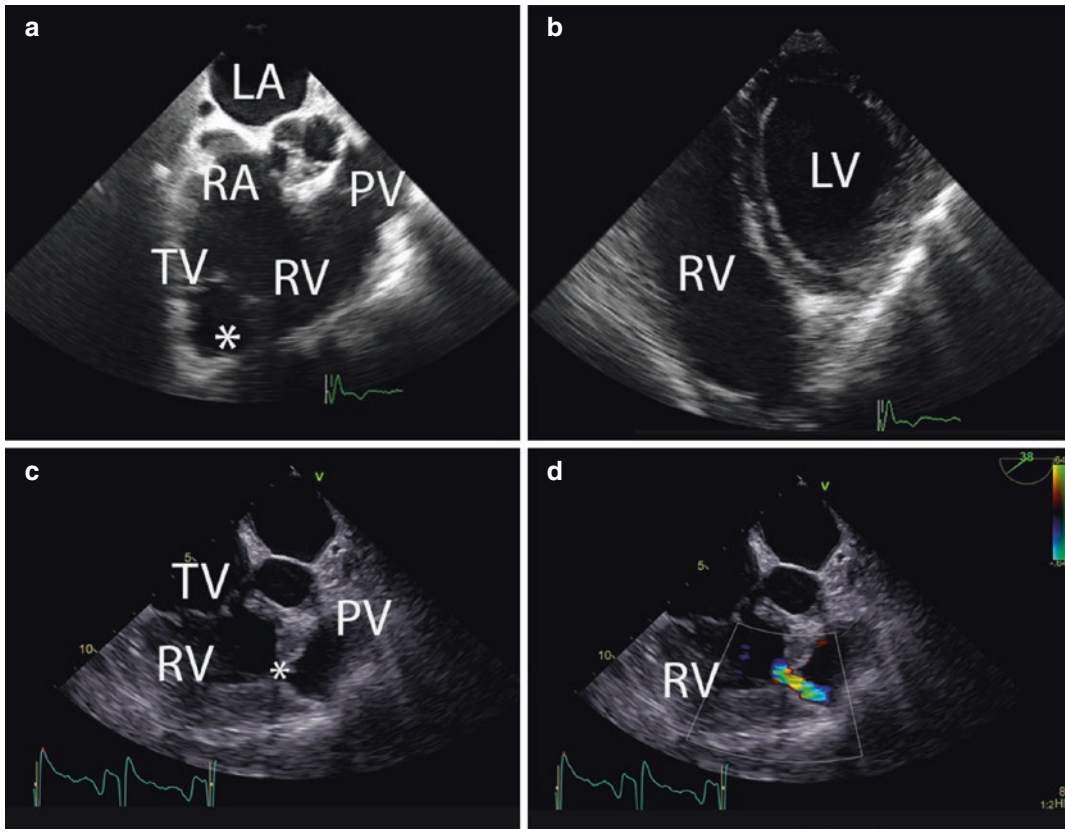

Fig. 34.3 Right ventricle infarction- to note right ventricle dilatation in inflow-outflow view (**a**) and transgastric short axis view focus on right ventricle (**b**). Regional wall motion abnormalities are also present with dyskinesia of mid part of the lateral wall (**a**,*). Right ventricle mid obstruction—to note hypertrophy of lateral right ventricle wall in inflow-outflow view (**c**, *), and the turbulent flow at this level (**d**) (*TV* tricuspid valve, *RV* right ventricle, *PV* pulmonary valve, *RVOT* right ventricle outflow tract, *LV* left ventricle)

Table 34.2 Right ventricle function assessment by TEE [3, 16]

Parameter	Definition	Recommended view	Cut off value for abnormality
Global function			
PW myocardial performance index or Tei index	The ratio between isovolumic relaxation time and isovolumic contraction time and ejection time calculated by PW Doppler	PW sample volume is placed at the level of tricuspid valve in four chamber view and just below the pulmonic valve in transgastric right ventricle outflow view	0.54
DTI myocardial performance index or Tei index	The ratio between isovolumic relaxation time and isovolumic contraction time and ejection time calculated by DTI Doppler	DTI sample volume placed lateral to tricuspid annulus in deep transgastric view or mid-esophageal inflow-outflow view	0.43
Right ventricle dp/dt	The rate of pressure rise in right ventricle	CW through tricuspid valve (best jet aligned view)	400 mmHg/s
Fractional area change	The percentage of difference between end-diastolic and end-systolic area to the end-diastolic area		35%
Ejection fraction	The percentage of difference between end-diastolic and end-systolic volume to the end-diastolic volume calculated by 3D TEE		45%
Longitudinal function			
TAPSE (Tricuspid Annulus Plane Systolic Excursion)	Systolic excursion of the lateral tricuspid annulus	M mode along lateral tricuspid annulus in deep transgastric view or mid-esophageal inflow-outflow view	17 mm
Systolic velocity of right ventricle free wall	Doppler tissue imaging of the right ventricle inflow velocities	DTI sample volume placed lateral to tricuspid annulus in deep transgastric view or mid-esophageal inflow-outflow view	9.5 cm/s
Global longitudinal strain	Global strain calculated by speckle tracking: Longitudinal deformation during cardiac cycle	Four chamber view	25% [28]
Regional function			
Peak regional strain and strain rate	Deformation imaging of the six segments of right ventricle	Four chamber view	

function, especially in perioperative settings [18] (Fig. 34.4). Fusini et al. proved a feasibility of 3D TEE analysis of RV was 98.7% for preoperative and 92.7% for postoperative TEE data set in patients with normal and dilated RV [23].

The cardiac index can be evaluated by VTI measurement: the Doppler cursor is positioned just below the pulmonary valve in transgastric outflow view. A value less than 12 cm has a sensibility of 85.7% and a specificity of 70.8% for low right heart cardiac output (less than 2.2 L/min) [24].

The regional function of right ventricle is generally visually estimated (Fig. 34.3). The segmentation used for right ventricle is the following: septum, anterior, inferior and lateral wall (also known as right ventricle free wall). Every wall has three segments- basal, mid and apical segment and their function is appreciated as normal, hypokinesia, akinesia or dyskinesia.

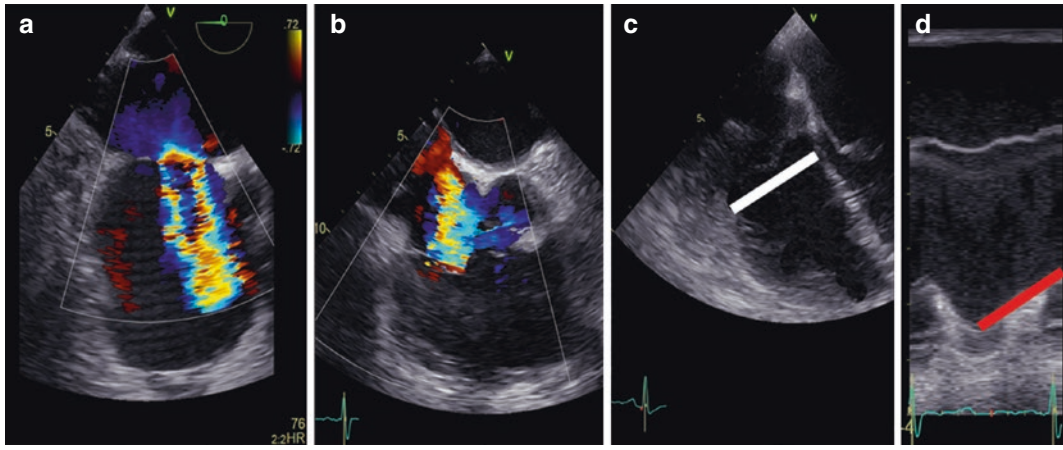

Fig. 34.4 Patient with interatrial septum defect visible in short axis view at the level of the great vessel, focus on interatrial septum (**a**) and moderate tricuspid regurgitation (**b**). To note de right ventricle dilatation based on basal diameter measure din four chamber view (**c**) and decreased systolic function based on low TAPSE value (**d**)

34.6 Importance of Transesophageal Echocardiography in Right Ventricle Assessment and Managing

As previously mentioned, TEE in not routinely used for the evaluation of right ventricle in every day clinical practice but this imaging tool is essential in some clinical scenarios. Its importance is evident especially when the others imaging modalities (TTE, cardiac MRI) are difficult to be used. Although it is a semi-invasive diagnostic method, TEE is cheap, moderately available and easily performed in perioperative settings or critically ill patients.

Given the importance of the right heart in perioperative morbidity and mortality, TEE is used for diagnostic purposes as well as for patient monitoring during cardiac or non-cardiac surgery [25]. Right ventricle dysfunction is a usual concern after cardiac surgery, and there are several possible causes: inadequate myocardial protection, increases in pulmonary vascular resistance, coronary air embolism, acute ischemia or acute valvular dysfunction [26].

It is also beneficial for evaluation and monitoring the patient in the intensive care unit. The presence of right ventricle infarction, pulmonary embolus, loculated pericardial effusion, extracardiac pathology such as masses may be revealed during TEE right ventricle evaluation in critically ill patient. Sometimes can be used for guidance of catheter placement, being an adjunctive method to conventional pressure waveform placement of pulmonary artery catheter placement [27].

TEE remains mandatory during the cardiac interventional procedures, and the right heart function and hemodynamic conditions can be analyzed during DSA closure, TAVI, Mitral Clip procedures. Another application of TEE is the guidance for implantation or the evaluation of cardiovascular implantable electronic devices, like device infection [28].

Conclusions

Although considered to have limited value in the evaluation of right heart cavities, TEE has its specific role in some specific clinical situations for diagnosis and monitoring purposes as well.

References

1. Ho SY, Nihoyannopoulos P. Anatomy, echocardiography, and normal right ventricular dimensions. Heart. 2006;92(Suppl 1):i2–i13.
2. Goor DA, Lillehei CW. Congenital malformations of the heart. 1st ed. New York: Grune and Stratton; 1975. p. 1–37.
3. Rudski LG, Lai WW, Afilalo J, et al. Guidelines for the echocardiographic assessment of the right heart in adults: a report from the American Society of Echocardiography endorsed by the European Association of Echocardiography. J Am Soc Echocardiogr. 2010;23(7):685–713.
4. Cho EJ, Jiamsripong P, Calleja A, et al. Right ventricular free wall circumferential strain reflects graded elevation in acute right ventricular afterload. Am J Physiol Heart Circ Physiol. 2009;96:H413–20.
5. Plunkett MD, Buckberg GD. Pathophysiologic implications of the helical ventricular myocardial band: considerations for right ventricular restoration. Semin Thorac Cardiovasc Surg Pediatr Card Surg Annu. 2007;10:68–75.
6. Hristov N, Liakopoulos OJ, Buckberg GD, Trummer G. Septal structure and function relationships parallel the left ventricular free wall ascending and descending segments of the helical heart. Eur J Cardiothorac Surg. 2006;29:S115–25.
7. Foale R, Nihoyannopoulos P, McKenna W, Kleinebenne A, Nadazdin A, Rowland E, Smith G. Echocardiographic measurement of the normal adult right ventricle. Br Heart J. 1986;56(1):33–44.
8. Greenbaum RA, Ho SY, Gibson DG, Becker AE, Anderson RH. Left ventricular fibre architecture in man. Br Heart J. 1981;45:248–63.
9. Pierpont GL, DeMaster EG, Cohn JN. Regional differences in adrenergic function within the left ventricle. Am J Physiol Heart Circ Physiol. 1984;246:H824–9.
10. Kühl HP, Hanrath P. The impact of transesophageal echocardiography on daily clinical practice. Eur J Echocardiogr. 2004;5(6):455–68.
11. Haddad F, Couture P, Tousignant C, Denault AY. The right ventricle in cardiac surgery, a perioperative perspective: I. Anatomy, physiology, and assessment. Anesth Analg. 2009;108:407–21.
12. Kasper J, Bolliger D, Skarvan K, Buser P, Filipovic M, Seeberger MD. Additional cross-sectional transesophageal echocar diography views improve perioperative right heart assessment. Anesthesiology. 2012;117:726–34.
13. Flachskampf FA, Wouters PF, Edvardsen T, et al. Recommendations for transoesophageal echocardiography: EACVI update 2014. Eur Heart J Cardiovasc Imaging. 2014;15(4):353–65.
14. Hahn RT, Abraham T, Adams MS, et al. Guidelines for performing a comprehensive transesophageal echocardiographic examination: recommendations from the American Society of Echocardiography and the Society of Cardiovascular Anesthesiologists. J Am Soc Echocardiogr. 2013;26(9):921–64.
15. Vegas A. Perioperative two-dimensional transesophageal echocardiography. Berlin: Springer; 2012.
16. Lang RM, Badano LP, Mor-Avi V, et al. Recommendations for cardiac chamber quantification by echocardiography in adults: an update from the American Society of Echocardiography and the European Association of Cardiovascular Imaging. Eur Heart J Cardiovasc Imaging. 2015;16(3):233–70.
17. Lang RM, Bierig M, Devereux RB, et al. Recommendations for chamber quantification: a report from the American Society of Echocardiography's guidelines and standards committee and the chamber quantification writing group, developed in conjunction with the European Association of Echocardiography, a branch of the European Society of Cardiology. J Am Soc Echocardiogr. 2005;18(12):1440–63.
18. Karhausen J, Dudaryk R, Phillips-Bute B, et al. Three-dimensional transesophageal echocardiography for perioperative right ventricular assessment. Ann Thorac Surg. 2012;94(2):468–74.
19. Fusini L, Tamborini G, Gripari P, et al. Feasibility of intraoperative three-dimensional transesophageal echocardiography in the evaluation of right ventricular volumes and function in patients undergoing cardiac surgery. J Am Soc Echocardiogr. 2011;24:868–76.
20. Xu Y, Wu W, Fang W, Chen H. Reproducibility and correlations of right ventricular end-diastolic volume index measured by real-time three-dimensional echocardiography. J Clin Ultrasound. 2014;42(2):81–8.
21. Maffessanti F, Muraru D, Esposito R, et al. Age-, body size-, and sex-specific reference values for right ventricular volumes and ejection fraction by three-dimensional echocardiography: a multicenter echocardiographic study in 507 healthy volunteers. Circ Cardiovasc Imaging. 2013;6(5):700–10.
22. Imada T, Kamibayashi T, Ota C, et al. Intraoperative right ventricular fractional area change is a good indicator of right ventricular contractility: a retrospective comparison using two- and three-dimensional echocardiography. J Cardiothorac Vasc Anesth. 2015;29(4):831–5.
23. Fusini L, Tamgorini G, Fripari P, et al. Feasibility of intraoperative three-dimensional transesophageal echocardiography in the evaluation of right ventricular volumes and function in patients undergoing cardiac surgery. JASE. 2011;24(8):868–77.
24. Ginghina C, Muraru D, Popescu BA. Hipertensiunea pulmonara si functia ventriculului drept. In: Ginghina C, Popescu BA, editors. Ecografia Doppler. Bucuresti: Editura Medicala; 2011.
25. Shah SB, Hariharan U, Bhargava AK. Utility of TEE in anesthesia for non cardiac surgery: a practical review. J Anesth Crit Care Open Access. 2015;3(4):00102.
26. Sreeram G, Mark J. Right ventricle, right atrium, tricuspid valve and pulmonic valve. In: Reeves S, editor.

A practical approach to transesophageal echocariography Perrino A. Philadelphia: Lippincott Williams & Wilkins; 2003.
27. Cronin B, Robbins R, Maus T. Pulmonary artery catheter placement using transesophageal echocardiography. J Cardiothorac Vasc Anesth. 2017;31:178–83.
28. Allred C, Crandall M, Auseon A. The important but underappreciated transgastric right ventricular inflow view for transesophageal echocardiographic evaluation of cardiac implantable device infections. Echocardiography. 2013;30(1):E1–3.

Computed Tomography

35

Harold Goerne and Prabhakar Rajiah

Abstract

Computed Tomography (CT) plays an important role in the evaluation of diseases of the right heart, both congenital and acquired. Advantages of CT include its wide availability, rapid turnaround time, good spatial and temporal resolutions, multi-planar reconstruction capabilities and wide field-of-view. Disadvantages of CT include the use of potentially nephrotoxic contrast media and ionizing radiation. In this chapter, we review the comprehensive role of CT in the evaluation of right heart, including techniques, protocols and pathologies.

Keywords

CT · Heart · Right heart · ARVD · Congenital Tumor · Cardiomyopathy · Infarction

H. Goerne
IMSS Western National Medical Center, Guadalajara, Jalisco, Mexico

CID Imaging and Diagnostic Center, Guadalajara, Jalisco, Mexico

P. Rajiah (✉)
Department of Radiology, Cardiothoracic Imaging, UT Southwestern Medical Center, Dallas, TX, USA

35.1 Introduction

The right heart can be evaluated by multiple imaging modalities, including radiography, echocardiography, magnetic resonance imaging (MRI), nuclear medicine and conventional invasive angiography. Computed tomography (CT) technology has progressed exponentially in the last couple of decades and is playing an increasingly important role in the evaluation of right heart diseases, both congenital and acquired. CT provides information both on the morphology and function of the right heart, with high image quality and low radiation dose.

In this chapter, we review the comprehensive role of CT in the evaluation of right heart, including techniques, protocols and pathologies.

35.2 Advantages and Disadvantages

A major advantage of CT is that it is widely available in many centers throughout the world and it has a rapid turnaround time. CT can be performed in all patients, including those who are severely ill and hemodynamically unstable. CT has good spatial resolution with isotropic reconstruction possible in multiple planes. With injection of intravenous contrast, there is high contrast between blood pool and myocardium. ECG-gated CT also has good temporal resolution for

S. I. Dumitrescu et al. (eds.), *Right Heart Pathology*, https://doi.org/10.1007/978-3-319-73764-5_35

evaluation of rapidly moving structures including the coronary arteries. The wide field-of-view allows evaluation of not only the heart but also extracardiac and other abnormalities. If an optimal heart rate is maintained, it is an excellent technique to exclude coronary stenosis, with a very high negative predictive value and sensitivity [1]. CT is however associated with the use of ionizing radiation, which has a theoretical risk of complications such as carcinogenesis. However, it should be noted that the data on the development of cancer from low-dose radiation is derived from atomic bomb survivors and there is no conclusive evidence on the causation [2]. In addition, latest scanners allow performance of CT at very low radiation doses. CT also uses iodinated contrast media, which are potentially nephrotoxic, particularly in patients with severe renal dysfunction. Allergic reactions ranging from minor to anaphylactic shock may be seen, but this can be minimized by premedication with steroids and antihistaminics [3].

35.3 CT Technology

CT technology has significantly improved in the last decade, now enabling rapid acquisition of data at low doses of radiation and contrast. CT scanners have an X-ray tube that rotates around the patient and a detector ring that captures the data after the X-ray beams pass through and attenuated by the patient. The current CT scanners are multi-detector scanners (MDCT), with multiple detectors capturing data from the single X-ray tube. Currently wide-array/volume scanners are available with up to 320 detector-rows, enabling craniocaudal (z) coverage of up to 16 cm in one tube rotation. This results in shorter acquisition times enabling shorter breath hold and less motion artifact. This also results into less contrast medium needed to opacify the cardiac chambers and lower radiation dose to the patient [4]. For performing a good quality cardiac CT scan, atleast 64 detectors are required [4]. The detector size is as small as 0.24 mm in some of the newer scanners, which significantly improves the spatial resolution, enabling visualization of small structures. In order to obtain diagnostic images without motion and to perform measurements accurately, CT scanners with a rotational speed that allow a sufficient temporal resolution to obtain motion-free images of the heart are required. The gantry rotation times are progressively improving, which not only allows shorter scan times, but also higher temporal resolutions, now as high as 66 ms in some scanners [5, 6].

Dual-source scanners have two X-ray tubes at 90° to each other, which when operated in the same tube current have high temporal resolution. High-pitch helical mode is a recently introduced CT technology that has value in cardiovascular imaging. The pitch represents the ratio of the table movement to the rotation of the gantry [7]. A pitch of one indicates that there is neither overlap or gap between the slices. With pitch <1, there is oversampling of information due to slower table movement with gantry rotation, which is required for evaluating cardiac structures. A pitch >1 indicates that the table movement is faster than the gantry rotation, resulting in gaps between the slices and is typically avoided in cardiac imaging. However, with the availability of high-pitch helical mode in the latest generation dual source scanners, it is possible to get high-quality cardiac scans at high pitch (up to 3.4), since the gaps in data are filled by data from the second X-ray beam. The high pitch allows rapid acquisition, resulting in lower motion, radiation and contrast doses [8].

Another development has been dual-energy/multi-energy/spectral CT technology, which allows additional material characterization, currently not possible with a conventional CT scanner. Since many elements have similar density although their elemental composition is different, they appear similar in conventional CT with similar Hounsfield units [9]. With dual-energy CT, data is obtained at two energy levels and since elements with different tissue composition react differently at different levels of energy, the materials can be distinguished. There are several technologies to obtain dual energy CT. The most commonly used in the dual source CT, in which two X-ray tubes are operated at two different energy levels. In rapid kVp-switching technology, there is only one X-ray tube, but the tube voltage is changed rapidly for each X-ray

projection between a high and low energy. With dual-spin technology using a volume scanner, the patient is scanned twice, consecutively at two different energy levels. In the split-beam technology, the X-ray beam is divided into two energy levels by using dedicated filters. With dual-layer CT, there is a single X-ray tube but there are two layers of detectors which separate high and low energy photons. Photon counting CT allows separation of multiple energy levels by using semi-conductor detectors [9]. With dual energy CT, multiple additional images are obtained including- iodine map (which shows only iodine); virtual non contrast (images without iodine, which mimick a true non-contrast acquisition); effective atomic number-based (color coding based on the atomic number) and virtual monoenergetic images (mimic a true monoenergetic image). Iodine maps are used in evaluating organ perfusion. VNC can save radiation dose by eliminating the need for true non contrast in multi-phasic studies and also helps in lesion characterization. Effective atomic number images also help in lesion characterization. VMI at low energies are useful in enhancing the contrast, which helps in salvaging suboptimal studies as well as allow the use of low dose of intravenous contrast. VMI at high energies are useful in decreasing several artifacts [10].

35.4 CT Technique for the Right Heart

Several parameters can be optimized for obtaining a good quality CT of the right heart, including the scanning mode, tube current & voltage, pitch, slice thickness, contrast bolus and timing and use of medications. For adults, the CT scan does not need anesthesia or sedation, but in children general anesthesia/sedation may be required if high quality images of the heart are required, especially for the coronary arteries. Premedication is required when motion-free images of the heart are required, particularly for assessment of the coronary arteries. Beta blockers, either oral (50–100 mg, 1 h prior to study) or intravenous (5 mg every 5 min, maximum 25 mg) are administered in patients with high heart rates. Please note that the ideal heart rate varies from scanner to scanner depending on its temporal resolution. For adequate visualization and evaluation of coronary arteries lumen, nitroglycerin 0.4–0.8 mg sublingual is used. In most cases where coronary arteries are not a concern, it is not necessary to administer these medications.

CT angiography is performed by intravenously injecting iodinated contrast, with the largest possible cannula to obtain a high flow rate. Low or iso-osmolar contrast media are used to minimize adverse reactions, with high concentrations of iodine (350 or 370 mg Iodine/mL) used for optimal opacification. For most studies, a biphasic injection protocol is used, with an initial bolus of contrast followed by saline injection at the same flow rate to wash out the contrast and reduce streak artifacts. Contrast volume varies from 20–150 mL (typically 1 mL/kg) depending on the clinical indication and body habitus. For children, 1–2 mL/kg of body weight of contrast is used. For visualization of the right ventricle, a triphasic injection protocol is preferred, where the initial contrast phase at high flow rate (5–7 mL/s) is followed by either a mixture of contrast/saline at same flow rate (50:50 or 60:40) or slow injection of contrast (2–3 mL/s) and finally a pure saline bolus. A split bolus protocol can be used in complex cases, with the first phase of slow contrast injection followed by a pause of 30–60 s, after which contrast is injected at high flow rate followed by saline. To achieve homogeneous opacification, a power injector is used, with flow rates up to 5–7 mL/s in adults with power ranging from 50 to 300 psi [11–13]. To time the contrast, a region of interest (ROI) is placed over the vessel of interest after contrat injection and when the attenuation in that vessel crosses a pre-set threshold (typically 100 HU above baseline), the scan is started. Iodinated contrast should not be administered in patients with acute/chronic severel renal dysfunction (GFR < 30 mL/min) or with previous major contrast reaction. In renal failure, contrast dose should be reduced and hydration may be used. Patients with contrast allergies should be premedicated for at least 24 h before the study. Metformin should be stopped for 48 h prior to contrast to avoid lactic acidosis [3].

Depending on the indication, the scan can be performed with or without ECG gating. For most of the structures, such as pulmonary arteries, scanning can be performed without ECG gating. ECG gating is required for high resolution motion-free images of the heart and coronary arteries. High-pitch helical mode (FLASH) with the dual-source scanner is another option, which allows motion free images at low contrast and radiation dose without ECG gating.

35.5 CT Protocols for the Right Heart

Depending on the clinical indication, dedicated and standardized protocols can be established to ensure data acquisition at peak enhancement without missing the contrast bolus. The following are some examples of standard protocols for the right heart.

(a) *Pulmonary embolism and pulmonary hypertension:* This is a commonly used protocol for the evaluation of pulmonary arteries. The entire chest is scanned after contrast injection, with bolus tracking on the main pulmonary artery. Images are reconstructed with a pitch <1. ECG gating or FLASH made minimizes motion artifacts. Dual-energy iodine maps helps in evaluating perfusión defects seen in pulmonary embolism pulmonary hypertension.

(b) *Congenital heart disease and masses*: If anatomical evaluation of these pathologies is desired, a prospective ECG-triggered mode can be used. A triphasic contrast injection protocol is used to visualize both the right and left heart. Scan coverage depends on the type of congenital heart disease and location of the mass.

(c) *Cardiomyopathies:* This protocol is similar to the above, with triphasic contrast injection protocol. Coverage is limited to the heart. Prospective ECG triggering is utilized for evlauation of morphology, but retrospective ECG gating is used if dynamic information or quantification is required. A delayed enhancement phase can be obtained to evaluate for scar/fibrosis

(d) *Retrospective ECG gating*: Retrospective ECG gating is utilized when there is a need for data from all the phases of cardiac cycle. This is useful in quantification of ventrcular function/volumes, especially in congenital heart disease and cardiomyopathies in patients who cannot have MRI. Wall motion and thickening can also be evaluated. It is also used in dynamic evaluation of masses as well as native and prosthetic valves.

(e) *Trauma protocol:* In patients with suspected chest trauma, an arterial and venous phase (1–2 min delay) are obtained. Venous phase is useful for evaluation of venous leaks and contrast extravasation. This does not require ECG gating. Improved quality may be obtained with high-pitch helical mode. This protocol can also be used for evaluation of venous obstruction, vasculitis and infection.

(f) *Clot protocol:* This protocol is used for evaluation of cardiovascular clots. Similar to a trauma protocol, this also has an arterial and venous phase. A common differential diagnosis for clot is slow-flow. While a clot is seen in both arterial and delayed phases, slow flow is seen only in the arterial phase. Another option for this protocol is to use the abovementioned split-bolus protocol. With dual-energy CT, quantification of iodine may help in distinguishing clot from slow flow.

(g) *Coronary artery protocol:* This protocol involves scanning the heart from the carina to the ápex, after biphasic contrast injection. Prospective ECG triggering is the default mode for eliminating cardiac motion at a low radiation dose. This requires a low heart rate, typically <60 bpm (dependent on the scanner). Nitroglycerine is also administered to dilate the coronary arteries. If the heart rate is high or irregular, retrospective ECG gating is used, which has higher radiation dose.

(h) *Triple rule-out protocol:* This protocol is used to evaluate coronary artery disease, pulmonary embolism and aortic dissection in patients with acute chest pain [10]. A triphasic injection of contrast is used to opacify all these structures in a single ECG-gated scan.

(i) *Myocardial perfusión protocol:* This protocol is used to evaluate for myocardial

ischemia and is performed with contrast administration before and after stress with pharmacological agents (adenosine, dipyridamole or regadenoson). This can be performed either in a static mode or a dynamic mode with multiple acquisitions at the same location. An additonal delayed enhancement phase can be added for looking at scar.

35.6 Image Reconstruction and Post Processing

Following data acquisition, CT images are reconstructed, post-processed and viewed in several different ways.

- *Axial source images*- For visualization of the heart, the CT images are obtained in the axial plane, usually at 0.5–0.75 mm, with 0.5 mm overlap. Thicker reconstructions are used in the evaluation of lungs as well as pulmonary embolism, typically 1 × 1 mm. While thinner slices provide higher isotropic spatial resolution which allows generation of multiplanar reconstructions, they are associated with higher noise. Thicker slices have lower noise but also lower spatial resolution, which however is adequate for the evaluation of lungs and other non-cardiovascular structures. Spatial resolution can also be improved by using a small field-of-view or high resolution filters.
- *Multi-planar reconstructions*- From the submillimeter isotropic voxels, 2d images can be reconstructed in sagittal and coronal plane, at any thickness. These can also be reconstruction in any plane, including cardiac planes such as 2-chamber, 3-chamber, 4-chamber and short axis planes.
- *Curved multiplanar reconstructions*- Curved multiplanar reconstructions straighten or strech out vascular structures, including the coronary arteries, aorta and pulmonary artery and allows to follow the course of a vessel from beginning to end following a centerline in the vessel. This is very useful to evaluate the luman as well as wall of the vessel, particularly in the evaluation of stenosis since it also provides transverse planes throughout the vessel.
- *Double oblique reconstruction*- A double oblique image is reconstructed from two orthogonal views. These views are also useful for accurate and reproducible measurements of vascular structures.
- *Maximal Intensity Projection*- Maximal Intensity Projection (MIP) display high-density voxels in a single plane, at a pre-determined thickness. This is useful for evaluation of small vessels and high attenuation structures such as contrast, calcification and grafts. MIP is useful for visualizing the course of vessels, but not for evaluating stenosis, as these can be underestimated in the case of non-calcified plaques or overestimated in case of calcified plaques. It is also extremely useful for screening of small pulmonary nodules
- *3d reconstructions*- 3d renderings of vascular structures can be derived by using either volumen-rendering or shaded-surface display. These reconstructions are valuable in providing a roadmap for surgeries and interventions, particularly in congenital heart disease.
- *Endoscopic view*- These images mimic the appearance of the heart as if it is looked from inside [14].
- *Cine images*- In studies obtained with retrospective ECG gating, it is possible to performe cine images of the heart using the multiple acquired phases. This can be used for evaluating the morphology as well as the global and regional wall motion, thickening, valve motion, and contrast flows through shunts. Using multi-phasic studies, quantifaction is performed for several factors including end-diastolic volumen, end-systolic volumen, stroke volumen, cardiac output, ejection fraction and mass.

35.7 Radiation Dose Reduction Strategies

High quality images can be obtained in CT by using the least posible radiation dose taking advantages of several radiation dose reduction

strategies. An important principle in radiology is ALARA ("as low as reasonably achievable"), which means that whenever radiation is used, it should be kept to the least possible to answer the clinical question. CT should be performed only when there is a clear clinical indication that has been evaluated using appropriateness criteria and the benefits outweigh the risk. The scan coverage should include only the area of interest and the examination should be protocolled to answer the clinical question. Non-ECG gated techniques are associated with lower radiation doses. Except in cases which absolutely require ECG gating, non-ECG gated techniques can be employed for other indications such as acute or chronic pulmonary embolism. If ECG gating is required, prospective ECG triggering is the default mode, particularly when only the morphology is evaluated, including that of coronary arteries. For evaluation of cardiac function, retrospective ECG gating is required, which is associated with higher radiation dose. This can be minimized by using ECG-based tube current modulation, in which a peak tube current is applied in a specific part of the cardiac cycle, whereas in other phases of the cardiac cycle, the tube is reduced to 30% of the máximum, which saves radiation dosess up to 50% [15].

The least possible tube current is used for the study, based on the body habitus. In addition, the tube current is also modulated based on the anatomy, with higher tube current delivered to larger body parts. The tube voltage is also kept to be the least possible, based on the body size. 120 kVp can be reserved for larger patients, with 100 kVp being the default in majority of the smaller patients (BMI < 30). 80 kVp or lower can be used in children. Obese patients may require 140 kVp. The tube current and voltage can be now automatically selected by the scanner based on the body size in topogram. Noise used be a limitation of low-radiation dose techniques. However, the use of advanced iterative reconstruction algorithms results in lower noise than the traditional filtered back projection, which allows the use of robust low radiation dose protocols [16]. The use of high-pitch helical mode of the latest generation of dual-source scanner also allows the use of low radiation and contrast doses [4, 17].

35.8 CT Anatomy

CT provides detailed and precise anatomical evaluation of the right heart. The right ventricle has a complex and irregular anatomy. Its inlet tract receives deoxygenated blood from the right atrium through the tricuspid valve. The RV body has multiple trabeculations and three papillary muscles (anterior, posterior and septal). The moderator band or septomarginal trabecula is a muscular band that crosses the cavity in its apical region, serves as a conduit of the nerve fibers that innervate the RV free wall. The crista supraventricularis separates the trabecular portion of the ventricle from the ventricular outflow tract or conus, a tubular structure with smooth walls and directs the blood from the RV into the main pulmonary artery. The most important anatomical characteristic that defines the right ventricle is the lack of fibrous continuity between the tricuspid valve and the semilunar valve [18] (pulmonary in a normal heart, aortic valve in transposition of great vessels). Moderator band, apical displacement of the atrioventricular valve and prominent trabeculations are also supportive features.

The right atrium (RA) has a triangular auricle (atrial appendage) with a broad base. The RA receives the deoxygenated blood through the superior and inferior vena cava and the coronary sinus. It has a muscular ridge, the crista terminalis in its posterior wall that is a muscular ridge, that divides the atrium into a more trabecular anterolateral portion with pectineus muscles and a smooth posterior wall. This structure may become very prominent and simulate a thrombus or tumor [19]. A thin interatrial septum divides the right from left atrium. Deposits of fat in the septum secundum can result in lipomatous hypertrophy of the atrial septum, which spares the fossa ovalis [20]. Persistent Eustachian valve is an anatomical variant located between the junction of the inferior vena cava and the right atrium, representing remnant of this valve whose function during fetal life is to redirect the oxygenated blood from the inferior vena cava into the foramen ovale [21]. This may be confused with Cor triatriatum dexter [22]. Thebesian valve is a thin structure that prevents retrograde blood flow into the coronary sinus. The

tricuspid valve divides right atrium and right ventricle, it has three valves (septal, anterior and posterior), which are visible in tomography only if it has an adequate contrast medium opacification.

35.9 Pathologies

CT is useful in the evaluation of several right heart disorders. In the following section, the common entities will be discussed briefly.

35.9.1 Pulmonary Embolism

CT pulmonary angiography (CTPA) timed to visualize the pulmonry arteries is now the standard of care in the evaluation of pulmonary embolism. In **acute pulmonary embolism,** partial or complete intraluminal filling defects are seen in the pulmonary arteries (Fig. 35.1a), forming an acute angle with the vessel wall [23–25]. The vessel is typically expanded. In iodine maps of dual energy CT, wedge shaped perfusión defects are seen in occlusive emboli (Fig. 35.1b), which can be useful in detecting small emboli and has prognostic value. CT also provides additional prognostic information for right heart strain, with dilated RV, flattening of interventricular septum and reflux of contras tinto IVC and hepatic veins [24, 25]. In **chronic pulmonary embolism**, a peripheral filling defect which makes an obtuse angle or linear irregularities or webs or calcifications are seen (Fig. 35.2a).

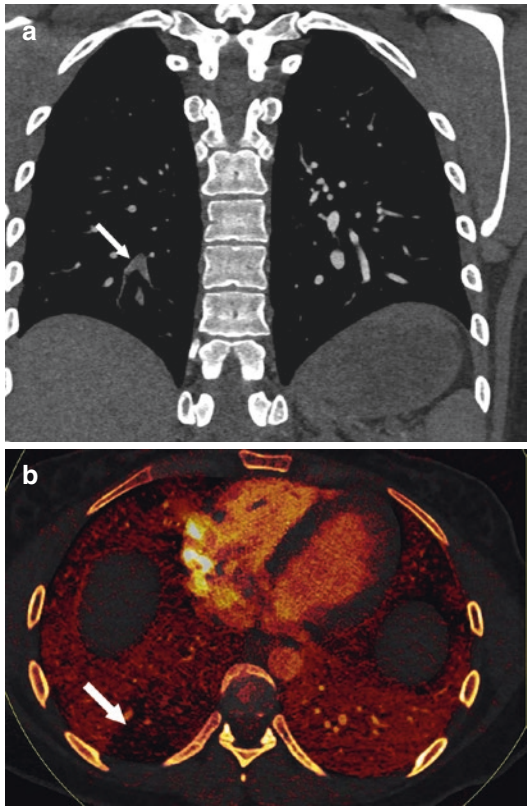

Fig. 35.1 Acute pulmonary embolism. (**a**) Coronal CTA image shows a filling defect in right lower lobe segmental branches (arrow), which is consistent with an acute occlusive pulmonary embolus. (**b**) Axial dual-energy iodine map in the same patient shows a wedge shaped perfusion defect in the right lower lobe (arrow)

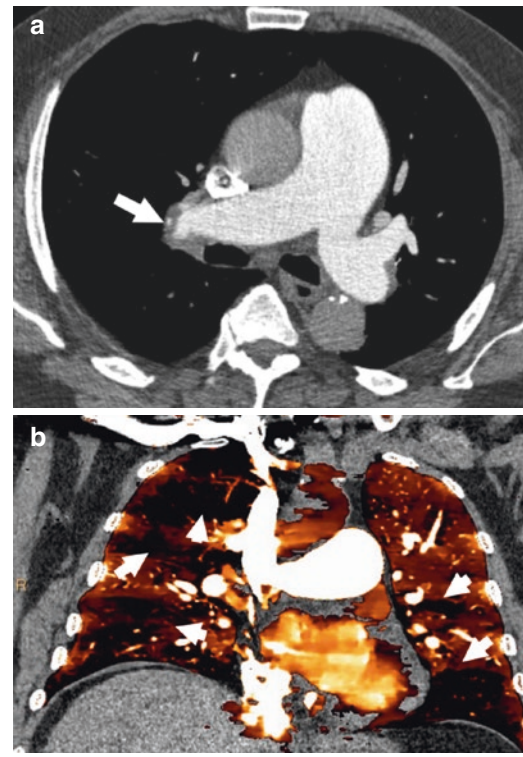

Fig. 35.2 Chronic pulmonary embolism. (**a**) Axial CTA image shows an eccentric filling defect with calcification in the right pulmonary artery (arrow), consistent with a chronic pulmonary embolus. The central pulmonary arteries are dilated due to pulmonary hypertension. (**b**) Coronal dual-energy lung perfusion map in the same patient shows multiple filling defects in bilateral lungs (arrows), caused by the chronic thromboembolism

Occlusion and tapering of vessel may also be seen. Dual energy CT shows perfusión defects, either in a mottled, mosaic or wedge pattern (Fig. 35.2b). Non-thrombotic causes of pulmonary embolism include catheter, fat, air, amniotic fluid, cement, talc, mercury, iodinated oil and cotton [26].

35.9.2 Pulmonary Hypertension

Pulmonary hypertension is defined as elevated mean pulmonary arterial pressure of greater than 25 mmHg. On CT, there is dilation of the central pulmonary arteries (Fig. 35.3a), with the main pulmonary measuring >29.5 mm and larger than diameter of the ascending aorta, with dilated segmental arteries. Other features include- Calcification of pulmonary artery; dilated RV (RV/LV ratio > 1); systolic flattening of ventricular septum (Fig. 35.3c); reflux of contrast into hepatic veins and IVC. The RV function and volumes can be quantified if a retrospective ECG gated acquisition is done. CT can also provide clues as to the etiology of PH, with the peripheral arteries pruned in arterial PH, while they are splayed in COPD. The pulmonary veins are small in the pre-capillary type, while they are large in post-capillary type of PH. Lung windows show underlying lung abnormalities including interstitial lung disease, whereas cardiac CT can show cardiac pathologies Septal lines and centrilobular ground glass nodules indicate venoocclusive disease, whereas only centrilobular ground glass nodules are seen in pulmonary capillary hemangiomatosis or colesterol granulomas.. Vacular signs of chronic PE are seen in CTEPH. Congenital abnormalites, includng shunts can be visualized [27]. Perfusion defects of different types are seen in PH with the dual energy CT scanners [28].

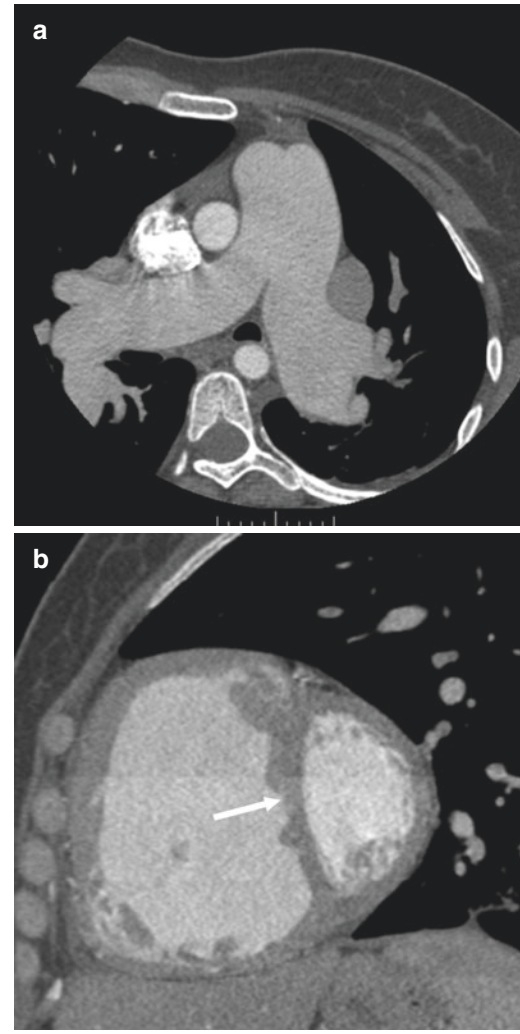

Fig. 35.3 Pulmonary hypertension. (**a**) Axial CTA image demonstrates severe dilation of the main, right and left pulmonary arteries, consistent with pulmonary hypertension. (**b**) Sagittal contrast enhanced CT image in another patient shows flattening of the interventricular septum in systole, also a feature of pulmonary hypertension

35.9.3 Congenital Heart Disease

CT is used in the evaluation of congenital heart disease, when the patient has contraindication to MRI or when MRI is associated with significant artifacts. CT can provide information on morphology, function, quantification and presurgical/interventional evaluation. Cardiac shunts, of the left-to-right type are associated with dilation of the right ventricle. Atrial septal defect can occur at the ostium secundum, ostium primum, sinus venosus or coronary sinus levels (Fig. 35.4a). Ventricular septal defect can occur either at the membranous, muscular, inlet or outlet levels. Patent ductus arteriosus is a

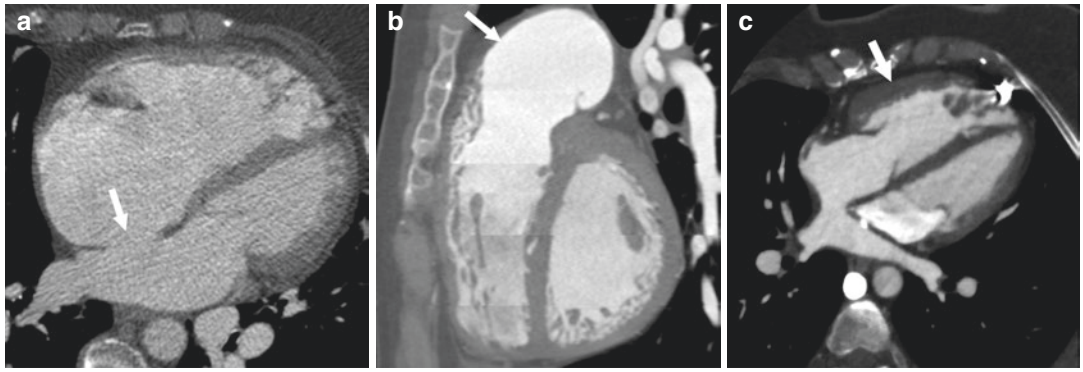

Fig. 35.4 Congenital heart disease. (**a**) 4-chamber contrast-enhanced CT image shows a large ostium secundum type of atrial septal defect (arrow), resulting in right atrial and ventricular dilation. (**b**) Short axis contrast enhanced CTA in a patient with repaired Tetralogy of Fallot shows aneurysmal dilation of the right ventricular outflow tract (arrow). (**c**) 4-chamber contrast-enhanced CT image in a patient with D-transposition of great arteries, status post atrial switch procedure (Mustard) shows hypertrophied and dilated systemic ventricle (morphological right ventricle)

communication between pulmonary artery and aorta at the level of ligamentum arteriosum and AP window is seen proximally. Tetralogy of Fallot is characterized by RV hypertrophy, RV obstruction, overriding aorta and VSD. After definitive treatment, it presents with RV dilation, RV dysfunction, pulmonary regurgitation and RVOT aneurysm (Fig. 35.4b), with CT providing good information except for pulmonary reguritation quantification. Tranposition of great arteries are also evaluated by CT, with ventriculoarterial discordance seen, with L-TGA showing additional atrioventricular discordance as well. Following surgeries for TGA such as arterial or atrial switch, CT can be used for evaluating complications (Fig. 35.4c). Ebstein anomaly is a condition in which there is apical displacement of the tricuspid valve by >8 mm/m^2, which results in atrialization of a portion of the right ventricle which does not contract effectively, resulting in significant tricuspid regurgitation, RV dilation and systolic dysfunction. In tricuspid atresia, the RV is small. Single ventricle conditions usually bypass the RV, with the creation of a Glenn and Fontan shunts [11–13]. CT is also useful in the evaluation of patients being considered for interventions such as percutaneous pulmonary valve placement for patients with abnormal valves.

35.9.4 Cardiomyopathies

CT is used in the evaluation of cardiomyopathies, when the patient has contraindications or artifacts associated with MRI or if echocardiogram is suboptimal. It is used for the evaluation of coronary arteries to exclude CAD as a cause of cardiomyopathy in these patients. It can provide functional and volumetric information, which is useful for diagnosis, managmeent and prognosis. Stress perfusión CT can be performed to evaluate for myocardial ischemia. Delayed iodine enhancement can show specific patterns of enhancement in different cardiomyopathies, although the contrast to noise ratio is lower than MRI [29]. Arrthythmogenic right ventricular dysplasia/cardiomyopathy (ARVD/C) is characterized by fibrofatty replacement of the myocardium (Fig. 35.5). Cine images show major wall motion abnormalities (aneurysm, akinesia, dyskinesia) along with either low ejection fraction (<40%) or dilated RV (EDV > 110 mL/m^2 in males, >100 mL/m^2 in females). Non ischemic cardiomyopathy, just as idiopathic form or sarcoidosis may manifest as linear or patchy mid myocardial or subepicardial enhancement. Amyloidosis shows myocardial thickening along with diffuse subendocardial/transmural enhancement. Hypertrophic cardiomyopathy is

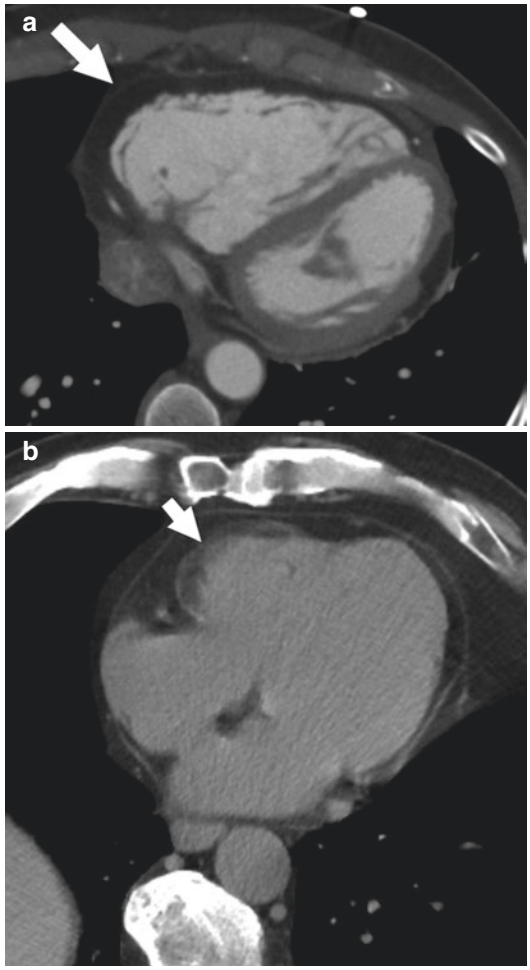

Fig. 35.5 Cardiomyopathy. (**a**) Axial contrast enhanced CTA image shows dilated right ventricle along with fat deposition in the right ventricular myocardium (arrow), indicative of arrhythmogenic right ventricular dysplasia. (**b**) Axial non contrast CT in another patient with ARVD shows fat in the RV myocardium (arrow)

characterized by asymmetric hypertrophy of the myocardium, and occasionally involves the RV. Prominent trabeculations are seen in non-compaction less commonly involving the RV and diagnosed when the trabeculations involve >75% of the RV myocardium [29]. Constrictive pericarditis is characterized by restriction of ventricular filling, which can be seen with cine CT. Pericardial thickening and calcification may also be seen [29]. In acute pericarditis, pericardial thickening, contrast enhancement and effusion are seen.

35.9.5 Masses

CT is used in the evaluation of cardiac masses when the patient has contraindications to MRI or claustrophobic or artifacts with MRI. CT can characterize the location, shape, size and extent of lesión along with extensión to adjacent organs and involvement of coronary arteries. CT is also ideal to evaluate for calcifications and feeding arteries, but has limited tissue characterization capabilities. Benign tumors are more common on the left, whereas malignant lesions are more common on the right. Benign lesions are usually small, well-defined, confined to one compartment without involvement of adjacent structures, do not have feeding artery and are not associated with pericardial effusion or metastasis. Malignant lesions are usually larger, ill-defined, have irregular margins, involve multiple compartments, extend to adjacent organs, may have a feeding artery and are associated with periardial effusion or metastasis. CT can distinguish normal variant structures from cardiac masses. Thrombus is the most common cardiac mass, which can be well evaluated with CT (Fig. 35.6a). Thrombus does not show significant iodine content in dual-energy iodine maps. Lipomatous hypertrophy shows fatty involvement of the atrial septum with sparing of the fossa ovalis. Pericardial cyst is seen as a fluid containing lesión in the cardiophrenic angle. Caseous mitral annular calcification is seen adjacent to the mitral valve. Benign primary neoplasms are more common than malignant primary lesions in the heart. Myxoma is the most common benign lesión originating commonly from the fossa ovalis and projecting into the left atrium. Lipoma, fibroma, hemangioma and paraganglioma are the other common primary neoplasms in adults, whereas rhabdomyoma and fibroma (Fig. 35.6b), are the common primary benign neoplasms in children. Metastasis is the most common malignancy to involve the heart and can present as nodules (single or multiple), diffuse infiltration or pericardial effusion. Tumors can also extend from adjacent structures such as lung and mediastinum directly or through lymphatics or vascular structures (renal, adrenal, liver) (Fig. 35.6c). Lymphoma

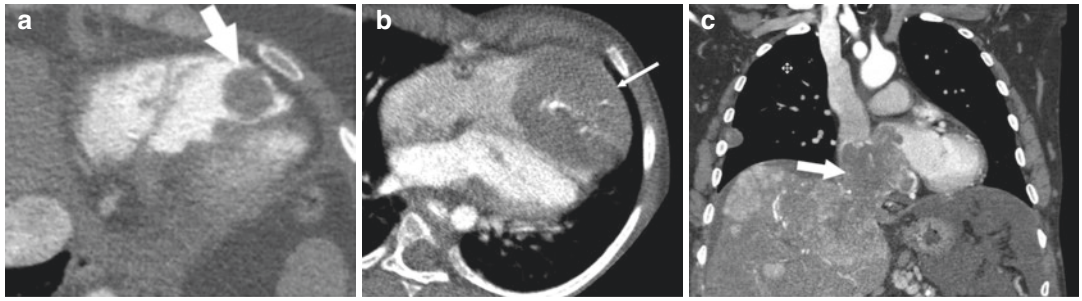

Fig. 35.6 Masses. (**a**) Axial contrast enhanced CTA shows a large thrombus (arrow) in the right ventricle. (**b**) 4-chamber CT in another patient shows a large mass containing central calcification (arrow), which was proven to be a fibroma. (**c**) Coronal contrast-enhanced CT image in a patient with hepatocellular carcinoma shows extension of this mass through the IVC into the right atrium

and leukemia can also involve the heart. Primary cardiac malignancies are rare and include sarcoms, with angiosarcoma the most common sarcoma [30].

35.9.6 Valvular Disorders

CT is not the primary modality for the evaluation of native valvular disorders, with echocardiography and MRI providing superior information. However, CT can provide morphological information on valves. For example, tricuspid stenosis is associated with leaflet thickening and calcification. Carcinoid syndrome typically affects the right heart valves, with thickening often the main manifestation. Valve motion and masses can be evaluated dynamically with cine images. Using differences in stroke volumes of the ventricles, regurgitation can be quantified if it is an isolated lesión without shunt. CT is valuable in the evaluation of prosthetic valves, particularly those with complications such as size mismatch, dehiscence, leak, pseudoaneurysm, endocarditis, abscess, structural failure, frozen leaflet, thrombus and pannus [31].

Conclusion

CT plays an important role in the evaluation of the right heart. CT is the most commonly used modality in the evaluation of acute as well as chronic pulmonary embolism. CT is also provides valuable information on the heart and lungs in pulmonary hypertension. CT is an alternative to MRI in the evaluation of cardiomyoapthies, congenital heart diseases and masses. With the latest technology, it is possible to obtain high quality images with low doses of radiation and contrast.

References

1. Cury RC, Abbara S, Achenbach S, et al. CAD-RADS(TM) coronary artery disease – reporting and data system. An expert consensus document of the Society of Cardiovascular Computed Tomography (SCCT), the American College of Radiology (ACR) and the North American Society for Cardiovascular Imaging (NASCI). Endorsed by the American College of Cardiology. J Cardiovasc Comput Tomogr. 2016;10(4):269–81.
2. Rajiah P, Abbara S. Radiation exposure from medical imaging must not be taken out of context. Trends Cardiovasc Med. 2016;26(1):66–7.
3. ACR Manual on contrast media. https://www.acr.org/~/media/37D84428BF1D4E1B9A3A2918DA9E27A3.pdf
4. Machida H, Tanaka I, Fukui R, et al. Current and novel imaging techniques in coronary CT. Radiographics. 2015;35(4):991–1010.
5. Abbara S, Blanke P, Maroules CD, et al. SCCT guidelines for the performance and acquisition of coronary computed tomographic angiography: a report of the society of Cardiovascular Computed Tomography Guidelines Committee: endorsed by the North American Society for Cardiovascular Imaging (NASCI). J Cardiovasc Comput Tomogr. 2016;10(6):435–49.
6. Rajiah P, Saboo SS, Abbara S. Role of CT in congenital heart disease. Curr Treat Options Cardiovasc Med. 2017;19(1):2.
7. Cody DD, Mahesh M. AAPM/RSNA physics tutorial for residents: technologic advances in multidetector

CT with a focus on cardiac imaging. Radiographics. 2007;27(6):1829–37.
8. Bogaard K, van der Zant FM, Knol RJJ, Reinders S, Krul MMG, van Rossum AC, et al. High-pitch prospective ECG-triggered helical coronary computed tomography angiography in clinical practice: image quality and radiation dose. Int J Cardiovasc Imaging. 2015;31(1):125–33.
9. McCollough CH, Leng S, Yu L, Fletcher JG. Dual- and multi-energy CT: principles, technical approaches, and clinical applications. Radiology. 2015;276(3):637–53.
10. Kalisz K, Halliburton S, Abbara S, et al. Update on cardiovascular applications of multienergetic CT. Radiographics. 2017;37:1955–74.
11. Rajiah P, Saboo SS, Abbara S. Role of CT in congenital heart disease. Curr Treat Options Cardiovasc Med. 2017;19(1):6.
12. Han BK, Rigsby CK, Hlavacek A, et al. Computed tomography in patients with congenital heart disease part 1: rationale and utility. An expert consensus document of the society of cardiovascular computed tomography (SCCT): endorsed by the Society of Pediatric radiology (SPR) and North American Society of Cardiac Imaging (NASCI). J Cardiovasc Comput Tomogr. 2015;9(6):475–92.
13. Han BK, Rigsby CK, Hlavacek A, et al. Computed tomography in patients with congenital heart disease part 2: technical recommendations: an expert consensus document of the society of cardiovascular computed tomography (SCCT): endorsed by the Society of Pediatric radiology (SPR) and North American Society of Cardiac Imaging (NASCI). J Cardiovasc Comput Tomogr. 2015;9(6):493–513.
14. Leipsic J, Abbara S, Achenbach S, et al. SCCT guidelines for the interpretation and reporting of coronary CT angiography: a report of the Society of Cardiovascular Computed Tomography Guidelines Committee. J Cardiovasc Comput Tomogr. 2014;8(5):342–58.
15. Raman SP, Johnson PT, Deshmukh S, Mahesh M, Grant KL, Fishman EK. CT dose reduction applications: available tools on the latest generation of CT scanners. J Am Coll Radiol. 2013;10(1):37–41. https://doi.org/10.1016/j.jacr.2012.06.025.
16. Halliburton S, Tanabe Y, Partovi S, Rajiah P. The role of advanced reconstruction algorithms in cardiac CT. Cardiovasc Diagn Ther. 2017;7(5):527–38.
17. Halliburton SS, Abbara S, Chen MY, Gentry R, Mahesh M, Raff GL, et al. SCCT guidelines on radiation dose and dose-optimization strategies in cardiovascular CT. J Cardiovasc Comput Tomogr. 2011;5(4):198–224.
18. O'Brien JP, Srichai MB, Hecht EM, Kim DC, Jacobs JE. Anatomy of the heart at multidetector CT: what the radiologist needs to know. Radiographics. 2007;27(6):1569–82.
19. Akcay M, Bilen ES, Bilge M, Durmaz T, Kurt M. Prominent crista terminalis: as an anatomic structure leading to atrial arrhythmias and mimicking right atrial mass. J Am Soc Echocardiogr. 2007;20(2):197.e9–10.
20. Laura DM, Donnino R, Kim EE, Benenstein R, Freedberg RS, Saric M. Lipomatous atrial Septal hypertrophy: a review of its anatomy, pathophysiology, multimodality imaging, and relevance to percutaneous interventions. J Am Soc Echocardiogr. 2016;29(8):717–23.
21. Gad A, Mannan J, Chhabra M, Zhang XXY, Narula P, Hoang D. Prominent eustachian valve in newborns: a report of four cases. AJP Rep. 2016;6(1):e33–7.
22. Hwang SH, Oh Y-W. Assessment of cor triatriatum dexter and giant eustachian valve with cardiac magnetic resonance. Circulation. 2014;130(19):1727–9.
23. Castaner E, Gallardo X, Ballesteros E, et al. CT diagnosis of chronic pulmonary thromboembolism. Radiographics. 2009;29:31–53.
24. Kirsch J, Brown RKJ, Henry TS, et al. Expert panels on cardiac and thoracic imaging, ACR appropriateness criteria® acute chest pain-suspected pulmonary embolism. J Am Coll Radiol. 2017;14(5S):S2–S12.
25. Schoepf UJ, Costello P. CT angiography for diagnosis of pulmonary embolism: state of the art. Radiology. 2004;230(2):329–37.
26. Rossi SE, Goodman PC, Franquet T. Non thrombotic pulmonary emboli. Am J Roentgenol. 2000;174(6):1499–508.
27. Pena E, Dennie C, Veinot J, et al. Pulmonary hypertension: how the radiologist can help. Radiographics. 2012;32:9–32.
28. Ameli-Renani S, Rahman F, Nair A, et al. Dual-energy CT for imaging of pulmonary hypertension: challenges and opportunities. Radiographics. 2014;34(7):1769–89.
29. Kalisz K, Rajiah P. Computed tomography of cardiomyopathies. Cardiovasc Diagn Ther. 2017;7(5):539–56.
30. Rajiah P, Kanne JP, Kalahasti V, Schoenhagen P. Computed tomography of cardiac and pericardiac masses. J Cardiovasc Comput Tomogr. 2011;5(1):16–29.
31. Pham N, Zaitoun H, Mohammed TL, et al. Complications of aortic valve surgery: manifestations at CT and MR imaging. Radiographics. 2012;32:1873–92.

Magnetic Resonance Imaging

36

Prabhakar Rajiah

Abstract

There is a broad spectrum of disease processes that affect the right ventricle. Multiple imaging modalities are available in the evaluation of the right ventricle. MRI plays a comprehensive role in the evaluation of right ventricular pathology and provides unique insights into the morphology and pathophysiology as well as accurate quantification of several parameters including volumes and function. In this chapter, we review the comprehensive role of MRI in the evaluation of right ventricle, including sequences, protocol and imaging appearances of common entities.

Keywords

MRI · Imaging · Right ventricle · ARVD Congenital · Tumor · Cardiomyopathy Infarction

36.1 Introduction

There is a broad spectrum of disease processes that affect the right ventricle. Multiple imaging modalities are available in the evaluation of the right ventricle. MRI plays a comprehensive role in the evaluation of right ventricular pathology and provides unique insights into the morphology and pathophysiology as well as accurate quantification of several parameters including volumes and function. In this chapter, we review the comprehensive role of MRI in the evaluation of right ventricle, including sequences, protocol and imaging appearances of common entities.

36.2 Advantages and Disadvantages

Compared to other imaging modalities, a major advantage of MRI is its ability to provide tissue characterization, which is made possible due to its inherent contrast resolution, which can be amplified by obtaining sequences at different weightings and by administration of gadolinium-based contrast agent. MRI also has good spatial resolution, which is important for morphological evaluation of small-sized structures. It has good temporal resolution, which is essential for evaluating motion, although it is not as good as echocardiogram. MRI can be obtained in any place and with suitable data, can also be reconstructed in any plane. It has a wide field-of-view which enables evaluation of extra-cardiac and vascular structures. MRI can provide comprehensive information including morphology, function, flow and tissue characterization. MRI is considered the gold standard in evaluation of function

P. Rajiah
Department of Radiology, Cardiothoracic Imaging, UT Southwestern Medical Center, Dallas, TX, USA

S. I. Dumitrescu et al. (eds.), *Right Heart Pathology*, https://doi.org/10.1007/978-3-319-73764-5_36

particularly for the right heart function, which is evaluated only to a limited extent in other imaging modalities such as echocardiogram due to limited acoustic windows. It can evaluate for shunts and help in quantification. MRI does not need ionizing radiation, which makes it preferable to CT.

Disadvantages of MRI include several contraindications including metallic devices. Pacemakers/ICDs used to be an absolute contraindication for the performance of MRI; however, recent pacemakers and some ICDs are MRI compatible or "conditional" and MRI can be safely performed if scanned within specified conditions. Some patients are claustrophobic and may need light sedation to the extent that breath hold is still possible. In children and uncooperative patients, general anesthesia may be required to keep the patient still. Gadolinium-based contrast is associated with the development of nephrogenic systemic fibrosis in patients with severe renal dysfunction [1]. Hence its use should be restricted in such patients. There are also reports of deposition of gadolinium in the brain with repeated use [2].

36.3 MRI Technology

In MRI, the patient is placed inside a magnet, typically of 1.5 of 3.0 T tesla field strength. Randomly oriented protons become aligned along the direction of the external magnetic field of this magnet, more than in the anti-parallel direction. The protons also precess around the axis of the magnetic field, with a frequency called the Larmor frequency, which is proportional to the B0 and gyromagnetic ratio. Following this, a radiofrequency pulse is applied using special coils placed in the magnet. Depending on the strength of this RF gradient, the protons will be tipped to varying angles away from the transverse plane, resulting in decay of longitudinal magnetization. The transverse magnetization undergoes free induction decay and generates a signal in a receiver, when is then converted to digital signal, amplified, and then undergoes a process of Fourier transformation to generate the MR images. Magnetic gradients are utilized in different directions to encode for the spatial location as well as frequency. With a spatial encoding magnetic gradient, a gradient of magnetic field is applied across the body, so that different protons in different locations of the body have different magnetic field strengths and hence the computer will be able to localize where they are. In addition, within a single slice, magnetic gradients are further used to encode frequency in one direction and phase in the other direction. The combination of the number of frequency and phase encoding steps is called as the matrix, which along with the field of view determines the spatial resolution of the scanner [3].

36.4 MRI Sequences

MRI sequences refer to the specific combination of application of the magnetic pulses. TR, i.e. repetition time refers to the time between RF pulses. TE refers to the time between the initial RF pulse and the time when the echo, ie the MR signal is collected. In the basic spin-echo sequence, an initial 90° pulse is applied, followed by a 180° pulse at TE/2. Then another 90° pulse is applied at TR and so forth, till all the phase encoding steps are completed. This means that higher the number of phase encoding steps, longer the scan. By varying the TR and TE, different tissues can be distinguished. T1, which is also called the spin-lattice relaxation is the time taken for the magnetic spins to restore longitudinal magnetization, whereas T2, also called the lattice-lattice relaxation is the time taken for the decay of transverse magnetization. Different tissues have different T1 and T2. By using a short TR and TE, a T1-weighted image can be obtained. By using a long TR and TE, a T2-weighted image can be obtained. By using a long TR and a short TE, a proton-density weighted image can be obtained. Different tissues appear differently in these sequences. For example, fluid appears dark in T1 and bright in T2. Soft tissue appears low in T1 and intermediate to right in T2. Fat appears bright in T1 and T2. With an inversion recovery pulse, a 180° pulse is applied before the 90, 180

sequence so that all the protons are flipped 180°. Then the protons will recover at different rates, proportional to their T1 number. Specific tissues can be suppressed if MR is acquired at the time when that tissue is at zero point in the relaxation curve. For example, in STIR image, the fat is suppressed and in FLAIR image, fluid is suppressed. Gradient echo sequence is another commonly used sequence where RF pulses of varying angles are used, but a refocusing 180° pulse is not used [3, 4].

36.5 Cardiac MRI Sequences

The following MRI sequences are useful in the evaluation of right heart pathology [3–5].

Cine sequences Cine sequences are performed using balanced steady state free precession (b-SSFP) sequence, which is a type of gradient-echo sequence. Since the signal in this sequence depends on the T2/T1 ratio, blood looks bright without administration of intravenous contrast. Cine images are obtained in a segmented k-space acquisition, which means that with each R-R interval, only few lines of k-space are filled and data is collected over multiple R-R intervals, depending on the spatial and temporal resolution desired. Typically, these are performed over a single breath-hold, approximately 15–20 heartbeats. The images are displayed as a cine loop and are obtained as average of multiple heartbeats. The cine images can be acquired in any plane. For the left ventricle, 2 chamber, 3 chamber, 4 chamber, and short axis views are the most commonly used. For the right ventricle, right ventricle long axis, horizonal long axis and outflow tract views provide evaluation. In patients with metallic devices, gradient echo sequence can be used instead of SSFP to minimize artifacts. In addition to evaluation of the morphology, the sequence can be used for qualitative evaluation of global and regional function (Fig. 36.1a).

In addition, contours can be drawn in the endocardium and epicardium in end systole and end systole in multiple slices (typically short axis), to obtain quantitative values of ventricular volumes, mass and function using the modified Simpson's formula (Fig. 36.1b). MRI has shown to be highly accurate and reproducible technique in the evaluation of ventricular parameters. Especially for RV, MRI is the ideal imaging modality since echocardiography is limited by acoustic windows [6]. SSFP images can also be obtained in static mode, which can be utilized for evaluating morphology.

Real time cine SSFP Cine images can also be obtained in real-time, which means that the data is not averaged over multiple cardiac cycles, but instead obtained in real-time as and when it is happening, similar to a fluoroscopic image. Real time cine imaging is commonly used when a regular ECG gated MRI cannot be performed or suboptimal due to the presence of extensive arrhythmia. Real time cine imaging is also useful in the evaluation of ventricular interdependence in patients with pericardial constriction, who show exaggerated diastolic septal flattening with inspiration [7].

3d whole heart SSFP 3d whole heart SSFP is similar to the 2d cine SSFP, but unlike the latter is a 3d volumetric acquisition. This can be performed in any plane and the extent can be customized depending on the clinical indication, from just the coronary arteries to the entire chest. Images are typically ECG-gated and can be obtained from any phase of the cardiac cycle, typically in diastole for coronary imaging. Images are also obtained with navigator-gating of the diaphragm, allowing to the patient to free breath, with the data being collected only in end-expiratory phase. For optimizing coronary arterial imaging, fat saturation and T2 prep pulse are also obtained, the former to null the fat and the latter to suppress the myocardial signal, both of which improve the contrast between coronary arteries and adjacent structures [8].

Strain imaging Strain refers to relative deformation of myocardium in response to an applied force. Strain imaging is useful in the evaluation of regional myocardial function, which is often abnormal in early stages of disease process

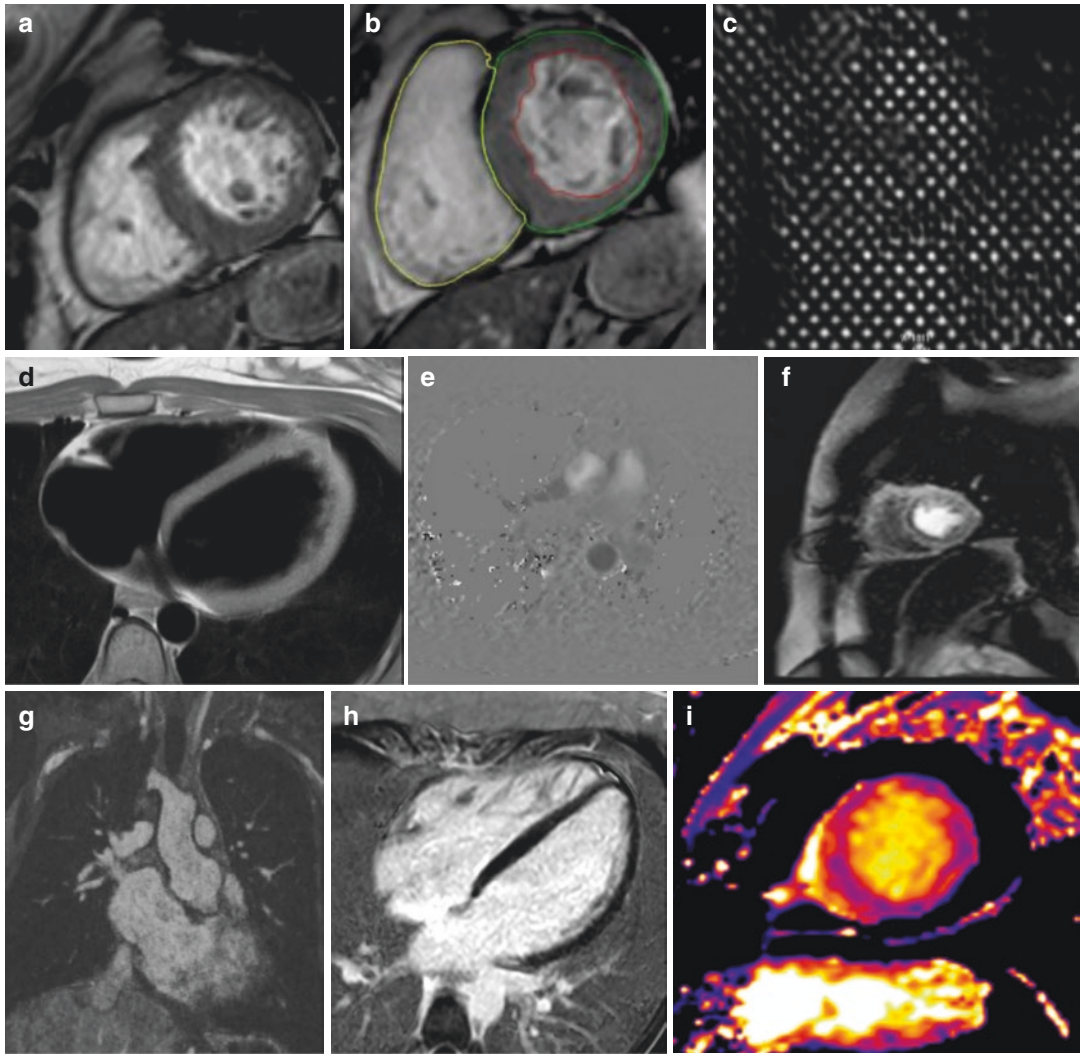

Fig. 36.1 MRI sequences. (**a**) Cine SSFP sequence in the short axis plane. (**b**) Quantification of right ventricular volumes and function using contours drawn in systole and diastole. (**c**) Myocardial tagging image for regional cardiac function. (**d**) Black-blood sequence. (**e**) Velocity encoded phase contrast image through the pulmonary artery. (**f**) Dynamic perfusion imaging. (**g**) MR angiography. (**h**) Late gadolinium enhancement through the myocardium. (**i**) T1 mapping through the heart

before there is obvious failure. For example, in chemotherapy induced cardiotoxicity, abnormalities are seen regionally much ahead of global systolic dysfunction. Strain evaluates regional deformation of myocardium in different directions, including radial, longitudinal and circumferential directions along with torsion. There are several sequences which can evaluate strain, including myocardial tagging, which uses grids or lines to tag the myocardium and quantifying the deformation using advanced software such as HARP (Fig. 36.1c). Feature tracking uses conventional cine SSFP sequence and evaluates strain by tracking the changes in feature of the images over the cardiac cycle. Other techniques include tissue velocity phase mapping, Strain-encoded imaging (SENC) and Displacement-Encoded imaging (DENSE) [9].

Black blood sequences Black blood sequences are used for evaluation of morphology, particularly of the myocardium and pericardium, as well for the evaluation of myocardial edema and characterization of masses. These are performed with prospective ECG-triggering and a double inversion recovery pulse. The first inversion pulse is applied throughout the scanned volume and flips all the protons by 180°. The second 180° pulse is applied only to the imaged slice. Thus any tissue in the slice will have encountered two 180° pulses with signal cancelling out each other. Blood however flows out and at the time of imaging, the blood in the image would have come from outside the slice and has encountered only one 180° pulse. The definitive image is then acquired when this blood reaches the zero point. After this T1, or T2 weighting can be obtained by optimizing the TR and TE (Fig. 36.1d). Fat saturation can also be obtained by using a triple inversion recovery pulse. Black blood images can also be obtained by using ultra-fast spin- echo T2 (single shot SSE, HASTE, etc), but these images have low resolution and are hence used limited to provide overview of the thoracic structures and not for fine detail [4].

Phase contrast Velocity-encoded phase contrast imaging utilizes two equal but opposite gradients (bipolar gradients). A static tissue in between these gradients undergoes phase shifts that cancel out each other. However, if there is flowing tissue such as blood, it undergoes phase shift due to the bipolar gradients and this phase shift is proportional to the velocity. In the phase contrast image, the signal is proportional the velocity. By obtaining images perpendicular to the vessel of interest, velocity can be calculated and flow derived by multiplying velocity with the area of the vessel. Pressure gradient can be calculated by modified Bernoulli equation, $\Delta P = 4v^2$ [3–5].

4d flow A recent advance in flow imaging is the development of 4d flow, in which phase contrast images are obtained with velocity encoding in all the three directions, along with acquisition of time information. This provides the ability to image large volumes of tissues using a single sequence without specific planning for specific vessels. Using computational fluid dynamic models, the flow patterns, including helices and turbulence can be evaluated in the heart or other vessels. Several abnormalities have shown early alterations in flow before the development of morphological abnormalities [10].

Perfusion imaging Dynamic first pass perfusion imaging is acquisition of images through the myocardium on the first phase of contrast through the myocardium. This is obtained using a gradient echo or SSFP readout following injection of gadolinium-based contrast media at high flow rate (Fig. 36.1f). Images are obtained both at rest and following stress, which may be either pharmacological (adenosine, dipyridamole, regadenoson) Myocardial ischemia demonstrates a perfusion defect in stress images, but no defect is seen at rest. This sequence can also be used for the evaluation of microvascular dysfunction as well cardiac masses [11].

MR angiography MR angiography is useful in the assessment of the vasculature, including pulmonary arterial and venous system. This is performed using a 3d T1-weighted spoiled gradient echo sequence, after administration of gadolinium based contrast agent, which shortens the T1. Hence the blood vessels which have the contrast appear bright. Timing of the acquisition is crucial since the images have to be obtained when the contrast is in the vessel of interest, which can be accomplished by using a MR fluoroscopic image which tracks the passage of contrast. Typically, two phases of contrast can be obtained, the first in pulmonary artery and the second in aorta (Fig. 36.1g). This can be accomplished on two breath-holds. However, with modern technologies, multiple phases with high temporal resolution can be obtained by using sequences such as time resolved MR angiography (TWIST, TRICKS, etc), in which only selective data is obtained at each time interval from the center of the k space, whereas the same data is used for the k-space periphery. In addition to high temporal resolution, this also provides perfusion images, including that of the lung [3, 4].

3d ultrafast gradient echo 3d ultrafast gradient echo is another technique for obtaining angiographic images of the thorax using a rapid 3d volumetric sequence such as VIBE, THRIVE or LAVA. Pre and post contrast images can be subtracted to optimize contrast enhancement.

Late Gadolinium enhancement This sequence is valuable in characterizing the cardiomyopathies, based on different patterns of enhancement. Abnormal myocardium, such as scar, fibrosis or tumor show contrast uptake with slow washout. Images are obtained 10–15 min after administration of gadolinium-based contrast, to optimize the difference in signal between normal and abnormal myocardium since in early phase both these show contrast enhancement, but at later phases, contrast washes out from normal myocardium, whereas it is retained in scar/fibrosis (Fig. 36.1h). This difference can be amplified by using inversion recovery sequence with the null time optimized to suppress signal from normal myocardium. Hence, a normal myocardium appears dark, whereas abnormal myocardium appears bright. The optimal nulling time is determined by using scout images at low resolution obtained at different inversion times and identifying which phase has the lowest signal [3–5].

T1 mapping T1 mapping is a novel technique in which the absolute T1 number of the myocardium can be obtained. LGE technique is not adequate in diffuse disease processes since it depends on identifying a normal myocardium which may be a challenge in diffuse processes. By using sequences such as MOLLI, SCHMOLLI, SASHA and others, which are either inversion or saturation-recovery based, images of the same slice are obtained at different inversion times. By fitting a curve and then solving the equation, the absolute number of T1 can be obtained. The images can also be color coded based on their T1 (Fig. 36.1i). Different pathological processes have different T1, both pre and post contrast. In native T1 mapping, high T1 values are seen in edema, fibrosis and amyloid whereas low T1 values are seen in fat and iron, including Fabry disease. After giving contrast, low T1 values are seen in tissues with fibrosis or amyloid. By obtaining real or synthetic hematocrit, the extracellular volume can be quantified, which is increased in several disease processes, correlating with prognosis [12].

T2 mapping Similar to T1 mapping, absolute T2 number can also be obtained by using sequences such as SSFP, ACU2TE, which obtain images in same slice at different TE. By plotting signal intensity against the time, the absolute T2 number can be obtained. Color maps can be obtained by color coding based on the T2 value. This is high in edema of myocarditis and myocardial infarction, which is more sensitive than routine T2 weighted sequences [12].

Multi-echo gradient echo imaging This sequence is used in the evaluation and quantification of myocardial iron. Images in the same slice are obtained at different echo times (TE). By plotting the signal intensities against the corresponding TE, the absolute T2* number can be obtained, which is inversely proportional to the myocardial iron, with values <20 ms associated with significant iron deposition [13]. This information can be used to initiate chelation therapy before the onset of advanced LV dysfunction [3, 4].

Advanced sequences **Arterial spin** labeling is technique in which perfusion images such that of the lung can be obtained without administering intravascular contrast. Localized RF pulses are used to invert pulmonary blood magnetization. Images obtained with and without arterial labeling are subtracted and thus perfusion images of the lungs can be obtained [14]. **MR spectroscopy can** evaluate for the metabolites in the myocardium, which can be abnormal in early phases of the disease. **Diffusion tensor imaging** evaluates for changes in the orientation of myocardial fibers, which is also seen in early stages of disease process [15]. **Ultra short echo TE** is a novel sequence, which may be useful in the evaluation of lungs. The lung parenchyma is usually not well-visualized in conventional MRI sequences due to short T2*. However, at

ultra-short TE times (i.e <500 μs), there is more inherent signal from MR parenchyma. This allows for potential quantification of interstitial tissue density/volume. The non-uniform disruption of lung architecture can be detected and characterized without radiation dose [16].

36.6 MRI Protocol

MRI protocol refers to the combination of the different MRI sequences that are utilized in a patient. Depending on the clinical indication, different sequences can be added. An optimal workflow involves having few pre-selected protocols making only minimal modifications if necessary. Examples of common protocols are shown in Table 36.1. For example, if there is need for evaluation of ARVD, cine sequences are performed in multiple planes, particularly right ventricular horizonal long axis; black blood T1-weighted images to evaluate for myocardial fat; and post-contrast late gadolinium enhancement images for fibrosis. 3d whole heart SSFP sequence is also performed to evaluate for coronary arterial origins and exclude anomalies. If a cardiomyopathy is considered, cine images, LGE, T2*, STIR and T1 mapping are performed. For cardiac masses, tissue characterization is performed using T1, T2, early contrast enhancement and late gadolinium enhancement are performed [5].

Table 36.1 MRI protocols for common right ventricular disorders

Disease	Protocol
Congenital heart disease	Cine SSFP- Multiple planes
	Phase contrast- Aorta, pulmonary & directly through the shunt if present
	MR angiography
	3d whole heart SSFP
	Late gadolinium enhancement
ARVD	Cine SSFP- RV planes
	Black blood T1- RV plane
	LGE- RV plane
	3d whole heart SSFP
Other cardiomyopathies	Cine SSFP- Multiple planes
	Phase contrast- Aorta & pulmonary
	Black blood- STIR
	Late gadolinium enhancement
	T1 mapping T2 mapping, T2* in iron overload
Pulmonary hypertension	Cine SSFP- multiple planes
	Phase contrast- Aorta & pulmonary
	MR angiography
	Late gadolinium enhancement
Masses	Axial cine SSFP-to locate the mass
	Mass- T1, T2, STIR, perfusion, LGE (regular and long inversion times)

36.7 Pathologies

MRI is useful in the evaluation of several pathologies of the right heart, with the following section discussing the common clinical conditions.

36.7.1 Congenital

MRI is an optimal imaging modality for congenital heart diseases (CHD), that provides comprehensive information, including morphology, function, quantification and pre-surgical/interventional evaluation. A morphologic right ventricle is identified by the presence of muscular tissue between the AV and semilunar valves, moderator band and prominent trabeculations. Left-to-right is a common cause for right ventricle dilation. Atrial septal defect can occur at the ostium secundum, ostium primum, sinus venosus or coronary sinus levels (Fig. 36.2a). Ventricular septal defect can occur at the membranous, muscular, inlet or outlet level. Patent ductus arteriosus is seen as a communication between the pulmonary artery and the descending aorta. MRI can not only evaluate the morphology of the abovementioned shunts it can also quantify the shunt either directly or by measuring Qp:Qs with phase contrast, which is used for surgical decision making. Tetralogy of Fallot is characterized by RV outflow obstruction, RV hypertrophy, VSD and overriding aorta. This is treated by

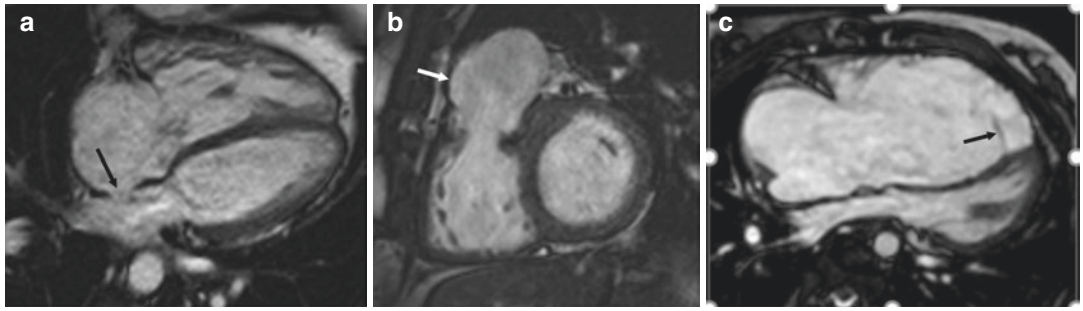

Fig. 36.2 Congenital heart disease. (**a**) 4-chamber cine SSFP image shows an atrial septal defect (arrow). (**b**) Sagittal MR image in a patient post repair of Tetralogy of Fallot shows aneurysmal dilation of the right ventricular outflow tract (arrow). (**c**) Ebstein anomaly, with apical displacement of the tricuspid valve leaflet (arrow)

definite surgical repair of RVOT. These patients are followed up with MRI, since they are at high –risk for developing pulmonary regurgitation. MRI is used to quantify the pulmonary regurgitation and as well as RV dilation and dysfunction (Fig. 36.2b). Extensive LGE in the RVOT or aneurysm are adverse prognostic indicators [17]. Ebstein anomaly is a condition in which there is apical displacement of the tricuspid valve by >8 mm/m^2, which results in atrialization of a portion of the right ventricle which does not contract effectively, resulting in significant tricuspid regurgitation, RV dilation and systolic dysfunction (Fig. 36.2c) [18]. In tricuspid atresia, the RV is small. Single ventricle conditions usually bypass the RV, with the creation of a Glenn and Fontan shunt [18, 19].

36.7.2 Cardiomyopathies

MRI is an important modality in the evaluation of cardiomyopathies. It helps in diagnosis, characterization, risk stratification and follow up after treatment. Infarction of the RV may be seen as subendocardial or transmural LGE in the myocardium (Fig. 36.3a). Arrthythmogenic right ventricular dysplasia/cardiomyopathy (ARVD/C) is a cardiomyopathy that affects the RV, characterized by fibrofatty replacement of the myocardium. On MRI, it is diagnosed by the presence of major wall motion abnormalities (aneurysm, akinesia, dyskinesia) along with either low EF (<40%) or dilated RV (EDV > 110 mL/m^2 in males, >100 mL/m^2 in females). This is combined with other clinical criteria to make a diagnosis. Presence of fat in the RV myocardium in black blood image is supportive, but not necessary. Late gadolinium enhancement may be seen in the RV. Dilated cardiomyopathy is characterized by dilated ventricle and global systolic dysfunction. Non ischemic cardiomyopathy, due to idiopathic cause, chronic myocarditis or sarcoidosis may manifest as linear or patchy mid myocardial or subepicardial enhancement. Amyloidosis shows myocardial thickening along with diffuse subendocardial/transmural LGE involving LV, RV, atria and atrial septa. There is also alteration of the T1 kinetics, with the myocardium appearing dark before the blood pool becomes dark, which is a reversal of the normal pattern. Hypertrophic cardiomyopathy is characterized by asymmetric hypertrophy of the myocardium, and occasionally involves the RV. Prominent trabeculations are seen in non-compaction less commonly involving the RV and diagnosed when the trabeculations involve >75% of the RV myocardium (Fig. 36.3b). Constrictive pericarditis is characterized by restriction of ventricular filling. On MRI, pericardial thickening is usually seen and there may be pericardial enhancement if there is inflammation. There is diastolic septal bounce, abrupt cessation of diastolic filing and exaggerated inspiratory diastolic septal flattening in real-time images [20].

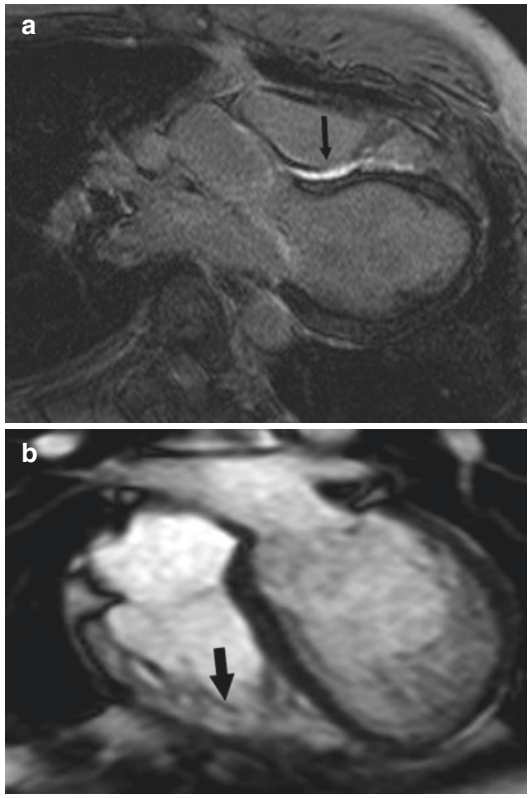

Fig. 36.3 Cardiomyopathies. (**a**) Right ventricular infarction showing subendocardial late gadolinium enhancement (arrow). (**b**) Prominent right ventricular trabeculations in a patient with ventricular non compaction (arrow)

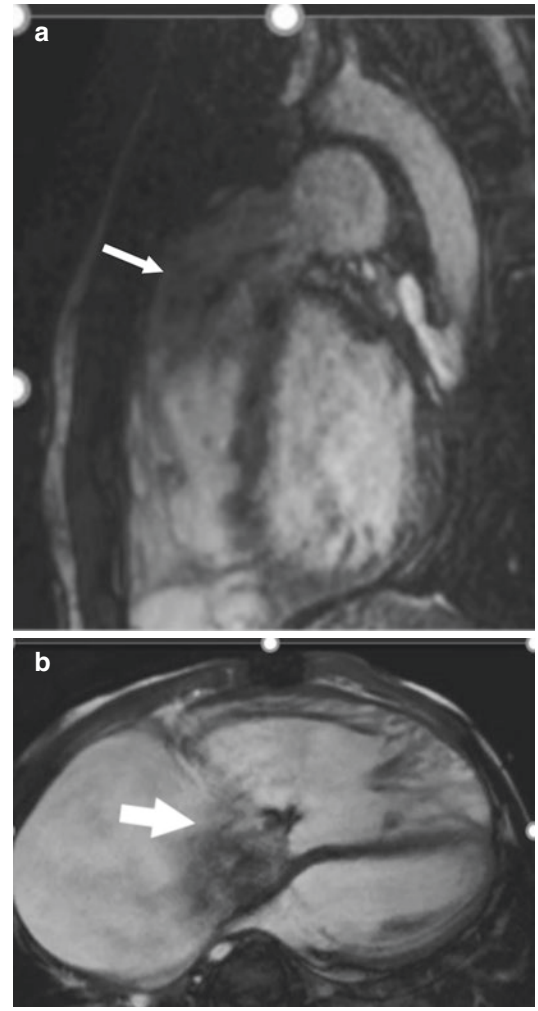

Fig. 36.4 Valvular heart disease. (**a**) Sagittal MRI image showing severe pulmonic regurgitation (arrow). (**b**) 4-chamber SSFP image showing severe tricuspid regurgitation (arrow)

36.7.3 Valvular Disorders

Valvular disorders produce significant effect on the right ventricle. Regurgitant lesions such as tricuspid and pulmonary valves result in dilation and increased stroke volume of the RV, with diastolic septal flattening in cine images. There is incomplete coaptation of the pulmonary valve in diastole and tricuspid valve in systole (Fig. 36.4). The regurgitation can be accurately quantified by using velocity encoded phase contrast imaging, which is useful in therapeutic decision making. Stenotic lesions such as pulmonary stenosis produces RV hypertrophy and systolic septal flattening. The valve leaflets appear thickened and there is restricted systolic opening of the pulmonic valve. The velocity of the stenotic jet and pressure gradient can be calculated using phase contrast imaging [21]. On MRI, the regurgitation is graded as mild (<15%), moderate (16–25%), moderate severe (26–48%) and severe (>48%) [22]. The velocity of stenotic jet is measured and using this pressure gradient can be calculated using modified Bernoulli equation, $\Delta p = 4v^2$ [21].

36.7.4 Pulmonary Hypertension

Pulmonary hypertension is characterized by elevation of the mean pulmonary arterial pressure (>25 mmHg). There are several causes of PH, Type 1- Pulmonary arterial hypertension; 2- left heart disease;3- lung disease;4- chronic thromboembolic hypertension; 5- unclear/multifactorial. MRI is used primarily in the quantification of right ventricular volume and function, which is challenging with echocardiography. There may be RV hypertrophy, RV dilation, systolic septal flattening and low systolic function. MRI can provide comprehensive information that may expedite the workup of PH and the need for multiple tests. Using composite scores, MRI can help in the diagnosis of pulmonary hypertension, although it is not commonly used for this purpose. Using interventricular septal angle and ventricular mass, metrics for diagnosis can be obtained. Estimated mPAP= (interventricular septal angle × 0.23) + (ventricular mass index × 16.3) − 4.6. Estimated PVR (in Woods units)- 19.38 − {4.62 × ln PA average velocity (cm/s)} − {0.08 × RVEF (%)} [2, 24].

There is dilation of the central pulmonary arteries (main pulmonary artery >2.8 cm, or larger than ascending aorta) (Fig. 36.5a), with or without pruning of the peripheral pulmonary arteries. The right ventricle is initially hypertrophied, but then fails resulting in systolic dysfunction. There is systolic flattening of the interventricular septum (Fig. 36.5b) [23]. Using phase-contrast imaging, the pulmonary and tricuspid regurgitation can be quantified. Decreased myocardial perfusion reserve is seen in pulmonary hypertension. LGE shows enhancement in RV insertion points. Altered hemodynamics can be seen, both in phase contrast and time resolved MRA. MRI can be used to establish the etiology of pulmonary hypertension which is vital for selecting appropriate therapy [23]. Shunts can be evaluated as described above. Left heart disease, including cardiomyopathies can be comprehensively evaluated with MRI. Using MR pulmonary angiography, chronic pulmonary embolism can be seen either as filling defect, webs or attenuation of vessel. With MR perfusion imaging, perfusion defects may be seen in chronic PE, which may be the only finding in chronic thromboembolic disease. Pulmonary veno-occlusive disease can also be evaluated with MRA. MRI also provides prognostic information. For example, altered hemodynamics with time resolved MRA has been shown to be associated with pulmonary arterial pressure and vascular resistance [25]. MRI can also be used to monitor the response to treatment.

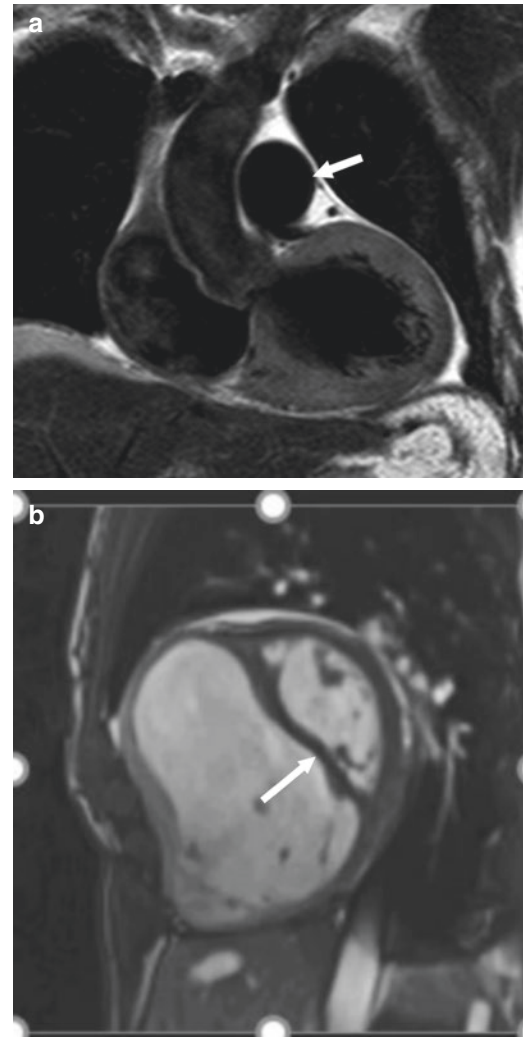

Fig. 36.5 Pulmonary hypertension. (**a**) Coronal MR Image shows several dilation of the central pulmonary arteries. (**b**) Systolic flattening of the interventricular septum towards the left ventricle (arrow)

36.7.5 Masses

Cardiac masses can be seen in the right heat and can be characterized with MRI by using a combination of T1, T2, perfusion and late enhancement sequences. The most common non neoplastic mass is a thrombus, which has low signal in all sequences. When there is question of thrombus, an additional LGE image is obtained at long inversion time (approximately 600 ms), at which point only thrombus has low signal. Pericardial cyst is seen in the right paracardiac region, in the cardiophrenic angle and has low signal in T1, high signal in T2 without contrast enhancement. Occasionally a prominent moderator band can mimic a mass, but can be distinguished from a true mass by evaluating it in multiple planes. Benign neoplasms usually are confined to the right ventricle, does not extend to other chambers or the pericardium, have smooth margins may have a stalk and are small while malignant lesions are larger, extend or involve more than one compartment. Benign tumors like myxoma, lipoma, fibroelastoma, hemangioma and paraganglioma are rare in the right ventricle. Myxoma may have a stalk and has heterogeneous signal. Fibroelastoma has a stalk that is attached to the tricuspid valve. Lipoma has fat signal in all the sequences. Hemangioma and paraganglioma have high T2 signal and vascular enhancement. Metastasis is the most common tumor to involve the heart and can present as a single nodule, multiple nodules or diffuse infiltration or pericardial effusion. Lymphoma can also have similar appearance. Angiosarcoma is the most common sarcoma in the heart, originating from the right atrium and extending to the ventricle with irregular margins and infiltration of adjacent structures [26, 27].

Conclusion

MRI provides comprehensive information on right heart pathology. It provides information on the morphology of several disorders. It is the most accurate and reproducible technique for quantification of function. Valvular and shunt quantification is performed using phase contrast imaging. Late gadolinium enhancement, T1 and T2 mapping are useful in characterization of several cardiomyopathies and masses. Different sequences are optimized and chosen to answer the specific clinical question.

References

1. Reiter T, Ritter O, Prince MR, et al. Minimizing risk of nephrogenic systemic fibrosis in cardiovascular magnetic resonance. J Cardiovasc Magn Reson. 2012;14:31.
2. Olchowy C, Cebulski K, Lasecki M, et al. The presence of gadolinium-based contrast agent depositions in the brain and symptoms of gadolinium neurotoxicity- a systematic review. PLoS One. 2017;12(2):30171704.
3. Ridway JP. Cardiovascular magnetic resonance physics for clinicians: part I. J Cardiovasc Magn Reson. 2010;12:71.
4. Biglands JD, Radjenovic A, Ridway JP. Cardiovascular magnetic resonance physics for clinicians: part II. J Cardiovasc Magn Reson. 2012;14:66.
5. Kramer CM, Barkhausen J, Flamm SD, et al. Standardized cardiovascular magnetic resonance protocols 2013 update. J Cardiovasc Magn Reson. 2013;15:91.
6. Geva T. Is MRI the preferred method for evaluating right ventricular size and function in patients with congenital heart disease. Circ Cardiovasc Imaging. 2014;7:190–7.
7. Francone M, Dymarkowski S, Kalantzi M, et al. Real-time cine MRI of ventricular septal motion: a novel approach to assess ventricular coupling. J Magn Reson Imaging. 2005;21(3):305–9.
8. Rajiah P, Setser RM, Desai MY, et al. Utility of free-breathing, whole-heart, three-dimensional magnetic resonance imaging in the assessment of coronary anatomy for congenital heart disease. Pediatr Cardiol. 2011;32(4):418–25.
9. Chitiboi T, Axel L. Magnetic resonance imaging of myocardial strain: a review of current approaches. J Magn Reson Imaging. 2017;46(5):1263–80.
10. Stankovic Z, Allen BD, Garcia J, et al. 4d flow imaging with MRI. Cardiovasc Diagn Ther. 2014;4(2):173–92.
11. Kellman P, Hansen S, Nielles-Vallespin S, et al. Myocardial perfusion cardiovascular magnetic resonance: optimized dual sequence and reconstruction for quantification. J Cardiovasc Magn Reson. 2017;19:43.
12. Messroghli DR, Moon JC, Ferreira VM, et al. Clinical recommendations for cardiovascular magnetic resonance mapping of T1, T2, T2* for extracellular volume: a consensus statement by the

Society for Cardiovascular magnetic resonance (SCMR) endorsed by the European Association for Cardiovascular Imaging (EACVI). J Cardiovasc Magn Reson. 2017;19:75.
13. Carpenter JP, He T, Kirk P, et al. On T2* magnetic resonance and cardiac ioron. Circulation. 2011;123:1519–28.
14. Li Z, Schar M, Wang D, et al. Arterial spin labeled perfusion imaging using three-dimensional turbo spin echo with a distributed spiral-in/out trajectory. Magn Reson Med. 2016;75(1):266–73.
15. Scott AD, Ferreira PF, Nielles-Vallespin S, et al. Optimal diffusion weighting for in vivo cardiac diffusion tensor imaging. Magn Reson Med. 2015;74(2):420–30.
16. Ohno Y, Koyama H, Yoshikawa T, et al. Pulmonary high-resolution ultrashort TE MR imaging: comparison with thin-section standard and low-dose computed tomography for the assessment of pulmonary arteries. J Magn Reson Imaging. 2016;43(2):512–32.
17. Etesami M, Gilkeson RC, Rajiah P. Utility of late gadolinium enhancement in pediatric cardiac MRI. Pediatr Radiol. 2016;46(8):1096–113.
18. Rajiah P, Tandon A, Greil GF, Abbara S. Update on the role of cardiac magnetic resonance imaging in congenital heart disease. Curr Treat Options Cardiovasc Med. 2017;19(1):2.
19. Ntsinjana HN, Hughes ML, Taylor AM. The role of cardiovascular magnetic resonance in pediatric congenital heart disease. J Cardiovasc Magn Reson. 2011;13:51.
20. Rajiah P, Raza S, Saboo SS, et al. Update on the role of cardiac magnetic resonance in acquired non ischemic cardiomyopathies. J Thorac Imaging. 2016;31(6):348–66.
21. Cawley PJ, Maki JH, Otto CM. Cardiovascular magnetic resonance imaging for valvular heart disease. Circulation. 2009;119:468–78.
22. Gelfand EV, Hughes S, Hauser TH, et al. Severity of mitral and aortic regurgitation as assessed by cardiovascular magnetic resonance: optimizing correlation with Doppler echocardiography. J Cardiovasc Magn Reson. 2006;8(3):503–7.
23. Swift A, Wild JM, Nagle S, et al. Quantitative magnetic resonance imaging of pulmonary hypertension: a practical approach to the current state of the art. J Thorac Imaging. 2014;29(2):68–79.
24. Garcia-Alvarez A, Fernandez-Friera L, Mirealis JG, et al. Non-invasive estimation of pulmonary vascular resistance with cardiac magnetic resonance. Eur Heart J. 2011;32(19):2438–45.
25. Peacock AJ, Crawley S, McLure L, et al. Changes in right ventricular function measured by cardiac magnetic resonance imaging in patients receiving pulmonary arterial hypertension-targeted therapy: the EURO-MR study. Circ Cardiovasc Imaging. 2014;7(1):107–14.
26. Sparrow PJ, Kurian JB, Jones TR, Sivanathan MU. MR imaging of cardiac tumors. Radiographics. 2005;25:1255–76.
27. Motwani M, Kidambi A, Herzog BA, et al. MR imaging of cardiac tumors and masses: a review of methods and clinical applications. Radiology. 2013;268(1):26–43.

Cardiac Catheterization and Angiography

37

Larisa Pinte, Florina Pinte, Ana Maria Cristian, Iancu Mocanu, Vasile Murgu, and Liviu Stan

Abstract

Cardiac catheterization is an invasive investigation which offers the benefit of a diagnostic certainty in congenital heart disease with, some of which having a great deal of complexity.

The investigation may also be useful in some cases of complicated valvular diseases, as well as in making differential diagnosis of some myocardial or pericardial lesions.

Using this invasive procedure, pressures and oximetries in the heart cavities and great vessels are recorded, thus determining transvalvular gradients, cardiac shunts and the severity of pulmonary hypertension. Cardiac angiography brings extra data about the anatomy of the heart and vessels, allowing accurate diagnostics.

Although there are major progresses in imaging performing echocardiographic exams, cardiac catheterization is still the "gold standard" in complex congenital heart diseases for determining sequential gradients, bidirectional cardiac shunts, as well as stenosis of the peripheral branches of the pulmonary artery.

Last but not least, it should be mentioned the major advantage that this invasive procedure has, it offers the possibility to solve some cardiac malformations (septal defects, valvular/vascular stenosis, etc.) in the same intervention.

Keywords

Cardiac catheterization · Indications · Contraindications · Complications · Congenital heart diseases · Angiography

L. Pinte
Internal Medicine Department, Colentina Clinical Hospital, Bucharest, Romania

F. Pinte (✉) • A. M. Cristian
Department of Interventional Cardiology, MEDLIFE – Angiolife, Bucharest, Romania

I. Mocanu
Department of Cardiovascular Surgery, SANADOR Hospital, Bucharest, Romania

V. Murgu
Department of ITU, Central Military Hospital, Bucharest, Romania

L. Stan
Department of Cardiovascular Surgery, Central Military Hos-pital, Bucharest, Romania

37.1 Introduction

Humans desire for knowledge was manifested from ancient times, but in this domain, the first description of the blood circulatory system was published in 1628 by William Harvey in his paper "De motu cordis," in which he describes the macrocirculation, the microcirculation and also the roles of the right side of the heart and the left side

S. I. Dumitrescu et al. (eds.), *Right Heart Pathology*, https://doi.org/10.1007/978-3-319-73764-5_37

of the heart [1]. Physiologist Claude Bernard in 1847 standardizes the techniques for measuring intracardiac pressure, introducing the name of 'cardiac catheterization.'

The first cardiac catheterization in humans was made in 1929 by Werner Forssman on himself. He had introduced under radiological guidance a urethral probe in the cubital vein up to the right atrium and he measured cardiac blood flow directly. A. Cournand and D. W. Richards improved the technique for clinical applicability in 1941, for which they received the Nobel Prize together with Forssman in 1956 [1–3].

From 1950 to 1960, cardiac catheterization laboratories developed rapidly as a necessity imposed by the launch of cardiac surgery based on the hemodynamic data obtained using catheterization for the purpose of therapeutic decision making in patients with congenital heart defects and those with valvular heart diseases.

37.2 Definition

Cardiac catheterization is the set of invasive diagnostic techniques involving the insertion of a percutaneous catheter in order to obtain hemodynamic data by performing direct measurement of blood pressures and oxygen saturation of the blood in various chambers of the heart, as well as anatomical data about the heart and vessels using a contrast injection agent.

Catheterization is an invasive diagnostic method that complements echocardiography and cardiac MRI used to collect as much hemodynamic and anatomic data as possible, in order to obtain a correct and accurate diagnosis, on the basis of which are elaborated strategies for treating congenital heart defects, valvular diseases and pericardial diseases.

In recent years, cardiac catheterization has been used less as a diagnostic method, considering that echocardiography and cardiac MRI provide enough information, but it remains the gold standard method for complex congenital cardiac diseases.

This method of diagnosis was the basis of interventional cardiology, and it involves methods of percutaneous and endovascular treatment for several cardiac diseases.

Depending on the insertion path of the probe and on the interest in the left or the right side of the heart catheterization, we may classify this investigation into [4]:

- venous or right heart catheterization, the approach of a vein brings hemodynamic data about pressures, valve gradients, the grade of pulmonary arterial hypertension and also cardiac shunts.
- arterial or left heart, the approach of an artery brings data about mitral and aortic valves gradients, the gradient in the aorta and eventually right to left shunts. It is also the approach used for performing coronarography in order to visualize the coronary arteries.
- right and left catheterization, the approach of an artery and vein simultaneously.

It is to be noted that insertion of a probe into heart chambers is performed with the following purposes: measuring hemodynamic parameters, such as pressure and oximetry (oxygen saturation of blood) in the chambers of the heart; angiography, which means injecting a contrast agent to visualize heart chambers, cardiac wall contractility, or to detect cardiac shunts; endocardial pacing and therapeutic interventional maneuvers [5].

37.3 Indications for Cardiac Catheterization

Cardiac catheterization has contributed decisively to the development of modern cardiology, both for diagnostic formulation and for percutaneous treatment methods, which have become very useful in treating congenital heart diseases at increasingly younger ages.

Initially, cardiac catheterization and angiography were methods of high accuracy in the diagnosis of congenital heart diseases, providing better understanding of complex diseases, which has led to effective treatment methods in this field.

The main objectives of catheterization and angiography are [6]:

- confirmation of clinical and echocardiographic diagnosis for some structures that are difficult to be visualized (peripheral branches of the pulmonary artery, coronary abnomalities, etc.)
- evaluation of the hemodynamic impact of the disease (quantification of valvular regurgitation,

cardiac shunts, stenotic orifice area, associated coronary abnormalities, etc.)
- assessment of biventricular dysfunction.
- assessment of postoperative consequences in some malformations, as follow-up (residual shunts, valvular insufficiencies and stenosis, stenosis of the aorta to pulmonary anastomosis or branches of the pulmonary artery).
- possibility of choosing the optimal interventional therapy, when possible.

Appropriate or acceptable indications for right heart catheterization according to cardiology and cardiac surgery societies, which try to cover current practice indications [7] (Table 37.1):

Indications of cardiac catheterization in congenital heart diseases are [6]:

Table 37.1 Indications of cardiac catheterization in cardiac pathologies

	Cardiac pathology
A. Diagnosticated or suspicious ischemic cardiomyopathy	1. Acute coronary syndrome (ACS):
	• Cardiogenic shock due to an ACS
	• ST elevation myocardial infarction (STEMI)
	• Unstable angina/non-ST elevation myocardial infarction
	• Suspicion of ACS with undiagnosed LV kinetics defect or with perfusion disorders diagnosed on recent scintigraphy
	2. Chronic ischemic heart disease without stress testing performed in patients with a high or intermediate clinical suspicion
	3. Chronic ischemic heart disease with positive results on stress testing
	4. Echocardiographic disorder of LV:
	• LV systolic dysfunction (EF below 40%), recently discovered
	• Recent segmental kinetic alteration with normal EF
	• Mechanical defects of possible ischemic etiology (mitral insufficiency or ventricular septal defect)
B. Known ischemic heart disease (history of ACS, revascularized by PCI or CABG, significant lesions on coronography)	1. Symptomatic patients receiving medicamentous treatment, having positive stress testing or accusing worsening of symptoms
	2. Revascularized patients using PCI or CABG showing worsening of symptom
C. Arrhythmias	• Patients resuscitated after cardiac arrest
	• Patients with sustained ventricular tachycardia
	• Syncope in a patient with aggregation of risk factors
	• Left bundle branch block, newly found
D. Preoperative evaluation before noncardiac surgery in stable patients	• Before transplantation
	• Before vascular surgery in patients with more than three risk factors
E. Valvulopathies	1. To determine comorbidities:
	• Preoperative coronarographic evaluation
	• Patients with severe pulmonary hypertension inconsistent with the severity of the valvulopathy
	• Patients with LV dysfunction inconsistent with the severity of the valvulopathy
	2. To assess the severity of the valvulopathy
	• The severity of the valvulopathy appreciated on imaging methods is inconsistent with clinical severity
	• Aortic stenosis of unclear severity /"low-gradient"—cardiac catheterization may be completed with dobutamine administration
	• Mitral insufficiency or acute aortic insufficiency when there is inconsistency with clinical severity

(continued)

Table 37.1 (continued)

F. Pericardial diseases	• Suspicion of cardiac tamponade
	• Suspicion of constrictive pericarditis or differentiation between restrictive cardiomyopathy and constrictive pericarditis
G. Cardiomyopathies	• Suspicion of arrhythmogenic right ventricular dysplasia
	• Known cardiomyopathy where the clinical picture has changed
H. Pulmonary hypertension (PH) or cardiac shunts	• Known or suspected cardiac shunt having unclear anatomy and flow
	• Suspicion of PH due to the increased pressure in the RV measured using a resting echocardiogram
	• Testing PH response to vasodilatator medication
	• Patient who underwent a heart transplant for myocardial biopsy
	• Evaluation of the circulating volume when other methods have unclear results

- complex congenital heart diseases.
- suspicion on echocardiography of other associated malformations.
- coronary artery anomalies.
- measuring with precision the severity of pulmonary hypertension, when applicable.
- establishing the opportunity for an interventional corrective or palliative procedure.
- for research purposes, when experimenting with new techniques or devices.

In newborns, a complete health assessment should be performed and careful risk-benefit assessment should be made as long as there are other diagnostic methods such as 2D and Doppler color echocardiography, MRI which may perform three-dimensional reconstruction of cardiac structures.

For some congenital heart diseases, is enough to make a diagnostic based on the two cited methods, unless an interventional procedure is intended.

Complex cardiac diseases require diagnostic cardiac catheterization with the recording of hemodynamic parameters and an angiography with contrast agent, which it may be or it may be not followed by an interventional procedure.

37.4 Contraindications

Cardiac catheterization and angiography have relative contraindications, imposed by the laboratory equipment and the experience of cardiac catheterization lab staff.

Table 37.2 Contraindication for cardiac catheterization

Relative contraindications for cardiac catheterization	• Severe decompensated heart failure or acute pulmonary edema
	• Acute renal failure
	• Chronic renal insufficiency with creatinine values greater than 2.5
	• Severe coagulation disorder
	• Anaphylactic reaction to iodinated contrast agents
	• Feverish condition
	• Sepsis or bacterial endocarditis
	• Malignant rhythm disorders, uncontrolled therapeutically
	• Acute stroke
	• Active digestive hemorrhage
	• Severe anemia
	• Severe comorbidities that significantly reduce lifespan

Relative contraindications refer to patients with severe diseases [8] (Table 37.2).

The only absolute contraindication of cardiac catheterization is the patient's refusal to perform the procedure [8].

37.5 Incidents and Accidents

Experience has demonstrated that the incidence of accidents during cardiac catheterization depends on: the technique used, duration of exploration, type of anesthesia, the overall condition of the patient and tolerance to the contrast agent.

37.5.1 Incidents Related to Injection of the Contrast Agent

The contrast agent may cause injuries to the lung and kidney parenchyma when injected in large quantities, in particular to newborns and children.

It is considered that the maximum dose that can be injected for an angiography is 4 mL/kg body weight in infants and 5–6 mL/kg body weight in bigger children, above which overdoses may put in danger the life of the patient. The dose of the contrast agent for adults is adjusted according to renal function and generally should not exceed 200–300 mL, when necessary, for a complex and complete diagnosis [10].

Incidents related to overdosed contrast agent are: cyanosis, bradycardia, metabolic acidosis, pulmonary hemorrhage, seizures coma and cardio-respiratory failure [11].

Adverse reactions to contrast agent can be categorized into two main groups (Table 37.3) [4, 9, 10].

These reactions may occur also to low doses of contrast agent in patients with renal failure, because there is a risk for accumulation [9].

37.6 Complications [12, 13]

See Table 37.4

37.7 Facilities and Equipment in Cardiac Catheterization Laboratory

Total space required in twenty-first century for a pediatric cardiac catheterization laboratory and the related areas is significantly higher reaching 80–100 m^2. Increased demand for space is a consequence of the dimensions of a modern biplane X-ray equipment that is equipped both with a set of angular X-ray tubes and sophisticated electronic auxiliary equipment, as well

Table 37.3 Adverse reaction to contrast agent

1. Physico-chemotoxic reactions	2. Idiosyncratic drug reactions
• Transient erythema	• Itching or rash
• Nausea or vomiting	• Maculopapular rash
• Hypotension	• Hyperhidrosis
• Headache, syncope, or even paralysis	• Conjunctival congestion
• Chills or hyperthermia	• Angioneurotic and facial edema
• Arrhythmia up to heart attack	• Respiratory disorders up to severe dyspnea

Table 37.4 Complications of cardiac catheterization

Complications at the puncture site	Complications during catheterization
– Local hemorrhage	– Arrhythmias, frequent ventricular fibrillation, ventricular or atrial extrasystoles, paroxysmal supraventricular tachycardia, temporary or permanent atrioventricular block of various degrees.
– Ecchymosis or hematoma	– Perforation of the heart and great vessels
– Infection	– Severe hypotension
– Dissection or rupture of the vessel	– Central nervous system lesions (stroke)
– Vascular thrombosis with subsequent occlusion of the vessel	– Pulmonary or systemic embolism
– Distal embolism or pulmonary thromboembolism	– Foreign body remaining in the body after rupture or knotting the catheter
– The formation of a pseudoaneurysma	– Infection up to sepsis
– Arterio- venous fistula, a direct communication between the artery and the vein due to the needle tract and then the sheath inserted in the vessel	– Allergy to the contrast agent
	– Secondary kidney failure
	– Dyspnea up to respiratory insufficiency requiring respiratory assistance
	– Death

as the increased number of complex procedures that are currently performed in these laboratories [14].

Adult laboratories require also large spaces due to the catheterization procedures that require additional voluminous equipment (such as anesthesia units, transesophageal and intracardiac ultrasounds, etc), which should be placed near the catheter table.

Catheterization room needs to be placed behind closed doors, with the exception of the control room which must be equipped with an air filter unit that maintains a positive pressure of the air circulation. At the same time, due to a permanent maintenance equipment and other adjacent units, the catheterization room is considered rather a clean space than a sterile area.

Location of catheterization room would be optimal in the immediate vicinity and with quick access to the operating blocks and intensive care.

37.7.1 Cardiac Catheterization Room

An ordinary ideal catheterization lab must be at least 4 m long and 3 m wide and the ceiling must be at least 2.5 m away from the floor to accommodate X-ray tube suspension equipment and the image intensifiers. The only fixed equipment is the catheter table and the X-ray tube suspension equipment as well as the monitors. The location of the catheterization table in the laboratory relative to the connecting routes with adjacent passage spaces, depends on the available space in close proximity to the catheterization lab [14] (Fig. 37.1).

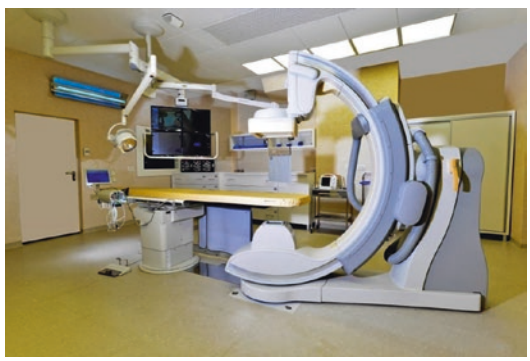

Fig. 37.1 Cardiac catheterization room in Angiolife Clinic—Bucharest

The control room for the X-ray system must be in close proximity to the catheterization room and have at least one access door to the catheterization room. The control room can be positioned at the end of the catheterization room, but operators in the control room should have a clear view of the patient on the table the catheterization.

The catheterization room should be one or two times as wide as the patient's door. Even if a patient may arrive on a narrow hospital bed, he must be able to leave the room together with supporting equipment and medical staff during the resuscitation or emergency period up to the operator block. It is important for the laboratory staff to clean up before the start of the program and even after each intervention.

37.8 Preparing the Patient in the Catheterization Laboratory Procedure Room

The patient is placed on the catheterization table and peripheral ECG is monitored. Then the skin area where the venous or artery puncture will be performed—either inguinal, subclavicular, cervical lateral or radial, as decided by the operator—is sterilized with iodine tincture.

For adults, sedation is rarely required, only when the patient is very anxious or in a poor hemodynamic state, and the procedure can be prolonged by performing an interventional maneuver (Fig. 37.2).

37.9 The Vascular Approach

Seldinger technique for catheterization of the femoral vein is used frequently, but other vascular approaches such as right internal jugular vein, umbilical vein, or transhepatic approach could be used, usually for newborns with malformations of the inferior vena cava system.

Seldinger technique consists in: puncturing the femoral vein and introducing a 0.021″ guidewire for children and a 0.035″ guidewire for adults. Into the guidewire is inserted the sheath with dilator, then the dilator is withdrawn and the guidewire and the sheath remains in place in the vessel.

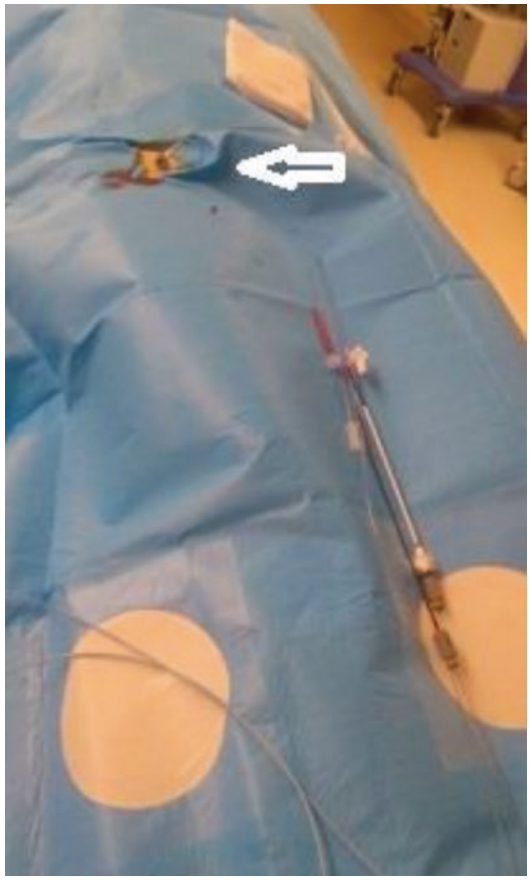

Fig. 37.2 Patient sitting on the catheterization table with venous puncture materials prepared for femoral approach. The femoral vein puncture is performed and the sheath is inserted into the right inguinal fold (arrow). On the sterile field, it can be seen a Seldinger needle, a 0.035′′ guidewire and the 5F sheath for the right femoral artery puncture

For adults, femoral vein approach is preferred for the right catheterization, and femoral or radial approaches are preferred for the left catheterization.

37.10 Cardiac Catheterization Technique

Once there is a venous or arterial access, catheter probes can be inserted to record pressures from different cavities, blood samples are taken, and angiography is performed to visualize the heart cavities and any existing shunts.

Right side of the heart catheterization is performed with several types of probe: Cournand probe, NIH probe and Swan—Ganz Catheter [15].

A few maneuvers for the insertion of the catheter into various chambers of the heart—into the right atrium, the right ventricle and the pulmonary artery—are described in Fig. 37.3.

When the approach is femoral, the probe is inserted into the heart from the inferior vena cava and there are required maneuvers aiming to insert the catheter into the superior vena cava for blood sampling and for detecting the existence of a right pulmonary vein with aberrant drainage into the superior vena cava.

From the right atrium, by pushing or by spinning, the diagnostic probe is inserted into the right ventricle and from there, by spinning, into the pulmonary artery.

These maneuvers should be performed with gentleness, especially in newborn's cord, in order not to produce severe arrhythmias in conditions of significant hypoxemia. In some cases, catheterization may be particularly difficult when there are abnormalities of the tricuspid valve implantation or significant infundibular stenosis.

Unsuspected anatomic abnormalities can be detected by an unusual catheter course—described in Fig. 37.4.

When approaching the internal jugular vein or subclavian vein, the diagnostic catheter is inserted through the superior vena cava and generally it requires fewer spinning maneuvers in order to insert the probe into the right ventricle and into the pulmonary artery. For these reasons, this approach, which may be easier, is preferred in some cases [4].

Right heart catheterization provides important hemodynamic data [6]:

- pressure in the right heart cavities guide us towards the existence of gradients in the tricuspid or pulmonary valve, as well as in the pulmonary artery branches.
- sequential gradients may be detected, such as the association of infundibular stenosis of the right ventricle with pulmonary valve stenosis.
- cardiac shunts are detected and their direction (left to right or right to left).
- existence of pulmonary hypertension and its degree.

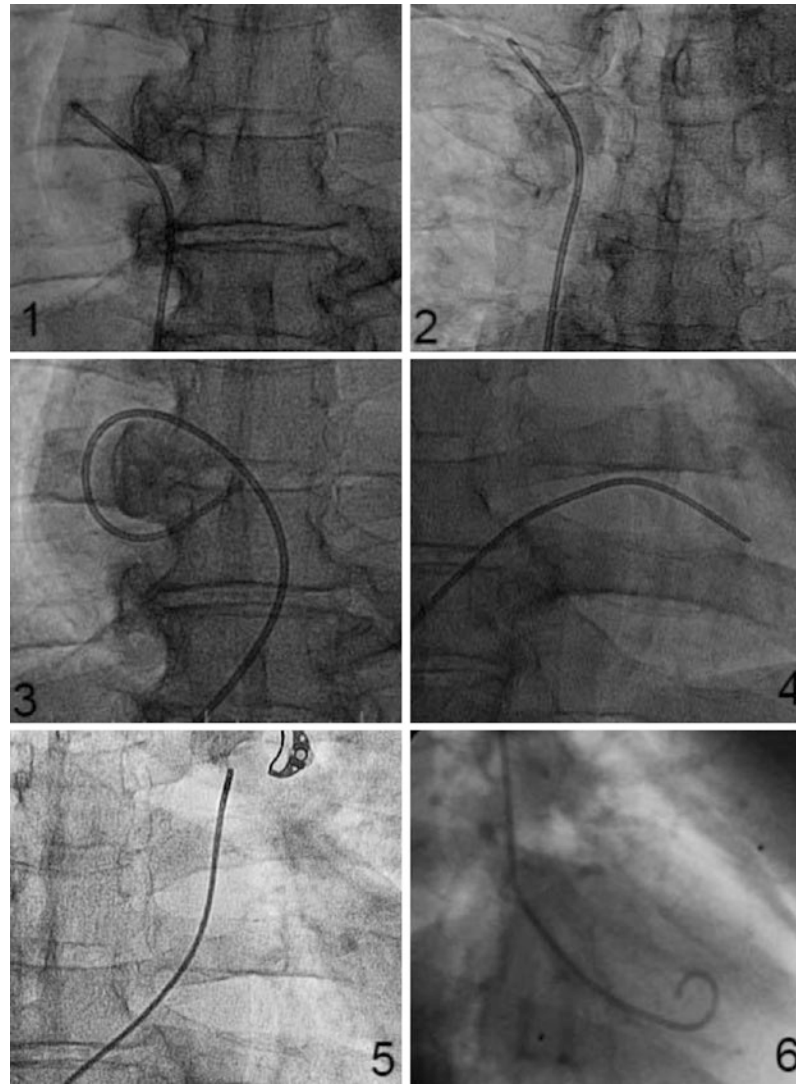

Fig. 37.3 Presentation of various maneuvers that may be performed during right heart catheterization. (1) the catheter in right atrium (RA). (2) the catheter in superior vena cava (SVC). (3) larger loop of probe in right atrium may be required to reach the tricuspid valve, maneuver useful in catheterization of a dilated right heart. (4) the probe in right ventricle (RV). (5) the catheter in pulmonary artery (PA). (6) Pigtail catheter in left ventricle (LV).

- indicate if there is a secondary right heart injury caused by overload, after an impaired left ventricular valve.

Right heart angiography provides information about the anatomy of the cavities and the pulmonary artery with its branches and it shows at what level left to right shunts exist and how significant they are angiographically [16].

Left heart catheterization has the two above-mentioned pathways as ways to approach and it is most often done by insertion of a Pigtail catheter from the femoral artery into the aorta and then into the left ventricle. Blood samples can be collected to determine if there are any right to left shunts, pressures are measured to determine aorta or aortic valve gradients (sometimes there may be sequence gradients to explain the great pressure overload of the left ventricle).

Aortography brings additional data about [6]:

- diameter of the aorta at various levels, highlighting the stenose or dilatation (very important in case of coarctation).
- aortic valve configuration (bi or tricuspid) and the mobility of the cusps.
- the existence of collateral vessels originating in the descending aorta, in the case of tetralogy of Fallot.

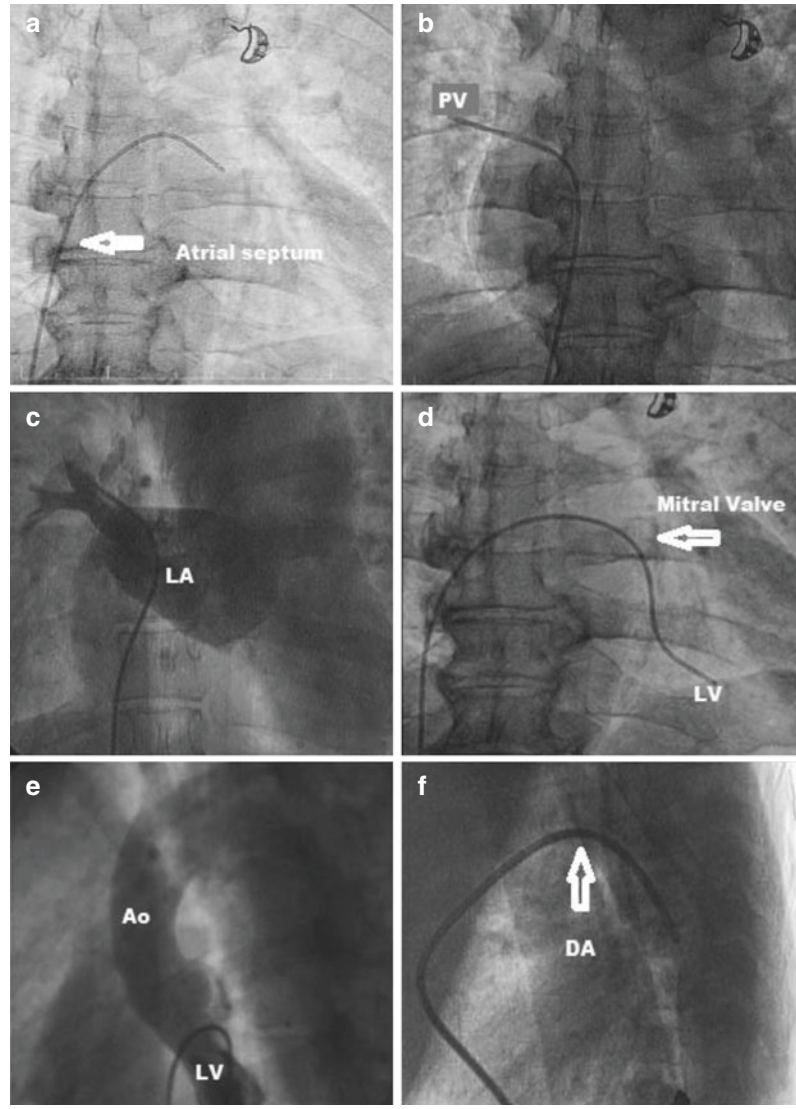

Fig. 37.4 Abnormal probe course. (**a**) the course of the catheter from right atrium (RA) passed into the left atrium (LA) (atrial septal defect). (**b**) the position of catheter is in the right pulmonary vein (PV). (**c**) injection of contrast agent in right pulmonary vein with drainage normal in left atrium (diagnosis PFO). (**d**) the course of the catheter from right atrium- left atrium and left ventricle. (**e**) contrast agent injected in left ventricle (LV) through atrial septum. (**f**) catheter crossing from the pulmonary artery (PA) to descending aorta (A0) by patent ductus arteriosus

- shows pulmonary circulation in duct dependent heart disease.
- highlights the existence of any aortopulmonary window.

37.11 Hemodynamics

Having hemodynamic data, we understand the recordings of blood pressures and oximetry from various cavities of the heart with the purpose of establishing the direction of a shunt (left to right, right to left or bidirectional), as well as its significance.

Absolute pressures are measured in mmHg, the hydrostatic point being 6 cm below the manubrium of the sternum or half the anteroposterior diameter of the chest [19].

Three types of pressure are recorded in each cavity: systolic pressure (S p), diastolic pressure (D p) and mean pressure (Mp).

Starting from the values of blood pressure, blood oximetry and oxygen consumption, the following hemodynamic data are calculated [6]:

- pulmonary and systemic blood flow.
- shunt flow (left to right, right to left).

Table 37.5 Normal values for intravascular pressure

Intravascular pressures in normal subjects (children and adults)				
Measured parameter	Symbol	Mean	S.E	S.D
Mean pressure in the right atrium	RA p	2	±1	±4
Right ventricular end-diastolic pressure	RVED p	3	±1	±5
Right ventricle systolic pressure	RVS p	20.0	±3	±10
Systolic gradient between the right ventricle and the pulmonary artery	RV/PA	3.8	±1	±3.8
Pulmonary artery systolic pressure	PAS p	20	±1	±10
Pulmonary artery diastolic pressure	PAD p	6	±1	±6
Mean pulmonary arterial pressure	PAM p	13	±1	±5
Pulmonary capillary mean pressure	PCW p	6	±4	±8
Aortic systolic pressure	AoS p	120	±30	±20
Aortic diastolic pressure	AoD p	70	±10	±20
Mean aortic pressure	Aom p	90	±10	±10
Left ventricle end-diastolic pressure	LVED p	9	±1	±7

There are no significant differences between different age groups [17]

- shunt location (atrial, ventricular, aortic-pulmonary or intrapulmonary).
- vascular resistance (total pulmonary, arteriolar pulmonary, capillary pulmonary, systemic).
- stenosis in valve area.

Normal values of pressures in the heart cavities and large vessels are listed in the table below (Table 37.5).

Pressure curves in cavities of the heart have different morphologies [4]:

- The morphology of the right atrial pressure curve may provide information about the barrier in front of the right ventricle when excessive diastolic pressure or high wave "v" which shows significant tricuspid insufficiency.
- Increased end-diastolic pressure in the right ventricle shows low compliance.
- high pressure curve with plateau in the right ventricle shows a barrier in the right ventricle ejection pathway (pulmonary valve stenosis).
- The flattened pulmonary artery pressure curve is recorded when there is a tight valvular stenosis that prevents optimal ventricular ejection.

Not all pressures in the cavities are important, but the followings should be remembered: right atrium mean pressure, systolic and end-diastolic pressure in the right ventricle, as well as systolic, diastolic and mean pulmonary artery pressures.

(A) Right atrium pressure curve. The normal right atrial pressure waveform is characterized by two positive waves, a (right atrial contraction) and, v(ventricular systole and in the same time the passive venous filling of the atrium, representing atrial diastole). The normal RA pressure waveform present three negative deflections: x, (atrial relaxation followed by atrioventricular valve closure), x, (combined effects of continued atrial relaxation and ventricular contraction).

(B) Right ventricle pressure curve. Normal is marked by a rapid rise during isovolumic contraction followed by the peak systolic pressure before isovolumetric relaxation (RVS p) and minimum diastolic pressure (RVED p) (arrow).

(C) Pulmonary artery pressure curve. The pressure wave is characterized by a relatively slow upstroke, peak systolic pressure (PAS p), a small dicrotic notch (arrow) and slow fall to end diastole (PAD p).

(D) Aortic pressure curve. It is systolic rise, peak aortic pressure (AoS p) and a variable dicrotic notch on the downstrocke (arrow) (Fig. 37.5).

When we want to know left atrial pressure and the interatrial septum is intact, we can indirectly measure it by measuring the pressure in pulmonary capillary with a free-tip diagnostic probe inserted into the pulmonary artery and pushed

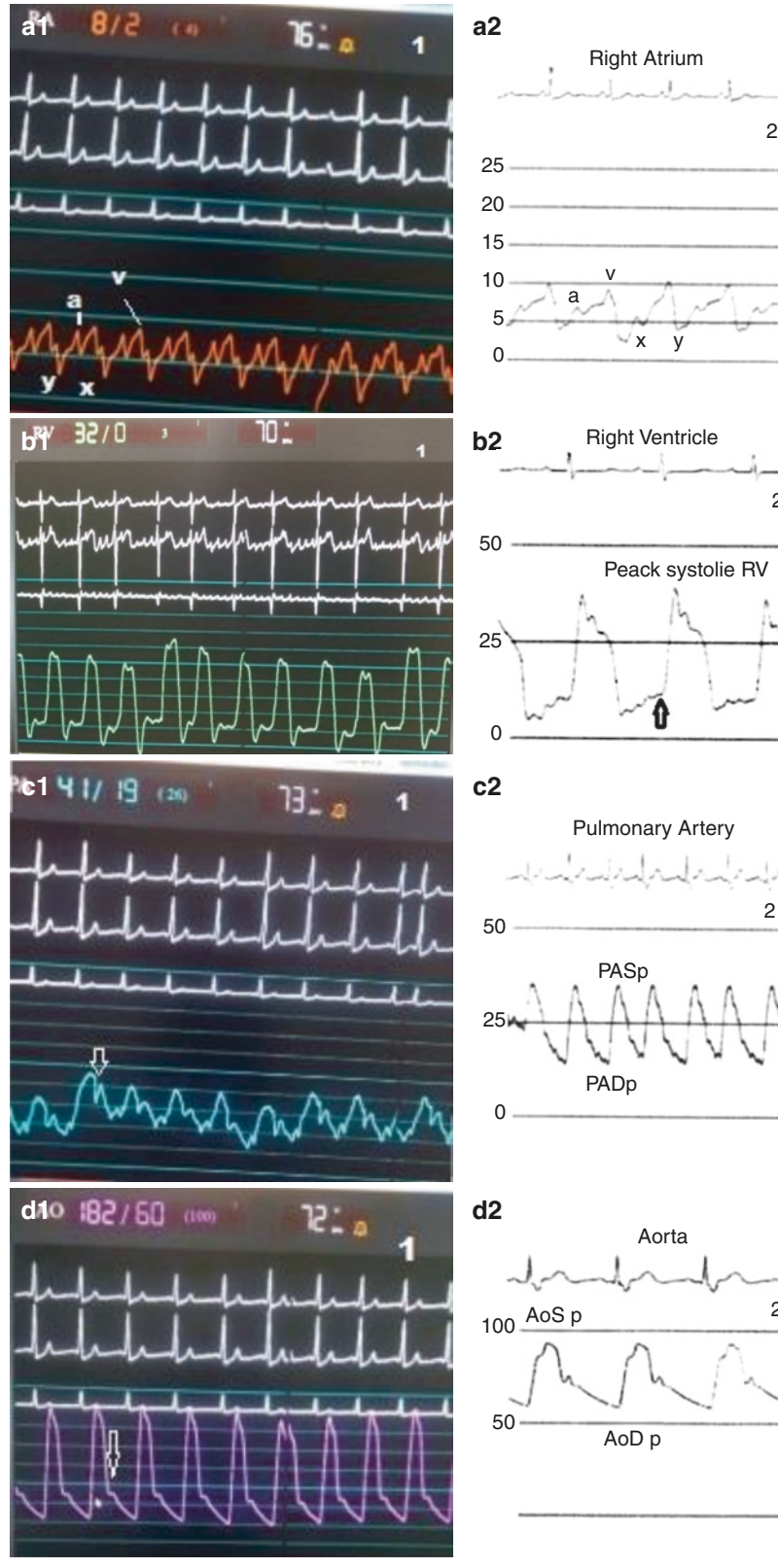

Fig. 37.5 (1) Waves of normal pressure recorded on the m.onitor in the control room within catheterization laboratory. (2). Normal pressure curves in various cavities of the heart: (**a**). Right atrium. (**b**) Right ventricle. (**c**) Pulmonary artery. (**d**) Aorta.

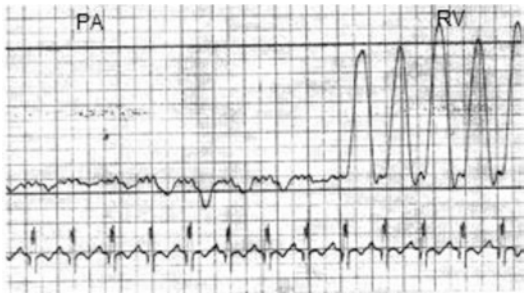

Fig. 37.6 Pull-back pressure pulmonary artery—right ventricle, pressure gradient of 180 mmHg, diagnosis of tight pulmonary valve stenosis

distally into a more peripheral branch. Pulmonary capillary pressure is also called "blocked" pressure, and its value is close to pulmonary arterial end-diastolic pressure [20].

In congenital malformations is important to measure accurately the pressures of the blood in the heart cavities in order to find: transvalvular pressure gradients or on the trajectory of some blood vessels (branches of the pulmonary artery or aorta) and insufficiencies (aortic, pulmonary, mitral or tricuspid).

Pull-back pressure from one cavity to another is important in order to determine valvular gradient, on a diagnostic probe (Fig. 37.6).

Thus, by withdrawing the catheter and by measuring the pressure, it can be determined [6]:

- pulmonary or aortic transvalvular gradients, at the level of branches of the aorta or pulmonary artery.
- the severity of stenosis, and if the gradient is high, a balloon dilation therapy is to be considered.
- location of stenosis, if it is in the valve or in the right ventricular ejection outflow tract.
- existence of seqential gradients at different levels and the severity of each one (valvular stenosis associated with infundibular stenosis).

37.12 Direct Oximetry

Measurement of the oxygen concentration in the blood collected through the diagnostic catheter can be done by chemical analysis (Van Slyke), electromechanical or photometrical in two wavelengths, red and infrared. Photometric method is the most common, because it is fast, convenient and requires small quantities of blood [4, 19, 20].

Oximetry is required to calculate the pulmonary blood flow according to Fick principle and to diagnose the shunts between the two circulations [15].

Blood samples are collected from the following cavities: inferior vena cava, superior vena cava, right atrium, right ventricle, pulmonary artery, aorta and left ventricle. The term shunt means a short circuit of the normal circuit that the blood has through different cavities of the heart.

Shunts in the heart can be divided into three major categories according to the direction that the blood flow has passing the short circuit and then, according to the level at which these shunts are located.

The three major categories are [4]:

- left to right shunt, consists in abnormal passing of a quantity of oxygenated blood from the cavities in the left side of the heart into cavities in the right side and it is marked with "y"
- right to left shunt, consists in abnormal passing of a quantity of non-oxygenated blood from the right cavities to the left ones and it is marked with "x"
- bidirectional, consists in passing of blood flow in both directions, left to right and right to left, simultaneously in a cavity and, usually, it signals a major pulmonary hypertension.

Left to right shunt leads, hemodynamically, to a volume overload with increased pulmonary blood flow in the lung. Increased pulmonary blood flow can cause, over time, an increase in pulmonary resistance consecutive with the increase in pulmonary arterial systolic pressure and the occurrence of secondary pulmonary hypertension.

Pulmonary hypertension by increased pulmonary blood flow occurs at young age when the shunt is large and located in the ventricle (large VSD) or lung (often, aortopulmonary window). Left to right shunt is detected by comparing the oximetry of the blood samples collected and, depending on the cavity where oximetry grows,

it is considered that there is an abnormal communication, as follows [6]:

- at the level of superior vena cava—partial or total anomalous pulmonary venous drainage.
- at the level of the right atrium (anomalous pulmonary venous drainage or atrial septal defect), marked with y.
- at the level of the right ventricle (ventricular septal defect)), marked with y'.
- at the level of the pulmonary artery (patent ductus arteriosus or aortopulmonary window), marked with y".

The oximetry difference between two successive cavities is significant, if it exceeds 10% for the right atrium, 7% for the right ventricle and 5% for the pulmonary artery [4].

Right to left shunt manifests by desaturation of left cavities at a certain level, systemic saturation decreasing below 93% [6]:

- at the level of the left atrium, in complex congenital maladies (tricuspid atresia, trilogy of Fallot, transposition of the great vessels with atrial septal defect) marked with x.
- at the level of the left ventricle in the outflow tract in the ventricular septal defect, marked with x'.
- at the level of the aorta (ventricular septal defect, tetralogy of Fallot) marked with x".
- at the level of the descending aorta in patent ductus arteriosus with Eisenmenger's syndrome.

It should be noted that not every child with cyanosis has a cardiac disease because there may be also peripheral cyanosis central cyanosis of noncardiac causes. In adults, peripheral arterial desaturation is often due to alveolar hypoventilation caused by increased sedation, pulmonary disease, pulmonary edema, cardiogenic shock [4, 18].

37.13 Cardiac Output

It should be measure the pulmonary blood flow (Q p), systemic blood flow (Q s) and eventually right to left shunt flow (Q x) or left to right shunt flow (Q y).

The most accurate method to determine cardiac output is based on the principle of Fick [19, 20]:

$$Q = \frac{Vo_2}{Co_2A - Co_2V}$$

where the numerator is the oxygen consumption, and the denominator the arteriovenous difference in blood oxygen which comes in and out of the body.

In patients without cardiac shunts, the pulmonary flow is equal to the aortic flow.

Determining shunts at different levels is based on a well-determined algorithm [19]:

1. Determine mixed venous saturation:

$$\text{Mixed venous saturation} = \frac{3(\text{SVC}) + (\text{IVC})}{4}$$

2. Calculated pulmonary blood flow (Q p):

$$Qp = \frac{\text{O2 consumption} \times \text{BSA}}{(\text{PV sat} - \text{PA sat})(\text{Hgb})(13{,}6)}$$

3. Calculate systemic blood flow (Q s):

$$Qs = \frac{\text{O2 consumption} \times \text{BSA}}{(\text{Ao sat} - \text{MV sat})(\text{Hgb})(13{,}6)}$$

4. Calculate shunt flow:

$$\text{Shut flow} = Qp - Qs$$

$$\text{Shut ratio} = Qp / Qs$$

Hemoglobin = Hgb
Superior vena cava = SCV
Inferior vena cava = ICV
Body surface area = BSA
Pulmonary vein = PV
Pulmonary artery = PA
Aorta = Ao

Simplified formula for determination of shunt ratio is [19, 20]:

$$\frac{\mathrm{Qp}}{\mathrm{Qs}} = \frac{(\mathrm{Aosat} - \mathrm{MVsat})}{(\mathrm{PVsat} - \mathrm{PAsat})}$$

In patients with left to right shunt, pulmonary flow is greater than systemic flow, because of systemic passage of oxygenated blood from the left cavities into the right ones [19].

$$\mathrm{Qp} = \mathrm{Qs} + \text{left-to-right shut flow}$$

In patients with right to left shunt, pulmonary flow is lower than systemic flow, because of the volume load of systemic blood flow with non-oxygenated blood [19].

$$\mathrm{Qs} = \mathrm{Qp} + \text{right-to-left shut flow}$$

After determining the hemodynamic significance of cardiac shunts, it can be established the therapeutic conduit, because trivial shunts without hemodynamic significance will not be closed either surgically or interventionally [6].

37.14 Vascular Resistance

The force of friction that the vascular wall opposes the passage of blood flow is called vascular resistance. It is determined by several factors: laminar or turbulent blood flow regimes, the elasticity of the great arteries, systolic blood pressure growth rate, but the most important factor remains friction between the blood and the walls of the vessels, friction that is directly proportional to the degree of narrowing of the vascular lumen [16].

The most important level, in terms of resistance, has the arteriole that has a much smaller diameter than the elastic arteries. The greatest variation in vascular resistance happen at arteriolar level, because of its ability to change the lumen depending on vasomotricity [4].

The hemodynamic formula that relates resistance (R) with cardiac output (Q) and pressure (P) is: [6].

$$R = \frac{P}{Q}$$

formula: [19].

$$R(din \cdot s \cdot cm^{-5}) = \frac{P\left(mmHg\right)}{Q\left(mls^{-1}\right)} \cdot 1332$$

where 1332 is the factor for converting.

Considering that, normally, the vascular resistance increase and decrease in order to counterbalance variations of blood flow, increases in resistance may be physiological or pathological due to increased pulmonary flow.

In practice, the most important pulmonary resistances are: total systemic resistance (SVR), total pulmonary resistance (PVR), pulmonary arterial resistance (PAR) and capillary resistance (PCWR).

Their calculation formulas are listed below: [4, 19].

$$SVR(din \cdot s \cdot cm^{-5}) = \frac{mean\ Aop\left(mmHg\right)}{QAo\left(mls^{-1}\right)} \cdot 1332$$

$$PVR(din \cdot s \cdot cm^{-5}) = \frac{mean\ PAp\left(mmHg\right)}{QPA\left(mls^{-1}\right)} \cdot 1332$$

$$PAR(din \cdot s \cdot cm^{-5}) = \frac{mean\ PAp - PCWp\left(mmHg\right)}{QPA\left(mls^{-1}\right)} \cdot 1332$$

$$PCWR(din \cdot s \cdot cm^{-5}) = \frac{mean\ PCWp\left(mmHg\right)}{QPA\left(mls^{-1}\right)} \cdot 1332$$

Normal values are: SVR 700–1500 $din \cdot s \cdot cm^{-5}$ and PAR < 2.5 Wood unit.

1 Wood unit = 80 $din \cdot s \cdot cm^{-5}$.

From the pulmonary resistance values, we can see the hemodynamic resonance that an increased pulmonary flow has on the vascular bed.

Pulmonary hypertension with increased flow is often a minor hypertension since pulmonary vascular bed adapts to the increased flow by dilating itself (decrease of resistance) [6].

Quantification of pulmonary hypertension is important for subsequent therapeutic conduit [16].

(a) Normal values <4 WU.
(b) Moderate PH 5–7 WU.
(c) Severe PH > 8 WU. Where WU is Wood units.

Any surgical or interventional maneuver in congenital heart disease is performed up to 8 WU, over this value corrective treatment is contraindicated [18].

37.15 Angiography

Angiography represents the injection of a contrast agent into a heart cavity in order to visualize the anatomy and blood flow in the heart cavities, it highlights cardiac shunts and their hemodynamic significance.

If a contrast agent is injected into the right ventricle, the pulmonary artery is visualized, but the left-side of the heart cavities can also be seen on the left angiography (especially useful for newborns, where it cannot be injected a large amount of contrast media). When performing angiography, iodine-based contrast agent is used, more commonly ionic and hyperosmolar preparations that may have side effects: allergic reactions, renal toxicity, bradycardia and myocardial depression.

Non-ionic and iso-osmolar contrast agents are used today in current practice, thus reducing the risk of side effects [16].

There are some standard angiographic projections that can visualize better the anatomical structures of the heart, that provide data for a correct diagnosis of complex congenital heart diseases.

Right ventricle and pulmonary artery can be visualized from postero-anterior (PA) projections, and the trunk and the branches of the pulmonary artery from left anterior oblique (LAO) view with Cranial projection. LAO 60° projection is frequently used to visualize ventricular septum, thus interatrial and interventricular septs run making possible to highlight shunts at these levels.

These angles of the image intensifier are most often used to highlight the heart structures and shunts, but sometimes they are not useful in special situations such as dextrocardia and mesocardia. In these situations, non-standard angles will be used to give a better image of the cavities and septs in order to highlight the shunts [6].

Angiography determines cardiac shunts and their size (Figs. 37.7, 37.8, 37.9 and 37.10).

Cardiac catheterization and angiography represents a very useful diagnostic tool in the diagnosis of congenital heart defects and, in the last years, an efficient method of treatment by interventional maneuvers.

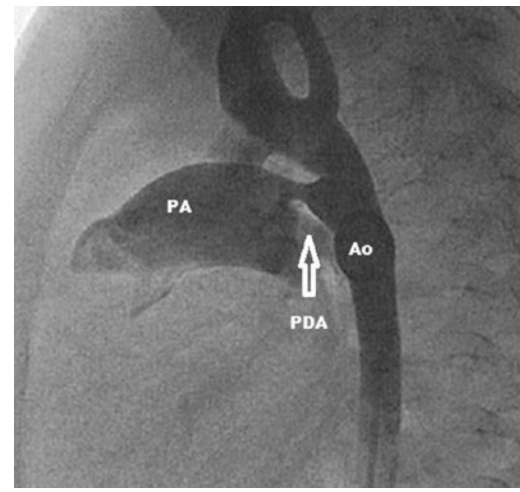

Fig. 37.7 Aortic angiography highlighting patent ductus arteriosus and loading of the pulmonary arterial trunk

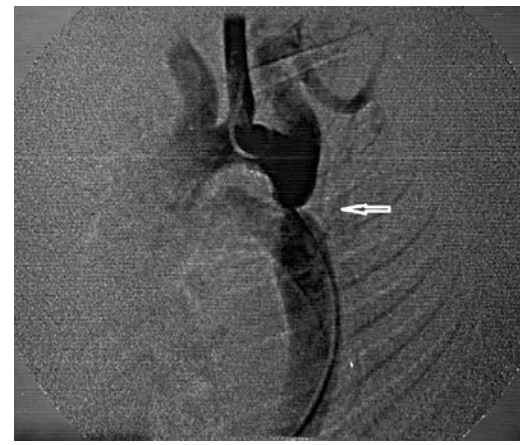

Fig. 37.8 Aortography that highlights tight diaphragmatic coarctation of the aortic isthmus (arrow)

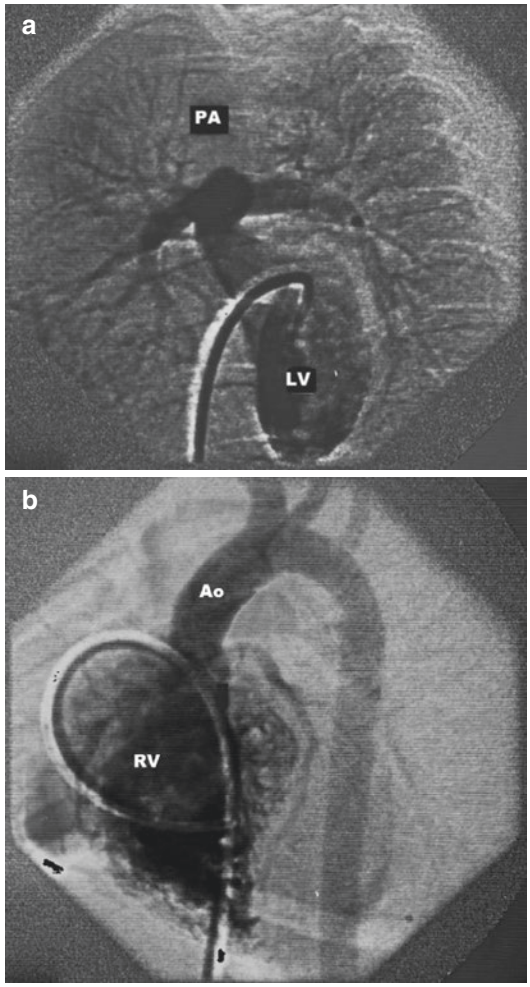

Fig. 37.9 (**a**) Injection into the left ventricle shows the pulmonary artery. (**b**) Injection into the right ventricle shows the aorta. Based on angiography, transposition of the great vessels may be diagnosed

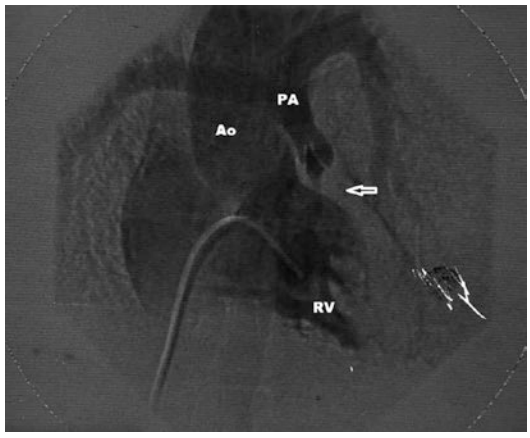

Fig. 37.10 Tetralogy of Fallot. Injection the contrast media in right ventricle with simultaneous visualization of pulmonary artery and aorta. It is very tight stenosis of the outflow tract of right ventricle (arrow)

References

1. Eeckhout E, Serruys PW, Wijns W, Vahanian A, van Sambeek M, de Palma R. Percutaneous interventional cardiovascular medicine. The PCR-EAPCI textbook, vol. l. Toulouse: Europa edition; 2012. ISBN 978-2-913628-62-5.
2. Mueller RL, Sanborn TA. The history of interventional cardiology: cardiac catheterization, angioplasty and related interventions. Am Heart J. 1995;129:146–72.
3. Nossaman BD, Scruggs BA, Nossaman VE, Murthy SN, Kadowitz PJ. History of right heart catheterization: 100 years of experimentation and methodology development. Cardiol Rev. 2010;18(2):94–101.
4. Carp C. Treaty of cardiology, vol. 1. Bucharest: Medical ed; 2002. p. 412–75. ISBN 973-8194-65-2.
5. Pinte F. Interventional treatment of congenital heart diseases in children, Modern Medicine no. 5; 1997.
6. Socoteanu I. Treaty of congenital heart diseases, vol. 1. Bucharest: Romanian Academy ed; 2010. p. 441–56. ISBN 978-973-27-1796-7.
7. Patel MR, Bailey SR, Bonow RO, et al. ACCF/SCAI/AATS/AHA/ASE/ASNC/HFSA/HRS/SCCM/SCCT/SCMR/STS 2012 appropriate use criteria for diagnostic catheterization. J Am Coll Cardiol. 2012;59(22):1995–2027.
8. Aviles RJ, Messerli AW, Askari AT, Penn MS, Topol EJ. Introductory guide to cardiac catheterization. Philadelphia: Lippincott Williams & Wilkins; 2004. ISBN 978-0-7817-5202-2.
9. Paun R. Treaty of internal medicine, Vol. 1, Part 1, Cardiovascular diseases, Medical ed; 1989. ISBN 973-39-0212-8.
10. Singh J, Daftary A. Iodinated contrast media and their adverse reactions. J Nucl Med Technol. 2008;36:69–74.
11. Tepel M, Aspelin P, Lameire N. Contrast-induced nephropathy: a clinical and evidence-based approach. Circulation. 2006;113:1799–806.
12. Davidson CJ, Bonow RO. Cardiac catheterization. In: Mann DL, Zipes DP, Libby P, Bonow RO, Braunwald E, editors. Braunwald s heart disease. A textbook of cardiovascular medicine. 10th ed. Philadelphia: Elsevier; 2015. p. 364–85. ISBN 976-1-4557-5133-4.
13. Hanna BE, Glancy DL. Practical cardiovascular hemodynamics. New York: Demos Medical; 2013. ISBN 978-1-936287-8.
14. Mullins CE. Cardiac catheterization in congenital heart disease. Oxford: Blackwell Futura; 2006. p. 1–25. 272-350, ISBN 978-1-4051-2200-9.
15. Grossman W. Cardiac catheterization, angiography and intervention. Philadelphia: Lippincott Williams & Wilkins; 2000. p. 75–8. ISBN 0-683-30741-X.
16. Apetrei E. Clinical cardiology, Callistro ed; 2015. p. 227–241. ISBN 978-606-8043-18-0.
17. Keith JD, Rowe RD, Vlad P. Heart disease in infancy and childhood. New York: The Med. Mil. Comp; 1988.
18. Hoffman JIE. Congenital heart disease. Ped Clin North Am. 1990;37: 45.
19. Ragosta M. Textbook of clinical hemodynamics Saunders Eselvier ed; 2008. p. 16–37, ISBN 978-1-4160-4000-2.
20. Bergersen L, Foerster S, Marshall A, Meadows J. Congenital heart disease the catheterization manual. Berlin: Springer; 2009. ISBN 978-0-387-77291-2.

3D Printing As a New Technique in Management of Right Heart Pathology

38

Zhonghua Sun

Abstract

Three-dimensional (3D) printing has shown great promise in recent years, with increasing applications in medicine. 3D printing in cardiovascular disease is another potential field with cardiovascular applications comprising the use of patient-specific 3D printed models for diagnosis, medical education and training, pre-surgical planning and simulation of complex interventional cardiovascular procedures. This chapter provides an overview of the usefulness of 3D printed models in cardiovascular disease with a focus on the applications in right heart diseases.

Keywords

Application · Cardiovascular disease · Education · Model · Simulation · Three-dimensional printing

38.1 Introduction

Three-dimensional (3D) printing technology was introduced in late 1980s [1], and the technique has grown rapidly over the last few years to include many applications in medicine with use of different manufacturing technologies. Several 3D printing technologies are used for printing 3D physical models in medicine, including stereolithography apparatus, fused deposition modelling, laminated object manufacturing, electron beam melting, selective laser melting or sintering and polyjet technology [1–4]. Of these technologies, stereolithography apparatus is the most widely used 3D technique in medicine, in particular in surgery due to its greatest accuracy and best surface finish for any 3D printing technology [4]. The 3D printed model with use of this technique is robust and relatively light [5, 6]. Polyjet is another technique that is commonly used in 3D printing of anatomy models as it is capable of producing highly complex models such as complicated cardiac anatomy with smooth surfaces and very thin layer (resolution up to 0.016 mm) [7]. This technique is also able to manufacture flexible, patient-specific models with different materials to replicate complex anatomical structures with high accuracy. Table 38.1 summarizes the 3D printers and materials that are currently available in medical field for 3D printing [8].

Due to complexity of cardiac anatomy and pathology, it is important to have advanced pre- and peri-procedural imaging tools to fully appreciate the complicated cardiovascular conditions by cardiologists or cardiac surgeons. Currently, 3D imaging datasets acquired with 3D echocardiography, cardiac computed tomography (CT)

Z. Sun
Department of Medical Radiation Sciences, Curtin University, Perth, WA, Australia
e-mail: z.sun@curtin.edu.au

S. I. Dumitrescu et al. (eds.), *Right Heart Pathology*, https://doi.org/10.1007/978-3-319-73764-5_38

Table 38.1 Overview of 3D printing techniques and medical applications

Techniques	Materials	Advantages	Limitations
Stereolithography	Photopolymers	High detail and precision, smooth surfaces	Moderate strength, high cost
Selective Laster sintering	Polymers, metals	High accuracy, good strength	High cost, powdery surface
Fused deposition Modeling	Thermoplastic materials or eutectic metals	Low cost, good strength	Low speed
Laminated object manufacturing	Layers of paper or plastic films	Low cost, material stock easy to obtain	High material waste, slower printing
Inkjet printing techniques (such as ZPrinter 450, PolyJet and PolyJet matrix)	Fine powers such as plaster or starch	Low cost, high speed, multiple materials	Moderate strength, fail to mimic true tissue properties

and magnetic resonance imaging (MRI) display the images on a two-dimensional (2D) flat screen which do not reflect the actual cardiac structures [9, 10]. Further, these images lack of providing precise information on structural depth of cardiac anatomy and pathology. To overcome these limitations, 3D printed-physical models have been proven to be effective in demonstrating patient's anatomy, simulating of surgical or interventional cardiac procedures and planning of highly complex procedures [11–14]. This chapter provides an overview of 3D printed models in cardiovascular disease, with a focus on the applications in right heart diseases.

38.2 Image Data Segmentation

The first step to create a patient-specific 3D printed model is to acquire high resolution images. An imaging dataset suitable for 3D printing must be isotropic of high spatial resolution (ideally slice thickness less than 1 mm). The 2D images are reconstructed into 3D volume rendering datasets which undergo the process of image processing, called segmentation in Digital Imaging and Communications in Medicine (DICOM) format. The purpose of segmentation is to separate cardiac structures of interest including pathologies from surrounding irrelevant structures such as bones, lungs or soft tissues. The use of contrast medium in cardiac CT and MRI imaging enables images to be displayed as high attenuation or high signal intensity which allows for differentiation of intracardiac or intravascular structures from the low intensities of adjacent tissues or structures [10, 11]. Further image processing of 3D volume data requires semi-automatic or manual process to improve the quality of the segmented images. In most of the cases, manual editing is necessary to confirm that all structures are delineated and the created geometry represents the true cardiac anatomy accurately.

When segmentation is complete, the digital model is saved as another standard called Standard Tessellation Language (STL) for 3D printing purpose because DICOM image file cannot be used by 3D printers. The STL file also undergoes some further postprocessing to fix some small 'openings' resulting from the conversion from DICOM to STL format. This process is performed to remove some particular structures or eliminate small 'opens' or 'openings' with the aim of demonstrating anatomy or pathology clearly [10, 15].

There are several commercial software platforms and some open-source freeware packages available to perform the above steps including image processing and segmentation. The most commonly used commercial software is the Mimics Innovation Suite (Materialise, Leuven, Belgium) which includes a comprehensive set of segmentation and computer-aided design tools, while Osirix (Pixmeo, Geneva, Switzerland) offers free software for these steps [10, 16–19]. Analyze 12.0 (AnalyzeDirect, Inc., Lexana, KS, USA) is another commercial biomedical software which provides a variety of functions for image processing and segmentation [20–24]. Figure 38.1 shows the steps of image processing, segmenta-

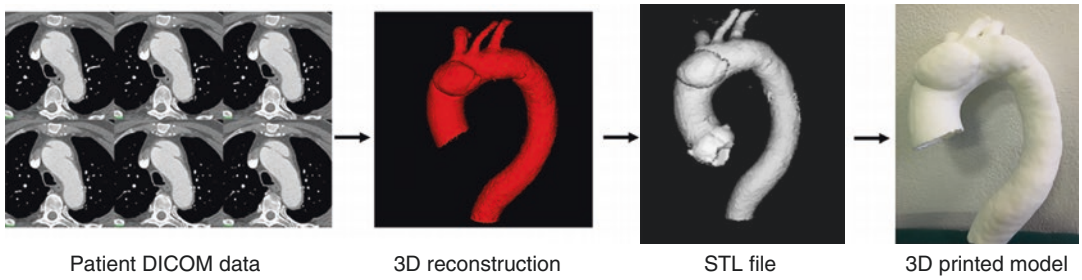

Fig. 38.1 Flow diagram shows the progress from original DICOM CT data to a 3D depiction of the aorta and aortic aneurysm, generation of STL file for 3D printing. Reprint under the terms of open access article from Ho D, Squelch A, Sun Z. Modelling of aortic aneurysm and aortic dissection through 3D printing. J Med Radiat Sci. 2017;64:10–17 [21]

tion and conversion to STL file in a sample cardiac CT dataset using Analyze 12.0.

38.3 3D Printed Models in Replicating Normal Cardiac Anatomy and Pathology

Patient-specific 3D printed models have been shown to accurately replicate complex cardiovascular anatomy and pathology, with excellent agreement or correlation having been reported in the literature [14, 20, 25–30]. This is demonstrated by correlating 3D printed models with echocardiographic, CT or MRI images in the diagnostic assessment of aortic disease, congenital heart disease and valvular diseases.

3D printed models based on 3D echocardiographic images are also feasible in demonstrating congenital heart disease with high accuracy [26–28]. In their early report, Binder et al. produced 3D models using 3D transesophageal echocardiographic datasets in 13 patients with mitral valve and other cardiac disease [26]. All 3D printed models accurately depicted mitral valve anatomy and pathology, with disease extent, morphology and location correlated to intraoperative findings reported by the surgeon. This is confirmed by Olivieri et al. in their study who generated 3D printed models based on 3D echocardiographic images from nine patients with congenital heart diseases (eight with ventricular septal defects and one with perivalvar leaks) [27]. Long- and short-axis measurements of these diseases were performed and compared between 2D echocardiographic images and 3D models, with high correlation noticed between the two groups (Pearson correlation coefficient of 0.988), and the mean error for each measurement was less than 1 mm, indicating high accuracy of 3D printed models.

Most of the 3D printed models are generated using high-resolution CT datasets with replication of cardiac anatomy and pathology (Figs. 38.2 and 38.3). A recent study has shown high accuracy in the measurements of aortic aneurysm and aortic dissection between 3D printed models and original CT images [20]. In addition to depicting the location of aneurysm in the aortic arch, aortic dissection, especially the intimal flap separating the true lumen from false lumen is also visualized on 3D printed models as shown in Fig. 38.4. With measurements taken at six anatomical sites of the ascending and descending aorta, 3D printed models were found to accurately replicate these anatomical structures with differences of less than 0.8 mm when compared to those measured on original CT angiographic images [20]. Other studies have demonstrated the usefulness of 3D printed models in aortic roots and implanted aortic valves [29, 31]. Ripley et al. produced 3D printed models of aortic valves based on CT data from 16 patients with nine having paravalvular aortic regurgitation and seven normal cases as the control group [31]. There was excellent agreement between 3D models and 2D CT data for annulus measurements, with mean difference less than 0.4 mm (95% limits of agreement ±1.3 mm)

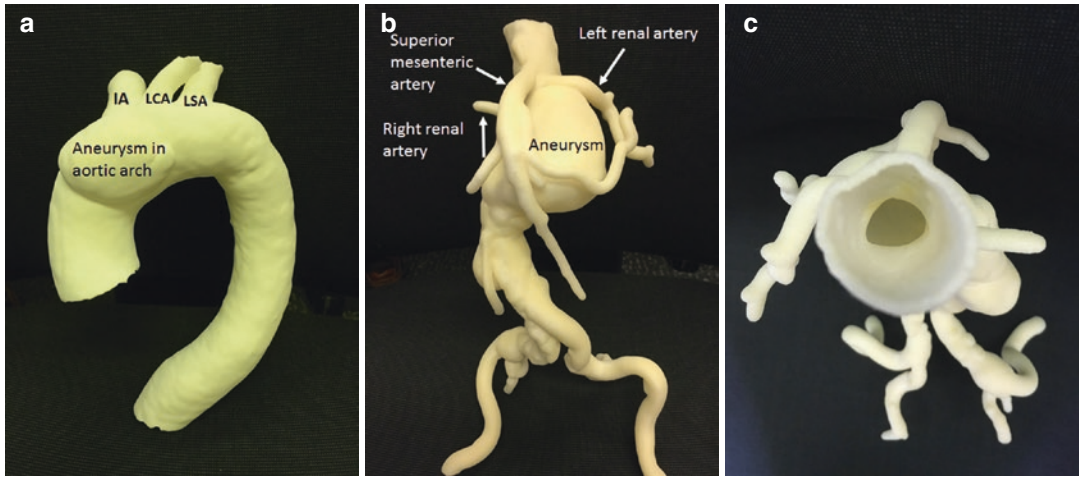

Fig. 38.2 3D printed models of aortic aneurysms. (**a**): 3D printed patient-specific model shows an aneurysm involving the ascending aorta and aortic arch. (**b**): Anterior view of a 3D printed model with an abdominal aortic aneurysm. (**c**): Superior view of the same 3D printed model as shown in (**b**) showing the hollow structure of the abdominal aorta. *IA* innominate artery, *LCA* left common carotid artery, *LSA* left subclavian artery

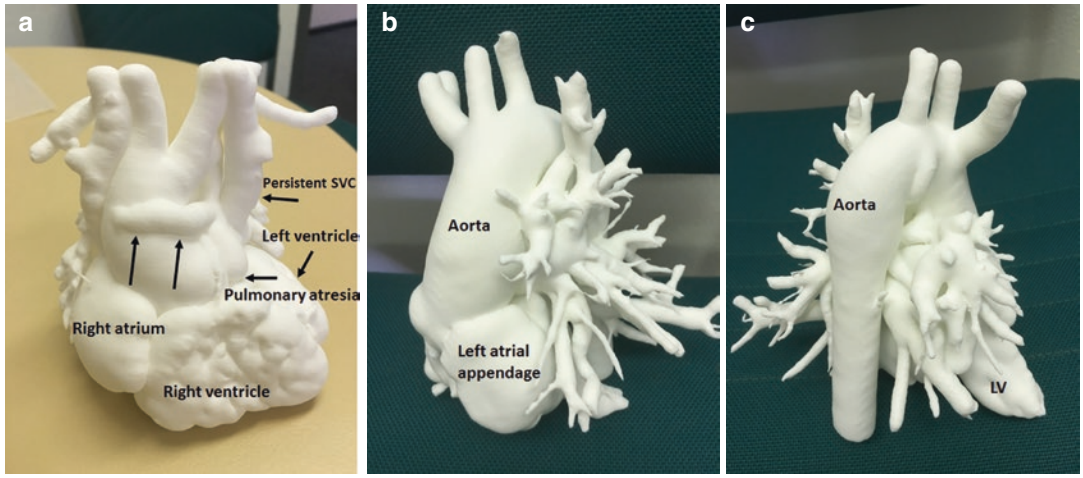

Fig. 38.3 3D printed models of congenital heart disease. (**a**): 3D printed model of a 3-year-old boy with congenital heart disease showing pulmonary atresia with ventricular septal defect. An artificial artery is noticed to attach to the anterior wall of ascending aorta (long arrows) following Blalock-Taussig (BT) shunt. (**b** and **c**) (anterior and posterior views): 3D printed model of an 8-year-old boy with congenital heart disease consisting of dextrocardia, pulmonary atresia and malposition of aorta. *LV* left ventricle, *SVA* superior vena cava

(Fig. 38.5). 3D printed models of valve prostheses were also found to be highly accurate with measured dimensions within 0.1 mm.

3D printed models based on MRI imaging datasets also showed high accuracy. Schievano and colleagues reported their experience of using MRI data to create 3D printed models [32]. Twelve patients' MR images were analysed and segmented to construct 3D models representing anatomical details and pathological changes. Excellent correlation was found between 3D printed models and 3D MR images in the measurement of narrowest dimensions of right ventricular outflow tract ($r = 0.97$, $p < 0.01$). Other case reports also confirmed the accuracy of 3D printed models based on MRI data to replicate complex cardiac anatomy and pathology [33–37].

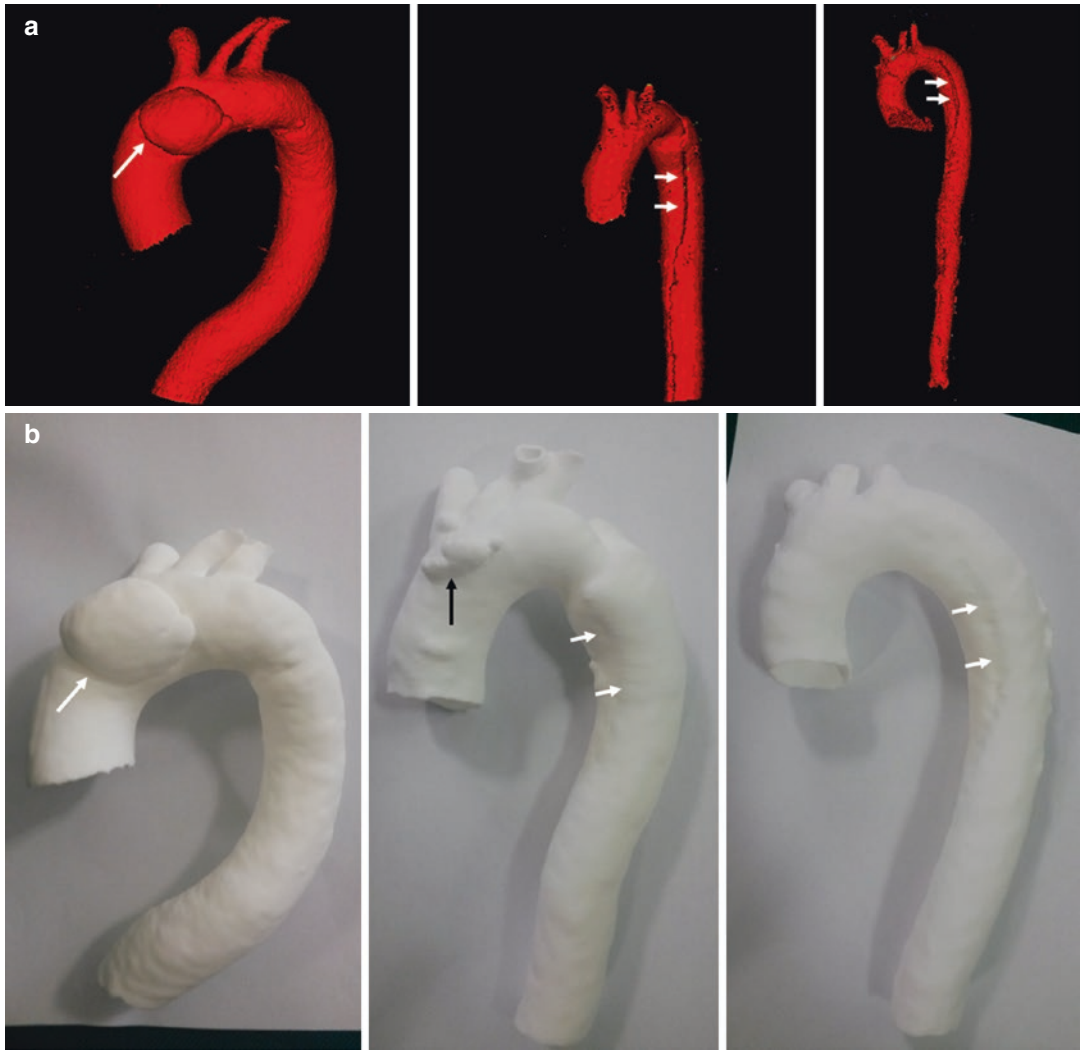

Fig. 38.4 3D printed patient-specific models of aortic aneurysm and aortic dissection. (**a**): 3D segmented reconstructions of aortic aneurysm (first image), and Stanford type B aortic dissection (second and third images) based on CT angiographic images. (**b**): 3D printed models of aortic aneurysm and aortic dissection. White long arrow refers to the aortic aneurysm in the first model, and short arrows indicate the intimal flap separating the true lumen from the false lumen in the second and third models with aortic dissection. Black long arrow indicates the artefact in the second model

38.4 3D Printed Models in Pre-procedural Planning

Due to difficulty in fully understanding complex cardiac anatomy and pathology, 3D printing may overcome the limitations of 2D or 3D image visualizations and play an important role in providing a comprehensive assessment of various cardiovascular diseases. Integration of 3D printed models into pre-operative planning increases efficiency of surgical interventions by decreasing operating time, reducing radiation exposure to patients during operative procedure, and assisting decision making in managing cardiovascular disease by selecting the appropriate device size and type for a specific patient, achieving better outcome with reduced complications.

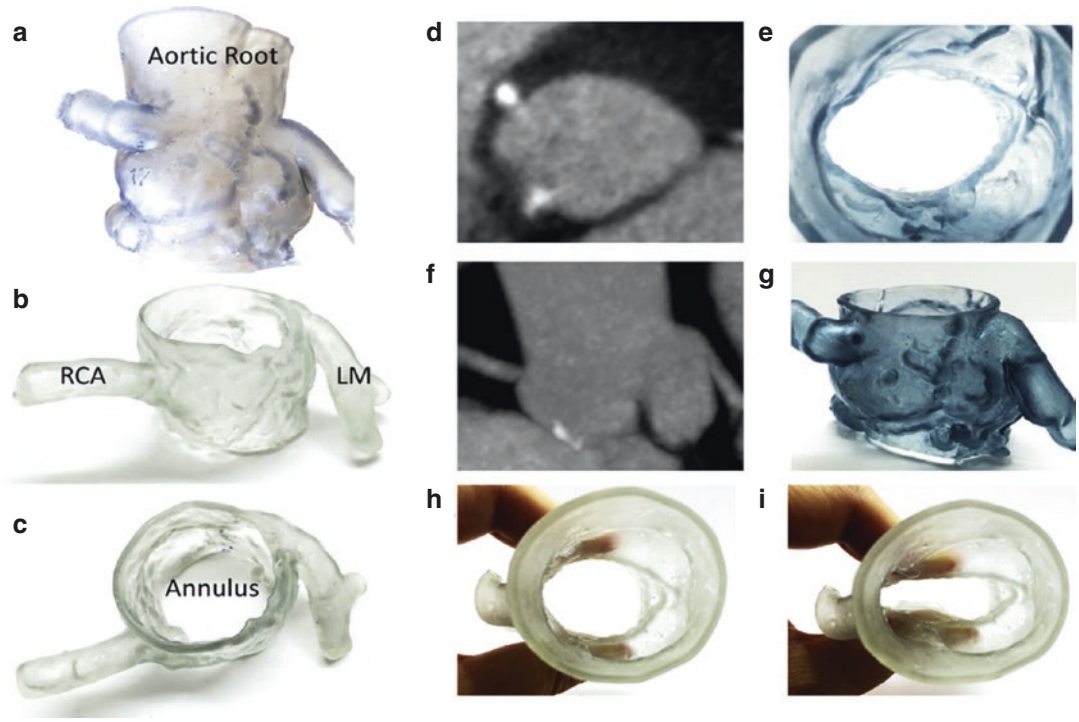

Fig. 38.5 3D printed models of the aortic root accurately depict morphology. (**a**–**c**): 3D printed aortic valve complexes from two different patients demonstrating anatomy included in the models. *RCA* right coronary artery, *LM* left main artery. (**d**–**e**): 3D printed model from an individual patient (**e**) reproduces the geometry of the annulus as seen on CT (**d**). (**f**–**g**): 3D printed model from another patient (**g**) reproduces the geometry of the sinuses of Valsalva and coronary artery take-offs as seen on CT (**f**). (**h**–**i**): 3D models were printed in flexible material to mimic the elastic properties of the aorta. Reprint with permission from Ripley B, Kelil T, Cheezum MK, et al. 3D printing based on cardiac CT assists anatomic visualization prior to transcatheter aortic valve replacement. J Cardiovasc Comput Tomor. 2016;10:28–36 [29]

With 3D printed physical models used in the operating room, complex cardiac structures were simplified by direct comparison between 3D printed models and the living heart, as reported by Mottl-Link et al. [38]. Their experience showed that the exact position of the pathologies such as ventricular septal defect could be localized accurately with physical models demonstrating views that could not be intraoperatively obtained. Further, virtual cuts could be performed on the physical models, thus assisting planning of the surgical approach or simulating interventional procedures. Ryan et al. reported the use of 3D printed model in a 1-day age of patient with congenital heart disease [39]. The model was shown to improve planning and guide placement of a central aortopulmonary shunt, with simulation of stent deployment in the printed models. The amount of fluoroscopy time could be reduced, hence reducing radiation exposure. 3D printed models also clearly depicted other pathologies involving the aortic arch or pulmonary vessels [37, 40].

Schmauss et al. presented their single centre experience in eight representative cases, showing the feasibility of using 3D printed models in preoperative planning and simulation [33]. 3D printing has proven value in both adult and pediatric patients for preoperative planning of a variety of complex cardiac diseases. Other case studies also reported that the 3D printed models were useful for planning surgical and transcatheter interventions through clear illustration of pathologies and facilitation of the simulation [30, 34, 35, 41, 42].

Schievano et al. evaluated 12 patients with pulmonary valve diseases for deciding the suitability of receiving percutaneous pulmonary valve implantation (PPVI) through comparison of 3D printed models with MR images [32]. Their results showed that patient selection for PPVI was more accurate with use of 3D physical models than with MR images alone. Two observers were involved in determining the suitability of patients for PPVI and their accuracy was found to be increased to 75% and 75%, respectively, with use of 3D printed models, however, the accuracy for both observers was only 50% when MR images were used for assessment. This highlights the increased certainty by 3D printed models in clinical decision making when compared to conventional MR findings alone.

Patient-specific 3D printed models have been found to play a role in pre-procedural planning of interventional procedures, such as development of the occluder device sizing for treatment of atrial septal defect (ASD) or ventricular septal defect (VSD) to ensure successful management of these congenital heart diseases (Fig. 38.6), and implantation of endovascular stent grafting (Fig. 38.7) [11, 43, 44]. Others reported the positive impact of 3D printed models on surgical management of cardiac tumors [45, 46].

38.5 3D Printed Models in Pre-surgical Simulation

3D printing serves as a valuable tool for pre-surgical simulation of cardiovascular and cerebrovascular diseases [14]. 3D printing has been reported to be advantageous over conventional approach based on image visualizations on computer screen in the simulation of surgical and interventional procedures of cerebral aneurysms [47–49]. Sodian et al. in their case report demonstrated the feasibility of simulating interventional procedure in an adult patient with replacement of aortic arch due to type A dissection, but developed pseudoaneurysm in the aortic arch [30]. They tested surgical customized implants on the 3D printed model with improvement of the surgeon's or interventionalist's understanding of complex cardiac anatomy and pathology, and assisted development of the optimal interventional approach to reduce complications that may arise. Simulation of the stenting interventional procedures is proven to be feasible in another study with hypoplastic aortic arch in a 15-year-old boy [37]. 3D printed models were found to be extremely helpful in pre-procedural planning of catheterization intervention, in particular,

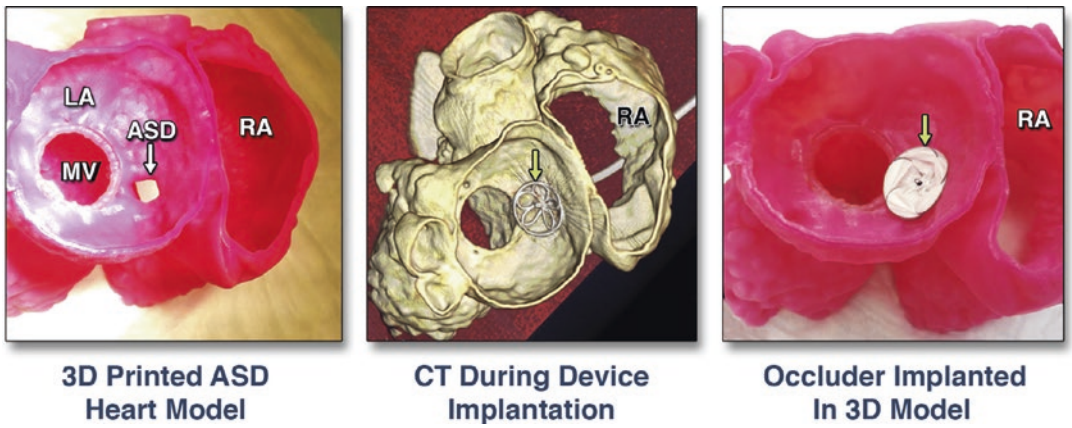

Fig. 38.6 3D-printed model of an atrial septal defect (ASD) imaged by CT (left). 3D-printed model with bench-top implanted septal occluder device (yellow arrows) (middle). CT scan of septal occluder implantation within the 3D-printed model. *LA* left atrium, *MV* mitral valve, *RA* right atrium. Reprint with permission from Vukicevic M, Mosadegh B, Min JK, Little SH. Cardiac 3D printing and its future directions. JACC Cardiovasc Imaging. 2017;10:171–184 [11]

assisting interventional trainees to test and practice the procedure, determine the best delivery site, and be aware of potential complications associated with the procedure. Further improvements in the 3D models in terms of replicating realistic vascular wall properties and hemodynamic flow are necessary.

Shiraishi et al. further demonstrated the significant impact of performing surgical simulations using 3D printed models on accurate diagnosis and treatment of complicated congenital heart disease (CHD) [41]. Twelve patient-specific 3D models were created from eight pediatric cases with complicated CHD in their study. Both solid epoxy and rubber-like flexible models were fabricated for surgical simulation. The rubber-like models allowed for surgical simulation of treating different cardiac diseases, such as performing cut and suture operative procedures on the aorta, pulmonary trunk or even intracardiac structures.

Deployment of stents can be simulated on 3D printed models, and this represents another unique application of 3D printing. Pre-operative simulation has been tested on a 3D printed model with complex cardiac disease showing the accuracy of depicting pathologies and improving successful procedure (Fig. 38.7) [13]. Other reports also confirmed the value of performing simulation on 3D printed models for appropriate patient selection for treatment [32, 37, 40].

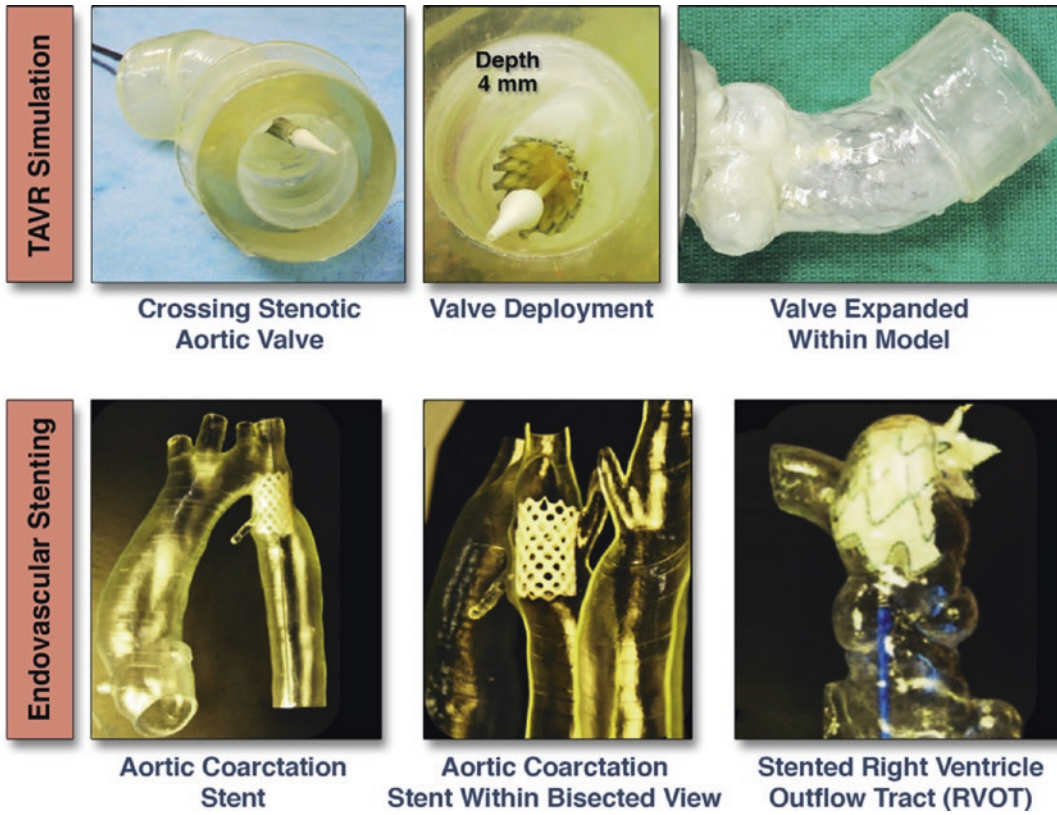

Fig. 38.7 Transcatheter valve and stent implantation within patient-specific models. Bench top transcatheter aortic valve replacement (TAVR) performed within a model of aortic valve stenosis (top). Endovascular stenting within models of aortic coarctation and a pulmonary artery (bottom). Reprint with permission from Vukicevic M, Mosadegh B, Min JK, Little SH. Cardiac 3D printing and its future directions. JACC Cardiovasc Imaging. 2017;10:171–184 [11]

38.6 3D Printed Models in Medical Education and Training

The role of 3D printing as a useful education tool has been reported in a number of studies [50–55]. Its applications are manifested in different areas such as for education and training of healthcare professionals and medical students, as well as facilitation of communication between parents and clinicians.

Biglino et al. first reported the benefit of patient-specific 3D models in the doctor-patient communication [50]. Forty-five participants were assigned to the model group who were presented with 3D printed patient-specific models of their children' heart diseases, and 52 participants to the control group who did not have any model during the consultation. Results showed that 3D printed models received higher scores indicating that they were very useful to improve communication between cardiologists and parents. A recent study by the same group evaluated young patient attitudes towards the 3D models and the impact of 3D models on their communication with cardiologists [51]. There were significant changes observed in knowledge, confidence and satisfaction ($p < 0.05$) among participants following consultation through the use of 3D models when compared to the responses from pre-consultation (Fig. 38.8). Most of the participants considered that the 3D models were fun, helped understanding of their condition and improved visits (Fig. 38.9).

Nurse education and training play an important role in providing high standards of care to patients with CHD [52, 53]. The usefulness of 3D printed models has been studied in nurse training in ophthalmology [54]. The same research group by Biglino et al. reported the advantages of 3D printed models for training cardiac nurses [55]. A total of nine models were presented to 100 cardiac nurses (65 pediatric cardiac nurses and 35 adult cardiac nurses) for assessment of the usefulness of the 3D models in terms of learning experience and facilitating understanding of cardiac anatomy. 3D printed models were considered useful to improve learning experience by 60% of participants,

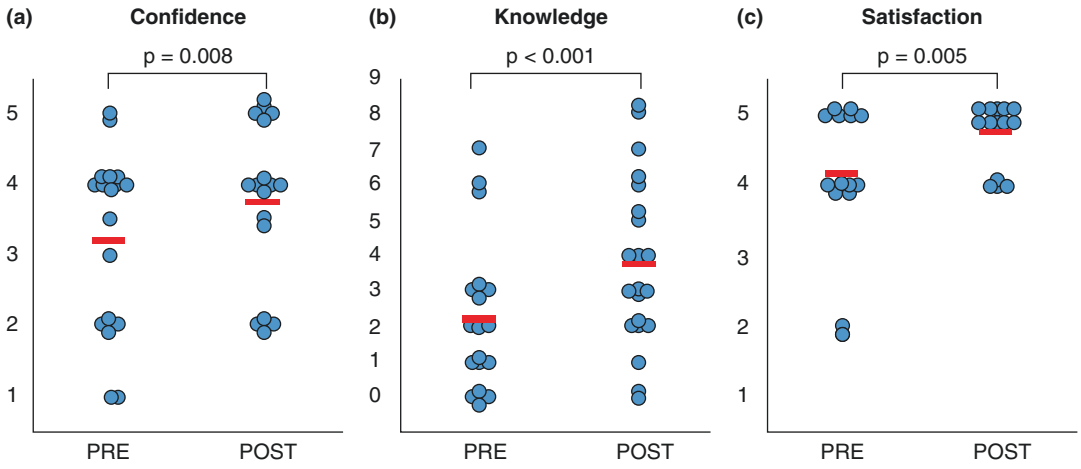

Fig. 38.8 Statistically significant changes were observed in confidence (**a**), knowledge (**b**) and satisfaction (**c**) amongst participants comparing responses before ("Pre") and after ("Post") their consultation. Note for (**a**) 1 = Not at all confident—5 = Very confident; for (**b**) each point represents a point in knowledge, as marked according to the correct name of primary diagnosis, correctly identified keywords and correct use of diagrams; for (**c**) 1 = Very dissatisfied—5 = Very satisfied. The *red lines* indicate average score. Reprint with permission under the open access from Biglino G, Koniordou D, Gasparini M, et al. Piloting the use of patient-specific cardiac models as a novel tool to facilitate communications during clinical consultations. Pediatr Cardiol. 2017;38:813–818 [51]

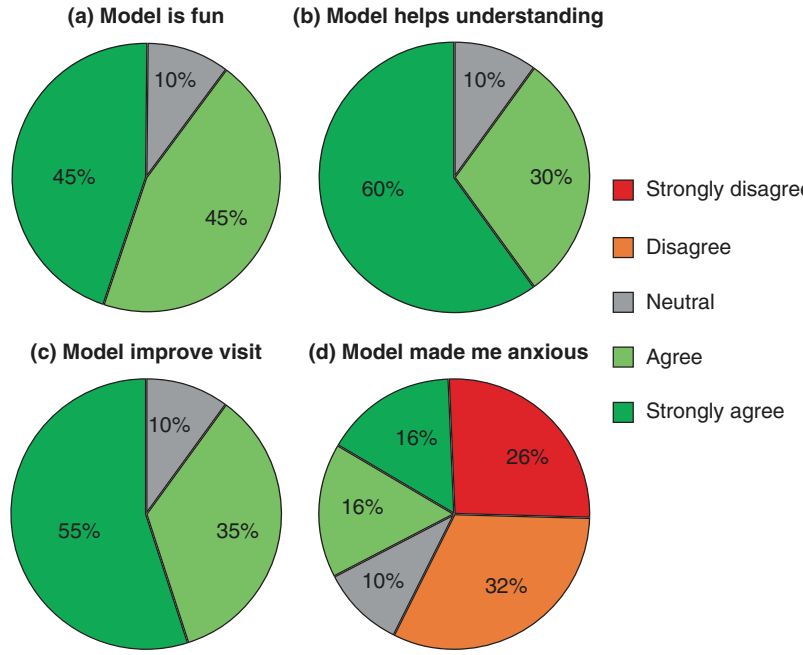

Fig. 38.9 Summary of participants' level of agreement to different statements on 3D models. Reprint with permission under the open access from Biglino G, Koniordou D, Gasparini M, et al. Piloting the use of patient-specific cardiac models as a novel tool to facilitate communications during clinical consultations. Pediatr Cardiol. 2017;38:813–818 [51]

provide more information than diagrams by 74% of participants. Further, the 3D models were found to understand the overall anatomy, spatial orientation and complex anatomy after treatment by 86, 70 and 66% of participants, respectively. Similarly, Costello et al. reported significant improvements in knowledge acquisition, knowledge reporting and structural conceptualization ($p < 0.05$) of VSDs by 29 premedical and medical students [56]. Using 3D printed models of VSDs, residents' ability to describe and manage postoperative complications in VDS patients was also improved.

Lim et al. conducted a randomized control trial to compare student performances with use of 3D printed models as opposed to the traditional cadaver-based curriculum [57]. 3D printed models only, cadaveric materials only and a combination of 3D models and cadaveric materials were presented to 16, 18 and 18 first year medical students, respectively for assessment of learning objectives in terms of identifying external cardiac anatomy (identification of cardiac surfaces and chambers, grooves, coronary arteries and veins, as well as great vessels in relation to the above-mentioned structures). Test scores were significantly increased in the 3D models only group when compared to the other two groups ($p < 0.05$). Surprisingly, no significant difference was found in the test scores between cadaveric materials only and the combined groups ($p = 0.080$). 3D printed models demonstrate advantages over cadaveric materials and may serve as supplements to traditional curriculum for anatomy teaching and learning.

38.7 Summary

3D printing has shown great promise in medicine. Patient-specific 3D printed models have been increasingly used in the diagnosis and preoperative planning of cardiovascular disease. The majority of 3D printing applications involve congenital heart diseases and great vessels and valvular diseases. This chapter has provided an overview of the applications of 3D printed models in a variety of cardiovascular diseases, which range from accurate replication of normal cardiac anatomy to delineation of cardiac pathology, pre-procedural planning and pre-surgical simulation of complex cardiac diseases, and to the assistance on medical education and training. Patient-specific 3D printed models are changing current clinical practice and may have significant impact on life-saving procedures in the near future.

References

1. Farooqi KM, Sengupta PP. Echocardiography and three-dimensional printing: sound ideas to touch a heart. J Am Soc Echocardiogr. 2015;28:398–403. https://doi.org/10.1016/j.echo.2015.02.005.
2. Sumida T, Otawa N, Kamata YU, et al. Custommade titanium devices as membranes for bone augmentation in implant treatment: clinical application and the comparison with conventional titanium mesh. J Craniomaxillofac Surg. 2015;43:2183–8. https://doi.org/10.1016/j.jcms.2015.10.020.
3. Aranda JL, Jimenez MF, Rodriguez M, Varela G. Tridimensional titanium-printed custom-made prosthesis for sternocostal reconstruction. Eur J Cardiothorac Surg. 2015;48:e92–4. https://doi.org/10.1093/ejcts/ezv265.
4. Kim GB, Lee S, Kim H, et al. Three-dimensional printing: basic principles and applications in medicine and radiology. Korean J Radiol. 2016;17:182–97. https://doi.org/10.3348/kjr.2016.17.2.182.
5. Choi JY, Choi JH, Kim NK, et al. Analysis of errors in medical rapid prototyping models. Int J Oral Maxillofac Surg. 2002;31:23–32. https://doi.org/10.1054/ijom.2000.0135.
6. Chang PS, Parker TH, Patrick CW Jr, Miller MJ. The accuracy of stereolithography in planning craniofacial bone replacement. J Craniofac Surg. 2003;14:164–70.
7. Ibrahim D, Broilo TL, Heitz C, et al. Dimensional error of selective laser sintering, three-dimensional printing and PolyJet models in the reproduction of mandibular anatomy. J Craniomaxillofac Surg. 2009;37:167–73. https://doi.org/10.1016/j.jcms.2008.10.008.
8. Sun Z, Squelch A. 3D printed models of complex anatomy in cardiovascular disease. Heart Res Open J. 2015;2:103–8. https://doi.org/10.17140/HROJ-2-118.
9. Valverde I. Three-dimensional printed cardiac models: applications in the field of medical education, cardiovascular surgery, and structural heart interventions. Rev Esp Cardiol. 2017;70:282–91. https://doi.org/10.1016/j.rec.2017.01.012.
10. Bartel T, Rivard A, Jimenez A, Mestres CA, Muller S. Medical three-dimensional printing opens up new opportunities in cardiology and cardiac surgery. Eur Heart J. 2017. https://doi.org/10.1093/eurheartj/ehx016. [Epub ahead of print].
11. Vukicevic M, Mosadegh B, Min JK, Little SH. Cardiac 3D printing and its future directions. JACC Cardiovasc Imaging. 2017;10:171–84. https://doi.org/10.1016/j.jcmg.2016.12.001.
12. Giannopoulos AA, Steigner ML, George E, et al. Cardiothoracic applications of 3-dimensional printing. J Thorac Imaging. 2016;31:253–72. https://doi.org/10.1097/RTI.0000000000000217.
13. Giannopoulos AA, Mitsouras D, Yoo SJ, Liu PP, Chatzizisis YS, Rybicki FJ. Applications of 3D printing in cardiovascular diseases. Nat Rev Cardiol. 2016;13:701–18. https://doi.org/10.1038/nrcardio.2016.170.
14. Sun Z, Lee SY. A systematic review of 3-D printing in cardiovascular and cerebrovascular diseases. Anatol J Cardiol. 2017;17:423–35. https://doi.org/10.14744/AnatolJCardiol.2017.7464.
15. Mitsouras D, Liacouras P, Imanzadeh A, et al. Medical 3D printing for the radiologist. Radiographics. 2015;35:1965–88. https://doi.org/10.1148/rg.2015140320.
16. Firouzian A, Manniesging R, Flach ZH, Risselada R, Kooten F, Sturkenboom M. Intracranial aneurysm segmentation in 3D CT angiography: method and quantitative validationwith and without prior noise filtering. Eur J Radiol. 2016;79:299–304. https://doi.org/10.1016/j.ejrad.2010.02.015.
17. Byrne N, Velasco FM, Tandon A, Valverde I, Hussain T. A systematic review of image segmentation methodology, used in the additive manufacture of patient-specific 3D printed models of the cardiovascular system. JRSM Cardiovasc Dis. 2016;5:2048004016645467. https://doi.org/10.1177/2048004016645467. eCollection 2016 Jan-Dec.
18. Oyama R, Jakab M, Kikuchi A, Sugiyama T, Kikinis R, Pujol S. Towards improved ultrasoundbased analysis and 3D visualization of the fetal brain using the 3D slicer. Ultrasound Obstet Gynecol. 2013;42:609–10. https://doi.org/10.1002/uog.12484.
19. Bauch T, Vijayaraman P, Dandamudi G, Ellenbogen K. Three-dimensional printing for in vivo visualization of his bundle pacing leads. Am J Cardiol. 2015;116:485–6. https://doi.org/10.1016/j.amjcard.2015.04.061.
20. Sun Z, Squelch A. Patient-specific 3D printed models of aortic aneurysm and aortic dissection. J Med Imaging Health Inform. 2017;7:886–9. https://doi.org/10.1166/jmihi.2017.2093.
21. Ho D, Squelch A, Sun Z. Modelling of aortic aneurysm and aortic dissection through 3D printing. J Med Radiat Sci. 2017;64:10–7. https://doi.org/10.1002/jmrs.212.
22. Xu L, Sun Z. Virtual intravascular endoscopy visualization of calcified coronary plaques: a novel approach of identifying plaque features for more accurate assessment of coronary lumen stenosis. Medicine. 2015;94:e805. https://doi.org/10.1097/MD.0000000000000805.
23. Sun Z, Ng C. High calcium scores in coronary CT angiography: effects of image post-processing on visualization and measurement of coronary lumen diameter. J Med Imaging Health Inform. 2015;5:110–6. https://doi.org/10.1166/jmihi.2015.1366.
24. Sun Z, Xu L, Fan Z. Coronary CT angiography in calcified coronary plaques: comparison of diagnostic accuracy between bifurcation angle measurement and coronary lumen assessment for diagnosing significant coronary stenosis. Int J Cardiol. 2016;203:78–86. https://doi.org/10.1016/j.ijcard.2015.10.079.
25. Farooqi K, Uppu SC, Nguyen K, et al. Application of virtual three-dimensional models for simulta-

neous visualization of intracardiac anatomic relationships in double outlet right ventricle. Pediatr Cardiol. 2016;37:90–8. https://doi.org/10.1007/s00246-015-1244-z.
26. Binder TM, Moertl D, Mundigler G, et al. Stereolithographic biomodeling to create tangible hard copies of cardiac structures from echocardiographic data: in vitro and in vivo validation. J Am Coll Cardiol. 2000;35:230–7. https://doi.org/10.1016/S0735-1097(99)00498-2.
27. Olivieri LJ, Krieger A, Loke YH, et al. Three-dimensional printing of intracardiac defects from three-dimensional echocardiographic images: feasibility and relative accuracy. J Am Sco Echocardiogr. 2015;28:392–7. https://doi.org/10.1016/j.echo.2014.12.016.
28. Samuel BP, Pinto C, Pietila T, Vettukattil JJ. Ultrasound-derived three-dimensional printing in congenital heart disease. J Digit Imaging. 2015;28:459–61. https://doi.org/10.1007/s10278-014-9761-5.
29. Ripley B, Kelil T, Cheezum MK, et al. 3D printing based on cardiac CT assists anatomic visualization prior to transcatheter aortic valve replacement. J Cardiovasc Comput Tomogr. 2016;10:28–36. https://doi.org/10.1016/j.jcct.2015.12.004.
30. Sodian R, Sschmauss D, Schmitz C, et al. 3-dimensional printing of models to create custom-made devices for coil embolization of an anastomotic leak after aortic arch replacement. Ann Thorac Surg. 2009;88:974–8. https://doi.org/10.1016/j.athoracsur.2009.03.014.
31. Maragiannis D, Jackson MS, Igo SR, et al. Replicating patient-specific severe aortic valve stenosis with functional 3D modelling. Circ Cardiovasc Imaging. 2015;8:e003626. https://doi.org/10.1161/CIRCIMAGING.115.003626.
32. Schievano S, Migliavacca F, Coats L, et al. Percutaneous pulmonary valve implantation based on rapid prototyping of right ventricular outflow tract and pulmonary trunk from MR data. Radiology. 2007;242:490–7. https://doi.org/10.1148/radiol.2422051994.
33. Schmauss D, Haeberle S, Hagl C, Sodian R. Three-dimensional printing in cardiac surgery and interventional cardiology: a single-centre experience. Eur J Cardiothorac Surg. 2015;47:1044–52. https://doi.org/10.1093/ejcts/ezu310.
34. Sodian R, Weber S, Market M, et al. Stereolithographic models for surgical planning in congenital heart surgery. Ann Thorac Surg. 2007;83:1854–7. https://doi.org/10.1016/j.athoracsur.2006.12.004.
35. Sodian R, Weber S, Markert M, et al. Pediatric cardiac transplantation: three-dimensional printing of anatomic models for surgical planning of heart transplantation in patients with univentricular heart. J Thorac Cardiovasc Surg. 2008;136:1098–9. https://doi.org/10.1016/j.jtcvs.2008.03.055.
36. Valverde I, Gomez G, Gonzalez A, et al. Three-dimensional patient-specific cardiac model for surgical planning in Nikaidoh procedure. Cardiol Young. 2015;25:698–704. https://doi.org/10.1017/S1047951114000742.
37. Valverde I, Gomez G, Coserria JF, et al. 3D printed models for planning endovascular stenting in transverse aortic arch hypoplasia. Catheter Cardiovasc Interv. 2015;85:1006–12. https://doi.org/10.1002/ccd.25810.
38. Mottl-Link S, Hubler M, Kuhne T, et al. Physical models aiding in complex congenital heart surgery. Ann Thorac Surg. 2008;86:273–7. https://doi.org/10.1016/j.athoracsur.2007.06.001.
39. Ryan JR, Moe TG, Richardson R, Frakes DH, Nigro JJ, Pophal S. A novel approach to neonatal management of tetralogy of Fallot, with pulmonary atresia, and multiple aortopulmonary collaterals. JACC Cardiovasc Imaging. 2015;8:103–4. https://doi.org/10.1016/j.jcmg.2014.04.030.
40. Olivieri L, Krieger A, Chen MY, Kim P, Kanter JP. 3D heart model guides complex stent angioplasty of pulmonary venous baffle obstruction in a mustard repair of D-TGA. Int J Cardiol. 2014;172:e297–e98. https://doi.org/10.1016/j.ijcard.2013.12.192.
41. Shiraishi I, Yamagishi M, Hamaoka K, Fukuzawa M, Yagihara T. Simulative operation on congenital heart disease using rubber-like urethane stereolithographic biomodels based on 3D datasets of multislice computed tomography. Eur J Cardiothorac Surg. 2010;37:302–6. https://doi.org/10.1016/j.ejcts.2009.07.046.
42. Vranicar M, Gregrory W, Douglas WI, Sessa PDI, Di Sessa TG. The use of stereolithographic hand held models for evaluation of congenital anomalies of the great vessels. Stud Health Technol Inform. 2008;132:538–43.
43. Biglino G, Capelli C, Taylor AM, Schivano S. 3D printing cardiovascular anatomy: a single-center experience. In: Shishkovsky IV, editor. New trends in 3D printing. Rijeka: IN-Tech Publishing House; 2016.
44. Kim MS, Hansgen AR, Wink O, et al. Rapid prototyping: a new tool in understanding and treating structural heart disease. Circulation. 2008;117:2388–94. https://doi.org/10.1161/CIRCULATIONAHA.107.740977.
45. Schmauss D, Gerber N, Sodian R. Three dimensional printing of models for surgical planning in patients with primary cardiac tumors. J Thorac Cardiovasc Surg. 2013;145:1407–8. https://doi.org/10.1016/j.jtcvs.2012.12.030.
46. Al Jabbari O, Abu Saleh WK, Patel AP, Igo SR, Reardon MJ. Use of three-dimensional models to assist in the resection of malignant cardiac tumors. J Card Surg. 2016;31:581–3. https://doi.org/10.1111/jocs.12812.
47. Mashiko T, Otani K, Kawano R, et al. Development of three-dimensional hollow elastic model for cerebral aneurysm clipping simulation enabling rapid and low

cost prototyping. World Neurosurg. 2015;83:351–61. https://doi.org/10.1016/j.wneu.2013.10.032.
48. Namba K, Higaki A, Kaneko N, Mashiko T, Nemoto S, Watanabe E. Microcatheter shaping for intracranial aneurysm coiling using the 3-dimensional printing rapid prototyping technology: preliminary result in the first 10 consecutive cases. World Neurosurg. 2015;84:178–86. https://doi.org/10.1016/j.wneu.2015.03.006.
49. Ngan EM, Rebeyka IM, Ross DB, et al. The rapid prototyping of anatomic models in pulmonary atresia. J Thorac Cardiovasc Surg. 2006;132:264–9. https://doi.org/10.1016/j.jtcvs.2006.02.047.
50. Biglino G, Capelli C, Wray J, et al. 3D-manufactured patient-specific models of congenital heart defects for communication in clinical practice: feasibility and acceptability. BMJ Open. 2015;5:e007165. https://doi.org/10.1136/bmjopen-2014-007165.
51. Biglino G, Koniordou D, Gasparini M, et al. Piloting the use of patient-specific cardiac models as a novel tool to facilitate communications during clinical consultations. Pediatr Cardiol. 2017;38:813–8. https://doi.org/10.1007/s00246-017-1586-9.
52. Royal College of Nursing. Children and young people's cardiac nursing: RCN guidance on roles, career pathways and competence development. 2014. Website. http://www.rcn.org.uk/__data/assets/pdf_file/0010/594658/004_121_web.pdf. Accessed 31 May 2017.
53. Royal College of Nursing. Adult congenital heart disease nursing: RCN guidance on roles, career pathways and competence development. 2015. Website. http://www.rcn.org.uk/__data/assets/pdf_file/0009/626877/004522.pdf. Accessed 31 May 2017.
54. Adams JW, Pacton L, Dawes K, Burlak K, Quayle M, McMenamin PG. 3D printed reproductions of orbital dissections: a novel mode of visualising anatomy for trainees in ophthalmology or optometry. Br J Ophthalmol. 2015;99:1162–7. https://doi.org/10.1136/bjophthalmol-2016-309848.
55. Biglino G, Capelli C, Koniordou D, et al. Use of 3D models of congenital heart disease as an education tool for cardiac nurses. Congenit Heart Dis. 2017;12:113–8. https://doi.org/10.1111/chd.12414.
56. Costello JP, Olivieri LJ, Su L, et al. Incorporating three-dimensional printing into a simulation-based congenital heart disease and critical care training curriculum for resident physicians. Congenit Heart Dis. 2015;10:185–90. https://doi.org/10.1111/chd.12238.
57. Lim KH, Loo ZW, Goldie SJ, Adams JW, McMenamin PG. Use of 3D printed models in medical education: a randomized controlled trial comparing 3D prints versus cadaveric materials for learning external cardiac anatomy. Anat Sci Educ. 2016;9:213–21. https://doi.org/10.1002/ase.1573.

Part III

Treatment

Inhaled Vasodilators in Right Heart Failure

39

Mahsa Elmi-Sarabi and André Denault

Abstract

This chapter presents a brief description for the use of inhaled vasodilators in the management of right ventricular failure (RVF) in cardiac surgical patients. The effects of inhaled vasodilators extend beyond the right heart and pulmonary circulation and can also be seen on the portal vein and on cerebral oxygenation. Agents such as milrinone and epoprostenol, which are typically administered intravenously, can exert a more localized effect when aerosolized. In this form, these drugs can selectively lower pulmonary pressures without exhibiting a systemic effect, thus showing to be beneficial in the management of right ventricular (RV) dysfunction.

The experiences described in this chapter originate from researchers at the Montreal Heart Institute (MHI) in Quebec, Canada. The MHI is an ultraspecialized hospital centre dedicated to care, research, teaching, prevention, rehabilitation, and the assessment of new technologies in cardiology. It is affiliated with Université de Montréal.

Keywords

Inhaled vasodilator · Milrinone · Epoprostenol Pulmonary hypertension · Cardiac surgery Near-infrared spectroscopy · Portal vein pulsatility

Abbreviations

CABG	Coronary artery bypass grafting
cAMP	Cyclic adenosine monophosphate
cGMP	Cyclic guanosine monophosphate
CO_2	Carbon dioxide
CPB	Cardiopulmonary bypass
ET-1	Endothelin-1
ICU	Intensive care unit
LV	Left ventricular
MHI	Montreal Heart Institute
MPAP	Mean pulmonary artery pressure
NIRS	Near-infrared spectroscopy
NO	Nitric oxide
OR	Operating room
PAP	Pulmonary artery pressure
PDE	Phosphodiesterase

M. Elmi-Sarabi · A. Denault (✉)
Department of Anesthesiology, Montreal Heart Institute, Université de Montréal, Montreal, QC, Canada
e-mail: andre.denault@umontreal.ca

S. I. Dumitrescu et al. (eds.), *Right Heart Pathology*, https://doi.org/10.1007/978-3-319-73764-5_39

PDE-3	Phosphodiesterase type 3
PDE-5	Phosphodiesterase type 5
PGI_2	Prostacyclin
PH	Pulmonary hypertension
Prv	Right ventricular pressure
RA	Right atrial
rSO_2	Regional oxygen saturation
RV	Right ventricle
RVF	Right ventricular failure
TEE	Transesophageal echocardiography
TTE	Transthoracic echocardiography
TXA_2	Thromboxane A_2

39.1 Inhaled Vasodilators: Mode of Action and Rationale for Combination Therapy

Pulmonary hypertension (PH) is a hemodynamic problem that can result in right ventricular failure (RVF). It has a complex pathophysiology and is associated with increased morbidity and mortality.

Cardiac surgical patients with PH carry a higher risk for surgery than those without PH [1–4]. Complications such as pneumonia, prolonged mechanical ventilation, renal failure, cardiac arrest, and multiple organ system failure occur more frequently with increasing mean pulmonary artery pressure (MPAP) [5]. In patients with severe PH, the incidence of major postoperative complications was previously reported at 32% [5]. Mortality in PH is most closely associated with RV hemodynamic function [6]. RVF after cardiac surgery has previously been reported with mortality rates varying from 37% to 90% [7–9]. Moreover, cardiogenic shock secondary to RVF can have mortality rates as high as 53% [10]. What will determine survival in the postoperative period is the ability of the right heart to cope with the added strain of augmented pulmonary pressure [11].

Management of patients with PH is particularly challenging. In recent years, despite the emergence of new therapies for PH, treatment of PH with or without RVF failure in the operating room (OR) and in the intensive care unit (ICU) remains a challenge and relies primarily on expert opinion [12]. Despite advances in perioperative management, registry data from the International Society of Heart and Lung Transplantation show that RV dysfunction accounts for 50% of all cardiac complications and 19% of all early deaths in patients after heart transplantation [13]. Treatment of patients with PH and RVF is particularly challenging since mechanical ventilation and volume resuscitation typically used may worsen hemodynamics [14]. In the cardiac surgery patients, although therapeutic strategies should focus on prevention of both acute perioperative PH and exacerbation of pre-existing PH, in the event of a sudden onset of perioperative PH, therapy should aim at resolution of PH and supportive therapy for the RV [15]. Appropriate management entails not only treatment of symptoms in order to avoid RVF but also parallel treatment of the underlying cause of PH so as to avoid its exacerbation, which could lead to the death of the patient [12].

39.1.1 Mode of Action of Inhaled Vasodilators

Intravenous vasodilators have traditionally been used in managing PH in heart surgery, but they lack specificity for the pulmonary circulation and their systemic hypotensive effects often limit their use [16]. This limitation highlights the need for selective pulmonary vasodilators for this cohort of patients. Nebulization of drugs could provide such localized pulmonary vasodilation with little or no clinically significant hypotension [17]. In addition, inhalation of drugs may improve ventilation/perfusion matching by promoting regional vasodilation in well-ventilated areas of the lungs thereby redirecting pulmonary blood flow away from poorly ventilated alveoli, whereas their intravenous administration may worsen ventilation/perfusion matching by causing non-selective pulmonary vasodilation [18–23].

Endothelial dysfunction plays a central role in the initiation and progression of PH. The endothelium releases a variety of growth factor, thromboregulatory and vasoactive mediators in response to physical and chemical stimuli, which

affect cell growth and proliferation as well as vascular contractility of pulmonary vessels [24]. Maintenance of pulmonary vascular tone is a critical function of the pulmonary endothelium, and is achieved through a balance between vasodilator, growth inhibitor and fibrinolytic/antiaggregant endothelial factors such as prostacyclin (PGI_2) and nitric oxide (NO), and vasoconstrictor, growth-promoting and thrombotic inducing factors such as endothelin-1 (ET-1) and thromboxane A_2 (TXA_2) [25, 26]. Endothelial dysfunction causes an imbalance of these factors leading to impaired production of PGI_2 and NO and prolonged overexpression of ET-1 and TXA_2, thus promoting pulmonary vasoconstriction and vascular remodelling [26, 27].

A fundamental understanding of the imbalance between these vasoactive mediators was key to identifying the three major pathways, endothelin, PGI_2 and NO, involved in the development and progression of PH, which in turn provided molecular targets for the development of new therapies [27–30].

39.1.2 Rationale for Combination Therapy

As stated above, the mechanisms promoting development and disease progression of PH involve multiple pathways. Given the complexity of the disease, treatment with a single therapeutic agent may not be sufficient to completely reverse or halt progression of pathologic changes. Therefore, combination therapy, using multiple drugs of different classes to simultaneously target different mechanistic pathways of the disease, is in theory an attractive option. The rationale behind combination therapy is threefold. Combining drugs with different mechanisms of action may not only have an additive effect but may also act in synergy to improve treatment success [31]. Furthermore, it is believed that by enhancing treatment efficacy, lower doses of each drug may be required in combination therapy, thereby decreasing toxicity and reducing the risk of adverse events [32]. Two systematic review and meta-analysis studies were recently published comparing the effects of combination therapy with monotherapy for the treatment of PH [33, 34]. Both studies reported that combined therapy for PH is associated with a significant reduction in clinical worsening compared with monotherapy. In addition, these meta-analyses showed that combination therapy improves pulmonary hemodynamics, exercise capacity, and functional status, while reducing the risk for admission to hospital, treatment escalation, and symptomatic progression.

As previously mentioned, either an additive or a synergistic effect can explain the amplified hemodynamic response obtained when combining therapies. As we will see below, an example for the additive effect is the combination of PGI_2 and a phosphodiesterase (PDE) type 3 (PDE-3) inhibitor, whereas the combination of PGI_2 and a type 5 PDE (PDE-5) inhibitor demonstrate the synergistic effect.

39.1.2.1 Additive Effect of Combination Therapy

Combining inhaled vasodilators with different mechanisms of action amplifies the pulmonary vasodilator response. The additive effect of a combination therapy can be attributed to the use of several drugs that act through different and complementary pathways [35]. Haraldsson et al. [36] were the first to report on the effects of inhaled milrinone in patients with PH in the context of cardiac surgery. Their study concluded that not only is inhaled milrinone a selective pulmonary vasodilator, it also seems to have an additive pulmonary vasodilator effect to epoprostenol, without systemic effects.

Furthermore, Schermuly et al. have shown in a series of animal studies that low-dose PDE inhibitors amplify the pulmonary vasodilator response to inhaled PGI_2 in experimental PH [37–39]. Authors first showed in a rabbit model of PH that a sub-threshold dose of an intravenous monoselective PDE-3 inhibitor causes significant amplification of the pulmonary vasodilatory response to inhaled PGI_2 without any systemic effects [37]. Since the intravenous administration of PDE-3 inhibitor alone was associated to a dose-dependent pulmonary vasodilation accompanied

by a decrease in systemic pressure, a sub-threshold dose, with no effect of PDE inhibition on the pulmonary vascular tone, was utilized in combination with inhaled PGI_2. PDE-3 inhibition enhanced the MPAP reduction and prolonged the post-nebulization vasodilatory effects of PGI_2 aerosolization. In addition, results of a sub-threshold level of a dual-selective PDE-3/PDE-4 inhibitor were comparable to those obtained with a mono-selective PDE-3 inhibitor. Furthermore, in a subsequent experiment, Schermuly et al. [38] showed that co-aerosolization of non-specific and dual-specific PDE inhibitors can also enhance the vasodilatory response to inhaled iloprost, a PGI_2 analogue. In contrast to intravenous PDE inhibitors, nebulization of sub-threshold doses neither amplified nor prolonged the iloprost-induced drop in MPAP. Nevertheless, when aerosolized in doses inducing a moderate decrease in MPAP, both non-specific and dual-specific (PDE-3/PDE-4) PDE inhibitors doubled the MPAP reduction in response to iloprost and significantly prolonged this response in the absence of any systemic effects or deterioration of gas exchange. However, a study by Ghofrani et al. [40] in patients with pre-capillary PH, showed that even sub-threshold (ineffective) doses of a PDE-3/4 dual selective inhibitor are effective at amplifying and prolonging the vasodilatory effects of inhaled iloprost in both infused and aerosolized forms. Therefore, even minute doses of a PDE-3/4 inhibitor are sufficient via the inhalative route to amplify the vasodilatory response to iloprost.

These data suggest that combination of a PGI_2 analogue and a PDE-3 inhibitor, even at sub-threshold doses, can amplify the vasodilatory hemodynamic response while maintaining pulmonary selectivity. This is explained by the fact that both PGI_2 analogues and PDE-3 inhibitors exhibit their vasodilatory effect through their action on the PGI_2 pathway. Both PGI_2 and iloprost cause vasodilation through an increase in cyclic adenosine monophosphate (cAMP) levels by stimulating the PGI_2 receptor thereby activating adenylate cyclase. PDE-3 inhibitors, on the other hand, will increase cAMP levels by preventing its degradation. cAMP is degraded by PDEs at a much faster rate than it is synthesized by adenylate cyclase. Thus, blocking the degradation of cAMP with a PDE-3 inhibitor will stabilize cAMP concentrations within the cell and amplify the vasodilatory response observed with PGI_2. Therefore, it is not surprising that an additive hemodynamic effect is observed when these two classes of drugs are combined, nor that lower doses are required to achieve response.

39.1.2.2 Synergistic Effect of Combination Therapy

Combination therapies may also amplify response through a synergistic effect where one therapy, acting on one pathway, may facilitate the action of another therapy acting on a different but complementary pathway [41]. This was shown in a rabbit model of experimental PH where a sub-threshold ineffective dose of sildenafil, a PDE-1/5/6 inhibitor, was able to significantly enhance iloprost-induced vasodilation. This response was comparable to that obtained with a sub-threshold ineffective dose of a mono-selective PDE-3 inhibitor [39]. Sildenafil exerts its effect through the NO pathway by inhibiting PDE-5, thereby increasing or stabilizing cyclic guanosine monophosphate (cGMP) levels in smooth muscle cells of the pulmonary vasculature. On the other hand, iloprost's mechanism of action is through the PGI_2 pathway, where it increases cAMP levels within smooth muscle cells. So how does a sub-threshold dose of sildenafil, which has no effect on the pulmonary vascular tone when administered alone, amplify the vasodilatory effect observed with iloprost? This observation is attributed to what is known as "crosstalk" between the cAMP and cGMP signalling pathways [42]. cGMP can regulate the activity of cAMP by inhibiting PDE-3 activity, thereby increasing cAMP levels [42, 43]. Therefore, a PDE-5 inhibitor that acts directly on the NO pathway can also potentiate the effects of a PGI_2 analogue by raising cGMP levels. Augmented levels of cGMP, in turn, inhibit PDE-3, thus further raising cAMP levels and enhancing sensitivity to inhaled PGI_2 (or its analogue) [39].

39.1.2.3 Safety of Combination Therapy

As with all therapies, monotherapy with PH medications is also linked to some toxicity and intolerable adverse events. Infusion of epoprostenol for instance, has previously been associated with dose-related side effects such as flushing, headache, nausea, and hypotension [44, 45]. Although reducing epoprostenol dosage may attenuate its side effects, doing so may also reduce the hemodynamic efficacy of the drug, thus rendering it less effective [46]. Low doses of epoprostenol cannot always improve hemodynamics in patients with severe PH, whereas high-dose therapy has previously been shown to cause important hemodynamic improvements [47]. A way to overcome the intolerance observed at the higher more efficacious doses would be to use combination therapy. Combining epoprostenol with a drug having a different mechanism of action may allow use of epoprostenol at lower doses, thus lessening its side effects, while potentiating its anticipated hemodynamic effects. In fact, addition of oral bosentan therapy, an endothelin receptor antagonist, to long-term epoprostenol infusion therapy in children with severe PH has allowed a dose reduction of epoprostenol and decreased its associated side effect without deteriorating any clinical or hemodynamic parameters [46].

39.2 Inhaled Vasodilators and Their Neurological Effect (Cerebral Oxygenation: NIRS)

Cerebral near-infrared spectroscopy (NIRS) is a non-invasive marker of tissue perfusion that can be used during non-pulsatile flow conditions not amenable to monitoring with pulse oximetry and non-invasive arterial pressure measurements [48]. It is a nonspecific method to evaluate whether cardiac output is sufficient to maintain adequate oxygen transport in relation to oxygen demand [49]. Cerebral regional oxygen saturation (rSO_2) monitoring using NIRS is a promising technology that could help anesthesiologists in meeting these goals during cardiac or noncardiac surgery. The monitor gives a baseline numerical value of the rSO_2 [49]. In the presence of RVF, NIRS signal will be reduced (Fig. 39.1). On the other hand, NIRS value will increase if RV function improves. The non-invasive and continuous nature of this type of monitoring is very useful in both the OR and the ICU [50].

Studies have shown that intraoperative NIRS values correlate with postoperative outcome in cardiac [51] and in noncardiac surgery [52]. Interventions to correct brain saturation can be associated with improved outcome [53, 54]. Finally, in a recent prospective trial, baseline cerebral NIRS values obtained before cardiac surgery were superior to the euroSCORE in predicting survival in cardiac surgery [55]. In the OR, NIRS trends are used to evaluate response to therapy, which is associated with normalization of this parameter. NIRS is particularly useful in RVF compared to thermodilution, as it is not influenced by tricuspid regurgitation [49]. The intraoperative NIRS signals of a patient with severe PH and RVF are shown in Fig. 39.2. Initial rSO_2 values after induction of anesthesia indicated 39% and 54% on the left and right forehead, respectively (Fig. 39.2a). Following the administration of 5 mg of inhaled milrinone and 75 μg of inhaled epoprostenol through the endotracheal tube with a nebulizer attached to the inspiratory limb, normalization of both left and right NIRS values were observed (Fig. 39.2b). The left sided value increased to 67% and the right to 78%.

39.3 Inhaled Vasodilators and Their Effect on the Portal Vein

Doppler interrogation of the portal and splenic veins is useful to assess the extracardiac congestive effects of right heart failure [50]. Hepatic interrogation is an area of greater interest in recent years and is currently being studied more comprehensively and current investigations are ongoing. Portal vein pulsatility has been described as a marker of congestive heart failure [56] and correlates with elevated right atrial (RA) pressure and worse New York Heart Association

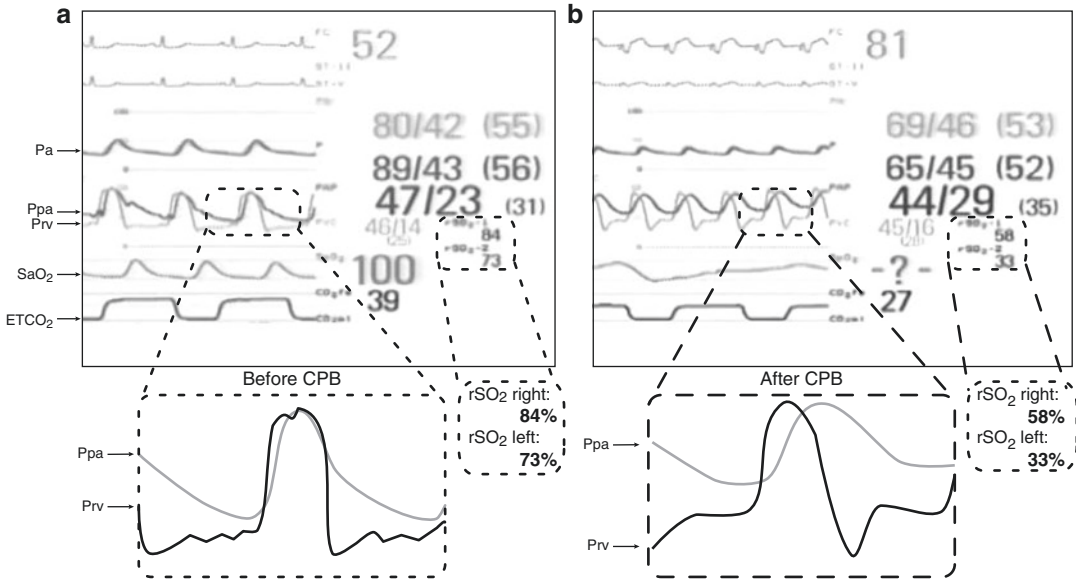

Fig. 39.1 Hemodynamic waveforms combined with regional near-infrared spectroscopy (NIRS) values obtained before (**a**) and after cardiopulmonary bypass (CPB) (**b**). The upper NIRS value was obtained from the right lower extremity and the lower NIRS value is from the brain. Note that after CPB, both values were reduced significantly. This was associated with failure to wean from CPB and significant hemodynamic instability. The cause was a result of acute right ventricular (RV) failure, demonstrated on the RV pressure (Prv) waveform. Note the change of Prv from a normal shape before CPB to a square root sign, with diastolic equalization after CPB. Note also that the pulmonary artery pressure (Ppa) systolic values were lower after CPB and nondiagnostic of acute RV failure. The right atrial pressure was 16 mmHg compared to 14 mmHg before CPB. *ETCO₂* end-tidal carbon dioxide, *Pa* arterial pressure, *rSO₂* regional oxygen saturation, *SaO₂* oxygen saturation (with permission of Denault et al. [49])

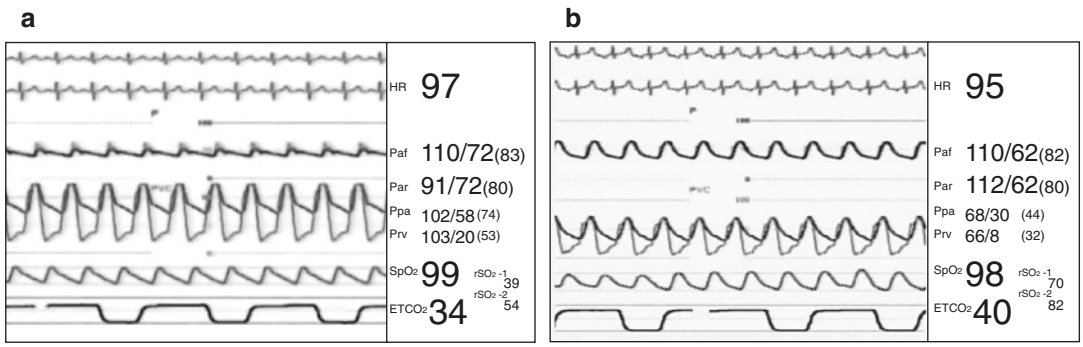

Fig. 39.2 Hemodynamic waveforms combined with regional near-infrared spectroscopy values obtained after induction of anesthesia (**a**) and during nebulization (**b**). During that time, the capnographic monitor was removed in order to prevent drug accumulation in the side-stream system. *HR* heart rate, *Paf* femoral artery pressure, *Par* radial artery pressure, *Ppa* pulmonary artery pressure, *Prv* right ventricular pressure, *SpO₂* oxygen saturation, *ETCO₂* end-tidal carbon dioxide, *rSO₂* regional brain oxygen saturation (with permission of St-Pierre et al. [71])

functional class [57]. In acutely decompensated heart failure, it has been reported that 89% of patients with a RA pressure higher than 8 mmHg have a pulsatile portal flow. Portal vein pulsatility has also been described as a sign of severe tricuspid regurgitation [58] and post-hepatic portal hypertension. Figure 39.3 illustrates different RV diastolic pressure profiles during cardiac surgery

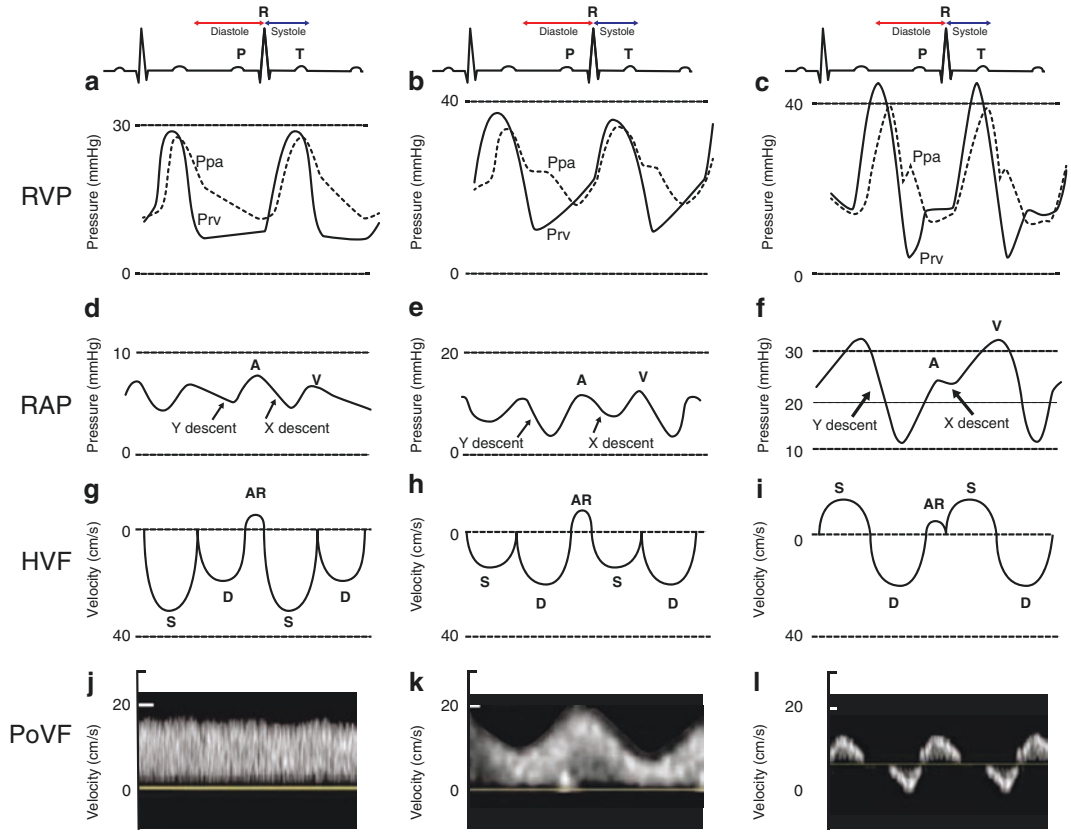

Fig. 39.3 Right ventricular pressure (RVP), right atrial pressure (RAP), hepatic venous flow (HVF) and portal venous flow (PoVF) in normal patients (**a**, **d**, **g**, **j**) and typical patterns commonly observed in patients with mild (**b**, **e**, **h**, **k**) and severe (**c**, **f**, **i**, **l**) right ventricular dysfunction. *AR* atrial reversal HVF velocity, *D* diastolic HVF Doppler velocity, *Ppa* pulmonary artery pressure, *Prv* right ventricular pressure, *S* systolic HVF velocity (with permission of Amsallem et al. [59])

and their RA pressure, hepatic and portal flow correlates [59].

In the next section, we report changes in portal vein pulsatility as a surrogate of venous congestion caused by RVF and describe a combination of inhaled milrinone and epoprostenol to reduce RV afterload.

39.3.1 Effect of Combined Inhaled Milrinone and Epoprostenol on Portal Vein Pulsatility

An 83-year-old man presented with acute chest pain. Coronary angiogram showed severe coronary artery disease with a 90% left main coronary artery stenosis [60]. Bedside transthoracic echocardiography (TTE) revealed a severely hypokinetic inferior left ventricular (LV) wall, an LV ejection fraction of 0.5, and moderate RV dysfunction.

The patient underwent urgent coronary artery bypass grafting (CABG) with complete revascularization. Weaning from cardiopulmonary bypass (CPB) required high doses of vasopressors and inotropes and use of an intra-aortic balloon pump.

On arrival in the surgical ICU, bedside TTE showed progressive RV dilation with diffuse hypokinesis, inferior vena cava enlargement without respiratory variation, and abnormal portal vein flow pulsatility with diastolic flow reversal (Fig. 39.4a). At this point, the patient was also anuric. A continuous infusion of furosemide was started, and in an attempt to reduce RV afterload, epoprostenol (60 μg) and milrinone (4 mg) were

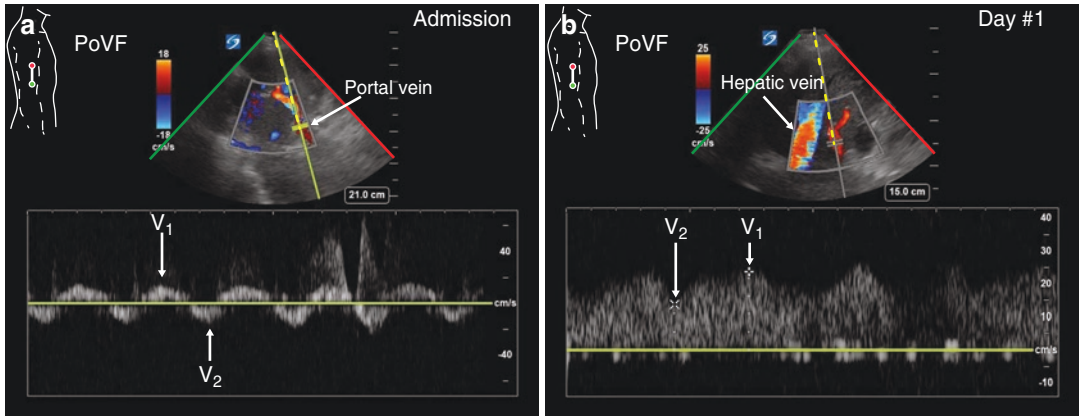

Fig. 39.4 Bedside transthoracic echocardiography upon intensive care unit admission, with posterior axillary line interrogation of the portal vein using spectral Doppler tracing. An abnormal pulsatile portal waveform with transient diastolic flow reversal is seen (V1: peak flow velocity; V2: trough flow velocity) (**a**). Transthoracic echocardiography, postoperative day 1. Note the significantly reduced pulsatility of the spectral Doppler tracing of the main portal vein (**b**). *PoVF* portal venous flow (with permission of Tremblay et al. [60])

administered via an ultrasonic nebulizer attached to the inspiratory limb of the ventilator. Administration of nebulized epoprostenol and milrinone was repeated 2 h later. At 6 h postoperatively, the patient was awakened and his trachea was extubated.

Vasopressor support was rapidly weaned off and stopped 12 h after ICU admission, and the intra-aortic balloon pump was removed. Pulmonary artery pressure (PAP) decreased and urine output was adequate without furosemide infusion. Twenty-four hours after admission, repeat focused TTE revealed mildly phasic portal vein and normal inferior vena cava (Fig. 39.4b). The patient was discharged from the ICU 36 h after admission and was discharged home uneventfully on postoperative day 6. Hemodynamic parameters, drug administration, and diuresis of this patient in the first 12 postoperative hours are summarized in Fig. 39.5.

39.4 Preliminary Experience with Inhaled Vasodilators at the Montreal Heart Institute

Inhaled milrinone or epoprostenol has been used at the MHI since 1999. Although initially in an exploratory fashion, their therapeutic success has since expanded their use as a standard of care for patients with or at risk of right heart failure during the intraoperative period. In this section, we will describe our preliminary experience with these agents, including animal and human studies.

39.4.1 Experience with Animal Studies

Animal experience from our institution has suggested that administration of inhaled epoprostenol or inhaled milrinone during CPB could prevent the pulmonary endothelial dysfunction observed after CPB [61, 62]. In a first animal study, the effects of prophylactic use of inhaled epoprostenol administered before CPB were demonstrated in a porcine model [61]. Three groups of Landrace swine were compared: (1) control without CPB; (2) 90 min of normothermic CPB; (3) 90 min of CPB preceded by a bolus of inhaled PGI_2 followed by continuous nebulization of PGI_2 until the end of CPB. The major findings of this study were that (1) inhaled PGI_2 prevents the increase of MPAP following CPB; (2) PGI_2 is associated with a lower increase of the alveolar-arterial oxygen gradient; (3) animals receiving PGI_2 have a maximal response of the pulmonary endothelium-dependent relaxation to bradykinin but no change in pulmonary

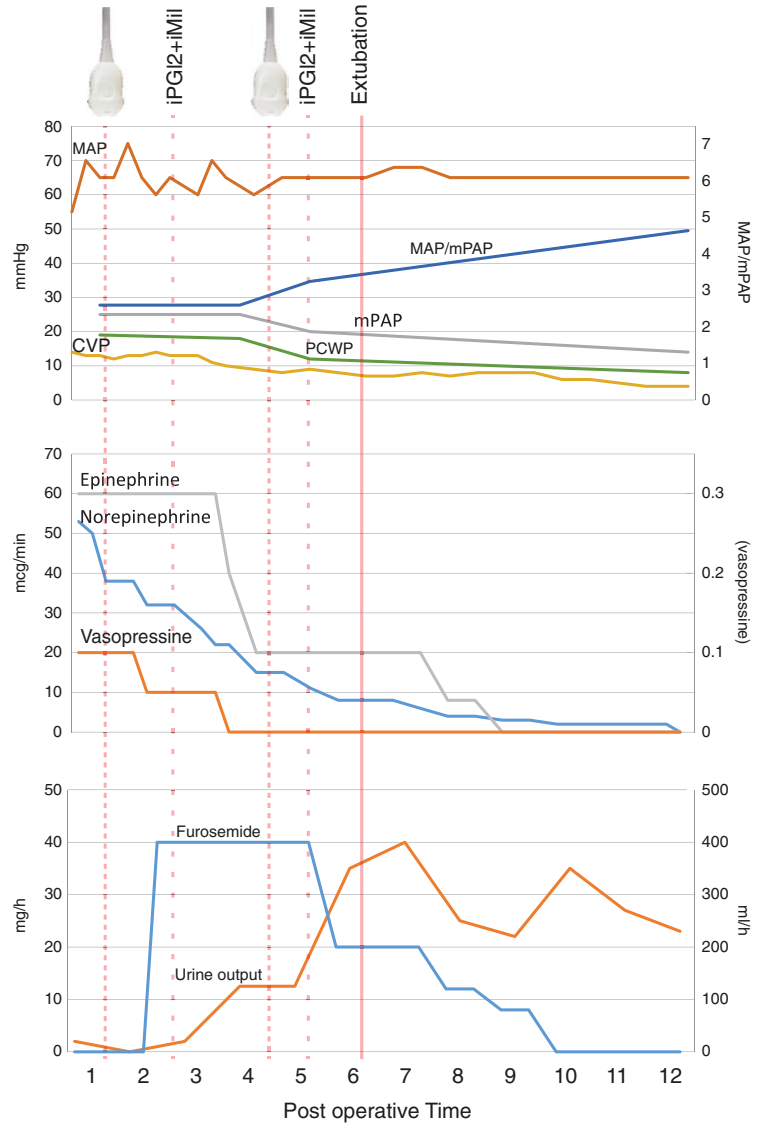

Fig. 39.5 Hemodynamic parameters, drug administration and diuresis in the first 12 postoperative hours. Both administrations of inhaled epoprostenol ($iPGI_2$) and inhaled milrinone (iMil) were followed by gradual reduction in the pulmonary capillary wedge pressure (PCWP), mean pulmonary artery pressure (mPAP), central venous pressure (CVP). The ratio of the mean arterial pressure (MAP) on the mean systemic arterial pressure (MAP/mPAP) increased throughout this period. In addition, significant reduction in perfusion rate of inotropes and vasopressors was observed. Urine output was sustained after discontinuation of the furosemide perfusion (with permission of Tremblay et al. [60])

endothelium-dependent relaxation to acetylcholine; and (4) the administration of PGI_2 is associated with preservation of pulmonary arterial cAMP content after CPB. In a second porcine study, inhaled and intravenous milrinone were compared for their effects on the pulmonary endothelium-dependent relaxations and hemodynamic and oxygenation parameters after CPB [62]. In this study, five groups of landrace swine were compared: (1) control without CPB; (2) 90 min of normothermic CPB; (3) 90 min of CPB preceded by a bolus of inhaled milrinone followed by continuous nebulization of milrinone until the end of CPB; (4) 90 min of CPB preceded by a bolus of intravenous milrinone; and (5) 90 min of CPB preceded by a bolus of inhaled saline solution. The major findings of this study were that (1) CPB induces a pulmonary endothelial dysfunction of the acetylcholine and bradykinin pathways that is reversed by administration of inhaled but not intravenous milrinone before CPB; (2) inhaled milrinone is associated with better hemodynamic and oxygenation profiles than intravenous milrinone, with less hypotension, a lower heart rate, and a lesser reduction in systemic vascular resistances;

and (3) intravenous milrinone causes an increase in the alveolar-arterial oxygen gradient. These animal studies show that the reduced PAP is secondary to a preservation of pulmonary arterial endothelial function and increased cAMP content in pulmonary artery cells, favouring vasodilation even in the setting of a reperfusion injury after CPB.

39.4.2 Preliminary Experience with Inhaled Milrinone

Preliminary experience with inhaled milrinone in cardiac surgery suggests that administration before initiation of CPB could help weaning from CPB. A retrospective analysis of 70 high-risk cardiac surgical patients receiving inhaled milrinone was conducted to evaluate its effects on clinical outcome and ventricular function [63]. Inhaled milrinone was administered before (n = 30) or after (n = 40) CPB. This study found that not only administration of inhaled milrinone before initiation of CPB is associated with a lower MPAP after CPB it is also associated with a lower rate of CPB reinitiation compared to those receiving inhaled milrinone after CPB.

The safety and efficacy of inhaled milrinone has been studies in two prospective randomized double-blind placebo-controlled trials at the MHI. The first, a pilot trial in 21 high-risk cardiac surgical patients with PH randomized to receive inhaled milrinone or placebo before the initiation of CPB [64]. The effects on ventricular function were evaluated by means of pulmonary artery catheterization and transesophageal echocardiography (TEE). In this cohort, the use of inhaled milrinone was not associated with systemic hypotension but with a reduced pulmonary vascular resistance and the prevention of the increase in right-sided cavity dimensions. The second study was a multicentre trial conducted in four Canadian University Medical Centres [65]. A total of 124 high-risk cardiac surgical patients with PH were randomized to receive inhaled milrinone or placebo before the initiation of CPB. Hemodynamic parameters and RV function were evaluated by means of pulmonary artery catheterization and TEE. The prophylactic use of inhaled milrinone was associated with favourable hemodynamic effects that did not translate into improvement of difficult or complex separation from CPB. Inhaled milrinone was also associated with a modest reduction in the hemodynamic severity of PH, an increased cardiac output with a modest overall reduction in systolic PAP, no systemic hypotension, and a gradual reduction in RA dimension. Nevertheless, these studies suggest that a prophylactic strategy using inhaled milrinone alone before CPB neither facilitates separation from CPB nor prevents post-CPB RVF.

39.4.3 Preliminary Experience with Inhaled Epoprostenol

Our experience with inhaled epoprostenol was first reported in a retrospective study of nebulized epoprostenol used in the OR or in the ICU [66]. A total of 35 patients with PH or hypoxia received inhaled epoprostenol over a one-year period. The results confirmed that inhaled epoprostenol could improve oxygenation in patients suffering from hypoxemia and help reduce PH. The effects of inhaled epoprostenol in cardiac surgical patients with PH were subsequently evaluated in a prospective randomized double-blind placebo-controlled exploratory trial [67]. Twenty patients were randomized to receive inhaled epoprostenol or placebo before the initiation of CPB. The effects on cardiac function were evaluated by means of pulmonary artery catheterization and TEE. Oxygenation and platelet aggregation studies were also performed. The prophylactic use of inhaled epoprostenol was associated with reduced pulmonary pressures and improvements in RV stroke work but had no effect on oxygenation. The study confirmed that inhaled epoprostenol was safe, with no systemic hypotension, does not increase platelet dysfunction or perioperative bleeding, and can be a selective pulmonary vasodilator. TEE findings also suggested a tendency toward improvement of left and RV systolic functions, as well as RV diastolic function.

39.4.4 Preliminary Experience with Combined Inhaled Epoprostenol and Milrinone

Our preliminary experience with combined inhaled epoprostenol and milrinone in cardiac surgical patients suggests that it could also reduce vasoactive requirements after CPB. A retrospective analysis of 40 high-risk patients operated at the MHI who received a combination of inhaled milrinone and inhaled epoprostenol before CPB was conducted [68]. The aim of this study was to determine whether the combined administration of milrinone and epoprostenol, given by inhalation before CPB, has a beneficial effect on vasoactive requirements during weaning from CPB and in the ICU in high-risk patients with PH. Results showed that administration of the combination before CPB reduced vasoactive requirements during the first 24 h in the ICU and reduced the severity of PH without systemic hypotension. Pre-emptive treatment with combined inhaled agents also increased cardiac index by reducing indices of RV afterload, which was associated with increase in the NIRS signal.

39.5 Case Studies with Inhaled Vasodilators

39.5.1 Case Study of Inhaled Epoprostenol

A 69-year-old man with unstable angina and a medical history of morbid obesity, hypertension, mild asthma, and dyslipidemia, presented for coronary arteriogram [69]. Coronary anteriography showed a 70% occlusion of the left anterior descending artery and a 60% stenosis of the circumflex artery. LV function was described as normal on the coronary angiogram. The patient was then scheduled for endoscopic saphenous harvesting and CABG without extracorporeal bypass.

Central venous and pulmonary artery catheters were then inserted after induction of general anesthesia. Catheterization showed a normal systolic and diastolic PAP (22/8 mmHg), and the cardiac output was 4.8 L/min (cardiac index, 2.3 L/min/m^2). The initial blood gas values were within normal limits. Initial TEE examination showed normal left and RV systolic function. Carbon dioxide (CO_2) insufflation was initiated at a flow of 2 L/min to obtain a pressure of 15 mmHg.

Soon after the beginning of the endoscopic dissection, systolic PAP suddenly increased to 65 mmHg, and the systemic blood pressure declined to 90 mmHg (Fig. 39.6a). Capnography showed an immediate increase of end-tidal CO_2 to 54 mmHg (Fig. 39.7). Simultaneously, numerous gaseous bubbles were seen with the TEE in the RV chamber, the right atrium, the pulmonary artery, and in the inferior vena cava confirming the infradiaphragmatic origin of the emboli. The four-chamber view showed a dilated right ventricle associated with septal shift and compression of the left ventricle.

CO_2 insufflation was immediately discontinued, and ventilatory rate and tidal volume were increased with an inspired oxygen fraction of 100%. Pharmacologic treatment was initiated consisting of nitroglycerine up to 83 μg/min, norepinephrine 20 μg/min, and inhaled epoprostenol 75 μg via a jet nebulizer attached to the inspiratory limb of the ventilator near the endotracheal tube. Nebulization was achieved with a bypass flow of oxygen at 8 L/min. Five minutes after the initiation of treatment, ST segment increase normalized, and PAPs returned to normal values (Fig. 39.6b).

No more gaseous bubbles were detectable using the TEE, and both left and RV function returned to normal. Postoperatively, the patient had an uneventful course. He was tracheally extubated approximately 8 h after surgery and discharged home the fourth postoperative day. This patient's systolic and diastolic PAPs remained high despite treatment with large doses of intravenous nitroglycerin. We found that inhaled epoprostenol is efficient in the treatment of PH secondary to CO_2 embolism and is beneficial in the hemodynamic stabilization, thus enabling completion of the off-pump CABG procedure.

In our previous experience with CO_2 embolism, the off-pump bypass procedure had to be converted to CABG with extra-corporeal circulation [70]. It is possible that the favourable response observed in the treatment of PH with

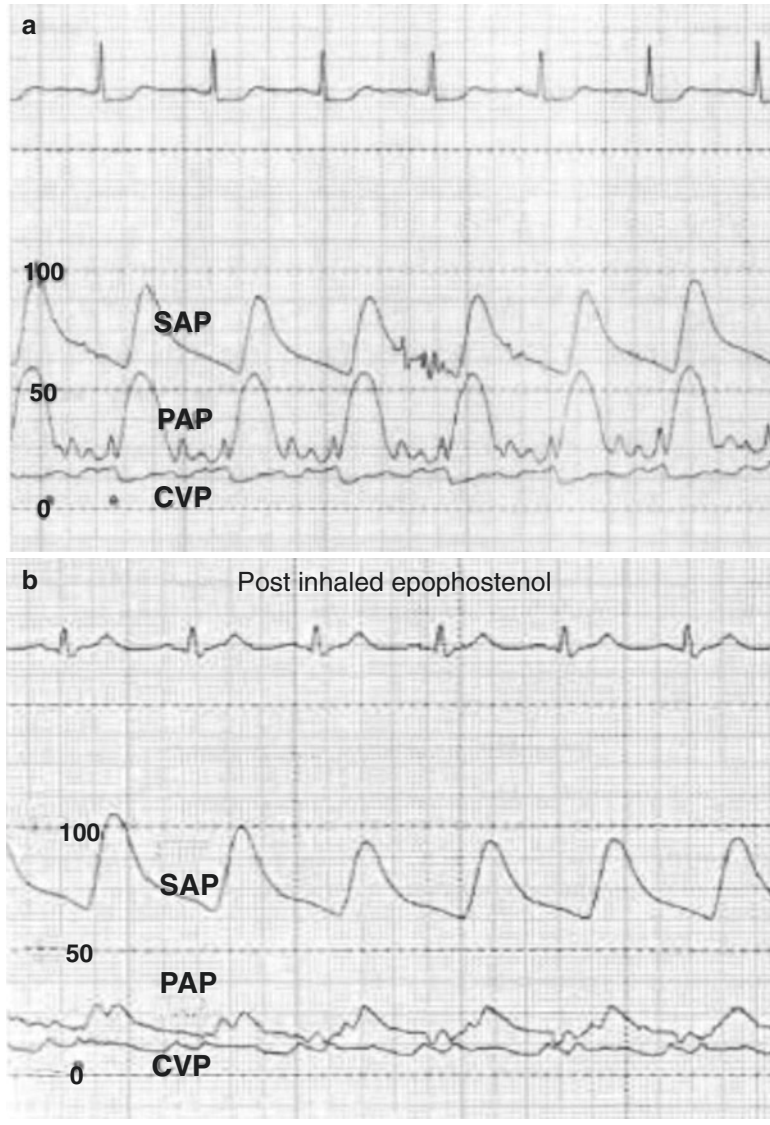

Fig. 39.6 Systemic (SAP), pulmonary (PAP), and central venous pressure (CVP) during the episode of CO_2 embolism (**a**) and after the use of epoprostenol (**b**) (with permission of Martineau et al. [69])

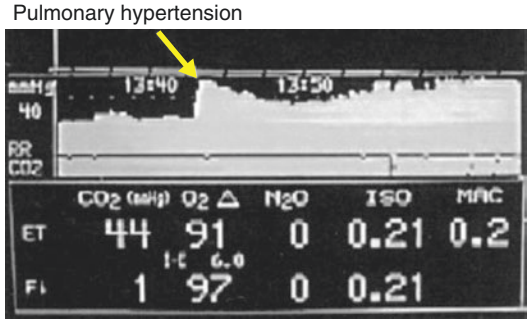

Fig. 39.7 Capnographic data wave form summary. There was a sudden increase in end-tidal CO_2 (yellow arrow) (with permission of Martineau et al. [69])

use of inhaled epoprostenol may have prevented us from using extra-corporeal circulation for circulatory support.

39.5.2 Case Study of Inhaled Milrinone

An example of the effect of inhaled milrinone on two patients with PH undergoing cardiac surgery with CPB is illustrated in Fig. 39.8 [64]. Patients were considered to have PH if the systolic PAP was greater than 30 mmHg or the MPAP above

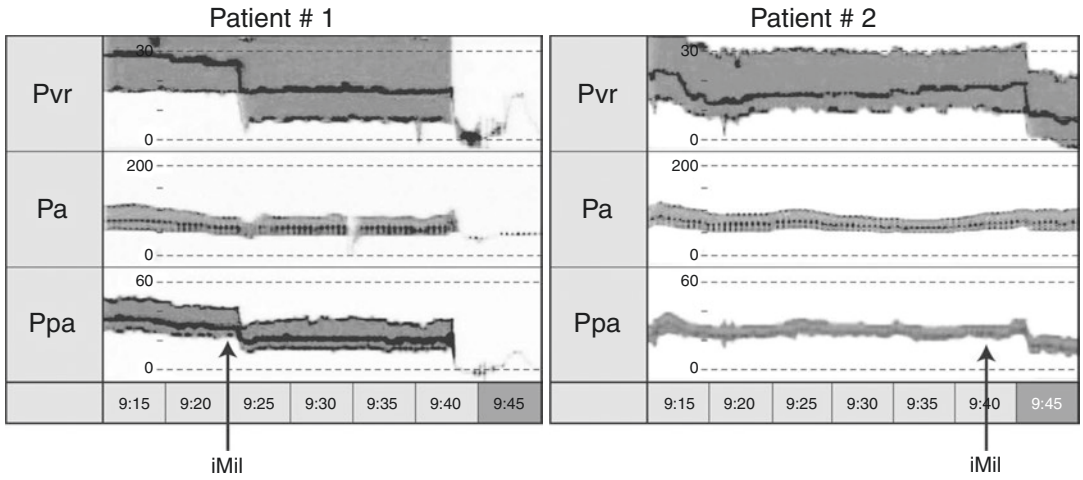

Fig. 39.8 Inhaled milrinone in two patients. Hemodynamic evolution of the right ventricular pressure (Prv), systemic arterial pressure (Pa) and pulmonary artery pressure (Ppa) in two patients after receiving inhaled milrinone (iMil) (arrow) before cardiopulmonary bypass. A reduction of the diastolic Prv and Ppa without any significant changes in Pa is observed (with permission of Denault et al. [64])

25 mmHg, as measured during the preoperative period or estimated by Doppler echocardiography. The diagnosis of PH was confirmed after insertion of a pulmonary artery catheter and before induction of general anesthesia. Inhaled milrinone was administered after the induction of anesthesia through a jet nebulizer attached to the inspiratory limb of the ventilator near the endotracheal tube with a bypass flow of oxygen at 10 L/min. Five milligrams (1 mg/mL) were administered, resulting in a dose ranging from 50 to 80 μg/kg, over 5 min. Hemodynamic evolution of the RV pressure (Prv), systemic arterial pressure (Pa) and PAP was monitored after receiving inhaled milrinone before CPB. Administration of inhaled milrinone was associated with a reduction of the diastolic Prv and PAP without any significant systemic hypotension.

39.5.3 Case Studies of the Combination of Inhaled Epoprostenol and Milrinone

39.5.3.1 Combined Inhaled Epoprostenol and Milrinone in the Operating Room

This next case describes the successful use of combined inhaled milrinone and epoprostenol for the intraoperative management of a high-risk patient with severe PH, RVF, and low NIRS [71]. A 26-year-old woman with no past medical history presented with progressive lower limb edema and fatigue. Physical examination revealed a heart rate of 101 beats/min, blood pressure of 110/79 mmHg, and bilateral leg edema. A diastolic "plop" and a low-frequency diastolic rumble were present on cardiac auscultation. Her electrocardiogram showed normal sinus rhythm. TTE revealed the presence of a large left atrial mass (4.9 8.1 cm, 31.8 cm^2 area) with dilated right-sided cavities (right atrium area 23.2 cm^2, RV area 34 cm^2) and an RV fractional area change of 15%. The patient was transferred to the tertiary care center for surgical removal of the tumor.

Invasive monitoring was inserted in the awake patient under local anesthesia upon arrival in the OR. Monitoring included a 5-lead electrocardiogram, pulse oximetry, peripheral venous catheter, radial and femoral arterial catheter, a 3-lumen central catheter, and a sheath introducer with a pulmonary artery catheter with a pacing port. The latter two were inserted into the internal right jugular vein, allowing a continuous display of Prv. General anesthesia was then induced. Before CPB, norepinephrine was infused at a rate of

8 mg/min to maintain mean arterial pressure above 60 mmHg and minimize reduction in systemic vascular resistance, considering the relatively fixed cardiac output from severe PH.

The intraoperative electrocardiographic and hemodynamic variables, capnographic, and NIRS signals are summarized in Fig. 39.9. Her initial hemodynamic values included sinus rhythm at 97 beats/min, arterial pressure at 110/72 with a mean of 83 mmHg. PAP and Prv were 102/57 (mean of 74 mmHg) and 102/20 with a cardiac index of 1.5 L/min/m^2. End-tidal CO_2 level was 34 mmHg. NIRS, which is used routinely in these cases, indicated 39% and 54% on the left and right forehead, respectively. Five mg of inhaled milrinone and 75 mg of epoprostenol were nebulized sequentially through the endotracheal tube with a nebulizer attached to the inspiratory limb. During nebulization, the PAP and Prv decreased to 96/44 (mean of 65) and 95/9 mmHg initially. Following inhaled drug administration, the systemic arterial pressure was 87/54 with a mean value of 66 mmHg. The Pap and Prv were 88/43 (mean of 59) and 83/11 mmHg, respectively. End-tidal CO_2 increased to 40 mmHg without any change in minute ventilation. In addition, normalization of both left and right NIRS values was observed. The left-sided value increased to 67% and the right to 78%. This was not associated with any significant changes in heart rate and no increases in norepinephrine perfusion rate were required. There was no significant change in the need for vasopressors while weaning the patient from CPB (norepinephrine at 7 mg/min). Neither inotropic nor vasodilatory agents were required to come off bypass. The cardiac output after CPB was 4.7 L/min with a cardiac index of 2.9 L/min/m^2. The RV systolic function improved but remained abnormal after CPB. The patient was extubated 5 h after surgery and discharged from the hospital 5 days later. Pathologic examination confirmed the diagnosis of left atrial myxoma. Administration of a combination of inhaled milrinone and epoprostenol after the induction of anesthesia, before going on CPB, improved the hemodynamic condition of the patient and was associated with an increase and normalization of the NIRS signal and an increase of the end-tidal capnographic signal as a surrogate of cardiac output.

39.5.3.2 Combined Inhaled Epoprostenol and Milrinone in the ICU

A 58-year-old woman with coronary and mitral valve disease presented for coronary revascularization and mitral valve repair. The patient was unstable in the ICU following the procedure. Her initial hemodynamic values are summarized in Fig. 39.10a. Arterial pressure was at 103/54 with a mean of 70 mmHg, PAP at 41/31 (mean of 34 mmHg), and Prv at 53/10 (mean of 25 mmHg). The square root appearance of the Prv waveform was indicative of RV dysfunction. Lactates were elevated at 4.0 mmol/L.

Sixty μg of inhaled epoprostenol and 4 mg of milrinone were nebulized sequentially through an ultrasonic nebulizer attached to the inspiratory limb of the ventilator near the endotracheal tube. As shown in Fig. 39.10b, administration of combined inhaled epoprostenol and milrinone resulted in normalization of the Prv waveform and reduction of lactate levels to 2.2 mmol/L, with no effect on systemic arterial pressure (101/52 with mean at 68 mmHg). The requirement for vasoactive agents was also reduced.

39.6 Intratracheal Milrinone

In acute RVF the administration of inhaled agents are limited by the availability of a nebuliser and also the time to administer them. In such situation, at the MHI we use intratracheal milrinone. Our preliminary experience has been described [72] and is being currently reviewed. An example of the use of intratracheal milrinone is illustrated in Fig. 39.11. An 80-year-old man presented with reduced biventricular function after revascularization. He was given 5 mg (1 mg/mL) of milrinone by direct administration into the tracheal tube using a 5 mL syringe. The acute effects of intratracheal milrinone on hemodynamic and transcranial Doppler variables are shown in Fig. 39.11. Administration of intratracheal

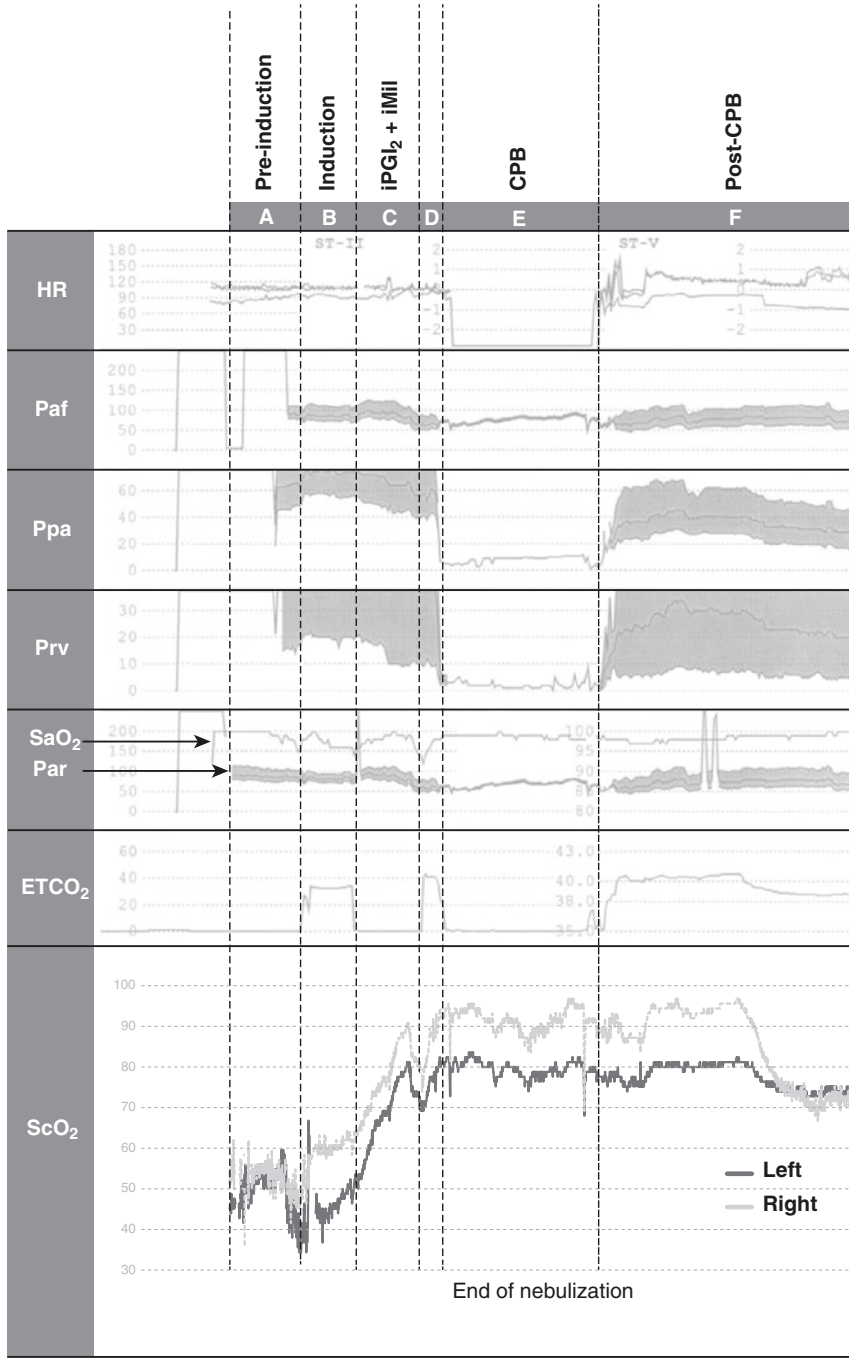

Fig. 39.9 Intraoperative summary. The heart rate (HR), femoral arterial pressure (Paf), pulmonary artery pressure (Ppa), right ventricular pressure (Prv), pulse oximetry (SaO_2), radial arterial pressure (Par), end-tidal carbon dioxide ($ETCO_2$), regional brain saturation signal of the right and left frontal hemispheres (ScO_2) are shown before induction of anesthesia (**a**), after induction (**b**), during administration of inhaled prostacyclin ($iPGI_2$) and inhaled milrinone (iMil) (**c**), following the administration if the inhaled drugs (**d**), during cardiopulmonary bypass (CPB) (**e**), and after CPB (**f**). Note the gradual increase in the ScO_2 signals during nebulization (period **c**) with corresponding reduction in the Ppa and Prv values (with permission of St-Pierre et al. [71])

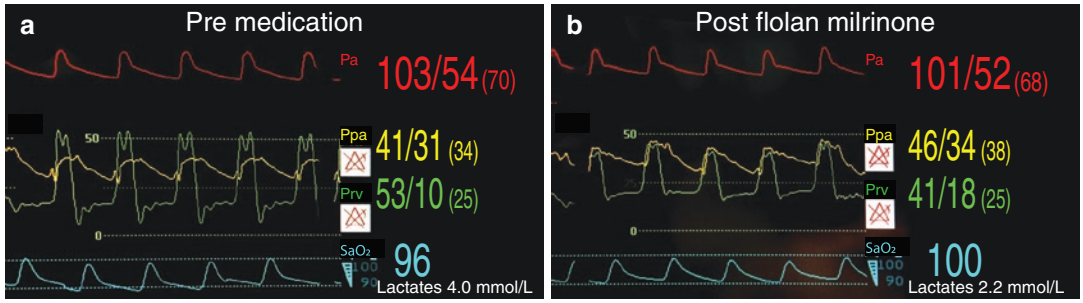

Fig. 39.10 Administration of combined flolan (epoprostenol) and milrinone in a 53-year-old woman with hemodynamic instability from right ventricular failure. Hemodynamic waveforms obtained before (**a**) and after treatment (**b**). Note the square root aspect of the right ventricular pressure (Prv) waveform, which normalised after treatment. *Pa* arterial pressure, *Ppa* pulmonary artery pressure, SaO_2 oxygen saturation

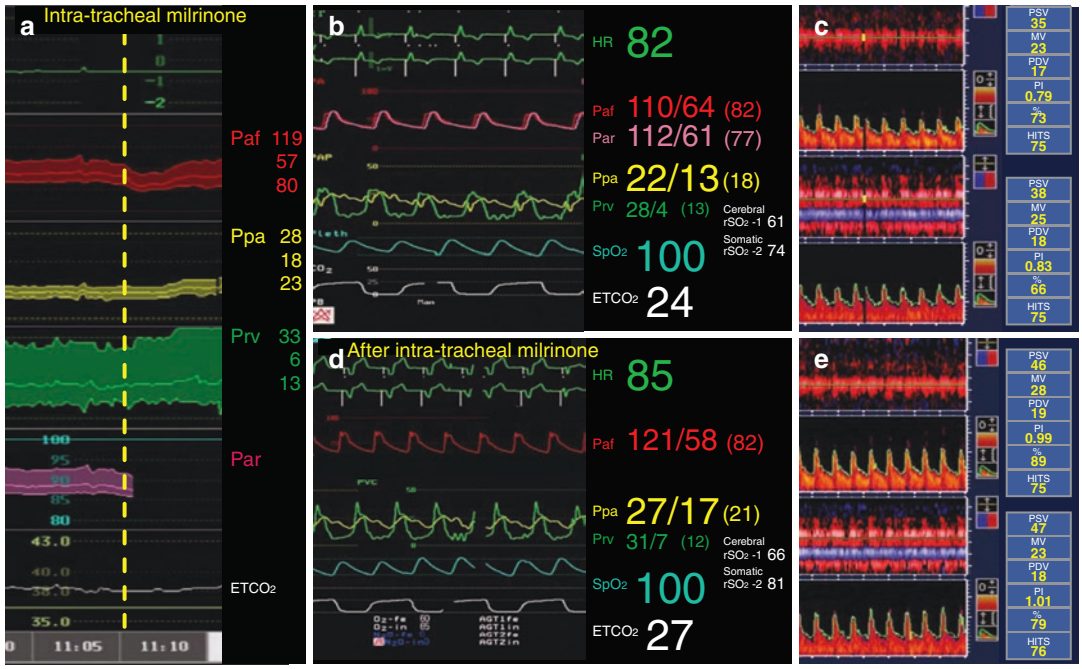

Fig. 39.11 Administration of intratracheal milrinone in an 80-year-old man after cardiopulmonary bypass (**a**) resulted in an increase in femoral arterial pressure (Paf), increase in pulmonary artery pressure (Ppa), right ventricular pressure (Prv) with an increase in pulse pressure. The hemodynamic waveform, cerebral and somatic regional oxygen saturation (rSO_2), end-tidal carbon dioxide ($ETCO_2$) and transcranial Doppler signal are shown before (**b**, **c**) and after (**d**, **e**) the administration of the drug through the intratracheal route. *HR* heart rate, *Par* radial arterial pressure, SpO_2 oxygen saturation, *PSV* peak systolic velocity, *MV* mean velocity, *PDV* peak diastolic velocity, *PI* pulsatility index, *HITS* high-intensity transient signals

milrinone resulted in an increase in the femoral arterial pressure, PAP, Prv, as well as transcranial Doppler signals values. Both cerebral and somatic rSO_2 increased following drug administration. Additionally, velocity time integral derived using TEE measured at the LV outflow tract went from 8 to 14 cm, and cardiac index increased from 1.3 to 1.8 L/m^2.

39.7 Meta-Analysis on Inhaled Vasodilators

In recent years, there has been a growing interest for using inhaled agents for the treatment of PH in cardiac surgery. The efficacy of these inhaled strategies, however, continue to be shown only through a limited number of small trials, case reports and series. A systematic review and meta-analysis was recently published comparing the efficacy of inhaled aerosolized agents with intravenously administered agents or placebo for the treatment and management of PH in patients undergoing cardiac surgery [73]. The purpose of this review was to summarize the state of the art in this field. Databases such as MEDLINE, CENTRAL, EMBASE, Web of Science, and clinicaltrials.gov were searched, which identified 2897 relevant citations. From those, 10 studies were included in the review and meta-analysis, comprising a total of 434 patients.

The primary outcome of the study was the incidence of mortality. Secondary outcomes were length of stay in hospital and in the ICU and evaluation of the hemodynamic profile. The meta-analysis revealed that inhaled aerosolized agents were associated with a significant decrease in pulmonary vascular resistance and a significant increase in mean arterial pressure and RV ejection fraction when compared to intravenously administered agents. No significant hemodynamically meaningful differences were observed between inhaled agents and placebo. However, an increase in length of stay in the ICU was shown with the use of inhaled aerosolized agents compared to placebo.

This systematic review and meta-analysis showed that the administration of inhaled aerosolized vasodilators is associated with improved RV performance when compared to intravenously administered agents for the treatment of PH during cardiac surgery. This study, however, did not show any benefit on mortality, nor did it support any benefit compared to placebo on major outcomes. The limitations of this review were the limited number of studies published on this topic and the small size of the trials. This review shows that more studies are required in this area of research and that these should focus on clinically significant outcomes.

Conclusion

In summary, inhaled vasodilators in patients with PH are first line therapy in our Institution mostly because of their significant hemodynamic advantage over intravenous agents. Combination therapy has now replaced the use of a single agent because the underlying mediators responsible for PH are often unknown. Therefore, targeting more than one pathway is more likely to be successful. Large trials in patients with PH comparing therapeutic strategies and analyzing their hemodynamic and their cardiac and extra-cardiac echocardiographic effects will help in better defining the role of inhaled agents in their ability to prevent and treat right heart failure in patients with PH.

References

1. Murali S, Kormos RL, Uretsky BF, Schechter D, Reddy PS, Denys BG, Armitage JM, Hardesty RL, Griffith BP. Preoperative pulmonary hemodynamics and early mortality after orthotopic cardiac transplantation: the Pittsburgh experience. Am Heart J. 1993;126(4):896–904.
2. Chen JM, Levin HR, Michler RE, Prusmack CJ, Rose EA, Aaronson KD. Reevaluating the significance of pulmonary hypertension before cardiac transplantation: determination of optimal thresholds and quantification of the effect of reversibility on perioperative mortality. J Thorac Cardiovasc Surg. 1997;114(4):627–34. https://doi.org/10.1016/s0022-5223(97)70053-9.
3. Reich DL, Bodian CA, Krol M, Kuroda M, Osinski T, Thys DM. Intraoperative hemodynamic predictors of mortality, stroke, and myocardial infarction after coronary artery bypass surgery. Anesth Analg. 1999;89(4):814–22.
4. Melby SJ, Moon MR, Lindman BR, Bailey MS, Hill LL, Damiano RJ Jr. Impact of pulmonary hypertension on outcomes after aortic valve replacement for aortic valve stenosis. J Thorac Cardiovasc Surg. 2011;141(6):1424–30. https://doi.org/10.1016/j.jtcvs.2011.02.028.
5. Kennedy JL, LaPar DJ, Kern JA, Kron IL, Bergin JD, Kamath S, Ailawadi G. Does the Society of Thoracic

Surgeons risk score accurately predict operative mortality for patients with pulmonary hypertension? J Thorac Cardiovasc Surg. 2013;146(3):631–7. https://doi.org/10.1016/j.jtcvs.2012.07.055.
6. D'Alonzo GE, Barst RJ, Ayres SM, Bergofsky EH, Brundage BH, Detre KM, Fishman AP, Goldring RM, Groves BM, Kernis JT. Survival in patients with primary pulmonary hypertension. Results from a national prospective registry. Ann Intern Med. 1991;115(5):343–9.
7. Reichert CL, Visser CA, van den Brink RB, Koolen JJ, van Wezel HB, Moulijn AC, Dunning AJ. Prognostic value of biventricular function in hypotensive patients after cardiac surgery as assessed by transesophageal echocardiography. J Cardiothorac Vasc Anesth. 1992;6(4):429–32. https://doi.org/10.1016/1053-0770(92)90008-U.
8. Davila-Roman VG, Waggoner AD, Hopkins WE, Barzilai B. Right ventricular dysfunction in low output syndrome after cardiac operations: assessment by transesophageal echocardiography. Ann Thorac Surg. 1995;60(4):1081–6. https://doi.org/10.1016/0003-4975(95)00526-Q.
9. Denault AY, Pearl RG, Michler RE, Rao V, Tsui SS, Seitelberger R, Cromie M, Lindberg E, D'Armini AM. Tezosentan and right ventricular failure in patients with pulmonary hypertension undergoing cardiac surgery: the TACTICS trial. J Cardiothorac Vasc Anesth. 2013;27(6):1212–7. https://doi.org/10.1053/j.jvca.2013.01.023.
10. Jacobs AK, Leopold JA, Bates E, Mendes LA, Sleeper LA, White H, Davidoff R, Boland J, Modur S, Forman R, Hochman JS. Cardiogenic shock caused by right ventricular infarction: a report from the SHOCK registry. J Am Coll Cardiol. 2003;41(8):1273–9.
11. Hill NS, Roberts KR, Preston IR. Postoperative pulmonary hypertension: etiology and treatment of a dangerous complication. Respir Care. 2009;54(7):958–68.
12. Gayat E, Mebazaa A. Pulmonary hypertension in critical care. Curr Opin Crit Care. 2011;17(5):439–48. https://doi.org/10.1097/MCC.0b013e32834a7619.
13. Stobierska-Dzierzek B, Awad H, Michler RE. The evolving management of acute right-sided heart failure in cardiac transplant recipients. J Am Coll Cardiol. 2001;38(4):923–31. https://doi.org/10.1016/S0735-1097(01)01486-3.
14. Zamanian RT, Haddad F, Doyle RL, Weinacker AB. Management strategies for patients with pulmonary hypertension in the intensive care unit. Crit Care Med. 2007;35(9):2037–50.
15. Riedel B. The pathophysiology and management of perioperative pulmonary hypertension with specific emphasis on the period following cardiac surgery. Int Anesthesiol Clin. 1999;37(2):55–79.
16. Goldman AP, Delius RE, Deanfield JE, Macrae DJ. Nitric oxide is superior to prostacyclin for pulmonary hypertension after cardiac operations. Ann Thorac Surg. 1995;60(2):300–5. https://doi.org/10.1016/0003-4975(95)00408-D.
17. Haj RM, Cinco JE, Mazer CD. Treatment of pulmonary hypertension with selective pulmonary vasodilators. Curr Opin Anaesthesiol. 2006;19(1):88–95. https://doi.org/10.1097/01.aco.0000192765.27453.5a.
18. Hillman ND, Meliones JN, Black DR, Craig DM, Cheifetz IM, Smith PK. In acute lung injury, inhaled nitric oxide improves ventilation-perfusion matching, pulmonary vascular mechanics, and transpulmonary vascular efficiency. J Thorac Cardiovasc Surg. 1995;110(3):593–9; discussion 599–600. https://doi.org/10.1016/s0022-5223(95)70089-7.
19. Walmrath D, Schneider T, Schermuly R, Olschewski H, Grimminger F, Seeger W. Direct comparison of inhaled nitric oxide and aerosolized prostacyclin in acute respiratory distress syndrome. Am J Respir Crit Care Med. 1996;153(3):991–6. https://doi.org/10.1164/ajrccm.153.3.8630585.
20. Olschewski H, Ghofrani HA, Walmrath D, Schermuly R, Temmesfeld-Wollbruck B, Grimminger F, Seeger W. Inhaled prostacyclin and iloprost in severe pulmonary hypertension secondary to lung fibrosis. Am J Respir Crit Care Med. 1999;160(2):600–7. https://doi.org/10.1164/ajrccm.160.2.9810008.
21. Rocca GD, Coccia C, Pompei L, Ruberto F, Venuta F, De GT, Pietropaoli P. Hemodynamic and oxygenation changes of combined therapy with inhaled nitric oxide and inhaled aerosolized prostacyclin. J Cardiothorac Vasc Anesth. 2001;15(2):224–7. https://doi.org/10.1053/jcan.2001.21974.
22. Lowson SM. Inhaled alternatives to nitric oxide. Anesthesiology. 2002;96(6):1504–13. https://doi.org/00000542-200206000-00034.
23. Ivy DD. Prostacyclin in the intensive care setting. Pediatr Crit Care Med. 2010;11(2 Suppl):S41–5. https://doi.org/10.1097/PCC.0b013e3181d10845.
24. Celermajer DS. Endothelial dysfunction: does it matter? Is it reversible? J Am Coll Cardiol. 1997;30(2):325–33.
25. Budhiraja R, Tuder RM, Hassoun PM. Endothelial dysfunction in pulmonary hypertension. Circulation. 2004;109(2):159–65. https://doi.org/10.1161/01.cir.0000102381.57477.50.
26. Veyssier-Belot C, Cacoub P. Role of endothelial and smooth muscle cells in the physiopathology and treatment management of pulmonary hypertension. Cardiovasc Res. 1999;44(2):274–82.
27. Humbert M, Sitbon O, Simonneau G. Treatment of pulmonary arterial hypertension. N Engl J Med. 2004;351(14):1425–36. https://doi.org/10.1056/NEJMra040291.
28. McGoon MD, Kane GC. Pulmonary hypertension: diagnosis and management. Mayo Clin Proc. 2009;84(2):191–207. https://doi.org/10.1016/S0025-6196(11)60828-8.
29. Agarwal R, Gomberg-Maitland M. Current therapeutics and practical management strategies for pulmonary arterial hypertension. Am Heart J. 2011;162(2):201–13. https://doi.org/10.1016/j.ahj.2011.05.012.

30. Lai YC, Potoka KC, Champion HC, Mora AL, Gladwin MT. Pulmonary arterial hypertension: the clinical syndrome. Circ Res. 2014;115(1):115–30. https://doi.org/10.1161/circresaha.115.301146.
31. Humbert M, Sitbon O, Simonneau G. Novel therapeutic perspectives in pulmonary arterial hypertension. Eur Respir J. 2003;22(2):193–4.
32. Benza RL, Park MH, Keogh A, Girgis RE. Management of pulmonary arterial hypertension with a focus on combination therapies. J Heart Lung Transplant. 2007;26(5):437–46. https://doi.org/10.1016/j.healun.2007.01.035.
33. Lajoie AC, Lauziere G, Lega JC, Lacasse Y, Martin S, Simard S, Bonnet S, Provencher S. Combination therapy versus monotherapy for pulmonary arterial hypertension: a meta-analysis. Lancet Respir Med. 2016;4(4):291–305. https://doi.org/10.1016/s2213-2600(16)00027-8.
34. Fox BD, Shtraichman O, Langleben D, Shimony A, Kramer MR. Combination therapy for pulmonary arterial hypertension: a systematic review and meta-analysis. Can J Cardiol. 2016;32(12):1520–30. https://doi.org/10.1016/j.cjca.2016.03.004.
35. Blaise G, Langleben D, Hubert B. Pulmonary arterial hypertension: pathophysiology and anesthetic approach. Anesthesiology. 2003;99(6):1415–32. https://doi.org/00000542-200312000-00027.
36. Haraldsson A, Kieler-Jensen N, Ricksten SE. The additive pulmonary vasodilatory effects of inhaled prostacyclin and inhaled milrinone in postcardiac surgical patients with pulmonary hypertension. Anesth Analg. 2001;93(6):1439–45.
37. Schermuly RT, Ghofrani HA, Enke B, Weissmann N, Grimminger F, Seeger W, Schudt C, Walmrath D. Low-dose systemic phosphodiesterase inhibitors amplify the pulmonary vasodilatory response to inhaled prostacyclin in experimental pulmonary hypertension. Am J Respir Crit Care Med. 1999;160(5 Pt 1):1500–6. https://doi.org/10.1164/ajrccm.160.5.9901102.
38. Schermuly RT, Krupnik E, Tenor H, Schudt C, Weissmann N, Rose F, Grimminger F, Seeger W, Walmrath D, Ghofrani HA. Coaerosolization of phosphodiesterase inhibitors markedly enhances the pulmonary vasodilatory response to inhaled iloprost in experimental pulmonary hypertension. Maintenance of lung selectivity. Am J Respir Crit Care Med. 2001;164(9):1694–700. https://doi.org/10.1164/ajrccm.164.9.2105060.
39. Schermuly RT, Inholte C, Ghofrani HA, Gall H, Weissmann N, Weidenbach A, Seeger W, Grimminger F. Lung vasodilatory response to inhaled iloprost in experimental pulmonary hypertension: amplification by different type phosphodiesterase inhibitors. Respir Res. 2005;6:76. https://doi.org/10.1186/1465-9921-6-76.
40. Ghofrani HA, Rose F, Schermuly RT, Olschewski H, Wiedemann R, Weissmann N, Schudt C, Tenor H, Seeger W, Grimminger F. Amplification of the pulmonary vasodilatory response to inhaled iloprost by subthreshold phosphodiesterase types 3 and 4 inhibition in severe pulmonary hypertension. Crit Care Med. 2002;30(11):2489–92. https://doi.org/10.1097/01.CCM.0000034559.25857.90.
41. Levinson AT, Klinger JR. Combination therapy for the treatment of pulmonary arterial hypertension. Ther Adv Respir Dis. 2011;5(6):419–30. https://doi.org/10.1177/1753465811411602.
42. Zaccolo M, Movsesian MA. cAMP and cGMP signaling cross-talk: role of phosphodiesterases and implications for cardiac pathophysiology. Circ Res. 2007;100(11):1569–78. https://doi.org/10.1161/circresaha.106.144501.
43. Murthy KS, Zhou H, Makhlouf GM. PKA-dependent activation of PDE3A and PDE4 and inhibition of adenylyl cyclase V/VI in smooth muscle. Am J Physiol Cell Physiol. 2002;282(3):C508–17. https://doi.org/10.1152/ajpcell.00373.2001.
44. Pickles H, O'Grady J. Side effects occurring during administration of epoprostenol (prostacyclin, PGI2), in man. Br J Clin Pharmacol. 1982;14(2):177–85.
45. Rich S, McLaughlin VV. The effects of chronic prostacyclin therapy on cardiac output and symptoms in primary pulmonary hypertension. J Am Coll Cardiol. 1999;34(4):1184–7.
46. Ivy DD, Doran A, Claussen L, Bingaman D, Yetman A. Weaning and discontinuation of epoprostenol in children with idiopathic pulmonary arterial hypertension receiving concomitant bosentan. Am J Cardiol. 2004;93(7):943–6. https://doi.org/10.1016/j.amjcard.2003.12.031.
47. Saito Y, Nakamura K, Akagi S, Sarashina T, Ejiri K, Miura A, Ogawa A, Matsubara H, Ito H. Epoprostenol sodium for treatment of pulmonary arterial hypertension. Vasc Health Risk Manag. 2015;11:265–70. https://doi.org/10.2147/vhrm.s50368.
48. Denault A, Lamarche Y, Rochon A, Cogan J, Liszkowski M, Lebon JS, Ayoub C, Taillefer J, Blain R, Viens C, Couture P, Deschamps A. Innovative approaches in the perioperative care of the cardiac surgical patient in the operating room and intensive care unit. Can J Cardiol. 2014;30(12 Suppl):S459–77. https://doi.org/10.1016/j.cjca.2014.09.029.
49. Denault AY, Haddad F, Jacobsohn E, Deschamps A. Perioperative right ventricular dysfunction. Curr Opin Anaesthesiol. 2013;26(1):71–81. https://doi.org/10.1097/ACO.0b013e32835b8be2.
50. Haddad F, Elmi-Sarabi M, Fadel E, Mercier O, Denault AY. Pearls and pitfalls in managing right heart failure in cardiac surgery. Curr Opin Anaesthesiol. 2016;29(1):68–79. https://doi.org/10.1097/aco.0000000000000284.
51. Fischer GW, Lin HM, Krol M, Galati MF, Di Luozzo G, Griepp RB, Reich DL. Noninvasive cerebral oxygenation may predict outcome in patients undergoing aortic arch surgery. J Thorac Cardiovasc Surg. 2011;141(3):815–21. https://doi.org/10.1016/j.jtcvs.2010.05.017.

52. Casati A, Fanelli G, Pietropaoli P, Proietti R, Tufano R, Montanini S, Danelli G, Nuzzi M, Mentegazzi F, Torri G, Martani C, Spreafico E, Fierro G, Pugliese F, De Cosmo G, Aceto P, Servillo G, Monaco F. Monitoring cerebral oxygen saturation in elderly patients undergoing general abdominal surgery: a prospective cohort study. Eur J Anaesthesiol. 2007;24(1):59–65. https://doi.org/10.1017/s0265021506001025.
53. Casati A, Fanelli G, Pietropaoli P, Proietti R, Tufano R, Danelli G, Fierro G, De Cosmo G, Servillo G. Continuous monitoring of cerebral oxygen saturation in elderly patients undergoing major abdominal surgery minimizes brain exposure to potential hypoxia. Anesth Analg. 2005;101(3):740–7. https://doi.org/10.1213/01.ane.0000166974.96219.cd.
54. Murkin JM, Adams SJ, Novick RJ, Quantz M, Bainbridge D, Iglesias I, Cleland A, Schaefer B, Irwin B, Fox S. Monitoring brain oxygen saturation during coronary bypass surgery: a randomized, prospective study. Anesth Analg. 2007;104(1):51–8. https://doi.org/10.1213/01.ane.0000246814.29362.f4.
55. Heringlake M, Garbers C, Kabler JH, Anderson I, Heinze H, Schon J, Berger KU, Dibbelt L, Sievers HH, Hanke T. Preoperative cerebral oxygen saturation and clinical outcomes in cardiac surgery. Anesthesiology. 2011;114(1):58–69. https://doi.org/10.1097/ALN.0b013e3181fef34e.
56. Gallix BP, Taourel P, Dauzat M, Bruel JM, Lafortune M. Flow pulsatility in the portal venous system: a study of Doppler sonography in healthy adults. AJR Am J Roentgenol. 1997;169(1):141–4. https://doi.org/10.2214/ajr.169.1.9207514.
57. Duerinckx AJ, Grant EG, Perrella RR, Szeto A, Tessler FN. The pulsatile portal vein in cases of congestive heart failure: correlation of duplex Doppler findings with right atrial pressures. Radiology. 1990;176(3):655–8. https://doi.org/10.1148/radiology.176.3.2202011.
58. Hosoki T, Arisawa J, Marukawa T, Tokunaga K, Kuroda C, Kozuka T, Nakano S. Portal blood flow in congestive heart failure: pulsed duplex sonographic findings. Radiology. 1990;174(3 Pt 1):733–6. https://doi.org/10.1148/radiology.174.3.2406781.
59. Amsallem M, Kuznetsova T, Hanneman K, Denault A, Haddad F. Right heart imaging in patients with heart failure: a tale of two ventricles. Curr Opin Cardiol. 2016;31(5):469–82. https://doi.org/10.1097/hco.0000000000000315.
60. Tremblay JA, Beaubien-Souligny W, Elmi-Sarabi M, Desjardins G, Denault AY. Point-of-care ultrasonography to assess portal vein pulsatility and the effect of inhaled milrinone and epoprostenol in severe right ventricular failure: a report of 2 cases. A A Case Rep. 2017;9(8):219–23. https://doi.org/10.1213/xaa.0000000000000572.
61. Fortier S, DeMaria RG, Lamarche Y, Malo O, Denault A, Desjardins F, Carrier M, Perrault LP. Inhaled prostacyclin reduces cardiopulmonary bypass-induced pulmonary endothelial dysfunction via increased cyclic adenosine monophosphate levels. J Thorac Cardiovasc Surg. 2004;128(1):109–16. https://doi.org/10.1016/j.jtcvs.2003.09.056.
62. Lamarche Y, Malo O, Thorin E, Denault A, Carrier M, Roy J, Perrault LP. Inhaled but not intravenous milrinone prevents pulmonary endothelial dysfunction after cardiopulmonary bypass. J Thorac Cardiovasc Surg. 2005;130(1):83–92. https://doi.org/10.1016/j.jtcvs.2004.09.011.
63. Lamarche Y, Perrault LP, Maltais S, Tetreault K, Lambert J, Denault AY. Preliminary experience with inhaled milrinone in cardiac surgery. Eur J Cardiothorac Surg. 2007;31(6):1081–7. https://doi.org/10.1016/j.ejcts.2007.02.019.
64. Denault A, Haddad F, Lamarche Y, Nguyen A, Varin F, Levesque S, Shi Y, Perrault P, Tardif J, Lambert J. Pilot randomized controlled trial of inhaled milrinone in high-risk cardiac surgical patients. Surg Curr Res. 2014;4(4):192.
65. Denault AY, Bussières JS, Arellano R, Finnegan B, Gavra P, Haddad F, Nguyen AQ, Varin F, Fortier A, Levesque S, Shi Y, Elmi-Sarabi M, Tardif JC, Perrault LP, Lambert J. Multicenter randomized-controlled trial of inhaled milrinone in high-risk cardiac surgical patients. Can J Anesth. 2016;63(10):1140–53.
66. Hache M, Denault AY, Belisle S, Couture P, Babin D, Tetrault F, Guimond JG. Inhaled prostacyclin (PGI2) is an effective addition to the treatment of pulmonary hypertension and hypoxia in the operating room and intensive care unit. Can J Anesth. 2001;48(9):924–9. https://doi.org/10.1007/bf03017361.
67. Hache M, Denault A, Belisle S, Robitaille D, Couture P, Sheridan P, Pellerin M, Babin D, Noel N, Guertin MC, Martineau R, Dupuis J. Inhaled epoprostenol (prostacyclin) and pulmonary hypertension before cardiac surgery. J Thorac Cardiovasc Surg. 2003;125(3):642–9. https://doi.org/10.1067/mtc.2003.107.
68. Laflamme M, Perrault LP, Carrier M, Elmi-Sarabi M, Fortier A, Denault AY. Preliminary experience with combined inhaled milrinone and prostacyclin in cardiac surgical patients with pulmonary hypertension. J Cardiothorac Vasc Anesth. 2015;29(1):38–45. https://doi.org/10.1053/j.jvca.2014.06.012.
69. Martineau A, Arcand G, Couture P, Babin D, Perreault LP, Denault A. Transesophageal echocardiographic diagnosis of carbon dioxide embolism during minimally invasive saphenous vein harvesting and treatment with inhaled epoprostenol. Anesth Analg. 2003;96(4):962–4.
70. Chavanon O, Tremblay I, Delay D, Bouveret A, Blain R, Perrault LP. Carbon dioxide embolism during endoscopic saphenectomy for coronary artery bypass surgery. J Thorac Cardiovasc Surg. 1999;118(3):557–8. https://doi.org/10.1016/s0022-5223(99)70196-0.
71. St-Pierre P, Deschamps A, Cartier R, Basmadjian AJ, Denault AY. Inhaled milrinone and epoprostenol in a patient with severe pulmonary hypertension, right ventricular failure, and reduced baseline brain saturation

value from a left atrial myxoma. J Cardiothorac Vasc Anesth. 2014;28(3):723–9. https://doi.org/10.1053/j.jvca.2012.10.017.

72. Gebhard CE, Desjardins G, Gebhard C, Gavra P, Denault AY. Intratracheal milrinone bolus administration during acute right ventricular dysfunction after cardiopulmonary bypass. J Cardiothorac Vasc Anesth. 2017;31(2):489–96. https://doi.org/10.1053/j.jvca.2016.11.033.
73. Elmi-Sarabi M, Deschamps A, Delisle S, Ased H, Haddad F, Lamarche Y, Perrault LP, Lambert J, Turgeon AF, Denault AY. Aerosolized vasodilators for the treatment of pulmonary hypertension in cardiac surgical patients: a systematic review and meta-analysis. Anesth Analg. 2017;125(2):393–402. https://doi.org/10.1213/ANE.0000000000002138.

40 Importance of Extra-Cardiac Manifestations of Right Heart Failure Using Bedside Ultrasound

William Beaubien-Souligny, Nadia Bouabdallaoui, and André Denault

Abstract

Organ ischemia in the context of right ventricular dysfunction are the result of the profound hemodynamic alterations caused by a decrease in cardiac output and an elevation in central venous pressure. Performing a focused extra-cardiac ultrasound examination can reveal the impact of right ventricular failure by identifying signs of venous congestion in distal organs and might provide clinically relevant information to personalise management.

Keywords

Point-of-care ultrasound · Doppler ultrasound Congestive heart failure · Right ventricular failure · Cardiorenal syndrome · Cardiointestinal syndrome · Venous congestion

W. Beaubien-Souligny
Department of Medicine, Université de Montréal, Montreal, QC, Canada

N. Bouabdallaoui
Department of Cardiology, Université de Montréal, Montreal, QC, Canada

A. Denault (✉)
Department of Anesthesiology, Montreal Heart Institute, Montreal, QC, Canada
e-mail: andre.denault@umontreal.ca

Abbreviations

ARDS	Acute respiratory distress syndrome
CI	Collapsibility index
CVP	Central venous pressure
EVLW	Extravascular lung water
ICP	Intra-cranial pressure
IJV	Internal jugular vein
IVC	Inferior vena cava
MCA	Middle cerebral artery
PF	Pulsatility fraction
PI	Pulsatility index
RAP	Right atrial pressure
TAPSE	Tricuspid annular plane systolic excursion

40.1 Introduction

The progressive increase in central venous pressure (CVP) in patients with right heart failure has a detrimental impact on organ function. The cardio-renal syndrome, the cardio-intestinal syndrome and the cardio-hepatic syndrome have all been attributed to an inadequate tissue delivery of oxygen and nutriments stemming from a combination of decreased cardiac output and increased venous pressures. While autonomic and hormonal

S. I. Dumitrescu et al. (eds.), *Right Heart Pathology*, https://doi.org/10.1007/978-3-319-73764-5_40

autoregulation is able to compensate for a reduced cardiac index to maintain adequate blood flow until it falls below a critical threshold [1], the presence of elevated venous pressure creates a synergy where interstitial edema and a reduced arterio-venous gradient is providing the "second-hit" resulting in organ dysfunction. Venous congestion appears to be one of the most important factors leading to adverse outcomes in patients with heart failure [2]. Additionally, it is now believed to be an important mediator of multiorgan complications in critically ill patients (Table 40.1). Consequently, finding new tools to tailor diuretic therapy in patients with right heart failure might be one of the most promising strategies to improve their prognostic.

In order to assess venous congestion, clinicians are used to rely on physical examination and on the dosage of B-type natriuretic peptide. While it can be useful in daily practice, lower extremity edema is not reliable to evaluate increased CVP [3]. Jugular venous pressure examination at the bedside has variable accuracy depending on the skills of the observer and can be impossible in some patients [4].

The use of a focused bedside ultrasound assessment has significantly enhanced clinical examination in various inpatients and outpatient's settings. The assessment of right heart function using echocardiography described in Chaps. 31 to 34 is important to establish the diagnosis and etiology of right heart failure but is of limited use for monitoring the effect of increased CVP on end-organs and is not helpful to guide diuretic therapy. The use of bedside ultrasound to assess signs of venous congestion directly in end-organs can provide important information in order to individualize management. This chapter focuses on the multisystemic ultrasound features associated with organ congestion from right heart failure.

Table 40.1 Adverse effects of organ congestion in critically ill patients

Involved systems	Clinical consequences	Evidence
Gastrointestinal	– Prolonged ileus – Bacterial endotoxin translocation: systemic inflammation – Impaired hepatic function and cholestasis – Impaired drug absorption	– A restrictive fluid strategy leads to shorter hospital stay after intestinal surgery [69] – Higher measurements of serum LPS in decompensated CHF patients [33] – Post-hepatic portal hypertension and hyperbilirubinemia in CHF patients [70] – Diuretic resistance in CHF patients [71]
Kidney	– Acute kidney injury	– Fluid overload is an independent risk factor for acute kidney injury in critically ill adults [72, 73] – Elevated CVP is a predictive factor of renal impairment in CHF patients [38] and in cardiac surgery patients [74]
Lungs	– Pulmonary edema – Decreased compliance – Increased work of breathing	– A restrictive fluid strategy has led to fewer ventilator days in patients with ARDS [75] – EVLW correlated with organ dysfunction and poor outcomes and with increased risk of re-intubation and respiratory failure [76]
Central nervous system	– Impairment in cognition and delirium	– Fluid overloaded patients could be at greater risk of delirium [77] – CHF after surgery is a risk factor for post-operative delirium [78] – In an animal model of intra-abdominal hypertension, intracranial pressure correlated with CVP values [56]
Heart	– Conduction abnormalities – Sub-endocardial ischemia	– Myocardial edema may contribute to increased risk of atrial fibrillation and bundle branch block in critically ill patients [79]
Soft tissues	– Impaired wound healing – Promote surgical site infections	– A restrictive fluid regimen reduced post-operative wound healing complications after colorectal surgery [80]

ARDS acute respiratory distress syndrome, *CHF* chronic heart failure, *CVP* central venous pressure, *EVLW* extravascular lung water, *LPS* lipopolysaccharide (endotoxin)

40.2 Assessment of Central Vessels

Ultrasound measurements of the inferior vena cava (IVC) have been used for the evaluation of fluid responsiveness in the hemodynamically unstable patient under the prerequisite that they are representative of right ventricular preload. The IVC diameter and collapsibility are now integrated in focused ultrasound assessment in trauma patients [5] and IVC collapse is the best predictor of hypotension following induction of anesthesia [6]. Some measurements may reflect abnormally high CVP (10–20 mmHg), such as an IVC diameter of more than 20 mm, a collapse of IVC (CI) of less than 50% with sudden inspiration [7], variation of less than 20% of IVC diameter upon normal inspiration [8], or a short diameter to long diameter ratio of more than 0.69 [9]. Many studies have evaluated the correlation between IVC diameter/collapsibility index and CVP with variable results, showing a moderate correlation and relatively fair accuracy to predict CVP [8, 10–13]. While ultrasonographic measurements of the IVC do not seem to be precise enough to estimate absolute CVP values, they can discriminate between normal/low CVP and high CVP [8, 11]. Consequently, finding a non-dilatated IVC presenting respiratory variations on bedside ultrasound can rule-out elevated CVP and therefore exclude cardiogenic venous congestion of end-organs while a dilated IVC without respiratory variations warrant for a more in-depth evaluation for the others signs of venous congestion.

The technique of evaluation is shown in Fig. 40.1. Longitudinal imaging of the IVC can

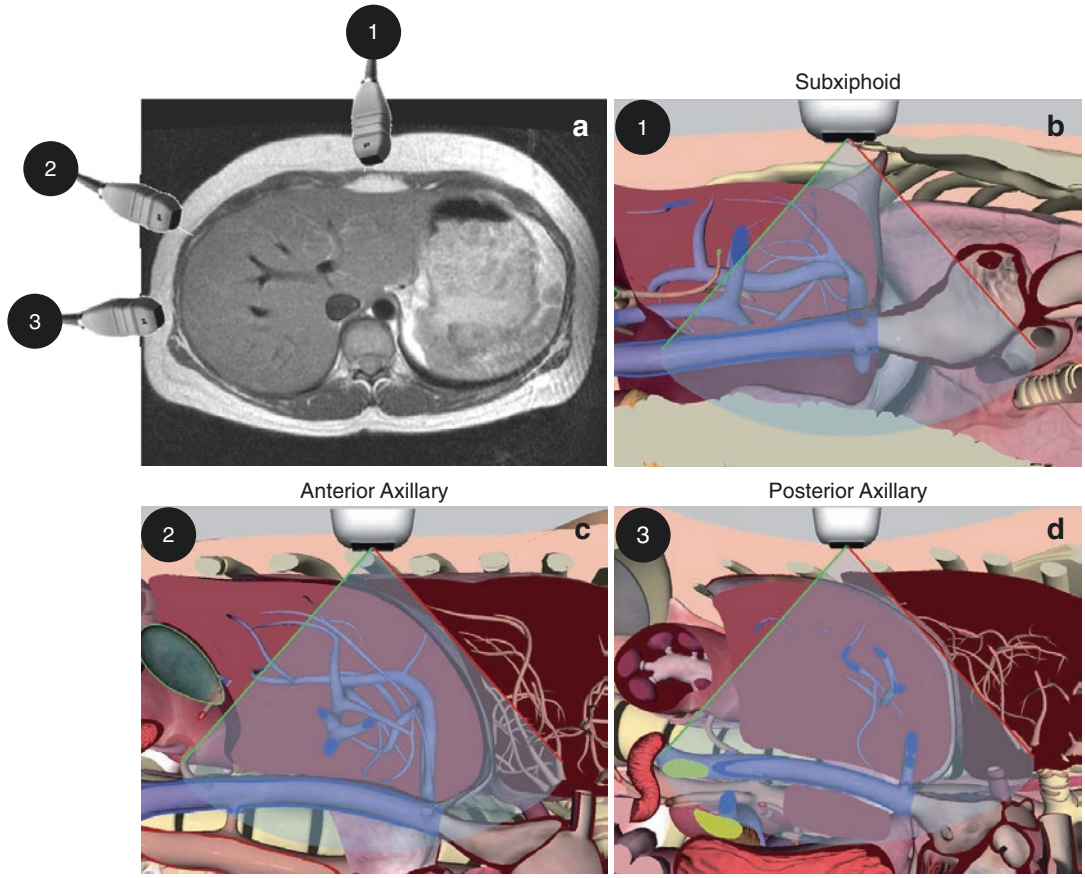

Fig. 40.1 Examination of the inferior vena cava (IVC): (**a**) Axial T1 weighted magnetic resonance image of the liver showing different positions of the ultrasound probe to obtain a longitudinal view of the IVC. The subxyphoid [1], anterior axillary line [2] and posterior axillary line [3]. The subxyphoid (**b**), anterior axillary line (**c**), posterior axillary line (**d**) position is shown using the Vimedix simulator (with permission of Denault et al. [82])

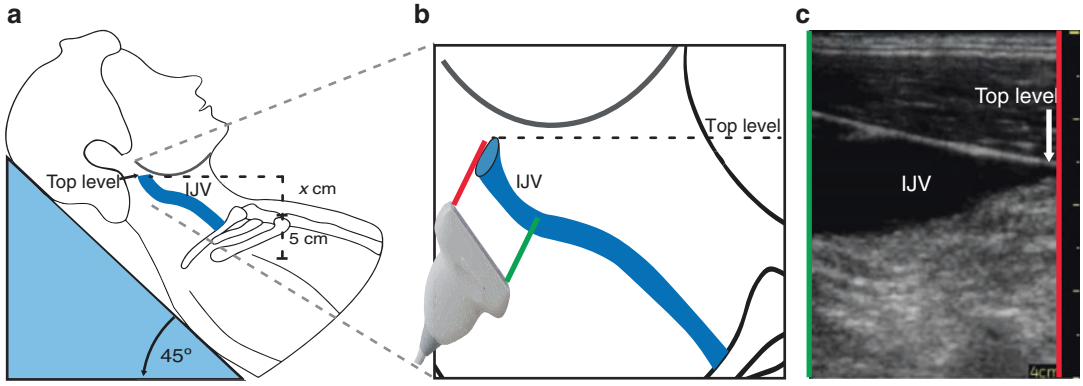

Fig. 40.2 Examination of the internal jugular vein (IJV) (**a**) Measurements of the vertical distance between the top of the IJV and the sternal angle. Central venous pressure is estimated by adding 5 cm to the measured height at a 30–45° angle [18]. (**b**) Linear probe position to obtain a longitudinal view of the IJV. (**c**) Visualization of the IJV taper point (with permission of Beaubien-Souligny et al. [84])

be done though the liver with a phased array transducer (cardiac probe) or a curved array transducer (abdominal probe) from the subxiphoid position down to the posterior axillary line providing a large window for adequate visualization. Using the liver as an acoustic window, the success rate in visualizing the IVC is very high even for clinicians with basic training [14]. It should be noted there is some limitation to the estimation of systemic venous pressure with this technique as any supra-diaphragmatic mechanical obstruction can impair venous return [9, 15]. Consequently, tamponade, pneumothorax, or direct obstruction of the IVC from stenosis or thrombus should the suspected according to the clinical context. Measurements of the IVC are modified by positive pressure ventilation and should be interpreted with caution in mechanically ventilated patients [10]. A high positive end expiratory pressure (PEEP) or lung hyperinflation can lead to a larger IVC size leading to potential overestimation of cardiac preload [16]. However, in mechanically ventilated patients, IVC distensibility >18% with passive respiration has been shown to predict fluid responsiveness [17]. In addition, measuring the IVC in both short- and long-axis plane is more accurate in terms of estimating CVP [9].

Bedside ultrasound can also be used to estimate jugular venous pressure non-invasively very quickly. The technique relies on the visualization of the right jugular vein tapering point as presented in Fig. 40.2. Using a linear probe, the right jugular vein can be located to obtain a longitudinal image. Minimal pressure must be applied to the probe as the internal jugular vein is easily collapsible. After identification of the taper point, CVP can be estimated by measuring the height as for physical examination [18]. This technique can predict CVP with moderate accuracy in a few seconds at the bedside [19]. It must be noted that this technique has been reported to underestimate CVP and should be interpreted with caution [20].

40.3 Assessment of Liver and Spleen

Doppler ultrasound of the liver offers the possibility to assess flow in the hepatic and portal veins. These can provide an important insight into the severity of right ventricular failure and hepatic congestion, respectively.

Hepatic venous flow can be used to evaluate right ventricular diastolic function [7] based on the aspect of the Doppler signal pattern [21, 22].

Hepatic vein flow can be obtained using a phased array probe or a curved array probe in the subxiphoid or lateral chest regions as presented in Fig. 40.3. Normal hepatic flow is directed away from the liver and fluctuates during the cardiac cycle as shown in Fig. 40.3a–d [23]. Systolic flow is usually of higher velocity than diastolic flow. This is due to downward motion of the tricuspid annulus during ventricular systole resulting in a rapid filling of the right atria. In patients with right heart failure, decreased tricuspid annulus plane systolic excursion (TAPSE) and/or tricuspid regurgitation during ventricular systole lead to a reduction of the velocity in systole and to a systolic-to-diastolic ratio less than 1 as shown in Fig. 40.3e–h [22, 24, 25]. In severe right heart failure or tricuspid regurgitation, the S wave appears to be completely reversed with backward flow in the hepatic veins during systole. While an abnormal hepatic vein flow waveform can be found in stable chronic heart failure patients and is not synonymous with organ congestion, its presence should prompt the clinician to consider the patient to have right heart failure and to be at increased risk of organ congestion.

Flow in the portal vein can be assessed using a phased array or a curved linear array probe positioned in a right mid-axillary coronal view as shown in Fig. 40.4 [26]. Venous flow through the portal vein is of low velocity (20 cm/s) because this circulation is isolated from the systemic circulation by the liver sinusoids and splanchnic capillary bed. Therefore, portal venous flow present minimal variations through the cardiac cycle. A difference between systolic and diastolic velocities (also named pulsatility fraction (PF)) of more than 50% can be considered abnormal and is called pulsatile portal flow.

$$PF\left(\%\right) = 100\left[\left(V_{Systole} - V_{Diastole}\right) / V_{Systole}\right]$$

Pulsatile blood flow is a sign of post-hepatic portal hypertension and has been studied as a sign of severity in patients with congestive heart failure. The presence of an abnormal portal pulsatility predicted increased CVP and worse functional class in heart failure patients [27–29]. Venous congestion resulting from congestive heart failure begins with an elevation of the CVP and dilatation of the IVC and its main tributaries such as the hepatic veins. When the dilatation becomes severe, the venous compliance of the IVC is decreased and pressure is transmitted through the hepatic sinusoids to the portal system. This results in a decrease in velocities in the portal system or, when severe, in a complete absence or reversal of portal flow. Doppler

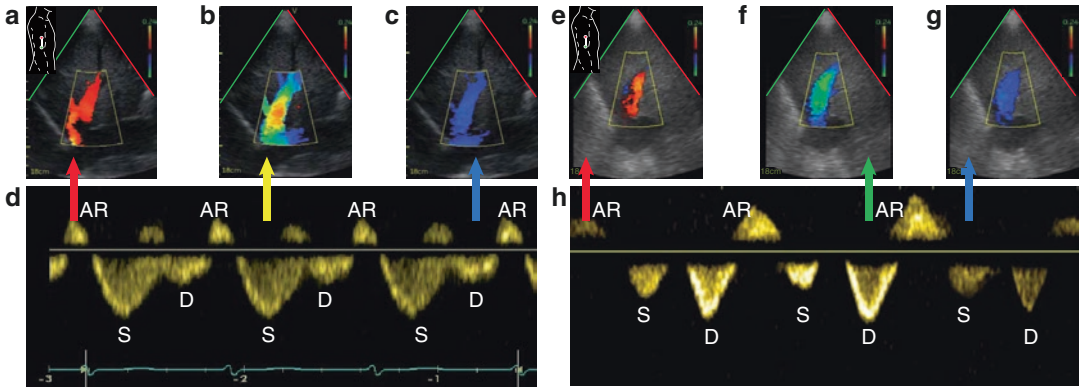

Fig. 40.3 Examination of hepatic venous flow. Triphasic Doppler hepatic venous flow obtained from a subxyphoid abdominal ultrasound image with color (**a**–**c**) and pulsed-wave Doppler (**d**) has an atrial reversal (AR) in red, a systolic (S) phase in blue/green which can be followed by a V wave, and a diastolic (D) phase in dark blue. Images **e**–**h** show abnormal hepatic venous flow in the context of right ventricular dysfunction. Notice the change in the D to S velocity ratio that is now less than 1 (with permission of Denault et al. [82])

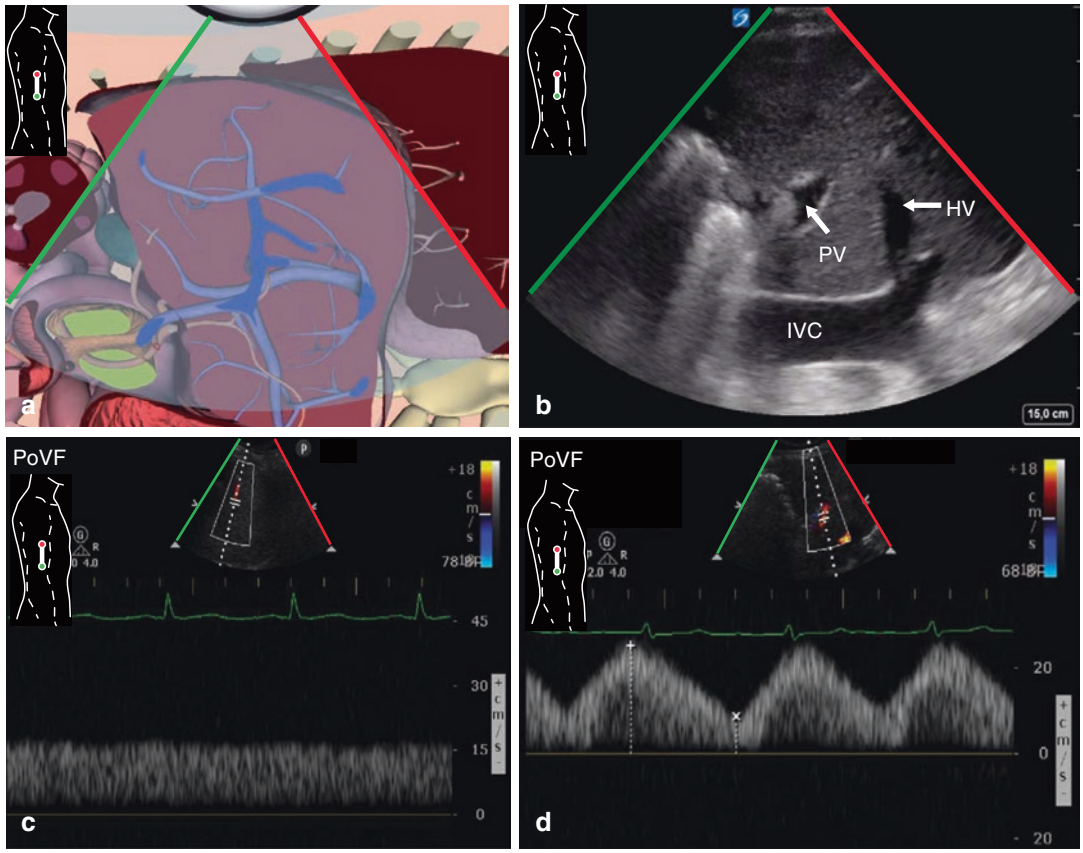

Fig. 40.4 Examination of portal venous flow. (**a**) Portal venous flow (PoVF) assessment from a posterior axillary line coronal view. (**b**) Using the same view, the inferior vena cava (IVC), portal vein (PV) and hepatic vein (HV) can be seen. Note the increased echogenicity of the PV wall. (**c**) Normal portal vein pulsed-wave Doppler has a monophasic signal indicating that blood is directed toward the transducer. Note the background pulsatile higher velocity of the hepatic artery, which is in the same direction. (**d**) Abnormal pulsatile portal flow with a pulsatility fraction (PF) of more than 50% (adapted from Denault et al. [26])

evaluation of the portal flow could be used as a marker of end-organ venous congestion. In decompensated heart failure, a portal pulsatility of more than 50% was the best predictor of increased serum bilirubin compared with hemodynamic parameters such as CVP and echocardiographic measurements such as TAPSE [30]. For the portal flow to be representative of central venous congestion, other causes of portal hypertension such as cirrhosis and portal thrombosis must be absent. A PF of more than 50% has also been reported in some individuals with low body mass index and normal cardiac function [31]. Consequently, this finding should be supported by other signs of elevated CVP such as IVC dilatation/non-collapsibility and an abnormal hepatic vein flow waveform.

40.4 Assessment of the Bowel

Bowel edema is believed to be one of the main determinant of the development of the cardiointestinal syndrome characterized by a chronic inflammatory state due to bacterial endotoxin translocation through an altered intestinal mucosa [32, 33]. Weight loss in patients with congestive heart failure identified as cardiac cachexia has been linked with the severity of right ventricular failure [34, 35]. Bowel wall thickness can be evaluated using bedside ultrasound. With a linear array transducer positioned over the abdominal area, a traverse and longitudinal view of different bowel regions can be obtained. The high resolution of the linear transducer is able to provide adequate

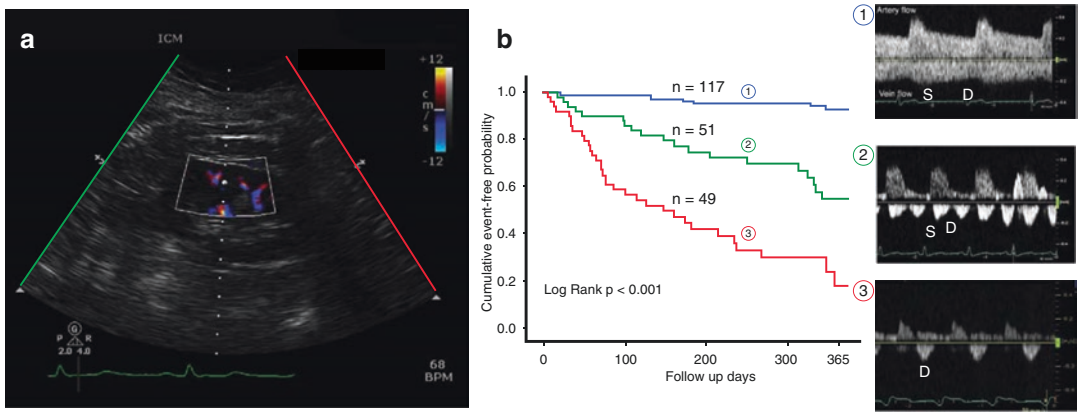

Fig. 40.5 (**a**) Examination of renal venous flow using color Doppler (**b**) Kaplan-Meier curves at 1-year follow-up for the probability of freedom from death from cardiac causes and unplanned hospitalizations for heart failure of three classifications of intrarenal venous flow which include the [1] continuous flow, [2] biphasic discontinuous flow and [3] monophasic discontinuous flow. D, diastolic; S, systolic (adapted with permission from Iida et al. [39])

definition in order to measure the thickness between the mucosa and the muscularis propria [36, 37]. However, this assesment requires considerable skill and experience from the ultrasonographer.

This parameter has been proved to be clinically important. In a prospective study by Valentova et al. bowel wall thickness was measured in 165 congestive heart failure patients with a reduced left ventricular ejection fraction (≤40%) [37]. Patients who presented a weight loss of ≥5% in the past 6 months had higher bowel wall thickness. When bowel wall thickness information was added to a model integrating right atrial pressure, TAPSE, New York Heart Association functional class, left ventricular ejection fraction, left atrial area and C-reactive protein, it resulted in a significant improvement in discrimination between cachexic and non-cachexic patients. These results suggest that directly assessing bowel congestion is a promising tool for the clinician as the individualisation of treatment in order to avoid chronic bowel edema might potentially prevent cardiac cachexia.

40.5 Assessment of the Kidneys

In decompensated heart failure patients, an elevated CVP is the best predictor of renal failure when compared to cardiac index, systolic blood pressure and pulmonary capillary wedge pressure [38]. The impact of elevated CVP on intrarenal hemodynamic can be assessed by Doppler ultrasound. In physiological condition, blood flow in the interlobar veins is continuous during the cardiac cycle. With high CVP, venous flow transforms into a discontinuous biphasic pattern similar to the Doppler pattern seen in the hepatic veins. With severe right heart failure, venous flow transforms into a monophasic discontinuous pattern with flow being present only during diastole (Fig. 40.5) [39]. Discontinuous flow in the interlobar renal veins can be linked to the CVP waveform during the cardiac cycle. As CVP increases and the IVC becomes non-compliant, the CVP waveform is transmitted deep into the renal parenchyma. Flow in the interlobar vein can be observed during the systolic and diastolic filling of the right atria (during the X and Y descent on CVP waveform). As right heart failure worsens, intrarenal venous flow becomes monophasic reflecting the predominance of the Y descent of the CVP waveform analogous to the variation in the S/D ratio in the hepatic vein waveform (decrease filling of the right atria during systole) [40].

Iida et al. has shown that the intrarenal venous flow pattern strongly correlated with death from cardiovascular disease and unplanned hospitalization for heart failure independent of renal resistance index, CVP and hemodynamic status including echocardiographic parameters [39]. In this study, patients with the monophasic discontinuous flow pattern also had lower estimated glomerular filtration rate (55 mL/min/1.73 m^2) compared

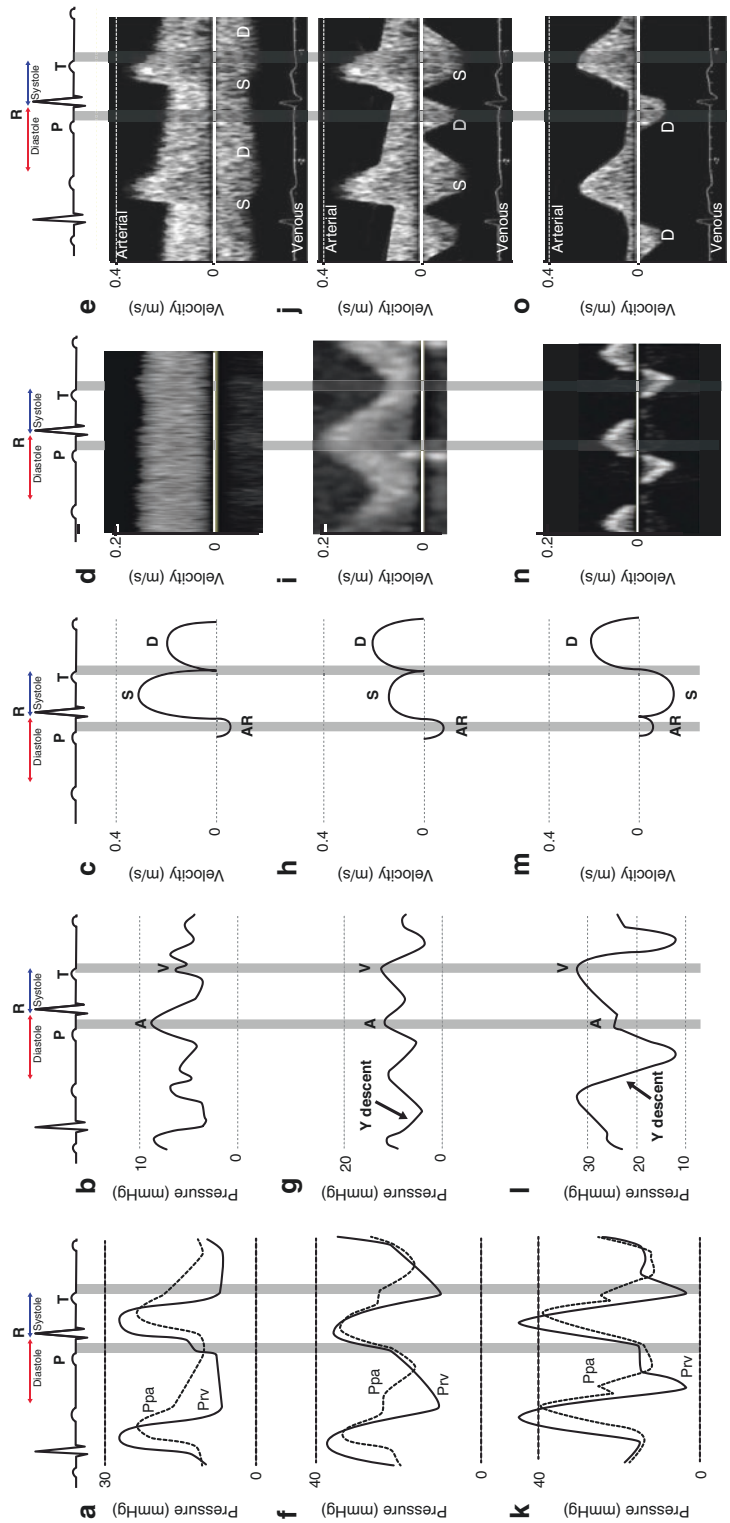

Fig. 40.6 Right ventricular pressure, right atrial pressure, hepatic venous flow (HVF), portal venous flow and interlobar renal veno-arterial flow in normal patients (**a**–**e**) and typical patterns commonly observed in patients with mild (**f**–**j**) and severe (**k**–**o**) right ventricular dysfunction. *AR* atrial reversal, *D* diastole, *Ppa* pulmonary artery pressure, *Prv* right ventricular pressure, *S* systole (adapted from Amsalem et al. [83])

with continuous and biphasic flow (67 mL/min/1.73 m^2) ($p = 0.005$). Figure 40.6 summarizes the relationship between right ventricular, central venous pressure waveforms and Doppler signals from the hepatic, portal and renal venous flow.

40.6 Assessment of the Lungs

While pulmonary edema is not a feature of isolated right heart failure, it can be present when a degree of left ventricular dysfunction or mitral insufficiency is present and can have an important clinical impact. Detection of sub-clinical pulmonary edema or increased extravascular lung water (EVLW) could avoid pulmonary complications and improve functional class. Bedside physical examination, CVP measurements and chest X-ray do not predict increased EVLW measured by transpulmonary thermodilution, suggesting that those techniques do not have sufficient sensitivity to detect early fluid overload [41]. While normal lung parenchyma cannot be visualized with ultrasound imaging because of air which is impermeable to ultrasound, the image generated by thickened interlobular septas produce an artefact called pulmonary B-lines also referred to as "comet tail artefacts" (Fig. 40.7). The detection of pulmonary B-lines is possible with a linear probe or a phased array probe placed over the parasternal, mid-clavicular, anterior axillary and mid axillary lines at the 2nd, 3rd, 4th and 5th intercostal spaces. Visualization of B-lines identifies the presence of alveolar-interstitial syndrome which can be explained by congestive pulmonary edema secondary to heart failure or acute respiratory distress syndrome (ARDS). Edema can be semi-quantitatively assessed by recording the number of B-lines present in multiple lung fields [42]. The presence of B-lines has been correlated to capillary wedge pressure and invasively measured EVLW [43]. B-lines have also been proven to be more reliable than chest X-ray for the evaluation of EVLW in patients with ARDS [44]. This information can be obtained within a few minutes with a short learning curve [45]. Lung ultrasound has been used for the evaluation of pulmonary congestion in a variety of different settings such as the differential diagnosis of dyspnea in the emergency department [46], the evaluation of chronic heart failure in an outpatient setting [47] and fluid status in hemodialysis patients [48]. In the intensive care setting, the predominance of pleural B-lines can predict elevated EVLW measured by transpulmonary thermodilution [43]. It is important to note that interstitial lung disease such as idiopathic pulmonary fibrosis can also produce B-lines on pulmonary ultrasound examination [49]. To avoid this pitfall, pulmonary ultrasound must be interpreted in the light of other findings from the patient's medical background, physical examination and ultrasound of the other systems.

Pleural effusions are usually present in patients with significant fluid overload. A pleural effusion can be detected on a posteroanterior chest X-ray at a volume of 200 mL [50]. Bedside pleural ultrasound examination can reliably detect pleural effusion with better sensitivity than the chest X-ray and chest auscultation [51]. An anechoic pleural effusion is compatible with a transudate that could be caused by congestive heart failure. Bilateral anechoic pleura effusions in a patient with normal serum albumin level are highly suggestive of fluid overload.

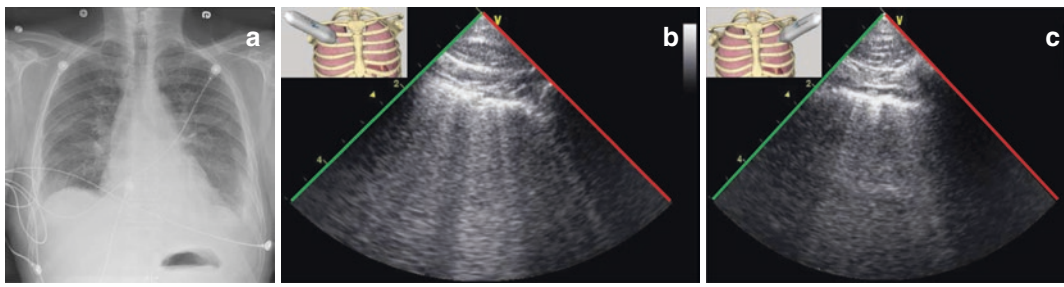

Fig. 40.7 Pulmonary congestion. (**a**) Chest radiograph of an 86-year-old man and lung ultrasound images (**b**, **c**) show diffuse B-lines in zones 1 and 5 (with permission of Denault et al. [82])

40.7 Assessment of Neurological Manifestations of Fluid Overload

While the utility of ultrasound examination of the nervous system in the setting of right heart failure is not yet clear, it should be an area of active investigation as cerebral congestion might be a contributing factor increasing the risk of cognitive dysfunction in chronic congestive heart failure patients [52, 53] and promoting delirium in hospitalized patients with acute decompensated heart failure [54, 55]. While the impact of right heart failure on the central nervous system has not been documented, it is plausible that elevated CVP could impair cerebral perfusion by increasing intra-cranial pressure (ICP) and decreasing the arteriovenous pressure gradient resulting in encephalopathy of varying severity [56, 57]. In an acute setting, severe venous congestion impairing cerebral perfusion could represent an indication for the urgent induction of a negative fluid balance.

Bedside ultrasound can be used to detect elevated ICP by the measurement of the optic nerve sheath. The technique is presented in Fig. 40.8.

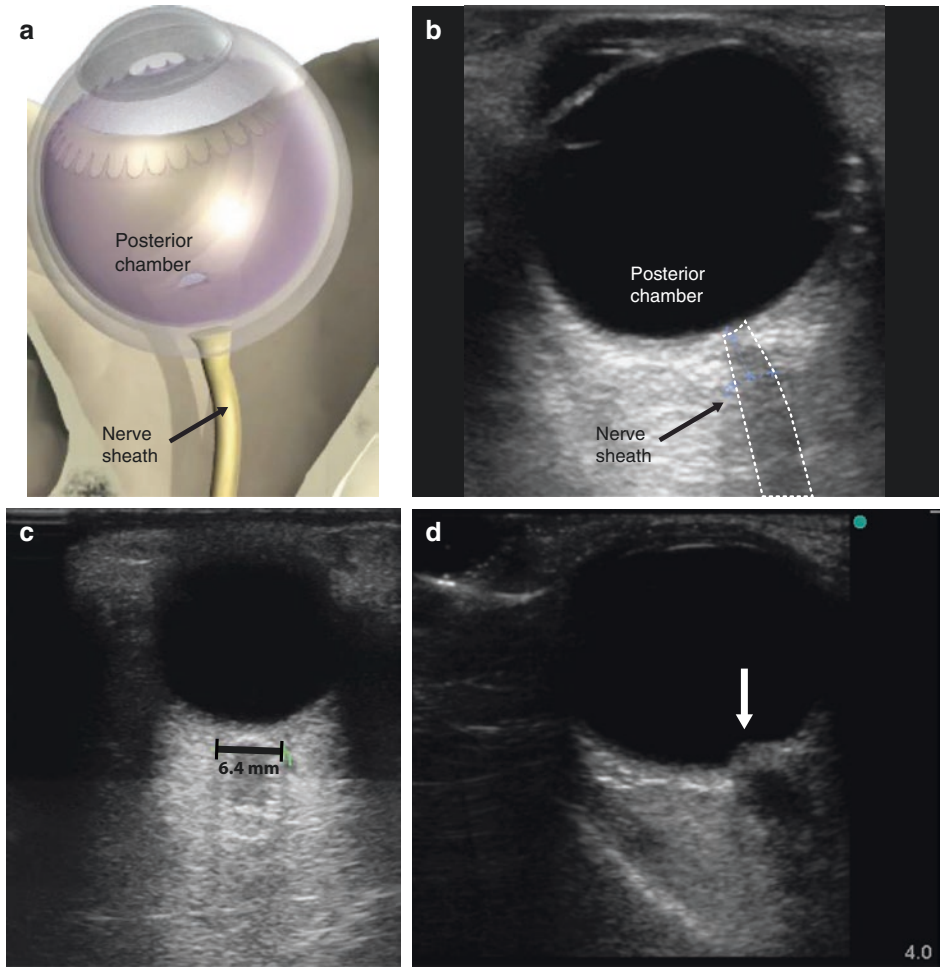

Fig. 40.8 Optic nerve sheath measurement. (**a**) The site for measuring the diameter of the optic nerve sheath is shown. A 3 mm perpendicular line is drawn from the middle of the optic nerve, at which point the transverse measurement of the optic sheath is performed. Note that the measurement includes the sheath and stops at the transition contrast between the optic nerve and surrounding tissue. (**b**) A 2D image displays the ocular structures and optic nerve sheath. (**c**) Ultrasound of the eye orbit from an 85-year-old patient after aortic valve replacement with significant post-operative fluid balance. The optic nerve diameter was 6.4 mm. (**d**) Optic nerve 2D images of papilledema (arrow) in a brain dead patient for organ donation (adapted with permission of Denault et al. [82])

The diameter threshold of 5.2–5.9 mm has been used to detect increased ICP. The diagnostic accuracy for the detection of intracranial hypertension has been assessed in multiples observational studies showing good diagnostic accuracy compared with invasive monitoring [58].

Transcranial Doppler offers the possibility to assess blood flow in the cerebral vessels when the probe is positioned in the temporal region. This technique has been used to monitor vasospasm in patients with subarachnoid hemorrhage, for the diagnostic of cerebral circulatory arrest and for the monitoring of cerebral embolism during surgery [59–61]. In the context of an increase in ICP, transcranial Doppler examination shows a reduction of flow velocity in diastole as shown in Fig. 40.9. Multiple studies have shown good correlation between the pulsatility index and elevated ICP [62–64]. While the relationship between CVP and cerebral blood flow has not been described systematically, our local experience suggests that significant venous congestion in an acute setting could impair diastolic blood flow in the cerebral arteries. Transcranial Doppler is a highly operator dependent technique and adequate imaging is impossible to achieve in up to 10% of patients due to inadequate temporal window. However using two-dimensional echography to identify the acoustic cranial window increases the success rate to 95% [65]. Anatomical variants of the circle of Willis can also alter the interpretation of the exam. Finally, transcranial Doppler waveform are known to be modified by other factors such as arterial pressure and steno-occlusive vessel disease.

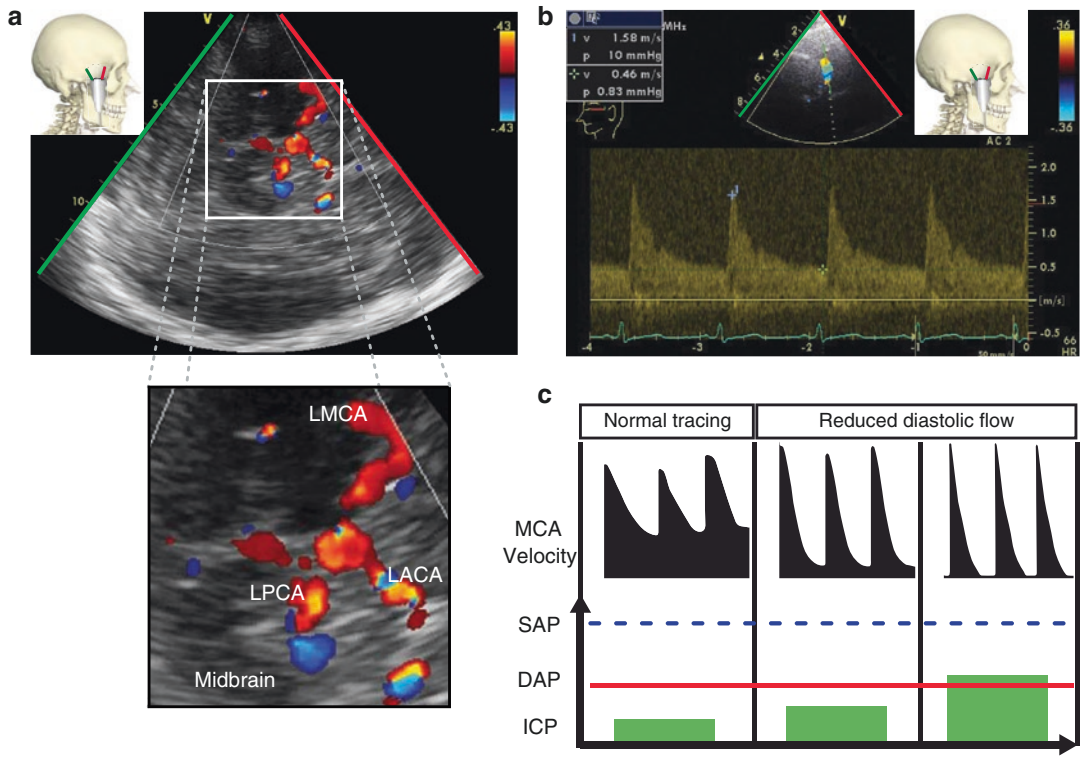

Fig. 40.9 Transcranial Doppler color-coded duplex sonography. The middle cerebral artery (MCA) is interrogated using a transthoracic probe positioned over the right temporal region. (**a**) A 2D image of the circle of Willis with color Doppler (Nyquist 43 cm/s) where flow interrogation is obtained. (**b**) Sample volume positioning in the vessel allows precise determination of the MCA velocity spectral Doppler profile. (**c**) Transcranial Doppler changes in the MCA mean flow with progressive increase in intracranial pressure (ICP) are shown compared with normal MCA flow trace and normal ICP. *LMCA* left middle cerebral artery, *LACA* left anterior cerebral artery, *LPCA* left posterior cerebral artery, *SAP* systolic arterial pressure, *DAP* diastolic arterial pressure (adapted with permission of Denault et al. [82])

40.8 Conclusion: Integrating Ultrasound Assessment into Practice

Clinical assessment of the congestive heart failure patient relies on the integration of multiple parameters having their own advantages and caveats (Table 40.2). As such, patient management should not be based on an individual finding in ultrasound assessment but enhancing physical examination with the use of bedside ultrasound offers the possibility for early detection of the impacts of venous congestion on end-organs. An overview of the proposed multisystem organ congestion evaluation using ultrasound is shown in Fig. 40.10E. This assessment can be repeated to monitor the response to therapy during hospitalization or during outpatient follow-up. The presence of multiple signs of organ congestion may predict adverse outcomes and this hypothesis is currently being studied in an acute setting. Two examples are presented in Figs. 40.11 and 40.12. It should be noted that central nervous system evaluation for congestion using transcranial Doppler and optic nerve measurement is based on local experience in selected cases and should be further studied before being used at the bedside. To be competent in the use of bedside ultrasound, clinicians should seek Point-of-care ultrasound training based upon current recommendations from expert statements [66–68].

The integration of the understanding of the pathophysiology of a clinical syndrome and ultrasonographic assessment as described in this chapter may help to individualize the diuretic management of patients with acute or chronic right heart failure to avoid the adverse effects of venous congestion.

Table 40.2 Clinical and ultrasound signs of fluid overload and their associated characteristics

Clinical signs of fluid overload	
Fluid balance and weight	– Advantages: Objective and included in routine care – Limitations: Does not consider cardiac function, not necessarily representative of end-organ congestion and can lead to misinterpretation of fluid status
Peripheral edema	– Advantages: Part of routine examination – Limitations: Can be caused by hypoalbuminemia, venous insufficiency and non-use, not necessarily representative of central organ congestion and can lead to misinterpretation of fluid status
CVP measurements	– Advantages: Usually available in critically ill patients – Limitations: Require a central venous access, important technical caveats and measurements are modified by pleural pressure in mechanically ventilated patients
Intra-abdominal pressure monitoring	– Advantages: Detection of intra-abdominal hypertension due to fluid overload is clinically important – Limitations: Intra-abdominal hypertension is not specific to fluid overload. A bladder catheter is required
Ultrasound signs of fluid overload	
IVC collapsibility and diameter	– Advantages: Short learning curve and non-invasive – Limitations: Can be modified by other factors such as positive pressure ventilation and other conditions impairing venous return to the right atria – Cut-off for CVP > 10 mmHg in spontaneously breathing patients [12]: CI < 40% (sensitivity: 73% specificity: 85%) or IVC diameter > 2.0 cm (sensitivity 73% specificity 84%)
JVP estimation	– Advantages: Rapid and non-invasive – Limitations: Same limitations as CVP. Has been reported to underestimate CVP [20] – PPV of 81.3% for CVP > 8 cm H_2O, NPV of 96.4% for CVP ≤ 5 cm H_2O [81]
Hepatic vein flow	– Advantages: Dynamic marker of central hemodynamics: A reduction in the systolic-to-diastolic ratio is observed with right heart failure and/or tricuspid regurgitation [25] – Limitations: Not necessarily representative of end-organ venous congestion

Table 40.2 (continued)

Pulsatile portal flow	– Advantages: Marker of hepatic venous congestion [30] – Limitations: Not studied in critically ill patients
Pulmonary B-lines	– Advantages: Marker of pulmonary congestion: able to detect early increase in EVLW [43] – Limitations: Can be present in ARDS and pulmonary fibrosis
Discontinuous intrarenal venous flow	– Advantages: Marker of the effect of elevated venous pressure on renal hemodynamics [39] – Limitations: not studied in critically ill patients
Optic nerve diameter	– Hypothesis: Potential marker of increased ICP caused by important cerebral congestion – Diameter > 5.2–5.9 mm: Sensibility: 90%, Specificity: 85% for intracranial hypertension [58]
Transcranial Doppler	– Hypothesis: Assessment of cerebral hemodynamics which could be altered by venous congestion – PI > 1.26–1.34: Sensitivity: 80–89%, Specificity 90–97% for intracranial hypertension [62]

ARDS acute respiratory distress syndrome, *CI* collapsibility index, *CHF* chronic heart failure, *EVLW* extra-vascular lung water, *ICP* intra-cranial pressure, *JVP* jugular venous pressure, *IVC* inferior vena cava, *NPV* negative predictive value, *PI* pulsatility index, *PF* pulsatility fraction, *PPV* positive predictive value

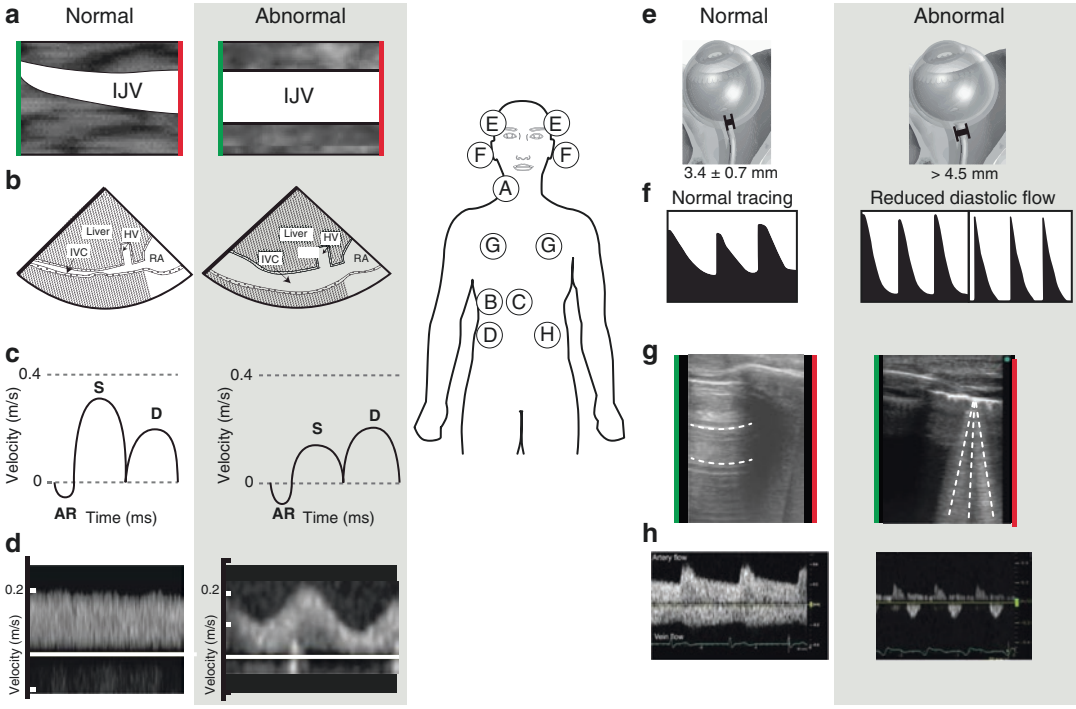

Fig. 40.10 Extra-cardiac ultrasound signs of fluid overload. (**a**) Internal jugular vein (IJV), (**b**) Inferior vena cava (IVC), (**c**) hepatic venous flow (HVF), (**d**) portal venous flow, (**e**) optic nerve diameter, (**f**) trans-cranial Doppler, (**g**) pulmonary B-lines and (**h**) renal interlobar vein Doppler [39]. *AR* atrial reversal, *D* diastolic velocity of HVF, *HV* hepatic vein, *RA* right atrium, *S* systolic velocity of HVF (adapted with permission from Iida et al. [39] and Beaubien-Souligny et al. [84])

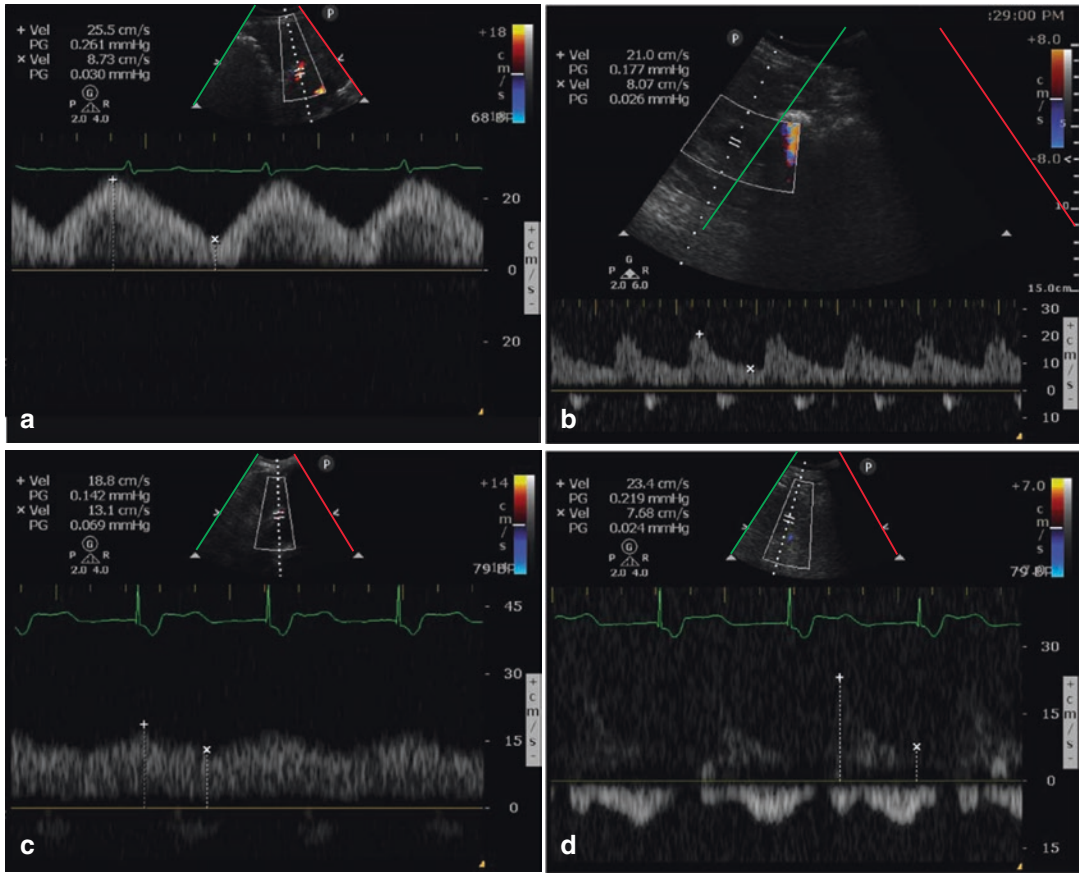

Fig. 40.11 Doppler assessment of portal and intra-renal flow in a 57 years-old female patient with chronic severe tricuspid valve insufficiency who underwent surgical repair. Before surgery, Doppler assessment showed: (**a**) portal flow pulsatility (pulsatility fraction (PF) of 66%) and (**b**) monophasic discontinuous intrarenal venous flow (only in diastole). Two days after surgery, Doppler assessment showed (**c**) minimal portal flow variations (PF: 27%) and (**d**) biphasic discontinuous intrarenal venous flow (both in systole and diastole). Renal function improved from a serum creatinine of 102 μmol/L before surgery (estimated glomerular filtration rate (eGFR): 47 mL/min/1.73 m^2) to 63 μmol/L (eGFR > 60 mL/min/1.73 m^2) 2 days after surgery

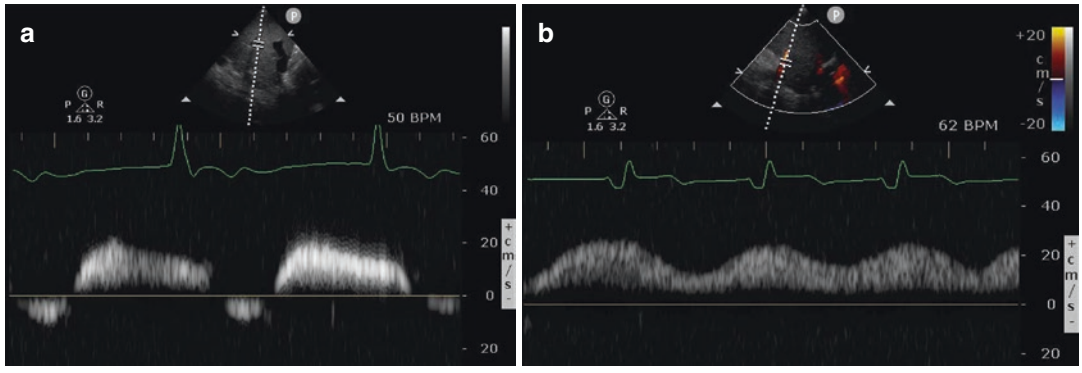

Fig. 40.12 Doppler assessment of portal flow in an 80 years-old male patient admitted for decompensated congestive heart failure with severe left and right ventricular dysfunction (LVEF: 20%), severe pulmonary hypertension (systolic PAP: 65 mmHg), significant tricuspid regurgitation (Grade III/IV) and elevated NT-Pro-BNP measurements (11,618 pg/mL, normal <300 pg/mL). (**a**) Upon admission, portal flow was reversed (PF > 100%). A negative fluid balance of 1.2 L was achieved during the first day with the use of IV furosemide. (**b**) The following day, Doppler assessment of the portal vein revealed moderate pulsatility without reversal (PF: 35–50%)

References

1. Ljungman S, Laragh JH, Cody RJ. Role of the kidney in congestive heart failure. Relationship of cardiac index to kidney function. Drugs. 1990;39(Suppl 4):10–21. discussion 2–4.
2. Damman K, van Deursen VM, Navis G, Voors AA, van Veldhuisen DJ, Hillege HL. Increased central venous pressure is associated with impaired renal function and mortality in a broad spectrum of patients with cardiovascular disease. J Am Coll Cardiol. 2009;53(7):582–8.
3. Breidthardt T, Irfan A, Klima T, Drexler B, Balmelli C, Arenja N, et al. Pathophysiology of lower extremity edema in acute heart failure revisited. Am J Med. 2012;125(11):1124.e1–8.
4. Vinayak AG, Levitt J, Gehlbach B, Pohlman AS, Hall JB, Kress JP. Usefulness of the external jugular vein examination in detecting abnormal central venous pressure in critically ill patients. Arch Intern Med. 2006;166(19):2132–7.
5. Gunst M, Sperry J, Ghaemmaghami V, O'Keeffe T, Friese R, Frankel H. Bedside echocardiographic assessment for trauma/critical care: the BEAT exam. J Am Coll Surg. 2008;207(3):e1–3.
6. Zhang J, Critchley LA. Inferior vena cava ultrasonography before general anesthesia can predict hypotension after induction. Anesthesiology. 2016;124(3):580–9.
7. Rudski LG, Lai WW, Afilalo J, Hua L, Handschumacher MD, Chandrasekaran K, et al. Guidelines for the echocardiographic assessment of the right heart in adults: a report from the American Society of Echocardiography endorsed by the European Association of Echocardiography, a registered branch of the European Society of Cardiology, and the Canadian Society of Echocardiography. J Am Soc Echocardiogr. 2010;23(7):685–713.
8. Stawicki SP, Braslow BM, Panebianco NL, Kirkpatrick JN, Gracias VH, Hayden GE, et al. Intensivist use of hand-carried ultrasonography to measure IVC collapsibility in estimating intravascular volume status: correlations with CVP. J Am Coll Surg. 2009;209(1):55–61.
9. Seo Y, Iida N, Yamamoto M, Machino-Ohtsuka T, Ishizu T, Aonuma K. Estimation of central venous pressure using the ratio of short to long diameter from cross-sectional images of the inferior vena cava. J Am Soc Echocardiogr. 2017;30(5):461–7.
10. Jue J, Chung W, Schiller NB. Does inferior vena cava size predict right atrial pressures in patients receiving mechanical ventilation? J Am Soc Echocardiogr. 1992;5(6):613–9.
11. Kircher BJ, Himelman RB, Schiller NB. Noninvasive estimation of right atrial pressure from the inspiratory collapse of the inferior vena cava. Am J Cardiol. 1990;66(4):493–6.
12. Brennan JM, Blair JE, Goonewardena S, Ronan A, Shah D, Vasaiwala S, et al. Reappraisal of the use of inferior vena cava for estimating right atrial pressure. J Am Soc Echocardiogr. 2007;20(7):857–61.
13. Nagueh SF, Kopelen HA, Zoghbi WA. Relation of mean right atrial pressure to echocardiographic and Doppler parameters of right atrial and right ventricular function. Circulation. 1996;93(6):1160–9.
14. Muniz Pazeli J, Fagundes Vidigal D, Cestari Grossi T, Silva Fernandes NM, Colugnati F, Baumgratz de Paula R, et al. Can nephrologists use ultrasound to evaluate the inferior vena cava? A cross-sectional study of the agreement between a nephrologist and a cardiologist. Nephron Extra. 2014;4(1):82–8.
15. Beigel R, Cercek B, Luo H, Siegel RJ. Noninvasive evaluation of right atrial pressure. J Am Soc Echocardiogr. 2013;26(9):1033–42.
16. Via G, Tavazzi G, Price S. Ten situations where inferior vena cava ultrasound may fail to accurately predict fluid responsiveness: a physiologically based point of view. Intensive Care Med. 2016;42(7):1164–7.
17. Barbier C, Loubieres Y, Schmit C, Hayon J, Ricome JL, Jardin F, et al. Respiratory changes in inferior vena cava diameter are helpful in predicting fluid responsiveness in ventilated septic patients. Intensive Care Med. 2004;30(9):1740–6.
18. Cook DJ, Simel DL. The Rational Clinical Examination. Does this patient have abnormal central venous pressure? JAMA. 1996;275(8):630–4.
19. Avcil M, Kapci M, Dagli B, Omurlu IK, Ozluer E, Karaman K, et al. Comparision of ultrasound-based methods of jugular vein and inferior vena cava for estimating central venous pressure. Int J Clin Exp Med. 2015;8(7):10586–94.
20. Deol GR, Collett N, Ashby A, Schmidt GA. Ultrasound accurately reflects the jugular venous examination but underestimates central venous pressure. Chest. 2011;139(1):95–100.
21. Vegas A, Denault A, Royse C. A bedside clinical and ultrasound-based approach to hemodynamic instability – part II: bedside ultrasound in hemodynamic shock: continuing professional development. Can J Anesth. 2014;61(11):1008–27.
22. Hulin J, Aslanian P, Desjardins G, Belaidi M, Denault A. The critical importance of hepatic venous blood flow Doppler assessment for patients in shock. A A Case Rep. 2016;6(5):114–20.
23. Abu-Yousef MM. Normal and respiratory variations of the hepatic and portal venous duplex Doppler waveforms with simultaneous electrocardiographic correlation. J Ultrasound Med. 1992;11(6):263–8.
24. Abu-Yousef MM. Duplex Doppler sonography of the hepatic vein in tricuspid regurgitation. AJR Am J Roentgenol. 1991;156(1):79–83.
25. Scheinfeld MH, Bilali A, Koenigsberg M. Understanding the spectral Doppler waveform of the hepatic veins in health and disease. Radiographics. 2009;29(7):2081–98.
26. Denault AY, Beaubien-Souligny W, Elmi-Sarabi M, Eljaiek R, El-Hamamsy I, Lamarche Y, et al. Clinical significance of portal hypertension diagnosed with bedside ultrasound after cardiac surgery. Anesth Analg. 2017;124(4):1109–15.
27. Hu JT, Yang SS, Lai YC, Shih CY, Chang CW. Percentage of peak-to-peak pulsatility of portal blood flow can predict right-sided congestive heart failure. World J Gastroenterol. 2003;9(8):1828–31.
28. Rengo C, Brevetti G, Sorrentino G, D'Amato T, Imparato M, Vitale DF, et al. Portal vein pulsatility ratio provides a measure of right heart function in chronic heart failure. Ultrasound Med Biol. 1998;24(3):327–32.

29. Catalano D, Caruso G, DiFazzio S, Carpinteri G, Scalisi N, Trovato GM. Portal vein pulsatility ratio and heart failure. J Clin Ultrasound. 1998;26(1):27–31.
30. Styczynski G, Milewska A, Marczewska M, Sobieraj P, Sobczynska M, Dabrowski M, et al. Echocardiographic correlates of abnormal liver tests in patients with exacerbation of chronic heart failure. J Am Soc Echocardiogr. 2016;29(2):132–9.
31. Gallix BP, Taourel P, Dauzat M, Bruel JM, Lafortune M. Flow pulsatility in the portal venous system: a study of Doppler sonography in healthy adults. AJR Am J Roentgenol. 1997;169(1):141–4.
32. Sundaram V, Fang JC. Gastrointestinal and liver issues in heart failure. Circulation. 2016;133(17):1696–703.
33. Niebauer J, Volk HD, Kemp M, Dominguez M, Schumann RR, Rauchhaus M, et al. Endotoxin and immune activation in chronic heart failure: a prospective cohort study. Lancet. 1999;353(9167):1838–42.
34. Melenovsky V, Kotrc M, Borlaug BA, Marek T, Kovar J, Malek I, et al. Relationships between right ventricular function, body composition, and prognosis in advanced heart failure. J Am Coll Cardiol. 2013;62(18):1660–70.
35. Valentova M, von Haehling S, Krause C, Ebner N, Steinbeck L, Cramer L, et al. Cardiac cachexia is associated with right ventricular failure and liver dysfunction. Int J Cardiol. 2013;169(3):219–24.
36. Allgayer H, Braden B, Dietrich CF. Transabdominal ultrasound in inflammatory bowel disease. Conventional and recently developed techniques--update. Med Ultrason. 2011;13(4):302–13.
37. Valentova M, von Haehling S, Bauditz J, Doehner W, Ebner N, Bekfani T, et al. Intestinal congestion and right ventricular dysfunction: a link with appetite loss, inflammation, and cachexia in chronic heart failure. Eur Heart J. 2016;37(21):1684–91.
38. Mullens W, Abrahams Z, Francis GS, Sokos G, Taylor DO, Starling RC, et al. Importance of venous congestion for worsening of renal function in advanced decompensated heart failure. J Am Coll Cardiol. 2009;53(7):589–96.
39. Iida N, Seo Y, Sai S, Machino-Ohtsuka T, Yamamoto M, Ishizu T, et al. Clinical implications of intrarenal hemodynamic evaluation by Doppler ultrasonography in heart failure. JACC Heart Fail. 2016;4(8):674–82.
40. Tang WH, Kitai T. Intrarenal venous flow: a window into the congestive kidney failure phenotype of heart failure? JACC Heart Fail. 2016;4(8):683–6.
41. Saugel B, Ringmaier S, Holzapfel K, Schuster T, Phillip V, Schmid RM, et al. Physical examination, central venous pressure, and chest radiography for the prediction of transpulmonary thermodilution-derived hemodynamic parameters in critically ill patients: a prospective trial. J Crit Care. 2011;26(4):402–10.
42. Jambrik Z, Monti S, Coppola V, Agricola E, Mottola G, Miniati M, et al. Usefulness of ultrasound lung comets as a nonradiologic sign of extravascular lung water. Am J Cardiol. 2004;93(10):1265–70.
43. Agricola E, Bove T, Oppizzi M, Marino G, Zangrillo A, Margonato A, et al. "Ultrasound comet-tail images": a marker of pulmonary edema: a comparative study with wedge pressure and extravascular lung water. Chest. 2005;127(5):1690–5.
44. Lichtenstein D, Goldstein I, Mourgeon E, Cluzel P, Grenier P, Rouby JJ. Comparative diagnostic performances of auscultation, chest radiography, and lung ultrasonography in acute respiratory distress syndrome. Anesthesiology. 2004;100(1):9–15.
45. Lichtenstein D, Meziere G. A lung ultrasound sign allowing bedside distinction between pulmonary edema and COPD: the comet-tail artifact. Intensive Care Med. 1998;24(12):1331–4.
46. Prosen G, Klemen P, Strnad M, Grmec S. Combination of lung ultrasound (a comet-tail sign) and N-terminal pro-brain natriuretic peptide in differentiating acute heart failure from chronic obstructive pulmonary disease and asthma as cause of acute dyspnea in prehospital emergency setting. Crit Care. 2011;15(2):R114.
47. Miglioranza MH, Gargani L, Sant'Anna RT, Rover MM, Martins VM, Mantovani A, et al. Lung ultrasound for the evaluation of pulmonary congestion in outpatients: a comparison with clinical assessment, natriuretic peptides, and echocardiography. JACC Cardiovasc Imaging. 2013;6(11):1141–51.
48. Mallamaci F, Benedetto FA, Tripepi R, Rastelli S, Castellino P, Tripepi G, et al. Detection of pulmonary congestion by chest ultrasound in dialysis patients. JACC Cardiovasc Imaging. 2010;3(6):586–94.
49. Hasan AA, Makhlouf HA. B-lines: transthoracic chest ultrasound signs useful in assessment of interstitial lung diseases. Ann Thorac Med. 2014;9(2):99–103.
50. Blackmore CC, Black WC, Dallas RV, Crow HC. Pleural fluid volume estimation: a chest radiograph prediction rule. Acad Radiol. 1996;3(2):103–9.
51. Xirouchaki N, Magkanas E, Vaporidi K, Kondili E, Plataki M, Patrianakos A, et al. Lung ultrasound in critically ill patients: comparison with bedside chest radiography. Intensive Care Med. 2011;37(9):1488–93.
52. Vogels RL, Scheltens P, Schroeder-Tanka JM, Weinstein HC. Cognitive impairment in heart failure: a systematic review of the literature. Eur J Heart Fail. 2007;9(5):440–9.
53. van den Hurk K, Reijmer YD, van den Berg E, Alssema M, Nijpels G, Kostense PJ, et al. Heart failure and cognitive function in the general population: the Hoorn Study. Eur J Heart Fail. 2011;13(12):1362–9.
54. Levin SN, Hajduk AM, McManus DD, Darling CE, Gurwitz JH, Spencer FA, et al. Cognitive status in patients hospitalized with acute decompensated heart failure. Am Heart J. 2014;168(6):917–23.
55. Honda S, Nagai T, Sugano Y, Okada A, Asaumi Y, Aiba T, et al. Prevalence, determinants, and prognostic significance of delirium in patients with acute heart failure. Int J Cardiol. 2016;222:521–7.
56. Scheuermann K, Thiel C, Thiel K, Klingert W, Hawerkamp E, Scheppach J, et al. Correlation of the

intracranial pressure to the central venous pressure in the late phase of acute liver failure in a porcine model. Acta Neurochir Suppl. 2012;114:387–91.
57. Kotlinska-Hasiec E, Czajkowski M, Rzecki Z, Stadnik A, Olszewski K, Rybojad B, et al. Disturbance in venous outflow from the cerebral circulation intensifies the release of blood-brain barrier injury biomarkers in patients undergoing cardiac surgery. J Cardiothorac Vasc Anesth. 2014;28(2):328–35.
58. Dubourg J, Javouhey E, Geeraerts T, Messerer M, Kassai B. Ultrasonography of optic nerve sheath diameter for detection of raised intracranial pressure: a systematic review and meta-analysis. Intensive Care Med. 2011;37(7):1059–68.
59. Sreeram GM, Grocott HP, White WD, Newman MF, Stafford-Smith M. Transcranial Doppler emboli count predicts rise in creatinine after coronary artery bypass graft surgery. J Cardiothorac Vasc Anesth. 2004;18(5):548–51.
60. Nakae R, Yokota H, Yoshida D, Teramoto A. Transcranial Doppler ultrasonography for diagnosis of cerebral vasospasm after aneurysmal subarachnoid hemorrhage: mean blood flow velocity ratio of the ipsilateral and contralateral middle cerebral arteries. Neurosurgery. 2011;69(4):876–83; discussion 83.
61. Chang JJ, Tsivgoulis G, Katsanos AH, Malkoff MD, Alexandrov AV. Diagnostic accuracy of transcranial Doppler for brain death confirmation: systematic review and meta-analysis. AJNR Am J Neuroradiol. 2016;37(3):408–14.
62. Wang Y, Duan YY, Zhou HY, Yuan LJ, Zhang L, Wang W, et al. Middle cerebral arterial flow changes on transcranial color and spectral Doppler sonography in patients with increased intracranial pressure. J Ultrasound Med. 2014;33(12):2131–6.
63. Prunet B, Asencio Y, Lacroix G, Montcriol A, Dagain A, Cotte J, et al. Noninvasive detection of elevated intracranial pressure using a portable ultrasound system. Am J Emerg Med. 2012;30(6):936–41.
64. Wakerley BR, Kusuma Y, Yeo LL, Liang S, Kumar K, Sharma AK, et al. Usefulness of transcranial Doppler-derived cerebral hemodynamic parameters in the noninvasive assessment of intracranial pressure. J Neuroimaging. 2015;25(1):111–6.
65. Couture EJ, Desjardins G, Denault AY. Transcranial Doppler monitoring guided by cranial two-dimensional ultrasonography. Can J Anesth. 2017;64(8):885–7. [Epub ahead of print]. https://doi.org/10.1007/s12630-017-0898-9.
66. Arntfield R, Millington S, Ainsworth C, Arora R, Boyd J, Finlayson G, et al. Canadian recommendations for critical care ultrasound training and competency. Can Respir J. 2014;21(6):341–5.
67. Mayo PH, Beaulieu Y, Doelken P, Feller-Kopman D, Harrod C, Kaplan A, et al. American College of Chest Physicians/La Societe de Reanimation de Langue Francaise statement on competence in critical care ultrasonography. Chest. 2009;135(4):1050–60.
68. Expert Round Table on Ultrasound in ICU. International expert statement on training standards for critical care ultrasonography. Intensive Care Med. 2011;37(7):1077–83.
69. Nisanevich V, Felsenstein I, Almogy G, Weissman C, Einav S, Matot I. Effect of intraoperative fluid management on outcome after intraabdominal surgery. Anesthesiology. 2005;103(1):25–32.
70. Gieling RG, Ruijter JM, Maas AA, Van Den Bergh Weerman MA, Dingemans KP, ten Kate FJ, et al. Hepatic response to right ventricular pressure overload. Gastroenterology. 2004;127(4):1210–21.
71. Brater DC, Day B, Burdette A, Anderson S. Bumetanide and furosemide in heart failure. Kidney Int. 1984;26(2):183–9.
72. Payen D, de Pont AC, Sakr Y, Spies C, Reinhart K, Vincent JL, et al. A positive fluid balance is associated with a worse outcome in patients with acute renal failure. Crit Care. 2008;12(3):R74.
73. Bouchard J, Soroko SB, Chertow GM, Himmelfarb J, Ikizler TA, Paganini EP, et al. Fluid accumulation, survival and recovery of kidney function in critically ill patients with acute kidney injury. Kidney Int. 2009;76(4):422–7.
74. Saito S, Uchino S, Takinami M, Uezono S, Bellomo R. Postoperative blood pressure deficit and acute kidney injury progression in vasopressor-dependent cardiovascular surgery patients. Crit Care. 2016;20(1):74.
75. Wiedemann HP, Wheeler AP, Bernard GR, Thompson BT, Hayden D, National Heart Lung and Blood Institute Acute Respiratory Distress Syndrome (ARDS) Clinical Trials Network, et al. Comparison of two fluid-management strategies in acute lung injury. N Engl J Med. 2006;354(24):2564–75.
76. Sakka SG, Klein M, Reinhart K, Meier-Hellmann A. Prognostic value of extravascular lung water in critically ill patients. Chest. 2002;122(6):2080–6.
77. Warrillow SJ, Weinberg L, Parker F, Calzavacca P, Licari E, Aly A, et al. Perioperative fluid prescription, complications and outcomes in major elective open gastrointestinal surgery. Anaesth Intensive Care. 2010;38(2):259–65.
78. Parente D, Luis C, Veiga D, Silva H, Abelha F. Congestive heart failure as a determinant of postoperative delirium. Rev Port V. 2013;32(9):665–71.
79. Madias JE. Apparent amelioration of bundle branch blocks and intraventricular conduction delays mediated by anasarca. J Electrocardiol. 2005;38(2):160–5.
80. Brandstrup B, Tonnesen H, Beier-Holgersen R, Hjortso E, Ording H, Lindorff-Larsen K, et al. Effects of intravenous fluid restriction on postoperative complications: comparison of two perioperative fluid regimens: a randomized assessor-blinded multicenter trial. Ann Surg. 2003;238(5):641–8.
81. Siva B, Hunt A, Boudville N. The sensitivity and specificity of ultrasound estimation of central venous

pressure using the internal jugular vein. J Crit Care. 2012;27(3):315.e7–11.
82. Denault AY, Couture P, Lamarche Y, Tardif JC, Vegas A. Basic transesophageal and critical care ultrasonography. London: CRC Press; 2017.
83. Amsallem M, Kuznetsova T, Hanneman K, Denault A, Haddad F. Right heart imaging in patients with heart failure: a tale of two ventricles. Curr Opin Cardiol. 2016;31(5):469–82.
84. Beaubien-Souligny W, Bouchard J, Desjardins G, Lamarche Y, Liszkowski M, Robillard P, et al. Extracardiac signs of fluid overload in the critically ill cardiac patient: a focused evaluation using bedside ultrasound. Can J Cardiol. 2017;33(1):88–100.

Interventional Procedures

41

Larisa Pinte, Florina Pinte, Daniel Niţa, Iancu Mocanu, and Vasile Murgu

Abstract

Interventional cardiology was developed more in the past 2–3 decades, especially with new treatment options for congenital heart disease such as atrial septal defect, patent ductus arteriosus, ventricular septal defect and pulmonary valve stenosis. These techniques avoid open-heart surgery. Good long-term results allow treated children to have a normal life.

Recent advances in interventional cardiology were due to the discovery of new techniques, some of them are revolutionary techniques, and also due to the technical improvement of materials used for procedures: new types of balloons, guidewires, devices to oclude intracardiac communications, which assured optimal results after the procedure.

In recent decades, with all medical advances, congenital heart diseases are also common in adults because some diseases in this category are well tolerated until adulthood and due to a specific pathology in patients who had undergone cardiac surgery in childhood (lung failure, residual shunts, or valve stenosis).

Keywords

Interventional cardiology · Atrial septal defect · Ventricular septal defect · Patent ductus arteriosus · Pulmonary valvuloplasty · Interventional procedures

41.1 Introduction

In recent years, interventional cardiology in congenital malformations has made real progress, some malformations being treated only by interventional maneuvers, and in complex malformations, with the help of a good collaboration with cardiac surgery, interventional procedures ensure survival of the infant until the age at which complete corrective surgery is possible.

The incidence of congenital heart defects is 0.6–1% of the annual number of live births, and the diagnosis is made today in utero via fetal ultrasound, making possible early treatment to ensure survival. When fetal echocardiography detects complex cardiac malformations

L. Pinte
Internal Medicine Department, Colentina Clinical Hospital, Bucharest, Romania

F. Pinte (✉)
Department of Interventional Cardiology, Medlife – Angiolife, Bucharest, Romania

D. Niţa
Interventional Cardiology Department, Central Military Hospital, Bucharest, Romania

I. Mocanu
Department of Cardiovascular Surgery, Sanador Hospital, Bucharest, Romania

V. Murgu
Department of ITU, Central Military Hospital, Bucharest, Romania

S. I. Dumitrescu et al. (eds.), *Right Heart Pathology*, https://doi.org/10.1007/978-3-319-73764-5_41

Table 41.1 IPCCC classification of congenital heart disease and most common diagnoses (International Pediatric and Congenital Cardiac Code (IPCCC) [1]

Classification category	Most common diagnoses
Abnormalities of position and connection of the heart	Dextrocardia
	Atrial situs inversus
	Double inlet left ventricle (DILV); double inlet right ventricle (DIRV)
	Transposition of the great arteries (TGA)
	Double outlet left ventricle (DORV); double outlet right ventricle (DORV)
	Common arterial trunk (CAT), aka truncus arteriosus (TA)
Tetralogy of Fallot and variants	Tetralogy of Fallot (TOF)
	Pulmonary atresia (PA) and ventricular septal defect (VSD)
Abnormalities of great veins	Superior vena cava (SVC) abnormality
	Inferior vena cava (SVC) abnormality
	Coronary sinus abnormality
	Total anomalous pulmonary venous connection (TAPVC)
	Partially anomalous pulmonary venous connection (PAPVC)
Abnormalities of atriums and atrial septum	Atrial septal defect (ASD)
	Patent foramen ovale (PFO)
Abnormalities of AV valves and AV septal defect	Tricuspid regurgitation (TR)
	Tricuspid stenosis (TS)
	Ebstein's anomaly
	Mitral regurgitation (MR)
	Mitral stenosis (MS)
	Mitral valve prolapse (MVP)
	Atrioventricular septal defect (AVSD)
Abnormalities of ventricles and ventricular septum	Single ventricle
	Ventricular imbalance: dominant LV + hypoplastic RV, or dominant RV + hypoplastic RV
	Aneurysm (RV, LV, or septal)
	Hypoplastic left heart syndrome (HLHS)
	Double chambered right ventricle (DCRV)
	Ventricular septal defect (VSD)
Abnormalities of VA valves and great arteries	Aortopulmonary window (AP Window)
	Pulmonary stenosis (PS), valvar or subalvar
	Pulmonary artery stenosis (PAS)
	Aortic stenosis (AS), valvar or subalvar
	Aortic insufficiency (AI)
	Bicuspid aortic valve (BAV)
	Supravalvar aortic stenosis (SVS)
	Coarctation of the aorta (COA)
	Interrupted aortic arch (IAA)
Abnormalities of coronary arteries, arterial duct and pericardium; AV fistulae	Anomalous origin of coronary artery from pulmonary artery (ALCAPA)
	Patent ductus arteriosus (PDA)

incompatible with long term survival after birth, therapeutic abortion is recommended.

The complexity of congenital heart diseases requires a classification of them, which is listed in Table 41.1.

41.2 Percutaneous Pulmonary Valvuloplasty

Percutaneous pulmonary valvuloplasty can be defined as the mechanical expansion of a valvular or supravalvular pulmonary stenosis by means of a percutaneous balloon catheter inserted into a peripheral vein, often the femoral vein.

Percutaneous pulmonary valvuloplasty (Seldinger technique) was performed for the first time by Semb et al. in 1975 using a Berman angiography catheter.

The technique was then improved by Kan for children in 1982 and Pepine for adults in the same year [2]. Experience in this field was enriched by Ali Kahn in 1986, who introduced the double balloon technique and by B. Maier in 1986, who described the technique of pulmonary valvuloplasty using a trifoil balloon catheter (three identical balloons of 15 mm mounted on a single shaft) [2].

From anatomical point of view, congenital pulmonary stenoses are classified as follows [3]:

- **valvular stenoses**, made by welding the pulmonary valve commissures and creating the appearance of "dome" shaped valve, making a punctiform orifice or a few millimeters orifice located centrally or eccentric. The cusps may have various structures: spongy, fibrous, collagenous or mixed. The number of cusps varies from one to three, making different degrees of stenosis in the valve opening. In a smaller percentage, there is a hypoplasia of the pulmonary valve ring and a dysplasia of the pulmonary valve [4].
- **supravalvular stenosis**, generally represented by a circular membrane formation located 2–3 cm above the valvular plane, which makes a pressure gradient at this level.
- **stenosis of the main branches** of the pulmonary artery or in the periphery of the lung fields.

To these types, it may be added an infundibular right ventricular stenosis, which is of two types: muscular (dynamic) or fibro-muscular [5].

Pulmonary valve anatomy is very important in the decision-making process, especially in the case of percutaneous balloon pulmonary valvuloplasty.

The severity of pulmonary valve stenosis can be quantified according to the following values of the pulmonary transvalvular pressure gradient [6]:

- mild up to 40 mmHg
- moderate 40–70 mmHg
- severe over 70 mmHg.

When pulmonary transvalvular pressure gradient is above 80 mmHg, there is a marked hypertrophy of the right ventricular walls, accompanied by tricuspid insufficiency of various degrees and frequent association of a patent oval foramen [7].

After divulsion of the pulmonary valve commissures, the pulmonary transvalvular pressure gradient is decrease, over the time the right ventricle hypertrophy will decrease. Because pulmonary flow will increase significantly, symptomatology improves after valvuloplasty [8].

Most of the time, pulmonary valve stenosis is associated with other malformations, particularly in complex cyanogenic diseases such as: tetralogy of Fallot, trilogy of Fallot, double outlet right ventricle, transposition of the great vessels etc. In these cases of complex congenital diseases, pulmonary valvuloplasty may be a palliative treatment until complete full surgical correction.

These diseases are accompanied by a very low pulmonary flow that can endanger the life of the newborn, pulmonary valvuloplasty increase the pulmonary flow, providing a better oxygenation of the blood and lowering right-left shunt through defects at various levels: atrial septal defect, ventricular septal defect and patent ductus arteriosus [9].

The indications of percutaneous pulmonary valvuloplasty are summarized in the following congenital maladies [7]:

- isolated pulmonary valve stenosis (not associated with other malformations)
- supravalvular pulmonary stenosis
- stenosis of the main branches of the pulmonary artery
- stenosis of the peripheral branches of the pulmonary artery
- pulmonary valve stenosis associated with cyanogenic complex malformations: tetralogy of Fallot, trilogy of Fallot, double outlet right ventricle and transposition of the great vessels and protected lung.
- pulmonary valve stenosis in non-cyanogenic diseases, in which it has the role to protect the lung against increased pulmonary blood flow: atrial septal defect, ventricular septal defect, anomalous pulmonary venous drainage.

Percutaneous pulmonary valvuloplasty is indicated for isolated pulmonary valve stenosis in the following cases: pulmonary transvalvular pressure gradient over 50 mmHg, electrocardiographic marked right ventricular hypertrophy and symptomatoms as: fatigue, dyspnea, angina and syncope (Table 41.2).

In cyanogenic congenital diseases, pulmonary valvuloplasty is recommended in the following situations [7]:

- pulmonary transvalvular pressure gradient over 40 mmHg
- low pulmonary blood flow, characterized by poor circulation on chest radiography
- progressive and marked hypoxemia and polycythemia
- frequent hypoxic seizures.

Although in this last category of malformations, pulmonary valvuloplasty is only a palliative treatment, it is very useful because it ensures a higher pulmonary flow, which leads to better oxygenation, to disappearance of hypoxic crisis and it prevents the death of the infant, making possible the corrective surgery after [9].

In order to select correctly the group of patients for percutaneous pulmonary valvuloplasty, a diagnostic catheterization is initially performed, which consists of:

- measurement of pressures in all right heart cavities, showing the degree of pulmonary stenosis by measuring transvalvular gradient peak (Fig. 41.1)
- taking oximetry samples from all cavities in order to detect intracardiac shunts
- angiography with contrast agent, to analyze the morphology of right ventricular, pulmonary valve aspect, pulmonary valve ring size

Table 41.2 Classification of pulmonic stenosis [10]

Class I	Exertional dyspnea, angna, syncope, presyncope
	Asymptomatic, normal cardiac output, peak gradient 50 mmHg
Class IIa	Asymptomatic, normal cardiac output, peak gradient 40–49 mmHg
Class IIb	Asymptomatic, normal cardiac output, peak gradient 30–39 mmHg
Class III	Asymptomatic, normal cardiac output, peak gradient <30 mmHg

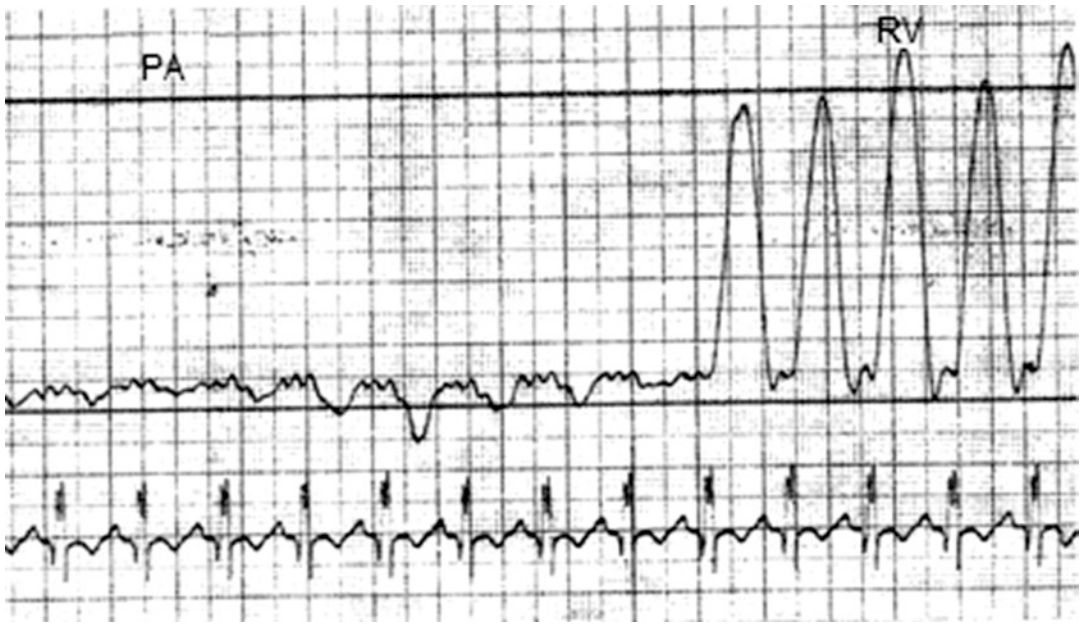

Fig. 41.1 Recording pullback pressure from pulmonary artery into the right ventricle

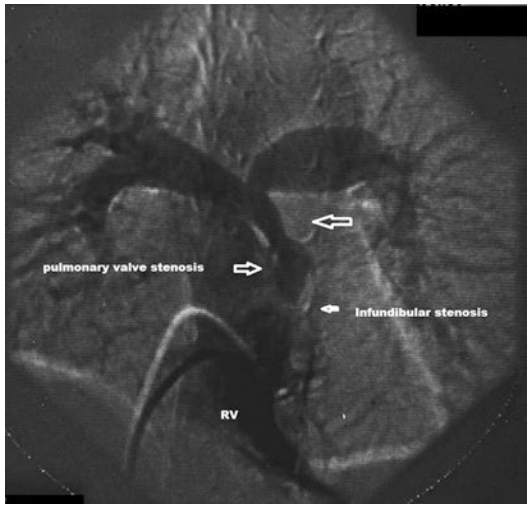

Fig. 41.2 Right ventricular angiography highlighting the stenosis of outflow of right ventricle, associated with pulmonary valve stenosis and hypoplasia of main pulmonary artery (arrow)

in order to choose the size of the balloon and the diameter of the pulmonary artery branches. The stenosis of the ejection tract is best seen when performing angiography of the right ventricle; it may be associated with pulmonary valve stenosis or hypoplasia of the pulmonary valve ring and/or of the pulmonary artery trunk (Fig. 41.2)

If the patient has indications for balloon valvuloplasty in the same session, dilation of the pulmonary valve is performed. Dynamic muscular stenosis of the right ventricular ejection tract does not benefit from balloon dilatation because ventricular muscles do not react favorably, on the contrary, it increases the infundibular gradient through mechanical irritation [11].

41.2.1 The Technique of Pulmonary Valvuloplasty

This procedure can be performed by several venous approaches, usually approaching the femoral vein, but also the transhepatic or jugular veins in newborns with anomalies of the venous system afferent to inferior vena cava.

Percutaneous pulmonary valvuloplasty consists in inserting on femoral vein sheath of a 5–7 F catheter with terminal hole into the pulmonary artery (Berman catheter or multi-purpose catheter), on which an extra stiff 0.035–0.038″ metallic guidewire is inserted up to one of the pulmonary artery branches, after which the probe is withdrawn and the guidewire remains in place [12].

The dilatation balloon with 5–9 F shaft is introduced on this guidewire, which is positioned in the pulmonary valve, the markers on the balloon help us to positionate it correctly.

The balloon catheters used in pulmonary valvuloplasty may be of several types [13]:

- a single balloon that has the disadvantage of stopping the pulmonary blood flow during inflation.
- two balloons, used when the diameter of the pulmonary valve ring is greater than 18–20 mm.

If two balloons are used during valvuloplasty, the following formula is used to calculate the actual balloon diameter [14]:

$$\text{Effective balloon diameter} = 0.82\left(\text{D1} + \text{D2}\right).$$

D1 and D2 are the diameters of the two balloons.

- Bifoil balloon
- Trifoil balloon that allows blood to pass through during inflating the balloon, moderate hypotension is recorded.
- The Inoue balloon is used in the last few years on a smaller scale, which has the advantage of increasing its diameter as needed so that post-valvuloplasty residual pressure gradient is as small as possible.

Choosing of the diameter of the dilatation balloon is based on the diameter of the pulmonary valve ring, which is measured angiographically, the optimal ratio diameter of the balloon/diameter of the pulmonary valve ring is 1.2–1.4 and for thickened pulmonary valves, it is 1.5 or even slightly over in the case of the dysplastic pulmonary valves [15, 16].

It is considered that dysplastic pulmonary valves have thick cusps with welded commissures. Even if a larger balloon diameter is introduced, it is taken into account the resistance opposed by the greater thickness of the cusp. Balloon diameter/pulmonary valve ring diameter ratio should not exceed 1.5 in order not to produce severe pulmonary insufficiency [17].

The recommended length of the balloon is 20 mm for infants and newborns, 30 mm for children and adolescents and 40 mm for adults [18].

Today there is a wide variety of pulmonary valvuloplasty balloons that are used depending on the age of the patient since the balloon shaft for infants should not be larger than F6 in order to avoid complications involving the femoral vein.

The balloon-catheter positioned in the pulmonary valve is inflated with diluted contrast agent 2–8.5 atm for 5–60 s, then it is deflated and withdrawn on the guidewire until the inferior vena cava (Fig. 41.3).

After pulmonary orifice dilation, the pulmonary transvalvular residual gradient is measured with a single-hole probe and it is appreciated if it is an optimal result or if it is necessary to change

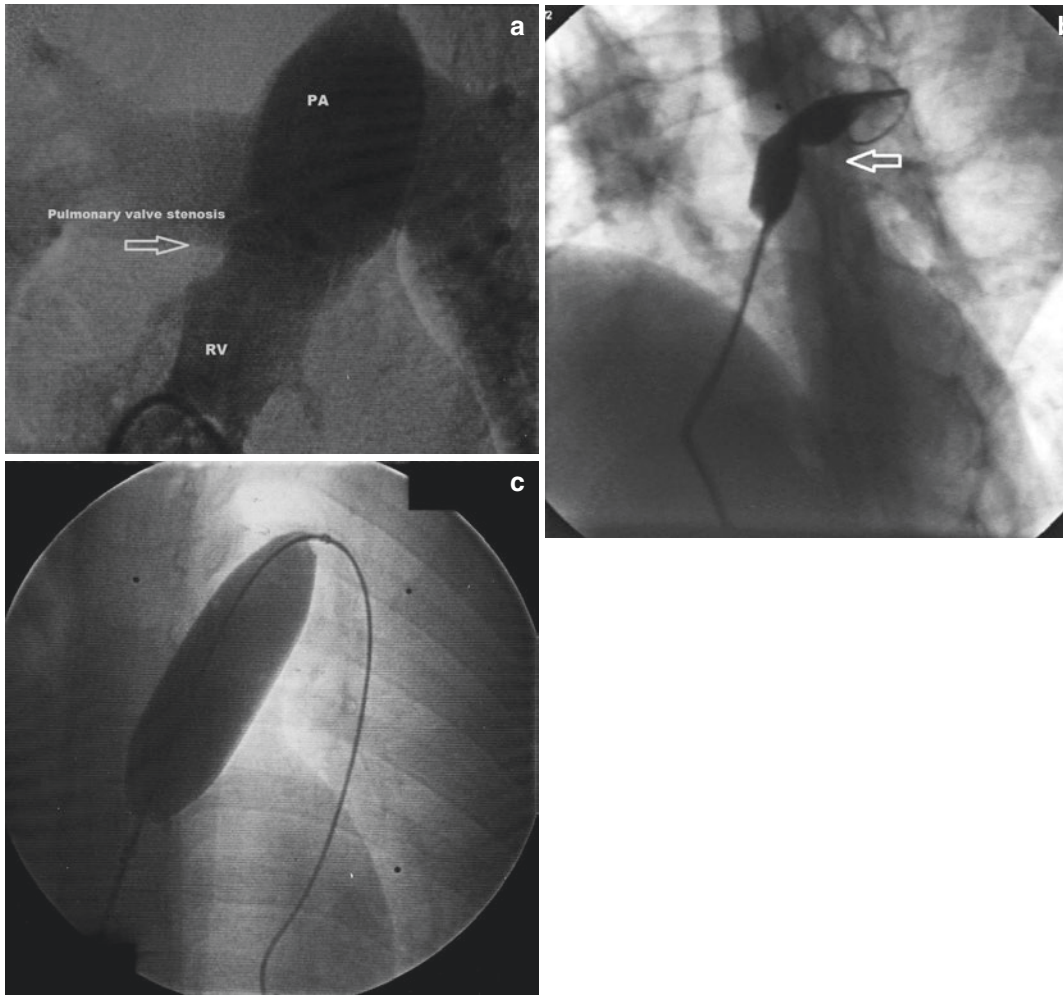

Fig. 41.3 (**a**) Angiography of the right ventricle reveals in dome shaped opening of the pulmonary valve. (**b**) Inflated balloon in the pulmonary valve with incision on the balloon—unique balloon technique. (**c**) Fully inflated balloon without incision

the balloon by a larger one when the residual pressure gradient is too high.

The immediate and long-term results of percutaneous pulmonary valvuloplasty both in isolated pulmonary stenoses and in those of complex cyanogenic congenital malformations are as follows [7]:

- decrease of right ventricular to pulmonary artery pressure gradient.
- increased pulmonary blood flow.
- decrease of the right to left oximetry shunt.
- increased peripheral arterial oximetry.
- possibility of remodeling the pulmonary vascular bed and left heart cavities.
- improving cyanosis, dyspnea and fatigue.
- better psychosomatic development for infants and children.

For complex cyanogenic congenital malformation, pulmonary valvuloplasty provides the opportunity for corrective surgical treatment after a period of time when the somatic development of the infant allows it, and the pulmonary vascular bed is already prepared to take a larger amount of blood from the venous circulation, without postoperative acute right heart failure.

In adults, the result of valvuloplasty is very effective and it persists for a long time, pulmonary valve restenosis was recorded in 8% of patients.

Complications of the pulmonary valvuloplasty are generally rare and frequently transient without compromising the patient's life. Death was quoted in 0.24% of patients who underwent percutaneous pulmonary valvular surgery [13].

Acute postprocedural complications may be:

- transient modifications were quoted with a frequency of 0.35%: hypotension when inflating the balloon, frequently when single balloon is used; bradycardia; heart blocks (1st or 2nd degree AV block); arrhythmias (tachycardia or ventricular fibrillation, cardiac arrest)
- breaking the balloon because of increased inflation pressure
- tricuspid insufficiency resulting from breakage the chordae tendineae of papillary muscles
- bleeding at the percutaneous puncture site, which rarely requires transfusion.

Late complications most commonly found are:

- occlusion of the femoral vein through local thrombosis especially in neonates and infants (cited as 19%).
- pulmonary valve insufficiency, which is often low grade and it can be quantified on echocardiography, but without hemodynamic influence on the right ventricle (if pulmonary insufficiency exceeds grade 2, the right ventricle responds by dilating its cavity). In rare cases, the severity of post-procedural pulmonary insufficiency is grade 3 and it is maintained over time, so it requires percutaneous implantation of a pulmonary valve.
- restenosis of the pulmonary valve is rare and it depends on certain factors.

Long-term studies have shown that pulmonary restenosis after valvuloplasty is rare, 10%, being dependent on two important factors [19]:

- the anatomy of pulmonary valve, thickened valves respond relatively well with commissures opening, while dysplastic valves exhibit an elastic recovery phenomenon (recoil) remaining after procedure with a high gradient, over 40–50 mmHg, often requiring surgical intervention
- optimally, balloon diameter/valvular ring diameter ratio must be between 1.2 and 1.5, so that immediately after valvuloplasty the gradient should be less than 30 mmHg.

After pulmonary valvuloplasty, the patient's follow-up is performed by Doppler echocardiography in order to track the evolution of the gradient.

It was found that, in general, if the gradient is only at the level of the valve, it remains almost unchanged over time, but if there is an associated infundibular reaction it is noted that the gradient decreases over time (in weeks or months) by reducing the dynamic muscle component, which is reversible [20, 21].

If right after procedure, the gradient at the level of the right ventricle outflow tract is greater

than 50 mmHg, β-blocker therapy is administered, after which at follow-up echocardiography made several months after, shows an important decrease of the pressure gradient at this level.

The follow-up protocol includes: physical examination, chest radiography, electrocardiography and echocardiography at 6 weeks and 6 months, then one examination per year (to measure the pressure gradient and check for restenosis phenomenon).

41.3 Angioplasty for Pulmonary Artery Branches

It should be noted another type of pulmonary stenosis, the stenosis of the main or distal pulmonary artery branch which in terms of the balloon dilatation technique it differs by choosing the diameter of the balloon, as well as by producing more marked elastic recoil than other types of stenosis.

For this type of stenosis, immediate results were suboptimale when was used balloon only and they became optimal when a stent is implanted.

Stenosis of the main and peripheral branches of the pulmonary artery occur with a frequency of 2–3% in congenital heart diseases, such as tetralogy of Fallot, and pulmonary atresia associated with ventricular septal defect [7].

Stenosis may be isolated or associated with long hypoplastic segments, it may be congenital or the result of a surgical correction, when they appear:

- at the anastomosis site of a shunt,
- in the terminal portion of an enlargement patch,
- at the anastomosis site of the unifocalization of the branches,
- torsion or stretching after arterial switch or Norwood surgery [13, 22] (Fig. 41.4).

In young children with pulmonary artery stenosis unassociated with other congenital heart diseases rarely appear symptoms and treatment under 5 years of age is not recommended in

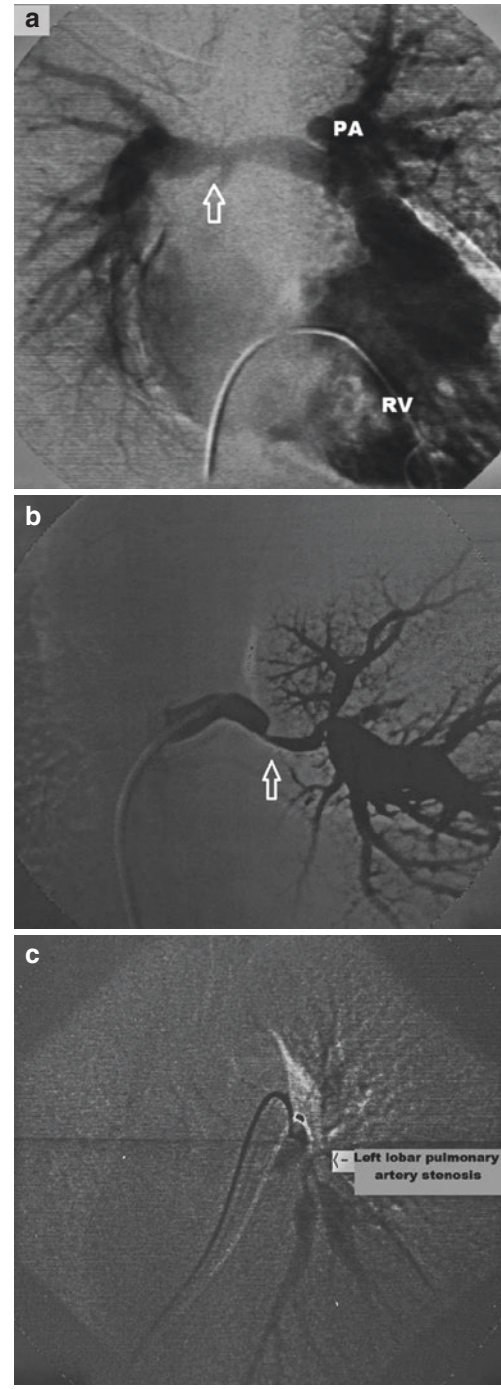

Fig. 41.4 Different localizations of stenoses of pulmonary artery branches. (**a**) Stenosis of the right pulmonary artery branch (pressure gradient 50 mmHg). (**b**) Stenosis of left inferior lobar pulmonary artery associated with poststenotic dilatation of distal artery (pressure gradient was 80 mmHg). (**c**) Stenoses of bifurcation of the left lobar pulmonary artery (patient 8 years old with William–Beuren syndrome)

asymptomatic patients [13]. Patients with associated congenital heart diseases may not tolerate relatively mild degrees of pulmonary artery stenosis if a surgery procedure is necessary [13]. Older patients with severe proximal stenosis or multiple distal stenoses may have normally distributed perfusion, but severely elevated main pulmonary artery and right ventricular pressure [13]. This patients have symptoms: dyspnea, limited ability to increase cardiac output with exercise and risk for sudden death.

Rarely, stenosis occurs together with inflammatory mediastinal disease (radiation or inflammatory mediastinitis) or extrinsic compression by tumoral mass.

In terms of pathophysiology, stenosis of a peripheral branch of the pulmonary artery decreases pulmonary blood flow in pulmonary parenchyma, with an increase in systolic pressure in the main pulmonary artery and right ventricle.

The more stenoses of peripheral branches, the higher the systolic pressure in the trunk of the pulmonary artery and secondary an overload of the right ventricle will appear. In these cases, symptoms related to the decrease of blood flow in the pulmonary parenchyma (dyspnea and poor development of pulmonary circulation associated with the stenosed segment) or the right overload (right heart failure, arrhythmias, sudden death) [23].

Treatment for pulmonary artery stenoses is **indicated** in patients:

- right ventricular pressure is more than 75% systemic
- significant symptoms.

41.3.1 Technique of Peripheral Pulmonary Angioplasty

Pulmonary angiography is the first step in the diagnosis of branch stenosis and it indicates the degree of stenosis and the distal diameter of the affected vessel.

A guiding catheter for coronary dilatation is inserted into main pulmonary artery or in the proximal pulmonary artery branch where the stenosis is; on it, a 0.014″ (for newborn and children) or 0.035″ guidewire is inserted through stenosis distal from the affected vessel. For each stenotic lesion the guidewire is advanced into a stable position with the stiff portion of the guidewire extended past the stenosis for support. The dilating balloon is advanced over the wire and positioned at the level of vessel stenosis. It is important to ensure that the balloon is not protruding into a small side branch (risk of vessel rupture) and is in a good position [13].

The balloon has two times the diameter of the vessel's distal diameter at a high pressure for 30–60 s if the patient it is hemodynamically stable. The recoil phenomenon (elastic recovery) occurs frequently due to the muscular structure of the vascular wall [12] (Fig. 41.5).

When the pulmonary branch stenosis is tough, often in the distal pulmonary branches, a special balloon with metal blades called "cutting balloon" is used to dilate fibromuscular stenosis [7]. This balloon has three or four microtome blades fastened along the length of the balloon, with inflation the blades protrude approximately 10 thousandths of an inch above the surface the balloon [13]. These blades will create three or four equally spaced micro-incisions than ideally extend through the thickened intima and into the media of the vessels [13]. The spaced weakened areas should be the areas of expansion during angioplasty. The recommended "cutting balloon" diameter is slightly less than the diameter for simple angioplasty balloon and should not be chosen one larger than 10% of the normal vessel diameter [13].

This type of balloon requires attention as it may cause vascular intimal injury or even rupture of the vessel, which would require emergency implantation of a covered stent.

A new era opened after implantation of stents, an era in which the resolution of peripheral pulmonary stenoses became reality. The stent implanted in a vessel with a muscular wall structure keeps the vessel open after the procedure with an optimal result because can not appear elastic recovery phenomenon.

Stents for children have small sizes, coronary stents between 4 and 6 mm in diameter are inserted using 0.014″ guidewire [11]. Proximal main branch pulmonary arteries in adult have

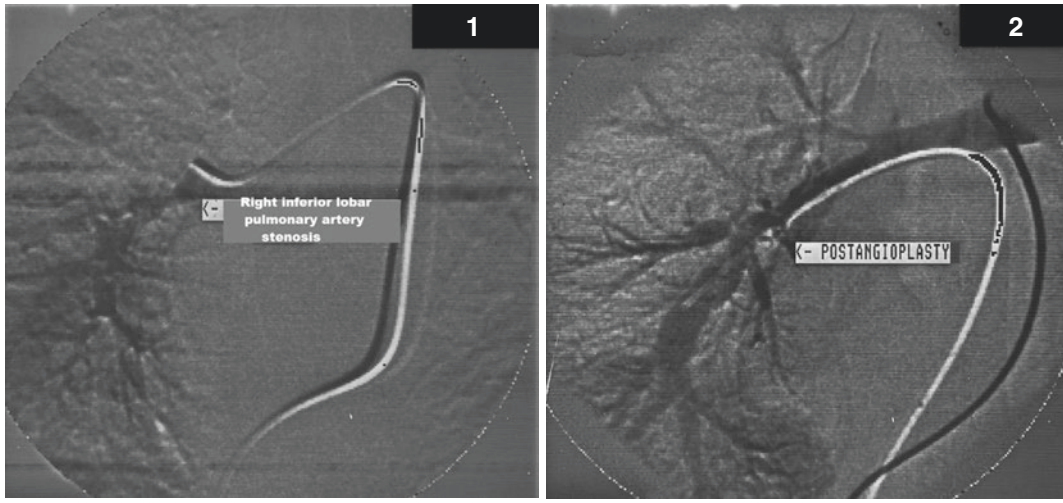

Fig. 41.5 (*1*) Right inferior lobar pulmonary artery stenosis (pressure gradient was 75 mmHg at a patient with William–Beuren syndrome). (*2*) The angiographic image of artery after dilatation with 6 mm balloon (pressure gradient after angioplasty is 7 mmHg)

16–20 mm diameter, sometime may be significantly larger. Primary lobar branch pulmonary arteries has typically 5–10 mm in diameter [13].

Sometimes stenoses are located at the bifurcation of two lobar branches and then the "kissing" technique is used, which consists in inflating simultaneously two stents, thus maintaining both vessels with optimal result. In this situation, a single Judkins right coronary guiding catheter 8 Fr is used, if is necessary to use two balloon technique, we must have two guiding catheters which are inserted through separate femoral approach [24].

If the stenoses are tough, due to a fibroelastic structure in the vascular wall, initially a cutting balloon is used (balloon which has cutter blades on its surface) for predilatation and then the stent is implanted. This type of balloon is used to cut the fibroelastic structure and it allows an optimal position of the stent in the vascular lumen.

41.3.2 Complications of Peripheral Pulmonary Angioplasty

Immediate complications [7]:

- dissection of tunica intima of the vessel, frequently recorded after using cutting balloon, it requires inflating the balloon for 5 min, and if the dissection maintains, it is necessary to implant a stent
- rupture of the vessel with haemorrhage in the related pulmonary parenchyma, which can be solved by implanting a covered stent or by occluding the vessel using Gianturco-Rubin coil
- acute development of an aneurysm of the vessel requires the implantation of a covered stent.
- stent migration to the distal portion of the vessel, which implies its withdrawal, some time can be difficult.

Late complications could be:

- pulmonary edema related to the dilated vessel, due to increased pressure of perfusion in distal part of the vessel
- intrastent restenosis possible because the diameter of the stent is small at this level.
- Obstruction caused by late thrombosis of the stent.

The benefits after pulmonary angioplasty are: a good perfusion of the lung segment, decrease the systolic pressure in main pulmonary artery and right ventricle, the patient became asymptomatic.

Follow-up of patient with pulmonary angioplasty is at 6 months: echocardiography, CT or MRI, quantitative radionuclide pulmonary perfusion scan and cardiac catheterization (if it is necessary a stent implantation).

41.4 Radiofrequency Treatment in Pulmonary Valve Atresia

Pulmonary atresia may be of two anatomical types, depending on which therapeutic approach is chosen [25]:

- pulmonary valve atresia—pulmonary valve is a fibrous membrane with the right ventricle infundibulum normally placed and located at a short distance from the trunk of the pulmonary artery. In this case, the pulmonary circulation is provided by the patent ductus arteriosus and the two branches of the pulmonary artery confluent with the existing pulmonary artery trunk are highlighted.
- pulmonary atresia associated with ventricular septal defect, where the right ventricle outflow tract is located at distance from the trunk of the pulmonary artery, if it exists.

In the first case, it can be made a passage through the membrane with a guidewire up to the pulmonary artery trunk and balloon dilatation, with restoration of the normal anterograde flow from the right ventricle to the pulmonary artery.

41.4.1 Technique

There are three techniques for introducing a guidewire from the infundibulum of the right ventricle into the trunk of the pulmonary artery:

- insert a guiding catheter for right coronary artery only through femoral approach to reach the infundibulum of the right ventricle, on which a 0.014″ guidewire is inserted with the hard side and pushed through the membrane.
- insert a laser guidewire into the guiding catheter that easily penetrates the membrane
- insert a radiofrequency wire, which perforates the membrane, reaching the trunk of the pulmonary artery.

After any of the three guidewires was introduced into the pulmonary artery, insert a 0.014″ guidewire and a 3 mm diameter coronary dilatation balloon, to create an orifice that allows introducing a balloon with larger diameter according to the diameter of the valve ring, which is frequently more than 7 mm [26].

Using a 0.035″ guidewire, the dilatation balloon is inserted according to the diameter of main pulmonary artery and an optimal orifice is created between the right ventricle and the pulmonary artery.

41.4.2 Complications

Major complications were cited in this type of interventional procedure:

- inability to pass through the membrane, with perforation in pericardium and secondary pericardial tamponade
- thromboembolic events
- infection
- death.

It is an interventional procedure that may increase the survival rate in newborns dependent on the arterial duct, which is maintained open with prostaglandins.

41.5 Transcatheter Valve Replacement of the Pulmonary Valve

A few years after surgery of tetralogy Fallot, severe pulmonary insufficiency may occur leading to dilatation of the right ventricle over time. In these cases, a pulmonary valve can be implanted percutaneously in the native pulmonary valve ring. Special attention is given to cases

with annuloplasty and pericardial patch that enlarges the main pulmonary artery and/or the major branches of the pulmonary artery.

Indications for pulmonary valve replacement are not very clearly defined:

- symptomatic patients with severe pulmonary regurgitation with right ventricle dysfunction and/or dilatation
- symptomatic arrhythmias and severe pulmonary regurgitation and dysfunction of the right ventricle
- severe pulmonary regurgitation with dysfunction of right ventricle and objective evidence of decreased exercise tolerance in asymptomatic patients
- moderate or severe pulmonary regurgitation with other associated lesions: residual ventricular septal defect, tricuspid regurgitation [13].

Very important for case selection are: electrocardiogram (right ventricular hypertrophy), Holter monitoring (ventricular or supraventricular arrhythmias), chest X-ray, echocardiography (right atrial and ventricular dilatation, severe pulmonary regurgitation) and MRI three-dimensional reconstruction (for selecting the site of implantation).

41.5.1 Technical Procedure

The procedure is performed with general anesthesia and monitoring ECG [13]:

- cardiac catheterization—the access is through femoral vein with 8 Fr sheath and femoral artery with 5 Fr sheath. With a Judkins right coronary catheter 5 Fr perform the right catheterization for hemodynamics. The Terumo 0.035 inch it is used to get a good distal position of the right or left pulmonary artery. Than exchange the catheter with an ultra—stiff wire 0.035 inch.
- Angiography must be performed in out flow tract of right ventricle and main of pulmonary artery for the site and size of pulmonary ring.
- Remove the 8 Fr sheath and dilate the femoral vein with 14 Fr and than with a 22 Fr dilatator for delivery system through the skin.
- The valve is washed 5 min in normal saline.
- The delivery system is prepared with the valve crimped over the BIB—balloon.
- The delivery system is advanced over the stiff guidewire 0.035 inch into out flow tract of right ventricle. Pulled back on the shaft of the outer sheath and performed an angiography on the side arm of the outer sheath to see the position of valve.
- The inner balloon is inflated and confirms its position in the pulmonary valve. Than the outer balloon is inflated to its full dimension to implant the valve stent assembly. Both balloons are deflated simultaneously.
- The delivery system is removed and the multitrack catheter is advanced over the wire for hemodynamics (right atrium, right ventricle, and pulmonary artery pressure, right ventricular out flow tract gradient).
- An angiography is performed above the valve to assess valvular and paravalvular regurgitation.

The delivery system is available 18, 20, 22 and 24 mm (indicates the size of the outer balloon of the BIB).

Follow-up is clinical, echocardiographic and chest X-ray at 6 month and 1 year.

41.6 Atrial Septostomy

Arial septostomy is a palliative interventional procedure used in transposition of the great vessels to save the life of the newborn from the very first days of life until complete corrective surgery is possible.

Transposition of the great vessels is a complex cyanogenic congenital diseases from birth, where survival is achieved by the shunts between the two circulatory paths, pulmonary and systemic (which are parallel) at interatrial or interventricular level.

When the link between the two circulatory paths is made only at the level of atrial septum, and this communication is small, restrictive, then the survival of the newborn is reduced to a few days after birth. If there are large interatrial or

interventricular communications, the child survives only a few years [12].

In the following images is presented the angiographic diagnosis of a transposition of the great vessels as follows: from the ventricle placed anteriorly which morphologically resembles the right ventricle, emerges the aorta which receives venous blood, and from the ventricle placed posteriorly which morphologically resembles the left ventricle emerges the pulmonary artery which receives oxygenated blood from the microcirculation through the pulmonary veins (Fig. 41.6) [7].

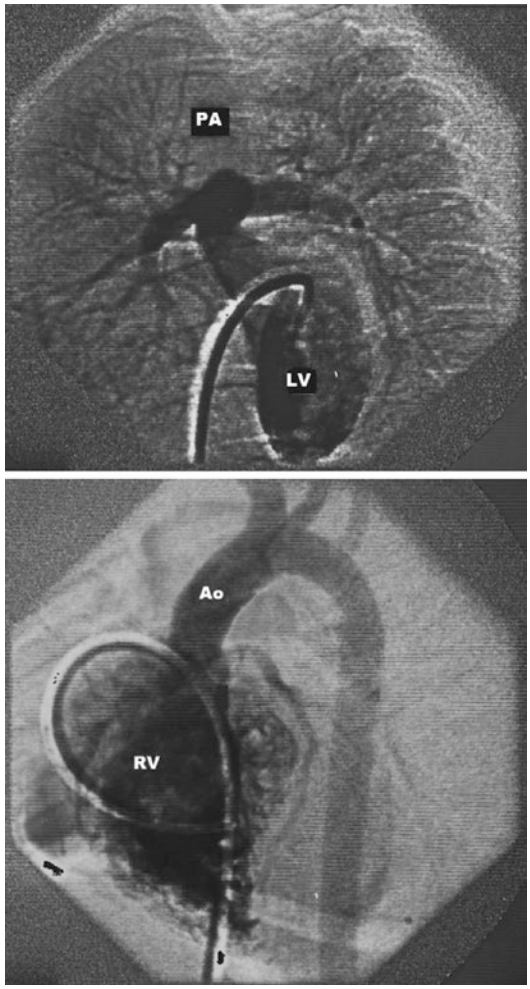

Fig. 41.6 The angiographic diagnosis of transposition of the great vessels, the aorta originates from the right ventricle and the pulmonary artery originates from the left ventricle

When there is a transposition of the great vessels with restrictive interatrial communication, there is a partial break in the atrial septum, thus increasing free bidirectional communication between the two atria, which leads to increase of oximetry in the right cavities of the heart with the reduction of cyanosis which is initially very big.

If atrial communication is restrictive and it does not allow good interatrial mixing, this may also be due to a large gradient between the measured pressures of the two atria, generally it exceeding 3–4 mmHg. This pressure gradient is significantly reduced if a corresponding septostomy balloon is inserted and optimal result means that remaining gradient is less than 2 mmHg [7].

Sometimes pressure gradient decreases transiently after inflating the balloon and then it grows a little bit in a few hours, due to the elastic recoil phenomenon of the atrial septum, which at that age behaves as an elastic membrane.

41.6.1 The Technique of Atrial Septostomy

The technique of atrial septostomy consists in inserting a balloon at the level of atrial septum and breaking it by inflating the balloon.

Initially, a diagnostic catheterization is performed with the measurement of pressures and oximetries in each heart cavity, followed by angiography with contrast agent which puts the diagnosis of certainty according to great vessels origin.

If there is an atrial communication, it should be measured the pressure gradient between the two atria, and if there is no such communication, oval fossa will be forced for septostomy using a Judkins right coronary catheter 4 Fr with guidewire 0.014″ to pass atrial septum [27].

The actual technique consists in introducing a diagnostic catheter with open end through interatrial communication through which a guidewire 0.014″ is inserted into left pulmonary vein or into left ventricle for stability.

A peripheral dilatation balloon having a convenient diameter according to the age of the newborn is inserted on the guidewire. This balloon inflates

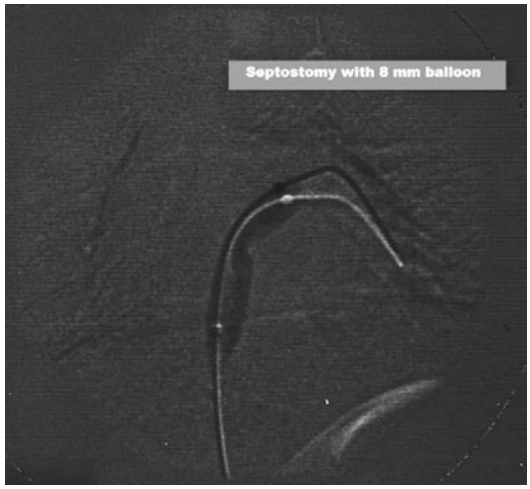

Fig. 41.7 The guidewire is inserted into right pulmonary vein and the balloon with the markers positioned at the level of atrial septum

at the level of the atrial septum, resulting in partial breakage of it with the achievement of large interatrial communication through which the blood circulates freely bidirectional (see Fig. 41.7) [27].

The following picture shows 8 mm balloon completely inflated at the level of atrial septum.

The peripheral balloon is not used anymore because the elastic recoil phenomenon was too high few hours after, so today septostomy is performed with a special Rashkind balloon that inflates in the left atrium and then withdrawn vigorously through the atrial septum, breaking it.

It is also possible to use a cutting balloon when the atrial septum is thick and it can not be broken only by the sudden withdrawn of the Rashkind balloon [27].

This interventional procedure was performed only in patients whose atrial communication was restrictive, with right to left atrial pressure gradient over 4 mmHg, and the residual gradient after septostomy 1–2 mmHg, allowing a good mixing at this level [28].

The left atrium pressure curve is presented with pullback of the catheter in the right atrium and recording a 1 mmHg gradient between them.

Aortic oximetry is important, initially it has very low levels, than it increases and provides better tissue oxygenation. In general, peripheral saturation in transposition of the great vessels is the smallest of all cyanogenic complex heart malformations reaching 75–79% SpO2 in the aorta, which favors the development of a major polycythemia, favoring thrombosis especially in intracranial circulation with consecutive cerebrovascular accident.

Peripheral saturation in the aorta increases significantly after the procedure, reaching values of 86–89% SpO2, which is the equivalent to the oximetry in severe tetralogy of Fallot, but it ensures the survival of the patient with these oximetric values.

41.6.2 Benefits of Atrial Septostomy

The benefits of atrial septostomy are [12]:

- ensures patient survival until corrective surgery
- better tissue oxygenation by increasing hemoglobin saturation in the aorta
- prevents cerebral thrombosis following a significant polycythemia.

41.6.3 Results

In the approached cases, survival rate was 90% and patients who were operated had favorable outcomes.

In conclusion, atrial septostomy may be a first palliative alternative for transposition of the great vessels, as a first step before complete surgical correction.

Worldwide today, it is performed echocardiography to diagnose the fetal disease and prostaglandins are administrated to the mother in order to maintain permeable the arterial duct after birth, thereby ensuring a new communication between systemic and pulmonary circulation [7].

41.7 Embolization

Systemic arterio-venous fistulas are a group of vascular anomalies characterized by abnormal communications between systemic arteries and veins without normal capillary development, with a left to right shunt from the high pressure arterial to the low pressure venous system [13].

Depending on the shunt volume, it may cause right ventricular overload, increased cardiac output and decrease of the peripheral vascular resistance.

Embolization is an accepted primary therapeutic approach in systemic arterio-venous fistulas, sometimes needing to be combined with surgery [13].

Embolization is an interventional maneuver useful in certain congenital heart diseases, and also in vascular malformation, as well as in anastomoses acquired in particular after trauma.

Of the cardiac malformations in which embolization with various embolization agents is frequently used, we can recall [7]:

- collateral bronchial circulation in tetralogy of Fallot
- pulmonary arteriovenous fistula
- coronary fistulas, when there is a coronary steal syndrome associated with angina
- arteriovenous fistulas at the level of different vessels
- aortopulmonary surgical derivation performed in extreme tetralogy of Fallot to provide a convenient pulmonary blood flow (Fig. 41.8)
- hypervascularized tumors (hemangiomas).

All therapeutic decisions should be made specific for every case, optimal closure technique is determined by the anatomy of fistula vessel.

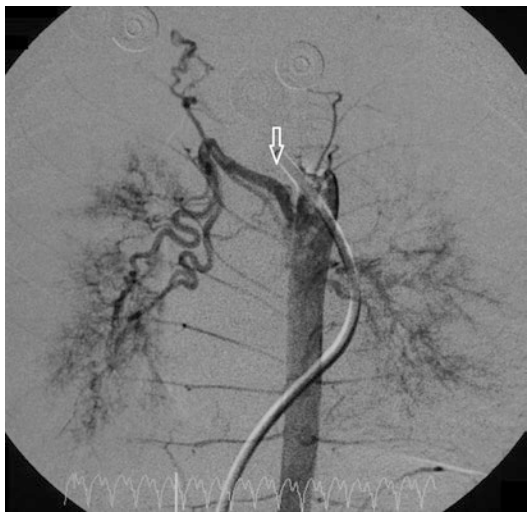

Fig. 41.8 Angiography shows a right bronchial artery collateral at a patient 4 year-old with Tetralogy of Fallot

Embolization material can be divided into two broad categories:

- **temporary embolization material** consisting of Gelfoam, the effect of this material generally lasts for about 10–12 days, after which the vessel is permeable again, but it is advantageous because in case of surgery only a small bleeding occurs in the wound.
- **permanent embolization material** consisting of:
  - liquid chemical agents represented by pure ethanol at a concentration of 90%, ivalon, agents containing cyanoacrylate monomers.
  - Special coils: different types of Gianturco coils, detachable coils, microcoils are used for permanent embolization of various malformations.
  - Device closure: Amplatzer vascular plug, Amplatzer duct occluder for vessels with large diameter.
  - Covered stent is not a typical embolization material, but it is useful in post-traumatic fistulous communication between big arteries and veins. Covered stent is implanted in the artery and can be balloon expandable or self-expandable.

In the catheterization lab, embolization was performed for congenital heart and vascular defects as follows [12]:

- bronchial collaterals in tetralogy of Fallot
- surgical aortopulmonary derivation
- hemangiomas with various localizations
- pulmonary arteriovenous fistula

In extreme tetralogy of Fallot where surgery is at high risk, a pulmonary derivation can be made in a first time in order to achieve a good blood flow in the pulmonary artery and in the same time to develop the pulmonary circulatory bed with the purpose to prepare it for corrective surgery [29].

In the following pictures is shown a case of occlusion of surgical aortopulmonary derivation prior to complete corrective surgery (Fig. 41.9).

This derivation has a calculated diameter of 7 mm and, depending on this, a Gianturco coil of 5 mm diameter was chosen. Calculation of the

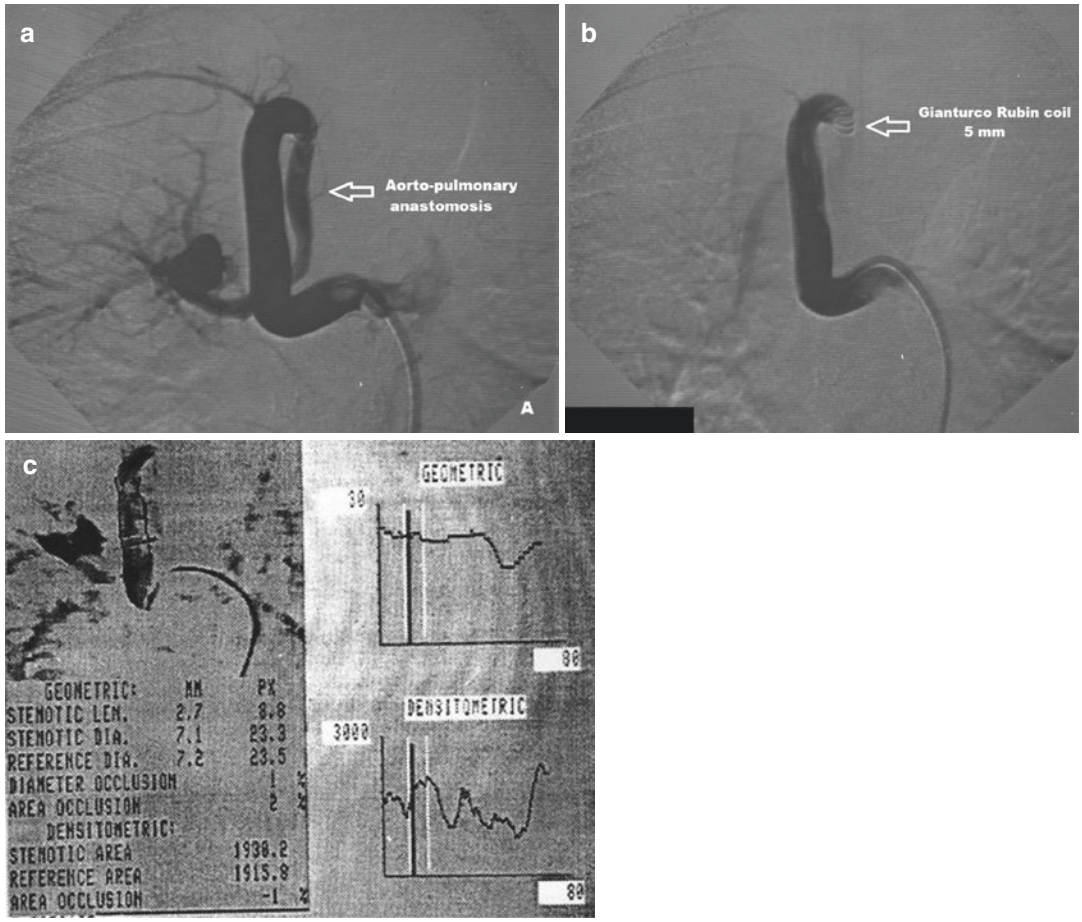

Fig. 41.9 (**a**) Selective angiography of aortopulmonary derivation. (**b**) Embolization of aortopulmonary derivation from the arterial side with the 5 mm diameter Gianturco coil. (**c**) Calculating the diameter of the device to be implanted

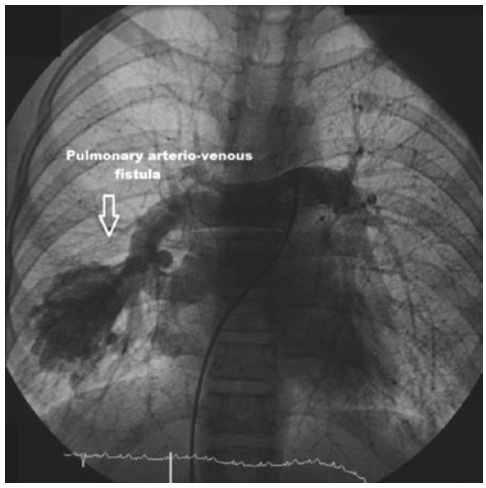

Fig. 41.10 Angiography before embolization of an arterio-venous pulmonary fistula

diameter of goretex prosthesis used in derivation is shown in Fig. 41.9.

Pulmonary arterio-venous fistulas is another congenital malformation that can be approached by embolization with Gianturco coils (see Fig. 41.10).

Complications which may occur in the embolization of a congenital malformation consist in:

- migration of embolization material distally into arterial tree
- tissue necrosis located distal from the embolization site
- hemolysis occurring only in significant residual flow and should be treated with additional embolization
- infection [30].

41.8 Closure of Atrial Septal Defect

Atrial septal defect is one of the most common congenital malformations seen in older patients and currently it can be solved without surgery, using interventional maneuvers through which various devices are implanted at the level of the atrial septum. In recent years, there has been a growing concern to make such devices that can be implanted to avoid surgery.

The concerns of interventionist cardiologists in this field have led to the invention of many types of devices, each of which has its advantages and disadvantages. Briefly, I will present some types of closure devices for atrial septal defects used quite often in today practice.

Anatomically atrial septal defect is of several types:

- ostium primum
- ostium secundum
- venous sinus type
- inferior cava type
- unique atrium
- cribriform (multiple communications in atrial septum).

These types are exemplified in the diagram below, which highlights how much atrial communication varies regarding their location in the septum, shape, and number [31].

Of these types of interatrial communication, only two are approachable interventionally: ostium secundum and cribriform type.

Patient selection for atrial septal defect interventional closure is performed by 2D and transesophagial echocardiography, which establishes [7, 32]:

- the anatomical type of communication
- the number of communications
- the type of communication, it is important to have an approximation in order to know if it can be covered with the device altogether or it will remain with shunt no matter how large the device would be.
- the atrial septum between communication and adjacent structures, generically called "rim"
- anomalies associated with atrial septal defect (pulmonary stenosis, partially anomalous pulmonary venous connection, aortic stenosis, mitral regurgitation, other).

At TEE, the rims are carefully monitored, they are necessary to allow the device to catch the remaining atrial septum and to be stable with low embolization risk [33, 34]:

- upper rim—to upper superior vena cava
- superoposterior rim—located close to the right pulmonary vein
- anterosuperior rim—to the aortic wall, which is often absent
- the lower rim—to the inferior vena cava, it is strictly necessary to exist.

If the patient has these rims, he meets the criteria for implanting a type of atrial septal defect closure device.

The final evaluation is based on diagnostic cardiac catheterization, considering: the degree of pulmonary hypertension, other associated malformations and the position of the inferior right pulmonary vein [12].

Indications for atrial septal defect device closure:

- symptomatic and hemodynamically significant shunt Qp/Qs > 1.5 or dilation of the right cavities
- patients with small atrial septal defect and a history of paradoxical embolism (stroke, TIA or peripheral embolism).

Contraindications for atrial septal defect device closure [13]:

- association of anomalous pulmonary venous drainage
- sinus venosus atrial septal defects
- ostium primum atrial septal defect
- rim deficiency below 5 mm to: superior vena cava, inferior vena cava, right pulmonary vein, coronary sinus and atrioventricular level.

- the association of other cardiac abnormalities requiring surgical intervention
- total pulmonary resistances greater than 8 Wood units
- sepsis
- contraindications for antiplatelet therapy.

41.8.1 The Technique for Inserting the Device to Close the ASD

The technique is broadly the same regardless of the type of device used and consists in [13, 35]:

- a diagnostic open tip catheter is inserted through the femoral vein up to the inferior vena cava–right atrium–left atrium–left superior pulmonary vein
- insert a 0.035″ stiff guidewire 260 cm long into the catheter and then retract the catheter
- insert a balloon on the guidewire to measure atrial communication, the balloon is inflated at the level of the atrial septum and looking at the incision on the balloon. This is measured and represents the diameter of the septum hole and implicitly the diameter according to which the device size is chosen.
- the balloon is withdrawn and on the guidewire in inserted a sheath having its size corresponding to the diameter of the device to be inserted.
- insert the device into the sheath, the device has a part which attaches to the left atrium, then it is gently withdrawn and detach the second part that attaches to the right atrium; atrial septum being between the two parts of the device.
- the device has a cable grip system that by counter-clockwise spinning, it detaches from the device, which must stay stable on the atrial septum.
- TEE and angiographic control is performed in order to check the position and stability of the device on the atrial septum and any eventually residual shunt (Fig. 41.11).

There are various types of devices: Starflex device, Amplatzer occluder and Helex device.

The disadvantage of Starflex device is that after implantation, a residual shunt may remain between the atria by separating the distal heads of the two parts of the device from the septum.

There is also another atrial septal device closure device, Helex device, which is made by a spiralling ring of nitinol, covered by Goretex, in the form of a double-helix which catches the atrial septum between its two parts.

In practice Amplatzer septal occluder has the advantage that there is no residual shunt after the procedure [7].

This closure system is made of a material with thermal memory—nitinol, which has the advantage of maintaining its initial shape without any deformation in any condition.

The Amplatzer device is selected depending on the on the atrial septum anatomy: if the defect has adequate rims (>5 mm), usually select a 2 mm larger than balloon stretched diameter. If the superior/anterior rim is deficient (5–7 mm) a device 4 mm larger that the balloon stretched diameter [13].

The echocardiographic image and transthoracic echocardiography after the implantation of the Amplatzer occluder shows that there is no left to right shunt in the atrial septum (Fig. 41.12).

41.8.2 Complications in ASD Device Closure

- embolization or migration of the device, which requires its withdrawal
- supraventricular arrhythmias, which often resolve spontaneously within the first 7 days after the procedure
- risk of erosion of the walls adjacent to the device, often when it was oversized [36, 37]
- pericardial effusion, requiring echocardiographic follow up
- impossibility of unloading the disc for right atrium if there is a protruding Eustachio valve.

Closing the atrial septal defect with various types of devices is a feasible alternative for some types of atrial septal defects [38].

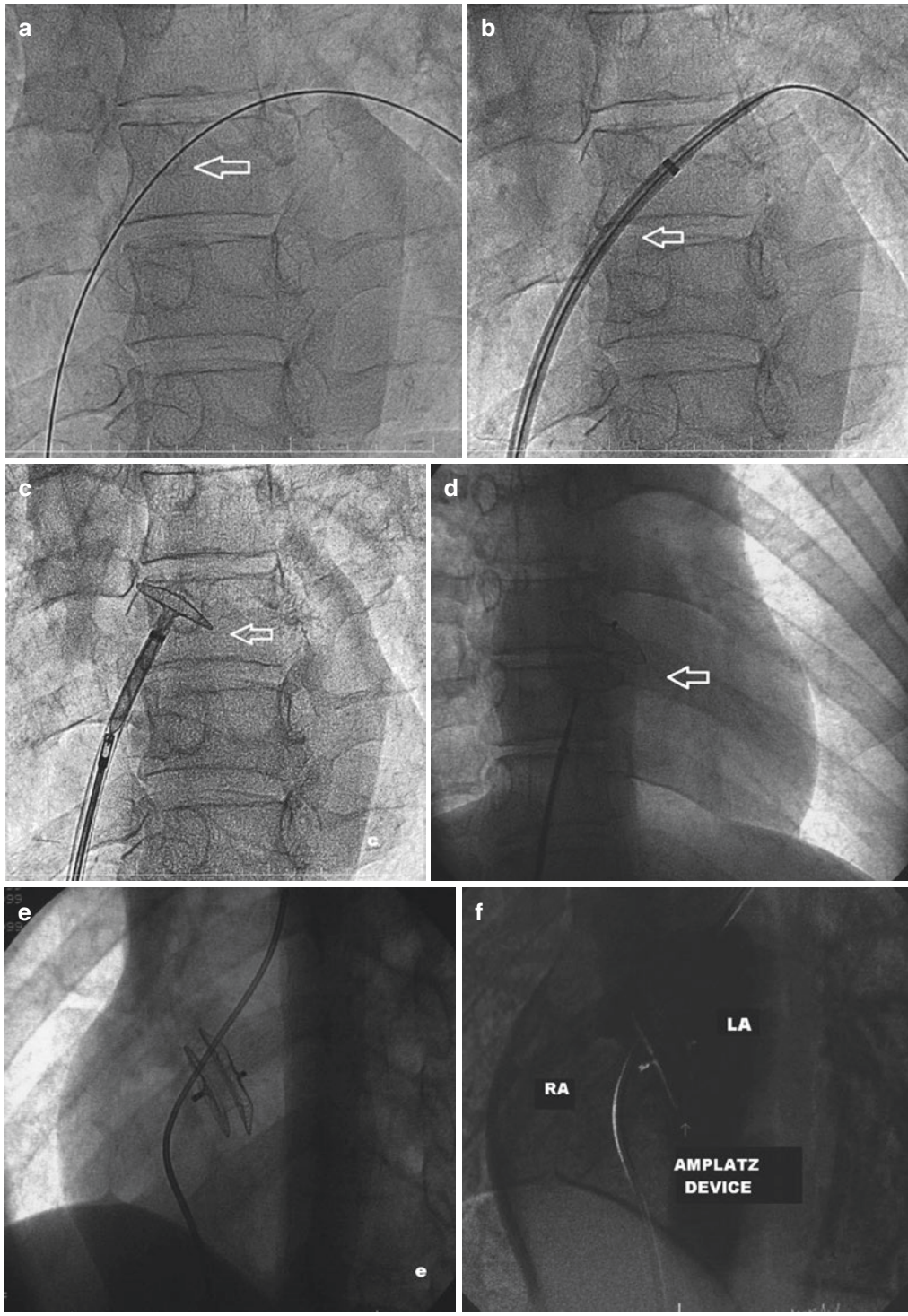

Fig. 41.11 Fluoroscopic images demonstrating the step of closure atrial septal defect with Amplatzer septal occluder. (**a**) Guidewire in left pulmonary vein through the atrial septum (arrow). (**b**) The 8 Fr sheath (arrow) advanced over the guidewire into left atrium. (**c**) The left atrial disk (arrow) has deployed in the left atrium. (**d**) Deployment of the right atrial disk (arrow) in the right atrium. (**e**) The device has been released from the delivery cable and it is stable on atrial septum. (**f**) Pulmonary levophase angiogram showing the device on the atrial septum and without left to right shunt at this level

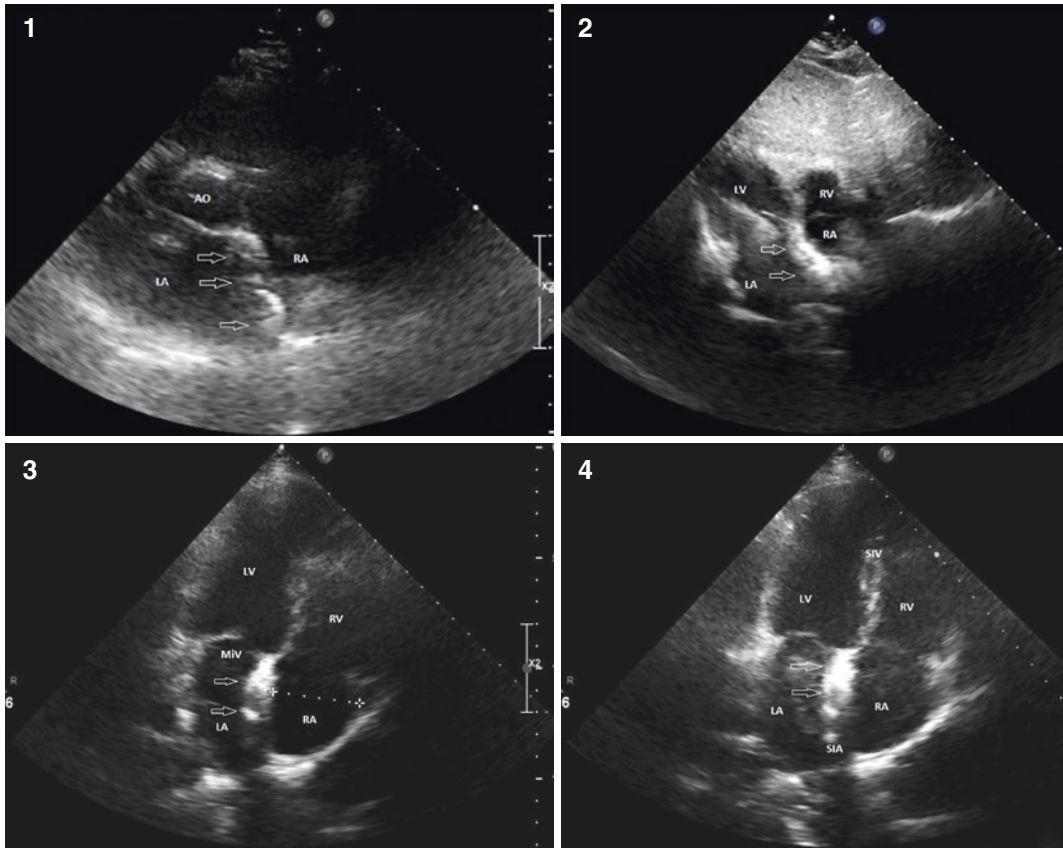

Fig. 41.12 The transthoracic echography views of the Amplatzer system implanted in the atrial septum. (*1*) Transverse section view (arrow). (*2*) Sub-xiphoid view (arrow). (*3*) and (*4*) Apical 4 chamber view (arrow).

After the procedure aspirin therapy 81–325 mg per day is administered for 6 months.

Follow up of the patient at 6 months includes: ECG (for cardiac arrhythmia), chest X-ray and TEE to see if the device is in the right position without residual shunt.

41.9 Closure Systems for Patent Ductus Arteriosus

Another interventional procedure used in pediatric and adult cardiology is the closure of patent ductus arteriosus with various devices, such as [39]:

- Amplatzer device of various sizes depending on the size of the duct
- detachable Jackson Coils
- Gianturco coil.

Each of this types of devices used for closing the patent ductus arteriosus is chosen according to the angiographic diameter of the arterial duct and as it follows [13]:

- if the duct has a diameter greater than 4 mm, the Amplatzer device is preferred
- if the arterial duct is below 2.5–3 mm, choose Gianturco coil or detachable coil.

Due to the different types and varied sizes of devices, today almost any patent arterial duct without pulmonary hypertension can be closed [39].

The advantage of implanting in the arterial duct of such a device is to avoid surgical intervention and to cancel the left to right shunt at this level.

Consideration should be given to the shape and diameter of the arterial duct, which can be determined by echocardiography and with a

greater accuracy by angiography, after injecting contrast agent into the descending aorta.

If the length of the duct is great, special attention will be given when choosing the device because there is an increased risk of embolization [7].

41.9.1 Implantation Technique of the Device in the Arterial Duct

First diagnostic cardiac catheterization is performed and then the angiography based on which the anatomical type of arterial duct, its diameter and length are established.

A Pigtail catheter 5 Fr is inserted through the femoral artery into the descending aorta for angiographic control and for some types of devices which can be introduced from the arterial side into the arterial duct.

For the majority of patent ductus arteriosus, especially with a conical shape the Amplatzer device size selected (the pulmonary end) should be at least 2 mm larger than the narrowest PDA diameter. The long sheath is recommended to be 7 or 8 Fr size depending on the size of the Amplatzer device [13].

Insert the long sheath through the femoral vein up to main pulmonary artery and then is guided by the guidewire through the arterial duct into the descending aorta. Through this sheath, the Amplatzer device is inserted into the descending aorta and it is withdrawn to the arterial duct, opening the arterial part anchored to the wall of the aorta and then the central part at the level of the duct (Fig. 41.13) [40].

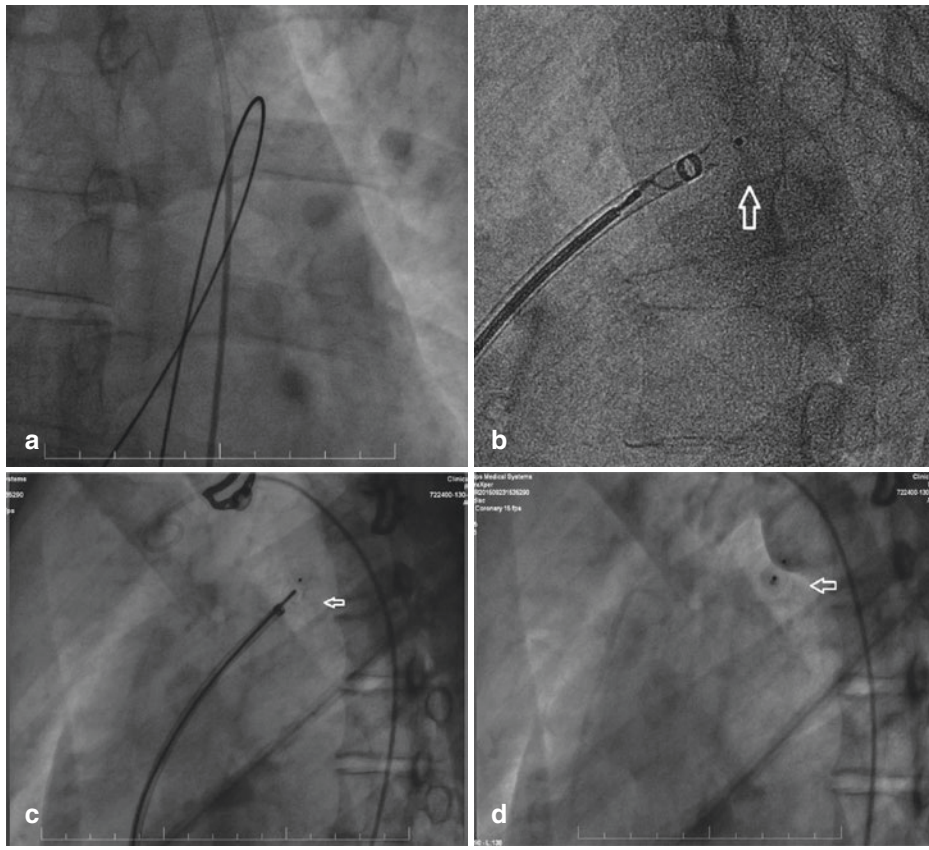

Fig. 41.13 Technique implantation of an Amplatzer device with a diameter of 8–10 mm in the patent ductus arteriosus. (**a**) The Pigtail catheter is positioned in descending aorta and we can see the guidewire from pulmonary artery through ductus arteriosus in descending aorta. (**b**) A partially deployment of Amplatzer device, only the arterial disk in aorta (arrow). (**c**) The sheath with device fully deployment in ductus arteriosus (arrow). (**d**) Device is detached and the angiography in aorta shows no left to right shunt through Amplatzer occluder

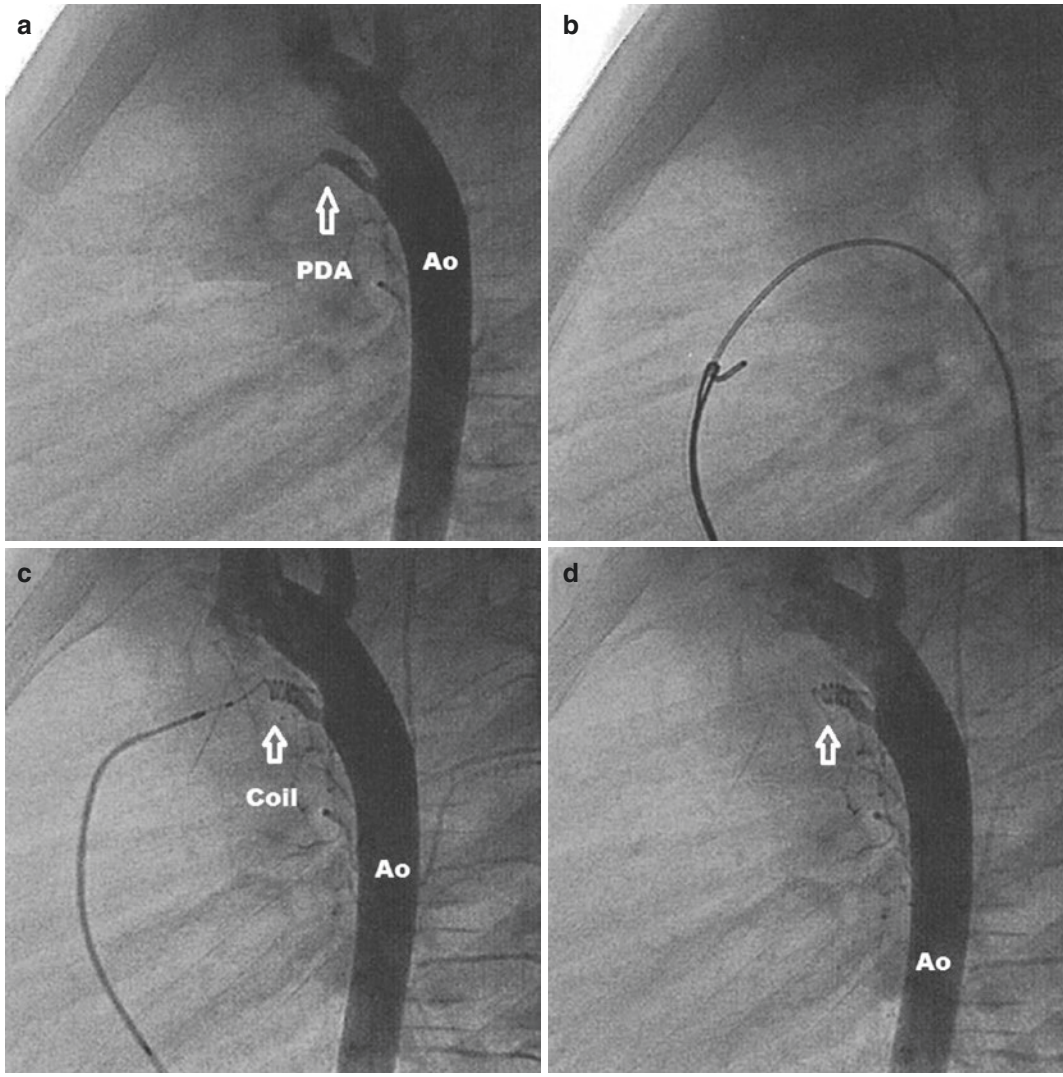

Fig. 41.14 Deployment sequence of detachable Jackson coil in a ductus arteriosus 2.5 mm diameter. (**a**) Angiogram obtain by a pigtail catheter in descending aorta—patent ductus arteriosus with a small diameter and left to right shunt (arrow). (**b**) Guidewire introduced from aortic root through ductus arteriosus it is snared in pulmonary artery and retrieved outside in the femoral vein. (**c**) The Jackson coil is positioned in ductus arteriosus (arrow) and angiogram shows that is in correct position. (**d**) The coil detached and occludes the duct without left to right shunt

In Fig. 41.14 PDA is shown by injecting a contrast agent into the aorta that initially opacifies also the pulmonary artery, but after the implantation of the coil inside the ductus arteriosus, the pulmonary artery is no longer highlighted.

41.9.2 Complications

The following complications are cited:

- bending of the long sheath inserted from the venous part at the levels of the infundibulum, the pulmonary artery trunk or the descending aorta with the impossibility of inserting the device [41–43]
- protrusion of the device in the aorta, narrowing the aortic lumen at this level (especially in young children) with a pressure gradient which usually is not hemodynamic significant.

- embolization of the device in the descending aorta or in a pulmonary artery branch [44–46]
- infection.

Some devices are in continuous refinement, such as the Amplatzer occluder, which now has a double-disk variant, which corresponds to the two ends of the arterial duct, it may be inserted on the venous end as well as on the arterial end.

41.10 Transcatheter Closure of Ventricular Defect

Ventricular septal defect (VSD) is the most common congenital heart disease 20%.

Ventricular septal defect may have various anatomic types, its localization in the ventricular septum can be determined by performing transthoracic echocardiogram in short axis parasternal view [13]:

- membranous septal defect—(defects are seen between 9 and 12 o' clock)
- perimembranous defect—(between 7 and 9 o' clock)
- supracristal or subpulmonary defect—(between 12 and 1 o' clock)

Muscular septal defects may be single or multiple ("Swiss—cheese").

Anatomically, depending on the opening of the defect in the right ventricle, the VSD may be [47, 48]:

- infracristal, it opens in the middle-superior portion of the septum in the proximity of the tricuspid valve (80%)
- supracristal, it opens in the right ventricle outflow tract located under the pulmonary valve (5–7%)
- muscular, located from the apex to the mid-muscular septum (5–20%) (Fig. 41.15)

In addition to congenital ventricular septal defect, it is also reported as a complication in acute myocardial infarction, after trauma and as residual defect after surgical closure of a congenital ventricular septal defect. In high defects with

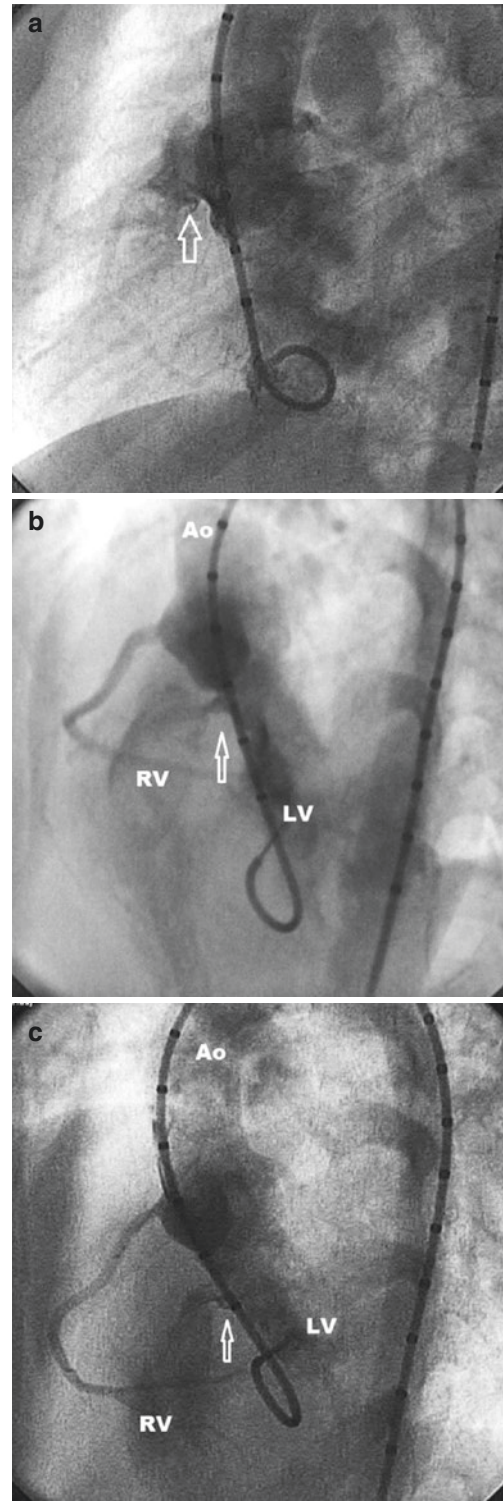

Fig. 41.15 Various types of ventricular septal defects. (**a**) Supracristal ventricular septal defect (arrow). (**b**) Membranous ventricular septal defect (arrow). (**c**) Muscular ventricular septal defect (arrow)

big shunt, aortic valve prolapse may occur (Venturi effect), causing aortic regurgitation or valvular aneurysm (Pezzi-Laubry syndrome).

Anatomic localization, left to right shunt quantification (normally Qp/Qs > 1.5), pulmonary hypertension and association with other malformations (atrial septal defect, aortic regurgitation, aortic stenose, double ventricular outflow tract, tetralogy of Fallot) are very important, to decide the indication for the procedure [49–51].

Indications for transcatheter closure of ventricular septal defect:

- membranous or muscular ventricular septal defect demonstrated by transthoracic echocardiography
- asymptomatic restrictive ventricular septal defect with significant left to right shunt (Qp/Qs > 1.5).

Contraindications of ventricular septal defect closure:

- distance of less than 4 mm between the aortic, pulmonary, mitral and tricuspid valves and ventricular defect.
- supracristal ventricular defect
- sepsis
- pulmonary vascular resistance >8 Wood units
- contraindication to antiplatelet therapy
- smaller patients, less than 5 kg.

Patient preparation consists in administrating Aspirin 81 mg for children and 325 mg for adults 48 h prior to the procedure. The procedure is performed under general anesthesia and under TEE tracing to determine defect localization and neighborhood relationships with the aortic, tricuspid and mitral valve before and after implantation of the device.

41.10.1 Device Implantation Technique

Femoral approach is performed by inserting a 4–5 Fr sheath into the femoral artery and the 7–9 Fr sheath into the femoral vein. Diagnostic catheterization will always be performed to determine the localization of the defect and its dimensions, as well as left to right shunts and pulmonary vascular resistance (less than 7 Wood units).

Left ventriculography is performed at 60° LAO 20° CR to determine the location and diameter of the ventricular septal defect.

4 or 5 Fr Judkins right coronary catheter is introduced by arterial route from the aorta into the left ventricle and it crosses the ventricular septal defect.

Most frequently for crossing ventricular defect is used a curved 0.035 inch Terumo glide wire which reaches the superior vena cava or a branch of the pulmonary artery. The catheter is advanced on the guide wire up to one of these two locations and then it is withdrawn and replaced by the noodle wire (AGA Medical) [52, 53].

This guide wire is snared using a gooseneck snare and exteriorized out through the right femoral vein, an arterio-venous wire loop is created starting from the femoral vein up to the femoral artery. TEE is very important in this moment to see if the loop passing through chordae or leaflets of valves [13].

Over the noodle wire, the delivery sheath is advanced from the femoral vein into the ascending aorta. From the femoral artery, a Judkins right coronary catheter is passed over the wire and touches the dilatator of the sheath. The dilatator is drawn back into the inferior vena cava and then the sheath is withdrawn by torquing it counterclockwise above the aortic valve and the noodle wire and the sheath are pushed into the left ventricle apex. Then the wire is retrieved from the Judkins catheter [13].

A proper device size is attached to the cable and with a pusher catheter it is advanced on the sheath in the apex of the left ventricle.

The left disk is deployed and the sheath is withdrawn over the pusher catheter, the platinum marker is checked carefully and it should be pointed towards patient's feet (correct position) [13].

When the left disk is confirmed to be in good position by angiography and TEE, the connecting waist and right disk of the device are deployed. If the position of the device is correct, the final step is to release the device rotating it counterclockwise and the cable should be immediately brought inside the sheath (see Fig. 41.16).

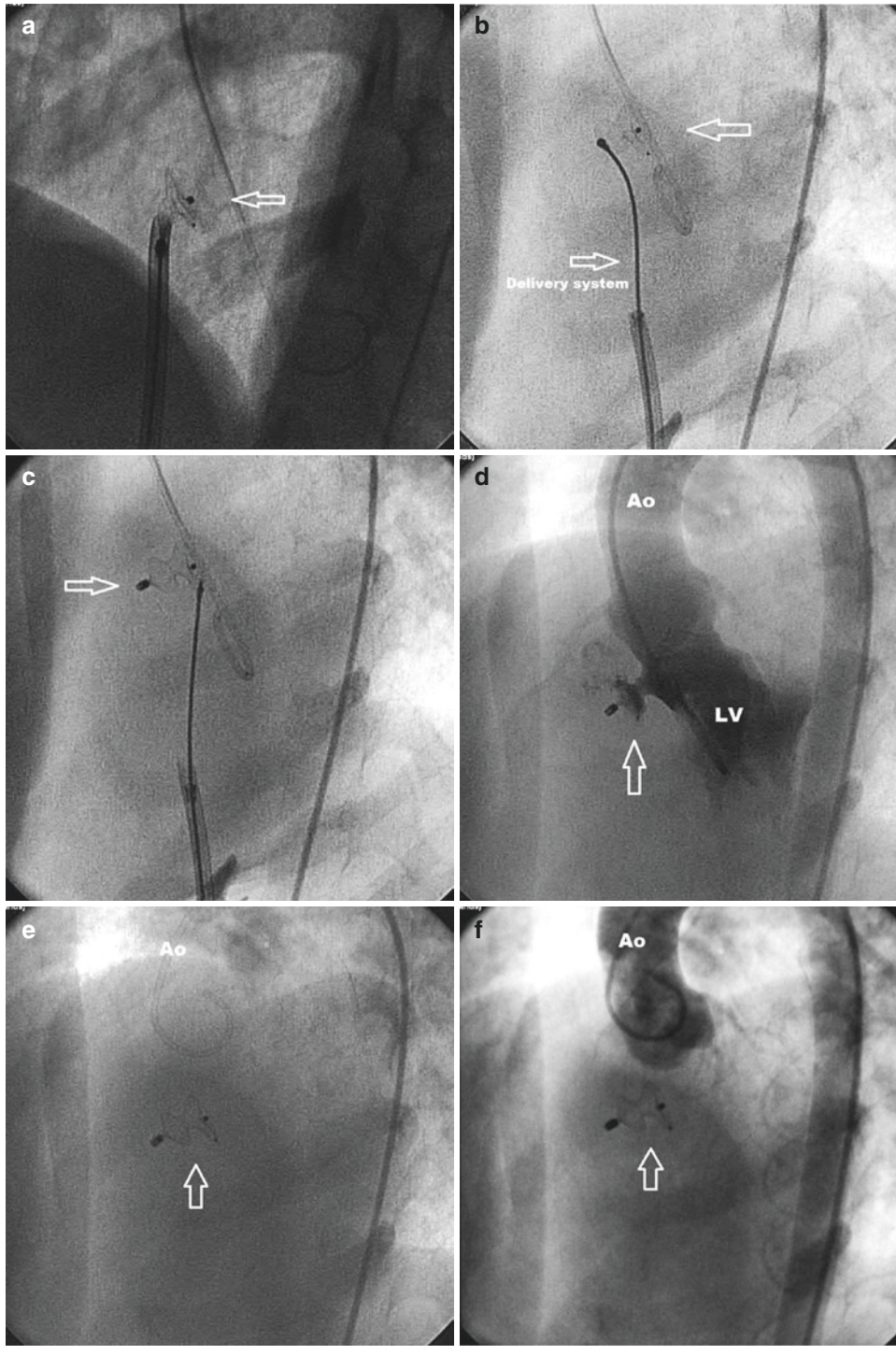

Fig. 41.16 The implantation technique of the Amplatzer device in the membranous ventricular septal defect. (**a**) Cine fluoroscopy image after the deployment of left ventricle disk (arrow) was brought close to the ventricular septum. (**b**) The Amplatzer occluder is fully deploy and is not detached (arrow). The platinum marker is orientated correctly towards the patient's feet. (**c**) Amplatzer occluder is detached (arrow). (**d**) Left ventriculography demonstrating good position of device at the ventricular septum without left to right shunt. (**e**) Amplatzer occluder is correctly positioned and stable (arrow). (**f**) Aortography without aortic regurgitation (arrow)

Echocardiography and left ventriculography highlight the correct position of the device in the ventricular septum and whether or not there is a residual shunt.

Complications of ventricular septal defect closure [54, 55]:

- device embolization or migration. It is a rare complication and the device may migrate to the left or right ventricle, aorta or pulmonary artery. The device can be snared and retrieved.
- arrhythmia, which may be a ventricular arrhythmia during catheter or device handling or conduction disorders up to complete atrioventricular block.
- air embolization is a rare complication.
- hemolysis is usually associated with residual shunt after device implantation.
- aortic, tricuspid or mitral valvular regurgitation may occur.
- pericardial effusion is a very rare complication, it appears when the guide wire perforates the ventricular wall during the procedure.

The follow-up protocol includes: physical examination, chest radiography, electrocardiography and echocardiography at 6 weeks and 6 months.

Interventional cardiology procedures are effective treatments for congenital heart diseases with a high rate of success, both for children and for adults.

References

1. Fahed AC, Nemer GM. Genetic causes of syndromic and non-syndromic congenital heart disease. Mutat Hum Genet Dis. 2012. https://doi.org/10.5772/48477. Available from: https://www.intechopen.com/books/mutations-in-human-genetic-disease/genetic-causes-of-syndromic-and-non-syndromic-congenital-heart-disease
2. Grossman W. Cardiac catheterization, angiography and intervention. 1997. p. 654. ISBN: 13: 978-1451127409.
3. Gikonyo BM, Lucus RV, Edwards JE. Anatomic features of congenital pulmonary valvar stenosis. Pediatr Cardiol. 1987;8:109–15.
4. Koretzky ED, Moller JH, Karns ME, et al. Congenital pulmonary stenosis resulting from dysplasia of the valve. Circulation. 1969;60:43–53.
5. Pinte F. Tratamentul interventional in malformatii le cardiace congenitale la copii, [Interventional treatment in congenital heart diseases in children]. Medicina Moderna nr. 5, [Modern Medicine no. 5]. Bucharest; 1997.
6. Pinte F. Valvuloplastia si angioplastia in bolile congenitale; Actualitati in cardiologie [Valvuloplasty and angioplasty in congenital heart diseases], Ed. Med. Amaltea [Amaltea Medical Editure]; 1998.
7. Socoteanu I. Tratat de cardiopatii congenitale, [Treaty of congenital cardiopathies] Editura Academiei Romane [Romanian Academy Editure], vol. II, Bucharest; 2010. ISBN: 978-973-27-1915-2; 1847-1885.
8. Narin A, Unal S. Percutaneous balloon valvulotomy. Circulation. 1995(78):86–91.
9. Pinte F. Valvuloplastia pulmonara percutana in bolile congenitale complexe, [Pulmonary valvuloplasty in complex congenital heart diseases] Rev. Rom. de Cardiologie [Romanian Journal of Cardiology] vol. V, No. 1; 1995.
10. Bergersen L, Foerster S, Marshall A, Meadows J. Congenital heart disease the catheterization manual. New York: Springer; 2009. ISBN: 978-0-387-77291-2
11. Jureidini SB. Pulmonary stenosis in the neonate. J Invasive Cardiol. 1996;8(7):16–19.
12. Carp C. Tratat de cardiologie [Treaty of cardiology], Editura Medicala Nationala [Medical Editure], vol. II. Bucharest; 2002. ISBN: 973-659-010-0, 730–739.
13. Sigvert H, Qurreshi S, Wilson N, Hijazi Z. Percutaneous interventions for congenital heart disease. London: Informa Healtcare; 2007. ISBN-10: 1 84184 556 6.
14. Rao PS. Influence of balloon size on short-term and long-term results of balloon pulmonary valvuloplasty. Tex Heart Inst J. 1987;14:57–61.
15. Rao PS. How big a balloon and how many balloons for pulmonary valvuloplasty? Am Heart J. 1988;116:577–80.
16. Rao PS. Further observations on the effect of balloon size on the short-term and intermediate-term results of balloon dilatation of the pulmonary valve. Br Heart J. 1988;60:507–11.
17. Rao PS. Late pulmonary insufficiency after balloon dilatation of the pulmonary valve. Cathet Cardiovasc Interven. 2000;49:118–9.
18. Rao PS. Balloon pulmonary valvuloplasty in children. J Invas Cardiol. 2005;17:323–5.
19. McCrindle B. Independent predictors of long-term rezults after balloon pulmonary valvuloplasty. Am Heart J. 1997.
20. Fontes VF, Esteves CA, Eduardo J, et al. Regression of infundibular hypertrophy after pulmonary valvotomy for pulmonic stenosis. Am J Cardiol. 1988;62:977–9.
21. Kraul U. Long-term rezults after balloon pulmonary valvuloplasty in adults. Am Heart J. 1997.

22. Rocchini A. Use of balloon angioplasty to treat peripheral pulmonary stenosis. Am J Cardiol. 1986.
23. Baumi D, et al. Congenital stenosis of the pulmonary artery. Circulation. 1995;43:56–63.
24. Pinte F, Socoteanu I, Iosifescu A. Valvuloplastia pulmonara in sindromul William–Beuren [Pulmonay valvuloplasty in William–Beuren Syndrome], Simpozionul de ecocardiografie Institutul "C.C. Iliescu" 1997. [Echocardiography Symposium of C.C. Iliescu Institute 1997].
25. Yoshimura N, Yamaguchi M, Ohashi H. Pulmonaryatresiawith intact ventricular septum: strategybased on right ventricular morphology. J Thorac Cardiovasc Surg. 2003;126(5):1417–26.
26. Siblini G. Transcatheter management of neonates with pulmonary atresia and intact ventricular septum. Catheter Cardiovasc Diagn. 1997;42(4):395–402.
27. Rashind WJ. Creation of an atrialseptal defect without thoracotomy: paleative approachto complete transpozition of the great arteries. JAMA. 1968;196(11):991–2.
28. Pinte F, Iacob M. Septostomia—o alternativa a tratamentului chirurgical in transpozitia de mari vase [Septostomy—an alternative of surgical treatment in transposition of the great arteries]. Balkan Pediatric Cardiology and Cardiac Surgery Congress; 1996.
29. Iosifescu A, Socoteanu I, Fotiade B. Embolizarea arterelor bronsice in tetralogia Fallot [Bronchial artery embolisation in Tetralogy of Fallot]. Balkan Pediatric Cardiology and Cardiac Surgery Congress; 1996.
30. Siblini G. Coilembolization in the management of cardiac problems in kilogram dren. J Invasive Cardiol. 1997;8(7):32–35.
31. Hamdan MA, Cao QL, Hijazi ZM. Amplatzer septal occluder. In: Rao PS, Kern MJ, editors. Catheter based devices for the treatment of non-coronary cardiovascular disease in adults and children. Philadelphia: PA Williams and Wilkins; 2003. p. 51–9.
32. Masura J, Gavora P, Formanek A, Hijazi ZM. Transcatheter closure of secundum atrial septal defects using the new self-centering Amplatzer septal occluder: initial human experience. Catheter Cardiovasc Diagn. 1997;42:388–93.
33. Hijazi ZM, Cao Q, Patel HT, et al. Transesophageal echocardiographic results of catheter closure of atrial septal defect in children and adults using the Amplatzer device. Am J Cardiol. 2000;85:1387–90.
34. Mazic U, Gavora P, Masura J. The role of transesophageal echocardiography in transcatheter closure of secundum atrial septal defects by the Amplatzer septal occluder. Am Heart J. 2001;142:482–8.
35. Harper RW, Mottram PM, McGaw DJ. Closure of secundum atrial septal defects with the Amplatzer septal occluder device: techniques and problems. Cathet Cardiovasc Interven. 2002;57:508–24.
36. Amin Z, Hijazi ZM, Bass JL, et al. Erosion of Amplatzer septal occluder device after closure of secundum atrial septal defects: review of registry of complications and recommendations to minimize future risk. Cathet Cardiovasc Interven. 2004;63:496–502.
37. Divekar A, Gaamangwe T, Shaikh N, et al. Cardiac perforation after device closure of atrial septal defects with the Amplatzer septal occluder. J Am Coll Cardiol. 2005;45:1213–8.
38. Kim JJ, Hijazi ZM. Clinical outcomes and costs of Amplatzer transcatheter closure as compared with surgical closure of ostium secundum atrial septal defects. Med Sci Monit. 2002;8:CR787–91.
39. Rao PS. Transcatheter occlusion of patent ductus arteriosus. J Invasive Cardiol. 1997;8(7):278–88.
40. Masura J, Walsh KP, Thanpoulous B, et al. Catheter closure of moderate-large sized patent ductus arteriosus using the new Amplatzer duct occlude: immediate and short-term results. J Am Coll Cardol. 1998;31:878–82.
41. Hijazi ZM, Geggel RL. Results of antegrade transcatheter closure of patent ductus arteriosus using single or multiple Gianturco coils. Am J Cardiol. 1994;74(9):925.
42. Hijazi ZM, Geggel RL. Transcatheter closure of large patent ductus arteriosus (> or = 4 mm) with multiple Gianturco coils. Heart. 1996;76:536–40.
43. Tometzki AJP, Arnold R, Peart N, et al. Transcatheter closure of patent ductus arteriosus with cook detachable coils. Heart. 1996;76:531–5.
44. Owada CY, Teitel DF, Moore P. Evaluation of Gianturco coils for closure of large (> or −3.5 mm) patent ductus arteriosus. J Am Coll Cardiol. 1997;30:856–62.
45. De Wolf D, Verhaaren H, Matthys D. Simultaneous delivery of two patent arterial duct coils via one venous sheath. Heart. 1997;78(2):201.
46. Sommer RJ, Gutirrez A, Lai WW, Mullins CE. Use of preformed nitinol snare to improve transcatheter coil delivery in occlusion of patent ductus arteriosus. Am J Cardiol. 1994;74:834–9.
47. Hijazi ZM. Device closure of ventricular septal defects. Cathet Cardiovasc Interven. 2003;60:107–14.
48. Lock JE, Block PC, McKay RG, et al. Transcatheter closure of ventricular septal defects. Circulation. 1988;78:361–8.
49. Rigby ML, Redington AN. Primary transcatheter umbrella closure of perimembranous ventricular septal defect. Br Heart J. 1994;72:368–71.
50. Kalra GS, Verma PK, Dhall A, et al. Transcatheter device closure of ventricular septal defects: immediate results and intermediate-term follow-up. Am Heart J. 1999;138:339–44.
51. Hijazi ZM, Hakim F, Haweleh AA, et al. Catheter closure of perimembranous ventricular septal defects using the new Amplatzer membranous VSD occluder: initial clinical experience. Cathet Cardiovasc Interven. 2002;56:508–15.
52. Bass JL, Kalra GS, Arora R, et al. Initial human experience with the Amplatzer perimembranous ventricular septal occluder device. Cathet Cardiovasc Interven. 2003;58:238–45.

53. Thanopoulos BD, Tsaousis GS, Karanasios E, et al. Transcatheter closure of perimembranous ventricular septal defects with the Amplatzer asymmetric ventricular septal defect occluder: preliminary experience in children. Heart. 2003;89:918–22.
54. Pedra CA, Pedra SR, Esteves CA, et al. Percutaneous closure of perimembranous ventricular septal defects with the Amplatzer device: technical and morphological considerations. Cathet Cardiovasc Interven. 2004;61:403–10.
55. Pawelec-Wojtalik M, Masura J, Siwinska A, et al. Transcatheter closure of perimembranous ventricular septal defect using an Amplatzer occluder—early results. Kardiol Pol. 2004;61:31–40.

Open Surgery for Pulmonary Thromboembolism

42

Ionel Droc

Abstract

Acute massive pulmonary embolism (PE) is a life threatening condition requiring quick diagnosis and intervention. The mortality rate in this acute entity is high despite progress in therapeutically strategies. Acute PE is the third most common cause of death among hospitalized patients. Currently, multidisciplinary teams with cardiovascular surgeons' involvement have introduced again the surgical embolectomy on cardiopulmonary bypass for high risk patients with PE and also for selected patients with intermediate-high risk, particularly if thrombolysis is contraindicated or failed. There is also recent evidence data that supports prompt multidisciplinary approach and individualized indication of surgery before hemodynamic collapse, while the mortality rates are of 6% or less. Complete removal of thrombotic material from pulmonary arteries is the best predictor to avoid persistent pulmonary artery hypertension. Acute pulmonary embolectomy on cardiopulmonary bypass is safe and it has good and long-lasting results in patients with severe right ventricular dysfunction.

Keywords

Pulmonary embolism · Pulmonary embolectomy · Cardiopulmonary bypass · Thrombolysis Deep vein thrombosis · Pulmonary thromboembolism

42.1 Introduction

Acute massive pulmonary embolism (PE) is a life threatening condition requiring quick diagnosis and intervention. The mortality rate in this acute entity is high despite progress in therapeutically strategies. Acute PE is the third most common cause of death among hospitalized patients [1–3]. In United States, it occur in approximately 530,000 cases of symptomatic PE annually and about 300,000 people die every year from acute PE [1, 2, 4].

The first surgeon who attempted pulmonary embolectomy for PE was Trendelenburg, the founder of German Surgical Society in 1905 via thoracotomy. This was before the time of cardiopulmonary bypass (CPB) used in cardiac surgery [5]. Kirschner, a disciple of Trendelenburg, performed the first successful pulmonary embolectomy in 1924. The results were discouraging and led many surgeons, especially in USA to develop other techniques. Ochsner and DeBakey advocated inferior vena cava ligation to prevent PE, and 2 years later Homans performed the first prophylactic venous ligation. The interruption of

I. Droc
Department of Cardiovascular Surgery, Central Military Hospital, Bucharest, Romania

S. I. Dumitrescu et al. (eds.), *Right Heart Pathology*, https://doi.org/10.1007/978-3-319-73764-5_42

inferior vena cava was accompanied by the decrease of cardiac output and lower extremities edema. To avoid this complications partial caval plication (by suture or special clips) were developed by Adams, DeWeese and Miles [6]. These procedures have also their complications, consequently the percutaneous caval filters were developed and used in the last two decades. These are highly effective, with good and durable results, and with low complications rates.

In 1932, after an unsuccessful attempt to save a patient with massive PE, Gibbon worked intensively for developing the extracorporeal circulation that was crucial in the development of heart surgery, including pulmonary trombembolectomy. During 1961, Cooley used the extracorporeal circulation for a PE, but only 1 year later Sharp successfully saved the first PE patient using CBP.

42.2 Current Approach: Short Outlines

Etiology The main etiology for PE is deep vein thrombosis. In the majority of cases (95%) the thrombus originates in the leg or pelvic veins. It can also arises from axillary—subclavian veins or renal veins [7]. Not unexpectedly, it may appear as redoubtable complication after main surgeries (within 1 month postoperatively) in orthopedics (25%), neurosurgery (24%) or general surgery (22%) [8, 9].

As the population is aging, the probability of a venous thrombembolic event at the age of 80 years is 10.7% [10]. From all acute pulmonary embolisms, 40% could develop submassive pulmonary embolism and only 5–10% massive pulmonary embolism [10, 11].

Diagnosis and Treatment: Brief Up to Date Acute massive PE is characterized by the reduction of more than 50% of the main pulmonary artery cross-sectional area or occlusion of two or more lobar arteries or clinically hemodynamic compromise or severe right ventricular dysfunction [11, 12]. These patients are instable and are predisposed to sudden cardiac arrest. The main goal of treatment is to eliminate the embolic material (thrombus) and the prevention of recurrent PE. There are no randomized trials supporting an ideal treatment strategy.

Importantly, the diagnosis of PE should be done rapidly by a multidisciplinary team approach, mainly based on echocardiography and CT angiography. However, CT is superior to classically pulmonary angiography. The rapid identification and selection of the appropriate candidates for surgery is crucial. The evidence based clinical practice of American College of Chest Physicians guidelines outlines the indications for surgery in patients with acute PE associated with hypotension when:

- Patients have contraindication for thrombolysis,
- Failure of thrombolysis or catheter based thrombectomy,
- State of shock,
- The team has expertise and access to resources [12].

Moreover, the 2014 ESC guidelines on PE recommend a practical and rapid procedure if acute PE is suspected based on individual early mortality risk (see Fig. 42.1 and Table 42.1) [13].

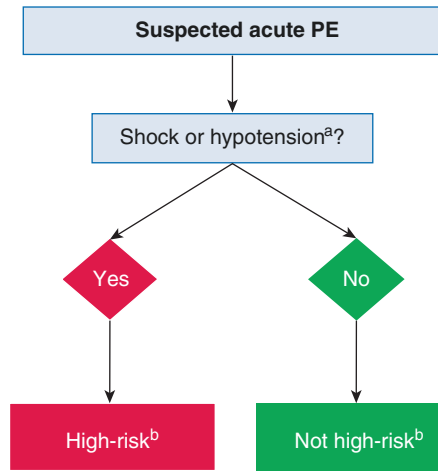

PE = pulmonary embolism.
[a]Defined as systolic blood pressure <90 mm Hg, or systolic pressure drop by ≥40 mm Hg, for >15 minutes, if not caused by new-onset arrhythmia, hypovolaemia, or sepsis.
[b]Based on the estimated PE-related in-hospital or 30-day mortality.

Fig. 42.1 Initial risk stratification of acute PE. From 2014 ESC guidelines of Acute Pulmonary Embolism [13] with permission

Table 42.1 Early mortality risk in PE. From 2014 ESC guidelines of Acute Pulmonary Embolism [13] with permission

Early mortality risk		Risk parameters and scores			
		Shock or hypotension	PESI class III.V or sPESI >I[a]	Signs of RV dysfunction on an imaging test[b]	Cardiac laboratory biomarkers[c]
High		+	(+)[d]	+	(+)[d]
Intermediate	Intermediate-high	–	+	Both positive	
	Intermediate-low	–	+	Either one (or none) positive[e]	
Low		–	–	Assessment optional; if assessed, both negative[e]	

PESI pulmonary embolism severity index, *sPESI* simplified pulmonary embolism severity index, *PE* pulmonary embolism, *PESI* Pulmonary embolism severity index, *RV* right ventricular, *sPESI* simplified Pulmonary embolism severity index

[a]PESI Class III to V indicates moderate to very high 30-day mortality risk; sPESI ≥1 point(s) indicate high 30-day mortality risk

[b]Echocardiographic criteria of RV dysfunction include RV dilation and/or an increased end-diastolic RV–LV diameter ratio (in most studies, the reported threshold value was 0.9 or 1.0); hypokinesia of the free RV wall; increased velocity of the tricuspid regurgitation jet; or combinations of the above. On computed tomographic (CT) angiography (four-chamber views of the heart), RV dysfunction is defined as an increased end-diastolic RV/LV (left ventricular) diameter ratio (with a threshold of 0.9 or 1.0)

[c]Markers of myocardial injury (e.g. elevated cardiac troponin I or -T concentrations in plasma), or of heart failure as a result of (right) ventricular dysfunction (elevated natriuretic peptide concentrations in plasma)

[d]Neither calculation of the PESI (or sPESI) nor laboratory testing are considered necessary in patients with hypotension or shock

[e]Patients in the PESI Class I–II, or with sPESI of 0, and elevated cardiac biomarkers or signs of RV dysfunction on imaging tests, are also to be classified into the intermediate-low-risk category. This might apply to situations in which imaging or biomarker results become available before calculation of the clinical severity index

Shortly, the mainly initial treatment of patients with PE is anticoagulation therapy, typically with intravenous heparin [14]. Conversely, a variety of invasive methods emerged for selected patients, such as catheter based or surgical therapies, each of them with their benefits and complications. Thrombolysis is considered the first line of treatment for instable PE patients [7, 9, 13]. Preoperative thrombolysis increases the bleeding risk, but is not anymore an absolute contraindication for surgery [15].

However, contraindications for thrombolytic therapy are prior intracranial hemorrhage, ischemic stroke (up to 3 months), aortic dissection, intracranial malignancies or arteriovenous malformations, recent head injuries, and bleeding disorders [16, 17].

Inferior vena cava filters (IVC) should be placed either preoperatively or in the first 24 h after surgery in order to prevent recurrence of embolization [6]. Retrievable filters are preferable because they have less complications rates [18].

The patient that comes with massive PE and cardiogenic shock should immediately start percutaneous cardiopulmonary support (ECMO—extracorporeal membrane oxygenation) in order to achieve hemodynamic stabilization [19].

Presently, multidisciplinary teams with cardiovascular surgeons' involvement have introduced again the surgical embolectomy on CBP for high risk patients with PE and also for selected patients with intermediate—high risk, particularly if thrombolysis is contraindicated [13].

Noteworthy, surgical pulmonary embolectomy is indicated for high risk pulmonary embolism patients with circulatory collapse.

Pulmonary embolectomy is done with median sternotomy with normothermic cardiopulmonary bypass or mild hypothermia. Also, it can be done with or without aortic clamping and cardiac arrest. The main pulmonary trunk is incised longitudinally, and the incision can be extended to the left pulmonary artery. The clots are removed under direct sight up to the lobar and segmental level. Clots are typically not adherent to the artery wall,

so they are easily removable with forceps and gentle suction. The pulmonary artery is closed usually using a pericardial patch (or synthetic one). A longer period of assistance on CPB is possibly need for the recovery of right ventricle function [20].

All patients should start systemic anticoagulation from first postoperative day via intravenously way with heparin, then warfarin. Importantly, they should be screened for prothrombotic diseases.

To sum up, anticoagulation with heparin is the first step, thrombolytic therapy, catheter thrombembolectomy, and now surgical embolectomy are methods to be individualized for every patient.

Prognosis The study of Takahashi et al. [19] on 24 patients with acute PE and circulatory collapse which undergone surgical embolectomy, reported a 30 days mortality rate of 12.5%. Of note, the survival rate at 5 years was 87.5% [19]. In same time, the analysis of 32 patients from a multicentre registry in Japan, published by Taniguchi in 2012 (60 institutes, 1661 cases of PE between 1994 and 2006, from which 32 (1.9%) with surgery, the overall mortality rate was 18.8%. It has to be mentioned, that 33% of patients were males and the mean age was 57 years. Conversely, the mortality rate raised to 30% if patients received preoperative percutaneos ECMO [21].

Later, Yavuz et al. [11] showed in a study of 13 patients with acute massive PE which undergone surgery that 61.5% males with an average age of 61.8 had in hospital mortality of 23.1%. Notably, as aetiology, the deep vein thrombosis was present in 69.2% of cases [11].

The mortality rates after this procedure is still high (30–40%) [19]. Preoperative conditions such as cardiac arrest affect early outcomes. Also, preoperative shock is associated with mortality rate between 11.1 and 57.1%, while cardiac arrest raises it between 25 and 75% [22]. Neely and colleagues reported in 2015 on a large study of 115 patients who underwent pulmonary embolectomy, a mean mortality rate of 6.6%. For unstable patients it was greater (10.2%) in comparison with stable patients (3.6%). The survival rates at 1 year and respectively 3 years were 68.4% and 65.8% for unstable patients, and respectively 86.7% and 80.4% for stable patients [9].

There are only a few studies that compared thrombolysis and surgical pulmonary embolectomy for acute PE. Particularly, they compared only all causes of mortality, which are not statistically significant even the surgical group has a lower mortality rate [23].

For instance, in the International Cooperative Pulmonary Embolism Registry study (ICOPER) the mortality rate at 3 months varies from 17.4 to 45.1% [24].

There are also recent reported studies that with a rapid multidisciplinary approach and individualized indication—surgery before hemodynamic collapse, the mortality rates are of 6% or less [13].

Hartman and colleagues from Texas Heart Institute published a study of 96 patients with consecutive surgeries for acute pulmonary embolism and severe right ventricle dysfunction with a 30 day overall mortality rate of 4.2% (1.4% for stable patients to 12.5% for unstable patients) [12].

Keeling published in 2016 the first and largest study on the outcomes of surgical pulmonary embolectomy on high volume centers all across the world, grouped as SPEAR working group (Surgical Pulmonary embolectomy as Routine Therapy). The postoperative mortality rate was 11.7% for the entire cohort. If the indication was for massive PE the rate was 23.7%, but it decreased dramatically if the surgery was done for submassive PE (9.1%). These results are lower than those reported by Nationwide Inpatient Sample (NIS) with a 27.2% overall mortality of 2700 patients who underwent surgical pulmonary embolectomy [10].

Recently, in 2017 a published meta-analyses by Kalra and colleagues on 56 studies with 1590 surgeries for PE found the hospital all-cause mortality rate of 26.3% [25].

Surgical Case Herein it is the case of a 46 years old man with an acute deep vein thrombosis (femuropopliteal), migrated to the right atrium

and very quickly the thrombotic material got into the trunk and main branches of the pulmonary artery. He was diagnosed with high risk PE (hypotension, ultrasound image of embolic material in the right atrium and right ventricle dysfunction, and elevated cardiac biomarkers) (Figs. 42.2, 42.3, and 42.4).

- dilated right femoral veins, with spontaneous contrast;
- right popliteal vein: thrombus 80% occlusion, partially compressible.

Further, emergency surgery was decided and the patient undergone surgery in our institution. We performed surgical embolectomy on CPB with success. The CPB setting was done with ascending aortic and bicaval cannulation with caval tapes. A mild degree of systemic hypothermia (32 °C) was used for CBP. The aortic clamping and cardiac arrest were used with antegrade cardioplegia. The clots were removed via a longitudinal incision on the pulmonary trunk. The arteriotomy was closed using a pericardial patch (Figs. 42.5, 42.6, and 42.7).

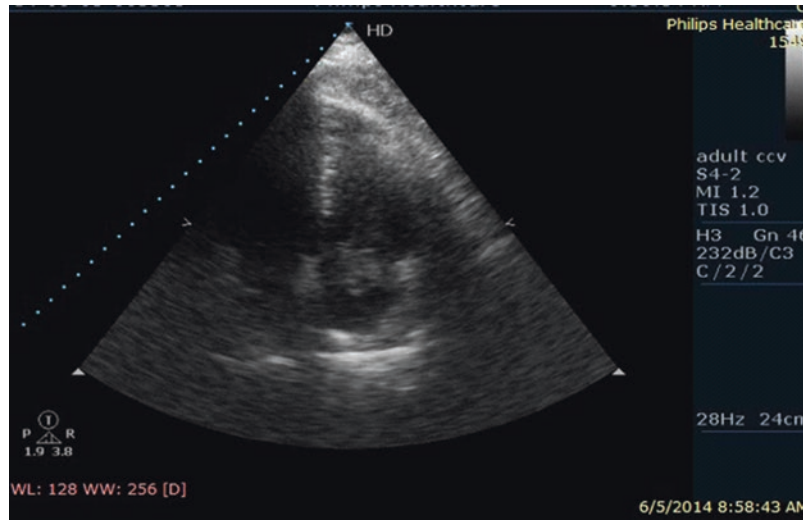

Fig. 42.2 Transthoracic echocardiography showing the thrombus in the right atrium, in the proximity of the tricuspid valve (migrated from the femoral veins)

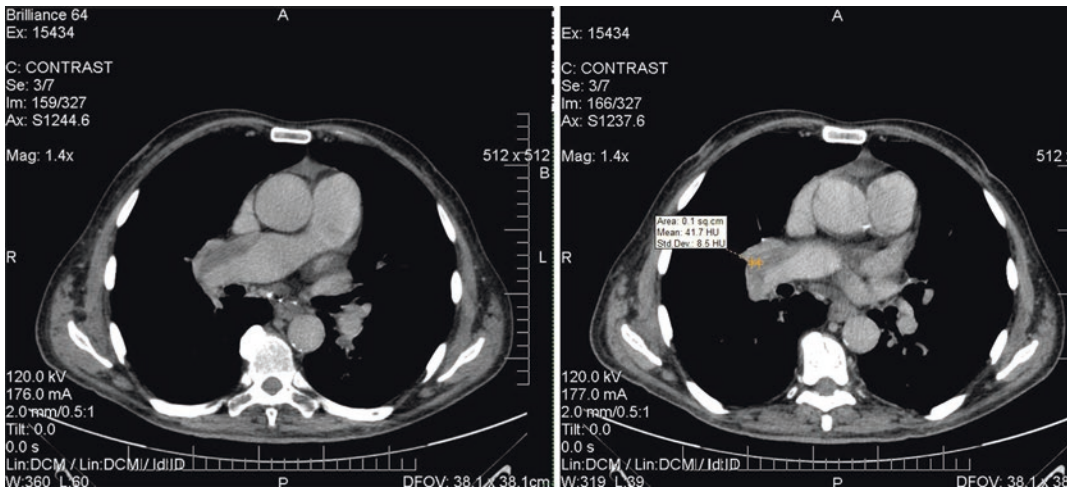

Fig. 42.3 Preoperative CT scan: thrombi in both pulmonary arteries and their proximal branches

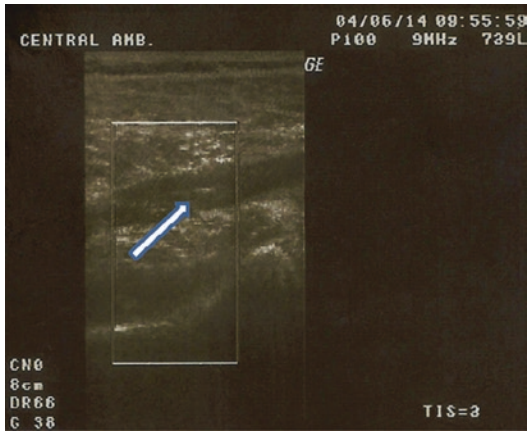

Fig. 42.4 Echo Doppler of lower limbs showing dilated right femoral veins, with spontaneous contrast: right popliteal vein: thrombus 80% occlusion

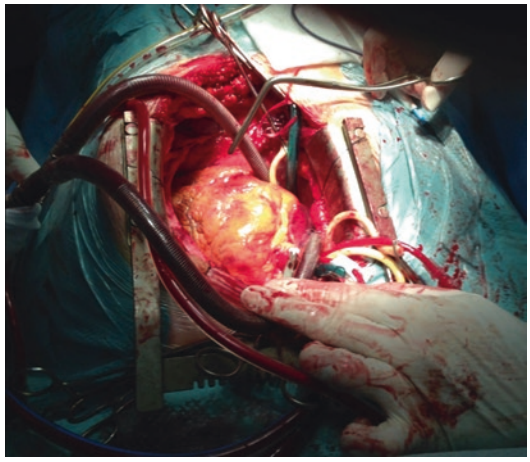

Fig. 42.5 Surgical technique, on-pump intervention

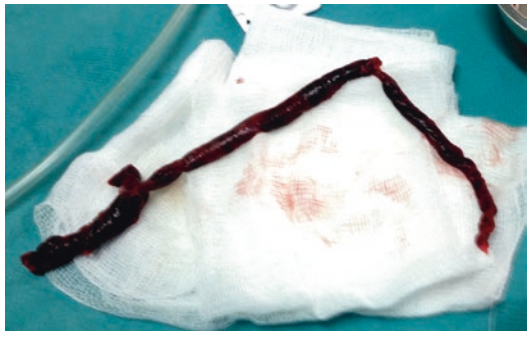

Fig. 42.6 Thrombus migrated from the femoral veins removed from the pulmonary trunk and branches

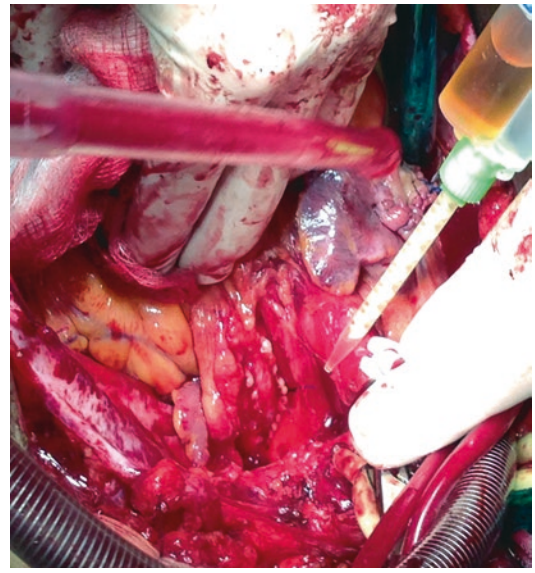

Fig. 42.7 Pulmonary trunk with pericardial patch angioplasty

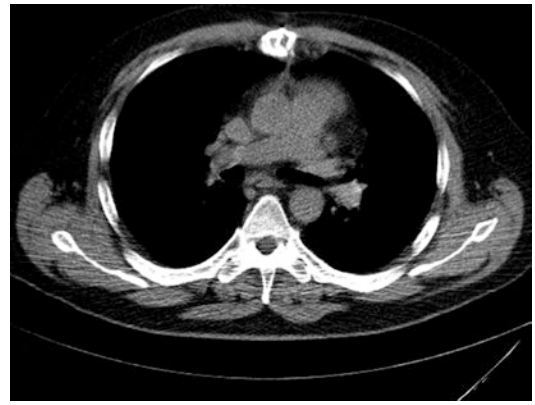

Fig. 42.8 Postoperative CT scan (2 months) pulmonary trunk and branches without any thrombotic material

The postoperative evolution was eventless and the patient was discharged after 7 days. The result is good after a follow up of 3 years with no recurrences, the patient being on chronic anticoagulation (Fig. 42.8).

To sum up, the complete removal of thrombotic material from pulmonary arteries is the best predictor to avoid persistent pulmonary artery hypertension.

Conclusions

Acute pulmonary embolectomy on CPB is safe and it has good and durable outcomes in patients with severe right ventricular dysfunction. The high volume cardiovascular surgery departments have better outcomes. Surgical pulmonary embolectomy should be increasingly considered in acute massive and submassive pulmonary embolism in patients. The fast identification and selection of the appropriate candidates is crucial.

References

1. Kuo WT. Endovascular therapy for acute pulmonary embolism. J Vasc Interv Radiol. 2012;23:167–79.
2. Pelliccia F, Schiariti M, Terzano C, Keylani AM, D'Agostino DC, Speziale G, Greco C, Gaudio C. Treatment of acute pulmonary embolism: update on newer pharmacologic and interventional strategies. Biomed Res Int. 2014;2014:410341.
3. Saxena P, Smail H, McGriffin DC. Surgical techniques of pulmonary embolectomy for acute pulmonary embolism. Oper Tech Thorac Cardiovasc Surg. 2017;21:80–8.
4. Tapson VF. Advances in the diagnosis and treatment of acute pulmonary embolism. F1000 Med Rep. 2012;4:9. https://doi.org/10.3410/M4-9.
5. Kodani N, Ohashi T, Iida H, Kageyama S, Furui M, Uchino G. Emergency pulmonary embolectomy using minimally invasive cardiac surgery. Ann Thorac Surg. 2016;101:1569–71.
6. McFadden MP, Ochsner JL. Aggressive approach to pulmonary embolectomy for massive acute pulmonary embolism: a historical and contemporary perspective. Mayo Clin Proc. 2010;85(9):782–4.
7. Streiff MB, Agnelli G, Connors JM, Crowther M, Eichinger S, Lopes R, McBane RD, Moll S, Ansell J. Guidance for the treatment of deep vein thrombosis and pulmonary embolism. J Thromb Thrombolysis. 2016;41:32–67.
8. Condliffe R, Elliot CA, Hughes RJ, Hurdman J, Maclean RM, Sabroe I, van Veen JJ, Kiely DG. Management dilemmas in acute pulmonary embolism. Thorax. 2014;69(2):174–80.
9. Neely RC, Byrne JG, Gosev I, Cohn LH, Javed Q, Rawn JD, Golhaber SZ, Piazza G, Aranki SF, Shekar PS, Leacche M. Surgical embolectomy for acute massive and submassive pulmonary embolism in a series of 115 patients. Ann Thorac Surg. 2015;100:1245–52.
10. Keeling WB, Sundt T, Leacche M, Okita Y, Binongo J, Lasajanak Y, Aklong L, Latouff OM, SPEAR Working Group. Outcomes after surgical pulmonary embolectomy for acute pulmonary embolus: a multi-institutional study. Ann Thorac Surg. 2016;102:1498–502.
11. Yavuz S, Toktas F, Goncu T, Eris C, Gucu A, Ay D, Erdolu B, Tenekecioglu E, Karaagac K, Vural H, Ozyazicioglu A. Surgical embolectomy for acute massive pulmonary embolism. Int J Clin Exp Med. 2014;7(12):5362–75.
12. Hartman AR, Manetta F, Lessen R, Pekmezaris R, Kozikowski A, Jahn L, Akerman M, Lesser ML, Glassman LR, Graver M, Scheinerman JS, Kalimi R, Palazzo R, Vatsia S, Pogo G, Hall M, Jen Yu P, Singh V. Acute surgical pulmonary embolectomy: a 9-year retrospective analysis. Tex Heart Inst J. 2015;42(1):25–9.
13. Konstantinides SV, Torbicki A, Agnelli G, Danchin N, Fitzmaurice D, Galiè N, Gibbs JS, Huisman MV, Humbert M, Kucher N, Lang I, Lankeit M, Lekakis J, Maack C, Mayer E, Meneveau N, Perrier A, Pruszczyk P, Rasmussen LH, Schindler TH, Svitil P, Vonk Noordegraaf A, Zamorano JL, Zompatori M, Task Force for the Diagnosis and Management of Acute Pulmonary Embolism of the European Society of Cardiology (ESC). 2014 ESC guidelines on the diagnosis and management of acute pulmonary embolism. Eur Heart J. 2014;35(43):3033–69.
14. Haaverstad R, Vitale N. Surgical pulmonary embolectomy: should we extend its role? J Thorac Cardiovas Surg. 2016;152:879–80.
15. Marti C, John G, Konstantinides S, Combescure C, Sanchez O, Lankeit M, Meyer G, Perrier A. Systemic thrombolytic therapy for acute pulmonary embolism: a systematic review and meta-analysis. Eur Heart J. 2015;36(10):605–14.
16. Azari A, Bigdelu L, Moravvej Z. Surgical embolectomy in the management of massive and sub-massive pulmonary embolism: the results of 30 consecutive ill patients. ARYA Atheroscler. 2015;11(3):208–13.
17. Rehman A, Yousaf S, Chugh A. Thrombolysis in submassive pulmonary embolism, prudent or puerile? BMJ Case Rep. 2013;2013. pii: bcr2012007549. https://doi.org/10.1136/bcr-2012-007549.
18. Jaber WA, Fong PP, Weisz G, Lattouf O, Jenins J, Rosenfield K, Rab T, Ramee S. Acute pulmonary embolism with an emphasis on an interventional approach. JACC. 2016;67(8):991–1002.
19. Takahashi H, Okada K, Matsumori M, Kano H, Kitagawa A, Okita Y. Aggressive surgical treatment of acute pulmonary embolism with circulatory collapse. Ann Trorac Surg. 2012;94:785–91.
20. Edelman JJ, Okiwelu N, Anvardeen K, Joshi P, Murphy B, Sanders LH, Newman MA, Passage J. Surgical pulmonary embolectomy: experience in a series of 37 consecutive cases. Heart Lung Circ. 2016;25:1240–4.
21. Taniguchi S, Fukuda W, Fukuda I, Watanabe K, Saito Y, Nakamura M, Sakuma M. Outcome of pulmonary embolectomy for acute pulmonary thromboembolism: analysis of 32 patients from a multicentre registry Japan. Interact Cardiovasc Thorac

Surg. 2012;14(1):64–7. https://doi.org/10.1093/icvts/ivr018.
22. Dauphine C, Omari B. Pulmonary embolectomy for acute massive pulmonary embolism. Ann Thorac Surg. 2005;79:1240–4.
23. Cho YH, Sung K, Kim WS, Jeong DS, Lee YT, Park PW, Kim DK. Management of acute massive pulmonary embolism: is surgical embolectomy inferior to thrombolysis? Int J Cardiol. 2016;203:579–83.
24. Sareyyupoglu B, Greason KL, Suri RM, Keegan MT, Dearani JA, Sundt TM. A more aggressive approach to emergency embolectomy for acute pulmonary embolism. Mayo Clin Proc. 2010;85(9):785–90.
25. Kalra R, Bajaj NS, Arora P, Arora G, Crosland WA, McGiffin DC, Ahmed MI. Surgical embolectomy for acute pulmonary embolism: systematic review and comprehensive meta-analysis. Ann Thorac Surg. 2017;103:982–90.

43 Surgical Management of Functional Tricuspid Regurgitation

Peter Sze Yuen Yu and Malcolm John Underwood

Abstract

Functional tricuspid regurgitation remains a dilemma in patients presenting with left sided valvular disease. The decision for intervening is not clear cut in patients with mild/moderate regurgitation and in patients with severe regurgitation, placement of an annuloplasty ring may not be sufficient for a durable result due to leaflet tethering. There is no doubt that there is a trend for earlier intervention in patients with a dilated tricuspid annulus but minimal regurgitation but longer term follow up is required to assess the impact of this on long term outcomes.

Keywords

Functional tricuspid regurgitation · Annuloplasty · Leaflet techniques · Tricuspid valve replacement

43.1 Introduction

The term "functional" indicates extra-valvular etiology of tricuspid regurgitation (TR). It is due to dilation of the tricuspid annulus or dysfunction of the right ventricle, distorting the normal coaptation of the tricuspid valve leaflets. The causation of functional TR includes atrial fibrillation ("atriogenic") [1], or pulmonary hypertension secondary to pulmonary or left heart pathologies (most notably mitral valve disease). These underlying conditions should be investigated and optimized before proceeding to surgical correction of the TR alone.

Severity of TR should be assessed by detailed echocardiographic examination. The leaflet morphology should be assessed to exclude primary TR. Malcoaptation of the tricuspid valve leaflets (edge-to-edge, edge-to-side, or absent coaptation) is the key feature of functional TR. The regurgitant jet is visualized by colour flow Doppler, which allows assessment of the vena contracta, proximal isovelocity surface area (PISA) radius, effective regurgitant orifice and regurgitant volume. The annular dilation is measured by the diameter of the tricuspid annulus during echocardiography, Tricuspid annular dimensions are measured at end-diastole in the modified apical four-chamber view to maximise right heart size. Right atrial (RA) major dimension is from the centre of the tricuspid annulus to the centre of the superior RA wall, parallel to the atrial septum. The RA minor dimension is from the mid-level of the RA free wall to the septum, perpendicular to the long axis.

P. S. Y. Yu · M. J. Underwood (✉)
Division of Cardiothoracic Surgery, Department of Surgery, The Chinese University of Hong Kong, Prince of Wales Hospital, Hong Kong SAR, China
e-mail: mjunderwood@surgery.cuhk.edu.hk

S. I. Dumitrescu et al. (eds.), *Right Heart Pathology*, https://doi.org/10.1007/978-3-319-73764-5_43

43.1.1 When Should the Functional TR Be Repaired?

Early historical studies believed that tricuspid regurgitation would resolve after surgical correction of left heart valvular disease [2, 3] but recently this view has been challenged. There has been gaining recognition that tricuspid regurgitation during mitral valve surgery cannot be ignored. Severe TR after left heart surgery is associated with worse long-term survival and quality of life [4–8]. Functional TR can persist after correction of left heart pathology or normalization of pulmonary arterial pressure [6, 9–12], and mild-to-moderate TR can progress into significant TR [13–15]. TR can also develop late after mitral valve surgery [16–19], especially in those with dilated tricuspid annulus [5], dilated atrium, and pulmonary hypertension [20]. The development of significant TR may be associated also with atrial fibrillation, a common linkage with mitral valve disease, but not mitral valve disease per se [21]. Reoperation for redo tricuspid valve surgery is high (up to 25%) [22–25], and the quality of life remains poor [22, 24, 25]. Concomitant correction of TR is not associated with increased operative mortality [26, 27], a contemporary concept overriding the historical hurdle [28]. Concomitant correction of at least moderate TR improves the freedom from congestive heart failure [29], better RV remodeling [30], and may be associated with better long-term survival [17, 31, 32]. Concomitant prophylactic (i.e. with not greater than moderate TR) tricuspid valve annuloplasty in patients with dilated tricuspid annulus may prevent tricuspid regurgitation progression, improved right ventricular remodeling, better functional outcomes [33, 34], and even long-term survival [27].

According to the latest European Society of Cardiology (ESC)/European Association for Cardio-Thoracic Surgery (EACTS) guideline, surgery for functional TR should be considered [35]:

1. In patients undergoing left-sided heart surgery with
   (a) Severe TR (I, C)
   (b) Mild or moderate TR with dilated annulus ($\geq$40 mm or $\geq$21 mm m^{-2} by 2D echocardiography) (IIa, C)
   (c) Mild or moderate TR with no dilated annulus, but with recent right heart failure (IIb, C)
2. In patients with severe TR after previous left-sided heart surgery: (IIa, C)
   (a) Symptomatic
   (b) Progressive right heart dilation/dysfunction
   (c) Absence of severe right heart dysfunction
   (d) Absence of severe left heart dysfunction
   (e) Absence of severe pulmonary vascular disease/pulmonary hypertension

43.1.2 Surgical Approach to Functional TR: General Considerations

Surgical correction of functional TR should be directed to tackle the pathogenesis: Annular Dilation and Leaflet tethering. In the initial phase of the pathogenesis, annular dilation may not lead to TR; however, as a progressive process, annular dilation worsens with time and subsequently leads to clinically-significant TR due to leaflet malcoaptation. The decision for intervention at this initial stage should be based on the annular dilation and not only the presence or absence of TR. Tricuspid annuloplasty at this stage addresses annular dilation and leaflet malcoaptation, and can effective correct the TR. Leaflet tethering occurs as the RV dilation and dysfunction progress, and annuloplasty alone cannot adequate correct the TR. Therefore, additional procedures may be necessary to tackle leaflet tethering. Leaflet augmentation, suture bicuspidalization, clover technique, and tricuspid valve replacement are the available options to address leaflet tethering.

Traditionally it has been assumed that enlargement of the tricuspid annulus mainly occurs along the free wall of the right ventricle, while the septal area of the annulus remains unaffected.

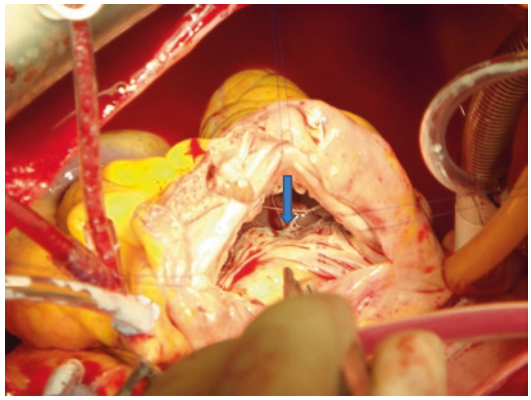

Fig. 43.1 Elongation of septal leaflet at surgery (arrow)

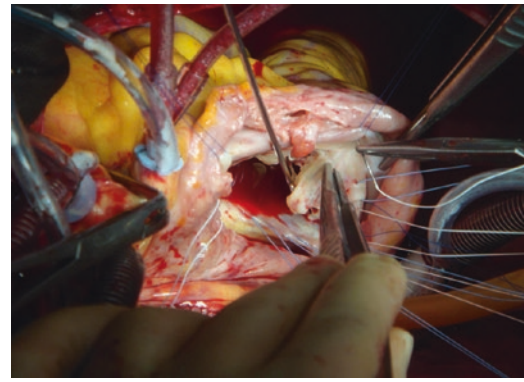

Fig. 43.2 Annuloplasty sutures inserted as horizontal mattress format

Sizing of the annulus is therefore based on the dimension of the septal leaflet [36]. However, in cases of late presentation it is very common to find elongation of the septal leaflet at surgery (Fig. 43.1). The atrioventricular node and bundle of His are located along the septal area of the annulus, which is bounded by the Triangle of Koch (Septal annulus, Tendon of Todaro, Coronary sinus). Any suture application or ring placement in this area is strictly forbidden to avoid conduction block.

The basic setup for tricuspid valve repair is cardiopulmonary bypass with bicaval venous cannulation with or without diastolic arrest of the myocardium. The vena caval snares should be applied to minimize venous return to the right atrium. The right atriotomy is created, and the right atrial exposure is maximized by retractors.

The tricuspid valve repair techniques can be grossly classified into:

1. Primary leaflet procedures:
   (a) Suture obliterating repair (Kay's procedure)
   (b) Edge-to-edge repair (Clover techniques)
   (c) Bicuspidalization
   (d) Leaflet patch augmentation
   (e) Cord cutting with artificial cord insertion
2. Annuloplasty:
   (a) Suture: DeVega procedure
   (b) Ring: Rigid/Semi-rigid/Flexible band
3. Tricuspid valve replacement/reconstruction

43.2 Annuloplasty

43.2.1 Ring Annuloplasty

The basic principles of tricuspid ring annuloplasty involve the following steps:

1. After cardiopulmonary bypass and right atriotomy, the anatomy and pathology of the tricuspid valve is directly assessed.
2. Multiple annular stitches are applied traveling parallel to the course of the annulus. Attention must be taken to avoid applying the stitches to the atrial wall, the leaflet tissue, and into the triangle of Koch (Fig. 43.2).
3. Size of the annuloplasty ring is selected by comparing the sizer to the surface area of the anterior and posterior TV leaflets, and to the length of the septal annulus. An equally-sized or undersized tricuspid annulus may be chosen (Fig. 43.3).
4. The annular stitches are sutured to the ring in a horizontal mattress manner.
5. The ring is parachuted down to the tricuspid annulus (Fig. 43.4)
6. The sutures are secured by hand-tying or specific knot-fastening device.
7. The competency of the tricuspid valve can be assessed by water injection (Fig. 43.5). This can be difficult unless the pulmonary artery is occluded and the veins of the right ventricle drain the saline very quickly so this test is not as durable for the mitral but will ensure any major leaks or leaflet tethering is recognized.

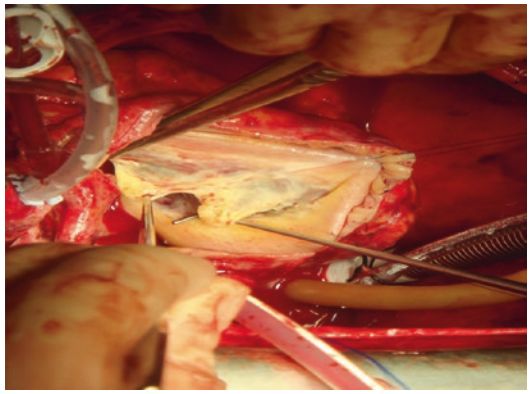

Fig. 43.3 Annuloplast ring sizing based on area of the non-septal leaflets

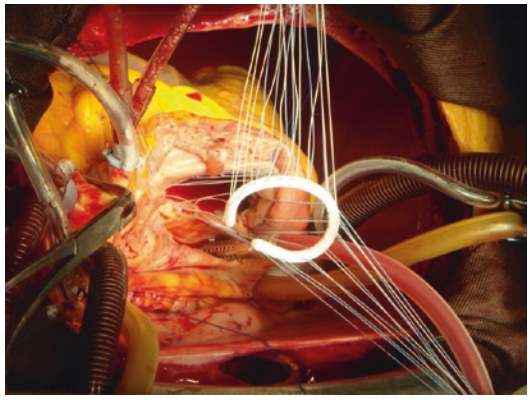

Fig. 43.4 Annuloplasty ring placement: parachute to level of the tricuspid

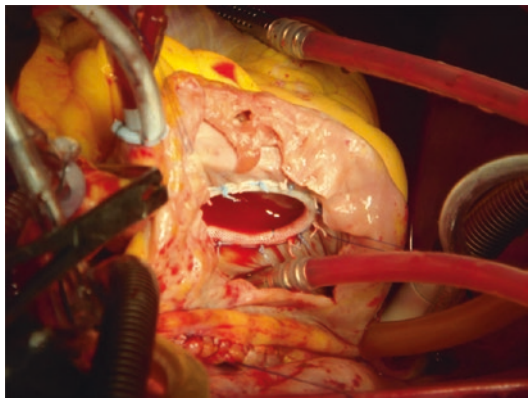

Fig. 43.5 Water test to ensure competency of the tricuspid valve

There are many different rings on the market. These rings can be different in size, configuration (i.e. complete vs. incomplete ring), and rigidity (i.e. rigid, semirigid, flexible band) and 2D versus 3D configurations. Incomplete rings sufficiently protect the anterior and posterior portion of the annulus which are most prone to progressive dilation. It also avoided suture application to the triangle of Koch, therefore can avoid conduction block. Complete rings have the advantage of additional stabilization of the septal area of the annulus, thereby completely protect the annulus from further dilation. Conduction block may be avoided by passing sutures through the base of the septal leaflet, instead of directly onto the annulus.

Rigidity of the annuloplasty ring is important to mechanically support the tricuspid annulus. Although the dynamic geometrical change of the annulus during cardiac cycles might be impaired, both the annular diameter and the annular saddle-shaped geometry can be effectively restored. These properties are especially important if the tricuspid annulus is severely dilated resulting in severe TR. There is currently no solid evidence to proof the pros and cons of each of the above choice. Both rigid rings and flexible bands provide satisfactory early results [37], but rigid ring annuloplasty had better long term freedom from TR [38, 39], and better reverse remodeling of the RV [40]. Use of rigid rings may increase the risk of subsequent ring dehiscence, especially at the septal leaflet part of the annulus [37], but this happens exclusively in the beating-heart annuloplasty [41]. This may be attributed to the increased shearing forces at the septal annulus during beating-heart procedure. There are also possibility of ring fracture [42, 43]. The annuloplasty may be performed using an autologous pericardial strip to structurally and functionally mimic an annuloplasty ring [44]. The recurrence after this method was also lower than purely suture-based annuloplasty. The flexible element may be integrated into a rigid or semirigid ring framework to combine the advantages of the two elements. The hybrid annuloplasty ring [Tri-Ad™ Adams, Medtronic, MN] comprises a semirigid component for implantation to the right ventricular

free wall aspect of the annulus to function as a remodeling ring, and flexible bands at the two ends of the semirigid component to restore the normal 3-dimensional elliptical shape of the annulus to reduce leaflet stress and tethering [45]. Early results showed that it is safe and effective for TR correction.

43.2.2 Suture Annuloplasty

The classic DeVega annuloplasty involves application of continuous sutures to form support to the anterior and posterior leaflets of the tricuspid valve. The principle steps involve:

1. A pledgeted 2/0 polypropylene suture is applied starting from the antero-septal leaflet commissure.
2. Sequential continuous sutures are applied through the tricuspid annulus in narrow bites
3. Suturing ends at the postero-septal commissure of the tricuspid valve.
4. The other end of the suture runs a second row of continuous suture just tangential to the tricuspid annulus
5. The two needles run through a second pledget felt.
6. A annuloplasty calibrator may be used to guide the degree of tightening of the suture annuloplasty. Water injection test can be done to test the tricuspid valve competency.
7. The sutures are tightened after confirmation of tricuspid valve competency.

Device-based annuloplasty had been unanimously shown to have superior long-term freedom from TR compared to suture-based surgery (6–17% vs. 33–61%) [46–51], although the most recent studies revealed no significant differences [52, 53]. Ring annuloplasty appears to have better long-term survival and freedom from TV reoperation [54]. The high and variable recurrence rate of TR after suture annuloplasty may be explained by the long suture line or the use of polypropylene suture, which is susceptible to disintegration as the annulus attempts to dilate.

43.3 Primary Leaflet Procedures

Nowadays annuloplasty is the mainstay of surgical treatment of function TR. Isolated leaflet procedures has been largely obsolete. The early techniques of leaflet procedures has been known to be ineffective and are no longer used. A few leaflet procedures, however, might still have some roles in correction of TR as isolated procedure or combined with annuloplasty.

43.3.1 Suture Bicuspidalization

Suture Bicuspidalization aims at reducing the annulus size by using a figure-of-eight mattress suture plication of the posterior leaflet from the anteroposterior to the posteroseptal commissures along the posterior annulus. This technique is effective in correction TR early post-op, while the recurrence of significant TR in the long-term ranges from 14–16% [46, 55].

43.3.2 Leaflet Augmentation

Severe leaflet tethering from right ventricle dilatation is a risk factor for recurrence of TR after annuloplasty [46, 56, 57]. Tricuspid valve leaflet augmentation is an adjunct to address severe tethering during tricuspid annuloplasty for functional TR [58, 59]. It can enlarge the surface area of leaflet coaptation and allow mobility of the leaflets. It is performed by detaching the anterior leaflet from the annulus, followed by attachment of a tailored pericardial patch to the annulus and to the detached anterior leaflet. The anterior leaflet is converted to be the coaptation surface, and the pericardial patch is made the main body of the leaflet. The size of the patch is tailored according to the width of incision and the suture width loss. Septal leaflet may also be augmented in the same way. The early and late correction results were promising (at most 9% recurrence of at least moderate TR at 4 years) [58–60].

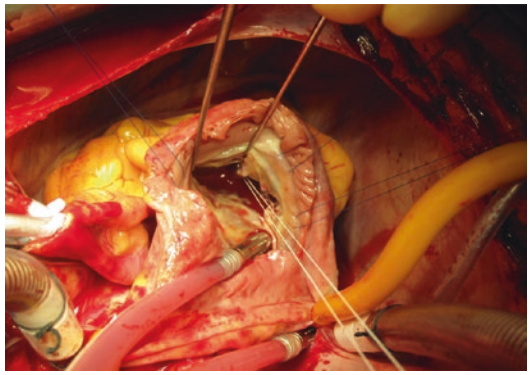

Fig. 43.6 Artificial cord being attached to a papillary muscle tip after cutting the primary restricted cords

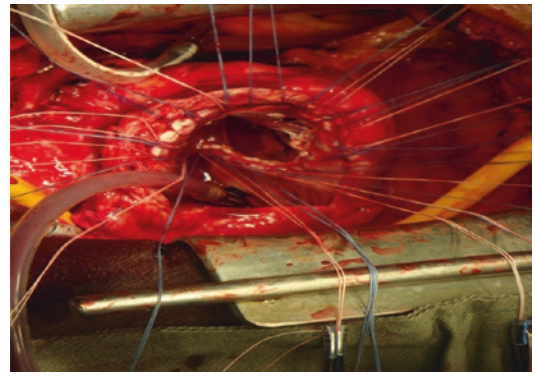

Fig. 43.8 Suture placement for tricuspid valve replacement

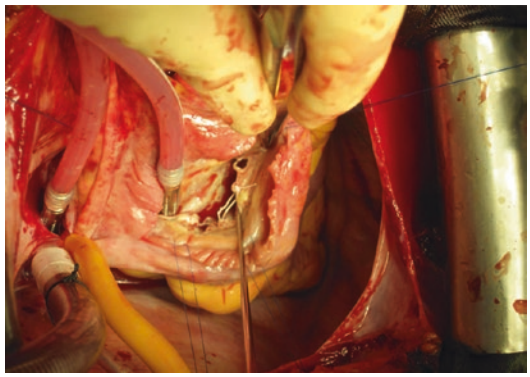

Fig. 43.7 Completed artificial cord from papillary muscle to leaflet edge

43.3.3 Cord Cutting and Replacement with Artificial Cords

This technique involves cutting any tethered primary cords and replacing them with artificial cords which are purposefully left longer. This is done so more leaflet tissue is available for coaptation in cases with leaflet tethering but there is very little in the published literature on long term outcomes or durability (Figs. 43.6 and 43.7).

43.4 Tricuspid Valve Replacement

The principle steps involved in TVR include:

1. The anterior, posterior, and part of the septal leaflet are excised. Septal leaflet should be preserved to allow attachment of prosthesis. Recently however, it is our routine to preserve all leaflets and place the valve in a supra-annular position using the leaflet tissue to reinforce the tricuspid annulus.
2. Valve annulus sizer is used to select the appropriate size of prosthesis
3. Multiple annular stitches are applied to the tricuspid annulus and to the septal leaflet. Needling of the septal annulus or the septal myocardium to avoid conduction block. To avoid this we place the sutures firstly through the free edge of the tricuspid leaflet and then anchor this a distance of 4–5 mm from the tricuspid annulus in the left atrium. This way, the conducting tissue is "tunneled" under the leaflet tissue avoiding heart block. (Fig. 43.8).
4. Horizontal mattress stitches are applied to the sewing cuff of the tricuspid prosthesis. Pledget felts may be used to reinforce the tissue anchorage of the sutures
5. Sutures are tightened to anchor the sewing cuff to the tricuspid annulus (Fig. 43.9)

TVR is prone to thromboembolic complications particularly for mechanical prosthesis (up to 1.28% patient/year) [61]. The operative mortality of TVR remained high (17–22%) [62–64]. TVR appeared to have less recurrence of moderate to severe TR, similar valve-related mortality or need of redo TV surgery compared to TV repair, but worse RV function [64, 65] and mid-term survival [64]. This may be

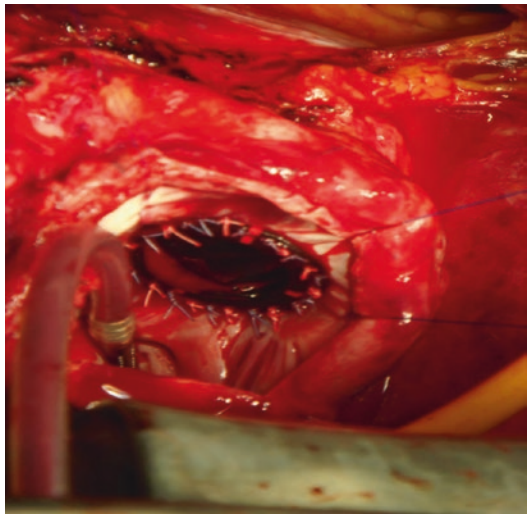

Fig. 43.9 Tricuspid valve replacement in-situ

explained by the placement of a large rigid prosthetic material in a low-pressure cavity leading to progressive RV dysfunction. Therefore, in the absence of organic TV pathologies, TV repair should be preferred over TVR. A high tenting volume or antero-posterior annular diameter measured on real-time three-dimensional echocardiography may predict severe residual TR after TV annuloplasty, and these patients may have TVR preferred as the initial operation [66].

43.5 Summary

Indication for correction of functional tricuspid regurgitation has changed now more is known about its pathophysiology and natural history. Moderate to severe TR should not be neglected during left-sided heart surgery, and prophylactic correction of mild to moderate TR associated with dilated tricuspid annulus may also improve outcomes. Annuloplasty is the mainstay for functional TR, but concomitant leaflet procedures may be indicated to address annular dilation or leaflet tethering. Tricuspid valve replacement provides the ultimate armament for correction of severe TR, but is associated with worse long-term survival.

References

1. Utsunomiya H, Itabashi Y, Mihara H, Berdejo J, Kobayashi S, Siegel RJ, Shiota T. Functional tricuspid regurgitation caused by chronic atrial fibrillation: a real-time 3-dimensional transesophageal echocardiography study. Circ Cardiovasc Imaging. 2017;10(1):e004897. https://doi.org/10.1161/CIRCIMAGING.116.004897.
2. Messer AL, Hurst JW, et al. A study of the venous pulse in tricuspid valve disease. Circulation. 1950;1(3):388–93.
3. Braunwald NS, Ross J Jr, Morrow AG. Conservative management of tricuspid regurgitation in patients undergoing mitral valve replacement. Circulation. 1967;35(4 Suppl):I63–9.
4. Groves PH, Lewis NP, Ikram S, Maire R, Hall RJ. Reduced exercise capacity in patients with tricuspid regurgitation after successful mitral valve replacement for rheumatic mitral valve disease. Br Heart J. 1991;66(4):295–301.
5. Groves PH, Ikram S, Ingold U, Hall RJ. Tricuspid regurgitation following mitral valve replacement: an echocardiographic study. J Heart Valve Dis. 1993;2(3):273–8.
6. Sagie A, Schwammenthal E, Palacios IF, King ME, Leavitt M, Freitas N, Weyman AE, Levine RA. Significant tricuspid regurgitation does not resolve after percutaneous balloon mitral valvotomy. J Thorac Cardiovasc Surg. 1994;108(4):727–35.
7. Izumi C, Iga K, Konishi T. Progression of isolated tricuspid regurgitation late after mitral valve surgery for rheumatic mitral valve disease. J Heart Valve Dis. 2002;11(3):353–6.
8. Ruel M, Rubens FD, Masters RG, Pipe AL, Bedard P, Mesana TG. Late incidence and predictors of persistent or recurrent heart failure in patients with mitral prosthetic valves. J Thorac Cardiovasc Surg. 2004;128(2):278–83. https://doi.org/10.1016/j.jtcvs.2003.11.048.
9. Sadeghi HM, Kimura BJ, Raisinghani A, Blanchard DG, Mahmud E, Fedullo PF, Jamieson SW, DeMaria AN. Does lowering pulmonary arterial pressure eliminate severe functional tricuspid regurgitation? Insights from pulmonary thromboendarterectomy. J Am Coll Cardiol. 2004;44(1):126–32. https://doi.org/10.1016/j.jacc.2003.12.058.
10. Hannoush H, Fawzy ME, Stefadouros M, Moursi M, Chaudhary MA, Dunn B. Regression of significant tricuspid regurgitation after mitral balloon valvotomy for severe mitral stenosis. Am Heart J. 2004;148(5):865–70. https://doi.org/10.1016/j.ahj.2004.05.017.
11. Simon R, Oelert H, Borst HG, Lichtlen PR. Influence of mitral valve surgery on tricuspid incompetence concomitant with mitral valve disease. Circulation. 1980;62(2 Pt 2):I152–7.
12. Shafie MZ, Hayat N, Majid OA. Fate of tricuspid regurgitation after closed valvotomy for mitral stenosis. Chest. 1985;88(6):870–3.
13. De Bonis M, Lapenna E, Pozzoli A, Nisi T, Giacomini A, Calabrese M, La Canna G, Pappalardo F, Miceli

A, Glauber M, Barili F, Alfieri O. Mitral valve repair without repair of moderate tricuspid regurgitation. Ann Thorac Surg. 2015;100(6):2206–12. https://doi.org/10.1016/j.athoracsur.2015.05.108.
14. Van de Veire NR, Braun J, Delgado V, Versteegh MI, Dion RA, Klautz RJ, Bax JJ. Tricuspid annuloplasty prevents right ventricular dilatation and progression of tricuspid regurgitation in patients with tricuspid annular dilatation undergoing mitral valve repair. J Thorac Cardiovasc Surg. 2011;141(6):1431–9. https://doi.org/10.1016/j.jtcvs.2010.05.050.
15. Kusajima K, Fujita T, Hata H, Shimahara Y, Miura S, Kobayashi J. Long-term echocardiographic follow-up of untreated 2+ functional tricuspid regurgitation in patients undergoing mitral valve surgery. Interact Cardiovasc Thorac Surg. 2016;23(1):96–103. https://doi.org/10.1093/icvts/ivw065.
16. Porter A, Shapira Y, Wurzel M, Sulkes J, Vaturi M, Adler Y, Sahar G, Sagie A. Tricuspid regurgitation late after mitral valve replacement: clinical and echocardiographic evaluation. J Heart Valve Dis. 1999;8(1):57–62.
17. Dreyfus GD, Corbi PJ, Chan KM, Bahrami T. Secondary tricuspid regurgitation or dilatation: which should be the criteria for surgical repair? Ann Thorac Surg. 2005;79(1):127–32. https://doi.org/10.1016/j.athoracsur.2004.06.057.
18. Matsuyama K, Matsumoto M, Sugita T, Nishizawa J, Tokuda Y, Matsuo T. Predictors of residual tricuspid regurgitation after mitral valve surgery. Ann Thorac Surg. 2003;75(6):1826–8.
19. De Bonis M, Lapenna E, Sorrentino F, La Canna G, Grimaldi A, Maisano F, Torracca L, Alfieri O. Evolution of tricuspid regurgitation after mitral valve repair for functional mitral regurgitation in dilated cardiomyopathy. Eur J Cardiothorac Surg. 2008;33(4):600–6. https://doi.org/10.1016/j.ejcts.2008.01.011.
20. Rajbanshi BG, Suri RM, Nkomo VT, Dearani JA, Daly RC, Burkhart HM, Stulak JM, Joyce LD, Li Z, Schaff HV. Influence of mitral valve repair versus replacement on the development of late functional tricuspid regurgitation. J Thorac Cardiovasc Surg. 2014;148(5):1957–62. https://doi.org/10.1016/j.jtcvs.2014.04.041.
21. Vaturi M, Kotler T, Shapira Y, Weisenberg D, Monakier D, Sagie A. Prevalence of late functional tricuspid regurgitation in degenerative mitral regurgitation surgery. J Heart Valve Dis. 2016;25(2):157–61.
22. Mangoni AA, DiSalvo TG, Vlahakes GJ, Polanczyk CA, Fifer MA. Outcome following isolated tricuspid valve replacement. Eur J Cardiothorac Surg. 2001;19(1):68–73.
23. Kwon DA, Park JS, Chang HJ, Kim YJ, Sohn DW, Kim KB, Ahn H, Oh BH, Park YB, Choi YS. Prediction of outcome in patients undergoing surgery for severe tricuspid regurgitation following mitral valve surgery and role of tricuspid annular systolic velocity. Am J Cardiol. 2006;98(5):659–61. https://doi.org/10.1016/j.amjcard.2006.03.047.
24. Staab ME, Nishimura RA, Dearani JA. Isolated tricuspid valve surgery for severe tricuspid regurgitation following prior left heart valve surgery: analysis of outcome in 34 patients. J Heart Valve Dis. 1999;8(5):567–74.
25. Kim YJ, Kwon DA, Kim HK, Park JS, Hahn S, Kim KH, Kim KB, Sohn DW, Ahn H, BH O, Park YB. Determinants of surgical outcome in patients with isolated tricuspid regurgitation. Circulation. 2009;120(17):1672–8. https://doi.org/10.1161/CIRCULATIONAHA.109.849448.
26. Badhwar V, Rankin JS, He M, Jacobs JP, Furnary AP, Fazzalari FL, O'Brien S, Gammie JS, Shahian DM. Performing concomitant tricuspid valve repair at the time of mitral valve operations is not associated with increased operative mortality. Ann Thorac Surg. 2017;103(2):587–93. https://doi.org/10.1016/j.athoracsur.2016.06.004.
27. Jeong DS, Park PW, Sung K, Kim WS, Lee YT. Determinants of late tricuspid regurgitation after aortic-mitral double valve replacement. Am J Cardiol. 2017;119(10):1643–9. https://doi.org/10.1016/j.amjcard.2017.02.013.
28. Rankin JS, Hammill BG, Ferguson TB Jr, Glower DD, O'Brien SM, DeLong ER, Peterson ED, Edwards FH. Determinants of operative mortality in valvular heart surgery. J Thorac Cardiovasc Surg. 2006;131(3):547–57. https://doi.org/10.1016/j.jtcvs.2005.10.041.
29. Chan V, Burwash IG, Lam BK, Auyeung T, Tran A, Mesana TG, Ruel M. Clinical and echocardiographic impact of functional tricuspid regurgitation repair at the time of mitral valve replacement. Ann Thorac Surg. 2009;88(4):1209–15. https://doi.org/10.1016/j.athoracsur.2009.06.034.
30. Bertrand PB, Koppers G, Verbrugge FH, Mullens W, Vandervoort P, Dion R, Verhaert D. Tricuspid annuloplasty concomitant with mitral valve surgery: effects on right ventricular remodeling. J Thorac Cardiovasc Surg. 2014;147(4):1256–64. https://doi.org/10.1016/j.jtcvs.2013.05.007.
31. Lee JW, Song JM, Park JP, Lee JW, Kang DH, Song JK. Long-term prognosis of isolated significant tricuspid regurgitation. Circ J. 2010;74(2):375–80.
32. De Meester P, De Cock D, Van De Bruaene A, Gabriels C, Buys R, Helsen F, Voigt JU, Herijgers P, Herregods MC, Budts W. Additional tricuspid annuloplasty in mitral valve surgery results in better clinical outcome. Heart. 2015;101(9):720–6. https://doi.org/10.1136/heartjnl-2014-306801.
33. Benedetto U, Melina G, Angeloni E, Refice S, Roscitano A, Comito C, Sinatra R. Prophylactic tricuspid annuloplasty in patients with dilated tricuspid annulus undergoing mitral valve surgery. J Thorac Cardiovasc Surg. 2012;143(3):632–8. https://doi.org/10.1016/j.jtcvs.2011.12.006.
34. Kim JB, Yoo DG, Kim GS, Song H, Jung SH, Choo SJ, Chung CH, Lee JW. Mild-to-moderate functional tricuspid regurgitation in patients undergoing valve replacement for rheumatic mitral disease: the influence of tricuspid valve repair on clinical and echocardiographic outcomes. Heart. 2012;98(1):24–30. https://doi.org/10.1136/heartjnl-2011-300403.

35. Baumgartner H, Falk V, Bax JJ, De Bonis M, Hamm C, Holm PJ, Iung B, Lancellotti P, Lansac E, Munoz DR, Rosenhek R, Sjogren J, Tornos Mas P, Vahanian A, Walther T, Wendler O, Windecker S, Zamorano JL. 2017 ESC/EACTS Guidelines for the management of valvular heart disease: The Task Force for the Management of Valvular Heart Disease of the European Society of Cardiology (ESC) and the European Association for Cardio-Thoracic Surgery (EACTS). Eur Heart J. 2017;38(36):2739–91. https://doi.org/10.1093/eurheartj/ehx391.
36. Yiwu L, Yingchun C, Jianqun Z, Bin Y, Ping B. Exact quantitative selective annuloplasty of the tricuspid valve. J Thorac Cardiovasc Surg. 2001;122(3):611–4. https://doi.org/10.1067/mtc.2001.113164.
37. Pfannmuller B, Doenst T, Eberhardt K, Seeburger J, Borger MA, Mohr FW. Increased risk of dehiscence after tricuspid valve repair with rigid annuloplasty rings. J Thorac Cardiovasc Surg. 2012;143(5):1050–5. https://doi.org/10.1016/j.jtcvs.2011.06.019.
38. Wang N, Phan S, Tian DH, Yan TD, Phan K. Flexible band versus rigid ring annuloplasty for tricuspid regurgitation: a systematic review and meta-analysis. Ann Cardiothorac Surg. 2017;6(3):194–203. https://doi.org/10.21037/acs.2017.05.05.
39. Wang H, Liu X, Wang X, Lv Z, Liu X, Xu P. Comparison of outcomes of tricuspid annuloplasty with 3D-rigid versus flexible prosthetic ring for functional tricuspid regurgitation secondary to rheumatic mitral valve disease. J Thorac Dis. 2016;8(11):3087–95. https://doi.org/10.21037/jtd.2016.11.97.
40. Gatti G, Dell'Angela L, Morosin M, Maschietto L, Pinamonti B, Benussi B, Forti G, Nicolosi GL, Sinagra G, Pappalardo A. Flexible band versus rigid ring annuloplasty for functional tricuspid regurgitation: two different patterns of right heart reverse remodelling. Interact Cardiovasc Thorac Surg. 2016;23(1):79–89. https://doi.org/10.1093/icvts/ivw047.
41. Pfannmuller B, Davierwala P, Misfeld M, Borger MA, Garbade J, Mohr FW. Postoperative outcome of isolated tricuspid valve operation using arrested-heart or beating-heart technique. Ann Thorac Surg. 2012;94(4):1218–22. https://doi.org/10.1016/j.athoracsur.2012.05.020.
42. Galinanes M, Duarte J, de Caleya DF, Garcia-Dorado D, Fdez-Aviles F, Elbal LM. Fracture of the Carpentier-Edwards ring in tricuspid position: a report of three cases. Ann Thorac Surg. 1986;42(1):74–6.
43. Kay HR, Hammond GL. Fracture of a prosthetic tricuspid annular ring. J Thorac Cardiovasc Surg. 1982;83(4):635.
44. Chang BC, Song SW, Lee S, Yoo KJ, Kang MS, Chung N. Eight-year outcomes of tricuspid annuloplasty using autologous pericardial strip for functional tricuspid regurgitation. Ann Thorac Surg. 2008;86(5):1485–92. discussion 1493. https://doi.org/10.1016/j.athoracsur.2008.07.007.
45. Milla F, Castillo JG, Varghese R, Chikwe J, Anyanwu AC, Adams DH. Rationale and initial experience with the Tri-Ad Adams tricuspid annuloplasty ring. J Thorac Cardiovasc Surg. 2012;143(4 Suppl):S71–3. https://doi.org/10.1016/j.jtcvs.2011.11.015.
46. McCarthy PM, Bhudia SK, Rajeswaran J, Hoercher KJ, Lytle BW, Cosgrove DM, Blackstone EH. Tricuspid valve repair: durability and risk factors for failure. J Thorac Cardiovasc Surg. 2004;127(3):674–85. https://doi.org/10.1016/j.jtcvs.2003.11.019.
47. Rivera R, Duran E, Ajuria M. Carpentier's flexible ring versus De Vega's annuloplasty. A prospective randomized study. J Thorac Cardiovasc Surg. 1985;89(2):196–203.
48. Matsuyama K, Matsumoto M, Sugita T, Nishizawa J, Tokuda Y, Matsuo T, Ueda Y. De Vega annuloplasty and Carpentier-Edwards ring annuloplasty for secondary tricuspid regurgitation. J Heart Valve Dis. 2001;10(4):520–4.
49. Tang GH, David TE, Singh SK, Maganti MD, Armstrong S, Borger MA. Tricuspid valve repair with an annuloplasty ring results in improved long-term outcomes. Circulation. 2006;114(1 Suppl):I577–81. https://doi.org/10.1161/CIRCULATIONAHA.105.001263.
50. Roshanali F, Saidi B, Mandegar MH, Yousefnia MA, Alaeddini F. Echocardiographic approach to the decision-making process for tricuspid valve repair. J Thorac Cardiovasc Surg. 2010;139(6):1483–7. https://doi.org/10.1016/j.jtcvs.2009.08.035.
51. Parolari A, Barili F, Pilozzi A, Pacini D. Ring or suture annuloplasty for tricuspid regurgitation? A meta-analysis review. Ann Thorac Surg. 2014;98(6):2255–63. https://doi.org/10.1016/j.athoracsur.2014.06.100.
52. Huang X, Gu C, Men X, Zhang J, You B, Zhang H, Wei H, Li J. Repair of functional tricuspid regurgitation: comparison between suture annuloplasty and rings annuloplasty. Ann Thorac Surg. 2014;97(4):1286–92. https://doi.org/10.1016/j.athoracsur.2013.10.037.
53. Hata H, Fujita T, Miura S, Shimahara Y, Kume Y, Matsumoto Y, Yamashita K, Kobayashi J. Long-term outcomes of suture vs. ring tricuspid annuloplasty for functional tricuspid regurgitation. Circ J. 2017;81(10):1432–8. https://doi.org/10.1253/circj.CJ-17-0108.
54. Guenther T, Mazzitelli D, Noebauer C, Hettich I, Tassani-Prell P, Voss B, Lange R. Tricuspid valve repair: is ring annuloplasty superior? Eur J Cardiothorac Surg. 2013;43(1):58–65. discussion 65. https://doi.org/10.1093/ejcts/ezs266.
55. Ghanta RK, Chen R, Narayanasamy N, McGurk S, Lipsitz S, Chen FY, Cohn LH. Suture bicuspidization of the tricuspid valve versus ring annuloplasty for repair of functional tricuspid regurgitation: mid-term results of 237 consecutive patients. J Thorac Cardiovasc Surg. 2007;133(1):117–26. https://doi.org/10.1016/j.jtcvs.2006.08.068.
56. Fukuda S, Gillinov AM, McCarthy PM, Stewart WJ, Song JM, Kihara T, Daimon M, Shin MS, Thomas JD, Shiota T. Determinants of recurrent or residual functional tricuspid regurgitation after tricuspid annuloplasty. Circulation. 2006;114(1 Suppl):I582–7. https://doi.org/10.1161/CIRCULATIONAHA.105.001305.

57. Park YH, Song JM, Lee EY, Kim YJ, Kang DH, Song JK. Geometric and hemodynamic determinants of functional tricuspid regurgitation: a real-time three-dimensional echocardiography study. Int J Cardiol. 2008;124(2):160–5. https://doi.org/10.1016/j.ijcard.2006.12.036.
58. Dreyfus GD, Raja SG, John Chan KM. Tricuspid leaflet augmentation to address severe tethering in functional tricuspid regurgitation. Eur J Cardiothorac Surg. 2008;34(4):908–10. https://doi.org/10.1016/j.ejcts.2008.07.006.
59. Pettinari M, Bertrand P, Van Kerrebroeck C, Vandervoort P, Gutermann H, Dion R. Mid-term results of leaflet augmentation in severe tricuspid functional tethering. Eur J Cardiothorac Surg. 2016;50(3):504–8. https://doi.org/10.1093/ejcts/ezw039.
60. Choi JB, Kim NY, Kim KH, Kim MH, Jo JK. Tricuspid leaflet augmentation to eliminate residual regurgitation in severe functional tricuspid regurgitation. Ann Thorac Surg. 2011;92(6):e131–3. https://doi.org/10.1016/j.athoracsur.2011.08.019.
61. Rizzoli G, Vendramin I, Nesseris G, Bottio T, Guglielmi C, Schiavon L. Biological or mechanical prostheses in tricuspid position? A meta-analysis of intra-institutional results. Ann Thorac Surg. 2004;77(5):1607–14. https://doi.org/10.1016/j.athoracsur.2003.10.015.
62. Ratnatunga CP, Edwards MB, Dore CJ, Taylor KM. Tricuspid valve replacement: UK Heart Valve Registry mid-term results comparing mechanical and biological prostheses. Ann Thorac Surg. 1998;66(6):1940–7.
63. Filsoufi F, Anyanwu AC, Salzberg SP, Frankel T, Cohn LH, Adams DH. Long-term outcomes of tricuspid valve replacement in the current era. Ann Thorac Surg. 2005;80(3):845–50. https://doi.org/10.1016/j.athoracsur.2004.12.019.
64. Singh SK, Tang GH, Maganti MD, Armstrong S, Williams WG, David TE, Borger MA. Midterm outcomes of tricuspid valve repair versus replacement for organic tricuspid disease. Ann Thorac Surg. 2006;82(5):1735–41. discussion 1741. https://doi.org/10.1016/j.athoracsur.2006.06.016.
65. Choi JW, Park EA, Lee W, Kim KH, Kim KB, Ahn H, Kim HK, Hwang HY. Changes in right ventricular volume and function after tricuspid valve surgery- tricuspid annuloplasty vs. tricuspid valve replacement. Circ J. 2016;80(5):1142–7. https://doi.org/10.1253/circj.CJ-15-1336.
66. Min SY, Song JM, Kim JH, Jang MK, Kim YJ, Song H, Kim DH, Lee JW, Kang DH, Song JK. Geometric changes after tricuspid annuloplasty and predictors of residual tricuspid regurgitation: a real-time three-dimensional echocardiography study. Eur Heart J. 2010;31(23):2871–80. https://doi.org/10.1093/eurheartj/ehq227.

Surgical Strategy in Tricuspid Valve Endocarditis

44

Horatiu Moldovan, Adrian Molnar, Victor Costache, and Ecaterina Bontaş

Abstract

Until recent years, the infective endocarditis of the right heart was considered extremely rare. In the last 20 years the incidence of this disease is increasing, especially for the isolated tricuspid valve infective endocarditis. Most frequent causes are: drug abuse, uterine infections, cardiac implantable electronic devices like pacemakers/defibrillators leads, other intracardiac devices or cardiac malformations. Medical treatment with antibiotics is the mainstay option but surgery is often required for a group of patients. Surgical interventions include valvectomy (total excision of the tricuspid valve without substitution), reconstruction or valve replacement. Surgical strategy in tricuspid valve endocarditis can produce satisfactory results. The clear indication and timing of surgery remain debatable. Association with intravenous antibiotics is of paramount importance. Conservative techniques are the first choice but replacement remains an option when repair is not feasible. However, there is no clear evidence supporting one technique over another.

Keywords

Endocarditis · Tricuspid valve · Tricuspid valve repair · Tricuspid valve re-placement · Right heart endocarditis · Intravenous drug abuser endocarditis · Intracardiac electronic devices endocarditis

H. Moldovan (✉)
Department of Cardiovascular Surgery, Titu Maiorescu University, Bucharest, Romania

Department of Cardiovascular Biomaterials, Department of Science and Engineering in Biomaterials, Politehnica University of Bucharest (UPB), Bucharest, Romania

Romanian Academy of Medical Sciences, Bucharest, Romania

Department of Cardiovascular Surgery, Sanador Clinical Hospital, Bucharest, Romania
e-mail: horatiu.moldovan@sanador.ro

A. Molnar
Department of Cardiovascular Surgery, University of Medicine and Pharmacy, Cluj-Napoca, Romania

Department of Cardiovascular Surgery, Heart Institute "Niculae Stancioiu", Cluj-Napoca, Romania

V. Costache
Department of Cardiovascular and Thoracic Surgery, POLISANO Hospital, Sibiu, Romania; http://www.clinicapolisano.ro

E. Bontaş
Department of Cardiology, "Prof. C.C. Iliescu" Emergency Institute for Cardiovascular Diseases Bucharest, Bucharest, Romania

44.1 Introduction

The infective endocarditis of the tricuspid valve is of uncertain frequency. There are studies that support tricuspid endocarditis as being of 5% of total numbers of infective endocarditis but other

S. I. Dumitrescu et al. (eds.), *Right Heart Pathology*, https://doi.org/10.1007/978-3-319-73764-5_44

reports consider a number up to 36% of cases. Moreover, there is evidence that the frequency of tricuspid endocarditis is increasing. The most important treatment is with large doses of intravenous antibiotics and it is generally successful. The surgical intervention is necessary in a relatively small number of patients in which the antibiotic therapy proven to be unsuccessful [1].

Surgical strategy includes:

- Tricuspid valve excision and replacement or partial excision of the infected tissue followed by valve reconstruction.
- Valvectomy alone without replacement is no more a viable solution [2].

44.2 Epidemiology

The most frequent predisposing factor for tricuspid endocarditis is the intravenous drug abuse followed by the cardiac implantable electronic devices (pacemakers, defibrillators leads, etc.) and long-term central venous access catheters for chemotherapy and dialysis [3–5].

Up to 86% of infective endocarditis among intravenous drug users is on the tricuspid valve [4, 6].

Another important condition that can generate tricuspid endocarditis is genital infection after birth or abortion in young women [7].

There is also infective endocarditis in congenital heart disease such as Ebstein's anomaly [1].

Importantly, there are many pathological agents involved in the etiology of right heart endocarditis. The most frequent is *Staphylococcus aureus*—up to 90% of cases. Nevertheless, it can be involved also: coagulase-negative Staphylococci, Streptococci, Enterococci and HACEK organisms (Haemophilus aphrophilus, Actinobacillus actinomycetemcomitans, Cardiobacterium hominis, Eikenella corrodens and Kingella kingae), Enterococci spp. and fungi [1].

In drug abusers can be also a mixed infection. The number of abusers is relatively constant, but the accessibility to intravenous drugs leads to increased number of tricuspid infective endocarditis [8].

In the last 25 years the number of patients with cardiac electronic implantable devices increased with 100%. Among these, there is also an increasing number of right heart infective endocarditis with tricuspid involvement between 5% and 8%. This form of endocarditis most frequently affects patients with various comorbidities.

There is an increase in the number of patients with congenital disease and previously repaired congenital heart disease, like Ebstein's anomaly who developes tricuspid infective endocarditis [9].

According to current evidence, tricuspid valve involvement is highly unusual in Libman–Sacks endocarditis (Fig. 44.1) [10, 11].

In a few words, Table 44.1 sum up the major differences between right sided infective endocarditis and left side infective endocarditis [12].

44.3 Indications for Surgery

The first step in the treatment strategy of tricuspid endocarditis is the antibiotic therapy. Patients treated only medical have an hospital mortality of less than 5%. There are only 20% who require surgical intervention [13, 14].

These situations are:

- Persistent right heart failure despite medical therapy.
- Recurrent pulmonary septic embolism.
- Pulmonary abscess.
- Intracardiac abscess, fistula, other mechanical complications.
- Septic shock.
- Failure of antibiotic therapy to control the infection.
- Right ventricular dilatation associated with severe tricuspid regurgitation [1].

Currently, the 2009 European Society of Cardiology (ESC) guidelines are based on limited evidence and suggest surgery according to [15]:

1. microorganisms (fungi or failure to eradicate bacterial infection);
2. vegetation over 20 mm with recurrent pulmonary emboli;
3. right heart failure due to severe tricuspid regurgitation with poor response to diuretic therapy.

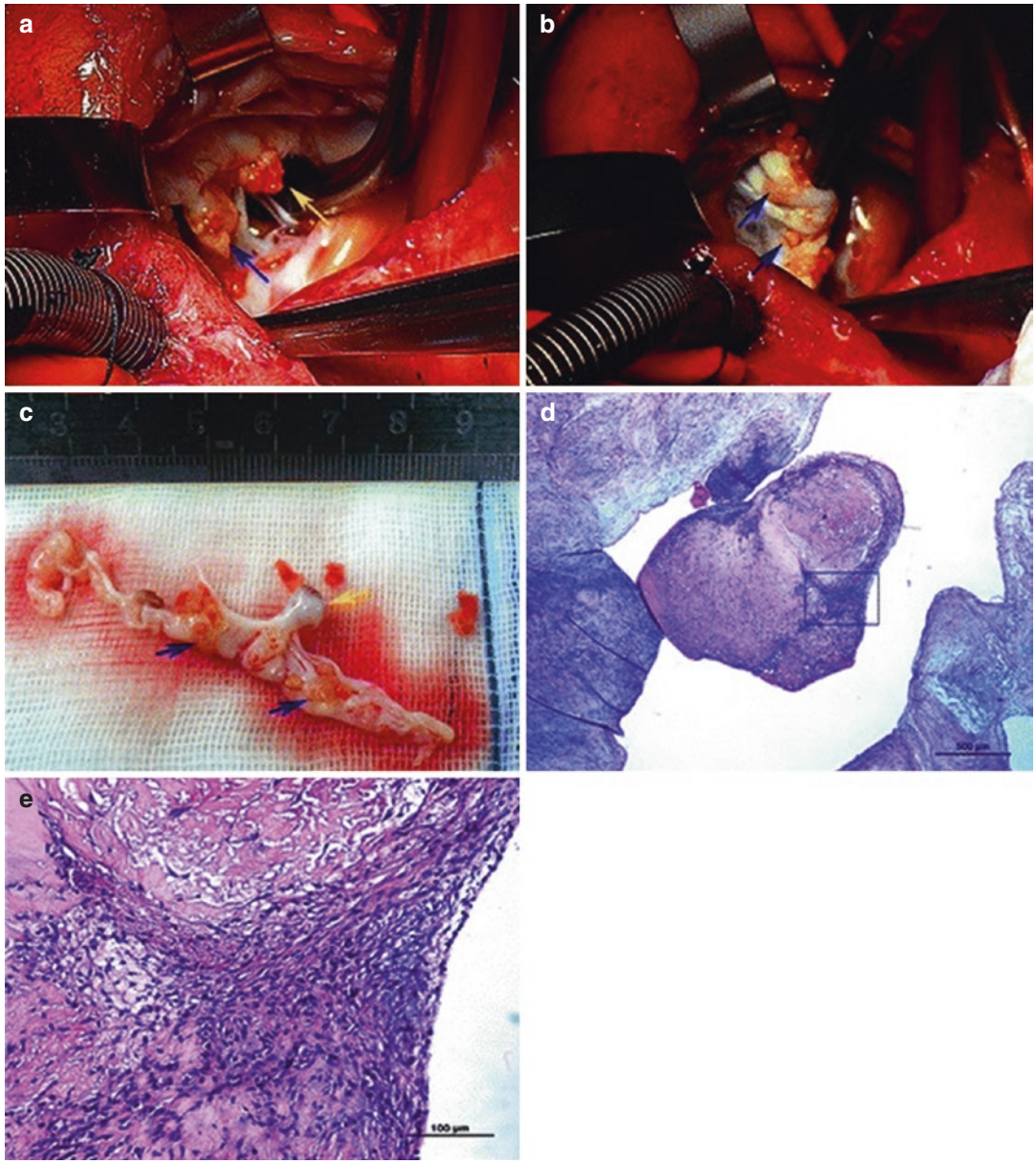

Fig. 44.1 Macroscopy and microscopy of the involved tricuspid valve and vegetation. (**a**) Yellow arrowhead: The large vegetation, Blue arrowhead: rupture mainchordae tendinae. (**b**) Blue arrowheads: Multiple verrucous nodular vegetation on the atrial surface of leaflet. (**c**) Resected tricuspid valve. Blue arrowheads: multiple small vegetations, Yellow arrowhead: rupture main chordae tendinae. (**d**) Microscopy of the vegetation adhered to the leaflet, Magnification 4×, Hematoxylin and Eosin stain. (**e**) Enlarged square area in (**e**) showing inflammatory cell infiltration and fibrin-platelet thrombi, Magnification 20×, Hematoxylin and Eosin stain. From Bai et al. [11]. It is an open access article

Also, they recommend similar medical or surgical strategies and perioperative approaches for intravenous drug abusers or non-intravenous drug abusers groups [15].

In 2014, "The American Heart Association/American College of Cardiology" guidelines do not describe precisely indications for surgical intervention in tricuspid valve infective endocarditis.

Table 44.1 Right versus left-sided infective endocarditis

Characteristics	Left	Right
Infective endocarditis	90%	5–10%
Predisposing factors	Acquired/congenital heart valve defects	IDU intravenous lines and wires (e.g. pacemakers—ICDs)
Microbiology	Streptococci and staphylococci	*S. aureus*
Pathogenesis	• Valvular endothelial damage followed by platelet-fibrin thrombus formation and adherence of bacteria	• Injecting matter endothelial damage with thrombus formation
		• Drug-induced pulmonary hypertension
		• IDU-related endothelial/immunologic abnormalities and microorganism preference
Clinical presentation	Fever, murmurs, anaemia, systemic emboli and/or left heart failure	Fever, cough, haemoptysis dyspnoea due to pulmonary emboli, anaemia; no systemic emboli
Diagnosis	Systemic symptoms and signs—duke criteria, blood culture, echocardiography (TTE and TEE)	Pulmonary symptoms and signs—chest X-ray, blood culture, echocardiography (TTE and TEE)
Prognosis	High rate of haemodynamic, embolic complications and mortality rate	Favourable outcomes, mortality <5%

IDU injecting drug user, *TTE* transthoracic echocardiography, *TEE* transesophageal echocardiography, *ICD* Implantable cardioverter defibrillator. From Akinosoglou et al. [12] with permission

They state: "Patients with infective endocarditis should be evaluated and managed with consultation of a multispecialty Heart Valve Team including an infectious disease specialist, cardiologist, and cardiac surgeon. In surgically managed patients, this team should also include a cardiac anesthesiologist" [16]. Moreover, newly updated guidelines from 2017 of "the American Heart Association/American College of Cardiology" [17] are unchanged.

44.4 Timing of Surgery

Despite the clear effectiveness of early surgery in left-sided infective endocarditis the indications and utility of early surgery are not clear for right heart infective endocarditis [18].

Early surgery is recommended in patients with pulmonary septic emboli or with persistent bacteraemia. In this group, there is a more effective solution of infection with improvement of the right ventricular function and more rapid evolution. It is also important to perform early surgery in patients with cardiac implantable electronic devices, in those infected with *Staphylococcus aureus* or fungi, in those with coexisting left-sided endocarditis and in those with no response to the antibiotic treatment or other complications [19].

There is also the opinion that surgical intervention should be delayed until the infection is in the healing phase (following completion of antibiotic therapy), thereby avoiding the severe inflammatory syndrome with high dose of norepinephrine support. This strategy, converting an active endocarditis in a healed one, can reduce the complication rates and improve outcomes. However, in the medical treatment group, a large proportion had long-term moderate to severe tricuspid regurgitation that may result in the development of right ventricular failure [19, 20].

In these days, there are no randomized controlled trials to address the benefit of early surgery or the indications for operative intervention in tricuspid endocarditis. More randomized multicenter trials may be necessary to solve this problem [18].

44.5 Surgical Techniques: Tricuspid Repair

There are three major principals in the strategy of the surgical intervention for tricuspid valve endocarditis:

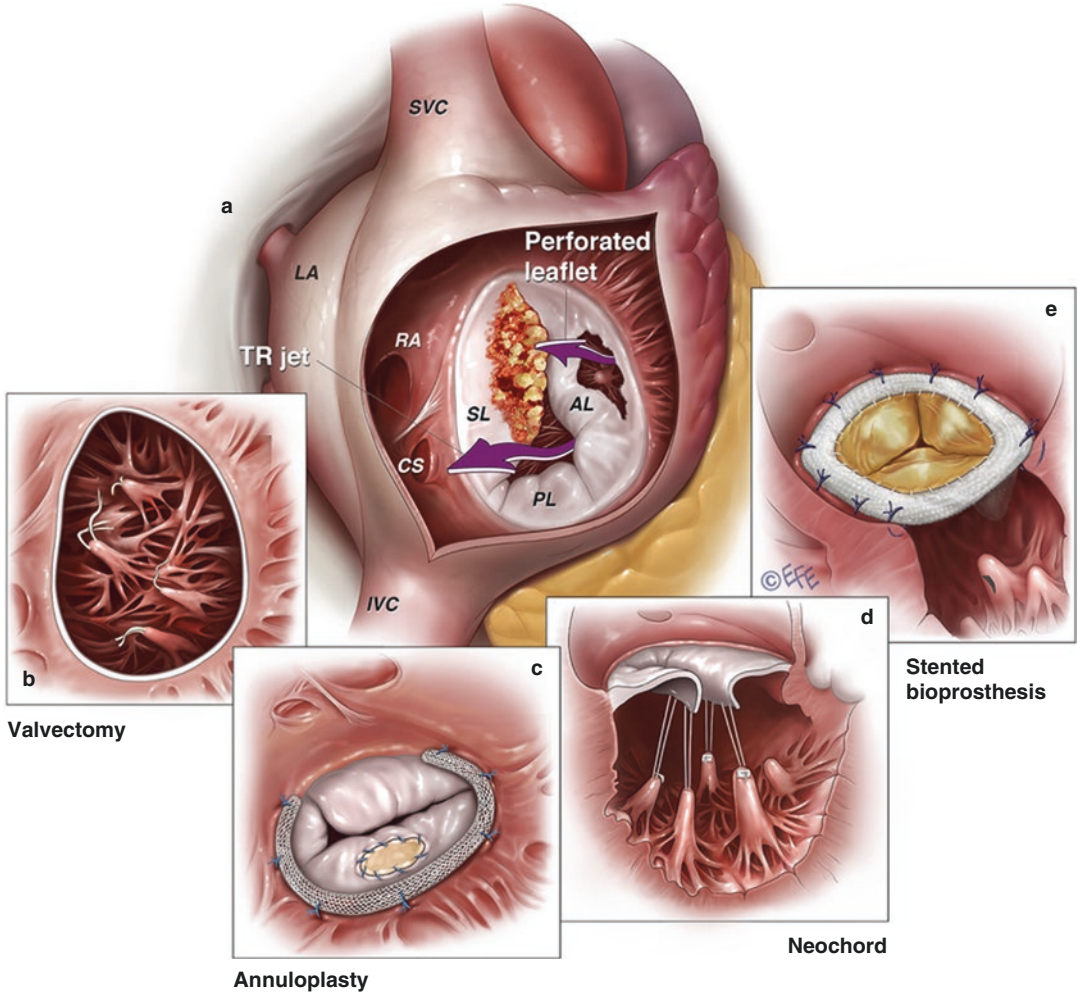

Fig. 44.2 (**a**) Anatomy of tricuspid valve and right atrium— surgeon's view. Findings include large perforation of the anterior leaflet, large vegetations on the septal leaflet, dilated tricuspid valve annulus and resultant severe tricuspid regurgitation. *AL* anterior leaflet, *CS* coronary sinus, *IVC* inferior vena cava, *LA* left atrium, *PL* posterior leaflet, *RA* right atrium, *SL* septal leaflet, *SVC* superior vena cava, *TR* tricuspid regurgitation. (**b**) Appearance of right atrium and ventricle following valvectomy. (**c**) Tricuspid valve repair following band annuloplasty and patch repair of the anterior leaflet. (**d**) Use of neochords to repair tricuspid valve. (**e**) Tricuspid valve replacement using a bioprosthetic valve. From Yong et al. [1] with permission

1. radical excision and debridement of the infected tissue of the valve and surrounding structures.
2. restoration of the valve function.
3. freedom from recurrent endocarditis [1, 21].

Figure 44.2 represents a general view of the surgeon [1].

Technical solutions:

1. Pericardial patch reconstruction (see Fig. 44.3) [12].

If it is possible it is important to avoid the use of any prosthetic materials. Small defects of one or two leaflets can be repaired by either direct closure or use of a pericardial patch. This patch can be made from autologous pericardium, fresh or treated with glutaraldehyde. It can be also made from bovine conserved pericardium [22].

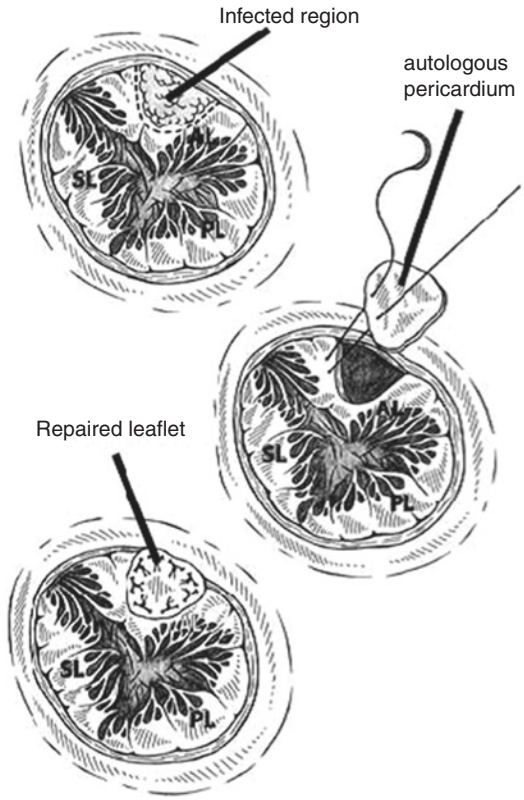

Fig. 44.3 Repair using autologous pericardium. After radical debridement of the infected region of the AL of the valve, a piece of autologous pericardium is sutured in the 'gap'. Modified from Akinosoglou et al. [12] with permission

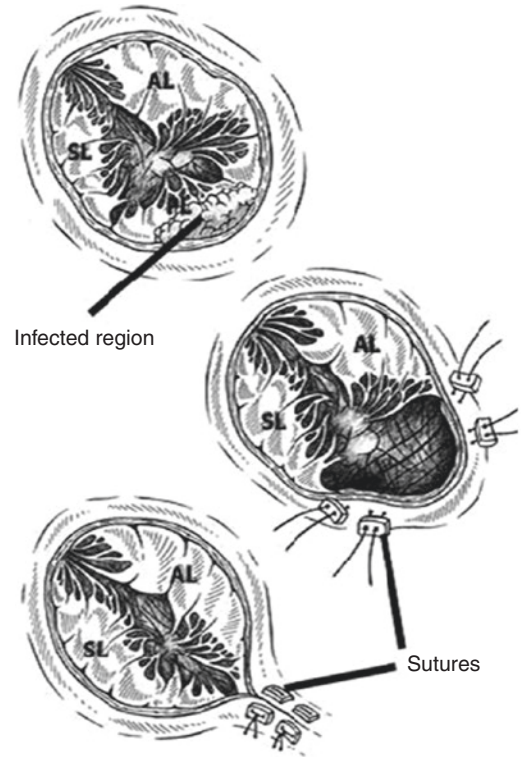

Fig. 44.4 Bicuspidalization of the repaired valve. In the case of profound destruction of one leaflet, and after its aggressive debridement, the remaining tissue is insufficient to restore the competence of the valve. Thus, the corresponding annulus of PL is obliterated by a few sutures, reinforced by pieces of autologous pericardium or pledges. Competence of the valve is re-obtained by cooptation (during systole) of the remaining AL and SL. Modified from Akinosoglou et al. [12] with permission

2. Conversion of the tricuspid into bicuspid valve (see Fig. 44.4) [12].

   This technique has the important advantage of non-using any artificial material, reducing the risk of recurrent endocarditis.

   Very well known as "Kay's plasty", it consists in a near complete excision of the infected leaflet, followed by placement of sutures in the corresponding segment of the annulus to reduce the annulus and orifice area and creation of a bileaflet valve. Insertion of an annuloplasty ring can aid in stabilizing the repair and achieving valve competence [1, 23].
3. Placement of artificial chord.

   It is a useful technique for improvement of leaflet support after resection of the infected tissue with the adjacent chords [1, 21].

Annuloplasty with prosthetic rings is necessary to stabilize the repair and to restore normal annular shape, orifice area and valve function (see Fig. 44.5) [12, 22, 24].

44.6 Surgical Techniques: Tricuspid Replacement

Considering the major disadvantage of recurrent endocarditis, replacement of the tricuspid valve with bioprosthesis is the last option. Valve replacement can be performed with either a mechanical or bioprosthetic valve, and both have

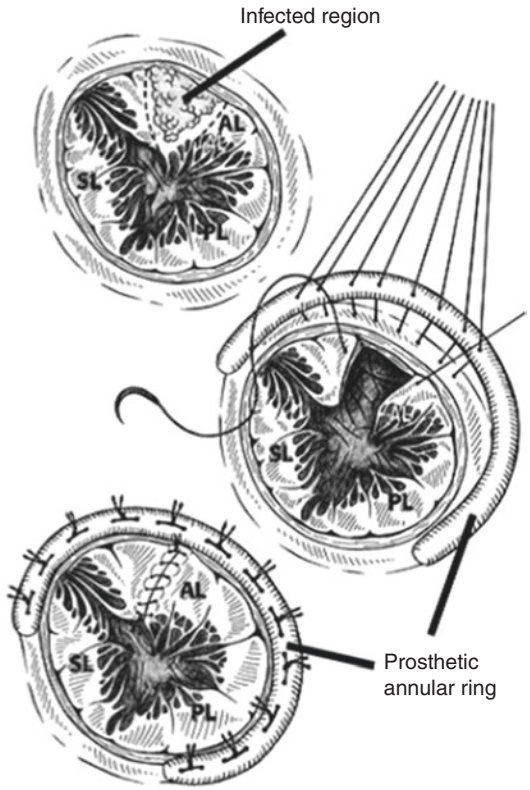

Fig. 44.5 Restoration of valve's competence using prosthetic annular ring. After extensive (>75%) debridement of the AL, the observed significant regurgitation of the valve may be eliminated by implantation of a prosthetic (or even pericardial) annular ring. *PL* posterior leaflet; AL: anterior leaflet; SL: septal leaflet. Modified from Akinosoglou et al. [12] with permission

similar survival outcomes and rates of valve-related complications [1, 21].

Mechanical valves are more durable compared to biological valves, but the main disadvantage is the exposure of patients to the long-term risk of anticoagulation. Very often the patients have atrial fibrillation or another condition, requiring long term anticoagulation, despite the type of prosthesis used to replace the valve. The overall long-term risks of thromboembolic or bleeding complications associated with mechanical and bioprosthetic valves in the tricuspid position are similar. There is also the possibility to use a cryopreserved mitral homograft [25].

44.7 Outcomes of Surgery

In the subset of patients with right-sided infective endocarditis treated surgically, the early, mid-term and long-term results are generally good [26]. Considering all patients undergoing surgery for infective endocarditis in the STS (Society of Thoracic Surgeons) Adult Cardiac Surgery Database, the overall surgical mortality is 8.2% within 30 days [1, 27]. There are several studies in the literature reporting results such as 0–10%, 30 days' mortality and survival rates of 30–58% at 20 years. Interestingly, they observed a high mortality rate 20% in the patients who were treated medically. As we see, the surgical risks of right sided infective endocarditis are similar those of the left-sided infective endocarditis [1, 26, 28].

The most important risk factors for adverse outcome are related to the type of microorganism involved: *Staphylococcus aureus* and fungi are associated with worse prognosis [29].

Also, the vegetation size correlates with early mortality: less than 20 mm—4%, more than 20 mm—24%. Association of large vegetation over 20 mm and fungal infection induce the worst prognosis in tricuspid valve endocarditis.

The association of tricuspid infective endocarditis with left-sided infective endocarditis has been found to be a risk factor for increased early and late mortality after surgery.

Adverse outcome, reduced survival rate of 35% at 10-years and higher re-interventions rates has been observed in drug abusers and in those with human immunodeficiency virus infection [29] (Fig. 44.6).

44.8 Choice of Surgical Approaches

Considering the recommendations of the guidelines (STS, ESC and EACTS)—the first choice is the infected tissue debridement and valve repair. (Class Ia) and the second choice is tricuspid valve replacement with a valvular prosthesis (Class IIa). It looks to be no major differences in outcomes between mechanical and stented bioprosthesis

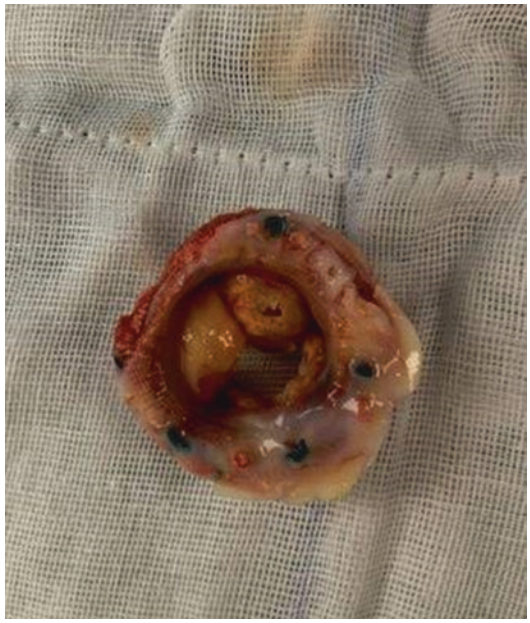

Fig. 44.6 The damaged bioprosthetic tricuspid valve with vegetations. From Chen et al. [30]. It is an open access article

[31, 32]. Despite these recommendations there is no clear evidence that promotes one surgical technique over another in tricuspid valve endocarditis. Comparisons are debatable due to the small frequency of the disease precluding large sample sizes, heterogeneous nature of the patients groups (abusers/no abusers, different surgery groups habits), pathological process, and so on.

During the last two decades, there have been an overall trend towards repair techniques in both tricuspid and mitral valve infective endocarditis [31].

It has been well documented that repair with ring annuloplasty in active tricuspid endocarditis correlates with excellent midterm results—practically none of the patients developed right heart failure. This fact can be explained by the observation that infection most often involves the free margin of the valve, rather than the annular region [29].

In mitral valve infective endocarditis repair techniques generates an important reduction in morbidity (need for reoperation, cerebrovascular events, and recurrent infective endocarditis) and 30 days mortality [32].

In the tricuspid valve endocarditis, there is a same trend except the incidence of reoperation that was observed. Heart block is more frequent in tricuspide valve replacement group. However, any statistically significant data are not available [33]. Tricuspid repair avoids the use of prosthetic material that can be an important risk factor for recurrence, reduces thromboembolic risk and avoids the need for long-term anticoagulation therapy. There are studies who demonstrated no difference in operative mortality or long-term survival in tricuspid repair versus replacement. Because valve repair is not always feasible, they recommend tricuspid valve replacement for patients with a high chance of recurrent regurgitation after repair [34, 35].

44.8.1 Management of Intravenous Drug Users and Patients with Cardiac Electronic Implantable Devices

There are two special situations that require particular management: intravenous drug abusers and patients with cardiac electronic implantable devices.

The management of tricuspid endocarditis in active intravenous drug abusers is difficult due to: non-compliant patients, late presentation in critical condition, left side valve involvement, mixed polymicrobial and fungal infection with resistant microorganisms such as: Candida species, Bartonella spp. or Tropheryma whipplei. The intravenous drug abusers dose not leave the habit and are always at risk of recurrence especially if a biological or mechanical prosthesis is implanted [12, 31]. The ESC guidelines recommend a conservative approach to surgery in these patients due to the high risk of recurrent infection. If valve replacement is needed, the use of tissue valves reduces the risk of thromboembolism and avoids the need for anticoagulant therapy at this subset of patients with very poor compliance to medical care. The younger age of these patients means that re-operation for valve degeneration will be necessary after a number of years.

The last option to valve repair or replacement in those patients with potential risk of re-infection is complete valvectomy. This technique avoids the implantation of prosthetic material and this may be an important advantage. The main limitation is the consequences of severe tricuspid regurgitation. There are studies who reported a 22-year survival of 64% among 53 drug abusers after complete valvectomy, up to 20% of patients who required reoperation to allow implantation of a prosthetic valve due to the development of right heart failure. Tricuspid valvectomy remains an extremely rare operation with only 66 cases out of 910 (7.3%) in the report by Gaca et al. [26]. The ESC guidelines recommend valvectomy in extreme cases followed by valve replacement once the infection has been cured.

In the subset of patients with cardiac implantable devices, the tricuspid valve endocarditis is related with the infection of the device and/or the conduction leads. The first step is the removal of the infected device and its leads. This goal can be achieved by the means of interventional cardiology (80%) or by surgery with extracorporeal circulation (20%). Margey et al. [36] reported complete device extraction in 82% of patients with no disease recurrence and a mortality rate of 7.4%. In patients who were managed with partial device removal or conservative therapy, disease recurrence occurred in 67% of patients with a mortality of 8.4%. The ESC guidelines recommend consideration of surgical device extraction when there is severe destructive tricuspid valve endocarditis (Class IIa recommendation) and in patients with vegetations >25 mm (Class IIb recommendation), while the American Heart Association guidelines recommend individualized decisions in patients with vegetations >20 mm [1, 12, 37, 38].

Conclusions

Right heart endocarditis is a sever condition with an increasing incidence. The involvement of the tricuspid valve generates possible complications: sepsis, intra-cardiac abscesses and fistulae, pulmonary thromboembolism, pulmonary abscess valve regurgitation and right ventricular dysfunction [31].

The incidence of the disease is increasing.

Most of the patients can be treated medically, the optimal indication and timing of surgery are debatable [39].

Repair techniques are preferable though there is no clear evidence supporting one method over another. The tricuspid infective endocarditis to the intravenous drug abusers is particularly difficult to treat considering the poor compliance of those patients.

There is a lack of consensus regarding the optimal treatment strategies for these patients. Many strategies are in use according to the case and the experience of the team. The lack of clear evidence-based guidelines highlights the recommendation that this condition should be treated by an "Endocarditis Team" [26, 33, 40].

References

1. Yong MS, Coffey S, Prendergast BD, Marasco SF, Zimmet AD, McGiffin DC, Saxena P. Surgical management of tricuspid valve endocarditis in the current era: a review. Int J Cardiol. 2016;202:44–8. https://doi.org/10.1016/j.ijcard.2015.08.211.
2. Cotrufo M, Carozza A, Romano G, De Feo M, Della Corte A. Infective endocarditis of native cardiac valves: 22 years' surgical experience. J Heart Valve Dis. 2001;10:478–85.
3. Yamashita S, Noma K, Kuwata G, Miyoshi K, Honaga K. Infective endocarditis at the tricuspid valve following central venous catheterization. J Anesth. 2005;19(1):84–7. https://doi.org/10.1007/s00540-004-0284-y.
4. Popescu GA, Prazuck T, Poisson D, Picu C. A "true" polymicrobial endocarditis: Candida tropicalis and Staphylococcus aureus—to a drug user. Case presentation and literature review. Rom J Intern Med. 2005;43:157–61.
5. Kale SB, Raghavan J. Tricuspid valve endocarditis following central venous cannulation: the increasing problem of catheter related infection. Indian J Anaesth. 2013;57:390–3. https://doi.org/10.4103/0019-5049.118564.
6. Carozza A, De Santo LS, Romano G, Della Corte A, Ursomando F, Scardone M, Caianiello G, Cotrufo M. Infective endocarditis in intravenous drug abusers: patterns of presentation and long-term outcomes of surgical treatment. J Heart Valve Dis. 2006;15:125–31.
7. Dupont P, Maragnes P, de la Gastine G, Jokic M, Morin M. Tricuspid valve endocarditis after umbilical piercing. Arch Mal Coeur Vaiss. 2006;99:629–31.

8. Rataj O, Martinkovičová L, Šetina M. Tricuspid valve infective endocarditis in intravenous drug abuser. Vnitr Lek. 2013;59:939–42.
9. Pachirat O, Chetchotisakd P, Klungboonkrong V, Taweesangsuksakul P, Tantisirin C, Loapiboon M. Infective endocarditis: prevalence, characteristics and mortality in Khon Kaen, 1990–1999. J Med Assoc Thail. 2002;85:1–10.
10. Unic D, Planinc M, Baric D, Rudez I, Blazekovic R, Senjug P, Sutlic Z. Isolated tricuspid valve libman-sacks endocarditis in systemic lupus erythematosus with secondary antiphospholipid syndrome. Tex Heart Inst J. 2017;44:147–9. https://doi.org/10.14503/THIJ-16-5856.
11. Bai Z, Hou J, Ren W, Guo Y. Diagnosis and surgical treatment for isolated tricuspid Libman-Sacks endocarditis: a rare case report and literatures review. J Cardiothorac Surg. 2015;10:93. https://doi.org/10.1186/s13019-015-0302-1.
12. Akinosoglou K, Apostolakis E, Koutsogiannis N, Leivaditis V, Gogos CA. Right-sided infective endocarditis: surgical management. Eur J Cardiothorac Surg. 2012;42:470–9. https://doi.org/10.1093/ejcts/ezs084.
13. Jassal DS, Hassan A, Buth KJ, Neilan TG, Koilpillai C, Hirsch GM. Surgical management of infective endocarditis. J Heart Valve Dis. 2006 Jan;15(1):115–21.
14. Kolek M, Brát R. Surgical treatment of infective endocarditis: 8 year experience. Cas Lek Cesk. 2006;145:718–24. discussion 724–5.
15. Habib G, Hoen B, Tornos P, Thuny F, Prendergast B, Vilacosta I, Moreillon P, de Jesus Antunes M, Thilen U, Lekakis J, Lengyel M, Müller L, Naber CK, Nihoyannopoulos P, Moritz A, Zamorano JL, ESC Committee for Practice Guidelines. Guidelines on the prevention, diagnosis, and treatment of infective endocarditis (new version 2009): the Task Force on the Prevention, Diagnosis, and Treatment of Infective Endocarditis of the European Society of Cardiology (ESC). Endorsed by the European Society of Clinical Microbiology and Infectious Diseases (ESCMID) and the International Society of Chemotherapy (ISC) for Infection and Cancer. Eur Heart J. 2009;30:2369–413. https://doi.org/10.1093/eurheartj/ehp285.
16. Nishimura RA, Otto CM, Bonow RO, Carabello BA, Erwin JP 3rd, Guyton RA, O'Gara PT, Ruiz CE, Skubas NJ, Sorajja P, Sundt TM 3rd, Thomas JD, ACC/AHA Task Force Members. 2014 AHA/ACC guideline for the management of patients with valvular heart disease: executive summary: a report of the American College of Cardiology/American Heart Association Task Force on Practice Guidelines. Circulation. 2014;129:2440–92. https://doi.org/10.1161/CIR.0000000000000029.
17. Nishimura RA, Otto CM, Bonow RO, Carabello BA, Erwin JP 3rd, Fleisher LA, Jneid H, Mack MJ, McLeod CJ, O'Gara PT, Rigolin VH, Sundt TM 3rd, Thompson A. 2017 AHA/ACC focused update of the 2014 AHA/ACC guideline for the management of patients with valvular heart disease: a report of the American College of Cardiology/American Heart Association Task Force on Clinical Practice Guidelines. Circulation. 2017;135:e1159–95. https://doi.org/10.1161/CIR.0000000000000503.
18. Denk K, Vahl CF. Infective endocarditis: considerations regarding optimal timing for surgical treatment. Herz. 2009;34:198–205. https://doi.org/10.1007/s00059-009-3232-7.
19. Poliakov VP, Shorokhov SE, Belyĭ VS, Goriachev VV, Kaganov II, Lias MN, Skuratova MA, Korytchenko VI, Suslina EA, Khokhlunov SM, Semagin AP. Surgical treatment of infective endocarditis of the right sections of the heart. Vestn Khir Im I I Grek. 2002;161:11–4.
20. Arbulu A, Holmes RJ, Asfaw I. Surgical treatment of intractable right-sided infective endocarditis in drug addicts: 25 years experience. J Heart Valve Dis. 1993;2:129–37. discussion 138–9.
21. Capoun R, Thomas M, Caputo M, Asimakopoulos G. Surgical treatment of tricuspid valve endocarditis: a single-centre experience. Perfusion. 2010;25:169–73. https://doi.org/10.1177/0267659110371857.
22. García-Rinaldi R. Tricuspid anterior leaflet replacement with autologous pericardium and polytetrafluoroethylene chordae, followed by edge-to-edge repair. Tex Heart Inst J. 2007;34:310–2.
23. Pomar JL, Mestres CA, Pare JC, Miro JM. Management of persistent tricuspid endocarditis with transplantation of cryopreserved mitral homografts. J Thorac Cardiovasc Surg. 1994;107:1460–3.
24. Tarola CL, Losenno KL, Chu MW. Complex tricuspid valve repair for infective endocarditis: leaflet augmentation, chordae and annular reconstruction. Multimed Man Cardiothorac Surg. 2015. https://doi.org/10.1093/mmcts/mmv006.
25. Sugimoto T, Okada M, Yamashita C, Ataka K, Yoshida M, Toyoda Y, Ozaki N. Surgical assessment of tricuspid valve replacement for severe tricuspid regurgitation without stenosis. Ann Thorac Cardiovasc Surg. 1999;5:300–3.
26. Gaca JG, Sheng S, Daneshmand M, Rankin JS, Williams ML, O'Brien SM, Gammie JS. Current outcomes for tricuspid valve infective endocarditis surgery in North America. Ann Thorac Surg. 2013;96:1374–81. https://doi.org/10.1016/j.athoracsur.2013.05.046.
27. Gottardi R, Bialy J, Devyatko E, Tschernich H, Czerny M, Wolner E, Seitelberger R. Midterm follow-up of tricuspid valve reconstruction due to active infective endocarditis. Ann Thorac Surg. 2007;84:1943–8. https://doi.org/10.1016/j.athoracsur.2007.04.116.
28. André C, Da Silva MM, Da Silva EJ, Souza MA, Bastos ES, Novis SA. Postoperative mortality in infective endocarditis: determinant factors. Arq Neuropsiquiatr. 1997;55:231–6.
29. Zhang L, Gao CQ, Jiang SL, Ren CL. Surgical treatment of isolated right-sided infective endocarditis. Zhonghua Wai Ke Za Zhi. 2010;48:342–4.

30. Chen Q, Cao H, Lu H, Qiu ZH, He JJ. Bioprosthetic tricuspid valve endocarditis caused by Acinetobacter baumannii complex, a case report and brief review of the literature. J Cardiothorac Surg. 2015;10:149. https://doi.org/10.1186/s13019-015-0377-8.
31. Fayad G, Modine T, Lions C, Polge AS, Azzaoui R, Larrue B, Decoene C, Leroy O, Senneville E, Beregi JP, Warembourg H. Conservative surgical treatment for active infective tricuspid valve endocarditis according to the "clover technique". Heart Surg Forum. 2008;11:E120–6. https://doi.org/10.1532/HSF98.20071188.
32. Gutierrez-Martin MA, Galvez-Aceval J, Araji OA. Indications for surgery and operative techniques in infective endocarditis in the present day. Infect Disord Drug Targets. 2010;10:32–46.
33. Jiang SL, Li BJ, Zhang T, Ren CL, Wang Y, Chen TT, Gao CQ. Surgical treatment of isolated right-sided infective endocarditis. Tex Heart Inst J. 2011;38:639–42.
34. Musci M, Siniawski H, Pasic M, Grauhan O, Weng Y, Meyer R, Yankah CA, Hetzer R. Surgical treatment of right-sided active infective endocarditis with or without involvement of the left heart: 20-year single center experience. Eur J Cardiothorac Surg. 2007;32:118–25. https://doi.org/10.1016/j.ejcts.2007.02.034.
35. Myerson M, Armstrong EJ, Poltavskiy E, Fefer J, Bang H. Tricuspid valve replacement in an HIV-infected patient with severe tricuspid regurgitation secondary to remote endocarditis. Tex Heart Inst J. 2016;43:514–6. https://doi.org/10.14503/THIJ-15-5354.
36. Margey R, McCann H, Blake G, Keelan E, Galvin J, Lynch M, Mahon N, Sugrue D, O'Neill J. Contemporary management of and outcomes from cardiac device related infections. Europace. 2010;12:64–70. https://doi.org/10.1093/europace/eup362.
37. Shetty N, Nagpal D, Koivu S, Mrkobrada M. Surgical and medical management of isolated tricuspid valve infective endocarditis in intravenous drug users. J Card Surg. 2016;31:83–8. https://doi.org/10.1111/jocs.12682.
38. Baddour LM, Epstein AE, Erickson CC, Knight BP, Levison ME, Lockhart PB, Masoudi FA, Okum EJ, Wilson WR, Beerman LB, Bolger AF, Estes NA 3rd, Gewitz M, Newburger JW, Schron EB, Taubert KA, American Heart Association Rheumatic Fever, Endocarditis, and Kawasaki Disease Committee; Council on Cardiovascular Disease in Young; Council on Cardiovascular Surgery and Anesthesia; Council on Cardiovascular Nursing; Council on Clinical Cardiology; Interdisciplinary Council on Quality of Care; American Heart Association. Update on cardiovascular implantable electronic device infections and their management: a scientific statement from the American Heart Association. Circulation. 2010;121:458–77. https://doi.org/10.1161/CIRCULATIONAHA.109.
39. Pang PY, Sin YK, Lim CH, Tan TE, Lim SL, Chao VT, Chua YL. Surgical management of infective endocarditis: an analysis of early and late outcomes. Eur J Cardiothorac Surg. 2015;47:826–32. https://doi.org/10.1093/ejcts/ezu281.
40. Chambers J, Sandoe J, Ray S, Prendergast B, Taggart D, Westaby S, Arden C, Grothier L, Wilson J, Campbell B, Gohlke-Bärwolf C, Mestres CA, Rosenhek R, Pibarot P, Otto C. The infective endocarditis team: recommendations from an international working group. Heart. 2014;100(7):524. https://doi.org/10.1136/heartjnl-2013-304354.

Heart, Lung, and Heart–Lung Transplant

45

Kaan Kırali

Abstract

Organ transplantation has evolved to become as gold standard therapy for patients with end-stage heart and/or pulmonary diseases. When medical or temporary circulatory supportive treatment modalities cannot ensure a patient's survival and improve quality of life, the only approach may be isolated heart or lung transplantation, or combined transplantation. The main indication for heart transplantation is reversible pulmonary dysfunction with irreversible right heart failure; similarly, isolated irreversible pulmonary dysfunction resulting temporary right heart dysfunction requires isolated lung transplantation. However, irreversible right heart failure combined with irreversible pulmonary dysfunction requires heart–lung transplantation. The last two decades have seen the resolution of many technical problems and the refinement of surgical techniques for heart and lung transplantation, but problems remain for heart–lung transplantation because of complications such as major bleeding, nerve injuries, and graft failure. Patients with dominant right ventricular failure referred to heart transplantation usually suffer from the left-sided heart failure, primary pulmonary hypertension, and congenital heart diseases; however, the frequency of isolated right heart failure with structural abnormalities has also been increasing recently. Despite regular revisions of the transplantation guidelines that have resulted in annual increases in recipient pool, the number of donors has not increased sufficiently. Advances in the fields of immunosuppression, infection prophylaxis, and surgical techniques have improved surgical outcomes and long-term survival rates. Future improvements in organ donation could increase the donor numbers and improve donor–recipient immunologic matching and the allocation of organs. Biomechanical and biotechnological advancement in long-term ventricular assist devices may prolong survival and improve the quality of life; however, although mechanical circulatory support technology is improving, transplantation remains the sole effective treatment for irreversible right heart pathologies.

Keywords

Right heart failure · Transplantation · Pulmonary hypertension · Cardiomyopathy · Bicaval · Biatrial · Heart transplantation · Mechanical circulatory support · Congenital heart defect · Immunosuppression · Donor · Recipient

K. Kırali
Department of Heart Transplantation and Mechanical Assist Devices, Koşuyolu Heart and Research Hospital, Istanbul, Turkey

S. I. Dumitrescu et al. (eds.), *Right Heart Pathology*, https://doi.org/10.1007/978-3-319-73764-5_45

45.1 History

The history of intrathoracic organ transplantation has involved overcoming a range of technical and immunologic hurdles. Allograft heart and lung transplantations were achieved only after the success of other organ transplantations. This was because of several specific problems that had to be resolved for intrathoracic organs: (1) the difficulty of realizing intrathoracic organ replacement; (2) ineligible surgical techniques and skills; (3) frequent rejection episodes; (4) patient survival of no more than weeks; (5) the lack of long-term alternative treatment modalities; and (6) the lack of life support therapies for the management of allograft rejection (like the use of hemodialysis for renal failure).

The first step toward intrathoracic organ transplantation was to demonstrate its feasibility. Working with dogs, Vladimir Demikhov implanted the first intrathoracic heterotopic heart and performed the first orthotopic heart-lung transplantation (HLTx) in 1946; he also demonstrated the feasibility of isolated orthotopic lung transplantation (LTx) in 1947, and performed the first orthotopic heart transplantation (HTx) in 1951 [1]. He concluded that the heart could only function actively when it was transplanted into the thorax; otherwise, it would not take an active part in the movement of blood and, if it was transplanted to the vessels of the neck or into the inguinal region, it would be living on the recipient's blood [2]. The first human-to-human LTx was performed by Hardy et al. [3] in 1963, but the patient died 18 days later. The first human-to-human orthotopic HTx was performed by Christian Barnard [4] in 1967, but the patient survived only for a few hours. The following year, Bernard performed the first long-term survived orthotopic HTx in which the patient survived for 18 months. The first human-to-human HLTx was performed by Cooley in 1968, but the patient, a child, survived for only 14 h [5]. The clinical use of intrathoracic organ transplantation then largely disappeared from clinical practice because of the high early mortality rate and unsuccessful mid- or long-term surveillance. Because recipients of orthotopic HTx did not survive postoperatively due to acute or hyperacute rejection, the preferred approach in the 1970s was heterotopic HTx to hemodynamically support the failed heart [6].

The second step in developing modern intrathoracic organ transplantation was to introduce transvenous endomyocardial biopsy; this opened up new possibilities for HTx because it allowed serial monitoring for cardiac allograft rejection [7]. The third step was the introduction in 1981of a new generation immunosuppressive agent, cyclosporine A, which encouraged the transition of intrathoracic organ transplantation from the experimental phase to the clinical treatment of patients with advanced cardiopulmonary failure [8]. The first successful HLTx was performed by Reitz et al. [9] in 1981, and the first successful isolated unilateral LTx by the Toronto Lung Transplant Group in 1983, who went on to perform the first successful bilateral LTx in 1986 [10]. An advantage of both unilateral and bilateral LTx is that they avoid the necessity for combined cardiac transplantation and allow the donor heart to be used for another recipient. The Domino Procedure is a sequential HLTx–HTx procedure that uses the explanted heart from an en-bloc heart–lung recipient as a donor organ for a second heart recipient; this was first performed by Yacoub et al. [11] in 1988. Even now, the Domino Procedure is extremely rare, primarily because en-bloc heart–lung transplantation is rare; but its selective use can improve and maximize organ allocation [12]. Heterotopic HTx is a surgical procedure in which allows the graft is connected in parallel to the native heart, providing a form of biological biventricular support. Its main use is in rare, selected cases, such as for patients with fixed pulmonary hypertension (PHT) to avoid heart–lung transplantation or for patients where there is a substantial mismatch in donor-recipient body-size [13].

45.2 Transplant Activity and Survival

The total number of HTx, LTx, and HLTx procedures has increased rapidly worldwide. The 2016 reports of the Registry of the International

Society for Heart and Lung Transplantation provide the latest data about intrathoracic transplant events, recipient and donor demographics, and survivals rates, representing an estimated two thirds of the thoracic transplant events worldwide. These reports provide a major impression of general thoracic transplantation activity performed up until July 2015. Over the decades, the number of HTx and LTx procedures increased while the number of HLTx declined. The data show that survival for all three transplantation procedures has improved over time because of improved survival in the early post-transplant period (Table 45.1). There were several serious morbidities that commonly developed after intrathoracic transplantations, but the main risks to long-term survival were coronary vasculopathy in the HTx group, obliterative bronchiolitis in the LTx and HLTx groups, and infections in all three groups.

Adult-HTx was performed for 113,472 patients at 457 heart transplant centers worldwide between 1982 and July 2015 [14]. The average annual activity was 10–20 HTx procedures in 163 (35.7%) centers and 20–29 in 115 (25.2%) centers, with 11 (<2.5%) centers performing <5 HTx annually. The median survival was 10.6 years for primary HTx and 6.2 years for re-transplantation; however, for recipients who survived the first year, the conditional median survival increased to 13.1 years for primary HTx and 11.2 years for re-transplantation. Risk factors for reduced survival were advanced age, elevated pulmonary vascular resistance (PVR) and PHT, and diabetes mellitus. In recent years, pre-transplant mechanical circulatory support has not adversely affected post-transplant survival, especially the use of left ventricular assist device (LVAD). A notable exception, however, has been extracorporeal membrane oxygenation (ECMO), which has resulted in distinctly worse post-transplant survival, with survival rates of 65% at 3 months and 50% at 3 years. LVAD was used as a bridge to HTx in >50% of adult and >30% of pediatric recipients, whereas bridging with ECMO has remained at <2.5% and <3% for adult and pediatric recipients, respectively. The cause of death varied with time after transplantation: graft failure, non-cytomegalovirus infection, and multiple organ failure were the most important causes in the first year postoperatively; malignancy, cardiac allograft vasculopathy, and renal failure were the main determinants of later deaths.

Pediatric-HTx was performed for 5,316 patients at 112 pediatric heart transplant centers in the same period [15]. More than 80% of centers performed <5 pediatric HTx procedures per year, on average, but the number of centers performing >5 has increased in the last decade, with

Table 45.1 Median long-term survival rates of intrathoracic organ transplantation

	Survival							
Transplant-type	3-month	1-year	3-year	5-year	10-year	15-year	20-year	25-year
Heart transplantation								
Adult HTx	88%	83%	75%	70%	52%	34%	20%	
Re-adult HTx	77%	69%	60%	54%	37%	25%	14%	
Pediatric HTx	89%	85%	78%	73%	61%	51%	43%	38%
Lung transplantation								
Adult LTx	89%	80%	65%	54%	32%			
Re-adult LTx	79%	66%	49%	39%	21%			
Pediatric LTx	92%	79%	62%	51%	37%	28%		
Single	68%	57%	40%	31%				
Bilateral	92%	82%	63%	53%				
Heart-lung transplantation								
Adult HLTx	71%	63%	52%	45%	32%			
Pediatric HLTx		<70%	<50%	<40%	<30%			

HLTx heart-lung transplantation, *HTx* heart transplantation, *LTx* lung transplantation

these centers now accounting for more than 75% of all pediatric-HTx procedures. The median survival after the procedure and the conditional median survival after the first year both depended on recipient age: 20.7 years for recipients aged <1 year, 18.2 and 21.5 years for those aged 1–5 years, 14 and 16.5 years for those aged 6–10 years, and 12.7 and 15.7 years for those aged 11–17 years.

Adult-LTx was performed for 55,795 patients at 253 lung transplant centers worldwide between 1985 and July 2015. Of these, 53,522 (95.9%) were primary procedures, 2187 (3.9%) secondary, and 86 (0.2%) tertiary [16]. Only 76 (30%) of the centers performed ≥30 procedures per year on average. The trend seen over the past three decades has been a considerable increase in the number of transplants, especially bilateral procedures. The median survival was 5.8 years following primary LTx and 2.8 years for re-transplantation; for recipients surviving after the first year, the conditional median survival increased to 8 years for primary and 6.5 years for re-transplants. The main causes of mortality in the first 30 days were graft failure and non-cytomegalovirus infections, multiple organ failure, and cardiovascular causes. After the first year, obliterative bronchiolitis, infections, and malignancy resulted in the most deaths. The rate of developing chronic rejection (bronchiolitis obliterans syndrome) was lower for primary LTx than for re-transplantation: 41% versus 63% at 5 years, and 76% versus 81% at 10 years. In 2014, the number of adult lung transplants reported was about 37 times greater than the number of pediatric lung transplants.

Pediatric-LTx, with approximately 10% receiving re-transplantation, was performed for 2,225 patients between 1986 and 2015; >70% of the patients were aged 11–17 years and 5% were aged <1 year [17]. Pediatric-LTx activity has increased over the last three decades. Nevertheless, >85% of the centers performed <5 pediatric LTx each year, on average, and together these accounted for nearly 60% of the total pediatric transplant activity. The median survival was 5.4 years, and freedom from chronic rejection was 88% at 1 year, 45% at 5 years, and 25% at 10 years.

Adult-HLTx was performed for 3,879 patients at 177 heart-lung transplant centers worldwide between 1982 and July 2015; only 57 (1.5%) of these were re-transplants [15]. The annual volume was very low, ranging between 50 and 100 procedures per year, with >50% of the centers performing only 1 or 2 HLTx procedures. The median survival was 5.8 years for primary HLTx, but conditional median survival exceeded 10 years for the recipients who survived the first year. The main causes of mortality during the first 30 days postoperatively were graft failure and technical complications. Lung-related causes were more dominant in early and late mortality. Long-term follow-up revealed chronic rejections because of the lungs (obliterative bronchiolitis) in 42 and 62% of patients at 5 and 10 years, respectively, and because of the heart (coronary artery vasculopathy) in 9 and 27% at 5 years and 10 years, respectively.

Pediatric HLTx was performed for 710 pediatric patients between 1985 and July 2015, of whom >60% were aged 11–17 years and <3% were aged <1 year [16]. Almost all pediatric HLTx centers performed <5 cases per year. The median survival was 1.5 years for recipients aged ≤5 years, and 3.4 years for those aged >5 years.

45.3 Recipient Evaluation

45.3.1 Clinical Diagnosis

Recently, there has been increased interest in isolated right heart failure (RHF) because of the associated deterioration in the patient's quality of life, the increased frequency of hospitalization, and the impairment of functional capacity. Isolated RHF is more resistant to cardiac decompensation or functional deterioration than is isolated left heart failure (LHF), because the normally functioning left ventricle can support and take over right ventricular functions over an extended period. For this reason, transplant therapy is always postponed for patients with isolated RHF. Right ventricular pathologies usually remain silent for several years, but they can appear with symptomatic low cardiac output

syndrome (LCOS) caused by a decrease in right heart ejection without PHT. Because these patients do not show LHF symptoms and signs (such dyspnea on exertion and/or at night, restricted capacity for effort, or pulmonary edema), most clinicians become aware of the severity of RHF. However, the thin-walled right ventricle (RV) pumps the entire systemic venous return through the pulmonary circulation for gas exchange; this implies the right side cardiac output should be equal to that of the left. Indeed, there have been several mistaken prejudices related to isolated symptomatic RHF: (1) that the left heart is often the focus of interest in cardiology; (2) that imaging of the left side is easier than that of the right; (3) that it is primarily the left heart that is influenced by leading causes of mortality and morbidity such as infarction, valvular pathologies, and myocardial failure; (4) that healthy left heart is adequate to salvage a significant part of right heart functions; and (5) that the right heart is a passive chamber.

Right heart failure represents a pathologic disturbance of any component of the right heart circulatory system. This consists of the venous system up to the level of the pulmonary capillaries and so has both systemic components (such as the systemic veins up to the level of the pulmonic valve) and pulmonary components (the precapillary pulmonary circulation). Myocardial involvement of the RV presents with myocardial stiffness or ventricular dilatation, and right ventricular failure (RVF) can develop primary to structural pathologies or secondary to PHT depending on the primary or secondary etiologies (pre-alveolar or post-alveolar diseases, respectively) [18]. Increased stiffness (i.e., non-dilated RVF) impairs diastolic filling, but the systolic function is often preserved or mildly depressed, and right atrial enlargement may be the only sign of RHF. In early PHT, the thin-walled crescent-shaped RV adapts to the increased pressure overload through hypertrophy, thereby maintaining cardiac output. At later stages, however, the increased afterload overwhelms the RV and cause dilatation. Ventricular dilatation (i.e., dilated RVF) usually impairs systolic and diastolic functions and presents with mild to severe RHF symptoms. The left ventricle may or may not be affected and the right heart pathology can be accompanied by a normal left ventricular ejection fraction (LVEF).

Symptomatic RHF can cause serious systemic venous congestion, which impairs the function of other organs and can result in the severe dysfunction of vital organs such as the liver and kidneys. Renal dysfunction is characterized by elevated serum creatinine level and decreased creatinine clearance, according to whether the renal involvement is intrinsic or extrinsic. The main reason for functional renal insufficiency in patients with severe RHF is the progression of LCOS, but increasing central venous pressure (CVP) with or without severe ascites can also be a primary determinant factor; this reduces effective renal circulation or renal function by compressing the renal veins [19]. Important markers of progressive RHF include high or increasing diuretic requirements, the elevation of renal insufficiency parameters (i.e., creatinine serum level >2.0 mg/dL or rising >0.3 mg/dL, and effective glomerular filtration rate <60 mL/min or decreasing >25 mL/min), persistent hyponatremia, and fluid retention. The main etiology for hepatic failure is elevated right atrial pressure not secondary to LHF, which increases pulmonary pressure at the same time [20]. The hepatocellular necrosis and dysfunction that accompany the deterioration of RHF are caused by sinusoidal congestion and the inadequate hepatic circulation. Long-standing venous stasis results in cardiac hepatopathy, particularly advanced hepatic fibrosis and cirrhosis. Cardiac hepatopathy is defined by elevation of the serum markers aspartate aminotransferase (>100 U/L), alkaline phosphatase (>200 U/L), and serum total bilirubin (>2.0 mg/dL). If patients with RHF develop a decreasing hepatic reserve and persistent hepatic dysfunction, despite relief from congestion, they should be considered for liver biopsy. Usually, decreasing CVP can resolve this pathologic vicious circle; otherwise, repetitive paracentesis can help to address the increasing intraperitoneal pressure and to improve renal and hepatic functions.

Evaluating the volume, structure, function, mechanics, and deformation of the RV in patients with RVF presents a considerable challenge due

to the anatomical complexity [21]. In everyday clinical practice, the preferred method for RV evaluation has been 2-dimensional echocardiography, although 3-dimensional echocardiography has started a completely new era in right ventricular imaging. Nevertheless, cardiac magnetic resonance remains the gold standard for assessing the RV. Diagnosis of RHF can be done by several methods, but transthoracic echocardiography with or without transesophageal echocardiography should be the first approach because it allows the measurement of several parameters related to ventricular, atrial, and major vascular structures. Cardiac magnetic resonance is the best method for measuring the volume, mass, and ejection fraction of the two ventricles; it is also the best modality when echocardiographic studies have not resulted in a diagnosis (particularly for imaging the right heart), or for patients with complex congenital heart diseases. Cardiopulmonary exercise testing provides more detailed information about cardiac and pulmonary conditions, and it is a good diagnostic test for differentiating between isolated and combined failure. Other cardiac diagnostic tests include coronary angiography or cardiac computed tomography to visualize the coronary anatomy, positron or single-photon emission computed tomography or gadolinium cardiac magnetic resonance, to assess myocardial viability, endomyocardial biopsies and genetic tests to confirm specific pathologies, right heart catheterization to establish hemodynamics, and the analysis of biochemical samples such as natriuretic peptides to establish the severity of RHF.

45.3.2 Indications

The evaluation of patients with advanced heart failure and the selection of potential candidates for intrathoracic organ transplantation should be undertaken by a multidisciplinary team, and no patient should be exposed to the risk of transplant surgery until all other viable treatment options have been exhausted (Table 45.2) [22]. The transplant committee at each transplantation center should develop its own scientific strategy for recipient selection based on local experience, following the principles set out in international guidelines. Patients with symptomatic RHF referred for possible heart and/or lung should be assessed to

Table 45.2 Indications of intrathoracic transplantation for RHF

• Isolated HTx
– Morphological (primary) RHF
Hypertrophic cardiomyopathy
Restrictive cardiomyopathy (sarcoidosis, endomyocardial fibrosis, familial hemochromatosis, or thalassemia major)
Infiltrative cardiomyopathies (amyloidosis or glycogen storage diseases)
Arrhythmogenic right ventricle dysplasia
–Functional (secondary) RHF
Left heart failure (ischemic and/or dilated cardiomyopathies)
Pulmonary failure (pulmonary vascular or intrinsic pathologies)
– After LVAD implantation
– Structural (congenital) RHF
Postoperative persistence of systemic ventricular failure (D-TGA with atrial switch; TOF with postoperative severe PR)
Failure of previously palliative or reparative surgery (Fontan circulation)
Single ventricle physiology
Uncorrectable congenital heart diseases (e.g., c-TGA, uncorrectable AVSD, coronary anomalies, neonatal Ebstein's anomaly, and severe multi-valvular pathologies)
Ongoing pulmonary hypertension (Eisenmenger syndrome)
Refractory life-threatening arrhythmias
• Isolated LTx
– Chronic obstructive pulmonary disease with or without α1-antitrypsin deficiency
– Interstitial lung diseases (idiopathic pulmonary fibrosis or scleroderma)
– Bronchiectasis with or without cystic fibrosis
– Idiopathic PAH
– Re-transplantation
• HLTx
– Congenital heart disease
– Idiopathic pulmonary arterial hypertension
– Cardiomyopathies with irreversible high PVR
– Cystic fibrosis

AVSD atrioventricular septal defect, *HLTx* heart-lung transplantation, *HTx* heart transplantation, *LTx* lung transplantation, *LVAD* left ventricular assist device, *PAH* pulmonary arterial hypertension, *PR* pulmonary regurgitation, *PVR* pulmonary vascular resistance, *RHF* right heart failure, *TGA* transposition of great arteries, *TOF* tetralogy of Fallot

Table 45.3 Potential transplant candidates for RHF

Irreversible cardiac and/or lung pathology
Intractable RHF symptoms with or without LHF syndrome
No more than borderline non-thoracic organ dysfunction secondary to the RHF
Non-recovery of functional capacity of the RV after appropriate medical therapy or LVAD implantation
Presence of prevalent transplant indications
Appropriate morphologic structures No irreparable thoracic malformations
No contraindication to intrathoracic organ transplantation

LHF left heart failure, *LVAD* left ventricular assist device, *RHF* right heart failure, *RV* right ventricle

Table 45.4 Contraindications to intrathoracic organ transplantation

• Blood group incompatibility in prospective cross-matching between donor and recipient
• Older age (>65 years)
• Anatomic inconveniences
• Morbid obesity (BMI > 35 kg/m^2 or body weight > 140% of the predicted ideal value)
• Uncontrolled diabetes mellitus (HbA_{1c} > 7.5%) with or without end-organ damage
• Active or incurable malignancy (within the previous 5 years)
• Hepatic insufficiency (bilirubin >2.5 mg/dL; transaminases > twice normal; cirrhosis on biopsy)
• Renal insufficiency (creatinine >2.5 mg/dL; eGFR <30 mL/min; ERPF <200 mL/min)
• Septicemia
• Severe peripheral and/or cerebrovascular disease
• Evidence of active mycobacterium tuberculosis or human immunodeficiency virus infection
• Active GIS bleeding
• Non-cardiac organ failure under ECLS or LVAD therapy
• Significant psychosocial problems
• Special risk factors for isolated HTx (e.g., COPD, PE, PI, or irreversible PVR > 5 wood units)

BMI body mass index, *COPD* chronic obstructive pulmonary disease, *ECLS* extracorporeal life support, *eGFR* effective glomerular filtration rate, *ERPF* effective renal plasma flow, *GIS* gastrointestinal system, *HTx* heart transplantation, *LVAD* left ventricular assist device, *PE* pulmonary embolism, *PI* pulmonary infarction, *PVR* pulmonary vascular resistance

ensure they meet the criteria listed in Table 45.3. For intrathoracic organ transplantation to be completely successful, the recipient must be entirely healthy except for end-stage heart and/or lung disease, because transplantation is not curative in itself and is associated with its own chronic morbidity and survival limitations. The non-thoracic organ dysfunctions accompanied to intrathoracic transplantation reduce its operative course, as well as patient and graft survival; for this reason, it should not be a key strategy to reserve intrathoracic transplantation only for the patients close to death due to end-stage cardiopulmonary failure. The best candidate transplant recipients are those who are in the best condition preoperatively. Patients on the waiting list with cardiogenic shock, respiratory insufficiency, a septic condition, or a deterioration of biochemical values should not be listed for transplantation until they have received sufficient medical treatment, with or without circulatory support. To improve post-transplant outcomes, it is essential to evaluate and manage the comorbidities of list patients with cardiac failure (Table 45.4). Advanced age, extreme obesity, uncontrolled diabetes mellitus with or without end-organ damage, and active malignancies are the primary comorbidities that endanger intrathoracic organ transplantations. Preoperative diagnostic parameters show the severity of the RHF, varying from compensated hypertrophy (RVD) to ventricular dilatation (RVF) (Table 45.5).

The general criteria for appropriate HTx recipients are regularly reconsidered and refined, and then established by consensus [23]. The severity of cardiac dysfunction is indicated by specific signs of RHF, such as hepatomegaly, ascites, renal dysfunction, and edema; HTx should be the treatment option only for patients with aggressive resistance to medical treatment or repeated hospitalization for heart failure (Table 45.6). The transplanted heart cannot tolerate an elevated systolic pulmonic afterload of more than 50 mmHg, and fatal RHF develops above a pressure of 55–60 mmHg. Therefore, the presence of PHT, defined as systolic pulmonary artery pressure (PAP) >60 mmHg, in association with reactive elevated primary or secondary PVR is a relative contraindication to isolated HTx. However, irreversible elevated PVR (>8 Woods) is a main indication for LTx in primary lung pathologies or for HLTx in secondary pathologies (such as left heart cardiomyopathies). Several uncommon structural pathologies result

Table 45.5 Right heart hemodynamic parameters for isolated RVD and RVF

	Normal	RVD	RVF
CVP	2–6 mmHg	≥16 mmHg	>18 mmHg
PCWP	6–12 mmHg	≤18 mmHg	≤18 mmHg
CVP/PCWP	<1/2	>2/3	>1
IVC diameter	<15 mm	>21 mm	>21 mm
IVC inspiration collapse	≥50%	<50%	Non
TAPSE	≥16 mm (16–30)	10–15 mm	<10 mm
RV basal diameter	≤40 mm (24–40)	41–45 mm	>45 mm
RAD	<40 mm	40–50 mm	>50 mm
TR	Non	≤moderate	>moderate
TA diameter	<40 mm	40–43 mm	>43 mm
TA peak systolic velocity	≥10 cm/s	5–10 cm/s	<5 cm/s
RVEDD/LVEED	<0.6	>0.75	>1
RVEF	≥45% (45–69)	30–44%	<30%
RVFAC	≥35% (35–63)	<35%	<35%
RVLS of the free wall	<−24%	−20 to −24%	>−20%
RVLS of the lateral wall	<−20%	−9 to −20%	>−9%
RVSWI	>0.4 mmHg/L/m^2	0.25–0.40 mmHg/L/m^2	<0.25 mmHg/L/m^2
RVIMP with tissue Doppler			>0.54%

CVP central venous pressure, *IVC* inferior vena cava, *LVEED* left ventricular enddiastolic diameter, *PCWP* pulmonary capillary wedge pressure, *RAD* right atrial diameter, *RV* right ventricle, *RVD* right ventricular dysfunction, *RVEED* right ventricular enddiastolic diameter, *RVEF* right ventricular ejection fraction, *RVF* right ventricular failure, *RVFAC* right ventricular fractional area change, *RVIMP* right ventricular index of myocardial performance, *RVLS* right ventricular longitudinal strain, *RVSWI* right ventricular stroke work index, *TA* tricuspid annular, *TAPSE* tricuspid annular plane systolic excursion, *TR* tricuspid regurgitation

in RHF with significant decompensation signs in the absence of PHT, and so can be treated with isolated HTx; these include congenital heart diseases that cannot be corrected or that fail after surgical repair, an arrhythmogenic RV, or isolated right side dilated cardiomyopathies. Isolated RHF is not a common pathology; it usually develops secondary to LHF or pulmonary dysfunction caused by pulmonary vascular or intrinsic pathologies. A RV whose function has been adversely affected can usually be left untouched (the non-transplanted period) and supported medically and/or through intervention (the supportive period); the condition may then resolve with time (the healing period) or after surgical treatment for specific etiologic-based pathologies (the surgical treatment period). If there is no decrease in cardiac index, the reversibility of elevated PVR is determined by a decrease in mean PAP of at least 20% and the restoration of pulmonary capillary wedge pressure (PCWP) below 25 mmHg and systolic PAP below 60 mmHg, with an improvement in PVR to below 2.5 Wood units. If medical therapy fails to achieve these acceptable hemodynamic values or effective left ventricular unloading with mechanical support including an intra-aortic balloon pump (IABP) and/or LVAD in patients with LHF, it is reasonable to conclude that the PHT is irreversible. Following LVAD implantation, the patient's hemodynamics should be reevaluated after 3–6 months to investigate the reversibility of PHT. If RHF symptoms continue or become aggravated, this indicates the irreversibility of PHT or structural damage of the RV; this is a serious situation and a priority indication for HLTx. Isolated lung pathologies resulting functional RHF can be treated with uni- or bilateral LTx; those associated with irreversible morphologic damage to the RV caused by the elevated afterload or irreparable right ventricular pathologies should be treated with HLTx.

Table 45.6 Acceptable isolated HTx criteria after adequate treatment for transplant candidates with isolated RHF.

A) Heart failure prognosis scores (estimated 1-year survival)	
– Seattle heart failure model (SHFM)	<80%
– Heart failure survival score (HFSS)	≥medium/high
B) Cardiopulmonary stress (exercise) testing	
– 6-min walking test	<300 m
– RER	>1.05
– Peak VO_2	
BMI >30 kg/m^2	≤19 mL/kg/min
ß-blocker (−)	≤14 mL/kg/min
ß-blocker (+)	≤12 mL/kg/min
LVAD (+)	≤10 mL/kg/min
Isolated RHF (LVEF ≥50%)	≤10 mL/kg/min
Age ≤50 years	≤50% predicted
C) Right heart catheterization (with preserved LVEF)	
– CVP	>15 mmHg
– PCWP	≤15 mmHg
– CVP/PCWP	>1
– mPAP	<25 mmHg
– TPG	<15 mmHg
– DPG	<10 mmHg
– PVR	<2.5 Woods
Without medication	*<3 Woods*
Reversible with sildenafil, IABP, or LVAD therapy	*3–6 Woods*
Irreversible (inoperable or candidate for HLTx)	*>6 Woods*
– RVSWI	<5 g/m^2/beat
D) Echocardiographic parameters	
– RVEDD (parasternal/basal)	>35/45 mm
– RVEF	<30%
– TAPSE	<10 mm
– IVC	>2.1 cm
– Plethora	+
– Lateral RV peak longitudinal strain	>−9%
E) Improved systemic biomarkers	
– Creatinine	≤2 mg/dL
– Bilirubin	≤2 mg/dL
– Albumin	≥3 mg/dL
– AST	≤80 IU/L
– INR	<2
– Na+	>135 mEq/dL
– Anemia (hemoglobin or hematocrit)	≥10 mg/dL or ≥30%
F) Healed clinical condition and signs	
– t-MCS	Non
– Anasarca edema	Non
– Cachexia	Non
– Cardiac-related hepatic fibrosis or cirrhosis	Non

(continued)

Table 45.6 (continued)

– Splenomegaly	Non
– Ascites	<minimal
– Hepatomegaly	≤minimal
– Peripheral edema	<moderate

AST aspartate aminotransferase, *BMI* body mass index, *CVP* central venous pressure, *DPG* diastolic pulmonary gradient, *HTx* heart transplantation, *HLTx* heart-lung transplantation, *IABP* intra-aortic balloon pump, *INR* international normalized ratio, *IVC* inferior vena cava, *LVAD* left ventricular assist device, *LVEF* left ventricular ejection fraction, *t-MCS* temporary mechanical circulatory support, *mPAP* mean pulmonary arterial pressure, *PCWP* pulmonary capillary wedge pressure, *PVR* pulmonary vascular resistance, *RER* respiratory exchange ratio, *RHF* right heart failure, *RVEED* right ventricle end-diastolic diameter, *RVEF* right ventricular ejection fraction, *RVSWI* right ventricle stroke work index, *TAPSE* tricuspid annular plane systolic excursion, *TPG* transpulmonary gradient, VO_2 oxygen consumption

Providing end-stage heart failure patients, who are ineligible for HTx, with circulatory support using LVAD is an effective therapy that enables them to become eligible for transplantation after physiologic improvement [24]. This approach is the first stage or gold standard treatment for patients with elevated PVR or severe comorbidities. These devices improve end-organ perfusion and functions, stabilize hemodynamics, reduce PVR, and improve survival before and after HTx. The LVAD improves the left side cardiac output and the unloading of the left ventricle, which reduces the right ventricular afterload and augments the interventricular septum at the midline, increasing the right ventricular preload via the venous return. However, septal displacement and the increased right ventricular preload may lead to post-LVAD RVF, especially in patients with pre-existing right ventricular dysfunction (see Chap. 47) [25]. Most patients referred for LVAD have some degree of right ventricular dysfunction preoperatively (Table 45.7); it can also be a serious complication after LVAD implantation. The incidence of early-onset post-LVAD RVF is 15–25% and the condition has several potential consequences: (1) it can require the prolonged use (>14 days) of inotropes and intravenous vasodilators with or without mechanical support; (2) it can lead to coagulopathy, altered drug metabolism, deteriorating nutritional status, and diuretic resistance; and (3) it can result in poor quality of life, increased length of hospitalization, and poorer survival even after HTx [26]. Late post-LVAD RVF, defined as developing >30 days after discharge from hospital, has an incidence >10% and is associated with substantially reduced survival after HTx. Transplant candidates with signs of late-onset post-LVAD RVF should be hospitalized well before transplantation for aggressive intravenous management to stabilize their hemodynamics. Interestingly, there is no correlation between early and late post-LVAD RVF, and more than 60% of patients develop it after the first year [27]. Post-LVAD RVF refractory to medical and circulatory supportive therapies is a major indication for HTx or HLTx.

Patients with congenital heart diseases, which could not be surgically treated and either were palliated or remained untreated, commonly end up with isolated RHF because of persistent intracardiac abnormalities, persistent intracardiac or palliative shunts, ongoing PHT due to the long-term left-to-right shunting, electrophysiological disturbances, valvular or myocardial dysfunction, and systemic ventricular failure [28]. Morphologic and functional single ventricle pathologies are highly resistant to medical therapy and so most transplant candidates with congenital heart disease have undergone failed prior palliative surgery for univentricular lesions [29]. A failed Fontan circulation procedure has two presentations: failed Fontan physiology (e.g., refractory ascites, pleural effusions, and protein-losing enteropathy) or univentricular failure. Patients with a failed Fontan circulation have a higher post-transplant mortality than those with other congenital heart diseases because of the risk of infection, bleeding, and post-transplant RHF [30]. With the recent improvement of outcomes after corrective congenital cardiac surgery, HTx has been used less frequently as a

Table 45.7 Mechanisms for RHF after LVAD implantation in HTx candidates

A) Preoperative RVD
– TAPSE <10 mm
– RV short/long axis ratio > 0.6
– RVEDD/LVEDD >0.75
B) Persistent elevated PVR (PVR ≥3 woods; mPAP ≥25 mmHg)
C) Increased right side preload (CVP ≥16 mmHg)
– Increased venous return by increased cardiac output from a LVAD
– Inadequate left ventricular unloading
– Excessive volume resuscitation
– Severe TR (untouched or newly developed)
– Elevated CVP/PCWP (>2/3)
D) Non-recoverable postoperative systolic RV dysfunction (TAPSE <8 mm; RVSWI <250 mmHg/mL/m^2)
– Preoperatively impaired RV (myocardial dysfunction)
– Excessive leftward shift of the IVS by overly aggressive left ventricular unloading (contributial dysfunction)
– Unaffected systolic ventricular interdependence by akinetic IVS (inoperative 20–40% addition for right ventricular output) (functional dysfunction)
E) Tachyarrhythmias (>100 irregular beats/min)
– Atrial fibrillation (10–20% decrease in left ventricular output)
– Ventricular fibrillation (40% decrease in left ventricular output)
F) Contagion of the left side pathology to the right side

CO cardiac output, *CVP* central venous pressure, *IVS* interventricular septum, *LVAD* left ventricular assist device, *LVEDD* left ventricular end-diastolic diameter, *mPAP* mean pulmonary artery pressure, *PCWP* pulmonary capillary wedge pressure, *PHT* pulmonary hypertension, *RHF* right heart failure, *PVR* pulmonary vascular resistance, *RV* right ventricle, *RVD* right ventricular dysfunction, *RVEDD* right ventricular end-diastolic diameter, *RVSWI* right ventricular stroke work index, *TAPSE* tricuspid annular plane systolic excursion, *TR* tricuspid regurgitation

primary therapy; nevertheless, it remains an established therapy for patients with end-stage cardiac disease for whom there are no suitable medical or surgical options, thereby accounting for >25% of all pediatric recipients and <2% of all adult recipients [31]. The biventricular form of end-stage congenital heart disease, which is found in a heterogeneous group of patients who underwent prior surgical curative repair, has three main indications for HTx: refractory cardiac failure, pathology that cannot be treated surgically, and life-threatening arrhythmia [32]. Three progressive scenarios can result in refractory cardiac failure: systemic right ventricular failure (e.g., c-TGA, D-TGA with the atrial switch procedure), native right ventricular failure (e.g., TOF, DORV, and severe Ebstein's anomaly), or systemic left ventricular failure (e.g., inoperable VSD, AVSD). Candidates for HTx with congenital heart disease should undergo a detailed assessment of the position and anatomy of their thoracic abnormalities using imaging techniques (e.g., cardiac magnetic resonance imaging, chest computed tomography, or echocardiography) to guide the surgical strategy; in addition, PHT should be evaluated, and all potential sources of circulation flow identified (Table 45.8). Specific anatomical abnormalities, such as of vascular and cardiac size, position, and situs, require innovative solutions, careful surgical planning, modifications involving surgical ingenuity and creativity, and adaptation of the recipient's complex anatomy to that of the normal donor [33].

Lung transplantation is the only treatment modality that can be used for isolated RHF caused by end-stage parenchymal lung disease or PHT. It is reasonable to list patients for LTx if their life expectancy would be limited without a transplant and the risk-to-benefit ratio favors LTx rather than conventional medical treatment [34]. Many preoperative criteria need to be met before a decision is made regarding the suitability of an individual patient for LTx (Table 45.9). Lung function mea-

Table 45.8 Risk factors for HTx candidates with congenital heart disease

• Pulmonary hypertension (progressive or irreversible)
• Aortopulmonary collaterals
• Pulmonary arterial pathologies (stenosis, thrombosis, or occlusion)
• Pulmonary vein anomalies (hypoplasia or scimitar syndrome)
• Central vein pathologies (stenosis, thrombosis, or occlusion; bilateral SVC)
• CHF after a previous corrective operation

CHF congestive heart failure, *HTx* heart transplantation, *SVC* superior vena cava

Table 45.9 Acceptance criteria for LTx candidates with RHF

A) *Lung failure prognosis scores*	
– Estimated 2-year survival	>50%
– Estimated 90-day survival after LTx	>80%
– Estimated 5-year survival	>80%
B) *Absence of thorax (chest wall, or spinal) deformity*	
C) *Right heart catheterization*	
– RAP	>15 mmHg
– LAP	≤15 mmHg
– RAP/LAP	>1
– PCWP	>15 mmHg
– mPAP	≥25 mmHg
– TPG	>15 mmHg
– DPG	>10 mmHg
– PVR	>6 woods
– CI	<2 L/min/m^2
– RVSWI	≥5 g/m^2/beat
D) *Spirometric tests*	
– PaO_2	<60 mmHg
– $PaCO_2$	>50 mmHg
– FVC	<80% predicted or declined >10% in 6 months
– DLCO	<40% predicted or declined >15% in 6 months
– FEV_1	<25% predicted
E) *Cardiopulmonary exercise testing*	
– Peak Vo_2	≤10 mL/min/kg
F) *Progressive RHF signs*	
– Renal insufficiency	Creatinine <2 mg/dL
– Hepatic insufficiency	Bilirubin <2 mg/dL
– Recurrent ascites	
– BNP	>100 pg/mL
– 6-min walking test	Distance <300 m or desaturation <88%

BNP brain natriuretic peptide, *CI* cardiac index, D_{LCO} diffusion capacity of the lung for carbon monoxide, *DPG* diastolic pulmonary gradient, FEV_1 forced expiratory volume in first second, *LAP* left atrial pressure, PaO_2 partial arterial oxygen pressure, $PaCO_2$ partial arterial carbon dioxide pressure, *PAP* pulmonary artery pressure, *PCWP* pulmonary capillary wedge pressure, *PVR* pulmonary vascular resistance, *RAP* right atrial pressure, *RHF* right heart failure, *RVSWI* right ventricular stroke work index, *TPG* transpulmonary gradient, Vo_2 oxygen consumption

surement, especially spirometric assessments of airflow obstruction and restriction, and, more importantly, their deterioration, should be used to determine the true timing of transplant referral, assessment, wait-listing, and transplant priority [35]. Appropriate LTx candidates should not have any significant thoracic wall deformity that could preoperatively affect or postoperatively impair, their lung functions. However, preoperative pulmonary rehabilitation with anti-PHT medication can be an effective therapy for LTx candidates on the waiting list, improving their quality of life and exercise capacity, as well as the postoperative course [36]. Chronic obstructive pulmonary disease and idiopathic pulmonary fibrosis are the most common etiologies for primary LTx; on the other hand, re-transplantation rate has increased recently [37]. Idiopathic PHT with a normal PCWP and left ventricular end-diastolic pressure in the absence of structural, parenchymal, vascular, or thrombotic cardiopulmonary diseases is a rare pathology with a poor outcome [38]. Prior to the LTx procedure, a transplant candidate with this condition should be treated medically with endothelin receptor antagonists (ambrisentan or bosentan), phosphodiesterase type five inhibitors

and guanylate cyclase stimulators (sildenafil, tadalafil, or verdanafil), and/or prostacyclin analogs and prostacyclin receptor agonists (iloprost, treprostinil, or selexipag) [39]. The high resistance of the diseased pulmonary vascular bed with idiopathic PAH can hinder right ventricular ejection, and patients often die from progressive RHF or sudden fatal arrhythmias; however, these can be postponed by atrial septostomy or a pulmonary artery–left atrial shunt [40]. Bilateral LTx seems to have better overall survival than single LTx, and lower chronic rejection (the bronchiolitis obliterans syndrome), in older recipients (>50 years), and in those with a higher lung allocation score, chronic obstructive pulmonary disease, idiopathic PAH, septic lung disease (e.g., cystic fibrosis or bronchiectasis), or idiopathic pulmonary fibrosis [41].

The initial, and remaining most common, diagnoses for HLTx are primary PHT and congenital heart disease with or without concomitant Eisenmenger's syndrome. In chronic lung diseases such as chronic obstructive pulmonary disease or idiopathic pulmonary fibrosis, the pathophysiology of PHT is complex and multifactorial. Hypoxia and chronic inflammation are the main factors, resulting in vasoconstriction, vascular remodelling, small vascular destruction and fibrosis, and elevated PVR due to endothelial dysfunction [42]. Overload of the right heart initially results in remodeling and hypertrophy, but it can then lead to cor pulmonale, i.e., dysfunction and dilatation with an increase in the release of cardiac natriuretic peptides, despite the preserved left ventricular function [43]. The best curative treatment for this pathology in patients with severe pulmonary vascular disease is bilateral LTx, but HLTx is the preferred approach for severe pulmonary vascular disease combined with end-stage heart failure [44].

45.3.3 Waiting-List Priorities

Over the last two decades, there have been 3,500 and 4,000 HTx procedures annually, with the shortage of donors preventing an increase in these numbers. The widening gap between the number of donors and waiting recipients has resulted in a continuing trend towards transplanting the candidates whose status is considered to be urgent. In July 2006, the United Network for Organ Sharing (UNOS) changed the organ allocation algorithm, allowing the broader regional sharing of available hearts to those in more immediate need before their allocation to local, less sick candidates; this change increased the allocation of hearts to patients with urgent status 1A/1B, especially favoring status 1A patients (Table 45.10). However, for the allocation of the limited number of donor organs to be truly equitable, objective, and medically justified, it should be redefined in favor of the patients with the greatest change of a favorable postoperative course. The Thoracic Organ Transplantation Committee has begun work on a new heart allocation system with an expanded number of allocation statuses: This new system will take into account the severity of illness and geographic variations in heart allocation, and will incorporate the emerging population of LVAD patients, with and without associated complications, as well as previously disenfranchised groups of patients, it will also focus on the candidates' underlying physiology rather than their diagnoses (Table 45.11) [45]. However, this proposed allocation system assigns priority to patients on the waitlist based solely on their risk of mortality, with no consideration of post-transplant outcomes; maybe, mechanical circulatory support devices can be a better alternative for them, with delivering comparable survival with HTx [46]. The new system is similar to the present UNOS system, and RHF patients with severe decompensation caused by congenital heart disease, isolated right ventricular cardiomyopathy (CMP), severe primary or secondary PHT, or restrictive or infiltrative CMP are also at a considerable disadvantage in the proposed system. These patients generally experience longer wait times and higher waitlist mortality than other CMP patients. Patients supported with veno–arterial ECMO are undoubtedly at the highest risk of death on the waitlist, but they also have the worst post-transplant outcomes. Because of their higher

Table 45.10 The United Network for Organ Sharing (UNOS) heart allocation system

Status	Current criteria	
1A	A- Patients in the ICU with	
	• Inotropic support under pulmonary arterial monitorization	
	• Mechanical circulatory support	
	– 30-day elective ventricular assist device time	LVAD
	– Total artificial heart	TAH
	– Intra-aortic balloon pump	IABP
	– Extracorporeal membrane oxygenation	ECMO
	• Mechanical ventilation	
	B- LVAD patients with	
	• Life-threating ventricular arrhythmia	
	• RVF	
	• RVAD	
	• Device malfunctions	
	– Mechanical failure	
	– Line failure	
	– Thrombosis and/or thromboembolism	
	– Infection	
	– Pump	
	– Line	
	– Mediastinitis	
	– Septisemia	
	C- Exception granted by the regional review board	
1B	A- Mechanical circulatory support beyond the 30-day interval	
	B- Continuous intravenous inotropic support	
	C- Exception granted by the regional review board	
2	Those who do not meet the criteria for status 1A or 1B	

ECMO extracorporeal membranous oxygenation, *IABP* intra-aortic balloon pump, *ICU* intensive care unit, *LVAD* left ventricular assist device, *RVAD* righty ventricular assist device, *RVF* right ventricular failure, *TAH* total artificial heart

risk of postoperatively mortality, it remains a major concern that patients on ECMO are prioritized into the highest status. The role of LVAD versus HTx in a subgroup of heart failure patients should be determined by clinical trials that directly compare the effectiveness of LVAD as a destination therapy and HTx [47]. Over the last decade, in the absence of donors, LVAD implantation has increased and taken the place of HTx or HLTx in end-stage heart failure patients with reversible PHT, particularly for patients of advanced ages or who are ineligible for transplantation [24]. With this strategy, the proportion of patients bridged to transplant with LVAD has increased from around 20% to approximately 50%.

Because the number of donors is currently decreasing and is unlikely to increase in the future, the waitlist algorithm for HTx should be revised so that it does not depend on the involvement of the heart (left, right, or biventricular failure should have equal priority) or the presence of any mechanical circulatory support; the listing priority should be intravenous treatment with or without intra-aortic balloon pump > total artificial heart > LVAD > ECMO. Conversely, to improve early and late survival, as well as graft patency, the top priorities for listing should be decided according to the following criteria: the severity of symptoms; with priority for any type of compensated heart failure; the type of CMP, with right side CMPs, congenital anomalies, and

Table 45.11 The new heart allocation system

New status	Criteria	UNOS status
1	1. ECMO	1. Status 1A(a)(iv)
	2. Mechanical ventilation	2. Status 1A(c)
	3. Non-dischargeable (surgically implanted) LVAD	3. Subset of status 1A(a)(i) and subset of status 1B(aa)
	4. MCS with life-threatening ventricular arrhythmia	4. Status 1A(b)(iv)
2	1. IABP	1. Status 1A(a)(iii)
	2. Ventricular tachycardia/ventricular fibrillation, mechanical support not required	2. Subset of status 1A exceptions
	3. MCS with device malfunction/mechanical failure	3. Status 1A(b)(iii)
	4. Total artificial heart	4. Status 1A(a)(ii)
	5. Dischargeable BiVAD or RVAD	5. Subset of status 1A(a)(i) and subset of status 1B(aa)
	6. Acute circulatory support	
3	1. Dischargeable LVAD for up to 30 days	1. Subset of status 1A(a)(i)
	2. Status 1A exception	2. Status 1A(e)
	3. Multiple inotropes or single high-dose inotropes with continuous hemodynamic monitoring	3. Status 1A(d)
	4. MCS with device infection	4. Status 1A(b)(ii)
	5. MCS with thromboembolism	5. Status 1A(b)(i)
	6. MCS with device-related complications other than infection, thromboembolism, device malfunction/ mechanical failure or life-threatening ventricular arrhythmia (e.g., hemolysis, mucosal bleeding)	6. Status 1A(b)(v)
4	1. Diagnosis of CHD with:	1. a. a. a. NA
	a. Unrepaired/incompletely repaired complex CHD, usually with cyanosis	
	b. Repaired CHD with two ventricles (e.g., TOF, TOGV)	
	c. Single ventricle repaired with Fontan or modifications	
	2. Diagnosis of CAD with intractable angina	2. NA
	3. Diagnosis of hypertrophic CMP	3. NA
	4. Diagnosis of restrictive CMP	4. NA
	5. Diagnosis of amyloidosis	5. NA
	6. Stable LVAD candidates after 30 days	6. Subset of status 1B(aa)
	7. Inotropes without hemodynamic monitoring	7. Status 1B(bb)
	8. Retransplant	8. NA
	9. Status 1B exceptions	9. Status 1B = exception
5	Approved combined organ transplants: heart-lung; heart–liver; heart–kidney	Not applicable
6	All remaining active candidates	Status 2
7	Inactive/unable to undergo transplant	Inactive

BIVAD biventricular assist device, *CAD* coronary artery disease, *CHD* congenital heart disease, *CMP* cardiomyopathy, *ECMO* extracorporeal membraneous oxygenation, *IABP* intra-aortic balloon pump, *LVAD* left ventricular assist device, *MCS* mechanical circulatory support, *RVAD* right ventricular assist device

restrictive CMPs having priority; associated non-cardiac pathologies, with priority for multiorgan transplantation given to end-stage lung, renal, or hepatic diseases; and the patient's present clinical condition, with priority given in the order elective (hospitalized stability) > urgent (invasive treatment modalities with or without device-related complications) > emergency (temporary left heart circulatory support). The best important factor for improving operative and postoperative outcomes is for the patients to be in the best preoperative condition without immunologic sensitization. End-stage heart failure patients with decompensated LCOS should first be treated with a temporary circulatory support devices (an IABP, ECMO, or LVAD) before being nominated for transplantation; and, after their clinical condition has stabilized and the multisystem disruptions have healed, these patients should then be added to the waitlist to be avoided the harmful effects of pre-existing non-healed non-cardiac organ dysfunctions. In the near future, it is expected that technologic and medical advances will simplify temporary and/or permanent mechanical circulatory support, with fewer complications and better outcomes, and that this would allow the suspension of early HTx in unsuitable recipients or patients in bad condition. Destination therapy with prosthetic devices would take the place of HTx in end-stage LHF patients, and appropriate donor organs would be allocated to patients with RHF or restrictive CMPs, or who are in better conditions.

Although the number of LTx procedures has been increasing, it remains inadequate for meeting the LTx requirements of all patients with end-stage lung disease resulting severe RHF. The waiting list algorithm for chronic lung diseases has been revised with priority given to patients with progressively disabling pulmonary pathologies who still have the capacity for full rehabilitation after LTx. Much of the current success in LTx relates to the presence of the degree of RVF, and especially its temporary nature, because pulmonary failure progresses faster than does secondary RHF and survival is shorter. Potential LTx candidates with primary RHF resulting from severe pulmonary vascular disease are rarely included on the LTx waitlist; these patients are not given priority for isolated LTx either by thoracic surgeons, because of the persistence of the RHF after transplantation, or by cardiac surgeons, who neglect these patients for HTx in favor of patients with LHF. These patients are more suitable for HLTx. However, patients with secondary RHF resulting from by end-stage lung disease can be referred for isolated LTx because of the high probability they will recover from the RHF after LTx.

45.3.4 Management Until Transplantation

Candidates on the waitlist with isolated RHF usually have preserved LVEF with non-elevated PAP, but their left ventricle cannot take on the right ventricular function and prevent LCOS. Aggravated symptoms result mostly from the decompensated RVF, which should be treated immediately in the intensive care unit. Aggressive intravenous medical treatment can often solve systemic failure, with the first stage treatment including volume replacement (of colloid or blood products), pulmonary vasodilators, right heart inotropes, and diuretics. If the decompensation of the right heart is not resolved, the next step should be mechanical circulatory support; peripheral veno–arterial ECMO is the best option to prevent circulatory failure, hypoxia, hypercapnia, and multiorgan failure. If the LVEF is preserved, the peripheral ECMO is created between the right femoral vein, percutaneously, to unload the RV and the left subclavian artery, surgically via a prosthetic graft, to maintain the systemic circulation. If the LVEF is not preserved, left heart unloading should be created and added to the ECMO through the left atrium (LA) percutaneously or surgically via a Kırali circuit [48]. Both of these ECMO procedures were detailed in Chap. 46. An alternative would be to insert a temporary mechanical circulatory support device into the LV through the femoral artery.

45.4 Donor Evaluation and Management

Because of the significant shortage of donor, donor evaluation is the most important and most difficult step in HTx [49]. Fortunately, using LVAD implantation as a bridge to HTx should make it easier for the transplant team to allocate the donor hearts to recipients who are more hemodynamically stable or younger. Several cardiothoracic criteria for donor intrathoracic organ approval are widely accepted (Table 45.12). The first criterion is that the donor should be younger than 60 and without any documented atherosclerotic artery disease. It is recommended that all potential donors older than 45 years should undergo coronary angiography; however, this may not be feasible when a center lacks an angiography unit, as is commonly the case, or the renal transplant team objects to the procedure.

Table 45.12 Donor heart selection criteria

Absence of any cardiac pathology
Short-term cardiac arrest (<10 min)
Hemodynamic stability with/without a single low dose inotropic infusion dobutamine or dopamine <10 μg/kg/min
Age (<40 years)
Absence of systemic infection (normal procalcitonin level)
Soft chest trauma (normal cardiac enzyme levels)
Matched body size
Donor height ≥90% recipient height with normal PVR in adults
Donor height ≥120% recipient with high PVR in adults
Donor height <120% recipient height in children
Donor weight ≥90% recipient weight
Matched ABO blood-type compatibility
Hemodynamic parameters
LVEF >55%
CI >2.4 L/min/m^2
MAP >60 mmHg
CVP <10 mmHg
PCWP <12 mmHg

CI cardiac index, *CVP* central venous pressure, *LVEF* left ventricular ejection fraction, *MAP* mean arterial pressure, *PCWP* pulmonary capillary wedge pressure, *PRA* panel reactive antibody, *PVR* pulmonary vascular resistance

Many centers therefore prefer younger donors (<40 years) because of the absence or low incidence of coronary artery disease at these ages. If an intraoperative evaluation reveals several calcific plaques in the coronary territory of the donor heart, this is an absolute contraindication to HTx, especially in diabetic and/or hypercholesterolemic donors. The final decision should therefore be made after direct visualization and manual examination of the donor heart during organ procurement. The second criterion is that the donor should not have experienced any prolonged episodes of profound hypotension without LCOS (< a few hours) or cardiac arrest requiring external massage support (<10 min). Echocardiography should be performed prior to harvesting to evaluate the cardiac structures, myocardial capacity, and valvular functions, as well as the presence and content of any presence and content pericardial fluid. Serum cardiac enzymes should be at normal levels or, at most, mildly elevated. The third criterion is that there should have been no blunt or penetrative thoracic trauma associated with rib fracture or pleural and/or pericardial hemorrhage.

Before procurement, careful medical management of the donor heart is essential because brain death is associated with autonomic and cytokine storms. Hypotension, hypothermia, and diabetes insipidus are frequent physiologic results of brain death and should be managed carefully. In addition, excessive fluid replacement can result in right ventricular distention and lung damage due to extravascular water. Low-dose inotropic support is usually given to sustain hemodynamic stability (with mean arterial blood pressure >60 mmHg and CVP 6–10 mmHg). If a higher dose of inotropic and catecholamine infusions is needed, this indicates myocardial distress; however, these agents can themselves cause myocardial injury. The period of hypothermic ischemia should not exceed 4 h and should preferably be for less than 3 h.

The donor selection criteria for LTx are similar, but pulmonary function tests are paramount for LTx and HLTx. The chest X-ray should be clear and the partial pressure of arterial oxygen

(PaO_2) should exceed 140 mmHg for a fraction of inspired oxygen (FiO_2) of 40% and 300 mmHg for an FiO_2 of 100%. Peak inspiratory pressure, use to estimate lung compliance should be less than 30 mmHg, and a bronchoscopic evaluation should confirm the absence of purulent secretions or signs of aspiration. Medical management is more difficult and delicate for donor lungs than for donor hearts because of the high risk of neurogenic pulmonary edema, aspiration, nosocomial infection, and contusion. Intravascular volume replacements to maintain the mean systolic arterial pressure should be limited so that CVP does not exceed 10 mmHg. Crystalloid fluid boluses must be avoided, and the hemoglobin concentration should be maintained at >10 g/dL to prevent pulmonary congestion. To prevent atelectasis, the ventilator should be set so that positive end-expiratory pressures is 3–5 cm H_2O.

45.5 Technique of Operations

45.5.1 Intrathoracic Organ Procurement

45.5.1.1 Donor Heart Procurement

The most common incision used for standard multiorgan procurement is a long midline incision from the jugular notch to the pubis. The heart procurement team performs a median sternotomy after preparing the donor at first and opens the pericardium to examine the heart for evidence of cardiac injury, structural anomalies, coronary lesions, and myocardial performance before harvesting intraabdominal organs by the abdominal organ procurement teams. If the team decides to use the heart, they inform the heart transplant team in the recipient hospital so that preparations can start for the recipient. On the other hand, repeat sternotomy and harvesting of the stick adhesions around the recipient heart, especially around the implanted LVAD, take more time than those of primary operation. The heart procurement team should therefore begin first with examining the heart and notifying the transplant team if it is suitable. The other organ-teams proceed after this. The goal of this strategy is to reduce or eliminate the ischemic waiting time in the operating room after the donor heart arrives at the recipient hospital.

Procurement begins with the full mobilization of the ascending aorta and the superior vena cava (SVC). Before the cardiectomy begins, 10,000 units of heparin is given and the SVC is tied as far distally as possible and divided (Fig. 45.1a). There are two possible strategies to achieve unloading of the left heart to prevent left ventricular distention: (1) if the donor's lungs will not be used, the right superior pulmonary vein (RSPV) is divided to allow the left heart drainage (Fig. 45.1b1); or (2) if the donor's lung are to be used, a left atriotomy incision is made on the interatrial sulcus close to the RSPV (Fig. 45.1b2). The inferior vena cava (IVC) is divided for the right heart drainage (Fig. 45.1c). After a few beats to allow complete emptying of the heart, the ascending aorta is cross-clamped just proximal to the brachiocephalic artery and 2 L (≥20 mL/kg) of profoundly hypothermic cardioplegic solution is infused through the ascending aorta (Fig. 45.1d); at the same time the pericardial cavity is filled with ice-cold saline or slush solution. There are several cardioplegic solutions for graft preservation classified as intra-

Fig. 45.1 Donor heart harvesting. (**a**) Procurement begins by dividing of the SVC. There are two strategies to unload the left heart: (**b**1) if the donor's lungs will not be used, the RSPV is divided for the left heart drainage; or, (**b**2) if the donor's lungs will be used, a left atriotomy incision is performed on the interatrial sulcus close to the RSPV. (**c**) The IVC is divided for right heart drainage. (**d**) The ascending aorta is cross-clamped and the hypothermic cardioplegic solution is infused. (**e**) Cardiectomy proceeds by dividing the RIPV and then the left pulmonary veins at the pericardial reflection. (**f**1) The pulmonary veins are divided from the LA in an islet shaped (right side) if a single lung is harvested; or (**f**2) as bilateral pulmonary vein cuffs with myocardial tissue if both lungs will be used. (**g**1) After the ascending aorta is divided at the cross-clamping site, the PA is divided with both branches if donor lungs are not used, or (**g**2) transected just below the bifurcation if the donor lungs will be used

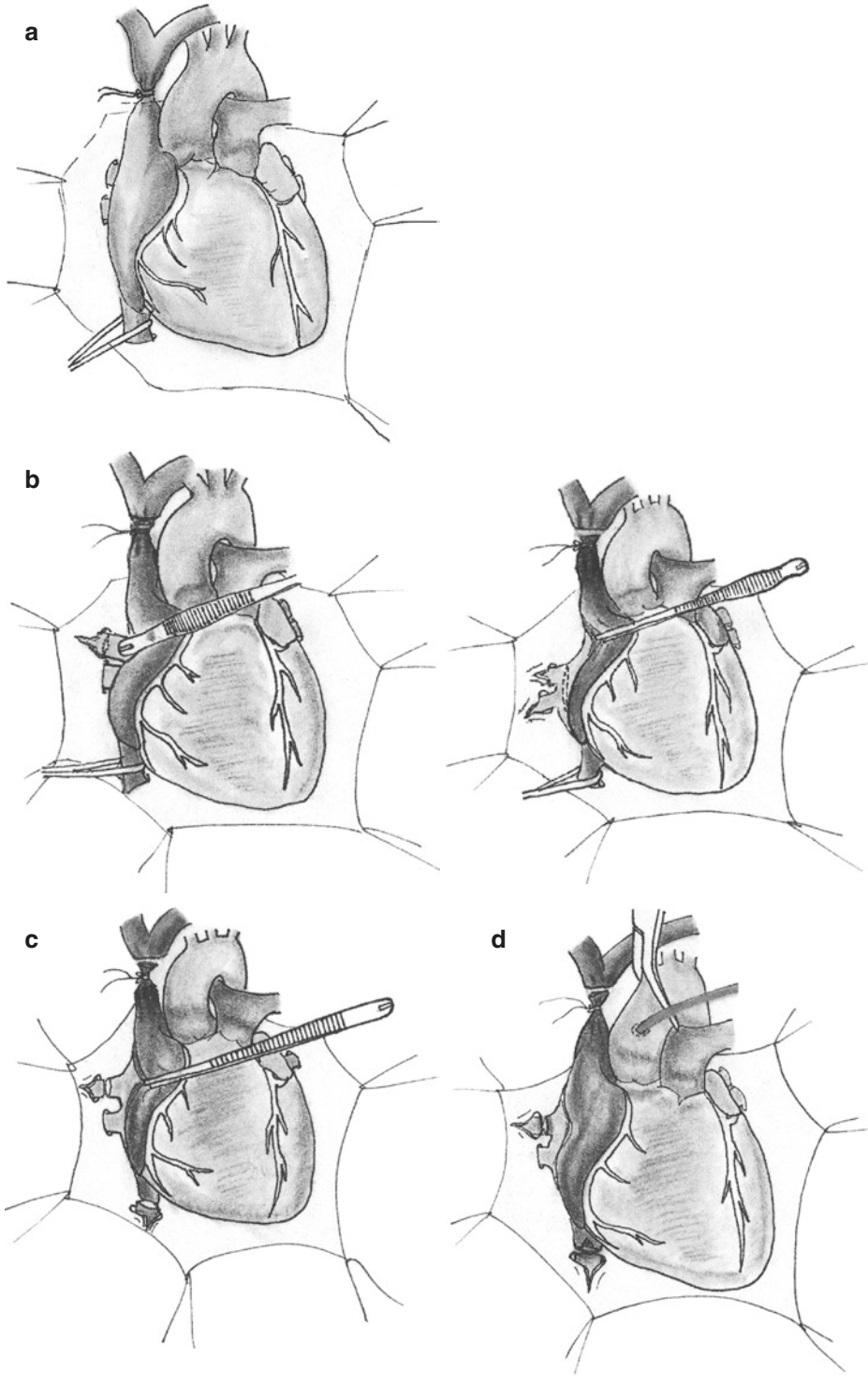
a
b
c
d

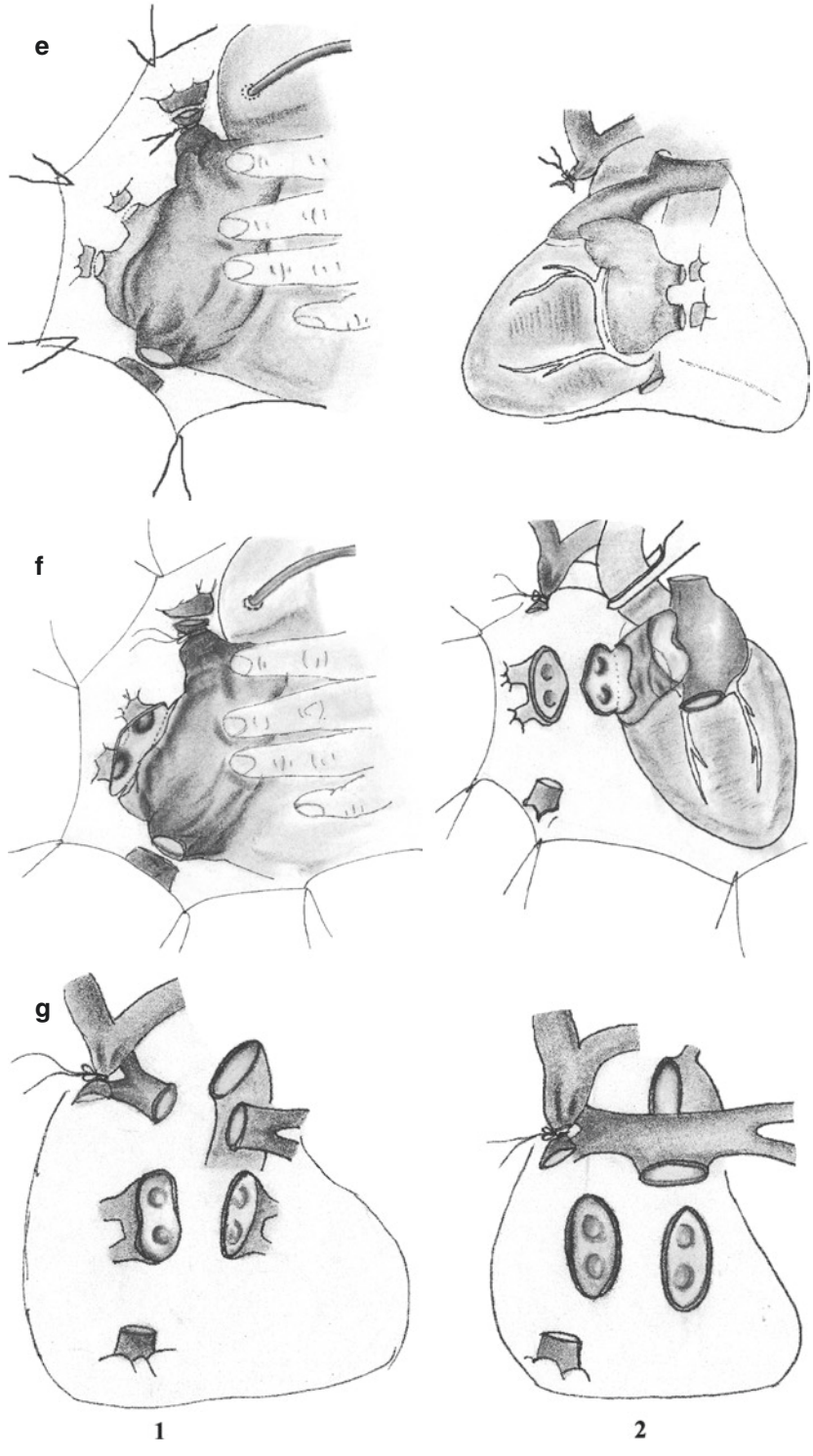

Fig. 45.1 (continued)

or extra-cellular, but Bretschneider's solution is the preferred cardioplegia in our clinic [50].

If neither lung is to be used, the cardiectomy proceeds with the division of the right inferior pulmonary vein (RIPV) and then the left pulmonary veins at the pericardial reflection (Fig. 45.1e). If one lung is used, the right pulmonary veins are divided from the left atrium (LA) in the shape of an islet (Fig. 45.1f1). If both lungs are used, the LA resection should be as broad as possible, leaving only the bilateral pulmonary vein cuffs with myocardial tissue (Fig. 45.1f2). After this, the ascending aorta is divided at the cross-clamping site. The pulmonary artery (PA) should be divided including both branches, if the donor lungs will not be used (Fig. 45.1g1), or transected just below its bifurcation if the lungs are to be harvested (Fig. 45.1g2). The heart is then removed from the body and placed in three sterile bags filled with cold preservation solution, and then into an icebox (at 4–10 °C) for transport. The donor heart can survive without structural or histological damage for 4–6 h, but it should be kept like this for as short a time as possible (preferably <3 h).

45.5.1.2 Donor Lung Procurement

During cardiac arrest, a large cannula should be inserted into the main PA through a horizontal incision approximately 1 cm wide just above the sinotubular junction; this achieves a more diffuse distribution of pulmoplegia (15 mL/kg/min for 4 min) (Fig. 45.2a). This strategy is essential for ensuring the pulmonary bifurcation with bilateral branches remain untouched for the LTx, as well as the main PA just below bifurcation for the HTx, after suturing the pulmoplegic incision. After the pulmoplegic and vasodilator solutions have been delivered, the lungs are deflated and the heart is removed first, leaving a sufficient rim of the LA (≥1 cm) as a cuff for both left- and right side pulmonary vein islets. After removing the heart from the mediastinum, en-bloc harvesting of both lungs should be started along the pre-esophageal plane above the carina (Fig. 45.2b). First, the inferior pericardium is transected in a U-shape, taking care not to injure the lung at its attachment with the pulmonary ligament. This structure should be transected carefully by cephalad traction on the double-lung bloc, and a sharp dissection is performed as high as possible between the esophagus and the posterior pericardium to separate the esophagus from the trachea. The right lung is moved across into the left pleural cavity and the azygos vein is transected; the same maneuver is then performed on the left side to divide the thoracic aorta from the left lung. Once all the attachments have been transected, the double-lung bloc remains connected only to the trachea. The endotracheal tube is suctioned and both lungs are gently inflated manually with 50% oxygen until all the atelectatic zones have been recruited; the trachea is then stapled at the highest possible point. After dividing the trachea between two parallel linear stapler lines, the inflated double-lung bloc is extracted from the body after spreading the sternal incision to its greatest extent and pulling down the diaphragm. If one or both lungs are used separately, the left and right PAs should be divided at the pulmonary bifurcation (Fig. 45.2c). The lungs are wrapped in sterile gauze pads and placed in ice-cold saline (at 2–4 °C).

45.5.1.3 Donor Heart–Lung Procurement

After administering the hypothermic cardioplegic and pulmoplegic solutions, the heart–lung block is removed from the donor's thoracic cavity with all vascular and respiratory structures, leaving behind only the distal ascending aorta and the IVC. Usually both lungs and the heart are harvested together for bi-lung and cardiac transplantation (Fig. 45.3a). If one lung may be sufficient for HLTx, then the right lung and the heart are harvested, and the left lung will be used for another isolated LTx (Fig. 45.3b).

45.5.2 Orthotopic Intrathoracic Organ Transplantation

45.5.2.1 Heart Implantation

There are two implantation techniques for orthotopic HTx according to implantation of the right

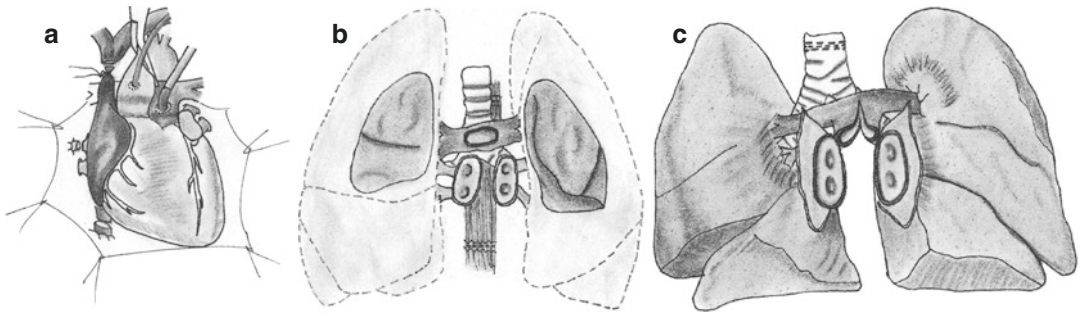

Fig. 45.2 Donor lung harvesting. (**a**) After cross-clamping the aorta pulmoplegia is given. (**b**) Both lungs are harvested. (**c**) If both lungs will be used separately, the PA is divided at the bifurcation level

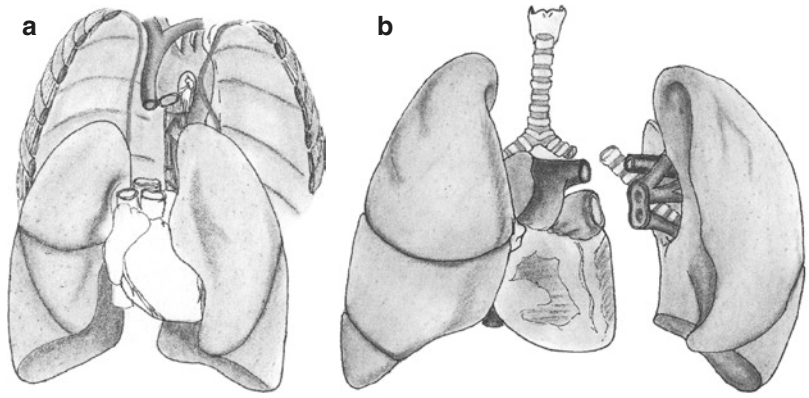

Fig. 45.3 (**a**) Donor heart and lung en-block harvesting. (**b**) The left lung is separated for another LTx

atrium (RA) [51]. The bicaval technique for orthotopic HTx is the preferred approach because of its simplicity, facility, and convenience [52]. This technique also has better early and late outcomes than the biatrial technique, especially with regard to maintaining the function of the atrioventricular valves [53]. The biatrial technique was the procedure we initially used in our clinic when we first started HTx [54, 55], but the bicaval technique has been our preferred technique over the last two decades [56].

After performing a median sternotomy and pericardiotomy, the recipient is heparinized and prepared for cardiopulmonary bypass (CPB).

The pericardium is divided like a bow from the lateral side of the PA to above the IVC in patients without prior intrapericardial interventions (cardiac or mediastinal surgery) or pericardial adhesions. This strategy is the exact opposite approach performed to prepare pericardial patch for septal defect closures or outflow tract enlargements. The main goal is to continue pericardial support for the transplanted heart after operation, especially for diastolic function.

The cannulation is first started with arterial cannulation through *the distal ascending aorta* using standard arterial cannula for standard cases or through *the arcus aorta* using ECMO arterial cannula via sliding technique for re-operations or recipients on LVAD. The next step is bicaval venous cannulation through the distal SVC just below the innominate vein and through the RA just above the atrio-IVC junction. The CPB is started before passing umbilical tape snares around both venae cavae and tightening them. After the donor heart arrives to the recipient hospital, the recipient should be cooled down to 28 °C.

The donor heart is taken into the operative field, trimmed, and prepared for implantation. First, the aorta is separated from the PA, and the PA is then opened below its bifurcation and trimmed. The ascending aorta is transected from at its widest diameter and trimmed. The right and left pulmonary veins are joined by incision, the LA is opened

posteriorly between these incisions to provide the maximum length for the left atrial suture line, and all weak tissues are removed. Finally, a retrograde cardioplegia cannula is inserted into the coronary sinus and the donor heart is preserved with retrograde continuous isothermic blood cardioplegia using "KK-polytropic" cardioplegia delivery system until the cross-clamp is released. The first blood cardioplegic volume (10 mL/kg) should be cooled down to 15°C and the latters should be cooled to the recipient's blood temperature at increasing temperature (2–3°C per each cyclus).

After the recipient's great vessels are dissected from each other, the ascending aorta is cross-clamped and a vent catheter is inserted into the LA via the RSPV. The recipient's heart is extracted and the donor heart is implanted using the preferred implantation technique, bicaval or biatrial.

Bicaval Technique

We prefer to use the standard bicaval technique with several variations of my clinic. There are several key points to avoid from surgical mismatches or deficiencies, purse-string effects, tension and torsion of anastomoses.

The SVC is transected at the atriocaval junction to the greatest extent possible without including atrial tissue. This approach provides the sufficient length of the native SVC without overly wide diameter for anastomosis and excludes the recipient's sinus node, resulting in postoperatively diagnostic mismatch of the presence or absence of the sinus rhythm.

The aorta and PA are then transected just above their sinotubular junctions (above commissural tops). This approach provides over-length native arterial structures, which can be trimmed according to donor arterial structures. If the recipient aortic length is excessive, the recipient aorta and also the donor aorta are trimmed until their midlevel, where each aorta has largest diameter, to prevent any anastomotic stenosis (purse-string effect, supravalvular stenosis, pseudocoarctation). If the recipient PA is long, it must be kept to avoid any injury of the recipient pulmonary bifurcation with or without branches, and the donor PA can be trimmed until its sinotubular junction to prevent any torsion or kinking of the anastomosis.

The LA resection is to begin at Sondergaard's plane, which starts on the left atrial wall anterior to the RSPV, as the standard left atriotomy incision. The left atrial incision is extended downwards under the IVC and upwards under the aorta; it is then completed in a semi-circular fashion by continuing above the left atrial appendage (LAA) and below the posterior mitral annulus. Before completing the total left atrial resection, the IVC should be transected with a generous cuff of the right atrial myocardium. If LA cavity is very enlarged, LA reduction is necessary and there are two approaches to reduce native left atrial cavity: LAA (for partial) or left atrial posterior wall between right and left pulmonary veins (for hudge) is resected as V-shape and both edges are sewn together with over-and-over technique. The LAA resection in a V-shape also prevents postoperative thrombosis due to removing the immobile recipient LAA.

The IVC is transected with a right atrial cuff. The incision should be started 2 cm above the inferior vena cannula on the anterior surface of the RA and extended immediately inferior to the coronary sinus orifice on the medial side and inferior to the RIPV on the lateral side; both ends are then joined to each other. The IVC cuff should be shaped like a broad-based funnel with an elliptic, concave tongue from bottom to front to prevent any stenosis of the IVC anastomosis.

The final step is to separate all attachments of the recipient heart to the underlying structures and remove it from the pericardial space. After then, all of the transected structures left behind should be prepared and trimmed for the upcoming anastomoses.

Implantation begins with the left atrial anastomosis, which starts with a double-armed 4/0 polypropylene suture at the lower sides of both LAAs (Fig. 45.4a). If native LAA is resected, then the sewn edges are sutured at the midlevel of the orifice of donor's LAA. Whenever possible, there should be mutual contact of the two left atrial surfaces to promote direct endothelial apposition and to prevent potential thrombus formation, and a running everything suture technique should be externally applied to avoid excessive protrusion of the tissue from the suture line. The two LAAs

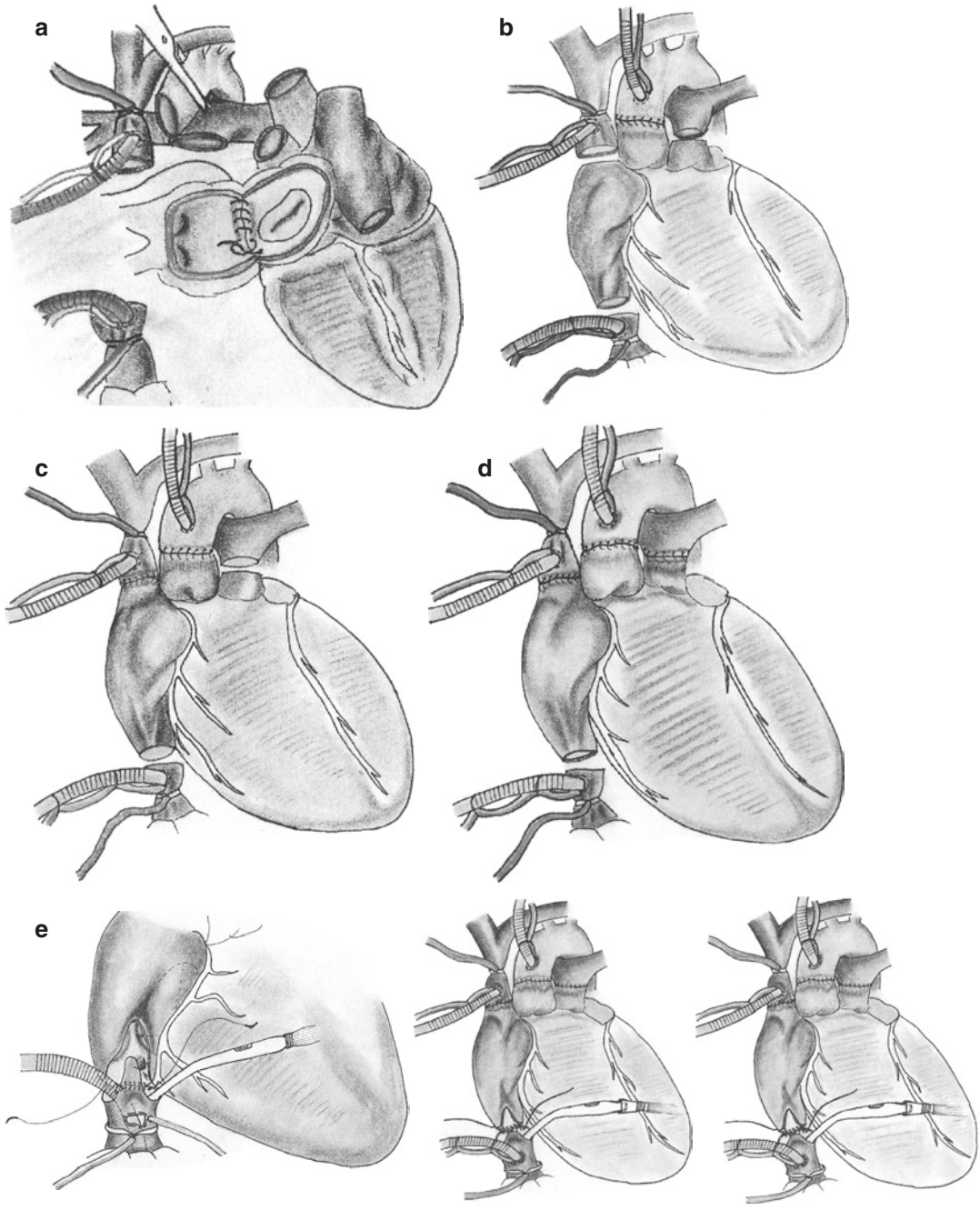

Fig. 45.4 Bicaval HTx. (**a**) Left atrial anastomosis is started at the appendage level. (**b**) Second step under cross-clamp is aortic anastomosis. (**c**) After removing cross-clamp, SVC anastomosis is performed. (**d**) The next step is pulmonary arterial anastomosis. (**e**) The last step is IVC anastomosis via open-suturing approach

are sewn to each other; this secures the appropriate geometric placement of the donor heart and the reciprocal placement of both SVCs, which is important for preventing any stenosis, torsion, tension, traction, or laceration of the superior caval anastomosis. When both arms of the suture are extended from both sides with the continuous suturing technique, a fixing loop should be per-

formed at every fifth or sixth stitch to ensure the tightness of the suture. When both arms of the suture reach the area of the right pulmonary veins, the LA is allowed to filling with blood by vigorous expansion of the lungs; the suture line is then secured and tied. The second anastomosis is performed as the same way between the two aortas, constructing a standard end-to-end anastomosis is by using a running double-armed 4/0 polypropylene suture that includes several fixing loops for suture tightness. It is rare for there to be an aortic mismatch but, in patients with annuloaortic ectasia, the donor ascending aorta cannot match the appropriate size of the dilated recipient aorta. A tubular graft must be interposed between the two aortas of different diameters to adapt the smaller outflow to the larger orifice [57]. Compatibility of the tubular arterial vasculatures is even more essential if recipient's aorta is markedly smaller, to avoid artificial aortic coarctation. Before securing the suture line, an antegrade cardioplegic needle should be inserted through the suture line or into the ascending aorta to de-air the left heart, and the suture line then secured. Rewarming and mechanical ventilation are started, the LA is filled, and the cross-clamp is removed after the left heart de-airing (Fig. 45.4b). The rest of the surgery is completed on the beating heart. The retrograde cardioplegia cannula is removed, and the left atrial and aortic anastomoses are both checked for any bleeding or dehiscence. The next step is the anastomosis of the PAs or SVCs depending on surgeon's preference. The SVC anastomosis is performed with a running double-armed 5/0 polypropylene suture, including several fixing loops to prevent the purse-string effect of the suture line. The key point is to avoid the reconstructed SVC being unnecessary long, because this causes a tunnel format that increases resistance and can result in SVC syndrome (Fig. 45.4c). The point to note is the length of the reconstructed PA to avoid folding and shrinking: the donor PA should be transected below its bifurcation, the recipient PA trimmed, and an end-to-end anastomosis constructed with a continuous double-armed 4/0 polypropylene suture, including several fixing loops for suture tightness (Fig. 45.4d). Finally, the IVC anastomosis is performed with a running double-armed 5/0 polypropylene suture, including several fixing loops to prevent the purse-string effect of the suture. The specific shape of the IVC cuff and the extended inferior orifice of the donor RA via a vertical front incision, made until the tricuspid annulus will be visible, both simplify inferior caval anastomosis by the continuous suturing technique without causing anastomotic stenosis. The attractive strategy during this anastomosis is the open suturing approach with releasing the tape around the native VCI, removing and inserting the inferior cava cannula directly into the VCI or leaving it as it is under negative vacuum, and aspirating the VCI with coronary suction cannula additionally (Fig. 45.4e).

Biatrial Technique

When using the biatrial technique, the recipient RA is incised just above the level of the entrance to the IVC and the incision is extended superiorly anterior to the sulcus terminalis. A second incision is made laterally at the interatrial membranous septum; this should continue superiorly until it meets the first incision in front of the SVC. The incision is then continued inferiorly around the coronary sinus until it meets the first incision in front of the IVC. The main difference of this technique from the bicaval technique is leaving both venae cavae intact below the cut surface, where the trabeculated RA is transected and the venous RA with both vena entrances is left untouched. The LA is resected, leaving a generous cuff above the entrances of both side pulmonary veins and the LAA.

The donor heart is prepared in a different way to the bicaval technique, especially with regard to the LA and the RA. A circular cuff for the LA, tailored to the recipient left atrial remnant, is created by incising through the pulmonary vein orifices and combining them. The RA is harvested as described for the bicaval technique, but the SVC is left as knotted during implantation. The RA is prepared by a curvilinear incision from the IVC orifice toward the base of the RA appendage, approximately equidistant from the sulcus terminalis and the atrioventricular groove to reduce the risk of injury on the sinoatrial node.

Implantation begins with the left atrial anastomosis, which starts with a double-armed 4/0 polypropylene suture at the lower sides of both LAAs. The rest of the anastomosis is completed as described for the bicaval technique, providing endothelium-to-endothelium apposition. When both arms of the suture are extended from both sides, a fixing loop should be performed by several time to ensure the tightness of the suture, and the suture arms tied together on the outside of the heart. Left atrial venting is stopped and the LA allowed to fill with blood by vigorous expansion of the lungs to de-air the left heart. The second anastomosis is proceeded with the RA anastomosis, which is constructed with a running double-armed 4/0 polypropylene suture, including several fixing loops for suture tightness. The third anastomosis is the aortic anastomosis, which is performed with a continuous double-armed 4/0 polypropylene suture. An antegrade cardioplegic needle is inserted through the suture line to de-air the left heart, and the suture line is then secured. Rewarming and mechanical ventilation are started, the LA is filled, and the cross-clamp is removed after de-airing the left heart. The pulmonary end-to-end anastomosis is constructed as described for the bicaval anastomosis (Fig. 45.5).

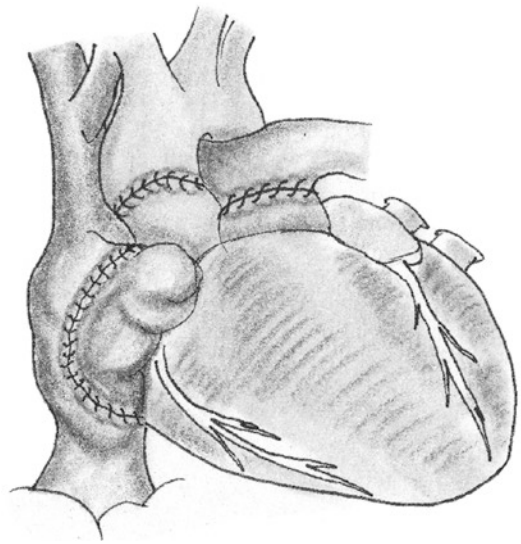

Fig. 45.5 Biatrial HTx

45.5.2.2 Lung Implantation

If the lungs are implanted separately without using CBP, a consecutive technique is preferred in which the functionally worse side is usually transplanted first with the better lung. Pneumonectomy of the recipient is performed in the standard fashion, stapling the pulmonary artery and veins, and the bronchus is prepared centrally and opened with a scalpel. Two 4/0 polydioxanone stay sutures are placed at the angles between the cartilaginous and membranous portions. The lung is then removed from the chest cavity, the pericardium is opened between the superior pulmonary vein and the phrenic nerve, and the LA is fully mobilized. The PA is prepared intrapericardially as centrally as possible to provide sufficient length for the anastomosis. The donor lung is then unpacked, all of the vascular structures are prepared, and the pulmonary artery is carefully inspected for any intraluminal embolic material. The bronchus is shortened such that only one cartilage ring remains after separating the upper lobe bronchus and careful preserving of the peribronchial tissue. The first step is the bronchial anastomosis, which starts at one end of the cartilaginous portion, passes over the membranous portion with a single running suture technique, and then uses the same single running suture for the anterior cartilaginous portion. If there is a bronchial size mismatch, the imbalance is adjusted over the whole circumference. Usually, the anastomosis is not covered with any additional tissue. The left atrium is then side-clamped intrapericardially with a Satinsky clamp and anastomosed at the level where there is myocardial muscle tissue present; this is because the tissue at the level of the veins is too fragile to allow a safe anastomosis. The final step is pulmonary artery anastomosis (Fig. 45.6). After administering the initial dose of immunosuppressants, retro- and antegrade flushing of the pulmonary vasculature to flush out the preservation solution, and de-airing the pulmonary vascular system, the sutures of the anastomoses are knotted. At this stage, protective ventilation is started without manual recruitment. If the procedure is performed without the use of extracorporeal support, controlled reperfusion

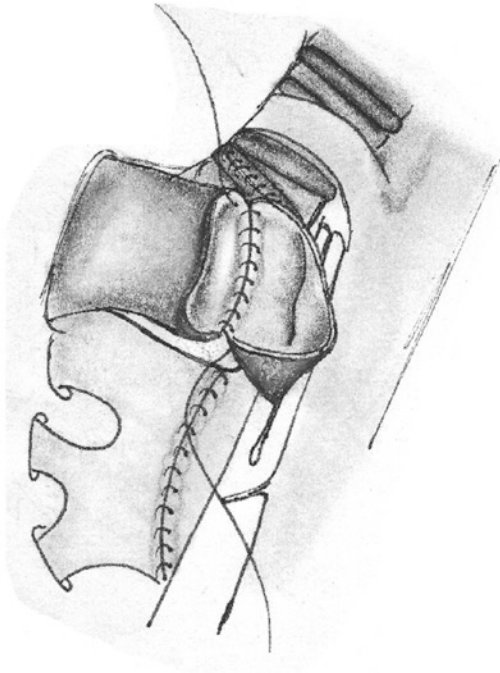

Fig. 45.6 Lung implantation

with partial manual compression of the PA should be performed for 10 min to avoid an initial volume overload of the newly implanted lung.

45.5.2.3 Heart and Lung En-Block Implantation

As with the procedure for orthotopic HTx, the HLTx recipient is prepared in the standard fashion and CPB is established through a median sternotomy. Both pleurae are opened widely. The native heart is excised first, as with the bicaval technique: all that remains are a cuff of the LA including bilateral pulmonary veins, the ascending aorta, and both venae cavae. The second step is to remove both lungs with the vascular structures, after dividing the pulmonary attachments. The bilateral bronchial stumps are mobilized to the level of the carina, and the trachea is transected just above the bronchial bifurcation. The donor's heart-lung block is prepared by dividing the trachea approximately 2 cm above the carina with the membranous portion longer than the cartilaginous portion. The lungs should be placed beneath the pericardial pedicle on each side. The

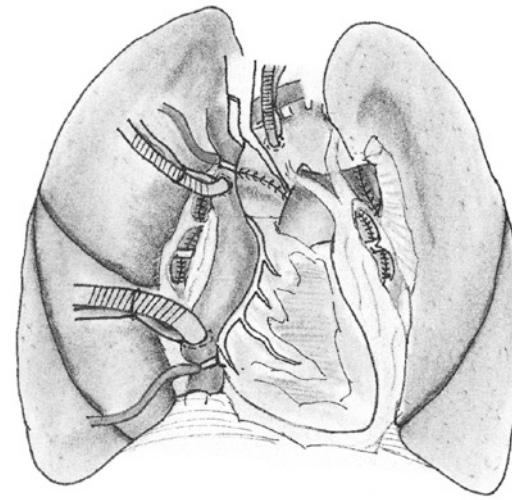

Fig. 45.7 Heart and lung en-block implantation

first anastomosis is the tracheal anastomosis using a continuous 3/0 polypropylene suture; the pericardium is then wrapped around it. The bicaval technique is used for the cardiac anastomosis (Fig. 45.7).

45.6 Immunosuppression

Each clinic designs its own immunosuppressive treatment, but the preferred regimen is usually triple medication with a calcineurin inhibitor (cyclosporine or tacrolimus), an antiproliferative agent (azathioprine or mycophenolate mofetil), and corticosteroids (Table 45.13). However, it is recommended that corticosteroids are discontinued at the 6th months post-HTx because of the numerous metabolic and cardiovascular side effects [58]. The early addition of an mTOR agent (sirolimus or everolimus) increases the effects of the calcineurin inhibitors and allows their dosage to be reduced to prevent renal impairment; these agents also reduce the progression of cardiac allograft vasculopathy. Induction therapy provides more intensive initial immunosuppression, with the aims of reducing the incidence of acute rejection and facilitating the maintenance of post-transplant immunosuppression [59]. Typically, this would comprise interleukin-2 antagonists (basiliximab) before surgery, corticosteroids

Table 45.13 Our immunosuppression protocol

A) Induction (preoperatively)				
Prednizolone (10–15 mg/kg iv bolus; usually total 1000 mg)				
Basiliximab (20 mg iv infusion/3 h)				
Mycophenolate (10–20 nmg/kg oral; usually total 1000 nmg)				
B) Post-surgery (during surgery, after cross-clamping)				
rATG (1–1.5 mg/kg infusion in 8 h; usually total 100 mg)				
C) Maintenance (during postoperative hospitalization)				
Cyclosporine (2 × 50 mg oral, increasing by 50 mg/daily until target blood level: 250–300 ng/mL) *or* [*Tacrolimus (2 × 0.5 mg oral, increasing by 0.5 mg/daily until target blood level: 8–10 ng/mL*)]				
Mycophenolate (2 × 500 mg oral, increasing by 250 mg/daily until target blood level: 1–3 ng/mL)				
Everolimus (2 × 0.5 mg oral, increasing by 0.25 mg/daily until target blood level: 6–8 ng/mL)				
(with/without Prednisolone 1 mg/kg oral, decreasing by 4 mg/daily until 2 × 4 mg)				
D) Maintenance (after discharge)				
Immunosuppressive	Total dose	Dosage	Target blood level	Duration
Cyclosporine	2–4 mg/kg/day	2 × 1/day	250–300 ng/mL	<6th month
			200–250 ng/mL	6–12th month
			<200 ng/mL	>12th month
or Tacrolimus	0.05–0.1 mg/kg/day	2 × 1/day	8–10 ng/mL	<3rd month
			5–8 ng/mL	>3rd month
Mycophenolate	10–20 mg/kg/day (max 2000 mg)	2 × 1/day	–	Life-long
Everolimus	1–2 mg/day	2 × 1/day	6 ± 1 ng/mL	Life-long
Prednisolon	4 mg	1 × 1 /day	–	<6 months

before and after surgery, antilymphocyte antibodies (thymoglobulin) after surgery.

The objectives of HTx management are the prevention of acute cellular and antibody-mediated rejection and cardiac allograft vasculopathy, and optimal preservation of the integrity and function of the donor organ. Valuable noninvasive diagnostic tests for the follow-up asymptomatic recipients include AlloMap molecular expression testing, graft-derived cell-free DNA testing, echocardiography and cardiac magnetic resonance imaging; however, endomyocardial biopsy remains the gold standard for clarifying allograft rejection in symptomatic patients [60]. Correlating with and supported by the other noninvasive methods, cytoimmunologic monitarization can be used a reliable method for screening of rejection phenomenon and infection, and may reduce the need of endomyocardial biopsies in heart transplant patients [61]. Electrocardiographic recordings from epicardial pacemaker leads left on the LV and the RV may be an assistive diagnostic method for early postoperative rejection [62]. However, the standard current practice for post-transplantation follow-protocol to detect allograft rejection consists of periodic echocardiographic controls with or without endomyocardial biopsy procurement [63].

45.7 Postoperative Complications

45.7.1 Acute Graft Failure

Primary cardiac allograft failure is the main cause of acute graft failure, accounting for more than 35% deaths in the first 30 days. This pathology is observed in 1.5–30% of recipients after HTx; its main manifestation is hemodynamical instability with LCOS [64]. Risk factors include ischemia–reperfusion, immunosensitization, elevated PVR, and blood group incompatibility. *Hyperacute humoral* rejection is infrequent, but it can be very severe. It is related to the presence of previously formed antibodies against the donor [the ABO system, human leukocyte antigens (HLA), or endothelium], and can be caused by ABO-incompatible transplantation or pre-transplant panel reactive antibodies. Treatment is difficult and is based on hemodynamic support with vasoactive and

inotropic drugs with or without mechanical circulatory assistance devices.

Primary lung allograft failure develops in at least one-third of LTx recipients within 1 year post-transplantation. Acute rejection, although rarely a direct cause of death, is the principal risk factor for chronic rejection, which is the greatest risk to long-term survival [65]. *Acute cellular rejection* is defined as perivascular or peribronchiolar lymphocytic infiltrates in the absence of infection; it is diagnosed primarily by bronchoscopic transbronchial biopsies. There is a strong correlation between the severity and frequency of acute cellular rejection and the risk of developing bronchiolitis obliterans syndrome. *Acute humoral rejection* remains poorly defined but is thought to involve anti-donor antibodies or allograft dysfunction; there is also pathological evidence of associated lung tissue injury or the deposition of complement.

45.7.2 Rejection

The main risk factor for impaired early- and long-term survival is rejection of the transplanted heart. Classically, there are three types of rejection: hyperacute, cellular and humoral. *Hyperacute rejection* is the main cause of early allograft failure, occurring within minutes to several hours after transplantation. *Acute cellular rejection* is the most frequent type of rejection in the first 6 months and is characterized by the presence of inflammatory cells in the myocardium. It is classified into four grades, 0R to 3R; grades 2R and 3R both require additional immunosuppressive treatment (corticosteroids and/or antilymphocyte antibodies). *Acute humoral rejection* is mediated by antibodies against the vascular endothelium of the allograft (mainly anti-HLA) and usually develops in patients who have become allosensitized (through exposure to transfusion, gestation, transplantation, or circulatory assistance devices). The true incidence of humoral rejection is estimated to be approximately 10–15% at the end of the first year post-transplantation. It is associated with worse clinical progress and requires aggressive therapy with corticosteroids, antilymphocyte antibodies, immunoglobulin, plasmapheresis, and drugs that block the production of antibodies by B lymphocytes (rituximab, bortezomib, or eculizumab).

45.7.3 Late Graft Failure

Cardiac allograft vasculopathy is the primary cause of late mortality more than 1 year after HTx, with an incidence rate of 8% in the first year, 30% at 5 years, and 50% at 10 years. There are several risk factors: the donor's age, the presence of anti-HLA antibodies, cytomegalovirus infection, dyslipidemias, diabetes mellitus, obesity, and smoking. The pathology has an atherosclerotic, obliterative, and diffuse nature with a faster rate of progression than primary coronary artery disease. It usually involves the entire coronary artery territory, including the intramyocardial arterioles. The main characteristics of its vasculopathy are smooth muscle cell proliferation, concentric intimal hyperplasia without calcification, perivascular infiltration, and the loss of endothelial continuity. Early symptoms usually include the typical clinical manifestations of atherosclerosis (arrhythmia, heart failure, and sudden death), but not angina pectoris because of the denervated allograft. Coronary angiography is the first choice for diagnosing this pathology and percutaneous revascularization the preferred treatment option [66]; however, heart retransplantation is the only definitive therapy.

Chronic lung allograft dysfunction has two phenotypes: bronchiolitis obliterans and restrictive allograft syndrome. Whether obstructive or restrictive, chronic lung allograft dysfunction is defined as a persistent, mostly irreversible, progressive and obstructive decline in pulmonary function after LTx (>20% decline in FEV_1 and/or FVC). It affects about 50% of recipients within 5 years postoperatively [67]. Radiologic findings typically demonstrate air trapping, mosaic attenuation, and hyperinflation. Pathologic examination reveals obliterative bronchiolitis lesions and pure obliteration of the small airways (<2 mm), with a relatively normal surrounding parenchyma and a damage-inducing epithelial repair response with activation of inflammatory and non-inflammatory mediators, leading to fibrosis [68].

45.7.4 Infection

Opportunistic infections are the second most frequent cause of mortality during the first year after transplant, accounting for 12% of deaths in the first 30 days and 29% between 1 month and 1 year. In the first 6 months, infections are mostly of bacterial origin related to hospital flora; after that, extra-hospital agents are more frequent. The lungs and urinary tract are the most common sites of infection during the first year [69].

45.7.5 Right Heart Failure

The most important cardiac dysfunction is RVF secondary to elevated right ventricular afterload (systolic PAP >60 mmHg, PVR >5 Wood units, and TPG >15 mmHg), which is characterized with hypoxia, acidosis and LCOS. It develops immediately after the discontinuation of CPB due to mechanical causes (such as anastomotic torsion or angulation of the PA), protamine reaction or gas embolism, or sinus node dysfunction. Right heart dysfunction accounts for up to 50% of all cardiac complications after HTx and almost 20% of deaths in the early postoperative period. Temporary RHF can usually be treated using simple treatment modalities such as optimization of the right ventricular preload, reduction of PVR (using nitroprusside, nitric oxide, prostacyclin, and sildenafil), augmentation of myocardial contractility (with milrinone, dobutamine, adrenaline, and isoproterenol), and procuration of heart rhythm (by atrio-ventricular pacing). If these approaches are not effective, mechanical ventilation to avoid hypoxia and elevated ventilatory pressures and/or mechanical circulatory support devices should be considered.

45.7.6 Neoplasms

Neoplastic disease can arise in the years following transplantation as a result of immunosuppressive medication, viral infections (with the Epstein–Barr virus, human herpes virus, human papilloma virus, hepatitis B and C viruses, etc.), or a preexisting malignancy. Chronic immunosuppression is associated with an increased incidence of malignancy (<5% during the first year, thereafter 4–18%). The most common malignancies are lymphoproliferative disorders and skin carcinoma [70].

Conclusion

Patients with dominant right ventricular failure referred to heart transplantation usually suffer from the left-sided heart failure, primary pulmonary hypertension, and congenital heart diseases; however, the frequency of isolated right heart failure with structural abnormalities has also been increasing recently. Biomechanical and biotechnological advancement in long-term ventricular assist devices may prolong survival and improve the quality of life; however, although mechanical circulatory support technology is improving, transplantation remains the sole effective treatment for irreversible right heart pathologies.

References

1. Konstantinov IE. A mystery of Vladimir P. Demikhov: the 50th anniversary of the first intrathoracic transplantation. Ann Thorac Surg. 1998;65(4):1171–7. pii: S0003-4975(97)01308-8.
2. Demikhov VP. Experimental transplantation of vital organs (authorized translation from the Russian by basil Haigh). New York: Consultant's Bureau; 1962.
3. Hardy JD, Webb WR, Dalton ML Jr, Walker GR Jr. Lung homotransplantation in man. JAMA. 1963;186(12):1065–74. https://doi.org/10.1001/jama.1963.63710120001010.
4. Barnard C. The operation. A human cardiac transplant: an interim report of a successful operation performed at Groote Schuur Hospital, Cape Town. S Afr Med J. 1967;41(48):1271–4.
5. Deuse T, Sista R, Weill D, Tyan D, Haddad F, Dhillon G, Robbins RC, Reitz BA. Review of heart-lung transplantation at Stanford. Ann Thorac Surg. 2010;90(1):329–37. https://doi.org/10.1016/j.athoracsur.2010.01.023.
6. Barnard CN, Barnard MS, Cooper DK, Curchio CA, Hassoulas J, Novitsky D, Wolpowitz A. The present status of heterotopic cardiac transplantation. J Thorac Cardiovasc Surg. 1981;81(3):433–9.
7. Caves PK, Stinson EB, Billingham ME, Rider AK, Shumway NE. Diagnosis of human cardiac allograft rejection by serial cardiac biopsy. J Thorac Cardiovasc Surg. 1973;66(3):461–6.

8. Kahan BD. Immunosuppressive therapy with cyclosporine for cardiac transplantation. Circulation. 1987;75(1):40–56. https://doi.org/10.1161/01.CIR.75.1.40.
9. Reitz BA, Wallwork JL, Hunt SA, Pennock JL, Billingham ME, Oyer PE, Stinson EB, Shumway NE. Heart-lung transplantation: successful therapy for patients with pulmonary vascular disease. N Engl J Med. 1982;306(10):557–64. https://doi.org/10.1056/NEJM198203113061001.
10. Toronto Lung Transplant Group. Unilateral lung transplantation for pulmonary fibrosis. N Engl J Med. 1986;314(18):1140–5. https://doi.org/10.1056/NEJM198605013141802.
11. Yacoub MH, Banner NR, Khaghani A, Fitzgerald M, Madden B, Tsang V, Radley-Smith R, Hodson M. Heart-lung transplantation for cystic fibrosis and subsequent domino heart transplantation. J Heart Transplant. 1990;9(5):459–66.
12. Shudo Y, Ma M, Boyd JH, Woo YJ. Current status of domino heart transplantation. J Card Surg. 2017;32(3):229–32. https://doi.org/10.1111/jocs.13104.
13. Flécher E, Fouquet O, Ruggieri VG, Chabanne C, Lelong B, Leguerrier A. Heterotopic heart transplantation: where do we stand? Eur J Cardiothorac Surg. 2013;44(2):201–6. https://doi.org/10.1093/ejcts/ezt136.
14. Lund LH, Edwards LB, Dipchand AI, Goldfarb S, Kucheryavaya AY, Levvey BJ, Meiser B, Rossano JW, Yusen RD, Stehlik J, International Society for Heart and Lung Transplantation. The registry of the International Society for Heart and Lung Transplantation: thirty-third adult heart transplantation report−2016; focus theme: primary diagnostic indications for transplant. J Heart Lung Transplant. 2016;35(10):1158–69. https://doi.org/10.1016/j.healun.2016.08.017.
15. Rossano JW, Dipchand AI, Edwards LB, Goldfarb S, Kucheryavaya AY, Levvey Rn BJ, Lund LH, Meiser B, Yusen RD, Stehlik J, International Society for Heart and Lung Transplantation. The registry of the International Society for Heart and Lung Transplantation: nineteenth pediatric heart transplantation report-2016; focus theme: primary diagnostic indications for transplant. J Heart Lung Transplant. 2016;35(10):1185–95. https://doi.org/10.1016/j.healun.2016.08.018.
16. Yusen RD, Edwards LB, Dipchand AI, Goldfarb SB, Kucheryavaya AY, Levvey BJ, Lund LH, Meiser B, Rossano JW, Stehlik J, International Society for Heart and Lung Transplantation. The registry of the International Society for Heart and Lung Transplantation: thirty-third adult lung and heart–lung transplant report-2016; focus theme: primary diagnostic indications for transplant. J Heart Lung Transplant. 2016;35(10):1170–84. https://doi.org/10.1016/j.healun.2016.09.001.
17. Goldfarb SB, Levvey BJ, Edwards LB, Dipchand AI, Kucheryavaya AY, Lund LH, Meiser B, Rossano JW, Yusen RD, Stehlik J, International Society for Heart and Lung Transplantation. The registry of the International Society for Heart and Lung Transplantation: nineteenth pediatric lung and heart–lung transplantation report-2016; focus theme: primary diagnostic indications for transplant. J Heart Lung Transplant. 2016;35(10):1196–205. https://doi.org/10.1016/j.healun.2016.08.019.
18. Kırali K, Özer T, Özgür MM. Pathophysiology in heart failure. In: Kırali K, editor. Cardiomyopaties: types and treatments. Crotia: InTech; 2017. p. 17–38. https://doi.org/10.5772/66887.
19. Mielniczuk LM, Chandy G, Stewart D, Contreras-Dominguez V, Haddad H, Pugliese C, Davies RA. Worsening renal function and prognosis in pulmonary hypertension patients hospitalized for right heart failure. Congest Heart Fail. 2012;18(3):151–7. https://doi.org/10.1111/j.1751-7133.2011.00275.x.
20. Megall S, Holtzman D, Aronow WS, Nazari R, Korenfeld S, Schwarcz A, Goldberg Y, Spevack DM. Predictors of cardiac hepatopathy in patients with right heart failure. Med Sci Monit. 2011;17(10):CR537–41. https://doi.org/10.12659/MSM.881977.
21. Tadic M. Multimodality evaluation of the right ventricle: an updated review. Clin Cardiol. 2015;38(12):770–6. https://doi.org/10.1002/clc.22443.
22. Ponikowski P, Voors AA, Anker SD, Bueno H, Cleland JG, Coats AJ, Falk V, González-Juanatey JR, Harjola VP, Jankowska EA, Jessup M, Linde C, Nihoyannopoulos P, Parissis JT, Pieske B, Riley JP, Rosano GM, Ruilope LM, Ruschitzka F, Rutten FH, van der Meer P. 2016 ESC guidelines for the diagnosis and treatment of acute and chronic heart failure. The task force for the diagnosis and treatment of acute and chronic heart failure of the European Society of Cardiology (ESC). Developed with the special contribution of the Heart Failure Association (HFA) of the ESC. Eur J Heart Fail. 2016;18(8):891–975. https://doi.org/10.1002/ejhf.592.
23. Mehra MR, Canter CE, Hannan MM, Semigran MJ, Uber PA, Baran DA, Danziger-Isakov L, Kirklin JK, Kirk R, Kushwaha SS, Lund LH, Potena L, Ross HJ, Taylor DO, Verschuuren EA, Zuckermann A. International Society for Heart Lung Transplantation (ISHLT) Infectious Diseases Council; International Society for Heart Lung Transplantation (ISHLT) Pediatric Transplantation Council; International Society for Heart Lung Transplantation (ISHLT) Heart Failure and Transplantation Council. The 2016 International Society for Heart Lung Transplantation: listing criteria for heart transplantation: a 10-year update. J Heart Lung Transplant. 2016;35(1):1–23. https://doi.org/10.1016/j.healun.2015.10.023.
24. Sajgalik P, Grupper A, Edwards BS, Kushwaha SS, Stulak JM, Joyce DL, Joyce LD, Daly RC, Kara T, Schirger JA. Current status of left ventricular assist device therapy. Mayo Clin Proc. 2016;91(7):927–40. https://doi.org/10.1016/j.mayocp.2016.05.002.

25. Meineri M, Van Rensburg AE, Vegas A. Right ventricular failure after LVAD implantation: prevention and treatment. Best Pract Res Clin Anaesthesiol. 2012;26(2):217–29. https://doi.org/10.1016/j.bpa.2012.03.006.
26. Lampert BC, Teuteberg JJ. Right ventricular failure after left ventricular assist devices. J Heart Lung Transplant. 2015;34(9):1123–30. https://doi.org/10.1016/j.healun.2015.06.015.
27. Rich JD, Gosev I, Patel CB, Joseph S, Katz JN, Eckman PM, Lee S, Sundareswaran K, Kilic A, Bethea B, Soleimani B, Lima B, Uriel N, Kiernan M, Evolving Mechanical Support Research Group (EMERG) Investigators. The incidence, risk factors, and outcomes associated with late right-sided heart failure in patients supported with an axial-flow left ventricular assist device. J Heart Lung Transplant. 2017;36(1):50–8. https://doi.org/10.1016/j.healun.2016.08.010.
28. Lin EY, Cohen HW, Bhatt AB, Stefanescu A, Dudzinski D, Yeh DD, Johnson J, Lui GK. Predicting outcomes using the heart failure survival score in adults with moderate or complex congenital heart disease. Congenit Heart Dis. 2015;10(5):387–95. https://doi.org/10.1111/chd.12229.
29. Michielon G, Carotti A, Pongiglione G, Cogo P, Parisi F. Orthotopic heart transplantation in patients with univentricular physiology. Curr Cardiol Rev. 2011;7(2):85–91. https://doi.org/10.2174/157340311797484259.
30. Stewart GC, Mayer JE Jr. Heart transplantation in adults with congenital heart disease. Heart Fail Clin. 2014;10(1):207–18. https://doi.org/10.1016/j.hfc.2013.09.007.
31. Kirklin JK. Current challenges in pediatric heart transplantation for congenital heart disease. Curr Opin Organ Transplant. 2015;20(5):577–83. https://doi.org/10.1097/MOT.0000000000000238.
32. Mora BN, Huddleston CB. Heart transplantation in biventricular congenital heart disease: indications, techniques, and outcomes. Curr Cardiol Rev. 2011;7(2):92–101. https://doi.org/10.2174/157340311797484196.
33. Hetzer R, Weng Y, Delmo Walter EM. State of the art in paediatric heart transplantation: the berlin experience. Eur J Cardiothorac Surg. 2013;43(2):258–67. https://doi.org/10.1093/ejcts/ezs588.
34. Weill D, Benden C, Corris PA, Dark JH, Davis RD, Keshavjee S, Lederer DJ, Mulligan MJ, Patterson GA, Singer LG, Snell GI, Verleden GM, Zamora MR, Glanville AR. A consensus document for the selection of lung transplant candidates: 2014. An update from the Pulmonary Transplantation Council of the International Society for Heart and Lung Transplantation. J Heart Lung Transplant. 2015;34(1):1–15. https://doi.org/10.1016/j.healun.2014.06.014.
35. Thompson BP, Westall GP, Paraskeva M, Snell GI. Lung transplantation in adults and children: putting lung function into perspective. Respirology. 2014;19(8):1097–105. https://doi.org/10.1111/resp.12370.
36. Hoffman M, Chaves G, Ribeiro-Samora GA, Britto RR, Parreira VF. Effects of pulmonary rehabilitation in lung transplant candidates: a systematic review. BMJ Open. 2017;7(2):e013445. https://doi.org/10.1136/bmjopen-2016-013445.
37. Whitson BA, Hayes D Jr. Indications and outcomes in adult lung transplantation. J Thorac Dis. 2014;6(8):1018–23. https://doi.org/10.3978/j.issn.2072-1439.2014.07.04.
38. Frost AE. The intersection of pulmonary hypertension and solid organ transplantation. Methodist Debakey Cardiovasc J. 2016;12(4 Suppl):10–3. https://doi.org/10.14797/mdcj-12-4s1-10.
39. Galiè N, Humbert M, Vachiery JL, Gibbs S, Lang I, Torbicki A, Simonneau G, Peacock A, Vonk Noordegraaf A, Beghetti M, Ghofrani A, Gomez Sanchez MA, Hansmann G, Klepetko W, Lancellotti P, Matucci M, McDonagh T, Pierard LA, Trindade PT, Zompatori M, Hoeper M. 2015 ESC/ERS guidelines for the diagnosis and treatment of pulmonary hypertension: the Joint Task Force for the Diagnosis and Treatment of Pulmonary Hypertension of the European Society of Cardiology (ESC) and the European Respiratory Society (ERS): endorsed by: Association for European Paediatric and Congenital Cardiology (AEPC), International Society for Heart and Lung Transplantation (ISHLT). Eur Respir J. 2015;46(4):903–75.
40. Keshavjee S. Lung transplantation for idiopathic pulmonary arterial hypertension: steps in the right direction. Circulation. 2013;127(25):2470–1. https://doi.org/10.1161/CIRCULATIONAHA.113.003386.
41. Puri V, Patterson GA, Meyers BF. Single versus bilateral lung transplantation: do guidelines exist? Thorac Surg Clin. 2015;25(1):47–54. https://doi.org/10.1016/j.thorsurg.2014.09.007.
42. Zangiabadi A, De Pasquale CG, Sajkov D. Pulmonary hypertension and right heart dysfunction in chronic lung disease. Biomed Res Int. 2014;2014:739674. https://doi.org/10.1155/2014/739674.
43. Collum SD, Amione-Guerra J, Cruz-Solbes AS, DiFrancesco A, Hernandez AM, Hammandlu A, Youker K, Guha A, Karmouty-Quintana H. Pulmonary hypertension associated with idiopathic pulmonary fibrosis: current and future perspectives. Can Respir J. 2017;2017:1430350. https://doi.org/10.1155/2017/1430350.
44. Schaffer JM, Singh SK, Joyce DL, Reitz BA, Robbins RC, Zamanian RT, Mallidi HR. Transplantation for idiopathic pulmonary arterial hypertension: improvement in the lung allocation score era. Circulation. 2013;127(25):2503–13. https://doi.org/10.1161/CIRCULATIONAHA.112.001080.
45. Meyer DM, Rogers JG, Edwards LB, Callahan ER, Webber SA, Johnson MR, Vega JD, Zucker MJ, Cleveland Jr JC. The future direction of the

adult heart allocation system in the United States. Am J Transplant. 2015;15(1):44–54. https://doi.org/10.1111/ajt.13030.
46. Fudim M. The future of the adult heart allocation system in the United States. http://www.acc.org/latest-in-cardiology/articles/2017/02/09/07/24/the-future-of-the-adult-heart-allocation-system-in-the-us?w_nav=Tab.
47. Kobashigawa JA. The future of heart transplantation. Am J Transplant. 2012;12(11):2875–91. https://doi.org/10.1111/j.1600-6143.2012.04223.x.
48. Kırali K, Yerlikhan ÖA, Hançer H. Invasive treatment in advanced (stage-d) heart failure. In: Kırali K, editor. Cardiomyopathies – types and treatments. Croatia: InTech; 2017. p. 405–57. https://doi.org/10.5772/67455.
49. Eren E, Kırali K, Güler M, Yakut C. Donor heart preservation in heart transplantation. Turk Gogus Kalp Dama. 2004;12(2):145–50.
50. Kırali K. Intrathoracic organ preservation (Turkish). In: Paç M, Akçevin A, Aka SA, Büket S, Sarıoğlu T, editors. Cardiovascular surgery. 2nd ed. Ankara: MN Medical and Nobel; 2013. p. 1457–70.
51. Yakut C, Kırali K, Sareyyüpoğlu B. Heart transplantation (Turkish). In: Erol Ç, editor. Internal medicine. 1st ed. Ankara: MN Medical and Nobel; 2008. p. 2119–32.
52. Kara I, Kırali K, Yakut C. A comparison of the results of the bicaval and biatrial surgical technique in orthotopic heart transplantation: a review and meta-analysis. Turk Gogus Kalp Dama. 2012;20(3):672–81. https://doi.org/10.5606/tgkdc.dergisi.2012.135.
53. Kara I, Mansuroğlu D, Kırali K, Güler M, Ömeroğlu SN, Eren E, Balkanay M, Alp M, Ipek G, Işık Ö, Yakut C. Early-term results of bicaval and biatrial techniques in orthotopic heart transplantation. Turk Gogus Kalp Dama. 2012;20(2):223–9. https://doi.org/10.5606/tgkdc.dergisi.2012.045.
54. Bayezid Ö, Balkanay M, Öztek İ, Carin M, Öcal A, Ener S, Sezer H, Işık I, Yakut Ç, Koçak T, Sezer S, Çağlar N, Özdemir M, Yakut C. The first successful heart transplantation in Turkey. Kosuyolu Heart J. 1990;1(1):3–10.
55. Kırali K, Mansuroğlu D, Ömeroğlu SN, Tuncer A, Eren E, Toker ME, Erdoğan HB, Rabuş MB, Erentuğ V, Göksedef D, Güler M, Dağlar B, Balkanay M, Akıncı E, İpek G, Koçak T, Berki T, Gürbüz A, Işık Ö, Yakut C. Heart transplantation:12-year Koşuyolu experience. Turk Gogus Kalp Dama. 2001;9(2):62–7.
56. Sareyyüpoğlu B, Kırali K, Göksedef D, Rabuş MB, Tuncer A, Erentuğ V, Mansuroğlu D, Yakut C. Factors associated with long-term survival following cardiac transplantation. Anadolu Kardiyol Derg. 2008;8(5):360–6.
57. Kırali K, Eren E, Mataracı İ, Çevirme D. Combined orthotopic heart transplantation and prophylactic ascending aorta replacement in a Marfan patient. Turk Gogus Kalp Dama. 2011;19(3):434–6. https://doi.org/10.5606/tgkdc.dergisi.2011.058.
58. Baraldo M, Gregoraci G, Livi U. Steroid-free and steroid withdrawal protocols in heart transplantation: the review of literature. Transpl Int. 2014;27(6):515–29. https://doi.org/10.1111/tri.12309.
59. Aliabadi A, Grömmer M, Cochrane A, Salameh O, Zuckermann A. Induction therapy in heart transplantation: where are we now? Transpl Int. 2013;26(7):684–95. https://doi.org/10.1111/tri.12107.
60. Mavrogeni SI, Athanasopoulos G, Gouziouta A, Leontiadis E, Adamopoulus S, Kolovou G. Cardiac transplantation: towards a new noninvasive approach of cardiac allograft rejection. Expert Rev Cardiovasc Ther. 2017;15(4):307–13. https://doi.org/10.1080/14779072.2017.1307734.
61. Mansuroğlu D, Kırali K, Güler M, Tuncer A, Eren E, Akıncı E, Gürbüz A, Işık Ö, Yakut C. Follow-up of rejection phenomenia by using cytoimmunologic monitorisation in the heart transplantations. Turk Gogus Kalp Dama. 1998;6(5):369–79.
62. Mansuroğlu D, Eren E, Kırali K, İpek G, Yakut C. Can epicardial electrocardiogram be used in diagnosis of rejection after heart transplantation during early period? Turk Gogus Kalp Dama. 2003;11(2):131–2.
63. Hullin R. Heart transplantation: current practice and outlook to the future. Swiss Med Wkly. 2014;144:w13977. https://doi.org/10.4414/smw.2014.13977.
64. Mangini S, Alves BR, Silvestre OM, Pires RV, Pires LJT, Curiati MNC, Bacal F. Heart transplantation: review. Einstein. 2015;13(2):310–8. https://doi.org/10.1590/S1679-45082015RW3154.
65. McManigle W, Pavlisko EN, Martinu T. Acute cellular and antibody-mediated allograft rejection. Semin Respir Crit Care Med. 2013;34(3):320–35. https://doi.org/10.1055/s-0033-1348471.
66. Çevirme D, Mataracı İ, Konukoğlu O, Kırali K, Balkanay M. Cardiac allograft vasculopathy and coronary artery disease development with orthotopic heart transplantation. Koşuyolu Heart J. 2012;15(2):75–9. https://doi.org/10.5578/kkd.3445.
67. Verleden GM, Vos R, Vanaudenaerde B, Dupont L, Yserbyt J, Van Raemdonck D, Verleden S. Current views on chronic rejection after lung transplantation. Transpl Int. 2015;28(10):1131–9. https://doi.org/10.1111/tri.12579.
68. Müller C, Andersson-Sjöland A, Schultz HH, Eriksson LT, Andersen CB, Iversen M, Westergren-Thorsson G. Early extracellular matrix changes are associated with later development of bronchiolitis obliterans syndrome after lung transplantation. BMJ Open Respir Res. 2017;4(1):e000177. https://doi.org/10.1136/bmjresp-2016-000177.
69. Mansuroğlu D, Tuncer A, Eren E, Kırali K, İpek G, Yakut C. Pulmonary abscess causing by aspergillus flavus after cardiac transplantation. Turk Gogus Kalp Dama. 2002;10(1):35–7.
70. Toyoda Y, Guy TS, Kashem A. Present status and future perspectives of heart transplantation. Circ J. 2013;77(5):1097–110. https://doi.org/10.1253/circj.CJ-13-0296.

46 Mechanical Circulatory Support for Right Ventricular Failure: RVADs

Kaan Kırali, Sabit Sarıkaya, and Mehmet Aksüt

Abstract

Heart failure is the basic and featured pathologic leading cause of death. From a clinical perspective, the most important objectives in caring for heart failure patients are diagnosis of the underlying mechanism and delivery of appropriate, effective treatment. In the majority of cases, the left ventricle is affected but the right ventricle functions normally until the end stage. Right ventricular failure (RVF) results from weakening of the right ventricular structures and/or by an increase in pulmonary vascular resistance. Post-implant RVF, a third type has been recognized in the last two decades. Right ventricular failure results in poor filling of the left ventricle and poor output, often necessitating additional right ventricular support in the form of inotropes or a mechanical right ventricular assist device (RVAD). Temporary mechanical support devices increase pulmonary blood circulation with or without extracorporeal oxygenation to provide adequate cardiac output. The preferred approach is to insert a temporary mechanical support device in percutaneous va-ECCPS configuration for acute RVF in the intensive care unit or in surgical vp-ECCS configuration for post-implant RVF in the operating room. For longer use, right ventricular or biventricular assist devices are used to provide circulatory support. Permanent RVADs provide a parallel or series artificial circulation to substitute for failed ventricles or they take over completely the pump function of a resected heart. Short-term RVADs are extracorporeal or paracorporeal pumps located outside the body, whereas durable RVADs are implanted inside the body. A novel development will be a true artificial heart without a need for anticoagulants; however, heart transplantation is still the gold standard for curative treatment.

Keywords

Mechanical circulatory support · Right heart failure · Extracorporeal membranous oxygenation · Extracorporeal circulatory support · Extracorporeal cardiopulmonary support · Left ventricular bypass · Right ventricular bypass · Biventricular bypass · Kırali circuit · Total artificial heart · Right ventricular assist device

46.1 Introduction

Heart failure (HF), particularly left heart failure (LHF), is the basic and featured pathologic leading cause of death worldwide and accounts for increas-

K. Kırali (✉) · S. Sarıkaya · M. Aksüt
Department of Heart Transplantation and Mechanical Assist Device, Kartal Koşuyolu Education and Research Hospital, Istanbul, Turkey

S. I. Dumitrescu et al. (eds.), *Right Heart Pathology*, https://doi.org/10.1007/978-3-319-73764-5_46

ingly large health care expenditures. From a clinical perspective, the most important objectives in caring for HF patients are diagnosis of the underlying mechanism and delivery of appropriate, effective treatment. Heart transplantation (HTx) remains the gold standard for curative treatment. In the majority of cases, the left ventricle (LV) is affected (causing LHF), but the right ventricle (RV) functions normally until the end stage of the pathology. In cases of right heart pathology or end-stage LHF, right ventricular failure (RVF) results from weakening of the right ventricular structures and/or by an increase in pulmonary vascular resistance (PVR). Right heart failure (RHF) can occur from primary right heart pathologies (e.g., congenital heart diseases, arrhythmogenic right ventricular dysplasia, right-sided valvular pathologies) or develop secondary to severe pulmonary arterial hypertension (PAH) caused by lung pathologies or LHF. Post-implant RVF, a third type of RHF type has been recognized in the last two decades (see Chap. 47). Several types of left ventricular assist device (LVAD) have been developed to maintain the cardiac cycle by continued drainage of the intercavitar ventricular blood volume into the arterial circulation. If the right heart cannot adapt to this nonphysiologic change, LVAD complications may arise, the most serious of which is newly developed or continued deterioration of RVF. This condition increases postoperative mortality and morbidity, end-organ dysfunction due to severe congestion (coagulopathy, malnutrition, renal and hepatic dysfunctions, edema, ascites, anasarca), the duration of hospitalization, and decreases the success of "bridge to HTx" therapy. The increasing number of LVAD implantations makes RVF a more common and challenging problem in HF clinics. Predicting post-implant RVF in LVAD patients becomes much more important because of the complex pathophysiology of post-operative RVF.

According to the International Right Heart Foundation Working Group, RHF is "a clinical syndrome due to an alteration of structure and/or function of the right heart circulatory system that leads to suboptimal delivery of blood flow (high or low) to the pulmonary circulation and/or elevated venous pressures—at rest or with exercise" [1]. The definition of RHF thus includes a dysfunction in any of the components of the right heart circulatory system, from systemic veins (post-systemic capillaries) to pulmonary arterial branches (pre-pulmonary capillaries). Post-implant RVF is defined by the Interagency Registry of Mechanically Assisted Circulatory Support (INTERMACS) as "symptoms and signs of persistent right ventricular dysfunction, central venous pressure >18 mmHg with a cardiac index <2.3 L/min/m^2 in the absence of elevated left atrial pressure or pulmonary capillary wedge pressure (>18 mmHg), tamponade, ventricular arrhythmias or pneumothorax; or requiring right ventricular assist device implantation; or requiring inhaled nitric oxide or inotropic therapy for a duration of more than one week at any time after LVAD implantation."

Left heart failure symptoms and concomitant RHF can be ameliorated by cardiac output provided by an LVAD. Increased stroke volume by the LVAD and ventricular unloading result in decreased mitral regurgitation and left ventricular end-diastolic pressure. Decreased pulmonary capillary wedge pressure (PCWP) and pulmonary arterial pressure (PAP) diminish the right ventricular afterload, improving right ventricular function. On the other hand, increased cardiac output lead to a much greater volume of venous return to the RV, where volume overloading may trigger distension of right ventricular myofibrils and tricuspid valve incompetence, resulting in RHF. Another cause for LVAD-related RHF is excessive unloading of the LV, causing a left-sided shift of the interventricular septum that can increase tricuspid regurgitation (TR) and cause progressive right ventricular dilation. Right ventricular dysfunction results in poor filling of the LV and poor LVAD output, often necessitating additional right ventricular support in the form of inotropes or a mechanical right ventricular assist device (RVAD). Optimal patient and device selection depends on the ability to predict which patients will tolerate isolated LVAD support. Several studies define preoperative risk factors and risk calculators for RVF development and optimal treatment strategies (Table 46.1) [2–6]. Individual risk scoring systems have been developed to identify independent predictors of post-

Table 46.1 Risk scores for post-implant RVF

1. Michigan RVF risk score

Matthews et al. [2] (*RVF rate: 35% in 197 patients*) evaluated over 80 pre-operative variables in LVAD patients to identify independent predictors of RVF, and all variables (i.e., clinical, echocardiographic, laboratory, and hemodynamic) with a univariable $p \leq 0.1$ for predicting RVF were entered into multivariable analyses. Remaining independent ($p \leq 0.1$) predictors of RVF were selected as the components of the RVF risk score. The score is calculated as the sum of the points awarded for the presence of each of the 4 pre-operative variables.

For each variable, if patients meet the "high-risk" criterion they are assigned with the score; if patients meet the "low-risk" criterion for a particular variable they are assigned a score of 0.

A threshold value of 5.5 (with a score <3 predicting successful LVAD support, and >5.5 predicting BiVAD) has an 80% positive predictive value of RV failure in LVAD candidates, reports an overall sensitivity of only 35%.

Variable	*OR (95%)*	*Cut-off level*	*Point*
Vasopressor requirement	3.9 (1.5–9.8)	+	4
Creatinine or dialysis	2.9 (1.1–7.7)	≥2.3 mg/dL	3
Bilirubin	2.4 (1.1–5.2)	≥2 mg/dL	2.5
AST	2.1 (0.96–4.5)	≥80 IU/L	2
Risk score	*RVF likelihood ratio (95% CI)*		
≤3	0.49 (0.37–0.64)		
4–5	2.8 (1.4–5.9)		
≥5.5	7.6 (3.4–17.1)		

2. Pennsylvania RVF risk score-1

Fitzpatrick et al. [3] (*RVF rate: 37% in 266 patients*) evaluated 23 pre-operative variables in LVAD patients to identify independent predictors of RVF, and all variables (i.e., clinical, laboratory, and hemodynamic) with a univariable $p \leq 0.05$ for predicting RVF were entered into multivariable analyses. Remaining independent ($p \leq 0.05$) predictors of RVF were selected as the components of the RVF risk score.

For each variable, if patients meet the "high-risk" criterion they are assigned with the score; if patients meet the "low-risk" criterion for a particular variable they are assigned a score of 0. The maximum possible score is 98, and the threshold is 50 points.

A threshold of 50 points (with a score <50 predicting successful LVAD support, and ≥50 predicting need for BiVAD), achieves sensitivity of 83% and specificity of 80%.

Variable	*OR (95% CI)*	*Cut-off level*	*Score*
CI	5.7 (1.3–24.4)	≤2.2 L/min/m^2	18
RVSWI	5.1 (2.1–12.2)	≤0.25 mmHg × L/m^2	18
Preoperative severe RVD	5 (2–12.5)	+	16
Preoperative creatinine	4.8 (1.9–12)	≥1.9 mg/dL	17
Previous cardiac surgery	4.5 (1.7–11.8)	+	16
Systolic blood pressure	2.9 (1.2–6.9)	≤96 mmHg	13
Risk score	*Prediction*		
< 30	LVAD		
< 50	LVAD		
≥ 50	BiVAD		
≥ 65	BiVAD		

3. Pennsylvania RVF risk score-2 (the CRITT score)

Atluri et al. [4] (*RVF rate: 23% in 167 patients*) evaluated 50 pre-operative variables in LVAD patients to identify independent predictors of RVF, and all variables (i.e., clinical, laboratory, echocardiographic, and hemodynamic) with a univariable $p \leq 0.05$ for predicting RVF were entered into multivariable analyses. Remaining independent ($p \leq 0.05$) predictors of RVF were selected as the components of the RVF risk score.

For each variable, if patients meet the criterion for a particular variable they are assigned with the score of 1; if patients do not meet the criterion they are assigned a score of 0.

(continued)

Table 46.1 (continued)

The CRITT score demonstrates a sensitivity of 87%, specificity of 75%, and negative predictive value of 93% for continuous flow LVADs.				
Variable	*OR (95% CI)*	*Cut-off level*		*Score*
CVP	2.0 (0.9–4.2)	>15 mmHg		1
RVD (severe)	3.7 (1.7–8.1)	+		1
Intubation *(mechanical ventilation)*	4.3 (1.9–9.6)	+		1
TR (severe)	4.1 (1.4–12.4)	+		1
Tachycardia	2.0 (0.9–4.3)	HR > 100 beats/min		1
Risk score	*Prediction*	*Sensitivity + Specificity + (−) PV*		
≤ 1	LVAD	87%	75%	93%
2–5	Grey zone	84%	63%	93%
≥ 4	BiVAD			
4. Utah RVF risk score				
Drakos et al. [5] (*RVF rate: 44% in 175 patients*) each of the 8-perioperative variables.				
Variable	*Cut-off level*	*Score*		
PVR				
Quartile 1	≤1.7 wood	1		
Quartile 2	1.8–2.7 wood	2		
Quartile 3	2.8–4.2 wood	3		
Quartile 4	≥4.3 wood	4		
IABP	+	4		
Destination therapy	+	3.5		
Inotrop dependency	+	2.5		
ACEI and/or ARB	+	2.5		
ß-blocker	+	2		
Obesity	+	2		
Risk score	*Risk for RVF*	*Prediction*		
≤5	Mild	LVAD		
5.5–8	Moderate	LVAD		
8.5–12	Moderate–high	Grey zone		
≥12	High	BiVAD		
5. Pittsburgh RVF risk score (Pittsburgh decision tree)				
Wang et al. [6] (*RVF rate: 15% in 183 patients*) evaluated 39 pre-operative variables in LVAD patients to identify independent predictors of RVF, and all variables (i.e., clinical, laboratory, and hemodynamic) were compared between RVAD (+) and RVAD (−) groups. Pearson product-moment pairwise analysis identified 2 variables that were significantly positively correlated with the need of post-RVAD individually: Female sex and elevated WBC count.				
Variable	*OR (95% CI)*	*Cut-off level*		
Sex	0.21 (0.07–0.35)	Female		
WBC count	0.18 (0.04–0.32)	≥9500 10^9/L		
In this model, TPG is the initial splitting feature with a breakpoint of 7 mmHg. The branch of TPG ≤ 7 mmHg predicts no need of RVAD support; and the branch of TPG > 7 mmHg leads to age as the secondary splitting feature with a breakpoint of 59. On the third level, there exist different thresholds of RAP depending on age: 18 mmHg (≤59 years), 10 mmHg (>59 years). The tree eventually terminates in a total of 14 leaves representing one of two outcomes (RVAD− or RVAD+). This model indicates that elevated INR and/or WBC are common to the branches with increased risk of the need of RVAD support. This model achieved 85% sensitivity, 83% specificity				

Table 46.1 (continued)

Decision tree parameters (8 parameters)			
Transpulmonary gradient; age; right atrial pressure; international normalized ratio; heart rate; white blood cell count; alanine aminotransferase; the number of inotropic agents			
6. Tokyo (Todai) RVF risk score (the TRV score)			
Shiga et al. [7] (*RVF rate: 37% in 197 patients*) evaluated 32 pre-operative variables in LVAD patients to identify independent predictors of RVF, and all variables (i.e., clinical, laboratory, and hemodynamic) with a univariable $p \leq 0.05$ for predicting RVF were selected as the components of the RVF risk score.			
For each variable, if patients meet the "high-risk" criterion they are assigned with the score; if patients meet the "low-risk" criterion for a particular variable they are assigned a score of 0. The maximum possible score is 45, and the threshold is 20 points.			
A threshold of 20 points (with a score > 20 predicting need for BiVAD), achieves sensitivity of 80% and specificity of 80%.			
Variable	*OR (95% CI)*	*Cut-off level*	*Score*
LVEDD	12.8 (1.4–118.4)	≤62 mm	13
CVP/PCWP	11.39 (1.2–111.4)	≥0.5	11
BNP	8.4 (0.9–76.7)	≥1200 pg/dL	8
BSA	7.3 (1.2–43.9)	≤1.40 m^2	7
CHDF	6 (1–34)	+	6
Risk score	*Prediction*		
≤20	LVAD		
>20	BiVAD		
7. Harefield RVF risk score			
Patil et al. [8] (*RVF rate: 23% in 152 patients*) evaluated 57 pre-operative variables in LVAD patients to identify independent predictors of RVF, and all variables (i.e., clinical, laboratory, echocardiographic, and hemodynamic) with a univariable $p \leq 0.1$ for predicting RVF were entered into multivariable analyses. Remaining independent ($p \leq 0.05$) predictors of RVF were selected as the components of the RVF risk.			
The TAPSE <12.5 mm score demonstrates a sensitivity of 84% and specificity of 75% for post-implant RVF.			
Variable	*OR (95% CI)*	*Cut-off level*	
TAPSE	0.6 (0.4–0.9)	<12.5 mm	
LAD	0.8 (0.7–0.9)	+	

ACEI angiotensin converting enzyme inhibitor, *ARB* angiotensin receptor blocker, *BiVAD* biventricular assist device, *BNP* brain natriuretic peptide, *BSA* body surface area, *CHDF* continuous hemofiltration, *CI* cardiac index, *CVP* central venous pressure, *HR* heart rate, *IABP* intra-aortic balloon pump, *INR* international normalized ratio, *LAD* left atrial diameter, *LVAD* left ventricular assist device, *LVEDD* left ventricular enddiastolic diameter, *OR* Odds ratio for multivariance analysis, *PCWP* pulmonary capillary wedge pressure, *RAP* right atrial pressure, *RVAD* right ventricular assist device, *RVD* right ventricular dysfunction, *RVF* right ventricular failure, *RVSWI* right ventricle stroke work index, *TAPSE* tricuspid annular plane systolic excursion, *TPG* transpulmonary gradient, *WBC* white blood cell

implant RVF [7, 8]. However, the current systems have only modest properties for RVF prediction after LVAD implantation. New RVF prediction scoring systems must be developed and validated for patient selection to optimize LVAD outcomes, potentially incorporating pre-operative echocardiographic data and reflecting contemporary patient characteristics, in studies using continuous-flow LVAD cohorts with a higher proportion of destination therapy cases [9–11].

Right ventricular failure has a specific pathophysiologic algorithm (Fig. 46.1). Increased afterload due to pressure overload of the pulmonary circulation prolongs systolic contraction of the RV. However, the RV is able to tolerate an increased preload due to volume overload. In the early phase of RVF, wall thickening and increased contractility are the first important responses of pressure overload, which causes adaptive remodeling with concentric hypertrophy and preserved right ventricular function. In chronic, higher afterload states, myocardial contractility is advanced yet the right ventricular functions decrease proportion-

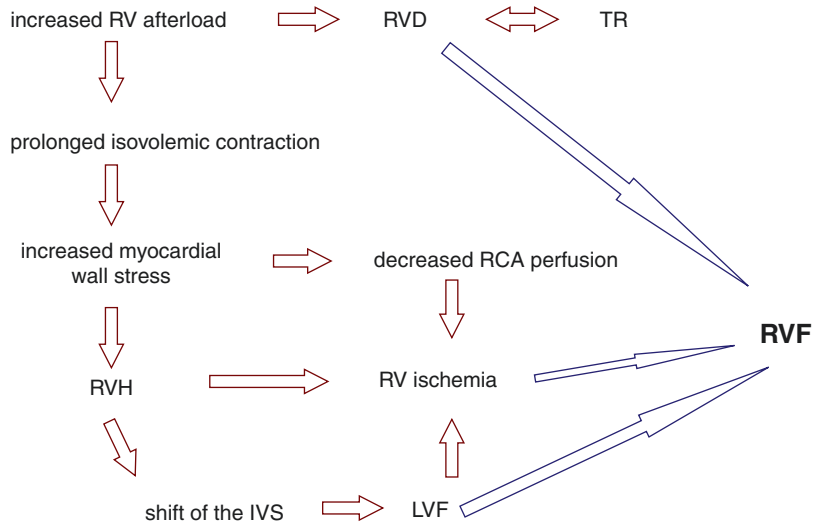

Fig. 46.1 Right ventricular pathophysiologic algorithm. *IVS* interventricular septum, *LVF* left ventricular failure, *RCA* right coronary artery, *RV* right ventricle, *RVD* right ventricular dysfunction, *RVF* right ventricular failure, *RVH* right ventricular hypertrophy, *TR* tricuspid regurgitation

ally, and the contractile dysfunction occurs later in the process. This remodeling process is sustained by the contribution of neurohormonal, genetic, and molecular components. Meanwhile, the RV dilates to provide adequate stroke volume, but this counter-effect leads to tricuspid annular dilatation, valve coaptation defect, and, eventually, significant TR. This process triggers maladaptive remodeling that causes eccentric hypertrophy and deteriorated right ventricular function. At the beginning of left ventricular diastole, the RV is contracting and the interventricular septum moves leftwards causing ventricular dyssynchrony. Ventricular dyssynchrony accelerates RVF or biventricular failure, with several fatal complications, including arrhythmia, hepatorenal failure, protein-losing enteropathy, and cardiac cachexia. Because RHF is a serious health issue causing poor quality of life, most of patients with uni- or biventricular HF are in the initial phase of the pathology allowing for successful medical intervention with newly developed agents and therapies to improve their quality of life. Advanced HF is usually treated, healed, and stabilized by pharmacologic and/or mechanical hemodynamic support, but end-stage HF is characterized by an increasing frequency of intervals of decompensation, re-hospitalization, and interventive therapy.

46.2 Mechanical Support of the RV

Acute RVF is an increasingly common clinical problem associated with significant morbidity and mortality. Acute exacerbations or decompensated end-stage HF patients should be hospitalized and treated more aggressively with intravenous inotropes, vasodilators, diuretics, and, if necessary, temporary mechanical support devices. Because the RV exhibits a greater capacity (up to 75%) for rapid recovery than the LV, refractory post-cardiotomy or post-transplant RVF should be managed using a temporary right ventricular assist device (RVAD) when optimal medical management has failed [12]. After stabilization of end-stage HF patients, they will be treated using a permanent RVAD or HTx if right ventricular recovery does not occur. Paracorporeal RVADs can be used for weeks or even months, but they are only approved for up to 4 weeks of use [13]. These devices can be combined easily with oxygenators when needed. If right ventricular function is not restored, the insertion of implantable continuous-flow ventricular assist devices is more effective in rare cases. Circulatory supports are categorized according to the involved cardiac chambers and lungs (Table 46.2). The principle function of mechanical support devices is very simple: to suck up circulatory blood and eject it into the sys-

Table 46.2 Definitions of t-MCS

I- Ventricular contribution:	To decrease ventricular unloading and work index
Ventricular assist:	Ventricular unloading through ventricular cavity directly *(after atrioventricular valve; series circulation)*
Ventricular support:	Ventricular preloading through atrial cavity *(before atrioventricular valve; parallel circulation)*
II-Cardiac relinquishment	
A. ECCS without external oxygenator:	To circulate blood out-of-heart
aa-ECCS (lv-bypass):	*atrio-arterial circulatory support without external oxygenation*
vp-ECCS (rv-bypass):	*veno-pulmonary circulatory support without external oxygenation*
bv-bypass:	*combined*
B. ECCS with external oxygenator:	To circulate and oxygenate blood out-of-heart
va-ECCPS (va-ECMO):	*veno-arterial circulatory support with external oxygenation*
va-a-ECCPS (va-a-ECMO):	*venoatrial-arterial circulatory support with external oxygenation*
aa-ECCPS (aa-ECMO):	*atrio-arterial circulatory support with external oxygenation*
vp-ECCPS (vp-ECMO):	*veno-pulmonary circulatory support with external oxygenation*

BV biventricular, *ECCPS* extracorporeal cardiopulmonary support, *ECCS* extracorporeal circulatory support, *ECMO* extracorporeal membranous oxygenation, *LV* left ventricular, *t-MCS* temporary mechanical circulatory support, *RHF* right heart failure, RV right ventricular

temic or pulmonary arterial circulation. The inflow cannula (temporary) or inlet pipe (permanent) is inserted into the related ventricle, and the outflow cannula (temporary) or outlet graft (permanent) is connected to the ventricle-associated main artery.

These devices have two different types of action: counterpulsatile or continuous flow. Counterpulsatile devices have a blood-compatible chamber and a moveable diaphragm that separates the chamber into blood and air spaces. The blood space is connected to the aorta or main pulmonary artery (PA) through a graft reinforced with a prosthetic valve. The air space is connected to a compressor console that provides power for counterpulsation through inflation and deflation. Devices working with nonpulsatile flow have a blood-compatible compartment and a frictionless, turnable rotor that directs the input flow to the related circulation. Continuous flow is the preferred approach, and is provided by one of two types of devices: extracorporeal or intracorporeal. These devices are designed to be small in through the use of two separate pump mechanisms: axial flow pumps with a pump rotor parallel to the blood path and centrifugal pumps with an impeller rotor perpendicular to the blood path. The rotor is magnetically levitated, and rotation is achieved without friction or wear, thus minimizing blood trauma, mechanical failure, and heat generation.

Designed to assist the native heart, mechanical support devices are differentiated according to the implant duration (short-term <10 days; mid-term 10–90 days; long-term >90 days); indication [temporary (bridge therapy) versus permanent (destination therapy)]; type (cardiopulmonary versus circulatory); approach (percutaneous versus surgical); location (extracorporeal versus intracorporeal); flow characteristic (pulsatile versus continuous); pump mechanism (volume displacement, axial, centrifugal); and the ventricle(s) supported (left, right, biventricular).

46.2.1 Temporary Mechanical Support

Temporary mechanical support devices increase pulmonary arterial blood circulation with or without extracorporeal oxygenation to support adequate right-sided cardiac output, which acts as a parallel artificial circulation to the physiologic circulation pattern (Table 46.3). These devices can successfully assist bridging to HTx or right

Table 46.3 t-MCS strategies for RHF

t-MCS strategies	Ventricular bypass	Type	Establishment between	Approach
A. ECCPS (with ECMO)				
va–ECCPS	*bv-bypass*	*veno-aortic* *veno-arterial*	RA – Ao (femoral and/or right jugular vein) – (left subclavian or femoral artery)	Sternotomy (median full/reverse T mini) Peripheral percutaneous
va-a–ECCPS	*bv-bypass*	*biatria-aortic* *venoatrio-aortic* *venoatrio-arterial*	(RA + LA) – Ao (femoral vein + LA) – Ao (femoral vein + LA) – (femoral or left subclavian artery)	Sternotomy (median full/reverse T mini) Peripheral percutaneous
aa–ECCPS	*lv-bypass*	*atrio-aortic* *atrio-arterial*	LA – Ao LA – (left subclavian or femoral artery)	Sternotomy (median full/reverse T mini) Peripheral percutaneous
vp–ECCPS	*rv-bypass*	*atrio-pulmonaric* *venopulmonaic*	RA – PA (femoral and/or jugular vein) – PA	Sternotomy (median full/reverse T mini) Peripheral percutaneous
B. ECCS (without ECMO)				
lv–ECCS (aa–ECCS)	*lv-bypass*	*atrio- or ventriculo-aortic* *atrio- or ventriculo-arterial*	(LA or LV) – Ao (LA or LV) – (left subclavian or femoral artery)	Sternotomy (median full/reverse T mini) Mini-thoracotomy
rv–ECCS (vp–ECCS)	*rv-bypass*	*atrio-pulmonic* *veno-pulmonic*	RA – PA (femoral and/or jugular vein) – PA	Sternotomy (median full/reverse T mini)
bv–ECCS	*bv-bypass*	Separately lv- and rv-ECCS	Combined	

ECCPS extracorporeal cardiopulmonary support, *ECCS* extracorporeal circulatory support, *ECMO* extracorporeal membranous oxygenation, *t-MCS* temporary mechanical circulatory support, *RHF* right heart failure
bv biventricular, *lv* left ventricular, *rv* right ventricular
Ao aorta, *LA* left atrium, *LV* left ventricle, *PA* pulmonary artery, *RA* right atrium

ventricular recovery in patients with post-implant, post-cardiotomy, or post-transplant RVF with evidence of improved hemodynamic stability. However, there is no clear evidence of the benefit of using an RVAD for any patient group because of the high mortality and morbidity rates. Therefore, RVADs must be carefully considered on an individual patient basis [14]. Because patients requiring temporary mechanical support with or without an external oxygenator for RHF are extremely ill and often suffer from multiple organ failure, the ideal device should be easy to implant and explant, provide adequate flow, and require minimal anti-coagulation. Two dominant approaches are used to support the failed RV: (1) va-ECMO, the preferred approach in emergency situations, particularly in the intensive care unit (ICU) or catheter laboratory; and (2) vp-ECCS, the preferred approach in all other cases and for intraoperative use as this method provides a more physiological transpulmonary blood flow and prevents left ventricular upload [15].

46.2.1.1 Temporary Mechanical Cardiorespiratory Support (t-MCRS for RHF)

Insufficient oxygenation by the lungs necessitates the use of an external oxygenator. Temporary mechanical cardiorespiratory support (t-MCRS) devices are designed to rapidly reestablish adequate organ perfusion and oxygenation. Univentricular t-MCRS is the most common approach to maintaining adequate right-sided cardiac output and oxygenation in the presence of severe RVF complicated with respiratory failure. However, biventricular t-MCRS may be the

preferred approach in the presence of significant LVF complicated with respiratory failure.

Cardiopulmonary Bypass (CPB for RHF)

The initial approach to life-supportive is cardiopulmonary bypass (CBP) using a roller or centrifugal pump for circulatory assistance and an oxygenator for respiratory reinforcement during open-heart surgery. Failure to wean from bypass after cardiac procedures prolongs the need for circulatory support via CPB. Because this approach is not suitable for short-term circulatory support or longer, CPB is used only for ultrashort-term (<1 day) circulatory assistance. Even with very short use of this extracorporeal circulation, serious side effects may arise including hemolysis, air embolism, generalized inflammatory reactions, and bleeding. In addition, lung injury is inevitable during CPB support because it causes increased pulmonary capillary permeability, interstitial lung fluid, and adverse inflammatory responses.

Extracorporeal Cardiopulmonary Support (t-ECCPS for RHF)

The term of these supports is accepted worldwide as extracorporeal membranous oxygenation (ECMO). However, when used for treatment in decompensated end-stage HF, the accurate term is extracorporeal cardiopulmonary support (ECCPS). In addition, the term "extracorporeal life support" (ECLS) describes similar support used during acute cardiogenic shock [16]. The main aim of ECCPS is to provide salvage therapy until recovery in patients with RHF and respiratory failure. An oxygenator is inserted into the extracorporeal circuit for gas exchange before return of the patient's venous blood, which is driven by a centrifugal pump, to the patient's pulmonary arterial circulation. If pulmonary functions are sufficient or pulmonary recovery occurs during t-ECCPS, the external oxygenator is not necessary and must be disconnected from the circuit. As ECMO offers prolonged cardiopulmonary support by way of a fast and simple surgical procedure, it is an option in almost all types of cardiopulmonary failure, including complex congenital cardiac anomalies, post-cardiotomy cardiogenic shock, and RHF for any reason. For patients with RHF, both veno-arterial (va) and veno-pulmonary arterial (vp) ECMO are potential alternatives. If the pathology affects the contractility of the RV, vp–ECMO can provide adequate hemodynamics. However, if the pathology involves the pulmonary arteries (like pulmonary hypertension or embolism) va–ECMO may provide better results [17, 18]. Post-implant RVF is a novel indication for vp–ECMO, and its use is growing with the increasing number of continuous-flow LVAD implantations. As new-generation LVADs are too large for young children, ECMO is the most-used circulatory support system in pediatric applications, particularly as a bridge to HTx. However, the mortality rate for patients younger than 18 years bridged to HTx using ECMO is over 50% with the worst outcome for those on ECMO for more than 28 days [19].

TandemHeart, Centrimag, Rotaflow, and other extracorporeal rotary pumps can be converted to ECMO in cases requiring concurrent respiratory support [20]. A hollow-fiber membrane oxygenator with an integrated heat-exchange system operated by a centrifugal pump provides circulatory, respiratory, and thermatory supports. They can be instituted via central or peripheral cannulation depending on the patient's clinical condition. Peripheral vp–ECMO may be preferred for patients who are in the ICU because it is fast and simple. This method uses an outflow cannula inserted through the right jugular vein into the PA and an inflow cannula inserted through the right femoral vein. However, central cannulation is the standard and preferred method intraoperatively, having a significantly lower incidence of major complications. This approach uses (1) an outflow cannula inserted through a tubular graft that is anastomosed to the PA; the cannula is then taken out of the chest through the second intercostal space; and (2) a femoral vein inflow cannula. After recovery of the RV, both approaches allow the patients to be disconnected from vp–ECMO in the ICU percutaneously, without opening the sternum. The outflow graft is tied and inserted into the mediastinum, and the peripheric vein is compressed externally to stop the bleeding.

t-ECCPS can be configured in several ways (Table 46.3).

va–ECCPS (va–ECMO) (biventricular bypass circuit) is the conventional ECMO system. This system comprises a biventricular bypass circuit with a centrifugal pump, which drives blood from the patient's venous circulation through an external membrane oxygenator for gas exchange before returning to the patient's systemic arterial circulation. Prolonged va–ECMO as a bridge to recovery or HTx is not ideal. Thus, va–ECCPS should be restricted to <1 week for adults and <14 days for children. If longer biventricular and respiratory support is needed, this t-MCPS approach should be converted to va–a–ECCPS to unload the LV.

va–a–ECCPS (va–a–ECMO) (biventricular bypass + unloading circuit; Kırali circuit) is a new-format biventricular assistance circuit (Kırali circuit) that includes biatrial drainage cannulas and an oxygenator-bypass line (Kırali line). This system assists and provides improved life-saving HF therapy using a configurable circuit, starting from the sophisticated immovable t-MCPS circuit to the simplest mobile t-MCS circuit. This system is particularly beneficial for biventricular HF patients, who are expected to recover the RV and respiratory functions within a few weeks. This biventricular unloading circuit includes a centrifugal pump that drives blood from both atria through an externalized membrane oxygenator for gas exchange before returning to the patient's systemic arterial circulation. This circuit has two venous cannulas: the first is inserted percutaneously (a multi-stage venous ECMO cannula) into the femoral vein or directly (standard venous cannula) into the right atrium (RA) for venous drainage; the second, a malleable one-stage venous cannula is placed into the left atrium (LA) to first provide left heart venting (drainage) and then left heart bypass (unloading). An arterial ECMO cannula is inserted into the distal ascending aorta or aortic arch, and the distal end of the cannula is placed distal to the cerebral branches. Both left heart cannulas with the RA cannula are taken out below the sternal incision, and the sternum is closed to prevent bleeding and to allow mobilization. Peripheric venous cannulation is the preferred method because decannulation of the percutaneously inserted femoral venous cannula is easy after brief support (<1 week). If more time (>1 week) to right ventricular recovery is expected, a small drainage cannula should be inserted distal to the outflow cannula at the femoral vein to prevent peripheral venous complications or central venous cannulation through the RA should be preferred. Each inflow line has its own tap to allow the withdrawal of blood samples to follow blood gas contents and pulmonary recovery. In addition, each inflow line can be controlled by partial or total clamping to manage adequate blood drainage from each atrium according to the relative ventricular dysfunction/recovery cascade. Right ventricular recovery is monitored using daily echocardiographic examination, and pulmonary recovery is followed with periodically blood samples taken from the left atrial inflow line.

Weaning from the t-MCPS protocol and converting to t-MCS protocol in end-stage HF patients with biventricular failure is easier than the other methods and does not require re-opening of the sternum or the establishment of a new circuit. The time between disconnection steps should be long enough to prevent respiratory failure recurrence or pulmonary complications. Decannulation of the peripheric venous cannula is very simple when the right ventricular recovery is completed. During this first stage, the circuit is converted to a left heart bypass system supported with an external oxygenator via removal of the right ventricular support (from va–a–ECCPS to aa–ECCPS). After pulmonary recovery, the oxygenator could be removed from the circuit. Weaning from the external oxygenator should be completed in ≥4 days, and the oxygenator should remain in the circuit in case of unexpected respiratory failure during the weaning period. First, the oxygenator bypass line is taken over pump flow gradually by partial declamping, and the full declamping of this line allows approximately three times more blood flow than that passing through the oxygenator due to the resistance of the oxygenator membrane. This strategy reduces oxygenator support and enables the native lungs to oxygenate most of the pumped blood flow. Finally, the oxygenator is switched off

and disconnected. At this stage, the circuit is converted to left heart bypass without the oxygenator (lv–ECCS). This simple lv–bypass system allows the patient to be discharged from the ICU and mobilized in the ward, and provides hemodynamically stable bridging to destination therapies (LVAD or HTx).

aa–ECCPS (aa–ECMO) (left ventricular bypass circuit) is a univentricular ECMO system with a left heart bypass circuit that uses a centrifugal pump to drive blood from the LA through an external membrane oxygenator for gas exchange before returning to the patient's systemic circulation. This approach is preferred in end-stage LHF patients complicated with respiratory failure, but without RVF or after right ventricular recovery, or as a part of va–a–ECCPS for biventricular HF patients. A common indication is acute pulmonary edema caused by acute decompensation of LVF.

vp–ECCPS (vp–ECMO) (right ventricular bypass circuit) is a univentricular ECMO system with a right heart bypass circuit using a centrifugal pump to drive blood from the patient's vena cava or RA through an external membrane oxygenator for gas exchange before returning to the patient's pulmonary circulation. This approach is preferred in RHF patients complicated with respiratory failure, but without LVF, who cannot be treated with fully mechanical ventilation. A common indication is respiratory failure accompanying post-implant RVF.

46.2.1.2 Temporary Mechanical Circulatory Support (t-MCS for RHF)

With sufficient spontaneous or mechanical ventilation, an oxygenator is not needed during t-MCPS for decompensated RHF (switch from ECCPS to ECCS). However, an external oxygenator can be added to the circuit if acutely respiratory decompensation develops (switch from ECCS to ECCPS). vp–ECCS is mostly often used in decompensated RVF, particularly after LVAD implantation. Timely establishment of right-sided temporary mechanical circulatory support (t-MCS) provided by a centrifugal pump is very important to prevent RHF-related multiorgan failure and death [21]. This approach is also the preferred method for weaning patients, who have had severe pulmonary failure, from vp–ECMO to vp–ECCS due to separation of the external oxygenator from the circuit after pulmonary recovery. In both situations, moribund patients should be treated and followed very carefully, and HTx must be not taken into consideration unless the patient shows significant recovery from multisystem organ failure. This type of t-MCS can be instituted via central or peripheral cannulation depending on the patient's clinical condition [16]. The vp–ECCS system is an acceptable method for maximizing survival and bridging to HTx, during which it can be used for many weeks to improve the patient's clinical status.

rv(vp)–ECCS (right ventricular bypass system) between the RA or femoral vein and the PA is rarely the preferred approach for isolated RVF because the normally-functioning LV can take over most of the right ventricular work and prevent right-sided cardiac output. The main indication of right heart bypass systems is acutely decompensated RVF after LVAD implantation. The inflow cannula is inserted into either the RA or femoral vein, and the outflow cannula is placed into the PA through a tubular graft extending outwards from the second intercostal space. Alternatively, completely percutaneous approaches for isolated RV support can be performed via an inflow cannula placed from the femoral vein into the RA and a flexible outflow cannula introduced from the right internal jugular vein into the PA. However, this approach requires fluoroscopy and is technically demanding [22].

lv(aa)–ECCS (left ventricular bypass system) between the LA and systemic arterial circulation is the most-preferred approach for the maintenance of end-stage HF patients with irreversible LVF but sufficient preserved right ventricular and pulmonary function. The inflow cannula is usually inserted into the LA. The longer ECMO outflow cannula is inserted into the distal ascending aorta or left subclavian artery [23]. One of several types of centrifugal pumps is chosen for this type of t-MCS for isolated LHF, and lv-ECCS can be used for long-term support (for several weeks).

bv–ECCS (biventricular bypass system) is a combination of both supports, but the indication for such a system is very limited. Most patients are supported by LVAD for left-sided dysfunction and a temporary right ventricular bypass system for right-sided dysfunction, as described above.

TandemHeart VAD (Cardiac Assist, Pittsburgh, PA, USA)

TandemHeart is an extracorporeal circulatory support system consisting of a small hydrodynamic centrifugal pump, which is approved as a short-term (up to 30 days) and life-saving t-MCS approach for acute LHF. This system also can be used for vp–ECCS and for ECCPS in end-stage HF patients with RVF [24]. Its first use was for right ventricular support in a patient with myocardial infarction [25]. This system is very versatile, can be easily deployed and discontinued, and can be applied surgically or percutaneously [26]. Percutaneous implantation is very practical and does not require reopening of the chest. For vp–ECCS, the right atrial cannulation is performed through the femoral vein, and the outflow cannula is directed into the PA. "Protek Duo" is another useful cannula with two lumens, which allows setting of the inflow in the RA and outflow in the PA to achieve right heart support via a single cannula [27]. When inserted percutaneously, the system can provide support up to 4 L/min; surgically implantation allows for a flow up to 8 L/min.

Rotaflow (Rotaflow; Maquet Gmbh & Co. KG, Rastatt, Germany)

Rotaflow is a new generation centrifugal pump with a magnetically levitated rotor capable of delivering 10 L/min. Because this device lacks bearings or seals, it causes much less trauma to blood elements and consequently less hemolysis than older generation devices [28]. This device has a spiral housing containing a spinning rotor with logarithmically curved flow channels that impart a rotary motion on the incoming blood, directing it toward the outlet. These features have been shown to allow improved continuous laminar flow, with fewer areas of stagnant flow or high shear stress. In addition, the permanent, stable radial magnetic field and low-friction, one-point sapphire bearing of the Rotaflow allow for reduced heat generation within the pump. Furthermore, the device can be configured to ECMO in cases of refractory respiratory failure by simply inserting an oxygenator into the system [29]. It can be used either with or without the oxygenator as t-MCS up to 6 h, but also, for longer period (up to 15 weeks) [30].

CentriMag (Thoratec, Pleasanton, CA, USA)

The CentriMag blood pump is a third generation ECCS device used for mid-term t-MCS (up to 30 days) in decompensated end-stage HF patients. This device provides hemodynamic support as a bridge to recovery or transplantation or mid-term ECMO to provide cardiorespiratory support [29, 31]. It is also approved for use as an RVAD in acute RVF to support patients up to 30 days. The CentriMag system consists of a continuous flow centrifugal blood pump, a primary console and motor, a flow probe, tubing, and cannulae. This mid-term support device is based on a 'bearingless motor' configuration, where the impeller is elevated magnetically to provide a contact-free environment to help minimize blood-related complications such as hemolysis and thromboembolism. It can provide a flowsupport of up to 10 L/min. The main advantage of this system is that it provides an adequate cardiac output even in patients with a high body mass index. The pump system can be used for longer time periods by changing the pumphead. Although the system is approved for 30 days of use, it can be used for longer support (up to 300 days) in uncertain conditions such as prolonged RVF subsequent to permanent LVAD implantation or bridged end-stage HF [32].

46.2.2 Intracorporeal Temporary Mechanical Circulatory Support

Intracorporeal t-MCS devices can be implanted surgically or percutaneously, but percutaneous devices are preferred for all indications because they avoid surgical cannulation of the RA and PA, which increase the risk of bleeding and infec-

tion and can necessitate additional surgery for device extraction [33]. Percutaneous t-MCSs are developed to unload the affected ventricle for better recovery and to maintain adequate cardiac output in patients who have acutely decompensated HF or have undergone high-risk cardiac interventions. A third indication is for transaortic left heart unloading in patients with postcardiotomy syndrome treated by peripheral va–ECMO. This device can also be used in acute decompensation of end-stage HF to improve end-organ function and to bridge to advanced HF treatments. A surgical intracorporeal t-MCS device also can be used as permanent RVAD.

46.2.2.1 Impella RP (Abiomed Impella, Danvers, MA, USA)

Impella RP is an axial-flow pump with a flow rate of up to 4 L/min that can be used as a novel percutaneous short-term RVAD for up to 14 days. This device is approved for decompensated RHF subsequent to LVAD implantation, heart transplantation, myocardial infarction, or open cardiac surgery [34]. Another indication is the management and treatment of serious RHF symptoms in acute right ventricular decompensation in the context of chronic biventricular HF refractory to pharmacologic therapy without significant LHF [35]. This device is inserted percutaneously into the PA through the femoral vein, and the inflow of the catheter must be placed in the inferior vena cava and the outflow must be in the PA. The Impella pumps blood directly from the systemic vein into the pulmonary trunk, thereby unloading the RV and increasing right-sided cardiac output. Transesophageal echocardiography and fluoroscopy are required for correct installation. The most important benefit of this system over other t-MCS devices is that it does not require a surgical procedure for implantation.

46.2.2.2 PERKAT (Percutaneous Catheterpump) (The Novapump GmbH, Jena, Germany)

The development and design of a novel, percutaneously implantable, and rapidly deployable pulsatile device for rapid percutaneous implantation with sufficient in vitro flow tests opens new possibilities for temporary right heart support, specifically for supporting the RV without the disadvantages of continuous flow systems [36]. The PERKAT device consists of a nitinol stent cage covered by flexible membranes containing numerous foil valves forming together the foil valve concept. A flexible outlet tube with a pigtail-shaped tip and outflow valves is attached to the distal end of the nitinol pumping chamber in the inferior vena cava. A standard intra-aortic balloon is then inserted into the pumping chamber and connected to a standard pump console. Blood flows from the vena cava and right atrium into the nitinol stent cage through the foil valves. During subsequent balloon inflation, the foil valves are closed from the pressure exerted on the blood by the helium-filled intra-aortic balloon, and blood is guided through the flexible outlet tube into the pulmonary trunk. The maximum flow-support can reach up to 3.9 L/min (highest flow with 40 mL balloon, 22 mmHg afterload, and 120 beats per minute) in a standardized in vitro model with blood analogs depending on the size of the IABP-balloon, the afterload setting, and the inflation/deflation frequency [37].

46.2.3 Permanent Mechanical Circulatory Support

Permanent mechanical pumps either provide a parallel artificial circulation for the failed pulmonary circulation or take over the pump function of the failed RV. Current RVADs usually operate in parallel with the native RV, altering the blood flow pattern and increasing RV afterload associated with high tension in cardiac muscles and long-term valve complications. The anterior location of the RA is preferable to that of the RV for implantation (RA to PA cannulation) to create permanent mechanical support of the failed RV with in-parallel RVAD. This approach provides a decrease in right ventricular preload but an increase in pulmonary afterload. In-series artificial circulation (RV to PA cannulation) can provide better right ventricular unloading and hemodynamic restoration to an overloaded or

failing RV. This type of device restores the balance between oxygen supply and demand in RHF patients through superior afterload and volume reduction [38, 39]. The standard use of permanent RVADs is as a biventricular ventricular assist device (BiVAD) in patients with circulatory decompensation caused by severe biventricular HF or post-implant RVF. The aim of this use is to bridge operable patients to HTx or inoperable patients to destination therapy. The options for biventricular support are total artificial heart (TAH) or pulsatile flow pumps, which are too large for hospital discharge and are limited by their large driver consoles to adequately restore patient mobility and improve quality of life; in addition, they have the highest mortality rate and lowest survival rate [40]. With advances in p-MCS design and miniaturization of pumps, the use of two continuous flow LVADs has been suggested for biventricular support [41]. This strategy has changed the treatment options, and different devices have been using for BiVAD therapy.

46.2.3.1 Pulsatil Dual Ventricular Assist Devices

Berlin Heart Excor (Berlin Heart AG, Berlin, Germany)

Berlin Heart Excor is a paracorporeal pulsatile pump used worldwide since 1996. The system is available for both pediatric patients and adults. Currently, this device is still the only choice for babies and young children with end-stage HF. The EXCOR system includes paracorporeal, pneumatically-driven polyurethane blood pumps, silicone cannulae, a stationary driving unit, and a mobile driving unit. The pumps are available in sizes of 50, 60, and 80 mL for adult patients, and 10, 15, 25, 30, 50, and 60 mL for pediatric patients. Pumps of all sizes have polyurethane valves, whereas mechanical valves are available only in 50, 60, and 80 mL pumps. Silicone cannulae are also available in various sizes. Pumps are produced from transparent material to allow visual inspection against thrombus formation or deformations of the interchamber membrane. The system can be used either for LVAD, RVAD or BiVAD. The blood flows from the cardiac cavities into Excor pumps through silicone cannulae, and the pump ejects blood into the aorta or PA. Suction and ejection of the pump are powered pneumatically by an air compressors unit. The Excor system can support patients from infants to adult-sized adolescents [42]. Loforte from Berlin reported a biventricular CentriMag cohort using Excor cannulas [43]. The goal of this strategy is to achieve an easy conversion from a short-term device to long-term support, with elimination of the potential risks of second surgery.

46.2.3.2 Continuous Dual Ventricular Assist Devices

Unlike pulsatile BiVAD and TAH, these LVADs are small light and do not require valves. In addition, they significantly restore patient mobility and allow discharge from the hospital because of their greater durability and longevity. While these devices are usually used as an LVAD combined with a paracorporeal t-MCS for RVAD for hybrid application as a BiVAD, the use of dual LVADs for both left and right ventricular support has increased recently. Third generation continuous flow ventricular assist devices are the choice for BiVAD achieved with dual devices; first and second generation devices are no longer in use. Widespread use of dual continuous-flow LVADs is limited because of logistical issues with separate controllers, reimbursement issues for the second pump, and the reported poor long-term prognosis compared with patients on isolated left ventricular support.

Heartware HVAD (HeartWare, Framingham, MA, USA)

Heartware HVAD is one of the commonly used 3rd generation LVADs. This centrifugal pump can provide a flow of 4–10 L/min with a pump speed of 2400–3200 rpm. The rotor of the pump is levitated magnetically and hydrodynamically. The inflow cannula is directly implanted into the ventricular cavity, and the outflow graft is anastomosed on the main arterial trunk. The inflow cannula can be placed either on the freewall, the

diaphragmatic wall of the RV, or the RA for RVAD implantation [44]. As a result of the lower PVR, the device can produce an extremely high flow because it is designed to work against systemic vascular resistance (SVR), which is at least three to four times higher than normal PVR. Some surgeons prefer to narrow the outflow graft to 5 mm in patients with lower PVR and 6–7 mm in those with higher PVR [41, 45]. However, it is preferable to use this device without any manipulations of the outflow graft [46].

HeartMate-3 (St. Jude Medical, St. Paul, MN, USA)

The Heartmate-III is a new third generation centrifugal LVAD designed for long-term circulatory support. Magnetic levitation technology is used to suspend the rotor for less shear stress and hemolysis. This device provides a blood flow of 2.5–10 L/min. Artificial pulse technology is used to prevent the formation of zones of recirculation and the stasis of blood. It also uses a textured blood-contacting surface to encourage endothelial tissue proliferation on the surfaces in contact with blood with the aim of reducing complications. This device is slightly larger than the HeartWare HVAD because of its greater displacement volume and profile, but it is still small enough to allow intrapericardial implantation for BiVAD [47]. In the case of direct anastomosis to the pulmonary artery, the narrowing may be achieved intraoperatively using hemostatic clips, depending on the pulmonary artery pressure and pump performance. We believe that no further constriction other than downsizing from 14 to 10 mm is necessary.

46.2.4 Total Artificial Heart

The total artificial heart is a permanent orthotropic pneumatic pulsatile system that enables biventricular support to maintain both the pulmonary and systemic circulation, providing a significant improvement for severe biventricular HF and allowing long-term hospital discharge. A total artificial heart consists of two pumps to replace the native ventricles. Patients with severe biventricular failure [48], complex non-repairable congenital structural disease [49], hypertrophic or restrictive cardiomyopathy, or severe rejection of transplanted heart are candidates for TAH.

46.2.4.1 The Syncardia TAH (SynCardia Systems, Inc., Tucson, AZ, USA)

The Syncardia TAH is the only FDA approved TAH available on the market for bridge-to-transplant indication [50]. The device is indicated in patients with the appropriate chest size (BSA 1.7–2.5 m^2 or >10 cm between the tenth thoracic vertebrae and the sternum) who are eligible for transplantation but not for LVAD or BiVAD [51]. This pneumatically driven device consists of two polyurethane pumps of 70-cc stroke volume for each ventricle. Each chamber contains two mechanical, single-leaflet tilting disc valves (SynHall, formerly Medtronic Hall; inflow, 27 mm; outflow 25 mm) to regulate flow direction. A smaller-sized model is also available that has 50-cc pumps for both sides. This model is made for patients with a BSA of 1.2–1.85 m^2, which is preferred for bridge to transplantation [52, 53]. To implant the SynCardia TAH, the left and right ventricles are excised, leaving a 1-cm rim of ventricular muscle around the mitral and tricuspid annulus. The mitral and tricuspid valve leaflets are also excised. The atrial septum must be checked to ascertain a patent foramen ovale. The artificial ventricles are attached to the atriums and great vessels via the quick connectors, which are previously sutured to the mitral, tricuspid, pulmonary and aortic annuli. Patients undergoing TAH implantation must take antiplatelet and anticoagulant therapy to prevent thromboembolic complications. The most common complications after TAH surgery include stroke, infections, bleeding, thrombosis, renal failure, and chronic anemia.

Conclusion

Right ventricular support is a novel area in the management of refractory RVF, and there is no perfect device for this therapy. Dual LVADs are preferred for biventricular p-MCS, but TAH will eventually take over this role. In

acute situations, va-ECMO or vp-ECCS is the best option to treat LVAD patients with refractory RVF. Isolated RVF is rare in patients with advanced LHF, and va-a-ECCPS is the preferred approach in such cases. Patients with preserved left ventricular function can be managed with isolated RVAD if t-MCS is insufficient.

References

1. Mehra MR, Park MH, Landzberg MJ, Lala A, Waxman AB, International Right Heart Failure Foundation Scientific Working Group. Right heart failure: toward a common language. J Heart Lung Transplant. 2014;33(2):123–6. https://doi.org/10.1016/j.healun.2013.10.015.
2. Matthews JC, Koelling TM, Pagani FD, Aaronson KD. The right ventricular failure risk score a preoperative tool for assessing the risk of right ventricular failure in left ventricular assist device candidates. J Am Coll Cardiol. 2008;51(22):2163–72. https://doi.org/10.1016/j.jacc.2008.03.009.
3. Fitzpatrick JR 3rd, Frederick JR, Hsu VM, Kozin ED, O'Hara ML, Howell E, Dougherty D, McCormick RC, Laporte CA, Cohen JE, Southerland KW, Howard JL, Jessup ML, Morris RJ, Acker MA, Woo YJ. Risk score derived from pre-operative data analysis predicts the need for biventricular mechanical circulatory support. J Heart Lung Transplant. 2008;27(12):1286–92. https://doi.org/10.1016/j.healun.2008.09.00.
4. Atluri P, Goldstone AB, Fairman AS, MacArthur JW, Shudo Y, Cohen JE, Acker AL, Hiesinger W, Howard JL, Acker MA, Woo YJ. Predicting right ventricular failure in the modern, continuous flow left ventricular assist device era. Ann Thorac Surg. 2013;96(3):857–63. https://doi.org/10.1016/j.athoracsur.2013.03.099.
5. Drakos SG, Janicki L, Horne BD, Kfoury AG, Reid BB, Clayson S, Horton K, Haddad F, Li DY, Renlund DG, Fisher PW. Risk factors predictive of right ventricular failure after left ventricular assist device implantation. Am J Cardiol. 2010;105(7):1030–5. https://doi.org/10.1016/j.amjcard.2009.11.026.
6. Wang Y, Simon MA, Bonde P, Harris BU, Teuteberg JJ, Kormos RL, Antaki JF. Decision tree for adjuvant right ventricular support in patients receiving a left ventricular assist device. J Heart Lung Transplant. 2012;31(2):140–9. https://doi.org/10.1016/j.healun.2011.11.003.
7. Shiga T, Kinugawa K, Imamura T, Kato N, Endo M, Inaba T, Maki H, Hatano M, Yao A, Nishimura T, Hirata Y, Kyo S, Ono M, Nagai R. Combination evaluation of preoperative risk indices predicts requirement of biventricular assist device. Circ J. 2012;76(12):2785–91. https://doi.org/10.1253/circj.CJ-12-0231.
8. Patil NP, Mohite PN, Sabashnikov A, Dhar D, Weymann A, Zeriouh M, Hards R, Hedger M, De Robertis F, Bahrami T, Amrani M, Rahman-Haley S, Banner NR, Popov AF, Simon AR. Preoperative predictors and outcomes of right ventricular assist device implantation after continuous-flow left ventricular assist device implantation. J Thorac Cardiovasc Surg. 2015;150(6):1651–8. https://doi.org/10.1016/j.jtcvs.2015.07.090.
9. Kalogeropoulos AP, Kelkar A, Weinberger JF, Morris AA, Georgiopoulou VV, Markham DW, Butler J, Vega JD, Smith AL. Validation of clinical scores for right ventricular failure prediction after implantation of continuous-flow left ventricular assist devices. J Heart Lung Transplant. 2015;34(12):1595–603. https://doi.org/10.1016/j.healun.2015.05.005.
10. Bellavia D, Iacovoni A, Scardulla C, Moja L, Pilato M, Kushwaha SS, Senni M, Clemenza F, Agnese V, Falletta C, Romano G, Maalouf J, Dandel M. Prediction of right ventricular failure after ventricular assist device implant: systematic review and meta-analysis of observational studies. Eur J Heart Fail. 2017;19(7):926–46. https://doi.org/10.1002/ejhf.733.
11. Dandel M, Krabatsch T, Falk V. Left ventricular vs. biventricular mechanical support: decision making and strategies for avoidance of right heart failure after left ventricular assist device implantation. Int J Cardiol. 2015;198:241–50. https://doi.org/10.1016/j.ijcard.2015.06.103.
12. Mulaikal TA, Bell LH, Li B, Wagener G, Takayama H. Isolated right ventricular mechanical support: outcomes and prognosis. ASAIO J. 2017. (in press). https://doi.org/10.1097/MAT.0000000000000597.
13. Harjola VP, Mebazaa A, Čelutkienė J, Bettex D, Bueno H, Chioncel O, Crespo-Leiro MG, Falk V, Filippatos G, Gibbs S, Leite-Moreira A, Lassus J, Masip J, Mueller C, Mullens W, Naeije R, Nordegraaf AV, Parissis J, Riley JP, Ristic A, Rosano G, Rudiger A, Ruschitzka F, Seferovic P, Sztrymf B, Vieillard-Baron A, Yilmaz MB, Konstantinides S. Contemporary management of acute right ventricular failure: a statement from the Heart Failure Association and the Working Group on Pulmonary Circulation and Right Ventricular Function of the European Society of Cardiology. Eur J Heart Fail. 2016;18(3):226–41. https://doi.org/10.1002/ejhf.478.
14. Lang SA, O'Neill B, Waterworth P, Bilal H. Can the temporary use of right ventricular assist devices bridge patients with acute right ventricular failure after cardiac surgery to recovery? Interact Cardiovasc Thorac Surg. 2014;18(4):499–510. https://doi.org/10.1093/icvts/ivt472.
15. Noly PE, Kirsch M, Quessard A, Leger P, Pavie A, Amour J, Leprince P. Temporary right ventricular support following left ventricle assist device implantation: a comparison of two techniques. Interact Cardiovasc Thorac Surg. 2014;19(1):49–55. https://doi.org/10.1093/icvts/ivu072.
16. Kapur NK, Paruchuri V, Jagannathan A, Steinberg D, Chakrabarti AK, Pinto D, Aghili N, Najjar S,

Finley J, Orr NM, Tempelhof M, Mudd JO, Kiernan MS, Pham DT, DeNofrio D. Mechanical circulatory support for right ventricular failure. JACC Heart Fail. 2013;1(2):127–34. https://doi.org/10.1016/j.jchf.2013.01.007.

17. Berman M, Tsui S, Vuylsteke A, Snell A, Colah S, Latimer R, Hall R, Arrowsmith JE, Kneeshaw J, Klein AA, Jenkins DP. Successful extracorporeal membrane oxygenation support after pulmonary thromboendarterectomy. Ann Thorac Surg. 2008;86(4):1261–7. https://doi.org/10.1016/j.athoracsur.2008.06.037.
18. Punnoose L, Burkhoff D, Rich S, Horn EM. Right ventricular assist device in end-stage pulmonary arterial hypertension: insights from a computational model of the cardiovascular system. Prog Cardiovasc Dis. 2012;55(2):234–243.e2. https://doi.org/10.1016/j.pcad.2012.07.008.
19. Merrill ED, Schoeneberg L, Sandesara P, Molitor-Kirsch E, O'Brien J Jr, Dai H, Raghuveer G. Outcomes after prolonged extracorporeal membrane oxygenation support in children with cardiac disease. Extracorporeal Life Support Organization registry study. J Thorac Cardiovasc Surg. 2014;148(2):582–8. https://doi.org/10.1016/j.jtcvs.2013.09.038.
20. Nagpal AD, Singal RK, Arora RC, Lamarche Y. Temporary mechanical circulatory support in cardiac critical care: a state of the art review and algorithm for device selection. Can J Cardiol. 2017;33(1):110–8. https://doi.org/10.1016/j.cjca.2016.10.023.
21. Saito S, Sakaguchi T, Miyagawa S, Nishi H, Yoshikawa Y, Fukushima S, Daimon T, Sawa Y. Recovery of right heart function with temporary right ventricular assist using a centrifugal pump in patients with severe biventricular failure. J Heart Lung Transplant. 2012;31(8):858–64. https://doi.org/10.1016/j.healun.2012.03.002.
22. Takayama H, Naka Y, Kodali SK, Vincent JA, Addonizio LJ, Jorde UP, Williams MR. A novel approach to percutaneous right-ventricular mechanical support. Eur J Cardiothorac Surg. 2012;41(2):423–6. https://doi.org/10.1016/j.ejcts.2011.05.041.
23. Kırali K, Yerlikhan ÖA, Hançer H. Invasive treatment in advanced (stage-D) heart failure. In: Kırali K, editor. Cardiomyopaties: types and treatments. Rijeka: InTech; 2017. p. 405–57. https://doi.org/10.5572/67455.
24. Herlihy JP, Loyalka P, Jayaraman G, Kar B, Gregoric ID. Extracorporeal membrane oxygenation using the TandemHeart System's catheters. Tex Heart Inst J. 2009;36(4):337–41. PMCID: PMC2720287.
25. Atiemo AD, Conte JV, Heldman AW. Resuscitation and recovery from acute right ventricular failure using a percutaneous right ventricular assist device. Catheter Cardiovasc Interv. 2006;68(1):78–82. https://doi.org/10.1002/ccd.20691.
26. Rajdev S, Benza R, Misra V. Use of Tandem Heart as a temporary hemodynamic support option for severe pulmonary artery hypertension complicated by cardiogenic shock. J Invasive Cardiol. 2007;19(8):E226–9.
27. Schmack B, Weymann A, Popov AF, Patil NP, Sabashnikov A, Kremer J, Farag M, Brcic A, Lichtenstern C, Karck M, Ruhparwar A. Concurrent left ventricular assist device (LVAD) implantation and percutaneous temporary RVAD support via CardiacAssist Protek-Duo TandemHeart to preempt right heart failure. Med Sci Monit Basic Res. 2016;22:53–7. https://doi.org/10.12659/MSMBR.898897.
28. Khani-Hanjani A, Loor G, Chamogeorgakis T, Shafii A, Mountis M, Hanna M, Soltesz E, Gonzalez-Stawinski GV. Case series using the ROTAFLOW system as a temporary right ventricular assist device after HeartMate II implantation. ASAIO J. 2013;59(4):456–60. https://doi.org/10.1097/MAT.0b013e318291d133.
29. Loforte A, Pilato E, Martin Suarez S, Folesani G, Jafrancesco G, Castrovinci S, Grigioni F, Marinelli G. RotaFlow and Centri Mag extracorporeal membrane oxygenation support systems as treatment strategies for refractory cardiogenic shock. J Card Surg. 2015;30(2):201–8. https://doi.org/10.1111/jocs.12480.
30. Khaliel F, Al Habeeb W, Saad E, Kjellman U. Use of Rotaflow pump for left ventricular assist device bridging for 15 weeks. Asian Cardiovasc Thorac Ann. 2014;22(2):205–7. https://doi.org/10.1177/0218492312469200.
31. Borisenko O, Wylie G, Payne J, Bjessmo S, Smith J, Yonan N, Firmin R. Thoratec CentriMag for temporary treatment of refractory cardiogenic shock or severe cardiopulmonary insufficiency: a systematic literature review and meta-analysis of observational studies. ASAIO J. 2014;60(5):487–97. https://doi.org/10.1097/MAT.0000000000000117.
32. Mohite PN, Zych B, Popov AF, Sabashnikov A, Sáez DG, Patil NP, Amrani M, Bahrami T, DeRobertis F, Maunz O, Marczin N, Banner NR, Simon AR. CentriMag short-term ventricular assist as a bridge to solution in patients with advanced heart failure: use beyond 30 days. Eur J Cardiothorac Surg. 2013;44(5):e310–5. https://doi.org/10.1093/ejcts/ezt415.
33. Cheung AW, White CW, Davis MK, Freed DH. Short-term mechanical circulatory support for recovery from acute right ventricular failure: clinical outcomes. J Heart Lung Transplant. 2014;33(8):794–9. https://doi.org/10.1016/j.healun.2014.02.028.
34. Anderson MB, Goldstein J, Milano C, Morris LD, Kormos RL, Bhama J, Kapur NK, Bansal A, Garcia J, Baker JN, Silvestry S, Holman WL, Douglas PS, O'Neill W. Benefits of a novel percutaneous ventricular assist device for right heart failure: the prospective RECOVER RIGHT study of the Impella RP device. J Heart Lung Transplant. 2015;34(12):1549–60. https://doi.org/10.1016/j.healun.2015.08.018.
35. Yan I, Grahn H, Blankenberg S, Westermann D. Right ventricular temporal assist device for cardiac recompensation. ESC Heart Fail. 2017;4(3):376–8. https://doi.org/10.1002/ehf2.12148.

36. Kretzschmar D, Lauten A, Ferrari MW. In vitro evaluation of a novel pulsatile right heart assist device - the PERKAT system. Int J Artif Organs. 2015;38(10):537–41. https://doi.org/10.5301/ijao.5000440.
37. Kretzschmar D, Schulze PC, Ferrari MW. Hemodynamic performance of a novel right ventricular assist device (PERKAT). ASAIO J. 2017;63(2):123–7. https://doi.org/10.1097/MAT.0000000000000464.
38. Hsu PL, McIntyre M, Boehning F, Dang W, Parker J, Autschbach R, Schmitz-Rode T, Steinseifer U. In-series versus in-parallel mechanical circulatory support for the right heart: a simulation study. Artif Organs. 2016;40(6):561–7. https://doi.org/10.1111/aor.12601.
39. Gregory SD, Pearcy MJ, Fraser J, Timms D. Evaluation of inflow cannulation site for implantation of right-sided rotary ventricular assist device. Artif Organs. 2013;37(8):704–11. https://doi.org/10.1111/aor.12067.
40. Shehab S, Newton PJ, Allida SM, Jansz PC, Hayward CS. Biventricular mechanical support devices. Clinical perspectives. Expert Rev Med Devices. 2016;13(4):353–65. https://doi.org/10.1586/17434440.2016.1154454.
41. Krabatsch T, Potapov E, Stepanenko A, Schweiger M, Kukucka M, Huebler M, Hennig E, Hetzer R. Biventricular circulatory support with two miniaturized implantable assist devices. Circulation. 2011;124(11 Suppl):S179–86. https://doi.org/10.1161/CIRCULATIONAHA.110.011502.
42. Morales DL, Almond CS, Jaquiss RD, Rosenthal DN, Naftel DC, Massicotte MP, Humpl T, Turrentine MW, Tweddell JS, Cohen GA, Kroslowitz R, Devaney EJ, Canter CE, Fynn-Thompson F, Reinhartz O, Imamura M, Ghanayem NS, Buchholz H, Furness S, Mazor R, Gandhi SK, Fraser CD Jr. Bridging children of all sizes to cardiac transplantation: the initial multicenter North American experience with the Berlin Heart EXCOR ventricular assist device. J Heart Lung Transplant. 2011;30(1):1–8. https://doi.org/10.1016/j.healun.2010.08.033.
43. Loforte A, Potapov E, Krabatsch T, Musci M, Wend Y, Pasic M, Hatzer R. Levitronix CentriMag to Berlin Heart Excor: a "bridge to bridge" solution in refractory cardiogenic shock. ASAIO J. 2009;55(5):465–8. https://doi.org/10.1097/MAT.0b013e3181b58c50.
44. Tran HA, Pollema TL, Silva Enciso J, Greenberg BH, Barnard DD, Adler ED, Pretorius VG. Durable biventricular support using right atrial placement of the HeartWare HVAD. ASAIO J. 2017. (in print). https://doi.org/10.1097/MAT.0000000000000645.
45. Shehab S, Macdonald PS, Keogh AM, Kotlyar E, Jabbour A, Robson D, Newton PJ, Rao S, Wang L, Allida S, Connellan M, Granger E, Dhital K, Spratt P, Jansz PC, Hayward CS. Long-term biventricular HeartWare ventricular assist device support--case series of right atrial and right ventricular implantation outcomes. J Heart Lung Transplant. 2016;35(4):466–73. https://doi.org/10.1016/j.healun.2015.12.001.
46. Bernhardt AM, De By TM, Reichenspurnera H, Deuse T. Isolated permanent right ventricular assist device implantation with the HeartWare continuous-flow ventricular assist device: first results from the European Registry for Patients with Mechanical Circulatory Support. Eur J Cardiothorac Surg. 2015;48(1):158–62. https://doi.org/10.1093/ejcts/ezu406.
47. Potapov EV, Kukucka M, Falk V, Krabatsch T. Biventricular support using 2 HeartMate 3 pumps. J Heart Lung Transplant. 2016;35(10):1268–70. https://doi.org/10.1016/j.healun.2016.07.013.
48. Cook JA, Shah KB, Quader MA, Cooke RH, Kasirajan V, Rao KK, Smallfield MC, Tchoukina I, Tang DG. The total artificial heart. J Thorac Dis. 2015;7(12):2172–80. https://doi.org/10.3978/j.issn.2072-1439.2015.10.70.
49. Villa CR, Morales DLS. The total artificial heart in end-stage congenital heart disease. Front Physiol. 2017;8:131. https://doi.org/10.3389/fphys.2017.00131.
50. Copeland JG. SynCardia Total Artificial Heart: update and future. Tex Heart Inst J. 2013;40(5):587–8. PMCID: PMC3853833.
51. Torregrossa G, Anyanwu A, Zucchetta F, Gerosa G. SynCardia: the total artificial heart. Ann Cardiothorac Surg. 2014;3(6):612–20. https://doi.org/10.3978/j.issn.2225-319X.2014.11.07.
52. Wells D, Villa CR, Simón Morales DL. The 50/50 cc total artificial heart trial: extending the benefits of the total artificial heart to underserved populations. Semin Thorac Cardiovasc Surg Pediatr Card Surg Annu. 2017;20:16–9. https://doi.org/10.1053/j.pcsu.2016.09.004.
53. Morales DLS, Lorts A, Rizwan R, Zafar F, Arabia FA, Villa CR. Worldwide experience with the Syncardia total artificial heart in the pediatric population. ASAIO J. 2017;63(4):518–9. https://doi.org/10.1097/MAT.0000000000000504.

POST-LVAD Right Ventricular Failure

47

Kaan Kırali, Tanıl Özer, and Emre Selçuk

Abstract

Patient selection and implantation timing are key determinants of success for therapy with a left ventricular assist device (LVAD). End-stage heart failure patients with stable disease on inotropic treatment are the best candidates, whereas patients with cardiogenic shock are considered too ill for LVAD support and should be receive temporary mechanical circulatory support devices to optimize their condition before LVAD implantation. However, if implantation is delayed, outcomes may worsen due to secondary organ damage caused by prolonged end-stage heart failure, with the potential for right heart failure to develop and lead to death. Most patients with advanced left ventricular failure assessed for LVAD implantation also have some degree of right ventricular dysfunction. Though LVADs are effective for treating left ventricular failure, they do not intrinsically treat, and in some instances may worsen, right ventricular failure (RVF). Indeed post-LVAD RVF is a major complication of device implantation and significantly increases postoperative morbidity and mortality. The etiology is often multifactorial, including pre-existing right ventricular dysfunction, leftward shifting of the interventricular septum, excessive volume overload, and suboptimal pulmonary afterload reduction. Different echocardiographic, hemodynamic, and biologic markers may help to the prevention, early diagnosis, and effective treatment of post-LVAD RVF. Specifically, post-LVAD RVF results in poor filling of the left ventricle and poor LVAD output that often necessitate additional right ventricular support with inotropes and pulmonary vasodilators, or rarely, a right-sided mechanical device. Additional treatments that can improve right ventricular function after LVAD implant include annuloplasty to reduce the severity of tricuspid regurgitation, aggressive diuresis to reduce volume overload, and treatment to maintain aortic valve patency in every cycle, to lower excessive left ventricular loading.

Keywords

Right ventricular failure · Right heart failure · Right ventricular dysfunction · Pulmonary hypertension · Pulmonary vascular resistance · Assist device · LVAD · Mechanical circulatory support · Leftward septal shift · Tricuspid regurgitation · Volume overloading · Septal contractility

K. Kırali (✉) · T. Özer · E. Selçuk
Department of Cardiovascular Surgery, Division of Heart Transplantation and Mechanical Assist Device, Kartal Koşuyolu Education and Research Hospital, Istanbul, Turkey

S. I. Dumitrescu et al. (eds.), *Right Heart Pathology*, https://doi.org/10.1007/978-3-319-73764-5_47

47.1 Introduction

The number of patients with heart failure (HF) is increasing worldwide due to advances in treatment for heart diseases, especially for coronary artery and valvular pathologies. Left heart failure (LHF) is now the most common type of end-stage HF, followed by biventricular HF and then right heart failure (RHF). Heart transplantation (HTx) is still the gold standard treatment for end-stage HF in eligible patients because new and effective developments in surgical techniques and immunosuppressive therapy have been associated with improved outpatient-care, long-term survival, and quality of life (see Chap. 45). As the prevalence of end-stage HF continues to rise, HTx is increasingly only available for a limited number of patients because of the shortage of suitable donors.

Shortages in available donors and increases in the waiting list for HTx have led to the need for novel treatment alternatives, with a particular focus on mechanical circulatory support (MCS) devices. Both short- and long-term MCS devices have been developed to ameliorate circulatory deterioration in end-stage HF patients and to act as a bridge to a better, more advanced, or definitive therapy. Acute left ventricular failure (LVF), regardless of whether there is cardiogenic shock, is fatal if not treated by hemodynamic support, which can be achieved by using short-term MCS devices. By contrast, chronic LVF has a more moderate course associated with circulatory decompensation if not supported with long-term MCS devices. In either case, a left ventricular assist device (LVAD) is the most effective means for mechanical support of cardiac output (CO) in hospitalized end-stage LHF patients, and can avoid pulmonary congestion and the need for respiratory support by mechanical ventilation or extracorporeal membranous oxygenation (ECMO). Preoperative new-onset pulmonary arterial hypertension (PAH) secondary by LHF prepares the right ventricle (RV) against increased afterload via resulting right ventricular hypertrophy, and therefore, early LVAD implantation can prevent the development of right ventricular dysfunction (RVD) and consequent right ventricular failure (RVF) due to reducing pulmonary afterload. However, almost all patients with advanced LHF have some degree of preoperative RVD, and because of long-standing elevated pulmonary afterload and pulmonary vascular resistance (PVR), can either tolerate or succumb to increased left-sided CO changes after LVAD implant.

Patients with advanced LHF are referred for LVAD implantation if they cannot wait for HTx because of severe clinical status, poor prognosis (1-year mortality of approximately 50%), poor quality of life due to symptoms even at rest, frequent hospitalizations, and difficultly managing complex drug regimens (Table 47.1). There are several indications for implanting an MCS device to keep end-stage HF patients alive or to bridge them to a more durable treatment modality; however, the indications for LVADs are more restricted (Table 47.2) [1]. Nevertheless, the use of LVADs is increasing annually among patients with advanced LHF, who cannot wait for HTx due to poor clinical statuses (*bridge to transplantation*) or who cannot become eligible for HTx due to severe additional risk factors (e.g., elevated PVR, advanced age, or severe non-cardiac pathologies) (*bridge to destination*), which is increasingly the case for life-long therapy [2]. Another area of clinical use for LVADs is in the evaluation of possible recovery of elevated PVR in end-stage HF patients and in the assessment of suitability for HTx (*bridge to candidacy*), but it can be difficult to predict this recovery capacity.

Patient selection and implantation timing are key determinants of success for LVAD therapy. The best candidates for LVAD implantation are those with advanced LHF, who are stable and receiving inotropic treatment. By contrast, patients in cardiogenic shock are unsuitable for LVADs because they are too sick, and should therefore be supported via percutaneous temporary MCS (t-MCS) devices to optimize their condition before LVAD implant [3]. If LVAD implantation is delayed, however, the outcome may worsen due to secondary organ damage caused by prolonged end-stage HF (e.g., poor nutritional status, low serum albumin, hepatic

Table 47.1 Indication and timing-criteria for LVAD implantation in patients with advanced LVF

1. Acceptable cardiac functions
(a) Severe left ventricular dysfunction (LVEF ≤25%; CI + <2 L/min/m^2; ± MR >2°)
(b) Adequate right ventricular function (TAPSE ≥1.0 cm; RAP ≤15 mmHg)
(c) Implantable pathologic cardiac anatomy
(d) Absence of non-cardiac contraindications
2. Worse functional status (NYHA IIIb–IV symptoms for at least 45 of the last 60 days)
3. Frequent hospitalizations (≥2 in the last 6 months)
4. INTERMACS status ≤4
5. Poor capacity for physical activity (6 min walking test <300 m)
6. Functional capacity reduction (peak VO_2 ≤14 mL/kg/min or continued need for intravenous inotropic therapy)
7. Inadequate pharmacologic support despite optimization (inotropic medications for ≥14 days)
8. Intractable ventricular arrhythmias
9. Aggressive therapy owing to severe congestive symptoms (e.g., LCOS, renal insufficiency, pulmonary congestion, or PVR)
10. Prolonged t-MCS without healing (IABP and/or va-ECMO support ≥7 days)
11. Prolonged va-a-ECCPS or lv-ECCS (≥14 days)

CI cardiac index, *va-a-ECCPS* venoatrial (biatrial)-arterial extracorporeal cardiopulmonary support, *lv-ECCS* left ventricle bypassing extracorporeal circulatory support, *ECMO* extracorporeal membranous oxygenation, *IABP* intra-aortic balloon pump, *INTERMACS* Interagency Registry for Mechanically Assisted Circulatory Support, *LCOS* low cardiac output syndrome, *LVAD* left ventricular assist device, *LVEF* left ventricular ejection fraction, *LVF* left ventricular failure, *t-MCS* temporary mechanical circulatory support, *MR* mitral regurgitation, *NYHA* New York Heart Association, *RAP* right atrial pressure, *RVD* right ventricular dysfunction, *VPR* vascular pulmonary resistance, *TAPSE* tricuspid annular plane systolic excursion, VO_2 oxygen consumption

and renal dysfunctions, and markers of RVF) [4]. Despite being a highly acclaimed treatment, LVAD is not a benign procedure, and patients with advanced LHF must overcome significant complications during the perioperative and postoperative periods (Table 47.3). Moreover, because many complications interact with severe RVF that develops after LVAD implant (i.e., post-LVAD RVF) being the most troublesome problem nowadays; maybe it will also in future.

Table 47.2 Targets of LVAD implantation

Bridge to recovery (BTR): *Salvage therapy*. Acute cardiogenic shock after a massive acute myocardial infarction with or without mechanical complications, acute myocarditis, or postcardiotomy syndrome can be fatal. The myocardium could be recovered by the LVAD unloading the left ventricle; with the main goal being to keep the patients alive while recovery occurs
Bridge to decision (BTD): *Supportive therapy*. Acute cardiac failure subsequent to acute decompensation of end-stage HF requiring optimal treatment by LVAD to keep patients alive, maintain cardiac output, and gain time until HTx or a decision for the destination therapy; with the main goal being to prevent non-cardiac organs deteriorating during the decision-making period
Bridge to candidacy (BTC): *Preparatory therapy*. Reversibility of the elevated PVR requires prolonged treatment, and recovery of PVR for HTx should be verified by invasive tests; with the main goal being to allow patients to continue in their daily lives
Bridge to transplantation (BTT): *Bridging therapy*. Candidates for HTx should undergo LVAD implantation due to serious life-threatening complications of advanced HF; with the main goal being to prevent patients alive until HTx
Bridge to destination therapy (BTDT): *Continuity therapy*. Long-term LVAD therapy is a durable treatment alternative to HTx in end-stage HF patients, who are not eligible for transplantation due to extracardiac diseases, irreversible elevated PVR, advanced age, or donor unavailability; with the main goal being to keep patients asymptomatic during their lives

HF heart failure, *HTx* heart transplantation, *LVAD* left ventricular assist device, *PVR* pulmonary vascular resistance

47.2 Right Ventricular Dysfunction After LVAD Implantation

The RV and left ventricle (LV) are anatomically, physiologically, and functionally distinct. There are two layers of right ventricular myocardium: the superficial muscle fibers are arranged circumferentially parallel to the atrioventricular groove in continuity with the LV, whereas the deep muscle fibers are aligned longitudinally, base to apex (in contrast to the LV where oblique fibers are found superficially, with longitudinal fibers on the endocardium and circumferential fibers between). The right heart circulatory

Table 47.3 Complications after LVAD implantation

(A) Device-related
(1) Post-implant RVD
(2) Major bleeding
(a) Surgical
(b) Hematological
(3) Thromboembolism
(a) Cerebral (stroke)
(b) Peripheral
(c) Intestinal
(d) Cardiac (acute coronary syndrome)
(4) Hemolysis
(5) Pump-thrombosis
(6) Aortic valve coaptation defect (AR)
(7) Infection
(a) Drive-line infection
(b) Mediastinitis
(c) Pump infection
(d) Sepsis
(B) Device independent
(1) Cardiac arrhythmias
(2) Pericardial fluid collection
(3) Wound dehiscence
(4) Hemorrhage
(a) Cerebral
(b) Gastrointestinal
(c) Mucosal
(5) Psychiatric episode
(6) Hepatic dysfunction
(7) Renal dysfunction
(8) Hypertension
(9) Respiratory failure
(10) Venous thromboembolism

AR aortic regurgitation, *LVAD* left ventricular assist device, *RVD* right ventricular dysfunction

system is comprised of the systemic veins up to the pulmonary arterioles, and RVF is defined as persistent signs and symptoms of dysfunction of the right heart circulatory system due to alteration of its structure and/or function, leading to suboptimal delivery of blood flow to the pulmonary circulation and/or elevated venous pressures at rest or with exercise [5]. The RV is the basic component of this circulatory system, and it is primarily affected by elevated PAH and PVR secondary to advanced LHF, either acutely or chronically. Functional deterioration in right ventricular ejection fraction (RVEF) is the initial scenario (i.e., RVD) following structural deterioration in the later phase (i.e., RVF). Anatomorphologic right ventricular pathologies, primarily pulmonary diseases or congenital anomalies resulting RVF, are outside of this definition.

Post-LVAD RVF, briefly, is the onset or exacerbation of right ventricular deterioration after LVAD implant, and is closely associated with postoperative mortality and morbidity. Therefore, it is important to give a clear definition to ensure accurate diagnosis. Different clinical definitions of post-LVAD RVF have been developed, based variously on hemodynamic parameters, echocardiographic measurements, and the requirement for a right ventricular assist device (RVAD). Interagency Registry of Mechanically Assisted Circulatory Support (INTERMACS) defines RVF as "persistent signs and symptoms of RVD evident by central venous pressure (CVP) >18 mmHg with a cardiac index (CI) <2.0 L/min/m^2 in the absence of increased left atrial pressure (LAP) or pulmonary capillary wedge pressure (PCWP) >18 mmHg, cardiac tamponade, ventricular arrhythmias, and/or pneumothorax, requiring either RVAD implantation, inhaled nitric oxide (NO), or inotropic therapy for ≥14 days after LVAD implantation" [6]. The spectrum of post-LVAD RVF ranges from mild dysfunction to life-threatening hemodynamic deterioration, and once RVD develops it is important to be alert for progression to severe RVF (Table 47.4). When a patient meets the criteria for this pathology, severity must be graded clinically based on persistent elevation of CVP and prolonged inotropic dependence (Table 47.5). Post-LVAD RVF mostly develops during the intraoperative and/or postoperative periods during hospitalization, but it can also emerge after discharge, defined as "late-onset RVF", which is a major reason for readmission with right heart related symptoms (i.e., edema, ascites, arrhythmia, renal and hepatic dysfunctions, coagulopathy, and malnutrition) despite adequate left ventricular support after hospital discharge [7]. Another group of patients, who are not included in the official classification, is the "subclinical" RVD, causing only limited exercise tolerance and impaired echocardiographic parameters;

Table 47.4 Severity of post-LVAD RVF

Hemodynamic (clinical-onset symptoms; post-LVAD RVF)	
Massive	Severe hypotensive (SAP <50 mmHg), low device flow alarm, stretched RA (CVP >20 mmHg), signs on TEE (mitral annular collapse, shrunken LV), deviation of IVS to the left; death due to RHF in hospital
Severe	Hypotensive (SAP <60 mmHg), CI <2 L/min/m^2, CVP >18 mmHg, low device flow, leftward shift of the IVS
Moderate	Borderline hypotensive (SAP 60–80 mmHg), CI 2–2.2 L/min/m^2, CVP 16–18 mmHg, leftward deviation of the IVS
Mild	Normotensive (SAP >80 mmHg), CI >2.2 L/min/m^2, CVP <16 mmHg, midline IVS
Therapeutic (healing-onset symptoms; after symptomatic RVF)	
Mild	Inotropic ± nitric oxide or vasodilators support for <7 days
Moderate	Inotropic ± nitric oxide or vasodilators support for 7–14 days
Severe	Inotropic ± nitric oxide or vasodilators support >14 days, RVAD
Postoperative (early-onset symptoms; after LVAD implantation)	
Hyperacute	Following excessive adjustment of the device speed
Acute	≤2 days
Early	3–14 days
Late	>14 days
Follow-up (late-onset symptoms; after discharge with an LVAD)	
Subclinical	Daily and/or exercise activity capability
Mild	No readmission after discharge
Moderate	Limited to one readmission for diuretic and/or vasodilator treatment
Severe	More than one readmission for inotropic and/or diuretic and/or vasodilator treatment; RVAD requirement; death due to RHF after discharge

CI cardiac index, *CVP* central venous pressure, *IVS* interventricular septum, *LV* left ventricle, *LVAD* left ventricular assist devices, *RA* right atrium, *RHF* right heart failure, *RVAD* right ventricular assist device, *RVF* right ventricular failure, *SAP* systemic arterial pressure, *TEE* transesophageal echocardiography

however, despite poor quality of life, this group typically has no history of hospital admissions due to major adverse events.

Table 47.5 Evidence of persistently elevated severe venous congestion

(a) CVP or RAP >18 mmHg (by right heart catheterization)
(b) IVC >2.5 cm with no inspiratory variation (by echocardiography)
(c) Worsening hepatic (total bilirubin >2.0 mg/dl) or renal (creatinine >2.0 mg/dl) dysfunction (by laboratory)
(d) Presence of ascites or palpable hepatomegaly (by diagnostic imaging)
(e) Elevated jugular venous distension at least half-way up the neck in an upright patient (by clinical findings)
(f) Peripheral and/or anasarca edema >2+ either new or unresolved (by physical examination)

CVP central venous pressure, *IVC* inferior vena cava, *RAP* right atrial pressure

Although LVAD implantations are effective for treating advanced LVF, they do not treat RVF intrinsically, and may in fact worsen RVF. The acceptable frequencies of early- and late-onset symptomatic post-LVAD RVF are approximately 20% and 10%, respectively [8]. However, prospective cohort studies have reported that the frequency of post-LVAD RVF may be as high as 35%, whereas heterogeneous studies have reported lower frequencies of up to 25% [9]. The reasons for this range are that different definitions have been used and the diagnosis of severe RVF is subjective, with different approaches used to determine prolonged inotropic requirement or aggressive management. Furthermore, patients' INTERMACS profiles, preoperative risk scores, and also postoperative management differences all contribute to the variability in incidence among populations. Severe post-LVAD RVF develops with a frequency <10% in patients with INTERMACS level 1 at implant, but this decreases to <4% for patients with INTERMACS levels 2–3 and to <2.3% for patients with INTERMACS levels 4–7 [10]. When comparing pulsatile and continuous flow devices, the overall incidences of post-LVAD RVF are similar in both groups [11]. The rate of unplanned RVAD use after LVAD implant is decreasing thanks to understanding of RV-LVAD relationship, better identification of risk profiles, and improved medical and surgical therapies. At present, approximately 10% of patients require an unplanned

RVAD for severe RVF immediately or late after LVAD implant, despite aggressive management [12]. The frequency of late-onset RVF is relatively low at 6–11%, but this should be treated by HTx.

47.3 Pathophysiology

Under normal physiological conditions, the anatomy, myocardial ultrastructure, and coronary physiology of the RV have the characteristics of a "high-volume/low-pressure" pump. The RV is not a mirror image of the LV, having its own anatomy, physiology, circulation, and hemodynamics. Despite the distinct embryologic origins of both ventricles, they are integrated rather than distinct structures that share the interventricular septum (IVS). The muscle mass of the RV is relatively less than that of the LV, because of a relatively thin (≤5 mm) free-wall. However, the RV can eject almost an equal stroke volume (SV) as the LV because it does so into a pulmonary circuit that has a lower afterloaded (low pressure and resistance) and is highly compliant, with a more complex contractile mechanism, requiring 75% less stroke work than the LV. The RV consists of separate ejection parts: passage (inlet) portion, pump (trabecular) portion, and throw (outlet) protion.

The trabecular portion is the main contractile part that has a crescent-shaped structure, including a concave free wall and a convex IVS. The systolic contraction of the RV includes longitudinal shortening, pressing of the free wall against the septum, contraction of the IVS, and a "wringing" action of the LV. The dominant part of contraction (80%) is achieved with longitudinal shortening (twisting) via oblique aligned septal myofibrils (superficial fibers), which are in continuation with fibers of the left ventricular free wall, and alone yield close to 60% of the RVEF. The rest of the contraction (20%) is achieved by short-axis shortening of the right ventricular free wall, which is attached to the IVS in the tricuspid annular plane, and yields approximately 30–35% of the RVEF. The contractile functions of both ventricles are closely related to biventricular anatomical and physiological interactions, defined as **ventricular interdependence** [13]. Anatomical interaction between both ventricles is more complicated: right ventricular contractility derived from the LV is significant (20–40%) and the LV contributes as much as 50% to the right ventricular pressure generation. Physiological dependence of both ventricles works according to the Frank–Starling mechanism: one is obliged to provide optimal preload to another to maintain circulation.

Right ventricular functions are more dependent on afterload than contractility and preload. ***Right ventricular afterload*** consists of two parameters: (1) opposing pulsatile flow (pulmonary vascular compliance, proximal vessel characteristic impedance, and wave reflections), which creates between 1/3 and 1/2 of the hydraulic power in the main pulmonary artery, and (2) opposing mean flow (i.e., PVR), which creates the rest of the hydraulic power. The working principles of afterload are bidirectional, with lower afterload making systolic ejection easier and unimpeded, but higher afterload resulting in systolic dysfunction as elevated resistance develops against ejection. Standard metrics such as PVR, the transpulmonary gradient (TPG), the diastolic pulmonary gradient (DPG), and LAP are used to describe right ventricular afterload. ***Contractility*** of the RV is weaker than that in the LV because of the lower myocardial mass, the crescent-shape cavity, and spindly papillary muscles; however, the structure of the trabeculae carneae in the RV gains power for ejection without requiring excessive concentric hypertrophy (>5 mm). The IVS, and its longitudinal shortening in particular, is the dominant component of right ventricular contractility under normal conditions, but septal involvement decreases significantly after cardiac surgery due to the effects of cardiopulmonary bypass (CPB) and pericardiotomy, resulting in a loss of pericardial restraint and a decline in the twisting motion of the LV, which is a significant portion of right ventricular systolic function. ***Right ventricular preload*** can also affect right ventricular function bidirectionally, with lower preload leading to decreased SV, and higher preload leading to increased

right-sided SV until pericardial constraint limits further augmentation to preserve the physiologic reserve of the RV.

Progression of LVF results in left ventricular remodeling via a vicious circle of complex changes of left ventricular hemodynamics on myocyte and nonmyocyte components of the myocardium. Irreversible pathologies of the LV lead to progressive loss of myofilaments, resulting progressive contractile dysfunction, and loss of collagen network connectivity, causing progressive cavity dilatation despite preserved structural integrity of the heart. Myocardial fibrosis interacts with other compartments to cause the following microvascular, mechanical, and electrical dysfunctions: (a) decreased perfusion reserve due to capillary rarefaction and perivascular fibrosis, (b) systolic and diastolic dysfunction due to myocardial stiffening from collagen expansion and increased filling pressures, (c) re-entrant arrhythmias and sudden death due to impaired electrical conduction from disarray in the collagen network architecture, and (d) impaired cardiomyocyte/mitochondrial energetics due to interposition of excess collagen between cardiomyocytes and capillaries. The enlargement of myocardial cells alters the LV from an elliptical to a spherical shape associated with increasing wall stress and mechanical energy that further aggravates left ventricular dilatation, wall thinning, and contractile dysfunction. This progressive dilatation also causes a "pull-apart" pathology of the papillary muscles that causes significant mitral regurgitation (MR) due to the inability of mitral valve coaptation. These left-sided pathologic changes result in pressure increase in the pulmonary vascular bed and increased right-sided filling pressures.

Pathophysiologically, RVF development is dependent on multiple risk factors (Chap. 11). Cardiomyopathic processes (maladaptive remodeling), elevated pulmonary pressure and resistance (pressure overloading), adverse left ventricular remodeling (ventricular dyssynchrony), accelerated resistance and/or obstructiveness against to coronary blood supply (myocardial hypoperfusion and/or ischemia), and inadequate diastolic filling (diastolic dysfunction) are mainly responsible for the development and progression of RVD before LVAD implant [14]. This remodelling process is sustained by the contribution of hemodynamic, neurohormonal, genetic, and molecular components. Because the RV is very sensitive to afterload, an acute increase in pulmonary afterload impairs the right heart circulatory system and the right-sided SV. *Maladaptive remodeling* of the RV is similar to that of the LV, being associated with increasing myocardial fibrosis, dilatation, wall thinning, atrioventricular valve regurgitation, and contractile failure. *Pressure overloading* in the pulmonary circulation increases afterload and prolongs the systolic contraction of the RV, and this increase in resistance can initially be tolerated due to preload overloading. In the early phase of RVD, wall thickening and enhanced contractility are the first important responses against pressure overloading, creating adaptive remodeling with concentric hypertrophy and preserved right ventricular function. As this progresses to a chronic phase, the higher afterload decreases the right pump function proportionally and contractile dysfunction eventually occurs despite advanced myocardial contractility induction. Meanwhile the RV dilates to provide adequate SV, but this leads to tricuspid annular dilatation, valve coaptation defects, and ultimately, significant tricuspid regurgitation (TR). This process triggers maladaptive remodeling that causes eccentric hypertrophy and deteriorated right ventricular function. *Ventricular dyssynchrony* by leftward movement of the IVS at the beginning of left ventricular diastole then accelerates RVD due to loss of left ventricular support. *Myocardial hypoperfusion* due to elevated intercavitary pressures of the RV, low cardiac output syndrome (LCOS) and/or coronary ischemia, may also functionally impact the highly compliant RV. *Diastolic dysfunction* can then develop due to the limited pericardial space, which accelerates the deleterious effects of the dilated LV with elevated end-diastolic pressure on the RV via rightward shift of the IVS. Impaired biventricular systolic function can also hinder right

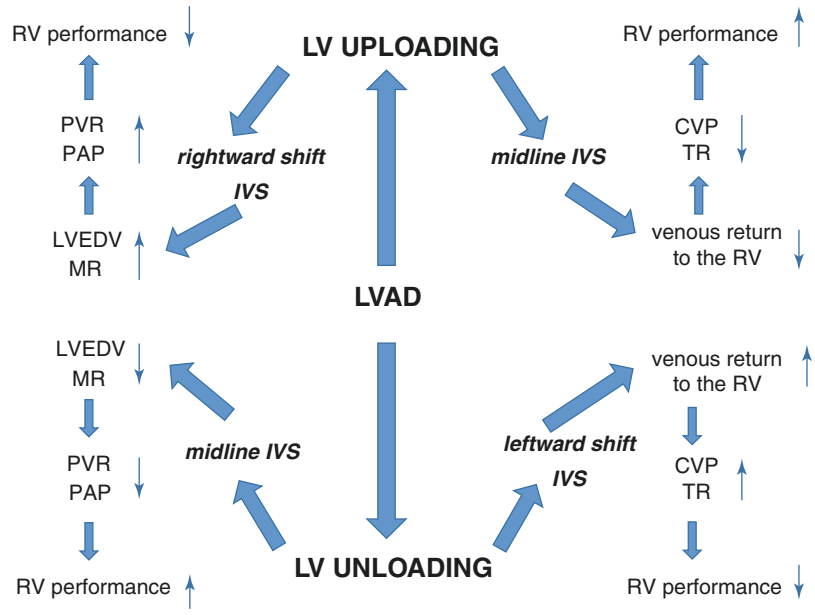

Fig. 47.1 The effects of an LVAD on an impaired RV. *CVP* central venous pressure, *IVS* interventricular septum, *LV* left ventricle, *LVAD* left ventricular assist device, *LVEDV* left ventricular end-diastolic volume, *MR* mitral regurgitation, *PAP* pulmonary artery pressure, *PVR* pulmonary vascular resistance, *RV* right ventricle, *TR* tricuspid regurgitation

ventricular unloading and precipitate diastolic dysfunction in that way.

Currently, the main indication for LVAD implantation in patients with advanced LHF is as a destination therapy, and this has both advantages and disadvantages for the RV [15]. Enhancement of CO by LVADs facilitates the recovery of end-organ dysfunction and ameliorates the biomarkers of target organ damage. By supporting the failing LV, an LVAD not only improves left-sided SV but also has reciprocal hemodynamic effects on the RV function (Fig. 47.1). Reducing left-sided filling pressures, and consequently MR, due to left ventricular unloading decreases, for example, the PVR and PAH. In turn, this contributes to right ventricular functions such as the RVEF, right ventricular stroke work index (RVSWI), and tricuspid annular plane systolic excursion (TAPSE) [16]. Finally, a marked reduction in right ventricular intercavitary pressure indirectly supports right ventricular myocardial perfusion, while reducing tricuspid annular tension decreases TR and the CVP, which can resolve congestive signs (e.g., edema, renal hypoperfusion, ascites, and hepatic congestion). Unfortunately, it is possible that post-LVAD RVF can develop or progress.

The etiology of post-LVAD RVF includes three main right-sided components: increased right-sided preload, impaired right ventricular contractility, and elevated pulmonic afterload (Fig. 47.2) [17]. After LVAD implant, several mechanisms influence these components, causing important changes in left and right ventricular geometries, and negatively affecting right-side CO (Table 47.6). Biventricular SVs must be equal for an unimpaired circulation, and normal RV function should be able to tolerate excessive volume displacements. However, patients with advanced LVF encounter early post-LVAD RVF regardless of whether right myocardial reserve is adequate preoperatively. In contrast to this, late-onset post-LVAD RVF clearly occurs due to progressive cardiomyopathy caused by ongoing severe PAH.

Preload increment is the first reason for aggravation of RVD after LVAD implant. Increased CO from the LV after LVAD implantation (approximately 100%) results in greatly increased venous return to the RV [18]. Equally, the administration of substantial amounts of blood products with or without fluids contributes to an elevation of the systemic venous return during the perioperative and/or early postoperative periods. This rapid increase in the preload can overstretch

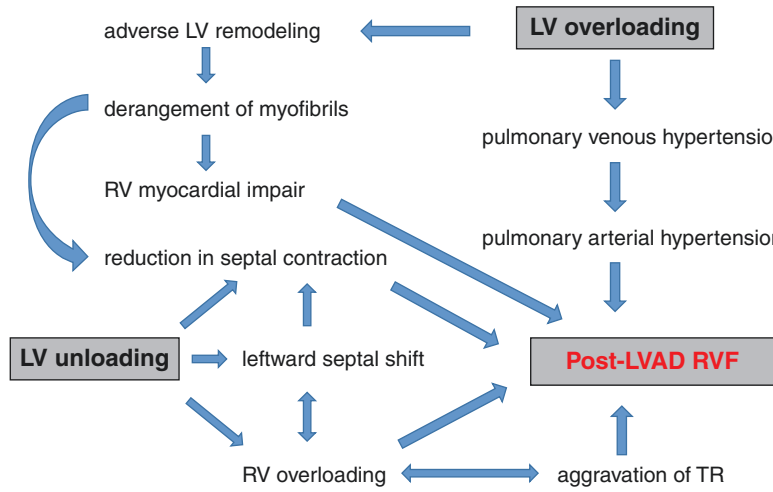

Fig. 47.2 The complex pathology of post-LVAD RVF. *LV* left ventricle, *LVAD* left ventricular assist device, *RV* right ventricle, *RVF* right ventricular failure, *TR* tricuspid regurgitation

Table 47.6 Determinants leading to post-LVAD RVF

1. Preload
a. Increased left ventricular output and venous return
b. Excessive administration of blood products and fluids
c. Decreased diuresis (renal failure)
d. Aggravated annular dilatation and tricuspid regurgitation
2. Contractility
a. Overstretched cardiac myofibrils (decreasing stroke volume)
b. Dyssynchrony of the IVS (non-contractile and/or leftward septal shift)
c. Impaired ventricular interdependence (LVF)
d. Intrinsic factors for RVF
e. Cardiopulmonary bypass with/without aortic cross-clamping
3. Afterload
a. Maintenance of pulmonary arterial hypertension
b. Inadequate unloading of the left ventricle by LVAD
c. Severe mitral regurgitation
d. Respiratory problems

IVS interventricular septum, *LVAD* left ventricular assist device, *LVF* left ventricular failure, *RVF* right ventricular failure

cardiac myofibrils in damaged RV, gradually aggravating the right ventricular and tricuspid annular dilatation, and resulting in worsening TR and right-sided SV. These adverse effects further increase right ventricular overdistension and filling pressures in a vicious circle.

Table 47.7 Classification of cardiorenal syndromes

Type	Clinical condition	Clinical etiology
I	Acute cardiorenal syndrome	Acute cardiogenic shock or acutely decompensated congestive heart failure leading to acute kidney injury
II	Chronic cardiorenal syndrome	Chronic congestive heart failure causing progressive and potentially permanent chronic kidney disease
III	Acute renocardiac syndrome	Acute kidney ischemia or glomerulonephritis causing acute cardiac failure or ischemia
IV	Chronic renocardiac syndrome	Chronic kidney disease contributing to decreased cardiac function
V	Secondary cardiorenal syndrome	Systemic condition (e.g., diabetes mellitus, sepsis) causing both cardiac and renal dysfunction

The cardiorenal syndrome (CRS) refers to a group of acute and chronic clinical conditions in which failure of either the heart or kidney initiates or aggravates failure of the other organ (Table 47.7) [19]. Most LVAD candidates have reversible preoperative renal dysfunction (CRS type II), which can be ameliorated quickly by improving systemic tissue perfusion with an LVAD. However, volume overloading caused by renal dysfunction, diuretic resistance, or excessive blood product replacement may lead

to deteriorated RV function in patients with renal dysfunction [20]. Worsening of right ventricular contractile function may also lead to additional kidney malperfusion via increased renal venous pressure due to elevated CVP and/or intraabdominal pressure due to severe ascites. Both can directly reduce the net filtration pressure, resulting in a decrease in the effective glomerular filtration rate (eGFR). Early improvement of renal dysfunction after LVAD implant is usually transient in end-stage HF patients with pre-existing renal insufficiency, and renal dysfunction frequently recurs during prolonged MCS because of inadequate systemic decongestion, a lack of pulsatility, and RVD [21]. Although eGFR generally remains above preimplant levels during follow-up, an initial large increase is followed by a proportionally larger decline a couple of months after LVAD implantation.

Impairment of contractility after LVAD implant may have several mechanisms. The 5 major mechanisms are likely as follows: (1) impairment of ventricular interdependence due to excessive left ventricular unloading, leftward septal shift, or left heart collapse, respectively; (2) the effect of pre-existing RVD; (3) the effect of advanced LVF with myocardial breakdown; (4) ventricular malign arrhythmias; and (5) the effect of CPB. Almost all patients with advanced LVF have PAH-induced subclinical right ventricular impairment. Pre-existing RVD aggravated by LVAD-dependent hemodynamic alterations limits postoperative hemodynamic adaptation of the RV and improvement of right ventricular contractile functions, and may be the main factor for the development of post-LVAD RVF. The intrinsic myocardial reserve of the RV is another key factor for right heart performance after LVAD implantation. In addition, various diseases directly damage the RV, such as congenital heart disease, myocarditis, arrhythmogenic right ventricular dysplasia, and coronary artery disease. The ongoing pathological process at the molecular level may cause late RVF: advanced LVF leads to myofibril derangement (reverse remodeling) and impairment of right ventricular contractile function, and reduced left ventricular contractility results in decreased the left ventricular contribution to the right ventricular systolic functions. Moreover, an LVAD can rapidly unload the LV, and may alter right ventricular geometry, so that right ventricular contractile functions are adversely affected despite decreasing pulmonary afterload. By contrast, excessive left ventricular unloading by an LVAD may result in a suction event and/or leftward septal shift, which causes bowing of the IVS into the LV that worsens right ventricular function as the RV becomes more spherical and aggravates TR. The worst situation is left heart collapse due to excessive hypovolemia in the LV, which can occur due to aggressive unloading by an LVAD. The left ventricular cavity then becomes smaller, new-onset subvalvular septal malposition creates subaortic stenosis, and the mitral valve apparatus shrinks on itself to form an intracardiac (left atrial) mass or thrombosis. Atrial tachyarrhythmia after LVAD implant occurs at a frequency of approximately 20% and can also impair right heart function [22]. Prolonged CPB time due to on-pump procedures on a beating heart (e.g., tricuspid annuloplasty, interatrial septal defect closure, aneurysmectomy, or coronary bypass) may contribute to transient myocardial dysfunction, with on-pump procedures under the cross-clamp (e.g., aortic valve replacement) potentially causing additional myocardial injury with or without cardiac failure.

Afterload elevation secondary to left-sided pathologies causes RVD in patients with advanced LVF. Chronically high left ventricular enddiastolic pressure with or without MR, eventually increases the LAP and causes pulmonary venous hypertension. This in turn, causes reactive pulmonary vasoconstriction that ends with secondary PAH. Elevated PVR may also increase the pulmonary afterload and RVD. However, the response of the pulmonary bed to significantly reduced left ventricular filling pressures is variable. A non-touch surgical strategy for significant MR can also aggravate PAH, despite sufficient unloading of the LV after LVAD implant. Pathologic remodeling of the pulmonary vasculature, insufficient left

ventricular unloading, primary PAH, or a combination of these may cause irreducible PVR. CPB-induced thromboxane A_2 release and elevated of cytokine levels after blood product transfusion, respiratory dysfunction, infection, or other pulmonary complications may also increase the PVR.

Post-LVAD RVF consists of two venous-side hemodynamic dysfunctions. These are elevated afterload that reduces volume delivery from the RV to the LVAD and elevated preload that causes systemic venous congestion. Even if left ventricular support is adequate, sufficient oxygenated blood cannot be pumped into the body due to the inadequate right-sided CO, which causes hypovolemic left-sided LCOS similar to preoperative advanced LVF. Systemic tissue hypoperfusion aggravates cardiac and non-cardiac organ failures to produce ischemic and biochemical byproducts that gradually impair right ventricular function. Overloading the RV results in systemic venous congestion due to elevation of the right atrial pressure (RAP) and worsening of TR. The severity of TR and the distorted geometry of the RV (increased short/long axis ratio) are primary predictors of RVD or the efficiency of the reserve capacity of the RV. However, the poor prognosis of patients with 'significant TR and silent MR' preoperatively compared to patients with 'severe MR' preoperatively reflects the predominant effect of significant TR over MR on RVD. Residual severe post-LVAD MR can only impair right ventricular functions and cause high mortality through persistent or elevated PAH, when left ventricular unloading by the LVAD is inadequate. This process (pulmonary and systemic venous congestion plus insufficient CO) results in dyspnea, intestinal angina and malabsorption, renal insufficiency, peripheral edema, and also systemic tissue hypoperfusion. Hepatobiliary failure, coagulopathy, ascites, and anasarca edema are seen in the late stage of this pathology, before irreversible end-organ damage develops. It should also be remembered that progressive right ventricular loading and left ventricular irritability by suction might lead to new-onset fatal tachyarrhythmias.

47.4 Preoperative Risk Evaluation

Post-LVAD RVF is associated with end-organ damage, prolonged hospital stays, more frequent readmissions, low quality of life, and reduced posttransplant survival. In the modern continuous flow device era, despite several pathophysiological processes being clarified, treatment options for severe RVF remain limited. Because RVF significantly increases perioperative and postoperative morbidity and mortality after LVAD implant, it is important to identify patients at elevated risk of post-LVAD RVF and to avert postoperative RVF by appropriate patient selection. Preoperative risk evaluation includes clinical condition, echocardiographic and hemodynamic measurements, biochemical markers, and device selection (univentricular or biventricular support). To detect high-risk candidates objectively, there are several risk scores developed based on combined multifactorial predictors (Table 47.8) [23–31]. These scoring systems do not include intraoperative events because they are based on patients' preoperative statuses. As new devices and management strategies have evolved over time, the validity of these risk scores has inevitably reduced [32]. However, uniform predictors have yet to be accepted widely, and the definition of RVF is often unclear; this is compounded by the fact that each patient should be assessed in detail according to his or her unique condition [33]. It is reasonable that patients with high-risk scores should be referred to alternative treatment methods such as HTx or operated after certain preparative therapies [34].

47.4.1 Clinical Condition

A poor preoperative clinical condition is related both to increased postoperative mortality and post-LVAD RVF (Table 47.9). Preoperative inotropic dependence is the primary risk factor, with intra-aortic balloon pump (IABP) requirement with or without a t-MCS device, also associated with an increased risk. Patients with poor INTERMACS profiles more frequently need right-sided support after LVAD implantation

Table 47.8 Risk scores of post-LVAD RVF

Risk score	Year	Clinical predictors	Biochemical markers	Hemodynamic predictors	Echocardiographic predictors	Criteria for post-LVAD RVF
Fitzpatrick et al.	2008	Previous cardiac surgery	Creatinine ≥1.9 mg/dL	CI <2.2 L/min/m^2 RVSWI ≤0.25 mmHg L/m^2 SBP ≤96 mmHg	Severe RVD	RVAD
Matthews et al.	2008	Need for vasopressor	AST >80 IU/L Bilirubin >2.0 mg/dL Creatinine >2.3 mg/dL			RVAD Inotropes >14 days Inhaled nitric oxide ≥48 h Inotrope requirement after discharge
Drakos et al.	2010	IABP requirement Inotrope dependency Obesity Destination therapy ACE/ARB usage Beta-blocker usage		PVR		RVAD Inotropes >14 days Inhaled nitric oxide ≥48 h
Kormos et al.	2010	Ventilator support	BUN >39 mg/dL Creatinine >1.7 mg/dL	RVSWI <300 (mmHg/mL)/m^2 CVP/PCWP >0.63 CVP >15 mmHg		RVAD Inotropes >14 days Need for inotrope after postoperative 14 day (late onset RVF)
Wang et al	2012	Number of inotropic agents	INR WBC ALT	TPG RAP		RVAD
Atluri et al.	2013	Heart rate >100 Preoperative intubation	Severe tricuspid regurgitation	CVP >15 mmHg	Severe RVD	RVAD
Aissaoui et al.	2015	INTERMACS <2			Em/S_{LAT} ≥18.5 Basal RVEDD ≥50 mm	RVAD
Loghmanpour et al.	2016	Late (>14 days) post-LVAD RVF Peripheral edema INTERMACS	Albumin BNP	PVR RVEF CO PAP RAP	MR TR LVEED	RVAD
Bellavia et al.	2017	Mechanical intubation Dialysis/CRRT	WBC, platelet ALT, AST INR NT-proBNP	RVSWI CVP	≥Moderate RVD RV/LV diameter ratio Low longitudinal sS of the RV free wall	

ACE angiotensin converting enzyme, *ALT* alanine transaminase, *ARB* angiotensin receptor blocker, *AST* aspartate transaminase, *CI* cardiac index, *CRRT* continuous renal replacement therapy, *CVP* central venous pressure, *Em* pulsed Doppler transmitral E wave, *INR* international normalized ratio, *INTERMACS* Interagency Registry for Mechanically Assisted Circulatory Support, *LV* left ventricle, *LVAD* left ventricular assist device, *PCWP* pulmonary capillary wedge pressure, *NT-proBNP* N-terminal pro-brain natriuretic peptide, *PVR* pulmonary vascular resistance, *RAP* right atrial pressure, *RV* right ventricle, *RVAD* right ventricular assist device, *RVD* right ventricular dysfunction, *RVEDD* right ventricular end-diastolic diameter, *RVF* right ventricular failure, *RVSWI* right ventricular stroke work index, S_{LAT} tissue Doppler lateral systolic velocity, *SBP* systolic blood pressure, *sS* systolic strain, *TPG* transpulmonary gradient, *WBC* white blood cell

Table 47.9 Preoperative clinical predictors for development of post-LVAD RVF

Inotrope independency (≥14 days) ± IABP (≥7 days) ± RVAD
INTERMACS status 1–2
Pre-existing RVD ≥ moderate (e.g., ascites, anasarca edema, or cardiac cirrhosis)
Malnutrition (hypoalbuminemia or cachexia)
Previous cardiac surgery
Mechanical ventilation
COPD
Continuous renal replacement therapy or dialysis
Advanced age
Frailty
Gender (female)
Obesity (BMI ≥30 kg/m^2)
Non-ischemic etiology

BMI body mass index, *COPD* chronic obstructive pulmonary disease, *IABP* intra-aortic balloon pump, *INTERMACS* Interagency Registry for Mechanically Assisted Circulatory Support, *LVAD* left ventricular assist device, *RVAD* right ventricular assist device, *RVD* right ventricular dysfunction, *RVF* right ventricular failure

Table 47.10 Interagency registry for mechanically assisted circulatory support

Status	Clinical profiles
INTERMACS	
1	Critical cardiogenic shock (crush and burn)
2	High dose intravenous inotropic support with or without t-MCS in instable condition
3	Low dose inotropic support with stable hemodynamics
4	Resting symptoms at home despite maximum oral therapy
5	Exertion intolerant
6	Exertion limited
7	Clinical stable advanced NYHA class III

INTERMACS Interagency Registry for Mechanically Assisted Circulatory Support, *t-MCS* temporary mechanical circulatory support, *NYHA* New York Heart Association Functional Classification

compared to patients with better profiles (Table 47.10) [35]. Preoperative nutrition is another key factor for patient performance after LVAD implantation. Obesity-related complications, such as cor pulmonale and respiratory failure, might increase the incidence of RVD [26]. But, many patients with advanced biventricular HF suffer from cardiac cachexia. Low albumin levels indicate poor nutritional statuses and are reported to be a significant risk factor for post-LVAD RVF [36]. In spite of clinicians are faced with older patients and have shown that advanced age is a risk factor, the precise role of age on post-LVAD RVF remains debatable. Pre-existing frailty (biological age rather than chronological age) is associated with higher mortality and morbidity due to limited capacity for organ recovery and vulnerability to LVAD-related complications [37]. Previous cardiac surgery, gender, non-ischemic etiology, and non-white ethnicity are other reported risk factors, but non have been confirmed consistently.

47.4.2 Echocardiographic Evaluation

Echocardiography is the simplest, but the most essential, imaging modality for determining pre-existing RVD and diagnosing post-LVAD RVF. Additionally, it can show important accompanying cardiac pathologies, such as TR, aortic incompetence, and intracardiac shunts. Unlike the case for the LV, it is difficult to establish standardized norms for RV assessment because of its complex geometrical structure and retrosternal position, as well as pacemaker/device-related artifacts, especially when using a transthoracic approach. Although many parameters have been developed to describe right heart systolic and diastolic functions in adults, most have limited prognostic significance for post-LVAD RVF (Table 47.11) [38–42].

Accurate assessment of quantitative parameters, especially the RVEF, is difficult on 2-D echocardiography due to the complex geometry of the RV, the heavily trabeculated endocardial surface, the bellows-like contractile pattern, and the increased RV/LV ratio. Furthermore, the reproducibility of these parameters is low because it is difficult to detect the right ventricular free wall and the precise endocardial border. The ability of 3-D echocardiography to assess right ventricular volumes and RVEF quantitatively, similar to cardiac magnetic resonance imaging, makes it a promising option for preoperative assessment among potential LVAD recipients [43]. TAPSE is

Table 47.11 Echocardiographic predictors of post-LVAD RVF

Parameters	Normal value	Diagnostic value
(1) M-mode		
(a) TAPSE	≥16 mm	<10 mm
(2) Two-dimensional measurements		
(a) LVEF	>60%	<20%
(b) RVEF	≥45%	<30%
(c) LAD/LVEDD		>2/3
(d) LVEDD	<50 mm	≥75 mm
(e) LA volume index	<34 mL/m^2	>38 mL/m^2
(f) RAD	<40 mm	>50 mm
(g) RVEDD (parasternal/basal)	<35/40 mm	>35/45 mm
(h) RV short/long axis	<0.5	>0.6
(i) RVEDD/LVEDD	<0.6	>0.75
(j) RVFAC	≥35%	<35%
(k) TA diameter	<40 mm	>43 mm (≥ 23 mm/m^2)
(l) IVC diameter	≤15 mm	>2.1 mm
(m) IVC collapse with sniff	≥50%	<50%
(3) Tissue Doppler		
(a) RV S'	≥10 cm/s	<5 cm/s
(b) RV-E/E'	≤6	>10
(c) Em/S_{LAT}		≥18.5
(4) Speckle tracking imaging		
(a) RV peak lateral longitudinal strain	< −20%	> −9%
(b) RV peak global longitudinal strain	< −25%	> −12%

E/E' trans-tricuspid filling velocity/early diastolic velocity ratio, *Em* pulsed Doppler transmitral E wave, *IVC* inferior vena cava, *LA* left atrium, *LAD* left atrial diameter, *LV* left ventricle, *LVAD* left ventricular assist device, *LVEDD* left ventricle end-diastolic diameter, *RA* right atrial diameter, *RV* right ventricle, *RVEED* right ventricular end-diastolic diameter, *RVEF* right ventricular ejection fraction, *RVF* right ventricular failure, *RVFAC* right ventricular fractional area change, *RV S'* tricuspid annular systolic velocity, S_{LAT} tissue Doppler lateral systolic velocity, *TA* tricuspid annulus, *TAPSE* tricuspid annular plane systolic excursion

the most basic and widely used echocardiographic parameter for assessing the systolic function of the RV and reflects right ventricular longitudinal systolic shortening. A very low TAPSE is a specific, but poorly sensitive predictor of post-LVAD RVF, especially when the RV is asymmetrically shaped due to inadequate presentation of global RVD. Despite a lack of standardization, both the strain and the strain rate have recently been highlighted as direct measures for assessing myocardial contractility independently of ventricular morphology and loading. Indeed, depressed right ventricular global and free-wall longitudinal strains are strong predictors of post-LVAD RVF. A dilated inferior vena cava with decreased or lost collapsibility (Plethora +) in subcostal window views indicates elevated RAP, and therefore suggests severe RVF. Tricuspid regurgitation is quite common in patients with pre-existing RVD, but its preoperative severity is often uncorrelated with post-LVAD RVF. In contrast to this, preoperative tricuspid annular dilatation (with or without severe TR) is not only a risk factor for postoperative RVD but also a predictor of poor mid-term outcomes [44]. Preoperative MR has not been demonstrated as a risk factor for post-LVAD RVF.

47.4.3 Hemodynamic Measurements

Invasive hemodynamic measurements focused on right heart function are recommended before implantation in all LVAD candidates (Table 47.12) [45]. Cardiac catheterization objectively reveals right and left filling pressures and hemodynamic evaluation demonstrates right ventricular preload and afterload. Moreover, information on right ventricular contractile functions can be obtained from these measurements. When taking measurements, it should be kept in mind that hemodynamic data may vary by volume status and by inotropic and vasodilator treatments, and that results reflect only the present profile of a patient. Therefore, cardiac catheterization should be repeated at regular intervals (e.g., annually) to detect hemodynamic alterations that occur over time.

Progression of left ventricular damage is liable for probable post-LVAD RVF. Therefore, end-stage HF patients with poor CIs are at increased risk of RVF, even though this

Table 47.12 Hemodynamic predictors for post-LVAD RVF

Parameters	Normal value	Diagnostic value
SV (EDV − ESV) (=CO/HR)	60–100 mL/beat	<50 mL/beat
SVI (=CI/HR)	35–47 mL/beat/m^2	
CO (=SV × HR)	4–8 L/min	<3.5 L/min
CI (=CO/BSA)	2.5–4 L/min/m^2	<2 L/min/m^2
Mixed venous oxygen saturation	60–80%	<55%
mABP	≥70 mmHg	≤60 mmHg
sPAP	15–30 mmHg	≥50 mmHg
CVP (=RAP)	2–6 mmHg	≥16 mmHg
PCWP	6–12 mmHg	≤18 mmHg
CVP/PCWP	<1/2	>2/3
PAPP (=sPAP − dPAP)		
mPAP	≤18 mmHg	≥25 mmHg
TPG (=mPAP − PCWP)	12 mmHg	>12 mmHg
DPG (=dPAP − PCWP)	≤7 mmHg	>7 mmHg
PVR [=80 × (TPG/CO)]	<250 dynes-s/cm^5	>250 dynes-s/cm^5 (≥3 wood)
RVSWI [=SVI × (mPAP − RAP) × 0.0136]	5–10 g/m^2/beat	<4.4 g/m^2/beat
PAPi (=PAPP/RAP)	>3.5	<2
PACi [=SV/PAPP/BSA]	>1 mL/mmHg/m^2	<0.85 mL/mmHg/m^2

mABP mean arterial blood pressure, *BSA* body surface area, *CI* cardiac index, *CO* cardiac output, *CVP* central venous pressure, *EDV* end-diastolic volume, *ESV* end-systolic volume, *HR* heart rate, *LVAD* left ventricular assist device, *d/m/sPAP* diastolic/mean/systolic pulmonary artery pressure, *PACi* pulmonary arterial compliance index, *PAPi* pulmonary artery pulsatility index, *PAPP* pulmonary artery pulse pressure, *PCWP* pulmonary capillary wedge pressure, *PVR* pulmonary vascular resistance, *RAP* right atrial pressure, *RVF* right ventricular failure, *RVSWI* right ventricular stroke work index, *SV* stroke volume, *SVI* stroke volume index, *TPG* transpulmonary gradient

assessment does not directly reveal right ventricular contractile functions. Most patients, who develop post-LVAD RVF, have elevated filling pressures preoperatively; elevated CVP accompanied by low PCWP is especially correlated with an increased risk of post-LVAD RVF. A more specific parameter, the RVSWI indicates the intrinsic function of the RV. Although the RVSWI is considered to reflect right ventricular contractile function almost directly, it relies on preload-dependent calculations that limit its prognostic value [46]. However, low RVSWI is certainly as a predictor for post-LVAD RVF.

Pre-existing PVR elevation is the most widely used risk factor for evaluating RVF before LVAD implantation, and its prognostic value is also valuable as a predictor of post-LVAD RVF. Improvement in pulmonary vascular overloading courtesy of significant left ventricular unloading after LVAD implant also results in a dramatic decrease in the PVR. This points to the reversibility of PAH and to the possible suitability for HTx (i.e., bridge to candidate). By contrast, continued elevation of the PVR indicates irreversibility (i.e., bridge to destination). A reduced pulmonary arterial capacitance index (PACi) is a better prognostic parameter than the PVR in patients with advanced LVF and pre-existing PAH, because the PVR may be insensitive to pulmonary vascular stiffening due to chronically elevated LAP [47]. Patients with a reduced PACi can have limited right ventricular reserve due to chronic pulsatile loading, which obstructs forward flow and results in a deterioration in RVF. At the same time, patients with a low PACi and higher CVP/PCWP ratio have an increased risk for post-LVAD RVF than patients with high PACi associated with a lower CVP/PCWP, which presents an adequate right heart response against pulsatile loading. The pulmonary artery pulsatility index (PAPi) is a novel invasive hemodynamic index that is a robust, independent predictor of post-LVAD RVF or the need for right heart MCS, especially in patients

receiving inotropes, and it remains valid regardless of the catheterization timing [48]. PAPi also indicates the severity of post-LVAD RVF [49]. Patients with slightly elevated pulmonary artery pressures (PAPs) despite a significant increase in PCWP (i.e., low TPG) need at least right-sided MCS after LVAD implant.

47.4.4 Biochemical Markers

Long-standing end-stage HF is usually present with several grades end-organ dysfunction caused by systemic hypoperfusion or venous congestion. End-organ damage is represented through elevations in several biochemical markers from cardiac and non-cardiac tissues, secondary to end-stage HF, and can be used to stratify patients at increased risk, to detect early signs of prognosis and treatment efficacy, and to select potential patients most likely to benefit from a given therapy (Table 47.13) [50–54]. Alone, they are not specific for cardiac failure, especially for RVF, but they can be meaningful predictors for post-LVAD RVF when interpreted in the context of echocardiographic and hemodynamic parameters showing HF. Biomarkers are available that reflect important and common pathophysiological processes in HF, but novel biomarkers are needed to improve the guidance of novel molecular targeted therapies for end-stage HF and post-LVAD RVF [55, 56].

The natriuretic peptides, with natriuretic, diuretic, and vasodilator effects, are the most important biomarkers of the existence, severity, and prognosis of decompensated end-stage HF. Atrial natriuretic peptide (ANP) is produced from atrial myocytes and brain natriuretic peptide (BNP) is mostly produced from ventricular myocytes [57]. Both are excreted in response to myocardial stretch caused by pressure and volume overload. However, the more durable mid-regional zone prohormone ANP (MR-proANP) and N-terminale prohormone BNP (NT-proBNP) can be detected more easily in the circulation and have greater diagnostic value. Using age-stratified cutoff levels for

Table 47.13 Biochemical predictors for post-LVAD RVF by pre-existing RVD in long-standing end-stage HF patients

	Normal value	Diagnostic value
A. Myocardial damage biomarkers		
(a) Myocardial stretch biomarkers		
BNP	<10 pg/mL	≥100 pg/mL
NT-proBNP	<450 pg/mL	≥1200 pg/mL
MR-proANP	<10 pg/mL	≥300 pg/mL
(b) Myocardial injury biomarkers		
hsTnT	<5 pg/mL	≥14 pg/mL
hsTnI	<5 pg/mL	≥30 pg/mL
(c) Oxidative injury biomarkers		
Myeloperoxidase		
MR-proADM		
Oxidize LDLs		
B. Cardiac remodeling biomarkers		
(a) Inflammation		
CRP		
Adinopectin		
TNF-α		
Interleukins		
Chemokine receptor downregulation (CCR3, CCR4, CCR6, CCR7, CCR8)		
Osteoprotegerin		
(b) Hypertrophy/fibrosis		
Collagen propeptides		
Soluble ST2		
Galectin 3		
(c) Apoptosis		
GDF-15		
C. End-organ damage biomarkers		
(a) Hepatic injury biomarkers		
AST	<40 IU/L	>80 IU/L (>2 × basal level)
ALT	<40 IU/L	>80 IU/L
Bilirubin	<1 mg/dL	>2.0 mg/dL
INR	<1.1	>1.5 (>50% basal level)
Albumin	>3.5 g/dL	<3.0 g/dL
(b) Renal damage biomarkers		
Creatinine	<1.2 mg/dL	≥2.0 mg/dL
BUN	<25 mg/dL	≥40 mg/dL

Table 47.13 (continued)

	Normal value	Diagnostic value
NGAL	<100 ng/mL	>100 ng/mL

ALT alanine aminotransferase, *AST* aspartate aminotransferase, *BUN* blood urea nitrogen, *CRP* C-reactive protein, *GDF* growth differentiation factor, *HF* heart failure, *INR* international normalized ratio, *LDL* low density lipoprotein, *LVAD* left ventricular assist device, *MR-proANP* mid-regional pro-atrial natriuretic peptide, *NGAL* neutrophil gelatinase-associated lipocalin, *NT-proBNP* N-terminal pro-brain natriuretic peptide, *RVD* right ventricular dysfunction, *RVF* right ventricular failure, *hs-Tn* high-sensitive troponin, *TNF* tumor necrosis factor

NT-proBNP (because serum concentrations increase with age) further improves the positive predictivity for acute cardiac failure, whereas it's acceptable cutoff level for chronic end-stage HF is even higher. Several clinical conditions are also known to affect NT-proBNP levels without causing obviously symptomatic cardiac failure. These include renal dysfunction (decreasing clearance), arrhythmias (increasing extraction), cardiotoxic agents, obesity (suppressing release), and heart muscles diseases (rising production).

Cardiac troponins T (TnT) and I (TnI) are the best diagnostic markers for acute myocardial injury. Furthermore, high-sensitive assays of both biomarkers can be used to detect cardiovascular and all-cause mortality risks in patients without acute cardiac injury such as those with chronic HF [58]. Basal elevations of cardiac troponin concentrations are associated with an increased risk for cardiovascular and all-cause mortality in the general population [59]. When detectable cardiac troponin levels by high-sensitive assay (hsTnT and hsTnI) exceed the 99th percentile of the reference population, there is a strong association with adverse cardiac outcomes and a threefold increase in the cardiovascular risk [60]. By contrast, minimally detectable levels (<5 pg/mL) have no strong association (1.3-fold) with cardiovascular risk, because they can also be physiological and reflect myocardial cell turnover and apoptosis within the normally aging heart.

Adrenomedullin is a potent vasodilator that induces NO synthesis under myocardial stress associated with a decreased LVEF, increased PAPs and diastolic dysfunction. This functions as a compensatory mechanism to reduce PCWP and improves the CI [61]. Mid-regional pro-adrenomedullin (MR-proADM) has a strong correlation with the global disease burden in end-stage HF and is a potent prognostic indicator for both cardiac and non-cardiac death.

Several inflammatory markers with prognostic and therapeutic inferences arise during the end-stage of HF. Injury of cellular elements triggers a proinflammatory state that causes further injury to cellular elements, including cardiomyocytes. The main predictors for release of these mediators are LCOS, pulmonary congestion, and systemic congestion, which mitigate the effects of myocardial stress and maladaptive cardiac remodeling. Several cytokines stimulate fibroblasts and initiate a process of collagen deposition in the cardiac interstitium (reactive interstitial fibrosis), which blocks cardiomyocyte oxygenation by constricting capillaries and triggering apoptosis. Abnormal chemokine activation (chemotactic cytokines) via chemokine receptors in the immunopathogenesis of HF plays a key role in modulating the cardiac response, and downregulation of these receptors in LVAD patients may be associated with worse post-implant RVF [62].

Renal dysfunction can depend on hypoperfusion, kidney tissue-congestion, pre-existing renal insufficiency, renotoxic treatment, or renal venous pressure elevation due to increased right-sided filling and/or intraabdominal pressures, and these processes can occur before or after LVAD implantation. Pre-existing renal dysfunction has an interesting behavior after LVAD implant. On the one hand, an effective glomerular filtration rate (eGFR) <60 mL/min/m^2 and renal perfusion will increase thanks to increased left-sided CO in the first month, before declining to the baseline level over the following 3 years. On the other hand, an eGFR >60 mL/min/m^2 will decline after the first month and remain worse than baseline over the following 3 years [63]. Elevated renal

biomarkers are important predictors for RVF, but they can also be used to indicate diuretic resistance, possible chronic renal disease, systemic hypoperfusion, and volume overload. Neutrophil gelatinase-associated lipocalin (NGAL) is a novel serum biomarker that can be used as an early predictor of renal failure, and has been shown to have a greater link to renal recovery after LVAD implant than serum creatinine [64].

Hepatic dysfunction caused by chronic CVP elevation, proinflammatory cytokine upregulation, and oxidative stress is a serious complication in patients with long-standing end-stage HF. Hepatic dysfunction begins asymptomatically with well-known laboratory abnormalities, but further progression of hepatic dysfunction and fibrotic transformation result in cardiac cirrhosis as the disease advances. The non-elastic capsule around the liver does not allow for the absorption of the elevated right heart filling pressures by the liver, and the resulting liver congestion causes hepatic stiffness, which can be used to indicate the severity of RVF [65]. However, hepatic stiffness may not resolve after treatment and can remain a significant predictor for post-LVAD RVF or irreversibility of hepatic injury, despite significant reduction of pulmonary afterload following successfully left-sided unloading by LVAD. The best marker of malnutrition, inflammation, hepatic dysfunction, and the overall catabolic state is hypoalbuminemia, which also predicts poor short- and long-term outcomes in patients with end-stage HF [36].

47.5 Management

The use of LVADs is now accepted as a mechanical supportive therapy for end-stage HF patients, especially as a bridge to HTx. After proving its therapeutic efficacy in non-HTx candidates, the implantation rate of these devices as a destination therapy has increased logarithmically in the last two decades. Successful decompression of the LV, as well as optimization of left-sided CO and peripheral perfusion, not only improve early- and long-term survival but also improve the quality of life of that survival, thanks to the amelioration of end-organ dysfunction. Furthermore, new devices have been developed that have reduced the rates of device-related complications such as bleeding, infection, malfunction, and thrombosis. However, the ability of LVADs to unload the RV and improve its functions remains controversial, primarily because LVAD therapy can cause post-LVAD RVF, which has a dramatic effect on postoperative morbidity and mortality. At the same time, effective LVAD treatment is the primary driver of improved right ventricular function through the resulting significant reduction in pulmonary afterload. Therefore, appropriate patients selection is the most important factor for predicting, preventing, and treating post-LVAD RVF, regardless of whether there is pre-existing RVD. The management of post-LVAD RVF can be more difficult, for example, in patients with pre-existing significant PAH and PVR [66]. A sound interdisciplinary approach, involving surgeons, cardiologists, anesthesiologists, critical care staffs, and nursing staffs, is therefore key issue to effective management.

In our clinic, specific treatment modalities, maneuvers, and techniques are preferred for optimizing patients with advanced LVF before LVAD implantation, managing them intraoperatively, and maintaining hemodynamic stability postoperatively. A few critical points during LVAD implantation positively influence the overall procedure (Table 47.14).

Table 47.14 Individual recommendations for managing LVAD patients against RVF

I. Preoperative patient selection and management
A. Preoperative appropriately compensated clinical condition (advanced LVF with compensated RVD)
1. NYHA class ≤IIIb without anasarca and peripheral edema at least 7 days
2. INTERMACS status 3–4 (–5)
3. Hospitalization for cardiac rehabilitation
a. Stabilization for pre-existing RVD with PCS
(i) Diuretic
(ii) Renodilator (dopamine)
(iii) Pulmonary vasodilator (sildenafil, iloprost)
(iv) Digoxin
(v) Inotrope (dobutamine, levosimendan)

Table 47.14 (continued)

(vi) Fluid removal (ultrafiltration, paracentesis, thoracentesis)
b. Stabilization for advanced LVF with t-MCHS
(i) IABP
c. Stabilization for biventricular failure with t-MCS
(i) ECCPS (respiratory insufficiency)
(i) va-ECMO (≤7 days)
(ii) va-a-ECMO (>7 days)
(ii) ECCS (respiratory competence)
(i) Biventricular-ECCS (LV-bypass and RV-bypass circuits)
B. Echocardiographic evaluation
1. LVEDD (>60 mm)
2. TAPSE (>10 mm)
3. Aortic valve coaptation (no AR)
4. Tricuspid valve coaptation with TA diameter
5. Interatrial shunt
6. Intracardiac thrombosis
C. Hemodynamic measurements
a. CI <2 L/min/m^2
b. PVR >3 woods
c. CVP ≤15 mmHg
d. PCWP ≥18 mmHg
D. End-organ functions' improvement
a. Nutritional adequacy (albumin ≥3.5 g/dL, Na^+ >135 mEq/L)
b. Hepatic performance (bilirubin ≤2 mg/dL, AST and ALT <40 IU/L)
c. Renal performance (creatinine ≤1.5 mg/dL)
d. Hematological suitability (Hct >30%, HGb >10 g/dL, platelet >100,000)
e. Hemorrhagical competence (INR <1.5, ACT <140 s)
E. Infection parameters
a. Procalcitonin
b. CRP
c. Sedimentation
II. Intraoperative management
A. Anesthesia-related complications (hypoxia, hypercarbia, acidosis)
B. Surgical process adequacy
1. Intervention
a. Primary
b. Re-operation
2. Surgical approach
a. Full sternotomy
b. Anterior left thoracotomy + reverse-T upper mini sternotomy

Table 47.14 (continued)

3. Implantation	
a. On-pump	
b. Off-pump	
c. On- and off-pump	
4. Outflow graft anastomosis	
a. Ascending aorta	
b. Descending aorta	
5. Augmentation of LVAD	
C. Post-implant medication	
1. Inotropes	
2. Vasodilators	
3. Anticoagulation	
III. Postoperatively	
A. Adequacy of left ventricular and septal systolic contractile functions	
B. Effective pulmonary vasodilatation	
C. Prevention of bleeding	
D. Close monitoring of hemodynamic parameters	
E. Early extubation and mobilization	
F. Vigilance for any grade post-LVAD RVF	
G. Multi-agents medical oral therapy with individualized daily dosages	
1. Digoxin	0.125 mg (1 × 1)
2. Sildenafil	10–20 mg (3 × 1)
3. Isosorbide mononitrate	50 mg (1 × 1)
4. Furosemide	20 mg (1–2 × 1)
5. Sacubitril/Valsartan (ARNI)	24/26 mg (2 × ½–1)
6. Warfarin	INR ≈ 2
7. Acetylsalicylic acid	300 mg (1 × 1)
8. Clopidogrel	75 mg (1 × 1)

ACT accelerated clotting time, *ALT* alanine aminotransferase, *AR* aortic regurgitation, *ARNI* angiotensin II receptor rlocker neprilysin inhibitor, *AST* aspartate aminotransferase, *CI* cardiac index, *ECCPS* extracorporeal cardiopulmonary support, *ECCS* extracorporeal circulatory support, *ECMO* extracorporeal membranous oxygenation, *HGb* hemoglobin, *IABP* intra-aortic balloon pump, *INR* international normalized ratio, *INTERMACS* Interagency Registry for Mechanically Assisted Circulatory Support, *LCOS* low cardiac output syndrome, *LVAD* left ventricular assist device, *LVEED* left ventricular end-diastolic diameter, *LVF* left ventricular failure, *t-MCS* temporary mechanical circulatory support, *t-MCHS* temporary mechanical counterpulsatile hemodynamic support, *MR* mitral regurgitation, *Na^+* sodium, *NYHA* New York Heart Association, *PCS* pharmacologic circulatory support, *PFO* patent foramen ovale, *PHT* pulmonary arterial hypertension, *PVR* pulmonary vascular resistance, *RVD* right ventricular dysfunction, *RVF* right ventricular failure, *TA* tricuspid annulus, *TAPSE* tricuspid annular plane systolic excursion, *TR* tricuspid regurgitation

47.5.1 Preoperatively

The development of post-LVAD RVF is closely related to patients' clinical conditions before surgery. Therefore, patients with RVD should be hospitalized for aggressive control before LVAD implantation, ensuring therapy optimizes right ventricular function before RVF develops or worsens. Cardiac rehabilitation alone is rarely sufficient for clinical recovery, so end-organ dysfunctions must be treated aggressively until LVAD implantation, according to the clinical situation of patients. Optimization of volume status is important for every patient, and diuresis and/or ultrafiltration must be regulated to reduce filling pressures on both sides and achieve a CVP <15 mmHg and PCWP <18 mmHg. Diuretic therapy is usually started with oral medication, although intravenous infusions are preferable during hospitalization because they have greater therapeutic efficacy. Daily follow-up of body weight, urine count, and fluid and sodium intake is essential when monitoring patients with pre-existing RVD. If diuretic therapy becomes ineffective or is associates with congestive symptoms (e.g., gastrointestinal angina, abdominal swelling, hepatomegaly, peripheral edema, or ascites), inotropic support can help to improve biventricular cardiac contractile function and ameliorate organ hypoperfusion during preoperative period. Different candidates for LVAD have different grades of RVD, and all receive standard treatment for congestive HF, including inotropes and pulmonary vasodilators, when they are referred to surgery. Inotropic support is initially provided via intravenous dobutamine with or without milrinone, which is a suitable option for decreasing pulmonary pressures and improving right ventricular performance. Sildenafil can also lead to a sufficiently significant decrease in the PAPs and PVR in patients with pre-existing PVR elevation before the LVAD is implanted [67]. Despite the direct effects of sildenafil on right ventricular contractility being uncertain, it is expected that there will be a significant improvement in the TAPSE caused by a reduction in the pulmonary afterload. Sildenafil therapy is generally used preoperatively, but it can also be continued postoperatively and during long-term follow-up. Elective IABP use can maintain significant cardiac support in severely ill candidates, and recover pre-existing RVD by unloading the LV, reducing PAPs, and increasing organ perfusion [68]. The preoperative INTERMACS scores of patients are closely related to mortality after LVAD treatment, and using t-MCS as bridge to LVAD can be more plausible than direct LVAD implantation in patients with high-risk INTERMACS profiles, such as those with cardiogenic shock [1].

47.5.2 Intraoperatively

For effective intraoperative management of LVAD implantation, strong and established task-sharing mechanisms should be in place for the transplant team at every stage of the operation. These include carefully anesthetic induction, invasive hemodynamic monitoring, real-time transesophageal echocardiography (TEE), optimal surgical techniques, weaning procedures, bleeding control, post-implant inotropic and pulmonary vasodilator management, and transfer to the intensive care unit.

Patients with advanced LVF who undergo LVAD implantation often have borderline hemodynamic statuses when they arrive in the operating room, and can be very sensitive to anesthesia-related fluctuations in hypoxia, hypercarbia, and acidosis. To protect the RV, avoidance of hypercapnic acidosis and hypoxic pulmonary vasoconstriction is very important during induction and after the procedure. Any excessive adrenergic stimulation should be managed to prevent LCOS caused by acute increases in the pulmonary afterload (i.e., acute PAH crises) and/or systemic afterload (i.e., by peripheral vasoconstriction), coldness in the operating room, exaggerated excitement, or extreme disturbance by percutaneous intravascular monitoring. Pulmonary artery catheterization is a basic and useful way to maintain minute-to-minute hemodynamic monitoring (e.g., CVP, PCWP, and mixed venous oxygen saturation). Detailed evaluation by TEE should be started immediately after induction to identify

aortic valve competency, intracardiac defects, tricuspid valve function, and any unknown cardiac pathologies. Device location, insertion, and positioning are performed under TEE guidance intraoperatively. Excessive fluid replacement should be avoided, as in standard cases, to prevent right ventricular overload, and fluid replacement should be done judiciously according to the hemodynamic parameters, TEE, and direct observation of the RV.

The precise surgical implantation technique varies according to the surgeons preferred approach. The least undesirable process is CPB, which can be mostly associated with elevated PVR, increased systemic inflammatory response, bleeding, kidney dysfunction, and lung dysfunction, and postoperative RVD. To avoid the side effects of prolonged CPB with or without aortic cross-clamping and cardioplegic arrest, the CPB period should be kept as short as possible.

On-pump implantation of LVADs, with or without cross-clamping the aorta, is the preferred approach for LVAD implantation with other cardiac procedures. All additional intracardiac surgical procedures, such as tricuspid annuloplasty, interatrial septal defect closure, and left ventricular aneurysmectomy with or without thrombectomy, can be performed on-pump without cardiac arrest (on the beating heart) if accompanied by full CPB perfusion; this keeps the aortic valve tightly closed and unloads the left heart very effectively when both venous cannulas are tightly snared. The left ventricular apex should be elevated during LVAD implantation performed through full median sternotomy, and CPB should be used to prevent left heart overloading, LCOS, and RVF during elevation.

To minimize the CPB time and avoid aortic cross-clamping, most implants that are done without an accompanying procedure can be performed off-pump, with only direct insertion of the device inflow cannula needing to be performed on-pump. Our preferred technique to implant an LVAD without additional cardiac procedure is left anterior thoracotomy, which is feasible and facilitated for off-pump surgery, combined with a reverse-T ministernotomy to anastomose the outflow graft to the proximal ascending aorta. This strategy allows to easy and full access to the left ventricular apex without changing the shape or location of the heart (though with appropriate position change of the operating table) during placing sutures for device implantation. The device insertion can be performed either on-pump or off-pump according to the surgeon preference.

Weaning from CPB is perhaps the most critical part of the operation. It should be performed under TEE-guidance to give detailed information about the global right ventricular function, IVS position, aortic valve opening, LV unloading, inflow position, and other valve functions. Before weaning, adequate pharmacologic support should be started using inodilators, inotropes, vasodilators, and vasoconstrictors. To start weaning, the LVAD is turned on and its flow speed is set at the lowest flow rate while the outflow graft is clamped. At this stage, de-airing of the LVAD and LV can be confirmed by detecting air bubbles with the aid of TEE, before both the partial aortic cross-clamp and full occlusion graft clamp are removed. When weaning starts, the main goal is then to balance MCS by CPB and LVAD without causing a shift of the IVS through inadequate (rightward shifting) or excessive (leftward shifting) unloading of the LV (Fig. 47.3). Both situations can cause massive hyperacute post-LVAD RVF due to decreased contribution of septal contractions to the RV and massive overloading or unloading of the LV. The best weaning protocol is to decrease the CPB machine form maximal flow to patient-specific full flow, then to ¾, ½, and ¼ flow, while increasing LVAD flow in the opposite direction. During calibration, pump speeds and CO should be adjusted to keep the IVS in the midline position, ensuring optimal loading of both ventricles. To prevent contractile assistance of the LV and IVS in the operating room, the rate of aortic valve opening should be at least 1:3, though preferably 1:1. The fluid status of the patient can be closely monitored using TEE and hemodynamic parameters, aiming to keep the CVP <15 mmHg (ideally between 10 and 12 mmHg) after CPB is discontinued. Fluid replacement, blood, and products are given very

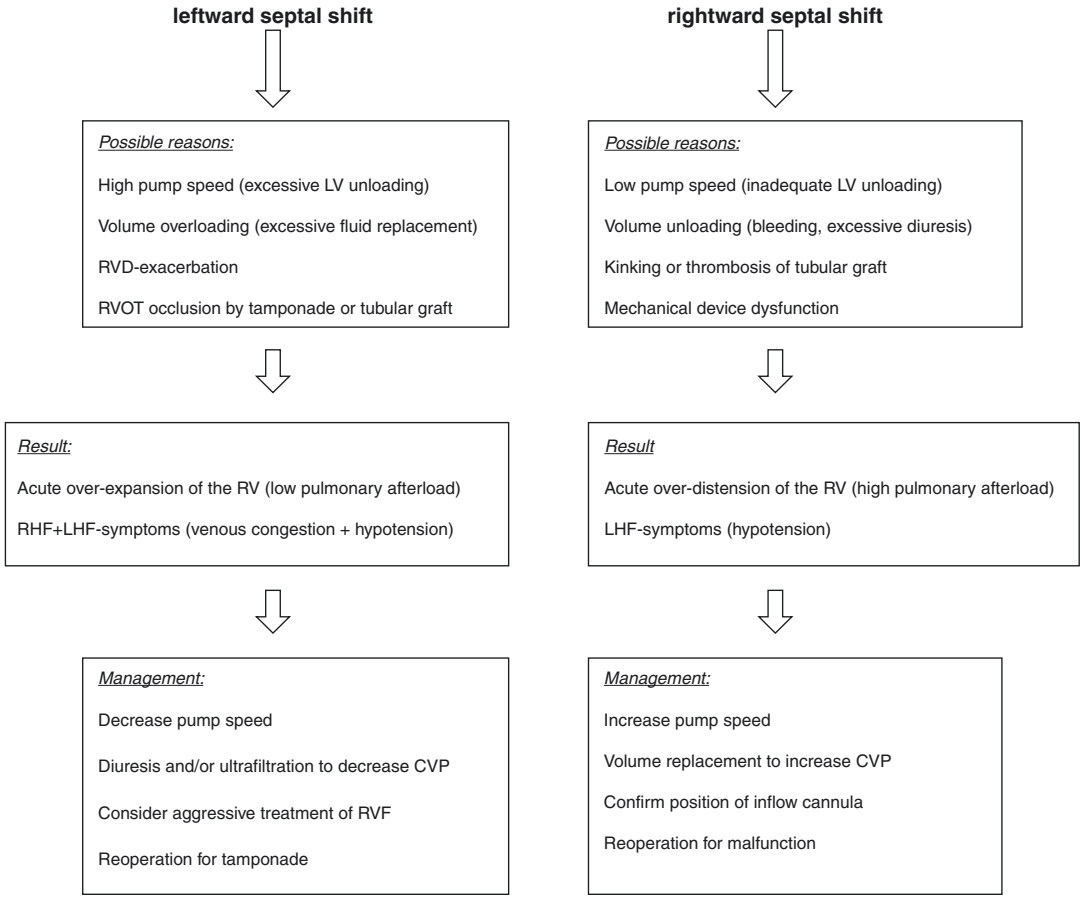

Fig. 47.3 The effects of the interventricular septum position. *CVP* central venous pressure, *LHF* left heart failure, *LV* left ventricle, *LVD* left ventricular dysfunction, *RV* right ventricle, *RHF* right heart failure, *RVD* right ventricular dysfunction, *RVF* right ventricular failure

carefully to avoid overloading the RV. Device malposition or excessive suction can cause inadequate unloading of the LV, can restrain the desired drop in filling pressures, and can cause continuity of elevated pulmonary afterload. Inappropriate short outflow grafts result in diastolic dysfunction by applying external pressure to the RV, whereas kinking or external tension by the sternum or surrounding tissue causes outflow graft compression, decreases or blocks LVAD flow, and results in LV overloading and systemic hypotension.

Tricuspid regurgitation, which causes systemic venous congestion and volume overload in the RV, is a common pathology in advanced LVF; moreover, the presence of TR associated with tricuspid annular dilatation is a possible risk factor for post-LVAD RVF [69]. Patients with advanced LVF most often suffer from progressive tricuspid annular enlargement and tricuspid valve leaflet tethering due to right ventricular enlargement (i.e., functional or secondary TR). Recommended surgical repair of moderate or severe TR with annular dilation is an acceptable treatment to reduce volume loading, improve right ventricular contractility, and break the vicious circle of progressive right ventricular enlargement [70]. However, several studies have been unable to demonstrate any significant relationship between tricuspid repair for any grade of pre-existing TR and early postoperative outcomes [71, 72]. There was also no significant difference in survival between patients who received tricuspid repair and those who did

not for pre-existing moderate TR [73]. By contrast, previous pacemaker lead insertion through the tricuspid valve can cause significant TR without annular dilatation via leaflet rupture or coaptation defect, thereby necessitating surgical exploration. There are two different surgical procedures for TR, with no consensus on the optimal surgical approach: tricuspid ring or suture annuloplasty. The tricuspid 3-dimensional rigid annuloplasty ring is the preferred approach in LVAD surgery, although the DeVega suture annuloplasty technique is another plausible approach that has a shorter CPB time and acceptable durability [74]. Despite the potential benefits to RV function, concomitant tricuspid surgery is associated with longer CPB times, postoperative renal failure, higher number of transfusion of blood products, and re-exploration for bleeding. In addition, tricuspid valve replacement is generally not recommended because of the need for prolonged CPB, but if repair is likely to be unsuccessful, the tricuspid valve should be replaced to prevent massive TR. Treatment of significant TR is the key point to prevent right-sided congestive signs and symptoms during post-discharge follow-up.

Patients with pre-existing RVD require inotropic and pulmonary vasodilator support to wean successfully from bypass and to maintain optimal hemodynamic parameters. All intravenous infusions should start before the outflow graft anastomosis.

Dobutamine, adrenaline, noradrenaline, and when necessary, milrinone, are the preferred pharmacological agents to improve myocardial contractility, increase systemic vascular resistance, and decrease PVR. Dobutamine increases biventricular contractility and provides mutual supports to each ventricle, providing support through IVS contraction. Adrenaline is used for myocardial chronotropy and inotropy to improve cardiac contractility and rhythm, as well as for peripheric vasoconstriction to raise systemic arterial pressure. Noradrenaline is usually used if severe vasodilatation cannot be prevented because of systemic circulatory collapse, milrinone and/or high-dose vasodilator usage. Finally, milrinone is provided as an inodilator to improve cardiac contractility directly and decrease PVR through pulmonary vasodilation.

Pulmonary vasodilators selectively decrease PVR with few systemic adverse effects. Intraoperative pulmonary vasodilator therapy includes NO and prostaglandin analogs. Nitric oxide, as an intrinsic vasodilator, diffuses into smooth muscle, activates cGMP, and relaxes vascular smooth muscles. Inhaled administration of NO selectively reduces the PVR without causing systemic hypotension, but the half-life of NO is quite short and specialized equipment is required to provide continuous nebulization. The optimal therapeutic dosage of NO is unclear, but treatment usually starts at 5–20 ppm. Prolonged NO therapy can lead to increased methemoglobin levels, that can be expected to drop immediately after the NO level is reduced. Weaning should be done gradually by monitoring pulmonary artery pressure and oxygen saturation, because sudden or rapid termination of treatment may cause rebound pulmonary hypertension [75]. Other available pulmonary vasodilators are prostacyclin and its analogs (e.g., epoprostenol, iloprost, and treprostinil), and intravenous infusion with these agens may reduce systemic vascular resistance and cause hypotension. Inhaled iloprost has a similar effect to NO on the pulmonary vascular circuit, effectively decreasing PVR and improving right ventricular performance. However, in contrast to NO, iloprost does not transform into toxic metabolites and does not cause in rebound pulmonary hypertension on withdrawal [76].

After discontinuing CPB and confirming bleeding control, there is a need for adequate and aggressive anticoagulation to prevent excessive bleeding. Successful anticoagulation is essential, because more bleeding than expected can be fatal. Adequate control of bleeding should be confirmed at every stage of device implantation, and both before and after weaning from CPB. When the device overtakes the whole circulation, pharmacologic agents should be given consecutively to treat several grades of pre-existing coagulopathies. Treatments will, therefore, include protamine sulfate (full dose for recovery of heparin), vitamin-K, tranexamic acid, cofactors (II, VII, IX, X), and if necessary,

fibrinogen, von Willebrand factor (factor VIII), platelets, and whole blood.

47.5.3 Postoperatively

The focus of management after LVAD implantation is to maintain adequate left ventricular contractility and appropriate systemic arterial pressure with optimum filling pressures by augmentation of LVAD flow with inotropic support, aggressive diuresis, and afterload reduction therapy. After discharge from hospital, circulatory support requires multi-agent oral pharmacotherapy at individualized dosages (Table 47.14).

Preventing left ventricular contractility is essential to maintaining stable hemodynamics. The most prominent benefit of an LVAD is biventricular unloading and decreased PAPs and PCWP, which improve RV function and prevent right-sided congestion. Device flow is arranged by paying attention to the CVP and PCWP in the early postoperative period, with CVP ideally maintained between 10 and 12 mmHg and fluid replacement should be done carefully without exceeding CVP >12 mmHg. Otherwise, diuretic management administered with caution to normalize elevated CVP value. To decrease the CVP, veno-venous hemofiltration or dialysis can be useful, but may lead to life-threatening hemodynamic fluctuation in the early postoperative period, especially if renal dysfunction develops. Device adjustment is essential in response to leftward (sudden suction and/or RVF) or rightward (lower speed or left ventricular overloading) shifting of the IVS, and should be monitored continuously in the intensive care unit. The aortic valve opening ratio is the best indicator of left ventricular contractility, provided systemic preload is sufficient to realize left ventricular ejection or to prevent device suction. After adequate systemic perfusion has been provided and the mean arterial pressure is >70 mmHg, the CVP is <12 mmHg, and the mixed venous oxygen saturation is >60%, the device speed can be periodically increased every 6 h until the aortic valve opening ratio reaches 1:3. However, optimal performance of the LV occurs when the opening of the aortic valve actualizes in each cardiac cycle (1:1) without right-sided LCOS, because this provides the best contractile status of the LV and IVS. The device speed should be increased until univentricular or biventricular LCOS have been resolved, but not to such a degree that it causes suction, even if the aortic valve cannot open. Another strategy is to monitor PAPs, and to increase the device speed to decrease right-sided pressures, especially until the systolic PAP decreases <40 mmHg and the PCWP <18 mmHg. Continuous flow obscures the pulse pressure by regulating nonpulsatile blood flow in the arterial system, where diastolic and systolic arterial pressures become closer to each other; however, the mean arterial pressure should be kept between 70 and 80 mmHg.

This strategy is usually effective for providing systemic perfusion, and inotropic support is needed to sustain adequate arterial pressure and LVAD flow. In this way, judiciously combining inotropes by monitoring hemodynamic changes is superior to monotherapy when preventing and treating post-LVAD RVF. Dobutamine, which leads to less pulmonary and systemic vasodilation, is the preferred inotropic agent for maintaining left and right ventricular contractile functions. Milrinone, another suitable agent, may cause clinically significant hypotension and systemic vasodilation in addition to the primary pulmonary vasodilatory effect, so should be assisted with other vasopressor agents. If LCOS is not present, vasopressor combinations (e.g., noradrenaline, epinephrine, or dopamine) should be avoided if possible because of the risk of triggering pulmonary vasoconstriction and PVR elevation. On the contrary, their use in combination is essential if hypotension continues due to significant peripheral vasodilatation.

The key to postoperative afterload reduction is pulmonary vasodilatation with NO, iloprost, and sildenafil. In combination, these agents significantly reduce PAPs and PVR, and improve RV function. Nitric oxide levels should subsequently be reduced by slow titration to avoid rebound pulmonary hypertension. Starting oral sildenafil on postoperative day 1 contributes to the reduction of pulmonary afterload and facilitates with-

drawal of inhaled therapy. Long-term sildenafil can maintain better hemodynamics by lowering the PVR. In addition, endothelin receptor antagonists can be used (e.g., bosentan), although they are not currently included in treatment guidelines.

Diuretics prevent the recurrence of fluid retention, volume overload, and congestion. The most common side effects of diuretic excess include fluid depletion, hypokalemia, hypomagnesemia, and azotemia. If the diuretic strategy is unsatisfactory or ineffective due to renal failure, ultrafiltration to remove water and small- to medium-weight solutes may be considered a primary volume-removal therapy. After the acute decompensation caused by volume overload resolves, combination oral diuretic therapy can be started with furosemide and/or thiazides, with or without spironolactone. Daily body weight recording is the best parameter to follow the effectiveness of diuretic treatment and to guide dose adjustment.

The natriuretic peptide system (NPS) counters the detrimental effects of renin–angiotensin–aldosterone system (RAAS) upregulation, inhibits arginine vasopressin secretion, modulates the autonomic nervous system, and antagonizes vasopressor effects in HF. This is achieve in 4 main ways: (1) activation of type A natriuretic peptide receptors, leading to vasorelaxation, natriuresis, and diuresis; (2) inhibition of the RAAS by blocking of renin secretion and the associated aldosterone production; (3) reducing adverse cardiovascular changes by triggering remodeling, apoptosis, ventricular hypertrophy, and fibrosis; and (4) enhancing myocardial relaxation. Natriuretic peptides are removed from the circulation through either clearance by natriuretic peptide clearance receptors (NPRC and NPRC3) or inactivation by neprilysin (a degrading endothelial enzyme). Blocking neprilysin alone does not completely inhibit the RAAS, because the system is also stimulated by the activated sympathetic nervous system, which will independently lead to increased secretion of renin and activation of angiotensin I to II by angiotensin converting enzyme. Combination of the neprilysin inhibitor sacubitril and the angiotensin receptor blocker valsartan has produced the first drug in a new class of angiotensin receptor neprilysin inhibitors (ARNi) that work by both inhibiting the NPS and blocking the angiotensin type-1 receptor. Low dose of ARNi can be given routinely after LVAD implantation, provided that the development of hypotension is closely monitored.

Conclusion

The use of LVADs is increasing annually among patients with advanced LHF for bridge to transplantation, bridge to destination, or bridge to candidacy. Patient selection and implantation timing are key determinants of success for LVAD therapy. The best candidates for LVAD implantation are stable advanced LHF patients receiving inotropic treatment. By contrast, patients in cardiogenic shock are unsuitable for LVADs because they are too sick, and should therefore be supported via percutaneous t-MCS devices to optimize their condition before LVAD implant. On the other hand, if implantation is delayed, outcomes may worsen due to secondary organ damage caused by prolonged end-stage heart failure, with the potential for RHF to develop and lead to death. Appropriate patients selection is the most important factor for predicting, preventing, and treating post-LVAD RVF, regardless of whether there is pre-existing RVD. Preoperatively, elective IABP use can maintain significant cardiac support in severely ill candidates, and recover pre-existing RVD by unloading the LV, reducing PAPs, and increasing organ perfusion. Postoperatively, the most important factor is to protect and maintain IVS-contractility at the optimum level, which is essential for right ventricular function.

References

1. Kırali K, Yerlikhan ÖA, Hançer H. Invasive treatment in advanced (Stage-D) heart failure. In: Kırali K, editor. Cardiomyopaties: types and treatments. Crotia: InTech; 2017. p. 405–57. https://doi.org/10.5772/67455.
2. Kirklin JK, Cantor R, Mohacsi P, Gummert J, De By T, Hannan MM, Kormos RL, Schueler S, Lund LH,

Nakatani T, Taylor R, Lannon J. First annual IMACS report: a global international society for heart and lung transplantation registry for mechanical circulatory support. J Heart Lung Transplant. 2016;35(4):407–12. https://doi.org/10.1016/j.healun.2016.01.002.
3. Englert JA 3rd, Davis JA, Krim SR. Mechanical circulatory support for the failing heart: continuous-flow left ventricular assist devices. Ochsner J. 2016;16(3):263–9.
4. Prinzing A, Herold U, Berkefeld A, Krane M, Lange R, Voss B. Left ventricular assist devices—current state and perspectives. J Thorac Dis. 2016;8(8):E660–6. https://doi.org/10.21037/jtd.2016.07.13.
5. Mehra MR, Park MH, Landzberg MJ, Lala A, Waxman AB. Right heart failure: toward a common language. J Heart Lung Transplant. 2014;33(2):123–6. https://doi.org/10.1016/j.healun.2013.10.015.
6. Kirklin JK, Naftel DC, Stevenson LW, Kormos RL, Pagani FD, Miller MA, Ulisney K, Young JB. INTERMACS database for durable devices for circulatory support: first annual report. J Heart Lung Transplant. 2008;27(10):1065–72. https://doi.org/10.1016/j.healun.2008.07.021.
7. Takeda K, Takayama H, Colombo PC, Yuzefpolskaya M, Fukuhara S, Han J, Kurlansky P, Mancini DM, Naka Y. Incidence and clinical significance of late right heart failure during continuous-flow left ventricular assist device support. J Heart Lung Transplant. 2015;34(8):1024–32. https://doi.org/10.1016/j.healun.2015.03.011.
8. Kimmaliardjuk DM, Ruel M. Cardiac passive-aggressive behavior? The right ventricle in patients with a left ventricular assist device. Expert Rev Cardiovasc Ther. 2017;15(4):267–76. https://doi.org/10.1080/14779072.2017.1308252.
9. Bellavia D, Iacovoni A, Scardulla C, Moja L, Pilato M, Kushwaha SS, Senni M, Clemenza F, Agnese V, Falletta C, Romano G, Maalouf J, Dandel M. Prediction of right ventricular failure after ventricular assist device implant: systematic review and meta-analysis of observational studies. Eur J Heart Fail. 2017;19(7):926–46. https://doi.org/10.1002/ejhf.733.
10. Kirklin JK, Naftel DC, Pagani FD, Kormos RL, Stevenson LW, Blume ED, Myers SL, Miller MA, Baldwin JT, Young JB. Seventh INTERMACS annual report: 15,000 patients and counting. J Heart Lung Transplant. 2015;34(12):1495–504. https://doi.org/10.1016/j.healun.2015.
11. Cheng A, Williamitis CA, Slaughter MS. Comparison of continuous-flow and pulsatile-flow left ventricular assist devices: is there an advantage to pulsatility? Ann Cardiothorac Surg. 2014;3(6):573–81. https://doi.org/10.3978/j.issn.2225-319X.2014.08.24.
12. Takeda K, Naka Y, Yang JA, Uriel N, Colombo PC, Jorde UP, Takayama H. Outcome of unplanned right ventricular assist device support for severe right heart failure after implantable left ventricular assist device insertion. J Heart Lung Transplant. 2014;33(2):141–8. https://doi.org/10.1016/j.healun.2013.06.025.
13. Santamore WP, Dell'Italia LJ. Ventricular interdependence: significant left ventricular contributions to right ventricular systolic function. Prog Cardiovasc Dis. 1998;40(4):289–308. https://doi.org/10.1016/S0033-0620(98)80049-2.
14. Houston BA, Shah KB, Mehra MR, Tedford RJ. A new "twist" on right heart failure with left ventricular assist systems. J Heart Lung Transplant. 2017;36(7):701–7. https://doi.org/10.1016/j.healun.2017.03.014.
15. Gustafsson F, Rogers JG. Left ventricular assist device therapy in advanced heart failure: patient selection and outcomes. Eur J Heart Fail. 2017;19(5):595–602. https://doi.org/10.1002/ejhf.779.
16. Morgan JA, Paone G, Nemeh HW, Murthy R, Williams CT, Lanfear DE, Tita C, Brewer RJ. Impact of continuous-flow left ventricular assist device support on right ventricular function. J Heart Lung Transplant. 2013;32(4):398–403. https://doi.org/10.1016/j.healun.2012.12.018.
17. Kırali K, Özer T, Özgür MM. Pathophysiology in heart failure. In: Kırali K, editor. Cardiomyopaties: types and treatments. Crotia: InTech; 2017. p. 17–38. https://doi.org/10.5772/66887.
18. Koprivanac M, Kelava M, Sirić F, Cruz VB, Moazami N, Mihaljević T. Predictors of right ventricular failure after left ventricular assist device implantation. Croat Med J. 2014;55(6):587–95. https://doi.org/10.3325/cmj.2014.55.587.
19. Tromp TR, de Jonge N, Joles JA. Left ventricular assist devices: a kidney's perspective. Heart Fail Rev. 2015;20(4):519–32. https://doi.org/10.1007/s10741-015-9481-z.
20. Hasin T, Topilsky Y, Schirger JA, Li Z, Zhao Y, Boilson BA, Clavell AL, Rodeheffer RJ, Frantz RP, Edwards BS, Pereira NL, Joyce L, Daly R, Park SJ, Kushwaha SS. Changes in renal function after implantation of continuous-flow left ventricular assist devices. J Am Coll Cardiol. 2012;59(1):26–36. https://doi.org/10.1016/j.jacc.2011.09.038.
21. Brisco MA, Testani JM, Cook JL. Renal dysfunction and chronic mechanical circulatory support: from patient selection to long-term management and prognosis. Curr Opin Cardiol. 2016;31(3):277–86. https://doi.org/10.1097/HCO.0000000000000278.
22. Brisco MA, Sundareswaran KS, Milano CA, Feldman D, Testani JM, Ewald GA, Slaughter MS, Farrar DJ, Goldberg LR. Incidence, risk, and consequences of atrial arrhythmias in patients with continuous-flow left ventricular assist devices. J Card Surg. 2014;29(4):572–80. https://doi.org/10.1111/jocs.12336.
23. Lampert BC, Teuteberg JJ. Right ventricular failure after left ventricular assist devices. J Heart Lung Transplant. 2015;34(9):1123–30. https://doi.org/10.1016/j.healun.2015.06.015.
24. Fitzpatrick JR 3rd, Frederick JR, Hsu VM, Kozin ED, O'Hara ML, Howell E, Dougherty D, McCormick RC, Laporte CA, Cohen JE, Southerland KW, Howard JL, Jessup ML, Morris RJ, Acker MA, Woo YJ. Risk score derived from pre-operative data analysis pre-

dicts the need for biventricular mechanical circulatory support. J Heart Lung Transplant. 2008;27(12):1286–92. https://doi.org/10.1016/j.healun.2008.09.006.
25. Matthews JC, Koelling TM, Pagani FD, Aaronson KD. The right ventricular failure risk score a preoperative tool for assessing the risk of right ventricular failure in left ventricular assist device candidates. J Am Coll Cardiol. 2008;51(22):2163–72. https://doi.org/10.1016/j.jacc.2008.03.009.
26. Drakos SG, Janicki L, Horne BD, Kfoury AG, Reid BB, Clayson S, Horton K, Haddad F, Li DY, Renlund DG, Fisher PW. Risk factors predictive of right ventricular failure after left ventricular assist device implantation. Am J Cardiol. 2010;105(7):1030–5. https://doi.org/10.1016/j.amjcard.2009.11.026.
27. Kormos RL, Teuteberg JJ, Pagani FD, Russell SD, John R, Miller LW, Massey T, Milano CA, Moazami N, Sundareswaran KS, Farrar DJ, HeartMate II Clinical Investigators. Right ventricular failure in patients with the HeartMate II continuous-flow left ventricular assist device: incidence, risk factors, and effect on outcomes. J Thorac Cardiovasc Surg. 2010;139(5):1316–24. https://doi.org/10.1016/j.jtcvs.2009.11.020.
28. Wang Y, Simon MA, Bonde P, Harris BU, Teuteberg JJ, Kormos RL, Antaki JF. Decision tree for adjuvant right ventricular support in patients receiving a left ventricular assist device. J Heart Lung Transplant. 2012;31(2):140–9. https://doi.org/10.1016/j.healun.2011.11.003.
29. Atluri P, Goldstone AB, Fairman AS, MacArthur JW, Shudo Y, Cohen JE, Acker AL, Hiesinger W, Howard JL, Acker MA, Woo YJ. Predicting right ventricular failure in the modern, continuous flow left ventricular assist device era. Ann Thorac Surg. 2013;96(3):857–63. https://doi.org/10.1016/j.athoracsur.2013.03.099.
30. Aissaoui N, Salem JE, Paluszkiewicz L, Morshuis M, Guerot E, Gorria GM, Fagon JY, Gummert J, Diebold B. Assessment of right ventricular dysfunction predictors before the implantation of a left ventricular assist device in end-stage heart failure patients using echocardiographic measures (ARVADE): combination of left and right ventricular echocardiographic variables. Arch Cardiovasc Dis. 2015;108(5):300–9. https://doi.org/10.1016/j.acvd.2015.01.011.
31. Loghmanpour NA, Kormos RL, Kanwar MK, Teuteberg JJ, Murali S, Antaki JF. A Bayesian model to predict right ventricular failure following left ventricular assist device therapy. JACC Heart Fail. 2016;4(9):711–21. https://doi.org/10.1016/j.jchf.2016.04.004.
32. Pettinari M, Jacobs S, Rega F, Verbelen T, Droogne W, Meyns B. Are right ventricular risk scores useful? Eur J Cardiothorac Surg. 2012;42(4):621–6. https://doi.org/10.1093/ejcts/ezs104.
33. Karimov JH, Sunagawa G, Horwath D, Fukamachi K, Starling RC, Moazami N. Limitations to chronic right ventricular assist device support. Ann Thorac Surg. 2016;102(2):651–8. https://doi.org/10.1016/j.athoracsur.2016.02.006.
34. Kalogeropoulos AP, Kelkar A, Weinberger JF, Morris AA, Georgiopoulou VV, Markham DW, Butler J, Vega JD, Smith AL. Validation of clinical scores for right ventricular failure prediction after implantation of continuous-flow left ventricular assist devices. J Heart Lung Transplant. 2015;34(12):1595–603. https://doi.org/10.1016/j.healun.2015.05.005.
35. Cowger J, Shah P, Stulak J, Maltais S, Aaronson KD, Kirklin JK, Pagani FD, Salerno C. INTERMACS profiles and modifiers: heterogeneity of patient classification and the impact of modifiers on predicting patient outcome. J Heart Lung Transplant. 2016;35(4):440–8. https://doi.org/10.1016/j.healun.2015.10.037.
36. Kato TS, Kitada S, Yang J, Wu C, Takayama H, Naka Y, Farr M, Mancini DM, Schulze PC. Relation of preoperative serum albumin levels to survival in patients undergoing left ventricular assist device implantation. Am J Cardiol. 2013;112(9):1484–8. https://doi.org/10.1016/j.amjcard.2013.06.023.
37. Dunlay SM, Park SJ, Joyce LD, Daly RC, Stulak JM, McNallan SM, Roger VL, Kushwaha SS. Frailty and outcomes after implantation of left ventricular assist device as destination therapy. J Heart Lung Transplant. 2014;33(4):359–65. https://doi.org/10.1016/j.healun.2013.12.014.
38. Rudski LG, Lai WW, Afilalo J, Hua L, Handschumacher MD, Chandrasekaran K, Solomon SD, Louie EK, Schiller NB. Guidelines for the echocardiographic assessment of the right heart in adults: a report from the American Society of Echocardiography endorsed by the European Association of Echocardiography, a registered branch of the European Society of Cardiology, and the Canadian Society of Echocardiography. J Am Soc Echocardiogr. 2010;23(7):685–713. https://doi.org/10.1016/j.echo.2010.05.010.
39. Potapov EV, Stepanenko A, Dandel M, Kukucka M, Lehmkuhl HB, Weng Y, Hennig F, Krabatsch T, Hetzer R. Tricuspid incompetence and geometry of the right ventricle as predictors of right ventricular function after implantation of a left ventricular assist device. J Heart Lung Transplant. 2008;27(12):1275–81. https://doi.org/10.1016/j.healun.2008.08.012.
40. Vivo RP, Cordero-Reyes AM, Qamar U, Garikipati S, Trevino AR, Aldeiri M, Loebe M, Bruckner BA, Torre-Amione G, Bhimaraj A, Trachtenberg BH, Estep JD. Increased right-to-left ventricle diameter ratio is a strong predictor of right ventricular failure after left ventricular assist device. J Heart Lung Transplant. 2013;32(8):792–9. https://doi.org/10.1016/j.healun.2013.05.016.
41. Kato TS, Farr M, Schulze PC, Maurer M, Shahzad K, Iwata S, Homma S, Jorde U, Takayama H, Naka Y, Gillam L, Mancini D. Usefulness of two-dimensional echocardiographic parameters of the left side of the heart to predict right ventricular failure after left ventricular assist device implantation. Am J Cardiol. 2012;109(2):246–51. https://doi.org/10.1016/j.amjcard.2011.08.040.

42. Grant AD, Smedira NG, Starling RC, Marwick TH. Independent and incremental role of quantitative right ventricular evaluation for the prediction of right ventricular failure after left ventricular assist device implantation. J Am Coll Cardiol. 2012;60(6):521–8. https://doi.org/10.1016/j.jacc.2012.02.073.
43. Kiernan MS, French AL, DeNofrio D, Parmar YJ, Pham DT, Kapur NK, Pandian NG, Patel AR. Preoperative three-dimensional echocardiography to assess risk of right ventricular failure after left ventricular assist device surgery. J Card Fail. 2015;21(3):189–97. https://doi.org/10.1016/j.cardfail.2014.12.009.
44. Kukucka M, Stepanenko A, Potapov E, Krabatsch T, Kuppe H, Habazettl H. Impact of tricuspid valve annulus dilation on mid-term survival after implantation of a left ventricular assist device. J Heart Lung Transplant. 2012;31(9):967–71. https://doi.org/10.1016/j.healun.2012.06.003.
45. Feldman D, Pamboukian SV, Teuteberg JJ, Birks E, Lietz K, Moore SA, Morgan JA, Arabia F, Bauman ME, Buchholz HW, Deng M, Dickstein ML, El-Banayosy A, Elliot T, Goldstein DJ, Grady KL, Jones K, Hryniewicz K, John R, Kaan A, Kusne S, Loebe M, Massicotte MP, Moazami N, Mohacsi P, Mooney M, Nelson T, Pagani F, Perry W, Potapov EV, Eduardo Rame J, Russell SD, Sorensen EN, Sun B, Strueber M, Mangi AA, Petty MG, Rogers J, International Society for Heart and Lung Transplantation. The 2013 International Society for Heart and Lung Transplantation Guidelines for mechanical circulatory support: executive summary. J Heart Lung Transplant. 2013;32(2):157–87. https://doi.org/10.1016/j.healun.2012.09.013.
46. Hayek S, Sims DB, Markham DW, Butler J, Kalogeropoulos AP. Assessment of right ventricular function in left ventricular assist device candidates. Circ Cardiovasc Imaging. 2014;7(2):379–89. https://doi.org/10.1161/CIRCIMAGING.113.001127.
47. Grandin EW, Zamani P, Mazurek JA, Troutman GS, Birati EY, Vorovich E, Chirinos JA, Tedford RJ, Margulies KB, Atluri P, Rame JE. Right ventricular response to pulsatile load is associated with early right heart failure and mortality after left ventricular assist device. J Heart Lung Transplant. 2017;36(1):97–105. https://doi.org/10.1016/j.healun.2016.06.015.
48. Kang G, Ha R, Banerjee D. Pulmonary artery pulsatility index predicts right ventricular failure after left ventricular assist device implantation. J Heart Lung Transplant. 2016;35(1):67–73. https://doi.org/10.1016/j.healun.2015.06.009.
49. Morine KJ, Kiernan MS, Pham DT, Paruchuri V, Denofrio D, Kapur NK. Pulmonary artery pulsatility index is associated with right ventricular failure after left ventricular assist device surgery. J Card Fail. 2016;22(2):110–6. https://doi.org/10.1016/j.cardfail.2015.10.019.
50. Yoshioka D, Takayama H, Colombo PC, Yuzefpolskaya M, Garan AR, Topkara VK, Han J, Kurlansky P, Naka Y, Takeda K. Changes in end-organ function in patients with prolonged continuous-flow left ventricular assist device support. Ann Thorac Surg. 2017;103(3):717–24. https://doi.org/10.1016/j.athoracsur.2016.12.018.
51. Zabarovskaja S, Hage C, Linde C, Daubert JC, Donal E, Gabrielsen A, Mellbin L, Lund LH. Adaptive cardiovascular hormones in a spectrum of heart failure phenotypes. Int J Cardiol. 2015;189:6–11. https://doi.org/10.1016/j.ijcard.2015.03.381.
52. Nymo SH, Aukrust P, Kjekshus J, McMurray JJ, Cleland JG, Wikstrand J, Muntendam P, Wienhues-Thelen U, Latini R, Askevold ET, Gravning J, Dahl CP, Broch K, Yndestad A, Gullestad L, Ueland T, CORONA Study Group. Limited added value of circulating inflammatory biomarkers in chronic heart failure. JACC Heart Fail. 2017;5(4):256–64. https://doi.org/10.1016/j.jchf.2017.01.008.
53. Sun RR, Lu L, Liu M, Cao Y, Li XC, Liu H, Wang J, Zhang PY. Biomarkers and heart disease. Eur Rev Med Pharmacol Sci. 2014;18(19):2927–35. https://doi.org/10.1007/s10741-015-9504-9.
54. Kramer F, Sabbah HN, Januzzi JJ, Zannad F, Peter van Tintelen J, Schelbert EB, Kim RJ, Milting H, Vonk R, Neudeck B, Clark R, Witte K, Dinh W, Pieske B, Butler J, Gheorghiade M. Redefining the role of biomarkers in heart failure trials: expert consensus document. Heart Fail Rev. 2017;22(3):263–77. https://doi.org/10.1007/s10741-017-9608-5.
55. Savic-Radojevic A, Pljesa-Ercegovac M, Matic M, Simic D, Radovanovic S, Simic T. Novel biomarkers of heart failure. Adv Clin Chem. 2017;79:93–152. https://doi.org/10.1016/bs.acc.2016.09.002.
56. Lichtenauer M, Jirak P, Wernly B, Paar V, Rohm I, Jung C, Schernthaner C, Kraus J, Motloch LJ, Yilmaz A, Hoppe UC, Christian Schulze P, Kretzschmar D, Pistulli R. A comparative analysis of novel cardiovascular biomarkers in patients with chronic heart failure. Eur J Intern Med. 2017;44:31–8. https://doi.org/10.1016/j.ejim.2017.05.027.
57. Gaggin HK, Januzzi JL Jr. Biomarkers and diagnostics in heart failure. Biochim Biophys Acta. 2013;1832(12):2442–50. https://doi.org/10.1016/j.bbadis.2012.12.014.
58. deFilippi CR, de Lemos JA, Christenson RH, Gottdiener JS, Kop WJ, Zhan M, Seliger SL. Association of serial measures of cardiac troponin T using a sensitive assay with incident heart failure and cardiovascular mortality in older adults. JAMA. 2010;304(22):2494–502. https://doi.org/10.1001/jama.2010.1708.
59. van der Linden N, Klinkenberg LJ, Bekers O, Loon LJ, Dieijen-Visser MP, Zeegers MP, Meex SJ. Prognostic value of basal high-sensitive cardiac troponin levels on mortality in the general population: a meta-analysis. Medicine. 2016;95(52):e5703. https://doi.org/10.1097/MD.0000000000005703.
60. Sze J, Mooney J, Barzi F, Hillis GS, Chow CK. Cardiac troponin and its relationship to cardiovascular outcomes in community populations: a systematic review

and meta-analysis. Heart Lung Circ. 2016;25(3):217–28. https://doi.org/10.1016/j.hlc.2015.09.001.
61. Morbach C, Marx A, Kaspar M, Güder G, Brenner S, Feldmann C, Störk S, Vollert JO, Ertl G, Angermann CE, INH Study Group and the Competence Network Heart Failure. Prognostic potential of midregional pro-adrenomedullin following decompensation for systolic heart failure: comparison with cardiac natriuretic peptides. Eur J Heart Fail. 2017;19(9):1166–75. https://doi.org/10.1002/ejhf.859.
62. Nayak A, Neill C, Kormos RL, Lagazzi L, Halder I, McTiernan C, Larsen J, Inashvili A, Teuteberg J, Bachman TN, Hanley-Yanez K, McNamara DM, Simon MA. Chemokine receptor patterns and right heart failure in mechanical circulatory support. J Heart Lung Transplant. 2017;36(6):657–65. https://doi.org/10.1016/j.healun.2016.12.007.
63. Brisco MA, Kimmel SE, Coca SG, Putt ME, Jessup M, Tang WW, Parikh CR, Testani JM. Prevalence and prognostic importance of changes in renal function after mechanical circulatory support. Circ Heart Fail. 2014;7(1):68–75. https://doi.org/10.1161/CIRCHEARTFAILURE.113.000507.
64. Sumida M, Doi K, Kinoshita O, Kimura M, Ono M, Hamasaki Y, Matsubara T, Ishii T, Yahagi N, Nangaku M, Noiri E. Perioperative plasma neutrophil gelatinase-associated lipocalin measurement in patients who undergo left ventricular assist device implantation surgery. Circ J. 2014;78(8):1891–9. https://doi.org/10.1253/circj.CJ-14-0008.
65. Kashiyama N, Toda K, Nakamura T, Miyagawa S, Nishi H, Yoshikawa Y, Fukushima S, Saito S, Yoshioka D, Sawa Y. Evaluation of right ventricular function using liver stiffness in patients with left ventricular assist device. Eur J Cardiothorac Surg. 2017;51(4):715–21. https://doi.org/10.1093/ejcts/ezw419.
66. Palmer B, Lampert B, Mathier MA. Management of right ventricular failure in pulmonary hypertension (and after LVAD implantation). Curr Treat Options Cardiovasc Med. 2013;15(5):533–43. https://doi.org/10.1007/s11936-013-0267-0.
67. Baker WL, Radojevic J, Gluck JA. Systematic review of phosphodiesterase-5 inhibitor use in right ventricular failure following left ventricular assist device implantation. Artif Organs. 2016;40(2):123–8. https://doi.org/10.1111/aor.12518.
68. Imamura T, Kinugawa K, Nitta D, Hatano M, Kinoshita O, Nawata K, Kyo S, Ono M. Prophylactic intra-aortic balloon pump before ventricular assist device implantation reduces perioperative medical expenses and improves postoperative clinical course in INTERMACS profile 2 patients. Circ J. 2015;79(9):1963–9. https://doi.org/10.1253/circj.CJ-15-0122.
69. Goldraich L, Kawajiri H, Foroutan F, Braga J, Billia P, Misurka J, Stansfield WE, Yau T, Ross HJ, Rao V. Tricuspid valve annular dilation as a predictor of right ventricular failure after ımplantation of a left ventricular assist device. J Card Surg. 2016;31(2):110–6. https://doi.org/10.1111/jocs.12685.
70. Brewer RJ, Cabrera R, El-Atrache M, Zafar A, Hrobowski TN, Nemeh HM, Selektor Y, Paone G, Williams CT, Velez M, Tita C, Morgan JA, Lanfear DE. Relationship of tricuspid repair at the time of left ventricular assist device implantation and survival. Int J Artif Organs. 2014;37(11):834–8. https://doi.org/10.5301/ijao.5000369.
71. Dunlay SM, Deo SV, Park SJ. Impact of tricuspid valve surgery at the time of left ventricular assist device ınsertion on postoperative outcomes. ASAIO J. 2015;61(1):15–20. https://doi.org/10.1097/MAT.0000000000000145.
72. Song HK, Gelow JM, Mudd J, Chien C, Tibayan FA, Hollifield K, Naftel D, Kirklin J. Limited utility of tricuspid valve repair at the time of left ventricular assist device implantation. Ann Thorac Surg. 2016;101(6):2168–74. https://doi.org/10.1016/j.athoracsur.2016.03.040.
73. Robertson JO, Grau-Sepulveda MV, Okada S, O'Brien SM, Matthew Brennan J, Shah AS, Itoh A, Damiano RJ, Prasad S, Silvestry SC. Concomitant tricuspid valve surgery during implantation of continuous-flow left ventricular assist devices: a Society of Thoracic Surgeons database analysis. J Heart Lung Transplant. 2014;33(6):609–17. https://doi.org/10.1016/j.healun.2014.01.861.
74. Akhter SA, Salabat MR, Philip JL, Valeroso TB, Russo MJ, Rich JD, Jeevanandam V. Durability of De Vega tricuspid valve annuloplasty for severe tricuspid regurgitation during left ventricular assist device implantation. Ann Thorac Surg. 2014;98(1):81–3. https://doi.org/10.1016/j.athoracsur.2014.03.022.
75. Potapov E, Meyer D, Swaminathan M, Ramsay M, El Banayosy A, Diehl C, Veynovich B, Gregoric ID, Kukucka M, Gromann TW, Marczin N, Chittuluru K, Baldassarre JS, Zucker MJ, Hetzer R. Inhaled nitric oxide after left ventricular assist device implantation: a prospective, randomized, double-blind, multicenter, placebo-controlled trial. J Heart Lung Transplant. 2011;30(8):870–8. https://doi.org/10.1016/j.healun.2011.03.005.
76. Antoniou T, Prokakis C, Athanasopoulos G, Thanopoulos A, Rellia P, Zarkalis D, Kogerakis N, Koletsis EN, Bairaktaris A. Inhaled nitric oxide plus iloprost in the setting of post-left assist device right heart dysfunction. Ann Thorac Surg. 2012;94(3):792–8. https://doi.org/10.1016/j.athoracsur.2012.04.046.

48 Pacemaker and ICD Implant Insertion Techniques: Venous Approach and Complications

Radu Ciudin

Abstract

Every year a few million people around the world will receive a cardiac implantable electronic device- either a pacemaker or an ICD (implantable cardioverter-defibrillator) or a device for cardiac resynchronization therapy. Elderly people is the fastest growing segment of population in the developed countries and is also responsible for most of the implanted devices in the world. Pacemakers and ICDs implants are prone to early or late procedure complications that need to be prevented and recognized. A better understanding and knowledge of clinical anatomy related to venous access for pacemaker and ICD leads insertion is needed to avoid complications. This 54th chapter is going to present clinical aspects related to venous approach of cardiac rhythm management devices implant procedure and also complications related to transvenous insertion and cardiac placement of devices leads.

Keywords

Pacemaker · ICD · Implant techniques · Venous approach · Complications

R. Ciudin
Cardiology Department, "Carol Davila" University of Medicine and Pharmacy, Bucharest, Romania

"Prof. C.C. Iliescu" Emergency Institute for Cardiovascular Diseases, Bucharest, Romania

48.1 Introduction

Pacemakers (PM) and implantable cardiodefibrillators (ICD) or cardiac resynchronization devices (CRT) implantation techniques are already a part of a subspecialty of cardiology on its own right -interventional cardiac electrophysiology and pacing.

The transvenous route is now the established technique used by the vast majority of cardiac implantable electronic devices (CIED), interventional electrophysiologists, or other device implanters including surgeons.

The usual venous route is by using upper extremities and neck veins, therefore knowing the anatomic structures of this area is compulsory and a training requirement [1]. Historically, the epicardial approach was the first route used for PM and ICD implantation. Mainly, it consist of placing/suturing the unipolar or bipolar electrodes directly on the heart—atrial or/and ventricular—epicardium. This is performed by the cardiovascular surgeon under general anaesthesia by having epicardial access. A novel approach is used for the leadless pacemakers. Nowadays the vast majority of CIED are implanted transvenously. In this chapter we are going to describe only the usual transvenous approach despite the fact that is almost impossible to cover theoretically all practical issues related to this topic.

S. I. Dumitrescu et al. (eds.), *Right Heart Pathology*, https://doi.org/10.1007/978-3-319-73764-5_48

48.2 Venous Anatomy

The venous anatomy important for CIED implantation is related to cephalic vein, axillary and subclavian veins and somewhat rarely external and internal jugular veins.

Cephalic vein/antecubital vein—is a superficial vein in the arm that drains to the axillary vein. Near the shoulder, the cephalic vein located along the anterolateral aspect of the biceps muscle passes between the deltoid and pectoralis major muscle into the deltopectoral groove. It empties into the axillary vein, sometimes by forming an arch (Fig. 48.1).

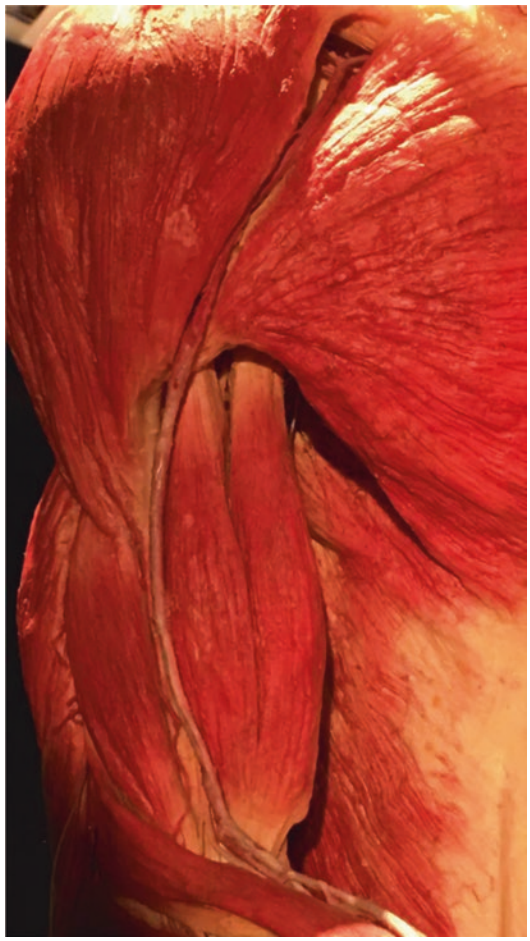

Fig. 48.1 Cephalic vein anatomy (R. Ciudin photo archive—taken from a plastinated body)

Axillary vein—it is a continuation of basilic and brachial veins and it drains blood from the axila, upper limb and lateral aspect of thorax. It ends at the lateral margin of the first rib where it becomes the subclavian vein. It lies medial to the axillary artery (Fig. 48.2).

Subclavian vein—is a continuation of the axillary vein from the outer border of the first rib and it joins the internal jugular vein forming the brachiocephalic vein or innominate vein. The thoracic duct that carries lymph also drains into the subclavian vein.

External jugular vein—is a superficial vein that drains blood from cranium and face—posterior, auricular and retromandibular areas and it runs from the angle of the mandible to the middle of the clavicle by the posterior area of the sternocleidomastoideus muscle. Its anatomy varies, sometimes it can be duplicated and it drains to the subclavian vein (Fig. 48.3).

Internal jugular vein—drains blood from the head and joins with the subclavian vein to form the brachiocephalic trunk. Left and right brachiocephalic trunks will form the superior vena cava.

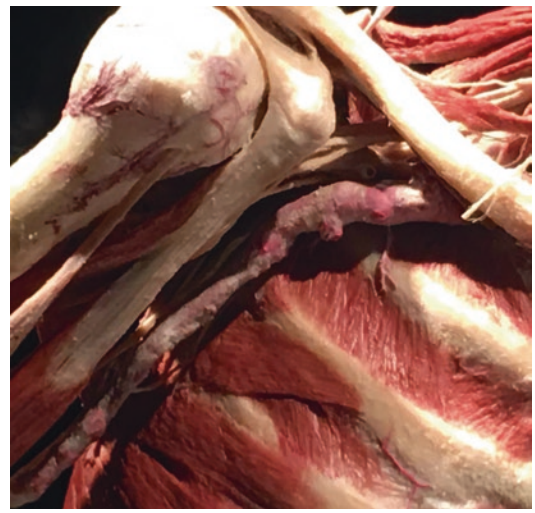

Fig. 48.2 Axillary vein anatomy (R. Ciudin photo archive- taken from a plastinated body)

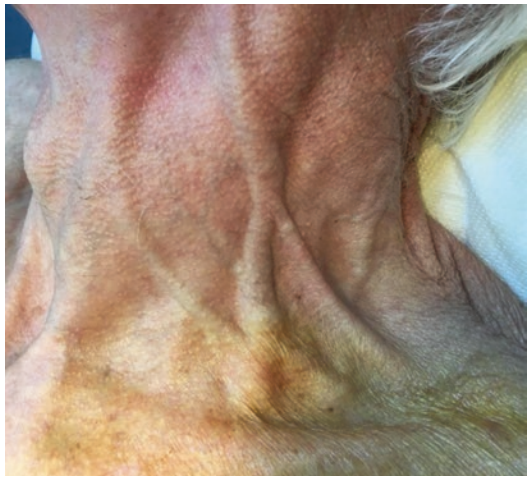

Fig. 48.3 Supraclavicular fossa veins - clinical anatomy (R. Ciudin photo archive)

48.3 Venous Approaches for CIED Implantation

CIED are usually implanted in the infraclavicular area. Following an incision of 4–5 cm in length parallel to the clavicula or in the deltopectoral groove a subcutaneous pocket is created above prepectoral fascia often by blunt dissection. More than 95% of centres prefer prepectoral subcutaneous implant but up to 10–12% use the subpectoral implant as well [2].

The venous approach could be done directly by blind percutaneous puncture using anatomical and/or radiological markers or using ultrasound or contrast substance venography as a guidance. A different approach is the direct cut down on the vein.

The first choice as a venous access for lead implantation is the cephalic vein in more than 60% of European centres [2], 40% start the procedure from the subclavian vein, 48% are using axillary vein through an extrathoracic access route and 52% by using an intrathoracic access route.

Cephalic vein access—It is a safe and effective technique to introduce pacing or defibrillation leads to the right heart [3, 4] or epicardial left ventricular leads via the coronary sinus [5].

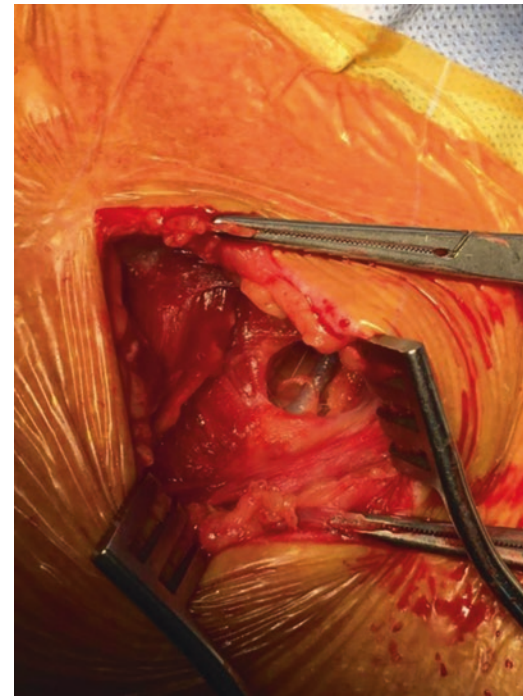

Fig. 48.4 Cephalic vein—deltopectoral groove—Intraprocedural aspect (R.Ciudin photo archive)

Cephalic vein is often large enough to accommodate two or sometimes three leads. Following skin incision and deltopectoral groove dissection (Fig. 48.4), as soon as the cephalic vein is isolated it can be used as a direct vein approach to introduce the lead through a small vein incision or a modified Seldinger technique using a J-shaped or hydrophilic guidewire to insert a peel-away introducer into the vein [4, 6]. It can be used to introduce contrast substance to visualize local venous anatomy as well. Cephalic vein cut down has some advantages and disadvantages: the cephalic vein is not always present or feasible as a venous approach (mainly due to its small diameter), it requires practice and may increase procedure time (Fig. 48.5).

Subclavian vein access—Could be done directly (by blind puncture) using anatomical landmarks, or guided by ultrasound techniques or

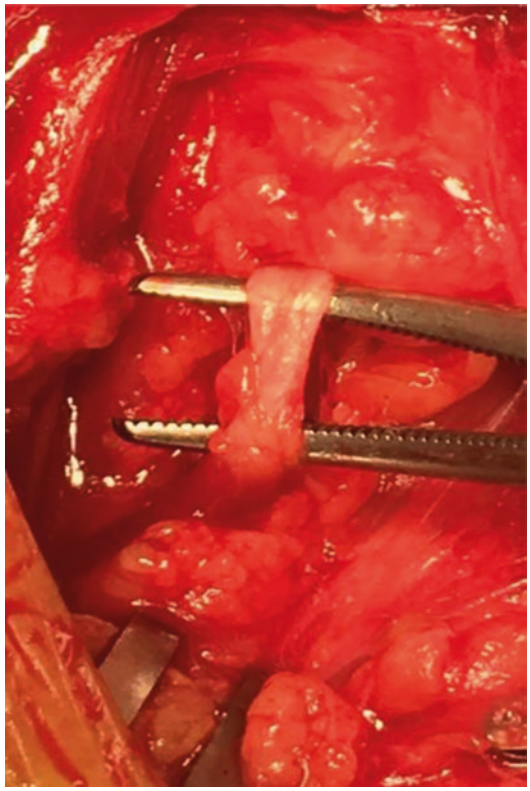

Fig. 48.5 Cephalic vein—procedural aspect (R.Ciudin photo archive)

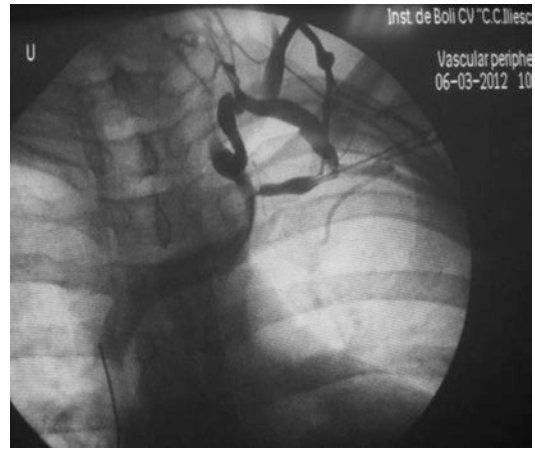

Fig. 48.6 Venography -Subclavian vein stenosis (R. Ciudin photo archive)

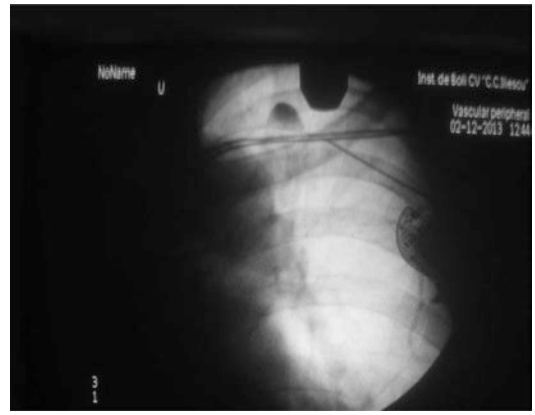

Fig. 48.7 X-Ray—Axillary vein puncture (R. Ciudin photo archive)

venography. It could be done percutaneously before making the skin incision or following the incision at a deeper level. After the skin puncture, the needle will travel through the clavicular head of the pectoralis major muscle toward the clavicula. Subclavian vein could be accessed from above as well (supraclavicular approach) [7]. Subclavian vein puncture has also some advantages: is almost always present (although stenosis or occlusions might occur, especially in patients with previously implanted leads—Fig. 48.6), is big enough for as many leads as we need and is usually quick to find. It has some disadvantages as well: there is a 1.5–2% risk of pneumothorax or hemothorax and also a risk of arterial puncture or nerve damage. Also if the puncture is too medial there is an increased risk of lead damage in the long-term (subclavian crush phenomenon).

Axillary vein access has been described first time in the late 1980s [8]. Since then several techniques have been described using anatomical and fluoroscopic landmarks or using as guidance vascular ultrasound or different catheters, guidewires or contrast substance introduced on upper limb veins or via the contralateral femoral vein [9–13]. Axillary vein approach is a favourable technique to avoid acute complications and to reduce lead fracture or insulation damage (Fig. 48.7).

External jugular vein access is now very rarely used as the lead should pass over the clavicula to reach the pulse generator pocket from the insertion site. However it has been used in the past as an alternative when cephalic vein or subclavian vein were inaccessible.

Internal jugular vein approach is used only in exceptional cases.

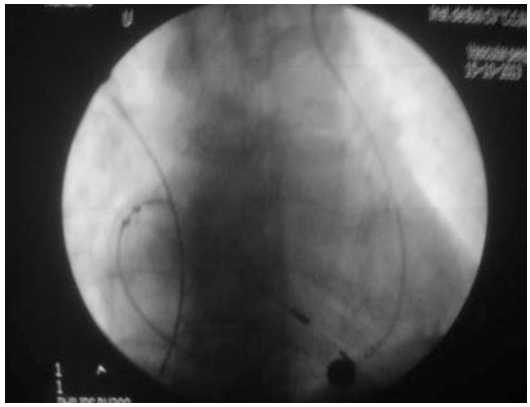

Fig. 48.8 X-Ray—Left superior vena cava pacemaker lead implant (R. Ciudin photo archive)

Other vein access for CIED implantation are the femoral vein, transhepatic with suprahepatic vein approach in rare venous anomalies or complex congenital heart diseases.

A special consideration should be offered to left superior vena cava approach to insert a pacemaker or ICD lead from the left side (Fig. 48.8).

As the left side approach for device implantation was reported as the preferred method by 79% of European centres [2] the chance to find a left superior vena cava variant is high, with a prevalence of 0.15–0.25% in the literature. Technically is more difficult to place the lead into the right ventricle as the lead needs a loop into the right atrium in order to go through the tricuspid valve and toward the right ventricular apex. Also the right atrial lead needs to be an active fixation lead to have enough stability into the desired atrial position.

48.4 Complications

The number of CIED implantations is increasing all over the world. Also the inevitable complications related to PM, ICD and resynchronization devices have also increased. This chapter addresses device implant insertion and venous access techniques—related complications and is not going to cover all sorts of potential complications related to CIED.

48.4.1 CIED Complications Classification

CIED complications could be classified in different ways. For example, we may have infectious and non-infectious complications [14] or early and late post implant complications.

As we are going to describe issues related to insertion and venous access techniques, we would preferred to use the following classification (modified after Yarlagadda et al. [15]):

- Pocket-related complications
- Insertion and Venous Access—related complications
- Pulse generator/ICD generator—related complications
- Leads-related complications
- CIED—infections
- Other complications

Most of the complications could be divided accordingly to the implant procedure in acute/intra procedural, early and late related complications.

48.4.1.1 Pocket: Related Complications

Early complications: local bruising, local hematoma, local pain, swelling, early infection.

Late complications: pocket related infection, pocket erosion, late/chronic pain at the site of the implant/generator.

48.4.1.2 Insertion and Venous Access: Related Complications

Early complications—Bleeding, hematoma, accidental arterial puncture or injury, accidental arterial guide wire or sheath/lead insertion, brachial plexus injury, pneumothorax, hemothorax, air embolism, lost guide wire, accidental large vein/atrial wall perforation by guidewire; hypotension, bradycardia and other vagal reactions.

Late complications—bleeding, large hematoma, venous occlusion, venous thrombosis, delayed pneumothorax or hemopneumothorax, infections.

48.4.1.3 Pulse Generator/ICD Generator: Related Complications

Malfunctions—sensing malfunctions-over and under sensing; pacing malfunctions -loss of capture, loss of output, inappropriate rate/mode pacing, pacemaker mediated tachycardia, early generator failure; pacemaker syndrome (single chamber pacemaker); pulse generator/ICD generator migration.

Early infections, acute endocarditis.

Late pulse generator/ICD generator related complications: infections (Fig. 48.9), malfunctions, Twiddler syndrome.

48.4.1.4 Lead-Related Complications

Early complications: lead micro or macro dislodgement, phrenic nerve and diaphragmatic stimulation, pectoral muscle stimulation (unipolar leads), cardiac chamber perforation and cardiac tamponade, tricuspid valve injury, loss of capture and sensing.

Late lead-related complications: systemic infection, endocarditis and lead vegetations; late/delayed cardiac chamber perforation; access vein thrombosis and obstruction; diaphragm or pectoral stimulation; tricuspid regurgitation; lead fracture, subclavian crush syndrome;

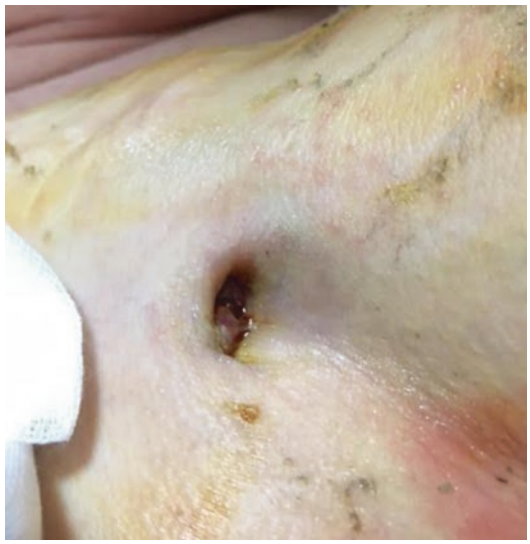

Fig. 48.9 Pacemaker pocket infection (R. Ciudin photo archive)

48.4.1.5 CIED: Related Infections

- Primary infection as a contamination during implant procedure (the device or pocket is the initial source of infection)
- Secondary infections (the device, leads and the pocket are contaminated late by bacteraemia from a different source)

48.4.2 Insertion and Venous Access: Related Complications

48.4.2.1 Lead Dislodgement

Lead dislodgement is probably the most common complication- atrial lead in dual chamber pacemaker implants and left ventricular lead via the coronary sinus in CRT devices being the most frequently seen types of dislodgement, from 1.6 to 4.4%, respectively up to 5–10% of patients [14, 16] but an acceptable dislodgement rate should probably be no more than 1% for right ventricular leads and less than 3% for atrial leads. Leads dislodgement can be diagnosed by testing the pacing or sensing function but not on X-ray (microdislodgements) or may be radiographically seen as a migration of the lead from its initial implant position in the same chamber or in a different heart chamber (macrodislodgement). Lead dislodgement and migration may be associated with other complications, not just pacing/sensing malfunction but also arrhythmias or thromboembolic complications.

48.4.2.2 Pneumothorax and Hemothorax

Pneumothorax as a result of inadvertent approach of pleural space is mainly related to the subclavian vein intrathoracic approach but it can rarely be seen in axilary vein approach as well. Pneumothorax is also related to operator experience. Its incidence ranges from 1 to 2–2.5% in the literature and is eliminated when cephalic vein cut-down technique is employed. Most of the pneumothorax complications are asymptomatic and detected on the following day after implantation on chest X-ray. When the pneumothorax is significant, during or just after the implant procedure it should be immediately treated by chest tube insertion.

Hemothorax and hemopneumothorax can occur when during venous puncture and lead insertion there is conocmitent vascular damage of the axilary or subclavian veins [17] or during up-grade of a pacing system that requires additional leads insertion and the superior vena cava is injured as well. It can also be seen in lead extraction procedures.

48.4.2.3 Bleeding, Hematoma and Local Venous Access Complications

Bleeding and local hematoma have been reported as up to 5% following CIED implantations and is been more often associated with antithrombotics-antiplatelet and anticoagulation therapy. In most of the cases, small hematoma can be treated conservatively by rest, local ice application and compression. Some patients require reintervention by opening the incision and evacuating the blood cloths (Fig. 48.10). Local hematoma and reoperation will increase the risk of infection.

In order to prevent bleeding and hematoma, use of electro-cautery and proper hemostasis has to be used to avoid back bleeding from the venous access and from the pocket itself, especially in patients on antithrombotic therapy. The risk of bleeding and hematoma is highest in patients taking dual antiplatelet therapy as aspirine and clopidogrel or even more in patients on ticagrelor -up to 18% [14] but is very commonly seen in patients on heparin (7%) as well. Recent (under 6 months) interventional procedures involving stent implant and dual antiplatelet therapy should be following CIED if possible or the device implant should be postponed until stopping the dual antiplatelet therapy could be done for few days before the CIED implant procedure.

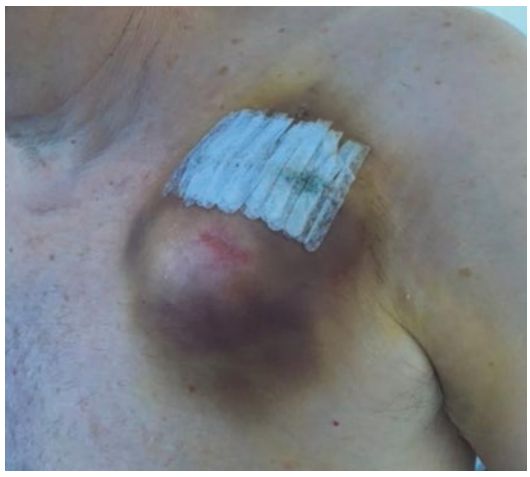

Fig. 48.10 Post ICD implant extensive hematoma (R. Ciudin photo archive)

48.4.2.4 Air Embolism

Air embolism is a consequence of air drawn into the venous system during lead insertion. Following a deep inspiration at the moment when the venous access is open can lead to a pressure gradient between the source of air and the venous pressure causing air aspiration into the venous system and right heart chambers. In most of the cases, an air embolus is asymptomatic and preventable by using introducers with haemostatic valves or asking patient to stop breathing few seconds if the peel-away sheath has no valve.

In rare cases there is a need to administrate 100% oxygen and some inotropic support.

48.4.2.5 Arrhythmias and Death

Death is a very rare event related to CIED implant procedure and occurs in less than 1% of pacemaker implantations. The most common causes are related comorbidities, with myocardial infarction as leading co-morbidity, but al-so stroke and heart failure.

Arrhythmias could be related to lead positioning—all sorts of supraventricular mechanically induced arrhythmias during atrial lead placement (atrial premature beats, atrial tachycardias, atrial fibrillation or flutter), atrio-ventricular conduction disturbances, right bundle branch block or ventricular arrhythmias during ventricular lead placement (ventricular premature beats, runs of mechanically induced ventricular tachycardia or ventricular fibrillation requiring resuscitation and external shock.

Intermittent 3rd degree atrio-ventricular block in patients with previous left bundle branch block has been seen commonly during coronary sinus ostium cannulation procedure for cardiac resyncronization. Pacemaker mediated tachycardia in patients with dual chamber devices is

not very rare seen. Rarely is been described leads related tachycardia long time following a CIED implant [18].

48.4.2.6 Cardiac Chambers Perforation and Tamponade

Cardiac perforation is a quite rare event during a CIED implant procedure, usually <1% [19, 20], but it can occur. There are three different types of factors that may influence the cardiac perforation ratio: lead design, physician's experience and patient—related factors. Any chamber of the heart can be perforated—right atrium or right ventricle, coronary sinus or left atrium or ventricle.

Pain, hypotension, decreased pulsatility of the cardiac silhouette monitored by fluoroscopy and increased size of cardiac silhouette or arrhythmias could be signs of perforation but pericardial effusion on echocardiography will accurately diagnose perforation and/or tamponade.

Delayed lead perforation is rare but cardiac tamponade or death have not been documented often (Fig. 48.11).

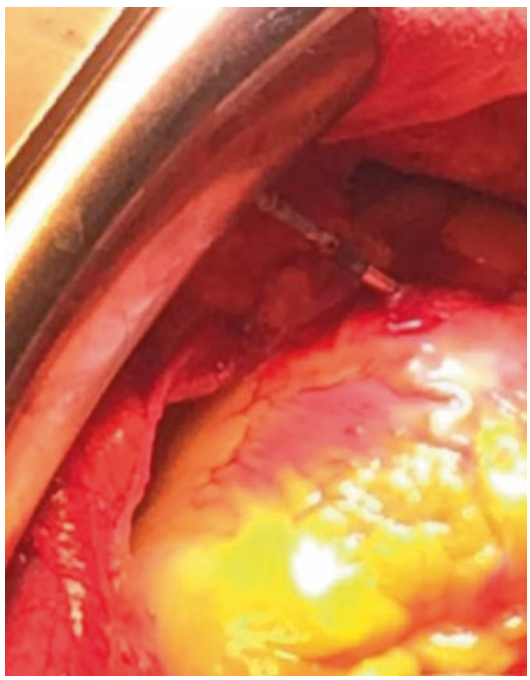

Fig. 48.11 Delayed perforation of an ICD lead: intraoperative aspect

Atrial leads can be more often than ventricular leads the cause of perforation and ICD leads may perforate more often than ventricular pacemaker leads [21].

Cardiac tamponade is an emergency and must be dealt with as soon as possible. It requires urgent pericardiocentesis and surgical intervention if the bleeding persists. Anticoagulation treatment is an important factor for maintaining bleeding and leading to tamponade.

48.4.2.7 Extracardiac Stimulation

Extracardiac stimulation is frequently seen. The usually susceptible sites are the diaphragm, the pectoral muscle or rarely intercostal muscles. Present use of bipolar leads have diminished the pectoral muscle stimulation but the atrial leads dislodgement stimulating the right phrenic nerve and right diaphragm or more often in nowadays left ventricular coronary sinus branch lead stimulating the left phrenic nerve and left diaphragm is been seen. Testing the lead during implant and using higher output energy can prevent extracardiac stimulation and patient discomfort [17]. Perforation could also be a cause for extracardiac stimulation.

48.4.2.8 Venous Thrombosis and Obstruction

Venous thrombosis and obstruction can occur early, but more often it appears late after CIED implantation procedures. In most of the patients venous thrombosis will remain silent and asymptomatic being discovered later during other procedures like lead extractions or up-grade procedures. Most of the patients will develop venous collaterals. Few percent (1–3%) of patients undergoing CIED devices will have any symptoms suggesting vein obstruction like upper arm swelling, oedema, discomfort or local cyanosis. Use of antiplatelet and anticoagulation therapy can be mandatory and interventional or surgical procedures are very rarely undertaken or necessary [16].

There are few prospective studies looking for venous obstruction in patients with previous CIED procedures [22]. Few factors are recognized as predictors of venous stenosis or obstructions:

multiple pacemaker or ICD leads, patient personal history of previous venous thrombosis, use of hormone therapy, use of temporary wire before implantation.

48.5 Conclusions and Future Perspectives

CIED—pacemakers, ICDs, CRT devices—have developed tremendously over the last two decades and the number of implant procedures is increasing constantly. More and more centres and cardiologists are taking up these implanting procedures. It will always be necessary to teach these young implanters about clinical anatomy related to venous access and how to prevent local and systemic complications related to the device implant procedure.

It is also an evolving and dynamic field. New technologies are now put in practice—see leadless pacemaker implant procedures or alternative energy—see ultrasound- driven devices. Different approaches are now alternatives for left ventricular leads implants—transseptal (atrial septum or interventricular septum!), epicardial or pericardial access, thoracoscopic minim invasive approach or transapical by surgeons. Subcutaneous ICD implants might become smaller and better and a real alternative to present trans-venous systems.

No matter what the developing technologies will bring in the future of cardiac rhythm management, the knowledge of clinical anatomy and prevention of new complications will always be needed.

References

1. Zipes PD, Calkins H, et al. 2015 ACC/AHA/HRS Advance Training Statement on Clinical Cardiac Electrophysiology (A Revision of the ACC/AHA 2006 Update of the Clinical Competence Statement on Invasive Electrophysiology Studies, Catheter Ablation, abd Cardioversion). Circ Arrhythm Electrophysiol. 2015;13:1–63.
2. Bongiorni MG, Proclemer A, Dobreanu D, et al. Preferred tools and techniques for implantation of cardiac electronic devices in Europe: results of the European Heart Rhythm Association survey. Europace. 2013;15:1664–8.
3. Furman S. Venous cutdown for pacemaker implantation. Ann Thorac Surg. 1986;41:438–9.
4. Ong LS, Barold SS, Lederman M, et al. Cephalic vein guide wire technique for im-plantation of permanent pacemakers. Am Heart J. 1987;114(4):753–6.
5. Watts TE, Pant S, Reddy S, et al. Cephalic vein cutdown foe left ventricular lead placement in biventricular device upgrades. J Innov Card Rhythm Manag. 2015;6:1906–7.
6. Kolettis TM, Lysitsas D, Apostolidis D, et al. Improved " cut-down" technique for transvenous pacemaker lead implantation. Europace. 2010;12(9):1282–5.
7. Patrick SP, Tijunelis MA, Johnson S, Herbert ME. Supraclavicular Subclavian vein catheterisation: the forgotten central line. West J Emerg Med. 2009;10(2):110–4.
8. Nickalls RWD. A new percutaneous infraclavicular approach to the axillary vein. Anaesthesia. 1987;42:151–4.
9. Belott P, Reynolds D. Permanent pacemaker and implantable cardioverter-defibrillator implantation in adults. In: Ellenbogen A, Wilkoff BL, Kay GN, Lau CP, Auricchio A, editors. Clinical cardiac pacing, defibrillation, and resynchronization therapy. 5th ed. Elsevier; 2017. p. 631–91.
10. Miglore F, Curnis A, Bertaglia E. Axillary vein technique for pacemaker and im-plantable defibrillator leads implantation: a safe and alternative approach? J Cardiovasc Med. 2014;15:309–13.
11. Sawasaki K, Sato T, Takayama Y, et al. Novel extrathoracic puncture techniques for pacemaker lead insertion: pitfalls of the conventional extrathoracic puncture method. J Arrhythm. 2012;28:111–3.
12. Yang F, Kulbak G. A new trick to a routine procedure: taking the fear out of the ax-illary vein stick using the 35 degree caudal view. Europace. 2015;17:1157–60.
13. Yeow KM, Kaufman JA, Rieumont MJ, et al. Technical innovation- axillary vein puncture over the second rib. AJR. 1998;170:924–6.
14. Carrillo R, Healy C. Prevention and management of procedural complications. In: Ellenbogen's clinical cardiac pacing, defibrillation, and resynchronization therapy. 5th ed. section 4, Chap. 32, Elsevier; 2017.
15. Yarlagadda C. Permanent pacemaker insertion technique. The heart.org Medscape site; 2014.
16. Gul EE, Kayrak M. Common pacemaker problems: lead and pocket complications, in modern pacemakers-present and future, Das R.M., InTech on www.intechopen.com, 2011.
17. Williams JL, Stevenson RT. Complications of pacemaker implantation, in urrent issues and recent advances in pacemaker therapy, editor. By Attila Roka, InTech on www.intechopen.com, 2012.
18. Witt CM, Asirvathan SJ, Warnes CA, McLeod CJ. Ventricular tachycardia secondary to abandoned epicardial pacemaker lead. HeartRhythm Case Rep. 2015;1(3):126–9.

19. Carlson MD, Freedman RA, Levine PA. Lead perforation: incidence in registries. Pacing Clin Electrophysiol. 2008;31:13–5.
20. Danik SB, Mansour M, Singh J, Reddy VY, Ellinor PT, Milan D, et al. Increased incidence of subacute lead perforation noted with one implantable cardioverter-defibrillator. Heart Rhythm. 2007;4:439–42.
21. Hirschl DA, Jain VR, Spindola-Franco H, Gross JN, Haramati LB. Prevalence and characterization of asymptomatic pacemaker and ICD lead perforation on CT. PACE. 2007;30:28–32.
22. Haghjoo M, Nikoo MH, Fazelifar AF, Alizadeh A, Emkanjoo Z, Sadr-Ameli MA. Predictors of venous obstruction following pacemaker or implantable cardiover-defibrillator implantation: a contrast venography study on 100 patients admitted for generator change, lead revision, or device upgrade. Europace. 2007;9(5):328–32.

Right Ventricular Dysfunction in Cardiac Surgery

49

Ovidiu Lazăr

Abstract

Right ventricular failure involves a great challenge due to the severity of this condition. In cardiac surgery RV failure is frequently associated with congenital disease and represent a high incidence among cardiac transplant patients when represent the main cause of graft failure. Appropriate hemodynamic monitoring and advanced pharmacological and mechanical support can reduce perioperative mortality in RV perioperative failure patients. Early postoperative care involves special measures to overcome compromised hemodynamics in RV failure cases.

Keywords

Right ventricular failure · Pulmonary hypertension · Hemodynamics · Transesophageal echocardiography · Near infrared spectroscopy (NIRS) · Ventricular assist devices (VAD) Extracorporeal membrane oxygenation (ECMO)

49.1 Introduction

Right heart failure can be defined in a very simply manner as a syndrome where the right heart is unable to fill or eject blood adequately to meet the circulatory needs of the body or can only do by increasing its filling pressures [1]. This is a simple definition emerged in the era before ventricular assist devices became so spread. Right ventricular (RV) dysfunction is an underdiagnosed clinical condition that has been associated with increased mortality in cardiac surgical patients [2]. It has a low incidence among non congenital cardiac surgery patients, is more likely associated with cardiovascular and pulmonary complications related to cardiopulmonary bypass (CPB) and is a cause of acute graft failure in cardiac transplant [3]. RV failure can be present before, during or after cardiac surgery. RV failure is a serious complication that may occur whether the surgery is done on the left or right cardiac cavities. It may also complicate any cardiac or noncardiac surgical procedures. There is growing evidence that RV dysfunction is a key determinant of bad prognosis in cardiac surgery, particularly in patients with pulmonary hypertension (PH) [4]. In cardiac surgery, PH is an important contributor to risk stratification as at least two popular models—the Parsonnet and Euroscore—considered it [5, 6]. The intraoperative diagnosis of this condition is mainly helped by the use of particular hemodynamic parameters and transesophageal echocardiography (TEE). Other diagnosis techniques (NIRS) are under current evaluation [7]. In cardiac surgery, RV failure leads to a difficult weaning from

O. Lazăr
Angiolife Unit, Anesthesia and Critical Care Department, "Life Memorial Hospital", Bucharest, Romania

S. I. Dumitrescu et al. (eds.), *Right Heart Pathology*, https://doi.org/10.1007/978-3-319-73764-5_49

cardiopulmonary bypass (CPB) and increased postoperative mortality and cost. The worst scenario is "impossible to wean patient" requiring mechanical assistance of the failed ventricle, biventricular assistance or ECMO [8]. Careful preoperative diagnosis, perioperative optimization of hemodynamic conditions (especially of pulmonary hypertension), proper anesthetic management and a short CPB time can contribute to a good prognosis after cardiac surgery in patients with RV dysfunction [9].

In perioperative cardiac surgery scenario the main causes of RV failure/dysfunction could precede de operation time. RV infarction secondary to a proximal right coronary artery (RCA) occlusion or severe coronary disease in a left dominant circulation could alter the already reduced capacity of RV to increase its work load. Pulmonary hypertension (PH) of any cause-mitral/aortic valvular disease, severe left ventricle (LV) dysfunction, lung disease, primary pulmonary hypertension- is the main pathological condition present before surgical time that can alter RV systolic function.

In most cases the right ventricle has a good systolic function in the preoperative settings but there are a lot of conditions that can emerge during cardiac surgery like poor myocardial protection—poor collateral circulation with an occluded RCA or due to exclusive use of retrograde cardioplegia, kinking of the RCA ostium in aortic root replacements, prolonged ischemic times, coronary embolism- or acute increased RV afterload—blood product transfusions during CPB with associated vasoactive substances release (transfusion related acute lung injury TRALI), severe LV dysfunction, protamine reaction, tension pneumothorax, pulmonary embolism, acute respiratory distress syndrome (ARDS), hypoxemia and acidosis [10].

The most common cause of RV systolic failure is afterload augmentation. Modest pressure increased at first mostly leads to increased RV contraction. However, RV is designed as a volume pump which keeps central venous (CVP) low and its ability to increase contractility is limited. The RV myocardium is thin compared with the left ventricle (LV) and the ejection relies more on longitudinal shortening and a "peristaltic" pattern one [11]. The RV is characterized by a high diastolic compliance and allows for a great variation in accommodation to venous return with little changes in end diastolic pressure. There are multiple etiologies for elevated pressure (beyond the normal values- mean pulmonary artery pressure <mPAP> ≥25 mmHg measured by right heart catheterization at rest) in the pulmonary circulation and PH could be defined as a hemodynamic state rather than a single disease entity. In summary preoperative causes of elevated PAP could be related to left heart diseases (ex. systolic or diastolic left ventricle dysfunction, valvular disease, congenital/acquired left heart inflow/outflow tract obstruction and congenital cardiomyopathies), due to lung diseases and/or hypoxia, chronic thromboembolic pulmonary hypertension [12].

Right heart catheterization and echocardiography are the best ways to evaluate the RV function. There are no clear hemodynamic criteria that can be used to diagnose PH by right heart catheterization even that method is superior to echocardiography to asses the RV function. However these topics are beyond the purpose of present chapter.

49.2 Perioperative Management and RV Failure in Cardiac Surgery

A careful evaluation is performed once a patient is considered a candidate for cardiac surgery including a detailed history and physical evaluation, current medication and comorbidities.

A detailed discussion with the patient and a comprehensive physical and echocardiography, right heart catheterism, chest radiography examination may revealed important information regarding preexisting symptoms and signs of cardiac failure, especially of right ventricle failure, history of pulmonary disease or left sided valvular disease, severe systolic left ventricular dysfunction, high left ventricular diastolic pressure or congenital anomalies with secondary PHT.

Typical clinical symptoms and signs such as dyspnea, hypotension, right upper quadrant discomfort and jugular vein distension, several electrocardiographic and radiographic clues should trigger further investigations. Electrocardiographic specific changes may include sinus tachycardia, T-wave inversion in III and aVF or in the precordial leads V1 to V4, right bundle branch block and a rightward axis. A right-sided precordial leads EKG is mandatory whenever a RV dysfunction is suspected [13]. Dilation of the proximal pulmonary arteries and RV enlargement (with filling of the retrosternal space) or right atrial enlargement is frequently found on standard chest radiography. Dilation of the inferior vena cava may be seen and pleural effusions are possible [14]. Troponin concentrations can increase in RV failure but its specificity is fair. B-type natriuretic peptide, can be used to differentiate cardiac and pulmonary acute dyspnea. In pulmonary hypertension, increasing concentrations of B-type natriuretic peptide may correlate with the degree of RV dysfunction but this correlation remains unclear [15]. There is no cut off value of B-type natriuretic peptide to sustain acute RV failure [16].

Echocardiography it has become the most important, noninvasive, bedside available tool in the evaluation of RV dysfunction and its associated conditions. Important findings include chamber dilatation, increased wall thickness (in chronic pulmonary hypertension) and wall motion abnormalities. Cardiac magnetic resonance investigation (MRI) may present more reproducible data than echocardiography but remains an alternative investigation tool [17]. Right heart catheterization with measurements of pulmonary artery, right-sided and left-sided pressures remains the gold standard for the diagnosis of pulmonary hypertension. These provide prognostic markers of survival. A comprehensive and detailed presentation of these diagnostic tools is beyond the purpose of present chapter.

Proper management of current medication is mandatory up to the time of scheduled surgery. Avoidance of tachycardia and increased pulmonary resistance can be done using the right dose of anxiolytics (short time action benzodiazepines) but great care should be taken to avoid respiratory depression. Preoperative oral sildenafil, tadalafil or other type V phosphodiesterase inhibitors, endothelin receptor antagonists, calcium channel blockers, inhaled nitric oxide and nebulized iloprost can be used to reduce pulmonary artery pressures. It is important that these chronic therapies are not interrupted in the perioperative period. Maintenance of sinus rhythm (e.g. electrical cardioversion of new onset atrial fibrillation) and optimal ventricular rate should be targeted to prevent RV dilatation and optimize ejection. When using beta blockers drugs to maintain sinus rhythm, associated negative inotropic and systemic vasodilatory side effects should not be neglected.

49.3 Intraoperative Monitoring and Anesthetic Management

Patients undergoing cardiac surgical procedures are extensively monitored. Standard monitoring in the operating room include five lead ECG system, arterial (radial or femoral) invasive blood pressure monitoring, pulse oximetry, end-tidal carbon dioxide measurement, a Swan-Ganz pulmonary artery catheter, cerebral oximetry, urinary Foley catheter, core body and peripheral temperature sensor. In some cases complex hemodynamic monitoring devices (pulse contour cardiac output PICCO or Vigileo Flow/Trac) can be used. Intraoperative TTE is already included in standard of care protocols in the majority of cardiac surgery centers because it is a fast, inexpensive, ready to use diagnostic tool. TTE should be a necessary diagnostic tool in every cardiac surgery operating room.

Swan Ganz pulmonary artery catheters are usually placed in the operating room before or after the induction of general anesthesia and these are used to measure the right atrial (central venous pressure CVP), the pulmonary arterial pressure (PAP) and the pulmonary capillary wedge pressure (PCWP) which can estimate the left sided atrial pressure and diastolic left ventricular pressure. Pulmonary artery pressure monitoring is the gold standard for the detection of PH; however, pulmonary artery pressure will

decrease as RV failure progress [18]. The severity of pulmonary hypertension can be determined by using absolute values of pulmonary artery pressure (PAP), calculation of pulmonary vascular resistance or by using relative values such as ratio medium PAP/medium systemic artery pressure. Normally this ratio (R) is <0.25. Increased values of R is a strong hemodynamic predictor of postoperative complications in cardiac surgery [19]. Usually these measures are performed at times not in a continuous manner. However, a new method was promoted from the Montreal Heart Institute that is the use of continuous RV pressure waveform monitoring. This method was first described as a tool in the diagnosis of right ventricular ischemia [20, 21].

The diagnosis of RV systolic or diastolic dysfunction and right ventricular outflow tract (RVOT) obstruction can be done using a new device (Paceport, Edwards Lifescience, Irvine, CA) able to continuously transducing the right ventricle and the pulmonary artery pressure instantaneously in a dynamic fashion [22]. Starting from the normal hemodynamic physiology of the right heart it is well known that the RV diastolic slope (volume-pressure diagram) is horizontal due to the normal right ventricular compliance which is much higher than the left ventricular one [23]. On a common recording pressure chart there should be no difference between the systolic RV pressure and the peak systolic pulmonary pressure. In right ventricular dysfunction there is a progressive change of diastolic slope which became oblique and then, as the right ventricle fails, will change to a square root slope. In severe cases, when RV has failed, the pulmonary systolic pressure and the RV pressure are equal. Another diagnosis that can be made using Paceport device is RVOT obstruction which is defined when the gradient pressure between pulmonary artery and the RV is greater than 6 mmHg. The mechanism of RVOT obstruction can be mechanical or dynamic. Mechanical RVOT obstruction can occur in the prone position [24], during sternal closure, in anterior pneumothorax [25] and after lung transplantation [26, 27]. In dynamic RVOT obstruction the pressure gradient is usually greater than 25 mmHg and complicates the evolution in 5% of patients undergoing cardiac surgery [23]. They are associated with hemodynamic instability and the management includes volume loading and beta blockers. It is contra-indicated to use adrenergic inotropic agents.

Echocardiographic evaluation of right heart function during cardiac surgical procedures is critical in hemodynamic management. Noninvasive TEE, simple measurements of RV function can be completed using several parameters. Tricuspid annular plane systolic excursion (TAPSE) is performed easy using ME 4C (mid-esophagus four chambers) or transgastric view. Its value is less preload dependent than other markers of RV function. TAPSE is determined using the M-mode cursor placed through the lateral annulus of tricuspid valve and the distance of annular motion during systole is measured longitudinally. A value of less than 16 mm correlates with a severe RV dysfunction [9]. Tissue Doppler Imaging (TDI) method is used to asses "s" wave (systolic motion) of RV. A value of "s" less than 10 cm/s is a sign of RV dysfunction. Other measurements of RV function include RV internal diameter in diastole (RVIDD) and fractional area change (FAC) using ME 4 C TEE. Both parameters need further evaluation in large randomized trials to be trustworthy [28]. More recently RV global longitudinal strain has emerged as diagnostic tool for RV systolic function assessment [28].

Pulmonary pressure can be also evaluated by calculating the RV-RA gradient and the RA pressure using the modified Bernoulli equation. Using ME 4 C view the regurgitate trans tricuspid jet can be aligned parallel to Doppler ultrasound beam giving a trusted value of RA-RV gradient pressure. The size of inferior vena cava is best measured using ME bicaval view in M mode and will estimate the RAP pressure. The value of pulmonary pressure is the sum of two pressures determined above.

Near infrared spectroscopy (NIRS) is a noninvasive method designed to offer information about the balance between tisular oxygen supply and consumption. This method is a nonspecific one since the information are collected in a strict limited area and cannot be generalized to

hole body. Also, apart form the older methods (mixed venous blood gas, lactate level), it can provide real time based information [29]. Regional cerebral oxygen saturation (rSO_2) monitoring using NIRS is a technology that could help meeting these goals during cardiac surgery. Studies have shown that intraoperative NIRS values correlate with postoperative outcome in cardiac surgery [30]. Combining right ventricular pressure waveform, echocardiography and NIRS monitoring allows the anesthesiologist to differentiate the compensated normal or abnormal RV (normal NIRS values 60–80) to the uncompensated failing RV (reduced NIRS values <60) [31]. In the operating room, end-tidal carbon dioxide and NIRS trends are used to evaluate response to therapy. They are useful in right ventricular failure compared to thermodilution, as they are not influenced by tricuspid regurgitation [32].

The anesthetic plan should avoid triggers of pulmonary vasoconstriction. Hypoxia, hypercarbia and acidosis should be aggressively managed. High-dose opioids have no direct effect on pulmonary vasculature and allow a reduction in anesthetic dosage, minimizing adverse effects. Low tidal volumes avoiding hyperinflation and low positive end expiratory pressure are both recommended for ventilation reducing any rise in pulmonary vascular resistance [33]. Induction agents most commonly used is a combination of 1–2 mg/kg of propofol or etomidate with sufentanyl 1 mcg/kg and a no depolarizing agent like rocuronium 0.5 mg/kg or vecuronium 0.01 mg/kg. Pancuronium 0.01 mg/kg is use mainly in pediatric patients. Anesthesia is maintained using subsequent doses of narcotics, muscle relaxants and an intravenous (propofol) or inhalators (sevoflurane) hypnotic agent. Bispectrality electroencephalographic (BIS) and neuromuscular monitoring (TOF guard) are useful tools to titrate dosage of anesthetic drugs. Dexmedetomidine is an $alpha_2$ adrenergic agonist with numerous properties including sedation, analgesia, anxiolysis and sympatholysis but no amnestic effect. During cardiac surgery it can be used to reduce the dosage of other medications allowing for early extubation [34].

After induction of anesthesia the arterial and venous lines are secured, TEE is inserted and prophylactic antibiotic (vancomycin or second generation cephalosporin) is administered. Steroids (methylprednisolone 30 mg/kg or dexamethasone 1 mg/kg) are administered before the cardiopulmonary by pass (CPB) according to team protocol. However the side effects of steroids should be kept in mind and balance the potential advantages of this therapy [35].

Antifibrinolytic drugs should be used for all on-pump procedures as long as has been demonstrated to reduce perioperative blood loss in cardiac surgery procedures [36]. Aprotinin was withdrawn from the market 10 years ago despite most of the criticism have been refuted and tranexamic acid 10 mg/kg in 20 min loading dose then 1 mg/kg/h infusion and epsilon aminocaproic acid are now the most used antifibrinolytic drugs. Avoidance of blood transfusion is mandatory because of risk of increasing pulmonary vascular resistance.

Anticoagulation is essential during CPB to minimize the generation of thrombin and fibrin monomers caused by interaction of blood with pump tubing. Unfractionated heparin remains the most used drug for this purpose. Once the activated clotting time is greater the value of 480 s (350 s in biocompatible circuits) the CPB is initiated.

49.4 Cardiopulmonary By-Pass, Myocardial Protection and Right Ventricular Failure

Extracorporeal circulation has evolved in terms of safety of technology and techniques so far that more complex cardiac surgery procedures are nowadays performed with great success. After decades of continuous improvement in terms of pump "driving force" technology and circuits the CPB is still a great challenge for any patient. There is a continuing improvement strategy to deal with the unsolved issues regarding CPB and patient safety: optimal hematocrit and transfusion strategy, temperature management, pH management, optimal anticoagulation, inflammatory response, glycemic control, organ protection strategy [37].

Transfusion strategy starts 3 weeks before surgery whenever is possible. Preoperative autologous blood donation is a feasible objective in a patient with stable angina or valvular heart disease but there are some limitations: emergency surgery, concerns about precipitating angina in patients' wits severe coronary lesions, questions about its cost-effectiveness, logistic blood bank considerations. This procedure should be combined with use of recombinant erythropoietin and iron supplementation [38]. Intraoperative autologous blood withdrawal before the institution of CBP provides a good quality blood available for post CBP period with excellent platelets and red blood cells and could be a valuable strategy in selected cases. However any strategy should maintain an optimal hematocrit during CBP and avoid unnecessary transfusion as long as a single pack unit of blood could trigger inflammatory systemic response and pulmonary hypertension with RV failure [39].

Contact of blood with the artificial surface of the CPB circuit, ischemia and reperfusion phenomena, along with hypo perfusion of various organs during periods of CPB may initiate and aggravate the systemic inflammatory response [40]. The systemic inflammatory response after bypass (SIRAB) is induced in nearly all patients but the severity of clinical manifestations is variable and include fever (core temperature over 38.5°C), tachycardia (ventricular rate over 120/min), low systemic vascular resistance, high pulmonary vascular resistance, myocardial edema and ventricular failure, arrhythmias, fibrinolysis, neurologic impairment. A lot of therapeutic avenues designed to reduce SIRAB has been imagined including pharmacologic manipulation (corticosteroids, aprotinin, neutrophil activation remodeling) and mechanical (depletion of leukocytes and inflammatory mediators, modified circuits) [41].

Myocardial injury in cardiac surgery is linked to ischemia-reperfusion lesion mechanism which can lead to permanent or reversible damage. Reversible injury is manifested by a transient depression in cardiac performance, myocardial edema and resolve without long term sequelae. Irreversible cardiac injury involves myocardial necrosis with permanent loss of ventricular contractile function. The term "myocardial protection" was linked to more generic term "organ protection" and includes a multitude of strategies designed to reduce the ischemia-reperfusion injury. The main strategy widely accepted and continuously improved is cardioplegic arrest using a large variety of cardioplegia solutions [41]. Cardioplegia can be delivered in a variety of ways (antegrade, retrograde, through bypass grafts, combined antegrade and retrograde) but the goal remains to provide adequate and uniform distribution of cardioplegia solution to the myocardium. There are some aspects that should not be forgotten in order to provide a good quality myocardial protection [41]:

- Antegrade cardioplegia delivery is simple, mimics normal coronary flow but requires competent aortic valve and is ineffective in advanced coronary disease (CAD) with left main or right ostium coronary disease.
- Retrograde cardioplegia delivery obviates limitations from aortic insufficiency and advanced CAD but catheter placement can be difficult (TEE can be utilized to help guide retrograde catheter placement).
- Retrograde delivery of cardioplegia to the left ventricle is very good but is poor to the right ventricle and the interventricular septum.
- Deep placement of the retrograde cannula could impede the venous drainage of right ventricle
- Excess retrograde cardioplegia pressure produces myocardial edema, hemorrhage and myocardial injury [42].
- Right ventricular protection can be challenging in reoperative patients owing to frequently occluded native coronaries supplying the right ventricle
- Persistent left superior vena cava should be identified and drain individually

In conclusion, independently on cardiac surgical procedure, RV dysfunction and high pulmonary vascular resistance at the conclusion of CPB could be a consequence of undesirable side effects that accompany the procedures of extracorporeal circulation.

49.5 CPB Weaning

The termination of bypass is a team effort requiring communication between surgeon, anesthesiologist and perfusionist and consists in:

- Rewarming- the core temperature should be returned to 37 °C; during rewarming the arteriovenous gradient temperature should be less than 10 °C to prevent bubble formation and coronary/cerebral emboli. The rewarming must proceed slowly, the recommended speed ranges from 0.1 to 0.4 °C/min and the team should consider weaning at temperatures around 37 °C because it has been proven that hyperthermia can exacerbate any neurological injury that occurs during surgery and accelerates neuronal death. Inadequate rewarming while on CBP can result in drop of patient temperature and precipitate subclinical shivering, hypercarbia, acidosis and increase in pulmonary vascular resistance [43].
- Correction of metabolic abnormalities-acidosis, diselectrolytemia, anemia, hyperglycemia.
- Ventilation must begin before discontinuation of bypass; the lungs must be manually reinflated to document bilateral inflation and elimination of atelectasis; hypoventilation and hypercarbia should be avoided since increase pulmonary vascular resistance.
- Calibrate pressure transducers (arterial, central venous pressure, pulmonary artery pressure); insert left atrial catheter if needed- useful to asses left ventricular end diastolic pressure and as a drugs line administration especially when adrenergic inotropic support is expected and excessive pulmonary vascular resistance is noted.
- Establish epicardial pacing if needed; ensure atrio-ventricular (third degree AV block) or atrio-biventricular (AV block and left/right bundle branch block) pacing [44].
- Start pharmacological (inotropes, vasodilators, vasoconstrictors)/mechanical (intraaortic balloon pump IABP, left and/or right ventricular assist device) hemodynamic support to ensure optimal cardiac output.
- Start protamine for heparin neutralization after CPB is off. Protamine reactions are unusual but could be life-threatening: type I (systemic hypotension), type II (anaphylactic reaction) or type III (catastrophic pulmonary vasoconstriction). In most cases pharmacologic measures can reverse these undesirable reactions but sometimes require systemic heparinization and turn on pump again with full CPB.

49.6 Intraoperative Right Ventricular Failure Management

Usually, in cardiac surgery, weaning from CPB is "the moment of truth." Typically, hemodynamic instability is associated with reduced cardiac output (cardiac index below 2 L/min/m^2) and low NIRS values indicating poor tissue perfusion.

Once the diagnosis of low cardiac output is done it is important to recognize the presence of right ventricular dysfunction. It is the role of surgeon to inspect the heart and to see if the right heart is "ballooning" and the myocardial contraction is weak. Direct observation of the right ventricle, right ventricular pressure waveform analysis and TTE should offer a comprehensive approach to RV dysfunction management.

The next step is to analyze the right ventricular pressure waveform and to exclude right ventricular output obstruction. The gold standard diagnosis in this situation is TEE. A gradient of more than 25 mmHg between the RV and the pulmonary artery correlates with the severity of hemodynamic instability and dynamic RVOT is the diagnosis. It must rule out the mechanical compression mechanism of RVOT (massive pneumothorax, other causes of pulmonary artery compression). In cardiac transplant receiver check the pulmonary anastomoses. If the cause of pressure gradient is not a mechanical one it must stopped/reduced inotropic support and a trial of fluid administration should begin. Short acting selective beta1 blockers may be administered (esmolol) in order to decrease the heart rate allowing for better RV preload [22].

Analysis of RV pressure waveform (oblique or square root slope) and TEE imaging is the next

step and will confirm right ventricular systolic or diastolic failure. General and goal directed measures should be taken as follows:

- Ensure optimal heart rate, rhythm (atrio-ventricular or atrio-biventricular sequential pacing, optimizes preload (fluids), afterload (reduce pulmonary/systemic hypertension, maintain normal pH, optimizes hematocrit.
- If ischemia and left ventricular dysfunction is suspected control coronary grafts, perform right coronary artery venous grafting, insert intraaortic balloon pump or ventricular assist device (VAD).
- If no ischemia/no left ventricular dysfunction reduce RV afterload (inhaled nitric oxide NO or prostacyclin, intravenous type III phosphodyesterase-milrinone, enoximone), improve RV contractility (milrinone, dobutamine levosimendane) [45].

49.7 Early Postoperative Management and RV Dysfunction

At the end of the surgery the patient is transferred, under the close attention of the surgical team, in the intensive cardiac care unit (ICCU). The local staff became now responsible for maintaining stable the vital signs and the protocols for early management are started. Focused on the main issue of this chapter we can divide these measures as general and specific.

49.7.1 General Measures

After cardiac surgical procedure most patients are transferred in the ICCU sedated and mechanically ventilated. Early extubation is one of the goals of fast track anesthesia and fast track care protocols. Nevertheless, mechanical ventilation weaning is one of the most critical moments when the cardiac output is redistributed including to respiratory muscles. Sometimes, when the cardiac output is marginal and maximal, the balance delivery/consumption of oxygen can be altered and myocardial ischemia can emerge.

Bases of fast track anesthesia and fast track care are created in the operating room and consist in type of anesthetic drugs, myocardial protection, and protocol of cardiopulmonary by-pass weaning, accuracy of surgical and nonsurgical hemostasis.

Neurologic complications (focal deficits or encephalopathy) represent dreaded sequelae of cardiac surgery and exclude the fast track care protocols. These complications delays ventilatory weaning and increase the general mortality.

49.8 Management of Temperature

Systemic hypothermia is routinely used in cardiac surgery, during cardiopulmonary bypass (CPB), in order to provide myocardial and cerebral protection [46].

The protective effect of hypothermia may be explained through several pathways:

- hypothermia decreases the metabolism by less oxygen and energy consumption and less carbon dioxide production (VO_2 slows down by 6%/1 °C reduction in body temperature)
- the cellular neuronal damage following activation of the neuro-excitatory cascade is reduced
- the ischemia induced by the inflammatory and the immune reactions is reduced
- hypothermia prevents the dysfunction of the blood brain barrier and reduces the vascular permeability [47].

Postoperative hypothermia is defined as core temperature <36 °C. During the early postoperative period, transient hypothermia is very common, but it's not associated with an increased mortality. On the other hand, persistent hypothermia is significantly and independently associated with an increased mortality [48]. Hypothermia induces vasoconstriction, increased pulmonary vascular resistance and right ventricular afterload, increased O_2 consumption, coagulopathies (especially platelet dysfunction), dysrhythmias, alterations in blood glucose homeostasis,

hypokalemia, hypocalcaemia, hypomagnesaemia, possibly immunosuppression [47].

The ideal postoperative rewarming method should be safe and enable fast, reliable and predictable rewarming, without causing burns [47].

The most commonly used warming techniques are:

- external and passive—they rely on the body's own heat-producing mechanism to restore the normal temperature (heated or reflective blankets, radiant heat sources from overhead or near the bed, raising the room temperature)
- active rewarming methods (heated mattresses and forced air tents—seem to be more effective and faster at raising core temperature)
- supplying warm fluids, Fortius catheter and Cool Gard 3000 heat exchange [49].
- circulating water system—it transferred more heat with the difference resulting from posterior heating [50].

During the rewarming there is a risk of mismatch between the total body oxygen demand and the oxygen delivery (rewarming shock). The increase in oxygen consumption happens mainly because of:

- the reperfusion of the areas of oxygen debt during hypothermia where lactate was generated and now reenters normal oxidative ways, consuming oxygen
- the inflammatory response to injury and free radical oxidation that leads to increased VO_2
- the shivering (a concerted reaction involving skeletal muscle contraction and peripheral vasoconstriction), associated with increased VO_2 and hemodynamic instability [47].

There are several rules that must be followed thoroughly in order to minimize the rewarming shock:

- Rewarming should be done slowly, in a controlled manner
- Sedation, controlling the pain, and preventing of shivering should limit the oxygen consumption
- The oxygen content and transport should be optimized—the anemia and hypoxemia must be avoided [47].

Rewarming and increased body O_2 consumption in the ICCU can be viewed as a heat and O_2 repayment of debt after surgery. The skin vasoconstriction and the increased muscle activity are considered to be appropriate thermoregulatory responses. Peripheral vascular resistance has been reported to be inversely related to central temperature [51].

In order to reduce the perioperative heat debt and to prevent and control the muscle hyperactivity related to hypothermia, beside physical methods, pharmacological means can be used [52]. Shivering is an involuntary, oscillatory muscular activity that augments metabolic heat production [53]. The Bedside Shivering Assessment Scale is a simple, validated four point scale that enables repeated quantification of shivering at the bedside [47].

In order to counteract shivering, the available active interventions are:

- meperidine possesses special antishivering properties; it decreases the shivering threshold twice as much as the vasoconstriction threshold, in contrast to other analgesic and sedative drugs [47, 53, 54].
- other opioids (morphine, fentanyl, alfentanyl, pentazocin) [47, 53, 54].
- centrally acting analgesics (tramadol, metamisol, nefopam) [47, 53, 54].
- α_2 agonist (clonidine) [47, 53, 54].
- correcting hypomagnesaemia with infusion of magnesium sulfate which produces vasodilation [47, 53, 54]
- doxapram [53, 54].
- ketanserin [53, 54].
- supplementing dexmedetomidine with buspirone (serotonin 5HT 1_A partial agonist) blocks shivering and causes minimal sedation; in combination with meperidine, they act synergistically (buspirone) or additively (dexmedetomidine) [55].
- propofol decreases vasoconstriction and shivering threshold [47, 56].
- neuromuscular blockade [47].

49.9 Management of Postoperative Bleeding

Postoperative bleeding after CPB is considered important if exceed 2 mL/kg/h and it affect approximately 8% of cardiac surgery procedures. Mediastinal bleeding after CPB is the main cause of early surgical reintervention. It can be categorized as surgical and medical (Table 49.1) but you never can draw a strict line between. Careful hemostasis at the end of surgery is crucial in reducing postoperative blood loss. If the initial coagulation tests are in normal range and the mediastinal drainage exceed 2 mL/kg/h, prompt mediastinal reexploration should be done. If the blood accumulates around the heart it impairs the filling causing cardiac tamponade and if severe hypotension or a cardiac arrest occurs, emergency sternotomy in the ICCU should be performed. Persistent bleeding will lead to "consumptive coagulopathy" that is self perpetuating [57].

Residual heparin or excessive protamine is the main medical cause of bleeding following cardiac surgery [58]. Heparin rebound is another cause of bleeding, especially in obese patients receiving large amounts of heparin. Close titration of protamine after cardiopulmonary bypass (CPB) based on activated clotting time (ACT) value and correcting the levels of III antithrombin (AT III) rather than giving extra heparin doses could prevent this situation [59].

Quantitative and qualitative platelet dysfunction is another cause of bleeding following cardiac surgery. Preoperative thrombocytopenia, cardiopulmonary by pass (CPB) and protamine administration reduce the platelet count up to 50%. Preoperative platelet dysfunction due to drugs administration, CPB exposure with alpha granule release and inadequate heparinization will reduce the function of thrombocytes [60].

Fibrinolysis occurs frequently after CPB and is caused by activation of coagulation and inflammatory pathways. Antifibrinolytic therapy is used in many cardiac surgery centers around the world and it includes drugs like epsilon aminocaproic acid, tranexamic acid and aprotinin. The last one is no longer used in USA and EU since 2007 because of fear of increased risk of stroke, renal failure and myocardial infarction even there is not strong evidence to sustain this fear [61].

The coagulation abnormality contributing to the bleeding can be identifying using conventional tests:

- prothrombin time measured as INR (international normalized ratio) should be less than 1.5; if exceed this value, fresh frozen plasma must be administered 10–20 mL/kg.
- partial thromboplastin time is usually increased in case of heparin rebound; protamine 25 mg/h until bleeding ceased could be the remedial.
- platelet count show usually a fall under 100,000/mmc. However, bleeding can occur even the number of platelets are beyond this value rising the suspicion of qualitative dysfunction. In both situations, if excessive bleeding is present, platelet transfusion became mandatory.
- coagulation factors level can now be individually measured and goal directed therapy can be provided. Fibrinogen promotes platelet-platelet interaction leading to platelet aggregation. However, preoperative fibrinogen levels are not associated with postoperative bleeding at 12 and 24 h after surgery [62].
- After a promising rescue solution in severe bleeding cardiac surgery patients, recombinant factor VIIa is no longer recommended because of fatal thrombotic episodes.
- Fibrinolysis, which is always present after CPB, can be highlight by elevated INR, PTT, a decreased level of factors I and VIII and the presence of fibrin splits products (D-dimer).

Table 49.1 Etiology of mediastinal bleeding

Surgical and medical causes of mediastinal bleeding
1. Surgical bleeding sites
2. Heparin effect-residual or rebound
3. Excessive protamine administration
4. Platelet dysfunction
5. Thrombocytopenia
6. Clotting factor deficiency
7. Fibrinolysis

Measuring the clot strength by different methods is the best way to make the right diagnostic of fibrinolysis. Administration of tranexamic acid 1 mg/kg/h until the bleeding cease could be a good option [63].

Even a lot of blood conservation techniques are generally approved today which include acute normovolemic hemodylution, hemofiltration blood, cell-saver, autotransfusion if excessive bleeding occurs after surgery blood and blood products must be used. Every component should be administered rationale, based on laboratory tests in conjunction with clinical judgement. Never use a blood product as a plasma expander to correct hypovolemia. However, you should have in mind that administering blood products can induce a state of hypervolemia—transfusion acute cardiac overload-(TACO) with a hemodynamic compromised situation especially on those patients with marginal ventricular reserve.

- Packed red blood cells are the rational option to increase the hemoglobin level. You have to keep in mind than any unit of transfused blood could precipitate catastrophic undesired reactions including acute pulmonary vasoconstriction crisis. The trigger level for transfusion must not be a number but rather a clinical situation which should include the preoperative associated pathology like obstructive chronic bronchopneumopathy, left and right ventricular function, age, rate and tendency of bleeding, work of breathing. Leukoreduction of red blood cells is beneficial in reducing nonhemolytic transfusion reactions including TRALI (transfusion related acute lung injury). It is preferred to give the freshest blood you have because of the low risk of bacterial infection and reduced incidence of renal dysfunction. Also, as fresh is the blood as high is the oxygen carrying capacity.
- Platelets should be given in a bleeding patient when the count number below 100,000/mmc or when we have the suspicion of platelets dysfunction
- Fresh frozen plasma (FFP) contains all coagulation factors at normal concentrations except factor I, factor V and factor VIII. It is recommended to administer 10–20 mL/kg of FFP if INR is greater than 1.5. In emergent cases, when the patient was on antivitamin K therapy prior to surgery you can use new products like prothrombin complex concentrates (PCC) Pronativ which contains factor II, VII, IX, X and proteins C and S. FFP should be used as AT III substitute only if there is not available AT III concentrate (Thrombate III).
- Cryoprecipitate contains factors important in primary hemostasis, mainly factor I, VIIIc and von Willebrand. The usual dose is 1 unit of cryo for every 8–10 kg of body weight.

Cardiac tamponade could be a complication of excessive postoperative bleeding and it represents a surgical emergency. Prompt mediastinal reexploration is mandatory. If cardiac arrest developed the chest must be opened in ICCU. There are some signs that should heighten the suspicion of cardiac tamponade:

- Significant mediastinal bleeding with sudden cessation
- Hemodynamic instability with persistent low cardiac output despite increasing inotropic and vasopressor support
- Micro voltage QRS complex, compensatory tachycardia, arrhythmia, electromechanical dissociation

Useful tools to diagnose cardiac tamponade:

- enlarged mediastinum on thoracic radio graphy
- transthoracic or transesophageal echocardio graphy

Early surgical reexploration for bleeding increased mortality and morbidity especially if the opening of the chest is performed in the ICCU. However, delayed reintervention in excessive bleeding is worst if low cardiac output persists and requirements for transfusion are high.

49.10 Respiratory Management and RV Failure after CPB

Ventilation mode selection is influenced by the patient's condition upon arrival in ICCU. Generally the patients need full ventilatory support, as they usually not demonstrate any inspiratory effort. Ventilatory support is provided either using volume ventilation or pressure ventilation. Each of these methods provides positive pressure ventilation. At the admission, the most used ventilation mode has to full support the work of breathing and allow the patient to gradually load the respiratory function and in this light synchronized intermittent mandatory ventilation (SIMV) could be the choice which is best for patient with normal or increased compliance but isn't optimal for stiff lung or bronchospastic airways. In these situations a pressure limited ventilation probably will provide better therapy. Regardless of the mode of ventilation, attention should be directed to mean airway pressure which is an expression of positive end expiratory pressure (PEEP), peak inflating pressure and the inspiratory time. High peak inspiratory pressures, as well as high levels of PEEP could produce barotrauma or compromise RV function by reducing preload (especially as these patients are usually hypovolemic) and increasing afterload.

Once the patient recovers from the anesthesia and regains inspiratory effort, a weaning protocol is indicated. It is important to decide when is possible to withdraw safety the ventilatory support and let the patient to breath spontaneously. Weaning process should be stopped if there are clinical and para clinical signs that are no well tolerated (somnolence or agitation, hemodynamic alteration, increase in respiratory rate, hypoxemia, and increase of lactate level). Oxygen consumption and cardiac index increase in patients during weaning from mechanical ventilation and the additional load on the cardiovascular system could be crucial in some patients.

There are studies that have evaluated the efficacy of one mode of ventilation in relation to other in this first postoperative period; commonly used methods of mechanical ventilation are SIMV, bi phase plateau airway pressure (BiPAP), pressure support ventilation (PSV). All three modes of ventilation were found to have similar effects on hemodynamic stability and gas exchange [64].

It could not determine the exact indication of a particular ventilation mode. This was left to the decision of the anesthetist based on his experience and patient pathology. Studies analyze and compare the benefits of a ventilation mode in relation to other. There are still debates about the appropriate protocol for ventilatory management in cardiac anesthesia.

49.11 Fluid Management and RV Failure

One of the main objectives in the early postoperative period is maintaining an adequate intravascular volume for an optimal cardiac output and a proper tissue perfusion. The CPB triggers a transient systemic inflammatory response that increases capillary membrane permeability (the capillary leak syndrome) and lead to decreased intravascular volume. Most often, maintaining intravascular volume occurs at the expense of expansion of the interstitial space. Postoperative bleeding and excessive administration of diuretics may also contribute to shrink the total blood volume. To counteract these phenomena, fluid therapy is an important part of treatment in the immediate postoperative period. Ideal fluid therapy should avoid both hypovolemia and hypervolemia and should be a goal directed therapy. Goal-directed hemodynamic therapy is an effective tool to reducing the incidence of postoperative complications after cardiac surgery and shortening hospital length of stay.

Adequate volume therapy involves the need for monitoring the hemodynamic parameters. Immediately after surgery, the patient is basic monitored with EKG, pulse oximetry, central venous pressure, pressure recording thru arterial lines, urinary flow and arterial blood gas analyze. Right heart failure requires advanced monitoring techniques like pulmonary artery catheter or trans pulmonary thermodilution and calibrated pulse contour analysis and TTE. Although Swan Ganz

pulmonary artery catheter is the gold standard for hemodynamic determinations, the new noninvasive or minimally invasive techniques can provide valuable information and they are less expensive and with fewer complications.

Vasoplegic syndrome is a common complication encountered immediately after surgery which can cover various aspects. When no longer can be managed by fluid therapy it requires vasopressor therapy like norepinephrine or vasopressin.

The fluid solutions used are either crystalloid or colloids.

Crystalloids solutions are given to every patient who undergoes surgery. Among crystalloids, balanced solutions are preferred because there are several advantages in their use. Balanced crystalloids solutions (Ringer lactate, Hartmann solution, Accusol, Normasol, Sterofundin, Plasma Lyte) contents slightly less Na, significant less chloride and have buffers such as lactate or acetate which determine a strong ion difference (SID) closer to that of plasma. They seem to be involved in maintaining renal blood flow, preventing metabolic acidosis and reducing the incidence of postoperative atrial fibrillation. A study to evaluate the effect of fluid therapy using Accusol showed that standard base excess was more stable in patients treated with Accusol. During the fluid therapy with crystalloids, one should keep in mind the risk of interstitial overload. The most important in this regard is increasing in extravascular lung water that can lead to pulmonary edema with its consequence on oxygenation. After the last warnings related to synthetic colloid, isotonic balanced crystalloids remains the fluid of choice immediately postoperative.

Colloids have better volume effect and stay longer in the intravascular space then crystalloids. Choices of colloids include either natural colloids (albumin) or synthetic (hydroxyethyl starch solutions, gelatins).

Starch solutions formed generally as 6% HES in normal saline (Hespan, Voluven) or in balanced electrolyte solution (Hextend), have greater oncotic pressure than crystalloids, so they could provide better volume expansion. Studies in connection with the use of HES have focused not only on volume expansion but also on possible side effects. HES solutions can be divided according to their molecular weight (MW) or their molar substitution ratio (MS) in older solutions and new low MW compounds. The higher the molar substitution ratio the greater the resistance to degradation. Thus older generation of HES (heptastarch) accumulate in the plasma unlike the latest tetrastarch and probably generate the renal complications. There are three starch solution in the USA licensed for intravascular use: Hespan (licensed in 1972), Hextend (1999) and the newest tetrastarch Voluven (licensed in 2007), but also other solutions available in Europe and Canada (Pentaspan). HES solutions are used since1978 but from 1993 have been reported renal dysfunctions and clotting disorders related to their use. In light of these trials the European Medicine Agency decide in 2013 that HES is no longer indicated in patients with sepsis, burn injuries or in critically ill patients because of the risk of kidney injury and rise in mortality [67]. FDA has analyzed recent data that indicate an increased risk of excess bleeding particularly in patients undergoing open heart surgery in association with cardiopulmonary bypass [65]. There is also a lack of robust long-term safety data in patients undergoing surgical procedures. HES solutions can be used only in hypovolemia due to acute blood loss, when treatment with crystalloids alone is not considered sufficient [67]. In conclusion in cardiac surgery patients, fluid therapy with perioperative administration of synthetic colloids carries a high risk of renal replacement therapy and blood loss and is not more effective than treating with only crystalloids [68]. As colloids are not associated with an improvement in survival and are considerably more expensive than crystalloids, it is hard to see how their continued use in clinical practice can be justified [68].

Albumin seems to be the best colloid solution used in any low volume state situation.

Pre-operative hypoalbuminemia is an independent risk factor for multiple poor outcomes in cardiac surgery and albumin administration may be valuable prior to cardiac surgery [69].

Values below 3.5 g/dL reveled worse long term survival after cardiac surgery [70]. The same applies to low albumin values in the postoperative period and albumin administration post-surgery may improve patient survival [71]. Albumin 5% is approximately five times more efficient as a plasma volume expander compared with normal saline in postoperative cardiac surgical patient and hyper oncotic albumin (with a volume effect of more than 100%) is a good option to recruit interstitially stored fluid toward the circulatory [72, 73]. Albumin, besides being a good volume expender, preserve coagulation and has oxygen free-radical scavenging and anti-inflammatory properties. It has found useful both as for pump priming and as a volume expender.

The studies performed till at issuing warning related to the use of HES, showed that albumin is better than HES on postoperative blood loss and as volume expender but it does not impair hemostasis after CPB [74]. Albumin may also have beneficial effects on renal function. It is the only colloid in which renal safety is supported by a large, multi-center, double-blind, randomized controlled trial in critically ill patients [75]. A recent study comparing chloride-liberal with chloride-restrictive intravenous fluid administration in critically ill patients demonstrated that a chloride-restrictive strategy with 20% albumin was associated with a significant decrease in the incidence of acute kidney injury and failure, and the use of renal replacement therapy [74, 75].

There are three types of new generation of gelatins currently used in the world: succinylated or modified fluid gelatins (Gelofusine, Plasmagel, Plasmion), urea-cross-linked gelatins (Polygeline) and oxypolygelatins (Gelifundol). They are cheaper compared with albumin or HES and do not have any upper limit of volume that can be infused. If the effect on blood loss is comparable with HES, induced renal changes are more important [74, 75].

Hypertonic solutions have attracted attention in last years because of the possibility of augmenting intravascular volume but also for their effects on immune system. Recent investigations have shown their role in decrease of inflammatory response and cytokines generation [76].

Studies lead by Jarvela and colleagues stated that administering a single dose of 4 mL/kg of 7.5% NaCl over 30 min to CABG patients during the postoperative rewarming phase resulted in intense diuretic effects and decreased fluid retention [76–78].

49.12 Metabolic and Endocrine Disturbances

The first 24 h after CPB represent to a period of major shift in metabolic and endocrine homeostasis.

Hyperkalemia is a common disturbance of homeostasis after cardiac surgery. High-potassium cardioplegia solutions combined with postoperative renal failure and low flow states are the main causes of hyperkalemia. The optimal level of kalium (K) after cardiac surgery is 3.8–4.2 mEq/L. Values higher than 5.5 mEq/L can induce life threating arrhythmias. Early ECG changes (peaked T waves, ST depression, increased PR interval, QRS widening) require emergent pharmacological interventions in order to decrease potassium level to a safe value: Calcium gluconate/calcium chloride, Insulin, Sodium bicarbonate, Furosemide, Hemodialysis.

Copious diuresis without proper replacement is the main cause of hypokalemia after CPB. Atrial, junctional, ventricular ectopy, AV block and ventricular tachycardia/fibrillation can be triggered if plasma kalium is below 3 mEq/L. Treatment consist of kalium replacement via intravenous route by giving KCl 1 M and check K level each 30 min.

Ionized calcium (Ca) should be monitored routinely in cardiac surgery patients and maintained in a tight range of 1.1–1.5 mmol/L. In the early period after CPB, ionized calcium level is decreased due to hemodylution, hypothermia, shift in pH and the use of citrated blood. Calcium gluconate or calcium chlorides are the pharmacological options to increase the serum calcium level. Clinical effects are: Increase SVR, increase inotropic, offset protamine vasodilator effects, increase clot strength and reduce bleeding.

Cardiopulmonary bypass (CPB) is associated with a metabolic acidosis of variable severity and it represents the main cause of acidosis in the first 24 h after cardiac surgery. Low flow states and the pump priming solutions with lactate buffer usually generate lactic acidosis (organic acidosis) whereas hypercloremic acidosis (inorganic acidosis) is created by pump priming solutions high chloride concentration. The recent studies indicates that the main cause of CPB induced acidosis is an iatrogenic one as it can be demonstrated using Stewart equation used to calculate the Strong Ion Difference (SID):

$$SID = Na^{++}K^{++}Ca^{+++}Mg^{++} - Cl^{-}$$

where each is expressed in mEq/L; normal value = 40–42 mEq/L.

Type A lactic acidosis is a sign of anaerobic metabolism secondary to impaired tissue oxygenation in low flow states. The treatment is addressed to increase the oxygen delivery and reduce the oxygen consumption by all pharmacological and mechanical means. A lactate level greater than 5 mmol/L at 24 h after CPB is associated with increased mortality.

Type B lactic acidosis occurs in the absence of hypoxia and is secondary to pyruvate accumulation resulted from free fatty acid metabolism. Glucose, insulin and reduce the level of catecholamine represent the first therapeutic option.

The treatment of hypercloremic acidosis consists in correcting pH using one of the following solutions: Sodium bicarbonate, Carbicarb (mixture of sodium bicarbonate and sodium carbonate), Tromethamine (Tris buffer).

Elevated levels of cortisol, catecholamine and activation of sympathetic nervous system are the main causes of hyperglycemia in the first 24 h after cardiac surgery. Hyperglycemia over 180 mg/dL is associated with increased mortality and morbidity in cardiac surgery patients.

Regular drip infusion of insulin is the only rationale treatment for hyperglycemia. The goal is to maintain serum glucose under 180 mg/dL while avoiding hypoglycemia. In order to reduce perioperative complications, tight glycemic control protocols were introduced in majority of ICCUs but abandoned since recent attempts to confirm these findings have not succeeded. Instead, they have increased the fear for negative consequences of hypoglycemia. Hypoglycemia is four to seven times more frequent in patients treated with strict glycemic control [79].

49.13 Specific Measures

49.13.1 RV Failure and Hemodynamic Support After CPB

The main goal of hemodynamic support after cardiac surgery is to maintain a minimum cardiac index (CI) of 2.2–2.4 L/kg/min. However, the optimal cardiac index after surgery has to be at least 50% higher than the minimum one to ensure weaning of ventilator support, optimal tissue oxygen delivery, avoiding organ dysfunction and proper wound healing. The inability to achieve an optimal CI in the first 24 h after ICCU admission increase the risk of developing multiple organ failure (MOF) increasing mortality, morbidity and costs. Ventilatory support (mechanical ventilation), mechanical hemodynamic support (cardiac assist devices), renal replacement therapies (dialyzer) are the main tools used, in a very expensive manner, to "gain more time" in the bad scenario of organs failure. Optimizing the preload, afterload, myocardial contraction and relaxation, ensuring the optimal heart rate and atrio-ventricular synchronism are the physiopathology options to increase the cardiac output. These are general measures applied in every case of low cardiac output scenarios. However, RV failure after CPB needs a particular approach even, like left ventricle, RV obeys the Frank-Starling law. RV, as we already outlined before, it has a thin wall with high dispensability and drains to a low pressure-low resistance pulmonary vascular system. With any abnormality in the preload, afterload or contractibility, a rapid dysfunction of the RV is produced [65, 66]. The specific physiopathology process of RV failure after cardiac surgery is more complex. Several mechanisms have been attributed to RV failure development, but according to the patient's

conditions, more than one mechanism may concur; among these mechanisms, preexistent PH, PH associated with CPB and ventricular interdependency are between the most relevant. Pulmonary vasoconstriction and acute increase in RV afterload after weaning from CPB may be due to inflammatory mediators that cause endothelial damage or due to ischemic and reperfusion mechanisms owing to bronchial arteries inadequate blood flow [65]. There is a lack of equilibrium between the vasodilation and vasoconstrictor endogenous substances with an imbalance between vasodilators (nitric oxide and prostacyclin) and vasoconstrictors (thromboxane A2 and endothelin) [65].

There are specific factors related to cardiac surgery that may cause PH and disturb the hemodynamic determinants of the RV, for example, administration of heparin and/or protamine, pulmonary micro embolism phenomena, ischemia of the RV, metabolic acidosis, hypercapnia, hypothermia, hydric overload, poor myocardial protection, long CPB time, obstruction of vascular grafts, and loss of auricular-ventricular synchrony [65].

Monitoring of cardiac output could be a difficult task after cardiac surgery. This include invasive hemodynamic monitoring (arterial, central venous, pulmonary artery and capillary wedge pressures, trans pulmonary thermodilution combined with pulse contour analysis PICCO), transthoracic or transesophageal echocardiography and provide values of systemic/pulmonary/cardiac pressures and cardiac volumes. Thereto TTE exam could provide direct 2D, 3D and Doppler values regarding RV function and pulmonary arterial pressure. All these values can be computed analyzed offering a lot of derived hemodynamic parameters (Table 49.2).

Based on direct monitoring and derived data it can be imagined an algorithm for ICCU management of post CPB RV failure:

- Check oxygenation, improve ventilation, assure adequate sedation/analgesia.
- High preload due to volume overload, valvular regurgitation or left-right shunt: reduce preload using pharmacological (nitroglycerine, morphine, diuretics) or mechanical means (ultrafiltration); close shunt, change/repair valve.
- Low preload due to hypovolemia. Optimizing preload in the early postoperative period could be a difficult task. A common approach to optimize preload is a clinical one by giving small amounts of fluids (ex. 250–500 mL) and look for the signs of increased cardiac output. Systemic inflammatory response, which is a common feature after CPB produce a capillary leak syndrome and can mask the clinical response to fluid challenge.
- Poor RV contractility due to:
  - Low inotropic due to previous RV dysfunction, poor myocardial protection, prolonged pump CPB, early sepsis, arrhythmia. A variety of inotropic and vasoactive medi-

Table 49.2 Hemodynamic measurement guide-normal values (after PULSION Medical Systems AG)

Parameter	Abbreviation	Range	Unit
Cardiac index	CI	3.0–5.0	L/min/m^2
Stroke volume index	SVI	40–60	mL/m^2
Global end-diastolic volume index	GEDI	680–800	mL/m^2
Intrathoracic blood volume index	ITBI	850–1000	mL/m^2
Stroke volume variation	SVV	<10	%
Pulse pressure variation	PPV	<10	%
Systemic vascular resistance index	SVRI	1970–2390	dyn s cm^{-5} m^2
Mean arterial pressure	MAP	70–90	mmHg
Extravascular lung water index	ELWI	<10	mL/kg

cations are used to provide hemodynamic support for the patients with inappropriate myocardial function. The most used in now days practice are:

Epinephrine is usually the first line drug for a marginal cardiac output; usually doses range 0.01–0.05 μg/kg/min; vasoconstrictor effect if the dose is 0.05–0.2 μg/kg/min;

Dobutamine increase cardiac output and decrease SVR; doses range 5–20 μg/kg/min; can induce tachyarrhythmia.

Dopamine may be considered a first line drug for low cardiac output state; increase SVR; doses 2–20 μg/kg/min.

PDE III inhibitors (amrinone, milrinone, enoximone) are considered "inodilators"; they improve contractility and decrease PVR and SVR; Drugs of choice in RV dysfunction; improve left ventricle diastolic function, altered after CPB.

Levosimendan is used especially in acute decompensated chronic heart failure; useful in combined procedure (valve and CABG) when the LV ejection fraction is <40% before surgery; loading dose 12–24 μg/kg followed by 0.1–0.2 μg/kg/min.

Norepinephrine is primary used to rise SVR; usually dose is 0.05–0.20 μg/kg/min; useful in low cardiac output state combined with low SVR after CPB; higher doses will reduce visceral blood flow. Increase PVR and can increase RV dysfunction.

Vasopressin is another drug used to rise SVR if the norepinephrine fails; it may compromise a marginal left ventricle and secondary induce RV failure.

– Coronary hypo perfusion due to coronary artery embolism, mechanical obstruction of the right coronary artery or LV failure with secondary right coronary hypo perfusion.

- High afterload due to:
  – Pulmonary vasoconstriction (hypoxia, hypercapnia, acidosis, blood transfusion, delayed protamine reaction).

    Correct factors that increase PVR

    There are a lot of drugs that reduce the pulmonary vascular tonus. None of them is an ideal one since each drug has adverse reactions.

    - Nitroso dilators (nitroglycerin and nitroprusside) have the potential to reduce the RV afterload but also the preload and the SVR and this combination could reduce the cardiac output.
    - Inhaled nitric oxide (NO) is a selective pulmonary vasodilator. The therapeutic dose is 10–40 ppm administered in the ventilatory circuit and you have to close monitor the levels of met hemoglobin (MetHb), the toxic metabolite of NO. Always you have to reduce the NO delivered to the patient very slowly in order to avoid rebound increase of PVR. NO can be stopped once 6 ppm is reached. The utility of this drug in adult cardiac patients is uncertain.
    - Prostaglandin and prostacyclin analogs can be delivered intravenous or via airway. They are very strong pulmonary arterial dilators, easy to titrate, rapid metabolized and without toxic metabolites.
    - Phosphodiesterase inhibitors (PDE) type V sildenafil, tadalafil, vardenafil, and the newer udenafil and avanafil are used primary for erectile dysfunction. Sildenafil given in small doses (25–50 mg) is used to wean patients from inhaled or intravenous pulmonary vasodilators.

  – Pulmonary congestion secondary to LV dysfunction

If pharmacologic support fails to increase the cardiac output beyond a cardiac index (CI) of 1.8–2.2 L/min/m^2 despite the optimal preload and afterload, mechanical hemodynamic support should be provided. There are some devices available now. Each of them offers benefits and has limitations.

Intra aortic Balloon Counter pulsation (IABP) "unload the heart," increase diastolic coronary perfusion and improves graft diastolic flow. Its benefit is very controversial for the RV. Boeken et al. described 79 patients with low cardiac output syndrome due to RV failure treated with IABP with a survival rate of 63% at 30 days and a significant increase of the cardiac index and median systemic arterial pressure. However, only 28% survived at 75 months follow-up [80].

Circulatory assist devices provide flow to support the systemic or/and pulmonary circulation while resting the heart allowing it to undergo metabolic and functional recovery or bridging the patient to transplantation or totally implantable artificial heart. These devices became smaller, smarter, more compatible with the human body allowing a greater independence. However, none is without adverse reactions, some of them life threatening.

As circulatory assist devices use became widespread there was a great concern about new diagnosis criteria of right heart failure including the cases with implanted left sided heart assist devices (Table 49.3). The use of RV mechanical circulatory support has seen advances in the recent years, and the field continues to evolve to provide novel solutions and meet the needs of a growing population with RHF. RV support could be needed in different clinical situations, such as postcardiotomy, heart transplantation or LVAD implantation. The right ventricle has a great potential for recovery especially in the acute setting. Most of the recent advances have been seen with temporary assist devices of the right ventricle, whereas more chronic RV support is accomplished using LVAD devices modified to adapt to the cardiopulmonary system.

Extracorporeal membrane oxygenation (ECMO) systems have proven to be valuable with the major advantage of supporting hypoxic patients, having the possibility of a peripheral cannulation strategy and being low cost compared with other options [81].

CentriMag (Levitronix LLC, Waltham, Massachusetts, USA) is another solution that utilizes central cannulation directly from the right atrium to the pulmonary trunk without an oxygenator allowing low anticoagulation level but requiring surgical implantation [82].

Table 49.3 Diagnostic criteria for right ventricular failure in cardiac surgery

Clinical situation	Definition criteria
Left ventricular assist device (LVAD)	Dispneea or impossible to wean ventilation, oliguria <0.5 mL/kg/min, right atrial pressure (RAP) >18 mmHg, CI < 2 L/min/m^2 in the absence of high left atrial pressure or high capillary wedge pressure >18 mmHg or tamponade or pneumothorax or ventricular arrhythmias requiring RVAD (severe) or requiring inhaled nitric oxide or prostaglandine E or inotropic therapy more than 1 week any time after LVAD implantation (moderate). Mild RV dysfunction: two of the following criteria: 1. RAP > 18 mmHg 2. CI < 2.3 L/min/kg 3. Ascites or peripheral edema 4. Vena cava inferior >2 cm without inspiratory collapse (echocardiograme)
Right heart failure with normal LV function	Dispneea or impossible to wean ventilation, oliguria <0.5 mL/kg/min, right atrial pressure (RAP) >18 mmHg, CI < 2 L/min/m^2 in the absence of high left atrial pressure or high capillary wedge pressure >18 mmHg or tamponade or pneumothorax or ventricular arrhythmias with preoperative PAH requiring pumpless interventional lung assist ventilator (severe) Mild RV dysfunction: two of the following criteria: 1. RAP > 18 mmHg 2. CI < 2.3 L/min/kg 3. Ascites or peripheral edema 4. Vena cava inferior >2 cm without inspiratory collapse (echocardiograme)
Right heart failure with severely depressed LV function	Severe RV enlargement in context of severely depresed CI

The Impella RP is an axial intracorporeal pump inserted through the femoral vein pumping blood from the inferior vena cava into the pulmonary artery [82].

The TandemHeart for RV support uses a dual lumen cannula removing blood from the right atrium and pumping back by an extracorporeal pump into the pulmonary artery. If needed, an oxygenator could be added to the TandemHeart system [82].

The pump less interventional lung assist membrane ventilator marketed by NovalungGmbH (Hechingen, Germany) is a low-gradient device that can allow complete CO_2 removal in patients with respiratory failure and adequate oxygenation [82].

Conclusions

There has been great progress in the evaluation and management of RHF in cardiac surgery in the last decade and further improvement will require well designed multicenter studies.

References

1. Vonk-Noordegraaf A, Haddad F, Chin KM, et al. Right heart adaptation to pulmonary arterial hypertension: physiology and pathobiology. J Am Coll Cardiol. 2013;62(25 Suppl):D22–33.
2. Ribeiro A, Lindmarker P, Juhlin-Dannfelt A, et al. Echocardiography Doppler in pulmonary embolism: right ventricular dysfunction as a predictor of mortality rate. Am Heart J. 1997;134:479–87.
3. Haddad F, Fisher P, Pham M, et al. Right ventricular dysfunction predicts poor outcome following hemodynamically compromising rejection. J Heart Lung Transplant. 2009;28:312–9.
4. Kaul TK, Fields BL. Postoperative acute refractory right ventricular failure: incidence, pathogenesis, management and prognosis. Cardiovasc Surg. 2000;8:1–9.
5. Nashef SA, Roques F, Michel P, et al. European system for cardiac operative risk evaluation (EuroSCORE). Eur J Cardiothorac Surg. 1999;16:9–13.
6. Bernstein AD, Parsonnet V. Bedside estimation of risk as an aid for decisionmaking in cardiac surgery. Ann Thorac Surg. 2000;69:823–8.
7. Murkin JM, Adams SJ, Novick RJ, et al. Monitoring brain oxygen saturation during coronary bypass surgery: a randomized, prospective study. Anesth Analg. 2007;104:51–8.
8. Denault AY, Belisle S, Babin D, et al. Difficult separation from cardiopulmonary bypass and delta PCO_2. Can J Anaesth. 2001;48:196–9.
9. McLaughlin VV, Archer SL, Badesch DB, et al. ACCF/AHA 2009 expert consensus document on pulmonary hypertension a report of the American College of Cardiology Foundation Task Force on Expert Consensus Documents and the American Heart Association developed in collaboration with the American College of Chest Physicians; American Thoracic Society, Inc.; and the Pulmonary Hypertension Association. J Am Coll Cardiol. 2009;53:1573–619.
10. Downing SW, Edmunds LH Jr. Release of vasoactive substances during cardiopulmonary bypass. Ann Thorac Surg. 1992;54:1236–43.
11. Haddad F, Hunt SA, Rosenthal DN, Murphy DJ. Right ventricular function in cardiovascular disease, part I: anatomy, physiology, aging, and functional assessment of the right ventricle. Circulation. 2008;117:1436–48.
12. Galiè N, Hoeper MM, Humbert M, et al. Guidelines for the diagnosis and treatment of pulmonary hypertension. Eur Heart J. 2009;30:2493–537.
13. Konstantinides S, Geibel A, Olschewski M, et al. Importance of cardiac troponins I and T in risk stratification of patients with acute pulmonary embolism. Circulation. 2002;106:1263–8.
14. Nagaya N, Nishikimi T, Okano Y, et al. Plasma brain natriuretic peptide levels increase in proportion to the extent of right ventricular dysfunction in pulmonary hypertension. J Am Coll Cardiol. 1998;31:202–8.
15. Nagaya N, Nishikimi T, Uematsu M, et al. Plasma brain natriuretic peptide as a prognostic indicator in patients with primary pulmonary hypertension. Circulation. 2000;102:865–70.
16. Kaczyńska A, Kostrubiec M, Ciurzyński M, Pruszczyk P. B-type natriuretic peptide in acute pulmonary embolism. Clin Chim Acta. 2008;398:1–4.
17. Kwong RY, Schussheim AE, Rekhraj S, et al. Detecting acute coronary syndrome in the emergency department with cardiac magnetic resonance imaging. Circulation. 2003;107:531–7.
18. Barash P, Cullen B, Stoelting R, et al., editors. Clinical anesthesia. 6th ed. Philadelphia: Lippincott Williams and Wilkins; 2009. p. 222.
19. Robitaille A, Denault AY, Couture P, et al. Importance of relative pulmonary hypertension in cardiac surgery: the mean systemic-to-pulmonary artery pressure ratio. J Cardiothorac Vasc Anesth. 2006;20:331–9.
20. Kinch JW, Ryan TJ. Right ventricular infarction. N Engl J Med. 1994;330:1211–7.
21. Goldstein JA, Barzilai B, Rosamond TL, et al. Determinants of hemodynamic compromise with severe right ventricular infarction. Circulation. 1990;82:359–68.
22. Denault AY, Chaput M, Couture P, et al. Dynamic right ventricular outflow tract obstruction in cardiac surgery. J Thorac Cardiovasc Surg. 2006;132:43–9.
23. Haddad F, Couture P, Tousignant C, et al. The right ventricle in cardiac surgery, a perioperative perspective: I. Anatomy, physiology and assessment. Anesth Analg. 2009;108:407–21.

24. Neira VM, Gardin L, Ryan G, et al. A transesophageal echocardiography examination clarifies the cause of cardiovascular collapse during scoliosis surgery in a child. Can J Anesth. 2011;58:451–5.
25. Denault AY. Difficult separation from cardiopulmonary bypass: importance, mechanism and prevention (PhD Thesis: www.mediaenligne.umontreal.ca/medclin/anesth/denault_phd.wmv) Montreal: Universitède Montrèal; 2010.
26. Denault AY, Couture P, Vegas A, et al. Transesophageal echocardiography multimedia manual, second edition: a perioperative transdisciplinary approach. New York: Informa Healthcare; 2010.
27. Denault AY, Ferraro P, Couture P, et al. Transesophageal echocardiography monitoring in the intensive care department: the management of hemodynamic instability secondary to thoracic tamponade after single lung transplantation. J Am Soc Echocardiogr. 2003;16:688–92.
28. Porter TR, Shillcutt SK, Adams MS, Desjardins G, Glas KE, Olson JJ, Troughton RW. Guide for the use of echocardiography as a monitor for therapeutic intervention in adults: a report from the American Society of Echocardiography. J Am Soc Echocardiogr. 2015;28:40–56.
29. Gomez CM, Palazzo MG. Pulmonary artery catheterization in anaesthesia and intensive care. Br J Anaesth. 1998;81:945–56.
30. Fischer GW, Lin HM, Krol M, et al. Noninvasive cerebral oxygenation may predict outcome in patients undergoing aortic arch surgery. J Thorac Cardiovasc Surg. 2011;141:815–21.
31. Maslow A, Stearns G, Bert A, et al. Monitoring end-tidal carbon dioxide during weaning from cardiopulmonary bypass in patients without significant lung disease. Anesth Analg. 2001;92:306–13.
32. Baraka AS, Aouad MT, Jalbout MI, et al. End-tidal CO_2 for prediction of cardiac output following weaning from cardiopulmonary bypass. J Extra Corpor Technol. 2004;36:255–7.
33. Zamanian RT, Haddad F, Doyle RL, Weinacker AB. Management strategies for patients with pulmonary hypertension in the intensive care unit. Crit Care Med. 2007;35:2037–50.
34. Carollo DS, Nossaman BD, Ramadhyani U. Dexmedetomidine: a review of clinical applications. Curr Opin Anesthesiol. 2008;21:457–61.
35. Halvorsen P, Raeder J, White PF, et al. The effect of dexamethasone on side effects after coronary revascularization procedures. Anesth Analg. 2003;96:1578–83.
36. McIlroy DR, Myles PS, Phillips LE, Smith JA. Antifibrinolytics in cardiac surgical patients receiving aspirin: a systematic review and meta-analysis. Br J Anesth. 2009;102:168–78.
37. Shann KG, Likosky DS, Murkin JM, et al. An evidence-based review of the practice of cardiopulmonary bypass in adults: focus on neurologic injury, glycemic control, hemodilution and the inflammatory response. J Thorac Cardiovasc Surg. 2006;132:283–90.
38. Alghamdi AA, Albanna MJ, Guru V, Brister SJ. Does the use of erythropoietin reduce the risk of exposure to allogeneic blood transfusion in cardiac surgery? A systematic review and meta-analysis. J Card Surg. 2008;21:320–6.
39. Chu D, Wei L, Subramaniam K. AATS/STS critical care symposium April 27; 2014.
40. Wan S, LeClerc JL, Vincent JL. Inflammatory response to cardiopulmonary bypass. Chest. 1997;112:676–92.
41. Gravlee GP, Davis RF, Stammers AH, Ungerleider RM. Cardiopulmonary bypass: principles and practice, vol. 15. Philadelphia: Lippincot Williams & Wilkins; 2008. p. 321–37.
42. Edwards R, Treasure T, Hossein-Nia M, et al. A controlled trial of substrate-enhanced, warm reperfusion ("hot shot") versus simple reperfusion. Ann Thorac Surg. 2000;69(2):551–5.
43. Nussmeir NA. Management of temperature during and after cardiac surgery. Tex Heart Inst J. 2005;32:472–6.
44. Berberian G, Quinn TA, Kanter JP, et al. Optimized biventricular pacing in atrioventricular block after cardiac surgery. Ann Thorac Surg. 2005;80:870–5.
45. Denault AY, Haddad F, Jacobsohn E, Deschamps A. Perioperative rigft ventricular dysfunction. Curr Opin Anesth. 2013;26:1–7.
46. Nussmeier NA. Management of temperature during and after cardiac surgery. Tex Heart Inst J. 2005;32(4):472–6.
47. Brauer A, Weyland W, Kazmaier S, Trostdorf U, Textor Z, Hellige G, et al. Efficacy of postoperative rewarming after cardiac surgery. Ann Thorac Cardiovasc Surg. 2004;10(3):171–7.
48. Karalapillai D, Story D, Hart GK, Bailey M, Pilcher D, Cooper DJ, Bellomo R. Postoperative hypothermia and patient outcomes after elective cardiac surgery. Anaesthesia. 2011;66(9):780–4.
49. Struijis A, De Ruiter F, Weijerse A, Klein J, Bogers AJJC. Intravenous device feasible for controlled cooling and rewarming of individuals with abnormal body core temperature. Available at https://www.zoll.com/uploadedFiles/Public_Site/Core_Technologies/Temperature_management/rewarmingpostcabg.
50. Taguchi A, Ratnaraj J, Kabon B, Sharma N, Lenhardt R, Sessler DI, et al. Effects of a circulating-water garment and forced-air warming on body heat content and core temperature. Anesthesiology. 2004;100(5):1058–64.
51. Licker M, Schweizer A, Ralley FE. Thermoregulatory and metabolic responses following cardiac surgery. Eur J Anaesthesiol. 1996;13(5):502–10.
52. Licker M, Hohn L, Ralley FE. Relation between oxygen uptake and tissue oxygen extraction following cardiac surgery. Eur J Anaesthesiol. 1996;13(6):562–70.
53. De Witte J, Sessler DI. Perioperative shivering: physiology and pharmacology. Anesthesiology. 2002;96(2):467–84.
54. Kranke P, Eberhart LH, Roewer N, Tramer MR. Pharmacological treatment of postoperative shivering: a quantitative systematic review of randomized controlled trials. Anesth Analg. 2002;94(2):453–60.

55. Lenhardt R, Orhan-Sungur M, Komatsu R, Govinda R, Kasuya Y, Sessler DI, et al. Suppression of shivering during hypothermia using a novel drug combination in healthy volunteers. Anesthesiology. 2009;111(1):110–5.
56. Presciutti M, Bader MK, Hepburn M. Shivering management during therapeutic temperature modulation: nurses' perspective. Crit Care Nurse. 2012;32(1):33–42.
57. Despotis GJ, Hogue CW Jr. Pathophysiology, prevention and treatment of bleeding after cardiac surgery: a primer for cardiologists and an update for the cardioyhoracic theam. Am J Cardiol. 1999;83:15B–30B.
58. Mc Laughlin KE, Dunning J. In patients post cardiac surgery do high doses of protamine cause increased bleeding? Interact Cardiovasc Thorac Surg. 2003;2:424–6.
59. Spiess BD. Treating heparin resistance with antithrombin or fresh frozen plasma. Ann Thorac Surg. 2008;85:2153–60.
60. Bojar RM. Manual of perioperative care in adult cardiac surgery. 2011;9:347–73.
61. Henry D, Carless P, Fergusson D, Lanpacis A. The safety of aprotinin and lysine derived antifibrinolytic drugs in cardiac surgery: analysis. CMAJ. 2009;180:183–93.
62. Jalali A, Ghiari M, et al. Can plasma fibrinogen levels predict bleeding after coronary artery bypass grafting? Res Cardiovasc Med. 2014;3(3):e19521.
63. Chauchan S, Gharde P, Bisoi A, Kale S, Kiran U. A comparison of aminocaproic acid and tranexamic acid in adult cardiac surgery. Ann Card Anaesth. 2004;7:40–3.
64. Samantaray A, Hemanth N. Comparison of two ventilation modes in post-cardiac surgical patients. Saudi J Anaesth. 2011;5(2):173–8.
65. Itagaki S, Hosseinian L, Varghese R. Right ventricular failure after cardiac surgery: management strategies. Semin Thorac Cardiovasc Surg. 2012;24(3):188–94.
66. Haddad F, Doyle R, Murphy DJ, Hunt SA. Right ventricular function in cardiovascular disease, part II: pathophysiology, clinical importance, and management of right ventricular failure. Circulation. 2008;117(13):1717–31.
67. Winterhalter M, Antoniou T, Loukanov T. Management of adult patients with perioperative pulmonary hypertension: technical aspects and therapeutic options. Cardiology. 2010;116(1):3–9.
68. Fries D, Kozek-Langenecker S, Friesenecker B, Lorenz I. Comments on perioperative fluid therapy with tetrastarch and gelatin in cardiac surgery--a prospective sequential analysis. Crit Care Med. 2014;42(7):e537–8.
69. Engelman DT, et al. Impact of body mass index and albumin on morbidity and mortality after cardiac surgery. J Thorac Cardiovasc Surg. 1999;118:866–73.
70. De la Cruz KI, et al. Hypoalbuminemia and long-term survival after coronary artery bypass: a propensity score analysis. Ann Thorac Surg. 2011;91:671–6.
71. Lee EH, et al. Postoperative hypoalbuminemia is associated with outcome in patients undergoing off-pump coronary artery bypass graft surgery. J Cardiothorac Vasc Anesth. 2011;25:462–8.
72. Ernest D, et al. Distribution of normal saline and 5% albumin infusions in cardiac surgical patients. Crit Care Med. 2001;29:2291–302.
73. Jacob M, et al. The intravascular volume effect of Ringer's lactate is below 20%: a prospective study in humans. Crit Care. 2012;16:R86.
74. Navickis RJ, et al. Effect of hydroxyethyl starch on bleeding after cardiopulmonary bypass: a meta-analysis of randomized trials. J Thorac Cardiovasc Surg. 2012;144:223–30.
75. The SAFE Study Investigators. A comparison of albumin and saline for fluid resuscitation in the intensive care unit. N Engl J Med. 2004;350:2247–56.
76. Yunos NM, et al. Association between a chloride-liberal vs chloride-restrictive intravenous fluid administration strategy and kidney injury in critically ill adults. JAMA. 2012;308:1566–72.
77. Wiedermann CJ, Joannidis M. Chloride-restrictive fluid administration and incidence of acute kidney injury. JAMA. 2013;309:543.
78. Boldt J, Brosch C, Röhm K, Papsdorf M, Mengistu A. Comparison of the effects of gelatin and a modern hydroxyethyl starch solution on renal function and inflammatory response in elderly cardiac surgery patients. Br J Anaesth. 2008;100(4):457–64.
79. Gandhi GY, Nuttall GA, Abel MD, et al. Intensive intraoperative insulin therapy versus conventional glucose management during cardiac surgery: a randomized controlled trial. Ann Intern Med. 2007;146:233–43.
80. Boeken U, Feindt P, Litmathe J, Kurt M, Gams E. Intraaortic balloon pumping in patients with right ventricular insufficiency after cardiac surgery: parameters to predict failure of IABP support. Thorac Cardiovasc Surg. 2009;57(6):324–8. https://doi.org/10.1055/s-0029-1185766. Epub 2009 Aug 25.
81. Fischer S, Hoeper MM, Tomaszek S, et al. Bridge to lung transplantation with the extracorporeal membrane ventilator novalung in the veno-venous mode: the initial hannover experience. ASAIO J. 2007;53:168–70.
82. Cheung AW, White CW, Davis MK, Freed DH. Short-term mechanical circulatory support for recovery from acute right ventricular failure: clinical outcomes. J Heart Lung Transplant. 2014;33:794–9.

Right Heart Dysfunction in Liver Transplantation

50

Gabriela Droc and Ecaterina Scărlătescu

Abstract

The heart and the liver are closely related; there are diseases of the heart affecting the liver (cardiac cirrhosis) and illnesses of the liver that involve the heart and finally disorders implicating both the heart and the liver (hemochromatosis, amyloidosis, alcohol abuse). Involvement of the cardio-pulmonary system in chronic liver disease can manifest as different clinical syndromes implicating the right ventricle: cirrhotic cardiomyopathy, hepatopulmonary syndrome, portopulmonary syndrome. These problems complicate the perioperative management and the postoperative evolution of liver transplant patients. Cirrhotic cardiomyopathy is characterized by intrinsic alterations in myocardial function. Even if right ventricle dysfunction is not included in the diagnostic criteria of cirrhotic cardiomyopathy, right ventricular diastolic dysfunction is a frequent finding in patients with chronic liver disease. Hepatopulmonary syndrome is defined as a triad of chronic liver dysfunction, intrapulmonary vasodilatation and hypoxemia that worsens with the erect posture. Portopulmonary hypertension is the association of pulmonary with portal hypertension. It is a rare condition but a life threatening one. Cirrhotic patients will be at higher risk of right heart failure due to pulmonary hypertension as we deal with decreased right ventricular contractility in cirrhotic cardiomyopathy or dilatation of the right ventricle secondary to volume overload. Liver transplantation can ameliorate conditions as cirrhotic cardiomyopathy or hepatopulmonary syndrome but does not really influence portopulmonary hypertension and is contraindicated in the severe form.

Keywords

Cirrhotic cardiomyopathy · Hepatopulmonary syndrome · Portopulmonary hypertension Liver transplant

50.1 Introduction

The heart and the liver are closely related; diseases affecting the heart can determine cardiac cirrhosis or congestive hepatopathy or even ischemic hepatitis as a result of cardiogenic shock. Illnesses of the liver will eventually determine malfunctions in the cardiopulmonary system affecting the heart and the pulmonary circulation

G. Droc (✉)
University of Medicine and Pharmacy "Carol Davila", Bucharest, Romania

Department of Anesthesia and Intensive Care, Fundeni Clinical Institute, Bucharest, Romania

E. Scărlătescu
Department of Anesthesia and Intensive Care, Fundeni Clinical Institute, Bucharest, Romania

S. I. Dumitrescu et al. (eds.), *Right Heart Pathology*, https://doi.org/10.1007/978-3-319-73764-5_50

with secondary effects involving the right ventricle. There are also systemic disorders (hemochromatosis, amyloidosis), infective diseases (HIV infection, Hepatitis C virus), as well as alcohol abuse implicating both the heart and the liver [1].

Involvement of the cardio-pulmonary system in chronic liver disease can manifest as different clinical syndromes implicating the right ventricle (RV): Cirrhotic cardiomyopathy (CCM), Hepatopulmonary syndrome (HPS) and Portopulmonary hypertension (POPH) [2].

These complications of liver disease increase the risk of liver transplant and worsen the intra operative evolution and postoperative outcome of the patients. A better understanding of those entities will lead to a better prognostic for the patients.

50.2 Cirrhotic Cardiomyopathy and RV Dysfunction

In end-stage liver disease (ESLD) patients, cardiac dysfunction was first described in alcohol-related cirrhosis [3]; however, cardiac impairment despite a high resting cardiac output was later observed irrespective of the causes of liver cirrhosis [4]. This syndrome is known as cirrhotic cardiomyopathy, defined as chronic cardiac dysfunction in patients with cirrhosis characterized by blunted contractile responsiveness to stress and/or altered diastolic relaxation with electrophysiological abnormalities, in the absence of known cardiac disease [4]. The prevalence of this syndrome is unknown, as it is under diagnosed because of near normal cardiac function at rest [4]. However, data from literature describe signs of cardiac dysfunction in about 50% of cirrhotic patients undergoing liver transplantation and deaths caused by overt heart failure in 7–21% of patients after orthotopic liver transplantation [4].

50.2.1 Pretransplant Assessment

The pretransplant diagnosis of this syndrome is very important, in order to avoid acute cardiac failure after liver transplantation [5]. In patients waiting for liver transplant screening of cirrhotic cardiomyopathy should be made irrespective of their cirrhosis severity, assessed by MELD or Child score [5].

Diagnosing CCM can be difficult, as the splanchnic arteriolar vasodilatation and the overall reduction in systemic vascular resistance lead to an increased cardiac output in the typical cirrhotic patient, masking the cardiac dysfunction. This hyperdynamic pattern gives the appearance of a normal to increased cardiac performance and even clinically significant cirrhotic cardiomyopathy may not be recognized [2]. However, when the patient is subjected to stress such as an acute decompensation of the liver disease, bacterial infections, TIPS or liver transplantation, this high output cardiomyopathy is revealed, resulting in cardiac failure and pulmonary hypertension [2, 4]. Baseline cardiac output is high and cannot adapt to stress by a further increase.

Echocardiography is useful to detect the subclinical systolic dysfunction and diastolic dysfunction [6]. The deformation of the longitudinal fibers, which is an early sign of systolic dysfunction can be detected by the use of tissue Doppler echocardiography [6, 7]; this technique is also useful for the diagnosis of early diastolic dysfunction [6, 7]. Electrophysiologic anomalies in cirrhotic patients, such as the prolongation of the QT interval corrected for the heart rate, are usually detected using a 12 lead electrocardiography [6]. Prolongation of the corrected QT interval is considered to be the earliest sigh of CCM [4, 8]. Cardiac biomarkers, such as NT pro-BNP plasma levels, are raised in patients with liver cirrhosis, correlate with the severity of the liver disease, with left atrial dilatation and with diastolic dysfunction on echocardiography [6, 9]. The evaluation of different cardiac biomarkers may be a useful tool in screening patients for the presence of cirrhotic cardiomyopathy [10].

There is no doubt that RV dysfunction correlates with increased morbidity in different clinical settings. The echocardiographic assessment of the right heart can reveal subclinical RV dysfunction. However, echocardiographic studies in liver transplant candidates mainly focus on the diagnosis and assessment of wall motion abnormalities, POPH or intrapulmonary shunts [11]. There are only a few publications evaluating right ventricular function in patients with chronic

liver disease [12]. In a recent study, Lopez-Candales et al. demonstrated that ESLD patients had increased values for the tricuspid annular plane systolic excursion (TAPSE), tricuspid annular tissue Doppler systolic velocity and RV fractional area change compared to healthy controls [11]. It is unclear if the same normal ranges for echocardiographic assessment of RV function should be used in the particular setting of hyperdynamic circulation of cirrhotic patients [11].

Even if RV dysfunction is not included in the diagnostic criteria of CCM, right ventricular diastolic dysfunction is a frequent finding in patients with chronic liver disease [12]. In a study focusing on echocardiography findings in cirrhotic patients with HPS, Karabulut et al. demonstrated that right ventricular end-diastolic diameter, right ventricle free wall thickness and right atrium were increased in cirrhotic patients without HPS compared to controls [12]. Using Doppler, they also revealed right ventricle diastolic dysfunction (defined as tricuspid E/A < 1 or increased tricuspid dt corrected for age) in cirrhotic patients without HPS [12]. As opposite to LV diastolic dysfunction which is known to be associated with ascites in cirrhotic patients, Karabulut et al. found no correlation between RV diastolic dysfunction and ascites in their study [12].

In a retrospective post-mortem study analyzing a large number of autopsy reports, Wehmeyer et al. found increased incidence of right ventricular hypertrophy and dilatation in cirrhotic patients compared to controls [13].

In a small study comparing echocardiography findings in cirrhotic patients with healthy controls, Soyoral et al. reported right ventricle diastolic dysfunction and biatrial dilatation with increased pulmonary artery pressures in the group of patients with cirrhosis [14]. A recent study on 216 liver transplant patients demonstrated using multivariate regression analysis that the pretransplant degree of tricuspid regurgitation was associated with increased mortality and graft failure [15].

In conclusion, data from the literature suggest that right heart dysfunction may be under diagnosed in liver cirrhosis patients and could be associated with or included in the entity of cirrhotic cardiomyopathy. RV dysfunction can be present in cirrhotic patients even in the absence of LV systolic or diastolic dysfunction [12]. Efforts should be made to increase the clinicians' awareness for cardiac dysfunction in cirrhotic patients, especially in liver transplant candidates [16]. When a patient develops CCM, the cardiac evaluation including transthoracic echocardiography should be undertaken regularly (every 3 months) prior to transplantation [17]. Pretransplant diagnosis of cardiac dysfunction mandates intraoperative and postoperative cardiovascular monitoring and efforts for minimizing excessive fluctuations in preload and afterload in order to avoid acute decompensation [17]. Pretransplant diagnosis of an underlying latent cardiac failure could also be a decision factor in graft choice, as it was demonstrated poor graft survival in patients with LV diastolic dysfunction, making the initial quality of graft more important in this patient category [17, 18].

50.2.2 Intraoperative Management

Liver transplant is associated with significant hemodynamic fluctuations due to increased blood loss, third space fluid loss and major vessel clamping depending on the surgical technique used [17]. During liver transplantation, patients can develop pulmonary edema because of impaired cardiac function in conjunction with volume replacement [19].

The reperfusion phase of liver transplantation is often associated with significant hemodynamic instability and during this phase right ventricular failure is not uncommon; intraoperative monitoring using trans esophageal echocardiography (TEE) is useful for the early detection of right ventricular failure [17, 20]. TEE allows direct visualization of the heart chambers and can identify earlier RV dysfunction better than by using a pulmonary artery catheter. Due to increased RV compliance leading to significant dilatation, changes in pressure occur at later stages, thus the RV dysfunction diagnosis by pressure measurements is delayed [17, 20]. Rosendal et al. demonstrated higher values for RV volumes and stroke volume measured by thermodilution using a pulmonary artery catheter compared to three-dimensional trans esophageal echocardiography, and concluded that more research is needed regarding the most

valuable monitoring technique for RV assessment during liver transplant surgery [21].

During the reperfusion of the graft, the release of cold, ischemic, hyperkalemic components and of inflammatory cytokines from the graft leads to marked hemodynamic instability by further increasing vasodilatation and decreasing myocardial contractility [17]. In patients with CCM undergoing liver transplantation, the use of strategies to limit excessive variations of preload and afterload and to minimize the reperfusion syndrome, such as the careful correction of acid-base and of electrolytes disturbances and the use of high-quality grafts are extremely important [17].

50.2.3 Post-transplant Evolution

Cardiac alterations diagnosed in cirrhotic patients, such as blunted response to stress, diastolic dysfunction and a mild degree of increased ventricular wall thickness are completely reversible after liver transplantation, with significant improvement of heart function parameters between 6 and 12 months after transplant surgery [22]. The hyperdynamic pattern is reversed the first year after transplantation [23]. In their study, Torregrosa et al. reported that the hyperdynamic syndrome disappeared, both systolic and diastolic functions improved at rest and during exercise and ventricular wall thickness decreased after 6–12 months after liver transplant surgery [22]. Even if the time interval necessary for the complete reversal of hemodynamic anomalies is still under debate, it is agreed that both hyperdynamic syndrome and portal hypertension are corrected after liver transplantation [5]. The reversibility of RV dysfunction after liver transplantation has not been specifically addressed.

50.3 Hepatopulmonary Syndrome

50.3.1 Pretransplant Assessment

Hepatopulmonary syndrome (HPS) was first described in 1977 by Kennedy and Knudson [24]. It is defined as a triad of chronic liver dysfunction (usually liver cirrhosis, but it can also include other causes of portal hypertension), intrapulmonary vasodilatation and hypoxemia that worsens with the erect posture [25].

HPS is due to the effect of liver impairment on pulmonary vascular endothelium and decreased arteriolar resistance leading to the formation of pulmonary vascular shunts that allow non-oxygenated blood to reach the systemic circulation [2]. In patients with HPS at rest, the blood that shunts the functioning alveoli represents at least 20% of the cardiac output and this percentage increases with exercise [19]. In the most common type of HPS (Type 1), the shunts are found diffusely in the lungs and the patients improve their oxygenation with supplemental oxygen [2, 26]. HPS Type 2 is not as frequent as HPS type 1 and is characterized by the development of a discrete arteriovenous malformation and is nonresponsive to supplemental oxygen administration [2, 26].

Initially, liver transplantation was contraindicated in patients with HPS; however, considering the reversibility of this syndrome after transplantation and the lack of effective medical treatment, it is now agreed that transplantation constitutes the only effective treatment of HPS; thus, HPS became an indication for liver transplant [27].

The reported prevalence of HPS was between 5 and 32% of patients undergoing pretransplant assessment, depending on the criteria used for arterial hypoxemia [26]. The finding of the pulmonary shunts was more frequent than hypoxemia; in a study, Abrams et al. detected pulmonary shunts in 38.0% of cirrhotic patients and gas abnormalities only in 17.5% of them [28].

The diagnosis of hypoxemia is based on decreased arterial oxygen partial pressure or increased alveolo-arterial oxygen gradient in patients at rest in sitting position [26]. The use of the alveolo-arterial gradient allows earlier detection of hypoxemia than the arterial partial pressure of oxygen, as it compensates for hypocarbia and hyperventilation, often encountered in cirrhotic patients [26]. An alveolo-arterial oxygen gradient higher than 15 mmHg (or 20 mmHg if older than 64 years) while breathing room air in

sitting position is a positive finding for the diagnosis of HPS [2, 26]. The alveolo- arterial oxygen gradient is increased in all cases of HPS, but the partial pressure of oxygen (PaO_2) in arterial blood ranges from low values (less than 50 mmHg) to only mild decreased values (higher than 80 mmHg).

Based on the decrease in oxygen partial pressure, HPS was classified into four categories: mild (with $PaO_2 \geq 80$ mmHg), moderate (with PaO_2 between 60 and 80 mmHg), severe (with PaO_2 between 50 and 60 mmHg) and very severe (PaO_2 less than 50 mmHg) [25] (Table 50.1).

Intrapulmonary vasodilatation is revealed by positive findings on contrast-enhanced echocardiography or macro aggregated albumin lung perfusion scan (99mTc-MAA). Using agitated saline (in order to produce micro bubbles) infused into a peripheral vein, the appearance of micro bubbles in the pulmonary veins and then in the left atrium within three to six cardiac cycles after right-atrial opacification was demonstrated in HPS patients [25]. This test indicates the presence of pulmonary shunts, as micro bubbles cannot pass through normal pulmonary capillaries. The intracardiac shunt is suspected if the micro bubbles appear earlier in the left atrium (within less than 3 cardiac cycles) and in this case, trans esophageal echocardiography is recommended [25].

The pathophysiology of HPS is not completely understood, but it seems that mediators such as nitric oxide (NO) and carbon monoxide (CO) are involved in pulmonary shunt formation [25, 26, 29]. Another possible mechanism is the release of endothelial growth factor and other similar molecules associated with angiogenesis [26, 29]. The increase in the alveolo-arterial gradient and hypoxemia in HPS patients are caused by three main mechanisms. The first is ventilation-perfusion mismatch due to the dilatation of blood vessels perfusing the normally ventilated alveoli; this mechanism is present even in mild cases of HPS [26, 29]. The other two mechanisms are described in moderate or severe cases of HPS and are represented by the development of intrapulmonary shunts and the reduction in the lung's diffusing capacity for CO (DLCO) [26, 29].

Table 50.1 Staging of HPS

	PaO_2 (mmHg)
Mild	>80
Moderate	60–80
Severe	50–60
Very severe	<50

The main clinical manifestation of HPS is dyspnea both at rest and on exertion, but this is quite unspecific, as the causes of dyspnea in a patient with chronic liver disease are multiple [26]. A pathognomonic finding in HPS is platypnoea, meaning the worsening of dyspnea when the patients moves from the supine to standing position [25]. This is associated with the objective finding of a decrease in PaO_2 of at least 5% or 4 mmHg with patient movement from supine to standing (orthodeoxia) [25]. This phenomenon is explained by the increased perfusion in the bases of the lungs in the erect position and by the reduced capacity of pulmonary blood vessels to perform vasoconstriction in response to a change in body position in cirrhotic patients with HPS [29].

The European Respiratory Society Task Force published in 2004 the screening tests for HPS recommended in liver transplant candidates and in patients with chronic liver dysfunction and dyspnea [25]. In recent studies, pulse oximetry is recommended as a first screening tool before the evaluation of arterial blood gas analysis, being the preferred method for starting the screening, especially in children [29, 30]. Patients free of respiratory symptoms and with peripheral oxygen saturation (SpO_2) of at least 96% will undergo monitoring at 12 months interval using pulse oximetry [29]. For symptomatic patients or if the peripheral oxygen saturation is less than 96%, arterial blood gas analysis is recommended as the next step [29]. However, SpO_2 can overestimate arterial oxygenation in cirrhotic patients, thus the use of pulse oximetry as a screening tool can miss the diagnosis in mild cases of HPS [30, 31]. If the alveolo-arterial gradient is increased with or without coexisting hypoxemia, contrast enhanced echocardiography and a set of pulmonary tests are performed [25, 29]. A negative result of the contrast enhanced echocardiography rules out HPS and the focus should turn to other

respiratory tests in order to investigate another pulmonary disease [25, 29]. In patients with mild or moderate HPS ($PaO_2 \geq 60$ mmHg), periodic follow-up is recommended at 6 months interval [25, 29]. Patients with severe HPS should be included on the transplant waiting risk as high-priority; in patients with very severe HPS, liver transplantation is considered on an individual basis after a careful assessment of the benefit-risk ratio [25, 29].

50.3.2 Intraoperative Management and Post-transplant Evolution

The mortality of HPS patients without liver transplant is reported to be higher compared to patients with HPS undergoing transplantation [32]. A study by Swanson et al. estimated a survival at 5 years of only 23% in HPS patients without liver transplant compared to 76% in HPS patients with liver transplant [32]. Reported survival at 10 years after liver transplantation in HPS patients was 64% [33]. The mortality in HPS patients is not associated with the severity of the liver disease as assessed by MELD score [33]. For this reason, a MELD exception rule was recommended since January 2002 in order to increase graft allocation and to improve survival in patients with very severe HPS and no contraindication for liver transplant [29, 34]. In a large cohort of HPS patients followed for a 25 years period, Yver et al. reported improved survival of HPS in the MELD exception era (since January 2002) compared to patients transplanted before 2002 [33]. In their study, 30-day mortality in HPS patients after liver transplantation was 11% and no intraoperative deaths were reported [33]. In a recent study, Goldberg et al. analyzed the outcomes of a large number of HPS patients followed over 10 years (from 2002 to 2012), concluding that HPS patients with MELD exception- graft allocation had lower overall mortality compared with other patients awaiting liver transplantation [35]. Due to these findings, the MELD exception rule policy is now debated and new recommendations might appear in the near future [29].

In patients with HPS oxygenation improves within 12 months after liver transplantation; however, perioperative mortality is increased and hypoxemia is often described in the immediate post-transplant period [32]. This risk is increased especially in patients with pre-transplant PaO_2 less than 50 mmHg [32]. Hypoxemic respiratory failure in the immediate post-transplant period was described by Gupta et al. in 23.8% of patients with HPS undergoing liver transplantation; in their small series of 30 patients, 6 months survival was 100% [36].

Severe post-transplant hypoxemia is a major complication in HPS patients and is defined as hypoxemia requiring the administration of 100% inspiratory oxygen to maintain a saturation of at least 85% [37]. In HPS patients, severe hypoxemia was described in 6–21% of patients after liver transplant and is associated with a mortality rate of 45%, accounting for the majority of post-operative deaths in this patient population [38]. This complication usually occurs in the first 24 h after transplant and the proposed mechanism is vasoconstriction of the pulmonary vessels and redistribution of blood flow as an effect of different mediators released from the graft [37, 38]. Dilated pulmonary vessels constrict less than normal non dilated vessels, leading to an increased blood flow through the pulmonary shunts [38]. The treatment is applied with the purpose of reducing blood flow through the pulmonary shunts to correct hypoxemia; the goal is to allow time for the post-transplant reversal of HPS to take place [38]. Treatment options include: Trendelenburg positioning, inhaled epoprostenol or nitric oxide or intravenous methylene blue [38]. The last line of therapies includes embolization of abnormal pulmonary vessels or extracorporeal life support (ECLS) [37–39]. The treatment should be individualized in each patient, as the responses to therapy are different [38].

Severe hypoxemia can occur immediately after induction of anesthesia in HPS patients and in this case the use of the therapies mentioned above should be considered intra-operatively for maintaining oxygenation during the liver transplant procedure [38]. The use of advanced hemodynamic monitoring and fluid restriction are also

recommended [38]. However, data from literature show that hypoxemia most often occurs in the first three postoperative days after liver transplant in HPS patients [37].

In the context of severe post-transplant hypoxemia, the graft function could be impaired and the reversal of HPS manifestations delayed [38]. The function of marginal grafts exposed to hypoxemia is worsened and for this reason the use of marginal grafts should be considered carefully in HPS patients at risk for severe post-transplant hypoxemia [38].

The reversibility of HPS is rapid, with a 95.8% reversal after 6 months (in mild or moderate cases) and complete reversal 1 year after transplantation [29]. Hypoxemia is reversed more rapidly than intrapulmonary shunts, as it was demonstrated by means of contrast echocardiography follow-up after liver transplant [29, 36]. CO diffusion capacity improved after liver transplant, but not in all patients [40].

Ideally, patients at risk for developing severe hypoxemic failure after liver transplantation should be identified preoperatively in order to make the arrangements for providing the special care required. HPS patients usually require prolonged mechanical ventilation and extended ICU stay post-transplant [41].

50.4 Porto-Pulmonary Hypertension

Pulmonary hypertension (PAH) is defined by high blood pressure in the pulmonary arteries as a consequence of vasoconstriction and thickening of the blood vessel's wall; the right heart will work under stress resulting in the end in right heart failure. Cirrhotic patients will be at higher risk of right heart failure due to PAH as we deal with decreased RV contractility in cirrhotic cardiomyopathy or dilatation of the RV secondary to volume overload [42].

POPH is defined as the association of PAH with portal hypertension. It is a rare condition but a life threatening one. The incidence of POPH in cirrhotic patients waiting for LT is 5.3–6.3% and is associated with female sex and autoimmune liver disease [43].

There is no linear correlation between PAH and the severity of the liver disease or between PAH and the severity of portal hypertension [44].

The pathophysiology of this syndrome is not yet very well understood but the pathological findings are similar to those of PAH of any origin. At first there is endothelial dysfunction with vasoconstriction of the pulmonary vessels reversible under medication, and then histopathological changes will progress leading to the narrowing of the vascular lumen, superimposed microthrombosis will narrow the vessel even more or even occlude it [42].

Diagnostic criteria are: mean arterial pulmonary pressure (mPAP) greater than 25 mmHg at rest and pulmonary vascular resistance (PVR) greater than 240 dyn s cm^{-5} with a pulmonary capillary wedge pressure (PCWP) less than 15 mmHg (Table 50.2). The transpulmonary gradient >12 mmHg (difference between the mPAP and the pulmonary arteriolar occlusion pressure) reflects obstruction to flow and differentiates the contribution of volume and resistance to the increase in mPAP [2].

In cirrhotic patients as a result of their hyperdynamic circulation and volume overload the mPAP can be elevated but with no increase in PVR which is inconsistent with the diagnosis of POPH [45, 46].

POPH is associated with 1 year poor survival without treatment and patients might die of right ventricular failure [46].

50.4.1 Pretransplant Assessment

All candidates for LT will undergo evaluation for POPH. Early clinical symptoms include dyspnea, palpitations, chest pain and signs of RV dysfunc-

Table 50.2 Diagnosis and staging of POPH

	mPAP (mmHg)	PVR (dyne s cm^{-5})
Diagnosis	>25	>240
Severity		
Mild	25–34	240–500
Moderate	35–44	500–800
Severe	>45	>800

tion as peripheral edema or jugular vein distension. All the signs however are non-specific. The chest x ray may show cardiomegaly and enlarged pulmonary arteries and possibly right bundle branch block or first degree atrio-ventricular block on the ECG, signs of right heart strain [42, 45]. RV insufficiency might determine elevation of BNP (B-type natriuretic peptide) and NT proBNP (N terminal proBNP).

The screening will start with a non-invasive method: transthoracic Doppler echocardiography (TTE) [47]. It does require the presence of a tricuspid regurgitant jet to evaluate the systolic pulmonary artery pressure (sPAP). The right ventricular systolic pressure (RVSP) is estimated to be equivalent to sPAP if no pulmonic stenosis or RV ventricular outflow tract obstruction [45]. A TTE showing normal values for sPAP rule out the POPH [44].

This method has a 97% sensitivity and 77% specificity for the diagnostic of moderate and severe POPH. If the value of RVSP exceeds 50 mmHg the next step will be right heart catheterization to measure pulmonary hemodynamics [42].

Right heart catheterization (RHC) is the gold standard for POPH diagnosis [1]. Indications for RHC are: RVSP greater than 50 mmHg, the presence of right atrial enlargement, the presence of RV enlargement or reduced systolic function of the RV. Some transplant centers consider RCH for RSVP greater than 40 mmHg. During RHC and direct measurement of pressures an acute vasodilator challenge with nitric oxide or intravenous epoprostenol; a positive answer will help staging severity [45].

While on the waiting list patients should be reevaluated for evolution of POPH at 6 or some authors suggest even 12 months; the optimal interval isn't yet clear [46].

In evaluating POPH it is very import not only to measure the pressures in the pulmonary arteries but also to evaluate the RV function. The success of the LT will depend on the capacity of the RV to deal with blood volume shifts and increases in PVR during surgery.

Most centers worldwide consider severe POPH as an absolute contraindication to LT; some consider even moderate POPH as a contraindication especially if it won't respond to medical treatment and have an impaired RV function.

Medical treatment might improve POPH as to make LT possible. Medication choices are: prostacyclin analogs (intravenous epoprostenol, intravenous or subcutaneous treprostinil, inhaled iloprost), phosphodiesterase 5 inhibitors (oral sildenafil) or endothelin receptor antagonists (oral bosentan) [46].

The success of the LT will not depend solely on the mPAP value but also on the quality of the RV function. A compromised RV will lead to liver congestion and poor graft function [42].

Patients presenting with mild or moderate form of POPH don't have an absolute contraindication to liver transplant but they still have an elevated perioperative mortality as high as 33–35% [48].

50.4.2 Intraoperative Issues

Each of the three stages of liver transplant surgery has its own hemodynamic challenges: during the pre-anhepatic phase the main risk is significant blood loss and reduction in the preload, in the anhepatic phase due to cross clamping there is a reduction of cardiac output than can reach 50% and the neohepatic phase will start with reperfusion of the new graft with hemodynamic instability as a result of hyperkalemia, and a variety of inflammatory and vasodilatatory mediators.

Hemodynamic monitoring needs to be invasive. As a special consideration to patients with POPH the use of pulmonary artery catheter (PAC) is mandatory. PAC is the only monitoring method that measures directly the pulmonary arterial pressures. If mPAP measured by PAC in the operating room is greater than 50 mmHg before incision, cancelation of the procedure is recommended [46]. In some centers [44] a RHC is performed on the anesthesia setting before the patient enters the operating room for transplant procedure and according to the pressure values the team decides whether or not to proceed to LT.

Specific therapy targeting pulmonary artery pressure is recommended during the whole transplant intervention [46].

To continuously evaluate RV function during surgery transesophageal echocardiography (TEE) is of use. TEE assesses in real time the preload of both left and right side of the heart and at the same time allows for detection of myocardial ischemia expressed by wall motion abnormalities. When the intravascular volume increases due to fluid overload the RV dilates resulting in no significant change in central venous pressure but the extra intravascular fluid determines liver congestion and might impair graft function [48].

During reperfusion of the liver there will be a sudden increase in intravascular volume as well as a release of cold fluid, cytokines and products of anaerobic metabolism that may worsen POPH syndrome by an acute rise in pulmonary artery pressure. The vasoconstriction of the pulmonary vessels will precipitate acute RV failure and determine liver congestion and delayed graft function or even graft failure [49]. A large number of interventions have been described: use of nitric oxide, intravenous prostacycline, milrinone to treat RV failure, ECMO [46].

Worse cases of cirrhosis with severe POPH may benefit from combined liver and lung transplantation [48, 50].

50.4.3 Post-transplant Evolution

POPH may improve, stabilize or even worsen after LT [43]. The evolution is highly impredictible [44]. Mortality remains pretty high: if preoperatively mPAP > 50 mmHg mortality is almost 100% making those patients unfit for LT. In case of values of mPAP of 35–50 mmHg mortality risk is as high as 50% [48]. With mild POPH survival of the patients is the same as of all other LT recipients.

If treated before with vasodilators transplant patients evolution is better. Pulmonary hypertension medication should be maintained posttransplant and POPH monitored with transthoracic Doppler echocardiography.

De novo development of POPH post LT has also been reported [46].

Conclusion

In summary the RV plays a key role in the ESLD patient and during liver transplant. His dysfunction must be recognized, quantified and monitored for a better understanding of the patients evolution while on the waiting list or during the transplantation procedure, a stressful hemodynamic period. He might be affected by the hyperdynamic syndrome of the cirrothic patient, the fluid overload, the cirrhotic cardiomyopathy or by the strain imposed by elevated pulmonary pressures in the portopulmonary syndrome. The postoperative evolution of those patients will also depend on a better understanding of RV behavior.

References

1. Moller S, Bernardi M. Interactions of the heart and the liver. Eur Heart J. 2013;34:2804–11.
2. Ramsay M. Cardiopulmonary disease in the liver transplant patient: the role of Doppler echocardiography. In: Fleming RM, editor. Establishing better standards of care in Doppler echocardiography, computed tomography and nuclear cardiology. Rijeka: InTech; 2011. p. 11.
3. Kowalski HJ, Abelmann WH. The cardiac output at rest in Laennec's cirrhosis. J Clin Invest. 1953;32(10):1025–33.
4. Zardi EM, Abbate A, Zardi DM, Dobrina A, Margiotta D, Van Tassell BW, et al. Cirrhotic cardiomyopathy. J Am Coll Cardiol. 2010;56(7):539–49.
5. Zardi EM, Zardi DM, Chin D, Sonnino C, Dobrina A, Abbate A. Cirrhotic cardiomyopathy in the pre- and post-liver transplantation phase. J Cardiol. 2016;67(2):125–30.
6. Licata A, Novo G, Colomba D, Tuttolomondo A, Galia M, Camma C. Cardiac involvement in patients with cirrhosis: a focus on clinical features and diagnosis. J Cardiovasc Med (Hagerstown). 2016;17(1):26–36.
7. Kazankov K, Holland-Fischer P, Andersen NH, Torp P, Sloth E, Aagaard NK, et al. Resting myocardial dysfunction in cirrhosis quantified by tissue Doppler imaging. Liver Int. 2011;31(4):534–40.
8. Bernardi M, Maggioli C, Dibra V, Zaccherini G. QT interval prolongation in liver cirrhosis: innocent bystander or serious threat? Expert Rev Gastroenterol Hepatol. 2012;6(1):57–66.
9. Licata A, Corrao S, Petta S, Genco C, Cardillo M, Calvaruso V, et al. NT pro BNP plasma level and atrial volume are linked to the severity of liver cirrhosis. PLoS One. 2013;8(8):e68364.

10. Wong F, Siu S, Liu P, Blendis LM. Brain natriuretic peptide: is it a predictor of cardiomyopathy in cirrhosis? Clin Sci. 2001;101(6):621–8.
11. López-Candales A, Menendez FL, Shah SA, Friedrich A. Measures of right ventricular systolic function in end stage liver disease patients awaiting transplant. Int J Cardiol. 2014;171(2):277–8.
12. Karabulut A, Iltumur K, Yalcin K, Toprak N. Hepatopulmonary syndrome and right ventricular diastolic functions: an echocardiographic examination. Echocardiography. 2006;23(4):271–8.
13. Wehmeyer MH, Heuer AJ, Benten D, Puschel K, Sydow K, Lohse AW, et al. High rate of cardiac abnormalities in a postmortem analysis of patients suffering from liver cirrhosis. J Clin Gastroenterol. 2015;49(10):866–72.
14. Soyoral Y, Süner A, Kidir V, Aritürk Z, Balakan O, Değertekin H. The effects of viral cirrhosis on cardiac ventricular function. Eur J Gen Med. 2004;1(2):15–8.
15. Kia L, Shah SJ, Wang E, Sharma D, Selvaraj S, Medina C, et al. Role of pretransplant echocardiographic evaluation in predicting outcomes following liver transplantation. Am J Transplant. 2013;13(9):2395–401.
16. Chen Y, Chan AC, Chan SC, Chok SH, Sharr W, Fung J, et al. A detailed evaluation of cardiac function in cirrhotic patients and its alteration with or without liver transplantation. J Cardiol. 2016;67(2):140–6.
17. Rahman S, Mallett SV. Cirrhotic cardiomyopathy: implications for the perioperative management of liver transplant patients. World J Hepatol. 2015;7(3):507–20.
18. Mittal C, Qureshi W, Singla S, Ahmad U, Huang MA. Pre-transplant left ventricular diastolic dysfunction is associated with post transplant acute graft rejection and graft failure. Dig Dis Sci. 2014;59(3):674–80.
19. Sawant P, Vashishtha C, Nasa M. Management of cardiopulmonary complications of cirrhosis. Int J Hepatol. 2011;2011:280–569.
20. Burtenshaw AJ, Isaac JL. The role of transoesophageal echocardiography for perioperative cardiovascular monitoring during orthotopic liver transplantation. Liver Transpl. 2006;12(11):1577–83.
21. Rosendal C, Almamat Uulu K, De Simone R, Wolf I, Deckert A, Martin EO, et al. Right ventricular function during orthotopic liver transplantation: three-dimensional transesophageal echocardiography and thermodilution. Ann Transplant. 2012;17(1):21–30.
22. Torregrosa M, Aguade S, Dos L, Segura R, Gonzalez A, Evangelista A, et al. Cardiac alterations in cirrhosis: reversibility after liver transplantation. J Hepatol. 2005;42(1):68–74.
23. Navasa M, Feu F, Garcia-Pagan JC, Jimenez W, Llach J, Rimola A, et al. Hemodynamic and humoral changes after liver transplantation in patients with cirrhosis. Hepatology. 1993;17(3):355–60.
24. Kennedy TC, Knudson RJ. Exercise-aggravated hypoxemia and orthodeoxia in cirrhosis. Chest. 1977;72(3):305–9.
25. Rodriguez-Roisin R, Krowka MJ, Herve P, Fallon MB. Pulmonary-hepatic vascular disorders (PHD). Eur Respir J. 2004;24(5):861–80.
26. Rodríguez-Roisin R, Krowka MJ. Hepatopulmonary syndrome — a liver-induced lung vascular disorder. N Engl J Med. 2008;358(22):2378–87.
27. Krowka MJ. Hepatopulmonary syndrome: recent literature (1997 to 1999) and implications for liver transplantation. Liver Transpl. 2000;6(4 Suppl 1):S31–5.
28. Abrams GA, Jaffe CC, Hoffer PB, Binder HJ, Fallon MB. Diagnostic utility of contrast echocardiography and lung perfusion scan in patients with hepatopulmonary syndrome. Gastroenterology. 1995; 109(4):1283–8.
29. Grilo-Bensusan I, Pascasio-Acevedo JM. Hepatopulmonary syndrome: what we know and what we would like to know. World J Gastroenterol. 2016;22(25):5728–41.
30. Kochar R, Tanikella R, Fallon MB. Serial pulse oximetry in hepatopulmonary syndrome. Dig Dis Sci. 2011;56(6):1862–8.
31. Abrams GA, Sanders MK, Fallon MB. Utility of pulse oximetry in the detection of arterial hypoxemia in liver transplant candidates. Liver Transpl. 2002;8(4):391–6.
32. Swanson KL, Wiesner RH, Krowka MJ. Natural history of hepatopulmonary syndrome: impact of liver transplantation. Hepatology. 2005;41(5):1122–9.
33. Iyer VN, Swanson KL, Cartin-Ceba R, Dierkhising RA, Rosen CB, Heimbach JK, et al. Hepatopulmonary syndrome: favorable outcomes in the MELD exception era. Hepatology. 2013;57(6):2427–35.
34. Fallon MB, Mulligan DC, Gish RG, Krowka MJ. Model for end-stage liver disease (MELD) exception for hepatopulmonary syndrome. Liver Transpl. 2006;12(12 Suppl 3):S105–7.
35. Goldberg DS, Krok K, Batra S, Trotter JF, Kawut SM, Fallon MB. Impact of the hepatopulmonary syndrome MELD exception policy on outcomes of patients after liver transplantation: an analysis of the UNOS database. Gastroenterology. 2014;146(5):1256–65.e1.
36. Gupta S, Castel H, Rao RV, Picard M, Lilly L, Faughnan ME, et al. Improved survival after liver transplantation in patients with hepatopulmonary syndrome. Am J Transplant. 2010;10(2):354–63.
37. Nayyar D, Man HS, Granton J, Gupta S. Defining and characterizing severe hypoxemia after liver transplantation in hepatopulmonary syndrome. Liver Transpl. 2014;20(2):182–90.
38. Nayyar D, Man HSJ, Granton J, Lilly LB, Gupta S. Proposed management algorithm for severe hypoxemia after liver transplantation in the hepatopulmonary syndrome. Am J Transplant. 2015;15(4): 903–13.
39. Fleming GM, Cornell TT, Welling TH, Magee JC, Annich GM. Hepatopulmonary syndrome: use of extracorporeal life support for life-threatening hypoxia following liver transplantation. Liver Transpl. 2008;14(7):966–70.
40. Pascasio JM, Grilo I, Lopez-Pardo FJ, Ortega-Ruiz F, Tirado JL, Sousa JM, et al. Prevalence and severity of hepatopulmonary syndrome and its influence on survival in cirrhotic patients evaluated for liver transplantation. Am J Transplant. 2014;14(6):1391–9.

41. Fauconnet P, Klopfenstein CE, Schiffer E. Hepatopulmonary syndrome: the anaesthetic considerations. Eur J Anaesthesiol. 2013;30(12):721–30.
42. Ramsay M. Portopulmonary hypertension and right heart failure in patients with cirrhosis. Curr Opin Anesthesiol. 2010;23:145–50.
43. Stauber RE, Olschewski H. Portopulmonary hypertension: short review. Eur J Gastroenterol Hepatol. 2010;22(4):385–90.
44. Aldenkortt F, Aldenkortt M, Caviezel L, Waeber JL, Weber A, Schiffer E. Portopulmonary hypertension and hepatopulmonary syndrome. World J Gastroenterol. 2014;20(25):8072–81.
45. Al-Naamani N, Roberts KE. Portopulmonary hypertension. Clin Chest Med. 2013;34:719–37.
46. Krowka MJ, Fallon MB, Kawut SM, Fuhrmann V, Heimbach JK, Ramsay MAE, Sitbon O, Sokol RJ. International liver transplant society guidelines: diagnosis and management of hepatopulmonary syndrome and portopulmonary hypertension. Transplantation. 2016;100(7):1440–52.
47. Zaky A, Lang JD. Cardiac dysfunction in liver transplantation. Austin J Anesth Analg. 2014;2(1):1007.
48. Rudnick MR, De Marchi L, Plotkin JS. Hemodynamic monitoring during liver transplantation: a state of the art review. World J Hepatol. 2015;7(10):1302–11.
49. Mangus RS, Kinsella SB, Marshall GR, Fridell JA, Wilkes KR, Tector AJ. Mild to moderate pulmonary hypertension in liver transplantation. J Surg Res. 2013;184:1150–6.
50. Grannas G, Neipp M, Hoeper M, Gottlieb J, Lück R, Becker T, Simon A, Strassburg CP, Manns MP, Welte T, Haverich A, Klempnauer J, Nashan B, Strueber M. Indications for and outcomes after combined lung and liver transplantation: a single center experience on 13 consecutive cases. Transplantation. 2008;85:524–31.

The Impact of Pneumonectomy on the Right Ventricular Function

51

Claudiu Nistor, Adrian Ciuche, Dragoş Săvoiu, Olivia Batog, and Ecaterina Bontaş

Abstract

Notably, pulmonary resection is used in much pathology and more frequently during last years, especially due to the increased incidence of the cases diagnosed with lung cancer. Pulmonary resection surgery varies from the detachment of a lung region (atypical resections, segmentectomy, lobectomy or bilobectomy) to complete unilateral pulmonary removing (pneumonectomy). Left pneumonectomy is usually better tolerated than right pneumonectomy and some authors further said that "the right pneumonectomy was a disease itself". Only that, this procedure has a proven impact on the heart function, particularly on the right ventricle performance. There is no doubt that pneumonectomy has consequences on the cardiac performance expressed by preload and afterload changes, as well as contractility adjustment by progressive dilatation of the right ventricle. Repercussions on the right ventricle function are the increase or reduction in volume or flow. Evaluation techniques are multiple but currently the mechanism of adaptation of the right ventricle to the conditions of pneumonectomy it is not precisely acknowledged. Deterioration of the right ventricle function begins after 6 months and is progressive to heart failure. Lobectomy and segmentectomy have fewer changes in the right ventricle performance due to the higher functional lung parenchyma remainder.

Keywords

Pneumonectomy · Segmentectomy · Lobectomy · Right ventricle dysfunction · Right ventricle treatment · Right heart · Pulmonary resection · Video-assisted thoracic surgery · Wedge resections · Lung resection

C. Nistor (✉)
"Carol Davila" University of Medicine and Pharmacy, Bucharest, Romania

Thoracic Surgery Department, "Carol Davila" Central Military Emergency University Hospital, Bucharest, Romania

A. Ciuche
Thoracic Surgery Department, "Carol Davila" Central Military Emergency University Hospital, Bucharest, Romania

D. Săvoiu
Cardiology Department, "Carol Davila" Central Military Emergency University Hospital, Bucharest, Romania

O. Batog
Thoracic Surgery Department, Oncology Institute "Alexandru Trestioreanu", Bucharest, Romania

E. Bontaş (✉)
Department of Cardiology, "Prof. C.C. Iliescu" Emergency Institute for Cardiovascular Diseases, Bucharest, Romania

S. I. Dumitrescu et al. (eds.), *Right Heart Pathology*, https://doi.org/10.1007/978-3-319-73764-5_51

51.1 Introduction

Historically, the first successful pneumonectomy was carried out by Graham and Singer at Barnes Hospital in St. Loius in 1933 [1, 2]. Later, lung resections such as lobectomies and segmentectomies were stated in the 1940s and 1950s followed by the first successful sleeve lobectomy for carcinoma in 1952 [3, 4]. Finally, the progress of surgical sutures and staplers in parallel with the development of specialised thoracic units and thoracic anaesthesia made lung resection be secure, more rapidly with a reduced amount of trauma, whereas surgical oncological rules are applied. Presently, surgeons apply broaden cancer resections to the chest wall and great vessels [5]. Nonetheless, improvements of new minimally invasive techniques permit surgeons to carry on lung resections even on patients with important cardiopulmonary comorbidities, patients with deficient pulmonary function or elderly patients [6].

Pulmonary resection surgery varies from the detachment of a lung region (atypical resections, segmentectomy, lobectomy or bilobectomy) to complete unilateral pulmonary removing (pneumonectomy). Only that, this procedure has a proven impact on the heart function, particularly on the right ventricle (RV) performance [7–10].

Notably, pulmonary resection is used in numerous pulmonary pathologies and quite often during last years, especially due to the increase of the incidence of diagnosed patients with lung cancer. It has to be underlined, that in case of patients with cancer, pneumonectomy is performed within oncological indications and it represents the best known method of treatment acknowledged until today for this serious illness.

Undoubtedly, as mentioned previously, the most frequent indications for lung resection is non-small cell lung cancer (NSCLC) [2]. Definitively, lung surgery is a vital stage in the complex therapy of patients with progressive lung cancer (stage III and IV) [6]. Other causes for pneumonectomy include pulmonary metastatic disease, pulmonary emphysema, inflammatory and infectious lung disease, secondary to thoracic trauma or because of congenital abnormalities of the lung (Table 51.1) [2, 11].

Table 51.1 Indications of pneumonectomies for benign disease

Indications	$N = 321$	Percent
Infection/abscess	114	37.1
Tuberculosis	47	15.3
Bronchiectasis	41	13.3
Aspergillus	33	10.7
Haemorrhage	26	8.5
Benign tumour	20	6.5
Rare indications: less than 2%		
Trauma	6	1.9
Congenital malformation	5	1.6
Emphysema	5	1.6
Radiation-induced lung damage	4	1.3
Marginal indications: less than 1%		
Candidosis	2	0.6
Silicosis/asbestosis	2	0.6
Sarcoidosis	1	0.3
Mucoviscidosis	1	0.3
Missing data	14	4.4

From Rivera et al. [11] with permission

Also, congenital disorders that need pneumonectomy in childhood comprise complicated cystic adenomatoid malformation of one lung, complicated hypoplastic lung, and chronic esophagobronchial communication with recurrent infections [12].

To sum up, pneumonectomies are the most frequent recommended surgery in lung cancer, however in case of benign lesions (Table 51.1) pneumonectomies are used only when there is no another alternative of treatment.

51.2 Perioperative and Postoperative Risk Stratification in Pneumonectomies

Pneumonectomy is associated with higher risk of postoperative morbidity and mortality, however after surgery there is a good long-lasting survival and good quality of life [2].

Risk stratification for death in thoracic surgery was rather simple until recently [13]. Within the period 2002–2007, the National Lung Cancer Audit (UK) reported 30-day mortality for pneumonectomy of 5.8% in comparison with the Society

of Thoracic Surgeons (STS) database that had the in-hospital mortality for pneumonectomy of 5.6% [14]. On the other side, the European Society of Thoracic surgeons (ESTS) risk model presented 3426 patients with 66 deaths and the Veterans Affairs risk model had 3516 patients with 184 deaths [15, 16]. Later, the French Society of Thoracic and Cardiovascular Surgery and the Society of Thoracic Surgeons (STS) formed based on databases with more than 15,000 patients each, "risk-adjustment models" to recognize predictors of mortality and most important complications caused by lung resections [17, 18]. These "risk-adjustment models" may help in clinical evaluation and to assess "risk-adjusted outcomes for quality improvement purposes" [6].

51.2.1 Perioperative Risk Stratification

Preoperative physiologic evaluation should comprise a cardiovascular examination, and spirometry tests to assess FEV1 and the diffusing capacity of carbon monoxide (DLCO) [19]. Firstly, respiratory evaluation by spirometry indexes as forced expired volume (FEV1) and diffusing lung carbon monoxide capacity (DLCO) should be determined. Evaluation of lung function is significant to analyse and approximate the risk of in-hospital mortality (i.e. respiratory failure). Nonetheless, it is important to appreciate the influence of lung resection on quality of life (i.e. long-term dyspnoea, permanent oxygen therapy). In case of FEV1 and DLCO are >60% from predicted value, there is a low risk for complications and lung or pulmonary resection can be done. If FEV1 and DLCO are <60% of predicted value, a quantitative lung scan is compulsory [20]. As already acknowledged as universal rule, it is established that a FEV1 of 40% of the predicted value was the cut-off for doing lung resection [21].

The risk of **perioperative complications** and death can be stratified by $V'O_2$max. If the exercise testing shows maximal oxygen uptake ($V'O_2$max) of >15 mL/kg, pulmonary surgery can be carry out, however if $V'O_2$max is <15 mL/kg, the surgery is forbidden [20]. Patients with a $V'O_2$max > 20 mL kg^{-1} min^{-1} are not at increased risk of complications or death; $V'O_2$max < 15 mL kg^{-1} min^{-1} indicates an increased risk of perioperative complications and $V'O_2$max < 10 mL kg^{-1} min^{-1} indicates a very high risk of perioperative complications and death [22]. Typically, patients who cannot go up a "flight of stairs" have a $V'O_2$max of 10 mL kg^{-1} min^{-1}. "Desaturation during exercise has been associated with an increased risk of perioperative complications" [22]. Clearly, all these tests has to be understood cautiously and the thoracic surgeon must do not overlook other anatomical factors like the weight and size of patients, the existence of a shunt and of correctable emphysema [6]. According to previously observations, patients with very poor lung function can endure lung resection associated with lung volume reduction. It is an exceptionally situation in patients with severe heterogeneous emphysema, especially when emphysema is restricted to the lobe enclosing the cancer [22]. In this case, it is rational to apply the criteria to choose patients for lung volume reduction surgery, with a lower limit of preoperative FEV1 or DLCO >20% predicted [13].

It seems that myocardial infarction is a most important cause of mortality after non-cardiac surgery and lung resection should be forbidden within 30 days of myocardial infarction [13]. In case of patients with stable angina, surgical revascularisation or coronary stenting would be discussed with a cardiologist preceding thoracic surgery [13]. Patients with good cardiac function and less than two risk factors can undergo surgery with no additional investigations. Cardiologic exam is compulsory in patients with over three risk factors or poor cardiac function [13]. Obviously, the pharmacological therapy in ischaemic heart disease before lung surgery should be optimised with anti-ischaemic treatment including aspirin, statins and β-blockers in the perioperative period [13].

To sum up, if both % ppo-FEV1 and %ppo-DLCO values are ≧60%, the patient has a low risk for anatomic lung resection. If both parameters are <60% of the predicted value, screening will continue with an exercise test. Also, if the execution of the exercise test is adequate, the patient is considered to have a low risk for anatomic lung resection [19].

51.2.2 Postoperative Risk Stratification

Quantitative ventilation and perfusion scintigraphy, quantitative CT scanning and dynamic perfusion MRI must be used to predict postoperative lung function [6]. Beckles et al. [22] suggests a various cardiopulmonary exercise tests to be applied routinely by thoracic surgeons to make easier the calculation of the risk of postoperative dyspnoea [22]. These comprise "stair climbing (usually two flights of stairs), 6 and 12 min walk tests, shuttle walk test and formal cardiopulmonary exercise testing with measurement of maximal oxygen uptake ($V'O_2$max)" [22]. Moreover, significant basic science work sustains the role of transfer factor as predictor of postoperative morbidity despite normal spirometry [23]. Therefore, a postoperative FEV1 or DLCO <40% suggests even an amplified risk of perioperative complications, including death, following lung cancer resection [22].

In case of patients with pulmonary resection with prophylactic diaphragm plication, the predicted postoperative lung function is related directly with the postoperative determined FEV1, FVC and gas transfer factor [24]. If it is of note, if transection of the phrenic nerve happens during lung resection and it is documented during surgery, prophylactic diaphragm plication is recommended [24].

On the whole, the postoperative pulmonary function depends on the size of parenchymal resection, location of resection, thoracotomy procedure, the severity of pulmonary emphysema and/or the postoperative progression of pulmonary fibrosis. Intriguingly, the postoperative pulmonary function carries on getting better during the first postoperative year the same as if the remaining parenchyma grows, however the mechanisms of this adaptable reaction is not established [25].

Postoperative lung function is estimated by the method of segment counting [21]. Lang-Lazdunski [6] made a very simple summary of "the method of segment counting". The total number of segments is 19 (9 left, 10 right). The number of segments obstructed (O) is measured by imaging (chest CT) and subtracted from 19 to obtain the number of functioning segments (T): T = 19-O. The residual number of segments (R) is estimated as: R = T—functioning segments to be resected. Typically, the number of segments per lobe is: right upper lobe n = 3, middle lobe n = 2, right lower lobe n = 5, left upper lobe n = 5, left lower lobe n = 4. The predicted postoperative (ppo) lung function is estimated by:

$$\text{ppo} = \left(\text{preoperative value} / \text{T}\right) \cdot \text{R}$$

Predicted postoperative (ppo) lung functions should be determined.

Postoperative respiratory complications are the most common, and preoperative respiratory disorders increase their frequency [26]. Established post-pneumonectomy complications comprise post pneumonectomy syndrome, bronchopleural fistula formation, cardiac herniation and recurrent pneumothorax [5]. Another important acknowledged postoperative complication after lung resection is acute respiratory distress syndrome (ARDS) [27]. It is defined by the acute beginning of hypoxemia with radiographic infiltrates consistent with pulmonary edema, but with no increases of the pulmonary capillary wedge pressure (PCWP) [27]. It is noteworthy that numerous studies showed that 2–5% of patients with lung resection could acquire ARDS with different degrees, and the mortality from ARDS following pulmonary resection is still elevated [27]. Importantly, ARDS following thoracotomy and lung resection has a poor prognosis with in-hospital mortality rates over 25% [27]. Presently, there is no acceptable predictor of postoperative cardiopulmonary complications, therefore postoperative morbidity and mortality are unchanged from a decade [26]. Only that, this procedure has a proven impact on the heart function, particularly on the RV performance [7–10].

51.3 The Technique of Pneumonectomy

The technique of pneumonectomy has known many evolutionary stages and unsuccessful attempts, until the current version that is today unanimously acknowledged and performed. The progress of the thoracic surgeon pioneers being helped by the

simultaneous progress of other specialities such as anesthesiology, cardiology, pneumonology, X-ray, including the development of antibiotherapy and blood transfusion techniques. Pulmonary resection surgery varies from the detachment of a lung region (atypical resections, segmentectomy, lobectomy or bilobectomy) to complete unilateral pulmonary removing (pneumonectomy). Surgical approach is usually thoracotomy, sternotomy and VATS.

Nonetheless, improvements of new minimally invasive techniques permit surgeons to carry out lung resections even on patients with important cardiopulmonary comorbidities, patients with deficient pulmonary function or elderly patients [6].

Pneumonectomy is the resection of a whole lung. It is usually applied to patients with central tumours, involvement of a mainstem bronchus, left or right pulmonary artery, and both superior and inferior pulmonary vein [6]. Pneumonectomy represented almost ~30% of lung resections for cancer in thoracic units until the 1990s [6]. Mortality, morbidity and complications of pneumonectomies are well acknowledged. Left pneumonectomy is usually better tolerated than right pneumonectomy and some authors went on to say that "the right pneumonectomy was a disease in itself" (**J. Deslauriers**) [6]. The mortality related with pneumonectomy continues to be important (5–10%) and the right pneumonectomy carries a higher risk of death or complications than the left pneumonectomy, mostly accredited to bronchopleural fistula [14, 18, 28].

In all pneumonectomies, first of all it is performed the pulmonary hill dissection with the identification of the pulmonary artery and of the two ipsilateral pulmonary veins (upper and lower) in order to assess their entirety (Fig. 51.1).

Depending on the disease and its severity, standard pneumonectomy is performed by the extrapericardial approach of the pulmonary vessels; pneumonectomy with the intrapericardial approach of the pulmonary vessels; extended pneumonectomies (with chest wall, vertebral bodies, diaphragm or pericardium resection); extensive pneumonectomies with cardiac wall resection (left atrium); extensive pneumonectomies with resection and reconstruction of superior vena cava; pneumonectomies with carina resection and tracheo-bronchoanastomosis; and pleuro-pneumonectomies. Nonetheless, in lung cancer, these types of pneumonectomies are also associated with mediastinal lymphadenectomy. It has to be underlined, that the increase of chemotherapy or chemoradiotherapy treatments, diminished pneumonectomy rates with important lower staging of large hilar tumours [29]. As a result, pneumonectomy rates are only 0–15% of lung resections for primary lung cancer in the most part of specialised thoracic units [6].

Sleeve resections are still a substitute to pneumonectomy as they result in lesser perioperative mortality and improved mid-term survival with outstanding long-term outcomes (Fig. 51.2)

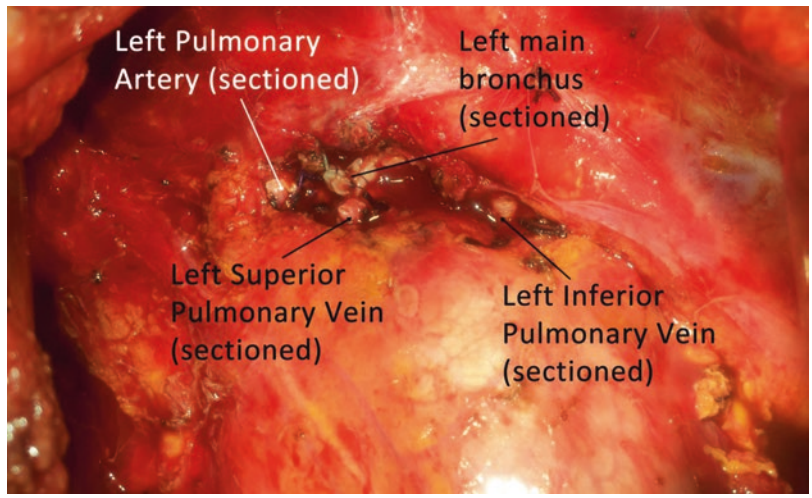

Fig. 51.1 Intraoperative left pneumonectomy appearance

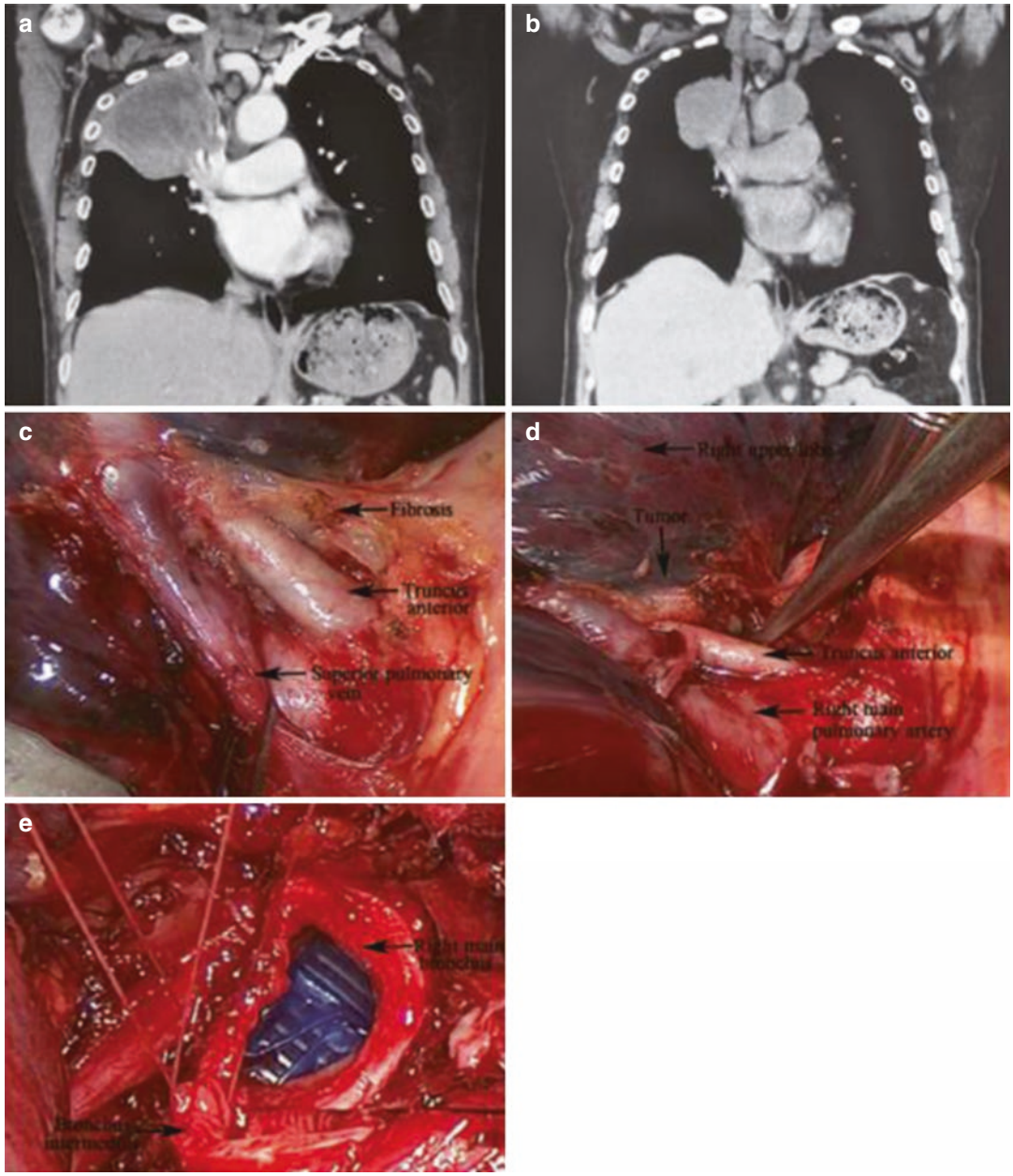

Fig. 51.2 The upper right pleural cavity was occupied by a large squamous carcinoma, and the right hilum had also been invaded (**a**). After neoadjuvant chemotherapy, the tumor shrank significantly (**b**). Although the induction therapy created fibrosis in the hilum (**c**), the truncus anterior was exposed and isolated successfully (**d**). Finally, the patient underwent right upper lobe sleeve resection without angioplasty (**e**). From Lv et al. [30]. This article is published under license to BioMed Central Ltd. This is an **Open Access article** distributed under the terms of the Creative Commons Attribution License (http://creativecommons.org/licenses/by/2.0), which permits unrestricted use, distribution, and reproduction in any medium, provided the original work is properly cited

[29–32]. Sleeve resections can simply implicate the bronchial tree or the ipsilateral pulmonary artery as well ("double sleeve or bronchovascular resection") [31, 33].

Sublobar resection is an old choice to lobectomy in the treatment of early-stage lung cancer in patients with preoperative poor pulmonary function. Presently, the data studies propose

sublobar resection must be considered in the treatment of lung cancer [34].

Lobectomy is defined as the surgical removal of a pulmonary lobe (upper, middle or lower) and represents the gold standard for most patients with an operable lung cancer. It represents ~60–70% of lung resections in most specific thoracic units [6]. The associated mortality is 2–3% in most part of thoracic units [16, 35]. Currently, large studies of robotic lobectomy for early-stage lung cancer have been published with excellent long-lasting oncological outcomes [36, 37]. It seems that robotic lobectomy has very decreased perioperative mortality, complication rates comparable to VATS lobectomy [36, 37]. Importantly, the mean surgery room period for a robotic lobectomy is still 4 h [36, 37]. Even if the cost of robotic lobectomy is higher than the cost of VATS lobectomy, however it is less than the cost of open lobectomy [38].

Bilobectomy is an alternative of lobectomy and applied only for right lung cancers (right upper and middle lobectomy, or right middle and lower lobectomy) (Fig. 51.3) [6, 30]. It is

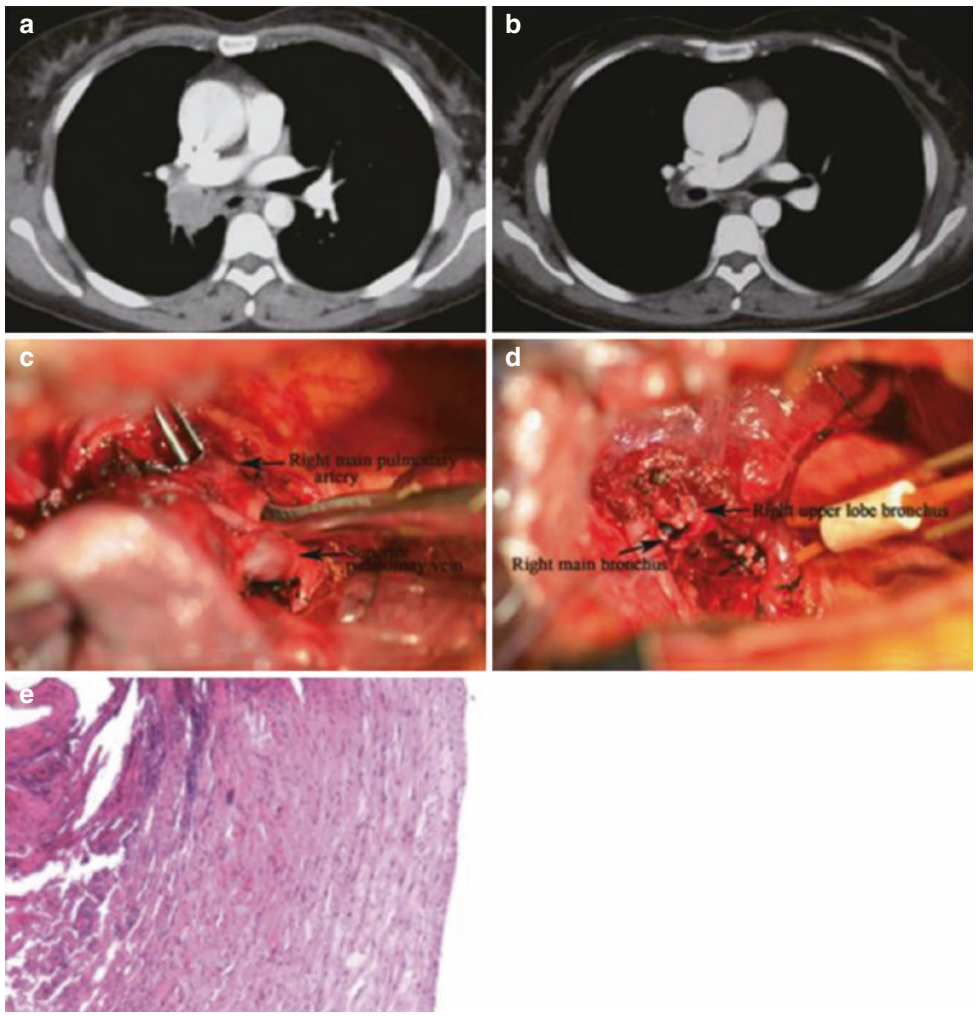

Fig. 51.3 To resect this centrally located tumor is also challenging (**a**), but two cycles of gemcitabine combined with cisplatin made it possible to preserve lung tissue and avoid pneumonectomy (**b**). During the resection, the right main pulmonary artery was successfully isolated and controlled (**c**). Finally, the **procedure of right middle and lower lobectomy** with bronchoplasty was performed (**d**), and the arterial margin was found to be free of tumor (**e**). From Lv et al. [30]. This article is published under license to BioMed Central Ltd. This is an **Open Access article** distributed under the terms of the Creative Commons Attribution License (http://creativecommons.org/licenses/by/2.0), which permits unrestricted use, distribution, and reproduction in any medium, provided the original work is properly cited

executed when all superior pulmonary veins have to be "sacrificed, when tumour or lymphadenopathy involves the bronchus intermedius, when the pulmonary artery is infiltrated in the fissure, or when the tumour crosses the major or minor fissure" [39]. Obviously, the mortality related with bilobectomy is same with to the one after lobectomy, but the morbidity is ≥71% in patients as the recent data studies confirmed [21, 23].

51.3.1 Segmentectomies

Accordingly, to thoracic surgeons both lungs have each 10 pulmonary segments. In case of segmental bronchi and vessels they can be separated by ligation and use of staplers [6]. It is of note, the segmental plan is not easy to be located and all more can be incomplete in most patients with important air leak [6]. Currently, the most part of thoracic surgeons will ventilate the lung following division of the segmental bronchus in order to locate this segment plan and put a stapler to reduce postoperative air leaks. A keynote factor is to place the stapler a few millimetres beyond the segmental plan fissure, continuing to the adjacent segment, containing the intersegmental lymphatic drainage of the involved segment in the resection ("extended segmentectomy") [6].

Presently, the major segmentectomies applied are the apical lower segment (segment 6); the lingulectomy (segment 4 and 5, left lung) equivalent to a middle lobectomy; the culmenectomy (segment 1, 2 and 3, left lung); and the basal segmentectomy (segments 7–10, right lung, or segments 8–10 left lung) [6]. It is important to mention that pulmonary segment is an anatomic structure of the lung with its own blood supply, bronchus and lymphatic drainage. Therefore, segmentectomy has to be considered as a suitable procedure in patients with small tumours, limited exactly to a segment but with lung function that doesn't allow lobectomy [6].

In case of patients with poor pulmonary function, **thoracoscopic segmentectomy** seems to diminish the length of hospitalization, diminish morbidity and lesser costs in comparison with an open anatomic segmentectomy. However, the oncological results were similar [40].

Wedge resections are non-anatomic lung resections defined by the surgical exclusion of the lung tumour with a rest of surgical edge as wide as possible to diminish the risk of local recurrence. It is well established that wedge resection is not a sufficient lung cancer surgery in most patients with lung cancer. However it may represent an alternative in patients with poor pulmonary function and no other choice, or in Asian patients with multiple peripheral ground-glass types of adenocarcinomas <20 mm [13, 41, 42]. In the absence of data proving the benefit of wedge resections, these procedures should be avoided as much as possible and the surgeon should always try to perform concomitantly a systematic lymph node dissection in order to obtain an adequate staging.

Extrapleural pneumonectomy (EPP) is used from the 1940s for the treatment of extensive infections of the lung and pleural space, such as tuberculous empyema [43]. Currently, EPP is applied to treat locally advanced malignant pleural mesothelioma (MPM) [43]. During procedure, it is utilized a patch with the important keynote, that in the operating room the patient has to be in supine position. A tight patch can cause constant hypotension with an increase of the filling pressures. In case of using a pericardial patch and diaphragmatic patch, cardiac or gastric herniation, complications can appear, as we discussed below (Fig. 51.4) [43].

VATS (**video-assisted thoracic surgery**) is the most recent minimally invasive surgical method utilized for both diagnostic and therapeutic lung cancer surgery.

It appears that VATS is correlated with decreased postoperative pain, diminished pulmonary dysfunction and diminished cytokines and acute-phase protein making in comparison with open surgery [44]. Furthermore, it diminishes the drainage period and in-hospital length after lung resection [45, 46]. Also, VATS lobectomy has same long-lasting results in comparison with open lobectomy in patients with stage I disease [47]. This is in line

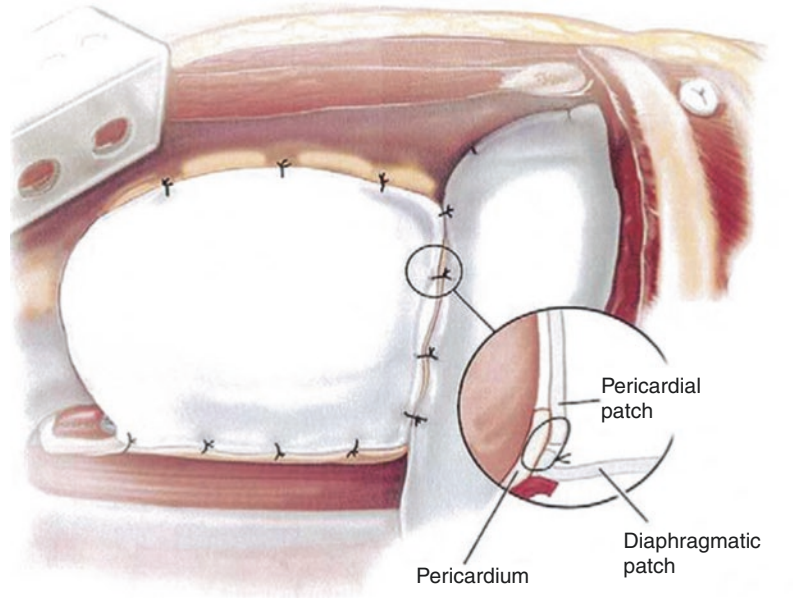

Fig. 51.4 Both patches should be sutured to the cut edge of the pericardium medially and the chest wall anterolaterally and posteriorly. If we fail to do so will result in cardiac or gastric herniation. Modified from Sugarbaker et al. [43] with permission

with two recently systematic reviews of the literature, that confirmed that VATS lobectomy is correlated with the improved survival in comparison with thoracotomy and lobectomy [46, 47]. Nonetheless, VATS has the potential to be applied in older population or in patients with poor pulmonary function [48, 49]. Additionally, patients who underwent VATS resections had lesser postpones in acceptance of adjuvant chemotherapy and surprisingly need lesser doses of chemotherapy [50]. Briefly, in 2004, Rocco described a new mini-invasive method, a uniportal technique based on a single anterior mini-thoracotomy together with VATs instruments and thoracoscope [51]. One year later, Gonzales-Rivas et al. [52] have applied with exceptional results a technique based on a uniportal video-assisted technique for lobectomy surgery, with a mean in-hospital length of 3 days, complications in 14% of patients and no 30-day mortality postoperatively [52].

Robotic video-assisted surgery (RVATS) has the same efficiency in comparison with video-assisted surgery (VATS) in lung resection (pneumonectomy, lobectomy, and segmentectomy) [53].

51.4 Physiopathology Outcomes Following Pneumonectomy

Lung resection that implies thoracic surgery severely modifies "the mechanical and fluid dynamic setting of the lung-chest wall coupling", also the water equilibrium in the pleural space and in the residual lung [26]. There is no information about adaptable lung growth in adults, however in children there are data studies of continuous lung growth over the first few years of life. Indices like a lower residual volume-to-total lung capacity (TLC) ratio and higher maximum breathing capacity observed practically in children, suggest recruitment of a new alveoli in the residual lung [54]. Moreover, Werner et al. [55] demonstrated a raise in lung volumes in most part of children who underwent pneumonectomy between ages of 1 week and 30 months, with a follow-up period of nearly 12 months [55]. Another study showed that on a group of children who underwent pneumonectomy between the ages of 1 day and 5 years had a postsurgery TLC of 96% of predicted value for two lungs at more than 30 years after surgery, signifying that the remaining parenchyma balances completely [56]. Conversely, young children and

adults after pneumonectomy turn up to develop overexpansion of the remaining lung instead of pulmonary reparation like lung growth [55].

Importantly, pneumonectomy decreases the pulmonary vascular system, modifies the location of the heart and large vessels, and further alters the **function of the heart**, during years after surgery [57]. Additionally, regardless of lung resection, RV and LV dysfunction arise with the decrease of cardiac output, but lobectomy has a lower effect on heart functions [58]. However, an important lung resection like pneumonectomy causes **in a short time** the diminishing of ventilatory function and has considerable side effects on right ventricular (RV) function [59–61].

There are many studies that evaluated the perioperative RV performance but currently they did not solved its adaptability in the conditions of an only one functional lung. On the other hand, other studies evaluated in pneumonectomies, the consequences of RV dysfunction on the left ventricle (LV) performance [62, 63]. As a result, these studies suggest that radical pulmonary surgery, for example pneumonectomies, affects much more the RV performance in comparison with limited lung resections—like lobectomies.

Right away after pneumonectomy, the RV dilates and RV ejection fraction diminishes [64, 65]. Okada et al. [65] suggested that after a significant lung resection the elevation of **RV afterload** secondary to increase of pulmonary artery pressure (PAP) and pulmonary vascular resistance (PVR) is the most important reason of this RV dysfunction [65]. Nonetheless, pneumonectomy is interrelated with postoperative increase of the pulmonary artery systolic pressure (PASP) and RV dilatation, in particular for right pneumonectomy [59]. Also, as mentioned above, preoperative and postoperative comparative studies showed the existence of RV dilatation and decreased contractility in varying degrees depending on the preexisting pulmonary and cardiac pathology and the extent of pulmonary resection. Kowalewski et al. [64] studied the RV function after pulmonary resection [64]. Same team observed that significant RV dilatation subsequent pneumonectomy is associated with increased RVEDP, RVESP, and diminished RVEF. Almost 50% from patients presented arrhythmias that further triggered higher RVEDV indexes and poorer RVEF. They summarized that these results are specific for postoperative enhances in RV afterload [64].

The greatest impact on morphology and function of the right ventricle in pneumonectomies are supraventricular arrhythmias, especially atrial fibrillation. In fact, supraventricular arrhythmias are the most common side effect after pneumonectomies (34%) [66].

51.5 Echocardiographic Evaluation of RV Dysfunction

As we have already stated, the most frequently used method in the assessment of RV function after pneumonectomies is echocardiography with all its variants. Currently, American Society of Echocardiography, the European Association of Echocardiography and Canadian Society of Echocardiography are considered to be the followed guidelines. The most used and accurate methods in appreciating the RV function are those recommended by the *Guidelines for the Echocardiographic Assessment of the Right Heart* in adult such as three-dimensional estimation of RV ejection fraction, tricuspid annular plane systolic excursion (TAPSE) and Tei index or RIMP (right ventricle index of myocardial performance), dP/dt (noninvasive Doppler evaluation of right ventricle pressure over time from tricuspid regurgitation jet), and speckle tracking echocardiography (STE) [67]. Furthermore, numerous studies approached RV performance in pneumonectomies through its hemodynamic parameters [64, 68–70] and by ultrasounds, especially through speckle tracking echocardiography [71, 72].

In addition to these highly specific methods for assessing RV function, there are classical techniques that can easily determine anatomical and functional parameters of cardiac performance. The exploration of RV function in these conditions is accomplished by several methods, among which multidetector CT (MDCT), catheterization, conventional contrast and radionuclide angiography, nuclear perfusion scintigraphy, single photon emission computed tomography (SPECT),

cardiac CT, MRI, positron emission tomography [73]. There are numerous studies showing that the above mentioned methods can prove the alteration of the RV performance after pneumonectomy, lesser in lobectomy, the production mechanism not being fully solved.

Recently, Wang et al. [58] studied in patients who underwent lung resection the main factors of cardiac performance obtained with classical methods: the left ventricular diastolic diameter, the left ventricular ejection fraction, the pulmonary artery pressure, the pulmonary artery diameter, the maximal velocity across pulmonary valve, the right ventricular diastolic diameter and the stroke volume. This study was the first performed on a relatively small group of patients that evaluated the biventricular myocardial strain using speckle tracking echocardiography (STE) in patients who underwent lung resection. Moreover, the study aimed to highlight differences in biventricular performance in patients with pneumonectomy and lobectomy, comparing preoperative and postoperative parameters as can be seen in the below table (Table 51.2) [58].

The results of Wang and colleagues showed statistically significant differences ($p < 0.05$) between the preoperative and postoperative heart rate measurements, in particular LVEF and pulmonary artery pressure (PAP), that further proved that both pneumonectomy and lobectomy have a negative effect on the cardiac performance of LV and RV (PAP). Furthermore, pulmonary resections can cause important upsurge in PAP ($p < 0.05$), this being explained by the removal from circulation of a larger volume of the vascular area in pneumonectomy [58].

In same study, Wang et al. [58] measured in the protocol of STE (Fig. 51.5) the circumferential strain (CS), longitudinal strain (LS), radial strain (RS), global CS (GCS) and global LS (GLS) in the RV and LV with intra and interobserver analysis [58].

The results also demonstrated the decline of LS, CS and RS values between preoperative and postoperative determinations ($p < 0.05$), respectively between pneumonectomy and lobectomy ($p < 0.05$) (Table 51.3) [58].

Furthermore, Smulders et al. [57] studied lung function, exercise tests and cardiac function on 15 consecutive patients who underwent over 5 years ago pneumonectomy. Further, the results of both ventricles function in pneumonectomy patients were evaluated with normal ventricular sizes by MRI from 25 patients healthy controls (Table 51.4) [57]. As can be seen in Table 51.3, the group with pneumonectomy comprised 6 patients with right pneumonectomy versus 9 patients with left pneumonectomy [57]. Cardiac performance output was quantified by classical transthoracic echocardiography parameters: cardiac output; heart rate; left ventricular end-diastolic volume; LVEDVI = LVEDV index; LVEF = left ventricular ejection fraction; LVM = left ventricular mass; right ventricular end-diastolic volume; RVEDVI = RVED index; right ventricular mass; stroke volume (Table 51.4) [57].

Between the healthy control group and the left and right pneumonectomy groups there was a decrease in SV, LVEF, LVM, RVEDV ($p < 0.05$). The same cardiac echocardiographic parameters were applied only in patients with left or right pneumonectomy, and there was a decrease in LVEDV and RVM after right pneumonectomy compared to the left pneumonectomy where LVEDV increases and LVEF decreases ($p < 0.05$). There were not significant differences looking the remainder of the functional parameters ($p > 0.05$) [57].

51.6 Right Ventricular Dysfunction in Early Pneumonectomy

The RV function is altered during surgery just immediately after the pulmonary artery is clamped, causing the concomitant rise of the right ventricular afterload, increased pulmonary vascular resistance and increased pulmonary artery pressure [64].

These changes are the result of lowering the cardiac output of the RV. These hemodynamic elements are also present during the first 3–4 days postoperative or may be permanent. However the above mentioned manifestations are not present in lobectomy or segmentectomy, maybe only transitory, well

Table 51.2 Traditional echocardiographic measurements of patients' pre and post lung resection

Groups	Conditions	LVDd, mm	SV, mL	LVEF, %	RVDd, mm	PA-D, mm	PV-Vmax, m/s	PAP, mmHg	HR, beats/min
Pneumonectomy (10)	Preop	42.83 ± 4.45	77.31 ± 37.27	66.64 ± 7.54	32.0 ± 4.5	19.6 ± 1.2	0.85 ± 0.51	21.4 ± 7.3 [74]	70.50 ± 18.46
	Postop	38.96 ± 3.80	62.57 ± 26.54	57.15 ± 6.52*	28.1 ± 3.8	21.3 ± 1.7	0.83 ± 0.13	28.8 ± 10.6* [63]	105.17 ± 12.12*
Lobectomy (20)	Preop	42.43 ± 3.02	75.41 ± 18.43	68.69 ± 4.2	31.4 ± 3.5	21.1 ± 1.5	1.00 ± 0.17	20.3 ± 6.7 [63]	70.08 ± 15.14
	Postop	43.11 ± 3.91	72.22 ± 26.41	63.28 ± 3.0.95*	29.2 ± 4.1	22.0 ± 1.9	0.99 ± 0.12	24.2 ± 9.1† [75]	87.86 ± 18.54*,†

HR heart rate, *LVDd* left ventricular diastolic diameter, *LVEF* left ventricular ejection fraction, *PAP* pulmonary artery pressure (cases of measurable PAP), *PV-D* pulmonary artery diameter, *PV-Vmax* maximal velocity across pulmonary valve, *RVDd* right ventricular diastolic diameter, *SV* stroke volume

*Comparison between preop and postop within the pneumonectomy group and within the lobectomy group ($P < 0.05$)

†Comparison between the pneumonectomy group and the lobectomy group ($P < 0.05$)

From Wang et al. [58]. **It is an open access article**

tolerated and obviously not allowed. It has to be underlined, that in case of the new hemodynamics, immediately postoperative RV dilatates and decreases in contractility and ejection fraction [64].

51.7 Right Ventricular Dysfunction Long Time After Pneumonectomy

Importantly, the postoperative progression of patients with pneumonectomy or lobectomy and segmentectomy is different. First of all, preload and afterload after pneumonectomy are more severely modified with triggering of biventricular dysfunction whereas in lobectomy and segmentectomy the compensatory mechanisms determine the normal function of LV and RV.

Venuta et al. [76] studied the right heart function on 36 patients with pneumonectomy and 15 patients with lobectomy using serial Doppler echocardiography in patients before surgery and 1 week, 3 months, 6 months, 1 year, and 4 years postoperatively (Table 51.5) [76].

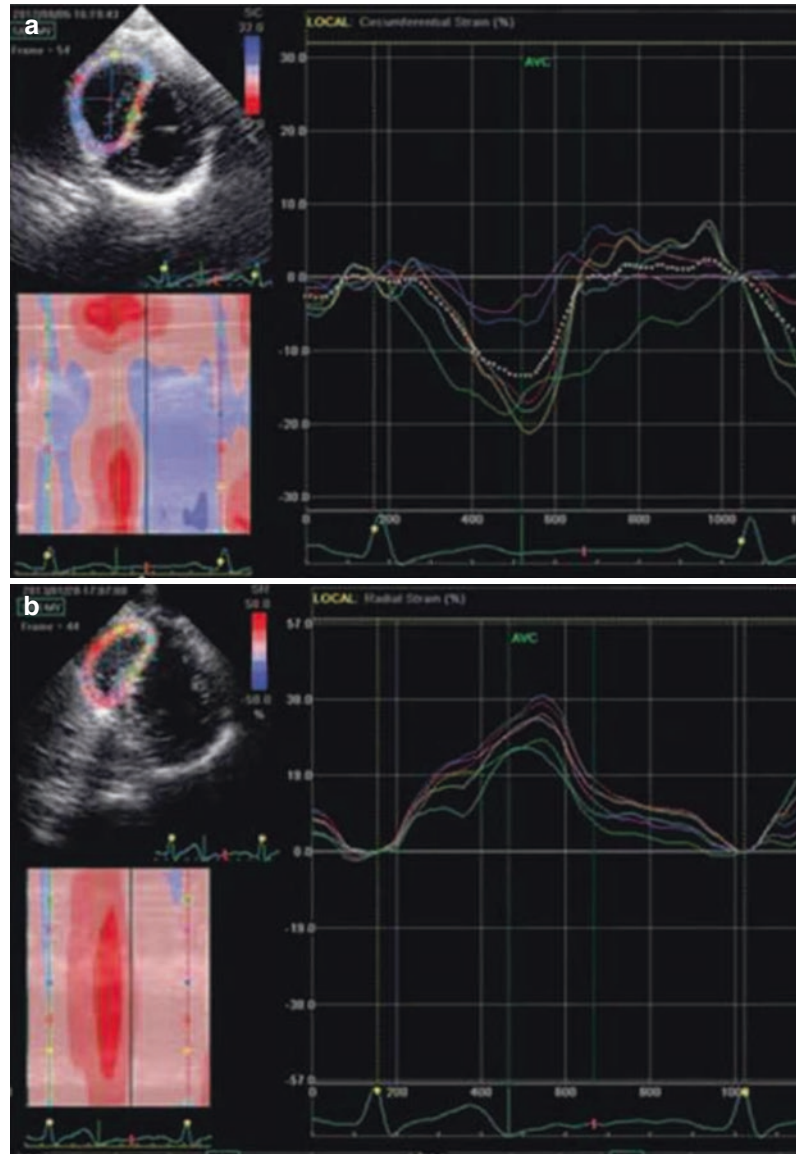

Fig. 51.5 Two-dimensional speckle tracking for strain values at both right and left ventricles. (**a**) Circumferential strain derived from mitral valve level of right ventricle; (**b**) radial strain derived from mitral valve level of right ventricle; (**c**) longitudinal strain derived from apical 4-chamber view of right ventricle; (**d**) longitudinal strain curves derived from apical 4 and 2-chamber view and apical long-axis view of left ventricle. From Wang et al. [58].

Fig. 51.5 (continued)

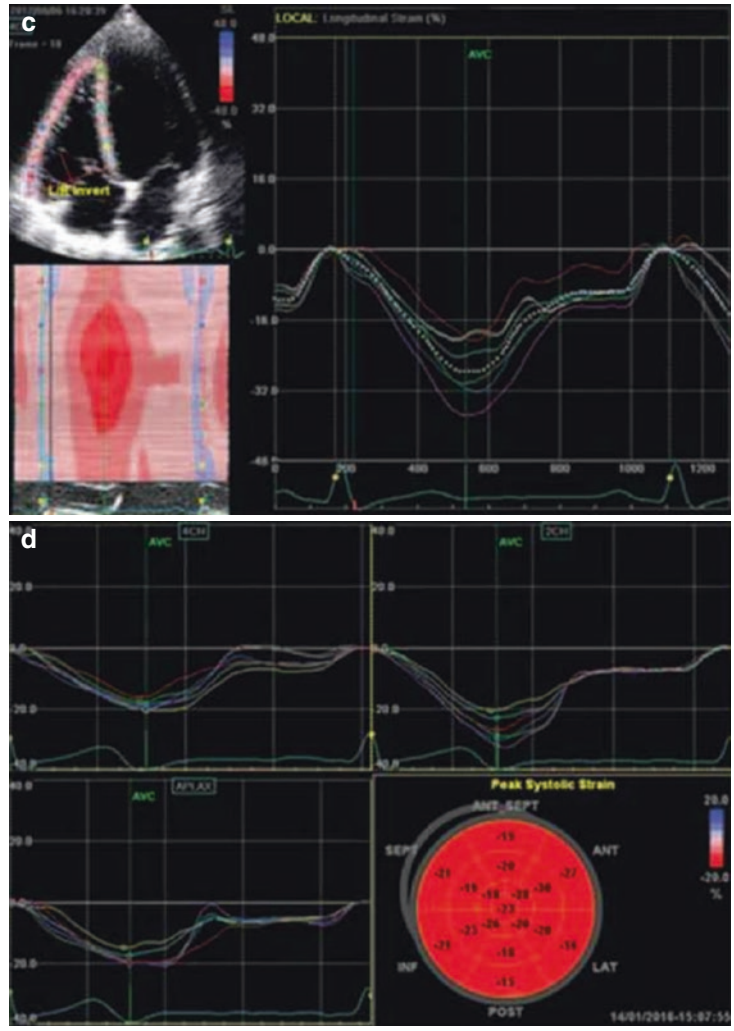

Table 51.3 Strain values derived from right ventricle preop and postop of lung resection

Groups (n)	Strain	Conditions	Right ventricular free wall	Septum	Global
Pneumonectomy (10)	LS (%)	Preop	−30.86 ± 5.88	−17.51 ± 7.11	−24.56 ± 5.32
		Postop	−11.77 ± 4.14*	−10.1 ± 5.92*	−12.04 ± 5.33*
	CS (%)	Preop	−14.69 ± 5.44	−16.34 ± 7.52	−15.01 ± 7.98
		Postop	−4.43 ± 3.56*	−5.06 ± 3.83*	−4.13 ± 2.86*
	RS (%)	Preop	33.86 ± 17.06	31.27 ± 17.78	32.56 ± 17.42
		Postop	11.36 ± 4.95*	11.23 ± 4.87*	11.29 ± 4.91*
Lobectomy (20)	LS (%)	Preop	−29.7 ± 6.23	−19.88 ± 5.92	−25.69 ± 4.71
		Postop	−18.03 ± 8.06*,†	−15.65 ± 6.40*,†	−17.07 ± 5.26*,†
	CS (%)	Preop	−14.30 ± 9.43	−14.34 ± 9.92	−14.13 ± 10.12
		Postop	−7.11 ± 4.84*	−6.54 ± 4.50*	−6.35 ± 4.85*
	RS (%)	Preop	32.71 ± 16.44	28.98 ± 15.15	30.8 ± 15.80
		Postop	18.14 ± 9.31*	16.10 ± 10.12*	17.12 ± 9.71*

CS circumferential strain, *LS* longitudinal strain, *RS* radial strain
*Comparison between preop and postop within the pneumonectomy group and within the lobectomy group ($P < 0.05$)
†Comparison between the pneumonectomy group and the lobectomy group ($P < 0.05$)

Table 51.4 Postoperative LV and RV function[a] comparing patients with healthy controls comparing patients after right- and left-sided pneumonectomy

	Patients n = 15	Healthy controls n = 25	p	Right n = 6	Left n = 9	p value
Age (yr)	64 ± 10	43 ± 14	0.0001			
HR (bpm)	80 ± 17	65 ± 12	0.006	89 ± 19	74 ± 13	0.099
SV (mL)	64 ± 12	83 ± 17	0.001	59 ± 14	67 ± 10	0.195
CO (L/min)	5.0 ± 0.9	5.4 ± 1.5	0.567	5.2 ± 1.2	4.9 ± 0.8	0.480
LVEF (%)	58 ± 14	72 ± 8	0.001	64 ± 11	54 ± 15	0.239
LVEDV (mL)	126 ± 67	120 ± 18	0.270	94 ± 23	148 ± 80	0.025
LVEDVI	64 ± 26	61 ± 10	0.645	52 ± 9	73 ± 31	0.059
RVEDV (mL)	123 ± 39	148 ± 32	0.043	99 ± 29	139 ± 38	0.059
RVEDVI	64 ± 17	75 ± 12	0.061	55 ± 14	70 ± 16	0.099
RVM (g)	48 ± 24	51 ± 20	0.434	33 ± 17	57 ± 24	0.018
LVM (g)	120 ± 41	148 ± 36	0.017	108 ± 45	127 ± 39	0.289

From Smulders et al. [57] with permission
CO cardiac output, *HR* heart rate, *LVEDV* left ventricular end-diastolic volume, *LVEDVI* LVEDV index, *LVEF* left ventricular ejection fraction, *LVM* left ventricular mass, *RVEDV* right ventricular end-diastolic volume, *RVEDVI* RVED index
From Smulders et al. [57] with permission
[a]Mean ± SD.

Table 51.5 Modifications of the echocardiographic variables during the 4 years of follow-up after pneumonectomy

Variable	Preop	1W	3M	6M	1Y	4Y	*p*-value
TVI	0.9 ± 0.7	0.9 ± 0.7	1.1 ± 0.7	1.2 ± 0.6	1.3 ± 0.5	1.3 ± 0.5	0.05
PASP	26.1 ± 2.8	31.8 ± 6.8	31.8 ± 6.8	32.6 ± 7.8	33.4 ± 7.9	34.3 ± 7.6	<0.00001
RVDD	26.4 ± 2.3	27.5 ± 2.6	28.2 ± 2.7	28.6 ± 3.7	29.6 ± 2.8	31.4 ± 3	<0.001
TRJ	2.3 ± 0.1	2.5 ± 0.1	2.5 ± 0.1	2.5 ± 0.1	2.6 ± 0.1	2.6 ± 0.1	<0.0001

From Venuta et al. [76] with permission
TVI tricuspid valve insufficiency, *PASP* pulmonary artery systolic pressure, *RVDD* right ventricle diastolic diameter, *TRJ* tricuspid regurgitation jet, *1W* 1-week follow-up, *3M* 3 months, *6M* 6 months, *1Y* follow-up at 1 year, *4Y* follow-up at 4 years

In fact, the team of Venuta showed that RV dysfunction begins after 6 months and continues to deteriorate progressively up to 4 years. The PASP increase begins after 7 days postoperatively and lasts up to 4 years ($p < 0.00001$ versus preoperative) explaining thus RVDD increase ($p < 0.001$). The most important parameter in the deterioration of RV performance is PASP and one reason that sustains this hypothesis is that after the right pneumonectomy, PASP is higher than the left one.

Another argument in favour of these hypotheses is that RV dilatation after pneumonectomy is higher than after lobectomy ($p < 0.001$) [59].

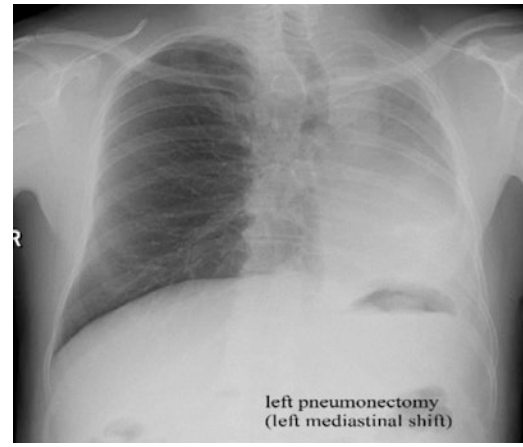

Fig. 51.6 Chest X ray—left pneumonectomy with cardiac shift on the operated side with left pleural cavity disappearance (4 years follow-up)

51.8 Herniation of the Heart

Nonetheless, after pneumonectomy, the pleural free cavity remains free. As the pressure of the residual lung increases with the dysfunction of the cardiac performance of the right ventricle and the left ventricle (Figs. 51.6, 51.7, and 51.8).

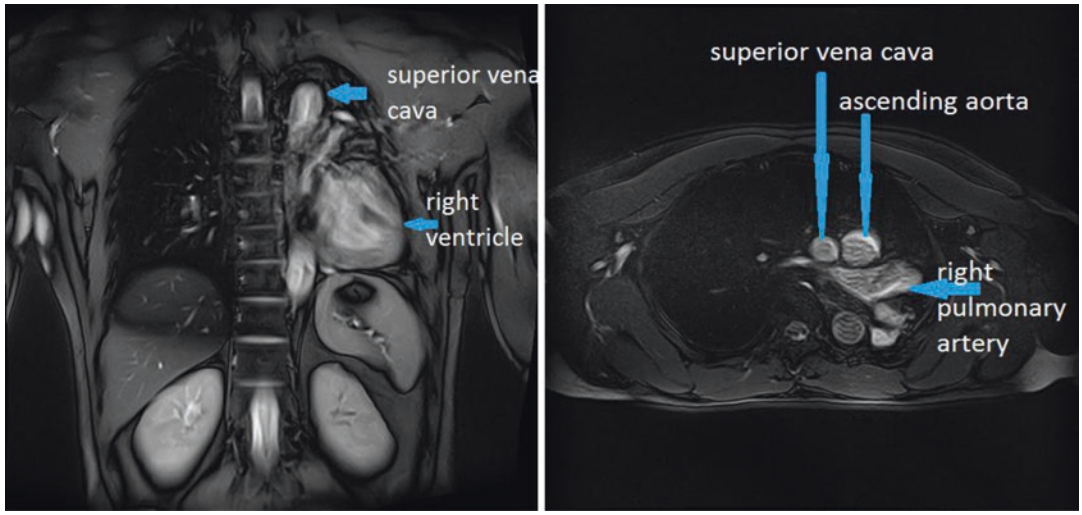

Fig. 51.7 Thoracic MRI—left pneumonectomy with cardiac displacement on the left side (4 years follow-up)

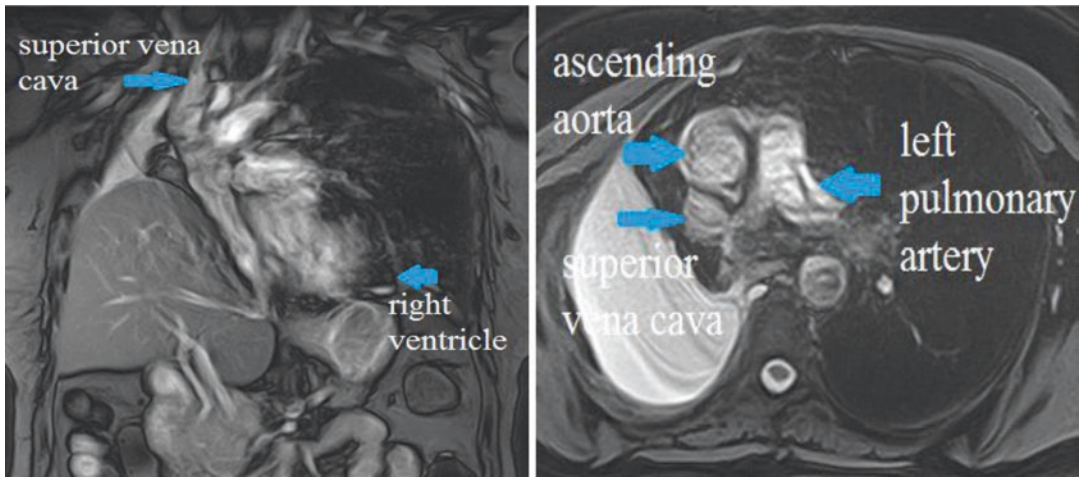

Fig. 51.8 Thoracic MRI Right pneumonectomy with cardiac displacement on the right side (1 year follow-up)

Of note, in the new anatomical conditions, there are changes of the ventilator function of lungs and biventricular cardiac performance. Smulders et al. [57] studied the dynamic magnetic resonance imaging of RV and LV according to the heart rate and noticed the increase of heart rate ($p = 0.006$) and decrease of stroke volume ($p = 0.001$) compared to the reference values in case of the displacement of the heart in the left hemithorax. After right pneumonectomy and the displacement of the heart into the right hemithorax, it produces a reduction in the EDV and maintains normal LVEF. Also, the left pneumonectomy with migration of the heart shows the decrease of the ejection fraction of LV andthe normal preservation of the ESV and EDV of RV [57].

Conclusions

There is no doubt that pneumonectomy has consequences on the cardiac performance expressed by preload and afterload changes, as well as contractility adjustment by progressive dilatation of RV. Repercussions on RV function are increase or decrease in volume or flow. Evalu-

ation techniques are multiple but the mechanism of adaptation of RV to the conditions of pneumonectomy is not yet precisely acknowledged. Deterioration of the RV function begins after 6 months and is progressive to heart failure. Lobectomy and segmentectomy have fewer changes in RV performance due to the higher functional remainder pulmonary parenchyma.

Without question, right ventricle modifications are obviously manifest after pneumonectomy and even if they do not show a clear clinical impact they should not be disregarded [76].

References

1. Evarts A, Graham MD, Singer JJ. Successful removal of an entire lung for carcinoma of the bronchus. JAMA. 1984;251:257–60.
2. Wood DE. Pulmonary resection after pneumonectomy. Thorac Surg Clin. 2004;14(2):173–82. https://doi.org/10.1016/S1547-4127(04)00006-4.
3. Jensik RL, Faber LP, Milloy FJ, et al. Segmental resection for lung cancer. A 15-year experience. J Thorac Cardiovasc Surg. 1973;66:563–72.
4. Thomas CP. The present position relating to cancer of the lung. Lobectomy with sleeve resection. Thorax. 1960;15:9–11.
5. Shields TW, LoCicero J III, Ponn RB, Daly BDT. Surgical treatment of non-small cell lung cancer. In: Shields TW, LoCicero J, Ponn RB, et al., editors. General thoracic surgery. 7th ed. Philadelphia: Lippincott Williams & Wilkins; 2009. p. 1311–41. ISBN: 0781779820.
6. Lang-Lazdunski L. Surgery for nonsmall cell lung cancer. Eur Respir Rev. 2013;22(129):382–404. https://doi.org/10.1183/09059180.00003913.
7. Gill Cryer H, Mavroudis C, Yu J, Roberts AM, Cue JI, Richardson JD, Polk HC. Shock, transfusion and pneumonectomy. Ann Surg. 1990;212:197–201.
8. Lewis JW Jr, Gabriel F, Bastanfar M, Servin J. Right ventricular performance in patients undergoing pneumonectomy. Chest. 1992;102:63S–7S.
9. Okada M, Okada M, Ishi N, Yamashita C, Sugimoto T, Okada K, Yamagishi H, et al. Right ventricular ejection fraction in the preoperative risk evaluation of candidates for pulmonary resection. J Thorac Cardiovasc Surg. 1996;112:364–70.
10. Reed CE, Spinale FG, Crawford FA Jr. Effect of pulmonary resection on right ventricular function. Ann Thorac Surg. 1992;53:578–82.
11. Rivera C, Arame A, Pricopi C, Riquet M, Mangiameli G, Abdennadher M, Dahan M, Le Pimpec Barthes F. Pneumonectomy for benign disease: indications and postoperative outcomes, a nationwide study. Eur J Cardiothorac Surg. 2015;48(3):435–40. ; discussion 440. https://doi.org/10.1093/ejcts/ezu439.
12. Conlan AA, Kopecf SE. Indications for pneumonectomy: pneumonectomy for benign disease. Chest Surg Clin N Am. 1999;9:311–26.
13. Lim E, Baldwin D, Beckles M, et al. Guidelines on the radical management of patients with lung cancer. Thorax. 2010;65(Suppl 3):iii1–iii27.
14. Shapiro M, Swanson SJ, Wright CD, et al. Predictors of major morbidity and mortality after pneumonectomy utilizing the Society for Thoracic Surgeons General Thoracic Surgery Database. Ann Thorac Surg. 2010;90:927–34.
15. Berrisford R, Brunelli A, Rocco G, et al. The European Thoracic Surgery Database project: modelling the risk of inhospital death following lung resection. Eur J Cardiothorac Surg. 2005;28:306–11.
16. Harpole DH Jr, DeCamp MM Jr, Daley J, et al. Prognostic models of thirty-day mortality and morbidity after major pulmonary resection. J Thorac Cardiovasc Surg. 1999;117:969–79.
17. Falcoz PE, Conti M, Brouchet L, et al. The thoracic surgery scoring system (THORACOSCORE): risk model for inhospital death in 15,183 patients requiring thoracic surgery. J Thorac Cardiovasc Surg. 2007; 133:325–32.
18. Kozower BD, Sheng S, O'Brien SM, et al. STS database risk models: predictors of mortality and major morbidity for lung cancer resction. Ann Thorac Surg. 2010;90:875–81.
19. Sawabata N, Nagayasu T, Kadota Y, Goto T, Horio H, Mori T, Yamashita S, Iwasaki A. Risk assessment of lung resection for lung cancer according to pulmonary function: republication of systematic review and proposals by guideline committee of the Japanese association for chest surgery 2014. Gen Thorac Cardiovasc Surg. 2015;63(1):14–21. https://doi.org/10.1007/s11748-014-0475-x.
20. Gaballo A, Corbo GM, Valente S, Ciappi G. Preoperative evaluation and risk factors of lung cancer. Rays. 2004;29(4):391–400.
21. Armstrong P, Congleton J, Fountain SW, et al. BTS guidelines: guidelines on the selection of patients with lung cancer for surgery. Thorax. 2001;56:89–108.
22. Beckles MA, Spiro SG, Colice GL, et al. The physiologic evaluation of patients with lung cancer being considered for resectional surgery. Chest. 2003; 123(Suppl 1):105S–14S.
23. Ferguson MK, Vigneswaran WT. Diffusing capacity predicts morbidity after lung resection in patients without obstructive lung disease. Ann Thorac Surg. 2008;85:1158–64.
24. Beattie GW, Dunn WG, Asif M. In patients with a tumour invading the phrenic nerve does prophylactic diaphragm plication improve postoperative lung function? Interact Cardiovasc Thorac Surg. 2016; 23(3):454–8. https://doi.org/10.1093/icvts/ivw091.
25. Ueda K, Hayashi M, Tanaka N, Tanaka T, Hamano K. Long-term pulmonary function after major lung

resection. Gen Thorac Cardiovasc Surg. 2014;62(1):24–30. https://doi.org/10.1007/s11748-013-0346-x.
26. Miserocchi G, Beretta E, Rivolta I. Respiratory mechanics and fluid dynamics after lung resection surgery. Thorac Surg Clin. 2010;20(3):345–57. https://doi.org/10.1016/j.thorsurg.2010.03.001.
27. Kometani T, Okamoto T, Yoshida S, Yoshino I. Acute respiratory distress syndrome after pulmonary resection. Gen Thorac Cardiovasc Surg. 2013;61(9):504–12. doi:https://doi.org/10.1007/s11748-013-0276-7
28. Darling GE, Abdurahman A, Yi QL, et al. Risk of a right pneumonectomy: role of bronchopleural fistula. Ann Thorac Surg. 2005;79:433–7.
29. Schirren J, Eberlein M, Fischer A, et al. The role of sleeve resections in advanced nodal disease. Eur J Cardiothorac Surg. 2011;40:1157–63.
30. Lv C, Ma Y, Wu N, Yan S, Zheng Q, Sun Y, Li S, Fang J, Yang Y. A retrospective study: platinum-based induction chemotherapy combined with gemcitabine or paclitaxel for stage IIB-IIIA central non-small-cell lung cancer. World J Surg Oncol. 2013;11:76. https://doi.org/10.1186/1477-7819-11-76.
31. Schirren J, Bolukbas S, Bergmann T, et al. Prospective study on perioperative risks and functional results in bronchial and bronchovascular sleeve resections. Thorac Cardiovasc Surg. 2009;57:35–41.
32. Tronc F, Gregoire J, Rouleau J, et al. Long-term results of sleeve lobectomy for lung cancer. Eur J Cardiothorac Surg. 2000;17:550–6.
33. Yildizeli B, Fadel E, Mussot S, et al. Morbidity, mortality and long-term survival after sleeve lobectomy for nonsmall cell lung cancer. Eur J Cardiothorac Surg. 2007;31:95–102.
34. Fields RC, Meyers BF. Sublobar resections for lung cancer. Semin Thorac Cardiovasc Surg. 2006;18(2):85–91.
35. Treasure T, Utley M, Bailey A. Assessment of whether in-hospital mortality for lobectomy is a useful standard for the quality of lung cancer surgery: retrospective study. BMJ. 2003;327:73.
36. Gharagozloo F, Margolis M, Tempesta B, et al. Robot-assisted lobectomy for early-stage lung cancer: report of 100 consecutive cases. Ann Thorac Surg. 2009;88:380–4.
37. Park BJ, Melfi F, Mussi A, et al. Robotic lobectomy for non-small cell lung cancer (NSCLC): long-term oncologic results. J Thorac Cardiovasc Surg. 2012;143:383–9.
38. Park BJ, Flores RM. Cost comparison of robotic, video-assisted thoracic surgery and thoracotomy approaches to pulmonary lobectomy. Thorac Surg Clin. 2008;18:297–300.
39. Fleisher LA, Beckman JA, Brown KA, et al. ACC/AHA 2007 guidelines on perioperative cardiovascular evaluation and care for non-cardiac surgery: a report of the American College of cardiology/American Heart Association task force on practice guidelines. J Am Coll Cardiol. 2007;50:e159–242.
40. Yang CF, D'Amico TA. Thoracoscopic segmentectomy for lung cancer. Ann Thorac Surg. 2012;94:668–81.
41. Mun M, Kohno T. Efficacy of thoracoscopic resection for multifocal bronchioloalveolar carcinoma showing pure ground-glass opacities of 20 mm or less in diameter. J Thorac Cardiovasc Surg. 2007;134:877–82.
42. Nakata M, Sawada S, Yamashita M, et al. Surgical treatments for multiple primary adenocarcinoma of the lung. Ann Thorac Surg. 2004;78:1194–9.
43. Sugarbaker DJ, Jaklitsch MT, Bueno R, et al. Prevention, early detection, and management of complications after 328 consecutive extrapleural pneumonectomies. J Thorac Cardiovasc Surg. 2004;128(1):138–46. https://doi.org/10.1016/j.jtcvs.2004.02.021.
44. Walker WS, Leaver HA. Immunologic and stress responses following video-assisted thoracic surgery and open pulmonary lobectomy in early stage lung cancer. Thorac Surg Clin. 2007;17:241–9.
45. Flores RM, Park BJ, Dycoco J, et al. Lobectomy by video-assisted thoracic surgery (VATS) versus thoracotomy for lung cancer. J Thorac Cardiovasc Surg. 2009;138:11–8.
46. Whitson BA, Groth SS, Duval SJ, et al. Surgery for early-stage non-small cell lung cancer: a systematic review of the video-assisted thoracoscopic surgery versus thoracotomy approaches to lobectomy. Ann Thorac Surg. 2008;86:2016–8.
47. Yan TD, Black D, Bannon PG, et al. Systematic review and meta-analysis of randomized and non-randomized trials on safety and efficacy of video-assisted thoracic surgery lobectomy for early stage non-small-cell lung cancer. J Clin Oncol. 2009;27:2553–62.
48. Cattaneo SM, Park BJ, Wilton AS, et al. Use of video-assisted thoracic surgery for lobectomy in the elderly results in fewer complications. Ann Thorac Surg. 2008;85:231–5.
49. Wolf AS, Richards WG, Jaklitsch MT, et al. Lobectomy versus sublobar resection for small (2 cm or less) non-small cell lung cancers. Ann Thorac Surg. 2011;92:1819–23.
50. Petersen RP, Pham D, Burfeind WR, et al. Thoracoscopic lobectomy facilitates the delivery of chemotherapy after resection for lung cancer. Ann Thorac Surg. 2007;83:1245–9.
51. Rocco G. One-port (uniportal) video-assisted thoracic surgical resections – a clear advance. J Thorac Cardiovasc Surg. 2012;144:S27–31.
52. Gonzales-Rivas D, Paradela M, Fernandez R, et al. Uniportal video-assisted thoracoscopic lobectomy: two years of experience. Ann Thorac Surg. 2013;95:426–32.
53. Emmert A, Straube C, Buentzel J, Roever C. Robotic versus thoracoscopic lung resection: a systematic review and meta-analysis. Medicine (Baltimore). 2017;96(35):e7633. https://doi.org/10.1097/MD.0000000000007633.
54. Stiles QR, Meyer BW, Lindesmith GG, et al. The effects of pneumonectomy in children. J Thorac Cardiovasc Surg. 1969;58:394–400.

55. Werner HA, Pirie GE, Nadel HR, et al. Lung volumes, mechanics and perfusion after pulmonary resection in infancy. J Thorac Cardiovasc Surg. 1993;105:737–42.
56. Laros CD, Westermann CJJ. Dilatation, compensatory growth, or both after pneumonectomy during childhood and adolescence. J Thorac Cardiovasc Surg. 1987;93: 570–6.
57. Smulders SA, Holverda S, Vonk-Noordegraaf A, van den Bosch HC, Post JC, Marcus JT, Smeenk FW, Postmus PE. Cardiac function and position more than 5 years after pneumonectomy. Ann Thorac Surg. 2007;83(6):1986–92. https://doi.org/10.1016/j.athoracsur.2007.01.036.
58. Wang Z, Yuan J, Chu W, Kou Y, Zhang X. Evaluation of left and right ventricular myocardial function after lung resection using speckle tracking echocardiography. Medicine (Baltimore). 2016;95(31):e4290. https://doi.org/10.1097/MD.0000000000004290.
59. Foroulis CN, Kotoulas CS, Kakouros S, Evangelatos G, Chassapis C, Konstantinou M, Lioulias AG. Study on the late effect of pneumonectomy on right heart pressures using Doppler echocardiography. Eur J Cardiothorac Surg. 2004;26:508–14. https://doi.org/10.1016/j.ejcts.2004.05.036
60. Schulman DS, Matthay RA. The right ventricle in pulmonary disease. Cardiol Clin. 1992;10:111–35.
61. Van Mieghem W, Demedts M. Cardiopulmonary function after lobectomy or pneumonectomy for pulmonary neoplasm. Respir Med. 1989;83: 199–206.
62. Çölkesen Y, Açıl T, Fındıkçıoglu A, et al. Tissue Doppler evaluation of the effects of major lung resection on cardiac functions. Turk Kardiyol Dern Ars. 2009;37:317–20.
63. Nojiri T, Maeda H, Takeuchi Y, et al. Predictive value of preoperative tissue Doppler echocardiographic analysis for postoperative atrial fibrillation after pulmonary resection for lung cancer. J Thorac Cardiovasc Surg. 2010;140:764–8.
64. Kowalewski J, Brocki M, Dryjanski T, Kapron K, Barcikowski S. Right ventricular morphology and function after pulmonary resection. Eur J Cardiothorac Surg. 1999;15:444–8.
65. Okada M, Ota T, Okada M, Matsuda H, Okada K, Ishii N. Right ventricular dysfunction after major pulmonary resection. J Thorac Cardiovasc Surg. 1994; 108:503–11.
66. Mitsudomi T, Mizoue T, Yoshimatsu T, Oyama T, Nakanishi R, Okabayashi K, Osaki T, Kume T, Yasumoto K. Sugimac postoperative complications after pneumonectomy for treatment of lung cancer: multivariate analysis. J Surg Oncol. 1996;61:218.
67. Rudski LG, Lai WW, Afilalo J, et al. Guidelines for the echocardiographic assessment of the right heart in adults: a report from the American Society of Echocardiography endorsed by the European Association of Echocardiography, a registered branch of the European Society of Cardiology, and the Canadian Society of Echocardiography. J Am Soc Echocardiogr. 2010;23:685–713.
68. Amar D, Burt ME, Roistacher N, et al. Value of perioperative Doppler echocardiography in patients undergoing major lung resection. Ann Thorac Surg. 1996;61:516–20.
69. Pedoto A, Amar D. Right heart function in thoracic surgery: role of echocardiography. Curr Opin Anesthesiol. 2009;22:44–9.
70. Roscher C, Reidy C, Augoustides JG. Progress in perioperative echocardiography: focus on safety, clinical outcomes, 3-dimensional imaging, and education. J Cardiothorac Vasc Anesth. 2011;25:559–64.
71. Sahn DJ, Zhang J, Tam L, et al. Evaluation of right ventricular mechanics with 4D echocardiography: an in vitro validation against sonomicrometry. J Am Coll Cardiol. 2013;61(Suppl 10):E892.
72. Yu HK, Li SJ, Ip JJ, et al. Right ventricular mechanics in adults after surgical repair of tetralogy of Fallot: insights from three-dimensional speckle-tracking echocardiography. J Am Soc Echocardiogr. 2014; 27:423–9.
73. Greyson CR. Evaluation of right ventricular function. Curr Cardiol Rep. 2011;13(3):194–202.
74. Vainshelboim B, Fox BD, Saute M, et al. Limitations in exercise and functional capacity in long-term postpneumonectomy patients. J Cardiopulmon Rehabil Prevent. 2015;35:56–64.
75. Leitman M, Lysyansky P, Sidenko S, et al. Two-dimensional strain: a novel software for real-time quantitative echocardiographic assessment of myocardial function. J Am Soc Echocardiogr. 2004;17: 1021–9.
76. Venuta F, Sciomer S, Andreetti C, Anile M, De Giacomo T, Rolla M, Fedele F, Coloni GF. Long-term Doppler echocardiographic evaluation of the right heart after major lung resections. Eur J Cardiothorac Surg. 2007;32(5):787–90. https://doi.org/10.1016/j.ejcts.2007.07.033.

Future Directions

52

Liviu Chiriac and Razvan Roşulescu

Abstract

The pulmonary system and the cardiovascular system are linked in multiple pathways such as in haemodinamics, physiological and pathological mechanisms, diseases complications and prognosis. The right ventricle is a vital heart chamber for the pulmonary and systemic mechanisms that contribute to sustain systolic and diastolic function. Due to the vastity and importance of pathologies that are involving mainly the left ventricule and the left heart valves represented by the mitral and aortic valves, the right heart was somehow like a Cinderella many years but as stated in the upper lines the right ventricule function and physiopathological implications are crucial for the normal function of the heart and cardiovascular system.

In this chapter we will attempt to illustrate the present and future directions of neurohormonal modulation in right heart failure, the present and future directions of three dimensional ultrasonographical assessment in the right heart pathology and the future perspectives given by 3D printed casts and materials.

Keywords

Right ventricule · Future direction · Physiopathology · Right heart system

52.1 Introduction

Cardiovascular diseases are the main global medical challenge because of the important residual morbimortality developed in our century [1].

The pulmonary system and the cardiovascular system are linked in multiple pathways such as in haemodinamics, physiological and pathological mechanisms, diseases complications and prognosis. There is a physiological interdependency in the normal functions of these two systems that some authors have named it ‘the cardiopulmonary bind system’ and further Guyton actually stated in his Textbook of Human Physiology that we should regard the pulmonary system as the fifth heart chamber [1].

The right ventricule is a vital heart chamber for the pulmonary and sistemic haemodinamical mechanism that contribute to sustain systolic and diastolic function.

Due to the vastity and importance of pathologies that mainly involve the left ventricule and the left heart system valves represented by the mitral and aortic valves, the right heart was some-

L. Chiriac (✉)
Cardiology Department, Central Emergency Universitary Military Hospital, Bucharest, Romania

R. Roşulescu
Cardiology Department, National Centre of Diagnosis and Treatment, Bucharest, Romania

S. I. Dumitrescu et al. (eds.), *Right Heart Pathology*, https://doi.org/10.1007/978-3-319-73764-5_52

how like a Cinderella many years but as stated in the upper lines the right ventricule function and physiopathological implications are definitive for the normal function of the heart and cardiovascular system.

In this chapter we will attempt to describe and to point into the direction of future development in pathology, laboratory diagnosis, evolving imagistic technics, bridging therapies of the right heart and right ventricule.

52.2 Future Direction in Neurohormonal Modulation in Right Heart Failure

It is well known scientifically by now that neurohormonal activation due to the high sympathetic system stimulation cause a pathophysiological chain of events that results in ventricular remodeling, myocardial fibrosis, modified systemic and pulmonar haemodynamics and in the end biventricular failure [2].

The question that is raised is if the same neurohormonal activation that contribute to the left ventricular dysfunction have the same relevant role in right ventricular remodelling, right ventricule failure and pulmonary hypertension [3].

There are depicted in the medical literature various similarities between precipitating factors that act as a triggering signal and the level of neuroendocrine response both in left and right ventricule [3].

Many studies revealed that neuroendocrine modulation is activated and maintained by systemic baroreceptors localised in the arteries wall that are responsive to hypotension and chemoreceptors sensitive to the variation of the oxygen levels in the bloodstream. Also the myocardial receptors localised with a higher density in the right atrium are modulated by variation of cardiac output and increased wall stretch [4].

All these mechanisms are responsible in the activation of mechanisms that generate right ventricular remodulation and failure [4].

Severe pulmonary hypertension due to the von Oiler mechanism and the angiotensin II vascular effects is a very important contributing factor for a decreased cardiac output resulting in systemic hypotension and hypoxia that can generate a mismatch between ventilation and perfusion affecting the microcirculation vascular section [4, 5].

There are studies that revealed an important role attributed to the neuroendocrine activation in the primary pulmonary hypertension.

Nootens et al. have developed a study in which were included 21 patient diagnosed with primary pulmonary hypertension. The levels of norepinephrine and renin were measured in the right atrium and in the bloodstream by femoral artery function [6].

The results revealed that the concentration of norepinephrine was higher in patients with pulmonary hypertension in comparison to the healthy group. In balance the renin activity was not modified in both central and peripheral determinations in the both groups.

So from this study has been postulated that the norepinephrine activity and the autonomic nervous imbalance can be estimated by using the heart rate variability.

This is a non-invasive method that it is obtained by measuring the variation of the heart rhythm on the surface 12 lead ECG during an interval of 15 minutes [7].

A very famous study in this regard has included a number of 75 patients with chronic heart failure involving predominantly right ventricule dysfunction. In the study group the levels of plasma norepinephrine were correlated significantly with the high heart rate variability [7].

In contrast in the control group where the levels of norepinephrine were almost in normal range the variability of the heart rate was very thin. In conclusion this study stated that heart rate variability can be used as a clinical parameter to assess the disautonomic imbalance and to suggest the presence of the right ventricular dysfunction.

Torbicki et al. in a study tried to give an answer to the question if there is any evidence of right ventricular cardiomyocites dysfunction on a molecular level from the increased activity of the sympathetic activity in patients suffering from pulmonary arterial hypertension [8].

All the patients with arterial pulmonary hypertension that presented elevated levels of troponin T have a worse prognosis compared with the patients with troponin T in normal range values.

The most important aspect is the fact that all patients regardless of their plasma troponin T levels have a high sympathetic activity revealed by high plasma concentrations of epinephrine and norepinephrine but only the patients group with increased levels of troponin T have the worse prognosis factors and the lowest survival on the Kaplan Myers charts.

Furthermore treatment with vasodilators and spironolactone have reduced significantly the levels of troponin T and the survival rate has increased in this category of patients.

The majority of patients have o high heart rate variability as a clinical marker of right ventricule dysfunction and hipersympathetic activity.

The most important pharmacological molecules that are efficient and approved in the current guidelines for reducing right ventricular dysfunction are spironolactone, digoxin and the increased oxygen input in cases of chronic hypoxia [9, 10].

Spironolactone is a very efficient modulator of the neuroendocrine pathological activation that can be used in isolated right ventricular failure or with other diuretics as combined therapy in arterial pulmonary hypertension [9].

Digoxin has demonstrated its usefulness when it is administred orally or by intravenous way in patients with pulmonary arterial hypertension and right ventricule dysfunction one of the effects being the lowering of the plasma norepinephrine [10].

External oxygen administration can be an option in acute and chronic hypoxia that can results in decreasing the pathological neuroendocrine activity and correct the metabolic acidosis [11].

52.3 Future Directions in 3D Echocardiography in Right Ventricular Pathology

The ultrasound technology has been improving for the last decade, cardiac ultrasonography being nowadays the most important imagistic feature to explore the cardiovascular system.

As a result of technological development of the bidimensional sectional ultrasonography the tridimensional ultrasounds have emerged and can be used for the expansion of diagnosis capabilities and to refine the stage of pathologies [12].

Three dimensional ultrasonography has a higher accuracy in the determination of ventricular muscle mass, depiction of valvular ultrastructure by obtaining a reconstruction of the anatomical cardiac sections from a series of rotational images that were obtained using a fixed point on the apical, coronal, sagittal or transverse axis.

The bidimensional ultrasound technics uses planes or incidences through which the ultrasounds pass making a 2D acquisition. In contrast the tridimensional ultrasonography has volumetric points of view making possible the study of cardiac morphology and functionality from external perspectives and from various internal views [12].

The main clinical applications of the 3D ultrasounds are cardiac chamber quantification, valvular structures depiction both in ambulatory or intraoperatory environments.

The right ventricular ultrasonographic assessment in bidimensional mode is very difficult and limited because of the characteristic pyramidal shape which it is nor a habitual technical geometric form in the ultrasonic acquisition. The reconstruction of the right ventricule by using 3D technology can be a suitable solution for the imagistic anatomic and functional evaluation of this heart chamber [13].

The main issue that could rise is the fact that the 3D reconstruction of the right ventricule is obtained from the offline processing and also we have to consider the fact that the images necessary for the postprocessing will be obtained by using bidimensional methods [13].

A very recent group of studies coordinated by Papavassilou et al. suggested the use of real time three dimensional echocardiography in the description of the anatomy and functionality of the right ventricule. A possible issue that can emerge is that the technique is still expensive and time consuming thereby with a relative narrow use in clinical practice [13].

With 3D echo and real time three dimensional echocardiography we can also describe heart valvular functionality. With the refined details obtained by valvular reconstruction techniques we can assess the best conditions for valvular reparing and replacement [14].

Three dimensional ultrasonography can also be used successfully in describing and assessing congenital heart diseases. It can be used for both isolated congenital disease but also in complex congenital cardiac anomalies.

In the preoperatory stage we can use 3D echo in the septal defects to describe the type of defect, the amount of the residual tissue and the morphology of the solution of continuity. So by using this innovative imagistic method we can assess with precision the type of cure interventional or surgical that is recommended [15]. A clinical practical application of three dimensional ultrasound is the evaluation of the therapeutic success and to find evidence of a possible residual shunt [15]. We can also estimate by 3D reconstruction the entire interventricular septum and analyse the color flow jet through the continuity solution and quantify its magnitude to better estimate the therapeutic cure [16].

By using 3D echo we can study with higher sensibility and specificity the diastolic and systolic function, the rotational and longitudinal strain of the left and right ventricle in the preoperative stage in a isolated or complex congenital heart disease [13].

We can also confirm the fact that three dimensional echo has a greater sensibility and is more reliable then bidimensional transoesophagial echocardiography during surgery providing additional information such as distorsion and folding of the tricuspidian annulus during valvular reconstruction and can better assess the potential residual valvular regurgitation.

In conclusion three dimensional echocardiography it is already used in the refined assessment of valvular heart disease, congenital heart conditions and anatomy and functionality of the left and right ventricules making reconstruction images in order to enhance the quality of the medical diagnosisis and therapeutic protocols.

52.4 Future Directions in 3D Printing in Right Heart Pathology

Three dimensional printing is a innovative method of obtaining models and casts of the entire human heart or from selected parts of it.

This modern method can be used in variate medical domains such as medical surgical training for a visual comprehension of the surgical methodology, protocols and also in the manufacturing of implants, patches, artificial valves and tissue engineering.

Three dimensional printed materials are obtained by reconstructing the heart structure using high resolution imagistic techniques such as advanced multi-slice computer tomography, cardiac magnetic resonance, 3D ultrasonography and real time 3D cardiac ultrasonography.

The main practical usage for three dimensional printing is represented by contribution for diagnosis and improved therapeutic methods in congenital heart disease.

Congenital heart disease are the most frequent birth anomaly, its incidence and prevalence with live birth being estimated in 7.5 per 1000 [17]. The haemodinamic consequences and the functional impairment caused by congenital heart disease put them on a public health importance [17].

The imagistic information provided by advanced computer tomography, cardiac magnetic resonance, 3D echocardiography is very accurate but the surgeon have to make a mental reconstruction of the congenital anomaly. In an isolated anomaly this process can be relatively easy but in a complex congenital heart disease this process can be complicated [18].

We can also state that the usage of ultraspecific medical terms between cardiologists, radiologists and cardiac surgeons may lead to misunderstanding the precise surgical anatomy and congenital anomaly description [19].

Medical data about 3D printed casts and materials with the intentional usage purposes was published in the early 2000 by Binder et al. describing the positive role of 3D structures in facilitating the diagnostic and therapeutic medical performance [19].

We will try to resume the current and possible application of 3D printed materials and the future direction in the medical management of the congenital heart disease.

Generally for the assessment of an isolated or complex congenital anomaly are used two types of heart models represented by blood pool models and wall models for the endocardial surface representation [20, 21].

The process of obtaining a suitable cast of the epicardial heart surface for the blood pool and of the inner endocardial surface can be time consuming up to a interval represented between 3 and 10 hours depending of the cardiac structure and of the size of it.

The main applications of the 3D printed cast models are in hands-on surgery training for the refinement of surgical techniques in young and not yet experienced surgeons without the risks involved on the surgical table [22].

For the most experienced cardiac surgeons the 3D printed casts can be use to try new surgical methods procedures and to refine their surgical skills for rare and very rare disease [23, 24].

Another practical application of 3D printed casts is the preoperatory three dimensional view of the congenital anomaly practical for establishing the timing of the procedures and the surgical gestures step by step adapted to each patient [25, 26].

Also 3D printed models can be used for educational means for patients suffering from congenital heart disease and undergoing interventional or surgical procedures for better understanding of the procedure, the risks involved and the target of their treatment [27].

Despite many limitations represented by obtaining the images, processing and postprocessing, printing the models, time challenges 3D printed materials can be a giant step forward into the direction of personalised medicine and refining interventional and surgical procedures [27].

References

1. Ferrara R, Mastrorilli F, Pasanisi G, Censi S, D'Aiello N, Fucili A, Valgimigli M, Ferrari R. Neurohormonal modulation in chronic heart failure. Eur Heart J Suppl. 2002;4:D3–D11.
2. Davila DF, Nunez TJ, Odreman R, de Davila CA. Mechanisms of neurohormonal activation in chronic congestive heart failure: pathophysiology and therapeutic implications. Int J Cardiol. 2005;101:343–6.
3. Chatterjee K. Neurohormonal activation in congestive heart failure and the role of vasopressin. Am J Cardiol. 2005;95:8B–13B.
4. Packer M. The neurohormonal hypothesis: a theory to explain the mechanism of disease progression in heart failure. J Am Coll Cardiol. 1992;20:248–54.
5. Voelkel NF, Quaife RA, Leinwand LA, Barst RJ, McGoon MD, Meldrum DR, Dupuis J, Long CS, Rubin LJ, Smart FW, Suzuki YJ, Gladwin M, Denholm EM, Gail DB. Right ventricular function and failure: report of a National Heart, Lung, and Blood Institute working group on cellular and molecular mechanisms of right heart failure. Circulation. 2006;114:1883–91.
6. Nootens M, Kaufmann E, Rector T, Toher C, Judd D, Francis GS, Rich S. Neurohormonal activation in patients with right ventricular failure from pulmonary hypertension: relation to hemodynamic variables and endothelin levels. J Am Coll Cardiol. 1995;26:1581–5.
7. Lucreziotti S, Gavazzi A, Scelsi L, Inserra C, Klersy C, Campana C, Ghio S, Vanoli E, Tavazzi L. Five-minute recording of heart rate variability in severe chronic heart failure: correlates with right ventricular function and prognostic implications. Am Heart J. 2000;139:1088–95.
8. Torbicki A, Kurzyna M, Kuca P, Fijalkowska A, Sikora J, Florczyk M, Pruszczyk P, Burakowski J, Wawrzynska L. Detectable serum cardiac troponin T as a marker of poor prognosis among patients with chronic precapillary pulmonary hypertension. Circulation. 2003;108:844–8.
9. Rousseau MF, Gurne O, Duprez D, Van MW, Robert A, Ahn S, Galanti L, Ketelslegers JM. Beneficial neurohormonal profile of spironolactone in severe congestive heart failure: results from the RALES neurohormonal substudy. J Am Coll Cardiol. 2002;40:1596–601.
10. Rich S, Seidlitz M, Dodin E, Osimani D, Judd D, Genthner D, McLaughlin V, Francis G. The short-term effects of digoxin in patients with right ventricular dysfunction from pulmonary hypertension. Chest. 1998;114:787–92.
11. Galie N, Torbicki A, Barst R, Dartevelle P, Haworth S, Higenbottam T, Olschewski H, Peacock A, Pietra G, Rubin LJ, Simonneau G, Priori SG, Garcia MA, Blanc JJ, Budaj A, Cowie M, Dean V, Deckers J, Burgos EF, Lekakis J, Lindahl B, Mazzotta G, McGregor K, Morais J, Oto A, Smiseth OA, Barbera JA, Gibbs S, Hoeper M, Humbert M, Naeije R, Pepke-Zaba J. Guidelines on diagnosis and treatment of pulmonary arterial hypertension. The Task Force on Diagnosis and Treatment of Pulmonary Arterial Hypertension of the European Society of Cardiology. Eur Heart J. 2004;25:2243–78.
12. Dekker DL, Piziali RL, Dong E Jr. A system for ultrasonically imaging the human heart in three dimensions. Comput Biomed Res. 1974;7:544–53.

13. Papavassiliou DP, Parks WJ, Hopkins KL, Fyfe DA. Three dimensional echocardiographic measurement of the right ventricular volume in children with congenital heart disease validated by magnetic resonance imaging. J Am Soc Echocardiodr. 1998;11:770–7.
14. Chauvel C, Bogino E, Clerc P, Fernandez G, Vernhet JC, Becat A, et al. Usefulness of three dimensional echocardiography fort the evaluation of mital prolaps. J Heart Valve Dis. 2000;9:341–9.
15. Sinha A, Nanda NC, Misra V, Khanna D, Dod HS, Vengala S, et al. Live three dimensional transthoracic echocardiographic assessment of transcatheter closure of atrial septal defect and patent foramen ovale. Echocardiography. 2004;21:749–53.
16. Ishii M, Hashino K, Eto G, Tsutsumi T, Himeno W, Sughara Y, et al. Quantitative assessment of severity of ventricular septal defect by three dimensional reconstruction of color Doppler imaged vena contracta and flow convergence region. Circulation. 2001;103:664–9.
17. Dolk H, Loane M, Garne E. Congenital heart defects in Europe: prevalence and perinatal mortality, 2000 to 2005. Circulation. 2011;123:841–9. https://doi.org/10.1161/CIRCULATIONAHA.110.958405.
18. Giroud JM, Jacobs JP, Spicer D, Backer C, Martin GR, Franklin RC, et al. Report from the international society for nomenclature of paediatric and congenital heart disease: creation of a visual encyclopedia illustrating the terms and definitions of the international pediatric and congenital cardiac code. World J Pediatr Congenit Heart Surg. 2010;1(3):300–13. https://doi.org/10.1177/2150135110379622.
19. Binder TM, Moertl D, Mundigler G, Rehak G, Franke M, Delle-Karth G, et al. Stereolithographic biomodeling to create tangible hard copies of cardiac structures from echocardiographic data: in vitro and in vivo validation. J Am Coll Cardiol. 2000;35:230–7.
20. Gilon D, Cape EG, Handschumacher MD, Song JK, Solheim J, VanAuker M, et al. Effect of three-dimensional valve shape on the hemodynamics of aortic stenosis: three-dimensional echocardiographic stereolithography and patient studies. J Am Coll Cardiol. 2002;40(8):1479–86.
21. Mottl-Link S, Boettger T, Krueger JJ, Rietdorf U, Schnackenburg B, Ewert P, et al. Images in cardiovascular medicine. Cast of complex congenital heartmalformation in a living patient. Circulation. 2005;112:e356–7.
22. Kim MS, Hansgen AR, Wink O, Quaife RA, Carroll JD. Rapid prototyping: a new tool in understanding and treating structural heart disease. Circulation. 2008;117(18):2388–94. https://doi.org/10.1161/CIRCULATIONAHA.107.740977.
23. Armillotta A, Bonhoeffer P, Dubini G, Ferragina S, Migliavacca F, Sala G, et al. Use of rapid prototyping models in the planning of percutaneous pulmonary valved stent implantation. Proc Inst Mech Eng H. 2007;221(4):407–16.
24. Costello JP, Olivieri LJ, Krieger A, Thabit O, Marshall MB, Yoo SJ, et al. Utilizing three-dimensional printing technology to assess the feasibility of high fidelity synthetic ventricular septal defect models for simulation in medical education. World J Pediatr Congenit Heart Surg. 2014;5(3):421–6. https://doi.org/10.1177/2150135114528721.
25. Kim MS, Hansgen AR, Carroll JD. Use of rapid prototypingin the care of patients with structural heart disease. Trends Cardiovasc Med. 2008;18(6):210–6. https://doi.org/10.1016/j.tcm.2008.11.001.
26. Jacobs S, Grunert R, Mohr FW, Falk V. 3D-Imaging of cardiac structures using 3D heart models for planning in heart surgery: a preliminary study. Interact Cardiovasc Thorac Surg. 2008;7(1):6–9.
27. Biglino G, Capelli C, Wray J, Schievano S, Leaver LK, Khambadkone S, et al. 3D-manufactured patient-specific models of congenital heart defects for communication in clinical practice: feasibility and acceptability. BMJ Open. 2015;5(4):e007165. https://doi.org/10.1136/bmjopen-2014-007165.

Index

S. I. Dumitrescu et al. (eds.), *Right Heart Pathology*, https://doi.org/10.1007/978-3-319-73764-5

I